NUCLEAR SCIENCE ABSTRACTS

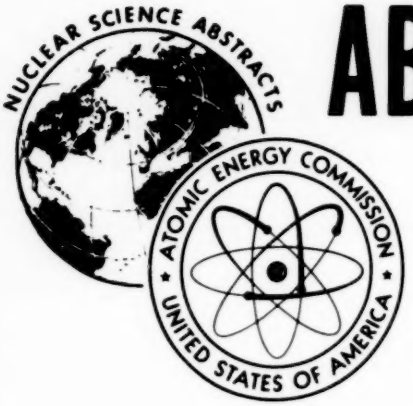

Volume 25 Number 15

Abstracts 34500-37258

August 15, 1971

UNITED STATES ATOMIC ENERGY COMMISSION
Division of Technical Information

REPORT COLLECTIONS IN THE UNITED STATES

The libraries listed below purchase and maintain microfiche collections of USAEC and foreign reports that are abstracted in *NSA*. Their collections also include *NSA* and its indexes, AEC's Technical Progress Reviews, AEC-sponsored translations, conference proceedings published by AEC, and various bibliographic tools. Most of these libraries have microfiche reader-printers or other photocopy facilities with which to reproduce enlarged copies from microfiche. Charges for reproduction services vary.

ALABAMA
Auburn, Auburn University
Tuskegee Institute, Tuskegee Institute

ALASKA
College, University of Alaska

ARIZONA
Tucson, University of Arizona

ARKANSAS
Fayetteville, University of Arkansas

CALIFORNIA
Davis, University of California
Los Angeles, University of California

COLORADO
Boulder, University of Colorado

DISTRICT OF COLUMBIA
Washington, Library of Congress (by deposit)

FLORIDA
Gainesville, University of Florida

GEORGIA
Atlanta, Georgia Institute of Technology

HAWAII
Honolulu, University of Hawaii

IDAHO
Pocatello, Idaho State University

ILLINOIS
Evanston, Northwestern University
Urbana, University of Illinois

INDIANA
Lafayette, Purdue University

IOWA
Ames, Iowa State University

KANSAS
Manhattan, Kansas State University

KENTUCKY
Lexington, University of Kentucky
Louisville, University of Louisville

LOUISIANA
Baton Rouge, Louisiana State University
New Orleans, Tulane University

MARYLAND
Baltimore, Johns Hopkins University
College Park, University of Maryland

MASSACHUSETTS
Cambridge, Massachusetts Institute of Technology
Worcester, Worcester Polytechnic Institute

MICHIGAN
Ann Arbor, University of Michigan

MISSISSIPPI
State College, Mississippi State University

MISSOURI
Kansas City, Linda Hall Library

NEVADA
Las Vegas, University of Nevada

NEW JERSEY
Princeton, Princeton University

NEW MEXICO
Albuquerque, University of New Mexico

NEW YORK
Albany, New York State Library
Albany, State University at Albany
Buffalo, State University of New York at Buffalo
Ithaca, Cornell University
New York, Columbia University
Rochester, University of Rochester
Syracuse, Syracuse University
Troy, Rensselaer Polytechnic Institute

NORTH CAROLINA
Raleigh, North Carolina State University

OHIO
Cincinnati, University of Cincinnati
Cleveland, Cleveland Public Library
Columbus, Ohio State University
Toledo, University of Toledo

OKLAHOMA
Norman, University of Oklahoma

PENNSYLVANIA
Philadelphia, University of Pennsylvania
Pittsburgh, Carnegie Library
University Park, Pennsylvania State University

PUERTO RICO
San Juan, University of Puerto Rico

SOUTH CAROLINA
Columbia, University of South Carolina

TENNESSEE
Knoxville, University of Tennessee
Nashville, Joint University Libraries
Oak Ridge, Oak Ridge Associated Universities

TEXAS
Austin, University of Texas
College Station, Texas A & M University
Houston, Rice University

UTAH
Salt Lake City, University of Utah

VIRGINIA
Blacksburg, Virginia Polytechnic Institute
Charlottesville, University of Virginia

WASHINGTON
Pullman, Washington State University
Seattle, University of Washington

WEST VIRGINIA
Morgantown, West Virginia University

WISCONSIN
Madison, University of Wisconsin

WYOMING
Laramie, University of Wyoming

The following governmental and international organizations offer for sale USAEC reports abstracted in *Nuclear Science Abstracts:*

National Technical Information Service, U. S. Department of Commerce
Springfield, Virginia 22151
International Atomic Energy Agency, Vienna, Austria
National Lending Library, Boston Spa, England

XUM

Volume 25, Number 15, August 15, 1971

NUCLEAR SCIENCE ABSTRACTS

A semimonthly publication of the USAEC Division of Technical Information, Edward J. Brunenkant, Director, Published by the USAEC Division of Technical Information Extension, Robert L. Shannon, Extension Manager.

Nuclear Science Abstracts provides the only comprehensive abstracting and indexing coverage of international nuclear science literature. *Nuclear Science Abstracts* covers scientific and technical reports of the U. S. Atomic Energy Commission and its contractors, other U. S. Government agencies, other governments, universities, and industrial and research organizations. In addition, books, conference proceedings, individual conference papers, patents, and journal literature on a worldwide basis are abstracted and indexed. Each issue of *Nuclear Science Abstracts* includes four indexes: subject, personal author, corporate author, and report number.

The following organizations scan and abstract the nuclear science literature in their respective countries:

Atomic Energy of Canada Limited
Australian Atomic Energy Commission
Danish Atomic Energy Commission
Finnish Atomic Energy Commission
French Atomic Energy Commission
Japan Atomic Energy Bureau–Atomic Energy Research Institute
Institutt for Atomenergi (Norway)
Aktiebolaget Atomenergi (Sweden)
United Kingdom Atomic Energy Authority

Numerous organizations, societies, and publishers throughout the world provide *Nuclear Science Abstracts* with advance page-proof copy of their publications, e.g., in the United States the American Institute of Physics provides page-proof copy of its publications.

A list of the journals scanned regularly and the abbreviations used appears in Issue 1 (January 15) of each volume of *Nuclear Science Abstracts* and is supplemented in Issues 7, 13, and 19. Issue 1 of each volume also describes the scope and arrangement of the subject matter covered in *Nuclear Science Abstracts*. The subject matter covered is also described in TID-4552, *Subject Scope of Nuclear Science Abstracts*, available free from the USAEC Division of Technical Information Extension, P.O. Box 62, Oak Ridge, Tennessee 37830. An outline of the subject categories appears in the Contents of each issue.

AVAILABILITY OF PUBLICATIONS ABSTRACTED

Public availability of all U. S. Atomic Energy Commission reports is indicated in the report number indexes. The availability of other reports, when known, is also indicated. The availability of some unnumbered reports is given in the abstract.

Dissertations abstracted in *Dissertation Abstracts* and included in *Nuclear Science Abstracts* are available from University Microfilms, Inc., 315 N. First Street, Ann Arbor, Michigan 48103.

Information on the availability of the published literature and unpublished conference papers abstracted in *Nuclear Science Abstracts* can be obtained from the USAEC Division of Technical Information Extension, P.O. Box 62, Oak Ridge, Tennessee 37830.

HOW TO OBTAIN NUCLEAR SCIENCE ABSTRACTS

Nuclear Science Abstracts is available to the public on a subscription basis from the Superintendent of Documents, U. S. Government Printing Office, Washington, D. C. 20402.

For the 24 regular issues, the yearly rate is $42.00 for domestic subscribers and $52.50 for foreign subscribers. A single issue costs $1.75, domestic rates, or $2.19, foreign rates. Domestic rates apply to the United States, Canada, Mexico, and Central and South American countries except Argentina, Brazil, Guyana, French Guiana, Surinam, and British Honduras.

For a yearly subscription to the cumulative indexes, the rates are $38.00 for domestic subscribers and $47.50 for foreign subscribers.

The following cumulative indexes are available:

From Johnson Reprint Corporation, 111 Fifth Avenue, New York, N. Y. 10003:

Vols. 1–4, Subjects and Authors (1948–1950), $30.00.

From Superintendent of Documents, U. S. Government Printing Office, Washington, D. C. 20402:

Vols. 5–10, Subjects and Authors (1951–1956), $5.25.

Vols. 11–15, Subjects (1957–1961), $19.00.
Vols. 11–15, Personal Authors (1957–1961), $14.25.
Vols. 11–15, Corporate Authors (1957–1961), $2.50.

Vols. 16–20, Subjects (1962–1966), $36.00.
Vols. 16–20, Personal Authors (1962–1966), $22.50.
Vols. 16–20, Corporate Authors (1962–1966), $3.75.

Vol. 21, Subjects and Authors (1967), $16.00.
Vol. 22, Subjects and Authors (1968), $26.00.
Vol. 23, Subjects and Authors (1969), $25.75.
Vol. 24, Subjects and Authors (1970), $22.50.

Cumulative Report Number Index, Vols. 1-15 Revised, $4.00.
Cumulative Report Number Index, Vols. 16-20 Revised, $5.50.
Cumulative Report Number Index, Vols. 21-24, $4.25.

Nuclear Science Abstracts is available on an exchange basis to universities, research institutions, industrial firms, and publishers of scientific information. Government agencies may obtain *NSA* free of charge. Inquiries should be directed to the USAEC Division of Technical Information Extension, P. O. Box 62, Oak Ridge, Tennessee 37830.

XUM

INDEXES TO NSA

Comprehensive indexes appear in each issue and are cumulated quarterly and annually. Multivolume cumulations have been issued as indicated above.

All documents abstracted are indexed by subjects and personal authors. Report literature is indexed also by corporate author and report number. Each of these indexes in every issue is preceded by an introduction explaining in detail the organization of the index and the principles by which it is compiled. The reader is referred to these explanations for information not found in the brief summary below.

Personal Authors

Each author's name is indexed in the form appearing on the document abstracted:

ISHIHARA, T., Accumulation of fallout ^{137}Cs in newborn infants, 23:50538
ISHIHARA, Toyokuki, Shielding effect of paraffin, water, soil, concrete, Fe, and Pb for high-energy neutrons, 23:51748

Subjects

The subject index consisting of specific materials, objects, and processes is arranged alphabetically. Modifying phrases specific to these subjects in turn are arranged alphabetically under the subjects.

MELPHALAN
  effects on proliferation of cultured antigen-stimulated spleen cells from mice, dose-response curve for, 23:50820
MEMBRANE FILTERS
  design for removal of cell-free Streptococcus faecalus from bacteria cultures in fermentation tank, 23:49996 (UCRL-18667, pp 322-9)
MENDELEVIUM
  separation from einsteinium and fermium by electrolysis, 23:49772 (UCRL-18667, pp 277-312)
  separation from sodium acetate solutions by solvent extraction using sodium amalgam, 23:49772 (UCRL-18667, pp 277-312)
  stability of divalent state of, 23:49772 (UCRL-18667, pp 277-312)

Corporate Authors

Technical report literature is indexed from the name of the organization or institution responsible for the issuance of the report.

51093 (LA-4164) FABRICATION OF BORON CARBIDE RINGS AND DISKS. Sheinberg, H.; Herrera, T.; Kostacopoulos, J. (**Los Alamos Scientific Lab., N. Mex.**). Apr. 25, 1969. Contract W-7405-eng-36. 11p. Dep. CFSTI.

is indexed as:

LOS ALAMOS SCIENTIFIC LAB., N. MEX.
  Fabrication of boron carbide rings and disks, 23:51093 (LA-4164)

Report Numbers

Technical report literature is also indexed by report numbers. This index includes information on where individual reports may be obtained. While not reports, patents and conference papers are indexed here as a matter of convenience.

JPRS-	**(Non-AEC)**	
46949	23-51587	CFSTI
48330	23-52305	CFSTI
48331	23-52451	CFSTI
48481	23-50889	CFSTI
48743	23-51034	CFSTI
49025	23-51706	CFSTI (U. S. Sales Only)
JUL-	**(German)**	
571-RG	23-52269	Dep
578-PP	23-51624	Dep. CFSTI (U. S. Sales Only)
581-FN	23-51079	Dep. CFSTI (U. S. Sales Only)
584-RG	23-52313	Dep
586-FN	23-51035	Dep. CFSTI (U. S. Sales Only)
K-		
1777	23-50987	Dep. CFSTI
1778	23-50988	Dep. CFSTI
KFK-	**(German)**	
743	23-52461	Dep
743	23-52447	For translation see EURFNR-613
781/I	23-52462	Dep
824	23-52397	Dep. CFSTI (U. S. Sales Only)

XUM

TABLE OF CONTENTS

Volume 25, Number 15, August 15, 1971

Category	Page
CHEMISTRY	3401
Analytical Chemistry	3401
Chemical and Spectral Procedures	3401
Isotope Dilution Procedures	3404
Radiometric and Radiochemical Procedures	3404
Activation Procedures	3405
Inorganic, Organic, and Physical Chemistry	3406
Chemical Properties	3406
Isotope Effects and Exchange	3408
Physical Chemistry	3411
Radiation and Nuclear Chemistry	3412
Radiation Effects	3412
Radiation Processes	3413
Radiolysis	3414
Radioisotope Production	3417
Recoil Production and Reactions	3418
Radiochemistry	3418
Separation Processes	3418
EARTH SCIENCES	3423
Geology and Hydrology	3423
Meteorology	3426
Mineralogy and Exploration	3426
Oceanography	3427
Seismology	3428
ENGINEERING	3429
Nuclear Explosions	3429
Facilities and Equipment	3429
Heat Transfer and Fluid Flow	3431
Isotope Technology	3433
Materials Testing	3434
Radioactive Material Handling	3436
Vacuum Engineering	3438
INSTRUMENTATION	3439
Radiation Detection Instruments	3439
General Detectors and Monitors	3439
Nuclear Spectroscopic Instrumentation	3443
High Energy Physics Instrumentation	3445
Radiation Dosimeters	3453
Radiometric Instruments	3454
Miscellaneous Instruments and Components	3455
Radiation Effects on Instruments and Instrument Components	3457
LIFE SCIENCES	3459
Biochemistry, Physiology, and Molecular Biology	3459
Basic Processes	3459
Metabolism, Physiology, and Toxicology	3459
Radiation Effects	3461
Immunology	3462
Ecology	3462
Genetics and Cytogenetics	3462
Health Physics and Safety	3464
Radioactive Contamination and Decontamination	3464
Dosimetry and Monitoring	3464

Category	Page
LIFE SCIENCES (Cont'd.)	
Radiation Protection	3465
Safety Procedures	3466
Medicine	3466
Protective Substances	3466
Radiodiagnosis	3467
Radiotherapy	3469
Radiation Effects on Animals	3470
Vertebrates	3472
Man	3475
Radiation Effects on Plants	3475
Radiation Effects on Microorganisms	3477
Radiosterilization and Radiopreservation	3478
METALS, CERAMICS, AND OTHER MATERIALS	3479
Metals and Alloys	3479
Corrosion and Erosion	3479
Preparation and Fabrication	3481
Properties Evaluations	3484
Structure and Phase Studies	3499
Radiation Effects	3501
Ceramics and Cermets	3503
Corrosion and Erosion	3503
Preparation and Fabrication	3504
Properties Evaluations	3506
Structure and Phase Studies	3508
Radiation Effects	3509
Plastics and Other Materials	3510
PHYSICS (GENERAL)	3511
Astrophysics and Cosmology	3511
Cosmic Ray Exposure Ages	3511
Stars	3511
Quasi-Stellar, Radio, and X-Ray Sources	3518
Solar Phenomena	3522
Galaxies	3528
Cosmology	3531
Planetary Phenomena	3533
Atomic and Molecular Physics	3534
Atomic, Electron, Ion, and Molecular Beams and Their Reactions	3534
Atomic and Molecular Properties	3535
Positronium, Muonium, and Mesic Atoms and Molecules	3536
Collision Phenomena	3536
Atomic Theory	3540
Cosmic Radiation	3540
Direct Energy Conversion	3544
Fluid Physics	3545
Geophysics (Upper Atmosphere)	3546
Low-Temperature Physics and Cryogenic Equipment	3553
Superfluidity	3553
Superconductivity	3554
Equipment and Devices	3559
Plasma and Thermonuclear Physics	3560
Confinement and Heating	3560
Diagnostics	3560

XUM

TABLE OF CONTENTS (continued)

Category	Page
PHYSICS (GENERAL) (Cont'd.)	
Kinetics (General)	3562
Kinetics (Experimental)	3563
Kinetics (Theoretical)	3564
Production	3565
Stability	3567
Thermonuclear Processes	3569
Wave Phenomena	3572
Shielding	3575
Solid-State Physics	3577
Radiation Effects	3577
Physical Properties	3582
Moessbauer Effects and NMR	3585
Theory	3586
Theoretical Physics	3586
PHYSICS (HIGH-ENERGY)	3589
Particle Interactions and Properties (Experimental)	3589
Electromagnetic	3589
Weak	3589
Strong (Baryon-Induced)	3590
Strong (Meson-Induced)	3591
Particle Interactions and Properties (Theoretical)	3593
General	3593
Electromagnetic	3594
Weak	3595
Strong (General)	3597
Strong (Baryon No. = 0)	3598
Strong (Baryon No. = 1)	3599
Strong (Baryon No. ≥ 2)	3601
Particle Invariance Principles and Symmetries	3603
General	3603
Applications (Electromagnetic and Weak)	3604
Applications (Strong)	3604
Field Theories	3604
General	3604
Quantum Field Theory	3604
Gravitation and General Relativity	3606
Scattering Theory	3607
Particle Accelerators	3608
PHYSICS (NUCLEAR)	3612
Neutron Interactions with Matter	3612
Nuclear Properties and Reactions, A ≤ 5	3613

Category	Page
PHYSICS (NUCLEAR) (Cont'd.)	
Nuclear Properties and Reactions, 6 ≤ A ≤ 19	3614
Nuclear Properties and Reactions, 20 ≤ A ≤ 89	3615
Nuclear Properties and Reactions, A ≥ 90	3618
Nuclear Theory	3627
REACTOR TECHNOLOGY	3631
Commercial Power Reactors	3631
Operation and Economics	3631
Safety and Siting	3633
Steam and Power Conversion Systems	3637
Power Reactor Development	3637
Kinetics and Dynamics	3638
Control Systems	3639
Shielding	3639
Cooling Systems	3639
Fuels	3641
Auxiliary and Emergency Systems	3642
Operation and Economics	3642
Safety and Siting	3643
Power Conversion Systems	3644
Research and Test Reactors	3644
Rocket and Space Reactors	3648
Process Heat and Desalination Reactors	3648
Marine and Portable Power Reactors	3648
Production Reactors	3649
Reactor Theory	3649
Kinetics	3650
Experimental Applications	3652
Reactor Components, Fuels, and Accessories	3653
GENERAL	3655
CORPORATE AUTHOR INDEX	INDEX-1
PERSONAL AUTHOR INDEX	INDEX-13
SUBJECT INDEX	INDEX-69
REPORT NUMBER INDEX	INDEX-165

XUM

STAFF OF NUCLEAR SCIENCE ABSTRACTS

John W. Norris
Managing Editor

Donald D. Davis
Assistant Managing Editor

David E. Bost
Production Manager

Sidney F. Lanier
Subject Heading Specialist

J. Paul Meredith
Descriptive Cataloging Specialist

Frederick E. Marsh, Jr.
Computer Index Coordinator

Clara L. Fox
Corporate Author Specialist

Helen W. White
Report Number Specialist

Section Editors

Everett J. Hoffman
Chemistry

Robert C. Kelly
Engineering; Earth Sciences; Metals, Ceramics, and Other Materials

Lee M. Thompson
General Physics

Charles E. Stuber
High Energy Physics; Instrumentation

Donald D. Davis
Life Sciences

Lawrence T. Whitehead
Nuclear Physics

James M. Jacobs
Reactor Technology

Evaluators

Thomas S. Chapman
Rose V. Jermain
John H. Mitchell
Mary H. Newman
Polly C. Summers

Abstractors

F. S. Armstrong*
Ellis R. Bedford
Mary M. Brown
Jane G. Buchanan
D. Lamar Cason
Gloria M. Caton
David C. Cunningham
James R. Dulaney
Helga B. Gerstner
Mary C. Grissom
Phyllis C. Hansen
Carolyn D. Houston
Elaine E. Huber
Rose V. Jermain
W. Hugh Kinser, Jr.
Lisbeth C. Lieberman
Betty L. McDowell
Patricia B. McEwen
Fay M. Martin
William D. Matheny
Dora H. Moneyhun
Jean F. Peckham
Henry D. Raleigh
Mona H. Raridon
Julia S. Redford
Jessie W. Rushing
Robert W. Rutkowski
Francis L. Sachs
Lila B. Smith
Anne G. Ward
Helen L. Ward
Milton O. Whitson
Juanita Wilson

*Atomic Energy of Canada, Ltd.

Charles R. Bruce
Publishing Coordinator

Communication concerning the editorial policy and content of *Nuclear Science Abstracts* should be addressed to the Managing Editor, *Nuclear Science Abstracts*, USAEC Division of Technical Information Extension, P. O. Box 62, Oak Ridge, Tennessee 37830.

Use of funds for printing this publication approved by the Director of the Bureau of the Budget, June 26, 1969.

XUM

Volume 25, Number 15 August 15, 1971

NUCLEAR SCIENCE ABSTRACTS

CHEMISTRY

Analytical Chemistry

Refer also to abstracts 35070 and 35303.

34500 METHODS FOR ANALYSIS OF THE RADIOACTIVITY IN THE SOIL. de Bortoli, M. C. (CCR-EURATOM, Ispra, Italy). Minerva Fisiconucl.; 13: 86-92(Jan-Mar 1969). (In Italian). (CONF-680535-10).

From fourteenth national conference of the Italian Association for Health Physics and Protection from Radiation; Formia, Italy (29 May 1968).

Some of the analytical methods used at the Protection Service of the Euratom Ispra Establishment for the surveillance of soil radioactivity are described. The radioisotopes of strontium, cesium, and plutonium can be determined on a single soil aliquot by appropriate chemical procedures. Measurements of the uranium concentration are performed through a fluorimetric technique. Some comments, deriving from the experience gained through the routine exploitation of the methods described, are reported. (auth)

Chemical and Spectral Procedures

Refer also to abstracts 34721, 34722, 35043, and 35057.

34501 (CEA-tr-X-667) POLAROGRAPHIC ANALYSIS OF HEXAVALENT URANIUM IN URANIUM DIOXIDE. Nakajima, F. Translated from Jap. Anal.; 9: 961-3(1960). 10p. (In French). Dep. NTIS (U. S. Sales Only).

A method for polarographic determination of U^{6+} in UO_2 and U_3O_8 was developed. The sample is boiled with concentrated phosphoric acid and then diluted. The U^{6+} is determined polarographically. The determination of U^{6+} in U_3O_8 gave a molar ratio of $U(VI)/(U)_t = 0.66$. U^{6+} is contained in U_3O_8 in the proportion $U(IV) : U(VI) = 1 : 2$. The results obtained for the ratio O/U in UO_2 are tabulated. The effects of the dilution method, degree of boiling, storage in air, and quantity of sample on the polarographic analysis were determined. (J.S.R.)

34502 (INR-1247) PHYSICO-CHEMICAL PROPERTIES OF THE LANTHANIDE COMPLEXES WITH THENOYLTRIFLUOROACETONE. I. THE HYDRATION-DEHYDRATION PROPERTIES AND THERMAL STUDY OF THE $Ln(TTA)_3.nH_2O$ COMPLEXES. Lis, S.; Siekierski, S. (Institute of Nuclear Research, Warsaw (Poland)). 1970. 14p. Dep. NTIS (U. S. Sales Only).

The complexes of all the lanthanides (excluding Pm) with thenoyltrifluoroacetone (TTA) of a general formula $Ln(TTA)_3 \cdot nH_2O$ were prepared. Results of elemental analysis and titration with K. Fischer reagent show a different degree of hydration from La to Lu. The dehydration process, its reversibility, and the thermal behavior of these compounds were studied. (auth)

34503 (NBL-256) SUMMARY OF THE RESULTS OF THE GENERAL ANALYTICAL EVALUATION PROGRAM, JANUARY-DECEMBER 1969. Rodden, C. J.; Jacob, E. H. (New Brunswick Lab. (AEC), N. J.). Sep 1970. 29p. Dep. NTIS.

Analytical results on PuO_2-UO_2 material were compared over a considerable range of plutonium content. Information was obtained on the stability of a mixed oxide containing 17.6% Pu by analyzing it at various times over the course of a year. Ten laboratories used various analytical methods and relative differences from the monthly mean are given. (M.C.G.)

34504 (NP-18865) SPECTROSCOPIC ANALYSIS OF URANIUM OXIDE: USE OF HALOGENATED CARRIERS. Ranquet, Pierre (Grenoble Univ. (France), Faculte des Sciences). 1970. 87p. (In French). Dep. NTIS (U. S. Sales Only).

Thesis.

In analysis of materials by emission spectroscopy, compounds were added to the sample subjected to the excitation of an electric arc in order to improve the precision of the determination. The mechanisms demonstrating the effect produced by the addition of these substances are discussed. The particular ease of determining the impurities in U_3O_8 was considered. After reviewing data on the continuous arc, the experimental methods used are described and some theoretical considerations from which the phenomena studied can be predicted are given. The experimental results are described: volatilization curves in the presence of silver halides, or silver halides and C; volatilization curves obtained with various carriers (chlorides, fluorides, $AgCl-SrF_2$ mixture). The effect of theoretical predictions on the choice of a carrier was examined. Some results on spectroscopic charge temperature and excitation conditions in the arc are described in an appendix. (France)

34505 (PG-Report-1020) ANALYTICAL METHOD FOR THE GENERAL GRAVIMETRIC DETERMINATION OF URANIUM IN ORES AND CONCENTRATES. (United Kingdom Atomic Energy Authority, Springfields (England). Production Group). 1971. 9p. Dep. NTIS (U. S. Sales Only).

Supersedes PG-Report-128.

A portion of the sample is dissolved in nitric acid, evaporated to dryness, and dissolved in a mixed nitrate solvent. The uranyl nitrate is eluted from a cellulose column while the impurities remain on the column. Uranium in the eluate is precipitated as ammonium diuranate, which is dried and ignited to U_3O_8. (auth) (UK)

34506 NEW REAGENTS FOR THE EXTRACTION-PHOTOMETRIC DETERMINATION OF TANTALUM. Tarayan, V. M.; Ovsepyan, E. N.; Barkhudaryan, S. R. (Erevan State Univ.). Arm. Khim. Zh.; 23: 596-601(1970). (In Russian).

The reaction of the fluorotantalate anion with three thiazine cation dyes, dimethylthionine (I), trimethylthionine (II), and toluidine blue (III), was investigated. The ratio of $[TaF_6]^-$/thiazine dye in the product was 1/1 in all cases. The resulting reaction mixtures were extracted with dichloroethane-trichloroethylene and dichloroethane-CCl_4, and the optimum acidity of the aqueous phase was established. Light absorption maxima for the three respective $[TaF_6]^-$ complexes were: I = 650 to 655, II = 660, and III = 665 to 660 nm, and the corresponding molar extinction coefficients were 3.6×10^4, 6.2×10^4, and 4.7×10^4. (tr-auth)

34507 INDIRECT COLORIMETRIC DETERMINATION OF EUROPIUM IN SAMARIUM AND OTHER RARE-EARTH OXIDES. Nowicka-Jankowska, Teresa; Szyszko, Helena (Inst. of Nuclear Research, Warsaw). Chem. Anal. (Warsaw); 16: No. 1, 3-8(1971).

The rare earth solution containing Eu ions is passed through a cadmium column into an excess of ferric chloride. Ferric ions equivalent to Eu(II) are reduced to ferrous ions and determined colorimetrically. Ce interferes and must be separated prior to the determination if its content is more than 5 times that of Sm. The determination of down to 0.02% Eu in SmO_2 was verified. (J.G.B.)

34508 ARSENATE METHOD FOR A MICRO IODOMETRIC DETERMINATION OF SCANDIUM. Shakhtakhtinskii, G. B.;

XUM

Baliev, B. S.; Aslanov, G. A.; Nadzhafkulev, N. A. (Inst. of Inorganic and Physical Chemistry, Baku). Azerb. Khim. Zh.; No. 3, 118-21(1970). (In Russian).

A volumetric determination of Sc by micro-iodometry is described. The micro method differs from the older macro method by incorporating a displacement of air by passage of CO_2 before titration with arsenic acid. Prolonged hot digestion of the precipitate is also recommended. For amounts of Sc less than 0.015 mg, precipitation is incomplete. (tr-auth)

34509 INVESTIGATION OF THE REACTION OF ACID COMPLEXES OF URANIUM(VI) WITH BASIC DYES: METHYL GREEN. Tarayan, V. M.; Ovsepyan, E. N.; Petrosyan, A. A. (Erevan State Univ.). Arm. Khim. Zh.; 23: 501-5(1970). (In Russian).

An extraction-photometric method for U determination is given. The reaction mixture of the benzoic acid complex of U(VI) with methyl green was extracted with benzene, and the molar coefficient of absorption was found to be 9.7×10^4. (tr-auth)

34510 GRAVIMETRIC DETERMINATION OF THE SUM OF NIOBIUM AND TANTALUM IN THE PRODUCTS OF TANTALUM ORE PROCESSING AFTER THEIR ISOLATION BY EXTRACTION. Chwastowska, Jadwiga; Szymczak, Swietlana (Inst. of Nuclear Research, Warsaw). Chem. Anal. (Warsaw); 16: No. 1, 144-51 (1971). (In Polish).

Extraction of niobium and tantalum from HF and H_2SO_4 solutions in the concentration range of 2 to 6M H_2SO_4 and 1 to 10M HF, respectively, was investigated with the aid of radioactive tracers ^{182}Ta and ^{95}Nb. The extraction of Nb and Ta was quantitative in the HF concentration range examined if the concentration of H_2SO_4 was not lower than 4M. Consequently the medium of 4M H_2SO_4 and 1M HF was chosen as an optimum one for quantitative extraction of Nb and Ta. Selectivity of extraction was examined by carrying out the extraction in the presence of iron, manganese, titanium, aluminum, and tin and controlling the purity of the Nb–Ta fraction spectrographically. It was found that if quantities of accompanying elements are of the same order as those of Nb and Ta (100 mg) the extraction should be carried out from a 3M HF to 4M H_2SO_4 medium to assure the desired purity of extracts. The final determination of the sum of Nb and Ta was carried out by precipitating hydroxides with concentrated ammonia in the medium of methyl isobutyl ketone with the addition of acetone as a dehydrating agent. The maximum error of determination did not exceed 1.5%. (auth)

34511 DIRECT SPECTROGRAPHIC DETERMINATION OF SMALL CONCENTRATION OF RARE EARTH ELEMENTS IN RARE EARTH OXIDES (CeO_2, La_2O_3, Nd_2O_3, Pr_6O_{11}, AND Sm_2O_3). Radwan, Zofia (Inst. of Nuclear Research, Warsaw). Chem. Anal. (Warsaw); 16: No. 1, 189-96(1971). (In Polish).

A mixture of rare earth oxides with graphite powder was excited in an atmosphere of oxygen and argon in a dc arc in the shallow crater of a graphite anode. Spectral lines of the matrix were selected as lines of internal standards. Background correction was necessary. Relative standard deviation s_r ranged from 0.1 to 0.2. Analytical data are tabulated. (auth)

34512 RAPID EXTRACTION OF ANTIMONY WITH TRIBUTYL PHOSPHATE. DIRECT PHOTOMETRIC DETERMINATION WITH BRILLIANT GREEN. Yadav, A. A.; Khopkar, S. M. (Indian Inst. of Tech., Bombay). Bull. Chem. Soc. Jap.; 44: No. 3, 693-6(Mar 1971).

A method was developed for the rapid extraction and direct photometric determination of antimony. With 20% TBP–toluene 3 to 15 μg of antimony is extracted from 2M hydrochloric acid containing 1M magnesium chloride. From the organic phase, antimony is directly determined photometrically at 640 nm as its complex with brilliant green. Antimony can be selectively extracted in the presence of a large number of cations and anions. The total operation requires only 20 min. (auth)

34513 SIMPLE AND INEXPENSIVE ELECTRONIC CONDUCTIVITY MANOMETER FOR MONITORING PRESSURE CHANGES. APPLICATION TO PRESSUREMETRIC TITRATIONS OF IODATE AND AMMONIUM IONS. Curran, D. J.; Swarin, S. J. (Univ. of Massachusetts, Amherst). Anal. Chem.; 43: 358-64(Mar 1971).

A novel pressure transducer system based on the electronic monitoring of the electrolyte level in a manometer with linear conductance circuitry has been developed. The instrument has a multirange capability and a high level dc output. It is simple in design and construction and can be built with readily available electronic units. Its response to the quantity of gas generated in a closed system is linear to within 2 to 4 parts per thousand. It was applied to the pressuremetric titrations of iodate with hydrazine sulfate and ammonium ion with electrogenerated hypobromite. Accuracies and precisions of a few parts per thousand have been obtained, down to the concentration level where only 12 μmoles of gas are evolved. (auth)

34514 DETERMINATION OF NITROGEN AND HYDROGEN AT PARTS-PER-MILLION LEVELS IN MILLIGRAM STEEL SAMPLES. Hargrove, G. L.; Shepard, R. C.; Farrar IV, Harry (Atomics International, Canoga Park, Calif.). Anal. Chem.; 43: 439-42(Mar 1971).

To determine hydrogen and nitrogen in steels that are to be exposed to fast neutrons, inert gas fusion methods were optimized and coupled with a high-sensitivity gas chromatograph to yield a micro inert gas fusion technique with more than the required sensitivity. By use of this technique, an analysis for both hydrogen and nitrogen contents, ranging from 1 to 1000 wt ppM, can be completed in 90 minutes. The technique is limited to samples where chemical decomposition is not required for the release of nitrogen and hydrogen, and therefore cannot be applied to the determination of nitrogen in Ti, Ta, and W. (D.P.O.)

34515 DETERMINATION OF ^{210}Po IN CIGARETTES AND TOBACCO. Lopes dos Santos, Pedro; Weinberg, Evelyn Miriam; Penna Franca, Eduardo (Istituto de Biofisica, Rio de Janeiro). Rev. Biol. Med. Nucl.; 2: 73-7(Jun-Oct 1970). (In Portuguese).

The process of natural fallout resulting from radon emanation from the soil, its decay in the atmosphere, and deposition of its long-lived daughter ^{210}Pb are the principal mechanisms by which leafy vegetables and tobacco are contaminated by ^{210}Pb. By its decay, ^{210}Po builds up in the vegetables. The ^{210}Po contents of tobacco leaves and products were determined. Since ^{210}Po is volatile at the temperature of a burning cigarette, part of its content in tobacco is inhaled by smokers. Therefore ^{210}Po may become the principal natural source of irradiation of bronchial epithelium of heavy smokers. ^{210}Po contents were determined in various tobacco products: cigarettes, cigars, and pipe tobacco of different brands manufactured in Brazil. The average contents of Brazilian cigarettes are about the same as the values found in the United States, Argentina, India, and Pakistan, above the ones observed in Indonesia, Turkey, and Greece, and below the ones found in Rhodesia, Australia, and Central America countries. (auth)

34516 SPECTROGRAPHIC DETERMINATION OF TUNGSTEN IN TUNGSTEN–MOLYBDENUM ALLOYS. Khlystova, A. D.; Kabesheva, E. T. Vestn. Mosk. Univ., Ser. II. Khim.; 12: 98-100(Jan-Feb 1971). (In Russian).

The spectrochemical determination of tungsten (20 to 50%) in tungsten–molybdenum alloys with preliminary chemical dilution was worked out. (auth)

34517 POTENTIOMETRIC DETERMINATION OF FREE NITRIC ACID IN THE PRESENCE OF URANYL, ALUMINUM, AND MAGNESIUM NITRATES. Chwastowska, Jadwiga; Skwara, Witold. Nukleonika; 15: 641-8(1970). (In Polish).

An alkalimetric method of determination of free nitric acid in the presence of uranyl, aluminum, and magnesium nitrates was developed. The end-point was recorded potentiometrically. Before titration the uranyl ions were complexed with ammonium sulfate and aluminum ions with potassium oxalate. The method makes possible the determination of nitric acid within the concentration range of 0.1 to 4 M in solutions containing 50 to 300 mg U/ml, 2 to 150 mg Al/ml, and 2 to 50 mg Mg/ml, respectively. The potentiometric curves showed a sharp pH kink at the equivalence point. (auth)

34518 ABSOLUTE ISOTOPIC SCALE FOR DEUTERIUM ANALYSIS OF NATURAL WATERS. ABSOLUTE D/H RATIO FOR SMOW. Hagemann, R.; Nief, G.; Roth, E. (CEN de Saclay, Gif-sur-Yvette, France). Tellus; 22: 712-5(1970).

The absolute isotopic ratios of the hydrogen content of two reference water standards called SMOW (Standard Mean Ocean Water) and SLAP (Standard Light Antarctic Precipitation) were measured to define an absolute isotopic scale. This isotopic scale can be used to normalize measurements of the natural isotopic variations in waters. The principle of the method used to define the zero of the scale is given. The absolute D/H ratios of SMOW and SLAP were measured by mass spectrometric comparison with calibration mixtures prepared in the laboratory. The following values are obtained: $(D/H)_{SMOW} = 155.76 \pm 0.05 \times 10^{-6}$, $(D/H)_{SLAP} = 89.02 \pm 0.05 \times 10^{-6}$, $\delta‰_{SLAP/SMOW} = 428.50 \pm 0.10$. Samples of about 20 cc of the reference standards SMOW and SLAP are available from the International Atomic Energy Agency, on request. (auth) (Sweden)

34519 CHEMICAL DETECTION OF ZIRCONIUM AND HAFNIUM. Sommer, L.; Katyal, M.; Pal, B. K.; Ryan, D. E. (Dal-

housie Univ., Halifax, Nova Scotia). Mikrochim. Acta; No. 6, 1181-9(1970).

Morin, 3-hydroxyflavone, and quercetin are suitable for the fluorescent detection of hafnium and zirconium under proper acidity and reagent concentration conditions. The most sensitive reagent for both metals is 3-hydroxyflavone. Substantially acid solutions are preferred for the reactions of hafnium and zirconium to increase selectivity despite decreasing reaction sensitivity. The hydroxylflavone hafnium chelates are more stable to acid than the zirconium chelates especially with morin and quercetin. The very low background fluorescence of quercetin permits the detection of hafnium in strong perchloric acid where the fluorescence of the other two reagents hinders detection. The effects of Al, In, Sc, Y, Sn, Ga, and Th ions on the procedure were studied. (auth)

34520 2-AMINOBENZOTHIAZOLE AS A GRAVIMETRIC REAGENT: MILLIGRAM LEVEL DETERMINATION OF MERCURY(II). Tandon, S. N.; Srivastava, P. K.; Joshi, S. R. (Univ. of Roorkee, India). Mikrochim. Acta; No. 6, 1208-13(1970).

Hg(II) was determined at the milligram level using 2-aminobenzothiazole as a gravimetric reagent. The interference of Pd(II) and V(V) can be suppressed by oxalate. Ag(I) and Au(III) interfere; the following ions do not: Na, K, Tl, Mg, Ca, Sr, Ba, Fe, Co, Ni, Cu, Zn, Pb, Cd, Mn, Sn, UO_2, Al, Cr, As, Sb, Bi, In, Ga, La, Sm, Sn, Th, Zr, Pt, and Mo. (J.G.B.)

34521 COLORIMETRIC DETERMINATION OF GOLD(III) USING 3-METHYL-4-VANILLIDINE ISOXAZOLONE-5. Hashmi, M. H.; Adil, A. Subhan; Viegas, A.; (and others) (Pakistan Council of Scientific and Industrial Research Labs., Lahore). Mikrochim. Acta; No. 6, 1214-19(1970).

A new colorimetric method for the determination of gold(III) was developed. Gold reacts with 3-methyl-4-vanillidine-isoxazolone-5 in basic media at 90° to produce a pink color which is specific. Cobalt and nickel do not interfere when present up to 4 fold. Maximum tolerable amounts of other metal ions, including UO_2^{2+}, Ru^{3+}, Ce^{3+}, Y^{3+}, Zr^{4+}, Ce^{4+}, and Mo^{6+}, were also studied. (auth)

34522 SEPARATION OF CERIUM FROM OTHER FISSION PRODUCTS BY EXTRACTION. Pfeifer, V. (Oesterreichische Studiengesellschaft fuer Atomenergie GmbH, Vienna). Mikrochim. Acta; No. 6, 1232-9(1970). (In German).

Trivalent cerium was separated from other fission products, utilizing the highly synergistic enhancement of its extraction by the mixture of thenoyltrifluoroacetone–trioctylphosphine oxide. Uranium, zirconium, and other elements that are also extracted remain in the organic phase when cerium is back-extracted into 1N acid solutions. Separation from other rare earth elements was not achieved. (Cesium and strontium were not among those elements extracted.) Optimal extraction conditions and the effects of various solvents and anions were investigated. Chloroacetate buffer can be used advantageously for adjusting the pH of the solution. High amounts of iron and cobalt interfere with the determination of cerium and must be separated by extraction of their thiocyanate complexes with methyl isobutyl ketone. (auth)

34523 ELECTRON BEAM MICROANALYSIS OF COMPLEX CARBIDES. Bloech, R.; Kulmburg, A. (Edelstahlwerke, Gebr. Boehler and Co., AG, Kapfenberg, Austria). Mikrochim. Acta; No. 6, 1240-6(1970). (In German).

Electron beam microanalysis makes possible the quantitative analysis of complex carbides in situ, if their particle diameter is not below 2 to 3 μm. In alloy systems with more than one species of carbide it is possible however to analyze each separately, provided that their proportion is not too low. A corresponding sample preparation, including specific etchings, especially potentiostatic etching, permits a simple differentiation of various carbides. In general, the quantitative analysis of the carbide-forming metals offers no great difficulties. An analysis of the C content of the carbides was not possible because the apparatus at our disposal was not suitable. Examples given are of carbides of the M_7C_3-type and MC in Fe–Cr–V–C cast alloys and also carbides of the M_6C-type and also MC in three hardened rapid steels. Cr, Mo, V, W, Co, and Fe contents were determined. (auth)

34524 REACTION OF URANYL NITRATE WITH ARSENAZO III IN NITRATE SOLUTION. Klygin, A. E.; Smirnova, I. D.; Kolyada, N. S. Zh. Neorg. Khim.; 15: 3304-9(Dec 1970). (In Russian).

It was established that, in nitrate solutions, uranyl nitrate forms the compound $UO_2(NO_3)_2H_3R$ with Arsenazo III, which has a formation constant of 3.36×10^4 and molar refraction coefficient of 6.16×10^4 at 650 nm. These data permitted optimum conditions to be established for determination of uranium using Arsenazo III. (tr-auth)

34525 SEPARATION OF Re FROM Mo AND W BY ACETONE EXTRACTION. Pilipenko, A. T.; Mubayadzhyan, M. A. Arm. Khim. Zh.; 23: 414-18(1970). (In Russian).

Acetone extraction of Re, W, and Mo from an alkaline medium was studied. The degree of removal of Re depends on the NaOH concentration, and attains a maximum at 20 to 25% NaOH. In agreement with this, complete removal of Re from Mo, W, and a number of other elements was achieved by a single scrubbing of an acetone extract with 20 to 25% NaOH solution. This work was made the basis of an analytical determination of Re. (tr-auth)

34526 POLAROGRAPHIC REDUCTION OF NIOBIUM IN HYDROCHLORIC ACID-THIOCYANATE MEDIUM. INFLUENCE OF FOREIGN CATIONS. Marchidan, Sofia; Dragulescu, C.; Facsko, Gh. (Center of Physical Chemistry, Bucharest). Rev. Roum. Chim.; 16: 399-409(Mar 1971).

The influence of some cations in the polarographic reduction of niobium in HCl-thiocyanate medium with acetone addition is considered. The action of iron, titanium, vanadium, molybdenum, tungsten, tantalum, and chromium from 1 : 0.1 to the 1 : 5 = Nb : M ratio was studied in order to establish the interference degree. Titanium, molybdenum, and chromium do not interfere. Tantalum does not noticeably modify the niobium wave up to the 1 : 0.5 ratio. Iron, vanadium, and especially tungsten cause interferences. (auth)

34527 ABSORPTION-SPECTROPHOTOMETRIC DETERMINATION OF CERTAIN RARE EARTH ELEMENTS IN THE AQUEOUS ACETONE SOLUTIONS OF DIBENZOYLMETHANE COMPLEXES. Kononenko, L. I.; Tishchenko, M. A.; Drobyazko, V. N. Zh. Anal. Khim.; 26: 729-34(Apr 1971). (In Russian).

Correlation between the intensity of the "supersensitive" absorption bands and the molecular weight of β-diketones was observed in aqueous acetone solutions of the rare earth complexes with certain β-diketones. In this case, the absorbance increased in aqueous acetone solutions as compared with benzene solutions of the complexes. A method is suggested for the highly sensitive determination of Pr, Nd, Eu, Ho, Er, and Tm in their mixture with other rare earth ions based on the measurement of the solution absorbance of the dibenzoylmethane complexes. (auth)

34528 EFFECT OF THE STRUCTURE OF MONO- AND BIFUNCTIONAL AZO COMPOUNDS ON THE ANALYTICAL PROPERTIES OF YTTRIUM AND RARE EARTH COMPLEX COMPOUNDS. Basargin, N. N.; Akhmedli, M. K.; Islamov, Sh. U. (Inst. of the Geology of Ore Deposits, Petrography, Mineralogy, and Geochemistry, Moscow. Azerbaydzhan State Univ., Baku). Zh. Anal. Khim.; 26: 722-8(Apr 1971). (In Russian).

Fifteen bisazo mono- and bifunctional reagents were synthesized and studied spectrophotometrically. The reagents contain substituents such as H, CH_3, SO_3H, AsO_3H_2 and NO_2 in the para-position to the azo group and a functional-analytical group (FAG) of the two perihydroxy groups (the I and II classes), and also a second FAG of the o-carboxyazo-o′-hydroxy group coupled with the first FAG (the III class). Such characteristics as pH_{50}, λ_{max}, $\Delta\lambda$, ϵ_{MeR}, ϵ_{HR}, the composition of the rare earth complexes, and the number of protons displaced on the reaction have been compared. The correlation between pK'_{OH} of the reagent and pH_{50} of the reaction with the rare earths, as well as between the substituent constant σ and pH_{50} has been established. The advantages of the III class reagents as compared with those of the I and II classes are due to the interaction of the rare earth ions by the o-carboxyazo-o′-hydroxy group and to the effect of substituents. (auth)

34529 FLAME-SPECTROPHOTOMETRIC MICRODETERMINATION OF SMALL AMOUNTS OF STRONTIUM AND BARIUM. Prudnikov, E. D.; Shapkina, Yu. S. (Leningrad State Univ.). Zh. Anal. Khim.; 26: 710-13(Apr 1971). (In Russian).

Methods were developed for the flame spectrophotometric microdetermination of strontium and barium in various materials. The sensitivity is down to 1×10^{-3}% of SrO and 0.1% of BaO at a sample weight of 10 mg, and down to 1×10^{-2}% of SrO and 0.1% of BaO for 1-mg samples. (auth)

34530 COLORIMETRIC DETERMINATION OF Ce^{4+} BY o-AMINOPHENOL. Suteu, A.; Hodisan, T.; Naumescu, Adriana. Stud. Univ. Babes-Bolyai, Ser. Chem.; 15: No. 2, 23-5(1970). (In French).

A new colorimetric method is suggested for the determination of Ce^{4+} using o-aminophenol, which with Ce^{4+} acquires a red-

XUM

orange coloring. The Beer–Lambert, law was verified for Ce^{4+} quantities ranging between 5.0 and 45.2 $\mu g/cm^3$. (R.V.J.)

34531 STUDIES IN THE FIELD OF THE ANALYTICAL CHEMISTRY OF URANIUM. COMMUNICATION 5. PHOTOMETRIC DETERMINATION OF URANYL IONS BY MEANS OF PHOSPHONAZO III AND CHLOROPHOSPHONAZO III IN STRONGLY ACID SOLUTIONS. Luk'yanov, V. F.; Lukin, A. M.; Duderova, E. P.; Barabanova, T. E. Zh. Anal. Khim.; 26: 772-6(Apr 1971). (In Russian).

The reaction of phosphonazo III and chlorophosphonazo III with uranium (IV) in a strongly acid medium was studied. It was found that the optical density of solutions of the uranium (IV) complexes is practically stable within HCl concentrations from 2.9 to 3.5 N on the use of phosphonazo III and within 2.5 to 3.5 N when chlorophosphonazo III is used. The interference of other elements with the uranium determination under the above conditions is essentially lower than in the case of uranium determination in weakly acid solutions. The determination of uranium (VI) by means of chlorophosphonazo III is recommended to be carried out in a medium containing 33% isopropanol, which is necessary to prevent precipitate deposition. (auth)

34532 STUDY OF THE COMPLEX FORMATION OF THORIUM WITH PHTHALEXON S AND THYMOLPHTHALEXON S. Cherkesov, A. I.; Argisheva, A. I.; Astakhova, N. K. (Saratov State Pedagogical Inst., USSR). Zh. Anal. Khim.; 26: 755-60(Apr 1971). (In Russian).

The complex formation of thorium with phthalexon S [a sodium salt of 3.3'-bis-N,N'-di(carboxymethyl)aminomethylphenolsulfophthalein] and thymolphthalexon S [a sodium salt of 3.3'-bis-N,N'-di(carboxymethyl)aminomethylthymolsulfophthalein] was studied. The composition of the complexes, their molar extinction coefficients, and pK of the conventional instability constants were determined. Phthalexon S and thymolphthalexon S are recommended for the spectrophotometric determination of small amounts of thorium. (auth)

34533 PECULIARITIES OF THE EXTRACTIVE-PHOTOMETRIC DETERMINATION OF TANTALUM BY BASIC DYESTUFFS. Tarayan, V. M.; Ovsepyan, E. N.; Barkhudaryan, S. P. (Erevan State Univ.). Arm. Khim. Zh.; 23: No. 10, 945-6 (1970). (In Russian).

The photometric determination of tantalum is improved by basing the method on an extraction of fluorotantalate anion with dyestuff cations. The presence of oxalate ion as a complexing agent did not significantly alter the outcome. An extract of the fluorotantalate with methyl green possessed a somewhat higher molar coefficient of light absorption (7.2×10^4 and 1.2×10^5) than when either methylene blue or acridine orange NO was employed. (K.S.W.)

34534 EXTRACTION OF URANIUM(VI)–BENZOIC ACID ANION COMPLEX BY SOME THIAZINE DYESTUFFS. Tarayan, V. M.; Ovsepyan, E. N.; Petrosyan, A. A. (Erevan State Univ.). Arm. Khim. Zh.; 23: No. 10, 957-8(1970). (In Russian).

Various derivatives of thionine were used in extractive-photometric determinations of uranyl ion: methylene green, azure I, and toluidine blue. Sodium benzoate provided the anion for complex formation of the U(VI). Molar coefficients of absorption for extracts of such U complexes were found to be: 7.3×10^4 for methylene green, 7.2×10^4 for azure I, and 8.4×10^4 for toluidine blue. (K.S.W.)

34535 USE OF N-FUROYLPHENYL HYDROXYLAMINE FOR AMPEROMETRIC TITRATION OF ZIRCONIUM. Gallai, Z. A.; Sheina, N. M.; Nifontova, N. V.; Kondratova, N. A. Vestn. Mosk. Univ., Ser. II. Khim.; 12: No. 1, 94-7(Jan-Feb 1971). (In Russian).

A method was developed for amperometric titration of zirconium by N-furoylphenylhydroxylamine solution using a graphite electrode. Large amounts of nickel, cobalt, zinc, magnesium, manganese(II), copper, cadmium, aluminum, and chromium(III) did not interfere with zirconium titration. (auth)

Isotope Dilution Procedures

Refer also to abstracts 34689 and 34924.

Radiometric and Radiochemical Procedures

Refer also to abstracts 34673, 34728, 34862, 34886, 34895, 34935, 35040, and 37015.

34536 (JUL-709-RG) METHOD FOR ANALYSIS OF COMPLEX AND SPECTRA IN SEMICONDUCTOR SPECTROSCOPY. Ewalds, Klaus (Kernforschungsanlage, Juelich (West Germany). Institut fuer Reaktorentwicklung). Oct 1970. 127p. (In German). Dep. NTIS (U. S. Sales Only).

A suitable measurement method by which the isotope composition of γ-active samples can be determined quantitatively was developed. The method is based on the γ-spectroscopic measurement of the samples using a Ge(Li) semiconductor. The construction of the γ spectrometer is described, and the theory of the spectral evaluation and the computer program are given. The preparation of calibration standards for all fission products considered is described. The measurement technique and the necessary correction are reported, and a second evaluation method based on the measurement of individual γ lines is also developed. The two methods are compared. (J.S.R.)

34537 DETECTION OF TRANSURANIC ELEMENTS IN THE pCi-RANGE. Schieferdecker, H. (Kernforschungszentrum, Karlsruhe, Ger.). Mikrochim. Acta; No. 6, 1283-6(1970). (In German).

The separation of the nuclides Pu, Am, Cm, and Cf in pCi amounts from biological material by extraction with bis(2-ethylhexyl)phosphate (DEHPA) is described. It is possible to identify individually the transuranic elements after joint carrier-free preparation by electrolytic deposition and subsequent α spectrometry. Amounts below 0.2 pCi of a nuclide can be determined by this method. (auth)

34538 DETERMINATION OF ^{10}B CONCENTRATIONS IN COMPOUNDS CONTAINING BORON BY MEANS OF THERMAL NEUTRON ABSORPTION MEASUREMENT TECHNIQUE. Gogitidze, O. A. (Scientific-Research Inst. for Stable Isotopes, Tbilisi, USSR). Kernenergie; 14: No. 3, 87-9(Mar 1971). (In Russian).

A new technique of analysis of compounds containing boron for ^{10}B by measuring the attenuation of the thermal neutron flux penetrating the volume with substance to be analyzed is described. The technique is based on the difference of effective thermal neutron capture cross section of the isotopes ^{10}B and ^{11}B and was used to determine ^{10}B concentration in liquid and gaseous compounds containing boron. The design of the apparatus is given. The method was used to determine ^{10}B concentration in the compound $(CH_3)_2O \cdot BF_3$ in the interval 5 up to 95 atomic percent. The error of determination is ±0.25 percent for the low concentration range, and ±0.5 percent for the high concentration range. (auth)

34539 GAMMA-RAY SPECTROMETRY OF ROCKS. Adams, John A. S.; Gasparini, Paolo. Methods in Geochemistry and Geophysics Series. Volume 10. New York; American Elsevier Publishing Company, Inc. (1970). 303p. $21.00.

Information necessary for designing a laboratory for γ spectrometry of natural samples, for planning a research program for mineral exploration, or for just dealing with natural radioactivity is summarized. Special emphasis was given to tables and figures through which the decay schemes of natural radioisotopes and the characteristics of different detectors are illustrated. A chapter is devoted to the main collaborative techniques and their auxiliary relationship to γ spectrophotometry is discussed. Case histories on the application of γ spectrometry to different geological problems are included. (B.L.M.)

34540 CHANNELS RATIO QUENCH CORRECTION USING CHERENKOV RADIATION FOR THE ASSAY OF ^{42}K IN BIOLOGICAL SAMPLES. Moir, A. T. B. (Univ. of Edinburgh). Int. J. Appl. Radiat. Isotop.; 22: 213-16(Mar 1971).

Results are given for efficiency of detection of ^{42}K by Cherenkov radiation in samples of whole blood, urine, and plasma from which it was concluded that for this isotope, at least, the most accurate estimate is given by using the channels ratio method. (UK)

34541 DETERMINATION OF ENRICHED URANIUM IN URINE. Efimova, A. N.; Andreeva, O. S. Gig. Sanit.; No. 12, 71-4(Dec 1970). (In Russian).

A simple method was developed for extraction of U from urine using tributyl phosphate (TBP) in 20% kerosene, ether, or trioctylphosphine oxide (TOPO) in cyclohexane. The best results for determining enriched uranium were obtained with TBP and TOPO. Considering that the daily MPC of low-solubility uranium compounds in urine is 40 pCi (~60 disint/min l) and for easily soluble uranium compounds is 200 pCi (~300 disint/min l), urine specimens containing 15 to 300 disint/min l were studied. The chemical yield of enriched uranium using TBP with aluminum or sodium nitrate salting-out averaged 85 to 86.5% with a maximum of 100%. The maximum sensitivity for the determination of enriched U in urine was 7 to 10 disint/min l. (R.V.J.)

XUM

Activation Procedures

Refer also to abstracts 34669 and 34670.

34542 (GA-9807) APPLICATIONS OF NEUTRON ACTIVATION ANALYSIS IN SCIENTIFIC CRIME INVESTIGATION. A Comprehensive Report Covering the Six-Year Period May 1, 1962 Through May 31, 1968. Guinn, V. P.; Lukens, H. R.; Schlesinger, H. L. (Gulf General Atomic, Inc., San Diego, Calif.). 30 Jun 1970. Contract AT(04-3)-167. 263p. Dep. NTIS.

The possible forensic applications of thermal neutron activation analysis (TNAA) and, to a lesser extent, other variations of activation analysis, were investigated and results are summarized. A means of ascertaining whether a person has fired a gun and the nondestructive characterization of a wide variety of evidence materials (such as paints and paper) through their major and trace element contents were established. This work has generally expanded the number of points by which evidence materials can be characterized and provided and in the establishment of statistical accuracies with which statements about evidence materials can be made. (auth)

34543 (NIM-1013) INSTRUMENTAL NEUTRON-ACTIVATION ANALYSIS OF SAMPLES TAKEN AT DIFFERENT LEVELS OF THE E.R.P.M. MINE. Sellschop, J. P. F.; Uken, E.-A.; Steele, T. W.; Erasmus, C. S. (National Inst. for Metallurgy, Johannesburg (South Africa)). 30 Sep 1970. 9p. Dep. NTIS (U. S. Sales Only).

Nondestructive neutron activation analysis was used to determine sodium, scandium, cobalt, rubidium, cesium, barium, lanthanum, cerium, europium, ytterbium, lutetium, hafnium, and tantalum in powdered rock samples taken at different levels of the mine of East Rand Proprietary Mines Ltd. A significant increase in concentration of the elements lanthanum, ytterbium, lutetium, and hafnium was noticed between the strata above and below the goldbearing main reef, suggesting that these elements could serve to indicate the location of the pay band. (auth)

34544 (NIM-1048) DETERMINATION, BY NEUTRON-ACTIVATION AND TRACER TECHNIQUES, OF THE LOSSES OF IRIDIUM DURING THE FIRE-ASSAY PROCEDURE FOR THE PLATINUM-GROUP METALS. Watterson, J. I. W.; Robert, R. V. D.; van Wyk, E. (National Inst. for Metallurgy, Johannesburg (South Africa)). 3 Sep 1970. 7p. Dep. NTIS (U. S. Sales Only).

A combined neutron activation and radioactive tracer technique was developed for study of the losses of iridium in the fire assay method for determination of the platinum group metals when lead is used as the collector. It was found that the losses during the fusion stage are small, but a large loss occurs during the cupellation stage. (auth)

34545 (THAI-AEC-36) SOIL ANALYSIS BY NEUTRON ACTIVATION METHOD. Nilubol, M. L. Anong; Sungtong, Prapai; Chamnirokasarnt, Darakarnt (Office of Atomic Energy for Peace, Bangkok (Thailand)). [nd]. 8p. Dep. NTIS (U. S. Sales Only).

Neutron activation analysis of soils for trace inorganic elements is discussed. Determination of Al, Mn, Na, Cu, and Zn is described and sensitivity is discussed. (M.C.G.)

34546 (THAI-AEC-39) INORGANIC ELEMENTS IN HUMAN STONES: A PRELIMINARY STUDY USING NEUTRON ACTIVATION TECHNIQUE. Siri-Upatham, Chyagrit (Office of Atomic Energy for Peace, Bangkok (Thailand)). Dec 1970. 15p. Dep. NTIS (U. S. Sales Only).

Human vesical, ureteral, and renal stones were broken, separated into layers, ground, and irradiated at 7.6×10^{10} n/cm^2/sec for 10 min or 10^{13} n/cm^2/sec for 7 hours. Gamma measurements were made at various time intervals. Elements found included P, Ca, Mg, Na, Zn, Hg, and Se. Cr, Cs, and N were identified qualitatively. (M.C.G.)

34547 (UARAEE-68) POSSIBLE TRENDS FOR PURITY CONTROL OF URANIUM BY NEUTRON ACTIVATION ASSAY. Abdel-Rassoul, A. A.; Wahba, S. S. (Atomic Energy Establishment, Cairo (Egypt). Nuclear Chemistry Dept.). 1968. 87p. Dep. NTIS (U. S. Sales Only).

Possible routes for purity control of uranium by neutron activation assay are discussed. Two analytical schemes were developed for general application, and used for simultaneous determination of the elements having atomic numbers from Z = 24 to 30 in different uranium samples, including metallic uranium, uranium concentrates, oxide, acetate, and nitrate and sodium uranate. The first scheme implies direct activation of test samples followed by adequate decontamination of gross fission product activities by adsorption on silica gel, removal of uranium by solvent extraction, separation of most carrier-free rare earth activities by coprecipitation with aluminum chloride and finally mutual separation of the elements by ion exchange elution chromatography. The method can assay ppM concentrations of chromium, iron, cobalt, and zinc in limited quantities of samples by scintillation γ spectrometric analysis within a reproducibility of 10 to 15%. The second scheme was developed for simultaneous determination of manganese, nickel, and copper. It is based on pre-separation of uranium by paper chromatography and subsequent determination of these elements in pile-irradiated residues by simple radiochemical operations. Reagent blank determinations are considered. The limits of detection sensitivity reveal possible determination of microgram quantities of elements with good precision. Evaluation of both schemes with regard to possible sources of error, nuclear interference, radiochemical purity of the preparations, and reliability of results, is included. (auth)

34548 DETERMINATION OF MAGNETIC IMPURITIES IN HIGH PURITY COPPER BY NEUTRON ACTIVATION ANALYSIS. Rodriguez, F. A. (Comision Nacional de Energia Nuclear, Mexico City. Univ. of Texas, Austin); Gage, S. J.; Gavenda, J. D. pp 505-9 of Materials Technology: An Interamerican Approach. New York; American Society of Mechanical Engineers (1968).

From Inter-American Conference on Materials Technology, San Antonio, Tex. See CONF-680513.

Neutron activation was used to determine trace impurity concentrations of Co in a Cu matrix. While concentrations of 4 to 6 ppM Co were determined, it was also experimentally verified that NAA could be used to determine even lower concentration levels. As for the effect of Co impurities on the electrical properties of dilute Cu–Co alloys, there is no correlation between the cobalt impurity levels reported and the resistivity ratios reported for the copper samples. Neutron activation analysis offers a simple and rapid technique for determination of Co concentrations at impurity levels of importance in the measurement of electrical properties of dilute Cu–Co alloys. It also promises to be useful in the determination of Ni in dilute Cu–Ni alloys. (auth)

34549 ACTIVATION-ANALYSIS DETERMINATION OF THE SILVER CONTENT IN MICROCRYSTAL CENTERS IN A PHOTOGRAPHIC EMULSION. Potap'eva, L. E.; Kalashnikova, V. I. This paper was summarized in At. Energ. (USSR); 29: 120(Aug 1970) as paper No. 413/5881. (In Russian).

The ability to determine the microscopic content of free silver (up to 10^{-8} g/cm^3 of emulsion) in grains of a photographic emulsion permits study of the formation of the latent image during exposure to various types of radiation and study of the physical mechanism responsible for the limiting sensitivity of the emulsion. A method was developed for determining the silver content in the centers by activation analysis, without the necessity for a preliminary fixation of the emulsion. The minimum silver content in the samples due to the presence of the salt AgBr in the photographic emulsion was $(8 \pm 2) \cdot 10^{-8}$ g/cc of solution. This is in good agreement with the value for the AgBr solubility in water. During the measurement of the silver in the latent-image centers or sensitivity centers, the content was determined to be 10^{-5} to 10^{-7} g. The experimental error was estimated from the scatter in the results to be 5 to 20%. This method was used to study the changes in the silver content in the surface sensitivity centers of a standard nuclear emulsion prepared by a type-R synthesis, but without any sensitizing additives, during its heating at a temperature suitable for chemical "ripening." On the basis of these measurements, recommendations were worked out for producing fog-free, highly sensitive nuclear emulsions. (M.C.G.)

34550 USE OF THE NUCLEAR MICROANALYSIS OF LIGHT ELEMENTS IN ELECTROCHEMISTRY APPLICATIONS TO ANODIC OXIDATION PROCESSES BY DIRECT DETERMINATION OF ^{16}O AND BY ^{18}O TRACING. Amsel, G. (Ecole Normale Superieure, Paris); Cherki, C.; Croset, M.; (and others). Collect. Czech. Chem. Commun.; 36: 883-9(Feb 1971).

The principles of the nuclear microanalysis of light elements in electrochemistry are described. Various applications to anodic oxidation processes in elemental analysis and by isotopic tracing are summarized. (auth)

34551 DETERMINATION OF MERCURY IN BIOLOGICAL AND ENVIRONMENTAL MATERIALS BY INSTRUMENTAL NEUTRON ACTIVATION ANALYSIS. Filby, R. H.; Davis, A. I.; Shah, K. R.; Haller, W. A. (Washington State Univ., Pullman). Mikrochim. Acta; No. 6, 1130-6(1970).

XUM

Mercury was determined by instrumental neutron activation analysis and Ge(Li) gamma spectroscopy in biological and environmental samples. Samples are sealed in polyethylene vials and irradiated with standards for 8 to 10 hours in a water-cooled assembly at a thermal neutron flux of 8×10^{12} neutrons/cm^2/second. High-resolution gamma spectroscopy allows the measurement of the 279-keV gamma ray of ^{203}Hg. Corrections are made for ^{203}Hg decay and for ^{75}Se interference on the 279-keV gamma ray. No interferences are important in biological or environmental samples and the problem of mercury volatilization and loss is eliminated by cooling during irradiation and the use of a sealed irradiation/counting container. The precision (counting statistics) of a single determination ranges from 0.4 to 15% (relative standard deviation). The detection limit for mercury varies with sample composition. For human blood the detection limit is 0.0035 ppM Hg. (auth)

34552 ACTIVATION ANALYSIS FOR DETERMINATION OF TRACES OF MAGNESIUM AND MANGANESE IN BIOLOGICAL MATRICES. Wald, M.; Kaysser, B. (Kernforschungsanlage, Juelich, Ger.). Mikrochim. Acta; No. 6, 1137-44(1970). (In German).

Ion exchange chromatography using Chelex-100 resin and elution with an acetate buffer (pH 6.25) was used for the separation of a mixture of Mg and Mn salts following irradiation with thermal neutron flux of 3.5×10^{13} n·cm^{-2}·sec^{-1} or 7×10^{13} n·cm^{-2}·sec^{-1}. Results show that both elements can be obtained in the pure form, or with a very small degree of contamination of magnesium with manganese. Application of the method for the determination of Mg and Mn content in rice is described. (auth)

34553 ABUNDANCE AND CERTAIN GENERAL CHARACTERISTICS OF THE GEOCHEMISTRY OF GOLD IN BAUXITES (ON THE BASIS OF NEUTRON-ACTIVATION ANALYSIS). Tenyakov, V. A.; Rakovskii, E. E.; Filippova, T. P. (All-Union Scientific Research Inst. of Mineral Raw Materials, Moscow. Central Geological Scientific Research Inst. for Explorations, Moscow). Dokl. Akad. Nauk SSSR; 195: 456-9(11 Nov 1970). (In Russian).

High-sensitivity neutron activation techniques were used to study the geochemical features of gold contained in bauxite samples of various ages. It was possible to detect amounts of 1×10^{-8}% with a precision of 15%. The occurrence of gold was found to be general; the metal was detected without exception in all of the bauxite samples in the study. The amount of gold varied within two orders of magnitude from 0.0004×10^{-4} to 0.0290×10^{-4}%. The samples from plateaus exhibited a mean gold content of 0.0049×10^{-4}% while those from geosynclinaloid regions contained 0.0036×10^{-4}%. A definite correlation was found between the gold content in primary bauxite ores; the concentration was always higher in bauxites originating from igneous or effusive rocks and was much lower in specimens which were genetically associated with clays or clay shales. It was concluded that the build-up factor of gold with respect to the terrestrial crust is about 1.0. The most probable means of entry of gold into bauxites is the mechanical accumulation of terrigenous impurities which contain it. (TTT)

34554 DETERMINATION OF V, Nb, AND S CONCENTRATIONS BY PROTON ACTIVATION ANALYSIS. Debrun, J. L.; Barrandon, J. N.; Albert, P. (CNRS, Vitry-sur-Seine, France). Ann. Chim. (Paris); 5: 357-66(Sep-Oct 1970). (In French).

In most cases S, V, and Nb cannot be determined at the lowest concentrations (<0.1 ppM) by neutron or photon activation. A method of analysis using charged particles was adopted. Concentrations of the order of 10^{-2} ppM of these elements were determined using the three reactions ^{34}S(p,n)^{34m}Cl, ^{51}V(p,n)^{51}Cr, and ^{93}Nb(p,n)^{43}Mo. The ^{34}S(p,n)^{34m}Cl and the subsidiary ^{35}Cl(p,pn)^{34m}Cl reactions were studied. The results show that the subsidiary reaction can be neglected at energies less than 13 MeV. Energies of less than 15 and 10 MeV were chosen, respectively, for the ^{51}V, and ^{93}Nb reactions, thus eliminating the subsidiary reactions ^{52}Cr(p,pn), and ^{94}Mo(p,pn)^{93}Mo. (France)

34555 RAPID ASSAY FOR NITROGEN IN GLUTEN AND USE OF REFERENCE NUCLIDES. Blake, Kenneth R. (Texas Nuclear Corp., Austin, Tex.); Hudspeth, Emmett L. Int. J. Appl. Radiat. Isotop.; 22: 233-41(Apr 1971).

Determination of the nitrogen content of a food product (samples of corn products were used) may be accomplished by fast neutron activation analysis. However, the activities induced in other elements commonly found in gluten interfere with the induced nitrogen activity. An analysis was made in a total elapsed time of approximately seven minutes by dealing directly with the problem of interfering elements; an empirically-determined effective half-life for such elements was used to separate their activity from that of the activity induced in nitrogen. Results indicate that this method should be competitive in accuracy with Kjeldahl determinations. A known amount of a reference nuclide (^{27}Al) was introduced into nitrogen samples. The activity induced in the nitrogen was compared with that induced in the reference nuclide. Since the reference nuclide is chosen so that activity induced in it has essentially the same half-life as the activity induced in the nitrogen, measurement of the specific neutron flux as a function of time or relative position of the sample is not required. (auth) (UK)

Inorganic, Organic, and Physical Chemistry

Chemical Properties

Refer also to abstracts 34502, 34639, 34680, 34698, 34699, and 35522.

34556 (EUR-4635) THERMOGRAVIMETRIC ANALYSIS (TGA) OF THE URANIUM OXIDE CARBOREDUCTION. Zamorani, E.; de Rijk, R.; Tocl, F. (European Atomic Energy Community, Karlsruhe (West Germany). Inst. of Transuranium Elements). Mar 1971. 21p. Dep. NTIS (U. S. Sales Only). EUR F.Fr. 4.45.

Kinetic investigations of uranium oxide carboreduction were made by thermogravimetric analysis (TGA). Two different starting mixtures of uranium oxides and carbon were used: UO_2 + C prepared by ammonia precipitation from uranyl nitrate solution containing dispersed carbon black followed by reduction at 500°C under N_2–8% H_2 and UO_2 or U_3O_8 + graphite, prepared by mechanical blending. In the thermobalance the material was placed into a W-crucible and the measurements were made under a vacuum of 10^{-5} torr either with a constant heating rate of 2°C/min, or isothermally at different temperatures. The kinetics of the carboreduction were affected by the characteristics of the starting material. The precipitation method improves the physical properties of the mixtures and can be used in the carbide preparation. In the oxide-carbon precipitated mixtures, the reaction started at 900°C. The activation energy was 66 ± 4 kcal/mole. In the mechanically blended material the carboreduction started at 1200°C. The activation energy was 83 ± 4 kcal/mole. The results are discussed and compared with those of previous workers. (auth)

34557 (KFK-1339) COMPLEX FORMATION OF HEXIVALENT URANIUM AND OF PENTAVALENT NEPTUNIUM WITH 1,3-DIKETONS AS WELL AS INVESTIGATIONS ON SEPTIVALENT NEPTUNIUM. Gross, J. (Kernforschungszentrum, Karlsruhe (West Germany). Institut fuer Radiochemie). Dec 1970. 98p. (In German). Dep. NTIS (U. S. Sales Only).

The extraction of hexavalent uranium by various 1,3-diketones in $CHCl_3$ always yields 1:2-chelates. Their $pH_{\frac{1}{2}}$-values, distribution coefficients, stability constants β_2, and extraction constants K_{Ex} were determined. The stabilities of these chelates are very different, their stability constants ranging over 18 orders of magnitude ($\log \beta_2 = 3.24$ for hexafluoroacetylacetone, $\log \beta_2 = 21.74$ for dibenzoylmethane at ionic strength $\mu = 0.1$ and T = 25°C). Synergistic effects were observed when methyl isobutyl ketone and diisobutyl ketone were added to the extraction systems UO_2^{2+}/thenoyltrifluoroacetone (HTTA) and UO_2^{2+}/benzoyltrifluoroacetone (HBTA). In the HTTA-systems 1:1- and 1:2-adduct chelates were obtained, and in the HBTA-systems 1:4-adduct chelates formed additionally. The corresponding adduct stability constants could be determined by graphical methods. A spectrophotometric titration of pentavalent neptunium with various 1,3-diketones shows always formation of 1:2-chelates except with trifluoroacetylacetone and hexafluoroacetylacetone, both forming only 1:1-chelates. As expected, the $\log \beta_2$-values of the NpO_2^+ chelates are about those of the UO_2^{2+} chelates, using the same chelating agent. The formation of the chelates in the system NpO_2^+ – acetylacetone was determined as function of the temperature. The thermodynamic data ΔG, ΔH, and ΔS of the reaction were calculated. The molar extinction coefficients of Np(VII) in alkaline solutions were determined ($\epsilon_{4120\,Å}$ = 1303.9 (1 N LiOH) or 1235.8 (0.1 N LiOH) 1/Mol · cm, $\epsilon_{6180\,Å}$ = 364.9 (1 N LiOH) or 356.8 (0.1 N LiOH) 1/Mol · cm at 25°C). The kinetics of the self reduction from Np(VII) to Np(VI) were investigated as functions of the concentration of OH^- ions. $[Co(en)_3]NpO_5 \cdot nH_2O$, $[Cr(NH_3)_6]NpO_5 \cdot nH_2O$, and $Ca_3(NpO_5)_2 \cdot nH_2O$ were prepared for the first time. The existence of $[Co(NH_3)_6]NpO_5 \cdot nH_2O$, $Sr_3(NpO_5)_2 \cdot nH_2O$, and $Ba_3(NpO_5)_2 \cdot nH_2O$ was proved additionally. (auth)

34558 (SRARI-P-92) THE INVESTIGATION OF THE COMPLEXING OF TETRAVALENT THORIUM, URANIUM, NEPTUNIUM AND PLUTONIUM WITH DIETHYLENTRIAMINPENTAACETIC ACID. Piskunov, E. M.; Rykov, A. G. (Scientific Research Atomic Reactor Inst., Melekess (USSR)). 1970. 20p. (In Russian). Dep. NTIS (U. S. Sales Only).

By pH-potentiometric and spectrophotometric methods it was found that tetravalent thorium, uranium, neptunium, and plutonium in solutions of diethylentriaminpentaacetic acid (DTPA, H_5A) form MA^- complexes. The pH-potentiometric titration method at 20°C and an ionic strength of $\mu = 0.5$ were used to determine the stability constants of MA^- complexes: $\lg \beta_{ThA^-} = 26.64 \pm 0.03$, $\lg \beta_{UA^-} = 28.76 \pm 0.09$, $\lg \beta_{NpA^-} = 29.29 \pm 0.02$, and $\lg \beta_{PuA^-} = 29.49 \pm 0.10$. (auth)

34559 (SRARI-P-94) EFFECT OF ACIDITY ON THE RATE OF CATION–CATION OXIDATION-REDUCTION REACTIONS OF ACTINIDE ELEMENTS. Rykov, A. G.; Timofeev, G. A. (Scientific Research Atomic Reactor Inst., Melekess (USSR)). 1970. 23p. (In Russian). Dep. NTIS (U. S. Sales Only).

On the basis of a hypothesis about the possibility of "the distant" transport of a charge in water and aqueous solutions, a model is suggested presenting the charge transport process as the sum of three stages: transport of a charge between the aquacomplex of the first cation–reactant and the solvent; transport of a charge along the system of intermolecular bonds of the solvent; and transport of a charge between the solvent and aquacomplex of the second cation–reactant. The model explains the totality of the experimental data for the acidity effect on the rate and thermodynamic characteristics of cation–cation reduction–oxidation reactions of actinides. (auth)

34560 INFLUENCE OF THE ADSORPTION OF THIOUREA ON ELECTRODE PROCESSES AT THE MERCURY ELECTRODE. Meuree, N.; Gierst, L. (Univ. Libre, Brussels). Collect. Czech. Chem. Commun.; 36: 389-403(Feb 1971).

The adsorption of thiourea at the mercury–water interface induces modifications in the state of the ionic diffuse part of the double layer, which were studied through their influence on the apparent reaction rates of faradaic processes. The polarographic investigation of the behavior of various depolarizers (chromate, uranyl carbonate, tetrathionate, trichloroacetate, europium(III), chromium(III), cobaltihexammine ions) leads to kinetic results which confirm the validity of the available electrocapillary data. It appears that the major role of thiourea is to shift the electrode charge density, which in turn controls the potential profile in the diffuse part of the double layer. Protons are catalytically reduced with an apparent rate constant which depends on both the extent of coverage by adsorbed thiourea molecules and the value of the potential. (auth)

34561 BEHAVIOR OF URANYL ION UPON REDUCTION FROM THE ETHYLENEDISULPHURDIACETIC ACID SOLUTION AT THE DROPPING MERCURY ELECTRODE. Suznjevic, D. Z.; Susic, M. V. (Univ. of Belgrade, Inst. for Chemistry, Tech., and Metallurgy, Belgrade). Collect. Czech. Chem. Commun.; 36: 935-9(Feb 1971).

At low uranyl concentration, only one wave exists, which varies linearly with concentration up to about 1.5×10^{-4} M where the other two waves start to appear. Each wave shows limited current saturation with increasing UO_2^{2+} ion concentration, and the total height of the waves is not proportional to concentration. Additional studies included: the effect of uranyl ion concentration on the electrocapillary curve of mercury, analysis of the current–time curves, reversibility of the electrode reaction and determination of number of electron consumption, calculation of the number of molecules adsorbed per unit area of mercury surface, and an evaluation of Langmuir Factor and free energy of adsorption. (D.P.O.)

34562 ELECTROCHEMICAL BEHAVIOR OF URANIUM ELECTRODE IN CONTACT WITH AQUEOUS SOLUTIONS AND THE NATURE OF THE PHASES FORMED AS A FUNCTION OF pH. Jouve, Gerard; Aucouturier, Marc; Lacombe, Paul (Univ. Paris, Orsay, France). Comp. Rend., Ser. C; 272: 598-601 (15 Feb 1971). (In French).

The dissolution potential of electrolytically or mechanically polished U settles at –1,200 V/S.C.E. and the sample becomes coated with a brown film of UO_3. The equilibrium potential of mechanically polished U varies with pH (from 1 to 7), with a slope of –0.06 V per unit pH. The U polarization curves were plotted for low $\Delta V/\Delta t$ values in acid and neutral solution at pH 2 (electrolytic polishing), pH 7 (mechanical polishing), and pH 7 (electrolytic polishing). The U polarization curves in basic NH_4OH solution at pH 11.6, 13, and 14 for $\Delta V/\Delta t = 700$ mV/h are given. In order to define the nature of the layers formed, the electron diffraction diagrams reflected from U were determined in acid and neutral solution at all potentials and in pH 13 solution at 700 mV/S.C.E. No diffraction diagram could be obtained on U treated at pH 11.6. (France)

34563 COMPLEX FORMATION OF PLUTONIUM(IV) IN SULFATE SOLUTIONS. Moskvin, A. I. Zh. Neorg. Khim.; 15: 3368-9(Dec 1970). (In Russian).

The equilibrium constants for reactions of Pu^{4+} with HSO_4^- were determined. The stabilities of the sulfate complexes of tetravalent actinides, Zr, and Hf are approximately identical. (M.C.G.)

34564 SPECTROPHOTOMETRIC INVESTIGATION OF COMPLEX FORMATION IN THE SYSTEM URANYL NITRATE–NITRIC ACID–WATER. Klygin, A. E.; Kolyada, N. S.; Smirnova, I. D. Zh. Neorg. Khim.; 15: 3300-3(Dec 1970). (In Russian).

Complex formation in the $UO_2(NO_3)_2$–HNO_3–H_2O system was studied spectrophotometrically. Existence of UO_2^{2+}, $UO_2(NO_3)_2$, $UO_2(NO_3)_2(HNO_3)$ and $UO_2(NO_3)^+$ was demonstrated. Formation constants were determined for $UO_2(NO_3)_2$ and $UO_2(NO_3)_2HNO_3$. (tr-auth)

34565 INTERACTION OF CERTAIN COMPOUNDS OF THORIUM WITH DIMETHYL SULFOXIDE. Molodkin, A. K.; Ivanova, O. M.; Belyakova, Z. V.; Kolesnikova, L. E. (Inst. of General and Inorganic Chemistry, Moscow). Zh. Neorg. Khim.; 15: 3245-8 (Dec 1970). (In Russian).

Reactions of dimethyl sulfoxide with $ThCl_4$, $ThBr_4$, ThI_4, $Th(NO_3)_4$, $Th(SO_4)_2$, and $Th(C_2O_4)_2$ hydrates were studied. Complexes containing 1 to 11 molecules of dimethyl sulfoxide and 0 to 4 molecules of water to one molecule of thorium compound were formed. The thermal stability, molecular electric conductivity, and absorption spectra of these compounds were studied. It was established that the coordination of dimethyl sulfoxide occurred at the expense of formation of the Th–O bond. (tr-auth)

34566 OXIDE CHEMISTRY OF PLUTONIUM IN MOLTEN FLUORIDES AND THE FREE ENERGY OF FORMATION OF PuF_3 AND PuF_4. Bamberger, C. E.; Ross, R. G.; Baes, C. F. Jr. (Oak Ridge National Lab., Tenn.). J. Inorg. Nucl. Chem.; 33: 767-76(Mar 1971).

The behavior of plutonium in molten fluorides in the presence of oxide ion was studied in order to establish, in a molten salt reactor (MSR) fuel salt, the conditions of redox potential and oxide concentration necessary to avoid the precipitation of plutonium oxides. Three salt mixtures, LiF–BeF_2 (66.7–33.3 mole %), LiF–BeF_2–ZrF_4 (65.7–29.3–5.0 mole %), and LiF–BeF_2–ThF_4 (72–16–12 mole %), containing PuF_3 were each equilibrated with the oxide that is stable in that media (BeO, ZrO_2, and ThO_2, respectively) under various redox conditions and different temperatures. Only in the ThF_4-containing melt, equilibrated with ThO_2 and NiO, did the PuF_3 concentration decrease. This was confirmed to be the result of the following reaction: $\frac{1}{2}NiO(c) + \frac{3}{4}ThO_2(ss) + PuF_3(d) \rightleftharpoons PuO_2(ss) + \frac{3}{4}ThF_4(d) + \frac{1}{2}Ni^\circ(c)$ where c, ss, and d denote respectively pure crystalline and solid solution phases, and components dissolved in the molten fluoride phase. The free energy of formation of PuF_3 was determined from the measured equilibria quotient of this reaction, the solubility of PuF_3, and the formation free energies available for $ThO_2(c)$, NiO(c), $PuO_2(c)$, and $ThF_4(d)$: $\Delta G^f_{PuF_3(c)} = -334.7 \pm 2.6$ and -333.1 ± 2.6 kcal/mole at 615° and 715°C. By combining this with literature data on the reaction of O_2 with PuF_3 $\Delta G^f_{PuF_4(c)} = -3.85.4 + 8.7\ (T/1000) \pm 2.8$ kcal/mole was obtained. From the results obtained it is concluded that no plutonium oxide would precipitate from the fuel of an MSR under normal operating conditions. (auth) (UK)

34567 RADIATIVE AND CHEMICAL EFFECTS OF ACCELERATED MULTICHARGED IONS ON GASEOUS NITROGEN-CONTAINING SYSTEMS. Gol'danskii, V. I.; Dzantiev, B. G.; Popov, V. N.; Gavrilov, K. A. At. Energ. (USSR); 30: 262-6(Mar 1971). (In Russian).

Flowing nitrogen-containing gaseous systems (N_2–O_2 and N_2–CH_4) were exposed to C^{6+}, N^{7+}, O^{8+}, Ne^{10+}, and Ar^{18+} at 7 MeV/n. The effects of temperature, ion type, and flow rate were determined. (auth)

34568 REACTIONS OF SODIUM N,N-DIETHYLDITHIOCARBAMATE WITH THE CHLORIDES AND BROMIDES OF NIOBIUM(V), TANTALUM(V), AND PROTACTINIUM(V). Heckley, P. R. (Lakehead Univ., Thunder Bay, Ont.); Holah, D. G.; Brown, D. Can. J. Chem.; 49: 1151-60(15 Apr 1971).

Reactions between niobium(V), tantalum(V), and protactinium(V) chlorides and bromides and sodium N,N-diethyldithiocarbamate

XUM

(Nadtc) were examined in nonaqueous, nonoxygenated organic solvents. Complexes obtained are of the types $Mdtc_4X$, $Mdtc_3X_2$, $Mdtc_3S$, $Mdtc_2X_3$, and $Mdtc_2X_3 \cdot nC_6H_6$ (n = 0.7–1.0); not all complexes were isolated for each metal. Within each group the niobium(V) and tantalum(V) complexes are isostructural; possible structures are discussed in the light of results from ir, and nmr spectra, molecular weight, and electrical conductivity measurements. (auth) (Canada)

34569 REDUCTION OF HEXAVALENT URANIUM WITH HYDROGEN SULFIDE IN AQUEOUS SOLUTION AT HIGH TEMPERATURES AND PRESSURES. Rafal'skii, R. P.; Osipov, B. S. At. Energ. (USSR): 30: 52-3(Jan 1971). (In Russian).

A solution of uranyl sulfate with an initial concentration of 9.8 g/l of uranium was frozen in a quartz ampule by immersion in liquid nitrogen. This freezing technique allowed the introduction of known amounts of H_2S from a gas buret. The quartz ampules were then sealed off, and held in an electric furnace for 75, 30, and 10 hours at temperatures of 100, 150, and 200°C respectively. These times were more than sufficient for attainment of equilibrium in the system. After heating, the ampules were opened, and the uranium dioxide was filtered off within 5 to 7 min before sampling for analysis. The formation of a noticeable amount of elementary sulfur was noted in all experiments. At 100 and 150°C the concentration of uranium in the filtrate increased with increasing amount of hydrogen sulfide in the ampule. The formation of uranium sulfide complexes is assumed. A more normal behavior was observed at 200°C with the concentration of uranium in solution decreasing, as the concentration of reducing agent (hydrogen sulfide) in the ampule was increased. With a solution containing 0.1N sodium bicarbonate and 0.05 g/l of uranium at 200°C for a period of 76 hr it was found that with low concentrations of H_2S the concentration of uranium in the acid and carbonate solutions was very close, but at high concentrations of H_2S the concentration of uranium in the bicarbonate solution was more than an order of magnitude higher than in the sulfate solution. The bicarbonate medium must also promote the formation of sulfide complexes. (TTT)

34570 TETRACIDO-TYPE OXALATE-PEROXO URANYL COMPOUNDS. Shchelokov, R. N.; Belomestnykh, V. I.; Somova, R. M. (Inst. of General and Inorganic Chemistry, Moscow). Dokl. Akad. Nauk SSSR; 196: 131-2(1 Jan 1971). (In Russian).

The conditions of formation of mixed oxalate-peroxouranyl compounds was examined, extending earlier studies on the synthesis of these complexes. Examination of the mutual substitution of ligands revealed that the peroxo group cannot be removed from the internal sphere of uranyl compounds even if an excess of oxalate ions is used. The previous synthesis of the compound $(NH_4)_2[UO_2(O_2)(C_2O_4)(OH_2)]$ was complicated by the substitution of the acid ligand in the starting compound; therefore, an approach was chosen using an excess of oxalate ions with $[UO_2(O_2)(OH_2)_2] \cdot 2H_2O$. Only the aquo group (or the fragment of crosslinked bond) was substituted in the starting compound, yielding a tetraacid-type compound; the insoluble material was dissolved in water in the presence of oxalate ions. The solubility of the aquo-peroxo-uranyl compounds was found to depend both on the oxalate ion concentration and on the nature of the cation. In the presence of the excess oxalate, the compounds were stable, making it possible to crystallize them by free evaporation of the solution at room temperature. Thus the difficult soluble uranyl compounds may be dissolved by introducing into the internal sphere the acido ligand that is less strongly coordinated than the ligand in the starting material. (TTT)

Isotope Effects and Exchange

Refer also to abstracts 34652, 34665, 34708, 36322, and 36323.

34571 (ANL-Trans-882) ISOTOPE EFFECT FOR THE DIFFUSION OF INTERSTITIAL ATOMS. Murtazin, I. A. Translated by S. J. Rothman (Argonne National Lab., Ill.), from Fiz. Tverd. Tela; 13: No. 1, 172-8(1971). 10p. Dep. NTIS.

An attempt was made to derive an expression for the quantity measured in the isotope effect and to investigate the role of the change in the vibration spectrum of the crystal, brought about by the diffusing atom, in the isotope effect. It was calculated that the value of the isotope effect increases with increasing temperature. (M.C.G.)

34572 (ORO-3234-23) TRACER AND ISOTOPE EFFECT STUDIES IN ORGANIC CHEMISTRY. Annual Progress Report. Fry, Arthur (Arkansas Univ., Fayetteville. Dept. of Chemistry). 1 Feb 1971. Contract AT(40-1)-3234. 66p. Dep. NTIS.

Research progress is reported on isotope effect studies in organic chemistry, gas-phase isotope effect studies, mechanisms of acid-catalyzed rearrangements of carbonyl compounds, ^{18}O and ^{15}N exchange studies, and ^{18}O and deuterium tracer studies in photochemical addition, reduction, and hydration reactions of double and triple bonds. (M.C.G.)

34573 (RLO-2230-T-2-2) DIFFUSION CONTROLLED REACTIONS AND EXCHANGE REACTIONS IN SOLUTION. Annual Progress Report. Noyes, Richard M. (Oregon Univ., Eugene). 2 Jun 1971. Contract AT(45-1)-1310. 10p. Dep. NTIS.

Work was completed on the polar exchange of isopropyl iodide with iodine in four aprotic solvents of moderate to high dielectric constant. It appears that this reaction can be used very effectively to test the abilities of different solvents to promote formation of transition states with large separation of charge. Work on measuring the diffusion coefficient of hydrogen atoms in water continues to be frustrated by an impurity that scavenges hydrogen atoms without itself being destroyed. A detailed chemical mechanism is proposed for a reaction in which concentrations of certain intermediate species oscillate repeatedly. (auth)

34574 EXACT TUNNELING CALCULATIONS. Truhlar, Donald G.; Kuppermann, Aron (California Inst. of Tech., Pasadena). J. Amer. Chem. Soc.; 93: 1840-51(21 Apr 1971). (CALT-767P4-60).

The transition state theory of chemical reactions rests on the assumption that motion along a reaction path is separable from motion in directions transverse to it and that the latter are adiabatic, i.e., that their quantum numbers are preserved as the reaction proceeds. This assumption requires that, in calculating quantum mechanical tunneling factors, the zero-point energy of the transverse motions be added to the potential energy along the reaction path to furnish an effective vibrationally adiabatic barrier which should be used in such calculations. All tunneling calculations reported so far have neglected such zero-point energy corrections or used unrealistic approximations for them, and most have also replaced the reaction barrier by approximate analytical fits for which transmission probabilities could be determined analytically. Accurate quantum mechanical calculations were performed by numerical techniques for the collinear exchange reactions of $H + H_2$ and $D + D_2$. The results of transmission probability and tunneling factor calculations from Eckart potential fits to the potential energy barrier lead to substantial systematic errors, especially at low temperatures, and therefore should not be used. Further, correcting Shavitt's calculations to eliminate his numerical approximations brings the model he used into better agreement with experiment. The results of calculations ignoring the zero-point energy of the transverse motion and its variation along the reaction path are dramatically different from the ones including it. Since the latter is in accord with the adiabatic derivation of transition state theory and the former is not, agreement of the latter with gas-phase experiments must be considered the result of fortuitous cancellations of errors and should not be construed as support for the assumption behind the theory. (auth)

34575 BRIDGED POLYCYCLIC COMPOUNDS. LXV. ELECTROPHILIC ADDITION OF HYDROGEN CHLORIDE, ACETIC ACID, AND THEIR DEUTERATED ANALOGS TO BENZONORBORNADIENE. Cristol, Stanley J.; Sullivan, John M. (Univ. of Colorado, Boulder. Eastern Michigan Univ., Ypsilanti). J. Amer. Chem. Soc.; 93: 1967-70(21 Apr 1971).

Addition of hydrogen chloride in acetic acid to benzonorbornadiene leads to mixtures containing 94% benzonorbornenyl chloride and 6% benzonorbornenyl acetate, with the composition invariant over a 90-fold variation in hydrogen chloride concentration. Addition of deuterated species leads to complete scrambling of deuterium between the positions randomized by Wagner–Meerwein rearrangements in the chlorides, but less than complete scrambling in the acetate. The data are consistent with competing mechanisms, one involving a nonclassical carbonium ion, and the other a synconcerted "molecular" addition, and are not consistent with any process in which it is necessary to assume that reaction of a carbonium ion with chloride ion is slower than that with acetic acid. (auth)

34576 PROTON TRANSFER AND HEAVY-ATOM REORGANIZATION IN AMIDE HYDROLYSIS. VALENCE-ISOMERIC TRANSITION STATES. Kershner, Larry D.; Schowen, Richard L. (Univ. of Kansas, Lawrence). J. Amer. Chem. Soc.; 93: 2014-24 (21 Apr 1971).

The hydrolysis in protium and deuterium oxides of ten ring-substituted trifluoro-N-methylacetanilides, $XC_6H_4N(CH_3)COCF_3$, in basic solution proceeds by rate-determining breakdown of tetrahedral intermediate to products with water catalysis (k_1

process) at low base concentrations, with hydroxide catalysis (k_2 process) at intermediate base concentrations, and by rate-determining formation of the tetrahedral intermediate (k_a process) at high base concentrations. The k_a process yields a linear free-energy relation (slope 0.35 in H_2O) with pK_b of the leaving-group aniline for all substituents (X = p-OCH_3 to m-NO_2) and occurs 1.2 to 1.7 times faster in deuterium oxide than in protium oxide. The k_1 and k_2 processes, on the other hand, exhibit biphasic free-energy relations with pK_b of the leaving group, with very small slopes (0.02 and 0.09 in H_2O, respectively) for $pK_b < 9$ and large slopes (0.3 and 0.7 in H_2O, respectively) for $pK_b > 9$. Solvent isotope effects for both processes decrease with increasing pK_b, in the case of the k_2 process dropping abruptly from normal to inverse values at $pK_b \sim 9$. Breakdown of the tetrahedral intermediate proceeds along two parallel pathways with valence-isomeric transition states, one involving mainly proton transfer from catalyst to nitrogen with generation of an ammonium intermediate and the other involving mainly C–N bond cleavage to give a hydrogen-bonded anilide ion intermediate. The former is favored by "poor" leaving groups (electron donors, $pK_b < 9$) and the latter by "good" leaving groups (electron acceptors, $pK_b > 9$). (auth)

34577 REVERSIBLE ADDITION OF BENZOYLOXY RADICALS TO BENZENE. Saltiel, Jack; Curtis, Howell C. (Florida State Univ., Tallahassee). J. Amer. Chem. Soc.; 93: 2056-8 (21 Apr 1971).

The photolysis of benzoyl peroxide in the presence of oxygen was carried out in ~1:1 mixtures of benzene-d_0 and benzene-d_6. Phenyl benzoate formation showed large apparent deuterium isotope effects at both oxygen concentrations studied (1.5 and 7.2×10^{-3} M), in contrast with much smaller isotope effect for biphenyl formation under the same conditions. These results substantiate the reversible addition of benzoyloxy radical to benzene. (D.H.M.)

34578 HYDROGEN ABSORPTION AND HYDROGEN EXCHANGE REACTIONS IN SOLUTION BY 1:2 ELECTRON DONOR–ACCEPTOR COMPLEXES OF ANTHRACENE WITH VARIOUS ALKALI METALS. Ichikawa, Masaru (Sagami Chemical Research Center, Sagamihara, Japan); Tamaru, Kenzi. J. Amer. Chem. Soc.; 93: 2079-80(21 Apr 1971).

The heterogeneous and homogeneous mechanisms of hydrogen activation by some electron donor-acceptor complexes of aromatic compounds and alkali metals were studied. It was found that anthracene–dianion complexes in solution catalyzed both hydrogen absorption and hydrogen exchange to a different extent, depending on the alkali metal cations. Exchange proceeded at higher rates in K and Rb solutions than in Na or Li solutions. (M.C.G.)

34579 HALIDE–HALIDE EXCHANGE AT ASYMMETRIC SILICON. NEW EVIDENCE AGAINST A SILICONIUM ION-PAIR MECHANISM. Sommer, L. H.; Homer, G. D.; Messing, A. W.; (and others) (Univ. of California, Davis). J. Amer. Chem. Soc.; 93: 2093-4(21 Apr 1971).

Evidence that the siliconium ion-pair mechanism originally proposed for the chloride–radiochloride exchange of optically active α-NpPhMeSi*Cl with $c\text{-}C_6H_{11}NH_3{}^{36}Cl$ is incorrect is presented. The data point to a mixture of inversion and retention mechanisms for the exchange. (M.C.G.)

34580 ISOTOPE EXCHANGE BETWEEN MOLECULAR OXYGEN AND SYNTHETIC ZEOLITES. Minachev, Kh. M.; Savost'yanov, E. N.; Kondrat'ev, D. A.; Chang, Zui N'yui; Antoshin, G. V. (Inst. of Organic Chemistry, Moscow). Izv. Akad. Nauk SSSR, Ser. Khim.; No. 4, 841-3(Apr 1971). (In Russian).

The kinetic properties of ^{18}O exchange at 600 to 700°C between O_2 and three specified zeolites were found to be closely similar. The zeolite samples had SiO_2/Al_2O_3 ratios of 2.45, approximately 4.0, and 11, respectively. During exchange of Na by Cu and Ag an increase in O mobility was observed in one of the zeolites. The oxygen of the zeolite structure was equivalent with respect to interchange with molecular oxygen. (tr-auth)

34581 FG MATRIX TREATMENT OF NORMAL VIBRATIONS IN ETHYLENE-LIKE AND NITROMETHANE-LIKE MOLECULES WITH FREE INTERNAL ROTATION. Papousek, D. (Inst. of Physical Chemistry, Prague); Sarka, K.; Spirko, V.; Jordanov, B. Collect. Czech. Chem. Commun.; 36: 890-905(Feb 1971).

The symmetry groups, transformation to symmetry coordinates, factorization of the FG matrices, and the form of the eigenvectors of the vibrational secular equation were discussed for the ethylene-like and nitromethane-like molecules with free internal rotation. An attempt was made at least squares refinement calculation of the quadratic force constants from the fundamental frequencies of vibrations of CH_3NO_2 and CD_3NO_2. (auth)

34582 ISOTOPIC EXCHANGE OF GASEOUS DEUTERIUM WITH LATTICE HYDROGEN OF HYDRIDES. Novakova, J.; Jiru, P.; Zavadil, V. (Inst. of Physical Chemistry, Prague). Collect. Czech. Chem. Commun.; 36: 520-7(Feb 1971).

Isotopic exchange of gaseous deuterium with saline hydrides (lithium, sodium, and calcium) and metal hydrides (titanium and zirconium) was studied in the temperature range of 20 to 400°C. The homophase equilibration was found to take place in the case of the lithium and titanium hydride. In the case of the other hydrides studied, the heterophase exchange, i.e., the exchange with lattice hydrogen, took place in addition to the homophase-exchange. The treatment used in the study of oxygen isotopic exchange with oxides was applied to the deuterium exchange with hydrides. (auth)

34583 ISOTOPIC EXCHANGE OF RADIOCHLORINE IN THE SYSTEM $(MoCl_6)^{3-}$–$^{36}Cl^-$. Wajda, Stanislaw; Zarzeczny, August (Univ., Wroclaw). Nukleonika; 15: 631-9(1970). (In Polish).

The exchange kinetics of radiochlorine in hexachloromolybdate (III) in formamide solution was studied. The exchange was found to proceed according to the S_{N2} association mechanism since the reaction order is equal to 2. On the basis of these data the mechanism of isotopic exchange is suggested. This mechanism is compared with the mechanism of isotopic exchange in the system $[Mo(CNS)_6]^{3-}$–$^{14}CNS^-$. The magnitude of the activation energy (36,5 kcal/mole) indicates that the Mo–Cl bonding is covalent. The exchange rate was determined by the formation of an association complex with the coordination number seven. (auth)

34584 STUDY OF KINETICS OF BENZOIC ACID EXTRACTION WITH TOLUENE BY ISOTOPIC EXCHANGE METHOD. Iofa, B. Z.; Nesmeyanov, An. N.; Kireev, G. I.; Kozlov, A. A. Vestn. Mosk. Univ., Ser. II. Khim; 12: 83-5(Jan-Feb 1971). (In Russian).

The rate of extraction and isotopic exchange on dimerization of benzoic acid in toluene were studied. The calculation of mass transfer factors for extraction and isotopic exchange was carried out. (auth)

34585 ISOTOPE EXCHANGE REACTIONS. VIII. VARIATION OF THE PARTITION FUNCTION RATIOS OF THE ISOTOPIC FORMS OF UNSUBSTITUTED HYDRIDES WITH CHEMICAL BOND CHARACTERISTICS. Knyazev, D. A.; Bantysh, A. N.; Ivlev, A. A. (Inst. of Chemical Engineering, Moscow). Russ. J. Phys. Chem. (Engl. Transl.); 44: 1264-7(Sep 1970).

The calculated partition function ratios (β factors) for the isotopic forms of straight-chain hydrides were interpreted quantitatively using a number of intramolecular characteristics, and the correlations obtained were used to estimate unknown β factors. (auth)

34586 ^{13}C HYPERFINE INTERACTION IN CD_2. Bernheim, R. A.; Bernard, H. W.; Wang, P. S.; Wood, L. S.; Skell, P. S. (Pennsylvania State Univ., University Park). J. Chem. Phys.; 54: 3223-5(1 Apr 1971).

A bond angle of 137.7° can be determined from measurement of the ^{13}C hyperfine interaction in CD_2. The main features of the EPR spectra of CD_2 containing only ^{12}C and of CD_2 containing a mixture of carbon isotopes, 62.1% ^{13}C and 37.9% ^{12}C, are the Y_2, X_2, and Z_1 lines. The ^{13}C hyperfine interaction is a splitting of the Y_2 and X_2 lines and a broadening of the Z_1 line. (D.P.O.)

34587 ROLE OF WAVE PROPERTIES OF ISOTOPES IN CHEMICAL KINETICS. Koch, F. Stud. Univ. Babes-Bolyai, Ser. Phys.; 15: No. 2, 53-5(1970).

The role of wave properties in respect to isotope effects is discussed. The effects of temperature on H and D exchange in N,N-dimethylformamide and the resulting internal rotation were studied by NMR spectral techniques. (J.G.B.)

34588 REGULARITIES IN INFRA-RED SPECTRA (AMIDE A, B, I, AND II BANDS) OF GLOBULAR PROTEINS IN D_2O. Abaturov, L. V.; Varshavskii, Ya. M. (Inst. of Molecular Biology, Moscow). Stud. Biophys.; 13: 47-52(1969).

The structure of globular proteins is too complex to permit any simple quantitative interpretation of their ir spectra. However, an attempt was made to elucidate regularities found in the shape and position of Amide A,B,I, and II peptide bands and to relate them with the conformation of the protein globules. This problem is of interest in connection with ir-spectroscopic studies on the kinetics of H–D exchange in globular proteins. (auth)

34589 HIGH-PRESSURE REGION OF THE RECOMBINATION $O + O_2 \rightarrow O_3$. Hippler, H.; Troe, J. (Univ., Goettingen, Ger.). Ber. Bunsenges. Phys. Chem.; 75: 27-32(Jan 1971). (In German).

XUM

The quantum yield of the NO_2 photolysis at 3660 Å was measured at room temperature for mixtures of NO_2 and O_2 in the carrier gas N_2. From the quantum yield the rate of recombination $O + O_2 \rightarrow O_3$ was derived. By variation of the carrier gas pressure between 1 and 200 atm the nearly complete transition of this recombination from a third order to a second order reaction could be observed. Limiting third order low pressure rate constants (with $M = N_2$) of $k_{e0} = 2.9 \cdot 10^{14}$ cm^6/mol^2 sec and second order high pressure rate constants of $k'_\infty = 10^{12}$ cm^3/mol sec were derived. Comparison of high pressure recombination rate constants, k_∞, and rate constants of isotope exchange, k_i, $\rightarrow k_i/k_\infty \approx 0.6$ for the O_3 system, whereas $k_i/k_\infty \approx 0.3$ for the NO_3 system and $k_i/k_\infty \approx 0.1$ for the NO_2 system was determined. O_3, NO_2, and NO_3 systems are compared in terms of different properties of the potential surfaces. (auth)

34590 INVERSE DEUTERIUM ISOTOPE EFFECT IN RADIATIONLESS ELECTRONIC TRANSITIONS. SINGLET → TRIPLET INTERSYSTEM CROSSING IN ANTHRACENE. Lim, E. C.; Bhattacharjee, H. R. (Wayne State Univ., Detroit). Chem. Phys. Lett.; 9: No. 3, 249-50(1 May 1971).

The rate of the singlet → triplet intersystem crossing in anthracene is enhanced, rather than retarded, by deuteration of the molecule. The "inverse" deuterium isotope effect on the intersystem crossing is interpreted to arise from the participation of a higher triplet state(s) in the radiationless transition. The lack of significant deuteration effect in fluorescence of aromatic hydrocarbons is attributed largely to the small energy gaps between the lowest excited singlet and triplet (including the lowest) states. (auth)

34591 VIBRATIONAL SPECTRA AND ANHARMONICITY OF H_2O, D_2O, AND HOD IN DILUTE SOLUTIONS. Burneau, A.; Corset, J. (Laboratoire de Spectrochimie Moleculaire, Paris). Chem. Phys. Lett.; 9: No. 2, 99-102(15 Apr 1971).

Absorption spectra of free H_2O, D_2O, and HOD molecules and HOH...B, DOD...B, DOH...B, HOD...B, B...HOH...B complexes (B stands for a base or anion) in binary or ternary solutions were studied between 1000 and 11,000 cm^{-1}. Calculation shows that the anharmonic constants depend on the symmetry of the interaction: for H_2O and D_2O, x_{13} decreases and x_{11} and x_{33} increase indicating decoupling of the vibrators. A new interpretation of the experimental results of Greinacher, Lüttke, and Mecke (1955) is given. (auth)

34592 OPTICAL STUDIES OF THE $^3(n,\pi^*)$ MAGNETIC SUBLEVELS IN BENZALDEHYDE. Koyanagi, M.; Zwarich, R.; Goodman, L. (Rutgers—The State Univ., New Brunswick, N. J.). Chem. Phys. Lett.; 9: No. 1, 74-6(1 Apr 1971).

Decay measurements at 1.68°K on several of the individual vibronic bands of benzaldehyde-h_6, $^3U(n,\pi^*) \rightarrow S_0$ phosphorescence yield two decays: 23.9 and 53.9 milliseconds. These are assigned from deuteration effects to the A′ magnetic sublevels. Deuteration at the aldehyde hydrogen nearly doubles the decay times indicating that second order vibronic spin orbit mechanisms involving aldehyde modes is the primary source of probability in benzaldehyde $^3U \rightarrow S_0$. The intersystem crossing selection rules $^1(n\pi^*) \nleftrightarrow {}^3(n\pi^*)$. $^1(n\pi^*) \longleftrightarrow {}^3(\pi\pi^*)$ are confirmed. (auth)

34593 DEUTERIUM EFFECT ON THE PHOSPHORESCENCE LIFETIME OF BIACETYL CRYSTAL AND VAPOR. Borkman, R. F. (Georgia Inst. of Tech., Atlanta). Chem. Phys. Lett.; 9: No. 1, 77-9(1 Apr 1971).

Phosphorescence lifetimes of biacetyl-h_6 and biacetyl-d_6 are reported for the vapor at room temperature and crystalline material at 77°K. Radiationless rate constants were calculated and the results are compared with data obtained in rigid EPA glass at 77°K. (auth)

34594 NOTE ON THE EMISSION BAND SPECTRUM OF THE CD^+ MOLECULE. Cisak, H.; Rytel, M. (Higher Pedagogical School, Rzeszow, Poland). Acta Phys. Pol.; A39: No. 5, 627-8(May 1971).

The emission spectra of the CD^+ molecule were obtained. Four bands of Douglas—Herzberg system were identified. The band origins, the band heads, and the first vibrational quantum of the lower state are given. (auth)

34595 NEW BAND SYSTEM IN THE CO MOLECULE EMISSION SPECTRUM: THE $E^1\Pi - A^1\Pi$ TRANSITION. Kepa, R.; Rytel, M. (Higher Pedagogical School, Rzeszow, Poland). Acta Phys. Pol.; A39: No. 5, 629-30(May 1971).

Three new bands in the emission spectrum of the $^{12}C^{16}O$ molecule and two new bands in the $^{13}C^{16}O$ molecule were obtained. These were identified as yet unobserved $E^1\Pi - A^1\Pi$ transition. The wavenumbers of band heads and some values of constants for the 0—1 band are presented. (auth)

34596 ISOTOPE-EXCHANGE REACTIONS OF OX HEART PHOSPHOFRUCTOKINASE. Hulme, E. C.; Tipton, K. F. (Cambridge Univ., Eng.). Biochem. J.; 122: 181-7(1971).

Ox heart phosphofructokinase catalyses isotope-exchange reactions at pH6.7 between adenosine 5′-diphosphate (ADP) and adenosine 5′-triphosphate (ATP), and between fructose 6-phosphate and fructose 1,6-diphosphate, the latter reaction being absolutely dependent on the presence of the magnesium complex of ADP. The reaction kinetics are hyperbolic with respect to substrate concentration for both exchange reactions (within the experimental error). The influence of pH, adenosine monophosphate, and citrate suggests that the fructose 6-phosphate—fructose 1,6-diphosphate exchange is subject to effector control, and is abolished by dissociation of the enzyme. These results are discussed in relation to the reaction mechanism of the enzyme. (auth) (UK)

34597 KINETICS AND MECHANISM OF THE REACTION OF NICKELOCENE WITH MERCAPTANS. Ellgen, Paul C.; Gregory, Carl D. (Univ. of California, Riverside). Inorg. Chem.; 10: 980-4(May 1971).

The kinetics of the reaction of bis(cyclopentadienyl)nickel with mercaptans to give bis(cyclopentadienyl)di-μ-mercaptodinickel have been studied in cyclohexane, tetrahydrofuran, cumene, and acetonitrile. Rate constants and activation parameters are insensitive to solvent and relatively insensitive to solvent and relatively insensitive to the nature of the mercaptan. For the reaction with thiophenol, $\Delta H^\ddagger = 12.7$ kcal/mol and $\Delta S^\ddagger = -26$ eu in cyclohexane while $\Delta H^\ddagger = 12.9$ kcal/mol and $\Delta S^\ddagger = -26$ eu in acetonitrile. Activation parameters for the reaction with cyclohexanethiol in cyclohexane are $\Delta H^\ddagger = 11.7$ kcal/mol and $\Delta S^\ddagger = -34$ eu. A primary kinetic isotope effect is observed when the rate constant for S-deuteriothiophenol is compared to that for thiophenol, $k_H/k_D = 2.8$. With thiophenol in cyclohexane, bis(methylcyclopentadienyl)nickel undergoes the analogous reaction at almost the same rate as unsubstituted nickelocene. The results are interpreted in terms of a mechanism proposed by Ustynyuk, et al., in which a $\pi-\sigma$ cyclopentadienyl rearrangement accompanies nucleophilic attack by mercaptan at nickel. (auth)

34598 ISOTOPIC EXCHANGE OF HYDROGEN α-POSITION OF ALKYL GROUPS OF AROMATIC HYDROCARBONS WITH DEUTEROTRIFLUOROACETIC ACID. Shubin, V. G.; Tabatskaya, A. A.; Kontyug, V. A. (Inst. of Organic Chemistry, Novosibirsk, USSR). Zh. Org. Khim.; 6: 2081-4(1970). (In Russian).

Mass spectrometric and proton magnetic resonance methods were used to show that α-hydrogen atoms of alkyl groups of aromatic hydrocarbons are capable of exchanging with deuterium in CF_3 COOD. The reaction mechanism is discussed. (R.V.J.)

34599 ISOTOPIC EXCHANGE REACTION OF HYDROGEN IN ARENYL IONS AND THEIR ANTECEDENTS. Shubin, V. G.; Tabatskaya, A. A.; Derendyaev, B. G.; Kopchagina, D. V.; Kopytyug, V. A. (Inst. of Inorganic Chemistry, Novosibirsk, USSR). Zh. Org. Khim.; 6: 2072-80(1970). (In Russian).

Mass spectrometry and proton magnetic resonance methods were used for determining in certain deuterated acids the behavior of nonsaturated polyalkyl compounds that are capable of converting into arenyl ions during protonization. It was found that α-hydrogen atoms of alkyl groups forming arenyl ions were capable of isotopic exchange with deuterium. The isotopic exchange of hydrogen between the hydrocarbon exo-methylene group (the antecedents of the arenyl ion) and the methyl groups of hexamethylcyclohexadiene with deuterioacetic acid was observed. The mechanism of the deuterium exchange reaction was investigated. (tr-auth)

34600 ELECTROPHILIC SUBSTITUTION ON AROMATIC CARBON ATOM. XIV. KINETICS OF PHENYLMERCUROBROMIDE ISOTOPIC EXCHANGE WITH $^{203}HgBr_2$ IN BENZENE. Zakharycheva, I. I.; Beletskaya, I. P.; Reutov, O. A. Zh. Org. Khim.; 5: 2081-7(1969). (In Russian).

The kinetics of isotopic exchange between phenylmercury bromide and $^{203}HgBr_2$ in benzene was studied at 20 to 50°C and reagent concentrations of 0.25 to 1×10^{-3} M. The reaction followed the second order. The activation energy was 11.9 ± 1 kcal/mole. Electron-donor substitutes in the para-position of the benzene ring accelerated the exchange and the electron acceptors slowed it down: $OCH_3 \gg CH_3 > H > Br \gg NO_2$. Additions of tetrabutylammonium bromide accelerated the exchange reaction 10^3 to 10^5 times. Under two anion catalytic conditions the rate of the exchange of para-substituted phenylmercury bromides (x = H, Br, and NO_2) with $^{203}HgBr_2$ was about identical. (tr-auth)

34601 RACEMIZATION AND ^{18}O EXCHANGE STUDIES OF HETEROCHELATE CHROMIUM(III) COMPLEXES. II. THE CATIONS OXALATOBIS(2,2′-BIPYRIDINE)CHROMIUM(III), OXALATOBIS(1,10-PHENANTHROLINE)CHROMIUM(III), AND

OXALATOBIS(ETHYLENEDIAMINE)CHROMIUM(III). Broomhead, J. A.; Kane-Maguire, N.; Lauder, I. (Australian National Univ., Canberra. Univ. of Queensland, St. Lucia, Australia). Inorg. Chem.; 10: 955-8(May 1971).

The kinetics of racemization and oxygen-18 exchange for $Cr(ox)bipy_2^+$, $Cr(ox)(phen)_2^+$, and $Cr(ox)(en)_2^+$ (where ox = oxalate ion, bipy = 2,2′-bipyridine, phen = 1,10-phenanthroline) have been studied in acid solution. Racemization of $Cr(ox)(bipy)_2^+$ is markedly acid dependent whereas $Cr(ox)(phen)_2^+$ shows little acid dependence. Both complexes show distinct racemization rate dependences on addition of various anions or cations. An intramolecular racemization mechanism accounts for the overall behavior. The $Cr(ox)(en)_2^+$ complex is hydrolyzed readily in acid media and this contributes largely to loss of optical activity. All three cationic complexes show acid-catalyzed exchange of all their oxalate oxygens with solvent water. The four oxalate oxygens are kinetically indistinguishable. The exchange reactions are uniformly first order in acid and in complex. Arrhenius parameters for oxygen exchange and for racemization have been measured. Two mechanisms for oxygen exchange are consistent with the data and involve either oxalate ring opening or rapid carbonyl-carboxyl oxygen interchange. (auth)

Physical Chemistry

Refer also to abstracts 34938, 34958, 34962, 34963, 35368, and 37106.

34602 (GAT-649) VAPOR PRESSURE-TEMPERATURE DATA FOR SELECTED HALOGEN-CONTAINING SUBSTANCES. Saraceno, A. J.; Willis, C. D. (Goodyear Atomic Corp., Piketon, Ohio). 10 Feb 1971. Contract AT(33-2)-1. 104p. Dep. NTIS.

Vapor pressure-temperature tables are presented for selected halogen compounds and other substances of interest to those working with uranium processing operations. The tables were prepared by computer printout of calculations based on vapor pressure-temperature equations either taken directly from the literature or derived by least squares fit of vapor pressure (P)-temperature (T) data available in the literature. In the latter case the data were fitted to equations of the form:

$$\ln P = A + \frac{B}{T} + \frac{C}{T^2} + \ldots$$

Each of the 58 substances given in the original listing has its vapor pressure in millimeters of mercury (mm Hg) tabulated as a function of temperature in degrees Kelvin (°K) in increments of one degree. (M.C.G.)

34603 (IJS-263) INVESTIGATION OF THE SYSTEMS OF URANIUM MONOSULFIDE WITH SOME ALKALINE EARTH SULFIDES. Komac, Milos (Institut Jozef Stefan, Ljubljana (Yugoslavia)). Jan 1971. 56p. (In Slovene). Dep. NTIS (U. S. Sales Only).

Thesis. Submitted to Univ. of Ljubljana, Yugoslavia.

Phase equilibria in the systems US-CaS, US-SrS, and US-BaS were investigated by x-ray diffraction, metallography, and electron-probe microanalysis. New ternary sulfides, $CaUS_2$, $SrUS_2$, and $BaUS_2$, which appeared in the corresponding systems, formed eutectic mixtures with primary solid solutions. Eutectic melting temperatures where determined in the systems US-CaS and US-SrS and proposed phase diagrams were constructed. Detailed crystal structure analyses of $CaUS_2$ and $SrUS_2$ were carried out. (auth)

34604 (JINR-P6-5683) DETERMINATION OF THE BOILING POINT OF SOME ISOALKYL ASTATIDES BY USING A GLASS GAS CHROMATOGRAPH. Gesheva, M.; Kolachkovskii, A.; Norseev, Yu. V. (Joint Inst. for Nuclear Research, Dubna (USSR). Lab. of Nuclear Problems). 1971. 12p. (In Russian). Dep. NTIS (U. S. Sales Only).

A gas chromatograph system with a glass working column and a detecting cell is described. It allows the determination of the boiling point of some isoalkyl astatides. The determinations were made on the basis of a linear dependence of the logarithm of retention time of $C_nH_{2n+1}At$ (n = 2 . . . 5) monoastatic derivatives on a gas chromatographic column on their boiling points. The boiling points for these isoalkyl astatides were found to be: isopropyl astatide, 112 ± 2°C; isobutyl astatide, 142 ± 3°C; isoamyl astatide, 163 ± 3°C; optically active amyl astatide 165 ± 3°C. (auth)

34605 (RFP-1608) PERMEATION OF HALOGENATED SOLVENTS THROUGH DRYBOX GLOVES. Johnson, Thomas C.; Merciez, W. Darrel (Dow Chemical Co., Golden, Colo. Rocky Flats Div.). 16 Apr 1971. Contract AT(29-1)-1106. 6p. Dep. NTIS.

The permeation of halogenated solvents through drybox gloves was experimentally investigated. Quantitative information on the permeation rates of six common halogenated solvents through five standard types of drybox gloves was developed. Drybox gloves exposed to both solvent liquid and saturated vapor were studied. Experimental methods were adapted from standard water vapor permeation tests. Permeation of a given solvent through gloves of the same thickness was the same, within the precision of the test. There were considerable differences in permeation rates of the different solvents through similar gloves. In general, methylene chloride permeated the gloves most rapidly, followed in order by trichloroethylene, carbon tetrachloride, methyl chloroform, perchloroethylene, and trichlorotrifluoroethane. (auth)

34606 DIRECT MEASUREMENT AT 1100°C OF THE PARTIAL MOLAR ENTHALPIES OF OXYGEN INCORPORATION IN PuO_{2-x} AND $(U,Pu)O_{2\pm x}$ BY MEANS OF A TIAN-CALVET HIGH-TEMPERATURE MICROCALORIMETER. Chereau, Pierre (CEA, Fontenay-aux-Roses, France); Dean, Guy; Gerdanian, Paul. Compt. Rend., Ser. C; 272: 512-15(8 Feb 1971). (In French).

Direct measurements of the partial molar enthalpy of oxygen incorporation in the Pu-O system reveal a sudden change of slope around O/Pu ~ 1.70. In the U-Pu-O system, a sharp variation is found for O/U + Pu = 2.00. (auth) (France)

34607 REGULARITIES ASSOCIATED WITH THE FORMATION OF LANTHANIDE AND ACTINIDE COMPLEXES. Wallace, R. M. (E. I. du Pont de Nemours and Co., Aiken, S. C.). Inorg. Nucl. Chem. Lett.; 7: 305-6(Apr 1971).

Reference is made to Siekierski (J. Inorg. Nucl. Chem. 32: 519 (1970)), who reported new regularities in the stability constants of trivalent lanthanide and actinide ions with a variety of ligands, and it is pointed out that these regularities may be a result of the method used in the studies, rather than an inherent property. It is stated that Siekierski's procedure, if applied in general, could have led to the sought-for regularities where none existed. (UK)

34608 RAMAN SPECTRA OF TECHNETIUM HEPTOXIDE. Selig, H.; Fried, S. (Argonne National Lab., Ill.). Inorg. Nucl. Chem. Lett.; 7: 315-23(Apr 1971).

Recent studies of the vibrational spectra of gaseous liquid and solid Re_2O_7 are briefly reviewed, and it was considered to be of interest to study the analogous Tc_2O_7. Details are given of the method of preparation of the Tc_2O_7 and determination of the Raman spectra. The Raman spectra of the solid, liquid, and gaseous oxide are shown graphically. It is evident that the liquid and vapor have similar structures which are, however, quite different from that of the solid phase. A striking observation is the one-to-one correspondence, except for small frequency shifts, of the corresponding spectra of Re_2O_7 and Te_2O_7. Monomeric Tc_2O_7 can therefore be assumed to have the same structure as Re_2O_7. The number of lines observed for the liquid and gas is far less than expected, indicating relatively high symmetry. It is also interesting to note that the spectra of Re_2O_7 and Tc_2O_7 appear very similar to those of pyramidal MO_3 species. The molecules behave as if they consist of MO_3 pyramids weakly coupled through an O-bridge of C_{2v} symmetry. As in the case of Re_2O_7 most of the Raman bands below 400 cm^{-1} consist of several superimposed bands, with depolarisation factors of about 0.8. Frequencies for solid, liquid and gaseous Tc_2O_7 are summarised in tabular form, with corresponding bands for Re_2O_7 and their assignments added for comparison. It was puzzling why the relatively intense and strongly polarised band at 60 cm^{-1} observed in the gas spectrum was not seen in the liquid. The spectra for solid Tc_2O_7 showed some similarity to those of Re_2O_7. Where Re_2O_7(s) showed more than ten high frequency Raman modes, only seven such modes were, however, observed for Tc_2O_7(s); this is consistent with the higher symmetry for the Tc_2O_7 units in the crystal structure of the solid. (UK)

34609 THERMODYNAMICS OF THE ACTINIDE ELEMENTS. PART III. HEATS OF FORMATION OF THE DICAESIUM ACTINIDE HEXACHLORO-COMPLEXES. Fuger, J. (Univ., Liege); Brown, D. J. Chem. Soc., A; No. 7, 841-6(1971).

The heats of solution in aqueous hydrochloric acid of the various dicesium actinide(IV) hexachlorides were measured at 25.00 ± 0.05°C. For the thorium, protactinium, uranium, neptunium, and plutonium compounds, the values are in 1M HCl, −31.37 ± 0.12, −23.94 ± 0.31, −19.91 ± 0.04, −20.16 ± 0.07, and −13.67 ± 0.19 kcal $mole^{-1}$, respectively, and in 6M HCl, −20.97 ± 0.06, −12.74 ± 0.24, −8.11 ± 0.05, −7.48 ± 0.10, and −0.18 ± 0.03 kcal $mole^{-1}$, respectively. The heat of solution of the plutonium compound in 1M $HClO_4$ is −17.74 ± 0.05 kcal $mole^{-1}$. Combination of these values with other thermodynamic data yields the following heats of formation at 298°K: $Cs_2ThCl_{6(c)}$, −508.7 ± 0.5 kcal $mole^{-1}$; $Cs_2UCl_{6(c)}$, −476.5 ± 1.1 kcal $mole^{-1}$; $Cs_2NpCl_{6(c)}$, −468.5 ±

XUM

0.4 kcal mole^{-1}, and $Cs_2PuCl_{6(c)}$, −466.9 ± 1.0 kcal mole^{-1}. (auth) (UK)

34610 CRYSTAL STRUCTURE OF PROTACTINIUM TETRABROMIDE. Brown, D. (Atomic Energy Research Establishment, Harwell, Eng.); Petcher, T. J.; Smith, A. J. J. Chem. Soc., A; No. 7, 908-10(1971).

The crystal structure parameters for $PaBr_4$ (isostructural with $ThCl_4$) were determined from quantitative x ray powder data and refined to R 0.123. The Pa−Br bond distances are 2.77 and 3.07 Å; a value of 1.63 Å was obtained for the covalent single-bond radius of Pa(IV). (auth) (UK)

34611 FLUORO COMPLEXES OF URANIUM(IV). Satapathy, K. C. (Univ. of Sambalpur, India); Sahoo, B. Indian J. Chem.; 8: 1031-2(Nov 1970).

Dimethylammonium and aminoguanidinium fluorides yield 1:1 complexes with uranium(IV) fluoride whereas di-sec-butylammonium and dimethylanilinium fluorides afford 1:2 complexes with uranium(IV) fluoride. The compounds are sparingly soluble in water and insoluble in common organic solvent. They are quite stable and can be stored for several days without appreciable decomposition. (auth)

34612 IR SPECTRA AND MAGNETIC SUSCEPTIBILITIES OF URANYL COMPLEXES. Sahakari, M. P.; Mukhedkar, A. J. (Univ. of Poona, India). J. Inorg. Nucl. Chem.; 33: 888-92(Mar 1971).

A series of UO_2^{2+} complexes was prepared, and an attempt was made to correlate their i.r. spectra and magnetic susceptibilities. These complexes included the guaicolate, oxinate, diethyldithiocarbamate, ethylenediamine complex, EDTA hydrate, dipyridine complex, cupferrate, tartrate, dianiline complex, salicylate, citrate, succinate, lactate, acetate, nitrate, tris-acetanilide complex, malate, mandelate, formate, hexamine complex, diquinoline complex, and oxalate. Antisymmetric and symmetric frequencies were characterized. The experimental results showed an excellent linear relationship between symmetric and antisymmetric O−U−O frequencies, and also a linear relations with a negative slope between the formal charge on U and the magnetic susceptibility of UO_2^{2+}. Visible and UV spectra showed bands at 15,350 and 9,320 cm^{-1}, indicating partial conversion to U(IV). Data for vibrational frequencies, molar magnetic susceptibilities, and U content are shown in tabular form, together with a plot of symmetric against antisymmetric frequencies and a plot of magnetic susceptibilities against antisymmetric O−U−O frequencies. (UK)

Radiation and Nuclear Chemistry

34613 (TID-25689) PRIMARY PROCESS IN RADIATION CHEMISTRY. Abrahamson, Edwin W. (Case-Western Reserve Univ., Cleveland, Ohio. Dept. of Chemistry). [1970]. Contract AT(11-1)-904. 41p. Dep. NTIS.

Research progress is reported on: quenching of excited iodine atoms and photosensitized production of excited singlet oxygen species ($^1\Sigma_g^+$ and $^1\Delta_g$) and their reactivity. The emission of $I(^2P_{\frac{1}{2}})$ at 1.315 μ following the flash photolysis of CF_3I−inert gas mixtures was monitored. The flash spectroscopy and photoreduction of phenazine were studied. Emission from $O_2(^1\Sigma_g^+)$ was detected following the flash photolysis of O_2 and 1-fluoronaphthalene mixtures. The quenching of $O_2(^1\Sigma_g^+)$ by the fluoronaphthalene was estimated to be $7.6 \pm 0.7 \times 10^8$ M^{-1} sec^{-1}. (M.C.G.)

34614 STUDIES ON NATURAL RUBBER LATEX SENSITIZED WITH METHANE HALIDES BY ELECTRON PARAMAGNETIC RESONANCE. PART II. EPR STUDIES OF THE GAMMA-IRRADIATED METHANE HALIDES AND THEIR SOLUTIONS IN NATURAL LATEX. Kosek, S.; Zielinski, W. (Inst. of Nuclear Research, Warsaw). Polim. Tworzywa; 13: 297-300(1968). (In Polish).

The gamma-irradiated CCl_4, $CHCl_3$, CH_2Cl_2, $CHBr_3$, CH_2I_2, and solutions of these compounds in latex of natural rubber were investigated. The EPR spectra obtained at the irradiation temperature (77°K) in the case of solutions of $CHBr_3$ and CH_2I_2 were similar to the spectrum of pure latex, contrary to the solutions of CCl_4, $CHCl_3$, and CH_2Cl_2, where the spectra were quite different. This fact was probably the consequence of the deficiency of a distinct signal from pure $CHBr_3$ and CH_2I_2 contrary to the chlorine derivatives of methane. The radicals of the chlorine derivatives of methane and of solutions of these compounds in latex were identified. Moreover, the formation of peroxide radicals during the heating of samples was confirmed in latex solutions. (auth)

34615 ADVANCES IN RADIATION CHEMISTRY. VOLUME 2. Burton, Milton; Magee, John L. (eds.). New York; John Wiley and Sons, Inc. (1970). 417p. $19.50.

This volume is divided into 3 sections: electron spin resonance of radiation-produced radicals, species in irradiated oxygenated water, and collisions of low-energy electrons with molecules: threshold excitation and negative-ion formation. Each section takes the form of a large review article. An abstract has been prepared for each section. (B.L.M.)

34616 ELECTRON SPIN RESONANCE SPECTRA OF RADIATION-PRODUCED RADICALS. Fessenden, Richard W.; Schuler, Robert H. (Carnegie-Mellon Univ., Pittsburgh). Advan. Radiat. Chem.; 2: 1-176(1970).

This survey of the place of ESR in radiation chemistry is limited to a treatment of topics required for the understanding of the application of ESR in radiation chemical researches. An attempt is made to illustrate the types of structural information available from the powerful coupling of radiation chemical and ESR spectrophotometric methods to produce and study free radicals. A brief chronology of important benchmarks in the development of ESR is given. Discussion of theoretical considerations, experimental techniques, results from ESR experiments, kinetic and magnetic aspects, and areas for future development are included. (311 references). (B.L.M.)

For abstracts of individual sections see: 34616−34618.

34617 SPECIES IN IRRADIATED OXYGENATED WATER. Bielski, Benon H. J.; Gebicki, Janusz M. (Brookhaven National Lab., Upton, N. Y. Australian National Univ., Canberra). Advan. Radiat. Chem.; 2: 177-279(1970).

All reactions considered in the formation of species in irradiated oxygenated water are tabulated. The importance of oxygen in this type system is considered in some detail. The formation, properties, and reactions of HO_2 and O_2^- are discussed in some detail. Since the reaction between oxygen and OH is of no importance except at very high pH, the chemistry of OH is omitted, but description of the formation of the ozonide ion formed by the reaction of O^- with O_2 is considered in some detail. Since all transients except O_2^- discussed at any length are derived from HO_2, and their formation is determined by the pH region in which the perhydroxyl radicals can exist, the main subdivisions of the subject matter fall naturally into two groups of species, those formed below pH 5 and those formed between pH 5 and 14. Results published after the preparation of the main manuscript are summarized in the addendum if they are deemed pertinent to the review. (292 references.) (B.L.M.)

34618 COLLISIONS OF LOW-ENERGY ELECTRONS WITH MOLECULES: THRESHOLD EXCITATION AND NEGATIVE-ION FORMATION. Compton, R. N.; Huebner, R. H. (Oak Ridge National Lab., Tenn. Atomic Energy Commission, Washington, D. C.). Advan. Radiat. Chem.; 2: 281-381(1970).

This report is concerned with low-energy electron−molecule collisions that are particularly important with regard to energy-loss mechanisms and the resultant species formed. The material is concerned specifically with processes occurring in the subionization region; namely, electron−molecule collision processes in which the incident electron energy just matches the excitation energy of one of the electronic states of a molecule or its corresponding molecular negative ion. Experimental studies are discussed under the following headings: electron-impact excitation of molecules, threshold electron-impact excitation: experimental, negative-ion formation in molecules, electron affinity of molecules, dissociative electron attachment, and temporary negative-ion states. (280 references.) (B.L.M.)

Radiation Effects

Refer also to abstract 36298.

34619 X-RAY STUDY OF NEUTRON IRRADIATED DIAMONDS. Vance, E. R. (University Coll., London). J. Phys., C (London); 4: 257-62(Mar 1971).

The diffuse x-ray maxima exhibited by single crystal diamonds, which had undergone a density decrease of about 6% on fast neutron irradiation, lay closer to the Bragg positions of the irradiated crystals than those of the unirradiated crystals. Annealing resulted in shifts of both the diffuse maxima and the Bragg positions. Diamonds in which the macroscopic density decrease on irradiation was less than about 12% recovered towards the original single crystal form on annealing. However, diamonds in which the density decrease on irradiation was more than about 12% reverted towards a semiamorphous state, the density of which was

XUM

about half that of unirradiated diamond, on annealing at temperatures below that required to produce significant graphitization in unirradiated diamond. Type I x-ray behavior was observed after annealing diamonds which had undergone density decreases on irradiation of up to 9%. (auth) (UK)

34620 LIGHT EMISSION FROM THE DISSOLUTION OF GAMMA IRRADIATED ALKALI HALIDES IN WATER. Mittal, J. P. (Bhabha Atomic Research Center, Trombay, India). Nature (London) Phys. Sci.; 230: 160(12 Apr 1971).

Some experimental evidence is reported for the involvement of triplet excitons of the Frenkel type in radiation chemical systems. When γ-irradiated alkali halides are dissolved in water, stored energy is transferred to the solvent, and light is emitted. This emitted light is due to a $T_1 \rightarrow S_0$ transition of the water molecule, indicated by the identification of the phosphorescent emission from added acceptors, a triplet state being invoked. It is believed that the emission from the triplet of the acceptors is due to their population via a triplet–triplet transfer from the solvent triplets. It was also found that when irradiated alkali halides are dissolved in pure water the emission is quenched by known triplet quenchers such as O_2 and paramagnetic ions such as Co^{2+}. A stable triplet excited state of water would be of great interest in radiation chemistry and photobiology. (UK)

34621 RADIATION STABILITY OF BeF_2 GLASSES ACTIVATED BY FLUORIDES OF RARE EARTH ELEMENTS. Margaryan, A. A. (Inst. of General and Inorganic Chemistry, Erevan. Leningrad Inst. of Technology). Arm. Khim. Zh.; 23: 404-9(1970). (In Russian).

The radiation stability of BeF_2–AlF_3–CaF_2 glasses with and without additives was investigated at dosages of 10^3, 10^5, and 10^6 roentgens. A 1.3-MeV ^{60}Co gamma source was used to irradiate samples of these transparent glasses containing 0.02 to 0.05 mole% of several rare earth fluorides. The results showed that the presence of SmF_3, YbF_3, and EuF_3 enhanced the radiation stability of such glasses, but that CeF_4 impaired it. (K.S.W.)

34622 RACEMIZATION OF α-AMINO ACIDS EXPOSED TO γ RADIATION. Kochetkov, N. K.; Kudryashov, L. I.; Senchenkova, T. M. (Inst. of Organic Chemistry, Moscow). Dokl. Akad. Nauk SSSR; 195: 410-12(11 Nov 1970). (In Russian).

It has been previously reported that the configuration of asymmetric carbon atoms is converted upon the irradiation of frozen solutions of monosaccharides. The effect of γ radiation on frozen solutions of L- and D-glutamic acid was investigated. The solutions containing 2 to 3×10^{-3} moles/l of L- and D-acid were irradiated at –78°C in a nitrogen atmosphere using a ^{60}Co source. It was found that the specific rotation of the irradiated solution of L-glutamic acid was greatly reduced with respect to the original solution. Paper chromatographic examination of the lyophilized residue revealed that the material did not differ from the starting solution. After fivefold fractional distillation two fractions were obtained, one of which was found to be identical with the pure L-acid, while the second had a much lower specific rotation and a lower melting point. It was concluded that the second fraction contained D-glutamic acid. Similar conversion was obtained by the irradiation of the D-glutamic acid. Although it was not found possible to evaluate quantitatively the racemization effect, it was concluded that the configuration of the asymmetric carbon atom was converted by exposure to γ radiation. (TTT)

34623 LUMINESCENCE OF WATER EXCITED BY AMBIENT IONIZING RADIATION. Quickenden, T. I.; Que Hee, S. S. (Univ. of Queensland, Brisbane). Radiat. Res.; 46: 28-35(Apr 1971).

A nondecaying weak luminescence of intensity 1.5 ± 0.1 photons sec^{-1} ml^{-1} was observed from purified water exposed to ambient ionizing radiation. The structured emission spectrum and the observed quenching by dissolved oxygen, indicated that a substantial portion of the luminescence was non-Cherenkov emission. Emission peaks were observed at 275 and 370 nm, and a broad emission band was observed between 400 and 700 nm. The peak at 275 nm was attributed to emission by excited triplet water molecules, and the peak at 370 nm was assigned to emission by OH radicals in the $^2\Sigma^+$ state. (auth)

34624 ROLE OF $CHCl_3$ AS A QUENCHER FOR γ- AND UV-EXCITED ORGANIC SOLUTIONS. Levin, E. (York Coll., Flushing, N. Y.); Pope, M.; Saperstein, D.; Oster, G. K. Chem. Phys. Lett.; 9: No. 3, 210-12(1 May 1971).

$CHCl_3$ dissolved in aromatic hydrocarbon solutions of fluorescent solutes is a specific quencher of fluorescence resulting from γ- or uv-excited upper electronic states of the solvent. $CHCl_3$ shows long-range electron-scavenging and short-range compact quenching properties. (auth)

34625 RADIATION EFFECTS WITH A MODEL LIPID MEMBRANE. Petkau, A. (Atomic Energy of Canada Ltd., Pinawa, Manitoba). Can. J. Chem.; 49: 1187-96(15 Apr 1971).

A cell is described that permits a model phospholipid membrane and the two adjacent aqueous compartments to be irradiated with a collimated beam of x rays. During a 2 hr irradiation a marked increase in $[H^+]$ in the aqueous phases is observed. A protonmotive force, given by the H^+ Nernst potential, is generated when one compartment only is irradiated or when both compartments separated by a membrane made structurally asymmetric by the adsorption of alamethicin, are irradiated equally. The results of irradiations in N_2O, N_2, and O_2 indicate that the membrane scavenges the superoxide O_2^-. The effect is discussed in terms of a clearing field that is derived from the potential at the membrane interfaces. (auth) (Canada)

Radiation Processes

Refer also to abstract 35532.

34626 GEL PERMEATION CHROMATOGRAPHIC INVESTIGATION OF IRRADIATED COPOLYMERS. Ferlauto, E. C. (Mobil Chemical Co., Edison, N. J.). J. Chromatogr.; 55: 45-54(17 Feb 1971).

From ninth international gel permeation chromatography seminar; Miami Beach, Fla. (4 Oct 1970). See CONF-701045.

Hot melt samples of γ-irradiated and nonirradiated ethylene–isobutyl acrylate copolymers and ethylene–vinyl acetate copolymers were examined with gel permeation chromatography and the gel content determined to investigate changes in polymer growth upon increasing radiation dosage. Variations in the molecular size and gel content of both copolymer systems studied suggested that the degree of crosslinking is inversely dependent upon the molecular size of the starting material and the rate of degradation is directly related to molecular size. It was demonstrated that these techniques can be employed to determine the optimum initial molecular size and polymer composition for selection of a copolymer system for irradiation. (auth)

34627 MODIFICATION OF FILLED VULCANIZED POLYISOPRENE (SKI-3) RUBBER BY RADIOINDUCED VINYL CHLORIDE GRAFTING. Tikhomirov, V. S.; Vasil'ev, E. V.; Serenkov, V. I. Vysokomol. Soedin., Ser. B; 13: 118-19(Feb 1971). (In Russian).

A possibility of improving the resistance of filled vulcanized rubber, SKI-3, to atmospheric wear by radiation grafting with vinyl chloride is discussed. A typical 60,000-Ci cobalt device was used as a source. The vinyl chloride was grafted by 100 rad/sec radiation. Tabulated data are given of physicomechanical parameters of the SKI-3 rubber irradiated in the presence of vinyl chloride and for ozone resistance of the modified vulcanized rubbers. (R.V.J.)

34628 RADIATION-CATALYTIC DEHYDROGENATION OF CYCLOHEXANE ON Al–Co–Mo CATALYST. Panchenkov, G. M.; Sokolov, L. F. Tr., Mosk. Inst. Neftekhim. Gazov. Prom.; No. 86, 142-50(1969). (In Russian).

An increase of catalytic activity of the Al–Co–Mo catalyst was observed in the radiation-catalytic dehydrogenation of cyclohexane in comparison with regular catalytic dehydrogenation at 360 to 465°C and γ dose rates of 0.1 to 1.5 Mrad/hr. The maximum increase in catalytic activity under the action of γ radiation at 0.3 Mrad/hr was observed at 380°C. Increases and decreases in temperature led to reduction of the effect. Above 465°C, the γ radiation had almost no effect on the rate of dehydrogenation. The action of γ radiation at 0.3 Mrad/hr caused a reduction in the activation energy of dehydrogenation from 48 ± 3 to 34 ± 2 kcal/mole. With the increase in dose rate in the range 0.1 to 1.5 Mrad/hr, the increase in rate of radiation-catalytic dehydrogenation of cyclohexane occurs with divergence from linear law. (tr-auth)

34629 DEHYDRATION OF ISOPROPYL ALCOHOL ON ALUMINUM OXIDE IRRADIATED BY ^{60}Co GAMMA RAYS. Panchenkov, G. M.; Sokolov, L. F. Tr., Mosk. Inst. Neftekhim. Gazov. Prom.; No. 86, 150-1(1969). (In Russian).

Experiments indicated an absence of effect of pre-gamma-irradiation on the catalytic activity of industrial aluminum oxide in the dehydration of isopropyl alcohol in the vapor phase at atmospheric pressure in a flow apparatus. (M.C.G.)

34630 EFFECT OF PRELIMINARY IRRADIATION ON CATALYST ACTIVITY IN DECOMPOSITION OF HYDROGEN PEROXIDE. Panchenkov, G. M.; Sokolov, L. F. Tr., Mosk. Inst. Neftekhim. Gazov. Prom.; No. 86, 151-4(1969). (In Russian).

The effects of previous irradiation with ^{60}Co γ rays on the

XUM

catalytic activity of Al–Co–Mo, Al–Mo–Si, NiO, and Al_2O_3 in the decomposition of H_2O_2 were studied. (M.C.G.)

34631 RADIATION-INDUCED GRAFTING OF STYRENE ONTO CROSS-LINKED BUTYL RUBBER. Dziedziela, W.; Kroh, J. (Technical Univ., Lodz, Poland). Polim. Tworzywa; 14: 63-6(1969). (In Polish).

Styrene was grafted on vulcanized butyl rubber using γ radiation with a dose intensity of 1.0×10^4, 2.1×10^5, and 1.1×10^6 rad/hr. The grafting rate increased with the increase in the dose intensity and was proportional to the 0.26 power of the dose intensity. Such a small value of the exponent power was attributed to the high viscosity of the medium. The high viscosity of the system was also the cause of the almost 8 times higher rate of the graft polymerization in comparison with polymerization of pure styrene. The degree of crosslinking changes on the course of grafting. The character of these changes depends on the intensity of radiation applied. In the case of irradiation with dose intensities lower than 10^6 rad/hr, no degradation of initial vulcanizate was observed and an increase in the network density was observed, which was attributed to the entanglements between the grafted-on chains and the vulcanizate chains. Irradiation at higher dose intensity caused degradation of vulcanizate with a simultaneous grafting. Thus, it was proved that the protective effect of styrene observed in the radiation degradation of polyisobutene depends on the radiation dose intensity. (auth) (NSA of Poland)

34632 RADIATION VULCANIZATION. Morganstern, Kennard H. (Radiation Dynamics, Inc., Westbury, N. Y.). Rubber Age (N. Y.); 103: No. 3, 49-54(Mar 1971).

The history and prospects of radiation vulcanization are reviewed. High power and low cost per usable kilowatt reduce costs to 1¢/lb. Radiation and thermal vulcanization are compared and the economics of radiation cures discussed. (M.C.G.)

34633 GAMMA-RAY-INDUCED POLYMERIZATION OF FLUORINE-CONTAINING PENTADIENE. Ito, Katsukiyo; Muramatsu, Hiroshige; Matsuda, Tatsuo (Government Industrial Research Inst., Nagoya, Japan). Kobunshi Kagaku; 27: 938-42(Dec 1970). (In Japanese).

The γ-induced bulk polymerizations of 3, 4, 5, 5, 5-pentafluoropentadiene-1, 3 (PFP) and 2-methyl-3, 4, 5, 5, 5-pentafluoropentadiene-1, 3 (MPFP) were investigated in the temperature range from +25 to –196°C. PFP was polymerized both in the liquid and solid states, and the structures of the resulting polymers was found to be 1,4-units. The intrinsic viscosity of the polymer obtained in the liquid-state polymerization was considerably higher than that in the solid-state polymerization. Poly-MPFP having 1,4-structure was obtained only in the liquid-state polymerization, and its rate was about one-tenth of PFP. These results suggest that 2-substituted methyl group in pentafluoropentadiene presumably reduces reactivity due to the steric effect. (auth)

Radiolysis

Refer also to abstracts 35103, 35106, 36277, and 36287.

34634 (COO–1385-37) ESR STUDIES OF RADIATION EFFECTS. Technical Report, January 1, 1970–December 31, 1970. ([Michigan State Univ., East Lansing. Dept. of Chemistry]). 6p. Dep. NTIS.

Single crystals of ammonium monofluoroacetate and ammonium difluoroacetate were irradiated at room temperature and ESR spectra of the $CFHCOO^-$ and CF_2COO^- radicals studied. Bromomalonic acid and mandelic acid were irradiated and radicals studied. Gamma-irradiated $KAsF_6$ and chloral hydrate and some neutron-irradiated compounds were also studied. Nuclear quadrupole resonance spectroscopy is also discussed. (M.C.G.)

34635 (NP–18810) RADIOLYSIS OF n-HEPTANE. Campos, Raul Montiel (Universidad Nacional Autonoma de Mexico, Mexico City. Facultad de Ciencias). 1970. 65p. (In Spanish). Dep. NTIS (U. S. Sales Only).

Thesis.

The radiolytic yield and the G value of the liquid products with n-alkane character in the radiolysis of n-heptane were investigated at doses from 1 to 1000 MRad. The possible reaction mechanisms that explain the distribution and the yields of the radiolytic products are discussed and analyzed. (J.S.R.)

34636 (ORO–3729-4) THE RADIOLYSIS OF WATER IN A WIDE RANGE RADIOLYSIS SOURCE. Progress Report, 1 September 1970–1 June 1971. Melton, Charles E. (Georgia Univ., Athens. Dept. of Chemistry). Contract AT(40-1)-3729. 39p. Dep. NTIS.

Research was carried out to develop and apply even more sophisticated theories and apparatus to research on the mechanism of a chemical reaction, specifically the radiolysis of water. During the past three years the mechanism involved in the radiolysis of water has been under investigation. The problem was approached from both an experimental and a theoretical point of view. The experimental approach involved the design and construction of two research mass spectrometers. Following initial testing of the instruments, attention was focused on the initial excitation processes occurring in the radiolysis of water. For negative species, ionizing radiation produces only three primary products, H^-, O^-, and OH^-. The OH^- species is produced only with high-energy radiation. Low-energy β particles (electrons) produce only H^- and O^- from water vapor. The processes whereby these negatively charged species are formed were essentially characterized within the past year. Cross sections, appearance potentials, and ionization efficiency curves were measured as a function of the energy of the ionizing medium. The resonance capture processes do not produce OH^- ions as a primary product. This means that only two negatively charged primary products, H^- and O^-, must be studied to completely characterize the role of negative ions in the overall reaction. At high electron energy (>300 eV) a quantum mechanical approach due to Born can be used to correctly predict the energy dependence of the ionization cross section for small molecules such as H_2, but the Born approximation can not be used for quantitative results in molecules such as H_2O. Because of mathematical and other difficulties in ab initio calculations, a semiempirical calculation must be used to obtain theoretical results. Values for H_2O ionization cross sections together with values obtained for Ar, CH_4, and n-C_4H_{10} were used to develop and test a semiempirical theory for calculating cross sections. Results from this semiempirical approach using a perturbation type model for some n-alkanes showed maximum deviation from experimental values of 6%. (M.C.G.)

34637 (ORO–4059-1) RADIATION CHEMISTRY OF HIGH POLYMERS. Progress Report No. 1, June 1, 1970–March 31, 1971. Dole, Malcolm; Welch, Robert A. (Baylor Univ., Waco, Tex.). 1 Apr 1971. Contract AT(40-1)-4059. 8p. Dep. NTIS.

Research is reported on development of computer techniques for data reduction, alkyl to allyl radical conversion in irradiated polyethylene, solubility of hydrogen in polyethylene, free radical decay in irradiated polyoxymethylene, and ESR spectra of irradiated polyoxymethylene. (M.C.G.)

34638 (RT/CHI–(70)35) AROMATIC HYDROCARBONS AS POTENTIAL SOURCE OF DILUENTS FOR NUCLEAR FUEL REPROCESSING TECHNOLOGY. RADIOLYTICAL AND CHEMICAL STABILITY. Baroncelli, F.; Brignocchi, A.; Gasparini, G. M. (Comitato Nazionale per l'Energia Nucleare, Rome (Italy)). 12 Oct 1970. 24p. Dep. NTIS (U. S. Sales Only).

The chemical and radiolytic stability of some pure and mixed aromatic hydrocarbons was examined to check their potential use as diluents in the nuclear fuel processing technology. Comparative tests in batches showed the pure compounds exhibit a better radiolitic and chemical stability than the mixtures. Mesitylene seems to behave better than the others as a potential alternative diluent for the liquid–liquid reprocessing of irradiated fuels. (auth)

34639 (USC–113-P-21-3) ESR STUDIES OF THIYL FREE RADICALS RELATION TO BIOLOGICAL EFFECTS OF RADIATION. Progress Report. Wolf, Walter (University of Southern California, Los Angeles). 1 Mar 1971. Contract AT(11-1)-113. 46p. Dep. NTIS.

The ESR characteristics of thiyl and related free radicals are being studied to achieve a better understanding of the role of mercapto-containing compounds, both in radiation damage and radiation protection processes. The oxidation of thiols with ceric ion, in solution, leads to a number of free radical signals, ascribable to at least six different species. Some of them, like the RS·, were conclusively identified, whereas others were only tentatively assigned. Further evidence is presented on the nature of "H" (g = 2.0050) as the alkoxy free radical, RO·, obtained possibly by an internal hydrogen migration. New instrumentation and systems were built, operational at carefully controlled temperatures and flow conditions. Attempts to identify a better oxidizing agent than the ceric ion were unsuccessful. Of major significance is the verification that the free radicals previously seen at pH = 2 are also observable in the pH 4 to 8 range, and thus have validity at physiological pH conditions. Also of great interest is the behavior of the free radicals arising on oxidation of glutathione, a potential model for more complex peptides. (auth)

34640 INFLUENCE OF MOLECULAR STRUCTURE AND EXTENT OF CROSSLINKING OF RUBBERS ON THE STABILIZATION OF RADICALS FORMED DURING LOW-TEMPERATURE RADIOLYSIS. Kozlov, V. T.; Evseev, A. G.; Kashevskaya, N. G.; Zubov,

XUM

P. I. (Scientific Research Inst. of Rubber Industry, Moscow). Vysokomol. Soedin., Ser. B: 13: 7-9(Jan 1971). (In Russian).

The kinetics of accumulation of combined radicals formed by ^{60}Co γ irradiation (at 77°K) in various nonlinked and linked (by radiation) rubbers were studied. (tr-auth)

34641 ELECTRON SPIN RESONANCE STUDIES OF FUNDAMENTAL PROCESSES IN RADIATION- AND PHOTO-CHEMISTRY. PART 6. THE RADIOLYSIS OF ACETIC ACID. Ayscough, P. B.; Mach, K.; Oversby, J. P.; Roy, A. K. (Univ. of Leeds, Eng.). Trans. Faraday Soc.; 67: 360-74(Feb 1971).

Matrix isolation studies on CH_3COOH, CH_3COOD, and CD_3COOD, using esr to identify trapped radicals, suggest a mechanism for the γ radiolysis of acetic acid at low temperatures. It is suggested that the primary anion, CH_3COOH^-, which is the only species observed at −196°C, dissociates into $CH_3CO_2^-$ and H, the latter reacting further to give CH_3CO and H_2O. The molecular cation CH_3COOH^+ is not observed, but the CH_3 radicals observed in acetic acid/water matrices are thought to be decomposition products, together with CO_2. The mechanism proposed for radiolysis of the solid is also compatible with product yields obtained from radiolysis of the pure liquid. (auth)

34642 ESR STUDIES OF RESTRICTED RANDOM MOTION OF NH_3^+ RADICALS IN γ-IRRADIATED AMMONIUM PERCHLORATE CRYSTALS. Janecka, J.; Fujimoto, M. (Univ. of Guelph, Ont.). J. Magn. Resonance; 4: 47-53(Feb 1971).

The ESR spectra of $^{14}NH_3^+$ radicals in γ-irradiated crystals of ammonium perchlorate were observed in the temperature range 77 to 300°K. It was found that the radicals rotate in random fashion about two distinct directions in the unit cell, jumping from one orientation to the other. The temperature variation of the correlation time for the nitrogen-14 hyperfine interaction was investigated. (auth) (UK)

34643 RADICAL PRODUCTS FROM THE RADIOLYSIS OF NITROALKANES IN ALKALINE ICE GLASSES. Forchioni, Alain; Chachaty, Claude (CEN de Saclay, Gif-sur-Yvette, France). Int. J. Radiat. Phys. Chem.; 2: 231-45(Dec 1970). (In French).

The scavenging by nitroalkanes of paramagnetic species formed under γ irradiation of alkaline ice glasses at 77°K was studied. Most of the experiments were carried out on a glassy solution of nitromethane and 2-nitro-2-methylpropanol in 10 mole dm^{-3} NaOH. The ESR spectra of radicals from nitroalkanes were attributed in the case of nitromethane to: $\cdot CH_2NO_2^{2-}$ (a_N = 21 G, $A_{N||}$ = 32 G, $A_{N\perp}$ = 16 G), $CH_3\dot{N}O_2^-$ (a_N = 26 G, $A_{N||}$ = 48.5 G, $A_{N\perp}$ = 15 G) and in the case of 2-nitro-2-methylpropanol to: $(CH_3)_2\dot{C}$ = NO· or

$$\begin{matrix} CH_3 \\ CH_2OH \end{matrix}\!\!>\!\dot{C} = NO\cdot \quad (a_N = 33\ G,\ A_{N||} = 48\ G,\ A_{N\perp} = 25\ G).$$

The radiochemical yield of these radicals reaches G = 4.5 for the highest concentration of scavenger used in this work (0.5 mole/dm^3). On the other hand, $G(\dot{O}^-)$ is roughly independent on the concentration of nitroalkanes. These results indicate that the effective yield of radiolysis of alkaline ice is noticeably higher than that measured by ESR in the absence of scavengers [$G(e_s^-)_0 \approx G(\dot{O}^-) \approx 2$] and that the radicals from nitroalkanes are only partly produced by the capture of solvated electrons. (auth) (UK)

34644 EFFECT OF ABSORBED DOSE ON THE YIELDS OF RADIOLYTIC PRODUCTS IN NEUTRAL AQUEOUS SOLUTIONS OF OXALATE ION AND OXYGEN. Micic, O. I.; Kosanic, M. M.; Nenadovic, M. T. (Boris Kidric Inst. of Nuclear Sciences, Vinca, Yugoslavia). Int. J. Radiat. Phys. Chem.; 2: 209-16(Dec 1970).

The radiation yields of hydrogen peroxide and carbon dioxide formed were measured in neutral oxygenated aqueous solution of oxalate ions over a wide range of absorbed doses. The values obtained depend on the dose absorbed. For the low absorbed dose range (2×10^{16} to 3×10^{17} eV g^{-1}) the results are consistent with radical yields $G_{e_{aq}^-} + G_H = 3.32 \pm 0.15$ and $G_{OH} = 2.6 \pm 0.1$, and they are higher than those previously reported for the same system. The hydrogen peroxide and carbon dioxide yields depend on the concentration of carbon dioxide, hydrogen peroxide, and oxygen present in the solution studied. From competition experiments $k_{OH,H_2O_2}/k_{OH,C_2O_4^{2-}} = 4.8 \pm 0.3$ was calculated. It was found that the molar extinction coefficient used in H_2O_2 determinations with KI method depends not only on the concentration of oxalate ion present, but also on the range of hydrogen peroxide concentration. (auth) (UK)

34645 MASS SPECTROMETRIC STUDY OF IONIC REACTIONS PERTINENT TO THE RADIATION CHEMISTRY OF METHANE. Aquilanti, V.; Giardini-Guidoni, A.; Volpi, G. G.; Zocchi, F. (Univ., Rome). Int. J. Radiat. Phys. Chem.; 2: 217-29(Dec 1970).

Several ionic processes of importance in the radiation chemistry of methane were studied by high pressure mass spectrometry. They include the chemistry of ions in pure methane, the reactions of the ions of all the five rare gases with methane, and the reactions of the methane ions with some organic (acetylene, methylacetylene, ethylene, ethane, propane) and inorganic (oxygen, nitrogen, NO, N_2O, CO, CO_2, water, ammonia) additives. (auth) (UK)

34646 PULSE AND γ-RADIOLYSIS OF BOROHYDRIDE ION IN AQUEOUS SOLUTION. Baxendale, J. H.; Breccia, A.; Ward, M. D. (Univ. of Manchester, Eng. CNR, Bologna). Int. J. Radiat. Phys. Chem.; 2: 167-76(Dec 1970).

Radiolysis of aqueous solutions of BH_4^- produces hydrogen, part of which (G = 6.8) is formed within the time for measurement, and the rest (G = 6.3) several hours after irradiation. Pulse radiolysis shows the presence of a transient species formed by the OH + BH_4^- reaction ($k = 1.2 \times 10^{10}$ dm^3 $mole^{-1}$ s^{-1}). It absorbs strongly in the uv (maxima at 260 nm and 400 nm) and decays by a bimolecular reaction ($k = 8.5 \times 10^8$ dm^3 $mole^{-1}$ s^{-1}) to give a second species (absorption maximum 250 nm) which disappears slowly by a first-order reaction ($k = 15$ s^{-1}). In the presence of oxygen the first species reacts ($k = 5.7 \times 10^9$ dm^3 $mole^{-1}$ s^{-1}) to give a product which also decays in two steps, one first order ($k = 3 \times 10^3$ s^{-1}) and the following second order ($k = 1.2 \times 10^5$ dm^3 $mole^{-1}$ s^{-1}). The nature of the species involved is discussed. (auth) (UK)

34647 FORMATION OF FREE RADICALS IN ALIPHATIC AND AROMATIC AMINO ACIDS BY TRAPPED ELECTRONS: AN ESR STUDY. Srinivasan, V. T.; van de Vorst, A. (Univ., Liege). Int. J. Radiat. Biol.; 19: 133-42(1971).

ESR spectroscopy was used to study the reactions of certain amino acids with the trapped electrons generated by x irradiation of alkaline solutions and photoionization of potassium ferrocyanide, $K_4Fe(CN)_6$, in alkaline solutions, both at 77°K. In the aliphatic amino acids, glycine and alanine, no radicals characteristic of the solute were induced during irradiation. However, thermal or photobleaching of the trapped electrons resulted in the formation of hydrogen abstraction radicals. In the presence of potassium nitrate, these radicals were not observed. In the case of aromatic amino acids, tryptophan, tyrosine, and phenylalanine, hydrogen addition radicals were seen immediately after irradiation. Potassium nitrate also suppressed these radicals. They were not observed in the photoionized system. (auth) (UK)

34648 ELECTRON PARAMAGNETIC RESONANCE SPECTRA OF IRRADIATED FROZEN AQUEOUS SOLUTIONS. PART 12. THE REACTIVITY OF MOBILE ELECTRONS RELATIVE TO HYDROGEN IONS IN AQUEOUS ACID GLASSES AT 77°K. Chernova, G. P.; Ershov, B. G.; Pikaev, A. K. (Inst. of Physical Chemistry, Moscow). Izv. Akad. Nauk SSSR, Ser. Khim.; No. 1, 43-8(Jan 1971). (In Russian).

The reactivity of migrating electrons was studied in a number of acidic electron acceptors in aqueous solutions irradiated with a ^{60}Co source at 77°K. These acceptors included CH_3COOH, FCH_2COOH, $ClCH_2COOH$, Cl_3COOH, $BrCH_2COOH$, and ICH_2COOH in 5 M $HClO_4$. The G(H) value for 5 M $HClO_4$ alone was found to be 3; and this decreased sharply with increase in acceptor concentration. A semiquantitative agreement was discovered between reaction velocity constants and electron constants in aqueous solution at room temperature. Hydronium ions (H_3O^+) in "glasses" at 77°K are characterized by anomalously low reactivity as regards free electrons. (K.S.W.)

34649 DIRECT OBSERVATION OF SOLVATION OF THE ELECTRON IN LIQUID ALCOHOLS BY PULSE RADIOLYSIS. Basendale, J. H.; Wardman, P. (Univ. of Manchester, Eng.). Nature (London); 230: 449-50(16 Apr 1971).

The electron solvation process was studied in liquid alcohols at low temperature by following the appearance of the optical absorption band of e_s^- ($\lambda_{max} \simeq 500$ to 800 nm), due to the solvated state, using nanosecond pulse radiolysis. Electron pulses from a 12-MeV linear accelerator were employed, giving doses of ~800 R/pulse, and absorptions were measured during and after the pulse, using equipment with a rise time of ~1 to 2 ns. The alcohols studies included CH_3OH, C_2H_5OH, n-C_3H_7OH, $(CH_3)_2CHOH$, and n-C_4H_9OH. The absorptions were time-dependent and showed distinct changes with time. Initially there was a structureless absorption curve rising steadily from <350 nm to >1,350 nm, attributable to a solvent environment which had not yet reacted to the presence of the charge. The subsequent changes are discussed and absorption curves are shown for n-propanol at 152°K at various times after a 5 ns, ~600 R electron pulse. Although all the alcohols showed the same qualitative behavior, the times during which the initial spectra changes occurred were markedly affected by temperature and varied as between alcohols, being most rapid in the alcohol with shortest dielectric relaxation time. An activation energy of 15 to 20 kJ/mole was estimated for

XUM

solvation of the electron, similar to that expected for H-bond rupture. An interesting observation was that about 50% of the equilibrium absorption at λ_{max} was present immediately after the pulse. Mechanisms are suggested. (UK)

34650 RADIATION RESISTANCE OF C–S BONDS OF MACROMOLECULAR SULFONE POLYELECTROLYTES UNDER THE ACTION OF γ RADIATION. Furnica, G.; Constantinescu, O. (Institut fuer Hygiene, Bucharest. Institut fuer Atomphysik, Bucharest). Rev. Roum. Chim.; 16: 433-7(Mar 1971). (In German).

In order to investigate the hypothesis on the radiation resistance of macromolecules, the electron spin resonance method was used to investigate the formation of free radicals in macromolecular sulfone polyelectrolytes. Ionizing radiation possesses the ability to split C–S bonds, whose stability depends on the electrochemical behavior of the mobile ions from the sulfone group ($R-SO_3^- + Na^+$). The Na^+ ions decrease the intensity of the ESR signal from the free radicals, and ions with increased valence cause the intensity of the signal to decrease even more. The radiation resistance of the macromolecule can be changed by a change in the stability of the chemical bonds in the molecule. The polyelectrolyte was irradiated using a ^{60}Co source with a dose of 8×10^{20} eV/g. (tr-auth)

34651 RADICAL PROCESSES FOLLOWING γ IRRADIATION OF FROZEN CONCENTRATED MATRICES OF HEPARIN AND DEXTRAN SULPHATE. Baugh, P. J.; Morgan, R. E.; Kershaw, K.; Phillips, G. O. (Univ. of Salford, Eng. Univ. of Alabama, Birmingham). Radiat. Res.; 46: 217-25(Apr 1971).

Unlike D-glucose and sucrose ices, frozen concentrated aqueous solutions of heparin and sodium dextran sulfate after γ-irradiation do not efficiently trap electrons ($G e_t^- < 0.1$). Radical yields were measured for these polyanion ices by ESR, and G(radical) was found to increase linearly with solute concentration. The radical yield, extrapolated from the concentrated polyanion ices to the solid state, is in good agreement with the experimental value determined at 77°K for γ-irradiated solid dextran sulfate. For heparin ices, however, the extrapolated value is approximately double the experimental value for the solid. The results indicate that whereas direct action effects adequately account for the radical production in dextran sulfate ices, there is evidence of electronic energy transfer from water molecules in association with the heparin which results in greater heparin degradation than from direct energy absorption. Similar effects could be responsible for the extreme sensitivity of the connective tissue matrix to radiation damage. (auth)

34652 IDENTIFICATION OF RADIATION-INDUCED HYDROGEN-ADDITION RADICALS IN ADENINE DERIVATIVES. Schmidt, Jack; Borg, Donald C. (Brookhaven National Lab., Upton, N. Y.). Radiat. Res.; 46: 36-51(Apr 1971).

Several crystalline N-9-substituted adenine derivatives which had been selectively deuterated at C-8 or at easily-exchangeable positions were exposed to hydrogen or deuterium atoms or to γ rays. The resulting free radicals were studied by electron spin spectroscopy. The radical formed by hydrogen addition on C-8 was always observed. In certain cases, the radical formed by hydrogen addition on C-2 was also present, but at a lower concentration. The source of hydrogen atoms in the γ-irradiation experiments appears to depend upon the molecular environment as determined by the crystal structure, and in one adenine derivative the source is different for the C-8 and C-2 hydrogen-addition radicals. (auth)

34653 INVESTIGATION OF RADIATION-THERMAL CRACKING OF n-TETRACOSANE AND n-HENEICOSANE IN THE LIQUID PHASE. Panchenkov, G. M.; Zhuravlev, G. I.; Polyakova, A. V.; Konstantinov, P. V. Tr., Mosk. Inst. Neftekhim. Gazov. Prom.; No. 86, 120-3(1969). (In Russian).

The radiation-thermal cracking of tetracosane and heneicosane was studied at 310, 330, 350, and 370°C and a γ dose of 80 rad/sec up to 1.3 Mrad. Chromatographic analysis of gaseous products showed that, with increasing temperature, the relative H_2 content of the gases decreased and the contents of CH_4 and olefins increased. Liquid products consisted basically of alkanes of lesser molecular weight than the starting material. (tr-auth)

34654 DOUBLE-STAGE MECHANISM OF THE FORMATION OF FREE RADICALS DURING THE RADIOLYSIS OF FROZEN AQUEOUS SOLUTIONS OF DNA AND ITS CONSTITUENT ELEMENTS. Abagyan, G. B. (Inst. of Physical Research, Erevan); Butyagin, P. Yu. Stud. Biophys.; 15-16: 291-8(1969).

From second international symposium on initial effects of ionizing radiation on a cell; Erevan, USSR (Oct-Nov 1968). See CONF-681087.

The method of Electron Spin Resonance (ESR) was applied to the study and analysis transforming the paramagnetic centers into γ-irradiated frozen aqueous solutions of 5-methylcytosine, thymidine, and DNA in ordinary and heavy water (temperature range 80 to 220°K). Electrons stabilized by the molecule of the base constituted the principal part of paramagnetic centers, to be found in the solution after the temperature has been raised up to 120°K. At 160 to 200°K those centers recombined with H^+ or D^+ resulting in radicals which were identical in structure with those arising from the combination of H or D atoms with the pyrimidine cycle. (auth)

34655 COENZYME-SUBSTRATE INTERACTIONS, ESR STUDY OF IRRADIATED SYSTEMS. Checcucci, A.; Depireux, J.; Lenci, F. (CNR, Pisa, Italy. Physics Inst., Liege). Stud. Biophys.; 13: 43-6(1969).

The radical yield (G_R) of x-irradiated coenzyme-substrate systems (glutamic acid, glutaric acid, and DPN) was determined in comparison with single components by the ESR method. G_R diminution and spectral modification of substrate in presence of its coenzyme are discussed on the basis of the H transfer mechanism. (auth)

34656 INTER AND INTRAMOLECULAR CHARGE AND EXCITATION TRANSFER OBSERVED IN IRRADIATED POLYVINYL CHLORIDE PARTICLES WITH SURFACE-COATED ADDITIVES. Ueda, Hisashi; Yashiro, Dairokuro (Government Chemical Industrial Research Inst., Tokyo). Bull. Chem. Soc. Jap.; 44: No. 3, 595-9(Mar 1971).

Particles of poly(vinyl chloride) (PVC) were coated with small amounts of various aromatic compounds from benzene solutions and were then γ-irradiated in a vacuum. The ESR spectra of the specimen thus obtained were recorded. Though the amount of the coated additives, in the ratio of 1 molecule for 100 monomer units of PVC, was small, strong effects on the ESR spectra were observed. The additives coated on the surface affect the ESR spectra in two ways. They cause a decrease in the total ESR absorption intensity; this was observed with all the additives studied. They also often transform the ESR spectrum; this was observed with several additive compounds, such as p-benzoquinone, tetramethylphenylenediamine-2·HCl, chrysene, hydroquinone, nitrosonaphthol, perylene, and diphenylpicrylhydrazine. Only the conduction of the excitations, holes and electrons formed in the bulk particles, to the surface of the particle can explain these results. On the surface of the particle, the excitation or the electric charge is transferred to the additive by means of an intermolecular interaction with it. The possibilities for the mechanism of the conduction of the excitation and the electric charges, and the ionization processes are discussed. (auth)

34657 STUDY OF THE OXIDATION AND REDUCTION OF $Ru(NH_3)_5N_2^{2+}$ BY γ- AND ELECTRON PULSE RADIOLYSIS. Baxendale, J. H.; Mulazzani, Q. G. (Univ. of Manchester, Eng.). J. Inorg. Nucl. Chem.; 33: 823-30(Mar 1971).

$Ru(NH_3)_5N_2^{2+}$ is oxidized to $Ru(NH_3)_5N_2^{3+}$ by OH radicals with a rate constant 4.8×10^9 M^{-1} sec^{-1}. The Ru(III) complex undergoes spontaneous aquation to $Ru(NH_3)_5OH^{2+}$ with a rate constant 250 sec^{-1}. $Ru(NH_3)_5N_2^{2+}$ reacts with e_{aq}^- with a rate constant 4.2×10^9 M^{-1} sec^{-1} to give the Ru(I) compound, $Ru(NH_3)_5N_2^+$. The latter undergoes dismutation in a bimolecular reaction with $2k = 2.7 \times 10^9$ M^{-1} sec^{-1} to give the original Ru(II) complex and a Ru^0 compound, which may originally be $Ru(NH_3)_5N_2$, but ultimately precipitates as ruthenium metal. Absorption spectra were obtained for all the species produced. (auth) (UK)

34658 FORMATION KINETICS OF THE PYRENE DIMER CATION OBSERVED BY PULSE RADIOLYSIS. Rodgers, M. A. J. (Univ. of Manchester, Eng.). Chem. Phys. Lett.; 9: No. 2, 107-8(15 Apr 1971).

The pyrene dimer cation is formed from the monomeric species in electron pulse radiolysis of pyrene in liquid acetone at –75°C with a rate constant close to the diffusion value. (auth)

34659 ALKOXY RADICAL PRODUCTION IN THE RADIOLYSIS OF t-BUTANOL (2-METHYL-2-PROPANOL). Verdin, D. (Atomic Energy Research Establishment, Harwell, Eng.). Int. J. Radiat. Phys. Chem.; 2: 201-8(Dec 1970).

The liquid products formed in the γ radiolysis of t-butanol (2-methyl-2-propanol) at 30°C are, in order of decreasing G value, acetone, isobutyraldehyde, di-t-butyl ether, t-butyl methyl ether, sec-butanol, 1,2-epoxy-2-methylpropane, and di-t-butyl peroxide. The influence of NaI, N_2O and 2,6-di-t-butyl-4-methylphenol on the yields of these products was examined in order to evaluate the contribution of tert-butoxy radicals to their formation. It is concluded that G(tert-butoxy) ≥ 2.3. The yields of H_2, CH_4, and C_2H_6 were also measured for pure t-butanol. (auth) (UK)

34660 RESISTANCE OF SOLID SUBSTANCES TO GAMMA RADIATION. Hangay, Gyorgy; Lukats, Bela (Pharmaceutical Works of Kobanya, Budapest). Acta Pharm. Hung.; 41: 10-19 (Jan 1971). (In Hungarian).

The radiation resistance of dihydrotriazine pamoate and ethionamide, two basic materials used in pharmaceutical preparations, was studied. Numerous physical, chemical and bacteriological tests were used to investigate samples irradiated with various doses and dose rates. The investigations revealed that these two heat-sensitive preparations remain unchanged after gamma irradiation, moreover, irradiation doses much larger than the effective sterilizing dose will not cause detectable decomposition in these substances. (JPRS)

34661 EFFECTS OF γ-IRRADIATION ON SODIUM SULPHACETAMIDE. Phillips, G. O.; Power, D. M.; Sewart, M. (Univ. of Salford, Eng.). Radiat. Res.; 46: No. 2, 236-50(May 1971).

The effects of γ-radiation on sodium sulfacetamide in aqueous solutions and in the solid state were studied. Pulse radiolysis and steady-state experiments demonstrate that hydrated electrons (e^-_{aq}) and hydroxyl radicals (OH) are mainly responsible for the degradation between 10^{-4} to 1.2 M solute concentrations. The reaction with e^-_{aq} yields sulfanilic acid and an additional unidentified product. Hydroxyl radicals give two products tentatively identified as monomeric and dimeric phenolic derivatives of sulfacetamide. Suitable e^-_{aq} and OH scavengers selectively remove these products. G(-sulfacetamide) is a maximum of 4.8 in aqueous solution and <0.01 for the solid. The implications of the results in the radiation sterilization of sulfacetamide formulations are discussed. (auth)

34662 EFFECT OF IONIZING RADIATION ON THE STABILITY OF SOME RADIOPAQUE IODINE COMPOUNDS. Perkowski, Edward; Szyszko, Edmund; Zagorski, Zbigniew Pawel; Wozniak, Wanda (Inst. for Drug Research and Control, Warsaw). Diss. Pharm. Pharmacol.; 23: 75-82(Jan-Feb 1971).

The radiopaque iodine compounds, diatrizoic acid and adipiodone, irradiated with 3.5 Mrad ^{60}Co do not undergo essential changes as shown by physical, physicochemical, and chromatographic investigations. The color was changed. N-methylglucamine irradiated with 2.5 and 3.5 Mrad showed a color change and a dose dependent increase of reducing sugars. Dry preparations containing diatrizoic acid and adipiodone salts decomposed in a dose dependent manner. (D.P.O.)

34663 CHEMICAL CONSEQUENCES OF THE (n,γ) REACTION IN POTASSIUM FERROCYANIDE. Meriadec, B.; Milman, M. (Department des Radioelements, Saclay, France. CEA, Gif-sur-Yvette, France). J. Inorg. Nucl. Chem.; 33: 915-35(Apr 1971).

The neutron irradiation of potassium ferrocyanide produced radioactive divalent and trivalent iron, potassium ferrocyanide, an and an insoluble fraction. The kinetic analysis of the post-irradiation thermal annealing showed that the reformation of the parent compound takes place exclusively at the expense of the Fe^{II} fraction. The presence of air does not profoundly affect the annealing process. The presence of water of crystallization accelerates the sample decomposition, has an oxidizing effect upon the divalent iron, but does not change the kinetics of the annealing. The kinetic study of the irradiation dose effect showed that an increase in does diminishes the potential number of atoms susceptible to annealing and diminishes the activation energy of the annealing process. The kinetics of the thermal macro-decomposition were also studied. (auth) (UK)

34664 RADIATION CHEMISTRY OF CARBOHYDRATES. XIV. FORMATION OF DEOXY-SUGARS BY RADIOLYSIS OF AQUEOUS SOLUTIONS OF CARBOHYDRATES. Kudryashov, L. I.; Yarovaya, S. M.; Voznesenskaya, S. V.; Kochetkov, N. K. Zh. Obshch. Khim.; 41: No. 2, 449-55(Feb 1971). (In Russian).

Deoxy-sugar formation from the irradiation of carbohydrates is a general phenomenon arising from radiolysis both of low-molecular-weight carbohydrates and carbohydrate-containing polymers. Oxygen-free aqueous solutions of sugars were given doses of 2.7×10^{16} ev/ml/sec from a ^{60}Co source. High yields of deoxy-sugars and the novelty of this reaction call attention to this process as evidently fundamental to radiation biology. (tr-auth)

34665 MECHANISMS OF HYDROGEN FORMATION IN THE RADIOLYSIS OF GASEOUS CH_3OH AND CD_3OH. Klosova, E.; Teply, J.; Prasil, Z. (Inst. of Nuclear Research, Rez, Czech.). Int. J. Radiat. Phys. Chem.; 2: 177-86(Dec 1970).

Radiation-chemical yields of hydrogen precursors — i.e., electrons, hydrogen atoms, and the unscavengeable (molecular) hydrogen — in the radiolysis of gaseous CH_3OH and CD_3OH were determined using SF_6, C_3H_6, and CCl_4 as scavengers. In the radiolysis of CD_3OH the isotopic composition of hydrogen originating from these precursors was measured and the corresponding isotopic separation factors were calculated. The experimental yields of hydrogen, carbon monoxide, and methane were compared with the yields calculated using the experimental mass spectra of CH_3OH and CD_3OH and the published data on ion-molecule reactions and on the uv photolysis of methanol vapor. It is concluded that hydrogen produced in reactions of electrons originates predominantly from the hydroxyl group, and that the scavengeable hydrogen atoms formed independently of reactions of electrons are produced in dissociations of excited ions and molecules. The unscavengeable hydrogen is produced also in decomposition of the excited ions and molecules and comes predominantly from the methyl group. Carbon monoxide and methane are formed mostly by the ionic mechanism and their yields are independent of the presence of SF_6 and /or C_3H_6. (auth) (UK)

34666 UNSTABLE INTERMEDIATES. PART LXXXV. ELECTRON SPIN RESONANCE STUDY OF γ-IRRADIATED SODIUM CHLORATE: LIBRATING CHLORINE DIOXIDE. Symons, M. C. R. (Univ. of Leicester, Eng.). J. Chem. Soc., A; No. 5, 698-700(1971).

The ESR spectrum of γ-irradiated sodium chlorate at 19°K shows features characteristic of chlorine dioxide. These change, reversibly, on warming to room temperature to give features previously assigned to chlorine trioxide. The two sets of data can be directly linked on the assumption that at room temperature, chlorine dioxide molecules are rotating about the C_{3v} axis of the chlorate ions from which they were derived. (auth) (UK)

34667 UNSTABLE INTERMEDIATES. PART LXXXVI. ELECTRON SPIN RESONANCE STUDIES OF THE EFFECT OF γ-RAYS ON POTASSIUM DIFLUOROPHOSPHATE: THE RADICAL PO_2F^-. Begum, A.; Subramanian, S.; Symons, M. C. R. (Univ. of Leicester, Eng.). J. Chem. Soc., A; No. 5, 700-2 (1971).

The magnetic parameters of PO_2F^- in potassium difluorophosphate show that this pyramidal radical is structurally similar to the isoelectronic radical PO_3^{2-}, the spin-density on phosphorus being slightly increased and the p : s ratio on phosphorus slightly reduced. The isotropic coupling to ^{19}F(165 G) is similar to that for CF_3. (auth) (UK)

34668 APPEARANCE OF H^+ IONS IN IRRADIATED LIQUID WATER. Kabakchi, S. A. (Inst. of Electrochemistry, Moscow); Kudryashov, L. I.; Bugaenko, L. T. Int. J. Radiat. Phys. Chem.; 2: 187-90(Dec 1970). (In Russian).

The transformation under irradiation of pH-indicators into their acid form was observed spectrophotometrically by pulse radiolysis of weakly alkaline aqueous solutions. The data prove the appearance of hydrogen ions by irradiation of liquid water. (auth) (UK)

Radioisotope Production

Refer also to abstract 36686.

34669 (JAERI-Memo-4279) IMPURITIES IN PROCESSED RADIOISOTOPES PRODUCED BY THE (n,γ) REACTION: PURITY OF ^{169}Yb. Kubota, M.; Amano, H. (Japan Atomic Energy Research Inst., Tokyo). Jan 1971. 15p. (In Japanese). Dep. NTIS (U. S. Sales Only).

Impurities in ytterbium oxide were determined in order to estimate the radiochemical purity of ^{169}Yb that is to be produced by neutron irradiation of this material. Impurities of 0.036 ppM Sc, 2.8 ppM Tm, 8.6 ppM Tb, and 7.2 ppM Eu were found in the ytterbium oxide by radioactivation analysis combined with ion-exchange separation. In spite of this high purity of the target material, the radiochemical purity of ^{169}Yb when irradiated for 130 hours in a neutron flux of 1×10^{18} n/cm^2 does not exceed 1.7% at the end of cooling for 24 hours after irradiation because of the formation of ^{175}Yb. Cooling for about 105 days is necessary to allow decay of the ^{175}Yb and ^{177}Lu formed from the β disintegration of ^{177}Yb, and to raise the radiochemical purity of ^{169}Yb to 99.9%. The specific activity of the product thus obtained was found to be 0.16 Ci/g Yb. (auth) (Japan)

34670 (JAERI-Memo-4280) IMPURITIES IN PROCESSED RADIOISOTOPES PRODUCED BY THE (n,γ) REACTION: PURITY OF ^{160}Tb. Kubota, M.; Amano, H. (Japan Atomic Energy Research Inst., Tokyo). Jan 1971. 16p. (In Japanese). Dep. NTIS (U. S. Sales Only).

Impurities in terbium oxide were determined in order to estimate the radiochemical purity of the ^{160}Tb radioisotope produced by neutron irradiation of this material. Radioactivation analysis combined with ion exchange separation showed the presence of

XUM

21 ppM of Gd, 135 ppM of Dy, 19 ppM of Ho, and 17 ppM of Er as impurities in the target material. From these results, the radiochemical purity for ^{160}Tb is calculated to be 95.8% at the time immediately after irradiation for 288 hours in a thermal neutron flux of 1×10^{13} n/cm^2 sec, and to be higher than 99.99% at 24 hours after the irradiation. While ^{165}Dy is a major shorter-lived impurity, ^{158}Gd and ^{169}Er become predominant among impurities after long term cooling; the proportion of both isotopes, however, do not exceed 1×10^{-3}% after cooling of even 100 days. (auth) (Japan)

34671 RAPID METHOD FOR PREPARATION OF ^{32}P APPLICATORS. Srobodova, J.; Kronrad, L.; Kolinska, J. (Czechoslovak Academy of Sciences, Prague). Int. J. Appl. Radiat. Isotop.; 22: 213(Mar 1971).

A method of using a plastic anion exchange resin in which ^{32}P is absorbed for use as applicators is described. It was found that a carrier-free solution of sodium phosphate–^{32}P solution produced the maximum though inhomogeneous absorption on Zerolitt F F foil. With 3mgP/ml carrier, homogeneous distribution was achieved and the absorption was about 60% after 10 hrs. The recommended procedure is given. (UK)

34672 CONTROL OF ELUTION AND ELUENT FROM ^{113m}In GENERATORS. Robles, Ana Maria; Servian, Jorge L.; Touya, Juan Jose. Rev. Biol. Med. Nucl.; 2: 78-81(Jun–Oct 1970). (In Spanish).

The normal elution curve in different isotopic generators of ^{113m}In was studied. The influence of variation of normality and pH of the eluent besides the temperature and velocity at which elution proceeds was determined. Such variations do not modify the elution curve to any appreciable extent. The characteristics of the eluate containing the indium were studied. The ^{113}Sn/^{113m}In ratio and the influence of the normality of the eluent upon it were determined. Also detected was the presence of other nuclides and zirconium. Finally the adsorption of ^{113m}In on glassware and the effect of silicone coating upon it were measured. (auth)

Recoil Production and Reactions

Refer also to abstracts 34674–34677.

Radiochemistry

Refer also to abstracts 34678, 34700, and 34863.

34673 (CEA-N-1440) CHARACTERISTICS OF VARIOUS SEALING MEMBRANES FOR ALPHA ACTIVITY MONITORING CELLS USED IN SOLUTIONS. Edeline, J. C.; Le Devehat, J. (Commissariat a l'Energie Atomique, Saclay (France). Centre d'Etudes Nucleaires). 6 Jan 1971. 44p. (In French). Dep. NTIS (U. S. Sales Only).

The membranes used in on line α activity measurement cells must possess the following characteristics: mechanical strength, transparency to α particles, resistance against chemical attack and contamination, and ease of decontamination. Various membranes were studied: polyamide, polyethylene, ethylene polyterephtalate, polytetrafluorethylene, and polypropylene. Only the polypropylene gave satisfactory results with nitric solutions. None of the membranes was entirely satisfactory against organic solvents. (France)

34674 CONSEQUENCES OF β-DECAY OF ^{129}Te IN SOME Te OXIDE COMPOUNDS. Lebedev, R. A.; Babeshkin, A. M.; Nesmeyanov, An. N. Vestn. Mosk. Univ., Ser. II. Khim.; 12: 113-15(Jan–Feb 1971). (In Russian).

The chemical state of ^{129}I atoms produced by β decay of ^{129}Te was studied by nuclear gamma resonance. The nuclear recoil and shake off effects on the chemical state of ^{129}I were found to be negligible. (auth)

34675 REACTIONS OF He^3H^+ IONS WITH GASEOUS HYDROCARBONS. IV. CYCLOBUTANE, CYCLOPENTANE, AND CYCLOHEXANE. Cacace, Fulvio; Guarino, Angelo; Possagno, Elvira (Univ., Rome). J. Amer. Chem. Soc.; 91: 3131-4 (4 Jun 1969).

Gaseous carbonium ions were produced from the protonation of cyclobutane, cyclopentane, and cyclohexane with helium tritide molecular ions, obtained from the β decay of molecular tritium. A fraction of the excited carbonium ions formed from the exothermic protonation are collision stabilized at pressures ranging from 100 to 400 Torr, and yield in all systems stabilized cycloalkanium ions. The latter can partially rearrange to the isomeric linear carbonium ions. The results obtained provide direct evidence for the existence of the gaseous cyclobutanium, cyclopentanium, and cyclohexanium ions. (auth)

34676 REACTIONS OF He^3H^+ IONS WITH GASEOUS HYDROCARBONS. III. CYCLOPROPANE, PROPANE, ISOBUTANE, AND n-BUTANE. Cacace, Fulvio; Caroselli, Marcello; Cipollini, Romano; Ciranni, Giovanna (Univ., Rome). J. Amer. Chem. Soc.; 90: 2222-7(24 Apr 1968).

The reactions of the He^3H^+ ions, formed from the decay of molecular tritium, with c-C_3H_6, C_3H_8, n-C_4H_{10}, and i-C_4H_{10} were investigated at the pressures of 20 and 760 torr, under conditions excluding the interference of radiolytic processes. The nature and the yields of the tritiated reaction products, determined by radio gas chromatography, are consistent with the hypothesis that the He^3H^+ ions attack the gaseous hydrocarbons, giving excited protonated species, which dissociate into neutral fragments and simpler ions along energetically allowed pathways. The formation of the observed labeled products can be rationalized taking into account the various fragmentation processes and the consecutive reactions of the fragment ions with the inactive hydrocarbon. The reaction of He^3H^+ ion with c-C_3H_6 yields labeled C_3H_6 hydrocarbons, whose formation requires the stabilization of a fraction of the protonated ions. Furthermore, the high yield of tritated c-C_3H_6 suggests a cyclic structure for the protonated ion and provides direct evidence for the existence of the cyclopropanium ion often postulated in different fields of chemistry. In the case of C_3H_8 and n-C_4H_{10}, on the other hand, the results can be interpreted without requiring the intervention of the stabilized protonated ions. (auth)

34677 REACTIONS OF He^3H^+ IONS WITH GASEOUS HYDROCARBONS. II. METHANE AND ETHANE. Cacace, Fulvio; Cipollini, Romano; Ciranni, Giovanna (Univ., Rome). J. Amer. Chem. Soc.; 90: 1122-6(28 Feb 1968).

The reactions of the He^3H^+ molecular ion, formed from the decay of gaseous tritium, with methane and ethane at atmospheric pressure were investigated under conditions ensuring that the labeled decay ions were the only source of the tritiated products, with no interference from radiolytic processes. The He^3H^+ exothermically protonate the methane, giving excited $CH_4{}^3H^+$ ions, that can be either collision stabilized at 760 torr or decompose into tritiated methyl ions and hydrogen. The stabilized ions react with CH_4 according to a thermoneutral proton-transfer process, which yields the observed tritiated methane, while the methyl ions react with CH_4 forming the highly unreactive ethyl ions, whose fate depends on the nature and the amount of the impurities contained in the system. The reaction of the He^3H^+ ions with ethane yields excited $C_2H_6{}^3H^+$ ions, which appear to decompose into labeled ethyl ions, without any appreciable stabilization. The thermoneutral hydride ion transfer from the C_2H_6 to the labeled ethyl ions leads to the formation of the observed tritiated ethane. (auth)

Separation Processes

Refer also to abstracts 34525, 34638, 34721, 34722, 34733, 34737, 34785, 34826, 34844, 35140, 36977, 37001, and 37106.

34678 (ARH-468(Rev.)) TECHNICAL CRITERIA FOR THE PREVENTION OF CRITICALITY. Tomlinson, R. E. (Atlantic Richfield Hanford Co., Richland, Wash.). 15 Apr 1971. Contract AT(45-1)-2130. 12p. Dep. NTIS.

Technical criteria are defined for use in developing the limits within which chemical processing facilities are to be designed and operated. Topics covered include: specifications, materials to be covered, assumptions, technical review, experimental basis, safety factors, safety mechanism limits, and fire fighting. (M.C.G.)

34679 (ARH-SA-58-RD) MACRORETICULAR ION EXCHANGE RESIN CLEANUP OF PUREX PROCESS TBP SOLVENT. Schulz, Wallace W. (Atlantic Richfield Hanford Co., Richland, Wash.). 1 Aug 1970. Contract AT(45-1)-2130. 26p. (CONF-710417-2). Dep. NTIS.

From International solvent extraction conference; The Hague, Netherlands (19 Apr 1971).

Strong base macroreticular ion exchange resins effectively remove both fission products and diluent and TBP degradation products from used Purex process solvent. Application of such resins in routine cleanup of Purex process extractant is potentially attractive to eliminate the large volumes of radioactive waste generated by presently used solvent wash procedures. The capacity of macroreticular resins for adsorbing extractant impurities is very high judging from batch and column data. Over 240 bed volumes of unwashed Hanford Purex plant first cycle solvent were passed downflow (at 40°C and 4 bed volumes/hr) through a 59-ml bed of 14- to 50-mesh resin without any detectable breakthrough of impurities. All the effluent solvent was water-white as opposed to the faint-yellow color of the feed; its fission product content and plutonium retention number were both substantially lower than

XUM

typical washed (alkaline permanganate) plant solvent. Elution of loaded resin with a few bed volumes of 3M HNO_3–0.05M HF and 4M NaOH removes all the adsorbed yellow color and ^{95}Zr–^{95}Nb activity but only 55 to 65% of the ^{106}Ru–^{106}Rh load. (auth)

34680 (CEA-R-4109) THE PRECIPITATION AND FILTRATION OF TRIVALENT PLUTONIUM OXALATE. Cheneau, Gilbert (Commissariat a l'Energie Atomique, Chusclan (France). Centre de Production de Plutonium de Marcoule). Feb 1971. 63p. (In French). Dep. NTIS (U. S. Sales Only).

The conditions of continuous precipitation and separation of Pu^{3+} oxalate on an industrial scale were investigated. The solubility of Pu^{3+} oxalate was measured as a function of nitric acidity, oxalic acid excess, and temperature. The most suitable precipitation and filtration conditions were defined from determinations of the sedimentation rate, the resistance to filtration, and the apparent density of the cake. A continuous precipitation and filtration pilot plant was built and tested. (France)

34681 (CONF-710417-1) OPTIMIZED USE OF MULTI-PURPOSE FUEL PROCESSING FACILITIES AT THE IDAHO CHEMICAL PROCESSING PLANT. Modrow, R. D.; Offutt, G. F.; Wheeler, B. R. (Idaho Nuclear Corp., Idaho Falls). [nd]. Contract AT(10-1)-1230. 23p. Dep. NTIS.

From International solvent extraction conference; The Hague, Netherlands (19 Apr 1971).

Three cycles of solvent extraction are used at the Idaho Chemical Processing Plant (ICPP) for purifying highly enriched uranium generated from reprocessing highly radioactive fuel elements in various head-end facilities. The first cycle of extraction usually employs TBP in this multi-purpose plant, and is followed by two extraction cycles using methyl isobutyl ketone (MIBK). Use of different solvents permits advantage to be taken of their respective characteristics for separating fission products from uranium; MIBK is more effective for zirconium whereas TBP is more effective for ruthenium. Five head-end systems are currently available for dissolving spent fuel elements. Currently, these systems at the ICPP are operated sequentially, along with a waste solidification facility, to permit optimum use of manpower and facilities to result in lowest possible reprocessing costs. The continuous aluminum process and the first extraction cycle are operated concurrently while the other facilities are in standby and the first cycle product is being collected and stored. Then the second- and third-extraction cycles and product denitration unit are operated concurrently. When these fuel processing facilities are in standby, the waste solidification facility is operated to convert the radioactive waste solutions from the solvent extraction system to a safer, more compact granular solid. (auth)

34682 (CONF-710509-1) TREATMENT OF RADIOACTIVE WASTE STREAMS AT THE IDAHO CHEMICAL PROCESSING PLANT BY EVAPORATION AND ION EXCHANGE. Rhodes, D. W.; Lohse, G. E. (Idaho Nuclear Corp., Idaho Falls). [1969]. Contract AT(10-1)-1230. 15p. Dep. NTIS.

From twenty-sixth annual Purdue industrial waste conference; Lafayette, Ind. (4 May 1971).

The systems and methods used for treating low- and intermediate-level wastes are described. The waste is received in an evaporator waste collection tank. In evaporation an appreciable decontamination factor was obtained for gross radionuclides. The condensate is pumped to an ion exchange system for additional decontamination. The need for regeneration of the system can be determined readily by monitoring for ^{137}Cs in the column effluent. (M.C.G.)

34683 (DOCKET-50201-73) WEST VALLEY REPROCESSING PLANT. Activity in Sanitary Waste System Effluent. (New York State Dept. of Environmental Conservation, Albany, N. Y.). 8 Jun 1971. 3p. Dep. NTIS.

Gross beta, ^{90}Sr, and tritium were determined in water at 4 points: the discharge pipe of the sanitary waste system, a warm water and a cold water discharge to a drainage ditch east of the plant, and surface water in a drainage ditch at the north end of the exclusion area. No uranium was found in the samples. Plutonium was present in a concentration of 4.1 pCi/l. (M.C.G.)

34684 (DOCKET-50268-8) MIDWEST FUEL RECOVERY PLANT. Preliminary Safety Analysis Report, Amendment 11 (Includes Technical Specifications). (General Electric Co., San Jose, Calif. Nuclear Energy Div.). 7 May 1971. 92p. (NEDO-14503). Dep. NTIS.

Technical specifications are submitted in support of application for an operating license. Safety limits, limiting conditions, surveillance requirements, equipment design features, and administrative requirements are discussed. (M.C.G.)

34685 (DOCKET-50268-9) MIDWEST FUEL RECOVERY PLANT. Preliminary Safety Analysis Report, Amendment 12. (General Electric Co., San Jose, Calif. Nuclear Energy Div.). 27 May 1971. 43p. Dep. NTIS.

An extension of the construction completion date from July 1, 1971 to April 1, 1972 is requested and information given in support of the operating license application. A copy of the General Electric Company 1970 Annual Report is included. (M.C.G.)

34686 (DOCKET-50332-18) BARNWELL NUCLEAR FUEL PLANT. Preliminary Draft of Supplementary Data for Seismic Structural Analysis. (Allied-Gulf Nuclear Services, Florham Park, N. J.). 4 Jun 1971. 59p. Dep. NTIS.

Design spectra, seismic soil data, and mathematical models for critical structures and equipment are given. (M.C.G.)

34687 (EUR-4614) PYROCHEMICAL HEAD END CONCEPTION FOR FAST BREEDER FUEL PROCESSING. Wurm, J. G.; Heylen, P. R.; De Beukelaer, R. C.; De Coninck, A. (Societe Belge pour l'Industrie Nucleaire, Brussels. Centre d'Etude de l'Energie Nucleaire, Mol (Belgium)). 6 Jul 1970. 20p. (CONF-700438-1). Dep. NTIS (U. S. Sales Only). EUR F.Fr. 4.55.

From Reactor meeting; Berlin, Germany (20 Apr 1970).

An integrated pyrochemical head end was developed. It is based on the decladding of the stainless steel canning in a liquid solvent alloy composed of Sb–Cu and followed by a disaggregation of the fuel in a molten oxidizing salt bath composed of alkaline nitrates. Two different Sb–Cu dissolution procedures are described and a materials balance is given for the liquid metal dissolution as well as for the molten salt disaggregation. (auth)

34688 (EUR-4615) FAST BREEDER FUEL PROCESSING PYROCHEMICAL HEAD END STUDY. Wurm, J. G.; David, C.; Heylen, P. R.; De Beukelaer, R. D.; De Coninck, A.; Verbeke, R. (Centre d'Etude de l'Energie Nucleaire, Mol (Belgium)). 27 Jul 1970. 24p. (CONF-700651-1). Dep. NTIS (U. S. Sales Only). EUR F.Fr. 4.45.

From European meeting of chemical engineering; Frankfurt am Main, Germany (17 Jun 1970).

Conceptual head-end studies were made for highly irradiated fast breeder fuel. The storage of short-cooled fuels in a hybrid sodium organic coolant storage pool and decladding experiments based on the Sb–Cu liquid metal dissolution technique are considered. A general design and layout of the hybrid Na organic storage pool is given and the inherent advantages over other storage facilities are discussed. The presence of Na during the liquid metal (Sb–Cu) dissolution procedure was investigated and it was shown on the basis of a small pilot scale experiment that sodium does not present a problem at this stage. Small-scale liquid metal dissolution experiments combined with filtration performed on small dummy fuel elements (19 pins) filled with ceramics proved the feasibility of the process. (auth)

34689 (IAEA-R-876-F) INVESTIGATION OF REPROCESSING INPUT MEASUREMENT USING TRACER TECHNIQUE. Final Report, December 15, 1960–July 14, 1970. Bokelund, H. (International Atomic Energy Agency, Vienna (Austria)). Oct 1970. 30p. NTIS (U. S. Sales Only).

The quantities of uranium and/or plutonium fed into a reprocessing plant are currently found by multiplying the dissolver solution batch size (volume or weight) by the concentrations of these elements as found by analyses of samples taken from the batch. An independent verification of the volume measurement using tracer techniques is proposed. The basic concept is that of isotope dilution mass spectrometry applied to the dissolver solution into which, at the outset, a known amount of ^{7}Li was mixed as tracer. Samples of the solution are spiked with ^{6}Li, ^{233}U, and ^{242}Pu for mass spectrometry. The measured ratio $^{6}Li/^{7}Li$ verifies the batch size (volume or weight), whereas the concentration ratios U/Li and Pu/Li give the quantities of these fissile materials, (kg), in the batch. The solution of the ^{6}Li spike is calibrated against a dilution of the ^{7}Li solution used to trace the dissolver solution; the batch size can thus be found merely as a ratio of two $^{6}Li/^{7}Li$ ratios, thereby circumventing the complicated absolute standardization of the ^{7}Li additive. The assets of the Li-concept are discussed in terms of process compatibility, analytical sensitivity, precision, and price. The chemical separation of Li from the dissolver solution prior to its determination by mass spectrometry is described. Results on simulated input solutions show the capability of the system under laboratory conditions to be about 0.3% relative standard deviation. (auth) (INIS)

34690 (IN-1457) CHEMICAL PROGRAMS DIVISION ANNUAL REPORT, FISCAL YEAR 1970. Bower, J. R. (ed.) (Idaho Nuclear Corp., Idaho Falls). Mar 1971. Contract AT(10-1)-1230. 109p. Dep. NTIS.

XUM

Operating experience in fuel processing and waste management at the ICPP for FY-1970 is summarized. Co-processing of aluminum and zirconium fuels was successfully demonstrated, as was startup of the Waste Calcining Facility using in-bed combustion of kerosene with oxygen to supply the necessary heat. Technical support activities dealing with current and proposed operations at the ICPP are also presented. These include: corrosion studies on processing equipment and fuel storage facilities; dissolution of aluminum fuel; fluidized-bed denitration of uranyl nitrate; combustion-dissolution of graphite fuels; developments in electrolytic dissolution; pilot plant calcination of varied waste solutions; evaluation of cleanup techniques for selected gaseous and liquid waste streams; studies on preparation and properties of uranium aluminide; and results of a study of a conceptual processing plant for high-temperature gas-cooled reactor fuel. (auth)

34691 (LA–4645) DESALINATION AND ION SEPARATION OF SODIUM AND POTASSIUM BY BROMINE REDOX ELECTROLYSIS. Onstott, E. I.; Thode, Edward F.; Holman, Kermit L. (Los Alamos Scientific Lab., N. Mex.). Jan 1971. Contract W-7405-eng-36. 16p. Dep. NTIS.

The important process operating parameters for desalination and ion separation in a bromine redox system were determined in two sets of experiments using mixed electrolytes of sodium and potassium chlorides. The results show that the change in concentration of potassium ion or sodium ion is directly proportional to the electric current and inversely proportional to the electrolyte flows through the porous electrodes. Ion separation is quantitatively in proportion to the mobility ratio. The empirical relations obtained in this study are in accord with the basic differential equations describing the transport phenomena involved and are also in accord with the simplified concept that this system, at steady state, may be considered to be the flow analog of the classical Hittorf method for determination of transport numbers. (auth)

34692 (NYO–4057-2) SEPARATION OF KRYPTON AND XENON FROM REACTOR ATMOSPHERES BY SELECTIVE PERMEATION. Comprehensive Progress Report, January 1, 1969–December 31, 1970. Stern, S. Alexander; Sen, S. K. (Syracuse Univ., N. Y. Dept. of Chemical Engineering and Metallurgy). 94p. Dep. NTIS.

Studies are being made to determine the most economical method of separating radioactive ^{85}Kr and $^{133-135}Xe$ from air within a nuclear reactor containment dome after an accidental release of fission products. A permeation cascade using asymmetric cellulose acetate membranes was evauated. Permeability, diffusion, and solubility coefficients were determined using nonradioactive krypton and xenon. It was confirmed that gas transport across cellulose acetate membranes occurs by a solution-diffusion mechanism. However, second-order transitions were found to affect the permeability. Permeation rates were much higher through asymmetric membranes than through symmetric ones, but the separation factors were very different. (M.C.G.)

34693 (ORNL–4574) MOLTEN-SALT FLUORIDE VOLATILITY PILOT PLANT: RECOVERY OF ENRICHED URANIUM FROM ALUMINUM-CLAD FUEL ELEMENTS. Carr, W. H.; King, L. J.; Kitts, F. G.; McDuffee, W. T.; Miles, F. W. (Oak Ridge National Lab., Tenn.). Apr 1971. Contract W-7405-eng-26. 78p. Dep. NTIS.

A molten-salt fluoride-volatility process for recovering decontaminated uranium from spent uranium–aluminum alloy ORR and LITR fuel elements clad in aluminum was successfully developed and demonstrated. The facilities and the process were essentially the same as those used for zirconium- and Zircaloy-clad fuels except that an aluminum-potassium-zirconium fluoride mixture was used as the carrier salt. The development program included the processing of both unirradiated and irradiated fuel elements. Fission product decontamination factors (fuel to UF_6 product) for the UF_6 products in the four hot runs were generally 10^6 to 10^{10}. The uranium concentration in the salt after fluorination ranged from less than 0.1 to 9 ppM; total nonrecoverable losses in scrubbers and waste salt averaged less than 0.9%. Dissolution of the fuel elements required 8 to 17 hr for 90% completion, and 12 to 25 hr for 100% completion; average dissolution rates were 0.6 and 0.4 kg of aluminum/hr, respectively. The release of fission products to the atmosphere during the first three hot runs was confined to 120 mCi of technetium, 5 mCi of ruthenium (which occurred in one run), undetectable amounts of ^{131}I, and 47 to 60 Ci (calculated) of ^{85}Kr. In the fourth run, an ORR element that had been cooled less than four weeks was processed. Radiation exposures to personnel were controlled within tolerable limits. The decontamination factors (DF's) in this run ranged from 2×10^5 to 10^8. Two major exceptions were the DF's for ^{99}Mo and ^{125}Sb, which were 36 and about 500 respectively. The product had a high radioactivity level due to the presence of ^{237}U. The uranium concentration in the salt after fluorination in this run was approximately 0.1 ppM, and the total nonrecoverable loss was 0.4%. In the short-cooled run (RA-4), 24 Ci of ^{85}Kr and 2260 Ci of ^{133}Xe (calculated) were released to the atmosphere during hydrofluorination; 20 Ci of technetium, along with barely detectable amounts of ^{131}I (10^{-2} Ci) and ruthenium (10^{-3} Ci), were released during fluorination. The ^{85}Kr and ^{133}Xe were released over an extended period so that actual ground-level concentrations did not exceed a small fraction of the maximum permissible concentrations (MPC's) at any time. (auth)

34694 (ORNL-TM–3138) ENGINEERING DEVELOPMENT STUDIES FOR MOLTEN-SALT BREEDER REACTOR PROCESSING NO. 3. McNeese, L. E. (Oak Ridge National Lab., Tenn.). May 1971. Contract W-7405-eng-26. 97p. Dep. NTIS.

Research progress is reported on: removal of protactinium from single-fluid MSBR, effect of chemical processing on nuclear performance of an MSBR, reductive extraction experiments in a mild steel flow-through facility, electrolytic cell development, analysis of mass transfer in electrolytic cells, axial mixing in packed columns with high-density fluids, removal of heat from packed-column contactors, and MSRE distillation experiment. (M.C.G.)

34695 (ORNL-tr–2397) SEPARATION OF TRANSITION ELEMENTS AND ACTINIDES BY MEANS OF ANIONITE AV-17. Mikulski, J.; Stronski, I. Translated by Lynda H. Kern (Oak Ridge National Lab., Tenn., from Kernenergie; 8: 178-80(1965). 7p. Dep. NTIS.

An abstract of this paper, prepared from the original language, appeared as NSA 19: 24449.

34696 (SZS–3/71 (pp 2-19)) FLOCCULATION AND SEDIMENTATION OF RADIOACTIVE TURBID MATERIAL FROM WASTE WATER UNDER CONTROL OF THE ZETA POTENTIAL. Johannsen, K.-H. (Staatliche Zentrale fuer Strahlenschutz, Berlin (East Germany)). (In German). Dep. NTIS (U. S. Sales Only).

The decontamination of waste water from nuclear plants was performed by coagulation with aluminum sulfate and flocculation with organic polymers of the STIPIX series controlling the zeta potential according to Riddick. The zeta potential, the sinking speed of the flocs, and the residual turbidity were determined in relation to the pH value and the quantity of flocculating agent. The results are discussed and the usefulness of controlling the flocculation by measuring the zeta potential is critically evaluated. (auth)

34697 (SZS–3/71 (pp 20-32)) RADIOACTIVE WASTE FROM THE REPROCESSING OF FAST REACTOR IRRADIATED FUEL. Sachse, G.; Anders, G. (Zentralinstitut fuer Kernforschung, Rossendorf bei Dresden (East Germany)). (In German). Dep. NTIS (U. S. Sales Only).

Radioactive wastes arising from the reprocessing of fuel elements of fast reactors are discussed. In addition to waste solutions originating from aqueous reprocessing, emphasis is given to the gaseous and solid wastes for nonaqueous processes. Because of the high residual heat, the highly radioactive wastes of the fluorinating reprocessing must be stored with cooling for at least two years. Thereafter they are incorporated into melted silicates to assure safe storage. Development of appropriate processes and problems of the ultimate storage of high-activity vitreous blocks are considered. (auth)

34698 (UJV–2291-Ch) PLUTONIUM HEXAFLUORIDE: PREPARATION AND PROPERTIES. Vanka, M. (Ceskoslovenska Akademie Ved, Rez. Ustav Jaderneho Vyzkumu). 1970. 67p. (In Czech). NTIS (U. S. Sales Only).

Preparation of PuF_6, its physical and chemical properties, separation from UF_6–PuF_6 mixtures, handling, and safety measures are reviewed. (INIS)

34699 PREPARATION OF CLEAR URANYL NITRATE SOLUTION BY FRACTIONAL DISSOLUTION OF SODIUM DIURANATE. Abrao, Alcidio; Franca, J. M. Jr. (Instituto de Energia Atomica, Sao Paulo, Brazil). pp 104-7 of Materials Technology: An Interamerican Approach. New York; American Society of Mechanical Engineers (1968).

From Inter-American Conference on Materials Technology, San Antonio, Tex. See CONF-680513.

A procedure for preparation of clear uranyl nitrate solutions by fractional dissolution of crude sodium diuranate (SDU) is described. The raw SDU used is obtained by industrial processing of monazite sand and contains some thorium, rare earth elements, iron, silicon, and phosphorus as main impurities. With the procedure here described, clear and stable uranyl nitrate solutions having 270 to 300 g/l U and exhibiting good filtration characteristics are obtained. The procedure allows a satisfactory removal

XUM

of thorium, rare earth elements, phosphorus, silicon, and iron. (auth)

34700 RAPID AND SIMPLE MICROSCALE SEPARATION OF PROTEINS AFTER RADIOIODINATION. Ceska, M.; Pihl, P.; Holmqvist, L.; Grossmueller, F. (Pharmacia Aktiebolaget, Uppsala). J. Chromatogr.; 57: 145-7(22 Apr 1971).

The method of gel filtration-centrifugation for the separation of radioactive iodide from radioiodinated proteins is especially useful when handling small volumes and high radioactivities, and is applicable to most proteins. With sample volumes up to 300 μl, the degree of "desalting" was over 99% and 90% desalting was still obtained with sample volumes up to 800 μl. (D.P.O.)

34701 EFFECT OF THE DILUENT ON THE PARTITION COEFFICIENT AND THE SINGLE-STAGE SEPARATION FACTOR IN THE EXTRACTION OF RUBIDIUM AND CESIUM SALTS BY PHENOL. Kuznetsova, E. M.; Klinovskaya, T. V.; Panchenkov, G. M. (Moscow State Univ.). Russ. J. Phys. Chem. (Engl. Transl.); 44: 1261-4(Sep 1970).

The partition coefficients of cesium and rubidium salts in their extraction by phenol solutions were determined in the following diluents: benzene, toluene, p-xylene, cymene, carbon tetrachloride, styrene, butyl alcohol, benzyl alcohol, pentyl alcohol, hexyl alcohol, cyclohexanol, and bromobenzene. The single-stage separation factors of these elements were determined. Experimental data were used to test an equation proposed previously in a study of diluents with a wide range of physicochemical parameters. (auth)

34702 HIGH-VOLTAGE ELECTROPHORETIC SEPARATION OF INORGANIC IONS WITH SPECIAL REGARD TO PLATINUM METALS. III. SEPARATION WITH SIMPLE CARBOXYLIC AND HYDROXYCARBOXYLIC ACIDS. Meier, H.; Zimmerhackl, E.; Albrecht, W.; (and others) (Staatliche Forschungsinstitut fuer Geochemie, Bamberg, Ger.). Mikrochim. Acta; No. 6, 1295-1305 (1970). (In German).

The high-voltage electrophoretic migration of the halogen complexes of the platinum metals and various inorganic ions by use of simple monocarboxylic acids (formic, acetic, chloroacetic, trichloroacetic, trifluoroacetic, glycine) hydroxycarboxylic acids (lactic, mandelic, α-hydroxyisobutyric acid (α-HIBA) sulfosalicylic acid, as well as several sodium salts of these acids, was investigated and the influence of the pH-value, the concentration of the substances, and the moistening of the paper strips were tested with respect to the migration. It was found that along with trichloroacetic acid, the hydroxycarboxylic acids or their salts (especially α-HIBA) can be introduced for the separation of mixtures containing platinum metals. (auth)

34703 REMOVAL OF RADIOACTIVE IODINE FROM MILK BY MEANS OF ION EXCHANGERS PRODUCED IN POLAND. Kornacki, Kazimierz; Poznanski, Stefan; Chojnowski, Wladyslaw. Nukleonika; 15: 683-92(1970). (In Polish).

The efficiency of ion exchangers produced in this country for removal of radioactive iodine from milk was tested. The composition of buffer solution for transforming the resins investigated to a chloride-citrate-phosphate form was established, and so were the thermodynamic conditions for milk decontamination. It was found that from among the four ion exchangers produced in Poland (LF, MG, FD, and GM-800), only LF is fully efficient in removing ^{131}I from milk. (auth)

34704 SAMPLER FOR CONCENTRATING RADIONUCLIDES FROM NATURAL WATERS. Silker, W. B.; Perkins, R. W.; Rieck, H. G. (Battelle-Northwest, Richland, Wash.). Ocean Eng.; 2: 49-55(Apr 1971).

A sampler that permits concentration of both particulate and dissolved radionuclides from large volumes of ocean and freshwater was developed and tested. The water sample passes through a filtration section for particle removal, then through a sorption section where the radionuclides of interest are removed on sorption or ion exchange beds. Components of the sampler that contact the water are of poly(vinyl chloride) construction, and flow rates of about 40 l/min are employed. This sampler was successfully employed in concentrating some twenty radionuclides from ocean and fresh waters. (auth)

34705 DISTRIBUTION OF TRANSURANIUM ELEMENTS BETWEEN MOLTEN LITHIUM CHLORIDE AND LITHIUM–BISMUTH SOLUTIONS. EVIDENCE FOR CALIFORNIUM(II). Mailen, J. C.; Ferris, L. M. (Oak Ridge National Lab., Tenn.). Inorg. Nucl. Chem. Lett.; 7: 431-8(May 1971).

The results of this preliminary study indicated that Cf(II) was present in the salt phase when the Li concentration in the Bi phase was greater than ~0.02 atom %. Details are given of the reagents and apparatus used, the procedure adopted, and the analytical work involved. Distribution coefficients at 640°C are tabulated and comparisons shown graphically with the behavior of Pu and Cm. Results are discussed. (UK)

34706 EXTRACTION OF SELECTED METALLIC CATIONS BY A HIGHLY HINDERED $(RO)_2PO(OH)$ EXTRACTANT IN TWO DIFFERENT DILUENTS FROM AN AQUEOUS CHLORIDE PHASE. Peppard, D. F.; Mason, G. W.; Bollmeier, A. F.; Lewey, S. (Argonne National Lab., Ill.). J. Inorg. Nucl. Chem.; 33: 845-56(Mar 1971).

A highly sterically hindered extractant, bis(2,6-dimethyl-4-heptyl) phosphoric acid, $(C_9H_{19}O)_2PO(OH)$, HD(DIBM)P, was shown to differentiate strongly in favor of U(VI) with respect to M(III) actinides, lanthanides, scandium, and yttrium and with respect to Th(IV). In the systems HD(DIBM)P (diluent) vs. 1.0F(NaCl + HCl), where the diluent is benzene or n-heptane, the extractions may be represented, operationally, by: $K = K_1F^2/[H^+]^2$, for UO_2^{2+}, i.e. U(VI), $K = K_3F^{2.5}/[H^+]^3$, for Sc(III), $K = K_3F^{2.5}/[H^+]^{3.5}$, for Th(IV), where F is the concentration in formality units of HD(DIBM)P in the organic phase and $[H^+]$ is the concentration of H^+ in the aqueous phase. From 0.025M HCl into 0.60F HD(DIBM)P in benzene measured K values are: U(VI), 2×10^4; Th(IV), 3; Sc(III), 6×10^2; Eu(III), Lu(III), Y(III) and Am(III), each less than 2×10^{-2}. The mutual separation of U(VI) and Th(IV) was demonstrated. For each of the elements studied, under comparable conditions, the K value is higher in n-heptane than in benzene. (auth) (UK)

34707 METHOD OF CALCULATING THE NUMBER OF THEORETICAL STAGES OF SEPARATION USING A SUBSTITUTING LINE. Dmitrevskaya, L. I.; Dmitrevskii, L. L.; Katal'nikov, S. G. (Moscow Order of Lenin Chemical-Engineering Inst.). Kernenergie; 13: No.12, 387-8(Dec 1970). (In Russian).

To calculate the number of theoretical stages of separation in binary two-phase systems exchanging with constant separation factor, an analytical method may be used according to which the equilibrium curve is substituted by a straight line. This line is proposed to be obtained by equalizing the number of theoretical stages determined from the true equilibrium curve and from the substituting line for zero-output operation. The method of determining the substituting line coordinate is elucidated. An equation is given for calculating the number of theoretical stages necessary for obtaining a given separation in operation with nonzero output. (auth)

34708 ISOTOPE EFFECTS IN CO_2 ADSORPTION ON ZEOLITES. Loseva, T. I.; Kochurikhin, V. E.; Zel'venskii, Ya. D. (Moscow Order of Lenin Chemical-Engineering Inst.). Kernenergie; 13: No.12, 389-91(Dec 1970). (In Russian).

An investigation was made of the isotope effects in adsorption of CO_2 molecules possessing high quadrupole moment on zeolites. Equilibrium separation factors of carbon and oxygen isotopes in CO_2 adsorption on various synthetic zeolites at temperatures in the range between 195 and 273°K were measured using a two-stage technique. The highest separation factor of oxygen isotopes equal to 1.010 was that for NaA zeolite. It was found that sorption of $^{13}CO_2$ is lower than that of $^{12}CO_2$ in some cases. Separation factors are compared with the thermodynamic functions of gaseous CO_2. Suggestions are made concerning factors which influence the magnitude of the isotope effect in adsorption on zeolites. (auth)

34709 SEPARATION OF ALKALINE EARTH METAL ISOTOPES BY ION EXCHANGE. PART I. STUDIES ON MAGNESIUM AND CALCIUM. Aaltonen, J. (Univ. of Helsinki). Suomen Kem.; 44B: No. 1, 1-4(1971).

Isotope separation studies were performed with Mg and Ca using a recycle ion exchange technique. The eluents used were ammonium lactate solution for Mg and ammonium α-hydroxyisobutyrate solution for Ca. The Mg and Ca contents of the fractions eluted were determined with an atomic absorption spectrophotometer. The fractions were analyzed on mass spectrometer. The isotope separation factors of Mg and Ca were calculated from the isotopic compositions of these eluted fractions. The separation factors obtained were $S_{26}^{25}(Mg) = 1.00016$ and $S_{44}^{42}(Ca) = 1.00087 \pm 0.00008$. (auth) (Finland)

34710 PROCESS FOR REMOVING CONTAMINANTS FROM ZIRCONIUM SURFACES. Konecny, Charles Richard (to General Electric Co.). British Patent 1,229,395. 21 Apr 1971. Priority date 20 Mar 1968, United States.

A method for removing chemically combined fluoride from the surface of Zr or Zr alloys comprises immersing the surface in an aqueous solution containing at least 500 g of an alkali metal hydroxide/l of H_2O, maintaining the surface in contact with this solution for a period of 1 to 120 min; removing the surface from the solution; and rinsing the surface with H_2O. The method is particularly applicable to the removal of film from Zr cladding of fuel elements. (B.L.M.)

XUM

34711 TREATMENT OF LIQUID RADIOACTIVE WASTE PRODUCTS IN THE REPROCESSING OF RADIOACTIVE FUEL. Bocola, W.; Donato, A. (CNEN, Rome). Minerva Fisiconucl.; 14: 7-16(Jan-Mar 1970). (In Italian). (CONF-690929-5; RT/PROT-(70)17).

From fifteenth national congress of the Italian Association for Health Physics and Protection Against Radiation; Cagliari, Italy (Sep-Oct 1969).

Owing to the growing importance of radioactive waste disposal problem, a solidification process of semicontinuous type has been developed by the CNEN's Sanitary Engineering Laboratory at Casaccia Center (ESTER program). The final product of the process is a phosphate glass obtained through concentration and denitration by formaldehyde, strong denitration by phosphorus, calcination, and melting of the initial solutions. The different steps of the process have been studied and the total flow-sheet set up. Using simulated solutions, a test on a bench scale plant was carried out. Ten solidification runs for an amount of more than 400 liters of solution were vitrified. The volume reduction factors ranged between 244 and 283. The ruthenium volatilization was kept under 1% by means of the strong reducing behavior of phosphorus. (auth)

34712 METHOD AND APPARATUS FOR THE CONTINUOUS DISSOLUTION OF CLAD NUCLEAR FUEL MATERIALS. Salviat, Jean (to Saint Gobain Techniques Nouvelles SA). French Patent 1,602,368. 16 Nov 1970. Filed 24 Sep 1968. (In French).

A continuous process is described for the treatment of irradiated elements made up of a cladding component and a nuclear fuel component. It includes the loading of these elements into a given number, at least two, of baskets immersed in a dissolution bath arranged at a fixed level and capable of dissolving one of the two components of the element. The method is to fill the first basket with irradiated elements at a constant feed-in rate, then repeat the process with another basket, until all the baskets are full. Meanwhile the elements in the first basket are transferred, after complete dissolution of one of their components, into a rinsing bath of attack liquid at a predetermined level. The level of the rinsing bath must be higher than that of the dissolution bath and the liquid from the former poured into the latter at a constant rate. (France)

34713 PROCESS AND DEVICE FOR FUEL REPROCESSING. Cherel, Guy (to Saint Gobain Techniques Nouvelles). French Patent 1,587,331. 9 Feb 1970. Filed 19 Jun 1967. (In French).

A procedure for reprocessing irradiated fuel elements is described. The elements considered are of the type having two inert ends and a body containing the nuclear fuel, enclosed in cartridges or cladding. The procedure consists of using a remote control handling assembly for transporting the fuel element from a storage area to a position between the scissor blades, the simultaneous sawing off of the inert ends of the element, the cutting up of the cartridge into pieces with the scissors, and the eventual distribution of the pieces in the bath, which dissolves the nuclear fuel. (France)

34714 SEPARATION OF LANTHANIDES BY CHROMATOGRAPHY ON SA-2 ION EXCHANGE PAPER. Dubuquoy, Claude; Gusmini, Simonne; Poupard, Danielle; Verry, Monique (CEA, Bruyeres-le-Chatel, France). J. Chromatogr.; 57: No. 3, 455-9 (19 May 1971). (In French).

Chromatography on SA-2 paper is of great interest in the purification of a single rare earth radioisotope. Likewise, it is of interest in the analyses of rare earths with small amounts of entrained material (150 μg per element): measurements of thin sources, liquid scintillation, the Cherenkov effect. Compared to the usual methods of analysis on a cation resin exchange column, the separation is more rapid and the apparatus simpler. However, the related problems (very painstaking prior chemical treatment, quality of the deposit, localization and elution of the separated elements) leads to a duration of the analysis analogous to that of the other method. Ammonium α-hydroxy-α-methylbutyrate shows good possibilities since it is possible to separate large amounts of impurities. (tr-auth)

XUM

EARTH SCIENCES

Geology and Hydrology

Refer also to abstracts 34539, 34683, 34743, 34767, 34845, 34846, 34862, 35600, and 35913.

34715 (BNWL-1502) ANALYSIS OF HYDROLOGICAL FACTORS INFLUENCING THE GABLE MOUNTAIN IRRIGATION PROJECT. Mudd, R. D.; Cearlock, D. B.; Reisenauer, A. E. (Battelle-Northwest, Richland, Wash. Pacific Northwest Lab.). Sep 1970. Contract AT(45-1)-1830. 11p. Dep. NTIS.

An analysis of the hydrological effects of continued long-range irrigation north of Gable Mountain on the chemical processing area waste management practices at Hanford, Washington are presented. Hydrological factors of the Hanford Reservation were evaluated as influenced by the operation of the Gable Mountain Irrigation Project. The study results indicate that there would be no significant hydrologic effect on the current chemical processing waste management practices. Changes in the groundwater piezometric surface were extremely small and generally confined to the irrigated area. The maximum area that could be irrigated safely was not determined nor was the maximum permissible application rate. Although an irrigated area of about 11,000 acres was studied the results indicate a much larger area could be safely considered. (auth)

34716 (CSIRO-Trans-10088) NEW METHOD OF INTERPRETING THE RESULTS OF GAMMA LOGGING OF BORFHOLES. Roesler, R. Translated by B. Bergmanis (Australian Atomic Energy Commission Research Establishment, Lucas Heights), from At. Energ. (USSR); 26: 337-40(1969). 12p. Dep. NTIS (U. S. Sales Only).

The problem of determining the content of radioactive elements in individual layers is reduced to the solution of an infinite system of equations. The calculation can be effected by the use of inverse matrix coefficients from counting rates at points equidistant from each other. The solving ability thus is dependent on the minimum thickness of elementary layers for which there still exists an inverse matrix. Interpretations of the results of γ-logging using this method are given. They are considered particularly applicable to potassium deposits because it is not necessary to account for radioactive equilibrium; however the method has been shown to be efficient for uranium also. (Australia)

34717 (EUR-4636) PRINCIPLES AND METHODS FOR THE DERIVATION OF A FORMULA FOR THE DISCHARGE OF RADIOACTIVE LIQUID WASTES IN SURFACE WATERS. Branca, G.; Breuer, F.; Cigna, A. A.; Amavis, R. (Comitato Nazionale per l'Energia Nucleare, Rome (Italy)). Apr 1971. 43p. Dep. NTIS (U. S. Salees Only). EUR F,Fr. 6,65.

In any nuclear project, it is essential to know exactly the maximum quantity of radioactive substances which may be disposed of in a specified environment. Many difficult problems are involved in the determination of a discharge formula: characteristics of radioactive wastes, characteristics of environmental media, various phenomena that may modify the distribution of radioactivity and all factors that influence the exposure to radiation for man. A mathematical solution is given for the problem of the distribution of radionuclides in the environments that are associated with surface waters. (auth)

34718 (KH-R-12) LONGITUDINAL DISPERSION IN LABORATORY AND NATURAL STREAMS. Fischer, Hugo B. (California Inst. of Tech., Pasadena. W. M. Keck Lab. of Hydraulics and Water Resources). Jun 1966. 250p.

The longitudinal dispersion of fluid particles which are initially distributed uniformly over one cross section of a uniform, steady, turbulent open channel flow was studied. The primary interest was the development of a method to predict the rate of dispersion in a natural stream. Taylor's method of determining a dispersion coefficient, previously applied to flow in pipes and two-dimensional open channels, was extended to a class of three-dimensional flows which have large width-to-depth ratios, and in which the velocity varies continuously with lateral cross-sectional position. Most natural streams are included. The dispersion coefficient for a natural stream may be predicted from measurements of the channel cross-sectional geometry, the cross-sectional distribution of velocity, and the overall channel shear velocity. Tracer experiments are not required. Large values of the dimensionless dispersion coefficient D/rU^* (where r is the hydraulic radius and r/rU^* the shear factor) are explained by lateral variations in downstream velocity. In effect, the characteristic length of the cross section is shown to be proportional to the width, rather than the hydraulic radius. The dimensionless dispersion coefficient depends approximately on the square of the width to depth ratio. A numerical program is given which is capable of generating the entire dispersion pattern downstream from an instantaneous point or plane source of pollutant. The program is verified by the theory for two-dimensional flow, and gives results in good agreement with laboratory and field experiments. Both laboratory and field experiments are described. Twenty-one laboratory experiments were conducted: thirteen in two-dimensional flows, over both smooth and roughened bottoms; and eight in three-dimensional flows, formed by adding extreme side roughness to produce lateral velocity variations. Four field experiments were conducted in the Green-Duwamish River, Washington. Both laboratory and flume experiments proved that in three-dimensional flow the dominant mechanism for dispersion is lateral velocity variation. For instance, in one laboratory experiment the dimensionless dispersion coefficient D/rU^* was increased by a factor of ten by roughening the channel banks. In three-dimensional laboratory flow, D/rU^* varied from 190 to 640, a typical range for natural streams. For each experiment, the measured dispersion coefficient agreed with that predicted by the extension of Taylor's analysis within a maximum error of 15%. For the Green-Duwamish River, the average experimentally measured dispersion coefficient was within 5% of the prediction. (auth)

34719 (NP-18737) ESTIMATION OF TRITIUM DISCHARGES INTO LLW-STREAMS. Hunzinger, W. (European Company for the Chemical Processing of Irradiated Fuels, Mol (Belgium)). Nov 1970. 17p. (ETR-267). Dep. NTIS (U. S. Sales Only).

The tritium transferred as LLW to the CEN waste treatment station and discharged to the Mol Nethe during the period January 1969 to July 1970 was compared with the calculated amount of ^3H produced by fission. The discharges are between 40 and 80% of the calculated quantities, if sources of ^3H production other than fission are neglected and a production rate of 16 mCi/MWd from fission of ^{235}U and 22 mCi/MWd from fission of ^{233}Pu is assumed. The time delay between fuel dissolution and arrival of the tritium in the river does not exceed 2 months. (auth)

34720 (NVO-1229-121) INTERIM SUMMARY OF RADIOCHEMICAL DATA FOR STS "A", AMCHITKA ISLAND, ALASKA, THROUGH JUNE 30, 1969. Essington, E. H.; Forslow, E. J.; Castagnola, D. C. (Teledyne-Isotopes, Palo Alto, Calif.). Jun 1970. Contract AT(29-2)-1229. 62p. Dep. NTIS.

Several sites on Amchitka Island, Alaska, are under consideration by the U. S. Atomic Energy Commission for underground nuclear experiments. Environmental samples from the vicinity of these sites were collected and analyzed. Programs are being conducted to generate essential data for radiological effects evaluations of future nuclear experiments. The programs include 1) determination of natural gross beta, gross alpha, and tritium radioactivities occurring in Amchitka's environmental waters and 2) determination and evaluation of radionuclide sorption, dispersion, and migration parameters for Amchitka's rock-water systems. The parameters include distribution and dispersion coefficients, and retardation factors for various radionuclides. Water source locations, sampling procedures, and analytical methods are briefly described. Results of determinations made through June 1969 of radioactivity levels and distribution coefficients are presented. (auth)

34721 (NYO-3912-3) COBALT SORPTION ON SURFACE REACTIVE MINERALS IN THE GLACIAL ENVIRONMENT. Progress Report, February-December 1970. Reynolds, R. C. Jr. (Dartmouth Coll., Hanover, N. H.). 25 Mar 1971. Contract AT(30-1)-3912. 21p. Dep. NTIS.

Progress is reported on a study of the distribution and compositions of natural waters in the South Cascade Glacier region, and on the regosols and stream and lake sediments in this alpine environment. New analytical techniques were developed for the analysis of Ca + Mg, K, Na, Cl^-, and SO_4^{-2} by means of ion sensitive electrodes. Work was performed in the laboratory that provides data on the cobalt and cesium sorption characteristics of natural silts in natural waters. Finally, progress was made toward the development of a quantitative model for cobalt sorption on vermiculite in the presence of interfering ions. (auth)

34722 (NYO-3912-4) COBALT SORPTION ON SURFACE REACTIVE MINERALS IN THE GLACIAL ENVIRONMENT. Three-year Summary Report, August 1967-February 1971. Reynolds, R. C. Jr. (Dartmouth Coll., Hanover, N. H.). 25 Mar 1971. Contract AT(30-1)-3912. 79p. Dep. NTIS.

XUM

Progress is reported covering the three year period of August, 1967 to February, 1971 on a study of the cobalt sorption on surface reactive minerals in a glacial environment. Results reported are: cationic denudation in the South Cascade Glacier Region is presently occurring at rates that are approximately three times the world average; the dominant driving force for chemical weathering consists of continuous carbonation of surface waters during their transit of the watershed; dominant clay mineral in the area is vermiculite, and it forms by the alteration of biotite; clays are sufficiently abundant to provide high cation exchange capacities in local sediments; ion sensitive electrodes can be used for the analysis of Ca + Mg, K, Na, Cl^-, and SO_4^{2-}. Preliminary data on cobalt and cesium sorption and the development of a quantitative model for cobalt sorption on vermiculite are also presented. (D.H.M.)

34723 (RLO-2225-T-20-3) RADIOCARBON IN THE SEA. Progress Report, August 15, 1968–May 1, 1971. Fairhall, A. W. (Washington Univ., Seattle. Dept. of Chemistry). Contracts AT(45-1)-2091; AT(45-1)-2225. 25p. Dep. NTIS.

Research progress is reported on a study of radiocarbon in the sea, including the design of a ^{14}C monitoring system, laboratory methods of analysis, geographical locations where most of the samples were collected, results of analysis, and discussion of the results. (D.H.M.)

34724 (RLO-2227-T-9-1) PHYSICO-CHEMICAL PROPERTIES OF SOILS FROM VOLCANIC ASH. Progress Report, September 1, 1970–May 31, 1971. Harward, M. E. (Oregon State Univ., Corvallis. Dept. of Soils). 31 May 1971. Contract AT(45-1)-2227. 9p. Dep. NTIS.

Ash soils are of scientific interest due to their unique properties and to the presence of large areas of volcanic ash deposits in countries surrounding the Pacific Ocean. Progress is reported in research for determining the sources of ash soil deposits, the applicability of instrumental neutron activation analysis to these studies, and the relationship of physico-chemical reactions to the internal porosity of particles. (L.C.L.)

34725 (STI/DOC-10/126) NUCLEAR WELL LOGGING IN HYDROLOGY. Technical Reports Series No. 126. (International Atomic Energy Agency, Vienna (Austria)). 1971. 95p. IAEA $3.00.

A comprehensive single-volume reference for practicing hydrologists with a limited knowledge of nuclear physics is presented which describes the physical principles of nuclear well logging methods, their applications to hydrogeological problems, and their limitations. Information on the following subjects is included: purpose of well logging in hydrology; hole construction and emplacement; instrumentation requirements; the equipment for and use of specific well logging methods such as natural gamma, gamma–gamma, neutron, and tracer; and how to interpret the well logging results. An appendix on the general characteristics of a nuclear well logging unit for hydrological purposes and personnel requirements is provided. (L.C.L.)

34726 (THAI-AEC-35, pp 9-20) ENVIRONMENTAL ISOTOPE INVESTIGATION IN THE TOTES GEBIRGE STYRIA, AUSTRIA. Yuthamanop, Anan (Office of Atomic Energy for Peace, Bangkok (Thailand)). Dep. NTIS (U. S. Sales Only).

During the panel on the Interpretation of the Environmental Isotope Data in Hydrology, it was decided to study a well-known karst region with the environmental isotope method to compare the results with those obtained by conventional tracer methods. The Totes Gebirge was selected for this study. Environmental isotope tracer studies of the ground waters in the Totes Gebirge began in Sept. 1968. The first group of 49 water samples from various lakes, springs, and water courses in the region were collected for ^3H, deuterium, and ^{18}O analysis. The water temperatures of the lakes, springs, and water courses at the sampling places were also recorded in order to establish the relationship between the isotope content and water temperature. Data is presented on the ^3H and ^{18}O content of the ground waters and the ^3H content of atmospheric precipitation in the region. It was concluded that most of the ground water samples have a transit time of 1 to 3 yr, with some having from 3 to 9 yr. This agreed well with previous calculations. (L.C.L.)

34727 (UCRL-72927) ESTIMATING NATURAL TERRESTRIAL BACKGROUND IN THE 17- AND 60-keV ENERGY REGIONS FROM THE COMPTON CONTINUUM PEAK. Lindeken, C. L.; Hodgkins, D. J.; Hoeger, T. O. (California Univ., Livermore. Lawrence Radiation Lab.). 1 Apr 1971. 12p. (CONF-710401-1). Dep. NTIS.

From Symposium on safety in plutonium-handling facilities; Rocky Flats, Colo. (13 Apr 1971).

A 1-yr study of terrestrial natural gamma background in the energy region of 10 to 100 keV showed that, whereas counting rates varied with geographical location, the percentage of the total activity within any given 10-keV interval was reproducible within about 5%. As a result, the 10 to 100 keV natural background gamma spectrum can be calculated from a counting rate measurement within this energy range. This technique, using thin NaI(Tl) crystals, is proposed for estimating natural background, which interferes in the detection of low-level plutonium surface contamination. Here detection is based on measurement of either the 17-keV x-ray band or the 60-keV gamma from ^{241}Am, the latter normally present through beta decay of ^{241}Pu. The 80-keV Compton continuum peak is used for calculating background contribution in these two energy regions, since it provides the best counting statistics and is above the plutonium contamination energies. Through the use of a pulse-rate meter having three switch-selected, high-voltage supplies, which permits detection of three separate energies, field tests demonstrate that natural background in the 17- and 60-keV regions can be estimated to within ±10%. (auth)

34728 (USGS-474-101) RADIOCHEMICAL ANALYSES OF WATER FROM SELECTED STREAMS, WELLS, SPRINGS, AND PRECIPITATION COLLECTED DURING REENTRY DRILLING, PROJECT RULISON. Voegeli, Paul T. Sr.; Claassen, Hans C. (Geological Survey, Denver, Colo.). 1971. Contract AT(29-2)-474. 14p. (PNE-R-48). Dep. NTIS.

Results of the analyses of stream, well, spring, and precipitation samples for tritium, gross alpha, and gross beta are presented. (D.H.M.)

34729 UNCONVENTIONAL METHODS IN EXPLORATION FOR PETROLEUM AND NATURAL GAS. A Symposium Under the Auspices of the Institute for the Study of Earth and Man, Dallas, Texas, September 12–13, 1968. Heroy, William B. (ed.). Dallas; Institute for the Study of Earth and Man (1969). 251p. $10.00. (CONF-680985).

Nineteen papers on unconventional methods of prospecting for petroleum and natural gas were presented at the conference and are included in this issue. A separate abstract was prepared for each of two. 17 were not within the scope of NSA. (L.C.L.)

For abstracts of individual papers see: 34730 and 34731.

34730 REVIEW OF RADIOMETRIC TECHNIQUES IN PETROLEUM EXPLORATION. Foote, R. S. (Texas Instruments, Inc., Dallas). pp 43-55 of Unconventional Methods in Exploration for Petroleum and Natural Gas. /Heroy, William B. (ed.). Dallas: Inst. for the Study of Earth and Man (1969).

From Symposium on Unconventional Methods in Exploration for Petroleum and Natural Gas, Dallas, Tex. See CONF-680985.

The literature on radiometric petroleum-prospecting techniques and results is reviewed, including both surface and subsurface gamma-radiation measurement patterns. Most of these studies have included the use of total gamma-ray flux-counting equipment. No accurate corrections were made in any studies for cosmic-ray contributions or for the gamma-ray flux from radon-daughter gamma-ray emitters in the atmosphere. Recently, highly sensitive airborne gamma-ray spectrometers have been developed which allow accurate determination of the separate contributors to the natural gamma-radiation flux: ^{214}Bi (uranium series), ^{208}Tl and ^{40}K. New methods include corrections for cosmic radiation and for contributions from radon in the atmosphere. These techniques make possible closely reproducible measurements and the development of meaningful low-order anomalies. Results from airborne-exploration programs for uranium minerals show that, for uranium minerals, 30% to 70% of the total measured gamma radiation from uranium daughters originate in the atmosphere, and that diurnal variations in total ^{214}Bi radiation may exceed 100%. The status of equipment-development and data-processing techniques, including correction for pedologic changes, is now sufficiently advanced to allow new, highly-controlled experimental verifications of the possible usefulness of gamma-radiation measurements in petroleum exploration. (auth)

34731 GEOLOGICAL, GEOPHYSICAL, AND CHEMICAL MODIFICATIONS OF SEDIMENTS IN THE ENVIRONMENT OF OIL FIELDS. Pirson, Sylvain J. (Univ. of Texas, Austin). pp 159-86 of Unconventional Methods in Exploration for Petroleum and Natural Gas. /Heroy, William B. (ed.). Dallas: Inst. for the Study of Earth and Man (1969).

From Symposium on Unconventional Methods in Exploration for Petroleum and Natural Gas, Dallas, Tex. See CONF-680985.

A water-borne process of hydrocarbon migration and accumulation is nearly universally accepted as the primary natural means of collecting oil and gas in structural as well as stratigraphic traps. This process calls for large volumes of fluid transfer

XUM

during the time elapsed from sedimentation to the present. It is postulated and it is verified by field examples that radioactive elements may be used as tracers of fluid motion throughout geologic time and that significant radioactive-mapping patterns are derivable from gamma-ray logs which are characteristic of hydrocarbon accumulations at depth. Hydrocarbons also leak from their loci of entrapment, thereby modifying the physicochemical properties of overlying sediments, more specifically their redox potential. (auth)

34732 TRITIUM CONTENT OF BEPPU HOT SPRING WATER. Koga, Akito (Kyushu Univ., Beppu, Japan); Kikkawa, Kyozo. Oita-ken Onsen Chosa Kenkyu-kai Hokoku; No. 21, 1-4(Mar 1970). (In Japanese).

Since 1952 the tritium content of rainwater has been increased by nuclear explosion. This tritium has been widely utilized for hydrography studies. If spring water originates from rainwater, the tritium content of spring water is varied, depending upon its underground circulation time. The longer the time, the less the tritium content. The tritium content of hot spring water at the several sites in Beppu City was studied. The results obtained were as follows: 35TU at Jizo Hot Spring, 50 TU at Uedanoyu-machi, 1 TU at Oniyama-Jigoku, 2 to 5 TU at Hacchogahara, and Tanikawa River water in Kuju district was 81 TU. It is presumed that the water at former two sites contains more groundwater from shallow strata, and that at latter two sites originates from the stored groundwater in deep strata. Furthermore, reciprocal proportion was recognized between tritium content and Cl-ion concentration in spring water. The tritium content of Jizo hot spring differs from that of Oniyama-Jigoku, although both are same acid hot spring. Therefore, the production mechanism of sulfuric acid in both seems to be different. In the shallow strata containing sufficient oxygen, sulfuric acid may be produced by the oxidation of hydrogen sulfide. On the other hand, in the deep strata depleted in oxygen, it seems to be produced by the self oxidative-reductive reaction of sulfurous acid. (Japan)

34733 RADIOACTIVE WASTES OF THE NUCLEAR CENTER IN MEXICO. HANDLING, TREATMENT, AND CONTROL. Morales Amado, A.; Ley-Koo, V.; Gomez Santamaria, E.; Avila Castillo, E. (CNEN, Mexico City). Rev. Mex. Fis., Supl. Reactor; 19: S99-105(1970). (In Spanish).

The processing of radioactive wastes in the liquid, solid, and gaseous form is described. Liquid wastes are transferred through special pipes to hold-up tanks, from where they can be discharged to the common drainage after they are monitored, or they are conducted to an evaporator which reduces their activity by a factor of 10^{-6}. The evaporator delivers concentrated wastes that are treated as solid wastes. Solid wastes are packed and buried. Gaseous wastes are released to the atmosphere after they are monitored. (auth)

34734 RADIOCHEMICAL PECULIARITIES OF GRANITOIDS OF THE GISSAR PLUTON (REGULARITIES OF U AND Th DISTRIBUTION IN ROCKS OF CENTRAL TAJIKISTAN). Mogarovskii, V. V.; Melnichenko, A. K.; Kozyrev, V. I. (Inst. of Geology, Dushanbe, USSR). Geokhimiya; No. 4, 406-14(Apr 1971). (In Russian).

In granitoids of the Gissar pluton uranium and thorium contents increase in intrusive phases 1 to 3 in rocks and then decrease in rocks of the following phases. These peculiarities of uranium and thorium distribution may be explained by their close connection with the volatile component fluorine. (auth)

34735 RECOMMENDED PRACTICE FOR STANDARD CALIBRATION AND FORM FOR NUCLEAR LOGS. API RP 33 1959. Dallas; American Petroleum Institute (1959). 12p. Available from American Petroleum Inst., Washington, D. C.

Specifications are presented for the API (American Petroleum Institute) Nuclear Logging Calibration facility for establishing standard API Gamma-Ray and API Neutron Units for nuclear logs, for calibrating logging tools in these units, and for a standard nuclear log form and heading. (L.C.L.)

34736 ^{226}Ra DISTRIBUTION IN HOT SPRINGS AND THE ORIGIN OF HIGHLY RADIOACTIVE SPRINGS. 5. Iwasaki, Iwaji (Tokyo Inst. of Tech.). Onsen Kogakkaishi; 7: No. 2, 109-14(Feb 1969). (In Japanese).

The origin of a highly radioactive spring in a region where a concentrated radioactive mineral is found is self evident. But in the cases of Masutomi, Ikeda, Arima and Brambach springs, no such mineral has been detected in granitic rocks. Some spring deposits contain an amount of Ra exceeding one thousand times as much as country rocks. The possibility of a highly radioactive spring being formed by the hot water flowing over a radioactive deposit was experimentally proved. It was concluded from many observations and experiments that the source of Rn in spring deposits must be found very near the surface. The process of highly radioactive spring formation may be summarized as follows. Original hot spring water that may or may not contain Ra and Rn, approaches the surface and is supplied with Ra and Rn on the way due to various chemical reactions. When it comes very near the escape channel, it may receive more Rn and Ra or lose a part or all of Ra as spring deposit. As the ascending thermal water approaches the surface, the reaction with underwater and oxygen leading to the formation of spring deposit is likely to be prominent. Thus the remaining Ra in the thermal water and Rn in hot spring gas well is released from the openings. Due to different chemical properties, chemical equilibrium is not obtained between Rn and Ra. This explains the existence of Rn hot springs that contain only Rn. (Japan)

34737 RESEARCH ON SORPTION OF THE RADIONUCLIDES ^{85}Sr, ^{137}Cs, AND ^{131}I BY UNCONSOLIDATED SEDIMENTS. SANDS FROM THE LOW-TERRACES OF THE RIVERS WESER, DONAU, ELBE/GERMANY. Puschmann, H. (Bundesanstalt fuer Gewaesserkunde, Coblenz, Ger.). Deut. Gewaesserk. Mitt.; 14: No. 3, 63-72(1970). (In German).

Fine-grained sediments from the Weser, Donau, and Elbe rivers were examined for their sorption behavior in respect to ^{85}Sr, ^{137}Cs, and ^{131}I. The experiments with closed systems give the course of the sorption and the possible sorption rate after the equilibrium has been established. The sorption rates are converted to grams of the element used per m^3 sand as used in the laboratory experiment. The results are compared with the sorption rates dealt with by Weisflog (1968), which were made with low-terrace sediments from the river Rhine. (auth) (INIS)

34738 ISOTOPIC COMPOSITION OF URANIUM AND THE CONTENT OF ACTINIUM IN MINERALS AND NATURAL WATERS. Kadyrov, N. B.; Issabayaev, E. A.; Assylbayaev, U. H.; Abildayaev, A. H.; Tscherdynzev, V. V. Z. Angew. Geol.; 16: 251-2 (May 1970). (In German).

The ratios of $^{234}U/^{238}U$, $^{235}U/^{238}U$, and $^{227}Ac/^{226}Ra$ in some minerals and natural waters were measured. The results are tabulated. Variations in the $^{234}U/^{238}U$ ratio was established in many minerals, but no significant change was found for $^{235}U/^{238}U$. An unusual activity in the energy range from 4.4 to 4.6 MeV was found in water from granites in Kazakhstan. It was attributed to the presence of transuranium isotopes. (J.S.R.)

34739 SIMPLE PROGRAMMER FOR AN RF INDUCTION HEATER, WITH PARTICULAR APPLICATION TO K–Ar DATING. Mussett, A. E. (Univ. of Liverpool). J. Phys., E (London); 4: No. 4, 329-30(Apr 1971).

A simple mechanical attachment is described for increasing the power of an r.f. induction heater over a period of tens of minutes, to a preset changeable program. There is no feedback from the object heated; the merit of the attachment is its simplicity. (auth) (UK)

34740 ISOTOPIC COMPOSITION OF LEAD IN VOLCANIC ROCKS FROM TENERIFE, CANARY ISLANDS. Oversby, V. M. (Australian National Univ., Canberra); Lancelot, J.; Gast, P. W. J. Geophys. Res.; 76: No. 14, 3402-13(10 May 1971).

Lead isotope compositions and lead and uranium concentration data are given for volcanic rocks from the Canary Islands. Isotopic compositions indicate a multistage history for the upper mantle under the Canaries. A linear relationship among Tenerife isotopic compositions is interpreted as a mixing line dominated by two components. The Pb–U system had an original heterogeneity of several per cent that has not been eliminated by homogenization during fractionation events. (auth)

34741 GEOLOGICAL SURVEY RESEARCH, 1970. U. S., Geol. Surv., Prof. Pap.; No. 700-A, 1-426(1970).

Geological Survey Research activities in 1970 are summarized and are categorized as: investigations of mineral and water resources in the U.S.; studies of geologic and hydrologic principles, processes, and techniques; applications of geology and hydrology to engineering and public welfare; astrogeologic research; development of remote sensing and advanced techniques; review of geologic and hydrologic investigations in other countries; topographic surveying and mapping; and computer applications in geology. Information is included on Th and U reserves in the U.S., the effects of radioactive wastes from nuclear facilities on the hydrologic environment, and the importance of geologic and hydrologic surveys to the siting of power reactors. (L.C.L.)

XUM

Meteorology

34742 (COO-1407-38) RAIN SCAVENGING STUDIES. Progress Report No. 7. Dingle, A. Nelson (Michigan Univ., Ann Arbor. Dept. of Meteorology and Oceanography). Dec 1970. Contract AT(11-1)-1407. 81p. Dep. NTIS.

In 1970 analytical work on samples collected in 1969 was completed, and some areas of analytical technique for the neutron-activation measurement of indium were worked out, and the procedures published. Field experiments were conducted during the period from May 15 to June 30 in the area of Clinton, Illinois, using the Illinois State Water Survey rain-gaging network augmented by our own samplers to a sampling density of about 1 per 3 sq. mi. Sequential sampling was done at the University of Michigan base station, and, by means of automatic samplers supplied by Argonne National Laboratory, at three additional stations. Six tracer experiments were conducted and samples were collected from a seventh storm system that passed the area at night. Although analysis has begun the results of the study are not ready for presentation at this time. Preliminary results for the case of June 1, 1970 are presented. (auth)

34743 (IS-2541) SURVEY OF ENVIRONMENTAL RADIOACTIVITY, JANUARY 1, 1970–DECEMBER 31, 1970. Voss, Milo D. (Ames Lab., Iowa). Feb 1971. Contract W-7405-eng-82. 37p. Dep. NTIS.

The environmental monitoring program of the Ames Laboratory of the USAEC for the Ames Laboratory Research Reactor (ALRR) is described. The environmental program consists of gross alpha and beta determinations of air, soil, vegetation, river water, ALRR outfall, bottom sediment, precipitation, well water, and pond samples. The ALRR reached full power on July 12, 1965. The ALRR had generated 105409 megawatt hours as of Dec. 31, 1969. A total of 34051 megawatt hours was generated in 1970. The data indicate that the ALRR has not contributed a significant amount of radioactivity to the environment in the Ames area. The conclusion is reached that radioactivity levels recorded for environmental samples represent background conditions from atmospheric fallout and naturally occurring radioactivity. (auth)

34744 (NP-18828) ANNUAL REPORT, 1969–70. (Commonwealth Scientific and Industrial Research Organization, Melbourne (Australia). Div. of Meteorological Physics). 41p. Dep. NTIS (U. S. Sales Only).

The 1969 to 1970 activities of the Division of Meteorological Physics of the Commonwealth Scientific and Industrial Research Organization, Melbourne, Australia are summarized. The main purpose of this research organization is to gain a more complete understanding of the basic physical processes which control weather and climate. A major field of study has been micrometeorology, including turbulence, which is interrelated with upper atmosphere research; air-sea interaction; agricultural meteorology including hydrology, evaporation, and plant-environment interaction; atmospheric pollution; and atmospheric and terrestrial radiation levels. Experimental research in each of these subjects is discussed. (L.C.L.)

34745 (NYO-4061-2) MEASUREMENT OF AIRBORNE RADIOACTIVITY AND ITS METEOROLOGICAL APPLICATION. Annual Report, April 1, 1969–March 31, 1970. Reiter, R.; Sladkovic, R.; Poetzl, K.; Carnuth, W.; Kanter, H.-J. (Fraunhofer-Gesellschaft, Garmisch-Partenkirchen (West Germany). Physikalisch-Bioklimatische Forschungsstelle). Contract AT-(30-1)-4061. 110p. Dep. NTIS.

A technique using stratospheric ^{7}Be and ^{32}P as tracers for studying the air mass exchange between stratosphere and troposphere is outlined. (auth)

34746 (RT/PROT-(70)42) SEVENTH ANNUAL METEOROLOGICAL REPORT OF THE CASACCIA CENTER FOR NUCLEAR STUDIES, 1968. Cagnetti, P.; Flenghi, C.; Giudici, G.; Martinelli, V. (Comitato Nazionale per l'Energia Nucleare, Rome (Italy)). 30 Nov 1970. 100p. (In Italian). Dep. NTIS (U. S. Sales Only).

Short description is presented of observed atmospheric phenomena and currently used climatological methods, with emphasis of the salient features of the meteorological year 1968. (auth)

34747 (SC-DC-70-5443) COMPARISON OF TURBULENCE INTENSITY AND STABILITY RATIO MEASUREMENTS TO PASQUILL TURBULENCE TYPES. Luna, R. E.; Church, H. W. (Sandia Labs., Albuquerque, N. Mex.). [1971]. 9p. (CONF-710406-1). Dep. NTIS.

From Conference on air pollution meteorology; Raleigh, N. C. (5 Apr 1971).

The intent of the Pasquill categories was that of estimating the diffusive properties of the atmosphere given only a minimum of measurements. The included data distributions show that in the mean, the categories are established in the proper sequence. However, the neutral class, D, does not seem to be an indicator of zero lapse rate of potential temperature. The distribution of standard deviation of azimuth (σ_A) and elevation angle (σ_E) determined by the stability classes have statistically different means, but the standard deviations are so large that almost any value of σ_A or σ_E could belong to any stability class. This large variability within any one category certainly suggests the need for measuring the σ_A, σ_E and wind speed (u) parameters directly with fast response vanes if possible. (auth)

34748 CONTENT OF ARTIFICIAL RADIOISOTOPES IN THE ATMOSPHERE OVER MOSCOW DURING 1962–1967. Zykova, A. S.; Telushkina, E. L.; Rublevskii, V. P.; Efremova, G. P.; Kuznetsova, G. A. Gig. Sanit.; No. 4, 50-3(Apr 1970). (In Russian).

In characterizing the radiological health situation in Moscow in relation to atmospheric contamination by global radioactive precipitation, the content of the major long-lived artificial radioisotopes (^{90}Sr, ^{137}Cs, ^{144}Ce, and ^{106}Ru) must be considered. Even the intensive radioactive fallout during 1962 and the first half of 1963 did not exceed the MPC incorporated in the health legislation (health standards for radioactive substances and ionizing radiation sources). From the second half of 1963 to 1967, a reduction in atmospheric radioactivity was observed. During the 5-yr period, the concentration of radioactive aerosols was reduced 40 times and the content of ^{137}Cs and ^{90}Sr approximately 10 times. (tr-auth)

Mineralogy and Exploration

Refer also to abstracts 34716, 34741, and 34761.

34749 (CEA-R-4034) URANIUM GEOCHEMISTRY AND GRANITIC DIFFERENTIATION IN THE URANIUM-BEARING PROVINCE OF THE NORD-LIMOUSIN. Ranchin, Guy (Commissariat a l'Energie Atomique, Fontenay-aux-Roses (France). Centre d'Etudes Nucleaires. Nancy Univ. (France)). Jan 1971. 397p. (In French). Dep. NTIS (U. S. Sales Only).

Thesis.

From the practical application point of view, there appears to be a promising future in the prospecting of new regions by the characterization of mineral-bearing granites. The typology of granitic mountain masses and the evolutionary processes they involve were studied from the basis of the petrographic and geochemical structures which have been shown to exist in these mountain masses. Uranium geochemistry and to a lesser degree, that of thorium, zirconium and the rare earths, and the behavior of these elements during the evolutionary processes dealt with in the first part were investigated. An attempt to classify trace elements is proposed. The study of uranium is based on numerous analyses (over one thousand); many of them were carried out using drilling techniques which have made it possible to establish the exact characteristics of the distribution of the primary uranium which was not affected by changes connected with the supergeneous degradation. (auth) (France)

34750 (COO-2024-1) CARBON, OXYGEN, AND SULFUR ISOTOPES AND THE ORIGIN OF SANDSTONE-TYPE URANIUM DEPOSITS. Final Report. Jensen, Mead LeRoy (Utah Univ., Salt Lake City. Dept. of Geological and Geophysical Sciences). 15 Feb 1971. Contracts AT(30-1)-2261; AT(11-1)-1553; AT-(11-1)-2024. 121p. Dep. NTIS.

Research on the isotopic geology of sandstone-type U deposits was continued with special emphasis on determining the significance of $\delta^{18}O$ values for oxides, quartz, clay minerals, and silicates, and the significance of these to the origin and redistribution of U deposits. Data from several hundred sulfur isotope analyses for $\delta^{34}S$ are included as well as data from less numerous measurements of $\delta^{13}C$, $\delta^{18}O$, $^{12}C/^{14}C$, and $^{32}C/^{34}C$. It is concluded that the use of isotope measurements for studying the genesis of sandstone-type U deposits is scientifically promising and may have practical economic significance. Specific recommendations are made for continuing and improving this research program. (L.C.L.)

34751 ECONOMIC ASPECTS OF PROSPECTION AND EXPLOITATION OF URANIUM ORES IN FRANCE. Gnojek, I. (Ustav Uzite Geofyziky, Prague); Vesely, T.; Sorf, F. Geol. Pruzkum; 12: 271-3(Sep 1970). (In Czech).

Information is given on the location of uranium ore fields and the individual important uranium deposits in France. A brief survey of the history of the development of prospecting and ex-

ploratory operations and their methods is presented. Also given are detailed data on deposition conditions, mining operations, radiometric apparatus used in mining, and data on ore dressing in the Vendée area. (auth) (INIS)

34752 OXIDATION–REDUCTION PROPERTIES OF ROCKS CONTAINING URANIUM ORES IN BLACK SHALES. Kurdyukov, A. A. Litol. Polez. Iskop.; No. 1, 130-3(Jan 1970). (In Russian).

Oxidation-reduction properties of uranium-bearing ores in black shale are analyzed. The deposits are related to the low-paleozoic era with variscite tectogenezis in the folding structures superimposed by faults. (tr-INIS)

34753 URANIUM DEPOSITS OF THE CENTRAL AND THE ARMORICAN MASSIFS IN FRANCE. Pouba, Z.; Vanecek, M. (Karlova Univ., Prague). Geol. Pruzkum; 12: 268-71(Sep 1970). (In Czech).

Information is given on uranium mineralization and age and genesis of uranium ores in the Central and Armorican Massifs in France. (INIS)

34754 METODY POISKOV URANOVYKH MESTOROZHDENII. (Methods of Prospecting for Uranium Deposits). Surazhskii, D. Ya. (ed.). Moscow; Izdatel'stvo Nedra (1969). 392p.

The book represents the second volume of the book published in 1964 under the title Geological Prerequisites in Prospecting for Uranium Deposits, V. I. Krasnikov ed. The first chapter discusses general prospecting methods including radiometric methods and devices, aerogeophysical surveys, gamma and emanation surveys, uranometric and biochemical surveys, γ-probing, γ-sampling and general physical prospecting methods. The second chapter deals with prospecting for uranium outcrops, prospecting for endogenic hidden deposits by geochemical studies of mineralization, and drilling in depth. The third and last chapter describes the geological method for prospecting and exploration for uranium deposits found in depth. Classifications and examples of deep radioactive anomalies, determination of primary and secondary deposition are discussed. (R.V.J.)

34755 URANIUM MARKET: THE SWISS OUTLOOK. Stobbs, J. J. (Electro-Watt Engineering Services Ltd., Zurich). Neue Tech., B; 12: 119-23(Aug 1970).

Switzerland has three commercial nuclear power stations operating or under construction and has already gained substantial experience in the purchase of uranium concentrates. The maximum rate of nuclear power installation through 1990 in Switzerland is defined. From these predictions the uranium requirements for the period were calculated and the influence of uranium and plutonium on annual and cumulative requirements is indicated. It is also shown that in comparison with the requirements of the total free world, the Swiss requirement is naturally very small which has the advantage of leaving Swiss utilities with substantial freedom to contract as desired on the market without fear of upsetting any supply-demand situation. Finally the way in which the uranium market trends, this freedom for contracting, and the personal preference of the utilities has affected the approach to contracting is briefly outlined. (auth)

34756 VARIOUS STRUCTURAL TYPES OF THE MOLYBDENUM–URANIUM ORES. Yakovlev, P. D. (Moscow Geological Exploratory Inst.). Izv. Akad. Nauk SSSR, Ser. Geol.; No. 8, 56-66(Aug 1970). (In Russian).

Six types of Mo–U ones were established: (1) volcanic fields with horizontal or bare stratified deposits, (2) volcanic cupolas and volcano-tectonic brachyanticlines, (3) craters, (4) elongated volcanic structures associated with deep fractures, (5) complex volcanic structures, and (6) fields of small intrusions, subvolcanic bodies and volcanic roots. In the first two formation types a localized mineralization plays a part in stratified dislocation as well as in volcanic and sedimentary rock. The role of volcanic and subvolcanic bodies as ore-controlling and ore-containing elements of the structure increases from the first type of ore to the last. (K.S.W.)

34757 URANIUM IN THE WORLD AT THE END OF 1970. Perilli, Maria L. Com. Naz. Energ. Nucl., Notiz.; 17: No. 1, 39-55(Jan 1971). (In Italian).

The activities of the main U producing countries and those which, though having a more limited production, are substantially interested in U are reviewed. (auth)

34758 URANIUM: PROSPECTS AND PROBLEMS. Brinck, Johan (EURATOM, Ispra, Italy). Euro-Spectra; 10: No. 1, 11-15(Mar 1971).

The European Community has suddenly become a self-supporting U producer. A June 18 and 19, 1970 symposium at Ispra focussed attention on the implications of this event, especially with respect to short-term marketing and long-term development of reserves. Data on current U reserves and forecasts on U reserves to 1993 in the western world are presented. Proposals for developing a free U market and for establishing and maintaining a permanent dialogue between U producers and their customers are described. (L.C.L.)

Oceanography

Refer also to abstract 34743.

34759 (NYO–2174-129) GENERAL SUMMARY OF PROGRESS, 1970–1971. Bowen, Vaughan T. (Woods Hole Oceanographic Institution, Mass.). Contract AT(30-1)-2174. 34p. Dep. NTIS.

The 1970 research activities of the Woods Hole Oceanographic Institute which were related to determining fallout distribution in oceans are described. These activities include: the analyses of reagent blanks for ^{137}Cs and ^{90}Sr; interlaboratory comparisons of results from reference sample analyses; measurement of ^{90}Sr content in Atlantic Ocean surface waters; and measurement of the vertical penetration of fallout in both seawater columns and ocean sediment columns. Data are presented on the ^{137}Cs and ^{90}Sr analysis of seawater samples, ^{90}Sr content of Atlantic Ocean waters; ^{137}Cs and ^{90}Sr vertical penetration in waters of Atlantic Ocean and Sargasso Sea; and ^{137}Cs, ^{239}Pu, and ^{90}Sr vertical profiles in both water columns and sediment cores from the North Atlantic and the western Mediterranean. (L.C.L.)

34760 STUDIES ON THE BEHAVIOR AND DISTRIBUTION OF RADIOACTIVE SUBSTANCES IN COASTAL AND ESTUARINE WATERS. Kimura, Yuichiro; Morishima, Hiroshige; Koga, Taeko; Kawai, Hiroshi; Honda, Yoshihide (Kinki Univ., Osaka). Kinki Daigaku Genshiryoku Kenkyusho Nenpo; 7: 21-31(1968). (In Japanese).

Low-level liquid radioactive wastes are continuously disposed of from fuel processing plants or radioisotope laboratories into coastal waters. For an estimation of the influence of these disposals on our environment, the variation of concentration of thorium and rare earth elements contained in coastal and estuarine waters was investigated with the tidal change. It was observed that the concentration of thorium and rare earth elements in coastal water varied widely with the tidal change. This seems to be not only due to simple dilution by the water mass but also to the various physicochemical conditions such as salinity, pH of water, wind, and tidal motion. Since thorium and rare earth elements are apt to be colloidal or particulate in seawater, this character is greatly different from the case of soluble elements. (auth) (Japan)

34761 URANIUM CONCENTRATION IN RECENT OCEANIC SEDIMENTS OF WATER UPRISE ZONES. Baturin, G. N.; Kochenov, A. V.; Senin, Yu. M. (Inst. of Oceanology, Moscow). Geokhimiya; No. 4, 456-62(Apr 1971). (In Russian).

Uranium concentration in recent oceanic sediments in water uprise zones (i.e., of permanent ascending currents) is several times higher near the shores of continents in comparison with deep-sea oceanic sediments. Biogenic and diagentic phosphates, which are present in these sediments, accumulate up to 10^{-3} to 10^{-2}% of uranium. In both cases uranium concentration occurs by the way of extraction from sea water. Uranium precipitation in these regions is connected with the accumulation of organic matter and phosphorus in bottom sediments and with hydrogen sulfide contamination of benthonic waters. The intensive supply of organic matter and phosphorus to sediments of shelf zones is conditioned by their high biological productivity and by periodical mass starvations of the fauna. (auth)

34762 PARTICULATE Pb, ^{210}Pb AND ^{210}Po IN THE ENVIRONMENT. Langford, J. C. (Battelle-Northwest, Richland, Wash.). Health Phys.; 20: 331-6(Mar 1971).

Particulate Pb, ^{210}Pb, and ^{210}Po were measured in a Pacific Ocean depth profile 350 miles west of Newport, Oregon and in Atlantic Ocean surface samples collected at various locations between the Bahama Islands and Sierra Leone, Africa. The specific activity of ^{210}Pb in the Pacific Ocean increased with depth mainly due to the rapidly decreasing concentrations of stable Pb with depth. Stable Pb deposited in the Pacific Ocean area represented atmospheric fallout over a period of about 27 yr. In the Atlantic Ocean the average particulate ^{210}Po concentration was 20% higher than the average ^{210}Pb concentration yet both isotopes were about one-tenth their radio-equilibrium concentrations from ^{226}Ra. The particulate stable Pb concentration in the Atlantic

XUM

Ocean decreased ninefold (2.23 ± 0.02 to 0.25 ± 0.03 μg/l) from 25°38′N lat, 72°20′W long. to 24°48′N lat. 59°20′W long. (auth) (UK)

Seismology

Refer also to abstract 34769.

34763 (CGS–746-10) ALEUTIAN/AMCHITKA SEISMIC PROGRAM. King, Kenneth W. (National Ocean Survey, Las Vegas, Nev.). 12 Mar 1971. 29p. Dep. NTIS.

The National Ocean Survey seismic program for determining and defining the seismicity of the Rat Island (Alaska) Group and for monitoring the possible changes in normal seismicity which occur during and after nuclear detonations on Amchitka Island is discussed. The seismic network installed in the Aleutian Islands for the purpose of investigating the seismicity of the area on and near Amchitka Island is described. The procedures and schedules for recording and analyzing the seismic data and for maintaining the equipment are included. (L.C.L.)

34764 SOURCE PARAMETERS OF THE SALMON AND STERLING NUCLEAR EXPLOSIONS FROM SEISMIC MEASUREMENTS. Healy, J. H.; King, Chi-yu; O'Neill, M. E. (National Center for Earthquake Research, Menlo Park, Calif.). J. Geophys. Res.; 76: No. 14, 3344-55(10 May 1971).

The source parameters for the Salmon and Sterling nuclear explosions can be approximated by an equivalent source involving a step function of pressure inside an elastic spherical cavity. The parameters of this theoretical model were determined for Salmon and Sterling by fitting the spectral ratios of the seismic signals. The elastic radius for Salmon is 169 meters; that for Sterling is 29 meters. The ratio of pressures at these radii is about 4. The values of the parameters determined from seismic data are in good agreement with the values determined from gages in the salt dome near the source. The success of this technique suggests that source parameters for small earthquakes might be determined from their spectral ratios. Estimates of the decoupling factor based on this model are in close agreement with values reported in the literature. (auth)

34765 ANALYSIS OF MARVEL: A NUCLEAR SHOCK-TUBE EXPERIMENT. Crowley, Barbara K.; Glenn, H. David; Marks, Robert E. (Univ. of California, Livermore). J. Geophys. Res.; 76: No. 14, 3356-74(10 May 1971).

Marvel, a nuclear-driven shock-tube experiment, consisted of a 2.2-kT nuclear explosive detonated 176 meters underground at one end of a 122-meter long, 1-meter diameter horizontal tunnel. Vaporization of material in the immediate vicinity of the explosive provided the source of high-energy driven gas. The driven gas was the ambient atmospheric air in the tunnel. Marvel was conducted as an experimental and calculational study of the time-dependent flow of energy in the tunnel and surrounding alluvium. Descriptions are given of: the design of Marvel, the dynamic and postshot experimental results; and a numerical simulation of the experiment. Experimental and calculational results indicate the following: the high-energy air shock traveled down the tunnel nearly 50 times faster than the shock in the surrounding alluvium; over the first 30 meters of the tunnel, the shock had a velocity of approximately Mach 380; during its 4-msec transit of the 122-meter tunnel, it attenuated to approximately Mach 30. Significant ablation of material from the tunnel walls had the primary effect in attenuating the air shock. The source energy was preferentially channeled down the tunnel, and a cone-shaped cavity resulted. (auth)

XUM

ENGINEERING

Nuclear Explosions

Refer also to abstracts 34720, 34728, 34763, 34765, 34817, 35058, and 35088–35090.

34766 (AECOP–632) COST-BENEFIT ILLUSTRATION FOR UNDERGROUND NUCLEAR NATURAL GAS STIMULATION. Aull, L. B.; Harrel, H. A.; Teleki, A.; Wood, P. M. (Atomic Energy Commission Combined Operations Planning, Oak Ridge, Tenn.). 17 Nov 1970. Contract W-7405-eng-26. 31p. Dep. NTIS.

An analysis is presented which is intended to illustrate potential economic advantages of developing the technology for the stimulation of natural gas by underground nuclear explosions. Estimates of the market for natural gas from various-sized fields in the Rocky Mountain area and wellhead price projections for several fields are included. The costs of nuclear devices and of developing commercial nuclear gas stimulation are discussed. It is concluded that, for the two Rocky Mountain area fields investigated, commercial exploitation of nuclear gas stimulation appears to be economically attractive under fairly conservative assumptions, and that, with productive periods of only 10 to 11 years, these ventures would result in a 10% return on investment. (L.C.L.)

34767 (BMI–171–129) AMCHITKA BIOENVIRONMENTAL PROGRAM ON LIMNOLOGY STUDIES, AMCHITKA ISLAND, ALASKA. Annual Progress Report, July 1, 1969–June 30, 1970. Koob, Derry D. (Battelle Memorial Inst., Columbus, Ohio). 1 Apr 1971. Contract AT(26-1)-171. 46p. Dep. NTIS.

Sixteen lakes were intensively studied immediately before Milrow, the underground nuclear test conducted on Amchitka Island, Alaska, on Oct. 2, 1969. During this preevent study, when all lakes had high water, the pH decreased in all except Clear Pond, and two underwent significant changes in water chemistry. Milrow produced structural changes in only 3 lakes, partially draining them. One of these, located 2.2 miles NNE of Surface Ground Zero (SGZ), showed multiple changes after Milrow. Its water level fell 10 inches, alkalinity decreased about 3.5 ppm, zooplankton abundance decreased, and suspended inorganic sediments increased. Most changes noted in the other lakes studied intensively after Milrow were minor and can be partly explained by seasonal changes and weather conditions. In these lakes, no significant changes in pH, alkalinity, zooplankton community structure or absolute abundance could be attributed to Milrow. That 12 lakes had lower suspended-sediment loads after Milrow is believed to be due to differences in weather conditions during the sampling periods before and after the nuclear test. In all lakes but two, rotifers, which dominated the zooplankton, decreased, but the decrease cannot be attributed to Milrow. (auth)

34768 (NCG-TR–15(Vol.1)) EMPIRICAL STUDY OF BEHAVIOR OF CLAY SHALE SLOPES. Fleming, R. W.; Spencer, G. S.; Banks, D. C. (Army Engineer Nuclear Cratering Group, Livermore, Calif.). Dec 1970. 101p. Dep. NTIS.

This study was undertaken to determine the factors that lead to instability in clay shale, and thus to provide a basis for assessing the probable long-term stability of high crater slopes in clay shales. The chief features contributing to the engineering behavior of clay shales are a degree of overconsolidation and lithology, both of which reflect geologic history. Local geologic structure and hydrologic conditions affect individual slopes. Weak layers may present slope hazards, while conversely a few stronger layers may materially strengthen an entire clay shale slope. Time-dependent phenomena are important in clay shale slopes, which may fail after standing apparently stable for many years. Intensive studies were made of natural slopes in five clay shale units in the upper Missouri Basin. The Claggett, Bearpaw, and Pierre formations, all marine-deposited shales of Late Cretaceous age, showed extensive slope failures; high slopes generally stood at overall inclinations of only 5 to 10°, inclinations comparable to the residual angles of internal friction of the materials. The Cretaceous Colorado group and Lower Tertiary Fort Union group showed steeper slopes with fewer failures. Intensive laboratory testing of the physical properties of all materials indicated that only gross differences in slope behavior can be related to any specific test or series of tests. Engineering practice in clay shale materials is customarily based on an empirical approach, attention being given to local site conditions and to the observed behavior of existing nearby slopes. Observations of experimental crater slopes in clay shale are limited. The conclusion is reached that future design crater slopes must be based on experiences with conventionally excavated slopes. Furthermore, the design of cratered slopes must be conservative, although no experience indicates that the slope inclination must be as flat as the residual angle of internal friction of the site materials. (auth)

34769 (UCRL–50987) TWO-DIMENSIONAL STRESS-INDUCED ADIABATIC FLOW. Cherry, J. T.; Sack, S.; Maenchen, G.; Kransky, V. (California Univ., Livermore. Lawrence Radiation Lab.). 30 Dec 1970. 62p. Dep. NTIS.

The TENSOR code provides a numerical solution to the propagation of a stress wave of arbitrary amplitude through a Lagrangian grid in two space dimensions. A detailed description of the code is presented. (auth)

34770 (UCRL–50993) PREDICTION OF UNDERGROUND NUCLEAR EXPLOSION EFFECTS IN WAGON WHEEL SANDSTONE. Terhune, Robert W. (California Univ., Livermore. Lawrence Radiation Lab.). 15 Jan 1971. Contract W-7405-eng-48 24p. Dep. NTIS.

Project Wagon Wheel is a study to investigate the technical concept of nuclear stimulation of a natural gas reservoir located near Pinedale, Wyoming. The results are presented of computer calculations, simulating the explosion effects, based on equation-of-state measurements of core samples taken from EPNG Wagon Wheel No. 1 hole at a depth between 8,000 to 12,000 ft. The shear failure envelope for Wagon Wheel sandstone is almost identical to that for Hoggar granite. A calculation for Wagon Wheel sandstone for one kt energy at a depth of 300 m duplicated cavity radius, shear fracture radius, stressed region, peak particle velocity, and peak acceleration data measured from the nuclear experiments conducted in the Hoggar granite by the French. The conclusion drawn from this comparison is that the Hoggar granite chimneys and regions of increased permeability provide a reasonable model to assume for Wagon Wheel. Cavity and chimney dimensions are predicted for a single explosive detonated at a depth of 10,000 ft. (auth)

34771 PEACEFUL USE OF NUCLEAR FISSION. Moulinier. Prot. Civ. Secur. Ind.; No. 180, 6-12(Oct 1969). (In French).

The principal peaceful application of nuclear fission are summarized. Its advantages and the dangers that can result are discussed. The politics of the major powers in the field of nuclear power plants are reviewed. (J.S.R.)

34772 PROCESS FOR STIMULATING PETROLIFEROUS SUBTERRANEAN FORMATIONS WITH CONTAINED NUCLEAR EXPLOSIONS. Bray, B. G.; Knutson, C. F.; Coffer, H. F. Canadian Patent 865,509. 9 Mar 1971.

The process for recovering hydrocarbons from a subterranean reservoir consists of detonating several horizontally spaced nuclear explosives or detonating a single nuclear explosive so that it does not break into any aquifer. (F.S.A.) (Canada)

Facilities and Equipment

Refer also to abstracts 34828, 34853, 35326, 36209, and 36229.

34773 (BNWL–B–51) ANALYSIS OF AIR PULSER PERFORMANCE FOR PULSED EXTRACTION COLUMNS. Kaser, J. D. (Battelle-Northwest, Richland, Wash. Pacific Northwest Lab.). Feb 1971. Contract AT(45-1)-1830. 19p. Dep. NTIS.

An expression was derived for determining the pulse amplitude in air pulsed columns as a function of reservoir air pressure and pulse frequency. Amplitudes calculated by this expression and by V. L. Hammond's simplified equation compare favorably with experimentally measured amplitudes and with amplitudes calculated by a lengthy numerical procedure. Plots of amplitude versus reservoir air pressure were calculated at several pulse frequencies for two-pulse column designs. (auth)

34774 (EUR–4629) MECHANICAL BEHAVIOUR OF COMPLEX STRUCTURES IN PRESENCE OF CREEP, THERMAL STRAINS AND IRRADIATION-INDUCED DIMENSIONAL CHANGES. Donea, J.; Giuliani, S. (European Atomic Energy Community, Ispra (Italy). Joint Nuclear Research Center). 10 Dec 1970. 66p. (In French). Dep. NTIS (U. S. Sales Only). EUR FF 9,45.

A numerical method of analysis and the associated computer program are presented for the determination of stresses and strains in complex structures encountered in the field of the nuclear technology. The method is based on the finite element technique. Plane stress, plane strain, and axisymmetric situations

XUM

can be investigated. Material anisotropy, general creep laws, thermal strains as well as irradiation-induced dimensional changes can be taken into account. Numerical examples are presented to demonstrate the validity of the proposed method of analysis. (auth)

34775 (EUR-4634) TEMPERATURE STABILIZATION IN HEAT EXCHANGE TUBES UNDER ALTERNATING HEAT FLUXES. Schlitt, K. R. (European Atomic Energy Community, Ispra (Italy). Joint Nuclear Research Center). Mar 1971. 78p. (In German). Dep. NTIS (U. S. Sales Only). EUR DM,920.

The use of heat pipes for stabilizing or controlling the temperature in heat exchanger tubes under conditions of variable heat flux was investigated. It was concluded that, if the heat pipes are partially filled with a rare gas, they can be used for controlling the heat flux. The experimental results of the change of temperature between heat fluxes of 0.5 and 1.0 kW are 0.5% for a self-controlled water-cooled heat pipe and 2.2% for a corresponding radiation-cooled heat pipe. The results also show that temperature stabilization is strongly influenced by the change of the rare gas temperature during operation, especially when the partial vapor pressure of the working fluid in this zone takes on a non-negligible value. (auth)

34776 (EURFNR-794) CONTRIBUTION TO EXPERIMENTAL THERMAL SHOCK ANALYSIS. Lang, W. (Kernforschungszentrum, Karlsruhe (West Germany). Institut fuer Reaktorentwicklung). Translation of report KFK-1168. 96p. Dep. NTIS.

Work Performed under United States–Euratom Fast Reactor Exchange Program.

A method for solving problems related to transient thermal stresses is described. The method is based on the experimental determination of frequency response functions and weighting functions for thermal stresses. Duhamel's integral is employed to determine the time curves of the temperatures and thermal stresses generated in a structural component as a result of fast variations of the coolant temperature during reactor operation. Moreover, it provides the means to evaluate the effects of cyclic thermal loads encountered in reactor operation which may cause fatigue of the structure in long-term operation. A representative structural component of reactor technology (hollow cylinder of 100 mm inside diameter with an abrupt change of wall thickness from 20 mm to 2 mm), which is particularly sensitive to thermal stresses, was equipped with thermocouples and strain gages and investigated in a helium circuit in order to test the proposed method. The validity of the method was demonstrated in a comparison of the results of a real thermal shock on the helium circuit with the results calculated in advance with the help of weighting functions which also had been determined experimentally. (auth)

34777 (ORNL-IIC-34) PATENT LITERATURE ON PROCESS RADIATION AND IRRADIATOR DESIGN. PART 1. UNITED STATES PATENTS 1950 THROUGH 1968. Greene, R. E.; Warren, H. S.; Baker, P. S. (Oak Ridge National Lab., Tenn.). Jun 1971. Contract W-7405-eng-26. 293p. Dep. NTIS.

A review of the United States patent literature from 1950 through 1968 on process radiation and irradiator design is presented. The search program for the identification of relevant patents is described, and information on more than 700 patents is included. For each patent the number, title, date of issue, date of filing, assignee, patentee, and either an abstract or the most descriptive patent claim are given. An analysis of the patent collection reflects industrial interest in present and potential applications of ionizing radiation. Subject and assignee indexes are included. Partial listings of 1969 and 1970 patents are appended. (auth)

34778 (ORNL-tr-2417) WAK: ADMINISTRATIVE BASIS AND COMMERCIAL REALIZATION. Tebbert, H.; Zuehlke, P. Translated by R. G. Mansfield (Oak Ridge National Lab., Tenn.), from Atomwirt., Atomtech.; 15: 77-9(1970). 7p. Dep. NTIS.

Economic aspects of design, construction, and operation of the WAK reprocessing plant are discussed. (J.R.D.)

34779 (TID-4103(Suppl.1)(Rev.2)) ENGINEERING MATERIALS LIST CUMULATIVE INDEX, 1968–1970. (Division of Technical Information Extension (AEC), Oak Ridge, Tenn.). Apr 1971. 40p. DTIE Free.

Cumulative subject and corporate author indexes are presented which cover all packages of AEC engineering materials that have been announced in the Engineering Materials List (TID-4100, Suppl. 43 through 61) from 1968 through 1970. A title list of packages arranged in CAPE-number sequence is also included. (L.C.L.)

34780 (UARAEE-54) MECHANICAL DECLADDING OF THE INCHAS FUEL. Abdel-Rassoul, A. A.; Higgy, H. R.; Hammad, F. H. (Atomic Energy Establishment, Cairo (Egypt). Nuclear Chemistry Dept.). 1968. 45p. Dep. NTIS (U. S. Sales Only).

The possible mechanical decladding of the Inchas fuel rod was investigated. The methods generally used for mechanical dejacketing of different fuel elements are briefly reviewed. Both mechanical and metallurgical properties of the Inchas fuel rod were studied in some details. This revealed that the Inchas fuel (enriched with ^{235}U), is a dispersed type of UO_2 in magnesium, manufactured by extrusion or by vibratory compaction techniques. Decladding by the rolling-straightener technique was studied both theoretically and experimentally. Successful decladding of respective models made from different mandril materials cladded with aluminum was realized. However, decladding of the tested fuel rod and some other designs as well are impractical, leading to nonuniform stresses due to the limited length of work pieces. Proper decladding, however, by the method investigated is not excluded. The decladding of the fuel by the proposed extrusion and shearing technique is expected to be feasibly realized without limitations. Necessary studies related to adequate design of proposed machine are also included. (auth)

34781 NUCLEAR METALLURGY CURRICULUM AT THE UNIVERSITY OF MISSOURI AT ROLLA. Leighly, H. P. Jr.; Edwards, D. R.; Bolon, Albert E. (Univ. of Missouri, Rolla). pp 586-9 of Materials Technology: An Interamerican Approach. New York; American Society of Mechanical Engineers (1968).

From Inter-American Conference on Materials Technology, San Antonio, Tex. See CONF-680513.

The Nuclear Engineering Curriculum at the University of Missouri at Rolla is described. The materials' portion of the curriculum is analyzed in considerable detail. The student receives substantially more of his education in the study of the properties and behavior of materials with particular emphasis on their application in nuclear reactor design and construction than in most similar curricula at other universities in the United States. This should permit him to be a very valuable member of a nuclear reactor design and construction group. With this background he could select employment with a company which fabricates and reprocesses fuel elements. In general, this graduate will be sought after. The careers of a number of recent graduates were analyzed with the results showing that most are working as metallurgists rather than as nuclear engineers. As the consequence, the curriculum was changed markedly to provide a stronger education in nuclear physics, reactor theory and reactor engineering. In the future the graduates will be more nearly nuclear engineers. (auth)

34782 URANIUM OXIDES TO UF_6 CONVERSION FACILITY (11 Feb 1971) (Engineering Materials). (Goodyear Atomic Corp., Portsmouth, Ohio). (CAPE-2083).

228 drawings.

A facility for producing UF_6 which is capable of processing purified U in its various oxide forms and as uranyl nitrate hexahydrate. The facility can produce 20,000 kg U/yr as UF_6 based on a processing rate of 4 kg U/hr with allowances for maintenance and inventory downtime, for a continuous seven-day week operation. The process consists of direct fluorination of U_3O_8 with elemental F in an air-cooled flame tower. The UF_6 in the off-gas stream is selectively frozen out in a 80°F cold trap. Traps are then heated and UF_6 is drained as a liquid into 5 in. product cylinders. Off-gas from the cold traps flows through NaF_2 traps (regenerated in situ) to bring the vent gas concentration below 5 ppM of U. A flame tower, which replaces the stirred-bed screw-type fluorination reactor formerly used is described. The flame tower and its associated subsystems, such as pneumatic unloading, transfer of oxide, feed screw and dispenser for the tower, ash removal, filtering, cold trapping, and liquid UF_6 cylinder loading, provide nuclear-safe geometry and maximum protection of personnel from radiation exposure. Pieces of equipment which are apt to release airborne radioactivity are enclosed in glove boxes. (For details see TID-4100 Suppl. 64) (see also 22-3577) (F.S.)

34783 TUBE CLEANING MACHINE (18 Mar 1970) (Engineering Materials). (Richland Operations Office (AEC), Wash.). (CAPE-2080).

6 drawings.

A brushing/rinsing machine for the removal of chlorinated polymers or chlorinated oils used as lubricants in the plug drawing of FTR fuel cladding is described. The machine incorporates a manifold to introduce a constant supply of clean rinse water to the bore of the tube while the rotating brushes are advanced and retracted under the control of timing and travel-limit switches. One end of the tube handling mechanism guides the brushes into the tube bore. Traveling shaft supports prevent whipping or deflection of the brush shafts as they rotate at ~100 rpm. The shafts themselves are covered with Teflon to protect the inner surface of the tubes. All parts of the machine contacting the tubes are made of plastic materials. Electrical controls are adjustable for cycle time and for length of stroke to 10 ft max. Operator labor is re-

XUM

duced to loading and unloading the machine. (For details see TID-4100 Suppl. 64) (See also 24: 8068) (F.S.)

34784 CHEMICAL PROCESSING EQUIPMENT (Dec 1970) (Engineering Materials). (Richland Operations Office (AEC). Wash.). (CAPE-2081).

46 drawings.

Operating equipment used in chemical processing facilities is described. Drum filters, reactor vessels, the chute from a drum filter to a calciner, calciner screw conveyor, and tanks from the plutonium processing facilities are described. Filtrate storage, condensate receiver, overflow, pre-reduction, and transfer head tanks are included. From the plutonium facility scrap dissolution equipment, dissolvers, and condensers are described. An offgas scrubber, incinerator, cyclone ash separator, and glove box for the cyclone ash separator from the incinerator facility are included. (For details see TID-4100 Suppl. 64) (F.S.)

34785 OFF-GAS HEATER AND SILVER REACTORS (17 Jan 1970) (Engineering Materials). (Richland Operations Office (AEC) Wash.). (CAPE-2082).

4 drawings.

Off-gas heaters and Ag reactors used in the Purex dissolver off-gas system are described. Gases leaving the dissolver contain ^{131}I which is absorbed on $AgNO_3$ and deposited on berl saddle packing. The heaters raise the off-gas temperature to the point where condensation is prevented. The reactor is a stainless steel vessel 4½ ft ID by 10½ ft tall. Silver nitrate-coated unglazed ceramic saddles are retained in two beds between grates and wire screens spaced 4 ft apart. A steam coil and insulation surround the packed reaction chamber to reduce heat losses. Preheated off-gas enters at the top of the reactor, flows downward through the beds, and leaves the reactor through the bottom outlet line. Regeneration or flush solutions are added through nozzles in the top head. Spent flush solutions are removed by the lower nozzles. Off-gas Ag reactors function efficiently but exposure to ammonia may be hazardous. (For details see TID-4100 Suppl. 64) (see also 25: 2416) (F.S.)

34786 STANDARD MARKING SYSTEM FOR VALVES, FITTINGS, FLANGES, AND UNIONS. MSS Standard Practice SP-25 1934. Arlington, Va.; Manufacturers Standardization Society of the Valve and Fittings Industry (1964). 24p. Avaiable from Manufacturers Standardization Society of the Valve and Fittings Industry, Arlington, Va.

This marking system applies to the various classes of valves (including cocks), flanges, fittings, and unions, hereinafter termed products, of whatever material made, which manufacturers recognize as regularly available products. Examples of marking regular products are illustrated. The term valve applies to such types as gate, globe, angle, cross, plug, needle, ball, butterfly, check of both the lift and swing type, and stop check. It is recommended that this marking system also be used in so far as possible for such products as pop, safety, relief, reducing, regulating, and other valves that require special markings to indicate the particular class of service for which the valve is made. (auth)

34787 REMOTE-CONTROLLED WELDING OF PRESSURE TUBES IN THE NIEDERAICHBACH NUCLEAR POWER PLANT. Steinkamp, E. Schweissen Schneiden; 22: 465-7(1970). (In German).

The welding of fillet welds lying within cooling tubes by means of the TIG method is reported. A description is given of the welding machine which works partly automatic and was developed especially for this work including the welding head. Information is given on welding tests. (INIS)

34788 AIR CONDITIONING IN THE NUCLEAR POWER PLANT. Morikawa, T. (Tokyo Shibaura Electric Co., Ltd., Kawasaki, Japan); Amamiya, N. Genshiryoku Kogyo; 16: No. 11, 48-56(Nov 1970). (In Japanese).

The air conditioning and ventilation in a nuclear power station has peculiar nature, because of radioactivity. The following are described mainly for a BWR power station: peculiarity of the air conditioning in nuclear power stations; radioactivity in the power station and the control; air conditioning and ventilation including the conditions of temperature and humidity for personnel and instruments, the air conditioning for dry-well, its ducts and auxiliaries in a reactor building, the air conditioning and temperature in a turbine building and operation floor, the storage rooms and a control room for radioactive wastes, and, finally, the service buildings, including laboratories, the power station control room, etc.; and automatic procedures for the air conditioning and ventilation in the reactor building and the central control room for normal conditions and during periods of high radioactivity. (auth) (Japan)

Heat Transfer and Fluid Flow

Refer also to abstracts 34775, 35549, 37000, 37008, 37009, 37020, 37035, and 37046.

34789 (ANL-7746) BUBBLE GROWTH AND COLLAPSE IN NARROW TUBES WITH NONUNIFORM INITIAL TEMPERATURE PROFILES. Ford, William Douglas (Argonne National Lab., Ill.). Dec 1970. Contract W-31-109-eng-38. 166p. Dep. NTIS.

Experimental data were obtained for both the bubble growth and collapse of Freon-113 in constant-diameter, vertical channels with nonuniform initial temperature profiles. The vapor growth was initiated by either rapid depressurization of the test section or pulsing an electrode following a slow depressurization. The experiment was recorded using high-speed photography. The experiments were divided into three series, each concerned with a portion of the expulsion (bubble growth) and reentry (bubble collapse) process. The first series was designed to obtain data for the slug expulsion from the hot portion of a constant-diameter test section. Data ranging in initial superheat from 59 to 128°F were obtained. In the second series, data were obtained, ranging in initial superheat from 30 to 100°F, for the expulsion from the hot portion into the cold portion of the test section. In addition, measurements of the void fraction during the expulsion process were made. The final series of experiments was designed to achieve reentry of the upper liquid-vapor interface within the constant-diameter portion of the test section. Reentry data were obtained for superheats ranging from 20 to 40°F. In addition to the experimental data, an analysis is given in which the momentum equation for the upper liquid slug and the energy equation for the vapor slug are coupled numerically to predict the growth of the vapor space. The energy equation accounts for not only the energy transported across the upper and lower liquid-vapor interfaces, but also that transported across the wall film-vapor interface. In computing the energy contribution of the wall film, a thin thermal boundary layer was assumed to exist, whose thickness as a function of exposure time and position along the vapor space was taken into account. The agreement between the experimental data and coupled solution was found to be good. (auth)

34790 (CONF-700557-4) NUMERICAL SOLUTION OF THE NAVIER-STOKES EQUATIONS TO CALCULATE INCOMPRESSIBLE CENTRIFUGE FLOWS. Krause, E. Translated from Stroemungsmechanische Vorgaenge in Graszentrifugen, DFVLR-Kolloquium, om 14 Mai 1970, Porz, Wahn, Germany. 17p. Dep. NTIS (U. S. Sales Only).

A new method is given for calculating the flow processes in gas centrifuges. The solution assumes that the flow can be described by a continuum concept. The non-steady Navier–Stokes equations and the energy equation form the starting point of this work. Using finite difference approximations the complete equations of motion are integrated in a cylindrical co-ordinate system. The axial symmetry of the problem is used to transform the original three-dimensional problem to a two-dimensional problem. Then a flow function can be introduced to satisfy the continuity equation. The tangential and radial velocities of the flow are determined as dependent on time. In a final calculation the Lagrange paths of the gas particles are determined. The throughput quantity and the width and arrangement of the throughput slits can be varied within definite limits. The method permits one to predict the effect of simple devices on the secondary flow. Previously, results for an incompressible centrifuge flow have been available. The results were for a closed pot-shaped centrifuge with a diameter/height ratio of 1 to 1. A slim tube was arranged concentric with the axis of rotation, turning with the same angular velocity as the centrifuge. Gas was fed in through a slit in the tube and removed through slits in the top and bottom of the centrifuge. The streamlines calculated give a detailed picture of the secondary flow in the centrifuge. (auth)

34791 (KFK-1332) EXPERIMENTAL INVESTIGATION OF THE RETARDATION OF BOILING OF SODIUM ON ARTIFICALLY ROUGHENED SURFACES. Schultheiss, G. F. (Kernforschungszentrum, Karlsruhe (West Germany). Institut fuer Reaktorentwicklung). Dec 1970. 100p. (In German). Dep. NTIS (U. S. Sales Only).

Results of investigations of thermo-hydraulic and physico-chemical influences on incipient boiling superheat of sodium are reported. The geometry of cylindrical-type artificial cavities was varied in depth and diameter. The sodium oxide concentration was varied and controlled by means of the cold trap temperature. All cavities tested were found to be extremely stable nucleation centers for months. They were not inactivated either by pressurization or by longtime boiling. Decreasing of depth to diameter ratio slightly increases the incipient boiling superheat. The incipient boiling superheat depends on oxide concen-

XUM

tration as well as on the test-surface material. For stainless steel superheat has a typical maximum at about 127°C cold trap temperature — corresponding to 2 ppM Na_2O — caused by the chromium content. Pure iron and nickel did not show such a maximum. Pure chromium behaves like stainless steel. Pure iron shows generally very small superheat not influenced by oxide concentration. For nickel superheat decreases with increasing oxide concentration and approaches the same constant value as stainless steel. (J.R.D.)

34792 (SC-DR-710084) SOLID PROPELLANT BURN TESTS. Baker, F. L. (Sandia Labs., Albuquerque, N. Mex.). Mar 1971. 95p. Dep. NTIS.

A series of solid propellant burn tests, utilizing the Titan III and Scout launch vehicle propellants, was conducted to provide data for a better understanding of the thermal environment that would result from such a fire. The fire test data and the analytical data utilized for deriving a thermal model are presented. (auth)

34793 (UARAEE-81) EXPERIMENTAL LOOP FOR TWO PHASE HEAT TRANSFER INVESTIGATIONS. El-Fouly, M. F.; Khattab, M. S. (Atomic Energy Establishment, Cairo (Egypt). Reactors Dept.). 1969. 50p. Dep. NTIS (U. S. Sales Only).

An experimental heat transfer loop was designed, manufactured, and erected for investigations of two phase heat transfer in a simulated BWR fuel channel. The test section, equipment, test procedures, measurements, and the experimental method for analysis are described. Recommendations for future work are listed. (auth)

34794 TWO-DIMENSIONAL ANALYSIS OF HEAT TRANSFER AND FLUID FLOW IN A ROD CLUSTER WITH SPECIAL ATTENTION TO ASYMMETRY. Chen, Ka-wei. Lafayette, Ind.; Purdue Univ. (1970). 301p. University Microfilms Order No. 71-2578. Thesis.

Theoretical predictions of laminar fully developed longitudinal flow and heat transfer performance characteristics under conditions of fully developed heat transfer for an axially uniform heat generation for a finite rod bundle in a tube are presented. A heat transfer analysis for slug flow is also presented. Two types of finite rod bundles are considered in this work. The first is with the rod cluster concentric with the tube, the second is with the rod cluster eccentric to the tube axis. No restrictions on equal rod diameters, equal heat generation in the rods or on symmetrical arrangement are imposed. This results in a more general approach than previously available. Two regions, the rod region and the flow region, are treated in the heat transfer problem. The energy equations together with a given flow field are solved to obtain the temperature field in each region. Flow distribution, friction factors, temperature and wall heat flux distributions, and Nusselt numbers are presented and discussed for example geometries. The computer code FAHS for the numerical calculations of these results is described. (Diss. Abstr. Int., B)

34795 HEAT TRANSFER AND HYDRAULIC RESISTANCE IN SMOOTH AND ROUGH TUBES AND CHANNELS FOR TURBULENT FLOW. Grunwald, G. (Zentralinstitut fuer Kernforschung, Rossendorf, Ger.). Kernenergie; 14: No. 3, 79-86 (Mar 1971). (In German).

Reichardt's method for calculating heat transfer in smooth tubes and channels for hydraulically and thermally developed turbulent flow based on the analogy of impulse and heat exchange is generalized for the case of rough tubes and channels. This calculation technique is of interest especially in reactor engineering, as a method for improving heat transfer in the reactor core, e.g., by roughening the fuel elements, an increase of power seems possible. A comparison of measuring and calculational results for heat transfer in smooth and rough tubes and channels shows good agreement for the ranges of Reynolds and Prandtl numbers studied. The new calculation technique for rough tubes and channels also gives velocity and temperature profiles in the turbulent flow. Finally, a semi-empirical equation for calculating the heat transfer for rib-like roughened tubes and channels is derived. (auth)

34796 CONTRIBUTION OF THE DEVELOPMENTS OF HEAT TRANSFER AND FLUID FLOW IN THE NUCLEAR FIELD TO OTHER USES, WITH PARTICULAR REFERENCE TO TWO-PHASE FLOW HEAT TRANSFER AND FLUID FLOW APPLICATIONS TO NON NUCLEAR FIELDS. Silvestri, M. (CISE, Milan. Politecnico, Milan). Energ. Nucl. (Milan); 18: 239-47(Apr 1971). (In Italian).

Special cases in which new developments in heat transfer and fluid flow are used are considered and include: problems of distillation related to seawater desalting; problems of conversion of thermal energy into mechanical energy by means of a gravimetric loop; and powder extraction from gaseous streams by means of annular flow. Some proposals for future developments of two-phase thermohydraulics are presented. (auth)

34797 ANNULAR-DISPERSED TWO-PHASE FLOW AND CRITICAL HEAT FLUX. Moeck, Edward Otto. Montreal; McGill Univ. (1970). National Library of Canada, Ottawa. Thesis.

Liquid film flow rates and critical heat fluxes were measured in a concentric, internally heated annulus in which steam and water flowed upwards at pressures and velocities of interest in nuclear reactors. Film growth rates were obtained from measurements of film flows on an unheated surface downstream of the heater. From these, droplet deposition fluxes were calculated and an equation for the entrainment flux is proposed. A theoretical expression for droplet velocity, obtained from droplet interchange between film and core, was linked with a critical Weber number to predict maximum stable drop diameters. These agreed with available data. A variable density film model, coupled with the core model, gave acceptable predictions of film thicknesses and crest velocities in air–water flow. (Diss. Abstr. Int., B)

34798 EXPERIMENTAL STUDY OF RADIATION-INDUCED BOILING IN SUPERHEATED LIQUIDS. El-Nagdy, M. M. (Babcock and Wilcox Ltd., London); Harris, M. J. J. Brit. Nucl. Energy Soc.; 10: 131-9(Apr 1971).

Conditions under which radiation-induced nucleation may occur in superheated liquids are discussed. An apparatus of the bubble chamber type, capable of achieving superheats as high as 100°C, was used to study bubble nucleation, induced by neutrons of energies 2.45 and 14.1 MeV, in superheated water, acetone and benzene. Special care was taken to suppress nucleation due to surface rugosities, suspended particles or dissolved gases, and this appears to have been achieved. It was found that for each liquid and each neutron energy there existed a superheat below which the liquid was insensitive to the radiation. A modified Lomer-type analysis suggests that the nucleation was induced by knocked-on oxygen and carbon ions. By adopting a new energy-deposition nucleation criterion derived from Rayleigh's perturbation wavelength criterion for the most rapid break up of a gas jet surrounded by liquid, it was found that calculated minimum superheats for neutron-induced nucleation were brought into closer agreement with the experimental values than had formerly been the case. (auth) (UK)

34799 THERMAL STRESSES IN ANNULAR DISKS. Miyazono, Shohachiro; Sakamoto, Fumio (Japan Atomic Energy Research Inst., Tokai). Hihakai Kensa; 19: No. 7, 356-60(Jul 1970). (In Japanese).

Liquid metal is used as coolant of a fast breeder, which is operated at high temperature of 500°C or higher. Consequently, a method of strain measurement in fused salt or liquid metal at high temperatures of 400°C or higher was investigated. As a first step, the characteristics of conventional strain gages for high temperature use were investigated. Temperature characteristics, value of zero point movement, and change of gage rate were measured. After the characteristics of strain gages were measured, thermal strains in SUS 27 annular disks were measured with these gages. As a result, it was confirmed that the measurement accuracy is comparatively high, if the zero point movement of each gage can be measured beforehand, and that the value of zero point movement depends on the aging temperature. (auth) (Japan)

34800 STABILITY OF LIQUID FLOW DOWN A HEATED INCLINED PLANE. Bankoff, S. George (Argonne National Lab., Ill.). Int. J. Heat Mass Transfer; 14: 377-85(Mar 1971).

The Yih Benjamin analysis of the stability to small surface perturbations of a thin liquid film flowing down an inclined wall is extended to take into account the effects of evaporation or condensation. Evaporation destabilizes the film. With vertical walls the flow is thus unstable at every Reynolds number under heating, but exhibits a critical Reynolds number under cooling. Above a critical heat flux the estimated time to develop thin spots decreases as the fourth power of the evaporation rate. (auth) (UK)

34801 QUALITY INFLUENCE IN POST-BURNOUT HEAT TRANSFER. Brevi, R.; Cumo, M. (CNEN, Rome). Int. J. Heat Mass Transfer; 14: 483-9(Mar 1971).

The analysis of many experimental results on post burnout heat transfer, obtained with a steam–water mixture flowing upward through a tubular duct at a pressure of 70 kg/cm^2 and at a specific mass flowrate of 220 g/cm^{2}s, led to the following main conclusions: In the post-burnout regime the heat flux φ goes partly to the liquid phase (φ_l) and partly to the vapor phase (φ_v): $\varphi = \varphi_l + \varphi_v$. The vapor heat flux is related to the wall-to-bulk temperature difference by a heat-transfer coefficient which is a linear

function of the quality. The liquid heat flux is directly proportional to the liquid quality of the mixture. (auth) (UK)

Isotope Technology

Refer also to abstracts 34777, 34790, 34879, 34923, and 36657.

34802 (BNL–50249) EXPLOITING THE PARENT-DAUGHTER RELATIONSHIP. Stang, Louis G. Jr. (Brookhaven National Lab., Upton, N. Y.). 20 May 1970. 17p. Dep. NTIS.
Brookhaven Lecture Series Number 93.

Methods of utilizing short half-life isotopes produced in radioisotope generators are described. The characteristics of radioisotope generators are discussed along with probable future developments in generators. Information is included on advantages and limitations of short half-life radioisotopes, growth and decay relations, ^{132}I generation, ^{99}Tc generation, ^{90}Y generation, and isomer generators. The characteristics of several isotope generators are tabulated. (J.R.D.)

34803 (BNWL–1308-5) PACIFIC NORTHWEST LABORATORY, DIVISION OF ISOTOPES DEVELOPMENT PROGRAMS QUARTERLY REPORT: NOVEMBER–JANUARY 1970–71. Hansen, J. E. (comp.) (Battelle-Northwest, Richland, Wash. Pacific Northwest Lab.). Mar 1971. Contract AT(45-1)-1830. 38p. Dep. NTIS.

Results of research conducted to develop isotopic fuels are reported. Information is included on progress in programs on: waste Cs and Sr sources; utilization of fission product Pd, Rh, Ru, and Tc; large scale uses of purified fission product Xe; fission product profitability studies; nondestructive testing of irradiation sources; neutron radiography using ^{252}Cf; advanced source development; radiation characteristics of circulatory support isotopic heat sources; and nuclear methods for seabed mineral exploration. (L.C.L.)

34804 (JAERI-Memo–4285) ANNUAL TECHNICAL PROGRESS REPORT IN THE DIVISION OF RADIOISOTOPE PRODUCTION, NO. 3. (1969 Fiscal Year). (Japan Atomic Energy Research Inst., Tokyo). Jan 1971. 60p. (In Japanese). Dep. NTIS (U. S. Sales Only).

The annual progress reports of technical developments in the Division of Radioisotopes Production for 1969 are summarized. Isotope production, processed isotopes, radiation sources, fission products, etc. are described. (auth) (Japan)

34805 (JINR–P6-5761) NEW METHOD FOR RARE-EARTH ISOTOPE SEPARATION. Beyer, G. J.; Piotrowski, A.; Raiko, V. J.; Tyrroff, H.; Herrmann, E. (Joint Inst. for Nuclear Research, Dubna (USSR). Lab. of Nuclear Problems). 1971. 10p. (In Russian). Dep. NTIS (U. S. Sales Only).

A new method is described for electromagnetic isotope separation of radioactive rare-earth elements. The chemically pure fractions of rare-earth elements obtained by cation-exchange chromatography technique and deposited in the process of cathode precipitation on a tungsten foil were loaded into a pipetype-surface-ionization ion source. Isotope separation time was approximately 3 min. The separation efficiency was approximately 80% for Nd and 66% for Dy. (auth)

34806 (JINR–P13-5757) ELECTROMAGNETIC SEPARATION OF SHORT-LIVED ISOTOPES OF Rn, Xe, AND Kr FOR SPECTROSCOPIC STUDIES. Afanasev, V. P.; Gromova, I. I.; Monchka, D.; Raiko, V. J. (Joint Inst. for Nuclear Research, Dubna (USSR). Lab. of Nuclear Problems). 1971. 13p. (In Russian). Dep. NTIS (U. S. Sales Only).

A technique for separating the short-lived Rn, Xe and Kr isotopes is described. The values of the separation efficiencies are given. The obtained isotopes were used in studies of α- and β-decay and γ-radiation of these isotopes. (auth)

34807 (MLM–1793) STABLE GASEOUS ISOTOPE SEPARATION AND PURIFICATION: OCTOBER–DECEMBER 1970. (Mound Lab., Miamisburg, Ohio). 7 May 1971. Contract AT-33-1-GEN-53. 29p. Dep. NTIS.

Results are reported for a study of stable gaseous isotope separation and purification, including carbon isotope separation by distillation, chemical exchange, and thermal diffusion; separation of the stable gaseous isotopes of neon, krypton, xenon, and chlorine; and thermal diffusion research (molecular beam scattering and transport properties, including column determination of α_T, thermal diffusion factor of $H_2-{}^4He$ and mutual diffusion coefficients). (D.H.M.)

34808 (ORNL-IIC–36) ^{90}Sr HEAT SOURCES. Shor, Roberta; Lafferty, Robert H. Jr.; Baker, P. S. (comps. and eds.) (Oak Ridge National Lab., Tenn.). May 1971. Contract W-7405-eng-26. 134p. Dep. NTIS.

Strontium-90 heat source production is described. This includes purification, transportation, preparation of fuel forms, analytical methods, densification, encapsulation, source testing, and examination of used sources. Details of source preparation, encapsulation, and testing are given. (auth)

34809 (ORNL-TM–3230) ISOTOPES KILOWATT PROGRAM: FUELED CAPSULE DESIGN AND EVALUATION. A SAFETY ANALYSIS. Haff, K. W. (Oak Ridge National Lab., Tenn.). May 1971. Contract W-7405-eng-26. 60p. Dep. NTIS.

A large heat source capsule design for the Isotopes Kilowatt Program meets the containment criteria for safe operation in terrestrial systems and probable accident conditions. The capsule presented here meets all the requirements of operational safety and the particular hazards to which it might be exposed in its operational environment and transportation to and from its use site. (auth)

34810 (ORNL-TM–3394) ISOTOPE KILOWATT PROGRAM QUARTERLY PROGRESS REPORT FOR PERIOD ENDING MARCH 31, 1971. (Oak Ridge National Lab., Tenn.). May 1971. Contract W-7405-eng-26. 26p. Dep. NTIS.

The organic capsule test continued during the quarter without an interruption and has accumulated 2180 hr as of the end of March. The detail design of the 1/4-scale organic fluid evaluation loop was completed. The heat block forging has been procured and the specifications for the pumps are out for bids. A glass loop has been built to mock-up the 1/4-scale organic fluid test loop. Results of operation experience analyses indicate that good startup, fluid flow stability, and control precision characterize the loop. Both startup and operating tests at 1000 to 1500°F were made on the heat pipe. No performance data were obtained because of the failure of a differential thermopile. A new thermopile has been fabricated and calibrated. The heat pipe for the thermoelectric module was completed. Fabrication of the thermoelectric module was completed and testing was initiated. The test was stopped 9 hr after startup because of the failure of two nickel wire leads to the heaters. Subsequent examination of the loop and chemical analysis of sections of the wire showed that the lead broke because of embrittlement by sulfur and possibly cadmium contamination. The test was shut down pending analysis of scrapings and fillings taken from various parts of the system to determine the extent to which other parts might have been adversely affected. The assembly of the test section for the next series of tests on the aluminum wire screen insulation was completed. Aluminum alloy 1100 has been selected for the fusible insulation for the organic and low-temperature (PbTe) thermoelectric units and an order placed for the material. Tests were started to determine the effective thermal conductivity of the aluminum screen insulation as a function of pressure. The design of the full-scale heat block-shield has been completed and the drawings have been sent out for bids. (auth)

34811 (ORNL-tr–2485) ISOTOPIC ELECTRIC GENERATORS. Laveissiere, Francoise (Commissariat a l'Energie Atomique, Saclay (France). Centre d'Etudes Nucleaires). Translated by Martha Gerrard (Oak Ridge National Lab., Tenn.), from report CEA-Bib–190. 10p. Dep. NTIS.

An abstract of this paper, prepared from the original language, appeared as NSA 25: 26423. (L.C.L.)

34812 (ORNL-tr–2492) SEDIMENT DYNAMICS AND RADIOACTIVE TRACERS; STATUS OF WORK IN FRANCE. Courtois, G. Translated by Martha Gerrard (Oak Ridge National Lab., Tenn.), from Houille Blanche; 25: 617-28(1970). 17p. Dep. NTIS.

The development and current status of radioactive tracer techniques for studying sediment dynamics are discussed with particular reference to current French experimental work for determining the possibilities of using tracers for measuring the movement of sands and muds, soil erosion, and massif stability, and for studying any problem of particle movement. (L.C.L.)

34813 (TID–25705) REPORT ON NATIONAL USES AND NEEDS FOR SEPARATED STABLE ISOTOPES. (National Academy of Sciences-National Research Council, Washington, D. C. Committee on Nuclear Science). 29 Jul 1968. 37p. Dep. NTIS.

A review is presented of scientific and technical uses of and needs for separated stable isotopes in the following fields: basic nuclear physics, applied nuclear physics, non-nuclear physics, chemistry, earth sciences, biology, and medicine. (D.H.M.)

XUM

34814 RADIATION AND RADIATION SOURCES INTENDED FOR USE IN THE PRODUCTION, PROCESSING, AND HANDLING OF FOOD. 21 CFR 121G 1970. Washington, D. C.; Superintendent of Documents, GPO (1970). 3p. Available from Superintendent of Documents, GPO, Washington, D. C.

Standards are presented for the safe use of radiation sources in the processing, production, and handling of food. Electron beam, gamma-ray, radiofrequency, ultraviolet, and x-ray radiation sources are included. (L.C.L.)

34815 SPECIFIC γ RAY CONSTANT AND γ SPECTRUM OF ^{182}Ta. Ninkovic, M.; Mladjenovic, M. (Boris Kidrich Inst. of Nuclear Sciences, Belgrade). Health Phys.; 20: 215-19(Feb 1971).

The value of the specific γ-ray constant for ^{182}Ta is tabulated together with all the data used for its calculation. The error of 4.9% is mainly due to the uncertainty of the calibration curve. The discussion shows that the value of the specific γ-ray constant = 0.69 can be used with confidence if one remembers that the error is about 5%. (UK)

34816 LABORATORY FOR PRODUCTION OF RADIOISOTOPES. Martinez, A. M.; Parra M, E.; Lezama C, J.; (and others) (CNEN, Mexico City). Rev. Mex. Fis., Supl. Reactor; 19: S85-97(1970). (In Spanish).

The facilities and equipment are described that are needed for isotope production, according to the chosen process that consists of the following stages: target preparation, canning, target irradiation, transport of samples to the processing laboratory, decanning, processing by dry or wet methods, final control of the isotope, and packing and distribution. The processing cells are constructed of steel and lucite plates, and it is possible to work in them with activities up to 1 Ci of gamma radiation with an average energy of 1 MeV. The biological shielding is provided by lead bricks and steel plates. In the first stage of work, the following isotopes were produced: ^{42}K, ^{24}Na, ^{89}Sr, ^{99}Mo, ^{18}F, ^{87m}Sr, ^{83}Kr, ^{197}Pt, ^{124}Sb, ^{129}Te, ^{131}I, ^{60}Co with a total activity of 795.88 mCi. (auth)

34817 PEACEFUL USES OF NUCLEAR ENERGY. A Collection of Speeches. Seaborg, Glenn T. Oak Ridge, Tenn.; Division of Technical Information Extension, Atomic Energy Commission (1970). 159p.

A compilation of speeches and excerpts of speeches made in recent years by Dr. Glenn T. Seaborg on benefits from the peaceful atom is presented. (D.H.M.)

34818 CURRENT STATUS OF RADIOACTIVITY STANDARDIZATION. Kawada, Yasushi. Nippon Genshiryoku Gakkaishi; 13: No. 4, 190-200(Apr 1971). (In Japanese).

The current status of radioactivity standardization is reviewed from the standpoints of both preparation and use of radioactivity standard samples. Absolute and relative methods used for radioactivity calibration are discussed. Considering the primary importance of the $4\pi\beta-\gamma$ coincidence method among a variety of the techniques, a detailed description is given of this useful method and its related techniques. The other methods also are surveyed briefly. Various associated techniques and practical considerations, such as handling of radioactive solutions and detection and elimination of radioactive impurities are considered. (auth)

34819 ENRICHED URANIUM: REPORT ON THE SITUATION IN SWITZERLAND. Enzmann, H. F. Neue Tech., B; 12: 127-9(Aug 1970).

Predictions are made as to the types and sizes of nuclear power plants which will be needed in Switzerland to 1990, and of the enriched U requirements for fueling these power reactors. It is concluded that the Swiss will continue to depend on the USAEC enrichment plants to supply their reactor fuels, but that alternative sources of supply should be investigated. (L.C.L.)

34820 INVESTIGATIONS OF SOLIDIFICATION FRONT AND THE DEPTH OF THE LIQUID PHASE IN CONCAST BILLETS BY THE TECHNIQUE OF RADIOACTIVE TRACES. Firganek, H. (Iron and Steel Research Inst., Gliwice, Poland); Labus, J.; Paczula, B.; Siewierski, J.; Raczka, K. Pr. Inst. Hutn.; 19: 373-9(1967). (In Polish).

Radioisotopes were used to investigate cast billets of H19N9Sp and H19N9Msp steel of 100 × 100 mm. As variables, steel temperatures and the speed of casting were taken. At the end stage of casting 10 radiation sources of ^{32}P of about 3 mCi activity distributed uniformly on a steel rod 3 m long were introduced into the molten steel in the mold. Studies of the solidification front were made by measuring the thickness of radioautographs taken at various distances from the metal level. The depth of the liquid phase was determined by the solidification front. Results of measurements indicate that there is a definite influence of the speed of casting on the surface thickness and the depth of the liquid phase. A conclusion may be drawn as to the depth of the liquid phase and the approximate limit on the speed of casting without the surface cracks below the continuous casting mold. (auth) (NSA of Poland)

Materials Testing

Refer also to abstracts 34774, 35366, 35367, and 35412.

34821 (CONF-701044-(Sect.2)) PAPERS OF THE V. CONGRESS ON MATERIAL TESTING. II. SECTION. NONDESTRUCTIVE TESTINGS, BUDAPEST 19–24 OCTOBER 1970. (Scientific Society of Mechanical Engineers, Budapest (Hungary)). 168p. (In English and German).

Twenty-four papers on materials testing were presented at the conference and are included in this section. A separate abstract was prepared for each of 3. Twenty-one were not within scope of NSA. (L.C.L.)

For abstracts of individual papers see: 34835–34837.

34822 EXPERIMENTAL GAMMA RADIOGRAPHY EQUIPMENT FOR DETERMINING DEFECTS IN CONSTRUCTION MATERIALS. Shlyak, M. P.; Lapshin, S. I.; Terekhin, L. N.; Gorin, A. I; Potapov, V. Ya. (All-Union Scientific-Research Inst. of Physics, Moscow). Defektoskopiya; No. 5, 125-6(1970). (In Russian).

Radiographic equipment used for detecting defects in construction materials is discussed. The design and operation of a recorder for the radiation detector using a photoelectric multiplier FEU-2 with a NaI(Tl) crystal are described. The main characteristics of the apparatus are: measured thickness working range of 90 g/cm^2; measuring accuracy of 1.5%; and duration of continuous use without adjustment of 8 hr. (R.V.J.)

34823 ISOTOPIC RADIOGRAPHY WITH RADIATION BACKGROUND CONDITIONS. Maiorov, A. N. Defektoskopiya; No. 5, 61-5(1970). (In Russian).

The effects of background radiation conditions on the performance of gamma radiographic equipment for inspecting welded components in nuclear power plants were studied. Basic calculations related to these effects are presented. Methods for reducing the influence of the background radiation on the performance of the radiographic instruments are discussed. (R.V.J.)

34824 SELECTION OF OPTIMUM THICKNESS OF METALLIC IMAGE-INTENSIFYING SCREENS FOR RADIOGRAPHIC INSPECTION USING BETATRON PMB-6. Gorbunov, V. I.; Krasin, L. G.; Titov, G. V. (Tomsk Polytechnical Inst., USSR). Defektoskopiya; No. 5, 56-61(1970). (In Russian).

Data for optimizing the process of radiographic inspection by means of a small-size betatron PMB-6 was studied. The effects of the thickness and type of material for the image-intensifying screens on the efficiency and sensitivity for detecting defects were investigated. The optimum thickness of screens for different types of x-ray film emulsions was determined. Experiments were performed with absorbers of steel and aluminum with maximum thicknesses of 200 and 500 mm respectively. (R.V.J.)

34825 APPLICATION OF FAST NEUTRONS IN RADIATION DEFECTOSCOPY. Gorbunov, V. I.; Elagin, V. B.; Pekarskii, G. Sh. (Tomsk Polytechnical Inst., USSR). Defektoskopiya; No. 5, 53-6(1970). (In Russian).

The results of experimental and theoretical investigations of the application of fast neutrons in defectoscopy are reported. A defectoscope designed for fast neutrons is described, and experimental results on thick layers of lead and three-layer products are presented. The results showed the high sensitivity of the instrument. (R.V.J.)

34826 MATERIALS TECHNOLOGY: AN INTERAMERICAN APPROACH. Interamerican Conference on Materials Technology, May 20–24, 1968, San Antonio, Texas. New York; American Society of Mechanical Engineers (1968). 647p. $27.00. (CONF-680513).

Seventy eight papers presented at the Interamerican Conference on Materials Technology are included. The papers are grouped under the following headings: general metallurgy, materials for nuclear energy production, design and materials, extraction and beneficiation of raw materials, production of metals and alloys, reinforced concrete, powder metallurgy, nondestructive testing, joining and welding, casting and forming, corrosion, fracture, machining, quality control programs and techniques, fatigue and fracture of materials, and materials education. A separate abstract was prepared for each of 22 papers. (M.C.G.)

For abstracts of individual papers see: 34548, 34699, 34781,

34827–34834, 35297, 35298, 35345, 35346, 35506, 35526–35528, 35550, 35551, and 36857.

34827 INVESTIGATION OF THE STRUCTURAL RELIABILITY OF HEAVY SECTION STEELS FOR LIGHT-WATER REACTOR PRESSURE VESSEL APPLICATIONS. Witt, F. J. (Oak Ridge National Lab., Tenn.). pp 42-51 of Materials Technology: An Interamerican Approach. New York; American Society of Mechanical Engineers (1968).

From Inter-American Conference on Materials Technology, San Antonio, Tex. See CONF-680513.

A program was initiated to study the structural behavior of very thick pressure vessels typical of current and future designs for boiling water and pressurized water power reactors. The program was identified as the Heavy Section Steel Technology Program (HSST) and is to be carried out in very close cooperation with the materials, fabrications, and design interests of the nuclear power industry. The total scope of the program is summarized and the objectives of the various tasks are identified. Initial results, mainly in the areas of fabrication, inspection, and materials properties, are presented. (auth)

34828 PROJECT CEMAN. da Costa, Jose Ribeiro. pp 127-32 of Materials Technology: An Interamerican Approach. New York; American Society of Mechanical Engineers (1968).

From Inter-American Conference on Materials Technology, San Antonio, Tex. See CONF-680513.

The development of the Experimental Center for Nuclear Materials (CEMAN) will be made in two important steps. The first step already begun is the Nuclear Materials Analysis Laboratory (LAMAN) where conventional analysis and tests will be made. Testing the application of special materials to heavy concretes and its aggregates for use in shielding and nuclear structures will be the LAMAN's first purpose. During this step, both the Irradiated Materials Laboratory (LAMIR) and the High-Flux Unit will be constructed. The work in the LAMAN is independent of these facilities. In a second step, the analysis and testing will be repeated after irradiation. Following these analyses data will be obtained about the behavior of the materials studied concerning: mechanical strength; the behavior of materials (change of physical and mechanical properties) under heating and temperature effects; and the same behavior, after irradiation, with or without heating and temperature effects. The principal objective of the CEMAN Project philosophy is to concentrate in a single center the studies about materials technology: conventional analysis, heating and temperature effects, and behavior of these materials under irradiation conditions. The cost of CEMAN buildings and equipment is estimated at about ten million dollars. (auth)

34829 NONDESTRUCTIVE TEST DEVELOPMENT FOR NUCLEAR REACTOR PROGRAMS AT THE OAK RIDGE NATIONAL LABORATORY. McClung, R. W. (Oak Ridge National Lab., Tenn.). pp 246-53 of Materials Technology: An Interamerican Approach. New York; American Society of Mechanical Engineers (1968).

From Inter-American Conference on Materials Technology, San Antonio, Tex. See CONF-680513.

Nondestructive testing (NDT) is an integral part of the nuclear reactor development program of the Oak Ridge National Laboratory. The NDT development includes study of the physical phenomena as well as development of equipment and specific techniques in such methods as eddy current testing, ultrasonics, and penetrating radiation methods. These are applied at many stages of reactor materials and component development, fabrication, and also for postoperation evaluation. (auth)

34830 NONDESTRUCTIVE TESTING IN CANADIAN GOVERNMENTAL SERVICES. Havercroft, W. E. (Dept. of Energy, Mines, and Resources, Ottawa). pp 254-9 of Materials Technology: An Interamerican Approach. New York; American Society of Mechanical Engineers (1968).

From Inter-American Conference on Materials Technology, San Antonio, Tex. See CONF-680513.

The growth of nondestructive testing in Canada is illustrated. The Government uses nondestructive testing as an inspection tool for various materials and applications, uses it in research and development, and has established education and training programs for nondestructive testing personnel. The program for the certification of industrial radiographers in Canada and radiation safety controls is discussed. (auth)

34831 NONDESTRUCTIVE TESTING IN INDUSTRY TODAY AND TOMORROW. Socky, Richard B. (General Electric Co., Philadelphia). pp 260-71 of Materials Technology: An Interamerican Approach. New York; American Society of Mechanical Engineers (1968).

From Inter-American Conference on Materials Technology, San Antonio, Tex. See CONF-680513.

Through application of nondestructive testing in industry today, part and piece serviceability is maintained at the same time that a 100% inspection is achieved. Unfortunately, the ability for 100% application of nondestructive testing principles is not always utilized resulting in only partial realization of product service life. System complexity and overall costs of service failures have become so great that it is imperative that the most effective nondestructive test methods be used and that they be applied throughout the product cycle. Now a program of total nondestructive testing is being implemented by industry. The underlying principle is that to provide genuine effectiveness, nondestructive testing must start with the design of the product and end only when the product, used by the customer, performs correctly for a satisfactory period of time. For the above purpose, product flow must be examined in its entirety. Design concepts are augmented through nondestructive testing research. Developments in nondestructive testing keep pace with product growth. Nondestructive testing development may also involve evaluation of materials variability. Nondestructive testing augments engineering detail by being factored into design criteria and drawing details. Standardization of nondestructive testing techniques and specifications for acceptance limits form an important part of engineering detail. Qualification testing may not only involve pieces and parts but is also applied to personnel. Nondestructive testing certification of in-house and supplier methods and personnel is commonplace. In the manufacturing area proper, nondestructive testing enjoys an inline function as a process control step. Testing of the finished product brings into play the unique abilities of nondestructive testing to evaluate the piece or part indirectly. Techniques have now been developed that are finding application to parts in service. Evaluations in use are being made through signature analysis concepts. Finally, analysis of performance and/or degradation in operation can also be made using nondestructive techniques to measure operation. Examples of nondestructive testing applications will be presented to illustrate the scope of work presently being accomplished. The problems, trends, and future applications of nondestructive testing in industry will also be covered. (auth)

34832 ROLE OF NONDESTRUCTIVE TESTING IN MATERIALS TECHNOLOGY AND ENGINEERING. Tenney, Gerold H. (Los Alamos Scientific Lab., N. Mex.). pp 344-52 of Materials Technology: An Interamerican Approach. New York; American Society of Mechanical Engineers (1968).

From Inter-American Conference on Materials Technology, San Antonio, Tex. See CONF-680513.

The history of nondestructive testing from the period before 1945, to the atomic age, to after the launching of Sputnik in 1957 is briefly given. The importance of nondestructive testing is seen by recognition by management, its use in the booming commercial reactor industry, and its participation in creating specifications, standards, and codes. Problems in the nondestructive testing profession including its position in laboratories and industry, education, and prediction of future uses of the technique are discussed. (G.M.C.)

34833 REVIEW OF SELECTED NONDESTRUCTIVE TESTING ACTIVITIES AT BATTELLE NORTHWEST LABORATORY. Worlton, D. C. (Battelle-Northwest, Richland, Wash.). pp 353-60 of Materials Technology: An Interamerican Approach. New York; American Society of Mechanical Engineers (1968).

From Inter-American Conference on Materials Technology, San Antonio, Tex. See CONF-680513.

Developments in three nondestructing testing programs at Battelle Northwest Laboratory are described. Acoustic emission is being developed to be an in-service inspection method possibly for nuclear reactors. Data suggest that there are basically three types of signals emitted by steel undergoing plastic deformation, ductile fracture, and brittle fracture. These high-signal frequencies permit ready discrimination of unwanted background noises. A two-frequency instrument for eddy current tests can distinguish between outside surface and inside surface defects. Upon processing the resulting composite signal the contributions from individual variables are isolated from each other at the instrument output. Critical angle ultrasonic tests utilize a heretofore unexploited property of ultrasonic waves. When a sound beam travelling through water is incident on a metal at the Rayleigh critical angle, a lateral displacement of the beam occurs along the metal surface. Data were obtained which correlate this displacement with nuclear irradiation damage and strongly suggest its potential use for the detection of shifts in nil ductility transition temperature. (G.M.C.)

34834 RADIOGRAPHY IN QUALITY CONTROL: A SEVENTY-YEAR PROGRESS REPORT. Turner, Ralph E. (Eastman

XUM

Kodak Co., Rochester, N. Y.). pp 530-4 of Materials Technology: An Interamerican Approach. New York; American Society of Mechanical Engineers (1968).

From Inter-American Conference on Materials Technology, San Antonio, Tex. See CONF-680513.

Industrial radiography is considered to be one of the best methods for nondestructive testing in a quality control program. Virtually any material, regardless of size, shape, and composition, lends itself to radiographic examination. A partial listing gives a brief description of 17 different radiography methods including: x-ray, gamma, panoramic, slit, layer type, flash, hot cell, neutron, multiple film, and color radiography. The versatility of equipment is also discussed. (G.M.C.)

34835 DEVELOPMENT HISTORY AND CURRENT STATE OF NONDESTRUCTIVE MATERIALS TESTING. Reti, P. pp I-XIII of Papers of the V. Congress on Material Testing. II. Budapest; Scientific Society of Mechanical Engineers (1970). (In German).

From fifth congress on material testing; Budapest, Hungary (19 Oct 1970). See CONF-701044-(Sect.2).

The historical development, particularly in the past three decades, and the current status of nondestructive materials testing methods are discussed. These methods include: x-ray inspection, gamma radiography, ultrasonic testing, eddy current testing, magnetic testing and chemical penetration testing. (L.C.L.)

34836 BETA-RAY BACK-SCATTERING METHOD FOR COATING THICKNESS MEASUREMENTS. Szepke, Ryszard. pp 85-6 of Papers of the V. Congress on Material Testing. II. Budapest; Scientific Society of Mechanical Engineers (1970).

From fifth congress on material testing; Budapest, Hungary (19 Oct 1970). See CONF-701044-(Sect.2).

The principles of a new beta back-scattering nondestructive method for measuring coating thickness are described. Using these principles an apparatus was developed for measuring the thickness of such coatings as Au on Cu, Ag on Cu, Au on Ag, and others. The measurements can be made on very small surfaces of from 1 to 20 mm^2 with an error of ±0.1 mu. (L.C.L.)

34837 APPLICATION OF ALPHA AND BETA-GAMMA AUTORADIOGRAPHY IN SHIELDED CELLS FOR THE EXAMINATION OF IRRADIATED NUCLEAR FUELS. Pugnetti, G.; Trezza, G. pp 109-14 of Papers of the V. Congress on Material Testing. II. Budapest; Scientific Society of Mechanical Engineers (1970).

From fifth congress on material testing; Budapest, Hungary (19 Oct 1970). See CONF-701044-(Sect.2).

Techniques used at the Casaccia Hot Laboratory for recording alpha and beta-gamma activity in samples of irradiated UO_2 and $UO_2 + PuO_2$ nuclear fuels are described. Fission products distribution was studied by beta-gamma autoradiography in connection with the problems of fission gas release and swelling of the fuel. The relation between bands of activity and grain structures and to the chemical compatibility between fuel and structural materials was also investigated. Alpha autoradiography, on the other hand, was used as a control on mechanical mixtures of fissile materials and as a test of diffusion of the heavy elements. The trend of both techniques is towards more quantitative results. For this purpose interpretation of the autoradiographic method is being performed by photometric and microscopic examinations. (auth)

34838 NONDESTRUCTIVE TESTING OF ADVANCED FIBER-REINFORCED COMPOSITES. Schultz, Arnold W. SAMPE; 2: No. 2, 31-7(Jan 1971).

Physical and mechanical strength properties of high modulus fiber-reinforced/epoxy matrix composites are influenced by their fabrication methods. The need for nondestructive testing (NDT) in evaluating these properties and their variabilities is now being recognized as requirement in most material development and application programs. The degrading effect of voids on mechanical properties, the property values themselves as a function of loading direction, and the degree of property inhomogeneity in fabricated composites are each of immediate concern to designers. Capabilities for nondestructively predicting and fully characterizing the mechanical properties of multidirectional fiber composites were developed. Methods, including a one-sided interval velocity technique, and procedures for evaluating carbon and boron fiber composites are discussed. (auth)

34839 ATTEMPTS TO APPLY RADIOGRAPHY IN THE TESTING OF THE GLASS-REINFORCED POLYESTER LAMINATES. Miduch, K. Polim. Tworzywa; 14: 78-9(1969). (In Polish).

Radiographic patterns obtained for plates of glass-reinforced polyester laminates prepared with a mat and with glass fabric were compared. It was found that this method makes it possible to detect air bubbles and unimpregnated places in the laminate. (auth) (NSA of Poland)

34840 RADIOGRAPHIC EXAMINATION OF WELDED T-JOINT IN FLUE AND SMOKE-TUBE BOILERS. Nohara, Ishimatsu (Ministry of Labour, Tokyo). Nippon Kikai Gakkai Rombunshu; 36: No. 291, 1944-53(Nov 1970). (In Japanese).

In order to obtain radiographic testing standards, specimens similar to the actual T-joints in a boiler were prepared, and tested for flaws. The T-joint is between a shell or a tubular flue and end plates and welded inside and outside. X radiation was used and the welding bead of the T-joint was irradiated from one side and from both sides. The relations of film exposure with weld thickness and image quality were also examined. It was found that it is desirable to make the irradiation test for both the inside and outside welds; that the suitable irradiation angle with respect to the tubular-body was 45°; the film should be as close to the weld as possible; the film must be chosen according to the weld thickness; and in order to have a clear bead width on the film, the boundary of bead and base metal should be marked. (Japan)

34841 INDUSTRIAL RADIOGRAPHY WITH RADIOISOTOPES. Chrimes, N. W. D. Coogee, Australia; Australian Atomic Energy Commission (1970). 48p.

Sections deal with the general principles of radiography, properties and production of radioisotopes, radiographic technique, interpretation of radiographs, and radiation protection dealing specifically with monitoring and shielding provisions based on local codes of practice. Characteristics of the principal radioisotopes used for radiography are tabulated and exposure techniques and instruments are illustrated. A bibliography of British and Australian codes and specifications and transport regulations is appended. (Australia)

34842 STANDARD METHOD OF TEST FOR SURFACE FLAMMABILITY OF MATERIALS USING A RADIANT HEAT ENERGY SOURCE. ASTM E 162-67. Philadelphia; American Society for Testing and Materials (1967). 12p. Available from American Society for Testing and Materials, Philadelphia.

This method, to be used for research and development purposes, covers the measurement of surface flammability of materials. It is not intended for use as a basis of ratings for building code purposes. (auth)

Radioactive Material Handling

Refer also to abstracts 34698, 34715, 34717, 34719, 34733, 34741, 34924, 35056, 35154, and 37048.

34843 (AECL-3804) SPECIAL ARRANGEMENT SHIPMENTS IN CANADA. Taylor, W. R. (Atomic Energy of Canada Ltd., Chalk River (Ontario). Chalk River Nuclear Labs.). Jan 1971. 5p. (CONF-710210-3; SM-147/38). Dep. NTIS (U. S. Sales Only). AECL $0.20.

From Seminar on test requirements for packaging for the transport of radioactive materials; Vienna, Austria (8 Feb 1971).

In Canada, special arrangement procedures have proven to be practical solutions to many awkward radioactive material shipments. Usually, the package was large or heavy and impact or thermal tests, which would prove package integrity, were costly and impractical. Operational controls, which offset package design deficiencies, were specified. This procedure maintained the overall safety of the shipments. The special arrangement shipments of irradiated fuel, of an active steam generator, and of tritiated heavy water are described. (auth)

34844 (CONF-700440-1) NUCLEAR POWER REACTOR WASTES AND OUR ENVIRONMENT. Barnes, R. G. (General Electric Co., San Jose, Calif. Reactor Fuels and Reprocessing Dept.). [nd]. 25p. Dep. NTIS (U. S. Sales Only).

From third annual national pollution control conference; San Francisco, Calif. (1 Apr 1970).

Methods used for minimizing the environmental effects of wastes from the reprocessing of fuels from power reactors are discussed. These wastes include solid fuel and cladding materials, and waste streams of solvents, water, and gases used in the chemical reprocessing. The Midwest Fuel Recovery Plant, under construction, is used as an example of how industry is designing facilities which will control and permanently isolate from the biosphere all the radioactive material involved in fuel reprocessing. (L.C.L.)

34845 (INR-1249) BITUMIZATION OF LIQUID RADIOACTIVE WASTES. Ksiazak, Z.; Heger, L. (Institute of Nuclear

Research, Warsaw (Poland)). 1970. 44p. (In Polish). Dep. NTIS (U. S. Sales Only).

Laboratory tests were carried out on the possibility of utilizing Polish bitumen for fixation of radioactive wastes, especially sludges after co-precipitation of liquid wastes and evaporated concentrates. Physicochemical properties of the final products were examined. Leach rates of ^{137}Cs from mixtures and the influence of surface-active substances that are present in liquid wastes on mixing conditions were investigated. (auth)

34846 (LA–4660) GEOLOGY AND HYDROLOGY OF MESITA DEL BUEY. Purtymun, William D.; Kennedy, William R. (Los Alamos Scientific Lab., N. Mex.). Nov 1970. Contract W-7405-Eng-36. 12p. Dep. NTIS.

Mesita del Buey is used for the disposal of wastes contaminated by radionuclides, of toxic or explosive chemicals, and of classified materials. These are buried in pits or shafts dug into the mesa surface. The mesa, covered by a clay-like soil, is underlain by a series of ashfalls of rhyolite tuffs from 240 to 590 ft thick. The tuffs are above the main aquifer of the Los Alamos area which lies at a depth of about 1,000 ft. Stream flow in adjacent canyons is intermittent. Water in the alluvium of the stream-connected aquifer in the canyon south of the mesa is recharged by storm runoff. The hydrologic characteristics and conditions of the soil, tuff, and seal material used to cover the wastes indicate no recharge to the stream-connected aquifer or main aquifer through the soil, buried wastes, or tuff as Mesita del Buey. (auth)

34847 (ORNL–4607) AN INTEGRATED SYSTEM OF NUCLEAR MATERIALS CONTROL AT OAK RIDGE NATIONAL LABORATORY. Cardwell, R. G.; Foster, B. E.; Gower, J. C. (Oak Ridge National Lab., Tenn.). Apr 1971. Contract W-7405-eng-26. 13p. Dep.

Current emphasis on development of fuels for breeder reactor application has necessitated frequent intermixing and compressing of ^{233}U, ^{235}U, and ^{239}Pu isotopes. To provide the highly accurate control system that assures safe operation of the facilities, all criticality, accountability, and radiation safety controls were integrated into a centralized system managed by a coordinator designated the Nuclear Materials Controller. Emphasis was placed on minimizing the spread of contamination and reducing the potential for a nuclear incident while at the same time maintaining a smooth, uninterrupted flow of materials with a minimum of paper work. The centralized system is composed of three integrated units: the Criticality Control Board—a visible, current record of all nuclear materials under control of the system, with magnetic, color-coded indicators that reflect values, location, and type of isotope in each approved laboratory to the nearest ½ g; the Nuclear Materials Flowboard—a modified, color-coded, industrial indicator that visibly reflects each temporary movement of the materials and their current location during processing; and the Flip-Sheet Ledger system—a concise version of the columnar accounting sheet that permits a great number of accounts to be filed and worked on overlays in an $8\frac{1}{2} \times 11$-in. ledger book. The system has effectively and efficiently met all control requirements and provided both necessary and desirable safeguards without hindering the processing of materials; in several instances it has expedited production. The detailed records of materials on hand by type and location provide a detailed, current inventory that has resulted in savings of time and money on materials procurement and that has brought to attention valuable, inactive quantities that could be returned to production channels. (auth)

34848 (ORNL–4680) TECHNICAL STATUS OF THE RADIOACTIVE WASTE REPOSITORY: A DEMONSTRATION PROJECT FOR SOLID RADIOACTIVE WASTE DISPOSAL. Culler, F. L. (Oak Ridge National Lab., Tenn.). Apr 1971. Contract W-7405-eng-26. 69p. Dep. NTIS.

The work that has been done to establish the suitability of bedded salt formations for the containment of radioactive solid wastes and the nature of the additional investigations that are either under way or are scheduled to be carried out are reviewed. It is believed that this work constitutes a valid technical justification for proceeding with the present plans to establish a demonstration repository at Lyons, Kansas. (auth)

34849 (RT/PROT–(70)36) STUDY ON THE RECEPTIVITY OF THE SITE SURROUNDING THE CASACCIA C.S.N. TO THE END OF THE DISPOSAL IN IT OF RADIOACTIVE WASTE. Frittelli, L. (Comitato Nazionale per l'Energia Nucleare, Rome (Italy)). 4 Jan 1971. 101p. (In Italian). Dep. NTIS (U. S. Sales Only).

The main exposure routes to man from the disposal of radioactive wastes into atmosphere and surface waters in the site surrounding the C.S.N. Casaccia are discussed. (auth)

34850 DEVICE FOR THE SEALING OF CYLINDRICAL CONTAINERS FOR RADIOACTIVE MATERIALS. Rothfuss, H. (to INTERATOM GmbH). German Patent 1,295,723. 22 May 1969. Filed 8 Oct 1963. (In German).

A device for the sealing of cylindrical transport containers for radioactive materials by means of lids applied by pressure from a cylindrical feed is described. The device is characterized by the placement of the feed arranged coaxially to the container to to be sealed and to receive a number of lids stacked on top of each other. The device is provided with a compression piston to seal the lids on the containers. (J.S.R.)

34851 DETAILED REGULATIONS GOVERNING RADIOACTIVE MATERIALS. 46 CFR 146.19 1969. Washington, D. C.; Superintendent of Documents, GPO (1969). 24p. Available from Superintendent of Documents, GPO, Washington, D. C.

Detailed regulations for the handling, packaging, and transport of radioactive materials are presented. (L.C.L.)

34852 TRANSPORTATION OF DANGEROUS ARTICLES AND MAGNETIZED MATERIALS. 14 CFR 103 1968. Washington, D. C.; Superintendent of Documents, GPO (1968). 15p. Available from Superintendent of Documents, GPO, Washington, D. C.

Standards for the safe air transport of dangerous articles and magnetized materials, including radioactive materials, are presented. (L.C.L.)

34853 FACILITIES HANDLING RADIOACTIVE MATERIALS, 1970. NFPA 801 1970. Boston; National Fire Protection Association (1970). 30p. Available from National Fire Protection Association, Boston.

Standards for the fire protection of facilities handling radioactive materials are presented in order to provide the fire protection specialist with certain fundamental information about radioactive materials and their handling and to provide designers and operators of such laboratories with guidance on practices necessary for fire safety. The subjects discussed include: radiation sources; nature of the fire problem; arrangement of facilities handling unsealed radioactive materials; service facilities; equipment for handling and processing radioactive materials; and protection against fire and explosion. (L.C.L.)

34854 HANDLING AND TRANSPORT OF IRRADIATED FUEL. Ribaux, P. A. (Ateliers des Charmilles SA, Geneva). Neue Tech., B; 12: 131-3(Aug 1970).

Data are given on the quantity, packaging, mode of transport, legal aspects, and operating experience of handling and shipping irradiated fuel elements from two research reactors and two commercial power plant reactors in Switzerland. (L.C.L.)

34855 APPARATUS FOR CARRYING OUT PROCESSES IN A CONTROLLED ENVIRONMENT. Evans, Charles Gervase Thorngate; Harris-Smith, Robbin (to National Research Development Corp.). British Patent 1,225,962. 24 Mar 1971. Filed 16 Dec 1966.

The apparatus described is intended for use in chemical and microbiological processes where the ingress or egress of noxious matter or contaminants must, as far as possible, be avoided, and as such is suitable for the processing of radioactive materials. In conventional glove box systems the transfer vessels are directly exposed to the outer atmosphere, leading to risks from faults in the flexible tubing or incomplete sealing between the tubing and the transfer vessel, or from damage to the transfer vessel, tubing or seal by accidental knocking or movement, or from the danger of implosion or explosion of the transfer vessel when suction or pressure is employed. The apparatus comprises an outer casing that encloses the process chamber, with means to prevent the ingress of air to the process chamber and the egress of contaminating material, together with a transfer chamber having a sealable door for allowing access for a transfer vessel. A communicating trap is provided between the process chamber and the transfer chamber, and means are provided for controlling processes within the process chamber and the transfer chamber from outside the outer casing. A pressure difference may be provided between the transfer chamber and the outer atmosphere. Accident wells may be provided below the process chamber and the transfer chamber to receive any spillage. (UK)

34856 HOSPITAL SOLID WASTE MANAGEMENT. Iglar, Albert F. (East Tennessee State Univ., Johnson City). CRC Crit. Rev. Environ. Contr.; 1: 507-50(Jan 1971).

The problem of solid waste management in U. S. hospitals is discussed in detail. Information is included on: classification of hospitals; quantities, sources, and types of solid waste; equip-

XUM

ment and methods for waste storage and transport in hospitals; waste treatment and disposal methods at hospitals; hazardous biological materials and microbe-containing matter; radioactive solid waste; transport of solid wastes from hospitals and community disposal thereof; and personnel requirements for the management of solid hospital wastes. (L.C.L.)

34857 PERMISSIBLE LIMITS FOR NUCLEAR FUELS ACCORDING TO ATOMIC LAW AND THE RELATED LEGAL ORDERS. Blechschmidt, M. PTB Mitt., 80: No. 3, 199-200 (Jun 1970). (In German).

The limitations imposed by the German Atomic Law and other pertinent legal restrictions on the maximum quantity or activity of nuclear fuels which may be transported or stored are summarized. (J.S.R.)

34858 TRANSPORT CONTAINERS FOR RADIOACTIVE MATERIALS. Lindsay, Graham Eades; Evans, Leslie Samuel (to United Kindom Atomic Energy Authority). U. S. Patent 3,575,601. 20 Apr 1971. Filed 11 Apr 19669.

A container for the transportation of radioactive material, specifically irradiated fuel elements, is described. The transport container consists of an outer shock-resistant steel container and an interfitted inner container constructed of a plurality of radioactive shielding inserts. (Official Gazette)

34859 CODE OF PRACTICE FOR THE CARRIAGE OF RADIOACTIVE MATERIALS BY ROAD. London; Her Majesty's Stationery Office (1970). 74p. £ 0.45. (NP-18760).

The carriage of radioactive materials by road in the UK is governed by the Radioactive Substances (Carriage by Road) (Great Britain) Regulations 1970 which are made under Section 5(2) of the Radioactive Substances Act, 1948. These regulations are mainly and purposely in general terms, requiring a proper course of conduct on the part of those concerned, but do not for the most part lay down precise technical requirements. Provisions for the control of radiation doses received by road transport workers in certain circumstances are contained in the Radioactive Substances (Road Transport Workers) (Great Britain) Regulations 1970. Advice on the storage of radioactive material in transit is contained in a Code of Practice issued jointly by the Department of the Environment, the Department of Trade and Industry and the Department of Employment. This Code of Practice is intended to assist all concerned, and consignors in particular, to discharge their obligations under the law. Although many provisions of the Code are explicitly dealt with in the Regulations, the Code does not purport to be the Regulations nor to give a legal interpretation of them. But, with that reservation, the Code is commended to those concerned as a proper standard by which to determine their course in order to fulfill their statutory obligations. The Code conforms generally to the International Atomic Energy Agency's Regulations for the Safe Transport of Radioactive Materials, as amended in 1967. (UK)

34860 PROBLEMS OF PROTECTIVE GAS TECHNOLOGY. Krauth, A. (Nuklear-Chemie und -Metallurgie GmbH, Wolfgang, Ger.). Kerntech. Atomprax.; 13: No. 4, 172-5(Apr 1971). (In German and English).

Techniques for handling toxic and pyrophoric materials is described with particular reference to nuclear fuels. (auth)

Vacuum Engineering

Refer also to abstract 35835.

INSTRUMENTATION

Radiation Detection Instruments

General Detectors and Monitors

Refer also to abstracts 34818, 35079, 36991, 36995, and 37086.

34861 (AERE-R-6776) REVISED POSITION SENSITIVE DETECTOR ARRAY FOR A CHARGED PARTICLE SPECTROGRAPH. Ansell, G. V.; Armitage, B. H. (Atomic Energy Research Establishment, Harwell (England)). Mar 1971. 6p. Dep. NTIS (U. S. Sales Only). UK 9p.

A modified position sensitive detector array (surface-barrier detectors) associated with a broad-range spectrograph is described which enables a continuous spectrum to be obtained when operated in two locations along the focal surface. (auth) (UK)

34862 (EGG-1183-1517) USE OF AERIAL SURVEYS FOR DETERMINING PLUTONIUM CONCENTRATION. Technical Report No. L-1030. Stuart, T. P. (EG and G, Inc., Las Vegas, Nev.). 29 Apr 1971. 10p. (CONF-710401-2). Dep. NTIS.

From Symposium on safety in plutonium-handling facilities; Rocky Flats, Colo. (15 Apr 1971).

A Pu aerial survey using an array of NaI detectors that are set up to sense the 60 keV γ-ray from ^{241}Am, a decay product of ^{241}Pu, is described. The detecting system was mounted inside an Air Force helicopter and flown over known concentrations at the Nevada Test Site. (auth)

34863 (HMI-B-108) NUCLEAR CHEMISTRY COMPENDIUM. PART I. NUCLEAR RADIATION MEASUREMENT TECHNIQUE. Moeller, P.; Zimen, K. E. (Hahn-Meitner-Institut fuer Kernforschung, Berlin (West Germany)). Apr 1971. 137p. (In German). Dep. NTIS (U. S. Sales Only).

The background material on nuclear radiation measurement techniques used in the nuclear chemistry course at the Hahn-Meitner Institute is presented. Corrections in counter measurements, statistical scattering and measurement error in counter measurements, measurement of half lives, measurement of decay rates, gamma spectrometry, and autoradiography are considered. The special measurement problems of soft β emitters and of very weak activities are discussed separately. Detector comparison and the selection of the measurement method are considered. (J.S.R.)

34864 (IFVE-SEF-70-17) A HODOSCOPE BASED ON SMALL PHOTOELECTRON MULTIPLIERS, FEU-85. Borisov, A. A.; Bugorskii, A. P.; Nurushev, S. B. (Gosudarstvennyi Komitet po Ispol'zovaniyu Atomnoi Energii SSSR, Serpukhov. Institut Fiziki Vysokikh Energii). 1970. 17p. (In Russian). Dep. NTIS (U. S. Sales Only).

The hodoscope system based on new small photomultipliers 85 is described. The hodoscope characteristics have been investigated. The possibility of constructing the hodoscope with operating cell dimensions of 3 mm for loading the particles up to $3 \cdot 10^6$ per 0.1 sec is presented. (auth)

34865 (JINR-P13-5696) HADAMARA: TRANSFORM SCINTILLATION COUNTER. Soroko, L. M. (Joint Inst. for Nuclear Research, Dubna (USSR). Lab. of Nuclear Problems). 1971. 16p. (In Russian). Dep. NTIS (U. S. Sales Only).

The Hadamard-transform scintillation counter designed to measure the angular and spatial distributions of nuclear and atomic particles in the presence of large noise from the photomultiplier is described. The gain in the effective signal-to-noise ratio achieved by this counter is the result of the spatial multiplexing, that is, of coding the spatial or angular distribution to be measured before counting it. The counter consists of a multi-element heterogeneous scintillator, two lightguides and two photomultipliers. The multi-scintillator consists of (2M-1) scintillation elements. The lightflashes can enter only into the lower or only into the higher lightguides. The (M-1) elements of multi-scintillator are out of the region of the lightguide. The counting to be measured is equal to the difference between the number of N (up) (i) events and the number of N (down) (i) events at all M positions ($1 \leq i \leq M$) of the moving multiscintillator relative to the lightguide. It is needed to perform M independent measurements. The spatial distribution of particles is undergoing the binary coding according to the Hadamard-transform algorithm. The system of multiplex Hadamard-transform detection is giving rise to the gain in the signal-to-noise ratio, being equal to $\sqrt{M}$, where M is the number of element-scintillators in the multiplex block scintillator. Neither the degradation of the angular distribution, nor the loss of the counting rate of the events to be measured, is taking place. The Hadamard-transform scintillator counter gives the direct economical gain in the time of particle accelerators and also in the cost of the equipment. (auth)

34866 (JINR-P13-5722) PSEUDO-NOISE SEQUENCES APPLICABLE TO MULTIPLEX SYSTEMS OF PARTICLE DETECTION. Soroko, L. M. (Joint Inst. for Nuclear Research, Dubna (USSR). Lab. of Nuclear Problems). 1971. 15p. (In Russian). Dep. NTIS (U. S. Sales Only).

The properties of pseudo-noise sequences used in the multiplex systems of particle detection are presented. The method for the generation of pseudo-noise sequences using the Hadamard matrix is given. The performance of the pseudo-noise sequences is discussed in the terms of the discrete Fourier transform. The multiplex systems of the particle detection are useful from the economical point of view, if the limit of the equipment is the background error. (auth)

34867 (NP-18849) FISSION TRACK SOLID STATE DETECTOR. (Ceskoslovenska Akademie Ved, Rez. Ustav Jaderneho Vyzkumu). [1968]. 9p. (In Czech). Dep. NTIS (U. S. Sales Only).

A brief introduction to the use of fission foils with dielectric track detectors for neutron dosimetry is presented, and a list of 46 references from NSA from 1961 to 1968 is given. (W.H.K.)

34868 (SZS-2/71, pp 1-6) REQUIREMENTS FOR PORTABLE INSTRUMENTS FOR DOSE RATE AND CONTAMINATION MEASUREMENTS. Herrmann, D. (Staatliche Zentrale fuer Strahlenschutz, Berlin (East Germany)). (In German).

For portable health physics instruments the permissible total error, the necessary measuring ranges, and the energy ranges to be recorded are given. Special emphasis is given to some universal health physics instruments available in the sphere of the Council for Mutual Economic Aid (COMECON). (auth)

34869 (SZS-2/71, pp 7-11) SPECIAL REQUIREMENTS FOR INSTRUMENTS FOR RADIATION PROTECTION MONITORING IN NUCLEAR POWER PLANTS. Willuhn, K. (Staatliche Zentrale fuer Strahlenschutz, Berlin (East Germany)). (In German).

On the basis of the problems of health physics instrumentation in a nuclear power plant and the radiation field to be surveyed and depending on the operational conditions, special requests are formulated on the instrumentation for the control of the observation of projected and existing parameters of radiation protection. (auth)

34870 (SZS-2/71, pp 12-22) PROBLEMS OF INSTRUMENTATION FOR RADIATION PROTECTION MONITORING OF WATERS. Stange, E. (Staatliche Zentrale fuer Strahlenschutz, Berlin (East Germany)). (In German).

The systematic errors are discussed occurring in the determination of the radioactivity of waters. The different problems of discontinuous and continuous monitoring are pointed out. For continuous activity measurements, the detection sensitivities of three Geiger counters, one proportional counter and one scintillation counter are graphically shown. Recommendations are given according to the question of which monitoring instrument should be used for a certain monitoring problem. (auth)

34871 (UARAEE-82) CHARACTERISTICS OF THE COLLIMATOR CONSTRUCTED FOR THE INCHASS WHOLE BODY MONITOR. Morsy, S. M.; Alloush, A. A. (Atomic Energy Establishment, Cairo (Egypt). Radiation Protection Dept.). 1969. 22p. Dep. NTIS (U. S. Sales Only).

The properties of a multi-slit collimator designed for the 8×4 in. crystal of the Inchass whole body monitor are given. The minimum detectable activity using the collimator is calculated at two different energies. Septa penetration was taken in consideration by assuming the activity to be represented by a line source in the mid line of the subject. Factors affecting the absolute activity determination are studied. (auth)

34872 (UCRL-20699) EIGHTY-LENS OPTICAL CAMERA FOR RECORDING DYNAMIC STUDIES WITH THE SCINTILLATION CAMERA. Anger, Hal O. (California Univ., Berkeley. Lawrence Radiation Lab.). May 1971. Contract W-7405-eng-48. 9p. Dep. NTIS.

An optical camera for continuous recording of information with a scintillation camera for dynamic studies is described. The 80-lens camera described eliminates the loss of information during frame advance that is inherent in other camera systems. (W.H.K.)

34873 (UCRL-50007-70-3) HAZARDS CONTROL PROGRESS REPORT NO. 38, SEPTEMBER-DECEMBER 1970. (California

XUM

Univ., Livermore. Lawrence Radiation Lab.). Contract W-7405-eng-48. 16p. Dep. NTIS.

The status of research activities in the fields of radiation protection, instrumentation, and environmental protection is briefly described. (W.H.K.)

34874 COMPOSITION FOR SCINTILLATION COUNTING. Sena, Edwin Andres. British Patent 1,222,112. 10 Feb 1971. Priority date 1 Feb 1967, United States.

A surfactant/cosurfactant composition is described which comprises at least one surfactant and a cosurfactant; the composition forms, when mixed with scintillation solvent, primary scintillator, and a radioactive sample, a sample-containing cocktail having high counting efficiency. It exhibits essentially no chemiluminescence or phosphorescence, is thermodynamically stable, and contains substantially no free internal phase fluid. (R.W.R.)

34875 METHOD OF MEASURING FAST NEUTRONS BY OBSERVING MULTIPRONGED TRACKS OF CHARGED PARTICLES FORMED IN CELLULOSE NITRATE. Price, Paul B.; Walker Robert M.; Fleischer, Robert L. (to General Electric Co.). U. S. Patent 3,564,250. 16 Feb 1971. Filed 3 Jan 1967.

A means for detection of fast neutrons by chemically drilling or etching out multipronged tracks of charged particles formed in cellulose nitrate test bodies by collisions of fast neutrons with nuclei including those of carbon, nitrogen, oxygen, and boron is described. (auth)

34876 GAS-FILLED SPARK CHAMBER RADIATION DETECTOR. Lansiart, Alain; Leloup, Jean; Lequais, Jean (to Commissariat a l'Energie Atomique). U. S. Patent 3,560,746. 2 Feb 1971. Priority date 26 Feb 1968, France.

A particle detector comprising a gas-filled chamber in which are disposed an anode and a cathode separated by a grid is described. These three electrodes are parallel, and the gap between the grid and the cathode is of sufficient width for the type of incident radiation. The filling gas is selected in order to ensure that a high proportion of the β radiation, which constitutes the incident particles or which is induced by incident particles at the cathode and/or within the gap, loses the larger part of its energy by the usual ionization process which results in the release of electrons. The detector has means for establishing between the anode and the grid a potential difference that is slightly smaller than the breakdown voltage and between the cathode and and the grid a voltage for collecting the electrons towards the grid–anode gap. The collection voltage is sufficiently low and the mesh of the grid is sufficiently large to ensure that only a negligible proportion of electrons is collected by the grid as the electrons pass through the grid. (auth)

34877 PROGRESS OF IN-CORE INSTRUMENTATION. Sekiguchi, Akira (Tokyo Univ.). Genshiryoku Kogyo; 16: No. 11, 33-9(Nov 1970). (In Japanese).

Advantages and disadvantages of the use of activation detectors, miniature ionization chambers, and thermocouples for in-core measurements are briefly discussed; and the development, operation, and performance of self-powered detectors are reviewed. (TSS) (Japan)

34878 IMPROVEMENTS IN OR RELATING TO DATA ANALYSING SYSTEMS. (to Packard Instrument Co., Inc.). British Patent 1,218,845. 13 Jan 1971. Priority date 28 Sep 1967, United States.

Improvements to scintillation spectral analysis of test samples containing n unknown isotopes by liquid scintillation spectral analysis techniques are described, along with equipment for analysis of samples containing n isotopes in a liquid scintillator. The techniques and equipment are wholly automatic in operation, and the counting conditions are automatically optimized for each sample in response to determination of the effective quench level for each sample, so that optimum counting conditions are attained irrespective of the actual quench level. (R.W.R.)

34879 MEASUREMENT OF NEUTRON FLUX AND SPECTRA FOR PHYSICAL AND BIOLOGICAL APPLICATIONS. National Bureau of Standards Handbook 72. Washington, D. C.; National Bureau of Standards (1960). 98p. (NCRP–23). Available from Superintendent of Documents, GPO, Washington, D. C.

The measurement of neutron flux and spectra is discussed, various methods are compared, and results of intercomparisons are given. Methods of measurement are discussed for the emission rate of radioactive neutron sources, thermal-neutron flux, epithermal-neutron flux, intermediate-neutron flux, fast-neutron flux, and neutron energy spectra. Neutron radiation instruments for area survey and personnel monitoring involving flux and spectrum measurements are included. Typical spectra of various neutron sources are shown. (auth)

34880 METHOD OF OPTIMIZATION OF PARAMETERS OF COLLIMATOR FOR RADIOISOTOPE SCANNING. Kostylev, V. A.; Fishman, L. Ya. (Inst. of Experimental and Clinical Oncology, Moscow). Med. Radiol.; 16: No. 3, 80-5(Mar 1971). (In Russian).

An objective method of optimization of the parameters of a single-canal collimator and multi-canal focusing ring collimator for radioisotope scanning is proposed. Using the known function of sensitivity of the system for a single-canal collimator one can prove the presence of such an optimum and thus the possibility of optimization of the collimator parameters. Optimization of the parameters of a multi-canal ring focusing collimator involves a relative significantly simplified solution which can be made by the method of dynamic programming. (auth)

34881 OFF-LINE COMPUTER INTERFACE FOR A RECTILINEAR SCANNER. Dowsett, D. J.; Ritchie, D. R. (Atkinson Morley's Hospital, London). Phys. Med. Biol.; 16: No. 2, 249-56(Apr 1971).

An off-line computer interface is described which, when coupled to a rectilinear scanner, automatically punches on paper tape the information necessary for subsequent computer analysis of the scan. The use of integrated micrologic results in a compact instrument which can be conveniently situated near the scanner. The interface functions without disturbing the scanning routine. Information is obtained from the interface at fast scanning speeds even when the scanner's visual displays cannot be used. (auth) (UK)

34882 NUCLEAR SEMICONDUCTOR DETECTOR AND ITS MANUFACTURE. Meuleman, Johannes (to RTC La Radiotechnique Compelec, SA). French Patent 1,598,473. 6 Jul 1970. Filed 17 Dec 1968. (In French).

A semiconductor crystal detector is described which consists of two external regions of different type separated by an intermediate lithium compensated region and a cavity made in one of the external regions. The plane back surface serves as the radiation receiving face; contact is effected by the external regions. The cavity has a parallelepiped form with a depth at least equal to the thickness of the external region in which it is made such that its bottom exists in the intermediate compensated region. (auth) (France)

34883 FISSION CHAMBER. Bouchard, Jacques; Guery, Marcel (to Commissariat a l'Energie Atomique). French Patent 1,593,960. 1 Jun 1970. Filed 3 Dec 1968. (In French).

A fission chamber is presented, which permits the measurement of local perturbations in the neutron flux. The chamber consists of a double cylindrical envelope containing, in an atmosphere of neutral gas, a coaxial tube with fissile material deposited on one of its faces. The tube and the envelope are electrically insulated from one another. They are connected to a linking coaxial cable with a measuring device. This fast counting device renders the measurement of the neutron pulses independent of the accompanying γ radiation. (auth)

34884 IONIZATION FISSION CHAMBER. Gaillet, Gerard; Guery, Marcel (to Commissariat a l'Energie Atomique). French Patent 1,596,082. 15 Jun 1970. Filed 13 Dec 1968. (In French).

This invention concerns an ionization fission chamber preserving the desirable characteristics of chambers of this type but being more suitable for mapping the neutron flux in a reactor. The casing is sealed and provides a joining plug connected by coaxial cable to the electric supply for the chamber, the amplifier, and the pulse counter. An electrically conducting tube whose diameter is significantly less than the one of the casing is sealed to the casing. Its length is greater than its diameter and the end remote from the casing either forms one of the electrodes or is connected to the annular electrode of the chamber. An electric conductor, whose end point is remote from the casing, is centralized in the tube and in relation to the cathode by insulators of radiation resistant material, forms the other electrode. One of the electrodes is at least partially coated with fissile material. The length–diameter ratio of the tube constituting the electrode is of the order of 1000. This tube and the parts inside are adapted for possible curving. (auth) (France)

34885 RADIO-ISOTOPE MACHINE. Sear, Reginald; Dean, Peter Mervyn (to National Research Development Corp.). British Patent 1,228,030. 15 Apr 1971. Filed 19 Jun 1968

Reference is made to radioisotope scanning machines, such as are used for medical purposes. The ability of the eye to discern features of diagnostic significance depends on the extent to which color or x-ray film density boundaries corresponding to different radiation levels are discernable, and the object of the machine described is to provide a display in which the boundaries between different regions are more readily discernable. (UK)

XUM

34886 AUTOMATIC LIQUID SCINTILLATION COUNTING SYSTEMS. (to Nuclear-Chicago Corp.). British Patent 1,230,031. 28 Apr 1971. Priority date 12 Jun 1968, United States.

An automatic liquid scintillation counting system is described including sample transport system, standard source system for calibration, and automatic gain adjustment system. (W.H.K.)

34887 IMPROVED CHARGED PARTICLE DETECTOR. Muga, Marvin Luis; Taylor, Howard E. (to United States Atomic Energy Commission). U. S. Patent 3,567,925. 2 Mar 1971. Filed 26 Jul 1968.

A new time-of-flight particle detector comprises an ultra thin plastic scintillator placed perpendicular to the face of a photomultiplier tube and sandwiched between two Lucite light pipes. The Lucite enclosure has a large hole for passage of fragments through the thin scintillator with a minimum energy loss, as small as 1 percent for fission fragments. A fission fragment, upon passing through the scintillator, triggers a light flash which traverses the film and light pipes and in turn is detected by the photomultiplier tube. Rise times of the order of 2 nanoseconds are achieved and the efficiency of detection is 100 percent for fission fragments. This detector has the great advantage of providing a clear distinction between time pulses and background noise. (auth)

34888 PREREGULATION OF HIGH VOLTAGE SUPPLY CIRCUIT FOR A MEDICAL NUCLEAR SPECTROMETER. Satterfield, Marion M.; Dyer, George R. (to United States Atomic Energy Commission). U. S. Patent 3,569,701. 9 Mar 1971. Filed 7 Mar 1969.

A modular, all transistorized, direct-coupled, pulse-height spectrometer for use in nuclear medical measurements is provided with means for the specific control of noise level, overloads, linearity and voltage regulation, together with compactness is described. These features make the present spectrometer substantially superior to the prior art tube-type spectrometers. (auth)

34889 LEAD IODIDE NUCLEAR PARTICLE DETECTORS. Roth, S.; Willig, W. R. (Siemens AG, Erlangen, Ger.). Appl. Phys. Lett.; 18: No. 8, 328-30(15 Apr 1971).

Semiconductor nuclear particle detectors have been made from lead iodide. Alpha particles and gamma quanta have been counted in the temperature range from −200 to +130°C. From α-particle pulse height the carrier mobility × carrier lifetime product has been estimated to be 2×10^{-8} cm^2/V. (auth)

34890 RESOLVING TIME OF A COUNTER BY THE METHOD OF PAIRED SOURCES. Castrillon, J. (Puerto Rico Nuclear Center). Contract AT(40-1)-1833. Radiochem. Radioanal. Lett.; 6: 249-56(24 Apr 1971).

The different formulas that have been proposed for the calculation of the resolving time of a counter by the paired sources method are examined. It is shown that the most widely recommended expression leads to errors that may reach 100%. A simpler formula applicable when both sources have approximately the same counting rate and which gives accurate results is described. (auth)

34891 RESPONSE OF SELF-POWERED GAMMA DETECTORS. Strindehag, Ove (Aktiebolaget Atomenergi, Studsvik, Sweden). Atomkernenergie; 17: No. 4, 267-70(Jul 1971).

Experimental results from an investigation of self-powered gamma detectors with emitters of lead, zirconium, Inconel 600, magnesium, and graphite are presented. The detectors are intended primarily for in-core applications in power reactors, and the detector design is the same as for a type of neutron sensitive self-powered detector previously utilized for in-core measurements. Detector sensitivities measured both in a ^{60}Co gamma cell and in a test reactor are given. For detectors with lead emitter the measured sensitivity in the gamma cell is $8 \cdot 10^{-16}$ A/Rh^{-1}, and for detectors with magnesium emitter $1{,}2 \cdot 10^{-16}$ A/Rh^{-1}. (auth)

34892 DOSIMETRY OF A GAMMA FLASH. Nemsmann, U.; Roose, U. J. (Univ., Kiel). Atomkernenergie; 17: No. 4, 274-6 (Jul 1971). (In German).

A silicon surface-barrier detector (Valvo BPY 83-200 A) has been investigated for dose- and doserate measurements in a pulsed gamma-ray-field. This detector offers two advantages: the absorbed dose and doserate can be determined directly and absolutely from the collected radiation induced charges in terms of rad(Si) and from the current in terms of rad(Si)/s respectively; and the timeresponse is in the nanosecond region. Application and operation of the detector as a dosimeter has been investigated. It can be used for doserate measurements in the range from 10^4 rad(Si)/s up to 10^7 rad(Si)/s and for registration of the integral dose per pulse in the range from 0.5 μ rad(Si) to 10 rad(Si). For measurements of higher doserates a similar detector will be constructed with a smaller sensitive volume and a higher collecting field. Finally the radiation field and the energy spectrum of a gamma-flash-generator have been determined. (auth)

34893 POCKET DOSIMETER. Herzog, Heinz (to Telefunken Patentverwertungsgesellschaft mbH). German Patent 1,514,804. 23 Oct 1969. Filed 30 Mar 1965. (In German).

A pocket dosimeter for the measurement of x, gamma, and neutron radiation made up of two cylindrical conductors under vacuum arranged concentrically and of different sensitivities to the electron energy is described. The exterior cylinder forms one part of a wall enclosing the vacuum. There is also an electrometer indicating the difference in potential between the two cylinders. A switching foil is arranged in the vacuum enclosure but maneuverable from outside the enclosure, serving to discharge the electrometer. (J.F.P.)

34894 RADIOLOGICAL MONITORING METHODS AND INSTRUMENTS. NCRP 10 1952. Washington, D. C.; National Bureau of Standards (1952). 33p. Available from NCRP Publications, Washington, D. C.

Topics include general principles of hazard control, airborne hazards, surface contamination, determination of hazards and personnel monitoring. Also, radiation detectors, measuring instruments, personnel monitoring instruments, and instrument requirements are discussed. General recommendations for radiation-survey methods are presented. (W.H.K.)

34895 LIQUID SCINTILLATION COUNTING USING AN RCA PHOTOMULTIPLIER TYPE C31 000D. Kolbe, W.; Schwerdtel, E. Int. J. Appl. Radiat. Isotop.; 21: 750-2(Dec 1970).

In the new RCA photomultipler type C31 OOOD, gallium phosphide is used for the first dynode of the multiplier which increases the multiplication factor from ~3 or 4 to ~40. Using these new photomultipliers it has been found that: (1) The spectrum of ^{3}H showed a large number of single electron pulses, which with quenched samples were predominant. (2) The pulse spectrum of ^{3}H showed a form which was only dependent to a small degree on the form of the ^{3}H energy spectrum. The larger part of the ^{3}H pulse spectrum was determined by the kind of multiplication in the multiplier. It is, therefore, incorrect to speak of an energy scale or of proportionality between pulse-height and beta energy, for ^{3}H spectrum. (3) The noise spectrum consisted only of single electron pulses. The single electron spectrum essentially showed a Gauss distribution. (4) By pulse summation the mean pulses were biased to the small and larger ones. The ^{3}H pulse spectrum was smaller. The separation of the pulses of one and two-electron pulses was blurred. (UK)

34896 SIMPLIFIED FABRICATION OF POSITION SENSITIVE DETECTORS. Nakamoto, Shunsuke (Chubu Inst. of Tech., Kasugai, Japan). Mem. Chubu Inst. Technol.; 6: 115-20(Dec 1970). (In Japanese).

The position sensitive detector (PSD) is fabricated from a 250Ω · cm n-type silicon by evaporating gold film on the front surface and by plating nickel terminals on the rear surface. The back layer is composed of the silicon itself between the nickel terminals, but the resistance is stable for a long time. The detector has a sensitive area of 3×11mm^2 and a junction capacitance of 40 pF at 100 V bias. The energy and position resolutions are 2.5 and 1% (100 μm), respectively. The fabrications of a larger PSD, a two-dimensional PSD, or a β- and γ-ray sensitive PSD are very promising by this method. (auth)

34897 INFLUENCE OF AMBIENTS ON THE REVERSE CURRENT OF SURFACE BARRIER DETECTORS. I. Aoki, Takashi (Chubu Inst. of Tech., Kasugai, Japan). Mem. Chubu Inst. Technol.; 6: 121-6(Dec 1970).

In order to obtain better semiconductor surface barrier nuclear particle detectors, an investigation of surface effects on the reverse current is made. Gold is vapor-deposited on the etched silicon surface, in the shape of concentric circles; one of which is a central solid circle, and the other an outer ring surrounding the former. The currents that flow between these two separated gold layers are measured as functions of ambients. It is then shown that the surface leakage current is a large component of the reverse current, and that the strong inversion layer is formed on the silicon surface, in vacuo, resulting in high surface current, and in room air atmosphere the depletion or accumulation layer is formed, though the formation of it is very sensitive to water vapor. (auth)

XUM

34898 SELF-QUENCHING OPEN-POINT COUNTER AS DETECTOR OF POSITIVE IONS. Reizer-Stepniowska, D.; Stepniowski, I.; Sujak, B. (Univ., Wroclaw). Acta Phys. Pol.; A39: No. 3, 343-50(Mar 1971).

It has been shown that a self-quenching open point counter, extensively used in the detection of exoelectrons, is also a good detector of slow positive ions in air when the point is negatively polarized. Use of the counter has revealed that during both the dehydration and hydration processes in quinine sulphate there are generated positive ions, besides the well known fact of exoelectron emission—emission of negative charge carriers. (auth)

34899 TIMING WITH SURFACE BARRIER DETECTORS USING CHARGE AND CURRENT PULSES. Emmerich, W.-D. (Univ., Erlangen, Ger.); Hofmann, A.; Philipp, G.; (and others). Nucl. Instrum. Methods; 93: No. 2, 397-401(1971).

For obtaining fast time marking signals from silicon surface barrier detectors the leading edge method and the method of constant fraction of pulse height triggering have been used. These two methods have been studied with a counter telescope using both the charge and the current pulses. The distribution of the time signals as a function of the particle energy has been investigated for protons and deuterons using a computer program for two dimensional analysis. (auth)

34900 EXPERIMENTAL AND CALCULATED PHOTOPEAK EFFICIENCIES FOR A COAXIAL Ge(Li) DETECTOR. Raeside, D. E.; Ludington, M. A. (Univ. of Michigan, Ann Arbor). Nucl. Instrum. Methods; 93: No. 2, 389-90(1971).

Experimental and calculated photopeak efficiencies have been obtained for a 32 cm^3 true coaxial Ge(Li) detector at four distances: 2, 5, 10 and 20 cm. A comparison of these results is presented. (auth)

34901 ASSOCIATED PARTICLE SYSTEM FOR POLARIZED NEUTRONS FROM THE T(d,n)^{4}He REACTION. Chisholm, A.; Garrett, R. (Univ. of Auckland, N. Z.). Nucl. Instrum. Methods; 93: No. 2, 365-7(1971).

An associated particle system for use with the T(d,n)^{4}He reaction at deuteron energies in the 6 MeV region is described. (auth)

34902 ENERGY THRESHOLD FOR NEUTRON DETECTION IN A MAKROFOL DIELECTRIC TRACK DETECTOR. Jozefowicz, K. (Inst. of Nuclear Research, Swierk, Poland). Nucl. Instrum. Methods; 93: No. 2, 369-70(1971).

The energy threshold for neutron registration in a Makrofol E particle track detector due to carbon recoil atoms is estimated at about 1.2 MeV. Monoenergetic neutron irradiations confirm this prediction. (auth)

34903 SYSTEM FOR PRECISE DETERMINATIONS OF ELECTRON–GAMMA DIRECTIONAL CORRELATIONS. Holmberg, L.; Cho, Z. H. (Univ. of Stockholm). Nucl. Instrum. Methods; 93: No. 2, 353-5(1971).

A three-detector setup for simultaneous measurements of electron-gamma and gamma-gamma directional correlations is described. Several sources of systematic errors are eliminated in this system. The angular positions of the detectors are shown to be of considerable importance. The system is applied to a study of the 208K–113γ directional correlation in ^{177}Hf. (auth)

34904 GEOMETRIC INVERSION AND ITS UTILIZATION IN X-RADIOMETRIC AND GAMMA–GAMMA METHOD. Leman, E. P.; Ochkur, A. P. Geofiz. App.; 43: 98-105(1970). (In Russian).

It was shown analytically that the inverse dependence of the intensity of secondary (characteristic or dispersed) radiations on changes of the distance between the detector and the surface of the medium studied is explained by the effect of the geometric factor, i.e., by the ratio of the length of the probe to the magnitude of this distance. The position of the point of inversion corresponds to the value of this ratio equal to unity. The aspects of applying this effect of geometric inversion in x-radiometric and gamma-gamma methods for creation of noise-free probes are described. In particular, it was shown that in double probes the limits of compensation of change of the distance between detector and the surface of the medium studied are determined by the position of the inversion points of small and large probes. (tr-auth)

34905 ELECTRON ENERGY DISTRIBUTION WITHIN A CURVED CHANNEL MULTIPLIER. Andresen, R. D.; Ho, S. T.; Page, D. E. (European Space Research and Tech. Centre, Noordwijk, Netherlands). Nucl. Instrum. Methods; 93: No. 2, 357-60(1971).

The energy distribution of electrons leaving a C-shaped channel multiplier has been experimentally determined. There exists a peaked distribution for relatively low voltages V_0 applied to the curved channel multiplier. The mean electron energy E_m shows a $E_m \sim V_0^5$ dependence as predicted by theory. (auth)

34906 MEASUREMENT OF NEUTRON MEAN ENERGIES OF EVAPORATION-TYPE NEUTRON SOURCES. Barrett, R. F.; Thies, H. H. (Univ. of Western Australia, Nedlands). Nucl. Instrum. Methods; 93: No. 2, 333-9(1971).

It is shown how one can calibrate and use a multi BF_3-counter neutron-detection system to measure accurately the mean energy of neutrons from evaporation-type neutron sources. The expediency of the method is demonstrated by a sample experiment. (auth)

34907 CALCULATION OF GAMMA-RAY PULSE HEIGHT SPECTRUM IN A SEMICONDUCTOR DETECTOR IN THE PRESENCE OF CHARGE CARRIER TRAPPING. Bell, R. O. (Tyco Labs., Inc., Waltham, Mass.). Nucl. Instrum. Methods; 93: No. 2, 341-8(1971).

An integral expression for the spectral distribution produced by monoenergetic gamma rays on a planar semiconductor radiation detector has been derived. The effect of the charge collection efficiency has been included by using the Hecht relation for mobile holes and electrons. The method of subtracting fwhm contributions by quadrature when attempting to separate the contribution produced by finite drift lengths from effects such as the electronic noise, pair creation statistics, material inhomogeneities, or other independent processes can be grossly in error. A FORTRAN program to numerically evaluate the integral and calculate a spectrum is included. (auth)

34908 EXPERIMENTAL DETERMINATION BY MEANS OF ACTIVATION MONITORS OF THE DISTRIBUTION OF THE GAMMA PHOTON BREMSSTRAHLUNG BEAM PRODUCED BY 25 TO 45 MeV ELECTRONS. Engelmann, Ch. (Centre d'Etudes Nucleaires de Saclay, Gif-sur-Yvette, France). Nucl. Instrum. Methods; 93: No. 2, 197-204(1971). (In French).

Ag and C activation monitors, evenly arranged behind platinum and aluminum targets, were used to determine the distribution of the part of the 25 to 45 MeV electron-induced bremsstrahlung beam spectrum involved in the activation of elements by (γ,n) reactions. The results are given in the form of curves representing the magnitude of the longitudinal and transversal (γ,n) activation gradients on the one hand, and on the other hand the irradiation positions where the activities induced are decreased by 0.5, 10^{-1}, 10^{-2}, 10^{-3} and 10^{-4} with respect to those corresponding to the maximum activation position immediately behind the target. (auth)

34909 SLOPE SENSITIVE ALARM FOR USE WITH FIXED FILTER AIR MONITORS. Singh, A. N.; Nair, N. B.; Pinto, R. (Bhabha Atomic Research Centre, Bombay). Nucl. Instrum. Methods; 93: No. 2, 227-34(1971).

An alarm system for fixed filter air monitors is described. The functioning of the alarm depends only upon the levels of air activity irrespective of the accumulated activity on the filter. The principle of the alarm is discussed in detail and the theoretical derivations have been verified experimentally. The performance of the alarm has been studied in actual operations and the results are presented. (auth)

34910 COOLED PREAMPLIFIERS WITH DIODE CURRENT LEAK. Ryan, R. D. (Australian Atomic Energy Commission Research Establishment, Sutherland). Nucl. Instrum. Methods; 93: No. 2, 241-3(1971).

A high resolution voltage sensitive cooled preamplifier for semiconductor radiation detectors has been operated with a Schottky barrier diode as the current leak. A resolution of less than 300 eV (fwhm Si) was realized. The charge sensitive mode of operation has also been used. (auth)

34911 PRINCIPLE OF FORMATION OF AMPLITUDE SPECTRA IN SEMICONDUCTOR NUCLEAR RADIATION COUNTERS. Strokan, N. B.; Lomashevich, C. A.; Makovskii, L. L.; Tisnek, N. I. (Ioffe Inst. of Physics and Tech., Leningrad). Nucl. Instrum. Methods; 93: No. 2, 277-84(1971).

The principle of amplitude spectra formation on the basis of representing the pulse formation stages as a successive series of independent processes has been suggested. Each one of them is characterized by a so-called response function which reflects distortions in the amplitude spectra, caused by a statistical character of the process considered. Main attention is paid to those response functions which are connected with incomplete charge collection of electron-hole pairs on the counter electrodes in spectrometric measurements of different kinds of radiation. The most interesting case of γ-quanta spectrometry has been analyzed taking into account double absorption events (Compton scattering in the first event and photoabsorption of the scattered γ-quanta).

XUM

Considerable distortions of the amplitude spectrum (comparison with the direct photoabsorption) are shown to appear even at charge losses occurring homogeneously all over the counter volume. (27 references) (auth)

34912 AUTOMATIC QUENCH COMPENSATION FOR LIQUID SCINTILLATION COUNTING SYSTEM. (to Beckman Instruments, Inc.). British Patent 1,226,834. 31 Mar 1971. Priority date 3 Jul 1967, United States.

A method of automatically compensating for spectral shift due to quench in a liquid scintillation nuclear counter is described. Alignment of the spectral energy end-point of an isotope with a selected discriminator level is accomplished by means of a voltage-controlled parameter. A voltage from a reference voltage source is established in proportion to the measure of quench on a sample prior to taking a sample count. The level of the voltage-controlled parameter is adjusted in accordance with the measure of quench in such a manner that the spectral energy end-point is substantially restored to the selected counting-window discriminator level, and the sample count is taken with the parameter automatically maintained at the adjusted level. (R.W.R.)

34913 APPARATUS FOR AUTOMATIC DRIFT STABILIZATION IN INTENSITY MEASUREMENTS OF NUCLEAR RADIATION BY α-PROBES. (to Laboratorum Professor Dr. Rudolph Berthold). British Patent 1,226,924. 31 Mar 1971. Priority date 13 Mar 1968, Austria.

An apparatus for automatic drift stabilization in intensity measurements of nuclear radiation by alpha particles is described. A radiation source having a ray energy that is at least equal to the maximum to be expected in the measured spectrum is located in a definite position relative to the counter. The design includes an integral discriminator and a control circuit for pulse amplification, the circuit maintaining the pulse rate recorded by the integral discriminator constant. The device can be used either for nuclear spectroscopy or as a radiometric gage. The source of calibrating radiation may be a discrete source or homogeneously distributed in the scintillator crystal. (R.W.R.)

34914 IMPROVEMENTS IN AND RELATING TO THE COUPLING OUT OF PULSES FROM NUCLEAR RADIATION DETECTORS. Michel, Horst-Stephan; Deckert, Harald (to Deutsche Akademie der Wissenschaften zu Berlin). British Patent 1,225,197. 17 Mar 1971. Filed 19 Jul 1968.

A method is described for coupling out pulses in nuclear radiation measurements with detectors of the avalanche type which utilize the electromagnetic radiation field set up in the detector plasma, and/or in the detector connection lines, on arrival of an ionizing particle, and employs a receiving antenna or other structural or electrical elements serving as an antenna, together with a conventional radio receiver. This avoids the unsatisfactory operation when conventional circuits are employed, if the detector and its connecting lines are not carefully shielded. The number of electronic components is reduced, and the apparatus is thus made simpler and cheaper. Another object is to provide a circuit arrangement that enables coupling out of pulses from multi-chamber counting tubes, even when the chambers are not completely functionally separate from each other, and using a working resistance common to all chambers. (UK)

Nuclear Spectroscopic Instrumentation

Refer also to abstracts 34536 and 36343.

34915 (ANU-P-438) GAMMA RAY ANALYSIS PROGRAMS. Ophel, T. R. (Australian National Univ., Canberra. Research School of Physical Sciences). Feb 1969. 5p. Dep. NTIS (U. S. Sales Only).

General-purpose gamma-ray-analysis programs in use at ANU are summarized, and brief descriptions of variants of the basic program for line-shape analysis are given. (Australia)

34916 (JINR-E14-5731) SYNCHRONIZED CHOPPER TIME-OF-FLIGHT SPECTROMETER AT THE DUBNA PULSED REACTOR IBR-30. Deme, S.; Horvath, J.; Kroo, N.; Szlavik, F.; Zsigmond, G. (Joint Inst. for Nuclear Research, Dubna (USSR). Lab. of Neutron Physics). 1971. 31p. Dep. NTIS (U. S. Sales Only).

A time-of-flight spectrometer has been constructed at the pulsed reactor in Dubna. The spectrometer works in the direct geometry with a phased chopper before the sample. The energy of the incoming neutrons can be varied in the 3 to 130 MeV range. Scattered neutrons can be analyzed simultaneously in 8 angles covering about 10° wide angular region. By moving the detector arm ±65° scattering angle region can be covered. (auth)

34917 (JUL-719-FF) DEVELOPMENT OF A FOUR-CRYSTAL MONOCHROMATOR AND A ROTATING MINIATURE COLLIMATOR FOR NEUTRON SPECTROSCOPY. Stockmeyer, R. (Kernforschungsanlage, Juelich (West Germany). Institut fuer Festkoerperforschung). Dec 1970. 27p. (In German). Dep. NTIS (U. S. Sales Only).

A multi-crystal monochromator and a miniature rotating collimator were developed for use with the time-of-flight spectrometer SV5c. The miniature collimator built for a chopper with short opening time can be used for triaxial spectrometers and double monochromators. The intensity yield factor 8.6 for the multi-crystal monochromator can not be expected for the very broad beam of the SV5c time-of-flight spectrometer. It was established however that the monochromatic beam can be so focused with 10 crystals that the spectrometer yields measurements with better resolution at the same intensity as previously in a large angular range than is possible without the multicrystal monochromator. (tr-auth)

34918 (LB/G-3034) ENERGY RESOLUTION OF MULTIPLYING SEMICONDUCTOR DETECTORS FOR SOFT γ SPECTROSCOPY AT ROOM TEMPERATURE. Ruge, I.; Berg, G.; Heuberger, A. Translated by W. G. Stripp (Atomic Energy Research Establishment, Harwell, Eng.), from Nucl. Instrum. Methods; 84: 55-60(1970). 11p. Dep. NTIS (U. S. Sales Only).

An abstract of this paper, prepared from the original language, appeared as NSA 24: 39323. (R.W.R.)

34919 (UARAEE-61) CALCULATION OF THE NEUTRON PULSE SHAPE, TRANSMISSION FUNCTION AND RESOLUTION FUNCTION IN A MECHANICAL TIME-OF-FLIGHT SPECTROMETER. El-Konsol, S.; Hussein, A.; Novikov, A.; Hamouda, I. (Atomic Energy Establishment, Cairo (Egypt). Reactor and Neutron Physics Dept.). 1968. 59p. Dep. NTIS (U. S. Sales Only).

The calculation of two important characteristics of the mechanical chopper (neutron pulse shape and transmission function) is described. The neutron pulse shape is defined as the time dependence of a neutron flux passing through a rotating slit. It is calculated for three different types of slits, namely: straight, curved and cigar-shaped. The transmission function was also calculated for the three types of slits and it can be noticed to vary for each type. Also, the calculation of the counting rate in the analyzer channel and the spectrometer resolution are studied. A function for the pulse shape is proposed to calculate the instrument spectral line. To optimize the relation between the counting rate and the resolution, a value called the specific area of the spectral line is derived. (auth)

34920 (UARAEE-91) MEASUREMENT OF CONTINUOUS FAST NEUTRON SPECTRA BY SCINTILLATION TECHNIQUE. Megahid, R.; Makarious, A. S.; Belov, S.; Hamouda, I. (Atomic Energy Establishment, Cairo (Egypt). Reactor and Neutron Physics Dept.). 1970. 25p. Dep. NTIS (U. S. Sales Only).

A fast neutron scintillation spectrometer with stilbene crystal was assembled, adjusted, and calibrated to measure continuous fast neutron spectra in the energy range 1 to 11 MeV. Insensitivity to gamma rays and electrons is achieved by utilizing differences in the pulse shapes of light pulses produced by electrons and protons. To check the working efficiency of the spectrometer as well as the energy scale and handling method used, the neutron spectra of a Po-α-Be source and the direct neutron spectrum from a horizontal beam channel of the UA-RR-1 and after passing through graphite filters of 18 and 50 cm thickness were measured. A reasonable agreement with other measurements was obtained. The spectrum of the fast neutrons of the reactor beam was compared with available calculation of the leakage neutron spectrum. After introduction of a number of experimental corrections both spectra were found to be in good agreement. (auth)

34921 (UARAEE-93) CALIBRATION OF A THREE-CRYSTAL-NaI-PAIR-SPECTROMETER. Abu-Zeid, H. M.; Hassan, A. M. (Atomic Energy Establishment, Cairo (Egypt). Reactor and Neutron Physics Dept.). 1970. 24p. Dep. NTIS (U. S. Sales Only).

The scintillation-pair-spectrometer is intended to yield energies and intensities of neutron capture gamma rays as precisely as possible. It is found possible to determine experimentally the relative peak-to-total ratio for a pair crystal spectrometer. (auth)

34922 (UARAEE-100) CONSTRUCTION OF A THREE-CRYSTAL SCINTILLATION PAIR SPECTROMETER. Hassan, A. M.; Abu-Zeid, H. M. (Atomic Energy Establishment, Cairo (Egypt). Reactor and Neutron Physics Dept.). 1970. 37p. Dep. NTIS (U. S. Sales Only).

The construction and tests of the three crystal scintillation pair spectrometer are reported. The design and construction of the ra-

XUM

diation shield and collimation of the thermal neutron beam are also described. It is found that the intensity of the collimated thermal neutron beam at the target is 10^6 neutron/cm^2 sec. The central scintillation head has an energy resolution ~7.5% for the ^{137}Cs line of 0.662 MeV, with a NaI(Tl) crystal of dimensions (1.75'' ϕ × 2'' L). The scintillation heads have a resolution of about 10% for NaI(Tl) crystals with the dimensions (3'' ϕ × 3'' L). The electronic equipment i.e., a pulse shaper for the fast coincidence input and another for the analyzer gate, a stabilized power supply and the matching cathode followers were locally constructed. The linearity of a (512 pulse Height Analyzer) and the two single P.H.A. was checked. In the fast-slow coincidence circuit, the resolving time used for the fast is about 50×10^{-9} sec., while that of the slow is 0.42×10^{-6} sec. The fast-slow coincidence was checked using a ^{22}Na standard source which indicates that the electronic equipment is satisfactory for a three-crystal pair spectrometer. Also, the gamma-ray spectrum following thermal neutron capture in natural lead is presented, as a check for the validity of the spectrometer. (auth)

34923 (UCRL-20476) GAMMA-RAY CALIBRATION STANDARDS. Jardine, Leslie J. (California Univ., Berkeley. Lawrence Radiation Lab.). Apr 1971. Contract W-7405-eng-48. 22p. Dep. NTIS.

A collection of γ-ray energies and intensities is given that are suitable for use in the calibration of high resolution γ-ray spectrometers. The energy range included in this tabulation is 25 keV < E_γ < 3452 keV. Adopted values are given for gamma-ray energies based on weighted averages of the author's stated uncertainties. Relative γ-ray intensities are also given for ^{133}Ba, ^{182}Ta, and ^{56}Co. No attempt was made to establish weighted averages for the intensity values. (auth)

34924 (WCAP-7562-3) PLANT INSTRUMENTATION PROGRAM QUARTERLY PROGRESS REPORT FOR THE PERIOD ENDING SEPTEMBER 30, 1970. Limpert, J. C. (Westinghouse Electric Corp., Pittsburgh, Pa. Nuclear Energy Systems Div.). Mar 1971. Contract AT(30-1)-64. 10p. Dep. NTIS.

The fuel rod transport device was set up and evaluated. Minor modifications were found to be necessary in order to reproduce the traversing time at rates less than 1 ft. per minute. These modifications are being made. Further characterization of the Westinghouse plutonium recycle fuel gamma spectra resulted in the identification of activity from the decay of daughters in the ^{232}Th chain. This contamination was traced to the incoming $Pu(NO_3)_4$. Passive waste assay studies were continued. Gamma energy ratio techniques for attenuation correction were examined. The assay of low-level waste in drums and packages has continued. Waste categories have been established and the relative standard error for the assay of Pu in 55-gallon drums and 5-gallon packages has been shown to be of the order of ±10 percent ±5 percent, respectively. (auth)

34925 SIMPLE NEUTRON SPECTROMETER. Liu, Yuen-chung; Tzeng, Huw-shing; Cheng, Vianney Kuo-chuan; Hsu, Wu-shiung (National Tsing Hua Univ., Hsinchu, Taiwan). Chin. J. Phys. (Taiwan); 8: 31-5(Oct 1970).

A simple neutron spectrometer was constructed by using an aluminum absorber coated with ^{6}LiF and a collimator and a gold-silicon surface barrier detector. The thermal-neutron spectrum was obtained with an energy resolution of 300 keV. (auth)

34926 STUDY OF THE PROPERTIES OF MARMET'S MONOKINETRON BY CALCULATION OF ELECTRON ENERGY DISTRIBUTION PROFILES. Roy, D.; Carette, J.-D. (Univ. Laval, Quebec). Rev. Sci. Instrum.; 42: No. 6, 776-82(Jun 1971).

A method of calculation of the electron energy distribution produced by various electrostatic spectrometers is applied to Marmet's monokinetron. Properties of this apparatus are verified and studied as functions of the main geometrical and electrical parameters in second order approximation. Electron motion calculations are performed from two dimensional considerations, but consequences of finite axial dimensions are studied. Results are in agreement with the experimental and theoretical determination of the resolution done by Marmet. (auth)

34927 ANALYSIS OF THE ENERGY DISTRIBUTION IN CYLINDRICAL ELECTRON SPECTROMETERS. Aksela, S. (Univ. of Oulu, Finland). Rev. Sci. Instrum.; 42: No. 6, 810-12(Jun 1971).

The cases of minimum trace width and second order focus for double focusing cylindrical electron spectrometers are investigated by calculating the energy distributions of transmitted electrons. It is shown that the base width of the electron energy distribution is appreciably smaller in the case of the minimum trace width condition than for the second order focusing arrangement. For high energy resolution, however, the second order focus is found advantageous because the distribution curve has a sharper peak and also a smaller full width at half-maximum for energy spreads (FWHM) less than 0.1%. (auth)

34928 ANTICOINCIDENCE GAMMA SPECTROMETER WITH SHIELDED SCINTILLATOR. Kireev, V. A.; Navalikhin, L. V.; Sattarov, M. G.; Talanin, Yu. N. (Inst. of Nuclear Physics, Tashkent). Izv. Akad. Nauk Uzb. SSR, Ser. Fiz.-Mat. Nauk; No. 4, 76-9(1970). (In Russian).

Descriptions are given of the design and performance of a scintillation anticoincidence spectrometer for recording low-energy (up to 1 MeV) γ-quanta. The spectrometer consists of a shielded plastic cylindrical scintillator 220 × 350 mm with a channel perpendicular to its axis with a 40 × 50 mm NaI(Tl) crystal detector and a well. The spectrometer is surrounded by a 100 mm thick lead shield. The performance of the anticoincidence spectrometer with the shielded crystal was tested with the mixture of isotopes ^{65}Zn (E_γ = 1.115 and 0.511 MeV), ^{196}Au (E_γ = 0.668, 0.426, 0.354, and 0.332 MeV) and ^{196m}Au (E_γ = 0.188, 0.149, and 0.084 MeV). The threshold of the main discriminator is 50 keV and the shielded 70 keV and the discriminator dead time by anticoincidence is 2 μsec. (R.V.J.)

34929 DOUBLE-STATISTICAL CHOPPER FOR ELIMINATION OF INELASTIC SCATTERED NEUTRONS IN TIME-OF-FLIGHT EXPERIMENTS. Pellionisz, P. (Institut Max von Laue-Paul Langevin, Grenoble, France). Atomkernenergie; 17: No. 4, 277-80(Jul 1971).

An experimental method is presented for time-of-flight measurement of elastic neutron scattering with the elimination of the inelastically scattered contribution. The polyenergetic incoming beam is pulsed with a chopper of statistical type; the time-of-flight spectrum of the scattered neutrons is regained with the usual correlation data-processing. Another statistical chopper is placed just in front of the sample. According to this on–off program—but on a lengthened time-scale, corresponding to the geometrical relations of the experiment—a binary separator function controls a regrouping of the detected neutrons. By the super-position of the correlation and separation process two time-of-flight spectra are collected in two parts of a multichannel memory (e.g. analyzer): one of the inelastically, the other of the inelastically plus elastically scattered neutrons. Their difference gives the pure elastically scattered spectrum. The introduction of the correlation-method at the separation arrangement increases its neutron-economy, and in most cases, gives a gain in statistical accuracy or in measuring-time compared to the conventional method. The gain, however, is always determined by the actual structure of the spectrum to be measured and background properties. (auth)

34930 LIQUID SCINTILLATION COUNTER FOR ALPHA-PARTICLE ENERGY RESOLUTION (3 Feb 1969) (Engineering Materials). (Oak Ridge National Lab., Tenn.). (CAPE-1879). 2 drawings.

Instrumentation for counting α particles with near 100% efficiency and good energy resolution is described. The equipment is used to investigate the chemistry of complex ions of actinides with high atomic numbers, such as Am, Cm, Bk, Cf, and Es, in aqueous media. A light guide made of Lucite is coupled to the face of the photomultiplier tube. A slot in the guide holds a pyrex vial containing the liquid scintillation mixture of 2,5-diphenyloxazole (PPO) and 1,4-bis-2-(4-methyl-5-phenyloxazolyl)-benzene (M_2POPOP) dissolved in toluene. Styrofoam placed behind the light guide reflects light into a photocathode. The radioactive material is contained in the vial also. Access to the dark chamber for changing samples is through a hinged door. The size and shape of the liquid scintillator samples influence the energy resolution. Sample size and contaminants in the sample-scintillation mixture limit energy resolution, while removal of O and H_2O from the sample-scintillation mixture improves the resolution. (F.S.)

34931 TRIPLE-CRYSTAL GAMMA SCINTILLATION SPECTROMETER WITH A PROTECTIVE ANTICOINCIDENT SCINTILLATOR. Marik, Petr; Vespalec, Rudolf. Jad. Energ.; 17: No. 4, 127-8(1971). (In Czech).

A gamma spectrometer with protective anti-coincidence is described which permits to a certain extent the suppression of continuous Compton background for improved efficiency and energy resolution. (tr-auth)

34932 Ge(Li)–Ge(Li) SUM COINCIDENCE: A BONUS FROM Ge(Li)–Ge(Li) MEGACHANNEL COINCIDENCE EXPERIMENTS. Giesler, G. C.; Kosanke, K. L.; Warner, R. A.; McHarris, Wm. C.; Kelly, W. H. (Michigan State Univ., East Lansing). Nucl. Instrum. Methods; 93: No. 2, 211-20(1971).

The sum-coincidence technique in Ge(Li)–Ge(Li) γ-ray spec-

troscopy is shown to be a viable and useful method for reducing Compton backgrounds and the resulting confusion they can cause. When used in conjunction with the digital readout from a two-dimensional "megachannel" coincidence experiment, many of the disadvantages and much of the tedium associated with the technique can be eliminated. It thus becomes a valuable, complementary technique to be used as needed in processing the data from a γ-γ coincidence experiment, requiring little or no additional experimental preparation. Examples of its use in a relatively simple (^{63}Zn) and a very complex (^{205}Bi) spectrum are presented. (auth)

34933 BETA- AND COMPTON-SUPPRESSION FOR THE INTERNAL CONVERSION STUDY. Ishii, M. (Japan Atomic Energy Research Inst., Tokai). Nucl. Instrum. Methods; 93: No. 2, 271-5(1971).

A method is described where internal conversion electrons are observed in coincidence with fluorescent x-rays subsequent to them. In this way it is possible to suppress almost all pulses produced in a detector by beta- and gamma-rays. An experimental measurement was performed on ^{124}Sb, and a beta- and Compton-spectrum was suppressed with a reduction factor of eighty by this method. (auth)

34934 ELECTRONIC DEVICE FOR MOESSBAUER SPECTROMETRY. Thenard, J.; Victor, G. (Centre d'Etudes Nucleaires de Saclay, Gif-sur-Yvette, France). Nucl. Instrum. Methods; 93: No. 2, 311-15(1971). (In French).

An electronic device for "Moessbauer" spectrometry is described. The goals of the research have been reliability, accuracy and ease of utilization. The device is composed of a calibrated generator which controls a vibrator by means of an electronic command system. The generator supplies symmetric or disymmetric sawtooth signals the periods of which are 80, 160 or 320 ms. For a given vibrator, the source and absorber motion speeds can be adjusted (from 0.1 to 4 cm/s) by varying the reference signal amplitude. Once this adjustment has been made for one speed, the calibration is correct for all others. The measurements which have been made on a ^{57}Fe spectrum with a velocity sweep of ±10 mm/s show that the widths between peak positions, when experimentally measured (the peaks being taken two by two), agree with theoretical results in a precision range of 0.01 mm/s. Finally, measurements performed at different temperatures ranging from 0 to 45°C show that the width drift between two spectral peaks is a linear function of the temperature ($\Delta W/\Delta T = 2 \times 10^{-4}$ per °C). (auth)

34935 LOW LEVEL Ge(Li) GAMMA-RAY SPECTROMETRY IN MARINE RADIOACTIVITY STUDIES. Lewis, S. R.; Shafrir, N. H. (Technion–Israel Inst. of Tech., Haifa). Nucl. Instrum. Methods; 93: No. 2, 317-32(1971).

A system has been designed, built, and put into continuous operation that is capable of unambiguous, accurate, qualitative and quantitative analysis of minute quantities of gamma-emitting radionuclides in complex mixtures. The desired results have been achieved without prohibitive expenditure. A large-volume (42 cm^3) Ge(Li) crystal serves as the main detector and is operated in anticoincidence with a 40 cm × 40 cm plastic scintillator assembly. The whole is enclosed in a cosmic-radiation shield of 10 cm thick lead walls. When operated in the anticoincidence mode, the background continuum is reduced to 0.3 cpm/keV at 100 keV and to less than 0.005 cpm/keV at 1000 keV for an average reduction of normal background of 99.5%. System resolution is 3.0 to 3.5 keV fwhm depending on gamma-energy. Sensitivity of the system permits detection of many radionuclides in environmental samples at levels below 0.02 pCi/g with no chemical separation prior to measurements. The accuracy of the counting is improved by the anticoincidence mode up to a factor 3 depending on the initial peak to background ratio. Results of illustrative measurements for ^{137}Cs content performed on several biota, sediment, and seawater samples are given. Total activities of biota samples ranged from 2.3 pCi to 48.5 pCi. Specific activities of ^{137}Cs ranged from 0.02 pCi/g to 0.15 pCi/g with statistical accuracies of 10 to 20%. Seawater measurements clearly showed a decrease in ^{137}Cs activity with increasing depth. (auth)

34936 SHAPE CALIBRATION AND PEAK-TO-TOTAL RATIO MEASUREMENTS OF A 5" x 6" NaI(Tl) SCINTILLATION DETECTOR. Ahmed, N.; Rahman, M. A.; Awal, M. A.; Khatun, S. (Atomic Energy Centre, Dacca, Pakistan). Nucl. Instrum. Methods; 93: No. 2, 381-3(1971).

A number of (p,γ) reactions have been used to obtain the single γ-ray spectra to obtain shape calibration curve and peak-to-total ratio for a 5" × 6" NaI(Tl) scintillation detector from 0.662 to 8.92 MeV of γ-ray energy. (auth)

High Energy Physics Instrumentation

Refer also to abstract 36431.

34937 (CERN-Trans–71-9) RELATIVISTIC INCREASE OF IONIZATION AND SENSITIVITY OF NUCLEAR EMULSIONS. Ermilova, V. K.; Kotenko, L. P.; Merzon, G. I. (Akademiya Nauk SSSR, Moscow. Institut Fiziki). Translated by R. Luther (CERN, Geneva, Switzerland), from Report No. 2, 26p. Dep. NTIS (U. S. Sales Only).

A quantitative explanation is given of the value found by experiment and the energy dependence of the track density of relativistic particles in a nuclear emulsion, based on the peculiarities of the ionization process for silver bromide and on the physico-chemical structure of emulsion. An understanding of these points is important for the identification of high-energy particles in nuclear emulsions, and also for an explanation of the activation mechanism of AgBr microcrystals. (tr-auth)

34938 (CONF-700623–(Vol.1)) PROCEEDINGS OF INTERNATIONAL CONFERENCE ON BUBBLE CHAMBER TECHNOLOGY, JUNE 10–12, 1970, ARGONNE NATIONAL LABORATORY. Derrick, M. (ed.) (Argonne National Lab., Ill.). 591p. Dep. NTIS.

Separate abstracts were prepared for 27 of the 28 papers in this volume. The remaining paper has already appeared as NSA 25: 8549. (R.W.R.)

For abstracts of individual papers see: 34939–34965.

34939 (CONF-700623–(Vol.1), pp 5-41) OPTIMIZATION OF BUBBLE CHAMBER DESIGN PARAMETERS FOR STRONG INTERACTION EXPERIMENTS. Fisher, C. M. (Rutherford High Energy Lab., Chilton (England)).

From International conference on bubble chamber technology; Argonne, Ill. (10 Jun 1970).

In Proceedings of international conference on bubble chamber technology.

The relation between the chamber parameters and the physics potential of the bubble chamber is discussed. The relation of errors in measurements of momenta and angles to the dimensions, field, and spatial precision of the chamber is considered. (R.W.R.)

34940 (CONF-700623–(Vol.1), pp 42-55) STRONG INTERACTION PHYSICS IN THE NAL BUBBLE CHAMBER. Lach, J. (National Accelerator Lab., [Batavia, Ill.]).

From International conference on bubble chamber technology; Argonne, Ill. (10 Jun 1970).

In Proceedings of international conference on bubble chamber technology.

Those properties that make a large bubble chamber a distinctive and unique instrument for the study of strong interactions are enumerated. Plots of the optimum track length needed to minimize angle errors versus the momentum of the particle are given for several values of the setting error. The possibility of using proportional wire chambers in order to define the beam angle with sufficient precision is presented. (R.W.R.)

34941 (CONF-700623–(Vol.1), pp 56-96) NEUTRINO PHYSICS WITH LARGE H_2 CHAMBERS. Stevenson, M. L. (California Univ., Berkeley. Lawrence Radiation Lab.).

From International conference on bubble chamber technology; Argonne, Ill. (10 Jun 1970).

In Proceedings of international conference on bubble chamber technology.

For high-energy neutrinos a H_2 bubble chamber as small as the one proposed for NAL (30 m^3) is marginal in its usefulness when track-sensitive targets (TST) are placed inside. (One needs ≈100 m^3.) The need to surround the TST with two conversion lengths of $Ne-H_2$ mixture makes the effective volume more than 10 times smaller than the full chamber volume. However, if provisions are made to place a quantometer between the downstream wall of the chamber and the superconducting coils, the π^0-photons can be detected externally with high efficiency (100%) and high precision ($\Delta E_\gamma/E_\gamma \approx 3\%$ for a 10 GeV photon). Included in this hybrid system would be a capability for identifying which of the outgoing charged particles is a muon and in some events for identifying which particle is the nucleon. (auth)

34942 (CONF-700623–(Vol.1), pp 97-116) PROPORTIONAL QUANTAMETER FOR THE 15-FOOT BUBBLE CHAMBER. Yount, D. (Hawaii Univ., Honolulu).

From International conference on bubble chamber technology; Argonne, Ill. (10 Jun 1970).

In Proceedings of international conference on bubble chamber technology.

The performance of a proportional quantameter to detect and

XUM

measure the energy of the neutral pions produced by neutrino interactions in the 15-foot bubble chamber is evaluated. The total energy is determined from the sum of a number of wire outputs, while spatial resolution is obtained by reading out other wire planes individually. (auth)

34943 (CONF-700623-(Vol.1), pp 123-35) NEUTRINO PHYSICS IN HEAVY LIQUID CHAMBERS. Perkins, D. (Oxford Univ. (England)).

From International conference on bubble chamber technology; Argonne, Ill. (10 Jun 1970).

In Proceedings of international conference on bubble chamber technology.

Heavy-liquid chambers are valuable in neutrino experiments when the work is of an exploratory nature or depends critically on good ν detection or the ability to recognize high-energy electrons or muons against a large background. The program for Gargamelle in 1971 is set forth: measurements are to be made on total ν and $\bar{\nu}$ cross sections at high energy, inelastic structure factors, diagonal interactions, intermediate boson production, and neutral currents. A table of expected event rates is given. (R.W.R.)

34944 (CONF-700623-(Vol.1), pp 136-44) PHYSICS PLANS FOR GARGAMELLE. Musset, P. (Ecole Polytechnique, Paris (France)).

From International conference on bubble chamber technology; Argonne, Ill. (10 Jun 1970).

In Proceedings of international conference on bubble chamber technology.

The properties of the bubble chamber Gargamelle are briefly reviewed, and early proposals for experiments are reported. (R.W.R.)

34945 (CONF-700623-(Vol.1), pp 196-255) ROUND TABLE ON EXPERIENCE WITH EXISTING CHAMBERS. Fields, T. H. (Argonne National Lab., Ill.).

From International conference on bubble chamber technology; Argonne, Ill. (10 Jun 1970).

In Proceedings of international conference on bubble chamber technology.

After introductory remarks by the moderator, six speakers recounted their experience with existing bubble chambers. These included chambers at Argonne National Laboratory, Brookhaven National Laboratory, CERN, Rutherford High Energy Laboratory, and the Stanford Linear Accelerator Center. (R.W.R.)

34946 (CONF-700623-(Vol.1), pp 256-73) USE OF A COMPUTER ON THE CERN 2M LIQUID HYDROGEN BUBBLE CHAMBER. Schmitt, M. (European Organization for Nuclear Research, Geneva (Switzerland)).

From International conference on bubble chamber technology; Argonne, Ill. (10 Jun 1970).

In Proceedings of international conference on bubble chamber technology.

The use of a PDP9 computer at the CERN 2-meter hydrogen bubble chamber is reviewed. Although first used merely for monitoring and alarm functions of the principal beam and chamber parameters, it was increasingly integrated into the chamber control system and now regulates the expansions of the chamber. The systematic recording of more objective information affords better preventive maintenance; i.e., it helps prevent accidents. By increasing the time between failures, it improved efficiency and produced a higher percentage of good-quality pictures. (R.W.R.)

34947 (CONF-700623-(Vol.1), pp 275-302) OPTICAL CONSTANTS FOR THE ANL 12-FOOT BUBBLE CHAMBER. Yuta, H. (Argonne National Lab., Ill.).

From International conference on bubble chamber technology; Argonne, Ill. (10 Jun 1970).

In Proceedings of international conference on bubble chamber technology.

The optics system for the 12-foot bubble chamber includes four wide-field angle lenses viewing the chamber through fish-eye windows. Because these lenses have large distortion, ordinary pinhole optics cannot be used. Four kinds of constants—lens constants, window constants, camera constants, and BC fiducials—are required to reconstruct space points and calculate the corresponding coordinates in such a way that conventional pinhole-optics methods can then be used. This report explains the meaning of these constants and describes briefly the procedures for obtaining them. The present constants are tabulated, but it is necessary for users to procure the latest set. (R.W.R.)

34948 (CONF-700623-(Vol.1), pp 303-11) TVGP FOR 12 FOOT CHAMBER. Campbell, J. (Argonne National Lab., Ill.).

From International conference on bubble chamber technology; Argonne, Ill. (10 Jun 1970).

In Proceedings of international conference on bubble chamber technology.

The changes made to TVGP, a computer program for analysis of data from conventional bubble chambers, in order to reconstruct points and tracks from film from the ANL 12-foot bubble chamber are described. Results are presented to show quantitatively the current state of the optical parameters needed for reconstruction. Only those modifications necessary to treat the new optical system correctly are made. (R.W.R.)

34949 (CONF-700623-(Vol.1), pp 312-24) TVGP FOR TRACK SENSITIVE TARGETS. Badewitz, R. C.; Christian, R. S. (Purdue Univ., Lafayette, Ind.).

From International conference on bubble chamber technology; Argonne, Ill. (10 Jun 1970).

In Proceedings of international conference on bubble chamber technology.

One method for reconstruction of tracks from a TST Bubble Chamber is presented. Changes necessary for a TVGP-type reconstruction program are indicated, and some preliminary results are discussed. (auth)

34950 (CONF-700623-(Vol.1), pp 325-33) MINIMIZING ANGLE ERRORS DUE TO MULTIPLE SCATTERING. Plano, Richard J.; Handler, Thomas (Rutgers-The State Univ., New Brunswick, N. J.).

From International conference on bubble chamber technology; Argonne, Ill. (10 Jun 1970).

In Proceedings of international conference on bubble chamber technology.

The usual assumption of equal errors at all points along a track is invalid for multiple scattering. It is found that the use of the full error matrix is important in reducing azimuth-angle errors for those tracks in which multiple scattering dominates over measurement errors. It is possible to reduce the angle errors by more than a factor of three when fitting peripheral protons that may be lengthy though slow in interactions up to the highest energies. In addition, prior knowledge of the curvature of a track can be used to reduce the angle error by a factor of up to $\sqrt{13}$ when the measurement error is dominant. (R.W.R.)

34951 (CONF-700623-(Vol.1), pp 334-44) PROJECTOR FOR GARGAMELLE'S PICTURES. Fiorini, E.; Negri, P. (Milan Univ. (Italy). Istituto di Fisica. Istituto Nazionale di Fisica Nucleare, Milan (Italy)).

From International conference on bubble chamber technology; Argonne, Ill. (10 Jun 1970).

In Proceedings of international conference on bubble chamber technology.

A projector for pictures taken with the heavy-liquid bubble chamber Gargamelle is described. An image inverter and movable and interchangeable objective lenses are incorporated into the design. (R.W.R.)

34952 (CONF-700623-(Vol.1), pp 346-75) RAPID CYCLING BUBBLE CHAMBER PROGRAM AT SLAC. Rogers, A. (Stanford Linear Accelerator Center, Calif.).

From International conference on bubble chamber technology; Argonne, Ill. (10 Jun 1970).

In Proceedings of international conference on bubble chamber technology.

Two important requirements for improving the performance of the bubble chamber are triggering and rapid cycling. The latter can be either of the conventional type, but powered by an electromagnetic shaker, or produced by sound pressure waves and powered by piezoelectric crystals. Work on both of these methods at SLAC is reviewed. The report concludes with some predictions for future developments. (R.W.R.)

34953 (CONF-700623-(Vol.1), pp 376-89) ULTRASONIC BUBBLE CHAMBER DEVELOPMENT AT CERN. Brown, R. C. A.; Harigel, G.; Hilke, H. J.; Jarman, P. D. (European Organization for Nuclear Research, Geneva (Switzerland)).

From International conference on bubble chamber technology; Argonne, Ill. (10 Jun 1970).

In Proceedings of international conference on bubble chamber technology.

Development work on ultrasonic bubble chambers using high frequencies and a plane radiation field are reviewed; results are given for helium, hydrogen, and freon 13 B1. The construction of a helium ultrasonic bubble chamber with high bubble densities and short recompression times is shown to be possible. To get high repetition rates the heat losses in the crystals must be reduced considerably. The possibility of nucleating sub-visible

XUM

bubbles on ionizing particles, sustaining them with a low-amplitude sound field, and then growing them to visible size with a large-amplitude field after an interesting particle has been identified is being investigated. (R.W.R.)

34954 (CONF-700623–(Vol.1), pp 390-407) RESULTS ACHIEVED WITH A RAPID-CYCLING HYDROGEN BUBBLE CHAMBER. Delcros, Philippe (Ecole Polytechnique, Paris (France)).

From International conference on bubble chamber technology; Argonne, Ill. (10 Jun 1970).

In Proceedings of international conference on bubble chamber technology.

An apparatus, built in 1967, for the purpose of investigating the possibility of increasing the repetition rate of a hydrogen bubble chamber, is described. The study was concerned with the local behavior of the fluid as a function of the cycling rate, the effect of differences of temperatures in the interior of the chamber, and the search for the thermodynamical equilibrium conditions of the chamber; from these results the conditions for fast cycling were determined. It was possible to sensitize the hydrogen up to a frequency of 45 pulses per second, but the distortion was rather large. A better temperature regulation should reduce this defect. The mechanical system seemed quite satisfactory and suitable for an operational chamber. (R.W.R.)

34955 (CONF-700623–(Vol.1), pp 408-17) CHARACTERISTICS OF A STANDING WAVE BUBBLE OR CLOUD CHAMBER. Shoemaker, V.; Walker, R. J. (Argonne National Lab., Ill.).

From International conference on bubble chamber technology; Argonne, Ill. (10 Jun 1970).

In Proceedings of international conference on bubble chamber technology.

The properties of a rapid-cycling bubble chamber were studied by taking advantage of the nodes and antinodes in a standing compressional wave. If the piston is placed at a pressure node in the standing wave, there should be no boiling at the piston, and the liquid should exert zero forces on the piston. A few preliminary results are given for freon 115. A rapid-cycling freon 115 cloud chamber was also investigated. In this case the piston is put at a pressure antinode and a velocity node; thus, a very small stroke produces a large pressure wave. The standing wave worked as expected; the limiting feature was the streaming losses in the center of the chamber. Freon is a poor cloud-chamber medium because of the low value of γ (ratio of specific heats); the pressure wave attained was insufficient. (R.W.R.)

34956 (CONF-700623–(Vol.1), pp 418-23) WISCONSIN RAPID CYCLING BUBBLE CHAMBER. Sviatslavsky, I.; Walker, W. D.; Binkley, M. (Wisconsin Univ., Madison).

From International conference on bubble chamber technology; Argonne, Ill. (10 Jun 1970).

In Proceedings of international conference on bubble chamber technology.

A brief description is given of the Wisconsin rapid-cycling bubble chamber, anticipated to work at 30 to 60 Hz and still produce good pictures. A fast expansion stroke will promote cleanliness (minimal irreversible work) and small size of bubbles. The difficulty with optics consisting of a simple mirror is that reflections of tracks are also visible. This situation can be alleviated somewhat by aluminizing both front and back surfaces. If the front surface is aluminized in strips and the back, totally, the reflected tracks will appear as a sequence of disconnected segments. (R.W.R.)

34957 (CONF-700623–(Vol.1), pp 424-48) INFLUENCE OF PARASITIC BOILING AND EXPANSION SPEED ON THE DYNAMIC PRESSURE IN A BUBBLE CHAMBER. Harigel, G. (European Organization for Nuclear Research, Geneva (Switzerland)); Horlitz, G.; Wolff, S. (Deutsches Elektronen-Synchrotron, Hamburg (West Germany)).

From International conference on bubble chamber technology; Argonne, Ill. (10 Jun 1970).

In Proceedings of international conference on bubble chamber technology.

The pressure reduction in bubble chambers is limited by parasitic boiling. A shift of the possible pressure minimum p_{min} to lower values can be obtained by increasing the expansion speed $\dot{\epsilon}$. The effect of this increase is partially cancelled by an increase of the instantaneous rate of evaporation with $\dot{\epsilon}$, especially in the low-pressure region. For large bubble chambers a compromise has to be found, which takes into account not only the gain in pressure drop but also the effort expended to achieve this gain, especially increasing costs and mechanical difficulties of high-speed expansion systems. A detectable delay of the order of milliseconds between the time at which the pressure passes the vapor pressure and the time when parasitic boiling starts was measured at 25 K. A fast-cycling bubble chamber that could complete one total expansion cycle within this delay time would certainly be a very interesting instrument. (auth)

34958 (CONF-700623–(Vol.1), pp 449-58) BUBBLE NUCLEATION ON SURFACES IMMERSED IN CRYOGENIC FLUIDS. Bailey, C. A.; Bland, M. E.; Davey, G. (Oxford Univ. (England)).

From International conference on bubble chamber technology; Argonne, Ill. (10 Jun 1970).

In Proceedings of international conference on bubble chamber technology.

Bubble nucleation from artificially prepared cavities in metal surfaces was studied in saturated liquid nitrogen and saturated liquid hydrogen. After nucleation was initiated on a copper or brass surface that had not been previously heated, the nucleating area spread very rapidly. Spreading appears to be caused by a vapor spreading mechanism in which a bubble from one site spreads over to another and activates it. If the superheat was created by a sudden decrease in the liquid pressure, nucleation did not occur from any unheated surfaces. If the surface was heated during the expansion pulse, boiling could be induced but in all cases the heat flux necessary to initiate nucleation was only very slightly below that which would have caused boiling without the pressure drop. (R.W.R.)

34959 (CONF-700623–(Vol.1), pp 460-76) GARGAMELLE TECHNICAL ASPECTS. Queru, P. (European Organization for Nuclear Research, Geneva (Switzerland)).

From International conference on bubble chamber technology; Argonne, Ill. (10 Jun 1970).

In Proceedings of international conference on bubble chamber technology.

The principal technical problems involved in the construction of the heavy-liquid bubble chamber Gargamelle are reviewed. Components included in the discussion are the magnet, the chamber body, the membranes, and the expansion system. (R.W.R.)

34960 (CONF-700623–(Vol.1), pp 477-510) TRACK SENSITIVE H_2 AND D_2 TARGETS IN NEON–HYDROGEN MIXTURES. Leutz, H. (European Organization for Nuclear Research, Geneva (Switzerland)).

From International conference on bubble chamber technology; Argonne, Ill. (10 Jun 1970).

In Proceedings of international conference on bubble chamber technology.

After a general introduction to the advantages of the composite chamber, the design features for the Big European Bubble Chamber (BEBC) are listed; both liquids in this chamber are to be sensitive to track formation. Experiments with the composite-chamber technique at the DESY 85-cm chamber and the RHEL 1.5-m chamber are described. Calculations of the properties of "composite BEBC" are discussed. A brief report on a target run with the 1-m BEBC model chamber ends the paper. (R.W.R.)

34961 (CONF-700623–(Vol.1), pp 511-31) BNL WORK ON NEON/H_2 TARGETS. Huson, F. R.; Cnops, A. M.; DiLullo, C.; Koehler, J. T.; Louttit, R. I.; Prodell, A. G.; Worwetz, H. A. (Brookhaven National Lab., Upton, N. Y.).

From International conference on bubble chamber technology; Argonne, Ill. (10 Jun 1970).

In Proceedings of international conference on bubble chamber technology.

The measurement of electron–positron pairs in heavy liquids and analysis of the results obtained are briefly described; it is apparent that π^0's can be measured quite well in heavy liquid. The design and testing of a track-sensitive target (TST) is discussed. Parameters of a TST under construction for the 80-inch BNL bubble chamber are given. (R.W.R.)

34962 (CONF-700623–(Vol.1), pp 532-42) NEON–HYDROGEN MIXTURES IN LARGE CRYOGENIC BUBBLE CHAMBERS. Gueseweil, D. (European Organization for Nuclear Research, Geneva (Switzerland)).

From International conference on bubble chamber technology; Argonne, Ill. (10 Jun 1970).

In Proceedings of international conference on bubble chamber technology.

Density and sound-velocity data and their consequences for the use of neon–hydrogen mixtures in large bubble chambers are discussed. The necessity of uniform mixtures in large bubble chambers and the means of accomplishing this are described. Good uniformity of dynamic pressure requires that the expansion duration should be at least 15 times greater than the travel time of pressure pulses across the chamber. The mechanical properties and working conditions of the different liquids that might be used in BEBC are tabulated. (R.W.R.)

XUM

34963 (CONF-700623-(Vol.1), pp 543-54) REFRACTIVE INDICES OF NEON AND NEON-HYDROGEN MIXTURES. Newport, R. W. (Rutherford High Energy Lab., Chilton (England)).
From International conference on bubble chamber technology; Argonne, Ill. (10 Jun 1970).
In Proceedings of international conference on bubble chamber technology.

Measurements of the refractive index of neon in the temperature range 24.95 to 32.50°K are reported, as well as some provisional results for neon-hydrogen mixtures for neon concentrations up to 22 mole%. The results indicate that there is likely to be little difference in the refractive indices of the mixtures for temperatures close to 20°K. This temperature is near the minimum operating temperature for mixtures in the range 50 to 85 mole% neon, and thus at this temperature a measurement of the refractive index is of no value for analysis of the mixture composition. (R.W.R.)

34964 (CONF-700623-(Vol.1), pp 555-66) AN IMPROVED BUBBLE CHAMBER DETECTION TECHNIQUE FOR GAMMA RAYS IN THE MOMENTUM REGION BELOW 1 GeV/c. Bierman, E.; Goshaw, A.; Sager, D. (Princeton Univ., N. J.); Colleraine, A. P. (Maryland Univ., College Park); Koehler, John; Prodell, A. (Brookhaven National Lab., Upton, N. Y.); Nauenberg, Uriel (Colorado Univ., Boulder).
From International conference on bubble chamber technology; Argonne, Ill. (10 Jun 1970).
In Proceedings of international conference on bubble chamber technology.

A technique that detects photons with momenta less than 1 GeV/c with reasonable efficiency and measures their momenta and direction with good resolution is described. The spatial and momentum resolution of the photons is shown. (R.W.R.)

34965 (CONF-700623-(Vol.1), pp 567-80) FOUR-INCH HYDROGEN TARGET FOR THE 40-INCH SLAC BUBBLE CHAMBER. Petersen, Henning O.; Skarpaas, Knut; Watt, Robert D. (Stanford Linear Accelerator Center, Calif.).
From International conference on bubble chamber technology; Argonne, Ill. (10 Jun 1970).
In Proceedings of international conference on bubble chamber technology.

The design and development of the four-inch track-sensitive target for the 40-inch SLAC bubble chamber are discussed. Graphs of the dynamic response of the target under different chamber conditions are given. (R.W.R.)

34966 (CONF-700623-(Vol.2)) PROCEEDINGS OF INTERNATIONAL CONFERENCE ON BUBBLE CHAMBER TECHNOLOGY, JUNE 10-12, 1970, ARGONNE NATIONAL LABORATORY. Derrick, M. (ed.) (Argonne National Lab., Ill.). 641p. Dep. NTIS.

Separate abstracts were prepared for 37 of the 38 papers in this volume. The remaining one has already appeared as NSA 24: 48319. (R.W.R.)

For abstracts of individual papers see: 34967-35003.

34967 (CONF-700623-(Vol.2), pp 582-92) NEUTRAL PARTICLE TAGGING FACILITY FOR THE ANL 30" BUBBLE CHAMBER. Gunderson, B.; Benvenuti, A.; Brush, A.; Erwin, A.; Mistretta, C.; Thompson, M. A.; Walker, W. D. (Wisconsin Univ., Madison).
From International conference on bubble chamber technology; Argonne, Ill. (10 Jun 1970).
In Proceedings of international conference on bubble chamber technology.

A counter-spark-chamber system was used to trigger the optics of the ANL 30" bubble chamber and to tag events with forward neutral particles during the course of a conventional bubble-chamber exposure. Trigger rates and general characteristics of the system are discussed. (auth)

34968 (CONF-700623-(Vol.2), pp 593-605) POSSIBLE COUNTER ARRAY FOR TRIGGERING A BUBBLE CHAMBER. Kalbfleisch, G. R. (Brookhaven National Lab., Upton, N. Y.).
From International conference on bubble chamber technology; Argonne, Ill. (10 Jun 1970).
In Proceedings of international conference on bubble chamber technology.

A method for observing multipronged events in a bubble chamber by means of arrays of scintillation counters is proposed. Five counters are arrayed as five faces of a cube. Preliminary results indicate that scintillation counters work at liquid-hydrogen temperatures, and the scheme seems feasible. (R.W.R.)

34969 (CONF-700623-(Vol.2), pp 606-16) COUNTER CONTROL OF BUBBLE CHAMBER PHOTOGRAPHY. Pless, I. A. (Massachusetts Inst. of Tech., Cambridge).
From International conference on bubble chamber technology; Argonne, Ill. (10 Jun 1970).
In Proceedings of international conference on bubble chamber technology.

A counter coincidence system is described for controlling the taking of bubble-chamber pictures. Counters are located in front of and behind the bubble chamber. If a particle is detected in the entrance counter and not in the exit counter, an interaction is presumed to have occurred and a photograph is taken. (R.W.R.)

34970 (CONF-700623-(Vol.2), pp 617-28) DESCRIPTION OF A SCINTILLATION COUNTER DATA ACQUISITION SYSTEM FOR USE WITH THE SLAC 40" HYDROGEN BUBBLE CHAMBER. Smart, W. M. (Stanford Linear Accelerator Center, Calif.).
From International conference on bubble chamber technology; Argonne, Ill. (10 Jun 1970).
In Proceedings of international conference on bubble chamber technology.

A data acquisition system for the SLAC 40" hydrogen bubble chamber (HBC), consisting of time-of-flight scintillation counters, associated electronics, and a PDP-9 computer, is discussed. The system is designed to give optimum timing resolution subject to the limitations of the HBC design, but it may also be used to trigger the HBC camera for only a certain class of events. A general description of the system is given, including a discussion of the major factors affecting the timing resolution and the expected results for use of the system in a K_2^0 beam. (R.W.R.)

34971 (CONF-700623-(Vol.2), pp 629-38) STUDY OF DIFFRACTIVE N* PRODUCTION IN A TRIGGERED-BUBBLE-CHAMBER EXPERIMENT. Dzierba, Alex R. (California Inst. of Tech., Pasadena).
From International conference on bubble chamber technology; Argonne, Ill. (10 Jun 1970).
In Proceedings of international conference on bubble chamber technology.

A proposed experiment on diffractive N* production with the SLAC 40" hydrogen bubble chamber operating in a triggered mode is described. The fast forward particle will be detected by using SAC wire chambers. If this particle has momentum such that the missing mass is above the threshold for pion production, the bubble chamber will be photographed. (R.W.R.)

34972 (CONF-700623-(Vol.2), pp 640-6) HYPERON BUBBLE CHAMBER HYBUC. Doble, N.; Gottstein, K.; Hahn, G.; Herynek, I.; Manz, A.; Matt, W.; Scheuing, V.; Settles, R. (Max-Planck-Institut fuer Physik, Munich (West Germany)).
From International conference on bubble chamber technology; Argonne, Ill. (10 Jun 1970).
In Proceedings of international conference on bubble chamber technology.

A general description of the hyperon bubble chamber HYBUC, to be built at CERN, is given. An unusual feature is that the beam will enter the chamber parallel to the optic and magnetic-field axes; this arrangement obviates the problems of getting the beam into the chamber through the high field and is advantageous for the physics of hyperon-magnetic-moment measurements. (R.W.R.)

34973 (CONF-700623-(Vol.2), pp 647-74) MIRABELLE. Prugne, P. (Commissariat a l'Energie Atomique, Saclay (France). Centre d'Etudes Nucleaires).
From International conference on bubble chamber technology; Argonne, Ill. (10 Jun 1970).
In Proceedings of international conference on bubble chamber technology.

A brief description of the bubble chamber Mirabelle and its construction is given. Nineteen full-page photographs and drawings are included. (R.W.R.)

34974 (CONF-700623-(Vol.2), pp 675-95) STATUS OF THE 12-FOOT HYDROGEN BUBBLE CHAMBER. Pewitt, E. G. (Argonne National Lab., Ill.).
From International conference on bubble chamber technology; Argonne, Ill. (10 Jun 1970).
In Proceedings of international conference on bubble chamber technology.

A brief history and status report for the ANL 12-foot hydrogen bubble chamber is given. Photographs of the major components of the system are shown; these include the magnet, chamber, expander, and optics. (R.W.R.)

34975 (CONF-700623-(Vol.2), pp 696-702) NAL PLANS. Fowler, W. (National Accelerator Lab., Batavia, Ill.).
From International conference on bubble chamber technology; Argonne, Ill. (10 Jun 1970).
In Proceedings of international conference on bubble chamber technology.

XUM

Present concepts in the design of the proposed NAL bubble chamber are reviewed. (R.W.R.)

34976 (CONF-700623-(Vol.2), pp 703-13) STATUS REPORT OF BEBC. Florent, R. (European Organization for Nuclear Research, Geneva (Switzerland)).

From International conference on bubble chamber technology; Argonne, Ill. (10 Jun 1970).

In Proceedings of international conference on bubble chamber technology.

A general description of the BEBC is given. The main parameters of the BEBC are tabulated. (R.W.R.)

34977 (CONF-700623-(Vol.2), pp 714-34) 1.5 METRE DIAMETER HIGH FIELD HYDROGEN CHAMBER. Thomas, D. B. (Rutherford High Energy Lab., Chilton (England)).

From International conference on bubble chamber technology; Argonne, Ill. (10 Jun 1970).

In Proceedings of international conference on bubble chamber technology.

The proposed 1.5-meter High Field Bubble Chamber (HFBC) at Rutherford High Energy Laboratory is described. Technical specifications are given for the HFBC, which uses liquid hydrogen and superconducting coils. Notable features included in the report are the 70-kG magnet, the four-channel fisheye optical system at the base of the chamber, the plastic expansion bellows and piston, the resonant expansion system (capable of operating at up to 10 cycles per second), and the provision for use of counters with the bubble chamber. (R.W.R.)

34978 (CONF-700623-(Vol.2), pp 735-49) 7-FOOT BUBBLE CHAMBER CONVERSION: 11-FOOT NEUTRINO AND TRACK-SENSITIVE TARGET FACILITY. Prodell, A. G. (Brookhaven National Lab., Upton, N. Y.).

From International conference on bubble chamber technology; Argonne, Ill. (10 Jun 1970).

In Proceedings of international conference on bubble chamber technology.

Plans for the conversion of the BNL 7-foot bubble chamber to one of 11 feet in diameter are described. Among the modifications involved is provision for track-sensitive targets. (R.W.R.)

34979 (CONF-700623-(Vol.2), pp 751-64) THE BIG HYDROGEN BUBBLE CHAMBER MIRABELLE CRYOGENICS EXPANSION: TESTS AND EXPERIMENTS. Lottin, J. C. (Commissariat a l'Energie Atomique, Saclay (France). Centre d'Etudes Nucleaires).

From International conference on bubble chamber technology; Argonne, Ill. (10 Jun 1970).

In Proceedings of international conference on bubble chamber technology.

The cryogenics system of the 12,000-liter, liquid-hydrogen bubble chamber Mirabelle is described; mounting, cooling loops, and refrigeration system are included. The expansion system is next discussed. The results of tests made with Mirabelle and a full-scale model are described. Although some minor problems still exist, Mirabelle was pronounced ready to start physics experiments. (R.W.R.)

34980 (CONF-700623-(Vol.2), pp 765-73) RESULTS FROM ANL 12 FT. CHAMBER. Tamosaitis, Anthony (Argonne National Lab., Ill.).

From International conference on bubble chamber technology; Argonne, Ill. (10 Jun 1970).

In Proceedings of international conference on bubble chamber technology.

Operational aspects rather than experimental results concerning the ANL 12-ft bubble chamber are described. Several of the problems encountered in the construction and testing of the chamber are reviewed. The chamber heat load is discussed. (R.W.R.)

34981 (CONF-700623-(Vol.2), pp 774-89) RESULTS FROM THE BNL 7-FOOT CHAMBER. Fowler, W. (National Accelerator Lab., Batavia, Ill.).

From International conference on bubble chamber technology; Argonne, Ill. (10 Jun 1970).

In Proceedings of international conference on bubble chamber technology.

The development of the Brookhaven 7-ft bubble chamber is discussed. Information is given on performance during track sensitivity and on the heat generated per pulse. Results on the quality of the tracks obtained are presented. The expansion system was redesigned to cut hydrogen loss. (R.W.R.)

34982 (CONF-700623-(Vol.2), pp 790-812) EXPERIMENTAL RESULTS WITH THE 1 M MODEL CHAMBER AT CERN . A. THERMODYNAMICS. Dauvergne, J. P.; Erdt, W.; Guesewell, D.; Schmid, J. (European Organization for Nuclear Research, Geneva (Switzerland)).

From International conference on bubble chamber technology; Argonne, Ill. (10 Jun 1970).

In Proceedings of international conference on bubble chamber technology.

Thermodynamics experiments with a 1-m test bubble chamber constructed as a model for the 3.7-m BEBC are reported. The experiments concern the following points: optimum cooling of the piston region; influence of reinforced piston cooling on spurious boiling and dynamic heat load; dependence of spurious boiling on the expansion-cycle length; location of the dynamic heat sources; and pressure distribution in the chamber. (R.W.R.)

34983 (CONF-700623-(Vol.2), pp 813-23) EXPERIMENTAL RESULTS WITH THE 1 M MODEL CHAMBER. B. OPTICS. Harigel, G.; Pouyat, F.; Reinhard, H. P. (European Organization for Nuclear Research, Geneva (Switzerland)).

From International conference on bubble chamber technology; Argonne, Ill. (10 Jun 1970).

In Proceedings of international conference on bubble chamber technology.

The optics problems investigated with the 1-m model of BEBC are discussed; these concern various technical problems (such as those concerning the fisheyes or the sticking of Scotchlite), track distortion due to thermal turbulence, and bright-field photography of tracks near the diffraction limit. (R.W.R.)

34984 (CONF-700623-(Vol.2), pp 824-35) RESONANT EXPANSION SYSTEM FOR THE PROPOSED HIGH FIELD BUBBLE CHAMBER. Swain, J. H. (Rutherford High Energy Lab., Chilton (England)).

From International conference on bubble chamber technology; Argonne, Ill. (10 Jun 1970).

In Proceedings of international conference on bubble chamber technology.

After a general introduction to the idea of a resonant expansion system for bubble chambers, the specific mechanism used in the proposed High Field Bubble Chamber (HFBC) at Rutherford High Energy Laboratory is described. The method of operation and the means of control are discussed. (R.W.R.)

34985 (CONF-700623-(Vol.2), pp 836-48) THE BEBC EXPANSION PISTON. Linser, G. (European Organization for Nuclear Research, Geneva (Switzerland)).

From International conference on bubble chamber technology; Argonne, Ill. (10 Jun 1970).

In Proceedings of international conference on bubble chamber technology.

Some of the design criteria for the expansion piston of the BEBC are discussed. Among the most important conditions that determine the design of the piston are the presence of eddy currents and the stiffness and weight of the piston to insure structural rigidity. (R.W.R.)

34986 (CONF-700623-(Vol.2), pp 849-62) DEVELOPMENT OF FIBREGLASS REINFORCED EPOXY RESIN BELLOWS. Diplock, B. R. (Rutherford High Energy Lab., Chilton (England)).

From International conference on bubble chamber technology; Argonne, Ill. (10 Jun 1970).

In Proceedings of international conference on bubble chamber technology.

The development program for the fiber-glass-reinforced epoxy-resin bellows for the High Field Bubble Chamber is described. Tests on the basic material are reviewed. The design, manufacture, and fatigue testing of the bellows are discussed. (R.W.R.)

34987 (CONF-700623-(Vol.2), pp 863-72) BEHAVIOUR OF TRANSDUCERS AND GAUGES IN HIGH MAGNETIC FIELDS AND AT LOW TEMPERATURES. Rau, G. (European Organization for Nuclear Research, Geneva (Switzerland)).

From International conference on bubble chamber technology; Argonne, Ill. (10 Jun 1970).

In Proceedings of international conference on bubble chamber technology.

The vacuum gages and pressure transducers that will be used in the BEBC were tested in high magnetic fields and at low temperatures. Penning gages are not influenced by low temperatures but show pronounced magnetic-field effects. Magnetic fields up to 40 kG do not adversely affect the pressure measurements with Pirani gages, but every heat loss other than by the thermal conductivity of the residual gas simulates a higher pressure. The dynamic-pressure transducers are not influenced by magnetic fields or temperature changes, but magnetic effects on the semiconductor strain gages used for determining the static pressure of the chamber must be taken into account. (R.W.R.)

XUM

34988 (CONF-700623–(Vol.2), pp 873-92) BEBC EXPANSION SERVO-SYSTEM. Bachy, G. (European Organization for Nuclear Research, Geneva (Switzerland)).

From International conference on bubble chamber technology; Argonne, Ill. (10 Jun 1970).

In Proceedings of international conference on bubble chamber technology.

The criteria for the selection of the BEBC expansion system and the solutions used to overcome the various problems encountered are considered. After a general description of the system and its operation, the main servo valve is dealt with in some detail: the frequency response of the main spool, tolerances of the spool valve, lateral forces impressed, and the expected performance are covered. The actuator, power consumption of the servo system, and problems due to the magnetic field are described. Information on the expected performance of the servo system concludes the report. (R.W.R.)

34989 (CONF-700623–(Vol.2), pp 893-900) BUBBLE DENSITY IN LIQUID HELIUM. Moffatt, J.; Peel, T. D.; Roaf, D. (Oxford Univ. (England). Nuclear Physics Lab.).

From International conference on bubble chamber technology; Argonne, Ill. (10 Jun 1970).

In Proceedings of international conference on bubble chamber technology.

The tracks of 2 GeV/c pions in liquid helium were used to investigate the variation of bubble density along the tracks with the thermodynamic state of the liquid helium at the time the particle beam passed through it. It was found that, within experimental error, the bubble density in the temperature range 3.0 to 3.5°K depends only on the "underpressure" $p_s - p$, where p is the operating pressure and p_s is the saturation vapor pressure at the operating temperature. (R.W.R.)

34990 (CONF-700623–(Vol.2), pp 902-14) THE WIDE ANGLE LENS FOR BEBC. Reinhard, H. P. (European Organization for Nuclear Research, Geneva (Switzerland)).

From International conference on bubble chamber technology; Argonne, Ill. (10 Jun 1970).

In Proceedings of international conference on bubble chamber technology.

The specifications, design, performance, and calibration of the wide-angle lens for BEBC are briefly described. (R.W.R.)

34991 (CONF-700623–(Vol.2), pp 915-42) DEVELOPMENT AND PERFORMANCE OF THE ANL 140° CAMERA LENS. Welford, W. T. (Imperial Coll. of Science and Tech., London (England)).

From International conference on bubble chamber technology; Argonne, Ill. (10 Jun 1970).

In Proceedings of international conference on bubble chamber technology.

The general principles leading to the design specifications for the ANL 140° camera lens are listed. After some comments on the final design, the aberrational performance of the manufactured lenses and the distortion and contrast are discussed. The construction of the exposure-equalizing mask is described, and the questions of choosing the relative aperture and optimum focal setting are treated. (R.W.R.)

34992 (CONF-700623–(Vol.2), pp 943-58) OPTICAL SYSTEM MIRABELLE. Comby, G.; Derre, J. (Commissariat a l'Energie Atomique, Saclay (France). Centre d'Etudes Nucleaires).

From International conference on bubble chamber technology; Argonne, Ill. (10 Jun 1970).

In Proceedings of international conference on bubble chamber technology.

The optical system for Mirabelle is reviewed. A general description of the stereoscopic base is given; 78% of the chamber volume will be seen by at least three cameras. The procedures to be used for optical calibration of the chamber are discussed. (R.W.R.)

34993 (CONF-700623–(Vol.2), pp 959-71) THE CALIBRATION OF THE GARGAMELLE OBJECTIVES. Price, M. (European Organization for Nuclear Research, Geneva (Switzerland)).

From International conference on bubble chamber technology; Argonne, Ill. (10 Jun 1970).

In Proceedings of international conference on bubble chamber technology.

The calibration procedure for the Gargamelle objectives is described. Photographs of a grid plate are taken at two different object distances; from these photographs the distortion law at the two different positions may be found, and equations may be formulated to relate points in chamber space to points on the film. Since calibration is done in air, the necessary modifications to the calibration data for actual running conditions are discussed. The magnitude and direction of the distortion produced by one of the Gargamelle lenses are shown. (R.W.R.)

34994 (CONF-700623–(Vol.2), pp 972-83) LENSES AND ILLUMINATION SYSTEM OF MIRABELLE. Bourdinaud, M. (Commissariat a l'Energie Atomique, Saclay (France). Centre d'Etudes Nucleaires).

From International conference on bubble chamber technology; Argonne, Ill. (10 Jun 1970).

In Proceedings of international conference on bubble chamber technology.

The characteristics of the lenses and illumination system of Mirabelle are discussed. Specifications are given for the objectives. The results of tests of the optical system are reviewed. It was concluded that the behavior of the optical system was satisfactory. (R.W.R.)

34995 (CONF-700623–(Vol.2), pp 984-96) FIDUCIAL LINES IN LARGE BUBBLE CHAMBERS PRODUCED BY LASER BEAMS. Muuss, Harry (Heidelberg Univ. (West Germany)).

From International conference on bubble chamber technology; Argonne, Ill. (10 Jun 1970).

In Proceedings of international conference on bubble chamber technology.

The mechanism of light scattering in liquid hydrogen was investigated from the point of view of using laser lines as fiducial lines. It was found that Rayleigh scattering is responsible for the visibility of laser lines in the chamber liquid. The scattered light intensity was determined in order to estimate the input intensity necessary to take pictures of the laser lines. The two primary applications for laser lines in bubble chambers are the calibration of the optical constants of the chamber and, combined with camera-based fiducial marks, determination of the film–space relation on each frame. (R.W.R.)

34996 (CONF-700623–(Vol.2), pp 997-1009) FISHEYE WINDOW CONCENTRICITY PROBLEMS. Welford, W. T. (Imperial Coll. of Science and Tech., London (England)).

From International conference on bubble chamber technology; Argonne, Ill. (10 Jun 1970).

In Proceedings of international conference on bubble chamber technology.

Problems in tolerances and alignment of the fisheye windows for the ANL 12-ft bubble chamber are discussed. After a general introduction, the basic tolerances for the individual windows and the window assembly are examined. It was found that the desired concentricity of the set of three windows could not be achieved. A method for calibrating the window assembly in an attempt to overcome this difficulty is described; however, this method is difficult in practice. A way of assembling windows that are individually eccentric to form a window assembly that does not need any corrections is then explained. (R.W.R.)

34997 (CONF-700623–(Vol.2), pp 1010-23) FISHEYE MOUNTING PROBLEMS. Edwards, B.; Turner, W. (Rutherford High Energy Lab., Chilton (England)).

From International conference on bubble chamber technology; Argonne, Ill. (10 Jun 1970).

In Proceedings of international conference on bubble chamber technology.

The problems of mounting the fisheye windows of the High Field Bubble Chamber are discussed. Solid flanges holding each fisheye rigidly in place must have a thermal expansion coefficient equal to that of the glass. The best material is ferromagnetic, but this would experience unacceptably high magnetic forces. It was decided to use thin Ni/Fe spinnings to hold the glass. This design is shown and the measurements made of the window concentricities when the system was cooled to liquid-hydrogen temperatures are described. It is concluded that gluing the thin spinnings to the glass with an aluminum-loaded epoxy provides an excellent means of making a good seal that is capable of thermal cycling without contamination of the vacuum interspaces. (R.W.R.)

34998 (CONF-700623–(Vol.2), pp 1024-38) BUBBLE CHAMBER HOLOGRAPHY. Welford, W. T. (Imperial Coll. of Science and Tech., London (England)).

From International conference on bubble chamber technology; Argonne, Ill. (10 Jun 1970).

In Proceedings of international conference on bubble chamber technology.

The required depth of focus in photography becomes increasingly difficult to achieve in ever-larger bubble chambers. Holographic recording offers a way around this difficulty, because a hologram optically records a volume in such a way that objects at all distances within the volume can be reconstructed in perfect focus. In

XUM

effect, in the reconstruction process one could vary a focus control and examine the complete range of depth of the chamber. Tracks at all depths would have the contrast expected for an in-focus track; moreover, the camera lens aperture can be opened much wider than in ordinary bubble-chamber photography. Progress in developing the holographic technique for use in bubble chambers is reviewed. (R.W.R.)

34999 (CONF-700623-(Vol.2), pp 1040-94) LARGE SUPERCONDUCTING MAGNETS FOR BUBBLE CHAMBERS AND OTHER DETECTORS. Prodell, A. G. (Brookhaven National Lab., Upton, N. Y.).

From International conference on bubble chamber technology; Argonne, Ill. (10 Jun 1970).

In Proceedings of international conference on bubble chamber technology.

Several large superconducting magnets for use with bubble chambers are described; those treated include the magnets for the 12-foot chamber at Argonne National Laboratory, the 7-foot chamber at Brookhaven National Laboratory, the Big European Bubble Chamber (BEBC) and Omega project at CERN, and the High Field Bubble Chamber at Rutherford High Energy Laboratory. Some innovations and advances made in the construction of these magnets are mentioned. (32 figures) (R.W.R.)

35000 (CONF-700623-(Vol.2), pp 1095-1125) MAGNETIZATION CURRENT EFFECTS IN COILS WOUND FROM MULTIFILAMENT STABILIZED SUPERCONDUCTOR. Clee, P. T. M.; Dean, M. W.; Thomas, D. B.; Trowbridge, C. W. (Rutherford High Energy Lab., Chilton (England)).

From International conference on bubble chamber technology; Argonne, Ill. (10 Jun 1970).

In Proceedings of international conference on bubble chamber technology.

It has been shown experimentally that magnetization currents in small coils made from composite superconducting strips decay so slowly that extrapolation to large coils such as those required for bubble chambers suggests decay time constants of months or years. The magnitude of the field distortions associated with these currents were calculated for one such coil, and these amount to several per cent in the working region. Since time-dependent distortions of this magnitude are unacceptable for the HFBG, twisted filament conductors were developed. Measurements with a variety of these conductors indicated that simple magnetic diffusion theory underestimates the decay time constants by a considerable factor, even after the lengthening effect in time constant due to inductive coupling between turns in the test coils has been taken into account. It is suggested that the reason for the observed discrepancy is to be sought in the geometry of the conductor itself; it probably depends on the proximity of filaments and their size and number. (auth)

35001 (CONF-700623-(Vol.2), pp 1126-49) BIG EUROPEAN BUBBLE CHAMBER (BEBC) MAGNET PROGRESS REPORT. Haebel, E. U.; Wittgenstein, F. (European Organization for Nuclear Research, Geneva (Switzerland)).

From International conference on bubble chamber technology; Argonne, Ill. (10 Jun 1970).

In Proceedings of international conference on bubble chamber technology.

A brief engineering and status report on the BEBC is first given. Work on the design of the conductor to minimize the effects of long-time-constant eddy currents is then described. Theoretical results were checked by experiment. It was found that persistent eddy currents could slightly influence the field distribution in the magnet volume, but that they could be destroyed by short heat pulses. As a result of these measurements a heater strip was included in the BEBC windings. (R.W.R.)

35002 (CONF-700623-(Vol.2), pp 1150-71) CALCULATION OF THE MAGNETIC FIELD MAP OF THE LARGE EUROPEAN BUBBLE CHAMBER FROM MEASUREMENTS MADE ON THE WALL OF THE CHAMBER BODY. Riche, J. (European Organization for Nuclear Research, Geneva (Switzerland)).

From International conference on bubble chamber technology; Argonne, Ill. (10 Jun 1970).

In Proceedings of international conference on bubble chamber technology.

The advantages of using probes fixed on the wall of the chamber for measuring the magnetic field in the BEBC are discussed. Several methods for calculation of the field are presented. Errors involved in making the measurements and the choice of the method of field reconstruction are discussed. (R.W.R.)

35003 (CONF-700623-(Vol.2), App.I) GARGAMELLE: SOME TECHNICAL ASPECTS. Alfille, L. (Commissariat a l'Energie Atomique, Saclay (France). Centre d'Etudes Nucleaires). 27p.

From International conference on bubble chamber technology; Argonne, Ill. (10 Jun 1970).

In Proceedings of international conference on bubble chamber technology.

Some technical aspects of the construction of Gargamelle are considered; illumination problems (reduction of light-source dimensions, masking to avoid direct illumination of objectives, and camera design) and the safety philosophy are emphasized. (R.W.R.)

35004 (JINR-P10-5762) AUTOMATIC PROCESSING OF INFORMATION FROM SPARK CHAMBERS. Volchenkov, N. G.; Golovin, B. M.; Preobrazhenskii, A. B. (Joint Inst. for Nuclear Research, Dubna (USSR)). 1971. 15p. (In Russian). Dep. NTIS (U. S. Sales Only).

Some mathematical problems of the automatic processing of experimental data from spark chambers are considered. The program system is based on the ideas of structural pattern recognition. It assumes the construction of a semiotic system containing grammar for the language describing the considered class of experiments. The system of programs is written in the language REFAL and realized in computer BESM-6. (auth)

35005 (JINR-P13-5751) INFLUENCE OF ULTRASOUND ON VAPOUR BUBBLE DYNAMICS IN LIQUID HYDROGEN. Tkachev, L. G.; Shestakov, V. D. (Joint Inst. for Nuclear Research, Dubna (USSR). Lab. of Nuclear Problems). 1971. 19p. (In Russian). Dep. NTIS (U. S. Sales Only).

The following assumptions are made: a bubble is spherical and homogeneous; vapor is in thermodynamical equilibrium with the surface layer of the liquid; and the liquid should be incompressible and isotropic. The system of equations takes into account heat and mass exchange between a bubble and the liquid. The state equation contains the second and third virial coefficients. The numerical solutions of the system of equations are given for the case of liquid hydrogen. Since the solutions are studied in the asymptotical region where the size of the bubble is 10^{-3} cm, the initial bubble is taken equal to $5 \cdot 10^{-4}$ cm, and the surface tension is neglected. The properties of solutions are discussed with the various values of thermodynamical and acoustical parameters corresponding to the working conditions of the ultrasonic bubble chamber. When the ultrasound is switched on, the initial bubble begins growing and after the finite number of pulsations, dynamical equilibrium is established and the average radius becomes constant. The mechanism of the bubble growth is rectified by heat diffusion. By taking into account the property of real gas one obtains a larger bubble compared to that of an ideal gas. It is shown that the qualitative behavior of small and big bubbles has the peculiarity due to the presence of the surface and volume terms in the equations. These peculiarities and the sign of vapor specific heat conductivity along the phase equilibrium curve are of importance when the dynamical equilibrium pulsations of the bubble are established. The natural frequency pulsations greatly affect the bubble behavior. (auth)

35006 (JINR-P13-5810) SHOWER EFFICIENCY OF SPARK CHAMBERS. Korenchenko, S. M.; Mitselmakher, G. V.; Nekrasov, K. G. (Joint Inst. for Nuclear Research, Dubna (USSR). Lab. of Nuclear Problems). 1971. 12p. (In Russian). Dep. NTIS (U. S. Sales Only).

A phenomenological model for developing of some break-downs in one gap of a spark chamber is suggested which takes account of the fluctuation in the streamer formation time. The shower efficiency can be determined with the help of two parameters: the efficiency of one particle recording and the shunting parameter. A satisfactory agreement with experimental data is obtained. (auth)

35007 (LNF-70/25) HEAVY GAS-LIQUID MIXTURE BUBBLE CHAMBER OF 70 LITERS VOLUME WITH HYDROGEN INTERNAL TARGET. Note No. 480. Argan, P. E.; Benvenuto, P.; Fabbri, D.; (and others) (Comitato Nazionale per l'Energia Nucleare, Frascati (Italy). Laboratori Nazionali di Frascati). 16 Jun 1970. 12p. (In Italian). Dep. NTIS (U. S. Sales Only).

A bubble chamber with a heavy gas–liquid mixture presently used with the γ beam of the Frascati electrosynchrotron is described. The bubble chamber was adapted for insertion in an analyzer magnet and provided with an internal gaseous hydrogen target at high pressure. The mechanical characteristic of the bubble chamber, the expansion and recompression apparatus, the analyzer magnet, the response optics, the command and control electronics, and operational characteristics of the chamber and the internal hydrogen target are described. (J.S.R.)

35008 (LNF-70/44) PRECISION OF AN OPTICAL SPARK CHAMBER WITH WIRE ELECTRODES. Note No. 491. Bisello,

XUM

D.; Ronga, F. (Comitato Nazionale per l'Energia Nucleare, Frascati (Italy). Laboratori Nazionali di Frascati). 5 Oct 1970. 9p. (In Italian). Dep. NTIS (U. S. Sales Only).

The precision obtainable in the determination of particle trajectories with an optical spark chamber with wire electrodes is studied. A better precision is obtainable with a chamber with a large gap, but a higher efficiency is obtained with a narrow-gap chamber. In order to obtain a good compromise between angular efficiency and precision, the internal chamber of the Adone Magnet Experiment was designed with alternating large and narrow bigaps. The analysis system adopted is described and discussed. (J.S.R.)

35009 (ORO-2504-172) 300 MEGACYCLE LOGIC WITH M.E.C.L. [PART] III. Technical Report No. 71-102. Risk, W. S. (Maryland Univ., College Park. Dept. of Physics and Astronomy). [1970]. 37p. Dep. NTIS.

Two high speed logic circuits developed for a high energy physics experiment have easily met or surpassed the performance of the best available commercial logic at a fraction of commercial costs. A four-fold coincidence-latch circuit and an eight-fold fanout circuit built with Motorola M.E.C.L. III integrated circuits demonstrate that discrete component logic even at the highest attainable speeds is fast approaching obsolescence. The output rise time of the coincidence circuit is 0.8 nsec with a pulse pair resolution of less than $3\frac{1}{2}$ nsec. The output rise time of the fanout is 1.0 nsec with a pulse pair resolution of 4 nsec. The circuits are completely D.C. coupled and N.I.M. compatible. The circuits were developed for use with a large, sectioned liquid scintillation detector. (auth)

35010 ANOMALOUS PULSE SPECTRUM OF A PLASTIC SCINTILLATOR AT SEA LEVEL. De, A. K.; Nath, M.; Mitra, S.; (and others) (Univ. of Calcutta). Nuovo Cim.; 3B: No. 1, 114-18(11 May 1971).

Scintillation counters 10 cm and 20 cm thick have been used to study the anomalous pulse spectra in the transition region observed at sea level. The experimental results may be explained in terms of the electromagnetic interactions of muons in the cosmic-ray beam. (auth)

35011 METHOD OF PROJECTING AND STUDYING THE SPATIAL IMAGE OF COMPLEX EVENTS RECORDED BY A SPARK CHAMBER. Abdullaev, A. M.; Azimov, S. A.; Beisembaev, P. U.; Yuldashbaev, T. S. (Inst. of Nuclear Physics, Tashkent). Izv. Akad. Nauk Uzb. SSR, Ser. Fiz.-Mat. Nauk; No. 4, 84-8(1970). (In Russian).

A method is suggested for spatial determination of interaction characteristics (in the absence of magnetic fields) in which the reduction of particle trajectory parameters was accomplished by simple geometrical equations. The suggested projection-graphical method for treating information obtained with spark chambers considerably lowered the precision requirement of the optical and measuring systems. Moreover, before reducing the spatial picture of the events on the independent projections it was possible to number the tracks and the parameters of particle trajectories. (R.V.J.)

35012 SOLID IRON MAGNETS USED IN THE DURGAPUR COSMIC RAY SPECTROGRAPH. Nandi, B. C.; Sinha, M. S. (Regional Engineering Coll., Durgapur, India). Proc. Indian Acad. Sci., Sect. A; 63: No. 2, 92-100(Feb 1971).

Two big solid iron magnets have been installed at Durgapur as a part of the cosmic ray spectrograph. The variation of magnetic induction with current and stability and uniformity of the flux inside the iron have been investigated. Near the saturation current, stability and uniformity of the flux have been found to be high enough, so that these magnets are useful in the accurate determination of momenta of particles. The leakage field outside the iron will not affect the accuracy of the measurement. (auth)

35013 EXPERIMENTAL FACILITIES AT THE KUM-BEL MOUNTAIN STATION FOR THE STUDY OF HIGH-ENERGY INTERACTIONS. Abdullaev, A. M.; Azimov, S. A.; Myalkovskii, V. M.; (and others) (Inst. of Nuclear Physics, Tashkent, USSR). pp 342-5 of Proceedings of the Eleventh Symposium on Cosmic Rays, Astrophysics, Geophysics and Elementary Particle Physics, 1969. Vol. II. Bombay; Department of Atomic Energy (1969).

From eleventh symposium on cosmic rays, astrophysics, geophysics and elementary particle physics; Delhi, India (7 Oct 1969). See CONF-691055-(Vol. 2).

The experimental station at Kum-bel Mountain, Uzbek S.S.R. Academy of Sciences Institute of Nuclear Physics, was constructed to study nuclear interactions at 10^{11} to 10^{13} eV. The apparatus consists of wide-gap spark chamber, thin Cerenkov counters, a total energy absorber, and the muon detector. (J.C.W.)

35014 BALLOON-BORNE INSTRUMENT FOR STUDYING X-RAY SOURCES IN 15- TO 150-keV RANGE. Agrawal, P. C.; Kamat, A. P.; Kunte, P. K.; (and others) (Tata Inst. of Fundamental Research, Bombay). pp 380-2 of Proceedings of the Eleventh Symposium on Cosmic Rays, Astrophysics, Geophysics and Elementary Particle Physics, 1969. Vol. II. Bombay; Department of Atomic Energy (1969).

From eleventh symposium on cosmic rays, astrophysics, geophysics and elementary particle physics; Delhi, India (7 Oct 1969). See CONF-691055-(Vol. 2).

A balloon-borne scintillation radiation detector was flown over Hyderabad to study high-energy x rays from discrete celestial sources in the 15- to 150-keV range. The intensity of x rays from a source is measured as it sweeps across the telescope by alternately looking at the source and then 180° away from it in a preset interval, thus eliminating uncertainties due to variations in background recordings. Measurements were made on Dec. 22, 1968 and Apr. 16, 1969. Intensity and energy spectra of background and various sources like Sco X-1 and Cyg X-1 have been obtained. (J.C.W.)

35015 DETECTING RADIATION WITH A SUPERCOOLED LIQUID. Dass, N.; Metra, S. K.; Singh, Om; Varshneya, N. C. (Univ. of Roorkee, India). pp 522-6 of Proceedings of the Eleventh Symposium on Cosmic Rays, Astrophysics, Geophysics and Elementary Particle Physics, 1969. Vol. II. Bombay; Department of Atomic Energy (1969).

From eleventh symposium on cosmic rays, astrophysics, geophysics and elementary particle physics; Delhi, India (7 Oct 1969). See CONF-691055-(Vol. 2).

The use of a supercooled liquid for detecting particle tracks is described. Some tracks due to cosmic rays were observed and are shown. Also some calculations for various liquids which could possibly be used as detectors are given. Included in these calculations are the minimum amount of supercooling needed for tracks to appear, the thermodynamic freezing temperature, and values for change in pressure to erase the tracks. (J.F.P.)

35016 NEW DIGITIZING AND MEMORY SYSTEM FOR WIRE SPARK CHAMBERS. Friday, R. G.; Leith, D. W. G. S.; Mauro, K. D.; Richter, B. (Stanford Univ., Calif.). Nucl. Instrum. Methods; 93: No. 2, 237-40(1971).

A new digitizing and memory system for use with magnetostrictive wire spark chambers has been developed. The system is based on the use of fast shift registers as the memory element, and appears to reduce the cost of readout systems for large spark chamber arrays by a factor of about 10. Circuitry is described for use with a large spark chamber system requiring the digitization and storage of 1000 sparks per event. The principle has applications in any situation requiring the digitization and storage of the arrival times of a burst of pulses. (auth)

35017 SIMPLE CAPACITOR READ-OUT FOR WIRE SPARK CHAMBERS IN MAGNETIC FIELDS. Pizer, H. I. (CERN, Geneva). Nucl. Instrum. Methods; 93: No. 2, 249-51(1971).

Multiwire spark chambers may be operated in magnetic fields using the simple memory circuit described. For each chamber wire a capacitor is used to store the spark information and a diode provides the readout facility. (auth)

35018 HIGH ENERGY PARTICLE IDENTIFICATION BY IONIZATION MEASUREMENTS USING SINGLE GAS PROPORTIONAL COUNTER. Lehraus, I.; Jeanne, D. (CERN, Geneva). Nucl. Instrum. Methods; 93: No. 2, 257-68(1971).

A high pressure gas proportional counter is described, which has an ionization resolution of 4% in the relativistic rise region up to 30 to 50 GeV/c. The counter is 0.5 cm diameter and 120 cm long, aligned along the beam axis. It was designed for tuning and monitoring of separated bubble chamber beams using fast ejection. Results of beam tests at 5.46 and 8.25 GeV/c show the statistical separation of protons and pions. (auth)

35019 SPARK COUNTER WITH LARGE AREA. Parkhomchuck, V. V.; Pestov, Yu. N.; Petrovykh, N. V. (Inst. of Nuclear Physics, Novosibirsk, USSR). Nucl. Instrum. Methods; 93: No. 2, 269-70(1971).

It is shown that spark counters with electrodes of an unlimited area, with time resolution better than 1 nsec, and with high charged-particle-detection efficiency may be constructed if one of the electrodes is made of high-resistive material. (auth)

35020 PRECISION OF TIME OF FLIGHT MEASUREMENTS USING LARGE (1 m^2) AREA SCINTILLATION COUNTERS. Ashton, F.; Edwards, H. J.; Kelly, G. N. (Univ. of Durham, Eng.). Nucl. Instrum. Methods; 93: No. 2, 349-51(1971).

Using two 5 cm thick 1 m^2 area scintillation counters each viewed edgewise on by single 2'' 56AVP photomultipliers it is found that time of flight measurements can be made to a pre-

XUM

cision of ±1.0 ns as long as the positions at which particles traverse the detecting scintillators are known. The arrangement used is much simpler than if isochronous counters had been used and the precision obtained is equally good. (auth)

35021 CHARACTERISTICS OF AN EXTERNAL ELECTRODE SPARK CHAMBER. Ashton, F.; Coats, R. B.; Simpson, D. A. (Univ. of Durham, Eng.). Nucl. Instrum. Methods; 93: No. 2, 395-6(1971).

The characteristics of an external electrode spark chamber suitable for use in a variety of different cosmic ray experiments is described. (auth)

35022 DESIGN AND CALIBRATION OF A GENERAL PURPOSE PULSE IONIZATION CHAMBER FOR MUON FLUX MEASUREMENT. Bhattacharya, P. K. (Inst. of Tech. and Science, Indore, India). Indian J. Pure Appl. Phys.; 9: No. 2, 115-18 (Feb 1971).

An account, using Enge's principles, of the effects of extended fringing field and short cutoff fringing field on electron trajectories inside a 60° double-focusing magnetic spectrometer is presented. The study has a significant bearing on the design of charged-particle beam-transport systems, with particular emphasis on the design of high-transmission (static-field) magnetic spectrometers. An intuitive grasp of the mechanism of second-order aberrations also results from this formalism and provides physical insight into the minimization or elimination of higher-order multipoles present. It seems that, for modest requirements of resolution and transmission, the first-order correction of optic-axis bending can be simply done satisfactorily by the shrouding of the beam from stray field with silicon-steel field clamps. (auth)

Radiation Dosimeters

Refer also to abstracts 34873, 34879, 34892, 35131, 35137, and 35139.

35023 (AEEW-M-962) EXPERIENCE IN THE USE OF THERMOLUMINESCENT DOSIMETERS FOR RADIATION DOSE CONTROL PURPOSES. Preston, H. E.; Clifton, J. J.; Hallett, C. D. (Atomic Energy Establishment, Winfrith (England)). Mar 1971. 8p. (CONF-700505-26). Dep. NTIS (U. S. Sales Only).

From second congress of the international radiation protection association; Brighton, England (3 May 1970).

In situations where doses to personnel must be controlled on a short term basis due to high levels of exposure, TLD dosimeters, using thermoluminescent lithium fluoride, with their rapid readout procedure, provide a useful method of dosimetry. Some results obtained in a variety of radiation environments are reported including soft x-rays and high energy gamma and beta rays. (UK)

35024 (AEEW-M-991) PROBLEMS OF HIGH TEMPERATURE ANNEALING OF PTFE/LITHIUM FLUORIDE DISCS USED FOR IONISING RADIATION DOSIMETRY. Preston, H. E. (Atomic Energy Establishment, Winfrith (England)). Apr 1971. 10p. Dep. NTIS (U. S. Sales Only).

The recommended annealing procedure for PTFE/LiF discs differs from that of LiF powder, due to the nature of PTFE. The maximum temperature to which PTFE may be raised during annealing is said to be 300°C. However, at this temperature the sensitivity of discs to ionising radiation decreases with use. By annealing at 400°C, in the same way as with powder, not only is the sensitivity of the discs enhanced, but it remains constant over many read/anneal cycles. (auth) (UK)

35025 (CEA-N-1435) MAINTENANCE PROGRAM FOR BABYLINE-20 DOSE RATE METERS MANUFACTURED BY NARDEUX. Pastre, Albert (Commissariat a l'Energie Atomique, Saclay (France). Centre d'Etudes Nucleaires). Apr 1971. 36p. (In French). Dep. NTIS (U. S. Sales Only).

Instructions for the maintenance of $\beta\gamma$ ion chamber exposure dosimeters of the Babyline-20 type are given. Three different levels of maintenance are considered. (auth) (France)

35026 (THAI-AEC-35, pp 21-3) STUDY ON THE THERMAL FADING CHARACTERISTICS OF SOME TSEE DOSIMETRY MATERIALS. Chantanakom, Nongnooch (Office of Atomic Energy for Peace, Bangkok (Thailand)). Dep. NTIS (U. S. Sales Only).

Thermal fading characteristics of LiF, BeO, and $CaSO_4$ irradiated with plutonium-239 alpha particles or cobalt-60 gamma radiation were studied. The materials were stored in different environmental conditions including vacuum, humid air, dry air, and normal laboratory air. (W.H.K.)

35027 DETERMINATION OF ABSORBED DOSE OF HIGH-ENERGY ELECTRONS BY LITHIUM FLUORIDE DETECTORS. Windelband, R.; Hegewald, H. (Humboldt-Univ., Berlin). Stud. Biophys.; 20: 9-16(28 Feb 1970). (In German).

Methods for obtaining the conversion factor of the absorbed dose in water to the exposure in air are summarized. The results of measurements which confirm the energy independence of thermoluminescence response up to an electron energy of 15 MeV are presented. The dependence of thermoluminescence response on the dose for different types and energies of radiation as given in literature was not found in the newer examined type of LiF. In two different powders of LiF (sublinear and supralinear) deviations from the dose response appear from 50 rad. Based on the tissue-equivalent absorption and scattering properties of LiF detectors, their use for the rapid check of the primary energy of electrons is suggested. (auth)

35028 SOLID STATE THERMOLUMINESCENT DOSIMETRY. Salton, D. G. M. (Hammersmith Hospital, London). Radiography; 37: 53-7(Mar 1971).

The operation of solid state thermoluminescent dosimeters is given and the handling and read-out techniques and conditions given. It is stated that they may be used to great advantage in measurement of skin and body cavity doses due to their small size, minimal shielding of underlying structures, and ease of handling. In radiation protection, finger doses may be measured without impairing the dexterity of the operator. In radiobiology, tissue equivalence and lack of absorption make this the method of choice for the measurement of dosage to samples. Interlaboratory comparisons of doses may be made providing the same batch of material is used and decay is allowed for by irradiations at both centers on the same day and reading-out both dosimeters consecutively on the same reader at a subsequent date. (UK)

35029 COLOR INDICATOR FOR THE VISUALIZATION OF RADIATION FIELDS AND THE BEAM ADJUSTMENT IN LARGE IRRADIATION PLANTS. Huebner, K.; Stolz, W.; Haberer, G. (Technische Univ., Dresden). Isotopenpraxis; 6: 332-4(Sep 1970). (In German).

A simple color indicator which gives in a very short time a visual survey of the radiation field and makes visible the flux density distribution of radiation beams is described. The organic color foil is obtained by evaporation of an aqueous solution of polyvinyl alcohol containing methyl orange as the color indicator agent, chloral hydrate as the halogen spender, and sodium tetraborate. Under the action of ionizing radiation the foil shows a sharp color change from yellow to red because of the release of HCl after a certain energy dose is reached. The presence of chloral hydrate and sodium tetraborate makes the color change sensitive to energy doses between 0.2 and 10 Mrad. An example of the results obtained with such foils is given. (J.S.R.)

35030 DETERMINATION OF THE QUALITATIVE COMPOSITION OF RADIATION AT THE DEPTH OF IRRADIATED MEDIUM. Frolova, A. V.; Titov, A. A.; Voloshko, E. N. (Moscow Research Inst. of X ray-Radiology). Med. Radiol.; 16: No. 3, 75-7(Mar 1971). (In Russian).

Phantom and scintillation detectors for determining the quality of radiation at the depth of the irradiated medium are described. The technique is based on the measurement with the aid of two pickups having a different energy dependence. The employment of the device is demonstrated by the evaluation of the qualitative composition of long-wave radiation in a water phantom. (auth)

35031 THERMAL RECEIVER OF ROENTGEN RADIATION. Kozyrev, B. P.; Sheveleva, T. Yu. (Leningrad Electrotechnical Inst.). Med. Radiol.; 16: No. 3, 72-4(Mar 1971). (In Russian).

A thermoelectric detector of roentgen radiation for the range of energies of 10 to 100 keV is described. The apparatus has no energy dependence and measures the intensity of radiation in the interval 5.10^{-7} to 5.10^{-2} wt/cm^2 with an error not exceeding 5%. The time constance of the apparatus is 10 seconds. (auth)

35032 INTRINSIC EFFICIENCIES OF SOME THERMOLUMINESCENT-DOSIMETRY PHOSPHORS. Lucke, William H. (Naval Research Lab., Washington, D. C.). J. Appl. Phys.; 42: No. 7, 3004-5(Jun 1971).

The intrinsic supralinear and linear efficiencies of LiF(TLD-100), CaF_2:Mn, $CaSO_4$:Mn, and Li_2B_4O:Mn thermoluminescent phosphors were measured and compared with values measured by other investigators. The methods used for correcting for PM-tube gain and uncertainties connected with the photocathode area and sensitivity are described. (W.H.K.)

XUM

35033 LOW ENERGY RADIATION DOSIMETRY METHOD IN THE RANGE OF 15 keV AND BELOW. Mallon, Barbara J.; Lorensen, Lyman E. (to United States Atomic Energy Commission). U. S. Patent 3,569,995. 9 Mar 1971. Filed 26 Aug 1968.

A method for measuring low-energy, high-flux radiation doses is described. Thin layers of poly-[3.3-bis (chloromethyl) oxacyclobutane] are exposed to ionizing radiation. Changes in physical properties of the layers are a measure of the radiation dose received. (auth)

35034 RELATIVE RESPONSE OF DOSIMETERS TO ^{60}Co AND 25 nsec PULSED ELECTRON IRRADIATIONS. Martin, J. A.; Jones, J. L.; Orehotsky, R. S. (Moleculon Research Corp., Cambridge, Mass.). Health Phys.; 20: No. 3, 267-75(Mar 1971).

The responses of a number of dosimeter materials to single 25 nsec pulses of two MeV electrons are compared with their corresponding responses, under vacuum, to cobalt-60 radiation. At a given total dose level, the responses to pulsed electrons were equal to or less than the corresponding cobalt-60 responses for all materials with the exception of the transvinylene double bond production in polyethylene, for which an over-response was found. Where the response of a material was found to be insensitive to environment (air vs. vacuum), the difference in response at the two sources was attributed to a dose rate effect; where the response was sensitive to the environment, synergistic effects were apparent. Experimental results are presented for polyethylene, a dyed cellophane system, a dyed cellulose acetate (Cinemoid) system, polyvinylchloride, polyvinylidenechloride (Saran), cobalt glass and high Z silver activated phosphate glass plates. (auth) (UK)

35035 THERMOLUMINESCENT DOSIMETER FOR PROVIDING A TOTAL RADIATION MEASURE OF RADIOACTIVITY IN A FLUID MEDIUM TO WHICH THE DOSIMETER IS EXPOSED. McCurdy, David E. (to United States Atomic Energy Commission). U. S. Patent 3,569,697. 9 Mar 1971. Filed 11 Feb 1969.

The present dosimeter includes a cylindrical housing having an intake port at one end and an exhaust port at the opposite end. A thermoluminescent disk and a radioactivity filter are coaxially and spatially mounted with respect to each other within the housing, with the thermoluminescent disk being mounted adjacent the intake port and having an aperture therethrough coaxially aligned with the intake port. The radioactivity filter is sealed to the interior walls of the housing. A pump draws a fluid medium through the ports of the housing to effect deposition of radioactive material of the fluid medium on the radioactivity filter. Energy from the radiation emitted by the ionizing radioactive material is absorbed by the thermoluminescent disk and stored. A heat source is provided to excite the thermoluminescent disk, the emitted light intensity therefrom being a measure of the detected radiation. (auth)

35036 RADIATION DOSIMETER. Mitchell, John P. (to United States Atomic Energy Commission). U. S. Patent 3,569,704. 9 Mar 1971. Filed 15 Aug 1968.

A dosimeter for measuring high energy ionizing radiation utilizes a metal-oxide-semiconductor (MOS) structure as the sensing element. Advantageously, the MOS structure comprises a silicon wafer a portion of one surface of which is oxidized and then provided with an aluminum electrode. In one embodiment, provision for heating the MOS structure and for measuring its temperature is incorporated in the MOS structure. After exposure to ionizing radiation the MOS structure is heated with an ammeter connected between the silicon wafer and aluminum electrode. The integrated current flow is then a measure of the radiation dose received by the structure. (auth)

35037 GLASS HAVING A BASE OF METAPHOSPHATES FOR DOSIMETERS WHICH ARE RESPONSIVE TO X-RAYS, γ-RAYS, AND THERMAL NEUTRONS. Carpentier, Serge; Chapuis, Anne Marie; Delarue, Roger; Francois, Henri (to Commissariat a l'Energie Atomique). British Patent 1,226,626. 31 Mar 1971. Priority date 24 Aug 1967, France.

The composition of a phosphate-glass dosimeter having adjustable sensitivity to thermal neutrons is described. It is possible, in addition, to equalize the sensitivity to thermal neutrons and the sensitivity to x and γ radiation. These properties are produced by regulating the amounts of ^{6}Li and ^{7}Li in the glass. Advantages of the new glasses include ease of manufacture, enhanced sensitivity, and smaller pre-dose. (R.W.R.)

Radiometric Instruments

35038 NUCLEONIC MEASURING APPARATUS WITH AUTOMATIC FIRE SAFETY RADIATION SOURCE SHUTTER CLOSING AND LOCKING MEANS RESPONSIVE TO HIGH TEMPERATURES FOR BLOCKING THE PATH OF THE SHUTTER MOVEMENT TO OPEN POSITION. Hatten, Bernard W. (to Industrial Nucleonics Corp.). U. S. Patent 3,560,748. 2 Feb 1971. Filed 27 Apr 1967.

A nucleonic measuring gage for cigarette tubing in which a housing contains a radiation source and has an aperture controlled by a sliding shutter is described. A U-shaped spring-steel shutter lock, positioned in the path of shutter movement, has leaves that are held in an open position by a quantity of meltable material; this arrangement permits the shutter to move between the leaves. The spring leaves are stressed to close together behind the shutter, thereby blocking the shutter in a closed position, upon occurrence of an abnormally high ambient temperature with the melting of the material. (auth)

35039 METHOD AND APPARATUS FOR CALIBRATING PULSED NEUTRON WELL LOGGING INSTRUMENT. Hopkinson, Eric C.; Youmans, Arthur H. (to Dresser Industries, Inc.). U. S. Patent 3,564,248. 16 Feb 1971. Filed 29 Nov 1967.

A well logging instrument having a pair of radiation-detector circuits and a pulsed neutron source coupled through a cable to the surface electronics and calibration controls is described. A first switch is provided at the surface for causing the neutron source to operate continuously, and a second switch is provided to effect a change in the gain of one of the radiation detector circuits—this provides means for comparison of the sensitivities of the two detection circuits. An adjustable observation gate in the surface electronics, in conjunction with a digital time-interval counter, is used to measure the time elapsed between sync pulses and the beginning and ending of each of the two detection gates. (auth)

35040 RADIOISOTOPIC ANALYSERS FOR DETERMINING SULPHUR CONTENT IN THE OIL-PRODUCTS AND THE EXPERIENCE IN THEIR EXPLOITATION. Drobiz, A. M.; Zolotarev, R. B.; Salakhov, Kh. N.; Khachaturov, Yu. G. Izotopy SSSR; No. 19, 12-18(1970). (In Russian).

Three types of automatic analyzers of sulfur in petroleum products are described. The first type is based on a radioisotopic γ-adsorption method. The γ-adsorption method may be modified by methods based on the absorption and reflection of β radiation by analyzed oil products. The β scattering method is used in the two other devices described. (tr-auth)

35041 INSPECTION AND/OR MEASURING APPARATUS USING RADIATION. Latter, Terence David Thomas; Crosby, Charles Edward (to Sel-Rex (UK) Ltd.). British Patent 1,228,149. 15 Apr 1971. Filed 8 Aug 1967.

Reference is made to apparatus employing β-radiation to measure the thickness of thin coatings or thin films. Commercially available "measuring tubes" for use in this technique employ a platen having an aperture located directly above the sensing surface of the detecting device, and suffer from the disadvantage that the shape and size of the aperture has to be chosen in accordance with the shape and size of the object being measured. Furthermore, with an object of non-uniform shape, when it is desired to measure the coating at several places, the use of a single size and shape of aperture is often insufficient. Changing of platens is time consuming and increases the risk of exposure of the operator to radiation. In the apparatus described a radiation window is provided, together with an elongated source holder which can be moved between first and second positions with respect to the radiation window. The arrangement is such that at the first source position radiation impinges on the specimen, whereas at the second position the specimen is substantially isolated from radiation. The source is located within a shielding sleeve when the source holder is at the rearward position. The end of the sleeve may be provided with a cap. A platen having at least one aperture may be provided. Various constructional alternatives are described. (UK)

35042 METHOD AND APPARATUS TO MEASURE THE WATER CONTENT OF A SNOW LAYER. Guillot, Pierre; Vuillot, Michel (to Electricite de France). French Patent 1,598,008. 29 Jun 1970. Filed 20 Dec 1968. (In French).

The special features of this invention are as follows: a radioactive source and a gamma ray detector are displaced in synchronism along vertical passages made inside the layer of snow, and the water content at various levels is deduced from the radiation intensities measured by the detector at these levels. The average displacement speed imparted to the source and the detector is set at a value proportional to the intensity measured at each level. The source and detector are moved in identical steps at time intervals corresponding each to the emission of a given number n of impulses by the detector. Each of the time intervals necessary for the detector to emit a given number of impulses N equal to or a multiple of n is measured and this corresponds

to the exploration of a section of the layer of given thickness, this time interval representing the water content of the section. The apparatus includes two fixed vertical tubes, a source of given activity travelling vertically in one and emitting a beam of gamma radiation in a horizontal plane, a radiation detector travelling vertically in the other, and a motor providing the synchronized movement of the detector and the source. (France)

35043 X-RAY FLUORESCENCE: DETECTION OF LEAD IN WALL PAINT. Laurer, Gerard R. (New York Univ., N. Y.); Kneip, Theo. J.; Albert, Roy E.; Kent, Frederick S. Science; 172: 466-8(30 Apr 1971).

An instrument has been developed for the in situ determination of lead on painted surfaces. It utilizes, as a source of gamma rays, radioactive cadmium-109 and its daughter silver-109 (metastable) to excite the K series x-rays of lead, and a solid-state, lithium-drifted germanium detector. The device, which is capable of detecting 0.26 milligram of lead per square centimeter of paint [approximately 3 percent (by weight) of lead in a single coat] beneath ten layers of leadfree paint, has been tested in a preliminary survey of several tenement apartments in New York City. (auth)

Miscellaneous Instruments and Components

Refer also to abstracts 34513, 34739, 34799, 34836, 34861, 34924, 34987, 35138, 35542, 36091, 36197, 36730, 37010, 37052, and 37146.

35044 (CEA-N-1439) NANOSECOND PULSE AMPLIFIER WITH AN ADJUSTABLE GAIN, WORKING IN BOTH POLARITIES. Lavaitte, A. (Commissariat a l'Energie Atomique, Grenoble (France). Centre d'Etudes Nucleaires). Mar 1971. 4p. (In French). Dep. NTIS (U. S. Sales Only).

A noninverter amplifier admitting positive and negative pulses is described. Its gain is continuously adjustable from 10 to 1,000 and its rise and fall time is 3 ns. (auth) (France)

35045 (CEA-N-1447) 200 MHz PULSE AMPLITUDE DISCRIMINATOR. Sentis, G.; Van Zurk, R. (Commissariat a l'Energie Atomique, Grenoble (France). Centre d'Etudes Nucleaires). Mar 1971. 7p. (In French). Dep. NTIS (U. S. Sales Only).

A fast d.c. coupled discriminator is described. Its threshold is continuously adjustable from 60 to 500 mV with an hysteresis of 50 mV and a stability better than 0.4 mV/°C. Its resolving time is 5 ns. Two 1 V complementary output signals are available with a common width adjustable by short circuited coaxial cable down to 2 ns. (auth) (France)

35046 (CEA-N-1448) BROAD BANDWIDTH DIFFERENTIAL AMPLIFIER. Lavaitte, A. (Commissariat a l'Energie Atomique, Grenoble (France). Centre d'Etudes Nucleaires). Apr 1971. 7p. (In French). Dep. NTIS (U. S. Sales Only).

A differential amplifier having a gain of 16 from DC to 150 MHz is presented. The rise and fall times are equal to 2 ns, the linearity is better than 1% and a high stability is obtained by using a D-C feedback system. (auth) (France)

35047 (CONF-700647) PROCEEDINGS OF THE FIFTH INTERNATIONAL SUMMER SCHOOL ON ELECTRONICS AND AUTOMATION, HERCEG-NOVI, JUNE 22-27, 1970. (Yugoslav Nuclear Energy Commission, Belgrade. Yugoslav Federal Council for the Coordination of Scientific Activities, Belgrade. Institut za Nuklearne Nauke Boris Kidric, Belgrade (Yugoslavia)). Nov 1970. 436p.

Separate abstracts were prepared for two of the papers in this volume. The remaining ones, dealing primarily with computer-aided design and on-line computer control of processes, are outside the scope of NSA. (R.W.R.)

For abstracts of individual papers see: 35048 and 35049.

35048 (CONF-700647-, pp 183-93) ON-LINE COMPUTER SYSTEM FOR NEUTRON PHYSICS EXPERIMENTS. Krajnik, J. (Institut Jozef Stefan, Ljubljana (Yugoslavia)).

From fifth international summer school on electronics and automation; Herceg-Novi, Yogoslavia (22 Jun 1970).

In Proceedings of the fifth international summer school on electronics and automation.

An on-line data acquisition system for neutron physics experiments based on the CDC 1700 computer is described. User requirements, computer configuration, system monitor, and future development are treated, with the operation of the interface and monitor considered in some detail. (R.W.R.)

35049 (CONF-700647-, pp 255-79) CENTRALIZED OUTPUT OF SPECTROMETRY DATA. Zamry, V. N. (Joint Inst. for Nuclear Research, Dubna (USSR)).

From fifth international summer school on electronics and automation; Herceg-Novi, Yogoslavia (22 Jun 1970).

In Proceedings of the fifth international summer school on electronics and automation.

When several physical experiments are performed simultaneously, the methods of centralized execution of similar functions and operations can be used. The peculiarities of centralized output of spectrometry data under the conditions of the measuring center are considered. The problems of concurrent work of many measurement systems and common output devices (productivity, efficient use of equipment, concordance, commutation, etc.) and also the demands on output units are discussed. It is shown that under certain conditions the method is rather effective. (auth)

35050 (PUC-937-396) RAD SWAPPING SYSTEM FOR NUCLEAR DATA ACQUISITION. Mead, William C. (Princeton Univ., N. J. Joseph Henry Labs.). Apr 1971. 13p. Dep. NTIS.

A set of Symbol programs, which utilizes a Sigma 2, a RAD, and RBM to provide approximately 50,000 channels of active storage for data from nuclear scattering experiments, is described. The swapping program and the data-collection activities for a prototype experimental configuration are discussed. (auth)

35051 STANDARD SPECIFICATION FOR THERMOCOUPLES, SHEATHED, TYPE K, FOR NUCLEAR OR FOR OTHER HIGH RELIABILITY APPLICATIONS. ASTM E 235-67. Philadelphia; American Society for Testing and Materials (1968). 12p. Available from American Society for Testing and Materials, Philadelphia.

The requirements for sheathed, Type K, thermocouples for nuclear applications are presented. General design, manufacturing, inspection, testing, and shipping aspects are considered. (R.W.R.)

35052 WIDE BAND CORRELATOR. Fukao, Masayuki (Kyoto Univ.). Rev. Sci. Instrum.; 42: No. 6, 783-8(Jun 1971).

A wide band correlator based on an orthogonal expansion of the correlation function to be analyzed is described. The resultant correlation function is displayed on an oscilloscope screen in "live" time. A frequency band from some kilohertz to 1 MHz can be dealt with only by changing the time constant of analyzing orthogonal filters. Some discussions about truncation error of orthogonal expansions and a treatment for the case of periodic functions are described. (auth)

35053 ULTRALINEAR 16-BIT DIGITAL-TO-ANALOG CURRENT CONVERTER. Zander, Dennis R. (Univ. of Illinois, Urbana). Rev. Sci. Instrum.; 42: No. 6, 797-800(Jun 1971).

The error analysis and the design of a 16-bit binary digital-to-analog converter are discussed. This method of conversion switches binary weighted constant current sources into a summing junction, in this case the yoke of a CRT. A conversion linearity of 0.00025% and a stability of 0.0004%/h were measured for a full scale current of 1 A showing that a converter linear to better than 16 bits can be constructed requiring no trimming of components. (auth)

35054 ECHELLE SPECTROGRAPH FOR HIGH RESOLUTION STUDIES OF THE SOLAR VACUUM ULTRAVIOLET SPECTRUM. Boland, B. C. (Astrophysics Research Unit, Culham, Eng.); Jones, B. B.; Engstrom, S. F. T. Solar Phys.; 17: No. 2, 333-54(Apr 1971).

An echelle grating spectrograph has been flown in Skylark sounding rockets to investigate the solar ultraviolet spectrum. The instrument can record a range of ~1000 Å, within the limits λ1000 to λ3000 Å, with a spectral resolving power of 10^5, and its use in the range λ1200 to λ2200 Å is described. Values are quoted for the spectral efficiency of the individual optical components, and for the complete instrument over a wide wavelength range, and a description is given of the method used to estimate and then to discriminate against the in-flight stray light when the solar disc is imaged onto the entrance slit. The mechanical arrangement of the components is described and some of the problems associated with the alignment and operation are discussed. (auth)

35055 DISCRIMINATION OF COMPOUND SIGNALS. Tanasescu, M. (Inst. of Nuclear Physics, Bucharest). Stud. Cercet. Fiz.; 22: 707-31(1970). (In Rumanian).

There are some industrial applications of radioisotopes in which it is necessary to discriminate a signal obtained at the output of a ratemeter circuit. In these cases the output signal

XUM

has two components: one with a determined variation in time due to the variation of the measured parameter, and the other with a random variation due to the statistical character of the radioactive desintegration. At the passing of this compound signal through the discrimination threshold at the output of the discrimination circuit, parasitic pulses due to the random component and available pulses due to the determined component may appear. The probability of obtaining available pulses at the output which carry the information is studied. This probability was calculated in connection with the influence of the electronic devices. Thus the discrimination circuit introduces as parameters the hysteresis and the sensitivity for electric charge, and the ratemeter circuit introduces the time constant. As a parameter for the determined component, the velocity of the rate variation at the discrimination threshold is considered and for the random component the standard deviation. Finally, the experimentation is described and theoretical and experimental curves plotted. (auth)

35056 INSTRUMENT FOR SLICING AND HANDLING RADIOACTIVE POLYACRYLAMIDE GELS. Malacinski, George M.; Gordon, Geoffrey (Indiana Univ., Bloomington). Chem. Instrum.; 3: No. 1, 89-96(1971).

The general features of an instrument designed for the precise slicing and safe handling of radioactive polyacrylamide gels are presented. Gels are maintained frozen by circulating coolant and positioned under a moving slicing blade by an adjustable ratchet mechanism. The gel slices are automatically deposited in a scintillation vial by a blast of air directed over the surface of the cutting blade. The instrument is designed to accommodate gels of various diameters and is easily dismantled for cleaning. (auth)

35057 X-RAYS. Stern, B. E.; Lewis, D. London; Pitman Publishing (1971). 313p. £ 3.50.

The subject is dealt with under the following sections; x-ray optics, x-ray emission spectra, absorption and scattering, measuring methods and instruments, calibration of x-ray sets, dosimetry, x-ray photography, radiography, radiotherapy, x-ray crystallography, x-ray chemical analysis, uses of large doses, x-ray equipment and radiation protection. (UK)

35058 IMPROVEMENTS IN OR RELATING TO APPARATUS FOR DETERMINING THE DIRECTION OF A NUCLEAR EXPLOSION. Fothergill, Reginald Allen; Sellek, William Harold; Norman, Kenneth George (to United Kingdom Atomic Energy Authority). British Patent 1,225,489. 17 Mar 1971. Filed 3 Oct 1967.

Apparatus is described for determining the direction of the radio-frequency transient associated with a nuclear explosion occurring at or above ground level, and thereby determining the direction of the explosion. It employs three non-directional aerials located at the apexes of a horizontal equilateral triangle, and spaced so that all three will intercept a substantially plane wavefront of the transient signal. The associated circuitry is described in detail, including triggering circuits and primary corrections, gating circuits, and means for determining time intervals between interception of wavefronts by the aerials. (UK)

35059 DEVICE FOR THE INVESTIGATION OF RELATIVE DOSE DISTRIBUTIONS. Akatkin, O. A.; Pozdnyakov, P. E. Med. Radiol.; 16: No. 3, 77-80(Mar 1971). (In Russian).

A detector positioning device for the investigation and recording of dose distributions in the field of gamma-radiation is described. The technique of graphic and mathematical treatment of the signal in transition to the true dose distribution is presented. The simplicity of the design of the apparatus enables to make it in any roentgenotechnical laboratory and useful for the evaluation of dose distributions. (auth)

35060 IONIZATION CHAMBER FOR A MASS-SPECTROMETER ION SOURCE. Gall, L. N. (Special Design Bureau for Analytic Instrument Construction, Leningrad). Sov. Phys.-Tech. Phys. (Engl. Transl.); 15: No. 9, 1545-7(Mar 1971).

Translated from Zh. Tekh. Fiz.; 40: No. 9, 1982-5(Sep 1970).

A method for determining the efficiency of an electron-impact ion source for a mass spectrometer as a function of the geometric dimensions of the ionization region in the ion source is described. Conclusions are presented for design optimization of electron-impact ion sources. (W.H.K.)

35061 INSTRUMENTATION FOR EARTHQUAKES. AEC Safety Guide 12 1971. Washington, D. C.; Atomic Energy Commission (1971). 2p. Available from United States Atomic Energy Commission, Washington, D. C.

A program of instrumentation is described for promptly determining the seismic response of a nuclear power plant and comparing such response with that used as the design basis. This comparison is needed to decide whether the plant can continue to be operated safely. (R.W.R.)

35062 BUBBLE CHAMBER FILM-ANALYSIS FACILITY. Subramanian, A. (Tata Inst. of Fundamental Research, Bombay). pp 274-6 of Proceedings of the Eleventh Symposium on Cosmic Rays, Astrophysics, Geophysics and Elementary Particle Physics, 1969. Vol. I. Bombay; Department of Atomic Energy (1969).

From eleventh symposium on cosmic rays, astrophysics, geophysics and elementary particle physics; Delhi, India (7 Oct 1969). See CONF-691055-(Vol. 1).

In the Tata Institute at Bombay a facility for the analysis of bubble chamber pictures is being set up. The facility will ultimately consist of three scanning machines and three measuring machines. The design and operation of the facility is described. (W.D.M.)

35063 CORRECTIVE TERMS TO THE HARTREE CORRECTION FORMULA. Grennberg, B.; Rytz, A. (Bureau International des Poids et Mesures, Sevres, France). Nucl. Instrum. Methods; 93: No. 2, 189-92(1971).

The validity of the Hartree correction formula for a semicircular spectrometer is discussed and some corrective terms proposed for the influence of anomalies in field direction and uniformity. A method of measuring the deviations from the ideal direction of field is demonstrated and the magnitude of the corrections for a particular case evaluated. (auth)

35064 CONSTANT FRACTION TIMING ADAPTER FOR A ZERO-CROSSOVER DISCRIMINATOR. Fullwood, R. R. (Los Alamos Scientific Lab., N. Mex.). Nucl. Instrum. Methods; 93: No. 2, 235-6(1971).

A 51 Ω passive adapter may be used to convert a zero-crossover discrimination to constant fraction timing. The time slowing is estimated to be less than 500 psec, and the reflection coefficient is ±5% with the major reflection less than 1 nsec in duration. (auth)

35065 VERSATILE ROUTING UNIT FOR MEASUREMENTS OF TIME-DEPENDENT PULSE-HEIGHT SPECTRA. Weitkamp, C. (Kernforschungszentrum, Karlsruhe, Ger.). Nucl. Instrum. Methods; 93: No. 2, 245-8(1971).

A routing unit for the sorting of pulse-height spectra into 16 different time groups is described. The widths of the time groups can be chosen independent of each other in increments of 10^{-4} of the total time range. Possible group widths are 10 μs to 10 s for use with the built-in 100 kHz oscillator and 100 ns to infinity using a suitable external pulse train generator. (auth)

35066 SLIDING PULSER FOR RAPID TESTING OF INTEGRAL LINEARITY. Takeuchi, S.; Shimura, T.; Nishino, O. (Tokyo Univ.). Nucl. Instrum. Methods; 93: No. 2, 253-5(1971).

The design and performance of a sliding pulser with high repetition rate ($\leq 10^6$ pps) is described. The output of this pulser is useful for rapid testing of integral linearity of analog pulse circuits. Generation of the sliding pulse is based on the DA converter technique. (auth)

35067 SIMPLE BINARY-TO-DECIMAL OR DECIMAL-TO-BINARY CONVERTER AND ADDING DEVICE. Schneider, R. H. (Bureau of Radiological Health, Rockville, Md.). Nucl. Instrum. Methods; 93: No. 2, 361(1971).

It is pointed out that a recently described system of binary-to-decimal conversion was previously used in some vacuum tube multi-channel pulse-height analyzers. (auth)

35068 POWER SUPPLY SYSTEM CONTROL. Brendle, M.; Briel, U. (Univ., Tuebingen, Ger.). Nucl. Instrum. Methods; 93: No. 2, 375-6(1971).

A control for a system containing many power supplies is described. If any power supply fails, the whole system is shut off. Other fault sensors (e.g., overtemperature sensors) can be connected to the control easily. (auth)

35069 ALIGNMENT TELESCOPE. Rogers, Benjamin T. (to United States Atomic Energy Commission). U. S. Patent 3,554,630. 12 Jan 1971. Filed 11 Sep 1968.

An alignment telescope for locating points along a line from a fixed point is described. A lens structure is used to establish a line from the fixed point, and a moveable mirror and eyepiece are then introduced into the device to locate points along the desired line. (auth)

35070 RESOLVING POWER AND MEASUREMENT OF ISOTOPIC ABUNDANCES BY A TIME-OF-FLIGHT MASS SPEC-

XUM

TROMETER WITH A LASER ION SOURCE. Bykovskii, Yu. A.; Dymovich, V. I.; Kozyrev, Yu. P.; Nevolin, V. N.; Sil'nov, S. M. (Engineering Physics Inst., Moscow). Sov. Phys.-Tech. Phys. (Engl. Transl.); 15: No. 11, 1877-9(May 1971).

Translated from Zh. Tekh. Fiz.; 40: No. 11, 2401-4(Nov 1970).

The resolving power of a time-of-flight mass spectrometer with a laser ion source and magnetic and electrostatic analyzers for measurement of isotopic abundances is discussed. The spatial resolution is limited mainly by aberrations of the optical system and the divergence of the laser radiation. (W.H.K.)

35071 PATTERN RECOGNITION STUDIES. Society of Photo-Optical Instrumentation Engineers Seminar Proceedings, New York, New York, June 9–10, 1969. SPIE Seminar Proceedings. Volume 18. Redondo Beach, Calif.; Society of Photo-Optical Instrumentation Engineers (1969). 230p. (CONF-690616).

Fifteen papers are presented on holographic and coherent optic techniques, pattern recognition techniques, and biomedical optical techniques. Two papers were previously included in NSA 23: 38525 and 23: 45545. The remaining 13 papers are not within the scope of NSA. (W.H.K.)

Radiation Effects on Instruments and Instrument Components

Refer also to abstract 36302.

35072 (HEDL-SA-152) EFFECTS OF FAST NEUTRON IRRADIATION ON CHROMEL/ALUMEL THERMOCOUPLES. Hoitink, N. C. (Hanford Engineering Development Lab., Richland, Wash.). 30 Mar 1971. Contract AT(45-1)-2170. 18p. (CONF-710510-1). Dep. NTIS.

From nineteenth annual northwest instrumentation conference; Richland, Wash. (20 May 1971).

Preliminary results obtained during early phases of a program to determine the effects of fast neutron irradiation on reactor-grade thermocouples being considered for use in the FFTF coolant measurement system are presented. The test program includes comparisons of pre- and post-irradiation calibration, wire resistance, insulation resistance and time response for twenty-two, 30-in. long, 0.0625 in. diameter, stainless steel sheathed, MgO insulated Chromel/Alumel thermocouples irradiated to 7×10^{21} nvt in EBR-II. The effects on performance of wire homogeneity and its importance in relation to radiation effects and reactor instrumentation is studied. (W.H.K.)

35073 METHOD OF CORRECTION OF AN OPTICAL SYSTEM BY IRRADIATION AND CORRECTED OPTICAL SYSTEM OBTAINED IN ACCORDANCE WITH SAID METHOD. Sinai, Philippe British Patent 1,223,888. 3 Mar 1971. Priority date 31 May 1967, France.

A method for producing an aberration-corrected optical lens is described. The lens is subjected to a neutron bombardment that varies with radius so as to obtain variations of the refractive index to produce a correction for aberrations of the lens. The irradiated lens is then subjected to a thermal decolorizing treatment at a temperature that is lower than the temperature necessary for recovery of the normal refractive index. (R.W.R.)

35074 DEVICE TO ELIMINATE UNDESIRABLE TRANSIENT EFFECTS ON COMPUTER OPERATIONS AND THE LIKE. Verbarg, Lawrence E.; Summers, Allan J. (to McDonnell Douglas Corp.). U. S. Patent 3,562,708. 9 Feb 1971. Filed 24 Jun 1968.

A device for preventing data signals that may be adversely affected by exposure to nuclear radiations or other transient conditions from replacing earlier received data signals in computers and like devices is described. Included are means for temporarily storing data signals in a condition in which they are relatively unlikely to be adversely affected by exposure to nuclear radiations and other transient conditions, comparing the temporarily stored data signals with later received data signals to determine the amount of difference between them, and substituting the temporarily stored data signals for the later received data signals whenever the amount of the difference between them exceeds a preestablished amount. (auth)

35075 USA AND IEEE GUIDE FOR CLASSIFYING ELECTRICAL INSULATING MATERIALS EXPOSED TO NEUTRON AND GAMMA RADIATION. ANSI N 4.1 1967. New York; Institute of Electrical and Electronics Engineers, Inc. (1968). 5p. Available from Institute of Electrical and Electronics Engineers, New York.

A guide to classify the environmental conditions of gamma radiation, neutron flux, and temperature in which electrical insulating materials must operate is presented. These environmental classifications are applicable to the specification and selection of the appropriate types of electrical insulation for nonmilitary equipment and devices that will be exposed to nuclear radiation. Maximum exposure limits are tabulated. (W.H.K.)

35076 SUPRALINEARITY AND SENSITIZATION OF THERMOLUMINESCENT PHOSPHOR LITHIUM FLUORIDE. Hwang, F. S. W. (Birmingham Univ., Eng.). J. Phys., D (London); 4: No. 4, 589-607(Apr 1971).

Two peaks were found in the high-temperature region for LiF thermoluminescent phosphor TLD-100. The total area of these two peaks increased with dose to a saturation value at about 4 Mrads. By extrapolation, a threshold dose of 1 krad was required to produce these two peaks. An investigation, using a thermal annealing technique, showed that these two peaks do not fit the Randall and Wilkins model. Evidence from optical absorption showed that these two peaks are probably connected with V-centres (hole traps). An attempt was made to correlate the supralinearity and sensitization behaviour to these two peaks. (auth) (UK)

35077 PROCESS FOR CORRECTING ABERRATIONS IN OPTICAL SYSTEM USING IRRADIATION AND CORRECTED OPTICAL SYSTEM OBTAINED BY THIS PROCESS. Sinai, Philippe. French Patent 1,592,906. 19 May 1970. Filed 22 Nov 1968. (In French).

The aberrations in optical systems may be corrected by a continuous and variable irradiation. A continuous variation in the refractive index of an element can be obtained from its center to its periphery; in this way the aberrations may be corrected in relation to a given law. The lenses must then be thermally decolorized; this process may be accelerated by exposure to ultraviolet radiation. The irradiation can be produced by neutrons, protons or fast ions. Irradiation can be used to modify the transmitting properties of optical materials. In this way variable transmittance screens can be produced. (France)

35078 IMPROVEMENTS IN AND RELATING TO THE MEASUREMENT OF COATING THICKNESS. Latter, Terence David Thomas; Crosby, Charles Edward (to Sel-Rex (UK) Ltd.). British Patent 1,228,150. 15 Apr 1971. Filed 1 Aug 1967.

Further constructional variations are presented with reference to the apparatus described in British Patent 1,228,149 for measuring the thickness of thin coatings or of thin films, employing β-radiation. (UK)

35079 GAMMA-RADIATION DAMAGE OF ORGANIC SCINTILLATION MATERIALS. Oldham, G.; Wave, A. R.; Salvaridis, P. (Loughborough Univ. of Tech., Eng.). J. Inst. Nucl. Eng.; 12: 4-6(Jan-Feb 1971).

Plastic scintillators consisting of p-terphenyl and 1,4 bis(5-phenyl-2-oxazolyl) benzene (POPOP) in a polyvinyltoluene base were irradiated using a ^{137}Cs source at 1570 rad per hour. The relationship between γ dose and radiation damage was measured by the percentage apparent energy change of a β-spectrum. The radiation damage was also measured by investigating the change in light absorption and the change in counting efficiency of the scintillator. The variation in those characteristics after recovery of the samples in air was also measured. The results indicated that the damage as measured by the percentage apparent energy change of the β spectrum end point followed an exponential growth curve. Over the range of dose investigated the damage measured by the other two methods show a linear relationship. Results show that significant damage is caused to this type of plastic scintillator at very low doses. (UK)

35080 EVOLUTION OF THE DISTRIBUTION OF INTERFACE STATES IN MOS STRUCTURES IRRADIATED WITH ELECTRONS AND SUBJECTED TO THE EFFECT OF A THERMAL TREATMENT IN AN ELECTRIC FIELD. Saminadayar, K.; Pfister, J. C. (CEN, Grenoble, France). Solid State Commun.; 8: 2135-9(15 Dec 1970). (In French).

The evolution of surface-state density of irradiated Al/SiO_2/Si capacitors during bias-temperature treatment is observed. Surface states due to irradiation are annealed by 200°C, 0 V treatment. During 200°C, −25 V treatment, two groups of surface states are created near the midgap and at 0.35 eV above the valence band of the semiconductor. In a nonirradiated capacitor, only the second group is created. (auth) (UK)

35081 MATERIALS FOR INSTRUMENTS IN RADIATION SERVICE. ISA RP 25.1 1957. Pittsburgh; Instrument Society of America (1957). 12p. Available from Instrument Society of America, Pittsburgh.

A general guide for the selection of materials for use in intense radiation fields such as those encountered in and around nuclear

XUM

reactors is presented. Information on the radiation resistance of various plastics and insulating materials is tabulated; and the radiation effects on structural metals including heat generation, atomic transmutations, and atomic displacements are discussed. Apparent radiation effects on properties of metals including hardness, tensile strength, impact strength, fatigue strength, density and dimensional stability, magnetic susceptibility, and electrical resistivity are discussed. Also, radiation effects on special components including thermocouples, ionization chambers, oils, and semiconductors and vacuum tubes are briefly discussed. In addition, a table is presented to aid in selecting shielding materials. (W.H.K.)

35082 INFLUENCE OF LARGE DOSES OF γ RADIATION ON OPTICAL PROPERTIES OF QUANTUM GENERATOR. Arifov, U. A.; Bedilov, M. R.; Khaidarov, K. (Inst. of Nuclear Physics, Tashkent). Dokl. Akad. Nauk Uzb. SSR; No. 8, 22-4(1970). (In Russian).

Effects of gamma radiation on stimulated emission of four-level optical quantum generators (OQG) with Nd^{3+}-activated glass were studied. Experiments with OQG irradiated with ^{60}Co γ radiation at 1.17 MeV and dose ranges up to 2×10^8 rad showed that the threshold pump energy, induced radiation energy, and efficiency of the facility were considerably increased. (R.V.J.)

XUM

LIFE SCIENCES

Biochemistry, Physiology, and Molecular Biology

Refer also to abstract 35829.

Basic Processes

Refer also to abstract 34588.

35083 METHODS AND USE OF RADIOIMMUNOASSAYS. Johannsen, B. (Zentralinstitut fuer Kernforschung, Rossendorf, Ger.). Isotopenpraxis; 6: 293-300(Sep 1970). (In German).

A bibliographic review is given of the methods and uses of radioimmunoassays. The preparation of tracers, production of antisera, methods for the separation of free and antibody-bound radioactivity, analysis procedures, specificity, sensitivity, and application examples are discussed. 165 references. (J.S.R.)

35084 THYROID ABLATION IN YOUNG MICE: A TECHNIQUE COMBINING SURGERY AND ^{131}I. Marks, Jnr.; Sandy, C.; Mitchell, Thomas G. (Naval Medical Research Inst., Bethesda, Md.). Int. J. Appl. Radiat. Isotop.; 22: 263-7(Apr 1971).

A technique is described and evaluated for producing young athyroparathyroid mice for studying the effects of thyroid and parathyroid hormones on bone formation. The method combines thyroparathyroidectomy at 2 days with ^{131}I irradiation (3.0 μCi per g body weight) of proliferating thyroid remnants at 7 days. It was found that the amount of isotope necessary for thyroid ablation when combined with previous surgery was one fifth that required in intact rodents. At these doses there was no observable cytologic damage to adjacent tissues. It is considered that the method could be used to produce thyroidless mice with functional parathyroids provided the parathyroids are transplanted to another site prior to isotope administration. (UK)

35085 MEASUREMENT OF THE CORONARY FLOW BY RADIOCARDIOGRAPHY. De Vernejoul, Pierre; Kellershohn, Claude (CEA, Orsay, France). Compt. Rend., Ser. D.; 272: No. 1, 137-40(4 Jan 1971). (In French).

By the simultaneous injection of rubidium 86 which is fixed selectively on the myocardium and of technetium 99m-labeled red blood cells, it is possible to obtain two radiocardiograms of which the difference, at the second peak corresponding to the left ventricle, measures the coronary flow. (France)

Metabolism, Physiology, and Toxicology

Refer also to abstracts 35116, 35133, 35134, 35144, 35189, and 35211.

35086 DEPOSITION AND RETENTION OF INHALED $^{152\ 153\ 154}Eu$ OXIDE IN THE RAT. Johnson, R. F. Jr.; Ziemer, P. L. (Purdue Univ., Lafayette, Ind.). Health Phys.; 20: 187-93(Feb 1971).

Uptake, distribution, retention, and excretion of $^{152-154}Eu$ were determined in the rat following a single, 20 min inhalation exposure to a radioactive aerosol of Eu_2O_3. The average activity median aerodynamic diameter, AMAD, of the aerosol was 2.50 μ and the geometric standard deviation, σ_g, was 1.85. Deposition of the aerosol averaged 66% of the inhaled activity. Early nasal deposition of radioeuropium was found to represent 3.4% of the initial inhaled body burden and was cleared in less than 12 hr. Thirty days following exposure the average lung burden was 4.8 ± 1.3% (±2S.D.) of the initial body burden per gram of lung tissue. Small traces of $^{152-154}Eu$ were found in the kidney, liver, blood, and bone at 30 days. Excretion of europium oxide was almost completely via the G.I. tract. Whole-body retention to 30 days could be described by two mathematical models: first, a dual term exponential function indicating half time values of 0.44 and 30.12 days and secondly, a power function with a time exponent of –0.389. (auth) (UK)

35087 EXPERIMENTAL DATA ON THE FATE OF ^{76}As IN THE BODY OF RABBITS INFECTED WITH SYPHILIS. Eremenko, S. A. (Minsk Medical Inst.). Vestsi Akad. Navuk BSSR, Ser. Biyal. Navuk: No. 4, 78-83(1969). (In Belorussian).

The quantity of ^{76}As in the blood, fluids, brain, and internal organs was studied in 97 male Chinchilla rabbits at various stages of syphilitic infection–incubational, solid chancre, and nonchancrous. The pathways for excretion of the isotope from the body were also studied. It was established that the majority of the arsenic was removed from the circulatory system of the animals during the first 15 min following intravenous injection. A significant difference was noted in the quantity of arsenic accumulated in the cerebrospinal fluid, brain tissues, and internal organ tissues of rabbits with solid chancres and those that were nonchancrous. The main pathways for excretion of the radioisotope from the body of the animals infected with syphilis were the kidneys and the gastrointestinal tract. (tr-auth)

35088 AVAILABILITY IN THE PECCARY PIG OF RADIONUCLIDES IN NUCLEAR DEBRIS FROM THE PLOWSHARE EXCAVATION BUGGY. Chertok, Robert J.; Lake, Suzanne (Univ. of California, Livermore). Health Phys.; 20: 313-16 (Mar 1971).

The biological availability of radionuclides produced by a nuclear event was studied in the peccary pig. Nuclear debris obtained from a fallout tray located 1000 ft from Project Buggy was given to two Tayassu tajacu in single oral doses. Urine and feces were collected daily and sealed in tuna cans. Both the pigs and the urine and feces samples were analyzed daily in a whole-body counter with a lithium-drifted germanium detector for the gamma-emitting radionuclides. The daily analyses continued until very low levels of activity were reached. Most of the ^{99}Mo, ^{141}Ce, ^{132}Te, ^{198}Au, ^{103}Ru, ^{122}Sb, ^{187}W, and $^{140}Ba/^{140}La$ were eliminated in the feces, generally in the first 2 or 3 days. Varying amounts of ^{99}Mo, ^{132}Te, ^{198}Au, ^{122}Sb, and ^{187}W were found in the urine. Apparently little or no ^{141}Ce, ^{103}Ru, or $^{140}Ba/^{140}La$ was absorbed across the gut wall. The only radionuclide absorbed to any large extent was ^{131}I (73% found in urine). (auth) (UK)

35089 BIOLOGICAL AVAILABILITY OF RADIONUCLIDES PRODUCED BY THE PLOWSHARE EVENT SCHOONER. II. RETENTION AND EXCRETION RATES IN PECCARIES AFTER A SINGLE ORAL DOSE OF DEBRIS. Chertok, Robert J.; Lake, Suzanne (Univ. of California, Livermore). Health Phys.; 20: 325-30(Mar 1971).

The biological availability of radionuclides produced by the Plowshare event Schooner was studied in two peccaries (Tayassu tajacu). Debris was obtained from a surface-atmospheric debris separator and collector that was located in the expected cloud path 0.9 miles from ground zero. The debris that contained particles ranging from 10 to 80 μ in diameter was administered in a single oral dose to two peccaries. The animals were then analyzed daily with a solid-state detector for all the γ-emitting radionuclides until the activities had reached very low levels (9 days). The daily collections of urine and feces were sealed in 200 cm^3 tuna cans and analyzed with the same detector. The major radionuclides detected were $^{188}W/^{188}Re$, ^{196}Au, ^{131}I, ^{103}Ru, ^{74}As, ^{58}Co, ^{54}Mn, and ^{88}Y. The $^{188}W/^{188}Re$, ^{196}Au, ^{103}Ru, ^{58}Co, ^{54}Mn, and ^{88}Y were excreted mostly in the feces; some $^{188}W/^{188}Re$ (16%), ^{196}Au (7%), and ^{103}Ru (3%) were excreted in the urine. Large amounts of ^{131}I (39%) and ^{74}As (43%) were excreted in the urine. (auth) (UK)

35090 BIOLOGICAL AVAILABILITY OF RADIONUCLIDES PRODUCED BY THE PLOWSHARE EVENT SCHOONER. I. BODY DISTRIBUTION IN DOMESTIC PIGS EXPOSED IN THE FIELD. Chertok, Robert J.; Lake, Suzanne (Univ. of California, Livermore). Health Phys.; 20: 317-24(Mar 1971).

The biological availability and the distribution of radionuclides were studied in young Yorkshire pigs exposed to radioactive fallout from the Plowshare Event Schooner. Eight pigs were exposed in metabolic cages at various distances from ground zero in the expected path of the cloud, so that they could inhale debris and eat contaminated food. Three days after the detonation, the two pigs that were in the most contaminated portion of the fallout field were dissected. The organs were immediately sealed in cans and sent for analysis for γ-emitting radionuclides. The air filters that sampled the air at the pig station during the period of exposure were also canned and analyzed in the same manner. The radionuclides detected in the air filters were $^{188}W/^{188}Re$, ^{132}Te, ^{196}Au, ^{131}I, ^{103}Ru, and ^{74}As; the short-lived ^{99}Mo, ^{203}Pb, and ^{198}Au, although detected in the tissues, were too low in concentration for quantitation because of decay. The major radionuclides found in the pig tissues were ^{99}Mo, $^{188}W/^{188}Re$, ^{187}W, ^{132}Te, ^{203}Pb, ^{196}Au, ^{198}Au, ^{131}I, ^{103}Ru, and ^{74}As. Comparisons between lungs, blood, and other tissues suggested that the lungs retained small amounts of ^{203}Pb, ^{198}Au, ^{103}Ru, and ^{74}As. There seemed to be no differential

XUM

concentration within the lung except perhaps for ^{198}Au, which was more highly concentrated in the posterior portions. Of the other nuclides detected in the tissues, ^{99}Mo was accumulated in kidney, liver, and gall bladder, $^{188}W/^{188}Re$ in kidney and bone, ^{187}W in kidney, ^{196}Au in the gall bladder, ^{198}Au in the salivary gland, ^{103}Ru in kidney, and ^{74}As in kidney, all in much higher concentrations than in blood. (auth) (UK)

35091 METABOLIC AND THERAPEUTIC STUDY OF RESPIRATORY CONTAMINATION BY CERTAIN ACTINIDES [Pu, Am, AND Cm] IN SOLUTION. Nenot, J. C.; Morin, M.; Lafuma, J. (CEA, Fontenay-aux-Roses, France). Health Phys.; 20: 167-77(Feb 1971). (In French).

Respiratory contamination by Pu, Am, and Cm soluble salts was studied from the point of view of the salt's solubility in the body and its distribution and clearance. Uptake processes were rapid: 15 min after exposure, 15 to 45% of the amount retained in the lung passed through the alveoli, and 10% of this fraction was deposited in the bone. Two months later, only the lung showed an appreciable burden. Urinary excretion was a function of the solubility of the salt considered. Treatment by DTPA was effected either by aerosol or intramuscular injection. When treatment was undertaken 24 hr after exposure, the lung burden was reduced by a factor of $1/10$, the bone burden by a factor of $1/6$ to $1/10$. DTPA diffused more slowly from the lung than from the muscle, thus resulting in a longer lasting plasma burden. These metabolic and therapeutic data enable us to specify a treatment sequence to be applied to man in case of respiratory exposure to Pu, Am, or Cm solutions: DTPA should be given as aerosol immediately after exposure, then by systemic administration. Afterwards, one aerosol administration a week should be enough. (auth) (UK)

35092 DISTRIBUTION OF ^{239}Pu IN INTACT SKIN IN ITS SURFACE CONTAMINATION. Ershov, E. B.; Osanov, D. P.; Rakova, V. A. Med. Radiol.; 15: No. 12, 44-6(Dec 1970). (In Russian).

The penetration of ^{239}Pu through the epidermis (up to 150 μm thick) during superficial contamination was studied using 22 piglets whose morphological skin structure is similar to human skin. The results of the specific activity into the depth of the epidermis at various periods of time of contact with ^{239}Pu are given in graphic form. It was found that at the beginning the specific activity was very rapidly increased at any fixed depth and after 12 hr of contact the tempo decreased and became balanced, i.e. that the amount of the absorbed and expelled radioactive preparation was equal. (R.V.J.)

35093 DIETARY INTAKE AND EXCRETION OF ^{137}Cs IN CHILDREN. Pietrzak-Flis, Zofia (Central Lab. for Radiological Protection, Warsaw). Nukleonika; 15: 693-700(1970).

The content of ^{137}Cs in diet, urine, and feces of 4 to 6 year-old children from Warsaw was determined in the period from April 1965 to December 1967 and in June 1969. The mean annual intake of ^{137}Cs with diet was 67.3 ± 5.7 pCi/day in 1965; 53.8 ± 5.6 pCi/day in 1966 and 26.2 ± 1.4 pCi/day in 1967. Excretion of ^{137}Cs with urine amounted to 83 per cent of the total excretion, and the ^{137}Cs in feces/^{137}Cs in urine ratio equalled 0.21 ± 0.02. The body burden of children in 1967 was estimated from the excretion and intake of ^{137}Cs and it was found to be 1.32 and 1.24 nCi ^{137}Cs, respectively. Daily excretion of ^{137}Cs with feces was estimated to be about 0.37 per cent of the body burden. The ^{137}Cs/K in urine/^{137}Cs/K in diet ratio was equal to 1.0 ± 0.01, that indicated a lack of discrimination of ^{137}Cs in respect to K in the children studied. (auth)

35094 TEMPERATURE DEPENDENCE OF THE GROWTH OF ESCHERICHIA COLI B IN HEAVY WATER. Winkler, E.; Jung, K.; Huebner, G. (Institut fuer Stabile Isotope, Leipzig). Stud. Biophys.; 13: 73-6(1969). (In German).

Investigations on the growth of Escherichia coli B showed a decline in the inhibitional action of heavy water with increasing temperature. At temperatures below the optimal growth temperature a marked prolongation of the growth phase in heavy water was found. At temperatures above 45°C, cultures of Escherichia coli B grew better in D_2O than in H_2O. (auth)

35095 ^{137}Cs CONTENT OF THE HUMAN BODY, PARTICULARLY IN AREAS OF UNUSUAL CESIUM ECOLOGY. Moiseev, A. A.; Romanov, L. R.; Darovskikh, V. F. Gig. Sanit.; No. 6, 92-3(Jun 1970). (In Russian).

A portable whole-body radiation counter (North; 13.8 kg), was used to measure the ^{137}Cs content of the human body in populations from selected geographical regions. The lowest measurements were recorded within a group of adult men. Correcting for an external gamma background rate of 10 μCi/hr, the result of a 10 min whole-body count approximated 10 μCi. The results of measurements in the age-related groups are tabulated. (tr-auth)

35096 STUDIES ON THE ARTIFICIAL RADIOACTIVITY OF FISH IN 1967 TO 1968. Randow, F.; Schulze, H.-A. (Univ., Rostock, Ger.). Nahrung; 15: No. 1, 81-9(1971). (In German).

During 1967 and 1968, ^{90}Sr, ^{137}Cs, and total beta activity were measured in the flesh of freshwater fish from lakes in the northern districts of the German Democratic Republic (Mecklenburg) and of saltwater fish from the Baltic and the North Atlantic. Total beta activity of the samples amounted to 2100 to 3100 pCi/kg. Radioanalysis revealed the following mean contaminations: bream (Abramis brama), 6 pCi ^{90}Sr/kg and 332 pCi ^{137}Cs/kg; pike (Esox lucius), 2 pCi ^{90}Sr/kg and 450 pCi ^{137}Cs/kg. Saltwater fish contained 1 to 7 pCi ^{90}Sr/kg and 120 pCi ^{137}Cs/kg (Baltic) or 24 pCi ^{137}Cs/kg (North Atlantic). The ^{90}Sr content of the bones varied between 1.0 to 2.0 pCi/g Ca (fish from the Baltic) and 4.0 to 6.4 pCi/g Ca (freshwater fish). By way of fish consumption the population of the northern districts ingests 22 pCi ^{90}Sr and 1120 pCi ^{136}Cs per capita per year, which is nearly 0.1% of the maximum allowance of yearly activity uptake. (auth)

35097 CONTENT OF STABLE IODINE IN NORMAL AND GOITER-DEGENERATED THYROID GLANDS AND ITS EFFECT ON THE UPTAKE OF ^{131}I. Malenchenko, A. F. (Inst. of Nuclear Power Engineering, Minsk). Vestsi Akad. Navuk BSSR, Ser. Biyal. Navuk; No. 2, 119-21(1970). (In Russian).

The greatest proportion of iodine found in goiter tissue was found in the colloidal form. In the parenchymal structures, the content was less. In order to compare the concentration of stable iodine in thyroidal tissues to that of goiter parenchyma, disregarding the clinical course of the illness and the histology of the tissues, it is necessary to consider the degree of expressiveness of the goiter and the functional activity of the tissues studied. A negative correlation was established between the iodine content of the gland and the iodine absorbing activity of the goiter. (tr-auth)

35098 RETENTION OF ORALLY ADMINISTERED ^{47}Ca IN MAN UNDER NORMAL AND DISEASED CONDITIONS STUDIED WITH A WHOLE-BODY COUNTER TECHNIQUE. Sjoeberg, Hans Erik (Karolinska Mediko-Kirurgiska Institutet, Stockholm). Acta Med. Scand., Suppl.; 509: 1-28(1970).

The retention of orally administered ^{47}Ca was studied using the whole-body counter technique. The technique allows direct measurement of the retention and repeated measurements at short intervals of extremely small doses of an isotope with a short half-time. The technique can also be used on ambulatory subjects and it causes very little discomfort to the patient. In 27 healthy subjects the retention of ^{47}Ca one week after administration was 35.7 ± 7.6% and after two weeks 29.3 ± 7.4% of the given dose. The error due to geometrical and biological variations was 1.7% of the given dose. The ^{47}Ca retention was also measured in malabsorption, maldigestion, malnutrition after gastrectomy, acromegaly, primary hyperparathyroidism, Cushing's syndrome, rheumatoid arthritis, and postmenopausal osteoporosis. It was decreased in patients with regional enteritis and in the rheumatoid patients, and was increased in the post-gastrectomy state, in acromegaly, and in primary hyperparathyroidism. In the remaining groups, the retention was within normal limits. A method is suggested for calculation of the total losses of endogenous calcium, based on the values for calcium retention at 7 and 14 days and the urinary losses of calcium. The therapeutic value of high doses of calcium salts was evaluated by increasing the carrier dose of stable calcium from 135 mg to 675 mg. The amount of retained stable calcium increased in all the subjects, even in those with malabsorption after intestinal resection for regional enteritis. (auth) (Sweden)

35099 RADIATION BURDENS IN INCORPORATION OF RADIOISOTOPES. Oberhausen, E. (Univ. des Saarlandes, Homburg, Ger.). Strahlenschutz Forsch. Prax.; 9: 45-9(1969). (In German).

From ninth conference of the Society of German Radiation Medicine; Aachen, Germany (11 Oct 1968). See CONF-681082.

Generally, the radiation burden to medical personnel can be kept below permissible levels in a well-organized nuclear medicine department because of the short half-lives involved. In industrial application, where long-lived radioisotopes often are used, the situation is more hazardous. The case of two chemists who incorporated ^{226}Ra, with an annual radiation burden to the bone of 30 to 90 Rem, is reported. In most of the industrial applications, ^{137}Cs plays a major role because of the fact that it is absorbed mainly in the gastrointestinal tract. The incorporation of ^{137}Cs in excessive amounts was observed in two cases. However, minor transgression of the permissible dose occurred in about 20 cases. (H.B.G.)

35100 INCIDENCES OF RADIOISOTOPE INCORPORATION IN THE STATE OF NORDRHEIN-WESTFALEN. Rahm, G. Strahlenschutz Forsch. Prax.; 9: 73-81(1969). (In German).

XUM

From ninth conference of the Society of German Radiation Medicine; Aachen, Germany (11 Oct 1968). See CONF-681082.

For Nordrhein-Westfalen, statistical analysis of radioisotope incorporation by professional personnel showed that ^{131}I represents the major hazard for medical personnel, while tritium represents the predominant risk in the production of fluorescent paints. Thus far, radiation injuries have not been observed. Monitoring by both whole-body counting and urinary excretion should be applied prior to the occurrence of injuries and, since August 1968, is mandatory for all employees handling openly certain amounts of these substances. (H.B.G.)

Radiation Effects

Refer also to abstracts 34625, 34639, 34654, 34655, 34664, 35196, and 35215.

35101 MOLECULAR NATURE OF RADIOBIOLOGICAL PHENOMENA. Davila Sanchez, Carlos A. (Junta de Energia Nuclear, Madrid). Energ. Nucl. (Madrid); 14: 31-9(Jan-Feb 1970). (In Spanish).

Using schematic representations of the historical evolution of radiobiological phenomena, it was shown that a causal relation for these phenomena could be described only if molecular mechanisms were considered. Estimations of the order of magnitude of energy contributions, assuming lethal doses, indicate that the response of the biological system is disproportional when total energy relations are considered. The responses of the system are conditioned by interactions at the molecular level revealing a high degree of hierarchy. The schematic representations show that DNA is the most important biological macromolecule in the hierarchy. The enzymatic mechanisms evolved for the protection of these macromolecules against ionizing radiations are considered. (tr-auth)

35102 BIOCHEMICAL AND PHYSIOLOGICAL CHANGES IN GAMMA-IRRADIATED WHEAT DURING GERMINATION. Ananthaswamy, H. N.; Vakil, U. K.; Sreenivasan, A. (Bhabha Atomic Research Centre, Trombay, India). Radiat. Bot.; 11: 1-12(1971).

Impaired seedling growth on germination of wheat irradiated with ^{60}Co gamma rays at 20 to 200 krad dose levels, was observed. Growth was inhibited by 50 to 62% at low doses from 20 to 40 krad and almost completely at higher doses. Presoaking of control and irradiated grains in 2×10^{-5} M gibberellic acid for 16 hr resulted in stimulation of seedling growth and synthesis of alpha-amylase and ribonuclease in control seeds; gibberellic acid caused its normal effects despite radiation treatment with low doses. Radiation or/and gibberellic acid treatment exerted no marked effects on 3'-nucleotidase activity. Decreased incorporation of ^{14}C leucine in nascent alpha-amylase in irradiated seeds during 4 days germination could be attributed to its impaired de novo synthesis. The relative permeability of ^{14}C leucine in wheat was not changed by radiation treatment. Endogenous amino acids pool sizes were significantly low in irradiated seeds, but, specific activity of ^{14}C leucine was high in irradiated seeds. (auth) (UK)

35103 TEMPERATURE DEPENDENCE OF RADIATION-INDUCED FREE-RADICAL DESTRUCTION. Horan, Paul Karl; Snipes, Wallace (Univ. of California, Berkeley). Int. J. Radiat. Biol.; 19: 37-43(1971).

The study of the temperature dependence of radiation-induced free-radical destruction in N-acetyl-DL-valine led to the conclusion that at least two processes were involved. One process was temperature-independent with a rate constant of 0.07 MR^{-1}. The second process had a temperature-dependent rate constant, and kinetic analysis yielded an activation energy of 0.71 kcal/mole. Irradiations were carried out with 6.5 MeV linear accelerator electrons at a dose rate of 0.5 mR 1 min. (auth) (UK)

35104 STUDIES ON THE METABOLISM OF NUCLEAR BASIC PROTEINS AFTER RADIATION IN VITRO. Ghosh, M. (Atomic Energy of Canada Ltd., Chalk River, Ont.). Can. J. Biochem.; 49: 456-62(Apr 1971). (AECL-3828).

Exposure of isolated rabbit lymphocytes to 1000 R γ-radiation results in an increased rate of incorporation of amino acids-^{14}C into cellular proteins during the first hour after irradiation. Fractionation of the proteins showed that the synthesis of basic proteins extracted from the nucleus was most affected. Two factors contributed to this apparent stimulation of protein synthesis by irradiation: a transient increase in the amount of amino acid-^{14}C available for protein synthesis in the cell; and an increase in concentration of sodium ions in the cell. It is suggested that much of the observed increase in amino acid incorporation after irradiation of the lymphocytes is caused by radiation-induced changes in cell permeability. (auth) (Canada)

35105 METABOLIC CHANGES IN TISSUES PREPARED FROM IRRADIATED SWEET POTATO ROOTS WITH REGARD TO ETHYLENE EFFECTS. Ogawa, M.; Uritani, I. (Nagoya Univ., Japan). Radiat. Bot.; 11: 67-71(1971).

The stimulation of peroxidase development by γ radiation and exogenous ethylene was investigated in sweet potato disks. Results showed that the stimulation of peroxidase development by γ irradiation was brought about by an unknown mechanism, independent of ethylene effect. Irradiation was at 30, 60 and 90 krad from a ^{60}Co radiation source (dose rate: 20.5 krad/hr). Concentrations of ethylene were from 0-1000 ppM. (auth) (UK)

35106 HEME-PROTEIN INTERACTION AND RADIORESISTANCE. Crippa, P. R.; Vecli, A. (Univ. of Parma, Italy). Stud. Biophys.; 13: 65-8(1969).

From the study of radical yield in myoglobin and cytochrome c irradiated with x rays, information was obtained concerning the role of the link between the protein and the heme in intramolecular excitation transfer. (auth)

35107 UV INACTIVATION OF NADH. Hanschmann, H.; Berg, H. (Deutsche Akademie der Wissenschaften, Berlin. Institut fuer Mikrobiologie und Experimentelle Therapie, Jena, Ger.). Stud. Biophys.; 13: 69-72(1969). (In German).

The irradiation of NADH by uv light (λ = 254 nm) inactivated the NADH coenzyme. Spectrophotometric, polarographic, and chemical investigations proved that the inactivation is caused by oxidative formation of a dimer compound. (auth)

35108 REGENERATION OF IN VITRO X-RADIATION-INDUCED INJURIES OF DNA BY POLYNUCLEOTIDE LIGASE. Postnova, T. I.; Glazer, V. M.; Shestakov, S. V. (Moscow State Univ.). Dokl. Akad. Nauk SSSR; 195: 976-8(1 Dec 1970). (In Russian).

The potential recovery from x-radioinduced breaks in DNA was investigated by using E. K. F. Bautz's method originally developed for phage transformation. Instead of the molecular weight change of the affected DNA, the level of its biological activity was used to determine the extent of radiation injury. It was found that even relatively low x-ray doses of 1 to 2 kR considerably lowered the transformation activity of DNA. The polynucleotide ligase (DNL) at its optimum concentration did not affect the transformation capacity of the original DNA and nearly completely regenerated the transformation activity of DNA inactivated by DNAase which caused the unifilar 5'P and 3'OH type breakdowns. Thus the results point to the potential recovery in the cell from x-radioinduced injuries by means of a single stage crosslinkage by DNL. (TTT)

35109 CHEMICAL AND ENZYMATIC PROPERTIES OF ^{60}Co γ-IRRADIATED SUBTILISIN BPN. Ohtsuki, Kozo; Fukuhara, Masakatsu; Sumizu, Koichiro; Hatano, Hiroyuki (Kyoto Univ.). J. Radiat. Res.; 11: 113-19(Sep-Dec 1970).

When subtilisin BPN' solutions were irradiated with ^{60}Co γ rays, three hydrolytic activities of the subtilisin toward N-acetyl-L-tyrosine ethyl ester (ATEE), N-benzoyl-L-arginine ethyl ester (BAEE), and casein were found to be lost at different rates with doses of 30 to 300 krads. The esterase activity toward ATEE was most radiosensitive and the protease activity toward casein was most radioresistant. Behavior of the irradiated subtilisins on electrophoresis showed that these enzymes had more electronegative charges than native ones. Two tyrosine, one tryptophan, one methionine, and one histidine residues were lost from the irradiated subtilisin which had 55% survival activity of the hydrolysis of ATEE after exposure to 110 krads of γ rays, but still had 70% BAEE, 75% casein hydrolytic activities, and 85% active site which was determined by using diisopropyl fluorophosphate. The results suggest that the radiolysis of these several amino acid residues in subtilisin carries about these new features of irradiated subtilisin against the three kinds of substrates. (auth)

35110 KINETIC AND CHEMICAL PROPERTIES OF ^{60}Co γ-IRRADIATED SUBTILISIN BPN IN AQUEOUS SOLUTION. Ohtsuki, Kozo (Kyoto Univ.). J. Radiat. Res.; 11: 120-6(Sep-Dec 1970).

The effects of ^{60}Co γ ray irradiation on subtilisin BPN' solutions were studied. Kinetic parameters of the enzyme toward N-acetyl-L-tyrosine ethyl ester and N-benzoyl-L-arginine ethyl ester were affected in a different way by the irradiation. Amino acid composition of γ-irradiated diisopropyl phosphoryl-subtilisin, which was separated from low molecular weight fractions by gel-filtration, showed that two tyrosine and about one tryptophan residues were damaged and one methionine residue was oxidized to methionine sulfoxide with dosage of 125 krads. Conformational changes of the irradiated enzyme were studied by

XUM

two methods. Modification with 5-diazo-1-H-tetrazole and hydrolysis with α-chymotrypsin of the irradiated diisopropyl phosphoryl-subtilisin indicated that the tertiary structure of the enzyme was less rigid than the native one. From these results, it was concluded that the radiation damage of a few amino acid residues in the enzyme brought about the conformational changes and the altered kinetic parameters of the irradiated enzyme. (auth)

Immunology

35111 RELATIVE EFFICACY OF INTRAPERITONEAL APPLICATION OF HAEMATOPOIETIC CELLS TO IRRADIATED MICE. Fiala, J.; Viktora, L.; Urbancova, Jaromira (Inst. of Haematology and Blood Transfusion, Prague). Folia Biol. (Prague); 17: No. 1, 37-40(1971).

An attempt was made to estimate the relative efficacy of the intraperitoneal (as compared to intravenous) route of application of hematopoietic cells to irradiated mice by comparing the respective numbers of spleen colonies detectable nine days after inoculation of similar numbers of cells. In addition, the morphological picture and the incidence of reticulocytes in the spleen of injected mice were compared in the two groups. The results obtained on the basis of these methods make it possible to estimate that the fraction of cells resorbed from the peritoneal cavity amounts only to $1/10$ to $1/6$ of the number of cells that reach the spleen when the inoculation is intravenous. (auth)

35112 REGULATION OF HOMOCYTOTROPIC ANTIBODY FORMATION IN THE RAT. II. EFFECT OF X IRRADIATION. Tada, Tomio; Taniguchi, Masaru; Okumura, Ko (Chiba Univ., Japan). J. Immunol.; 106: 1012-18(Apr 1971).

Homocytotropic antibody (HTA) formation, as measured by the passive cutaneous anaphylaxis (PCA) test, was enhanced and prolonged by 400 R whole-body x irradiation given shortly before immunization of rats with dinitrophenylated Ascaris extracts (DNP-As) plus killed Bordetella pertussis. Delayed enhancement and prolonged production were most striking when x irradiation was given 1 day before to 2 days after initial immunization. An adjuvant effect of 400 R was produced in rats immunized with DNP-As alone omitting B. pertussis. As evidenced by passive hemagglutinin titers after 2-ME treatment, the production of γG antibody was greatly suppressed by 400 R x irradiation. Two possible pathways to account for the irradiation effects on HTA formation were postulated, i.e., the enhancement of γM antibody and the suppression of 7S γG antibody resulted in a defective humoral feed back regulation, and the depletion of certain populations of lymphoid cells, probably of thymic origin, caused cellular regulatory disturbances. (auth)

35113 ATTEMPTS TO ABOLISH TOLERANCE OF SKIN HOMOGRAFTS IN MICE WITH X-IRRADIATED PLASMA FROM SPECIFICALLY SENSITIZED DONORS. Lubaroff, David M.; Silvers, Willys K. (Univ. of Pennsylvania, Philadelphia). J. Immunol.; 106: 1122-4(Apr 1971).

The ability of plasma from sensitized, lethally x-irradiated mice to abolish tolerance of skin homografts was investigated. The graft was destroyed in only 1 of 12 tolerant mice that received plasma. A somewhat higher incidence (4/10) occurred in mice inoculated with serum from unirradiated donors. In contrast, all mice injected with sensitized lymphoid cells rejected their grafts. (auth)

35114 TRANSFER OF EXPERIMENTAL AUTOIMMUNE THYROIDITIS OF THE MOUSE BY SERUM. Vladutiu, Adrian O.; Rose, Noel R. (State Univ. of New York, Buffalo). J. Immunol.; 106: 1139-42(Apr 1971).

Female CF-1 mice, 8 weeks old, immunized with thyroid extract were x irradiated with a dose of 920 R, 9 days after the first injection of antigen. They were killed 3 days later and the sera pooled. Six female CF-1 mice, 8 weeks old, were injected with a serum pool, 0.5 ml in the tail vein and 0.5 ml intraperitoneally, and were killed 9 days later. None of them had thyroid antibodies or lesions, which suggested that lymphoid cell breakdown did not increase levels of the circulating pathogenic agent in donor mice. The results indicate that a circulating serum factor can provoke thyroiditis 2 weeks after transfer. The lesions were identical in appearance to those seen after active immunization, but were less severe. Radiothyroidectomy increased the percentage of successful transfers but not the severity of the lesions. (P.B.M.)

Ecology

Refer also to abstracts 37104 and 37105.

35115 (BNWL-1543) BIBLIOGRAPHY OF ECOLOGICAL PUBLICATIONS SUPPORTED BY THE ATOMIC ENERGY COMMISSION RELATED TO COLUMBIA RIVER THERMAL EFFECTS STUDIES. Templeton, William L.; Coutant, Charles C. (Battelle-Northwest, Richland, Wash. Pacific Northwest Lab.). 1 Mar 1971. Contract AT(45-1)-1830. 23p. Dep. NTIS.

Hanford publications from 1946 through 1970 that are relevant to thermal effects questions are listed. Many reports included are annual reports or special laboratory reports that are available either from the National Technical Information Service, Springfield, Virginia, or from the Librarian, Biology Library, Battelle-Northwest, P. O. Box 999, Richland, Washington. Others are articles published in the open literature. The reports offer a chronicle of relevant environmental studies that can be matched by few industrial enterprises in this country. The ecological effects of Columbia River temperatures have been studied in the field and laboratory at Hanford for nearly 25 years. Ecological research in the first two decades centered on the consequences of releasing radioactive materials in reactor cooling water discharges. The nearly complete paucity of radiological information necessitated this emphasis. However, the effects of temperature increases and chemical toxicity of effluents were also studied as significant aspects of the total environment. Thermal studies were expanded in 1966 coincident with rising national concern for environmental effects of electric power production and development of waterways as cooling water sources. The Hanford complex of nuclear reactors was seen as a useful prototype for studying many of the ecological effects anticipated from nuclear power plants. In addition, proposed development of the Columbia's apparent cooling water potential exposed serious concern over the capacity of this river to absorb heat, both additional and that already emanating from Hanford. Difficulties inherent in establishing temperature criteria for the Columbia led in 1968 to a cooperative, interagency Columbia River Thermal Effects Study with the AEC, the FWQA (now Environmental Protection Agency), and the Bureau of Commercial Fisheries (now National Marine Fisheries Service), as research participants, with other federal, state, and industrial interests serving on an Advisory Committee. This Thermal Effects Study has further stimulated research efforts. Some reports in the final stages of preparation are included. (auth)

35116 MEASUREMENTS OF ^{60}Co ORGAN BURDENS IN RATS AND THEIR USE IN CALCULATIONS OF EQUILIBRIUM DOSE-RATES TO VARIOUS ORGANS OF MAN. Smith, T.; Thompson, B. D.; Barnaby, C. F. (University Coll. Hospital Medical School, London). Health Phys.; 20: 195-204(Feb 1971).

The amount of ^{60}Co absorbed by rats given $^{60}CoCl_2$ in drinking water was only about one quarter of the amount absorbed by rats given $^{60}CoCl_2$ by gastric intubation. When allowances were made for this difference, retention data obtained in single-administration studies, in which rats were given $^{60}CoCl_2$ by gastric intubation, closely predicted the organ burdens acquired by rats allowed to drink ^{60}Co-water continuously for given periods. The subsequent whole-body retention of ^{60}Co by rats restored to normal drinking water was also accurately predicted and this result confirmed the value of the half-life of the long-term whole-body retention component observed in single-administration studies. Using the values of organ burdens at equilibrium, derived from the results of this study, calculations were made of the dose rates that would be delivered to organs of man if the metabolism of cobalt were similar in rat and man. On this basis the lower large intestine (LLI) would be the critical organ for ingested ^{60}Co and the maximum permissible concentration (MPC) of ^{60}Co in drinking water, applicable to individual members of the public, would be 4.5×10^{-5} μCi/ml. This MPC agrees with the presently accepted IGRP value. The possible differences between actual dose rates to organs of man and those predicted by extrapolation from rat data are discussed. (auth) (UK)

35117 MORSKAYA RADIOEKOLOGIYA. (Marine Radioecology). Polikarpov, G. G. (ed.). Kiev; Izdatel'stvo Naukova Dumka (1970). 276p.

Investigative methods for studying various fields of marine biology and oceanography are described in the book. The dynamics and the nature of radioactive and chemical metabolism among the hydrobionts of this medium are analyzed as well as the radioisotopes in marine animals, radiosensitivity of embryonal mitosis, and radioecology of seas and oceans and their tropical regions. The hydrobiological and ecological behavior of Ru and Rd, the uptake and retention of ^{137}Cs, ^{90}Sr, ^{95}Zr, ^{95}Nb, and ^{65}Zn by marine organisms (plankton, fish, shellfish, etc.), and the distribution of Cu in marine waters are also discussed. An extensive bibliography is included. (R.V.J.)

Genetics and Cytogenetics

Refer also to abstracts 35202 and 35230.

35118 SOME REACTIONS OF THE ORGANISMS TO RADIATION IN DIFFERENT OXYGEN PRESSURES. Avakyan, Ts. M.; Semerdzhyan, S. P.; Nor-Arevyan, N. G.; Hagyan, H. (Inst. of Physics, Erevan. Inst. of Zemledeliye, Ecmiadzin, USSR). Stud. Biophys.; 15-16: 211-22(1969).

From second international symposium on initial effects of ionizing radiation on a cell; Erevan, USSR (Oct-Nov 1968). See CONF-681087.

Experiments carried out on 3 day old roots of Vicia faba under x irradiation with a dose of 200 R showed that oxygen in pressures of 0.2 to 0.7 atm increases radiation injury of chromosomes, while higher pressures of 1.5 to 5 atm lowered injury. Further increase in pressure led to some increase in chromosome aberrations. (P.B.M.)

35119 TWO ASPECTS OF OXYGEN INFLUENCE IN A RADIOBIOLOGICAL EXPERIMENT. Atayan, R. R. (Inst. of Agriculture, Ecmiadzin, USSR). Stud. Biophys.; 15-16: 327-35(1969).

From second international symposium on initial effects of ionizing radiation on a cell; Erevan, USSR (Oct-Nov 1968). See CONF-681087.

The influence of post irradiation hydration of pea seeds in an oxygen atmosphere on radiation damage was studied. Dose response and time response curves for chromosome aberrations were determined. Data show that radiation injury takes place when pea seeds are hydrated in the presence of oxygen. Within 30 min after hydration the damage reached a maximum, and further exposure of seeds to oxygen did not modify the primary yield of chromosome aberrations. (P.B.M.)

35120 FAR-RED LIGHT EFFECT ON ULTRAVIOLET LIGHT INDUCED CHROMATID ABERRATIONS IN POLLEN TUBES OF TRADESCANTIA. Ma, Te Hsiu; Snope, A. J.; Chang, Tsai Ying (Smithsonian Institution, Washington, D. C.). Contract AT(30-1)-2373. Radiat. Bot.; 11: 39-43(1971).

A total dose of 7.65×10^5 erg cm^{-2} of far-red light (730 nm) was administered immediately after a total dose of 10^6 erg cm^{-2} of ultraviolet light (253 nm) treatment to mature dry pollen of Tradescantia paludosa. Three control groups were maintained: uv alone (uv), far-red alone (fr), and dark control (DC), in order to determine the effect of far-red light on uv-induced chromatid aberrations (uv + fr). Chromatid aberrations, including exchanges, chromatid and isochromatid breaks, were scored from metaphase figures of 18 hr old pollen tube culture grown on lactose agar medium supplemented with 0.02% colchicine. The average results of duplicated experiments indicated that the uv + fr group had about 46 percent lower aberration rate than the uv group, while the fr and DC groups yielded similar background aberration rates. The lower rate of aberration in uv + fr group was postulated to be either the result of mitotic cessation for uv + fr induced aberrant cells which therefore failed to reach metaphase stage to be scored for aberrations, or far-red light enhanced reparation of uv-induced breakage. (auth) (UK)

35121 INDUCTION OF MUTATION BY γ IRRADIATION IN THE PRESENCE OF OXYGEN OR NITROGEN. Alderson, T.; Scott, B. R. (Medical Research Council, Harwell, Eng.). Nature (London) New Biol., 230: 45-8(10 Mar 1971).

Experiments were made to show the effect of γ irradiation (16, 32, 48, 66 Kr) in the presence of oxygen or nitrogen on the reversion of the Meth GI strain of Aspergillus nidulans. Further experiments showed the effect of γ irradiation (32, 54, 80 Kr) on the frequency and distribution of 2-thioxanthine resistant mutants (2-TxR, hx, uaY and cnx) in the presence of oxygen or nitrogen. The results with both mutational systems showed a greater forward mutational response of gene loci to γ irradiation carried out in aqueous suspension in the presence of oxygen rather than nitrogen. The effect appeared independent of conidial survival levels. The interlocus specificities for mutation were shown to be dependent on the gas present at the time of irradiation; bubbling with the alternative gas immediately afterwards did not change the prevailing conditions. (UK)

35122 NEUTRON-INDUCED MUTANTS OF PISUM SATIVUM AND THEIR COMPARISON WITH X-RAY-INDUCED GENOTYPES. Chen, R.; Gottschalk, W. (Univ., Bonn). Angew. Bot.; 44: 325-42(Jan 1970). (In German).

Mutants (161) of Pisum sativum were selected after irradiation of dry seeds with neutrons. The chimerical nature of the M1 plants already known from x ray treatment was confirmed after neutron irradiation. The proportion of lethal mutants was considerably lower following neutron treatment than with x rays. Only 14% of all neutron-induced mutants were lethals while the corresponding proportion in x ray experiments was 27%. In the same trial some genes mutated several times; furthermore, at least 11 neutron-induced mutants were identical with genotypes obtained by x irradiations. It was concluded, that on principle many genes of the Pisum genome show the same response to the action of neutrons and x rays. The seed production of the fertile mutants varied between 200 and 10% of the original line. (auth)

35123 EFFECT OF CYSTAMINE ON THE CHROMOSOME ABERRATIONS OF LYMPHOCYTES OF PERIPHERAL HUMAN BLOOD IN THE CASE OF FRACTIONAL LOCAL γ IRRADIATION. Berlin, L. B. (Academy of Military Medicine, Leningrad). Dokl. Akad. Nauk SSSR; 195: 998-1000(1 Dec 1970). (In Russian).

The influence of cystamine on the frequency of chromosome aberrations in the lymphocytes of the peripheral blood was investigated in 36 female, 34- to 72-yr old patients afflicted with tumors. After removal of the uterus because of malignancy, the patients were treated weekly by γ teletherapy at a rate of ~500 rad per session. Some of the patients were administered 0.8 g cystamine one hour before the treatment. Within 12- to 24-hr after the 1st, 3rd, 5 to 6th, 10 to 11th, and 16 to 17th session, 10 ml of venal blood were collected for leukocyte culture to determine the metaphase chromosomes. The results revealed that the unirradiated patients exhibited 1.5% of cells with chromosome aberrations; this rose to 2.6% for patients irradiated once and to only 1.6% to those who were administered cystamine before the radiation treatment. Upon further exposure, the cells with aberrations showed a linear relation; the number of such cells in patients who received cystamine was always much lower. No mutagenic effect of cystamine was found; administration of this agent after irradiation did not change the number of chromosome aberrations. (TTT)

35124 X-RAY INDUCED 8-AZAGUANINE-RESISTANT CELLS IN L POPULATION. Adomaitene, D. (Inst. of Cytology, Leningrad). Tsitologiya; 13: 368-73(Mar 1971). (In Russian).

Non-treated L cells and those treated with the selective HAT medium to remove spontaneous 8-azaguanine resistant variants were x-irradiated at a dose of 300 R (LD_{50}). The analysis of the dynamics of frequency appearence of 8-azaguanine resistant cells revealed a mutagenic aftereffect on the irradiated cellular populations. No radioinduced 8-azaguanine resistant variants were found when the selective agent was injected immediately after irradiation; these were found some days after the mutagenic treatment. The frequency of x ray-induced 8-azaguanine-resistant cells rose with the increase of the time interval between the radiation and 8-azaguanine injection. An increased frequency of 8-azaguanine resistant variants was registered in the irradiated populations during 2 months after mutagenic treatment (it was about 10 times as high as that in the untreated control). X ray-induced 8-azaguanine resistant subline L/AG-R was isolated. After several months cultivation in drug free medium the L/AG-R cells retained their resistance to the selective agent which confirmed a hereditary nature of the marker. No karyological changes were found in the L/AG-R cells as compared with the spontaneous 8-azaguanine resistant ones. The subline L/AG-R was as radiosensitive as L cells. L/AG-R cells were unable to utilize exogeneous hypoxanthine while cultured on the HAT medium. (auth)

35125 EFFECT OF THERMAL HARDENING OF THE SPROUTS OF WHEAT AND ONION ON THE FREQUENCY OF CHROMOSOME ABERRATIONS CAUSED BY X-RAY IRRADIATION. Babayan, R. S.; Zavaryan, E. L. (Lab. of Induced Mutagenesis of Plants, Erevan). Tsitologiya; 13: 348-54(Mar 1971). (In Russian).

Sprouting seeds, prior to x irradiation, were subjected to 40°C for 10 to 15 min. Such an effect resulted in the decrease of the quantity of chromosome aberration in the cells of wheat sprouts and onion radicles. Different cell stages in the onion radicles reacted differently to the heating effect. It is supposed that the protective effect of the heating is realized at phases G_2 and S. (auth)

35126 EFFECT OF DONOR IRRADIATION ON THE FREQUENCY OF APPEARANCE OF PROXIMAL NONSELECTIVE MARKERS. Novitskaya, M. A.; Troitskii, N. A.; Bylinskii, A. F. (Inst. of Genetics and Cytologies, Minsk. Minsk State Univ.). Vestsi Akad. Navuk BSSR. Ser. Biyal. Navuk; No. 2, 106-8(1970). (In Russian).

Escherichia coli K-12, acting as a donor, was neutron-irradiated at a dose of 650 rads and crossed with AB 1157 F − recipients. Recombinants, selected for Arg^+ Sm^+, were analyzed for the presence of nonselective markers. Neutron irradiation of the donor increased significantly the yield of recombinants for selective markers and altered to a certain degree the frequency of the appearance of nonselective markers. The appearance of nonselective markers was increased in the progeny of the irradiated donors in proportion to the length of the segment selected. It is suggested that following neutron irradiation, two types of donor chromosome damages were induced—one led to an increase in the possibility of inclusion of

XUM

larger segments of the donor chromosome, while the other led to an increase in the degree of crossing over occurring at the point of damage. (tr-auth)

35127 RADIATION-INDUCED TRANSLOCATIONS IN PRUNUS AVIUM CV. LAMBERT. Whelan, E. D.; Hornby, C. A. (Univ. of British Columbia, Vancouver). Can. J. Bot.; 49: 623-30(Apr 1971).

Meiosis, pollen viability, and growth changes were investigated in two of six radioinduced reciprocal translocation mutants of Lambert sweet cherry (Prunus avium L). Meiosis in mutant 19-23-1CL was characterized by a quadrivalent which was evident from pachynema to metaphase I. A circle-4 configuration normally was observed, and alternate and adjacent configurations occurred with equal frequency. Pollen stainability tests indicated 28% normal pollen, as compared to 58% for the parental Lambert clone. Changes in growth habit were evident, the onset of meiosis and flowering were delayed, and only 2% of the blossoms set fruit. Any fruit retained was poor in color, noticeably pointed, and had a prominent longitudinal dorsal ridge. Meiosis in mutant 16-4E was more complex than in 19-23-1CL. Quadrivalents rarely were observed, and most meiocytes contained a trivalent and a centric fragment, or a univalent and centric fragment. Meiotic abnormalities associated with these defects frequently were evident throughout meiosis. Pollen stainability tests indicated about 34% normal pollen. No marked changes in growth habit, onset of meiosis, or flowering were evident. Fruit drop was about four times that of normal Lambert. Fruit retained appeared normal. (auth) (Canada)

35128 STRUCTURAL MUTATION INDUCED BY ^{137}Cs GAMMA IRRADIATION OF PHASE G. CHROMOSOMES IN THE CELLS OF CREPIS CAPILLARIS SHOOTS. Khalikov, P. Kh. (Inst. of General Genetics, Tashkent). Dokl. Akad. Nauk Uzb. SSR; No. 6, 58-60(1970). (In Russian).

Tabulated data are given on chromosome injuries in the cells of Crepis capillaris shoots in the G(1) phase induced by ^{137}Cs γ radiation with doses from 0 to 1,024,000 R. It was found that the appearance of cells with injured chromosomes and the frequency of chromosome reconstruction increased linearly with increased dose. After exposure to the 16,000 to 256,000 R all chromosomes in the cells of the shoots were injured. (R.V.J.)

35129 INCIDENCE OF DOMINANT LETHAL MUTATIONS AFTER X-IRRADIATION OF SPERMATOZOA OF MICE AND RATS. Gilliavod, Norberto; Leonard, Alain (Centre d'Etude de l'Energie Nucleaire, Mol, Belgium). Strahlentherapie; 141: No. 3, 351-3(Mar 1971).

Male mice from the BALB/c strain and male rats from the Wistar strain received whole-body irradiation with 400 R x rays. After irradiation, each male was mated for a period of 7 days with 3 virgin females in order to estimate the rate of dominant lethality induced in spermatozoa. On the seventeenth day after beginning of the mating, all females were dissected, and the number of corpora lutea and living and dead embryos was recorded. It was found conclusively that the incidence of dominant lethality induced by 400 R of x-irradiation given to spermatozoa was about 50% higher for rats than for mice. The genetic radiosensitivity of the rat appeared to be intermediate between the radiosensitivity of the hamster and the mouse. (auth)

Health Physics and Safety

Refer also to abstracts 34792, 34803, 34849, and 35088–35092.

35130 RADIATION PROTECTION FROM UNSEALED RADIOACTIVE MATERIAL AND EFFECT OF RADIATION ON THE CELL STRUCTURE. Ninth Conference of the Society of German Radiation Medicine, Aachen, Germany, October 11–12, 1968. Braun, Heribert; Frik, Wolfgang; Haage, Horst; (and others) (eds.). Strahlenschutz Forsch. Prax.; 9: 1-120(1969). (In German). (CONF-681082).

Separate abstracts were prepared for all twelve papers included in the conference proceedings. (H.B.G.)

For abstracts of individual papers see: 35099, 35100, 35134, 35150, 35151, 35153, 35154, 35179, 35189, 35209, 35210, and 35258.

Radioactive Contamination and Decontamination

35131 HEALTH PHYSICS ASPECTS OF THE DECONTAMINATION OF A HIGH LEVEL ACTIVITY CELL LINE. Clayton, R. F.; Smith, J. W. (Atomic Energy Research Establishment, Harwell, Eng.). Health Phys.; 20: 153-65(Feb 1971).

During the preparation of ^{90}Sr titanate sources, the general purpose high activity cell line at A.E.R.E., Harwell became heavily contaminated, resulting in surface beta dose-rates up to 10^5 rad/hr. Some remote cleaning was done, but for effective decontamination, controlled cell entries were made by operators. The report describes the methods used to assess the hazards to persons centering the cell-line, to prevent the spread of surface and airborne contamination from the cell-line, and to control the radiation exposure of the personnel employed. Of the approximately 250 men employed, who between them made about 440 cell entries, only 18 received surface doses in excess of the relevant permitted 13 week level, and none took a significant amount of radioactive material into his body. The necessity for wearing an array of dosimeters on the body when working in beta radiation fields is demonstrated. An attempt was made to use the large numbers of results (9000 thermoluminescent dosimeters and 2000 film dosimeters) to provide information on the relative performance of the dosimeters under difficult operational conditions. Thermoluminescent dosimeters generally under-read compared to film dosimeters by 10 to 34% depending upon the position on the body although in the overexposure cases it was noted that this was so only in eight of the nineteen comparisons made. The possible causes of these variations are discussed in detail. (auth) (UK)

35132 RADIOACTIVE CONTAMINATION OF THE ATMOSPHERE AROUND VALENCIA MEASURED FROM JANUARY 1966 TILL APRIL 1968. Catala, J.; Diez, R.; Perez, R.; Senent, F. (Inst. of Corpuscular Physics, Valencia). Rev. Agroquim. Tecnol. Aliment.; 10: 540-9(Dec 1970). (In Spanish).

Data are presented on the fallout radioactivity of atmospheric dust and rain around Valencia, monitored from January 1966 until April 1968. Various aspects of fallout from nuclear tests and the fallout from the stratosphere into the troposphere are discussed. (tr-auth)

35133 ^{131}I IN THYROIDS OF CATTLE AND SHEEP OF PORTUGAL. Simoes, Jose Henriques; Teixeira, Manuel Ribau (Servico de Proteccao Contra Radiacoes, Sacavem, Portugal). Zentralbl. Veterinaermed., Beih.; No. 11, 101-9(1970). (LFEN–115).

After the 3rd Chinese nuclear weapon test, a survey on ^{131}I in thyroids of pasture-fed livestock from the Portugese Mainland and the Azores Islands was conducted. Samples of 100 g of thyroid tissue were counted by γ spectrometry. The data obtained showed higher specific activities in sheep than in cattle glands. The first noticeable detection of ^{131}I after the Chinese weapons tests was 14 days after the 3rd and 5th, 11 days after the 4th and 9 days after the 7th. After the sixth test, the first thermonuclear one, no noticeable radioactivity increase in the glands was observed. During the survey, some samples, collected in an area in the north of the country showed a γ spectrum very different from those usually observed. Their total spectrum was similar to that of the not separated ^{226}Ra spectrum, with the 0.352-MeV photopeak of the ^{214}Pb interfering with the 0.364-MeV photopeak of ^{131}I. (auth)

35134 PRESENTLY AVAILABLE METHODS FOR ELIMINATION OF RADIOISOTOPES FROM THE BODY AND THEIR PRACTICAL APPLICATION. Moehrle, G. (Kernforschungszentrum, Karlsruhe, Ger.). Strahlenschutz Forsch. Prax.; 9: 67-73(1969). (In German).

From ninth conference of the Society of German Radiation Medicine; Aachen, Germany (11 Oct 1968). See CONF-681082.

Radioisotope removal from the organism by chelating agents is discussed. DTPA administration is the treatment of choice for a large number of radionuclides, such as lanthanum, thorium, uranium, and the transuranium elements. Appropriate doses for acute and chronic treatment are given. In the case of incorporation of a fission product mixture, selection of suitable chelating agents depends on the strontium content. For low strontium concentrations, DTPA seems to be superior, while for high radiostrontium levels, BAETA is indicated. If radiostrontium is absorbed through the gastrointestinal tract, administration of sodium alginate is presently the best countermeasure. With respect to ^{137}Cs removal, none of the chelating agents is effective; however, gastrointestinal absorption can be inhibited by oral administration of Prussian Blue. Superiority of DTPA in comparison with EDTA is discussed. (H.B.G.)

Dosimetry and Monitoring

Refer also to abstracts 34869–34871, 34879, 34894, 35023, 35030, 35059, 35116, and 35211

35135 (CNAEM–77) MANUAL FOR TURKISH FILM DOSIMETRY STANDARDS, 1962–1969. Goeksel, Selahattin A.; Senkon, Hasret (Cekmece Nuclear Research Center, Istanbul

(Turkey)). 1970. 19p. (In Turkish). Dep. NTIS (U. S. Sales Only).

The research and monitoring program of the film dosimetry service at the Cekmece Health Physics Division is described, indicating the results of film-dosimetry-based radiation monitoring surveys carried out at the Center and elsewhere in the country. The eight-year study permitted the accumulation of general data on the distribution of the radiation exposure doses among persons who handle radioactive material. This is of special importance because it made possible the identification of individuals who received excessive irradiation. The working environment of these persons who changed and more effective means of protection against radiation were recommended. (TTT)

35136 CONTRIBUTION TO DOSIMETRY IN COBALT-THERAPY. GRAPHIC METHODS FOR ESTABLISHING ISODOSE CURVES IN FIXED FIELDS AND CYCLOTHERAPY. Dutou, L. (Centre Leon-Berard, Lyon). Ann. Radiol.; 12: R929-63(1969). (In French).

A method permitting the tracing of isodose curves of fixed fields and a method for the rapid calculation of isodoses in cyclotherapy are presented. The theoretical bases, practical development, and a critical evaluation of each method are given. (J.S.R.)

35137 PHYSICAL ASPECTS OF IRRADIATION. National Bureau of Standards Handbook 85. Washington, D. C.; National Bureau of Standards (1964). 114p. (ICRU-10b). Available from Superintendent of Documents, GPO, Washington, D. C.

Various techniques for the measurement of absorbed dose and exposure are discussed. Characteristics of radiation (x, γ, and neutron) instrumentation are covered in some detail, including the more sophisticated work on standards. The specification and measurement of radiation quality of incoming beams and γ- and x-ray spectra are considered. Available data for stopping-power ratios and the average energy (W) required to produce an ion pair in a gas were reviewed. On this basis modifications of about 1 or 2 percent in stopping-power ratios and up to 1 percent in W are required. (R.W.R.)

35138 RADIOLOGICAL HAZARDS OF TRITIUM-ACTIVATED LUMINOUS DEVICES. Knapton, John D.; Comer, Richard H. (Ballistic Research Labs., Aberdeen Proving Ground, Md.). Health Phys.; 20: 345-9(Mar 1971).

The possible acute exposure of personnel to oxides of tritium should a tritium pressurized (⅔ to 2 atm) device be broken accidently in a confined space was estimated. The detection of such tritium oxide using a low temperature glass bead adsorption trapping system (Commer and Knapton 1968) was compared with detection by a water bubbler trapping system. (UK)

35139 EXPERIENCES WITH A THERMOLUMINESCENCE DOSIMETER. Allewaert, J.; Werkleider, Sc. (Kliniek voor Radiotherapie en Kerngeneeskunde, Ghent). J. Belge Radiol.; 53: 481-3(Nov-Dec 1970). (In Dutch).

Some experiences are reported concerning the use of a lithium-fluoride thermoluminescent dosimeter. (auth)

35140 IMPACT OF FUEL REPROCESSING ON THE HEALTH PHYSICS PROFESSION. Keely, Richard B.; Wenstrand, Terry K. (Nuclear Fuel Services, West Valley, N. Y.). Health Phys.; 20: 143-51(Feb 1971).

Finely divided fuel particles in work areas adjacent to the fuel chopping cell give significant exposures to the extremities and are resuspended into breathing zones. Empirical factors of 10X and 30X were found necessary to correct survey instrument readings to true dose rate. Resuspension factors for particles ranged from $5(10^{-6})$ m^{-1} to 10^{-3} m^{-1} depending upon air flow and worker's activity. Once particles were inhaled, a method was developed to correct in vivo counts for other beta emitters and low energy gamma emitters not easily identified using thick crystals. Plutonium inhalation experiences are described from urine, fecal, and in vivo counting data. Urine excretion of plutonium from a single uptake followed a 1.8 day half-life. (auth) (UK)

35141 IAEA POSTAL DOSE COMPARISON PROGRAM. Balamutov, V.; Eisenlohr, H. H.; Moos, W. S.; Nagl, J. (International Atomic Energy Agency, Vienna). Stud. Biophys.; 20: 189-92(31 Aug 1970).

The international Atomic Energy Agency has been performing an absorbed dose comparison program by mail for radiotherapy institutions in its Member States. Small capsules filled with LiF powder are used for ^{60}Co and ^{137}Cs radiations, and glass ampoules filled with Fricke solution are used for high-energy electrons. Reports have indicated that the use of ionizing radiation for therapeutic purposes is not accurately applied by many institutions. It was found that from the 102 participants in the program, 35% showed deviations in excess of 10% from the reference value, and 13% had deviations of over 30%. (F.M.M.)

35142 DOSE BURDEN DURING FLUOROSCOPY WITH IMAGE INTENSIFIER. Stieve, F. E. (Univ., Munich). Radiologe; 10: 357-67(Sep 1970). (In German).

The literature is equivocal about the fact whether image intensifiers reduce the radiation burden to patient and examiner. It is concluded that the most favorable conditions for low radiation burden are automatic brightness stabilizer, short distance between patient and image intensifier, collimation corresponding to size of object, and restriction of fluoroscopy time. If these conditions are maintained, image intensifiers lead to a significant reduction of radiation during fluoroscopy as well as radiography. (tr-auth)

35143 RADIATION BURDEN DURING ROENTGEN KINEMATOGRAPHY. Widenmann, L. (Univ., Munich). Radiologe; 10: 367-72(Sep 1970). (In German).

X-ray kinematography yields information that cannot be obtained by other diagnostic methods. In spite of image intensifiers, the procedure still requires relatively high doses that should be taken into account for each individual case. Means to assess the administered dose are discussed. Up to now, such assessments have been based mainly on phantom measurements because instruments permitting continuous doses were not available as yet. Nevertheless, the availability is strongly indicated because of uncertainties about voltage and current caused by the automatic brightness stabilizers of image intensifiers. (tr-auth)

35144 RADIOMETRIC DETERMINATION OF THE INTENSITY OF RADIATION OF THE UTERUS AND ITS APPENDAGES DURING ADMINISTRATION OF ^{32}P. Porai-Koshits, K. V. (Moscow Medical Inst.). Akush. Ginekol.; 46: No. 8, 6-9(Aug 1970). (In Russian).

The radioactivity of the uterus and appendages removed during surgery were investigated. In the tissues studied, the absolute quantity of impulses per min and the coefficient in percentage in respect to the uterine surface were determined. An absence of augmented ^{32}P accumulation in the wall of the uterus and ovaries was established. An increased accumulation was noted in the mucous membrane of the uterine tube, cervical canal, and uterus. Particularly high indexes of coefficient and its variability were revealed. The data derived testify to the possibility of calculating the coefficient in respect to the uterus for determining the malignancy of the process in the ovaries. (auth)

35145 DESCRIPTION OF RADIATION FIELDS BY SEPARATION OF PRIMARY AND SCATTERED RADIATION. IV. CALCULATION OF THE SCATTERING DISTRIBUTION FOR PARALLEL PHOTON BEAM FIELDS. Schoknecht, Guenter (Freie Univ., Berlin). Strahlentherapie; 141: No. 3, 326-31(Mar 1971). (In German).

Based on the scattered dose distribution of a pencil beam, it is possible to calculate by a convolution integral the scattered dose of extended fields. This was done for circular and rectangular fields of ^{60}Co parallel beams in a perpendicular incidence on a water phantom. The results were obtained by electronic computers and useful approximations are discussed. (auth)

35146 MEASURING OF THE STANDARD IONIC DOSE IN COMPACT AND LIQUID MEDIA DURING X-RAY AND GAMMA IRRADIATION BY ENERGIES BETWEEN 50 keV AND 3 MeV. VI. INVESTIGATION ON THE INFLUENCE OF THE VOLUMES OF IONIZATION CHAMBERS. Rakow, Adalbert; Will, Wolfram (Medizinisch-Biologische Forschungszentrum, Berlin). Strahlentherapie; 141: No. 3, 332-5(Mar 1971). (In German).

The distortion in dose distribution during x-ray and γ irradiation caused in water phantoms by the introduction of the volume of air of the ionization chamber was studied. The effect seemed to be that a higher dose was measured than really existed. The correction factors for cylindric chambers were measured depending on the radiation quality, the field surface, and the depth within the phantom. (auth)

Radiation Protection

Refer also to abstracts 34605, 34873, 35166, and 35179.

35147 TRAINING AND CONTINUOUS EDUCATION IN THE RADIATION PROTECTION FIELD FOR MEDICINE. Betz, B.; Niklas, K. (Gesellschaft fuer Strahlenforschung mbH, Munich). Radiologe; 10: 391-5(Sep 1970). (In German).

Problems involved in the fact that the radiation burden of a total population through artificial sources essentially is deter-

XUM

mined by medical application of ionizing radiation are discussed. These circumstances necessitate special emphasis for radiation protection in medicine. In spite of the current increase in the application of ionizing radiation, somatic and genetic risks must be held as low as possible through intensification of radiation protection. Proposals are made for dissemination of knowledge concerning both theoretical bases and practical procedures for radiation protection. (tr-auth)

35148 SAFETY PRECAUTIONS IN RADIOACTIVE CEMENT STORAGE. Bazhenov, Yu. M.; Volkova, O. I.; Dukhovich, F. S.; (and others). Izotopy SSSR; No. 17, 17-22(1970). (In Russian).

Practical information is given on the radiation protection and safety measures in the handling and storage of radioactive cement containing ^{137}Cs and ^{90}Sr. (tr-auth)

35149 STATE OF RADIATION PROTECTION IN FIRE DEPARTMENTS. Schenk, Max (Feuerwehr der Stadt, Essen). Tech. Ueberwach.; 10: 414-16(Dec 1969). (In German).

In the case of nuclear accidents, special operation methods and equipment are necessary for fire fighting groups. Smaller accidents of this kind fall under the competency of professional fire brigades. The training, equipment, and operation methods of the troops working in this field are described. Preventive fire protection necessitates special measures in works where there is a danger of nuclear accidents. (auth)

35150 CLINICAL CONSIDERATIONS OF RADIATION PROTECTION IN THE HANDLING OF OPEN RADIOACTIVE MATERIAL. Hellriegel, W. (Katharinenhospitals, Stuttgart). Strahlenschutz Forsch. Prax.; 9: 1-9(1969). (In German).

From ninth conference of the Society of German Radiation Medicine; Aachen, Germany (11 Oct 1968). See CONF-681082.

Reported are factors that must be considered in the establishment and operation of a nuclear medicine department within a hospital. Stressed are considerations of liability insurance. As far as radiation protection of personnel is concerned, individual exposure to radiation is discussed for stable and mobile treatment rooms. Difficulties of early detection of radiation injury as well as contamination with and incorporation of radioisotopes are mentioned. Emphasized is the fact that patients treated therapeutically with radioisotopes should be located in special rooms and should be handled in a special manner. (tr-auth)

35151 ORGANIZATIONAL AND ARCHITECTURAL CONSIDERATIONS OF RADIATION PROTECTION DURING ESTABLISHMENT OF A NUCLEAR MEDICINE DEPARTMENT. Schumacher, W. (Abtielungen Strahlentherapie und Nuklearmedizin, Berlin). Strahlenschutz Forsch. Prax.; 9: 10-16(1969). (In German).

From ninth conference of the Society of German Radiation Medicine; Aachen, Germany (11 Oct 1968). See CONF-681082.

Since April 5, 1968, a nuclear medicine department has been in operation at the Rudolph Virchow hospital in Berlin. The installation worked successfully and satisfactorily. Architectural designs concerning walls and floors are discussed. By proper arrangements, including monitoring by television, radiation exposure of medical personnel was reduced by 90%. (H.B.G.)

Safety Procedures

Refer also to abstract 35100.

35152 INSTITUTE OF OCCUPATIONAL HYGIENE IN THE URANIUM INDUSTRY. Decrees No. 15 and 16 of the Czechoslovak Ministry of Health, 1968). Vestn. Min. Zdrav.; 16: Nos. 7-8, 76-7(Jun 1968). (In Czech).

The decrees represent the basic regulations concerning health aspects in the uranium industry. The powers of the chief hygienist are delegated to the Institute of Occupational Hygiene for all questions pertaining to the uranium industry. The Institute carries out research for protecting employees engaged in production work involving uranium. Its responsibilities cover matters of labor hygiene and radiation toxicology. Detailed regulations concerning the working conditions are issued by the representative of the chief hygienist in consultation with local authorities. Due attention is paid to the protection of the environment. These decrees replace the June 2, 1960 decree of the Ministry of Health concerning sanitary inspections in uranium plants. (TTT)

35153 SAFETY PRINCIPALS IN THE HANDLING OF RADIOPHARMACEUTICALS AND RADIOISOTOPE-LABELED PHARMACEUTICALS. Ladner, H.-A. (Univ., Mainz). Strahlenschutz Forsch. Prax.; 9: 20-8(1969). (In German).

From ninth conference of the Society of German Radiation Medicine; Aachen, Germany (11 Oct 1968). See CONF-681082.

The fact that a physician should not only know the properties of radiopharmaceuticals but also their quality standard as established by the producer is discussed. The increasing application of short-lived isotopes causes uncertainty about values derived from long-lived isotopes. Concise concepts about effects of small radiation doses still do not exist. In individual cases, biological factors must be considered which can change considerably the radiation burden. Pharmaceuticals labeled with long-lived isotopes should be administered only with the consent of an expert group and in facilities with long-term radiation monitoring. (H.B.G.)

35154 HAZARDS AND MONITORING PROCEDURES IN THE HANDLING OF OPEN RADIOACTIVE MATERIAL IN NUCLEAR INSTALLATIONS. Keller, H. Strahlenschutz Forsch. Prax.; 9: 29-45(1969). (In German).

From ninth conference of the Society of German Radiation Medicine; Aachen, Germany (11 Oct 1968). See CONF-681082.

Incorporation hazards to industrial personnel handling radioactive materials are discussed. Considered are toxic amounts of incorporation, toxic amounts in the environment, and the effective incorporation factor. Protective procedures are discussed with respect to general safety, shielding properties of equipment, organizational structure, and monitoring procedures. (H.B.G.)

Medicine

Refer also to abstracts 35099, 35150, 35151, and 35153.

35155 NATIONAL CONFERENCE ON THE CONTRIBUTIONS OF NUCLEAR MEDICINE TO DIAGNOSIS AND THERAPY. CLINICAL APPLICATIONS OF THE NEUTRON ACTIVATION TECHNIQUE, TURIN, ITALY, 20-21 OCTOBER 1969. Minerva Med.; 60: 4059-4166(17 Oct 1969). (In Italian). (CONF-691029).

Nine papers are included; separate abstracts were prepared for each. (J.S.R.)

For abstracts of individual papers see: 35156, 35157, 35180–35185, and 35190.

35156 SERVICE OF NUCLEAR MEDICINE, ORGANIZATIONAL, AND TECHNICAL ASPECTS. Lin, S. (Ospedali Riuniti, Trieste, Italy). Minerva Med.; 60: 4063-81(17 Oct 1969). (In Italian).

From Conference on the Contributions of Nuclear Medicine to Diagnosis and Therapy, Turin, Italy. See CONF-691029.

The general organization criteria for a nuclear medical service are outlined and the organization established in Italy is described in detail. The types of information attributed to a nuclear medical service, nuclear medicine in the framework of socialized medicine, and radiopharmaceutics are also discussed. (J.S.R.)

35157 RADIOISOTOPIC DAIGNOSIS AND THERAPY IN HEMATOLOGY. Sacchetti, C.; Ponassi, A. (Univ., Genoa). Minerva Med.; 60: 4141-52(17 Oct 1969). (In Italian).

From Conference on the Contributions of Nuclear Medicine to Diagnosis and Therapy, Turin, Italy. See CONF-691029.

The diagnostic and therapeutic applications of radioisotopes in hematology are reviewed. Radioisotopic methods for the study of erythrocytes, neutrophil granulocytes, and platelets are described. The therapeutic uses are almost completely limited to the use of sodium phosphate-^{32}P in some myeloproliferative disorders such as polycythemia. (J.S.R.)

Protective Substances

Refer also to abstracts 35204, 35213, 35214, and 35264.

35158 RADIOLOGICAL ASPECTS OF POST-RADIOTHERAPEUTIC COLITIS. Jeanmart, L.; Bollaert, A.; Dagnelie, J.; (and others). J. Belge Radiol.; 53: 429-36(Nov-Dec 1970). (In French).

A statistical review of the complications following radiotherapy for neoplastic lesions of the cervix is given. The radiological symptomology of the complications is specific and resembles the lesions observed in ulcero-hemorrhagic recto-colitis. The early post-irradiation phase is characterized by anarchic plicature of the intestinal mucosa, with interruption of the mucous protective border, whereas the later phase shows a tabulated, rigid recto-sigmoid without haustration. Radiological investigation alone does not permit definite diagnosis. Data obtained by the anamnesis, clinical investigation, and radiological and rectoscopic examination are necessary for exact diagnosis. (auth)

35159 STUDIES ON THE ANTI-TUMOUR ACTIVITY OF ALIPHATIC ALDEHYDES. IV. RADIOSENSITIZING PROPER-

XUM

TIES OF L-ERYTHRO-α, β-DIHYDROXYBUTYRALDEHYDE ON E. COLI B AND EHRLICH ASCITES TUMOUR CELLS. Ciaranfi, E.; Perin, A.; Sessa, A.; (and others) (Univ., Milan). Eur. J. Cancer; 7: 17–24(Feb 1971).

A test of radiosensitivity carried out with γ radiation on Escherichia coli B indicated that L-erythro-α,β-dihydroxybutyraldehyde (DHBA) enhanced the effect of radiation in non-toxic and toxic conditions, giving respectively a Dose Modifying Factor of 1.3 and 1.7. In in vitro/in vivo experiments, carried out with the adenocarcinoma Ehrlich ascites cells, DHBA displayed a marked radiosensitizing action at non-toxic doses (1 or 5 mM), in air and nitrogen. The combined action of DHBA and x rays led to a slowdown of tumour growth with increased survival of the animals (mice). The presence of DHBA during radiation was necessary. The addition of aldehyde to irradiated cells appeared to be without effect on the cytokynetics of tumour growth. Immunological processes played a negligible role under the experimental conditions described. (UK)

35160 STRUCTURE-FUNCTION STUDIES OF THE AMINOTHIOL RADIOPROTECTANTS. THE EFFECT OF CARBON CHAIN LENGTH IN MERCAPTOETHYLAMINE HOMOLOGS. Swartz, Harold M.; Copeland, Edmund S.; Richardson, Earl C. (Walter Reed Army Inst. of Research, Washington, D. C.). Radiat. Res.; 45: 542-56(Mar 1971).

The relation between chemical structure and physicochemical radiation protection in E. coli has been studied in a series of aminothiols. The aminothiols used in this study were β-mercaptoethylamine and its propyl, butyl, pentyl, and hexyl homologs. The experiments were designed to minimize physiological and metabolic effects of the test compounds. The biological effects were determined by measuring survival (ability to form visible colonies) of E. coli irradiated in the presence of 0.1 M protectant either at 1°C or 77°K with ^{60}Co γ radiation. Prior to irradiation, samples were equilibrated with 100% oxygen or nitrogen. Effects of the compounds on free radical formation and interaction were observed by electron spin resonance spectroscopy of the bacteria preparations irradiated at 77°K. No abrupt reduction in radioprotection was observed when the carbon chain separating amino and thiol groups was lengthened from three to four or more units. From both bacteriological and free radical studies, the data indicate a gradual reduction in efficacy with no change in mechanism of action either in oxygen or nitrogen as might be expected for a homologous series. These findings suggest that the aminothiols protect by specific interactions with cell components in addition to acting via a more general, nonspecific radical scavenging and/or repair mechanism. (auth)

35161 DIFFERENCES IN THE EFFECT OF HYPOXIA ON THE RADIATION SENSITIVITY OF THE BONE MARROW AND THE INTESTINE IN MICE. Hornsey, Shirley (Hammersmith Hospital, London). Brit. J. Radiol.; 44: 357-60(May 1971).

Oxygen enhancement ratios, OERs, are reported for the bone marrow tissue assayed by animal survival 30 days after whole-body irradiation or by endogenous spleen nodule counts 11 days after wholebody irradiation for TO female mice and by endogenous spleen nodule counts for F1 hybrid ($C_3H \times C_{57}B1$) mice. For both strains of mice the OER was 2.0. This was shown to be different from the OERs obtained for intestinal tissues assayed by animal survival four days after wholebody irradiation. The OER for intestinal damage was 2.5 – 2.7. It is not known whether these differences in OER are due to differences in the response of the circulation of these tissues to hypoxia or to intrinsic differences in the radiosensitivity in the cells of these tissues. (auth) (UK)

35162 INFLUENCE OF SODIUM FLUORACETATE (FAc) ON THE SHIFT OF THE LD 50/30 VALUE. Hosek, B.; Novak, L.; Sikulova, J. (Biophysics Inst., Brno). Stud. Biophys.; 13: 1-6(1969). (In German).

In male mice, H strain, a significant shift of the LD 50/30 value was found after intraperitoneal injection of sodium fluoroacetate (FAc). While in the control group the LD 50/30 value was 648 R. After the administration of 5 and 7.5 mg FAc/kg 3 hours before x irradiation the LD 50/30 value increased to 822 and 998 R. After the administration of 5 mg of FAc/kg 1 hour before irradiation the protection was higher (LD 50 935 R) than after the same dose applied 3 hours before irradiation. (auth)

35163 ROLE OF HYPOTHERMY IN THE MECHANISM OF RADIOPROTECTIVE ACTION OF SODIUM FLUOROACETATE. Misustova, J.; Novak, L. (Inst. of Biophysics, Brno). Stud. Biophys.; 13: 7-14(1969).

The role of hypothermy in the mechanism of protective action of sodium fluoroacetate (FAc) was studied. In the course of intoxication by FAc (5 mg/kg), male mice of H-strain, 9 to 12 weeks old, were exposed to slight cool stress (17°C) inducing significant deepening of hypothermy and speeding up its start. In this state the animals were irradiated by 800 R exposure. It was found that the additional decrease in the level of respiratory exchange and body temperature during irradiation, induced by the change of ambient temperature, did not affect the degree of protection or its time course. The opinion is given that the primary blockade of akonitase caused by FAc and the corresponding decrease of metabolic processes are responsible for the degree of protection. The additional deepening of hypothermia had no effect. (auth)

35164 EFFECT OF INSULIN ON FUNCTIONAL STATE OF SOME ENDOCRINE GLANDS IN RATS IRRADIATED ON THE 25 MeV BETATRON. Pegel, V. A.; Dokshina, G. A.; Potapova, A. I. (Tomsk State Univ., USSR). Vop. Med. Khim.; 17: 125-8 (Mar-Apr 1971). (In Russian).

The administration of insulin (0.5 Units/kg) into rats irradiated with 25 MeV electrons from the betatron at a dose of 1000 rad increased the glucocorticoid level 2-fold and insulin like activity of blood plasma 3.5-fold, and partially restored the content of glycogen in the liver and sugar level in the blood. The protective effect of insulin was provided through the enhanced functioning of the adrenal cortex and the stimulation of the processes of gluconeogenesis. (auth)

35165 EFFECT OF RADIOPROTECTOR CYSTAMINE ON THE ACTIVITY OF MONOAMINE OXIDASE AND CATECHOL-O-METHYLTRANSFERASE. Kulinskii, V. I.; Shmuter, G. M. (Inst. for Advanced Training of Physicians, Kharkov). Vop. Med. Khim.; 17: 148-52(Mar-Apr 1971). (In Russian).

Administration of cystamine to albino rats at a radioprotective dose of 169 mg/kg (calculated per base) markedly inhibited activity of monoamine oxidase and catechol-O-methyltransferase at early stages. The activity of catechol-O-methytransferase returned to normal level within 45 min, while that of monoamine oxidase returned more slowly. The irradiation of rats with a dose of 860 rad 5 min after the administration of cystamine did not change its influence on the enzymatic activities studied. When given at a lower dose (101 mg/kg), cystamine inhibited only the catechol-O-methyltransferase activity. The possible role of inhibition of enzymes by thisamines in the mechanism of their protective action is discussed. (auth)

35166 FEATURES OF PHYSICO-CHEMICAL PROTECTION AGAINST EXTERIOR RADIATION. Kaul, A. (Freie Univ., Berlin). Isotopenpraxis; 6: 437-47(Dec 1970). (In German).

Discussed are: basic processes of biological radiation effects; basic processes of physical radiation effects; interpretation of direct and indirect radiation effects on the basis of target theory; mechanisms of shielding materials; and the practical importance of chemico-biological radiation protection. (auth)

Radiodiagnosis

Refer also to abstracts 34872, 34880, 34881, 34885, 34888, 35142, and 35143.

35167 TISSUE PERFUSION MEASURED USING THE RATIO OF ^{81}Rb TO ^{81m}Kr INCORPORATED IN THE TISSUE. Jones, T. (Hammersmith Hospital, London); Matthews, C. M. E. Nature (London); 230: 119-20(12 Mar 1971).

A possible new method for measuring tissue perfusion is discussed, based on the intravenous administration of cyclotron produced ^{81}Rb. This nuclide decays with a half-life of 4 hr. 34 min. to ^{81m}Kr, which in turn decays with a half-life of 13sec. to stable ^{81}Kr. The rate of removal of the Kr from tissues is dependent on the perfusion of the tissue, the equilibrium relationship being $\lambda 1/(\lambda 2 + K)$, where λ1 and λ2 are the disintegration rate constants of ^{81}Rb and ^{81m}Kr, respectively, and K is the perfusion rate constant. Since ^{81m}Kr gives only a single γ ray of 190 keV it is possible to obtain the ^{81m}Kr/^{81}Rb ratio spectroscopically, and there are calibration advantages in using a ratio to provide a measure of tissue perfusion compared with methods involving absolute uptake. The method would require only a single injection of ^{81}Rb in order to make a series of blood flow measurements on one or more organs. The technique, furthermore, utilizes a static measurement, thus potentially affording better statistics. The method, however, is applicable only to organs of relatively high blood flow. An inaccuracy is observed in the geometrical dependence of the ratio, necessitating equivalent measurements in a phantom if absolute perfusion values are required. Some experimental work is described. (UK)

35168 APPLICATION OF MATHEMATICAL MODELS FOR THE QUANTITATIVE INTERPRETATION OF RADIOISOTOPE

XUM

RENOGRAMS. Shchekina, G. D.; Shchekin, Yu. K. (Inst. of Nuclear Power Engineering, Minsk). Vestsi Akad. Navuk BSSR, Ser. Biyal. Navuk; No. 4, 54-61(1969). (In Belorussian).

Experimental blood-clearance curves obtained following unilateral renography using ^{131}I-labeled hippuran were found to fit a one exponent function rather than a two exponent function. A mathematical model of the blood–kidney–tissue system was constructed and analyzed to determine the structure of the single exponential curve. The model took into consideration the removal of activity from the blood directly by the tissue. It revealed the existence of a constant component that was dependent on the accumulation of activity in the tissue and hence referred to as tissue background. Following determination of the quantitative parameters of the constant, this quantity was subtracted from the two exponent curve resulting in a blood-clearance curve described entirely by one exponent. Also, the parameters of each one exponent curve (one for each kidney) coincided with the parameters for that exponent describing blood clearance in all cases of the same disease, and characterized the overall rate of removal of activity from the blood. (tr-auth)

35169 COMPARISON OF THE RESULTS OBTAINED IN THYROID SCINTIGRAPHY USING ^{99m}Tc AND ^{131}I. Massin, J. P.; Karam, J.; Savoie, J. C. (Groupe Hospitalier La Pitie-Salpetriere, Paris). Ann. Endocrinol. (Paris); 31: 962-8(Sep–Oct 1970). (In French).

The two isotopes ^{99m}Tc and ^{131}I were simultaneously administered to seventy patients suffering from various thyroid disorders. The corresponding thyroid scintigrams were examined. In all but five cases the results were comparable, particularly for establishing the variety of a thyroid nodule. In general, the quality of the scintigrams were similar although sometimes better images were obtained with ^{131}I. (France)

35170 USE OF RADIOACTIVE Xe IN THE EVALUATION OF REGIONAL PULMONARY FUNCTIONS IN PATIENTS WITH INTERSTITIAL PULMONARY EDEMA. Ruff, F.; Hughes, J. M.; McCarthy, D.; (and others) (Royal Victoria Hospital, Montreal). Union Med. Can.; 100: 496-500(Mar 1971). (In French).

Methods for studying regional pulmonary function using radioactive xenon were applied to patients with hepatic cirrhosis whose history suggested the presence of interstitial pulmonary edema. The results demonstrated that in patients with hepatic cirrhosis, there is increased gas trapping in the lungs which is probably caused by closure of airways in the dependent parts of the lungs. Consequently, these lower lung zones have a very low ventilation-perfusion ratio which contributes significantly to the arterial hypoxemia manifested by these patients suffering from hepatic cirrhosis. (auth) (Canada)

35171 MEASUREMENT OF BONE DENSITY IN THE FINGER WITH A ^{125}I-PROFILE-SCANNER. SEPARATE CALCULATION OF COMPACT AND CANCELLOUS BONE DENSITY BY A SENSITIVE METHOD. Moll, E.; Boerner, W.; Grehn, S.; Rauh, E. (Medical Univ., Wuerzburg, Ger.). Stud. Biophys.; 20: 211-17(31 Aug 1970). (In German).

A method is given for the separate calculation of mineral density of the cancellous bone. By this method it is possible to show even small alterations in the hydroxylapatite content of the finger that means a considerable improvement in the sensitivity of calculating bone density. (auth)

35172 RADIONUCLIDE CISTERNOGRAPHY. Harbert, John C. (Georgetown Univ., Washington, D. C.). Semin. Nucl. Med.; 1: 90-106(Jan 1971).

Radionuclide cisternography is a sensitive indicator of altered formation, flow, and reabsorption of CSF protein. The interest in cisternography is due to its applications to the study of hydrocephalus. The techniques of injection and scanning are discussed in detail. While ^{131}I-HSA has and continues to be the most widely used tracer, newer labels, particularly ^{99m}Tc-DTPA and ^{99m}Tc-HSA have significant promise. A classification of cisternographic patterns based upon the flow of CSF and rate of protein reabsorption is presented. Correlation of patterns with clinical results of surgical shunting allows not only a prognosis to be established, but indicates the type of shunt most likely to produce satisfactory results. (auth)

35173 INTRAVENOUS AND INTRACAROTID RADIONUCLIDE CEREBRAL ANGIOGRAPHY. Rosenthall, Leonard (Montreal General Hospital). Semin. Nucl. Med.; 1: 70-84(Jan 1971).

A comparison of cerebral hemispheric transit of intravenously injected radiopertechnetate appeared to be most useful in acute strokes, before the static scintiphotographs demonstrated a focal concentration of activity. However, interpretation could not be made out of clinical context as the older age group, in which this affliction is commonest, also had the greatest degree of asymmetric athero- and arteriosclerotic vascular disease, that may yield an equal or reduced transit on the side contralateral to the lesion. Disparate perfusion may occur in patients, particularly in advanced years, who did not suffer a stroke nor display neurological deficits. Increased perfusion on the side of a positive static scintiphotograph generally implies the presence of a tumor. This combination is not pathognomonic as three out of 96 strokes exhibited the same dynamics. Tumors can also be associated with reduced ipsilateral radioactive transit. Uncomplicated arteriovenous malformations were fairly characteristic as they showed the highest concentration with the initial entrance of the bolus of radioactive material that rapidly diminished during the washout and was seen later as a vascular pool of lesser concentration than the first bolus. Intracarotid injections of radiopertechnetate were found to be a useful adjunct to contrast angiography. Although lacking the resolution of radiography the radionuclide method was more sensitive to the presence or absence of the microcirculation. Time-activity curves over regional areas of the brain derived from a direct store video system are presented from intravenous and intracarotid studies. (auth)

35174 SEQUENTIAL BRAIN IMAGING AS AN AID IN UNDERSTANDING DISEASE ETIOLOGY. Handa, Jyoji; Handa, Hajime; Hamamoto, Ken; Torizuka, Kanji; Kousaka, Tadako (Kyoto Univ.). Semin. Nucl. Med.; 1: 56-69(Jan 1971).

Sequential cerebral scintiphotography was performed with a γ scintillation camera and intravenously administered ^{99m}Tc pertechnetate. The results of the serial scans were correlated with the disease etiology as determined by angiography and surgery. Abnormal foci noted in sequential scinti-photographs revealed either a regressive or progressive course of radionuclide uptake. When the differential uptake was determined digitally, it was possible to classify chronologic patterns of nuclide accumulation into four groups. In Group 1, the uptake ratio reached the maximum value immediately or soon after administration of the tracer and then decreased rapidly. Vascular anomalies, angiomas, and meningiomas belonged to this group; angiography and ^{133}Xe or ^{131}I-MAA scanning data all demonstrated high blood content and blood flow in the lesions. In Group 2, the uptake ratio showed a progressive increase with time. Gliomas of low grade malignancy, cerebral infarctions and abcesses showed this pattern. In Group 4, the uptake ratio did not exceed unity. This type of lesion was rare and was observed in large intracerebral hematomas and cysts. In Groups 2 and 4, the foci proved to be avascular at surgery or by other diagnostic methods. Group 3 included more or less vascular malignant tumors; namely glioblastomas, carcinomas, or sarcomas. The uptake ratio showed an initial increase that was followed by a secondary decrease. In addition to the morphological characteristics of the brain scan such as the size, shape, margin, location, density, homogeneity, and multiplicity of the radioactive foci, the dynamic analysis of time course of nuclide uptake appeared to improve the diagnostic accuracy and provided useful information concerning the nature of the lesion. (auth)

35175 VALUE OF THE VERTEX VIEW IN BRAIN SCANNING. Holmes, Richard A. (Marquette Univ., Milwaukee). Semin. Nucl. Med.; 1: 48-55(Jan 1971).

Although the vertex projection views more of the cerebral cortex than most combinations of brain scan views, it is generally used to detect superior brain lesions. When ^{99m}Tc pertechnetate ($^{99m}TcO_4$) is used to scan the brain, its uptake by the mucosa and salivary tissues obscures the frontal area on the vertex view. Atropine administration suppresses this activity and because of its transient effect the vertex view must be scanned first. Atropine has not been necessary for vertex flow studies or when other brain scanning agents are used. The prone position with the neck extended is employed to complete the vertex view advocated in conscious patients and the supine position, using the camera, in unconscious patients. Superior and midcortical brain lesions commonly rely on the vertex view for their definitive detection. Peripheral brain lesions are much more difficult to characterize on the vertex view due to the convexities of the head. Cystic brain lesions show as negative defects on the brain scan and are more easily detected on the vertex view because it compares contralateral regions. The inconsistency of detecting some basilar brain lesions is the most serious limitation of the vertex view. The major advantage of the vertex view is its lack of restricted regionalization for localizing brain lesions. When the vertex view was used as a fifth brain scan view and compared to the other views, it detected a greater number of the lesions than any other single view. The vertex view is recommended as a routine view in all brain scan studies. (auth)

35176 SCANNING IN CEREBRAL VASCULAR DISEASE. DeLand, Frank H. (Johns Hopkins Medical Institutions, Baltimore). Semin. Nucl. Med.; 1: 31-40(Jan 1971).

XUM

The detection of cerebral vascular accidents (CVAs) by brain scanning can be improved by correlating the characteristic appearance and location of the abnormal activity with the anatomical distribution of specific cerebral vessels. The relative consistency of the vascular distribution of the anterior, middle, and posterior cerebral arteries and major branches of the middle cerebral artery permits correlation with the abnormal radioactivity seen in CVAs. Characteristic vascular distribution of activity is more frequently seen in ischemic infarctions rather than hemorrhagic infarctions or hematomas. Positive brain scans are seen less frequently and later after the onset of symptoms in patients with ischemic infarctions than with the hemorrhagic type. Cerebral nuclear angiography is frequently helpful in detecting decreased blood flow in an otherwise normal brain scan. Diagrams of the vascular distribution of the major cerebral vessels are given for the various views used in brain scanning. Typical brain scans illustrate the characteristic abnormal activity seen in CVAs that involve different cerebral vessels. (auth)

35177 CURRENT STATUS OF BRAIN SCANNING. O'Mara, Robert E.; Mozley, James M. (State Univ. of New York, Syracuse). Semin. Nucl. Med.; 1: 7-30(Jan 1971).

Radionuclide scanning of the brain has grown from an experimental laboratory procedure to a widely used screening procedure in the study of neurological disorders. Considerable information may be elicited in such conditions as primary and secondary neoplasms, cerebrovascular disease, arteriovenous malformations, abscess, subdural hematoma, and calvarial lesions, especially when the scanning studies are correlated with other radiographic procedures. The addition of dynamic studies of the blood flow of the brain has added a new aspect to the usual static imaging procedure. Despite the drawbacks of present-day radionuclides and instrumentation, the overall accuracy of scanning approaches that of cerebral angiography, falling between 80 and 90%. Unfortunately, a significant number of lesions are difficult to detect or missed entirely. It is hoped that this accuracy will increase as a result of the development of biologically more suitable radiopharmaceuticals, instruments with greater resolution, and an increasing knowledge of the basic mechanisms by which radionuclides accumulate within lesions of the central nervous system. (68 references). (auth)

35178 CLINICAL APPLICATIONS OF BRAIN BLOOD FLOW STUDIES. Oldendorf, William H. (Wadsworth Hospital, Los Angeles, Univ. of California, Los Angeles). Semin. Nucl. Med.; 1: 107-19(Jan 1971).

Considerable quantitative information about brain hemodynamics can be obtained by external counting of γ emitters passing through various brain compartments. These γ-emitting radionuclides may be introduced intravenously, by inhalation, or into the carotid system. The merits of the various routes of administration and calculation are discussed. In view of the wide availability of rapid imaging γ cameras, the early distribution of nondiffusible radionuclides administered intravenously has the widest potential application. It requires only a minor modification of standard brain scanning technique. Utilization of these radionuclides techniques in clinical management of brain infarction is of value in assisting the clinician in understanding pathophysiology. They remain an important tool in research studies of the pathophysiology of brain circulatory disease. (auth)

35179 RADIOISOTOPE SELECTION IN DIAGNOSTIC NUCLEAR MEDICINE FROM THE STANDPOINT OF MINIMAL RADIATION BURDEN. Winkler, C. (Univ., Bonn). Strahlenschutz Forsch. Prax.; 9: 17-20(1969). (In German).

From ninth conference of the Society of German Radiation Medicine; Aachen, Germany (11 Oct 1968). See CONF-681082.

The selection of the most suitable radioisotopes for various organs in clinical diagnosis, with emphasis on thyroid and brain functions, is discussed. Whole-body and gonadal radiation burdens were analyzed for various isotopes. (H.B.G.)

35180 CONTRIBUTION OF RADIOISOTOPE TECHNIQUES TO THE DIAGNOSIS OF LUNG MORPHOLOGY. Englaro, G. C.; Zecchin, R.; Di Chiara, F.; Barbina, V. (Istituto di Radioterapia e Medicina Nucleare, Udine, Italy). Minerva Med.; 60: 4082-8 (17 Oct 1969). (In Italian).

From Conference on the Contributions of Nuclear Medicine to Diagnosis and Therapy, Turin, Italy. See CONF-691029.

The importance of scintigraphy in pulmonary pathology by means of the use of ^{131}I- or ^{99m}Tc-labeled albumin macroaggregates or crystalline aggregates of ferric oxide labeled with ^{113m}In lies in the fact that the method is simple, harmless, easily repeatable, and capable of showing alterations of a functional and organic nature of the pulmonary blood perfusion. Evidences of pulmonary circulatory alterations are visible by scintigraphy because of areas of hypodistribution or of total absence of the preparation injected. Typical scintigraphs obtained by this method are given and discussed to illustrate its applicability and sensitivity. (J.S.R.)

35181 CONCEPTUAL IMPORTANCE AND CLINICAL SIGNIFICANCE OF VARIOUS METHODS OF EXPLORING CARDIO-RESPIRATORY FUNCTION WITH RADIOACTIVE TRACERS. Cellerino, A. F.; Boario, U.; Banaudi, C. (Univ., Turin). Minerva Med.; 60: 4089-94(17 Oct 1969). (In Italian).

From Conference on the Contributions of Nuclear Medicine to Diagnosis and Therapy, Turin, Italy. See CONF-691029.

The various methods of exploring cardio-respiratory function with radioactive tracers are based implicitly on a conceptual distinction between the topographic and analytical distribution of the tracer. This is discussed in relation to different methods. (J.S.R.)

35182 POSSIBILITIES AND LIMITATIONS OF NUCLEAR MEDICINE IN INFANT DIAGNOSTICS. Gomirato Sandrucci, M.; Mussa, G. C.; Martini Mauri, M.; Bacolla, D. (Univ., Turin). Minerva Med.; 60: 4095-4105(17 Oct 1969). (In Italian).

From Conference on the Contributions of Nuclear Medicine to Diagnosis and Therapy, Turin, Italy. See CONF-691029.

The applications and limitations of radioisotopes in the diagnosis of the central nervous system, liver, pancreas, parathyroid, digestive function, hemolymphatic system, spleen, thyroid, skeleton, respiratory apparatus, cardio-circulatory apparatus, and uropoietic system in infants are reviewed on the basis of literature data and experimental work at the Pediatric Clinic of the University of Turin. (J.S.R.)

35183 EXPERIENCES WITH THE SHIELDED WHOLE-BODY COUNTER OF THE INSTITUTE OF RADIOLOGY OF THE UNIVERSITY OF ROME. Bompiani, C.; Giacco, G.; Scarpa, G.; Tomiselli, A.; Vignoni, A. (Univ., Rome). Minerva Med.; 60: 4111-22 (17 Oct 1969). (In Italian).

From Conference on the Contributions of Nuclear Medicine to Diagnosis and Therapy, Turin, Italy. See CONF-691029.

The shielded whole-body counter is briefly described. The background radiation, absolute calibration for ^{137}Cs and ^{40}K and the confidence limits, behavior of the counter efficiency as a function of radiation energy, and linearity of the response of the counter were studied. Measurements on normal patients for ^{137}Cs and K contents are described. (J.S.R.)

35184 DIAGNOSIS OF KIDNEY FUNCTION AND STRUCTURE BY MEANS OF RADIOISOTOPES. Mombelli, L. (Univ., Milan). Minerva Med.; 60: 4123-40(17 Oct 1969). (In Italian).

From Conference on the Contributions of Nuclear Medicine to Diagnosis and Therapy, Turin, Italy. See CONF-691029.

The morphological and functional aspects of the use of radioisotopes for kidney diagnosis are considered. The methods of quantitative and qualitative diagnosis or radionephrograms are described and the problem of flux determinations with clearance methods is discussed. Clearance is considered with particular emphasis on the estimation of the glomerular filtrate. (J.S.R.)

35185 CURRENT POSSIBILITIES IN THE DIAGNOSIS OF TUMORS BY MEANS OF RADIOISOTOPES. Riccioni, N.; Becchini, M. F.; De Giorgio, L. (Univ., Pisa, Italy). Minerva Med.; 60: 4153-65(17 Oct 1969). (In Italian).

From Conference on the Contributions of Nuclear Medicine to Diagnosis and Therapy, Turin, Italy. See CONF-691029.

The use of radioisotopes in the diagnosis of tumors is based on the detection of differences of the concentration of the radioactivity between the neoplasia and continguous tissues. The possibilities and limitations of scintigraphy are discussed. The use of radioisotopes in the diagnosis of neoplasms of bone, brain, and liver is described. (J.S.R.)

35186 LYMPHOSCINTIGRAPHY, GAMMA-VENOGRAPHY, AND HISTOLOGICAL EVIDENCE IN RADICAL OPERATION. Groenroos, M.; Voutilainen, A.; Ruponen, S. (Univ., Turku, Finland). Strahlentherapie; 141: No. 3, 346-50(Mar 1971). (In German).

The results of lymphoscintigraphy and gamma venography were compared with findings during lymphadenectomy for different gynecological carcinomas. There was a positive correlation of the lymphoscintigraphy with the microscopy in 77% of the cases, and with macroscopy in 55%. There was also a positive correlation between gamma-venography and microscopy in 75%. Optimum results were obtained for both methods combined in 83% of the cases. Thus, the best results were obtained when both methods were applied. (auth)

Radiotherapy

Refer also to abstracts 35057, 35136, 35141, 35145, 35240, and 35243.

XUM

35187 RADIATION TREATMENT OF METASTATIC BONE DISEASE. Blake, Damon D. (Wake Forest Univ., Winston-Salem, N. C. North Carolina Baptist Hospital, Winston-Salem, N. C.). Clin. Orthop.; 73: 89-100(Nov-Dec 1970).

Radiation treatment of metastatic malignant bone disease is generally very effective in controlling pain, and often in stopping the local destructive process. More frequent use should be made of external immobilization or support of involved bones during the radiation course as a means of reducing pain and preventing fractures. When a pathologic fracture has occurred in a long bone, internal fixation followed by radiation treatment usually constitutes the optimal management. Spinal cord compression can often be relieved by radiation without resorting to decompression surgery if the diagnosis is known, the tumor is radiosensitive, and the compression is not due primarily to severe collapse of bony structure. Radioisotopic bone scans will demonstrate the majority of metastatic bone lesions, often before a roentgenographic abnormality appears. The roentgenographic picture of late radiation changes in bone can simulate metastatic disease. (auth)

35188 IRRADIATION OF EARLY CARCINOMA OF THE LARYNX. SIGNIFICANCE OF TUMOR EXTENT. Perez, Carlos A.; Mill, William B.; Ogura, Joseph H.; Powers, William E. (Washington Univ., St. Louis). Arch. Otolaryngol.; 93: 465-72(May 1971).

Radiotherapy of early carcinoma of the larynx in 100 patients has produced 5-yr cure rates of 82% in $T^{(1)}$ lesions and 77% in $T^{(2)}$ lesions. The local control rates from ^{60}Co γ-radiation were 88 and 72%, respectively. Although irradiation was not as effective in controlling $T^{(2)}$ lesions, the results were comparable to those obtained by hemilaryngectomy. The majority of the patients failing after radiotherapy presented with local recurrence, making early diagnosis of the recurrent lesions critical, since about 75% of these patients can subsequently be cured with hemilaryngectomy. The major complications observed in these patients appeared in the group treated with orthovoltage therapy. Supervoltage irradiation has allowed the delivery of higher doses with only transient complications. (auth)

35189 PERIPHERAL BLOOD PICTURE AND PLASMA PROTEIN FRACTIONS FOLLOWING THERAPEUTIC INCORPORATION OF RADIOISOTOPES. Pfannenstiel, P. (Univ., Freiburg i. B.). Strahlenschutz Forsch. Prax.; 9: 49-66 (1969). (In German).

From ninth conference of the Society of German Radiation Medicine; Aachen, Germany (11 Oct 1968). See CONF-681082.

It was demonstrated that the effects of oral and endolymphatic ^{131}I therapy on cellular and protein components of human blood are negligible. The doses administered corresponded to a whole-body irradiation of 20 Rad. Therefore, within this range, blood studies are not suitable as biological dosimeters. It is found that annual blood tests fail to reveal low-grade exposure and are valuable only to detect high radiation incidents. (H.B.G.)

35190 CONTRIBUTION OF ISOTOPES TO THE SURGERY OF THE THYROID. Biancalana, L.; Maggi, G. (Univ., Turin). Minerva Med.; 60: 4106-10(17 Oct 1969). (In Italian).

From Conference on the Contributions of Nuclear Medicine to Diagnosis and Therapy, Turin, Italy. See CONF-691029.

The use of radioisotopes in the treatment of neoplasms of the thyroid, either before or after surgery, is discussed and illustrated with some specific cases. (J.S.R.)

35191 POSTOPERATIVE IRRADIATION OF BREAST CANCER BY FAST ELECTRONS. Hellriegel, W.; Schopka, H.-J. (Katharinenhospital, Stuttgart). Strahlentherapie; 141: No. 3, 263-70(Mar 1971). (In German).

A procedure and its practical application that makes pendulum irradiations of cylindrical and elliptical bodies possible is described. Because of the limited penetration of the electrons into matter, the pendular movement of the source of electrons around its center within the body allows a symmetric and homogeneous spreading of the irradiation energy within a layer formed by the body surface and by maximum penetration of the electrons. The lymph nodes in the axilla and the supra- and infraclavicular and cervical regions are irradiated from two additional fixed fields. The postoperative electron irradiation of breast cancer is very well tolerated and is not followed by reactive changes in the periphery of the lung. (auth)

35192 ^{60}Co THERAPY OF CARCINOMATA OF URINARY BLADDER: FIVE-YEAR RESULTS. Reinhard, B.; Fischedick, O. (Knappschafts-Krankenhauses, Dortmund, Ger.). Strahlentherapie; 141: No. 3, 271-5(Mar 1971). (In German).

One-hundred-forty-five patients with bladder carcinomas were treated with telecobalt. The tumor dose administered was 7000 R in two series. The mean survival time for a patient treated by combined surgery and radiation was 19 months. For the more radiosensitive papillary cancer it was 22.6 months and for the more resistant epidermoid cancer it was 16.3 months. The complication rate for telecobalt is much lower than for orthovoltage radiation. (auth)

35193 ^{60}Co THERAPY OF RENAL TUMORS. Heinze, H. G.; Schwaerzler, B. (Univ., Munich). Strahlentherapie; 141: No. 3, 276-83(Mar 1971). (In German).

Tumors of the kidney are relatively benign neoplasms. Survival of 50% after five years can be achieved. The prognosis is influenced by the extension of the tumor. Patients in stages I and II have the same survival as normal population, if they survive two years following ^{60}Co therapy. Invasion of the paraaortic lymph nodes (second lymph node station) has an unfavorable prognosis. The prognosis is more favorable in men than in women. Patients older than 50 years have a better prognosis than younger ones. The combined treatment of surgery followed by high energy radiotherapy yields 20% better results than surgery alone. (auth)

35194 CONFORMATION RADIOTHERAPY FOR NASOPHARYNGEAL TUMOR. Kitabatake, Takashi; Hinata, Hiroshi; Inakoshi, Hideki (Niigata Univ., Japan). Strahlentherapie; 141: No. 3, 300-5(Mar 1971).

According to pathological considerations, the nasopharyngeal cavity, surrounding lymphoid tissues, and upper cervical region should be primarily and homogeneously irradiated in patients with nasopharyngeal tumors. Also, to avoid radiation injury, such as radiation cataract and myelitis, eyeballs and spinal cord should be protected from harmful excess radiation. Such an ideal irradiation technique can be performed by conformation technique. A planning procedure and actual dose distribution is described in conformation technique using 10-MeV x rays and electrons. (auth)

35195 IRRADIATION PLANNING BY MEANS OF A PROGRAMMABLE TABLE COMPUTER. Wendhausen, Henning (Radiologische Univ., Kiel). Strahlentherapie; 141: No. 3, 306-10(Mar 1971). (In German).

A program is described for a table desk computer for the planning of telecobalt radiation therapy. Two different methods were analyzed: the static field method and the moving beam method. (auth)

Radiation Effects on Animals

Refer also to abstracts 35124 and 35258.

35196 INITIAL EFFECTS OF IONIZING RADIATION ON A CELL. II. Papers of the Second International Symposium, Erevan, USSR, October 29th–November 3rd, 1968. Stud. Biophys.; 15-16: 1-406(1969). (CONF-681087).

Separate abstracts were prepared for each of 27 papers included on radiation injury to cells. (P.B.M.)

For abstracts of individual papers see: 34654, 35118, 35119, 35197–35206, 35212–35218, 35245–35247, and 35259–35262.

35197 DNA ROLE IN THE CELL INITIAL RADIATION INJURY. Shekhtman, Ya. L.; Strazhevskaya, N. B.; Moiseenko, E. V.; (and others) (Inst. of Biological Physics, Pushchino, USSR). Stud. Biophys.; 15-16: 9-21(1969).

From second international symposium on initial effects of ionizing radiation on a cell; Erevan, USSR (Oct-Nov 1968). See CONF-681087.

It was found that irradiation of DNA solutions brought about a number of significant changes in its structure, single and double strand breaks, destruction of bases, and breaking of hydrogen bonds. Evidently, the radiobiological effect is of a complex nature and includes modifications of nitrogenous bases and single breaks connected with local denaturation injuries in the DNA structure. As a result of these injuries the native bond in the cell nucleus chromatin can be damaged and a nonspecific interaction of histon and DNA may occur which, in its turn, can be one of the causes of radiation death of the cell. (P.B.M.)

35198 SOME NEW ASPECTS OF THE EFFECT OF IONIZING RADIATION ON DEOXYRIBONUCLEOPROTEINS OF SOMATIC CELLS. Tseitlin, P. I.; Spitkovskii, D. M.; Pisarevskii, A. N.; (and others) (Inst. of Experimental Biology, Moscow). Stud. Biophys.; 15-16: 23-38(1969).

From second international symposium on initial effects of ionizing radiation on a cell; Erevan, USSR (Oct-Nov 1968). See CONF-681087.

Data are presented on the relationship between the single breaks

of the polynucleotide chains of DNP macromolecules and the structural damages of the supermolecular DNA system caused by low doses of ionizing irradiation. The role of both types of damages in the disturbance of genetic structure in vivo caused by irradiation is discussed. Analysis of primary lesions in deoxyribonucleoproteins (DNP) of somatic cell nuclei presents a fairly complex problem, involving the singling out of primary lesions from secondary ones determined by the development of metabolic disorders which undoubtedly contribute to the total picture of lesions of nuclear DNP. (P.B.M.)

35199 HIT AND TARGET PRINCIPLES IN RADIOBIOLOGY. Timofeev-Resovskii, N. V. (Inst. of Medical Radiology, Obninsk, USSR). Stud. Biophys.; 15-16: 39-46(1969).

From second international symposium on initial effects of ionizing radiation on a cell; Erevan, USSR (Oct-Nov 1968). See CONF-681087.

The hit and target principles characterize the primary physical processes which initiate radiochemical and radiobiological reactions in irradiated cells. The main concepts and uses of hit and target principles for building up hypotheses and theories explaining mechanisms of elementary responses of organisms to irradiations and deactivation of some biologically active macromolecules are discussed. (P.B.M.)

35200 ROLE OF PRIMARY RADIOTOXINS IN RADIATION DAMAGE OF A CELL. Kuzin, A. M.; Goncharenko, E. N.; Kudryashov, Yu. B.; (and others) (Inst. of Biological Physics, Moscow. Moscow State Univ.). Stud. Biophys.; 15-16: 47-62 (1969).

From second international symposium on initial effects of ionizing radiation on a cell; Erevan, USSR (Oct-Nov 1968). See CONF-681087.

The role of primary radiotoxins (RT) in cell damage development was studied. Water soluble radiotoxins of semiquinoid nature that actively react with nucleoproteids cause the formation of auxotrophic mutants and lysogeny in Escherichia coli. According to changes in ultrastructure and functional activity of mitochondria and hystohematic barriers an effect of radiotoxins mainly on intracellular membranes was detected. It was also found that the radioprotectors AET and cysteamine decrease formation and biological effect of primary radiotoxins. (auth)

35201 CHEMILUMINESCENCE AS INFORMATION SOURCE ABOUT PRIMARY REACTIONS IN BIOLIPIDS BY IRRADIATION. Tarusov, B. N. (Moscow State Univ.). Stud. Biophys.; 15-16: 79-85(1969).

From second international symposium on initial effects of ionizing radiation on a cell; Erevan, USSR (Oct-Nov 1968). See CONF-681087.

Ionizing radiation induces in biolipids two independent primary reactions of different nature. The first is oxidation, which predominates in biolipid systems of mitochondria and leads to the destruction of antioxidants. The second which predominates in lysosomes is accompanied by increase of antioxidative activity. Generally the second reaction is masked by the first reaction which is much more intensively developed. The kinetics of chemiluminescence intensity gave information on functional membrane stability. (P.B.M.)

35202 PART PLAYED BY RADICALS IN RADIATION DAMAGE OF BIOCHEMICAL COMPONENTS OF CELLS. Emanuel, N. M. (Inst. of Chemical Physics, Moscow). Stud. Biophys.; 15-16: 87-99(1969).

From second international symposium on initial effects of ionizing radiation on a cell; Erevan, USSR (Oct-Nov 1968). See CONF-681087.

The effects of free radicals on radioinduced cell damage are reviewed. Kinetic regularities for variations in the content of free radicals formed in biochemical components of cells under the action of irradiation are considered. (P.B.M.)

35203 FREE RADICALS INDUCED IN CELL PROTEINS BY IONIZING RADIATION AND THEIR ROLE IN RADIATION DAMAGE. Kayushin, L. P; L'vov, K. M.; Pulatova, M. K.; Pasoyan, V. G. (Inst. of Biological Physics, Pushchino, USSR). Stud. Biophys.; 15-16: 101-11(1969).

From second international symposium on initial effects of ionizing radiation on a cell; Erevan, USSR (Oct-Nov 1968). See CONF-681087.

A study on the free radical nature in proteins under uv and γ irradiation revealed that in irradiated proteins at 77°K complex primary ESR spectrum is observed. This spectrum is conditioned by trapped electrons, ion radicals of aromatic amino acids, ion radicals of sulphur containing amino acids, and radicals of the peptide chain. At 300°K the ESR doublet observed was determined by the free radical with the localization of unpaired electrons on the oxygen atom of the hydrogen bond. The properties of protein free radicals depend on distribution regularity of peptide hydrogen bonds. The possible role of protein free radicals in biological damage of cells is considered. (auth)

35204 INTRACELLULAR RELEASE OF GLUTATHIONE: A POSSIBLE MECHANISM OF ACTION OF RADIOPROTECTIVE SULPHYDRYL CONTAINING COMPOUNDS. Modig, Hans G. (Karolinska Institutet Medical School, Stockholm). Stud. Biophys.; 15-16: 181-96(1969).

From second international symposium on initial effects of ionizing radiation on a cell; Erevan, USSR (Oct-Nov 1968). See CONF-681087.

The mechanism of action of sulfur containing radioprotective chemical compounds is still not completely understood. Based upon experimental evidence different mechanisms can be considered, several of which may act in the living system. Treatment of Ehrlich ascites tumor cells in vitro with increasing concentrations of the radioprotectors cysteamine and AET caused a proportional increase of the intracellular nonprotein bound sulfhydryl (NPSH) level. The NPSH increase in the cells was found to have a value similar to the dose reduction factor, which characterizes the particular protector at corresponding concentrations. About 45 and 25% of the NPSH increase after cysteamine and AET treatment, respectively, was found to be due to an increase of the cellular glutathione (GSH) content. (auth)

35205 SOME PROBLEMS OF THE MECHANISM OF INJURY AND RECOVERY OF CELLS. Eidus, L. Kh.; Vygodskaya, A. L.; Ganassi, E. E.; Plotnikova, E. D. (Inst. of Biological Physics, Pushchino, USSR). Stud. Biophys.; 15-16: 311-26 (1969).

From second international symposium on initial effects of ionizing radiation on a cell; Erevan, USSR (Oct-Nov 1968). See CONF-681087.

The problem of radiation injury and recovery of the living cell includes 3 main aspects; the regularity of injury and recovery of the cell by itself, the regularity of injury and recovery of the whole pool of a given cell type, and the regularity of injury and recovery of a cell system of vital importance consisting of cells of various types. A review is presented on all three aspects with special attention the analysis of injury and recovery of the hematopoietic system. (P.B.M.)

35206 EARLY STRUCTURAL DISTRUBANCES OF NUCLEOPROTEINS IN RADIOSENSITIVE AND RADIORESISTANT CELLS EXPOSED TO IONIZING RADIATION. Manteifel, V. M.; Zotikov, A. A.; Meisel, M. N. (Inst. of Molecular Biology, Moscow). Stud. Biophys.; 15-16: 347-59(1969).

From second international symposium on initial effects of ionizing radiation on a cell; Erevan, USSR (Oct-Nov 1968). See CONF-681087.

The early changes in nucleoproteins induced by irradiation in cells with different radiosensitivity, lymphocytes, amnion cells in culture, and Tetrahymena pyriformis were investigated by means of different fluorescent microscopic methods. The early reaction of the deoxyribonucleoprotein to ionizing radiation was an increase in their secondary fluorescence intensity as the result of an additional binding of acridine orange with free phosphate groups of DNA. The most severe disturbances were accompanied by the shift of the maximum of the fluorescence spectrum to the longer wavelengths. Obviously this shift was connected with the change in the secondary structure of nucleic acid. The response of the cell cytoplasm to irradiation was also found by means of primary uv fluorescence measuring in the wavelength range of 320 to 380 nm. The significance of these changes is discussed. (auth)

35207 MOLECULAR WEIGHT OF THE DNA SYNTHESIZED IN L-CELLS CONTAINING PYRIMIDINE DIMERS IN THEIR DNA. Klimek, M.; Zemanova, L. (Inst. of Biophysics, Brno). Neoplasma; 18: 87-97(1971).

An investigation into the molecular weight of the DNA synthesized after uv irradiation in L cells (partially synchronized by 5-fluoro-2-deoxyuridine) was made. These cells were either uv irradiated (254 nm) by a dose of 80 erg/mm^2 or 650 erg/mm^2, respectively or nonirradiated. Molecular weight of the DNA synthesized at 1 to 24-hr after DNA synthesis was unblocked (and the cells irradiated) was estimated. The data show that the DNA molecules originating from uv irradiated cells were at first much shorter, probably proportionally to the dose of uv light. But gradually these molecules grew longer and at 24-hr there was only a small difference between the molecular weight of the DNA originating from non-irradiated cells and cells irradiated by 80 erg/mm^2. With a delay, and to a smaller extent, this process was found

XUM

even in cells irradiated by a dose as high as 650 erg/mm^2. The results showed the existence of a postreplication repair mechanism in the uv irradiated L cells, which probably gradually repairs gaps in the daughter strand, located opposite unexcised pyrimidine dimers. (auth)

35208 HORMONOGENESIS IN THYROID BY LOCAL IRRADIATION. Ablyaeva, N. Kh.; Bekmukhametova, Z. U.; Turakulov, Ya. Kh. (Inst. of Biochemistry, Tashkent). Uzb. Biol. Zh.; No. 6, 5-7(1970). (In Russian).

It was found that by local irradiation, iodine absorption by the thyroid gland is not essentially changed, but the synthesis of thyroid hormones is depressed. (auth)

35209 RADIATION EFFECTS ON CELL STRUCTURE. Braun, H. (Univ., Freiburg i. B.). Strahlenschutz Forsch. Prax.; 9: 81-99(1969). (In German).

From ninth conference of the Society of German Radiation Medicine; Aachen, Germany (11 Oct 1968). See CONF-681082.

Radiation effects on cellular fine structure and the associated biochemical and physical processes are reviewed. Emphasized are alterations occurring 24 hours following radiation exposure. Membrane structure, permeability, and various enzymatic systems are discussed. (H.B.G.)

35210 RADIATION EFFECTS ON BIOLOGICAL MEMBRANES. Bergeder, H. D. (Institut fuer Biophysik, Bonn). Strahlenschutz Forsch. Prax.; 9: 100-14(1969). (In German).

From ninth conference of the Society of German Radiation Medicine; Aachen, Germany (11 Oct 1968). See CONF-681082.

The possibilities of explaining cellular injury following radiation as membrane effects are reviewed. As examples, erythrocytes, nerve fibers, and other structures are discussed. Also presented are theories concerning cellular and intracellular membrane structure with respect to their susceptibility to ionizing radiation. (H.B.G.)

Vertebrates

Refer also to abstracts 35112–35114, 35129, 35159, and 35161–35165.

35211 RELATIONSHIP BETWEEN INTRAMEDULLARY DOSE AND ^{59}Fe UPTAKE IN THE BONES OF RATS EXPOSED TO WHOLE-BODY 250 kVp X IRRADIATION. Maillie, H. D.; Mermagen, H. (Univ. of Rochester, N. Y.). Health Phys.; 20: 179-85(Feb 1971). (UR-49-1211).

Studies were performed to examine the effects of 250 kVp x-irradiation on the uptake of ^{59}Fe in irradiated animals. Such experiments showed that certain bones, e.g., those of the skull, paws, or tail, showed no change in uptake with increasing exposure. The remaining bones showed a definite and consistent decrease in uptake with increasing radiation. The humeri, femurs, and the spinal column of rat carcasses were implanted with thermoluminescent dosimeters and the intramedullary dose in rads determined per unit of midline air exposure. A good correlation was found between intramedullary dose and the decrease in ^{59}Fe uptake in those bones in irradiated live rats. This correlation was then used to estimate the intramedullary dose in all of the bones of rats irradiated to a given midline air exposure. (auth) (UK)

35212 CELLULAR ASPECTS OF RADIATION-INDUCED BONE-MARROW FAILURE. Silini, Giovanni (CNEN, Rome). Stud. Biophys.; 15-16: 145-61(1969).

From second international symposium on initial effects of ionizing radiation on a cell; Erevan, USSR (Oct-Nov 1968). See CONF-681087.

The relationships between radioinduced damage to the bone marrow stem cells and the lethality of irradiated mice were reexamined in view of providing some quantitative basis for a mathematical model of bone marrow death. Data are reported to show that within the dose range considered the survival of the mice is well correlated with the number of stem cells surviving the radiation treatment. Evidence consistently pointed to the conclusion that when the stem cell pool of irradiated mice is reduced to less than 100 cells per animal, the probability that those animals survive for 30 days is around 50%. (auth)

35213 SULFHYDRYL GROUPS AND RADIOSENSITIVITY. Graevskii, E. Ya.; Konstantinova, M. M.; Tarasenko, A. G. (Inst. of Developmental Biology, Moscow). Stud. Biophys.; 15-16: 163-80(1969).

From second international symposium on initial effects of ionizing radiation on a cell; Erevan, USSR (Oct-Nov 1968). See CONF-681087.

A distinct correlation was drawn between the radiosensitivity of mammals and the content of thiols in their hemopoietic tissues on whose reaction to irradiation depends on the outcome of radiation injury. Individual differences in the radiosensitivity of rats proved to correspond well to the total content of sulfhydryl groups in their bone marrow. For animals with an average content of sulfhydryl groups of 0.36 micromole/25 mg of bone marrow tissue, LD 50/30 amounted to 559 R. For rats with an average content of sulfhydryl groups equal to 0.56 micromole, LD 50/30 was considerably greater and amounted to 685 R. (P.B.M.)

35214 DUAL EFFECT OF OXYGEN. Revesz, Laszlo; Littbrand, Bo (Karolinska Institutet, Stockholm). Stud. Biophys.; 15-16: 197-210(1969).

From second international symposium on initial effects of ionizing radiation on a cell; Erevan, USSR (Oct-Nov 1968). See CONF-681087.

Chinese hamster cells, derived from 1 day-old or 7-day-old cultures were exposed to x rays in argon to which oxygen was added in an amount varying between 50 to 960 ppM. Controls were treated in argon containing less than 2 ppM oxygen. The survival ratio of the cells determined after treatment with a single dose and with the same dose split in two equal fractions and given 18 hr apart, was the same in the controls, and increased with increasing concentrations of oxygen. With cells derived from the older culture, this increase closely parallelled the increase in oxygen consumption of Ehrlich ascites cells at corresponding oxygen concentrations. The results support the conclusion that oxygen has a dual effect on radiation survival. Depending upon the x ray dose delivered, oxygen at different concentrations may have a protective or a sensitizing effect on the net survival. (P.B.M.)

35215 SIGNIFICANCE OF THE INTRACELLULAR DISTRIBUTION OF ENZYMES IN EARLY CHANGES OF THEIR ACTIVITIES AFTER IRRADIATION IN VIVO. Dancewicz, Antoni M. (Inst. of Nuclear Research, Warsaw). Stud. Biophys.; 15-16: 243-54(1969).

From second international symposium on initial effects of ionizing radiation on a cell; Erevan, USSR (Oct-Nov 1968). See CONF-681087.

Rats were x-irradiated with a dose of 750 R and killed at 0 or 2 hr after exposure. The liver and spleen of control and irradiated animals were excised, homogenized, and analyzed for the activity of a chosen set of enzymes. The activity of enzymes was determined and their intracellular distribution calculated. Changes in the biosynthesis of enzymes and in their regulation, changes in the relationships between the enzyme molecule and its surrounding, and between enzyme and structural elements of the cell organization are suggested as radiation effects which may account for the resulting changes in enzymatic activities after exposure of a living system to ionizing radiation. (P.B.M.)

35216 EARLY BIOCHEMICAL AND STRUCTURAL CHANGES IN LIVER MITOCHONDRIA OF IRRADIATED RATS. Romantsev, E. F.; Cherkasova, L. S.; Kozyreva, E. V.; (and others). (Inst. of Physiology, Minsk. Belorussian State Univ., Minsk.). Stud. Biophys.; 15-16: 273-90(1969).

From second international symposium on initial effects of ionizing radiation on a cell; Erevan, USSR (Oct-Nov 1968). See CONF-681087.

The effects of low and high radiation doses on the processes of oxidative phosphorylation in liver and brain mitochondria of rats were investigated. Certain changes in physicochemical characteristics of mitochondria were found after x irradiation of animals with a dose of 40-R, spontaneous swelling and swelling after addition of trypsin, natrium desoxylate, ATP, and nonorganic phosphate. Mitochondria isolated from the brain of rats were more stable to swelling than liver mitochondria. After irradiation of animals with 1000-R, early changes in a functional state of mitochondria acquired a soft coupled state, their ultrastructure changed. (auth)

35217 EFFECT OF RADIATION ON THE REPRODUCTION OF CELLS OF HEMOPOIETIC ORGANS IN VARIOUS SPECIES OF LABORATORY ANIMALS ACCORDING TO THEIR RADIOSENSITIVITY. Papoyan, S. A.; Ohanzhanyan, E. E.; Fichizhyan, B. S.; Sahakyan, Zh. G. (Dept. of Radiobiology, Erevan). Stud. Biophys.; 15-16: 299-310(1969).

From second international symposium on initial effects of ionizing radiation on a cell; Erevan, USSR (Oct-Nov 1968). See CONF-681087.

The defect of post radiation recovery of hemopoiesis may be connected with early destructions of reticular cells and chromosomal aberrations. According to the investigation of aberrant mitosis the degree of radiosensitivity and resistance of hemopoietic organs of different experimental animals are not identical. (auth)

XUM

35218 EFFECT OF IRRADIATION CONDITIONS ON THE RECOVERY OF SOMATIC CELLS IN MAMMALIAN ORGANISM. Yarmoneko, S. P.; Olshevskaya, O. P. (Inst. of Experimental and Clinical Oncology, Moscow). Stud. Biophys.; 15-16: 337-46(1969).

From second international symposium on initial effects of ionizing radiation on a cell; Erevan, USSR (Oct-Nov 1968). See CONF-681087.

The results of experiments on the radiosensitivity of mice and blood-forming cells in early postirradiation period were compared. The correlation in time and in character of animals and stem bone marrow cells radiosensitivity within the first 24 hr after irradiation is given. When chronic and fractionating irradiation was used the number of the damaged liver cells was less than that of momentary irradiation. In the interval of dose rate from 39 rad/min to 3.5×10^{-3} rad/min the degree of damage effect weakening was not changed; it began to increase after further lowering of dose rate. The results indicated the reality of the repair phenomenon of the cell viability and chromosome structure in vivo. (auth)

35219 CHANGES IN THE QUANTITY OF ASCORBIC ACID IN THE SOFT TISSUES OF THE ORAL CAVITY IN THE CHRONIC RADIATION DISEASE. Zlateva, M.; Dachev, B.; Antov, G. Stomatologiia (Sofia); 52: 107-11(Mar-Apr 1970). (In Bulgarian).

The changes in ascorbic acid content in the gingiva, oral mucosa, tongue, and the striated muscle of the cheek in experimentally induced radiation disease were investigated. The changes were compared with those that occur in the liver. It was found that the quantity of ascorbic acid in the tissues of experimental animals (liver, gingiva, the striated muscle of the cheek, tongue) submitted to progressively increased doses of x irradiation was considerably reduced. This drop in ascorbic acid testifies to grave disturbances in the oxidation-reduction processes in the tissues of the experimental animals. (auth)

35220 NUMBER OF EPITHELIAL CELLS AS MEASURE OF THE RADIATION DAMAGE AND REGENERATION OF THE SMALL INTESTINES. Kabakov, E. N. (Inst. of Medical Radiology, Obninsk, USSR). Stud. Biophys.; 13: 27-34(1969). (In Russian).

The number of epithelial cells of the rat small intestines was determined after irradiation. A suspension of the surface layer of intestines was prepared and the cells were counted by Celloscope. The maximal depletion of the epithelial cells at 500 and 750 R was observed in 48 hours after the irradiation and the regeneration was completed in 5 days. The number of epithelial cells at different doses of irradiation decreased exponentially at doses of 0 to 1000 R and was close to constant during further increase of irradiation dose (1100 to 5000 R). It was concluded that the method can be used for rapid evaluation of the radiation damage level in small intestine. (auth)

35221 POST-TRAUMATIC REGENERATION IN LIVER AFTER INTERNAL IRRADIATION. Tokin, I. B.; Filimonova, G. F.; Merkushev, G. N. (Leningrad Inst. of Radiation Protection). Arkh. Anat., Gistol. Embriol.; 60: No. 3, 66-73(Mar 1971). (In Russian).

Regeneration processes were studied in the liver of irradiated Wistar rats 45 days after intraperitoneal administration of ^{144}Ce in a dose of 200 mCi following partial hepatectomy. Animals were decapitated at 6 a.m. having been operated on 2 to 48 hr previously. RNA and DNA syntheses were investigated autoradiographically; mitotic activity was also determined. Mechanisms of irradiation effects on processes of liver regeneration are discussed. All disturbances due to irradiation were found to be of relatively short duration and the generation process was not much delayed as compared to control. The delay in posttraumatic regeneration of irradiated liver as an organ did not coincide with depression in hepatocyte reparation. As shown in electron microscopic studies under these conditions reparative processes in hepatocytes proceeded at a higher level as compared to the rate of reparation of nonirradiated liver cells. Thus reparative processes at the cellular level may differ significantly from those at organ level. (auth)

35222 REGULATION OF FRACTIONAL COMPOSITION OF 11-OCS BY THE LIVER OF DOGS IRRADIATED WITH GAMMA RAYS. Fedotov, V. P.; Pantyushina, N. N. (Moscow Inst. of Experimental Endocrinology and Chemistry of Hormones. Moscow Inst. of Biophysics). Probl. Endokrinol.; 17: 105-8(Jan-Feb 1971). (In Russian).

A study was made on the effects of γ radiation (350 R) on the capacity of the liver to control the fractional composition of corticosteroids in the blood plasma during hormonal loads (ACTH, hydrocortisone). Investigations were carried out on angiostomized dogs with skin cannulae on the portal and hepatic veins. The intensity of retention of free corticosteroids by the liver was noted. As in healthy animals the hormones bound with plasma proteins passed through the liver in unchanged form; the binding capacity of plasma proteins diminished, however. No significant alteration of hepatic retention in glucuronides was found. (auth)

35223 EFFECTS OF IONIZING RADIATIONS ON OXYGEN UPTAKE BY RAT LIVER SLICES, MITOCHONDRIA, AND MITOCHONDRIAL MEMBRANES. Jordana, R.; Lopez, Natalia; Alonso, A.; Santiago, E.; Ponz, F. (Univ. of Navarra, Pamplona, Spain). Rev. Espan. Fisiol.; 27: No. 1, 63-7(Mar 1971).

X irradiation caused a decrease in oxygen consumption in rat liver slices. Electron microscopy of the irradiated tissue revealed marked swelling of mitochondria accompanied by a decrease in the density of the matrix, as well as by vesiculation of the rough and smooth endoplasmic reticulum. In the jejunum irradiation caused a shortening of the microvilli and a reinforcement of the microfilaments of the terminal web. It was also found that in suspensions of mitochondria from irradiated rat liver slices, irradiated mitochondria, and irradiated inner mitochondrial membranes there was a faster onset of swelling and lysis provoked by ascorbate. It was also found that irradiation of the inner mitochondrial membranes caused the formation of lipid peroxides. (auth)

35224 REJOINING OF SINGLE BREAKS OF DNA INDUCED BY X-RAYS IN MAMMALIAN CELLS: EFFECTS OF METABOLIC INHIBITORS. Tsuboi, Atsushi; Terasima, Toyozo (National Inst. of Radiological Sciences, Chiba, Japan). Mol. Gen. Genet.; 108: 117-28(28 Sep 1970).

The effects of metabolic inhibitors on the rejoining of broken single strands of DNA in mouse L cells induced by x irradiation were studied by the sucrose gradient sedimentation method. Inhibitors of protein and DNA syntheses, such as cycloheximide and 5-fluorodeoxyuridine, could not suppress the rejoining of broken strands, when they were introduced into cultures at the time of irradiation. However, 2.5-hr pretreatment of cells with 5-fluorodeoxyuridine was capable of reducing the rate of rejoining. In addition, proflavin, one of DNA binding substances tested, prevented the rejoining. These results suggest that preexisting DNA-related enzymes, for instance, DNA polymerase and ligase, are responsible for the process. (auth)

35225 ALLOMETRY OF BODY WEIGHT AND TAIL LENGTH AFTER HEAD X-IRRADIATION IN RATS. Mosier, H. David Jr.; Jansons, Regina A. (Univ. of California, Irvine. Memorial Hospital Medical Center, Long Beach, Calif.). Growth; 35: No. 1, 23-31(Mar 1971).

Bilateral x irradiation of the head of the 2 day old Long Evans rat with 600 R produced a disturbance of the allometric relationship of body weight and tail length. This was greatest between 9 and 30 days of age in most of the experiments. There was a tendency toward recovery of normal proportions even in the presence of permanent stunting of body weight and tail length. The bearing of the findings on the problem of the control of proportionate growth is discussed. (auth)

35226 HYPOXANTHINE DYNAMICS IN BRAIN FOLLOWING NEUTRON IRRADIATION. Gamezo, N. V. (Inst. of Physiology, Minsk). Vestsi Akad. Navuk BSSR, Ser. Biyal. Navuk; No. 2, 116-18(1970). (In Russian).

The hypoxanthine content of brain tissues was studied in Wistar rats 1 hr to 30 days following irradiation of the animals with intermediate neutrons at a dose of 13.5 rads. The content of the compound underwent phasic changes reaching its lowest point through 12 hr postirradiation and then increasing through the seventh day. (tr-auth)

35227 EFFECT OF CORTISOL ON THE OPTICAL DENSITY OF SARCOSOMES IN INTACT AND ADRENALECTOMIZED ANIMALS FOLLOWING RELATIVELY SMALL DOSES OF IONIZING RADIATION. Nasirov, R. A. (Inst. of Physiology, Minsk). Vestsi Akad. Navuk BSSR, Ser. Biyal. Navuk; No. 2, 112-15 (1970). (In Russian).

It was established that the ultrastructure of the mitochondrial membranes in cardiac muscle depends on the primary functional state of the hypothalamo-hypophyseal-adrenal systems. The conclusion was based on the dissimilarity of the changes occurring in the optical density of the irradiated mitochondria in both intact and adrenalectomized animals when subjected to the action of cortisol in vitro. (tr-auth)

35228 CONTENT OF COPPER AND ALUMINUM IN FUNCTIONALLY AND MORPHOLOGICALLY DIFFERENT TISSUES OF THE SPINAL CORD AFTER X IRRADIATION OF ANIMALS. Tsegel'nik, L. I.; Reva, A. D. (Dnepropetrovsk State Univ.,

XUM

USSR). Byull. Eksp. Biol. Med.; 71: No. 2, 40-2(Feb 1971). (In Russian).

Spectrography was employed to determine the content of copper and aluminum in morphologically and functionally different parts of the lumbar thickening of the spinal cord, grey matter of anterior and lateral horns (motor zones), grey matter of posterior horns (sensitive zone), white substance, and anterior and posterior cerebrospinal radicles during the period ranging from 1-hr to 8 to 10 days after x irradiation of animals at a dose of 1200 R. Ionizing radiation caused essential changes in the concentration of trace elements in the above mentioned structures of the spinal cord. In local irradiation of the lumbar region of the spinal cord the changes were the same as those noted in total irradiation. (auth)

35229 INFLUENCE OF URANIUM NITRATE ON THE MORPHOFUNCTIONAL STATE OF RABBIT THYROID GLAND. Malenchenko, A. F.; Bakhanovich, V. I.; Radyuk, K. A. (Inst. of Nuclear Energy, Minsk). Byull. Eksp. Biol. Med.; 71: No. 3, 36-8(Mar 1971). (In Russian).

Under the effects of uranium nitrate, a decline in the values of radioiodine accumulation in the thyroid gland, values of $SB^{131}I$, degree of conversion, and thyroxine test occurred in rabbits. Along with this, autoantibodies to the thyroid gland appeared in the blood in titers of up to 1:512. In the thyroid gland, a picture of micro and mediofollicular colloidal goiter was found with the development of adenoma of parenchymatous structure. (auth)

35230 TRANSPLANTATION OF THE BONE MARROW TO IRRADIATED MONKEYS: CHROMOSOMAL ABERRATIONS IN DONOR CELLS. Udalov, G. A.; Chertkov, I. L. (Central Inst. of Hematology and Blood Transfusion, Moscow). Byull. Eksp. Biol. Med.; 71: No. 2, 97-101(Feb 1971). (In Russian).

Allogenic bone marrow from females was transplanted to thymectomized male baboons and Macaca rhesus after irradiation with doses of 800 to 1000 R. Ten to 15 days after irradiation, up to one third of donor hematopoietic cells showed structural lesions of chromosomes, chromatid, and isochromatid fragments. In 3 weeks the content of injured cells decreased. Analogous chromosomal injuries in the hematopoietic cells were also revealed after autotransplantation of the bone marrow. (auth)

35231 GROWTH AND TRANSFORMATION OF CRYSTALLINE EPITHELIUM IN IMPLANTS FOLLOWING WHOLE-BODY X-IRRADIATION OF THE DONOR WITH A SUBLETHAL DOSE. Dunaev, P. V.; Agarkov, V. A. (Tyumen Medical Inst., USSR). Byull. Eksp. Biol. Med.; 71: No. 3, 91-4(Mar 1971). (In Russian).

The crystalline epithelium of mature albino rats was implanted 24 hr after total x irradiation of the donor with a dose of 800 R. In 1 to 90 days of the experiment the implants were studied histochemically for DNA, RNA, and neutral and acid mucopolysaccharides. Implantation growth processes of differentiation of the crystalline epithelium were disturbed as the result of the direct effect of x rays on the nuclear and cytoplasmic components of the cell. Histochemically this was manifested by an impaired glycogen synthesis. The equatorial and preequatorial zones of the crystalline epithelium were most sensitive to x rays. (auth)

35232 CHOLINESTERASE ACTIVITY IN SUBCELLULAR FRACTIONS OF THE BRAIN OF WHITE RATS FOLLOWING X IRRADIATION IN RELATION TO THE FUNCTIONAL STATES OF THE HYPOPHYSEAL AND ADRENAL SYSTEMS. Khrypchanka, I. P.; Kakhnyuk, V. I. (Minsk State Univ.). Vestsi Akad. Navuk BSSR, Ser. Biyal. Navuk; No. 2, 90-3(1970). (In Belorussian).

Cholinesterase activity in subcellular fractions (supernatant, nucleus, and mitochondria) isolated from 10% homogenates of the cerebral hemispheres of white rats was studied. The experimental design included the use of intact animals and adrenalectomized animals with subsequent hormone therapy plus x irradiation. It was found that under conditions of surgical interference, enzyme activity was increased in all fractions studied. Following subsequent hormonal modification by introduction of hydrocortisone acetate and adrenalin in combination or singly, the regulating role of the adrenal cortex by an acetylcholine-cholinesterase system was demonstrated. This was manifested especially under conditions of irradiation. (tr-auth)

35233 COMBINED ACTION OF CARBON MONOXIDE AND IONIZING RADIATION UNDER PROLONGED CONDITIONS. Kustov, V. V.; Tiunov, L. A.; Vasil'ev, G. A.; Keizer, S. A.; Ivanova, F. A. Gig. Tr. Prof. Zabol.; No. 5, 36-8(May 1971). (In Russian).

Experiments with 30 white rats chronically exposed for 85 days to the combined effects of 0.012 mg/l CO and ionizing γ radiation (^{60}Co) with 0.05 rem/day doses revealed a series of disturbances in the health of animals. However, exposures to 0.005 mg/l CO concentration and 0.05 rem/day γ radiation did not produce any negative effects in the examined rats. (R.V.J.)

35234 EFFECT OF UV IRRADIATION ON HEXOKINASE ACTIVITY IN SKIN. Smirnova, M. G. (Arkhangelsk State Medical School, USSR). Vop. Med. Khim.; 17: 145-8(Mar-Apr 1971). (In Russian).

Within 1, 4, 24 hrs, and 6 days after uv irradiation hexokinase activity in animal skin sharply decreased. This phenomenon might be explained by an increased concentration in the blood of corticosteroid hormones which inhibit hexokinase activity. Insulin administered 30 min before irradiation prevented the inhibition of hexokinase activity. (auth)

35235 EFFECT OF IONIZING RADIATION ON THE INDUCED BIOELECTRICAL ACTIVITY OF THE BRAIN OF THE RAT. Gezalyan, L. S.; Podachin, V. P. (Ministry of Public Health, Erevan. Inst. of Higher Nervous Activity and Neurophysiology, Moscow). Biol. Zh. Arm.; 23: No. 7, 32-9(Jul 1970). (In Russian).

Changes in the radioinduced potential were determined at time periods up to 3 weeks after exposure. White rats were subjected to whole-body irradiation doses of 300 to 700 R. The electric activity of the brain was recorded within 24 hr to 3 weeks after irradiation at the medulla oblongata, the thalamus, and the crust of the cerebellum by means of a microelectrode with a resistance of 10 to 5 ohm. The excitation stimulus was applied at the right front paw of the animal. No reliable observation could be made about disturbing effects during the first few days after irradiation. An increase in the latent period of the induced potential and the observed decrease of the amplitude indicated a slowing down of the neurons. In the cerebellum, an increase in the amplitude of the response was noted at first; during the 3rd week both components of the response were affected and the latent period was increased, indicating a similar weakening of the nerve cells. (TTT)

35236 FIBROSARCOMA INDUCED BY ALPHA PARTICLE IRRADIATION. de Estable-Puig, R. F.; de Estable-Puig, J. F.; Auger, C. (Laval Univ., Quebec). Virchows Arch., B; 6: 367-9(1970).

A report is given on the first observation of a fibrosarcoma induced in rats by a beam of alpha particles. The alpha particles had a 48-MeV energy and were delivered by a 60 inch cyclotron through a 14.3 mm aperture at a dose rate of 1000 rad/min. One year after irradiation, a tumor measuring $0.75 \times 0.5 \times 0.6$ cms was observed in the scalp within the locus of irradiation. Under the electron microscope, the main cellular component of the tumor had the features of a neoplastic fibroblast. (P.B.M.)

35237 HISTOLOGICAL CHANGES IN THE UTERUS AND OVARY OF ALBINO RATS AFTER IRRADIATION AND SIMULTANEOUS ADMINISTRATION OF SYNTHETIC ESTROGENS AND PROGESTOGENS. Pompili, G.; Roseo, B. (Ospedale Maggiore, Milan). Osp. Magg.; 63: 571-8(May 1968). (In Italian).

The results of research on the possible histologic alterations caused by x rays and hormone treatment in the uterus and the ovary of female albino rats at various periods of time after irradiation are given. Interactions between ionizing radiations and progestative and estrogenic hormones were not found in the in the organs studied by histologic techniques. (auth)

35238 AUTORADIOGRAPHIC STUDIES ON ^3H-THYMIDINE INCORPORATION IN THE LIVER AND KIDNEYS OF IRRADIATED MICE. Unger, Emil; Gidali, Julia (Frederic Joliot-Curie National Research Inst. for Radiobiology and Radiohygiene, Budapest). Strahlentherapie; 141: No. 3, 354-7(Mar 1971).

The incorporation of ^3H-thymidine into the liver- and renal tubulus cells of mice whole-body irradiated with 200, 450, and 700 R, respectively, was studied immediately post irradiation, and again after 4, 24, 72 hours, and 6 or 9 days. It was established that as a result of irradiation, the count of DNA-synthesizing cells generally decreased both in the resting liver and the kidneys, within 72 hours in direct proportion to the time elapsed since irradiation. Six and nine days after irradiation the labeling index rose again but failed to reach the control level. (auth)

35239 CELL POPULATION KINETICS IN ACUTE INTESTINAL RADIATION DEATH. Okumura, Yutaka; Matsuzawa, Taiju (Aichi Cancer Center Research Inst., Nagoya, Japan). Strahlentherapie; 141: No. 3, 358-62(Mar 1971).

A mechanism of the denudation of the epithelial cells after x-irradiation inducing acute intestinal death was analyzed by developing a model of the intestinal epithelium which has two cell compartments. These, the proliferative and the functional compartments, are located in the crypts and on the villi, respectively.

After irradiation, the cell number in the proliferative compartment decreased exponentially. As change of the cell number of the functional compartment is expressed by influx- and efflux-cell number, the lack of the proliferative compartment caused depletion of the functional compartment subsequently. There was good agreement of the results between the calculation on this model and the experimental data obtained by germ-free and conventional CFW mice. It was found that the model indicates the mechanism of the denudation of the epithelial cells as a cell renewal system after irradiation. (auth)

Man

Refer also to abstracts 35123, 35144, and 35158.

35240 ORIGIN AND KINETICS OF GOBLET CELLS IN THE HUMAN JEJUNUM DURING IRRADIATION. Wiernik, George; Plant, Mary (Oxford Univ.). Brit. J. Radiol.; 44: 348-56(May 1971).

The data obtained from multiple serial biopsies of the jejunal mucosa of patients receiving post-operative irradiation were analyzed. These have demonstrated an inverse relationship between mitotic activity in the crypt and the number of goblet cells. From this and other evidence the conclusion was reached that a single stem-cell system in the mucosal crypt gives rise to both epithelial and goblet cells and that the latter are a product of differentiation and are not derived from an independent stem-cell population. (auth) (UK)

35241 AGING IN HIROSHIMA AND NAGASAKI ATOMIC BOMB SURVIVORS: ACCUMULATION OF CARDIAC LIPOFUSCIN. Anderson, Robert E. (Univ. of New Mexico, Albuquerque); Yamamoto, Tsutomu; Oshida, Kenzo; Thorslund, Todd. J. Amer. Geriat. Soc.; 19: 193-8(Mar 1971).

Report is given on the amount of age dependent lipofuscin in the myocardium (left ventricle) as found at autopsy in a group of 54 persons who were exposed proximally (1,400 meters from the hypocenter) to the Hiroshima and Nagasaki atomic bombs of 1945. The subjects were matched by sex and age decade of death with a similar number of subjects who were in neither city at the time of the explosions. The results failed to demonstrate an accelerated accumulation of pigment in the proximally exposed group. Although the difference was not statistically significant, the majority of the exposed group appeared to accumulate lipofuscin more slowly than did the nonexposed group. The possible implications are discussed. (auth)

35242 EFFECT OF FRACTIONATED X IRRADIATION ON THE CELLS DERIVED FROM HUMAN BONE TUMOR IN TISSUE CULTURE. Takase, Buhei; Yamazaki, Anro; Manabe, Shohei; Yasumoto, Saburo; Miaki, Hiroshi (Kanazawa Univ., Japan). Cent. Jap. J. Orthop. Traumatic Surg.; 12: 1107-10(Dec 1969). (In Japanese).

Experimental observations were made on the effects of fractionated x irradiation on cultured cells by using the OST line cells (cells isolated from the osteosarcoma of femur and established as a culture cell line). A commercial synthetic medium, TCM 199, added with calf serum was used. Irradiation was given once directly after serial transfer and the second time after 12, 24, or 36 hr. Culture cell number was counted after the end of the second irradiation for subsequent 120 hr at 12-hr intervals by the leucocyte counting method. In the A group given fractionated irradiation of 100 R, cell number decreased after the second irradiation while that in the B group increased. With a dose above 400 R, cell number was large when the second irradiation was given at the 24 hr interval and smaller when irradiated after 36 hr. The appearance of mitotic figures was observed from 12 hr after serial transfer and was seen in 3 to 5% of the cells. The period of appearance after the first irradiation was prolonged with an increase in dose. In the B group irradiated with a fractionated dose of 100 R, mitosis appeared uniformly after 12 hr. Appearance of megakaryocytes was in approximate proportion with the number of cells but was not proportional with the increase in dose. It was found that inhibition of cell proliferation was most effective when irradiation with large doses was followed by a small dose, with an interval of 12 hr between the two doses. (Japan)

35243 PROBLEM OF RADIOTHERAPY OF THE PERIPHERAL INOPERABLE BRONCHIAL CARCINOMA. Freise, G. (Staedt. Krankenhauses Heckeshorn, Berlin). Strahlentherapie: 141: No. 3, 291-9(Mar 1971). (In German).

After surgery and radiotherapy for peripheral bronchial carcinomas, some modifications occur in the tissues, causing a reduction of the pulmonary function. By examining the mean survival times, it was found that for surgery and radiotherapy the complications and mortality are essentially the same. Bad results are obtained by both methods, when cardiopulmonary function is already reduced before treatment begins. The results, however, are better when radiotherapy is done over small fields. Survival is then higher and complications are lower than if large fields are used or a complementary mediastinal irradiation. (auth)

Radiation Effects on Plants

Refer also to abstracts 35102, 35118–35120, 35122, 35125, 35127, 35128, 35196, and 35199.

35244 CYTOPLASMIC INJURY IN THE SHOOT APEX OF MAIZE AFTER GAMMA IRRADIATION. Graham, E. T.; Generoso, Estela E. (Univ. of Tennessee, Knoxville). Contract AT(40-1)-GEN-242. Radiat. Bot.; 11: 73-4(1971).

Generative cells of maize shoot apices developed irregularly-shaped dense condensates in cytoplasm during 12 hr after acute gamma irradiation. The condensates were clearly delineated by stains having high affinity for RNA but were not revealed by protein stains. This evidence of cytoplasmic change receded after 12 hr. Irradiation was by exposure to ^{60}Co gamma radiation, 5000R at 50R/min. Stains used were azure B toluidine blue, methyl green-pyronine, Safranin fast green and hematoxylin. (auth) (UK)

35245 RADIATION INJURY OF MOLECULAR MECHANISMS OF THE RNA MATRIX SYNTHESIS. Tokarskaya, V. I. (Inst. of Biophysics, Pushchino, USSR). Stud. Biophys.; 15-16: 63-78 (1969).

From second international symposium on initial effects of ionizing radiation on a cell; Erevan, USSR (Oct-Nov 1968). See CONF-681087.

It was found that γ irradiation leads to the disturbance of regulation of the genome function which is accompanied by the decrease in the number of active cistrons on which the AU type RNA is synthesized, simultaneously with the activation of regions of the DNA matrix, responsible for the synthesis of rRNA. (auth)

35246 RADIOSENSITIVITY OF CELL REPAIR SYSTEMS. Paribok, V. P. (Inst. of Cytology, Leningrad). Stud. Biophys.; 15-16: 113-26(1969).

From second international symposium on initial effects of ionizing radiation on a cell; Erevan, USSR (Oct-Nov 1968). See CONF-681087.

Examples of γ and x radiation effects on repair systems of Escherichia coli and Vicia faba are given. It was found that the repair system of chromosomal breaks of Vicia faba is resistant to radiation. Even after doses of 200 and 400 R, the reparation rate remained the same. The photoreactivation system of Escherichia coli B s-1 though not altered during x irradiation was damaged by γ rays. (P.B.M.)

35247 EARLY STRUCTURAL, ULTRASTRUCTURAL, AND FUNCTIONAL DISTURBANCES IN RADIOSENSITIVE AND RADIORESISTANT YEAST CELLS UNDER THE INFLUENCE OF IONIZING RADIATION. Meisel, M. N.; Biryuzova, V. I.; Galtsova, R. D.; (and others) (Inst. of Microbiology, Moscow). Stud. Biophys.; 15-16: 223-41(1969).

From second international symposium on initial effects of ionizing radiation on a cell; Erevan, USSR (Oct-Nov 1968). See CONF-681087.

Studies on the radiosensitivity of yeast cells have revealed that not only different cells, but even their various structural and biochemical components are unequally sensitive to radiation. Radiosensitive cultures and strains of yeasts differed from radioresistant ones in that they had more labile nucleoproteins, contained lower molecular acid insoluble polyphosphate and sulfhydryl groups, had a richer reserve of free amino acids, and their cells released more amino acids and group B vitamins. Consequently, the genetic conditionality of radiosensitivity manifested itself not only in the structural peculiarity of the DNA and the chromosomes of the cell, but also in the lowered resistance of the nucleoproteins connected with it, as well as in a number of enzymatic systems which regulate the carbohydrate, protein, phosphorus, fat, and sterol metabolism. (auth)

35248 CONTRIBUTIONS TO RADIATION STIMULATION. III. INFLUENCE OF TEMPERATURE ON RADIATION-INDUCED GROWTH STIMULATION IN LEMNA MINOR L. Feldmann, A. (Kernforschungsanlage, Juelich, Ger.). Radiat. Bot.; 11: 59-65 (1971). (In German).

Radiation-induced acceleration of development in Lemna minor was modified by temperature in a similar way as that caused by exposure to light. With increasing stimulation, increased doses

XUM

had to be applied to cause damage. Compared with exposure to light, the influence of temperature was, less pronounced. Exposure to light led to a maximal increase of frond production of 32.4%, whereas in temperature experiments the maximal value was 21.7 percent. The threshold values varied between about 400 R and 600 R for the light experiments. In contrast to exposure to light at suboptimal conditions, no increase in surface and weight of single segments could be found in temperature experiments. (auth) (UK)

35249 EFFECT OF A CHRONIC EXPOSURE TO GAMMA RADIATION ON THE SHRUB EPHEDRA NEVADENSIS IN THE NORTHERN MOJAVE DESERT. Kaaz, H. W.; Wallace, A.; Romney, E. M. (Univ. of California, Los Angeles). Radiat. Bot.; 11: 33-7(1971).

A 33,600 Ci ^{137}Cs source which was differentially shielded to increase the uniformity of the distribution of radiation was set up on a 15-m tower in the center of a 9-ha plot in January 1964 in the Rock Valley area of the northern Mojave Desert. In the spring of 1969 the large majority of 5000 Ephedra nevadensis Wats. shrubs (Mormon Tea) within the plot failed to produce flowers and very little vegetative growth occurred on the species in contrast to a control plot and to other nonirradiated areas. The 5-year cumulative radiation exposure throughout about 85 percent of the plot ranged from 3.9 to 9.8 kR. Radiation effects on other species were nonexistent or doubtful. E. nevadensis has a higher interphase chromosome volume than do the other shrub species. (auth) (UK)

35250 GYMNOSPERM SEEDLING SENSITIVITY TO GAMMA RADIATION: ITS RELATION TO SEED RADIOSENSITIVITY AND NUCLEAR VARIABLES. Rudolph, T. D. (Inst. of Forest Genetics, Rhinelander, Wis.). Radiat. Bot.; 11: 45-51(1971).

Newly germinated seedlings of Larix laricina, Picea glauca, Picea mariana, Pinus banksiana, Pinus contorta, Pinus resinosa, and Thuja occidentalis were gamma irradiated at exposures of 150, 300, 450, 600, 900, 1200, 1800, 2400 and 3600 R. Number of leaves produced and shoot dry weight were determined 50 days after irradiation and survival and shoot dry weight after 130 days. Of the 4 endpoints scored, shoot dry weight at 50 days showed greatest radiosensitivity with a D_{50} ranging from 195 R for Pinus resinosa to 380 R for Picea mariana. Except for shoot dry weight at 50 days, all endpoints showed a sharp response over a relatively narrow range of exposures, generally between 600 and 900 R. The 7 species differed in seedling radiosensitivity by a factor of less than 2 for all endpoints. Comparison with seed radiosensitivity of the same populations showed that seedlings are from 7 to 15 times more sensitive than seeds. Correlation analyses showed that the only relationship among the endpoints studied was between D_{50} for number of leaves at 50 days and shoot dry weight at 130 days: the seedlings with the greatest number of leaves at 50 days had the greatest dry weight at 130 days. No relation was found between the D_{50} following seedling irradiation and the D_{50} for irradiated seed previously reported for the same populations of the 7 species. The observed seedling radiosensitivity was not correlated with predicted mature plant sensitivity. Seedling radiosensitivity as determined from 3 of the 4 endpoints studied was related to DNA content per cell determined cytophotometrically in Feulgen absorption units, but unrelated to DNA content determined chemically or to nuclear volume. (auth) (UK)

35251 ANTAGONISTIC ACTION OF IODACETATE AND ETHANOL ON THE RECOVERY IN YEAST. Mosin, A. F. (Inst. of Medical Radiology, Obninsk, USSR). Stud. Biophys.; 13: 21-6 (1969).

The role of various pathways of glucose catabolism during the recovery of γ- and uv-irradiated Saccharomyces vini was investigated. It was found that if cells were treated after γ irradiation with both ethanol and iodacetate, the inhibitive effect of ethanol on recovery was removed to a great extent. The restoration of viability in S. vini after uv irradiation was less sensitive to ethanol and insensitive to iodacetate. (F.M.M.)

35252 TRACER STUDIES ON SYNTHESIS OF FREE NUCLEOTIDES IN YEAST AFTER β-IRRADIATION. Altmann, H.; Stehlik, G. (Reactor Centre, Seibersdorf, Austria). Stud. Biophys.; 13: 59-64(1969).

The effects of ^{90}Sr β irradiation on the synthesis of free nucleotides in Saccharomyces cerevisiae were investigated. A double label method was used, i.e., the incorporation of ^{3}H and ^{14}C from labeled glucose into the free nucleotides was examined. The uv spectra and radioactivity of the nucleotides were measured following paper chromatographic and high voltage electrophoretic separation. (F.M.M.)

35253 VARIATION IN LIPASE ACTIVITIES DURING GERMINATION (IN DARK) OF γ-IRRADIATED CASTOR-SEEDS. Thanki, R. J.; Patel, K. C.; Patel, R. D. (Sardar Patel Univ., Vallabh Vidyanagar, India). Lipids; 5: 519-23(Jun 1970).

A special variety of Ricinus communis has two types of lipases. One of these is active at pH 4.5 and another at pH 6.8. The acid lipase was maximum in dry seeds. The control and γ-irradiated seeds when germinated in dark showed a decrease in acid lipase. The decrease in acid lipase was dependent on the period of germination and the applied irradiation dose. The presence of a de novo synthesis of another activity measured at pH 6.8 was found after 24 hr of germination of the control as well as the irradiated seeds. The new activity termed as a neutral lipase showed a gradual increase with the period of germination. Irradiation played a characteristic role in the production of this activity. (auth)

35254 EFFECTS ON THE ALKALOID CONTENT OF POTATOES GROWN FROM SEEDS SUBJECTED TO LOW-DOSE GAMMA IRRADIATION. Sutton, William R.; Agarwala, Om Prakash; Pigott, George M. (Univ. of Washington, Seattle). J. Food Sci.; 36: 416-18(Apr 1971).

The effects of low-dose γ irradiation of seeds on alkaloid content, proximate composition, and yield of the potato tubers were studied. Increase in yield with irradiation of seeds was inconclusive. Changes in proximate composition of Russet potatoes grown from tubers irradiated at 1500 rads were found to be insignificant. Varietal differences in solanine content were more pronounced than those due to γ irradiation. In all cases the solanine content in potatoes grown from irradiated seeds was found to be far below the toxic level for human beings. (auth)

35255 USE OF IRRADIATED POLLEN FOR THE LONG-TERM HYBRIDIZATION OF TULIPS. Kudrautsava, V. M. Vestsi Akad. Navuk BSSR. Ser. Biyal. Navuk; No. 2, 64-7(1970). (In Belorussian).

The effects of γ irradiation on the viability of pollen of certain species and varieties of tulips were studied along with the possibility of overcoming non cross breeding by using irradiated pollen for the long term hybridization of tulips. Tulip pollen manifests individual (in relation to varieties) radiosensitivities. For some of the varieties studied, doses of 4000 to 6000 R were lethal. The optimum doses for efficient pollen interbreeding and formation of normal length pollen tubes were 1000 to 2000 R. It was not possible to overcome non cross breeding in the Tulipa using irradiated pollen. In all combinations tested, the control plants as well as the irradiated pollen set seeds. At the same time, the yield of hybrid seeds was not determined by the method of pollination, but rather by the crossing combination. (tr-auth)

35256 IRRADIATION INDUCED PHYSIOLOGICAL AND MORPHOLOGICAL VARIATION IN COLLETOTRICHUM CAPSICI, INCITANT OF ANTHRACNOSE OF CHILLIES. Chatrath, M. S.; Raychaudhuri, S. P.; Gupta, J. P. (Indian Agricultural Research Inst., New Delhi). Mycopathol. Mycol. Appl.; 43: 217-22(1971).

With the aid of radioactive phosphorus and gamma rays, a number of morphological and biochemical mutants of Colletotrichum capsici were induced and these showed a wide range of variability. Biochemical mutants mostly induced by means of ^{32}P irradiation showed deficiency of amino acids or vitamins. Specific deficiency analysis of some of the biochemical mutants revealed requirements for lysine, methionine, glycine or serine, and biotin. These biochemical mutants could not be distinguished from the wild type in morphological characters when grown on complete or otherwise suitable supplemented media. (auth)

35257 REPAIR OF STRAND BREAKS IN CHLORELLA-DNA CAUSED BY GAMMA IRRADIATION. Cabela, E.; Wawra, E.; Altmann, H. (Reaktorzentrum, Seibersdorf, Austria). Biophysik; 7: 200-4(1971). (In German).

DNA repair after γ irradiation was investigated in a stage of synchronous Chlorella cells in which no active DNA synthesis occurs. A modified method of alkaline sucrose gradient centrifugation was used. A complete repair within 30 min after irradiation could be observed up to 100 krad. Repair after 300 and 500 krad with a dose rate of 500,000 rad/hr was very poor. (auth)

35258 EFFECTS OF ULTRA-HIGH-ENERGY RADIATION (600 TO 6000 MeV) ON THE CELL NUCLEUS. Linden, W. (Univ., Hamburg). Strahlenschutz Forsch. Prax.; 9: 114-20 (1969). (In German).

From ninth conference of the Society of German Radiation Medicine; Aachen, Germany (11 Oct 1968). See CONF-681082.

After radiation application to seeds of barley and beans with relativistic protons (600 MeV) and 6,300-MeV Bremsstrahlung, nearly the same qualitative and quantitative effects were observed as those occurring following irradiation with 200 kV x rays or ^{60}Co gamma radiation. As judged by the incidence of aberrant

metaphases and anaphases, the RBE was found to range between 2.4 and 2.5 when comparing relativistic protons with x rays or γ rays. High-energy radiation in comparison with conventional radiation led to significant enhancement of chromosome break recombination; this difference is explained as the effect of localized high-energy densities. Whereas, relativistic protons offer themselves as therapeutic tools because of their favorable depth dose distribution, photon irradiation beyond 100 MeV apparently yields no advantages over ultrahard betatron x rays. (H.B.G.)

Radiation Effects on Microorganisms

Refer also to abstracts 35126, 35159, 35160, 35196, and 35246.

35259 ALTERATIONS IN THE DNA STRUCTURE IN IRRADIATED PHAGES. Hagen, Ulrich (Kernforschungszentrum, Karlsruhe, Ger.). Stud. Biophys.; 15-16: 3-8(1969).

From second international symposium on initial effects of ionizing radiation on a cell; Erevan, USSR (Oct-Nov 1968). See CONF-681087.

When bacteriophages were irradiated in nutrient broth, a single hit inactivation curve was observed. The loss of the plaque forming ability can be due to various radiation effects. Results indicated that about one-third of the inactivated phages are hindered in their ability to inject their genome into the bacterial cell. The molecular alterations in the phage responsible for the loss of plaque forming ability after irradiation in nutrient broth were localized mostly in the DNA molecule whereas the energy absorbed in the protein coat contributed far less to the inactivation. (P.B.M.)

35260 RADIATION INDUCED DAMAGES TO CELLS. Korogodin, V. I.; Korogodina, Yu. V.; Myasnik, M. N.; Sokurova, E. N. (Inst. of Medical Radiology, Obninsk, USSR). Stud. Biophys.; 15-16: 127-44(1969).

From second international symposium on initial effects of ionizing radiation on a cell; Erevan, USSR (Oct-Nov 1968). See CONF-681087.

A summary is given of five main kinds of manifestations of lethal effects of ionizing radiation on cells of Escherichia coli and yeast. Survival curves are also given for the organisms. It was found that the qualitative peculiarities of cell responses to γ radiation damages may be determined mainly by their biological properties, that is, by ploidy, genotype, cell cycle phase, and physiological state. (P.B.M.)

35261 RADIOSENSITIVITY OF VIRUS-SYNTHESIZING FUNCTION OF CELLS IRRADIATED IN VITRO AND IN VIVO. Kamalyan, L. A.; Ter-Pogosyan, R. A. (Ministry of Health Protection, Erevan). Stud. Biophys.; 15-16: 255-62(1969).

From second international symposium on initial effects of ionizing radiation on a cell; Erevan, USSR (Oct-Nov 1968). See CONF-681087.

The effects of x irradiation on the replication of virus in primary tissue culture cells from chick embryos were studied. It was found that the increase in the reproduction of various viruses in the irradiated organism is caused by a disturbance in the antiviral immunity mechanism. (P.B.M.)

35262 ENHANCEMENT OF RADIATION LETHALITY OF BACTERIAL CELLS BY SOME SENSITIZERS: A RADIOCHEMICAL APPROACH. Singh, B. B.; Shenoy, M. A.; Gopal-Ayengar, A. R. (Bhabha Atomic Research Centre, Trombay, India). Stud. Biophys.; 15-16: 263-72(1969).

From second international symposium on initial effects of ionizing radiation on a cell; Erevan, USSR (Oct-Nov 1968). See CONF-681087.

Evidence is presented that radiolytic transients are involved during the process of radiosensitization of Staphlococcus aureus and Escherichia coli by iodoacetic acid, vitamin K, and its degradation products. In order to obtain maximum sensitization, a prolonged treatment of cells with the sensitizer is not necessary. It was noticed that if the sensitizer was removed from the cell suspension following irradiation, the effect was slightly reduced indicating that the sensitizer continued to exert some effect even after irradiation. (P.B.M.)

35263 RELATIONSHIP OF RADIORESISTANCE TO BALANCED GROWTH-RATE IN MICROCOCCUS RADIODURANS. Freedman, M. L.; Bruce, A. K. (State Univ. of New York, Buffalo). Int. J. Radiat. Biol.; 19: 111-21(1971).

The changes in the macromolecular composition of Micrococcus radiodurans with increasing medium-determined growth-rate were similar to such alterations in more radiosensitive bacterial strains. As the growth-rate and quantity of cellular macromolecules increase, the x-radiation sensitivity tended to increase when measured by the D_0 or the LD_{90} exposure. The amounts of endogenous, possibly radioprotective sulphydryls did not account for the increased radiosensitivity. It was found that the assay of cells on minimal agar improved the survival after irradiation. The findings in M. radiodurans suggested that damage to DNA and to the division mechanisms of the cells may account for the heightened radiosensitivity found in condition of rapid growth. (auth) (UK)

35264 POTENTIATION BY HALOGEN COMPOUNDS OF THE LETHAL ACTION OF γ RADIATION ON SPORES OF BACILLUS CEREUS. Gould, G. W. (Unilever Research Lab., Bedford, Eng.). J. Gen. Microbiol.; 64: 289-300(Dec 1970).

Spores of Bacillus cereus were inactivated by γ-radiation more effectively in the presence than in the absence of a variety of halogen compounds. Where homologous series of compounds were used, activity decreased in the order I > Br > Cl and F. Activity did not depend upon affinity of the compounds for thiol groups. Potassium iodate was the most active compound tested. Iodate and iodoacetamide, and to a lesser extent iodide, were most effective at low pH values, but potentiation by 3,5-diiodo-L-tyrosine was hardly affected by pH. Survival curves of spores irradiated in water plus iodoacetamide or iodate were convex, suggesting that potentiation increased with increase in γ-radiation dose. The compounds tested were all more effective potentiators of radiation inactivation of spores in water than in sodium phosphate buffers or in complex media, and potentiation was greater with low than with high spore concentrations. Histidine antagonized the potentiation of radiation inactivation by iodate, iodide and iodoacetamide. Potentiation decreased with decrease in temperature, and was not shown at −15°. The results suggested that potentiation resulted from toxicity to spores of halogen-free radicals, and to a lesser extent free halogen, formed by reaction of the compounds with the radiolytic products formed from water during irradiation. Radiation was at 0.8 Mrad/h and ranged up to 1.25 Mr. (auth) (UK)

35265 INACTIVATION AND DIVISION DELAY OF ESCHERICHIA COLI B/r BY COMBINED TREATMENT WITH UV AND VACUUM. Buecker, H.; Horneck, G.; Wollenhaupt, H. (Univ., Frankfurt am Main). Biophysik; 7: 217-22(1971).

UV-irradiated in vacuum (10^{-6} torr) stationary phase cells of Escherichia coli B/r showed an increased uv-sensitivity regarding the inactivation of colony forming ability. The enhancement factor of the D_{10} values was 12.8, that of the slopes of the survival curves was 6.1. This increased uv sensitivity in vacuum was not caused by selection of uv sensitive mutants by vacuum treatment. Photoenzymatic repair of the lethal uv lesions obtained in vacuum was not detectable, though the photoreactivating enzyme was shown to be intact. In contrast there was no enhanced sensitivity concerning the delay of the first cell division after uv irradiation in vacuum. The division delay was additive regarding the single effects of uv and vacuum. It was assumed that after uv irradiation in vacuum the uv-induced inactivation is caused by still unknown non or less repairable photoproducts and the uv-induced division delay is due to pyrimidine dimers. (auth)

35266 MARKER RESCUE WITH ULTRAVIOLET-INACTIVATED INFLUENZA VIRUS. Sugiura, A.; Ueda, M. (Inst. of Publich Health, Tokyo). J. Virol.; 7: 499-503(Apr 1971).

Influenza A1/CAM virus undergoes abortive growth in FL cells, whereas X-3311, a recombinant virus clone from the cross between CAM and NWS, is capable of complete replication in FL cells and plaque formation on FL monolayers (FL-marker). Clone 1-5C-4 cells are permissive for both viruses. When either clone 1-5C-4 or FL cells, which were mixedly infected with both uv-irradiated X-3311 and active CAM viruses, were plated on FL monolayers, infective centers far exceeding in number those expected from the surviving X-3311 virus were observed, i.e., the FL-marker of the irradiated parent was rescued. The significantly lower radiation sensitivity of FL-marker than that of infectivity indicated that only part of the genome is responsible for the FL-marker. The capability of X-3311 virus to produce NP antigen and its infectivity were lost at the same time when the former was assayed under the condition of low multiplicity of infection. This suggests that only infectious virus is capable of producing NP antigen and that no stepwise inactivation of the viral genome occurs. It is also suggested that any lethal uv damage inflicted upon the viral genome prevents the expression of the portion of the genome coding for NP antigen. (auth)

35267 INACTIVATION OF T ANTIGEN-FORMING CAPACITIES OF SIMIAN VIRUS 40 AND ADENOVIRUS 12 BY ULTRAVIOLET IRRADIATION. Yamamoto, Hiroshi; Shimojo, Hiroto (National Inst. of Health, Tokyo). J. Virol.; 7: 419-25(Apr 1971).

Methods to measure T antigen forming capacities of Simian

XUM

virus 40 (SV40) and Adenovirus 12 (Ad12) were investigated, and a method to measure the capacity in terms of T antigen forming units was employed by the use of cytosine arabinoside. Plaque forming units and T antigen forming units of SV40, SV40 deoxyribonucleic acid, or Ad12 were inactivated by uv irradiation at the same rate, roughly following a single hit curve. T antigen formation by uv-irradiated SV40 and Ad12 was enhanced in cells multiply infected and in cells in a growing state. These observations showed that it was difficult or impossible to estimate the size of the gene for T antigen by uv inactivation. (auth)

35268 GAMMA-RAY INDUCED STRAND BREAKAGE OF BACILLUS SUBTILIS DNA IRRADIATED IN VIVO. Dugle, D. L.; Dugle, J. R. (Atomic Energy of Canada Ltd., Pinawa, Manitoba). Can. J. Microbiol.; 17: 575-83(May 1971). (AECL-3835).

Evidence is presented for the isolation of DNA having a molecular weight of $31 \pm 5 \times 10^8$ from Bacillus subtilis strain 23 Thy^- cells. This accounts for the total DNA content of the genome. Single strand and double strand breaks induced by ^{60}Co γ rays were measured by sucrose density centrifugation. The occurrence of repair of single strand and possibly double strand breaks at 0°C is inferred from survival data and the effects of pre or post-irradiation heating. (auth) (Canada)

35269 MECHANISM OF INACTIVATION OF TRANSFORMING DEOXYRIBONUCLEIC ACID BY X RAYS. Randolph, M. L.; Setlow, Jane K. (Oak Ridge National Lab., Tenn.). J. Bacteriol.; 106: 221-6(Apr 1971).

Transforming DNA from Haemophilus influenzae was exposed to x rays either in phosphate buffer or in 10% yeast extract. Relations between determinations of biological inactivation, DNA uptake by competent H. influenzae, integration of DNA into the competent cell genome, and induced single and double strand breaks indicated that transforming DNA is inactivated by the direct and the indirect effect of x radiation primarily because integration of DNA is prevented as a result of the production of double strand breaks. (auth)

35270 MUTANTS OF STAPHYLOCOCCUS AUREUS WITH INCREASED SENSITIVITY TO ULTRAVIOLET RADIATION. Goering, R. V.; Pattee, P. A. (Iowa State Univ., Ames). J. Bacteriol.; 106: 157-61(Apr 1971).

Nitrosoguanidine (NG) mutagenesis of Staphylococcus aureus resulted in the isolation of 8 mutants exhibiting 3 to 28 times greater sensitivity to uv radiation. These mutants were further characterized by their ability to repair uv-irradiated bacteriophage, to act as recipients in the transduction of antibiotic resistance, and their sensitivity to NG. Based on the available data, 6 of these mutants were reduced in their ability to perform host cell reactivation. It is also believed that one of the remaining 2 mutants may be deficient in postreplication repair. (auth)

35271 PROPERTIES OF F' FACTOR DEOXYRIBONUCLEIC ACID TRANSFERRED FROM ULTRAVIOLET-IRRADIATED DONORS: PHOTOREACTIVATION IN THE RECIPIENT AND THE INFLUENCE OF recA, recB, recC, and uvr GENES. Cole, Ronald S. (Yale Univ., New Haven). J. Bacteriol.; 106: 143-9(Apr 1971).

UV-irradiated Escherichia coli K-12 F lac^+ donors transferred damaged F' factors when mated with female cells. Exposure of the zygotes to white light after mating can cause the photoreactivation of the damaged transferred F' factors. Insofar as the photoreactivation is specific for pyrimidine dimers, these experiments indicated the presence of uv-induced dimers in the transferred F' factor DNA. These damaged F' factors were remarkably stable in recA recipients, having a half-life for susceptibility to photoreactivation of 1.5 to 2 hr. This was judged by the formation of Lac^+ colonies, all of which were male secondary donors. In crosses with wild type and uvrA, recB, or recC mutant recipients, however, the Lac^+ colonies were predominantly recombinants and photoreactivation was not detected. The extent of DNA synthesis resulting from transfer of F' episomers from irradiated donors suggests that a complementary strand is formed on the damaged template. Photoreactivation behavior and sedimentation properties were used to deduce properties of such damaged episomes. It was concluded that the complementary strand is discontinuous directly opposite dimers in the transferred strand. This structure may be an intermediate in the recombinational event sequence in Rec^+ recipients. (auth)

Radiosterilization and Radiopreservation

35272 STUDIES ON THE COMBINED EFFECT OF GAMMA RADIATION AND COOKING ON THE NUTRITIONAL VALUE OF FISH. Kennedy, T. S.; Ley, F. J. (Atomic Energy Research Establishment, Harwell, Eng.). J. Sci. Food Agr.; 22: 146-8 (Mar 1971).

The effect of irradiation (0.6 Mrad), cooking and a combination of both treatments was measured on the protein nutritive value and on the B-complex vitamins, nicotinic acid, riboflavin and thiamine, in cod fish fillets. Microbiological assay methods were used throughout. Protein nutritive value was unaffected by irradiation, whereas cooking caused a 9% loss; this loss was not increased by prior irradiation treatment. Irradiation did not affect nicotinic acid and a 4% loss caused by cooking was again not increased by a combination of treatments. Riboflavin was reduced 6% by radiation, 9% by cooking, and 16% after both treatments, while for thiamine the losses were 47% by radiation, 10% by cooking and 54% combined treatment. It was concluded that irradiation followed by cooking produced a total loss which was the sum of the losses produced by each treatment. The importance of loss of nutrients in fish due to radiation processing is discussed. (auth) (UK)

35273 PRESERVATION OF FRUITS BY RADIOPASTEURIZATION. Wilska, J. (Technical Univ., Lodz, Poland). Przem. Spozyw.; 23: No. 2, 48-51(1969). (In Polish).

The principal problems in fruit radiopasteurization are discussed. The choice of radiation source and dose and the influence of some parameters such as fruit maturity, temperature of irradiation, storage and nutritive value of the irradiated fruits were considered. The influence of irradiation on the principal components of fruits and on the wholesomeness of the irradiated food is described. (NSA of Poland)

35274 IRRADIATION OF CALIFORNIA FRUITS AND VEGETABLES. Maxie, E. C.; Sommer, N. F.; Mitchell, F. G. (Univ. of California, Davis). Calif. Agr.; 24: No. 12, 14-15(Dec 1970).

In 1954, research was started on the effects of ionizing radiation on fresh fruits and vegetables. A summary of 15-yr of work is given along with the commercial potential for irradiation of some major California commodities. Gamma rays from a ^{60}Co source were used, but the results would be comparable with other types of radiation. Only one California commodity, strawberries, showed promise for commercial application of radiation and even with this crop its use would depend on major changes in marketing conditions. (P.B.M.)

METALS, CERAMICS, AND OTHER MATERIALS

Metals and Alloys

Refer also to abstract 34826.

Corrosion and Erosion

Refer also to abstracts 35546, 37028, and 37038.

35275 (ANL–7777) LITHIUM/CHALCOGEN SECONDARY CELLS FOR COMPONENTS IN ELECTRIC VEHICULAR PROPULSION GENERATING SYSTEMS. Interim Technical Summary Report No. 3, May 23–November 22, 1970. Cairns, E. J.; Gay, E. C.; Kyle, M. L.; Tevebaugh, A. D.; Trevorrow, L. E.; Walsh, W. J.; Webster, D. S. (Argonne National Lab., Ill.). Mar 1971. Contract W-31-109-eng-38. 62p. Dep. NTIS.

Activities in a program to develop the technology for construction and testing of 50-kW lithium/chalcogen secondary batteries for the propulsion of electrically driven military vehicles are summarized. The immediate goals are the testing of single lithium/chalcogen cells followed by the testing of small (near 1 kW) batteries. Twenty-eight cells were tested during this reporting period. Tests of selenium-thallium and sulfur-thallium mixtures showed promise of achieving the required short-time peak power density of 1 to 3 W/cm^2 and showed no indications of cathode-material transport to the anode. A procedure has been developed for fabrication of 7.5-cm diameter paste electrolytes by the molten salt infiltration of disks pressed from pure powdered lithium aluminate. The important property of disks made by this procedure is the low permeability to helium, less than 0.04 ml (STP) min^{-1} cm^{-2} atm^{-1} for 0.25-cm thickness. A number of disks of this type were fabricated for use in cell tests to determine whether the selenium transport rate was less than for previously tested pastes. Chromium, aluminum, and beryllium were the most corrosion-resistant materials tested in the Li–Se alloys at 375°C in 600-hour tests. (auth)

35276 (GEAP–13539-16) SODIUM TECHNOLOGY DEVELOPMENT PROGRAM: MASS TRANSFER INVESTIGATIONS IN LIQUID METAL SYSTEMS. Quarterly Progress Report No. 16, December 1970–February 1971. (General Electric Co., Sunnyvale, Calif. Breeder Reactor Development Operation). Mar 1971. Contract AT(04-3)-189. 43p. Dep. NTIS.

In the current phase of the program, the number of materials studied has been extended to include cladding candidates for oxide fuel (Types-304, -316, and -347 stainless steels and Incoloy 800). The temperature range of testing has been increased to 1300°F, and temperature profiles, loop geometry, and sodium purity controls have been established to better represent environments of large fast reactors. Oxygen concentration has been maintained less than 5 ppM, well within recommended prototypic values. Increasing emphasis has been placed on improving sodium impurity monitoring and control. In-line devices are used to obtain rapid and, where possible, continuous indications of impurity changes. These include chromatography for cover gas, replaceable flow-through sodium samplers, electrochemical cells for oxygen activity, diffusion cells for hydrogen concentration in sodium and on-line distillation. Two cold traps for control of sodium purity in test loops have been modified with electromagnetic stirring devices to increase cleanup rate. Automatic controls have been added on all operating loops for continuous and unattended operation with an accuracy of ±2°F. (auth)

35277 (NP–18833) OXIDATION KINETICS OF PURE OR ALLOYED ZIRCONIUM WITH OXYGEN OR WATER VAPOR. Leclercq, Michel (Lyon Univ. (France). Faculte des Sciences). 1969. 177p. (In French). Dep. NTIS (U. S. Sales Only).

Thesis.

The various isothermal oxidation stages of very pure Zr were studied in the temperature range 600 to 800°C under oxygen pressures of 6, 10, and 16 torr for limited reaction times (320 mn). The observation of the oxide layer growth and thickness as a function of time by metallographic microscopy and of the oxygen penetration depth by microhardness measurements were made under the same conditions. The Zr–water vapor, Zircaloy-2–O_2 and Zircaloy-2–water vapor couples were studied. A theoretical model taking the competitive processes of oxygen diffusion into account was established and compared to metallographic and microgravimetric results. Oxygen diffusion coefficients in zirconia and zirconium were measured with this model and by microhardness measurements. The oxidation process was investigated under thermodynamically reversible conditions. The metal was subjected to gas pressures lower than 10^{-6} torr. The flash heating method of the filament was used. The pressure variations near the metallic filament, rapidly heated by Joule effects to a high temperature, are plotted. The desorption spectrum of the previously sorbed gases supplies information on the thermodynamic conditions and the gas adsorption processes at the metallic surface. (France)

35278 (UARAEE–72) EFFECT OF HEAT-TREATMENT AND COLD WORK ON THE OXIDATION OF Zr–1 PERCENT Nb ALLOY IN AIR AND PRESSURIZED STEAM AT 450–650°C. El-Shanshoury, I. A.; Rudenko, V. A.; El-Dahshan, M. E. (Atomic Energy Establishment, Cairo (Egypt). Dept. of Metallurgy). 1969. 46p. Dep. NTIS (U. S. Sales Only).

The effect of various treatments ($\alpha + \beta$ and β annealing and cold rolling) on the corrosion behavior of zirconium–1% Nb alloy was studied in air and pressurized steam at 450 to 650°C. Cold rolled alloy was found to show the best corrosion resistance in air and pressurized steam. Annealing of the alloy at 900°C (β–phase) resulted in higher weight gains during corrosion tests than annealing in $\alpha + \beta$ phase. The initial stages of the corrosion process in air and steam follow the parabolic rate law. The activation energies were calculated to be 38.5 and 25.3 kcal/mole for air and steam respectively. The activation energy of the process was independent of the treatment. The only variable is the constant of the Arrhenius equation. Differences in oxidation rates were attributed to the differences in the structure of the alloy due to treatment. (auth)

35279 ANALYSIS OF FREQUENCY AND AMPLITUDE EFFECTS ON CORROSION FATIGUE CRACK PROPAGATION IN Ti–8Al–1Mo–1V. Meyn, D. A. (Naval Research Lab., Washington, D. C.). Met. Trans.; 2: 853-65(Mar 1971).

Crack growth rates were measured in Ti-8Al-1Mo-1V, which exemplifies titanium alloys susceptible to transgranular stress-corrosion cracking (SCC). A wide stress intensity amplitude (ΔK) range, with R = 0, was employed at ½ to 30 cps in H_2O, 3½% NaCl solution, and methanol; at 10 to 30 cps in air; and at 20 to 30 cps in vacuum, the reference environment. Crack growth was augmented by two kinds of environmental effects. The first, Type A corrosion fatigue (cyclic SCC), was effective at low frequencies in the liquid environments when $K_{max} \geq K_{Iscc}$, intensified with increasing amplitude, but diminished with increasing frequency. In addition to fatigue striations, cleavage on a plane 15° from $(0001)_\alpha$ was observed. The second kind, Type B corrosion fatigue, was effective at low amplitudes and in all the environments, diminished at higher amplitudes, was unaffected by changes in cyclic frequency, and was not related to the SCC susceptibility of the alloy. Striated cleavage facets on $(0001)_\alpha$ and on a plane 15° from $(0001)_\alpha$ occurred at low amplitudes, while ordinary ductile striations occurred at higher amplitudes. Fatigue in vacuum did not produce fractographic fatigue striations. (auth)

35280 MICROGRAVIMETRICS OF THE OXIDATION OF POLYCRYSTALLINE NIOBIUM SAMPLES UNDER THE CONDITIONS IN WHICH THIN FILMS ARE FORMED. Dalibard, Gerard; Mollimard, Daniel; Bardolle, Jean (Univ., Orleans, France). Compt. Rend., Ser. C; 272: No. 12, 1119-22(22 Mar 1971). (In French).

A device for measuring the oxidation of polycrystalline niobium samples by microgravimetry under the conditions in which thin films are formed was constructed. The reaction temperatures lie between 300 and 500°C and the pressures between 5.10^{-3} and 225 torr. The kinetic laws were determined: at a 75 torr pressure and between 300 and 500°C, the first step is linear with an activation energy of 5.7 kcal. $mole^{-1}$; the second one is logarithmic (activation energy of 8 kcal. $mole^{-1}$). The effect of pressure was established. A mechanism was proposed in order to explain these results. (auth) (France)

35281 CORROSION INDUCED BY LIQUID SODIUM. Furukawa, Kazuo; Nihei, Isao (Japan Atomic Energy Research Inst., Tokai). Boshoku Gijutsu; 18: 503-11(Dec 1969). (In Japanese).

Studies on liquid sodium-induced corrosion of stainless steel, especially 18–8 stainless steel are reported. The corrosion induced by liquid metal can be divided into two phenomena. One is the phenomenon that the constituent elements of solid materials dissolve into liquid metals and therefore, corrosion progresses. The other is the phenomenon that a part of solid metal breaks away as oxides, carbides, hydrides, etc., reacting with the impurities in liquid metal such as oxygen, carbon, and hydrogen and induces corrosion. In sodium–cooled fast breeders, the problems that exist in connection with the corrosion induced by liquid sodium are the mass transfer phenomenon induced by temperature difference in fuel cladding tubes and structural materials and the

XUM

chemically-induced mass transfer phenomenon in a sodium-heated steam generator. Recent experimental studies on these problems in Japan and foreign countries are reviewed. (Japan)

35282 OXIDATION KINETICS OF NIOBIUM–TITANIUM ALLOYS. Perrin, Christian; Bardolle, Jean; Mollimard, Daniel (Univ., Orleans, France. CNRS, Orleans-la-Source, France). Compt. Rend., Ser. C; 272: 929-32(8 Mar 1971). (In French).

The oxidation of an alloy containing 20.15 per cent Ti at an oxygen pressure of 100 torr in the temperature range 600 to 1300°C was studied. The reaction kinetics were parabolic up to 800°C. At higher temperatures, a linear law was found. The oxide $Nb_2O_5TiO_2$ which is formed at all temperatures, was analyzed. The appearance of the oxide layer and the metal after oxidation were investigated by micrography. (auth) (France)

35283 HYDROGEN ABSORPTION BY ZIRCONIUM ALLOY. Nagai, Nobuyuki (Kobe Steel, Ltd., Japan). Boshoku Gijutsu; 18: 496-502(Dec 1969). (In Japanese).

Some problems are summarized concerning hydrogen absorption by zirconium alloys, e.g., hydrogen absorption which appears in fuel cladding and pressure tubes and on the problem of hydrogen absorption induced by corrosion. (TSS) (Japan)

35284 INFLUENCE OF ELECTROLYTES AND PRE-TREATMENTS ON THE INITIAL GROWTH OF ANODIC OXIDE FILMS ON Ti, Ta, AND Zr. Baba, Nobuyoshi; Fujiwara, Katsutoshi; Tajima, Sakae (Tokyo Metropolitan Univ.). Denki Kagaku; 39: 42-7(Jan 1971). (In Japanese).

Anodic behavior of Ti, Ta, and Zr in aqueous or nonaqueous electrolytes was investigated under galvanostatic anodizing conditions using the voltage-time (V–T) transient techniques. The V–T curves obtained were classified into five types: straight line, increasing slope, decreasing slope, break-down, and periodically vibrating. In aqueous solutions V–T curves of all five types were observed, whereas in nonaqueous solutions Type 4 was predominant. In the case of Ti, Type 2 was often observed, indicating that the resistivity of the oxide film being formed was increasing. Since the calculated values of $M/nF\rho$ for Ti, Ta, Zr, and Al were 5 to 6×10^{-3} and since the initial slopes of the V–T curves for these metals were not greatly different, the resistivity of the oxide films was not greatly different from one another. The effect of pre-treatment on the initial slope of the V–T curves for Ti was attributed to the presence of the mechanically deformed surface layer (so called the Beilby layer). It was also found that the variation of the initial slope of the V–T curves for these metals was partly due to the variation of the surface roughness factor, which determined the true current density at the film growing area. (auth) (Japan)

35285 PERSPECTIVES ON CORROSION OF MATERIALS. THE 1970 EDWARD DeMILLE CAMPBELL MEMORIAL LECTURE. Fontana, Mars G. (Ohio State Univ., Columbus). Corrosion; 27: No. 4, 129-45(Apr 1971).

Perspectives on corrosion are presented that look back ten years or so and into the seventies. General ignorance by many engineering disciplines and others and resultant costly failures are emphasized. The scope of the corrosion problem is described. Discussed are forms of corrosion and methods for combating; secondary reactions; effects of materials structure; advances in techniques for measuring corrosion; important developments; and needs for the 1970's. Need for involvement by metallurgists is emphasized. (auth)

35286 GRAIN BOUNDARY GROOVING OF TYPE 304 STAINLESS STEEL AND ARMCO IRON DUE TO LIQUID SODIUM CORROSION. Borgstedt, Hans U. (Nuclear Research Center, Karlsruhe, Ger.). Corrosion; 27: 113-14(Mar 1971).

Liquid sodium was flowed past surfaces of Type 304 stainless steel and Armco iron at 500 to 600°C. It was found that the corrosion rates of the two materials were approximately the same but the width of grain boundary grooves on Armco iron was greater than on stainless steel. It appears that the corrosion rates of these materials do not depend simply on a single component element, for example iron, in the corrosion action. (J.R.D.)

35287 CORROSION OF TITANIUM–6Al–4V IN HCl–METHANOL. Takimoto, H. H.; Denault, G. C.; Marsh, P. A. SAMPE J.; 6: No. 3, 65-8(Apr-May 1970).

The dissolution of Ti–6Al–4V in HCl–methanol was investigated. Under the conditions studied, the corrosion rate increased with a higher concentration of HCl, whereas water inhibited the corrosion. The presence of cold-worked edges in the test specimen also enhanced the rate. Replacement of HCl with NaCl as a catalyst and changing the solvent from methanol to isopropyl alcohol greatly decreased the rate of dissolution of the metal. (Metals Abstr.)

35288 OXIDATION PROTECTION OF A CHROMIUM ALLOY BY NICKEL-ALLOY CLADDINGS. Williams, D. N.; Ernst, R. H.; English, J. J.; Bartlett, E. S. (Battelle Memorial Inst., Columbus, Ohio). J. Less-Common Metals; 24: 41-54(May 1971).

The utility of nickel-alloy claddings to protect a chromium alloy from oxidation and nitrogen absorption during cyclic exposure in air at 2100 and 2300°F was examined. Several cladding systems were evaluated, all of which were applied to the chromium-alloy substrate by gas pressure bonding. The best system of those studied consisted of a 5 mil thick Ni–20Cr–20W–5Al cladding alloy separated from the chromium alloy by a 1.5 mil thick tungsten barrier layer. Although none of the systems was completely satisfactory, several of the cladding systems provided good oxidation protection at 2100°F for 600 hr and at 2300°F for at least 300 to 400 hr, and prevented nitrogen contamination at 2100°F. However, bend ductility was reduced during cyclic exposure as a result of interdiffusion of metallic elements through the barrier layer. The successful development of this type of protection system for chromium alloys will be dependent upon improving the effectiveness of the barrier layer. Methods for improving this layer are suggested. (auth)

35289 OXIDATION OF Ni–V ALLOYS IN AIR. Kramer, K. H.; Borgstedt, H. U. (Kernforschungszentrum, Karlsruhe, Ger.). Werkst. Korros.; 21: 804-9(Oct 1970). (In German).

The stability of Ni–V alloys with 2 to 16 wt % V was investigated at high temperatures in air. The composition of the oxides in the oxide layer, the effect of the V content on the oxidation kinetics, and the analogies to the behavior of Ni–Cr alloys were determined. Ni–V alloys form a typical multilayer oxidation zone, whose individual layers are clearly different in composition. The formation of the oxidation zone is analogous to that of Ni–Cr alloys. A parabolic law was determined for the air oxidation. The vanadium content affects the size of the scaling constant and can be explained by the reduction of defect electron concentrations and the increase in the number of Ni ion vacancies. (J.S.R.)

35290 BIBLIOGRAPHIC SURVEY OF CORROSION, 1960. A Compilation of Corrosion Abstracts. Hunt, W. T. Houston, Tex.; National Association of Corrosion Engineers (1971). 522p. $35.00.

The survey consists of about 3400 abstracts plus alphabetical subject and author indexes. (J.R.D.)

35291 SECONDARY OXIDATION OF METALS AFTER HYDROGEN ANNEALING. Karakozov, E. S.; Shabalin, I. N.; Shmykov, A. A. Fiz. Khim. Obrab. Mater.; No. 4, 151-5(Jul-Aug 1970). (In Russian).

Thermodynamic calculations showed that oxidation of Fe, Mo, Ni, and W in atmospheres of H_2 plus O_2 is possible. Thermogravimetric analyses showed that the secondary oxidation of Fe formed maximum thickness layers when the O content was less than 0.01%. Superfine films were formed on Ni at O contents of more than 0.1%. (R.V.J.)

35292 EFFECT OF NITROGEN ON THE LINEAR OXIDATION OF NIOBIUM. Catella, C.; Streiff, R. (CNRS, Nancy). J. Electrochem. Soc.; 118: No. 6, 1006-9(Jun 1971).

The oxidation of niobium at a constant oxygen partial pressure both with and without nitrogen was investigated. The effects of 10 to 90% nitrogen on the niobium oxidation behavior in 0.1 to 1 atm oxygen and at 450 to 1000°C are illustrated. Nitrogen caused a reduction in the linear oxidation rate at all temperatures. The retardation was not strongly influenced by the percentage of nitrogen. Likewise, the reduction in the rate was not dependent on temperature ranges on both sides of the minimum rate where a stronger effect was observed. (G.M.C.)

35293 ^{18}O STUDY OF THE SOURCE OF OXYGEN IN THE ANODIC OXIDATION OF SILICON AND TANTALUM IN SOME ORGANIC SOLVENTS. Croset, M. (CNRS, Orsay, France); Petreanu, E.; Samuel, D.; Amsel, G.; Nadai, J. P. J. Electrochem. Soc.; 118: 717-27(May 1971).

The anodic oxidation of silicon and tantalum in organic solvents containing small quantities of dissolved salts (KNO_2 and KNO_3) and water has been studied. The source of oxygen in the oxide layer has been determined using ^{18}O-labeled materials. The isotopic exchange of oxygen between the various components of the electrolyte under thermal and electrolytically induced conditions was measured using mass spectrometric analysis and found to be extremely slow. Nuclear methods of analysis of isotopic oxygen were used to determine the source of oxygen in the oxide layer on both metals. It was found that over 80% of the oxygen of the oxide comes from water, the rest from the salt. The small extent of incorporation of nitrogen-containing anions in the oxide layers was also measured by a nuclear method. (auth)

35294 STUDY OF THE OXYGEN GROWTH LAWS OF ANODIC OXIDE FILMS OF ALUMINUM AND TANTALUM USING NUCLEAR MICROANALYSIS OF ^{16}O AND ^{18}O. Seijka, J.; Nadai, J. P.; Amsel, G. (Ecole Normale Superieure, Paris). J. Electrochem. Soc.; 118: 727-37(May 1971).

The oxygen growth laws of anodic oxide films on aluminum and tantalum were studied using the nuclear microanalysis of the ^{16}O and ^{18}O isotopes. The influence of current density and surface preparation on the growth laws has been demonstrated. The correlation of the results of nuclear microanalysis of ^{16}O and of coulometric measurements allowed the determination of the dissolution current density during anodic oxidation of aluminum. This dissolution current was shown to be purely electrochemical. The values of the intercepts with the potential axis of the linear growth laws show that the overpotentials at the interfaces are smaller than 0.1V for current densities from some $\mu A/cm^2$ to 10 mA/cm^2. Measurements of isotopic exchange of oxygen using ^{18}O as a tracer allowed direct estimation of the oxygen exchange current without applied field. The results show that oxygen transfer at the oxide-solution interface, enhanced by field-induced oxygen vacancies, is responsible for the growth of the anodic film. (auth)

35295 ANODIZATION OF VANADIUM. Keil, R. G.; Ludwig, K. (Univ. of Dayton, Ohio). J. Electrochem. Soc.; 118: No. 6, 864-6(Jun 1971).

A study was made of the relationship between ion current migrating through anodic oxide films on vanadium and the electrostatic field across the dielectric over a potential range of some 100V utilizing the open-circuit transient method. The results show that the relationship between the formation current density, i, and the formation potential, V, is of the form $i = i_0 \exp(V/V_0)$, where i_0 and V_0 are parameters resulting from analysis. V_0 was found to be a linear function of the formation voltage. The quantity, θ, was found to be essentially equal to zero, a result which departs from results previously reported for other metals, for example tantalum, iron, and bismuth. (auth)

35296 STUDY OF THE ANODIC OXIDATION OF VANADIUM. Ellis, B. H.; Hopper, M. A.; De Smet, D. J. (Univ. of Alabama, University). J. Electrochem. Soc.; 118: No. 6, 860-4(Jun 1971).

The anodic oxidation of vanadium in acetic acid-sodium tetraborate solutions containing small amounts of water was studied over a potential range of 100V using the open-circuit transient analysis technique. An anodic layer which showed bright uniform interference colors was found to grow on the metal surface. Results of these experiments indicate that the dependence of the oxidation current density, i, on the formation potential, V, is expressible in the form $i = i_0 \exp(V/V_0)$, where i_0 and V_0 are parameters determined from the data analysis. The parameter i_0 is found to depend on the applied current density, while the parameter V_0 varies directly with the formation potential during galvanostatic oxidation. A result in this form implies that the electric field in the oxide is a function of the applied current density. These results show similarities to results previously obtained by others for the anodic oxidation of bismuth, tantalum, and iron. (auth)

Preparation and Fabrication

Refer also to abstracts 34787, 34819, 34820, 36316, and 36336.

35297 PROPERTIES, PREPARATION, AND HANDLING OF PURE RARE EARTH METALS. Spedding, F. H.; Beaudry, B. J.; Croat, J. J.; Palmer, Paul E. (Ames Lab, Iowa). pp 151-80 of Materials Technology: An Interamerican Approach. New York; American Society of Mechanical Engineers (1968).

From Inter-American Conference on Materials Technology, San Antonio, Tex. See CONF-680513.

The results of studies over the past 20 years on the preparation and properties of the individual rare earth metals and their alloys are reviewed. Some of the techniques needed in order to produce very pure rare earth metals and to keep them pure after they have been produced are pointed out. (auth)

35298 EXPLOSIVE CLADDING AND WELDING FOR LOW CAPITAL INVESTMENT FABRICATION. Wittman, R. H. (Battelle Memorial Inst., Columbus, Ohio). pp 326-33 of Materials Technology: An Interamerican Approach. New York; American Society of Mechanical Engineers (1968).

From Inter-American Conference on Materials Technology, San Antonio, Tex. See CONF-680513.

Explosive bonding is a metallurgical joining technique. The mechanism of bonding and methods of application are such that several process advantages combine to result in a unique and versatile metals joining technique. There are several generally recognized advantages of explosive bonding. A high-strength metallurgical bond can be formed not only between similar metals but also between those dissimilar metals classified as incompatible when fusion or diffusion joining methods are used. Bonding can be achieved between alloys without significantly disturbing the effects of cold work, dispersions, or precipitates that are necessary to strengthen various alloys. The explosive energy is self-contained, cheap, safe to handle, and for many special applications can be portable. Bonding can be achieved quickly in applications involving bond areas from less than 1 $in.^2$ to over 100 ft^2. Only a simple, inexpensive capital facility is required. One important reason that explosive-bonding applications have been limited thus far in the United States is because large sums of money are invested in other processes and equipment, and there is a natural reluctance to abandon existing techniques if the cost or technical advantages of a new process are only marginal. The result is that new applications of explosive bonding in the United States generally involve situations in which explosive bonding can give a great technical advantage in high performance, high cost systems such as found in the aerospace or nuclear industries. However, in nations with expanding industrial economies, the explosive-bonding process might find widespread acceptance as a fabrication technique for low and medium cost assembly if other cladding or bonding processes are not firmly entrenched particularly because of the low capital investment required to build an explosive cladding facility. (auth)

35299 PREPARATION AND PULVERIZATION OF HYDROGENATED NIOBIUM. Sasaki, Yasuo; Amano, Muneyuki (National Research Inst. for Metals, Tokyo). J. Jap. Inst. Metals; 35: 77-81(Jan 1971). (In Japanese).

Alloys containing 3.8 at.%, 7.2 at.% and 14.5 at.% hydrogen were prepared and were pulverized with a ball mill. The particle size distribution of the powders was measured by screen analyses, and microscopic observation of the particle shape was carried out. The main results obtained were: the alloys were brittle enough to be pulverized readily; cracking and fragmentation of the alloys were enhanced by thermal cycling in the hydrogenation process; with increasing hydrogen content in the alloys, a higher percentage of fine particles was obtained; and particle shape varies with the hydrogen content of the alloys. Rounded or irregular particles are obtained from the lower concentration alloys and acicular or angular particles from the higher concentration alloy. (auth) (Japan)

35300 THERMOMECHANICALLY-PRODUCED CARBIDE DISPERSION-STRENGTHENED AUSTENITIC STAINLESS STEEL WITH IMPROVED HIGH-TEMPERATURE TENSILE AND CREEP-RUPTURE PROPERTIES. Levy, I. S. (Battelle-Northwest, Richland, Wash.). Contract AT(45-1)-1830. pp 943-6 of Second International Conference on the Strength of Metals and Alloys, Pacific Grove, California, 30 August-4 September 1970. Vol. III. Metals Park, Ohio; American Society for Metals (1970).

From second international conference on the strength of metals and alloys; Pacific Grove, Calif. (Aug-Sep 1970). See CONF-700819-(Vol.3).

Preparation of improved Type 348 stainless steel by addition of Nb, C, and Mo is described. These additions were accompanied by full deformation which produced increased yield strengths with no reduction in ductility. The improved strength with good ductility leads to superior creep-rupture properties. (J.R.D.)

35301 BASIC PROBLEMS UNDERLYING HIGH-TEMPERATURE MATERIALS DEVELOPMENT. VerSnyder, F. L. (Pratt and Whitney Aircraft, Middletown, Conn.). pp 1013-27 of Second International Conference on the Strength of Metals and Alloys, Pacific Grove, California, 30 August-4 September 1970. Vol. III. Metals Park, Ohio; American Society for Metals (1970).

From second international conference on the strength of metals and alloys; Pacific Grove, Calif. (Aug-Sep 1970). See CONF-700819-(Vol.3).

Development of columnar grain and single crystal high-temperature gas turbine elements through directional solidification is described. Discussions are included on various aspects of directional solidification. It is concluded that this process as practiced in precision investment casting is a method of obtaining desired structure and properties in intricate shapes. (J.R.D.)

35302 STRENGTHENING OF NICKEL-BASE SUPERALLOYS BY PRECIPITATION OF A BODY-CENTERED TETRAGONAL γ' PHASE. Kotval, P. S. (Cabot Corp., Kokomo, Ind.). pp 1042-6 of Second International Conference on the Strength of Metals and Alloys, Pacific Grove, California, 30 August-4 September 1970. Vol. III. Metals Park, Ohio; American Society for Metals (1970).

From second international conference on the strength of metals and alloys; Pacific Grove, Calif. (Aug-Sep 1970). See CONF-700819-(Vol. 3).

XUM

The precipitation strengthening of body-centered-tetragonal γ'' phase in Ni-base alloys was investigated. Precipitation of γ'' phase Ni_3Nb was shown to have a useful strengthening effect in Ni-base superalloys without the presence of γ' $Ni_3(Al + Ti)$ phase. Another similar phase, Ni_3Ta, was also found useful in precipitation strengthening of Ni-base superalloys. (J.R.D.)

35303 SPECTROPHOTOMETRIC COMPOSITIONAL ANALYSIS OF TANTALUM–ALUMINUM ALLOY FILMS. Huber, F.; Jaffe, D. (Bell Telephone Labs., Inc., Allentown, Pa.). J. Vac. Sci. Technol.; 8: No. 3, 480-7(May-Jun 1971).

A comparative technique suitable for the rapid and reliable compositional analysis of sputtered tantalum–aluminum alloy films in the range of 0 to 68 at. % Al is described. The technique is based on spectrophotometric reflection measurements of anodically formed oxides of the alloys. Oxides formed at a given anodization voltage on different alloys exhibit different reflection spectra due to the compositional dependence of their refractive indexes and thicknesses. Empirical calibration curves were established between Al content (as determined independently by electron microprobe analysis) and minima of the reflection spectra. The calibration curves were linear in the range of approximately 0 to 55 at. % Al with regression limits (95% confidence level) of $\leq \pm 0.82$ at. % Al in the range of 20 to 55 at. % Al. (auth)

35304 REFABRICATION OF NUCLEAR FUEL ELEMENTS: FUNDAMENTALS, PLANTS, TECHNOLOGY. Steinkopff, H., Schumann, Z.; Krompass, R. (Zentralinstitut fuer Kernforschung, Rossendorf, Ger.). Kernenergie; 14: No. 1, 6-15(Jan 1971). (In German).

Refabrication fundamentals and the place of the refabrication process in the nuclear fuel cycle are discussed. The consequences of nuclear physics fundamentals in the fuel cycle and the structure of a type of fuel element selected as an example on the layout of refabrication processes and plants described. Finally, a description of refabrication plants and of the principal technological refabrication processes known so far are given. (auth)

35305 PRODUCTION OF TYPE 316 STAINLESS STEEL CLADDING TUBES FOR FAST BREEDER REACTOR. Nakamura, Hisashi; Matsuura, Nobuo; Yui, Shinroku; Ota, Kunio (Sumitomo Metal Industries, Ltd., Amagasaki, Japan). Sumitomo Kinzoku; 22: No. 4, 509-15(Oct 1970). (In Japanese).

The Power Reactor and Nuclear Fuel Development Corporation has been developing a fast breeder reactor as a national project in Japan. A Fast Breeder Reactor requires various kinds of more severely specified steel tubes and pipe than a light-water reactor. Fuel cladding tubes are one of the most important materials requiring high-quality tubing. The production method and quality control for fuel cladding tubes were established. The production method, quality control or test results on the products are described. (auth) (Japan)

35306 NEW RETENTIVE ALLOYS OF COBALT AND RARE EARTH METALS. Schuchert, H. (Fried Krupp GmbH, Essen). Tech. Mitt. Krupp, Forschungsber.; 28: 121-6(Dec 1970). (In German).

Development of a group of rare earth metal–cobalt intermetallic magnetic alloys during the past ten years is reviewed. The high anisotropic field strength resulting from crystal anisotropy is the main cause of the excellent permanent magnet properties. Successful application of the melting and powder metallurgical processes is essential. The powder metallurgical process is preferable if optimum magnet values are to be attained. With pure RCo_5 compounds (R = rare earth metal), particularly with $SmCo_5$, the theoretically attainable values are almost reached. Developments in the area of misch metal compounds are only in the initial phase. (auth)

35307 MACHINING METHODS OF DEPLETED ALLOYED OR WEAKLY ALLOYED URANIUM. Mach. Outil Fr.; 36: 169-75 (Mar 1971). (In French).

The characteristics of depleted U were improved by alloying the uranium. Its origin and machining were studied e.g., turning, lathe-cutting, drilling, cylinder boring, tapping, milling, and electro-erosion. Machining according to these methods allowed pieces of quality 7 with a 0.8 μ surface to be made. The manufacturing of depleted U necessitates safety precautions. (France)

35308 WELDING FERROUS MATERIALS FOR NUCLEAR POWER PIPING. AWS D10.5-59 1959. New York; American Welding Society (1959). 14p. Available from American Welding Society, New York.

The changes that are necessary in welding procedures because of the application to nuclear power service of ferrous materials now used for conventional pressure piping systems in nonradioactive service are indicated. The report represents a compilation and review of many welding procedures and specifications for nuclear and non-nuclear power piping applications. No major changes in many existing welding procedures for materials in high pressure piping are necessary, except for increased cleanliness and crevice elimination. The emphasis should be on conforming to present specifications completely and as intended. In any case, no limitations or additions should be made to existing specifications unless they actually contribute to better service or are improvements that are significant enough to justify any increased cost. In addition, such variations in specifications must be attainable practically. The most obvious differences in service conditions are in increased thermal shock if liquid metal coolants are used, greater corrosion potential for certain aqueous or molten fuel systems, and possible changes in material properties because of radiation effects. In addition, there is a biological hazard from radiation and the effects of particles of radioactive materials, which makes any leakage dangerous and maintenance difficult or even, in some cases, impossible. Because of factors such as these, the highest quality product possible and practical is desired. (auth)

35309 MOLYBDENUM DECARBURIZATION BY ANNEALING AT LOW OXYGEN PRESSURES. Touboul, Jean-Paul; Minel, Lea; Langeron, Jean-Paul (CNRS, Vitry-sur-Seine, France). Compt. Rend., Ser. C; 272: No. 12, 1109-11(22 Mar 1971). (In French).

The carbon content in 1 mm thick molybdenum was reduced less than $0.3 \cdot 10^{-4}$ by annealing for an hour at 1800°C at an oxygen pressure of 2.10^{-5} torr. The decarburization kinetics are dependent on the carbon diffusion through the metal. (auth) (France)

35310 PLUTONIUM. Schumacher, H. (Swiss Federal Inst. for Reactor Research, Wuerenlingen). Neue Tech., B; 12: 129-31(Aug 1970).

The cumulative amount of Pu which will be produced in Swiss power reactors to 1990 is predicted, and programs for the future development of reactors and fuel reprocessing plants for using this Pu are briefly described. (L.C.L.)

35311 WELDING PECULIARITIES IN THE FABRICATION OF FUEL ELEMENTS FOR THE SUPERHEAT REACTOR GROSSWELZHEIM. Zutz, L.; Busch, H. Schweissen Schneiden; 22: 461-4(1970). (In German).

The welding procedures employed for the fabrication of fuel elements for the HDR are described. Most of the welds are mechanized according to the TIG method. The materials to be welded are Inconel 625 and Inconel 625 with chromium-nickel steel corresponding to material Nr. 4981 S. (INIS)

35312 BEHAVIOR OF BORON-ALLOYED SINTERED MOLYBDENUM IN ELECTRON BEAM WELDING. Benesovsky, F.; Koeppe, A. (Univ., Stuttgart). Planseeber. Pulvermet.; 18: 84-90(Jun 1970). (In German).

Electron beam welding tests were carried out on sheets of sintered molybdenum with maximum boron content of 360 ppM. Compared with pure molybdenum, the boron-alloyed material had a finer-grained structure and excellent ductility of the welding seam and transition zone, probably due to the grain refining and desoxidizing effect of the boron. Excessive boron contents cause segregations of borides which has an unfavorable effect on the welding behavior. The structure investigation on the welding seams was carried out by means of a novel texture-revealing color etching method. (auth)

35313 FUEL MANUFACTURING, SWISS ASPECTS. Naegelin, R. (Sulzer Brothers Ltd., Winterthur, Switzerland). Neue Tech., B; 12: 124-6(Aug 1970).

Up to the year 1969 only minor amounts of nuclear fuel for research and experimental reactors were used in Switzerland. The construction of three power reactors of the light-water type caused a rapid increase in the fuel element demand. A quantity of about 40 metric tons per year will be needed in the first half of the coming decade and about 70 tons per year in its second half. Free market conditions for fuel element manufacturers will come up in this second period, when the fuel ordered initially from the reactor designers of the three first power reactors will be used. At present there is no fuel element factory in Switzerland. Although the fuel consumption within the country is still relatively small, it will soon reach the output of one production line. Preconditions for fuel element fabrication in Switzerland seem to be rather favorable. The industry is used to precision manufacturing of expensive components under clean conditions and also the development of tool machines for special purposes. Specific technological knowledge has been acquired in the course of reactor development programs in

XUM

industry and at the Swiss Federal Institute for Reactor Research. Finally, other favorable conditions such as relatively low capital cost and low strike risk may also be mentioned. (auth)

35314 COATING OF NIOBIUM AND NIOBIUM ALLOYS WITH ALUMINUM. PART II. HOT-DIPPED COATINGS. Slama, G.; Vignes, A. (Univ., Nancy). J. Less-Common Metals; 24: 1-21(May 1971).

Coupons of niobium and niobium alloys were hot-dipped in molten aluminum. For niobium, a critical temperature of 1200°C was found. Above this temperature an adherent coating is formed. This coating consists of a thick layer of $NbAl_3$, a thin layer of Nb_2Al and, for prolonged dipping times, a very thin layer of Nb_3Al. Below this temperature, a biphase zone of $NbAl_3$ grains in an aluminum matrix if formed at the niobium surface. For niobium alloys, the critical temperatures vary with the composition of the alloy. As in the case of pack-cementation of niobium and niobium alloys, the mechanical characteristics of the substrate determine the structure of the coating and therefore the critical temperature. The growth kinetics of the coatings were also studied. (auth)

35315 STUDIES OF STAINLESS STEEL CLADDING. Inagaki, Michio (Japan Welding Engineering Society, Tokyo). Koatsuryoku; 8: No. 5, 2102-13(Sep 1970). (In Japanese).

Stainless steel cladding for light-water reactor structures was studied. The base metal for cladding was plates of ASTM A533B steel. The cladding material was Type 309L or 308L; the carbon and ferrite contents were varied systematically. The welding method used was covered arc welding or band electrode automatic welding. The metallurgy of stainless steel cladding related to factors such as the behavior of ferrite and carbide, the transfer of carbon, and the precipitation of sigma-phase was clarified. The band electrode automatic welding presented more stable and uniform cladding than covered arc welding. Postwelding heat treatment over 650°C at 20 hrs adversely influenced the cladding. Five percent ferrite was sufficient to prevent weld cracking in both methods. To inhibit embrittlement after heat treatment, it was found that the Cr content should be less than 21%, thereby preventing the formation of sigma phase. (Japan)

35316 BONDING BERYLLIUM–COPPER ALLOYS WITH HIGH TEMPERATURE THERMOPLASTIC. A REPORT OF A PROGRAM UNDERTAKEN TO MEET THE PROBLEMS CONFRONTING POTENTIAL USERS. Magariello, E.; Hannon, M. (AVCO, Stratford, Conn.). Adhes. Age; 14: No. 3, 24-7(Mar 1971).

A program was conducted to study methods of joining Be–Cu for an assembly that incorporated a thin cover bonded to a frame. The adhesive acts as a sealer in forming a pressure tight component. Useful adhesive values were obtained over a wide temperature range of −65 to 400°F in the bonding of beryllium-copper using a thermoplastic polysulfone resin. This resin exhibited excellent resistance to various chemicals and water at room temperature; however, immersion in boiling water reduced lap shear strength by approximately 50 percent. A linear relationship exists between lap shear strength and temperature over the range of 75 to 500°F. (J.R.D.)

35317 MACHINING ZIRCONIUM. pp 12-13 of Engineering Information and Data. Zirconium and Hafnium. Akron, N. Y.: AMAX Specialty Metals Div. (1971).

It is noted that Zr has a marked tendency to gall and work harden during machining. For these and other reasons, special machining techniques are required in Zr fabrication. A review of methods is presented for turning, drilling, milling, grinding, and sawing Zr. (J.R.D.)

35318 WELDING AND JOINING ZIRCONIUM. pp 14-15 of Engineering Information and Data. Zirconium and Hafnium. Akron, N. Y.: AMAX Specialty Metals Div. (1971).

It is noted that most Zr applications require welding, and since it is a reactive metal, welds must be shielded and active gases cannot be used in joining. Information is included on inert gas welding, equipment for proper fabrication, welding operations, shielding, and inspection. (J.R.D.)

35319 FABRICATING ZIRCONIUM. pp 16-17 of Engineering Information and Data. Zirconium and Hafnium. Akron, N. Y.: AMAX Specialty Metals Div. (1971).

A review of fabrication procedures involving forming, tube bending, deep drawing, punching, annealing casting, powder metallurgy, and electroplating is presented. (J.R.D.)

35320 BORON STAINLESS STEEL FOR JMTR FUEL FOLLOWERS. Watanabe, Ringe (Furukawa Electric Co. Ltd., Tokyo). FAPIG (Tokyo); No. 52, 248-52(Feb 1969). (In Japanese).

The material testing reactor in Oarai Laboratory, JAERI, is a light water-moderated, cooling tank-type reactor with the thermal output of 50 MW, using ETR-type fuel plates. The standard core is composed of 20 to 22 normal fuel elements and 5 to 7 fuel followers. When control rods are withdrawn from the reactor, the fuel followers connected to the control rods take their places. An aluminum part provides the connection of fuel follower and control rod, and may cause the peaking of neutron flux, therefore, highly enriched boron stainless steel plate is used as an absorber at the top end of fuel plate in the fuel follower. Boron stainless steel embrittles when the boron concentration increases; ^{10}B with a large neutron absorption cross section was enriched to more than 90%, and the enriched boron stainless steel was used for the fuel followers of JMTR. Boron stainless steel is produced by melting or powder metallurgical methods. The irradiation specimens manufactured by the powder metallurgical method was highly enriched boron stainless steel equivalent to SUS 27 containing 1% of 90% enriched boron. The mechanical properties and the radiation damage of this material are discussed. (Japan)

35321 WELDING OF VARIOUS SOLID STATE METALS. Suganeev, Yu. S.; Shorshorov, M. Kh.; Yakutovich, M. V. Fiz. Khim. Obrab. Mater.; No. 4, 99-106(Jul-Aug 1970). (In Russian).

Experimental studies were made of the process of welding solid-state Mo with Y considering the absolute rate of the reaction process. The results of creep and deformation measurements and of electronographic and x-ray structure analyses made during the formation of the alloys are presented. (R.V.J.)

35322 WELDING PROBLEMS CONNECTED WITH THE FABRICATION OF THE MODERATOR TANK FOR THE NIEDERAICHBACH NUCLEAR POWER PLANT. May, R. Schweissen Schneiden; 22: 467-70(1970). (In German).

A description is given of the welding procedures applied to the stiffening and bearing rings and to the connection between shield sleeves and sealing membrane. This welding is a part of the fabrication process for a reactor under construction. (INIS)

35323 STAINLESS STEEL. (to Japan Atomic Energy Research Inst.). British Patent 1,224,114. 3 Mar 1971. Priority date 19 Mar 1968, Japan.

Thermomechanical treatments for austenitic stainless steel are described for preparation of radiation- and temperature-resistant materials. Stainless steel, prepared by methods described, is especially suitable for use in fast neutron breeder reactors. The steels improved by the thermomechanical treatments include AISI numbers 301 to 317. (J.R.D.)

35324 PECULIARITIES OF FORMATION OF INTERMETALLICS IN EXPLOSION-PRODUCED COPPER–TITANIUM COMPOUNDS. Grabin, V. F.; Gurevich, S. M.; Dzykovich, I. Ya.; Zamkov, V. N.; Sabokar, V. K. Fiz. Khim. Obrab. Mater.; No. 6, 65-9(Nov-Dec 1970). (In Russian).

Microscopic analysis was used for studying the appearance of intermetallics in the contact zone of Cu with Ti during blast fusion. The effect of Nb on the formation of the intermetallics during the β welding of Ti with Cu is discussed. (R.V.J.)

35325 EFFECTS OF DIFFUSION INTERACTION COMPONENTS ON NIOBIUM–TITANIUM ALLOYS. Vergasova, L. L.; Lazarev, E. M. Fiz. Khim. Obrab. Mater.; No. 6, 46-9(Nov-Dec 1970). (In Russian).

A thermodiffusion process is described for preparing Nb alloys with from 5 to 50 wt % Ti. Studies of the process showed that a redistribution of the components in the alloy and coating occurs and results in diffusion of Ti in the coating surface. The oxidation resistance of coatings was measured at 1100 and 1200°C, and the composition of the corrosion products was determined. It was shown that alloying of $NbAl_3$ compounds with Ti increases the heat resistance. Consequently it was recommended that heat-resistant Nb alloys be coated with Ti to improve the heat resistance properties. (tr-auth)

35326 WELDING AND BRAZING TECHNIQUES IN THE FABRICATION OF FACILITIES FOR NUCLEAR EXPERIMENTS. Lehrheuer, W.; Lison, R. (Kernforschungsanlage, Juelich, Ger.). Kerntech. Atomprax.; 13: No. 4, 157-63(Apr 1971). (In German and English).

The facilities required for irradiation experiments are discussed. This is followed by a discussion, on the basis of specific examples, of the materials and of the connection techniques used, including high temperature brazing in vacuum, electron beam welding, diffusion welding, and welding under inert gas; this latter in the particular form of welding in an inert gas chamber. Brazing facilities developed for specific brazing applications are described. A diffusion-welded connection between stainless steel 1.4541 and $AlMg_3$ is discussed. (auth)

XUM

35327 HIGH TEMPERATURE BRAZING OF REACTOR COMPONENTS. Iversen, K. (International Atomreaktorbau GmbH, Bensberg, Ger.). Kerntech. Atomprax.; 13: No. 4, 164-71(Apr 1971). (In German and English).

High-temperature brazing with working temperatures above 800°C is a technique for joining materials by means of seams, which is finding an increasing number of applications for highly stressed components in the construction of motors, aircraft, and reactors. Using this technique, it is possible to fabricate optimally from both the technical and the economic points of view, especially in mass fabrication, complex components, including components in superalloys and in high hot strength steels, in vacuum or in protective gas furnaces without the use of fluxes. The technique of vacuum brazing with nickel-based brazing filler metals is described and the properties of high temperature brazed connections are discussed. The use of high temperature brazing in reactor engineering is illustrated on an example. (auth)

35328 PREPARATION AND ELECTRICAL RESISTIVITY OF ULTRAHIGH PURITY NIOBIUM. Meyerhoff, R. W. (Union Carbide Corp., Tarrytown, N. Y.). J. Electrochem. Soc.; 118: No. 6, 997-1001(Jun 1971).

Niobium samples with residual resistivity ratios greater than 20,000 were prepared via a two-step process. First, a fused salt electroplating process was used to prepare niobium having an exceptionally high purity with respect to the substitutional transition metal impurities tantalum and tungsten. Second, this electroplated niobium was vacuum degassed to remove the interstitial impurities, oxygen, nitrogen, and hydrogen. The major contributions to the residual resistivity after vacuum degassing were from the impurities nitrogen, tantalum, and tungsten. The electrical resistivity of these ultrahigh purity niobium samples can be calculated from the relation $\rho_T = \rho(T) + 10.0 \times 10^{-6}\ C_{N2} + 2.49 \times 10^{-7}\ C_{Ta} + 11.0 \times 10^{-7}$ Cw ohm-cm where $\rho(T)$ represents the thermal contribution to the resistivity at the temperature T and C_{N2}, C_{Ta}, and Cw represent respectively the concentrations in atomic per cent of nitrogen, tantalum, and tungsten. The value of C_{N2} for the vacuum degassed samples is given by $C_{N2} = 6.2 \times 10^{-4}\ (p_{N2})^{1/2} \exp(23{,}000/T)$ where p_{N2} represents the partial pressure (torr) of nitrogen in the vacuum system and T represents the temperature (K) of the sample during outgassing. (auth)

35329 HYDRIDING RESISTANT ZIRCONIUM ALLOY COMPONENTS. Boulton, John (to Atomic Energy of Canada Ltd.). U. S. Patent 3,575,806. 20 Apr 1971. Filed 24 Nov 1967.

Materials for nuclear reactor components in an organic coolant circuit formed from a zirconium alloy containing 0.1 to 0.3% Sn, 0.05 to 0.2% Fe, 0.05 to 0.2% Ni, 0.05 to 0.2% Nb by weight with the remainder zirconium are described. The alloy exhibits a high resistance to hydriding when exposed to a hydriding atmosphere such as that provided by organic coolant. (AEC)

35330 SAFETY IN WELDING AND CUTTING. USAS Z49.1 1967. New York; American Welding Society, Inc. (1968). 70p. Available from American Welding Society, New York.

A standard for the protection of persons from injury and illness and the protection of property (including equipment) from damage by fire and other causes arising from welding and cutting is presented. Specific provisions are included for gas welding, shielded metal-arc welding, submerged arc welding, gas shielded-arc welding, brazing, and resistance welding. However, the requirements of this standard are generally applicable to other welding processes. No attempt has been made to include all particular hazards which may be inherent when welding and cutting equipment is used in special industries. (auth)

Properties Evaluations

Refer also to abstracts 34809, 34827, 36326, 36331, 37006, 37011, 37016, and 37139.

35331 (AWRE-O-25/71) SURVEY OF THE EFFECTS OF POROSITY ON THE ELASTIC MODULI AND STRENGTH OF BRITTLE MATERIALS WITH PARTICULAR REFERENCE TO BERYLLIUM. Cooper, R. E.; Rowland, W. D.; Beasley, D. (Atomic Weapons Research Establishment, Aldermaston (England)). Apr 1971. 18p. Dep. NTIS (U. S. Sales Only). UK 15p.

The effects of porosity on the elastic and strength properties of brittle materials are surveyed and compared with data obtained on beryllium. It is shown that beryllium exhibits monotonic decreases in its elastic moduli and various strength properties with increasing porosity but that its Poisson's ratio remains constant. The mechanical properties at high strains are more strongly dependent on porosity than those at lower strains and reasons for this are suggested. (auth)

35332 (BMI-X-604) EVALUATION OF BERYLLIUM FOIL SUBJECTED TO BIAXIAL STRESSES. Final Report. Gelles, S. H.; Rudnick, A. (Battelle Memorial Inst., Columbus, Ohio). 10 Aug 1970. Contract W-7405-eng-92. 60p. Dep. NTIS.

For Univ. of California, Lawrence Radiation Lab., Livermore.

The uniaxial and biaxial tensile properties of five sources of beryllium foil nominally 0.004 in. thick were evaluated. Three of the materials were fabricated from ingot and two via the powder route. The materials displayed a grain size range between 10 and 45 μ and degrees of preferred orientation between essentially random to approximately eight times the random level. A plane-strain tensile test was successfully applied to the evaluation of the beryllium foil. Through this test and well-instrumented uniaxial tensile tests, both conducted in the rolling and transverse directions, it was possible to establish yield and fracture loci for combined tensile stresses. The asymmetry of the texture in the plane of the sheet and the degree of texture significantly affected both the uniaxial and biaxial mechanical properties of the foil. Grain size sensitively affected the yield and fracture strengths, whereas its effect on the ductility was small. The data generated in this program seem to support the hypothesis that there is an optimum nonrandom texture for maximum ductility in foil subjected to balanced biaxial stresses. (auth)

35333 (CEA-CONF-1760) CHEMICAL DIFFUSION AND KIRKENDALL EFFECT IN THE BODY-CENTERED CUBIC PHASE OF THE SYSTEM PLUTONIUM/ZIRCONIUM. Remy, C.; Dupuy, M.; Calais, M. D. (Commissariat a l'Energie Atomique, Fontenay-aux-Roses (France). Centre d'Etudes Nucleaires). [nd]. 4p. (CONF-690724-2). Dep. NTIS (U. S. Sales Only).

From Conference on quantitative relation between properties and microstructure; Haifa, Israel (27 Jul 1969).

The Kirkendall effect can occur in solid-state diffusion in a gradient of chemical concentration. It is observed during diffusion treatment as a movement of diffusion couple interfaces, marked by inert wires, towards the element which diffuses more rapidly. Chemical diffusion and Kirkendall effect were studied in the $\epsilon\beta$ body-centered cubic phase of the system Pu-Zr by the welded couple technique. (auth)

35334 (EUR-4637) LABORATORY GUIDE FOR THE SELECTION OF BRAZING MATERIALS. Cappelletti, C. (European Atomic Energy Community, Ispra (Italy). Joint Nuclear Research Center). 15 Dec 1970. 14p. Dep. NTIS (U. S. Sales Only). EUR F.Fr. 4.45.

Orientating experiments were carried out on the wetting of various metals by different brazing alloys. The difference of behavior of refractory metals submitted to brazing at low temperature ($\leq$1,300°C) and at high temperature ($\geq$1,300°C) is noted. In the first case wetting will be obtained by adding small amounts of metal, which alloys easily with the base metal (mainly Ni). In the other case the compatibility between the brazing metal and the base metal plays its own important role. In order to avoid a too vigorous attack of the base metal, a judicious choice of the geometry of the parts to be joined and of the right brazing procedure is necessary. (auth)

35335 (HSSTP-TR-14) GROSS STRAIN CRACK TOLERANCE OF A533-B STEEL. Randall, P. N. (TRW Systems Group, Redondo Beach, Calif.). 1 May 1971. Contract W-7405-eng-26; Subcontract 3134. 56p. Dep. NTIS.

For Oak Ridge National Lab., Tenn.

Gross strain crack tolerance is a measure of fracture toughness that is useful where yielding precedes fracture yet flaw size must be treated quantitatively. In these tests, rectangular bars containing surface fatigue cracks were pulled in tension at several temperatures. Strains were measured at the edges of the specimen on a gage length spanning the plane of the crack, and also in the gross section above and below the crack. Gross strain crack tolerance is the strain at maximum load on the gage length designated. It is a function of crack size, constraint and temperature, and perhaps other variables. In A533-B steel, the plots of all of the displacement measurements versus temperature showed a sharply defined transition temperature. The effects of crack size are reported in terms of the temperature at which the strain in the net section reached 1.5%, or the temperature at which gross section yielding occurred. The two were essentially the same. Tests of three sizes of surface cracks in geometrically similar specimens have shown that increasing the crack size causes significantly higher temperatures to be required to reach the above criteria for gross strain crack tolerance. (auth)

35336 (INR-1255) PROPERTIES OF STAINLESS STEEL 1H18N9T AFTER AGING IN THE POWER REACTOR TEMPERATURE RANGES. PART II. MICROSTRUCTURE. Seyna, F.; Mizera, E.; Chyczewski, M. (Institute of Nuclear Research,

XUM

Warsaw (Poland)). 1970. 12p. (In Polish). Dep. NTIS (U. S. Sales Only).

Metallographic examinations of the material in the initial and aged condition were carried out by optical and electron microscopy techniques. The experimental results are discussed. (auth)

35337 (NYO-3975-3) ENVIRONMENT AND FRACTURE. Progress Report. Johnson, H. H. (Cornell Univ., Ithaca, N. Y. Dept. of Materials Science and Engineering). 20 Mar 1971. Contract AT(30-1)-3975. 6p. Dep. NTIS.

The results of studies of the effects of hydrogen and hydrogen-oxygen mixtures on the fracture of a high strength H11 steel in the pre-cracked configuration at −28 to +100°C and various pressures are reported. Electrochemical permeation measurements on biaxially stressed iron and steel membranes exposed to a hydrogen-containing environment verified that the chemical potential of an interstitial solute depends only upon the hydrostatic component of an imposed stress state. This same apparatus is being used to study hydrogen brittleness. Exploratory studies of the effects of hydrogen on the mechanical properties of iron whiskers are reported. (G.M.C.)

35338 (ORNL-TM-3316) EFFECT OF BORON ON THE DUCTILITY AND STRENGTH OF INCONEL 600 AND TYPES 304 AND 316 STAINLESS STEEL AT HOT METALWORKING TEMPERATURES. Chakraborty, A. K.; DuBose, C. K. H.; Martin, W. R. (Oak Ridge National Lab., Tenn.). May 1971. Contract W-7405-eng-26. 15p. Dep. NTIS.

Inconel 600 and Types 304 and 316 stainless steel containing 0.0005 to 0.02% B were tensile tested at 900 to 1300°C. Boron had little effect on Inconel 600, but the stainless steels were weakened somewhat at higher temperatures for the higher boron contents. All alloys lost ductility at the highest temperatures for the higher boron concentrations. (auth)

35339 (ORNL-tr-2479) MEASUREMENT OF THE CONCENTRATION OF OXYGEN DISSOLVED IN TANTALUM. Anuchkin, A. M.; Volkov, A. K.; Kidin, I. N.; Rozhnova, T. M.; Shtremel, M. A. Translated for Oak Ridge National Lab., Tenn., from Izv. Vyssh. Ucheb. Zaved., Chern. Met.; 13: No. 1, 140-2(Jan 1970). 4p. Dep. NTIS.

An abstract of this paper, prepared from the original language, appeared as NSA 25: 6862.

35340 (UARAEE-55) MECHANICAL BEHAVIOUR OF Ni-BASED ALLOYS AT ELEVATED TEMPERATURES. El-Shanshoury, I. A.; Voronin, I. M.; Gadallah, F. I. (Atomic Energy Establishment, Cairo (Egypt). Dept. of Metallurgy). 1968. 39p. Dep. NTIS (U. S. Sales Only).

An investigation of different factors which effect the short-time tensile properties of three unirradiated Ni-based alloys (60 Ni−17 Cr−Fe, 40 Ni−17 Cr−Fe, 80 Ni−19 Cr−Fe) and the precipitation hardened alloy 75 Ni−20 Cr−Fe−Ti−Al in the temperature range 25 to 850°C is discussed. High-temperature decrease in elongation to fracture was obtained. The decrease in ductility was found to be enhanced by increasing the test time, the grain size of the specimens, and ability of the material to precipitate. The different causes of embrittlement and ways to improve the high-temperature ductility properties of Ni-based alloys are discussed. (auth)

35341 (UCRL-50962) AN AC TEMPERATURE TECHNIQUE FOR MEASURING THE HIGH-TEMPERATURE SPECIFIC HEAT OF METALS. Finnila, Ronald Matti (California Univ., Livermore. Lawrence Radiation Lab.). 7 Dec 1970. Contract W-7405-eng-48. 71p. Dep. NTIS.

Thesis.

An ac temperature technique for measuring the specific heat of electrical conductors was developed. This technique can be used to measure the specific heat of small wire or foil samples in the temperature range of a few hundred degrees Kelvin to temperatures near the melting point of the sample. The accuracy of the specific heat data obtained using this technique is limited solely by the accuracy of the measurement of the sample's temperature coefficient of resistance. This ac temperature technique was used to measure the specific heat of tungsten in the temperature range 800 to 3400°K. A method for analyzing specific heat data to determine the contribution of lattice mono-vacancies was also developed. This method was used to determine the following data for tungsten: the energy of formation of mono-vacancies, $\Delta E_V = 3.90 \pm 0.30$ eV; the entropy of formation of mono-vacancies, $\Delta S_V/k = 8.4 \pm 1.3$; the concentration of mono-vacancies at the melting point, $c_{mp} = 2.1 \pm 0.7$ mole percent; the migration energy for mono-vacancies, $E_M = 2.74 \pm 0.56$ eV; and the anharmonic-lattice specific heat (800°K < T < 3400°K), $c_A \approx -0.48 + (0.57 \times 10^{-3})T + (0.015 \times 10^{-6})T^2$ cal/mole-°K. (auth)

35342 (UCRL-51035) A TECHNIQUE FOR MEASURING THE PRESSURE, VOLUME, ENTHALPY, AND RESISTANCE OF EQUILIBRIUM THERMODYNAMIC STATES OF LIQUID METALS AT HIGH TEMPERATURES AND PRESSURES. Henry, Kenneth W. (California Univ., Livermore. Lawrence Radiation Lab.). Apr 1971. Contract W-7405-eng-48. 203p. Dep. NTIS.

Thesis.

A method for overcoming the temperature and pressure limitations of conventional techniques for measuring equilibrium thermodynamic data has been developed. It can be applied to conducting materials that can be resistively heated and that do not disassociate in the liquid phase. This makes its application to the determination of pure liquid−metal thermodynamic data of great value. A material specimen in the form of a wire 1 mm in diameter by 25 mm long is mounted between two current leads such that it is axially concentric with a high-pressure cell. The cell is filled with helium to the desired working pressure. A current pulse of controlled magnitude and duration, from the overdamped discharge of a high-voltage capacitor bank, heats the wire to the desired state at a rate such that its expansion is nearly isobaric. The energy deposited in a segment of the sample is calculated from data obtained by measuring the current through the sample and the potential difference between two probes spaced about 5 mm apart near the center of the specimen. These data also allow calculation of the sample resistance during a major portion of the time that current flows. The thermodynamic specification of the high-temperature state is completed by measuring the expanded diameter of the sample, using flash x-radiographic techniques. The principal unique feature of this technique that succeeds in overcoming the limitations of previous techniques is the use of a rare gas to transmit pressure to the portion of the sample measured. The technique has been applied extensively to lead, successfully reaching temperatures exceeding 5000°K, at pressures up to 2 kbar. However, a large scatter in this lead data, probably due to oxide-impurity-induced nonuniformities in deposited energy, prevents claiming the full accuracy capability of the technique. A very limited application to uranium has been made. These data are insufficient to conclusively test their thermodynamic validity, but the repeatability of the data appears better than obtained with lead. (auth)

35343 (WANL-TME-1857) COMPARISON OF INCONEL 718 AND INCONEL 750 FOR ELEVATED TEMPERATURE SERVICE IN A PUMPED NaK SYSTEM. Svedberg, R. C.; Keeton, A.; Ammon, R. L. (Westinghouse Electric Corp., Pittsburgh, Pa. Astronuclear Lab.). Sep 1968. Contract AT(30-1)-3584. 44p. Dep. NTIS.

Inconel 718 and Inconel 750 tubular sections were fabricated using electron beam and TIG welding techniques. These test specimens were incorporated into a NaK loop operating in the temperature range of 1050 to 1310°F for 6000 hours. After exposure, these test sections were compared with identical unexposed samples to determine the effect of a liquid metal environment on the alloys. Results indicated that the only degradation in properties of the alloys was caused by aging at the elevated temperatures. There was no evidence of liquid metal corrosion or erosion. (auth)

35344 (Y-1788) MECHANICAL BEHAVIOR OF A UNIAXIALLY ALIGNED TUNGSTEN WIRE-REINFORCED LEAD COMPOSITE SYSTEM. Courtright, E. L. Jr. (Union Carbide Corp., Oak Ridge, Tenn. Y-12 Plant). 9 Apr 1971. Contract W-7405-eng-26. 105p. Dep. NTIS.

A study of the mechanical behavior of tungsten reinforced-lead matrix composites tested in uniaxial tension at room temperature revealed that variations in the strain hardening exponent of the matrix were at least partially responsible for synergistic departures from rule-of-mixtures behavior. The degree of synergism appeared to increase with the volume fraction of fiber as well as with the magnitude of the strain hardening exponent. Efforts were made to separate the axial stress contribution due solely to the matrix from which it was observed that the stress-strain behavior of the unreinforced matrix tested by itself would not adequately represent matrix behavior in the composite. This lack of representation was due to the rheological interaction between the constituent phases which developed a state of triaxial stress in the matrix, and thus enabled the matrix to bear a much larger stress loading that, in turn, increased with the volume fraction of fiber. The axial component of stress in the matrix was not found to be a monotonically increasing function of the axial strain, and inflections were observed at the Stage I and Stage II proportional limits. An analytical model was used to calculate the axial and transverse stress distribution in the matrix as a function of axial strain in the composite. The model was used to predict an increase in each of the three stress components with increasing volume fraction of fiber; and, as a result, it provides a more useful tool for predicting composite behavior than does the more conventional rule-of-mixtures formula. (auth)

XUM

35345 BERYLLIUM PRODUCTS FOR NUCLEAR, AEROSPACE, AND ELECTRONIC APPLICATIONS. Beaver, Wallace W. (Brush Beryllium Co., Cleveland). pp 181-9 of Materials Technology: An Interamerican Approach. New York; American Society of Mechanical Engineers (1968).

From Inter-American Conference on Materials Technology, San Antonio, Tex. See CONF-680513.

The employment of beryllium, its alloys, and its compounds as engineering materials in the electronics, nucleonics, and aerospace industries is reviewed in relation to such of their properties which make this family of materials particularly unique. Specific alloys and compounds in commercial use are covered as well as developmental materials having particular properties of interest to these fields. Growth indications in the engineering application of these materials to other industries are described. (auth)

35346 STRESS CYCLING INDUCED CHANGES IN THE YIELD PROPERTIES OF MOLYBDENUM. Dubensky, R. G.; Stephens, R. I. (Univ. of Iowa, Iowa City). pp 510-15 of Materials Technology: An Interamerican Approach. New York; American Society of Mechanical Engineers (1968).

From Inter-American Conference on Materials Technology, San Antonio, Tex. See CONF-680513.

The upper yield point of low carbon steel can be removed under certain precycling stress conditions. This investigation presents the hypothesis that similar changes are induced in the yield behavior of other bcc metals that exhibit an upper yield point. The hypothesis was partially verified by showing an enclosed region on the S-logN diagram where fully reversed stress precycling completely eliminated the upper yield point in a subsequent monotonic tensile test. The yield behavior is discussed in terms of localized cumulative inelastic strains due to precycling. A model of this process is explained in terms of cyclic induced mobile dislocation generation. (auth)

35347 DISSOCIATION ENERGY OF DIATOMIC CERIUM AND PREDICTED STABILITY OF GASEOUS INTERMETALLIC CERIUM COMPOUNDS. Gingerich, K. A.; Finkbeiner, H. C. (Texas A and M Univ., College Station). J. Chem. Phys.; 54: 2621-6 (15 Mar 1971).

The Knudsen-cell mass spectrometric method was used to study gaseous equilibria over the Au–Ce–CeS–BN–C system. The third-law enthalpies, ΔH_0°, in kcal mol^{-1}, of the reactions: (1) 0.5 $Ce_2(g)$ + 0.5 $Au_2(g)$ = CeAu(g), (2) $Ce_2(g)$ + Au(g) = CeAu(g) + Ce(g) and (3) $Ce_2(g)$ = 2 Ce(g), were found to be 24.7 ± 0.14, 23.0 ± 0.16, and 58.0 ± 1.5, respectively. The corresponding second-law value for Reaction (3) is 53.4 ± 10. The reaction enthalpies for Reactions (1) and (2) were combined with the literature value for D_0° (Au_2) and the value of D_0° (CeAu) obtained in the present investigation to yield the dissociation energy of diatomic cerium. The selected value for the dissociation energy of Ce_2 is D_0° = 57 ± 4 or D_{298}° = 58 ± 4 kcal mol^{-1}. Using the latter value and the literature value for the standard heat of sublimation of cerium, $\Delta H_{v,298}^\circ$ = 101 ± 1 kcal mol^{-1}, the standard heat of formation, $\Delta H_{f,298}^\circ$, of diatomic cerium was calculated as 144 ± 6 kcal mol^{-1}. The stability of selected gaseous intermetallic cerium compounds was predicted on the basis of the Pauling model of a polar bond and the experimental value for the dissociation energy of diatomic cerium. A reassessment of the dissociation energies, D_0°, of LaAu, CeAu, PrAu, and NdAu [J. Chem. Phys., 52: 2956(1970)] resulted in the values of 79.5 ± 5, 77.0 ± 3.5, 72.0 ± 5, and 70.6 ± 5, kcal mol^{-1}, respectively. (auth)

35348 INTERRELATIONSHIP OF FRACTURE TOUGHNESS AND MICROSTRUCTURE IN A Ti-5.25Al-5.5V-09Fe-0.5Cu ALLOY. Greenfield, M. A.; Margolin, H. (New York Univ., N. Y.). Met. Trans.; 2: 841-7(Mar 1971).

Fracture toughness of an $\alpha-\beta$ titanium alloy heat treated to a constant yield strength was found to depend upon the morphology of α produced or remaining after the initial solution treatment. In equiaxed α structures, fracture toughness depends linearly upon the grain boundary area per unit volume, S_v, and is independent of equiaxed α particle size or spacing. In a grain boundary α structure fracture toughness depends both on S_v and, within limits, linearly on the thickness of the α. Explanations are offered for the observed propagation of cracks at $\alpha-\beta$ interfaces and for the observation that high fracture toughness can accompany low tensile ductility. (auth)

35349 RELATIONSHIP BETWEEN ALPHA GRAIN SIZE AND CRACK INITIATION FATIGUE STRENGTH IN Ti-6Al-4V. Lucas, J. J.; Konieczny, P. P. (Sikorsky Aircraft, Stratford, Conn.). Met. Trans.; 2: 911-12(Mar 1971).

During the course of investigating the effects of processing variables and heat treat conditions on the mechanical properties of Ti–6Al–4V, a general relation was observed between α grain size and the high cycle (10^5) fatigue strength for both smooth (K_t = 1.0) and notched (K_t = 1.8) specimens. This relation is presented. Limited data on solution treated and aged (STA) Ti–6Al–6V–2Sn is also presented. The finer α grain sizes were obtained in the barstock and in the STA forging materials and these materials exhibit the higher fatigue strengths. (auth)

35350 MASS SPECTROMETRIC EVIDENCE FOR THE EXISTENCE OF GASEOUS INTERMETALLIC COMPOUNDS OF HIGH STABILITY AS PREDICTED BY THE BREWER–ENGEL METALLIC THEORY. Gingerich, Karl A.; Grigsby, Ronald D. (Texas A and M Univ., College Station). Met. Trans.; 2: 917-18(Mar 1971).

From eighth electronic materials conference; New York, N. Y. (Aug-Sep 1970).

A spark source mass spectrometer was used to obtain evidence of the existence and high stability of gaseous intermetallic compounds between platinum metals and Group IV transition metals. The following compounds were observed: TiRu, TiRh, TiPd, TiPt, Ti_2Pt, ZrRu, ZrRh, ZrPd, ZrPt, and HfPt. These observations were taken as an evidence of the expected high bond energies in the sense of the Brewer-Engel theory. (G.M.C.)

35351 WROUGHT STAINLESS STEEL BUTT-WELDING FITTINGS. INCLUDING REFERENCE TO OTHER CORROSION RESISTANT MATERIALS. MSS Standard Practice SP-43 1950. Arlington, Va.; Manufacturers Standardization Society of the Valve and Fittings Industry (1959). 12p. Available from Manufacturers Standardization Society of the Valve and Fittings Industry, Arlington, Va.

This standard covers overall dimensions, tolerances, and marking for wrought stainless steel butt-welding fittings. In this standard wrought is used to denote fittings made of pipe, tubing, plate, bar, sheet, strip or forgings. This standard covers only fittings made for use with Schedule 5S or 10S pipe except that short pattern stub ends suitable for use with Schedule 40S pipe are also shown. Stainless steel fittings for butt welding to standard wall or heavier pipe should be produced in accordance with ASA B16.9. (auth)

35352 EFFECT OF DISSOLVED OXYGEN ON THE TENSILE BEHAVIOR OF POLYCRYSTALLINE α ZIRCONIUM BETWEEN 25 AND 700°C. Com-Nougue, Jacques; Beranger, Gerard (Ecole Nationale Superieure des Mines, Paris). Compt. Rend., Ser. C; 272: 999-1002(15 Mar 1971). (In French).

The oxygen in solution in α Zr (between 0.3 and 12 at. %) increases the rupture strength and the yield strength of Zr up to a critical value C(c) which increases with the deformation temperature. This temperature strongly influences the yield strength, for oxygen contents ≥1.5 at. %; moreover the yield strength is a linear function of the oxygen content at a given high temperature. The yield strength and rupture strength decrease with increasing grain size (hardening effect), whereas the oxygen dissolution induces a grain growth annealing effect. These two opposing effects are evaluated. (France)

35353 FARADAIC YIELD OF THE ELECTROLYTIC DISSOLUTION OF Al AND Be. Garreau, Michel (CNRS, Paris). Metaux (Corros.-Ind.); 45: 425-47(Dec 1970). (In French).

The essential parameters of the anodic dissolution of Be and Al and their influence on the faradaic dissolution yield are examined. The effects of temperature, anode voltage, diffusion, water content of the electrolyte, surface state, and physical state of the anode are studied in turn. The reduction products formed at the anode are given. For each parameter are outlined the reasons why its influence was foreseen, the direction in which the yield may be expected to change in the different mechanisms proposed, and the measurements and observations carried out in the laboratory in order to compare experimental and theoretical results. (auth) (France)

35354 SINTERING PROCESS FOR Ni–P ALLOY COATED TUNGSTEN. Ito, Hiroshi (Nippon Tungusten Co. Ltd., Fukuoka); Mihashi, Yasuo; Tamagusuku, Susumu. J. Jap. Inst. Metals; 35: 6-10(Jan 1971). (In Japanese).

To lower the sintering temperature of tungsten to a technically acceptable level, elements of Group VIII in the periodic system, particularly nickel, were used. The addition of small amounts of Ni–P alloy to tungsten powder markedly accelerated low-temperature sintering of tungsten compared with nickel additions. To investigate the effects of Ni–P alloy addition to tungsten on low-temperature sintering, several experiments, mainly on the diffusion phenomenon, were performed. Results were: the liquid phase of Ni–P alloy that occurred at about 900°C accelerated sintering of tungsten; wetting of Ni–P alloy to tungsten was sat-

isfactory; and when nickel coexists with phosphorus, the diffusion rate of nickel in tungsten was markedly large compared with the case devoid of phosphorus. (auth) (Japan)

35355 LOW TEMPERATURE HEAT CAPACITIES OF PrBi, PrSb, LaBi, AND LaSb, CRYSTAL FIELD EFFECTS IN PrBi AND PrSb. Wallace, W. E.; Deenadas, A. W.; Thompson, A. W.; Craig, R. S. (Univ. of Pittsburgh). J. Phys. Chem. Solids; 32: 805-13 (Apr 1971).

The heat capacities of PrBi, LaBi, PrSb, and LaSb were measured between 7 and 300°K. While the results on LaBi and LaSb showed only vibrational and electronic contributions, PrBi and PrSb exhibit Schottky-type thermal anomalies which are attributed to excitation within the crystal field states. The entropy changes associated with the anomalies were in approximate agreement with the theoretical value of $R\ln(2J + 1) = R\ln 9$. The overall splitting associates with the crystal field heat capacity is found to be 280°K in both cases. (auth) (UK)

35356 WELDING OF TANTALUM AND NEWLY DEVELOPED TANTALUM-CLAD STEEL. Nishio, Y.; Omae, T.; Yoshida, Y.; Oka, T. (Mitsubishi Heavy Industries, Ltd., Hiroshima). Mitsubishi Juko Giho; 8: No. 1, 90-7(Jan 1971). (In Japanese).

Research was conducted to find a solution to the problems encountered in welding of tantalum and tantalum clad steel. The results are as follows: (1) A new sandwich type clad steel with titantium inserted between carbon steel and tantalum was developed. This clad steel is free from weld cracking and its weld has the same high corrosion resistance as its base metal. (2) Pores are liable to occur on tantalum weld obtained by TIG welding. However, this defect could be prevented by pretreatment, i.e., pickling and acetone degreasing. Neither contamination of air during welding nor grain coarsening of the weld had any effect on its corrosion resistance. (auth) (Japan)

35357 ADSORPTION OF CO ON THE (110) PLANE OF TUNGSTEN. Kohrt, Carl; Gomer, Robert (Univ. of Chicago). Surface Sci.; 24: 77-103(Jan 1971).

Sticking coefficients, desorption spectra, and isothermal desorption rates for CO on a macroscopic (110) plane of tungsten were determined by an extension of the method of Bell and Gomer. Sticking coefficients can be fitted by a Kisliuk isotherm with $K = 0.1$ for $300°K \leq T \leq 600°K$. Initial sticking coefficients S_0 range from 0.96 at 100°K to 0.72 at 600°K. The function $\log[(1 - S_0)/S_0]$ versus $1/T$ is linear from 300 to 600°K. Desorption spectra show the existence of virgin, beta and alpha states, as on polycrystalline tungsten. The abundances are beta/virgin = 0.4, alpha/beta = 1.0. Virgin desorption occurs at 200 to 450°K and obeys complex kinetics, suggesting competition between desorption and conversion to beta, with the latter predominating at low θ. Two beta states, beta-1 desorbing at 850 to 1000°K, and beta-2 desorbing at 975 to 1250°K were found, with beta-1/beta-2 $\approx$ 0.25. Arguments are made for the genuineness of beta-1. The desorption of both beta-1 and beta-2 is first order. The activation energy for beta-1 could only be determined as being between 40 to 55 kcal. The data for beta-2 give $\nu = 10^{12}$ sec^{-1} and $E = 67 \pm 2$ kcal with good accuracy. Alpha states, formed by readsorption on a beta layer, desorb from 100 to 450°K, with a highly coverage dependent energy spectrum. Models for the adsorption states are discussed. (auth)

35358 RADIOTRACER AND PHOTOEMISSION STUDIES OF CO CHEMISORBED ON Mo(100). Matthews, Lee D. (Univ. of Vermont, Burlington). Surface Sci.; 24: 248-54(Jan 1971).

Using a combination of photoelectric work function and radiotracer techniques, the adsorption and desorption of carbon monoxide from the (100) single crystal face of molybdenum were studied. The clean surface work function was found to be 4.67 ± 0.03 eV. Upon adsorption of carbon monoxide the work function increased to a maximum of 5.27 eV. Desorption studies led to the identification of several binding states corresponding to desorption energies of 2.85, 3.05, 3.24, 3.35, and 3.54 eV/mole. A photoelectric work function was associated with each of the states, and the corresponding values were 5.05, 5.05, 5.01, 4.92, and 4.87 eV. The three higher desorption energies are similar to those observed previously on polycrystalline molybdenum and are attributed to adsorption on surface defects. (auth)

35359 CONTACT POTENTIAL MEASUREMENTS OF THE ADSORPTION OF ALKALI METALS ON Ta(110) AND W(100) CRYSTALS. Fehrs, D. L. (Electronics Research Center, Cambridge, Mass.); Stickney, R. E. Surface Sci.; 24: 309-31(Jan 1971).

The adsorption of Cs, K, and Na on Ta(110) and of Cs and K on W(100) was studied under ultrahigh vacuum conditions using an ion gun to deposit the alkali metals and an electron gun to measure the resulting change in work function, $\Delta\phi$. Since the ion-deposition technique leads to a quantitative determination of n, the number (coverage) of alkali atoms adsorbed per cm^2, it was possible to obtain data on $\Delta\phi$ versus n. The crystal was at room temperature (~300°K) during deposition and measurements, but was flashed to ~2500°K between runs to desorb impurities. The principal observations are: (i) the initial dipole moments, μ_0, determined from the slope of $\Delta\phi$ versus n in the limit $n \to 0$, are in fair agreement with those based on the classical image-potential model; (ii) for Cs or K on W(100) or Ta(110), the minimum work functions observed showed no apparent dependence on substrate structure or properties; (iii) in the high coverage limit, the work functions are approximately equal to the values corresponding to bulk alkali metal crystals; (iv) the maximum coverages are approximately equal to the densities of surface atoms of an alkali metal crystal having the same orientation as the substrate. The last two points suggest that, in the high coverage limit, the surface properties tend toward those of the surface of an alkali metal crystal having the same BCC orientation of the substrate surface, although the adsorbate unit cell need not be coherent with that of the substrate. (auth)

35360 STANDARD SPECIFICATION FOR NICKEL–CHROMIUM–IRON ALLOY PLATE, SHEET, AND STRIP. ASTM B 168-70. Philadelphia; American Society for Testing and Materials (1970). 13p. Available from American Society for Testing and Materials, Philadelphia.

This specification is general and covers rolled nickel–chromium–iron alloy plate, sheet, and strip. Provision is made herein for material suitable for the general run of drawing, forming, stamping, bending, joining operations, and all other common methods of fabrication. Since the material may be used for purposes where the requirements of the operations are too particular to be prescribed in a general specification, it is advisable in these instances for the purchaser to submit samples or detailed information to the manufacturer and secure an adjustment of processing to suit the conditions for which the material is intended. (auth)

35361 STANDARD SPECIFICATION FOR SEAMLESS NICKEL AND NICKEL ALLOY CONDENSER AND HEAT EXCHANGER TUBES. ASTM B 163-66. Philadelphia; American Society for Testing and Materials (1967). 12p. Available from American Society for Testing and Materials, Philadelphia.

This specification covers seamless cold-drawn tubes of nickel and nickel alloys for use in condenser and heat-exchanger service. Provision is made for two carbon levels in nickel (only) in order that the low-carbon nickel may be selected for corrosive and elevated temperature applications where it may be preferred to that of commercially pure, wrought nickel. The sizes covered by this specification are 3 in. and under in outside diameter with minimum wall thicknesses of 0.148 in. and under, and with average wall thicknesses of 0.165 in. and under. Tubes shall be specified to two dimensions only, for example, outside diameter and minimum wall thickness or outside diameter and average wall thickness. The inside diameter shall not be specified. (auth)

35362 STANDARD SPECIFICATION FOR TITANIUM AND TITANIUM ALLOY STRIP, SHEET, AND PLATE. ASTM B 265-69. Philadelphia; American Society for Testing and Materials (1969). 7p. Available from American Society for Testing and Materials, Philadelphia.

This specification covers annealed titanium and titanium alloy strip, sheet, and plate as follows: Grades 1 to 4–unalloyed titanium; Grade 5–titanium alloy (6 percent aluminum, 4 percent vanadium); Grade 6–titanium alloy (5 percent aluminum, 2.5 percent tin); and Grade 7–unalloyed titanium plus palladium. (auth)

35363 STANDARD SPECIFICATION FOR FERRITIC AND AUSTENITIC STEEL CASTINGS FOR HIGH-TEMPERATURE SERVICE. ASTM A 351-70. Philadelphia; American Society for Testing and Materials (1970). 7p. Available from American Society for Testing and Materials, Philadelphia.

This specification covers ferritic and austenitic steel castings for valves, flanges, fittings, and other pressure containing parts intended for high-temperature and corrosive service. One grade of ferritic and 17 grades of austenitic steel castings are included in this specification. Selection will depend on design and service conditions, mechanical properties, and the high-temperature and corrosion-resistant characteristics. (auth)

35364 STANDARD SPECIFICATION FOR NICKEL–CHROMIUM–IRON ALLOY ROD AND BAR. ASTM B 166-70. Philadelphia; American Society for Testing and Materials (1970). 8p. Available from American Society for Testing and Materials, Philadelphia.

XUM

This specification covers nickel–chromium–iron alloy in the form of hot-finished and cold-drawn rounds, squares, hexagons, and rectangles. This specification is general. Provision is made herein for material suitable for hot- and cold-working operations, machining, and all other common methods of fabrication. Since the material may be used for purposes where the requirements of the operations are too particular to be prescribed in the general specification, it is advisable in these instances for the purchaser to submit samples or detailed information to the manufacturer and secure an adjustment of processing to suit the actual conditions for which the material is intended. (auth)

35365 SPOT FACING FOR BRONZE, IRON, AND STEEL FLANGES. MSS Standard Practice SP-9 1929. Arlington, Va.; Manufacturers Standardization Society of the Valve and Fittings Industry (1970). 4p. Available from Manufacturers Standardization Society of the Valve and Fittings Industry, Arlington, Va.

This MSS standard applies primarily to the spot facing of pipe flanges in brass, iron, or steel when cast integral with valves and fittings, as well as the companion flanges used with these products. (auth)

35366 STANDARD SPECIFICATION FOR SEAMLESS AUSTENITIC STEEL PIPE FOR HIGH-TEMPERATURE CENTRAL-STATION SERVICE. ASTM A 376-70. Philadelphia; American Society for Testing and Materials (1970). 7p. Available from American Society for Testing and Materials, Philadelphia.

This specification covers seamless austenitic steel pipe intended for high-temperature central-station service. Among the ten grades covered are five H grades which are specifically intended for high-temperature service. Optional supplementary requirements specify additional tests which will be made only when stated in the order, together with the number of such tests required. (auth)

35367 STANDARD SPECIFICATION FOR ELECTRIC-FUSION-WELDED AUSTENITIC CHROMIUM–NICKEL ALLOY STEEL PIPE FOR HIGH-TEMPERATURE SERVICE. ASTM A-358-70. Philadelphia; American Society for Testing and Materials (1970). 6p. Available from American Society for Testing and Materials, Philadelphia.

This specification covers electric fusion-welded austenitic chromium–nickel alloy steel pipe suitable for corrosive or high-temperature service, or both. (Although no restrictions are placed on the sizes of pipe which may be furnished under this specification, commercial practice is commonly limited to sizes not less than 8-in. nominal diameter.) This specification covers seven grades of alloy steel. The selection of the proper alloy and requirements for heat treatment shall be at the discretion of the purchaser, dependent on the service conditions to be encountered. Two classes of pipe are covered as follows: Class 1–all welded joints to be completely examined by radiography; and Class 2–no radiographic examination required. Optional requirements of a supplementary nature are provided for pipe where a greater degree of examination is desired. These supplementary requirements call for additional tests to be made and, when desired, one or more of these may be specified in the order. (auth)

35368 THERMODYNAMICS OF SOLUTION OF Ti, V, Cr, Fe, AND Co IN LIQUID TIN. Bowersox, David F. (Los Alamos Scientific Lab., N. Mex.). Met. Trans.; 2: 916-17(Mar 1971).

The partial molar enthalpies and entropies of solution of Ti, V, Cr, Re, and Co in liquid Sn were calculated from solubility data in two different approaches with the equation, $2.303\ R \log_{10}X = \Delta\bar{S} - \Delta\bar{H}/T$, where R is the gas constant and X is the mole fraction of solute in a saturated solution at absolute temperature T. In one approach the entropy and enthalpy of solution are considered independent of temperature in the temperature range of interest and the equation is differentiated in respect to T. The partial enthalpies were then calculated. In the second approach the excess entropy of solution was assumed to be negligible and the equation was rewritten as $\Delta\bar{H} = T(\Delta S_f - 2.303\ R \log_{10}X)$, where ΔS_f is the entropy of fusion of the solute. (G.M.C.)

35369 SECOND INTERNATIONAL CONFERENCE ON THE STRENGTH OF METALS AND ALLOYS, PACIFIC GROVE, CALIFORNIA, 30 AUGUST–4 SEPTEMBER 1970. VOLUME I. Metals Park, Ohio; American Society for Metals (1970). 399p. (CONF-700819–(Vol.1)).

Sixty-two of the papers presented at the conference are included in Volume 1. A separate abstract was prepared for each of 21 papers. One paper was previously abstracted in NSA as 25: 651. Papers for which no abstracts were prepared were considered not in the scope of NSA. These papers are concerned with plastic deformation, solid solutions, and solute effects. (J.R.D.)

For abstracts of individual papers see: 35370–35389 and 35485.

35370 PLASTIC DEFORMATION OF BCC METALS. Christian, J. W. (Oxford Univ.). pp 31-70 of Second International Conference on the Strength of Metals and Alloys, Pacific Grove, California, 30 August–4 September 1970. Vol. I. Metals Park, Ohio; American Society for Metals (1970).

From second international conference on the strength of metals and alloys; Pacific Grove, Calif. (Aug-Sep 1970). See CONF-700819–(Vol.1).

A review of investigations of bcc metal plasticity is presented. It seems well established that there is both a shear stress asymmetry and a variation of dislocation mobility with other components of the stress tensor, but the details of the orientation dependence and the $\psi(\chi)$ curves are not well understood. There is also no current explanation for the anomalous slip observed only in very pure niobium. Most results indicate that screw dislocations control the macroscopic flow at low temperatures, but not necessarily the micro-strain. Distributions of screw dislocations are observed at high stress levels, and are associated with more crystallographic slip, coarser slip lines, and parabolic rather than three-stage hardening. In a given alloy system, these parameters necessarily vary with a single parameter, the level of the flow stress. The three main models for thermally activated flow can individually all be fitted to most of the experimental results on flow stress, and to measurements of the activation parameters. Agreement with results of experiments is thus often a test of the general applicability of the rate equation, rather than of any specific model. Differentiation between the models depends on much more detailed experiments in which the many relevant variables are controlled carefully; such experiments are now beginning to be reported. (auth)

35371 INTERSTITIAL HARDENING AND THE PEIERLS STRESS IN TANTALUM. Mitchell, T. E.; Smialek, R. L. (Case Western Reserve Univ., Cleveland). pp 73-7 of Second International Conference on the Strength of Metals and Alloys, Pacific Grove, California, 30 August–4 September 1970. Vol. I. Metals Park, Ohio; American Society for Metals (1970).

From second international conference on the strength of metals and alloys; Pacific Grove, Calif. (Aug-Sep 1970). See CONF-700819–(Vol.1).

The additive behavior of Peierls stress and interstitial hardening stress in interstitial Ta–N alloys was investigated by measuring the strain-rate sensitivity of the flow stress. Results of these measurements are presented graphically. The thermal activation parameters of these reactions are calculated and their meaning discussed. (J.R.D.)

35372 EFFECT OF INTERSTITIAL NITROGEN ON THERMALLY ACTIVATED FLOW IN NIOBIUM SINGLE CRYSTALS. Taylor, G. (Oxford Univ.); Bowen, D. K. pp 78-82 of Second International Conference on the Strength of Metals and Alloys, Pacific Grove, California, 30 August–4 September 1970. Vol. I. Metals Park, Ohio; American Society for Metals (1970).

From second international conference on the strength of metals and alloys; Pacific Grove, Calif. (Aug-Sep 1970). See CONF-700819–(Vol.1).

Niobium crystals containing N at doping levels of 0.3 to 150 ppM were deformed in compression. Temperature and strain rate changes were imposed at intervals and the consequential changes in flow stress were measured. Discussions of results, presented graphically, are included along with descriptions of experimental techniques. (J.R.D.)

35373 STRENGTH DIFFERENTIAL EFFECT IN NIOBIUM–OXYGEN SOLID SOLUTIONS. Ravi, K. V. (Motorola Inc., Phoenix, Ariz.); Gibala, R. Contract AT(11-1)-1676. pp 83-7 of Second International Conference on the Strength of Metals and Alloys, Pacific Grove, California, 30 August–4 September 1970. Vol. I. Metals Park, Ohio; American Society for Metals (1970).

From second international conference on the strength of metals and alloys; Pacific Grove, Calif. (Aug-Sep 1970). See CONF-700819–(Vol.1).

The role of interstitials in slip anisotropy of bcc metals at low temperatures was investigated using Nb and Nb–O solid solutions. Results show that slip anisotropy depends on and increases with interstitial content. It appears that the stress-differential effect is also largely interstitial. Ways in which interstitials may contribute to or control slip anisotropy in bcc metals are discussed. (J.R.D.)

35374 SOLUTION SOFTENING IN Fe–Mo ALLOYS. Sakuma, T.; Karashima, S. (Tohoku Univ., Sendai). pp 88-92 of Second International Conference on the Strength of Metals and Alloys, Pacific Grove, California, 30 August–4 September 1970. Vol. I. Metals Park, Ohio; American Society for Metals (1970).

XUM

From second international conference on the strength of metals and alloys; Pacific Grove, Calif. (Aug-Sep 1970). See CONF-700819-(Vol.1).

Results of tensile tests on vacuum melted specimens of Fe and Fe-Mo alloys are presented and discussed. Addition of these small quantities of solute produces solution softening, characterized by reduction in strain and/or flow stress. Experimental results were interpreted as an indication that solution softening in such substitutional alloys is due to a decreased Peierls energy during alloying. (J.R.D.)

35375 EXPERIMENTAL CONFIRMATION OF AN ASYMMETRIC PEIERLS BARRIER IN THE TEMPERATURE DEPENDENCE OF YIELD STRESS IN TANTALUM AND TUNGSTEN. Mukherjee, A. K.; Misro, S. C.; Sato, R. T. (Univ. of California, Davis). pp 93-7 of Second International Conference on the Strength of Metals and Alloys, Pacific Grove, California, 30 August-4 September 1970. Vol. I. Metals Park, Ohio; American Society for Metals (1970).

From second international conference on the strength of metals and alloys; Pacific Grove, Calif. (Aug-Sep 1970). See CONF-700819-(Vol.1).

An evaluation is presented of the validity of a pseudo-Peierls model used to elucidate the effects of temperature and strain rate on the yield stress behavior of monocrystals of Ta and W for a particular orientation. Arguments are offered to support the major assumptions. It is noted that the curve representing effective tensile stress vs temperature is insensitive to acceptable alterations to the major suppositions. (J.R.D.)

35376 DISLOCATION SUBSTRUCTURE AND STRENGTH PROPERTIES OF NIOBIUM SINGLE CRYSTALS. Raghuram, A. C. (Univ. of Maryland, College Park); Reed, R. E.; Armstrong, R. W. pp 99-102 of Second International Conference on the Strength of Metals and Alloys, Pacific Grove, California, 30 August-4 September 1970. Vol. I. Metals Park, Ohio; American Society for Metals (1970).

From second international conference on the strength of metals and alloys; Pacific Grove, Calif. (Aug-Sep 1970). See CONF-700819-(Vol.1).

Strength properties of niobium single crystals were correlated with the dislocation subgrain structure produced during their fabrication. The quantitative results which were obtained indicate that the polycrystal flow strength of niobium material is very strongly influenced by the presence of dislocation subgrain boundaries. (auth)

35377 DEFORMATION OF BODY-CENTERED-CUBIC TITANIUM-VANADIUM SINGLE CRYSTALS. Paton, N. E.; Williams, J. C. (North American Rockwell Corp., Thousand Oaks, Calif.). pp 108-12 of Second International Conference on the Strength of Metals and Alloys, Pacific Grove, California, 30 August-4 September 1970. Vol. I. Metals Park, Ohio; American Society for Metals (1970).

From second international conference on the strength of metals and alloys; Pacific Grove, Calif. (Aug-Sep 1970). See CONF-700819-(Vol.1).

Results of an investigation of deformation modes in bcc Ti-V alloy monocrystals are presented. Resolved shear stresses in these specimens were also studied as function of temperature and composition. Results indicate that at 300°K and lower there is a yield drop, a negative work hardening rate, and inhomogeneous yielding marked by well defined slip bands. Experimental results are presented graphically and discussed. (J.R.D.)

35378 HETEROGENEOUS DEFORMATION OF NIOBIUM SINGLE CRYSTALS AT VERY LOW TEMPERATURES. Kubin, P.; Jouffrey, B. (Faculte des Sciences, Orsay, France). pp 123-4 of Second International Conference on the Strength of Metals and Alloys, Pacific Grove, California, 30 August-4 September 1970. Vol. I. Metals Park, Ohio; American Society for Metals (1970).

From second international conference on the strength of metals and alloys; Pacific Grove, Calif. (Aug-Sep 1970). See CONF-700819-(Vol.1).

Results of Nb monocrystal tensile testing at 2.17 to 17°K are presented. At 4.2°K and below deformation proceeds by jerky flow corresponding to macroscopic shearing of the sample. Jerky flow is thought to be caused by an adiabatic temperature rise during deformation. (J.R.D.)

35379 PLASTIC ANISOTROPY IN BCC METALS. Crutchley, D. E. (Univ. of Birmingham, Eng.); Reid, C. N.; Webster, T. H. pp 127-31 of Second International Conference on the Strength of Metals and Alloys, Pacific Grove, California, 30 August-4 September 1970. Vol. I. Metals Park, Ohio; American Society for Metals (1970).

From second international conference on the strength of metals and alloys; Pacific Grove, Calif. (Aug-Sep 1970). See CONF-700819-(Vol.1).

Variations in plastic anisotropy among bcc metals characterized by the extent to which flow strength of crystals vary with direction or directions of stressing were investigated. The plastic anisotropies of Cr, Mo, V, and Nb mono-crystals were compared under conditions where all the metals are compelled to undergo the same change in shape. Results indicate that the Group VIA metals do not obey the Taylor postulate, which predicts a specific amount of plastic anisotropy, because they violate the premise that shear stress required to continue slip depends only on the accumulated shear strain. (J.R.D.)

35380 THERMALLY ACTIVATED FLOW IN IRON, LOW CARBON STEEL, AND OTHER BODY-CENTERED CUBIC METALS (V AND Ta). Gokyu, I.; Kihara, J.; Hayashi, H. (Tokyo Univ.). pp 146-50 of Second International Conference on the Strength of Metals and Alloys, Pacific Grove, California, 30 August-4 September 1970. Vol. I. Metals Park, Ohio; American Society for Metals (1970).

From second international conference on the strength of metals and alloys; Pacific Grove, Calif. (Aug-Sep 1970). See CONF-700819-(Vol.1).

The relations between activation energy and the effective stress to move dislocations as found in Fe, low-C steel, V, and Ta were examined. It was found that the activation energy-effective dislocation movement stress relation is not affected by the presence of interstitial impurities in solutes in Fe and steel. The thermally-activated flow in Fe is rate determined at stresses higher than 20 to 25 kg/mm^2 by a process different from that at lower stress. The thermally-activated flow in V and Ta is rate-determined by a process that is independent of the effective stress. (J.R.D.)

35381 ASYMMETRY OF SLIP IN TANTALUM AND TANTALUM ALLOYS. Rogausch, K. D.; Mordike, B. L. (Univ. of Liverpool). pp 168-72 of Second International Conference on the Strength of Metals and Alloys, Pacific Grove, California, 30 August-4 September 1970. Vol. I. Metals Park, Ohio; American Society for Metals (1970).

From second international conference on the strength of metals and alloys; Pacific Grove, Calif. (Aug-Sep 1970). See CONF-700819-(Vol.1).

Results are given from an investigation directed to determining a curve representing the relations between the (101) crystal plane in Ta and Ta alloys, the maximum resolved shear stress in these crystals, and the observed slip plane. Rhenium and Mo were the alloying elements used in the investigations of temperature effects and alloying element effects on the asymmetry of slip and the slip line morphology. Analytical discussions of slip morphology and deformation modes are included. (J.R.D.)

35382 SLIP AND TWINNING IN α URANIUM. Daniel, J. S. (Ecole Polytechnique, Montreal); Lesage, B.; Lacombe, P. pp 185-8 of Second International Conference on the Strength of Metals and Alloys, Pacific Grove, California, 30 August-4 September 1970. Vol. I. Metals Park, Ohio; American Society for Metals (1970).

From second international conference on the strength of metals and alloys; Pacific Grove, Calif. (Aug-Sep 1970). See CONF-700819-(Vol. 1).

Results are reported from an investigation conducted to compare quantitatively the ease of operation of the various twinning modes in α-U. The importance of shear, shuffles, and dislocation mechanisms was evaluated. Results indicate that dislocations of the $\frac{1}{2}$ [1$\bar{1}$0] type play an important role in (1$\bar{3}$0) twinning. Predeformation by (110) slip leaves a high density of $\frac{1}{2}$ [110] dislocations which can assist (1$\bar{3}$0) twin propagation by the above mechanism. In freshly grown crystals, where the density of $\frac{1}{2}$ [1$\bar{1}$0] dislocations is much lower, lateral growth of (1$\bar{3}$0) twins depends on the ease with which these dislocations can move towards the twin under the influence of the applied stress. (J.R.D.)

35383 EFFECT OF THE SUPERCONDUCTING TRANSITION ON THE PLASTICITY OF METALS. Startsev, V. I.; Pustovalov, V. V.; Soldatov, V. P.; Fomenko, V. S.; Vainblat, T. I. pp 219-23 of Second International Conference on the Strength of Metals and Alloys, Pacific Grove, California, 30 August-4 September 1970. Vol. I. Metals Park, Ohio; American Society for Metals (1970).

From second international conference on the strength of metals and alloys; Pacific Grove, Calif. (Aug-Sep 1970). See CONF-700819-(Vol.1).

Results of investigations on the increased plasticity at the transition to superconducting state in crystalline Pb, In, Tl, Sn,

XUM

and Pb–In alloys are presented. Analyses of results are included. It is noted that further research is likely to reveal the concrete physical mechanisms which are responsible for the effect of superconducting transition on metal plasticity. (J.R.D.)

35384 SOLID SOLUTION HARDENING OF TANTALUM-BASE ALLOYS. Mordike, B. L.; Rogausch, K. D. (Univ. of Liverpool). pp 258-61 of Second International Conference on the Strength of Metals and Alloys, Pacific Grove, California, 30 August–4 September 1970. Vol. I. Metals Park, Ohio; American Society for Metals (1970).

From second international conference on the strength of metals and alloys; Pacific Grove, Calif. (Aug-Sep 1970). See CONF-700819–(Vol.1).

Parameters controlling solid solution hardening in Ta-base binary alloys containing less than 6 at. % Mo, W, Nb, Hf, Re, or Ru as the additive element were examined. Single crystals of the alloys were deformed in compression at 77 to 2000°K. Analytical discussions of the results are included. (J.R.D.)

35385 INFLUENCE OF VARIOUS ORDERED STATES ON THE MECHANICAL PROPERTIES OF VANADIUM–COBALT–NICKEL TERNARY ALLOYS. Liu, C. T.; Inouye, H. (Oak Ridge National Lab., Tenn.). pp 283-7 of Second International Conference on the Strength of Metals and Alloys, Pacific Grove, California, 30 August–4 September 1970. Vol. I. Metals Park, Ohio; American Society for Metals (1970).

From second international conference on the strength of metals and alloys; Pacific Grove, Calif. (Aug-Sep 1970). See CONF-700819–(Vol.1).

The effects of various ordered states on the properties of V–Co–Ni alloys were studied using alloys capable of long-range ordering and others incapable of long-range ordering. It was found that the viscous glide of superdislocations is the rate-controlling process in ordered alloys, and dislocation climb in disordered alloys. (J.R.D.)

35386 CROSS SLIP IN FCC ALLOYS. Nakada, Y.; Tisone, T. C. (Bell Telephone Labs., Inc., Allentown, Pa.). pp 288-93 of Second International Conference on the Strength of Metals and Alloys, Pacific Grove, California, 30 August–4 September 1970. Vol. I. Metals Park, Ohio; American Society for Metals (1970).

From second international conference on the strength of metals and alloys; Pacific Grove, Calif. (Aug-Sep 1970). See CONF-700819–(Vol.1).

Information is presented to show that in three fcc alloy systems the ease of cross slip is not a unique function of γ/Gb, where γ is the stacking fault energy, G is the shear modulus, and b is the Burgers vector. For example, the Ag–Li system exhibits a planar dislocation arrangement at $\gamma/Gb = 2 \times 10^{-3}$ whereas the Co–Fe system shows a cellular dislocation tangle at the same value of γ/Gb. On the other hand Ni–Mo alloys with $\gamma/Gb \sim 8.3 \times 10^{-3}$ exhibited difficult cross slip. Since the effect of solute on the difficulty of cross slip does not manifest itself until relatively high solute content is reached, it is proposed that the local curvatures produced on the dislocation lines by small regions of short range order (SRO) rather than by individual solute atoms cause the difficulty of cross slip. Furthermore, the destruction of the SRO by the leading dislocation lowers the glide stress for the subsequent dislocations, thus making the cross slip energetically unfavorable. Both of these factors result in planar glide when a high degree of SRO exists in fcc alloys. (auth)

35387 PLASTIC DEFORMATION OF SINGLE CRYSTALS OF INDIUM SOLID SOLUTIONS IN MAGNESIUM. Escaravage, C.; Bach, P.; Champier, G. (Laboratoire de Physique du Solids, Nancy). pp 299-303 of Second International Conference on the Strength of Metals and Alloys, Pacific Grove, California, 30 August–4 September 1970. Vol. I. Metals Park, Ohio; American Society for Metals (1970).

From second international conference on the strength of metals and alloys; Pacific Grove, Calif. (Aug-Sep 1970). See CONF-700819–(Vol.1).

Results of research on the solute effect in In–Mg solid solutions on basal slip are reported. It was found that the alloying effect of indium on critical resolved shear stress for basal slip of magnesium can be explained by elastic interaction between dislocations and foreign atoms; unique or repeated yielding are attributed to short range order occurring in this alloy. Prismatic slip of indium–magnesium solid solution is very similar to prismatic slip of beryllium. Further experiments on nonbasal slip and twinning of pure magnesium and magnesium alloys are necessary to understand the exact influence of indium on twinning inhibition, and narrow splitting of dislocations on prismatic planes. (J.R.D.)

35388 STRENGTHENING MECHANISM IN VANADIUM–TITANIUM ALLOYS. Boehm, Horst (Kernforschungszentrum, Karlsruhe, Ger.). pp 341-5 of Second International Conference on the Strength of Metals and Alloys, Pacific Grove, California, 30 August–4 September 1970. Vol. I. Metals Park, Ohio; American Society for Metals (1970).

From second international conference on the strength of metals and alloys; Pacific Grove, Calif. (Aug-Sep 1970). See CONF-700819–(Vol.1).

The stress rupture strength of binary vanadium–titanium-alloys at 650 to 850°C shows a maximum at a titanium content of 1 to 3%. Various results indicate that the high strength is due to an interaction between titanium and oxygen, which leads to the precipitation of TiO particles. The dependence on the Ti content of the creep properties can be explained by the dependence of the oxygen solubility and the conditions for coherent precipitation of TiO on the titanium content. The influence of ternary alloying elements on the long time stress rupture properties of V–Ti-alloys can also be described by considering the change in conditions for coherent precipitation of TiO due to changes in lattice parameters. (auth)

35389 CHANGE IN FLOW STRESS DUE TO THE SUPERCONDUCTING-NORMAL TRANSITION. Alers, G. A.; Buck, O.; Tittmann, B. R. (North American Rockwell Corp., Thousand Oaks, Calif.). pp 368-72 of Second International Conference on the Strength of Metals and Alloys, Pacific Grove, California, 30 August–4 September 1970. Vol. I. Metals Park, Ohio; American Society for Metals (1970).

From second international conference on the strength of metals and alloys; Pacific Grove, Calif. (Aug-Sep 1970). See CONF-700819–(Vol.1).

Recent measurements of the decrease in mechanical strength which accompanies the appearance of superconductivity are reviewed. The simplest explanation in terms of an electronic contribution to the viscous drag on moving dislocations is found to be inconsistent with the data. Qualitative agreement with the hypothesis of a change in dislocation pinning point strength can be demonstrated. (auth)

35390 SECOND INTERNATIONAL CONFERENCE ON THE STRENGTH OF METALS AND ALLOYS, PACIFIC GROVE, CALIFORNIA, 30 AUGUST–4 SEPTEMBER 1970. VOLUME II. Metals Park, Ohio; American Society for Metals (1970). 423p. (CONF-700819–(Vol.2)).

Sixty-eight of the papers presented at the conference are included in Volume 2. A separate abstract was prepared for each of 12 papers. Five papers were previously abstracted in NSA as 25: 4812, 25: 6882, 25: 13661, 25: 16594, and 25: 19252. Papers for which no abstracts were prepared were considered not in the scope of NSA. These papers are concerned with dislocation structures, strengthening effects of second phase particles, and precipitation hardening. (J.R.D.)

For abstracts of individual papers see: 35486, 35487, 35391–35394, 35507–35511, and 35573.

35391 INFLUENCE OF TITANIUM ON THE STRENGTHENING OF A Ni–Mo–Cr ALLOY. Sessions, C. E.; Stansbury, E. E.; Gehlbach, R. E.; McCoy, H. E. Jr. (Oak Ridge National Lab., Tenn.). pp 626-30 of Second International Conference on the Strength of Metals and Alloys, Pacific Grove, California, 30 August–4 September 1970. Vol. II. Metals Park, Ohio; American Society for Metals (1970).

From second international conference on the strength of metals and alloys; Pacific Grove, Calif. (Aug-Sep 1970). See CONF-700819–(Vol.2).

The strengthening mechanism in this alloy was investigated in studies directed to correlation of structures with high temperature creep and tensile properties. Particular attention is given to correlation of microstructures and mechanical properties. (J.R.D.)

35392 TEXTURE AND ELEVATED TEMPERATURE MECHANICAL PROPERTIES OF DISPERSION-STRENGTHENED Ni–20Cr ALLOYS. Killpatrick, D. H. (McDonnell Douglas Astronautics Co., Huntington Beach, Calif.). pp 649-53 of Second International Conference on the Strength of Metals and Alloys, Pacific Grove, California, 30 August–4 September 1970. Vol. II. Metals Park, Ohio; American Society for Metals (1970).

From second international conference on the strength of metals and alloys; Pacific Grove, Calif. (Aug-Sep 1970). See CONF-700819–(Vol.2).

The effects of texture on the strength of dispersion-strengthened Ni–20Cr alloys at 2,000°F were studied and its contribution to the indirect strengthening was determined. Three isotropic alloys in the form of 0.020-in. sheet were studied. These alloys had nom-

XUM

inal compositions of Ni–20Cr, Ni–20Cr–2ThO_2, and Ni–20Cr–4ThO_2. The cube textured alloy was in the form of 0.030-in. sheet and had a nominal composition of Ni–20Cr–2ThO_2. All samples were tested in air. The tensile data is an average of at least two separate tests. The 100-hr stress-rupture strength was determined from the results of at least five samples. Longitudinal-tensile and stress-rupture properties of the texture and isotropic alloys were obtained. The directional dependence of the properties of the textured alloy was also determined. Two different types of microstructure were observed in the alloys studied. The first type of structure is typical of that found in the isotropic alloys, where the twins are randomly oriented and extend across the entire grain. The second type of structure was observed in the textured, 2% ThO_2 alloy. This structure is typified by numerous fine, fragmented twins within an individual grain. These twins intersect at right angles, an indication of the strong cube texture present in the alloy. The presence of the texture was verified by a pole figure and was similar to that observed in a previous investigation. The comparison of the 0.02% yield strength, ultimate strength, and 100-hr stress-rupture strength of the textured and untextured alloys shows a nearly linear relationship between these properties and the amount of dispersed ThO_2 for the untextured alloys. However, the comparison shows that the textured alloy was nearly twice as strong as would be expected from the isotropic alloys. The differences between the strength of the textured and isotropic alloys can also be seen in the stress-strain curves for the 2% ThO_2 alloys. The textured alloy has a high yield and ultimate but limited elongation, typical of a high strength alloy. The isotropic alloy, however, yields at a very low stress and has considerably more elongation, typical of a lower strength alloy. (J.R.D.)

35393 STRENGTHENING Nb–Hf ALLOYS BY α PRECIPITATION. Carpenter, R. W.; Liu, C. T. (Oak Ridge National Lab., Tenn.). pp 674-8 of Second International Conference on the Strength of Metals and Alloys, Pacific Grove, California, 30 August–4 September 1970. Vol. II. Metals Park, Ohio; American Society for Metals (1970).

From second international conference on the strength of metals and alloys; Pacific Grove, Calif. (Aug–Sep 1970). See CONF-700819–(Vol. 2).

Results of an investigation are presented on the changes in hardness and strength and the attendant changes in microstructure of Nb–Hf alloys aged at temperatures from 600 to 1000°C. Two types of phase diagram for the Nb–Hf system are reported: a β-isomorphous diagram and a monotectoid-miscibility gap type (similar to the Nb–Zr system). The equilibrium precipitation products in this system were also examined. The alloy compositions of present interest indicated 38 and 54 at. % Hf. (J.R.D.)

35394 WORK HARDENING IN POLYCRYSTALLINE ALPHA ZIRCONIUM. Ells, C. E.; Cheadle, B. A. (Atomic Energy of Canada Ltd., Chalk River, Ont.). pp 758-62 of Second International Conference on the Strength of Metals and Alloys, Pacific Grove, California, 30 August–4 September 1970. Vol. II. Metals Park, Ohio; American Society for Metals (1970).

From second international conference on the strength of metals and alloys; Pacific Grove, Calif. (Aug–Sep 1970). See CONF-700819–(Vol.2).

Results of investigations on work hardening of Zr alloys are reported. Work hardening in polycrystalline Zr alloys was found to be dependent on an interaction between grain size and texture. Work hardenability of Zr irradiated at about 300°C is increased by dilute additions of Nb. (J.R.D.)

35395 SECOND INTERNATIONAL CONFERENCE ON THE STRENGTH OF METALS AND ALLOYS, PACIFIC GROVE, CALIFORNIA, 30 AUGUST–4 SEPTEMBER 1970. VOLUME III. Metals Park, Ohio; American Society for Metals (1970). 443p. (CONF-700819–(Vol.3)).

Sixty-eight of the papers presented at the conference are included in Volume 3. A separate abstract was prepared for each of seventeen papers. Papers for which no abstracts were prepared are considered out of scope for NSA. These papers are concerned with strengthening of metals and alloys, thermomechanical processing, high strain-rate phenomena, high-temperature alloy properties, and composites. (J.R.D.)

For abstracts of individual papers see: 35300–35302, 35396–35402, 35488–35491, and 35556–35558.

35396 HARDENING MECHANISMS IN MULTIPHASE ALLOYS. Drapier, J. M.; Viatour, P.; Coutsouradis, D.; Habraken, L. (Centre National de Recherches Metallurgiques, Liege). pp 830-4 of Second International Conference on the Strength of Metals and Alloys, Pacific Grove, California, 30 August–4 September 1970. Vol. III. Metals Park, Ohio; American Society for Metals (1970).

From second international conference on the strength of metals and alloys; Pacific Grove, Calif. (Aug-Sep 1970). See CONF-700819–(Vol.3).

The hardening mechanisms responsible for MP35N alloy having a nominal composition of 35Co–35Ne–20Cr–10Mo are described. Results of investigations show that holding the material at temperatures between 500 and 600°C, i.e., in the $\alpha + \epsilon$ field of the equilibrium diagram, causes the Mo atoms to segregate on preferred sites. Localization of the segregated Mo atoms, then of the precipitates, at the interfaces between the α matrix and the primary ϵ platelets retards the intervention of the dislocation sources; this accounts for the improved strength of the cold-worked MP35N alloy after holding in the $\alpha + \epsilon$ field. (J.R.D.)

35397 THERMOMECHANICAL PROCESSING OF MOLYBDENUM ALLOYS. Raffo, Peter L. (Illinois Inst. of Tech., Chicago). pp 925-6 of Second International Conference on the Strength of Metals and Alloys, Pacific Grove, California, 30 August–4 September 1970. Vol. III. Metals Park, Ohio; American Society for Metals (1970).

From second international conference on the strength of metals and alloys; Pacific Grove, Calif. (Aug-Sep 1970). See CONF-700819–(Vol.3).

The relations between thermomechanical processing and the mechanical properties of Mo-base-Hf–C alloys were investigated. It was found that the strain-aged alloys are characterized by coarser subgrains. Stronger Mo alloys can be produced by allowing carbide precipitation and strain hardening to occur simultaneously during processing. (J.R.D.)

35398 INFLUENCE OF THERMOMECHANICAL PROCESSING ON THE STRUCTURE AND PROPERTIES OF EXTRUDED BETA III TITANIUM. Adair, Attwell M.; Roberson, James A. (Air Force Materials Lab., Wright-Patterson AFB, Ohio. Aerospace Research Labs., Wright-Patterson AFB, Ohio). pp 932-6 of Second International Conference on the Strength of Metals and Alloys, Pacific Grove, California, 30 August–4 September 1970. Vol. III. Metals Park, Ohio; American Society for Metals (1970).

From second international conference on the strength of metals and alloys; Pacific Grove, Calif. (Aug-Sep 1970). See CONF-700819–(Vol.3).

High temperature thermomechanical processing of the Beta III titanium alloy which combines a 10.9 to 1 reduction by extrusion followed immediately by water quenching, effectively retains a significant amount of the dislocation structure produced. The dislocation structure retained promotes the formation of a fine distribution of the alpha phase during aging and suppresses the tendency for the omega phase to form. Direct aging of specimens from water quenched extrusions favors a greater amount of the alpha phase than when an intermediate solution treatment is used. An increased quantity and more favorable distribution of alpha phase obtained in this manner increase the ultimate tensile stress and the capacity for work hardening without seriously affecting the ductility. For specimens from the lowest temperature water quenched extrusion which were directly aged, the yield stress is significantly increased as well. The fracture toughness of Beta III is greater than that of most other titanium alloys when tested at the same strength level and under the same testing conditions. Although K_{IC} values for water quenched extrusion were somewhat lower than air cooled extrusions at the same yield stress level, the rate of crack propagation in the water quenched extrusion specimens was significantly lower. The extrusion forces for the Beta III Ti alloy are significantly below other titanium alloys at lower extrusion temperatures, and the difference between Ti–13V–11Cr–3Al is maintained over the temperature range investigated. (auth)

35399 INFLUENCE OF STRAIN RATE ON FLOW STRESS OF TANTALUM. Hoge, K. G. (Univ. of California, Livermore). pp 996-1000 of Second International Conference on the Strength of Metals and Alloys, Pacific Grove, California, 30 August–4 September 1970. Vol. III. Metals Park, Ohio; American Society for Metals (1970).

From second international conference on the strength of metals and alloys; Pacific Grove, Calif. (Aug-Sep 1970). See CONF-700819–(Vol.3).

The influence of strain rate on the flow stress of 99.9% pure, fully recrystallized tantalum was examined. Stress-strain curves in both tension and compression are obtained at strain rates from 10^{-5} to 5000 sec^{-1}. The dependency of the upper and lower yield stress on strain rate is closely predicted by the Johnston–Gilman model. However, this model does not adequately describe post-

XUM

yield hardening behavior. The Dorn–Rajnak model appears to describe the dynamic behavior better; it not only predicts yield behavior accurately but provides an excellent description of post-yield behavior. (auth)

35400 STRUCTURAL STUDIES AND PROPERTIES OF A NEW CAST HIGH STRENGTH CORROSION RESISTANT SUPERALLOY. Bieber, C. G.; Mihalisin, J. R. (International Nickel Co., Inc., Suffern, N. Y.). pp 1031-6 of Second International Conference on the Strength of Metals and Alloys, Pacific Grove, California, 30 August–4 September 1970. Vol. III. Metals Park, Ohio; American Society for Metals (1970).

From second international conference on the strength of metals and alloys; Pacific Grove, Calif. (Aug-Sep 1970). See CONF-700819–(Vol.3).

IN-738 is a balanced alloy composition possessing an excellent combination of high strength and ductility over a wide range of temperatures, excellent hot salt corrosion and oxidation resistance, and freedom from sigma formation. (auth)

35401 HIGH TEMPERATURE FLOW STRESS AND SUBSTRUCTURE STRENGTHENING OF POLYCRYSTALLINE α-ZIRCONIUM. Luton, M. J.; Jonas, J. J. (McGill Univ., Montreal). pp 1100-5 of Second International Conference on the Strength of Metals and Alloys, Pacific Grove, California, 30 August–4 September 1970. Vol. III. Metals Park, Ohio; American Society for Metals (1970).

From second international conference on the strength of metals and alloys; Pacific Grove, Calif. (Aug-Sep 1970). See CONF-700819–(Vol. 3).

Results of an investigation are presented in which the yield strength and the steady-state flow stresses of α–Zr were determined in a single operation. A method of analysis which applies to both types of data was used. (J.R.D.)

35402 ANALYSIS OF L AND Y TILT BOUNDARY INTERSECTIONS FORMED DURING CREEP IN MOLYBDENUM. Clauer, A. H. (Battelle Memorial Inst., Columbus, Ohio); Hirth, J. P. pp 1113-17 of Second International Conference on the Strength of Metals and Alloys, Pacific Grove, California, 30 August–4 September 1970. Vol. III. Metals Park, Ohio; American Society for Metals (1970).

From second international conference on the strength of metals and alloys; Pacific Grove, Calif. (Aug-Sep 1970). See CONF-700819–(Vol.3).

Results of the investigation show that the L and Y junctions observed in Mo single crystals and in various polygonized structures can be modeled as local equilibrium configurations on the basis of the theoretical stress fields of finite tilt walls. The equilibrium is consistent with that deduced from superdislocation analogs, suggesting that such analogs can be usefully applied to other small angle boundary configurations. (J.R.D.)

35403 BERYLLIUM COMES INTO ITS OWN. Goggin, William R. (Perkin-Elmer Corp., Pomona, Calif.). Opt. Spectra: 5: No. 4, 30-1(Apr 1971).

Properties of Be for use in optical materials are discussed. Information and discussions are included on state-of-the-art of Be mirror technology. It is noted that physical properties of Be are the basis for its usefulness in mirrors for precision optical systems and other critical instrumentation. (J.R.D.)

35404 INTERNAL FRICTION DUE TO OXYGEN-SUBSTITUTIONAL IMPURITY ATOM COMPLEXES IN ZIRCONIUM. Mishra, S.; Asundi, M. K. (Bhabha Atomic Research Centre, Trombay, India). Trans. Indian Inst. Metals; 23: No. 3, 73-9 (Sep 1970).

Internal friction peaks are observed in hcp metals like hafnium and titanium, which contain both interstitial and substitutional impurities. The present study is an investigation on the effect of tungsten–oxygen complex on the internal friction behavior of zirconium. Activation energy for the relaxation process was calculated and interpreted in terms of the diffusion process involved. (auth)

35405 SUPERPLASTICITY IN ALUMINUM–ZINC AND TIN–CADMIUM EUTECTOID ALLOYS. Darekar, V. S.; Chaudhari, R. D. (Coll. of Engineering, Poona). Trans. Indian Inst. Metals; 23: No. 3, 56-60(Sep 1970).

The superplasticity in Al–Zn and Sn–Cd eutectoid alloys was studied under the conditions of metastability postulated by Presnyakov. The results obtained on the two alloys are compared and discussed. The Sn–Cd alloy did not show superplasticity under the conditions of metastability as compared with the Al–Zn alloy. The Sn–Cd alloy was heavily worked and recrystallized at room temperature, to produce a fine grained structure and superplasticity was achieved. Superplasticity was found to depend on the prior degree of reduction and hence on the grain size produced after recrystallization. The effects of testing temperature, testing speed, and grain size were also studied and dependence of superplasticity on the strain rate sensitivity index m was found. (auth)

35406 DIFFUSION OF ^{95}Nb INTO COPPER. Saxena, M. C.; Sharma, B. D. (Bhabha Atomic Research Centre, Trombay, India). Trans. Indian Inst. Metals; 23: No. 3, 16-19(Sep 1970).

Present theories of solute diffusion in noble metals are based on size effect or on solute-vacancy interactions, which involve use of valence. The valence of transition metals for screening purposes is not well established and as such, solute-vacancy interaction terms cannot be evaluated with confidence. Furthermore, due to lack of sufficient data on the diffusion of transition elements in monovalent metals, a coherent picture of valence or size effect in such cases is not available. The diffusion data for ^{95}Nb into copper is reported. The results indicate that the diffusion of Nb in Cu is similar to those of Fe, Co and Ni in copper. (auth)

35407 FERRITIC Cr–Mo-STEEL WITH NIOBIUM ADDITION USABLE FOR THE CONSTRUCTION OF SODIUM-COOLED NUCLEAR REACTORS. Lorenz, K.; Kranz, E.; Fabritius, H. Klepzig Fachber.; 78: 564-8(1970). (In German).

Presupposition for the use of ferritic steels in combination with austenitic materials in sodium-cooled reactors is the inhibition of carbon transfer from the ferritic steel elements to the austenitic material. Systematic diffusion experiments using alloyed steels with niobium, titanium, and vanadium demonstrated that the addition of niobium and titanium inhibits the carbon transfer. In different steels alloyed with niobium the separated phases were isolated. Further experiments were carried out with steel containing completely stabilized niobium. The transition behavior and the mechanical properties were studied with respect to heat treatments. (NIS)

35408 STANDARD SPECIFICATION FOR ALLOY-STEEL AND STAINLESS STEEL BOLTING MATERIALS FOR HIGH-TEMPERATURE SERVICES. ASTM A 193-70. Philadelphia; American Society for Testing and Materials (1970). 8p. Available from American Society for Testing and Materials, Philadelphia.

This specification covers alloy and stainless steel bolting material for pressure vessels, valves, flanges, and fittings for high-temperature service. The term bolting material as used in this specification covers bars, bolts, screws, studs, and stud bolts. The bars may be hot-rolled, forged, centerless ground, or cold-drawn ferritic steels, or carbide-solution treated (annealed) annealed and strain-hardened austenitic stainless steels. Eight grades are covered, including four ferritic steels and four austenitic stainless steels. Selection will depend upon design, service conditions, mechanical properties, and high-temperature characteristics. Nuts for use with this bolting material are covered. (auth)

35409 EFFECT OF CARBON AND OXYGEN CONCENTRATIONS ON THE RUPTURE CHARACTERISTICS OF POLYCRYSTALLINE MOLYBDENUM. Minel, Lea; Langeron, Jean-Paul. (CNRS, Vitry-sur-Seine, France). Compt. Rend., Ser. C; 272: No. 13, 1204-7(29 Mar 1971). (In French).

The behavior of carbon and oxygen concentrations as low as 10^{-6} was studied by microfractography. These two impurities have a similar behavior in the precipitation and chemisorption processes. They, however, have opposite effects on molybdenum brittleness: the carbon reinforces the cohesion of the grain boundaries in relation to the matrix while the oxygen decreases it. (France)

35410 INTERNAL FRICTION PEAKS DUE TO OXYGEN IN Nb–4.6 Ti ALLOYS. Vercaemer, Claude; Heulin, Bernard (Ecole Nationale Superieure de Chimie, Strasbourg). Compt. Rend., Ser. C; 272: No. 13, 1200-3(29 Mar 1971). (In French).

The internal friction peaks of $Nb^{-4.6}$ Ti–O alloys were measured as a function of the oxygen content. The decomposition of the spectrum into elementary peaks revealed that four were due to oxygen. An interpretation of the various peaks is proposed. (France)

35411 DEFORMATION ANISOTROPY AND TEXTURE OF MOLYBDENUM. Palme, Ch.; Benesovsky, F.; Simader, F. (Metallwerk Plansee, Reutte/Tyrol, Austria). Planseeber. Pulvermet.; 18: 149-65(Sep 1970). (In German).

The deformation behavior of sheet is frequently characterized by the strain ratio $r = \epsilon_b/\epsilon_d$ (decrease in width ϵ_b and thickness ϵ_d during the tensile test), the so called r-value. Measurements of the r-value have not been previously carried out on pure molybdenum. Sheets of pure sintered molybdenum and one sheet specimen of boron-alloyed molybdenum rolled and annealed under different conditions were used in the present study. The r-values were determined for three preferred directions (0,

45, and 90° to the rolling direction); the maxima were found in nearly all cases for angles under 45°. This is the direction in which earing is observed during deep drawing of molybdenum sheet. The directional dependence of the r-values can be qualitatively explained by means of the x-ray texture study of the known preferred crystal orientations and the calculations of the r-values carried out by other authors. A more quantitative evaluation of the x-ray pole figures confirmed the increase in the r-value, previously observed in steels, through increase in the {111} texture at the expense of the {100} orientations. (auth)

35412 STANDARD SPECIFICATION FOR ALLOY STEEL FORGINGS FOR SEAMLESS DRUM, HEADS, AND OTHER PRESSURE VESSELS. ASTM A 336-70a. Philadelphia; American Society for Testing and Materials (1970). 8p. Available from American Society for Testing and Materials, Philadelphia.

This specification covers forged alloy steel hollow drums, headers, barrels, nozzles, and similar parts for use in pressure vessels and also alloy steel forgings for heads, covers, plugs, and other component parts for pressure vessels. Sixteen classes are covered, including ten ferritic steels, and six austenitic steels. Forgings made of steel grades listed in ASTM Specification A 335 seamless ferritic alloy steel pipe for high-temperature service may also be ordered under this specification. The chemical, tensile, heat treatment, and marking requirements of Specifications A 335 shall apply except the forgings shall conform to the chemical requirements of Specifications A 335 only with respect to ladle analysis. On check analysis they may deviate from these limits to the extent permitted in this specification. For closed-in forgings the requirements of this specification shall apply. (auth)

35413 STANDARD SPECIFICATION FOR NICKEL–CHROMIUM–IRON ALLOY SEAMLESS PIPE AND TUBE. ASTM B 167-70. Philadelphia; American Society for Testing and Materials (1970). 9p. Available from American Society for Testing and Materials, Philadelphia.

This specification covers nickel-chromium-iron alloy in cold-drawn and hot-finished seamless pipe and tube intended for general corrosive service and for heat-resisting applications. Cold-drawn pipe and tube is available in sizes of 6⅝ in. and under in outside diameter, and 0.382 in. and under in wall thickness. Cold-drawn pipe is available in various schedules. Hot-finished tube is available in sizes 9¼ in. and under in outside diameter, and 1.0 in. and under in wall thickness. Pipe and tube may be specified to two dimensions only as follows: outside diameter and average wall, outside diameter and inside diameter, or inside diameter and average wall. (auth)

35414 STANDARD SPECIFICATION FOR TITANIUM SPONGE. ASTM B 299-69. Philadelphia; American Society for Testing and Materials (1969). 3p. Available from American Society for Testing and Materials, Philadelphia.

This specification covers virgin titanium metal melting stock. This virgin metal is commonly designated as sponge titanium because of its porous, spongelike texture. (auth)

35415 STANDARD SPECIFICATION FOR SEAMLESS AND WELDED AUSTENITIC STAINLESS STEEL TUBING FOR GENERAL SERVICE. ASTM A 269-69. Philadelphia; American Society for Testing and Materials (1969). 5p. Available from American Society for Testing and Materials, Philadelphia.

This specification covers grades of stainless steel tubing for general corrosion resisting and low- or high-temperature service. (auth)

35416 STANDARD SPECIFICATION FOR WELDED AUSTENITIC STEEL BOILER, SUPERHEATER, HEAT-EXCHANGER, AND CONDENSER TUBES. ASTM A 249-65. Philadelphia; American Society for Testing and Materials (1968). 5p. Available from American Society for Testing and Materials, Philadelphia.

This specification covers welded tubes made from austenitic steels with various grades intended for such use as boiler, superheater, heat exchanger, or condenser tubes. Grades TP304H, TP316H, TP321H, TP347H, and TP348H are modifications of grades TP304, TP316, TP321, TP347, and TP348, and are intended for high-temperature service such as for superheaters and reheaters. This specification covers tubes ½ to 5 in., inclusive, in outside diameter and 0.035 to 0.320 in., inclusive, in minimum wall thickness. (auth)

35417 STANDARD SPECIFICATION FOR SEAMLESS AND WELDED AUSTENITIC STAINLESS STEEL PIPE. ASTM A 312-70a. Philadelphia; American Society for Testing and Materials (1970). 8p. Available from American Society for Testing and Materials, Philadelphia.

This specification covers seamless and welded austenitic steel pipe intended for high-temperature and general corrosive service. Sixteen grades are covered. Grades TP 304H, TP 316H, TP 321H, TP 347H, and TP 348H are modifications of Grades TP 304, TP 316, TP 321, TP 347, and TP 348, and are intended for high-temperature service. Optional supplementary requirements are provided for pipe where a greater degree of testing is desired. These supplementary requirements call for additional tests to be made and, when desired, one or more of these may be specified in the order. (auth)

35418 STANDARD FINISHES FOR CONTACT FACES OF PIPE FLANGES AND CONNECTING-END FLANGES OF VALVES AND FITTINGS. MSS Standard Practice SP-6 1929. Arlington, Va.; Manufacturers Standardization Society of the Valve and Fittings Industry (1963). 4p. Available from Manufacturers Standardization Society of the Valve and Fittings Industry, Arlington, Va.

Several types of contact faces for flanges are illustrated. The standard finishes for contact faces of pipe flanges and connecting-end flanges of valves and fittings of bronze, cast iron, and steel or ductile iron are described. (G.M.C.)

35419 STANDARD SPECIFICATION FOR GENERAL REQUIREMENTS FOR CARBON, FERRITIC ALLOY, AND AUSTENITIC ALLOY STEEL TUBES. ASTM A 450-70. Philadelphia; American Society for Testing and Materials (1970). 8p. Available from American Society for Testing and Materials, Philadelphia.

This specification covers a group of common requirements which, when specified in the purchase order or in an individual specification, shall apply to hot-finished and cold-drawn, welded and seamless carbon steel, and ferritic and austenitic alloy steel under each of the specifications issued by the American Society for Testing and Materials. (auth)

35420 STANDARD SPECIFICATION FOR CENTRIFUGALLY CAST AUSTENITIC COLD-WROUGHT PIPE FOR HIGH-TEMPERATURE SERVICE. ASTM A 452-65. Philadelphia; American Society for Testing and Materials (1966). 7p. Available from American Society for Testing and Materials, Philadelphia.

This specification covers austenitic steel pipe made by the centrifugal casting process, subsequently cold worked, and given a recrystallizing anneal. Pipe ordered to this specification is suitable for use in high-pressure, high-temperature services and shall be suitable for bending and other forming operations and for fusion welding. Selection will depend on design, service conditions, mechanical properties, and high-temperature characteristics. Several grades of austenitic steels are covered. Optional supplementary requirements are provided which call for additional tests, and when desired, shall be so stated in the purchase order together with the number of such tests required. (auth)

35421 STANDARD SPECIFICATION FOR SEAMLESS AND WELDED TITANIUM TUBE FOR CONDENSERS AND HEAT EXCHANGERS. ASTM B 338-65. Philadelphia; American Society for Testing and Materials (1965). 5p. Available from American Society for Testing and Materials, Philadelphia.

This specification covers six grades of seamless and welded titanium tubes intended for use in surface condensers, evaporators, and heat exchangers. (auth)

35422 STANDARD SPECIFICATION FOR TITANIUM AND TITANIUM ALLOY FORGINGS. ASTM B 381-69. Philadelphia; American Society for Testing and Materials (1969). 4p. Available from American Society for Testing and Materials, Philadelphia.

This specification covers seven grades of annealed titanium and titanium alloy forgings as follows: Grade F-1 to F-4 unalloyed titanium, Grade F-5—titanium alloy (6 percent aluminum, 4 percent vanadium), Grade F-6—titanium alloy (5 percent aluminum, 2.5 percent tin), and Grade F-7—unalloyed titanium plus palladium. (auth)

35423 STANDARD SPECIFICATIONS FOR REMELTED LITHIUM METAL IN INGOT FORM. ASTM B 357-66. Philadelphia; American Society for Testing and Materials (1967). 1p. Available from American Society for Testing and Materials, Philadelphia.

These specifications cover one grade of remelted lithium metal in ingot form. (auth)

35424 THERMAL CONDUCTIVITY OF NEPTUNIUM AT 300°K. (Los Alamos Scientific Lab., N. Mex.). J. Less-Common Metals; 24: 106-7(May 1971).

XUM

Thermal conductivities derived from measurements of thermal diffusivities are reported for unalloyed alpha-plutonium, a delta-plutonium alloy (96.65 at. % Pu-3.35 at. % Ga), and for unalloyed (alpha phase) neptunium. These measurements were made at room temperature (300°K) using a flash diffusivity apparatus whose description has appeared in the literature. The specimens were 0.6 cm diameter foils. Spot-welded to one surface on each foil was a Platinel thermocouple. The opposite surface was mounted on a microscope slide glass, and the foils were then sealed to the slide with an air-tight silicone plastic. The mounted specimens, prepared in this manner, were handled without undue attention in a clean laboratory, which suffered no contamination of a radioactive nature during the course of the experiments. Thermal conductivities, λ, were computed from the measured thermal diffusivities, α, by $\lambda = \alpha\rho C_p$, where ρ is the density and C_p is the heat capacity. (auth)

35425 CYCLIC YIELD BEHAVIOR OF POLYCRYSTALLINE NIOBIUM. Agrawal, S. K.; Stephens, R. I. (Univ. of Iowa, Iowa City). J. Less-Common Metals; 24: 93-101(May 1971).

Previous investigations have shown the room temperature upper and lower yield point stress of bcc iron and molybdenum can be completely removed by initially elastic cyclic stressing above the fatigue limit. The described work shows that the upper and lower yield point stresses in niobium can also be removed under these same conditions. The cyclic stress–strain curve of niobium was found cyclically to strain soften at small strain amplitudes and cyclically to strain harden at larger strains. Under constant cyclic strain amplitudes in the inelastic region, niobium cyclically strain hardens and quickly reaches a stable hysteresis loop. The cyclic yield point behavior described is explained in terms of localized cumulative multiplication of mobile dislocations. (auth)

35426 STANDARD SPECIFICATION FOR CENTRIFUGALLY CAST AUSTENITIC STEEL PIPE FOR HIGH-TEMPERATURE SERVICE. ASTM A 451-66. Philadelphia; American Society for Testing and Materials (1966). 6p. Available from American Society for Testing and Materials, Philadelphia.

This specification covers austenitic alloy steel pipe made by the centrifugal casting process intended for use in high-temperature or nuclear-pressure service. Several grades of austenitic stainless steel are covered. Optional supplementary requirements are provided which call for additional tests to be made if desired. (auth)

35427 DIFFUSION STUDY OF CHROMIUM–MOLYBDENUM SYSTEM BY VAPOR-SOLID COUPLES. Ruud, Clayton Olaf. Denver; Univ. of Denver (1970). 99p. University Microfilms Order No. 71-8031.

Thesis.

Diffusion of Cr–Mo in the solid solution range was studied in ⟨100⟩ direction from pure Cr to pure Mo using vapor-solid couples and single crystal Mo. The composition-distance data were obtained using an electron microprobe and correcting the data mathematically. The activity of the Cr vapor at the vapor-solid diffusion couple interface was varied between 1.00 and 0.48. However, the exact location of the final vapor-solid interface was so critical in the calculation of the diffusion coefficients for those samples in which the a_{Cr} was much less than unity, that the values were questionable. Consequently, only diffusion coefficients from samples with vapor-solid interface chromium activities near unity were used to calculate the activation energies and frequency functions reported. These values are reported from 0.10 to 0.98 atomic fraction Cr in the temperature range from 1440 to 1603°C. A computer method to calculate the diffusion coefficient by a modified Matano method was devised. The values of the diffusion coefficients were found to vary approximately two orders of magnitude from 0.10 to 0.98 atomic fraction chromium. The activation energies and frequency functions varied 69.2 kcal/gm. atom and approximately ten orders of magnitude over this same range of compositions, respectively. The Hall graphical method for finding diffusion coefficients was found to be inferior to the computer methods used in this study. No miscibility gap in the Cr–Mo solid solution was seen in the microprobe traverses. (Diss. Abstr. Int., B)

35428 FATIGUE FAILURE IN HIGH STRENGTH METALS. Tomkins, B. (United Kingdom Atomic Energy Authority, Springfields, Eng.). Phil. Mag.; 23: 687-704(Mar 1971).

A recently developed theory of fatigue crack propagation in ductile metals is extended to high-strength metals. The basic fatigue laws for such materials are derived and their behavior compared with that of more ductile metals. (auth) (UK)

35429 NITROGEN SOLUBILITY IN TUNGSTEN AT HIGH TEMPERATURES. Fromm, Eckehard; Jehn, Hermann (Institut fuer Sondermetalle, Stuttgart). Z. Metallk.; 62: No. 5, 378-81 (May 1971). (In German).

The solubility of nitrogen in tungsten was investigated in the pressure range 15 to 400 torr N_2 and in the temperature range 2400 to 3050°C. The equilibrium solubility is very low and increases with temperature (0.001 to 0.01 at. %). It can be represented by the equation (at. %, torr, °K): $c_N = \sqrt{p_{N_2}} \times 0.92 \cdot \exp(-46{,}700/RT)$. Gibbs free energy for solution is given by (atm, mole fraction, °K): $\Delta G^0_L = +46{,}700 + 2.75\ T$. (auth)

35430 EQUILIBRIA IN MOLYBDENUM–NITROGEN SOLID SOLUTIONS. Fromm, Eckehard; Jehn, Hermann (Institut fuer Sondermetalle, Stuttgart). Z. Metallk.; 62: No. 5, 372-7 (May 1971). (In German).

The solubility of nitrogen in molybdenum was investigated in the pressure range 15 to 400 torr N_2 and in the temperature range 1600 to 2400°C. The equilibrium solubility is very low and increases with temperature (0.01 to 0.1 at. %). It can be represented by the equation (at. %, torr, °K): $c_N = \sqrt{p_{N_2}} \times 0.3 \cdot \exp(-22{,}600/RT)$. The Gibbs free energy for solution is given by (atm, mole fraction, °K): $\Delta G^0_L = +22{,}600 + 5.03\ T$. In the molybdenum-nitrogen system an estimate of the solid solubility limit is given by $c_{N,max} = 3.1 \times 10^3 \exp(-36{,}200/RT)$. (auth)

35431 FRENCH RESEARCH ON METALLIC MATRIX COMPOSITES. Sindzingre, Michel (Ecole des Mines, Paris. Ecole des Mines, Corbeil, France). Z. Metallk.; 62: No. 5, 365-71(May 1971).

The mechanical properties of composites consisting of an aluminum matrix reinforced by boron fibers are presented. The experimental and control techniques used are described. The different structures obtained by unidirectional eutectic solidification of nickel and cobalt based alloys are shown. The resistance to tensile deformation and creep of these alloys is reported. Finally some investigations of new composite materials which are not reinforced unidirectionally but rather isotropically within a plane are described. (auth)

35432 MEASUREMENTS OF HEATS OF MIXING IN LIQUID GOLD BINARY ALLOYS. Itagaki, Kimio; Yazawa, Akira (Tohoku Univ., Sendai). J. Jap. Inst. Metals; 35: No. 4, 389-94(Apr 1971). (In Japanese).

Using the adiabatic calorimeter, heats of mixing in the binary liquid alloys consisting of gold and silver, aluminum, gallium, indium, germanium, or tin were determined at 1100°C. The experimental results obtained are discussed. Some systematic correlations were found between heats of mixing in the gold alloys and positions of the considered couples on the periodic table, but the correlation in a given group is quite different from that in the silver or copper alloys. The ξ function of the gold alloys having compounds in a solid phase shows a linear dependence on the gold concentration like that in subregular solution. This behavior is different from that of the silver or copper alloys, in which ξ shows a markedly negative value in the silver or copper rich region, owing to the larger electronegativity factor in the gold alloys. (auth)

35433 MEASUREMENTS OF HEATS OF MIXING IN LIQUID COPPER BINARY ALLOYS. Itagaki, Kimio; Yazawa, Akira (Tohoku Univ., Sendai). J. Jap. Inst. Metals; 35: No. 4, 383-9 (Apr 1971). (In Japanese).

Using the adiabatic calorimeter, heats of mixing in binary liquid alloys consisting of copper and silver, gold, aluminum, gallium, indium, germanium or tin were determined at 1100°C. The experimental data obtained were represented by the following ξ function: $\xi = \Delta H/X_{Cu}(1 - X_{Cu})$. The behavior of heats of mixing and some systematic correlations between heats of mixing and positions of the considered couples on the periodic table in the copper alloys are similar to those in the silver alloys. The heats of mixing in the copper alloys are closely related to the phase diagrams, suggesting that the atomic bonding in the solid copper alloys are retained partly in the liquid alloys. Since the ξ function of copper alloys having secondary solid solutions in solid phase decreases markedly with increasing copper concentration, it is considered that the interaction energy depends considerably on copper concentration. This dependence seems to be explained well by Engel's hypotheses for the electron distribution in copper and its alloys. (auth)

35434 ANOMALIES IN THE TENSILE PROPERTIES AT ELEVATED TEMPERATURES OF METASTABLE BETA TITANIUM ALLOYS. Otani, Shitoshi; Nishigaki, Minoru; Tokuda, Shoichi Kobe Steel, Ltd., Japan). J. Jap. Inst. Metals; 35: No. 4, 378-82(Apr 1971). (In Japanese).

Two anomalies in the tensile properties at elevated temperatures were observed in the metastable beta Ti–Mo alloy annealed

in the beta field. The one is the existence of a peak on the flow stress-temperature curve in the vicinity of 400°C and the other is the existence of a serration on the load-elongation curve in the range of 200° to 400°C. In order to procure more detailed information on these two anomalies tensile tests at elevated temperatures were carried out on metastable beta titanium alloys of different stability such as Ti–12 Mo–6 Sn, Ti–11.5 Mo–6 Zr–4.5 Sn, Ti–15 Mo–0.2 Pd, Ti–15 Mo–5 Zr, Ti–15 Mo–5 Zr–3 Al, Ti–15 Mo–5 Zr–3 Al–2 V, and Ti–13 V–11 Cr–3 Al. At the same time the effect of strain rates and annealing conditions on these two anomalies were examined. These two anomalies were not observed in the stable beta alloy, Ti–13 V–11 Cr–3 Al, and Ti–15 Mo–5 Zr, prestabilized by annealing at 400 or 500°C for 8 hr before tensile testing. The new type of serration observed in this study is different from the one due to the Portevin–Le Chatelier effect which has been suggested for mild steel and aluminum alloys. It is concluded from this investigation that both the peak of flow stress at 400°C and the serration on the load-elongation curve in metastable beta titanium alloys are due to the transformation of the metastable beta to the omega phase which took place during deformation. (auth)

35435 INFLUENCE OF HIGH HYDROSTATIC PRESSURE ON THE FLOW STRESS OF ZINC AND ZIRCONIUM POLYCRYSTALS. Oguchi, Atsushi; Yoshida, Susumu; Nobuki, Minoru (National Research Inst. for Metals, Tokyo). J. Jap. Inst. Metals; 35: No. 4, 371-7(Apr 1971). (In Japanese).

The influence of high hydrostatic pressure on the flow stress of zinc and zirconium polycrystals was investigated at room temperature. Pressurizing under a pressure of 12,000 kg/cm^2, tensile tests using the differential pressure method between atmospheric pressure and 12,000 kg/cm^2, and tensile tests under a constant hydrostatic pressure of 12,000 kg/cm^2 were carried out. The tensile load was measured by a magnetostrictive load cell in the high pressure chamber. Both the materials belong to the hexagonal close-packed system and are anisotropic in their elastic constants. Therefore, it is expected that shear stresses are generated at grain boundaries when they are subjected to high hydrostatic pressure and cause the pressurizing effect. The effect of pressurizing, however, is very small and is within the error of measurement for both the materials at atmospheric pressure. It seems that for zinc the most part of work-hardening caused by pressurizing disappears rapidly due to recovery before tensile testing and for zirconium the shear strain due to pressurizing remains in the elastic region. But it is presumed that a pressurizing effect will remain latently under high hydrostatic pressure if the annealed material is not returned to atmospheric pressure after being pressurized. In the differential pressure method, the change of flow stress with the ambient pressure includes the latent pressurizing effect. At large strains where the latent pressurizing effect decreases and becomes negligibly small, the rate of change of flow stress between 12,000 kg/cm^2 and atomospheric pressure is shown to be about 8% for zinc and about 3% for zirconium. These values coincide with the rates of change of shear modulus of the materials by hydrostatic pressure which are estimated theoretically. The work-hardening is enhanced for these materials under hydrostatic pressure. In the case of zirconium, the tendency of enhancement is similar to that observed with cubic metals. That is, at first it increases and then becomes saturated. For zinc, the enhancement continues to increase with increasing strain in the strain range tested. This seems to be due to the fact that recovery is suppressed under hydrostatic pressure, while it takes place actively at atmospheric pressure. (auth)

35436 SOLUTION HARDENING AND SOFTENING IN NIOBIUM–MOLYBDENUM AND NIOBIUM–RHENIUM ALLOYS. Statham, C. D.; Christian, J. W. (Oxford Univ.). Scr. Met.; 5: 399-405 (May 1971).

Data and information are presented on solution hardening and softening of single crystals composed of substitutional alloys of niobium with molybdenum or rhenium. Data are included on the resolved shear stress in compression for various Mo contents with axes corresponding to the ⟨100⟩ and ⟨011⟩ axes. Data are also included on the solute content dependence of the resolved shear stress on the (1̄01) [111] systems for crystals of specified orientation along with data on solution hardening of Nb produced by Re as function of temperature. (J.R.D.)

35437 ENGINEERING INFORMATION AND DATA. ZIRCONIUM AND HAFNIUM. Akron, N. Y.: AMAX Specialty Metals Division (1971). 36p.

Twelve articles and briefs are presented in the booklet. A separate abstract was prepared for each of six articles. Articles for which no abstracts were prepared are concerned with Zr and Hf products, applications in the chemical industry, Hf preparation, and quality control. (J.R.D.)

For abstracts of individual papers see: 35317–35319, 35438, 35439, and 35497.

35438 ZIRCONIUM FOR THE NUCLEAR INDUSTRY. pp 6-7 of Engineering Information and Data. Zirconium and Hafnium. Akron, N. Y.: AMAX Specialty Metals Div. (1971).

Properties of Zr and Zr alloys for use in the nuclear industry are reviewed. It is noted that strength, corrosion resistance, and low neutron cross section are important properties; data are included on neutron cross sections of common reactor materials. Properties of Zircaloy-2 and Zircaloy-4 are briefly discussed. (J.R.D.)

35439 ZIRCONIUM AND ALLOYS. PHYSICAL AND MECHANICAL PROPERTIES. pp 22-5 of Engineering Information and Data. Zirconium and Hafnium. Akron, N. Y.: AMAX Specialty Metals Div. (1971).

The physical and mechanical properties of Zr and Zr alloys are tabulated and presented graphically. (J.R.D.)

35440 SOLID STATE DIFFUSION: FAMILIAR EXAMPLES AND MODERN PROBLEMS. Kelly, J. W. (Australian Atomic Energy Commission Research Establishment, Lucas Heights). At. Energy Aust.; 14: No. 1, 2-7([1971]).

A review is given of the evolution of the theory of solid state diffusion. Diffusion mechanisms are described as well as experimental methods of determination of diffusion coefficients. The Kirkendall and Soret effects are outlined. Some correlation factors for isotope systems are given, as well as applications of the Soret effect in the nuclear field, such as the temperature gradient established between unstressed fins attached to a zirconium pressure tube, and the hot stressed tube itself, whereby hydrogen concentration in the tube is diminished. (Australia)

35441 REVIEW OF SOME SODIUM/WATER REACTION EXPERIMENTS. Bray, J. A. (Dounreay Experimental Reactor Establishment, Thurso, Scotland). J. Brit. Nucl. Energy Soc.; 10: 107-19(Apr 1971).

A summary is given of the experimental work carried out at Dounreay to endorse the PFR steam generator design. It is mainly concerned with the effects of complete tube failures in which full bore water flow passes into the sodium heat transfer fluid. Test work on the Na/H_2O (NOAH) and SUPER-NOAH rigs is described, together with some work on small water leaks. (auth) (UK)

35442 DETERMINATION OF THE THERMODYNAMIC PROPERTIES IN Zn–In LIQUID SOLUTIONS. Moser, Z. (Inst. of Metallurgy, Krakow). Rev. Roum. Chim.; 16: 327-41(Mar 1971).

The emf method of concentration in cells was used in the studies. The measurements were performed for the zinc concentration X_{Zn} = 0.01 to 0.9 mole fractions at 714, 757, and 805°K. Experimental results were used in the calculation of the partial functions for zinc. In order to determine the partial function for indium and the functions for 1 mole of the Zn–In liquid solutions, Krupkowski's formulas were applied. Zn–In liquid solutions were found as semi-regular; in this case the partial heat of solution of zinc and partial entropies were independent of temperature. (auth)

35443 ANISOTROPY OF THE ACTIVATION ENERGY OF DISLOCATION MOTION IN MONOCRYSTALS OF MOLYBDENUM AND NIOBIUM. Polotskii, I. G.; Prokopenko, G. I.; Trefilov, V. I. (Inst. of Metal Physics, Moscow). Fiz. Metal. Metalloved.; 31: No. 2, 410-11(Feb 1971). (In Russian).

Results of correlation of activation energy determined by various methods indicated that the spectrum of dislocation relaxation in Mo and Nb is related to the anisotropy of mechanical properties of these metals. (R.V.J.)

35444 STANDARD SPECIFICATIONS FOR FORGED OR ROLLED STEEL PIPE FLANGES, FORGED FITTINGS, AND VALVES AND PARTS FOR HIGH-TEMPERATURE SERVICE. ASTM A 105-68. Philadelphia; American Society for Testing and Materials (1968). 4p. Available from American Society for Testing and Materials, Philadelphia.

These specifications cover forged or rolled steel pipe flanges, forged fittings, and valves and parts for high-temperature service. The term forgings shall be understood to cover one or all of the products mentioned above, either forged or rolled. Two grades of material are covered, designated grades I and II, respectively, and are classified in accordance with their mechanical properties. (auth)

35445 STANDARD SPECIFICATIONS FOR SEAMLESS CARBON STEEL PIPE FOR HIGH-TEMPERATURE SERVICE. ASTM A 106-68. Philadelphia; American Society for Testing and Materials (1968). 10p. Available from American Society for Testing and Materials, Philadelphia.

XUM

These specifications cover seamless carbon steel pipe for high-temperature service in nominal sizes ⅛ to 26 in. inclusive, with nominal (average) wall thickness as given in ANSI B36.10-1959. Pipe having other dimensions may be furnished provided such pipe complies with all other requirements of these specifications. Pipe ordered under these specifications shall be suitable for bending, flanging, and similar forming operations. Supplementary requirements of an optional nature are provided for seamless pipe intended for use in central stations having steam service pressures of 400 psi and over and high temperatures or other applications where a superior grade of pipe is required. These supplementary requirements call for additional tests to be made. (auth)

35446 STANDARD SPECIFICATION FOR COLUMBIUM AND COLUMBIUM ALLOY STRIP, SHEET, FOIL, AND PLATE. ASTM B 393-64. Philadelphia; American Society for Testing and Materials (1965). 7p. Available from American Society for Testing and Materials, Philadelphia.

This specification covers unalloyed niobium and niobium alloy strip, sheet, foil, and plate as follows: Type 1.—reactor grade unalloyed niobium, Type 2.—commercial grade unalloyed niobium, and Type 3.—reactor grade niobium alloy containing 1% zirconium. (auth)

35447 STANDARD SPECIFICATION FOR COLUMBIUM AND COLUMBIUM ALLOY INGOTS. ASTM B 391-64. Philadelphia; American Society for Testing and Materials (1965). 5p. Available from American Society for Testing and Materials, Philadelphia.

This specification covers unalloyed niobium and niobium alloy ingots prepared by fusion, compressing and sintering of powder, or other suitable means to produce consolidated metal for processing to various basic shapes. The materials covered by this specification are: Type 1.—reactor grade unalloyed niobium, Type 2.—commercial grade unalloyed niobium, and Type 3.—reactor grade niobium alloy containing 1% zirconium. When an alloy not listed in this specification is desired, the purchaser may specify changes in chemical composition and other requirements needed to obtain the desired material. (auth)

35448 STANDARD SPECIFICATION FOR COLUMBIUM AND COLUMBIUM ALLOY BAR, ROD, AND WIRE. ASTM B 392-64. Philadelphia; American Society for Testing and Materials (1965). 6p. Available from American Society for Testing and Materials, Philadelphia.

This specification covers unalloyed niobium and niobium alloy bar, rod, and wire as follows: Type 1.—reactor grade unalloyed niobium, Type 2.—commercial grade unalloyed niobium, and Type 3.—reactor grade niobium alloy containing 1% zirconium. (auth)

35449 STANDARD SPECIFICATION FOR PRIMARY COLUMBIUM METAL. ASTM B 383-64. Philadelphia; American Society for Testing and Materials (1965). 5p. Available from American Society for Testing and Materials, Philadelphia.

This specification covers primary niobium metal, including virgin niobium metal for consolidation or melting. It also covers powder, roundels, beads, sponge, and other forms in which the primary metal may be produced. Two grades, reactor and commercial, are included. (auth)

35450 STANDARD SPECIFICATION FOR ELECTRIC-FUSION-WELDED STEEL PIPE FOR HIGH-PRESSURE SERVICE. ASTM A 155-70. Philadelphia; American Society for Testing and Materials (1970). 7p. Available from American Society for Testing and Materials, Philadelphia.

This specification covers electric-fusion-welded steel pipe suitable for high-pressure service and for use at high, intermediate, or lower temperatures, depending upon grade of material specified, in outside diameters 16 in. and larger with wall thicknesses up to 3.000 in. Pipe having other dimensions may be furnished provided such pipe complies with all other requirements of this specification. Pipe ordered under this specification shall be suitable for bending, flanging (vanstoning), corrugating, and similar forming operations. Several grades of carbon steel and alloy steel plates are covered, of different minimum specified tensile strengths and of flange or firebox quality; also, two different classes of welded joint quality as defined by heat treatment and radiographic requirements. Two classes of pipe are covered as follows: Class 1—all pipe to be heat treated and radiographed and Class 2—all alloy steel pipe to be heat treated and carbon steel pipe ¾ in. and over in thickness to be heat treated. (auth)

35451 STANDARD SPECIFICATION FOR CARBON AND ALLOY STEEL NUTS FOR BOLTS FOR HIGH-PRESSURE AND HIGH-TEMPERATURE SERVICE. ASTM A 194-69. Philadelphia; American Society for Testing and Materials (1969). 8p. Available from American Society for Testing and Materials, Philadelphia.

This specification covers steel nuts for bolts used in high-pressure or high-temperature service, or both. Twelve grades of material for services varying in degree of severity are covered: Grades 3, 4, 6, 7, 8, 8C, 8M, 8T, and 8F for service under the most severe conditions, and Grades 1, 2, and 2H for less severe service conditions. (auth)

35452 STANDARD SPECIFICATION FOR SEAMLESS FERRITIC AND AUSTENITIC ALLOY-STEEL BOILER, SUPERHEATER, AND HEAT-EXCHANGER TUBES. ASTM A 213-70. Philadelphia; American Society for Testing and Materials (1970). 7p. Available from American Society for Testing and Materials, Philadelphia.

This specification covers seamless ferritic and austenitic steel boiler and superheater tubes and austenitic steel heat exchanger tubes, designated Grades T 5, TP 304. Grades TP 304 H, TP 316 H, TP 321 H, TP 347 H, and TP 348 H are modifications of Grades TP 304, TP 316, TP 321, TP 347, and TP 348, and are intended for high-temperature service such as for superheaters and reheaters. This specification covers tubes ½ to 5 in., inclusive in outside diameter and 0.035 to 0.500 in., inclusive, in minimum wall thickness. (auth)

35453 RE-HEAT CRACKING IN HIGH NICKEL ALLOY HEAT-AFFECTED ZONES. McKeown, D. (Welding Inst., Cambridge, Eng.). Weld. J. (N. Y.); 50: No. 5, 201s-5(May 1971).

Postweld heat treatment (re-heat) cracking of high nickel alloys was studied by mechanical testing and metallography. The susceptibility of various alloys was determined with a test based on constant load rupture. The microstructural changes occurring during aging were related tentatively to the cracking problem as it exists in British commercial alloys. The conclusion reached was that cracking occurred after precipitation of the hardening phase, γ', and apparently before grain boundary carbide precipitation became an important factor. The susceptibility test offers a possible quantitative basis for comparing materials although some development of the technique might be required to give a correlation with practice. (auth)

35454 DEFORMATION OF LAMINAR SYSTEMS OF COPPER–MOLYBDENUM AND COPPER–TUNGSTEN AT INCREASED TEMPERATURES. Reznichenko, V. V.; Somov, A. I.; Tron, A. S.; Chernyi, O. V. Fiz. Khim. Obrab. Mater.; No. 6, 93-6 (Nov-Dec 1970). (In Russian).

Results are given of studies of the effects of composition on the strength and ductility of laminar systems at temperatures from 20 to 600°C. The systems were prepared by impregnation of blocks of Mo or W by melted Cu. (R.V.J.)

35455 EFFECTS OF COMPOSITION ON THE STRENGTH OF COPPER–MOLYBDENUM LAMINATES. Gindin, I. A.; Somov, A. I.; Starodubov, Ya. D.; Chernyi, O. V. Fiz. Khim. Obrab. Mater.; No. 6, 82-6(Nov-Dec 1970). (In Russian).

The effects of composition on the strength and plasticity of multilayered laminated Cu–Mo systems obtained by impregnating Mo plates with melted copper were studied. It was found that with a Mo content from 0 to 25%, the maximum strength of the system varied inconsistently with the content, reaching a maximum magnitude with 10 vol % Mo. Systems containing 90 vol % Cu plus 10 vol % Mo had ductility 50% higher than systems without the copper envelope. (R.V.J.)

35456 HIGH-TEMPERATURE THERMOMECHANICAL TREATMENT OF MAGNESIUM–ZINC–ZIRCONIUM ALLOYS. Drits, M. E.; Sviderskaya, Z. A.; Oreshkina, A. A. Fiz. Khim. Obrab. Mater.; No. 6, 70-5(Nov-Dec 1970). (In Russian).

The effects of high-temperature thermomechanical treatment on the mechanical properties and structure of Mg–Zn–Zr alloys were studied. It was determined that to obtain strength characteristics which permit up to 87% deformation, the alloy should be artificially aged by heating to 480°C for 2 hr, followed by cooling in air, and then compressed at 150°C. This heat treatment resulted in a 10 to 20% increase in the strength of the alloy at room temperature. Microstructural studies, using specific electric resistance measurements and x-ray methods, were performed to investigate the structural changes which occur as a result of the heat treatment, and showed that hardening is a function of: the deformation of the crystalline lattice of the solid solution; the Mg enrichment; and the kinetic processes of recrystallization and decomposition of the supersaturated solution. (R.V.J.)

XUN

35457 EFFECT OF HYDROGEN ON DEFORMATION AND FRACTURE PROCESSES IN HAFNIUM. Seelinger, S. M.; Stoloff, N. S. (Rensselaer Polytechnic Inst., Troy, N. Y.). Contract AT(30-1)-3719. Met. Trans.; 2: No. 5, 1481-4(May 1971).

Considerable effort has been devoted to examining the mechanical properties and fracture mechanisms of zirconium and its alloys. Very little information, however, has been published concerning hafnium, which is crystallographically and chemically similar. Zirconium and hafnium both crystallize in the hcp structure at room temperature and transform to bcc at elevated temperatures. The axial ratio is 1.589 for zirconium and 1.583 for hafnium. Similar etching techniques can be used for the two metals and they are believed to form similar hydrides. Limited torsion tests revealed that hafnium deforms predominantly by prismatic slip and twinning on $\{10\bar{1}2\}$ and $\{11\bar{2}1\}$ at low temperatures. This investigation determined the operative deformation modes and hydride habit planes and studied the effects of hydrogen on fracture phenomena in polycrystalline hafnium tested in tension between 77°K and room temperature. (auth)

35458 MEASUREMENT OF PARTICLE–MATRIX INTERFACE STRENGTH IN TD-NICKEL. Olsen, R. J.; Judd, G.; Ansell, G. S. (Rensselaer Polytechnic Inst., Troy, N. Y.). Met. Trans.; 2: No. 5, 1353-7(May 1971).

A technique was developed for the determination of the particle-matrix interface strength in dispersion-strengthened alloys. The procedure involves very rapid resistance heating, which results in the nucleation of voids by the effect of differential thermal expansion between the metal matrix and the dispersed phase particles. The interface stresses during heating are a function of temperature, and thus determination of minimum temperature at which decohesion occurs permits the estimation of interface strength. This determination was accomplished by tensile testing immediately after heating and the findings supported by transmission electron microscopy of quenched samples. The strength of the Ni–ThO_2 interface in a TD–Nickel alloy was found to be approximately 30,100 psi. (auth)

35459 EFFECTS OF TEMPERATURE AND STRAIN RATE ON THE STRENGTH OF BERYLLIUM SHEET. Conrad, H.; Cooke, F. W. (Franklin Inst. Research Labs., Philadelphia). Met. Trans.; 2: No. 5, 1307-13(May 1971).

The stress-strain behavior and the deformation dynamics of compression rolled and hot upset beryllium sheet prepared from secondarily refined powder were investigated in tension over the range 25 to 355°C. The true stress-true strain curves were approximated by the relation $\sigma = \sigma(0) + h\epsilon^{\frac{1}{2}}$. Both $\sigma(0)$ and h decreased with temperature. $\sigma(0)$ was higher at all temperatures for the compression rolled sheet, whereas h was the same for the two materials. The difference in $\sigma(0)$ was in the athermal component of the stress. The effects of temperature and strain rate on the flow-stress of the polycrystalline sheet agreed with those for prism slip in single crystals. Thermal activation analysis of the deformation dynamics yielded values of 123 to 158b^3 for the activation volume, 1.5×10^7 sec^{-1} for the preexponential factor and 1.8 eV (0.18 μb^3) for the activation energy, H_0. (auth)

35460 EFFECT OF MOLYBDENUM AND HARDENER CONTENT ON GAMMA-PRIME SOLVUS TEMPERATURE IN A Ni20Cr BASE HEAT-RESISTANT ALLOY. Maniar, G. N.; Bridge, J. E. Jr.; James, H. M. (Carpenter Tech. Corp., Reading, Pa.). Met. Trans.; 2: No. 5, 1484-7(May 1971).

The effect of molybdenum and hardener content on the γ' solvus and the γ' solutioning rate of Ni-20 Cr base alloys is described quantitatively. It is shown that by increasing the hardener content, the γ' solvus temperature and volume fraction increase greatly, while the addition of molybdenum has a very small effect on these parameters. The γ' solutioning rate, however, is unaffected by molybdenum and hardener additions. (auth)

35461 MECHANICAL RESPONSE OF THE Ni–Ni_3Nb EUTECTIC COMPOSITE. PART I. MONOTONIC BEHAVIOR. Hoover, W. R.; Hertzberg, R. W. (Lehigh Univ., Bethlehem, Pa.). Met. Trans.; 2: No. 5, 1283-8(May 1971).

To understand the mechanical behavior of the Ni-Ni_3Nb eutectic composite, it was necessary to determine the operative deformation and fracture mechanisms in the Ni_3Nb intermetallic phase. It was found that Ni_3Nb deforms primarily by twinning along $\{112\}$ planes and $\{011\}$ planes when tension and compression, respectively, are applied parallel to the [100] growth direction. The $\{112\}$ twins were observed to serve as crack nucleation sites with cracks forming along the twin boundaries. The monotonic response of the Ni-Ni_3Nb eutectic composite was investigated with tension and compression tests, metallography, and electron fractography. Room temperature tensile testing of the Ni-Ni_3Nb composite revealed this material to be capable of sustaining tensile strains in excess of 11%. This large composite ductility was associated with extensive $\{112\}$ twinning of the Ni_3Nb lamellae and subsequent twin boundary cracking. When amassed in sufficient numbers in a given cross-section, these $\{112\}$ twin boundary fissures initiated composite rupture. The room temperature ultimate tensile and compressive strengths of the alloy were found to be 109 and 235 ksi, respectively. (auth)

35462 MECHANICAL RESPONSE OF THE Ni–Ni_3Nb EUTECTIC COMPOSITE. PART II. CYCLIC BEHAVIOR. Hoover, W. R.; Hertzberg, R. W. (Lehigh Univ., Bethlehem, Pa.). Met. Trans.; 2: No. 5, 1289-92(May 1971).

In an effort to more fully understand fatigue crack propagation in composite materials, tension-tension fatigue studies of the Ni-Ni_3Nb eutectic composite were conducted. This composite displayed excellent fatigue resistance in notched configuration by exhibiting an endurance limit of 55% of the 108.7 ksi smooth bar tensile strength. Under high stress-low cycle fatigue conditions, the fatigue resistance of the composite was controlled by the $\{112\}$ twinning and subsequent twin boundary fracture of the Ni_3Nb phase. However, under low stress-high cycle fatigue conditions, Stage I crack propagation was observed in the nickel matrix. It was concluded that the nickel matrix controls the high cycle fatigue resistance of the composite. The fatigue behavior of the Ni-Ni_3Nb eutectic composite was compared with that of the Al-Al_3Ni composite. The similarity in the operative crack growth mechanisms in these two composites suggests a trend which may apply to all composites. (auth)

35463 EFFECT OF PURITY AND PROCESSING PROCEDURE ON THE MECHANICAL PROPERTIES OF BERYLLIUM SHEET. Cooke, F. W.; Herman, M.; Conrad, H. (Franklin Inst. Research Labs., Philadelphia). Met. Trans.; 2: No. 5, 1297-1305(May 1971).

The purpose of this research was to assess what improvements might be obtained in the bend ductility of beryllium sheet by starting with high purity commercial powder and consolidating it into sheet by techniques that minimized deformation and texturing. Sound sheet was achieved with reduction ratios from 2 : 1 to 12 : 1 at temperatures from 700 to 1050°C by forging, upsetting and compression rolling. Compression rolling is accomplished by successively changing the rolling direction by 30° after each pass so that no preferred rolling direction was developed. It was found that as the plastic bend ductility increased (up to 4%) the yield strength decreased. The higher bend ductilities corresponded to lower reduction ratios, lower degrees of preferred orientation and a larger subgrain size as determined by transmission electron microscopy. Sheet prepared by commercial rolling practices from the less pure commercial powder exhibited similar behavior. The ductile-to-brittle transition temperature for bending decreased with improved purity and reduced texture. (auth)

35464 STRESS DEPENDENCE OF HIGH-TEMPERATURE CREEP IN Fe–Mo AND Fe–Co ALLOYS. Watanabe, Tadao (University Coll., Swansea, Eng.); Karashima, Seiichi. Met. Trans.; 2: No. 5, 1359-65(May 1971).

The stress dependence of high-temperature creep and the alloying effects on it were investigated both in the ferromagnetic and the paramagnetic temperature regions of alpha iron and Fe-Mo and Fe-Co alloys. The steady-state creep rate, $\dot{\epsilon}_S$, of alpha iron was found to obey a power law relationship, $\dot{\epsilon}_S \propto \sigma^n$(n: constant) in the temperature range above 0.5 T_m(T_m : the melting temperature). The stress exponent, n, was 4.6 at all the temperatures examined. By addition of molybdenum n decreased to 3, while it remained unchanged by addition of cobalt. It seems that the change in n due to alloying is mainly attributed to the change in activation area for creep, A*, which results in the change in stress dependence of dislocation velocity. The magnetic transformation was found not to influence the stress dependence of $\dot{\epsilon}_S$. (auth)

35465 INFLUENCE OF GRAIN SIZE ON THE HARDNESS OF ALPHA PLUTONIUM. Merz, M. D.; Nelson, R. D. (Battelle Memorial Inst., Richland, Wash.). Contract AT(45-1)-1830. Met. Trans.; 2: No. 5, 1399-1402(May 1971).

The effect of grain size on the hardness of alpha plutonium was measured at temperatures between 77 and 373°K. The observations were: fine-grained metal had the lowest hardness at 373°K, fine-grained metal had the highest hardness at 77°K, and fine-grained metal had the greatest temperature dependence of hardness. At room temperature, fine-grained α-plutonium (1 μm) had a hardness of 235 dph, whereas coarse-grained metal (2000 μm) had a hardness of 310 dph. At 373°K fine-grained metal had a hardness of 120 120 compared to 225 dph for the coarse-grained metal. At 77°K the hardness values were 505 and 475 dph, the fine-grained metal being harder at this temperature. The hardness was estimated to be independent of grain size at 140°K. Above 140°K, grain bound-

XUM

aries have a softening effect due to the contribution of grain boundary sliding to deformation. (auth)

35466 TECHNICAL NOTE: FATIGUE CRACK PROPAGATION IN ZIRCALOY-2 WELD METAL. Ferrill, D. A. (General Electric Co., Schenectady, N. Y.). Weld. J. (N. Y.); 50: No. 5, 206s; 230s; 234s(May 1971).

The fatigue crack propagation characteristics of zircaloy weld metal were studied. This study was undertaken to gain insight into the growth characteristics of defects under cyclic loadings, since in service, this material would inevitably contain sources for crack initiation, such as structural discontinuities and weld defects. (auth)

35467 STANDARD SPECIFICATION FOR CARBON STEEL PLATES FOR PRESSURE VESSELS FOR INTERMEDIATE AND HIGHER TEMPERATURE SERVICE. ASTM A 515-70. Philadelphia; American Society for Testing and Materials (1970). 5p. Available from American Society for Testing and Materials, Philadelphia.

This specification covers carbon–silicon steel plates in four tensile strength ranges, designated Grades 55, 60, 65, and 70, intended primarily for intermediate or high temperature service in boilers and other pressure vessels. It is expected that plates will be manufactured in accordance with coarse grain practice. The maximum thickness plates of Grade 55 shall be 12 in.; and of Grade 60, 65, and 70 shall be 8 in. This material is intended for fusion welding. Welding technique is of fundamental importance and it is presupposed that welding procedure will be in accordance with approved methods. (auth)

35468 STANDARD SPECIFICATION FOR CARBON STEEL PLATES FOR PRESSURE VESSELS FOR MODERATE AND LOWER TEMPERATURE SERVICE. ASTM A 516-70a. Philadelphia; American Society for Testing and Materials (1970). 5p. Available from American Society for Testing and Materials, Philadelphia.

This specification covers carbon–manganese–silicon steel plates in four tensile strength ranges, designated Grades 55, 60, 65, and 70, intended primarily for service at temperatures in pressure vessels where improved notch toughness is important. The maximum thickness of plates of Grade 55 shall be 12 in.; and of Grades 60, 65, and 70 shall be 8 in. This material is intended for fusion welding. Welding technique is of fundamental importance and it is presupposed that welding procedure will be in accordance with approved methods. (auth)

35469 STANDARD SPECIFICATION FOR STAINLESS AND HEAT-RESISTING CHROMIUM AND CHROMIUM–NICKEL STEEL PLATE, SHEET, AND STRIP FOR FUSION-WELDED UNFIRED PRESSURE VESSELS. ASTM A 240-70. Philadelphia; American Society for Testing and Materials (1970). 6p. Available from American Society for Testing and Materials, Philadelphia.

This specification covers chromium–nickel stainless and heat-resisting steel plate, sheet, and strip for fusion-welded unfired pressure vessels. (auth)

35470 STANDARD SPECIFICATIONS FOR FORGED OR ROLLED ALLOY-STEEL PIPE FLANGES, FORGED FITTINGS, AND VALVES AND PARTS FOR HIGH-TEMPERATURE SERVICE. ASTM A 182-69. Philadelphia; American Society for Testing and Materials (1969). 9p. Available from American Society for Testing and Materials, Philadelphia.

These specifications cover forged or rolled alloy-steel pipe flanges, forged fittings, and valves and parts intended for high-temperature service. The term forgings shall be understood to cover one or all of the products mentioned above, either forged or rolled. Twenty-five grades are covered including eleven ferritic steels and fourteen austenitic steels. Selection will depend upon design and service conditions, mechanical properties, and the high-temperature characteristics. The H grades of the 300 series are modifications of the standard 300 grades and intended for service above 1000°F. (auth)

35471 TENTATIVE SPECIFICATION FOR UNALLOYED URANIUM CASTINGS. ASTM B 419-64T. Philadelphia; American Society for Testing and Materials (1965). 7p. Available from American Society for Testing and Materials, Philadelphia.

A specification covering unalloyed uranium castings prepared from primary and secondary melting stock, or both, is presented. (auth)

35472 STANDARD SPECIFICATION FOR PRIMARY HAFNIUM METAL SPONGE AND OTHER FORMS. ASTM B 414-67. Philadelphia; American Society for Testing and Materials (1968). 4p. Available from American Society for Testing and Materials, Philadelphia.

A specification is presented covering virgin hafnium metal commonly designated as sponge because of its porous, sponge-like texture; it may also be in other forms such as chunklets. The specification does not cover crystal bar. (auth)

35473 STANDARD SPECIFICATION FOR MANGANESE–MOLYBDENUM AND MANGANESE–MOLYBDENUM–NICKEL ALLOY STEEL PLATES FOR PRESSURE VESSELS. ASTM A 302-70. Philadelphia; American Society for Testing and Materials (1970). 5p. Available from American Society for Testing and Materials, Philadelphia.

A specification covering manganese-molybdenum and manganese-molybdenum-nickel steel plates, in two high tensile strength ranges, designated Grades A, B, C, and D, for use in boilers and other pressure vessels is presented. The minimum thickness of plates to be furnished to this specification is $\frac{1}{4}$ in. The maximum thickness is limited only by the capacity of the selected composition to respond to the heat treatment and meet the specified mechanical tests. Welding technique is of fundamental importance and it is presupposed that welding procedure shall be in accordance with approved methods for this class of material. (auth)

35474 STANDARD METHOD OF TEST FOR DENSITY IN AIR OF MANUFACTURED CARBON AND GRAPHITE ARTICLES BY PHYSICAL MEASUREMENTS. ASTM C 559-69. Philadelphia; American Society for Testing and Materials (1969). 2p. Available from American Society for Testing and Materials, Philadelphia.

A method covering the determination of the density of manufactured articles of carbon and graphite from measurements of weight and dimensions in air at 25°C is described. The method is also applicable to boronated carbon or graphite, a dispersion of boron in either carbon or graphite shapes, used for control rods and neutron shielding in nuclear technology. (auth)

35475 TENTATIVE SPECIFICATION FOR UNALLOYED URANIUM MELTING STOCK. ASTM B 420-64T. Philadelphia; American Society for Testing and Materials (1965). 6p. Available from American Society for Testing and Materials, Philadelphia.

A specification covering unalloyed primary and secondary uranium melting stock, or both, is presented. (auth)

35476 TUNGSTEN BASE METAL–CERAMIC ALLOY. Tsukerman, S. A.; Chernukho, B. M.; Kvin, V. E.; Kravchenko, A. T.; Kirpichankov, V. A. (to Inst. of Metallurgy). Russian Patent 240,206. 21 Mar 1969. Filed 26 Jul 1967. (In Russian).

Recrystallization and mechanical properties of tungsten alloy with 0.1 to 5 wt % Mn were studied at 1800 to 2000°C. (R.V.J.)

35477 HIGH-SPEED (SUBSECOND) MEASUREMENT OF HEAT CAPACITY, ELECTRICAL RESISTIVITY, AND THERMAL RADIATION PROPERTIES OF TANTALUM IN THE RANGE 1900 TO 3200 K. Cezairliyan, A.; McClure, J. L.; Beckett, C. W. (National Bureau of Standards, Washington, D. C.). J. Res. Nat. Bur. Stand.; 75A: 1-13(Jan-Feb 1971).

Measurements of heat capacity, electrical resistivity, hemispherical total and normal spectral emittances of tantalum above 1900°K by a pulse-heating technique are described. Duration of an individual experiment, in which the specimen is heated from room temperature to near its melting point, is less than one second. Temperature measurements are made with a photoelectric pyrometer. Experimental quantities are recorded with a digital data acquisition system. Time resolution of the entire system is 0.4 msec. Results on the above properties of tantalum in the range 1900 to 3200°K are reported and are compared with those in the literature. Estimated inaccuracy of measured properties in the above temperature range is 2 to 3 percent for heat capacity, 0.5 percent for electrical resistivity, 3 percent for hemispherical total emittance, and 2 percent for normal spectral emittance. (auth)

35478 STANDARD SPECIFICATION FOR COLUMBIUM AND COLUMBIUM ALLOY SEAMLESS AND WELDED TUBES. ASTM B 394-70. Philadelphia; American Society for Testing and Materials (1970). 6p. Available from American Society for Testing and Materials, Philadelphia.

This specification covers wrought niobium and niobium alloy seamless and welded tubes as follows: Type 1— reactor grade unalloyed niobium, Type 2— commercial grade unalloyed niobium, and Type 3— reactor grade niobium alloy containing 1 percent zirconium. (auth)

35479 AMERICAN STANDARD: NUCLEAR GRADE, URANIUM METAL MELT STOCK; NUCLEAR GRADE, URANIUM DIOXIDE, SINTERABLE; NUCLEAR GRADE, URANIUM DIOXIDE, COM-

XUM

PACTIBLE. ANSI N 5.4, 5.5, 5.6 1965. New York; American Institute of Chemical Engineers (1965). 40p. Available from American National Standards Inst., New York.

A specification is given for unalloyed nuclear-grade primary uranium metal stock which includes depleted, natural, or enriched uranium metal of an available ^{235}U content in the form of derbies, buttons, or cut pieces. Specifications for nuclear-grade uranium dioxide as sinterable powder or compactible material cover depleted, natural, or enriched material of any available ^{235}U content. The physical and chemical requirements are defined. (G.M.C.)

Structure and Phase Studies

Refer also to abstracts 36318, 36329, 36330, and 36338.

35480 INFLUENCE OF IRON AND ALUMINUM ON THE PRECIPITATION OF METASTABLE Ni_3Nb PHASES IN THE Ni–Nb SYSTEM. Quist, W. E. (Boeing Co., Seattle); Taggart, R.; Polonis, D. H. Met. Trans.; 2: 825-32(Mar 1971).

The effect of additions of aluminum and iron on the formation of transitional phases was examined for alloys of the Ni–Nb system. It was established that metastable phases of approximate composition Ni_3Nb will not form in binary Ni–Nb alloys under normal conditions of quenching and aging, but that iron or iron and aluminum additions promote their formation when certain size and electronic factors are satisfied. In Ni–Nb–Fe alloys containing more than ~12 at. % Nb, iron promotes the formation of a bct ($D0_{22}$) Ni_3Nb precipitate. Aluminum additions to these Ni–Nb–Fe alloys promote the precipitation of fcc ($L1_2$) Ni_3NB γ', initially together with the bct phase, but at higher aluminum concentrations the tetragonal phase disappears. The appearance of both precipitates followed the Hagel–Beattie requirement for interfacial mismatch of < or ~ 1% between the matrix and the precipitate. The presence of both precipitating phases can be predicted on the basis of the Engel–Brewer correlations. The preferred e/a ratio for the stability of the bct ($D0_{22}$) phase is 2.50 to 2.62. In the present investigation this phase precipitates only in the presence of iron (bcc e/a ratio = 1.5), and only when the lattice constant of the matrix is greater than 3.600Å. The preferred e/a ratio for the stability of the γ' having a fcc $L1_2$ structure is between ~2.75 and 3.0. Precipitation of this phase occurred only when aluminum (e/a) ratio = 3.0) was present, and when the matrix lattice constant was greater than 3.589Å. (auth)

35481 TWIN–SLIP AND TWIN–TWIN INTERACTIONS IN Mo–35 AT. PERCENT Re ALLOY. Mahajan, S. (Atomic Energy Research Establishment, Harwell, Eng.). Phil. Mag.; 23: 781-94(Apr 1971).

The crystallographic features of a twin–slip and of intersecting twins having like and unlike shear vectors were studied in detail using transmission electron microscopy. The observations suggest that a slip dislocation on penetrating a twin dissociates into a glide dislocation in the twin and a complementary twinning dislocation; these results are consistent with the suggestion of Sleeswyk and Verbraak (1961). The intersection of twins having the same shear vector causes the cessation of widening of the crossed twin on the side which makes an obtuse angle with the boundary of the crossing twin. This observation was rationalized in terms of the geometrical incompatibility of the atom movements necessary for simultaneous widening of both twins. The crystallographic features observed, viz. slip across planes in the matrix and the crossed twin, after the intersection of twins of different shear vectors, could have been caused by the penetration of the crossed twin by the glide dislocations which may result from the dissociation of twinning partials comprising the non-coherent boundary of the crossing twin. Based on these results it is suggested that in this alloy the crossed twins are unlikely to be very effective obstacles either to the slip dislocations or to the crossing twins. (auth) (UK)

35482 STRUCTURE MODIFICATIONS OF A Nb–Ti ALLOY DURING ITS OXIDATION. Perrin, Christian (Univ., Orleans, France). Compt. Rend., Ser. C; 272: 1026-9(15 Mar 1971). (In French).

Samples oxidized in the temperature range 600 to 1300°C under an oxygen pressure of 100 torr, and observed by microscopy, reveal an external zone with well defined grain boundaries. The growth kinetics of this layer were established and the oxygen penetration deduced from these measurements; the diffusion coefficient of oxygen in the alloy was then measured using microhardness curves. The concentration of solved oxygen and the distribution of Nb and Ti were determined by electron microprobe analysis. (auth) (France)

35483 MECHANISM OF PRECIPITATION AND PLASTIC DEFORMATION OF NICKEL–CHROMIUM ALLOYS HARDENED BY NIOBIUM AND TANTALUM PRECIPITATION. Royer, A.; Gantois, M. (Ecole Nationale Superieure de Metallurgie et de l'Industrie des Mines, Nancy). Mem. Sci. Rev. Met.; 68: 1-14 (Jan 1971). (In French).

Alloys containing 80 at. % Ni, 12 at. % Cr, 8 at. % Nb or 8 at. % Ta were studied. After tempering in water from 1250°C followed by annealing at 700°C, two kinds of Ni_3Nb precipitates appear successively. In the first stage, the precipitate P has a Do_{22} type tetragonal unit cell and appears in the form of thin platelets. In the second stage this tetragonal precipitate disappears in favor of a Do_a type orthorhombic precipitate in the form of large flakes. The respective orientations of each of these precipitates with the matrix, the divergences from coherence and the nature of the interfaces are determined. Stacking faults were revealed in the precipitates and the mechanism of the tetragonal → orthorhombic transformation is discussed. Three modes of plastic deformation were observed by electron microscopy at different stages of annealing: deformation by slip of the matrix and the tetragonal precipitates; deformation by slip of the matrix and the orthorhombic precipitates when these are in the form of fairly thin flakes (start of precipitation); and deformation by twinning of the matrix and the precipitates when the flakes have thickened. (France)

35484 FORMATION OF STACKING FAULTS IN MAGNESIUM–THORIUM ALLOYS. Noble, B.; Pike, T. J.; Crook, A. (Univ. of Nottingham, Eng.). Phil. Mag.; 23: 543-54(Mar 1971).

Trace additions of zinc to Mg–Th alloys result in the formation of stacking faults on (0001) planes when the quenched alloys are aged in the temperature range 300 to 400°C. The faults are intrinsic and bounded by $\frac{1}{3}\langle 10\bar{1}0\rangle$ partial dislocations. The mechanism of fault formation is discussed and it is proposed that the trace addition reduces the interfacial energy which promotes the formation of wide extended dislocations. (auth) (UK)

35485 MOBILITY OF DISLOCATIONS IN MOLYBDENUM SINGLE CRYSTALS. Das, G. C.; Pratt, P. L. (Imperial Coll. of Science and Tech., London). pp 103-7 of Second International Conference on the Strength of Metals and Alloys, Pacific Grove, California, 30 August–4 September 1970. Vol. I. Metals Park, Ohio; American Society for Metals (1970).

From second international conference on the strength of metals and alloys; Pacific Grove, Calif. (Aug-Sep 1970). See CONF-700819–(Vol.1).

The velocity of edge dislocations in Mo single crystals moving on {110} planes was measured as a function of applied stress and temperature, and the results are compared with those obtained by indirect experimental techniques. Discussions are included on slip systems for dislocation motion stress dependence of dislocation velocity, temperature dependence of dislocation velocity, comparisons of flow stress and stress to move fresh dislocations. (J.R.D.)

35486 OBSERVATION OF DISLOCATIONS IN CADMIUM BY OPTICAL, X-RAY, AND ELECTRON MICROSCOPY. Puttick, K. E. (Univ. of Surrey, Eng.). pp 464-7 of Second International Conference on the Strength of Metals and Alloys, Pacific Grove, California, 30 August–4 September 1970. Vol. II. Metals Park, Ohio; American Society for Metals (1970).

From second international conference on the strength of metals and alloys; Pacific Grove, Calif. (Aug-Sep 1970). See CONF-700819–(Vol.2).

Results of investigations on dislocations in Cd single crystals are presented. Attention is particularly directed to the dislocation structure in Cd crystals deformed homogeneously by basal glide and to sessile dislocations which may act as barriers to the movement of edge dislocation walls. (J.R.D.)

35487 AGING RESPONSE OF A Mg–8.7 PERCENT Y ALLOY. Mizer, D.; Peters, B. (Dow Chemical Co., Midland, Mich.). pp 669-73 of Second International Conference on the Strength of Metals and Alloys, Pacific Grove, California, 30 August–4 September 1970. Vol. II. Metals Park, Ohio; American Society for Metals (1970).

From second international conference on the strength of metals and alloys; Pacific Grove, Calif. (Aug-Sep 1970). See CONF-700819–(Vol. 2).

Results of an investigation of the precipitation process in the Mg–Y system conducted to identify the phase responsible for the age hardening reaction, and to gain insight into the mechanism of inhibition of $\{10\bar{1}2\}$ twinning are presented. It was found that the observed aging response in the Mg–Y system is the result of the precipitation of a coherent metastable phase that occurs at low aging temperatures. Directional strain in a second phase and second-phase ordering on the Mg lattice appear to be important in the process of $\{10\bar{1}2\}$ twinning. (J.R.D.)

XUM

35488 MICROSTRUCTURAL ANALYSIS OF A HIGH STRENGTH MARTENSITE-BETA TITANIUM ALLOY. Crossley, F. A.; Lindberg, R. W. (Lockheed Missiles and Space Co., Palo Alto, Calif.). pp 841-5 of Second International Conference on the Strength of Metals and Alloys, Pacific Grove, California, 30 August–4 September 1970. Vol. III. Metals Park, Ohio; American Society for Metals (1970).

From second international conference on the strength of metals and alloys; Pacific Grove, Calif. (Aug-Sep 1970). See CONF-700819– (Vol.3).

The Ti–2Al–11.5V–2Sn–11.3Zr alloy represents a new type of titanium alloy which consists of submicroscopic martensite in a β matrix in the annealed condition. The alloy is highly ductile in the annealed condition due at least partially to the occurrence of stress induced transformation. The alloy can be age hardened or isothermally transformed to strengths up to 200 ksi or more. The primary age hardening reaction appears to be rapid growth of the submicroscopic α. A secondary hardening reaction appears to be the precipitation of submicroscopic particles of $ZrFe_2$ formed from the 0.1 wt % Fe impurity. (auth)

35489 EQUILIBRIUM AND PRECIPITATION EFFECTS IN Co-RICH ALLOYS OF THE Co–Cr–W SYSTEM. Barrows, R. G.; Newkirk, J. B. (Univ. of Denver). pp 1047-51 of Second International Conference on the Strength of Metals and Alloys, Pacific Grove, California, 30 August–4 September 1970. Vol. III. Metals Park, Ohio; American Society for Metals (1970).

From second international conference on the strength of metals and alloys; Pacific Grove, Calif. (Aug-Sep 1970). See CONF-700819– (Vol.3).

A portion of the phase boundary configurations for the Co–Cr–W phase diagram was determined at 1350°C. Although it is unlikely that a cobalt-base alloy would ever be used at this temperature it is possible that these alloys would receive heat treatments in this temperature region. A previously unreported TCP-type phase was found to exist in this system with the approximate composition $Co_{23}Cr_{15}W_{15}$. The intermetallic compound has the R-phase crystal structure and hexagonal lattice parameters of $a_0 = 10.882$ A and $c_0 = 19.25$ A. Results of experimental work indicated that in the vicinity of 1350°C, the alpha–Co phase field increases in area with increasing temperature. (auth)

35490 MICROSTRUCTURAL ASPECTS OF FRACTURE TOUGHNESS IN A COBALT-BASE SUPERALLOY. Woodford, D. A. (General Electric Co., Schenectady, N. Y.); McMahon, C. J. Jr. pp 1067-71 of Second International Conference on the Strength of Metals and Alloys, Pacific Grove, California, 30 August–4 September 1970. Vol. III. Metals Park, Ohio; American Society for Metals (1970).

From second international conference on the strength of metals and alloys; Pacific Grove, Calif. (Aug-Sep 1970). See CONF-700819– (Vol.3).

The microstructural aspects of fracture at room temperature in MAR-M-509 cobalt-base alloy were examined. It was found that under the conditions of three heat treatments used in the experiments there were sufficient large carbide inclusions present to cause cracking after the onset of plastic deformation. It is noted that further research is needed on ways to remove the large carbides. (J.R.D.)

35491 STACKING FAULT FORMATION AND MECHANICAL TWINNING PROCESSES IN A NICKEL-BASE SUPERALLOY DURING TENSILE DEFORMATION AT HIGH TEMPERATURE. Guimier, A.; Strudel, J. L. (Ecole des Mines, Paris). pp 1145-9 of Second International Conference on the Strength of Metals and Alloys, Pacific Grove, California, 30 August–4 September 1970. Vol. III. Metals Park, Ohio; American Society for Metals (1970).

From second international conference on the strength of metals and alloys; Pacific Grove, Calif. (Aug-Sep 1970). See CONF-700819– (Vol.3).

In high-temperature tensile tests at low rates or during creep, the development of intrinsic stacking fault (S-ISF) in the precipitates instead of antiphase (APB) appears as the most common mode of deformation in Was alloy. Similar results were obtained on Udimet 500. At higher rates and/or for large deformations, mechanical microtwins originating in the precipitates spread to the matrix. High temperature is required for both mechanisms. Lowering of the stacking fault energy due to selective segregation effects may take place. (auth)

35492 POINT DEFECTS IN BODY-CENTERED CUBIC TRANSITION METALS. Kimura, Hiroshi (Tohoku Univ., Sendai). Nippon Kinzoku Gakkai Kaiho; 9: No. 11, 709-23(Nov 1970). (In Japanese).

A review of basic properties and behavior of point defects in body-centered cubic transition metals such as iron molybdenum, tantalum, niobium, vanadium, tungsten, etc., is presented, including formation energy of the vacancies, activation energy of their movement (recovery process of point defects), aggregate of vacancies and interaction between impurities and vacancies. In some properties, there is a clear distinction between niobium and tantalum and tungsten and molybdenum. If the difference in the point defects is confirmed between these two groups, the relation between them and the electron structure will be clarified together with an interpretation of the difference in other properties. (Japan)

35493 X-RAY STUDIES OF THE TENDENCY OF NIOBIUM TOWARD FORMATION OF STACKING FAULTS. Ivanov, A. N.; Popkov, Yu. M. (Inst. of Steel and Alloys, Moscow). Fiz. Metal. Metalloved.; 31: No. 2, 401-4(Feb 1971). (In Russian).

X-ray diffraction lines were analyzed for determining the dimensions of coherent scattering at the (100) and (110) surfaces of Nb with various oxygen contents and deformed by machining. The observed anisotropy of the area of coherent scattering was the result of the stacking faults. (tr-auth)

35494 INFLUENCE OF PRIOR COLD WORK ON THE DISCONTINUOUS PRECIPITATION IN COPPER–2 WT. PERCENT Be. Kreye, Heinrich (Bell Telephone Labs., Inc., Murray Hill, N. J.). Z. Mettalk.; 62: No. 5, 441-4(May 1971).

The discontinuous precipitation of the equilibrium γ phase in copper–2 wt % Be is in the range 20 to 50% RA increased due to an increase in the density of the reaction fronts. Additional reaction fronts are formed at deformation bands. In the range 50 to 90% RA the competition with the continuous precipitation of γ in front of the reaction front leads to a decrease in the rate of the discontinuous reaction. After cold work of more than 90% RA no discontinuous precipitation is found. At higher annealing temperatures (470°C) the rate of discontinuous reaction decreases in the range 0 to 20% RA as the mobility of the reaction front is decreased by the presence of larger metastable γ particles. (auth)

35495 CRYSTAL STRUCTURE OF RARE-EARTH ALUMINUM COMPOUNDS R_2Al. Buschow, K. H. J.; van der Goot, A. S. (Philips Research Labs., Eindhoven, Netherlands). J. Less-Common Metals; 24: 117-20(May 1971).

In previous investigations the phase diagrams of most of the rare-earth aluminium systems have been studied. The compounds occurring at the highest rare-earth concentration are of the type R_3Al for the light rare-earth elements and of the type R_2Al for the heavy rare-earth elements. For the elements Pr, Nd, and Sm, the compounds R_2Al occur together with the compounds R_3Al. In general, six intermetallic compounds are observed in each binary R–Al system and apart from the phase R_2Al the structure of these compounds is well established. The x-ray diagrams of these latter compounds could tentatively be indexed with an orthorhombic unit cell containing 10 formula units R_2Al but a structure determination on this basis was not possible. Successful determinations of the crystal structures of the compounds Sc_2Al and Y_2Al led to the reinvestigation of the crystallographic properties of the compounds R_2Al. (auth)

35496 STRUCTURE OF THE COMPOUNDS AG_4Sc, Ag_2Sc, Au_4Sc, Au_2Sc, AND Ag_3YB. Reule, H. (Max-Planck Institut fuer Metallforschung, Stuttgart); Steeb, S.; Donolato, C. J. Less-Common Metals; 24: 108-12(May 1971).

Continuing earlier studies on the structure of the binary alloy phases formed between silver or gold with Group IIIA metals, the phases Ag_4Sc, Ag_2Sc, Au_4Sc, Au_2Sc, and Ag_3Yb were investigated. Starting with the elements Au (99.99 at. %), Ag (99.999 at. %), Sc (main impurities, La, 0.03; Ce, 0.05; Fe, 0.03; Si, 0.02, and Al, 0.02 at. %), and Yb (> 99.0 at. %) the alloys were prepared by arc melting as described previously. After homogenization, powders were produced, annealed at 750°C and finally investigated by x-ray diffraction in a Guinier–de Wolff-type camera with CuKα-radiation. (auth)

35497 METALLURGY AND METALLOGRAPHY OF ZIRCONIUM. pp 18-19 of Engineering Information and Data. Zirconium and Hafnium. Akron, N. Y.: AMAX Specialty Metals Div. (1971).

Aspects of Zr metallurgy are discussed. Information is included on effects of alloying elements on allotropic behavior, properties of Zr alloys, and use Zr as an alloying metal. The metallography of Zr is also reviewed. (J.R.D.)

35498 OCCURRENCE OF SIGMA-TYPE PHASES IN HEAT-RESISTING ALLOYS, WITH SPECIAL EMPHASIS ON THE Co–Cr-W SYSTEM. Barrows, Richard Gridley. Denver; Univ. of Denver (1970). 162p. University Microfilms Order No. 71-8023. Thesis.

Although the Co–Cr–W system is the basis of several commerically important cobalt-base superalloys, the ternary phase diagram has not been well-defined. This phase diagram was determined for cobalt-rich alloys at 1350°C. Experimental alloy compositions were examined by light microscopy, quantitative electron microprobe analysis, x-ray diffraction, and microhardness measurements. In addition to the known σ and μ phases (from existing Co–Cr and Co–W binary diagrams respectively) a previously unreported R-phase was found to be in equilibrium with the fcc α-Co solid solution. This R-phase, with the approximate composition $Co_{23}Cr_{15}W_{15}$, has space group $C_{3i}^{3}-R\bar{3}$ with 159 atoms per hexagonal unit cell, and lattice constants of a_0 = 10.8819 + 0.0004 Å and c_0 = 19.254 + 0.001 Å. The identification of the R-phase was confirmed by the excellent agreement of observed d-spacing and line intensities with data from R-phases known to exist in other alloy systems. The R, μ and σ phases are members of the crystallographically related group of intermetallic structures known as topologically-close-packed (tcp) phases. The precipitation of tcp phases in a high-temperature superalloy is undesirable, since experience has shown that their presence often coincides with deterioration of properties such as stress-rupture life. A new method is proposed for predicting tcp phase stability. It is based on modifications of previous methods which involve electron-vacancy correlations for tcp phase control. The new method has been applied to experimentally determined residual matrix compositions (i.e., the composition of a matrix after all early precipitates have formed) of nickel- and cobalt-base superalloys. It exhibits a greater range of applicability to various austenitic alloy compositions than do current electron-vacancy prediction tools. (Diss. Abstr. Int., B)

35499 AGING BEHAVIOR OF Fe–30 Ni ALLOYS CONTAINING NIOBIUM. Leitch, K.; Chaturvedi, M. (Univ. of Manitoba, Winnipeg). Met. Trans.; 2: No. 5, 1407-13(May 1971).

A study was made of the precipitation reactions in Fe-30 wt % Ni alloys containing up to 5 wt % Nb. The as-quenched structures of these alloys consist of austenite, martensite in twinned as well as in massive form, and Ni_3Nb and Fe_2Nb precipitates. On aging at 700 and 800°C the main precipitation reaction results in the formation of hexagonal Laves phase Fe_2Nb, but Ni_3Nb in both bct and orthorhombic structures also precipitates. The precipitation of Fe_2Nb is a heterogeneous process and results in a considerable increase in the hardness of the alloy. (auth)

35500 RELATIONSHIP OF MICROSTRUCTURE TO WORKABILITY IN A HIGH STRENGTH NICKEL-BASE SUPERALLOY. Oblak, J. M.; Owczarski, W. A.; Duvall, D. S. (Pratt and Whitney Aircraft, Middletown, Conn.). Met. Trans.; 2: No. 5, 1499-1501 (May 1971).

It has been shown that at temperatures above the γ' precipitate solvus (~2070°F) little deformation of the nickel-base superalloy Udimet 700 is possible before fracture occurs by grain boundary separation. On the other hand, if the alloy is first precipitation-aged (to form γ' particles approximately 0.3 μ in size) and then swaged or rolled at 1950°F where the precipitate phase is stable, then large reductions can be routinely accomplished. Metallographic examination of samples prior to and after deformation showed that the microstructures and mode of deformation differed considerably for the two temperature regimes noted above. The results of the structure study are consistent with the hypothesis that fracture occurs during working at temperatures above the γ' solvus because of the relative ease of grain-boundary sliding with a resultant stress concentration and crack initiation at grain-boundary triple lines. In contrast, precipitation of γ' alters the grain-boundary structure and makes it much more resistant to sliding. therefore, stress concentrations at triple lines are greatly reduced. For this reason nickel-base superalloys such as Udimet 700 are more easily worked in the two phase γ-γ' condition. (auth)

35501 ELECTRICAL RESISTIVITY MEASUREMENTS OF DEFORMED METALS AFTER LOW-TEMPERATURE NEUTRON IRRADIATION. Takamura, Saburo (Japan Atomic Energy Research Inst., Tokai); Hanada, Reimon; Okuda, Shigeo. J. Phys. Soc. Jap.; 30: No. 5, 1360-6(May 1971).

The effect of deformation before and after fast neutron irradiation at about 10°K on the recovery spectra of Cu, Al, and Au is studied by measurements of residual resistivity. In Cu specimen deformed at 4.2°K after irradiation, the recovery below 43°K is retarded. But this retardation can not be observed in Al and a small reduction is observed in Au. On the other hand, the stages II and III are enhanced by deformation in all three metals. Two mechanisms are discussed in relation with these observations, namely, the recovery of stage I defects and the transformation of stage I defects through interactions with moving dislocations. (auth)

35502 CO-PRECIPITATION OF $\gamma'(Ni_3Al)$ AND α-Cr IN A NICKEL-BASE ALLOY. Lemaire, L.; Fornwalt, D. E.; Kear, B. H. (Pratt and Whitney Aircraft, Middletown, Conn.). Microstructures; 2: No. 1, 13-16(Dec-Jan 1971).

Co-precipitation of $\gamma'(Ni_3Al)$ and α-Cr in a nickel base superalloy subjected to various heat treatments was studied by transmission electron microscopy and x-ray diffraction. It is demonstrated that nickel-base alloys, containing a large volume fraction of γ' and high Cr levels, are susceptible to precipitation of α-Cr by a microsegregation phenomenon. The phenomenon involves rejection of Cr by the growing γ' particles during cooling through the precipitation temperature range. At the appropriate level of supersaturation α-Cr particles nucleate heterogeneously at γ/γ' interface dislocations and subsequently grow with a 110 platelet morphology. It is also shown that the composition of the extracted γ' changes little with the heat treatment of the alloy, while the quantity of precipitated α-Cr increases with a decrease in the aging temperature. Data reported also indicate the constrained γ/γ' misfit is approximately an order of magnitude less than the unconstrained misfit. (auth)

Radiation Effects

Refer also to abstracts 36270 and 36286.

35503 (HEDL-SA-193) HELIUM PRODUCTION IN STAINLESS STEEL AND ITS CONSTITUENTS AS RELATED TO LMFBR DEVELOPMENT PROGRAMS. McElroy, W. N. (WADCO Corp., Richland, Wash.); Farrar IV, H. (Atomics International, Canoga Park, Calif.). May 1971. Contracts AT(45-1)-2170; AT(04-3)-824. 63p. (CONF-710601-2). Dep. NTIS.

From International conference on radiation-induced voids in metals; Albany, N. Y. (9 Jun 1971).

It is well known that helium can severely limit the ductility of austenitic stainless steels at temperatures greater than half the melting point temperature, and that in the presence of a high fast-neutron flux, helium atoms can serve as void nuclei. As a factor causing dimensional instabilities, void formation has become a critical problem in the development of liquid-metal fast-breeder reactors (LMFBR's). Therefore, the rate of helium production in a fast neutron environment is important. Information on helium production in stainless steel and its constituents to provide a basis for predicting helium generation rates for the correlation and interpretation of irradiation effects data is presented. (auth)

35504 (ORO-3912-4) COMPUTER EXPERIMENT STUDIES ON MECHANISMS FOR IRRADIATION INDUCED DEFECT PRODUCTION AND ANNEALING PROCESSES. Progress Report for Period Ending May 31, 1970. Beeler, J. R. Jr. (North Carolina State Univ., Raleigh). Jun 1970. Contract AT(40-1)-3912. 23p. Dep. NTIS.

Research is reported on a program that attempts to describe primary damage state production and annealing in impure polycrystalline materials during neutron irradiation. Qualitative descriptions are given for 3 new investigations, the evolution of a damage state via the accumulation of independently produced Frenkel Pairs; the stability of void edges and corners; and the effect of impurity atoms on the Frenkel Pair recombination region. (D.H.M.)

35505 (ZJE-99) INFLUENCE OF SOME METALLURGICAL VARIABLES ON THE RADIATION DAMAGE SENSITIVITY OF PRESSURE VESSEL STEELS. Brumovsky, M. (Skoda Concern, Pilsen (Czechoslovakia). Nuclear Power Plants Div.). 1971. 31p. (CONF-700630-2). Dep. NTIS (U. S. Sales Only).

From Symposium on effects of radiation on structural materials; Niagara Falls, Ontario, Canada (29 Jun 1970).

Studies of binary and ternary alloys of Fe–C–Mn type were performed to understand the mechanism of radiation hardening and embrittlement in nuclear reactor low-carbon pressure vessel steels. Results of static tensile tests showed the substantial effect of carbon and manganese contents. Carbon, with respect to pearlite content in alloys, increases the resistance against radiation damage during irradiation at 80 to 100°C, while manganese content higher than 0.5 to 1.0 wt % decreases this resistance. Supersaturation connected with the decrease of yield strength was observed in iron and Fe–C type alloys at neutron doses higher than 5×10^{19} n/cm^2. Influence of the initial yield strength value upon its increase during irradiation was shown for low-carbon steel with various heat-treatment or cold work value. (auth)

35506 IRRADIATION EFFECTS ON THE MECHANICAL PROPERTIES OF REACTOR STRUCTURAL AND CLADDING ALLOYS. Claudson, T. T. (Battelle-Northwest, Richland, Wash.). pp 22-36 of Materials Technology: An Interamerican

XUM

Approach. New York; American Society of Mechanical Engineers (1968).

From Inter-American Conference on Materials Technology, San Antonio, Tex. See CONF-680513.

Recent data are described which relate the effects of environment and irradiation in fast and thermal reactors on the tensile, creep, and creep-rupture properties and fracture characteristics of zirconium, stainless steel, nickel-base alloys and A302-B pressure vessel steels used as reactor structural and cladding materials. Correlations of the material microstructure (as viewed by thin film microscopy) with mechanical property data are made to explain the high temperature hardening and low ductility observed in austenitic stainless steel alloys irradiated in both the EBR-II and ETR facilities. The in-reactor creep properties of cold-worked Zircaloy-2 and heat treated Zr-2.5 wt% Nb alloys were obtained over a 300 to 450°C temperature range and at stress levels to 55,000 psi. These data indicate a region temperature and stress at which the in-reactor creep rate is independent of test conditions. The creep rate of austenitic stainless steel seems to be unaffected by irradiation under the present test conditions. Evidence of both strain-induced and irradiation-induced precipitation of carbide phases is presented and the effects of this metallurgical instability on the stress-to-rupture properties of Hastelloy X-280 are given. Also described are improvements in the stress-rupture life and ductility of this material through preirradiation commercial mechanical/thermal treatments. Efforts are presently being directed toward the development of adequate fracture mechanics specimens for irradiation studies on pressure vessel materials. Presented are data, obtained using a double cantilever beam (DCB) specimen, which show the effects of neutron irradiation, material microstructure, and environment on the fracture toughness (K_{I_c}) of A302-B pressure vessel plate material. (auth)

35507 RADIATION HARDENING AND RADIATION-ANNEAL HARDENING IN BODY-CENTERED CUBIC METALS. Ohr, S. M. (Oak Ridge National Lab., Tenn.); Wechsler, M. S.; Chen, C. W.; Hinkle, N. E. pp 742-6 of Second International Conference on the Strength of Metals and Alloys, Pacific Grove, California, 30 August–4 September 1970. Vol. II. Metals Park, Ohio; American Society for Metals (1970).

From second international conference on the strength of metals and alloys; Pacific Grove, Calif. (Aug-Sep 1970). See CONF-700819– (Vol.2).

Aspects of radiation hardening in bcc metals are described. Radiation effects on the relations between yield stress and temperature is examined along with radiation-anneal hardening. It was found that higher radiation doses are necessary in less pure single crystals and polycrystals before effective barriers become active at short range. Radiation-anneal hardening in bcc metals appears to be due to the motion of interstitial impurities. (J.R.D.)

35508 MODEL FOR THE EMBRITTLEMENT AND ANNEALING OF IRRADIATED STEEL. De Meester, P. (Katolieke Univ., Louvain, Belg.). pp 752-7 of Second International Conference on the Strength of Metals and Alloys, Pacific Grove, California, 30 August–4 September 1970. Vol. II. Metals Park, Ohio; American Society for Metals (1970).

From second international conference on the strength of metals and alloys; Pacific Grove, Calif. (Aug-Sep 1970). See CONF-700819– (Vol.2).

Radiation effects on Type A302B steel tested in BR3/Vulcain reactor are reported. Irradiation at various fluences and subsequent annealing treatments were performed on specimens of the same heat. A comparison of existing hypotheses on radiation-induced change in mechanical properties of steel is included. (J.R.D.)

35509 EFFECTS OF FAST NEUTRON IRRADIATION ON THE TENSILE PROPERTIES OF AUSTENITIC STAINLESS STEELS. Bloom, E. E.; Stiegler, J. O. (Oak Ridge National Lab., Tenn.). pp 768-72 of Second International Conference on the Strength of Metals and Alloys, Pacific Grove, California, 30 August–4 September 1970. Vol. II. Metals Park, Ohio; American Society for Metals (1970).

From second international conference on the strength of metals and alloys; Pacific Grove, Calif. (Aug-Sep 1970). See CONF-700819– (Vol.2).

Results of radiation testing to determine the changes in tensile properties of due to irradiation at 600 to 800°C are reported. Tensile specimens of Type 304 stainless steel were irradiated in EBR-II. Tensile and microstructural observations and measurements were made which were in qualitative agreement. Discussions are included on radioinduced defects and results of tensile measurements. (J.R.D.)

35510 EFFECTS OF THERMAL AGING AND NEUTRON IRRADIATION ON INCOLOY 800. Harman, D. G. (Westinghouse Electric Corp., Tampa, Fla.). pp 778-82 of Second International Conference on the Strength of Metals and Alloys, Pacific Grove, California, 30 August–4 September 1970. Vol. II. Metals Park, Ohio; American Society for Metals (1970).

From second international conference on the strength of metals and alloys; Pacific Grove, Calif. (Aug-Sep 1970). See CONF-700819– (Vol.2).

Results of radiation testing of Incoloy 800 at 350 to 700°C in ORR are reported. The Ti content of the Incoloy specimens was varied and controlled along with the content of Al and C. It was found that Ti improves Incoloy 800 resistance to irradiation damage and that further ductility improvements can be obtained by treating to finer grain sizes. The importance of grain boundary freedom from impurities was confirmed. (J.R.D.)

35511 VOID FORMATION DURING IRRADIATION. Wiedersich, H. W. (North American Rockwell Corp., Thousand Oaks, Calif.). pp 784-8 of Second International Conference on the Strength of Metals and Alloys, Pacific Grove, California, 30 August–4 September 1970. Vol. II. Metals Park, Ohio; American Society for Metals (1970).

From second international conference on the strength of metals and alloys; Pacific Grove, Calif. (Aug-Sep 1970). See CONF-700819– (Vol.2).

Aspects of radioinduced void growth in materials are discussed. Attention is directed to the steady state conditions which develop in materials under irradiation for specified initial structural states, and the growth of voids and dislocation loops under steady state conditions. Results of analysis of crystal incorporation or recombination with opposites for point defects, interstitials, or vacancies conducted using rate equations are summarized along with results of similar analyses of sink annihilation. (J.R.D.)

35512 RADIATION-ENHANCED DIFFUSION IN THE Au–Ag SYSTEM. Spreng, Daniel Theodor. Evanston, Ill.; Northwestern Univ. (1970). 82p. University Microfilms Order No. 71-10,194. Thesis.

Interdiffusion was measured in a Au–Ag alloy during electron irradiation at ~90°K and during subsequent warm-up to room temperature. The diffusivities were determined from the rate of decay of composition modulations (of 10–20Å wave-length) in vapor-deposited films. The rate of decay was measured by x-ray diffraction and electrical resistivity. At an irradiation energy of 2.0 MeV and a flux of 2 $\mu A/cm^2$ an interdiffusion coefficient $\tilde{D} = 1.5 \times 10^{-22 \pm 0.5}$ cm^2/sec was observed in a 37 Au-63 Ag alloy. The results are consistent with the hypothesis that interstitialcies migrate during irradiation at ~90°K. Between 90 and 420°K, isochronal anneals of irradiated samples showed a single annealing stage in which interdiffusion occurred. This stage located at about 250°K and extending over 40 degrees is due to vacancy migration, the activation energy being (0.63 ± 0.05) eV. The amount of diffusion during irradiation was about half of that during subsequent warm-up to room temperature. (Diss. Abstr. Int., B)

35513 INFLUENCE OF IRRADIATION ON CORROSION. Morozumi, Takashi (Hokkaido Univ., Sapporo). Boshoku Gijutsu: 18: 512-19(Dec 1969). (In Japanese).

The effects of radiation on the corrosion of nuclear materials are reviewed. The relation between the radiation of various kinds and the effect is discussed. Radiochemical effects on corrosion are also discussed. Corrosion in the in-pile environment, mainly the corrosion of zirconium and its alloys, is described in detail. Corrosion in solutions where nuclear fission reactions exist is described. Nuclear fission reactions accelerate corrosion. The effects of radiation on corrosion by hot water are also described. High-temperature water corrosion is generally accelerated by radiation. Several theories on the acceleration effect of irradiation on corrosion are introduced. The effect of irradiation on hydrogen absorption is reviewed. Radiation-enhanced corrosion in plants for nuclear fuel reprocessing is described. (Japan)

35514 DISLOCATION-PINNING MEMORY-EFFECT IN γ-IRRADIATED AND STRESS-ANNEALED COPPER. Lenz, D.; Edenhofer, B.; Luecke, K. (Technische Hochschule, Aachen). Scr. Met.; 5: 387-94(May 1971).

The action of external shear stress on dislocations pinned by point defects or point defect clusters in irradiated Cu to cause the defects to be torn loose from their pinning points was investigated. Results indicate that by a suitable stress-annealing treatment, well defined dislocation pinning point configurations can be produced which subsequently cause dips in the measured $\alpha-\tau$ curves. This memory-effect always appears with fresh dislocations (torn away or newly created dislocations) and, at the same time, point defects which are able to diffuse to these dislocations and form pinning points there. The break-away of the dislocations from their pinning points is connected with a loss of stability of these now free pinning points. (J.R.D.)

XUM

35515 EXPLOSION-LIKE PROCESSES DURING IMPULSED TREATMENT OF MATERIALS BY ELECTRON BEAMS. Noskov, D. A.; Pankovets, N. G. Fiz. Khim. Obrab. Mater.; No. 4, 16-20(Jul-Aug 1970). (In Russian).

Processes for removing substances by the intensive impulse bombardment of solids are discussed. The removal of substances by the beam has explosion-like characteristics. In most metals, the thermal explosion results in metal spallation during which metal is thrown out from the point of bombardment in the form of fine drops. The processes which occur during the bombardment of ceramics, diamonds, and glasses are described. (R.V.J.)

35516 STUDY OF VOID FORMATION IN FAST NEUTRON-IRRADIATED METALS. Harkness, S. D.; Li, Che-yu (Argonne National Lab., Ill.). Met. Trans.; 2: No. 5, 1457-70(May 1971).

Experimental observations on the temperature dependence of void formation in Type 304 stainless steel are presented. The average void size is seen to increase while the void number density decreases with increasing irradiation temperature. The total void volume reaches a maximum at an intermediate temperature (~500°C). A thermodynamically based model for void formation was developed in an effort to understand these and other experimental observations. The model is a quasi-steady-state approach that attempts to describe the void and dislocation loop nucleation and growth rates as a function of temperature, neutron flux, and type and density of point-defect sinks. The model was written in the form of a computer routine which iterates over small time steps and is fitted to experimental observations of void formation in irradiated austenitic stainless steel by adjustment of material constants within reasonable limits. Good agreement was obtained for a wide range of experimental results. Development of the model has emphasized that some kind of preferential attraction between one type of sink and one type of point defect is necessary in order for void growth to occur. The preferential attraction suggested is that between the stress field of a dislocation and the misfit strain of an interstitial. The model also pointed out the necessity of separating the neutron flux and time of irradiation when reporting information on void formation. It is expected that quite different dependences of void size and number density on the total neutron dose would be obtained depending on whether the experimental information was obtained under constant flux or under constant time conditions. It was also concluded that the magnitude and temperature dependence of dislocation loop formation would have a marked effect on void formation. (auth)

35517 ELECTRON BOMBARDMENT OF NIOBIUM CONTAINING INTERSTITIAL IMPURITIES. Igata, N. (Tokyo Univ.); Kohyama, A.; Dollins, C. C. Met. Trans.; 2: No. 5, 1490-1(May 1971).

The interaction between solute nitrogen or oxygen atoms and simple point defects in electron irradiated niobium and the relation between yield stress and irradiation induced complex defects were investigated. At room temperature an interstitial niobium atom migrates to an interstitial impurity atom and produces a complex defect. These complex defects are destroyed at about 230°C, a slightly lower temperature than in the case of neutron irradiation. This is due either to thermally activated unbonding between the interstitials or to annihilation of a self interstitial and a vacancy. There is little difference between a nitrogen atom and an oxygen atom in ability to bind an interstitial niobium atom. The hardening and its recovery corresponds to the behavior of the complex defects. (auth)

35518 ELECTRON MICROSCOPE INVESTIGATIONS OF THE DISLOCATION ARRANGEMENT OF DEFORMED COPPER SINGLE CRYSTALS IN THE STRESS-APPLIED STATE. III. A COMPARISON OF SOME CHARACTERISTIC QUANTITIES OF THE DISLOCATION STRUCTURE IN THE STRESS-APPLIED AND STRESS-REMOVED STATES. Mughrabi, H. (Max-Planck-Institut fuer Metallforschung, Stuttgart). Phil. Mag.; 23: 931-47(Apr 1971). (In German).

Copper single crystals oriented for single glide were deformed in tension at 78°K and irradiated before load-removal with fast neutrons at 4 or 20°K. It was shown in two preceding papers (Mughrabi 1971) that the dislocation arrangements of these crystals which were thus stabilized in the stress-applied state differ in stages I and II from the dislocation arrangements of similarly deformed crystals irradiated in the unloaded state. The dislocation densities in the stress-applied and stress-removed states, as determined by electron microscopy, are compared. It is found that in both cases in stage II the primary dislocation density ρ_p increases linearly with flow stress τ whereas the secondary dislocation density ρ_s increases quadratically with τ and that the dislocation densities are of comparable magnitude in the stress-applied and in the unloaded state. The density of free primary dislocations, however, is about twice as large in the stress-applied state (where a substantial number of primary dislocation groups are observed) as in the unloaded state. It is suggested that the linear increase of ρ_p with τ may be explained in part by taking into account that deformation occurs not only by the glide of newly generated dislocations but also by the glide of the existing dislocations. The densities of free primary dislocations can be used to estimate the reversible and irreversible contributions to reverse dislocation glide upon unloading and the corresponding elastic modulus defects in the stress-applied and in the unloaded states. The results are in qualitative agreement with other investigations. (auth) (UK)

35519 ELECTRON MICROSCOPE INVESTIGATIONS OF THE DISLOCATION ARRANGEMENT OF DEFORMED COPPER SINGLE CRYSTALS IN THE STRESS-APPLIED STATE. II. THE DISLOCATION ARRANGEMENT IN STAGE II. Mughrabi, H. (Max-Planck-Institut fuer Metallforschung, Stuttgart). Phil. Mag.; 23: 897-929(Apr 1971). (In German).

Copper single crystals orientated for single glide were deformed in tension at 78°K and irradiated before load-removal with fast neutrons at 4 or 20°K. The dislocation arrangement which was thus stabilized in the stress-applied state was investigated extensively by transmission electron microscopy and compared with the results of corresponding investigations on unloaded crystals. In stage II dislocation braids and dislocation grids (sheets) were observed both in the stress-removed and the stress-applied states. Groups of primary dislocations of the same sign, however, are a representative feature of the dislocation arrangement in the stress-applied state only. It is concluded from the observations that the grids are formed by secondary slip at the head of piled-up groups and are capable of growth. The observed spatial change in the curvature of free primary dislocations in the stress-applied state points directly to the existence of a quasi-periodic long-range internal stress field whose amplitude is of the order of the applied stress and whose wavelength is closely correlated to the number of dislocation groups. A quantitative analysis of the observed dislocation groups is in fair agreement with the long-range stress theory of work-hardening in stage II. (auth) (UK)

35520 ELECTRON MICROSCOPE INVESTIGATIONS OF THE DISLOCATION ARRANGEMENT OF DEFORMED COPPER SINGLE CRYSTALS IN THE STRESS-APPLIED STATE. I. THE DISLOCATION ARRANGEMENT AT THE END OF STAGE I. Mughrabi, H. (Max-Planck-Institut fuer Metallforschung, Stuttgart). Phil. Mag.; 23: 869-95(Apr 1971). (In German).

Copper single crystals oriented for single glide were deformed in tension at 78°K and irradiated before load-removal with fast neutrons at 20°K. The dislocation arrangement which was thus pinned in the stress-applied state was investigated by transmission electron microscopy and compared with the results of corresponding investigations on unloaded crystals. In the stress-applied state, in stage I, the majority of the dislocations are primary dislocations which frequently form dipoles and planar multipoles. Free primary dislocations are usually curved, the curvature corresponds to the applied stress. Some isolated screw dipoles which were retained by virtue of the pinning at low temperatures were also observed. Mechanisms of microscopic cross-slip are discussed. It is concluded from the observations that the work-hardening in stage I is due primarily to the short-range elastic interaction between primary dislocations of opposite sign. The dislocation reactions which initiate the transition to stage II are discussed. (auth) (UK)

Ceramics and Cermets

Corrosion and Erosion

Refer also to abstracts 34826, 35390, and 35395.

35521 CORROSION BEHAVIOR OF ALUMINUM–BORON COMPOSITES IN AQUEOUS CHLORIDE SOLUTIONS. Sedriks, A. J.; Green, J. A. S.; Novak, D. L. (Martin Marieta Corp., Baltimore). Met. Trans.; 2: 871-5(Mar 1971).

A study was made of the corrosion behavior of diffusion bonded 2024 aluminum alloy–unidirectional boron filament composites in aqueous chloride solutions. Compared with the 2024 alloy, the composites suffer greater localized corrosion, both in the presence and absence of applied stress, when the environment is in contact with transverse section surfaces (i.e., surfaces containing exposed boron filament ends and diffusion bonds). The electrochemical behavior of such surfaces indicates that the lowered corrosion resistance is not due to galvanic action between the filament and matrix, but results from an increase in the number of anodic sites, the latter being associated with the filament-matrix interfaces and the diffusion bonds between the alloy foils. (auth)

XUM

35522 CHEMICAL PROPERTIES OF NITRIDES OF SOME TRANSITION METALS. Lyutaya, M. D.; Kulik, O. P. (Inst. of Materials Science, Kiev). Sov. Powder Met. Metal Ceram. (Engl. Transl.); No. 10, 821-6(Oct 1970).

Translated from Porosh. Met., Akad. Nauk Ukr. SSR; No. 10, 48-54(Oct 1970).

To obtain a basis for comparison of the chemical stability of nitrides of some transition metals in liquid aggressive media, data on the stability of the metals in the same reagents are given. The chemical stability is given for the nitrides in water, alkali solutions, and acids. The decomposition rate for the nitrides is given. (D.P.O.)

Preparation and Fabrication

Refer also to abstracts 34556, 34782, 35290, and 35373.

35523 (AECL-3462) FABRICATION AND BURST TESTING OF REACTION-BONDED SILICON CARBIDE TUBES. Phillips, E.; Hutchings, W. (Atomic Energy of Canada Ltd., Pinawa (Manitoba). Whiteshell Nuclear Research Establishment). Feb 1971. 51p. Dep. NTIS (U. S. Sales Only). AECL $1.50.

The fabrication of silicon carbide discs, rods, tubes, and slabs by reaction-bonding is described. The effects of silicon carbide particle size, graphite type and content, and fabrication pressure on the ease and uniformity of silicon impregnation during reaction-bonding are discussed. Microstructures and hoop tensile strengths obtained from hydrostatic burst tests on reaction-bonded tubes are presented and compared with results obtained with commercially available reaction-bonded tubes. The best WNRE tubes had an average grain size of 5 μm, contained less than 10 wt % free silicon and broke at an average hoop tensile stress of 21,800 lbf/in^2. (auth)

35524 (RT/ING-(70)22) UTILIZATION OF VIBRATIONAL COMPACTION FOR NUCLEAR FUEL. Ferrari, S.; Giaquinto, L.; Petrucciani, N. (Comitato Nazionale per l'Energia Nucleare, Rome (Italy)). 2 Oct 1970. 29p. (CONF-700556-4). Dep. NTIS (U. S. Sales Only).

From Italian-Polish meeting; Warsaw, Poland (26 May 1970).

The first attempts of utilizing vibrational compaction technique in the field of nuclear energy began about ten years ago. From that time, this technique has been developed so as to represent an alternative to the most traditional and characteristic processes of powder metallurgy, such as pelleting and sintering. In the vibrational compaction technique a great importance must be attributed to the preparation of dense material. The application of the method to some types of dense oxides is discussed. Also, an original process for the preparation of UO_2, whose in-pile tests are in progress, is described. (auth)

35525 LAWS OF FORMATION OF SINGLE CRYSTALS OF SOLID SOLUTIONS OF BINARY RARE-EARTH OXIDES, GROWN BY THE VERNEUIL METHOD. Popova, A. A. (Inst. of Crystallography, Moscow). Sov. Phys.-Cryst. (Engl. Transl.); 15: No. 6, 1060-4(May-Jun 1971).

Translated from Kristallografiya; 15: No. 6, 1214-18(Nov-Dec 1970).

Some results are given of an investigation of binary systems of rare-earth sesquioxides of a nonisostructural series. The oxides used are: La_2O_3, Nd_2O_3, Sm_2O_3, Gd_2O_3, Dy_2O_3, Ho_2O_3, Er_2O_3, Tm_2O_3, and Yb_2O_3. The regions of formation of single crystals of solid solutions of the A, B, and C structural types are determined. (auth)

35526 MULTISPECIMEN HOT PRESSING OF UO_2. Dusek, J. T.; White, G. D.; de Freitas, C. Trench (Argonne National Lab., Ill.). pp 133-5 of Materials Technology: An Interamerican Approach. New York; American Society of Mechanical Engineers (1968).

From Inter-American Conference on Materials Technology, San Antonio, Tex. See CONF-680513.

A procedure for multispecimen hot pressing of urania disks was developed as a preliminary step in manufacturing $(U_{0.8}Pu_{0.2})O_2$ fuel plates for the Zero Power Plutonium Reactor (ZPPR). Hot pressing is a technique which is generally used to produce a small number of pieces, and is feasible for large production only if several specimens can be pressed at one time. The technique is amenable to close dimensional control and produces specimens having a fine grained structure. Pressings of five specimens each were made at 1400, 1500, and 1625°C, and one pressing of eleven specimens was made at 1625°C. Density variation of specimens within one pressing was approximately 0.5%. Specimen densities over the range of temperatures were from 76.2 to 88.9% of theoretical. Plate thickness was maintained within ±0.005 of an inch, and the diameters were maintained within a smaller tolerance. Carbon pickup was from 165 to 508 ppM on the as-pressed specimens, which, after a hydrogen anneal at 1550°C, contained from 25 to 44 ppM carbon. Photomicrographs are presented to show the difference in reaction of the UO_2 with two grades of graphite mold. (auth)

35527 SOME NUCLEAR DEVELOPMENTS IN ARGENTINA. Araoz, C.; Biondo, C. D.; Martinez Vidal, C. A. (Atomic Energy Commission, Buenos Aires). pp 144-50 of Materials Technology: An Interamerican Approach. New York; American Society of Mechanical Engineers (1968).

From Inter-American Conference on Materials Technology, San Antonio, Tex. See CONF-680513.

Some technological developments in the field of nuclear materials at the Atomic Energy Commission of Argentina are described in the following examples of fuel element fabrication. An extrusion method was developed for RA-1 reactor Argonaut type plates with a U_3O_8-Al core fuel, 20% enriched. The picture frame technique was used and the rolling procedure is described for the fabrication of the core for the RA-3 reactor. This is a 5000 MW, water-cooled reactor with MTR-type 90% enriched fuel. U-Al master alloy for this core was prepared in a one step operation from UF_6. This method of direct reduction of UF_6 with molten Al is described. The second and third core fabricated for the RA-1 reactor, where power was raised to 100 kW, consists of a 75% UO_2-25% core rod clad with Al. Conversion of UF_6 to UO_2 and the extrusion method are described. Due to the small amount of fuel elements to be fabricated, emphasis was put on the development of techniques which need a minimum of capital investment. A well trained basic team was engaged to deal with this problem. In some cases non-traditional solutions were found. (auth)

35528 TECHNIQUES FOR THE FABRICATION OF HIGH-STRENGTH, HIGH-MODULUS, LOW-DENSITY FILAMENT-REINFORCED METAL MATRIX COMPOSITES. Alexander, J. A.; Cunningham, A. L.; Withers, J. C. (General Technologies Corp., Reston, Va.). pp 301-7 of Materials Technology: An Interamerican Approach. New York; American Society of Mechanical Engineers (1968).

From Inter-American Conference on Materials Technology, San Antonio, Tex. See CONF-680513.

Metal matrix composite materials are demonstrated to exhibit mechanical properties which are two to four times those of conventional structural alloys on a density-normalized basis. Various techniques for the fabrication of high-performance sheet, plate, rod, tape, and surface-of-revolution forms of composite materials are discussed together with representative mechanical properties. The experimental achievement of predicted strength and modulus is demonstrated for the most advanced composite system, hot-pressed Al-B. Strength retention at 500°F is excellent with the 100-hour stress-rupture life at that temperature exceeding 100,000 psi. In fatigue, the material shows a 10^7 cycle life at a combined stress in excess of 100,000 psi at both 70° and 500°F. The most obvious applicational possibilities from a property, form, and economic standpoint are discussed. The presentation serves as a summary of what can be achieved now in composite materials. (auth)

35529 FABRICATION AND PROPERTIES OF LANTHANIDE TUNGSTATES. Millet, J. (Electricite de France, Paris); Provost, G. Bull. Soc. Fr. Ceram.; No. 89, 47-53(Oct-Dec 1970). (In French).

The tungstates studied in the research on electrically conducting electrodes for MHD nozzles were those with a fusion point above 1700°C. The synthesis, sintering, and corrosion resistance to potassium salts of the selected lanthanide tungstates were studied. The investigation of thermal expansion and electrical resistivity was made up to 1500°C with two materials: $3Er_2O_3 \cdot WO_3$ and $3Y_2O_3 \cdot WO_3$. (France)

35530 REINFORCED ABLATIVE COMPOSITES FOR EXTREME ENVIRONMENTS. Speyer, Fred B. SAMPE; 2: No. 2, 12-17(Jan 1971).

A concept of in-situ carbiding in ablative composites has been prognosticated and by combining an organo-metallic synthesis with a composite fabrication process, extreme environmental material properties have been accomplished. Refractory metal carbides have been formed within the fiber bundles of graphite cloth and throughout the fiber bonding matrix of laminate molded, pyrolyzed and carburized composites. Refractory metal alkoxide and glykoxide solutions were prepared and used to saturate graphite cloth. The saturated cloth, after heat treating to provide polymetalloxanes within the fiber bundles, was impregnated with phenolic resin and laminate molded into composites. Carburized composites were also fabricated using refractory metalhydride dispersed phenolic resin matrices. Phrolyzation, reimpregnation (densification) and carburization of the composites were per-

XUM

formed. Resultant (graphite-refractory metal carbide-carbon) composites were machined into test specimens, plasma flame treated and evaluated for high temperature, oxidation erosion resistance. (auth)

35531 FORMATION PROCESS OF WC–TiC POWDER. Hara, Akio; Miyake, Masaya (Sumitomo Electric Industries Ltd., Itami, Japan). Funtai Oyobi Funmatsuyakin; 17: No. 5, 206-13 (Jan 1971). (In Japanese).

The mechanism of formation of (W-Ti)C powder, one of the most important raw materials for cemented carbides, was studied by microscopy, x ray and XMA analyses. Various combinations of starting powders, i.e., W, WC, TiO_2, TiC, and carbon black, were used. Coarse powders were used for optical microscopic observations. The results obtained were as follows: (1) for all combinations of starting powders, the dissolution of W and Ti began after W had almost changed to WC. When TiO_2 was used as a starting powder, the formation of solid solution was assumed to begin at the temperature where TiC was formed from TiO_2. (2) With an increase in the heating temperature, (W-Ti)C was formed at the surface of WC particles, and the carbide particles showed shell structure of (W-Ti)C as observed in the cross sections. (3) The mechanism of formation of (W-Ti)C in the solid state reaction was considered as follows; Ti(TiC) diffuses on the surface of the WC particle very rapidly and reacts with WC on the particle surface. The reason for such rapid diffusion of Ti(TiC) on the carbide surface was discussed. (4) When the carbide particle with WC in the core was heated with cobalt above the eutectic temperature, the WC that remained as a result of insufficient diffusion in the solid solution reaction, dissolved into the liquid eutectic and W diffused into TiC from the surface. As a result, (W-Ti)C phase formed in the shape of ring around TiC particle. (auth) (Japan)

35532 9th INTERNATIONAL GEL PERMEATION CHROMATOGRAPHY SEMINAR, MIAMI BEACH, FLORIDA, OCTOBER 4–7, 1970. Almquist, Ph. W.; Lederer, M.; Macek, K. (eds.). J. Chromatogr.; 55: 1-220(17 Feb 1971). (CONF-701045).

Twenty-six papers were presented at the conference. A separate abstract was prepared for each of two papers. The remaining 24 papers are concerned with various applications of gel permeation chromatography that are not within scope of NSA. (R.C.K.)

For abstracts of individual papers see: 34626 and 35533.

35533 USE OF GEL PERMEATION CHROMATOGRAPHY IN THE DEVELOPMENT OF HIGH-QUALITY GRAPHITE. Dickinson, J. M.; Wewerka, E. M. (Los Alamos Scientific Lab., N. Mex.). J. Chromatogr.; 55: 25-31(17 Feb 1971).

From ninth international gel permeation chromatography seminar; Miami Beach, Fla. (4 Oct 1970). See CONF-701045.

Many graphites to be used for nuclear, aerospace or high-temperature applications are now being made with synthetic components rather than with the traditional mixtures of coke filler and pitch binder. This additional control of raw materials results in a higher quality and more reproducible graphite. One class of synthetic polymers finding considerable use as graphite binder materials is furfuryl alcohol resins. The molecular size distributions of furfuryl alcohol resin binders as determined by gel permeation chromatography have been shown to play an important role in determining the physical properties of the resulting graphites. Gel permeation chromatographic data were related to graphite physical properties by two methods. In the first, the amount of material in a given molecular size interval was computed, and the effect of each size interval on the properties of graphite was determined using a graphical method. Secondly, the total molecular size distribution was then related to the physical properties of graphite by a statistical method, which was used to calculate parameters describing the gel permeation chromatographic data. The results of these studies have led to a more thorough understanding of the role played by furfuryl alcohol resins as related to their use in the manufacture of graphites, and to specifications for the synthesis of an improved furfuryl alcohol resin for use as a graphite binder material. (auth)

35534 EXPERIMENTAL STUDY ON THE SINTERING OF TUNGSTEN CARBIDE POWDER WITH VARIOUS METAL BINDERS. Choi, Hyung Sup; Kee Soon. J. Korean Inst. Metals; 6: No. 1, 9-14(1968).

The tungsten carbide powder was sintered with various metal binders in order to get the necessary information for the manufacture of tungsten carbide tips. The experimental results showed that a good quality of sintered product was obtained when the tungsten carbide powder, mixed with cobalt powder, was pressed at a pressure of 5 ton/cm^2 and sintered at 1350°C for 2 hours. However, the quality of product, using iron or nickel powder as a binder instead of cobalt, was not satisfactory. It is also found that the properties of sintered product, obtained using various binders, seem mainly to result from the characteristics of grain growth caused by solution and precipitation phenomena during sintering. (Korean Sci. Abstr.)

35535 RECRYSTALLIZATION OF HIGH-MELTING CARBIDES. Samsonov, G. V.; Boschko, S. A. Planseeber. Pulvermet.; 18: 166-77(Sep 1970). (In German).

The secondary recrystallization of titanium, zirconium, and niobium carbides within their homogeneity ranges was investigated on loose powders and on hot-pressed specimens following strain hardening by grinding. The activation energies of these processes as a function of the carbon deficiency of the carbide lattice were determined. The results are discussed on the basis of the known electronic structure of these carbides. (auth)

35536 STUDIES ON THE FORMATION PROCESS OF TUNGSTEN CARBIDE POWDER FROM TUNGSTEN POWDER. Hara, Akio; Miyake, Masaya (Sumitomo Electric Industries, Ltd., Itami, Japan). Planseeber. Pulvermet.; 18: 91-110(Jun 1970).

In order to study the formation process of WC powder for cemented carbide from tungsten powder, the cross section and the surface state of the powder carburized at temperatures between 1000 and 1900°C were observed with microscopes. Relations in microstructure between the WC powder and the cemented carbide were studied. The coarse WC powder which is carburized from coarse W powder often has grain boundaries in its particles. The WC crystal size in the cemented carbide depends on the single crystal size in the particle. The single crystal size increases with an increase in the carburization temperature. Carbon diffuses inward from the periphery of the W particle and three phases of WC, W_2C, and W are formed at the initial stage of carburization. Grain growth by sintering is observed in the case of fine W powder but is rarely observed in the case of coarse W powder. (auth)

35537 FORMATION PROCESS OF (W,Ti)C POWDER. Hara, Akio; Miyake, Masaya (Sumitomo Electric Industries, Ltd., Itami, Japan). Planseeber. Pulvermet.; 18: 227-45(Dec 1970).

The mechanism of formation of (W, Ti)C powder, one of the most important raw materials for cemented carbides, is not yet elucidated. A study of the mechanism utilized microscopic observation, x-ray, microprobe, and carbon analysis. Various combinations of starting powders, i.e., W, WC, TiO_2, TiC, and carbon black, were used. For optical microscopic observation coarse powders were used. With any combination of starting powders, the solid solution reaction of W and Ti began after W had almost changed to WC. Where TiO_2 was used as a starting powder, the solid solution reaction was assumed to begin at the temperature where TiC was formed from TiO_2. With an increase in the heating temperature, (W, Ti)C was formed at the periphery of a WC particle, and one result was that in the cross section the carbide particle showed a ring structure of (W, Ti)C. The formation mechanism of (W, Ti)C in the solid state reaction appears as follows; Ti(TiC) diffuses on the surface of the WC particle very rapidly and reacts with WC on the particle surface. The reason for such rapid diffusion of Ti(TiC) on the carbide surface is discussed. When the carbide particles with WC in the core were heated with cobalt above the eutectic temperature, the WC which remained as the result of insufficient diffusion in the solid state dissolved into the liquid eutectic and W diffused into TiC from the periphery. As a result (W, Ti)C phase formed in the shape of a ring around the TiC particle. (auth)

35538 PHYSICAL PROPERTIES OF PLASMA-SPRAYED CARBIDES. Zil'berberg, V. G.; Kutsenok, T. G.; Sharivker, S. Yu. Fiz. Khim. Obrab. Mater.; No. 4, 49-52(Jul-Aug 1970). (In Russian).

The electroconductivity and coefficients of thermal expansion of sprayed Nb and Zr carbides were studied at temperatures to 1000°C. It was shown that the properties of the sprayed materials are identical to the properties of sintered materials with the exception of the electroconductivity of ZrC. (R.V.J.)

35539 MICROSPHERES. (to W. R. Grace and Co.). British Patent 1,224,012. 3 Mar 1971. Priority date 13 Jun 1967, United States.

A process is described for forming microspheres from aqueous feeds containing particles of UO_2, UO_3, ThO_2, PuO_2, PuO_3, ZrO, Y_2O_3, rare earth oxides, BeO, or mixtures of these compounds. Colloidal carbon may also be incorporated. The feed is dispersed in droplets by ultrasonic vibration. (J.R.D.)

35540 URANIUM–SILICON FUEL ELEMENTS FOR A NUCLEAR REACTOR. Feraday, Melville Albert (to Atomic Energy of Canada Ltd.). U. S. Patent 3,567,581. 2 Mar 1971. Filed 4 Jun 1968.

XUM

A nuclear reactor fuel element using delta phase (U_3Si) uranium–silicon alloy to provide a low aqueous corrosion rate together with low parasitic neutron absorption is described. The nuclear fuel is provided with a central hollow core or uniformly dispersed porosity or a combination of both having a volume in the range 3 to 25% of the volume of the core and sheathed width corrosion-resistant material. (Official Gazette)

35541 PREPARATION OF ^{241}Pu OXIDE SAMPLES FOR NEUTRON CROSS SECTION MEASUREMENTS. Del Bino, G.; Lauer, K. F.; Verdingh, V. (Central Bureau for Nuclear Measurements, Geel, Belg.). Nucl. Instrum. Methods; 93: No. 2, 205-9(1971).

A description of the preparation of samples of $^{241}PuO_2$ for several types of neutron cross section measurements is given. The experimental set-up including the chemical treatment, the purification, the preparation of the samples, the vacuum canning, and the decontamination as well as the yield and quantitativity is outlined. (auth)

35542 METHOD FOR PRODUCING TEMPERATURE SENSITIVE RESISTOR COMPRISING VANADIUM OXIDE. (to Hitachi Ltd.). British Patent 1,168,107. 22 Oct 1969. Priority date 14 Sep 1966, Japan.

A method is described for making a thermistor or a thermally sensitive resistor that has a large negative temperature coefficient of resistance in a particular temperature range. A mixture of V_2O_5 and another oxide is crushed and heated at about 400°C in a reducing atmosphere with the result that the mean value of the O/V ratio of the mixture is between the true stoichiometric values of V_2O_5 and V_2O_4. The mixture is formed into a desired shape and sintered at 1000 to 1300°C. (G.M.C.)

35543 TRANSPARENT THORIA-BASE CERAMICS CONTAINING Y_2O_3 AND METHOD FOR PRODUCING SAME. Anderson, Richard C. (to General Electric Co.). U. S. Patent 3,574,645. 13 Apr 1971. Filed 17 Mar 1969.

The preparation of high density thoria-base ceramic bodies containing up to about 5 mole percent of Y_2O_3 is disclosed. These bodies have high orders of in-line transmission of light and are prepared by pressing the mixed powders and sintering in a hydrogen-water vapor atmosphere until theoretical density is achieved. (auth)

35544 MANUFACTURING OF FUEL ELEMENTS FOR THE THTR AND AVR REACTORS. Hackstein, K. G. (NUKEM Nuklear-Chemie und -Metallurgie GmbH, Hanau, Ger.). Atomwirt., Atomtech.; 16: 245-6(May 1971). (In German).

Although the type of fuel elements is common to both reactors, the THTR in comparison with the AVR requires significant changes in the production process. Annual recharging of fuel elements in the THTR lies higher by a factor of 10, and that of heavy metals nearly by a factor of 20. Consequently, more components must be produced which necessitates a continuous manufacturing process with large scale automation. In addition, automatic controls of intermediate and final products become necessary. With establishment of this production line, a significant step toward large scale production will be achieved. (tr-auth)

35545 REGULARITY IN THE FORMATION OF SOLID SOLUTIONS OF OXIDES IN ZnO_2–MeO_n SOLUTIONS. Leonov, A. I. Zh. Neorg. Khim.; 16: No. 2, 295-300(Feb 1971). (In Russian).

Properties of solid solutions of oxides may be predicted from such physico-chemical constants of the parent oxides as their ionization potentials, cation dimensions, and melting points. This technique was applied to solid solutions of ZrO_2 in Groups I to VIII oxides of the periodic system. Perfect isomorphism was apparently conditional upon both cation dimensions and their electric fields. (tr-auth)

Properties Evaluations

Refer also to abstracts 34837, 34838, 35392, 35398, 35411, 35431, 35479, 36310, 36320, 36334, 36335, and 37006.

35546 (AWRE-O-42-69) ELECTRICAL METHOD OF ASSESSING THE SUITABILITY OF SILICON NITRIDE COMPONENTS FOR USE WITH MOLTEN PLUTONIUM. Barlow, H. C. (Atomic Weapons Research Establishment, Aldermaston (England)). Sep 1969. 22p. Dep. NTIS (U. S. Sales Only).

Silicon nitride components are frequently used in contact with molten plutonium. Contamination of the metal with silicon sometimes occurs due to the presence of unreacted silicon in the silicon nitride matrix. A nondestructive electrical method for determining the content of the silicon and hence the quality of the silicon nitride is described. The effects of moisture content on the electrical parameters are given and the results obtained are compared with the metallographic evidence. (auth)

35547 (GEAP-12182) THERMODYNAMIC DATA PROGRAM INVOLVING PLUTONIA AND URANIA AT HIGH TEMPERATURES. Quarterly Report No. 14, November 1, 1970–January 31, 1971. Aitken, E. A.; Adamson, M. G.; Evans, S. K.; Ludlow, T. E. (General Electric Co., Pleasanton, Calif. Nucleonics Lab.). Contract AT(04-3)-189. 14p. Dep. NTIS.

Work progress is reported in the continuing scope of work related to vaporization of urania in urania–plutonia solid solutions, oxygen activities at high temperatures, oxygen redistribution in a temperature gradient, Pu/U segregation and sodium-fuel interactions. (auth)

35548 (ORNL-4503(Vol.3)) THORIUM CERAMICS DATA MANUAL. VOLUME III. CARBIDES. Peterson, Sigfred; Curtis, C. E. (Oak Ridge National Lab., Tenn.). Apr 1971. Contract W-7405-eng-26. 34p. Dep. NTIS.

The thorium–carbon system is reviewed. Properties are listed for the monocarbide and dicarbide alone and in combination with other carbides, notably those of uranium and plutonium. Literature through April 1970 is covered, and 91 references are cited. Since the main interest in thorium carbides is for nuclear fuel, nearly as much information is available on the thorium–uranium carbides as on the pure carbides. Uncertainties in composition and impurity content lead to disagreement on many key properties. (auth)

35549 (TID-25696) THE DESIGN OF A TEST PROGRAM TO EVALUATE THE RE-ENTRY PROTECTION PERFORMANCE OF A METAL IMPREGNATED FOAMED ZIRCONIA THERMAL SWITCH MATERIAL FOR THE ZrH REFERENCE DESIGN REACTOR. (Weiner Associates, Inc., Baltimore, Md.). Aug 1970. Contract AT(30-1)-4145. 23p. (WAI-TR-70.5/AEC). Dep. NTIS.

Analyses were performed on ZrO_2-silver foam material with 8 inches of LiH as a backup. It was found that the LiH front face reaches 950°F at impact, which is below the LiH melt temperature. The value of thermal conductivity used to account for switching is also shown. The LiH does not melt primarily due to the thermal soaking capability of the LiH biological shield. Since 4 to 5 inches of LiH is required to absorb sufficient heat to prevent surface melting, based on this analysis, the arc tunnel model would have to be 4 to 5 inches thick and approximately 5 inches in diameter (to get a reasonably uniform front face heating distribution). The maximum attainable heating rates for present NASA and Sandia facilities are 100 to 200 $BTU/ft^2\text{-}sec/\sqrt{R}$. The ZrH reference design reactor produces reference peak heating rates of 500 to 700 $BTU/ft^2\text{-}sec/\sqrt{R}$ for earth orbital decay. Therefore some scaling of results will be necessary. It is anticipated that the model could be run at the lower heating rates and compared with a TAP-4 thermal analysis run under the same heating conditions. At present, the ability to simulate pressure and shear forces in the arc tunnel is impossible. (auth)

35550 EL DEVELOPMENT FOR POWER REACTORS. Ferrari, H. M.; Allio, R. J. (Westinghouse Electric Corp., Pittsburgh). pp 52-66 of Materials Technology: An Interamerican Approach. New York; American Society of Mechanical Engineers (1968).

From Inter-American Conference on Materials Technology, San Antonio, Tex. See CONF-680513.

The fuels used in major power reactor programs are briefly described. The major U.S. effort in fuel development is currently aimed at obtaining a better understanding of the phenomena which occur with contemporary fuels. Key technical problems relative to specific fuel types are discussed including: fuel swelling in oxide, carbide, and metallic fuels; fission gas release in oxide, carbide, metallic, molten salt fuels, and coated carbides; fuel-cladding chemical interactions in oxide, carbide, and molten salt fuels. Chemical interactions between the fuel and the environment are also considered for: water and oxide fuels; sodium and oxide fuels; and sodium and carbide fuels. (G.M.C.)

35551 STRENGTHS OF SOME URANIUM COMPOUNDS. Beals, R. J.; Handwerk, J. H. (Argonne National Lab., Ill.). pp 136-43 of Materials Technology: An Interamerican Approach. New York; American Society of Mechanical Engineers (1968).

From Inter-American Conference on Materials Technology, San Antonio, Tex. See CONF-680513.

The strength of ceramic materials is almost always limited by brittle fracture. Yet, ceramic materials deform plastically at stress levels and temperatures at which dislocations are sufficiently mobile. The high temperature strength of ceramic nuclear materials affects their utilization as reactor fuels. In this study, the dependence of maximum fiber stress upon temperature, stress levels, composition and physical properties of some uranium compounds was investigated. Sintered specimens of uranium dioxide, uranium monosulfide and uranium monophosphide were tested by

four-point load cross bending from room temperature up to 1900°C. Urania behaved as a high strength, brittle solid up to 1250°C in vacuo, became increasingly ductile at 1500°C and was highly plastic at 1750°C. The maximum modulus of rupture was 1760 ± 100 kg/cm² at 1250°C under a controlled strain rate. Uranium monosulfide undergoes a brittle-to-ductile transition around 1000°C, reaches a maximum strength at 1250°C and becomes highly ductile at 1750°C. The strength of 93% dense US at 1250°C in vacuo was 900 ± 55 kg/cm². Uranium monophosphide undergoes this transformation near 1275°C, at which the maximum strength was achieved. The modulus of rupture of UP at 1275°C in vacuo was 1540 ± 100 kg/cm². The mechanism of failure appeared to be crack propagation caused by movement and collection of pores at the grain boundaries as well as possible intragranular slip. (auth)

35552 STUDIES ON ULTRA-CLEAN CARBON SURFACES. III. KINETICS OF CHEMISORPTION OF HYDROGEN ON GRAPHON. Bansal, R. C.; Vastola, F. J.; Walker, P. L. Jr. (Pennsylvania State Univ., University Park). Carbon; 9: 185-92(Mar 1971).

The chemisorption of hydrogen on activated Graphon was studied over the range 80 to 600°C at a hydrogen pressure of 0.10 torr and at 500°C over the pressure range 0.020 to 0.47 torr. The Graphon was activated by preoxidation in oxygen to 18.6% wt loss at 625°C. The oxidized sample had a BET surface area of 100 m²/g. Prior to adsorption measurements, the sample was outgassed at 1000°C at residual pressures $<10^{-6}$ torr. Adsorption was followed for times up to 24 hr. Plots of amount of hydrogen adsorbed vs log of time showed linear regions. In all, four linear regions were identified. The activation energy for chemisorption changed little within a linear region. However, it changed abruptly between linear regions, increasing over-all from 5.7 kcal/mole for the first linear region to 30.4 kcal/mole for the last. It is concluded that each linear region represents chemisorption on different discrete configurations of sites on the carbon surface. (auth) (UK)

35553 OXYGEN SELF-DIFFUSION AND ELECTRICAL TRANSPORT PROPERTIES OF NONSTOICHIOMETRIC CERIA AND CERIA SOLID SOLUTIONS. Steele, B. C. H.; Floyd, J. M. (Imperial Coll. of Science and Tech., London). Proc. Brit. Ceramic Soc.; 19: 55-76(Mar 1971).

The self-diffusion of oxygen in non-stoichiometric ceria and ceria–yttria solid solutions was measured as a function of composition by observing the rate of depletion of ^{18}O from an isotopically enriched gas phase in the temperature range 850 to 1150°C. The diffusion data confirmed that the predominant defects in oxygen-deficient ceria are anion vacancies. The activation energy for motion for oxygen ions varied from about 24 kcal. in near-stoicheiometric ceria to around 4 kcal. for $CeO_{1.8}$, while in ceria–yttria solid solutions the corresponding activation energy was virtually independent of composition and had the value of 20 kcal. The oxygen diffusion results were used to provide an explanation of discrepancies in the reported electrical conductivity data for ceria, and a model was derived to account for observed values of the ionic transference number in ceria as a function of temperature and oxygen partial pressure. (auth) (UK)

35554 CURRENT AND POTENTIAL OPAQUE CERAMIC ARMOR MATERIALS. Ruh, Robert; Stiglich, J. J.; Rankin, D. T. SAMPE; 2: No. 2, 46-50(Jan 1971).

The fabrication and properties of opaque ceramic armor materials which have been investigated for lightweight armor applications are reviewed. Mechanical properties which are related to ballistic performance are discussed briefly. Potential new materials are examined, some fabricated by conventional processing techniques and some by new and novel processes. New concepts for ceramic armor are also discussed. (auth)

35555 COMPRESSIVE CREEP OF YTTRIA RARE EARTH STABILIZED ZIRCONIA STORAGE HEATER REFRACTORIES. Fehrenbacher, L. L.; Bailey, F. P.; McKinnon, N. A. SAMPE; 2: No. 2, 18-30(Jan 1971).

The compressive creep behavior of 10.4 wt% yttria rare earth stabilized zirconia specimens was determined using incremental (DORN) and conventional tests over a temperature and stress range of 800 to 7500 psi and 1400 to 1535°C, in order to make credible predictions of creep rates at various operating conditions in a ceramic storage heater. The experimental temperature (ΔH = 110K cal/mole) and stress (approximately linear) dependencies of the secondary creep rates supplemented by microstructural analysis suggested that grain boundary sliding was controlled by diffusion of Zr and Y cations in a boundary second phase. From the experimental data, stress-time to failure curves were plotted and correlated with storage heater idling temperatures (2500 to 2800°F) and stresses (10 to 50 psi). These time to 3% strain failure extrapolations indicated that creep of 95% dense cored brick in the 2500 to 3000°F range appears negligible. Calculations of creep rates and times to failure in the high temperature (4000°F)–low stress (10 to 20 psi) regions of a heater were based on the experimental deformation equation and a theoretical modified Nabarro–Herring equation, the latter providing an estimation of the grain size influence. These results revealed that fairly high creep rates and short life expectancies might be experienced at the maximum operating conditions. (auth)

35556 HIGH-TEMPERATURE CREEP OF POLYCRYSTALLINE GRAPHITE. Green, W. V. (Los Alamos Scientific Lab., N. Mex.); Weertman, J.; Zukas, E. G. pp 1160-4 of Second International Conference on the Strength of Metals and Alloys, Pacific Grove, California, 30 August–4 September 1970. Vol. III. Metals Park, Ohio; American Society for Metals (1970).

From second international conference on the strength of metals and alloys; Pacific Grove, Calif. (Aug-Sep 1970). See CONF-700819–(Vol.3).

A theory for use in modeling high-temperature creep of graphite based on crack opening mechanisms and other experimental data interpretations relevant to creep in graphite is presented. An outline of the theory is included and results of experiments are compared with theoretical predictions. (J.R.D.)

35557 STRENGTHENING OF METALS AND ALLOYS BY REFRACTORY FIBERS GROWN FROM THE MELT. Bibring, H.; Seibel, G.; Rabinovitch, M. (Office National d'Etudes et de Recherches Aerospatiales, Chatillon, France). pp 1178-82 of Second International Conference on the Strength of Metals and Alloys, Pacific Grove, California, 30 August–4 September 1970. Vol. III. Metals Park, Ohio; American Society for Metals (1970).

From second international conference on the strength of metals and alloys; Pacific Grove, Calif. (Aug-Sep 1970). See CONF-700819–(Vol.3).

A method of strengthening metals and alloys by in-situ growth of refractory fibers having whisker-like characteristics is described. Composites prepared in this manner are well reinforced by relatively low volume fractions of fibers, displaying high ultimate tensile strength (UTS) coupled with good ductility. The method is illustrated using data on TaC incorporated in various refractory alloy composites. (J.R.D.)

35558 MECHANICAL PROPERTIES OF TiC–VC ALLOYS. Hollox, G. E.; Novak, D. L.; Huntington, R. D. (Martin Marietta Corp., Baltimore). pp 1192-6 of Second International Conference on the Strength of Metals and Alloys, Pacific Grove, California, 30 August–4 September 1970. Vol. III. Metals Park, Ohio; American Society for Metals (1970).

From second international conference on the strength of metals and alloys; Pacific Grove, Calif. (Aug-Sep 1970). See CONF-700819–(Vol.3).

Results of measurements of the mechanical strength of single-crystal TiC–VC alloys are reported. Data and discussions are included on room temperature hardness, high temperature deformation, and uses of these alloys. (J.R.D.)

35559 INFLUENCE OF SUBSTOICHIOMETRIC CARBON CONTENTS OF THE CARBIDE PHASE ON THE PROPERTIES OF TiC–Mo_2C–Ni REFRACTORIES. Kieffer, R.; Fister, D. (Technische Hochschule, Vienna). Planseeber. Pulvermet.; 18: 246-53(Dec 1970). (In German).

The properties of cemented carbides of TiC–Mo_2C-Ni versus Mo_2C and carbon content of the primary solid solutions were investigated. Optimal properties were found at a content of 15 to 25 wt % Mo_2C in the solid solution. With decreasing carbon content the transverse rupture strength and the hardness showed a pronounced maximum. The influence of the carbon content on the properties of the applied solid solutions can be observed between 10 and 40 wt % Mo_2C in the solid solution. The optimal carbon content is found near 90 to 96% of the theoretical carbon content of the carbide phase. (auth)

35560 CONCENTRATION CHANGES AND METAL LOSSES DURING DEGASSING BY ANNEALING OF BINARY DILUTE METAL-GAS SOLUTIONS. II. DISCUSSION OF THE CONCENTRATION CHANGES AND METAL LOSSES IN THE SYSTEMS OF THE GROUP VA METALS WITH OXYGEN OR NITROGEN. Hoerz, Gerhard (Institut fuer Sondermetalle, Stuttgart). Z. Metallk.; 62: No. 5, 416-18(May 1971). (In German).

The concentration changes and metal losses during degassing by annealing of dilute metal-gas solutions of the V–O, Nb–O, Ta–O, Nb–N, and Ta–N systems (thin specimens) are discussed. In the oxygen systems degassing is theoretically possible down to a gas concentration x = 0 whereas in the nitrogen systems there is a limiting concentration $x = x_g$. In practice, however, the final

XUM

gas concentrations are determined by the residual gas pressure in the degassing apparatus. In the V–O system large metal losses are observed even at small degrees of degassing. On the other hand the metal losses in the Nb–O and Ta–O systems are negligible up to very high degrees of degassing, in the Nb–N and Ta–N systems up to high degrees of degassing. (auth)

35561 PIEZO-ELECTRIC CERAMICS CONTAINING ANTIMONY AND NIOBIUM OR TANTALUM. (to Nippon Electric Co., Ltd.). French Patent 2,002,111. 3 Oct 1969. Priority date 17 Feb 1968, Japan. (In French).

Piezoelectric ceramics suitable for ceramic filter elements and transducer elements of mechanical filters where a factor of electromechanical coupling and a mechanical quality factor are necessary are described. They are composed essentially of a solid solution of $Pb(Sb_{\frac{1}{4}}Z_{\frac{3}{4}})O_3$, $PbTiO_3$, $PbZrO_3$, and MnO in quantity between 0.10 and 3.0 wt %. Z represents either Nb or Ta and up to 25 at. % of Pb can be replaced by Ba, Sr, or Ca. (J.S.R.)

35562 GRAPHITE AS A NEUTRON MODERATOR AND REFLECTOR MATERIAL. Baker, D. E. (Battelle-Northwest, Richland, Wash.). Nucl. Eng. Des.; 14: 413-44(Feb 1971).

The properties of graphite and its uses in nuclear engineering are examined. Information is included on production and fabrication, preparation processes, physical, nuclear, electric, and mechanical properties, radiation effects, and gas–graphite systems. (J.R.D.)

35563 DIFFERENTIAL CAPACITANCE STUDY OF STRESS-ANNEALED PYROLYTIC GRAPHITE ELECTRODES. Randin, Jean-Paul; Yeager, Ernest (Case Western Reserve Univ., Cleveland). J. Electrochem. Soc.; 118: 711-14(May 1971).

The differential capacity of the basal planes on pyrolytic graphite was studied in aqueous solutions using ac impedance bridges. It was found that the differential capacitance of the basal planes of stress-annealed pyrolytic graphite–electrolyte interface is abnormal and that the space charge characteristics of graphite must be considered in resolving the electrochemical properties of this material. (J.R.D.)

35564 PREPARATION AND PROPERTIES OF PYROLYTIC ZIRCONIUM DIOXIDE FILMS. Tauber, R. N.; Dumbri, A. C.; Caffrey, R. E. (Bell Telephone Labs., Inc., Allentown, Pa.). J. Electrochem. Soc.; 118: 747-54(May 1971).

Zirconium dioxide films in the thickness range of 500 to 8000 Å have been prepared by chemical vapor deposition in the temperature range of 800 to 1000°C. The films were identified as fine-grained (~325Å), nearly stoichiometric, monoclinic ZrO_2, using electron microprobe analysis, infrared absorption, and transmission electron microscopy. The films exhibited resistance to most aqueous acids and bases, although slight etching occurred in hot (220°C) phosphoric acid. The deposits had an index of refraction of 2.1 ± 0.1 at 546 nm and an optical energy gap of 5.12 eV. ZrO_2 deposited on silicon offered little resistance to Na diffusion at 600°C, while films deposited on thermal SiO_2 were a good barrier due to pile-up of the Na near the ZrO_2/SiO_2 interface. The current density, J, depended on the field, E, as $J = AE^n$, where n was 6 for the metal biased negatively and 2.75 or 5, depending on the magnitude of the field, for the opposite polarity. The dielectric constant in the frequency range of 5×10^2 to 1×10^5 Hz was relatively independent of frequency near 300°K and equal to approximately 18, however some dispersion was noted near 573°K. The ac conductivity could be represented by $\sigma_{ac} = Cf^{\beta}$ where f is the measuring frequency and β a temperature dependent parameter, decreasing from ~1 at 300°K to ~0.5 at 573°K. The dielectric strength of the films varied between 1 to 2×10^6 V/cm, independently of thickness and polarity. High frequency (1 MHz) C–V measurement results indicated the presence of negative surface charge, which varied between -6×10^{11} to -1×10^{12} cm^{-2}. The structures exhibited instability under negative bias, indicative of negative charge being injected into the insulator. C–V measurements on the double dielectric system (ZrO_2/SiO_2) showed that the presence of ZrO_2 caused a flatband voltage displacement ≈+0.8V. In addition, the flatband voltage shifted as a function of time under negative bias and was found to obey the relationship $\Delta V_{FB} = K \log t$. (auth)

35565 CONTACT INTERACTION OF TITANIUM DIBORIDE WITH TITANIUM, ZIRCONIUM, AND VANADIUM IN A VACUUM. Strashinskaya, L. V.; Stepanchuk, A. N. (Inst. of Material Studies, Kiev). Fiz.-Khim. Mekh. Mater.; 6: No. 6, 76-9(1970). (In Russian).

The reactions of TiB_2 at 900 to 1700°C with Ti, Zr, and V were studied in a vacuum of 5×10^{-5} mm Hg. Microscopic examination and x-ray powder analyses showed that the initial reaction temperature increased with increase in melting point of the metals and their degree of compaction. (tr-auth)

35566 SOLUBILITY OF OXYGEN IN HAFNIUM NITRIDE. Nechaev, Yu. A.; Kamyshov, V. M. Zh. Neorg. Khim.; 15: 3249-53(Dec 1970). (In Russian).

During oxidation of HfN under equilibrium conditions substitutional solid solutions having a cubic structure are formed. In equilibrium with these solid solutions at specific compositions of the gaseous phase, HfO_2 is found. The activities of component solid solutions in the $HfN–HfO_2$ system were determined at 1023 to 1073°K along with the heats of mixing, isobaric potentials, and entropies. (tr-auth)

35567 BEHAVIOR OF FISSION CESIUM IN GRAPHITE-CONTAINING FUEL ELEMENTS. Merz, E.; Scharf, H. (Kernforschungsanlage, Juelich, Ger.). Atomkernenergie; 17: No. 4, 287-92(Jul 1971). (In German).

In order to prove the existence of cesium graphite intercalation compounds at the operation temperatures of high-temperature gas-cooled reactors, an improved experimental technique was applied. Support was gained from disintegration isotherms, diffusion curves (under the consideration of a superimposed chemical reaction) as well as from vapor pressure measurements of cesium graphite compounds. Deciding factors were evaluated stressing the existence of compounds representing the formula $C_{4m}Cs$, m = 2, 3, 4. The threshold vapor pressure postulated by Salzano and Aronson could be verified experimentally for the first time. (auth)

Structure and Phase Studies

35568 (ORNL-TM-3362) STATISTICAL TECHNIQUE FOR DETERMINING SOURCES OF VARIATION IN $(U,Pu)O_2$ OXYGEN-TO-METAL RATIO. Lackey, W. J.; Bradley, R. A.; Pechin, W. H.; Hebble, T. L. (Oak Ridge National Lab., Tenn.). Jun 1971. Contract W-7405-eng-26. 21p. Dep. NTIS.

With a statistically designed experiment it was demonstrated that gravimetric determinations of the oxygen-to-metal ratio of $(U,Pu)O_2$ depend strongly on the day of analysis, slightly on the particular sintering run, and not detectably on position in either the sintering furnace or the analysis furnace. The average oxygen-to-metal ratio of a single sintering run can be determined to a precision of ±0.005 at the 95% confidence level. (auth)

35569 CONCERNING THE ARTICLE "SOME PHYSICO-CHEMICAL PROPERTIES OF CODEPOSITED HYDROXIDES OF HOLMIUM AND ZIRCONIUM, AND HOLMIUM AND HAFNIUM" BY I. N. BELYAEV AND S. M. ARTAMONOVA. Spiridonov, F. M. (Moscow State Univ.). Inorg. Mater. (USSR) (Engl. Transl.); 6: 1222-3(Jul 1970).

Translated from Izv. Akad. Nauk SSSR, Neorg. Mater.; 6: 1385-6(Jul 1970).

Comments are given on a paper published previously concerning the physicochemical properties of codeposited hydroxides of holmium and zirconium, and holmium and hafnium. The paper was abstracted in NSA as 24: 6277. (G.M.C.)

35570 REPLY TO THE ARTICLE BY F. M. SPIRIDONOV. Belyaev, I. N.; Artamonova, S. M. Inorg. Mater. (USSR) (Engl. Transl.); 6: 1224(Jul 1970).

Translated from Izv. Akad. Nauk SSSR, Neorg. Mater.; 6: 1387 (Jul 1970).

A rebuttal is given to Spiridonov [Inorg. Mater. (USSR) (Engl. Transl.), 6: 1222-3(1970)] concerning his comments on a paper dealing with the physicochemical properties of codeposited hydroxides of holmium and zirconium, and holmium and hafnium (previously published and abstracted in NSA as 24: 6277). (G.M.C.)

35571 L_3GaS_6 COMPOUNDS (L = Dy, Ho, Er, AND Y), AND THE PHASE DIAGRAM OF THE $Y_2S_3–Ga_2S_3$ SYSTEM. Lozac'h, Anne-Marie; Jaulmes, Sylvie; Guittard, Micheline (Univ., Paris). Compt. Rend., Ser. C; 272: No. 12, 1123-6 (22 Mar 1971). (In French).

Four new orthorhombic L_3GaS_6 compounds with Ccmm, $Ccm2_1$ or Ccm2 space groups are described. The phase diagram of the $Y_2S_3–Ga_2S_3$ system demonstrates the existence of the Y_3GaS_6 compound, which presents a peritectic decomposition. A $Y_6Ga_{10/3}S_{14}$ compound with a $P6_3$ hexagonal structure which is only stable at high temperatures was investigated and an eutectic with the $Y_2S_32Ga_2S_3$ composition was found at 940°C. (auth) (France)

35572 STUDY OF PHASE TRANSFORMATIONS IN ZIRCONIUM-RICH Zr–Nb ALLOYS CONTAINING OXYGEN. Kubit, Charles John. Pittsburgh; Univ. of Pittsburgh (1970). 115p. University Microfilms Order No. 71-9028.

Thesis.

A controversy exists in the literature concerning the exact placement of phase boundaries in the Zr–Nb system, particularly the maximum solid solubility of niobium in alpha zirconium. This point, which is variously accepted as 0.6 or 6.5% Nb, is of practical importance in interpreting the behavior of commercially useful alloys. The DTA method, supported by x-ray diffractometry, was used to determine the phase boundaries in commercial purity Zr–Nb alloys. The resulting data, as well as thermodynamic calculations, support the higher value of the solid solubility maximum. The effects of impurities, notably oxygen, were principally to raise the monotectoid horizontal. Published supporting data are presented and discussed. (Diss. Abstr. Int., B)

35573 CONTRIBUTION TO THE STUDY OF COHERENCY OF VANADIUM CARBIDE WITH THE MATRIX OF ALPHA IRON. Prnka, Tasilo (Vitkovice Steelworks, Ostrava, Czech.). pp 590–4 of Second International Conference on the Strength of Metals and Alloys, Pacific Grove, California, 30 August–4 September 1970. Vol. II. Metals Park, Ohio; American Society for Metals (1970).

From second international conference on the strength of metals and alloys; Pacific Grove, Calif. (Aug-Sep 1970). See CONF-700819–(Vol.2).

On the basis of theoretical calculations, supplemented by an analysis of the orientation relation, and experimental results, it is possible to determine the critical diameter of vanadium carbide V_4C_3 diameter in the plane $(100)_{V_4C_3}$. If the diameter is greater than the critical one, the vanadium carbide V_4C_3 may be expected to be non-coherent with the matrix of alpha iron. The computed critical diameter values and the measured ones are mutually compared in a table. The results demonstrate that vanadium carbide V_4C_3 with a diameter greater than ~150 Å in the $(100)_{V_4C_3}$ plane will already be non-coherent with the alpha iron matrix. (auth)

35574 LATTICE PARAMETERS OF (U,Pu)N SOLID SOLUTIONS. Tennery, V. J.; Bomar, E. S. (Oak Ridge National Lab., Tenn.). J. Amer. Ceram. Soc.; 54: No. 5, 247-9(May 1971).

The lattice parameters of the cubic solid solutions from the system $(U_{1-x}Pu_x)N$ were measured at 25°C. The lattice constant, α_0, of UN was 4.88918 ± 0.00017 Å and that of PuN was 4.90476 ± 0.00008 Å. The parameter of the solid solution does not depend linearly on the composition parameter, x. The x-ray specimens contained from 600 to 1200 ppM total O + C as impurities; thus, these samples had much lower impurity levels than those of previous investigators. The compositions of the x-ray specimens were corroborated by quantitative chemical analysis. The significant deviation from Vegard's relation and the small variation observed for α_0 in this system are discussed in terms of the strongly hybridized electron f–d bands that were calculated for these compounds. (auth)

35575 THIN FILMS OF PRASEODYMIUM SESQUIOXIDE: MARTENSITIC CHARACTER OF THE MONOCLINIC TO HEXAGONAL PHASE TRANSFORMATION. Boulesteix, C. (Faculte des Sciences, Orsay, France); Caro, P.-E.; Gasgnier, M.; La Blanchetais, Ch. H.; Schiffmacher, G. Phys. Lett.; 34A: 437-8(19 Apr 1971).

In thin films of A-type praseodymium sesquioxide (hexagonal), B-phase (monoclinic) domains can be produced. The B-to-A transformation has a martensitic character. (auth)

35576 THERMAL EQUILIBRIA OF THE PHASES IN THE SYSTEM $MgO–TiO_2–V_2O_5$. Solacolu, S.; Dinescu, R.; Zaharescu, Maria (Center of Physical Chemistry, Bucharest). Rev. Roum. Chim.; 16: 351-6(Mar 1971). (In French).

The thermal equilibrium diagram of the phases of the system was established, and the areas of primary crystallization of the single and binary compounds were delimited. It was also established that there are no ternary compounds in this system. (tr-auth)

35577 KINETICS OF INTERACTION OF TANTALUM DISILICIDE WITH TANTALUM AND OTHER METALS. Schwartz, L. J.; Kolodney, M.; Graff, R. A. (City Coll., New York). Met. Trans.; 2: No. 5, 1429-32(May 1971).

The rate of growth of Ta_5Si_3 in the $Ta–TaSi_2$ system was measured with good accuracy in the temperature range of 1150 to 1370°C using couples consisting of dense wafers of the components. The isothermal growth is shown to be parabolic and the temperature dependence of the growth constant is given by $k = 5 \exp(-77{,}000/RT)$. It was shown that tantalum diffusion is negligible by comparison with silicon diffusion. The Ta_5Si_3 was found to exist in both tetragonal and hexagonal forms. A more limited investigation of silicon loss from $TaSi_2$ to W, Mo, Nb, Zr, Ti, and Re indicates that none of these is superior to tantalum in limiting the degradation of the tantalum disilicide. In most instances a layer of composition M_5Si_3 forms on the metal side of the couple. (auth)

35578 PHASE DIAGRAMS OF THE SYSTEMS $MoO_3–MeMoO_4$ (Me = Mg, Ca, Sr, Ba). Zhukovskii, V. M.; Tkachenko, E. V.; Rakova, T. A. (Ural State Univ., Sverdlovsk, USSR). Zh. Neorg. Khim.; 15: 3326-8(Dec 1970). (In Russian).

Thermographic and roentgenographic methods were used to construct phase diagrams of $MoO_3–MeMoO_3$, where Me = Mg, Ca, Sr, or Ba. All systems examined were eutectic. The systems $MoO_3–BaMoO_4$ and $MoO_3–MgMoO_4$ contain $BaMo_2O_7$, which melts at 653°C, and $Mg_2Mo_3O_{11}$, which melts at 826°C. (tr-auth)

35579 STUDIES ON THE URANIUM DICARBIDE PHASE. Tagawa, Hiroaki; Fujii, Kimio; Sasaki, Yasuichi (Japan Atomic Energy Research Inst., Tokai). J. Nucl. Sci. Technol. (Tokyo); 8: No. 5, 244-9(May 1971).

The lattice parameters of UC_2 are examined as a function of carbon content and annealing conditions on sintered carbides between $UC_{1.5}$ and $UC_{2.2}$ (7.0 to 10.0 wt % of carbon). The values of UC_2 obtained under equilibrium state are around $a_0 = 3.5253$ Å and $c_0 = 5.9994$ Å. The lattice parameter measurements were made also on UC_2 obtained under non-equilibrium conditions by arc-melting and carbothermic reaction of UO_2. The lattice parameters were appreciably smaller than on the specimens obtained under equilibrium. With annealing, both the lattice parameter and the combined carbon content showed a tendency to increase. (auth)

35580 CdP_2–Sn SYSTEM AND SOME PROPERTIES OF $CdSnP_2$ CRYSTALS. Buehler, E. (Bell Telephone Labs., Murray Hill, N. J.); Wernick, J. H.; Shay, J. L. Mater. Res. Bull.; 6: 303-9 (May 1971).

Phase relations in the $CdP_2–Sn$ system were determined. $CdSnP_2$ forms peritectically at approximately 570°C and crystals of this semiconductor can be grown successfully from tin solutions containing CdP_2 concentrations of less than 10 mole percent. Some electrical and optical results on Ag and Cu doped crystals are presented. (auth)

35581 PHASE DIAGRAM OF THE SYSTEM $PbO–MoO_3$. Bukhalova, G. A.; Manakov, V. M.; Mal'tsev, V. T. Zh. Neorg. Khim.; 16: No. 2, 530-1(Feb 1971). (In Russian).

Thermal and x-ray analysis of the $PbO–MoO_3$ system demonstrated the existence of two congruently melting compounds $2\,PbO \cdot MoO_3$ and $PbO \cdot MoO_3$ (mp 950 and 1070°C respectively). Eutectic compositions at 14, 37.5, and 79.5 mole percent MoO_3 melted at 744, 910, and 660°C. The two compounds were identified by synthesis. (tr-auth)

35582 $Y–YH_2$ PHASE DIAGRAM AT ROOM TEMPERATURE. Landin, N. A.; Izhvanov, L. A.; Chernikov, A. S.; Kalinin, V. P. Zh. Neorg. Khim.; 16: No. 2, 519-22(Feb 1971). (In Russian).

Phase boundaries were established for the system $Y–YH_2$ at room temperature by metallographic and x-ray techniques. Changes in microhardness, Vickers hardness, electrical conductivity, and the density of Y as a function of H content were also contributing factors. (tr-auth)

35583 REGION OF HOMOGENEITY OF A ZIRCONIUM OXYNITRIDE OF NaCl STRUCTURE AT 1500°C. Zainulin, Yu. G.; Alyamovskii, S. I.; Shveikin, G. P.; Gel'd, P. V. Zh. Neorg. Khim.; 16: No. 2, 315-17(Feb 1971). (In Russian).

A Zr compound of cubic structure (NaCl) with the formula ZrN_xO_y has a finite region of homogeneity ($y_{max} \simeq 0.3$) at 1500°C and 10^{-5} mm of Hg. The constants for the ZrN_xO_y lattice vary insignificantly (between 4.574 and 4.578 Å). The unoccupied lattice sites of the oxynitride ZrN_xO_y are typical of both a sublattice metal and a nonmetal. (tr-auth)

Radiation Effects

Refer also to abstracts 35511, 35515, 36268, 36278, 36279, 36308, 36314, 36977, 36978, 37017, and 37018.

35584 THRESHOLD ENERGY FOR THE DISPLACEMENT OF SURFACE ATOMS IN GRAPHITE. Montet, G. L.; Myers, G. E. (Argonne National Lab., Ill.). Carbon; 9: 179-85(Mar 1971).

The energy required to displace a C atom from a site in the surface of a graphite crystal was determined by the detection of surface vacancies resulting from the displacement process. Cleaved fragments, a few hundred Angstrom units thick from annealed natural crystals of graphite containing less than 10^{-10} vacancies per C atom were irradiated at room temperature with electrons of selected energies in the range from 100 to 200 keV. Preparation of these fragments by an etch-decoration

XUM

technique and subsequent examination in an electron microscope indicated that irradiation by electrons possessing an energy of 150 keV was sufficient to produce vacancies in the surface of graphite; this corresponds to a threshold displacement energy of 31 eV, which is the value found for production in the interior. It was necessary to take extreme precautions to protect the surface from chemical attack. (auth) (UK)

35585 IRRADIATION-INDUCED DIMENSIONAL CHANGES AND CREEP OF ISOTROPIC CARBON. Kaae, J. L.; Bokros, J. C. (Gulf General Atomic Inc., San Diego, Calif.). Carbon; 9: 111-22(Mar 1971).

An investigation is described of the dimensional behavior of unrestrained and spherically restrained isotropic carbons deposited at both high temperatures (>1500°C; HTI carbons) and low temperatures (<1500°C; LTI carbons) during irradiation at 600, 1000, and 1250°C to fast-neutron fluences near 2×10^{21} n/cm^2 (E > 0.18 MeV). The investigation covered, in particular, the effect of the initial density on the unrestrained dimensional changes and on the total strain accommodated without fracture in the spherically restrained specimens. For isotropic carbons (Bacon anisotropy factor <1.1), the unrestrained dimensional changes were primarily those due to irradiation-induced densification, and the strain accommodated consisted mostly of irradiation-induced creep strain. The largest dimensional changes and highest total strains accommodated were in low-density carbons. At 1000°C the accommodated strain rates were 0.04 per 10^{21} n/cm^2 and 0.05 per 10^{21} n/cm^2 for LTI and HTI carbons, respectively. At 600°C the respective accommodated strain rates were 0.028 per 10^{21} n/cm^2 and 0.025 per 10^{21} n/cm^2. At 1250°C both an upper and a lower limit on the density of the restrained LTI carbons that survived irradiation were observed. The lower density limit apparently revealed the maximum densification strain rate that can be tolerated. The existence of the upper density limit is discussed. (auth) (UK)

35586 RADIATION-INDUCED CREEP IN PYROCARBON. Voice, E. (Atomic Energy Establishment, Winfrith, Eng.). Nature (London) Phys. Sci.; 230: 47-8(8 Mar 1971).

It is stated that creep strains of up to 10% were measured in pyrocarbon, with fixed restraint, so that no actual specimen extension occurred. It is an open question as to how much creep strain can be ultimately accommodated or what net extension could occur. In polycrystalline graphite it is possible that shape change of the crystallites will eventually destroy their cohesion, reducing the tensile strength below the applied load, but for pyrocarbon no evidence exists. A crack in the outer pyrocarbon layer of a coated fuel particle caused by fast neutron damage is illustrated and discussed, together with cracks caused by fission fragment damage. It is evident that although the bulk may fail by cracking at low strains, parts of the structure are extremely ductile under irradiation and can extend by several thousand per cent, at temperatures which alone would allow no thermal creep. (UK)

35587 EFFECTS OF NEUTRON IRRADIATION ON STRAIN-AMPLITUDE DEPENDENT INTERNAL FRICTION IN SODIUM CHLORIDE SINGLE CRYSTALS. French, I. E.; Harris, R. W. (Univ. of New South Wales, Kensington, Australia). J. Phys., C (London); 4: 331-7(Mar 1971).

A method was developed which allows the dependence of internal friction on strain amplitude for a crystal to be measured in a period of 30 s. This method was used to study the variation of internal friction with strain amplitude in sodium chloride single crystals as a function of neutron irradiation. The results were found to agree with the Granato–Lücke theory of strain-amplitude dependent internal friction and this theory was used to examine the variation of pinned dislocation loop length with irradiation time. It was found that the loop-length variation from amplitude-dependent results was different to that from amplitude-independent results. An explanation is offered for this difference. (auth) (UK)

35588 LOW TEMPERATURE IRRADIATION STUDIES ON IRON–BORON ALLOYS. Kitajima, Kazunori; Futagami, Koji; Abe, Hironobu; Koiwa, Masahiro; Yoshida, Hiroyuki (Kyushu Univ., Fukuoka, Japan). Bull. Res. Inst. Appl. Mech., Kyushu Univ.; No. 34, 109-23(1970). (In Japanese).

The internal friction of Fe–B alloys damaged by neutron irradiation was measured using a low-temperature irradiation facility of the lateral vibration-type with coil magnets. A stable relaxation peak caused by interstitial atoms appeared at 170°K and its activation energy was 0.285 ± 0.011. This relaxation peak agreed with that of 120°K obtained by other workers. Other peaks appeared at 100 and about 200°K. It was assumed that the peak of 100°K was due to the recombination of close pairs, and the peaks at about 200°K were not a result of point defects. Measurement of internal friction inside of the loop was made at 11°K; its precision was as high as that of out-of-loop measurement. From measurement of electrical resistivity, it was found that 200 ppM natural boron doped in iron increase the resistivity to a higher level than that of pure iron when irradiated at 11°K. (auth) (Japan)

35589 SELF-RADIATION EFFECT ON THE LATTICE PARAMETER OF $^{244}CmO_2$. Noe, M.; Fuger, J. (Univ., Liege). Inorg. Nucl. Chem. Lett.; 7: 421-30(May 1971).

Changes in the lattice parameter of $^{244}CmO_2$ as a function of time were studied. At room temperature, expansion reached a saturation value within a few days. It was found that the expansion in a vacuum of 10^{-6} torr was slightly different than under 0.75 atm of oxygen. At liquid nitrogen temperature, a further expansion was observed with samples sealed in O_2; this low-temperature expansion annealed out at room temperature within 2 days, whereas complete annealing of the initial room-temperature expansion needed 10 days at 360°C. Freshly prepared samples kept in 0.75 atm oxygen for a month at 360° did not show any lattice expansion. Details are given of the Cm purification, oxide preparation, and x-ray technique and calculations. Results are tabulated and discussed. The discrepancy between the samples stored in O_2 and those vacuum-sealed could involve a differential loss of O_2, possibly as a result of radiation damage. This loss could be smaller with oxygen-stored specimens. At liquid nitrogen temperature, the O_2 loss would proceed and the expansion continues. When the sample was brought back to room temperature, contraction of the lattice could then denote an absorption of oxygen, and not simply a recovery from radiation damage. Such an explanation could also account for room-temperature changes being much faster than annealing at 300°C of room temperature defects. (UK)

Plastics and Other Materials

Refer also to abstracts 34627, 34839, 35316, 37006, and 37007.

35590 CHANGES IN STRUCTURE AND PROPERTIES IN γ-IRRADIATED CRYSTALLIZABLE CHLOROPRENE RUBBER. Makhlis, F. A.; Nikitin, L. Ya.; Volkova, A. K.; Tikhonova, M. N. Vysokomol. Soedin., Ser. A; 13: 596-602(Mar 1971). (In Russian).

The influence of the phase state of nairite B rubber on structural changes after γ-irradiation at different temperatures was studied. The density of cross-linking, the speed of continuous and steady state relaxation tension, and thermomechanical properties were measured. Intramolecular cross-links are formed mainly in the crystalline regions of the polymer, and intramolecular cross-links are formed mainly in the crystalline regions of the polymer, and intramolecular cross-links are formed in the amorphous regions. Structure formation and degradation takes place in amorphous regions more easily than in crystalline regions. Heating after radiation increases the density of cross-linking in crystalline samples. The determination of the extent of structure formation and degradation by gel-zol analysis and by equilibrium swelling in rubbers containing a large degree of crystallinity gives false results. The capacity of the elastomer to sequential recrystallization depends on its phase condition during irradiation. (auth)

35591 EFFECT OF THE TYPE OF POLYETHYLENE ON THE GRAFTING OF STYRENE ONTO POLYTEHYLENE. III. THE CROSSLINKING EFFECT IN THE GRAFTING BY PRE-IRRADIATION IN VACUUM. Dobo, J. (Research Inst. of Plastics, Budapest); Ranogajec, F.; Dvornik, I. Croat. Chem. Acta; 42: 551-6(1970).

The graft-copolymerization of styrene on free radicals trapped in vacuum-irradiated polyethylene was investigated. By an increase of the rigidity of the foils, the grafting rate is also increased, because the termination of the growing chains becomes more hindered; but further increase of the rigidity causes grafting to stop at comparatively low values. Crosslinking of the foils also increases this rigidity, while raising of grafting temperature partially eliminates its effect. Some kinetic and structural factors governing the grafting reactions are discussed and some former theories are revised. (auth)

PHYSICS (GENERAL)

Astrophysics and Cosmology

Refer also to abstracts 35892 and 35893.

35592 EXISTENCE OF SUPER-HEAVY NUCLEI. Bhattacherjee, S. K. (Tata Inst. of Fundamental Research, Bombay). pp 159-68 of Proceedings of the Eleventh Symposium on Cosmic Rays, Astrophysics, Geophysics and Elementary Particle Physics, 1969. Vol. I. Bombay; Department of Atomic Energy (1969).

From eleventh symposium on cosmic rays, astrophysics, geophysics and elementary particle physics; Delhi, India (7 Oct 1969). See CONF-691055-(Vol. 1).

The possibility of the existence of an island of stability associated with nuclear magic numbers somewhat beyond the presently accessible regions of stable nuclei has been extensively discussed in the literature. Topics considered here include: the predicted atomic properties of element 114, existence in nature, and experimental efforts to produce these nuclei in the laboratory or find them in nature. (W.D.M.)

35593 INTERPRETATION OF EXTRA-TERRESTRIAL LYMAN-ALPHA OBSERVATIONS. Blum, P. W.; Fahr, H. J. (Univ., Bonn). Nature (London); 231: 171-3(21 May 1971).

Recent observations and measurements in this field are reviewed, and results are interpreted. (UK)

Cosmic Ray Exposure Ages

35594 ^{244}Pu: CONFIRMATION AS AN EXTINCT RADIOACTIVITY. Alexander, E. C. Jr.; Lewis, R. S.; Reynolds, J. H.; Michel, M. C. (Univ. of California, Berkeley). Science; 172: No. 3985, 837-40(21 May 1971).

The mass spectrum of xenon from spontaneous fission in a laboratory sample of plutonium-244 is precisely what meteoriticists predicted it would be; this discovery completes a web of proof that this nuclide is a bona fide extinct radioactivity of galactic origin, that r-process nucleosynthesis was ongoing in the Galaxy at the time of the birth of the Sun, and that the early meteoritic abundances of plutonium-244, heretofore tentative, can be utilized with confidence in models for the chronology of galactic nucleosynthesis. The search for an explanation for anomalous fission-like xenon in carbonaceous chondrites can now be narrowed. (auth)

35595 HOW WELL DO WE KNOW COSMIC ABUNDANCES? Anders, Edward (Univ. of Chicago. Univ., Bern). Geochim. Cosmochim. Acta; 35: No. 5, 516-2(May 1971).

Five lines of evidence suggest that Cl chondrites closely approximate the condensable fraction of primordial solar-system matter: continuity of isotopic and elemental abundance trends, agreement with solar and cosmic-ray abundances, fractionation patterns among chondrites, and absence of chondrules. Maximum differences between Cl abundances and true solar-system abundances are estimated as factors of 2 to 5 for individual elements and a factor of 1.5 or less for groups of 10 or more elements. (auth) (UK)

35596 MEASUREMENT AND INTERPRETATION OF THE LUMINOUS EFFICIENCIES OF IRON AND COPPER SIMULATED MICROMETEORS. Becker, D. G.; Friichtenicht, J. F. (TRW Systems Group, Redondo Beach, Calif). Astrophys. J.; 166: No. 3, 699-716(15 Jun 1971).

The photographic luminous efficiency τ_{pg} was measured in the laboratory for simulated iron and copper micrometeors at velocities $11 \leq v \leq 47$ km sec^{-1} interacting with air in free-molecule flow. Both τ_{pg}(Fe) and τ_{pg}(Cu) varied similarly with v, first increasing and then decreasing as v increased; but their detailed behavior showed significant differences. Peak values were τ_{pg}(Fe) = 2.3×10^{-12} sec erg^{-1}, 0 mag at $v \simeq 18$ km sec^{-1}, and τ_{pg}(Cu) = 9.5×10^{-14} sec erg^{-1}, 0 mag at $v \simeq 13.5$ km sec^{-1}, where $\tau_{pg}(\mathrm{Fe}) \propto v^{-\frac{1}{2}}$ and $\tau_{pg}(\mathrm{Cu}) \propto v^{-\frac{1}{2}}$ at higher velocities. Above 20 km sec^{-1}, $\tau_{pg}(\mathrm{Fe})/\tau_{pg}(\mathrm{Cu}) > 20$. The fact that the τ_{pg}(Fe) results agreed well with reported data for Harvard meteors 1242 and 19,816 and with data on artificial Fe and Ni meteors at $10 \leq v \leq 16$ km sec^{-1} implies that the experiment properly simulates atmospheric entry conditions. The conclusion $\tau_{pg}(\mathrm{Fe}) \propto v^{-\frac{1}{2}}$ for $v > 18$ km sec^{-1} agreed with a prediction by Öpik for dust-ball meteors, however, it is shown that there is not necessarily any correspondence between the velocity dependence of τ_{pg}(Fe) and that of the luminous efficiency of natural meteors. The latter can be obtained as a sum of τ_{pg} values for the various constituent radiators in the meteoroid, which fact was a principal motivation for these experiments. (auth)

35597 MEASUREMENTS OF THE IONIZATION PROBABILITY OF Cu AND LaB_6 SIMULATED MICROMETEORS. Friichtenicht, J. F.; Becker, D. G. (TRW Systems Group, Redondo Beach, Calif.). Astrophys. J.; 166: No. 3, 717-24(15 Jun 1971).

The ionization probability β, related to the radiometeor ionizing efficiency τ_q by the relation $\tau_q = (2\phi/\mu v^2)\beta$, where ϕ, μ, and v are respectively the ionization energy, mass, and velocity of the meteor atom being ionized, was measured as a function of velocity v_0 for simulated micrometeoroids composed of copper and lanthanum hexaboride (LaB_6) interacting with an air target gas under conditions of free molecule flow. The range of the experiment was $16 \leq v_0 \leq 38$ km sec^{-1} for Cu, selected for comparison with results previously published for Fe at 20 to 45 km sec^{-1}, and $20 \leq v_0 \leq 112$ km sec^{-1} for LaB_6, chosen for its ability to be accelerated to ultrahigh velocities. It was found that $\beta(\mathrm{Cu}) = 2.17 \times 10^{-35} v_0^{5.24}$ (v_0 in cm sec^{-1}) and $\beta(LaB_6) = 6.31 \times 10^{-21} v_0^{-0.8}$ over the respective velocity ranges. It was also found that $\beta(LaB_6) > 1$ for $v_0 > 40$ km sec^{-1}, $\beta(LaB_6) \approx 50$. This result implies the existence of appreciable atmospheric ionization. The possibility that heavy, high-velocity meteor atoms or molecules may produce significant ionization of the atmosphere and may have $\beta > 1$ is not generally considered in current meteor theory, which may therefore be in need of modification. (auth)

35598 MECHANISM FOR PRODUCING MAGNETIC REMANENCE IN METEORITES AND LUNAR SAMPLES BY COSMIC-RAY EXPOSURE. Butler, Robert F.; Cox, Allan V. (Stanford Univ., Calif.). Science; 172: No. 3986, 939-41(28 May 1971).

An irradiation of 3×10^{17} neutrons cm-2 in a reactor core produced an increase in the coercive force of iron and kamacite of 16 to 21%. The ac demagnetization spectrum of saturation isothermal remanence was shifted toward higher coercive forces. Similar neutron fluences produced by cosmic-ray exposure may be capable of converting soft isothermal remanence in meteorites and lunar samples to remanence with a higher coercive force. (auth)

35599 PRODUCTION RATES OF ^{22}Na AND ^{3}H IN STONE METEORITES BY COMIC RAYS. Trivedi, B. M. P.; Goel, P. S. (Indian Inst. of Tech., Kanpur). pp 316-19 of Proceedings of the Eleventh Symposium on Cosmic Rays, Astrophysics, Geophysics and Elementary Particle Physics, 1969. Vol. II. Bombay; Department of Atomic Energy (1969).

From eleventh symposium on cosmic rays, astrophysics, geophysics and elementary particle physics; Delhi, India (7 Oct 1969). See CONF-691055-(Vol. 2).

Samples from three thick silicate target systems resembling stone meteorites in chemical composition and bombarded by 0.44-, 1.0-, and 3-GeV protons were used in studying and calculating the production rates of sodium-22 and tritium. Similarities are noted in the nuclide distributions in this study with those found in thick iron targets. Tritium and sodium-22 production rates calculated using the measured cosmic-ray intensity agree well with the meteoritic measurements and indicate that the observed galactic cosmic-ray intensity is sufficient to produce tritium and sodium-22 as observed in meteorites. (J.C.W.)

35600 ORBITAL VELOCITIES OF SOME STONE METEORITES. Bhandari, Narendra (Tata Inst. of Fundamental Research, Bombay). pp 327-31 of Proceedings of the Eleventh Symposium on Cosmic Rays, Astrophysics, Geophysics and Elementary Particle Physics, 1969. Vol. II. Bombay; Department of Atomic Energy (1969).

From eleventh symposium on cosmic rays, astrophysics, geophysics and elementary particle physics; Delhi, India (7 Oct 1969). See CONF-691055-(Vol. 2).

Cosmic-ray heavy-nuclei fossil tracks in meteoritic minerals reveal information about the composition and energy spectrum of the cosmic rays, but also phenomena about the meteorites. It has been found that stone meteorites are heavily ablated during atmospheric transit. With some of its regions only slightly ablated, and excluding meteoritic orientation, it is possible to gain some knowledge about the orbits of the meteorites and their orbital velocity with the help of a relation developed by Whipple and Opik. The technique involves taking samples from many locations on the surface and finding the ablation. The velocity of Pribram is photographically known, and the track method given agrees well with the results. (J.C.W.)

Stars

Refer also to abstracts 36140, 36263, and 36577.

XUM

35601 MAGNETOHYDRODYNAMICS IN NEUTRON STARS. Rostron, Ira Ralph. Provo, Utah; Brigham Young Univ. (1970). 119p. University Microfilms Order No. 71-8860.

Thesis.

A theoretical study of some of the properties of neutron stars was made. The principal interest was in magnetohydrodynamic behavior in the presence of gravitational potentials and large magnetic fields. Expressions are derived from Maxwell's equations, the energy equation, the momentum equation, and the equation for electric charge in the presence of gravitational potentials. The relativistic equation of continuity and an equation of state are then selected to complete the necessary equations. Magnetohydrodynamic behavior is considered in the static case and expressions are obtained for magnetic pressure, viscosity, magnetic energy, and Poynting vector. Wave behavior is considered in incompressible matter and in compressible matter. A dipole-like magnetic field is considered in the regions outside the neutron star. Finally, a general magnetic field is obtained for the regions outside and inside the star and the two fields are matched at the surface. (Diss. Abstr. Int., B)

35602 LUMINOSITY OF THE PECULIAR WHITE DWARF ROSS 640. van Altena, W. F. (Univ. of Chicago, Williams Bay, Wis.). Astron. J.; 76: No. 5, 484-5(Jun 1971).

A new trigonometric parallax for the peculiar (DF_p) white dwarf Ross 640 determined from plates taken with the Yerkes Observatory 40-inch refractor is presented. When combined with a recent Allegheny parallax, an average value of π_{abs} = +0.0626 ± 0.004″ (p.e.) is obtained. The corresponding absolute magnitude is M_V = +12.84 ± 0.13 mag (p.e.), which when combined with its measured colors (B − V = +0.18, U − B = −0.68, b − y = +0.141), places Ross 640 either 0.29 ± 0.13 mag (p.e.) above the lower white dwarf sequence in the M_V versus U − V diagram, or about 0.2 mag below the single white dwarf sequence in the M_V versus b − y diagram. (auth)

35603 RELATIVE PROPER MOTIONS IN THE REGION OF THE OPEN CLUSTER NGC 2168 (M35). Cudworth, Kyle M. (Univ. of California, Santa Cruz). Astron. J.; 76: No. 5, 475-83(Jun 1971).

Relative proper motions of 763 stars in the region of NGC 2168 were determined from two plate pairs taken at the Allegheny Observatory. The epoch difference of 41 years yielded centennial proper motions with a mean error from two plate pairs equal to ±0.11″. The probability of cluster membership was derived for each star with the conclusion that about 513 members were measured. (auth)

35604 INTERNAL MOTIONS IN PRAESEPE. Jones, Burton F. (Univ. of California, Santa Cruz). Astron. J.; 76: No. 5, 470-4(Jun 1971).

New relative proper motions were determined for 91 stars in Praesepe. The proper-motion dispersions showed that the velocity distribution in Praesepe is more isotropic than in the Pleiades. The velocity dispersion in one coordinate was 0.46 km/sec, assuming a distance of 160 pc to the cluster. A virial mass of 550 $M_\odot$ was obtained. The dependence of the velocity dispersion with magnitude was similar to that of the Pleiades. (auth)

35605 PRELIMINARY PHOTOMETRY OF THE OPEN CLUSTER NGC 609. Lee, Vincent J.; Burkhead, Martin S. (Indiana Univ., Bloomington). Astron. J.; 76: No. 5, 467-9(Jun 1971).

Preliminary photometric observations of the cluster NGC 609 indicate it is similar to M11. A color excess, E_{B-V} = 0.95, and a distance modulus of 12.45 yield (R = 3.0) a distance of 3.1 kpc and a linear diameter of 2.7 pc. The age is determined to be ~2×10^8 yr. (auth)

35606 PHOTOMETRIC STUDIES OF NORTHERN GALACTIC CLUSTERS. I. ROSLUND NO. 5. Lee, Paul D.; Perry, Charles L. (Louisiana State Univ. Observatory, Baton Rouge). Astron. J.; 76: No. 5, 464-6(Jun 1971).

UBV photometry is presented for 46 stars in the vicinity of the suspected galactic cluster Ros 5. The analysis shows that it is unlikely that Ros 5 is a bona fide open cluster but, rather, it is only a slightly obscured area with a background of relatively early-type stars at a mean distance of approximately 300 pc with a mean reddening of approximately 0.07 mag. (auth)

35607 PHOTOMETRIC ELEMENTS OF THE ECLIPSING BINARY EE PEGASI. Ebbighausen, E. G. (Univ. of Oregon, Eugene). Astron. J.; 76: No. 5, 460-4(Jun 1971).

New photometric orbital elements are given for the eclipsing binary EE Peg based on 1635 B observations made at the Pine Mountain Astrophysical Observatory of the University of Oregon. The secondary eclipse is total and shallow and results from the eclipse of the smaller, darker star by the larger Am star. Primary eclipse is annular. The peculiarities of the spectrum of the Am star are discussed. The limb-darkening coefficient of the Am component is determined. The rectification procedure is studied with considerable care in part because the A_1 coefficient of the cos θ term is positive. (auth)

35608 PHOTOELECTRIC OBSERVATIONS OF UU PISCIUM. Johnston, K. J. (Georgetown Coll. Observatory, Washington, D. C.). Astron. J.; 76: No. 5, 455-59(Jun 1971).

UU Piscium was monitored in the V color. The amplitude of the light variation was 0.03 mag. This is caused by the elliptical shapes of the component stars of UU Piscium. The phase of secondary minimum occurred at 0.55. The cause of this may be that the period of rotation of the component stars of UU Piscium is not synchronized with their orbital revolutions, or their orbit is elliptical. Previous observations of UU Piscium by Magalashvili and Kumsishvili seem to indicate that the orbit is elliptical. (auth)

35609 NEW PHOTOMETRIC SOLUTION FOR TW CASSIOPEIAE. McCook, George P. (Villanova Univ., Pa.). Astron. J.; 76: No. 5, 449-54(Jun 1971).

A new solution for TW Cassiopeia based on 649 yellow and 651 blue photoelectric observations was found to differ significantly from previously published solutions. The primary eclipse is shown to be a partial occultation. The system is semidetached and probably consists of a B9 and a G5 star. (auth)

35610 PHOTOMETRY OF VARIABLES IN GLOBULAR CLUSTERS. II. M13. Demers, Serge (Laurentian Univ., Sudbury, Ont.). Astron. J.; 76: No. 5, 445-8(Jun 1971).

U, B, V photographic photometry of three Population II Cepheids, one long-period variable, and two RR Lyrae stars in M13 are presented. The mean (B − V) colors of the Population II Cepheids are bluer than previously believed, and their magnitudes are fainter. The RR Lyrae variable 8 has normal magnitude and color for its type. The long-period variable is probably the brightest star in the cluster since it falls at the tip of the giant branch. The color effect derived in Paper I is not real; corrected magnitudes and colors of the M2 variables are presented. (auth)

35611 INTRINSIC POLARIZATION IN K AND M GIANTS AND SUPERGIANTS. Dyck, H. Melvin; Jennings, Mark C. (Kitt Peak National Observatory, Tucson, Ariz.). Astron. J.; 76: No. 5, 431-44(Jun 1971).

Multicolor polarimetry of 55 cool stars is presented. The location of intrinsic polarization in the H−R diagram is more precisely defined. The frequency of the phenomenon is high among K and M supergiants, showing no correlation with temperature. For luminosity class III stars the frequency is high for stars of spectral type M4 or later. The wavelength dependence of intrinsic polarization is discussed; it is argued that the polarization in giants and supergiants must be of circumstellar origin and that the mechanism is solid particles. (auth)

35612 uvby PHOTOMETRY OF Ap STARS: THE NATURE OF THE LIGHT VARIATIONS. Wolff, Sidney Carne; Wolff, Richard J. (Univ. of Hawaii, Honolulu). Astron. J.; 76: No. 5, 422-30(Jun 1971).

Four-color (uvby) observations of eight Ap stars were obtained at the Mauna Kea Observatory. For Ap stars cooler than about spectral type B9, large-amplitude light variations appear to occur only in those objects that also show pronounced spectrum variations. It is suggested that photometric variability may result from a redistribution of energy, which is caused by variable absorption in the region below about λ3000. (auth)

35613 SECONDARY UBV COMPARISON STARS NEAR SOME SOUTHERN GLOBULAR CLUSTERS. II. STARS BRIGHTER THAN 13th MAGNITUDE. White, Raymond E. (Univ. of Arizona, Tucson). Astron. J.; 76: No. 5, 419-21(Jun 1971).

The results for UBV-system magnitude sequences observed photoelectrically near six southern globular star clusters (NGC 3201, IC 4499, NGC 5986, 6316, 6266, and 6388) are assembled. Identification charts for the sequence stars are included. (auth)

35614 STRUCTURE OF DENSE STARS. PART II. THEORY OF STABILITY AGAINST RADIAL PULSATIONS. Abramowicz, M. A. Postepy Astron.: 19: No. 1, 19-43(Jan-Mar 1971). (In Polish).

A review is given of the classic papers by Chandrasekhar, Thorne, Wheeler, and coworkers concerning the theory of stability against centrally symmetric perturbations of very dense (relativistic) stars. The convective stability criterion is given, and the difficulties of the theory of stability against nonradial pulsations are briefly discussed. (auth)

35615 ELECTRIC CHARGE OF STARS. Shvartsman, V. F. State Astronomical Inst., Moscow. (Inst. of Applied Mathematics, Moscow). Zh. Eksp. Teor. Fiz.; 60: No. 3, 881-4(Mar 1971). (In Russian).

Stars possess electric charges, the sign and magnitude of which are determined by exchange processes between the stars and the surroundings. For compact objects (neutron stars, bodies below their gravitational radius) the corresponding potential difference may reach tens of billions of volts and may be capable of accelerating positrons produced near the compact objects up to the energies mentioned. (auth)

35616 RADIO EMISSION FROM FLARE STARS NEAR THE ORION NEBULA. Slee, O. B.; Higgins, C. S. (CSIRO, Epping, Australia). Aust. J. Phys.; 24: No. 2, 247-62(Apr 1971).

An experiment performed to detect the radio emission from energetic flares on some of the many flare stars in the Orion stellar aggregate is described. Radio emission in the metre waveband was probably detected from seven flares. Some possible mechanisms for both the optical and radio emissions are discussed. The high radio brightness temperatures of 10^{18} to 10^{20}°K cannot be due to incoherent synchrotron emission because of limitations due to self-absorption. The coherent mechanisms of plasma oscillations and amplification of gyro or synchrotron radiation can account for the radio observations without invoking the presence of abnormally dense particle streams, strong magnetic fields, or high ambient electron densities. The intense optical continuum may be generated by the incoherent synchrotron mechanism. (auth) (Australia)

35617 UBV, NARROW-BAND u(3580A), b(4250A), v(5050A), org(5905A), AND Hbeta PHOTOMETRY OF THE ECLIPSING SYSTEMS R CANIS MAJORIS AND V1010 OPH. Guinan, Edward Francis. Philadelphia; Univ. of Pennsylvania (1970). 347p. University Microfilms Order No. 71-7810.

Thesis.

U, B, V, narrow-band, and Hβ photoelectric photometry of the eclipsing systems R CMa and V1010 Oph was done with the 16-inch Cassegrain telescope at Mount John University Observatory in New Zealand. The observations were made on 32 nights during 1967-68. Nine hundred and ninety-five observations of R CMa and 1,271 observations of V1010 Oph were secured in 9 filters. Light curves, improved light elements, and orbital solutions were obtained for both systems. The orbital solutions were made using the method of Russell and Merrill. B − V, U − B, and Hβ indices were computed for the components of each system from their respective photometric solutions. The spectral types of the components were found from their color and Hβ indices. (TSS) (Diss. Abstr. Int., B)

35618 ELLIPTICAL POLARIZATION OF STARLIGHT. Wolf, George William. Philadelphia; Univ. of Pennsylvania (1970). 147p. University Microfilms Order No. 71-7872.

Thesis.

A survey search for elliptical polarization was undertaken on objects observable from the northern hemisphere. The 64 objects observed include O and B stars with a low ratio of polarization to interstellar absorption, and stars with intrinsic polarization, peculiar spectra, high linear polarization, wavelength dependence of position angles of polarization, and high magnetic fields. Several galaxies, planetary nebulae, reflection nebulae, and the Crab Nebula were also included. All observations were made at Kitt Peak National Observatory during December 1969 and January 1970. The final results list the linear polarization and position angle, the ellipticity, and the normalized Stokes parameters Q/I, U/I and V/I for all objects observed. No definite case of a significant circular component in the observed polarization of any of the survey objects was found. A few possible cases are discussed. Since the objects in the survey represent a fairly wide cross section, it must be concluded from the observational results that a circular component in the polarization of starlight is very small or nonexistent. (Diss. Abstr. Int., B)

35619 PHOTOELECTRIC OBSERVATIONS OF H-ALPHA IN LATE-TYPE STARS. Caplan, James Gerald. Evanston, Ill.; Northwestern Univ. (1970). 116p. University Microfilms Order No. 71-10,100.

Thesis.

A photoelectric investigation of the Hα absorption lines in G, K, and M stars is described that was undertaken with a pressure-scanning, echelle grating plus Fabry−Perot, spectrophotometer. After a review of some aspects of Hα in late-type stars, the instrumentation which was constructed for this study is discussed. Observations of some line profiles using the Fabry−Perot étalon, and also direct measurements of equivalent width using the grating system alone, are presented for 32 stars. It is concluded that a direct measurement of Hα equivalent width, in conjunction with an R−I color index, provides a potentially useful method of luminosity discrimination. The pressure-scanned grating provides a good method of making such observations. The more detailed profiles observed with the Fabry−Perot were not as useful for luminosity determination. However, experience suggests that this type of instrumentation could be quite successful for various stellar observations with modifications that are proposed. (Diss. Abstr. Int., B)

35620 $^{12}C/^{13}C$ AND THE CN/C_2 RATIO IN THE CARBON STARS 19 PSC AND Y CVN. Marenin, Irene Renate. Bloomington, Ind.; Inidana Univ. (1970). 176p. University Microfilms Order No. 71-6876.

Thesis.

The two carbon stars 19 Psc (C6,2) and Y CVn (C5,4) were studied in the near-infrared region (λλ 7680 to 7800 Å) in order to determine the isotopic ratio of $^{12}C/^{13}C$ and the molecular ratio of CN/C_2. The calibrated high-dispersion spectrograms (6 Å/mm) were compared to synthetic spectra calculated by assuming a Milne−Eddington (M−E) model atmosphere. The parameters of the model (temperature, abundance ratios, etc.), were varied till the difference between the two spectra was minimized. It was found that 19 Psc was best represented by a temperature of T_v = 2300° ± 150°K and T_r = 2100° ± 200°K. For Y CVn a temperature of T_v = 2700° ± 200°K and T_r = 2600° ± 200°K were assumed. The M−E model is inadequate for fitting all features by one temperature. A model atmosphere that takes the exact variations in temperature and molecular abundance (due to dissociation) with height in the atmosphere into account should be used in order to obtain better fits. The weak $^{13}C^{14}N$ features in 19 Psc imply an isotopic ratio of 12 to 22, whereas the strong $^{13}C^{14}N$ features in Y CVn imply a ratio of 2.5 to 4. Lines of the (3,0) band of the C_2 Phillips system could not be identified. Hence, $CN/C_2 > 100$ in 19 Psc and $CN/C_2 > 35$ in Y CVn. The nitrogen-to-carbon ratio was estimated as N/C > 50 (19 Psc). (Diss. Abstr. Int., B)

35621 ORIGIN OF MAGNETIC FIELDS IN WHITE DWARFS AND NEUTRON STARS. O'Connell, R. F.; Roussel, K. M. (Louisiana State Univ., Baton Rouge). Nature (London) Phys. Sci.; 231: 32-3(10 May 1971).

It is stated that the origin of magnetic fields in degenerate matter is of particular interest because of the discovery of large magnetic fields in some white dwarfs, and because of the even higher fields of the order of the critical magnetic field, thought to exist in pulsars, accepting the rotating neutron star theory. An interesting question is also why some, but not all, white dwarfs are magnetic. The fact that some supernovae do not have associated pulsars might also lead to the speculation that perhaps the collapse of all supernovae results in a neutron star, but that not all neutron stars are magnetic. These topics are discussed in terms of the magnetic moment of electron gas, Gibbs free energy, Helmholtz free energy, and metastable and unstable states. The results of Lifshitz and Kosevich (Sov. Phys. JETP 2: 636(1956)) are applied, with some necessary modifications, to consider the energy eigenvalues of a relativistic electron, but the same basic conclusions are reached for a non-relativistic electron gas; for making the analysis less cumbersome, further consideration is confined to the latter. (UK)

35622 PHOTOELECTRIC PHOTOMETRY OF HO TELESCOPII AND KZ PAVONIS. Shaw, James Scott. Philadelphia; Univ. of Pennsylvania (1970). 125p. University Microfilms Order No. 71-7853.

Thesis.

Photoelectric photometry was made in the ultraviolet, blue, and yellow on two newly discovered eclipsing binaries HO Telescopii and KZ Pavonis. Light curves, improved light elements and orbital solutions were obtained. HO Telescopii is a detached system consisting of two similar early A-type stars. A consistent solution was found in all three wavelength regions. KZ Pavonis is a semi-detached system in which primary is a very deep total eclipse. In the analysis a substantial amount of third light due to two visual companions was removed. A consistent solution was found in all three wavelength regions. (Diss. Abstr. Int., B)

35623 EVOLUTIONARY CONSIDERATIONS INVOLVING THE INTERNAL DENSITY CONCENTRATION PARAMETER OF BINARY STARS. Petty, Alan Frederick. Philadelphia; Univ. of Pennsylvania (1970). 141p. University Microfilms Order No. 71-7844.

Thesis.

The evolutionary changes that occur in the internal density concentration parameter k_2 for a star of given mass and initial composition were examined in detail. The express purpose of this analysis was to ascertain whether or not such an approach leads to a reduction in the differences now noted between the

XUM

theoretically derived values of k_2 and the observational values as derived from the orbital motion in close eclipsing binary systems. A series of stellar models of mass 0.5, 0.7, 1.0, 2.0, 5.0, 10.0, and 20.0 $M_\odot$, with an initial compositional mixture of X = 0.739, Y = 0.24 and Z = 0.021, was employed. These models cover an evolutionary range from a point in time where the stars have just completed the Hayashi phase of their pre-main-sequence contraction through their entire main-sequence phase to a point in time at which hydrogen depletion in the core is complete. In three cases, 1.0, 2.0, and 5.0 $M_\odot$, the evolutionary sequence was carried somewhat further along in time from the point of hydrogen-core depletion into the hydrogen shell-burning phase. For each model, a value of k_2 was determined by numerically integrating Radau's equation and using the values of $\rho(a)/\bar{\rho}$, the ratio of the star's density at point (a) to its mean density, as taken from the models. The result was the time history of k_2 for each stellar mass over the evolutionary range of interest. The results were then summarized in the (log k_2, log T_e) plane which for the first time, quantatively indicates the variation in k_2 as a function of the evolutionary state of the star. A comparison is presented between these theoretically derived values of k_2 and a selected set of observationally determined ones. It is apparent that the evolutionary variation in k_2 plays an extremely important role in any comparison between theory and observation. Though the present theory provides a satisfactory explanation for the known discrepancies in the determinations of k_2, there now exists the problem of accurately pinpointing the evolutionary state of the observed binary system. (Diss. Abstr. Int., B)

35624 EXTENDED MODEL ATMOSPHERES FOR THE CENTRAL STARS OF PLANETARY NEBULAE. Cassinelli, Joseph Patrick. Seattle; Univ. of Washington (1970). 122p. University Microfilms Order No. 71-8470.

Thesis.

Procedures were developed for the construction of spherical stellar model atmospheres. These procedures were applied to the calculation of grey and nongrey model atmospheres for the central stars of planetary nebulae. The models were calculated under the classical assumptions of hydrostatic, radiative, and local thermodynamic equilibrium. Spherical geometry and the $1/r^2$ dependence of gravity were taken into account. The spherical geometry hydrostatic equilibrium equation was solved including the effects of the radiative pressure gradient. Iteration of the hydrostatic calculation was required to obtain models with a predefined total optical thickness. A boundary condition on the hydrostatic equation was developed which clearly reduces to the plane parallel expression in the limit in which gravity is constant over the atmospheric layers. The radiative transfer equation was solved using the discrete S_N method of Carlson and Lathrop (1968) and a difference form of the diffusion approximation equation. The atmospheres were brought to radiative equilibrium using modifications to spherical geometry of the flux correction procedure of Unsöld (1951), for the grey case, and of the temperature correction procedure of Lucy (1964), for the nongrey case. Models which have radiative flux constancy of less than 1.5% were calculated using these procedures. (TSS) (Diss. Abstr. Int., B)

35625 INFRARED EXCESS OF W CEPHEI AND SIMILAR STARS. Wallerstein, George (Univ. of Washington, Seattle). Astrophys. J.; 166: No. 3, 725-9(15 Jun 1971).

Emission lines in W Cep were analyzed to yield an electron temperature of 5000 to 6000°K and an electron density of 2 to 4×10^9 electrons cm^{-3}. Much of the infrared excess can be explained by free–free emission from an envelope of radius 15 AU and the parameters listed above. The upturn in the emission from 8.4 to 11.0 μ cannot be due to free–free emission but must be due either to dust at a temperature less than 300°K or to emission lines. It is suggested that objects with infrared excesses can be placed into a sequence running from almost pure-dust envelopes as in NML Cygnus to pure-gas envelopes as in the Be stars. (auth)

35626 HYDROGEN-RICH MODELS FOR HORIZONTAL-BRANCH AND POST-HORIZONTAL-BRANCH STARS. Shipman, H. L. (Carnegie Institution of Washington, D. C. California Inst. of Tech., Pasadena). Astrophys. J.; 166: No. 3, 587-91(15 Jun 1971).

Hydrogen-rich model atmospheres in the temperature and gravity range applicable to old novae, sdO, DO, DA, and blue horizontal-branch stars are presented with emergent fluxes, hydrogen-line profiles, and helium-line equivalent widths. (auth)

35627 ABUNDANCES IN OPEN CLUSTERS: MODEL-ATMOSPHERE ABUNDANCE ANALYSIS OF STARS IN THE PLEIADES AND HYADES CLUSTERS. Chaffee, Frederic H. Jr. (Smithsonian Astrophysical Observatory, Cambridge, Mass.); Carbon, Duane F.; Strom, Stephen E. Astrophys. J.; 166: No. 3, 593-603(15 Jun 1971).

Detailed analysis of six F and G dwarfs in the Pleiades and fourteen in the Hyades indicates that the Fe/H ratio in the Hyades is 50% higher than that in the Pleiades, the latter yielding the solar value. To gain insight into the cause of the differences in observed narrow-band photometric indices between the clusters, a grid of blanketed model atmospheres was computed. The models provide estimates of the changes in the Strömgren four-color indices caused by variations in the metal abundance z and the microturbulent velocity ξ. The trajectories in the (m_1, b − y)-plane resulting from either of these variations are similar and difficult to distinguish observationally. The trajectories in the (c_1, b − y)-plane, however, differ significantly, and in some cases this may permit these two atmospheric parameters to be distinguished by the photometry alone. In the case of the Pleiades and Hyades, it appears that the observed differences in ξ and z can explain the photometric differences between the clusters. However, the effects of initial helium content and stellar evolution considerably complicate the interpretation of the Strömgren diagrams of these clusters; interpretation is even more difficult for more heterogeneous samples of stars. (auth)

35628 REALIZATION OF ACCURATE CLOSE-BINARY LIGHT CURVES: APPLICATION TO MR CYGNI. Wilson, Robert E.; Devinney, Edward J. (Univ. of South Florida, Tampa). Astrophys. J.; 166: No. 3, 605-19(15 Jun 1971).

A general procedure for computing monochromatic light curves of close eclipsing-binary systems is presented, with allowance for rotational and tidal distortion, the reflection effect, limb darkening, and gravity darkening. All basic techniques used to compute light curves are specified. Solution of the inverse problem (finding the elements from observations) is accomplished by differential corrections, and probable errors are obtained for all adjustable parameters. No rectification of any kind is used or needed. Because of the basic flexibility of the scheme, present limitations (e.g., synchronous rotation only, black-body physics) may be improved upon with reasonable convenience, as time permits. The procedure has been applied to B and V observations of MR Cyg, and the results of the differential corrections adjustments are given. With the use of available spectroscopic observations and model-atmosphere results by Mihalas, the components are placed in the H − R diagram. Although the primary seems to be on the main sequence, the secondary is found to be above the main sequence — an observation which suggests that the secondary may still be in the gravitational-contraction phase. (auth)

35629 NONLINEAR PULSATIONS AND STABILITY OF UNIFORMLY ROTATING SPHEROIDS. Tassoul, Jean-Louis; Tassoul, Monique (Univ. of Montreal). Astrophys. J.; 166: No. 3, 621-5(15 Jun 1971).

Finite-amplitude axisymmetric motions of a uniformly rotating, gaseous spheroid of uniform density are considered. Nonlinear adiabatic pulsations are described by means of Lagrangian variables. Conservation of energy then provides a criterion for discussing the stability of these motions. According to the linear analysis, the adiabatic exponent γ at which dynamical instability sets in, γ_L, is smaller than $4/3$ when rotation is present; γ_L thus unequivocally delineates stable from unstable infinitesimal oscillations. This work shows that nonlinear motions are indeed stable when $\gamma \geq 4/3$, and unstable when $\gamma \leq \gamma_L$; however, in the range $\gamma_L < \gamma < 4/3$ they can also grow in time, if the amount of energy needed to sustain them becomes too large. Allowance for finite-amplitude motions thus lessens the stabilizing influence of rotation predicted in the linear analysis. (auth)

35630 GALACTIC NEBULA YM 29. Terzian, Yervant (Cornell Univ., Ithaca, N. Y.). Astrophys. J.; 166: No. 3, 559-61(15 Jun 1971).

Radio observations at 318 and 606 MHz of the galactic nebula YM 29 are presented. It is shown that this nebula has a thermal radio spectrum and is probably a planetary nebula of low density. Balmer-line fluxes are predicted which indicate that these emission lines should be observable. (auth)

35631 FORMATION OF CONDENSATIONS IN PLANETARY NEBULAE. I. Capriotti, Eugene (Ohio State Univ., Columbus. Ohio Wesleyan Univ., Delaware). Astrophys. J.; 166: No. 3, 563-72(15 Jun 1971).

The condensations in planetary nebulae are considered in terms of the "mock gravitational" instability that may arise from shadowing effects on radiation. The nebulae are assumed to contain dust particles which provide an energy sink for L_α radiation. Apparently, ionized regions are stable against L_α pressure-induced condensation whereas neutral regions are not, in general, stable

against such condensations. However, conditions in the neutral parts of young planetary nebulae are probably unfavorable to Lα pressure-induced condensation. The condensations are also considered in terms of gravitational stability. Surprisingly, the gas in a very young planetary nebula may be gravitationally unstable. The Jeans wavelength, however, is never significantly smaller than the dimensions of the nebula, and it is doubtful that gravitational instability could be responsible for the small-scale structure of planetary nebulae. (auth)

35632 HYADES MEMBERSHIP OF THE WHITE-DWARF ECLIPSING SYSTEM BD +16°516. Young, Arthur; Capps, Richard, W. (San Diego State Coll., Calif.). Astrophys. J.; 166: No. 3, L81-3(15 Jun 1971).

Evidence is presented that indicates that this important eclipsing binary is a member of the Hyades Cluster. (auth)

35633 CHEMICAL COMPOSITION OF THE SYMBIOTIC STARS. Boyarchuk, A. A. Izv. Krym. Astrofiz. Observ.; 41-42: 264-74(1970). (In Russian).

From an investigation of the relative intensities of the emission lines, it was found that the chemical composition of the nebulae of the symbiotic stars AG Dra, Z And, AX Per, CI Cyg, BF Cyg, and MH_α 328-116 does not differ from that of the planetary nebula NGC 7027. (auth)

35634 THREE-COLOR PHOTOELECTRIC OBSERVATIONS OF Z AND FROM 1962 TO 1967. Belyakina, T. S. Izv. Krym. Astrofiz. Observ.; 41-42: 275-82(1970). (In Russian).

During 1964–1967 three-color photoelectric observations of Z And were carried out in the system similar to UBV. For the period from 1962 to 1967 a composite photoelectric light curve was constructed in the instrumental system. The considerable synchronous light variations of Z And were noted; the amplitude of light variations is 2.1 m for yellow light, 2.6 m for the blue, and 2.7 m for the ultraviolet. Light variations of Z And in yellow light were compared to its corresponding displacements on a two-color diagram. From the beginning of the observations up to J. D. 2438975, the yellow and blue region radiation of the spectrum was subjected to larger variations than the ultraviolet while from J. D. 2438998 to the end of the observations the latter showed the largest ones. It was determined qualitatively that photoelectric observations were in good agreement with the hypothesis of the composite construction of Z And (M2 III + hot star + gas). The rough estimation of the hot-component amplitude was 5 m in yellow light. It was calculated that the luminosity of a cold component without interstellar absorption was 11.0 m in yellow light, that of a hot component in minimum was about 14 m. (auth)

35635 STUDY OF THE ATMOSPHERES OF SUPERGIANTS. II. QUANTITATIVE ANALYSIS OF γ CYG AND ε PEG. Zeinalov, S. K. Izv. Krym. Astrofiz. Observ.; 41-42: 298-341(1970). (In Russian).

Using the curve-of-growth method, an analysis of physical parameters characterizing the atmospheres of Ib supergiants γ Cyg (F8) and ε Peg (K2) was carried out. In 1964, eight spectra with a dispersion of 1.0 to 2,07 Å/mm taken at the coudé focus of the 2.6-m reflector of the Crimean Astrophysical Observatory were used. In the region of λλ3660 to 6845 Å about 2250 and 2000 lines were identified, and equivalent widths were obtained for each star. The increase of excitation temperature (T_e) with the mean excitation potential was confirmed. The excitation temperatures of neutral atoms were higher than those of the ions. The inequality $\overline{T}_e < T_{eff}$ was valid. It was found that the microturbulent velocity for the lines of ions was larger on the average than for the lines of neutral atoms. With excitation potential increasing, the microturbulent velocities decrease to a certain minimum. (auth)

35636 SPECTROPHOTOMETRIC STUDY OF FOUR K STARS. Boyarchuk, M. E.; Voikhanskaya, N. F. Izv. Krym. Astrofiz. Observ.; 41-42: 342-56(1970). (In Russian).

The physical characteristics and chemical composition of the atmospheres of four K stars, 70 Oph K0 V, ε Peg K2 Ib, 61 Cyg A K5 V, and ξ Cyg K5 Ib were analyzed by the curve-of-growth method. Forty-five spectrograms with a dispersion of 33 Å/mm at λλ6800 to 5300 Å and 14 Å/mm at λλ5000 to 3800 Å were used. The equivalent widths were determined for 280 absorption lines of the metals. The turbulent velocities, excitation temperatures, and electron densities were obtained for the dwarfs and supergiants. A comparison of the relative chemical composition of the stellar atmospheres studied showed that the abundance of lithium in the atmospheres of 61 Cyg A and of ξ Cyg is less by a factor of 30 than in the atmospheres of 70 Oph and ε Peg. The abundance of Sr, Y, and Ba in the atmospheres of the stars studied is more by a factor of 3 than that in the solar atmosphere. The relative chemical abundances of the other elements do not differ from that of the solar atmosphere. (auth)

35637 POLARIMETRIC MEASUREMENTS OF UV CETI-TYPE STAR FLASH RADIATION. Efimov, Yu. S. Izv. Krym. Astrofiz. Observ.; 41-42: 357-66(1970). (In Russian).

The problem of the polarimetric measurements of flash-star radiation during the flare is considered. It is suggested that the observations be carried out with a one-channel photoelectric polarimeter. The method of the continuously rotating analyzer and digital pulse-counting system are used. It is shown that polarization measurements will not be distorted by the influence of light variation during the observation if the frequency of the analyzer rotation f is higher than $f_{min} = 0.20\ \overline{r}_m/\Delta p$, where $\overline{r}_m$ is the mean rate of the magnitude of star change during the observation and Δp is the acceptable error of polarization measurement in the case. The influence of the statistical fluctuation of the signal on the signal on the accuracy of observation was estimated. The dependence of the accuracy of photoelectric polarization measurements on the observational conditions was found. Using AD Leo as an example, it is shown that an accidental error in the percentage polarization is of the order of ±0.2% and about ±6° in the polarization position angle if the observations are made with the 2.6-m telescope for 10 or 20 seconds. It is concluded that the polarimetric observations of some flash stars during the flare are possible under certain conditions. (auth)

35638 TV OBSERVATIONS OF SN 1966 (NGC 3198) AND SN1967 (NGC 3389). Prokof'eva, V. V. Izv. Krym. Astrofiz. Observ.; 41-42: 367-71(1970). (In Russian).

Seventy TV observations of two supernovae were made with the 20- and 50-cm telescopes during a 3-month period. The exposure were 30 sec. The accuracy of one estimation of stellar brightness is ±0.10 to ±0.15 m. (auth)

35639 TV SYSTEM USED FOR THE OBSERVATIONS OF FAINT VARIABLE STARS AT THE CRIMEAN ASTROPHYSICAL OBSERVATORY. Abramenko, A. N.; Istomin, L. F.; Prokof'eva, V. V. Izv. Krym. Astrofiz. Observ.; 41-42: 372-83(1970). (In Russian).

The highly sensitive TV system mounted on the 0.5-m telescope allows observations of 16 to 17 m variable stars. The exposure time is from 20 to 120 sec. The accuracy obtained is compared to that of the photographic method. Regular TV observations of short-period variables in star clusters are being carried out. It took only 20 hours to make 850 TV observations of the open cluster NGC 188. Light curves of W UMa type variables S 8279 (ER Cep) and S 8280 (ES Cep) are given. (auth)

35640 VSPYSHKI KRASNYKH KARLIKOVYKH ZVEZD. (Flares of Red Dwarf Stars). Gershberg, R. E. Moscow; Izdatel'stvo Nauka Glavnaya Redaktsiya Fiziko-Matematicheskoi Literatury (1970). 168p.

The results of observations and theoretical studies of the flare activity of UV-Cet-type red dwarfs were critically analyzed. The analysis includes photometric, colorimetric, spectral, polarimetric, and radio-astronomical investigations, results of which were published before autumn 1969. Luminosity curves of the flares of different stars are illustrated, and tables include statistical data for the flare frequency of different objects. The results are used to construct a simple phenomenological scheme of UV-Cet-type flares. Attention is given to different hypotheses for the flare mechanism, including the hot spot, external excitation, scintillation of relativistic electrons ejection of matter from the interior, internal electromagnetic forces, stimulated emission of nonequilibrium plasma, and Compton scattering on thermal photons. A nebular model of flares is constructed, and the overall flare activity of low-mass stars is related to other features of stellar instability and stellar evolution. (IAA)

35641 PULSARS AND TYPE II SUPERNOVAE. Shkovskii, I. S. (Space Research Inst., Moscow). Astrophys. Lett.; 8: No. 2, 101-3(Apr 1971).

Most pulsars originate from Type II supernova explosions. From this identification it follows that several empirical characteristics of exploding massive stars may be obtained. Some difficulties arise from the large masses and fast rotation of these stars. To overcome these difficulties it is necessary to suppose that ejection of mass during explosion takes place by the loss of rotational stability. (auth)

35642 RADIO RECOMBINATION LINE IN NGC 7027. Rubin, R. H. (Univ. of Illinois, Urbana); Palmer, Patrick. Astrophys. Lett.; 8: No. 2, 79-82(Apr 1971).

The H85α recombination line at 10522.04 MHz in the planetary nebula NGC 7027 was observed. A signal somewhat larger than the peak-to-peak noise was observed, and the inferred physical pa-

XUM

rameters were consistent with those obtained from optical work. (auth)

35643 NARROW BAND FILTER PHOTOGRAPHS AND SPECTRA OF THE PLANETARY NEBULA NGC 7009. Ford, W. Kent Jr.; Rubin, Vera C. (Carnegie Institution of Washington, D. C.). Astrophys. Lett.; 8: No. 2, 67-71(Apr 1971).

Photographs of NGC 7009 were obtained with 10 Å interference filters centered at wavelengths of selected emission lines. The appearance of the nebula is strikingly different in the light of [O III] and Hα from that in [N II] and [S II]. Spectra across the disk and in the knot at the E end of the ansae indicate that this difference is due to the large variations in intensities of the lines in the various regions. Spectra indicate a systematic variation in velocity across the nebula. By use of a model for NGC 7009 developed by Wilson (1958) and Weedman (1968) it is possible to explain the line-of-sight velocities as projections of the expansion velocities in the nebular shell. (auth)

35644 ATOMS IN A SUPERSTRONG MAGNETIC FIELD. Kadomtsev, B. B.; Kudryavtsev, V. S. JETP Lett. (USSR) (Engl. Transl.); 13: No. 1, 42-4(5 Jan 1971).

Translated from Zh. Eksp. Teor. Fiz., Pis'ma Red.; 13: No. 1, 61-4(5 Jan 1971).

It has been shown (Kadomtsev, 1970) that in the magnetic field region $Z^4 < B < Z^3$ the ground state of a very heavy atom can be described within the framework of the modified Thomas–Fermi model. The atom retains spherical symmetry, and its radius varies as $Z^{-1}B^{-1}$. The same article contains qualitative ideas concerning the possible conservation of spherical symmetry also when $B > Z^3$, when not more than one electron remains at each level. However, the latter statement turns out to be incorrect—the more accurate quantitative analysis presented here for the limiting case $B > Z^3$ shows that, in this case, the ground state with minimum energy corresponds not to a spherical electron density distribution, as in the case when $B < Z^3$, but to a distribution strongly elongated in the direction of the magnetic field. In this sense the case $B \gg Z$ corresponds to the hydrogen atom at $B \gg 1$. (W.D.M.)

35645 MOLECULES IN AN ULTRASTRONG MAGNETIC FIELD. Kadomtsev, B. B.; Kudryavtsev, V. S. JETP Lett. (USSR) (Engl. Transl.); 13: No. 1, 9-12(5 Jan 1971).

Translated from Zh. Eksp. Teor. Fiz., Pis'ma Red.; 13: No. 1, 15-19(5 Jan 1971).

In a very strong magnetic field (10^9 Oe) an atom becomes strongly stretched along the magnetic field. Such atoms have a large electric quadrupole moment and should become bound into stable molecules. This makes possible the formation of molecules of a highly extraordinary type, in which the electron cloud becomes common, and all the electrons form a negatively charged "needle," with the nuclei lying on its axis. The binding energy of such a molecule is determined approximately, disregarding the interaction of the atoms at large distances. (W.D.M.)

35646 CATALOGUE OF STARS MEASURED IN THE GENEVA OBSERVATORY PHOTOMETRIC SYSTEM. Rufener, F. G. (Geneva Observatory). Astron. Astrophys., Suppl. Ser.; 3: No. 3, 181-252(Mar 1971).

A compilation of the photoelectric measurements in the Geneva Observatory seven-color system ($UBVB_1B_2V_1G$) is presented. The catalogue includes data for 1406 stars. The pass-band profiles and the internal accuracy of the measurements are dealt with. (auth)

35647 DERIVATION OF THE ORBIT OF A DOUBLE STAR FROM OBSERVATIONS MADE WITH AN INTENSITY INTERFEROMETER. Herbison-Evans, D. (Sydney Univ.). Comput. Phys. Commun.; 2: No. 2, 59-78(Feb-Mar 1971).

The data from a stellar intensity interferometer, consisting of a set of observations of the correlation of the light from two optical reflectors with a given separation (the baseline), was used to determine the orbit of α Vir. (W.D.M.)

35648 LIGHT CURVE AND PHOTOMETRIC ELEMENTS OF β AURIGAE. Johansen, K. T. (Copenhagen Univ. Observatory, Brorfelde, Denmark). Astron. Astrophys.; 12: No. 2, 165-74 (May 1971).

Photoelectric observations of the eclipsing binary β Aur were carried out in B and V in four spectral regions close to the Strömgren u, v, b, y system and in two Hβ regions. Several solutions for the photometric elements can be obtained since the eclipses are very shallow. However, from spectroscopic work it turns out that the two components are almost identical. Photometric elements were therefore computed assuming the ratio of the radius of the eclipsing star to the radius of the eclipsed star in primary minimum equal to 1.1, 1.0, or 0.9. (auth)

35649 MODEL-ATMOSPHERE ANALYSIS OF FIVE APPARENTLY SUPER-METAL-RICH K GIANTS. Strom, S. E.; Strom, K. M.; Carbon, D. F. (State Univ. of New York, Stony Brook. Smithsonian Astrophysical Observatory, Cambridge, Mass.). Astron. Astrophys.; 12: No. 2, 177-89(May 1971).

Recent work by Spinrad and Taylor has led to the conclusion that there exists a class of "super-metal-rich" (SMR) stars among field and cluster K giants. The results of this paper suggest that φ Aur, μ Leo, λ Hya, and 20 Cyg, four field representatives of this class, have abundances within 0.2 in the log of normal values for K giants. The star μ Aql appears to be overabundant by 0.3 in the log compared to normal K giants and could be called SMR. These conclusions are based on model-atmosphere abundance analyses for these stars relative to the normal field giant ε Vir and the Hyades giants γ Tau, δ Tau, and ε Tau. It is suggested that some of the observable phenomena attributed to super-metal richness may result in part from an increase in the turbulent-velocity parameter. For example, results based on blanketed model atmospheres indicate that variations in turbulence can produce significant changes in the broad-band photometric indices. These changes cannot be distinguished easily by broad-band photometry alone from those caused by metallicity variations. Finally, the computations suggest that a decrease in the boundary temperature of a K giant can produce selective enhancements of Ca, Na, Mn, and V line strengths. It is just these elements that appear to show the most abnormal behavior in the SMR stars. A boundary temperature decrease relative to normal K giants could be caused by the increased strengths of the CO and/or CN bands in the SMR stars. The results of this work suggest that the stars selected by Spinrad and Taylor as SMR are a mixed group having one or more of the following characteristics: (a) higher turbulence; (b) enhanced CO and/or CN band strengths, which contribute to lowering the stellar boundary temperature; or (c) a slight increase in metal content. (auth)

35650 FINE STRUCTURE OF NEBULAR EMISSION LINES. Dyson, J. E.; Meaburn, J. (Univ. of Manchester, Eng.). Astron. Astrophys.; 12: No. 2, 219-22(May 1971).

The effect of fine structure on the profile of Hα in diffuse nebulae is discussed in detail. Published electron temperatures derived from a comparison of the line widths of Hα and [N II] at 6584 Å are critically evaluated. (auth)

35651 VARIABILITY OF A AND F MAIN SEQUENCE STARS. Joergensen, H. E. (Copenhagen Univ. Observatory); Johansen, K. T.; Olsen, E. H. Astron. Astrophys.; 12: No. 2, 223-31(May 1971).

Ninety-four bright stars mostly of spectral type A and F in the southern sky were tested for short-period variability. Three new δ Scuti variables were found. Further, six stars showed systematic variations less than 0.01 magnitude, but no decision on intrinsic variability of these stars could be made. (auth)

35652 SECULAR STABILITY. I. A POPULATION I STAR NEAR THE MAIN SEQUENCE. Aizenman, M. L.; Perdang, J. (Univ., Liege). Astron. Astrophys.; 12: No. 2, 232-9(May 1971).

The evolution of a Population I star of 1.13 $M_\odot$ was studied, and its secular spectrum was examined. It was found that, near the main sequence, the star has stable eigenvalues with the lowest modes complex. As evolution proceeds away from the main sequence, new modes become complex as well. Eigenvalues and eigenfunctions for the models considered were calculated. (auth)

35653 DETAILED ANALYSIS OF THE METALLIC-LINE STAR 15 VULPECULAE. Faraggiana, R.; van't Veer-Menneret, C. (Osservatorio Astronomico, Trieste, Italy. Institut d'Astrophysique, Paris). Astron. Astrophys.; 12: No. 2, 258-63(May 1971).

The differential curve-of-growth analysis of 15 Vulpeculae confirmed its marginal metallic-line star type, with the characteristics of a subgiant of luminosity class III, in agreement with recent photometric results and an earlier analysis by Miczaika et al. (1956). Other cases of metallic-line stars that appear to be subgiants on the basis of photometric criteria are discussed. The following atmospheric parameters were found to be the best to explain the observations: $\theta = 0.63$, $\log g = 3.5$. The abundance analysis showed a very slight underabundance of calcium and scandium, iron normal, and a weak but real overabundance of heavier elements. (auth)

35654 UBV PHOTOMETRY OF THE ECLIPSING BINARY ZETA PHOENICIS. Dachs, J. (Ruhr Univ., Bochum, Ger.). Astron. Astrophys.; 12: No. 2, 186-96(May 1971).

Two-hundred photoelectric observations of ζ Phe in the UBV system, along with recent radial velocity measurements by Popper (1970), were used to derive an improved set of elements of this eclipsing binary system with detached components. The colors of the components corresponded to stars of spectral types B7V and B8.5V, respectively. The radii of the individual

XUM

components of the system were: $R_1 = 2.96 \pm 0.05$, $R_2 = 1.96 \pm 0.06$ (solar radii). The observed radii were compared to radii computed from the theory of stellar interiors by various authors, for stars of masses as measured by Popper (1970) for the components of ζ Phe ($M_1 = 3.85 \pm 0.2$, $M_2 = 2.5 \pm 0.1$ solar masses). The best agreement for the radii was obtained with the stellar models of Mathis (1967). The evolutionary age of the system was estimated from the increase of radii as compared to age zero models and was about 1.0×10^8 years. The observed values of the magnitudes and colors of the components of ζ Phe and theoretical results for the luminosities and effective temperatures are discussed. A difference of the depths of the primary minimum was found between the spectral ranges V, B, and U. This difference of depths may be explained by a faint extended envelope surrounding the smaller component of the system and giving rise to continuous absorption in the U spectral band. The line of apsides was found to rotate by at least 120 or 240° within 20 years. A rotation of the line of apsides of 240° within 20 years was in quantitative agreement with the amount of apsidal motion predicted by Mathis (1967) for a system like ζ Phe. (auth)

35655 PHOTOELECTRIC OBSERVATIONS OF LUNAR OCCULTATIONS. Pansch, E.; de Vegt, Chr. (Hamburger Sternwarte, Hamburg). Astron. Astrophys.; 12: No. 2, 310-11(May 1971).

Photoelectric timings of lunar occultations observed at the Hamburg Observatory during 1970 with the 60 cm refractor are quoted. Those stars that need further observations for final decision on possible double star nature are specified. (auth)

35656 RAPID EVOLUTION OF LkHα 190. Welin, G. (Uppsala Astronomical Observatory). Astron. Astrophys.; 12: No. 2, 312(May 1971).

A very rapid period of evolution in the star LkHα 190 in which a large increase in luminosity occurred in November 1969 is discussed briefly. (W.D.M.)

35657 STELLAR CHROMOSPHERES. Bappa, M. K. V. (Kodaikanal Observatory, India). pp 79-86 of Proceedings of the Eleventh Symposium on Cosmic Rays, Astrophysics, Geophysics and Elementary Particle Physics, 1969. Vol. I. Bombay; Department of Atomic Energy (1969).

From eleventh symposium on cosmic rays, astrophysics, geophysics and elementary particle physics; Delhi, India (7 Oct 1969). See CONF-691055-(Vol. 1).

A study of the chromospheres of stars is capable of shedding much light on the phenomena prevalent in the atmospheres that produce these characteristics. Much can be learned also from a study of the solar chromosphere and extrapolating the results to stellar chromospheres. These two approaches are briefly discussed. (W.D.M.)

35658 INFRARED ASTRONOMY. Vardya, M. S. (Tata Inst. of Fundamental Research, Bombay). pp 87-99 of Proceedings of the Eleventh Symposium on Cosmic Rays, Astrophysics, Geophysics and Elementary Particle Physics, 1969. Vol. I. Bombay; Department of Atomic Energy (1969).

From eleventh symposium on cosmic rays, astrophysics, geophysics and elementary particle physics; Delhi, India (7 Oct 1969). See CONF-691055-(Vol. 1).

The difficulties inherent in infrared astronomy consist of lack of sensitive detectors, background radiation, terrestrial absorption, and atmospheric transparency uncertainties. Despite these difficulties solid results have been obtained. Selected results are briefly discussed. (W.D.M.)

35659 HIGHLIGHTS OF NEW ASTRONOMIES. Sreekantan, B. V. (Tata Inst. of Fundamental Research, Bombay). pp 100-29 of Proceedings of the Eleventh Symposium on Cosmic Rays, Astrophysics, Geophysics and Elementary Particle Physics, 1969. Vol. I. Bombay; Department of Atomic Energy (1969).

From eleventh symposium on cosmic rays, astrophysics, geophysics and elementary particle physics; Delhi, India (7 Oct 1969). See CONF-691055-(Vol. 1).

Developments are briefly summarized in the fields of microwave astronomy, masers, infrared astronomy, ultraviolet astronomy, x-ray astronomy, gamma-ray astronomy, and pulsars. (W.D.M.)

35660 COLLAPSED OBJECTS. Chitre, S. M. (Tata Inst. of Fundamental Research, Bombay). pp 130-42 of Proceedings of the Eleventh Symposium on Cosmic Rays, Astrophysics, Geophysics and Elementary Particle Physics, 1969. Vol. I. Bombay; Department of Atomic Energy (1969).

From eleventh symposium on cosmic rays, astrophysics, geophysics and elementary particle physics; Delhi, India (7 Oct 1969). See CONF-691055-(Vol. 1).

The physics of white-dwarf and neutron-star formation is reviewed, and the radiation emission mechanism for pulsars is discussed. The possible origin of cosmic radiation in pulsars is considered. (W.D.M.)

35661 PRESSURE EFFECT AND ABSORPTION COEFFICIENT OF H^-. Tarafdar, S. P.; Vardya, M. S. (Tata Inst. of Fundamental Research, Bombay). pp 431-5 of Proceedings of the Eleventh Symposium on Cosmic Rays, Astrophysics, Geophysics and Elementary Particle Physics, 1969. Vol. II. Bombay; Department of Atomic Energy (1969).

From eleventh symposium on cosmic rays, astrophysics, geophysics and elementary particle physics; Delhi, India (7 Oct 1969). See CONF-691055-(Vol. 2).

An attempt was made to determine the bound-free absorption coefficient of H^- incorporating the effect of interparticle interaction in the Debye-Hueckel approximation. The absorption of radiation by H^- is important as a source of opacity in the atmosphere of late-type stars, specifically dwarf stars. Most investigations assume that the absorption by H^- takes place without the interference by other particles, which is valid only at low densities, and it is in this attempt that modifications are made at high densities. (J.C.W.)

35662 PHOTOELECTRIC ELEMENTS OF ECLIPSING SYSTEM WX CEPHEI. Kandpal, C. D.; Sirvastava, J. B. (Uttar Pradesh State Observatory, Naini Tal, India). pp 436-9 of Proceedings of the Eleventh Symposium on Cosmic Rays, Astrophysics, Geophysics and Elementary Particle Physics, 1969. Vol. II. Bombay; Department of Atomic Energy (1969).

From eleventh symposium on cosmic rays, astrophysics, geophysics and elementary particle physics; Delhi, India (7 Oct 1969). See CONF-691055-(Vol. 2).

The star system WX Cep was observed on 20 nights from 1966 to 1968 to study the photoelectric elements of the eclipsing system. The star BD + 62°2094 was used as a comparison star. The geometrical, photometric, and absolute elements determined are tabulated. The Roche constants for the equipotential surfaces of the system are given, and it appears that the WX Cep system is a detached one. (J.C.W.)

35663 SIZE-DEPENDENT RESONANCE IN MIE THEORY OF SCATTERING AND UNIDENTIFIED INTERSTELLAR BANDS. Shah, G. A. (Tata Inst. of Fundamental Research, Bombay). pp 440-2 of Proceedings of the Eleventh Symposium on Cosmic Rays, Astrophysics, Geophysics and Elementary Particle Physics, 1969. Vol. II. Bombay; Department of Atomic Energy (1969).

From eleventh symposium on cosmic rays, astrophysics, geophysics and elementary particle physics; Delhi, India (7 Oct 1969). See CONF-691055-(Vol. 2).

Some exact calculations on Mie theory of scattering are given for small smooth single metallic spheres to help explain a strong unidentified interstellar band that occurs at 4430 A with full bandwidth of 40 to 150 A and half width of 19 to 26 A. It is concluded that sodium, potassium, and calcium may be important in producing some of the interstellar bands. (J.C.W.)

35664 ROTATIONAL VELOCITIES AND MAGNETIC FIELDS OF A_p STARS. Babu, G. S. D. (Uttar Pradesh State Observatory, Naini Tal, India). pp 451-3 of Proceedings of the Eleventh Symposium on Cosmic Rays, Astrophysics, Geophysics and Elementary Particle Physics, 1969. Vol. II. Bombay; Department of Atomic Energy (1969).

From eleventh symposium on cosmic rays, astrophysics, geophysics and elementary particle physics; Delhi, India (7 Oct 1969). See CONF-691055-(Vol. 2).

Information on the magnetic-field strengths is available for 72 stars. For nine of these stars, the values of V sin i are available from the literature. The maximum modulus of the effective magnetic-field strength and the V sin i of these 9 stars are tabulated. From a plot of these figures it is suggested that, for rotating magnetic stars, a linear relationship apparently exists between the two parameters. Using a least-squares solution, a relationship is given. (J.C.W.)

35665 RELATIVE MOTION OF TWO SPHEROIDAL RIGID BODIES. II. Lanzano, Paolo (North American Rockwell Corp., Downey, Calif.). Astrophys. Space Sci.; 11: No. 2, 191-221(May 1971).

An isolated binary system is considered whose components are bodies: (1) of comparable size; (2) of constant density; and (3) having the shape of an oblate ellipsoid of revolution with small meridional eccentricity. The equations that determine the relative motion of the centroids and the angular motion for the two sets of body axes constitute a simultaneous system of seven nonlinear, second-order differential equations for which solutions are obtained as power series in the two meridional eccentricities. A recurrent procedure is formulated to ascertain

XUM

the various approximations in terms of lower-order terms; it gives rise to linear differential equations with constant coefficients for the angular variables and to differential equations of the Hill type for the other coordinates. The zero-order approximation for the motion of the centroids is assumed to be a Kepler elliptic orbit of small eccentricity. The following contributions are made: (1) the general solution to the zero-order approximation of the rotational motion is obtained in terms of elementary functions; (2) certain functionals, related to the Kepler motion and depending on two parameters, are expressed in terms of the mean anomaly up to the sixth power of the orbital eccentricity in order to evaluate the lower-order terms of the various approximations; (3) secular terms are eliminated from the first-order approximation; (4) the second-order approximation is also obtained; and (5) an alternate procedure is suggested that might be more appropriate for achieving higher-order approximations. (auth)

35666 LIGHT CURVE AND ORBITAL ELEMENTS OF V 337 AQUILAE. Catalano, F. A.; Catalano, S.; Rodono, M. (Univ., Catania, Italy. Consiglio Nazionale delle Richerche, Catania, Italy). Astrophys. Space Sci.; 11: No. 2, 232-43(May 1971).

From photoelectric observations of V 337 Aql, a new solution was carried out. Transit at primary eclipse in disagreement with the Wright–Dugan results was found. Both Russell–Merrill and Kitamura methods of light curve solution were used. The slight period variation and the distortions of the light curve would support the idea that a mass exchange could be in action. (auth)

35667 CORONAE OF COOL STARS. de Jager, C. (Astronomical Inst., Utrecht); de Loore, C. Astrophys. Space Sci.; 11: No. 2, 284-7(May 1971).

With the hypothesis generally adopted as responsible for the heating of the solar corona, an attempt was made to predict the coronal temperature for a few cool stars. Stars with effective temperatures between 2500 and 3700 K, with log g-values of 3 or 4, appear to have coronal temperatures only 600 to 25,000 K higher than T_{eff}. In order to determine the possibility of coronal heating caused by sound waves, a comparison was made between the frequency of the sound waves and the cutoff frequencies. (auth)

35668 REVIEW OF RADIO OBSERVATIONS OF PLANETARY NEBULAE. Heckathorn, Joy (Northwestern Univ., Evanston, Ill.). Astrophys. Space Sci.; 11: No. 2, 309-21(May 1971).

The observational data for planetary nebulae in the radio region of the spectrum is reviewed and summarized. The methods of determining interstellar extinction, electron temperatures, and turnover points in the spectrum for these observations are given, as are the tests for the recombination theory and a discussion of the validity of several models of these objects. (auth)

35669 SHORT-PERIOD MAGNETIC VARIABLE HD 133029. Steinitz, Raphael; Pyper, Diane M. (Tel-Aviv Univ., Israel). Astrophys. Space Sci.; 11: No. 2, 322-9(May 1971).

It is shown that the magnetic measurements of HD 133029 exhibit a correlation of magnetic intensity with exposure length. Due to this effect a re-examination of the star's period was undertaken, resulting in a new value of 0.168. The significance of such a short period is discussed. It is argued that this short variation cannot be due to an oblique rotator. (auth)

35670 A–K SUPERGIANT STARS AND INTERSTELLAR ABSORPTION IN THE DIRECTION OF THE LARGE MAGELLANIC CLOUDS. Lenoble, Jacqueline (Univ., Lille). Compt. Rend., Ser. B; 272: No. 14, 873-6(5 Apr 1971). (In French).

The spectral classification and UBV photometry of 42 supergiant stars of advanced spectral types enabled the interstellar absorption in the direction of the Large Magellanic Clouds to be determined ($\bar{A}_v = 0.24 \pm 0.02$). This result completes that obtained from hot star observations ($A_v = 0.30 \pm 0.02$). (France)

35671 *VARIABLES IN NGC 1466.* Wesselink, A. F. (Radcliffe Observatory, Pretoria). Mon. Notic. Roy. Astron. Soc.; 152: 159-63(1971).

The variables of the Magellanic Cloud globular cluster NGC 1466, are discussed. In all, 43 RR Lyrae variables were discovered. Periods and light curves are presented for six of these. Five are of Bailey class a, and one is a c type. The mean apparent magnitude of the variables is 19.1. The corresponding apparent distance modulus is 18.6. (auth) (UK)

35672 VARIABILITY OF M STARS. Stokes, N. R. (Australian National Univ., Canberra). Mon. Notic. Roy. Astron. Soc.; 152: 165-95(1971).

The photometry at 5500, 6500, and 8700 Å of seventy-nine HD stars of type M is described. Eleven of these stars are known variables. Forty-five of the remaining 68 were also found to be variable. These observations indicate that about one-third of the HD stars of type Ma and four-fifths of those of type Mb are variable. The transformation of the photometry at 5500, 6500, and 8700 Å to the VRI system is given, and luminosities are obtained from the (M_I, R – I) relation of Eggen. Proper motions were collected for about 70% of the stars and used to obtain space motion components. Population discrimination is made using the position of the stars in the (U, V) plane. The spatial distribution of the different populations agrees with that of Eggen. Observations of fifteen K5 stars in one region suggest that the proportion of field giants of lower metal abundance in that region is small. (auth) (UK)

35673 ANALYSIS OF THE SPECTRUM OF THE LARGE MAGELLANIC CLOUD SUPERGIANT HD 32034. Przybylski, A. (Australian National Univ., Canberra). Mon. Notic. Roy. Astron. Soc.; 152: 197-208(1971).

In a coarse analysis, the Large Magellanic Cloud supergiant HD 32034 was compared with η Leo and 13 Mon. It was found that, if the assumptions normally made in curve of growth analysis are applicable, then: the helium content of HD 32034 is probably normal, and metals are deficient by a factor of 6. (auth) (UK)

35674 OBSERVATIONS OF RAPID BLUE VARIABLES. I. TECHNIQUES. Nather, R. Edward; Warner, Brian (Univ. of Texas, Austin). Mon. Notic. Roy. Astron. Soc.; 152: 209-17 (1971).

An instrumental system designed to obtain data from rapid variables at high time resolution is described. The central element of the system is a small general-purpose digital computer, which controls the data acquisition process and records the data under the direction of internally stored programs. The basic architecture of these programs is outlined, some constraints on the process of high-speed photometry are briefly discussed, and examples of recent results are presented to illustrate the potential of the method. (auth) (UK)

35675 OBSERVATIONS OF RAPID BLUE VARIABLES. II. U GEMINORUM. Warner, Brian; Nather, R. Edward (Univ. of Texas, Austin). Mon. Notic. Roy. Astron. Soc.; 152: 219-29 (1971).

A new model is described for the binary dwarf nova U Geminorum, based on high-time-resolution photometric observations during normal light. These demonstrate the nature of the light flickering around the orbit. Flickering disappears during primary eclipse. It is suggested that the previously known bright spot in the U Gem system is the source of all flickering during normal light and that it is situated on the nebulous ring that surrounds the hot component. Infalling material from the cool star, which fills its Roche lobe, provides the energy needed to maintain the bright spot as a stable feature. The primary eclipse is interpreted as an eclipse of the bright spot plus nebulosity. The inclination of the orbit is then such that the hot component is not eclipsed. Thus, either component can be the source of the dwarf nova outbursts, in contrast with the model proposed by Krzeminski, which requires that the seat of eruption be in the cool star. (auth) (UK)

35676 SUSPECTED SUPERNOVA IN A.D. 1181. Stephenson, F. R. (Univ. of Newcastle upon-Tyne, Eng.). Quart. J. Roy. Astron. Soc.; 12: No. 1, 10-38(Mar 1971).

A new star that appeared in Cassiopeia in A.D. 1181 attracted considerable attention in the Far East. It was visible for about six months, and its position was carefully recorded by the Chinese and Japanese astronomers. Their observational evidence favors identification of the star as a supernova of type I. It is proposed that the radio source 3C 58 is a remnant of that star. (auth) (UK)

Quasi-Stellar, Radio, and X-Ray Sources

Refer also to abstract 35014.

35677 SPLITTING OF A PHOTON IN A MAGNETIC FIELD AND POLARIZATION OF HARD RADIATION FROM PULSARS. Gal'tsov, D. V.; Skobelev, V. V. JETP Lett. (USSR) (Engl. Transl.); 13: No. 3, 122-3(5 Feb 1971).

Translated from Zh. Eksp. Teor. Fiz., Pis'ma Red.: 13: No. 3, 173-5(5 Feb 1971).

Starting from CP-invariance considerations and from the energy-momentum conservation law, with allowance for the polarization of vacuum, Adler et al. (Phys. Rev., 25: 1061(1970)) showed that the process $\gamma \rightarrow 2\gamma$ in a magnetic field of 4.41×10^{13} G should lead to polarization of hard γ radiation. It is emphasized here that, owing to the specific kinematics of the $\gamma \rightarrow 2\gamma$ process (the momenta of all three photons are parallel), gauge invariance imposes weak limitations on the possible form of the matrix element, and consequently the conclusions by Adler et al. are inconsistent. (W.D.M.)

XUM

35678 POSSIBLE OBSERVABLE EFFECTS OF ELECTRON PAIR PRODUCTION IN QSOs. Bonometto, S.; Rees, M. J. (Cambridge Univ.). Mon. Notic. Roy. Astron. Soc.; 152: No. 1, 21-35(1971).

The energy distribution of the electrons produced in the annihilation of γ rays by softer ambient photons is calculated, assuming different possible spectra for the soft photons. The relevance of this process to quasars is discussed, and the effects of the electrons produced in this way are quantitatively studied in the frame of simplified models. Some results about the spectral index, and possible bends of the photon spectrum, are obtained. (auth) (UK)

35679 PHOTOELECTRIC SEQUENCES FOR THE BRIGHTER QSO's. Angione, Ronald J. (Univ. of Texas, Austin). Astron. J.; 76: No. 5, 412-18(Jun 1971).

UBV photoelectric sequences were measured for 22 of the brighter QSO's and four other objects. The results and finding charts are presented. (auth)

35680 H I CLOUDS WITH SPIN TEMPERATURES LESS THAN 25°K. Verschuur, G. L. (National Radio Astronomy Observatory, Green Bank, Va.); Knapp, Gillian R. Astron. J.; 76: No. 5, 403-8(Jun 1971).

Narrow-bandwidth neutral-hydrogen observations of two cold clouds around $l = 230°$, $b = +45°$ and near-zero velocity reveal that the emission spectra from these objects may be closely approximated if the spin temperature of the clouds is between 10 and 20°K and if the optical depth is in the range 1 to 2. The possible existence of expansion, contraction, or turbulence in these clouds was investigated. (auth)

35681 PERIOD–LUMINOSITY FUNCTION FOR PULSARS. Cavallo, G. (Laboratorio TESRE, Bologna). Nature (London) Phys. Sci.; 231: 35-6(10 May 1971).

The possibility that pulsar distance estimates based on dispersion measure (DM) are unreliable is discussed, and arguments to support this contention are advanced. A period luminosity function is tentatively introduced, leading to new distance determinations. The computed radio luminosity L was plotted against the Period P for 34 pulsars for which L could be estimated, P being directly observable whereas L could only be estimated from the received radio flux (which was poorly known) and an assumed distance D. The distance is unknown and could only be based on the observed DM. If the pulsars are ordered according to distance classes it is found that the closest are the faintest and the most distant are the brightest. The first obvious suggestion is that the pulsars can be classified according to luminosity classes, but although the farthest pulsars are expected to be particularly bright, it is not clear why there should be a lack of very bright pulsars in the nearer neighbourhood; almost 50% of the plotted pulsars belong to the two highest luminosity classes. This appears to be evidence that the distances are somewhat inaccurate, most distances below 400 ps being probably underestimated, whilst above 800 ps they are probably overestimated. If the proposed period–luminosity relationship is valid, it would lead to the conclusion that there are more visible pulsars than at present thought. A period–age relationship consistent with the period–luminosity relationship would be $p \propto t^{0.8}$. (UK)

35682 OBSERVATIONS AT 408 MHz OF RADIO SOURCES FROM 4C CATALOGUE. I. DECLINATION RANGE -7° TO -3°. Munro, R. E. B. (Univ. of Sydney). Aust. J. Phys.; 24: No. 2, 263-91(Apr 1971).

Radio sources from the Fourth Cambridge (4C) catalogue were observed at 408 MHz using the Molonglo radio telescope. Details of the observation and analysis techniques are given. The measured positions and flux densities at 408 MHz of 351 of the sources in the declination range –7° to –3° are listed. Optical identifications are suggested for 100 of these sources. (auth) (Australia)

35683 *ELECTRON TEMPERATURES OF H II REGIONS.* Simpson, Janet Pagdin. Berkeley, Calif.; Univ. of California (1970). 79p. University Microfilms Order No. 71-9923. Thesis.

A numerical model of the Orion Nebula was constructed to agree with observations of the radio continuum, the optical forbidden lines, and the optical hydrogen recombination lines. It was found that large temperature and density fluctuations are necessary to make the predicted radio and optical line and continuum intensities agree with the observations. The model was used to predict intensities of the radio recombination lines under LTE conditions and under non-LTE conditions. It was found that the observed recombination line intensities are significantly smaller than the predicted line intensities derived from the model and the non-LTE of b_α computed by Sejnowski and Hjellming (1969). Additional observations of Orion A, M17, and W3 were made at the National Radio Astronomy Observatory to look for non-Doppler line broadening in the α, β, γ hydrogen recombination lines at 22 cm. This Stark broadening was indeed found, and it has such a large effect on the line profiles that fitted Gaussian profiles must not be used to measure the area of the lines. The effects of fitting Voigt profiles on theoretical profiles derived from the model H II regions are discussed. Using least-squares-fitted Voigt profiles, it was found that line intensities at 22 cm agree with the intensity ratios predicted by the LTE theory. The anomalous recombination lines were also analyzed and compared to observations at higher frequencies. (Diss. Abstr. Int., B)

35684 SUPERNOVA REMNANT NEAR GX 5-1. Milne, D. K.; Dickel, J. R. (CSIRO, Sydney). Nature (London) Phys. Sci.; 231: 33-5(10 May 1971).

A suggestion that the x-ray source GX 5−1 is associated with a newly discovered supernova remnant (No. 56 in Milne's catalogue) is discussed. Measurements by Bradt and others (Nature, 229: 96(1971)), however, indicated that the x-ray source is 13′ from the centre of the supernova remnant, and these authors did not admit Milne 56 as an identification of GX 5−1. The present authors consider that this decision was premature, since the relatively large angular extent of Milne 56 was ignored; they find that GX 5−1 lies near the edge of the shell of the supernova remnant. Observations were made with the 64-m Parkes telescope to obtain 5,000- and 2,700-MHz total power isotherms and polarization vectors of this region, and results are shown in tabular and graphical form. Milne derived a distance of 3.4 kps for the source, but the present observations indicate a larger angular diameter than previously adopted, and if this is taken to be 30′, the distance must be reduced to 2.4 kps; the diameter at this distance is 20 ps and the total radiated power at 1,000 MHz is 3×10^{16} W/Hz, and the source is intrinsically similar to some other supernova remnants that are sources of x-ray emission. (UK)

35685 TIMING OBSERVATIONS OF THE CRAB NEBULA PULSAR AT THE ARECIBO OBSERVATORY. Roberts, J. A.; Richards, D. W. (Arecibo Observatory, Puerto Rico). Nature (London) Phys. Sci.; 231: 25-8(10 May 1971).

Accurate radio observations of the Crab pulsar were used to examine the long-term slowing down of the pulsar and the more irregular perturbations in the periodicity. (auth) (UK)

35686 OBSERVATIONS OF 3C 273 RADIO SOURCE AT 8 mm WITH THE MASER. Efanov, V. A.; Zagatin, V. I.; Moiseev, I. G.; Misezhnikov, G. S.; Shteinshleiger, V. B. Izv. Krym. Astrofiz. Observ.; 41-42: 248-52(1970). (In Russian).

The main parameters of the traveling-wave maser with the radiometer attached to the 22-meter antenna of the Crimean radio telescope are given. The use of the maser allowed the fluctuation sensitivity (0.07 to 0.09)°K at $\tau = 1$ sec to be determined, and as a result the radio telescope sensitivity at 8 mm increased tenfold. The observations of 3C 273 showed that the flux density of emission in October 1968 was $(50 + 1.5) \times 10^{-26}$ W m^{-2} Hz^{-1}. As compared to earlier observations with the same radio telescope there is a tendency to a decrease of flux density for the period of April–October, 1968, while from October, 1967 to May, 1968 the fluctuations were not observed within the limits of the accuracy of observations. (auth)

35687 *ESTIMATION OF HIGH-ENERGY γ-RADIATION* FLUXES FROM SOME COSMIC OBJECTS. Vladimirskii, B. M.; Stepanyan, A. A. Izv. Krym. Astrofiz. Observ.; 4142: 198-*202(1970). (In Russian)*

Gamma fluxes with energies $\geq 5 \times 10^{12}$ eV originating from bremsstrahlung and inverse Compton effect of high-energy electrons are estimated for several cosmic objects. These fluxes are 10^{-11} to 10^{-13} cm^{-2} sec^{-1} for the remnants of Type I supernovae and 10^{-13} to 10^{-16} cm^{-2} sec^{-1} for those of Type I and some radio galaxies. The detection probability of the high-energy γ-ray sources associated with supernovae, novae, and eruptive stars is estimated. It is possible to detect a γ-ray burst for near novae (<1000 ps) and eruptive stars (<30 ps) using the technique of Cherenkov flash count for γ-quantum observations. (auth)

35688 FURTHER COMMENT ON THE DUST-RADIATION INSTABILITY IN IONIZED NEBULAE. Nordsieck, Kenneth H. (Univ. of California, San Diego). Astrophys. J.; 166: No. 3, 731-3(15 Jun 1971).

Correction of an error in a previous paper on the formation of inhomogeneities in ionized nebulae significantly alters the growth times reported there. However, inhomogeneities of observable size will still form in planetary nebulae, whereas they grow too slowly to be of importance in most H II regions. (auth)

XUM

35689 MULTIPATH DELAY DISTORTION OF RADIO PULSES FROM NP 0532. Counselmann III, C. C. (Massachusetts Inst. of Tech., Cambridge); Rankin, J. M. Astrophys. J.; 166: No. 3, 513-23(15 Jun 1971).

The multipath-scattering delay distribution function for radio pulses received from the Crab Nebula pulsar NP 0532 is recovered by Fourier analysis of periodic "pulse" wave forms observed simultaneously at different radio frequencies. The derived distribution function, which scales in delay as f^{-4}, accounts well for the change of pulse shape, the reduction of pulsed flux, and the excess delay of the pulse centroid relative to the Df^{-2} plasma-dispersion law, which are observed at lower frequencies. The form of the derived function is inconsistent with that expected for Gaussian angular scattering by either a single thin screen or by many screens in the propagation path. A model in which scattering occurs in just two widely separated regions along the path is compatible with expectations, however, and suggests that most of the interstellar scattering occurs in two localized clouds or perhaps in the separate Orion and Perseus arms of the Galaxy. (auth)

35690 EVIDENCE FOR MULTIPLE PERIODICITY IN THE X-RAY EMISSION FROM CYGNUS X-1. Holt, S. S. (Goddard Space Flight Center, Greenbelt, Md.); Boldt, E. A.; Schwartz, D. A.; Serlemitsos, P. J.; Bleach, R. D. Astrophys. J.; 166: No. 3, L65-8(15 Jun 1971).

X-ray data from a rocket-borne exposure to Cyg X-1 confirm indications of periodicity obtained from Uhuru. However, the data are inconsistent with a single periodic component at 73 ms, and are most easily reconciled in terms of at least two harmonic components at lower frequencies. (auth)

35691 DETECTION OF A HIGH-ENERGY X-RAY FLARE FROM A SOURCE IN CRUX. Lewin, Walter H. G.; McClintock, Jeffrey E.; Ryckman, Stanley G.; Smith, William B. (Massachusetts Inst. of Tech., Cambridge). Astrophys. J.; 166: No. 3, L69-72(15 Jun 1971).

On April 16, 1969, balloon x-ray observations were carried out from Australia (energies above 18 keV). A strong x-ray flux in the range 18 to 36 keV from a source at $l^{II} = 301° \pm 3°$, $b^{II} = -2° \pm 3°$ was detected. During the observations the x-ray flux flared up by about a factor of 3. The flare lasted for a period of about $1\frac{1}{2}$ hours. There is also some evidence for a flux change in less than 10 minutes. The average observed flux was about 2 keV cm^{-2} sec^{-1}, which is at least a factor of 7 higher than that observed about one month earlier on March 20, 1969, at which time no evidence for x-ray emission from this region of the sky was found by Lewin, McClintock, and Smith. The average flux is about as high as that observed by Lewin, Clark, and Smith on October 15, 1967, from a source at $l^{II} = 304°.8 \pm 1°.5$, $b^{II} = -1°.5 \pm 2°$. (auth)

35692 RAPID FLUCTUATIONS IN THE HIGH-ENERGY X-RAY FLUX FROM A SOURCE IN CRUX. McClintock, Jeffrey E.; Ricker, George R.; Lewin, Walter H. G. (Massachusetts Inst. of Tech., Cambridge). Astrophys. J.; 166: No. 3, L73-6(15 Jun 1971).

On October 15-16, 1970, balloon x-ray observations were carried out from Australia (energies above 15 keV). A rapidly varying flux from a source at $l^{II} = 300.7° \pm 0.5°$, $b^{II} = -2.2° \pm 2.7°$ (GX 301-2) was detected. Several flares with rise and decay time of a few minutes were recorded. A flux change of about a factor of 5 was recorded in 2.5 minutes. The highest flux observed in the energy range from 15 to 32 keV was ~10 keV cm^{-2} sec^{-1}. This is at least a factor of 35 higher than the average flux from this region of the sky measured on March 20, 1969, by Lewin, McClintock, and Smith. The lowest flux measured from GX 301-2 during the October 1970 observation is ~2 keV cm^{-2} sec^{-1}. In the same energy range a source at $l^{II} = 303.8° \pm 0.8°$, $b^{II} = -1.2° \pm 2.5°$ (GX 304-1) was also observed. The flux from this source was about 1 keV cm^{-2} sec^{-1}. (auth)

35693 RELATIVE CORRELATION OF LARGE- AND SMALL-REDSHIFT QUASI-STELLAR OBJECTS WITH CLUSTERS OF GALAXIES. Bahcall, John N. (California Inst. of Tech., Pasadena); Bahcall, Neta A.; Burbidge, G. R. Contract AT(11-1)-68. Astrophys. J.; 166: No. 3, L77-80(15 Jun 1971).

The importance of investigating the relative probability that large- and small-redshift QSOs appear in the direction of catalogued clusters of galaxies is discussed. This relative probability is determined for a large sample of QSOs with respect to both Zwicky and Abell clusters of galaxies. The results are summarized in three general conclusions. (auth)

35694 RUNAWAY STARS AND THE PULSARS NEAR THE CRAB NEBULA. Trimble, Virginia; Rees, Martin J. (Inst. of Theoretical Astronomy, Cambridge, Eng.). Astrophys. J.; 166: No. 3, L85-90(15 Jun 1971).

It has been suggested that the pulsars 0527 and 0531 are the remnants of two supernova explosions of stars which once formed a close-binary system in the I Geminorum association. Considerations of mass exchange in such a system and the measured proper motion of 0531 and the Crab Nebula place severe constraints on the masses and initial separation of the stars. The time elapsed since the disruption of the binary system greatly exceeds the slowing-down time scale of 0527, except in cases when the member stars are too small to have evolved to the supernova stage if they were formed at the same time as the association. (auth)

35695 OPTICAL TIME-OF-ARRIVAL MEASUREMENTS FROM THE CRAB PULSAR: COMPARISON OF RESULTS FROM FOUR OBSERVATORIES. Horowitz, Paul (Harvard Univ., Cambridge, Mass.); Papaliolios, Costas; Carleton, Nathaniel P.; (and others). Astrophys. J.; 166: No. 3, L91-3(15 Jun 1971).

A comparison of data from four observatories on the optical timing of the Crab pulsar shows the observed site arrival times to be consistent. Possible errors introduced in reducing these data to an inertial frame are discussed, and previously reported departures of the period decay from a simple slowdown law are confirmed as intrinsic to the pulsar. (auth)

35696 OH-LINE ABSORPTION AT 1665 AND 1667 MHz IN THE DIRECTION OF THE OMEGA NEBULA. Gardner, F. F.; McGee, R. X. (Commonwealth Scientific and Industrial Research Organization, Sydney). Astrophys. Lett.; 8: No. 2, 83-7(Apr 1971).

With the 12.2 arc min beam of the Parkes 210-ft telescope the OH line absorption at 1665 and 1667 MHz was found to be displaced well to the west of the continuum peak. Four main velocity groups at about 11.5, 17, 19.5, and 23 km/sec could be distinguished, centered on different positions. The one of most interest at 17 km/sec had the largest displacement, at least 2.5 arc min in right ascension and 1.5 arc min in declination to the northwest of the continuum peak, and appeared to have the lowest 1667/1665 intensity ratio. Since the OH absorption "centers" are in a region of high optical obscuration, there is no possibility of comparison with optical data. Comparisons were made with H I, CH_2O, and excited H-line radiation observed in the direction of the nebula. (auth)

35697 SEARCH FOR INTERSTELLAR SH AT RADIO FREQUENCIES. Heiles, C. E. (Arecibo Observatory, Puerto Rico); Turner, B. E. Astrophys. Lett.; 8: No. 2, 89-91(Apr 1971).

A new search for the two ground-state main-line transitions of interstellar SH at 111 MHz was unsuccessful. Five sources, including three H II regions that show anomalous OH emission, a supernova remnant, and a dust cloud all yielded upper limits for the abundance of SH that are small enough to suggest that SH is under-abundant relative to OH in the interstellar medium. In addition, upper limits of 0.7 flux units for the two principal 70-cm lines of NO were established in the galactic center. (auth)

35698 ANOMALOUS OH EMISSION FROM NEW TYPES OF GALACTIC OBJECTS. Turner, B. E. (National Radio Astronomy Observatory, Green Bank, W. Va.). Astrophys. Lett.; 8: No. 2, 73-7(Apr 1971).

Anomalous OH emission was found in the direction of the planetary nebula NGC 2438 and the optically radio-weak galactic nebulae S 247, S 269, IC 2162, and NGC 2264. The OH emission from NGC 2438 appears to arise from neutral condensations distributed fairly uniformly throughout the planetary nebula. (auth)

35699 PULSAR WOBBLE. Chau, W. Y.; Henriksen, R. N. (Queen's Univ., Kingston, Ont.). Astrophys. Lett.; 8: No. 2, 49-52(Apr 1971).

The wobble and the alignment time-scales of the oblique-rotator model for the pulsar were studied both from the conventional geophysicist's point of view and on the basis of the 2-component model proposed by Baym et al. In particular, the complications arising from a possibly oblate core are discussed. (auth)

35700 OBSERVATION OF γ QUANTA WITH ENERGY GREATER THAN 100 MeV FROM THE RADIO SOURCE 3C 120. Volobuev, S. A.; Gal'per, A. M.; Kirillov-Ugryumov, V. G.; Luchkov, B. I.; Ozerov, Yu. V. (Moscow Engineering Physics Inst.). JETP Lett. (USSR) (Engl. Transl.); 13: No. 1, 28-31(5 Jan 1971).

Translated from Zh. Eksp. Teor. Fiz., Pis'ma Red.; 13: No. 1, 43-6(5 Jan 1971).

Gamma telescopes on Kosmos 251 and Kosmos 264 are described and the techniques used for obtaining the primary gamma flux from the galactic anticenter region are discussed. There was

XUM

some indication that an excess flux came from a discrete source. The sources 3C 120 and 3C 93 were considered to be the prime candidates as sources of this excess flux. (W.D.M.)

35701 POSSIBLE RADIO IDENTIFICATION OF CYGNUS X-2. Braes, L. L. E.; Brouw, W. N. (Leiden Observatory). Astron. Astrophys.; 12: No. 2, 320-1(May 1971).

An observation at 1415 MHz with the Westerbork synthesis telescope showed a variable radio source that is possibly connected to the x-ray source Cyg X-2. An optical identification remains in doubt. (auth)

35702 DISTANCE AND SPECTRUM OF 3C 391. Caswell, J. L.; Dulk, G. A.; Goss, W. M.; Radhakrishnan, V.; Green, Anne J. (CSIRO, Sydney. Univ. of Sydney). Astron. Astrophys.; 12: No. 2, 271-7(May 1971).

The angular structure and low-frequency spectrum of 3C 391 were investigated with new high-resolution observations at 80 and 408 MHz. The spectrum has a turnover near 408 MHz. An H I absorption kinematic distance shows that the source is at least 8.5 kpc distant. The new data are compatible with the conclusion that 3C 391 is a supernova remnant. (auth)

35703 SATELLITE EXPERIMENTS IN X-RAY ASTRONOMY. Naranan, S. (Tata Inst. of Fundamental Research, Bombay). pp 143-58 of Proceedings of the Eleventh Symposium on Cosmic Rays, Astrophysics, Geophysics and Elementary Particle Physics 1969. Vol. I. Bombay; Department of Atomic Energy (1969).

From eleventh symposium on cosmic rays, astrophysics, geophysics and elementary particle physics; Delhi, India (7 Oct 1969). See CONF-691055-(Vol. 1).

The few small extrasolar x-ray experiments carried by satellites are described. Experimental details of SAS-A and the results expected therefrom are discussed in some detail. (W.D.M.)

35704 ENERGY SPECTRUM OF SCO X-1 IN THE REGION 15 TO 120 keV. Agrawal, P. C.; Biswas, S.; Gokhale, G. S.; (and others) (Tata Inst. of Fundamental Research, Bombay). pp 383-5 of Proceedings of the Eleventh Symposium on Cosmic Rays, Astrophysics, Geophysics and Elementary Particle Physics, 1969. Vol. II. Bombay; Department of Atomic Energy (1969).

From eleventh symposium on cosmic rays, astrophysics, geophysics and elementary particle physics; Delhi, India (7 Oct 1969). See CONF-691055-(Vol. 2).

The flux and energy spectrum of Scorpious X-1 was measured in the energy range of 15 to 120 keV during three balloon flights launched from Hyderabad on Apr. 28 and Dec. 22, 1968 and Apr. 16, 1969, using identical detector systems. A single exponential spectrum cannot be fitted into the entire energy range. Forms are given for 15- to 40-keV range and from 40 to 120 keV. Sudden changes in the intensity of Sco X-1 by as much as a factor of 5 have been obtained. (J.C.W.)

35705 SEARCH FOR HIGH-ENERGY GAMMA RAYS FROM PULSARS. Chatterjee, B. K.; Murthy, G. T.; Murthy, P. V. Ramana; Sreekantan, B. V.; Tonwar, S. C. (Tata Inst. of Fundamental Research, Bombay). pp 394-6 of Proceedings of the Eleventh Symposium on Cosmic Rays, Astrophysics, Geophysics and Elementary Particle Physics, 1969. Vol. II. Bombay; Department of Atomic Energy (1969).

From eleventh symposium on cosmic rays, astrophysics, geophysics and elementary particle physics; Delhi, India (7 Oct 1969). See CONF-691055-(Vol. 2).

The suggestion that pulsars are a source of high-energy cosmic rays has led to an attempt to detect the emission of high-energy gamma rays in the pulsed mode. During April 1969, a search was made for nanosecond-duration Cherenkov light flashes due to electrons of electromagnetic cascades generated by the gamma rays in the atmosphere. Attempts were made to detect the high-energy gamma rays ($\gtrsim 10^{13}$ eV) from CP 0950, CP 1133, AP 1541, and PSR 1642. Pulsar CP 0950 may possibly emit pulsed gamma rays and may possibly be the nearest-known pulsar. (J.C.W.)

35706 CONSEQUENCES OF INTENSE PHOTON FIELD AROUND PULSAR NP 0532. Rengarajan, T. N. (Tata Inst. of Fundamental Research, Bombay). pp 410-13 of Proceedings of the Eleventh Symposium on Cosmic Rays, Astrophysics, Geophysics and Elementary Particle Physics, 1969. Vol. II. Bombay; Department of Atomic Energy (1969).

From eleventh symposium on cosmic rays, astrophysics, geophysics and elementary particle physics; Delhi, India (7 Oct 1969). See CONF-691055-(Vol. 2).

The pulsar NP 0532 has been observed to pulsate in radio, optical, and x-ray frequencies. The surface brightness of the source is so large that effects like inverse Compton scattering, γ-γ interaction and synchrotron self-absorption become important. The radiation process may be so coherent that hardly any interaction takes place. It is unlikely that no interaction takes place, though, so the radiation and charged particles will be confined in a finite volume and collisions between the various components should be important and the consequences of the collisions are investigated. The production of x rays, absorption of high-energy γ rays by γ-γ interaction, and synchrotron self-absorption are discussed. (J.C.W.)

35707 OPTICAL IDENTIFICATION OF PKS 0320-37. Whiteoak, J. B.; Gardner, F. F. (CSIRO, Sydney). Nature (London); 231: 108-9(14 May 1971).

It has been suggested that the large extended radio source PKS 0320-37 (Fornax A), identified for many years with the tenth magnitude SO galaxy NGC 1316, should really be identified with a seventeenth magnitude blue stellar object, but it is argued in the present communication that this new identification should not be accepted, and it is recommended that identification with NGC 1316 should be retained. The structure and scale of the radio source are typical of a radio galaxy and not of any known QSO. Total intensity and linear polarization distributions at 6 cm, obtained with the Parkes 64-m telescope at a resolution of 4.0′, are shown graphically. The distribution consists basically of two highly polarized components straddling the galaxy NGC 1316. (UK)

35708 SEARCH FOR INTERSTELLAR H_2CS. Davies, R. D.; Booth, R. S.; Pedlar, A. (Univ. of Manchester, Jodrell Bank, Eng.). Mon. Notic. Roy. Astron. Soc.; 152: 7-8(1971).

A search was made for the 1046.48-MHz line of H_2CS during a recombination-line-observing session on May 6-7, 1970. This line is the $I_{10} \rightarrow I_{11}$ transition, which is the same as that giving the 4830-MHz line of formaldehyde (H_2CO). The observations were made with the 250-ft radio telescope, using a travelling-wave tube receiver followed by a 256-channel autocorrelation spectrometer. No absorption or emission features were detected at the frequency of the H_2CS transition in the directions of Sag A, Sag B2, M17, or Cas A. Estimates are made of the expected optical depth of H_2CS in terms of that of H_2CO, and the results are discussed. It was clear that the abundance ratio H_2CS/H_2CO is less than the cosmic abundance ratio of S to O, suggesting that the processes leading to the formation of H_2CS are less efficient than those producing H_2CO. (UK)

35709 INTERFEROMETRIC OBSERVATIONS WITH A BASELINE OF 127 KILOMETRES. II. Donaldson, W.; Miley, G. K.; Palmer, H. P. (Univ. of Manchester, Jodrell Bank, Eng.). Mon. Notic. Roy. Astron. Soc.; 152: 145-58(1971).

Further observations at frequencies of 1422 and 2694 MHz with an interferometer baseline of 127 km are described for 12 sources whose fringe visibilities varied with hour angle. Five of these sources, 3C 119, 3C 287, 3C 286, LHE 210, and 3C 446 are only partially resolved at both frequencies. PKS 1938-15, 3C 237(1422 MHz), and 3C (2694 MHz) are shown to have double structures, and further evidence is presented for a physical association between the sources 3C 343 and 3C 343.1. Fine structure was observed in both Virgo A and Cygnus A. (auth) (UK)

35710 NEW SOFT X-RAY SOURCE IN THE ARIES-TAURUS REGION. Hayakawa, S. (Nagoya Univ., Japan). Nature (London) Phys. Sci.; 231: No. 21, 76(24 May 1971).

Observations carried out from a sounding rocket launched on September 19, 1970 revealed a new soft x-ray source in the Aries-Taurus region. A tentative exponential spectrum is given that is consistent with the observations, and the energy flux of the source in the measured energy range was $\sim 2 \times 10^{-9}$ erg/cm^2/s. (UK)

35711 STARK BROADENING IN HIGH-QUANTUM-NUMBER RECOMBINATION LINES OF HYDROGEN. Pedlar, A.; Davies, R. D. (Univ. of Manchester, Jodrell Bank, Eng.). Nature (London) *Phys. Sci.; 231: No. 20, 49-51(17 May 1971).*

Some previous studies in this field are first described, followed by some measurements of high-quantum-number recombination lines in H II regions, using the 250-ft telescope at Jodrell Bank. There were indications that the broadening was significantly less than predicted theoretically. Further theoretical analysis of the problem is clearly desirable, and some improved observational techniques are suggested. (UK)

35712 ROCKET OBSERVATIONS AND THE COSMIC X-RAY BACKGROUND. Fabian, A. C.; Sanford, P. W. (University Coll., London). Nature (London) Phys. Sci.; 231: No. 20, 52-3(17 May 1971).

A rocket-borne proportional counter was used to sample x rays coming from nine areas of the sky, chosen for the absence of known cosmic x-ray sources. Analysis of the data and some possible interpretations are discussed. (auth) (UK)

XUM

35713 LONG-TERM INTENSITY OBSERVATIONS ON PULSARS. Hesse, K. H. (Cavendish Lab., Cambridge, Eng.). Nature (London) Phys. Sci.; 231: No. 20, 54-5(17 May 1971).

The day-to-day intensity variations of the seven strongest pulsars at 81.5 MHz were studied over periods ranging from 15 to 34 months (CP 0328, 0808, 0834, 0950, 1133, 1919; HP 1506). A power-spectrum analysis for frequencies less than 45 cycles per year indicated a predominance of frequencies in the range 0 to 6 cycles per year; these are considered to be intrinsic source variations, and there was little evidence for any regular long-term behavior. There was a distinct excess of power in the lower frequencies of the power spectra. Observations at 81.5 MHz are being continued and have been commenced at 151 MHz; this should assist in determining the relative intensity and the phase relationship of any long-term intensity variations as a function of frequency. (UK)

Solar Phenomena

Refer also to abstracts 35054, 35914, and 35987.

35714 SUBMILLIMETRE-WAVE SOLAR OBSERVATIONS USING A DOUBLE-OUTPUT MICHELSON INTERFEROMETER. Burroughs, W. J.; Chamberlain, J. (National Physical Lab., Teddington, Eng.). Infrared Phys.; 11: No. 1, 1-23(Apr 1971).

A double-output Michelson-type interferometer having Golay cell detectors was used at an altitude of 3580 m to study, by means of Fourier spectrometry, the atmospheric absorption of solar radiation in the submillimeter-wave region. Spectra having 0.5, 0.25, and 0.125 cm^{-1} resolution were obtained. The 0.5 cm^{-1} results were compared with spectra obtained with the same instrument in the laboratory using a mercury-lamp source. At higher resolution the spectroscopic results revealed features due to atmospheric oxygen and ozone, and also showed that quantitative estimates of the integrated water content of the absorption path can be made from measurements of experimentally determined profiles of single submillimeter-wave lines. At lower resolution the atmospheric absorption at 8 cm^{-1} attributed to dimers of the water molecule appears to have a doublet structure. Anomalous signal levels in the region of 22 and 28 cm^{-1} were confirmed. A study of the sources of noise in the observations showed that in a system using Golay cells the dominant source of noise is the detectors, and that atmospheric modulation of the signal is, by comparison, negligible. (auth) (UK)

35715 CENTER LIMB OBSERVATIONS OF INHOMOGENEITIES IN THE SOLAR ATMOSPHERE. II. THE Na D AND Na 5688 DOUBLETS AND THE MgI 4571 LINE. Cannon, C. J.; Wilson, P. R. (Univ. of Sydney). Solar Phys.; 17: No. 2, 288-303 (Apr 1971).

Center-limb observations of line-center intensity fluctuations in the Na D and Na 5688 doublets and the Mg 4571 line are described. For small-scale structures, the rms distributions for the photospheric lines show maxima of 20% at a heliocentric angle of 40° (Mg 4571) and 9% at 20° (Na 5688). The rms values for Na D range between 10 and 13%, but show no significant maximum. Values for large-scale structures are somewhat less. Autocorrelation curves show a range of structures from 4000 to 30,000 km. Brightness-velocity cross-correlation curves and the actual brightness and velocity tracings from a region near disk-center are also studied. A new method of classifying cross-correlation coefficients calculated over many different ranges within the sample enables one to distinguish the existence and extent of regions of significant cross-correlation within the sample and this is applied both to the results for the Na D lines and for the Mg b lines given in Paper I. It is found that regions of significant correlation may extend for lengths of order 25,000 km, after which the correlation may abruptly change sign or become negligible. The suggestion made in Paper I that these abrupt changes may occur at the supergranule boundaries is further supported. The relation between these small-scale structures and the 5-min oscillations is investigated. The question of the reproducibility of these statistical data from day to day and at different positions of the Sun at the same heliocentric angle is discussed and the need for further independent observations is stressed. (auth)

35716 FORMATION OF THE Ca II K-LINE CORE WITH ARBITRARY TEMPERATURE MINIMA. Beebe, Herbert A. (Indiana Univ., Bloomington). Solar Phys.; 17: No. 2, 304-15(Apr 1971).

The formation of the solar Ca II K-line core is studied under the assumption of a two-component chromosphere for many atmosphere models, which are tested by comparing observed and calculated average intensity profiles at several places on the solar disk. Non-LTE-line profile calculations are made using model atoms of two and three bound levels while the value and depth of the temperature minimum and turbulent velocity gradient are varied. A critique of several broad types of models is provided. Limb darkening of the entire core, a K1 radiation temperature of 4300°K and increasing limbward separation of the K2 peaks are predicted by a combination of a "cool" component, covering 90% of the solar disk, and a "hot" component, representing the bright calcium network. The optimum cool component is characterized by a 4200°K temperature minimum and low (≈1 km/sec) microturbulent velocities. The hot component begins its outward temperature rise in the photosphere at 4300°K and is never more than 500°K hotter than the cool component. (auth)

35717 K EMISSION-LINE WIDTHS AND THE SOLAR CHROMOSPHERE. Bappu, M. K. V.; Sivaraman, K. R. (Astrophysical Observatory, Kodaikanal, India). Solar Phys.; 17: No. 2, 316-30 (Apr 1971).

Closely spaced microphotometer tracings parallel to the dispersion of one excellent frame of a K-line time sequence were utilized for a study of the nature of the K_{2V}, K_{2R} intensities in the case of the solar chromosphere. It is concluded that bright fine mottling is responsible for the relation, found by Wilson and Bappu, between K emission line widths and absolute magnitudes of the stars. The solar cycle equivalents that stellar chromospheres can demonstrate are discussed and a possible line of approach for successful detection of cyclic activity in stellar chromospheres is indicated. (W.D.M.)

35718 APPARENT DIFFERENCES IN MAGNETIC FIELD STRENGTHS MEASURED FROM ZEEMAN SPLITTINGS OF MOLECULAR LINES AND Fe I λ 5250.2 A. Staude, Juergen (Zentralinstitut fuer Solar-Terrestrische Physik, Potsdam, Ger.). Solar Phys.; 17: No. 2, 331-2(Apr 1971).

Recently Wöhl (1969) and Mallia (1970) reported on observations of Zeeman splittings of molecular lines within sunspots. An explanation is offered for the discrepancies noted in the aforementioned papers. (W.D.M.)

35719 PHYSICAL PROPERTIES OF SOLAR SPICULES. Krat, V. A. (Pulkovo Astronomical Observatory, Leningrad); Krat, T. V. Solar Phys.; 17: No. 2, 355-68(Apr 1971).

New observations of solar spicules at Pulkovo, made simultaneously in four spectral regions, are described. The profiles of the Hα, D3, Hβ, H and K lines were derived for 23 spicules. The spicules occur usually in narrow bundles and can be resolved into separate objects only due to a dispersion of radial velocities inside the bundle. The spicules in D3 are diffuse with faint interspicular emission. The emission of hydrogen, helium, and Ca II originate in different parts of spicules with different radial and "turbulent" velocities. The core of a spicule with Ca II emission is a narrow rope several tens of km in diameter for the normal section. The optical thickness of a spicule in Hα is approximately 1.0 and the atomic density varies from 10^{11} to 10^{12} cm^{-3}. The helium emission in spicules seems to be produced by different mechanisms, one of them being the external radiation of corona and subcoronal matter. The model of a solar spicule is discussed. (auth)

35720 RADIO MODEL OF THE TRANSITION LAYER IN SOLAR ACTIVE REGIONS. Chiuderi, Claudio (Goddard Space Flight Center, New York); Chiuderi Drago, Franca; Noci, Giancarlo. Solar Phys.; 17: No. 2, 369-78(Apr 1971).

A model of the transition layer of an active region of the Sun, based on radio observations, is presented. The model is deduced by using the Laplace transform of the brightness temperature and the hydrostatic equilibrium equation. A rational function, well-behaved in the coronal region, was used to represent the observed brightness temperature. The model indicates the existence of a very steep temperature gradient and suggests the presence of a constant conductive flux from the corona into the chromosphere. Both these conclusions are quantitatively in very good agreement with those deduced from the uv emission-line observations, thus removing a previous discrepancy between radio- and optical-based models. It is also shown that the presence of a weak magnetic field does not alter the above conclusions. (auth)

35721 SOFT X-RAY EMITTING REGIONS IN THE SOLAR CORONA. Landini, M.; Monsignori Fossi, B. C. (Arcetri Astrophysical Observatory, Florence). Solar Phys.; 17: No. 2, 379-88 (Apr 1971).

The soft x-ray emission of the solar corona was investigated by comparison of the signals of several broad-band photometers carried on the Solrad 9 satellite, and sensitive to the region 0.5 to 20 Å. Temperatures from 1.5×10^6 to 25×10^6°K were measured, with "emission measure" $\int N_e^2\, dV$ ranging between 10^{50} cm^{-3} to 10^{47} cm^{-3}. By means of the observational data, and assuming magnetic confinement and hydrostatic equilibrium, the model of an active region was investigated. For temperatures larger than 10^7°K, the emission is due to flare activity and two sets of emis-

XUM

sion measure were observed that appear to be related to the evolution of flares. (auth)

35722 EVIDENCE FOR THE PHOTOSPHERIC ORIGIN OF THE FLARE OPTICAL CONTINUUM. Machado, Marcos E. (Astronomical Inst., Ondrejov, Czech.). Solar Phys.; 17: No. 2, 389-91(Apr 1971).

Recently, Grossi et al. (1971) studied the line excitation in a flare of 3b importance that occurred on Mar. 12, 1969 near the western limb. Further work on this material was done in order to determine the location of the continuum. (W.D.M.)

35723 TYPE III SOLAR RADIO BURST STORMS OBSERVED AT LOW FREQUENCIES. III. STREAMER DENSITY, INHOMOGENEITIES, AND SOLAR WIND SPEED. Fainberg, Joseph; Stone, R. G. (Goddard Space Flight Center, Greenbelt, Md.). Solar Phys.; 17: No. 2, 392-401(Apr 1971).

Analysis of a storm of type-III solar radio bursts observed in August 1968 between 5 and 0.2 MHz by the RAE-1 satellite yielded the storm morphology, a possible relation to meter and decameter storms, and an average exciter speed of 0.37 c between 10 and 40 $R_\odot$ (Fainberg and Stone, 1970a, b). A continuation of the analysis, based on the apparent dependence of burst drift rate on heliographic longitude of the associated active region, now provides a distance scale between plasma levels in the streamer, an upper limit to the scale size of coronal streamer density inhomogeneities, and an estimate of the solar-wind speed. By fixing one level, the distance scale is utilized to determine the electron density distribution along the streamer between 10 and 40 $R_\odot$. The streamer density is found to be 16 times that expected for the solar-minimum quiet solar wind. An upper limit to the scale size of streamer density inhomogeneities is estimated to be of the order of 1 or 2 $R_\odot$ over the same height range. From the progressive delay of the central meridian passage (CMP) of the lower-frequency emission, a streamer curvature is inferred that in turn implies an average solar-wind speed of 380 km/sec between 14 and 36 $R_\odot$ within the streamer. (auth)

35724 THREE YEARS STATISTICS OF SIMPLE 3 SOLAR BURSTS. Matsuura, Oscar T.; Marques dos Santos, P. (Mackenzie Univ., Sao Paulo, Brazil). Solar Phys.; 17: No. 2, 402-7 (Apr 1971).

A plasmoid may be ejected during a flare and condensed by a radiative instability. The spectral shape of the mean fluxes of Simple 3 (or long-enduring) solar events is interpreted in terms of a thermal emission from this transient condensation in the higher levels of the solar atmosphere. This condensation is thick enough to block the radiation from the underlying S-component. This explanation fits the observed polarization changes, as well as the thermal character of the bursts time profiles. A clue for solar activity forecasting, as well as for detailed studies of active sources, is indicated. (auth)

35725 OBSERVATIONS OF A SOLAR RADIO BURST ON SEPTEMBER 27, 1969. Tanaka, Haruo; Enome, Shinzo (Nagoya Univ., Toyokawa, Japan). Solar Phys.; 17: No. 2, 408-11(Apr 1971).

A weak broad-band radio burst associated with a flare of importance 3B or 3N was observed on Sept. 27, 1969 at Toyokawa, Mitaka, and Hiraiso. The observations are briefly described, with the position of the source of the burst being emphasized. (W.D.M.)

35726 10 TO 100 keV ELECTRON ACCELERATION AND EMISSION FROM SOLAR FLARES. Lin, R. P. (Univ. of California, Berkeley); Hudson, H. S. Solar Phys.; 17: No. 2, 412-35 (Apr 1971).

An analysis is presented of spacecraft observations of nonthermal x rays and escaping electrons for 5 selected small solar flares in 1967. OSO-3 multi-channel energetic x-ray measurements during the nonthermal component of the solar-flare x-ray bursts were used to derive the parent electron spectrum and emission measure. IMP-4 and Explorer-35 observations of >22-keV and >45-keV electrons in the interplanetary medium after the flares provided a measure of the total number and spectrum of the escaping particles. The ratio of electron energy loss due to collisions with the ambient solar flare gas to the energy loss due to bremsstrahlung was derived. The total energy loss due to collisions was then computed from the integrated bremsstrahlung energy loss during the nonthermal x-ray burst. (W.D.M.)

35727 RELATIVISTIC ELECTRONS IN SOLAR PARTICLE EVENTS. Datlowe, Dayton (Univ. of Chicago). Solar Phys.; 17: No. 2, 436-58(Apr 1971).

Results of the first systematic study of electrons of energies greater than 10 MeV associated with solar flares are presented. Direct measurements of the frequency with which these particles are found in solar-flare-related events, the spectra of the particles, and the evolution of the spectra during these events were made. In addition, the nature of the propagation of these electrons was studied and the degree of anisotropy in their diffusion was measured for the first time. The observations were made aboard the spacecraft OGO-5 from March 1968 through August 1969. It was found that electrons in the energy range 12 to 45 MeV are normally present in major solar particle events. The time–intensity profiles of the fluxes indicate diffusive propagation; and the time-to-maximum intensity is found to vary with solar longitude in a way that can only be the result of anisotropic propagation with the perpendicular diffusion coefficient comparable in magnitude to, but smaller than, the parallel diffusion coefficient. Spectra during the observed events fit the power law $AE^{-\gamma}$ with $2.5 \leq \gamma \leq 3.8$. The time evolution of the spectrum throughout the course of the four most intense events shows that the spectrum steepens rapidly during the initial phase but retains a constant slope through the decay phase. Events that behave in a manner not described by the normal diffusion picture are also discussed. These examples show phenomena other than direct flare injection followed by anisotropic diffusion. (auth)

35728 ACCELERATION AND PROPAGATION OF SOLAR COSMIC RAYS AS DEDUCED FROM THE RELATIVE ABUNDANCE OF PROTONS TO HELIUM NUCLEI. Sakurai, Kunitomo (Goddard Space Flight Center, Greenbelt, Md.). Solar Phys.; 17: No. 2, 459-67(Apr 1971).

Except for protons, the chemical composition of solar cosmic rays is very similar to the abundance of the elements at the photosphere of the Sun. If the relative abundance ratio of protons to α particles (P/α) at constant rigidity is considered, this ratio is highly variable from one solar cosmic-ray event to another. This ratio observed at the Earth, however, decreases monotonically with time from the onset of solar flares and, furthermore, is dependent on the heliocentric distance of the parent flares from the central meridian of the solar disk. P/α's, which have been measured before the onset of SC geomagnetic storms, change from 1.5 to 50 or more, being a function of the westward position of the source from the east limb of the Sun. These variations with respect to time and heliocentric distance suggest that the propagation of solar cosmic rays is strongly modulated in the interplanetary space. The major part of the α particles seems to propagate as if they are trapped within the magnetic clouds that produce SC geomagnetic and cosmic-ray storms at the Earth. The chemical composition and rigidity spectra of solar cosmic rays suggest that solar cosmic rays are mainly accelerated by the Fermi mechanism in solar flares. The observed variation of P/α's is produced mainly through the difference between the propagation characteristics of protons and α particles. (auth)

35729 OBSERVATION OF SOLAR WIND HEAVY IONS. Cattaneo, M. B.; Formisano, V.; Moreno, G.; (and others) (CNR, Rome. Univ., Rome). Solar Phys.; 17: No. 2, 468-72(Apr 1971).

A plasma experiment on board the ESRO satellite HEOS-1 observed heavy ions with energy per unit charge 2.5 and 4 times higher than protons. Observations refer to the driving piston of the interplanetary shock that occurred on March 31, 1970. (auth)

35730 EFFECT OF A BOUNDED INTERPLANETARY DIFFUSION MEDIUM ON THE PROPAGATION OF SOLAR FLARE COSMIC RAYS. Feit, Julius (Queensborough Community Coll., Bayside, N. Y.). Solar Phys.; 17: No. 2, 473-90(Apr 1971).

An analysis of solar-flare data indicates that the graph of log $(nt^{3/(2-\beta)})$ deviates late in the solar event from the straight line predicted for the infinite, unbounded interplanetary medium. It is shown by mathematical analysis, utilizing a model based on the radial diffusion coefficient $D = Mr^\beta$, with $\beta \simeq 1$, that the deviation can be ascribed to the loss of flare particles through an external boundary at about 5 to 6 AU from the Sun. An inner region terminating at 5 to 6 AU, followed by an extensive region of increasingly less resistance to the diffusion of flare particles is also feasible, and it is shown that measurements taken at the Earth cannot predict the extent of this outer region. The results are applicable to either the isotropic or highly anisotropic models. The constant diffusion model is shown to be inadequate since it requires a boundary $\leq$1.5 AU from the Sun. In view of the present and previous studies of solar-flare data, it is asserted that the fundamental principle governing the diffusion of solar-flare particles through interplanetary space is the radial diffusion coefficient mode of propagation. (auth)

35731 SOLAR EFFECTS ON THE COSMIC RAY INTENSITY OBSERVED AT 70 M.W.E. UNDERGROUND. Antonucci, E.; Cini Castagnoli, G.; Dodero, M. A. (Univ., Turin). Solar Phys.; 17: No. 2, 491-8(Apr 1971).

Intensity decreases in the galactic component of cosmic rays observed at the Earth were correlated with solar phenomena. It

XUM

was found that there exist intensity decreases detected underground, which are probably associated with long-lived interplanetary streams and which are not directly associated with single flares. One can expect to detect the streams with underground monitors before the arrival of the streams at the Earth. The early detection will be in the northern or in the southern hemisphere, depending on the sign of the interplanetary field. (auth)

35732 VARIATIONS IN THE SOLAR WIND SPEED ALONG THE EARTH'S ORBIT. Gosling, J. T. (High Altitude Observatory, Boulder, Colo.). Solar Phys.; 17: No. 2, 499-508(Apr 1971).

Comparison of solar-wind speed data obtained from the Pioneer 6 and 7 and Vela 3, 4, and 5 satellites from January 1969 through July 1970 was undertaken. The distribution of measured speeds was similar for all satellites, despite wide separations along the Earth's orbit. For satellite separations (along the Earth's orbit) of 0.5 AU or less, the speeds measured by different satellites were closely correlated, i.e., it was usually possible to predict (to within ±100 km sec^{-1}) the arrival of a particular solar-wind speed at one satellite on the basis of earlier measurements at another. For separations larger than ≈1.0 AU it was usually not possible to make accurate predictions in this manner. This appears to be evidence that: (1) the boundary conditions on the coronal expansion at the base of the corona are a sensitive function of latitude and/or (2) the boundary conditions at any one point on the Sun evolve sufficiently in ≈4 days to alter significantly the speed of the wind at 1 AU. (auth)

35733 SOLAR CHARGE AND THE PERIHELION MOTION OF 1566 ICARUS. Burman, R. (Univ. of Western Australia, Perth). J. Proc. Roy. Soc. N. S. W.; 103: No. 1, 1-3(1970).

If, as suggested by Bailey, the Sun possesses a net charge, it will induce a dipole moment in a planet or other body. The resulting electrostatic force leads (using nonrelativistic mechanics) to an advance of perihelion, which is calculated here for an orbit of arbitrary eccentricity. The formula obtained is applied to observational results for Icarus. (auth) (Australia)

35734 FLUCTUATIONS IN THE INTERPLANETARY PLASMA. Buckley, R. (Univ. of Adelaide). Planet. Space Sci.; 19: No. 5, 421-36(May 1971).

Spacecraft-based observations of fluctuations in the interplanetary magnetic field and solar-wind speed yield dominant spatial scales of the order 10^6 km, and negligible structure below about 500 km. Earth-based observations of the angular broadening and scintillation of cosmic radio sources were interpreted in terms of electron-density scales of order a few hundred km. It is suggested that for scales below a few hundred km, there exists an enhanced level of small scale-density fluctuations not accompanied by comparable magnetic variations. This proposal is shown to be consistent with radio observations, the contribution of the much-larger electron-density irregularities being quite negligible. A physical mechanism that might account for the small-scale fluctuations is described. (auth) (UK)

35735 80-MHz OBSERVATIONS OF A HARMONIC TYPE-II SOLAR BURST ACCOMPANYING A LIMB FLARE. Dulk, G. A. (CSIRO, Epping, Australia). Aust. J. Phys.; 24: No. 2, 177-83 (Apr 1971).

A flare near the Sun's west limb on October 3, 1969 resulted in a Type-II burst with a weak fundamental radiation and a strong harmonic radiation. At 80 MHz, the sources of both bands of radiation appeared $0.6R_\odot$ above the limb in a tangentially extended source region. K-coronameter observations showed a dense streamer in the vicinity of the source. It is suggested that the observed positions can be explained in terms of direct fundamental radiation and backward refracted harmonic radiation from near the 80- and 40-MHz plasma levels, respectively. The weakness of the fundamental band is attributed to the difficult escape conditions encountered by plasma from near the limb; without the streamer, no fundamental radiation would have been seen. (auth)

35736 SOLAR TYPE-II BURST OF OCTOBER 13, 1969. Dulk, G. A.; Smerd, S. F. (CSIRO, Epping, Australia). Aust. J. Phys.; 24: No. 2, 185-91(Apr 1971).

A solar Type-II burst observed with the 80-MHz Culgoora radioheliograph on October 13, 1969 is attributed to an explosive flare behind the west limb. The source of the Type-II burst was an extended arc with three emission peaks. The weak radiation between the peaks is attributed to scattering and the large radial extent of the source to defocusing. Computed 80-MHz-ray paths through a model corona, which includes a streamer structure compatible with electron-density enhancements observed with the K-coronameter of the High Altitude Observatory, support the conclusion that the observed Type-II radiation was second-harmonic and was emitted backward from the direction of propagation of the Type-II disturbance. (auth)

35737 OBSERVATIONS OF HARMONIC STRUCTURE IN TYPE-III SOLAR RADIO BURSTS. Labrum, N. R. (CSIRO, Epping, Australia). Aust. J. Phys.; 24: No. 2, 193-9(Apr 1971).

Two examples of Type III-bursts with fundamental and second-harmonic structure were studied with the aid of the Culgoora radioheliograph. There is clear evidence of harmonic radiation being received after reflection in the lower corona and, in one case, both the reflected and the direct rays are observed. In both instances the harmonic is much more intense at 80 MHz than the fundamental. (auth)

35738 RADIOHELIOGRAPH OBSERVATIONS OF HARMONIC TYPE-III SOLAR BURSTS. McLean, D. J. (CSIRO, Epping, Australia). Aust. J. Phys.; 24: No. 2, 201-7(Apr 1971).

Observations made with the Culgoora radioheliograph and spectrograph of Type-III bursts show clear fundamental and harmonic components. The significance of these observations is discussed. (auth)

35739 BIPOLAR STRUCTURE IN A MOVING TYPE-IV SOLAR RADIO BURST. Stewart, R. T. (CSIRO, Epping, Australia). Aust. J. Phys.; 24: No. 2, 209-15(Apr 1971).

A moving Type-IV solar radio burst is described in which two oppositely polarized sources appear to lie on an expanding arch moving outwards from the flare region. Analysis suggests that the moving sources are initiated by a shock wave ejected from the flare region. One of the moving sources eventually becomes a highly polarized jet. It is concluded that the radio emission can be completely attributed to synchrotron radiation from mildly relativistic electrons. (auth)

35740 MOTIONS AND POLARIZATION OF A SOLAR TYPE-IV BURST RELATED TO A MAGNETIC ARCH. Dulk, G. A. (CSIRO, Epping, Australia). Aust. J. Phys.; 24: No. 2, 217-27 (Apr 1971).

A solar radio event recorded on August 29–30, 1969 included a polarized moving Type-IV source, seemingly at the top of an expanding magnetic arch, and two stationary sources closer to the Sun but separated by about 1 $R_\odot$, presumably near the feet of the magnetic arch. As the Type-IV source moved outward, it split into two components with opposite circular polarizations. These components expanded and then faded rapidly. It is suggested that the polarization, the peculiar source structure, and the rapid fade-out result from the dissipation of the magnetic arch and the consequent deceleration of synchrotron-emitting electrons. (auth)

35741 MOVING TYPE-IV SOLAR BURST ON OCTOBER 10, 1969. Smerd, S. F. (CSIRO, Epping, Australia). Aust. J. Phys.; 24: No. 2, 229-38(Apr 1971).

A moving Type-IV burst was observed with the Culgoora radioheliograph to develop from a single to a double and, eventually, a triple source. All three source components had the same sense but differing degrees of circular polarization. The direction of movement of the original source changed rapidly during the event. In the late fading stages the sources moved apart. It is suggested that the initiating event occurred behind the Sun and that a disturbance traveled first along an arch and then continues outwards between the open magnetic field lines of a helmet structure. The disturbance was probably a plasmoid or possibly an advancing front in the form of a magnetohydrodynamic or shock wave. While this sequence accounts for most of the observed features, it does not explain the appearance, late in the event, of the third source. (auth)

35742 MEANDERING SOLAR TYPE-IV BURST ON DECEMBER 17, 1969. Dulk, G. A.; Stewart, R. T.; Black, H. C.; Johns, I. A. (CSIRO, Epping, Australia). Aust. J. Phys.; 24: No. 2, 239-45(Apr 1971).

A 2B solar flare on December 17, 1969 produced two moving Type-IV sources and a stationary Type-IV source. Culgoora radioheliograph observations at 80 MHz show one Type-IV source moved for 30 min along a curved path approximately 0.6 $R_\odot$ above the limb. It then stopped and became nearly 100% R.H. polarized. The second moving Type-IV source, 100% L.H. polarized, traveled slowly outward along an approximately straight path for 1 hr. The stationary Type-IV source, 100% R.H. polarized, developed late in the event at a projected position on the disk devoid of active regions. Interferometer observations at 158 MHz show similar movements in the early stage of the event but imply a more-rapid fading of the moving sources and earlier development of the stationary Type-IV source. It is suggested that the first and second sources were each associated with plasmoids moving along closed and open field lines, respectively, and containing synchrotron-emitting mildly relativistic electrons. (auth)

35743 NEW TYPE OF SUPERSONIC SOLUTION FOR THE INVISCID EQUATIONS OF THE SOLAR WIND. Durney, B. (National Center for Atmospheric Research, Boulder, Colo.). Astrophys. J.; 166: No. 3, 669-73(15 Jun 1971).

The transition from a supersonic to a subsonic corona was investigated by increasing the density N_0 (initially $N_0 = 9.3 \times 10^7$ cm^{-3}) at the base of the corona while keeping the temperature T_0 constant ($T_0 = 2.1 \times 10^6$°K). As the density was increased, the energy flux at infinity due to thermal conductivity, ϵ_∞^c, steadily decreased and vanished for $N_0 \sim 1.17 \times 10^8$ cm^{-3}. However, the total energy flux at infinity ϵ_∞ remained different from zero. From somewhat higher values of the density up to $N_0 \sim 3 \times 10^8$ cm^{-3} a new type of supersonic solution was found; the temperature behaving as $(1/r)^{\frac{4}{3}}$ for large distances. It is expected that this type of supersonic solution will exist up to a value of the density for which subsonic solutions are possible ($N_0 > 10^9$ cm^{-3}) Thus for the chosen value of T_0, there is not a direct transition from the Parker-type supersonic solution to the subsonic solution (as N_0 increases from its initial value); instead, there is first a transition to a supersonic flow characterized by a $(1/r)^{\frac{4}{3}}$ asymptotic behavior for the temperature. (auth)

35744 EMPIRICALLY CORRECTED CALCULATIONS OF CORONAL VISIBLE LINES FROM THE $3p^53d$ CONFIGURATION. Wagner, William J. (Univ. of Colorado, Boulder); House, Lewis L. Astrophys. J.; 166: No. 3, 683-98(15 Jun 1971).

A laboratory study of extreme-ultraviolet spectral lines provided empirical data on the $3p^53d$ configuration in high ionization stages of the Ar I sequence. Using a three-electrode spark source with variable inductance, twelve $3p^53d - 3p^54f$ transitions were identified in each of the ions V VI to Fe IX. A least-squares procedure gave a fit of Slater integrals, spin-orbit parameters, and interactions of the type $\alpha L(L+1)$ to the extreme-ultraviolet wavelengths. Using these empirically corrected energy parameters, the energy levels of the $3p^53d$ configuration were recalculated. Within $3p^53d$, it is suggested that six magnetic-dipole transitions may be associated with visible emission lines observed in the solar corona: λ3021, Ni XI, $^3F_3 - {}^1D_2$; λ3167, Fe IX, $^3F_2 - {}^1F_3$; λ3534, Fe IX, $^3F_2 - {}^3D_2$; λ3643, Fe IX, $^3F_3 - {}^1D_2$; λ3801, Ni XI, $^3F_2 - {}^1D_2$; λ4359, Fe IX, $^3F_2 - {}^1D_2$. (auth)

35745 MOTIONS OF FINE STRUCTURE FEATURES IN THE SUNSPOT PENUMBRAS. Steshenko, N. V.; Shcherbakov, A. G. Izv. Krym. Astrofiz. Observ.; 41-42: 3-14(1970). (In Russian).

High-definition ground-level photographs of sunspots (resolution better than 1″) and photographs previously published were used for measuring transverse motions of fine-structure features in the penumbra of sunspots. No penumbra features with permanently directed motions were found at a velocity of ≥2 km/sec. Motions of the pulsations in the radial direction along the penumbra filaments were observed. The displacement of penumbra features took place for a short time (of the order of one minute) at a velocity of about 4 to 8 km/sec; within the next ~10 minutes most of the features change the direction of their motions for the opposite one. The results are in good agreement with spectral data, which show the complicated and rapidly changing structure of the spectral lines of sunspot penumbras. (auth)

35746 VELOCITY FIELD AT DIFFERENT LEVELS IN THE SOLAR-ACTIVE REGIONS. Gopasyuk, S. I.; Tsap, T. T. Izv. Krym. Astrofiz. Observ.; 41-42: 15-24(1970). (In Russian).

The velocity field in 13 active regions near the central meridian were studied. The recordings were made in the K_3Ca^+, H_α, H_β, H_γ, H_δ, Mg I λ5184 Å, Na I D_1, Ca I λ4227 Å, Ca I λ6103 Å, Fe I λ5250 Å, and Fe I λ4808 Å lines with the double magnetograph. It is shown that there is a good correlation between velocities at the neighboring levels in the active region. The correlation decreases with the distance increasing between the levels and disappears for the velocities recorded in the H_α and λ5250 Å lines. The fastest decrease of this correlation takes place in the transitional region between the photosphere and chromosphere. In this region the velocities of ascending and descending gases are equal and have minimum value. Upwards and downwards from the transitional region the velocities of descending gas increase faster with distance than those of ascending gas. (auth)

35747 FORMS OF MOTIONS IN THE CHROMOSPHERIC FLARES. Ogir, M. B. Izv. Krym. Astrofiz. Observ.; 41-42: 25-44(1970). (In Russian).

The motions in a number of limb and disk flares are discussed by means of Hα films. (W.D.M.)

35748 DEVELOPMENT OF THE SOLAR FLARE ON JULY 11, 1966. Babin, A. N. Izv. Krym. Astrofiz. Observ.; 41-42: 45-52 (1970). (In Russian).

A large flare that appeared outside the west solar limb on July 11, 1966 is described. Observations were made with the 12-cm coronagraph in H_α light; in addition, 2 pairs of simultaneous spectroheliograms (in Ca II K_{232} and H_α) were taken with the spectroheliograph. The elevation of a bright flare filament at a velocity of ~10 km/sec and its bifurcating a few minutes later were observed. The observations demonstrate the ejection of plasma out of the flare in opposite directions: from the photosphere at the flare front and to the photosphere from its tail part. Attention is called to the unusual behavior of the Ca II K_{232} line in some flare parts. They are seen to be brighter than the undisturbed solar disk in H_α light and darker (or invisible) in Ca II K_{232}. An attempt is made to explain this effect by the fairly large width of the H_α line in comparison with the calcium one (in flares) and Doppler shift of flare emission. The evidence of Doppler displacement of flare emission to the blue is given. The transient brightening of the flare base was observed, and 45 seconds later the flare-front velocity showed a sudden rise from 40 to 160 km/sec (acceleration up to 10^6 cm/sec^2). If both processes were caused by an invisible disturbance traveling along the flare, its velocity was ~10^3 km/sec. In the late stages of development the flare showed fine, jet-threadlike (filamentary) structure. (auth)

35749 SOLAR RADIO EMISSIONS AT 10 cm AND 1.5 m AND THE CHROMOSPHERIC FLARE OF JULY 11, 1966. Yurovskii, Yu. F.; Babin, A. N. Izv. Krym. Astrofiz. Observ.; 41-42: 53-8(1970). (In Russian).

Radio emissions at 10 cm and 1.5 m were compared with the development of a large limb flare in H_α light. The first pulsed centimetric burst occurred a few minutes after the start of the flare and correlated with the brightening of the flare basis. The second gradually rising burst showed time coincidence with the violent growth of flare ejection. It is shown that the occurrence of a "negative" centimetric burst correlates with the bright matter passage at the heights of 3×10^4 km. There is no time correlation between the appearence of separate bursts at 1.5 m and the dynamic peculiarities of the flare. (auth)

35750 TEMPORAL VARIATIONS OF THE PHOTOSPHERIC VELOCITY FIELD IN THE ACTIVE REGION. Gopasyuk, S. I.; Kartashova, L. G. Izv. Krym. Astrofiz. Observ.; 41-42: 59-66 (1970). (In Russian).

The peculiarities of temporal variations of the photospheric velocity field in a developed active region were examined. The recordings of radial velocities were obtained with the magnetograph in Fe I line λ5250 Å. Two domains with 8-hour oscillations of velocity were found in the active region. During all the observations one of these domains coincided with high magnetic field strength of the leading spot and its vicinity, while the other one coincided with high magnetic field strength of all the other spots of the active region. The oscillations of velocity in both domains were in opposite phase. (auth)

35751 MAGNETIC FIELD AND ELECTRIC CURRENTS OF THE UNIPOLAR SUNSPOT. Kotov, V. A. Izv. Krym. Astrofiz. Observ.; 41-42: 67-88(1970). (In Russian).

Photoelectric recordings of the total field vector H in a large unipolar sunspot were made simultaneously in the λ4808 Fe I and λ6102.7 Ca I lines, and the $H_\parallel$ field was obtained in H_α. The chromospheric longitudinal field $H_\parallel$ is comparable to the photospheric value. The magnetic vector H is vertical at both photospheric levels (λ4808 and λ6102.7) in a very small central region, which has the size of the order of a second of arc. The presence of a strong $H_\perp$ field within the spot and the great (up to 90°) change of vector $H_\perp$ orientation with depth in some parts of the spot are noted. An observable azimuthal component at both levels shows a clockwise twist of the field. The gradient $\partial H_\parallel / \partial z$ determined from the equation div H = 0 is equal to ~0.6 G/km in the spot middle. An analysis of gradients shows that observation apparently corresponds to the transparent spot models best of all. The vertical electric current density is $j_z \sim 10^3$ to 10^4 CGSE. The mean quantity of j_z at the lower level λ4808 is twice that at the upper level λ6102.7. The total currents directed upwards and downwards compensate each other at both levels. The transverse current ($j_\perp \sim 10^4$ CGSE) is mainly perpendicular to the vector $H_\perp$. The electromagnetic force $f = j \times H/c$ in the spot on Michard's model is comparable with gravitation and equal to ~10^{-3} CGSE. There is a displacement strain directed mainly along the longitude in the horizontal plane. The force f_z directed downwards prevails in the spot, and it is accompanied by the principal fall of matter observed in the line λ6102.7. (auth)

35752 VERTICAL DISTRIBUTION OF MAGNETIC FIELD IN THE SUNSPOT UMBRA. Guseinov, M. Dzh. Izv. Krym. Astrofiz. Observ.; 41-42: 89-96(1970). (In Russian).

Thirty-four Fraunhofer lines were used for measuring absolute values of the magnetic field strength in the umbra of a unipolar

XUM

medium-size sunspot. The vertical gradients of magnetic field dH/dh are calculated according to Michard's ($-0,4 \leq dH/dh \leq +0,5$ G/km) and Mattig's ($-5,0 \leq dH/dh \leq +6,0$ G/km) models. It is found that the numerical values of the vertical gradient of the magnetic field in the umbra depend on the sunspot model and change with depth. The vertical gradient of the magnetic field in the sunspot investigated changes its sign at optical depth $\tau = 0.060$. The consideration of vertical gradients of a spot magnetic field investigated, as well as those investigated earlier, shows that the vertical gradients change with time. The values dH/dh are considerably larger for young spots than for the old ones. It is determined that the maximum values of dH/dh correspond to the phase of maximum flare activity of a spot group. (auth)

35753 MAGNETIC FIELDS AND PROTON FLARES 6 JULY AND 2 SEPTEMBER 1966. Zvereva, A. M.; Severnyi, A. B. Izv. Krym. Astrofiz. Observ.; 41-42: 97-157(1970). (In Russian).

Longitudinal and transverse components as well as the total vector of the solar magnetic field in two active spot groups produced proton flares of July 7, 1966 and Sept. 2, 1966. Records were examined for the time interval before and after the flares. In both cases it was found that the field gradients for some specific directions, the magnetic energy, and the total magnetic flux increase appreciably before the flares. (W.D.M.)

35754 MAGNETIC FIELDS AT DIFFERENT DEPTHS OF THE ACTIVE REGIONS OF SOLAR ATMOSPHERE. Tsap, T. T. Izv. Krym. Astrofiz. Observ.; 41-42: 158-67(1970). (In Russian).

The strengths of the longitudinal magnetic fields recorded at different depths of active regions with a double magnetograph of of the Crimean Astrophysical Observatory are compared. It is shown that there is a close correlation between the longitudinal magnetic fields at different levels. It is noted that the correlation between transverse magnetic fields is a little less than that of the longitudinal fields. (auth)

35755 NONUNIFORM CONDUCTIVITY AND FORCE-FREE MAGNETIC FIELDS. I. Gopasyuk, S. I. Izv. Krym. Astrofiz. Observ.; 41-42: 168-73(1970). (In Russian).

The influence of nonuniform conductivity on the structure of a force-free magnetic field is examined. Using Maxwell's equations and Ohm's law, it is shown that the magnetic field can not be force-free if conductivity is nonuniform. A force-free configuration exists in the case of uniform conductivity. Assuming axial symmetry, the general solution of the equation describing a force-free magnetic field is given. Both integrals for the equations of the lines of force are found. This solution shows that the magnetic field decreases exponentially with height. (auth)

35756 GAS PRESSURE GRADIENT AND TRANSPARENCE OF SUNSPOTS. Baranovskii, E. A. Izv. Krym. Astrofiz. Observ.; 41-42: 174-9(1970). (In Russian).

The profiles of the lines D_2 Na I and λ5173 Mg I were obtained for five spots. The wings of these lines were used for the derivation of the magnitude and the gradient of the gas pressure. The temperature and electron pressure, necessary for such a derivation, were obtained by measuring the equivalent widths of a number of weak lines. The transparency of spots was calculated, and the influence of the additional absorption in the continuum on transparency was investigated. The gradient of gas pressure was found to be larger than that in Michard's and Mattig's sunspot models. The transparency of the spots calculated with the derived values of T, p_e, and P_g is a little lower compared to that of Michard's model if no additional absorption is assumed. The calculated model becomes more transparent if continuous absorption is assumed to be larger than that due to the negative hydrogen ions. (auth)

35757 COMPUTATION OF CONTRIBUTION FUNCTIONS. Dubov, E. E. Izv. Krym. Astrofiz. Observ.; 41-42: 180-93 (1970). (In Russian).

Different kinds of contribution functions are compared. It is concluded that the contribution function for the variable $I_\mu/I_0 = 1 - r_\mu$ is the most convenient one to find the depth of a layer producing the emission in any part of a line profile, or to interpret the corresponding spectroheliogram. While calculating the contribution function the often-used partial integration changes somewhat the physical meaning of the contribution function and leads to the overestimation or underestimation of the role of different layers producing observable spectral line emission (especially in the wing of the line). For several $\Delta\lambda$ of three Fe I and one Mg I lines, different contribution functions are computed. The corresponding depths, where escaping radiation is produced, are found. It is noted that brightness distribution on spectroheliograms used to get the information about the structure of some parts of the solar atmosphere (velocity field, distribution of hotter or more dense elements) may reflect the structure of two different layers simultaneously. At some frequencies these two layers may be separated sometimes by a layer giving, in fact, no escaping radiation. Thus, the quanta of the same frequency sometimes carry information about the structure of two different layers, depending on the process of their formation: "bound–bound" or "free–free" or "free–bound" or similar "continuum" transitions. (auth)

35758 LIST OF PROTON FLARES, POLAR CAP ABSORPTIONS, AND SOLAR MICROWAVE RADIO BURSTS. Levitskii, L. S. Izv. Krym. Astrofiz. Observ.; 41-42: 203-29(1970). (In Russian).

The observational data of the lowest radio-wave reflection frequency (f_{min}) at the ionospheric stations of the northern and southern polar caps were analyzed. As a result of this analysis and the study of some published data (up to 1966) a list of solar proton events with particle energies from several MeV to several BeV was compiled for the period 1859 through 1964. The list contains about 300 cosmic-ray effects as well as information on the flares, radio bursts, and magnetic storms associated with these events. The dependence of solar proton events on microwave radio bursts and SC magnetic storms is considered. The distribution of proton flares and radio bursts in solar cycles was investigated for the northern and southern solar hemispheres separately. The conclusions were: (1) the generation of protons with energy $\geq$10 MeV apparently takes place in all chromospheric flares; (2) there is a dependence of the proton flux generated in the flare on the energy (or intensity) of a microwave radio burst of the same flare; (3) the correlation between the cosmic-ray flux and the radio burst (λ 3 to 10 cm) is broken when the Earth is in the equatorial zone of the Sun ($\pm 2^\circ$ helio latitude); and (4) the amount of small (>0.1%) cosmic-ray bursts at sea level apparently does not exceed several hundred events per solar cycle. (auth)

35759 FEATURES OF THE INTERPLANETARY PLASMA AND MAGNETIC FIELD IN THE PLANE OF SOLAR EQUATOR. Vladimirskii, B. M.; Levitskii, L. S. Izv. Krym. Astrofiz. Observ.; 41-42: 240-7(1970). (In Russian).

Some features of the propagation of solar cosmic rays in the solar equatorial zone ($\pm 2^\circ$ helio latitude) were investigated on the basis of the study of galactic cosmic-ray variations. It is shown that solar-wind bulk velocity is lower in this zone. As a consequence, an angle between the Sun–Earth line and a force line of the interplanetary magnetic field is larger in this layer. The decrease of the convection of galactic cosmic-ray particles in the equatorial plane results in the half-year variation of the intensity. The radial component of the solar diurnal anisotropy as well as an azimuthal component increase in this zone, thus the amplitude of the diurnal variation for the zone ($\pm 2^\circ$ helio latitude) is larger (15 to 20%) than for higher helio latitudes. This phenomenon may indicate the larger regularity of the magnetic field in the equatorial region. It was revealed that the mean delay time of the sudden commencement of a magnetic storm depends on the position of the flare and the Earth relative to the equatorial layer. If the shock front crosses the equatorial layer (or propagates along it) the delay time increases by 4 to 10 h. This effect may be caused by the enhanced density of the plasma in the equatorial zone. (auth)

35760 OBSERVATIONS OF SOLAR RADIO EMISSION AT 3,15 cm WITH THE 22-METER RADIOTELESCOPE OF THE CRIMEAN ASTROPHYSICAL OBSERVATORY. Eryushev, N. N.; Tsvetkov, L. I. Izv. Krym. Astrofiz. Observ.; 41-42: 253-9(1970). (In Russian).

Some observational results on solar radio emission at a wavelength of 3.15 cm are given. The association between the radio brightness of local sources and areas of sunspot groups are considered. For this purpose the data at wavelengths of 1.75; 7.5, and 21 cm were used. The change of flux density of the radio emission at 1.75 cm seemed to be correlated with a real area of sunspot groups, but at 7.5 and 21 cm it is correlated with a visible area of sunspot groups. This confirms the fact that, in the first case, the radio source is optically thin. In the second case, the optical thickness is considerable; that is why the directivity of emission takes place at these wavelengths. At 3.15 cm, the optical properties of the radio source are intermediate. During the solar flare of August 29, 1967, the radio burst appeared away from the center of the local source. In two other cases the burst sources, with a gradual rise and fall, coincided with the center of a local source. (auth)

35761 SUMMARY OF SKY BRIGHTNESS MEASUREMENTS DURING ECLIPSES OF THE SUN. Sharp, W. E. (Univ. of Colo-

rado, Boulder); Silverman, S. M.; Lloyd, J. W. F. Appl. Opt.; 10: No. 6, 1207-10(Jun 1971).

A selected group of measurements of the sky brightness during total solar eclipses was used to determine a standard light curve during the period from no obscuration to totality. It was found that the sky light may be considered as attenuated sunlight up to at least 99.8% obscuration. During totality, the sky light consists of multiply scattered light from outside the umbral region. The effects of solar elevation angle, cloud cover, and albedo and the variability of the light curve during totality are discussed. (auth)

35762 ZENITH SKY BRIGHTNESS AND COLOR CHANGE DURING THE TOTAL SOLAR ECLIPSE OF NOVEMBER 12, 1966 AT SANTA INES, PERU. Velasquez, D. A. (Instituto Geofisico del Peru, Huancayo). Appl. Opt.; 10: No. 6, 1211-14(Jun 1971).

Observations of the zenith sky brightness around totality at 5580 and 6300 Å during the eclipse of November 12, 1966 are reported. The observations were carried out at Santa Ines, Huancavelica, Peru, using interference filter photometers. The color change and the variation of the sky brightness at zenith were determined and are presented. (auth)

35763 MEASUREMENTS OF THE ZENITH SKY INTENSITY AND SPECTRAL DISTRIBUTION DURING THE SOLAR ECLIPSE OF NOVEMBER 12, 1966 AT BAGE, BRAZIL AND ON AN AIRCRAFT. Lloyd, J. W. F.; Silverman, S. M. (Air Force Cambridge Research Labs., Bedford, Mass.). Appl. Opt.; 10: No. 6, 1215-19(Jun 1971).

Measurements of the zenith sky intensity and spectral distribution during the solar eclipse of November 12, 1966 at Bage, Brazil, and on an aircraft over the Atlantic are reported. These, together with measurements reported elsewhere from Santa Ines, Peru, and Quehua, Bolivia, were used to define the intensities and changes in spectral distribution during totality and to discuss the dependence of these on such factors as height and terrain. (auth)

35764 DAY SKY BRIGHTNESS AND POLARIZATION DURING THE TOTAL SOLAR ECLIPSE OF 7 MARCH 1970. Dandekar, B. S.; Turtle, J. P. (Air Force Cambridge Research Labs., Bedford, Mass.). Appl. Opt.; 10: No. 6, 1220-4(Jun 1971).

Zenith sky brightness at totality was observed to be about four orders of magnitude lower than that for a normal day sky. The spectral distributions in terms of an effective blackbody temperature for the range 4100 to 8000 Å were 5000, 9000, and 11,000K for the twilight, control day sky, and totality, respectively, indicating a shift toward the shorter wavelength at totality. The polarization measured in the Sun's vertical plane 90° away from the Sun was 4% and 0.6% at 4750 Å and 6000 Å, respectively. Both colors showed a change in the plane of polarization of about 50° at the time of totality. From the change in the plane of polarization the component due to primary scattering reduced by about an order of magnitude at totality of the eclipse. (auth)

35765 SPECTRAL CHANGES IN THE ZENITH SKYLIGHT DURING TOTAL SOLAR ECLIPSES. Hall, W. N. (Air Force Cambridge Research Labs., Bedford, Mass.). Appl. Opt.; 10: No. 6, 1225-31(Jun 1971).

The relative spectral intensity of the zenith sky was measured with an optical scanning spectrometer at Nantucket Island, Massachusetts, during the total solar eclipse of March 7, 1970. The spectral ratios I(5100 Å)/I(4300 Å) and I(5900 Å)/I(5100 Å) at Nantucket remained unchanged for 96% or less obscuration of the Sun by the Moon. The results are compared with other recent relative spectral intensity measurements made during total solar eclipses. Comparison with other eclipse measurements for solar elevation angle at totality less than 45° shows a blue color shift consistent with Rayleigh scattering. Eclipses with solar elevation angles at totality greater than 45° do not show consistent color shifts. This inconsistency may be due to difficulty in establishing a suitable reference spectrum for comparison with the spectral distribution of the zenith sky at totality. Selection of a suitable reference spectrum is discussed. (auth)

35766 GRAZING-INCIDENCE SPECTRA OF Ne VII AND Ne VIII. Tondello, G.; Paget, T. M. (Culham Lab., Abingdon, Eng.). J. Phys., B (London); 3: 1757-61(Dec 1970).

About 90 lines of Ne VII and Ne VIII were observed in the region 50 to 140 Å with a θ-pinch discharge as a light source. Use was made of a rotating shutter in front of the spectrograph to eliminate impurity lines. (auth) (UK)

35767 PIONEER 9 ELECTRIC FIELD EXPERIMENT. PART 2. OBSERVATIONS BETWEEN 0.75 AND 1.0 AU. Scarf, F. L. (TRW Systems Group, Redondo Beach, Calif.); Siscoe, G. L. Cosmic Electrodyn.; 2: No. 1, 44-59(Apr 1971).

A general survey is presented of the deep space data for solar rotations 1851-1858 (November 11, 1968 to June 14, 1969). The response for twenty selected storm periods is analyzed covering a time interval from November 16, 1968 to May 11, 1969, and a heliocentric distance range from 1.0 to 0.75 AU. It is shown that the two low-frequency channels have disparate storm response characteristics that vary monotonically with radial distance, indicating that the turbulent E-field spectrum in the disturbed solar wind has a significant radial gradient. (auth)

35768 STUDY OF CORONAL CONDENSATIONS BY MEANS OF THEIR XUV LINE SPECTRUM. Chambe, G. (Observatoire, Meudon, France). Astron. Astrophys.; 12: No. 2, 210-18(May 1971). (In French).

An interpretation of the xuv resonance line spectrum of the coronal condensations is given in terms of thermal emission from inhomogeneous regions, i.e., with a continuous range of temperatures. It is shown that the temperature and the emission measure derived from the measured intensities of two lines depend on the coupling of lines in such a way that an isothermal model cannot account for wide ionization and excitation potential ranges. Besides, the formation temperature domain of each line is not narrow enough to allow one to neglect the variation of the emission measure inside it. Therefore, Pottasch's approximate method, valid for the quiet corona, is not suitable to the active centers. In that case a rigorous treatment is done. The calculation was fitted to the observed intensities of the Fe XV, XVI, lines at ≈300 Å, the Si VIII to XII lines in the 40 to 70 Å band, and the O VII, VIII, Ne IX, X and Fe XVII, XVII lines between 10 and 25Å. As there are no simultaneous observations for these spectral ranges, microwave data were used to select a set of xuv spectra corresponding to similar solar conditions. It is believed that this sample is typical of the case when two or three rather small condensations are present. (W.D.M.)

35769 COMPUTATION OF SHOCK HEATED MODELS FOR THE SOLAR CHROMOSPHERE AND CORONA. Ulmschneider, P. (Univ., Wuerzburg, Ger.). Astron. Astrophys.; 12: No. 2, 297-309(May 1971).

Theoretical models are computed for the chromosphere and corona starting at a height of 800 km. The observational chromospheric models can be reproduced very well up to 1400 km, assuming weak shock waves with periods of around 27 s. At greater heights, the Hα and Lyman continuum radiation loss regions can presently not be treated adequately. The observed Ly-α and xuv line fluxes are used to extend the theoretical model computation into the transition region and lower corona. Acoustic waves of periods between 100 and 200 s are shown to develop into strong shocks in the lower corona. The heating of these waves determines the theoretical models up to the coronal temperature maximum. The notion that short-period waves of around 27 s heat the chromosphere while long-period waves of around 100 to 200 s heat the corona was found to be consistent with the acoustic-wave fluxes and frequencies of spectra given by Stein (1968). (auth)

35770 BROADENING BY NEUTRAL HYDROGEN IN THE SOLAR ATMOSPHERE. Roueff, E.; Van Regemorter, H. (Observatoire de Paris, Meudon, France). Astron. Astrophys.; 12: No. 2, 317-19(May 1971).

The broadening cannot be given by the van der Waals interaction, increasing the C_6 constant arbitrarily, as it is assumed in a recent paper by Holweger (1971). A reply by Holweger is included. (W.D.M.)

35771 SOLAR CORPUSCULAR RADIATIONS AND THE INTERPLANETARY MAGNETIC FIELD. Tandon, J. N. (Univ. of Delhi). pp 62-78 of Proceedings of the Eleventh Symposium on Cosmic Rays, Astrophysics, Geophysics and Elementary Particle Physics, 1969. Vol. I. Bombay; Department of Atomic Energy (1969).

From eleventh symposium on cosmic rays, astrophysics, geophysics and elementary particle physics; Delhi, India (7 Oct 1969). See CONF-691055-(Vol. 1).

The interactions between the solar corpuscular radiation and the interplanetary magnetic field are considered. Particles of 200 eV to 20 keV are of primary importance in these interactions, and this review is centered around them. (W.D.M.)

35772 SEARCH FOR ENERGETIC NEUTRONS EMITTED DURING SOLAR FLARES. Daniel, R. R.; Gokhale, G. S.; Joseph, G.; Lavakare, P. J.; Sekhon, B. S. (Tata Inst. of Fundamental Research, Bombay). pp 311-12 of Proceedings of the Eleventh Symposium on Cosmic Rays, Astrophysics, Geophysics and Elementary Particle Physics, 1969. Vol. II. Bombay; Department of Atomic Energy (1969).

From eleventh symposium on cosmic rays, astrophysics, geophysics and elementary particle physics; Delhi, India (7 Oct 1969). See CONF-691055-(Vol. 2).

Balloon flights on Feb. 26, 1969 were made from Hyderabad,

XUM

India to detect possible high-energy neutron emissions during solar flares. Flares of classes 2B and 1N occurred, but no perceptible flare-associated increase in the counting rate was observed. (J.C.W.)

35773 OBSERVATIONS ON THE SCATTERING OF DECAMETER RADIO WAVES BY SOLAR CORONA. Sastry, Ch. V. (Astrophysical Observatory, Kodaikanal, India). pp 418-23 of Proceedings of the Eleventh Symposium on Cosmic Rays, Astrophysics, Geophysics and Elementary Particle Physics, 1969. Vol. II. Bombay; Department of Atomic Energy (1969).

From eleventh symposium on cosmic rays, astrophysics, geophysics and elementary particle physics; Delhi, India (7 Oct 1969). See CONF-691055-(Vol.2).

The occultations of the radio sources Tau A and Vir A were observed using a phase-switching interferometer at a wavelength of 12 meters. As radio waves pass through the solar corona they are scattered due to the fact that the electron density varies from point to point. The effect of scattering is manifested by an apparent increase in the angular diameter of the source. (J.C.W.)

35774 HOMOLOGOUS MICROWAVE BURSTS AND ASSOCIATED SOLAR FLARES. Gopala Rao, U. V. (Kodaikanal Observatory, India). pp 424-7 of Proceedings of the Eleventh Symposium on Cosmic Rays, Astrophysics, Geophysics and Elementary Particle Physics, 1969. Vol. II. Bombay; Department of Atomic Energy (1969).

From eleventh symposium on cosmic rays, astrophysics, geophysics and elementary particle physics; Delhi, India (7 Oct 1969). See CONF-691055-(Vol. 2).

Optical homologous characteristics associated with homologous radio bursts are reviewed. Two homologous radio bursts occuring on Aug. 21 and 23, 1968 are studied. According to the existing ideas the radio emission associated with solar flares is caused directly by the movement of the disturbance from the chromospheric levels where the optical flares originate into the corona from where the radio emission originates at different levels. It is to be expected that optical and radio homologies occur together. (J.C.W.)

35775 CORONAL LINE PROFILES OBSERVED BY MEANS OF CORONAGRAPHS AND A FABRY-PEROT SPECTROMETER. Henderson, G.; Larsen, A.; Marshall, P. M. (Heriot-Watt Univ., Edinburgh). Nature (London) Phys. Sci.; 231: No. 21, 77-8(24 May 1971).

Some results of observations of the λ5303 Å (Fe XIV) and λ6374 Å (FeX) emission line profiles in the solar corona are reported, using the 26-cm coronagraph at Pic-du-Midi, Hauts Pyrenees, and the 20 cm coronagraph at Wendelstein, Ober Bayern. Observations are also described that represent a continuation of the development of the application of the Fabry-Perot spectrometer to the study of coronal emission lines. Analysis of the data is proceeding, with a view to obtaining values for the temperature distribution in the observed coronal regions. (UK)

35776 SOLAR CHROMOSPHERIC ACTIVITY AT 400, 800, AND 1,200 μ. Ade, P. A. R.; Beckman, J. E.; Clark, C. D. (Queen Mary Coll., London). Nature (London) Phys. Sci.; 231: No. 20, 55-7(17 May 1971).

Observations using the 1.05-m Cassegrain telescope at the Pic-du-Midi Observatory, together with a He-cooled Rollin detector of mm and sub-mm radiation and suitable interference filters are described. The observations were made on February 8, 1971 with a view to producing isophote maps of active regions of the solar chromosphere. The raster scanning technique was employed. Isophotes were drawn at intervals of 50K, representing ~1% of the disk brightness temperatures, and enhanced temperatures in the active regions were calculated. Limb brightening was indicated in all three passbands, increasing with wavelength, and the "peak" temperature rose by 75% between 400 and 1,200 μm. These are considered to be the first sub-mm solar measurements to provide spatial as well as spectral resolution, and the data should enable the derivation of improved models of chromospheric active regions. (UK)

35777 DIAGNOSIS OF CORONAL MAGNETIC STRUCTURE BY FLARE-ASSOCIATED HYDROMAGNETIC DISTURBANCES. Uchida, Yutaka (Tokyo Univ., Mitaka, Japan). Publ. Astron. Soc. Jap.; 22: 341-64(Oct 1970).

Mechanical diagnosis of the coronal magnetic structure by the use of flare-associated hydromagnetic disturbances is proposed. By using a canonical-type formulation for the propagation of hydromagnetic disturbances in nonuniform, anisotropic media in WKB approximation, the expected shape and motion of the locus of simultaneous reentry of wave packets, which are emitted into the corona by a flare-explosion and reflected back onto the chromosphere, are calculated numerically for various model coronas having global and local structures. In particular, a series of calculations is made for model coronas with an aggregate of model local structures mimicking the realistic situation on the day of a particular typical Moreton-wave event. By comparing the calculation with the observed Moreton-wave distortion, it is concluded that the enhancement in the magnetic-field strength inside the diffuse coronal structure extending high above the general plage area (coronal streamer) is weaker than the enhancement in the square root of density, while the situation is naturally reversed for the strongly localized mound-like structure immediately above sunspot groups (coronal condensation). This result may be interpreted by considering that, though the enhancement in density above an active region may be originally induced by the magnetic enhancement, the density enhancement is maintained even after the magnetic enhancement has decreased markedly as the sunspot disappears leaving only the quieter plage region during the later history of an active center. (auth) (Japan)

35778 GEGENSCHEIN. Roosen, Robert G. (Goddard Space Flight Center, Greenbelt, Md.). Rev. Geophys. Space Phys.; 9: No. 2, 275-304(May 1971).

A comprehensive review is made of the observational history of the gegenschein with emphasis on its physical parameters: size, shape, brightness, spectrum, position, and parallax. The theories that have been considered tenable until recently are critically discussed. The libration point, gas tail, and dust tail hypotheses can be disproved, whereas the heliocentric dust-cloud hypothesis is consistent with all evidence available. At present, the asteroid belt seems to be the most likely source of the material producing the gegenschein. A short discussion of the false zodiacal light is included. (auth)

Galaxies

35779 NEW RADIAL VELOCITIES OF GALAXIES FROM IMAGE-TUBE SPECTRA. Kintner, Eric C. (Wesleyan Univ., Middletown, Conn.). Astron. J.; 76: No. 5, 409-11(Jun 1971).

Seventy-nine radial velocities of extragalactic objects were obtained from 88 spectra taken with the Carnegie image-tube spectrograph at the 84-inch telescope of the Kitt Peak National Observatory. Sixty-eight of these objects have no previous radial-velocity determinations. The accuracy of this study is similar to previous radial-velocity surveys. (auth)

35780 FAR-INFRARED ASTRONOMY AND THE GALACTIC CENTER. Frederick, Carlton. New York; Yeshiva Univ. (1970). 236p. University Microfilms Order No. 71-5682.

Thesis.

On the night of July 30, 1968, a far-infrared flux from a region roughly coincident with the galactic center, was detected. The shape of the source, as far as could be specified, was less than 2.3° on the direction perpendicular to the galactic plane, and greater than 6.5° in extent along the galactic plane. The flux density integrated over the extent of the source was $1.8 \pm 0.8 \times 10^{-19}$ W m^{-2} Hz^{-1}. Under the assumption that the source was indeed the galactic center, the total emission in the 40-μ band centered about 100 μ integrated over the source was 2.7×10^{42} ergs/sec, or 7×10^{8} $L_{\odot}$. This was approximately 3% of the total luminosity of the galaxy. The mass in the region was about 10% of the galactic mass. The 100 μ mass-to-luminosity ratio was then 12 $M_{\odot}/L_{\odot}$. It is difficult to find a mechanism other than that of degradation of starlight by grains to explain the high observed flux. The observation was performed by means of a balloon-borne telescope that utilized a liquid-helium-cooled detector with a NEP of about 10^{-13} watts. The telescope used a quartz, one-inch, f1.1 lens. The energy throughout to the detector was about 12%. The observation of the Moon during the same balloon flight was used to calibrate the galactic center source. (Diss. Abstr. Int., B)

35781 INTERPRETATION OF OBSERVATIONS OF NEUTRAL HYDROGEN IN EXTERNAL GALAXIES. Wright, Melvin C. H. (National Radio Astronomy Observatory, Green Bank, W. V.). Astrophys. J.; 166: No. 3, 455-64(15 Jun 1971).

A reanalysis was made of interferometer observations of neutral hydrogen in external galaxies. An interpretation, consistent with optically derived rotation curves, showed that the neutral-hydrogen distribution is wider than the total mass or H II region distribution, and that a fractional minimum of neutral hydrogen to total mass exists at the center of these galaxies. High-resolution pencil-beam observations are also discussed, and it is shown that the interpretation of minor-axis profiles is not unique. Both ring and Gaussian distributions of hydrogen are discussed, and it is not possible to decide between them. (auth)

35782 DENSITY-WAVE THEORY OF GALACTIC SPIRALS. III. COMPARISONS WITH EXTERNAL GALAXIES. Shu, Frank H.; Stachnik, Robert V.; Yost, Jonathan C. (State Univ. of New York, Stony Brook). Astrophys. J.; 166: No. 3, 465-81(15 Jun 1971).

A semi-empirical study was undertaken of the spiral patterns of three model galaxies constructed from the observed rotation curves of M33, M51, and M81. Consistent with the proposal that density waves are initiated in the outer regions of a galaxy, a good fit was found to result for the observed spiral structure if a pattern speed equal to the rotation speed was chosen where the distribution of H II regions is seen to end. The circumferential bands containing the most prominent H II regions are located in qualitative agreement with a mechanism in which star formation is triggered by spiral galactic shocks. A suggestion is made for M51 for the coexistence of short and long trailing waves traveling with the same pattern speed. (auth)

35783 RANDOM GRAVITATIONAL ENCOUNTERS AND THE EVOLUTION OF SPHERICAL SYSTEMS. II. MODELS. Spitzer, Lyman Jr.; Hart, Michael H. (Princeton Univ. Observatory, N. J.). Astrophys. J.; 166: No. 3, 483-511(15 Jun 1971).

The evolution of several model spherical star systems was followed numerically in time, using a new method for computing the velocity perturbations produced by stellar encounters. The integrations extended over 10 to 100 relaxation times at the center of the system. In every case a contracting, nearly isothermal, core of high star density develops at the center of the system, while stars in elongated orbits accumulate in a surrounding extended halo; the contraction as a whole is far from homologous. These results show clearly how the tendency to establish a Maxwellian velocity distribution produces a gradual evolution through two effects: (a) the stars diffuse in velocity space toward zero energy, populating the halo in elongated orbits with some escaping from the system altogether, and (b) stars heavier than the average lose energy to the lighter stars and fall toward the center of the system. In the model systems with a single mass component, the loss of energy to escaping stars is comparable with the loss of energy to those which accumulate in the halo; the relative importance of escaping stars would presumably be even greater if the tidal force of the Galaxy, which sets an upper limit on the apocenter of a bound stellar orbit, were considered, or if the occurrence of relatively close encounters, with large resultant velocity changes, were taken into account. The particular initial conditions assumed might also modify this ratio. In systems with several mass components the contraction of the core of heavier stars is in rough agreement with simple theory. If 10% of the system's mass is in stars with 5 times the mass of the lighter stars, the density in the central core increases to about 50 ρ_h, where ρ_h is the mean density for the inner half of the system's mass, during a time interval equal to t_{rh}, where t_{rh} is the dynamical relaxation time at the density ρ_h. Calculations were also carried through for the mass distribution anticipated in old stellar systems such as globular clusters, in which stars of 0.625, 0.25, and 0.1 $M_\odot$ represent one-half, one-third, and one-sixth the total mass, respectively; in this model the central density increases to 150 ρ_h in 2 t_{rh}, and the lighter stars move outward. Since t_{rh} equals about 8×10^9 years for a typical cluster, pronounced mass stratification should be present for the lower-mass stars in at least some of these systems. The structure and evolution of all these models depend only on t/t_{rh}, with no strong dependence on N, the total number of stars in the system, over the limited range of values, between about 10^3 and 10^4, assumed in the calculations. (auth)

35784 HEATING OF THE INTERSTELLAR MEDIUM BY X RAYS AND BY COSMIC RAYS. Habing, H. J. (Univ. of California, Berkeley); Goldsmith, D. W. Astrophys. J.; 166: No. 3, 525-41(15 Jun 1971).

The efficiency of the heating produced in the interstellar medium when soft x rays ionize hydrogen and helium, liberating "primary" electrons with energies of several hundred electron volts was calculated. Some of this energy is lost in excitation and ionization processes, but part of the energy is recovered through elastic collisions with thermal electrons in the interstellar gas. Using both an analytic treatment of the Boltzmann equation and a Monte Carlo calculation of the degradation of the primary electron's energy, the fraction of the primary's energy (taken to be either 70 or 300 eV) that is available to heat the gas was found. This efficiency increases with increasing ionization fraction, from ~0.3 at $n_e/n_H = 10^{-3}$ to ~0.95 at $n_e/n_H = 0.3$. These heating efficiencies were employed to calculate the equilibrium temperature-density and pressure-density relations for a given value of $\zeta_{pr}(H^0)$, the primary ionization rate of hydrogen by x rays. The general form of these curves is the same as that found for the case of cosmic-ray heating, although the x rays are less efficient than cosmic rays in heating the intercloud medium. Field et al., used a rate of primary cosmic-ray ionization $\zeta_{pr}(H^0) = 4 \times 10^{-16}$ sec^{-1} to obtain the best fit to the observational data. The required x ray ionization rates are $\zeta_{pr}(H^0) = 1.4 \times 10^{-16}$ sec^{-1} for 70-eV x rays and $\zeta_{pr}(H^0) = 3.5 \times 10^{-17}$ sec^{-1} for 300-eV x rays, several times greater than those found by extrapolating the spectrum suggested by Silk and Werner to 70 eV. Additional galactic sources of soft x rays (E < 150 eV) are required. (auth)

35785 FAR-ULTRAVIOLET INTERSTELLAR ABSORPTION IN ORION AND MONOCEROS. Weber, Stephen V. (Naval Research Lab., Washington, D. C.); Henry, Richard C.; Carruthers, George R. Astrophys. J.; 166: No. 3, 543-57(15 Jun 1971).

Eleven groups of hot stars and 206 individual such stars were examined in the ultraviolet at 1500 Å. Ten exhibit strong ultraviolet reddening according to a law $E(m_{1500} - V) = 6.0\ E(B - V)$, and about fifteen more are weakly reddened in a manner not inconsistent with that law, which is similar to laws derived by others. Most supergiants are fainter in the ultraviolet (relative to the visible) compared with main-sequence stars of the same B − V color, in agreement with previous work. There is a very weak and perhaps not significant tendency for giant stars also to be slightly dim. Two star groups appear to be reddened in an anomalous manner. One group of stars, and six single stars, all unreddened or slightly reddened, are anomalously bright at 1500 Å by about 1.3 mag. The two anomalously reddened objects could actually be examples of this new ultraviolet-bright class of stars, reddened in accord with the same reddening law as the other stars. (auth)

35786 KINEMATIC-DYNAMO THEORY. I. Lerche, I. (Univ. of Chicago). Astrophys. J.; 166: No. 3, 627-38(15 Jun 1971).

General kinematic-dynamo equations are derived that give the rate of generation of a large-scale magnetic field by a random velocity field, with or without large-scale shear. It is demonstrated that under the "short-sudden" approximation for the turbulent flow, the general kinematic-dynamo equations reduce to those previously derived by Parker. Under the "long-slow" approximation, the equations reduce to dynamo equations of the Braginskiĭ type. It is demonstrated that the helicity of the turbulent Lorentz force is the basis for all turbulent-dynamo equations. That part due to helicity in the velocity turbulence was first isolated under the "short-sudden" approximation by Steenbeck, Krause, and Radler as a direct cause of dynamo action on its own (their "α-effect"). A prescription is also given for handling small bulk velocities, and small bulk-velocity shear, occurring in the general kinematic-dynamo equations. (auth)

35787 KINEMATIC-DYNAMO THEORY. II. DYNAMO ACTION IN INFINITE MEDIA WITH ISOTROPIC TRUBULENCE. Lerche, I. (Univ. of Chicago). Astrophys. J.; 166: No. 3, 639-49(15 Jun 1971).

The general kinematic-dynamo equations derived in an earlier paper are applied to infinite media. It is demonstrated that under homogeneous, isotropic, and stationary velocity turbulence, an infinite, stationary medium possesses large-scale magnetic-field components which are stationary, and of a scale much larger than the correlation length of the weak random velocity turbulence. It is further shown that in the vicinity of each stationary mode (of the mean magnetic field) there exist both growing and decaying dynamo states. And whether the growing dynamo states lie to the long-wavelength side or the short-wavelength side of the stationary states is determined by the relative sizes of the resistivity and the turbulent-velocity field. It is also shown that inclusion of a small bulk velocity converts the stationary modes, and the regenerative and degenerative modes in their vicinity, into progressive dynamo waves which propagate (the stationary modes), propagate and grow (the regenerative modes), or propagate and decay (the degenerative modes). A prescription is also given for reducing the reduced dynamo equation derived elsewhere (valid for small bulk velocities and small bulk-velocity shears) even further under the "short-sudden" approximation. This reduction is of practical significance since it enables various terms in the dynamo equations to be singled out and investigated for their direct contribution (if any) to dynamo action. (auth)

35788 STRUCTURE AND POLARIZATION OF 3C 459 AT 610 MHz. Wardle, J. F. C. (National Radio Astronomy Observatory, Green Bank, W. Va.). Astrophys. Lett.; 8: No. 2, 53-5(Apr 1971).

The structure and distribution of linear polarization of the N-type galaxy 3C 459 were determined with a long-baseline interferometer at 610 MHz. The source consists of two small components: a relatively weak one with 8.8% linear polarization and a strong component with ≤0.3% polarization. It is likely that the

XUM

stronger component coincides with the nucleus of the galaxy and that the weaker component corresponds to an optically visible "jet". (auth)

35789 NEUTRAL HYDROGEN ABSORPTION AND EMISSION IN NGC 5128 (CENTAURUS A). Whiteoak, J. B.; Gardner, F. F. (Commonwealth Scientific and Industrial Research Organization, Sydney). Astrophys. Lett.; 8: No. 2, 57-60(Apr 1971).

The 21-cm line profiles of NGC 5128 (Centaurus A) show eight discrete absorption and two emission components, extending over a velocity range of ~500 km/sec. The absorption does not show measurable beam-broadening and is centered on the optical center of NGC 5128, suggesting that a source in the nuclear region is being absorbed. The two emission components are located ~10 arc min apart along the dust lane of the galaxy. The results suggest that NGC 5128 possesses many of the features of a spiral galaxy. (auth)

35790 INTERSTELLAR GRAIN TEMPERATURES. EFFECTS OF GRAIN MATERIALS AND RADIATION FIELDS. Greenberg, J. Mayo (Leiden Observatory). Astron. Astrophys.; 12: No. 2, 240-9(May 1971).

Temperatures of interstellar grains of various types were calculated in normal interstellar H I regions and in regions of abnormally low ultraviolet stellar radiation. Intermediate estimates and lower bounds were established for the temperatures in a variety of physical conditions. (auth)

35791 INTERSTELLAR GRAIN TEMPERATURES. EFFECT OF SHAPE. Greenberg, J. Mayo (Leiden Observatory); Shah, G. A. Astron. Astrophys.; 12: No. 2, 250-7(May 1971).

Emissivities calculated for small spheroids give a strong indication that shape considerations may be generally neglected in the determination of the temperature of small interstellar particles. Grain temperature calculations are also performed, using exact scattering theory for an infinite circular cylinder of radius a = 0.1 μ under a variety of radiations. Comparison made with a similar set of calculations for spheres shows small differences. The extremes represented by the infinite cylinder, as well as the very thin needle-shaped and flat disk-shaped spheroids, are generally about 10% cooler than spheres under the radiation conditions reached in interstellar space. Exceptional situations are shown to be attainable for metallic particles but under somewhat unlikely circumstances. (auth)

35792 LYMAN ALPHA EMISSION FROM THE GALAXY. Adams, T. F. (Univ. of Colorado, Boulder). Astron. Astrophys.; 12: No. 2, 280-5(May 1971).

The radiative transfer problem describing the diffusion of Lyman alpha through the Galaxy is formulated and then solved by Feautrier's method. The solutions are used to derive an upper limit to the Lyman-alpha emission expected in the galactic plane. This upper limit is comparable to the observed upper limit to the galactic component of the Lyman-alpha sky background. (auth)

35793 GRAVITOHYDROMAGNETIC INSTABILITY IN CONTRASTREAMING PLASMAS. Talwar, S. P. (Univ. of Delhi). Cosmic Electrodyn.; 2: No. 1, 60-77(Apr 1971).

The hydromagnetic stability of a composite system composed of infinitely conducting gravitating fluids is investigated by the normal mode analysis. The effects of hydromagnetic and gravitational coupling between the component fluids are studied in an initially static and a contrastreaming configuration. It is found that an N-component static nongravitating system allows, in general, (N + 1) magnetosound modes in addition to a pure Alfven mode. The gravitational coupling in a static composite medium results in an instability leading to an incipient fragmentation, whose size depends on the densities and the sound speeds of the individual components in the composite medium. The conditions for contrastreaming instability in gravitating plasmas are derived in view of their likely importance in galactic dynamics and star formation from primordial matter. Finally, the analysis is extended to include dilute plasmas with anisotropic pressure, obeying the "double-adiabatic" CGL equations. (auth)

35794 21-cm NEUTRAL HYDROGEN LINE AND CONTINUUM STUDY OF THE GALAXY MAFFEI 2. Bottinelli, L.; Chamaraux, P.; Gerard, E.; (and others). (Observatorie, Meudon, France). Astron. Astrophys.; 12: No. 2, 264-70(May 1971).

The Maffei 2 object was observed with the Nancay radio telescope in the 21-cm line of neutral hydrogen and in the continuum at 1415 MHz. Its main physical properties were determined, and it appears that this object is a medium spiral galaxy. It is probably located beyond the Local Group in the southern part of the Ursa Major–Camelopardalis cloud of galaxies. (auth)

35795 OBSERVATIONAL EVIDENCE FOR PARKER'S INSTABILITY OF THE INTERSTELLAR GAS AND MAGNETIC FIELD. Appenzeller, I. (Univ., Goettingen, Ger.). Astron. Astrophys.; 12: No. 2, 313-15(May 1971).

In order to test Parker's theory of the interstellar gas and magnetic field the structure of the local magnetic field in the vicinity of the α-Persei cluster is determined from polarimetric observations of nearby stars. The result agrees well with Parker's predictions. (auth)

35796 ESCAPE OF STARS FROM COLLIDING GALAXIES. Sastry, K. Shankara; Aliadin, Saleh Mohamed (Osmania Univ., Hyderabad, India). pp 428-30 of Proceedings of the Eleventh Symposium on Cosmic Rays, Astrophysics, Geophysics and Elementary Particle Physics, 1969. Vol. II. Bombay; Department of Atomic Energy (1969).

From eleventh symposium on cosmic rays, astrophysics, geophysics and elementary particle physics; Delhi, India (7 Oct 1969). See CONF-691055–(Vol. 2).

A theory was developed to estimate the percentage of stars that would escape from a galaxy by virtue of the energy gained by them during the collision and the energy associated with the escaping stars. The theory utilizes the estimates for the exchange of gravitational energy during a collision of two galaxies assuming that the galaxies may be regarded as spherical stellar systems whose over-all structure remains unchanged during a collision and the internal motions of the stars may be neglected during the encounter. (J.C.W.)

35797 ESTIMATION OF THE TOTAL KINETIC ENERGY OF CLUSTERS OF STARS OR GALAXIES. Sher, D. (Cincinnati Observatory). Astrophys. Space Sci.; 11: No. 2, 337-43(May 1971).

The kinetic energy of some model clusters was estimated by simulated observation of the line-of-sight velocities of the members, and this estimate was then compared with the actual kinetic energy which was known for each model. The model clusters were all self-consistent and had ellipsoidal velocity distributions of the type first discussed by Eddington some sixty years ago and give a reasonable run of density with distance from the center of the cluster. Estimates of the total kinetic energy varied with the part (as seen in the plane of the sky) of the cluster sampled, since velocity distributions of this sort have a preponderance of velocities along a radius of the cluster at great distances from the center. Overestimates of the total kinetic energy—even by as much as a factor of 2—were found to be rare; and, in practice, a factor of 1.5 would be a fair summary of the more extreme results obtained from samples near the apparent center. These results were found to be fairly insensitive to the degree of anisotropy in the velocity distribution. Since the mass of a cluster as determined from the virial theorem is directly proportional to the estimated kinetic energy, these same factors represent the systematic overestimation of the total mass of the cluster due to a lack of isotropy in the cluster's velocity field. (auth)

35798 KINEMATICS OF THE SCORPIO–CENTAURUS ASSOCIATION AND GOULD'S BELT. Jones, D. H. P. (Australian National Univ., Canberra). Mon. Notic. Roy. Astron. Soc.; 152: 231-59(1971).

The convergent points of the proper motions of all stars in the FK_4 catalogue, Gould's belt and the Scorpio–Centaurus association have been discussed on a maximum likelihood basis. About 10% of them seem to form an expanding group with vertex $l^{II} = 240°$, $b^{II} = -23°$, but the exact membership is vague and the group cannot be used for calibrating luminosity criteria. Confining the discussion to the neighborhood of Scorpio–Centaurus greatly improves the concentration of co-movers and a firm list of 47 stars can be isolated. Their vertex is $l^{II} = 236.5°$, $b^{II} = -25.0°$. The uncertainty is ±6° in the most important coordinate, which produces a negligible uncertainty in the luminosities. The K term is uncertain by a factor of two because of the uncertainty of the vertex. The discussion is in good accord with Bertiau (Astrophys. J., 128: 553(1958)) except that the FK_4 proper motions are about 20% bigger than the N30 proper motions used by him and consequently all the luminosities are about 0.4m fainter. The distances correlate well with galactic longitude; the residual scatter is 18% at most. Luminosities derived from hydrogen line indices and spectral types are re-discussed. The changes in luminosity produced by rotation, predicted by Hardorp and Strittmatter (Astrophys. J., 151: 1057(1968) and 153: 465(1968)) are compared with observation. Of the double stars, one visual binary, γ Lup, provides a measure of mass and two others should provide orbits if carefully followed. The eclipsing binary μ^1 Sco is a member and provides a measure of mass, radius, luminosity, and surface brightness. (auth) (UK)

35799 X RAYS FROM THE COMA CLUSTER OF GALAXIES. Meekins, J. F. (Naval Research Lab., Washington, D. C.);

Fritz, G.; Chubb, T. A.; Friedman, H.; Henry, R. C. Nature (London); 231: 107-8(14 May 1971).

Although the Coma cluster of galaxies is usually considered to contain insufficient matter to be gravitationally bound, nevertheless its high degree of symmetry and the presumed age of its galaxies suggest that it is, in fact, gravitationally bound. It is possible that the missing mass takes the form of ionized intracluster gas, but from the observational evidence of x-ray emission described the amount of hot intracluster gas is limited to less than 2% of that required for gravitational binding. The observations were made on March 14, 1969 from an Aerobee 150 rocket launched from the White Sands Missile Range, New Mexico, using methane/organic filled proportional counters. Count rates near the Coma cluster are shown tabulated, and a pulse-height analysis of the data is shown graphically. An approximately 5σ x-ray enhancement over the sky background from the direction of the cluster was indicated. Estimated upper limits of the photon flux from Coma are also shown tabulated for the wavelength bands 44 to 60 Å, 18 to 24 Å, 2 to 17 Å, and 1 to 3 Å. The way in which the x-ray data can be used to test the hypothesis that the cluster is gravitationally bound by an optically thin hot intracluster gas is described, and it is concluded that only if the total mass is about 2% of that required for gravitational binding can the x-ray observations in the various wavelength bands be reconciled. The possibility that individual galaxies within the Coma are responsible for the observed x rays is considered unlikely. (UK)

35800 GALACTIC SPURS AS POSSIBLE SOURCES OF SOFT X RADIATION. Shklovskii, I. S. (Inst. of Space Research, Moscow); Sheffer, E. K. Nature (London); 231: 173-4(21 May 1971).

It was suggested (1960) that the North Polar Spur of the Galaxy is the remnant of a supernova outburst that occurred in close vicinity of the Sun, at a distance of 20 to 30 pc. If this is so, the presence of soft x radiation can be expected at a significant intensity level in the spur region. A comparison is made of some observations of the soft x-radiation background in the range 44 to 60 Å with the distribution of spurs over the celestial sphere, and it is conjectured that increased intensity in this range coincides with the spur regions. Further observations, however, are necessary; in the region of even softer x radiation (80 to 100 Å) similar variation of background intensity, although somewhat weaker, would be expected, and such measurements would be a deciding factor in the verification of the validity of the hypothesis. (UK)

35801 ARE THE MAFFEI GALAXIES MEMBERS OF THE LOCAL GROUP. Van den Bergh, S. (Univ. of Toronto). Nature (London); 231: 35-6(7 May 1971).

It is suggested that the highly obscured galaxy IC 342 might be associated with Maffei 1 and 2. It is separated from Maffei 1 by less than 12° which, at a distance of 2 Mpc, would correspond to a projected separation of only 0.4 pc. It was also thought that IC 342 might possibly be a Local Group member, but it is probably too distant for this. A distance of about 2 Mpc would place the Maffei objects somewhat beyond the generally accepted limits of the Local Group. (UK)

35802 RADIO-CONTINUUM OBSERVATIONS OF MAFFEI 2. Webber, J. C.; Willis, A. G. (Univ. of Illinois, Urbana). Nature (London); 231: 36(7 May 1971).

The area containing the possible galaxies Maffei 1 and 2 was mapped at a wavelength of 11 cm using the 300-ft transit telescope of the National Radio Astronomy Observatory at Green Bank, W. Virginia over the period January 28–31, 1971. No emission was detected from the suspected position of Maffei 1. At the position right ascension 02h 38 m 12.3 ± 1s and declination +59° 23′ 03 ± 30″, the small-diameter source found by Bell and others (Astrophys. J. Lett., 161: L.13(1970)) was detected, with flux density 0.60 ± 0.03 fu. In an examination of the records at 49 cm from the 400-ft telescope of the Vermillion River Observatory of the University of Illinois, a source possibly larger than 16′ of arc in right ascension at the position of Maffei 2, with a flux density of 1.5 ± 0.5 fu was observed. A spectrum that decreases at short wavelengths is indicated, which is not unusual for ordinary extragalactic sources. In addition to the small-diameter source, a very weak extended source was detected at 11 cm, surrounding the former. The integrated flux density of the extended region was ~0.5 fu; it might have been merely an increase in the background radiation or some weak source within the Galaxy, but it is believed that it may be associated with Maffei 2. (UK)

35803 RADIO SPECTRUM OF MAFFEI 2. Caswell, J. L. (CSIRO, Sydney). Nature (London); 231: 35(7 May 1971).

There is considerable interest in Maffei 1 and 2 in that they may be previously unrecognized nearby galaxies. Observations are reported here that were obtained during a radio survey using the Cambridge 178-MHz pencil-beam synthesis instrument. A source with flux density 4.2 ± 1.0 f.u. was detected at right ascension 02h 38m 10s and declination + 59°20′5″, identical with that previously detected at higher frequencies and identified with Maffei 2. A recent measurement at 1,415 MHz gave a flux density of 1.08 ± 0.10 f.u. for Maffei 2 which, when combined with the values 4.2 at 178 MHz, gave a spectral index of 0.65 ± 0.1. Earlier, a spectral index of 1.30 ± 0.05 was obtained for frequencies between 10,700 and 3,200 MHz, but such a steep spectrum does not continue to low frequencies, since a flux density of 20 f.u. at 178 MHz would then be expected. Thus, the spectrum appears to steepen at high frequency. The steepness of the high-frequency spectrum may, however, have been overestimated due to noncorrection of the flux densities for the finite size of the source. The earlier search at 1,415 MHz revealed a previously uncatalogued radio source ~15′ north of Maffei 1 with a flux density of 0.427 ± 0.001 f.u. This source was also present on the 178-MHz records, with a flux density of 2.5 ± f.u., appearing to be nonthermal, with spectral index ≈0.9, but its separation from the center of Maffei 1 suggests that it is an unrelated background source. (UK)

35804 SPECTROPHOTOMETRY OF THE NGC 3351 GALAXY NUCLEUS FROM 3,300 TO 7,000 A. Alloin, Danielle (CNRS, Paris). Compt. Rend., Ser B; 272: No. 15, 909-12(14 Apr 1971). (In French).

The results of photometric observations of the nucleus of NGC 3351 are presented. A detailed description of the optical emission and absorption spectra is given. (France)

Cosmology

Refer also to abstract 35903.

35805 DENSITY PERTURBATION IN A UNIVERSE OF COLLISIONLESS PARTICLES. McCone, Alan Ivins Jr. College Park, Md.; Univ. of Maryland (1970). 182p. University Microfilms Order No. 71-10,477.

Thesis.

The coupled Einstein–Boltzmann equations are derived using Fourier techniques and solved numerically for density perturbations on a conformally flat expanding universe filled with collisionless radiation particles. Linear perturbation theory is used. The model approximately describes conditions between proper time 1.1 second and proper time 300 years in the evolution of the Universe, during which interval collisionless neutrinos probably contributed between 63 and 14% of the mass–energy in the Universe. The metric gage choice is one in which the observer with fixed background comoving coordinates is approximately a Newtonian observer. The initial perturbation in the Boltzmann distribution $f(\eta_0)$ is taken to have the same isotropic momentum spectrum as the appropriate background distribution function. The approach is similar to that of Lyle, who derived and examined the self-consistent equations for rotational and gravitational wave perturbations as well, but whose density perturbation equations seemed in intractable form. It also supplements the work of Bardeen, who treats photons by the relativistic radiative transfer (Boltzmann) equation with matter present, but who ignores cosmological neutrinos. A review of the literature on hydrodynamic and kinetic theory calculations of galaxy formation is provided as an introduction. Lindquist's exposition of relativistic kinetic theory is followed in the derivation of the perturbation equations. The numerical calculations show that the density contrast for long wave modes will grow until the particle horizon distance becomes comparable to the wavelength. After that, the contrast diminishes faster than $S(\eta)^{-1}$, where S is the expansion parameter. Because all modes eventually decay, it is unlikely that perturbations that went through a maximum during the epoch from one second to 300 years can be observed today. (Diss. Abstr. Int., B)

35806 CONSTRUCTION OF A RELATIVISTIC MODEL OF THE UNIVERSE. Heller, Michal. Postepy Astron.; 19: No. 1, 45-56(Jan-Mar 1971). (In Polish).

The method of constructing homogeneous, isotropic, relativistic world models is described. In particular, the implicit and explicit assumptions used in relativistic cosmology are discussed. It turns out that, from the point of view of logic, one should make a difference between the cosmological principle limiting the possible density distributions (the cosmological principle for the substratum) and the cosmological principle imposing symmetry conditions upon the geometric space (the cosmological principle for the geometry). These two principles are independent assumptions. A short review of the Robertson–Walker type of cosmological models is given. (auth)

35807 RADIO-EMISSION BACKGROUND OF THE METAGALAXY. Tokarev, Yu. V. (Inst. of Radio Physics and Elec-

tronics, Novosibirsk, USSR). Izv. Vyssh. Ucheb. Zaved., Radiofiz.; 13: No. 10, 1571-4(1970). (In Russian).

The spectral indices and luminosities of normal galaxies were compiled for a frequency of 178 MHz, using the data to calculate the mean spectral indices for frequencies <1000 MHz. Determination of the spectral index of the Metagalaxy, α, requires knowledge of the luminosity distribution of the sources. The value of α, calculated by using Sholomitskii's radio-emission formula, was found to be $\alpha = 0.55 \pm 0.05$. This value may be obtained independently from spectral measurements of the cosmic radio-emission distribution through a series of frequencies, using a two-temperature dependence to determine T, the temperature of the radio-emission of the Metagalaxy. (TTT)

35808 COSMOLOGICAL WORLD MODELS AND OBSERVATIONAL DATA. Raja, Shanker. Lafayette, Ind.; Purdue Univ. (1970). 134p. University Microfilms Order No. 71-9456. Thesis.

The observables of cosmology are z(the redshift), m(the apparent magnitude of a "standard candle"), θ(the angular diameter of a "standard" extended source of radiation), and n(the number of "uniformly" distributed discrete objects). Each of the three-parameter family of general relativistic world models and the steady-state model predicts a different relationship between these observables. "Accurate" data on the "ideal" objects of theory could then decide which, if any, of the models explain the data. Various uncertainties in the available cosmological data allow merely the labeling of models as more or less likely. A method is developed whereby a realistic appraisal of the uncertainties in the data can be translated into "relative likelihoods" of the various world models. The utility of the method is demonstrated by applying it to sample data taken from recent literature. As the data currently available are not sufficiently numerous or detailed, the results discussed are only illustrative. It is shown how one could narrow down the range of likely models and answer some of the interesting questions of cosmology when data of the requisite accuracy are forthcoming. It is to be hoped that observational cosmologists may use this method together with their better knowledge of the uncertainties in their data to "squeeze" out the maximum information from their observations. (Diss. Abstr. Int., B)

35809 STUDY OF THE MOTION OF A PARTICLE IN A GRAVITATIONAL MONOPOLE-QUADRUPOLE FIELD IN NEWTONIAN MECHANICS AND THE GENERAL THEORY OF RELATIVITY. Armenti, Angelo Jr. Philadelphia; Temple Univ. (1970). 234p. University Microfilms Order No. 71-10,560. Thesis.

The motion of particles in a gravitational monopole-quadruple field is considered, both in Newtonian mechanics and the general theory of relativity. The Newtonian calculations are based on the first and third terms in the familiar multipole expansion of Laplace for axially symmetric matter; the relativistic ones are based on the Erez-Rosen metric, an exact solution of Einstein's vacuum field equations. A complete classification of the exact orbits in a Newtonian equatorial monopole-quadrupole field is given. The motions are all quasi-Keplerian, except for a curious subclass of orbits corresponding to a form of two-body capture. The equatorial geodesics in the general-relativistic case are found in two different approximations. To lowest order, the solutions are essentially a superposition of relativistic monopole (Schwarzschild) and Newtonian quadrupole contributions. In higher order, purely relativistic cross terms appear. The results are used to study the effect of a solar oblateness on the three classical tests of general relativity. A class of exact relativistic solutions consisting of circular motion with constant angular velocity in planes parallel to the plane of symmetry of the quadrupole is found and discussed, analogous to those discovered by Havas in Newtonian physics. The properties of these noncoplanar motions are similar in both theories, the major difference being the appearance of certain existence- and stability-threshold values of the quadrupole moment in the relativistic case, which arise from the finiteness of the velocity of light (Diss. Abstr. Int., B)

35810 GLOBAL STRUCTURE OF THE UNIVERSE AND DISTRIBUTION OF QUASI-STELLAR OBJECTS. Paal, G. (Konkoly Observatory, Budapest). Acta Phys. Acad. Sci. Hung.; 30: No. 1, 51-4(1971).

Periodicities in the frequency distribution of quasars according to their redshifts (as well as other proposed regularities in their distribution) are shown to be compatible with the cosmological interpretation of the redshifts: they may be apparent geometrical phenomena in world models with multiply connected space sections. It is therefore a misconception that significant regularities would necessarily imply the existence of intrinsic redshift components in the spectra of quasars — as generally stated in the astronomical literature. Some further remarks on the connectivity properties of cosmological models are also made. (auth)

35811 DENSITY OF MATTER IN THE UNIVERSE AND THE EPOCH OF GALAXY FORMATION. Sunyaev, R. A. (Inst. of Applied Mathematics, Moscow). Astron. Astrophys.; 12: No. 2, 190-5(May 1971).

A possible way of determining a lower bound to the density of matter in the Universe is discussed in which theoretical results on the delayed growth of density perturbations in open universes are compared with the observed counts of radio sources and quasars. The latter imply the intense formation of objects at a redshift $z \approx 2$ to 4. The proposed model of the condensation and formation of sources satisfies the results of the source counts and explains the absence of absorption corresponding to the Ly-α line in the spectra of quasars having $z > 23$. (auth)

35812 MISSING MASS AND THE GRAVITATIONAL LENSE EFFECT. Reinhardt, M. (Univ., Bonn). Astron. Astrophys.; 12: No. 2, 196-8(May 1971).

It is shown that, if there is a large amount of mass in clusters of galaxies in the form of massive dark objects, it is quite hopeless to detect those objects by the gravitational lense effect. (auth)

35813 RELATIVISTIC EXTENSION OF NEWTON'S THEORY OF GRAVITATION. Spieweck, F. Astron. Astrophys.; 12: No. 2, 278-9(May 1971).

It is shown that Newton's theory of gravitation can be extended by introducing the "relativistic mass" and by adding a vector potential of gravitation. The resulting vector theory of gravitation is built up in analogy to the Maxwell-Lorentz theory. The equations of motion show the same dependence of inertia on the gravitational potential as in the general theory of relativity. (auth)

35814 COSMOLOGICAL SOLUTION OF THE JORDAN-DICKE FIELD EQUATIONS AND OBSERVATION DATA. Mandzhos, A. V. (Kiev State Univ.). Ukr. Fiz. Zh. (Russ. Ed.); 16: 413-22(Mar 1971). (In Russian).

The homogeneous isotropic cosmological problem at zero pressure is solved in the framework of the Jordan-Dicke field equations. It is shown that, in all, there are seven types of solutions. Each has a singularity: the state of infinite density and zero radius of curvature. The open model of the negative curvature corresponds to the modern observational data. The dependence of the radius of curvature and gravitational scalar on time are found numerically. The time scale of the expansion agrees better with the evolution time scale, than in the case of general relativity. A decrease in the gravitation scalar has an asymptotic limit, to which the modern value of the gravitational scalar is close. (auth)

35815 NONLINEAR EFFECT OF COSMIC FLUID IN AN EXPANDING UNIVERSE. II. REFINEMENT AND EXTENSION OF THE FORMALISM. Nariai, Hidekazu (Hiroshima Univ.). Progr. Theor. Phys. (Kyoto); 45: No. 1, 61-9(Jan 1971).

A formalism for dealing with various nonlinear effects of cosmic fluid which is important in the process of galaxy formation is refined by introducing a new shearing tensor q_{ij} such as $q_{ij} = 0$. It is shown that, even in the local analysis around an equilibrium point, the dynamical equation for q_{ij} contains a nonlocal gravitational term which does not necessarily vanish even in the case of density fluctuations with spherical symmetry. A global approach to the problem of galaxy formation is, therefore, presented by considering a rotating gaseous spheroid with uniform density and diagonal shearing. Basic equations for dealing with hydrodynamical instability before the decoupling time of matter from the primordial radiation are also derived by taking into account the viscosity effect due to Thomson's scattering at that stage. (auth)

35816 SCALE FACTOR IN COSMOLOGICAL HOMOGENEOUS MODELS. Agnese, A. G.; Wataghin, A. (Univ., Genoa. Istituto Nazionale di Fisica Nucleare, Genoa). Lett. Nuovo Cim.; 1: No. 21, 857-60(22 May 1971).

An alternative cosmological scale is discussed in which the possibility exists that the speed of light and the unit of time may have changed. This can give an age of the universe which tends to infinity. (W.D.M.)

35817 HIERARCHICAL BIG-BANG COSMOLOGY. de Vaucouleurs, G. (Univ. of Texas, Austin); Wertz, J. R. Nature (London); 231: 109(14 May 1971).

A reply is given to the comments by McCrea (Nature 228: 21 (1970)) on the communication of de Vaucouleurs (Science, 167: 1203(1970)) concerning evidence for hierarchical clustering in the Galaxy distribution. It is stated to be incorrect to assume that the criticisms of de Vaucouleurs concerning "current big-

bang cosmology" were directed at "big-bang" models; the principal intention was to indicate the need to study the impact on cosmological theories of hierarchical structure in the distribution of matter. Hierarchical cosmology attempts to replace the idealized homogeneous isotropic models by more realistic models, that have explicit structure on large scales; it is in no way opposed, in principle, to "big-bang," steady-state, or other current theories, and a "big-bang" hierarchical model has indeed been described. It is hoped that cosmologists will not continue to insist that the Universe must be homogeneous and isotropic merely because theories are made easier by such an assumption; observational evidence indicates that the real Universe is not built that way. (UK)

35818 INFRARED BACKGROUND AND UNIVERSAL COSMIC RAYS. Setti, G.; Woltjer, L. (Univ., Bologna). Nature (London) Phys. Sci.; 231: No. 20, 57-9(17 May 1971).

It is stated that the fact that the energy densities of the infrared background radiation and of local cosmic rays are of the same magnitude permits the development of a reasonable universal cosmic-ray theory, and an attempt is made to show that the energetic arguments frequently advanced against a universal theory for the origin of cosmic rays can be countered. The only outstanding difficulty appears to be that the intergalactic gas density has to be lower than generally assumed. No intergalactic gas has, in fact, been detected, and high estimates of its density have been based only on very indirect arguments. In the simple model discussed, the infrared emission from a source would be a direct measure of its cosmic-ray production. (UK)

35819 MAGNETIC FIELD OF A ROTATING CLOUD AND MAGNETO-ROTATIONAL EXPLOSIONS. Ozernoi, L. M.; Somov, B. V. (Lebedev Inst. of Physics, Moscow). Astrophys. Space Sci.; 11: No. 2, 264-83(May 1971).

The contraction of a massive rotating plasma cloud with the magnetic field perpendicular to the axis of rotation and extending to infinity is considered. At some stage the contracting cloud reaches a state of dynamic quasi-stationary equilibrium. The change of the magnetic field in the cloud atmosphere before its arrival at the quasi-stationary state (stage I) and also in the process of quasi-equilibrium (stage II) are studied. At stage I an essential change of the external magnetic field geometry occurs, namely the formation of zero (neutral) lines and the transformation of the field into a quasi-radial one. Given certain conditions, the reconnection of the field lines in neutral X-type points may occur with the formation of closed loops. In this case the flux of field lines, which connect the contracting cloud with infinity, decreases asymptotically as $(R/R_i)^{\frac{1}{2}}$, where R/R_i is the ratio of the present radius to initial one. After the cloud arrives at the state of dynamic equilibrium (stage II) a considerable increasing of the magnetic field occurs due to twisting of the field lines by rotation. The field strength increases up to some threshold after which instability suddenly occurs. As a result of cumulation occurring in the zero-line direction, and the subsequent dynamic dissipation, the ejection of relativistic particles and plasma in both directions along the rotational axis takes place. The magnetic field restores itself rapidly due to the continual twisting, and this leads to the appearance of repeated explosions. The tension of the magnetic field lines as well as plasma outflow carry away the angular momentum. Its diminution determines the rate of secular gravitational contraction. During the contraction the rotational energy increases so that recurrent bursts, being of magneto-rotational nature, are based, finally, on the gravitational energy reservoir. According to calculations of the time interval for repetition of explosions, the energy output, and certain other parameters, repeated bursts in the nuclei of galaxies and quasars can be explained. (auth)

35820 BLACK AND WHITE HOLES. Hjellming, R. M. (National Radio Astromomy Observatory, Green Bank, W. Va.). Nature (London) Phys. Sci.: 231: 20(3 May 1971).

The term "black holes" in the present context refers to singularities by which matter "disappears" from the Universe and "white holes" are singularities from which matter and energy emerge, usually in the centers of quasars and galaxies, and it seems natural to suggest that the two are genitively related, on the basis of the dominance of conservation laws in physics. Either the "black holes" of our Universe could supply our "white holes," or our "black holes" could supply another Universe with "white holes" and vice versa; consideration of symmetry and conservation probably favor the latter. With a system of multiply connected Universes "black-hole"–"white-hole" transition could involve matter on one side and antimatter on the other, and thus the transition of matter through the singularity is an analogue of particle–antiparticle creation; it is then possible to speculate further that the initial creation of the known Universe was part of the creation of a Universe–antiuniverse pair, which thereafter remains connected only by the exchange of matter and energy through "black-hole"–"white-hole" singularities. In this context a generalization of the "expanding balloon" model, frequently used to illustrate the concept of an expanding Universe, is discussed. The concept of "white holes" has been invoked by Hoyle and Narlikar to identify the sites at which matter is "created" in a steady-state cosmology, and a genitive relation between "black holes" in another Universe and "white holes" in our Universe could also be involved in our cosmology. This model would be particularly attractive if the entropy function for matter and energy passing through the "black-hole"–"white-hole" singularity were reset to zero; our Universe would not then "run down," as implied by the second law of thermodynamics. An interesting area of research would be the behavior of matter and radiation when emerging from "white holes." The origin of cosmic rays, x rays, radio jets, the double radio source phenomena, etc., could possibly be traced to the behavior of systems of "white holes" interacting with the surrounding medium. Circumstances by which "white holes" could attain large velocities might help to explain some of the peculiar phenomena seen in some galaxies and clusters of galaxies. (UK)

35821 RELATIVITY EXPERIMENTS IN SPACE VEHICLES. Schiff, L. I. (Stanford Univ., Calif.). Rev. Geophys. Space Phys.: 9: No. 2, 407-15(May 1971).

Experiments that make use of space vehicles for the quantitative study of gravitation are reviewed. Several experiments are discussed that can be performed in Earth orbit, and others that require deep-space probes. It is anticipated that the decade of the 1970's will place the relativistic theory of gravitation on a firm experimental basis. (auth)

Planetary Phenomena

35822 DETERMINATION OF THE MASS OF PLUTO. Seidelmann, P. K.; Klepczynski, W. J.; Duncombe, R. L.; Jackson, E. S. (Naval Observatory, Washington, D. C.). Astron. J.; 76: No. 5, 488-92(Jun 1971).

Transit circle observations of Neptune from its discovery to the present are rediscussed. An analysis of these observations indicates a reciprocal mass of Pluto of 3,000,000 (0.11 earth mass), with a mean error of 500,000. If 6400 km is accepted as the diameter of Pluto, then this value for the reciprocal mass implies a density of about 4.86 g/cm^3 (0.88 times the Earth's density). (auth)

35823 PALES (49) AND THE MASS OF JUPITER. Doggett, LeRoy E. (Naval Observatory, Washington, D. C.). Astron. J.; 76: No. 5, 486-7(Jun 1971).

The motion of Pales (49) was analyzed to determine an improved value of the mass of Jupiter. Because of unresolvable discrepancies between old and recent observations, the solution based on twentieth century observations was adopted: $1/m = 1047.340 \pm 0.013$ m.e. (auth)

35824 THERMOLUMINESCENCE OF LUNAR SAMPLE 10084 APOLLO 11. Hess, B.; Hueber, R.; Herr, W. (Univ., Cologne). Mod. Geol.: 2: No. 1, 55-60(Feb 1971).

The thermoluminescence (TL) of the lunar surface sample 10084, Apollo 11 was investigated over the temperature range −196°C to 450°C, as well as the implications for TL as a tool for further lunar studies. Natural TL was not detected, whereby it is not quite clear, whether there was none originally or if it had decayed by thermal annealing below the limit of detection. The artificial TL reaches saturation at doses of the order of 10^6 to 10^7 Rad of γ, p, and α radiation. The LET of the radiation was found to have little effect on the glow curve. The influence of grain size and repeated exposure followed by heating to 450°C was examined. It was observed that well over 50% of the TL induced at −196°C was emitted below ambient temperatures. All measured glow curves were complex, i.e., consisted of a number of overlapping glow peaks. These could not be resolved by examining the spectral distribution of the glow. In view of the innate complexity of the TL curves obtained it seems doubtful whether TL measurements on lunar dust from this site will yield unambiguous information on the lunar radiation history. The luminescence and thermoluminescence efficiency of this material is too low to contribute significantly to the luminosity of the lunar surface. (auth)

35825 TERRESTRIAL PLANETS AND STAGES OF THEIR EVOLUTION. Benes, Konrad (Ostrava Mining Inst., Czech.); Katterfeld, Gennadii N. Mod. Geol.: 2: No. 2, 129-31(Apr 1971).

An overall view of the terrestrial planets is presented with the intention of bringing attention to similarities and differences. A theory is proposed which calls for several evolutionary stages in

XUM

the terrestrial planets. The stages, and representative planets, are: cosmogonic, pre-geological (Moon and Mercury), pre-geosynclinal (Mars, Venus), geosynclinal, platformic (Earth). (auth)

35826 TABLES OF AUXILIARY FUNCTIONS FOR THE NONCONSERVATIVE RAYLEIGH PHASE MATRIX IN SEMI-INFINITE ATMOSPHERES. Abhyankar, K. D.; Fymat, A. L. (California Inst. of Tech., Pasadena). Astrophys. J., Suppl. Ser.; 23: No. 195, 35-101(May 1971).

Tables of $H^1(\mu)$, $H^2(\mu)$, $H^1_V(\mu)$, $H^1_V(\mu)$, and $N(\mu)$ functions appropriate for semi-infinite atmospheres scattering according to the nonconservative Rayleigh phase matrix are given for thirty values of the albedo for single scattering $\Omega = 0$ (0.1) 0.6 (0.05) 0.8 (0.025) 0.9 (0.01) 0.98 (0.005) 0.995 (0.001) 0.999, at intervals of $\mu = 0$ (0.01) 1.0 to six significant figures. They can be used for computing the emergent diffuse radiation field corresponding to an incident illumination in an arbitrary state of polarization. (auth)

35827 DAYSIDE IONOSPHERE OF VENUS. Herman, J. R.; Hartle, R. E.; Bauer, S. J. (Goddard Space Flight Center, Greenbelt, Md.). Planet. Space Sci.; 19: No. 5, 443-60(May 1971).

Theoretical modeling of the daytime Venus ionosphere is used to augment the measurements of Mariner V made during its 1967 flyby of Venus. The equations of heat transport for the electron, ion, and neutral gases are simultaneously solved, along with the associated momentum and chemical equations for the ion and neutral gas densities. When solutions are constrained by the observations from Mariner V, the resulting temperature and density profiles can be used to estimate the possible magnetic-field strength within the Venus ionosphere and concentration of neutral helium at 100-km altitude. Several alternate models are presented to account for the effects of eddy diffusion in the neutral atmosphere and solar-wind heating. In all these models the resulting solutions lead to an approximately horizontal magnetic field in the topside ionosphere of strength 10 to 20 γ and a neutral helium density of order 10^8 cm^{-3} at 100-km altitude. (auth) (UK)

35828 TWO MAGNETIC TAIL MODELS FOR URANUS. Siscoe, G. L. (McDonnell Douglas Astronautics Co., Santa Monica, Calif.). Planet. Space Sci.; 19: No. 5, 483-90(May 1971).

The magnetic tail configurations are considered appropriate to a planet with its dipole axis parallel to the solar wind. Such configurations would apply to Uranus if it proves to have a dipole moment approximately parallel to its rotation axis. The topology of the neutral sheet depends on whether the mechanism assumed to create the tail is a viscous or a magnetic force acting on the boundary. In the former case, the neutral sheet is a cylinder with its axis parallel to the tail axis, whereas the latter assumption requires the neutral sheet to connect to the tail boundary, as in the case of the Earth. Dynamics of the concentric cylinder model of the tail are derived and found to be similar to that of the geomagnetic tail. (auth) (UK)

35829 SOLAR SYSTEM BEYOND MARS: AN EXOBIOLOGICAL SURVEY. Sagan, Carl (Cornell Univ., Ithaca, N. Y.). Space Sci. Rev.; 11: 827-66(Mar 1971).

Beyond Mars lie the asteroids, the Jovian planets and their moons, Pluto, and the comets. The vast bulk of the angular momentum of the solar system resides here as well as most of the nonsolar mass. Past the region of the inner or terrestrial planets lie these objects of great importance for exobiology. Physical properties, coloration and meteorology, temperatures, radio spectrum, molecular constituents, coloration and organic molecules, uv spectra, the Great Red Spot, the possibility of life, projected space missions, and the satellites of the Jovian planets are discussed for the Jovian planets. Asteroids, presumed to be the parent bodies of most of the meteorites recovered on Earth, are discussed. The properties, observations, and origin of the comets are discussed. (J.C.W.)

35830 POTASSIUM–URANIUM SYSTEMATICS OF APOLLO 11 AND APOLLO 12 LUNAR SAMPLES AND OF SOME DEEP EARTH ROCKS. Fisher, David E.; Fanale, Fraser P.; Nash, Douglas B. (Univ. of Miami, Fla. California Inst. of Tech., Pasadena). Science; 172: No. 3988, 1166-7(11 Jun 1971).

Fanale and Nash (1971) discussed the K–U systematics of lunar, chondritic, and terrestrial samples. They discerned distinct trend lines for Apollo 11 and 12 samples and for terrestrial rocks and showed that chondrites are not members of these trend lines. Their conclusion that the Moon must have a reservoir of K and U depleted material is questioned. A reply by Fanale and Nash is included. (W.D.M.)

35831 ^{222}Rn EMANATION AND THE HIGH APPARENT LEAD ISOTOPE AGES IN LUNAR DUST. Adams, J. A. S.; Barretto, P. M.; Clark, R. B.; Duval, J. S. (Rice Univ., Houston, Tex.). Nature (London); 231: 174-5(21 May 1971).

It was found that U–Pb and Th–Pb ages for Apollo 11 and 12 lunar samples did not match, and that the dust samples appeared older than the rocks. These observations are generally thought to require some source of parentless Pb. It is proposed that escape of ^{222}Rn, ^{219}Rn, and ^{220}Rn produced in the ^{238}U, ^{235}U, and ^{232}Th decay chains may be a significant mechanism for a partial redistribution of the post-radon lead daughters. Preliminary experiments showed that ^{222}Rn readily escapes from lunar materials, and some data are given for samples of lunar dust; the ratio of the emanation rate to the production rate was found to be 0.48, with an estimated accuracy better than 50%. This result indicates that there is substantial migration of ^{222}Rn above and below the lunar surface, and there may also be significant migration of ^{220}Rn and ^{219}Rn. The different half-lives will result in isotopic fractionation, which may have an important influence on the apparent U–Th–Pb ages. It is considered that emanation rates should be measured for all types of lunar samples. (UK)

35832 MASS DISTRIBUTION OF PLANETS ON PARTICLE ACCRETION. Mitra, Ved (M. N. R. Engineering Coll., Allahabad, India). Astrophys. Space Sci.; 11: No. 2, 330-6(May 1971).

The mass distribution of planets was obtained on the basis of the accretional theory of their formation recently developed by the author. The results agree fairly well with the observations. (auth)

Atomic and Molecular Physics

Atomic, Electron, Ion, and Molecular Beams and Their Reactions

Refer also to abstracts 36248, 36280, and 36640.

35833 (ORO–3027-19) EXCITATION AND IONIZATION OF IONS BY ELECTRON IMPACT. Technical Progress Report, September 1, 1970–May 31, 1971. Hooper, J. W.; Feeney, R. K.; Majure, J. C.; McPherson, D. (Georgia Inst. of Tech., Atlanta. Engineering Experiment Station). 31 May 1971. Contract AT(40-1)-3027. 34p. Dep. NTIS.

Development of the microwave transient response technique for magnetoplasma diagnostics is described. Diagrams of the experimental arrangement are shown. An outline of research on energy losses of Li particles in thin films of carbon at incident energies between 2 and 10 keV is presented. Some preliminary data on energy distributions of Li particles emerging from carbon films are included. A survey of possible sources of highly charged ions for collision experiments indicated that the electron-cyclotron source and the hot-electron plasma source merit further study. (A.G.W.)

35834 ENERGY SHIFT OF CHARACTERISTIC X RAYS INDUCED IN COLLISIONS BETWEEN 15- to 60-MeV I IONS AND Mo, Yb, AND Au TARGETS. Mokler, P. H. (Kernforschungsanlage, Juelich, Ger.). Phys. Rev. Lett.; 26: 811-13(5 Apr 1971).

X rays emitted in collisions between heavy atomic particles were analyzed with a highly resolving Si(Li) detector. L and M x-ray spectra are shown for collisions of I ions with Mo, Yb, and Au at ion energies of 17.6, 34.0, and 57.0 MeV. The L x rays of both colliding particles are shifted to higher energies compared with photon-induced characteristic x rays. (auth)

35835 SURFACE AND VACUUM PHYSICS INDEX. VOLUME 6, NO. 3, 1971. Bibliography, Author Index, Subject Index in Alphabetical Order, Cumulative Subject Index in Logical Order. Frankfurt am Main; Zentralstelle fuer Atomkernenergie-Dokumentation (1971). 68p.

This listing includes 276 references on various aspects of surface and vacuum physics. (A.G.W.)

35836 METHOD FOR PRODUCING POLARIZED ATOMS. Kaminsky, Manfred S. (to United States Atomic Energy Commission). U. S. Patent 3,569,705. 9 Mar 1971. Filed 1 Aug 1969.

A polarized beam of atoms is generated by passing, in a partial vacuum, a collimated atomic beam through a magnetically saturated monocrystalline material parallel to a lattice channel of the material. The monocrystalline material effects a charge-transfer reaction with the atomic beam to produce a polarized atomic beam, the nuclei of which are subsequently polarized by hyperfine interaction in a weak external magnetic dipole field. (auth)

35837 INJECTOR FOR FAST HYDROGEN ATOMS. I. MAGNETO-OPTICS. Kulygin, V. M.; Panasenkov, A. A.; Sveshnikov,

A. B.; Semashko, N. N. Sov. Phys.-Tech. Phys. (Engl. Transl.); 15: No. 10, 1628-34(Apr 1971).
Translated from Zh. Tekh. Fiz.; 40: No. 10, 2091-8(Oct 1970).

An injector is described that produces a current of 15- to 30-keV hydrogen atoms at an intensity equivalent to more than 0.5 A. The current of atoms is formed by charge exchange in an ion beam incident on a gas target of magnesium vapor. The ion beam is produced and formed in a gas-discharge ion source operating in a transverse magnetic field which is also the focusing element for the ion beam. Calculations of the magneto-optical system are presented, and the particle motion is analyzed by numerical methods. An experimental injector based on the calculations was constructed, and the results are compared with the calculated values. (auth)

35838 INSTABILITY OF RING CURRENTS. Grigor'ev, V. P.; Didenko, A. N. Sov. Phys.-Tech. Phys. (Engl. Transl.); 15: No. 11, 1782-6(May 1971).
Translated from Zh. Tekh. Fiz.; 40: No. 11, 2283-8(Nov 1970).

A self-consistent field analysis is used to study the stability of a ring current in the presence of a focusing magnetic field. The region in which the beam is stable against resonant instabilities is determined. The dependence of the growth rate on the number of particles, on the energy spread, on the figure of merit of the system, and on the frequency of the oscillation is investigated. It is shown that the high-frequency growth rate of the instability is maximized at the frequency $\omega = 3\Omega^0\gamma^3/2$. (auth)

35839 MEASUREMENT OF IONIZATION YIELDS OF MOLECULAR AND ATOMIC IODINE ON TUNGSTEN, TUNGSTEN (1.6 PERCENT ThO_2), AND PLATINUM (8 PERCENT W) SURFACES. Rosenkranz, F.; Wagner, H. Gg. (Univ., Goettingen, Ger. Univ., Bochum, Ger.). Z. Phys. Chem. (Frankfurt); 68: 317-20(Dec 1969). (In German).

The ionization yields of molecular and atomic iodine on tungsten, tungsten (1.6% ThO_2), and platinum (8% W) surfaces were measured at temperatures from 1300 to 2000°K to determine whether the molecular and atomic yields differ from each other. The results obtained are tabulated and show that, whereas the measured temperature dependence of the ionization yield for I and I_2 on W agrees well with the values calculated by the Saha-Langmuir formula, the ionization on W(1.6% ThO_2) and Pt(8% W) have great deviations. Between 1800 and 1850°K the ionization yields of I_2 and I vary by an order of magnitude so that a discrimination between these appears possible. (J.S.R.)

35840 ELECTRON EMISSION FROM MONOCRYSTALS OF ALKALI-METAL HALIDE COMPOUNDS BOMBARDED BY ION AND ATOMS OF INERT GASES. Arifov, U. A.; Rakhimov, R. R.; Gaipov, S. Izv. Akad. Nauk SSSR, Ser. Fiz.; 35: 562-6 (Mar 1971). (In Russian).

Potential and kinetic emission of electrons from KBr, NaCl, and LiF bombarded by ions and atoms of He, Ne, Ar, and Kr was studied in the energy range from 0.2 to 6.0 keV at specimen temperature of ~350 to 380°C. A regular growth of coefficients of ion-electron and atom-electron emission was observed with increase of energy. (R.V.J.)

35841 INFLUENCE OF NONRADIATIVE TRANSITIONS ON THE LUMINESCENCE SPECTRA OF EXCITED PARTICLES KNOCKED OUT OF SOLID TARGETS BY FAST ARGON IONS. Gritsyna, V. V.; Kiyan, T. S.; Gutt, R.; Koval, A. G.; Fogel, Ya. M. Izv. Akad. Nauk SSSR, Ser. Fiz.; 35: 578-84(Mar 1971). (In Russian).

The influence of resonance ionization on the luminescence spectra emitted by excited particles knocked out from the solid targets of metal (Cu), semiconductor (Si), and dielectric (Al_2O_3) by 20-keV Ar^+ ions was studied. It was found that the resonance processes of excitation loss, taking place during the emission of excited particles from the solid state surface, exerted a strong influence on the particle luminescence spectra and must be considered in energy-level determination in solids. (R.V.J.)

35842 PRODUCTION OF HIGH-INTENSITY K X-RAY BEAMS. Motz, J. W.; Dick, C. E.; Lucas, A. C.; Placious, R. C.; Sparrow, J. H. (National Bureau of Standards, Washington, D. C.). J. Appl. Phys.; 42: 2131-3(Apr 1971).

Higher K x-ray beam intensities can be obtained by direct electron excitation of K x rays in a primary target, and the bremsstrahlung contamination may be reduced by observing the K x rays at large angles. This method was used in measurements made on Be, C, Al, Ti, Cu, Ag, and Au, and conditions for maximum K x-ray output and purity are given. The effects of incident electron energy and target atomic number on the yield and purity are discussed. (D.L.C.)

35843 PRODUCTION OF NEGATIVE HYDROGEN IONS IN A PLASMA WITH A DOUBLE SHEATH. Demirkhanov, R. A.; Kursanov, Yu. V.; Lazarev, N. F.; Blagoveshchenskii, V. M. Sov. Phys.-Tech. Phys. (Engl. Transl.); 15: No. 9, 1489-92 (Mar 1971).
Translated from Zh. Tekh. Fiz.; 40: No. 9, 1911-15(Sep 1970).

The mass-energy spectrum of negative hydrogen ions, H^-, taken from a discharge bounded by double sheaths, was studied. The H^- ions are produced in a plasma region having a low electron temperature. One of these regions is in the immediate vicinity of the anode, while the others are on the cathode side of the double sheaths. Such a discharge has been used in an ion source to produce a 200-μA current of H^- ions with an emission aperture 1 mm in diameter. (auth)

Atomic and Molecular Properties

Refer also to abstracts 35644, 35645, 35766, 36567, 36571, and 37108.

35844 (SC-RR-70-406) CALCULATED GENERALIZED OSCILLATOR STRENGTHS FOR THE ATOMS He-Na. McGuire, Eugene J. (Sandia Labs., Albuquerque, N. Mex.). May 1971. 84p. Dep. NTIS.

Tables of generalized oscillator strengths for excitation and ionization of the atoms He through Na are presented. (auth)

35845 CALCULATION OF THE DECAY RATE FOR $2^3S_1 \rightarrow 1^1S_0$ + ONE PHOTON IN HELIUM. Feinberg, G. (Columbia Univ., New York); Sucher, J. Phys. Rev. Lett.; 26: 681-4(22 Mar 1971).

The amplitude for the one-photon transition $2^3S_1 \rightarrow 1^1S_0$ in helium is shown, from quantum electrodynamics, to be computable in terms of the nonrelativistic wave functions. Numerical evaluation gives a decay rate of 1.2×10^{-4} sec^{-1}. (auth)

35846 PRELIMINARY LEVEL ANALYSIS OF THE FIRST AND SECOND SPECTRA OF DYSPROSIUM, Dy I AND Dy II. Conway, John G. (Univ. of California, Berkeley); Worden, Earl F. J. Opt. Soc. Amer.; 61: 704-26(Jun 1971).

Accurate wavelengths and wave numbers of over 22,000 dysprosium lines were measured in the wavelength region 2300 to 11,400 Å. By comparison of relative intensities of the lines from sources under various conditions, 85% of the lines were assigned as Dy I or Dy II spectrum lines. From the energy-level analysis, 141 even and 197 odd levels of Dy I are known. Combinations between these levels account for 1952 lines. For Dy II, 14 even and 214 odd levels are known, with 1000 lines classified. The ground levels of Dy I and Dy II are $4f^{10}6s^2\ ^5I_8$ and $4f^{10}6s\ ^6I_{8½}$, respectively. The lowest level of the $4f^95d6s^2$ configuration of Dy I lies 7565.62 cm^{-1} above the ground level. The g values for most of the levels of both spectra are given. (auth)

35847 NEW ENERGY LEVELS OF TRIPLY IONIZED PRASEODYMIUM. Sugar, Jack (National Bureau of Standards, Washington, D. C.). J. Opt. Soc. Amer.; 61: 727-32(Jun 1971).

Measurements of the spectrum of triply ionized praseodymium produced by a 500-A sliding-spark discharge revealed new high-lying energy levels of both even and odd parity. Nearly all levels of the 4f5f configuration were found as well as portions of 4f6d, 4f7s, and 5d6p. Radial parameters were fitted to 4f5f and 4f6d. A value for the ionization limit of 314,200 ± 200 cm^{-1} was deduced from the 4f6s, 7s series. (auth)

35848 RELATIVE LINE INTENSITIES IN THE LYMAN BANDS OF HD AND H_2. Becker, K. H.; Fink, E. H. (Univ., Bonn). Z. Naturforsch.; 26a: 319-20(Feb 1971).

Relative intensities of P(J' + 1) and R(J' − 1) lines were measured in the (v' = 3, v'') progressions of the Lyman bands of HD and H_2. The intensity ratios are in good agreement with previous experimental data and with the results of theoretical calculations that account for the centrifugal distortion. (auth)

35849 DETERMINATION OF LIFETIMES FOR MULTIPLY CHARGED HEAVY IONS EXCITED IN COLLISIONS WITH LIGHT GASES. Betz, H. D. (Massachusetts Inst. of Tech., Cambridge); Grodzins, L.; Wittkower, A.; Ryding, G. Phys. Rev. Lett.; 26: 871-3(12 Apr 1971).

A technique is presented for determining average radiative lifetimes of multiply charged heavy ions predominantly excited in collisions with light-gas atoms. The method utilizes the measurement of ionic charge-state distributions as a function of target density. Average lifetimes ranging from more than 65 to 0.76 nsec were determined for chlorine ions with charge states +1 to +6, respectively. (auth)

XUM

35850 TWO-PARTICLE FRACTIONAL PARENTAGE COEFFICIENTS AND THEIR APPLICATION TO ATOMIC SPECTRA. Donlan, Vincent Louis. Columbus, Ohio; Ohio State Univ. (1970). 443p. University Microfilms Order No. 70-26,275.

Thesis.

In developing the theory of two-particle fractional parentage coefficients (cfp), an equation was derived expressing the two-particle cfp in terms of the one-particle cfp of Racah. This equation was coded for numerical computations on an IBM 7094 computer. With the aid of this program, the two-particle cfp for the p^3, d^3, d^4, d^5, f^3, f^4, f^5, f^6, and f^7 configurations were calculated and stored on magnetic tape. A complete listing, reproduced directly from computer outputs, of these cfp in powers-of-primes format is included. The orthogonality and charge-conjugation rules for the two-particle cfp are derived and compared with the corresponding relationships for the one-particle cfp. The unique symmetries of the cfp of four- and eight-particle configurations are derived and discussed. Equations for calculating matrix elements of two-particle scalar and tensor operators in terms of the two-particle cfp are derived. The equation for two-particle scalar operators is used to display numerous relationships among the cfp. The equation for calculating the matrix elements of two-particle tensor operators was programed to generate the complete spin–spin and spin–other-orbit matrices of the f^N configurations for the first time. These matrix elements, parametrized in terms of Marvin's radial integrals, were used to compare calculated and experimental energy levels of the lanthanide series of ions in aqueous solution. The optimized values of Marvin's integral M^0 (M^2/M^0 and M^4/M^0 were assumed to be hydrogenic) and the spin–orbit constant, in units of cm^{-1}, were found for the following lanthanides: For $Pr^{3+}(f^2)$, $M^0 = 1.55$, $\zeta = 769.3$; for $Nd^{3+}(f^3)$, $M^0 = 1.89$, $\zeta = 900.5$; for $Eu^{3+}(f^6)$, $M^0 = 0.45$, $\zeta = 1333$; for $Gd^{3+}(f^7)$, $M^0 = 1.35$, $\zeta = 1525$; for $Tb^{3+}(f^8)$, $M^0 = 0.69$, $\zeta = 1713$; for $Er^{3+}(f^{11})$, $M^0 = 2.46$, $\zeta = 2421$; for $Tm^{3+}(f^{12})$, $M^0 = 2.49$, $\zeta = 2673$. (TSS) (Diss. Abstr. Int., B)

35851 SINGLE-CENTER CALCULATIONS ON THE ELECTRONICALLY EXCITED STATES OF EQUILATERAL H_3^+ ION. Kawaoka, Kenji; Borkman, Raymond F. (Georgia Inst. of Tech., Atlanta). J. Chem. Phys.; 54: No. 10, 4234-8(15 May 1971).

A theoretical investigation of the excited electronic states of the equilateral triangular H_3^+ ion is reported. Ab initio calculations were performed for the lowest energy states of symmetries $^3A_1'$, $^1A_2''$, $^3A_2''$, $^1E'$, and $^3E'$, using the single-center expansion configuration-interaction method. For each state the potential-energy curve in D_{3h} symmetry was obtained. The calculated state energies are expected to be in error by a most 0.01 hartree (6 kcal/mole). Two of the excited states $^1E'$ and $^3E'$ were found to be purely repulsive with respect to the totally symmetric nuclear coordinate, while three excited states, $^1A_2''$, $^3A_2''$, and $^3A_1'$, showed minima with respect to the totally symmetric nuclear coordinate. However, arguments based on group-theoretical correlation between the calculated D_{3h} state energies and the energies of possible dissociation products suggest that none of the excited states considered achieves an absolute energy minimum in D_{3h} symmetry. For the allowed electric dipole transitions $^1A_2'' \leftarrow {}^1A_1'$ and $^1E' \leftarrow {}^1A_1'$ the vertical (Franck–Condon) transition energies, oscillator strengths, and polarizations were calculated. The nature of the excited-state energy curves, at the ground-state equilibrium geometry, indicates that in every case only continuum absorption from the $^1A_1'$ ground state would be observed experimentally. (auth)

Positronium, Muonium, and Mesic Atoms and Molecules

Refer also to abstract 36539.

35852 CHEMICAL SHIFTS OF THE μ^+: A COMMENT. Williams, R. W. (Univ. of Washington, Seattle). Phys. Lett.; 34B: 63-4(18 Jan 1971).

Correction of an error in a recent paper of the above title by Breskman and Kanofsky reduces the calculated difference of chemical shift between μ^+ and proton by $2\sqrt{2}$. The possibility of reducing the chemical-correction uncertainty in muon-moment measurements is discussed. (auth)

35853 POSITRONIUM ATOM IN ORGANIC LIQUIDS. Buchikhin, A. P.; Gol'danskii, V. I.; Tatur, A. O.; Shantarovich, V. P. (Inst. of Chemical Physics, Moscow). Zh. Eksp. Teor. Fiz.; 60: No. 3, No. 3, 1136-40(Mar 1971). (In Russian).

Correlation curves and time spectra for positron annihilation in a number of organic liquids were studied experimentally. The results are interpreted on the basis of the "bubble" model according to which positronium atoms interacting with molecules of the liquid push them apart thus forming a "bubble" or potential well with a certain depth and radius. Both parameters are evaluated on the basis of the data obtained by the two methods (correlation and time methods). In both cases practically identical quantities are obtained; this indicates that the model is essentially correct (in hydrocarbons, alcohols, and bromides the well radius is 4 to 4.5 Å and well depth 0.7 to 1 eV). (auth)

35854 PIONIC X-RAY YIELDS AND LEVEL BROADENING IN LOW-Z ATOMS. Sapp, William Wade Jr. Williamsburg, Va.; Coll. of William and Mary (1970). 106p. University Microfilms Order No. 71-9605.

Thesis.

Absolute intensities of pionic and muonic x-ray transitions in ^6Li, ^9Be, C, O, Mg, and Ti were measured in thin elemental targets (except for H_2O) using Si(Li) and Ge(Li) spectrometers. The pionic K transitions in targets with $Z \leq 8$ and L transitions in all targets except ^6Li were examined in order to study the absorption process of negative pions in complex nuclei. A pionic-cascade calculation, which was constrained to reproduce the observed yields, predicted population probabilities for the lower levels of the mesic atoms and gave values for the strong-interaction level widths. It was also used to predict a nuclear capture schedule for π^- in ^6Li. The 2p-level broadenings are 0.015 ± 0.005 eV for ^6Li, 0.16 ± 0.03 eV for ^9B, 2.6 ± 0.9 eV for ^{12}C, and 12 ± 4 eV for ^{16}O. The latter two results are a factor of 2.5 larger than the values obtained in a recent experiment that employed somewhat different techniques. The present results are in satisfactory agreement with predictions based on a phenomenological optical potential whose constant parameters had been determined from selected pionic x-ray data. The parameters for the imaginary part of this potential are larger by a factor of two than those predicted by the quasi-deuteron absorption model. (Diss. Abstr. Int., B)

Collision Phenomena

Refer also to abstracts 36255 and 36256.

35855 (UCRL–20099) TOTAL LOSS CROSS SECTIONS FOR D_2 MOLECULES PASSING THROUGH H_2 GAS. Oliver, Young Pinckney (California Univ., Berkeley. Lawrence Radiation Lab.). Apr 1971. Contract W-7405-Eng-48. 26p. Dep. NTIS.

Thesis.

Total loss (attenuation) cross sections for 3- to 45-keV D_2 molecules and D^0 atoms passing through H_2 gas were measured. A light ion accelerator with an ion source operating in the PIG mode produced a 10^{-8}-A D_2^+ current. Hydrogen gas in gas cell I neutralized a portion of the primary beam. Hydrogen in gas cell II reionized a fraction of the particles that had passed through the target cell. The target pressures varied between 0 and 25 mtorr. All beam-current measurements were made with Faraday cups and electrometers with integrators. The values for the total loss cross sections for D_2 increased monotonically from 1.7×10^{-16} cm^2 at 3.3 keV D_2 energy to 3.0×10^{-16} cm^2 at 45 keV. (auth)

35856 PROMOTION OF L-SHELL ELECTRONS TO HIGHER BOUND STATES IN Ar^+–Ar COLLISIONS. Del Boca, R. (Univ. of Connecticut, Storrs); Hayden, H. C.; Thomson, G. M. Phys. Rev. Lett.; 26: No. 23, 1417-19(7 Jun 1971).

The Ar^+ + Ar collision was studied for evidence that an L-shell electron may be promoted to a higher bound level. An ion–ion coincidence apparatus was used on events where the incident energy T_0 was 25 keV and the scattering angle θ was 16°. Those inner-shell vacancy-producing collisions in which no purely outer-shell autoionization processes took place and in which only one electron was ejected per vacancy were successfully sought. For such an event to occur the inner-shell electron must be promoted to a bound state. This effect can be accounted for by use of the promotion model of Fano and Lichten; it provides additional evidence of the model's validity. (auth)

35857 POLARIZATION-FREE VACUUM-ULTRAVIOLET EXCITATION OF HELIUM BY ELECTRONS. McConkey, J. W.; Donaldson, F. G.; Hender, M. A. (Univ. of Windsor, Ont.). Phys. Rev. Lett.; 26: No. 23, 1413-15(7 Jun 1971).

"Polarization-free" excitation cross sections for the 1^1S-n^1P transitions of He were measured from threshold to 2 keV using a crossed-beam technique. Results were made absolute using the accurately known oscillator strengths. Maxima in the cross sections for the n^1P levels occurred around 100 eV and were found to be 106×10^{-19} cm^2 (2^1P), 31×10^{-19} cm^2 (3^1P), and 13×10^{-19} cm^2 (4^1P). (auth)

XUM

35858 DIFFERENTIAL MEASUREMENT OF THE He 3^3P EXCITATION, IN He^+–He COLLISIONS BY USING AN ION–PHOTON COINCIDENCE METHOD. Rahmat, G.; Vassilev, G.; Baudon, J.; Barat, M. (Univ. Paris, Orsay, France). Phys. Rev. Lett.; 26: No. 23, 1411-13(7 Jun 1971).

In order to determine the differential cross section for excitation at a given radiative level in ion–atom collisions, the scattered ions are detected at a given angle in coincidence with the photons emitted by the excited target atoms. The method has been applied to the He^+–He collision at laboratory energies of 200, 300, and 350 eV in the angular range 5 to 18 deg, for the 3^3P level of He. At 200 and 300 eV, the differential cross sections exhibit an interference pattern characteristic of a curve crossing. The behavior is more complicated at 350 eV, possibly because more than two molecular states are involved. (auth)

35859 1s–3d EXCITATION OF ATOMIC HYDROGEN BY ELECTRON AND PROTON IMPACT. Bhadra, Kalidas; Ghosh, A. S. (Indian Association for the Cultivation of Science, Calcutta). Phys. Rev. Lett.; 26: 737-9(29 Mar 1971).

The Glauber approximation was applied to calculate the total and the differential cross sections of 1s–3d excitation of the hydrogen atom by electron and proton impact. The results obtained are compared with other existing theoretical findings. (auth)

35860 MEASUREMENT OF HELIUM–HELIUM SCATTERING CROSS SECTION AT LOW TEMPERATURES. Oates, Daniel E.; King, John G. (Massachusetts Inst. of Tech., Cambridge). Phys. Rev. Lett.; 26: 735-7(29 Mar 1971).

The ^4He–^4He scattering cross section was measured at 2.1°K by an atomic-beam method. The value found for the averaged total effective cross section Q_{eff} with both beam and scattering gas at 2.1°K is 144 Å^2, with an estimated accuracy of 12%. The total effective cross section was also measured as a function of beam velocity, $Q_{eff}(v)$, with v ranging from 70 to 210 m/sec. These measurements were made with the scattering gas at 2.1°K. (auth)

35861 NEW RESONANCES IN THE TOTAL CROSS SECTION OF ELECTRONS ON CO AND O_2. Sanche, L.; Schulz, G. J. (Yale Univ., New Haven). Phys. Rev. Lett.; 26: 943-6(19 Apr 1971).

A transmission experiment is used to observe the structure in the total electron-impact cross section for CO and O_2. The structure in the cross sections is enhanced by measuring directly the derivative of the transmitted current. An isolated resonance in CO is observed at an electron energy of 10.04 ± 0.03 eV. In O_2, structure is observed which correlates well with the absorption spectra in the energy range 8 to 10 eV. In addition, two very sharp resonances (30-MeV width) are observed at 8.02 ± 0.03 and at 8.25 ± 0.03 eV. (auth)

35862 POLARIZATION OF THE H_α LINE PRODUCED IN $He^+ + H_2$ COLLISIONS. Nathan, R. D.; Isler, R. C. (Univ. of Florida, Gainesville). Phys. Rev. Lett.; 26: 1091-3(3 May 1971).

Van Brunt and Zare have noted that polarized spectral lines might be observed from many types of dissociative collisions that produce excited atomic fragments and that studies of this polarization could prove to be valuable in determining the angular distribution of the fragments. It was observed that such polarization does, indeed, exist in the H_α line produced by dissociative charge transfer in $He^+ + H_2$ collisions. Measurements were made at 90° to the beam direction in the energy range from 45 to 700 eV. (auth)

35863 SCATTERING OF CHARGED PARTICLES BY ATOMS. Franco, Victor (Brooklyn Coll., N. Y.). Phys. Rev. Lett.; 26: 1088-91(3 May 1971).

The (3Z + 2)-dimensional integral for scattering of charged particles by Z-electron atoms, which is obtained in the Glauber approximation, is reduced to a one-dimensional integral. Consequently, the approximation may be applied with relative ease to elastic and inelastic transitions of a wide variety of atoms. (auth)

35864 NEW DATA ON THE VELOCITY DISTRIBUTION OF H(2S) ATOMS PRODUCED BY DISSOCIATIVE EXCITATION OF H_2. Czarnik, J. W.; Fairchild, C. E. (Oregon State Univ., Corvallis). Phys. Rev. Lett.; 26: 807-10(5 Apr 1971).

New structure was observed in the time-of-flight distribution of H(2S) atoms produced by electron bombardment of H_2. The observed time-of-flight peaks are so located as to agree with the interpretation that the dissociative excitation proceeds predominantly through predissociation of intermediate bound states. (auth)

35865 MULTIPLE IONIZATION OF CESIUM AND BARIUM BY SUCCESSIVE ELECTRON IMPACTS. Redhead, P. A.; Gopalaraman, C. P. (National Research Council of Canada, Ottawa). Can. J. Phys.; 49: 585-93(1 Mar 1971).

The electron energy dependence of the multiply charged ion currents of cesium and barium (up to Cs^{10+} and Ba^{10+}) was measured in a trapped-ion-source mass spectrometer. Approximate values of the higher ionization potentials were measured, which agree with the values predicted by extrapolation methods to within the combined uncertainty of the experimental and extrapolation methods (~5 V), except for the ionization potential of Ba^{9+}. Improved estimates of higher ionization potentials of ions with atomic number 53 through 56 were obtained by the extrapolation method. The energy levels of some long-lived metastable states of Cs and Ba ions were estimated from the measured appearance potential curves. (auth) (Canada)

35866 CHARGE-EQUILIBRIUM FRACTIONS AND CHARGE-EXCHANGE CROSS SECTIONS FOR FAST IONS IN NITROGEN AND ARGON. Ormrod, J. H.; Michel, W. L. (Atomic Energy of Canada Ltd., Chalk River, Ont.). Can. J. Phys.; 49: 606-20 (1 Mar 1971). (AECL–3772).

Charge-equilibrium fractions and charge-exchange cross sections were measured in nitrogen and argon targets for ions with $Z \leq 11$ and energies 20 to 80 keV. A lower bound to the stopping by charge exchange was calculated using these measurements. At constant velocity, this calculated minimum rate of energy loss from charge-changing collisions varies with atomic number in the same periodic manner as the electronic stopping cross sections, and the charge-exchange contribution may account for most of the variation. (auth) (Canada)

35867 TOTAL CROSS SECTIONS FOR COLLISIONAL DETACHMENT OF ONE OR TWO ELECTRONS FROM H^- ON H_2O. Baribaud, Michel; Monte, Jacqueline; Zadworny, Francois (Univ. Grenoble, France). Compt. Rend., Ser. B; 272: 457-60(22 Feb 1971). (In French).

During experiments on the neutralization of a beam of H^- ions, the total cross sections σ_{-0} and σ_1 for the respective $\bar{1}0/0e0$ and $\bar{1}0/1ee0$ reactions, representing the collisional detachment occurring when H^- ions collide with vapor molecules, were measured for 5-keV H^- ions. (auth) (France)

35868 ELASTIC SCATTERING OF PROTONS AND ELECTRONS FROM HELIUM ATOMS IN THE GLAUBER APPROXIMATION. Johnson, James D.; Brolley, John E. (Los Alamos Scientific Lab., N. Mex.). Progr. Theor. Phys. (Kyoto); 44: 1700-1(Dec 1970).

A simple wave function ($c_1 = c_2 = c_3 = c_4 = c_5 = 0$) adjusted to fit $\bar{r}^2_m$ obtained from diamagnetism measurements was used to evaluate the Glauber amplitude for elastic scattering of electrons by He atoms at 100 and 700 eV. The fit is good at 700 eV. Use of the function in calculation of small-angle proton scattering resulted in larger cross sections than those obtained by use of a similar function used by Hylleraas. (A.G.W.)

35869 ANGULAR DISTRIBUTIONS FOR THE EXCITATION OF VIBRONIC STATES BY RESONANT ELECTRON–MOLECULE REACTIONS. Andrick, D.; Read, F. H. (Univ., Trier-Kaiserslautern, Ger. Univ. of Manchester, Eng.). J. Phys., B (London); 4: 389-96(1971).

In resonant reactions of electrons with molecules, vibronic transitions that influence the angular distribution of the scattered electrons may occur. General expressions were obtained for these angular distributions, and these were applied to some recent measurements on CO_2, in which the angular distributions were seen to depend on the vibronic symmetry of the final molecular state. (auth) (UK)

35870 IMPORTANCE OF THE KINETIC ENERGY EXPRESSION FOR THE BOUND ELECTRON IN THE BINARY COLLISION THEORY OF IONIZATION. Tripathi, D. N.; Rai, D. K. (Banaras Hindu Univ., India). J. Phys., B (London); 4: 365-7(1971).

Electron-impact ionization cross sections of alkali metal atoms were calculated using Gryzinski, Vriens, and Burgess formulae. Kinetic energy of the bound electron was estimated by Slater's rule. Comparison with experimental results was made. (auth) (UK)

35871 VIRIAL THEOREM FOR VARIATIONAL FUNCTIONS IN COLLISION THEORY. Heaton, M.; Moiseiwitsch, B. L. (Queen's Univ., Belfast). J. Phys., B (London); 4: 332-42(1971).

It is proved that if a scaling parameter α contained in a trial function u_T is optimized using Kohn's variational principle, then the virial theorem is satisfied by the optimized variational function and the variationally determined phase shift, provided that the asymptotic form of u_T does not depend upon α. By considering the cases of the scattering of electrons by the static potential of atomic hydrogen and the scattering of particles by screened

XUM

Coulomb potentials, it is shown that the virial theorem provides a valuable method for determining the optimum value of the scaling parameter and estimating the accuracy of the variationally determined trial function. (auth) (UK)

35872 OBSERVATION OF SUPERELASTIC ELECTRON SCATTERING FROM EXCITED MERCURY ATOMS. Killpatrick, Allen Ross. Provo, Utah; Brigham Young Univ. (1970). 58p. University Microfilms Order No. 71-8853.
Thesis.

Observation of superelastic scattering of low-energy electrons from excited mercury atoms is reported. The atoms are excited using an optical pumping scheme. The electron beam is orthogonal to the optically pumped atomic beam, and the scattered current is measured by a technique that eliminates the primary beam and the elastically scattered electrons from detection. Estimates of the superelastic scattering cross section are made. The $^3P_0$ and $^3P_2$ excited states of mercury were the only metastable states present in the scattering region. (Diss. Abstr. Int., B)

35873 OPTICAL SPECTRA OBSERVED DURING ION–MOLECULE COLLISIONS WITH LOW-ENERGY N_2^+ AND Ar^+ BEAMS. Liu, Chelcie Bosland. Santa Barbara, Calif.; Univ. of California (1969). 212p. University Microfilms Order No. 70-24,237.
Thesis.

A spectroscopic study was made of the light emitted during ion–molecule collisions using Ar^+ and N_2^+ beams at laboratory energies ranging from 10 to 1000 eV. Target gases for both ions included H_2, D_2, CO, N_2, O_2, NO, N_2O, CO_2, CH_4, and C_3H_2; in addition, He, Ne, Ar, and Kr were used as N_2^+ targets. Preliminary spectra of the reactions $He^+ + CO_2$ and $Ar^+ + Ar$ also were obtained. Photon emission in the visible and near ultraviolet was found to be a common occurrence for ion–molecule reactions in this energy range. Several different types of reactions were found, which lead to electrically, rotationally, and vibrationally excited states. Absolute cross sections for the production of some of the bright features observed in these reactions were measured. They were in the range of 10^{-17} to 10^{-16} cm^2 at beam energies of several hundred eV and decreased with decreasing beam energy. For some of the reactions, structure was observed in the cross section versus energy curves. Rotational and vibrational excitations of the collision products were studied. In general, the rotational excitation increased as the energy of the bombarding ion decreased. A "billiard ball" model of the collision is presented, which gives a semiquantitative explanation of the dependence of rotational excitation on the energy and identity of the incident ion for "grazing" collisions. The degree of vibrational excitation and its energy dependence depended on the reaction partners. (Diss. Abstr. Int., B)

35874 CROSS SECTIONS FOR THE DESTRUCTION OF 1- TO 25-keV/NUCLEON $X^1\Sigma_g^+$ AND c $^3\Pi_u$ HYDROGEN MOLECULES IN COLLISIONS WITH H_2 GAS. Morgan, Thomas J.; Berkner, Klaus H.; Pyle, Robert V. (Univ. of California Berkeley). Phys. Rev. Lett.; 26: 602-4(15 Mar 1971).

Measurements of the cross sections for the total loss and the ionization of $X^1\Sigma_g^+$ H_2 [1 ≤ E (keV/nucleon) ≤ 25] and $c^3\Pi_u H_2$ molecules [3 ≤ E (keV/nucleon) ≤ 20] in collisions with H_2 gas are reported. The $c^3\Pi_u$ molecules were formed by electron capture by H_2^+ ions in Mg vapor. The total-loss cross section of the $c^3\Pi_u$ state is about 5 times larger than the total-loss cross section of the $X^1\Sigma_g^+$ state. (auth)

35875 COHERENCE TRANSFER IN A PENNING IONIZING COLLISION. Schearer, L. D.; Riseberg, L. A. (Texas Instruments Inc., Dallas). Phys. Rev. Lett.; 26: 599-601(15 Mar 1971).

Modulation of the intensity of light emitted by $Sr^+(^2P_{\frac{1}{2}})$ ions at the resonance frequency of metastable helium atoms was observed, demonstrating that coherence was transferred in the Penning collision. The coherent excitation of the Penning ions suggests that the techniques of "coherence spectroscopy" such as level-crossing and Hanle experiments can be extended to excited states of Penning ions currently inaccessible by means of optical excitation. (auth)

35876 OSCILLATIONS OF THE TOTAL CROSS SECTIONS FOR INELASTIC PROCESSES IN ATOMIC COLLISIONS. Ankudinov, V. A.; Bobashev, S. V.; Perel, V. I. (Ioffe Inst. of Physics and Tech., Leningrad). Zh. Eksp. Teor. Fiz.; 60: No. 3, 906-19(Mar 1971). (In Russian).

The simplest model of collision of two atomic particles resulting in oscillations of the total cross sections for processes with a large resonance defect is considered. In accordance with the Rosenthal hypothesis the oscillations are the result of interference of two energetically close inelastic channels arising as a consequence of term interaction at large internuclear distances. It is assumed that the two vacant excited levels are consecutively occupied from the ground state according to the Landau–Zener scheme and interact when the particles fly apart. Conditions for appearance of oscillations of the total cross sections are analyzed, and expressions are obtained for their amplitudes, periods, and phases. It is shown that under certain conditions the oscillations are harmonic in the inverse velocity scale. The oscillation phase depends on the nature of the interaction between the excited terms on flying apart of the particles. Two types of such an interaction are considered, involving intersection and close approach of terms. More complex models are discussed, which include the interaction of several terms at large internuclear distances, and it is shown that to each closed "loop" formed by the terms there corresponds an oscillation mode in the collision cross sections. A comparison with experimental data is presented. (auth)

35877 STUDY OF ELECTRON CHARGE TRANSFER PROCESSES BY PHOTON–NEUTRAL-PARTICLE COINCIDENCE TECHNIQUES. McKnight, Ronald Hugh. Lincoln, Neb.; Univ. of Nebraska (1970). 170p. University Microfilms Order No. 71-9576.
Thesis.

Studies of charge-transfer processes were made for the scattering systems $H_1^+ + Ar$ and $H_1^+ + He$ by use of delayed coincidence techniques. Differential cross sections and probabilities of charge transfer into the 2p state of hydrogen may be related to the number of coincidences between Lyman-α photons emitted in the decay of the 2p state and the resulting fast hydrogen atoms. A beam of fast protons was introduced into a gas-filled scattering chamber, and the scattered beam and the Lyman-α radiation produced in the scattering region were observed with suitable detectors. Coincidence circuitry employing crossover timing and a resolving time of 100 nsec was used to determine the number of protons that acquired an electron in the 2p state and were simultaneously scattered through an angle Θ. Results were obtained for the system $H_1^+ + He$ for the condition ΘE = 20 keV deg, which corresponds to an impact parameter of 0.138 au. When the probability of charge transfer into the 2p state, P_{2p}, is plotted as a function of 1/v, where v is the velocity of the incident proton, an oscillatory structure is observed. The coupled-state calculation of Sin Fai Lam, which incorporates n = 1 and 2 atomic states as the basis for expansion of the system wave function, properly predicts the location of the maxima and minima in the graph but overestimates the magnitude of P_{2p} by an order of magnitude. Similar results are obtained for scattering in which E = 6.25 keV and Θ varies between 1 and 5 deg. The comparison between experiment and theory casts considerable doubt on the reliability of coupled-state calculations for differential scattering processes that use atomic orbitals as an approximation to the more appropriate molecular wave functions. For the $H_1^+ + Ar$ system, the total charge-transfer probability has a quasi-resonant behavior that is not observed in a comparable measurement of P_{2p}. (Diss. Abstr. Int., B)

35878 CALCULATIONS OF ELECTRON AND PROTON COLLISIONS BY ATOMIC HYDROGEN. Tai, Hsiang. Pittsburgh; Univ. of Pittsburgh (1970). 229p. University Microfilms Order No. 71-9033.
Thesis.

In the first part of this thesis, the Glauber approximation was applied to excitation of the 2s, 2p, 3s, and 3p levels of the hydrogen atom by electron impact. The differential and integrated excitation cross sections predicted by Glauber theory were compared with experiment and with other calculations. The Glauber approximation is a considerable improvement over the Born approximation at energies < ~100 eV. At energies > ~100 eV the Glauber total excitation cross sections approach the Born, even though at large scattering angles (>40°) the Glauber differential cross sections may be very different from the Born. At intermediate energies (~30 to 100 eV) the Glauber predictions are surprisingly good; at energies < ~20 eV the Glauber integrated cross sections are rather smaller than observed experimentally. The Glauber approximation was extended to the calculation of excitation of atomic hydrogen by proton and positron impact. In the Glauber approximation of elastic or excitation scattering of atomic hydrogen, positron impact yields results identical to results of electron impact. The proton impact also yields very good results in the Glauber approximation. In the second part of this thesis, the multistate impact–parameter formulation was applied to the proton–hydrogen scattering problem with the following approximations: (1) the protons describe constant-velocity straight-line classical trajectories; (2) the spinless electronic wave function is expanded in terms of a finite subset of traveling hydrogenic wave functions centered about either proton. The one-electron ex-

XUM

change integrals that arise in the theory of heavy-particle collisions are expressed as the solutions of a set of first-order differential equations integrated numerically along with the scattering amplitudes with respect to time. Two calculations were made. In the first, the 1s, 2s, and 3s states but not the 2p states were coupled. It was found that the inclusion of the 3s state gave negligible contributions. In the second calculation, the 1s, 2s, $2p_0$, and $2p_{\pm1}$ states are included but not the 3s state. The inclusion of 2p state in the direct and exchange channel gives overall much better results. The unitary condition and the detailed balancing theorem are well demonstrated by these results. (Diss. Abstr. Int., B)

35879 HARRIS-METHOD CALCULATION OF ELECTRON AND POSITRON SCATTERING BY HYDROGEN ATOMS. Shimamura, Isao (Tokyo Univ.). J. Phys. Soc. Jap.; 30: No. 6, 1702-8(Jun 1971).

The Harris method of obtained scattering phase shifts is applied to the s-wave elastic electron and positron scattering by hydrogen atoms by use of Schwartz-type correlated trial functions with 50 and 56 terms, respectively. Kohn-method calculations with the same trial functions are also carried out at the same energies. The agreement between the Harris-method results and the Kohn-method results is good especially at low energies. In the electron-scattering case, two kinds of errors cancel each other to some extent, but in the positron case, they add to make the agreement between the Harris-method and Kohn-method results somewhat worse. (auth)

35880 IONIZATION OF THE L-SHELL OF ALUMINUM BY FAST CHARGED PARTICLES. Manson, S. T. (Georgia State Univ., Atlanta). Phys. Lett.; 35A: No. 2, 89-91(17 May 1971).

Cross sections for ionization of 2s and 2p electrons in aluminum by proton impact were calculated in the Born approximation using Hartree–Slater wave functions. Large differences at small energy loss from previous hydrogen-like calculations are found. (auth)

35881 CALCULATION OF THE EXCITATION CROSS SECTION $3s \rightarrow 3p$ OF SODIUM SUBJECTED TO ELECTRON IMPACT. Felden, Madeleine (Univ., Nancy). Compt. Rend., Ser. B; 272: No. 11, 641-3(15 Mar 1971). (In French).

The first Born approximation was used to calculate the excitation cross section $\sigma_{3s\rightarrow 3p}$ of sodium subjected to electron impact with two types of wave functions: those of Fock and Petrashen, and those of Bates and Damgaard. The results are compared, and the small difference between them shows that the Bates and Damgaard wave function can be used for general cases. (auth)

35882 EXCITATION OF n = 2 HELIUM LEVELS BY LOW-ENERGY ELECTRONS (30 TO 50 eV). ANGULAR DISTRIBUTION OF THE SCATTERED ELECTRONS. Hall, Richard Ian; Joyez, Gerard; Mazeau, Jean; Reinhardt, Jean; Schermann, Catherine (Univ., Paris). Compt. Rend., Ser. B; 272: No. 12, 743-6(22 Mar 1971). (In French).

The angular dependence of the ratio of the intensities of optically forbidden transitions to allowed transitions is investigated. The results indicate that in high-angle scattering probabilities for forbidden and allowed transitions are equal. (auth) (France)

35883 INELASTIC ELECTRON SCATTERING FROM FORMALDEHYDE. Weiss, M. J.; Kuyatt, C. E.; Mielczarek, S. (National Bureau of Standards, Washington, D. C.). J. Chem. Phys.; 54: No. 10, 4147-50(15 May 1971).

The electron scattering spectrum of H_2CO was determined in the energy-loss range between 0 and 16.0 keV. Three Rydberg series in the region 7 to 11 eV can be identified with the s, p, and d series reported in the literature by ultraviolet absorption studies. Oscillator strengths are determined for some of the Rydberg states and comparison is made with recent ultraviolet absorption work employing photoelectric methods of detection. A serious disagreement exists between the f values obtained by the two methods for the $3sa_1$ Rydberg. Another Rydberg series, probably converging to the third ionization potential of H_2CO is observed in the electron scattering spectrum in the energy-loss region 12.4 to 14.0 eV. Erratic behavior of the quantum defects of the first Rydberg series as well as failure to detect the $\pi \rightarrow \pi^*$ transition in H_2CO is discussed in the light of recent theories involving valence states that can seriously perturb members of a Rydberg series. (auth)

35884 COLLISION-INDUCED VIBRATIONAL EXCITATION AND DISSOCIATION OF HYDROGEN WITH ALKALI ATOMS AND IONS FROM 2 TO 50 eV. Dittner, Peter F.; Datz, Sheldon (Oak Ridge National Lab., Tenn.). J. Chem. Phys.; 54: No. 10, 4228-33(15 May 1971).

Inelastic energy losses for Na^0, Na^+, K^0 and K^+ backscattered from H_2 and D_2 were measured. At center-of-mass energies below ~15 eV for Na and ~20 eV for K, the collisions yield vibrational excitations, which are compared with the one-dimensional exact classical calculations of Secrest. The vibrational excitation in the Na^+-H_2 and Na^0-H_2 system is in excellent agreement with three-dimensional classical calculations of Cheng and Wolfsberg. Above these energies the molecules are dissociated but the energy-loss distribution of the alkali projectile remains sharp and in the case of Na–H approaches the maximum loss possible at 50 eV. (auth)

35885 EFFECTS OF SURFACE CROSSING IN CHEMICAL REACTIONS: THE H_3^+ SYSTEM. Preston, Richard K.; Tully, John C. (Yale Univ., New Haven). J. Chem. Phys.; 54: No. 10, 4297-4304(15 May 1971).

Approximate potential-energy surfaces for the two lowest singlet states of H_3^+ are calculated using the diatomics-in-molecules approach. The nonadiabatic terms that couple these surfaces can be directly computed in this approximation. From the magnitudes of these coupling terms it is apparent that, for excitation energies below about 10 eV, nonadiabatic transitions must be confined almost entirely to a region localized at the avoided crossing of the two surfaces. This fact suggests the following simplified picture of the dynamics of the $H^+ + H_2$ reaction: As the H^+ and H_2 approach, they remain on the lower potential surface (there is no initial electron jump). They continue to follow adiabatically the lower surface in the close-collision region, so the probability of a nonadiabatic transition does not appear to be related to the lifetime of the collision complex. It is while the products are receding that electronic transitions become important. Consequences of this model on the threshold for formation of H_2^+ and on the partition of vibrational energy in the products are discussed, and a comparison with recent experiments of Krenos and Wolfgang is included. (auth)

35886 INTERPRETATION OF ALKALI–INERT-GAS BEAM SCATTERING WITH THE BUCKINGHAM–CORNER POTENTIAL. Okel, J. G. R.; van de Ree, J. (Univ. of Tech., Eindhoven, Netherlands). J. Chem. Phys.; 54: No. 10, 4259-68(15 May 1971).

It is shown that recent measurements of alkali-metal–inert-gas beam scattering cross sections can be fit by a four-parameter Buckingham–Corner potential with the same accuracy as with previously proposed four- to seven-parameter models. The Buckingham–Corner model contains a single Born–Mayer repulsive term and two attractive terms, the ordinary Van der Waals attraction and the second term in the London dispersion series. This model gives the correct broadening of the potential well. In addition some of the terms can be calculated theoretically. A fit of the measured total and differential cross sections for the systems Na–Xe and Na–Kr yields a set of form parameters assumed to be characteristic of the alkali-metal–inert-gas interaction. Using these one can deduce well parameter values for each particular combination. Since the fit of the Buckingham–Corner potential is determined from the oscillatory structure of thermal beam measurements, its validity is confirmed only in the attractive region. A possible application of the model to the interaction between two inert gas atoms is discussed. (auth)

35887 INTERPRETATION OF HIGH-ENERGY CROSS SECTIONS FOR MOLECULAR SCATTERING. Wartell, M. A.; Cross, R. J. Jr. (Yale Univ., New Haven). J. Chem. Phys.; 54: No. 10, 4519-20(15 May 1971).

Calculations based on the sudden approximation for $He-H_2$ scattering are used to show that high-energy molecular scattering measurements may be interpreted in terms of a spherically symmetric potential and that this potential is the true potential evaluated at the most probable vibrational coordinate and averaged over orientations. These conclusions are not valid if dissociation occurs or if a crossing of electronic energy surfaces is involved. (A.G.W.)

35888 IONIZATION OF NOBLE GASES BY PROTONS. Parks, James Edgar. Lexington, Ky.; Univ. of Kentucky (1970). 121p. University Microfilms Order No. 71-8594.

Thesis.

A new W-value experiment was developed to measure the total ionization produced when protons interact with gases. This new experiment has three advantages: (1) W measurements can be made over a wide range of pressures, (2) the interactions take place at a definite particle energy, and (3) the experiment can be placed in tandem with a light-emission cell so that studies of the excitation and ionization of gases with protons can be directly correlated. As opposed to other W-value experiments in which the total energy of a particle is absorbed by the gas, this is a differential-W experiment where only a fraction of the proton's energy is absorbed by the gas. In this new method, protons are Rutherford scattered by a thin gold foil into the W cell consisting of a parallel-plate ionization chamber, while most of the protons are allowed to pass on through to the light-emission cell where the

XUM

electronic excitation of the gas may be studied with a vacuum-ultraviolet scanning monochromator. The number of protons scattered into the W cell is measured with a silicon surface-barrier detector, and the energy lost to the gas is calculated from known stopping-power data. Gases to be studied are flowed simultaneously through the two cells so that the proton interactions take place at nearly the same pressure, energy, and path length. W values for 4-MeV protons interacting with the noble gases are measured as a function of pressure. At 400 torr for pure gases, the following values of W (eV per ion pair) were found: He, 45.2 ± 0.2; Ne, 39.3 ± 0.2; Ar, 26.6 ± 0.2; Kr, 23.0 ± 0.2; Xe, 20.5 ± 0.2; N_2, 36.6 ± 0.2. No appreciable pressure dependence was observed for the pure gases. The Jesse effect, which is the increase in ionization observed when impurities are added to certain gases, is studied as a function of concentration and pressure. W measurements are reported for mixtures of C_2H_4, C_2H_2, CO_2, and Kr with Ar and are correlated with the quenching of continuous emission data. W values are also studied as a function of pressure and concentration for mixtures of Ne, Ar, Kr, and Xe with He. A pressure dependence is observed for the mixtures with small concentrations of impurities. The Jesse effect in argon was also investigated by performing novel experiments using trinary mixtures. The W-value results are used with new and old supplementary evidence to extend a model for the Jesse effect in argon. A model is proposed which suggests that the energy for the Jesse effect comes from intermediate molecular states of argon. (Diss. Abstr. Int., B)

Atomic Theory

35889 PERTURBATION TREATMENT OF THE HARTREE–FOCK EQUATIONS FOR THE GROUND STATES OF 3- TO 10-ELECTRON ATOMS. Wilson, R. G. (London Univ.). J. Phys., B (London); 4: 311-13(1971).

The first-order Hartree–Fock (HF) equations for the ground state of atomic systems with 4 to 10 electrons are deduced from the corresponding unrestricted (UHF) equations given previously. The second-order HF energies are given exactly and the third-order energies very accurately. Each atom is treated as a special case of a general scheme. The third-order energy of lithium is calculated very accurately, completing Linderberg's calculation. The HF ground-state energies of atoms with 3 to 10 electrons are shown to differ very little from the corresponding UHF energies previously given. The zero- and first-order expectation values of various operators are related to their corresponding UHF values. (auth) (UK)

35890 MULTI-CONFIGURATION FROZEN-CORE APPROXIMATION. I. EIGENSTATES OF THE TWO-ELECTRON ATOM. Calvert, J. McI.; Davison, W. D. (Queen's Univ., Belfast). J. Phys., B; 4: 314-31(1971).

A generalization of the "frozen core" approximation is described in which several configurations are employed, each containing a fixed core function chosen where possible from physical considerations. This multiconfiguration frozen-core (MCFC) procedure is applied to the ground ^1S states of He and H^- and to the singly excited ^1S, ^3S, ^1P, ^3P, ^1D, and ^3D states of He (up to principal quantum number n = 7), two of the core functions being chosen so as to take account of the dipole and quadrupole components of the long-range correlation. Eigenenergies of high accuracy are obtained using at the most five core functions: expectation values of several operators are also calculated. The success of a special case of the MCFC method, the generalized polarized orbital approximation, confirms in a striking way that short-range correlation is of little importance in all except the ^1S series. It is concluded that for many purposes the MCFC method may possess some distinct advantages when compared with other configuration-interaction procedures. (auth) (UK)

35891 MODEL FOR γ DECAY OF ATOMIC OR NUCLEAR SYSTEMS. Razavy, M.; Henley, E. A. Jr. (Univ. of Alberta, Edmonton). Can. J. Phys.; 48: 2399-2410(15 Oct 1970).

An exactly solvable quantum-mechanical model for interaction of a spinless bound particle with the electromagnetic field is studied. This model is used to calculate the electromagnetic transition in atomic and nuclear systems. Some general results as to the dependence of line width and level shift on the binding potential are obtained. (auth) (Canada)

Cosmic Radiation

Refer also to abstracts 35010, 35012, 35014, 35704, 35712, 35759, 35818, 35974, 36378, 36383, 36394, and 36416.

35892 (CONF-691055-(Vol.1)) PROCEEDINGS OF THE ELEVENTH SYMPOSIUM ON COSMIC RAYS, ASTROPHYSICS, GEOPHYSICS AND ELEMENTARY PARTICLE PHYSICS, UNIVERSITY OF DELHI, OCTOBER 7–11, 1969. VOLUME I. INVITED TALKS. (Department of Atomic Energy, Bombay (India). Cosmic Rays, Astrophysics and Geophysics Committee). 1969. 315p.

A separate abstract was prepared for each of the twenty-four papers included in this volume. (W.D.M.)

For abstracts of individual papers see: 35062, 35592, 35657–35660, 35703, 35771, 35904–35909, 35997, 36427, 36452, 36467, 36479, 36480, 36500, 36516, 36533, and 36584.

35893 (CONF-691055-(Vol.2)) PROCEEDINGS OF THE ELEVENTH SYMPOSIUM ON COSMIC RAYS, ASTROPHYSICS, GEOPHYSICS AND ELEMENTARY PARTICLE PHYSICS, UNIVERSITY OF DELHI, OCTOBER 7–11, 1969. VOLUME II. CONTRIBUTED PAPERS. (Department of Atomic Energy, Bombay (India). Cosmic Rays, Astrophysics and Geophysics Committee). 1969. 263p.

A separate abstract was prepared for each of the 58 papers included in this volume; also, four "abstracts only" of papers are given but are not included here for NSA. Thirty related papers given at the symposium are listed, but manuscripts were received too late for publication in the proceedings. (J.C.W.)

For abstracts of individual papers see: 35013–35015, 35599, 35600, 35661–35664, 35704–35706, 35772–35774, 35796, 35910–35923, 35998–36001, 36239, 36240, 36383, 36400–36404, 36416–36418, 36453, 36468–36470, 36481, 36501, 36517–36520, 36534, 36535, and 36546.

35894 MODULYATSIYA KOSMICHESKIKH LUCHEI V MEZHPLANETNOM PROSTRANSTVE. (Modulation of Cosmic Rays in Interplanetary Space). Krymskii, G. F. Moscow; Izdatel'stvo Nauka (1969). 152p.

Interplanetary modulation of cosmic rays is discussed in an anisotropic diffusion approximation on the basis of a diffusion equation containing additional terms that take into account the transport of cosmic rays and their energy variation in a moving magnetized medium. Methods of determining the energy spectrum of cosmic-ray variations are described, and the mechanisms of cosmic-ray modulation are examined. A quantitative characteristic for the magnetic-field irregularity is introduced. An interpretation of cosmic-ray effects associated with chromospheric flares is given, and the energy spectrum of Forbush effects is obtained. Assuming that the effects are caused by the magnetic sheath, an energy relation for the transparency of its walls is derived from observation data. Three models for the propagation of cosmic rays are studied that correspond to the three flares of February 23, 1956 and May 4 and November 12, 1960. Estimates of the diffusion coefficient of particles are obtained as a function of their energy and the distance to the Sun. A model for the diurnal variations of cosmic rays, based on the mechanism of anisotropic diffusion, is proposed, and a critical analysis of the mechanism relating the 11-year variations with superposed Forbush effects is presented. The nature of the hysteresis of the 11-year variations is studied, and the solar-wind parameters are evaluated. The modulation of cosmic rays is studied as a function of solar-wind geometry. A special chapter is devoted to the general picture of cosmic-ray modulation in interplanetary space. Modulation equations are derived, and their applicability range is examined. (IAA)

35895 CHEMICAL COMPOSTION AND THE ENERGY SPECTRUM OF HEAVY NUCLEI IN THE COSMIC RADIATION ABOVE 10 GeV/NUCLEON. Saito, Takeshi (Tokyo Univ.). J. Phys. Soc. Jap.; 30: No. 6, 1535-45(Jun 1971).

A total of 7695 heavy nuclei was located in the Brawley emulsion stack. The error in energy estimation was about 30% and that in charge estimation was 0.25 units of charge for nuclei with $Z \leq 9$ and 0.5 for the iron group. The flux values for respective charge groups at the top of the atmosphere at energies above 10 GeV/nucleon are $J^0_M = 0.686 \pm 0.117$, $J^0_H = 0.241 \pm 0.032$, $J^0_{LH} = 0.166 \pm 0.022$, $J^0_{MH} = 0.015 \pm 0.004$, and $J^0_{VH} = 0.060 \pm 0.012$ particles/$m^2 \cdot$ sec $\cdot$ sterad. The integral energy spectra of the individual charge groups have the same exponent of $\gamma = 1.60$ up to several hundreds of GeV/nucleon. On the basis of the results, mechanisms of cosmic-ray acceleration and the amount of matter traversed by the cosmic rays are discussed. (auth)

35896 RADIO NOISE GENERATION BY SCATTERING OF PLASMA WAVES. Windsor, Robert Anthony. Minneapolis; Univ. of Minnesota (1970). 82p. University Microfilms Order No. 71-8235.

Thesis.

A new process is proposed for generating radio noise in cosmic sources. The mechanism envisioned is the scattering of plasma waves by a flux of ultrarelativistic electrons passing through the plasma. In view of its similarity to the mechanism of inverse Compton scattering, this process is called inverse plasmon scattering. It is found that the electric field strengths due to thermal fluctuations in the plasma are several orders of magnitude below the levels needed to generate detectable levels of radiation. Hence, the mechanism is only interesting in unstable plasmas where the electric fields may grow to sufficient levels. The frequency dependence of inverse plasmon scattering is similar to that found for the mechanisms of synchrotron radiation and inverse Compton scattering, in that all three of these mechanisms exhibit the same power-law decrease of intensity with increasing frequency. But the frequency bands into which the power is radiated vary from one mechanism to the next. The frequency band for inverse Compton scattering will generally fall far beyond those of the other two mechanisms and thus will not cause any problems in identifying radiation from these different mechanisms. The frequency bands of inverse plasmon scattering and synchrotron radiation will generally overlap, with radiation from inverse plasmon scattering extending past the high-frequency cutoff for synchrotron radiation. Thus, this high-frequency tail of inverse plasmon scattering is, in principle, detectable. It is possible that the radiation at the highest frequencies seen from synchrotron sources is generated by inverse plasmon scattering instead of synchrotron radiation. If this is true, it would not be necessary to postulate continuous injection of high-energy electrons into the source in order to explain the discrepancy between the age of the source and the particle lifetimes, as calculated from the synchrotron radiation formulas. The radiation from inverse plasmon scattering has small, but definite, amounts of linear polarization. The polarization is calculated, assuming that the electric field of the plasma wave is either fixed in direction or randomly oriented along the line of sight in the plasma. (Diss. Abstr. Int., B)

35897 STUDY OF COSMIC-RAY MODULATION WITH NEUTRON MULTIPLICITY ANALYZERS. Singh, Partap. Durham, N. H.; Univ. of New Hampshire (1971). 162p. University Microfilms Order No. 71-10,244.

Thesis.

Neutron multiplicity data were utilized to study the cosmic-ray intensity–time variations. For this purpose, the neutron multiplicity spectra were recorded continuously at the Mt. Washington and Durham neutron monitors during 1968–69. The recorded data were corrected for the probable coincidences and dead-time losses in the neutron multiplicity analyzer and for the atmospheric-pressure variations. The corrected data were analyzed to study the neutron multiplicity (or equivalently the rigidity) dependence of the 11-year variation, Forbush-decrease variation, and the daily variation of the cosmic-ray intensity. It was found that the 11-year variation and the Forbush decreases during the period of investigation do depend upon the neutron multiplicity but the dependence appears to be the same for the two types of cosmic-ray intensity variations. Similar results obtained from the cosmic-ray records of several neutron monitors indicate that the rigidity dependence of the 11-year variation is slightly larger than that of the Forbush decreases considered. The magnitude and the direction of the anisotropy in the cosmic-ray flux as inferred from the neutron multiplicity spectrum are found to be practically independent of the multiplicity but consistent with the results obtained from neutron monitor records. (TSS) (Diss. Abstr. Int., B)

35898 MOMENTUM AND ZENITHAL DEPENDENCE OF THE CHARGE RATIO OF ENERGETIC COSMIC-RAY MUONS NEAR SEA LEVEL. Bateman, Benjamin Jefferson Jr. College Station, Tex.; Texas A and M Univ. (1970). 166p. University Microfilms Order No. 71-8864.

Thesis.

The result of a measurement and a theoretical calculation of the effect of the geomagnetic field on the charge ratio as a function of energy and zenith angle in the geomagnetic west are presented and compared. The theoretical calculations are unique in that they consider the dipole nature of the geomagnetic field and the distributed source of muons. The experimental results are unique because this is the first work to be reported that uses three wide-gap spark chambers with high spatial resolution in conjunction with two separate magnets. These features allow the complete identification of about 99% of the events. A quantitative comparison of the experiment and the theoretical calculation shows excellent agreement. (Diss. Abstr. Int., B)

35899 PHENOMENOLOGICAL APPROACH TO THE SOLAR MODULATION OF COSMIC RAYS. Burger, J. J. (Kamerlingh Onnes Laboratorium, Leiden). Astrophys. J.; 166: No. 3, 651-67(15 Jun 1971).

The interstellar electron spectrum is derived from the galactic nonthermal radio volume emissivity. Comparison with the electron spectrum observed near the Earth yields the magnitude of the modulation $K(R, r_E, 1968)$ at the Earth in 1968. $K(R, r_E, 1968)$ is applied to the proton and α-particle spectra observed in 1968 using the simple diffusion-convection theory. The use of this theory at $R > 0.5$ GV is justified by the characteristics of the simultaneous intensity of variations of electrons, protons, and α particles. The demodulated proton and α-particle spectra are compared with interstellar equilibrium spectra calculated for injection spectra, following power laws in kinetic energy T, total energy W, or rigidity R. The fit between the demodulated spectra and the equilibrium spectra from the rigidity power-law injection spectra is good for protons as well as α particles with a kinetic energy above ~100 MeV per nucleon. The fit is equally good if source spectra for protons and α particles similar to the derived electron spectrum, taking the rigidity as the appropriate parameter are assumed. The deviations occurring below a kinetic energy of ~100 MeV per nucleon are attributed either to local components present in the observations near the Earth or to energy-loss processes complicating the modulation at these energies. The rigidity dependence of $K(R, r_E, 1968)$ below 2 GV differs significantly from the rigidity dependence of the time variations of the cosmic rays at the Earth. Hence the cosmic-ray diffusion coefficient D cannot be a separable function of R and heliocentric distance r. Instead, a new model is proposed for D(R,r), which is based on a decrease of the magnetic bending power in the average magnetic irregularity present in the solar wind with increasing r. An observational justification of this basis is discussed in some detail. This new model implies that (1) the time variations of the cosmic rays near the Earth arise mainly from changes in the conditions in local interplanetary space; (2) the rigidity dependence of the time variations reflects the rigidity dependence of the local scattering mean free path λ_E, which has a transition rigidity R_0 below which λ_E is independent of R and above which $\lambda_E \propto R$; (3) R_0 is a decreasing function of r. With this model a satisfactory match of the rigidity dependences of $K(R, r_E, 1968)$ and the time variations is obtained. The specific r-dependence of R_0 and λ, which reconciles the observed rigidity dependences suggests that λ for $R < R_0(r)$ is not only independent of R but also independent of r. The numerical values of the various parameters required in this model are in good agreement with the current estimates. (auth)

35900 EFFECT OF PLASMA INSTABILITIES IN COLGATE'S COSMIC-RAY MODEL. McKee, Christopher F. (Univ. of California, Livermore). Astrophys. J.; 166: No. 3, 573-86(15 Jan 1971).

The interaction between the interstellar plasma and cosmic rays ejected from a supernova in Colgate's model was analyzed in order to determine if the cosmic rays can escape. The expansion of the cosmic rays is described, and the effects of both the stellar and interstellar magnetic fields are discussed. Applying the results of a one-dimensional computer simulation of instabilities between counterstreaming plasmas, it is concluded that a significant fraction of the cosmic rays can escape along the interstellar magnetic field, although the energy spectrum may be altered in the process. (auth)

35901 COSMIC-RAY DIURNAL VARIATION FOR THE PERIODS OF 1962 AND 1964–1965. Pankratov, A. K. Izv. Krym. Astrofiz. Observ.; 41-42: 230-9(1970). (In Russian).

The diurnal variation amplitude and phase data of the cosmic-ray neutron component for the periods of August–December 1962, and 1964–65 and the hard component for the period of January 1964–April 1965 were obtained. The qualitative analysis of these data, as well as the same data for the period of the IGY, and underground measurement data shows that, during minimum sunspot activity, significant changes in configuration of the cosmic-ray modulation region take place in the direction of high helio latitudes. (auth)

35902 COMPOUND DIFFUSION OF COSMIC RAYS. Lingenfelter, R. E. (Univ. of California, Los Angeles); Ramaty, R.; Fish, L. A. Astrophys. Lett.; 8: No. 2, 93-7(Apr 1971).

The combined effects of the one-dimensional diffusion of cosmic rays along interstellar magnetic field lines and the three-dimensional random walk of these field lines due to interstellar turbulence are considered. The resulting compound diffusion can account for the observed low anisotropy of cosmic rays in terms of a correlation length of a few tens of parsecs, which is consistent with the observational data on the scale of the interstellar turbulence. (auth)

35903 COSMIC GAMMA-RAY BACKGROUND. Bhatia, V. B.; Tandon, J. N. (Delhi Univ.). Astrophys. Lett.; 8: No. 2, 99-100 (Apr 1971).

XUM

The cosmic γ-ray background flux for photon energies greater than 100 MeV was evaluated by considering Compton collisions between the 3°K background photons and high-energy electrons in the halo. It is shown that the computed flux is in agreement with the revised upper limit for γ rays with $E \geq 100$ MeV. (auth)

35904 WHAT IS NEW IN COSMIC RAYS. Pal, Yash (Tata Inst. of Fundamental Research, Bombay). pp 1-23 of Proceedings of the Eleventh Symposium on Cosmic Rays, Astrophysics, Geophysics and Elementary Particle Physics, 1969. Vol. I. Bombay; Department of Atomic Energy (1969).

From eleventh symposium on cosmic rays, astrophysics, geophysics and elementary particle physics; Delhi, India (7 Oct 1969). See CONF-691055-(Vol. 1).

Attention is concentrated on the development of cosmic rays as an astronomical signal. Topics discussed include: distribution of cosmic rays; x rays and gamma rays; highest-energy cosmic rays, low-energy nucleonic component; origin of cosmic rays; superheavy nucleic; cosmic-ray accelerators; and secondary cosmic rays. (W.D.M.)

35905 CONFINEMENT OF COSMIC RAYS. Daniel, H. R. (Tata Inst. of Fundamental Research, Bombay). pp 24-38 of Proceedings of the Eleventh Symposium on Cosmic Rays, Astrophysics, Geophysics and Elementary Particle Physics, 1969. Vol. I. Bombay; Department of Atomic Energy (1969).

From eleventh symposium on cosmic rays, astrophysics, geophysics and elementary particle physics; Delhi, India (7 Oct 1969). See CONF-691055-(Vol. 1).

In the past the galactic halo has been generally assumed as the confinement region of cosmic rays seen in the vicinity of the Earth. Recent observations, in particular the intensity of diffuse gamma rays of energy greater than 100 MeV, have clearly shown that cosmic rays are of galactic origin and confinement, and observations on the energy spectrum of electrons above 100 GeV strongly indicate that cosmic rays are confined to the galactic disk and have a residence time of 0.5 to 1×10^6 years. (W.D.M.)

35906 COSMIC-RAY PROPAGATION IN INTERPLANETARY SPACE: INVITED REVIEW. Rao, U. R. (Physical Research Lab., Ahmedabad, India). pp 39-52 of Proceedings of the Eleventh Symposium on Cosmic Rays, Astrophysics, Geophysics and Elementary Particle Physics, 1969. Vol. I. Bombay; Department of Atomic Energy (1969).

From eleventh symposium on cosmic rays, astrophysics, geophysics and elementary particle physics; Delhi, India (7 Oct 1969). See CONF-691055-(Vol. 1).

Some of the major results are presented on particle propagation and modulation in the interplanetary field that have been obtained from experiments on various spacecraft and also from ground-based instruments during the last two or three years. The interaction between the spiral field and the solar wind has a considerable effect on the propagation and modulation of cosmic particles in interplanetary space. The major effects on modulation of primary cosmic particles are dealt with and an attempt is made to infer the electromagnetic conditions of interplanetary space through the propagation characteristics of low-energy cosmic particles of solar origin. (W.D.M.)

35907 MODULATION OF GALACTIC COSMIC RAYS: REVIEW. Kane, R. P. (Physical Research Lab., Ahmedabad, India). pp 53-61 of Proceedings of the Eleventh Symposium on Cosmic Rays, Astrophysics, Geophysics and Elementary Particle Physics, 1969. Vol. I. Bombay; Department of Atomic Energy (1969).

From eleventh symposium on cosmic rays, astrophysics, geophysics and elementary particle physics; Delhi, India (7 Oct 1969). See CONF-691055-(Vol. 1).

An interplanetary space model is discussed and its effect on cosmic-ray intensity variations is considered in terms of the 11-year cycle, seasonal changes, 27-day recurrences, diurnal and semidiurnal changes, micropulsations, Forbush decreases, day-to-day changes, and sudden increases. (W.D.M.)

35908 TIFR BALLOON FACILITY. Daniel, R. R.; Gokhale, G. S.; Redkar, R. T. (Tata Inst. of Fundamental Research, Bombay). pp 289-95 of Proceedings of the Eleventh Symposium on Cosmic Rays, Astrophysics, Geophysics and Elementary Particle Physics, 1969. Vol. I. Bombay; Department of Atomic Energy (1969).

From eleventh symposium on cosmic rays, astrophysics, geophysics and elementary particle physics; Delhi, India (7 Oct 1969). See CONF-691055-(Vol. 1.).

Topics discussed include polyethylene film, balloon making, launching, recovery operations, flying season, balloon capacities, ground facilities, hydrogen requirements, and special launchings. (W.D.M.)

35909 RESEARCH ACTIVITY AT HIGH ALTIDUDE RESEARCH LABORATORY, GULMARG. Razdan, H. (High Altitude Research Lab., Gulmarg, India). pp 296-9 of Proceedings of the Eleventh Symposium on Cosmic Rays, Astrophysics, Geophysics and Elementary Particle Physics, 1969. Vol. I. Bombay; Department of Atomic Energy (1969).

From eleventh symposium on cosmic rays, astrophysics, geophysics and elementary particle physics; Delhi, India (7 Oct 1969). See CONF-691055-(Vol. 1).

Facilities at Gulmarg are listed along with experiments conducted during the past 3 to 4 years. (W.D.M.)

35910 CHARGE COMPOSITION OF COSMIC-RAY NUCLEI OF ELEMENTS FROM Ne TO Ni. Bhatia, V. S.; Biswas, S.; Chohan, V. S.; Kainth, P. S.; Pabbi, S. D. (Panjab Univ., Chandigarh, India). pp 300-3 of Proceedings of the Eleventh Symposium on Cosmic Rays, Astrophysics, Geophysics and Elementary Particle Physics, 1969. Vol. II. Bombay; Department of Atomic Energy (1969).

From eleventh symposium on cosmic rays, astrophysics, geophysics and elementary particle physics; Delhi, India (7 Oct 1969). See CONF-691055-(Vol. 2).

The results of an experiment are reported on the measured charge distribution of cosmic-ray nuclei from neon to nickel in the energy intervals at 250 to 1000 MeV/nucleon and >1000 MeV/nucleon. Two emulsion stacks, each consisting of 120 emulsions of three different sensitivities, were used. Use was made of Fowler-Perkin's parameter for measuring the primary ionization in the case of majority of tracks. The detector does not show saturation at high values of ionization. (J.C.W.)

35911 ULTRA-HEAVY NUCLEI IN COSMIC RAYS FROM METEORITE STUDIES. Rajan, R. S. (Tata Inst. of Fundamental Research, Bombay). pp 304-5 of Proceedings of the Eleventh Symposium on Cosmic Rays, Astrophysics, Geophysics and Elementary Particle Physics, 1969. Vol. II. Bombay; Department of Atomic Energy (1969).

From eleventh symposium on cosmic rays, astrophysics, geophysics and elementary particle physics; Delhi, India (7 Oct 1969). See CONF-691055-(Vol. 2).

The composition of ultra-heavy nuclei in cosmic radiation was investigated by using fossil-track measurements in meteorites. Attempts were made to study whether the tracks were fully etched on the long tracks. On tracks considered fully etched, it is concluded that tracks greater than 200 μ are genuinely scarce and that the longest track recorded is 495 μ. These results are in good agreement with plastics and emulsion measurements on contemporary cosmic rays. (J.C.W.)

35912 RELATIVE ABUNDANCE OF DEUTERONS IN COSMIC RAYS AND ITS ASTROPHYSICAL SIGNIFICANCE. Biswas, S.; Radhakrishnan, B.; Ramadurai, S. (Tata Inst. of Fundamental Research, Bombay). pp 307-10 of Proceedings of the Eleventh Symposium on Cosmic Rays, Astrophysics, Geophysics and Elementary Particle Physics, 1969. Vol. II. Bombay; Department of Atomic Energy (1969).

From eleventh symposium on cosmic rays, astrophysics, geophysics and elementary particle physics; Delhi, India (7 Oct 1969). See CONF-691055-(Vol. 2).

Deuteron-to-helium ratios in cosmic rays were calculated using a regular model. The H^2/He^4 ratio is expected to be independent of solar modulation, as the mass-to-charge ratio of these nuclei is the same, and hence, the ratio measured near the Earth would be the same as in local interstellar space. These data furnish information on the propagation of cosmic-ray hydrogen and helium nuclei in interstellar and interplanetary space. The deuteron-to-helium ratios were calculated as a function of path length for different energies and determine the amount of matter traversed by low-energy cosmic-ray nuclei. (J.C.W.)

35913 INTERPLANETARY DUST. Venkatavaradan, V. S. (Tata Inst. of Fundamental Research, Bombay). pp 320-6 of Proceedings of the Eleventh Symposium on Cosmic Rays, Astrophysics, Geophysics and Elementary Particle Physics, 1969. Vol. II. Bombay; Department of Atomic Energy (1969).

From eleventh symposium on cosmic rays, astrophysics, geophysics and elementary particle physics; Delhi, India (7 Oct 1969). See CONF-691055-(Vol. 2).

Interplanetary-space dust particles of the size of a few microns or less are very unstable in their orbit around the Sun. If the particles are too small, so that the radiation pressure overwhelms the gravitational attraction, the particles will be thrown out of the

solar system. If they are sufficiently large, they will spiral in towards the Sun and ultimately fall into the Sun. They may be captured by the Earth or other planets during their shrinkage if they intercept a planet's orbit. Cosmic rays induce radioactivities in meteorites and in the Earth's atmosphere. Variations are shown of the estimates of dust influx into the Earth. Concentrations of aluminum-26, manganese-53, and nickel-59 are given from recent analyses of ocean sediments. (J.C.W.)

35914 VARIATION OF LIMITING ENERGY OF COROTATING COSMIC RAYS WITH THE SOLAR CYCLE. Agrawal, S. P.; Rao, U. R. (Physical Research Lab., Ahmedabad, India). pp 332-8 of Proceedings of the Eleventh Symposium on Cosmic Rays, Astrophysics, Geophysics and Elementary Particle Physics, 1969. Vol. II. Bombay; Department of Atomic Energy (1969).

From eleventh symposium on cosmic rays, astrophysics, geophysics and elementary particle physics; Delhi, India (7 Oct 1969). See CONF-691055-(Vol. 2).

Diurnal variation is shown by cosmic radiation in the energy range 1 to 200 GeV. During the 1958-1968 solar cycle, the diurnal variation is constant, but the amplitude shows small variations that can be attributed to the change in the limiting energy of corotation. The amplitude change in 1965, a sunspot minimum year, is concluded to be due to the decrease in the scale size and number of the interplanetary-field irregularities that can cause an increase in the gradient of cosmic-ray density in the perpendicular plane that can cancel a part of the anisotropy. (J.C.W.)

35915 FORBUSH DECREASE IN VARIOUS MULTIPLICITIES IN GULMARG NEUTRON MONITOR. Bemalkhedkar, M. M. (Physical Research Lab., Ahmedabad, India). pp 339-41 of Proceedings of the Eleventh Symposium on Cosmic Rays, Astrophysics, Geophysics and Elementary Particle Physics, 1969. Vol. II. Bombay; Department of Atomic Energy (1969).

From eleventh symposium on cosmic rays, astrophysics, geophysics and elementary particle physics; Delhi, India (7 Oct 1969). See CONF-691055-(Vol. 2).

A neutron monitor responds mainly (90%) to secondary neutrons and protons in the atmosphere and the minor contributions come from muons captures and in flight, and pions and showers. Events of various multiplicities have been shown to be a function of the energy of the nucleon impinging on the monitor. Two Forbush decreases studied occurred on Oct. 29, 1968 and May 14, 1969. The regression coefficients indicate less depression in higher multiplicities for the October event. The May event showed a decrease of about 6%. (J.C.W.)

35916 ENERGY SPECTRUM OF N COMPONENT OF COSMIC RAYS AT SEA LEVEL FROM ION CHAMBER MEASUREMENTS. Ganguly, S. R. (Jadavpur Univ., Calcutta). pp 356-8 of Proceedings of the Eleventh Symposium on Cosmic Rays, Astrophysics, Geophysics and Elementary Particle Physics, 1969. Vol. II. Bombay; Department of Atomic Energy (1969).

From eleventh symposium on cosmic rays, astrophysics, geophysics and elementary particle physics; Delhi, India (7 Oct 1969). See CONF-691055-(Vol. 2).

Nuclear interactions producing bursts in an unshielded ion chamber are used to evaluate the energy spectrum of the N-component of cosmic rays at sea level. The integral size-frequency distribution of bursts, a comparison of burst and star data, and the differential energy spectrum of the N-component are shown. The intensity of the N-component is also deduced. (J.F.P.)

35917 PION PRODUCTION SPECTRUM AT 12°N GEOMAGNETIC LATITUDE. Bhattacharyya, D. P. (Presidency Coll., Calcutta). pp 359-62 of Proceedings of the Eleventh Symposium on Cosmic Rays, Astrophysics, Geophysics and Elementary Particle Physics, 1969. Vol. II. Bombay; Department of Atomic Energy (1969).

From eleventh symposium on cosmic rays, astrophysics, geophysics and elementary particle physics; Delhi, India (7 Oct 1969). See CONF-691055-(Vol. 2).

An experiment is described to measure the integral muon spectrum determined by a counter-controlled neon hodoscope in order to calculate the pion production spectrum near the geomagnetic equator ($\lambda = 12°N$) and to observe whether there is any significant dependence of the pion intensity on the geomagnetic latitude. Comparison of some other results shows a significant increase in the muon intensity with increase of geomagnetic latitude and it may be attributed to continuous decrease of the vertical cutoff rigidity of the primaries. (J.C.W.)

35918 DURGAPUR COSMIC-RAY SPECTROGRAM WITH TWO SOLID-IRON MAGNETS. Nandi, B. C.; Sinha, M. S. (Regional Engineering Coll., Durgapur, India). pp 363-8 of Proceedings of the Eleventh Symposium on Cosmic Rays, Astrophysics, Geophysics and Elementary Particle Physics, 1969. Vol. II. Bombay; Department of Atomic Energy (1969).

From eleventh symposium on cosmic rays, astrophysics, geophysics and elementary particle physics; Delhi, India (7 Oct 1969). See CONF-691055-(Vol. 2).

A vertical cosmic-ray spectrograph with two big solid-iron magnets was installed at Durgapur for the measurement of momentum spectrum and charge ratio of cosmic-ray muons at sea level and 12°N geomagnetic latitude. The spectrograph can be used for the measurement of momentum spectrum of muons in the region 3 GeV/c to 1000 GeV/c. (J.C.W.)

35919 MOMENTUM SPECTRUM AND THE CHARGE RATIO OF VERTICAL MUONS AT SEA LEVEL. Nandi, B. C.; Sinha, M. S. (Regional Engineering Coll., Durgapur, India). pp 369-72 of Proceedings of the Eleventh Symposium on Cosmic Rays, Astrophysics, Geophysics and Elementary Particle Physics, 1969. Vol. II. Bombay; Department of Atomic Energy (1969).

From eleventh symposium on cosmic rays, astrophysics, geophysics and elementary particle physics; Delhi, India (7 Oct 1969). See CONF-691055-(Vol. 2).

Preliminary results are presented of the momentum spectrum and charge ratio of vertical muons at sea level and 12°N geomagnetic latitude in the momentum range 3 to 834 GeV/c. (J.C.W.)

35920 HIGH-ENERGY COSMIC-RAY ELECTRONS. Anand, K. C.; Daniel, R. R.; Stephens, S. A. (Tata Inst. of Fundamental Research, Bombay). pp 374-9 of Proceedings of the Eleventh Symposium on Cosmic Rays, Astrophysics, Geophysics and Elementary Particle Physics, 1969. Vol. II. Bombay; Department of Atomic Energy (1969).

From eleventh symposium on cosmic rays, astrophysics, geophysics and elementary particle physics; Delhi, India (7 Oct 1969). See CONF-691055-(Vol. 2).

A description is given of the apparatus used to study the cosmic electron spectrum at 200 GeV and greater than 200 GeV. The detector was flown by balloon over Hyderabad, India on May 4, 1968. The present evidence suggests a steepening of the electron spectrum at about 200 GeV. A balloon flight was made with equipment aboard to study the charge composition of cosmic-ray electrons between 12 to 30 GeV using a vertical stack of pure nuclear emulsions. The flight was made above Hyderabad, India on Mar. 30, 1966. (J.C.W.)

35921 ENERGY SPECTRUM OF DIFFUSE COSMIC X RAYS IN THE ENERGY RANGE 20 TO 120 keV. Agrawal, P. C.; Biswas, S.; Gokhale, G. S.; (and others) (Tata Inst. of Fundamental Research, Bombay). pp 386-8 of Proceedings of the Eleventh Symposium on Cosmic Rays, Astrophysics, Geophysics and Elementary Particle Physics, 1969. Vol. II. Bombay; Department of Atomic Energy (1969).

From eleventh symposium on cosmic rays, astrophysics, geophysics and elementary particle physics; Delhi, India (7 Oct 1969). See CONF-691055-(Vol. 2).

Two balloon flights were made from Hyderabad, India on Apr. 28 and Dec. 22, 1968 to observe the diffuse background x rays in the energy range 20 to 120 keV. The diffuse background counts were obtained by subtracting the atmospheric background from the total number recorded. The data seem to indicate a break in the diffuse background x-ray spectrum around 60 to 80 keV. (J.C.W.)

35922 LOW-ENERGY GAMMA-RAY SPECTRUM IN SPACE. Anand, K. C.; Joseph, George; Lavakare, P. J. (Tata Inst. of Fundamental Research, Bombay). pp 397-9 of Proceedings of the Eleventh Symposium on Cosmic Rays, Astrophysics, Geophysics and Elementary Particle Physics, 1969. Vol. II. Bombay; Department of Atomic Energy (1969).

From eleventh symposium on cosmic rays, astrophysics, geophysics and elementary particle physics; Delhi, India (7 Oct 1969). See CONF-691055-(Vol. 2).

Low energy gamma-ray data are shown from balloon, satellite, and deep-space probe measurements in the energy region 0.1 to 10 MeV. Photon counts and flux measurements between 0.1 and 10 MeV energy interval have been made by using omnidirectional gamma-ray spectrometers with a charged-particle anticoincidence shield. Satellite and balloon data show that there exists a flattening of spectrum at ~1 MeV. Calculations were extended to generate a set of respond functions for the entire gamma-ray energy region of 0.2 to 10 MeV. (J.C.W.)

35923 GAMMA RADIATION FROM THE GALACTIC CENTER: FUTURE EXPERIMENTS. Anand, K. C.; Damle, S. V.; Daniel, R. R.; (and others) (Tata Inst. of Fundamental Research, Bombay). pp 400-4 of Proceedings of the Eleventh Symposium on

XUM

Cosmic Rays, Astrophysics, Geophysics and Elementary Particle Physics, 1969. Vol. II. Bombay; Department of Atomic Energy (1969).

From eleventh symposium on cosmic rays, astrophysics, geophysics and elementary particle physics; Delhi, India (7 Oct 1969). See CONF-691055-(Vol. 2).

Two balloon experiments are explained that are planned to look for the photon flux from the galactic center direction in the energy range 0.2 to 100 MeV. The region 0.2 to 4 MeV will be covered by an electronic detector system and the region 10 to 100 MeV will be explored by the nuclear-emulsion technique. The flights will be made from Hyderabad, India. (J.C.W.)

35924 ENERGY LOSSES AND MODULATION OF GALACTIC COSMIC RAYS. Gleeson, L. J. (Monash Univ., Clayton, Australia); Urch, I. H. Astrophys. Space Sci.; 11: No. 2, 288-308 (May 1971).

Numerical solutions of the cosmic-ray transport equation for the interplanetary region and including the effects of diffusion, convection, and energy loss, were obtained for a galactic differential number-density spectrum of Gaussian form, central kinetic energy T_0, and a width at half-height maximum of 0.1 T_0. These solutions were used to show the redistribution in energy, and the reduction in number density, within the solar cavity. The mean energy loss is shown to be usefully approximated by the force-field potential Φ when $\Phi/T_0 \leq \frac{1}{2}$. The principal finding was that galactic cosmic-ray protons and helium nuclei, with kinetic energies less than about 80 MeV/nucleon, are virtually completely excluded from near Earth by convective effects. As a result of this exclusion, it was found that it is not possible to demodulate the proton and helium-nuclei spectra, observed in 1964-65, to obtain information about low-energy galactic cosmic rays. (auth)

35925 COSMIC-RAY PROPAGATION IN THE ATMOSPHERE. O'Brien, K. (Atomic Energy Commission, New York, N. Y.). Nuovo Cim.; 3A: No. 3, 521-47(1 Jun 1971).

An essentially analytical theory of atmospheric cosmic-ray propagation is developed on the basis of a phenomenological model of hadron-nucleus collisions. This model correctly predicts the sea level cosmic-ray nucleon, pion, and muon spectra, the cosmic-ray ionization profile in the atmosphere, and neutron flux and density profiles in the atmosphere. It is concluded that the large-scale properties of atmospheric cosmic rays can be predicted accurately on the basis of a purely nucleonic cascade, as a result of which all secondaries are mediated by pion production. Implications for energy independence of cross sections, the recent 70-GeV results from Serpukhov, and nucleonic relaxation rates in the atmosphere are discussed. (auth)

Direct Energy Conversion

Refer also to abstract 37090.

35926 EFFECTS OF BOUNDARY LAYERS UPON CURRENT DISTRIBUTION AND INTERNAL RESISTANCE IN SEGMENTED MAGNETOHYDRODYNAMIC CHANNELS. Taylor, R. E.; Wu, C. L.; Denzel, D. L. (Univ. of Tennessee, Tullahoma). J. Appl. Phys.; 42: No. 7, 2689-2700(Jun 1971).

The effects of nonuniform properties of an equilibrium plasma in a segmented magnetohydrodynamic generator are investigated. The current distribution is distorted more for laminar flow than for turbulent flow. The shape of the current streamlines depends strongly on wall temperature, free stream Mach number, and boundary-layer thickness. For fine segmentation ratio ($s/h \approx 0.1$), the current densities are uniform at distances 10% of the channel height away from the walls. Since the two-dimensional effects are confined to this narrow region, the changes of the current distribution outside this region are due to changes in flow properties. The current distribution on the electrode is most sensitive to the electrode temperature. For hot walls, current shorting between adjacent electrodes is important and is significantly affected by the boundary-layer type and free-stream Mach number. Boundary layer thickness is of minor importance. Shorting decreases as the wall temperature decreases and eventually disappears when the walls are sufficiently cold. The internal resistance of the channel is within 70% of its uniform-property value for hot wall (2700°K) conditions for both laminar and turbulent flows. In the cold wall case (1500°K), the internal resistance increases about 3 times over its constant property value for turbulent flow but as high as 350 times for laminar flow. For cold-wall laminar flow, the internal resistance increases almost linearly with boundary layer thickness. The comparison with experiments is favorable. (auth)

35927 CHAR BURNING MHD SYSTEMS. Way, S. Combustion; 42: No. 11, 27-35(May 1971).

The levels of plant thermal efficiency that might be anticipated from three MHD systems (two burning char and oxygen, one burning char and air) are indicated, featuring reaction of the char and CO_2 leading to a CO-rich gas that would then be oxidized to give virtually ash-free working fluid. The plants analyzed also featured recirculation of combustion products, somewhat analogous to the semiclosed gas-turbine cycle. (auth)

35928 EXPERIMENTAL STUDY OF GAS HEATING EFFICIENCY IN SECTIONED PLASMA GENERATOR WITH CHANNEL ADJUSTMENT. Stel'makh, G. P.; Ryabtsev, E. I.; Chesnokov, N. A.; Kosarenkov, V. A. Inzh.-Fiz. Zh.; 20: No. 3, 522-6(Mar 1971). (In Russian).

The thermal efficiency of gas heating in a sectioned plasma generator was studied, considering especially the pressure in the channel created with the help of nozzle diaphragms. Relationships are obtained for calculation of the thermal efficiency of plasma generators of similar types. (auth)

35929 ZHIDKOMETALLICHESKIE INDUKTSIONNYE MGD-MASHINY. (Liquid-Metal MHD Induction Machines). Lielpeter, Ya. Ya. Riga; Izdatel'stvo Zinatne (1969). 247p.

The basic theory of three-phase induction machines with a liquid-metal working fluid is discussed, specifically magnetohydrodynamic (MHD) pumps and generators with fixed operating channels. The following problems are elucidated: basic designs of MHD machines, theory of ideal machines, the effect of higher spatial harmonics on typical equipment, longitudinal and transverse boundary effects, and MHD phenomena in a moving magnetic field. Energy conversion in MHD machines is discussed in the electrodynamic approximation, neglecting velocity distributions. MHD phenomena are examined with suitable adjustment to electrodynamic theory. The text is provided with data from actual working designs of induction pumps and generators. (216 references) (tr-auth)

35930 EFFECT OF ARGON ON THERMIONIC CONVERTER OPERATION AT LOW CESIUM PRESSURES. Kucherov, R. Ya.; Nevolin, V. K.; Tkeshelavshili, G. I.; Tsiberev, V. P. Sov. Phys.-Tech. Phys. (Engl. Transl.); 15: No. 11, 1937-9(May 1971).

Translated from Zh. Tekh. Fiz.; 40: No. 11, 2472-4(Nov 1970).

An experimental investigation of the effect of argon on a low-pressure cesium arc discharge is described. When the cesium atoms satisfy only the electron space-charge neutralization function and electron emission is facilitated by a low effective work function material, the addition of argon can improve the output characteristics. (auth)

35931 EFFECT OF PATCHINESS AND INCREASES IN CATHODE EMITTING AREA ON THERMIONIC CONVERTER CHARACTERISTICS. Baksht, F. G.; Korobova, I. L.; Moizhes, B. Ya. (Inst. of Semiconductors, Leningrad). Sov. Phys.-Tech. Phys. (Engl. Transl.); 15: No. 11, 1940-3(May 1971).

Translated from Zh. Tekh. Fiz.; 40: No. 11, 2474-8(Nov 1970).

Theoretical results are presented for the plasma state and the voltage-current characteristics of a thermionic converter with patchy and developed surface cathodes. (M.O.W.)

35932 PERFORMANCE OF A LARGE-SCALE, NONEQUILIBRIUM MHD GENERATOR WITH RARE GASES. Zauderer, B.; Tate, E. (General Electric Co., King of Prussia, Pa.). AIAA (Amer. Inst. Aeronaut. Astronaut.) J.; 9: No. 6, 1136-43(Jun 1971).

An experimental study was performed of the operating characteristics of a shock-tunnel driven, supersonic MHD generator. The following major results were obtained: (1) uniform preionization was required at the generator entrance to achieve appreciable generator power output; (2) the open-circuit, induced voltages were in good agreement with the theory; (3) the electrical characteristics and plasma properties of the loaded, Faraday generator were in agreement with the predictions of the one-dimensional electron conservation equations and Ohm's low if the conductivity was computed on the assumption that the plasma was homogeneously turbulent; (4) when the slope of the axial velocity and pressure gradients changed signs, a nonstationary shock wave formed in the generator leading to boundary-layer separation and eventual generator current cutoff; (5) the maximum generator power of 500 kW was equal to 7½% of the thermal power input; (6) the electrical performance of the present generator was similar to that measured in a generator having 2% of the volume of the present generator. It is concluded that electrode conduction losses and shock-wave formations were the two major factors limiting the efficiency of this generator. (auth)

35933 EFFECTS OF ELECTRODE SIZE ON THE PERFORMANCE OF A COMBUSTION-DRIVEN MHD GENERATOR. Rubin,

E. S.; Eustis, R. H. (Stanford Univ., Calif.). AIAA (Amer. Inst. Aeronaut. Astronaut.) J.; 9: No. 6, 1162-9(Jun 1971).

Electrode sizes with length-to-pitch ratios of 0.23, 0.50, and 0.79 were tested in a generator section simulated by three molybdenum electrode pairs located at the downstream end of an MHD channel. Voltage probe data were obtained for electrode surface temperatures between 500 and 1600°K, with gas conductivity in the electrode boundary-layer regions established independently by either a hot (2200°K MgO brick) or cold (750°K water-cooled plate) upstream wall. At a given load current, larger electrodes were found to have lower voltage losses for similar conditions of surface and gas boundary-layer temperatures. For dissimilar boundary layers, reflecting coupling between electrode and boundary-layer temperatures in a cold-electrode generator, total voltage losses for a large electrode pair were equal to or greater than those of a small electrode pair at the same surface temperature. Experimental boundary-layer resistances at anodes were in good agreement with analytical predictions, based on both an approximate and more exact gasdynamic model, for electrode temperatures above about 800°K. At lower temperatures, anodes were believed to be influenced by solidification of seed compounds on the electrode surfaces, resulting in higher losses. For cathodes, the boundary-layer resistance was gasdynamic for the case of a hot upstream wall for electrode current densities below that of saturated thermionic emission at the electrode temperature. In all other cases, the presence of cathode surface-sheath effects was indicated. (auth)

35934 PROSPECTS AND ECONOMY OF LIQUID-METAL MHD–STEAM BINARY POWER PLANTS. Prem, L. L.; Parkins, W. E. (Atomics International, Canoga Park, Calif.). Combustion: 42: No. 3, 29-38(Sep 1970).

The status of the technology of liquid-metal MHD is described with emphasis on potential future application as a topping cycle for central station plants. The choice of metal working fluid, the various MHD cycles previously investigated, possible nuclear reactor or fossil-fueled furnace designs to serve as heat source, the electrical generator design, and candidate materials of construction are all discussed. A proposed large liquid metal MHD–steam binary plant is then described, together with estimates of its capital and operating costs. The economics are compared with those of a modern conventional coal-fueled central station plant. (auth)

35935 ELECTRICAL EFFECTS IN THE INSULATING-WALL BOUNDARY LAYER IN FARADAY-TYPE MHD GENERATOR. Celinski, Zdzislaw N. (Inst. of Nuclear Research, Swierk, Poland). Nukleonika; 15: 613-21(1970).

Some interesting physical phenomena occur in the gas in the Faraday-type MHD generator when the gas parameters vary in the direction of the magnetic field. They will concentrate first of all in the wall boundary layers where the largest gradients of the gas velocity and gas temperature are attained. The distributions of the electrical quantities in the wall boundary layers are calculated, and some physical effects occurring there are discussed. (auth)

35936 POST IRRADIATION EXAMINATION OF A THERMIONIC CONVERTER. Enderlein, H. (Gesellschaft fuer Kernforschung, Karlsruhe, Ger.); Zoeller, R. Kerntech. Atomprax.; 13: 24-9(Jan 1971). (In German and English).

Within the scope of the ITR project (incore Thermionic Reactor), the Central Research Laboratory of Brown, Boveri, & Cie AG is conducting irradiation tests for the development of thermionic fuel rods. A thermionic converter was irradiated for 3750 h in the reactor FR 2 of the Nuclear Research Center, Karlsruhe. The performance of the fuel and of the structural materials was investigated in hot cells. The investigation methods used and the results obtained are reported. (auth)

35937 THERMIONIC REACTOR ION PROPULSION SPACECRAFT FOR UNMANNED OUTER PLANET EXPLORATION. Mondt, J. F.; Davis, J. P. (Jet Propulsion Lab., Pasadena, Calif.). J. Spacecraft Rockets; 8: 295-7(Mar 1971).

The external-fuel thermionic reactor concept provides the potential for developing a useful 70-lb/kw$_e$, 70-kw$_e$ electric propulsion system. The side-thrust propulsion system isolates the science payload from the high-temperature, the nuclear-radiation, and the mercury-exhaust environments. A spacecraft arrangement using side-thrust propulsion allows a 4π steradian field of view during the entire mission. The Titan III-D/Centaur launch vehicle, being developed for other unmanned missions, has the capability to launch the 70-kw$_e$ spacecraft to Earth escape. (auth)

Fluid Physics

Refer also to abstract 36103.

35938 (UCRL-51010) CALCULATION TECHNIQUES FOR ESTIMATING THE PRESSURE LOSSES FOR CONDUCTING FLUID FLOWS IN MAGNETIC FIELDS. Hoffman, M. A.; Carlson, G. A. (California Univ., Livermore. Lawrence Radiation Lab.). 4 Feb 1971. Contract W-7405-eng-48. 40p. Dep. NTIS.

Simple analytical relations are proposed for rapid estimation of the various ordinary and magnetic pressure drops for conducting fluid flows in magnetic fields. The relations are based on various theoretical and experimental investigations. Effects considered include magnetic suppression of turbulence and electrical eddy currents induced in the fluid due to spatial variations of either the fluid velocity or the magnetic field strength. The relations are used to estimate the upper bound on the pressure drops of lithium flow in a hypothetical fusion reactor blanket. The results indicate that the pressure drops are very sensitive to the choice of path which the pipes follow through the magnetic field region. In particular, the pressure drops can span a range of values over six orders of magnitude from <0.1 to >100,000 psi, depending on the path and pipe wall conductance. Based on these results, it appears that the pressure drop in a Li blanket can be made acceptably small, but only through careful design. (auth)

35939 ELECTROHYDRODYNAMIC STABILITY OF A THIN LIQUID LAYER IN UNIFORM SHEARING MOTION INDUCED BY A TRAVELING ELECTRIC POTENTIAL-WAVE. Kim, Moonuhn; Lee, Chung-oh; Kim, Chul-soo (Seoul National Univ.). J. Phys. Soc. Jap.; 30: No. 6, 1744-56(Jun 1971).

Pumping of a slightly conducting thin liquid layer by means of a traveling electric-potential wave and the electrohydrodynamic stability problem for the flow, which has a linear velocity profile, and is bounded by a fixed wall and an infinitely extended insulating liquid are dealt with experimentally and theoretically. It is shown that the induction pumping is successful in getting the film Reynolds number of the order of a few hundreds and that the limitation on the uniform flow results from flow instability. The stability problem is solved asymptotically for large values of the Reynolds number. The neutral stability curves are presented in an α vs R plane; the critical Reynolds number and its corresponding wave number are found. The comparison of the theory with experimental data on the interface velocity of laminar flow, the voltage corresponding to the critical Reynolds number, and the most unstable wavelength of the disturbance is proved to be satisfactory. (auth)

35940 LAMINAR UNSTEADY MAGNETOHYDRODYNAMIC FLOW IN A POROUS ANNULAR CHANNEL UNDER A RADIAL MAGNETIC FIELD. Singh, G. S. J. Sci. Eng. Res. (India); 13: No. 1, 182-9(Jan 1969).

Gupta and Mital [App. Mech. Rev., 19(1966), Rev. 5873] discussed the unsteady magnetohydrodynamic flow in an annular channel under a radial magnetic field. Their problem is extended here by taking the annulus as porous. The effect of suction or injection either on the velocity field or on the magnetic field is not discussed. The suction parameter does not appear in the boundary conditions or in the solution. (App. Mech. Rev.)

35941 STATIONARY PROBLEM OF CYLINDRICAL MAGNETOACOUSTIC WAVE SCATTERING BY AN IDEAL CONDUCTING CYLINDER. Selezov, I. T.; Krivonos, Yu. G. (Inst. of Cybernetics, Kiev). Dopov. Akad. Nauk Ukr. RSR, Ser. A; No. 2, 169-73(Feb 1971). (In Ukrainian).

The problem of a wave scattering in a medium of finite electric conductivity is solved. A magnetic Reynolds number $\ll 1$ and nonperturbated magnetic pressure $P_H \gg 1$ are assumed. The medium is described by magnetohydrodynamic equations in the linear acoustic approximation. The asymptotic solutions are obtained for far fields in a long-wave approximation. The influence of electromagnetic effects is investigated. (auth)

35942 OPTIMIZATION OF ENERGY EXCHANGES BETWEEN AN UNIDIRECTIONAL MAGNETIC FIELD AND A THIN CONDUCTING LAYER WITH FINITE DIMENSIONS. Kant, Michel (Univ. Paris, Fontenay-aux-Roses, France). Compt. Rend., Ser. B; 272: No. 14, 821-4(5 Apr 1971). (In French).

The idea of the complex efficiency of the electromechanical conversion is introduced using the Poynting theorem. The expression for the efficiency includes two terms, the energy term and the magnetic term. A method for optimizing the energy efficiency term in relation to the distribution of an electromotive field variation is presented. (France)

35943 STUDY OF THE LAMINAR FLOW OF AN INCOMPRESSIBLE CONDUCTING FLUID IN A SLIGHTLY DIVERGENT MAGNETOHYDRODYNAMIC CHANNEL. Kant, Michel; Robert, Jack; Bonnefille, Robert (Univ. Paris, Fontenay-aux-Roses, France). Compt. Rend., Ser. A; 272: No. 13, 915-18(29 Mar 1971). (In French).

XUM

A method for calculating the velocity profile of a conducting fluid moving in a slightly divergent channel in a magnetic field of arbitrary frequency, is proposed. (France)

35944 PROPAGATION AND GROWTH OF WEAK DISCONTINUITIES IN MAGNETOGASDYNAMICS IN THE PRESENCE OF DISSIPATIVE MECHANISMS. Mishra, R. S.; Babu, Ram (Banaras Hindu Univ., India). Indian J. Pure Appl. Math.; 1: 506-11(Oct 1970).

Based on the theory of singular surfaces Thomas (1957) proved that moving a weak discontinuity in gasdynamics, if compressive, must terminate into a shock. Using the compatibility conditions, Nariboli and Secrest (1967) studied the corresponding problem of magnetogasdynamics. Here, the propagation and growth of weak discontinuities in the presence of finite electrical and thermal conductivity were studied. The critical time was also calculated when the weak discontinuity generates the shock wave. The theory of rays (Luneberg 1964) was used frequently for calculations. (auth)

35945 GENERALIZED MHD COUETTE FLOW WITH HEAT TRANSFER BETWEEN CONDUCTING WALLS. Soundalgekar, V. M.; Dhavale, A. T. (Indian Inst. of Tech., Bombay). Indian J. Pure Appl. Math.; 1: 608-24(Oct 1970).

The fully developed generalized MHD Couette flow in a transverse magnetic field between two finitely electrically conducting plates was studied. Closed-form solutions for the velocity and temperature field are obtained. It is observed that the separation at the stationary plate may be avoided by choosing the upper plate of large electrical conductance ratio compared to that of the lower plate. In the case of walls of equal electrical conductance ratios, at large M, there occurs a transition from laminar to turbulent flow. For finite value of ϕ_u, ϕ_l the viscous drag, mass flow rate, the force to move the upper plate are not affected by the pressure-induced flow superimposed on the simple shear flow when M is large (greater than 6). (auth)

35946 HYDROMAGNETIC STABILITY OF A NONUNIFORMLY ROTATING FLUID. Brahme, A. (Kungliga Tekniska Hoegskolan, Stockholm). Phys. Scr.; 2: 108-12(1970).

The stability of nonuniformly rotating mercury was studied experimentally in the presence of an axial magnetic field. A cylindrically symmetric flow of mercury was driven by a volume force originating from the magnetic field and radial currents in the fluid. Concentric electrodes at the bottom of the mercury container made it possible to vary the current distribution and thus to produce different types of velocity profiles in the fluid. The electric field induced in the rotating mercury was used to measure the fluid velocity. The results of the experiments can be explained by a criterion for stability being deduced by approximate methods. It is a modification of a criterion given by Chandrasekhar for a dissipative Couette flow. (auth) (Sweden)

35947 MAGNETOHYDRODYNAMIC LAMINAR FLOW BETWEEN POROUS DISKS. Chandrasekhara, B. C.; Rudraiah, N. (Balgalore Univ., India). Appl. Sci. Res. (The Hague); 23: No. 1/2, 42-52(Oct 1970).

The steady two-dimensional laminar flow of an incompressible conducting fluid between two parallel circular disks in the presence of a transverse magnetic field is investigated. A solution is obtained by perturbing the creeping flow solution, and it is valid only for small suction or injection Reynolds numbers. Expressions for velocity, induced magnetic field, pressure, and shear stress distribution are determined and are compared with the creeping flow and hydrodynamic solutions. It is found that the overall effect of the magnetic field on the flow is the same as that in the Hartmann flow. (auth)

35948 MAGNETOHYDRODYNAMIC COUETTE FLOW WITH TRANSPIRATION COOLING. Tan, C. W. (Cooper Union for Advancement of Science and Art, New York). Appl. Sci. Res. (The Hague); 23: 167-84(Dec 1970).

Transpiration cooling with magnetohydrodynamic effects is studied in a porous-wall Couette flow of a steadily moving, incompressible, electrically conducting fluid. The flow, induced by the motion of the moving wall, is subject to a uniform transverse magnetic field. A coolant fluid, with the same properties as the main-stream fluid, is uniformly injected into (or extracted from) the flow through a porous stationary wall. Solutions are presented for the velocity and induced magnetic field distributions across the parallel walls, the pressure difference induced by the magnetic drag, and the friction factor in such a flow configuration. Considerations are further given to the heat-transfer characteristics, wherein viscous and Ohmic heating are significant. In this connection, the recovery factor and the Nusselt number are also presented over a wide range of blowing and suction rates. (auth)

35949 HYDROMAGNETIC FLUCTUATING FLOW PAST AN INFINITE POROUS PLATE IN SLIP FLOW REGIME. Soundalgekar, V. M. (Indian Inst. of Tech., Bombay). Appl. Sci. Res. (The Hague; 23: 301-14(Dec 1970).

The effect of a uniform external magnetic field on the laminar, incompressible rarefied gas flow along an infinite porous flat plate is studied under the following conditions: (1) there is uniform suction, (2) the external flow velocity varies periodically with time in magnitude but not in direction, (3) the magnetic Reynolds number is small, and (4) the current occurs under slip-flow boundary conditions. Expressions for the velocity and temperature fields in the boundary layer are obtained. The response of skin friction and heat transfer to the fluctuating stream is studied for variations in the rarefaction parameter h_1, the magnetic field parameter M, and the frequency of the fluctuating stream. (auth)

35950 RAYLEIGH PROBLEM IN SLIP FLOW WITH TRANSVERSE MAGNETIC FIELD. Nath, G. (Indian Inst. of Science, Bangalore). Appl. Sci. Res. (The Hague); 23: 315-23(Dec 1970).

An analytical continuum solution of the Rayleigh problem in slip flow with applied magnetic field is obtained, using a modified initial condition and slip boundary conditions. The results are uniformly valid for all times, and show that the velocity slip and the local skin friction coefficient remain almost unaffected by the imposition of the magnetic field for short times. They increase, however, with the magnetic field for large times. The present results reduce to the corresponding results of the hydrodynamic case when there is no magnetic field. (auth)

35951 QUADRATIC ARTIFICIAL VISCOSITY IN NUMERICAL MAGNETIC GAS DYNAMICS. Lutzky, M. (Naval Ordnance Lab., White Oak, Md.). J. Comput. Phys.; 7: 172-7(Feb 1971).

A form of artificial viscosity, which is quadratic in the velocity gradient, has been used extensively in numerical gas dynamics since its introduction by von Neumann and Richtmeyer. Its chief virtue is that it produces a shock transition whose width is constant (in Lagrangian coordinates) and independent of both the shock strength and the initial state of the medium. To what extent these desirable properties are preserved when a quadratic viscosity is used for magnetogasdynamic shock problems is investigated. The case of a plane shock in an initially uniform, infinitely conducting fluid is considered, together with an initially uniform magnetic field aligned perpendicularly to the shock velocity. The treatment of von Neumann and Richtmeyer is followed, and the structure of the steady-state shock is analyzed by looking for running-wave solutions of the Lagrangian equations of motion. (M.H.R.)

Geophysics (Upper Atmosphere)

Refer also to abstracts 35772, 35892, 35893, 35915, 35917–35920, and 36367.

35952 (NBS-TN-326) AN ATLAS OF SOLAR FLARE EFFECTS IN THE IONOSPHERE OBSERVED WITH A HIGH-FREQUENCY DOPPLER TECHNIQUE, SEPTEMBER 1960–DECEMBER 1962. Baker, Donald M. (Institute for Telecommunication Sciences and Aeronomy, Boulder, Colo.). 1 Dec 1965. 116p. GPO $0.60.

Records of selected solar flare effects (sudden frequency deviations) in the ionosphere detected by a high frequency Doppler technique from September 1960 through December 1962 are presented. When available, records of short wave fadeouts (SWF) are also given. (auth)

35953 KINETIC APPROACH TO SELF MODULATION OF AN AMPLITUDE-MODULATED WAVE IN MAGNETOPLASMAS. Sodha, M. S.; Sawhney, R. L. (Indian Inst. of Tech., New Delhi). Radio Sci.; 6: No. 5, 593-601(May 1971).

A rigorous theory for the self-modulation of an amplitude-modulated electromagnetic wave propagating along the direction of the magnetic field is developed; the effects of self-interaction and mutual interaction for both extraordinary and ordinary modes of propagation are considered simultaneously. It is shown that the ordinary mode of propagation becomes demodulated and that the extraordinary mode shows strong over-modulation during its propagation through the medium, when the carrier frequency equals the electron gyrofrequency. (auth)

35954 RESPONSE OF THE MAGNETOSPHERE TO SUNSPOTS AS INDICATED BY GEOMAGNETIC STORMINESS LEVELS. Chernosky, Edwin J. (Air Force Cambridge Research Labs., Bedford, Mass.). Radio Sci.; 6: No. 5, 579-82(May 1971).

The rather well-defined level of geomagnetic activity that occurs with developing sunspots was examined by using 38 years of daily geomagnetic Ap activity indices and sunspot number Rz. It is found that the Ap values between about 70 and 160 are characteristically associated with sunspots that develop rapidly and reach a peak in number about three days before the occurrence of these levels of Ap. The daily Kp sums from about 45 to 55 were found earlier to be similarly associated with Rz. This relationship predominates at this Ap level during the years in which the average annual Rz is above 50 or more. In quieter solar years some of this range of Ap values tend to be part of a broad recurrence tendency for Rz that peaks about a week before this level of geomagnetic activity is attained; this pattern is a characteristic of a lower level of geomagnetic disturbance. The rapidly developing spots with their high association with solar flares apparently contribute to the magnetospheric energy budget through enhanced electromagnetic radiation. The broad recurrence tendency of a lesser disturbance that peaks six to eight days earlier would probably be predominantly due to the Chapman–Ferraro compression of the magnetosphere by corpuscular emission from the solar M regions of Bartels. (auth)

35955 CHARACTERISTIC SIGNATURES OF THE MIDLATITUDE IONOSPHERE OBSERVED WITH A NARROW-BEAM HF BACKSCATTER SOUNDER. Hunsucker, Robert D. (Inst. for Telecommunication Sciences, Boulder, Colo.). Radio Sci.; 6: No. 5, 535-48(May 1971).

Over 18,000 frames of data acquired with a narrow-beam azimuth and elevation-scan high-frequency backscatter sounder located at Boulder, Colorado, during the period October 1964 through June 1968 were examined and classified. Analysis of these data revealed that the irregular structure of the midlatitude ionosphere is the rule rather than the exception. Irregularities of varying scale size and apparent motion were present in about 90% of the observations made during almost one-half a sunspot cycle. The signatures observed by this hf radar system were categorized into eight generic types that have been labeled with names roughly describing their appearance on the range-azimuth scan record. The relative diurnal and seasonal occurrences, as well as the qualitative sunspot cycle and geomagnetic correlation of these signatures, are presented. (auth)

35956 SIMULTANEOUS STORM-TIME INCREASES OF THE IONOSPHERIC TOTAL ELECTRON CONTENT AND THE GEOMAGNETIC FIELD IN THE DUSK SECTOR. Papagiannis, M. D. (Boston Univ.); Mendillo, M.; Klobuchar, J. A. Planet. Space Sci.; 19: No. 5, 503-11(May 1971).

Using the Faraday-rotation technique with the ATS-3 satellite, it was possible to monitor changes in the total electron content (N_T) of the midlatitude ionosphere during the first day of 20 geomagnetic storms. The analysis showed that, during the positive phase ($\Delta N_T > 0$) of ionospheric storms, the absolute magnitude of the increase in N_T exhibits a very pronounced maximum near sunset. The mean value of ΔN_T at 17:00 LT is more than five times the average ΔN_T value at local noon. This effect is basically independent of the storm-commencement time and is usually associated with substantial local enhancements of the total geomagnetic field. The N_T enhancements are discussed in terms of a contraction and draining of the plasmasphere. A model is presented in which the dawn–dusk electric field responsible for the magnetospheric convection slows down the corotational motion of the plasmaspheric ionization in the dusk sector. This braking action causes a pile up of the plasma and the magnetic field along the entire dusk sector. (auth) (UK)

35957 CONJUGATE AND CLOSELY SPACED OBSERVATIONS OF AURORAL RADIO ABSORPTION. V. ALTERNATION OF AURORAL PARTICLE PRECIPITATION BETWEEN HEMISPHERES. Hargreaves, J. K. (Univ. of Lancaster, Eng.). Planet. Space Sci.; 19: No. 5, 513-19(May 1971).

Short-term differences of auroral radio absorption in conjugate regions are investigated by means of specific absorption events observed with spaced riometer systems at Great Whale River and Byrd. It is demonstrated that some of the observed conjugate differences cannot be explained by displacement of the conjugate point, and probably arise from an inter-hemispheric difference of particle precipitation in which the flux of auroral particles is enhanced alternately in the northern and southern hemispheres. The phenomenon occurs mainly in the night sector, and the alternation periods are tens of minutes to an hour or two. The observations may be indicative of the behavior of magnetospheric electric fields aligned parallel to the geomagnetic field. (auth) (UK)

35958 ZONES OF CORPUSCULAR PRECIPITATIONS AND STRUCTURE OF THE MAGNETOSPHERE. Pudovkin, M. I.; Barsukov, V. M. (Leningrad State Univ.). Planet. Space Sci.; 19: No. 5, 525-31(May 1971).

The configuration of geomagnetic-field lines in the magnetotail is considered. It is suggested that disappearance of the polar-cap aurorae during a storm is associated with disruption of the field lines in the neutral sheet. (auth) (UK)

35959 STORM-TIME VARIATIONS IN THE HIGH-LATITUDE FLUXES OF LOW-ENERGY ELECTRONS INFERRED FROM O I (λ 6300 A) OBSERVATIONS. Stromman, J. R. (Norwegian Defense Research Establishment, Kjeller); Maehlum, B. N.; Oleson, J. K. Planet. Space Sci.; 19: No. 5, 540-3(May 1971).

In order to investigate the time variations in the red emission inside the polar cavity, two sets of two-channel photometers were installed at Ny Aalesund, Svalbard (invariant latitude $\Lambda = 75°$) and at Thule (Qanaq) Greenland ($\Lambda = 85°$). The instruments that are essentially identical to the tilt-filter photometer presented by Eather and Reasoner (1969) were in operation from November 1969 to March 1970, measuring continuously during the dark hours the luminosities of the atomic oxygen line $\lambda = 6300$ Å and the molecular nitrogen band $\lambda = 4278$ Å in the zenith. Some results pertaining to the geomagnetic control of the red emission are presented that have bearing on the time variations in the zone of low-energy electron precipitation. (auth) (UK)

35960 ION AND NEUTRAL COMPOSITION CHANGES IN THE THERMOSPHERIC REGION DURING MAGNETIC STORMS. Chandra, S. (Goddard Space Flight Center, Greenbelt, Md.); Stubbe, P. Planet. Space Sci.; 19: No. 5, 491-502(May 1971).

The structural differences of the ion and neutral composition in the thermospheric region are studied by solving a system of basic ionospheric and atmospheric equations. The study shows that the compositional changes during a magnetic storm arise largely as a result of changes in the neutral composition at the turbopause. A decrease in $[O]/[N_2]$ in the lower atmosphere triggers a complex chain of events that results in an increase of the neutral gas temperature, depletion of the O^+ layer and enhancement of NO^+. The relative changes in these layers occasionally produce a sequence of electron-density profiles, giving rise to the so-called G condition. It is shown that, compared to the neutral atmosphere, the ionosphere is much more sensitive to the changes in $[O]/[N_2]$ in the lower thermospheric region. Since the ionospheric parameters can be measured much more accurately than the atmospheric parameters, it is argued that they should form an integral part of the observational data required to construct the atmospheric models. (auth) (UK)

35961 RESULTS FROM A MERIDIAN CHAIN OF OBSERVATORIES IN THE ALASKAN SECTOR. I. Akasofu, S.-I.; Wilson, C. R.; Snyder, L.; Perreault, P. D. (Univ. of Alaska, College). Planet. Space Sci.; 19: No. 5, 477-82(May 1971).

Some new results of auroral morphology obtained from a meridian chain of observatories through Central Alaska are presented. Magnetic records from the chain of stations also confirmed an intense westward jet when a positive change of the H-component occurs at an auroral zone station in the afternoon sector. (auth) (UK)

35962 SIGNATURE PROFILES OF O(^{1}S) IN THE AIRGLOW. Hernandez, G. (Environmental Science Services Administration, Boulder, Colo.). Planet. Space Sci.; 19: No. 5, 467-76 (May 1971).

The spectral-line shapes, or signature profiles, of O(^{1}S) proceeding from the dissociative recombination of $O_2^+(^2\pi_g)$ in the upper atmosphere were optically observed in the nightglow at the geomagnetic equator with a Fabry–Perot spectrometer. The results indicate that the recombination leading to O(^{1}S), O(^{3}P) and 2.79 eV excess energy is favored relative to that leading to O(^{1}S), O(^{1}D) and 0.83 eV excess energy by at least a factor of 5 to 1. Partial thermalization of the profile was observed, indicating energy exchange with the medium. From this, a relaxation time of about 3 sec or a collision cross section of about 6×10^{-16} cm^2 can be derived, depending on the mechanism invoked for thermalization. (auth) (UK)

35963 ROCKET MEASUREMENTS OF LOW-ENERGY AURORAL ELECTRON SPECTRA. Rearwin, Stephen Dearborn. San Diego, Calif.; Univ. of California (1970). 90p. University Microfilms Order No. 71-8989.

Thesis.

A Nike–Tomahawk flown from Fort Churchill into a widespread, diffuse (~2 kR at 3914 Å), stable aurora detected highly thermal (kT ~ 3.2 keV) electron fluxes from 1 to 30 keV at 60 to 120° pitch angles. Peak fluxes were ~10^7 el/cm^2 sec sr keV. The total electron flux in this energy range was very nearly a linearly decreasing function of pitch angle; the temperature was roughly

XUM

constant for $\alpha < 90°$ and decreased steadily with increasing pitch angle for $\alpha \geq 90°$. Analysis of 230 seconds of data from altitudes above 200 km revealed no coherent time variations with periods $3 \text{ sec} \leq \tau \leq 100$ sec. It is suggested that the electrons measured in this experiment had been convected toward the Earth from the magnetospheric tail region. (Diss. Abstr. Int., B)

35964 ORIGIN OF LONG-PERIOD MICROPULSATIONS IN THE GEOMAGNETIC FIELD. Luke, Stacy Wenzel. Provo, Utah; Brigham Young Univ. (1970). 137p. University Microfilms Order No. 71-8859.

Thesis.

The possible interplanetary origin of 2- to 8-min micropulsations in the Earth's magnetic field is explored. Power spectra obtained from Mariners II, IV and V magnetic data are compared with micropulsations observed on the Earth at College, Alaska; Reykjavik, Iceland; and Sodankyla, Finland. An approximate one-to-one correspondence is found between the periods of micropulsations in the Earth's magnetic field and the periods of oscillations in the interplanetary magnetic field. A dispersion equation is derived to show that these periodic oscillations in the interplanetary magnetic field could be transverse waves propagating along field lines. Damping lengths of 10^{11} meters to over 10^{39} meters are obtained. It is suggested from the evidence of the study that waves in the interplanetary medium interact with the geomagnetic field generating micropulsations of approximately the same period. (Diss. Abstr. Int., B)

35965 TELEVISION IMAGING OF FAST AURORAL WAVES. Scourfield, M. W. J.; Parsons, N. R. (Univ. of Calgary, Alberta). Planet. Space Sci.; 19: No. 5, 437-42(May 1971).

Fast auroral waves were recorded with an image intensifier–TV system, and a new characteristic of this phenomenon was revealed, namely, an abrupt transition from wave motion equatorwards to an E to W motion associated with an auroral band. For equatorward motion, speeds ranged from 15 to 150 km/sec, which is significantly lower than values previously reported. For the E to W motion, speeds ranged from 20 to 90 km/sec. (auth) (UK)

35966 ELECTRON ECHO EXPERIMENT: A NEW MAGNETOSPHERIC PROBE. Hendrickson, R. A.; McEntire, R. W.; Winckler, J. R. (Univ. of Minnesota, Minneapolis). Nature (London); 230: 564-6(30 Apr 1971).

A controlled method of investigating the trapping of particles in the Earth's magnetosphere is described. Instruments in the separated nose cone of a rocket were used to detect electromagnetic radiation from electrons injected into the magnetosphere from the rocket and magnetically reflected. (auth) (UK)

35967 CONTROLLED EXPERIMENT ON WAVE–PARTICLE INTERACTIONS IN THE IONOSPHERE. Cartwright, D. G.; Kellogg, P. J. (Univ. of Minnesota, Minneapolis). Nature (London) Phys. Sci.; 231: 11-12(3 May 1971).

A comparison experiment to the electron echo experiment described (Nature, 230: 564(1971)) was designed with a view to studying the electric component of waves generated by the electron beam, and a preliminary report on the observations is presented. A high-sensitivity experiment was necessary, as calculations indicated that the radiation from the beam would be weak. The experiments were launched on an Aerobee 150 sounding rocket at the NASA Wallops Island firing range on Aug. 13, 1970, and were mounted in the fibreglass nose cone, which was ejected from the electron accelerator payload at 140 km. An antenna consisting of two stainless steel bands was riveted to the outside of the nose cone, and two receivers covered the frequency range 16 Hz to 10 MHz. The nose cone was separated from the accelerator payload 95 sec after launch and 15 sec later the gun commenced to emit electron pulses of energy 35 to 45 keV and beam current about 70 mA. The spectrum of emissions detected at the nose cone over the frequency range 0 to 10 MHz is shown and its features are discussed; the most striking feature is the double-humped profile of the high-frequency radiation between 5 and 7 MHz. The obvious explanation for the plasma-frequency radiation is that the beam electrons generate Cherenkov-like emission into wave modes with low phase velocity, and a similar explanation is offered for the observed whistler radiation. Many of the details are puzzling and remain to be explained, but it was found that the beam did not lose a significant part of its energy to instabilities or to wave emissions; also, the energy radiated by the beam was easily detected by receivers within about 500 m, and the waves radiated were those with phase velocities low enough to interact strongly with the beam. (UK)

35968 PROPOSED ANNUAL AND SUNSPOT CYCLE VARIATION OF THE PLASMASPHERE OF THE EARTH. Oksman, J. (Max-Planck-Inst. fuer Aeronomie, Lindau/Harz, Ger.). Nature (London) Phys. Sci.; 231: 12-13(3 May 1971).

The plasmasphere surrounding the Earth is known to have a noncircular equatorial cross section with an outward bulge in the evening sector, causing a local-time variation in the observed distance to the plasmapause. The plasmasphere is also known to respond to geomagnetic disturbances of solar origin, contracting with increasing geomagnetic activity and expanding with decreasing geomagnetic activity. Little is known, however, about its longer-term variations. The present communication discusses the possibility of annual and sunspot-cycle variations. Long-term changes in whistler paths might be used as indicators of movements of the plasmapause, as might also observed long-term changes of the periods of micropulsations of the geomagnetic field; some previous studies in these fields are discussed, and criticisms are offered on conclusions reached. It is suggested that the observed mean movement of whistler paths and most of the observed variation of the mean periods of Pc4 pulsations can be explained by assuming a mean annual and sunspot-cycle secular variation in the size of the plasmasphere, which appears to be largest during the December solstice and during high solar activity, and it can be estimated that the yearly variation of the equatorial radius of the plasmasphere may be as large as one Earth radius. It may be safely assumed that the secular variation is smaller than the annual variation. It is thought that the possible annual variation in size of the plasmasphere may be linked with the changing tilt angle of the geomagnetic axis to the ecliptic plane. If this is so, it may help in solving the puzzling problems concerning annual variations of some geophysical quantities, such as the annual anomaly of the F2 layer, the E layer, and the neutral gas temperature. The changing tilt angle of the geomagnetic axis might modulate particle precipitation from the magnetosphere, causing corresponding electron-density and temperature variations in the ionosphere; through the coupling between the lower ionosphere and the protonosphere, the electron density of the plasmasphere would vary accordingly. (UK)

35969 REAPPEARANCE OF A MULTIPLE MIDLATITUDE AURORAL ARC (6300A). Old, T.; Okuda, M.; Kim, J. S. (State Univ. of New York, Albany). Nature (London) Phys. Sci.; 231: 14-15(3 May 1971).

During the 1957–58 solar activity maximum, monochromatic midlatitude auroral arcs of 6300 Å (0 I) were seen for about 20% of the observation time; these arcs were, however, chiefly single, multiple arcs occurring infrequently. During the present maximum solar-activity year no multiple arcs had been reported. The present authors, however, observed reappearance of the multiple-arc system on the night of March 8–9, 1970, during the recovery phase of a geomagnetic storm. The 6300 Å arcs and a visible aurora to the far north were observed simultaneously from two stations, at Whiteface Mountain, New York, and the Leander McCormick Observatory, Virginia. The instruments employed were two identical multicolor meridian-scanning photometers with narrow-band interference filters centered on 5577, 6300, 5300 and 6100 Å lines. The multiple arcs comprised two relatively stable 6300 Å arcs, with the occasional appearance of a third unstable 6300 Å arc. The arcs were of very low intensity, but there was a sharp temporary enhancement accompanied by an isolated geomagnetic bay-like disturbance during the recovery phase of the geomagnetic storm. A temporary but pronounced northward movement of the arcs was observed during the bay-like disturbance. Strong correlations were found between the variation in position and intensity of the arcs and changes in the H and D components of the concurrent magnetic bay-like disturbance. The intensities of the arcs decreased throughout the night, with some fluctuation. The variations in position and intensity are shown tabulated with the recorded variation of the geomagnetic field. (UK)

35970 EQUATORIAL IONOSPHERIC ABSORPTION AT DIFFERENT LONGITUDES. Mbipom, E. W. (Ahmadu Bello Univ., Zaria, Nigeria). Nature (London) Phys. Sci.; 231: 15-16(3 May 1971).

Some ionospheric absorption measurements by the pulse-reflection technique at vertical incidence made at Ibadan and Colombo using frequencies of 2.0 to 7.5 MHz are described. These two locations have almost the same geographical latitude and magnetic dip, but differ in longitude by about 76°. The effect of the difference in longitude is discussed; good agreement was found between results for the two stations, and the difference in longitude did not seem to affect the form of the diurnal variation, a result expected. Plots are shown of the diurnal variation of absorption with local time and virtual height of the reflecting layer, monthly median values of noon absorption, and variation of absorption with sunspot number. There was clearly a semi-annual variation with equinoctial peaks and solstitial minima. Data obtained during the rising phase of the solar cycle (1966–68) showed an increase in absorption with increasing solar activity. (UK)

35971 TWILIGHT FLASH OF SODIUM. Peterson, Alan W.; Kieffaber, Lois M. (Univ. of New Mexico, Albuquerque). Sky Telesc.; 41: No. 6, 344-5(Jun 1971).

The mechanism responsible for generating the twilight flash of sodium is described. An absorption-line spectrum is presented and the grating spectrograph is discussed briefly. (W.D.M.)

35972 VLF WAVE AMPLIFICATION BY WAVE–PARTICLE INTERACTION. Singh, R. N.; Singh, R. P. (Banaras Hindu Univ., India). Phys. Lett.; 35A: No. 2, 105-6(17 May 1971).

A charged-particle beam is assumed to move through the magnetosphere. It is shown that the vlf waves propagating at nonzero angles with the beam are amplified. (auth)

35973 INFLUENCE OF SOLAR FLARES ON THE TROPOSPHERIC CIRCULATION. Statistical Indications, Tentative Explanation, and Related Anomalies of Weather and Climate in Western Europe. Schuurmans, C. J. E. Mededelingen en Verhandelingen, No. 92. The Hague; Staatsdrukkerij (1969). 122p. f. 19,00. (NP–18733).

The relation between the eruptions on the Sun and the circulation in the upper air was investigated. Solar activity as a cause of long-term weather anomalies was studied. The statistical study is based upon a sample of 81 flares, occurring during July 1957 to Dec. 1959, IGY–IGC. The investigation concerns the response to solar flares of contour heights of several constant-pressure levels between the ground and the 50-mbar level. For one level (500 mbar) the investigation covers the whole northern hemisphere north of 10°N and the southern hemisphere south of 20°S; results are given and analyzed. A physical theory is presented that makes it possible to give a quantitative explanation of the influence of solar flares on the tropospheric circulation. An estimate is given of the importance of the tropospheric flare effect on the weather and climate in Western Europe. (J.C.W.)

35974 POSSIBLE CORRELATION BETWEEN ATMOSPHERIC OZONE CONTENT AND COSMIC-RAY INTENSITY VARIATIONS. Alexander, Saramma; Chatterjee, S. D. (Jadavpur Univ., Calcutta). J. Atmos. Terrest. Phys.; 33: 831-3(May 1971).

A comparative study of the diurnal cosmic-ray meson intensity variations at Calcutta and the concomitant variations of the atmospheric ozone content at a neighboring station indicated a correlation between the two events. This is more evident on magnetically undisturbed days. (auth) (UK)

35975 RELATION BETWEEN SUDDEN COMMENCEMENT AMPLITUDE AND INITIAL PHASE DURATION OF GEOMAGNETIC STORMS. Ranganayaki, P. R. (National Geophysical Research Inst., Hyderabad, India). J. Atmos. Terrest. Phys.; 33: 835-9(May 1971).

Dependence of the initial phase duration of geomagnetic storms on the sudden commencement amplitude is investigated with the help of 45 well-developed storms recorded at Hyderabad during 1966–68. It is found that there is an inverse relationship between the two, namely storms with large sudden commencement amplitudes have small initial phase durations, and vice versa. Considering the initial phase duration as the time required for the formation of the ring current after the impact of the enhanced solar wind on the magnetosphere, the above observation seems to be in accord with the theory of viscous interaction between the solar wind and the Earth's magnetosphere as the source of input energy during magnetic storms as developed by Axford and Hines (1961). (auth) (UK)

35976 EFFECT OF ENERGY SPECTRA ON SYNCHROTRON RADIATION FROM THE MAGNETOSPHERE. Singh, R. P.; Misra, K. D.; Singh, R. N. (Banaras Hindu Univ., India). J. Atmos. Terrest. Phys.; 33: 825-30(May 1971).

The effect of the power spectrum of energetic electrons on the synchrotron radiation was studied. The synchrotron power for four different energy spectra of radiating electrons was calculated. The radiated synchrotron power is found to change with the energy spectrum of the radiating electrons. The calculated synchrotron power is compared with available experimental results. It is concluded that the measured synchrotron power is capable of giving the nature of the energy spectra of radiating electrons. (auth) (UK)

35977 PHASE-HEIGHT FLUCTUATIONS IN THE IONOSPHERE BETWEEN 130 AND 250 km. Tolstoy, I. (Florida State Univ., Tallahassee); Montes, H. J. Atmos. Terrest. Phys.; 33: 775-81(May 1971).

Power spectra of c–w phase-path sounders operating at 6.0, 4.8, and 2.4 MHz often display peak or slope changes at periods in the 5- to 20-min range. Plots of these periods vs real height tend to follow mean Väisälä frequency curves calculated from Standard Atmosphere models. This suggests that statistical properties of c–w phase-path sounder fluctuation can be used to monitor certain mean physical parameters of the upper atmosphere. (auth) (UK)

35978 REFLECTION OF RADIO WAVES FROM IONOSPHERIC IRREGULARITIES AT VERTICAL INCIDENCE. Hibberd, F. H. (Max-Planck-Institut fuer Aeronomie, Lindau/Harz, Ger.). J. Atmos. Terrest. Phys.; 33: 783-95(May 1971).

When a radio wave is reflected at vertical incidence from a horizontally stratified ionosphere that contains random irregularities of electron density, the downcoming wave consists of a cone of rays apparently scattered back to the receiving point by the irregularities. It is suggested here that the oblique rays are partially or totally reflected in the backwards direction from irregularities situated at or near the apex of the ray trajectories. The width of the angular spectrum of the downcoming wave is determined by the intensity $\Delta N/N$ of the irregularities; $\Delta N/N$ is deduced to be of the order of 0.01. The rays received at the ground appear to come from a virtual diffracting screen located at the virtual height of reflection. When field-aligned irregularities are present, reflection occurs where the rays are perpendicular to the elongation. This restricts the angular spectrum in the meridian plane and produces a north–south elongation of the ground pattern with an axial ratio r = cosec I, where I is the magnetic dip. An explanation is given of why a ground pattern produced by transmission is more elongated than one produced by reflection. (auth) (UK)

35979 IMPORTANCE OF DIFFUSION PROCESSES IN INTERACTION BETWEEN NEUTRAL WAVES AND IONIZATION. Testud, J.; Francois, P. (Centre National d'Etudes des Telecommunications, Issy-les-Moulineaux, France). J. Atmos. Terrest. Phys.; 33: 765-74(May 1971).

A study was made of how a gravity wave can perturb the ionization in the F2-layer. In particular, the perturbed state of the ion velocity and electron density are calculated when the diffusion processes are taken into account. The importance of these processes is pointed out. Results are compared with experimental data provided by the French incoherent scatter facility. (auth) (UK)

35980 ELECTRIC CURRENTS AND POLARIZATION FIELDS AT THE BASE OF THE MAGNETOSPHERE. Wagner, C.-U. (Central Inst. for Solar-Terrestrial Physics, Berlin). J. Atmos. Terrest. Phys.; 33: 751-64(May 1971).

A series of Ba-ion cloud measurements and simultaneous ground-based measurements of the variation of the geomagnetic field were investigated in detail. For undisturbed conditions these investigations lead to the conclusion that the main part of the electric polarization field at the base of the magnetosphere can be explained by the atmospheric dynamo theory, i.e., it is of ionospheric origin. Even at auroral-zone latitudes, at most a small fraction of the field vector is due to processes acting in the magnetosphere and in the tail. For disturbed conditions the investigations prove that, even during small bay disturbances, a considerable part of the currents flowing in the ionosphere is due to polarization fields transferred from the magnetosphere. (auth) (UK)

35981 FORMATION OF FIELD-ALIGNED IRREGULARITIES IN THE MAGNETOSPHERE. Cole, K. D. (La Trobe Univ., Bundoora, Australia). J. Atmos. Terrest. Phys.; 33: 741-50(May 1971).

The general physics of field-aligned irregularities in the magnetosphere is studied. A specific mechanism is then proposed for formation of irregularities. It involves a spatially varying electrostatic field orthogonal to B and operates in conjunction with irregularities of conductivity in the E region, and field-aligned currents caused by mismatch of conjugate ionopheric potentials. The mechanism functions most easily at night and in equatorial regions. An application to the formation of spread F is discussed. (auth) (UK)

35982 MORPHOLOGY OF AURORAL ELECTRON ENERGETIC AND ANGULAR DISTRIBUTIONS ACCORDING TO COSMOS 261 MEASUREMENTS. Fedorova, N. I.; Temny, V. V.; Galperin, Yu. I. (Inst. of Space Research, Moscow). J. Atmos. Terrest. Phys.; 33: 731-40(May 1971).

For tangential passes of northern and southern auroral zones average characteristics of diffuse background electron precipitations for the energy range 1 to 150 keV and more were obtained. Pitch-angle distribution and spectral characteristics of this background remained constant for the satellites trajectories up to 5000 to 6000 km. The pitch-angle electron distributions for eight

XUM

energy intervals, spectral characteristics over auroral zones and in polar caps, and diurnal variations of auroral electron distribution intensity as a function of geomagnetic activity were obtained. (auth) (UK)

35983 PHASE-HEIGHT MEASUREMENTS OF THE E REGION. Schrader, D. H.; Hower, G. L. (Washington State Univ., Pullman). J. Atmos. Terrest. Phys.; 33: 723-9(May 1971).

A phase-path sounder with spaced receivers and not requiring ultrastable oscillators is described. Measurements of the morning variation in the E-layer height using this equipment are reported. From these measurements made in March 1968, a scale height of about 7 km is calculated. (auth) (UK)

35984 CONCENTRATION AND TRANSPORT OF MINOR CONSTITUENTS IN THE MESOSPHERE AND LOWER THERMOSPHERE (70 TO 110 km) DURING PERIODS OF ANOMALOUS ABSORPTION. Manson, A. H. (Univ. of Saskatchewan, Saskatoon). J. Atmos. Terrest. Phys.; 33: 715-21(May 1971).

The concentrations of minor constituents required to produce the winter anomaly of midlatitude radio-wave absorption are evaluated. Between 85 and 100 km, increases above presently measured values are by a factor of 30 to 150 for nitric oxide or $\sim 10^3$ for metastable oxygen ($O_2(^1\Delta_g)$). Nitric oxide transported from the auroral zone has been suggested as a possible source of minor constituent; such a process would require ratios of $n(NO)/n(O_2) > 0.1$ near 115 km. The January 1963 stratospheric warmings and associated ionospheric and thermospheric (90 to 100 km) changes are consistent with this hypothesis. (auth) (UK)

35985 SOME ASPECTS OF IONOSPHERIC DRIFTS USING PARTIAL AND TOTAL REFLECTIONS FROM THE LOWER IONOSPHERE. Golley, M. G.; Rossiter, D. E. (Univ. of Adelaide). J. Atmos. Terrest. Phys.; 33: 701-14(May 1971).

Two different aspects of ionospheric drifts are discussed. The effect of the receiver triangle size on the drift parameters derived from full correlation analysis is investigated when partial reflections from altitudes near 90 km are used. It is found that, for frequencies near 2 MHz, the scale of the diffraction pattern on the ground is of the order of 100 m and drift parameters show little dependence on triangle size for aerial separations greater than 100 m. In addition, a number of drift records obtained using both partial and total reflections were analyzed by a dispersion method in order to look for any systematic variation of the drift velocity with fading frequency. It is shown that dispersion is present in only a minority of records but that it occurs more frequently for the partial reflection examples than for records of totally reflected waves from the E region. (auth) (UK)

35986 NUMERICAL COMPUTATION OF THE IONIZATION REDISTRIBUTION EFFECT OF THE WIND IN THE NIGHTTIME IONOSPHERE. Fujitaka, K. (Tokyo Univ.); Ogawa, T.; Tohmatsu, T. J. Atmos. Terrest. Phys.; 33: 687-700(May 1971).

The effect on the ionization redistribution in the nighttime ionosphere of the neutral atmospheric wind was studied quantitatively by using the sound-rocket data of the electron density by L. G. Smith (1966, 1970), and of the neutral wind by Constantinides and Bedinger (1971). The hydrogen and helium ultraviolet emissions from the geocorona and the interplanetary space were considered as the source of the ionization in the nighttime ionosphere between 90- and 220-km levels. The general behavior of the so-called intermediate layer — its generation mechanism and motion — were analyzed in terms of the convergence effect of the ionization due to the vertical shear of the horizontal neutral wind. The structures of the multiple sporadic-E layers between the altitudes of 90 and 110 km are discussed in connection with the history of the wind structure in the observed night. (auth) (UK)

35987 MEASUREMENT OF SOLAR PROTON ANISOTROPIES. Balogh, A. (Imperial Coll. of Science and Tech., London). Planet. Space Sci.; 19: No. 5, 533-6(May 1971).

The results show that four-quadrant measurements of solar-proton anisotropy can be misleading when the intensity distribution contains third and higher harmonics of significant amplitude. They also show that, during the period of equilibrium anisotropy during the February 25, 1969 event, the measured amplitude and phase agree very well with that expected on the basis of solar-wind convection as treated by Forman (1970). (UK)

35988 SEREBRISTYE OBLAKA. (Noctilucent Clouds). Bronshten, V. A.; Grishin, N. I. Moscow; Izdatel'stvo Nauka Glavnaya Redaktsiya Fiziko-Matematicheskoi Literatury (1970). 360p.

The first chapter gives a brief review of the discovery of noctilucent clouds and the research carried out by various international organizations. Propagation range and frequency of appearance of noctilucent clouds are described in the second chapter. The morphology, dynamics, and luminescence of the clouds are discussed in the third and fourth chapters. The properties and composition of the clouds and their relation to solar and ionospheric phenomena are covered in the fifth chapter. The sixth and last chapter reviews the presence of noctilucent clouds on other planets. A supplementary table of i_1, i_2 scattering functions is included. 589 references. (R.V.J.)

35989 DAS MODELL DES SYMMETRISCHEN ATMOSPHAERISCHEN DYNAMOS UND SEINE ANWENDUNG ZUR BESTIMMUNG DER LEITFAEHIGKEIT DES IONOSPHAERENPLASMAS AUS DEN GEOMAGNETISCHEN Sq-VARIATIONEN. (Model of the Symmetrical Atmospheric Dynamo and Its Application to the Determination of the Conductivity of the Ionospheric Plasma from the Geomagnetic Sq Variations). Wagner, Christian-Ulrich. Deutsche Akademie der Wissenschaften zu Berlin, Geomagnetisches Institut Potsdam, Abhandlung Nr. 37. Berlin; Akademie-Verlag (1968). 155p.

The efficiency of the symmetrical atmospheric dynamo model was developed to explain quiet-day geomagnetic variations. An attempt is made, using the dynamo theory and geomagnetic measurements, to determine the physical parameters of the ionospheric plasma, particularly the electrical conductivity and its temporal variations. It is found that the model described is a good approximation. Improvement in the theory of the symmetrical atmospheric dynamo could lead to substantial improvement over present models of Sq variations. (Meteorol. Geoastrophys. Abstr.)

35990 MORPHOLOGY OF THE GEOMAGNETIC FIELD VARIATIONS AND A STUDY OF THE INTERPLANETARY MAGNETIC FIELD FLUCTUATIONS IN RELATION TO THE DAILY VARIATION OF THE GEOMAGNETIC FIELD AT LOW LATITUDES. Sarabhai, V.; Nair, K. N. (Physical Research Lab., Ahmedabad, India). Cosmic Electrodyn.; 2: No. 1, 3-21(Apr 1971).

It is suggested that ΔH, the daily variation of the horizontal component of H at a low latitude station outside the influence of the equatorial electrojet is caused by (1) the dynamo current, mainly at the ionospheric E region, (2) the surface currents at the magnetopause, and (3) the tail currents, the eccentric ring current, and the partial ring current in the magnetosphere. Analysis of data from Honolulu and Guam confirms the contention that ΔH is largely due to a reduction of the field on the night side, suggesting a major contribution from magnetospheric currents. The study of the variability of H at different hours related to day-to-day changes of the daily variation, confirms the view that there are two independent processes contributing to ΔH even during quiet days and that the variance, due to both the factors, is larger during years of high solar activity than when the Sun is quiet. From the study of the observed interplanetary magnetic field parameters from satellites IMP-1, IMP-3, and Explorer-33, it is shown that σB_z, the fluctuation of the north–south component of the interplanetary magnetic field is linearly correlated with ΔH. The relationship between the two remains relatively unaltered during the solar cycle from 1963–64 (IMP-1) through 1965 (IMP-3) to 1967–68 (Explorer-33). In the light of the experimental evidence, it is shown that the time dependent azimuthal electric field in the magnetosphere and the azimuthal asymmetry of the outer magnetosphere play a very important part in populating the inner shells of the magnetosphere. These enhance the eccentric and the partial ring currents, and the tail currents, lowering H during night time and contributing to an increase in ΔH. 66% of the variance of $(\Delta H)^2$ can be attributed to changes in KE density and $(\sigma B_z)^2$ of the interplanetary plasma. This leaves 34% of the variance of $(\Delta H)^2$ attributable to other causes such as ionospheric currents. The experimentally observed shift of the time of minimum of H, from dawn hours during quiet days to dusk hours during disturbed days, is explained as a consequence of the drift motion of charged particles injected from the tail of the distorted magnetosphere in the presence of a corotational electric field and geomagnetic field gradients. (auth)

35991 FLUX CONTENT AND FORM OF THE GEOMAGNETIC TAIL. Sonett, C. P. (Ames Research Center, Moffett Field, Calif.); Mihalov, J. D.; Klozenberg, J. P. Cosmic Electrodyn.; 2: No. 1, 22-33(Apr 1971).

A model for the longitudinal magnetic field gradient of the distant geomagnetic tail is derived, using pressure balance between tail field and plasma and the solar-wind field and plasma pressure. It is shown that, for negligible internal plasma pressure, the tail field gradient is integrable in closed form and is represented by a power law with index $-\frac{2}{3}$. The more general equation, including all pressure effects, is numerically integrated to obtain the tail field gradient; the results are compared to experimental

data and are shown to yield estimates of tail field gradient compatible with reasonable estimates of the expected solar-wind plasma properties. Lastly, these estimates are related to the total flux in the tail and changes in flux content and its connection with the latitude of the auroral oval. (auth)

35992 MODEL OF TRANSVERSE STRUCTURE OF THE GEOMAGNETIC TAIL AND THE RECONNECTION PROCESS. Hruska, A. (High Altitude Observatory, Boulder, Colo.). Cosmic Electrodyn.; 2: No. 1, 34-43(Apr 1971).

A magnetodynamic description of the structure of the undisturbed magnetotail is formulated using recent results on the variation of the tail magnetic field, B, in a plane perpendicular to the x-axis of the solar magnetospheric coordinates. The lines of constant B, drawn in a plane perpendicular to the x-axis, are streamlines for any systematic plasma motion that can exist in the model of magnetotail in which the magnetic lines of force are straight lines parallel to the axis x. No reconnection of the field lines can occur in this idealized magnetotail. A slow steady-state reconnection does not seem to be excluded in the actual magnetotail where the field lines deviate from straight lines. Rapid reconnection can take place only if the structure of the magnetotail changes with time. (auth)

35993 NEW APPROACH TO THE THEORY OF THE MAGNETOSPHERE. Alfven, H.; Faelthammar, C.-G. (Royal Inst. of Tech., Stockholm). Cosmic Electrodyn.; 2: No. 1, 78-88(Apr 1971).

The solar-wind–magnetosphere interaction, usually discussed in hydrodynamic terms, is reconsidered from the point of view of electric fields and currents. A simple model of the transfer of solar-wind energy to the magnetosphere is presented. The case of magnetic-field reversal at the magnetopause is discussed in terms of an idealized current-sheet model. The energy release by magnetopause and magnetotail currents depends on magnetic topology. Southward interplanetary magnetic fields favor release of energy that may drive geomagnetic activity. (auth)

35994 ADIABATIC FLOW MODEL OF A NEUTRAL SHEET. Cowley, S. W. H. (Imperial Coll. of Science and Tech., London). Cosmic Electrodyn.; 2: No. 1, 90-104(Apr 1971).

A self-consistent model of a noiseless magnetic neutral sheet of finite width is given. Particles flow adiabatically into the thin reversal region under the action of electric fields, become trapped about the neutral plane, and then are accelerated along it by the electric field. These particles provide the current of the reversal region, but it is shown that their charge density may also be important, leading to an inhomogeneous electric field and possible breakdown of the adiabatic flow approximation outside the sheet. (auth)

35995 RING CURRENT AS THE SOURCE REGION FOR PROTON AURORAS. Eather, R. H. (Boston Coll., Chestnut Hill, Mass. Lockheed Palo Alto Research Labs., Palo Alto, Calif.); Carovillano, R. L. Cosmic Electrodyn.; 2: No. 1, 105-32(Apr 1971).

A phenomenological approach suggests the ring current as a likely source region for proton auroras. A review of wave–particle interactions suggests pitch-angle diffusion driven by ion-cyclotron resonance as the most likely loss mechanism. Lifetimes for energetic protons to diffuse to the loss cone are calculated for a model magnetosphere and for an experimentally measured power spectral density of hydromagnetic waves. These lifetimes are much shorter than charge-exchange lifetimes. The energy loss during the diffusion process is calculated, and the resulting precipitated spectrum is in good agreement with experiment. Calculated Hβ intensities in the resulting proton aurora also agree with ground measurements. It is proposed that the ion-cyclotron waves are self-generated through the ring-current region, but magnetospheric particle distributions are not defined completely enough to allow a confident calculation of the precise region where wave growth can occur (at a rate to balance wave losses). The calculated lifetimes are consistent with experimental observations of asymmetric ring currents at higher L values (quiet time), and symmetric ring currents at lower L (latter phases of magnetic storms). An investigation of azimuthal drifts and proton-aurora morphology suggests the injection region should be in the evening–midnight sector. It is proposed that charge-exchange decay cannot explain many features of the recovery phase of magnetic storms, and the loss rate of ring-current protons is much faster so that the recovery phase of storms would reflect a diminishing source function. The increased energy association with storms may lead to easier particle access to "closed" field lines by enhanced merging. (auth)

35996 EFFECT OF ELECTRON ANISOTROPY ON WHISTLERS LEADING STRONG COLLISION-FREE SHOCKS. Schindler, Karl; Rogister, Andre (ESRIN, Frascati, Italy. Cosmic Electrodyn.; 2: No. 1, 133-8(Apr 1971).

Using the linear Vlasov theory, it is shown that whistlers propagating obliquely to the magnetic field in a homogeneous plasma are unstable if the electron thermal anisotropy is sufficiently large in either direction. Some implications of this effect for whistlers leading strong collision-free shock waves are discussed. (auth)

35997 SPACE RESEARCH IN INDIA. Chitnis, E. V. (Physical Research Lab., Ahmedabad, India). pp 277-88 of Proceedings of the Eleventh Symposium on Cosmic Rays, Astrophysics, Geophysics and Elementary Particle Physics, 1969. Vol. I. Bombay; Department of Atomic Energy (1969).

From eleventh symposium on cosmic rays, astrophysics, geophysics and elementary particle physics; Delhi, India (7 Oct 1969). See CONF-691055–(Vol. 1).

The various space research programs and facilities throughout India are briefly discussed. (W.D.M.)

35998 ATMOSPHERIC NEUTRONS AND THE VAN ALLEN RADIATION BELT. Daniel, R. R.; Gokhale, G. S.; Joseph, George; Lavakare, P. J. (Tata Inst. of Fundamental Research, Bombay). pp 313-15 of Proceedings of the Eleventh Symposium on Cosmic Rays, Astrophysics, Geophysics and Elementary Particle Physics, 1969. Vol. II. Bombay; Department of Atomic Energy (1969).

From eleventh symposium on cosmic rays, astrophysics, geophysics and elementary particle physics; Delhi, India (7 Oct 1969). See CONF-691055–(Vol. 2).

An experiment to measure energetic neutron flux in the high atmosphere near the geomagnetic equator is described. The neutron-induced reactions give rise to slow protons and alpha particles as a result of inelastic collisions, and gamma rays give rise to fast electrons through electromagnetic processes. A pulse-shape discrimination technique distinguishes the particle events. The neutron flux in the energy region of 10 to 500 MeV was measured at various depths in the atmosphere during a high-altitude balloon flight. The calculated flux does not explain the CRAND process for the origin of the radiation-belt proton flux, and the Cosmic-ray Albedo Neutron Decay Theory is not adequate. (J.C.W.)

35999 GENERATION OF BREMSSTRAHLUNG X RAYS IN THE LOWER IONOSPHERE. Prasad, R. Y.; Singh, R. N. (Banaras Hindu Univ., India). pp 389-93 of Proceedings of the Eleventh Symposium on Cosmic Rays, Astrophysics, Geophysics and Elementary Particle Physics, 1969. Vol. II. Bombay; Department of Atomic Energy (1969).

From eleventh symposium on cosmic rays, astrophysics, geophysics and elementary particle physics; Delhi, India (7 Oct 1969). See CONF-691055–(Vol. 2).

X-ray spectra were calculated from electron–atom and electron–ion collisions in the lower ionosphere. The height profile of x-ray flux was calculated for 30 to 140 km. The total x-ray flux generated by electron–ion collisions is found to increase with increasing heights, and the total x-ray flux due to electron–atom collisions is found to decrease with increasing heights. Calculations show that the observed x-ray intensity in the auroral zone is mostly generated by bremsstrahlung processes. (J.C.W.)

36000 ATMOSPHERIC GAMMA-RAY SPECTRUM UP TO 6 GM CM^{-2} OVER 7.6°N GEOMAGNETIC LATITUDE. Kasturirangan, K. (Physical Research Lab., Ahmedabad, India). pp 405-7 of Proceedings of the Eleventh Symposium on Cosmic Rays, Astrophysics, Geophysics and Elementary Particle Physics, 1969. Vol. II. Bombay; Department of Atomic Energy (1969).

From eleventh symposium on cosmic rays, astrophysics, geophysics and elementary particle physics; Delhi, India (7 Oct 1969). See CONF-691055–(Vol. 2).

The measurements on the atmospheric gamma-ray spectrum between 135 and 1125 keV over Hyderabad, India at equatorial latitudes were reported. The fluxes of gamma rays measured for the continuous background were consistently lower than the corresponding values for high latitudes. At 6 g cm^{-2}, and in the 300 keV region, an intensity of $2 \pm .23$ photons cm^{-2} sec^{-1} MeV^{-1} was measured, whereas over Minneapolis, measurements yield 6 photons cm^{-2} sec^{-1} MeV^{-1}. (J.C.W.)

36001 SYNCHROTRON RADIATION FROM ELECTRONS OF VARIOUS ENERGY SPECTRA. Singh, R. P.; Misra, K. D.; Singh, R. N. (Banaras Hindu Univ., India). pp 414-17 of Proceedings of the Eleventh Symposium on Cosmic Rays, Astrophysics, Geophysics and Elementary Particle Physics, 1969. Vol. II. Bombay; Department of Atomic Energy (1969).

From eleventh symposium on cosmic rays, astrophysics, geo-

XUM

physics and elementary particle physics; Delhi, India (7 Oct 1969). See CONF-691055-(Vol. 2).

The effects of four different forms of energy spectra for electrons in the ionosphere and magnetosphere on the theoretical calculation of total radiated power by the synchrotron process have been studied. The electromagnetic waves in the rf range have been detected on the ground and at high altitudes by rockets and satellites. It is proposed that these waves are generated by the process of synchrotron radiation from electrons trapped in the Van Allen belt. The theoretical and experimental results can be compared if total synchrotron radiated power is calculated from all the electrons taking part in the radiation process. It has been shown that the synchrotron noise is directly proportional to the electron influx and magnetic field. (J.C.W.)

36002 ENERGY DEPENDENCE OF THE EQUATORIAL PITCH ANGLE DISTRIBUTION OF TRAPPED PROTONS Watari, Nobuo; Kamiyama, Hiroshi (Tohoku Univ., Sendai). Rep. Ionosphere Space Res. Jap.: 24: No. 2, 127-34(Jun 1970).

The energy dependence of the equatorial pitch-angle distribution for protons trapped in the radiation belt is discussed on the basis of the adiabatic theory. When an exponential form is assumed for the energy spectrum at the source, even if the 1-folding energy is constant regardless of the pitch angle, a conclusion is reached from the theory that the inward transport of particles due to the violation of the third adiabatic invariant results in the energy dependence of the equatorial pitch-angle distribution. From the comparison of the theoretical results with the observations, a suggestion is given that the equatorial pitch-angle distribution at the source is approximated by $\sin^{1.5}\alpha$. When the source energy spectrum is assumed to be given by a power-law form, the pitch-angle distribution is shown to be independent of the energy. The observational facts indicate that the proton energy spectrum in the outer radiation zone is expressed by an exponential form rather than a power law. (auth) (Japan)

36003 IRREGULARITIES IN THE QUIET IONOSPHERE AND THEIR EFFECT ON PROPAGATION. Fialer, Philip Anthony. Stanford, Calif.; Stanford Univ. (1970). 140p. University Microfilms Order No. 71-2758.

Thesis.

A class of large, weak ionospheric irregularities in certain circumstances significantly affects long-distance hf radio-wave propagation. The relative practical importance of the diffraction produced by these inhomogeneities, in relation to their influence of other mechanisms such as Faraday rotation and scattering by small irregularities is determined. Measurements of quasi-periodic variations in phase-path length were made on a 2600-km one-hop lower-ray F-region path. Variations of 8 to 75 wavelengths were regularly observed during winter daylight hours. They have a pseudo-period of about 20 minutes. Correlations of measurements made at spaced-receiver locations indicate that these variations in phase-path length are produced by irregularities having a horizontal scale size of about 35 km. Multiple-frequency measurements show a vertical scale size of about 15 km, with a maximum in the lower F region. A lower limit of 65 m/sec is determined for the horizontal velocity of the irregularities. A downward vertical velocity of 30 to 40 m/sec is observed. The irregularities limit achievable bandwidth and spatial resolution for one-hop hf ionospherically propagated waves under quiet ionospheric conditions. A model of the irregularities was used to predict the signal-strength fluctuations that would result from propagation through a medium described by the model. Two classes of signal-strength behavior are predicted and observed experimentally, depending on the relative magnitude of the phase-path variations within the limits mentioned. (TSS) (Diss. Abstr. Int., B)

36004 IRREGULAR GEOMAGNETIC MICROPULSATIONS ASSOCIATED WITH GEOMAGNETIC BAYS IN THE AURORAL ZONE. Tartaglia, Nunzio Anthony. Pittsburgh; Univ. of Pittsburgh (1970). 669p. University Microfilms Order No. 71-3526.

Thesis.

Ten magnetic-bay events were analyzed using data from the digitally reconstructed rapid-run magnetograms recorded at Pt. Barrow and College, Alaska. The irregular pulsations were separated from the bay using a 16-minute sliding average. The dynamic power spectra of the pulsations were calculated for the H, D, and Z components. During the onset of individual substorms, a multiple band structure is observed, from which discrete bands were extracted by digital band-pass filters. Three-dimensional polarizations of the pulsations were analyzed. Five periods at 680, 484, 344, 271, and 193 seconds occurred most frequently at both stations independent of local time on the night side. This discrete band structure is quite similar to that of long-wave, linear oscillations of a magnetic tube excited by mirroring particles of monochromatic kinetic energy. Of 26 transverse pulsations analyzed (H-D plane), 21 had periods less than 300 seconds. The longer periods were predominantly tilted downward in a west-to-east, north-to-south geomagnetic direction at College with an average tilt of 35°, while at Barrow the downward tilt averaged 20° in a west-to-east and slightly south-to-north direction. These observations cannot be explained by the seacoast effect. There is seen a definite relation between the peak energy in the substorm and the peak power in the associated pulsations. (Diss. Abstr. Int., B)

36005 MORPHOLOGY OF AURORAL HYDROGEN EMISSIONS DURING AURORAL SUBSTORMS. Montbriand, Leslie Edward J. Saskatoon; Univ. of Saskatchewan (1969). 354p. University Microfilms Order No. 71-3234.

Thesis.

A chain of four stations near geographic longitude 100°W and providing complete coverage over a corrected geomagnetic latitude (CGT) range from 57° to 79°N was operated during 1963, 1964, and 1965 to study the behavior of aurora and auroral hydrogen. Spectrographs, all-sky cameras, and magnetometers were operated. Over 75,000 spectrograms and 2 million all-sky camera photographs were used to examine the model of the auroral substorm proposed by Akasofu and detailed by Akasofu, Kimball and Meng. Although this model was not completely satisfactory for explaining the behavior of auroral hydrogen, it provided an excellent basis for a more detailed description of the auroral substorm. This detailed description includes new morphological features, illustrations and descriptions of the development of the substorm for different magnitudes, placement of the boundaries of the hydrogen-emission zone on the substorm illustrations, and descriptions of the hydrogen behavior for the different substorm magnitudes. New morphological features include the north-south segments (NSS) which occur within the polar bulge between 10 and 15 minutes after the substorm onset, isolated band segments of hydrogenic aurora which break away from the equatorward part of the hydrogen region in the area of the westward traveling surge (WTS), and very early evening, low latitude, non-hydrogenic, cirrus cloud-like patches which appear after passage of the WTS. Observations were made of the relationships between the occurrence of the auroral type absorption of cosmic noise (AA) and (a) visual aurora and (b) substorm aurora. Results of these relationships were used to indicate on diagrams of the substorm those forms below which conditions exist to produce intense AA. Some relations between magnetic variations and the principal features of the auroral substorm are noted. Various substorm effects which theoretical models must satisfy are indicated. (TSS) (Diss. Abstr. Int., B)

36006 CORRELATIVE STUDY OF RADIO AURORA AND AURORAL ELECTROJET CURRENTS. Harris, Frank Richard. Saskatoon; Univ. of Saskatchewan (1968). 226p. University Microfilms Order No. 71-3209.

Thesis.

The results of detailed, space-time coincident studies of radio aurora and auroral-zone currents are reported. It is shown that auroral-echo Doppler shift is directly proportional to the cosine of the supplement of the angle contained between the direction of the auroral-zone current and the propagation vector of the radar. This is interpreted as evidence that auroral-radar echoes may not arise from scattering by acoustic plasma waves. The Doppler-shift results appear to be in better agreement with an irregularity drift model of radio aurora. The study shows that simultaneous range-time and Doppler-shift measurements of motions of radio aurora provide differing results at times. Range-time radars map outlines of active volumes of the ionosphere. Doppler radars detect apparent motions inside these volumes. The results indicate that auroral-radar echoes and enhancements of the auroral-zone current occur in the same general area at the same time. It is also shown that local magnetic bays are correlated with zenithal echo amplitudes. It is shown that the southernmost edge of detectability of radio aurora and the location of the auroral-zone current are similar functions of magnetic disturbance. Furthermore, it is shown that auroral motions, pertinent to Doppler shift, undergo three phases that are coincident with three phases of the motions of negative charge presumed to be the auroral zone current. (TSS) (Diss. Abstr. Int., B)

36007 DETERMINATION OF PLANETARY ENERGY INTRODUCED BY GALACTIC COSMIC RAYS INTO THE IONOSPHERE AND ATMOSPHERE. Velinov, P. (Inst. of Geophysics, Sofia). Compt. Rend. Acad. Bulg. Sci.: 23: 1485-8(1970).

A mathematical determination is given for energy flux released by galactic cosmic rays into the ionospheric D region and the upper atmosphere. Percentage calculations are given for galactic cosmic-ray energy releases in the D region and the atmosphere for

latitude areas of 0 to 30, 30 to 45, 45 to 55, and 55 to 90 degrees. The greatest energy releases in both cases are in the higher latitudes. (J.C.W.)

36008 SOLAR X-RAY AND PARTICLE RADIATION IN CONNECTION WITH GEOMAGNETIC DISTURBANCES IN LATE SEPTEMBER 1969. Nestorov, G. (Geophysical Inst., Sofia). Compt. Rend. Acad. Bulg. Sci.; 23: 1481-4(1970).

A medium geomagnetic storm began on Sept. 28, 1969 and increased significantly the next 2 days, calming on Oct. 1. The preceding month had been geomagnetically calm. At these times, ionospheric phenomena may be assessed readily. Data on hard x rays measured by Explorer 37 assess to the cause of the sudden increase of absorption on Oct. 1 in the lower ionosphere, testifying to an ionization agent of nonelectromagnetic origin. The profile for the electron production at a given height for Oct. 1 was calculated in accordance with the heightened absorption on that day. Since no solar flares which, as a rule, accompany highly intensified hard x rays were recorded at this time, this is another confirmation of the particle origin of the disturbance. (J.C.W.)

36009 GEOMAGNETIC MODELS FROM SATELLITE SURVEYS. Cain, Joseph C. (Goddard Space Flight Center, Greenbelt, Md.). Rev. Geophys. Space Phys.; 9: No. 2, 259-73(May 1971).

The use of satellite scalar magnetic-field data to produce geomagnetic-field models is reviewed. There have been nine separate spacecraft that have acquired observations of the geomagnetic field from low (<1500 km) satellite altitudes since 1958. The magnetic-field models produced from such data have not been sufficiently compared with surface vector data to firmly establish their validity. One comparison has indicated that satellite-derived models are as valid overall as those produced from surface data. Variations in the field components are shown to be larger than those in scalar field by factors of 4 to 10. Recent satellite models indicate an increase in dipole decay to $-27\ \gamma$/year, a value that may be plausible, judging from extrapolation of earlier surface-derived models. Also noted is a recent slowing of eccentric dipole westward drift. (auth)

36010 DYNAMICAL ASPECTS OF LUNAR ORIGIN. Kaula, William M. (Univ. of California, Los Angeles). Rev. Geophys. Space Phys.; 9: No. 2, 217-38(May 1971).

According to tidal-friction calculations in which estimates of the current dissipation factor are used, the Moon was close to the Earth less than two billion years ago. The most plausible solution to this time-scale problem appears to be a much lesser extent of shallow seas in the past; a coupling of the Moon's orbit with Venus is also a possibility. The same calculations indicate that the Moon had an inclination of at least 10° to the equator, and that the Earth's rotation period was five hours. Fission theories are unsatisfyingly episodic: matter must first lose angular momentum to fall into the Earth, and then regain it to separate. All capture hypotheses are inherently improbable, particularly if the Moon came from a different enough part of the solar system to account for the Moon's density difference. The least implausible capture hypothesis, by Urey and MacDonald, entails collision with a pre-existing Earth satellite at 30 to 40 Earth radii, but the reasoning behind it is not compelling. Most compatible with the idea that formation of the Moon is closely connected to the formation of the Earth are hypotheses that the Moon formed out of a geocentric swarm of matter to which matter from heliocentric orbit was continually added. The theory of Ruskol seems to incorporate most of the dynamical essentials. A possibly severe constraint on the distance from the Earth at which the Moon's formation was completed is a systematic ellipticity of lunar craters pointed out by Opik; it should be re-examined after oriented metric photographs from Apollo 15–17 flights are obtained. (auth)

36011 SOLAR-WIND INTERACTION WITH PLANETARY ATMOSPHERES. Michel, F. Curtis (Rice Univ., Houston, Tex.). Rev. Geophys. Space Phys.; 9: No. 2, 427-35(May 1971).

Several quite dissimilar models have been proposed for the direct interaction of the solar wind with planetary ionospheres, based, respectively, on the assumption of (1) restricted flow into the ionosphere, (2) an interface between the solar wind and the ionospheric plasma, or (3) a magnetic-field barrier (induced magnetopause). All three require the existence of a standing bow shock in the solar wind. These models, their individual limitations, and observational data are reviewed. (auth)

36012 NEW POLAR MAGNETIC DISTURBANCES: S_q^P, SP, DPC, AND DP 2. Nishida, A.; Kokubun, S. (Tokyo Univ.). Rev. Geophys. Space Phys.; 9: No. 2, 417-25(May 1971).

The analyses that have led to the finding of a new polar magnetic disturbance are reviewed, and a unified picture is presented. Although the new disturbance was reported under various names, an essential common feature is that the disturbance does not originate from the auroral electrojet. The high correlation observed between the disturbance and the orientation of the interplanetary magnetic field suggests that the disturbance reflects a basic interaction process between the solar wind and the magnetosphere. (auth)

36013 CRITICAL REVIEW OF ULTRAVIOLET PHOTOABSORPTION CROSS SECTIONS FOR MOLECULES OF ASTROPHYSICAL AND AERONOMIC INTEREST. Hudson, R. D. (Univ. of Colorado, Boulder). Rev. Geophys. Space Phys.; 9: No. 2, 305-406(May 1971).

A critical review is given of photoabsorption cross sections for molecules of aeronomic and astrophysical interest at wavelengths less than 3000 A. A discussion of the relative merits of various experimental techniques is given along with possible systematic and random errors that may be associated with them. The problems in data analysis associated with finite spectral band widths are reviewed, with special emphasis on the interpretation of published absorption cross sections. Prepared figures are used to compare the results of several determinations or to point out where difficulties of interpretation might arise. (auth)

Low-Temperature Physics and Cryogenic Equipment

Refer also to abstracts 35383 and 35389.

Superfluidity

Refer also to abstract 36843.

36014 INFLUENCE OF IMPURITIES ON THE LASER INDUCED BREAKDOWN IN LIQUID ^{4}He. Hunklinger, S.; Leiderer, P. (Technical Univ., Munich). Z. Naturforsch.; 26a: 587-8 (Mar 1971).

The threshold power of the laser-induced optical breakdown of liquid ^{4}He increases by one order of magnitude when the temperature is cooled from T_λ to 1.5°K. Evidence is presented that this effect is not caused by the electronic scattering rate, but rather by the impurity content. An injection of electrons from a hot cathode had no influence on the threshold power. When the liquid was maintained at 1.9°K for 30 min, the threshold power increased by one order of magnitude, but decreased again by the same amount if the liquid was stirred to prevent impurity sedimentation. (D.L.C.)

36015 ROTON VISCOSITY AND THERMAL CONDUCTIVITY OF SUPERFLUID HELIUM. Fomin, I. A. (Inst. of Theoretical Physics, Moscow). Zh. Eksp. Teor. Fiz.; 60: No. 3, 1178-84 (Mar 1971). (In Russian).

It is shown that kinetic equation for the roton part of viscosity and thermal conductivity in superfluid helium with a complete collision integral can be reduced to an equation in the τ approximation. An expression is derived for the roton viscosity and thermal conductivity in terms of an unknown cross section for scattering of rotons by rotons. (auth)

36016 LIQUID ^{4}He. I. BINDING ENERGY AND EXCITATION ENERGY SPECTRUM FROM TWO-BODY CORRELATIONS. Oestgaard, E. (Institut Max von Laue–Paul Langevin, Garching, Ger.). J. Low Temp. Phys.; 4: No. 3, 239-62(Mar 1971).

As a first step in a theoretical study of the properties of liquid ^{4}He, the binding energy was calculated from two-body correlations in the system. Using an effective interaction matrix obtained by a modified Brueckner theory, low-temperature properties such as the binding energy, the elementary excitation energy spectrum, and the velocity of first (ordinary) sound are calculated or estimated. For simplicity, the approximation of a reference energy spectrum with a quadratic momentum dependence for the input single-particle energy spectrum was used, which in principle should be fitted to self-consistent single-particle energies. The intermediate-state potential energies are, however, chosen to be equal to zero. Hence, the three-body energy contribution and also higher-order energy contributions must be estimated by separate calculations. A self-consistent solution is obtained through the depletion of the zero-momentum state, which is also calculated. The calculations are done for two different two-body potentials, an Yntema–Schneider potential given by Brueckner and Gammel and a Frost–Musulin potential given by Bruch and McGee. The theoretical results are –3.1 to –4.0°K for the binding energy, 39 to 44% for the depletion, and 176 to 217 m/sec for the sound velocity. The corresponding experimental results are –7°K, 83%, and 238.3

XUM

m/sec, respectively, i.e., the difference is generally within a factor of two. The agreement with experimental results is reasonably good (or bad), especially since three-body and higher-order cluster terms are not included in this first approximation. (auth)

36017 MEASUREMENT OF THE PROBABILITY OF NUCLEATION OF A VORTEX RING IN HELIUM II. Strayer, Donald M.; Donnelly, Russell J. (Univ. of Oregon, Eugene). Phys. Rev. Lett.; 26: No. 23, 1420-3(7 Jun 1971).

An experiment is described that determines the probability of nucleation of a quantized vortex ring by an ion as a function of the ion velocity. The "lifetime edge" produced by a series of such measurements is compared with the theoretical predictions of Donnelly and Roberts. [Phys. Rev. Lett., 26: 165(1971)] (auth)

Superconductivity

Refer also to abstract 36315.

36018 (CONF-700341-7) METALLURGY OF SUPERCONDUCTORS. New Superconducting Materials and Some Developments. Blanc, J. M. (Thomson-CSF, Orsay (France)). 1970. 30p. (In French). Dep. NTIS (U. S. Sales Only).

From Panel on superconductors; Paris, France (17 Mar 1970).

The fundamental properties of superconductors are reviewed, enumerating the different categories of superconductors. Among the industrial superconductors, particular attention is given to the alloy Nb–Ti and the intermetallic compound Nb_3Sn. The manufacturing process and methods of stabilization employed in the production of Nb–Ti are presented: use of a conducting matrix, hollow conductor, and intrinsic stabilization. The physical properties of Nb_3Sn are described, and the processes whereby the tin is diffused into the niobium are discussed. The mechanical and superconducting properties obtained are described. (France)

36019 (CONF-700341-8) PENETRATION OF THE MAGNETIC INDUCTION, ELECTRIC FIELD, AND LOSSES IN IMPURE SUPERCONDUCTORS OF THE SECOND KIND WITH SURFACE CURRENTS. Fournet, G.; Mailfert, A. (Paris Univ. (France). Laboratoire de Genie Electrique). 1970. 26p. (In French). Dep. NTIS (U. S. Sales Only).

From Panel on superconductors; Paris, France (17 Mar 1970).

The penetration of magnetic induction into very impure Type-II superconductors traversed by a low-frequency alternating electric current or subjected to a low-frequency alternating magnetic field, is studied. Experiments performed permitted the critical surface and volume currents for various samples to be determined. A theoretical expression for the electric field, in the material, at any point during the sinusoidal cycle, was deduced. The predicted curves are in good agreement with those experimentally obtained. The analytic expressions for the electric field enabled the losses to be calculated. Formulas obtained for the losses associated with the type of penetration observed in practice (Kim law) are new. It is shown that surface currents present themselves in the loss expression in a complicated manner and that part of the loss is localized in the surface of the sample. The expression enables the losses occurring at the surface of the sample to be separated from those occurring in the volume. In the case of the superconductors studied, the small depth associated with volume losses justifies the hypothesis proposed for samples subjected to magnetic fields with complex configurations. For sufficiently weak external magnetic fields, all the losses can be considered to take place at the surface. (auth) (France)

36020 THEORY OF ULTRASONIC ATTENUATION IN TWO-BAND SUPERCONDUCTORS. Tang, I-ming (Reed Coll., Portland, Oreg.). Solid State Commun.; 9: No. 9, 547-9(1 May 1971).

The ultrasonic attenuation coefficient for longitudinal waves is formulated for two-band superconductors. The resulting expression differs from that previously obtained by Fal'ko, 1967. (auth) (UK)

36021 PRESSURE EFFECT ON THE MAGNETIC PROPERTIES OF SUPERCONDUCTING La AND La–Ce. Takata, Mitsuhiro; Oshida, Soichi (Osaka Univ.). J. Phys. Soc. Jap.; 30: No. 6 1640-4(June 1971).

The pressure dependence of the thermodynamic critical field of La was measured, and the pressure effect on the electronic density of states at the Fermi surface is calculated. The value of $d\ln N(0)/d\ln v$ is found to be -4.54 ± 1.67, where $N(0)$ and v are the density of states at the Fermi surface and the volume, respectively. From the pressure dependence of $N(0)$ and T_c of La–1.0% Ce, $d\ln J/d\ln v$ is calculated to be -4.3 (J is the exchange interaction parameter). From the experimental result, the mechanism of superconductivity of La at high pressure is discussed. (auth)

36022 HEAT CAPACITY AND AC SUSCEPTIBILITY MEASUREMENTS ON PRESSED-POWDER COMPACTS OF V_3Si. McCarthy, S. L.; Viswanathan, R. (Univ. of California, San Diego). Contract AT(11-1)-34. Solid State Commun.; 9: No. 9, 569-72(1 May 1971).

Results of heat capacity and susceptibility measurements confirm the existence of residual-stress-induced superconductivity in V_3Si, with a transition temperature near 8°K. (auth) (UK)

36023 SUPERCONDUCTIVITY INDUCED BY PRESSURE. Gandel'man, G. M.; Fedorov, M. A. JETP Lett. (USSR) (Engl. Transl.); 13: No. 3, 127-8(5 Feb 1971).

Translated from Zh. Eksp. Teor. Fiz., Pis'ma Red.; 13: No. 3, 180-2(5 Feb 1971).

An attempt is made to explain pressure-induced superconductivity from the point of view of the change of the band structure of the elements under pressure. The authors predict that pressure-induced superconductivity should be observed in Rb, Sr, K, Ca, and Sc. (L.M.T.)

36024 NONLINEAR ELECTRICAL CONDUCTIVITY OF SUPERCONDUCTING FILMS BELOW THE TRANSITION TEMPERATURE. Kajimura, Koji (Electrotechnical Lab., Tanashi, Japan); Mikoshiba, Nobuo; Yamaji, Kunihiko. Phys. Rev., B; 4: No. 1, 209-16(1 Jul 1971).

The Langevin equation for the superconducting order parameter above the transition temperature T_c proposed by Schmid is modified to calculate the nonlinear excess conductivity $\sigma'(T,E)$ slightly below T_c. The electric field dependence of $\sigma'(T,E)$ is described approximately by the same function of $E/E_c(T)$ as Schmid's function above T_c, with a newly defined characteristic field $E_c(T)$ below T_c. The experimental results of the nonlinear electrical conductivity of aluminum films below T_c are in fairly good agreement with the theory. (auth)

36025 MAGNETIZATION OF DIRTY SUPERCONDUCTORS NEAR THE UPPER CRITICAL FIELD. Usadel, Klaus D. (Univ. of Montreal). Phys. Rev., B; 4: No. 1, 99-110(1 Jul 1971).

The magnetic behavior of a type-II superconductor with very short electron mean free path (dirty limit) near its upper critical field $B_{c2}(T)$ is investigated. A calculation of the magnetization up to the second order in the difference between $B_{c2}(T)$ and the external magnetic field, which is valid for all temperatures, is presented. A triangular and a square lattice of flux lines are considered. A numerical calculation suggests that the triangular lattice remains stable despite the fact that the difference in the thermodynamical potentials between the two lattices decreases due to these second-order terms. (auth)

36026 PRESSURE DEPENDENCE OF THE SPECIFIC HEAT OF A SUPERCONDUCTOR DERIVED FROM CRITICAL-MAGNETIC-FIELD DATA. Carbotte, J. P. (McMaster Univ., Hamilton, Ont.). Phys. Rev., B; 4: No. 1, 82-4(1 Jul 1971).

The low-temperature variation of the critical magnetic field of a superconductor is related to the normal-state electronic specific-heat coefficient γ. Measurements of the critical magnetic field at zero and finite pressure are used to obtain a value for the volume Ω dependence of γ. It is shown that strong-coupling corrections must be included in such an analysis. For example, in Pb, ignoring such corrections leads to an error of almost a factor of 2 in $d\ln\gamma/d\ln\Omega$. (auth)

36027 FLUX-FLOW EFFECT IN JOSEPHSON TUNNEL JUNCTIONS. Barone, A. (CNR, Naples). J. Appl. Phys.; 42: No. 7, 2747-51(Jun 1971).

Experimental results exhibiting the displaced linear slope effect in the volt–ampere characteristics of large Josephson junctions are reported. These data substantially confirm theoretical predictions based on the effect of magnetic flux flow. (auth)

36028 NATURE OF THE TRANSITION AT H_{c2}. Doidge, P. R.; Eastham, A. R. (Univ. of Surry, Guildford, Eng.). Solid State Commun.; 9: No. 9, 543-5(1 May 1971).

A small discontinuity in the magnetization of low-κ superconducting alloys at H_{c2} in increasing fields is found to depend on surface conditions, and is attributed to a change in surface pinning rather than to a bulk first-order phase change at H_{c2}. (auth) (UK)

36029 MEASUREMENT OF THE SURFACE INDUCTANCE AND PENETRATION DEPTH OF SUPERCONDUCTING ALUMINUM. Tedrow, P. M.; Faraci, G.; Meservey, R. (Massachusetts Inst. of Tech, Cambridge). Phys. Rev., B; 4: No. 1, 74-82(1 Jul 1971).

The inductance of a pure-aluminum wire was measured as a function of temperature in the superconducting state at a frequency of 10 MHz. The temperature dependence of the penetration depth calculated from these measurements does not agree with that predicted by the BCS theory for aluminum, an extreme nonlocal superconductor. It is shown that the present measurements agree with previous results at higher frequencies and have a temperature dependence very close to the BCS local theory. It is concluded that there is no rigorous way of obtaining an absolute value of the penetration depth from this or previous measurements of the temperature dependence of the inductance (or the penetration depth). (auth)

36030 GAP ENERGY OF SUPERCONDUCTING NIOBIUM CARBIDE. Shacklette, L. W.; Radosevich, L. G.; Williams, Wendell S. (Univ. of Illinois, Urbana). Phys. Rev., B; 4: No. 1, 84-7(1 Jul 1971).

The first estimate of the superconducting energy gap in a transition-metal carbide was recently made from thermal conductivity data on $NbC_{0.96}$. The quantity $2\epsilon(0)/kT_c$ was treated as an adjustable parameter in fitting the data to Bardeen–Rickayzen–Tewordt (BRT) theory, and a good fit was found for $2\epsilon(0)kT_c = 4.0$. The resulting value of the gap energy has now been verified by tunneling measurements using both probe and thin-film techniques. The best value is $2\epsilon(0) = 3.2 \pm 0.1$ MeV. The result supports the applicability of BRT theory to the transition-metal carbides having low vacancy concentrations and demonstrates that under favorable circumstances, which may be unique to nonstoichiometric compounds, thermal conductivity data can be used to evaluate the gap energy of a superconductor. (auth)

36031 SUPERCONDUCTIVITY OF A SEMICONDUCTOR PLACED IN A LASER LIGHT FIELD. Blazhin, V. D.; Selivanenko, A. S. (Lebedev Inst. of Physics, Moscow). Sov. Phys.-Solid State (Engl. Transl.); 12: No. 11, 2610-13(May 1971).
Translated from Fiz. Tverd. Tela; 12: No. 11, 3229-33(Nov 1970).

A theoretical study was made of a model of a strongly doped semiconductor with a complex conduction band. The electron scattering in the conduction band arising from the Coulomb interaction with electrons of the valence band was calculated, taking the effect of the light field into account simultaneously. It is shown that, under certain conditions, such scattering can lead to the appearance of superconductivity at temperatures of the order of 100°K. (auth)

36032 CREEP IN TYPE-II SUPERCONDUCTORS. Vainblat, T. I.; Soldatov, V. P.; Startsev, V. I. (Physical-Technical Inst. of Low Temperatures, Kharkov). Sov. Phys.-Solid State (Engl. Transl.); 12: No. 11, 2727-9(May 1971).
Translated from Fiz. Tverd. Tela; 12: No. 11, 3357-60(Nov 1970).

The results of a study of creep in a Pb–10 at.% In alloy are presented. The polycrystalline samples were prepared from 99.999% pure lead and indium. After annealing and chemical polishing, the samples were subjected to tensile strain in the creep made at 4.2°K. The deformation as a function of the magnetic field and the relation between the jump in deformation and the magnetic field going from the normal and intermediate to the superconducting state are shown graphically. (M.H.R.)

36033 THEORY OF SUPERCONDUCTORS WITH OVERLAPPING BANDS IN THE PRESENCE OF NONMAGNETIC IMPURITIES. II. Chow, W. S. (Univ. of Cincinnati). Phys. Rev., B; 4: No. 1, 111-15(1 Jul 1971).

The transition temperatures of two-band superconductors containing nonmagnetic impurities are further investigated. It is found that because of interband impurity scattering in an impure two-band superconductor, the s-band transition temperature T_{cs} is identical to the d-band transition temperature T_{cd}. That is, for an impure two-band superconductor, there is only one transition temperature. This result is in agreement with the recent experimental findings of Hafstrom and MacVicar. Further, it is noted that the perturbing processes due to the interband impurity scattering are similar to the perturbing processes due to the phonon-exchange interaction between the electrons of the two bands, previously considered by Suhl, Matthias, and Walker. (auth)

36034 THEORY OF SUPERCONDUCTORS CONTAINING MAGNETIC IMPURITIES: CRYSTALLINE FIELD EFFECTS. Keller, Joachim (Univ. of Maryland, College Park); Fulde, Peter. J. Low Temp. Phys.; 4: No. 3, 289-98(Mar 1971).

A previous calculation of crystalline field effects in superconductors containing rare-earth impurities is extended to finite concentrations. The computations, which have to be done numerically, apply to non-Kramers ions as well as Kramers ions. A comparison between theory and available experimental data is made. (auth)

36035 NUCLEATION FIELD OF A THIN SUPERCONDUCTING FILM ON A THICK NORMAL LAYER. Fink, H. J. (Swiss Federal Inst. of Tech., Zurich. Univ. of California, Davis); Martinoli, P. J. Low Temp. Phys.; 4: No. 3, 305-15(Mar 1971).

The nucleation field H_0 of a normal/superconducting double layer is calculated when the normal layer is thick and the thickness of the superconducting film is varied and is of the order of magnitude of the coherence length in the superconducting metal. The results are general and are exact when the transition temperatures of the two metals are not too different. The above theory is extended to metal layers having very different transition temperatures. When both metal layers are thick, the agreement with experiments by Fischer and Klein on lead/copper films is good. (auth)

36036 PROXIMITY EFFECT IN GADOLINIUM-BACKED LEAD FILMS. Smith, R. O.; McLean, W. L.; Serin, B. (Rutgers–The State Univ., New Brunswick, N. J.). J. Low Temp. Phys.; 4: No. 3, 317-29(Mar 1971).

Measurements of the surface reactance at a frequency of 100 MHz and at various temperatures were used to study some aspects of the proximity effect in lead films in contact with gadolinium. It was found that, although the normal metal in this case is magnetic, an adequate explanation of the experimental results cannot be obtained by assuming that the Ginzburg–Landau order parameter vanishes at the NS interface. The microscopic theory that allows the boundary condition $(\nabla\Psi)_n = \Psi/b$ (where n indicates the normal component of the gradient, Ψ is the order parameter, and b is called the extrapolation length) does agree well with both the dependence of the transition temperature T_{cNS} on the thickness of the superconducting layer and variation of the surface reactance with temperature. (auth)

36037 FIZIKO-KHIMIYA, METALLOVEDENIE, I METALLOFIZIKA SVERKHPROVODNIKOV. TRUDY IV VSESOYUZNOGO SOVESHCHANIYA. (Physical Chemistry, Metallography, and Metal Physics of Superconductors. Report of the Fourth All-Union Conference). Savitskii, E. M.; Baron, V. V. (eds.). Moscow; Izdatel'stvo Nauka (1969). 160p.

Twenty-four papers are included; a separate abstract was prepared for each. (M.H.R.)

For abstracts of individual papers see: 36038–36056, 36076–36079, and 36321.

36038 SUPERCONDUCTING METALLIC COMPOUNDS OF RHENIUM. Savitskii, E. M.; Khamidov, O. Kh. pp 3-8 of Fiziko-Khimiya, Metallovedenie, i Metallofizika Sverkhprovodnikov. /Savitskii, E. M. (ed.). Moscow; Izdatel'stvo Nauka (1969). (In Russian).

The critical temperature was determined for intermediate phases of the scandium–rhenium and iron–rhenium systems and systems of rhenium with certain rare-earth metals (gadolinium, terbium, holmium, and erbium). The compounds of rhenium with transition metals primarily relate to three types: σ-phases with the structure β – U, λ-phases with the structure $MgZn_2$, and χ-phases with the structure α – Mn. It was established that in proportion to the proximity of an alloying element to rhenium in the periodic system, the increase of the number of valence electrons and, consequently, the complications of the electronic structure of their atoms, an increase in the critical temperature of metallic compounds of rhenium is observed for σ-, λ-, and χ-phases. It was shown that the largest transition temperatures are for phases with the $MgZn_2$ phases. (tr-auth)

36039 EFFECTS OF IMPURITIES AND DIVERGENCES FROM STOICHIOMETRY ON CERTAIN PROPERTIES OF THE Nb_3Sn PHASE. Medvedev, S. A.; Kiseleva, K. V.; Lykhin, V. A.; Denker, B. I. pp 8-15 of Fiziko-Khimiya, Metallovedenie, i Metallofizika Sverkhprovodnikov. /Savitskii, E. M. (ed.). Moscow; Izdatel'stvo Nauka (1969). (In Russian).

Polycrystalline Nb_3Sn of stoichiometric composition was obtained by the method of the self-soluble crucible, which was subjected to vacuum heat treatment to assure gradual change of composition. As a result the evaporation of a certain quantity of tin occurred; changing the time of heat treatment made it possible to regulate the loss of tin. The following were obtained: (1) chemical composition, (2) transition temperature T_c (3) the parameter α of the crystalline lattice, and (4) the degree of filling of sites in the niobium and tin sublattices. It was shown that the range of existence of the superconducting phase $Nb_{3+\delta}Sn$ constitutes approximately 3 at. %, from 75 up to 78.16 at. % Nb. (M.H.R.)

36040 EFFECTS OF ALLOYING ON TRANSITION TEMPERATURE OF SUPERCONDUCTING COMPOUNDS V_3Ga, V_3Si, AND

XUM

Nb_3Sn. Efimov, Yu.; Baron, V. V.; Savitskii, E. M. pp 15-23 of Fiziko-Khimiya, Metallovedenie, i Metallofizika Sverkhprovodnikov. /Savitskii, E. M. (ed.). Moscow; Izdatel'stvo Nauka (1969). (In Russian).

About 30 alloys were studied, which are the compound V_3Ga with the addition of 5 at. % of an alloying element. Transition metals of groups III and VIII were introduced at the expense of vanadium, metals in the main subgroups II and V at the expense of gallium, and the introduced elements at the expense of both compound components, the ratio of which remained constant at 3:1. At the composition of the compound V_3Ga, optimum conditions for the maximum superconducting transition temperature are realized. The replacement of atoms of vanadium or gallium in the lattice of the compound by atoms of any element apparently leads to a decrease in T_c. The degree of lowering of the critical temperature with equal percent of addition is different for different alloying elements. (tr-auth)

36041 SUPERCONDUCTIVITY OF NIOBIUM DISELENIDE. Antonova, E. A.; Kiseleva, K. V.; Kalyuzhnaya, G. A.; Medvedev, S. A. pp 23-8 of Fiziko-Khimiya, Metallovedenie, i Metallofizika Sverkhprovodnikov. /Savitskii, E. M. (ed.). Moscow; Izdatel'stvo Nauka (1969). (In Russian).

Niobium diselenide and solid solutions with it as a base were synthesized by a new method, which uses a self-soluble crucible. Samples of the composition $NbSe_{(2-x)}$ with different selenium contents and also substitutional solid solutions of the niobium–selenium–tellurium system were obtained. Monocrystals of these compounds were grown by a gas transport reaction method. The relation of the composition to the transition temperature of the superconducting state was studied for the given compounds. The transition temperature of the compound, close to the stoichiometric composition $NbSe_2$, is in the vicinity of 7°K. (tr-auth)

36042 TRANSITION TEMPERATURE IN SUPERCONDUCTING STATE IN SYSTEMS ZIRCONIUM–VANADIUM AND ZIRCONIUM–VANADIUM–NIOBIUM NEAR ZrV_2. Matveeva, N. M.; Malakhova, T. O. pp 28-36 of Fiziko-Khimiya, Metallovedenie, i Metallofizika Sverkhprovodnikov. /Savitskii, E. M. (ed.). Moscow; Izdatel'stvo Nauka (1969). (In Russian).

The superconducting transition temperature T_c of V–Zr–Nb alloys near the composition ZrV_2 was determined in connection with the equilibrium diagram of the alloys. In the binary system V–Zr for single-phase alloys with cubic structure of the $MgCu_2$-type, T_c is between 7.05° and 7.35°K. A change in the lattice constant of the compound ZrV_2 from 7.427 to 7.410 Å indicates the possibility of dissolution of the excess component in the compound. Alloying the compound ZrV_2 with niobium leads to the formation of γ-solid solutions on a cubic structure base. With a constant zirconium content, the substitution of vanadium by niobium leads to a lowering of T_c; with the substitution of the sum of the atoms (2V + Zr) by niobium a change in T_c is not observed. At the composition 18 at. %, 33.4 at. % Zr, and 48.6 at. % V, the triple Laves phase is formed with the composition $ZrNb_{0.5}V_{1.5}$ and $MgZn_2$ structure. T_c of this new compound is 4.34°K. (tr-auth)

36043 OBTAINING THE SUPERCONDUCTING COMPOUND V_3Ga BY MEANS OF DIFFUSION. Kunakov, Ya. N.; Vorob'eva, N. S.; Tochenova, I. N. pp 36-44 of Fiziko-Khimiya, Metallovedenie, i Metallofizika Sverkhprovodnikov. /Savitskii, E. M. (ed.). Moscow; Izdatel'stvo Nauka (1969). (In Russian).

The formation conditions were studied for the superconducting compound V_3Ga and other intermediate phases in the V–Ga system in diffusion layers which were obtained in the temperature range 450 to 1350°C. The investigation was conducted with x-ray structure, metallographic, and x-ray spectral methods. First, the method of anode oxidation of the produced phases was worked out for the vanadium–gallium alloys. As a result of the work conducted, the temperature ranges of the existence of the compound V_3Ga and other phases in the vanadium–gallium system were determined. The strong influence of "the third elements" (such as silicon, aluminum, oxygen) interacting with samples on the formation of the compound V_3Ga was found. Under certain annealing conditions, in the interaction with "a third element" the compound V_3Ga can undergo an allotropic transformation. (tr-auth)

36044 PLASMOCHEMICAL METHOD OF SYNTHESIS OF SUPERCONDUCTING COMPOUNDS WITH STRUCTURE OF A15 TYPE. Bashkirov, Yu. A.; Medvedev, S. A. pp 44-50 of Fiziko-Khimiya, Metallovedenie, i Metallofizika Sverkhprovodnikov. /Savitskii, E. M. (ed.). Moscow; Izdatel'stvo Nauka (1969). (In Russian).

The method described consists of reduction by hydrogen of a mixture of chlorides in the plasma of a high-frequency electrodeless gas discharge. A diagram of the apparatus and a description of its most important points are presented. As an example the binary vanadium–silicon system showed that, under specific conditions, the composition of the final product repeats the composition of the initial gas mixture. Crystals of binary systems with a vanadium base were obtained: V_3Si, V_3Ge, and other compounds of the A-15 structural type. The following parameters were found for the tetragonal phase V_5Si_3: a = 9.429 Å, c = 4.757 Å and for the A-15 phase V_3Si: a = 4.734 Å. The transition temperature measured by the induction method was T_c = 17.1°K for V_3Si and T_c = 6.5°K for V_3Ge. (tr-auth)

36045 INVESTIGATION OF COMPOUNDS IN THE NIOBIUM–TIN SYSTEM OBTAINED BY MEANS OF DIFFUSION. Kunakov, Ya. N.; Tochenova, I. N.; Volkov, I. G. pp 50-3 of Fiziko-Khimiya, Metallovedenie, i Metallofizika Sverkhprovodnikov. /Savitskii, E. M. (ed.). Moscow; Izdatel'stvo Nauka (1969). (In Russian).

The formation of intermediate compounds in the niobium–tin system, obtained with different diffusion annealings, was studied. The investigation was conducted on a coil of thin (50-μ diameter) niobium wire cable covered with tin, and on special samples of closed niobium containers with tin inside. The phases produced were studied by metallographic, x-ray structural, and micro-x-ray-spectral analyses. The color metallography method was used, with which the different colorations of the phases formed were obtained by anode oxidation. It was established that in the temperature range studied, 600 to 1600°C, only three intermediate phases are formed in diffusion layers: Nb_3Sn, Nb_4Sn_5, and $NbSn_5$. (tr-auth)

36046 EXPERIMENTAL INVESTIGATION OF MAGNETIZATION OF CERTAIN TYPE-II SUPERCONDUCTORS. Baron, V. V. pp 53-61 of Fiziko-Khimiya, Metallovedenie, i Metallofizika Sverkhprovodnikov. /Savitskii, E. M. (ed.). Moscow; Izdatel'stvo Nauka (1969). (In Russian).

Magnetization curves recorded at 4.2°K in an external magnetic field of samples of the compound Nb_3Sn prepared by different methods (thermodiffusion, etc.) after different thermal treatment are presented. The magnetization of niobium and a niobium–zirconium alloy is also reported. (tr-auth)

36047 PHASE COMPOSITION, STRUCTURE, AND MAGNETIC HYSTERESIS OF NIOBIUM–TIN ALLOYS. Potapov, N. N.; Zaikina, G. I. pp 61-8 of Fiziko-Khimiya, Metallovedenie, i Metallofizika Sverkhprovodnikov. /Savitskii, E. M. (ed.). Moscow; Izdatel'stvo Nauka (1969). (In Russian).

According to the results of a study of the magnetic hysteresis of superconducting sintered Nb–Sn (72 to 84 at. % Nb) alloys, cooled to 4.2°K in a magnetic field, a concentration dependence was constructed for the main hysteresis characteristics: residual induction (frozen magnetic flux), coercive force, and maximum magnetic energy. A study of phase composition and structural anomalies of the alloys was conducted to explain this relation. It was shown that, in phase relations, the samples of different composition scarcely differ from each other qualitatively, but it is not possible to relate the difference in the volumetric content of the different phases to the hysteresis value. Frozen-in-magnetic-flux samples conform well with the crystalline lattice parameter of Nb_3Sn, and the coercive force and maximum magnetic energy with the number of intergranular boundaries of the Nb_3Sn phase. It was concluded that the grain boundaries contain structural defects that determine the cause and amount of hysteresis in the Nb–Sn alloys. (tr-auth)

36048 CRITICAL CHARACTERISTICS OF SUPERCONDUCTING ALLOYS OF TYPE NT-I IN A WIDE RANGE OF MAGNETIC FIELDS AT DIFFERENT TEMPERATURES. Savitskii, E. M.; Baron, V. V.; Goncharov, I. N.; (and others). pp 69-75 of Fiziko-Khimiya, Metallovedenie, i Metallofizika Sverkhprovodnikov. /Savitskii, E. M. (ed.). Moscow; Izdatel'stvo Nauka (1969). (In Russian).

The structure and superconducting characteristics of alloys of the types NT-1 and NT-2 (niobium–titanium systems) were studied. The critical currents of the alloys were studied in fields from 10 to 80 kG. The measurements of critical characteristics were conducted on cold-deformed and hot-worked alloys, on samples both with a copper coating and without it. The regimes of alloy treatment were established that provide best characteristics in fields of larger strength. (tr-auth)

36049 INFLUENCE OF TIME AND TEMPERATURE OF ANNEALING ON STRUCTURE AND SUPERCONDUCTING PROPERTIES OF RECRYSTALLED AND DEFORMED ALLOYS OF NIOBIUM WITH 75 AT. PERCENT TITANIUM. Bychkova, M. I.; Baron, V. V.; Savitskii, E. M.; Sudareva, S. V.; Buinov, N. N. pp 76-86 of Fiziko-Khimiya, Metallovedenie, i Metallofizika Sverkhprovodnikov. /Savitskii, E. M. (ed.). Moscow; Izdatel'stvo Nauka (1969). (In Russian).

XUM

Effects of heat treatment on the structure and properties of alloy NT-1 (Nb–75 at. % Ti), which possesses a high critical magnetic field and good technology, were investigated. The alloy structure was studied using the electron microscope and thin metallic films: The observed microstructures are compared with the corresponding values of the critical current density, and the relationship is noted. (tr-auth)

36050 CRITICAL CURRENT OF SUPERCONDUCTING ALLOY 65BT IN FIELDS UP TO 80 kOe. Davydov, A. A.; Prokoshin, A. F.; Sokolov, V. I.; Fedotov, L. N. pp 92-6 of Fiziko-Khimiya, Metallovedenie, i Metallofizika Sverkhprovodnikov. /Savitskii, E. M. (ed.). Moscow; Izdatel'stvo Nauka (1969). (In Russian).

Results are cited of an investigation of the relation of critical current to magnetic field in Type-II superconductors. It was found for samples of superconducting alloy 65BT that heat treatment has a different effect on the critical current in the region of low fields than in fields close to critical. An opinion is expressed concerning the expediency of special heat treatment for ribbon 65BT, used in the internal sections of the solenoids. A diagram of a simple apparatus for study of superconducting alloys in fields up to 80 kOe is presented. (tr-auth)

36051 CONCERNING THE PHASE TRANSFORMATIONS IN ALLOY 65BT. Kadykova, G. N.; Surovaya, G. N. pp 96-104 of Fiziko-Khimiya, Metallovedenie, i Metallofizika Sverkhprovodnikov. /Savitskii, E. M. (ed.). Moscow; Izdatel'stvo Nauka (1969). (In Russian).

Dilatometric, electron-microscopic, and x-ray analyses showed that, in alloy 65 BT, the separation of the second phase occurs in the process of deformation and tempering after deformation at temperatures below 600°C; this contributes to an enhancement of the superconducting properties. (tr-auth)

36052 STUDIES OF THE BEHAVIOR OF FOIL SPECIMENS OF NT-TYPE ALLOYS IN AN EXTERNAL MAGNETIC FIELD. Moskvitin, A. I.; Savitskii, E. M.; Baranov, V. V.; Blinkov, E. L.; Bychkova, M. I. pp 104-7 of Fiziko-Khimiya, Metallovedenie, i Metallofizika Sverkhprovodnikov. /Savitskii, E. M. (ed.). Moscow; Izdatel'stvo Nauka (1969). (In Russian).

Superconducting specimens of Nb alloyed with Ti (three compositions from 14 to 61% Ti) were studied in order to prepare magnetic screens of complex configuration. The behavior of these alloys in a strong magnetic field was analyzed by means of InAs Hall detectors. The curves describing the variations in the emf of the Hall detectors as functions of magnitudes of the magnetic field and the current at liquid helium temperature are included as well as the curves of the alloy behavior in external fields of various intensities. Data obtained were compared with data on pure niobium. Certain peculiarities of the alloyed foil material were observed. (tr-auth)

36053 CONCERNING THE FINE STRUCTURE OF SUPERCONDUCTING ALLOYS OF ZIRCONIUM WITH NIOBIUM. Bychkov, Yu. F.; Sokolov, N. A.; Chuprin, V. A. pp 108-13 of Fiziko-Khimiya, Metallovedenie, i Metallofizika Sverkhprovodnikov. /Savitskii, E. M. (ed.). Moscow; Izdatel'stvo Nauka (1969). (In Russian).

The change in the half-width of the lines of the β solid solution by plastic deformation of alloys of zirconium with 25 to 100% niobium, and zirconium–50% niobium with subsequent tempering, was studied. The changes in the dimensions of the units of coherent scattering and microdistortions in the lattice of the β-phase with deformation and tempering were determined by the method of harmonic analysis. The question of interdependence of critical currents and fine structure is discussed. (tr-auth)

36054 EFFECTS OF HEAT TREATMENT ON THE SUPERCONDUCTING PROPERTIES OF NIOBIUM–TANTALUM ALLOYS. Pakhomov, V. Ya.; Ovcharenko, O. N.; Lainer, D. I. pp 113-19 of Fiziko-Khimiya, Metallovedenie, i Metallofizika Sverkhprovodnikov. /Savitskii, E. M. (ed.). Moscow; Izdatel'stvo Nauka (1969). (In Russian).

The effect of heat treatment on the superconducting properties of Nb–Ta alloys with 25 and 50 at. % tantalum was studied. The Nb–25 at. % Ta melted in an electron-beam furnace contained only half as much oxygen as that after arc melting (am). After strong cold deformation (drawing μ ~1600) with heat treatment and optimum temperature, the critical current density of all samples is doubled in a magnetic field 0.32 H_{c2} which is 0.8, 1.65, and 2.1 kG for alloys Nb–50 Ta (am), Nb–25 Ta (el), and Nb–25 Ta (am), respectively. Strongly deformed samples near fields have higher critical current density than after optimum annealing for I_c in fields of 0.32 H_{c2}. In the investigation of magnetic properties of alloys (magnetization) it was established that even low-temperature heat treatment at 450°C reduces the critical field H_{c2} 5 to 7% in comparison with the strongly deformed state. The results of experiments show that high-purity alloys of the Nb–Ta system with unlimited solubility at the optimum temperature of heat treatment increase the critical current density. Investigations were made on wire samples 0.25 mm in diameter at 4.2°K. (tr-auth)

36055 DETERMINATION OF SPECIFIC RESIDUAL ELECTRICAL RESISTANCE IN S $\rightleftharpoons$ N TRANSITION ASPECTS OF WIRE FORMS FROM SUPERCONDUCTING MATERIALS BY THE RESISTIVITY METHOD. Kozlova, N. D.; Myzenkova, L. F.; Baron, V. V. pp 120-5 of Fiziko-Khimiya, Metallovedenie, i Metallofizika Sverkhprovodnikov. Sanitskii, E. M. (ed.). Moscow; Izdatel'stvo Nauka (1969). (In Russian).

Apparatus was set up for recording the curve S $\rightleftharpoons$ N of the transition of wire samples from superconducting materials in the temperature range 4.2 to 20°K in the absence of a magnetic field. The specific and also the residual electrical resistances of samples of niobium, zirconium, and vanadium and a niobium–zirconium alloy were measured after various treatments to determine the effect of deformation and phase composition of the material on the electrical resistance. (tr-auth)

36056 SUPERCONDUCTING ELECTROLYTIC FILMS OF NIOBIUM. Savitskii, E. M.; Baron, V. V.; Mikhailov, B. P. pp 128-8 of Fiziko-Khimiya, Metallovedenie, i Metallofizika Sverkhprovodnikov. /Savitskii, E. M. (ed.). Moscow; Izdatel'stvo Nauka (1969). (In Russian).

Superconducting niobium films were obtained by electrodeposition of niobium from melted salts. The effect of cathode current density, temperature, and process continuity on the structure, thickness, purity, and transition temperature of superconducting niobium films was studied. It was established that thickness of the films from 33 to 90 μ has little effect on the superconducting transition temperature. The obtained critical temperatures of the films (8.9 to 8.8°K) are commensurate with the transition temperature of vacuum-melted (about 9°K) niobium. (tr-auth)

36057 SUPERCONDUCTIVITY AND DISLOCATION CELL STRUCTURE IN NIOBIUM: STRESS EFFECTS. Hill, D. C.; Rose, R. M. (Massachusetts Inst. of Tech., Cambridge). Met. Trans.; 2: No. 5, 1433-7(May 1971).

To investigate the mechanism for the development of large anisotropic resistive critical fields in deformed niobium, the dependence of the parallel critical field $H_{||}$ on stress σ was measured in both compression and tension for severely deformed niobium composites. The magnitude of $\partial H_{||}/\partial\sigma$ increased with strain up to a value of 27 times that of annealed niobium. Also, both tension and compression increased $H_{||}$. Both of these discrepancies from the thermodynamic predictions can be ascribed to the presence of double-ended dislocation pileups in the cell walls. (auth)

36058 FLUX FLOW AS FUNCTION OF FILM THICKNESS IN TYPE-I SUPERCONDUCTORS. Takayama, Tetsunobu; Ogushi, Tetsuya; Shibuya, Yoshio (Kyushu Univ., Fukuoka). J. Phys. Soc. Jap.; 30: 1083-90(Apr 1971).

The flux flow in type-I superconducting Pb film was measured as a function of film thickness. The vortex state is stable in the films perpendicular to the magnetic field, provided the films are thinner than the critical thickness, d_c, which is about 9,000 Å at 4.2°K, while the theoretically predicted one is about 2,200 Å. The flux flow pattern changes gradually with the change of film thickness around d_c. The flow resistivity of the films, the thickness of which is thinner than d_c, is nearly linear against the magnetic field H for $H/H_{c\perp} > 0.5$. On the other hand the I–V plots in perpendicular field for films much thicker than d_c start from the origin and show characteristic "knick" at certain values of current in weak fields. This result can be explained by assuming that in strong fields these films have an effective laminar structure and in weak fields they have a bundle structure in addition to an effective laminar structure. The experimental results are consistent with those of Van Gurp by a different method of measurement, i.e., the flux-flow noise measurement. (auth)

36059 BAND STRUCTURE IN THE EXCITATION SPECTRUM OF TYPE-II SUPERCONDUCTORS. Schattke, W. (Univ., Kiel). Z. Naturforsch.; 26a: 228-32(Feb 1971).

The periodic structure of the mixed state leads to some band splitting in rough analogy to the electrons in a metal. The density of states for tunneling perpendicular to the flux lines shows an appreciable depression at energies $\hbar\omega \approx (\hbar^2/2m)\, k_F\, |l|$, l being a reciprocal lattice vector of the flux lattice normal to the tunneling surface. (auth)

36060 REMARKS ON THE ISOTOPIC VOLUME EFFECT IN SUPERCONDUCTORS. Nakajima, Tetsuo (Tohoku Univ., Sendai). J. Phys. Soc. Jap.; 30: 932-40(Apr 1971).

XUM

One possible manner in which the change in isotopic volume contributes to the isotope effect in superconductors is discussed with relation to the empirical formula of Olsen et al., $\alpha = 0.25 + 0.1\phi$, which represents a relation between the exponent α in $T_c \propto M^{-\alpha}$ and the volume dependence of the transition temperature, $\phi = \partial \ln [T_c/\theta]/\partial \ln V \cdot \{\ln(0.85\theta/T_c)\}^{-1}$. Here, the volume effect being taken into consideration, α is expressed in terms of the mass and volume effects of the Debye temperature θ and those of the phonon mediated electron–electron interaction N(0)J in the BCS relation. In addition to this, the limitations of the argument concerning the relation between the isotope effect and the volume dependence of the transition temperature are briefly examined in connection with the isotopic volume in some isotopic compounds. (auth)

36061 INVESTIGATION OF TIME-DEPENDENT FLUX TRANSPORT VOLTAGES IN NIOBIUM FOILS. Heiden, C.; Friedrich, H. P. (Univ., Muenster, Ger.). Solid State Commun.; 9: 323-6(1 Mar 1971).

Power spectra of time-dependent voltages due to flux transport across superconducting niobium foils are measured at 4.2K for various separations of the voltage probe contacts. The results are in qualitative agreement with theoretical predictions of Burgess and of Clem. The variation of the low-frequency power density with contact separation reveals a considerable correlation of flux transport fluctuations throughout the foil. (auth) (UK)

36062 PHOTOLUMINESCENCE STUDIES OF SUPERCONDUCTING Nb_3Sn. Fraas, L. M.; Williams, P. F.; Porto, S. P. S. (Univ. of Southern California, Los Angeles). Solid State Commun.; 8: 2113-15(15 Dec 1970).

Some experimental results are reported that indicate the feasibility of photoluminescence studies of the superconducting energy gap. Experimental techniques, results and difficulties are discussed. The results and the extrapolation of the results of others indicate that useful information about the energy gap comes from photoluminescence. Existing theoretical papers discussing the light scattering cross section for the observation of the superconducting energy gap should be extended to account for resonant optical interband transitions. (auth) (UK)

36063 ENTROPY OF VORTICES IN HIGH-κ TYPE II SUPERCONDUCTORS. Vidal, F. (CNRS, Paris). Solid State Commun.; 8: 2147-50(15 Dec 1970).

The entropy per unit length of flux-line $s_i(B, T) = \phi_0(\partial^2 F/\partial B \partial T)$ is calculated from the free energy forms, for high-κ Type II superconductors throughout the entire temperature and magnetic field range. The agreement with the calorimetric measurements reported by many authors seems satisfactory. (auth) (UK)

36064 JOSEPHSON JUNCTIONS WITH SUPERCONDUCTING BARRIERS. Yamafuji, Kaoru; Ezaki, Tadao; Matsushita, Teruo (Kyushu Univ., Fukuoka). J. Phys. Soc. Jap.; 30: 965-71(Apr 1971).

Dc characteristics of Josephson junctions with thin superconducting barriers are discussed with the aid of the Ginzburg–Landau equations. The main difference of the present junctions from the Josephson junctions proposed so far lies in the fact that the barrier is composed of a thin superconductor in the superconducting state. It is shown that maximum dc current densities of present junctions can be at most 10^5 times of those of typical Josephson junctions with dielectric barriers. The oscillating powers of present elements are expected to be greatly increased from those of typical Josephson oscillators. (auth)

36065 SUPERCONDUCTING TRANSITION TEMPERATURES OF RF-SPUTTERED NbN FILMS. Keskar, K. S.; Yamashita, Tsutomu; Onodera, Yutaka (Tohoku Univ., Sendai). Jap. J. Appl. Phys.; 10: 370-4(Mar 1971).

NbN films are examined with respect to their electrical and superconducting properties. The films are deposited by rf reactive sputtering technique under argon gas atmosphere added with nitrogen. The films obtained have a wide range of resistivities and transition temperatures depending upon the partial nitrogen pressure in the argon atmosphere and the substrate temperature at which the films were deposited. The maximum transition temperature obtained is 17.3°K, higher by 0.9°K than the highest one reported so far. (auth)

36066 IMPROVEMENTS IN SUPERCONDUCTORS. Clayton, Anthony Robert King; Barber, Anthony Clifford (to Imperial Metal Industries (Kynoch) Ltd.). British Patent 1,164,816. 24 Sep 1969. Filed 4 May 1966.

A method of manufacturing a superconductor is described that comprises as a first step cold working a ductile superconductor material to effect a reduction in the cross-sectional area of the material of at least 10% and then heat treating the material at 100 to 500°C for at least ten minutes to produce a primary product. At least one further step of cold working the primary product is included to effect a reduction in the cross-sectional area of at least 5% and then heat treating at 100 to 500°C for at least ten minutes for each of the further steps, there being a minimum total reduction in the cross-sectional area of the material of 95%. (M.H.R.)

36067 THEORY OF RESONANCE EFFECTS IN METALS. I. ELECTRON SPIN RESONANCE IN TYPE I SUPERCONDUCTORS. II. HIGH FREQUENCY WAVES AND LANDAU FERMI-LIQUID EFFECTS IN NOBLE METALS. Aoi, Koya. Bloomington, Ind.: Indiana Univ. (1970). 160p. University Microfilms Order No. 71-6821.

Thesis.

Part I. For the purpose of determining whether electron spin resonance in type-I superconductors is experimentally possible, Dyson's theory was extended to the case of a superconductor taking into account the penetration depth of electromagnetic fields, the change in phase of the surface impedance and the change in group velocity and relaxation time of the quasi particles compared to the normal case. Line shapes and magnitudes of power absorbed and rf field transmitted for various frequencies and temperatures of thin film superconductors were calculated. From the calculation, the optimum temperatures and frequencies were determined, and it is concluded that even for these conditions, the experiment would be difficult. Part II. Dispersion relations of the high-frequency wave (HFW) were calculated. In order to include the Landau Fermi-liquid interaction, the symmetry relations of Landau function $f(\underline{k},\underline{k}')$ were investigated by the group-theoretic method, and then a theorem was derived concerning the symmetry of expansion coefficients of $f(\underline{k},\underline{k}')$. The theorem is applicable for systems of any symmetry. It is applied for noble metals, and then dispersion curves of the ordinary mode of HFW were calculated for copper for small q values where q is the wave vector of HFW. It is assumed that the static magnetic field is in the [001] direction and q is in the [100] direction. The velocity distribution and analytical representation of the noble metal Fermi surface derived by Halse were used. Qualitative differences between dispersion curves of HFW in alkali and noble metals are seen. (Diss. Abstr. Int., B)

36068 AC JOSEPHSON EFFECT IN Nb–Hg CONTACTS. Angadi, M. A.; Graham, G. M. (Univ. of Toronto). Can. J. Phys.; 49: 629-31(1 Mar 1971).

Some experiments with Nb/Hg contacts are described which suggest that these may be the basis of practical microwave systems. (auth) (Canada)

36069 CONTRIBUTION TO THE THEORY OF WEAK-COUPLING SUPERCONDUCTORS. Leavens, C. R.; Carbotte, J. P. (McMaster Univ., Hamilton, Ont.). Can. J. Phys.; 49: 724-46 (15 Mar 1971).

The Eliashberg equations for the case of weak-coupling superconductors are simplified. Further, an explicit approximate analytic solution of the simplified equations is obtained for the zero temperature gap edge. An expression for the critical temperature is also given. It is found to be of the BCS form and allows the BCS parameter N(0)V to be identified with a simple function of the normal state properties. The validity of these simplified integral equations and of this analytic solution is established by comparison with numerical solutions of the complete Eliashberg equations. The equations are used to discuss the effect of pressure on the gap, the isotope effect, as well as other properties. (auth) (Canada)

36070 SUPERCONDUCTING POINT CONTACT HAVING THE PROPERTIES OF A JOSEPHSON JUNCTION. Bondarenko, S. I.; Balanov, E. I.; Kolin'ko, L. E.; Narbut, T. P. (Physical Tech. Inst. of Low Temperatures, Kharkov). Cryogenics; 10: 508-10 (Dec 1970).

A method for producing point contacts between two superconductors is described. The contacts have properties of Josephson junctions between 3.8 and 1.5°K if their resistance at 300°K lies in the range 0.02 to 10 Ω. After being kept at room temperature for a month, the resistance changes by about 20% and the current–voltage characteristics by not more than 30%. After many cooling and warming cycles between 1.5 and 300°K there was practically no change in the contact properties. Although the positions of both pressed contacts and point contacts on superconductors can be accurately determined, the point contacts are much smaller. (UK)

36071 GENERALIZED LANGEVIN APPROACH TO EVALUATE ULTRASONIC ATTENUATION RATE IN SUPERCONDUCTORS. Leung, M. C. (Univ. of British Columbia, Vancouver). Physica; 48: 597-604(30 Sep 1970).

The longitudinal ultrasonic attenuation rate is derived by means of Mori's generalized Langevin equation. For most of the temperature range, earlier results obtained by perturbation theory are reproduced. However, when $\Delta \lesssim 1/\tau$, where τ is the relaxation time of quasi-particle density, it is shown that the Cooper pairs begin to participate in ultrasonic absorption, even when $\omega < 2\Delta$, as a result of fluctuation of the order parameter. (auth)

36072 EFFECT OF THE SUPERCONDUCTING STATE ON STRESS RELAXATION IN LEAD-TEMPERATURE DEPENDENCE. Suenaga, M.; Galligan, J. M. (Brookhaven National Lab., Upton, N. Y.). Scr. Met.; 5: 63-70(Jan 1971).

Some recent studies have shown that plastic flow of crystals is relatively easier in a crystal in the superconducting state than in the normal state. There are two possible mechanisms for such a difference, the first involving a change in an activation barrier, such as a pinning site, while the second involves a retardation of the dislocation motion by an electron viscosity or electron drag. The electron drag on a dislocation motion can be varied in a superconductor by varying the density of paired electrons, through the known temperature dependence of this density. It was expected that the barrier model would also show a temperature dependence, but not necessarily the same as the electron drag model. Experiments that bear on this question are presented for the case of pure lead. Lead single crystals were grown by standard Bridgeman techniques in graphite molds in a helium gas atmosphere. All tests below 4.2°K were performed in a liquid helium bath with a superconducting magnet surrounding the specimen. Above 4.2°K the tests were conducted in a variable-temperature cryostat, with the temperature controlled by an exchange gas of helium or a flowing helium gas. The results are discussed. (M.H.R.)

Equipment and Devices

Refer also to abstracts 34966, 34999–35001, 36607, and 36614.

36073 (CEA-CONF–1734) STATE OF THE ART OF PRODUCING STRONG MAGNETIC FIELDS. Bronca, G. (Commissariat a l'Energie Atomique, Saclay (France). Centre d'Etudes Nucleaires). 1970. 9p. (In French). (CONF-700341–1). Dep. NTIS (U. S. Sales Only).

From Panel on superconductors; Paris, France (17 Mar 1970).

The progress made during the last few years and the studies to be undertaken in the future concerning the use of Type-II superconducting materials in producing strong magnetic fields in large volumes are reviewed. The simple solution due to Stekly on the degradation of superconducting material is recalled. Results obtained from studies of loss and flux jumps are given. Some of the difficulties encountered in the development of superconducting coils are enumerated, and some of the superconducting magnets existing in Europe are described. (France)

36074 (CEA-CONF–1736) USE OF SUPERCONDUCTORS FOR ENERGY STORAGE AND DISCHARGE. Sole, J. (Commissariat a l'Energie Atomique, Limeil-Brevannes (France). Centre d'Etudes). 1970. 14p. (In French). (CONF-700341–5). Dep. NTIS (U. S. Sales Only).

From Panel on superconductors; Paris, France (17 Mar 1970).

The various processes connected with energy storage and discharge using superconductors are briefly studied. The processes of charging by external or internal generators, with or without any electric connections, and the associated storage processes are examined as well as the optimized value of the stored energy, the process involved in the transfer of the stored energy into the output circuit by direct connection or inductive coupling, according to the nature of the output circuit. (France)

36075 VACUUM BREAKDOWN BETWEEN SUPERCONDUCTING ELECTRODES. Williams, W. T. (University Coll., Swansea, Wales). Nature (London) Phys. Sci.; 231: 42-4(10 May 1971).

Preliminary results are reported on an investigation of prebreakdown current–voltage characteristics of superconducting electrodes in a high vacuum. The electrodes employed were machined from zone-refined (99.99% pure) Ta, placed in a Pyrex-glass discharge tube with a gap separation of 0.043 cm; a pressure of $\lesssim 10^{-8}$ torr was maintained in the discharge chamber. The current was measured as a function of applied voltage, which was increased in small steps until breakdown occurred and varied from $\sim 10^{-11}$ to 10^{-3} A. Measurements were made at 297, 77.2, 4.2, and 3.8 K and the data were analyzed in terms of the Fowler–Nordheim field equation (Proc. Roy. Soc., A119: 173(1928)). Straight-line Fowler–Nordheim graphs were obtained at 297, 72, and 4.2 K. When the temperature was lowered to 3.8 K, however, a discontinuity was observed; the variation of prebreakdown current with applied field at 4.2 and 3.8 K is shown graphically and, for a given applied field, the current at 3.8 K was greater than that at 4.2 K, the increase being as much as an order of magnitude at the lowest field values. Values of β, the enhancement factor of the applied electric field due to small projections on the cathode surface, are also given. Since the transition temperature of Ta is 4.5 K, the data suggest that the emitting sites on the cathode surface were only in the superconducting state for currents $< 5 \times 10^{-8}$ A, and transition from the superconducting state may have occurred at even lower currents. There appeared to be no obvious reason for the large change in β at 3.8 K, but a possible explanation might be a change in the work function of the surface. Further clarification is desirable because of the implications in the use of superconducting cables and vacuum insulation. (UK)

36076 PROBLEMS OF DESIGN AND CONSTRUCTION SUPERCONDUCTING SOLENOIDS FOR PHYSICAL INVESTIGATIONS. Krainskii, I. S.; Gruznov, Yu. A. pp 129-33 of Fiziko-Khimiya, Metallovedenie, i Metallofizika Sverkhprovodnikov. /Savitskii, E. M. (ed.). Moscow; Izdatel'stvo Nauka (1969). (In Russian).

Relations $I_c = f(B)$ were determined for short samples and small solenoids ($d_{ID} = 6$ mm, $d_{OD} = 16$ to 14 mm, $l = 15$ mm), made from the same wire, and placed in an external field. Several solenoids $d_{ID} = 16$ to 48 mm, $l = 45$ to 300 mm were made; good agreement was obtained for $I_c = f(B)$ for both small and large solenoids. The distribution of field in the short-circuited regime and also the distribution of residual field were measured. The maximum field is 80 kG in a 16-mm opening. (tr-auth)

36077 MACHINE ESTIMATE OF HOMOGENEITY OF MAGNETIC FIELDS OF SOLENOIDS. Kurochkin, V. I.; Yadroshnikov, V. A.; Vatulin, I. F.; Kulik, I. A. pp 133-40 of Fiziko-Khimiya, Metallovedenie, i Metallofizika Sverkhprovodnikov. /Savitskii, E. M. (ed.). Moscow; Izdatel'stvo Nauka (1969). (In Russian).

The method is described, and machine calculations of the strength and homogeneities of the magnetic field of the solenoid in the specified volume are presented. The data obtained were used for the production of a superconducting solenoid with correcting rings. The results of the measurement of the axial homogeneity of the magnetic field are cited, and the data obtained are compared with calculation. (tr-auth)

36078 INVESTIGATION OF TRANSITION PROCESSES OF SUPERCONDUCTING SOLENOID INTO STATE WITH NORMAL CONDUCTIVITY. Savitskii, E. M.; Moskvitin, A. I.; Baron, V. V.; Blinkov, E. L. pp 140-5 of Fiziko-Khimiya, Metallovedenie, i Metallofizika Sverkhprovodnikov. /Savitskii, E. M. (ed.). Moscow; Izdatel'stvo Nauka (1969). (In Russian).

The transitions of a four-quadrant solenoid from the superconducting to the normal state were studied to determine the characteristic causes of the transition process. The appearance of a signal made possible a system of detection of the pre-breakdown regime to control the solenoid artificially. Oscillograms were made of the transition process of the solenoid, that originates in a series of natural production factors. Attention is called to the fact that, in every case before the solenoid transition, an increase in the field strength in the first section of the solenoid occurs. The separation of the signal from the variation of field strength or its derivative for the first section in the static regime is possible for not more than 0.1 sec. This time is sufficient for the synchronization of an electronic system of automatic outward flow of magnetic energy from the superconducting apparatus. (tr-auth)

36079 ALL-PURPOSE LABORATORY COMPLEX FOR PRODUCING HIGHLY HOMOGENEOUS MAGNETIC FIELDS BY MEANS OF SUPERCONDUCTING MAGNETIC SYSTEMS. Kurochkin, V. Ya.; Vatulin, I. F.; Podteteneva, A. I.; Demisheva, A. G. pp 145-51 of Fiziko-Khimiya, Metallovedenie, i Metallofizika Sverkhprovodnikov. /Savitskii, E. M. (ed.). Moscow; Izdatel'stvo Nauka (1969). (In Russian).

A laboratory installation for producing magnetic fields of 0 to 32 kOe with homogeneity in the solenoid center in a cylinder (8 mm in diameter and 30 mm long) no worse than 10^{-5} is described. Calculations are given for the cryogenic section of the installation. Experiments carried out at liquid-helium and room temperature are discussed. (tr-auth)

36080 NEUTRON DIFFRACTION CRYO-ORIENTER. Heaton, L.; Mueller, M. H.; Adam, M. F.; Hitterman, R. L. (Argonne National Lab., Ill.). J. Appl. Crystallogr.; 3: 289-94(1970).

The cryo-orienter is used for neutron-diffraction studies of single crystals between liquid helium and room temperatures. It combines a double Dewar cryostat with a three-circle goniostat. The temperature of the crystal is controlled by a combination of exchange gas and a bridge circuit to a stability of ±0.01°K. A ring assembly allows the cryostat to be angularly displaced ±50° from vertical (χ), and to be rotated 360° (φ), which provides crystal

XUM

motion about two axes with ±0.01° precision. The ring assembly can be rotated about the diffraction vector. Crystals can be mounted along a nonmajor zone and sufficient data can then be collected with one crystal mounting. The ARCADE computer system controls the entire data collection. (auth) (Denmark)

Plasma and Thermonuclear Physics

36081 TECHNOLOGY INDEX FOR PLASMAPHYSICS RESEARCH AND FUSION REACTORS. VOLUME 5, NO. 4, 1971. Bibliography, Author Index, Subject Index, Appendix. Frankfurt am Main; Zentralstelle fuer Atomkernenergie-Dokumentation (1971). 47p.

This listing includes 247 articles on various aspects of the title subjects. (M.O.W.)

36082 PLASMA PHYSICS INDEX. VOLUME 6, No. 4, 1971. Bibliography, Author Index, Subject Index. Frankfurt am Main; Zentralstelle fuer Atomkernenergie-Dokumentation (1971). 149p.

This listing contains 565 articles on various aspects of the subject. (M.O.W.)

Confinement and Heating

Refer also to abstract 36178.

36083 CONCERNING ONE MORE METHOD OF MAGNETIC ENERGY PUMPING INTO A TURBULENT PLASMA. Akhiezer, A. I.; Alaksin, V. F.; Khodusov, V. D. (Kharkov State Univ.). JETP Lett. (USSR) (Engl. Transl.); 13: No. 3, 114-17(5 Feb 1971).

Translated from Zh. Eksp. Teor. Fiz., Pis'ma Red.; 13: No. 3, 164-6(5 Feb 1971).

Increasing plasmon energy by modulating the external parameters on which their frequencies depend is discussed. The energy change during three-plasmon interactions is described. (M.O.W.)

36084 EFFECT OF AN ELECTRIC FIELD ON THE MOTION OF PARTICLES IN HELICAL FIELDS. Popryadukhin, A. P. (Lebedev Inst. of Physics, Moscow). Sov. Phys.-Tech. Phys. (Engl. Transl.); 15: No. 9, 1435-43(Mar 1971).

Translated from Zh. Tekh. Fiz.; 40: No. 9, 1839-50(Sep 1970).

The effect of an electric field on the motion of various particles in systems with helical magnetic fields is investigated. It is shown that the electric field leads to the rearrangement of particles in velocity space. If the equipotentials do not coincide with the magnetic surfaces, the trajectories can be displaced over distances greater than the Larmor radius. (auth)

36085 ION ENERGY SPECTRA AND LIFETIMES IN A MULTIPOLE MAGNETIC TRAP. Demidenko, I. I.; Lomino, N. S.; Padalka, V. G. Sov. Phys.-Tech. Phys. (Engl. Transl.); 15: No. 11, 1823-7(May 1971).

Translated from Zh. Tekh. Fiz.; 40: No. 11, 2335-40(Nov 1970).

Ion energy spectra in a plasma confined in a quadrupole magnetic trap were studied. Measurements were made by means of a retarding potential. Ion energy distribution functions were obtained for various times, and the Maxwellian nature of the distribution was demonstrated. The time variation of ion temperature and the energy dependence of ion lifetime in the trap were determined. The nature of this dependence indicated that the main mechanism for particle loss from the system was the loss of plasma in the mechanical supports of the current-carrying windings. (auth)

36086 PLASMA TRANSPORT IN A MAGNETIC QUADRUPOLE FIELD. Demidenko, I. I.; Lomino, N. S.; Padalka, V. G. Sov. Phys.-Tech. Phys. (Engl. Transl.); 15: No. 11, 1816-22(May 1971).

Translated from Zh. Tekh. Fiz.; 40: No. 11, 2326-34(Nov 1970).

Plasma motion in a linear magnetic quadrupole field was studied in order to determine the feasibility of plasma transport. The magnetic field was produced by currents flowing in the same direction through two parallel conductors. The plasma motion along the axis of the magnetic multipole field is drift motion in the crossed polarized electric and magnetic fields. The structure of the polarization potential and the plasma density distribution in the plane perpendicular to the direction of the plasma motion were studied. Localization of the plasma is governed by the MHD-stability region of the plasma. In a magnetic quadrupole field of sufficient intensity, the plasma is transported without loss over distances up to 150 cm, and the plasma density becomes significantly larger than in the absence of a magnetic field. In the absence of MHD stability, fluctuations in the potential and plasma density are observed; these represent the initial stage of the development of a flute instability. (auth)

36087 HIGH-FREQUENCY PLASMA HEATING NEAR THE LOWER HYBRID FREQUENCY. Galaktionov, B. B.; D'yachenko, V. V.; Shcherbinin, O. N. (Ioffe Inst. of Physics and Tech., Leningrad). Sov. Phys.-Tech. Phys. (Engl. Transl.); 15: No. 11, 1809-12(May 1971).

Translated from Zh. Tekh. Fiz.; 40: No. 11, 2317-21(Nov 1970).

Experimental results on high-frequency heating of a hydrogen plasma are described. As a function of the magnetic field, plasma heating has a threshold near the lower hybrid frequency; below this frequency the power transferred to the plasma is reduced noticeably. The value of the plasma density corresponding to the maximum heating efficiency was determined. From an analysis of the curves giving the drop of the diamagnetic signal along the axis of the apparatus, it is possible to separate the diamagnetic effects due to the ions and electrons. Electron and ion temperatures measured during the high-frequency power transfer are approximately equal. (auth)

36088 EFFECT OF ELECTRON HEATING ON OVERALL EFFICIENCY OF CONCEPTUAL MIRROR FUSION REACTORS. Lazar, N. H.; Haste, G. R. (Oak Ridge National Lab., Tenn.). Plasma Phys.; 13: 433-7(May 1971).

The principal limitation to fuel confinement in conceptual mirror reactors is the rapid scattering of the ions into the loss cone following cooling by the trapped electron distribution. The ion confinement time and nuclear reaction rate are estimated as functions of electron energy assuming the space potential resulting from the hotter electrons can be controlled. It is shown that values of Q (nuclear power produced/power injected) ≈ 3 to 4 can be attained for the principal reacting region. These values would be sufficient to obtain significant fuel heating from charged reaction products so that the overall Q could approach 10. (auth) (UK)

Diagnostics

Refer also to abstracts 35833 and 36208.

36089 (KHFTI-69/51) MEASUREMENT OF THE DENSITY OF A PLASMA WITH THE AID OF AN OPEN RESONATOR. Ulshmid, I.; Bez'yazychnyi, I. A. (Akademiya Nauk Ukrainskoi SSR, Kharkov. Fiziko-Tekhnicheskii Institut). 1970. 18p. (In Russian). Dep. NTIS (U. S. Sales Only).

The application of classical interferometers to measurement of plasma density is hampered significantly for devices with metallic chambers, which lead to the emergence of reflections and deformations in the measurement results. These difficulties are increased in proportion to the decrease of the radial dimensions of the vacuum chambers. In devices of relatively greater dimensions, the most reliable method is the application of the Fabry–Perot resonator, which combines the advantages of classical interferometers with resonator-sensitivity methods and allows density measurements in a wide range with good spatial resolution. For the measurement of plasma density N_e in devices with metal chambers $L \gg 2a$ (L is the length, a is the radius of the chamber), it is possible to use directly a certain part of the chamber, forming an opened cylindrical resonator. A great disadvantage of such a resonator is the averaging of density values N_e along the whole system. The methodology of determining plasma parameters (electron density N_e and the electron–ion collision frequencies ν_{ei}) does not differ from that used in the case of closed resonators. However, the open resonator has a discharge spectra that allows measurements to be conducted simultaneously on several highly differing frequencies. The use of types of oscillations with different radial field distributions gives the possibility of determining the radial distribution of plasma density. (tr-auth)

36090 (MATT-838) SPECIAL DIAGNOSTIC DEVICES. Christie, R. S.; Knutson, D. S. (Princeton Univ., N. J. Plasma Physics Lab.). May 1971. Contract AT(30-1)-1238. 12p. (CONF-710418-9). Dep. NTIS.

From fourth symposium on engineering problems of fusion research; Washington, D. C. (20 Apr 1971).

Several of the special diagnostic devices, designed to solve particular positioning and measurement problems, are described and illustrated. In particular, the problems associated with achieving the various mechanical movements within a vacuum, and the methods employed in controlling the coaxial conductors from the probe tip to the vacuum feedthrough are discussed. (auth)

36091 (UARAEE-95) INSTRUMENTS FOR MEASUREMENT OF THE SPECTRAL LINES PROFILE AND SHIFT. El-Khalafawy, T. A.; Hafez, L. A.; Nofal, E. E.; Volkov, Ja. F. (Atomic Energy

XUM

Establishment, Cairo (Egypt). Dept. of Accelerators and Plasma Physics Research). 1970. 21p. Dep. NTIS (U. S. Sales Only).

Two spectral instruments for fast-discharge investigation are described. One of these represents a device for a grating spectrograph (Jarrel–Ash) for recording line profiles via an 8-channel fiber bundle array covered with the line under investigation. The other device may be used with any type of spectrograph or monochromator by using a Fabry–Perot interferometer. Light from a plasma passes through the Fabry–Perot etalon and spectrograph and is reflected from a profile dividing mirror to eight photomultipliers. Formulas are presented for calculating the width or shift of the spectral line. The device adjustment is described. (auth)

36092 (UARAEE–101) EXPERIMENTAL STUDIES ON SHOCK WAVES PROPAGATED THROUGH A LONGITUDINAL MAGNETIC FIELD IN ELECTRODELESS DISCHARGE TUBES. Mahmoud, H. M.; El-Khalafawy, T. A.; Masoud, M. M.; El-Gwaily, M. S.; Volkov, Ya. (Atomic Energy Establishment, Cairo (Egypt). Dept. of Accelerators and Plasma Physics Research). 1970. 40p. Dep. NTIS (U. S. Sales Only).

A microwave-reflection method is applied to study the interaction mechanisms of shock waves propagated through an axial external magnetic field. It is found that the velocity damping factor $\alpha(B)$ increases linearly with increasing uniform magnetic fields according to the relation $\alpha = aH$ where $a \cong 0.25$ per kG. The microwave-interferometer method was used to determine the average electron density distribution; the maximum electron density measured approaches a value of 1.7×10^{13} cm^{-3}, which represents the theoretical cutoff density. The above microwave methods are used in the Q-band range (8 mm wave length). A double electrical probe (Langmuir probe) is used to determine the density within the shock front and its variation with the external magnetic field along the tube axis. It is found that the shock front density decreases with increasing magnetic field in both positive and negative directions, only in the region where B is variable it also decreases with increase of distance. The plasma is produced by electromagnetically driven shock waves in hydrogen gas at pressure of 70 m torr. The velocity reaches a value of 10^6 cm/sec. A superimposed axial magnetic field of intensity 6.7 kG is applied to the path of the shocks. (auth)

36093 ELECTRON BEAM AS A METHOD OF FINDING THE POTENTIAL DISTRIBUTION IN A CYLINDRICALLY SYMMETRIC PLASMA. Stallings, Charles H. (Univ. of Wisconsin, Madison). J. Appl. Phys.; 42: No. 7, 2831-4(Jun 1971).

An electron beam was used to determine the plasma potential and charge density as a function of radius for an inertially confined tenuous plasma. The column of plasma was formed by a collimator in front of a plasma gun. The observations showed a positive charge density inside the region of approximately uniform ion density but with the net charge density having a peak well inside the plasma column. A significant negative charge density was observed outside the column of ions. An inversion of the integral equation relating the deflection of the electron beam to the internal electric field was performed. This inversion gave the plasma potential as a function of radius. The deflection of the electron beam at a constant-impact parameter oscillated as a function of distance from the collimator for the plasma cylinder. This oscillation was evident only in certain regions and the wavelength was not a constant. (auth)

36094 OPTICAL MEASUREMENT OF A HIGH-FREQUENCY ELECTRIC FIELD IN A WEAKLY IONIZED PLASMA. Takamura, S.; Kodama, T.; Aihara, S. (Nagoya Univ., Japan). J. Appl. Phys.; 42: No. 7, 3014-15(Jun 1971).

The intensity of the light (He I 4471Å) emitted from helium plasma increases in a high-frequency electric field. The intensity of the rf electric field estimated by the increment of the light intensity agrees with the result obtained from the sheath plasma series resonance characteristic. (M.O.W.)

36095 PLASMA DIAGNOSTIC TECHNIQUES. Fuhs, A. E. (Naval Postgraduate School, Monterey, Calif.). AGARD Conf. Proc.; No. 38, 501-44(1970).

From Conference on new experimental techniques in propulsion and energetics research; Munich, Germany (11 Sep 1967). See CONF-670999.

The following diagnostic techniques are reviewed: transducer design from active magnetic probes; observation of radiation excited by a high-energy electron beam; electrostatic probes in static plasma; interferometry, including holographic interferometry; giant pulse lasers as source suitable for visualization, namely schlieren and shadowgraph; microwave determination of electron density profiles; and a method based on excitation of electro-acoustic waves. (M.O.W.)

36096 INTERNAL PHYSICAL MEASUREMENTS IN MHD PLASMA ACCELERATORS. Lovberg, R. H. (Univ. of California, San Diego, La Jolla). AGARD Conf. Proc.; No. 38, 545-57(1970).

From Conference on new experimental techniques in propulsion and energetics research; Munich, Germany (11 Sep 1967). See CONF-670999.

A restricted set of correlated measurements is described in which the electromagnetic field structure and the electron density distribution are determined, and inferences concerning the efficiency of acceleration and partitioning of electron and ion currents are made. The apparatus employed for this research is an inductive "theta pinch". Electric and magnetic fields are measured by the use of probes, and the electron density distribution is determined through the use of a modified schlieren photographic technique. Current partitioning is inferred through insertion of the experimental data into the generalized Ohm's law. (auth)

36097 SPATIAL DISTRIBUTION OF ION TEMPERATURES IN TOKAMAK DEVICES. Shcheglov, D. A.; Kuznetsov, E. I. Sov. Phys.-Tech. Phys. (Engl. Transl.); 15: No. 9, 1453-7(Mar 1971).

Translated from Zh. Tekh. Fiz.; 40: No. 9, 1863-8(Sep 1970).

To determine the spatial distribution of ion temperatures in the plasma of the Tokamak-5 device, measurements were made of the broadening of individual spectral lines of atoms and ions by means of a Fabry–Perot interferometer. Hydrogen atomic temperatures averaged over the length of the discharge are 0.5 to 0.9 eV. The measured distribution of ion temperatures along the minor radius of the plasma is approximated by $(1 - \rho^2)^2$. A feature of this distribution is the smooth drop in ion temperature at the edge of the plasma, indicating a region with cold ions. (auth)

36098 EFFECT OF COLLISIONS ON THE DIFFUSION ELECTRON CURRENT TO A CYLINDRICAL PROBE IN A MAGNETIZED PLASMA. Litvinov, I. I. Sov. Phys.-Tech. Phys. (Engl. Transl.); 15: No. 9, 1572-3(Mar 1971).

Translated from Zh. Tekh. Fiz.; 40: No. 9, 2018-20(Sep 1970).

The various types of collisions that make a diffusion contribution to the probe current are studied. The necessary criteria are derived. (M.O.W.)

36099 PLASMA CAMERA DIAGNOSTICS IN THE STUDY OF WAVE EVOLUTION. Cataldo, Joseph C.; Tao, Chia-hwa (City Coll., New York). Rev. Sci. Instrum.; 42: No. 6, 897-8(Jun 1971).

A plasma camera, designed for high-resolution photography of a columnar plasma cross section, was adopted for sequential high-speed photography in a single-ended Q machine. The plasma camera consists of a 50% transmissive stainless steel screen and an aluminum-coated scintillator. The camera and its use are described. (M.O.W.)

36100 THEORY OF A CYLINDRICAL PHOTOIONIZATION CHAMBER OF HIGH DENSITY. Groenig, Hans (Technische Hochschule, Aachen). Z. Naturforsch.; 25a: 1053-62(Jul 1970). (In German).

The theory of a cylindrical photo-ionization chamber with high density and small ionization degree is developed. Under the basic assumptions made, the problem can be reduced to the simultaneous solution of the continuity equations for ions and electrons containing production terms and of the Poisson equation. Physically, the region between the electrodes is characterized by three zones: both space-charge boundary layers at the electrodes and the quasi-neutral area. Mathematically, it appears as an analogous distribution by an asymptotic development of the dimensionless basic equations according to a very large parameter α. Explicit solutions are obtained for the current–voltage characteristics, the saturation current, and the particle density. The knowledge of these sizes makes it possible to use the photoionization chamber for the calibration of Langmuir probes. (tr-auth)

36101 LIMITS IN DETECTION OF RADIATION SCATTERED BY A PLASMA. Pyatnitskii, L. N.; Korobkin, V. V. Sov. Phys.-Tech. Phys. (Engl. Transl.); 15: No. 11, 1914-17(May 1971).

Translated from Zh. Tekh. Fiz.; 40: No. 11, 2449-52(Nov 1970).

The region in which the scattering of electromagnetic radiation can be used for plasma diagnostics is determined. The effect of the plasma properties (collective effects) on the aperture broadening of the satellites in the scattering spectrum is considered. It is shown that a limiting value of the solid angle of observation exists; this value depends on the plasma parameters, the accuracy of the plasma measurements, and the scattering angle. Relationships obtained between the limiting solid angle, the plasma properties, and the scattering angle limit the regions in which experi-

XUM

ments can be carried out. Similar relationships are presented for the case in which the aperture broadening can be neglected. The effect in question can be important in laboratory plasmas and plasmas in the upper layers of the atmosphere. (auth)

36102 USE OF THE SAHA EQUATION FOR THE SIMULTANEOUS DETERMINATION OF TEMPERATURE AND ELECTRON CONCENTRATION. Vujnovic, V. (Univ., Zagreb). Fizika (Zagreb); 3: No. 2, 105-8(Apr 1971).

The Saha equation is applied for the simultaneous determination of temperature and electron concentration using a suitable representation of the relative line intensities of spectral lines emitted by ionized and neutral atoms. An illustration of the method is shown. (auth)

Kinetics (General)

Refer also to abstracts 36560, 36636, and 36640.

36103 (DLR-FB-70-13) ON THE FLOW OF COMPRESSIBLE PLASMAS IN THE SELF-INDUCED MAGNETIC FIELD OF ARC DISCHARGES. Huegel, H. (Deutsche Forschungs- und Versuchsanstalt fuer Luft- und Raumfahrt E. V., Stuttgart (West Germany). Institut fuer Plasmadynamik). Feb 1970. 117p. (In German). Dep. NTIS (U. S. Sales Only).

Flow of compressible plasmas in axisymmetric channels under the influence of electromagnetic body forces and Joule heating is described within the framework of magnetogasdynamics. The existing electric and magnetic fields originate as the electric field and self-induced magnetic field from a dc discharge. For the flow parameters velocity, Mach number, pressure, density, and temperature, the quasi-one-dimensional analysis yields coupled first-order differential equations that are solved by numerical integration. At arc currents of 500 to 3,000 A, measured values of thrust and Mach numbers show satisfactory agreement with theoretical results. (auth)

36104 (NP-18772) EQUILIBRIUM COMPOSITIONS AND THERMODYNAMIC PROPERTIES OF MIXED PLASMAS. II. ARGON-OXYGEN PLASMAS AT 10^{-2} TO 10 ATMOSPHERES, BETWEEN 2,000°K AND 35,000°K. Capitelli, M.; Ficocelli V., E.; Molinari, E. (Consiglio Nazionale delle Ricerche, Bari (Italy). Centro di Studio per la Chimica dei Plasmi. Bari Univ. (Italy). Istituto di Chimica General ed Inorganica). 1970. 139p. Dep. NTIS (U. S. Sales Only).

Thermodynamic and transport data are presented of mixtures of diatomic gases with rare gases up to 35,000°K. The results are given in tabular form for equilibrium calculations of the system argon–oxygen between 2,000 and 35,000°K at 10^{-2}, 10^{-1}, 1, and 10 atmospheres. Numerical values are reported for every 1,000°K and for compositions between 0 and 100% O_2 at intervals of 20%. (M.O.W.)

36105 IMPROVEMENTS IN OR RELATING TO PLASMA ACCELERATORS FOR GENERATING PROPULSION THRUST. Maes, Michel Emil (to Rocket Research Corp.). British Patent 1,181,431. 18 Feb 1970. Filed 11 Jan 1967.

A pulsed plasma accelerator wherein a vaporizable ionizable propellant is injected into a plasma accelerating chamber open only at one end is described. The accelerating chamber is generally rectangular in configuration and bounded by electroconductive surfaces and insulative surfaces in alternating pattern. (TSS)

36106 INVESTIGATION OF ION SHOCK WAVES IN A COLLISIONLESS PLASMA. Alikhanov, S. G.; Belan, V. G.; Kichigin, G. N.; Chebotaev, P. Z. (Inst. of Nuclear Physics, Novosibirsk, USSR). Zh. Eksp. Teor. Fiz.; 60: No. 3, 982-92(Mar 1971). (In Russian).

The problem of propagation of a stationary shock wave in a collisionless plasma with warm ions ($T_i \neq 0$) in the absence of a magnetic field is solved. The shock wave velocity dependence on potential is found for a temperature ratio $T_e/T_i = 10^1$ to 10^3. The minimal value $T_e/T_i = 5$ for which the waves can exist is found. Results of experiments on propagation of finite-amplitude ion shock waves in a laboratory plasma ($T_e/T_i = 20$ to 50) are presented. The initial stage of wave formation and dynamics of ion reflection from the wave front are studied. The ion distribution function in a plasma for waves with various amplitudes and velocities is measured. Evolution of a large-amplitude wave in conditions close to the experimental ones is studied by carrying out a numerical experiment with a computer plasma. Results of the theoretical analysis are compared with the experimental data. In all cases considered, the calculations and experiments indicate that the Mach numbers do not exceed 1.6. (auth)

36107 NEW EXPERIMENTAL TECHNIQUES IN PROPULSION AND ENERGETICS RESEARCH. Technical Meeting Held in Munich, September 11–15, 1967. Andrews, David; Surugue, Jean (eds.). AGARD Conference Proceedings No. 38. Slough, Eng.; Technivision Services (1970). 637p. (CONF-670999).

Separate abstracts were prepared for 4 of the 29 papers. The remaining papers were not in the scope of NSA and hence omitted. (M.O.W.)

For abstracts of individual papers see: 36095, 36096, 36108, and 36202.

36108 MAGNETOGASDYNAMIC PROPERTIES OF STATIONARY SUPERSONIC PLASMA JETS. Huegel, J. (Deutsche Versuchsanstalt fuer Luft und Raumfarht eV, Stuttgart). AGARD Conf. Proc.; No. 38, 559-80(1970).

From Conference on new experimental techniques in propulsion and energetics research; Munich, Germany (11 Sep 1967). See CONF-670999.

A device, similar to an arc-jet engine, was operated stably within a current range of 500 to 3000 amps at an ambient pressure of 0.5 mm Hg. With argon and nitrogen as working gases mass flow rates of 0.075 to 0.6 g/sec were applied. The velocity produced resulted from two mechanisms namely aerodynamic acceleration due to heating and expansion processes, and electromagnetic acceleration due to self-magnetic body forces. The latter originate from the interaction of the arc current with its self-induced magnetic field. The relative importance of both effects is found to depend on arc current, mass flow rate and electrode and nozzle configuration. The exit Mach number of the plasma flow increased with increasing current. A mean magnetic Reynolds number calculated from the experimental data exhibited a stronger than linear dependence on arc current and reached values of the order of one at high currents. The magnetic pressure number (Cowling number) of the flow inside the nozzle is a marked function of arc current and mass flow rate. With increasing current this quantity increases to attain constant values for flow conditions with predominant self-magnetic velocity production. (auth)

36109 INFLUENCE OF TRIPLE ELECTRON AND ION COMBINATION ON ELECTRODYNAMIC PLASMA ACCELERATION. Kolesnikov, P. M.; Stolovich (Inst. of Heat and Mass Exchange, Minsk). Inzh.-Fiz. Zh.; 20: No. 3, 467-75(Mar 1971). (In Russian).

The integral characteristics of plasma are determined, taking into account triple electron and ion recombination as well as mass-transfer processes and resistance forces. The appropriate sets of differential equations describing such plasma acceleration are solved on digital computer. The solutions are analyzed. (auth)

36110 OCCURRENCE AND BEHAVIOR OF CURRENT SPOKES IN MPD ARCS. Cochran, Robert A.; Fay, James A. (Massachusetts Inst. of Tech., Cambridge). AIAA (Amer. Inst. Aeronaut. Astronaut.) J.; 9: No. 5, 886-93(May 1971).

A pulsed MPD arc was operated to experimentally determine the occurrence of the rotating-spoke mode of operation and to investigate voltage characteristics and spoke frequency of the MPD arc. It was found that the single rotating current spoke occurs at intermediate current levels above a critical magnetic field strength. A comparison of the spoke frequency measurements with the actuator-disk theory of Fay and Cochran shows that the actuator-disk model gives a satisfactory prediction of the behavior of the spoke frequency until a limiting frequency is reached, after which the spoke approaches a constant rotational speed which is the same for all gases. The variation in the electrode voltage was found to obey the correlation of Patrick and Schneiderman when the arc was operated in the diffuse mode at low power levels. In the spoke mode, voltages several times this prediction were measured and can be explained in terms of the emf generated by the rotating spoke. Several criteria are suggested for prediction of the observed spoke/no-spoke boundaries. (auth)

36111 PROPERTIES OF THE ROTATING SPOKE IN AN UNSTABLE PULSED MPD ARC. Kribel, R.; Eckdahl, C.; Lovberg, R. (Univ. of California, San Diego, La Jolla). AIAA (Amer. Inst. Aeronaut. Astronaut.) J.; 9: No. 5, 893-9(May 1971).

A modified magnetoplasmadynamic (MPD) arc was operated in a pulsed mode to permit internal probing of the arc region. The arc attains steady-state operation that strongly resembles the behavior of the more-conventional continuous MPD arcs. Spatial surveys with magnetic probes and small Rogowski coil probes show the current distribution to have the form of a well-defined radial spoke which rotates azimuthally. The rotation frequency is typically about 40 kc with argon. Observations with double-plane Langmuir probes measuring plasma flow indicate that the

rotating current spoke corresponds to an actual plasma rotation. The spoke exhibits an internal structure. The plasma in the leading edge is streaming radially outward, while that in the trailing edge is counterstreaming inward towards the cathode. Most of the arc current flows in the trailing section, and the ions there seem to carry about 30% of the total arc current. (auth)

36112 TRANSITION FROM DISTRIBUTED EMISSION TO A CATHODE SPOT IN AN ARC. Moizhes, B. Ya.; Rybakov, A. B. (Semiconductor Inst., Leningrad). Sov. Phys.-Tech. Phys. (Engl. Transl.); 15: No. 9, 1574-6(Mar 1971).

Translated from Zh. Tekh. Fiz.; 40: No. 9, 2020-3(Sep 1970).

It is assumed that the cathode spot appears during the voltage increase when a negative-slope region appears on the current–voltage characteristic, the latter being caused by cathode heating and the Schottky effect. Diagrams relating currents and voltages are shown. (M.O.W.)

36113 PLASMA ACCELERATION WITH AN AUXILIARY STATIONARY MAGNETIC FIELD . Churaev, V. A.; Popov, N. F. Sov. Phys.-Tech. Phys. (Engl. Transl.); 15: No. 9, 1449-52(Mar 1971).

Translated from Zh. Tekh. Fiz.; 40: No. 9, 1858-62(Sep 1970).

The effect of an additional stationary magnetic field on the conditions under which the acceleration of a plasmoid takes place in an inductive conical source was studied. A theoretical analysis of the acceleration process is carried out. An experimental study is also performed and the results are in qualitative agreement with the calculation. It is shown that the presence of an external field with a strength of ~200 Oe can triple the plasmoid velocity. (auth)

36114 MASS AND VELOCITY SPREAD OF PLASMOIDS IN PULSED PLASMA ACCELERATORS. Derevshchikov, V. A.; Struchkov, A. I. Sov. Phys.-Tech. Phys. (Engl. Transl.); 15: No. 9, 1458-62(Mar 1971).

Translated from Zh. Tekh. Fiz.; 40: No. 9, 1869-74(Sep 1970).

Using a low-inertia, platinum thermal probe, a study was made of the velocity distribution of plasmoids in end-type (electrode erosion) and coaxial (dielectric erosion) pulsed plasma accelerators. The masses and velocities of individual plasmoids are determined, and the mean-mass velocity is calculated. (auth)

36115 EXPERIMENTAL STUDY OF A TWO-LENS ACCELERATOR. Zubkov, I. P.; Kislov, A. Ya.; Morozov, A. I. Sov. Phys.-Tech. Phys. (Engl. Transl.); 15: No. 11, 1796-1800(May 1971).

Translated from Zh. Tekh. Fiz.; 40: No. 11, 2301-6(Nov 1970).

A high-current accelerator in which crossed electric and magnetic fields are used for plasma acceleration with "closed" electron drift is described. Results obtained from studies of the potential and magnetic fields in the accelerator are also presented. (auth)

36116 TWO-PHASE SEEDING IN LOW-DENSITY PLASMA FLOW. Lien, Hwachii; Stepakoff, Gerald (Avco Systems Div., Wilmington, Mass.). AIAA (Amer. Inst. Aeronaut. Astronaut.) J.; 9: No. 6, 1129-35(Jun 1971).

Numerical solutions of a typical boundary-layer seeding problem at low pressure are presented to demonstrate the important roles played by the interaction of heterogeneous fluid flow and chemical processes. A physico-chemical model is developed for the investigation of the coupling of heterogeneous vaporization kinetics in a rarefied atmosphere, with the distribution of ionic and neutral species and homogeneous gas-phase chemistry. It is found that the seeding effectiveness, as indicated by the evaporation efficiency and the degree of ionization for a given injection mass flow rate, is essentially controlled by the initial droplet size, the velocity and the direction of injection, kinetics of vaporization, and chemical processes. (auth)

Kinetics (Experimental)

36117 (UARAEE-106) EXPERIMENTAL STUDIES ON MAGNETICALLY DRIVEN SHOCK WAVE PASSING THROUGH A LONGITUDINAL MAGNETIC FIELD. El-Khalafawy, T. A.; Volkov, Ya. F.; El-Menshawy, M. F.; Masoud, M. M.; El-Masry, M. A. (Atomic Energy Establishment, Cairo (Egypt). Dept. of Accelerators and Plasma Physics Research). 1970. 40p. Dep. NTIS (U. S. Sales Only).

The main interest is focused on studying the effect of an external magnetic field on the shock wave produced by a conical pinch discharge of peak current 250 kA, charging voltage = 20 kV and time of half cycle 1.5 μsec. The external magnetic field of 6.8 kG is produced by capacitor bank (charging voltage 10 kV and time of half cycle 1 m sec). The shock-wave capacitor bank is fired near maximum magnetic field. Hydrogen gas is used at initial pressure 70 m torr, and the shock-wave produced has maximum velocity 10^7 cm/sec. The analysis of the variation of shock wave velocities due to the presence of a magnetic field shows that the propagation factor of the shock-wave is proportional linearly with the magnitude of the constant axial magnetic field and to the square of the gradient magnetic field. The magnetic probe measurement shows the presence of a rotating current within the front, which is also a source of energy given to the front within propagation. (auth)

36118 PARAMETERS OF PLASMA PRODUCED BY FAST ELECTRON BEAM IN A MAGNETIC FIELD. Zhilinskii, A. P.; Liventseva, I. F. (Leningrad Polytechnical Inst.). Sov. Phys.-Tech. Phys. (Engl. Transl.); 15: No. 10, 1621-7(Apr 1971).

Translated from Zh. Tekh. Fiz.; 40: No. 10, 2082-90(Oct 1970).

The parameters of a plasma (electron temperature and density) produced by a pulsed beam of fast electrons in a magnetic field (up to 1000 Oe) are discussed. The measurements were made by probe and resonator methods. The beam current was varied from a few milliamperes to hundreds of milliamperes. Data are presented for helium at pressures of 8×10^{-3} to 10^{-1} mm Hg. It is shown that anomalously high electron temperatures can be obtained under certain conditions. Under these conditions the maximum effective energy transfer from the beam electrons to the plasma occurs. The results are compared with estimates of the plasma parameters based on the balance equations. (auth)

36119 ELECTRON ENERGY DISTRIBUTION IN THE POSITIVE COLUMN OF A HELIUM DISCHARGE. Bessonova, K. F.; Oreshak, O. N.; Stepanov, A. F.; Stepanov, V. A. Sov. Phys.-Tech. Phys. (Engl. Transl.); 15: No. 9, 1481-2(Mar 1971).

Translated from Zh. Tekh. Fiz.; 40: No. 9, 1900-2(Sep 1970).

In a tube 60 mm in diameter a region of helium pressure is found in which a uniform positive column can exist in a discharge. A deviation from the Maxwellian distribution is observed at 17 or 18 eV because of inelastic collisions of electrons with helium atoms in the uniform positive column. At low currents a deviation from a Maxwellian occurs in the low-energy region because of increased elastic collisions of electrons with atoms. (auth)

36120 METHOD OF OBTAINING SHORT DENSE PLASMOIDS. Gol'ts, E. Ya; Khodzhaev, A. Z. (Lebedev Inst. of Physics, Moscow). Sov. Phys.-Tech. Phys. (Engl. Transl.); 15: No. 10, 1688-9(Apr 1971).

Translated from Zh. Tekh. Fiz.; 40: No. 10, 2164-6(Oct 1970).

A method is described for obtaining short dense plasmoids with small cross section by cutting off portions of a plasma jet using a transverse electric field. By choosing appropriate shutter geometry, it is possible to avoid discharges and to raise substantially the density of the plasma jet that is cut off. Plasmoids with a density of 10^{15} cm^{-3} and a time length of 0.1 μsec were obtained. (auth)

36121 ACHIEVING LOCAL THERMODYNAMIC EQUILIBRIUM STATES IN LASER-INDUCED XENON PLASMAS. Hugenschmidt, Manfred (Deutsch-Franzoesisches Forschungsinstitut, Saint-Louis, France). Z. Angew. Phys.; 30: 350-7(1971). (In German).

An examination was made of the initiation and expansion as well as the detailed development of the parameters of a laser-induced breakdown in xenon. Optical methods were used to visualize the geometrical structure of the plasma, especially during the first few nanoseconds of the expansion, so that thermodynamic calculations could be carried out on the plasma parameters. The spatial and temporal development of the electron density was obtained by an optical-interferometric method which showed, for example, that the central value, 9 nsec after initiation, was 1.7×10^{19} cm^{-3}. An estimation of the electron temperature was obtained by a spectroscopic method, measuring the luminosity of plasma in the near-uv spectral region. It was found that between 20 and 400 nsec the electron temperature decreases from about 50,000 to 15,000°K. With these experimental data (electron density and temperature) it was possible to calculate the relaxation times necessary to establish local thermodynamic equilibrium, which is achieved because of the high values of electron densities 10 to 15 nsec after the beginning of the cascade in the inner central part of the plasma. (auth)

36122 INVESTIGATION OF THE AZIMUTHAL CURRENT AND MICROWAVE RADIATION IN A THETA PINCH. Adamov, I. Yu.; Berezhnyi, V. L.; Dushin, L. A.; Kononenko, V. I. Sov. Phys.-Tech. Phys. (Engl. Transl.); 15: No. 11, 1787-91(May 1971).

Translated from Zh. Tekh. Fiz.; 40: No. 11, 2289-94(Nov 1970).

It was shown earlier that, for initial discharge pressures of 10^{-3} to 10^{-2} torr, an instability develops in a theta pinch, and as a result, electromagnetic radiation and hard x rays appear. The electromagnetic radiation was recorded, both at the electron plasma

XUM

frequency and at harmonics of the electron cyclotron frequency. The intensity of the radiation exceeds considerably the level of thermal radiation in the plasma. The results of a study of the plasma radiation using sensitive superheterodyne receivers are presented. The discharge pressures were 10^{-2} to 10^{-1} torr. The process of azimuthal current growth and its cross correlation are described. (auth)

36123 ANOMALOUS SCATTERING OF LASER LIGHT FROM A MAGNETIZED ARC PLASMA. Ludwig, D.; Mahn, C. (Max-Planck-Institut fuer Plasmaphysik, Garching, Ger.). Phys. Lett.; 35A: No. 3, 191-2(31 May 1971).

The spectrum of light scattered from fluctuations perpendicular and parallel to a magnetic field in a hydrogen arc plasma (n_e = 1.2×10^{16} cm^{-3}; $T_e = 7 \times 10^4$ °K; $\alpha = 0.47$; B = 10 kG) reveals considerable deviations from the thermal spectrum. It has a peaked structure with enhanced cross sections at multiples of half the plasma frequency and is the same for both directions. (auth)

36124 RADIATION EMITTED BY AN ARGON PLASMA PRODUCED BY A LOW-PRESSURE TORCH DISCHARGE. Triche, H.; Tabassian, M.; Besombes-Vailhe, J. (Univ., Toulouse). Method. Phys. Anal.; 7: No. 1, 68-73(Mar 1971). (In French).

Radiation from a high-frequency inductive discharge in argon at low pressure was studied. Disappearance of the continuous spectra and the appearance of intense argon II emission lines were observed. Variations in the principal parameters of the discharge, power, pressure, and argon flow were related to the emission lines from argon II and subsequently to the excitation temperature of the discharge. This temperature increases with the electrical power supplied by the generator and with the reduction of the number of atoms in the source. (France)

36125 ISOMAGNETIC DISCONTINUITY IN A COLLISIONLESS SHOCK WAVE IN A PLASMA. Eselevich, V. G.; Es'kov, A. G.; Kurtmullaev, R. Kh.; Malyutin, A. I. (Nuclear Physics Inst., Novosibirsk, USSR). JETP Lett. (USSR) (Engl. Transl.); 13: No. 2, 49-51(20 Jan 1971).

Translated from Zh. Eksp. Teor. Fiz., Pis'ma Red.; 13: No. 2, 73-6(20 Jan 1971).

The electrostatic discontinuity in a collisionless shock front in a plasma was investigated. The relative amplitude of the discontinuity is shown for Mach numbers 3 to 6. (M.O.W.)

Kinetics (Theoretical)

36126 (NYO-1480-173) NUMERICAL SOLUTION OF THE BOLTZMANN EQUATION. Chorin, Alexandre Joeel (New York Univ., N. Y. AEC Computing and Applied Mathematics Center). Apr 1971. Contract AT(30-1)-1480. 49p. Dep. NTIS.

A numerical method for solving the full nonlinear Boltzmann equation is presented, and applied to the problem of shock structure in a gas of elastic spheres. The success of the method hinges on the systematic use of Gaussian quadrature and Hermite interpolation. (auth)

36127 (UARAEE-65) DIELECTRIC TENSOR OF INHOMOGENEOUS PLASMA TO SECOND ORDER WITH RESPECT TO SPACE DERIVATIVES. El-Siragy, N. M. (Atomic Energy Establishment, Cairo (Egypt). Dept. of Accelerators and Plasma Physics Research). 1968. 43p. Dep. NTIS (U. S. Sales Only).

General expressions for all the components of the dielectric tensor are obtained, taking into consideration the second-space derivatives of the equilibrium plasma parameters. General expressions for polarization vector components are also obtained. Integration with respect to the velocities is carried out for the case of a Maxwellian distribution of the particles. (auth)

36128 (UARAEE-78) BOUNDARY CONDITIONS IN THE CASE OF ADJACENT PLASMA STREAMS. El-Naggar, I. A.; Pakhomov, V. I.; Zayed, K. E. (Atomic Energy Establishment, Cairo (Egypt). Dept. of Accelerators and Plasma Physics Research). 1969. 26p. Dep. NTIS (U. S. Sales Only).

The comprehensive and rigid derivation of boundary conditions for adjacent streams of cold plasma in the presence of an external magnetic field is carried out. The cases of plane and cylindrical geometries are considered. Expressions are obtained for the dielectric permeability tensor-operator components for cold inhomogeneous plasma in the presence of a certain profile of the equilibrium particle velocities. (auth)

36129 (UARAEE-102) STUDY OF DYNAMICS OF THE Θ-PINCH DISCHARGE WITH A SUPERIMPOSED AZIMUTHAL MAGNETIC FIELD. El-Khalafawy, T. A.; Youssef, A. M.; Diatlov, V. G.; Volkov, Ya. F. (Atomic Energy Establishment, Cairo (Egypt). Dept. of Accelerators and Plasma Physics Research). 1970. 26p. Dep. NTIS (U. S. Sales Only).

A magnetohydrodynamic steady-flow model, on the assumption of ideal plasma conductivity, is used for the theoretical consideration. The pressure balance with the inclusion of the time variations of the external, trapped, and azimuthal magnetic fields is considered in order to estimate the discharge radius. The plasma radial oscillations are shown to be of a magnetohydrodynamic nature. Its period is of the order of the ion-ion self-collision time. The measurements of an axial electric polarization and the azimuthal magnetic field made it possible to determine the discharge boundary motion velocity and that of any inner plasma layer. High-speed photographic techniques were also used. (auth)

36130 NONLINEAR THEORY OF RELAXATION OF A MONOENERGETIC BEAM IN A PLASMA. Shapiro, B. D.; Shev'chenko, V. I. (Physical-Technical Inst., Kharkov). Zh. Eksp. Teor. Fiz.; 60: No. 3, 1023-35(Mar 1971). (In Russian).

The dynamics of relaxation of an initially monoenergetic beam in a plasma are investigated. It is shown that instability of beam particles, captured in the oscillation potential well, play an important role in the relaxation process. Equations are derived that describe oscillation excitation and diffusion in the beam with allowance for instability. An inspection of the equations reveals that the distribution function is almost plateau-like for times $t \sim \omega_p^{-1} n_0/n_1$ (ω_p is the plasma frequency and n_1, n_0 the beam and plasma densities, respectively). During the following relaxation stage for which the characteristic time is $t \sim \Omega^{-1} n_0/n_1$ ($\Omega = \omega_p (n_1/n_0)^{1/3}$ is the oscillation frequency of the captured particles), accelerated particles appear in the beam, and a velocity distribution is established that is similar to a Maxwellian. (auth)

36131 THERMOKINETIC EXPANSION THEORY. Dawson, John M. (Princeton Univ., N. J.). pp 355-63 of Laser Interaction and Related Plasma Phenomena. /Schwarz, Helmut J. (ed.). New York; Plenum Publishing Corp. (1971).

From Laser interaction and related plasma phenomena meeting; East Windsor Hill, Conn. (9 Jun 1969). See CONF-690622.

A model for the expansion of a spherical ball of plasma is discussed. Solutions for the model are outlined. (M.O.W.)

36132 RESULTS OF THE SELF-SIMILARITY MODEL. Hora, Heinrich (Rensselaer Polytechnic Inst., Troy, N. Y. Institut fuer Plasmaphysik, Garching, Ger.). pp 365-82 of Laser Interaction and Related Plasma Phenomena. /Schwarz, Helmut J. (ed.). New York; Plenum Publishing Corp. (1971).

From Laser interaction and related plasma phenomena meeting; East Windsor Hill, Conn. (9 Jun 1969). See CONF-690622.

The self-similarity model of expanding laser-produced plasma is derived from the hydrodynamic equations. An analytical iterative solution, taking into account the varying plasma diameter, results in remarkably higher electron temperatures. Numerical iteration with the condition of total transfer of the radiation to the plasma in overdense states shows a good agreement with measurements of Engelhardt et al. at large spherical suspended targets and agreement with measurements of Sigel et al. at hydrogen foils. On the basis of detailed numerical calculations of Mulser et al., either heating by self-focusing or higher thermal conductivity than Spitzer's values is concluded due to collective effects at conditions of high density, if conditions of degeneration and Coulomb logarithms less than unity are present. (auth)

36133 CALCULATION OF THE ION TRAJECTORIES IN A PENNING DISCHARGE. Ivanova, T. I.; Pustovalov, G. E. (Moscow State Univ.). Sov. Phys.-Tech. Phys. (Engl. Transl.); 15: No. 10, 1646-51(Apr 1971).

Translated from Zh. Tekh. Fiz.; 40: No. 10, 2112-18(Oct 1970).

Using the method of finite differences and a BTsÉM computer, the potential distribution in Penning discharges with various geometries was examined. The trajectories of ions moving toward the cathode with zero initial velocity from a point located inside the anode are found by numerical integration. Inside the anode there are regions from which ions fall into a central hole of fixed radius drilled in the cathodes. Space charge is ignored. (auth)

36134 ELECTRON DISTRIBUTION FUNCTION IN A LOW-TEMPERATURE PLASMA. Lukovnikov, A. I.; Fetisov, E. P.; Trekhov, E. S. (Engineering Physics Inst., Moscow). Sov. Phys.-Tech. Phys. (Engl. Transl.); 15: No. 9, 1493-1500(Mar 1971).

Translated from Zh. Tekh. Fiz.; 40: No. 9, 1916-26(Sep 1970).

The method of solution of the transport equation proposed by Kovrizhnykh is extended to the case of a weakly ionized molecular plasma in an electric field E. The symmetric part of the distribution $f_0(\epsilon)$ is found in analytic form, allowance being made for the different types of inelastic collisions of electrons with the neutral particles (molecules). A numerical calculation of

$f(\epsilon)$ is given and the average electron energy in a nitrogen plasma is found for various values of the ratio of electric field to the neutral density. (auth)

36135 KINETIC THEORY OF THE PINCH EFFECT. Kasatkin, A. P.; Kon'kov, V. L. (Gorky Physicotechnical Research Inst., USSR). Sov. Phys.-Tech. Phys. (Engl. Transl.); 15: No. 10, 1612-15(Apr 1971).

Translated from Zh. Tekh. Fiz.; 40: No. 10, 2070-4(Oct 1970).

Joint Coulomb and magnetic interactions between electrons are calculated for systems in which collisions play a significant role. The system is neutral overall; ion mobility is neglected. The particles are contained in an infinite cylinder of specified radius in a longitudinal electric field. Stationary solutions of the system composed of the kinetic equation and Maxwell's equations are given in the form of a series with respect to the external fields. An expression is obtained for the first four approximations to the distribution function. A method is given for determining the equilibrium density of the current-carrying particles and the relaxation times with respect to the measured radial electric field. (auth)

36136 EFFECTIVE NUMBER OF IONIZATION AND RECOMBINATION EVENTS IN THE POSITIVE COLUMN. Kagan, Yu. M.; Lyagushchenko, R. I. (Leningrad State Univ.). Sov. Phys.-Tech. Phys. (Engl. Transl.); 15: No. 9, 1568-9(Mar 1971).

Translated from Zh. Tekh. Fiz.; 40: No. 9, 2013-15(Sep 1970).

Expressions are derived for the effective number of ionization and recombination events in the positive column of a glow discharge. The effective recombination constant may be noticeably smaller than the recombination constant found from the cross section for the elementary process. (auth)

36137 COMPTON FOKKER-PLANCK EQUATION FOR HOT PLASMAS. Cooper, Gilbert (Univ. of California, Livermore). Phys. Rev., D; 3: No. 10, 2312-16(15 May 1971).

The Fokker–Planck equation for Compton scattering in a plasma is developed without recourse to a nonrelativistic expansion. Using calculated energy exchange rates for scattering in a relativistic Maxwellian plasma, an equation is obtained that is valid for electron temperatures up to 100 keV and photon energies up to 1 MeV. Numerical comparisons presented show excellent agreement between Fokker–Planck and Monte Carlo calculations. Results using the nonrelativistic Fokker–Planck, valid to only 20 keV, are also presented to indicate the improvement made. (auth)

36138 EXPLANATION OF THE ANOMALOUS SKIN EFFECT. Gupta, R. M. (Univ. of Rajasthan, Jaipur, India). Acta Phys. Pol.; A39: No. 3, 267-72(Mar 1971).

Landau studied the longitudinal field penetration into a semi-bounded plasma, considering specularly reflecting electrons at the boundary. Kurilko and Popov and Gorman and Mason examined the same problem, considering a fraction p of all incident electrons reflecting specularly and the remaining portion diffusely. Here, the penetration of transverse electromagnetic waves into magnetoactive semi-bounded plasma is studied and the electric field for specular reflection of electrons is obtained. The results are used to explain the phenomenon of the anomalous skin effect. (auth)

36139 THEORY OF A ROTATING PLASMA IN CROSSED ELECTRIC AND MAGNETIC FIELDS. Vrba, P. (Inst. of Plasma Physics, Prague). Czech. J. Phys.; 21: No. 6, 636-50(1971).

The behavior of a weakly ionized gas confined by cylindrical electrodes and dielectric fronts is studied. An ionized gas is given rotational movement by transverse electric and longitudinal magnetic fields. Quantities describing a plasma in the stationary state are obtained by solving a system of macroscopic equations. Some of them are compared with experimental data. (auth)

36140 THOMSON SCATTERING IN A STRONG MAGNETIC FIELD. Canuto, V. (Goddard Space Flight Center, New York); Lodenquai, J.; Ruderman, M. Phys. Rev., D; 3: No. 10, 2303-8 (15 May 1971).

The effect of a strong magnetic field on neutron stars or white dwarfs is calculated for Thomson scattering in a fully ionized collisionless plasma. The photon mean free path can be greatly extended for propagation nearly parallel or, for the extraordinary mode, nearly perpendicular to the field. (auth)

36141 ELECTRONIC THERMAL CONDUCTIVITY IN A TOROIDAL PLASMA LOOP. Artsimovich, L. A. JETP Lett. (USSR) (Engl. Transl.); 13: No. 2, 70-3(20 Jan 1971).

Translated from Zh. Eksp. Teor. Fiz., Pis'ma Red.; 13: No. 2, 101-5(20 Jan 1971).

Using data on the energy balance of the electron component of Tokamak plasmas and the distribution of electron temperature, an expression is derived for the thermal conductivity coefficient. A discussion of this coefficient is given. (M.O.W.)

36142 NUMERICAL SOLUTION OF THE QUASI-LINEAR EQUATIONS FOR A BEAM–PLASMA SYSTEM. Nemchinskii, V. A. (Inst. of Semiconductors, Leningrad). Sov. Phys.-Tech. Phys. (Engl. Transl.); 15: No. 11, 1927-9(May 1971).

Translated from Zh. Tekh. Fiz.; 40: No. 11, 2462-5(Nov 1970).

Steady-state one-dimensional solutions are obtained for the dynamic relaxation of an electron beam in a plasma. (M.O.W.)

36143 POLARIZED RADIATION TRANSFER IN A COLLECTIVE PLASMA. Heyvaerts, J. (CNRS, Paris). J. Phys. (Paris); 32: No. 2-3, 145-55(Feb-Mar 1971). (In French).

Proper modes phase-correlation effects are analyzed using a Liouville-equation perturbation method. The equations obtained are reduced to a simpler form in the high-frequency limit. (auth) (France)

36144 LIGHT SCATTERING IN A MARGINALLY STABLE PLASMA. Joyce, Glenn (Univ. of Iowa, Iowa City); Salat, Albert. Plasma Phys.; 13: 359-64(May 1971).

The density fluctuations in a marginally stable, or slightly unstable plasma are considered. A kinetic equation for the density fluctuations is derived, and the cross section for light scattering is calculated. In general, it is a function of the distribution function and the growth rate of the least stable mode at all previous times. (auth) (UK)

36145 ANOMALOUS RESISTIVITY OF A TURBULENT PLASMA. Dum, Christian T. (Cornell Univ., Ithaca, N. Y.). Plasma Phys.; 13: 399-413(May 1971).

The conductivity tensor of a turbulent plasma is computed from the coherent response to an external test wave. The enhanced resistivity arises from wave–particle interactions and nonlinear coupling between the test wave and the turbulent spectrum. Nonexpandable effects due to scattering of particles by the turbulent fluctuations and the modification of dielectric properties by turbulence are included. The conditions under which these effects may become significant, even at low levels of turbulence, are discussed. The possibility of a hydrodynamic description of the turbulent plasma is also discussed and effective collision frequencies for the resistivity are introduced. The dipole and reactive approximation commonly used in calculations of high frequency conductivity are re-examined in the context of the new theory. An improved kinetic equation for waves is proposed. (auth) (UK)

36146 ANALYTICAL EXPRESSIONS OF THE ELECTRON ENERGY DISTRIBUTION FUNCTION IN A WEAKLY IONIZED GAS, TAKING INTO ACCOUNT INELASTIC COLLISIONS. Segur, Pierre; Gaillard, Joelle (Univ., Toulouse). Compt. Rend., Ser. B; 272: No. 16, 917-20(19 Apr 1971). (In French).

Some analytical expressions of the energy distribution function are obtained, taking into account inelastic collisions by using the technique of asymptotic resolution of differential equations proposed by Feschenko et al. (France)

Production

Refer also to abstract 36211.

36147 LASER INTERACTION AND RELATED PLASMA PHENOMENA. Proceedings of the First Workshop, Held at East Windsor Hill, Connecticut, June 9–13, 1969. Schwarz, Helmut J.; Hora, Heinrich (eds.). New York; Plenum Publishing Corporation (1971). 520p. $25.00. (CONF-690622).

Separate abstracts were prepared for 12 of the included papers. The remaining papers were not in the scope of NSA and hence omitted. (M.O.W.)

For abstracts of individual papers see: 36131, 36132, 36148–36156, and 36203.

36148 INTRODUCTORY COMMENTS TO LASER INTERACTION AND RELATED PLASMA PHENOMENA. Harteck, Paul (Rensselaer Polytechnic Inst., Troy, N. Y.). pp 1-10 of Laser Interaction and Related Plasma Phenomena. /Schwarz, Helmut J. (ed.). New York; Plenum Publishing Corp. (1971).

From Laser interaction and related plasma phenomena meeting; East Windsor Hill, Conn. (9 Jun 1969). See CONF-690622.

First work on stimulated emission by Einstein and Planck is briefly discussed. The historical developments of laser radiation are reviewed. Some use of laser radiation for plasma studies is briefly mentioned. (M.O.W.)

36149 LINEAR AND NONLINEAR LASER-INDUCED EMISSION OF IONS FROM SOLID TARGETS WITH AND WITHOUT MAGNETIC FIELD. Schwarz, Helmut (Rensselaer Polytechnic Inst., East Windsor Hill, Conn.). pp 207-22 of Laser Interaction and Related Plasma Phenomena. /Schwarz, Helmut J. (ed.). New York; Plenum Publishing Corp. (1971).

From Laser interaction and related plasma phenomena meeting; East Windsor Hill, Conn. (9 Jun 1969). See CONF-690622.

A survey of some of the first laser experiments involving ion emission from irradiated solid targets is given. Ion emission in the absence and presence of magnetic fields is also considered. A brief theoretical discussion of the problem is also given. (M.O.W.)

36150 KINETIC AND IONIZATION PHENOMENA IN LASER-PRODUCED PLASMAS. Sklizkov, G. V. (Lebedev Inst. of Physics, Moscow). pp 235-57 of Laser Interaction and Related Plasma Phenomena. /Schwarz, Helmut J. (ed.). New York; Plenum Publishing Corp. (1971).

From Laser interaction and related plasma phenomena meeting; East Windsor Hill, Conn. (9 Jun 1969). See CONF-690622.

Experiments on heating solids by powerful laser radiation are discussed. The parameters of high-temperature, high-density plasma with effective ion charge $q > 1$ were studied. All experiments were separated into three groups. (M.O.W.)

36151 FREE TARGETS. Witkowski, S. (Institut fuer Plasmaphysik, Garching, Ger.). pp 259-71 of Laser Interaction and Related Plasma Phenomena. /Schwarz, Helmut J. (ed.). New York; Plenum Publishing Corp. (1971).

From Laser interaction and related plasma phenomena meeting; East Windsor Hill, Conn. (9 Jun 1969). See CONF-690622.

Techniques for laser beam irradiation of a single solid particle in vacuum are reviewed. They include experiments at Culham, Frascati, and Garching. (M.O.W.)

36152 EXPERIMENTAL RESULTS OF FREE TARGETS. Hora, Heinrich (Rensselaer Polytechnic Inst., Troy, N. Y. Institut fuer Plasmaphysik, Garching, Ger.). pp 273-88 of Laser Interaction and Related Plasma Phenomena. /Schwarz, Helmut J. (ed.). New York; Plenum Publishing Corp. (1971).

From Laser interaction and related plasma phenomena meeting; East Windsor Hill, Conn. (9 Jun 1969). See CONF-690622.

Plasmas produced from free small (5 to 10μ radius) electromagnetically suspended LiH targets showed in the first measurements a quite symmetric expansion but finally an asymmetry with a preferential direction against the laser. Preheating by tailored laser pulses re-established conditions of the self-similarity model of a symmetric expansion and heating up to temperatures of few hundred eV. Aluminum balls of 50- to 150-μ radius showed two groups of plasma, a slow spherical inner core fulfilling thermokinetic properties describable by the self-similarity model, and an asymmetric outer shell expanding preferentially against the laser due to a nonlinear surface process. Free-hydrogen targets of the larger size expand symmetrically and drift slowly into the direction of the laser radiation, indicating a recoil by a surface acceleration against the laser. Magnetic fields decrease the expansion velocity and increase the duration of luminosity in some experiments. Emission of microwave radiation can be explained, but many effects are unsolved (increase of ion energy, increase of electric resistivity, instabilities etc.). (auth)

36153 SHOCK-WAVE PROCESS AND NUMERICAL CALCULATIONS. Witkowski, S. (Institut fuer Plasmaphysik, Garching, Ger.). pp 339-53 of Laser Interaction and Related Plasma Phenomena. /Schwarz, Helmut J. (ed.). New York; Plenum Publishing Corp. (1971).

From Laser interaction and related plasma phenomena meeting; East Windsor Hill, Conn. (9 Jun 1969). See CONF-690622.

Two models for plasma production by irradiating solids with laser beams are considered in which the spatial inhomogeneity of the absorption process is taken into account. The first model was treated by dimensional methods and gives the order of magnitude of averaged values of the plasma parameters. The second model takes into account the locally varying plasma properties and gives numerical results for different laser intensities. (M.O.W.)

36154 NONLINEAR EFFECT OF EXPANSION OF LASER-PRODUCED PLASMAS. Hora, Heinrich (Rensselaer Polytechnic Inst., Troy, N. Y. Institut fuer Plasmaphysik, Garching, Ger.). pp 383-426 of Laser Interaction and Related Plasma Phenomena. /Schwarz, Helmut J. (ed.). New York; Plenum Publishing Corp. (1971).

From Laser interaction and related plasma phenomena meeting; East Windsor Hill, Conn. (9 Jun 1969). See CONF-690622.

At light intensities exceeding $I^* = 10^{14}$ W/cm^2 (for ruby and neodymium glass lasers), nonlinear effects start to become efficient. One of these effects at plasma densities close to the cutoff case is the creation of a force directed towards lower plasma density that exceeds the thermokinetic forces. An elementary description of the force is given, showing a drift of the oscillating electrons where only the nonlinear longitudinal oscillation has to be included. The general derivation of the force is given by the equation of motion of the Lorentz theory for nonrelativistic plasma with or without collisions at oblique incidence of the radiation and at total reflection. The transferred momentum can be expressed by a nonlinearly increased radiation pressure, and the resulting ion energy of translatory motion is equal to the increased oscillation energy of the electrons in the plasma. The evaluation of the threshold I^* for the nonlinear effect is based on a nonlinear intensity dependence of the inverse bremsstrahlung. A self-focusing mechanism in plasma has a threshold at laser powers of only 1 MW. It results in light filaments with electromagnetic energy densities exceeding the thermokinetic values ($I > I^*$), which can explain measured filament diameters in gas breakdown and nonlinear effects in the usual cases of laser-produced plasma. It cannot be excluded that the high-energy, nonthermal ions at laser-produced plasmas (Linlor effect) are due to the described nonlinear acceleration after self-focusing occurred. (auth)

36155 APPLICATION OF LASER-PRODUCED PLASMAS FOR CONTROLLED THERMONUCLEAR FUSION. Hora, Heinrich (Rensselaer Polytechnic Inst., Troy, N. Y. Institut fuer Plasmaphysik, Garching, Ger.). pp 427-45 of Laser Interaction and Related Plasma Phenomena. /Schwarz, Helmut J. (ed.). New York; Plenum Publishing Corp. (1971).

From Laser interaction and related plasma phenomena meeting; East Windsor Hill, Conn. (9 Jun 1969). See CONF-690622.

A review is given on earlier theoretical estimations of laser-produced fusion plasmas. The optimum fusion efficiencies are given for densities of 6×10^{22} cm^{-3} of 50:50 D–T plasmas. The fusion efficiency of one is reached at laser energies E_0 of 10^4 joules of the fusion reactions during the heating where assumptions are included in an optimistic way, while E_0 is 10^6 joules if only the fusion during free-plasma expansion is effective. Experiments of Sun et al. and Basov et al. are reviewed and the problems are discussed for laser-produced fusion plasmas due to nonlinear acceleration and other nonlinear effects, starting at laser intensities of 10^{14} W/cm^2. If overdense plasmas are irradiated at nonlinear conditions, the nonlinear acceleration can be used for a confinement by a nonlinearly increased radiation pressure of the interior of a spherical plasma, being sufficiently heated and having not too much loss of plasma by the blowoff process. The Lawson criterion of fusion can be reached within a factor of 3. The laser intensities should be below 10^{15} W/cm^2 and of about 0.1- to 10-nsec length. (auth)

36156 HIGH-DENSITY AND HIGH-TEMPERATURE LASER-PRODUCED PLASMAS. Floux, Francis (CEA, Villeneuve-Saint-Georges, France). pp 447-68 of Laser Interaction and Related Plasma Phenomena. /Schwarz, Helmut J. (ed.). New York; Plenum Publishing Corp. (1971).

From Laser interaction and related plasma phenomena meeting; East Windsor Hill, Conn. (9 Jun 1969). See CONF-690622.

Theoretical and experimental studies are described on the heating of massive solid targets by powerful laser pulses. The purpose of the experiments was a comprehensive investigation of the parameters of high-density and high-temperature plasmas with low-z ionic charge and particularly solid deuterium targets. The experiments and results are described. (M.O.W.)

36157 PLASMA EFFECTS IN THE INTERACTION OF INTENSE ELECTRON BEAMS WITH MATTER. Ledovskoi, V. P.; Mladenov, G. M. (Leningrad Electrotechnical Inst.). Sov. Phys.-Tech. Phys. (Engl. Transl.); 15: No. 10, 1766-7(Apr 1971).

Translated from Zh. Tekh. Fiz.; 40: No. 10, 2260-2(Oct 1970).

The interaction of intense electron beams with matter and the effects of the produced plasma are discussed. At a certain critical intensity at the focal spot, ion focusing causes a reduction in the transverse cross section of the beam. The diameter of the plasma-filled hollow channel in the liquid phase is an order of magnitude smaller than the initial beam diameter for most materials. (auth)

36158 MOTION AND COLLISION OF PLASMA BLOBS PRODUCED BY GIANT PULSE LASER IN A TRANSVERSE MAGNETIC FIELD. Matoba, Tohru; Ariga, Seiichi (Kyoto Univ.). J. Phys. Soc. Jap.; 30: No. 5, 1477-87(May 1971).

The properties of plasma created by the 200-MW giant pulse ruby laser irradiation on the lithium plate were investigated. Measurements of the variation of the shape and size of the plasma

blob with and without the existence of the uniform magnetic field, its density, temperature, pressure, velocity of the motion and the electric field due to the charge separation were made. The phenomena occurring at the head-on collision of two blobs across the uniform magnetic field were also investigated, confirming that the electric field could be canceled out at the colliding region. (auth)

36159 IONIZATION INSTABILITY OF A SELF-SUSTAINING LOW-PRESSURE DISCHARGE IN A STRONG TRANSVERSE MAGNETIC FIELD. Erofeev, V. S.; Sanochkin, Yu. V. Sov. Phys.-Tech. Phys. (Engl. Transl.); 15: No. 9, 1413-17(Mar 1971).
Translated from Zh. Tekh. Fiz.; 40: No. 9, 1810-16(Sep 1970).

The stability of the sheath at the anode of a low-pressure discharge with magnetized electrons is investigated. It is shown that, as the pressure increases and a vacuum regime is converted into a regime with strong ionization, the discharge becomes unstable with respect to long-wave perturbations with period much longer than the ion transit time. The perturbation is due to the loss of balance between the ionization rate in the sheath and the loss of ions from the sheath. Criteria are obtained for the instability, and the phase velocity of waves is determined. The critical density of neutral particles depends only on the kind of gas, and is proportional to the strength of the applied magnetic field. These results can be used in the interpretation of cutoff phenomena and in the discharge readjustment observed in experiments with Penning discharges or inverse magnetrons. (auth)

36160 PRODUCTION OF A HIGH-DENSITY PLASMA BY MICROWAVES IN A MAGNETIC FIELD. Krivosheev, M. V. (Leningrad Polytechnic Inst.). Sov. Phys.-Tech. Phys. (Engl. Transl.); 15: No. 11, 1805-8(May 1971).
Translated from Zh. Tekh. Fiz.; 40: No. 11, 2312-16(Nov 1970).

In an earlier paper by the author, the interaction of the microwave fields in a waveguide with the plasma in a straight discharge in a magnetic field was studied. The experiments were carried out over a wide range of microwave energies with the microwave power supplied to the plasma being smaller than that dissipated in a constant current. Here, investigations were made in which the microwave energy exceeds the energy dissipated in the discharge with no microwave field ((2 to 6) $\times 10^{-2}$ W/cm^3) by at least two orders of magnitude. (auth)

36161 DYNAMIC VOLTAGE-CURRENT CHARACTERISTICS OF d. c. PLASMA GENERATORS AT LARGE AND SMALL AMPLITUDES AND RATES OF CURRENT VARIATION. Sergienko, A. S.; Shashkov, A. G. (Inst. of Heat and Mass Exchange, Minsk). Inzh.-Fiz. Zh.; 19: 669-77(Oct 1970). (In Russian).

From the study of dynamic voltage–current characteristics of a plasma generator with an interelectrode insertion and operating with air, at large amplitudes (I_D = 70 A) and small amplitudes (dI/dt = 1.5 to 5 A/sec) of current variation, the presence of electric hysteresis and difference of these characteristics from the static voltage–current one was established. By the method of small disturbances, dynamic voltage–current characteristics of plasma generator with fixed length of an arc burning in argon atmosphere were obtained. It is shown that, within the frequency range from 0.2 to 2.0 kc, the arc resistance is inductive, and with increasing frequency from 2.0 to 20 kc, of capacitive nature. (auth)

36162 EXPLORATORY TESTS ON A DOWNSTREAM-CATHODE MPD THRUSTER. Burkhart, James A. (Lewis Research Center, Cleveland). J. Spacecraft Rockets; 8: 240-4 (Mar 1971).

Substantial improvement in the thrust performance of a low-power MPD arc thruster has been achieved in the specific impulse range of 600 to 2100 sec. The thruster tested utilizes a cathode positioned in the exhaust beam, downstream of the anode, as opposed to the conventional position upstream of the anode. Xenon is the propellant used, and testing is conducted in a background pressure of 1.6×10^{-5} torr. Operation achieved in the above specific impulse range is at thrust levels from 6 to 16 mN, power levels of 180 to 720 w, and thrust efficiencies of 13 to 24%. (auth)

Stability

36163 (CTO–737) REPORT OF EXPERIMENTS ON THE SUPPRESSION OF FLUTE INSTABILITY BY MEANS OF A FEEDBACK SYSTEM IN PHOENIX II. Chuyanov, V. A. (Institut Atomnoi Energii, Moscow (USSR)). Translated by J. B. Sykes (U.K.A.E.A., Culham Lab., Abingdon, Eng.), from report IAE–2012. 57p. Dep. NTIS (U. S. Sales Only).

Experiments are described relating to the stabilization of flute instability in the Phoenix II plasma at densities $\approx 10^9$ cm^{-3}, using a one-electrode feedback system. A detailed comparison is made between the experimental results and computer calculations based on a theory that takes account of the frequency response of the feedback system. (auth)

36164 (TID–25713) NONLINEAR THEORY OF MACROINSTABILITIES AND ENHANCED TRANSPORT IN PLASMAS. Weinstock, Jerome; Williams, Robert H. (Environmental Science Service Administration, Boulder, Colo. Aeronomy Lab.). 7 Jul 1970. Contract AT(49-8)-2976. 31p. Dep. NTIS.

A method is described for solving the MHD equations for nonlinear plasma waves and turbulence due to macroinstabilities. It is argued that the dominant nonlinear effect for macroinstabilities is the scattering of fluid elements of charge by plasma waves. The consequent wave–fluid interaction causes an enhanced diffusion coefficient in the continuity equation and an identical enhanced viscosity coefficient in the momentum equation. This enhanced plasma transport is analogous to the "eddy" transport and Reynolds stress of neutral turbulence. A nonlinear dispersion relation is obtained from the linear dispersion relation by simply adding the enhanced diffusion term to the frequency. It is shown that linear macroinstabilities are stabilized by the enhanced diffusion and viscosity terms. As examples, the enhanced diffusion coefficients and density and electric field fluctuations are calculated for resistive instabilities. (auth)

36165 (UCRL–51030) COMPUTATION OF PLASMA EQUILIBRIA AND STABILITY IN ASTRON AND MINIMUM-B MIRROR SYSTEMS. Anderson, David Vincent (California Univ., Livermore. Lawrence Radiation Lab.). Apr 1971. Contract W-7405-Eng-48. 112p. Dep. NTIS.
Thesis.

For the Astron, the equilibrium equation for the E layer and plasma reduces to a single scalar elliptic equation in two dimensions. The finite-difference form of this equation is solved by the ADI (alternating direction implicit) algorithm. Stability of the equilibria found are checked by the fluid energy principle of Bernstein; the numerical analysis of this is carried out by integrating a Sturm–Liouville equation along flux lines. A restriction of this stability analysis is that all toroidal fields vanish. A generalization of the analysis to include toroidal fields is considered, but then rejected as computationally impractical. Two codes were developed for Astron. The first is in cylindrical coordinates, and the second one is in toroidal coordinates. The latter of these is more general than Astron and can treat other configurations such as Tokomak and Levitron. The mirror configurations have open field lines and are generally lacking the symmetry required for a two-dimensional representation. The equilibrium equation for tensor pressure reduces to one scalar equation in three dimensions, which is assumed to be elliptic. A generalization of the ADI algorithm is required to solve the finite-difference form of this equation. Stability of the equilibria are checked by the Hastie–Taylor criteria for hydromagnetic stability in the guiding-center theory. The mirror instability places a limit on the maximum plasma pressure. Examples of mirror devices that can be modeled here include Ioffe bar experiments, Baseball II, 2-X-II, and the proposed mirror fusion experiment (MFX). (auth)

36166 (CONF-710607–1) LOSS-CONE MODES IN INHOMOGENEOUS MIRROR MACHINES. Baldwin, D. E.; Beasley, C. O. Jr.; Berk, H. L.; Farr, W. M.; Harding, R. C.; McCune, J. E.; Pearlstein, L. D.; Sen, A. (California Univ., Livermore. Lawrence Radiation Lab.). 30 Apr 1971. 30p. (CN-28/G-13; UCRL–73135). Dep. NTIS.
From fourth conference on plasma physics and controlled nuclear fusion research; Madison, Wis. (17 Jun 1971).

Loss-cone modes in inhomogeneous mirror geometries are discussed with emphasis placed on the drift-cone mode, the effects of ion and electron thermal motion on the negative energy wave, and electromagnetic corrections. Thermal motion affects the density threshold for stability of nonflute loss-cone modes and determines the criterion for stability of flute-like negative energy modes. In a fluid model it is necessary to assume that electron Landau damping absorbs energy of outgoing waves near the mirror ends. It is shown that the numerical solution of a linear integral equation derived from a Vlasov model verifies this assumption. The Vlasov model gives the stability threshold as a function of density and scale length. When the electron drift term is neglected it is found that, for long plasmas ($L/a_i \gg (M_i/M_e)^{1/2}$), the worst modes are generally the absolute loss-cone modes. As the scale length decreases, the plasma modes change character to negative energy modes. Most of these modes eventually stabilize at a length $L/a_i \sim (M_i/M_e)^{1/2}$. One remnant negative energy mode persists below the critical length and evolves into a negative energy flute-like mode

XUM

at frequencies below the central cyclotron frequency. This mode is destabilized by electron dissipation that arises from electron damping. Stabilization arises when inverse dissipation due to ion transit effects dominate at sufficiently short scale lengths. The flute-like drift-cone mode is unstable and insensitive to thermal corrections and, therefore, it is particularly dangerous to mirror confinement. The dispersion relation for a finite-size and finite-mirror-ratio machine yields stability density thresholds and growth rates that are qualitatively similar to infinite-medium theory. The flute modes can be stabilized by nonlinear currents flowing at the ends. (auth)

36167 THEORY OF THE BEAM CYCLOTRON INSTABILITY IN PLASMAS. Lampe, M.; McBride, J. B.; Orens, J. H.; Sudan, R. N. (Naval Research Lab., Washington, D. C.). Phys. Lett.; 35A: No. 2, 131-2(17 May 1971).

Important new aspects of the linear theory of the beam cyclotron instability in a magnetized plasma are discussed. (auth)

36168 EXPERIMENTAL INVESTIGATION OF A TOROIDAL DIFFUSE PINCH. Wilhelm, R.; Zwicker, H. (Max-Planck-Institut fuer Plasmaphysik, Garching, Ger.). Phys. Lett.; 35A: No. 2, 99-100(17 May 1971).

In a toroidal screw-pinch device a radial magnetic field distribution was established that theoretically, should be MHD-stable. The experiment showed however, after 3 μsec, a very-fast-growing instability might be of the resistive-type. (auth)

36169 STABILITY OF RELATIVISTIC ELECTRON BEAMS IN PLASMA AND THE PROBLEM OF CRITICAL CURRENTS. Bogdankevich, L. S.; Rukhadze, A. A. (Lebedev Inst. of Physics, Moscow). Usp. Fiz. Nauk; 103: No. 4, 609-40(Apr 1971). (In Russian).

The theory of stability of restricted relativistic electron beams in plasma is surveyed. Critical currents are established by the origin of electrostatic instability, and are attained in compensated electron beams. In such beams, focused by a terminal longitudinal magnetic field, critical currents are dependent on a current-convective instability, and increase with stronger magnetic fields. In a system consisting of an electron beam and a dense plasma, the plasma density becomes a critical parameter and determines the system's stability. Thus, instability develops under conditions whereby the plasma density is greater than critical and is accompanied by a high-frequency plasma oscillation. Recent experimental data are discussed and found to compare satisfactorily with theory. (tr-auth)

36170 QUASILINEAR DESTABILIZATION OF DISSIPATIVE PARAMETRIC PLASMA INSTABILITY IN A HIGH FREQUENCY ELECTRIC FIELD. Kirii, A. Yu. (Lebedev Inst. of Physics, Moscow). Zh. Eksp. Teor. Fiz.; 60: No. 3, 955-64(Mar 1971). (In Russian).

Quasi-linear action on parametric dissipative instability is studied, and it is shown that the formation of a plateau in the velocity distribution function results in a decrease of Cherenkov dissipation and corresponding increase of the instability increment. It is also shown that during the destabilization time, the plasma conductivity, which determines the energy growth of the excited plasma oscillations, considerably increases. (auth)

36171 EQUILIBRIUM OF FINITE-β TOROIDAL HELICES. Ikuta, Kazunari (Nagoya Univ., Japan). J. Phys. Soc. Jap.; 30: No. 6, 1709-11(Jun 1971).

The equilibrium shift of the finite-β fat-snake configurations with sharp plasma surfaces is calculated analytically and is found to be finite under the influence of the toroidal perturbation. (auth)

36172 FREQUENCY SHIFT AND SUPPRESSION OF ION-WAVE INSTABILITY BY HIGH-FREQUENCY ELECTRIC FIELD. Aihara, S.; Takamura, S. (Nagoya Univ., Japan). Appl. Phys. Lett.; 18: No. 9, 375-7(1 May 1971).

The frequency of an ion wave decreases in an rf electric field. At the same time strong suppression of the ion-wave instability occurs. The frequency shift is explained by the additional pressure produced by the spatial modulation of the rf field by the ion wave. (auth)

36173 SAUSAGE INSTABILITIES IN A TRANSPARENT PLASMA OF FINITE CONDUCTIVITY. Rukhadze, A. A.; Triger, S. A. (Lebedev Inst. of Physics, Moscow). Sov. Phys.-Tech. Phys. (Engl. Transl.); 15: No. 9, 1418-22(Mar 1971).

Translated from Zh. Tekh. Fiz.; 40: No. 9, 1817-22(Sep 1970).

The problem of axisymmetric sausage instabilities in a self-constricted discharge (pinch effect) in a dense but optically transparent plasma is solved. Cases of high and low plasma conductivity are examined. The fact that the discharge lacks a clearly defined boundary because of the free escape of radiation is responsible for the disappearance of the most dangerous surface mode of unstable oscillations typical of a discharge in an opaque plasma. The growth rates of three-dimensional longwave sausage instabilities fall off with decreasing plasma conductivity, tending to zero in the limit $\sigma_0 \to 0$. (auth)

36174 INSTABILITIES IN A DOUBLE-STREAM PLASMA WITH COULOMB COLLISIONS. Rabinovich, M. I.; Fainshtein, S. M. Sov. Phys.-Tech. Phys. (Engl. Transl.); 15: No. 9, 1423-30(Mar 1971).

Translated from Zh. Tekh. Fiz.; 40: No. 9, 1823-33(Sep 1970).

High-frequency plasma oscillations in electron streams moving in a uniform ion background are considered. It is assumed that the mechanism by which the oscillations grow in the electron stream is associated with the presence of a falling section in the nonlinear friction characteristic (runaway electrons). Different classes of stationary oscillations are investigated in infinite and bounded systems, terminated by electron beams. The analysis is carried out in the hydrodynamic approximation. (auth)

36175 OSCILLATIONS IN A MAGNETIZED AFTERGLOW PLASMA WITH A TRANSVERSE CURRENT. Bulanin, V. V.; Zhilinskii, A. P.; Yakovlev, V. N. (Leningrad Polytechnic Inst.). Sov. Phys.-Tech. Phys. (Engl. Transl.); 15: No. 10, 1616-20(Apr 1971).

Translated from Zh. Tekh. Fiz.; 40: No. 10, 2075-81(Oct 1970).

Plasma instability in a radial electric field is investigated. The electric field is perpendicular to a homogeneous magnetic field. It is shown that the instability develops from one of the drift modes. The instability occurs for a magnetic field which exceeds a critical value at which the ratio of the cyclotron gyrofrequency to the ion–neutral collision frequency is approximately unity. The amplitude of the oscillations is proportional to the radial electric field. (auth)

36176 STABILITY OF A HIGH-β PLASMA WITH A WEAK PRESSURE GRADIENT. Mikhailovskii, A. B. Sov. Phys.-Tech. Phys. (Engl. Transl.); 15: No 10, 1597-9(Apr 1971).

Translated from Zh. Tekh. Fiz.; 40: No. 10, 2050-3(Oct 1970).

Low-frequency longwave magnetic perturbations of an inhomogeneous collisionless plasma with $\beta \gg 1$ and $\partial \ln p_0/\partial \ln n_0 \simeq 1/\beta$ are investigated ($\beta \equiv 8\pi p_0/B_0^2$ is the ratio of the pressure of the magnetic field, n_0 is the plasma density). The lines of force of the magnetic field are approximated by straight lines. It is proved that if $\partial \ln p_0/\partial \ln n_0 > 0$ the plasma is stable with respect to all longwave magnetic perturbations except those whose longitudinal phase velocity exceeds the electron thermal velocity. The latter are sensitive to collisions and are not generated if the frequency of electron–ion collisions exceeds the characteristic drift frequency. (auth)

36177 DRIFT INSTABILITIES IN A PLASMA IN A HIGH-FREQUENCY ELECTROMAGNETIC FIELD. Krivorutskii, E. N.; Tsytovich, V. N. (Moscow Pedagogical Inst.). Sov. Phys.-Tech. Phys. (Engl. Transl.); 15: No. 10, 1600-7(Apr 1971).

Translated from Zh. Tekh. Fiz.; 40: No. 10, 2054-64(Oct 1970).

The nonlinear properties of drift oscillations in a plasma subject to intense electromagnetic waves are investigated. It is shown that nonlinear effects can suppress the drift instabilities in a certain range of the parameters. Effects arising from nonlinear drift instabilities are studied in this connection, and a number of problems concerning the interaction of intense high-frequency fields with a plasma are investigated. (auth)

36178 THERMAL STABILITY OF A FUSION REACTOR. Ohta, Mitsuru (Japan Atomic Energy Research Inst., Tokai); Yamato, Harumi; Mori, Shigeru. Nippon Genshiryoku Gakkaishi; 13: No. 5, 259-66(1971). (In Japanese).

The stability of equilibrium plasma is discussed for a steady-state D-T fusion reactor operated without any dynamic control. A critical temperature above which the reactor is stable may be determined from the dependence of the durations of energy and particle confinement on the temperature and density. If the confinement duration is independent of these parameters, the critical temperature is given by the minimum value of $n\tau_E$, the product of density and energy confinement duration, which is a function of temperature. This critical temperature is about 28 keV in a charged-particle-heated reactor. When the confinement durations are proportional to $1/T$, as in Bohm diffusion, the critical temperature is lower than in the previous case, and higher on the other hand, if the confinement durations are proportional to $T^{1/2}n^{-1}$ as in classical diffusion. A wider range of stable operating temperature can be expected in an injection-heated reactor. The time-dependent behavior of the plasma density and temperature in a fusion reactor with charged particle heating was studied. (auth)

36179 STABILIZATION OF THE DRIFT-DISSIPATIVE INSTABILITY IN A PLASMA BY rf MAGNETIC AND ELECTRIC FIELDS. Alcock, M. W.; Keen, B. E. (United Kingdom Atomic Energy Authority, Culham, Eng.). Phys. Rev. Lett.; 26: No. 23, 1426-9(7 Jun 1971).

The experimental results presented show the stabilization of the drift-dissipative instability in an afterglow plasma. Stabilization was achieved by means of an applied azimuthal rf magnetic field perpendicular to the main containing axial magnetic field or, alternatively, by an applied rf axial electric field parallel to the dc magnetic field. The results obtained at various applied frequencies are compared with a previous theory, and some points of agreement and disparity are noted. (auth)

36180 THEORY OF TRAPPED PARTICLE INSTABILITY. I. GENERAL FORMULATION AND ANALYSIS FOR WEAK COUPLING LIMIT. Mima, Kunioki; Nishikawa, Kyoji (Kyoto Univ.). J. Phys. Soc. Jap.; 30: No. 6, 1722-43(Jun 1971).

A general formulation is developed to investigate the stability of a collisionless, one-dimensional plasma that sustains a large-amplitude, monochromatic electron plasma wave. A nonlinear dispersion relation is derived that governs the stability of a small-amplitude test wave. It is shown that untrapped electrons can produce a significant modification to the Kruer–Dawson–Sudan dispersion relation, which was derived by considering only the effect of trapped electrons on the test wave. As an application, a weak-coupling limit is considered. It is shown that in this limit waves can grow in the distinct wavenumber regions given by $|\Delta k| = \sqrt{2n + 1}k_B (n = 0, 1, 2, \ldots)$, and $|\Delta k| \ll k_B$, where Δk is the difference of the wave numbers of the test wave and the original large-amplitude wave and k_B the bounce frequency divided by the phase velocity of the large-amplitude wave. Various characteristics of the growing waves are obtained. (auth)

36181 EQUILIBRIUM AND STABILITY OF CURRENT-CARRYING PLASMAS IN TOROIDAL SYSTEMS. Rosinskii, S. E.; Rukhlin, V. G. (Lebedev Inst. of Physics, Moscow). Sov. Phys.-Tech. Phys. (Engl. Transl.); 15: No. 11, 1769-76(May 1971).
Translated from Zh. Tekh. Fiz.; 40: No. 11, 2265-75(Nov 1970).

The instabilities of current-carrying plasmas in toroidal systems are examined. The instabilities of interest are due to trapped particles and slowly drifting particles. Criteria are found for the stabilization of unstable modes by radial electric fields, longitudinal (current) particle drifts, finite Larmor radius, finite particle drift orbits, and shear. It is shown that familiar trapped-particle flute instabilities are stabilized by shear if the rotational transform is such that the maximum wavelength along the magnetic field $\lambda_{||}$ is smaller than the distance between local magnetic mirrors L. In this case, the effective fraction of trapped particles goes as $(\lambda_{||}/L)^{\frac{1}{2}}$. A comparison is made between current-carrying toroidal systems (tokamaks) and stellarators. (auth)

36182 EXPERIMENTAL PROOF OF MIRROR INSTABILITIES IN THE ISAR I THETA PINCH. Kaufmann, M.; Neuhauser, J.; Roehr, H. (Institut fuer Plasmaphysik GmbH, Garching, Ger.). Z. Phys.; 244: No. 2, 99-116(1971).

In the Isar I linear theta pinch, m = 0 instabilities were observed and experimentally investigated. The variation of the plasma parameters over a wide range ($\tau_{ii} = 10^{-2}$ to 10^{2} μsec) showed that the m = 0 instabilities occurred only in sufficiently hot and thin plasmas; therefore, they are most probably due to the anisotropic pressure of the ions and should be mirror instabilities. Perturbations of the plasma limited in space and time were observed by measuring the continuum radiation, by 90° laser scattering measurements, and by measuring the magnetic field and the local neutron rate. All measurements showed distinct, correlated, local perturbations of the plasma cylinder. These perturbations were accompanied by bulging of the plasma cylinder and increasing density. The extent in the axial direction was of the order of the plasma diameter. It may be assumed that the observed instabilities contribute appreciably to relaxation of the anisotropic ion pressure and increase the end losses. (auth)

36183 INFLUENCE OF THE HELICON WAVE UPON SOME ELECTROSTATIC INSTABILITIES OF PLASMAS. Teichmann, J. (International Centre for Theoretical Physics, Trieste, Italy); Ivanov, A. A.; Krlin, L. Plasma Phys.; 13: 415-17(May 1971).

The influence of the drift, caused by the electric component of the helicon-type electromagnetic wave together with the action of the time oscillating magnetic component is considered for the stabilization of electrostatic microinstabilities in a nonuniform plasma. (auth) (UK)

36184 FEEDBACK STABILIZATION OF A PLASMA INSTABILITY BY A REMOTE MODULATED SOURCE AT THE ELECTRON CYCLOTRON RESONANCE FREQUENCY. Keen, B. E.; Fletcher, W. H. W. (Culham Lab., Abingdon, Eng.). Plasma Phys.; 13: 419-31(May 1971).

It was demonstrated that the ion sound instability can be stabilized by a remote feedback technique. The instability was sensed by a photo-diode detector outside the plasma, and the suppressor element was an electron cyclotron resonance (E.C.R.) structure remote from the plasma. Power from this causes local heating of the electrons, and feedback is effected by modulation of the E.C.R. power level at the instability frequency. A theory is developed that predicts the variation of the instability amplitude and frequency in terms of the change in electron temperature ΔT, fractional modulation of the E.C.R. power f, and phase change in the loop φ. Comparison between theory and experiment shows good agreement. (auth) (UK)

36185 EFFECT OF A TRANSVERSE ELECTRIC FIELD ON THE STABILITY OF A WEAKLY IONIZED PLASMA IN A MAGNETIC FIELD. Zhilinskii, A. P. (Leningrad Polytechnic Inst.). Sov. Phys.-Tech. Phys. (Engl. Transl.); 15: No. 11, 1918-20 (May 1971).
Translated from Zh. Tekh. Fiz.; 40: No. 11, 2453-5(Nov 1970).

The influence of the transverse ion conductivity on the stability of a bounded plasma in a magnetic field is determined. The hydrodynamic approximation is used; the finite thermal conductivities of the electrons and ions are neglected. It is shown that ion drift with respect to the electrons can, in a transverse electric field, give rise to a drift instability under certain conditions. (auth)

Thermonuclear Processes

Refer also to abstract 35837.

36186 (CTO–746) FAST HYDROGEN ATOM INJECTOR. Kulygin, V. M.; Panasenkov, A. A.; Sveshnikov, A. G.; Semashko, N. N. (Institut Atomnoi Energii, Moscow (USSR)). Translated by J. B. Sykes (U.K.A.E.A., Culham Lab., Abingdon, Eng.), from report IAE–1952. 33p. Dep. NTIS (U. S. Sales Only).

The injector described produces a flux of hydrogen atoms with energy 15 to 30 keV and intensity above 0.5 A eq. A proton beam is produced and shaped in a gas-discharge source operating in a transverse magnetic field, which also focuses the ion beam. The flux of atoms is formed by charge exchange of the protons on a magnesium vapor target. Calculations of the magneto-optical system are given and the particle motion is analyzed numerically. An experimental injector was constructed on the basis of the calculations, and the results of measurements are compared with the theory. Experiments on the production and shaping of the proton beam and intense fluxes of fast atoms are described. (auth)

36187 (MATT–837) VACUUM TUBE COMPENSATED FLAT TOP HIGH-CURRENT PULSE SUPPLY FOR SYMMETRICAL TORUS MACHINE. Turitzin, N. M.; Chandler, H. M. Jr. (Princeton Univ., N. J. Plasma Physics Lab.). Apr 1971. Contract AT(30-1)-1238. 10p. (CONF-710418-7). Dep. NTIS.
From fourth symposium on engineering problems of fusion research; Washington, D. C. (20 Apr 1971).

The conversion of the Model C Stellarator to a symmetrical torus machine produced a longer plasma confinement time. This, in turn, required a longer ohmic heating current pulse than could be supplied by the existing vacuum tube system controlling the total energy flow. A new energy supply, consisting of a high-voltage capacitor bank and crowbar coupled with a low-voltage pulse-forming network of electrolytic capacitors, was added in parallel with the existing vacuum tube system such that the two are complementary. The composite supply is capable of producing longer pulses with a greater amplitude and, at the same time, permits modulation of the flat top. (auth)

36188 (MATT–839) FLOATING RING STABILIZATION SYSTEM. Pelovitz, M.; Heim, W. J.; Murray, J. G. (Princeton Univ., N. J. Plasma Physics Lab.). May 1971. Contract AT-(30-1)-1238. 9p. Dep. NTIS.

The necessity of magnetically levitating a superconducting, current-carrying ring without mechanical supports requires an electrical stabilizing system. The ring, when supported, has only one equilibrium position, and this position is one of unstable equilibrium. The ring is free to move with up to six degrees of freedom. Two degrees are dictated by the ability of the ring to move in any direction in the plane of the ring. Additionally, the ring can be tilted, requiring three more reference points to determine a new plane. The sixth degree of freedom is the ability of the ring to rotate upon its own axis, but because external forces tending to cause this rotation can, in principal, be eliminated, a

XUM

restoring supply is not provided. Each of the five identical stabilizing supplies in this system has a feedback loop composed of the following segments. The position detector element is an optical head that sends a light beam across an optical edge on the ring, the reflection of which is sensed on a photo diode. This diode voltage signal, proportional to the ring position, is the input to an amplifier whose output is a signal proportional to position, velocity, and ring acceleration. A 50-V, 100-A, bidirectional dc transistor power supply is activated from this signal, which in turn powers the appropriate stabilizing coil located near the floating current-carrying ring. A $J \times B$ force is produced in a direction to restore the ring to its equilibrium position, at which time the stabilizing coil currents return to approximately zero, minimizing any effect upon the experiment. The design and construction details of this system are discussed. (auth)

36189 (MATT-840) THE OPTICAL SENSORS IN FM-1. Foote, V. S. Jr. (Princeton Univ., N. J. Plasma Physics Lab.). May 1971. Contract AT(30-1)-1238. 12p. (CONF-710418-10). Dep. NTIS.

From fourth symposium on engineering problems of fusion research; Washington, D. C. (20 Apr 1971).

In the PPL FM-1 Machine, the plasma containment volume is shaped, in part, by a levitated superconducting ring, which is stabilized and positioned by servoed currents in stationary tilt and slide coils. The instantaneous position of the ring is sensed, in the required five degrees of freedom, by external noncontacting reflex optical sensors. Design and construction of these sensors are described, and results of performance tests, both off and on the FM-1, are presented. (auth)

36190 (MATT-841) STELLARATOR-MIRROR MACHINE TARGET PLASMA REACTOR. Dawson, J. M.; Furth, H. P.; Tenney, F. H. (Princeton Univ., N. J. Plasma Physics Lab.). May 1971. Contract AT(30-1)-1238. 11p. Dep. NTIS.

The stellarator configuration appears particularly well-suited as a container of target plasma for energetic ions trapped in a local mirror section. (auth)

36191 (MATT-844) LAWSON CRITERIA. Mills, R. G. (Princeton Univ., N. J. Plasma Physics Lab.). May 1971. Contract AT(30-1)-1238. 6p. (CONF-710418-12). Dep. NTIS.

From fourth symposium on engineering problems of fusion research; Washington, D. C. (20 Apr 1971).

The Lawson criterion is a minimum condition on the product of ion density, n_i, and mean residence (confinement) time, τ, of the energetic ions within a reacting plasma if it is to be useful as a source of thermonuclear power. This criterion is a function of temperature, T, and energy recovery efficiency, η. The curve originally presented by Lawson, for a single efficiency of 1/3, is actually the lower side of a closed contour in the n_i,T plane. This is readily generalizable to a cup-like surface in n_i,T,η space. There is a forbidden region within which a steady-state reactor cannot operate. The Lawson efficiency, η, should not be confused with the thermal efficiency of the associated energy conversion device, which may have a lower value. Examples for selected fuel cycles are given. (auth)

36192 (MATT-846) LEAD SHIELDED DEWAR DEVELOPMENT. Martin, G. D.; Willard, J. W. (Princeton Univ., N. J. Plasma Physics Lab.). May 1971. Contract AT(30-1)-1238. 11p. (CONF-710418-11). Dep. NTIS.

From fourth symposium on engineering problems of fusion research; Washington, D. C. (20 Apr 1971).

Results of a recent development program to increase operating time of levitated rings are presented. Fabrication and cryogenic and mechanical testing of 20- and 36-in. major-diameter lead-shielded toroidal Dewars are described. Thirty to sixty pounds of lead shielding was applied to a glass epoxy and fiberglass substructure separated by a vacuum gap from the inner chamber. A typical installation consisted of lead-copper sheet laminates applied to a tinned copper base. Cooling of the lead jacket was accomplished by a separate cooling loop or by vent gases from the inner chamber. Mechanical integrity of the lead shield assembly was evaluated by shock testing the assembly in excess of 10 g's at 77°K. Test results indicate that the addition of 32 lbs of lead shielding increases the isochoric operating time of a typical 36-in. ring by a factor of 2.5 or more. (auth)

36193 (ORNL-TM-3401) NEW DATA SYSTEM FOR INTEREM. Francis, J. E.; Yonts, O. C. (Oak Ridge National Lab., Tenn.). May 1971. 76p. Dep. NTIS.

The new data system for INTEREM that uses a PDP-12 computer is described. Listings of the control program and subroutines along with interface wiring diagrams are included as appendices. (auth)

36194 (UCRL-51042) PROPOSAL FOR MIRROR FUSION EXPERIMENT (MFX). (California Univ., Livermore. Lawrence Radiation Lab.). 7 May 1971. Contract W-7405-eng-48. 115p. Dep. NTIS.

This is a proposal to construct at LRL, Livermore, a large facility for the study of mirror-confined fusion plasmas. The facility, called MFX for Mirror Fusion Experiment, is to be readied for first operation in FY 75. MFX is the successor to the present mirror experiments, 2X II and Baseball II. It has two main goals: (1) to extend mirror confinement studies from their present plasma parameter limits to reactor-like average ion energies (≥100 keV) and reactor densities (~10^{14} ions/cm^3) and (2) if adequate confinement is achieved, to demonstrate with a reacting plasma all of the essential functions of a mirror-reactor—i.e., injection, confinement, and energy recovery. (M.O.W.)

36195 (UCRL-73030) AUTOMATIC DATA PROCESSING SYSTEM FOR 2X II. Tyler, George C. (California Univ., Livermore. Lawrence Radiation Lab.). 5 Apr 1971. 9p. (CONF-710418-8). Dep. NTIS.

From fourth symposium on engineering problems of fusion research; Washington, D. C. (20 Apr 1971).

The 2X II automatic data system is composed of an analog disc connected to a small computer system. The multichannel analog disc is the principal intermediate means of recording the data, which are then digitized and stored permanently on magnetic tape. Reading of the data is accomplished by scanning all of the disc channels with a single analog-to-digital converter and transferring the data into the computer's magnetic core memory. This scanning of the analog disc is done automatically by the computer's software program, but it can also be done either manually from the disc control panel or remotely from a teletype terminal. A software program is under development that will put the digitized data on magnetic tape in a form that can be retrieved by both on-line mini-computer and by LRL's large computers for more complex analysis such as calculation of auto and cross correlations, Fourier analysis, statistical variations, etc. The system hardware was developed with the capability for expansion to 2 μs resolution of the data if it is required in the future. (auth)

36196 (UCRL-73031) 2X II 10-MEGAJOULE IGNITRON CROWBAR. Headley, F. B. (California Univ., Livermore. Lawrence Radiation Lab.). 2 Apr 1971. 18p. (CONF-710418-2). Dep. NTIS.

From fourth symposium on engineering problems of fusion research; Washington, D. C. (20 Apr 1971).

A 10-MJ Ignitron Crowbar Array for the 2X II fusion machine was installed and is now in operation. It is designed to handle about three times the energy of the previous array used with the 2X machine, which has been supplanted by the 2X II. In addition, this array is expected to be considerably more reliable than previous designs. Furthermore, the floor utilization of the assembly is considerably improved, access to all components is better, and the overall cost per kilojoule is substantially reduced. Two insulated identical main pulse coils are incorporated in the 2X II machine. Similarly, the crowbar array is split into two equal parts, with each connected permanently across its pulse coil. The crowbar array is expected to handle 10 MJ at 40 kV. However, because of reliability limitations of the capacitor banks above 30 kV, operation above this value is not planned except for possible special tests. With the present coils, the decay time constant of current to I/ϵ of its peak value will be about 7 msec. A mechanical switch, actuated by exploding a copper foil against one electrode, was built and installed within a foot of the coil terminals. It has not yet been perfected adequately for use, but calculations indicate that it could extend the time constant above 20 msec. (auth)

36197 (UCRL-73047) 12-KILOWATT OUTPUT SWITCHING-TYPE POWER AMPLIFIER. Rossow, Terry L. (California Univ., Livermore. Lawrence Radiation Lab.). 15 Apr 1971. 5p. (CONF-710418-5). Dep. NTIS.

From fourth symposium on engineering problems of fusion research; Washington, D. C. (20 Apr 1971).

High-power-output servoamplifiers using switching devices to control instantaneous output power can provide significant performance and cost advantages over conventional amplifiers. Of special interest is the silicon controlled rectifier when used as a low-cost, high-power switch in such an amplifier. A typical design for this type of amplifier is illustrated. (auth)

36198 (UCRL-73059) ASTRON MECHANICAL ENGINEERING EFFORT. Hurley, C. A.; Bulmer, R. H.; Hibbs, S. M. (California Univ., Livermore. Lawrence Radiation Lab.). 13 Mar 1971. 13p. (CONF-710418-4). Dep. NTIS.

From fourth symposium on engineering problems of fusion research; Washington, D. C. (20 Apr 1971).

The two major components of the Astron machine, namely, the accelerator and main chamber, were modified. In two successive steps, the accelerator was increased in energy from 4 to 5 MeV, and then from 5 to 6 MeV, with a final beam current of approximately 800 A. This increased energy required a major modification to the radiation shielding. Additional hardware and refined diagnostics were added to the accelerator to improve its performance. Among these is a unique on-line energy analyzer, a 60-MHz rf modulator, a new method for measuring current and beam position, and the use of titanium to minimize sparking in the electron gun. Optimization of the beam transport included redesign of the solenoid magnets and the installation of a 65-ft-long continuous solenoid. Main-chamber changes included the repair and installation of both cantilevers with the addition of a device to bridge between the cantilevers. New geometric arrangements were made to the static resistors, which are part of the E-layer trapping mechanism. A method for quickly and accurately measuring the magnitude and configuration of the magnetic field for the main chamber solenoid is also described. (auth)

36199 (UCRL-73060) ENGINEERING DESIGN OF THE 2X II. Anderson, C. J.; Batzer, T. H.; Calderon, M. O.; Vogtlin, G. E. (California Univ., Livermore. Lawrence Radiation Lab.). 12 Mar 1971. 19p. (CONF-710418-1). Dep. NTIS.

From fourth symposium on engineering problems of fusion research; Washington, D. C. (20 Apr 1971).

The engineering aspects of the facility, including the magnetic and mechanical design of the magnet system, the attendant structure, and the vacuum system are described. Material problems are discussed as well as the scheduling, fabrication, and assembly of the facility. Design problems associated with the injection of a neutral beam are included. (auth)

36200 (UCRL-73067) ENGINEERING THE BASEBALL MAGNET SYSTEM. Henning, C. D.; Nelson, R. L.; Chargin, A. K.; Denhoy, B. S.; Harshbarger, F. (California Univ., Livermore. Lawrence Radiation Lab.). 1970. 11p. (CONF-710418-3). Dep. NTIS.

From fourth symposium on engineering problems of fusion research; Washington, D. C. (20 Apr 1971).

The Baseball II magnet system has satisfactorily completed engineering testing at LRL. Over a three-day period the magnet was lowered to 30°K by a helium refrigerator. Then the magnet was filled with liquid helium from the 10,000-liter storage dewar and energized to about 75% of its capability. The electrical and magnet quench systems performed satisfactorily. However, helium loss rates were greater than necessary because the permanent heat shield was not installed. A plasma beam line is being completed that incorporates superconducting magnetic shielding to protect the injected beam from the Baseball II fringe field. (auth)

36201 (UCRL-73129) RECENT CHANGES IN THE ASTRON FAST PULSING SYSTEM. Smith, Mark E. (California Univ., Livermore. Lawrence Radiation Lab.). 15 Apr 1971. 27p. (CONF-710418-6). Dep. NTIS.

From fourth symposium on engineering problems of fusion research; Washington, D. C. (20 Apr 1971).

Two major changes were made in the Astron Fast-Pulsing System since June 1970. The hard-tube modulators used to charge the accelerator PFN's were changed to a resonant-charge system and completely rebuilt. While no comparative reliability records are available, it is obvious that the new system is at least ten times more reliable than the old system. The pulse-to-pulse regulation of the new system is not as good as was hoped for, but it seems to be adequate for reasonable performance of the accelerator. Furthermore, significant improvement should be simple and of negligible cost. The second major change was the building of a new power supply for the core-reset system. The old system had relatively poor voltage regulation (15 or 20%). Two problems existed: the power supply and cabling system were inherently poorly regulated, and an already too-small substation was shared with another pulsed load of comparable size. Instead of about 90 small power supplies, the new system uses one large series-pass transistor supply, operated on its own 1.5-MVA substation. The new supply consists of a 340-V brute-force rectifier unit with a 1-F capacitor bank, followed by a series-pass transistor bank (about 2,000 transistors) feeding a distributed 1.3-F bank at 260 V. Rated output current is 7500 A. Output voltage is sensed at the most distant part of the load, and a loop gain of 1,000 is planned for the system. The major components are completed, and the substation and 13.8-kV switchgear are installed and have been tested at no load. The transistor bank is now being tested in small segments. Completion of the new system is expected in May of this year. (auth)

36202 ANALYSIS OF THE CURRENT FLOW OF A CONDENSER DISCHARGE OF AN ELECTRODELESS MHD MOTOR. Meert, A. (Deutsche Versuchsanstalt fuer Luft und Raumfahrt eV, Stuttgart). AGARD Conf. Proc.; No. 38, 581-92(1970).

From Conference on new experimental techniques in propulsion and energetics research; Munich, Germany (11 Sep 1967). See CONF-670999.

An analysis of the time dependence of the current due to a high-current condenser discharge permits the determination of the magnitude of losses in the discharge circuit as well as of the energy input into the plasma. The problems associated with the measurement of the discharge current are known, and some of them are mentioned. Difficulties arise in the correct evaluation of the curves of the discharge current. A procedure based on a mathematical abstraction permits a very precise analysis of the current to be made. Some procedures for the measurement of the discharge current are discussed. (auth)

36203 NEUTRONS PRODUCTION IN SOLID-DEUTERIUM LASER-CREATED PLASMAS. Floux, Francis (CEA, Villeneuve-Saint-Georges, France). pp 469-75 of Laser Interaction and Related Plasma Phenomena. /Schwarz, Helmut J. (ed.). New York; Plenum Publishing Corp. (1971).

From Laser interaction and related plasma phenomena meeting; East Windsor Hill, Conn. (9 Jun 1969). See CONF-690622.

The production of neutrons when a 4-GW laser beam is focused onto a solid deuterium target is discussed. Neutron spectra are given. (M.O.W.)

36204 TANDEM PLASMA ACCELERATION IN COAXIAL SYSTEMS. Komel'kov, V. S.; Modzolevskii, V. I. Sov. Phys.-Tech. Phys. (Engl. Transl.); 15: No. 10, 1674-80(Apr 1971). Translated from Zh. Tekh. Fiz.; 40: No. 10, 2147-55(Oct 1970).

A method for analyzing two-stage acceleration of a plasma stream is described. An additional discharge current is superimposed on the moving stream, causing one part of the stream to be accelerated and the other to be retarded. This procedure makes it possible to evaluate the effects of the parameters of the discharge circuit, the masses of the front and tail of the stream, and the initial plasma velocity on the accelerated plasmoid. The calculated data are compared with experiment. (auth)

36205 NONSTATIONARY THREE-DIMENSIONAL PLASMA FLOW IN A HOMOPOLAR DEVICE. Gannitskii, A. I.; Drobyshevskii, E. M.; Rozov, S. I. (Ioffe Inst. of Physics and Tech., Leningrad). Sov. Phys.-Tech. Phys. (Engl. Transl.); 15: No. 10, 1681-7(Apr 1971).

Translated from Zh. Tekh. Fiz.; 40: No. 10, 2156-63(Oct 1970).

Theoretical and experimental investigations of the flow of a weakly ionized plasma in a homopolar device are described. The nonstationary flow of an incompressible viscous plasma is analyzed numerically, taking account of the inhomogeneity of the electric current distribution and the Hall conductivity. Attention is focused on the evolution of secondary cross flows in the process of plasma acceleration and the effect of these on the ionization—diffusion balance. A comparison of the solutions with the measurements of the velocity field in a homopolar device confirms the strong influence of the anisotropy in the conductivity on the hydrodynamics. The results of an experimental investigation of the plasma flow in an inhomogeneous skew magnetic field are presented. (auth)

36206 ASYMMETRIC HELICAL MAGNETIC CONFIGURATIONS. Loktinov, Yu. M.; Sebko, V. P. Sov. Phys.-Tech. Phys. (Engl. Transl.); 15: No. 9, 1444-8(Mar 1971).

Translated from Zh. Tekh. Fiz.; 40: No. 9, 1851-7(Sep 1970).

Two or more stellarator windings with different multipolarities (l number) and different small radii reduce to a single winding when superposed. If the pitches of the helices in each of the windings are equal, it is possible to obtain a helical winding that corresponds to asymmetric conductors and unequal currents. The determination of the magnetic configuration created by such a system of currents is considerably simplified by the helical symmetry. The properties of magnetic fields generated by asymmetric windings in combination with a longitudinal field are described. It is shown that closed magnetic configurations with shear and minimum B can exist near the three-dimensional magnetic axis. (auth)

36207 ELECTRODE EROSION IN PULSED PLASMA ACCELERATORS. Khizhnyak, N. A.; Safronov, B. G.; Vereshchagin, V. L.; Popov, N. P. Sov. Phys.-Tech. Phys. (Engl. Transl.); 15: No. 11, 1828-31(May 1971).

Translated from Zh. Tekh. Fiz.; 40: No. 11, 2341-5(Nov 1970).

Studies were made of the erosion of electrode material in a conical, pulsed plasma source. A 200-μF condenser bank is discharged into the source electrodes, which are separated by

XUM

a heat-resistant dielectric. The inductance of the circuit is 0.08 μH. The dependence of mass on current has three characteristic regions corresponding to different erosion mechanisms: cathode, anode, and jet disintegration. It is shown that the efficiency of energy transformation into plasma kinetic energy is very low for jet disintegration. Currents for which electrode jet disintegration begins were determined experimentally. On this basis, a number of metals were arranged in order of their erosion resistance in a pulsed electric discharge: Sn, Pb, Cd, Al, Mg, D16, brass, bronze, Cu, and Ti. (auth)

36208 DETERMINATION OF MAGNETIC SURFACES WITH A DIELECTRIC GRID. Popryadukhin, A. P. (Inst. of Physics, Moscow). Sov. Phys.-Tech. Phys. (Engl. Transl.); 15: No. 11, 1792-5(May 1971).

Translated from Zh. Tekh. Fiz.; 40: No. 11, 2295-2300(Nov 1970).

A fast method of determining magnetic surfaces is described in which an electron beam is used to induce charges in a dielectric grid. Surfaces found in the Tor-2 stellarator are described. (auth)

36209 ONE-MEGAJOULE INDUCTIVE ENERGY STORAGE SYSTEM (28 Jul 1970) (Engineering Materials). (Princeton Univ., N. J.). (CAPE-2039).

59 drawings.

An inductive energy storage system, which utilizes ignitrons for rectifiers and for the major switching element, stores one MJ at 2000 A and is able to transfer this energy to an inductive load in a fraction of a second at voltages up to 20,000 V. An inverter limits the voltage developed during energy transfer. Energy transfer is accomplished by inverting the direct current of the inductor to an alternating triangular voltage wave form. The voltage is then rectified, filtered, and applied to the load. Advantages of the system are: there are no moving parts in the system and all parts are static; the inductor may be crowbarred at any time in the charge-transfer cycle, thus insuring system safety; the storage inductor and the load are in separate loops, making it possible to transfer all the stored energy; and initial system costs are lower than those for capacitive storage systems of equivalent size. The energy-storage inductor, a water-cooled air-core coil with an 80-in. OD and 41-in. ID, has an inductance of 0.5 H and a resistance of 0.167 Ω. The inductor, which is horizontally oriented with a height of 20 in. has 24 layers with 26 turns each, a total of 624 turns. Weight of Cu is 9.5 tons and the conductor length is 10,000 ft. A $\frac{3}{4}$-in.^{2} Cu bus with a $\frac{1}{4}$-in. circular hole and insulated with four layers of 3.5-mil Mylar tape is used as the conductor. The inductor is charged from a three-phase, full-wave bridge operating from a 480-V, 60-Hz bus. Four ignitrons in series disconnect the charger when the inverter action begins. The theoretical energy efficiency is unity and the practical energy efficiency exceeds 90%. (For details see TID-4100 Suppl. 61). (see also NSA 24: 37490) (F.S.)

36210 PROPERTIES OF MAGNETIC SURFACES IN THE MODEL C STELLARATOR. Hosea, J. C.; Sheffield, G. V.; Sinclair, R. M.; Tamano, T. (Princeton Univ., N. J.). Plasma Phys.; 13: 365-72(May 1971).

The magnetic field of the Model C stellarator was mapped by a new technique using the long-term storage of low-energy electrons. The properties of the field (such as the existence of surfaces and realistic values of their average radius and transform) can be correlated with the plasma behavior in the device. (auth) (UK)

36211 FUSION BY LASER. Lubin, Moshe J.; Fraas, Arthur P. Sci. Amer.; 224: No. 6, 21-33(Jun 1971).

The current status of the development of high-power pulsed lasers is reviewed. The mechanism by which the energy from a laser beam interacts with a dense medium is described. The possibility of an operating thermonuclear power plant by focusing laser radiation on a frozen pellet of fuel is discussed. (M.O.W.)

36212 PROBLEM OF CONTROLLED THERMONUCLEAR FUSION. Lehner, G. (Institut fuer Plasmaphysik, Garching, Ger.). pp 290-321 of 35. Physikertagung 1970 Hannover. Stuttgart; B. G. Teubner (1970). (In German).

From thirty-fifth physicists conference; Hanover, Germany (Sep-Oct 1970). See CONF-700954.

The characteristics of plasmas and the problems of controlled thermonuclear fusion are reviewed. The mechanism of nuclear fusion is described. The magnetic confinement of plasma, the macroscopic instabilities, and abnormal diffusion are discussed. The fusion reactor is considered in conclusion. (J.S.R.)

36213 CONTROLLED NUCLEAR FUSION: STATUS AND OUTLOOK. Rose, David J. (Oak Ridge National Lab., Tenn.). Science; 172: No. 3985, 797-808(21 May 1971).

The status of controlled nuclear fusion may be summarized as follows: (1) measurements of reaction energies and rates between hydrogen isotopes and other light elements that show, under proper conditions, large energy releases are possible; (2) the well-known laws of single-particle physics seem to show how an assembly of high-energy ions and electrons can be confined in magnetic fields long enough to establish proper conditions; (3) the radioactive ingredients and by-products of fusion appear to be much less hazardous than those associated with nuclear fission; and (4) deuterium is a fusion fuel in plentiful supply. The reaction of deuterium (D) and tritium (T) $D + T \rightarrow {}^4He + n + 17.6$ MeV is discussed. Confinement of plasma by magnetic fields is included in the present scientific effort. Environmental and technological factors are presented. (J.C.W.)

Wave Phenomena

Refer also to abstracts 35896 and 36167.

36214 (DEMO-71/5) GROUP VELOCITY OF HIGH AMPLITUDE SURFACE WAVES IN VACUUM-PLASMA INTERFACES. Nicolis, J. S.; Athanassoula, E. (Democritus Nuclear Research Center, Athens (Greece)). Mar 1971. 6p. Dep. NTIS (U. S. Sales Only).

The behavior of the refractive index and group velocity for strong electromagnetic surface waves propagating along a vacuum–overdense plasma plane interface is investigated. (auth)

36215 (DEMO-71/6) RELATIVISTIC DOPPLER EFFECT AND GROUP VELOCITY IN HOMOGENEOUS NONLINEAR AND INHOMOGENEOUS PLASMA. Nicolis, J. S.; Athanassoula, E. (Democritus Nuclear Research Center, Athens (Greece)). Mar 1971. 39p. Dep. NTIS (U. S. Sales Only).

The variations of the received frequencies (complex Doppler effect) from a source moving uniformly in a homogeneous isotropic plasma and emitting a uniform electromagnetic plane wave with amplitude E_0, as a function of ω_e/E_0 where ω_e is the plasma frequency, are studied. The ratio of the velocity U of the source over the group velocity U_{gr} of the transmitted wave is then calculated from the slope of the Doppler curves. When the plasma is inhomogeneous (one-dimensional stratification) the Doppler effect depends on the particular profile of the refractive index and its higher (even) derivatives with respect to the direction of stratification z. In this case, the ratio $U/U_{gr} = f(z)$ is given as the solution of a higher-order differential equation, with the inhomogeneous part depending on the slope of the Doppler curve with respect to frequency. Typical cases involving symmetrical and transition profiles are examined. (auth)

36216 (ITF-70-56) NONLINEAR ECHO PHENOMENA IN PLASMA. Sitenko, A. G. (Akademiya Nauk Ukrainskoi SSR, Kiev. Institut Teoreticheskoi Fiziki). 1970. 17p. Dep. NTIS (U. S. Sales Only).

Echo effects are considered in plasma conditioned by an undamped character of the distribution function oscillations that appear under the influence of perturbations shifted in time. The cases of two and three external perturbations are studied. The high- and low-frequency echo oscillations appearing in plasma under the influence of the external charges are investigated, particularly considering the echo effects associated with the oscillation transformation. It is shown that for echo phenomena associated with oscillations, the dispersion of which is determined by the character of the distribution function, external perturbations are possible. The possibility of third-order echo oscillations is shown if the wave vectors of perturbations lie in one plane; even in the case of longitudinal perturbations, the echo oscillation field contains both longitudinal and transverse components. (tr-auth)

36217 (UARAEE-88) STUDY OF LONGITUDINAL NONLINEAR OSCILLATIONS OF A HOT ELECTRON MAGNETIC PLASMA. El-Naggar, I. A. (Atomic Energy Establishment, Cairo (Egypt). Dept. of Accelerators and Plasma Physics Research). 1970. 20p. Dep. NTIS (U. S. Sales Only).

Longitudinal nonlinear oscillations of a hot electron plasma in the presence of an external magnetic field were investigated by applying Krylov–Bogolyubov–Mitropolskii perturbation method. The second harmonic was added to the solution of the linear problem in the first approximation. The expressions for frequency and wavenumber shifts were derived from the second approximation. (auth)

36218 (UARAEE-92) AXIALLY SYMMETRIC WAVES IN VACUUM CHANNEL IN PLASMA. Pakhomov, V. I.; Rizk, H. M. (Atomic Energy Establishment, Cairo (Egypt). Dept. of Accelera-

tors and Plasma Physics Research). 1970. 31p. Dep. NTIS (U. S. Sales Only).

Axially symmetric electromagnetic waves propagating along a round cylindrical vacuum channel in an unbounded magnetoactive plasma are investigated. The external magnetic field is parallel to the channel axis. The general dispersion equation is obtained. For some specific cases (the absence of the external magnetic field, the infinite magnetic field, quasi-static approximation) a detailed investigation of the dispersion equation is made. (auth)

36219 (UARAEE-97) STUDY OF ELECTROMAGNETIC SURFACE WAVES IN ADJACENT PLASMA FLOWS. Hussein, A. M.; Pakhomov, V. I. (Atomic Energy Establishment, Cairo (Egypt). Dept. of Accelerators and Plasma Physics Research). 1970. 35p. Dep. NTIS (U. S. Sales Only).

A dispersion equation describing electromagnetic waves that propagate along a plane boundary of contiguous plasma streams was obtained. The external magnetic field is parallel to the unperturbed velocities of the streams and is homogeneous in the whole space. In the general case, the plasma streams are relativistic ones. The longitudinal thermal motion of the plasma particles is taken into consideration. In the direction perpendicular to the boundary the thermal motion of the particles is supposed to be absent. Thus, the present investigation is applicable for the oscillations whose transverse wavelength is much larger than the Larmor radius of particles with velocities $v_{T\perp}$. The excitation of surface waves in the half-bounded plasma by the adjacent beam of charged particles was investigated in detail. The expressions for the amplification coefficients, both for the case of the cold beam and for the beam with great spread of the longitudinal particle velocities, were obtained. (auth)

36220 INVESTIGATION OF COLLECTIVE OSCILLATIONS IN A SYNTHETIC PLASMA COMPOSED OF POSITIVE AND NEGATIVE ION BEAMS. Gabovich, M. D.; Naida, A. P. (Inst. of Physics, Kiev). Zh. Eksp. Teor. Fiz.; 60: No. 3, 965-71(Mar 1971). (In Russian).

It is shown that oscillation amplification occurs in a synthetic plasma consisting of mutually interpenetrating beams of positive and negative ions moving in a given direction with various velocities. The experimental results are in qualitative agreement with the conclusion of the linear theory. (auth)

36221 SPONTANEOUS LOW-FREQUENCY LONGITUDINAL WAVE PROPAGATION IN A PLASMA COLUMN. Fisher, Roger Edwin. Riverside, Calif.; Univ. of California (1970). 90p. University Microfilms Order No. 71-8795.

Thesis.

Spontaneous plasma density fluctuations in discharge tubes are too large to be explained as the result of thermal noise. This fact suggests the existence of a strong collective process in the plasma. The nature of these spontaneous fluctuations is examined with correlation measurement techniques, whereby it is established that the fluctuations propagate toward the anode with a velocity appropriate to the well-known ion acoustic mode. The presence of such a wave suggests that the ion acoustic mode is unstable in the discharge tube because of the relative drift velocity between ions and electrons. Through the use of Boltzmann's equation for the single-particle distribution functions for the plasma particles, the longitudinal electromagnetic properties of the plasma are described by a dielectric constant $K_L(\omega,k)$ (where ω is the angular frequency and k is the wave number). It is shown that the roots of K_L in the complex k-plane for real ω determine the predicted spatial growth or damping of the wave. As results of this study, the following were obtained: (1) a self-consistent set of experimental data, (2) agreement between a band of minimum damping as predicted by the theory and the band of frequencies within which ion waves are observed, and (3) agreement between the theoretical and experimental phase velocities. (Diss. Abstr. Int., B)

36222 LONGITUDINAL ION-WAVE PROPAGATION IN A MAGNETIZED PLASMA. Berry, Lee Allen. Riverside, Calif.; Univ. of California (1970). 77p. University Microfilms Order No. 71-8790.

Thesis.

Longitudinal ion-wave propagation perpendicular to an applied magnetic field was theoretically investigated. The Boltzmann equation was used to describe the plasma. It was found that the usual approximation of $(kT_i/m_i)^{1/2} \ll (\omega/\beta\sin\theta) \ll (kT_e/m_e)^{1/2}$ holds over a sufficiently wide range of angles as to be experimentally accessible. Dispersion relations for this regime can be adequately obtained from a quadratic (in β^2) approximation to the longitudinal dielectric constant. The experimental dispersion relations for propagation below the ion cyclotron frequency and θ about one radian, however, can only be explained by exact calculations. For perpendicular propagation, the effect of ion-neutral and ion-ion collisions was studied using, respectively, a BGK and a model Fokker-Planck collision operator. The dispersion relations calculated from these models indicated that the backward modes are heavily damped by both types of collisions. The forward branch is damped to a lesser degree by ion-neutral and not at all by ion-ion collisions. (TSS) (Diss. Abstr. Int., B)

36223 DAMPING OF PLASMA WAVES IN THE BORN APPROXIMATION. Warner, David Charles. Columbia, Mo.; Univ. of Missouri (1970). 91p. University Microfilms Order No. 71-8404.

Thesis.

Methods are presented for calculating the damping of plasma oscillations in the Hartree approximation due to electron-neutral collisions. The linearized equation of motion for the one-electron density matrix is employed in deriving a transport equation. The classical limit of the transport equation is solved in conjunction with Poisson's equation in order to obtain the damping decrements in the Born approximation. Time-dependent perturbation theory is then used to obtain the damping for the same model. This calculation results in a frequency dependence unlike that resulting from use of the density matrix. (Diss. Abstr. Int., B)

36224 THEORY OF LINEAR TRANSFORMATION OF WAVES IN AN INHOMOGENEOUS PLASMA. Davydova, T. A. (Inst. of Nuclear Research, Kiev). Zh. Eksp. Teor. Fiz.; 60: No. 3, 1001-11(Mar 1971). (In Russian).

Linear transformation of waves in an inhomogeneous plasma described by a fourth-order differential equation with inhomogeneous coefficients is considered. It is shown that, in the vicinity of points at which the second-derivative coefficients vanish, a quasi-surface wave may arise that travels perpendicular to the density gradient. It is demonstrated in the magnetohydrodynamic approximation that, when the sound velocity considerably exceeds the Alfvén velocity in the inhomogeneity region, there also occurs a sharp change in the shape and polarization of the initial magnetosonic wave. The conditions for formation of surface waves at the sharp boundary between two plasma media, which is perpendicular to the magnetic field, are elucidated. The reflection and refraction coefficients and, also, the magnetohydrodynamic wave transformation coefficient at the boundary are determined. (auth)

36225 SELF-TRAPPING OF POWERFUL ELECTROMAGNETIC WAVES IN A DENSE PLASMA. Brodskii, Yu. Ya.; Eremin, B. G.; Litvak, A. G.; Sakhonchik, Yu. A. JETP Lett. (USSR) (Engl. Transl.); 13: No. 3, 95-7(5 Feb 1971).

Translated from Zh. Eksp. Teor. Fiz., Pis'ma Red.; 13: No. 3, 136-9(5 Feb 1971).

Direct observations of the passage of intense electromagnetic waves through a dense plasma are reported. The experimental apparatus is briefly described, and it is shown that the experimental results agree with theoretical predictions on self-trapping. (M.O.W.)

36226 SELF-FOCUSING OF A VECTOR FIELD. Eleonskii, V. N.; Silin, V. P. (Lebedev Inst. of Physics, Moscow). JETP Lett. (USSR) (Engl. Transl.); 13: No. 3, 117-19(5 Feb 1971).

Translated from Zh. Eksp. Teor. Fiz., Pis'ma Red.; 13: No. 3, 167-70(5 Feb 1971).

It was shown earlier that nonlinear action of an electromagnetic field on a plasma medium can give rise to spatially localized distributions of the field, which were called self-trapping or self-focusing. It is shown here that self-focused field distributions exist also for TM waves when there are two components of the electric field (the vector case). (M.O.W.)

36227 SPATIALLY GROWING PLASMA WAVES AND THEIR NONLINEAR EFFECTS BY BEAM MODULATION. Nagashima, Takashi (Tokyo Univ. of Education). J. Phys. Soc. Jap.; 30: No. 6, 1712-18(Jun 1971).

Spatial behavior of electron plasma waves due to beam-plasma instability was studied with a waveguide antenna that did not give any disturbance on the plasma. The observed growth rates are in agreement with those obtained by linear theory considering the plasma temperature. The criteria of validity of linear theory and the saturation of wave amplitude are also discussed. The electron beam modulated with microwave frequency gives rise to a strong electron plasma wave that shows the amplitude oscillation phenomena. The experimental value of its wavelength agrees with the theoretical one in order of magnitude. The modulation was applied to the beam; the intensity of waves showed a dip when the modulation frequency was varied near the receiving frequency. (auth)

36228 INHOMOGENEOUS PLASMAS: ON THE REFLECTION AND TRANSMISSION OF FIELDS OF ARBITRARY POLARIZATION.

XUM

Taylor, Clayborne D. (Mississippi State Univ., State College); Harrison, Charles W. Jr. J. Appl. Phys.; 42: No. 7, 2676-81(Jun 1971).

A simple numerical procedure was developed to determine the electromagnetic field penetration through a slab many hundreds of wavelengths in thickness of cold plasma with collisions. The electron-density-collision frequency profiles may be arbitrary but must contain only a finite number of discontinuities. The solution of this problem leads to a differential equation of the Riccati type. Other objectives are to evaluate exactly the transmission loss through the aforementioned inhomogeneous plasma and to determine the field variation within the plasma slab when the incident field is of arbitrary polarization. This is accomplished by solving the E and H plane incidence problems separately and then employing superposition. The results are in the form of an integral involving the reflection coefficient. The differential equations for the reflection coefficient and the transmission integrals are easily evaluated to practically any desired degree of accuracy by computer. Analytical and numerical results are presented for a plasma half-space with an exponential electron-density distribution. (auth)

36229 LUMPED ELEMENT LINE GENERATOR FOR LOW rf SINUSOIDAL OSCILLATIONS. Hoegger, B.; Weise, E. (Univ., Fribourg, Switzerland). Z. Naturforsch.; 26a: 597-8(Mar 1971).

A lumped-element line generator is described for exciting magneto-acoustic waves in a plasma. A ringing circuit is used as an rf power source; an axially periodic rf field with a frequency of 300 kHz is excited in the plasma. Schematic diagrams of the generator are presented, showing it to be made up of assembled capacitors and inductors, with the elements isolated by spark gaps. Its operation is described. (D.L.C.)

36230 NONLINEAR THEORY OF ELECTROMAGNETIC-WAVE TRAPPING IN A PLASMA. Alanakyan, Yu. R. Sov. Phys.-Tech. Phys. (Engl. Transl.); 15: No. 9, 1405-6(Mar 1971).

Translated from Zh. Tekh. Fiz.; 40: No. 9, 1799-1801(Sep 1970).

A monochromatic wave traveling along a helix is considered. It is shown that a tubular waveguide channel can be formed as a result of the interaction of the wave field with a plasma. Equilibrium conditions for a self-sustaining toroidal waveguide are discussed. (auth)

36231 ION-ACOUSTIC OSCILLATIONS AND TRANSPORT PROCESSES IN A LOW-TEMPERATURE CESIUM PLASMA. Pashchenko, V. P.; Slobodyanyuk, V. A.; Volkov, N. V.; Gus'kov, Yu. K.; Lebedev, M. A. Sov. Phys.-Tech. Phys. (Engl. Transl.); 15: No. 10, 1690-6(Apr 1971).

Translated from Zh. Tekh. Fiz.; 40: No. 10, 2167-74(Oct 1970).

Oscillations in a bounded cesium plasma are analyzed. The local plasma parameters are determined in the region in which the oscillations appear, and the applicability of various generation mechanisms is discussed. The spectrum is analyzed; data are presented that indicate the effect of the oscillations on transport processes in the ionized region. (auth)

36232 WAVE INTERACTION IN A MAGNETIZED PLASMA. Repalov, N. S.; Khizhnyak, N. A. Sov. Phys.-Tech. Phys. (Engl. Transl.); 15: No. 10, 1608-11(Apr 1971).

Translated from Zh. Tekh. Fiz.; 40: No. 10, 2065-9(Oct 1970).

The energy transfer between two independent degrees of freedom of a cold plasma in a uniform magnetic field is investigated. When resonance conditions are satisfied, this interaction can be used for frequency multiplication. (auth)

36233 WAVE KINETICS IN AN ANISOTROPIC PLASMA. III. Suramlishvili, G. I. Sov. Phys.-Tech. Phys. (Engl. Transl.); 15: No. 9, 1407-12(Mar 1971).

Translated from Zh. Tekh. Fiz.; 40: No. 9, 1802-9(Sep 1970).

The Lagrangians for three- and four-wave interactions were used to calculate the matrix elements for magneto-acoustic waves. Estimates are made of certain parameters of a plasma in which such waves are excited in sufficient number so that the statistical approach is valid. (auth)

36234 EFFECT OF INHOMOGENEITIES IN A PLASMA WAVEGUIDE ON THE PROPAGATION OF SLOW WAVES AND ON ELECTRON BEAM INTERACTIONS. Rogashkova, A. I.; Tseitlin, M. B. Sov. Phys.-Tech. Phys. (Engl. Transl.); 15: No. 9, 1463-70(Mar 1971).

Translated from Zh. Tekh. Fiz.; 40: No. 9, 1875-86(Sep 1970).

The propagation of slow waves in a waveguide containing a plasma with a nonuniform electron density is investigated. In certain special cases, analytic solutions of the wave equation are obtained; these give the phase velocity along the plasma waveguide and the distribution of the field amplitude. The interaction of an electron beam with a slow wave propagating in a plasma waveguide is investigated for both linear and nonlinear spatial variations of plasma density. It is shown that a variation in plasma density in the direction of propagation leads to a change in gain and to a broadening of the pass band in the linear case. For large amplitudes, a reduction in electron density and in the magnitude of the magnetic field along the axis leads to a decrease in the saturation length and to an increase in efficiency. (auth)

36235 EXCITATION OF ELECTROMAGNETIC WAVES IN A BEAM–PLASMA SYSTEM WITH COULOMB FRICTION. Rabinovich, M. I.; Fainshtein, S. M. Sov. Phys.-Tech. Phys. (Engl. Transl.); 15: No. 9, 1431-4(Mar 1971).

Translated from Zh. Tekh. Fiz.; 40: No. 9, 1834-8(Sep 1970).

In a beam–plasma system with nonlinear electron–ion friction, it is possible for plasma waves to be converted to transverse waves. Results of investigations of steady-state oscillations in a one-dimensional resonator are reported here. (auth)

36236 PERTURBATION APPROACH TO NONLINEAR VLASOV EQUATION. III. STATIONARY NONLINEAR OSCILLATION. Kawakami, Ichiro; Sanuki, Heiji (Nihon Univ., Tokyo). J. Phys. Soc. Jap.; 30: No. 5, 1488-1503(May 1971).

One-dimensional stationary nonlinear electrostatic waves, periodic in space, are investigated by use of the perturbation method. The distribution functions are derived; for these functions, some conditions under which periodic waves exist are determined. (auth)

36237 INTENSE OSCILLATIONS IN THE PLASMA HEATING BY THE LARGE ELECTRIC FIELD. Hamada, Yasuji (Tokyo Univ.). J. Phys. Soc. Jap.; 30: No. 6, 1719-21(Jun 1971).

In 0.2 μs after a large electric field (up to 60 V/cm) was induced electromagnetically on a toroidal plasma, an anomalous resistivity and intense uhf and vhf bursts around $\frac{1}{2}(M/m)^{1/4}\omega_{pi}$ up to 50 V_{p-p} were observed. The lower part of the frequency spectrum of plasma oscillations was ascribed to the Buneman instability. Its dependence on the plasma density was observed and was in agreement with the theoretical predictions. (auth)

36238 DETERMINATION OF THE LIMITING FREQUENCY FOR PLASMA ABSORPTION OF HIGH-FREQUENCY WAVES AT FREQUENCIES BETWEEN THE ELECTRON CYCLOTRON FREQUENCY AND THE LOWER HYBRID FREQUENCY. Galaktionov, B. V.; Golant, V. E.; D'yachenko, V. V.; Shcherbinin, O. N. (Ioffe Inst. of Physics and Tech., Leningrad). Sov. Phys.-Tech. Phys. (Engl. Transl.); 15: No. 11, 1813-15(May 1971).

Translated from Zh. Tekh. Fiz.; 40: No. 11, 2322-5(Nov 1970).

The limiting frequency for the absorption of high-frequency waves by a plasma was measured, and the conditions for its existence were determined experimentally. Some critical values of the plasma parameters, which correspond to a sharp decrease of the plasma density, were measured. These results can be related to the prediction of a theory that assumes linear conversion of the wave energy. (auth)

36239 COLLECTIVE OSCILLATIONS IN A DENSE ELECTRON GAS CONTAINING A FIXED POINT CHARGE. Tripathy, D. N. (Visva-Bharati Univ., Santinikentan, India). pp 443-6 of Proceedings of the Eleventh Symposium on Cosmic Rays, Astrophysics, Geophysics and Elementary Particle Physics, 1969. Vol. II. Bombay; Department of Atomic Energy (1969).

From eleventh symposium on cosmic rays, astrophysics, geophysics and elementary particle physics; Delhi, India (7 Oct 1969). See CONF-691055–(Vol. 2).

A new method is presented for obtaining a single-particle Schrodinger equation to describe the collective oscillations in a dense electron gas containing a fixed-point charge. It has been shown previously that the equation has solutions corresponding to a continuous spectrum of free plasmons and to a discrete spectrum of bound plasmons. Physically, a bound plasmon means a density wave trapped at the impurity site, and it exists only if the impurity charge is negative. The new method is based on the methods of quantum-field theory to many-particle systems, in which an expression of the dielectric constant of this system was obtained in the random-phase-approximation (RPA). (J.C.W.)

36240 WAVE PROPAGATION IN COLD PLASMA IN PRESENCE OF CORIOLIS FORCE. Uberio, C.; Das, G. C. (Indian Inst. of Science, Bangalore). pp 447-50 of Proceedings of the Eleventh Symposium on Cosmic Rays, Astrophysics, Geophysics and Elementary Particle Physics, 1969. Vol. II. Bombay; Department of Atomic Energy (1969).

From eleventh symposium on cosmic rays, astrophysics, geophysics and elementary particle physics; Delhi, India (7 Oct 1969). See CONF-691055–(Vol. 2).

XUM

Wave propagation was studied in cold plasma in the presence of external magnetic field and Coriolis force when the magnetic field and the axis of rotation are in the same direction. Collisional effects were taken into account, but the main emphasis was to study the effects of rotational frequency on resonance and cutoff frequencies of the waves. (J.C.W.)

36241 ELECTRON CYCLOTRON WAVE AND ELECTROSTATIC WAVE IN BOUNDED PLASMAS. Ohkubo, K.; Yamamoto, Y.; Tanaka, S. (Kyoto Univ.). Phys. Lett.; 35A: No. 3, 189-90(31 May 1971).

A probe antenna was used to excite the electrostatic wave in a low electron density region and the electron cyclotron wave in a high-density region in a plasma column. The transition region between two modes is interpreted from the theory of plasma waveguides. (auth)

36242 OSCILLATIONS IN A LOW-PRESSURE PENNING DISCHARGE. Smirnitskaya, G. V.; Nosyreva, I. A. (Moscow State Univ.). Sov. Phys.-Tech. Phys. (Engl. Transl.); 15: No. 11, 1832-8(May 1971).

Translated from Zh. Tekh. Fiz.; 40: No. 11, 2346-53(Nov 1970).

An experimental study was made of the dependence of the electron-bunch rotation frequency (at $p < 10^{-4}$ torr) and the plasma rotation frequency (at $p > 10^{-4}$ torr) on the physical and geometric parameters in a Penning discharge in various gases. The radial potential drop is determined by the "ion-kinetic" method of Reikhrudel' et al. The positive space charge is shown to affect the potential distribution and the oscillation frequency at large H. The theoretical functional dependences are in satisfactory agreement with experiment. (auth)

36243 WAVE PROPAGATION NEAR THE UPPER-HYBRID FREQUENCY IN A MIRROR-CONFINED UNSTABLE PLASMA. Porkolab, M.; Brennan, M. H.; Sinnis, J. (Princeton Univ., N. J.). Plasma Phys.; 13: 353-8(May 1971).

Experimental measurements of the upper hybrid waves in a mirror-confined plasma are presented. The waves are generated by an instability in the device. The present work shows that (a) the waves are absorbed upon reaching the mirror region, rather than being reflected, and (b) the instability is a convective one that is believed to be associated with a small group of energetic electrons having a loss-cone-type distribution. (auth) (UK)

36244 OPTIMUM THIRD-HARMONIC GENERATION IN MAGNETOPLASMAS. Sodha, M. S.; Singh, A.; Sawhney, R. L. (Indian Inst. of Tech., New Delhi). Plasma Phys.; 13: 373-86(May 1971).

Using the Boltzmann transfer equation and Maxwell's equation, an explicit expression is obtained for the third harmonic component in the reflected and transmitted waves from a magnetoplasma slab when an electromagnetic wave of frequency ω is normally incident. These expressions for the third harmonic component in the reflected and transmitted waves are used to obtain the optimum conditions under which the conversion efficiency of the third harmonic is maximum. (auth) (UK)

36245 EFFECT OF PRESSURE DRIFTS ON THE PLASMA-COLUMN EDGE OSCILLATIONS. Cataldo, Joseph C. (City Coll., New York). Plasma Phys.; 13: 393-7(May 1971).

By applying a dc voltage to the aperture limiter plate in a Q-machine, the radial density gradient and plasma frequency were varied. The frequency shift was attributed to a $\nabla p \times B$ azimuthal drift velocity. An increase of less than 2 V also changes the plasma column from a turbulent to a quiescent state. (auth) (UK)

Shielding

Refer also to abstracts 36373 and 36610.

36246 (ANL-7796) EMPIRICAL FORMULA FOR INTERPOLATION OF TABULATED PHOTON PHOTOELECTRIC CROSS SECTIONS. Smith, Donald L. (Argonne National Lab., Ill.). Mar 1971. Contract W-31-109-eng-38. 23p. Dep. NTIS.

The empirical formula $\sigma_\tau(E_\gamma) = \exp[p_1 + (\Sigma_{i=2}^{k} p_i E_\gamma^{i-2}) \ln E_\gamma]$ has been useful in the calculation of total photoelectric cross sections for photon energies E_γ not listed in tables. The parameters p_i are determined by least-squares fitting of the formula to tabulated values at neighboring energies. The number of parameters required for a satisfactory fit depends upon the atomic number of the element, the photon-energy range over which the formula is to be applied, and the desired accuracy. This formula was used to fit total photoelectric cross sections for elements Z = 1 to 100 from E_γ = 1 keV to 100 MeV photon energy. An agreement between the formula and the tabulated values of better than ±3% was sought and obtained. The parameters p_i extracted from the analysis are presented in this report. (auth)

36247 (CTC-48) RADIATION SHIELDING INFORMATION CENTER USER DOCUMENTATION. Jones, J. G.; Green, R. O.; Yount, S. L. (Union Carbide Corp., Oak Ridge, Tenn. Computing Technology Center). 25 May 1971. Contract W-7405-eng-26. 143p. Dep. NTIS.

The Radiation Shielding Information Center (RSIC) information storage and retrieval system is described in detail. The system was designed and implemented for use on the IBM 360/50-65 computer configuration. Bibliographic data are input primarily via an IBM Magnetic Tape Selectric Typewriter (MT/ST) and Digi-Data Corporation's Model 1420 Recorder and Model 1670 Coupler. The converted input data and authority files are stored on IBM 2321 Data Cells; the customer and document master files are stored on magnetic tape. The system provides for flexible searching of both the customer and document master files. A selective dissemination of information (SDI) search provides a current awareness service to RSIC customers. (auth)

36248 (GIPR-41) INFLUENCE OF THICKNESS AND SCATTERING ANGLE ON THE STOPPING CROSS SECTIONS OF NITROGEN, NEON, AND ARGON IONS IN THIN CARBON FOILS. Hoegberg, G. (Chalmers Tekniska Hogskola, Goteborg (Sweden). Institutionen for Fysik). Nov 1970. 28p. Dep. NTIS (U. S. Sales Only).

The mean stopping cross sections $\bar{S}$ of thin carbon foils for nitrogen, neon, and argon ions are determined. The dependence of stopping cross section of foil thickness and scattering angle is reported. The energy of the incident ions ranged from 12 to 56 keV. The electronic S_e and nuclear S_n stopping cross sections were deduced from the experimentally determined stopping cross section $\bar{S} = S_e + \bar{S}_n$ by putting $S_e = \lim_{t \to 0} \bar{S}(t)$, where t is the foil thickness. The reported values of S_e are in reasonably good agreement with previously published results. The mean nuclear stopping cross section in the forward direction is found to reach a saturation value in foils thicker than about 8 $\mu g/cm^2$. The increase of $\bar{S}$ with scattering angle is parabolic at small scattering angles and linear at large scattering angles. (auth) (Sweden)

36249 (LA-4624) BREMSSTRAHLUNG EMISSION MEASUREMENT FROM THICK TUNGSTEN TARGETS IN THE ENERGY RANGE 12 TO 300 kV. Storm, Ellery; Israel, Harvey I.; Lier, Douglas W. (Los Alamos Scientific Lab., N. Mex.). Nov 1970. Contract W-7405-eng-36. 25p. Dep. NTIS.

X-ray spectral measurements were made using four commercial, tungsten-target, x-ray units operating between 12 and 300 kV. The absolute intensity and the spectral distribution were measured. The effects of varying the tube current, target aperture, and detector aperture were investigated. The intensity from two constant-potential units was proportional to the tube current, but two self-rectified units displayed a departure from linearity as the tube current increased. As the target aperture area was increased, the photon intensity increased rapidly at first, but then leveled off to a constant value. The intensity was found to vary directly with the area of the detector aperture, but the spectra became distorted when the aperture was increased to where the counting rate exceeded 1.2×10^4 counts/sec. Sodium iodide scintillators, germanium and silicon semiconductors, and a xenon proportional counter were used to measure the spectra. The measurements were corrected for Gaussian broadening, efficiency, escape peak losses, Compton scattering, and energy linearity to obtain an estimate of the undistorted spectra incident on the detectors. The estimate was used as the input to a computer program that simulated the detectors. The estimate was revised until the calculation gave satisfactory agreement with the spectral measurements of all four detector types. The best estimates of the spectra incident on the detector were corrected for the attenuation of the intervening air, Mylar windows, detector windows, and inherent filtration. After correcting for the solid angle subtended by the detector, the absolute intensity and spectral distribution emitted from the target was obtained for each x-ray unit operating between its minimum and maximum potentials. The total photon and energy fluxes in the L lines, K lines, and continuum are given, as well as the jump ratio at the K edge. The x-ray production efficiency was found to increase from 0.025% at 12 kV to 1% at 300 kV. The constant of proportionality varied in the range $(0.22 \text{ to } 0.74) \times 10^{-6}$ $(kV)^{-1}$. (auth)

36250 (ORNL-TM-3364) ORNL-SNAP SHIELDING PROGRAM. Mynatt, F. R.; Clifford, C. E.; Muckenthaler, F. J.; Gritzner, M. L. (Oak Ridge National Lab., Tenn.). 1 Apr 1971. 29p. (CONF-710304-12). Dep. NTIS.

From Symposium on natural and manmade radiation in space; Las Vegas, Nev.

XUM

The effort in the ORNL–SNAP shielding program is directed toward the development and verification of computer codes using numerical solutions to the transport equation for the design of optimized radiation shields for SNAP power systems. A brief discussion is given for the major areas of the SNAP shielding program which are: cross-section development, transport code development, and integral experiments. Detailed results are presented for the integral experiments utilizing the TSF–SNAP reactor. Calculated results are compared with experiment for neutron and gamma-ray spectra from the bare reactor and as transmitted through slab shields. (auth)

36251 (UARAEE–86) NEUTRON TRANSMISSION THROUGH DUCTS PERPENDICULAR TO NEUTRON BEAM AXIS IN WATER SHIELDS. Sayed Ahmed, F. M.; Belov, S.; Megahid, R.; Hamouda, I. (Atomic Energy Establishment, Cairo (Egypt). Reactor and Neutron Physics Dept.). 1969. 17p. Dep. NTIS (U. S. Sales Only).

The thermal neutron flux distributions were measured along the axis of hollow, cylindrical, air-filled ducts of diameters D = 29, 58, and 100 mm. The ducts were placed in a water-filled tank positioned at one of the horizontal beam channels of the UA-RR-1 reactor so that the duct axis was perpendicular to the beam axis. The distributions obtained were approximated by exponential functions of the distance along the duct axis and the duct effect, defined as the ratio of the neutron flux at a point on its axis to the neutron flux in water at the same place when the duct is filled with water, and are approximately described by an exponential with parameter dependent on $D^{0.75}$. (auth)

36252 (UARAEE–104) TRANSMISSION OF SLOW NEUTRONS IN MULTIPLE-SEGMENT DUCTS IN A WATER SHIELD. Sayed Ahmed, F. M.; Hamouda, I. (Atomic Energy Establishment, Cairo (Egypt). Reactor and Neutron Physics Dept.). 1970. 20p. Dep. NTIS (U. S. Sales Only).

The transmission of slow neutrons in air-filled cylindrical duct segments joined at 90° angles in a water shield was studied. Three duct diameters were investigated, namely 29, 58, and 100 mm, and the ducts were bent through two angles of 90°, in two different directions. The central-segment length varied from 2.9 to 20 cm. The ducts were located in a water-filled tank placed in front of one of the horizontal beam channels of the UA–RR–1 reactor, with the axis of the first segment coinciding with the axis of the neutron beam. The transmission was taken as the ratio between the flux at the end of each segment of the duct, and the incident flux. The transmission at the end of the second bend was found to decrease with the increase in offset length and to increase with the increase of duct diameter. The ratio of the flux measured at the end of the multiple-segment duct to the entrance flux was compared with calculations based on a Simon–Clifford formula for fast neutrons. It was found that the formula is not applicable, and a semi-empirical formula based on the Simon–Clifford formula was obtained to allow for the difference in source geometry and for the energy range of neutrons considered. The results also lead to derivation of an empirical formula, indicating that the duct effect at the end of third segment is a function of the product of the effect at the end of the preceding two segments, duct diameter, and the offset length L_2. (auth)

36253 INCOHERENT SCATTERING OF GAMMA RAYS IN HEAVY ATOMS. Whittingham, I. B. (Monash Univ., Clayton, Australia). J. Phys., A (London); 4: 21-37(Jan 1971).

Exact relativistic differential cross sections for the incoherent scattering of gamma rays by the inner shell electrons of heavy atoms are developed from the second order S matrix element for the electron–photon interaction in the Furry picture. Electron binding is accounted for completely by using the bound electron propagator and Dirac eigenfunctions for the initial and final electron states. A pure Coulomb potential is used to calculate the energy spectrum and the differential cross section for 662-keV gamma rays scattered by the K electrons of lead. In contrast with the results of Di Lazzaro and Missoni, the energy spectrum maximum is displaced by 10% from the Compton energy towards higher photon energies, and there is no increase in the spectrum at the low-energy end. The relativistic results for the ratio of the bound electron to free electron cross sections are larger than the incoherent scattering function calculations and exceed unity for scattering angles above 52°. (auth) (UK)

36254 NANOSECOND STUDIES OF FLUORESCENCE IN GASES EXCITED BY FISSION FRAGMENTS. Calo, Joseph Manuel. Princeton, N. J.; Princeton Univ. (1970). 197p. University Microfilms Order No. 71-1587.

Thesis.

A versatile pulse-sampling apparatus that has a unique excitation source—a few microcuries of the spontaneously fissioning nuclide ^{252}Cf—was developed and applied to the measurement of fluorescent lifetimes and energy transfer rates in gases. A stochastic analysis of distortion effects demonstrates that the random risetimes and amplitudes of the excitation pluses cause negligible distortion in comparison to that produced by the photomultiplier tube. Observations of unfiltered light from the nitrogen Second Positive Group (SPG: $C^3\Pi_u \rightarrow E^3\Pi_g$) yielded a natural radiative lifetime of 40.5 ± 1.3 nsec and a quenching cross section of 1.98 ± 0.02 A^2 for the $C^3\Pi_u$ state. Kinetic and luminosity measurements of filtered light from the $v' = 0$ and $v' = 1$ levels of this state indicated a vibrational relaxation cross section of 2.5 ± 0.7 A^2 for N_2 ($C^3\Pi_u$) $v' = 1$. An interesting result of the kinetic analysis is that, although the total lifetime of the $C^3\Pi_u$ state increases with v', vibrational relaxation reduces the gross, unfiltered SPG luminosity to a single exponential characteristic of the $v' = 0$ level. The energy transfer cross section for the excitation of the $C^3\Pi_u$ state by $Ar(^3P_2,o)$ metastable atoms, determined by kinetic analysis of SPG luminosity following excitation of N_2–Ar mixtures, is 5.0 ± 0.4 A^2. The rate constant for three-body quenching of argon metastables by ground-state argon atoms, obtained from the same analysis, is 10.7 ± 1.2 sec^{-1}-$torr^{-2}$. Values of the ratio of the quenching rate constant to the natural transition probability, k', were determined for CO_2 and CO by a kinetic analysis of luminosity data for these two gases. The results are $k'(CO_2)$ = 0.28 ± 0.05 $torr^{-1}$ and $k'(CO)$ = 0.046 ± 0.008 $torr^{-1}$. Fission-fragment electronic ranges, R_e, in N_2, CO_2, and CO were determined from a kinetic model based on the square law for energy deposition, viz. $E = E_0(1 - r/R_e)^2$, where E is the energy of a fission fragment of initial energy E_0 which has traveled a distance r. A method was also developed that yields predictions of electronic ranges for use with the square law to determine energy deposition in most gases. Results from these calculations show good agreement with available experimental data. Some preliminary data on other gases and a comparison of relative luminosities of all the gases studied are also included. (Diss. Abstr. Int., B)

36255 STOPPING CROSS SECTIONS OF GASES FOR α PARTICLES FROM 0.3 TO 2 MeV. Bourland, P. D.; Chu, W. K.; Powers, D. (Baylor Univ., Waco, Tex.). Phys. Rev., B; 3: 3625-35(1 Jun 1971).

Stopping cross sections for α particles were measured in a differentially pumped gas-cell system from 300 keV to 2 MeV in 13 gaseous compounds: H_2, N_2, O_2, NH_3, N_2O, CO, CO_2, CH_4, C_2H_2, C_2H_4, C_2H_6, C_3H_6, and $(CH_2)_3$. The probable random error of the measurements varied from 1 to 2%. Independent measurements were also made with a sealed gas cell in a scattering chamber for N_2 and H_2, and are found to agree with the differentially pumped gas-cell measurements to within 2.7%. Tests for water-vapor adsorption on thin carbon films used by Chu and Powers were also made and show that a deviation no greater than 3.8% would occur in their original dE/dx measurements. (auth)

36256 ATOMIC STOPPING CROSS SECTION OF H_2, D_2, He, N_2, AND Ar FOR α PARTICLES IN THE CHARGE EXCHANGE REGION ($0.5 \leq E_\alpha \leq 2$ MeV). Hoyer, U.; Waeffler, H. (Max-Planck Institut fuer Chemie, Mainz). Z. Naturforsch.; 26a: 592-5(Mar 1971). (In German).

Measurements of the atomic stopping cross section of the gases H_2, D_2, He, N_2, and Ar for α particles in the energy range from 0.5 to 2 MeV are described. The values obtained are in good agreement with the data given by Weyl for energies up to 0.5 MeV, and also with those from Whaling's compilation for energies beyond 2 MeV. (auth)

36257 POSSIBLE EVIDENCE FOR DOUBLE PLASMONS IN ELECTRON ENERGY-LOSS SPECTRA. Spargo, A. E. C. (Univ. of Melbourne). Nature (London) Phys. Sci.; 230: 195(26 Apr 1971).

Reference is made to Crick and Misell (Nature, 227: 484 (1970)), who gave energy-loss spectra of fast electrons passing through thin films of Ge, with a large peak at 15.6 eV representing the single scattering single plasmon excitation process, and a small broad peak with a maximum near 33 eV that they interpret as being due to the $M_{4,5}$ x-ray absorption edge of Ge at 32 eV, and which is usually obscured by the multiple-loss peak due to the double-scattering single-plasmon excitation process. It is suggested here, however, that the broad peak at 33 eV could be composite, consisting of the single-particle x-ray transitions and also containing a contribution from the single-scattering double-plasmon excitation process. The small peak can be decomposed into a narrow double-plasmon peak at 31.5 eV and a broader peak due to single-particle transitions above 32 eV. A comparison of the areas of the two peaks then gives a measure of the relative probabilities of the two processes. (UK)

36258 ASPECTS OF DEGRADATION SPECTRA. Klots, Cornelius E.; Wright, Harvel (Oak Ridge National Lab., Tenn.). Int. J. Radiat. Phys. Chem.; 2: No. 4, 191-200(Dec 1970).

Monte Carlo calculations are presented of degradation spectra associated with 100-keV electrons slowing down in model physical systems. The resultant spectra are compared with those predicted by the continuous approximation, and the differences are discussed. Transition yields in mixtures are obtained and found amenable to a linear representation. (auth) (UK)

36259 PHOTON ATTENUATION COEFFICIENTS FOR ORGANIC MATERIALS. Atwater, H. F. (Los Alamos Scientific Lab., N. Mex.). Health Phys.; 20: 213-15(Feb 1971).

Because of the disagreements in the existing data, a new set of theoretical attenuation coefficients for hydrogen and valence carbon was developed for photon energies from 1 to 1000 keV. The results are presented in this paper. (auth) (UK)

36260 ATTENUATION OF 14-MeV NEUTRONS IN CALCIUM-BASED CONCRETE AND THE RESULTANT PRODUCTION OF RADIOACTIVITY. Greene, D. (Christie Hospital and Holt Radium Inst., Manchester, Eng.): Major, D.; Croft, J. R.; Roberts, G. C. Brit. J. Radiol.; 44: 116-19(Feb 1971).

The broad-beam attenuation of 14-MeV neutrons in a concrete made from limestone aggregate, limestone dust, and cement was measured, and shown to be exponential with a tenth-value thickness of 46 cm. The γ ray dose rate from activation of this concrete was compared with that from ordinary concrete, made from gravel aggregate, sand, and cement. The data for these measurements were used to estimate the γ-ray exposure rates, in the periods when the neutron generator is switched off, in irradiation rooms constructed from each of these two concretes, and it is shown that the use of the limestone concrete will reduce this radiation hazard by a factor of 5. (auth) (UK)

36261 THEORY OF EFFECTIVE CHARGE AND STOPPING POWER OF HEAVY IONS. Bloom, Stewart D. (Univ. of California, Davis. Univ. of California, Livermore); Sauter, George D. Phys. Rev. Lett.; 26: 607-10(15 Mar 1971).

The Knipp–Teller theory of stopping power for heavy ions is reviewed and revised. The basic idea of using the Thomas–Fermi theory to describe the electron charge around the moving ion is retained. The major alteration introduced is in relating the degree of ionization to the velocity of the ion. The zero-order term of the resulting theory comes within 10% or so of predicting observed mean electronic stopping powers for ions with $z > 6$ and $\epsilon/z^{4/3} > 0.002$, where z is the atomic number of the ion and ϵ its kinetic energy in million electron volts per atomic mass unit. (auth)

36262 RANGE AND RANGE STRAGGLING OF 97-keV ^{224}Ra PARTICLES IN GASES. Leon, J.; Steiger-Shafrir, N. H. (Technion-Israel Inst. of Tech., Haifa). Can. J. Phys.; 49: 1004-17(15 Apr 1971).

High-precision range and straggling measurements of 96.5-keV ^{224}Ra recoil particles, obtained from α disintegration of ^{228}Th, in various gaseous media are described. Special emphasis is placed on the development of a uniform and nondegrading recoil source in order to insure accurate range determination and to prevent broadening of the straggling results by the source. Excellent symmetry for the range distribution curves for all gases was obtained. The performance of the measurements in gases, where successive collisions can be considered as uncorrelated, enabled a detailed comparison with theoretical treatments of the nuclear stopping mechanism dominating in this energy region. The results obtained were compared with the Lindhard theory and show good agreement, especially for the medium-mass gases. (auth) (Canada)

36263 SPECTRUM OF HIGH-ENERGY ELECTRONS UNDERGOING KLEIN–NISHINA LOSSES. Blumenthal, George R. (Univ. of California, San Diego, La Jolla). Phys. Rev., D; 3: No. 10, 2308-11(15 May 1971).

A solution is presented for the spectrum of high-energy electrons confined to a region where the main energy-loss mechanism is Compton scattering in the extreme Klein–Nishina limit. The solution is valid in the steady-state limit, assuming the region under consideration is optically thin to the emitted photons. (auth)

36264 RANGE OF FISSION PRODUCTS IN CARBON. Chinaglia, B.; Demichelis, F.; Tartaglia, A. (Politecnico, Turin). Lett. Nuovo Cim.; 4: 1185-90(19 Dec 1970).

Ranges were measured in isotropic, 1.8-g/cm^2 pyrocarbon disks for nine products of thermal neutron fission of ^{235}U. The enriched U was introduced as uranyl nitrate into the disks by diffusion, and the irradiation was carried out in conjunction with catcher foils. After irradiation, the activities of the catcher foils and disks were determined by γ counting. The fission fragments whose ranges were measured are: ^{95}Zr, ^{99}Mo, ^{103}Ru, ^{131}I, ^{132}Te–I, ^{133}I, ^{140}Ba–La, ^{143}Ce, and ^{147}Nd. The ranges and energies were converted into dimensionless units; the ranges were plotted as functions of energy and mass number and compared with theoretical predictions. (D.L.C.)

36265 ONE-GROUP METHOD FOR CALCULATING DOSE FIELDS FROM SOURCES OF γ-RADIATION WITH A COMPLEX SPECTRUM. Dunaev, L. M.; Drozdov, V. E.; Orlenko, N. I. This paper was summarized in At. Energ. (USSR); 28: 493-4(Jun 1970) as paper No. 396/5558. (In Russian).

Experiments and calculations indicated the possibility and desirability of setting up a single-group method, greatly simplifying the determination of the dose fields of γ radiation arising from sources with a complex spectrum. Effective energies E_{eff} were obtained for various fuel elements as a function of the thickness of the irradiated material and the values of t_r (reactor working time) and t_d (decay after stopping the reactor). A value of $E_{eff} = 1.25$ MeV may be thus used in determining the a.d.r. (absorbed dose rate) arising from the isotopes ^{116}In and ^{56}Mn for H_2O targets with thicknesses of 0 to 60 cm and iron targets with thicknesses of 0 to 3 cm. The a.d.r. values calculated by the single- and many-group methods and those obtained experimentally are all in excellent agreement. (TSS)

36266 NUMERICAL SOLUTION TO SPACE-ANGLE ENERGY-DEPENDENT NEUTRON INTEGRAL TRANSPORT EQUATION. Takeuchi, Kiyoshi (Ship Research Inst., Tokyo). J. Nucl. Sci. Technol. (Tokyo); 8: 141-52(Mar 1971).

A numerical approach to the steady-state, space-, angle- and energy-dependent neutron transport equation is presented for neutron shielding calculations. The scattering integral, with anisotropic treatment of elastic scattering and isotropic treatment of inelastic scattering, is evaluated by the use of Gaussian and straightforward quadratures. A system of coupled one-group integral equations for all the energy meshes of interest, converted from the energy-dependent integral transport equation, is calculated by performing a line integration along the neutron path in the direction of motion. For this purpose, the direction of neutron motion is represented by discrete-ordinate directions Ω_{pq} on the unit sphere. The final presentation of the integral transport equation is derived in a difference form convenient for machine computation. A computation program PALLAS was written in Fortran IV for IBM 360-75 computer to perform neutron transport calculations based on this approach. Comparisons are given of the numerical solutions with analytical solutions for unscattered fluxes in various geometries such as plane, spherical and two-dimensional cylindrical, for volume sources with self absorption, and with experimental spectra for angular neutron fluxes in graphite, polyethylene, and water shields. Excellent agreement is obtained between the present calculations and analytical or experimental results. (auth)

36267 RADIATION TRANSPORT IN A FREE-ELECTRON ATMOSPHERE. Domke, H. (Zentralinstitut fuer Astrophysik, Potsdam, Ger.). Monatsber. Deut. Akad. Wiss. Berlin; 12: 448-52(1970). (In German).

Equations were derived for radiation transport in a free-electron atmosphere. The Milne problem was considered as a special case. (J.S.R.)

Solid-State Physics

Refer also to abstracts 35835 and 36380.

Radiation Effects

Refer also to abstracts 34907, 34911, and 36348.

36268 (NYO-3504-50) DEFECT STRUCTURE OF DEPLETED ZONES IN IRRADIATED TUNGSTEN. Beavan, L. A.; Scanlan, R. M.; Seidman, D. N. (Cornell Univ., Ithaca, N. Y. Dept. of Materials Science and Engineering). 22 Mar 1971. 28p. Dep. NTIS.

A quantitative field-ion-microscope study was made of the defect structure of two depleted zones detected in high-purity ($\leq 1.5 \times 10^{-6}$ at.fr.) tungsten specimens irradiated in situ under ultrahigh-vacuum conditions at a specimen temperature of 18°K with 20-keV W^+ ions to a dose of $\sim 1 \times 10^{13}$ W^+ ions cm^{-2}. The irradiated specimens were examined by the pulsed-field evaporation technique at 18°K, hence their structure is characteristic of this temperature. The depleted zone detected in the (111) plane had a local vacant site concentration of ~8.7 at. % and a self-interstitial atom concentration (SIA) of ~0.92 at. %, while the depleted zone detected in the (141) plane of a second specimen had values of ~10 at. % and ~0.5 at. % for these same quantities.

XUM

The SIAs found locally were on the peripheral surfaces of the depleted zones. In addition to this large local imbalance in point defect concentrations, the depleted zones were elongated along ⟨011⟩ directions. It was found that each of these depleted zones was created by a single incident ion, and a comparison of the number of displaced atoms in each zone with the value predicted by the Kinchin–Pease model showed that this model overestimates strongly the number of displacements created per incident ion. For the depleted zone detected in the (111) plane, it was demonstrated that 23 of 25 SIAs found in the lattice around this zone could have been propagated away from it along ⟨011⟩ and ⟨111⟩ directions as focused replacement sequences. The measured distances of these SIAs away from the depleted zone along ⟨011⟩ and ⟨111⟩ directions were between 45 to 150Å, and 45 to 85Å, respectively. The upper and lower values of these distances were determined by a geometric sampling problem. (auth)

36269 (SC-B-710148) ION IMPLANTATION: A SELECTIVE BIBLIOGRAPHY. Mazzio, Joann (Sandia Labs., Albuquerque, N. Mex.). May 1971. 186p. Dep. NTIS.

This bibliography of titles and abstracts was selected primarily from the periodical literature. It covers the research on ion implantation from January 1967 through September 15, 1970. References are given to earlier studies that trace the historical development of ion-implantation technology. (auth)

36270 (UCRL-51009) RADIATION DAMAGE FROM INTERNAL ALPHA DECAY IN THORIUM. Schmidt, Dorn (California Univ., Livermore. Lawrence Radiation Lab.). Feb 1971. Contract W-7405-eng-48. 93p. Dep. NTIS.

Thesis.

A promising new technique was investigated for producing radiation damage in metals by homogeneously doping the metal (in this case thorium) with some short-lived atomic species whose decay produces sufficient radiation damage to permit study by conventional techniques. The relative advantages and disadvantages are discussed. Radiation damage was accumulated at 4.2°K, and a rough isochronal anneal covering the temperature range 4.2 to 1150°K was performed. Additional isochronal and isothermal recovery studies were performed in the temperature range 4.2 to 80°K. The upper boundaries of the various stages are as follows: Stage I (48°K), Stage II (230°K), Stage III (400°K), Stage IV (1100°K). Total Stage I recovery was only 30%. Stage I was found to have five substages with assignments of substage sources being the same as in copper. Long-range interstitial migration in Stage I_E was clearly demonstrated, but distinction between various interstitial models was not possible. Activation energies were determined for the following stages: I_B (0.021 ± 0.002 eV), I_D (0.0875 ± 0.002 eV), I_E (0.0869 ± 0.002 eV), and, subject to assumptions discussed herein, II_A (0.100 ± 0.01 eV) and II_B (0.182 ± 0.01 eV). (auth)

36271 DECHANNELING OF MeV PROTONS FROM AXIAL AND PLANAR CHANNELS OF GERMANIUM CRYSTAL. Morita, Kenji; Itoh, Noriaki (Nagoya Univ., Japan). J. Phys. Soc. Jap.; 30: No. 5, 1430-8(May 1971).

Energy spectra of protons backscattered from the surface of germanium single crystals are measured. The dechanneling rate of channeled protons into random direction and the stopping power ratio of the aligned to the random beam are obtained. The stopping-power ratios for 1.5-MeV protons in the ⟨112⟩, ⟨111⟩, and ⟨100⟩ directions are 0.31 ± 0.04, 0.40 ± 0.06, and 0.43 ± 0.06, respectively. The dechanneling rate of 1.5-MeV protons at the axial channel in which atoms in the row are uniformly spaced is proportional to the reverse of the square of the critical angle. The theoretical values of the dechanneling rate are calculated, using the diffusion model, and compared with the experimental values. The experimental dechanneling rate in the ⟨111⟩ direction is considerably lower than the theoretical value. (auth)

36272 DAMAGE DEPTH DISTRIBUTION OF 15-keV Kr IMPLANTED IN RbCl AS OBTAINED FROM DIFFUSION MEASUREMENTS. Pronko, P. P.; Kelly, R. (McMaster Univ., Hamilton, Ont.). Appl. Phys. Lett.; 18: No. 8, 335-7(15 Apr 1971).

The steady-state trapping model for inert-gas diffusion in alkali halides is used to obtain direct experimental information on the damage depth distribution resulting from 15-keV Kr bombardment of RbCl. The average damage concentration falls to 5% at about 350 Å (in rough agreement with random stopping theory) but does not reach 1% until about 650 Å (suggesting that channeled stopping also plays a role). Beyond 1200 Å, the implanted damage merges with the background concentration of traps. The traps are shown to be single vacancies by comparing diffusion and conductivity measurements for pure and doped specimens. (auth)

36273 ELECTRON IRRADIATION EXPERIMENTS ON TANTALUM. INFLUENCE OF SPONTANEOUS RECOMBINATION PROCESSES ON THE PRODUCTION OF FRENKEL DEFECTS AT 4.5°K. Meissner, D.; Schilling, W. (Kernforschungsanlage, Juelich, Ger.). Z. Naturforsch.; 26a: 502-11(Mar 1971). (In German).

In high-purity Ta foils, the damage production during electron irradiation at 4.5°K was studied, using electrical resistivity measurements. The observed dose curves show a strong saturation effect, i.e., the effective damage rates decrease with increasing defect densities. Two mechanisms contribute to this radiation annealing effect: (1) spontaneous recombination of newly produced interstitials or vacancies with vacancies or interstitials already present in the crystal (direct recombinations) and (2) spontaneous recombination of close Frenkel pairs under the influence of nearby low-energy recoil events (subthreshold events). The contribution of both direct recombinations and subthreshold events can be separated by subthreshold test irradiations as well as by radiation-doping experiments. Both methods yield mutually consistent results. From these one can deduce a value of the spontaneous recombination volume of about 50 atomic volumes and a value for the cross section for the spontaneous recombination of a close Frenkel pair by subthreshold energy transfers from 1.2-MeV electrons of about 90,000 barns. (auth)

36274 EFFECTS OF ELECTRON IRRADIATION ON PHOTOLUMINESCENCE SPECTRA OF Si-DOPED MELT-GROWN n-GaAs. Jeong, Manu; Shirafuji, Junji; Inuishi, Yoshio (Osaka Univ.). Jap. J. Appl. Phys.; 10: 656(May 1971).

The isochronal annealing behavior of the photoluminescence spectrum in Si-doped n-type GaAs after irradiation with 1.7-MeV electrons was studied. Before irradiation, two strong bands (1.51 and 1.2 eV) and three weak bands (1.47, 1.415, and 1.36 eV) were observed. Irradiation reduced drastically their intensity, and annealing below 470°K did not have any effect. Annealing at 520°K, however, resulted in almost complete recovery of the bands, with a remarkable growth in the 1.415-eV band. Some possible reasons for the observations are discussed. (D.L.C.)

36275 STUDY OF CRYSTALLINE DEFECTS BY CHANNELING. Quere, Y. (CEA, Fontenay-aux-Roses, France). Ann. Phys. (Paris); 5: 105-38(Mar-Apr 1970). (In French).

After a brief survey on the slowing down of particles in amorphous matter, particular cases of the effect of the crystalline state on this slowing down are recalled. The main characteristics of sheet and axial channeling are rapidly discussed, as well as most classical experimental procedures that allow the investigation of this phenomenon. Experiments using a beam of parallel particles (by transmission or backscattering) are distinguished from those using an isotropic flux of particles. The main dechanneling parameters (dechanneling coefficient, opacity . . .) are then defined. It is shown that most crystal defects cause dechanneling. The order of magnitude of the dechanneling probability is given for some classical defects. Results are obtained analytically for the simplest cases or by computer simulation. Dechanneling is much greater when the lattice distortions are large; it is more evident when the temperature is lower. Finally, a certain number of experiments are reviewed that show dechanneling, especially by grain boundaries, stacking faults, dislocations, interstitial atoms, and Guinier–Preston zones. These experiments prove that theoretical assessments made within the scope of classical mechanics are generally correct. In some cases, they allow the configuration of defects to be determined. (France)

36276 ESR STUDIES ON P^+ ION-IMPLANTED Si. Hasegawa, Seiichi; Kontani, Ryozo; Shimizu, Tatsuo (Kanazawa Univ., Japan). Jap. J. Appl. Phys.; 10: 655(May 1971).

An investigation was made of the depth distribution of ESR centers and the effects of annealing in 100-keV P^+-implanted Si. The distribution was determined from the decrease of ESR intensity with successive layer removal. The spectrum did not change with temperature, annealing, or layer removal, but the spin density per area decreased with annealing and layer removal. The region of the depth distribution roughly agrees with the amorphous region (0 to 2000 Å) determined by LEED. It is concluded that the ESR signal originates in the amorphous region. (D.L.C.)

36277 PARAMAGNETIC DEFECTS INDUCED IN NAPHTHALENE AND ANTHRACENE SINGLE CRYSTALS BY NEUTRON IRRADIATION AT LOW TEMPERATURE. Akasaka, Youichi; Masuda, Kohzoh; Namba, Susumu (Osaka Univ.). J. Phys. Soc. Jap.; 30: No. 6, 1686-9(Jun 1971).

Radiation-induced defects in naphthalene and anthracene single crystals irradiated with reactor neutrons at 10 to 17°K were stud-

ied by ESR at 4.2°K, 77°K, and room temperature. The initial radicals produced in naphthalene at low temperature were identified to be α-naphthyl radical and isolated hydrogen atoms, whereas in anthracene, 9-anthryl radical and isolated hydrogen atoms were detected. At room temperature the ESR signals of these radicals disappear, and α-hydronaphthyl radicals and dibenzo-cyclohexadienyl radicals were detected in naphthalene and anthracene, respectively. The results indicate the following processes in the radiation damage in naphthalene and anthracene: RH + neutron → R + H, RH + H → RH_2. (auth)

36278 PARAMAGNETIC CENTRES IN IRRADIATED, OXIDISED, AND REDUCED SODIUM SILICATE GLASSES. Mackey, J. H.; Boss, J. W.; Kopp, M. (Carnegie-Mellon Univ., Pittsburgh). Phys. Chem. Glasses; 11: 205-12(Dec 1970).

Four paramagnetic color centers are observed by EPR spectroscopy in sodium silicate glasses free from metal impurity with 5 to 30% Na_2O, and all result from hole trapping. The occurrence of these centers correlates with changes in the equilibrium between network nitrogen and silanol groups. Two of them (H_2^+ and H_3^+) have been reported in the past; their envelopes (centered at g = 2.0106) overlap so strongly that they have not been resolved. These centers are found in oxidised glass and are responsible for optical absorption bands at 460 and 620 nm; evidence is given that H_2^+ and H_3^+ are in reversible equilibrium at higher temperatures and have a common structural precursor. The other two hole centers (H_4^+ and H_5^+) are found only in reduced (nitrided) glass. The H_4^+ center has a large and anisotropic nitrogen hyperfine splitting (2 to 36 Oe); it was assigned to a π-radical at a nitrogen bridge between two silicons. Interpretation of the EPR spectrum of this center requires a wide distribution of the Si–N–Si bond angle. The H_5^+ spectrum is nearly isotropic (g = 2.0026) and shows only small ^{29}Si hyperfine splitting. No model for this center is yet established. The defects H_4 and H_5 are partly responsible for the ultraviolet sensitivity of reduced glass. (auth) (UK)

36279 *HIGH RESOLUTION INFRA-RED SPECTRA OF DIAMOND.* Runciman, W. A.; Carter, T. (Atomic Energy Research Establishment, Harwell, Eng.). Solid State Commun.; 9: 315-17(1 Mar 1971).

Narrow infrared absorption lines were found in some type Iα diamonds. The main lines, possibly due to X–H bonds, are at 1405 cm^{-1} (7.115 μm) and 3107 cm^{-1} (3.218 μm) with half-widths of 2 cm^{-1} and 4 cm^{-1} respectively. Another line at 1450 cm^{-1} (6.895 μm) with a half-width of 4 cm^{-1} was produced by irradiating type Iα diamonds with 1-MeV electrons to a dose of 6×10^{18} electrons cm^{-2}. (auth) (UK)

36280 PHONON SCATTERING OF FAST ELECTRONS BY CRYSTALS. Earney, J. J. (Univ. of Sussex, Eng.). Phil. Mag.; 23: 577-84(Mar 1971).

The imaginary potential for fast electrons scattered thermally by crystals is evaluated exactly in Born approximation in terms of a correlation function. This result gives the correct temperature dependence for the imaginary potential. The previously obtained one-phonon approximate result has an incorrect temperature dependence. Numerical evaluations of the imaginary potential for copper and lead are given (for an Einstein model). (auth) (UK)

36281 STUDY BY MAGNETIC ANISOTROPY OF DEVELOPMENT OF ORDER OF A 50–50 Fe–Ni ALLOY IRRADIATED BY NEUTRONS. Chamberod, A.; Barruel, F.; Pauleve, J. (CEN, Grenoble, France). J. Phys. Chem. Solids; 32: 881-7(Apr 1971). (In French).

The energy of magnetic anisotropy that develops in a 50–50 iron–nickel single crystal during in-pile irradiation at 250°C with a magnetic field was studied. The experiments enable one to follow the development of order in its initial state. A satisfying interpretation can be given in terms of the formation of nuclei of order corresponding to the disturbed zones characteristic of fast-neutron irradiation. At the onset of ordering these nuclei would be isolated in the disordered matrix in which, however, the directional order is produced by defect migration. This latter type of order is established much more rapidly than the long-range order. The three types of ordered Fe–Ni crystallites, corresponding to the three orientations of the tetragonal axis, may develop in almost the same way regarding volume and degree of order. When the applied magnetic field is parallel to one of these orientations, the resulting slight disequilibrium is sufficient to account for the observed anisotropy energy of tetragonal symmetry. (auth) (UK)

36282 CONCENTRATION PROFILES OF ROOM-TEMPERATURE ION-IMPLANTED INDIUM IN SILICON. Gamo, Kenji (Osaka Univ.); Iwaki, Masaya; Masuda, Kohzoh; (and others). Jap. J. Appl. Phys.; 10: 523-5(Apr 1971).

Antimony-doped Si crystals with a resistivity of less than 0.01 Ω cm were implanted with ~10^{15} In ions/cm^2 at 20 to 80 keV. The profiles were measured by neutron activation, anodization, and stripping. They are in good agreement with calculations from the theory of Lindhard, Scharff, and Schiott, but moments of higher order are needed to describe the asymmetric profiles exactly. (D.L.C.)

36283 EPR IDENTIFICATION OF THE NEUTRAL CHARGE STATE OF THE BERYLLIUM VACANCY IN IRRADIATED BeO. Maffeo, B.; Herve, A.; Cox, R. (CEN, Grenoble, France). Solid State Commun.; 8: 2169-71(15 Dec 1970).

An electron-irradiated BeO single crystal studied by EPR at liquid helium temperatures (1.5 to 4.2°K) shows an anisotropic spectrum corresponding to a spin-1 hole center. It is identified as the neutral charge state of the beryllium vacancy. (auth) (UK)

36284 SHUBNIKOV–de HAAS OSCILLATIONS IN NEUTRON-IRRADIATED GRAPHITE. Cooper, J. D.; Smith, J. P.; Woore, J.; Young, D. A. (Imperial Coll. of Science and Tech., London). J. Phys., C (London); 4: No. 4, 442-52(29 Mar 1971).

Shubnikov–de Haas oscillations were observed in $\rho_{xx}(H)$ with single-crystalline graphite and in $\rho_{zz}(H)$ with well-oriented pyrolytic graphite. Exposure to fast-neutron bombardment at ~303°K up to a total dose of 1.12×10^{17} nvt produces electron acceptors which lower the Fermi energy, thus expanding the hole Fermi surface and contracting the electron Fermi surface. The long period (ca. 2.1×10^{-5} G^{-1}) previously associated with majority electrons ($m_c^* = 0.039\ m_0$) is reduced by pre-irradiation, while the short period (ca. 1.6×10^{-5} G^{-1}) which had been attributed to majority holes ($m_c^* = 0.061\ m_0$) is increased. Electron and hole assignments must therefore be interchanged, with electron states now appearing at point K and hole states near point H of the Brillouin zone. The introduction of acceptors increases the Dingle temperature for both carriers. Results are variable, but the reciprocal relaxation time for electrons in the single crystal is proportional to acceptor concentration after allowance has been made for other sources of scattering. (auth) (UK)

36285 USE OF HIGH ENERGY ION BEAMS FOR CRYSTAL ANALYSIS OF ION IMPLANTED DIAMOND. Davidson, Lewis Arthur. Stanford, Calif.; Stanford Univ. (1970). 112p. University Microfilms Order No. 71-2752.

Thesis.

The implanted layers were analyzed by means of the channeling technique to determine the state of crystalline order and the atomic location of the implanted impurities. Backscattered ions and characteristic x rays produced by high-energy ion-beam bombardments were used for this crystal analysis. An annealing procedure was developed that was shown to restore the diamond cubic-lattice structure in the implanted layer. For room-temperature 8- to 70-keV phosphorous-ion bombardment of Type IIa diamond, it was found that doses of 3×10^{13}/cm^2 did not significantly affect the crystalline order, whereas a dose of 3×10^{14}/cm^2 destroyed the crystalline order. The damaged layer was found to be disordered carbon, not graphite. The anneal procedure consisted of one hour at 950°C in an ampoule initially evacuated to approximately 5×10^{-6} torr. It was found that (1) the diamond retained the implanted phosphorous atoms during this anneal, (2) the implanted phosphorous atoms did not assume either substitutional or tetrahedral interstitial sites, (3) the measured projected range for 70-keV phosphorous in diamond of 450 ± 115 Å was consistent with theoretical range calculations, and (4) a stable monolayer of oxygen atoms (5.5×10^{15}/cm^2) exists on the (111) surface of implanted and annealed diamond. Optical and electrical measurements on the implanted diamonds revealed (1) a degradation of the band-gap and sample coloration, (2) no optical absorption levels that would be characteristic of hydrogenic ionization levels, (3) resistivity activation energies of 0.2 to 0.3 eV independent of the ion specie, and (4) no measurable Hall Effect. The results of the crystal analysis show that these electrical and optical properties are dominated by the radiation damage and not substitutional doping mechanisms. (Diss. Abstr. Int., B)

36286 RADIATION DAMAGE STUDIES USING THE LOW TEMPERATURE IRRADIATION FACILITY. II. ELECTRICAL RESISTIVITY MEASUREMENT OF PURE ALUMINUM AND AN ALUMINUM ALLOY. Kino, Takao; Notsu, Shuzo; Yoshida, Hiroyuki (Kyoto Univ.). Annu. Rep. Res. Reactor Inst., Kyoto Univ.; 3: 202-4(1970).

The damage production rate during neutron irradiation at low temperatures for intermediate doses in the 4 to 20×10^{18} n/cm^2 range was investigated for high-purity Al and Al containing 150 ppM Mg. The irradiations were conducted at 11 and 18°K, and the resistivity was measured during the irradiation. The results show that the resistivity increased linearly with dose. The production rates, ~5 to 6×10^{-25} ohm · cm/n/cm^2, are lower than those reported by Swanson and Piercy for low doses. (D.L.C.)

XUM

36287 RADIATION DAMAGE STUDIES USING THE LOW TEMPERATURE IRRADIATION FACILITY. VI. RADIATION INDUCED DEFFECTS IN ANTHRACENE AND NAPHTHALENE SINGLE CRYSTALS. Akasaka, Youichi; Masuda, Kohzoh (Kyoto Univ.). Annu. Rep. Res. Reactor Inst., Kyoto Univ.; 3: 216-19(1970).

Crystals of naphthalene and anthracene were irradiated by neutrons at 10°K, and the ESR spectrum was measured at 77°K and room temperature. The ESR spectrum of irradiated naphthalene at 77°K showed lines of hydrogen atoms and naphthyl radicals, while the spectrum of hydronaphthyl radical was observed at room temperature, indicating the reactions $C_{10}H_8 \xrightarrow{\text{irrad.}} C_{10}H_7 + H$ at low temperature and $C_{10}H_8 + H \rightarrow C_{10}H_9$ at room temperature. Similar results were obtained for the dibenzocyclohexadienyl radical in anthracene. (D.L.C.)

36288 DAMAGE PRODUCTION AND RECOVERY IN LOW TEMPERATURE IRRADIATED ZINC. Maury, F.; Lucasson, A.; Lucasson, P. (CNRS, Orsay, France). Cryst. Lattice Defects; 2: 47-54(Feb 1971).

Experimental data obtained at 4.4°K, 4.9°K, and 7.6°K in electron-irradiated zinc are compared and discussed in the aim of obtaining a better understanding of the atomic displacement processes. From the 4.4°K data, a higher limit of 13.5 eV is found for the Frenkel pair production absolute threshold. A single-step displacement probability function cannot account for the experiments. A double-step function with threshold energies at $T_1 = 13.5$ eV and $T_2 = 18$ eV may be used to fit the results. As concerns the irradiations at 7.6°K, it is proposed that the recombination of the most unstable Frenkel pairs results in a modification of the function's shape. (auth)

36289 ION MASS EFFECT IN DECHANNELING RATE. Morita, K.; Itoh, N. (Nagoya Univ., Japan). Phys. Lett.; 34A: 359-60(19 Apr 1971).

The dependence of the dechanneling rate on the projectile ion mass is studied experimentally using H^+, D^+, and $^4Hr^+$ in Ge single crystals at 1.5 MeV, and the contribution of the electron collisions to the dechanneling is separated from that of the nuclear collisions. (auth)

36290 RADIATION DAMAGE STUDIES USING THE LOW TEMPERATURE IRRADIATION FACILITY. V. COLOR CENTERS IN SOME IONIC CRYSTALS. Nakagawa, Masuo; Atobe, Kozo; Okada, Moritami; (and others) (Kyoto Univ.). Annu. Rep. Res. Reactor Inst., Kyoto Univ.; 3: 211-15(1970).

Absorption spectra were measured at 77°K in TlCl, LiF, and MgF_2 single crystals after neutron irradiation at 13 to 15°K. For TlCl, two absorption peaks appeared at 426 and 460 nm after a 1.5×10^{16} nvt dose, and their thermal bleaching was studied. For LiF, after a dose of 6×10^{15} nvt, the M band at 445 nm was observed, and warming produced another band at 630 nm. For MgF_2, a dose of 2.5×10^{16} nvt at 15°K produced a main band at 253 nm and two weak bands at 300 and 320 nm, but the 371-nm band previously reported was not seen. Effects of thermal bleaching were also studied. (D.L.C.)

36291 MAGNETIC CIRCULAR DICHROISM OF BANDS ASSOCIATED WITH THE F^+ CENTER IN SrO. Modine, F. A.; Izen, E. H.; Kemp, J. C. (Univ. of Oregon, Eugene). Phys. Lett.; 34A: 413-14(19 Apr 1971).

A technique that combined magnetic circular dichroism and electron spin resonance was used to associate optical absorption bands in neutron-irradiated SrO with the F^+ center. It is hypothesized that these bands are analogous to bands observed in the alkali halides. (auth)

36292 IMPROVEMENTS IN OR RELATING TO ION SOURCES. Collins, Leslie Edward (to the United Kingdom Atomic Energy Authority). British Patent 1,220,449. 27 Jan 1971. Filed 31 Jul 1967.

This invention relates to methods of positive ion production and to ion sources for producing such ions to use in ion implantation techniques. The method of producing positive ions of a solid material consists of locating the material within the aperture of, or including the material in the material forming the aperture of, the intermediate electrode of a duoplasmatron source and applying a negative voltage to the intermediate electrode relative to the anode sufficient to cause sputtering of the material by gaseous ions produced in the source. (UK)

36293 DEFECT PRODUCTION IN n-TYPE GERMANIUM BY ELECTRON IRRADIATION AT LOW TEMPERATURES. Whitehouse, J. E. (Univ. of Reading, Eng.). J. Phys. Chem. Solids; 32: 677-83(Mar 1971).

During electron irradiation the damage rate is determined by the rates of atom displacement and of simultaneous radiation annealing. Three cases are considered in which the annealing takes place by (1) recombination of close vacancy–interstitial pairs over a unique potential barrier; (2) recombination of isolated vacancies and interstitials following diffusion of one or the other; and (3) recombination of close vacancy–interstitial pairs in which the barrier to recombination is affected by the charge state of the defects. Three expressions are obtained for the number of defects as a function of the temperature of irradiation. Examining the experimental results for n-type germanium irradiated at various low temperatures, one may eliminate case (1) but may not distinguish between cases (2) and (3). It is suggested that unaccounted factors entered into similar experiments described elsewhere. (auth) (UK)

36294 MAGNETIC RELAXATION IN HIGH-PURITY IRRADIATED IRON. I. NEUTRON IRRADIATION. Blythe, H. J.; Kronmueller, H. (Max-Planck-Institut fuer Metallforschung, Stuttgart). Phys. Status Solidi (a); 4: 603-18(16 Mar 1971).

The magnetic after-effect, observed as a time decrease of the initial susceptibility, was measured in high-purity, neutron-irradiated iron. Integrated doses varied from 1.1×10^{17} to 1.1×10^{19} neutrons cm^{-2} ($E > 0.1$ MeV) and the irradiation temperature was about 80°C. Strong relaxation peaks were observed at –65 and –15°C; these were analyzed quantitatively and interpreted as being due to the reorientation of interstitial–impurity clusters and to impurity interstitials. Above 0°C, a relaxation peak occurs at 70°C and is complicated by the occurrence of an annealing process. This peak is attributed to an impurity–vacancy cluster. The relaxation peaks anneal out between 70 and 200°C. This is attributed to the migration of vacancies and vacancy–impurity clusters. During the annealing of these relaxation peaks, another relaxation peak below –150°C is built up and is identified with the cold-work peak of hydrogen atoms that have been detrapped from defect clusters during the annealing process. (auth)

36295 ANOMALOUSLY HIGH COLLECTION OF COPPER IONS IMPLANTED IN ALUMINUM. Arminen, E.; Fontell, A.; Lindroos, V. K. (Univ. of Helsinki. Inst. of Tech., Otaniemi, Finland). Phys. Status Solidi (a); 4: 663-73(16 Mar 1971).

Polycrystalline aluminum was bombarded with 30- and 60-keV Cu ions in an electromagnetic isotope separator. The quantity of copper collected as a function of the bombardment dose was measured by elastic backscattering of 1.8-MeV He^+ ions. From the scattering spectra, the composition of the Cu–Al alloy formed was calculated. At a current density of 20 $\mu A/cm^2$, a collection curve with an anomalously high maximum was obtained, this being about 3.5 times the value of the final steady state attained after prolonged bombardment. The alloy composition at the maximum was about Cu_2Al, while the final composition was about $CuAl_2$. If oxygen gas was sprayed onto the specimen surface during the ion bombardment, a steady state with a composition of roughly Cu_2Al was also obtained at the higher current densities. The bombarded specimens were examined using transmission electron microscopy; precipitates of the various possible phases are observed. (auth)

36296 EPR INVESTIGATIONS ON X-RAY AND PHOTO-INDUCED PROCESSES IN ZnO COATING MATERIAL. Born, G. K. (Univ., Giessen, Ger.); Hofstaetter, A. B.; Scharmann, A. O.; (and others). Phys. Status Solidi (a); 4: 675-84(16 Mar 1971).

The use of zinc oxide (ZnO) powder as a thermal-control coating material for spacecraft was investigated by electron paramagnetic resonance (EPR) technique. The EPR signal of the photosensitive donor at $g = 1.9557$ is shown to be influenced by x rays, temperature, and light irradiation. The activation energy (trap depth) is deduced from isothermal decay experiments, applying the cross-cut method. The estimated value of $E = 0.52$ eV corresponds to optical data. After x-ray irradiation at 88°K, the EPR signal is no longer photosensitive; increasing temperature causes an annealing of this x-ray-induced effect. The annealing process is correlated with the thermoluminescence glow curve. The excitation spectra and photoquenching of the EPR signal were measured. Radiation damage after high-dose irradiation is investigated with regard to the degradation process. (auth)

36297 CHANGE OF DEFECT FORMATION ENERGIES AND RELATED PROPERTIES IN IRRADIATED POLYMORPHIC MATERIALS DETERMINED BY THERMODYNAMIC EVALUATION OF TRANSITION DATA. Unger, S. (Zentralinstitut fuer Kybernetik und Informationsprozesse, Berlin); Schenk, M. Phys. Status Solidi (a); 4: 693-9(16 Mar 1971).

The changes of the thermodynamic properties of polymorphic substances containing lattice defects due to phase transformations are treated thermodynamically. The phase transition is assumed to be diffusionless and reversible. The crystal-lattice defects are considered to be radiation-created point defects; the treatment,

XUM

however, should also be valid for defects generated by means of quenching, cold working, and doping. The lattice defects cause transition point shifts and variations of the transformation heats. The defect-induced changes of the thermodynamic quantities are calculated from appropriate measurements on $PbZrO_3$ and $PbTiO_3$ irradiated with neutrons. (auth)

36298 THERMOLUMINESCENCE INDUCED IN THICK TARGETS BY 3 GeV PROTONS. Lalou, Claude; Brito, Ubirajara; Nordemann, Daniel; Mary, Monique (CEN de Saclay, Gif-sur-Yvette, France. CNRS, Gif-sur-Yvette, France). Compt. Rend., Ser. B; 270: 1706-8(29 Jun 1970). (In French).

The artificial thermoluminescence induced in meteorite powder irradiated with 3-GeV protons was measured. The variation in the intensity of the thermoluminescence with respect to the target depth was determined for a 1-m-long target; the dominant role of secondary particles generated in the target by nuclear reactions is demonstrated. (France)

36299 GROWTH OF DEFECT CLUSTERS IN THIN NICKEL FOILS DURING ELECTRON IRRADIATION. I. Urban, K. (Max-Planck-Institut fuer Metallforschung, Stuttgart). Phys. Status Solidi (a); 4: 761-72(16 Mar 1971).

Thin nickel foils were irradiated with 650-keV electrons in a Hitachi high-voltage electron microscope at temperatures between 20 and 650°C. The formation of interstitial dislocation loops was observed during irradiation in the temperature range from 20 to about 540°C. In an intermediate temperature region from above 200 to 420°C, vacancy-type defect clusters were also found. Vacancy dislocation loops only grew on the compression side of an edge dislocation. The growth of interstitial dislocation loops at elevated temperatures is interpreted under the following assumptions: (i) the point defect concentrations are mainly determined by mutual annihilation and diffusion to the foil surfaces, and (ii) the interaction of a dislocation with an interstitial is stronger than that with a vacancy. (auth)

36300 DISORDER IN IMPLANTED SEMICONDUCTORS: ENERGY DEPENDENCE AND PENETRATION DEPTH. Della Mea, G. (Univ., Padua); Drigo, A. V.; Mazzoldi, P.; Nardelli, G.; Zannoni, R. Phys. Status Solidi (a); 4: 797-804(16 Mar 1971).

The energy dependence of lattice disorder produced by implanting Hg ions of energy 10 to 200 keV into Si crystals was studied at room temperature. The damage produced was studied by means of the channeling technique with 2.0- and 3.0-MeV $^4He^+$ beams. The number of Si atoms displaced per implanted ion was observed to increase linearly with the implantation energy over the whole range studied, in agreement with the Kinci..n–Pease theory. The slope of this linear relationship is (53 ± 6) keV^{-1}. The penetration depth of lattice disorder produced by ^{200}Hg, ^{131}Xe, and ^{84}Kr in Si and ^{200}Hg implanted in Ge was measured in the energy interval 10 to 200 keV. A comparison is presented between the disorder penetration depth and the implanted ion range. (auth)

36301 IRRADIATION DAMAGE IN NICKEL AND IRON IN A HIGH-VOLTAGE ELECTRON MICROSCOPE AND THRESHOLD ENERGY DETERMINATION. Bourret, A. (CEN, Grenoble, France). Phys. Status Solidi (a); 4: 813-25(16 Mar 1971).

Iron and nickel thin foils were irradiated in a high-voltage electron microscope. Interstitial dislocation loops are observed as a result of agglomeration of point defects produced by electrons. Comparison with theoretical results deduced from chemical reaction rate theory shows that nucleation is impurity-controlled for nickel and that the binding energy of di-interstitials is low for iron. Measurements of the total cross section for producing free interstitials as a function of the incident electron energy were performed. Comparison with calculated curves following the method developed by v. Jan and Seeger gives for threshold energies in the three directions the values $T_{110} = 21$ eV, $T_{100} = 38$ eV, and $T_{111} > 60$ eV for nickel. (auth)

36302 RAPID ANNEALING OF PULSE-RADIATION-INDUCED SPACE CHARGE IN SILICON DIOXIDE. Simons, M. (Research Triangle Inst., Research Triangle Park, N. C.); Hughes, H. L. J. Appl. Phys.; 42: No. 7, 3000-1(Jun 1971).

To study possible rapid charge annealing in SiO_2 in the sub-second time regime, MOS samples of thermal oxides grown on p-type Si were exposed at room temperature to 3-nsec electron pulses. The positive oxide space charge was monitored during the 1-msec to 1-sec interval by oscilloscope display of capacitance vs voltage data. The results show flat-band voltage displacements at −14.2 V after 1 msec, 3.6 V after 40 msec, −12.4 V after 23 msec, and 2.8 V after 1 sec. The approximate linearity of the annealing curves is consistent with previous models, and the annealing slope between 10 and 100 msec is $\sim 3.2 \times 10^{-8}$ C/cm^2. The charge present after 1 msec exceeds that after 1 sec by ~75%. (D.L.C.)

36303 EFFECT OF IONIZING RADIATION OF IMPURITY-VACANCY DIPOLES IN LEAD-DOPED NaCl AND KCl. Stott, J. P.; Crawford, J. H. Jr. (Univ. of North Carolina, Chapel Hill). Phys. Rev., B; 4: No. 2, 639-47(15 Jul 1971).

The radiolytic behavior of NaCl : Pb and KCl : Pb upon exposure to 1.5-MeV electrons at various temperatures was investigated by means of optical absorption and ionic thermocurrent (ITC) methods. Irradiation decreases the Pb^{2+} A band at 272 nm and introduces two narrow bands at 207(210) and 253 nm in NaCl (KCl). Since the new bands decrease in amplitude when holes are released by warming the crystals into the range where they become mobile, and increase in amplitude at the expense of the A band when electrons are released by F-band excitation, it is concluded that they are associated with Pb states of lower positive charge, i.e., Pb^0 and/or Pb^+. Irradiation also decreases the height of the Pb^{2+}-cation-vacancy ITC relaxation peak near 227°K and introduces small ITC peaks at lower temperature, which are not produced by similar irradiation doses in pure KCl. One of these, at 175°K in NaCl and near 200°K in KCl, anneals at 300°K but is enhanced by F-band bleaching at lower temperatures. It is proposed that this new ITC peak is associated with the relaxation of a pseudodipole composed of a cation vacancy bound by elastic forces to a Pb^+ ion. (auth)

36304 EFFECTS OF X IRRADIATION ON THE IONIC CONDUCTIVITY OF DOPED SrF_2 CRYSTALS. Kristianpoller, N.; Kirsh, Y. (Tel-Aviv Univ., Israel). Phys. Rev., B; 4: No. 2, 635-8(15 Jul 1971).

The ionic conductivity of SrF_2 doped with various concentrations of Nd^{3+} and Tb^{3+}, as well as of nominally pure SrF_2 crystals, was measured in the extrinsic region. The conductivity was found to increase with the concentration of the dopant, and was attributed mainly to F^- interstitials. The conductivity of the Tb-doped crystals was considerably higher than that of the Nd-doped samples. The difference is attributed to the difference in association between these rare-earth ions and the F^- interstitials. The effect of x irradiation at 80°K on the extrinsic ionic conductivity was investigated. The x irradiation caused a decrease in the conductivity of the pure and the slightly doped samples, but did not notably influence the conductivity of the heavily doped specimens. The activation energies were not affected by the x irradiation. After annealing to about 600°K, the original conductivity of all the x-rayed samples was restored. It is assumed that, as a result of the x irradiation at low temperature, F^- interstitial ions transformed to F^0 atoms. During the heating of the samples, these atoms recombined with electrons trapped at the sites of rare-earth ions and re-formed F^- interstitials. (auth)

36305 ELECTRON-IRRADIATION EFFECTS IN SILICON AT LIQUID-HELIUM TEMPERATURES USING ac HOPPING CONDUCTIVITY. McKeighen, R. E.; Koehler, J. S. (Univ. of Illinois, Urbana). Phys. Rev., B; 4: No. 2, 462-76(15 Jul 1971).

Changes in ac hopping conductivity with electron irradiation were measured in n-type, p-type, and high-purity silicon. Irradiations were carried out at both 5.0 and 1.6°K, with measurements made at reference temperatures of 4.2 and 1.3°K, respectively. In the p-type crystals, the changes in ac hopping conductivity depend strongly on the concentration of chemical acceptors, indicating a concentration dependence on impurities in the defect production rate. The production rates at 1.6°K were generally very similar to those for a 5.0°K irradiation. No significant thermal annealing stages below room temperature were observed in any of the crystals. No radiation annealing effects due to a beam of either 0.500- or 0.350-MeV electrons were observed, either at 4.5 or 1.45°K. The possibility of athermal effects leading to interstitial migration is suggested. (auth)

36306 RECOVERY OF PURE PLATINUM AND DILUTE PLATINUM–GOLD ALLOY ELECTRON-IRRADIATED AT LIQUID-NITROGEN TEMPERATURE. Doyama, M. (Argonne National Lab., Ill.); Koehler, J. S.; Lwin, Y. N.; Ryan, E. A.; Shaw, D. G. Phys. Rev., B; 4: No. 2, 281-91(15 Jul 1971).

Pure platinum, platinum−0.1 at. % gold alloy, and platinum with various supersaturations of vacancies were irradiated at approximately 90°K by 3-MeV electrons. The production of damage for these samples did not follow the simple power law widely used. Isothermal annealing in 10°C temperature intervals in the range −150 to 100°C revealed annealing peaks at −75, 0, and 25°C. The activation energies of these peaks were determined to be 0.48 ± 0.04, 0.74 ± 0.06, and 0.74 ± 0.06 eV. In addition, the annealing was continued to higher temperatures in 25°C intervals to investigate the stage at 325°C. From the dependence of the various peaks upon the pre-irradiation vacancy concentration, dose, and the results for

XUM

the alloy samples along with the activation energies, it is suggested that the annealing process at 325°C (activation energy of 1.45 ± 0.06 eV) associated with the migration of vacancies should be called stage III. In this way the physical phenomenon associated with this stage will correspond to that in other metals, such as Al and Au. The stage around −75°C is strongly impurity-dependent, being completely suppressed in the 0.1 at.% alloy. (auth)

36307 DECHANNELING OF α PARTICLES BY DISLOCATIONS OCCURRING IN ALUMINUM. Leteurtre, J.; Housseau, N.; Quere, Y. (CEA, Fontenay-aux-Roses, France). J. Phys. (Paris); 32: No. 2-3, 205-9(Feb-Mar 1971). (In French).

The origin of particle dechanneling due to dislocations is briefly recalled. An experiment is then described in which the dislocation density for a slightly cold-worked aluminum sample and the fraction of α particles dechanneled by these dislocations are measured. In the case of 5-MeV α particles channeled along dense {111} planes, the mean dechanneling width of dislocations is found to be (140 ± 40) Å. This value is in correct agreement with a theoretical evaluation of 175 Å. (auth) (France)

36308 FORMATION OF BANDS OF ADDITIONAL ABSORPTION IN RUBY CRYSTALS DUE TO X RADIATION. Niklas, A. (Higher Pedagogical School, Opole, Poland); Sujak, B. Acta Phys. Pol.; A39: No. 3, 351-62(Mar 1971).

The effect of x radiation on the formation of additional optical absorption bands and on photostimulated (exo)electron emission N/t as a function of stimulating light wavelength was examined for ruby crystals with Cr_2O_3 concentrations of 10^{-4} and 3×10^{-2} percent. By resolving the curves of additional absorption into Gaussian curves, the following respective absorption bands were obtained for the 10^{-4} and 3×10^{-2}% Cr_2O_3 concentrations: 222, 298, and 410 nm, and 219, 286, 375, and 474 nm. The data obtained from measurements of the additional absorption bands and photostimulated exoelectron emission $N/t = f(\lambda)$ imply that the absorption band in the vicinity of 470 nm should rather be assigned to Cr^{2+} ions. (auth)

Physical Properties

Refer also to abstracts 35328, 35477, 35553, 35563, 35564, 35580, and 36080.

36309 (AAEC/TM-578) PROGRAMS FOR THE MANAGEMENT AND PROCESSING OF NEUTRON DIFFRACTION DATA. Elcombe, M. M.; Cox, G. W.; Pryor, A. W.; Moore, F. H. (Australian Atomic Energy Commission Research Establishment, Lucas Heights). Feb 1971. 56p. Dep. NTIS (U. S. Sales Only).

This report described the programs developed over about five years at Lucas Heights for the processing of crystallographic data from manual and computer-controlled diffractometers. The description, theory, and input and output formats are given, but not the program listings. Sections 2 and 3 describe the programs for handling, editing, and reducing the 5-hole tape produced by manually operated machines. Section 4 describes the revised versions of the programs associated with the computer-controlled diffractometers; it replaces the previous report, AAEC/E191, as an operating manual for these instruments. Section 5 describes the programs for sorting, absorption-correcting, and evaluating standard deviations. Section 6 describes the Job-Control procedures (auth) (Australia)

36310 (HEDL-SA-119) RESISTIVITY MEASUREMENTS OF INSULATORS USING THE FOUR-PROBE TECHNIQUE. Schemmel, R. R.; Gordon, R. L. (Hanford Engineering Development Lab., Richland, Wash.). 21 Apr 1971. Contract AT(45-1)-2170. 23p. (CONF-710415-1). Dep. NTIS.

From seventy-third annual meeting of the american ceramics society; Chicago, Ill. (26 Apr 1971).

Discrepancies existing in published bulk-resistivity values for refractory oxides result from sample differences and experimental techniques. This paper discusses difficulties encountered in attempts to employ four-probe insulation measurement techniques. Constant application of voltage or current causes polarization of ionic conductors. Experiments reported here indicate charge-density collection at interfaces sufficient to vary potential distributions across a sample with time, thus causing nonlinearities between sample current and probe voltage. At elevated temperatures, thermally emitted electrons increase the electron density and/or ion concentration surrounding a sample, causing net currents in the gas phase and erroneous sample current measurements. Actual measured emission currents approximated apparent sample currents at these temperatures, and conductivity curves indicated that parallel paths through the atmosphere "shunt" sample currents. The monitored potential distribution across the sample surrounded by an equipotential shield indicated direct coupling between the shield and sample at elevated temperatures. Above 1100°C measured potentials approach shield voltages. (auth)

36311 (NP-18845) TABLES OF MAGNETIC STRUCTURES DETERMINED BY NEUTRON DIFFRACTION. PART III. RHOMBOHEDRAL AND HEXAGONAL SYSTEMS. ELABORATION AND REDACTION. Oles, A.; Bombik, A.; Kajzar, F.; Kucab, M. (Institute of Nuclear Techniques, Krakow (Poland)). Jan 1971. 86p. (INT-7). Dep. NTIS (U. S. Sales Only).

Tables of the Magnetic Structures Determined by Neutron Diffraction were elaborated on the basis of the original papers. The tables contain the chemical symbol of the substance, its space group, crystallographic data, cation distribution, temperatures of magnetic transitions, a brief description of magnetic structure including some figures, magnetic moments and their directions, effective magnetic moments, and references on magnetic additional properties. Magnetic space groups for stoichiometric compounds are indicated. The third part of the tables contains compounds and alloys belonging to the rhombohedral and hexagonal systems at room temperature. (auth)

36312 ELECTRONIC SPECIFIC HEAT OF AN IMPURE TUNGSTEN SAMPLE. Potton, R. J.; Brewer, D. F. (Univ. of Sussex, Brighton, Eng.). Phys. Lett.; 35A: No. 2, 85-6(17 May 1971).

A specific heat anomaly, probably of hyperfine origin, was observed in a sintered tungsten sample. Decomposition of the specific heat into hyperfine, lattice, and electronic terms suggests that the electronic specific heat is also anomalous. (auth)

36313 QUASI-ELASTIC SCATTERING OF NEUTRONS FOR THE STUDY OF RANDOM MOTIONS IN SOLIDS. Stiller, H.; Springer, T. (Kernforschungsanlage, Juelich, Ger.). Z. Naturforsch.; 26a: 575-84(Mar 1971).

Investigations on motions of hydrogen atoms in metals, on rotational diffusion in molecular solids, and on fluctuations of protons at hydrogen bonds are reviewed as examples for experiments with incoherent neutron scattering requiring high resolution. (auth)

36314 ANNEALING EFFECTS ON GALVANOMAGNETIC PROPERTIES OF HEAVILY RADIATION-DAMAGED GRAPHITE. Tsuzuku, Takuro; Arai, Shiro (Nihon Univ., Chiba, Japan). Jap. J. Appl. Phys.; 10: 580-8(May 1971).

An annealing study of radiation damage in graphite was made through the observation of the changes in electrical resistivity, Hall coefficient, and magnetoresistance at room and liquid-nitrogen temperatures. The specimen examined is a pile-grade polycrystalline graphite bombarded with fast neutrons at 30°C to total dose of 5.8×10^{20} nvt. The isothermal annealing is performed in a stepwise manner at temperatures from 200 up to 2400°C. The recovery diagrams are characterized by the presence of two major stages lying on the annealing temperature axis; the relatively small one around 300°C and the bigger around 1300°C. Based on a parabolic two-band representation for the electronic structure, thorough analyses are made of the whole data, which lead to a coherent description of the recovery process in terms of the following parameters; the density and mobility of conduction carriers, the overlap of upper and lower bands and the location of the Fermi level. Discussions are also given in relation to the defect structure. (auth)

36315 ELECTRICAL RESISTIVITY MEASUREMENTS OF VANADIUM AND IRON DEFORMED AT 4.2°K. Takamura, Saburo (Japan Atomic Energy Research Inst., Tokai). J. Phys. Soc. Jap.; 30: No. 5, 1367-73(May 1971).

The recovery of electrical resistivity in polycrystalline vanadium and iron, deformed at 4.2°K, was studied in the temperature range of 4.2 to 440°K. The initial recovery stage (Stage I) is attributed to the dislocation rearrangement and the stage II recovery is also considered to be due to the migration or dissociation of interstitial clusters in fcc metals (Cu, Au, and Al). The effect of a deformation on the flux line in the mixed state of a type-II superconductor is also studied. The movement of flux lines in the medium containing defects is discussed as analogous to movement of dislocations. (auth)

36316 HOMOGENEOUS NUCLEATION DURING CRYSTALLIZATION OF SUPERCOOLED TIN. Skripov, V. P.; Koverda, V. P.; Butorin, G. T. (Ural Polytechnic Inst., Sverdlovsk, USSR). Sov. Phys.-Cryst. (Engl. Transl.); 15: No. 6, 1065-9 (May-Jun 1971).

Translated from Kristallografiya; 15: No. 6, 1219-25(Nov-Dec 1970).

A criterion for homogeneous nucleation is proposed. Experi-

mental data on the supercooling of small tin drops have been obtained and the temperature dependence of the nucleation frequency I_1 between 7×10^4 and 3×10^8 cm^{-3}. sec^{-1} with a supercooling $\Delta T = 121$ to 131°C has been measured. Analysis of the results shows the fluctuational origin of crystallization centers. (auth)

36317 X-RAY LUMINESCENCE AND THERMOLUMINESCENCE OF SrF_2 AND BaF_2 CRYSTALS ACTIVATED BY Gd^{3+} AND Dy^{3+} IONS. Luks, R. K.; Stolov, A. L. Opt. Spectrosc. (USSR) (Engl. Transl.); 29: 170-3(Aug 1970).
Translated from Opt. Spektrosk.; 29: 322-7(Aug 1970).

A study was made of the x-ray luminescence and thermoluminescence (TL) spectra of Gd^{3+} and Dy^{3+} ions in SrF_2 and BaF_2 crystals, and of the kinetics of the initial stages of luminescence decay. It was shown that x-irradiation excites the rare earth ions which constitute centers with localized and nonlocalized charge compensation. Glow curves were obtained for centers of cubic and trigonal symmetry. (auth)

36318 CRYSTALLOGRAPHIC AND MAGNETIC PROPERTIES OF COMPOUNDS OF COBALT AND LUTETIUM. Givord, Francoise; Lemaire, Remy (CNRS, Grenoble, France). Solid State Commun.; 9: 341-6(1 Mar 1971). (In French).

Intermetallic compounds observed in the lutetium–cobalt system were Lu_3Co, Lu_4Co_3, $LuCo_2$, $LuCo_3$, and Lu_2Co_{17}. The Lu_2Co_7 and $LuCo_5$ compounds do not exist. (in French) the ratio between the atomic radii of lutetium and cobalt is too small. The three richest lutetium compounds exhibit only a high Pauli paramagnetism. The two others are ferromagnetic. The magnetic behavior of cobalt essentially depends on the number of alloyed lutetium atoms. On the other hand, the differences between interatomic distances in compounds with lutetium and with yttrium have minor effects on magnetic properties, while they determine the magnetic behavior of iron in similar compounds. (auth) (UK)

36319 LATTICE VIBRATIONAL SPECTRA AND PHYSICAL CHARACTERISTICS OF METALS WITH CUBIC STRUCTURE. Plendl, J. N. (Air Force Cambridge Research Labs., Bedford, Mass.); Gielisse, P. J.; Plendl, H. S.; Kromhout, R. A.; Mansur, L. C. Appl. Opt.; 10: No. 6, 1444-50(Jun 1971).

A recently developed method for obtaining the absorbed energy spectrum and calculating its absorption frequencies from elastic constant data was applied to metals, using cold neutron spectra in absence of infrared data. The emitted spectrum from incoherent neutron scattering becomes, through Kirchhoff's law, directly related to the absorbed energy spectrum. The cold neutron spectra examined were for the metals Al, V, Ni, Pd, and Pb. The numerical data of the T and L modes were compared with those calculated from elastic constant data, including their interpretations. The agreement was within experimental error. Interesting differences occur between metals and dielectrics with respect to the intensity of the various T modes. The damping of lattice vibrations in metals was of the same order of magnitude as in dielectrics with ionic binding, i.e., much higher than the damping in dielectrics with covalent binding. (auth)

36320 DETECTION OF REACTIONS TAKING PLACE IN PULVERIZED OXIDE MIXTURES OF THE SYSTEM La_2O_3–TiO_2–ZrO_2 BY MEASUREMENT OF THE ELECTRIC RESISTANCE. Solacolu, S.; Barbulescu, A. (Institut Polytechnique, Bucharest). Rev. Roum. Chim.; 15: 1851-5(Dec 1970). (In French).

In studying the variation of the electric resistance when the temperature of an intimate mixture of oxides is raised progressively, it is possible to detect the solid-phase reactions that take place. It is in this manner that the phenomena that appear during the heating of oxide mixtures having a strong chemical reactivity that constitute the system La_2O_3–TiO_2–ZrO_2 have been demonstrated. A special technique of sample preparation as well as the advantages resulting from it are described. The results obtained confirm the potential possibilities of applying this method to the study of reactions in the solid phase. (tr-auth)

36321 ELECTRICAL RESISTANCE OF Ti–Nb ALLOYS AT HIGH PRESSURES. Fedotov, L. N.; Kirshenina, I. I.; Zarubina, O. A.; Kuznetsov, V. V. pp 86-92 of Fiziko-Khimiya, Metallovedenie, i Metallofizika Sverkhprovodnikov. /Savitskii, E. M. (ed.). Moscow; Izdatel'stvo Nauka (1969). (In Russian).

The electrical resistance of Ti–Nb alloys containing 20 to 56 at. % niobium was measured as a function of hydrostatic pressure up to 15 katm. at room temperature. The results are discussed from the point of view of possible phase transformations in these alloys. (tr-auth)

36322 LATTICE VIBRATIONS IN DEUTERATED AMMONIUM CHLORIDE AT 85°K. I. EXPERIMENTAL. Teh, H. C.; Brockhouse, B. N. (McMaster Univ., Hamilton, Ont.). Phys. Rev., B; 3: 2733-43(15 Apr 1971).

Dispersion curves for the [00ζ] (Δ), [ζζ0] (Σ), [ζζζ] (Λ), and [$1\frac{1}{23}$ζ] (T) directions in ND_4Cl were measured at 85°K by inelastic scattering of slow neutrons using the McMaster triple-axis crystal spectrometer at Chalk River. The single crystals were grown from solution. A torsional (librational) branch, flat within about 2%, with an average frequency of 8.3×10^{12} cps, was found. Results are compared with a modified rigid-ion-model calculation based on Parlinski's formulation. Symmetry points and branches in the dispersion curves are classified according to their symmetry species. The Lyddane–Sachs–Teller relation as generalized by Cochran holds within experimental accuracy. (auth)

36323 LATTICE VIBRATIONS IN DEUTERATED AMMONIUM CHLORIDE AT 85°K. II. THEORETICAL. Cowley, E. R. (McMaster Univ., Hamilton, Ont.). Phys. Rev., B; 3: 2743-50 (15 Apr 1971).

A shell model is shown to provide a good fit to the phonon dispersion curves in ND_4Cl. The model contains 22 parameters of which 13 are fitted to the experimental measurements. The ionic charge on the chlorine, and the electronic polarizabilities of the ions, are not fitted to the experiments. The ND_4 group is not treated as rigid, but it is shown that an effective dynamical matrix can be set up, which does not contain the internal coordinates explicitly, but which describes their effect on the external dispersion curves to a very good approximation. The dispersion curves in NH_4Cl are also calculated. A group-theoretical analysis of the symmetry of the normal modes is given. (auth)

36324 HALL EFFECT STUDIES ON STRONTIUM AND YTTERBIUM UNDER HIGH PRESSURES. Holzapfel, W. B. (Technische Univ., Munich); Severin, D. Phys. Lett.; 34A: 371-3 (19 Apr 1971).

Hall coefficients of strontium and ytterbium under pressures between 0 and 50 kbar are presented. The data further support the general picture of close similarities in the band structure of Sr and Yb. (auth)

36325 INTERACTION BETWEEN POINT DEFECTS IN METALS. March, N. H.; Rousseau, J. S. (Univ. of Sheffield, Eng.). Cryst. Lattice Defects; 2: 1-46(Feb 1971).

Both experiments and basic theory that lead to knowledge of the interactions between defects and impurities in metals are surveyed. The areas dealt with include the study of interaction energies from nonequilibrium production of defects, the deductions that can be made from impurity-diffusion experiments, and the screening theory of the charge-displaced round defects. Electron theory allows one to understand the smaller values that are now appearing for impurity–vacancy binding energies, at least in relatively simple polyvalent matrices like Al. Earlier results, in which large impurity–vacancy interaction energies were being obtained from quenching experiments, need reinterpreting in terms of solute clustering and it seems likely that these will then fall into line with the smaller binding energies referred to above. Diffusion experiments in close-packed metals also support small impurity–vacancy binding energies, though the migration energy changes involved in addition, comparing with measured activation energies, are still not known quantitatively. In open body-centered-cubic metals however, great care is going to be needed, for it now seems highly probable that, in some of these metals at least, self-diffusion proceeds via interstitials at low temperatures. Finally, some directions of promise in combining electron theory with the Kanzaki method of treating relaxation round defects are pointed out. In particular, it is emphasized that the Kanzaki method characterizes a defect by forces acting on the other atoms in the crystal, while electron theory works in terms of the charge displaced by a defect, or a defect complex. It is shown how one can relate the Kanzaki forces to the displaced charge and this offers promise of a very basic calculation of defect interaction energies. The problem of mapping out the anisotropy of the displaced charge around an isolated defect and its possible relation to the anisotropy of activation energies for impurity diffusion in Zn and other hexagonal metals is also emphasized as an important direction for future work. (auth)

36326 EFFECT OF WIRE PARAMETERS ON THE EMISSION OF HARD X RAYS FROM EXPLODING WIRES. Stenerhag, B.; Haendel, S. K.; Goehle, B. (Uppsala Univ.). J. Appl. Phys.; 42: 1876-82(Apr 1971).

Tungsten wires, 20 to 80 mm long and 0.05 to 0.20 mm dia, were exploded in vacuum (1×10^{-5} torr) by means of a 0.4-μF capacitor charged to 30 kV. A pronounced dip and peak in the dI/dt and voltage oscillograms, respectively, corresponded in time to each other and to an ultrafast x-ray pulse. Calculations showed that the wire temperature reached melting point at the same moment. It was

XUM

found that for a constant wire length, the magnitude of the voltage peak attained a weak maximum at a diameter of about 0.10 mm. In addition, for a constant wire diameter, this magnitude increased with increasing wire length. The x-ray output was measured by a scintillator–photomultiplier (PM) combination and an x-ray film. The PM pulses (half-width 20 nsec) depended only slightly on the wire parameters. Their peak values plotted against wire length and diameter showed the same feature as the peak voltage diagram did. Furthermore, studies of the film blackening indicated that various wire dimensions gave rise to various rates of blackening. It was also found that the higher the voltage peak (or PM pulse), the more dense the blackening on the film. A model, based on Ohmic heating of the wire with accompanying thermionic electron emission, which qualitatively explains the generation of the ultrafast x-ray pulse, is presented. In addition, it was found that the electron currents which gave rise to the x-ray burst were up to 10 times higher than those predicted by Richardson's formula. (auth)

36327 STUDY OF THE LINE SHAPES FOR THE RADIO-FREQUENCY SIZE EFFECT IN CADMIUM. Boudreau, D. A.; Goodrich, R. G. (Louisiana State Univ., Baton Rouge). Phys. Rev., B; 3: 3086-93(15 May 1971).

The behavior of the line shapes of the radio-frequency size effect was observed in cadmium both below and in the vicinity of the surface-impedance singularities as a function of surface condition and temperature. It is shown that recent theoretical line-shape calculations based on phenomenological parameters give quantitative and qualitative agreement with experiment, and on the basis of this, inferences on the role of surface scattering in measurements of the radio-frequency surface impedance are outlined. Comments concerning the implications of the present results on past measurements are given. (auth)

36328 TEMPERATURE DEPENDENCE OF ELECTRON MEAN FREE PATHS IN CADMIUM AND COPPER. Cox, W. Royall; Gavenda, J. D. (Univ. of Texas, Austin). Phys. Rev., B; 3: 3577-9(15 May 1971).

A T^{-5} temperature dependence of electron mean free paths is deduced from high-field and open-orbit ultrasonic attenuation data in cadmium and copper. (auth)

36329 COMPARISON OF MODEL CALCULATIONS OF LOW-ENERGY-ELECTRON-DIFFRACTION INTENSITIES FROM Be(0001) AND Al(001). Duke, C. B. (Univ. of Illinois, Urbana. General Electric Research and Development Center, Schenectady, N. Y.); Tucker, C. W. Jr. Phys. Rev., B; 3: 3561-8(15 May 1971).

Low-energy-electron-diffraction (LEED) intensity profiles are calculated using the phenomenological s-wave inelastic-collision model for electrons incident on Be(0001) and Al(001). The predicted intensity profiles are compared both with those obtained in two recent calculations (performed using "realistic" potentials) and with experimental data. When strong inelastic-collision damping is included in the model, the correspondence between the two types of calculations is comparable to that between either of the calculations and the experimental data. This result remains valid over wide ranges of values of the parameters used in the inelastic-collision model. It reflects an insensitivity of certain qualitative features of the model predictions to the values of the "material" parameters used in the calculation. This insensitivity is fortunate because an examination of the realistic potential models suggests that they fail to consider several surface and many-body phenomena that seem to be of significance in determining the intensity profiles. (auth)

36330 LOW-ENERGY ELECTRON-DIFFRACTION INTENSITY CALCULATIONS FOR BERYLLIUM WITH A REALISTIC CRYSTAL POTENTIAL. Strozier, J. A. Jr. (State Univ. of New York, Stony Brook. Cornell Univ., Ithaca, N. Y.); Jones, R. O. Phys. Rev., B; 3: 3228-43(15 May 1971).

The band-matching approach is used to calculate low-energy electron-diffraction intensity–voltage curves for the basal cleavage plane of beryllium. An approximation to the exact theory, made possible by the presence of strong inelastic scattering, enables these curves to be calculated very rapidly for general angles of incidence and with a detailed nonlocal potential. The potential is constructed from first principles, includes thermal and inelastic-scattering effects, and has no adjustable parameters. Over a wide range of incident angles, the calculated curves show marked agreement with recent experiments. A test of the sensitivity of the calculations to changes in the scattering-potential parameters shows that the absolute intensity, rather than peak position or peak width, should be the best experimental probe of the scattering processes. A new approximation for core–valence exchange used in the calculation is described. (auth)

36331 LOW-TEMPERATURE ELECTRICAL AND THERMAL RESISTIVITIES OF TUNGSTEN. Wagner, D. K. (Cornell Univ., Ithaca, N. Y.); Garland, J. C.; Bowers, R. Phys. Rev., B; 3: 3141-9(15 May 1971).

Measurements of ρ and WT (ρ is the electrical resistivity and W is the thermal resistivity) of high-purity single-current specimens of tungsten were performed in the temperature range 1.5 to 6.0°K. The temperature dependence of ρ and WT was found to be predominantly quadratic, in agreement with observations in other transition metals. This behavior is attributed to electron–electron scattering between different branches of the Fermi surface. The validity of Matthiessen's rule for impurity and boundary scattering was investigated to determine whether the contributions of electron–electron scattering ρ_e and W_eT could be meaningfully separated from the total resistivities ρ and WT. In those samples in which boundary scattering contributed least to the total resistivities, Matthiessen's rule was found to be reasonably well obeyed for the electrical resistivity, while deviations were observed for the thermal resistivity. The Lorentz number for electron–electron scattering, $L_e = \rho_e/W_eT$, for these samples was found to range from 0.2×10^{-8} to 0.4×10^{-8} WΩ/K². (auth)

36332 MICROSTRUCTURE EFFECT ON HYPERFINE INTERACTIONS IN Yb-Ag. Beraud, R.; Berkes, I.; Daniere, J.; Haroutunian, R.; Marest, G.; Rougny, R. (Lyon Univ., Villeurbanne, France). J. Phys. (Paris); 31: 1025-31(Nov-Dec 1970). (In French).

Differential and integral measurements of the ($\gamma\gamma$) angular correlations associated with $^{169}Yb \rightarrow {}^{169}Tm$ decay enabled the determination of the electronic relaxation time at ambient temperature in a dilute Ag–Yb alloy and in a source produced by isotope implantation. The existence in the alloy of an electric field gradient acting on the ^{169}Tm nucleus was demonstrated. The results are interpreted assuming the precipitation of Yb in the alloy and the subsequent formation of $YbAg_5$. (auth) (France)

36333 SIMPLE MODEL OF LATTICE DYNAMICS FOR MAGNESIUM, COBALT, AND YTTRIUM. Czachor, A. (Inst. for Nuclear Research, Swierk, Poland); Rajca, A. Acta Phys. Pol.; A39: No. 5, 555-66(May 1971).

A simple model of lattice dynamics for hexagonal, close-packed-structure crystals is proposed. Parameters of the model can be derived from the elastic constants data. The model was successfully tested by evaluating phonon frequencies for magnesium and comparing them with experimental ones. Using the model, phonon dispersion curves and frequency spectra for magnesium, cobalt, and yttrium are calculated. (auth)

36334 PRESSURE DEPENDENCE OF THE ELECTRICAL RESISTIVITY OF GRAPHITE POWDER AND ITS MIXTURES. Marinkovic, S.; Suznjevic, C.; Djordjevic, M. (Boris Kidrich Inst. of Nuclear Sciences, Belgrade). Phys. Status Solidi (a); 4: 743-54(16 Mar 1971).

Using an experimental equipment which made possible electrical resistivity measurements of powders in dependence on pressure up to 250 kp/cm², the relations between resistivity, pressure, and apparent density of graphite powder were investigated, as well as the resistivities of graphite mixtures containing different portions of a nonconductive component. It was found that the electrical resistivity ρ of graphite powder diminishes with pressure P according to the relation $\rho = k\,P^{-s}$. From the pressure dependence of the powder volume V, which is found to satisfy a relation of the same type, a contribution of 0.25 in the exponent s due to the packing of the particles was determined, applying Mrozowski's relation $\rho \approx V^{\frac{1}{2}}/P^{\frac{1}{2}}$ to the case of graphite. The relatively strong pressure dependence of the apparent density, as compared to carbon powders, is explained in terms of the greater orientation tendency of lamellar graphite particles, which is verified by orientation measurements. The pressure dependence of the electrical resistivity of graphite containing different portions of ZnO or SiO_2 could be expressed by curves analogous to those for pure graphite but parallel shifted to greater resistivity values. The orientation of the graphite crystallites in compressed mixtures is considerably smaller than in pure graphite and decreases progressively with increasing content of the nonconductive component. (auth)

36335 WORK FUNCTION OF TANTALUM CARBIDE AND THE EFFECTS OF ADSORPTION AND SPUTTERING OF CESIUM. Baxter, William J. (General Motors Corp., Warren, Mich.). J. Appl. Phys.; 42: No. 7, 2682-8(Jun 1971).

The work function of "unactivated" tantalum carbide is 4.22 ± 0.06 eV. The decrease of work function produced by the so-called "activation" process is attributed to a loss of carbon. The deposition of low-energy cesium ions (2 to 5 eV) reduced the work function to a minimum value of 1.40 ± 0.02 eV. Cesium ions with

energies of 7 to 28 eV sputter previously adsorbed cesium in the form of neutral atoms. The energy required to produce this sputtering decreases with increasing cesium coverage. (auth)

36336 COBALT–MISCHMETAL–SAMARIUM PERMANENT MAGNET ALLOYS: PROCESS AND PROPERTIES. Benz, M. G.; Martin, D. L. (General Electric Research and Development Center, Schenectady, N. Y.). J. Appl. Phys.; 42: No. 7, 2786-9 (Jun 1971).

Several authors have reported successful fabrication of high-energy product (15–20 MGOe) Co_5R-type cobalt–samarium permanent magnets. The authors above have described preparation of such magnets by a liquid-phase sintering process sequence that includes powder preparation, magnetic alignment, pressing, sintering, and magnetizing; they have also described preparation of ternary compositions, primarily Co–Sm–Pr, by this process. In an effort to utilize more abundant rare-earth metals, the cobalt–mischmetal–samarium system was studied. Initial results indicate that a substantial fraction of the samarium may be replaced with mischmetal and still obtain high magnetic properties (BH_{max} = 20 MGOe). Complete documentation of magnetic properties, i.e., saturation, remanence, coercive force, intrinsic coercive force, $(BH)_{max}$, and temperature coefficients, is presented along with a discussion of the fabrication techniques utilized for preparation of the samples. (auth)

36337 TEMPERATURE VARIATION OF SUSCEPTIBILITY OF SOME AMORPHOUS ANTIFERROMAGNETIC OXIDES. Simpson, A. W.; Lucas, J. M. (Univ. of Sussex, Brighton, Eng.). J. Appl. Phys.; 42: 2181-5(May 1971).

The temperature dependences of the susceptibilities of amorphous magnetic oxides with various iron/yttrium and iron/gadolinium stoichiometries were studied between 4.2 and 320°K. The reciprocal susceptibilities of the iron/yttrium oxides exhibited an unusual downward curvature at low temperatures. These measurements are interpreted by means of a simple effective field model for amorphous antiferromagnetic materials recently proposed by one of the authors. Good agreement between the experimental results and the theory is obtained. The analysis enables certain broad conclusions to be drawn about the number and distribution of interacting pairs of magnetic atoms. (auth)

36338 STRUCTURAL AND ELECTRICAL PROPERTIES OF TANTALUM FILMS SPUTTERED IN OXYGEN–ARGON MIXTURES. Westwood, W. D.; Waterhouse, Neil (Bell-North Research, Ottawa). J. Appl. Phys.; 42: No. 7, 2946-52(Jun 1971).

The dependence of the structural and electrical properties of sputtered tantalum films on the rate at which oxygen is leaked into the system has been investigated. The films were deposited on glass and polycrystalline alumina substrates, and both structural and electrical measurements were made on the same samples. While some films deposited in argon contained both the bcc and tetragonal β phases of tantalum, those deposited in the presence of oxygen consisted of the β phase. Increasing oxygen content of the films caused an expansion of the tetragonal lattice and changed the preferred grain orientation from (200) to (202). Increases in the oxygen content from 10 to 50 at. % decreased the film density by 2 g/cm^3, increased the resistivity ρ from 200 to 5000 $\mu\Omega$ cm, and decreased $\Delta\rho/\Delta T$ from 0 to −3.5 $\mu\Omega$ cm/°C. While the activation energy for conduction was small, it increased with the changing orientation of the β–Ta. This may indicate that ρ is due to the semiconducting nature of β–Ta and that the band structure of β–Ta is anisotropic. (auth)

36339 ELECTRONIC TRANSITIONS IN NEAR-EQUIATOMIC VANADIUM–RUTHENIUM ALLOYS. Chu, C. W.; Bucher, E.; Cooper, A. S.; Maita, J. P. (Bell Telephone Labs., Murray Hill, N. J.). Phys. Rev., B; 4: No. 2, 320-6(15 Jul 1971).

The electrical resistivity, the magnetic susceptibility, and the Knight shift of ^{51}V have been studied as a function of temperature in near-equiatomic V–Ru alloys. Electronic transitions were observed as evidenced by the following anomalies: Over a narrow temperature range, the resistivity increases sharply, the susceptibility decreases rapidly, and the Knight shift increases during cooling. At the same time, a tetragonal crystallographic distortion occurs, as found by Marezio et al. The low-temperature specific heat and the superconducting transition temperature were found to vary drastically over the concentration region of interest in agreement with the results of previous work. These changes in electronic properties can be consistently interpreted as arising from a substantial reduction in the Fermi-surface area and of the effective number of carriers associated with the tetragonal distortion. This further suggests that the tetragonal phase is stabilized by the reduction of the electronic free energy. (auth)

36340 MAGNETIC-SUSCEPTIBILITY AND LOW-TEMPERATURE SPECIFIC-HEAT STUDIES OF Ti, Zr, AND Hf. Collings, E. W.; Ho, J. C. (Battelle Memorial Inst., Columbus, Ohio). Phys. Rev., B; 4: No. 2, 349-56(15 Jul 1971).

The results of magnetic-susceptibility and low-temperature specific-heat measurements of high-purity Zr and highest-obtainable-purity Hf are presented, together with earlier data for high-purity Ti. The observed susceptibility components of the Zr single crystal ($\chi_{||}$ = 1.656, $\chi_{\perp}$ = 1.092 μemu/g) confirm the results of another recent measurement, and susceptibility data for Hf single crystals ($\chi_{||}$ = 0.531; $\chi_{\perp}$ = 0.354 μemu/g) are reported for the first time. With the aid of the calorimetric data, values of χ_{orb} are deduced to be 125, 100, and 75 μemu/mole for Ti, Zr, and Hf, respectively. A possible mechanism for the susceptibility temperature dependence in these metals is suggested. (auth)

Moessbauer Effects and NMR

Refer also to abstract 34934.

36341 INTERPRETATION OF THE VARIATIONS WITH RESPECT TO TEMPERATURE OF QUANTITIES MEASURED, USING ESR, FOR A FAMILY OF NEUTRON-IRRADIATED CARBON BLACKS. Carmona, Francois; Delhaes, Pierre (Univ. Bordeaux, Talence, France). Compt. Rend., Ser. B; 272: No. 11, 649-52(15 Mar 1971). (In French).

A phenomenological model accounting for interactions between two spin systems enables the variations with temperature (4.2 to 300°K) of the g factor and the line width associated with neutron-irradiated P33 carbon black to be determined. (France)

36342 ANISOTROPIC BEHAVIOR OF DILUTE MAGNESIUM–GADOLINIUM ALLOYS. Tao, L. J.; Davidov, D.; Orbach, R.; Shaltiel, D.; Burr, C. R. (Univ. of California, Los Angeles). Phys. Rev. Lett.; 26: No. 23, 1438-40(7 Jun 1971).

The electron spin-resonance spectrum of Mg : Gd single-crystal alloys in the concentration range 50 to 1000 ppM exhibits a single anisotropic line. Both the field for resonance and the angular variation of linewidth can be described in terms of unresolved fine structure, but with substantially different values for the axial crystalline field constant. A possible explanation for this difference is proposed. Discrepancies between the conclusions and those of Salamon on a similar system are discussed. (auth)

36343 YADERNYI GAMMA-REZONANS (APPARATURA I METODIKA). (Nuclear Gamma Resonance (Apparatuses and Methods)). Irkaev, S. M.; Kuz'min, R. N.; Opalenko, A. A. Moscow; Izdatel'stvo Moskovskogo Universiteta (1970). 208p.

Nuclear gamma resonance (NGR) spectroscopy is surveyed with particular emphasis on the Moessbauer effect. A mathematical introduction to NGR spectroscopy is offered with coverage of spectral parameters, sources of γ resonance energy, and standardization of resonance line position. Decay schemes are discussed for ^{191}Ir, ^{57}Fe, ^{119}Sn, ^{197}Au, ^{125}Te, and ^{121}Sb. Common gamma detectors and their functioning are described as a prelude to a detailed discussion of the construction and operation of Moessbauer spectrometers, types and requirements, and specialized NGR equipment. Tables of the absorption edges for the K and L series and of characteristics of Moessbauer isotopes are presented. 288 references. (K.S.W.)

36344 MOESSBAUER ISOMER SHIFTS AND HYPERFINE SPLITTING OF THE 145.4 keV γ-RAYS OF ^{141}Pr. Kapfhammer, W. H.; Maurer, W.; Wagner, F. E.; Kienle, O. (Technical Univ., Munich). Z. Naturforsch.; 26a; 357-67(Mar 1971).

The Moessbauer scattering of the 145.4-keV γ rays of ^{141}Pr was observed in a number of praseodymium compounds. From the isomer shifts between trivalent and tetravalent fluorine compounds, the value $\Delta\langle r^2\rangle = +12 \times 10^{-3}$ fm^2 was derived for the change of the nuclear charge radius. The magnetic moment of the 145.4-keV state, $\mu_3 = (2.8 \pm 0.2)\ \mu_N$, was deduced from the magnetic hyperfine pattern observed with scatterers of antiferromagnetic PrO_2. (auth)

36345 GAS PHASE ESR SPECTRA OF ^{31}P, ^{75}As, ^{121}Sb, AND ^{123}Sb. Zijlstra, W. G.; Henrichs, J. M.; Mooy, J. H. M.; van Voorst, J. D. W. (Univ., Amsterdam). Chem. Phys. Lett.; 7: 553-6(1 Dec 1970).

The ESR spectra of ^{31}P, ^{75}As, ^{121}Sb, and ^{123}Sb in the $^4S_{\frac{3}{2}}$ ground state are reported. The free gaseous atoms were obtained in a vacuum cavity by reaction of atomic hydrogen with the vapor of PCl_3, $AsCl_3$, and $SbCl_3$ respectively, at total pressures below 0.8 torr. A possible reaction mechanism is proposed. The ob-

XUM

served hyperfine coupling and quadrupole coupling constants and g_J-values are for ^{31}P: A = 55.15(6) MHz, B = 0, g_J = 2.0020(2); for ^{75}As: A = 66.2(1) MHz, B = 0.13(3) MHz, g_J = 1.9983(1); for ^{121}Sb: A = 298.6(1) MHz, B = 0.86(8) MHz, g_J = 1.9708(1) and for ^{123}Sb: A = 162.3(3) MHz, B = 1.3(1) MHz, and g_J = 1.9708(1). (auth)

36346 SCATTERING OF THE BREMSSTRAHLUNG BY THE MOESSBAUER NUCLEI. Kuz'min, R. N.; Kolpakov, A. V.; Zhdanov, G. S. Vestn. Mosk. Univ., Ser. III. Fiz. Astron.; No. 3, 99-103(May-Jun 1969). (In Russian).

X-ray tube bremsstrahlung scattering by nuclei with low-resonance levels was studied. It was shown by means of a crystalline monochromator containing such nuclei that it is possible to separate from the solid spectra supermonochromatic radiation with band width of the order of the resonance width. The intensity of monochromatic radiation was estimated. (tr-auth)

36347 SPIN–LATTICE RELAXATION BY NUCLEAR MAGNETIC RESONANCE ON ORIENTED NUCLEI. Barclay, John Arthur. Berkeley, Calif.; Univ. of California (1969). 110p. University Microfilms Order No. 70-17,505.

Thesis.

Nuclear magnetic resonance was detected at 0.004 to 0.010°K by perturbation of the gamma-ray anisotropy of ^{60}Co in Fe, Co, and Ni. Shirley's work on the response functions describing the perturbation in the presence of homogeneous broadening is extended to include inhomogeneous broadening. The existence of a "hard core" value at resonance is demonstrated in this case also. Frequency modulation of the inhomogeneous line was necessary in order to perturb all of the spin packets in the broadened lines. The optimum conditions for frequency modulation were found by varying the modulation bandwidth and modulation frequency. A simple model is proposed to explain the observed degree of perturbation. In addition, nuclear spin–lattice relaxation times were measured in the 0.004 to 0.010°K temperature range. The data were interpreted by fitting the data with a sum of exponentials. Precise T_1 results are obtained, but the accuracy is uncertain due to the uncertainty of the initial conditions. (Diss. Abstr. Int., B)

36348 NUCLEAR SPIN–LATTICE RELAXATION AND DYNAMIC POLARIZATION IN γ-IRRADIATED LiF. Valentine, K. M.; Nolle, A. W. (Univ. of Texas, Austin). Phys. Rev., B; 4: No. 1, 15-21(1 Jul 1971).

The spin–lattice relaxation at 13.6 MHz of ^{19}F nuclei in γ-irradiated LiF was investigated at 300, 77, and 4.2 to 1.7°K. The crystals used had optically determined F-center concentrations of 7.0×10^{17}, 2.0×10^{18}, and 3.5×10^{18} cm^{-3}. The relaxation in the temperature range 4.2 to 1.7°K was found to be characterized by a spin-diffusion regime intermediate to the slow- and rapid-diffusion cases. At 300°K, the nuclear spin–lattice relaxation is found to be predominantly controlled by F-center spin–lattice relaxation. However, for the F-center concentrations used, temperature-independent F-center spin–spin relaxation is found to control the nuclear spin–lattice relaxation below 10°K. The variation of the ^{19}F dynamic polarization as a function of microwave power at 1.7°K is investigated for microwave magnetic field amplitudes up to 2.6 G. For this range of fields, the dynamic polarization process also is characterized by an intermediate spin-diffusion regime. Existing theory yields an expression giving the variation of the dynamic polarization time with microwave power, which is used to estimate the correlation time of the F-center-nucleus dipole–dipole interaction at 1.7°K. Estimates are also obtained for the F-center spin–lattice relaxation time at 300°K. (auth)

36349 NUCLEAR SPIN–LATTICE RELAXATION IN PURE AND IMPURE INDIUM. I. NORMAL STATE. MacLaughlin, D. E. (Univ. of California, Riverside); Williamson, J. D.; Butterworth, J. Phys. Rev., B; 4: No. 1, 60-70(1 Jul 1971).

Transient nuclear spin–lattice relaxation measurements were made in indium metal and the InCd, InTl, InSn, and InPb dilute alloy systems using the ^{115}In nuclear-quadrupole-resonance (NQR) spectrum. The theory of spin–lattice relaxation in NQR is described for both magnetic and quadrupolar contributions to the relaxation. Precautions were taken to avoid eddy-current heating. A slight dependence of the relaxation rate on NQR transition was observed. Several explanations of this effect were considered, none of which proved satisfactory. In particular, no evidence was found for quadrupolar relaxation. The relaxation rate increased in the alloys at a rate of a few percent/(at. % solute) for all alloy systems studied. No extrema in relaxation rate in the concentration range 0.5 to 1 at. % solute were found, in contrast to the behavior of the Knight shift as measured by Hewitt and coworkers. The observed increase in relaxation rate in the alloys may be due either to increased enhancement of the contact relaxation, or to an increase in the noncontact contribution to the total relaxation rate. (auth)

36350 NMR MEASUREMENTS IN THE PARAMAGNETIC STATE OF URANIUM–PHOSPHORUS COMPOUNDS. I. LINE SHIFTS OF ^{31}P IN UP AND IN $UP_{1-x}S_x$. Friedman, F.; Grunzweig-Genossar, J. (Technion–Israel Inst. of Tech., Haifa). Phys. Rev., B; 4: No. 1, 180-91(1 Jul 1971).

NMR line shifts ΔH of ^{31}P in the antiferromagnetic semimetal UP and in its solid solutions $UP_{1-x}S_x$ ($x \simeq 0$, 1/4, 1/2, 3/4) in the paramagnetic state are proportional to the magnetization of the solid: $K = \Delta H/H = K_0 + \alpha\chi_M$, where the parameters are nearly independent of composition x and fall within a narrow range $K_0 = (-35 \pm 15) \times 10^{-4}$; $\alpha = 5.2 \pm 0.5$ (emu/mole)$^{-1}$. This line shift is interpreted as superhyperfine (shf) polarization transferred through U–P bonds, where the shf coupling constants are $A_s = -32.4 \pm 1.0$ MHz and $A_p = +3.6 \pm 0.6$ MHz. Although the U–U magnetic coupling is carried by conduction electrons (Ruderman–Kittel–Kasuya–Yosida interaction), the U–P magnetic coupling is through bonds of localized electrons. The results are compared with NMR line shifts in rare-earth monopnictides and with electron-nuclear double-resonance experiments on rare-earth ions. (auth)

Theory

Refer also to abstracts 36358, 36509, and 36846.

36351 FIELD-GRADIENT CALCULATIONS IN SOME METALS OF HEXAGONAL CLOSE-PACKED STRUCTURE. Kantimati, B. (Andhra Univ., Waltair, India). Indian J. Pure Appl. Phys.; 8: 458-61(Aug 1970).

Expressions are derived for the evaluation of the field gradients in the case of metals of hexagonal close-packed structure, following the method due to W. W. Simmons and C. P. Slichter [Phys. Rev., 121: 1580(1961)]. The field gradients are calculated for six metals, viz. lithium, beryllium, rhenium, α-cobalt, sodium, and zinc. The results are compared with those of F. W. deWette [Phys. Rev., 123: 103(1961)] obtained by the method of plane-wise summation. The values of q vary linearly with the axial ratio c/a, although the constants involved in this linear relation are different from those reported earlier. (auth)

36352 NONRELATIVISTIC ENERGY BANDS OF DOUBLE HEXAGONAL CLOSE-PACKED LANTHANUM. Ghosh, Aparna; Kumar, Santosh; Das, K. C. (Saha Inst. of Nuclear Physics, Calcutta). Indian J. Pure Appl. Phys.; 8: 685-90(Nov 1970).

The results of a detailed investigation of the nonrelativistic band structure of double hexagonal close-packed lanthanum, using the symmetrized augmented plane wave (APW) methods, are reported. The crystal potential was constructed with an accuracy of 0.1% in muffin-tin form. The energy eigenvalues were computed for the equivalent of 1152 points in the first Brillouin zone. From these calculations, the Fermi energy was obtained as 0.410 rydberg with respect to the zero of the scale at −1.178 rydbergs, the constant potential in between the APW spheres. The intersections of the Fermi surface with quite a few planes in the reciprocal space were determined. The density of states at the Fermi energy was found to be 20.8 electrons/atom rydberg, which is quite close to that obtained by the relativistic APW calculation. This value is, however, smaller by a factor of approximately 2.5 compared to those obtained from the experimental data of electronic specific heat and paramagnetic susceptibility. This indicates that the electron–phonon interaction is more important than the relativistic effects as far as the density of states in lanthanum is concerned. (auth)

Theoretical Physics

Refer also to abstracts 36126 and 36813.

36353 (ITF-70-61-E) LOGIC OF CONCLUSIVE EXPLICATION OF THE QUANTUM THEORY. Lomsadze, Yu. M. (Akademiya Nauk Ukrainskoi SSR, Kiev. Institut Teoreticheskoi Fiziki). 1970. 28p. Dep. NTIS (U. S. Sales Only).

Based only on the general principles of the quantum theory (on linearity and unitarity of the evolutional operator $\hat{S}$, the usual interpretation of the state vector as probability amplitude and finiteness of velocity of any perturbation spreading), directly on experiment, and on the fundamental thesis of dialectic materialism about primacy of matter with respect to cognition, the uniqueness of explication of this theory is shown. The explication obtained confirms in its turn the deep dialecticity of man's cognition of nature. (auth)

36354 (JINR-P4-5734) EFFECT OF THE OPTICAL PARAMETERS OF THE MEDIUM ON THE YIELD OF TRANSITION RADIATION OF NON-RELATIVISTIC PARTICLES. Kobzev, A. P.; Michalak, S.; Rutkowski, J.; Frank, I. M. (Joint Inst. for Nuclear Research, Dubna (USSR). Lab. of Neutron Physics). 1971. 16p. (In Russian). Dep. NTIS (U. S. Sales Only).

The effect of the values of real and imaginary parts of the refraction index on the yield and angular distribution of the transition radiation of nonrelativistic charged particles is considered. (auth)

36355 (NP-18818) IMPROVED RELATIVISTIC CORRECTIONS TO FERMI-CONTACT HYPERFINE HAMILTONIAN. Pyykkoe, P.; Pajanne, E. (Helsinki Univ. (Finland). Research Inst. for Theoretical Physics). Feb 1971. 12p. Dep. NTIS (U. S. Sales Only).

Following an idea of Breit, a relativistic correction factor to the Fermi-contact hyperfine Hamiltonian is derived for arbitrary principal quantum number n. This n-dependent factor agrees better with an explicit relativistic calculation than the commonly used Racah correction factor. (auth)

36356 STATISTICS OF COMPOSITE BOSONS. Su, Derruenn; Lin, Tzuen-shyan (National Taiwan Univ., Taipei). Chin. J. Phys. (Taiwan); 8: 64-70(Oct 1970).

Quasi-spin formalism is applied to construct a composite boson system that has a definite spin J and a definite z component of spin M. The statistics of two such kinds of composite boson are thus investigated. It is found that the statistics are J- and M-dependent in general. Therefore, the statistics of composite bosons are different from any kinds of presently known statistics and is very complicated. Finally, it is concluded that the Slater determinant is not enough to represent an antisymmetric fermion-antifermion system. (auth)

36357 DELPHI-SPEAKEASY SYSTEM. I. OVERALL DESCRIPTION. Cohen, Stanley (Argonne National Lab., Ill.). Comput. Phys. Commun.; 2: 1-10(Jan 1971).

DELPHI is a modular computer program designed to aid scientists in their day-to-day research. Originally intended to serve the field of nuclear shell-model studies, it has since become a generalized program for theoretical physics. A user-oriented language called SPEAKEASY, included to make the system easily used, is itself becoming a powerful research tool. This paper, the first in a series, is intended to provide a general description of the program. A brief description of nuclear shell-model calculations is included. (auth)

36358 VARIATIONAL CALCULATION OF ELECTRONIC- OR NUCLEONIC-ORDERED SYSTEMS. Coldwell, Robert Lynn. Seattle; Univ. of Washington (1969). 126p. University Microfilms Order No. 70-14,746.

Thesis.

A variational calculation was made of the ground-state energy of an electronic or nucleonic many-body system using Mathieu functions of fractional order as orthogonal single-particle wave functions. This produced a system trial wave function capable of approximating either a system of uniform density or a crystal-like system, depending on the value of a variational parameter, q, present in the Mathieu functions. A new lowest upper bound to the energy of an electron system was found for r_s greater than 12 and to the energy of a nucleon system for r_0 between .2 fm and 1.0 fm. The correlation function for various values of q and hence for the wave functions giving the minimum energy for various values of r_s and r_0 is presented largely to decide if the crystallization implied is real in the sense that the system could reasonably be expected to be crystalline or apparent in the sense that the true wave function would not be expected to be of this type. The evidence favors crystallization in the electron system for r_s greater than 5 and in the nucleon system for r_0 between .4 fm and .8 fm, although the variational nature of the calculation precludes rigorous statements. (Diss. Abstr. Int., B)

36359 ELEMENTARY EXCITATIONS IN A SYSTEM OF CHARGED PARTICLES IN MAGNETIC FIELD. Petru, Z. K. (Univ., Wroclaw). Bull. Acad. Pol. Sci., Ser. Sci., Math., Astron Phys.; 19: No. 2, 159-64(1971).

A system of interacting charged particles (bosons or fermions) in homogeneous magnetic field is studied with the aid of Green's functions method in the hydrodynamical approximation. The full magnetohydrodynamical equations are obtained, and their linearized form is solved. In this way, the explicit form of the retarded Green's function is calculated, and it is found that the elementary excitations are the combination of acoustic and Lamor types. (auth)

36360 FIELD OF A CHARGED PARTICLE MOVING OVER A PERIODIC DIELECTRIC STRUCTURE. Mergelyan, O. S. Sov. Phys.-Tech. Phys. (Engl. Transl.); 15: No. 10, 1592-3 (Apr 1971).

Translated from Zh. Tekh. Fiz.; 40: No. 10, 2043-5(Oct 1970).

The radiation from a charged particle moving in an isotropic medium parallel to the boundary separating this medium from a medium whose dielectric properties are periodic functions of the coordinate is investigated. Perturbation-theory approximations are derived for the fields and angular distribution. (auth)

36361 INTRODUCERE IN MECANICA TEORETICA MODERNA. (Introduction to Modern Theoretical Mechanics). Ionescu-Pallas, Nicolae. Bucharest; Editura Academiei Republicii Socialiste Romania (1969). 234p.

The principles of theoretical mechanics are described from a modern point of view. The following three chapters are included: (1) physics and geometry, (2) relativistic dynamics of a single body, and (3) classical interactions and the many-body problem. (M.O.W.)

36362 EXISTENCE OF ATOMS IN n-DIMENSIONAL SPACE. Gurevich, L.; Mostepanenko, V. (Physical Technical Inst., Leningrad). Phys. Lett.; 35A: No. 3, 201-2(31 May 1971).

The Coulomb interaction of Gaussian type is studied between electron and a proton in n-dimensional space with $n > 3$. The corresponding Schrödinger equation is investigated. It turns out that the energy spectrum of the bounded electron extends to $-\infty$, and the atomic structure of matter does not exist. (auth)

36363 RELATIVISTIC MOTION OF A RADIATING POINT CHARGE IN A CONSTANT ELECTROMAGNETIC FIELD. Mitchell, Thomas P.; Chirivella, Jose; Lingerfelt, J. E. (Univ. of California, Santa Barbara). Plasma Phys.; 13: 387-91(May 1971).

The attenuating influence of the radiation recoil momentum on the motion in constant uniform-arbitrarily directed electric and magnetic fields is exhibited in detail by solving the relativistic Lorentz-Dirac equation to first order in the parameter $2e^2/3mc^3$. The geometry of the trajectory is also elucidated. (auth) (UK)

36364 APPROACH TO THE QUANTUM MECHANICAL FOUR-BODY BOUND-STATE PROBLEM. II. GENERALIZATIONS TO INCLUDE IDENTICAL PARTICLES. Jambor, Cs.; Magyari, E. (Univ., Craiova, Rumania). Acta Phys. Pol.; A39: No. 3, 255-65(Mar 1971).

This paper is closely related to its previous part (E. Magyari, Acta Phys. Polon., A38: 703(1970)). Sets of integral equations were derived for four-particle bound-states systems including 2, 2 + 2, 3, and 4 identical particles, respectively. In the last three cases it was ascertained, as a consequence of the exchange symmetry requirements, that the Eyges "two-body orbital" decomposition of the space parts of the total wave function may be applied only to a restricted class of four-particle bound states. (auth)

36365 THEORY OF DEGENERATE FERMI GAS IN AN EXTERNAL FIELD. Shnol, E. E. (Inst. of Applied Mathematics, Moscow). Teor. Mat. Fiz.; 4: 239-45(Aug 1970). (In Russian).

The change of density $\delta\rho(x,E)$ of a degenerate ideal Fermi gas under a local change of external field V(x) is considered. It is shown that the continuous dependence of $\delta\rho$ on δV is not disturbed by the appearance (or disappearance) of discrete levels far from E. In particular, if there is an energy gap (E_1, E_2) where $E_1 < E < E_2$, then the appearance of discrete levels does not reduce the rate of exponential decrease of $\delta\rho(x,E)$ as $|x| \to \infty$. (auth)

36366 ANGULAR MOMENTUM COUPLING COEFFICIENTS. Tamura, Taro (Univ. of Texas, Austin). Comput. Phys. Commun.; 1: 337-42(Sep 1970).

A computer program for calculating the geometrical coefficients is described; examples are the Clebsch-Gordan coefficient, Racah coefficient, 9-j symbol, etc., occurring in the quantum theory of angular momentum. Logarithms of factorials are calculated and stored at the beginning of the main routine; symmetry properties of the coefficients are used to optimize the speed of the calculation. The program, written in FORTRAN IV for the CDC 660, requires 5358 60-bit words of storage. Average time to calculate a typical coefficient, with the arguments ranging from zero to twenty, is a few tenths of a millisecond on a CDC 660. (R.W.R.)

36367 PROPAGATION OF ELECTROMAGNETIC PERTURBATION OVER A PLANE SURFACE. Ivanov, V. V.; Chernyi, G. P. Zh. Prikl. Mekh. Tekh. Fiz.; No. 5, 22-30(Sep-Oct 1970). (In Russian).

Knowledge of the propagation of an electromagnetic pulse along a plane impedance surface helps to interpret the results derived

XUM

from the observation of electromagnetic fields which vary in time intervals of the order of 10 μsec. In view of the theory of reciprocity, the determination of the distortion of a dipole with arbitrary orientation requires the solution of four functions k_{vv}, k_{hv}, k_{hh}, and M; these designations correspond to the vertical component polarized in a plane normal to the surface of the dipole, its vertical and horizontal components, polarized in the plane of observation, parallel to the surface of the Earth, and polarized in the direction normal to the plane of propagation, respectively, without limiting the latter case to terrestrial propagation. Only the first three equations were examined, because the M function of practically all altitudes leads to a Fresnel function. The dimensions of the pulse functions are those of negative time. (TTT)

36368 VELOCITY OPERATOR IN MANY-BOSON SYSTEMS. Sunakawa, Sigenobu; Yamasaki, Shuichiro; Kebukawa, Takeji (Osaka Univ.). Progr. Theor. Phys. (Kyoto); 44: 819-20(Sep 1970).

The usual commutation relation describing the collective behavior of Bose systems has been shown to be inconsistent with the nonnegative character of the density operator. It is shown that it is still possible to define the velocity operator in such a way (as a canonical conjugate variable for the density-fluctuation operator) that no contradiction with the commutation relation results. (R.W.R.)

36369 ELECTRONS IN STRONG EXTERNAL FIELDS. Reinhard, P.-G. (Univ., Frankfurt am Main); Greiner, W.; Arenhoevel, H. Nucl. Phys.; A166: 173-97(1971).

The problems that arise in the treatment of electrons in strong external fields are discussed. In particular, a method for calculation of field corrections without an expansion in powers of the external field is established. A renormalization procedure is proposed for the divergencies that occur. (auth)

36370 SOLUTION OF AN EXACTLY SOLVABLE QUANTUM MECHANICAL N-BODY PROBLEM. Katriel, J.; Adam, G. (Nuclear Research Centre, Negev, Israel). Amer. J. Phys.; 39: 334-6(Mar 1971).

The classical solution of the N-body problem is reviewed briefly. The transition to the classical Hamiltonian formalism and the possibility of performing the normal-mode transformation in it are indicated, from which the transition to quantum mechanics can be established; also, the possibility of performing the whole normal-mode analysis within quantum-mechanical formalism in the Heisenberg representation is discussed. (M.H.R.)

36371 RELATIVISTIC GROUND-STATE ENERGY EIGENVALUES OF AN ELECTRON-DIPOLE SYSTEM. Turner, J. E.; Anderson, V. E. (Oak Ridge National Lab., Tenn.). Nuovo Cim.; 1B: 149-54(11 Feb 1971).

Relativistic corrections to the ground-state energy eigenvalues of an electron in the field of a stationary, finite electric dipole have been calculated to order α^2 (α = fine-structure constant). Relativistic terms in the Hamiltonian that arise from the Dirac equation are treated as a perturbation of the nonrelativistic Schroedinger equation, which has been solved previously. At large values of the dipole moment D = eR, where −e = electronic charge and R = separation of dipole charges in Bohr radii a_0, the relativistic correction approaches the hydrogenic limit $-(\alpha^2/4)$ Ryd. The magnitude of the correction decreases monotonically to zero as D decreases from very large values to the minimum value, D = 0.639, required nonrelativistically for electronic binding. The relative magnitude of the correction, however, is largest in the region $D = 1.2ea_0$. The critical value $D = 0.639ea_0$ is also apparently implied by the Dirac equation. (auth)

36372 TIME SCALES AND THE PROBLEM OF MEASUREMENT IN QUANTUM MECHANICS. Lanz, L. (Univ., Milan. Istituto Nazionale di Fisica Nucleare, Milan); Prosperi, G. M.; Sabbadini, A. Nuovo Cim.; 2B: 184-92(11 Apr 1971).

A contribution is given to the attempts towards a solution of the measurement problem in quantum mechanics. In order to justify the possibility of a macroscopic description of the measuring apparatus, a relevant hypothesis is found to be the separation of two characteristic times: the decay time for the kernel of a generalized master equation and the characteristic time for the evolution of macroscopic quantities of the measuring device. (auth)

36373 SPACE–TIME PAIR CORRELATION FUNCTION OF A MAXWELL–BOLTZMANN FLUID IN THE T-APPROXIMATION FOR TEMPERATURE GREEN'S FUNCTIONS. I. THEORY. Leribaux, Henri R.; Pope, Noel K. (Royal Military Coll. of Canada, Kingston, Ont.). Phys. Rev., A; 3: 1752-63(May 1971).

A many-body theory is presented here for the Van Hove pair (or density) correlation function, in a quantum fluid obeying Boltzmann statistics, of which the Fourier transform $S(q, \omega)$ determines the differential cross section for inelastic coherent scattering of slow neutrons. The theoretical formalism of two-particle thermodynamic Green's functions is based on Baym and Kadanoff's conserving T-matrix approximation, developed for strong short-range (intermolecular) potentials. The only other approximations made are: (i) the smallness of the activity or fugacity $z \ll 1$, which implies Boltzmann statistics for the single-particle states; and (ii) the T matrices are replaced by elastic scattering amplitudes. The results for $S(q, \omega)$ developed to order z^2 are found to consist of Boltzmann averages of Lorentzian distributions in the energy transfer $\hbar\omega$ (except for a three-particle scattering term which is developed in the δ-function limit of the Lorentzians). The results are general enough to satisfy detailed balancing at all stages and are found to generalize Van Leeuwen and Yip's results for the classical case. The only unknown in the results is the intermolecular scattering amplitude or phase shifts. The results seem, however, to break down in the hydrodynamic limit (ω and $q \to 0$) since each term in the expansion diverges in this limit. (auth)

36374 ENERGY LEVELS AND LORENTZ INVARIANCE. Landsberg, P. T.; Hindmarsh, J. L. (University Coll. of South Wales, Cardiff). Nature (London); 229: 332-3(29 Jan 1971).

The relativistic soundness of the quantum theoretical formula $h\nu = E' - E$ was questioned by Synge (Nature, 228: 271(1970)) who derived instead the formula $H\nu = (m'^2 - m^2)c^2/2m'$ where m' was the relativistic mass of the system (atom) in its initial state S' in the initial rest frame (the center-of-mass frame) and m was the lower energy state S of the system. The energies E' and E were measured in the initial and final rest frame of the system. While not disagreeing with Synge, a slightly different formulation of this question is given that preserves the original equation by giving it an interpretation fully consistent with Synge's equation. This requires all the energies in the first equation to be measured in the same frame. (UK)

36375 MONTE-CARLO SOLUTION OF SCHROEDINGER'S EQUATION. Grimm, R. C.; Storer, R. G. (Flinders Univ. of South Australia, Bedford Park). J. Comput. Phys.; 7: 134-56 (Feb 1971).

A new Monte-Carlo method is presented for the calculation of the ground-state wavefunction and energy value of the many-body Schroedinger equation. Several refinements to the iterative scheme, including the use of variational wave functions to improve the energy estimate and a variance-reducing technique, are also discussed. The method allows for a straightforward treatment of repulsive potentials. It is applied to several problems, including the three-nucleon problem with simple two-body forces. (auth)

36376 HOW TO AVOID SECULAR TERMS IN CLASSICAL AND QUANTUM MECHANICS. Kummer, M. (Univ. of Toledo). Nuovo Cim.; 1B: 123-48(11 Feb 1971).

Perturbation theories in classical and quantum mechanics which avoid secular terms are discussed. It is shown that the "averaging" method put forward by Bogolyubov, Mitropolsky, and Kruskal can, in many cases, be replaced by a method constructing a formal transformation, which brings the Hamiltonian into a normal form. The transformation bears great resemblance to the Foldy–Wouthuysen transformation of the Dirac equation. (auth)

36377 ANGULAR MOMENTUM COHERENT STATES. Atkins, P. W.; Dobson, J. C. (Oxford Univ.). Proc. Roy. Soc. (London), Ser. A; 321: 321-40(23 Feb 1971).

The work of Carruthers & Nieto (1965, 1968) on the harmonic oscillator coherent states is combined with Schwinger's construction of angular momentum to produce the angular momentum coherent states. It is shown that these states become the vector representatives of angular momentum in the classical limit, and so are particularly useful for discussing the transition from quantum to classical angular momentum. The uncertainty relations for angle and angular momentum are described and are compatible with the classical limit. Under rotations the coherent states transform in a manner that, in the classical limit, is equivalent to the transformation of vectors, and in the same limit, the root mean square variation of the expectation values of the components of angular momentum becomes negligible in comparison with the expectation values themselves. The coupling of two angular momenta in the classical limit is investigated: it is shown that, although the product of two coherent states is not itself a coherent state, it does represent a packet similar to a true coherent state, and centered on the direction of the classical resultant of the two component vectors. The properties and implications of hyperbolic angular momentum space are discussed. (auth) (UK)

XUM

PHYSICS (HIGH ENERGY)

Particle Interactions and Properties (Experimental)

Refer also to abstracts 35892, 35893, and 36419.

36378 SEARCH FOR TACHYONS IN THE COSMIC RADIATION. Murthy, P. V. Ramana (Tata Inst. of Fundamental Research, Bombay). Lett. Nuovo Cim.; 1: No. 22, 908-12(29 May 1971).

An experiment is described for the search for tachyons in cosmic extensive air showers. An upper limit is set on the observed number of tachyons. It is concluded that the frequencies of tachyon occurrence in the EAS are less $3(10)^{-4}$ to 10^{-5} relative to that of electrons. (J.F.P.)

Electromagnetic

36379 (CERN-Trans-71-10) SEARCH FOR ELEMENTARY PARTICLES BEARING A MAGNETIC CHARGE. An Experimental Design in the Form of a Modified Variant. Blagov, M. I.; Isakov, A. I.; Murashova, V. A.; Petukhov, V. A.; Samoilov, A. V.; Syreishchikova, T. I.; Tel'nov, Yu. Ya.; Frolov, A. M.; Usachev, Yu. D.; Yakimenko, M. N. (Akademiya Nauk SSSR, Moscow. Institut Fiziki). Translated by B. Hodge (CERN, Geneva, Switzerland), from Report No. 46. 23p. Dep. NTIS (U. S. Sales Only).

An experiment is proposed for the study of a range of possible monopole charges from 1 e to 70 e in a mass range from 4.8 downwards. The statement of the problem, behavioral characteristics of monopoles with a large charge used in well-known experiments for their detection, identification of monopoles with small charges, general description of the experiment, overcoming the background, the recording apparatus, and the expected results are discussed. (J.F.P.)

36380 (JINR-E3-5713) NEUTRON-ELECTRON INTERACTION STUDIED BY NEUTRON DIFFRACTION ON A SINGLE CRYSTAL OF ^{186}W. Alexandrov, Yu. A. (Joint Inst. for Nuclear Research, Dubna (USSR). Lab. of Neutron Physics). 1971. 19p. Dep. NTIS (U. S. Sales Only).

Experiments performed on the study of n^+e scattering by neutron diffraction on a single crystal of ^{186}W, whose nuclear scattering amplitude is very small, are analyzed and summarized. Subsequent results obtained at the fast pulsed reactor in Dubna are presented. Some perspectives on future research on the n^+e interaction are considered. (auth)

36381 INELASTIC ELECTRON-PROTON SCATTERING IN THE REGION OF THE $\Delta(1236)$ RESONANCE. Bartel, W.; Buesser, F.-W.; Dix, W.-R.; (and others) Deutsches Elektronen-Synchrotron Univ., Hamburg). Phys. Lett.; 35B: No. 2, 181-4 (10 May 1971).

Electron-proton inelastic scattering cross sections were measured at four momentum transfers q^2 between 0.4 and 0.8 $(GeV/c)^2$ by detecting electrons scattered at 86°. The range of invariant mass W of the hadronic final state was 1.10 to 1.35 GeV. The data were combined with the results of an earlier experiment performed at small electron scattering angles and analyzed in terms of the cross sections σ_T and σ_L for the absorption of transverse and longitudinal photons. (auth)

36382 DYNAMIC RADIATION GENERATED IN CRYSTALS BY PARTICLES WITH ULTRARELATIVISTIC ENERGIES. Alikhanyan, A. I.; Garibyan, G. M.; Lorikyan, M. P.; Shikhlarov, K. K. JETP Lett. (USSR) (Engl. Transl.): 13: No. 4, 142-4(20 Feb 1971).

Translated from Zh. Eksp. Teor. Fiz., Pis'ma Red.; 13: No. 4, 201-5(20 Feb 1971).

Strong evidence is given that a new mechanism for radiation by a fast charged particle, wherein the number of photons generated in the investigated frequency interval increases with increasing primary-particle energy, unlike the bremsstrahlung mechanism, was observed. The physical mechanism for the production of such radiation is connected with the diffraction of the field of the charged particle moving at constant velocity by the individual atoms of the crystal lattices, for fields whose wavelengths are much shorter than the interatomic distances. Measurements were made of the number of photons produced from 1.3- to 4.0-GeV electrons passing through a crystal. (J.F.P.)

36383 INVESTIGATIONS ON THE HIGH-ENERGY N COMPONENT OF EXTENSIVE AIR SHOWERS USING A LARGE MULTIPLATE CLOUD CHAMBER. Chatterjee, B. K.; Gopalakrishnan, N. V.; Sreekantan, B. V.; Vatcha, R. H. (Tata Inst. of Fundamental Research, Bombay). pp 350-5 of Proceedings of the Eleventh Symposium on Cosmic Rays, Astrophysics, Geophysics and Elementary Particle Physics, 1969. Vol. II. Bombay; Department of Atomic Energy (1969).

From eleventh symposium on cosmic rays, astrophysics, geophysics and elementary particle physics; Delhi, India (7 Oct 1969). See CONF-691055-(Vol. 2).

A preliminary analysis of data on hadron lateral distribution and charge to neutral ratio in extensive air showers, studied using a large multiplate cloud chamber, is given. Muon bundles were also studied. (J.F.P.)

Weak

36384 (COO-1195-213) ANNUAL PROGRESS REPORT ON [ELEMENTARY PARTICLE PHYSICS]. Wattenberg, A.; Simmons, R. O. (Illinois Univ., Urbana. Dept. of Physics). Apr 1970. Contract AT(11-1)-1195. 27p. Dep. NTIS.

A brief outline is given of experiments on the strong and weak interactions in elementary particle physics performed at various high-energy particle accelerators. A list of publications issued during the period is included. (J.F.P.)

36385 (IAE-1947) MEASUREMENTS OF ANGULAR CORRELATION OF NEUTRON SPIN AND ANTINEUTRINO MOMENTUM IN THE DECAY OF POLARIZED NEUTRONS. Erozolimskii, B. G.; Bondarenko, L. N.; Mostovoi, Yu. A.; (and others) (Institut Atomnoi Energii, Moscow (USSR)). 1970. 16p. (In Russian). Dep. NTIS (U. S. Sales Only).

The magnitude of the B-constant between vectors of neutron spin and antineutrino momentum in β decay of polarized neutrons was measured. The magnitude B obtained was equal to 0.995 ± 0.34 and was found within the limits of one standard error of measuring at the magnitude 0.99 predicted by V-A-variation of the weak-interaction theory. (R.V.J.)

36386 (UCRL-20264) STRINGENT LIMITS ON THE DECAYS $K_L^0 \to \mu^+\mu^-, e^+e^-, \mu^\pm e^\pm$. Frisch, Henry Jonathan (California Univ., Berkeley. Lawrence Radiation Lab.). 24 Mar 1971. Contract W-7405-Eng-48. 109p. Dep. NTIS.

Thesis.

A search was performed at the Bevatron for the decays $K_L^0 \to \mu^+\mu^-, e^+e^-, \mu^\pm e^\pm$. The search was made with a double arm spectrometer comprised of picture frame magnets and wire spark chambers: data were accumulated with an on-line PDP-9 computer. Running conditions included both helium and vacuum in the decay volume. Approximately 1,041,000 $K_L^0 \to \pi^+\pi^-$ decays were observed: these determine the normalization for the dilepton decay modes. No e^+e^- or $e^\pm\mu^\pm$ events were observed, resulting in an upper limit for the branching ratio for each of the above modes of 1.6×10^{-9} (90% C.L.). One possible $\mu^+\mu^-$ event and at least four background events were detected in the data taken with helium in the decay volume. No $\mu^+\mu^-$ events were detected in the much larger data sample from the evacuated decay volume. If one chooses to ignore the helium data, the vacuum data alone determines a limit on the branching ratio for the decay $K_L^0 \to \mu^+\mu^-$ of 1.82×10^{-9} (90% C.L.). If one regards the one event in the helium as real, the branching ratio is determined to be 6.8×10^{-10}. In either case our result is in conflict with the theoretical lower "unitarity" limit of 4.8×10^{-9} for the $K_L^0 \to \mu^+\mu^-$ branching ratio. (auth)

36387 WEAK INTERACTIONS: ON THE EXISTENCE OF NEUTRAL LEPTONIC CURRENTS. Johnson, Rolland Paul. Berkeley, Calif.; Univ. of California (1970). 73p. University Microfilms Order No. 71-9838.

Thesis.

New upper limits to the branching ratios for $K_L^0 \to \mu^+\mu^-$, $K_L^0 \to e^+e^-$, and $K_L^0 \to \mu^\pm e^\pm$ are set. A two-armed spectrometer system for the simultaneous detection of these decay modes and the normalizing $K_L^0 \to \pi^+\pi^-$ mode is described. No events of the $\mu\mu$, ee, or μe type were observed. Twenty three thousand $K_L^0 \to \pi^+\pi^-$ events with detection efficiency corrections then determine new branching ratio upper limits relative to all K_L^0 modes of 1.1×10^{-7} (90% C.L.) for all three leptonic modes. (Diss. Abstr. Int., B)

XUM

Strong (Baryon-Induced)

Refer also to abstracts 36533 and 36539.

36388 (ITJ–3) ESTIMATION OF ENERGY AND MEAN INELASTICITY OF NUCLEAR INTERACTIONS AT ENERGIES ABOVE 3.10^{12} eV USING A SIMPLIFIED VERSION OF IONIZATION SPECTROMETER. Massalski, Jerzy; Suszycki, Leszek; Warczewski, Jerzy. (Institute of Nuclear Techniques, Krakow (Poland)). Nov 1970. 25p. Dep. NTIS (U. S. Sales Only).

An analysis of 111 events obtained at the mountain laboratory on Mount Aragac was performed using a Monte Carlo method for simulating nuclear-electromagnetic cascades. Using a digital computer 1036 simulated events were obtained. A method for determination of the energy of high-energy particles using a simplified version of ionization spectrometers was worked out. The energy spectrum of individual nuclear active particles at the altitude of Mount Aragac was determined. The exponent of the spectrum was found to be $\gamma = 2.0^{+0.2}_{-0.3}$. The flux of the particles was $I(>3.10^{12}\ eV) = (1.6 \pm 0.6) \cdot 10^{-9} cm^{-2} s^{-1} sr^{-1}$. For mean inelasticity coefficients for collisions of nucleons with the nuclei of lead and graphite the values $\langle K_{Pb} \rangle = 0.7 \pm 0.1$ and $\langle K_C \rangle = 0.5 \pm 0.1$, respectively, were obtained. (auth)

36389 (ITJ–5) DISTRIBUTIONS AND MEAN VALUES OF INELASTICITY COEFFICIENT K_{π^0} FOR LEAD AND GRAPHITE. Massalski, Jerzy; Suszycki, Leszek; Warczewski, Jerzy (Institute of Nuclear Techniques, Krakow(Poland)). Nov 1970. 11p. Dep. NTIS (U. S. Sales Only).

An analysis of the experimental material obtained in the mountain laboratory on Mount Aragac is performed using a digital computer. Distributions and mean values of inelasticity coefficient for the production of neutral pions for lead and graphite are obtained. The mean values obtained are $\langle K_{\pi^0} \rangle_{Pb} = 0.24 \pm 0.02$ and $\langle K_{\pi^0} \rangle_C = 0.29 \pm 0.14$, respectively. It is found that large energy transfer to neutral pions occurs, at most, in 6% of all interactions. (auth)

36390 (JINR–P1–5743) DEPOLARIZATION IN 612 MeV ELASTIC pn-SCATTERING. Glonti, L. N.; Kazarinov, Yu. M.; Khayatov, M. R. (Joint Inst. for Nuclear Research, Dubna (USSR). Lab. of Nuclear Problems). 1971. 25p. (In Russian). Dep. NTIS (U. S. Sales Only).

Depolarization in 612-MeV elastic pn-scattering was measured to fill in the lack of experimental data in the pn-system necessary for the unambiguous determination of the 600 to 650 MeV nucleon–nucleon scattering amplitude. The experimental set up permitted measurements at two angles. The proton beam extracted from the accelerator was scattered on carbon at 6.3°. The obtained polarized beam with the 0.332 ± 0.011 polarization underwent second scattering on deuteron neutrons (the difference effect of CD_2 and hydrogen was measured). The events of quasi-elastic pn-interactions were determined by the C1 + C2 + C3 – AC and C1′ + C2′ + C3′ – AC′ for two scattering angles, respectively, by means of fast coincidence–anti-coincidence circuits. The third analyzing scattering on carbon occurred in spark chambers. The pn-event selection was regulated by means of small spark chambers. The measurements were performed with four combinations of the first and second scattering to reject systematic errors. The pictures obtained from spark chambers were measured with semiautomatic scanners and then the unknown D_{pn} parameters were determined by the maximum likelihood method. The analysis of possible systematic errors was made. The results of experiments are shown. The comparison of the obtained values of D_{pn} with the angular dependence $D_{pn}(0)$ calculated by a previous most probable phase shift is shown. Rather a good fit is obtained. Also the previous results of D_{pn} measurement at an angle of 112.3° are shown. (auth)

36391 (UCRL–20632) CHARGED PION PRODUCTION IN PROTON–PROTON INTERACTIONS BETWEEN 13 AND 28.5 GeV/c. Smith, Dennis Baird (California Univ., Berkeley. Lawrence Radiation Lab.). Mar 1971. Contract W-7405-Eng-48. 109p. Dep. NTIS.

Thesis.

Multiparticle production is examined using 40,000 inelastic proton–proton interactions seen in the B. N. L. hydrogen bubble chamber at five incident beam momenta: 13, 18, 21, 24, and 28.5 GeV/c. Cross sections are presented for various inelastic topologies. Using the sample of positively charged track momenta, it is found that one can estimate both the π^+ and proton momentum distributions. The cross sections for π^- production in the reaction $pp \rightarrow \pi^- +$ anything are given. For small values of π^- laboratory momentum, it is found that the π^- production differential cross section is independent of beam energy, indicating that the hypothesis of limiting fragmentation already holds at these energies. The transverse and longitudinal center-of-mass momentum distributions of both π^+'s and π^-'s are given for each inelastic topology and for each beam momentum. One parameter functions successfully describe each distribution. The topology and beam energy dependence of all the longitudinal c.m. momentum spectra can be described by two parameters. The transverse momentum distributions are consistent with a high energy limit that is independent of topology and that agrees well with a picture of "hadronic boiling." (auth)

36392 NEW APPROACH FOR THE ANALYSIS OF SHOWER PARTICLES PRODUCED IN HIGH-ENERGY INTERACTIONS. Bhowmik, B.; Singh, S.; Jha, S. K. (Univ. of Delhi). Nuovo Cim.; 3A: No. 2, 250-8(21 May 1971).

The proposed method is based essentially on the characteristics of the p_t/M distribution of shower particles, which shows clearly resolved peaks for the most copiously produced particles—protons and pions. This distribution is obtained (through the relation $p_t/M = \gamma\beta \sin\theta$) by measuring the values of the emission angle θ and estimating γ from a precise measurement of the blob density. Distribution factors, which give the relative number of different types of particles, are computed for each measured shower particle and thus the distributions of various dynamical quantities are obtained. The method was applied for the analysis of 22.8-GeV/c p-n interactions and the results were found to be in very good agreement with those obtained by the usual (g^*,$p\beta$) method. (auth)

36393 ANGULAR DISTRIBUTION OF PARTICLES AT ENERGIES OF 10 GeV. Takibaev, Zh. S.; Temiraliev, T. T. Izv. Akad. Nauk Kaz. SSR, Ser. Fiz.-Mat.; No. 6, 29-34(Nov-Dec 1970). (In Russian).

A study was made of the angular distribution of particles and of the mechanism of particle generation in two-modal jets. Nearly 700 four–pp-interactions recorded in a 81 cm hydrogen bubble chamber, irradiated a 10 GeV proton momentum. It is shown that the dynamic characteristics of secondary charged particles for various groups of showers (D > 0, D = 0, D < 0) agree within the limits of statistical error. The distribution of effective masses of the ($p\pi$) system has a sharp peak in the region of mass $\Delta(1236)$. This shows that two-modal showers are associated with simultaneous production of isobars with subsequent decay. Dual modality occurs in those events in which excited baryons are strongly collimated. (tr-auth)

36394 INTERACTION MEAN FREE PATHS AND THE FRAGMENTATION PROBABILITIES OF COSMIC HEAVY NUCLEI AT ENERGIES ABOVE 10 GeV/NUCLEON. Saito, Takeshi (Tokyo Univ.). J. Phys. Soc. Jap.; 30: No. 5, 1243-51(May 1971).

A total of 7695 tracks of heavy nuclei were located in a systematic scanning of a stack of Brawley nuclear emulsion, and of the heavy nuclei with energies greater than 10 GeV/nucleon, 497 events were accepted for the present investigation. The error in energy estimation was 30% and that in charge estimation by δ-ray counting was 0.25 units of charge for M-nuclei and about 0.5 units of charge for iron-groups. The interaction mean free paths and the fragmentation probabilities of heavy nuclei at energies above 10 GeV/nucleon in nuclear emulsion were obtained and those in air and in hydrogen were deduced with reasonable accuracy. The interaction mean free paths and the fragmentation probabilities do not indicate any noticeable energy dependence over the wide energy range of a few GeV/nucleon to several hundred GeV/nucleon for heavy nuclei and of about 0.1 GeV/nucleon to several hundred GeV/nucleon for α-particles. (auth)

36395 HADRON INTERACTIONS AT VERY HIGH ENERGIES. Truemper, J. (Christian-Albrechts Univ., Kiel). Phys. Bl.; 25: No. 3, 119-25(Mar 1969). (In German).

Investigations on air shower nuclei at Kiel have concentrated on the distribution of very high energy hadrons ($\gtrsim$1000 GeV) and of the lower energy electrons. A brief review is given of these experiments and the results obtained. Studies on the structure of the electron distribution are critically analyzed. (J.S.R.)

36396 STUDY OF QUASI-TWO-PARTICLE REACTIONS IN PROTON–PROTON INTERACTIONS AT 10 GeV/c. Takibaev, Zh. S.; Boos, E. G.; San'ko, L. A.; Temiraliev, T. (Inst. of High Energy Physics, Moscow). JETP Lett. (USSR) (Engl. Transl.); 13: No. 3, 83-6(5 Feb 1971).

Translated from Zh. Eksp. Teor. Fiz., Pis'ma Red.; 13: No. 3, 122-5(5 Feb 1971).

Quasi-two-particle interactions of the type $p + p \rightarrow p + N^*(\Delta)$, and $p + p \rightarrow \Delta + N^*(\Delta)$ at 10.01 GeV/c in a hydrogen bubble chamber were studied. The momentum transfer distributions and cross sections are discussed. (J.F.P.)

36397 MEASUREMENT OF np(pp) TRIPLE SCATTERING PARAMETERS R^T(R AND R'^T(R′) 510 TO 670 MeV. Leung,

XUM

Kwok-chu. Berkeley, Calif.; Univ. of California (1970). 58p. University Microfilms Order No. 71-9854.

Thesis.

Wolfstein triple scattering parameters R and R′ for the proton–proton system and R^t and R'^t for the neutron–proton system were measured. The p–p data were measured at three angles at 510, 600, and 670 MeV, and the n–p data were measured at four angles at 510 and 600 MeV. No strong energy dependence is observed in either case. A spark chamber spectrometer system was used to analyze the second and third scattering. Polarized proton and neutron beams were produced by scattering the primary proton beam off liquid hydrogen and liquid deuteron targets respectively. Good agreement between the proton–proton data and the published data at 430 and 660 MeV is found. Phase shift predictions are compared to the results. (Diss. Abstr. Int., B)

36398 MISSING MASS SPECTROMETER SURVEY OF I = 1, 0 MESONS BELOW 1.1 GeV^2. Groves, Eric Stedman. Philadelphia; Univ. of Pennsylvania (1970). 114p. University Microfilms Order No. 71-7809.

Thesis.

During the spring and summer of 1969 a Jacobian-peak missing mass spectrometer was constructed at the Princeton–Pennsylvania Accelerator. This spectrometer employed the reaction p + d → ^{3}He + missing mass (X^0) to survey the mass region of I = 0, 1 mesons from 0.0 to 1.1 GeV^2. A description is given of the experimental apparatus, plots of $(d\sigma_{X^0}/d\Omega)$ versus $M_{X^0}{}^2$ for 2 and 3 GeV incident protons, cross sections for π^0, η, ω and X (952) production for 3-GeV incident protons, and cross sections at 2 GeV for π and η production. It also contains a discussion of the π^0 cross section dependence upon various variables and empirical formulas suitable for π^0 cross section predictions at higher energies, a discussion of the 2π threshold enhancement effect (ABC effect) seen also by previous experimenters, and a discussion of a theoretical SU-3 prediction of the relations between the π^0, η, and η' cross sections. (Diss. Abstr. Int., B)

36399 EVIDENCE FOR THE EXISTENCE OF A NARROW anti pn BOUND STATE. Gray, L.; Hagerty, P.; Kalogeropoulos, T. (Syracuse Univ., N. Y.). Phys. Rev. Lett.; 26: No. 24, 1491-4(14 Jun 1971).

A method of search for an $\bar{N}N$ bound state is pointed out and evidence is presented for the existence of a $\bar{p}n$ bound state. It is produced in $\bar{p}d$ annihilations at rest and has been observed decaying into four and six pions. The binding energy is 83.3 ± 1.4 MeV and the width ≤8 MeV at the 95% confidence level. (auth)

36400 SOME ASPECTS OF K^- ABSORPTION AT REST IN EMULSION NUCLEI. Gurtu, A.; Swami, M. S. (Panjab Univ., Chandigarh, India. Aligarh Muslim Univ., India). pp 509-11 of Proceedings of the Eleventh Symposium on Cosmic Rays, Astrophysics, Geophysics and Elementary Particle Physics, 1969. Vol. II. Bombay; Department of Atomic Energy (1969).

From eleventh symposium on cosmic rays, astrophysics, geophysics and elementary particle physics; Delhi, India (7 Oct 1969). See CONF-691055–(Vol. 2).

Properties of charged Σ hyperons produced in single-nucleon capture of stopping K^- mesons in emulsion nuclei were studied. Distributions for the kinetic energy of the hyperon, the space angle between Σ and π, the invariant mass of the Σ and π, and the total momentum of the Σπ system are shown graphically. (J.F.P.)

36401 HYPERNUCLEI RESONANT STATES ^{5}He, ^{6}Li, AND ^{9}Be. Gurtu, A.; Rao, N. K.; Singh, M. B.; Swami, M. S. (Panjab Univ., Chandigarh, India). pp 512-16 of Proceedings of the Eleventh Symposium on Cosmic Rays, Astrophysics, Geophysics and Elementary Particle Physics, 1969. Vol. II. Bombay; Department of Atomic Energy (1969).

From eleventh symposium on cosmic rays, astrophysics, geophysics and elementary particle physics; Delhi, India (7 Oct 1969). See CONF-691055–(Vol. 2).

In order to detect the narrow resonant state hyperfragments Λ-^{5}He, Λ-^{6}Li, and Λ-^{9}Be the Q-value distribution for the respective decay schemes must be studied. For this purpose an emulsion stack was exposed to a slow K^- beam, and the residual ranges of the emitted hyperfragments and those of the tracks associated with them at the K^- absorption center and the space angles of these tracks with respect to the hyperfragments were measured. The measured Q-value distributions are shown and compared with the background. It is concluded that the production frequencies of these narrow resonance states are rather small. (J.F.P.)

36402 NEW METHOD FOR IDENTIFICATION OF SHOWER PARTICLES IN HIGH-ENERGY INTERACTIONS. Bhowmik, B.; Singh, S.; Jha, S. K. (Univ. of Delhi). pp 527-30 of Proceedings of the Eleventh Symposium on Cosmic Rays, Astrophysics, Geophysics and Elementary Particle Physics, 1969. Vol. II. Bombay; Department of Atomic Energy (1969).

From eleventh symposium on cosmic rays, astrophysics, geophysics and elementary particle physics; Delhi, India (7 Oct 1969). See CONF-691055–(Vol. 2).

A method for the identification of shower particles is given whereby the transverse momentum distribution to secondary particle rest mass p_t/M ratio distribution is plotted for a large number of produced shower particles to be identified. The peaks are then assigned to different identities, the first peak corresponding to the largest-mass particles. The parameter p_t/M for a produced particle can be calculated without knowing its identity by means of the relation $p_t/M = \gamma\beta\sin\theta$, where β is the velocity, θ the emission angle with respect to the primary, and $\gamma = (1-\beta^2)^{-\frac{1}{2}}$. This method eliminates the necessity of making scattering measurements and provides a quick and fairly accurate means of identification. The p_t/M distribution of the showers produced in the interactions of 22.8-GeV/c protons with emulsion nuclei is found using this method. (J.F.P.)

36403 EMISSION OF DEUTERONS IN 24-GeV/c PROTON INTERACTIONS WITH EMULSION NUCLEI. Shafi, M.; Ansari, A. R.; Lal, K. B.; Naqvi, A. H.; Zafar, M. (Aligarh Muslim Univ., India). pp 534-9 of Proceedings of the Eleventh Symposium on Cosmic Rays, Astrophysics, Geophysics and Elementary Particle Physics, 1969. Vol. II. Bombay; Department of Atomic Energy (1969).

From eleventh symposium on cosmic rays, astrophysics, geophysics and elementary particle physics; Delhi, India (7 Oct 1969). See CONF-691055–(Vol. 2).

An investigation is made of the emission of deuterons in the reactions of 24-GeV/c protons with nuclei in emulsions. There were 79 deuterons observed in the energy interval from 50 to 700 MeV. The angular distributions of deuterons and protons are shown. The pick-up and the N(N,π)d processes were found to explain the observed deuteron frequency. (J.F.P.)

36404 STUDY OF NEUTRAL PIONS PRODUCED IN 5-GeV/c ANTIPROTON INTERACTIONS. Bhowmik, B.; Singh, S. (Univ. of Delhi). pp 540-4 of Proceedings of the Eleventh Symposium on Cosmic Rays, Astrophysics, Geophysics and Elementary Particle Physics, 1969. Vol. II. Bombay; Department of Atomic Energy (1969).

From eleventh symposium on cosmic rays, astrophysics, geophysics and elementary particle physics; Delhi, India (7 Oct 1969). See CONF-691055–(Vol. 2).

A method of kinematical analysis is described for study of the properties of neutral pions produced in high-energy interactions by the observation of any one of the electron pairs originated in the process $\pi^0 \to 2\gamma$, $\gamma \to e^+ + e^-$. Some results for neutral pions produced in 5 GeV/c antiproton interactions with emulsion nuclei obtained from this method are presented. These results include the angular and momentum distributions for neutral pions. (J.F.P.)

Strong (Meson-Induced)

36405 (JINR-P1-5781) $\pi^-p \to \pi^0\pi^0n$ REACTION AT 447 MeV. Dainet, V.; Myuller, G.; Shmitt, D.; (and others). (Joint Inst. for Nuclear Research, Dubna (USSR)). 1971. 24p. (In Russian). Dep. NTIS (U. S. Sales Only).

Differential cross sections for the neutrons resulting from the reaction $\pi^-p \to \pi^0\pi^0n$ at 447 MeV were measured for the angle range 20 to 60° in the lab system. The experiment was performed at the CERN proton synchrotron using the missing-mass spectrometer combined with optical spark chambers. The experimental effective mass spectrum of $\pi^0\pi^0$-system has a noticeable enhancement over the phase space distribution in the region of large and small masses and a dip in the middle of the spectrum. The angular distribution for neutrons in the c.m.s. has sharp asymmetry with the prevailing backward escape of neutrons. The total cross section of the reaction $\pi^-p \to \pi^0\pi^0n$ at 447 MeV is found to be 1.90 + 0.25 mb. (auth)

36406 (NP-18873) MEASUREMENT OF THE A AND R POLARIZATION PARAMETERS IN π^- PROTON ELASTIC SCATTERING AT 6 AND 16 GeV/c. Amblard, Bernard (Paris Univ. (France). Faculte des Sciences). 1971. 87p. (In French). Dep. NTIS (U. S. Sales Only).

The π^- proton elastic scattering was studied at momenta of 6 and 16 GeV/c and at transfer momenta of −0.2 and 0.5 $(GeV/c)^2$. The A and R polarization parameters and the scattering amplitude terms were calculated. The results obtained for the parameters were compared with the Cohen–Tannoudji diffraction model and the Barger and Philips per Regge model. The interpretation of the results is still very difficult. (France)

XUM

36407 MEASUREMENT OF THE X^0 CROSS-SECTIONS IN π^-p INTERACTIONS AT 1.6 GeV/c AND DETERMINATION OF THE BRANCHING RATIO $(X^0 \rightarrow \text{NEUTRALS})/(X^0 \rightarrow \text{TOTAL})$. Basile, M.; Bollini, D.; Dalpiaz, P.; (and others) (CERN, Geneva. Istituto Nazionale di Fisica Nucleare, Bologna. Univ., Bologna. Centre National de Recherches Scientifiques, Strasbourg). Nuovo Cim.; 3A: No. 2, 371-84(21 May 1971).

The reactions $\pi^-p \rightarrow n + (X^0 \rightarrow \text{total})$ and $\pi^-p \rightarrow n + (X^0 \rightarrow \text{neutrals})$ were studied at 1.6 GeV/c with the Bologna-CERN neutron missing-mass spectrometer. Both reactions were detected without the use of visual techniques. The results are: $\sigma(X^0 \rightarrow \text{total}) = (108 \pm 14)$ μb and $\sigma(X^0 \rightarrow \text{neutrals}) = (20.0 \pm 3.5)$ μb, giving a branching ratio $\Gamma(X^0 \rightarrow \text{neutrals})/\Gamma(X^0 \rightarrow \text{total}) = (18.5 \pm 2.2)\%$. The branching ratio for other possible, so far undetected, neutral decay modes of the X^0 turns out to be $(2.4 \pm 1.9)\%$. (auth)

36408 DETERMINATION OF C NUCLEUS RADIUS BY INTERACTION WITH π^- AT 7 GeV. Munteanu, G.; Caramihu, D.; Moldoveanu, S. Bul. Inst. Politeh. Brasov, Ser. B; 12: 345-7 (1970). (In Rumanian).

Scanning was carried out three times on 200 frames obtained with the Dubna 51-cm bubble chamber. The radius $r_c = 8.04(10)^{-13}$ cm was obtained with an average scanning efficiency $\bar{\epsilon} = 0.967$. (tr-auth)

36409 STUDY OF THE A_2^- FROM THE REACTION $\pi^-p \rightarrow K_S^0 K^-p$ AT 4.5 GeV/c. Crennell, D. J.; Gordon, H. A.; Lai, Kwan-wu; Scarr, J. M. (Brookhaven National Lab., Upton, N. Y.). Phys. Lett.; 35B: No. 2, 185-8(10 May 1971).

A study of $A_2^- \rightarrow K_S^0 K^-$ from the reaction $\pi^-p \rightarrow K_S^0 K^-p$ at 4.5 GeV/c in the 82-in. hydrogen bubble chamber is presented. From a sample of 542 events from this final state, the mass (and its possible fine structure), width, production distribution and decay correlations of A_2^- are examined. (auth)

36410 DIFFERENTIAL CROSS SECTION AND POLARIZATION OF THE REACTION $\pi^+p \rightarrow K^+\Sigma^+$ FROM 2.75 TO 14 GeV/c. Fischer, Glen Charles. Madison, Wis., Univ. of Wisconsin (1970). 106p. University Microfilms Order No. 70-22,643.

Thesis.

A high statistics study was made of the reaction $\pi^+p \rightarrow K^+\Sigma^+$ at Brookhaven AGS. Gas Cherenkov counters identified the mesons. The kaon momentum and the scattering angle were measured by a wire spark chamber spectrometer. A liquid hydrogen target was used and side counters detected the charged particle from the Σ^+ hyperon decay. Results are given for the forward differential cross section and polarization from 2.75 to 5 GeV/c in 0.25 GeV/c steps and at 5.5, 6, 10 and 14 GeV/c. The extreme forward peak ($-t < 0.2$ $(\text{GeV/c})^2$) at each momentum is fitted to an exponential distribution and is further expressed as a function of s and t by: $d\sigma/dt = 9.3\ s^{-1.20}\ e^{(9.2 \pm 9.3 \ln s)t}$ mb/$(\text{GeV/c})^2$. A dip at very small $-t$ indicating a spin-flip contribution to the differential cross section is not observed. No significant structure is observed in the partial cross section as given by: $\sigma = \int_{-\infty}^{t_{min}} (d\sigma/dt)\ dt$ leading to the conclusion that there is no strong s channel contribution to the differential cross section. The polarization is consistent with zero at all momenta for $-t < 0.2$ $(\text{GeV/c})^2$. At 6, 10 and 14 GeV/c, where data were obtained for larger $-t$, the slope of the differential cross section decreases abruptly at $-t \approx 0.45$ $(\text{GeV/c})^2$. A large positive polarization is observed for $-t > 0.4$ $(\text{GeV/c})^2$. The data are discussed in terms of Regge-pole models and the t channel exchange of $K^*(890)$ and $K^{**}(1450)$ resonances. The $\pi^+p \rightarrow K^+\Sigma^+$ differential cross section is compared with that of the line reversed reaction, $K^-p \rightarrow \pi^-\Sigma^+$. Results appear inconsistent with the predictions of equal differential cross sections at high energy by exchange degeneracy and a single pole Regge model. (Diss. Abstr. Int., B)

36411 A_2^+ MASS SPECTRUM IN π^+p INTERACTIONS AT 3.7 GeV/c. Barnham, K. W. J.; Abrams, G. S.; Butler, W. R.; (and others) (Univ. of California, Berkeley). Phys. Rev. Lett.; 26: No. 24, 1494-8(14 Jun 1971).

A study of the A_2^+ mass spectrum in π^+p interactions at 3.7 GeV/c is presented. For a cut of $t' = 0.1-2.0$ GeV^2 and on eliminating the Δ^{++} it is found that the three-pion mass spectrum in the A_2^+ region is fitted by the dipole formula with a confidence level of 53% and a single Breit-Wigner formula with a confidence level of 11%. The result thus favors A_2^+ splitting although a single Breit-Wigner fit cannot be ruled out. The A_2^+ decay branching fractions measured over all t' values are also reported. They are 0.78 ± 0.05, 0.15 ± 0.04, 0.06 ± 0.03, and <0.02 for $\rho\pi$, $\eta\pi$, $K\bar{K}$, and $\eta'\pi$, respectively, in good agreement with other experiments. (auth)

36412 MOMENTUM DEPENDENCE OF THE 180° π^-p CHARGE EXCHANGE CROSS SECTION. Kistiakowsky, V. (Massachusetts Inst. of Tech., Cambridge); Triantis, F. A.; Yamamoto, R. K.; (and others). Phys. Rev. Lett.; 26: No. 24, 1498-1501(14 Jun 1971).

The differential cross sections for π^-p charge exchange at 180° are given as a function of π^- momentum from 1.8 to 6.0 GeV/c. Below 4 GeV/c there is a resonancelike structure. Above 4 GeV/c the data are in excellent agreement with a smooth exponential drop. A modification of the Igi model gives a good fit to the data. The momentum dependence of the moduli of the isospin $-\frac{1}{2}$ and $-\frac{3}{2}$ amplitudes and their relative phase is presented. (auth)

36413 OFF-MASS-SHELL Kpi SCATTERING PHASE SHIFTS. Yuta, H. (Argonne National Lab., Ill.); Derrick, M.; Engelmann, R.; (and others). Phys. Rev. Lett.; 26: No. 24, 1502-5(14 Jun 1971).

The final states $K^-\pi^+n$ and $\bar{K}^0\pi^-p$ were measured in a K^-p experiment at 5.5 GeV/c. The data on the angular distribution of the outgoing K meson in the $K\pi$ rest system at low momentum transfer were analyzed by a simple model including $I = \frac{3}{2}$ s-wave and $I = \frac{1}{2}$ s-, p-, and s-wave amplitudes. The results show that the phase shift for the $I = \frac{3}{2}$ s wave is negative. The two solutions obtained for the $I = \frac{1}{2}$ s-wave off-mass-shell phase shift are consistent with an s-wave resonance at either ~0.85 or ~1.2 GeV. (auth)

36414 EVIDENCE FOR SPLITTING IN THE Q REGION OF $K^+pi^+pi^-$ MASS. Garfinkel, A. F. (Purdue Univ., Lafayette, Ind.); Holland, R. F.; Carmony, D. D.; (and others). Phys. Rev. Lett.; 26: No. 24, 1505-8(14 Jun 1971).

A splitting was observed in the $K^+\pi^+\pi^-$ mass spectrum in K^+d interactions at 9 GeV/c. A mass of 1243 ± 8 MeV/c^2 and a width of 70^{+26}_{-18} were found for the lower mass state, and a mass of 1344 ± 8 and a width of less than 60 MeV/c^2 were found for the higher mass state. The isospin of both states is determined to be $\frac{1}{2}$. The results can be interpreted as evidence for the mixing of two $J^P = 1^+$ K^* states. (auth)

36415 STUDY OF $Y_1^*(1385)$ π PRODUCTION NEAR THE $Y_1^*(1520)$ RESONANCE. Chan, Shu-bon. Amherst, Mass.; Univ. of Massachusetts (1970). 148p. University Microfilms Order No. 71-8751.

Thesis.

The production mechanism of the reaction $K^-p \rightarrow Y_1^*(1385)$ π with total energy in the vicinity of the $Y_1^*(1520)$ resonance was studied. Two different analysis techniques were used: partial waves and moments. The results establish the decay mode $Y_1^*(1520) \rightarrow Y_1^*(1385)$ π. The observation of this decay mode indicates that $Y_1^*(1520)$ is not a pure SU(3) singlet but a mixed state between a $\frac{3}{2}^-$ singlet and the I = 0 member of the $\frac{3}{2}^-$ octet. The two different ways of calculating the mixing angle gave two values: $|\theta| = (16 \pm 3)°$ and $|\theta| > (23 \pm 3)°$. (Diss. Abstr. Int., B)

36416 PROGRAM FOR THE STUDY OF HIGH-ENERGY NUCLEAR INTERACTIONS OF COSMIC RAYS AT THE KUM-BEL MOUNTAIN STATION. Abdullaev, A. M.; Azimov, S. A.; Myalkovskii, V. M.; (and others) (Inst. of Nuclear Physics, Tashkent, USSR). pp 346-9 of Proceedings of the Eleventh Symposium on Cosmic Rays, Astrophysics, Geophysics and Elementary Particle Physics, 1969. Vol. II. Bombay; Department of Atomic Energy (1969).

From eleventh symposium on cosmic rays, astrophysics, geophysics and elementary particle physics; Delhi, India (7 Oct 1969). See CONF-691055-(Vol. 2).

An experiment is prepared for the study of nucleon-nucleon and pion-nucleon interactions in the energy range 10^{11} to 10^{13} eV. The average characteristics of the interactions and the angular distributions will be studied. Also studied will be the direct production of muons. (J.F.P.)

36417 K-MESON-NUCLEON PHASE SHIFTS NEAR 600 MeV/c. Ray, A. K. (Carnegie-Mellon Univ., Pittsburgh); Burris, R. W.; Fisk, H. E.; (and others). pp 517-21 of Proceedings of the Eleventh Symposium on Cosmic Rays, Astrophysics, Geophysics and Elementary Particle Physics, 1969. Vol. II. Bombay; Department of Atomic Energy (1969).

From eleventh symposium on cosmic rays, astrophysics, geophysics and elementary particle physics; Delhi, India (7 Oct 1969). See CONF-691055-(Vol. 2).

Kaon-nucleon phase shifts were determined from K^0 angular distributions and proton polarization in $K^+ + n \rightarrow K^0 + p$ interactions at 600 MeV/c in a deuterium bubble chamber. It is concluded that a simple description of K-N interactions near 600 MeV/c requires s- and p-wave scattering for both T = 0 and 1 channels as described by the phase shift solution. (J.F.P.)

36418 SOME CHARACTERISTICS OF 17.2-GeV π^- INTERACTIONS WITH EMULSION NUCLEI. Kohli, J. M. (Panjab Univ., Chandigarh, India). pp 531-3 of Proceedings of the Eleventh Sym-

XUM

posium on Cosmic Rays, Astrophysics, Geophysics and Elementary Particle Physics, 1969. Vol. II Bombay; Department of Atomic Energy (1969).

From eleventh symposium on cosmic rays, astrophysics, geophysics and elementary particle physics; Delhi, India (7 Oct 1969). See CONF-691055-(Vol.2).

A study is made of 17.2-GeV π^- reactions with nuclei in emulsions. Angular, scattering, and ionization measurements were made. Among the properties discussed are the average shower multiplicity, the pion and proton angular distributions, the average transverse momentum, the momentum distribution, total energy distribution of pions, the total energies carried by pions and protons, and the coefficient of inelasticity. (J.F.P.)

Particle Interactions and Properties (Theoretical)

General

Refer also to abstracts 35892, 35893, and 36568.

36419 (NYO-3178-8) RESEARCH IN ELEMENTARY PARTICLE PHYSICS. Technical Progress Report. Kirsch, Lawrence; Schnitzer, Howard J. (Brandeis Univ., Waltham, Mass. Dept. of Physics). 31 May 1971. Contract AT(30-1)-3178. 12p. Dep. NTIS.

Research on the theoretical and experimental properties of elementary particles from September 1, 1970, to April 30, 1971, is summarized. A list of publications is included. (J.F.P.)

36420 (UCSD-10-P-10-78) TRIPLE POMERON VERTEX, DUALITY, AND DIFFRACTION DISSOCIATION. Ting, Peter D.; Yesian, Harry J. (California Univ., La Jolla, San Diego. Dept. of Physics). [1971]. Contract AT(11-1)-Gen-10. 11p. Dep. NTIS.

By invoking duality for the Reggeon-particle absorptive part, the triple Reggeon coupling is related to the low missing-mass spectrum in diffraction dissociation. Existing experimental data are analyzed and suggest that the triple Pomeron coupling is small. (auth)

36421 FIXED-ANGLE LIMIT IN INCLUSIVE EXPERIMENTS. White, A. R. (Cambridge Univ., Eng.). Phys. Lett.; 35B: No. 2, 175-7(10 May 1971).

The fixed-angle, fixed scaled longitudinal momentum, limit of the inclusive single particle distribution is related to a fixed-angle limit of the six-particle amplitude. A straightforward derivation of the lower bound exp[-c slog s] for the inclusive distribution, in such a limit, can then be given, based on the assumptions of multi-Regge theory. Possible generalizations of the Orear and Krisch fits to the four-particle amplitude are also discussed. (auth)

36422 SOME CALCULATIONS IN TWO-BODY AND MULTI-BODY SCATTERINGS. Chiang, Soong Tao. Los Angeles; Univ. of California (1970). 140p. University Microfilms Order No. 71-10,637.

Thesis.

A relativistic equation based on analyticity and unitarity in the equivalent potential approach is solved by iteration and approximation by Padé approximants. The equivalent potential is a relativistic generalization of a local energy-dependent potential in contrast with the generalization of a nonlocal energy-independent potential. This potential is constructed from the low-t part of the Veneziano amplitude in the crossed channel, and the free parameters of the Veneziano amplitude are determined self-consistently in this model. The output resonant masses and widths of the rho and f^0 are found to agree with the experimental values. The calculated Regge trajectories of both isospin I = 1 and I = 0, seem to be indefinitely rising in an approximately linear way. The partial cross section with KK produced in the final state in πN and NN interactions are found to have certain distinct features when compared with the same interactions but with $\pi\pi$ produced in the final state. These features are: strangeness suppression, a threshold shift, and a violation of quark model sum rules. A generalized multiperipheral model is constructed to compute these cross sections and is found to be able to explain these features within experimental error. (Diss. Abstr. Int., B)

36423 CORRELATION BETWEEN THE TRANSVERSE AND *LONGITUDINAL MOMENTA IN MULTIPLE GENERATION.* Roinishvili, N. N.; Sherrer, E. N. (Inst. of Physics, Tbilisi, USSR). JETP Lett. (USSR) (Engl. Transl.); 13: No. 5, 171-4 (5 Mar 1971).

Translated from Zh. Eksp. Teor. Fiz., Pis'ma Red.; 13: No. 5, 243-6(5 Mar 1971).

It is proven that the responsibility for the $p_t - p_l$ correlation lies not in the matrix element of the interaction but in its phase volume. It is concluded that at experimental accuracy on the correlations between p_t and p_l, it can be asserted that the interaction matrix element produces practically no connection between these two parameters. (J.F.P.)

36424 LANDAU EQUATIONS FOR A CONTINUOUS MEDIUM AND THE KOBA-NIELSEN KERNELS IN THE GENERALIZED VENEZIANO FORMULA. Minami, Masatsugu (Kyoto Univ.). Progr. Theor. Phys. (Kyoto); 45: No. 1, 208-26(Jan 1971).

It is pointed out that the Poisson equation governing the four-position x in a continuous medium, which is a generalization of the Feynman graph, corresponds to one of the Landau equations for the graph: The solution of the equation with a given boundary condition is inserted into the action integrand of the Feynman integral to give Koba and Nielsen's kernels in the generalized Veneziano representation. It is also shown that one can get the same results if one works consistently with the four-position x^* of a dual of the original Feynman graph, the four-position x^* also satisfying the Laplace equation inside the medium. If x is regarded as a potential, the function x^* is as a stream function. (auth)

36425 MASS EQUATION FROM TADPOLES: NONPOLYNOMIAL LAGRANGIANS. Caianiello, E. R. (Imperial Coll. of Science and Tech., London. CNR, Naples); Marinaro, M. Lett. Nuovo Cim.; 1: No. 22, 899-902(29 May 1971).

A formalism, based on the consideration of the whole set of Green functions corresponding to interactions other than of the standard renormalizable types, is established for the case of a scalar particle interacting with itself through a given Lagrangian. The role of tadpoles is studied in assessing the value of the physical mass or masses of a particle dressed by the given Lagrangian. (J.F.P.)

36426 MASS EQUATIONS OF NUCLEAR PARTICLES. Majid Mian, A. (Peshawar Univ., Pakistan). J. Natur. Sci. Math.; 10: No. 1, 131-52(Apr 1970).

An exact mathematical formulation of the mass equation is given whose characterization gives matter particles in the form of a spectrum. In this formulation the linear formulation of Dirac which describes the external behavior of a matter particle is followed closely. It is found that for the exact description and quantization one must incorporate the principles of the general theory as conditioned to the requirement of quantum mechanics along with the contents of SU_3. Each section is done briefly avoiding mathematical calculations as much as possible. Result of the theory can be compared in each case with the experimental results. The subject of primary or base particles only is considered. The subject of complex mesons and hyperons which form part of the present theory is left out entirely. (auth)

36427 ANOMALIES IN WARD IDENTITIES AND CURRENT COMMUTATORS. Choudhury, S. Rai (Univ. of Delhi). pp 215-28 of Proceedings of the Eleventh Symposium on Cosmic Rays, Astrophysics, Geophysics and Elementary Particle Physics, 1969. Vol. I. Bombay; Department of Atomic Energy (1969).

From eleventh symposium on cosmic rays, astrophysics, geophysics and elementary particle physics; Delhi, India (7 Oct 1969). See CONF-691055-(Vol. 1).

A review is given of anomalies in Ward identities and current commutators for particles. The electrodynamics of a spin-$\frac{1}{2}$ system is considered. Also the vector current in the presence of an axial-vector field is discussed. (J.F.P.)

36428 PARAMETRIZATION OF THE PHASE SPACE OF N RELATIVISTIC PARTICLES. Sokolov, S. N. (Inst. of High-Energy Physics, Serpukhov, USSR). Teor. Mat. Fiz.; 7: No. 2, 217-18(May 1971). (In Russian).

A parametrization of the phase space of N relativistic particles is proposed which transforms the surfaces E_i = const into spheres and makes the factor of a phase volume equal to 1. (auth)

36429 VECTOR DOMINANCE AND DECREASE OF DIFFERENTIAL CROSS SECTION OF LEPTON PAIR PRODUCTION AT HIGH ENERGY AND LARGE SCATTERING ANGLES. Mestvirishvili, M. A. (Inst. of High-Energy Physics, Serpukhov, USSR). Teor. Mat. Fiz.; 7: No. 2, 192-4(May 1971). (In Russian).

It is shown that the vector dominance hypothesis taken together with analyticity and unitarity implies the decrease of differential cross section of lepton pair production at high energy in the region of large scattering angles. (auth)

XUM

36430 35. PHYSIKERTAGUNG 1970 HANNOVER. PLENARVORTRAEGE. (35th Physicists Conference, Hanover. Plenary Papers). Conference Held at Hanover, Germany, September 28–October 3, 1970. Stuttgart; B. G. Teubner (1970). 349p. (In German and English). (CONF-700954).

The 15 plenary papers presented at the 35th Physicists Conference at Hanover are compiled. Individual abstracts were prepared for 5 of the 15 papers. (J.S.R.)

For abstracts of individual papers see: 36212, 36539, 36549, 36576, and 36585.

Electromagnetic

Refer also to abstracts 36571 and 36610.

36431 (ITJ–6) MONTE CARLO SIMULATION OF THE NUCLEAR-ELECTROMAGNETIC CASCADE DEVELOPING IN AN IONIZATION SPECTROMETER. Massalski, J.; Suszycki, L.; Warczewski, J. (Instiute of Nuclear Techniques, Krakow (Poland)). Dec 1970. 26p. Dep. NTIS (U. S. Sales Only).

The Monte Carlo method was applied to the analysis of the development of nuclear-electromagnetic cascades in an ionization spectrometer. The calculations were performed for 830 cascades with an average energy ~4 TeV using various values of inelasticity coefficients. The energy balance and the total ionization as a function of depth were obtained. It has been found that nuclear disintegrations and the ionization by $\pi^{\pm}$ mesons contribute significantly to the total ionization. An experimental method for the determination of the energy of the primary hadron by ionization sampling is discussed. The effect of nuclear disintegrations is found to induce underestimation of the energy of about 29% whereas statistical fluctuations introduce an error of about 8%. (auth)

36432 (LA–4663) A NEW METHOD OF SAMPLING THE KLEIN–NISHINA PROBABILITY DISTRIBUTION FOR ALL INCIDENT PHOTON ENERGIES ABOVE 1 keV. Everett, C. J.; Cashwell, E. D.; Turner, G. D. (Los Alamos Scientific Lab., N. Mex.). Apr 1971. Contract W-7405-Eng-36. 4p. Dep. NTIS.

A Monte Carlo method is given for accurate determination of scattered photon energy in the distribution required by the Klein–Nishina cross section for Compton collisions. The relative error does not exceed 2.2% for all incident energies above 1 keV. (auth)

36433 (LNF-71/1) MULTIPLE e.m. PROCESSES IN HIGH ENERGY e^-e^+ COLLISIONS. Greco, M. (Comitato Nazionale per l'Energia Nucleare, Frascati (Italy). Laboratori Nazionali di Frascati). 8 Jan 1971. 14p. Dep. NTIS (U. S. Sales Only).

The production of electron and muon pairs is studied in high energy e^-e^+ collisions. Total and differential cross sections are discussed with special regard to experimental implications. Hadron production via photon-photon scattering is also studied, and suggestions are made for present and next future experiments. (auth)

36434 (LNF-71/5) e^+e^- ANNIHILATION INTO HADRONS IN THE PREASYMPTOTIC REGION AND $\mu^+\mu^-$ PRODUCTION IN PROTON COLLISIONS. Parisi, G. (Comitato Nazionale per l'Energia Nucleare, Frascati (Italy). Laboratori Nazionali di Frascati). 3 Feb 1971. 4p. Dep. NTIS (U. S. Sales Only).

Parton model predictions are compared with the Adone data. The relevance of the parton antiparton threshold is stressed and a simple explanation is given for the structure recently observed in the production of high mass $\mu^+\mu^-$ pairs in proton collisions. (auth)

36435 (NYO–1932(2)-189) SCALING PROPERTIES IN e-p SCATTERING. Lee, T. D. (Columbia Univ., New York). Apr 1971. Contract AT(30-1)-1932. 16p. Dep. NTIS.

The discussion of scaling properties in e + p scattering covers the structure functions, results of SLAC experiments, scale, soft and hard mesons, multiplicity, and an SU(2) phenomenological Lagrangian model calculation. (J.F.P.)

36436 (ORO–3992-28) A MODEL FOR DIPOLE ELECTROMAGNETIC FORM FACTORS. Yamada, Masao (Texas Univ., Austin. Dept. of Physics). [1970]. 25p. (CPT–79; AEC–28). Dep. NTIS.

A model of the electromagnetic form factor of the scalar π meson is discussed in which the π meson is a bound state of scalar nucleon-antinucleon system. Starting from an exact integral representation of the form factor, which is well defined in a space like region of the momentum transfer squared, q^2, an analytic continuation of the representation is performed under some plausible assumptions on dynamics and a simple pole definition of a resonance in the π-N scattering amplitude. It is shown that the singularities of the form factor corresponding to resonances turn out to be dipoles and not simple poles contrary to the widely held belief. A generalization to the other hadron cases is discussed in the quark model scheme. (auth)

36437 ASYMPTOTIC NUCLEON FORM FACTORS FROM CURRENT ALGEBRA AND THE REGGE MODEL. Dominguez, C. A.; Zandron, O. (Univ. of Buenos Aires). Nuovo Cim.; 3A: No. 2, 298-308(21 May 1971).

Current algebra identities and the Regge model are used in order to obtain the asymptotic behavior of the electric and magnetic nucleon form factors. This is done for the scattering of an axial current on a spin-$\frac{1}{2}$ target. It is shown that the scattering amplitude can be decomposed into a set of suitable invariant scalar amplitudes, free of kinematical singularities, for which a pure Regge model can be safely assumed in both s and $\bar{s}$ channels. In this way, the relevant amplitudes furnish an asymptotic expression for the nucleon form factors, whose behavior for large t is $\beta_1(-t)^{\alpha(s=M^2)-\frac{1}{2}n_1} + \beta_2(-t)^{\alpha(\bar{s}=M^2)-\frac{1}{2}n_2}$, where $\alpha(s)$ and $\alpha(\bar{s})$ are the trajectories exchanged in the baryonic channels, M the nucleon mass and n_1, n_2 odd integer numbers. (auth)

36438 ANNIHILATION REACTION OF A PAIR OF POLARIZED PARTICLES WITH SPIN 1/2. Khoze, V. A. (Inst. of Physics, Erevan). Izv. Akad. Nauk Arm. SSR, Ser. Fiz.; 5: 159-64(1970). (In Russian).

On the basis of invariance with respect to rotations and reflections, CP-invariance and conservation of helicity of ultrarelativistic electrons, the reactions of polarized spin-$\frac{1}{2}$ pair annihilation are investigated. Polarization effects in reactions of identical mesons pair creation in electron-positron collisions are considered. (auth)

36439 QUARK SELECTION PRINCIPLE. II. PSEUDOSCALAR MESON FORM FACTOR. Schiff, L. I. (Stanford Univ., Calif.). Ann. Phys. (N. Y.); 63: No. 1, 248-60(Mar 1971).

The quark selection principle proposed earlier is applied to the calculation of the elastic electromagnetic form factor of a pseudoscalar meson. The Bethe–Salpeter equation is inapplicable, and it is assumed instead that the quark–antiquark wavefunction satisfies a free Dirac equation for each particle. A spatial boundary condition is applied instantaneously in the rest system, and the dependence on relative time is inferred by adapting an argument given previously. Initial and final states are then obtained by applying appropriate Lorentz boosts to the resulting rest-system wavefunction. It is found that the form factor falls off for large momentum transfer like $1/q^2$. (auth)

36440 LARGE ANGLE ELECTROPRODUCTION OF ELECTRON–POSITRON PAIRS. Baier, V. N.; Fadin, V. S. (Inst. of Nuclear Physics, Novosibirsk, USSR). Phys. Lett.; 35B: No. 2, 156-8(10 May 1971).

Cross section of electron-positron pair electroproduction for large angles with the colliding e^+–e^- beams is calculated. The result obtained is in good agreement with the experiment. (auth)

36441 DUALITY, MESON TRAJECTORIES, AND REMARKS ON THE REGGE-POLE MODEL FOR $\pi^0(\eta)$ PHOTOPRODUCTION. Minami, Shigeo (Osaka City Univ.). Progr. Theor. Phys. (Kyoto); 45: No. 1, 104-10(Jan 1971).

In the description of photo-reactions on the basis of the Argonne Regge cut model, it is pointed out that the effect due to the ω trajectory plays a role of the primitive Regge amplitude in the $\gamma + p \rightarrow \pi^0 + p$ reaction and as the primitive-Regge amplitude for the $\gamma + p \rightarrow \eta + p$ reaction, it is not appropriate to consider the ρ- or ω-exchange amplitude whose magnitude turns out to be zero at about $t = -0.5$ $(GeV/c)^2$, and the Regge amplitude due to a meson trajectory with unnatural parity can be regarded as one of the candidates. Moreover, a possible degeneracy pattern for the unnatural parity trajectories is suggested. (auth)

36442 EFFECTS OF A FINITE ρ WIDTH ON THE ELECTROMAGNETIC MASS DIFFERENCE OF PIONS. Wakano, Masami (Kyoto Univ.). Progr. Theor. Phys. (Kyoto); 45: No. 1, 317-18 (Jan 1971).

A calculation for the electromagnetic mass difference of pions is performed in which the one-pion intermediate state alone is kept so that one must supplement it with the contribution from the one-A_1 meson in order to obtain a complete mass shift. (J.F.P.)

36443 ELECTROMAGNETISM AND GEODESICS OF AN EINSTEIN CONNECTION. Burman, R. R. (Univ. of Western Australia, Perth). Progr. Theor. Phys. (Kyoto); 45: No. 1, 321 (Jan 1971).

The paths of charges in general relativity theory are expressed as goedesics of an affine connection satisfying a basic principle of Einstein unified field theory. (J.F.P.)

36444 DEEP INELASTIC STRUCTURE OF e-p SCATTERING AND RELATIVISTIC EXTENDED PARTICLE MODEL BASED ON THE QUARK MODEL. Fujimura, Kimio; Kobayashi, Tsunehiro (Waseda Univ., Tokyo. Tokyo Univ. of Education). Progr. Theor. Phys. (Kyoto); 45: No. 1, 227-42(Jan 1971).

The structure functions for deep inelastic electron–proton (e–p) scattering are investigated in a quark model with the relativistic extended internal structure. Bjorken's conjecture for the structure functions, W_1 and νW_2, can be reproduced under a certain condition for the total decay widths of resonances. The ratios of σ_L/σ_T and $MW_1/\nu W_2$ are studied for the test of the current in the model. The level structure of resonances is also discussed. (auth)

36445 STRUCTURE OF THE PROTON AND THE NEUTRON. Kendall, Henry W.; Panofsky, Wolfgang K. H. Sci. Amer.; 224: No. 6, 60-6; 71-4; 76-7(Jun 1971).

The discussion of the internal structure of the proton and neutron from the way ultrahigh-energy electrons are scattered by protons and neutrons covers elastic and inelastic scattering, the Stanford electron accelerator, nucleon form factors, real and virtual particles, and the parton model. (J.F.P.)

36446 ANOMALOUS BEHAVIOR OF $\gamma\gamma \rightarrow n\pi^0$ IN EFFECTIVE LAGRANGIANS. Abers, Ernest S.; Fels, Stephen (Univ. of California, Los Angeles). Phys. Rev. Lett.; 26: No. 24, 1512-14 (14 Jun 1971).

A recent result of Aviv, Hari Dass, and Sawyer, relating the anomalous value of $\gamma\gamma \rightarrow$ (any odd number of pions) to the anomalous rate of $\pi^0 \rightarrow 2\gamma$, is demonstrated by conventional graph techniques. It is also shown that the neutral mode $\gamma\gamma \rightarrow n\pi^0$ is suppressed for all odd n. (auth)

36447 PION PHOTOPRODUCTION ON NUCLEON NEAR THRESHOLD AND THE CONTRIBUTION FOR VECTOR-MESON EXCHANGE. Radutskii, G. M.; Serdyutskii, V. A. (Tomsk Polytechnic Inst., USSR). JETP Lett. (USSR) (Engl. Transl.); 13: No. 6, 205-7(20 Mar 1971).
Translated from Zh. Eksp. Teor. Fiz., Pis'ma Red.; 13: No. 6, 288-90(20 Mar 1971).

It is shown that in the framework of the pole approximation in dispersion relations and the vector dominance hypothesis, it is impossible to obtain agreement with experimental data on the magnitude of the multipole amplitude for vector meson contributions to pion photoproduction on nucleons near threshold. (J.F.P)

36448 ELECTROPRODUCTION IN COLLIDING-BEAM EXPERIMENTS. Baier, V. N.; Fadin, V. S. (Inst. of Nuclear Physics, Novosibirsk, USSR). JETP Lett. (USSR) (Engl. Transl.); 13: No. 6, 208-12(20 Mar 1971).
Translated from Zh. Eksp. Teor. Fiz., Pis'ma Red.; 13: No. 6, 293-7(20 Mar 1971).

A more complete analysis of the pair-electroproduction process is presented. The exchange diagrams for e^-e^- collisions and the annihilation diagrams for e^+e^- collisions are considered separately. (J.F.P.)

36449 BARYON ELECTROMAGNETIC MASSES. Katsumori, Hiroshi (Chubu Inst. of Tech., Kasugai, Japan). Mem. Chubu Inst. Technol.; 6: 105-9(Dec 1970).

The problem of the baryon electromagnetic masses is reinvestigated in the framework of conventional dispersion theory. The Cottingham formula is studied with a particular emphasis on possible core contributions. Assumption is made of a very small and nearly hard core, whose existence is not inconsistent with the available experimental data on the high energy electron-proton scattering. The scaling form factor relations are used together with the SU(3) magnetic moment relations. Thus the correct signs and approximate relative ratios of the observed electromagnetic mass differences among baryons are reproduced by theory. (auth)

36450 ELECTROMAGNETIC INTERACTIONS OF PARTICLES WITH SPIN. I. ELASTIC SCATTERING. Waldenstroem, S.; Olsen, H. (Univ. of Trondheim, Norway). Nuovo Cim.; 3A: No. 3, 491-504(1 Jun 1971).

Cross sections for scattering of two different-spin particles are given. The projectile particle with spin s (s = 0, ½, 1, ⅔) is taken to be a point particle without electromagnetic structure, while the effects of the structure of the target particle with spin J (J = 0, ½, 1, ⅔) are described in terms of (2J + 1) phenomenological form factors. (auth)

36451 EXPERIMENTAL CONDITIONS FOR $\gamma\gamma$ COLLISIONS WITH ALMOST REAL PHOTONS. Parisi, J. (Univ., Paris): Arteaga-Romero, N.; Jaccarini, A.; Kessler, P. Lett. Nuovo Cim.; 1: No. 23, 935-40(5 Jun 1971).

Experimental conditions for photon–photon collisions in electron-positron storage rings are examined. Numerical calculations are performed of cross sections for $e^-e^+ \rightarrow e^-e^+A^-A^+$ (A = e, μ, π, K), taking into account the cut-off effects of a minimal angle for the particles produced and of a minimal relative energy loss. The feasibility of $\gamma\gamma$ collisions of this type is demonstrated. (L.B.S.)

36452 RECENT THEORETICAL DEVELOPMENTS IN ELECTROPRODUCTION OF HADRONS. Das, Tapas (Tata Inst. of Fundamental Research, Bombay). pp 263-73 of Proceedings of the Eleventh Symposium on Cosmic Rays, Astrophysics, Geophysics and Elementary Particle Physics, 1969. Vol. I. Bombay; Department of Atomic Energy (1969).
From eleventh symposium on cosmic rays, astrophysics, geophysics and elementary particle physics; Delhi, India (7 Oct 1969). See CONF-691055–(Vol. 1).

A review is given of the structure functions and cross sections for deep inelastic e + p interactions with hadron production. The parton and vector dominance models are considered. (J.F.P.)

36453 REGGE TRAJECTORIES IN NUCLEAR PHOTOPRODUCTION. Rej, A. K. (Indian Statistical Inst., Calcutta). pp 475-7 of Proceedings of the Eleventh Symposium on Cosmic Rays, Astrophysics, Geophysics and Elementary Particle Physics, 1969. Vol. II. Bombay; Department of Atomic Energy (1969).
From eleventh symposium on cosmic rays, astrophysics, geophysics and elementary particle physics; Delhi, India (7 Oct 1969). See CONF-691055–(Vol. 2).

It is suggested that if one considers inelastic photoproduction processes leading to appropriately chosen excited states of the nuclear system and uses linearly polarized photons, the different Regge trajectories entering into the amplitudes can be isolated. Carbon-12 and oxygen-16 are considered. (J.F.P.)

Weak

36454 (IAE–1944) LEPTON DECAY OF THE HYPERNUCLEUS ^{3}H. Lyul'ka, V. A. (Institut Atomnoi Energii, Moscow (USSR)). 1970. 15p. (In Russian). Dep. NTIS (U. S. Sales Only).

Lepton decays for the $\Lambda - {}^3H$ hypernucleus were studied. Recoil spectra of ^{3}He, and angular lepton-neutrino correlation in the decays of $\Lambda - {}^3H \rightarrow {}^3He + l^- + \bar{\nu}$ were estimated. Calculations were made of the longitudinal and transverse polarization in the plane of the M-meson decay. The lifetime of the decays was determined. A brief analysis was also made of the leptonic decays of $\Lambda - {}^3H$ into four particles. (R.V.J.)

36455 (ORO–3992-24) DEEP INELASTIC NEUTRINO–NUCLEON INTERACTIONS. Clark, Robert Beck; Yamada, Masao (Texas Univ., Austin. Center for Particle Theory). 10 Nov 1970. 11p. (CPT–75). Dep. NTIS.

Deep inelastic neutrino-nucleon interactions are discussed under the assumptions of conserved axial vector current and equal time commutation relations of currents. It is shown that the structure functions W_1 and W_2 for vector and axial vector currents are equal in the average sense with respect to the variable ν and are equal in the limit $\nu \rightarrow \infty$. The resulting expressions are then used to predict relations connecting deep inelastic neutrino and electron scattering. (auth)

36456 (ORO-3992-39) MODEL FOR K_{l3} FORM FACTORS AND CABIBBO ANGLE. Yamada, Masao (Texas Univ., Austin. Dept. of Physics). Feb 1971. 15p. (CPT-90). Dep. NTIS.

A quark model of K_{l3} form factors is discussed using Regge pole theory. It is shown that $\xi(t) = f_-(t)/f_+(t)$ for $0 < t < 7\mu_\pi^2$ can be fitted and that there is a dip in $f(t) = f_+(t) + tf_-(t)/\mu_K^2 - \mu_\pi^2$. Within the same model, the Cabibbo angle is also calculated to be 0.26, assuming that the SU(3) breaking is significant for masses in a multiplet but not for the strong couplings. (auth)

36457 TEST OF THE WEAK INTERACTION RULE $\Delta S = \Delta Q$ IN THE TIME DISTRIBUTION OF LEPTONIC K^0 DECAYS. Mann, William Anthony. Amherst, Mass.; Univ. of Massachusetts (1970). 124p. University Microfilms Order No. 71-9335.

The time distribution of 198 neutral K meson decays into $\pi l\nu$ and $\pi\pi\gamma$ channels was searched for amplitudes which violate the weak interaction selection rule $\Delta S = \Delta Q$. The sample contains $92 - K \rightarrow \pi^+e^-\nu$, $24 - K \rightarrow \pi^+\mu^-\nu$, $10 - K \rightarrow \pi^+l^-\nu$, l mass ambiguous, and $72 - K \rightarrow \pi l\nu$ and $K \rightarrow \pi^+\pi^-\gamma_{90}$, $k_\gamma > 90$ MeV/c in kaon

XUM

CM. A maximum-likelihood determination of the amplitude ratios $x_1 = A_1(\Delta S = -\Delta Q)/A_1(\Delta S = \Delta Q)$ was performed. The 92 charge-identified K^0_{e3} decays yield Re $x_e = +0.19^{+0.9}_{-0.21} - \text{Im}\ x_e = +0.16^{+0.9}_{-0.18}$. From 24 charge-identified $K^0_{\mu 3}$ events Re $x_\mu = 0.35^{+0.8}_{-1.0} - \text{Im}\ x_\mu = +0.42^{+0.8}_{-0.28}$ are found. The above results are compatible with $\mu - e$ universal leptonic currents and with negligible induced scalar interaction in $K^0_{\mu 3}$ decays. Assuming these hypotheses, the parameter $x = x_e = x_\mu$ was determined from all 126 of the charge-identified kaon decays: Re $x = +0.26^{+0.9}_{-0.14} - \text{Im}\ x = +0.21^{+0.8}_{-0.12}$. (1) The $\Delta S = \Delta Q$ prediction Re x = Im x = 0 lies on the 2.4 standard deviation contour of the most likely value. The result when combined with results from charge-identified K^+_{l3} samples of two previous light-liquid bubble chamber experiments, yields Re $x = +0.19 \pm 0.16 -$ Im $x = +0.01 \pm 0.05$. (2) The combined average indicates Im $x \simeq 0$, which implies that substantial CP nonconservation does not arise from $\Delta S = \Delta Q$-violating amplitudes which are 90° out of phase with allowed ones. However, the combined average does indicate a violation of the $\Delta S = \Delta Q$ rule at the three-standard-deviation level in positive Re x. (Diss. Abstr. Int., B)

36458 STRONG INTERACTIONS AND THE WEAK PARITY VIOLATING NUCLEAR POTENTIAL. Pignon, D. (Laboratoire de Physique Theorique et Hautes Energies, Orsay, France). Phys. Lett.; 35B: No. 2, 163-5(10 May 1971).

The one-pion exchange weak, parity non-conserving, potential is calculated, taking into account the effect of strong interactions in the lowest order. The corrections are estimated and compared with the rho-exchange potential. (auth)

36459 EFFECTIVE-DIPOLE FORM-FACTORS FOR THE K_{13}-DECAY. Chhajlany, S. C.; Pandit, L. K.; Rajasekaran, G. (Tata Inst. of Fundamental Research, Bombay). Phys. Lett.; 35B: No. 2, 166-8(10 May 1971).

To describe the latest experimental situation on the K_{13} decays (which shows large $\lambda_+ \approx 0.07$ along with a $\xi \approx -0.9$), effective-dipole form-factors, satisfying exact results of first order breaking of the chiral $SU_3 \otimes SU_3$ symmetry down to SU_2, are proposed. To the same order in the symmetry breaking the relation, $F_+(t) + tF_-(t)/(m_K^2 - m_\pi^2) = F_+(0)$, holds for a wide enough range of t, so that soft-meson current-algebra constraints are automatically satisfied to that order. (auth)

36460 EFFECT OF FORM FACTORS ON HIGH-ENERGY NEUTRINO REACTIONS. Elkhishen, M.; Mansour, H. M. (Cairo Univ.). Acta Phys. Acad. Sci. Hung.; 30: No. 1, 93-7 (1971).

Weak boson theory is used to study for effect of various form factors in the reaction $\bar{\nu} + p \rightarrow n + \mu^+$ at high energies. (J.F.P.)

36461 EFFECTIVE-RANGE FORMULA FOR THE FORM FACTOR $f_+(s)$ IN K_l DECAY. Chan, F. C. P. (Saginaw Valley Coll., University Center, Mich.). Lett. Nuovo Cim.; 1: No. 22, 903-7(29 May 1971).

An effective-range formula for $f_+(s)$ for three-body leptonic kaon decay without using K^* dominance is proposed. The problem is formulated using broken chiral SU(3) × SU(3) model. (J.F.P.)

36462 HEAVY LEPTONS AND NEUTRINO ASTRONOMY. Pontecorvo, B. (Joint Inst. for Nuclear Research, Dubna, USSR). JETP Lett. (USSR) (Engl. Transl.); 13: No. 6, 199-201(20 Mar 1971).

Translated from Zh. Eksp. Teor. Fiz., Pis'ma Red.; 13: No. 6, 281-3(20 Mar 1971).

The problem of neutrino oscillations for the case when heavy leptons exist is considered. The discussion covers the case when each new charged lepton has its own corresponding neutrino and all the neutrinos are strictly longitudinal, the case when in spite of the existence of a large number of charged leptons there are only the two already known types of neutrinos, and the case when there are N types of charged particles as well as N types of neutrinos but the neutrinos are not strictly longitudinal and, in addition, there is no exact conservation of the lepton charges. (J.F.P.)

36463 POLARIZATION EFFECTS IN LEPTONIC THREE-BODY DECAYS OF BARYONS. Uliu, F. S.; Gabos, Z. Stud. Univ. Babes-Bolyai, Ser. Phys.; 15: No. 2, 63-7(1970).

The transversal and longitudinal polarization of the final baryon in the decay of a baryon into a final baryon, a lepton and an anti-neutrino is determined. (J.F.P.)

36464 MODEL FOR WEAK INTERACTIONS. Shito, Okiyasu (Nihon Univ., Narashino, Japan). Progr. Theor. Phys. (Kyoto); 45: No. 1, 166-85(Jan 1971).

Three kinds of weak vector boson octet are assumed to exist. It is shown that certain modifications of the Michel theory for weak interactions, based on the new postulates for such weak boson octets, not only lead to the same results as the Cabibbo theory of the leptonic decays of hadrons, but also produce reasonable predictions for the nonleptonic decays of pseudoscalar mesons which satisfy the $\Delta I = 1/2$ rule with small violations. In particular, with specific parameter fits, the model can give $G^\beta(\beta\text{-decay})/G^\mu(\mu\text{-decay}) = 0.980$ and the same prediction as that of Cronin for K_{l4} decay. Further, for the slopes of the $K \rightarrow 3\pi$ decays and violations of the $\Delta I = 1/2$ rule in K-meson weak decays, it gives predictions with a very good fit to experiment. In the model, one can make a reasonable description of the meson weak decays in a unified manner. (auth)

36465 COMMENT ON A MODEL OF PARITY-VIOLATING NONLEPTONIC DECAYS. Trofimenkoff, N. N. (Univ. of Calgary, Can.). Progr. Theor. Phys. (Kyoto); 45: No. 1, 319-20 (Jan 1971).

A model of parity-violating nonleptonic decays within the framework of chiral dynamics with gauge fields in which the weak interaction, that consists of products of gauge fields, is interpreted as nondiagonal mass terms was proposed previously. It was claimed that diagonalization of these mass terms yields an enhancement of the octet part of the weak interaction sufficient to overcome the suppression due to the Cabibbo angle. Contrary to this claim, it is shown that the diagonalization does not give the necessary enhancement. The decays of hyperons and $K \rightarrow 2\pi$ decays are considered. (J.F.P.)

36466 DYNAMICAL STRUCTURE OF MASS MATRIX OF $K^0 - \bar{K}^0$ COMPLEX. Nakagawa, Masami; Watanabe, Keiji (Nagoya Univ., Japan). Progr. Theor. Phys. (Kyoto); 45: 1, 126-46(Jan 1971).

Dynamical structure of mass matrix of $K^0 - \bar{K}^0$ complex is examined in terms of combined contributions from a direct $\Delta S = 2$ interaction (the super weak model, if it exists), pseudoscalar meson poles and 2π continuum with both CP conservation and nonconservation but with CPT invariance. Numerical calculations are performed explicitly on these contributions based on as realistic model as possible. For the contributions from the second order effect of $\Delta S = 1$ interaction, an unsubtracted dispersion relation is discussed for the self-energy function. Assumption's made in calculation of 2π state contribution are: no intrinsic structure for vertices of the weak interaction other than that of $\pi\pi$ scattering, constant CP phases for the vertices with $\Delta S = 1$ transition, and introduction of a cutoff $\nu_c = 45$ in the dispersion integral. The main conclusions are the following: To get a correct sign and magnitude for $\delta m(L - S)$, mass difference K_L and K_S, the phase shift for I = J = 0, $\pi\pi$ scattering involving a resonance with mass ≅ 700 MeV – 1 GeV is favorable. This situation is unaltered when one takes into account the pole contributions from mesons of either an octet or a nonet multiplets. The best fit solution with the world data for δ_0 involving a resonance with mass ≅ 720 MeV yields the result $\delta m(L - S)/(1/2\Gamma_S) \cong 3.1$, which is brought into a good agreement with the observed value ≅ 1 by combining with the pole contribution which is ≅ −1.9. CP violation in the pseudoscalar meson poles with a milli weak strength gives rise to a correct order of magnitude for Re ϵ and a phase of about 43° for a CP mixing parameter ϵ. The 2π state contribution to ϵ is shown to be negligibly small. Possible CP violating models are examined; if experiment manifests $\eta_+ = \eta_{00}$ in the Wu-Yang parameters, it means the validity of the super weak model as well as a milli weak CP violation both in the $K^0 \nrightarrow$ meson vertex and in the $K - 2\pi$ vertex. If, however, $\eta_+ \neq \eta_{00}$, it still means the validity of a milli weak CP violation for the $K^0 \nrightarrow$ meson vertex but of a deci weak CP violation for the $K^0 - 2\pi$ vertex. Thus the models are different from the Truong model. Finally an argument is given for neglecting the higher configuration state contributions and also for a possible Hamiltonian model with a milli weak CP violation. (auth)

36467 MODELS IN WEAK INTERACTIONS. Mani, H. S. (Indian Inst. of Tech., Kanpur, India). pp 255-62 of Proceedings of the Eleventh Symposium on Cosmic Rays, Astrophysics, Geophysics and Elementary Particle Physics, 1969. Vol. I. Bombay; Department of Atomic Energy (1969).

From eleventh symposium on cosmic rays, astrophysics, geophysics and elementary particle physics; Delhi, India (7 Oct 1969). See CONF-691055-(Vol. 1).

Some models for weak interactions are described and their difficulties stated. Two specific models discussed are the Gell-Mann, Goldberger, Kroll, and Low model and the Segre model. (J.F.P.)

36468 RENORMALIZABLE MODEL OF WEAK INTERACTION. Rae, Anil C. (Indian Inst. of Tech., Kanpur). pp 488-92 of Proceedings of the Eleventh Symposium on Cosmic Rays, Astro-

physics, Geophysics and Elementary Particle Physics, 1969. Vol. II. Bombay; Department of Atomic Energy (1969).

From eleventh symposium on cosmic rays, astrophysics, geophysics and elementary particle physics; Delhi, India (7 Oct 1969). See CONF-691055-(Vol. 2).

A renormalizable model of weak interactions is derived considering W boson theories. It is noted that the electromagnetic corrections to n and μ decay are both finite in this theory and that the S-matrix is unitary. (J.F.P.)

36469 COMMENTS ON THE SIGN OF THE STRUCTURE-DEPENDENT FORM FACTORS IN $\pi \rightarrow l\nu\gamma$. Das, Tapas (Tata Inst. of Fundamental Research, Bombay). pp 497-9 of Proceedings of the Eleventh Symposium on Cosmic Rays, Astrophysics, Geophysics and Elementary Particle Physics, 1969. Vol. II. Bombay; Department of Atomic Energy (1969).

From eleventh symposium on cosmic rays, astrophysics, geophysics and elementary particle physics; Delhi, India (7 Oct 1969). See CONF-691055-(Vol. 2).

It is pointed out that the sign as well as the magnitude of the ratio of the structure-dependent axial-vector to the vector form factor for the $\pi \rightarrow l + \nu + \gamma$ decays can be predicted. This ratio is found to be +0.48. (J.F.P.)

36470 ON THE $e-\mu$ UNIVERSALITY IN $|\Delta|S = 1$ PROCESSES. Sarma, K. V. L. (Tata Inst. of Fundamental Research, Bombay). pp 500-4 of Proceedings of the Eleventh Symposium on Cosmic Rays, Astrophysics, Geophysics and Elementary Particle Physics, 1969. Vol. II. Bombay; Department of Atomic Energy (1969).

From eleventh symposium on cosmic rays, astrophysics, geophysics and elementary particle physics; Delhi, India (7 Oct 1969). See CONF-691055-(Vol. 2).

The validity of the $e-\mu$ universality hypothesis is examined. A table is given showing the ratio of the decay rate of the electronic mode to that of the muonic mode for $K^{\pm}_{e3}$, K^{0}_{e3}, K_{2e}, and π_{2e} decays. From the table it is found that a small violation of $e-\mu$ universality can be assumed for the $\Delta S = 1$ decays. Some consequences of this assumption are discussed. (J.F.P.)

36471 WEAK INTERACTIONS AT HIGH ENERGIES. Pais, A. (Rockefeller Univ., New York). Contract AT(30-1)-4204. Ann. Phys. (N. Y.); 63: No. 2, 361-92(Apr 1971).

Semi-leptonic phenomena induced by high-energy neutrino beams are surveyed. The determination of elastic form factors from differential cross sections and from polarizations is discussed, including second-class current effects and possible T violations. Scaling and sum rules for deep inelastic scattering are reviewed, as are results which go beyond the quasi-two-body description for inelastic description for inelastic phenomena. (auth)

Strong (General)

Refer also to abstract 36599.

36472 (NYO-4070-14) RESEARCH IN THEORETICAL PHYSICS. Annual Report, April 1, 1970-March 31, 1971. (Johns Hopkins Univ., Baltimore, Md. Dept. of Physics). Dec 1970. Contract AT(30-1)-4076. 15p. Dep. NTIS.

Research on the structure of hadrons is summarized covering purely hadronic and semileptonic processes. A list of publications is included. (J.F.P.)

36473 STRONG INTERACTIONS DYNAMICS WITH PADE APPROXIMANTS. Zinn-Justin, J. (Centre d'Etudes Nucleaires de Saclay, Gif-sur-Yvette, France). Phys. Rep.; 1C: No. 3, 1-102(May 1971).

Some elementary mathematical properties of the Padé approximants are first presented. A detailed study is made of how this method can be used to construct scattering amplitudes in potential scattering and in the case of the Bethe-Salpeter equation, where numerical solutions are known, and then in a particular field-theoretical model, the $\lambda\phi^4$ interaction between pions. A short review is given of different Lagrangian models in which the Padé approximation has been applied to compute two-body scattering amplitudes. (L.B.S.)

36474 GENERAL LEVEL STRUCTURE IN THE DUAL-RESONANCE MODEL. Ida, M. (Tokyo Univ.); Soffer, J. Nuovo Cim.; 3A: No. 2, 355-64(21 May 1971).

The simultaneous diagonalization of the residues of the signaturized and unsignaturized propagators is performed. This is done by means of an orthogonal decomposition of the space of the nonspurious states lying on arbitrary daughter trajectories. (auth)

36475 OPERATOR VERTICES AND PROPAGATORS IN DUAL THEORIES. Olive, D. I. (Cambridge Univ., Eng.). Nuovo Cim.; 3A: No. 2, 399-411(21 May 1971).

A modified version of Lovelaces' N-Reggeon vertex is derived. This new vertex factorizes precisely with no extraneous gauge factors and can be joined with both twisted or untwisted propagators. Since the operatorial duality conditions now involve the Kikkawa, Sakita and Virasoro change of variables, the theory seems to be the closest operatorial realization of the KSV graphical theory. A possible defect is that the spectrum of this theory may be larger than usual and may not always have a particle interpretation (though the leading trajectory is unaffected). (auth)

36476 MULTIPLICITY DEPENDENCE OF ONE-PARTICLE MOMENTUM DISTRIBUTIONS. Suranyi, P. (Johns Hopkins Univ., Baltimore). Phys. Lett.; 35B: No. 2, 169-74(10 May 1971).

The explicit form of the one-particle momentum distributions in multiperipheral models is found for large multiplicities, $\nu \gg 1$; $\nu = n/\log(E/E_0)$, where n is the secondary multiplicity, E is the primary energy and E_0 is an appropriate constant. Experimental data show a remarkable agreement with the theoretical distributions. (auth)

36477 SUPER EXCLUSION PRINCIPLE FOR HADRONIC PROCESSES. I. Bando, Masako; Machida, Shigeru (Kyoto Univ.). Progr. Theor. Phys. (Kyoto); 45: No. 1, 147-65(Jan 1971).

Hadrons are assumed to be composed of urbaryons which obey definite statistics. The exclusion principle, acting between pairs of urbaryons or antiurbaryons contained in the different hadrons in the s-, t- and u-channels, gives definite contributions to reaction amplitudes for hadronic processes (which may be called the "super exclusion principle"). Calculations are performed, assuming that the urbaryons are represented by a local field with the Fermi-Dirac statistics for definiteness. Effects of the super exclusion principle are expressed, in the short range approximation by the original amplitude smoothed by the convolution with the Fourier transform of the internal wave function of the hadron. Effects depend critically on the number of urbaryons and antiurbaryons contained in the hadrons and are shown generally to appear in the low partial waves at low energies. The largest effect appears in the S-state with the sign inverse to the original S-wave amplitude. By using the Veneziano amplitude as the original amplitude, it is shown that the effects of the super exclusion principle damp very rapidly at high energies. An exception is the case of meson-meson scattering where the effects have the same energy dependence as the original amplitude. Therefore one expects the existence of the low partial wave (or S-wave) anomaly for most hadronic processes. This anomaly seems to exist actually for KN, πN and NN scatterings, and is considered to be the strong support for the composite theory of hadrons. Comparison of the effects of the super exclusion principle with experimental data are made semi-quantitatively for KN, $\bar{K}$N, πN and NN scatterings. Unitary spin is considered and it is shown that the deviation from the Okubo-Iizuka rule is small for the strong decay of a meson into two mesons. Analytic properties of the contribution of the super exclusion principle are also investigated. It is shown that they give an imaginary part for exotic channels as well as for nonexotic channels and destroy duality. (auth)

36478 REMARKS ON INCLUSIVE EXPERIMENTS AND HIGH-ENERGY MODELS. Boldrighini, C. (Univ., Rome); Lusanna, L.; Sertorio, L. Lett. Nuovo Cim.; 1: No. 23, 973-8(5 Jun 1971).

The application of various models, namely, the multiperipheral model and the multi-Regge model, to inclusive experiments is discussed. The average multiplicity and the average perpendicular momentum of the final-state particles are considered as important features of the interaction and represent average properties connected to the general properties of the model. The relation between these quantities and to the asymptotic behavior of the elastic absorptive amplitude is discussed. (L.B.S.)

36479 RECENT DEVELOPMENTS IN STRONG-INTERACTION THEORY. Roy, S. M. (Tata Inst. of Fundamental Research, Bombay). pp 199-214 of Proceedings of the Eleventh Symposium on Cosmic Rays, Astrophysics, Geophysics and Elementary Particle Physics, 1969. Vol. I. Bombay; Department of Atomic Energy (1969).

From eleventh symposium on cosmic rays, astrophysics, geophysics and elementary particle physics; Delhi, India (7 Oct 1969). See CONF-691055-(Vol. 1).

Some new exact results are discussed obtained in the S-matrix

XUM

framework without any hypothesis about the singularity structure in the angular momentum plane. Also the radical strong interaction Veneziano model is briefly considered. (J.F.P.)

36480 TOTAL CROSS SECTIONS AND ELASTIC SCATTERING AT HIGH ENERGIES. Sarma, K. V. L. (Tata Inst. of Fundamental Research, Bombay). pp 229-42 of Proceedings of the Eleventh Symposium on Cosmic Rays, Astrophysics, Geophysics and Elementary Particle Physics, 1969. Vol. I. Bombay; Department of Atomic Energy (1969).

From eleventh symposium on cosmic rays, astrophysics, geophysics and elementary particle physics; Delhi, India (7 Oct 1969). See CONF-691055-(Vol. 1).

The review of total cross sections at high energies covers the Pomeranchuk theorems, experimental properties, SU(3) symmetry, and the Regge pole theory. The review of the elastic scattering of hadrons in the forward direction covers the Regge pole theory, the experimental properties, polarization, structure, cross sections, diffraction, and the proton electromagnetic form factor. (J.F.P.)

36481 STRONG-INTERACTION DYNAMICS BASED ON A CLASS OF NONLINEAR LAGRANGIAN MODELS. Khare, Avinash V.; Pradhan, T. (Saha Inst. of Nuclear Physics, Calcutta). pp 454-7 of Proceedings of the Eleventh Symposium on Cosmic Rays, Astrophysics, Geophysics and Elementary Particle Physics, 1969. Vol. II. Bombay; Department of Atomic Energy (1969).

From eleventh symposium on cosmic rays, astrophysics, geophysics and elementary particle physics; Delhi, India (7 Oct 1969). See CONF-691055-(Vol. 2).

An investigation is made of the dependence of the scattering length calculations on the type of symmetry breaking terms in the Lagrangian, the threshold behavior of scattering amplitudes obtained in the tree diagram approximation, and the validity of the Weinberg spectral function sum rules. (J.F.P.)

Strong (Baryon No. = 0)

Refer also to abstract 36582.

36482 (NYO-2262-TA-241) COMMENT ON CURRENT ALGEBRA BEYOND THE TREE APPROXIMATION. Jen, Chian-li (Brown Univ., Providence, R. I. Dept. of Physics). Apr 1971. 12p. Dep. NTIS.

The Schnitzer solution for the s-wave $\pi\pi$ scattering amplitudes was improved so as to satisfy the crossing relations of Roskies' and the Martin inequality relations. (auth)

36483 (SU-1206-241) GENERAL TREATMENT OF CHIRAL AND SCALE BREAKING IN THE SU(3) SIGMA MODEL. Schechter, J.; Ueda, Y. (Syracuse Univ., N. Y. Dept. of Physics). Jan 1971. 61p. (NYO-3399-241). Dep. NTIS.

The model of nine scalar and nine pseudoscalar fields interacting by means of the most general nonderivative chiral SU(3) × SU(3) invariant and any particular symmetry breaker is studied. Two basic "generating" equations which express the complete content of chiral symmetry are derived. The masses and coupling constants of arbitrary order for this model are simply found by differentiating the "generating" equations an arbitrary number of times and using an equation which expresses the stability of the "ground" state. In this way, previous results on this model can be easily recaptured and a systematic framework for the investigation of different symmetry breakers is provided. Numerical estimates are made for scalar meson widths, $\pi\pi$ and πK scattering lengths, and $\eta' \to \eta 2\pi$ decays. The consequences of imposing scale invariance on the invariant part of the interaction are also investigated by writing down a scale invariance "generating equation". Finally, the relation between this approach and the method of using the divergences of currents and trace of the energy momentum tensor is discussed. (auth)

36484 MODEL FOR THE s-WAVE PION-PION PHASE SHIFTS. Jen, C.-L.; Kang, K. (Brown Univ., Providence). Nuovo Cim.; 3A: No. 2, 425-40(21 May 1971).

The s-wave $\pi\pi$ phase shifts were obtained up to around 1 GeV, from the Chew-Mandelstam program but with the inputs restricted by the conditions derived from the Veneziano model. These solutions satisfy the elastic unitarity exactly and the five Roskies crossing conditions up to the order of 10^{-2} and further are consistent with the available experiments. (auth)

36485 N-POINT DUAL FUNCTIONS FOR MESONS WITH PHYSICAL TRAJECTORIES. Dorren, J. D. (Weizmann Inst. of Science, Rehovot, Israel); Rittenberg, V.; Rubinstein, H. R. Nuovo Cim.; 3A: No. 2, 385-98(21 May 1971).

A graphical formalism is presented from which the corresponding dual function for N scalar mesons can be written. The technique can accommodate the most general N-point functfon of the type in which the integrand of the basic function B_N is modified by a polynomial in α_{ij} and u_{ij}, the Regge trajectory in the ij channel and the corresponding integration variable respectively. Solutions can then be selected which have the correct isospin structure, have no ghosts on the leading trajectory, and satisfy the bootstrap principle. A thorough analysis was made of the odd-G unnatural-parity trajectories and the even-G natural-parity trajectories. A novel feature associated with physical amplitudes is that the leading trajectory may be degenerate. The rules for the other cases are indicated and the theoretical and phenomenological implications of the results are briefly discussed. (auth)

36486 DUALITY-BREAKING AND MESON SPECTRUM. Logan, R. K.; Roy, D. P. (Univ. of Toronto). Nuovo Cim.; 3A: No. 2, 241-9(21 May 1971).

The observed masses of the vector and tensor meson notets are incompatible with the constraints of duality and the absence of exotic resonance, unless one invokes a very peculiar type of SU_3 breaking in coupling strengths. Further, the masses of the pseudoscalar mesons are incompatible with these hypotheses irrespective of any SU_3 considerations. Thus, in the absence of exotic resonances, the mesonic mass spectrum seems to suggest a strong breaking of duality even for meson-baryon scatterings. (auth)

36487 DISPERSION RELATIONS AND ASYMPTOTIC BEHAVIOR OF THE VENEZIANO PARTIAL-WAVE AMPLITUDE IN THE COMPLEX s PLANE. Park, Robert Turner. Riverside, Calif.; Univ. of California (1970). 62p. University Microfilms Order No. 71-8801.

The asymptotic behavior of the Veneziano partial-wave amplitude is studied in the complex s plane for physical l values. Conditions under which partial-wave dispersion relations can be written are determined and the importance of dispersion relations in the development of the relativistic theory of strong interactions is stressed. A method for applying these results is suggested. Crossing symmetry, Bose statistics and isospin conservation are used to write the three relativistically invariant $\pi\pi$ scattering amplitudes, $A^I(s,t,u)$, in the Euler beta function representation of Veneziano. The ρ and f^0 Regge trajectories are assumed to be exchange degenerate and the Pomeranchuk is ignored. Then the $\pi\pi$ system is described by a single Regge trajectory which takes the form $\alpha(s) = as + b$. The standard series expansions of the beta function are used to calculate the partial-wave amplitudes, $V_l^I(s)$, which exhibit a branch cut along the negative real s axis—the so called left-hand cut. The discontinuity across the cut is calculated. For I = 0 or I = 2, disc $V_l^I(s)$ diverges exponentially as $s \to -\infty$ due to the unsatisfactory behavior of the partial-wave projection of the Veneziano t-u term. This behavior is unphysical and excludes the existence of partial-wave dispersion relations for I = 0 or I = 2. For I = 1, the discontinuity across the left-hand cut oscillates and, if $b < 1$, then, asymptotically, disc $V_l^I(s) \sim o(s^{-2b-4am_\pi^2})$. For the ρ-trajectory, with $a \simeq 1$ GeV^{-2} and $b \simeq \frac{1}{2}$, disc $V_l^I(s)$ goes to zero faster than $1/s$ along the left-hand cut. The series expansion for $V_l^I(s)$, which was used to investigate the discontinuity across the left-hand cut, converges only if $\mathrm{Re}\alpha(s) < l$. It is therefore replaced by an integral representation which is defined in the entire complex s plane. For $b < 1$ and $3b + 4am_\pi^2 > 1$, the integral representation is used to show that, asymptotically, $V_l^I(s) \sim o(s^{b-l})$. Under the same conditions, the resonance partial widths for fixed l have the property $\Gamma s_R \sim o(s_R^{b-\frac{1}{2}})$. In the case $-2am_\pi^2 < b < 1$, disc $V_l^I(s) \to 0$ as $s \to -\infty$ and $V_l^I(s) \to 0$ as $|s| \to \infty$, and $V_l^I(s)$ can be written in the form of unsubtracted partial-wave dispersion relations, i.e., as an integral along the left-hand cut plus the sum of an infinite number of poles along the right-hand real axis. Thus for the particular case of the ρ-trajectory, an unsubtracted dispersion relation can be written. (Diss. Abstr. Int., B)

36488 DIE SYSTEMATIK DER RESONANZEN. (Systematics of Resonances). Weckering, Rudolf. Stereophysik, Band VIII. Luxemburg; Buchdruckerei Hermann s.e.n.c. (1970). 74p.

The nodic field theory is briefly reviewed as an introduction to the understanding of resonances. Nature understood on the basis of the nodic field theory and the types of origin of resonances are discussed. The origin of resonances in scattering processes is considered separately. The preparation of resonance mass diagrams and the results obtained from the resonance line systems prepared are discussed. The spatial structure of various light syno- and anti-element particles are described. The spatial structure of resonances is considered in conclusion. (J.S.R.)

36489 NUCLEAR ABSORPTION OF LOW-ENERGY PIONS. Beder, D. A. (Univ. of Brisith Columbia, Vancouver). Can. J. Phys.: 49: 1211-14(1 May 1971).

An expression is derived for the mean free path of low energy π's traversing nuclear matter, with the assumption that absorption is dominantly on nucleon pairs. Relating the absorption cross section to the data for the inverse reaction NN → NNπ makes this susceptible to numerical calculation. The problem of nucleon Fermi motion in calculating the absorption rate is also discussed. (auth) (Canada)

36490 DUAL RESONANCE MODELS FOR VECTOR CURRENTS. Weis, Joseph Herman. Berkeley, Calif.; Univ. of California (1970). 78p. University Microfilms Order No. 71-9953.

Thesis.

Recent work on dual Reggeized resonance models for vector currents is discussed. The properties vector current amplitudes in such models are expected to possess are first described in some detail; i.e., (i) factorization, (ii) divergence conditions, and (iii) good large-q^2 behavior. Presently existing models fall into two classes: factorizable models that emphasize (i) and (ii) at the expense of (iii), and phenomenological models that emphasize (iii) at the expense of (i) and (ii). These models are discussed and a new phenomenological model is proposed that incorporates exponentially falling form factors, a property believed that dual resonance models should possess. The partial successes described are found a source of optimism for an eventual complete solution of the problem. (Diss. Abstr. Int., B)

36491 EFFECTS OF THE RESONANCE-SCATTERING AMPLITUDE IN NUCLEON–ANTINUCLEON REACTIONS. Hattori, Toshihiko (Univ. of Tokushima, Japan). Progr. Theor. Phys. (Kyoto); 45: No. 1, 111-25(Jan 1971).

The effects of direct channel resonances are investigated for $\bar{p}p$ elastic and charge exchange scatterings at intermediate energies. In this approach for the resonance amplitude, the effect of the phase shift caused by the background amplitude is considered. Among five independent helicity amplitudes, the resonance amplitude with the Regge recurrence of B resonance shows the dip-bump behavior at the desired position of the scattering angle in the differential cross section of $\bar{p}p$ elastic scattering. The amplitude with several infinite series of resonance level of the Chew–Frautschi plot reproduces the energy dependence of the secondary maximum of the differential cross section up to 6 GeV/c. The real to imaginary ratio of the scattering amplitudes is estimated to be negative and very small at t = 0. Also the differential cross section is calculated for $\bar{p}p$ charge exchange scattering in terms of the resonance amplitude with the same parameters in the case of $\bar{p}p$ elastic scattering. From the calculation of the polarization parameter, the contribution of the helicity single flip amplitude ϕ_5 is determined. (auth)

36492 DUAL AMPLITUDE WITH MANDELSTAM ANALYTICITY. Bugriia, A. I.; Jenkovskii, L. L.; Kobylinskii, N. A. (Inst. for Theoretical Physics, Kiev). Lett. Nuovo Cim.; 1: No. 22, 923-6(29 May 1971).

A procedure for the introduction of an imaginary part in the amplitude is presented. It allows the construction of a dual crossing-symmetric amplitude satisfying a Mandelstam representation with correct double-spectral-function boundaries, second-sheet poles, and Regge asymptotic behavior. The amplitude is applied to elastic ππ scattering. (J.F.P.)

36493 GENERALIZED VENEZIANO MODEL WITH NONLINEAR TRAJECTORIES. Golden, J. (Dublin Inst. for Advanced Studies). Lett. Nuovo Cim.; 1: No. 22, 893-8(29 May 1971).

The sort of trajectories and amplitudes that are allowed if one imposes the constraints that the residue functions be polynomials of correct degree and that superconvergence relations hold is considered. The $\pi^+\pi^-$ elastic scattering is discussed. (J.F.P.)

36494 POSSIBLE METHOD OF X^0 (960) MESON SPIN–PARITY DETERMINATION. Rembielinski, J.; Tybor, W. (Univ., Lodz, Poland). Acta Phys. Pol.; A39: No. 3, 389-90(Mar 1971).

A suggestion is made to make use of the forward scattering $\pi N \to X^0 N^*$ to establish the X^0 spin-parity. The measurement of the angular distribution of the decay $N^*(1236) \to N\pi$ may exclude the possibility of the $J^P(X^0) = 0^-$. (auth)

36495 MOMENTUM DEPENDENCE OF THE $\pi\rho\omega$ VERTEX. Pocsik, G.; Ferenczi, G. (Roland Eoetvoes Univ., Budapest). Acta Phys. Acad. Sci. Hung.; 30: No. 1, 81-2(1971).

Assuming that the $\pi\rho\omega$-vertex function defines a momentum-dependent coupling, it is shown that in current algebra there is a possibility of explaining the ratio $\Gamma(\omega \to \pi^0\gamma)/\Gamma(\pi^0 \to 2\gamma)$. (J.F.P.)

36496 K^+–K^0 MASS DIFFERENCE AND THE A_2 REGGE POLE. Morishita, Norikazu (Chubu Inst. of Tech., Kasugai, Japan). Mem. Chubu Inst. Technol.; 6: 127-30(Dec 1970).

The contribution of the A_2 Regge pole to the $K^+ - K^0$ mass difference is estimated. The usual Regge asymptotic behavior of the amplitude of $t_1(q^2,\nu)$ and the finite energy sum rule proposed previously which decides the explicit form of the A_2 Regge residue are assumed. The result obtained is $-\delta m^R(K^+ - K^0) \lesssim 0.7$ MeV. (auth)

36497 BOUND-STATE MODELS AND THE SPLITTING OF THE A_2. Gell, Y. (Tel Aviv Univ., Israel). Nuovo Cim.; 3A: No. 3, 457-66(1 Jun 1971).

A dynamical model is proposed describing a $J^P = 2^+$, I = 1 state as an $\omega\rho$ bound state. Using the Faddeev equations it is shown that two such bound states appear at 1525 and 1485 MeV. (auth)

36498 ZEROS IN ππ AMPLITUDES. Pennington, M. R.; Pond, P. (London Univ.). Nuovo Cim.; 3A: No. 3, 548-60(1 Jun 1971).

It is shown that the zeros which must exist in the physical ππ amplitudes are those implied by the Adler self-consistency condition, even if this condition is not explicitly imposed. This explains why all low-energy ππ models obtain approximately the same values for the s-wave scattering lengths. (auth)

36499 SMOOTHED VENEZIANO MODELS AND APPLICATIONS TO PION–PION SCATTERING. Burkhardt, H.; Cottingham, W. N.; Phua, K.-K. (Univ. of Birmingham, Eng.). Nuovo Cim.; 3A: No. 3, 584-602(1 Jun 1971).

Linear smoothing of the Veneziano formula is investigated and models are developed with the second-sheet resonance poles, unitarity branch cuts, and proper partial-wave threshold behavior, which retain many of the usual desirable analytic and asymptotic properties. A simple version of the model is applied phenomenologically to pion–pion scattering, and is shown to be in qualitative agreement with most of the data. (auth)

36500 RESONANCE PHENOMENOLOGY. Raghavan, R. (Tata Inst. of Fundamental Research, Bombay). pp 243-9 of Proceedings of the Eleventh Symposium on Cosmic Rays, Astrophysics, Geophysics and Elementary Particle Physics, 1969. Vol. I. Bombay; Department of Atomic Energy (1969).

From eleventh symposium on cosmic rays, astrophysics, geophysics and elementary particle physics; Delhi, India (7 Oct 1969). See CONF-691055-(Vol. 1).

A review is given of meson and baryon resonances in the quark model. The overall situation is presented and certain trends are indicated. (J.F.P.)

36501 FIELD-CURRENT IDENTITIES IN A GAUGE-INVARIANT FORMULATION OF MASSIVE GAUGE FIELDS. Ghose, Parthasarathy (Visva-Bharati Univ., Santiniketan, India). pp 471-4 of Proceedings of the Eleventh Symposium on Cosmic Rays, Astrophysics, Geophysics and Elementary Particle Physics, 1969. Vol. II. Bombay; Department of Atomic Energy (1969).

From eleventh symposium on cosmic rays, astrophysics, geophysics and elementary particle physics; Delhi, India (7 Oct 1969). See CONF-691055-(Vol. 2).

A previous formulation of the field–current identities is applied to the ρ and A_1 mesons. It is shown that some celebrated current algebra results follow from the Lagrangian density determined by requiring $\delta L = 0$, the vector part to give rise to a conserved current but the axial-vector part to a partially conserved current, and the universality of the bare weak couplings of the ρ and A_1 mesons. (J.F.P.)

Strong (Baryon No. = 1)

36502 (CALT-68-300) TESTS OF AN EMPIRICAL RULE FOR CUTS AND DISCUSSION OF LINE REVERSAL RELATIONS. Chiu, Charles B. (California Inst. of Tech., Pasadena). [1971]. Contract AT(11-1)-68. 53p. (CONF-710316-1). Dep. NTIS.

From Workshop on particle physics at intermediate energies; Pasadena, Calif. (29 Mar 1971).

The empirical rule, that cuts are important in the s-channel nonflip amplitude and relatively unimportant in the flip amplitude, consistently distinguishes the success and the failure of the Regge pole model for natural parity meson exchanges. Measurements on the density matrix elements of the ω in the reaction $\pi^+p \to \omega\Delta^{2+}$ will be helpful in understanding the underlying reason for such systematics. A discussion on the line reversal relation is also presented. A prediction of the absorption model on the Λ and the Σ polarizations in $\pi^+p \to K^+\Sigma^+$ and $\pi^-p \to K^0\Lambda$ and the line reversed reactions is discussed. Measurement of polarizations at

XUM

high energies will provide a direct test on the present absorption picture. (auth)

36503 (INR-P-1265) AFST MODEL WITH $\pi\pi$ AND πp PHASE SHIFTS AND DURR-PILKUHN FORM FACTORS APPLIED TO THE REACTION $\pi^+p \rightarrow p3\pi^+2\pi^-$ AT 8 GeV/c. Jurewicz, A.; Michejda, L.; Namyslowski, J.; Turnau, J. (Institute of Nuclear Research, Warsaw (Poland)). 1970. 56p. Dep. NTIS (U. S. Sales Only).

A previous multiperipheral model is used to perform calculations without any essential approximation for one definite channel $\pi^+ + p \rightarrow 3\pi^+ + 2\pi^- + p$ and one definite energy 8 GeV/c, for which the chosen channel represents about the average multiplicity. This numerical calculation was performed with $\pi\pi$ and πp phase shifts and the off-shell extrapolation for the studied reaction. Only pion exchange was considered. (J.F.P.)

36504 (JINR-E2-5770) THE STUDY OF SPIN EFFECTS AT HIGH ENERGY IN THE QUASIPOTENTIAL APPROACH. Garsevanishvili, V. R.; Goloskokov, S. V.; Matveev, V. A.; Slepchenko, L. A. (Joint Inst. for Nuclear Research, Dubna (USSR). Lab. of Theoretical Physics). 1971. 15p. Dep. NTIS (U. S. Sales Only).

Meson-nucleon scattering at high energies was considered in the quasipotential approach. For the scattering amplitude a representation of the eikonal type was obtained. The corrections of the relative order 1/p as compared to the leading contributions were calculated. (auth)

36505 (PAM-71.1) LOCAL MODELS FOR ANTIKAON-NUCLEON COLLISIONS. Benayoun, M.; Leruste, Ph. (College de France, Paris. Laboratoire de Physique Atomique et Moleculaire). Feb 1971. 42p. (In French). Dep. NTIS (U. S. Sales Only).

A local model built from the D/D formalism and valid in the neighborhood of the $\bar{K}N$ threshold is deduced. Since the local analysis of this process involves zero and one total isospin states, models for two or three channels are given and the equivalence between this D/D local model and the Dalitz-Tuan one is proved. The conclusions given turn out to be of the same kind as those previously deduced from the analysis of the rational approximation; these conclusions are the same as those of Dalitz deduced by a nonrelated method. Concerning the coupling constant of the Y_0^* (1405) resonance, the nature of the resonances is still unknown and the question is still unsolved as to whether the poles are of T- or K-matrix. (France)

36506 (TID-25726) πN PARTIAL-WAVE AMPLITUDES: A COMPILATION. Herndon, David J.; Barbaro-Galtieri, Angela; Rosenfeld, Arthur H. (California Univ., Berkeley. Lawrence Radiation Lab.). Feb 1970. 86p. Dep. NTIS.

A collection of the results of ten partial-wave analyses performed on the elastic π^+p and π^-p scattering at 0 to 2 GeV/c is presented. The amplitudes and some parameters deduced from the amplitudes are plotted and tabulated. (J.F.P.)

36507 LOW, INTERMEDIATE, AND HIGH ENERGIES IN THE VENEZIANO MODEL FOR KN SCATTERING. Namyslowski, J. (Univ., Warsaw); Rek, Z.; Swiecki, M. Nuovo Cim.; 3A: No. 2, 412-24(21 May 1971).

The low-energy contraints — consistency of the two Adler-Weisberger sum rules, the Adler requirement, and the isospin-zero KN scattering length equal to zero — are built in the Veneziano-type model, with no unobserved parity doublets of particles with spin $\leq 3/2$, and no unobserved daughters of $Y(3/2^+, 1382)$. Predictions of the amplitude are checked with the experimental data for the elastic widths of resonances, differential cross sections of the charge exchange process $K^+n \rightarrow K^0p$, and the elastic backward K^+p scattering, at energies ranging from 1 GeV up to 12.3 GeV. A reasonable qualitative agreement is found at all energies. The stability of the results, and the role of the PCAC condition are discussed. (auth)

36508 BACKWARD DISPERSION RELATIONS FOR $\pi N \rightarrow \pi\Delta$ SCATTERING AND $N\Delta\gamma$ COUPLINGS. Baacke, J. (Freie Univ., Berlin); Kleinert, H. Phys. Lett.; 35B: No. 2, 159-62(10 May 1971).

Using unsubtracted dispersion relations for the invariant amplitudes of the process $\pi N \rightarrow \pi\Delta$ in forward and backward direction, sum rules relating t channel to s and u channel resonances are derived. These sum rules are saturated by ρ, N, and Δ and values for the ρ coupling constants are obtained. Assuming vector meson dominance of the electromagnetic vertex $N\Delta\gamma$ these become the values of the Gourdin-Salin coupling constants in reasonable agreement with experiment. (auth)

36509 TOTAL $\pi^+\pi^-$ CROSS-SECTION FOR DIPION ENERGIES ABOVE 1.5 GeV. Caso, C. (Univ., Genoa. Istituto Nazionale di Fisica Nucleare, Genoa); Conte, F.; Tomasini, G.; (and others). Nuovo Cim.; 3A: No. 2, 287-97(21 May 1971).

The OPE model is applied to the reaction $\pi^-p \rightarrow n\pi^+\pi^-$. A sample of 1565 fitted events at an incident momentum of 11 GeV/c was used to obtain an order-of-magnitude estimate for the elastic and total $\pi^+\pi^-$ cross sections at $\pi\pi$ masses above 1.5 GeV. The assumption is made that the forward amplitude for $\pi\pi$ elastic scattering is purely imaginary at t = 0 (where $|t| = \Delta^2(\pi^-_{in}/\pi^-_{out})$). The elastic differential cross section is then extrapolated to t = 0 and with the help of the optical theorem the total $\pi\pi$ cross-section is derived for different mass intervals of the $\pi\pi$ system. (auth)

36510 POTENTIAL OF PION-NUCLEON SCATTERING. Chan, Lydia Sing-chai. Montreal; McGill Univ. (1970). National Library of Canada, Ottawa.

Thesis.

A Born approximation potential is derived from the one-boson-exchange model with the ρ-meson and the f^0-meson exchanges, together with the direct and exchange pole terms of the $\pi-N$ scattering. A "cut off" mass is introduced to regularize the singular part of the potential. The potential is inserted into the Klein-Gordon equation and the equation is then solved for the phase shifts. The coupling constants $G^2/4\pi$, $g_{\rho\pi\pi}g_{\rho NN}/4\pi$, $g_{f\pi\pi}g_{fNN}/4\pi$ and the "cut off" mass m_c are treated as adjustable parameters to fit the CERN phase shifts. The best solution obtained in the 0 to 700 MeV energy range includes three resonances; P_{33}(194 MeV), P_{11}(600 MeV) and D_{13}(616 MeV). The solutions are consistent with the CERN phase-shift analysis especially for large positive phase shifts such as P_{11}, P_{33}, D_{15}, and D_{13}. The P_{31}, P_{13} and D_{33} cannot be accurately predicted in the model. (Diss. Abstr. Int., B)

36511 VERIFICATION OF MODELS OF THE ASYMPTOTIC BEHAVIOR OF π^+p SCATTERING AMPLITUDES. Dumbrais, O. V. (Joint Inst. for Nuclear Research, Dubna, USSR). JETP Lett. (USSR) (Engl. Transl.); 13: No. 6, 224-6(20 Mar 1971).

Translated from Zh. Eksp. Teor. Fiz., Pis'ma Red.; 13: No. 6, 315-16(20 Mar 1971).

It is shown that by using a simple sum rule the number of different parametrizations in models for the $\pi^+ + p$ and $\pi^- + p$ amplitude asymptotic behavior can be greatly limited. (J.F.P.)

36512 MODEL FOR POMERANCHUKON COUPLINGS. Carlitz, R.; Green, M. B.; Zee, A. (Inst. for Advanced Study, Princeton, N. J.). Phys. Rev. Lett.; 26: No. 24, 1515-18(14 Jun 1971).

A model is presented for the Pomeranchukon which relates its couplings to those of the f and f' trajectories. Several features of total-cross-section data are successfully explained and s-channel helicity conservation at high energies in πN scattering and ρ photoproduction are discussed but it is not expected to be a feature of all diffractive processes. (auth)

36513 WARD-IDENTITY TECHNIQUES AND LOW-ENERGY PION-NUCLEON SCATTERING. Osypowski, Edward Thomas. Madison, Wis.; Univ. of Wisconsin (1970). 107p. University Microfilms Order No. 70-22,659.

Thesis.

The low-energy s- and p-wave πN partial-wave amplitudes calculated from an expansion of the on-mass-shell πN scattering amplitude to second order in the pion four-momenta are examined. The starting point for the expansion is an expression for the scattering amplitude obtained by applying Ward-identity techniques to three- and four-point functions composed of isotopic vector currents and nucleon field operators obeying postulated equal-time commutation rules. Numerical estimates for the three important expansion parameters are obtained by comparing the sum of the known N, ρ, N*(1236) contributions to the s- and p-wave scattering lengths and the s-wave effective ranges with experiment. The resultant amplitudes give good agreement with the experimentally determined partial-wave amplitudes at T_π = 58 MeV. The values obtained for the non-pole parameters imply a significant contribution from the σ-commutator. (Diss. Abstr. Int., B)

36514 REDEMPTION OF THE DUAL DESCRIPTION OF PRODUCTION PROCESSES BY UNITARITY. THE RELEVANCE OF THE EIKONAL MODEL. Gunion, John Francis. San Diego, Calif.; Univ. of California (1970). 93p. University Microfilms Order No. 71-8988.

Thesis.

A modified Baker-Blankenbecler type formalism is defined which is used to apply unitarity corrections to the Veneziano model and its generalization to many point functions. As a result an eikonal-like pole-cut model for elastic scattering and for production processes is obtained. The dip at t = -0.9

XUM

GeV^2 in K^-p scattering is particularly well described. The processes $K^-p \to \pi^- Y^{*+}$ and $\pi^+p \to K^+Y^{*+}$ are considered in detail, and it is found that inclusion of unitarity corrections allows one to retain the assumptions of factorization, exchange degeneracy and duality in contrast to the previous applications of the generalized Veneziano model to these reactions and leads to substantial improvement in the agreement with data. The extension of the model to include spin leads in a natural way to the conservation of s-channel helicity by the Pomeranchuk. (Diss. Abstr. Int., B)

36515 GAUGE INVARIANCE, SOFT PIONS TECHNIQUE, AND PION–NUCLEON INELASTIC SCATTERING. Tataru, P. I. Stud. Univ. Babes-Bolyai, Ser. Phys.; 15: No. 2, 9-13(1970).

Constraints between the nonpole part of the pion production amplitude and the pion–nucleon scattering amplitude are derived using a gauge condition for zero four-momentum pion amplitudes. (J.F.P.)

36516 SURVEY OF RESONANCE PHYSICS. Mitra, A. N. (Univ. of Delhi). pp 183-98 of Proceedings of the Eleventh Symposium on Cosmic Rays, Astrophysics, Geophysics and Elementary Particle Physics, 1969. Vol. I. Bombay; Department of Atomic Energy (1969).

From eleventh symposium on cosmic rays, astrophysics, geophysics and elementary particle physics; Delhi, India (7 Oct 1969). See CONF-691055–(Vol. 1).

A survey is given of the essential aspects of resonance physics including some latest trends of thought. The topics covered include SU(3) and SU(6) symmetries, the quark model, Regge pole theory, exchange degeneracy, duality, and the Veneziano model. (J.F.P.)

36517 πN CHARGE EXCHANGE POLARIZATION IN VENEZIANO MODEL. Maharana, J.; Ramachandran, R. (Indian Inst. of Tech., Kanpur). pp 458-62 of Proceedings of the Eleventh Symposium on Cosmic Rays, Astrophysics, Geophysics and Elementary Particle Physics, 1969. Vol. II. Bombay; Department of Atomic Energy (1969).

From eleventh symposium on cosmic rays, astrophysics, geophysics and elementary particle physics; Delhi, India (7 Oct 1969). See CONF-691055–(Vol.2).

For πN charge exchange polarization the Veneziano model has the appropriate Regge limit and resonance structure at low energies suggesting that at intermediate energies contributions include interferences between the two pieces. It is examined whether such interference yields the observed polarization. A polarization of the same order of magnitude as that found experimentally is found in the results; but whereas the degenerate case and that using backward scattering have the right sign, the finite-energy sum rule data indicate a polarization of opposite sign. (J.F.P.)

36518 MESON–BARYON SCATTERING IN THE QUARK MODEL. Sastry, C. V.; Misra, S. P. (Regional Engineering Coll., Rourkela, India). pp 463-6 of Proceedings of the Eleventh Symposium on Cosmic Rays, Astrophysics, Geophysics and Elementary Particle Physics, 1969. Vol. II. Bombay; Department of Atomic Energy (1969).

From eleventh symposium on cosmic rays, astrophysics, geophysics and elementary particle physics; Delhi, India (7 Oct 1969). See CONF-691055–(Vol. 2).

A model with two-body quark–quark and quark–antiquark interaction with T_3^3 type of violation in quark space, proposed earlier, is used to obtain many sum rules for meson–baryon scattering amplitudes and cross sections. The mesons are treated with the usual quark–antiquark configuration. (J.F.P.)

36519 VECTOR-MESON DOMINANT SUM RULES AND LOW-ENERGY KAON–NUCLEON SCATTERING. Pundari, S. Baba; Dutta-Roy, B.; Banerjee, H. (Saha Inst. of Nuclear Physics, Calcutta). pp 467-70 of Proceedings of the Eleventh Symposium on Cosmic Rays, Astrophysics, Geophysics and Elementary Particle Physics, 1969. Vol. II. Bombay; Department of Atomic Energy (1969).

From eleventh symposium on cosmic rays, astrophysics, geophysics and elementary particle physics; Delhi, India (7 Oct 1969). See CONF-691055–(Vol. 2).

Assuming unsubtracted dispersion relations in the forward and backward directions, sum rules are derived for the kaon–nucleon scattering amplitude at low energies. (J.F.P.)

36520 PION PHASE SHIFTS FROM BACKWARD PION–NUCLEON DISPERSION RELATIONS. Menon, V. J. (Saha Inst. of Nuclear Physics, Calcutta). pp 478-82 of Proceedings of the Eleventh Symposium on Cosmic Rays, Astrophysics, Geophysics and Elementary Particle Physics, 1969. Vol. II. Bombay; Department of Atomic Energy (1969).

From eleventh symposium on cosmic rays, astrophysics, geophysics and elementary particle physics; Delhi, India (7 Oct 1969). See CONF-691055–(Vol. 2).

In order to evaluate the low-energy $\pi\pi$ phase shifts in the isospin I = 0 and 1 channels an analysis is made of the once-subtracted backward πN dispersion relations for certain amplitudes. The solutions for the $\pi\pi$ phase shifts show resonance production. (J.F.P.)

36521 HIGH ENERGY DIFFRACTIVE DISSOCIATION OF PIONS AND THE A_1. Henley, E. M. (Univ. of Washington, Seattle). Ann. Phys. (N. Y.); 63: No. 2, 541-8(Apr 1971).

The diffractive dissociation of a pion into five pions via $A_1\rho$ production is used to study the Drell–Hiida–Deck effect at very high energies. It is shown that the predicted cross section for diffractive dissociation violates unitarity, so that (absorptive) corrections must be taken into account. (auth)

Strong (Baryon No. ≥ 2)

Refer also to abstract 36847.

36522 IMPROVEMENTS IN TESTS OF LONG-RANGE CHARGE INDEPENDENCE. Breit, G.; Tischler, M.; Mukherjee, S.; Lucas, J. (State Univ. of New York, Buffalo). Proc. Nat. Acad. Sci. U. S. A.; 68: No. 5, 897-900(May 1971).

The procedure used to determine the pion–nucleon coupling constant g^2 from multi-energy fits to nucleon–nucleon (N–N) scattering data has been shortened without a material loss of accuracy. The g^2 presetting effect is discussed in connection with the limited accuracy of g^2 determinations in general and the possibilities of the "optimized polynomial expansions." The desirability of the Yale graded introduction of one-pion exchange (OPE)-to-"searched" transition energies (E_{tr}) is brought out. Corrections for virtual discontinuities in phase-shift-energy dependence at the E_{tr} decreased the violation of long-range charge independence (LRCI). The effect of two-pion exchange (TPE) has been calculated on the ps theory as ≈ 1 for $g_0^2(p-p) - g_0^2(n-p)$, $g_0^2 = g^2/\hbar c$; a result consistent with LRCI. Searching all phase parameters including g^2 for both isospin values I in g^2 determinations from n–p data, but with fixed I = 1 non-OPE phases as deduced from p–p data in the base search with frozen g^2, the OPE effect of the neutral pion, π^0, was separated from that of the charged pion, π^c. The g^2 for π^c in n–p scattering is determined with much better statistical accuracy than that for π^0. The overall n–p value of g^2 is nearly equal to that for π^c. The results suggest that the distinction between p–p and n–p values of g^2, if present, is in first approximation that arising from the difference between π^0–N and π^c–N couplings. Some limitations on the validity of the conclusions are mentioned. (auth)

36523 IMPROVEMENT TO THE MULTIPLE-SCATTERING EXPANSION OF THE THEORETICAL OPTICAL POTENTIAL. Giannini, M. M. (Univ., Genoa. Istituto Nazionale di Fisica Nucleare, Genoa). Nuovo Cim.; 3A: No. 2, 365-70(21 May 1971).

An approximation, which is introduced in Watson's derivation of the theoretical optical potential, is discussed. This approximation consists of neglecting the projection operator on the target ground state in the equations which define the "single-scattering" matrices. Comparison with the calculations made by Johnston and Watson shows that this approximation is equivalent to neglecting, in the optical-potential expansion, a term which is of second order in the scattering matrices and of order 1/A. (auth)

36524 ALLOWANCE FOR THE COULOMB INTERACTION IN THE SCATTERING OF A FAST CHARGED PARTICLE BY A NUCLEUS. Kondratyuk, L. A.; Kopeliovich, V. P. JETP Lett. (USSR) (Engl. Transl.); 13: No. 3, 123-6(5 Feb 1971).

Translated from Zh. Eksp. Teor. Fiz., Pis'ma Red.; 13: No. 3, 176-9(5 Feb 1971).

On the basis of the assumption that the Glauber formula for the scattering amplitude holds when account is taken of only the strong interactions with the pion with nucleons of a given nucleus, it is proven that to take into account the Coulomb interaction of the pion with protons it is sufficient to make the substitution $\delta^p(\vec{\rho}) \to \delta^p(\vec{\rho}) + \delta^c(\rho)$, where $\delta^p(\rho)$ and $\delta^c(\rho)$ are respectively the nuclear and Coulomb phases for the scattering of the pion by the free proton, and $\vec{\rho}$ is the impact parameter. Charged pion reactions with helium-4, carbon-12, oxygen-16, and calcium-40 are considered. (J.F.P.)

36525 SOFT PIONEERING DETERMINATION OF THE INTERMEDIATE RANGE NUCLEON–NUCLEON INTERACTION. Brown, G. E.; Durso, J. W. (NORDITA, Copenhagen. State Univ. of New York, Stony Brook). Contract AT(30-1)-4032. Phys. Lett.; 35B: No. 2, 120-4(10 May 1971).

XUM

It is shown that the nucleon-nucleon interaction in the range $r \approx \hbar/2\mu c$, where μ is the pion mass, is determined by the behavior of the (analytically continued) pion-nucleon scattering amplitudes for small pion momenta nine. This latter behavior is determined from soft-pion theorems. (auth)

36526 NUCLEON–NUCLEON SCATTERING IN HIGH WAVES AND PION–PION DYNAMICS. Chemtob, M. (Univ. of Copenhagen); Riska, D. O. Phys. Lett.; 35B: No. 2, 115-19(10 May 1971).

The two-pion exchange contribution to NN scattering in high waves is calculated within the framework of dispersion theory. The effect of πN resonances and of various available models for the $N\overline{N} \to 2\pi$ helicity amplitudes $f^J_\lambda (J = 0,1)$ on the NN phase parameters is discussed. (auth)

36527 MULTIPLE-SCATTERING THEORY FOR PION–NUCLEUS SCATTERING NEAR THE 3,3 RESONANCE. Charlton, L. A.; Eisenberg, J. M. (Univ. of Virginia, Charlottesville). Ann. Phys. (N. Y.); 63: No. 1, 286-308(Mar 1971).

Multiple-scattering theory is used to calculate differential and total cross sections for the elastic scattering of pions on closed-shell nuclei in the energy range near the 3,3 resonance. A separable form for the fundamental pion–nucleon interaction is used. Results are presented for ^{4}He and ^{16}O, and several of the standard approximation techniques are assessed. Indications are that for all but the lightest of nuclei the multiple-scattering series may not converge near the 3,3 resonance, so that an approach is necessary—such as that used—which allows for an approximate summation of the series. (auth)

36528 $S_{\frac{1}{2}}$ DOUBLETS IN HYPERNUCLEAR AND NUCLEAR PHYSICS. Walecka, J. D. (Stanford Univ., Calif.). Ann. Phys. (N. Y.); 63: No. 1, 219-47(Mar 1971).

Some remarks on the spectroscopy of heavy hypernuclei are developed. In particular, the ground-state $S_{\frac{1}{2}}$ doublets of $^A_\Lambda Z$ hypernuclei with an odd number of core nucleons are examined in detail. Using the present knowledge of the $\Lambda - N$ force, it is shown that the lower member of the doublet can be expected to satisfy the rule $\Pi = (-1)^J$ and predictions are made for the doublet splittings throughout the periodic table. The magnetic moments of the doublet states are predicted as well as the M-1 transition rate between them. A similar analysis is carried out for the known $S_{\frac{1}{2}}$ doublets in odd-odd nuclei, and a comparison with experiment in this case yields some insight into the validity of the various predictions for hypernuclei. (auth)

36529 SHELL-MODEL ANALYSIS OF Λ BINDING ENERGIES FOR THE p-SHELL HYPERNUCLEI. I. BASIC FORMULAS AND MATRIX ELEMENTS FOR ΛN AND ΛNN FORCES. Gal, A. (Hebrew Univ., Jerusalem); Soper, J. M.; Dalitz, R. H. Ann. Phys. (N. Y.); 63: No. 1, 53-126(Mar 1971).

A uniform intermediate-coupling shell model is formulated for the p-shell Λ hypernuclei, those belonging to the configuration $\{(1s)^4_N(1p)^{A-5}_N(1s)_\Lambda\}$, using NN parameters obtained from previous fits to the corresponding core nuclei. The physical origins of the ΛN forces are discussed, with special attention to the noncentral components, and the characteristics of the three-body double-OPE ΛNN interaction are reviewed briefly. Expressions are derived for all the ΛN and ΛNN matrix elements needed for the discussion of these configurations. Attention is drawn particularly to their qualitative characteristics. For the purpose of orientation, numerical estimates of them are given for all possible types of ΛN forces and for all the constituents of the double-OPE ΛNN interaction, using explicit forms for the radial wave functions, as a basis for the purely phenomenological analysis (now complete) of the data available on the p-shell hypernuclei. (auth)

36530 MODEL FOR THE PRODUCTION OF PARTICLES WITH SUPERSTRONG INTERACTIONS: ESTIMATES OF LOWER BOUNDS ON THE QUARK AND MONOPOLE MASSES. Newmeyer, J. L.; Trefil, J. S. (Univ. of Virginia, Charlottesville). Phys. Rev. Lett.; 26: No. 24, 1509-12(14 Jun 1971).

When particles like quarks and magnetic monopoles are produced in pairs, there is a suppression of the production due to the superstrong attractive forces which exist between the constituents of the pair. An approximate way of incorporating this effect into a production model is presented and lower bounds on the masses of the particles are estimated from present experimental data using our method in conjunction with the standard statistical model. (auth)

36531 IMPORTANCE OF USING EXACT FORMS FOR SCATTERING AMPLITUDE IN REGGE POLE THEORY. Krasznovszky, S.; Nemeth, G.; Pinter, Gy. (Central Research Inst. for Physics, Budapest). Acta Phys. Acad. Sci. Hung.; 30: No. 1, 83-7(1971).

It is shown that the asymptotic forms for the Legendre functions in the expression for the scattering amplitude may lead in some cases to substantially different results from those obtainable using forms which agree in the critical regions with the exact values within 1%. The measurement considered covered the differential cross section for p + p elastic scattering observed at a fixed angle of 90° in the cms system as a function of the squared four-momentum transfer at large values when the angular momentum of the incoming protons varied from 5 to 13.4 GeV/c. (J.F.P.)

36532 OPTIMIZED POLYNOMIAL REPRESENTATION OF SCATTERING AMPLITUDES AND ITS APPLICATION TO ANALYSIS OF p–p AND K^+–p SCATTERINGS. Chao, Yung-an. Pittsburgh; Carnegie-Mellon Univ. (1971). 109p. University Microfilms Order No. 71-9676.

Thesis.

The theory on optimized polynomial representations of scattering amplitudes and Cutkosky's model of estimating truncation errors are described. The formalism for applying these new techniques to the p–p phase-shift analysis is worked out. Examination of self-consistency of the Livermore energy-dependent solutions of p–p phase-shift analyses are made. Reanalyses at single energies, 210 MeV and 330 MeV, by using the Livermore second derivative matrices are carried out, and significant improvements over the Livermore results are found. Differential cross section data on p–p and K^+ – p scatterings are analyzed by this new method to estimate forward nonspinflip amplitudes and coupling constants in pole terms. (Diss. Abstr. Int., B)

36533 RECENT INTEREST IN HADRON–NUCLEUS COLLISIONS. Subramanian, A. (Tata Inst. of Fundamental Research, Bombay). pp 250-4 of Proceedings of the Eleventh Symposium on Cosmic Rays, Astrophysics, Geophysics and Elementary Particle Physics, 1969. Vol. I. Bombay; Department of Atomic Energy (1969).

From eleventh symposium on cosmic rays, astrophysics, geophysics and elementary particle physics; Delhi, India (7 Oct 1969). See CONF-691055–(Vol.1).

In this review of hadron reactions with nuclei at high energies, the Glauber theory is mainly considered. Various experiments are also briefly described. It is pointed out that the main interest in these studies is the density distribution of nucleons in nuclei and also information on total cross sections on nucleons of unstable particles and resonances. (J.F.P.)

36534 LARGE-ANGLE PROTON–PROTON SCATTERING AT HIGH ENERGIES. Ammiraju, P. (Tata Inst. of Fundamental Research, Bombay). pp 483-7 of Proceedings of the Eleventh Symposium on Cosmic Rays, Astrophysics, Geophysics and Elementary Particle Physics, 1969. Vol. II. Bombay; Department of Atomic Energy (1969).

From eleventh symposium on cosmic rays, astrophysics, geophysics and elementary particle physics; Delhi, India (7 Oct 1969). See CONF-691055–(Vol. 2).

An attempt was made to fit the π^-p data at 9.85 GeV/c for the angular distributions. Also a formula is used for cross sections of large-angle proton–proton elastic scattering. The results are shown graphically. (J.F.P.)

36535 MONTE CARLO CALCULATIONS AND THE LIFETIME OF HEAVY HYPERFRAGMENTS. Singh, Triyug (Jammu Univ., India); Prakash, Y.; Bhalla, K. B.; Lokanathan, S. pp 505-8 of Proceedings of the Eleventh Symposium on Cosmic Rays, Astrophysics, Geophysics and Elementary Particle Physics, 1969. Vol. II. Bombay; Department of Atomic Energy (1969).

From eleventh symposium on cosmic rays, astrophysics, geophysics and elementary particle physics; Delhi, India (7 Oct 1969). See CONF-691055–(Vol.2).

The results of Monte Carlo calculations simulating the production and decay of hyperfragments are presented, and the lifetimes are calculated. A comparison is made with experimental results of 1.5 and 3.5 GeV/c K^- meson interactions. (J.F.P.)

36536 POTENTIALS WITH HARD-CORE REPULSION AND NUCLEAR THREE-BODY PROBLEM. Belyaev, V. B.; Zubarev, A. L. (Joint Inst. of Nuclear Research, Dubna, USSR). Fizika (Zagreb); 3: No. 2, 77-89(Apr 1971). (In Russian).

Several alternative approaches are considered for calculation of the three-particle systems consisting of particles, interacting with the help of the potential with the hard core repulsion at small distances. It is established that the phase of scattering on the "hard shell" potential is invariant with respect to the arbitrary function added inside the shell. The Bateman method for the potentials with the hard core repulsion is generalized. The doublet length for n–d scattering and the tritium binding energy for such potentials are calculated. (auth)

36537 INTERACTION POTENTIAL BETWEEN α-PARTICLE TAKING INTO ACCOUNT THEIR MEASUREMENT. Yanavichyus, A. I. (Pedagogical Inst., Shaulyai, USSR). Liet. Fiz. Rinkinys; 10: No. 4 513-20(1970). (In Russian).

Regge theory is applied to obtain interaction potential between two α-particles. The main assumption which allows one to get numerical results is that potential crosses zero at the distance 1–2 F. Previous experimental data were used. The obtained potential has a repulsive barrier and reasonable depth. (auth)

36538 INVESTIGATION OF NUCLEON–NUCLEON CORRELATIONS BY MEANS OF HIGH-ENERGY SCATTERING. Kofoed-Hansen, O. (CERN, Geneva); Wilkin, C. Ann. Phys. (N. Y.); 63: No. 2, 309-18(Apr 1971).

The possible effects of short-range dynamical nucleon–nucleon correlations on high-energy hadron scattering on ^{4}He are examined. The Glauber theory of multiple scattering is used as the basis for the computations. The conclusion is that very small effects are to be expected for elastic and sum total inelastic scattering of commonly available projectiles. (auth)

36539 K-MESIC ATOMS AND HYPERNUCLEI. Mitter, H. (Univ., Tuebingen, Ger.). pp 121-35 of 35. Physikertagung 1970 Hannover. Stuttgart; B. G. Teubner (1970). (In German).

From thirty-fifth physicists conference; Hanover, Germany (Sep-Oct 1970). See CONF-700954.

A review is presented of the latest experimental and theoretical data on K-mesic atoms and hypernuclei. The physical data that can be obtained from a study of these two types of particles are indicated. (J.S.R.)

Particle Invariance Principles and Symmetries

General

Refer also to abstracts 36711 and 36844.

36540 A POSSIBLE TEST OF THE VALIDITY OF TIME REVERSAL. Logan, B. A. (Univ. of Ottawa). Can. J. Phys.; 49: 1162-6(1 May 1971).

A possible test of the validity of symmetry under time reversal is discussed. It is proposed to investigate time reversal by measuring any imaginary component of the mixing ratio in the mixed dipole–quadrupole transitions between nuclear levels. The experimental method is based on measurements of the angular correlation of a cascade from a level which is oriented by the inelastic scattering of polarized protons. The method is capable of improving on the accuracy of previous investigations. (auth) (Canada)

36541 BROKEN CONFORMAL INVARIANCE. Katz, J. (Purdue Univ., Lafayette, Ind.). Nuovo Cim.; 3A: No. 2, 263-70(21 May 1971).

The equal-time commutator algebra satisfied by the generators of the broken conformal group is derived. These expressions are then used to discuss Coleman's theorem for dilatations and conformal transformations and to give necessary and sufficient conditions in order for all the components of a local operator to have the same dimension. (auth)

36542 BROKEN SCALE INVARIANCE IN PARTICLE PHYSICS. Carruthers, P. (California Inst. of Tech., Pasadena). Phys. Rep.; 1C: No. 1, 1-29(Mar 1971).

The general theoretical questions such as the proper way to describe the breaking of scale invariance, and the relation to short distance behavior in field theory, are reviewed. The possible role of scale and conformal transformations in the strong interactions is discussed. Topics covered include: the energy momentum tensor in canonical theories; effects of renormalization on scaling; approximate scale invariance; relation between violation of scale invariance and of SU(3) × SU(3); and scaling laws in deep inelastic electroproduction. (L.B.S.)

36543 BARYON–LEPTON CORRESPONDENCE AND SYMMETRY BREAKING. Kaneko, Takao (Meijo Univ., Nagoya, Japan). Progr. Theor. Phys. (Kyoto); 45: No. 1, 326-8(Jan 1971).

A previously proposed scheme in which some ideal SU(3) × SU(3) symmetrical world is broken in two chains is discussed on a more physical basis in accordance with the unified model of elementary particles, especially the baryon–lepton correspondence. The bare mass of urbaryons is also estimated. (J.F.P.)

36544 NEW VIEWPOINT ON THE SPACE–TIME MODEL OF ELEMENTARY PARTICLES. I. Heskia, Said (London Univ.). Progr. Theor. Phys. (Kyoto); 45: No. 1, 277-94(Jan 1971).

An attempt was made to describe the pseudo-unitary group U(3,1) of particle physics on the basis of a classical formulation of the nonlocal theory of Yukawa in contrast to quantum mechanical approach of Takabayasi, Shin and others. This is done by describing the group U(3,1) as the structural group of the frame bundle of the eight-dimensional classical relativistic space $B_{8,2} = (X,y)$ (where X denotes the external co-ordinates of Yukawa). Such a classical approach to the group U(3,1) has the novel feature of enabling one to interpret the gauge vector fields and the gauge tensor fields, which are associated with the gauge extension of this group, as the manifestation of the local connection and the local curvature of the classical space $B_{8,2}$. This is achieved by postulating that the classical gauge fields give rise to a strong inhomogeneity in the neighborhood of a point of the $B_{8,2}$ space so that there exists a y-dependent Riemann curvature in this space. Then by interpreting the group U(3,1) as the group of holonomy of $B_{8,2}$ it is shown that the expansion coefficients of the connection and curvature of the tangent bundle of $B_{8,2}$, which are elements of the holonomy group of $B_{8,2}$, constitute the bilocal generalization of the gauge vector field and the gauge tensor field of Yang and Mills, respectively. (auth)

36545 PROJECTION OPERATOR TECHNIQUES FOR SU(n) AND AN SU(9) THEORY OF ELEMENTARY PARTICLES. Schott, John T. Bronx, N. Y.; Fordham Univ. (1970). 156p. University Microfilms Order No. 71-8740.

Thesis.

General projection operator techniques for SU(n) are developed and a physical application of the unitary groups, employing the particular group SU(9), is presented. A review of the fundamental properties of continuous groups and SU(n), in particular, as well as the general projection operator for arbitrary compact Lie groups, is given. A theorem of Shapiro allows the matrix elements of this projection operator between product states, to be related to matrix elements of P^0, the projector onto the identity representation. Specializing to SU(n), an expression for $P^0(n)$, in terms of the generators of SU(n), is sought. Using the chain SU(n) ⊃ SU(n – 1) ⊃ ... ⊃ SU(2), a simple expression is found in terms of $P^0(n-1)$ and an operator R(n) which involves only one generator and its adjoint and ultimately, by iteration, in terms only of R(1) for $1 = 2, \ldots, n$. The Gel'fand basis is introduced and a formalism is developed for the calculation of matrix elements of $P^0(n)$ relative to a product basis of Gel'fand states. Tables can be constructed of certain polynomial coefficients, f^j_{ji}, from which matrix elements can easily be found for any number of states in a product basis. A simple example is worked out. The magnetic monopole theories of Schwinger and Dirac and the dyon model of Schwinger are reviewed. The group SU(9) is developed in terms of its subgroup SU(3) × SU(3) and is applied to the dyon model. Particle assignments in SU(9) (and its extension SU(1C)) are made which allow any SU(3) or SU(6) results to be reproduced. A study of mass formulas, related to an attempt to make further particle assignments in multiplets containing magnetically charged states, leads to a qualitative model for the observed spectrum of SU(3) multiplets of baryons and mesons. Examples of SU(9) ⊃ SU(3) × SU(3) calculations are given. (Diss. Abstr. Int., B)

36546 IS TIME-REVERSAL INVARIANCE VIOLATED IN ELECTROMAGNETIC INTERACTIONS? Ramachandran, G. (Indian Statistical Inst., Calcutta). pp 493-6 of Proceedings of the Eleventh Symposium on Cosmic Rays, Astrophysics, Geophysics and Elementary Particle Physics, 1969. Vol. II. Bombay; Department of Atomic Energy (1969).

From eleventh symposium on cosmic rays, astrophysics, geophysics and elementary particle physics; Delhi, India (7 Oct 1969). See CONF-691055-(Vol.2).

The elastic scattering of electrons on deuterons is considered for T-violation effects. It is shown that it is possible to account for the observed experimental deviations in the cross sections on the basis of the phase difference hypothesis without the need for T violation in electromagnetic interactions. (J.F.P.)

36547 GENERALIZED O(2,1) EXPANSION FOR ASYMPTOTICALLY GROWING AMPLITUDES. Jones, C. Edward; Low, F. E.; Young, J. E. (Massachusetts Inst. of Tech., Cambridge. Los Alamos Scientific Lab., N. Mex.). Contract AT(30-1)-2098. Ann. Phys. (N. Y.); 63: No. 2, 476-96(Apr 1971).

It is shown how the conventional O(2,1) expansion for square integrable many-particle amplitudes may be generalized to functions which grow no faster than a power of the energy. The method is somewhat analogous to the use of the Laplace transform for O(1,1) (Fourier) expansions. Simple derivations of the

XUM

needed properties for the O(2,1) representations are included. Mathematical details are given. Expansions of the type considered may be of use in diagonalizing dynamical equations. (auth)

36548 INTRINSICALLY SELF-CONJUGATE BOSON STRUCTURE: THE SYMPLECTON. Biedenharn, L. C. (Duke Univ., Durham, N. C.); Louck, James D. Ann. Phys. (N. Y.); 63: No. 2, 459-75(Apr 1971).

By explicit construction a primitive minimal realization of the SU(2) ≅ Sp(2) symmetry group in terms of a single boson operator is demonstrated. The construction denies the usual "boson calculus rule" $(\bar{a}\,|\,0\rangle \equiv 0)$ and as such constitutes a generalization of the boson calculus. The resulting inherently conjugation symmetric structure is denoted as a symplecton. (auth)

36549 ELEMENTARY PARTICLES AND SYMMETRY. Wild, Wolfgang (Technische Hochschule, Munich). pp 90-120 of 35. Physikertagung 1970 Hannover. Stuttgart; B. G. Teubner (1970). (In German).

From thirty-fifth physicists conference; Hanover, Germany (Sep-Oct 1970). See CONF-700954.

The classification of elementary particles from the viewpoint of the SU_2, SU_3, and SU_6 symmetries has led to a very extensive understanding of the uniformities in the meson and baryon spectra. Whether these symmetries have their dynamic basis in a structure of the elementary particles from more simple building stones (quarks) must be considered as still unresolved. The symmetry principles derived from phenomenology have not yet been correlated into a relativistic, invariant, self-consistent, dynamic theory. (tr-auth)

Applications (Electromagnetic and Weak)

Refer also to abstract 36466.

36550 (COO-1749-24) SEARCH FOR A CP-NONCONSERVING ASYMMETRY IN THE DECAY $K_L^0 \to \pi^+\pi^-\pi^0$. Levit, Lawrence B. (Case-Western Reserve Univ., Cleveland, Ohio. Dept. of Physics). Jan 1971. 94p. Dep. NTIS.

Thesis.

The purpose of this experiment was to test CP symmetry in the decay $K_L^0 \to \pi^+\pi^-\pi^0$. A search was made for a charge asymmetry revealing itself as a difference between the π^+ and π^- transverse momentum spectra. The experimental configuration was three hodoscopes in line and a momentum analyzing magnet. The experimental limit set by this experiment was calculated from the data for which both charged π mesons were detected, and one γ-ray from the π^0 decay was identified. This constitutes 400,000 events. The experimental data were analyzed by a Monte Carlo fitting procedure. The best value obtained for the CP violating parameter, $\sigma\pm$, was 0.0001 ± 0.0009. Estimates of all biases that could mask the asymmetry are included in the uncertainty quoted above. Two previous experiments have shown no asymmetry to a precision of 0.02, and one experiment exhibited a $2\frac{1}{2}$ standard deviation effect of 0.04. The result of this experiment is consistent with CP invariance. (auth)

Applications (Strong)

36551 $\eta-X$ MIXING IN THE GMOR MODEL. Dutt, R.; Eliezer, S. (Technion-Israel Inst. of Tech., Haifa). Lett. Nuovo Cim.; 1: No. 22, 918-22(29 May 1971).

The $\eta-X$ mixing in the broken chiral SU(3) × SU(3) model is studied. A way of obtaining the mixing angle in this model avoiding the use of the mass formula and the mass of the κ meson is presented. (J.F.P)

36552 TEORIYA UNITARNOI SIMMETRII. (Theory of Unitary Symmetry). Rumer, Yu. B.; Fet, A. I. Moscow; Izdatel'stovo Nauka Glavnaya Redaktsiya Fiziko-Matematicheskoi Literatury (1970). 400p.

A mathematical introduction, unitary classification of hadrons, and mass formulas are given. The main facts from the theory of complex linear spaces and construction over them, the main properties of groups, algebras, and their representations are presented. In the discussion the accurate formulations of the definitions and theorems are given; the proofs of the theorems are as a rule omitted. Numerous comments are included, which explain the significance and formulation of the given results. The detailed investigation of these special groups (and their representations) is described which are necessary for the description of strong interaction symmetry, i.e. the groups SU(2), SU(3), SU(4), and SU (6). Attention is given to the physical aspects of the theory. The derivation of mass formulas is treated in a way which is more physical than mathematical. A new proof for the mass formulas is proposed, which permits a more extensive treatment. (tr-auth)

36553 NEW SU(3) CLASSIFICATION OF VECTOR MESONS. Chand, Prakash (Colorado State Univ., Fort Collins). Fizika (Zagreb); 3: No. 2, 71-6(Apr 1971).

The Gell-Mann–Okubo mass formula for vectons is examined. It is shown that if one includes the B-mesons in the list of vectons, the G-O mass formula is exactly satisfied. This leads to the existence of two octets of vectons and suggests that the $\omega-\varphi$ mixing can be abandoned. Further consequences of this assumption are considered. (auth)

Field Theories

General

36554 EXACT SOLUTION CORRESPONDING TO A SPECIAL FIELD STRUCTURE IN SCHROEDINGER'S UNIFIED FIELD THEORY. Tiwari, R. N. (Indian Inst. of Tech., Kharagpur). Tensor; 22: No. 1, 82-6(Jan 1971).

A general solution for the Schroedinger para-form field equations is obtained. The derivation of the solution is based on a previously obtained solution. The Schroedinger field equations and their solutions and the derivation of the solution of the Einstein weak form equations are treated. (J.F.P.)

36555 SPECIAL SOLUTION OF THE FIELD EQUATIONS IN THE CASE OF THE CHARACTERISTIC [(211)]. Isaak, S. (Univ. of South Florida, Tampa). Tensor; 22: No. 1, 48-52(Jan 1971).

A sufficient condition is established for a reduction of the number of unknown on which $g_{\lambda\mu}$ depends to 2 and a reduction of the number of Cauchy data to 3. (J.F.P.)

36556 CLASSICAL FIELDS, PARTICLES, AND THE THEORY OF RELATIVITY. Davis, William R. New York; Gordon and Breach, Science Publishers, Inc. (1970). 412p. $27.50.

An attempt is made to give a logical presentation that stresses the fundamental principles tending to unify all physics. Kinematical methods are stressed, and methods using orthonormal vector tetrads are used. The topics covered are space–time and the Lorentz group, introduction to relativistic mechanics, Lorentz covariant classical theory of fields, the Maxwell–Lorentz electrodynamics and radiating classical electrons, and introduction to the general theory of relativity. (J.F.P.)

36557 INFINITE-COMPONENT WAVE EQUATION AND SCATTERING AMPLITUDE. Goto, Tetsuo; Otokozawa, Jun (Nihon Univ., Tokyo). Progr. Theor. Phys. (Kyoto); 45: No. 1, 263-76(Jan 1971).

The scattering amplitude of an infinite component field under a scalar external field is calculated in the lowest order diagram. It is explicitly shown that from the crossed diagram the Regge pole does not arise and, therefore, two amplitudes corresponding to ordinary and crossed diagrams cannot be continued analytically from one to another. (auth)

36558 GAUGE FIELDS IN THE NONLINEAR REALIZATION OF A GROUP ON ITS SUBGROUP. Okabayashi, Takao; Watanabe, Tadashi (Tokyo Univ.). Progr. Theor. Phys. (Kyoto); 45: No. 1, 243-62(Jan 1971).

The commutability of the boosting procedure with the process to localize the group parameters is discussed based on the formalism of the nonlinear realization of a group on its sub-group developed previously. It is concluded that any gauge fields cannot be introduced into the scheme consistently. (auth)

36559 HOMOGENEOUS NONSTATIC SOLUTIONS OF EINSTEIN–MAXWELL FIELD-EQUATIONS FOR AN ISOTROPIC SPACE–TIME. Iyengar, V.; Mohan, K. (Osmania Univ., Hyderabad, India). Istanbul Univ. Fen Fak. Mecm., Seri A; 32: 33-6 (1971).

Solutions of the Einstein–Maxwell field-equations in vacuo for spatially homogeneous electromagnetic fields are considered. It is found that, except for certain times, the metric is regular everywhere, there is no magnetic-field and there is an electric-field of equal strength in the x, y and z directions which increases with time. (auth)

Quantum Field Theory

Refer also to abstracts 36378 and 36591.

36560 (ITF-70-96-P) ABSOLUTE, CONVECTIVE AND GLOBAL UNSTABILITIES, AMPLIFICATION AND NON-TRANSMISSION OF VIBRATIONS. Akhiezer, A. I.; Polovin, R. V. (Akademiya Nauk Ukrainskoi SSR, Kiev. Institut Teoreticheskoi Fiziki). 1970. 94p. (In Russian). Dep. NTIS (U. S. Sales Only).

The review of criteria of the absolute, convective and global instability and criteria of the amplification and nontransmission of vibrations is presented. (auth)

36561 (JINR-P2-5716) CONFORMAL-COVARIANT INTERACTIONS. Tagirov, E. A. (Joint Inst. for Nuclear Research, Dubna (USSR). Lab. of Theoretical Physics). 1971. 16p. (In Russian). (CONF-700342-1). Dep. NTIS (U. S. Sales Only).

From second international conference on the linear and nonlocal quantum field theory; Dubna, USSR (15 Mar 1970).

Necessity and consequences of approximate conformal covariance of field equations are considered. A connection between conformal covariance and gauge invariance of interactions is established. (auth)

36562 (JINR-P2-5760) PARTIAL ELIMINATION OF INFRARED DIVERGENCES IN THE MODEL OF QUANTUM FIELD THEORY WITH DEGENERATED VACUUM. Zastavenko, L. G. (Joint Inst. for Nuclear Research, Dubna (USSR). Lab. of Theoretical Physics). 1971. 16p. (In Russian). Dep. NTIS (U. S. Sales Only).

The model of a scalar charged field with self-action in two-dimensional space-time is considered for the case when the vacuum is degenerated. In the quantum field theory with degenerated vacuum the particles with zero rest mass are necessarily present which induces the appearance of infrared divergences. It is shown that taking account of some class of diagrams together with each divergent diagram determining this class leads to annihilation of the divergences in the expressions for mean values; in this case in the expansion over small parameter $1/\beta$ there appear nonanalytical terms $\approx \ln \beta/\beta$ when $1/\beta = 0$. (auth)

36563 (ORO-3992-26) ANALYTICITY, COVARIANCE, AND UNITARITY IN INDEFINITE METRIC QUANTUM FIELD THEORIES. Gleeson, A. M.; Moore, R. J.; Rechenberg, H.; Sudarshan, E. C. G. (Texas Univ., Austin. Center for Particle Theory). Dec 1971. Contract AT(40-1)-3992. 38p. (CPT-77; AEC-26). Dep. NTIS.

The general properties of analyticity, covariance, and unitarity are studied in quantum field theories regularized by finite-mass indefinite norm states. After reviewing the general status of indefinite metric theories, a relativistic scalar model is analyzed for covariance and analyticity. This model shows that a commonly accepted prescription for treating the negative norm states is not covariant, and more sophisticated methods are required. A modified prescription obtained as a limit of the previous result is tested in a more complicated diagram and found to be inadequate for the correction of unitarity difficulties. The general technique of shadow states developed elsewhere is reviewed in order to show their relevance to this problem. (auth)

36564 (ORO-3992-30) INDEFINITE METRIC AND SHADOW STATES IN QUANTUM FIELD THEORY. Sudarshan, E. C. G. (Texas Univ., Austin. Center for Particle Theory). Nov 1970. 13p. (CPT-81; AEC-30). Dep. NTIS.

Fundamental questions in relativistic quantum field theories are discussed. It is argued that the introduction of states with negative norm provides a way out of the divergence difficulties in realistic quantum field theories. In order to assure the probability interpretation the concept of shadow states and ideas from an action-at-a-distance theory are introduced. (auth)

36565 PERTURBATIVE SOLUTIONS OF RENORMALIZATION GROUPS. Irac-Astaud, M. (College de France, Paris). Nuovo Cim.; 3A: No. 2, 323-46(21 May 1971).

The functional equations of the renormalization "groups" formulated in a preceding paper do not contain much physical information. It is shown that they can lead to interesting consequences when accompanied by suitable hypothesis. (auth)

36566 COVARIANT QUANTUM ELECTRODYNAMICS IN TERMS OF A POSSIBLE ETHER FLOW. Brevik, I. Ark. Fys. Seminar Trondheim: No. 4, (1971).

Three topics are examined. First it is shown that the fundamental reason for the difficulties met in the quantization of the free electromagnetic field should not be considered to lie in the incompatibility between the Lorentz condition and the canonical commutation rules. Rather, the difficulties arise already on the level of Maxwell's equations, as these equations (solved in terms of the potentials) get into conflict with generally accepted postulates of relativistic quantum field theory. Secondly, by permitting the existence of an extra parameter $V\mu$ of the nature of a four-velocity in the formalism, it is shown that a covariant quantum electrodynamic theory can be constructed which reconciles Maxwell's equations with the general field theoretical postulates. With the use of a set of covariant basis vectors the Fourier components of the potential become Lorentz invariants. For each value of the photon momentum only two of these components are subject to quantization, the remaining c-number components being unphysical and adjustable by restricted gauge transformations. Finally the possibility of associating $V\mu$ with the four-velocity of an ether is investigated. This cannot reasonably be done in classical terms, as an ether of such a kind would destroy the isotropy of space in a vacuum. The isotropy can be restored, however, by picturing the ether as a quantal object. In this way there will be no conflict between the ether hypothesis and the principle of relativity. Possible influence from the ether on observable phenomena is discussed. The final conclusion with respect to the ether hypothesis is that, although the evidence for the actual existence of an ether at present is meagre, the hypothesis is nevertheless in accordance with fundamental physical principles and deserves attention. (auth)

36567 RECOIL CORRECTIONS MADE EASY. Bodine, Norman Ralph. Seattle; Univ. of Washington (1970). 132p. University Microfilms Order No. 71-8459.

Thesis.

A new approximation procedure for treating the two-body problem in quantum electrodynamics was developed. It is useful when one of the two particles can be well approximated to be infinitely massive. By means of an expansion about the limit of an infinitely massive particle, the amplitude for the interaction of a relativistic particle with a heavy nonrelativistic particle is treated to first order in the ratio of the masses of the two particles in the approximation where photon-photon interactions and radiative corrections to the heavy particle are ignored. A Green's function is found for this situation which is applicable to both scattering problems and bound state problems. The Lamb shift in hydrogen is investigated using this approach and is found to agree with previous calculations of this number. In this investigation both radiative corrections and recoil corrections are treated together. (Diss. Abstr. Int., B)

36568 METHODS OF THE BETHE-SALPETER EQUATION. Kershaw, David Stanley. Berkeley, Calif.; Univ. of California (1970). 61p. University Microfilms Order No. 71-9842.

Thesis.

As a step toward being able to do practical bootstrap calculations in elementary particle physics, a new method of solving the Bethe-Salpeter equation was developed. The Bethe-Salpeter equation is solved in space-time and the method of solution closely parallels the simplest methods for solving the Schrödinger equation. The Bethe-Salpeter is a fourth order, linear hyperbolic equation in two variables (after rotational invariance has been exploited). The usual mathematical treatments draw a sharp distinction between hyperbolic and elliptic differential equations because of the different type of boundary condition with which they are usually associated. For the Bethe-Salpeter equation, however, the natural boundary condition is a "radiation" condition and under the transformation which takes the real time into a negative imaginary time, the boundary conditions remain well defined and go over into natural boundary conditions for the Wick rotated, elliptic Bethe-Salpeter equation. It is shown that this Wick rotation of the time axis is valid for all energies. It is the Wick rotated elliptic Bethe-Salpeter equation which is actually solved. A slight generalization of the usual method of power series solution is used to generate a complete set of solutions to the homogeneous equation which are regular or irregular at the origin. The same method is used to generate a complete set of solutions to the inhomogeneous equation, regular at the origin. Then, from the known Green's function for the physical problem, one determines the free solutions which satisfy the boundary conditions at infinity, as a sum of the free origin solutions with appropriate coefficients. The wave function is then uniquely determined by requiring it to be regular at the origin and at infinity. Using a C.D.C. 6600 high accuracy bound state eigenvalues and scattering phase shifts are found with excellent convergence. (Diss. Abstr. Int., B)

36569 BORCHERS CLASS OF A LOCAL FIELD. Rosenberg, Allan Peter. Durham, N. C.; Duke Univ. (1970). 69p. University Microfilms Order No. 71-10,419.

Thesis.

A quantum field A(x) is an operator-valued tempered distribution. For such distributions powers of A are generally undefined. It follows that equations of motion for A, such as $(\Box + m^2)A(x) = gA^3(x)$ by means of which one might hope to set up a theory of interacting quantum fields, do not make mathematical sense. It would be very desirable to have a procedure for construction of

XUM

distributions which have the physical meaning of terms like $A^n(x)$ but which are mathematically well-defined. One approach to the problem of defining powers of a field is studied. It is assumed that with any useful definition $A^n(x)$ will be local with respect to A(x); it will thus be a member of the Borchers class of A. Next operator-valued distributions defined by their action on the vacuum state are considered, and it is asked under what conditions can they be extended to fields locai with respect to the given field A, and which coincide with the original distribution on the vacuum. Since members of a Borchers class are uniquely labeled by their action on the vacuum, if such an extension exists it is necessarily unique. A set of necessary and sufficient conditions are given. Unfortunately no prescription has yet been found for constructing operator-valued distributions which satisfy these conditions. The possibility of defining local fields in this manner does suggest a particular approach to the problem of defining powers, which is successful for the case of a massive free field. Difficulties of the general case are discussed. It is shown that a scalar product can be defined for members of the Borchers class of A. Some speculations are given about the role of this scalar product in associating with every operator-valued distribution a unique local field. (Diss. Abstr. Int., B)

36570 FIELD THEORETIC CRITERION FOR PARTICLES TO HAVE MASS ZERO. Petzold, Joachim; Gerlach, Bernd (Univ., Marburg, Ger.). Z. Phys.; 244: No. 2, 129-39(1971). (In German).

A new inequality is investigated. This inequality allows one, without use of any field equation, to decide if particles of a certain ensemble have mass zero or not. (auth)

36571 POSSIBLE OBSERVATION OF THE SKEW-SYMMETRIC TENSOR GAUGE FIELD. Miyamoto, Shikao; Nakano, Tadao (Osaka City Univ.). Progr. Theor. Phys. (Kyoto); 45: No. 1, 295-311(Jan 1971).

When the translational gauge transformation for spinning particles, is considered, a vier-bein field is needed in order to keep invariance of the theory. There is a possibility that a skew-symmetric tensor field appears by a linear approximation and maintains its proper position in physical phenomena. It is discussed how to find out effects by this new field. From elastic neutrino scattering experiments one can discuss the existence of the skew-symmetric field. (auth)

36572 VACUUM VECTOR OF THE YUKAWA$_2$ MODEL. Park, Y. (Indiana Univ, Bloomington). Lett. Nuovo Cim.; 1: No. 23, 946-8(5 Jun 1971).

Proof is given of various conditions for the uniqueness of the vacuum vector of the Hamiltonian in Yukawa field theories for small values of the coupling constant. (L.B.S.)

36573 LOWER BOUNDS AND SELF-ADJOINTNESS OF HAMILTONIANS FOR A CLASS OF MODELS. Tirapegui, E. (Univ. of Chile, Santiago de Chile). Nuovo Cim.; 3A: No. 3, 561-83 (1 Jun 1971).

The problem of the existence of a lower bound for the Hamiltonians of a class of models in quantum field theory is studied. The relation of this property to self-adjointness is investigated. (auth)

36574 GEOMETRICAL DESCRIPTION OF THE GENERALIZED GAUGE FIELDS. I. Heskia, S. (London Univ.). Nuovo Cim.; 3A: No. 3, 625-44(1 Jun 1971).

An attempt is made to give a geometrical description of the generalized gauge vector and tensor fields of the group SU_3 in terms of the Riemann connexion and curvature of a six-dimensional almost-Hermitian space. This is achieved by allowing the linear Hermitian space of the almost-Hermitian space, which carries a set of Hermitian connexion and curvature forms, to play the role of an abstract fibre of the space-time manifold and then taking a fibre vector around a loop on this manifold. This gives rise to the internal group of holonomy $H_{int} \subseteq SU_3$ of the event space in such a way that the expansion coefficients of the connexion and the curvature of the internal bundle, which are elements of $H_{int} \subseteq SU_3$, constitute the generalized gauge vector and tensor fields of Yang and Mills, respectively. (auth)

36575 GEOMETRICAL DESCRIPTION OF THE GENERALIZED GAUGE FIELDS. II. Heskia, S. (London Univ.). Nuovo Cim.; 3A: No. 3, 645-56(1 Jun 1971).

As the chiral partners of the internal bundle connexions and curvatures the axial bundle connexions and curvatures are introduced by endowing the linear internal vector space $\hat{T}_6 = (\varphi_\alpha(X), \varphi_{\alpha^*}(X))$ of the event space with the γ_5 matrix of Dirac. This leads to a chiral extension of the internal holonomy group $H_{int} \subseteq SU_3$. The connexion to chiral current algebra is discussed. (auth)

36576 ROLE OF QUANTUM FIELD THEORY IN THE PHYSICS OF THE LAST DECADE. Haag, R. (Univ., Hamburg). pp 20-9 of 35. Physikertagung 1970 Hannover. Stuttgart; B. G. Teubner (1970). (In German).

From thirty-fifth physicists conference; Hanover, Germany (Sep-Oct 1970). See CONF-700954.

The quantum field theory is broadly considered. It is shown as a synthesis between the principles of quantum physics and the special relativity theory. Its applicability is found first of all in the phenomena of elementary particle physics. Its mathematic apparatus is functional analysis. (J.S.R.)

Gravitation and General Relativity

Refer also to abstracts 35821 and 36443.

36577 CERTAIN TYPE OF EINSTEIN'S SPACE–TIMES. Jakubowicz, Antoni (Inst. of Mathematics, Szczecin, Poland. Technical Univ., Szczecin, Poland). Tensor; 22: No. 1, 73-6 (Jan 1971).

The discussion of a certain type of Einstein space–times covers the equations of motion and field equations. These space times have applications in general relativity theory, the theory of an isolated star, and in the gravitational field of the greater part of the cosmos. (J.F.P.)

36578 SOME SOLUTIONS OF THE INTERNAL PROBLEM IN GENERAL RELATIVITY. Bray, Marcel. Compt. Rend., Ser. A; 272: No. 12, 841-4(22 Mar 1971). (In French).

Some solutions of Einstein's equations in cylindrical coordinates are given. (auth)

36579 CANONICAL FORM OF THE GRAVITATIONAL FIELD EQUATIONS. Bray, Marcel. Compt. Rend., Ser. A: 272: No. 11, 757-9(15 Mar 1971). (In French).

A canonical form of the Einstein equations was established for a special case. (auth)

36580 COMPLETE SCHWARZSCHILD SOLUTION. Rosen, Nathan (Technion–Israel Inst. of Tech., Haifa). Ann. Phys. (N. Y.); 63: No. 1, 127-33(Mar 1971).

Some remarks are made about the complete Schwarzschild solution, consisting of the interior and exterior solutions, joined together. It is pointed out that, if the complete solution is put into the isotropic form, the metric tensor and its first derivatives are everywhere continuous, and the space described by it is topologically equivalent to that of special relativity, provided the radius of the particle of given mass is larger than a certain value. (auth)

36581 MUST IT REALLY BE E = 0? Horsky, J.; Novotny, J. (Purkyne Univ., Brno). Acta Phys. Pol.; A39: No. 3, 369-70 (Mar 1971).

Two expressions for the total mass of a closed static system in general relativity theory are compared. It is concluded that the total mass of the system is different from the Schwarzschild mass for a covariant Lagrangian. (J.F.P.)

36582 MASSIVE SCALAR (MESON) FIELDS IN GEOMETRODYNAMICS. Nagaraj, Muppinaiya (Bangalore Univ., India). Tensor; 22: No. 1, 53-63(Jan 1971).

The inherent geometric properties are discussed in the problem of the geometrization of a massive scalar meson field represented by a real-valued scalar function ϕ, which is defined over a region of the Einstein–Riemann space of general relativity. The admissible Weierstrass characteristic for the scalar field ϕ and energy considerations for the geometrodynamical massive scalar meson field are considered. (J.F.P.)

36583 COMPOSITE SPHERE IN GENERAL RELATIVITY. Bohra, M. L.; Mehra, A. L. (Jodhpur Polytechnic, India). Acta Phys. Acad. Sci. Hung.; 30: No. 1, 89-92(1971).

A solution of the field equations of general relativity which gives the internal structure of a composite sphere having a core of a certain radius and density surrounded by a shell of a different density is described. (J.F.P.)

36584 GRAVITATIONAL WAVES: FACT OR FANTASY. Subbaraman, M. S. (Tata Inst. of Fundamental Research, Bombay). pp 169-82 of Proceedings of the Eleventh Symposium on Cosmic Rays, Astrophysics, Geophysics and Elementary Particle Physics, 1969. Vol. I. Bombay; Department of Atomic Energy (1969).

From eleventh symposium on cosmic rays, astrophysics, geophysics and elementary particle physics; Delhi, India (7 Oct 1969). See CONF-691055–(Vol.1).

Some properties of gravitational waves which arise from a study of the solutions and equations in the weak-field approximations are discussed. The production and detection of gravitational waves, the earth as a gravitational detector, the Weber Maryland detector and preliminary experiments, and the Maryland–Argonne experiment are considered. (J.F.P.)

36585 GRAVITATIONAL RADIATION EXPERIMENTS. Weber, J. (Univ. of Maryland, College Park). pp 191-222 of 35. Physikertagung 1970 Hannover. Stuttgart; B. G. Teubner (1970).

From thirty-fifth physicists conference; Hanover, Germany (Sep-Oct 1970). See CONF-700954.

An account is given of recent experimental research on gravitational radiation together with some discussion of the instrumentation. (auth)

Scattering Theory

36586 (JINR–E2-5771) RELATIVISTIC THREE-PARTICLE PROBLEM IN TERMS OF THREE-DIMENSIONAL VARIABLES. Kvinikhidze, A. N.; Stoyanov, D. Ts. (Joint Inst. for Nuclear Research, Dubna (USSR). Lab. of Theoretical Physics). 1971. 27p. Dep. NTIS (U. S. Sales Only).

Using the retarded part of the two-time Green function of three particles the equations determining the relativistic scattering amplitudes of all possible 16 transitions in three-body system are obtained. These equations do not contain the relative energies and are the relativistic generalization of the Faddeev equations. The equations for the wave functions of three-particle bound state are also derived. (auth)

36587 (JINR–P2-5768) FUNCTIONAL INTEGRATION AND REGGE-EIKONAL REPRESENTATION OF THE SCATTERING AMPLITUDE. Barbashov, B. M.; Nesterenko, V. V. (Joint Inst. for Nuclear Research, Dubna (USSR). Lab. of Theoretical Physics). 1971. 14p. (In Russian). Dep. NTIS (U. S. Sales Only).

In scalar model $g\psi^2\phi$ by the functional integration method in the straight-line way approximation the Regge-eikonal representation was obtained for the amplitude of high-energy particle scattering. All kinds of ladder diagrams with the "multi-tower" exchange were summed within the given approximation. (auth)

36588 COLLIDING POLE AND BRANCH POINT AS A MODEL FOR A SELF-CONSISTENT POMERANCHUK SINGULARITY. Branson, D. (Univ. of Essex, Colchester, Eng.). Nuovo Cim.; 3A: No. 2, 271-86(21 May 1971).

The multiperipheral integral equation of Chew, Goldberger and Low, restricted to the case of forward scattering, is modified in order to accommodate a Regge cut or multiple pole as input. It is shown that the leading output singularity is either a simple pole or a branch point, depending on the nature of the input singularity and the strength of its coupling. The mean multiplicity of particle production is discussed in each case. For a particular value of the coupling strength a self-consistent solution is obtained corresponding to an asymptotic behavior $s/(\log s)^{\beta}$, where $\beta = \frac{2}{3}$ if the input trajectory is flat and $\beta = \frac{1}{3}$ if the trajectory rises linearly. Examination of the nonforward case shows that the output singularity should be regarded as a pole and a branch point which coincide in the forward direction, the pole residue vanishing at that point. (auth)

36589 USE OF THE GREEN FUNCTION METHOD FOR THE SCATTERING OF A PARTICLE ON A SYSTEM OF BOUND PARTICLES. Janev, R. K.; Zivanovic, D. (Boris Kidric Inst., Belgrade). Fizika (Zagreb); 3: 29-40(1971).

A method for treating elastic and inelastic scattering of a particle on a system of bound particles, using the many-body techniques, is presented. The optical potential model for the elastic scattering is discussed, and the way of direct inclusion of the self-consistent incoherent terms is given. Analogous procedure for the inelastic scattering is described. (auth)

36590 HIGH ENERGY APPROXIMATIONS IN POTENTIAL SCATTERING THEORY. Rihan, T. H. (Atomic Energy Establishment, Cairo). Phys. Lett.; 35B: No. 2, 133-4(10 May 1971).

The relation between the Glauber eikonal and the Blankenbecler and Goldberger impact parameter representation is discussed on the basis of a separable potential model for the scattering amplitude. In this way a correction to both approximations is proposed. (auth)

36591 ALGEBRAIC TREATMENT OF SUBSIDIARY CONDITIONS IN DUAL RESONANCE MODELS. Fubini, S.; Veneziano, G. (Massahchusetts Inst. of Tech., Cambridge). Contract AT(30-1)-2098. Ann. Phys. (N. Y.); 63: No. 1, 12-27(Mar 1971).

The Ward-like identities previously proposed in order to eliminate unphysical states (ghosts) from dual amplitudes and generalized previously are investigated within the context of the projective operator language. One can generalize further this result to the case of amplitudes with different internal trajectories and release the unphysical condition on the external masses. A purely algebraic treatment of the problem of ghost cancellation is also presented and shown to provide cancellation of ghosts up to to the third excited level. (auth)

36592 VENEZIANO AMPLITUDES FOR FIRST-EXCITED SCALARS. Oyanagi, Yoshio (Tokyo Univ.). Progr. Theor. Phys. (Kyoto); 45: No. 1, 203-7(Jan 1971).

From the factorization of the residue associated with the spinless particle lying on the first daughter trajectory in the multiparticle Veneziano model, it is shown that the amplitude including any number of such particles as external lines is expressed by the ordinary one-term multi-point amplitude if any two of them do not lie next to each other. The possibility of the off-shell extrapolation of the Veneziano amplitude is also discussed. (auth)

36593 PROPER TIME FORMULATION FOR THE GENERAL DUAL AMPLITUDE. Kobayashi, Tsunehiro (Tokyo Univ. of Education). Progr. Theor. Phys. (Kyoto); 45: No. 1, 314-16 (Jan 1971).

The general dual amplitude with the general vertex is derived in the proper time formulation. (J.F.P.)

36594 TWISTING INVARIANT FACTORIZATION IN DUAL RESONANCE MODEL. II. DUALITY IN THE GENERAL DIAGRAM. Sakai, Sunao (Tokyo Univ. of Education). Progr. Theor. Phys. (Kyoto); 45: No. 1, 186-202(Jan 1971).

The Feynman-like rules to construct any planar and non-planar diagrams satisfying duality in the new base vectors which are eigen-states of twisting transformation are obtained. The general vertex is factorized, and it is shown explicitly that the planar and nonplanar general Born terms satisfy duality. The gauge property of dual resonance amplitudes plays an essential role in obtaining these results. Since the general vertex and twisting operator have a simple form compared with the conventional one obtained in the $P^{(n)}$ factorization, it will be useful to construct the general planar and nonplanar diagrams, in the formalism. (auth)

36595 HELICITY CONSERVATION AND DUALITY. Mueller, H. J. W. (Univ., Munich). Lett. Nuovo Cim.; 1: No. 22, 927-30(29 May 1971).

It is pointed out that for diffractive dissociation processes duality is compatible with conservation of t-channel helicity. The argument is a geometrical extension of a previous argument. (J.F.P.)

36596 DUAL-RESONANCE AMPLITUDE FOR SPINNING PARTICLES. Rosenzweig, C.; Sukhatme, U. P. (Massachusetts Inst. of Tech., Cambridge). Contract AT(30-1)-2098. Nuovo Cim.; 3A: No. 3, 511-20(1 Jun 1971).

A nonoperational, dual-resonance amplitude is obtained for the scattering of an arbitrary number of spinning particles on the mass shell. (auth)

36597 MERGING OF ANALYTICITY AND STATISTICS IN EXTRAPOLATIONS AND REPRESENTATIONS OF DATA. Presnajder, P. (Comenius Univ., Bratislava); Pisut, J. Nuovo Cim.; 3A: No. 3, 603-24(1 Jun 1971).

Basic ideas of the Cutkosky theory of the representation of data by analytic functions together with some additions are applied to some problems of analytic extrapolations. The data and hypotheses about the behavior of the extrapolated function are understood as determining the probability in a suitable space of analytic functions. Quantities of interest (values of a function in a point, or average values over an arc) appear as expectation values obtained by the continuum (Wiener) integration over the space of analytic functions. The corresponding errors are defined in an unambiguous and "statistical" way as a generalization of usual standard deviations. The problems dealt with as applications of the formalsim are of relevance for the determination of coupling constants from dispersion relations and for extrapolations of the Chew-Low-Goebel type. (auth)

36598 OFF-MASS-SHELL EXTRAPOLATION OF THE DUAL-RESONANCE AMPLITUDE. Rebbi, C. (Univ., Trieste, Italy). Lett. Nuovo Cim.; 1: No. 23, 967-72(5 Jun 1971).

An off-mass-shell extrapolation of the dual resonance amplitude is proposed. The explicit forms of the amplitudes with three and four external lines are presented. (L.B.S.)

XUM

36599 PHASE INSTABILITY IN SCATTERING ON RANDOM POTENTIAL. Pukhov, N. M.; Chernavskii, D. S. (Lebedev Inst. of Physics, Moscow). Teor. Mat. Fiz.; 7: No. 2, 219-29(May 1971). (In Russian).

A model nonrelativistic problem is considered of phase function stability in the scattering on random stationary potential. It is shown that the phase functions can be stable as well as unstable, which depends on the values taken by the parameters of the problem. In the case of instability the usual quantum-mechanical treatment is incorrect and the additional averaging procedure must be applied. This is the necessary feature of the statistical nature of the system. The obtained criterion of instability is used in the discussion of the properties of intermediate compound-systems in hadron–hadron and hadron–nucleus interactions. (auth)

36600 CONSTRAINTS ON GROWTH POWER OF THE BINARY PROCESS AMPLITUDE. Ezhela, V. V.; Mestvirishvili, M. A. (Inst. of High-Energy Physics, Serpukhov, USSR). Teor. Mat. Fiz.; 7: No. 2, 195-202(May 1971). (In Russian).

The Kinoshita–Loeffel–Martin's method is extended on helicity amplitudes. The upper bound at fixed scattering angle is obtained for the differential cross section decreasing with the energy for binary reactions including particles with nonzero spin. (auth)

36601 REPRESENTATION FOR THE RELATIVISTIC SCATTERING AMPLITTUDE AT HIGH ENERGIES. Garsevanishvili, V. R.; Kadyshevskii, V. G.; Mir-Kasimov, R. M.; Skachkov, N. B. (Joint Inst. for Nuclear Research, Dubna, USSR). Teor. Mat. Fiz.; 7: No. 2, 203-16(May 1971). (In Russian).

In the framework of quasipotential approach the representation is obtained for relativistic scattering amplitude at high energy. The key-point of the method used is the Fourier-analysis on the three-parameter nonabelian translation group embedded as a subgroup in the Lorentz group. The representation obtained is the generalization of the eikonal approximation in quantum mechanics. (auth)

36602 SYMMETRY OF AN EXACT THREE-BODY SOLUTION. Coffou, E. (Inst. Ruder Boskovic, Zagreb). Fizika (Zagreb); 3: No. 2, 91-7(Apr 1971).

The symmetry of the solution of an exactly solvable three-body problem was considered. A three-body wave function invariant under permutations of the particle numeration was constructed. The uniqueness of the solution was proved. (auth)

Particle Accelerators

Refer also to abstracts 35069, 35541, 35838, 36292, and 36738.

36603 (IFVE-SKU-70-20) INCREASE OF THE EFFECTIVENESS OF SYNCHRONIZED CAPTURE DURING BUNCHING OF THE BEAM OUTSIDE THE SEPARATRIX. Gurov, G. G.; Myae, E. A.; Pashkov, P. T.; Yakovlev, K. A. (Gosudarstvennyi Komitet po Ispol'zovaniyu Atomnoi Energii SSSR, Serpukhov. Institut Fiziki Vysokikh Energii). 1970. 18p. (In Russian). Dep. NTIS (U. S. Sales Only).

The results of the calculation on the analog computer of a capture factor of particles into a synchrotron acceleration process for the case of preliminary bunching of the beam out of a bucket are given. The beam energy spread was taken into account in the calculations which have been carried out for the 70 GeV IHEP PS. The cases of particle injection above the bucket as well as below it were treated. The experimental data on the trapping efficiency growth, which are in principle agreed with the calculation, are given. The experimental methods are described. (auth)

36604 (JINR-P9-5645) KINETIC MODEL OF THE PLANE HIGH-CURRENT ELECTRON-ION BEAM. Rubin, S. B. (Joint Inst. for Nuclear Research, Dubna (USSR)). 1971. 14p. (In Russian). Dep. NTIS (U. S. Sales Only).

An example of a precise solution of the self-consistent Vlasov equations for a two-component system consisting of ions and electrons is considered. The solution is found in the form of a plane relativistic beam. The solution is provided for when observing the Budker condition for relativistic beams. Consideration of the distribution of particle and current densities shows that the value of the total current per unit of the beam width can be great. (auth)

36605 (JINR-P9-5724) SYSTEM FOR DEPRESSION OF THE MAGNETIC FIELD PULSATIONS IN THE DUBNA SYNCHROPHASOTRON. Smirnov, A. A.; Belyaev, L. N.; Doroshenko, A. Z.; Kalmykov, D. P. (Joint Inst. for Nuclear Research, Dubna (USSR). Lab. of High Energy). 1971. 11p. (In Russian). Dep. NTIS (U. S. Sales Only).

The scheme, connected by means of an L C-filter thyratron, forms the basis of the system for depression of the magnetic field pulsations in the Dubna synchrophasotron. The system has a rather high coefficient of depression for the components of 500, 1000 and 1500 Hz, etc. of the accelerator magnetic field (for the component of 500 Hz the depression coefficient is 100). In order to reduce the capacity of the recharging rectifier and to save the power, the resistor is switched on with the help of an additional thyratron. The shielding of the depression system equipment is described. (auth)

36606 (LAL-1249) DEVICE FOR MEASURING THE LUMINOSITY OF THE ORSAY STORAGE RING. Augustin, J. E.; Buon, J.; Haissinski, J.; Lalanne, D.; Marin, P.; Petroff, P.; Rumpf, F.; Silva, E. (Paris Univ., Orsay (France). Laboratoire de l'Accelerateur Lineaire). Apr 1971. 28p. (In French). Dep. NTIS (U. S. Sales Only).

A precise monitoring device for the luminosity is used at the Orsay e^+e^- storage ring (ACO). Two lead-scintillator sandwich counters detect the photons emitted at small angles in the double bremsstrahlung reaction $e^+e^- \rightarrow e^+e^-\gamma\gamma$. The detection thresholds of these two counters are accurately determined by a tagging method of the bremsstrahlung photons. (auth)

36607 (LNF-70/19) TECHNICAL-ECONOMIC INFORMATION ON SUPERCONDUCTORS AND CONDUCTORS FOR HIGH FIELD MAGNETS. Note No. 475. Pasotti, G.; Sacerdoti, G. (Comitato Nazionale per l'Energia Nucleare, Frascati (Italy). Laboratori Nazionali di Frascati). 15 May 1970. 6p. (In Italian). Dep. NTIS (U. S. Sales Only).

Technical-economic data are presented for four cases: copper conductors operating at room temperature, copper conductors operating at 20°K, aluminum conductors operating at 20°K, and superconductors operating at 4.2°K. Cost factors for different current densities and fields are tabulated. (J.S.R.)

36608 (NP-18855) ELECTROSTATIC SYSTEMS FOR ION TRANSPORT. Excoffon, Jacques (Conservatoire National des Arts et Metiers, Paris (France)). Dec 1970. 61p. (In French). Dep. NTIS (U. S. Sales Only).

Two electrostatic ion transport devices are described. The mathematical analysis used for their construction is given; only first order terms were considered in the study of the trajectories and images, and the geometrical aberrations were not taken into account. The on-line device of the Orsay Nuclear Physics Institute and that of CERN at Geneva are described. (France)

36609 (NP-18860) CALCULATION OF THE INTERNAL STRUCTURE OF NON-LAMINAR AXIALLY-SYMMETRIC INTENSIVE BEAMS OF CHARGED PARTICLES. Kuznetsov, V. S.; Bogdanova, V. I.; Komarov, O. L. (Scientific Research Inst. of Electro-Physical Apparatus, Leningrad (USSR)). 1970. 20p. (In Russian). Dep. NTIS (U. S. Sales Only).

A statistical method to calculate non-laminar beams is considered. A set of equations, describing internal structure of charged particle non-laminar beams is derived. A non-laminar model of the beam with non-zero angular velocities is considered and it is shown that this model describes properties of real beams better than non-laminar models with zero angular velocities. Results of concrete calculations of internal structure of the intense non-laminar beams, focused by homogeneous longitudinal magnetic fields, are given. (auth)

36610 (ORNL-TM-3353) MUON TRANSPORT AND THE SHIELDING OF HIGH-ENERGY (≤ 500 GeV) PROTON ACCELERATORS. Alsmiller, R. G. Jr.; Alsmiller, F. S.; Barish, J.; Shima, Y. (Oak Ridge National Lab., Tenn.). 12 Apr 1971. 41p. (CONF-710423-1). Dep. NTIS.

From International congress on protection against accelerator and space radiation; Geneva, Switzerland (26 Apr 1971).

Calculated results on the muon shielding required around high-energy (200 GeV and 500 GeV) proton accelerator targets are presented. The calculations differ from those presented previously in that, in addition to the angular scattering of the muons due to Coulomb elastic collisions, an estimate of the angular scattering of the muons due to bremsstrahlung production, pair production, and nonelastic nuclear collisions is included. It is found that the angular scattering of the muons due to bremsstrahlung production, pair production, and nonelastic nuclear collisions does not have a pronounced effect on the shield dimensions and therefore for many design purposes may be neglected. The calculations also differ from those presented previously in that the case of laminated shields is considered. (auth)

36611 (SLAC-130) TWO-MILE ACCELERATOR PROJECT. Quarterly Status Report, October 1–December 31, 1970. (Stanford Linear Accelerator Center, Calif.). Mar 1971. Contracts AT(04-3)-400; AT(04-3)-515. 69p. Dep. NTIS.

A status report on the Stanford Linear Accelerator Project covering the period October 1, 1970 to December 31, 1970 is presented. Topics included are accelerator and research area operations, accelerator and research area equipment, and physics research equipment development. (auth)

36612 (UARAEE-76) USE OF A CONTROL COMPUTER FOR THE ANALYSIS AND MEASUREMENT OF BEAM QUALITY IN A 50-MeV ACCELERATOR. Abdelaziz, M. E. (Atomic Energy Establishment, Cairo (Egypt). Dept. of Accelerators and Plasma Physics Research). 1969. 17p. Dep. NTIS (U. S. Sales Only).

A multiplexed ADC and a high-speed buffering system linked to a control computer are used in a new technique to analyze and study the beam quality, or so-called beam emittance, of the 50-MeV proton linear accelerator (linac) that is used as injector for the Zero Gradient Synchrotron (ZGS) at Argonne National Laboratory. This method permits beam sampling at a speed of one microsecond such that phase-space variations during the beam pulse as well as pulse-to-pulse variations can be detected. Beam profiles can also be obtained both from computer stored data and from oscilloscope traces. (auth)

36613 (UARAEE-87) DESIGN AND CONSTRUCTION OF A SINGLE GAP HIGH GRADIENT COLUMN. Abdelaziz, M. E. (Atomic Energy Establishment, Cairo (Egypt). Dept. of Accelerators and Plasma Physics Research). 1969. 28p. Dep. NTIS (U. S. Sales Only).

A design study for a single-gap, high gradient acceleration column to be used as a high current injector supplying a pulsed 300 keV beam of 200 m.A. protons is described. The facility, when completed, will be utilized in plasma ignition to a high temperature. The high current injector will be also used in the study of improved beam quality, or so-called beam emittance, due to the effect of reduced space charge forces resulting from high gradient acceleration. This problem is of vital importance when we consider beam injection from an acceleration column into an accelerator of given acceptance. The emittance-acceptance matching is a necessity in the development of accelerators capable of accepting a large proportion of the injected beam. (auth)

36614 (UCRL-20299) FACTORS WHICH WILL AFFECT THE COST OF A SUPERCONDUCTING SYNCHROTRON. Green, Michael A. (California Univ., Berkeley. Lawrence Radiation Lab.). 17 Feb 1971. Contract W-7405-eng-48. 25p. (CONF-710111-1). Dep. NTIS.

From HEPAP subpanel on advance accelerator technology; Berkeley, Calif. (7 Jan 1971).

The effects of the more important machine parameters on synchrotron cost are studied. As a start, published cost estimates of the LRL and BNL superconducting synchrotron studies are presented. These costs are compared with published cost data for the NAL conventional synchrotron. Some rough conclusions about the effects of aperture and dipole magnet field can be drawn from these already published cost data. In order to show more clearly the effects of machine parameters on cost, consistent cost-estimating procedures are applied to a wide variety of machines with various dipole magnetic fields, magnet apertures, and machine cycle times. The cost of machines using a highly advanced nonexistent β tungsten type of material (Nb_3Sn, V_3Ga, etc.) is compared with machines using a practical Nb-Ti material now available. The basic assumptions used in the cost-estimating process are described. The basic machine parameters used in the estimate are discussed. The results of consistent cost calculations using the CDC 6600 computer are presented in tabular and graphical form. The costs for a number of these machines are broken down into component costs so that the effect of various machine parameters can be seen in each of the important machine components. The effect of various machine parameters on the 10-year cost of electric power is also presented. It is shown that the capital plus power cost of a superconducting synchrotron can be expected to be lower by a factor of 2 or 3 than the best of the conventional synchrotrons. The superconducting machine would also have a gain in energy of 2 or 3 over the conventional machine of the same radius. The lowest-cost machines will have dipole magnetic inductions of the order of 40 to 50 kG, the machine cycle times are likely to be 5 to 15 seconds. The report also makes it clear that no one thing is going to have a dramatic effect on machine cost. In short, one is going to use the best economically justified technology that is available to him at the time of construction of the synchrotron. (auth)

36615 (UCRL-Trans-1434) EXPERIMENTS ON ACCELERATION OF α-PARTICLES BY THE COLLECTIVE METHOD. Sarantsev, V. P.; Rasherskii, V. P.; Kaminskii, A. K.; Mironov, V. I.; Fartushnyi, V. P.; Sergeev, A. P.; Novikov, V. G.; Tyutyunnikov, S. I.; Kaminskaya, A. M. (Joint Inst. for Nuclear Research, Dubna (USSR)). Translated by G. Brodell for Univ. of California Lawrence Radiation Lab., Berkeley, from report JINR-P9-5558. 19p. Dep. NTIS.

An abstract of this paper, prepared from the original language, appeared as NSA 25: 12305. (W.H.K.)

36616 (UCRL-Trans-1440) ELECTRON-ION BUNCH DIAGNOSTICS BY MEANS OF BREMSTRAHLUNG. Iovnovich, M. L.; Sarantsev, V. P.; Fiks, M. M. (Joint Inst. for Nuclear Research, Dubna (USSR)). Translated for Univ. of California Lawrence Radiation Lab., Berkeley, from report JINR-P9-4850. 8p. Dep. NTIS.

An abstract of this paper, prepared from the original language, appeared as NSA 25: 9908. (W.H.K.)

36617 (UCRL-Trans-1443) COLLECTIVE BEAM ACCELERATION. Tsytovich, V. N. (Joint Inst. for Nuclear Research, Dubna (USSR)). Translated for Univ. of California Lawrence Radiation Lab., Berkeley, from report JINR-P9-5091. 10p. Dep. NTIS.

An abstract of this paper, prepared from the original language, appeared as NSA 24: 35731. (W.H.K.)

36618 MAGNETIC FLECTION COILS OF THE BATAVIA ACCELERATOR. Goyer, J. P. (Alsthom, Paris). Energ. Nucl. (Paris); 13: No. 1, 39-41(Jan-Feb 1971). (In French).

The National Accelerator Laboratory, which is constructing the most powerful (400 GeV) proton accelerator in the world near Chicago, ordered a large part of the coils for the principal flection magnets from Alsthom after international competition. The new design of these magnets and the particularly high irradiation rate to which they are subjected required exceptional fabrication precautions. (auth) (France)

36619 MAGNETIC LENS FOR FOCUSING A BEAM OF CHARGED PARTICLES. (to Atomic Energy of Canada Ltd.). British Patent 1,229,469. 21 Apr 1971. Priority date 10 Nov 1967, Canada.

The design of multipole permanent magnet lenses for focusing charged particle beams is described. (W.H.K.)

36620 DEPOLARIZATION OF PROTONS IN A PHASOTRON WITH SPATIAL VARIATION OF THE MAGNETIC FIELD. Plis, Yu. A.; Soroko, L. M. This paper was summarized in At. Energ. (USSR); 29: No. 2, 122-3(Aug 1970) as paper No. 416/5568. (In Russian).

The depolarization of protons as a function of magnetic field in the 700-MeV synchro cyclotron is estimated for the purpose of establishing the tolerances for deviation from the theoretical value of the field. If the amplitudes of the deviation harmonics are about 1 mm, a depolarization of about 10% is expected. In order to achieve this, the accuracy on the magnetic field required is 10^{-4}. A value of 2% was obtained for the depolarization in an extraction system consisting of a regenerator, an exciter, and a magnetic channel. (R.W.R.)

36621 TRAJECTORIES OF PARTICLES IN AN ISOCHRONOUS CYCLOTRON IN THE PRESENCE OF ACCELERATION. Khokhlov, Yu. K. This paper was summarized in At. Energ. (USSR); 29: No. 1, 39-40(Jul 1970) as paper No. 408/5358. (In Russian).

A flat trajectory of a particle accelerated in an isochronous cyclotron with an arbitrary number and placement of the accelerating gaps is considered. It is shown that, for constant energy-gain per gap, the action of the gaps is to excite oscillations having the same frequency and amplitude variations as those of free betatron oscillations and to create a "quasi-constant displacement" that decreases smoothly with increasing n as n^{-5} and has no oscillations at the frequency $2\pi(\nu_r - 1)$, where ν_r is the frequency of radial betatron oscillations. The first of these effects can be compensated for completely by correct choice of initial conditions for particle injection. As a result of this choice, the particle will move on an "ideal trajectory" consisting of a uniformly unwinding spiral that does not have the usual condensations and rarefactions. (R.W.R.)

36622 TARGETS FOR PARTICLE ACCELERATORS. Fabian, H. (Nuklear-Chemie und -Metallurgie GmbH, Wolfgang, Ger.). Kerntech. Atomprax.; 13: No. 4, 176-8(Apr 1971). (In German and English).

Accelerator target types and arrangements, requirement imposed on targets, and the manufacturing of targets are discussed. (W.H.K.)

XUM

36623 FEATURES OF A DOUBLE-BEAM ACCELERATING STRUCTURE. Bomko, V. A.; Ovsyannikov, V. M.; Revutskii, E. I. (Physical-Technical Inst., Kharkov). Sov. Phys.-Tech. Phys. (Engl. Transl.); 15: No. 9, 1471-3(Mar 1971).

Translated from Zh. Tekh. Fiz.; 40: No. 9, 1887-91(Sep 1970).

The features of a double-beam accelerating system, which is a cylindrical resonator excited in the TM_{110} mode and loaded with two rows of drift tubes, are described. The frequency dependences, the Q, and the shunt resistance are studied. The high-frequency power and efficiency are evaluated. (auth)

36624 FOCUSING PROPERTIES OF A HELICAL QUADRUPOLE LENS. Kartashev, V. P.; Kotov, V. I.; Rzaev, R. A. Sov. Phys.-Tech. Phys. (Engl. Transl.); 15: No. 9, 1535-9(Mar 1971).

Translated from Zh. Tekh. Fiz.; 40: No. 9, 1969-75(Sep 1970).

The properties of a helical quadrupole lens are studied for focusing parallel beams and for focusing a beam from a point source into a point image. Also, the shaping of μ-meson beam by a helical lens is discussed. (W.H.K.)

36625 MEASUREMENT OF MAGNETIC FIELD INDEX N OF THE 5 MeV BETATRON BY AN AC POTENTIOMETER. Bhiday, M. R.; Bhoraskar, V. N. (Univ. of Poona). J. Phys., E (London); 4: No. 4, 330-2(Apr 1971).

The ac potentiometer method described determines the field index n of the betatron at different radial distances in its median plane by simply measuring the length of the potentiometer wire. This method is independent of the stability of the betatron magnet current as well as of the constants of the search coils used. The accuracy achieved is sufficient for the purpose of the beam extraction. (auth) (UK)

36626 CRYOGENIC PUMPING GAS TARGET SYSTEM. Strang, R. M.; Ritter, R. C. (Univ. of Virginia, Charlottesville). Nucl. Instrum. Methods; 93: No. 2, 221-6(1971).

A small-volume gas-target system has been built which uses immersion of one of two like chambers into liquid helium for contaminant-free pumping. An unlimited number of gas exchanges can be made without opening the system. Hence, rapid cycling of "gas in-gas out" measurements can be made with expensive gases which are returned to the reservoir. This operation is practical with total gas quantities of 10 cm^3 STP or more. Reliability in six experiments to date has been such that no gas loss or contamination has been measured and only one leak, before startup, has appeared. (auth)

36627 CONCEPT AND QUALITY MEASUREMENTS OF THE MAGNETIC FIELD IN CONNECTION WITH THE IMPORTANT PROPERTIES OF THE OPTICAL SYSTEM CONSIDERED. Ribes, M.; Turck, B. (Centre d'Etudes Nucleaires de Saclay, Gif-sur-Yvette, France). Nucl. Instrum. Methods; 93: No. 2, 285-93 (1971). (In French).

This study is the second and last part of the work. The first part about the influence of measurement errors of the magnetic field in an optical system was previously published. It is pointed out that the effect of some errors is related to the direction along which the probe is moved, and that if the errors at each point of measurement are not quite independent, the overall effect may be in some cases practically negligible. Therefore measurement accuracy is not so critical as usually specified. As a conclusion, some general considerations about conceiving measuring systems in a real case are drawn. (auth)

36628 ON THE EQUATION DEFINING THE PROFILE OF NON-RELATIVISTIC BEAMS WITH SPACE-CHARGE FORCES AND FINITE EMITTANCE. Ciuti, P. (Univ., Trieste, Italy). Nucl. Instrum. Methods; 93: No. 2, 295-9(1971).

A differential equation is obtained for the profile of a non-relativistic beam with finite emittance and space charge, subject to linear focusing realized by electric and magnetic fields. An approximate method of solution is described and two applications are reported. (auth)

36629 THREE-MAGNET SYSTEM FOR MEASUREMENT OF ELECTRON SCATTERING THROUGH 180°. van Niftrik, G. J. C.; de Vries, H.; Lapikas, L.; de Vries, C. (Inst. for Nuclear Physics Research, Amsterdam). Nucl. Instrum. Methods; 93: No. 2, 301-9(1971).

A three-magnet system permitting measurement of electron scattering through 180° is described. An important feature of this system is that the direction of the outgoing electron beam is the same as in "normal" scattering experiments, which facilitates beam handling and current integration. Some of the calculated optical properties of this system have been checked by experiment. Emphasis is given to the optical properties of the circular pre-target magnet in conjunction with the spectrometer. By appropriate beam steering the scattering angle can be varied by up to 6°. The system has so far been used for experiments on the magnetization distributions of several $1f_{\frac{7}{2}}$-shell nuclei and of ^{7}Li. (auth)

36630 NOMOGRAMS FOR CALCULATING THE OPTICAL PARAMETERS OF WEAK MAGNETIC QUADRUPOLAR LENS SYSTEMS CONCERNING ANTISYMMETRICAL DOUBLET AND SYMMETRICAL TRIPLET, FOR ELECTRONS IN THE 1 TO 10 MeV ENERGY RANGE. Nemes, M. (Inst. for Atomic Physics, Bucharest). Nucl. Instrum. Methods; 93: No. 2, 363-4(1971).

Nomograms for calculating the optical parameters of weak magnetic quadrupolar lens systems concerning antisymmetrical doublet and symmetrical triplet, for electrons in the 1 to 10 MeV energy range, are described and the conditions in which they are valid are given. (auth)

36631 PRE-TARGET MONITOR FOR THE INTENSITY AND TIME DISTRIBUTION OF A PROTON BEAM. Santoro, R. T.; Wachter, J. W.; Love, T. A. (Oak Ridge National Lab., Tenn.). Nucl. Instrum. Methods; 93: No. 2, 371-3(1971).

A relative proton beam monitor is described which measures the intensity and time distribution of a proton beam from the flux of protons scattered from a thin Mylar film using an ionization chamber and a plastic scintillator detector. (auth)

36632 IMPROVED ELECTRONIC CONTROL UNIT FOR A MOTOR TYPE BEAM SCANNER. Boving, R.; Elskens, M. (Univ., Louvain, Belg.). Nucl. Instrum. Methods; 93: No. 2, 391-3(1971).

A circuit has been developed, providing a stable and almost perfect proportionality between the deflection of the scanner needle and the X-deflection of the oscilloscope, visualizing the beam profile. (auth)

36633 GAS TARGET FOR PRODUCTION OF MONOENERGETIC NEUTRONS. Cramer, D. S.; Cranberg, L. (Univ. of Virginia, Charlottesville). Nucl. Instrum. Methods; 93: No. 2, 405-7(1971).

A new design of gas target cell is described for neutron production. Results are given on effects attributed to diffusion of tritium gas from the cell into the window material. (auth)

36634 THERMOELECTRIC COOLING IN THE SCATTERING CHAMBER 800 OF THE HAMBURG ISOCHRONOUS CYCLOTRON. Abels, C.; Pegel, C. (Univ., Hamburg). Nucl. Instrum. Methods; 93: No. 2, 409-10(1971).

A cooling apparatus with Peltier thermocouples for semiconductor detectors for temperatures up to −72°C is described. The method of production is discussed in detail. (auth)

36635 CHARGED PARTICLE ACCELERATOR. Schmidt, Fritz; Matthaeus, Guenther (to Siemens AG). German Patent 1,564,583. 4 Sep 1969. Filed 28 Apr 1966. (In German).

A device is described in which the particles are drawn from a source by a tubular acceleration electrode. This tubular electrode is surrounded at least partially by a second concentric electrode, and a continuous voltage is applied between the two electrodes. (J.F.P.)

36636 THREE VARIANTS OF THE FERMI MODEL OF PARTICLE ACCELERATION. Zoler, D. (Technical and Physical Research Centre, Iasi). Phys. Lett.; 35A: No. 3, 163-4(31 May 1971).

Three variants of charged particle acceleration are suggested, in which magnetic mirrors perform an oscillation movement. (auth)

36637 FEASIBILITY STUDY TO INCREASE THE AVAILABLE TAMVEC PROTON AND DEUTERON ENERGIES. Poulsen, Niel Bowman. College Station, Tex.; Texas A and M Univ. (1970). 88p. University Microfilms Order No. 71-8904.

Thesis.

Computer studies made of high-energy proton and deuteron beams indicated that protons to 80 MeV and deuterons to 70 MeV could be achieved if the radio-frequency range were extended to 18.75 MHz and additional flutter were available. It was determined that the needed flutter could be obtained, essentially, by rewiring the valley coils to act as flutter coils. Studies made on a quarter-scale model of radio-frequency system indicated that, by adding a radio-frequency driver and slightly modifying the resonator-tank panels, the frequency could be extended even beyond the needed 18.75 MHz. The studies showed that the deuteron energy was limited at 70 MeV by the maximum main magnet coil current, and that the proton energy was limited at 80 MeV by the amount of flutter that could be obtained without overheating the flutter coils. (Diss. Abstr. Int., B)

36638 POSSIBLE METHOD OF ACCELERATING HEAVY IONS. Tarantin, N. I. This paper was summarized in At. Energ.

(USSR); 29: No. 2, 122(Aug 1970) as paper No. 415/5489. (In Russian).

This method, a modification of the Alvarez method, can be summarized as follows: Heavy ions are accelerated in a cyclotron at resonance at one of the lower harmonics. Under these conditions the orbit of the ions is shifted along the accelerating gap in such a way that, after the ions have been stripped as a result of passing through a target mounted in the accelerating gap and the orbital radius has been reduced, the ion source turns out to be inside the orbit and does not interfere with further acceleration of the ions. This feature allows the use of the most modern ion sources, which produce ions of relatively high charge. After stripping, the ions are accelerated at resonance at the fundamental frequency. The usual problems of a conventional cyclotron, a circular drift of the orbit center and weakening of axial focusing, are eliminated by applying the appropriate plane-symmetrical magnetic field. Use of this method in a cyclotron having a final orbital radius of 200 cm for $B_0 = 7$ kG enables the production of ions having an energy of 8 to 12.5 MeV per nucleon and a fairly high intensity. This can be achieved, for example, by using preliminary acceleration at the third harmonic and stripping of $^{40}Ar^{2+}$, $^{84}Kr^{4+}$, $^{132}Xe^{6+}$, $^{200}Hg^{8+}$, and $^{238}U^{10+}$. (R.W.R.)

36639 OPERATION OF A GLOW DISCHARGE ION GUN USED FOR SPECIMEN THINNING. Holland, L.; Hurley, R. E.; Laurenson, L. (Edwards High Vacuum International, Crawley, Eng.). J. Phys., E (London); 4: 198-200(Mar 1971).

The operation of a cold-cathode ion source with perforated cathode and anode plates was studied. The source is of the Paulus and Reverchon type commonly used for thinning electron microscope specimens by sputtering. The ion source was operated with an anode–cathode spacing of 1.5 mm at an applied voltage of 6 kV. Calculations indicated that the operating pressure and current density for argon were 0.5 torr and 0.5 A cm^{-2} respectively. It is shown that under these conditions, the current flowing is limited to less than 1 mA and the glow discharge is localized in the region of the perforations where the electron ionizing paths are greatest. A stable discharge is obtained when the diameter of an anode hole is two to four times that of a cathode hole. (auth) (UK)

36640 COULOMB COLLISIONS IN DENSE BEAMS. Globenko, Yu. G.; Koshkarev, D. G.; Barkhudaryan, A. V. Sov. Phys.-Tech. Phys. (Engl. Transl.); 15: No. 11, 1880-6(May 1971).

Translated from Zh. Tekh. Fiz.; 40: No. 11, 2405-14(Nov 1970).

Coulomb collisions in dense beams are studied by numerical integration of the Fokker–Planck equation in a limited range for three initial distribution functions. These collisions lead to a relaxation of the initial distribution function into $\delta(\epsilon)$. The process is illustrated by a sequence of curves for each initial distribution function and by the time dependences of the total number of particles and the average energy, which contain information about the relaxation rate. The particle loss is shown to depend on the initial distribution function and is greatest for distributions which increase toward the boundary. When such distributions occur in storage rings the lifetime of intense beams is limited. An equation is found for the relaxation time of a spherically symmetric system. This relaxation time is shown to depend only on the mass of the colliding particles and the density in phase space. (auth)

36641 ISOCHRONOUS BENDING MAGNET FOR A LINOTRON. Gapanovich, V. G. (Lebedev Inst. of Physics, Moscow). Sov. Phys.-Tech. Phys. (Engl. Transl.); 15: No. 11, 1909-11(May 1971).

Translated from Zh. Tekh. Fiz.; 40: No. 11, 2443-6(Nov 1970).

Equations are derived for the calculation of isochronous bending magnets for a linotron accelerator. The quadrupole doublets, bending magnets, and field-free regions are calculated. (W.H.K.)

36642 INTENSE BEAMS WITH AN ARBITRARY PHASE-DENSITY DISTRIBUTION IN EXTERNAL FOCUSING FIELDS. Kuznetsov, V. S.; Fidel'skaya, R. P. Sov. Phys.-Tech. Phys. (Engl. Transl.); 15: No. 10, 1635-9(Apr 1971).

Translated from Zh. Tekh. Fiz.; 40: No. 10, 2099-2105(Oct 1970).

A method described previously for treating beams with an arbitrary phase-density distribution is generalized to the case in which there are external magnetic and electric fields. Conditions are derived and formulated under which the general stationary six-dimensional problem of determining the particle-density distribution in phase can be reduced to a nonstationary four-dimensional problem. The results of concrete calculations are reported to illustrate the fundamental properties of beams having a phase-density distribution different from microcanonical. In particular, it is shown that the projection of the four-dimensional phase volume on the plane of the Cartesian coordinates x, x′ can be increased in such beams. (auth)

36643 MAGNETIC LENSES WITH PARABOLIC, TRIANGULAR AND TRAPEZOIDAL DISTRIBUTIONS OF LINEAR AMPERE-TURN DENSITY. Basin, L. A.; Bobykin, B. V.; Davydovskii, V. Ya.; Kel'man, V. M. (Inst. of Nuclear Physics, Alma-Ata, USSR). Sov. Phys.-Tech. Phys. (Engl. Transl.); 15: No. 10, 1640-5(Apr 1971).

Translated from Zh. Tekh. Fiz.; 40: No. 10, 2106-11(Oct 1970).

The focal lengths, foci, and spherical aberration are calculated for iron-free lenses with windings in which the linear density of ampere-turns is determined by a simple law. The data are shown in the form of tables. The electron-optical parameters of the lenses are like those of lenses with a bell-shaped field distribution. (auth)

36644 CURRENT LOADING AND DISPERSION IN AN IRIS-LOADED LINEAR ELECTRON ACCELERATOR. Makhnenko, L. A.; Ivanov, G. I. Sov. Phys.-Tech. Phys. (Engl. Transl.); 15: No. 10, 1745-9(Apr 1971).

Translated from Zh. Tekh. Fiz.; 40: No. 10, 2236-41(Oct 1970).

The effect of the space charge of the electron beam on the dispersion properties of iris waveguides is considered. Theoretical relations are obtained for determining the phase velocity in an iris-loaded waveguide in the small-signal approximation when the beam radius is smaller than the radius of the iris aperture. The phase velocity is calculated as a function of the current for two versions. For phase velocities less than 0.7 of the velocity of light, the correction due to the actual value of the beam radius is negligible. The theoretical results are compared with the experimental data. (auth)

36645 METHOD OF MEASURING THE POLARIZATION OF AN ORIENTED HYDROGEN TARGET. Kovalev, A. I.; Komar, A. P.; Parfenov, L. B.; Prokof'ev, A. N.; Shklyarevskii, G. M. Sov. Phys.-Tech. Phys. (Engl. Transl.); 15: No. 10, 1750-3 (Apr 1971).

Translated from Zh. Tekh. Fiz.; 40: No. 10, 2242-7(Oct 1970).

A new method is described for measuring the polarization of an oriented hydrogen target. The method is based on simultaneous frequency modulation of the Q meter and the magnetic field, so the proton magnetic resonance (PMR) can be separated from the signal due to the frequency dependence of the impedance of the Q meter; no integration or computation is needed. The apparatus is described. (auth)

36646 DESIGN OF CROSSED ELECTRON-OPTICAL LENSES. Yavor, S. Ya. (Ioffe Inst. of Physics and Tech., Leningrad). Sov. Phys.-Tech. Phys. (Engl. Transl.).; 15: No. 10, 1763-5(Apr 1971).

Translated from Zh. Tekh. Fiz.; 40: No. 10, 2257-60(Oct 1970).

The properties of crossed electron-optical lenses, which can be formed from cylindrical lenses by rotating electrodes (every other pair), by 90°, are studied. The focusing equations are obtained. It is shown that crossed lenses can be diverging and achromatic. (auth)

XUM

PHYSICS (NUCLEAR)

Neutron Interactions with Matter

Refer also to abstracts 34879, 34901, 34906, 36266, 36313, 36633, 37118, 37119, 37123, 37129, and 37132.

36647 (ANL–7779) SURVEY OF APPROXIMATION PROCEDURES FOR THE NUMERICAL SOLUTION OF THE NEUTRON TRANSPORT EQUATION. Kaper, Hans G.; Leaf, Gary K. (Argonne National Lab., Ill.). Apr 1971. Contract W-31-109-eng-38. 55p. Dep. NTIS.

Various methods for the numerical solution of the stationary one-group neutron transport equation are evaluated. Emphasis is on these methods that are applicable to transport calculations for multidimensional, heterogeneous reactor configurations under realistic boundary conditions; in particular, attention is focused on the formulation aspects of these approximate procedures. The first part of the report deals with synthesis techniques (spherical harmonics method, moment methods); the second part with discrete-ordinates techniques. (auth)

36648 (CEA-R-4145) RESEARCH OF A BIASING SYSTEM FOR THE TREATMENT OF THE DEEP PENETRATION OF NEUTRONS BY THE MONTE-CARLO METHOD. Lanore, Jeanne-Marie (Commissariat a l'Energie Atomique, Fontenay-aux-Roses (France). Centre d'Etudes Nucleaires). Jan 1971. 73p. (In French). Dep. NTIS (U. S. Sales Only).

Thesis. Submitted to Univ. of Paris, France.

The Monte-Carlo method can be successfully applied to the study of the deep penetration of neutrons, by means of a biasing system using an asymptotic solution of the adjoint transport equation as an importance function. This system enabled a reduced and constant variance at every point in a phase space, which was rigorous in a special case and almost rigorous in the general case, to be obtained. Neutron spectra at a very great distance from the source were thus accurately derived, and an absolute upper limit of the variance could be calculated. (auth) (France)

36649 (CONF-710302–11) RAFFLE MONTE CARLO CODE AND ITS USE TO OBTAIN CORRELATED ESTIMATES OF COLLAPSED CROSS SECTIONS. Vesely, W. E.; Wheeler, F. J.; Marsden, R. S. (Idaho Nuclear Corp., Idaho Falls). [1971]. 23p. Dep. NTIS.

From Meeting on new development in reactor mathematics and applications; Idaho Falls, Idaho (29 Mar 1971).

An overall description is given of the RAFFLE code, a general-purpose Monte Carlo neutron-transport code. Features of the code described include the use of uniform interval number tables by which no logs, sines, or cosines are ever computed during a neutron history; the flexibility of handling pointwise and multigroup cross section data; and the flexibility of having three scoring estimators instead of the usual one particular estimator. A correlation technique incorporated in RAFFLE is described, by which collapsed group cross sections and the complete P_0 and P_1 group-to-group transfer matrices can be obtained. These collapsed group constants are analogous to those obtained from any cross section code and have the virtue of containing the exactness of the Monte Carlo technique. Particular applications are described to illustrate the RAFFLE code in general and to illustrate, in particular, the feasibility of obtaining group constants by means of Monte Carlo. (auth)

36650 (UARAEE–60) ENERGY-DEPENDENT MILNE PROBLEM. Hussein, A.; El-Konsol, S.; Novikov, A.; Hamouda, I. (Atomic Energy Establishment, Cairo (Egypt). Reactor and Neutron Physics Dept.). 1968. 57p. Dep. NTIS (U. S. Sales Only).

Previous work on the energy-dependent Milne problem for thermal neutrons is reviewed; the behavior of thermal-neutron spectra at the boundary with vacuum or "black" body is considered. Only thermal-energy region, non-multiplying media and a plane medium–vacuum boundary are investigated. The extrapolation distance is shown, for media with $\lambda_s \neq$ const., for infinite half-space and as a function of buckling. The spatial behavior of neutron temperature, the average energy of the spectrum near the boundary region, and the investigation of the integral and differential leakage spectra at the moderator surface are discussed. Finally, the behavior of the neutron space–energy distribution and its angular dependence studied in the experiments near a "black" sheet immersed in the moderator are considered. (R.W.R.)

36651 (UARAEE–107) RAM-1, MULTIGROUP NEUTRON DIFFUSION CODE FOR THE IBM-1130. Nassar, S. F.; Abu-Leilah, M. M. (Atomic Energy Establishment, Cairo (Egypt). Reactor and Neutron Physics Dept.). 1970. 21p. Dep. NTIS (U. S Sales Only).

The code RAM-1, for solving the time-independent neutron diffusion problem, is written in a FORTRAN language for the IBM-1130 Data Processing System. The code is memory-contained and requires no tapes. It can handle up to 11 energy groups, four different regions, and 55 spatial mesh points. Among its features are high-order differencing of the differential equation, a power extrapolation technique, and an energy-dependent extrapolation-length boundary condition at the outer boundary. The code was tested on two fast reactor assemblies. The first was ZPR-III cylindrical type reactor; the second was EBR-II spherical type reactor. The results were in excellent agreement with those already reported in literature. (auth)

36652 (WAPD-TM–991) SPATIAL DISTRIBUTION OF THE INDIUM ACTIVATION IN WATER USING A ^{252}Cf SOURCE (LWBR DEVELOPMENT PROGRAM). Semans, J. P. (Bettis Atomic Power Lab., Pittsburgh, Pa.). Mar 1971. Contract AT-11-1-GEN-14. 28p. Dep. NTIS.

An experiment was conducted to measure the indium activation distribution in water as a function of distance from a ^{252}Cf fission source. The experiment was compared with a Monte Carlo calculation and a higher approximation of a one-dimensional multigroup P-3 calculation, and an attempt was made to infer an experimental age. The intensity of the source limited the experiment to a maximum radius of approximately 29 centimeters. The RECAP and P3MG1 calculations are in reasonable agreement with the experiment. P3MG1 calculations for extrapolation beyond the last experimental point give an age of 30.4 ± 0.5 cm^2 for a water density of 0.9982 g/cm^3. (auth)

36653 NEUTRON ESCAPE FROM WATER-MODERATED TANKS. De Volpi, A. (Argonne National Lab., Ill.). J. Nucl. Energy; 24: 577-86(Jan 1971).

Integral measurements were made to determine neutron escape fractions from water-moderated tanks. Initial measurements of source strength were made with a manganese-bath sphere of 48-cm effective radius. Source-induced counting rates from a sphere of 28.2-cm radius and a cylinder of apparent effective radius of 36.7-cm gave leakage fractions up to ten times greater than the large tank. These experiments were performed primarily for ^{252}Cf, Ra–Be (α,n), and Am–Be (α,n) sources, with some additional data from Pu–Be (α,n) and Ra–Be (γ,n). Data were also obtained at both a dense and a dilute concentration of manganous sulfate. Measurements of the reflection coefficient were obtained. It was possible to fit the observations to a simple two-component model which allows interpolation and extrapolation with an accuracy adequate for >½% absolute neutron calibrations. If the leakage values obtained in this paper are used, a number of discrepancies existing in published calibrations of international sources may be rectified to produce a more uniform pattern of consistency. This improvement also applies to reported measurements of the fission parameters $\bar{\nu}$ and η. (auth) (UK)

36654 SOLUTION OF THE NEUTRON TRANSPORT EQUATION IN A DOUBLY-PERIODIC ARRAY OF SINGULAR ABSORPTION LINES. Aviram, Ira (Nuclear Research Centre-Negev, Beer-Sheva, Israel); Yeivin, Yehuda. J. Nucl. Energy; 24: 593-606(Jan 1971).

Periodic solutions are derived for the one-velocity transport equation in an infinite two-dimensional lattice of absorption lines in a moderating medium. The angular distribution of scattering is given by a truncated Legendre series. The unit cell of the lattice may be an arbitrary parallelogram so that the most common reactor lattices (square, hexagonal, triangular) are included as particular cases. The angular flux is expanded in a double Fourier series over the primitive cell. The coefficients are functions of the angular variable and can be expressed in terms of their spherical moments which, in turn, are solutions of a system of algebraic equations whose order is determined by the length of the truncated Legendre series. The terms of the double Fourier series exhibit an asymptotic behavior of the type $(m^2 + n^2)^{-\frac{1}{2}}$, and are therefore, only conditionally convergent. The solutions possess a $1/r$ singularity at the location of the absorption lines. (auth) (UK)

36655 PULSED NEUTRON AND DIFFUSION LENGTH STUDY IN BISMUTH. Bhushan, Vidya (Safdarjang Hospital, New Delhi); Trikha, S. K. J. Nucl. Energy; 25: 41-50(Jan 1971).

It is shown that the long-standing discrepancy between the calculated values of cold-neutron scattering cross sections in bismuth at room temperature and the experimentally observed re-

sults can be resolved if a Debye distribution is assumed for the lattice frequencies with a Debye temperature θ_D = 260°K, instead of the usual 120°K. It is also shown that this high value of θ_D is supported by specific heat data. For the scattering kernel the first term of the Placzek expansion with θ_D = 260°K was used. The pulsed-neutron and diffusion-length were studied, and attempts were made to compare the results with the experimental data of STARR and PRICE [NSA 17: 15200]. It was found that the experimental measurements do not represent the asymptotic state. Some results of the time-dependent and space-dependent studies are also reported. (auth) (UK)

36656 NEUTRON GENERATORS. Croitoru, Petrica (to Institutul de Fizica Atomica). British Patent 1,228,814. 21 Apr 1971. Priority date 10 Apr 1967, Rumania.

A T(d,n) type neutron generator is described. The ion beams are accelerated onto a hollow cylindrical target so that a sample placed in the hollow interior of the target may be irradiated by an intense flux of neutrons. (W.H.K.)

36657 VARIABLE RATE NEUTRON SOURCE. Silver, Gary L. (to United States Atomic Energy Commission). U. S. Patent 3,571,595. 23 Mar 1971. Filed 15 Apr 1969.

A variable-rate neutron source is described. It includes an alpha radiation source, a neutron-emitting target material normally separated from said alpha source, and means for cycling the target material between its separated location and contact with the alpha source. (auth)

Nuclear Properties and Reactions, A≤ 5

Refer also to abstracts 35050, 36408, 36527, 36719, 36732, 36733, 36737, 36738, and 36811.

36658 (CERN-Trans-71-13) ELASTIC ELECTRON SCATTERING ON ^{4}He AT ENERGIES BETWEEN 30 AND 59 MeV. Erich, U.; Frank, H.; Haas, D.; Prange, H. Translated by H. MacCabe (CERN, Geneva), from Z. Phys.; 209: 208-18(1968). 24p. Dep. NTIS (U. S. Sales Only).

The cross section of ^{4}He for elastic electron scattering has been measured relative to that of the proton using a gas target with helium, hydrogen, or a mixture of both gases. Scattering angles were between 56° and 130°, and the energy varied from 30 to 59 MeV. A model-independent r.m.s. charge radius of (1.63 ± 0.04) fm has been evaluated for the α particle. (auth)

36659 (INR-P-1234) BINDING ENERGY OF ^{3}H AND n-d DOUBLET SCATTERING LENGTH WITH RANK FOUR SEPARABLE POTENTIAL. Dabrowski, J.; Dworzecka, M. (Institute of Nuclear Research, Warsaw (Poland)). 1970. 56p. Dep. NTIS (U. S. Sales Only).

Separable charge-independent nucleon–nucleon potentials containing an attraction and a hard-core repulsion in the $^1S_0$ state and the Yamaguchi tensor interaction in the $^3S_1 + {}^3D_1$ state are used to calculate the ^{3}H ground-state energy E_T and the n–d doublet scattering length ^2a. The potential that gives the best fit to the nucleon–nucleon data is $E_T = -8.81$ MeV, $^2a = 0.58$ F. All results fall on the Phillips line. A derivation of the system of coupled integral equations for the bound state and for the scattering problem for an arbitrary-rank potential acting in the $^1S_0$ and $^3S_1 + {}^3D_1$ states is included. (auth)

36660 (LA-4574) EVALUATED NUCLEAR DATA FOR HYDROGEN IN THE ENDF/B-II FORMAT. Stewart, L.; LaBauve, R. J.; Young, P. G. (Los Alamos Scientific Lab., N. Mex.). Dec 1970. Contract W-7405-eng-36. 18p. (ENDF-141; EANDC(US)-151-A). Dep. NTIS.

The following nuclear data are given for hydrogen in the energy range from 1.0×10^{-5} eV to 20.0 MeV. The general information file includes a brief description of the data to follow. Values for nuclear spin and effective scattering radius are given in the resonance file. Smooth cross-section data are given for the total cross section, the free-atom elastic scattering cross section, and the radiative capture cross section; data for $\bar{\mu}$, ξ, and γ are also included. The angular distributions for elastic scattering are given as probability vs cosine of the scattering angle. The free-atom-scattering cross section is the only information provided at thermal. Secondary gamma-ray production multiplicities for capture, which are equal to one, are given. Gamma-ray angular distributions are provided for the single radiative capture gamma ray. (auth)

36661 (UCRL-20295) (n,p) ELASTIC SCATTERING: A FITTING EXPRESSION FOR THE DIFFERENTIAL CROSS SECTIONS IN THE ENERGY RANGE BETWEEN 22.5 AND 400 MeV. Rindi, Alessandro; Lim, Chun Bin; Salmon-Cinotti, Tullio (California Univ., Berkeley. Lawrence Radiation Lab.). 20 Nov 1970. Contract W-7405-eng-48. 18p. Dep. NTIS.

The differential cross sections for n + p elastic scattering at energies where the scattering is no longer isotropic in the cm system (i.e. for energies higher than about 10 MeV) are very often required for measurements of neutron fluxes and spectra. The literature provides a good amount of experimental data, but no simple empirical formula has yet been proposed that allows one to calculate the values of this cross section at any energy and at any angle. Metropolis and Gammel have proposed two semi-empirical formulas that fit the total n + p elastic scattering cross section with an acceptable approximation for, respectively, energies higher than 71 MeV and energies up to 71 MeV. Using these formulas, Hajnal has proposed a rather sophisticated empirical expression for fitting the differential cross section data up to about 600 MeV. With some of the Hajnal results as a basis, a simpler expression fitting the experimental data with a better approximation is found. (auth)

36662 CHARGE-SYMMETRY STUDY WITH THE REACTIONS ^{2}H(t,τ)nn AND ^{2}H(τ,t)pp. Gross, E. E.; Hungerford, E. V.; Malanify, J. J. (Oak Ridge National Lab., Tenn.). Nucl. Phys.; A164: 376-84(1971).

The ^{3}He spectra at 5° lab to a 22.0-MeV triton beam from the reaction ^{2}H(t,^{3}He)nn and the t-spectra at 5° lab to a 19.9 MeV ^{3}He beam from the reaction ^{2}H(^{3}He,t)pp were measured. An analysis of these charge-symmetric reactions with the comparison method gives an unrealistic n-n scattering length. A charge asymmetry is also noted in the absolute yields. Both effects are attributed to the influence of the sequential decay process $^3\text{He} + {}^2\text{H} \rightarrow {}^4\text{He}^*(20.3\text{ MeV}) + p \rightarrow {}^3\text{He} + p + p$. (auth)

36663 EVIDENCE FOR A T = $\frac{1}{2}$ RESONANCE IN THE ^{3}He SYSTEM. van der Woude, A. (Oak Ridge National Lab., Tenn.); Halbert, M. L.; Bingham, C. R.; Belt, B. D. Phys. Rev. Lett.; 26: 909-12(12 Apr 1971).

Evidence for a broad resonance in the ^{3}He system was found in the excitation function for the radiative capture of deuterons by protons. Supporting evidence is provided by the behavior of the angular distributions. The resonance is centered at (19.5 ± 0.5)-MeV excitation, has a width of about 2 MeV, and is most likely characterized by $(L^\pi, S, T) = (1^-, \frac{1}{2}, \frac{1}{2})$.

36664 EXCHANGE MAGNETIC MOMENTS OF LIGHT NUCLEI. Verde, Mario; Francovicchio, Paolo (Univ., Turin). Atti Accad. Sci. Torino. I. Cl. Sci. Fis., Mat. Natur.; 103: 951-7(Nov-Dec 1969).

The exchange currents in light nuclei are difficult to detect from experimental measurements because of their negligible role in the presence of normal currents. A polarization phenomenon that depends directly on exchange currents and allows an eventual confirmation of their prevalent isovector character is studied. (tr-auth)

36665 p–p FINAL-STATE INTERACTION IN THE ^{3}He(d,t)2p REACTION. Rutkowski, R. W.; Gross, E. E. (Oak Ridge National Lab., Tenn.). Phys. Lett.; 35B: No. 2, 151-2(10 May 1971).

The final-state-interaction peak for the reaction ^{3}He(d,t) 2p at 5° lab. 23.5 MeV c.m. is analyzed with the Born approximation. Using an effective-range wave function for the di-proton system, we extract $\gamma = 0.360 \pm 0.015$ fm^{-1} for the Gaussian range parameter describing the charge distribution in ^{3}He. (auth)

36666 NEUTRON CHANNEL IN MUON CAPTURE ON ^{4}He. Eramzhyan, R. A.; Fetisov, V. N.; Salganic, Yu. A. (Joint Inst. for Nuclear Research, Dubna, USSR). Phys. Lett.; 35B: No. 2, 143-4(10 May 1971).

The neutron channel in muon capture by ^{4}He is calculated. It is shown that asymmetry of the neutron angular distribution when polarized muons are captured is essentially due to the relativistic terms in the muon–nucleon Hamiltonian. Those terms also contribute significantly to the capture rate. The final-state interaction changes the neutron energy spectrum and the asymmetry of the angular distribution. (auth)

36667 ENERGY DEPENDENCE OF QUASIFREE SCATTERING IN THE ^{2}H(p,pn)p REACTION. Braithwaite, W. J.; Calarco, J. R.; Cameron, J. M.; Storm, Derek W. (Univ. of Washington, Seattle). Nucl. Phys.; A166: 515-24(1971).

The cross section for the reaction ^{2}H(p, pn)^{1}H was measured at 14, 17, 20, and 23 MeV incident energies. The proton and neutron counter angles were chosen to emphasize the quasi-free p–n scattering process. The neutron-counter efficiency was measured in order to obtain the absolute differential cross sections. The ex-

XUM

perimental results agree well with a modified simple impulse approximation, which is discussed. (auth)

36668 INELASTIC SCATTERING OF NEUTRONS BY HYDROGEN-BONDED FERROELECTRICS. Novakovic, L.; Stamenkovic, S. (Boris Kidric Inst. of Nuclear Science, Belgrade). pp 177-84 of Research Reactor Utilization. Vol. 1. Vienna; International Atomic Energy Agency (1970). (CONF-700204-9).

From IAEA meeting on research reactor utilization; Rome, Italy (2 Feb 1970).

An inelastic differential scattering cross section of slow neutrons scattered by hydrogen-bonded ferroelectrics (KDP and isomorphous substances) is presented in the temperature region above the Curie point. It is predicted that the intensity spectrum of a coherent part of the scattering behaves like $I_{coh} \propto T\,(T - T_c)^{-1}$, where T_c denotes the Curie temperature. (auth) (INIS)

36669 NUCLEON–NUCLEON QUASI-FREE SCATTERING IN THE p + d → p + n REACTION AT LOW BOMBARDING ENERGIES. Valkovic, V.; Rendic, D.; Otte, V. A.; von Witsch, W.; Phillips, G. C. (Rice Univ., Houston, Tex.). Nucl. Phys.; A166: 547-72(1971).

Proton–proton and proton–neutron quasi-free scattering (QFS) contributions in the p + d → p + p + n reaction were measured for proton bombarding energies 4.5 to 13.0 MeV. The impulse approximation gives a good description of the measured spectral shapes for $\theta_1 = -\theta_2 = 30°$ and, when normalized (with a factor ≈0.2 for p–p QFS and a factor ≈0.3 for n–p QFS), describes the peak cross-section energy dependence surprisingly well. The ratio of the peak cross sections $(\sigma_{np}/\sigma_{pp})_{exp}$ is ≈2.0 for most of the bombarding energies, while the simple impulse approximation predicts $(\sigma_{np}/\sigma_{pp})_{imp} \approx 1.3$. Coulomb effects are found not to be significant. The influence of the final-state interaction on the measured spectra is discussed. (auth)

36670 ^{2}H(p,pn)p REACTION AT 9.0 MeV. Jackson, W. R.; Valkovic, V.; Emerson, S. T.; (and others) (Rice Univ., Houston, Tex). Nucl. Phys.; A166: 525-33(1971).

The ^{2}H(p,pn) reaction was studied at a bombarding energy of 9.0 MeV and several coincidence detection angles. The energies of the detected, coincident particles were determined using a solid-state surface barrier detector for the proton and time-of-flight measurement on the neutron. The contributions of the neutron–proton final-state interaction and neutron–proton quasi-free scattering were observed. The final-state-interaction contribution is reproduced by the theory of Phillips, Griffy, and Biedenharn [Nucl. Phys., 21: 327(1960)]. The shape of the spectrum due to the quasi-free-scattering contribution is in reasonable agreement with the simple-impulse-approximation prediction. The absolute value of cross section is smaller than predicted by spectator-model calculations. (auth)

36671 TWO-BODY PHOTODISINTEGRATION OF ^{4}He UP TO 80 MeV. Busso, L.; Garfagnini, R.; Piragino, G.; Ronchi Della Rocca, S.; Zanini, A. (Univ., Turin. Istituto Nazionale di Fisica Nucleare, Turin). Lett. Nuovo Cim.; 1: No. 23, 941-5(5 Jun 1971).

The photodisintegration of ^{4}He was studied with a diffusion cloud chamber for energies up to 80 MeV. From an analysis of 9000 ^{4}He(γ,^{3}He)n and 9600 ^{4}He(γ,^{3}He)p events, the following were measured: the photoproduction emission cross section, the energy spectra of the photoprotons and photoneutrons, and the behavior of the asymmetry coefficient. Comparison is made with other experimental data. (L.B.S.)

Nuclear Properties and Reactions, 6≤A≤19

Refer also to abstracts 34915, 35050, 36298, 36527, 36707, 36710, 36712, 36719, 36732, 36733, 36737, 36738, 36783, 36799, 36811, 36815, 36836, 36837, 36847, 36848, and 37110.

36672 (LAL–1243) STUDY OF THE ^{11}B NUCLEUS BY ELECTRON SCATTERING. Riskalla, R. ([Paris Univ., Orsay (France). Laboratoire de l'Accelerateur Lineaire]). Feb 1971. 103p. (In French). Dep. NTIS (U. S. Sales Only).

Thesis.

The scattering of electrons by a natural boron target (80.22% ^{11}B and 19.78% ^{10}B) was studied. The experimental equipment and its use are described in detail. The details concerning the handling of the experimental data are given (cross section calculations, shift of the elastic peak, physical corrections, counting losses, error, and the determination of longitudinal and transverse components of the form factor). The energy spectra of electrons scattered by ^{11}B were measured for incident energies between 100 and 300 MeV and for angles between 30 and 135°. A spectroscopic analysis was made of the ^{11}B levels at excitation energies of 2.13, 4.46, 6.76, and 8.57 MeV. The fact that the ground state and the 4.46- and 6.76-MeV levels form a rotational band indicates the rotational or collective nature of the ^{11}B nucleus. In addition, the fact that the configuration of the individual particle agrees to some extent with the experimental points of the first excited state indicates the special nature of this transition. These two facts confirm the validity of hypotheses of the unified model. (France)

36673 PROTON INDUCED REACTIONS ON MASS-14 NUCLEI. Curtis, T. H.; Lutz, H. F.; Heikkinen, D. W.; Bartolini, W. (Univ. of California, Livermore). Nucl. Phys.; A165: 19-32(1971).

Targets of ^{14}N and ^{14}C were bombarded with 14.5 MeV protons. The ^{14}N was in the form of natural N_2 gas, which is 99.6% ^{14}N, while the ^{14}C was in the form of CO_2 with a ^{14}C enrichment of 91.4%. Particles from the (p,p′), (p,d) and (p,t) reactions on these nuclei were identified and analyzed using conventional solid-state detectors and electronics. The overall energy resolution was 70 keV. Angular distributions were taken from 20° to 150° for the (p,p′) reaction and from 20° to 110° for the (p,d) and (p,t) reactions. For ^{14}N, 18 levels were seen below 10 MeV excitation energy in the (p,p′) reaction and one transition to the ground state of ^{13}N in the (p,d) reaction. The (p,t) reaction is energetically forbidden. For ^{14}C, 5 levels were seen below 8.5 MeV excitation but it was not possible to obtain angular distributions because of masking due to excited states of ^{16}O. Also for ^{14}C, 3 levels were seen in the (p,d) reactions and the (p,t) reaction leading to the ground state of ^{12}C. The (p,p′) data were analyzed assuming a microscopic model of the nucleus and a two-body interaction, which included a tensor component for the study of the 2.31 MeV level of ^{14}N. The DWBA code DRC was used for the (p,p′) analyses. The (p,d) data were analyzed using the code DWUCK to extract spectroscopic factors. (auth)

36674 ^{19}F(^{3}He,^{6}Li)^{16}O REACTION AT 40 MeV. A STUDY OF THE MULTI-PARTICLE–MULTI-HOLE STRUCTURE OF ^{16}O EXCITED STATES. Detraz, C.; Moss, C. E.; Zafiratos, C. D.; Zaidins, C. S. (Univ. of Colorado, Boulder). Nucl. Phys.; A167: 337-51(1971).

The ^{19}F(^{3}He, ^{6}Li)^{16}O reaction has been studied at 40.7 MeV from $\theta_{lab} = 5°$ to 170°. Excitation functions have been measured at 20°, 70° and 165°. The reaction mechanism is found to be predominantly direct, except at backward angles where a compound-nucleus process dominates. Zero-range DWBA calculations fail to account for the shape of the angular distributions. The role of finite-range effects is discussed, and satisfactory fits to the angular distributions are obtained by assuming a fixed-range interaction between the ^{3}He and the transferred triton-like fragment. Because of the observed selective population of the ^{16}O excited states, several conclusions about their multi-particle-multi-hole structure can be derived. In particular, a test of current shell-model wave functions is provided for the low-lying excited states, and the role of $p_{\frac{1}{2}}^{-1}$ configurations is pointed out. (auth)

36675 ANGULAR DISTRIBUTIONS FROM THE REACTION ^{12}C(α,γ_0)^{16}O IN THE 13 MeV EXCITATION REGION OF ^{16}O. Kernel, G.; Mason, W. M.; von Wimmersperg, U. (Nuclear Physics Lab., Oxford). Nucl. Phys.; A167: 352-68(1971).

Angular distributions of gamma rays from the reaction ^{12}C (α,γ)^{16}O in the energy region E_α = 7.6 to 8.1 MeV were measured with good accuracy. The coefficients of the Legendre polynomial expansion of the angular distributions are given as functions of energy. Some resonance parameters are extracted. (auth)

36676 ISOBARIC ANALOGUE STATES IN NUCLEI. Jones, G. A. (Oxford Univ.). Phys. Bull. (London); 22: 137-40(Mar 1971).

The history and general concepts underlying the subject are first discussed; this introduction is followed by discussions of direct and exchange reactions, reactions proceeding via the compound nucleus, stripping and compound-nucleus reactions, and particle–hole excitations. Depicted graphically are energy levels for mass 14, neutron spectra from the reactions V(p,n) and Co(p,n) at E_1 = 17 MeV, neutron yields for ^{89}Y(p,n) and ^{88}Sr(p,n) as a function of proton energy, and proton elastic scattering yields from ^{92}Mo as a function of proton energy; a schematic representation of an isobaric analogue state for target nucleus (T,T) is also given. It is stated that the accurate locations of analogue states has determined the Coulomb displacement energy over a wide range of nuclei and the relative distributions of protons and neutrons in large nuclei. The examples relate to proton bombardments, but other bombarding particles have also been employed. The knowledge that such states can be extremely sharp has stimu-

lated a new attack on the light elements, and states of width ~100 eV at excitations of ~10 MeV have been located, as well as "double analogue states". (UK)

36677 CALCULATION OF ISOSPIN MIXING IN ^{8}Be WITH CORRELATED WAVE FUNCTIONS. Anderson, R. K.; Goldhammer, Paul (Univ. of Kansas, Lawrence). Phys. Rev. Lett.; 26: 978-80(19 Apr 1971).

Isospin mixing in the 2^+, 1^+, and 3^+ states of ^{8}Be is calculated with correlated radial wave functions obtained from reference-spectrum solutions of the Bethe–Goldstone equation. The off-diagonal matrix elements are approximately a factor of 2 larger than those calculated with oscillator wave functions and provide a very reasonable interpretation of the experimental data. (auth)

36678 INTERMEDIATE STRUCTURE AND THE GIANT-DIPOLE RESONANCE IN ^{16}O. Shakin, C. M. (Case Western Reserve Univ., Cleveland); Wang, W. L. Phys. Rev. Lett.; 26: 902-6(12 Apr 1971).

A projection-operator theory of photodisintegration is developed. It is shown that the coupling of 3p–3h (three-particle, three-hole) modes to the 1p–1h modes can explain the intermediate structure of the giant resonance in oxygen when the 1p–1h states are treated as "doorways" for γ-ray absorption and for particle emission. The structure problem is treated using the interacting-boson approximation of Iachello and Feshbach. (auth)

36679 DIFFRACTION EFFECTS IN THE HIGH ENERGY (p,2p) REACTION. Jackson, D. F. (Univ. of Surrey, Guildford, Eng.). Phys. Lett.; 35B: No. 2, 99-100(10 May 1971).

Differential cross sections for the (p,2p) reaction at 600 MeV show marked dependence on the recoil angle of the residual nucleus. It is shown that this dependence can be interpreted in terms of diffraction effects. (auth)

36680 ALPHA CLUSTERING AND ANGULAR MOMENTUM PROJECTION BEFORE AND AFTER VARIATION. Friedrich, H. (Univ., Freiburg i. B.); Weiguny, A. Phys. Lett.; 35B: No. 2, 105-8(10 May 1971).

By starting with α-cluster wave functions, angular-momentum projection before (PB) and after (PA) variation yields excitation energies of light 4N nuclei in good agreement with experiment. In contrast to PA, the results of PB show more pronounced α-clustering and a cutoff in rotational bands. (auth)

36681 SIZE OF ^{12}C IN THE α-PARTICLE MODEL. Borysowicz, J. (Michigan State Univ., East Lansing). Phys. Lett.; 35B: No. 2, 113-14(10 May 1971).

It is found that the radius of ^{12}C predicted in the α model is much larger than the experimental radius of the ground state. (auth)

36682 ELECTRON SCATTERING FROM ^{13}C. Yang, Chiensheng. Saskatoon, Saskatchewan; Univ. of Saskatchewan (1970). 186p. University Microfilms Order No. 71-6021.

The 140-MeV Saskatchewan electron linear accelerator was used to measure electron scattering from carbon-13. The experimental results for the elastic and inelastic scattering and theoretical calculations of the inelastic form factors based on various nuclear models are presented. The results of elastic electron scattering experiment using a $^{13}CH_4$ gas target showed that the ratio of the rms charge radius of the ^{13}C nucleus to that of ^{12}C is .975 ± 2% which is consistent with the result .96 ± 1% of Crannell et al. This confirms the somewhat surprising finding that the rms charge radius of ^{13}C is smaller than that of ^{12}C. Inelastic electron scattering was studied up to about 20 MeV excitation energy and for momentum transfers ranging from 0.627 to 0.935 fm^{-1} using both solid and gas targets. Eleven levels at excitation energies of 3.69, 7.55, 8.25, 8.86, 9.50, 11.70, 11.97, 12.32, 13.76, 15.11 and 19.15 MeV were observed. The spectra showed that the normal parity states are strongly excited especially the levels at 3.69 MeV ($3/2^-,1/2$), 7.55 MeV ($5/2^-,1/2$) and 15.11 MeV ($3/2^-,3/2$) and special attention has been paid to these levels. The values for the form factors of these levels are consistent with the previous extrapolation of the low momentum transfer data. The wave functions from the intermediate coupling shell model and the wave functions derived from the effective interaction calculation are the best wave functions available at this stage for the normal parity states. These wave functions are used to calculate the form factors for the ground state ($1/2^-,1/2$) to the ($3/2^-,1/2$) ($5/2^-,1/2$) ($7/2^-,1/2$) and $3/2^-,3/2$) excited state transitions. The results of these predictions are compared with the experimental form factors for the three levels mentioned above. The previous predictions are very close together and it is found that these wave functions can only roughly predict the form factors for the 3.69 and 7.55 MeV levels but agree fairly well for the 15.11 MeV level. However the configurations are restricted to the 1p shell, and it may be possible to improve the theoretical predictions by including 2s – 1d shell configurations. (Diss. Abstr. Int., B)

36683 NEUTRON SCATTERING FROM ^{15}N. II. COUPLED CHANNEL CALCULATIONS. Dover, C. B. (Univ., Heidelberg. Max-Planck-Institut fuer Kernphysik, Heidelberg); Cierjacks, S.; Kirouac, G. J.; (and others). Nucl. Phys.; A166: 461-78 (1971).

The total and differential cross sections for the scattering of neutrons from ^{15}N in the energy region $0 \leqq E_n \leqq 12$ MeV are analyzed by the method of coupled channels in a 1p–1h configuration space. The 1^- and 2^- resonances observed experimentally at E_n = 2.3 and 2.9 MeV, respectively, are identified with the $(d_{\frac{5}{2}}p_{\frac{1}{2}}^{-1})_{1-2^-}$ coupling in the p–h model. The absolute cross sections and angular distributions are in reasonably good agreement with experiment in the region $2 \leqq E_n \leqq 3$ MeV of the $d_{\frac{5}{2}}$ single-particle resonance. Some of the other particle–hole resonances predicted by theory are tentatively identified with broad peaks seen in the energy-averaged total cross section. (auth)

36684 NEUTRON SCATTERING FROM ^{15}N. I. R-MATRIX AND PHASE-SHIFT ANALYSES. Zeitnitz, B. (Univ., Hamburg); Dubenkropp, H.; Putzki, R.; (and others). Nucl. Phys.; A166: 443-60(1971).

The total neutron cross section of ^{15}N was measured in the neutron energy range 0.9 to 32 MeV. Between 0.8 and 3.1 MeV angular-distribution and polarization measurements were performed. Assignments for levels in ^{16}N up to E_x = 6.7 MeV could be determined using R-matrix and phase-shift analyses. The positions of the $d_{\frac{5}{2}}$ single-particle resonances were established. Above E_x = 6.7 MeV estimates of the angular momenta were obtained from the total cross section by the 2J + 1 rule. (auth)

Nuclear Properties and Reactions, 20 ≤ A ≤ 89

Refer also to abstracts 34915, 35050, 36676, 36679, 36680, 36718, 36719, 36732, 36733, 36737, 36738, 36741, 36757, 36783, 36798, 36799, 36811, 36816, 36834–36836, 36845, and 36848.

36685 (AWRE-O-3/71) ELASTIC AND INELASTIC SCATTERING OF 5.0 MeV NEUTRONS BY SODIUM. Coles, R. E. (Atomic Weapons Research Establishment, Aldermaston (England)). Feb 1971. 12p. Dep. NTIS (U. S. Sales Only). UK 10p.

The time-of-flight method was used to study 5.0 MeV neutron elastic and inelastic scattering by sodium. Differential cross sections at ten angles between 30° and 135° were measured for elastic scattering and for inelastic scattering to seven levels up to 3.88 MeV excitation in the target nucleus. This work was originated to provide information on the shape of the elastic angular distribution and where appropriate, comparisons are made with existing data in the UKAEA Nuclear Data File No. 182 for sodium. (auth)

36686 (CONF-680986-1) RADIONUCLIDE PREPARATION THROUGH (n,p) AND (n,α) REACTIONS WITH FAST REACTOR NEUTRONS. Braun, H. (Kernforschungszentrum, Karlsruhe (West Germany). Institut fuer Radiochemie). [1960]. 7p. (In German). Dep. NTIS (U. S. Sales Only).

From Meeting on preparative radiochemistry production of radionuclides and labelled compounds; Lindau Im Bodensee, Germany (5 Sep 1968).

For the production of radionuclides of high specific activity in reactors, cross sections for (n,p) or (n,α) reactions are mostly unknown or must be determined for each reactor individually. If the energy distribution of fast neutrons does not differ significantly from that of fission neutrons, cross sections of the former are proportional to the latter. Reactor cross sections, therefore, can be estimated from tables of fission-neutron cross sections. In the FR-2, Karlsruhe, (n,p) and (n,α) reactions were used, and the proportionality factors were determined for the production of ^{51}Cr, ^{54}Mn, ^{56}Mn, ^{59}Fe, ^{58}Co, ^{86}Rb, and ^{89}Sr. (tr-auth)

36687 (LYCEN-7087) REACTIONS (d,α) WITH ^{54}Fe AND ^{51}V. Grossiord, Jean-Yves (Lyon Univ. (France). Institut de Physique Nucleaire). Dec 1970. 56p. (In French). Dep. NTIS (U. S. Sales Only).

Thesis.

The two-nucleon transfer reactions ^{54}Fe(d,α)^{52}Mn and ^{51}V(d,α) ^{49}Ti, produced by 28-MeV incident deuterons, were studied. The excitation spectra and the angular distributions of the levels of

XUM

^{52}Mn and ^{49}Ti were established. The experimental results are given, and they are analyzed in the framework of the shell model with independent particles. The shape of the angular distributions depends upon the well depth in the α channel, and characterizes the transferred angular momentum L for a transfer occurring in the same shell. For a target nucleus with zero spin (^{54}Fe) the spin of the final state in the residual nucleus can be determined when the restriction J = L or J = L + 1 is imposed. The results obtained for ^{52}Mn and ^{49}Ti are compared with those obtained by other workers for the same nuclei by means of different reactions. The spin and parity of some already known levels are confirmed. (France)

36688 (N-70-43042) ABSOLUTE NEUTRON CROSS SECTIONS FOR THE PRODUCTION OF ^{24}Na ISOMER FROM MAGNESIUM AND ALUMINUM. Final Report. Salaita, George N. (Southern Methodist Univ., Dallas, Tex. Dept. of Physics). Oct 1970. 39p. (NASA-CR-110933; SMU-83-24). NTIS.

The cross sections for the ^{24}Mg(n,p)^{24m}Na and ^{27}Al(n,α)^{24m}Na reactions were measured using the cyclic activation technique and a high resolution Ge(Li) gamma-ray detector. The absolute activation cross sections were also measured for the ^{27}Al(n,p)^{27}Mg and ^{27}Al(n,α)^{24}Na reactions at 14.8 MeV neutron energy. The results were ^{24}Mg(n,p)^{24m}Na, 138 ± 14 mb; ^{27}Al(n,α)^{24m}Na, 65 ± 6 mb; ^{27}Al(n,p)^{27}Mg, 75 ± 6 mb; and ^{27}Al(n,α)^{24}Na, 111 ± 9 mb. These results are compared with similar measurements of other authors. (auth) (STAR)

36689 (NP-18820) STUDY OF THE SPALLATION OF MEDIUM-MASS NUCLEI. Regnier, Serge (Bordeaux Univ. (France). Faculte des Sciences). 1971. 38p. (In French). Dep. NTIS (U. S. Sales Only).

Thesis.

The cross sections for the production of ^{26}Al in Fe and Si by 600-MeV and 24-GeV protons were measured. The cross sections obtained in Fe and Si were, respectively, 0.36 ± 0.07 mb and 11.1 ± 1.1 mb at 600 MeV, and 2.3 ± 0.5 mb and 6 ± 1.2 mb at 24 GeV. The spallation cross sections were computed using a two-stage model. The evaporation stage was calculated using the RUDSTAM analytical method, and a simple approximation method was used to calculate the internuclear cascade. The principal characteristics of spallation for targets of medium mass were found. It is shown that these calculations explain the variations in the spallation cross sections with the charge and the mass of the products, the target, and the energy of the incident protons. The relative rates of production of spallation residues in Fe and Cu, and the dependence of the variations in the cross sections of ^{22}Na, ^{24}Na, and ^{32}P with the charge of the target were computed. The results obtained are fairly consistent with experiment. (France)

36690 (NP-18824) STUDY OF ISOBARIC ANALOGUE STATES BETWEEN 4 AND 8 MeV FOR THE REACTION ^{48}Ca(p,p)^{48}Ca. Estrada Tinajero, Pedro (Instituto Politechnico Nacional, Mexico City. Escuela Superior de Fisica y Matematicas). 1970. 79p. (In Spanish). Dep. NTIS (U. S. Sales Only).

Thesis.

Relative excitation functions for proton elastic scattering by ^{48}Ca at 4 to 8 MeV were measured. Resonances in ^{49}Sc were observed that are isobaric analogs to levels in ^{49}Ca. (R.W.R.)

36691 (ORNL-tr-2481) β^+ DECAY OF ^{47}V. Daniel, H. Translated by J. J. Pinajian (Oak Ridge National Lab., Tenn.), from Z. Naturforsch., A; 9: 974(1954). 5p. Dep. NTIS.

With the use of a magnetic spectrometer, ^{47}V was found to have only a simple allowed β spectrum with an end-point energy of 1.89 ± 0.01 MeV; the decay leads to the ground state of ^{47}Ti. (auth)

36692 (UARAEE-103) THERMAL NEUTRON CAPTURE GAMMA-RAYS IN IRON. Hassan, A. M.; Abu-Zeid, H. M.; Hamouda, I. (Atomic Energy Establishment, Cairo (Egypt). Reactor and Neutron Physics Dept.). 1970. 19p. Dep. NTIS (U. S. Sales Only).

Thermal neutron capture gamma radiation from natural iron sample was investigated with the aid of a three-crystal scintillation pair spectrometer. Previously unreported lines in natural iron of energies 6.95, 6.75, 5.35, and 5.18 MeV were observed. (auth)

36693 (WARD-4181-2) STATUS REPORT ON EVALUATION OF SODIUM CROSS SECTIONS FOR ENDF/B. Paik, N. C.; Pitterle, T. A. (Westinghouse Electric Corp., Madison, Pa. Advanced Reactors Div.). Feb 1971. Contract AT(30-1)-4181. 18p. Dep. NTIS.

The status of the evaluation of the total, scattering, and reaction cross sections of ^{23}Na for ENDF/B is examined. Detailed curves of the total cross section from 100 eV to 15 MeV are given. (L.T.W.)

36694 LOW-LYING LEVELS OF ^{58}Co. Robertson, R. G. H.; Summers-Gill, R. G. (McMaster Univ., Hamilton, Ont.). Can. J. Phys.; 49: 1186-1204(1 May 1971).

The odd-odd nucleus ^{58}Co was investigated experimentally by the ^{59}Co(d,t)^{58}Co and the ^{55}Mn(α,nγ)^{58}Co reactions. In the pickup studies deuteron energies of 15 and 16.5 MeV were used, and levels at 0, 25, 52, 112, 365, 375, 456, 888, 1043, and 1078 keV were observed. DWBA analysis showed mixed l_n = 1 and 3 transfers for all levels except the last named, which is pure l_n = 3. High-resolution gamma-gamma coincidence work using the (α,nγ) reaction revealed the decay properties of a large number of levels up to 1.5 MeV, including all those seen in (d,t) and allowed tentative spin assignments for a comparison with the theoretical calculations of Vervier. Qualitatively, the agreement is good. (auth) (Canada)

36695 INELASTIC ELECTRON SCATTERING FROM SEVERAL Ca, Ti, AND Fe ISOTOPES. Heisenberg, J.; McCarthy, J. S.; Sick, I. (Stanford Univ., Calif.). Nucl. Phys.; A164: 353-66(1971).

Differential cross sections for inelastic electron scattering from ^{40}Ca, ^{42}Ca, ^{44}Ca, ^{46}Ti, ^{48}Ti, ^{50}Ti and ^{56}Fe have been measured. The cross sections for the strongly excited 2^+, 3^-, 4^+ and 5^- levels have been measured over a range of momentum transfer q of 0.4 to 2.6 fm^{-1}. The data have been fitted using two representations for the transition charge, (i) to hydrodynamic liquid drop, and (ii) a phenomenological model. (auth)

36696 ^{39}K(^{3}He,^{3}He)^{39}K AND ^{39}K(^{3}He,d)^{40}Ca REACTIONS AT 29.3 MeV. Cage, M. E.; Johnson, R. R.; Kunz, P. D.; Lind, D. A. (Univ. of Colorado, Boulder). Contract AT(11-1)-535. Nucl. Phys.; A162: 657-72(1971).

The ^{39}K(^{3}He, d)^{40}Ca reaction has been employed to study proton particle-hole states of ^{40}Ca. A ^{39}K(^{3}He, ^{3}He)^{39}K elastic scattering experiment was also performed to obtain ^{3}He optical-model parameter sets necessary for a DWBA analysis of the (^{3}He, d) data. The ^{39}K(^{3}He, d)^{40}Ca reaction provided information on the ground state of ^{40}Ca and 17 excited states. Angular distributions, partial strengths and spectroscopic factors were extracted for 14 of these states, and agreed generally with the results found by Erskine, Seth et al., and Forster et al. at lower bombarding energies. Proton particle-hole states, presumed to have $(1d_{\frac{5}{2}}^{-1}f_{\frac{7}{2}})_{T=0}^{J=2,3,4,5}$ and $(1d_{\frac{5}{2}}^{-1}2p_{\frac{1}{2}})_{T=0}^{J=1,2,3}$ configurations, were observed. The results compare favorably with the ^{39}K(d,n)^{40}Ca work of Fuchs et al. and the shell-model predictions of Gerace and Green, but not with the calculations of Gillet and Sanderson. (auth)

36697 ELASTIC AND INELASTIC SCATTERING OF α PARTICLES ON ^{20}Ne AND ^{22}Ne. Labie, E.; Leleux, P.; Macq, P. Ann. Soc. Sci. Brux. Ser I; 84: 240-52(30 July 1970). (In French).

The elastic and inelastic scattering of 22.5-MeV α particles on ^{20}Ne and ^{22}Ne was measured between 15° and 80° in the laboratory system. The results were analyzed by the Blair-Drozdov model. The interaction radius for ^{20}Ne, the values of β_2 for ^{20}Ne and ^{22}Ne, and the nuclear scattering for ^{20}Ne and ^{22}Ne were determined and compared with the results of other studies. (J.S.R.)

36698 SPIN-PARITY COMBINATIONS IN ^{22}Ne. Ollerhead, R. W. (Univ. of Guelph, Ont.); Allen, G. F. R.; Baxter, A. M.; Gillespie, B. W. J.; Kuehner, J. A. Can. J. Phys.; 49: 594-600(1 Mar 1971).

Detection of inelastically scattered alpha particles near 180° from the reaction ^{22}Ne(α,α')^{22}Ne was used to identify natural-parity levels in ^{22}Ne. Energy spectra were recorded for ten incident energies from 16.5 to 21.0 MeV in steps of 500 keV. Levels at 4.46, 5.52, and 5.92 MeV were identified as having n natural parity, this result leading to definite assignments of 2^+, 4^+, and 2^+, respectively. Levels at 5.14 and 5.64 MeV were identified as having unnatural parity, this result implying assignments of 2^- and 3^+, respectively. Tentative assignments are suggested for other levels, and the implications of the present assignments with regard to the identification of band structure in ^{22}Ne are discussed. (auth) (Canada)

36699 STUDY OF THE E_p = 1.724 MeV RESONANCE IN THE ^{27}Al(p,γ)^{28}Si REACTION. Lam, S. T.; Litherland, A. E.; Azuma, R. E. (Univ. of Toronto). Can. J. Phys.; 49: 685-703(15 Mar 1971).

The 13.245-MeV level in ^{28}Si was populated by resonant proton capture at 1.724 MeV in the ^{27}Al(p,γ)^{28}Si reaction. Gamma-ray angular distributions and linear polarizations were measured, respectively, with a coaxial and a planar Ge(Li) counter. Branching ratios were extracted from the angular distributions. Spins were assigned to the levels of ^{28}Si with the help of the angular distribution and linear polarization results. The spin and parity of the 13.245- and 9.699-MeV levels are most probably 5^- with

T = 1 and 0, respectively. The assignment $J^{\pi} = 4^-$ for the 8.411-MeV level is in agreement with the present data. A spin and parity of 3^- for both the 13.245- and 9.699-MeV levels also fits the data but with more adjustable parameters. Arguments are presented to show that these assignments are unlikely. Relative measurements of the gamma-ray yields from a thick target give a value of (7.5 ± 1.5) eV for $(2J + 1)\Gamma_\gamma\Gamma_p/\Gamma$ of the resonance. The M1 transition strength between the 13.245- and the 9.699-MeV levels is then deduced to be (0.7 ± 0.15) W.u. The known properties of the 9.699-MeV level suggest that it may be associated with an E5 oscillation of the ground state of ^{28}Si. (auth) (Canada)

36700 DECAY OF ^{34}P AND ^{34m}Cl. Ward, T. E.; Kuroda, P. K. (Univ. of Arkansas, Fayetteville). J. Inorg. Nucl. Chem.; 33: 609-15(Mar 1971).

The decay of 12.4-sec ^{34}P and 32.0-min ^{34m}Cl was studied using a Ge−Li spectrometer and β- and γ-ray scintillation detectors. Approximately 40 per cent of the total decay of ^{34m}Cl was determined to decay through the 145.7-keV isomeric transition to 1.56-sec ^{34g}Cl. The ground-state to ground-state β branching of ^{34}P was measured to be 85 ± 2 per cent. Decay schemes are presented and discussed. (auth) (UK)

36701 ^{26}Mg(d,α)^{24}Na REACTION AT LOW ENERGIES. Lin, E. K.; Wang, W. N.; Kiang, G. C.; (and others) (Tsing Hua Univ., Taiwan. Academia Sinica, Taiwan). Chin. J. Phys. (Taiwan); 8: 36-43(Oct 1970).

The reaction ^{26}Mg(d,α)^{24}Na was investigated with incident deuteron energies ranging from 2.5 to 3.0 MeV. A total of seven alpha-particle groups, corresponding to levels in ^{24}Na up to 1.88 MeV excitation, were observed. Data were taken at thirteen angles from 40° to 160° at E_d = 2.5, 2.7, 2.8, 2.9, and 3.0 MeV to obtain angular distributions. Excition functions in 25-keV steps between 2.5 and 3.0 MeV were measured at θ = 140° lab. The measured angular distributions of all alpha-particle groups were found to be nearly isotropic, and the measured excitation functions indicate the predominance of the compound-nucleus mechanism in this region of deuteron energies. (auth)

36702 METHOD FOR PREDICTING THE GROUND STATE SHAPES OF 2s–1d SHELL NUCLIDES. Ruehl, Franklin R, Jr. (Univ. of California, Los Angeles). Chin. J. Phys. (Taiwan); 8: 53-7(Oct 1970).

A general method for determining ground-state shapes of light nuclides is outlined. Two possible avenues of application are then analyzed with respect to nuclides in the 2s−1d shell. (auth)

36703 PHONON-PARTICLE DOORWAY STATES IN (n,γ) REACTIONS ON NUCLEI WITH A < 80. Knatko, V. A.; Rudak, E. A. (Inst. of Physics, Minsk). Nucl. Phys.; A164: 417-21 (1971).

The role of phonon-particle doorway states is studied in the de-excitation of the excited state following (n,γ) reactions on nuclei with A < 80. Anticorrelation cases are considered between the reduced widths of E1 γ-transitions from the excited state and the reduced widths of final state p-levels. (auth)

36704 MULTIWIRE-PROPORTIONAL-COUNTER MEASUREMENT OF THE M/L ORBITAL-ELECTRON-CAPTURE RATIO IN ^{71}Ge DECAY. Genz, H.; Renier, J. P.; Pengra, J. G.; Fink, R. W. (Georgia Inst. of Tech., Atlanta). Phys. Rev., C; 3: 172-9(Jan 1971).

The M/L orbital-electron-capture ratio in ^{71}Ge decay has been measured in a wall-less multiwire proportional counter containing the gaseous radioactive compound $^{71}GeH_4$. The counter was filled to 6 atm with argon containing 15 cm Hg propane. Recent advances in proportional-counter spectrometry below 500 eV have extended the sensitivity for precision measurement to the detection of single- and few-electron events down to essentially zero energy, even in the presence of high intensities of more energetic radiation. These improvements are the result not only of the sophistication of the low-noise electronic system, but also of the present investigation of the degradation spectrum (low-energy tails and afterpulses) from spectral peaks, and of the resolution from each other of single- and few-electron spectra by using computer analysis. A fully transistorized electronic system was developed which includes a special dc-coupled logic unit with zero-time recovery (updating) to perform the following operations: (i) to ensure proper anticoincidence functioning of the ring counter; (ii) to provide paralysis pulses necessary to block possible afterpulses following an ionizing event in either the ring or central counter; and (iii) to eliminate the phenomenon of front- and back-edge clipping of large pulses into small ones by the action of the anticoincidence gate. Measurements were made of the K, L, and M peaks, having mean energies of 10.37 keV, 1298, and 158 eV, respectively, and the resulting orbital-electron-capture ratios were determined to be P_L/P_K = 0.117 ± 0.001 and P_M/P_L = 0.162 ± 0.003. These ratios are compared with theoretical results. Whereas the present L/K capture ratio is in closer agreement with theory corrected for exchange according to Bahcall, the theoretical prediction of the M/L ratio by Bahcall with correction for exchange lies approximately 7% above the present value, which agrees well with a recent theoretical calculation by Vatai. The half-life of ^{71}Ge was found by least-squares fitting to be 11.15 ± 0.15 days, by following the decay of K x rays from a solid source with a Ge(Li) x-ray detector. (auth)

36705 MIDSTREAM EVALUATION, A = 88. Goodman, C. D. (Oak Ridge National Lab., Tenn.); Hughes, T. A.; Johns, M. W. Nucl. Data, Sect. A; 8: 345-71(Dec 1970).

Data on the A = 88 nuclides, reported since the publication of the last Nuclear Data Sheets in this region (1960), are studied and evaluated. Decay and level schemes, as well as summaries of the experimental data on which the adopted values are based, are presented. Literature available in June 1969 and important papers appearing up to June 1970 are included. (auth)

36706 NUCLEAR DATA SHEETS FOR A = 87. Verheul, H. (Vrije Univ., Amsterdam. Oak Ridge National Lab., Tenn.). Nucl. Data, Sect. B; 5: 457-85(May 1971).

Level schemes and decay characteristics are presented for all nuclei with mass number A = 87. The available experimental data are extracted from the literature, compared, and evaluated. Inconsistencies and discrepancies are discussed. The adopted level schemes and decay characteristics are based on data received before September 1970, although some articles received after that date were added in proof. (auth)

36707 KERNEL FOR THE SCATTERING OF NEUTRONS FROM AN EXCITED NUCLEAR STATE. Beynon, T. D. (Univ. of Birmingham, Eng.). J. Nucl. Energy; 24: No. 11, 565-72(Dec 1970).

A kernel, describing the inelastic scattering of neutrons from a single excited level, is derived and converted into a form suitable for transport-theoretic and transport-numeric studies. The validity of the model is established by comparisons with recent scattering measurements from the 845-keV level in ^{56}Fe. (auth) (UK)

36708 SPIN DEPENDENCE IN THE EXCITATION OF THE FIRST 2^+ STATE OF ^{54}Fe. Tesmer, J. R.; Schmidt, F. H. (Univ. of Washington, Seattle). Phys. Rev. Lett.; 26: 857-60 (5 Apr 1971).

Proton−γ angular-correlation measurements at 19.6 MeV, together with asymmetry data for excitation of the first 2^+ state of ^{54}Fe, yield strong evidence for the full Thomas form of the spin-dependent collective-coupling potential. In addition, the agreement between these data and calculations is improved when the spin-dependent deformation $\beta_{s.o.}$ is twice β_2, the deformation parameter for the central potential. (auth)

36709 EXPERIMENTAL EVIDENCE FOR PROTON-PAIR CORRELATION IN Ti AND Cr LOW-LYING EXCITED STATES. Lemaire, M. C.; Loiseaux, J. M.; Mermaz, M. C.; Papineau, A.; Faraggi, H. (CEA, Saclay, France). Phys. Rev. Lett.; 26: 900-2(12 Apr 1971).

The two-proton-transfer reactions ^{44,48}Ca(^{16}O, ^{14}C)^{46,50}Ti and ^{48,50}Ti(^{18}O, ^{14}C)^{50,52}Cr studied at 48-MeV ^{16}O incident energy show that the first excited states must include strong proton-pair components. It appears that the (^{18}O, ^{14}C) two-proton-transfer reaction is a new and useful spectroscopic tool. (auth)

36710 PROPERTIES OF ^{13}B AND ^{20}Na: THE SECOND-CLASS CURRENT PROBLEM. Wilkinson, D. H. (Brookhaven National Lab., Upton, N. Y. Univ. of Washington, Seattle); Alburger, D. E.; Goosman, D. R.; (and others). Nucl. Phys.; A166: 661-6(1971).

The half-lives of ^{13}B and ^{20}Na were measured: $t_{\frac{1}{2}}(^{13}B)$ = 17.33 ± 0.17 ms; $t_{\frac{1}{2}}(^{20}Na)$ = 442 ± 5 ms. The mass difference was measured: ^{20}Na − ^{20}Ne = 13.892 ± 0.007 MeV. Combined with other data, these measurements lead to $(ft)^+/(ft)^-$ = 1.166 ± 0.026 for A = 13 and 1.054 ± 0.023 for A = 20. If these numbers are directly interpreted in terms of second-class currents, the values for the induced tensor coupling constant are $g_{1T}(13) = (2.6 \pm 0.5) \times 10^{-3}$; $g_{1T}(20) = (1.5 \pm 0.6) \times 10^{-3}$. (auth)

36711 POLYNOMIAL BASIS FOR THE IRREDUCIBLE REPRESENTATIONS OF U_6 IN THE CHAIN $U_6 \supset R_6$. Prasad, L.S.R.K.; Venkatarayudu, T. (Andhra Univ., Waltair, India). Proc. Indian Acad. Sci., Sect. A; 73: 42−50(Jan 1971).

Explicit polynomial basis for the irreducible representation (IR) (K_1, K_2, K_3) of U_6 containing an IR (λ_1, λ_2, λ_3) of R_6 is obtained. These polynomials are useful in calculating the nuclear energy levels in the 2s−1d shell. (auth)

XUM

36712 COULOMB ENERGY DIFFERENCES IN MIRROR NUCLEI IN THE HARTREE–FOCK APPROXIMATION. Nguygen Van Giai (Institut de Physique Nucleaire, Orsay, France); Vautherin, D.; Veneroni, M.; Brink, D. M. Phys. Lett.; 35B: No. 2, 135-9(10 May 1971).

Coulomb energy differences are studied by the Hartree–Fock approximation. Corrections due to isospin impurity of the core are found to be too small to explain the experimental differences. (auth)

36713 STUDY OF MECHANISMS FOR 13.6-MeV DEUTERON DISINTEGRATION BY NUCLEI. Nemets, O. F.; Pugach, V. M.; Sokolov, M. V.; Struzhko, V. G. (Inst. for Nuclear Research, Kiev). Ukr. Fiz. Zh. (Russ. Ed.); 16: 403-9(Mar 1971). (In Russian).

Measurements of the angular and energy (d,pn) correlations from 13.6-MeV deuteron disintegration by ^{16}O, ^{27}Al, ^{40}Ca, Ti, ^{59}Co, Ni, Cu, Ag, Au, $^{58,60,61,62,64}Ni$, and ^{63}Cu isotopes were performed. The experimental data testified that the Coulomb disintegration when E_d = 13.6 MeV is essential only for heavy nuclei (Ag, Au). The diffraction process prevails for the middle-weight nuclei. Cross sections were found to change irregularly with mass number: this phenomenon is explained in the framework of the diffraction theory [Yadern. Fiz. 6: 1197(1967)] by the surface-diffusivity dependence on the structure of external nuclear shells. (auth)

36714 MIDSTREAM EVALUATION, A = 89. Johns, M. W. (McMaster Univ., Hamilton, Ont.); Park, J. Y.; Shafroth, S. M.; Van Patter, D. M. Nucl. Data, Sect. A; 8: 373-405(Dec 1970).

Data on the A = 89 nuclides, reported since the publication of the last Nuclear Data Sheets in this region (1960), are studied and evaluated. Decay and level schemes, as well as summaries of the experimental data on which the adopted values are based, are presented. Literature available in June 1969 and important papers appearing up to June 1970 are included. (auth)

36715 SEARCH FOR 72.5$_s$ ^{30m}Al. Grench, H. A.; Jones, A. D.W.; Nightingale, R. W. (Lockheed Palo Alto Research Lab., Calif.). Nucl. Phys.; A166: 670-2(1971).

A search was made for a previously reported 72.5-sec isomeric state in ^{30}Al. No such activity was found. An upper limit of 0.2 mb is placed on the $^{30}Si(n,p)^{30m}Al$ cross section at 15 MeV. (auth)

36716 STUDY OF THE $^{48}Ti(\alpha,p)^{51}V$ and $^{50}Ti(^3He,d)^{51}V$ REACTIONS. Maheshwari, P. N. (Bhabha Atomic Research Centre, Bombay); Gupta, U. C.; St-Pierre, C. Can. J. Phys.; 49: 1053-65(15 Apr 1971).

The reactions $^{48}Ti(\alpha,p)^{51}V$ at ten bombarding energies between 8.25 and 10.75 MeV and $^{50}Ti(^3He,d)^{51}V$ at 10 MeV bombarding energy were studied. Energy levels of ^{51}V up to 4.85 and 6.17 MeV were observed by (α,p) and $(^3He,d)$ reactions, respectively. The (α,p) reaction yielded many new energy levels. The angular distributions for deuterons were measured at lab angles between 15° and 120°, and compared with predictions of DWBA calculations using the TSALLY code from which the transferred angular momenta and spectroscopic factors were deduced. These experimental results are examined from the viewpoint of shell-model and strong-coupling rotator-model calculations. The effect of changing various optical-model parameters is also discussed. (auth) (Canada)

36717 REACTIONS $^{26}Mg(d,p\gamma)^{27}Mg$ AND $^{26}Mg(d,n\gamma)^{27}Al$ AND THE DECAY OF ^{27}Mg. Skaali, B. (Univ., Oslo). Phys. Norv.; 4: No. 1, 45-51(1970).

Excitation energies and γ-branchings of bound states of ^{27}Mg and ^{27}Al and the β-branching of ^{27}Mg were determined from Ge(Li) γ-ray spectra from the reactions $^{26}Mg(d,p\gamma)^{27}Mg$, $^{26}Mg(d,n\gamma)^{27}Al$ and $^{27}Mg(\beta^-)^{27}Al$. New information was obtained on the decay of the ^{27}Mg levels at 3561, 3762, 3786 and 4819 keV. (auth)

Nuclear Properties and Reactions, A ≥ 90

Refer also to abstracts 34915, 35050, 36264, 36298, 36332, 36369, 36676, 36707, 36712, 36713, 36817, and 36836.

36718 (AAEC/TM-585) TABLES OF GAMMA RAYS FROM (n,γ) PRODUCED NUCLIDES. Greig, R. A.; Porritt, R. E. J.; Bone, S. J. (Australian Atomic Energy Commission Research Establishment, Lucas Heights). Feb 1971. 64p. Dep. NTIS (U. S. Sales Only).

A rearrangement of gamma-ray energy tables (Lederer et al.) is made to enable rapid identification of gamma spectra. Tables are arranged thus: (1) major gamma rays ordered by energy (each energy followed by all other gamma rays from that particular nuclide); (2) all gamma rays ordered by energy; (3) gamma rays from mass-ordered nuclides. (Australia)

36719 (BNL–50274) DATA FORMATS AND PROCEDURES FOR THE ENDF NEUTRON CROSS SECTION LIBRARY. Drake, M. K. (ed.) (Brookhaven National Lab., Upton, N. Y.). Oct 1970. 220p. Dep. NTIS.

The philosophy of the Evaluated Nuclear Data File (ENDF) and the data formats and procedures to be used for entering data into the ENDF library are described. The first several sections review the general features of the ENDF libraries, the relation between ENDF and CSISRS (Cross Section Information Storage and Retrieval System), and the relation between ENDF and its secondary libraries. The next section details the standard formats used in all record types. The arrangement of the various types of data are then discussed. The file is illustrated for elastic scattering by natural He. (R.W.R.)

36720 (CONF-710301–4) FAST-NEUTRON CAPTURE INTEGRAL MEASUREMENTS OF ^{99}Tc, ^{109}Ag, AND OTHER FISSION PRODUCTS. Harker, Y. D. (Idaho Nuclear Corp., Idaho Falls). [1970]. 9p. Dep. NTIS.

From third conference on neutron cross sections and technology; Knoxville, Tenn. (15 Mar 1971).

The Coupled Fast Reactivity Measurement Facility (CFRMF) has a neutron spectrum approximating that of a typical LMFBR; it is used in this work to measure fast-neutron integral capture cross sections. These integral measurements provide important checks for evaluating differential cross section data and calculations. Reported here are the measurements for ^{99}Tc, ^{107}Ag, ^{109}Ag, ^{115}In, ^{133}Cs, ^{141}Pr, ^{165}Ho, and ^{169}Tm. The measurements are compared with calculated integrals derived mainly from the predicted cross sections reported by Benzi. For ^{99}Tc a systematic approach was applied to get an approximate differential cross section whose integral compared very well with the measured value. (auth)

36721 (DP-MS–70-95) NEUTRON-INDUCED FISSION CROSS SECTIONS FOR ^{244} ^{248}Cm AND ^{249}Cf. Benjamin, R. W.; MacMurdo, K. W.; Spencer, J. D. (Du Pont de Nemours (E. I.) and Co., Aiken, S. C. Savannah River Lab.). [1970]. 6p. (CONF-710301–12). Dep. NTIS.

From third conference on neutron cross sections and technology; Knoxville, Tenn. (15 Mar 1971).

Thermal fission cross sections and fission resonances integrals have been measured for ^{249}Cf and $^{244-248}Cm$ with both dual fission chambers and plastic fission-track recorders. Measurements were made in the core and thermal column of a research reactor. Cross sections were determined through direct comparison with the ^{235}U cross sections, σ_0^f (effective) = 561.5 b and I^f = 268 b. The low-energy cutoff for the resonance integral was adjusted to 0.625 eV. (auth)

36722 (IA–1208) FLUCTUATION FACTORS FOR THEORETICAL EVALUATION OF AVERAGE NEUTRON CROSS SECTIONS OF FISSILE NUCLEI IN THE UNRESOLVED RESONANCES REGION. Gur, Y.; Yiftah, S. (Israel Atomic Energy Commission, Tel Aviv). Sep 1970. 48p. Dep. NTIS (U. S. Sales Only).

In the course of evaluating elastic, fission, and capture cross sections one has to compute, from basic data, dimensionless quantities called "fluctuation factors". These factors are expressed as zero-to-infinity integrals. The role that these factors play in cross-section evaluation is discussed, and a full representation of their values in the entire range needed is given in both graphical and tabular form. The inappropriateness of the Gauss–Laguerre or Hermite–Chebyshev methods of integration for evaluating the factors is discussed, and a method is described that cuts down the computer time needed for the Simpson integration by a factor of about 40 compared with the straightforward method of Simpson integrations. (auth)

36723 (JINR–P1-5530) RELATIVE YIELDS OF SECONDARY [(p,xn)α] REACTIONS ON Bi IN THE RANGE E_p = 120–660 MeV. Chi, Li Tsun; Maltseva, N. S.; Mekhedov, V. N. (Joint Inst. for Nuclear Research, Dubna (USSR). Lab. of Nuclear Problems). 1970. 14p. (In Russian). Dep. NTIS (U. S. Sales Only).

The yields of the astatine isotopes $^{203-210}At$ were determined relative to ^{211}At as a function of proton energy by measuring the α spectra of astatine by using a semiconductor α spectrometer. (auth)

36724 (JINR–P6-5673) DECAY OF ^{139}Nd. Buttsev, V. S.; Vylov, Ts.; Kalinnikov, V. G.; Tikhonov, N. A.; Herrmann, E.

(Joint Inst. for Nuclear Research, Dubna (USSR). Lab. of Nuclear Problems). 1971. 21p. (In Russian). Dep. NTIS (U. S. Sales Only).

The decay of ^{139}Nd was investigated by means of semiconductor γ spectrometers and magnetic β spectrometers. It is shown that in 14.3% of the cases the 5.5-hour state of ^{139}Nd is de-excited by the 231.15-keV γ transition of the M4 type and in other cases undergoes $\epsilon + \beta$ decay. The maximum kinetic energy of emitted positrons (E = 1170 ± 50 keV) is determined. The decay scheme of ^{139m,g}Nd is constructed. Quantum characteristics are assigned to a number of ^{139}Pr excited states. The ^{139}Pr nucleus structure is discussed. (auth)

36725 (JINR-P6-5674) INVESTIGATION OF DECAYS OF NEODYMIUM AND PRASEODYMIUM NUCLIDES WITH MASS NUMBER A = 138. Afanas'ev, V. P.; Butsev, V. S.; Gromova, I. I.; Kalinnikov, V. G.; Tikhonov, N. A. (Joint Inst. for Nuclear Research, Dubna (USSR). Lab. of Nuclear Problems). 1971. 18p. (In Russian). Dep. NTIS (U. S. Sales Only).

Decay of ^{138}Nd and ^{138g,m}Pr was studied using the semiconductor γ spectrometers and magnetic β spectrometers. The schemes of ^{138}Pr and ^{138}Ce were completed with the previously unknown levels. The quantum characteristics were assigned to a number of levels. The nature of the ground and excited states of ^{138}Pr and ^{138}Ce is discussed. (auth)

36726 (JINR-P6-5681) INVESTIGATION OF SHORT-LIVED ISOMERS OF THE TERBIUM ISOTOPES: ^{148}Tb, ^{149}Tb, ^{150}Tb, AND ^{152}Tb. Arl't, R.; Beyer, G.; Kuznetsov, V. V.; (and others) (Joint Inst. for Nuclear Research, Dubna (USSR)). 1971. 15p. (In Russian). Dep. NTIS (U. S. Sales Only).

A number of new γ transitions produced in the decay of ^{149}Tb and ^{152}Tb isomers, as well as in the decay of the previously unknown isomers of ^{150}Tb ($T_{1/2}$ = (6.0 ± 0.1) min) and ^{148}Tb ($T_{1/2}$ = (2.1 ± 0.1) min), were observed. Partial decay schemes for the investigated isotopes are suggested. (auth)

36727 (JINR-P6-5704) DECAY OF ^{173}Ta. Bochev, B.; Broda, R.; Zvolskii, I.; Molnar, J.; Nenov, N. (Joint Inst. for Nuclear Research, Dubna (USSR). Lab. of Nuclear Problems). 1971. 15p. (In Russian). Dep. NTIS (U. S. Sales Only).

Spectra of conversion electrons, γ-rays, fast and delayed $\gamma-\gamma$ coincidences, and triple $\beta^+-\gamma$ coincidences were studied. The decay scheme of ^{173}Ta to ^{173}Hf is suggested. The bands of the states $1/2^-$ /521/ (ground state), $5/2^-$ /512/ (107.2 keV), and $7/2^+$ /633/ (197.3 keV) were observed, as well as states at 785 keV, 872 keV, 942.1 keV, 1209 keV, 1248 keV, and 1450 keV. The half-lives of the states with E = 107.2 keV and E = 197.3 keV were determined to be $T_{1/2}$ = 180 ± 8 nsec and $T_{1/2} \approx$ 170 nsec, respectively. (auth)

36728 (KFKI-71-9) SURVEY OF MEASUREMENTS OF THE FISSION NEUTRON SPECTRUM OF ^{252}Cf. Jeki, L.; Kluge, Gy.; Lajtai, A. (Magyar Tudomanyos Akademia Kozponti Fizikai Kutato Intezete, Budapest). [1970]. 15p. Dep. NTIS (U. S. Sales Only).

The background sources arising in different techniques for measuring fission-neutron energies were studied in detail, and the background due to the detection of delayed gamma rays was calculated. The proposed value of the Maxwellian temperature for the energy distribution of neutrons from the spontaneous fission of ^{252}Cf is about T = 1.57 MeV. (auth)

36729 (N-70-41999) NEUTRON CAPTURE CROSS SECTIONS OF MOLYBDENUM, TANTALUM, AND ^{238}U. Final Report. Friesenhahn, S. J.; Lopez, W. M.; Fricke, M. P.; Costello, D. G.; Carlson, A. D. (Gulf General Atomic, Inc., San Diego, Calif.). 5 Jun 1970. Contract NAS3-11844. 94p. (NASA-CR-72745; GA-10194). NTIS.

Absolute neutron capture cross sections for natural molybdenum, tantalum, and ^{238}U were measured from approximately 1 to 1000 keV energy using the time-of-flight technique. The neutron flux spectrum was monitored with ^{3}He proportional counters that were calibrated against measurements based on the ^{10}B(n,α)^{7}Li cross section below 80 keV and on the neutron + proton scattering cross section at higher energies. The measured energy variation of the capture cross sections above 80 keV relies solely upon the neutron + proton cross section; the cross sections are normalized directly to resolved resonances at low (eV) energies. (auth) (STAR)

36730 (NP-18829) FISSION INVESTIGATION USING ON-LINE MASS SPECTROMETRY. Chaumont, Jacques (Paris Univ., Orsay (France). Faculte des Sciences). 1970. 97p. (In French). Dep. NTIS (U. S. Sales Only).

Thesis.

The mass spectrometer used is described and the following points emphasized: construction of the target, elimination of contamination due to naturally occurring elements, recording of mass spectra. The characteristics of an experiment made with an external beam from the EL3 pile at Saclay on U and proton beams with uranium, thorium, and tantalum targets at 156 MeV and 24 GeV are discussed. All the 220 cross sections for the isotopes of Rb and Cs were measured; the results obtained are discussed. Although only two elements are considered, the results are very detailed and lead to a good understanding of fission mechanisms. There is good agreement between calculation and experiment on the distribution of Cs isotopes in the fission products produced by 156-MeV protons. (France)

36731 (NP-18835) STUDY OF THE ^{153}Sm → ^{153}Eu DECAY. Patin, Yves (Paris Univ., Orsay (France). Faculte des Sciences). 1970. 70p. (In French). Dep. NTIS (U. S. Sales Only).

The ^{153}Sm isotope was produced by neutron irradiation of a Sm sample enriched in ^{152}Sm (98.18 p.%). The internal conversion electron spectrum was obtained using a 180° magnetic spectrometer; and the gamma ray spectrum, using Ge(Li) detectors; the two-dimension $\gamma-\gamma$ coincidence spectrum was also determined. The results obtained were interpreted. The ^{153}Eu nucleus is in the mass region described by the Nilsson model. It represents a special case, being a highly deformed nucleus in spite of being situated at the utmost limit of this region. A level scheme is proposed in which the levels are grouped in two clusters, one between 0 and 300 keV, the other above 600 keV. The results are compared with those recently obtained for ^{155}Eu. (France)

36732 (NRL-7230) FORTRAN PROGRAMS FOR (p,γ) YIELD CALCULATIONS BASED ON VAVILOV'S THEORY OF ENERGY LOSS DISTRIBUTIONS. Dunning, K. L. (Naval Research Lab., Washington, D. C.). 29 Mar 1971. 84p.

Two Fortran programs are described for the analysis of (p,γ) resonance yield curves for targets that may be thick compared to resonance width but which have a total energy loss small compared to the energy of the incident particle. For the sake of definiteness (p,γ) reactions are discussed, but the programs may be used for some other incident particles as well. The programs are designed with several kinds of usage in view; in each, calculated and experimental yield curves are to be compared. A subprogram for plotting yield curves on a Calcomp plotter facilitates this comparison. Other subprograms provide plots that are useful in insuring that suitable parameters have been chosen as input data. Among the uses envisioned are the extraction of resonance widths and energies from experimental (p,γ) yield data from homogeneous targets and for targets that have a layer of inert matter or matter that contributes to the yield but which is different from that of the target; the determination of the energy-loss characteristics of a layer of matter on a target that produces a reaction with a sharp resonance of known properties; the determination of target thickness, e.g., for solid targets used in neutron production; the determination of the atomic composition of certain kinds of thin films; the calculation of energy-loss distributions; and the calculation of the beam energy distributions after the beam has passed through a slab of matter. The necessary energy-loss distributions for the target are calculated by means of a theory due to P. V. Vavilov (Zh. Eksp. Teor. Fiz. 32: 320(1957)), which gives a mathematically rigorous solution of an integro-differential equation for the many-collision energy-loss fluctuations experienced by a charged particle as it penetrates matter. This solution is based on a free-electron single-collision energy-loss probability density; the consequences of this assumption are discussed. (auth)

36733 (ORNL-4564) INSTRUCTIONS FOR THE OPERATION OF CODES ASSOCIATED WITH MECC-3, A PRELIMINARY VERSION OF AN INTRANUCLEAR-CASCADE CALCULATION FOR NUCLEAR REACTIONS. Bertini, H. W.; Guthrie, M. P.; Hermann, O. W. (Oak Ridge National Lab., Tenn.). May 1971. Contract W-7405-eng-26. 53p. Dep. NTIS.

Instructions for the operation of MECC-3 and associated editing codes are given. MECC-3 will operate over the ranges of 1 to 3500 MeV for incident nucleons and 1 to 2500 MeV for incident π^+ and π^- mesons for targets ranging from ^{4}He to ^{239}Pu. The calculation is expected to be valid, however, only over the range from about 100 to 2000 MeV for targets heavier than carbon. The programs operate on the IBM 360/75 and 360/91 computers. (auth)

36734 (ORNL-TM-3331) NEUTRON MULTIPLICITY FOR ^{239}Pu RESONANCE FISSION. Weston, L. W.; Todd, J. H. (Oak Ridge National Lab., Tenn.). Apr 1971. Contract W-7405-eng-26. 12p. (CONF-710301-14). Dep. NTIS.

From third conference on neutron cross sections and technology; Knoxville, Tenn. (15 Mar 1971).

Measurements were carried out in an attempt to resolve the

discrepancy in the spin dependence of the fission-neutron multiplicity ($\bar{\nu}$) for resonances in ^{239}Pu between Weinstein et al. [IAEA, SM-122/113] (1969) at Rensselaer Polytechnic Institute and Ryabov et al. [JINR Report P3-5297 (1970)] at Dubna. For the present measurements fission neutrons from a fission chamber were detected with low efficiency by using fast-neutron detectors rather than counting with high efficiency by using thermal-neutron detectors. The data do not indicate any statistically significant separation into two groups of multiplicity values according to spin state of the resonance between 14 and 200 eV. Where previous results indicated an average difference of 3% to 5% in neutron multiplicity for resonances of different spin, the present results indicate no difference outside the ~1/4% uncertainty of the experiment. (auth)

36735 (SGAE-PH-104/1971) MASS SPECTROMETRIC DETERMINATION OF THE NEUTRON CAPTURE CROSS SECTION OF ISOTOPES OF THE RARE EARTHS. Dobrozemsky, R.; Pichlmayer, F.; Viehboeck, F. P. (Oesterreichische Studiengesellschaft fuer Atomenergie G.m.b.H., Seibersdorf. Physik-Institut). [nd]. 31p. (In German). Dep. NTIS (U. S. Sales Only).

For the determination of neutron-capture cross sections of rare earth isotopes, the corresponding elements were electromagnetically separated, and the highly enriched isotopes were irradiated with and without Cd shielding in the ASTRA reactor to an integrated neutron flux of about 10^{20} n cm^{-2}. Before and after irradiation the isotopic abundances were measured by mass spectrometry. The pile capture cross section, the thermal capture cross section, and the effective resonance integral for ^{147}Sm, ^{148}Sm, ^{154}Gd, ^{156}Gd, ^{160}Dy, ^{161}Dy, ^{162}Dy, ^{163}Dy, ^{166}Er, ^{167}Er, ^{170}Yb, ^{171}Yb, ^{172}Yb, and ^{173}Yb were obtained. (auth)

36736 (THAI-AFC-35, pp 1-8) HIGH ENERGY PHOTOFISSION CROSS SECTIONS OF URANIUM AND THORIUM. Methasiri, Thamrong (Lund Inst. of Tech. (Sweden). Dept. of Nuclear Physics). Dep. NTIS (U. S. Sales Only).

The photofission cross sections of uranium and thorium were measured in the bremsstrahlung energy range 200 to 900 MeV. A glass detector was used to detect the fission fragments. Fission cross sections are obtained from the integrated cross section by using Penfold and Leiss's method. It is found that the photofission cross sections of both uranium and thorium show resonance peaks at a photon energy of 350 MeV, with peak values of 80 and 60 mb, respectively. It is suggested that, in a high energy fission, the fission mechanism can, at least in part, be due to photomeson production processes. (auth)

36737 (TID-25690) ENDF/B CROSS SECTION PREPARATION AND TESTING IN THE JOSHUA SYSTEM. Finch, D. R.; Honeck, H. C.; Stewart II, J. W.; Baxter, W. V. (Du Pont de Nemours (E. I.) and Co., Aiken, S. C. Savannah River Lab.). Mar 1971. Contract AT(07-2)-1. 8p. Dep. NTIS.

The features of the JOSHUA Cross Section Subsystem and the JOSHUA Operating System of prime importance to the user are described. The Cross Section Subsystem provides cross-section and cell-spectrum modules to perform averaging, weighting, group collapsing, and spectrum calculations as required. The JOSHUA Operating System provides execution of function commands from the terminal facilities and data sets to store information both temporarily and for longer periods. The benefits to the user are to reduce the load of purely manipulative tasks and to reduce the total time required to perform a sequence of operations on cross section data. The Cross Section Subsystem allows the evaluator of cross sections to perform more calculations and more meaningful calculations with a set of cross section data. To the routine user of cross sections, the subsystem provides facilities for creating a set of cross sections for any purpose. (R.W.R.)

36738 (UCLA-10-P-18-23) RESEARCH PROGRAM OF THE NUCLEAR CONSORTIUM AT THE UCLA CYCLOTRON LABORATORY, JULY 1970. Report AR 5. Richardson, J. Reginald; Wright, Byron T.; Forster, Harriet H.; Eisberg, Robert M. (California Univ., Los Angeles. Dept. of Physics). Contract AT(11-1)-Gen-10. 195p. Dep. NTIS.

ANTIMONY-110—beta decay scheme, (E)
ANTIMONY-111—beta decay scheme, (E)
ANTIMONY-112—beta and electron-capture decay scheme, (E)
ANTIMONY-113—beta and electron-capture decay scheme, (E)
ANTIMONY-114—beta decay scheme, (E)
CARBON-12—proton reactions (p,Li-6) at 36, 41, and 45 MeV, angular distributions for, (E)
CYCLOTRONS—research of Nuclear Consortium at UCLA
—beam transport and analyzing system for UCLA
FLUORINE-19—proton reactions (p,He-3) and (p,t) with, angular distributions for, (E)
—proton reactions (p,pd) and (p,pt) with, summed energy spectra from, (E)
GOLD-197—proton reactions (p,np) at 25 to 45 MeV, proton spectra and differential cross sections for, (E)
HELIUM-3—proton reactions (p,pd) and (p,2p) at 35 MeV, kinematic analysis of, (E)
—proton reactions (p,d) at 12 and 46 MeV, energy spectra for, (E)
—neutron reactions (n,d) at 14.4 MeV, angular distributions for, (E)
LEAD-208—proton reactions (p,np) at 30.5 MeV, angular distributions for, (E)
NICKEL—proton reactions at 10 to 40 MeV, activation cross sections for, (E)
NICKEL-58—proton reactions (p,d) and (p,t) at 22 to 40 MeV, differential cross sections for, (E)
TANTALUM-181—proton reactions (p,np) at 25 to 45 MeV, proton spectra and differential cross sections for, (E)
TRITIUM—proton reactions (p,pd) and (p,2p) at 35 MeV, kinematic analysis of, (E)
—neutron reactions (n,d) at 14.4 MeV, angular distributions for, (E) (J.W.R.)

36739 (UCRL-73090) STRUCTURE IN THE ^{235}U keV FISSION CROSS SECTION. Bowman, C. D.; Sidhu, G. S.; Stelts, M. L.; Browne, J. C. (California Univ., Livermore. Lawrence Radiation Lab.). 11 Mar 1971. 9p. (CONF-710301-11). Dep. NTIS.

From third conference on neutron cross sections and technology; Knoxville, Tenn. (15 Mar 1971).

The structure in the keV fission cross section, which was reported at the Helsinki meeting, has been remeasured using the 250 meter flight path at the new Livermore 100 MeV electron linac. The resolution is nominally about 0.15 nsec/meter. (auth)

36740 (WAPD-T-2411) TOTAL AND DIFFERENTIAL CROSS SECTION FOR NEUTRONS SCATTERED FROM ^{90}Zr AND NAT. Zr. Stooksberry, R. W.; Anderson, J. H.; Goldsmith, M. (Bettis Atomic Power Lab., Pittsburgh, Pa.). [1969]. 21p. Dep. NTIS.

Total neutron cross sections for C, Zr, and ^{90}Zr are tabulated and plotted for 18 energies between 0.433 and 2.37 MeV. The differential elastic scattering cross sections (and cos θ_l) are given for ^{90}Zr at 2.1 and 5.17 MeV and θ = 17.5° to 157.4°. (L.T.W.)

36741 (WHAN-SA-107) NEUTRON ENERGY DEPENDENT CROSS SECTION EVALUATION BY A MULTIPLE FOIL ACTIVATION METHOD. McElroy, W. N.; Simons, R. L.; Ulseth, J. A.; Kellogg, L. S. (Hanford Engineering Development Lab., Richland, Wash.). [1970]. Contract AT(45-1)-2170. 10p. (CONF-710301-13). Dep. NTIS.

From third conference on neutron cross sections and technology; Knoxville, Tenn. (15 Mar 1971).

The timely evaluation and definition of energy-dependent reaction cross sections σ(E) in the energy region above ~10^{-5} MeV is important for the Liquid Metal Fast Breeder Reactor program. Previous studies demonstrated the feasibility of a multiple-foil-activation iterative method for σ(E) definition and evaluation. Recent applications of this method have produced evaluations of σ(E)'s for such reactions as ^{197}Au(n,γ)^{198}Au and ^{63}Cu(n,α)^{60}Co. Energy-dependent cross sections, based on monoenergetic measurements and theoretical estimates, are generally inconsistent with activation measurements, which are inherently of an integral nature. Energy-dependent cross sections determined by activation methods as described here can detect and remove such inconsistency. The large discrepancy between recent monoenergetic and integral measurements for ^{63}Cu(n,α)^{60}Co emphasizes the need for removing such inconsistencies. (auth)

36742 MULTIPOLE ADMIXTURES OF TRANSITIONS FROM BETA, GAMMA, AND OCTUPOLE VIBRATIONAL STATES IN ^{154}Gd. Whitlock, L. C. (Vanderbilt Univ., Nashville. Mississippi Coll., Clinton); Hamilton, J. H.; Ramayya, A. V. Phys. Rev., C; 3: 313-25(Jan 1971).

A NaI-Ge(Li) detector arrangement has been used to measure γ-γ directional correlations in ^{154}Gd from the decay of ^{154}Eu. From the NaI detector, gates were selected to span the 123-keV $2^+ \rightarrow 0^+$, and 248-keV $4^+ \rightarrow 2^+$ transition, and an equivalent region of the Compton distribution at 320 keV to obtain the background contribution to each gate. These gates opened 20488 channels of the memory of a 4096-channel analyzer for storage of data at 90, 135, and 180° from the Ge(Li) detector. The well-known 1274-123-keV and 873-123-keV correlations were used to obtain attenuation and Ge(Li) solid-angle corrections for cascades that involve the 123-keV 2^+ state. The following correlations (in keV) were measured, with the A_2 and A_4 coefficients, respectively,

XUM

in parentheses: 692-123, $2^+_\beta \rightarrow 2^+_g \rightarrow 0^+(-0.145 \pm 0.022, 0.311 \pm 0.040)$; 1005-123, $3^+_\gamma \rightarrow 2^+_g \rightarrow 0^+(-0.239 \pm 0.018, -0.073 \pm 0.026)$; 1494-123, $3^- \rightarrow 2^+_g \rightarrow 0^+(-0.075 \pm 0.029, -0.022 \pm 0.044)$; 1597-123, $2^- \rightarrow 2^+_g \rightarrow 0^+(0.196 \pm 0.013, -0.017 \pm 0.021)$; 757-248, $3^+_\gamma \rightarrow 4^+_g \rightarrow 2^+_g(0.161 \pm 0.004, -0.174 \pm 0.006)$, 677-248, $4^+_\beta \rightarrow 4^+_g \rightarrow 2^+_g(-0.168 \pm 0.020, 0.178 \pm 0.029)$, 444-248, $2^+_\beta \rightarrow 4^+_g \rightarrow 0^+(0.196 \pm 0.009, 0.095 \pm 0.011)$; 625-248, $2^+_\gamma \rightarrow 4^+_g \rightarrow 2^+(0.187 \pm 0.014, 0.108 \pm 0.019)$; 893-248, $4^+_\gamma \rightarrow 4^+_g \rightarrow 2^+(-0.037 \pm 0.010, 0.160 \pm 0.013)$; 881-248, $3^- \rightarrow 4^+_g \rightarrow 2^+(-0.132 \pm 0.058, -0.059 \pm 0.086)$; 1188-248, $4^- \rightarrow 4^+_g \rightarrow 2^+(0.224 \pm 0.028, -0.010 \pm 0.041)$; and 1246-248, $3^- \rightarrow 4^+_g \rightarrow 2^+(-0.151 \pm 0.007, 0.010 \pm 0.008)$. The following M1 admixtures (in keV) were found in the transition from the β and γ bands: 692, $2^+_\beta \rightarrow 2^+_g(99.2^{+0.7}_{-1.7}\%$ E2); 677, $4^+_\beta \rightarrow 4^+_g(>80\%$ E2 for 2σ limits); 1005, $3^+_\gamma \rightarrow 2^+_g(99.78^{+0.39}_{-0.23}\%$ E2); 757, $3^+_\gamma \rightarrow 4^+_g(97.0 \pm 0.3\%$ E2); and 893, $4^+_\gamma \rightarrow 4^+_g(95.2 \pm 0.8\%$ E2). The transitions from the odd-parity states studied to the even-parity ground-state band are all $99.9 \pm 0.1\%$ E1. (auth)

36743 SPECTRUM OF PHOTONS EMITTED IN COINCIDENCE WITH FISSION OF ^{235}U BY THERMAL NEUTRONS. Peelle, R. W.; Maienschein, F. C. (Oak Ridge National Lab., Tenn.). Phys. Rev., C; 3: 373-90(Jan 1971).

The absolute energy spectrum of prompt photons emitted from the fission of ^{235}U by thermal neutrons was measured in the range from 0.01 to 10 MeV by using single-crystal, Compton, and pair NaI(Tl) scintillation spectrometers. Each was operated in ≤69-nsec coincidence with a fission chamber exposed to thermal neutrons from a reactor. The pulse-height response functions of the spectrometers were constructed in detail by exposing the spectrometers to radioactive sources of known disintegration rates. These data were used to "unfold" the measured pulse-height spectra to give the absolute differential energy spectrum and its random uncertainties. A careful analysis of systematic uncertainties was also performed. The average number of photons per fission is 8.13 ± 0.35 and the average photon energy release per fission is 7.25 ± 0.26 MeV, both over the energy region from 10 keV to 10.5 MeV. The results obtained here are in approximate agreement with the recent measurement by Verbinski and Sund in the energy region above 140 keV. From 1.5 to 4 MeV the calculation of Zommer, Savel'er, and Prokofiev gives results which are close to the measurements. The observed total energy release in photon emission per fission has been predicted by two published calculations which treated statistical evaporation theory in different ways to enhance the emission of photons. The K-shell x-ray intensities for the light- and heavy-fragment groups were found to be 0.08 ± 0.02 and 0.23 ± 0.02 photons/fission, respectively. The x-ray intensities are consistent with internal conversion of the observed γ-ray spectrum for various assumed mixtures of E1, E2, and M2 transitions, including roughly equal E1−E2 mixtures; the intensities are not consistent with all the transitions having any single multipolarity. (auth)

36744 EXPERIMENTAL STUDIES OF NEUTRON-DEFICIENT GADOLINIUM ISOTOPES. III. THE STRANGE CASE OF /sup 145g/Gd. Eppley, R. E.; McHarris, Wm. C.; Kelly, W. H. (Michigan State Univ., East Lansing). Phys. Rev., C; 3: 282-95(Jan 1971).

The γ rays emitted following the decay of 21.8-min ^{145}Gd have been studied using Ge(Li) and NaI(Tl) detectors in a variety of singles, anticoincidence, pair-coincidence, and two-dimensional ("megachannel") coincidence experiments. Of the 38 γ rays attributed to this decay, 27 (accounting for >97% of the intensity) have been placed in a consistent decay scheme that includes 20 states in ^{145}Eu. All of the single-proton states between Z = 50 and 82 are seen (including the $h_{11/2}$ state populated directly by the decay of ^{145m}Gd), and the associated β and γ transitions are accounted for quite well using simple shell-model arguments. In addition, and explanation is proposed for the abrupt change in decay properties of the N = 81 isotones that occurs at ^{145}Gd, viz., the lack of observable population directly to the ^{145}Eu ground state but 72.6% of its decay going to states at 1757.8 and 1880.6 keV. With a $(\nu s_{1/2})^{-1}$ ground state for ^{145}Gd, these "fast" β transitions can be represented as $(\pi h_{11/2})^{2n}(\nu s_{1/2})^{-1} \rightarrow (\pi h_{11/2})^{2n-1}(\nu h_{9/2})(\nu s_{1/2})^{-1}$, making the final states another example of three-quasiparticle states being populated by the β^+/ϵ decay of nuclei below N = 82. (auth)

36745 MEASUREMENT AND EQUILIBRIUM STATISTICAL-MODEL CALCULATION OF EXCITATION FUNCTIONS OF THE ^{197}Au(α,xn) REACTIONS IN THE ENERGY RANGE FROM 16 TO 103 MeV. Kurz, H. E.; Jasper, E. W.; Fischer, K.; Hermes, F. (Univ., Bonn). Nucl. Phys.; A168: No. 1, 129-38(1971).

The excitation functions of the reactions ^{197}Au(α,xn)$^{201-x}$, x = 1 to 8 were obtained by irradiation of stacked foils with α particles of 104 MeV and subsequent measurement and analysis of the γ-ray spectra. A Monte Carlo calculation was carried out on the basis of the equilibrium statistical model and satisfying agreement with the measured cross sections in the complete range of energies was reached. (auth)

36746 FISSION OF U, Np, Pu, AND Am ISOTOPES EXCITED IN THE (d,p) REACTION. Back, B. B.; Bondorf, J. P.; Otroschenko, G. A.; Pedersen, J.; Rasmussen, B. (Univ. of Copenhagen). Nucl. Phys.; A165: 449-74(1971).

Fission cross sections measured by the (d,pf) reaction on ^{233,235}U, ^{237}Np, ^{236,239,241}Pu and ^{241,243}Am are reported. The fission probability was calculated assuming a double-humped fission barrier. Damping of the vibrational states in the second minimum was treated by means of an imaginary potential. In this way it was possible to explain the observed resonance structure for the even nuclei and the lack of resonances for the doubly odd nuclei. The heights and transparencies of the inner and outer barriers were extracted. (auth)

36747 α DECAY OF SPHERICAL NUCLEI. Kadmenskii, S. G.; Kalechits, V. E.; Martynov, A. A. (Voronezh State Univ., USSR). Yadern. Fiz.; 13: 300-13(Feb 1971). (In Russian).

Absolute α decay widths for 18 nuclei in the vicinity of ^{208}Pb are calculated in the framework of the recently developed version of the α-decay theory, with no fitting parameter R_0, which explicitly takes into account the interaction of the α particle with the daughter nucleus. The theoretical values of the absolute widths obtained for the case of pure shell configurations differs from experimental ones not more than by a factor of about 100 for even isotopes and not more than by 34 for odd isotopes of Po. The account of configuration mixing for characteristic transitions in α decay of ^{210}Po, ^{211}Po, ^{210}Bi, ^{211}Bi puts the theoretical values of the absolute widths in agreement with the experimental ones. The calculations performed are in agreement with the α particle optical potentials with ~200 MeV depth of the real part and with the radius close to one-nucleon. (auth)

36748 MEASUREMENT OF CROSS SECTION RATIO OF RADIATIVE CAPTURE AND FISSION (α) FOR ^{235}U AND ^{239}Pu IN RESONANCE REGION. Kurov, M. A.; Ryabov, Yu. V.; Suo Ton Sik, At. Energ. (USSR); 30: 258-61(Mar 1971). (In Russian).

The cross section ratio of radiative capture and fission (α) for ^{235}U and ^{239}Pu is measured by the time-of-flight method in the neutron energy region of 0.1 to 30 keV with resolution of 60 nsec/m. (auth)

36749 UNIFIED MODEL CALCULATIONS FOR THE N = 83 NUCLEI. Vanden Berghe, G.; Heyde, K.; Waroquier, M. (State Univ., Ghent). Nucl. Phys.; A165: 662-72(1971).

Level schemes of the N = 83 nuclei ^{137}Xe, ^{139}Ba, ^{141}Ce and ^{143}Nd are obtained in a unified model calculation. Spectroscopic factors for (d,p) reactions are calculated and compared with experimental data. Magnetic dipole and electric quadrupole moments of the ground state are calculated. Some (M1 + E2) transition rates are discussed in ^{141}Ce. (auth)

36750 DECAY OF ^{195m}Hg AND ^{195}Hg TO LEVELS IN ^{195}Au. Frana, J.; Spalek, A.; Fiser, M.; Kokes, A. (Nuclear Research Inst., Rez, Czech.). Nucl. Phys.; A165: 625-40(1971).

The radioactive decay of ^{195}Hg ($T_{1/2}$ = 10 h) and ^{195m}Hg ($T_{1/2}$ = 41 h) was studied using Ge(Li) detectors and Ge(Li) γγ coincidence spectrometers; conversion electron spectra were measured with a Si(Li) detector and a double-focussing magnetic β-ray spectrometer. In the γ-ray spectrum of both isomers 80 transitions were found, of which 19 were incorporated into the decay scheme for the first time. The γγ coincidence experiment and energy relations indicate the existence of 28 excited levels, eight of which were proposed for the first time. The internal conversion intensity ratios for L and M subshells yielded the multipolarity of 8 transitions. The α_K internal conversion coefficients were determined by comparing internal conversion and γ-ray intensities for 30 transitions. Transition probabilities for the low excited states of ^{195}Au were compared with theoretical estimates. (auth)

36751 MEASUREMENT OF THE CIRCULAR γ-POLARIZATION AFTER n-CAPTURE IN ^{141}Ce, ^{144}Nd, AND ^{140}La USING Ge(Li) DETECTORS. Djadali, F.; Eichler, J. (Kernforschungszentrum, Karlsruhe, Ger. Univ., Karlsruhe, Ger.). Nucl. Phys.; A165: 560-8(1971).

By applying the circular polarization technique spins of nuclear levels were investigated. For the 0.662 MeV level of ^{141}Ce the spin $5/2^-$ was deduced. The spin of the 1.56 MeV and 1.31 MeV levels of ^{144}Nd are confirmed $I^\pi = 2^+$, 3^+ (or 5^+) and 4^+ (or 3^+). Further the spins for the 0.32 MeV and 0.064 MeV states in ^{140}La were determined $I^\pi = 3^-$ (or 4^-) and 3^- or 4^-, respectively. (auth)

36752 HALF-LIFE MEASUREMENTS OF EXCITED LEVELS IN ^{121}I AND ^{123}I. Hoeglund, A. (Univ. of Stockholm); Malmskog,

XUM

S. G.; Muennich, F.; Schrader, H. Nucl. Phys.; A165: 513-23 (1971).

The half-lives of some low-lying levels in ^{121}I and ^{123}I were measured using delayed coincidence techniques. Using the information from the level schemes as obtained in parallel work, the partial half-lives were deduced and compared with the single-particle estimates. (auth)

36753 INTERACTION OF ONE-PARTICLE AND COLLECTIVE EXCITATIONS IN ODD NUCLEI NEAR Pb. Isakov, V. I.; Kozhamkulov, T. A. (Ioffe Inst. of Physics and Tech., Leningrad). Yadern. Fiz.; 13: 512-20(Mar 1971). (In Russian).

Properties of odd "double magic ±1" nuclei are considered in the framework of a model assuming a weak interaction of nucleons with collective excitations of the nuclear core that are defined as phonons with various multipolarities. Nucleon–phonon scattering processes and the phonon decays into particle-hole pairs are taken into account. The results are compared with experiments. (auth)

36754 EFFECT OF EXCITATION ENERGY ON YIELDS AND KINETIC ENERGIES OF FRAGMENTS AT THE FISSION OF ^{239}Pu BY NEUTRONS. Akimov, N. I.; Vorob'eva, V. G.; Kabenin, V. N.; (and others). Yadern. Fiz.; 13: 484-91(Mar 1971). (In Russian).

Mass and kinetic energy distributions of fragments from the fission of ^{239}Pu by neutrons of 0 to 5.5 MeV in steps of 100 keV were studied. From the measured results one can see that the mean kinetic energy of fragments shows the trend to decrease with increasing E_n. At the 0.6 and 1.1 MeV neutron energy there is a sharp decrease of kinetic energy of fragments of approximately 200 keV. Within the neutron energy range under investigation the fragment yields suffer inessential changes. The effects observed indicate the possible effect of fissile transient states on the mass and kinetic energy distribution of fragments. (auth)

36755 GIANT DIPOLE RESONANCE ON NUCLEI IN TRANSITION REGION N ≈ 90. Vasil'ev, O. V.; Semenov, V. A.; Semenko, S. F. (Saratov State Univ., USSR. Lebedev Inst. of Physics, Moscow). Yadern. Fiz.; 13: 463-72(Mar 1971). (In Russian).

Photoneutron cross sections in the region of the giant dipole resonance for ^{146}Nd, ^{148}Sm, ^{152}Gd, ^{154}Gd, ^{156}Gd, ^{158}Gd, ^{151}Eu, and ^{153}Eu were measured. The comparison of the photoabsorption curves of Gd isotopes shows that the splitting of the giant resonance appears at N numbers which are less than those at which large static deformations arise. Possible ways for interpretation of the observed phenomena are discussed in the frame of collective models. (auth)

36756 PARAMETERS OF THE NEUTRON RESONANCES OF ^{233}U, ^{235}U, AND ^{239}Pu. Ryabov, Yu. V.; Suo Ton Sik, N.; Chikov, N. Yaneva, N. (Joint Inst. for Nuclear Research, Dubna, USSR). Yadern. Fiz.: 13: 457-62(Mar 1971). (In Russian).

Total cross sections for ^{233}U, ^{235}U and ^{239}Pu and fission and radiative capture cross sections for ^{235}U and ^{239}Pu were measured using the time-of-flight method with resolutions of 40 and 55 nsec/m. A liquid boron-including scintillation detector was used to detect the resonance neutrons in measurements of the total cross sections by means of the transmission method. The measurements of the fission cross sections, capture, and the total cross sections, using the self-indication method, were fulfilled with a large liquid scintillation detector with Cd incorporated into the solution. The parameters $g\Gamma_n$, Γ, Γ_f and Γ_c were calculated by means of the area method for 78 levels of ^{235}U and 32 levels of ^{239}Pu, and $g\Gamma_n$ and Γ for 13 levels of ^{233}U. (auth)

36757 SPECTROSCOPY OF STATES IN ^{91}Zr FROM γ-RAY TRANSITIONS OBSERVED IN THE ^{88}Sr(α,nγ)^{91}Zr REACTION. Glenn, J. E.; Baer, H. W.; Kraushaar, J. J. (Univ. of Colorado, Boulder). Nucl. Phys.; A165: 533-44(1971).

Levels below an excitation energy of 3.1 MeV in ^{91}Zr and 3.6 MeV in ^{90}Zr were studied through the prompt γ-radiation in the ^{87,88}Sr(α,nγ)^{90,91}Zr reactions. Gamma-ray spectra were recorded in a 25 cm^3 Ge(Li) detector at 90° to the beam using $^{87,88}SrCO_3$ targets and α-particle energies of 10.3–13.5 MeV. The γ-rays observed for transitions in ^{90}Zr are consistent with the known level structure, although some more accurate energy values were measured. In ^{91}Zr, a higher level density was observed in the 2.0–3.1 MeV region than had previously been revealed by charged particle reaction experiments. Spins for some of these states are suggested by comparing the variations in γ-ray yields with α-particle energy with Hauser–Feshbach calculations. A new level scheme is proposed for ^{91}Zr which suggests that some previous interpretations of the low-lying states in terms of simple vector-coupled states of the $2d_{5/2}$ neutron with 2^+ and 3^- core states of ^{90}Zr may need to be modified. (auth)

36758 ANOMALOUS ELECTRON SCATTERING FROM $^{142\ 146\ 150}$Nd. Madsen, D. W.; Cardman, L. S.; Legg, J. R.; Bockelman, C. K. (Yale Univ., New Haven). Nucl. Phys.; A168: No. 1, 97-128(1971).

Properties of the ground state charge distributions and some low-lying states in ^{142,146,150}Nd have been investigated using the Yale University Electron Accelerator. The incident energy was varied between 15 MeV and 60 MeV while angular distribution measurements were obtained at angles between 70° and 150° inclusive. If the ground state charge distribution is described in terms of a half-density radius and a skin thickness, a conventional phase-shift analysis of the present results, in the context of spherically symmetric static charge distributions, indicates anomalously small values of the skin thickness in all three neodymium isotopes. Measured cross sections differ by as much as 40% from those expected for these nuclei on the basis of the results of muonic x-ray and high-energy electron scattering experiments. Estimates by Rawitscher of the effect of virtual nuclear excitations suggest that these excitations (neglected in the analysis) may be responsible for the observed anomalies. Reduced γ-transition probabilities have been deduced for the following low-lying levels: ^{142}Nd, 1.57 MeV (2^+), 2.09 MeV (3^-, (2^+?)); ^{146}Nd, 0.45 MeV (2^+); ^{150}Nd, 0.13 MeV (2^+). (auth)

36759 ANGULAR ANISOTROPY OF FISSION FRAGMENTS IN TERNARY FISSION OF ^{235}U AND ^{238}U INDUCED BY 14-MeV NEUTRONS. Kovacs, I.; Nagy, L.; Vinnay, I. (Central Research Inst. for Physics, Budapest). Acta Phys. Acad. Sci. Hung.; 29: No. 2-3, 239-41(1970).

The angular anisotropy of fission fragments of ^{235}U and ^{238}U with respect to the direction of 14-MeV neutrons was found to be larger in ternary than in binary fission. (auth)

36760 E0 AND E0+M1+E2 TRANSITIONS OF ^{178}Hf. Ohlsson, Harriet; Gizon, Jean (Univ., Grenoble, France). Compt. Rend., Ser. B; 272: 633-6(8 Mar 1971). (In French).

The line intensities of the E0 and E0 + M1 + E2 transition electrons were measured. The internal conversion coefficients were determined and the E0 electron emission of the E0 + M1 + E2 transition was studied. (auth)

36761 ^{96}Zr(p,2n)^{95}Nb ISOMERIC RATIO AT 400 MeV. Church, L. B. (State Univ. of New York, Buffalo). Nucl. Phys.; A162: 643-7(1971).

The isomeric ratio resulting from the ^{96}Zr(p,2n)^{95}Nb reaction with 400 MeV proton has been re-examined. A corrected ratio for the population of the $^9/_2^+$ to $^1/_2^-$ states of ^{95}Nb is 3.2 ± 0.8. This ratio is compared to a set of statistical calculations and the spin on the excited ^{96}Nb intermediate is estimated to be about 3.5 ħ units. The estimated change in spin due to the (p,n) event is in close agreement with the calculated spin-change resulting from a similar (p,p′) event which was the first part of a (p,pn) reaction. (auth)

36762 TRANSITION PROBABILITIES FOR LOW-LYING STATES IN ^{92}Nb. Cochavi, S.; Fossan, D. B. (State Univ. of New York, Stony Brook). Phys. Rev., C; 3: 275-81(Jan 1971).

Low-lying states in ^{92}Nb have been studied using the ^{92}Zr(p,nγ)^{92}Nb reaction at E_p = 6.3 MeV. A Ge(Li) γ spectrum was measured in coincidence with neutrons to identify low-lying states and their γ transitions. The mean lifetime of the 357-keV state was measured as τ = 2.73 ± 0.09 nsec by a neutron-γ delayed-coincidence technique. The mean lifetime of the 227-keV 2^- state obtained from a γ–γ delayed-coincidence measurement is τ = 6.2 ± 0.7 μsec. An upper limit of τ ≤ 0.8 nsec was measured for the mean lifetime of the 501-keV state. These lifetime results and observed γ transitions established for the predicted $[\pi,{}^9/_2^+]\otimes[\nu(2d_{5/2})]J^+$ configuration the level sequence 7^+, 2^+, 3^+, 5^+, 4^+, 6^+. A B(E2) = 50.9 e^2 F^4 was deduced for the $5^+ \rightarrow 7^+$ (357 → 0 keV) transition from the lifetime of the 357-keV state; effective E2 charges for the mass-90 region are compared. The lifetime of the 2^- state implies an E1 hindrance of 10^7 for the $2^- \rightarrow 2^+$ (227 → 135 keV) γ transition relative to single-particle estimates. (auth)

36763 ANGULAR CORRELATION OF ^{97}Nb γ RADIATION. Begzhanov, R. B.; Kobilov, O. Sh.; Radzhanov, P. S.; Sabinov, Kh. S. (Inst. of Nuclear Physics, Tashkent). Dokl. Akad. Nauk Uzb. SSR; No. 7, 20-2(1970). (In Russian).

Angular correlations of the ^{97}Nb γ cascades (355–1750), (602–1148), (704–1148), (855–508), (830–1275), (971–1275), and (254–1852) keV were studied; and spins and parities of levels in ^{97}Nb were determined by means of fast–slow coincidences with a resolving time of 2×10^{-9} sec. A source of ^{97}Zr($T_{\frac{1}{2}}$ = 17 hr) was produced by irradiating zirconium dioxide (enriched to 96% in

^{96}Zr) in a reactor by a thermal-neutron flux of 1.8×10^{13} n · cm^{-2} sec^{-1}. Angular correlation coefficients for cascades from levels at 2247, 2106, 1852, 1750, 1276, 1250, and 1148 keV were obtained; and the spin assignments were determined. (R.V.J.)

36764 BETA ENERGY RELEASE FOLLOWING THE THERMAL NEUTRON INDUCED FISSION OF ^{233}U AND ^{235}U. Scobie, J.; Scott, R. D.; Wilson, H. W. (Scottish Research Reactor Centre, Glasgow). J. Nucl. Energy; 25: 1-10(Jan 1971).

Measurements were made of the relative beta energy release rates following the therma-neutron-induced fission of ^{233}U and ^{235}U. The results are presented as a ratio of the ^{235}U release rate to that of ^{233}U as a function of time following an irradiation of 10^4 sec duration. Calculations of the above ratio were performed using calculated independent yields and the decay schemes of the various nuclides. The calculation is limited to times >60 sec after irradiation because of lack of knowledge of the decay schemes, and half-lives, of the short-lived fission products. The absolute beta energy release rates are given for the two cases and compared, in the case of ^{235}U, with some previous calculations and experiments. Theory and experiment agree qualitatively in that the ^{235}U to ^{233}U ratio is initially >1 and decreases with time to reach values <1. However, the time found experimentally at which the ratio equals 1 is not reproduced in the calculation. Further, both experiment and theory indicate that at long times (>10^4 sec) after irradiation the ratio increases again to a value >1. (auth) (UK)

36765 DECAY OF ^{142}La. Tong, S. L.; Prestwich, W. V.; Fritze, K. (McMaster Univ., Hamilton, Ont.). Can. J. Phys.; 49: 1179-85(1 May 1971).

The energies of the gamma rays following the beta decay of 92.5-min ^{142}La were precisely measured, and a coincidence measurement with a NaI(Tl) and Ge(Li) system was made by gating the NaI(Tl) at 641 keV. With these results, the decay scheme of ^{142}Ce derived by Prestwich and Kennett was modified. The beta branching ratios of the decay of ^{142}La to the ground and excited states of ^{142}Ce were obtained by simultaneous gamma and 4π beta countings with a 3 in. × 3 in. NaI(Tl) detector and a 4π proportional counter. (auth) (Canada)

36766 LEVEL STRUCTURE OF ^{143}Pm AND ^{142}Nd. Hayashibe, Shogo (Tohoku Univ., Sendai); Endo, Yorimasa; Miyata, Takamoto; Tazawa, Hisashi; Yoshikawa, Nobuharu. Kakuriken Kenkyu Hokoku; 2: No. 2, 59-68(Dec 1969). (In Japanese).

In the present work, Sm_2O_3 samples, in which the enrichment of $^{144}_{62}Sm_{82}$ was 75%, were irradiated with γ-rays of $E_{\gamma max}$ = 30 MeV, 50 MeV and 60 MeV; and the radiation emitted from ^{143}Sm and ^{142}Sm, which were formed by (γ,n) and (γ,2n) reactions respectively, was measured. The singles spectrum was measured with a Ge(Li) detector. The $\gamma-\gamma$ coincidence spectrum was measured with Ge(Li)–NaI(Tl), and the spectrum of internal conversion electrons was measured with a magnetic β-ray spectrometer. By measuring these radiations, the level structures of $^{143}_{61}Pm_{82}$ and $^{142}_{60}Nd_{82}$ were investigated. (Japan)

36767 FAST NEUTRON SPECTRA FROM NATURAL URANIUM TARGET BOMBARDED WITH HIGH ENERGY ELECTRONS. Kimura, Itsuro; Hayashi, Shu A.; Kobayashi, Katsuhei; Yamamoto, Shuji; Shibata, Toshikazu (Kyoto Univ.). J. Nucl. Sci. Technol. (Tokyo); 8: 173-5(Mar 1971).

The energy spectra of fast neutrons emitted from a natural U target bombarded with electrons at 18.5, 20, and 23 MeV were measured by the time-of-flight method; and the results were analyzed phenomenologically. Neutrons produced by electron bombardment of natural uranium targets exhibit a much harder spectrum than fission neutrons. It is found that each spectrum is clearly composed of two components with different nuclear temperatures. (R.W.R.)

36768 SMALL-ORDER DEVIATIONS OF ^{90}Y AND ^{32}P. Nagarajan, T. (Univ. of Madras); Ravindranath, M.; Reddy, K. Venkata. Nuovo Cim.; 2A: 662-78(1 Apr 1971).

The shape of ^{90}Y is studied as an overall check of the spectrometer response. The measured form factor of ^{90}Y, viz. $(q^2 + 9L_1/L_0) \cdot \{1 - (0.001 \pm 0.003)\ W\}$ indicates that the spectrometer is free from any distorting effect to within 0.3% per m_0c^2. This agrees very well with the conclusion arrived at by a direct study of the instrumental effects. The large hyperbolic terms reported for ^{90}Y and a few other allowed and 1st unique spectra are characteristic of only 180° spectrometers whose line-shapes are highly asymmetrical. The shape deviation of ^{32}P for optimal base position is found to be small ($a = -0.006 \pm 0.005$) in spite of its large log ft value. Wrong positioning of the entrance base resulted in large hyperbolic deviation and shape with double slopes. These anomalies resembled some of the results reported in the literature. The two prevailing approaches, viz. l-forbiddenness and cancellation effect in allowed matrix elements, to explain the large log ft value, small linear-shape deviation, and longitudinal polarization of $(-p/W)$ are only qualitatively successful. (auth)

36769 STUDY OF DELAYED STATES IN ^{94}Nb, ^{108}Ag, AND ^{110}Ag. Gujrathi, S. C.; d'Auria, J. M.; Korteling, R. G. (Simon Fraser Univ., Burnaby, B. C.). Can. J. Phys.; 49: 747-55 (15 Mar 1971).

The lifetimes and energies associated with low-energy gamma transitions from the ^{93}Nb(n,γ)^{94}Nb, ^{107}Ag(n,γ)^{108}Ag, and ^{109}Ag(n,γ)^{110}Ag reactions were studied using a high-resolution Ge(Li) x-ray spectrometer. New weak transitions are observed in the decay of ^{110}Ag at 30.84, 38.19, 41.78, and 136.65 keV, while intense gamma transitions at 105.6, 235.8, and 266.95 keV are resolved into doublets. The half-lives of the states involving the intense 117.47-keV transition in ^{110}Ag and the 215-keV transition in ^{108}Ag are confirmed as 36.5 ± 2.0 ns and 54 ± 8 ns, respectively, while a new delayed state associated with the gamma transition of 99.404 keV ($T_{\frac{1}{2}}$ = 30 ± 5 ns) in ^{94}Nb is observed for the first time. The upper limits for the half-lives involving most of the intense transitions in all the three isotopes are also reported. A level scheme is proposed and discussed for ^{108}Ag. (auth) (Canada)

36770 ^{235}U–^{207}Pb AND ^{238}U–^{206}Pb MASS DIFFERENCES. Kerr, Donald P.; Bainbridge, Kenneth T. (Harvard Univ., Cambridge, Mass.). Can. J. Phys.; 49: 756-60(15 Mar 1971).

The Harvard University mass spectrometer with the lock-in amplifier method of peak matching was used to measure the mass differences ^{235}U–^{206}PbC$_2$H$_3$, ^{235}U–^{206}Pb^{32}S, ^{238}U–^{238}U, and ^{206}PbH–^{207}Pb. The mass differences ^{235}U–^{207}Pb and ^{238}U–^{206}Pb derived from the data are compared with the values obtained using the total energies released in the respective decay series. (auth) (Canada)

36771 MEASUREMENT OF THE L/K ELECTRON CAPTURE RATIO IN THE DECAY OF ^{159}Dy. Leiper, W.; Jolly, O. P. (Dalhousie Univ., Halifax, Nova Scotia). Can. J. Phys.; 49: 582-4(1 Mar 1971).

NaI(Tl) crystals containing $DyCl_3$ were used to measure the L/K electron capture ratio in the decay of ^{159}Dy to the ground state of ^{159}Tb. The experimental result was 0.198 ± 0.009. Agreement with theory is obtained if any exchange correction of 1.062 ± 0.046 is used. Bahcall's calculated value for the exchange correction is 1.046. (auth) (Canada)

36772 β DECAY AND NUCLEAR STRUCTURE IN A = 99 NUCLEI. Nagarajan, T.; Ravindranath, M.; Reddy, K. Venkata (Andhra Univ., Waltair, India). Phys. Rev., C; 3: 247-54(Jan 1971).

An analysis of the β spectrum of ^{99}Mo taking into account the correct shape of the outer β group revealed β groups with end points 1214 ± 1 (84%), 840 ± 5 (2%), 450 ± 10 (14%) keV. The shape of the outer β group ($\frac{1}{2}^+ \rightarrow \frac{1}{2}^-$) feeding the 142-keV level in ^{99}Tc is expected to be statistical, obeying the ξ approximation. The measured shape-factor coefficient a is −0.01 ± 0.007. On the basis of shell-model matrix elements, the conserved-vector-current prediction for Λ gave a positive value for a, whatever the value of Λ_0. Treating both Λ and Λ_0 as free parameters, a fit to the experimental shape gave $3.4 \leq \Lambda \leq 5$ and $2.3 \leq \Lambda_0 \leq 3.7$. The shape of the inner group (840 keV) was found to be consistent with first-forbidden nonunique character, and within experimental accuracy it was consistent with the shell-model prediction, even though the 514-keV ($\frac{5}{2}^-$) level fed by this β group is considered as arising from the weak coupling of $p_{\frac{1}{2}}$ proton to the 2^+ first excited state of the core. But the large log ft value of this transition may perhaps be explained by a detailed "microscopic" picture of the core. (auth)

36773 EXPERIMENTAL TEST OF THE KUMAR–BARANGER PAIRING-PLUS-QUADRUPOLE FORCE MODEL IN THE A = 190 REGION THROUGH E2-M1 MIXING AMPLITUDES. Krane, K. S.; Steffen, R. M. (Purdue Univ., Lafayette, Ind.). Contract AT(11-1)-1746. Phys. Rev., C; 3: 240-7(Jan 1971).

The E2/M1 multipole mixing ratios $\delta(\gamma)$ of γ transitions in even–even osmium and platinum isotopes have been measured in order to test the predictions of the pairing-plus-quadrupole theory of Kumar and Baranger. The mixing ratios $\delta(\gamma)$ were determined from directional-correlation measurements on γ transitions in ^{188,188,190}Os (populated in the decay of ^{188,188,190}Ir) and in ^{194,196}Pt (populated in the decay of ^{194,196}Au). The radioactive iridium isotopes were produced by Re(α,xn) reactions, and the gold isotopes were produced by Pt(d,xn) reactions. The equipment employed for the $\gamma-\gamma$ directional-correlation measurements consisted of two coaxial 30-cc Ge(Li) detectors and appropriate electronic equipment for high-resolution pulse-height analysis and timing analysis. The observed directional corre-

XUM

lations were analyzed in terms of the appropriate E2/M1 mixing ratios, which are defined explicitly. The following results were obtained (predictions of the Kumar–Baranger theory are listed in square brackets): $\delta(^{186}Os, 630\ keV) = -(10^{+5}_{-\infty})$ [−14.7], $\delta(^{186}Os, 773\ keV) = -(13^{+\infty}_{-5})$ [−13.5], $\delta(^{188}Os, 478\ keV) = -12.3 \pm 2.8$ [−9.5], $\delta(^{188}Os, 635\ keV) = -6.9 \pm 3.2$ [−10.5], $\delta(^{190}Os, 371\ keV) = -8.5 \pm 1.0$ [−7.6], $\delta(^{190}Os, 569\ keV) = -9.0 \pm 1.5$ [−9.9], $\delta(^{194}Pt, 293\ keV) = +14.3 \pm 2.1$ [+19.9], $\delta(^{196}Pt, 333\ keV) = -5.7 \pm 0.3$ [−101.4]. Except for the 333-keV transition in ^{196}Pt the agreement of the experimental mixing ratios with the values and signs predicted by the Kumar–Baranger model is excellent. (auth)

36774 SPECTRUM SHAPE OF K-ORBITAL SHAKEOFF ELECTRONS AND ACCOMPANYING NUCLEAR BETA PARTICLES IN THE DECAY OF ^{143}Pr. Fischbeck, H. J.; Wagner, F.; Porter, F. T.; Freedman, M. S. (Argonne National Lab., Ill.). Phys. Rev., C; 3: 265-74(Jan 1971).

The composite (K-orbital shakeoff plus nuclear) electron spectrum shape in coincidence with K x rays in the pure β emitter ^{143}Pr (E_0 = 930 keV) was measured with the Argonne magnetic-lens spectrometer and a NaI scintillation x-ray spectrometer. It yields an ordinary Kurie plot nearly linear from E_{max} = 888 ± 5 keV [930 keV − (K binding energy)] to ~160 keV, below which, the contribution from the K shakeoff spectrum appears as a sharply rising component down to <30 keV. This composite coincidence spectrum agrees fairly well with the recent relativistic shakeoff theory of Stephas and Crasemann, but only if their formulation for the square of the atomic matrix element is multiplied by a factor of W/p. Significant differences of both component shapes with this modified theory remain. Comparison of the measured shape to that calculated from the formulation of Feinberg for direct collision indicates that this process contributes negligibly to the decay. The ratio of the higher-energy Kurie component (mainly the nuclear β component) of the composite spectrum to the singles intensity gives a total K-ionization probability $P_K = (2.95 \pm 0.3) \times 10^{-4}$; relativistic self-consistent-field wave-function overlap integrals give 3.0×10^{-4}. (auth)

36775 STUDY OF ^{150}Gd. Kewley, D.; Eastham, D. A.; Forsyth, P. D.; (and others) (Univ. of Liverpool). Nucl. Phys.; A165: 56-72(1971).

Intensities and energies of conversion electrons and γ-rays following the reaction $^{151}Eu(p,2n)^{150}Gd$ have been measured at various proton energies and multipolarities of decay transitions have been made on the basis of measured internal conversion coefficients. A conversion electron–γ-ray coincidence experiment was used to establish the decay scheme. Measurements of the angular distributions of the most prominent γ-rays have been used to ascertain spin values. Levels of the following energies and spin-parities have been determined: 638.1 ± 0.2, 2^+, 1134.6 ± 0.03, 3^-, 1288.3 ± 0.3, (4^+), 1430.2 ± 0.2, (2^+), 1518.4 ± 0.3, 1700.7 ± 0.3 and 1947.4 ± 0.4 keV. (auth)

36776 DIRECTIONAL CORRELATION MEASUREMENTS OF THE GAMMA RAYS EMITTED IN THE DECAY OF ^{160}Tb. Krane, K. S.; Steffen, R. M. (Purdue Univ., Lafayette, Ind.). Contract AT(11-1)-746. Nucl. Phys.; A164: 439-48(1971).

The decay of ^{160}Tb to levels in ^{160}Dy has been investigated by measuring the gamma–gamma directional correlations using two 30 cm^3 coaxial Ge(Li) detectors in conjunction with multichannel coincidence and routing electronics. A detailed analysis was performed in order to correct for the effects on the measured correlations of Compton-scattered radiation. The results of the sixteen measured directional correlations served to verify the current spin assignments, and in addition yielded values for the E2/M1 and M2/E1 multipole mixing ratios of the gamma transitions, given in terms of explicitly defined reduced matrix elements. Values obtained for the mixing ratios $\delta(\gamma)$ are (energies in keV): $\delta(215) = -0.18 \pm 0.10$, $\delta(299) = +0.005 \pm 0.010$, $\delta(392) = +0.005 \pm 0.070$, $\delta(765) = -(7^{+\infty}_{-5})$, $\delta(879) = -11.5 \pm 1.9$, $\delta(962) = -18.0 \pm 5.0$, $\delta(1178) = +0.02 \pm 0.02$, $\delta(1272) = -0.03 \pm 0.03$. The results are discussed in terms of collective rotational nuclear motion. (auth)

36777 ANALYSIS OF THE (p,^{3}He) AND (d,α) REACTIONS ON ^{209}Bi. Kolata, J. J.; August, L. S.; Shapiro, P. (Naval Research Lab., Washington, D. C.). Phys. Rev., C; 3: 296-307(Jan 1971).

The single-neutron-hole states of ^{207}Pb have been studied by means of the (p,^{3}He) and (d,α) reactions on ^{209}Bi at 40 and 20 MeV, respectively. Angular distributions were obtained for five of the six well-known neutron-hole states. The sixth state, the $(1h_{9/2})^{-1}$ level at 3.43 MeV, was not adequately separated from a group of unresolved, strongly excited states between 3.5- and 7.5-MeV excitation energy in ^{207}Pb. The data were compared with microscopic- and cluster-model two-nucleon-transfer calculations in the context of the distorted-wave Born approximation. Good agreement was found with theoretical predictions of the shapes and relative magnitudes of the angular distributions for the (d,α) reaction. However, it was necessary to introduce a radial lower cutoff at 8.3 F to reproduce the shape of the (p,^{3}He) angular distributions. The experimental absolute normalization constants were computed and compared with theoretical predictions and with a previous experimental determination. The sensitivity of these normalization constants to various parameters of the theory was investigated. (auth)

36778 IDENTIFICATION OF THE ATOMIC NUMBER OF NOBELIUM BY AN X-RAY TECHNIQUE. Dittner, P. F.; Bemis, C. E. Jr.; Hensley, D. C.; Silva, R. J.; Goodman, C. D. (Oak Ridge National Lab., Tenn.). Phys. Rev. Lett.; 26: 1037-40(26 Apr 1971).

A daughter x-ray identification scheme, in the original spirit of Moseley [Phil. Mag. 26: 1024(1913) and 27: 703(1941)] was applied to the identification of element 102, nobelium. The identification scheme is based on the coincident observation of K-series x rays from the daughter element, fermium in this case, with the α particle from the decay of the parent element, nobelium. The technique provides an unequivocal identification of atomic number for the transfermium elements. (auth)

36779 SEARCH FOR SUPERHEAVY ELEMENTS IN TERRESTRIAL MATTER. Grimm, W.; Herrmann, G.; Schuessler, H.-D. (Univ., Mainz). Phys. Rev. Lett.; 26: 1040-3(26 Apr 1971).

Negative results were obtained in a search for spontaneously fissioning superheavy nuclei by neutron counting of a large variety of samples. An upper limit of about 10^{-11} g/g is estimated for the presence of such nuclei with a half-life of about 10^9 yr. (auth)

36780 N-SHELL CONVERSION ELECTRONS FROM THE 2.33-keV TRANSITION IN ^{205}Pb. Johnston, W. C.; Kelly, W. H.; Haynes, S. K.; Kosanke, K. L.; McHarris, Wm. C. (Michigan State Univ., East Lansing). Phys. Rev. Lett.; 26: 1043-6(26 Apr 1971).

The N_{II} and N_{III} conversion electrons from the ≈2.33-keV transition in ^{205}Pb were measured with a $\pi\sqrt{2}$, iron-free, double-focusing β-ray spectrometer; the energy of this transition was determined to be 2.328 ± 0.007 keV. An N_{II}/N_{III} ratio of 0.70 ± 0.25 for this transition and a ratio $(N_{II} + N_{III})/L_I$, where the L_I is from the 26.22-keV M2 isomeric transition in ^{205}Pb, of $0.48^{+0.16}_{-0.08}$ were obtained. These are in very good agreement with predicted conversion ratios and represent the first test of theoretical calculations for the N shell at such low energies. (auth)

36781 SPONTANEOUSLY FISSIONING ISOMERS OF TRANSURANIC NUCLEI. Vilcov, N. (Inst. of Nuclear Physics, Bucharest). Stud. Cercet. Fiz.; 22: 795-819(1970). (In Rumanian).

The experimental technique is considered including the recoil, pulsed-beam, and fission-in-flight methods. The spectroscopic properties of isomeric states are discussed covering excitation energy and angular momentum. Also treated are isomeric states at high deformation including the spontaneously fissioning isomer population through the capture reactions, shell effects at high deformations, and shape isomerism. (J.F.P.)

36782 AVERAGE KINETIC ENERGIES OF FISSION PRODUCTS FROM THE SPONTANEOUS FISSION OF ^{238}Pu. Nikolaev, V. A. Izv. Akad. Nauk SSSR, Ser. Fiz.; 35: No. 1, 180-2(1971). (In Russian).

The diameter of a fission-product track in glass depends on the specific energy loss at the glass surface. The distribution of fission-product track diameters has the form of a double-humped curve, the humps corresponding to the light and heavy fragments of the fission products. The fission fragments must be filtered through 10 mm of argon or 1.5 mg/cm^2 of Al (equivalent to 10 mm of argon). The track diameter was measured with an ocular micrometer. The average energies of the light and heavy peaks were estimated to be 98.5 ± 2.5 MeV and 67.5 ± 1.5 MeV, respectively. The corresponding average masses are 97 and 141, and the average total kinetic energy is 166 ± 4 MeV, which is smaller for ^{238}Pu than for ^{239}Pu (174 MeV). (TTT)

36783 QUASI-GROUND, QUASI-BETA, AND QUASI-GAMMA BANDS. Sakai, Mitsuo (Tokyo Univ.). Nucl. Data, Sect. A; 8: 323-43(Dec 1970).

For even–even nuclei a list is presented of the probable members of quasi-ground, quasi-beta, and quasi-gamma bands of the spherical regions and the corresponding ground, beta, and gamma bands of the deformed regions. For simplicity the term "quasi" is used for both regions. References are given to the experimental data basic to the level assignments. The literature is covered through February 1970. (auth)

36784 FISSION-EXCITATION FUNCTIONS IN INTERACTIONS OF ^{11}B, ^{12}C, ^{14}N, AND ^{19}F WITH VARIOUS TARGETS. Sikkeland, Torbjoern; Clarkson, Jack E.; Steiger-Shafrir, Naftali H.; Viola, V. E. (Univ. of California, Berkeley). Phys. Rev., C; 3: 329-37 (Jan 1971).

Fission cross sections for the systems $^{169}Tm + ^{11}B$, $^{175}Lu + ^{11}B$, and ^{12}C, $^{174}Yb + ^{12}C$, $^{182}W + ^{12}C$, $^{165}Ho + ^{14}N$, and $^{159}Tb + ^{19}F$ have been measured for heavy-ion bombarding energies up to 10.4 MeV per nucleon. The experimental technique consisted of counting coincident fission-fragment pairs with two gold-surface-barrier silicon-diode detectors. For the above systems, fission takes place only in reactions in which a compound nucleus is formed between the incident projectile and the target nucleus. Values of the compound-nucleus cross sections for these reactions are estimated from other data in order to account for surface reactions which occur in heavy-ion bombardment. The difference between the cross section for compound-nucleus formation and that for fission is assumed to be equal to the cross section for neutron-evaporation products. The ratio of the fission cross section to that for neutron evaporation is then taken to be equal to $\langle \Gamma_f/\Gamma_n \rangle$, the ratio of the level widths for the two competing processes averaged over the various reaction channels. A theoretical fit to the $\langle \Gamma_f/\Gamma_n \rangle$ values is obtained for the low-energy region of the excitation function, where first-chance fission is highly probable. The ratio of the level-density parameter for fission to that for neutron emission was found to be 1.2 ± 0.1, and values for the fission barrier are in agreement with those predicted by Myers and Swiatecki. (auth)

36785 HIGH-ENERGY (γ,xn) REACTIONS IN ^{197}Au. Lindgren, K.; Johnsson, G.G. (Lund Inst. of Tech., Sweden. Univ. of Lund, Sweden). Nucl. Phys.; A166: 643-60(1971).

The bremsstrahlung-induced yields of some (γ,xn) reactions, $1 \leqq x \leqq 15$, in gold were measured in the energy region 75 to 900 MeV. The mean cross sections in the energy region 300 to 900 MeV were determined. The number of valence neutrons available in the (γ,n) reaction was estimated. The experimental cross sections for the more complex reactions are compared with cascade–evaporation calculations based upon the free-nucleon photopion cross sections. Fission competition must be taken into account to explain the experimental cross sections. The experimental result is consistent with the idea that fission is most probable at low excitation energy after the emission of several neutrons. Fission fragments were observed in a catcher-foil experiment, and the relative yields were determined. For two reactions the isomeric yield ratios were determined. (auth)

36786 PROMPT NEUTRON YIELD IN ^{235}U FISSION BY NEUTRONS WITH ENERGIES UP TO 1.5 MeV. Prokhorova, L. I.; Bagdasarov, R. E.; Kotukhov, I. I.; (and others). At. Energ. (USSR): 30: 250-7(Mar 1971). (In Russian).

A relative method was used to measure the dependence of $\bar{\nu}$, the mean number of prompt neutrons per ^{235}U fission, on the energy of bombarding neutrons, E_n, in the range from 0 to 1.5 MeV. The value of $\bar{\nu}$ for ^{252}Cf spontaneous fission served as a basic value. The neutron detector consisted of 24 ^3He counters in a paraffin tank. This detector had an efficiency of about 20%, and was characterized by the neutron mean lifetime of about 50 μsec. The data, obtained with an accuracy of 0.8 to 1%, revealed considerable discrepancies with a linear dependence. From an analysis of the data found in the literature, the recommended curve $\bar{\nu}(E_n)$ was obtained. (4 figures, 3 tables, 30 references.) (auth)

36787 LOW-LYING CONFIGURATIONS IN ^{210}Bi. Motz, H. T.; Jurney, E. T.; Shera, E. B.; Sheline, R. K. (Los Alamos Scientific Lab., N. Mex.). Phys. Rev. Lett.; 26: 854-6(5 Apr 1971).

The configurations $\pi h_{9/2} \nu g_{9/2}$ and $\pi h_{9/2} \nu i_{13/2}$ in ^{210}Bi were studied using the γ-ray spectra recorded following thermal-neutron capture in ^{209}Bi. Comparison of the experimental energies of these configurations with those calculated by Kim and Rasmussen [Nucl. Phys. 47: 184(1963)] indicates a remarkable agreement. (auth)

36788 ELECTRON–PHOTON CASCADES IN LEAD AT PRIMARY ENERGIES OF 100, 200, AND 400 MeV. Brockmann, R.; Keil, P.; Knop, G.; Wucherer, P. (Univ., Bonn). Z. Phys.; 243: 464-79(1971). (In German).

Electron-initiated showers in compact lead plates at primary energies of 100, 200, and 400 MeV were measured by means of a propane bubble chamber. Cut-off energies of the shower electrons were measured from 1.5 to 7.5 MeV by the range in propane. The wide-spread range distribution was related to energy by a Monte Carlo calculation. The results are compared with shower calculations of Nagel [Z. Phys. 186: 319(1965)]. The electron numbers show good agreement at depths between 2 and 15 radiation lengths. Radial and angular distributions agree also but cannot be measured with the same precision as the numbers. (auth)

36789 EXPERIMENTAL DETERMINATION OF PENETRATION PARAMETER FOR M1 CONVERSION AND THE E2 ADMIXTURES FOR 77 AND 191 keV TRANSITIONS IN ^{197}Au. Krpic, D.; Stepic, R.; Bikit, I.; Milanovic, J.; Vukanovic, R. (Boris Kidric Inst., Belgrade). Z. Phys.; 243: 452-63(1971).

The L-subshell conversion for the 77-keV transition and the K-, L_1-, and L_2-shell conversion for the 191-keV transition in ^{197}Au, as well as the K-shell conversion for the 158-keV transition in ^{199}Hg, were measured by means of a $\pi\sqrt{2}$ iron-free electron spectrometer. Relative gamma-ray intensities were determined by a Ge(Li) spectrometer. From these measurements the α_K conversion-coefficient value is deduced for the 191-keV transition as $\alpha_K(191\text{ keV}) = 0.86 \pm 0.03$. This value shows that the spin of the level at 268 keV in ^{197}Au is $\frac{3}{2}^+$. For the penetration parameter (λ) and intensity ratio ($\delta^2 = \langle E2 \rangle^2 / \langle M1 \rangle^2$) the following values are obtained: $\lambda = 3.4 \pm {}^{1.0}_{0.7}$, $\delta^2 = 0.11 \pm 0.03$ for the 77-keV transition; and $\lambda = 3.2 \pm {}^{0.8}_{0.6}$, $\delta^2 = 0.17 \pm 0.04$ for the 191-keV transition. The agreement of these results with the predictions of De Shalit model is discussed. (auth)

36790 DECAY MODES AND LIFETIMES OF THE LEVELS IN THE ($\pi h_{9/2} \cdot \nu g_{9/2}$) MULTIPLET IN ^{210}Bi. Ellegaard, C. (Carnegie-Mellon Univ., Pittsburgh); Barnes, P. D.; Eisenstein, R.; Canada, T. R. (Phys. Lett.; 35B: No. 2, 145-7(10 May 1971).

The decay scheme for the ten levels of the ($\pi h_{9/2}, \nu g_{9/2}$) multiplet in ^{210}Bi is determined by utilizing the $^{209}Bi(d,p\gamma)^{210}Bi$ reaction. The halflives of the 433.3- and 438.7-keV levels were measured to be 58 ± 6 nsec and 38 ± 6 nsec, respectively. The spin sequence within the multiplet is deduced from these data. (auth)

36791 EVIDENCE FOR LONG-RANGE FISSION FRAGMENTS INDUCED BY IRRADIATION WITH ELECTRONS. Maly, J. (Institut de Physique Nucleaire, Orsay, France). Phys. Lett.; 35B: No. 2, 148-50(10 May 1971).

In search of natural superheavy elements, long-range fission fragments penetrating up to 73 μm of mylar were observed when thick metallic foils of U, Pb, and W, covered with six mylar foils, were irradiated with 550-MeV or 1300-MeV electron beams. The cross section is of the order of 10^{-30} cm^2. The effect is produced in natural U, Pb, W, and similarly in mass separated ^{208}Pb and ^{186}W isotopes—not by fission of a superheavy element. (auth)

36792 880 ns ISOMERIC STATE IN ^{144}Sm. Kownacki, J.; Rensfelt, K. G. (Research Inst. for Physics, Stockholm). Phys. Lett.; 35B: No. 2, 153-5(10 May 1971).

The half-life of the 2323-keV state (6^+) in ^{144}Sm is determined to be 880 ± 25 ns. (auth)

36793 ENERGY SURFACES OF ^{238}U IN PARAMETRIZATION OF CASSINIAN OVALOIDS. Adeev, G. D.; Cherdantsev, P. A.; Gamalya, I. A. (Tomsk Polytechnic Inst., USSR). Phys. Lett.; 35B: No. 2, 125-8(10 May 1971).

The three-dimensional energy surface of ^{238}U was calculated by the Strutinsky method by using a two-centre single-particle potential whose equipotential surfaces describe various shapes: spheres; ellipsoids of different sizes; Cassinian ovaloids; and other, more general, asymmetric shapes. (auth)

36794 SPECTROSCOPIC STUDY OF (p,t) REACTIONS FROM NEUTRON-MAGIC NUCLEI IN TERMS OF THE COUPLED-CHANNEL BORN APPROXIMATION. Udagawa, T. (Univ. of Texas, Austin); Tamura, T.; Izumoto, T. Phys. Lett.; 35B: No. 2, 129-32(10 May 1971).

It is shown that the coupled-channel Born approximation explains well the data of $^{142}Nd(p,t)^{140}Nd$ with very natural assumptions made on the structure of the two nuclei involved. (auth)

36795 FISSION ISOMERS IN Cm AND Bk ISOTOPES. Repnow, R. (Max-Planck Institut fuer Kernphysik, Heidelberg); Metag, V.; von Brentano, P. Z. Phys.; 243: 418-30(1971).

A new, extremely short-lived fission isomer, presumably in ^{245}Bk, was detected following the bombardment of ^{243}Am with ^4He particles at 26 MeV. Proton bombardment of ^{243}Am gives some evidence for the excitation of two short-lived fission activities, which are tentatively assigned to isomers in $^{241,242}Cm$. In irradiation of targets of ^{237}Np, ^{241}Am, and ^{243}Am with deuterons in the energy range from 12 to 20 MeV, previously known isomers are observed. Excitation functions are given for the production of these fission isomers. (auth)

36796 NEW ISOTOPE ^{180}Lu. Swindle, D. L.; Ward, T. E.; Kuroda, P. K. (Univ. of Arkansas, Fayetteville). Contract AT(40-1)-3235. Phys. Rev., C; 3: 259-65(Jan 1971).

XUM

Irradiation of enriched ^{180}Hf with 14.7-MeV neutrons was found to produce a new radioactive nuclide which was assigned to ^{180}Lu. The following radiation characteristics were observed to belong to the decay of ^{180}Lu: half-life 5.8 ± 0.2 min; γ-ray energies 93.3 ± 0.8, 215.3 ± 0.8, 316.8 ± 0.8, 408.4 ± 0.8, 464.4 ± 0.8, 1065.2 ± 1.5, 1106.8 ± 0.8, 1197 ± 1, 1199.5 ± 0.8, 1298.8 ± 0.8, 1315.0 ± 1.0, 1433.6 ± 1.0, 1514.3 ± 0.8, and 1873.9 ± 2.0 keV; and a β ray of 1.45 ± 0.10 MeV. A tentative decay scheme is presented and discussed. (auth)

36797 (p,xn) REACTIONS INDUCED IN ^{169}Tm, ^{181}Ta, AND ^{209}Bi WITH 20 TO 45 MeV PROTONS. Birattari, C.; Gadioli, E.; Grassi Strini, A. M.; (and others) (Univ., Milan. Istituto Nazionale di Fisica Nucleare, Milan). Nucl. Phys.; A166: 605-23(1971).

Excitation functions for the reactions ^{169}Tm, ^{181}Ta, ^{209}Bi (p,xn) for x = 3, 4 were measured at proton energies from 20 to 45 MeV. The experimental curves are analyzed in terms of a sum of statistical and pre-compound contributions, the last one evaluated according to the model proposed by Griffin [Phys. Rev. Lett. 17: 488(1966); Phys. Lett. 24B: 5(1967)] and Blann [Phys. Rev. Lett. 21: 1357(1968)]. The cross section for pre-compound neutron and proton emission appears to constitute a significant portion of the total reaction cross section σ_R in the entire energy interval examined. Correspondingly, the fraction of σ_R accounted for by the compound-nucleus-formation cross section is found to be as low as some 30% for $30 \lesssim E_p \lesssim 40$ MeV. (auth)

36798 ELECTRIC DIPOLE TRANSITIONS IN ^{88}Sr AND ^{90}Zr. Vergados, J. D.; Kuo, T. T. S. (State Univ. of New York, Stony Brook). Phys. Lett.; 35B: No. 2, 93-8(10 May 1971).

Electric-dipole transitions in ^{88}Sr and ^{90}Zr were studied using realistic two-body interactions. Shell-model wave functions of definite isospin were used, and both the T-upper and the T-lower transitions were calculated. In the case of ^{90}Zr the pairing effect in the ground state was taken into account and, in addition to the ground-state E1 widths $\Gamma_{\gamma 0}$, the first-excited-state widths $\Gamma_{\gamma 1}$ were obtained. The results are in good agreement with experiment. (auth)

36799 MEASUREMENT OF INTERMEDIATE ENERGY GAMMA-RAY CROSS SECTIONS. Henry, L. C.; Kennett, T. J. (McMaster Univ., Hamilton, Ont.). Can. J. Phys.; 49: 1167-78(1 May 1971).

Gamma-ray cross sections for 30 well-distributed energies from 121 keV to 10.827 MeV in 9 target elements ranging from carbon to uranium were measured with an accuracy of better than 1%. Deviations from recently quoted theoretical cross sections were observed in the energy region from 6–11 MeV, particularly for high-Z target materials. The approximately Z^2 dependent deviations are certainly associated with the elastic pair-production process, the present opinion being that they arise from an overestimation of the effects of atomic–electron screening on the pair cross section in the intermediate energy region. (auth) (Canada)

36800 BACKGROUND REPORT ON FISSION PHYSICS. Ben-David, G. (Israel Atomic Energy Commission, Yavne). pp 209-24 of Research Reactor Utilization. Vol. 1. Vienna; International Atomic Energy Agency (1970). (CONF-700204-8).

From IAEA meeting on research reactor utilization; Rome, Italy (2 Feb 1970).

The present state of the art in fission physics research is reviewed. The main developments during the last few years, both in experimental techniques and in fission theory, are discussed. The scope of application of the liquid-drop model and shell corrections leading to the Strutinsky double-hump barrier picture are given special emphasis, and trends of future research are indicated. (auth) (INIS)

36801 MIDSTREAM EVALUATION, A = 90. Ball, J. B. (Oak Ridge National Lab., Tenn.); Johns, M. W.; Way, K. Nucl. Data, Sect. A; 8: 407-36(Dec 1970).

Data on the A = 90 nuclides, reported since the publication of the last Nuclear Data Sheets in this region (1960), are studied and evaluated. Decay and level schemes, as well as summaries of the experimental data on which the adopted values are based, are presented. Literature available in June 1969 and important papers appearing up to June 1970 are included. (auth)

36802 STUDIES OF PROTON-INDUCED NUCLEAR FISSION. Hageboe, E. Oslo; University of Oslo ([1971]). 30p.

Radiochemical studies on the interaction of protons with heavy nuclei, mostly uranium, leading to products generally far from the target are summarized. (Norway)

36803 STATIC QUADRUPOLE MOMENT OF THE COLLECTIVE OCTUPOLE VIBRATION IN ^{208}Pb. Soerensen, B. (Univ. of Copenhagen). Phys. Lett.; 35B: No. 2, 101-4(10 May 1971).

The static quadrupole moment of the ^{208}Pb 3^- state at 2.62 MeV is calculated with inclusion of anharmonic couplings to 2^+ states. Surface-peaked quadrupole and octupole interactions are used. The resulting static moment is not in agreement with the one existing measurement. (auth)

36804 K CONVERSION COEFFICIENT OF THE NEAR THRESHOLD M3 TRANSITION IN ^{191}Os. Campbell, J. L.; O'Brien, P.; McNelles, L. A. (Univ. of Guelph, Ont.). Can. J. Phys.; 49: 1066-9(15 Apr 1971).

The K conversion coefficient of the predominantly M3 transition at 74.37 keV in ^{191}Os was measured to be 75 ± 8. This differs both from the theoretical value of 160 and a recent measurement giving 38.4. (auth) (Canada)

36805 LOW-ENERGY BAND STRUCTURE IN ^{187}Os. Malmskog, S. G. (Aktiebolaget Atomenergi, Studsvik, Sweden. Univ. of Stockholm); Berg, V.; Fogelberg, B.; Baecklin, A. Nucl. Phys.; A166: 573-93(1971).

The level structure of ^{187}Os was investigated in the decay of ^{187}Ir (11 hr) produced in 600-MeV proton spallation at CERN and mass-separated in the ISOLDE on-line facility. Special emphasis is put on the study of absolute transition rates from low-lying levels in ^{187}Os by means of high-resolution electron and γ-ray spectroscopy and half-life measurements using the delayed-coincidence technique. The observed transition rates are used to assign Nilsson quantum numbers to different levels. The large B(E2) values for some interband transitions are accounted for through a Coriolis coupling calculation. Through an extensive investigation of the γ-ray spectrum from ^{187}Ir three new levels at 190.70, 332.94 and 586.40 keV are proposed. (auth)

36806 APPROXIMATE TREATMENT OF CORRELATIONS IN NUCLEAR SPECTROSCOPY. I. STRUCTURE OF THE LEAD ISOTOPES. Vary, James; Ginocchio, J. N. (Yale Univ., New Haven). Nucl. Phys.; A166: 479-514(1971).

As a result of the successes of the pairing-vibration model, the two-nucleon random phase approximation (2N RPA) is used to calculate properties of nuclei in the lead region. The spectra, wave functions, single-particle densities, spectroscopic factors, electromagnetic properties, and correlation energy resulting from a two-neutron RPA calculation are presented and compared with available experimental data and with results of the shell-model (SM) limit. (auth)

36807 LIFETIME OF THE 91.5 keV STATE IN ^{151}Sm. Hofmann, S.; Steiner, P. Weyer, G. (Freie Univ., Berlin). Nucl. Phys.; A166: 436-42(1971).

The γ transitions in ^{151}Sm following the β decay of 28-hr ^{151}Pm were studied with a high-resolution Ge detector. No evidence for levels proposed earlier at 245.6 keV and 280 keV could be found, while weakly populated levels at 306.7 and 395.6 keV were confirmed. On the basis of γ-γ delayed-coincidence measurements using NaI(Tl) detectors, the half-life of the 91.5-keV level is determined to be $T_{\frac{1}{2}} = 78 \pm 1$ nsec. An upper limit of 0.5 nsec for the half-lives of the states at 65.8, 69.7 and 104.9 keV and of 0.4 nsec for the states at 168.4 and 167.7 keV is found. (auth)

36808 NUCLEAR DATA SHEETS FOR A = 110. Bertrand, F. E.; Raman, S. (Oak Ridge National Lab., Tenn.). Nucl. Data, Sect. B; 5: 487-530(May 1971).

The 1960 version of the Nuclear Data Sheets for A = 110 is revised on the basis of experimental data received to January 1971. Over 200 papers were considered, and the data from 160 were actually used in constructing the adopted level schemes. The A = 110 chain consists of 7 nuclei (Rh, Pd, Ag, Cd, In, Sn, and Sb) and also probably Tc and Ru. The decay of 2504-d ^{110}Ag has been studied extensively, with the result that the γ-energies are now known to within 20 to 50 eV and the relative γ intensities to within 2 to 8%. By combining the extensive decay and reaction data pertaining to the 40 known levels in ^{110}Cd, it is possible to assign 9 definite and 24 tentative J^π values. The present detailed compilation should serve as a basis for further experiments and theoretical calculations. (auth)

36809 NUCLEAR DATA SHEETS FOR A = 203. Auble, R. L. (Oak Ridge National Lab., Tenn.). Nucl. Data, Sect. B; 5: 531-60 (May 1971).

Nuclear structure data for A = 203 are compiled, and adopted level schemes and decay properties are presented. Inconsistencies in the data, as well as areas where the need for further study is apparent, are noted. In general, where several measurements of a given quantity have been reported, only the more accurate values are listed. References for those values not listed are given under

XUM

"other measurements." The adopted level properties and gamma-ray properties, which follow the compiled data for each nucleus, are based on data available through December 1970. Data from later references are added in proof but are not used in constructing the adopted level schemes. (auth)

36810 PRECISION MEASUREMENT OF GAMMA RAYS FROM ^{94}Nb DECAY. East, L. V. (Los Alamos Scientific Lab., N. Mex.). Nucl. Instrum. Methods; 93: No. 2, 193-5(1971).

Gamma rays resulting from the ground state beta-decay of ^{94}Nb were studied using high resolution Ge(Li) detectors. The energies of the cascade gamma rays from the 1.57 MeV excited state of ^{94}Mo were determined to be 702.630 ± 0.030 and 871.104 ± 0.035 keV, with relative intensities of (0.98 ± 0.02)/1.00. No new gamma ray transitions were found. An upper limit of 0.015% was established for the 1.57 MeV crossover transition probability. (auth)

36811 EFFECT OF NONUNIFORM TARGETS ON CROSS SECTIONS OBTAINED IN NEUTRON TRANSMISSION EXPERIMENTS. Stoler, P. (Rensselaer Polytechnic Inst., Troy, N. Y.). Nucl. Instrum. Methods; 93: No. 2, 377-80(1971).

Errors in cross sections due to sample nonuniformities in transmission experiments are discussed. Resulting errors for some specific types of nonuniformities with various degrees of nonuniformity, and for various ratios between neutron beam diameter and sample diameter are presented. (auth)

Nuclear Theory

Refer also to abstracts 35891, 36366, 36489, 36523, 36528, 36529, 36538, 36599, 36733, and 36800.

36812 (AAEC/TM-586) SOLUTION OF THE INVERSE REACTION PROBLEM FOR COMPLEX POTENTIALS. Bertram, W. K.; Cook, J. L. (Australian Atomic Energy Commission Research Establishment, Lucas Heights). Feb 1971. 5p. Dep. NTIS (U. S. Sales Only).

A method is given for solving the inverse reaction problem to obtain complex potentials as in the optical model of the nucleus. The method will reproduce reaction data to the accuracy with which the reaction matrix can be least-squares fitted to a sum of simple poles. (auth) (Australia)

36813 (ANU-P-439) COMPUTER SUBPROGRAMS FOR SCATTERING PROBLEMS. Treacy, P. B. (Australian National Univ., Canberra. Dept. of Theoretical Physics). 1969. 9p. Dep. NTIS (U. S. Sales Only).

Transcendental functions in FORTRAN IV (E) for an IBM 360/50 are described. Several subprograms are described for both the Born approximation with Yukawa potential (gamma function for complex argument; psi-function for complex argument; Gaussian hypergeometric function for real argument and complex parameters; and the Gaussian hypergeometric function in the logarithmic case), and for potential scattering with complex angular momentum (ingoing and outgoing Coulomb wave functions for complex angular momentum; Coulomb function regular at the origin; Whittaker function for real argument; and Basset function for real argument). (Australia)

36814 (ANU-P-451) OPTICAL MODEL CODE JIB3 (VERSION PEREY 3). Baugh, D. J.; Bourke, W. P. (Australian National Univ., Canberra. Research School of Physical Sciences). 1969. 9p. Dep. NTIS (U. S. Sales Only).

A description is given of the optical model program JIB3 written by Perey and adapted for use on the ANU IBM 360/50. Additional routines which enable grid searches, plotted output and averaging over the experimental angular resolution are included. A solution to the Schroedinger equation for V(r) is obtained. (Australia)

36815 (JINR-E2-5797) Q-VALUE DEPENDENCE OF MULTINUCLEON TRANSFER REACTIONS. Toepffer, Christian (Joint Inst. for Nuclear Research, Dubna (USSR). Lab. of Theoretical Physics). 1971. 10p. Dep. NTIS (U. S. Sales Only).

The regular behavior of multinucleon-transfer cross sections in reactions between heavy ions as a function of the Q values, Q_{gg}, for the ground-state transitions is explained in the molecular-wave-function method. The coupled equations of the scattering problem are solved analytically. (auth)

36816 (JINR-P2-5719) INTERACTION OF HIGH-ENERGY RADIATION WITH MATTER. Barashenkov, V. S.; Sobolevskii, N. M.; Toneev, V. D. (Joint Inst. for Nuclear Research, Dubna (USSR)). 1971. 17p. (In Russian). Dep. NTIS (U. S. Sales Only).

On the basis of the cascade-evaporation model of nuclear reactions a statistical (Monte Carlo) method is developed for calculating the interactions of particles having energies from several dozens of MeV to several dozens of GeV with matter. The ionization losses, meson-production processes, and π-meson decay are taken into account. Spread of low-energy neutrons is described by means of a multigroup system of constants used in calculating nuclear reactors. The method can be applied to blocks of matter of practically any composition and configuration. The results are compared with the available experimental data and with the published results obtained by other authors. (auth)

36817 (JINR-P4-5744) GAMOV-TELLER 1^+ EXCITATIONS IN ODD-ODD NUCLEI. Gabrakov, S. I.; Kuliev, A. A.; Salamov, D. I. (Joint Inst. for Nuclear Research, Dubna (USSR). Lab. of Theoretical Physics). 1971. 12p. (In Russian). Dep. NTIS (U. S. Sales Only).

In the framework of the Random Phase Approximation β-decay properties of highly excited 1^+ states in odd-odd deformed nuclei are investigated. These states are collectivized by a charge-exchange residual interaction of the $\kappa_\beta \tilde{\sigma}_1 \tilde{\sigma}_2 \tilde{\tau}_1 \tilde{\tau}_2$ type. The calculations show that for β^--transitions the collective state (the Gamow-Teller resonance) is at an excitation energy of the order of 20 MeV. The calculations of the strength functions for the Gamow-Teller transitions show that this state exhausts the main part of the allowed transition (≈95%). The strength of β^+ transition is concentrated in the energy region of bound states. (auth)

36818 (KFK-1333) IMPROVED VERSION OF TAMURA'S CODE FOR COUPLED CHANNEL CALCULATIONS: "JUPITOR KARLSRUHE VERSION." Rebel, H.; Schweimer, G. W. (Kernforschungszentrum, Karlsruhe (West Germany). Zyklotron-Laboratorium). Feb 1971. 78p. Dep. NTIS (U. S. Sales Only).

The coupled-channel code JUPITOR 1 is modified and improved. The most important modification is an automatic parameter search option for the best fits. The treatment of the rotational model is improved by expanding the deformed optical potential in terms of Legendre polynomials up to order 8, thereby including all terms that contribute to the excitation of the 4^+ rotational state. Coulomb excitation is included in the same manner. In the original version some programming errors occurred, which in some cases caused drastic effects on the calculated cross sections. After an adequate correction the results agree with calculations done in the case of the rotational model by the coupled-channel program CCP1 (Oxford). The differential cross sections published by T. Tamura reproduced for the rotational model. Differences are found in some cases for the vibrational model and when the original treatment of the Coulomb excitation is used. The origin of these differences was not fully clarified. A Fortran IV listing of the modified code is presented. (8 references) (auth)

36819 ANATOMY OF THE HARTREE-FOCK PROCEDURE IN A SIMPLE MODEL. Harvey, M.; Jensen, A. S. (Atomic Energy of Canada Ltd., Chalk River, Ont.). Nucl. Phys.; A164: 641-57(1971).

The Hartree-Fock procedure is examined in detail for the simple problem of two particles in a four-dimensional function space for which the exact solution can be found. Conditions are determined for the stability of the iterative procedure used to solve the Hartree-Fock set of equations. The problem of drawing the energy surface using the constrained Hartree-Fock method is discussed. (auth)

36820 EFFECTIVE OPERATORS FOR THE NUCLEAR SHELL MODEL. III. E2 EFFECTIVE CHARGE WITH REALISTIC REACTION MATRICES. Khanna, F. C.; Lee, H. C.; Harvey, M. (Atomic Energy of Canada Ltd., Chalk River, Ont.). Nucl. Phys.; A164: 612-30(1971).

The structure of effective operators is determined in time-dependent perturbation theory and compared with the approach using Bloch-Horowitz theory discussed in paper I. The E2 effective charges in the spherical shell model arising from the core polarization in the oxygen and calcium regions are calculated with the G-matrices of Kahana et al. (auth)

36821 VOLUME, SURFACE, AND SYMMETRY TERMS IN THE SEMI-EMPIRICAL MASS FORMULA. Mavromatis, H. A. (Univ. of Sussex, Brighton, Eng.). Nucl. Phys.; A162: 648-56 (1971).

The coefficients of the volume, surface, and symmetry terms in the semi-empirical mass formula are extracted from a first-order shell-model calculation using the Sussex matrix elements and closed oscillator shell nuclei. The results especially for the volume term are satisfactory. The effect on these results of second-order contributions to the binding energy are also examined. (auth)

XUM

36822 STABILIZATION OF THE AXIALLY SYMMETRIC SHAPE AND $(pf)^2$ MIXING IN sd SHELL NUCLEI. Strottman, D. (State Univ. of New York, Stony Brook. Univ. of Copenhagen); Arima, A. Contract AT(30-1)-4032. Nucl. Phys.; A162: 605-23(1971).

Two-particle excitations into the pf shell from the sd shell are shown to be important to make nuclei such as ^{22}Ne and ^{24}Mg more axially symmetric. The level structure of ^{22}Ne can be reasonably understood, but a complete understanding of the level structure and electromagnetic properties of ^{24}Mg is still lacking. Two-hole eight-particle states are also considered in ^{22}Ne. (auth)

36823 COMPARATIVE STUDY OF FRENCH'S SPECTRAL DISTRIBUTION AND THE RANDOM MATRIX THEORY. Ullah, Nazakat (Tata Inst. of Fundamental Research, Bombay). Nucl. Phys.; A164: 658-63(1971).

A comparative study of French's spectral distribution and the random matrix theory is carried out. By using a similarity between the two, an expression is given for the volume element in the space of the expansion coefficients. Using this volume element an exact expression is derived from the mixing of two symmetries. For the case of small mixing this expression reduces to the one which is obtained using perturbation approximation. (auth)

36824 NUCLEAR SURFACE. Jones, G. A. (Oxford Univ.). Rep. Progr. Phys.; 33: 645-89(Jul 1970).

The nuclear surface cannot be sharply defined since the nuclear density is a continuous function of radius. By convention, one defines a surface thickness parameter as the width of the region in which the nuclear density falls from 90% to 10% of the central density. This parameter is known to be approximately 2.5 fm for the whole range of spherical nuclei, at least for those nuclei for which a central region of roughly constant density has meaning, that is above, say, A = 40. Experimentally it is an ill-defined parameter and appears to be independent of mass number—again this statement applies only to spherical nuclei. It is a matter of some speculation whether or not the constitution of this surface region is the same as that of the interior. Theoretically a preponderance of neutrons (i.e. a neutron/proton ratio greater than N/Z) is desirable in the surface, and the experimental measurements are consistent with a "neutron skin" of perhaps 0.2 to 0.3 fm. Though the size of the nuclear charge distribution has been determined with great precision, the nuclear matter distribution is known with much less certainty, and one still cannot rule out the possibility that protons and neutrons have a common distribution. One must also consider the possibility that nucleons in the nucleus are clustered into sub-units such as α-particles. Experiments designed to test this by knocking out these clusters look specifically at the nuclear surface since the mean free path of these sub-units in the central region must be too small to allow them to escape even if struck by a deeply penetrating probe. The results of such experiments seem to indicate that the nuclear matter in the surface region is largely condensed into α-particles. Another class of experiments involving meson-probes indicates a degree of spatial correlation of nucleons in the nuclear surface which is consistent with α-particle clustering. Recently doubt has been thrown on the interpretation of these experiments, so clustering into α-particles cannot be considered to be established. (auth) (UK)

36825 PAIR CORRELATIONS AND COLLECTIVE 0^+ STATES OF NUCLEI. I. Dzholos, R. V. (Joint Inst. for Nuclear Research, Dubna, USSR). Teor. Mat. Fiz.; 6: 403-14(Mar 1971). (In Russian).

The boson representation is obtained for the Hamiltonian of the microscopic model with pair residual forces. It is shown by using this representation that the connection of the collective pair branches of the excitation with noncollective ones is weak. The collective Hamiltonian describing pair excitations is constructed. It is shown how one can to pass from the collective Hamiltonian written in terms of the boson operators to differential equations similar to those of the generalized model of the nucleus. (auth)

36826 USA STANDARD: GLOSSARY OF TERMS IN NUCLEAR SCIENCE AND TECHNOLOGY. ANSI N 1.1 1967. New York; United States of America Standards Institute (1967). 111p. Available from American National Standards Inst., New York.

Standard definitions for the terms appearing in nuclear science and technology are given. (R.W.R.)

36827 RECENT ADVANCES IN THE THEORY OF NUCLEAR FISSION. Perez Belles, Rafael (Oak Ridge National Lab., Tenn.). Energ. Nucl. (Madrid); 14: 403-11(Sep-Oct 1970). (In Spanish).

The Bohr–Wheeler model is reviewed and used to analyze the probability of producing a nuclear reaction leading to fission. Some problems that have not been solved by the liquid-drop model are reported. The possibility of the existence of superheavy elements and their spontaneous-fission properties are considered. Some of these phenomena are studied in the light of the theory of nuclear orbits and the works of Strutinsky. An expression for the effective fission cross section is given. Some practical consequences of the infrathreshold structure and the possible existence of transactinide elements are discussed. (tr-auth)

36828 FINITE-RANGE CALCULATION OF THE TWO-NEUTRON TRANSFER REACTION. Bayman, B. F. (Univ. of Minnesota, Minneapolis). Contract AT(11-1)-1764. Nucl. Phys.; A168: No. 1, 1-16(1971).

Distorted-wave Born approximation calculations have been done for two-neutron transfer reactions, in which the total angular momentum transferred was zero. A finite-range interaction was used, which acted between the proton and each transferred neutron. The results support the conclusions of zero-range calculations, both with respect to the shapes of the angular distributions, and the relative cross sections for transfer into different shells. However, the absolute cross sections, calculated for the ^{40,48}Ca(t,p)^{42,50}Ca(g.s.) reactions, were only about a third as large as those observed. (auth)

36829 DIAGRAMMATIC METHOD OF THE PARTICLE-VIBRATION COUPLING MODEL. I. Paar, V. (Univ. of Copenhagen. Inst. Ruder Boskovic, Zagreb). Nucl. Phys.; A164: 576-92(1971).

A diagrammatic method of the particle-vibration coupling model based on Goldstone and Jucys–Bandzaitis–Vizbaraite formalisms is developed. (auth)

36830 PARTICLE-HOLE STATE DENSITY IN THE UNIFORM SPACING MODEL. Williams, Frederick C. Jr. (Univ. of Rochester, N. Y.). Nucl. Phys.; A166: 231-40(1971).

A new method is used to derive an accurate but simple formula for the state density for fixed numbers of particles and holes in the uniform spacing model. The calculation is extended to the case where two kinds of particles are present. The results are compared with exact numerical calculations. Direct numerical calculation of particle-hole state densities, asymptotic summation of the approximate formula, and angular momentum distribution of states are discussed in the appendices. (auth)

36831 NUCLEON–NUCLEON CORRELATION AND TWO-PION-EXCHANGE THREE-BODY FORCE IN NUCLEAR MATTER. Loiseau, B. A. (Institut de Physique Nucleaire, Orsay, France); Nogami, Y.; Ross, C. K. Nucl. Phys.; A165: 601-24(1971).

The contribution of the two-pion-exchange three-body force to the binding energy of nuclear matter is examined, and cutoffs between all the pairs of nucleons are introduced. The cutoffs are meant to simulate the nucleon–nucleon correlation at short distances, and also separate the effect of the better known long-range part of the force from that of the unknown short-range part. The contribution is found to be much reduced compared with that obtained in a recent paper by Bhaduri, Nogami and Ross. With reasonable cutoffs and pionic form factor the contribution is found to be of the order of 2 MeV attraction per particle. The similar ΛNN three-body force is also discussed, and a serious difficulty concerning the binding mechanism of a Λ-particle in nuclear matter is pointed out. (auth)

36832 MODEL SPACE CALCULATION OF THE QUASI-PARTICLE INTERACTION FOR NUCLEAR MATTER. Poggioli, R. S.; Jackson, A. D. (State Univ. of New York, Stony Brook). Nucl. Phys.; A165: 582-92(1971).

Landau's theory of Fermi liquids is outlined and a microscopic approach to the calculation of the quasiparticle interaction $f(k_1,k_2)$ for nuclear matter is detailed. A model space is introduced in order to take especial care of the contribution of low-lying states to $f(k_1,k_2)$. The model space is constructed to include only those states in which all particles have momentum less than 2k . The effect of the high momentum states is absorbed into the definition of the effective interaction to be used within the model space. An examination of Brueckner–Bethe theory leads to the choice of a truncated G-matrix as a good approximation for this model interaction. A simple perturbative approach is attempted within the model space. The quasiparticle interaction is calculated to second order (in the model interaction). Good values are obtained for the effective mass and symmetry energy, but the calculated compression modulus is too small. It is hoped that third-order corrections will improve the results, but no definitive statement about the convergence of this approach is possible at this stage. (auth)

36833 ISOSPIN CONSERVATION AND β DECAY OF HEAVY NUCLEI. Zaretskii, D. F.; Nersesov, E. A. (Moscow Engineering Physics Inst.). Yadern. Fiz.; 13: 499-504(Mar 1971). (In Russian).

On the basis of the theory of finite Fermi systems calculations are carried out for matrix elements for $0^+ - 0^+$ transitions between the grounds states of heavy deformed nuclei. Nucleon pairing in the nuclei is taken into account consistently. The obtained values of the matrix elements are compared with experimental results and with those obtained by other authors. (auth)

36834 EFFECT ON PHONON + PARTICLE DOORWAY STATES IN (n,γ) REACTION. Knat'ko, V. A.; Rudak, E. A. (Inst. of Physics, Minsk). Yadern. Fiz.; 13: 521-4(Mar 1971). (In Russian).

The effect of the "phonon + particles" doorway states is investigated for deexcitation of the capture state in the (n,γ) reaction on nuclei with $A < 80$. An attempt is made to explain the anticorrelation between the reduced neutron widths of the p levels and the reduced probabilities of the E1 γ transitions ^{57}Fe, ^{63}Ni, ^{65,67}Zn, and ^{71,73}Ge. (auth)

36835 EXCITATION OF ANALOGUE-DIPOLE STATES. Clement, C. F. (Atomic Energy Research Establishment, Harwell, Eng.); Perez, S. M. Nucl. Phys.: A165: 569-81(1971).

A collective theory is developed for the direct excitation of "analog-dipole" states which have been seen as bumps in (p,n) and (n,p) reaction spectra. The magnitudes of the excitation processes are given by V_1, the isospin optical model potential, and matrix elements which are obtained by evaluating a new model-independent dipole sum rule. The general behavior of the cross sections obtained is discussed and some estimates are made of their magnitude. Some distorted wave fits are obtained to data on the ^{58}Ni(n,p)^{58}Co reaction. (auth)

36836 HINDRANCE OF CHARGE EXCHANGE E1 TRANSITION. Ejiri, H. (Univ. of Copenhagen). Nucl. Phys.; A166: 594-604(1971).

The hindrance of the charge-exchange E1 transition is studied in terms of the core polarization, namely, coherent admixtures of many 1p–1h states. The mixing coefficients are calculated by using the random-phase approximation. The calculated E1 matrix element for the transition from the $2f_{\frac{5}{2}}$ neutron state in ^{141}Ce to the $2d_{\frac{5}{2}}$ proton state in ^{141}Pr is found to be reduced by a factor three compared with the pairing-model estimation. This value agrees with the value measured in the (p,γ) reaction through the $2f_{\frac{5}{2}}$ isobaric analog resonance. (auth)

36837 MEASURING THE PARAMETERS OF TWO-PARTICLE RESONANCE SCATTERING IN THREE-PARTICLE REACTIONS. Lazarev, L. M. Izv. Akad. Nauk SSSR, Ser. Fiz.; 35: No. 1, 207-10(1971). (In Russian).

A good method of studying quasi-stationary states is the investigation of cascade decomposition of a nuclear system into three parts in reactions on light nuclei: $a + A \rightarrow X^* \rightarrow 1 + Y^* \rightarrow 1 + 2 + 3$. However, experimental level parameters of the unstable nucleus Y^* are different from experimental parameters obtained from scattering of two particles $2 + 3 \approx Y^*$. This fact is due to correlation of the quasi-stationary states of X^* and Y^*. When the compound nucleus X^* is not formed, no changes in the parameters of resonance scattering of $2 + 3$ is noted experimentally. In order to understand the main qualitative regularities in the effect of a third body on the parameters of two-particle resonance scattering, it is sufficient to determine the energy dependence of the amplitude of the three-particle reaction near the resonance of the $2 + 3$ scattering. This problem is solved in the simplest case for three different neutral particles without spin. Jacoby coordinates and reduced masses are used. A contraction in widths of resonance states is noted in ^{8}Be and ^{12}C, and this is explained by the derived formulas as due to resonance interaction between two states. (TTT)

36838 NOTE ON THE WAVE FUNCTIONS OF NON-LOCAL SEPARABL POTENTIALS. Husain, D. (Dacca Univ., Pakistan). Nucl. Phys.; A166: 667-9(1971).

The wave functions of a nonlocal, separable potential are compared with the wave functions of an equivalent local potential. It is shown that the amplitudes of wave functions in an attractive nonlocal, separable potential are not always smaller than the amplitudes of wave functions in an equivalent local potential. (auth)

36839 COLLECTIVE EXCITATIONS IN NUCLEI. Belyaev, S. T. Documents on Modern Physics. New York; Gordon and Breach, Science Publishers, Inc. (1968). 80p. $5.50.

This book is a reprint in full, with corrections, of an item that first appeared as NSA 21: 30053. (R.W.R.)

36840 GROUND STATE CORRELATIONS AS VARIATIONAL PARAMETERS IN THE NUCLEAR MANY-BODY PROBLEM. Dreizler, R. M. (Univ. of Pennsylvania, Philadelphia); Klein, Abraham; Krejs, F. R.; Dreiss, Gerard J. Nucl. Phys.; A166: 624-42(1971).

It is shown that amplitudes which normally occur in the random-phase approximation (RPA) can be considered as variational parameters in an approximate theory of the ground state, arbitrary 2p–2h excitations of a Hartree–Fock substrate being allowed. These amplitudes obey equations that differ in detail from the RPA, although the two sets are shown to coincide in the weak-coupling limit. All the desirable mathematical and physical properties of the RPA have their counterpart in the new theory; but, in addition, correlations are guaranteed to be given correctly near the weak-coupling limit. The method is applied to an exactly soluble model, and some comparison with other approximation methods is made. (auth)

36841 SHAPE AND AVERAGE ENERGY OF BETA-PARTICLE SPECTRA. Murthy, M. S. S. (Univ. of Kansas, Kansas City). Int. J. Appl. Radiat. Isotop.; 22: No. 2, 111-23(Feb 1971).

The degree of distortion produced in a beta-particle spectrum due to the forbiddenness of the transition is discussed. By approximating the Fermi function appearing in the Fermi theory of beta decay to a three-term polynomial, equations are developed to calculate the average energy of various beta emitters having allowed as well as some forbidden transitions. The contribution to electron energy per decay, by the internal-conversion electrons, is also discussed. (auth) (UK)

36842 SPATIAL GENERALIZATION OF NOMOGRAPHS WITH AN ORIENTED TRANSPARENCY GRID, AND THEIR USE IN THE KINEMATICS OF NUCLEAR REACTIONS. Potetyunko, G. N. This paper was summarized in At. Energ. (USSR); 29: 124(Aug 1970) as paper No. 418/5765. (In Russian).

The theory developed is applied to the kinematics of nuclear reactions producing three particles for the case where the trajectories of the impinging particle and of the reaction products lie in a common plane. Inequalities defining the boundaries of the continuous spectrum of observed particles are given for several different observation conditions. (R.W.R.)

36843 LANDAU, BRUECKNER–BETHE, AND MIGDAL THEORIES OF FERMI SYSTEMS. Brown, G. E. (NORDITA, Copenhagen. State Univ. of New York, Stony Brook). Contract AT-(30-1)-4032. Rev. Mod. Phys.; 43: 1-14(Jan 1971).

The Landau theory for infinite Fermi systems is discussed, and it is then shown how one can apply the Landau technique of functional differentiation of the energy with respect to quasi-particle occupation numbers to obtain the effective interaction, by beginning from the Brueckner–Bethe approximation to the energy. Calculations of this effective interaction by Bäckman from a nucleon–nucleon potential are discussed and criticized. Results of Bäckman's calculation are compared with the parameters in Migdal's effective force, evaluated at the center of the nucleus, the latter parameters having been derived phenomenologically by fitting various nuclear phenomena. There is a large discrepancy between the calculated value of the compressibility of nuclear matter and that obtained phenomenologically. The advantages of introducing a model space in order to improve the accuracy of the calculated results is discussed, and it is pointed out that such an introduction would also be advantageous in recent calculations by Barrett and Kirson of third-order terms in the effective interaction. A model space is effectively introduced in recent calculations with the Migdal theory when it comes to deriving the quadrupole–quadrupole interaction. Calculation of the effective force between two atoms in ^{3}He is discussed briefly, and it is pointed out that this is a much more ambitious task than in nuclear matter. Calculations carried out within the Brueckner–Bethe formalism are reviewed. (auth)

36844 REACTION SYMMETRIES FOR MULTIPLET PRODUCTION. Robson, D. (Florida State Univ., Tallahassee); Richter, A. Ann. Phys. (N. Y.); 63: No. 1, 261-85(Mar 1971).

A theorem concerning nuclear reaction symmetries for isospin multiplet production involving complex nuclei is proved and generalized. The general formalism of possible symmetry violations is presented. Elastic scattering, multiparticle production in the final state, symmetry relations for polarizations, and substructure symmetries are discussed within the framework of the theorem. It is shown that the theorem has an extension in the case of multiplet production involving elementary particles. It is studied briefly in the case of SU(3) and SU(n) multiplets. Finally, some general remarks are made about approximate symmetries for multiplet production. (auth)

36845 GIANT MONOPOLE STATE: ISOSPIN MIXING IN NUCLEAR GROUND STATES. Noble, J. V. (Univ. of Pennsylvania, Philadelphia). Phys. Lett.; 35B: No. 2, 140-2(10 May 1971).

The Coulomb-induced $\Delta T = 1$ admixture in nuclear ground states is evaluated by assuming that the mixing is entirely through the giant monopole state $|\Phi\rangle \propto (\Sigma_p r_p^2 - \Sigma_n r_n^2)|g.s.\rangle$. (auth)

XUM

36846 TRANSIENT FIELDS ACTING ON HEAVY IONS DURING SLOWING-DOWN IN MAGNETIZED MATERIALS. Lindhard, Jens; Winther, Aage (Univ. of Aarhus, Denmark. Univ. of Copenhagen). Nucl. Phys.; A166: 413-35(1971).

The theory of transient fields acting on the nucleus of an energetic ion during slowing-down in magnetized materials is treated. The enhancement of density, at the ion nucleus, of atomic electrons scattered by the ion is $\chi \approx 10^2$ to 10^3. This implies a strong magnetic field from polarized electrons in a ferromagnetic material. Estimates of the enhancement and knowledge of energy loss permit a calculation of the total magnetic precession of a nucleus during slowing-down. Effects of screening are discussed, and the sizable relativistic correction is computed. Fluctuation phenomena are also treated, as well as transient electric field gradients due to electron scattering. There is good agreement with the trend of experimental results, and relative values in different ferromagnetics agree within experimental error. But the measurements remain ~50% above the formulas. The discrepancy may be due to some of the more complicated corrections, which have not yet been estimated. (auth)

36847 NONLOCAL POTENTIALS; THREE-BODY MODELS OF ${}^{9}_{\Lambda}$Be, ${}^{6}_{\Lambda\Lambda}$He, ${}^{3}_{\Lambda}$H, ${}^{5}_{\Lambda}$He, ^{9}Be, AND ^{6}Li; AND CLUSTER MODEL OF THE REACTION ^{6}Li(π^-,nn)^{4}He. Rickett, Joe Pat. Waco, Tex.; Baylor Univ. (1970). 334p. University Microfilms Order No. 71-6034.

Thesis.

Nonlocal, separable two-body potentials are studied. Emphasis is given to the interpretation of such potentials by means of equivalent local potentials. For example, the modern Tabakin potential is found to correspond to an equivalent local potential that has a repulsive core and is strongly attractive inside the core. The exponential local potential is compared with the NLS potential with an exponential form factor, and the Perey effect and energy-dependent nature of NLS potentials are demonstrated. A wave-function method is applied to the following six three-body systems: ${}^{9}_{\Lambda}$Be, ${}^{6}_{\Lambda\Lambda}$He, ${}^{3}_{\Lambda}$H, ${}^{6}_{\Lambda}$He, ^{9}Be, and ^{6}Li. These involve the six two-body interactions: N−N, $\alpha-\alpha$, $\alpha-\Lambda$, N−Λ, N−α, and Λ−Λ. The three-body binding energies of ^{6}Li, ^{9}Be, ${}^{3}_{\Lambda}$H, and ${}^{6}_{\Lambda}$He are found to be 4.7 MeV, 5.7 MeV, 2.8 MeV, and 2.9 MeV, respectively, when N−α, N−N, and N−Λ interactions are used that are common to pairs of these nuclei. The two-body interactions and three-body binding energies are found to be consistent with each other. When the all-attractive Yamaguchi $\alpha-\Lambda$ interaction is used for ${}^{9}_{\Lambda}$Be, a large binding energy of 18 MeV is obtained; and it is shown that it is possible to decrease this value to the experimental one (9.14 MeV) when a rank-two potential that includes repulsion is used. By means of a three-body determination with ${}^{6}_{\Lambda\Lambda}$He the strength of the Λ−Λ interaction is determined to be $\lambda_{\Lambda\Lambda} = 35\ \alpha_0^7$ ($\alpha_0 = .2316\ F^{-1}$). The theoretical distribution of recoil momentum and angle of the alpha particle in the reaction ^{6}Li(π^-,nn)^{4}He for the case in which the two neutrons are emitted in opposite directions is computed by using a cluster-model wave function, and it is found to be possible to fit the experimental data to within experimental error. Rescattering in the pion absorption mechanism and the final-state neutron−neutron interaction are included. It is found that the intercluster parameter alone controls the position of the first node in the distribution and that the deuteron cluster parameter determines the relative magnitude of a second peak in the theoretical distribution. The possible existence of a corresponding second peak in the experimental distribution is emphasized. (Diss. Abstr. Int., B)

36848 EFFECTS OF STRONG BINDING IN ELASTIC AND INELASTIC SCATTERING OF DEUTERONS BY NUCLEI. Korbetskii, E. V.; Neplyuev, V. M.; Sokolov, L. S. Izv. Akad. Nauk SSSR, Ser. Fiz.; 35: No. 1, 183-6(1971). (In Russian).

Calculated cross sections in the generalized model are compared with cross sections calculated by a simple optical model (for elastic scattering) and by the method of distorted waves (for inelastic scattering). Only even−even nuclei are considered. Their excited states with spin I and parity π are represented by a collective (vibration) model. The binding of elastic and inelastic processes are effected by a deformed optical potential whose real part is in the form of a Woods−Saxon potential, and whose imaginary part is in the form of a derivative of the real part. The parameters of the potential are listed. The effect of inelastic scattering of 13.6-MeV deuterons to the first excited states of ^{12}C and ^{60}Ni on the differential cross section is presented. The differences between calculations by the optical model and by the method assuming binding are greater for ^{12}C than for ^{60}Ni. This is due to the large value of the quadrupole deformation for ^{12}C. Calculations are presented for six sets of parameters for the potential. The character and absolute value of the differential cross section for inelastic scattering are not determined by the energy of the excited state. If the nature of the level is given, the scattering cross section of a previous level can be predicted without knowing its energy precisely. (TTT)

36849 THREE-NEUTRON RESONANCE IN THE REACTION ^{3}He(π^-,π^+)3n. Reitan, A. Ark. Fys. Seminar Trondheim; No. 6, (1971).

There has recently arisen interest in quasi-bound resonances in systems of three nucleons, and attention is here focussed on the ^{3}He(π^-,π^+)3n reaction. From previously published results it is found that such a resonance may best be studied at very, low energies, and an estimate of how large an effect to expect is attempted. The result leads one to conclude that it will be very difficult to use the ^{3}He(π^-,π^+)3n reaction to obtain accurate information on the structure of such a resonance. (Norway)

36850 CORRELATIONS BETWEEN REDUCED NEUTRON WIDTHS AND PARTIAL RADIATIVE WIDTHS IN RESONANCES. Solov'ev, V. G. (Joint Inst. for Nuclear Research, Dubna, USSR). Phys. Lett.; 35B: No. 2, 109-12(10 May 1971).

The cases in which there can be significant correlations between reduced neutron widths Γ^0_{ni} and reduced partial radiative widths $\Gamma^0_{\gamma if}$ in resonances are investigated. Some suggestions are given for the experimental study of these correlations. (auth)

36851 SINGULAR CORE INTERACTIONS AND THREE-BODY THEORY. Brayshaw, D. D. (Stanford Univ., Calif. Columbia Univ., New York). Phys. Rev. Lett.; 26: 659-61(15 Mar 1971).

It is shown that the Faddeev formalism must and can be modified when the short-range two-body behavior is specified by a hard core or boundary-condition model. A new integral equation is formulated for this purpose which, in the special case of boundary-condition model or hard core alone, reduces to an equation in a single vector variable. This feature provides an apparently unique example of a nonseparable interaction for which the three-body equations can be solved exactly. (auth)

36852 SPECTROSCOPIC INFORMATION FROM ISOBARIC ANALOG RESONANCES. Clarkson, R. G. (Univ. of Oregon, Eugene); von Brentano, P.; Dost, M. Phys. Rev. Lett.; 26: 656-8(15 Mar 1971).

The shell-model expressions for the partial widths of analog resonances are reformulated to demonstrate that the widths are functions primarily of asymptotic parameters; in particular, it is shown that the widths depend strongly on the asymptotic normalization of the neutron wave function rather than the spectroscopic factor, and that the dependence on the proton potential parameters is, in fact, a dependence on the phase shift. (auth)

36853 N–N INTERACTION MATRIX ELEMENTS FROM PHASE SHIFTS AND THE JOST FUNCTION. Ripa, P.; Maqueda, E. (Comision Nacional de Energia Atomica, Buenos Aires). Nucl. Phys.; A166: 534-46(1971).

An improvement of the Born approximation based on properties of the Jost function is tested by calculating N−N potential matrix elements from experimental phase shifts. Satisfactory results are obtained with a simple plane-wave method even for the S-channel. (auth)

REACTOR TECHNOLOGY

Commercial Power Reactors

Refer also to abstracts 34755, 34771, 34780, 34817, 34819, 34826, 35313, 37001, and 37092.

36854 (DOCKET-50003-73) INDIAN POINT STATION, UNIT NO. 1. Revised Schedule and Plan of Work on Emergency Core Cooling System. (Consolidated Edison Co. of New York, Inc., New York). 2 Jun 1971. 3p. Dep. NTIS.

36855 (NP-18846) ENERGY OUTLOOK IN THE COMMUNITY. Situation 1969; Perspectives 1970. (European Communities, Brussels (Belgium). Commission). Jan 1970. 174p. (In French). Dep. NTIS (U. S. Sales Only).

The energy production in the European Communities during 1969 is analyzed, trends for 1970 are described, and the principal problems in future energy production are examined. Energy requirements are discussed, and the fuel supply situation for coal, petroleum, and natural and product gas is described. Electric power production by conventional and nuclear power stations is summarized. (H.D.R.)

36856 (NP-18847) ENERGY OUTLOOK IN THE COMMUNITY. Situation 1970; Perspectives 1971. (European Communities, [Luxembourg]. Commission). 58p. (In French). Dep. NTIS (U. S. Sales Only).

The energy supply situation in the European Communities during 1970 is summarized and energy development perspectives and problems for 1971 are discussed. The petroleum, coal, gas, and nuclear fuel supply is summarized, and electric power production by conventional and nuclear power stations is reviewed. (H.D.R.)

36857 IN-REACTOR INSPECTION AND REPAIR PROCEDURES FOR THE BONUS NUCLEAR POWER PLANT. Wylie, Robert D. (Southwest Research Inst., San Antonio); Iriarte, Modesto Jr. pp 37-41 of Materials Technology: An Interamerican Approach. New York; American Society of Mechanical Engineers (1968).

From Inter-American Conference on Materials Technology, San Antonio, Tex. See CONF-680513.

During the early operating history of the BONUS reactor, leaks developed in the piping supplying the preheater which preheats the steam prior to inlet to the nuclear superheater fuel. The inspection procedures, the analysis techniques, and the in-reactor procedures for replacement of the pipes are described. (H.D.R.)

36858 NUCLEAR POWER REACTORS AND MOBILE NUCLEAR INSTALLATIONS. Wiesenack, Guenter (Technische Ueberwachungs-Vereine, Essen). VDI (Ver. Deut. Ing.) Z.; 113: No. 6, 426-30(Apr 1971). (In German).

The development of power reactors in the Federal Republic of Germany is reviewed. (55 references) (D.D.C.)

36859 SUBSTANCE AND MEANING OF THE NUCLEAR FUEL INDUSTRY AND ECONOMY. Wenzel, P. (Institut fuer Kraftwerke, Berlin). Kernenergie; 14: No. 1, 1-6(Jan 1971). (In German).

Erecting large nuclear power plants for meeting the continuously increasing requirements of electric and thermal power calls for evolution of a long-term industry and economy of nuclear fuel in order to realize and organize optimum fuelling in a developing nuclear power system with respect to resources of raw fuel material, simultaneous production of nuclear power and fissile material in power reactors and to all essential economical and political restrictions in a country. The fuel strategy for the different types of reactors present in the system which may qualitatively be divided into the two groups of converters and breeders is analyzed. (23 references) (auth)

36860 CONSTRUCTION PLAN FOR A NUCLEAR POWER PLANT OF THE CHUBU ELECTRIC POWER COMPANY. Suzuki, Shigema (Chubu Electric Power Co. Inc., Nagoya, Japan). Denryoku Shinpo; 16: No. 11, 61-3(Nov 1970). (In Japanese).

Construction plans for the Hamaoka Power Reactor are described. The site in Shizuoka prefecture faces the Pacific, and has hills in the background. The power station employs a BWR of electric output 540,000 kW. Construction of the power station will be started in November 1970, and will be completed in November 1974. The following are described: site topography, nuclear reactor, power distribution, sea-water intake, construction materials transport, construction schedule, nuclear fuel, and works up to the present. (Japan)

36861 EFFECT OF ESCALATION ON FUTURE FUEL COSTS. Hauser, Louis G. Pub. Util. Fortn.; 87: No. 12, 68-74(10 Jun 1971).

A detailed analysis is made of the cost components for coal and nuclear fuel in the electric utility fuel market. The effects of industry trends and escalation upon each of the cost factors for these two fuels are projected through 1985. A direct comparison is made between the projected behavior of coal and nuclear fuel market prices. The conclusion is reached showing the sensitivity of coal costs to escalation factors. Uranium fuel does not exhibit this characteristic. (auth)

Operation and Economics

36862 (BNWL-462) ALTHAEA: A ONE-DIMENSIONAL TWO-GROUP DIFFUSION CODE WITH AN EFFECTIVE FOUR-GROUP BURNUP. Merrill, E. T. (Battelle-Northwest, Richland, Wash. Pacific Northwest Lab.). May 1971. Contract AT(45-1)-1830. 111p. Dep. NTIS.

The ALTHAEA code systems calculate nuclear reactor fuel burnups with reasonable accuracy and at computer speeds sufficient for preliminary economic analysis of fuel cycle costs. This first version of the code describes four neutron energy groups, and collapses these to two groups for one-dimensional space diffusion calculations. It provides for cross shielding of the epithermal resonances. It is written in FORTRAN II for the IBM 7090, or FORTRAN IV for the Univac 1108 computer. 27 references. (auth)

36863 (CONF-700653-1) NUCLEAR POWER IN GREAT BRITAIN. Booth, E. S. (Central Electricity Generating Board, London (England)). 1970. 20p. Dep. NTIS (U. S. Sales Only).

From Jubilee meeting of the association of large boiler plant operators; Essen, Germany (1 Jun 1970).

A description of electricity generation and transmission systems in Britain is followed by a brief historical survey of nuclear power programs. The pattern of Britain's fuel policy and her policy for siting nuclear stations are outlined. Operational experience with the Magnox stations is described. There is a discussion of the program for AGR's and of future prospects for Mark III gas-cooled reactors and other reactor types. Nuclear power is shown to be already competitive with some contemporary coal-fired stations. (UK)

36864 (CONF-700956-2) OPERATING EXPERIENCE OF NUCLEAR POWER-STATIONS IN UNIPEDE MEMBER COUNTRIES. Sani, Luciano (Ente Nazionale per l'Energia Elettrica, Rome (Italy)); Stolz, Jean (Electricite de France, Paris); Weeks, Robert (Central Electricity Generating Board, London (England)). [nd]. 14p. Dep. NTIS (U. S. Sales Only).

From fifteenth international congress of the international union of producers and distributors of electrical energy; Cannes, France (13 Sep 1970).

A summary of the operating experience acquired with nuclear power-stations and general observations concerning the experience acquired regarding the primary circuit component performance, the fuel performance, and the control of radiation and contamination are presented. (auth)

36865 (DOCKET-1155-115) LA CROSSE BOILING WATER REACTOR. Unplanned Reactor Shutdown. (Dairyland Power Cooperative, La Crosse, Wis.). 13 May 1971. 2p. (DPC-71-9). Dep. NTIS.

An unplanned reactor shutdown on May 11, 1971 is described. The scram was actuated by a high frequency noise which caused the power-flow safety channels signals to spike to greater than the scram set points. The scram actuating noise was produced by a power tool plugged into a non-interruptible 110 volt AC outlet. (D.C.C.)

36866 (DOCKET-1155-120) LA CROSSE BOILING WATER REACTOR. Monthly Operating Report, March 1971. (Dairyland Power Cooperative, La Crosse, Wis.). 11 Jun 1971. Contract AT(11-1)-851. 40p. (DPC-851-24). Dep. NTIS.

36867 (DOCKET-50171-85) PEACH BOTTOM ATOMIC POWER STATION, UNIT 1. Monthly Operations Report No. 61, March 1971. (Philadelphia Electric Co., Pa.). 24 May 1971. 14p. Dep. NTIS.

36868 (DOCKET-50206-113) SAN ONOFRE NUCLEAR GENERATING STATION, [UNIT 1]. Operation Report, May 1970.

(Southern California Edison Co., Los Angeles). Jun 1970. Contract AT(30-1)-3270. 7p. (NYO-3270-38). Dep. NTIS.

36869 (DOCKET-50213-109) CONNECTICUT YANKEE ATOMIC POWER PLANT. Operation Report No. 71-4, April 1971. (Connecticut Yankee Atomic Power Co., Haddam). 25 May 1971. Contract AT(30-1)-3250. 15p. (NYO-3250-59). Dep. NTIS.

36870 (DOCKET-50219-135) OYSTER CREEK NUCLEAR POWER PLANT, UNIT NO. 1. Isolation Condenser System Time Delay Relay Failure. (Jersey Central Power and Light Co., Morristown, N. J.). 17 May 1971. 2p. Dep. NTIS.

36871 (DOCKET-50219-137) OYSTER CREEK NUCLEAR POWER PLANT, UNIT NO. 1. Summary Technical Report: Primary Containment Leakage Rate Test, October 1970. (Jersey Central Power and Light Co., Morristown, N. J.). May 1971. 11p. Dep. NTIS.

36872 (DOCKET-50237-172) DRESDEN NUCLEAR POWER STATION, UNIT 2. Unplanned Release of Radioactivity. (Commonwealth Edison Co., Chicago, Ill.). 28 May 1971. 1p. Dep. NTIS.

36873 (DOCKET-50237-173) DRESDEN NUCLEAR POWER STATION, UNIT 2. Summary Technical Report of Secondary Containment Leak Rate Tests, October 1970-March 1971. (Commonwealth Edison Co., Chicago, Ill.). 28 May 1971. 15p. Dep. NTIS.

36874 (DOCKET-50244-71) ROBERT EMMETT GINNA NUCLEAR POWER PLANT, UNIT NO. 1. Possible Excessive Gas Effluent Release. (Rochester Gas and Electric Corp., N. Y.). 11 Jun 1971. 3p. Dep. NTIS.

36875 (DOCKET-50245-59) MILLSTONE NUCLEAR POWER STATION, UNIT 1. Abnormal Occurrence Report No. A0-71-6. (Millstone Point Co., Hartford, Conn.). 2 Apr 1971. 2p. Dep. NTIS.

On March 25, 1971 the reactor underwent a high flux trip as a result of turbine control valve test while at 80% of full power. The trip was initiated by closing the control valve too fast during the test. (D.C.C.)

36876 (DOCKET-50245-60) MILLSTONE NUCLEAR POWER STATION, UNIT 1. Abnormal Occurrence Report No. A0-71-7. (Millstone Point Co., Hartford, Conn.). 8 Apr 1971. 2p. Dep. NTIS.

On March 31, 1971, while performing ten day surveillance test, the motor on the Loop A LPCI injection valve failed. Corrective maintenance is described. (D.C.C.)

36877 (DOCKET-50245-61) MILLSTONE NUCLEAR POWER STATION, UNIT 1. Abnormal Occurrence Report No. A0-71-5. (Millstone Point Co., Hartford, Conn.). 3 Mar 1971. 1p. Dep. NTIS.

On February 21, 1971, the gas turbine generator emergency power system failed to start following a reactor scram and trip of the main turbine. The gas turbine generator failed to start due to a blown tachswitch power supply fuse. (D.C.C.)

36878 (DOCKET-50245-67) MILLSTONE NUCLEAR POWER STATION, UNIT 1. Abnormal Occurrence Report No. A0-71-8. (Millstone Point Co., Hartford, Conn.). 29 Apr 1971. 2p. Dep. NTIS.

Inoperability of the gas turbine generator emergency power system due to incorrect operating procedures is described. On April 22, 1971 during a shutdown mode for the gas turbine, a turbine lube oil reservoir low level alarm was received due to an incorrect position for the turbine lube oil pump switch. (D.C.C.)

36879 (DOCKET-50245-81) MILLSTONE NUCLEAR POWER STATION, UNIT 1. Abnormal Occurrences No. A0-71-9 and No. A0-71-10. (Millstone Point Co., Hartford, Conn.). 12 May 1971. 2p. Dep. NTIS.

On May 2, 1971 a failed bypass valve motor was discovered on the cleanup system. On May 5, 1971 a failed pump suction valve motor was observed in the shutdown cooling system. Corrective maintenance required for both motor failures is described. (D.C.C.)

36880 (DOCKET-50261-60) H. B. ROBINSON UNIT NO. 2. Routine Operating Report No. 1, September 20, 1970-March 20, 1971. (Carolina Power and Light Co., Raleigh, N. C.). 3 Jun 1971. 68p. Dep. NTIS.

36881 (DOCKET-50266-49) POINT BEACH NUCLEAR PLANT, UNIT 1. Abnormal Occurrence Report: Improper Lineup of Safety Injection Pump Breaker. (Wisconsin Electric Power Co., Milwaukee). 14 May 1971. 3p. Dep. NTIS.

36882 (DOCKET-50289-36) THREE MILE ISLAND NUCLEAR STATION, UNIT 1. Preliminary Safety Analysis Report, Amendment 21 (Includes Additions and Revisions to Application for Reactor Operating License). (Metropolitan Edison Co., Reading, Pa. Jersey Central Power and Light Co., Morristown, N. J. Pennsylvania Electric Co., Johnstown). 26 May 1971. 7p. Dep. NTIS.

Additional information is presented concerning estimated operating costs for 1973 to 1977. (D.C.C.)

36883 (DOCKET-50354-14) NEWBOLD ISLAND NUCLEAR GENERATING STATION, UNITS 1 AND 2. Preliminary Safety Analysis Report, Amendment 7. (Public Service Electric and Gas Co., Newark, N. J.). 21 May 1971. 275p. (DOCKET-50355-14). Dep. NTIS.

Revised and additional information concerning design parameters and operations aspects of the reactor is presented. (D.C.C.)

36884 (IAEA-127) OPERATING EXPERIENCE WITH NUCLEAR POWER STATIONS IN MEMBER STATES. A Review Prepared in September 1970. Ristic, M.; Khan, M. (International Atomic Energy Agency, Vienna (Austria)). 1970. 244p. NTIS (U. S. Sales Only).

A survey of the operating experience with 63 nuclear power plants comprising 84 power reactors, located in 14 Member States of the International Atomic Energy Agency is presented. It covers the period until December 31, 1969. Most of the information was taken from official sources, but other sources were used to supplement the data. For each reactor type a short review is given, summarizing the general performance of the particular system. The types covered include light water-cooled, pressurized water, boiling water, and heavy water moderated. For each station data sheets are provided giving pertinent information, such as location; owner, contractor and operator; technical parameter of the core, moderator and coolant; dates of start of construction, criticality, first generation of electricity and commercial operation; the main plant characteristics; the power generating history until the end of 1969, giving the load, the authorized and average outputs, the capacity and plant availability factors, the annual and cumulative electricity generation and a short description of the main causes of outages and other technical problems. A set of tables on gross electrical generation and a summary table on power reactor characteristics, including the approximate time elapsed from start to connection to grid conclude the report. (auth) (INIS)

36885 (JUL-705-RG) TECHNICAL AND ECONOMIC STATE AS WELL AS PROSPECTS OF ATOMIC ENERGY IN THE ECONOMY OF THE FEDERAL REPUBLIC OF GERMANY. PART I. STUDIES COMMISSIONED BY FEDERAL MINISTER OF RESEARCH AND DEVELOPMENT. Kraemer, H.; Bergmann, B.; Wagemann, K. (Kernforschungsanlage, Juelich (West Germany). Institut fuer Reaktorentwicklung). Oct 1970. 55p. (In German). Dep. NTIS (U. S. Sales Only).

The present technical and economic situation of the LWR nuclear power plant is investigated in comparison with fossil-fuel power plants. After a brief consideration of the energy balance in the German Republic, the state of the techniques and development tendencies in conventional and LWR power plants is summarized. The economy of individual power concepts is compared, and the fossil and nuclear fuel markets are analyzed. A prognosis is made of the future development of the power economy in the 70's. 55 references. (J.S.R.)

36886 (ORNL-TM-3223) OAK RIDGE SYSTEMS ANALYSIS CODE (ORSAC) USER'S MANUAL. Welfare, F. G.; Culberson, O. L.; Durfee, R. C.; Gift, E. H.; Jacobs, S. C.; Nichols, J. P.; Salmon, R. (Oak Ridge National Lab., Tenn.). Jun 1971. Contract W-7405-eng-26. 118p. Dep. NTIS.

ORSAC consists of a combination of SYSCO, a code developed at Oak Ridge National Laboratory, and MPS/360, an IBM-developed mathematical programming package. These codes, used together, allow the calculation of the combination of power plants which will provide a given electrical capacity in the United States at the minimum cost. Intermediate results include the economic and fuel utilization characteristics of each nuclear or fossil plant type being considered in the system. A full description of the ORSAC code is presented. 6 references. (auth)

36887 (TID-23762) BIG ROCK POINT NUCLEAR PLANT. Monthly Operations Report No. 52, January 1967. (Consumers

Power Co., Jackson, Mich.). 15 Feb 1967. Contract AT(11-1)-932. 20p. (DOCKET-50155-27). Dep. CFSTI.

36888 (TID-23819) BIG ROCK POINT NUCLEAR PLANT. Monthly Operations Report No. 53, February 1967. (Consumers Power Co., Jackson, Mich.). 15 Mar 1967. Contract AT(11-1)-932. 23p. (DOCKET-50155-28). Dep. CFSTI.

36889 (UARAEE-98) STATION STAFFING REQUIREMENTS FOR OPERATION OF A 150 MWe NUCLEAR STATION IN THE U.A.R. El-Fouly, M. F. (Atomic Energy Establishment, Cairo (Egypt). Reactors Dept.). 1970. 18p. Dep. NTIS (U. S. Sales Only).

Problems of staffing a nuclear power station in a developing country are discussed. The personnel requirements and their qualifications for operating a 150 MW(e) power plant are described. (H.D.R.)

36890 (WAPD-MRP-135) PRESSURIZED WATER REACTOR (PWR) PROJECT. Technical Progress Report, October 24, 1970-January 25, 1971. (Bettis Atomic Power Lab., Pittsburgh, Pa.). Contract AT-11-1-GEN-14. 18p. Dep. NTIS.

Plant operations and testing on two, three and four reactor coolant loops continued satisfactorily during the period and the total operating time with PWR-2 Seed 2 was increased to approximately 4760 equivalent full power hours (EFPH). The reactor plant was operated at full power (150 MW(e)) at about 4700 EFPH for the third time during Seed 2 lifetime to demonstrate full power capability. PWR-2 Seed 2 power capability was re-evaluated for swing load and full power operation for the interval from 4000 to 5500 EFPH using a modified control rod program and revised operating limits were implemented. Measured coolant flows at all core locations remained in excess of design values. (auth)

36891 OPERATION RESULTS OF THE RHEINSBERG NUCLEAR POWER PLANT UP TO 4th REFUELLING. Brune, W. (VEB Kernkraftwerk, Rheinsberg, Ger.). Kernenergie; 14: No. 2, 43-6(Feb 1971). (In German).

The Rheinsberg nuclear power plant operations are reviewed. Power was increased from 70 to 80 MW(e) in long-term tests. Availability is described. High stability and reliability of the main components have been utilized for maximum power supply, especially in the winter months. Mean burnup of fuel elements discharged during 4th refuelling was above 12,000 MWd/t. (auth)

36892 PROBLEMS POSED BY THE OPERATION OF NUCLEAR POWER STATIONS. Metteil, A. (Electricite de France, Paris). Energ. Nucl. (Paris); 13: No. 1, 28-38(Jan-Feb 1971). (In French).

Experience in the operation of nuclear power stations in France is based mainly on knowledge acquired on graphite-gas reactors. Running problems are the direct result of the large power units, which require a high degree of operational safety, and of the low marginal cost, which sets its use at the base of the cost diagram. The normal maintenance of the nuclear sections proves to be comparable in cost to that of standard installations. The accident problem is examined through three examples: Chinon 1, Chinon 2, and St-Laurent 1. The difficulties encountered in present installations originate from the problems of intervention in active media, from their prototypal character and from the deficiencies of certain protection equipment. (auth) (France)

36893 INTERACTIONS BETWEEN NUCLEAR PLANT LOADING CHANGES AND NUCLEAR FUEL COSTS. Bonk, G. J.; Crowther, R. L.; Thompson, O. A. Nucl. News; 14: No. 6, 53-7(Jun 1971).

The effects of uncertainties on the optimization of nuclear power plant operating and fuel cycle strategies are examined. The importance of flexibility in utility system optimizations to provide for unexpected outages or load changes, delays in new unit startups or fuel availability, and associated revision of unit capacity factors and planned refueling dates is discussed. (H.D.R.)

36894 OPERATIONAL EXPERIENCE WITH THE STEAM GENERATING HEAVY WATER REACTOR. McKeague, R. (United Kingdom Atomic Energy Authority, Risley, Eng.). Elec. Eng. (Sydney); 48: No. 2, 14-17(Feb 1971).

A summary is made of the operational history of the Winfrith power station. The load factor for the first two years was approximately 43%, with an availability of 76% omitting losses due to experimental features, fuel defects and the research and development program. Initial fuel element leakages due to overheating of cans as a result of copper-rich crud deposited on fuel during commissioning and early operation were identified and rectified. The main shutdown of 1969 was extended to enable the removal and replacement of 6 experimental Zr-Nb pressure tubes and to allow chemical decontamination of one coolant circuit. Access to the plant and ability to replace components were thus convincingly demonstrated. Chemical control has been generally good following initial poor performance of the clean-up plant in the feed train. Operational flexibility has been confirmed by the success of the power cycling program. (Australia)

Safety and Siting

36895 (DOCKET-1155-116) LA CROSSE BOILING WATER REACTOR. Nuclear Instrumentation Automatic Gain Control System, Third Addendum. (Allis-Chalmers Mfg. Co., Bethesda, Md. Atomic Energy Div.). 20 May 1971. 28p. (ACNP-70503.3). Dep. NTIS.

For Dairyland Power Cooperative, La Crosse, Wis.

36896 (DOCKET-1155-117) LA CROSSE BOILING WATER REACTOR. Water Level Instrument Behavior During Main Steam Bypass Valve Malfunction Incident. (United Nuclear Corp., Elmsford, N. Y. Research and Engineering Center). 28 May 1971. 60p. Dep. NTIS.

For Dairyland Power Cooperative, La Crosse, Wis.

36897 (DOCKET-1155-118) LA CROSSE BOILING WATER REACTOR. Automatic Gain Control System: Power Testing I, Corrected Pages 5 and 7. (Dairyland Power Cooperative, La Crosse, Wis.). 7 Jun 1971. 3p. Dep. NTIS.

36898 (DOCKET-1155-119) LA CROSSE BOILING WATER REACTOR. Request for Technical Specification Changes Relative to Respiratory Protection Equipment. (Dairyland Power Cooperative, La Crosse, Wis.). 28 May 1971. 11p. Dep. NTIS.

36899 (DOCKET-50016-114) ENRICO FERMI ATOMIC POWER PLANT, UNIT 1. Request Increase in Maximum Allowable Nitrogen Dewpoint From Minus 35 F to 0 F. (Power Reactor Development Co., Detroit, Mich.). 8 Jun 1971. 2p. Dep. NTIS.

The technical specifications concerning the dewpoint of the nitrogen in the Fermi Fast Breeder Reactor primary shield tank are requested to be changed. (H.D.R.)

36900 (DOCKET-50016-115) ENRICO FERMI ATOMIC POWER PLANT, UNIT 1. License No. DPR-9; Request for Authorization of Change No. 28 in the Technical Specifications. (Power Reactor Development Co., Detroit, Mich.). 10 Jun 1971. 2p. Dep. NTIS.

Changes are requested in the maximum allowable dewpoint of nitrogen in the primary shield tank and in the frequency of leak rate testing of the primary shield tank of the Fermi Fast Breeder Reactor. (H.D.R.)

36901 (DOCKET-50133-57) HUMBOLDT BAY POWER PLANT, UNIT NO. 3. Change No. 33 to the Technical Specifications of the Provisional Operating License No. DPR-7. (Division of Reactor Licensing (AEC), Washington, D. C.). 14 May 1971. 15p. Dep. NTIS.

Operating limits and reactivity worth of control elements are presented. Design parameters of Type 2 and Type 3-2 and 3 fuel assemblies are listed. (D.C.C.)

36902 (DOCKET-50146-76) SAXTON REACTOR. Change No. 42 to Technical Specifications of Provisional Operating License No. DPR-4. (Division of Reactor Licensing (AEC), Washington, D. C.). 13 May 1971. 3p. Dep. NTIS.

A revised leak rate testing schedule for the containment vessel is presented. Also, revised release limits for radioactive effluents are included. (D.C.C.)

36903 (DOCKET-50146-78) SAXTON REACTOR. License No. DPR-4; Technical Specifications Change Request No. 44, Amendment No. 1. (Saxton Nuclear Experiment Corp., Pa.). 10 Jun 1971. 5p. Dep. NTIS.

Revised core configurations for test fuel elements are illustrated. (D.C.C.)

36904 (DOCKET-50146-79) SAXTON REACTOR. License No. DPR-4; Technical Specifications Change Request No. 45. (Saxton Nuclear Experimental Corp., Pa.). 10 Jun 1971. 5p. Dep. NTIS.

Revised technical specifications are presented concerning an increase in the allowable hydrogen concentration in the primary coolant. (D.C.C.)

36905 (DOCKET-50146-80) SAXTON REACTOR. License No. DPR-4; Technical Specifications Change Request No. 46.

XUM

(Saxton Nuclear Experimental Corp., Pa.). 10 Jun 1971. 4p. Dep. NTIS.

Revised technical specifications are presented concerning the use of two test fuel assemblies in the core periphery without a flux thimble in the center rod position. (D.C.C.)

36906 (DOCKET-50155–82) BIG ROCK POINT NUCLEAR PLANT. Operating with Control Rod Drive C-3 at Notch 17. (Consumers Power Co., Jackson, Mich.). 7 Jun 1971. 2p. Dep. NITS.

36907 (DOCKET-50213–107) CONNECTICUT YANKEE ATOMIC POWER PLANT. Change No. 17 to Technical Specifications of Provisional Operating License No. DPR-14. (Division of Reactor Licensing (AEC), Washington, D. C.). 15 May 1971. 11p. Dep. NTIS.

Revised technical specifications are presented for periodic testing requirements for steam-driven auxiliary boiler feed pumps, and in-service inspection requirements for pressure vessel and primary cooling system. (D.C.C.)

36908 (DOCKET-50213–108) CONNECTICUT YANKEE ATOMIC POWER PLANT. Change No. 19 to Technical Specifications of Provisional Operating License No. DPR-14. (Division of Reactor Licensing (AEC), Washington, D. C.). 15 May 1971. 5p. Dep. NTIS.

Revised technical specifications are presented concerning maximum safety settings for protective instrumentation, and periodic testing requirements for ECCS and emergency power system. (D.C.C.)

36909 (DOCKET-50213–112) CONNECTICUT YANKEE ATOMIC POWER PLANT. Request to Reevaluate Personnel Exposures to ^{131}I on April 18–22, 1971. (Division of Compliance (AEC), Washington, D. C.). 11 Jun 1971. 12p. Dep. NTIS.

36910 (DOCKET-50219–134) OYSTER CREEK NUCLEAR POWER PLANT, UNIT NO. 1. Notice of AEC Consideration of Issuance of Amendment to Provisional Operating License. (Division of Reactor Licensing (AEC), Washington, D. C.). 3 Jun 1971. 4p. Dep. NTIS.

Notice of AEC consideration of steady-state maximum power increase to 1930 MW(t) is presented. (D.C.C.)

36911 (DOCKET-50237–166) DRESDEN NUCLEAR POWER STATION, UNIT 2. Facility License DPR-19; Proposed Change No. 11 to Appendix A. (Commonwealth Edison Co., Chicago, Ill.). 11 May 1971. 6p. Dep. NTIS.

Revised technical specifications are presented concerning APRM and IRM scram settings. (D.C.C.)

36912 (DOCKET-50237–167) DRESDEN NUCLEAR POWER STATION, UNITS 2 AND 3. Additional Information Relative to Safety Analysis Report, Amendments 9 and 10. (Commonwealth Edison Co., Chicago, Ill.). 13 May 1971. 3p. (DOCKET-50249–66). Dep. NTIS.

Additional information is presented concerning transient responses for loss of electrical load tests. (D.C.C.)

36913 (DOCKET-50237–168) DRESDEN NUCLEAR POWER STATION, UNIT 2. Additional Information Concerning Operation. (Commonwealth Edison Co., Chicago, Ill.). 14 May 1971. 30p. Dep. NTIS.

Additional information is provided on the following topics: corrective actions for limitorque operators; corrective actions for ECCS water hammer problem; drywell pneumatic supply system; and recirculation system operation limits. (D.C.C.)

36914 (DOCKET-50237–169) DRESDEN NUCLEAR POWER STATION, UNIT 2. Supplementary Information to Special Report No. 12: Torus Paint Problems. (Commonwealth Edison Co., Chicago, Ill.). 21 May 1971. 5p. Dep. NTIS.

Maintenance problems for the torus paint are described. (D.C.C.)

36915 (DOCKET-50237–170) DRESDEN NUCLEAR POWER STATION, UNIT 2. Facility License DPR-19; Supplementary Information to Proposed Change No. 11 to Appendix A. (Commonwealth Edison Co., Chicago, Ill.). 21 May 1971. 3p. Dep. NTIS.

Additional information concerning revised scram settings for APRM and IRM systems is presented. (D.C.C.)

36916 (DOCKET-50237–171) DRESDEN NUCLEAR POWER STATION, UNIT 2. Facility License DPR-19; Technical Specifications Proposed Change No. 12 to Appendix A. (Commonwealth Edison Co., Chicago, Ill.). 21 May 1971. 13p. Dep. NTIS.

The revised technical specifications described include: assurance of core spray, LPCI, and HPCI discharge lines water level; maintaining long-term capability of core cooling systems; elimination of jet pump riser vibrations; and isolation valves provided with drywell pneumatic supply system. (D.C.C.)

36917 (DOCKET-50237–174) DRESDEN NUCLEAR POWER STATION, UNITS 2 AND 3. Report No. 4: Modifications to Off-Gas System. (Commonwealth Edison Co., Chicago, Ill.). 1 Jun 1971. 15p. (DOCKET-50249–71). Dep. NTIS.

36918 (DOCKET-50237–175) DRESDEN NUCLEAR POWER STATION, UNIT 2. Abnormal Occurrence Report: Unplanned Release of Radioactive Material. (Commonwealth Edison Co., Chicago, Ill.). 4 Jun 1971. 2p. Dep. NTIS.

On May 27, 1971, a pipe ruptured during a surveillance test of the high pressure coolant injection system. An estimated 15,000 gallons of condensate storage tank water containing approximately 10^4 pCi/liter were released to the Illinois River. The HPCI steam supply valve also failed to close completely following the test. (H.D.R.)

36919 (DOCKET-50237–179) DRESDEN NUCLEAR POWER STATION, UNIT 2. Change No. 12 to Technical Specifications of Provisional Operating License No. DPR-19. (Division of Reactor Licensing (AEC), Washington, D. C.). 15 Jun 1971. 11p. Dep. NTIS.

The technical specifications concerning the core cooling system pump discharge lines, availability of the core spray system, vibration of the jet pump riser, and drywell pneumatic supply system containment isolation valves are updated. (H.D.R.)

36920 (DOCKET-50249–67) DRESDEN NUCLEAR POWER STATION, UNIT 3. Facility Operating License No. DPR-25; Technical Specifications Proposed Change No. 3 to Appendix A. (Commonwealth Edison Co., Chicago, Ill.). 11 May 1971. 6p. Dep. NTIS.

Revised technical specifications are presented concerning APRM and IRM scram settings. (D.C.C.)

36921 (DOCKET-50249–68) DRESDEN NUCLEAR POWER STATION, UNIT 3. Facility Operating License No. DPR-25; Supplementary Information to Technical Specifications Proposed Change No. 3 to Appendix A. (Commonwealth Edison Co., Chicago, Ill.). 21 May 1971. 3p. Dep. NTIS.

Additional information concerning revised scram settings for APRM and IRM systems is presented. (D.C.C.)

36922 (DOCKET-50249–70) DRESDEN NUCLEAR POWER STATION, UNIT 3. Facility Operating License No. DPR-25; Technical Specifications Proposed Change No. 4 to Appendix A. (Commonwealth Edison Co., Chicago, Ill.). 24 May 1971. 11p. Dep. NTIS.

Revised technical specifications are presented concerning limiting conditions for ECCS discharge piping, for long-term core cooling capability, and for isolation valves on the drywell pneumatic supply system. (D.C.C.)

36923 (DOCKET-50249–72) DRESDEN NUCLEAR POWER STATION, UNIT 3. Change No. 2 to Technical Specifications of Facility Operating License No. DPR-25. (Division of Reactor Licensing (AEC), Washington, D. C.). 10 Jun 1971. 5p. Dep. NTIS.

The technical specifications for in-service inspection of reactor vessel closure studs and nuts, closure head cladding, and support attachments for piping, valves, and pumps are revised. (H.D.R.)

36924 (DOCKET-50249–73) DRESDEN NUCLEAR POWER STATION, UNIT 3. Change No. 3 to Technical Specifications of Facility Operating License No. DPR-25. (Division of Reactor Licensing (AEC), Washington, D. C.). 14 Jun 1971. 13p. Dep. NTIS.

The technical specifications are changed to add a scram function during startup/hot standby operation and in the event of a failure in the control system for the turbine generator. (H.D.R.)

36925 (DOCKET-50250–44) TURKEY POINT PLANT, UNITS NO. 3 AND NO. 4. Preliminary Safety Analysis Report, [Amendment 35], Suppl. 35 (Includes Final Safety Analysis Report, Rev. 14). (Florida Power and Light Co.). 24 May 1971. 63p. (DOCKET-50251–40). Dep. NTIS.

Revised and additional data on the design parameters and operations aspects of the reactors are presented. (D.C.C.)

XUM

36926 (DOCKET-50250-46) TURKEY POINT PLANT, UNITS NO. 3 AND NO. 4. Preliminary Safety Analysis Report, [Amendment 36], Suppl. 36 (Includes Final Safety Analysis Report, Rev. 15). (Florida Power and Light Co.). 4 Jun 1971. 22p. (DOCKET-50251-42). Dep. NTIS.

Revised and additional data on the Turkey Point Plant design parameters and operations aspects are presented. (H.D.R.)

36927 (DOCKET-50250-47) TURKEY POINT PLANT, UNITS NO. 3 AND NO. 4. Preliminary Safety Analysis Report, [Amendment 37], Suppl. 37 (Includes Final Safety Analysis Report, Rev. 16). (Florida Power and Light Co.). 11 Jun 1971. 53p. (DOCKET-50251-43). Dep. NTIS.

Revised and additional information is presented concerning meteorological data and core instrumentation. (D.C.C.)

36928 (DOCKET-50254-37) QUAD-CITIES STATION, UNITS 1 AND 2. Preliminary Safety Analysis Report, Amendment 23, Request for Additional Information. (Division of Reactor Licensing (AEC), Washington, D. C.). 24 May 1971. 2p. (DOCKET-50265-34). Dep. NTIS.

Additional information is requested concerning fuel cask drop, instrument line failures, and pipe whip analysis. (D.C.C.)

36929 (DOCKET-50255-41) PALISADES PLANT. Preliminary Safety Analysis Report, Amendment 22 (Includes Additions and Revisions to Final Safety Analysis Report). (Consumers Power Co., Jackson, Mich.). 28 May 1971. 103p. Dep. NTIS.

Revised information is presented concerning the use of boric acid containment spray buffered with sodium hydroxide. Additional information is also presented concerning financial protection, financial qualifications, and corporate data. The 1970 Annual Report for the Consumers Power Company is included. (D.C.C.)

36930 (DOCKET-50255-42) PALISADES PLANT. Failure of Tube in Cooling Water Heat Exchanger. (Consumers Power Co., Jackson, Mich.). 3 Jun 1971. 2p. Dep. NTIS.

36931 (DOCKET-50261-59) H. B. ROBINSON UNIT NO. 2. Change No. 3 to Technical Specifications of Provisional License No. DPR-23. (Division of Reactor Licensing (AEC), Washington, D. C.). 27 May 1971. 3p. Dep. NTIS.

Revised technical specifications are presented concerning part-length requirements of control rod banks during initial physics testing. (D.C.C.)

36932 (DOCKET-50261-61) H. B. ROBINSON UNIT NO. 2. Environmental Monitoring Report, October 1, 1970-March 31, 1971. (Eberline Instrument Corp., Santa Fe, N. Mex. Dept. of Nuclear Sciences). 3 Jun 1971. 31p. Dep. NTIS.

For Carolina Power and Light Co., Raleigh, N. C.

The results of background radioactivity surveys and environmental radioactivity monitoring are summarized. (H.D.R.)

36933 (DOCKET-50266-48) POINT BEACH NUCLEAR PLANT, UNITS 1 AND 2. Preliminary Safety Analysis Report, Amendment 12 (Includes Additions and Revisions to Final Facility Description and Safety Analysis Report). (Wisconsin Electric Power Co., Milwaukee. Wisconsin Michigan Power Co., Appleton, Wis.). 21 May 1971. 52p. (DOCKET-50301-31). Dep. NTIS.

Revised design parameters and operations aspects to reduce the radioactive effluents from the reactors are described. Revised technical specifications for the radioactive waste disposal system are presented. (D.C.C.)

36934 (DOCKET-50266-50) POINT BEACH NUCLEAR PLANT, UNITS 1 AND 2. Sensitized Stainless Steel in Nozzles of Pressurizer Safety Valves. (Wisconsin Electric Power Co., Milwaukee). 7 Jun 1971. 2p. (DOCKET-50301-33). Dep. NTIS.

A review of the materials and process used in manufacturing safety and relief valves indicates that there is no significant furnace sensitization. (H.D.R.)

36935 (DOCKET-50267-30) FORT ST. VRAIN NUCLEAR GENERATING STATION, UNIT 1. Plans for Cooperation with Bureau of Sport Fisheries and Wildlife and Colorado Game, Fish and Parks Department. (Public Service Co. of Colorado, Denver). 27 May 1971. 3p. Dep. NTIS.

Additional information concerning the environmental radiation monitoring program is presented. Availability and distribution list for radiation survey data are described. (D.C.C.)

36936 (DOCKET-50271-53) VERMONT YANKEE NUCLEAR POWER STATION. Preliminary Safety Analysis Report, Amendment 27 (Includes Additions and Revisions to Final Safety Analysis Report). (Vermont Yankee Nuclear Power Corp., Rutland). 27 May 1971. 44p. Dep. NTIS.

Seismic analysis for Class 1 piping systems is presented. Qualifications of power operation test program personnel are listed. Additional data on the reactor requested by the Division of Reactor Licensing are also included. (D.C.C.)

36937 (DOCKET-50277-20) PEACH BOTTOM ATOMIC POWER STATION, UNITS 2 AND 3. Environmental Report, Operating License Stage. (Philadelphia Electric Co., Pa.). 4 Jun 1971. 358p. (DOCKET-50278-20). Dep. NTIS.

Information concerning chemical, radioactive, and thermal discharges from the reactor is presented. The effects of reactor operations on the environment are analyzed. Geological, hydrological, and meteorological data for the site are included. (D.C.C.)

36938 (DOCKET-50280-40) SURRY POWER STATION, UNITS 1 AND 2. Preliminary Safety Analysis Report, Amendment 22 (Includes Additions and Revisions to Final Safety Analysis Report, Part B). (Virginia Electric and Power Co., Richmond). 28 May 1971. 107p. (DOCKET-50281-40). Dep. NTIS.

Revised and additional data on the design parameters and operations aspects of the reactors are presented. Revised technical specifications are included. (D.C.C.)

36939 (DOCKET-50282-35) PRAIRIE ISLAND NUCLEAR GENERATING PLANT, UNITS 1 AND 2. Preliminary Safety Analysis Report, Amendment 10. (Northern States Power Co., Minneapolis, Minn.). 3 Jun 1971. 5p. (DOCKET-50306-35). Dep. NTIS.

Requested information on the Prairie Island Station operating costs for the initial five year period and costs for maintaining the facility in a safe condition if permanent shutdown occurs is presented. (H.D.R.)

36940 (DOCKET-50285-45) FORT CALHOUN STATION, UNIT NO. 1. Preliminary Safety Analysis Report, Amendment 25 (Includes Final Safety Analysis Report, Suppl. No. 8). (Omaha Public Power District, Nebr.). 28 May 1971. 340p. Dep. NTIS.

Revised design parameters of the Fort Calhoun Power Reactor Unit 1 are presented. Included also are additional data on the reactor requested by the Division of Reactor Licensing. (D.C.C.)

36941 (DOCKET-50286-34) INDIAN POINT NUCLEAR GENERATING UNIT NO. 3. Environmental Report. (Consolidated Edison Co. of New York, Inc., New York). 14 Jun 1971. 162p. Dep. NTIS.

Environmental aspects of the Indian Point Station, Unit 3 site and its environs are presented. Releases of heat, chemicals, and radioactivity from the plant are described and their impact on the area environment are discussed. (H.D.R.)

36942 (DOCKET-50286-35) INDIAN POINT NUCLEAR GENERATING UNIT NO. 3. Environmental Report, Appendices, Vol. 1. (Consolidated Edison Co. of New York, Inc., New York). 14 Jun 1971. 644p. Dep. NTIS.

The hydrology and meteorology of the area surrounding the Buchanan, New York, site of the Indian Point Nuclear Power Station are described. The expected temperature distribution effects of plant cooling water discharge on the Hudson River are analyzed. (H.D.R.)

36943 (DOCKET-50286-36) INDIAN POINT NUCLEAR GENERATING UNIT NO. 3. Environmental Report, Appendices, Vol. 2. (Consolidated Edison Co. of New York, Inc., New York). 14 Jun 1971. 586p. Dep. NTIS.

The potential ecological impact of the Indian Point Nuclear Power Plant on the Hudson River is examined. Included are studies of the ecology of thermal and radionuclide additions, fish protection measures, and environmental monitoring surveys. (H.D.R.)

36944 (DOCKET-50289-35) THREE MILE ISLAND NUCLEAR STATION, UNIT 1. Preliminary Safety Analysis Report, Amendment 20 (Includes Appendix 13A and Final Safety Analysis Report Modifications). (Metropolitan Edison Co., Reading, Pa. Jersey Central Power and Light Co., Morristown, N. J. Pennsylvania Electric Co., Johnstown). 26 May 1971. 447p. Dep. NTIS.

Revised and additional data are presented under the following main headings: cooling system; engineered safeguards; instrumentation and control; initial tests and operations; safety analysis; and technical specifications. (D.C.C.)

XUM

36945 (DOCKET-50309-35) MAINE YANKEE ATOMIC POWER STATION. Preliminary Safety Analysis Report, Amendment 24. (Maine Yankee Atomic Power Co., Westboro, Mass.). 28 May 1971. 72p. Dep. NTIS.

Revised design parameters of the Maine Yankee Power Reactor are presented. Included also are additional data on the reactor requested by the Division of Reactor Licensing. Pre-operational tests for reactor systems are listed. (D.C.C.)

36946 (DOCKET-50309-36) MAINE YANKEE ATOMIC POWER STATION. Preliminary Safety Analysis Report, Amendment 25 (Includes Additions and Revisions to Final Safety Analysis Report). (Maine Yankee Atomic Power Co., Westboro, Mass.). 4 Jun 1971. 34p. Dep. NTIS.

Revised and additional information on design parameters and operations aspects of the Maine Yankee Station is presented. (H.D.R.)

36947 (DOCKET-50313-30) ARKANSAS NUCLEAR ONE, UNIT 1. Environmental Report, Operating Permit Stage. (Arkansas Power and Light Co., Little Rock). 8 Jun 1971. 321p. Dep. NTIS.

Information concerning chemical, radioactive, and thermal discharges from the reactor is presented. The effects of reactor operations on the environment are analyzed. Meteorological and hydrological data for the reactor site are included. (D.C.C.)

36948 (DOCKET-50315-35) DONALD C. COOK NUCLEAR PLANT, UNITS 1 AND 2. Preliminary Safety Analysis Report, Amendment 14 (Includes Application for Transfer of Construction Permit). (Indiana and Michigan Electric Co., Fort Wayne, Ind.). 25 May 1971. 8p. (DOCKET-50316-35). Dep. NTIS.

36949 (DOCKET-50333-22) JAMES A. FITZPATRICK NUCLEAR POWER PLANT. Environmental Report, Operating License Stage. (Power Authority of the State of New York). 22 May 1971. 161p. Dep. NTIS.

Information concerning chemical, radioactive, and thermal discharges from the reactor is presented. The effects of reactor operations on the environment are analyzed. Hydrological and meteorological data for the site are included. (D.C.C.)

36950 (DOCKET-50336-22) MILLSTONE NUCLEAR POWER STATION, UNIT 2. Construction Permit No. CPPR-76, Amendment No. 1. (Division of Reactor Licensing (AEC), Washington, D. C.). 11 Jun 1971. 8p. Dep. NTIS.

The Millstone Point Unit 2 construction permit is amended to ensure the applicants will observe standards for protection of the environment. (H.D.R.)

36951 (DOCKET-50348-20) JOSEPH M. FARLEY NUCLEAR PLANT, UNITS 1 AND 2. Preliminary Safety Analysis Report, Amendment 15. (Alabama Power Co., Birmingham). 3 Jun 1971. 168p. (DOCKET-50364-14). Dep. NTIS.

Revised design parameters of the Joseph M. Farley Power Reactor Units 1 and 2 are presented. Included also are additional data on the reactor requested by the Division of Reactor Licensing. (D.C.C.)

36952 (DOCKET-50352-13) LIMERICK GENERATING STATION, UNITS 1 AND 2. Preliminary Safety Analysis Report, Amendment 7. (Philadelphia Electric Co., Pa.). 10 Jun 1971. 201p. (DOCKET-50353-13). Dep. NTIS.

Revised and additional data are presented on the design parameters and operations aspects of Limerick Station, Units 1 and 2. (H.D.R.)

36953 (DOCKET-50358-17) WM. H. ZIMMER NUCLEAR POWER STATION, UNIT 1. Preliminary Safety Analysis Report, Amendment 11. (Cincinnati Gas and Electric Co., Ohio. Columbus and Southern Ohio Electric Co., Columbus, Ohio. Dayton Power and Light Co., Ohio). 26 May 1971. 221p. Dep. NTIS.

Revised data on the reactor are presented under the following headings: structures and buildings; control and instrumentation; electrical power systems; and containment systems. Included also are additional data on the reactor requested by the Division of Reactor Licensing. (D.C.C.)

36954 (DOCKET-50358-18) WM. H. ZIMMER NUCLEAR POWER STATION, UNIT 1. Preliminary Safety Analysis Report, Amendment 12. (Cincinnati Gas and Electric Co., Ohio. Columbus and Southern Ohio Electric Co., Columbus, Ohio. Dayton Power and Light Co., Ohio). 11 Jun 1971. 521p. Dep. NTIS.

Revised and additional data on the design parameters and operations aspects of the William H. Zimmer Power Reactor Unit 1 are presented. (D.C.C.)

36955 (DOCKET-50361-17) SAN ONOFRE NUCLEAR GENERATING STATION, UNITS 2 AND 3. Preliminary Safety Analysis Report, Amendment 9. (Southern California Edison Co., Los Angeles. San Diego Gas and Electric Co., Calif.). 26 Mar 1971. 241p. (DOCKET-50362-16). Dep. NTIS.

Revised and additional information requested by the Division of Reactor Licensing is presented. (D.C.C.)

36956 (DOCKET-50363-15) FORKED RIVER NUCLEAR GENERATING STATION, UNIT 1. Preliminary Safety Analysis Report, Amendment 10. (Jersey Central Power and Light Co., Morristown, N. J.). 11 Jun 1971. 33p. Dep. NTIS.

Earthquake response spectra for the Forked River site are presented. (H.D.R.)

36957 (DOCKET-50367-14) BAILLY GENERATING STATION, NUCLEAR I. Preliminary Safety Analysis Report, Amendment 7. (Northern Indiana Public Service Co., Hammond). 26 May 1971. 549p. Dep. NTIS.

Revised design parameters of the Bailly Power Reactor Unit I are presented. Additional data on the reactor requested by the Division of Reactor Licensing are also presented. Seismic analysis of structures and equipment is included. (D.C.C.)

36958 (DOCKET-50367-15) BAILLY GENERATING STATION, NUCLEAR I. Preliminary Safety Analysis Report, Amendment 8. (Northern Indiana Public Service Co., Hammond). 3 Jun 1971. 200p. Dep. NTIS.

Revised design parameters of the Bailly Power Reactor Unit I are presented. Included also are additional data on the reactor requested by the Division of Reactor Licensing. (D.C.C.)

36959 (DOCKET-50367-16) BAILLY GENERATING STATION, NUCLEAR I. Preliminary Safety Analysis Report, Amendment 9. (Northern Indiana Public Service Co., Hammond). 10 Jun 1971. 191p. Dep. NTIS.

Requested additional information is presented on design parameters and operations aspects of Bailly Station, Unit 1. (H.D.R.)

36960 (DOCKET-50368-11) ARKANSAS NUCLEAR ONE, UNIT 2. Preliminary Safety Analysis Report, Amendment 6. (Arkansas Power and Light Co., Little Rock). 2 Jun 1971. 53p. Dep. NTIS.

Revised design parameters of the Arkansas Nuclear One Power Reactor Unit 2 are presented. Included also are additional data on the reactor requested by the Division of Reactor Licensing. (D.C.C.)

36961 (DOCKET-50369-10) McGUIRE NUCLEAR STATION, UNITS 1 AND 2. Preliminary Safety Analysis Report, Amendment 6. (Duke Power Co., Charlotte, N. C.). 10 Jun 1971. 84p. (DOCKET-50370-9). Dep. NTIS.

Revised design parameters of the McGuire Power Reactor Units 1 and 2 are presented. Included also are additional data on the reactor requested by the Division of Reactor Licensing. (D.C.C.)

36962 (DOCKET-50389-8) HUTCHINSON ISLAND PLANT, UNIT NO. 2. Notice of Receipt of Application for Construction Permit and Facility License. (Division of Reactor Licensing (AEC), Washington, D. C.). 28 May 1971. 3p. Dep. NTIS.

36963 (DOCKET-50389-9) HUTCHINSON ISLAND PLANT, UNIT NO. 2. Preliminary Safety Analysis Report, Amendment 1. (Florida Power and Light Co.). 11 Jun 1971. 5p. Dep. NTIS.

Revised information concerning cooling water systems is presented. (D.C.C.)

36964 (DOCKET-50390-1) WATTS BAR NUCLEAR PLANT, UNITS 1 AND 2, RHEA COUNTY, TENNESSEE. License Application. (Tennessee Valley Authority, Knoxville). 14 May 1971. 103p. (DOCKET-50391-1). Dep. NTIS.

Financial data on the owners of the Watts Bar Power Reactor Units 1 and 2 are presented in support of the application for construction permit and operating license. The 1970 Annual Report for the Tennessee Valley Authority is included. (D.C.C.)

36965 (DOCKET-50390-2) WATTS BAR NUCLEAR PLANT, UNITS 1 AND 2. Preliminary Safety Analysis Report, Vol. 1. (Tennessee Valley Authority, Knoxville). 14 May 1971. 665p. (DOCKET-50391-2). Dep. NTIS.

Information on Watts Bar Power Reactor Units 1 and 2 is presented under the following headings: site and environment; and reactor. (D.C.C.)

XUM

36966 (DOCKET-50390–3) WATTS BAR NUCLEAR PLANT, UNITS 1 AND 2. Preliminary Safety Analysis Report, Vol. 2. (Tennessee Valley Authority, Knoxville). 14 May 1971. 507p. (DOCKET-50391–3). Dep. NTIS.

Information on Watts Bar Power Reactor Units 1 and 2 is presented under the following headings: reactor coolant system; containment; engineered safety features; and instrumentation and control. (D.C.C.)

36967 (DOCKET-50390–4) WATTS BAR NUCLEAR PLANT, UNITS 1 AND 2. Preliminary Safety Analysis Report, Vol. 3. (Tennessee Valley Authority, Knoxville). 14 May 1971. 328p. (DOCKET-50391–4). Dep. NTIS.

Information on Watts Bar Power Reactor Units 1 and 2 is presented under the following headings: electrical systems; auxiliary systems; steam and power conversion; waste disposal and radiation protection; conduct of operations; and initial tests and operations. (D.C.C.)

36968 (DOCKET-50390–5) WATTS BAR NUCLEAR PLANT, UNITS 1 AND 2. Preliminary Safety Analysis Report, Vol. 4. (Tennessee Valley Authority, Knoxville). 14 May 1971. 528p. (DOCKET-50391–5). Dep. NTIS.

Information on Watts Bar Power Reactor Units 1 and 2 is presented under the following headings: safety analysis; technical specifications; quality assurance program; design criteria and classifications; functional evaluation of components shared by both units; and general design criteria. (D.C.C.)

36969 (DOCKET-50390–6) WATTS BAR NUCLEAR PLANT, UNITS 1 AND 2. Draft Environmental Statement. (Tennessee Valley Authority, Knoxville). 18 May 1971. 124p. (DOCKET-50391–6). Dep. NTIS.

Information concerning chemical, radioactive, and thermal discharges from the reactor is presented. The effects of reactor operations on the environment are analyzed. (D.C.C.)

36970 ECOLOGICAL FACTORS IN THE SITING, DESIGN, AND OPERATION OF A NUCLEAR POWER STATION. Davy, D. R.; Giles, M. S.; Charash, E. (Australian Atomic Energy Commission Research Establishment, Lucas Heights). At. Energy Aust.; 13: No. 4, 16-28(Oct 1970).

Consideration is given to ecological factors in relation to both accident conditions and to normal plant operation. The mechanisms, effects and limits of airborne and liquid effluent dissipation are outlined. Dry deposition from a plume, which is primarily dependent on particle velocity, is compared diagrammatically with the washout from wet precipitation. Diffusion of liquid effluents varies with water turbulence but vertical diffusion in particular is small relative to that in the atmosphere. The effects on marine environment of the physical movement of large volumes of water, discharge of normal power plant wastes, heat and radioactivity are outlined. The setting of discharge limits for radioactivity is discussed within the framework of critical groups, dose limit, biological concentration factor, acceptable risk and accident conditions. Dose rates from some power plant contaminants are compared. (Australia)

36971 LOCATION PROBLEMS FOR NUCLEAR POWER STATIONS. Ailleret, Pierre (Union Internationale des Producteurs det Distributeurs d'Energie Electrique, Paris). Energ. Nucl. (Paris); 13: No. 1, 22-7(Jan-Feb 1971). (In French).

The location size limits for various types of power stations (conventional, light water reactors, super breeders) resulting from the heating of river water are summarized. The problem is not the same according to whether it concerns a single power station or several power stations in service on the same river. The possible consequences of limits to the use of rivers as a cold source are shown, as well as a certain number of thoughts concerning the specific definition of the cost of a site and the factors that can limit the concentration of units in a minimum number of locations. The fear that public opinion has concerning possible accidents in nuclear power stations is discussed. (auth) (France)

36972 LICENSING OF PRODUCTION AND UTILIZATION FACILITIES. 10 CFR 50 1969. Washington, D. C.; Superintendent of Documents, GPO (1970). 43p. Available from Superintendent of Documents, GPO, Washington, D. C.

Minimum requirements for quality assurance in the design of U.S. nuclear power plants employing water-cooled reactors are presented. (H.D.R.)

36973 FOUR BIG FEARS ABOUT NUCLEAR POWER. Lapp, Ralph E. N. Y. Times Mag.; 16-35(7 Feb 1971).

The potential hazards involved with operating nuclear power plants and disposing of radioactive wastes from these plants are discussed. Precautions taken to provide public safety are described. Basic technology related to nuclear power plants is reviewed. (D.C.C.)

Steam and Power Conversion Systems

36974 PAST AND FUTURE OF HEAT POWER PLANTS. Malek, Emil. Energetika; 21: No. 1, 7-9(Jan 1971). (In Czech).

The development of heat power plants is reviewed. The problems which heat power engineers have had to overcome in the past are described. Current developmental trends are analyzed. In the case of nuclear power plants it will be necessary to switch over from steam to gas turbines which will become the mainstay of the whole power system. (auth)

36975 PRESENT STATE OF TURBO-GENERATORS FOR NUCLEAR POWER PLANTS. Kai, Takashi (Mitsubishi Electric Corp., Kobe, Japan). Karyoku Hatsuden; 21: No. 12, 1322-42(Dec 1970). (In Japanese).

Primary difference in turbo-generators for thermal and nuclear power plants is that, while bipolar generators are used for the former, quadrupole generators (1,800 or 1,500 rpm) are employed for nuclear power plants. The world situation of nuclear power generation is reviewed. Turbo-generators for nuclear power plants are described concerning characteristics of the nuclear turbo-generators cooling methods for the nuclear turbo-generators including cooling of coils for the rotors and stators; excitation methods for the nuclear turbo-generators; and construction and performance of the nuclear turbo-generators of 400 to 1,400 MVA. Trends of the nuclear turbo-generators in future are summarized. (Japan)

Power Reactor Development

36976 (CONF-680818) FAST REACTORS AND THE UNIVERSITY. Proceedings of an ASEE–AEC Short Topical Conference Conducted at Rensselaer Polytechnic Institute, August 28–30, 1968. Becker, Martin (ed.) (American Society for Engineering Education, Urbana, Ill. Atomic Energy Commission, Washington, D. C.). 460p. Dep. NTIS.

The emergence of fast reactor development as a major U. S. program and its implications for both curricular and research activities in academic nuclear engineering programs are discussed. Included are presentations on general aspects of fast reactor development, specific technical disciplines pertinent to fast reactors, and academic aspects of fast reactor engineering programs. (H.D.R.)

36977 (GA–10501) HTGR BASE PROGRAM QUARTERLY PROGRESS REPORT FOR THE PERIOD ENDING FEBRUARY 28, 1971. (Gulf General Atomic Co., San Diego, Calif.). 30 Mar 1971. Contract AT(04-3)-167. 107p. Dep. NTIS.

GRAPHITE — radiation effects on boronated and hafnated, neutron, (E)
NEUTRONS — effects on boronated and hafnated graphite, (E)
REACTOR FUEL ELEMENTS — reprocessing cycle development for gas cooled, (E)
— fabrication of coated particle gas cooled, for recycle testing
REACTOR FUELS — radiation effects testing of coated particle
— reprocessing of coated particle, fluid bed oxidation procedures in, (E)
REACTORS, GAS COOLED — development of 1000 MW(e) HTGR concept during December 1970 through February 1971
— fission product release and transport in high temperature, (E/T)
— fuel elements for high temperature, fabrication and irradiation testing of recycle, (E/T)
— fuel elements for high temperature, plant designs and costs for reprocessing
REACTORS, POWER — development of 1000 MW(e) HTGR concept during December 1970 through February 1971 (H.D.R.)

36978 (GA–10560) PUBLIC SERVICE COMPANY OF COLORADO 330-MW(E) HIGH-TEMPERATURE GAS-COOLED REACTOR RESEARCH AND DEVELOPMENT PROGRAM. Quarterly Progress Report for the Period Ending March 31, 1971. (Gulf General Atomic Co., San Diego, Calif.). 30 Apr 1971. Contract AT(04-3)-633. 112p. Dep. NTIS.

XUM

BOILERS—testing of gas cooled reactor, pressure and temperature
BORON CARBIDES—oxidation in high temperature water vapor and helium environment
BURNABLE POISONS—performance of boron carbide (B_4C) in high temperature water vapor and helium
FORT ST. VRAIN POWER REACTOR, UNIT I—remote handling and viewing equipment for, pressure and temperature testing of in-vessel
—fuel cycle management program for, initial loading requirements for optimum
—control elements for, reactivity worth of
—core physics for
—fuels for, irradiation testing of coated particle
—fuel elements for, properties and irradiation stability of graphite in
—core for, properties and irradiation stability of graphite in
—boilers for, pressure and temperature testing of
—control elements of, performance of boron carbide (B_4C) burnable poison
GRAPHITE—radiation effects on, fast neutron
NEUTRONS, FAST—effects on coated particle fuels
—effects on properties of graphite
REACTOR FUELS—radiation effects on coated particle, fast neutron
REMOTE-HANDLING EQUIPMENT—testing of gas cooled reactor in-vessel, pressure and temperature,
REMOTE-VIEWING EQUIPMENT—testing of gas cooled reactor in-vessel, pressure and temperature
THORIUM CARBIDES—ThC_2–UC_2, irradiation testing of coated particles
URANIUM CARBIDES—ThC_2–UC_2, irradiation testing of coated particles (D.C.C.)

36979 (IRS-T-18(1970), pp 205-15) APPLICATION OF STATISTICAL METHODS FOR THE DESIGN OF REACTOR SYSTEMS. Voigt, O. (Technischer Ueberwachungs-Verein e. V., Cologne (West Germany). Institut fuer Reaktorsicherheit). 1970. (In German). NTIS (U. S. Sales Only).

The methods used at AEG and the work done in this field are presented in typical examples. (INIS)

36980 (JUL-725-RG) TEMPERATURE DISTRIBUTION AND CORROSION IN THE CORE OF AN ADVANCED HIGH-TEMPERATURE REACTOR. Drescher, Hans-Paul (Kernforschungsanlage, Juelich (West Germany). Institut fuer Reaktorentwicklung). Jan 1971. 95p. (In German). Dep. NTIS (U. S. Sales Only).

The design of a pebble-bed reactor for coupling in a process heat installation is considered. The core design and the damage to the core and primary circuit by corrosion are studied. The power density and temperature distributions in the core are determined. A theoretical model on the corrosion and reactor behavior is developed and applied to the high-temperature reactor. The prospects for a reactor outlet temperature of 1200°C are considered. 38 references. (J.S.R.)

36981 (ORNL-tr-2474) CONCEPT OF THE MARINE NUCLEAR POWER COMPLEX. Yoda, Yoichi. Translated for Oak Ridge National Lab., Tenn., from Genshiryoku Kogyo; 16: No. 6, 4-9(1970). 15p. Dep. NTIS.

The concept of placing nuclear power plants in the sea and developing a vast complex centered around this power plant is discussed. The problem of thermal pollution of the seas and how this may considerably complicate the concept of effective utilization of the sea are examined. (auth)

36982 TRANSVERSE OSCILLATION OF RIBBED RODS WITH A HELICAL PITCH. Novak, Josef; Votruba, Josef (State Inst. of Scientific Research on Machine Design, Bechovice, Czech.). Jad. Energ.; 17: No. 3, 73-80(Mar 1971). (In Czech).

The effect of helical pitch on transverse oscillation was investigated for isolated rods and rods in a bundle. Air or water was permitted to flow past the rods which were fastened at one end and supported at the other. Deformation, deflection, and vibration frequency were determined for Reynolds numbers in the region 1.2×10^4 to 4.3×10^4 for air, and for Reynolds numbers between 1.2×10^4 and 6.6×10^4 for water. It was established that the deflection of the individual rods increased with increase of the angle of slope (α) of the rod only between 0 to 2°. Deflection of rods in a bundle increases more slowly with α than in the case of the individual rods. For equal turbulence and similar Re values the deflection of the bundle is smaller than for the individual rods. Turbulence is a fundamental source of vibration, both for isolated rods and rods in a bundle. (tr-auth)

36983 HIGH TEMPERATURE GAS-COOLED REACTORS (HTR OR HTGR). Energ. Nucl. (Paris); 13: No. 1, 7-14(Jan-Feb 1971). (In French).

The technique of the H.T.R. may be considered as an extension of that of the graphite-gas reactors. The essential characteristics consist of the elimination of metallic cladding, the widest possible scattering of the fuel in the moderator and the use of helium as the coolant. The H.T.R. potential permits direct energy output from a helium turbine. (auth) (France)

36984 STATE OF DEVELOPMENT OF NUCLEAR POWER PLANTS WITH PRESSURIZED-WATER REACTORS IN CAPITALISTIC COUNTRIES. Nagel, D. (Institut fuer Kraftwerke, Berlin). Kernenergie; 13: No.12, 369-76(Dec 1970). (In German).

Starting from the position taken on pressurized-water reactor power plants in capitalistic countries, the most essential features of the plants built and planned are described. After presenting the technological state of development, the recent level of costs of these plants is briefly dealt with. 20 references. (auth)

36985 GAS CORE NUCLEAR REACTOR. Rom, Frank E. (to National Aeronautics and Space Administration). U. S. Patent 3,574,057. 6 Apr 1971. Filed 27 May 1968.

A gas passes through a previous liner into a gaseous core nuclear reactor. This gas cools the liner and is then heated by a fissionable gas in the core. The heated gas is discharged from the reactor. (auth)

Kinetics and Dynamics

36986 (AEEW-M-985) REACTOR PHYSICS CHARACTERISTICS OF THE HIGH TEMPERATURE REACTOR. Tyror, J. G. (Atomic Energy Establishment, Winfrith (England)). Mar 1971. 9p. (CONF-700608-37). Dep. NTIS (U. S. Sales Only).

From American Nuclear Society meeting; Los Angeles, Calif.

A brief description is given of the physics aspects of the UK high-temperature gas-cooled reactor, together with details of first phase physics experiments including resonance capture measurements in ^{238}U in a typical HTR lattice. Results of these measurements are summarized. (UK)

36987 (ANL-7788) SPACE-DEPENDENT TRANSFER-FUNCTION ANALYSIS OF LARGE NUCLEAR-REACTOR POWER SYSTEMS. Habegger, L. J.; Hsu, C. (Argonne National Lab., Ill.). Mar 1971. Contract W-31-109-eng-38. 63p. Dep. NTIS.

The importance of spatial effects in proposed transfer-function measurements in large, fast reactors was investigated. A general theoretical formulation of space-dependent transfer functions is derived which includes the effects of spatial characteristics of input and output devices. A quantitative indication of spatial effects is given by numerical simulation of measured transfer functions in a Liquid Metal Fast Breeder Reactor (LMFBR). A general space-time reactor model and approximate method of solution using the Galerkin's procedure were developed in conjunction with the investigation. A quasilinearization procedure was used to obtain the equilibrium states which were the solution of multipoint, boundary-value problems. 45 references. (auth)

36988 (BNWL-1561) MEASUREMENT OF THE TEMPERATURE DEPENDENCE OF K_∞ FOR A $^{233}UO_2$–ThO_2 HTGR LATTICE. Lippincott, E. P. (Battelle-Northwest, Richland, Wash. Pacific Northwest Lab.). May 1971. Contract AT(45-1)-1830. 92p. Dep. NTIS.

Information on the temperature dependence of k_∞ for a $^{233}UO_2$–$^{232}ThO_2$–C fuel mixture in a HTGR is presented. The infinite medium multiplication factor was found to decrease by .0350 ± .0015 from 20°C to 1000°C. This result provides direct information necessary in the design of the control system and in the safety analysis for advanced high-temperature gas-cooled reactors. 22 references. (auth)

36989 (CEA-N-1398) CALCULATION METHODS FOR HETEROGENEITIES IN REACTORS OF THE NATURAL URANIUM–GRAPHITE–GAS TYPE. Charbonneau, Serge (Electricite de France, Clamart); Lefebvre, Jean-Claude (Electricite de France, Paris). Jan 1971. 98p. (In French). Dep. NTIS (U. S. Sales Only).

The principal methods used at the CEA for neutron flux and reactivity calculations concerning natural uranium graphite moderated reactors are described. The problem of the typical heterogeneities encountered in this type of reactor, such as control rods, empty channels, and burnup variations in fuel elements, is considered. The principal theoretical aspects of the methods are presented. Practical applications and accuracy are discussed. The experimental results were obtained in the

MARIUS and CESAR critical assemblies at the Cadarache nuclear center, and in the power plants of Chinon and Saint-Laurent-des-Eaux. (43 references) (auth)

36990 (DLR-FB-70-18) RADIATIVE ENERGY TRANSPORT IN A PLASMA REACTOR (GAS-CORE REACTOR). Kelm, S. (Deutsche Forschungs- und Versuchsanstalt fuer Luft- und Raumfahrt E. V., Stuttgart (West Germany). Institut fuer Plasmadynamik). May 1970. 54p. (In German). Dep. NTIS (U. S. Sales Only).

At first the basic theory for the calculation of the radiation field and radiation flux is treated for a known temperature distribution in the plasma. Secondly, the temperature distribution is determined in the plasma of an uranium-plasma reactor using the energy equation in which the radiation flux and energy sources are considered. The calculations yield a temperature of 22,000°K for the middle of the reactor. The total radiative power which leaves the plasma is reduced considerably despite the very high temperatures at the middle of the reactor, because the temperature of the black body radiation near the walls is lower than 7000°K and because reflecting walls (liquid lithium) are assumed. The results show that the optical radiation in such a reactor does not destroy the inner walls and thus, such an energy-system can be realized if the only problem is that of optical radiation. 28 references. (auth)

36991 (GULF-RT-10523) FAST REACTOR SPECTRUM MEASUREMENTS. Technical Summary Report, February 1, 1970–January 31, 1971. Young, Jack C.; Borgonovi, G. M.; Neill, J. M.; Slaggie, E. L.; Crosbie, K. L. (Gulf Radiation Technology, San Diego, Calif.). 16 Mar 1971. Contract AT(04-3)-167. 123p. Dep. NTIS.

A continuing program of fast neutron spectrum measurements by time-of-flight methods in a subcritical facility (STSF) is described. Results of measurements and calculations for the STSF-1A, STSF-8, and STSF-9 systems are presented. Studies of techniques for measuring spectra with proton recoil detectors are also described. 45 references. (auth)

36992 (JAERI-Memo-4331) KINETICS PARAMETER CALCULATION CODE: (ARGO). Ikawa, Koji (Japan Atomic Energy Research Inst., Tokyo). Jan 1971. 40p. (In Japanese). Dep. NTIS (U. S. Sales Only).

ARGO is a one-dimensional (slab, cylinder, sphere), multigroup diffusion code for use in fast reactor criticality and kinetics parameter analysis. Three cross section sets, i.e., JAERI-FAST-SET, ABBN-SET and RCBN-SET, of 25 energy groups, are prepared for the code as library tapes. The outline of the code and its input format are described. 5 references. (auth) (Japan)

36993 (KFK-1337) INVESTIGATION OF THE NATURAL FREQUENCY OF THE NORMAL AND ELONGATION FUNCTION, AND OF THE DAMPING OF THE INSTRUMENTED MODEL FUEL RODS OF THE Na ½ MODEL SUBASSEMBLIES. Krueger, W.; Schwemmle, R. (Kernforschungszentrum, Karlsruhe (West Germany). Institut fuer Reaktorentwicklung). Dec 1970. 54p. (In German). (EUR-4572). Dep. NTIS (U. S. Sales Only).

Investigations on free lateral vibration of fuel pins of the instrumented subassembly mock-up of the sodium-cooled fast breeder reactor design Na-1 are described. The influence of the axial distribution of spacer grids on natural frequencies and the corresponding vibration modes was calculated and verified by experiments. The influence of the radial clearance in cells of spacer grids on the change of the normal modes was investigated experimentally. The frequency response functions of the miniature pressure transducers were measured. The transducers were mounted in one pin and in the subassembly sheath for the detection of the boundary layer pressure fluctuations in the subassembly. Experimental arrangements, results of investigations, and instrumentation of the subassembly mock-up are described in detail. 8 references. (auth)

Control Systems

36994 (INIS-mf-33) VERSUCHSATOMKRAFTWERK KAHL; CRACKS IN LENGTHENING RODS OF CONTROL ROD DRIVING SHAFTS. (Technischer Ueberwachungs-Verein e. V., Cologne (West Germany). Institut fuer Reaktorsicherheit). 1970. 3p. (In German). NTIS (U. S. Sales Only).

Flaw detection and location in ASME 304 lengthening rods, crack investigation, and exchange of control rod driving shafts in the VAK Reactor are described. In October 1969 during the routine inspection, flaws in the lengthening rod of the Position E4 control rod drive were detected by the color penetration method. Cracks were thought to be caused by tension crack corrosion. The whole of 21 control rod driving shafts were exchanged. Further flaws were detected in 7 lengthening rods. An improved design without welded and contraction joints was installed in the reactor. (INIS)

36995 (WCAP-7669) NUCLEAR INSTRUMENTATION SYSTEM: TOPICAL REPORT. Lipchak, J. B.; Stokes, R. A. (comps.) (Westinghouse Electric Corp., Pittsburgh, Pa. Nuclear Energy Systems [Div.]). Apr 1971. 56p.

The Nuclear Instrumentation System (NIS) is an integral part of the nuclear steam supply system provided for pressurized water reactor power plants. It monitors the power level of the reactor at all times and is used primarily for plant protection. It also provides appropriate alarm functions during plant operating and shutdown conditions. In addition it provides a secondary control function, and indicates reactor status during start-up and power operation. The three overlapping ranges of instrumentation (source, intermediate and power) provide overpower trip protection at increasing levels during startup and at power operation. A functional description of the standard nuclear instrumentation system used on PWR plants is presented. The sensor types and the signal processing equipment for each of the channels are described. (auth)

36996 REACTOR INSTRUMENTATION. Schruefer, Elmar (AEG-Telefunken, Frankfurt am Main). VDI (Ver. Deut. Ing.) Z.; 113: No. 6, 433-7(Apr 1971). (In German).

Reliability considerations for reactor protection system instrumentation are presented. (36 references) (D.D.C.)

36997 NUCLEAR REACTOR STRUCTURE. Thorp II, Arthur G. (to Westinghouse Electric Corp.). U. S. Patent 3,576,717. 27 Apr 1971. Filed 24 Jan 1968.

The fuel assemblies in a reactor are fixed arrays of fuel rods without the usual omissions for control rod slots. Instead, a number of fuel rods are omitted in the pattern on a nearly uniform grid throughout the core to provide spaces for pressure thimbles to house control elements of neutron absorbing material, such as a chain or bead type. The control elements are driven in or out of the core by such means as wire rope cables which are grouped to be driven by one mechanism per assembly. The thimbles are sealed at their lower ends and the interior thereof is isolated from the internal pressure of the reactor vessel so that the control elements operate in air or other gas, for example helium. (auth)

36998 CONTROL ROD ARRANGEMENT FOR LIGHT WATER NUCLEAR REACTORS. Soedergard, Bengt Martin (to Allmanna Svenska Elektriska Aktiebolaget). U. S. Patent 3,574,059. 6 Apr 1971. Priority date 3 Mar 1967, Sweden.

In a light water reactor, a control rod is of cruciform cross-section and runs in a cruciform gap between fuel assemblies arranged in a square, and in a guide tube arranged below the fuel assembly. The guide tube has a somewhat greater diameter than the span of the control rod across the cruciform section. The control rod is joined to an operating device arranged under the guide tube. At the lower end of the control rods the points of the control rod cross are provided with guide plates rounded off at the points facing the guide tube. The guide plates may consist of graphite or be coated on the surface facing the guide tube with a hard material such as stellite. The rounding off of the guide plates has a slightly smaller radius of curvature than the guide tube. (auth)

Shielding

36999 TECHNOLOGY OF REACTOR THERMAL SHIELDS. PART 1. Burman, G. C. (Royal Naval Coll., Greenwich, Eng.); Lakey, J. R. A. J. Inst. Nucl. Eng.; 12: 31-5(Mar-Apr 1971).

The technology of thermal shield design is reviewed both from the physics and engineering aspects as applied to a steel/water shielding system. Headings are as follows: sources of neutron and gamma radiation; estimation of neutron and gamma heating rates; determination of neutron flux and resulting gamma radiation; calculation methods available; gamma sources due to capture of thermal neutrons; determination of gamma flux and resulting heat source distribution; calculation of temperature distribution; temperature distribution and induced thermal stress in thermal shields; heat transmission in shields of slab form with experimental heat source; and induced thermal stress. (UK)

Cooling Systems

37000 (AAEC/LIB/Bib-286) BURNOUT IN FORCED CONVECTION BOILING HEAT TRANSFER. A Bibliography. Geue, Jean (comp.) ([Australian Atomic Energy Commission Research

XUM

Establishment, Lucas Heights]). May 1971. 23p. Dep. NTIS (U. S. Sales Only).

One hundred and twenty-two references are listed chronologically by year and alphabetically by author within each year. The search was restricted to NSA between 1962 and 1971. Emphasis is on uniformly and non-uniformly heated systems such as single rods, annuli and rod bundles. (Australia)

37001 (AECL-3787) AECL RESEARCH IN ENGINEERING. (Atomic Energy of Canada Ltd., Chalk River (Ontario)). 1971. 18p. Dep. NTIS (U. S. Sales Only). AECL $0.50.

Reviews are presented of engineering research at Atomic Energy of Canada Limited on heavy water production using amine–hydrogen isotopic exchange; CANDU reactor closure seal analysis; vibration of reactor fuel elements; the use of freon to model dry-out in a high-pressure boiling water system; in-core flux detectors for nuclear power reactors; and use of digital computation techniques. (D.H.M.)

37002 (AECL-3858) VALVES FOR PRIMARY HEAT TRANSPORT SYSTEMS FOR CANADIAN POWER REACTORS. Dixon, D. F. (Atomic Energy of Canada Ltd., Chalk River (Ontario). Chalk River Nuclear Labs.). Mar 1971. 23p. Dep. NTIS (U. S. Sales Only). AECL $1.00.

The economics of Canadian power reactor operation places stringent requirements on valve performance. Low leakage to atmosphere, dependability and maintainability are of particular interest. Most commercially available valves have weaknesses in one area or another, so test and development work was necessary to select and improve valve hardware. Test programs have screened out poor equipment and identified some problem areas. The development work has uncovered new technology which is presently being applied to existing reactor valve problems. 10 references. (auth)

37003 (CONF-710317-1) COLIBRI: A COMPUTER CODE FOR SUBCHANNEL ANALYSIS. Devold, I.; Persson, N.-O. (ASEA-ATOM, Vasteras (Sweden)). [1971]. 28p. Dep. NTIS (U. S. Sales Only).

From sixteenth nuclear congress; Rome, Italy (25 Mar 1971).

A code, COLIBRI, was developed, which takes into account the different mechanisms in the axial and the radial directions of the rod bundles. Three mixing mechanisms for transport of energy between two channels are discussed. The experiments on two types of fuel assemblies, heavy-water and light-water, are described. Features of the COLIBRI code are given, and comparisons of the COLIBRI-program with experiments are made. (Sweden)

37004 (JAERI-Memo-4330) SECOND POSTOPERATION INSPECTION ON JPDR REACTOR PRESSURE VESSEL. (Japan Atomic Energy Research Inst., Tokyo). Jan 1971. 49p. (In Japanese). Dep. NTIS (U. S. Sales Only).

The methods and results of the second JPDR reactor pressure vessel inspections are described. The inner surface of the bottom head and around the east forced circulation nozzle were inspected by borescope and resistance probe system. Inspection by borescope has detected no presence of crack in the cladding on the bottom head and circulation nozzle, but some indications equivalent to up to 1.8 millimeters depth have been detected by the resistance probe system on both surfaces. The cracks in the cladding on the cylindrical wall and the top head were also inspected by dye-penetrant method. As the result of the inspection, no evidence was found of crack propagation, but some pin-holes were found in the cladding of cylindrical wall. (auth) (Japan)

37005 (KFK-1379) INHERENT PROPERTIES OF THE DIFFERENT PRIMARY CIRCUITS OF SODIUM-COOLED REACTORS. Mueller, R. A. (Kernforschungszentrum, Karlsruhe (West Germany). Institut fuer Reaktorentwicklung). Mar 1971. 27p. (In German). Dep. NTIS (U. S. Sales Only).

The fundamental structure of the system "primary circuit of sodium-cooled reactors" is analyzed. On the basis of a general description found by abstraction, additional parameters are introduced stepwise so that the variants under consideration approach the real engineered designs. The method yields a consistent scheme comprising all possible variants up to a defined degree of refinement. The inherent properties are clearly attributed to the individual variants indicated. All designs investigated and realized so far can be placed on specific positions in this "family tree" and thus can be definitely recognized as the specific solutions of the general system. (auth)

37006 (ORNL-TM-2929) SURVEY OF THE MATERIALS AND DESIGN OF INSULATION FOR PRESTRESSED-CONCRETE VESSELS FOR GAS-COOLED REACTORS. Holcomb, R. S. (Oak Ridge National Lab., Tenn.). May 1971. Contract W-7405-eng-26. 92p. Dep. NTIS.

A survey was made of the materials, design, and performance of insulation for prestressed-concrete reactor vessels (PCRV) for gas-cooled nuclear power plants. The survey included a review of information available on the characteristics of materials currently being used in PCRV applications, the performance of insulation materials and systems in operating plants, the development programs for plants under construction, relevant high-temperature insulation development for other applications, and the methods for calculating the thermal conductivity of insulation. The needs for future development are defined. The survey revealed that there are four types of insulation being employed for PCRV applications: reflective metal, fibrous ceramics, metallic gauze, and pumice concrete. Fibrous ceramic insulation appears to be the most promising for future development, but metallic gauze offers some advantages for certain applications. Silica foam, alumina foam, and graphite cloth are the most promising materials for the temperature range 2000 to 3000°F. 36 references. (auth)

37007 (ORNL-tr-2470) EFFECT OF RADIATION ON THE MECHANICAL PROPERTIES OF CONCRETE. Stoces, B.; Otopal, P.; Juricka, V.; Gabriel, J. (Ceskoslovenska Akademie Ved, Rez. Ustav Jaderneho Vyzkumu). Translated for Oak Ridge National Lab., Tenn., from report UJV-2390-RT. 66p. Dep. NTIS.

In the frame of a design study of a HWGR power reactor for a 500 MW power plant a prestressed concrete pressure vessel has been studied. The type of concrete for the pressure vessel is studied for the neutron radiation effects during the plant life. Irradiation of series of concrete patterns and detailed measurements show that changes of mechanical properties of the patterns for doses up to $3 \cdot 10^{18}$ n/cm^2 for neutrons of E > 1 MeV are negligible. 10 references. (auth)

37008 (UARAEE-50) HEAT TRANSFER IN ANNULAR REACTOR CHANNELS: STEADY STATE FORCED CONVECTION IN THE TRANSITION AND TURBULENT REGIONS. Hilal, M. M.; Raafat, N. M.; Mitry, A. M. (Atomic Energy Establishment, Cairo (Egypt). Reactors Dept.). 1968. 34p. Dep. NTIS (U. S. Sales Only).

An experimental study of heat transfer through the inner walls of concentric smooth-walled annular passages under steady state operation is described. A fixed inner pipe dimension is maintained while the outer pipe inside diameter takes the values 15.50, 17.50, and 19.75 mm. Tests were conducted for different heating fluxes (up to 1.975×10^5 K.cal/hr m^2) in the transition and turbulent regions of flow ($2.1 \times 10^3 \leq N_{Re} \leq 1.0 \times 10^5$). Correlations describing experimental data obtained on heat transfer are established. 16 references. (auth)

37009 (UARAEE-110) COOLING OF A SIMULATED FUEL ELEMENT BY A FLOW OF NATURALLY CIRCULATED BOILING WATER. Raafat, N.; El-Fouly, M.; Gaddis, E. S.; Khattab, M. (Atomic Energy Establishment, Cairo (Egypt). Reactors Dept.). 1971. 52p. Dep. NTIS (U. S. Sales Only).

The cooling of a uniformly heated tube, forming the heating surface of an annular space and simulating a fuel element, by naturally circulated boiling water was investigated. It was shown that accurate prediction of the surface temperature of the heater cannot be made without taking into consideration entrance and end effects. The wall surface temperature in the subcooled region can be predicted by a knowledge of the heat transfer coefficient in the convection and nucleate boiling regions. The rate of increase of coolant mass flow rate with increase in inlet coolant temperature (also with increase in power) increased considerably once net boiling started in the test section. However, this rate of increase decreased to a low level, once the steam quality at the exit exceeded a certain value. At atmospheric conditions, the corresponding exit steam quality can be as low as 0.03, and is attributed to the high void fraction and low rate of its increase at such low steam quality. Such behavior can be important in predicting the performance of natural circulation boiling reactors. The effect of diameter ratio on the temperature distribution of the heater was insignificant, and was mainly in the entrance region. The coolant mass flow rate showed a maximum at the intermediate diameter ratio. (auth)

37010 (WCAP-7671) PROCESS INSTRUMENTATION FOR WESTINGHOUSE NUCLEAR STEAM SUPPLY SYSTEMS (4 LOOP PLANTS). Nay, J. A. (Westinghouse Electric Corp., Pittsburgh, Pa. Nuclear Energy Systems Div.). Apr 1971. 83p.

Process instrumentation includes measuring devices, power supplies, alarm actuating devices, controllers, signal conditioning devices, etc. which are necessary for operation of the nuclear steam supply system and for monitoring the plant and providing

XUM

initiation of protective functions upon approach to unsafe plant conditions. The devices used for process parameter measurements, the interconnection of these devices into instrumentation systems, and the application of the devices are described. (H.D.R.)

37011 SAFETY PROBLEMS OF FAST BREEDER SODIUM COOLANT LOOPS. Teske, K.; Pridoehl, E. (Zentralinstitut fuer Kernforschung, Rossendorf, Ger.). Kernenergie; 14: No. 2, 29-33(Feb 1971). (In German).

Sodium safety is a considerable problem of sodium cooled fast breeder reactors. Special physical and chemical properties of Na call for appropriate solutions in safety layout of coolant loops and their components, safety instrumentation, emergency and fire protection. The status of development in this field is described, and some trends of development are pointed out, followed by some arguments on problems of operation connected with safety technique. (14 references) (auth)

37012 CONSTRUCTIVE ASSEMBLY AND SAFETY PRINCIPLES FOR THE PRIMARY CIRCUIT OF LARGE PRESSURIZED WATER REACTORS. Ruf, R. (Siemens AG, Erlangen, Ger.). Neue Tech., B; 12: 135-41(Aug 1970). (In German).

A review on the experience made in manufacturing, erecting and operation of the primary circuit components of the light water reactors delivered by Siemens is presented. The practical application of this experience for the construction and the safety aspects related to the big power stations to be constructed by Siemens are discussed. (auth)

37013 STEAM COOLED REACTOR OPERATION. Ripley, Charles C. (to General Electric Co.). U. S. Patent 3,575,807. 20 Apr 1971. Filed 29 Jan 1968.

A steam circulating system for a steam cooled nuclear reactor is disclosed. This system includes a startup technique in which a steam thermopresser acts first as a contact condenser while the reactor is preheating then as a jet pump while the reactor coolant circulation is initiated, and finally as a thermopresser during normal reactor operation. (auth)

37014 IMPROVEMENTS RELATING TO NUCLEAR REACTOR INSTALLATIONS. (to Sulzer Brothers Ltd.). British Patent 1,232,767. 19 May 1971. Priority date 21 Apr 1969, Switzerland.

PUMPS—design parameters of turbine
REACTORS, BOILING—cooling system for, description of turbine pump (D.C.C.)

Fuels

Refer also to abstract 34566.

37015 (BNWL-1568) DESTRUCTIVE AND NONDESTRUCTIVE BURNUP DATA FROM NATURAL UO_2 FUEL. Christensen, D. E.; Matsen, R. P. (Battelle-Northwest, Richland, Wash. Pacific Northwest Lab.) May 1971. Contract AT(45-1)-1830. 156p. Dep. NTIS.

Experimental burnup data collected from spent UO_2 fuels which were irradiated in the PRTR are documented. One hundred sixty-five fuel samples were chemically analyzed to obtain total U and Pu concentrations, U and Pu isotopic compositions and fission product concentration data. Three fuel rods were nondestructively analyzed by gamma scanning which included both continuous scanning of the fuel rods to obtain axial gamma ray activity profiles and incremental scanning to obtain high resolution gamma ray spectra at selected points. Preliminary analyses of the data were done as well as documentation of additional information necessary for complete analysis and correlations between experiment and theory. 10 references. (auth)

37016 (CONF-700211-9) PROBLEMS ABOUT FUEL CLADDING MATERIALS. Mishima, Yoshitsugu (Tokyo Univ. (Japan)). [nd]. 3p. Dep. NTIS (U. S. Sales Only).

From Atomic energy society meeting; Tokyo, Japan (13 Feb 1970).

The use of Ti-V for fuel element cladding in fast breeder reactors is discussed. The effects of liquid Na on corrosion of Ti-V are described. (D.C.C.)

37017 (CONF-710414-1) EFFECTS OF BURNUP ON FUEL PIN THERMAL PERFORMANCE. Biancheria, A.; Nayak, U. P.; Beck, M. S. (Westinghouse Electric Corp., Madison, Pa. Advanced Reactors Div.). [1970]. Contract AT(30-1)-4210. 30p. Dep. NTIS.

From Conference on fast reactor fuel element technology; New Orleans, La. (13 Apr 1971).

The development of models for analyzing the thermal performance of fast reactor mixed-oxide fuel pins throughout life is presented. The models provide a capability for examining the interrelationship between the various kinetic phenomena occurring in fuel pins. Emphasis is placed on gap conductance behavior. The factors which influence thermal behavior as burnup proceeds are discussed. Preliminary application of the models to fast reactor operating conditions is presented. The results reveal the competing effects on thermal performance of fission gas dilution of the bond gas, fission gas pressure, gap closure rates and restructuring kinetics. The importance of a restraint-dependent fuel swelling model to thermal behavior was also revealed by these studies. 32 references. (auth)

37018 (JUL-701-RW) IRRADIATION EXPERIMENT FOR TESTING SPHERICAL FUEL ELEMENTS FOR HIGH-TEMPERATURE REACTORS (TEST SK 1 IN STUDSVIK R 2). Groos, E.; Pott, G.; in der Schmitten, W.; Theymann, W. (Kernforschungsanlage, Juelich (West Germany). Institute fuer Reaktorwerkstoffe) Sep 1970. 34p. (In German). Dep. NTIS (U. S. Sales Only).

For testing spherical fuel elements that were pressure cast for the AVR nuclear power station, two elements of this type were irradiated in Studsvik R 2 under conditions corresponding to those of AVR. During the experiment, the release of various fission gas nuclides was measured. In the last reactor period, a thermal cycling was performed. At a temperature of 1000°C on the surface of the spheres, a burnup was achieved which reached about 11% of the fissionable material, and a maximum fast rate of 2.2×10^{21} cm^{-2}. Release of ^{133}Xe remained below specified limits. Following irradiation, no damage could be observed on fuel elements as well as fuel particles. (H.B.G.)

37019 (ORNL-TM-3386) COMPARISONS BETWEEN PREDICTED AND MEASURED FUEL PIN PERFORMANCE. Homan, F. J.; Cox, C. M.; Lackey, W. J. (Oak Ridge National Lab., Tenn.). May 1971. Contract W-7405-eng-26. 26p. (CONF-710414-3). Dep. NTIS.

From Conference on fast reactor fuel element technology; New Orleans, La. (13 Apr 1971).

The FMODEL computer code is being developed to predict and analyze the irradiation performance of stainless steel clad $(U,Pu)O_2$ LMFBR fuel pins in terms of thermal and mechanical performance. Detailed comparisons were made between predicted and measured fuel pin performance in terms of cladding deformation, oxide fuel restructuring, and fuel temperatures. Reasonable agreement was obtained in each of these comparisons without resorting to the use of artificially adjusted parameters to fit the data. It is concluded that, while added sophistication will improve the performance predictions, the current version of FMODEL is a reliable tool for design analysis and interpretation of irradiation tests. 28 references. (auth)

37020 (WHAN-SA-76) ROTATING WIRE SPACER MODEL IN LARGE BUNDLE THERMAL-HYDRAULICS. Kolesar, Donald C. (WADCO Corp., Richland, Wash.). Mar 1971. Contract AT(45-1)-2170. 18p. Dep. NTIS.

Extensions of the "COBRA" heat transfer codes to large liquid Na cooled pin bundles and coolant mixing effects due to the presence of fuel pin spacer wires are described. Bundle sizes of up to 217-pins are considered. Wire rotation models which require only a few input parameters to characterize the complete set of interchannel mixing rates are proposed. Movement of the fluid along the duct (fuel pin container) wall in the direction of wire rotation is predicted by the models. Limitations on the code parameters due to the simulation of a boundary value problem with an initial value problem are discussed. Comparisons of the new COBRA results with experimental data have been successful where attempted. 13 references. (auth)

37021 REACTOR-PHYSICAL AND ECONOMICAL ASPECTS OF FUEL BURNUP CALCULATION. Meyer, K. (VEB Kraftwerksanlagenbau, Berlin). Kernenergie; 14: No. 1, 15-20(Jan 1971). (In German).

Data and requirements for accuracy in predicting reactor operations are compared with each other and related to expenditures for fuel. Relevance of technological and economical studies on this subject is pointed out. (9 references) (auth)

37022 CONSIDERATIONS OF THE COSTS FOR THE MANUFACTURE OF FUEL ELEMENTS WITH OXIDE FUEL FOR POWER REACTORS. Ortmayer, Rudolf Max; Braatz, Ullrich (Reaktor-Brennelemente GmbH, Wolfgang, Ger.). VDI (Ver. Deut. Ing.) Z.; 113: No. 6, 430-3(Apr 1971). (In German).

Cost analysis for manufacturing UO_2 fuel elements for power reactors is presented. (15 references) (D.D.C.)

37023 IMPROVEMENTS IN OR RELATING TO NUCLEAR REACTOR FUEL ELEMENTS. (to Le Carbone Lorraine). Brit-

XUM

ish Patent 1,230,520. 5 May 1971. Priority date 6 Dec 1968, France.

REACTOR FUELS—fabrication of graphite shell particle type, for high temperature gas cooled reactors
REACTORS, GAS-COOLED—fuels for high temperature, fabrication of graphite shell particle type (D.C.C.)

37024 PRODUCTION AND TESTING OF SUPERHEATER FUEL ELEMENTS. Tolson, G. M.; Kirstowsky, E. C.; Bogardus, B. J. (Union Carbide Corp., Oak Ridge, Tenn.). Mater. Eval.: 29: 75-80; 87(Apr 1971).

The program, undertaken to develop a manufacturing process for fabricating the fuel rods without vent holes, for eight fuel rod assemblies to supplement the BONUS system, is described. High integrity fuel rods were fabricated on a production basis by strict adherence to tight material and work specifications, backed up by rigid nondestructive and destructive test techniques and appraisals. The completed fuel rods passed leak test requirements of 1×10^{-10} std. cc/sec of helium. (auth)

37025 NUCLEAR REACTOR FUEL ASSEMBLIES. Binns, Ian Mason; Lewis, Robert Alec (to United Kingdom Atomic Energy Authority). British Patent 1,232,811. 19 May 1971. Filed 19 Jan 1968.

The fuel assembly described comprises a group of parallel spaced cylindrical fuel elements disposed with their centers in linear array to form a prismatic arrangement with a ring of fuel elements at least some of which are of elongated cross-section, arranged about the periphery of the main group to form a cylindrical cluster. Such a design finds particular application in a light water pressure tube reactor wherein either natural or slightly enriched fuel is employed. Because the interspaces between the fuel elements can be smaller for a linear array than for a circular array a higher fuel/coolant ratio is attainable for the same cross sectional area. The elongated elements provide additional fuel occupying parts of the segmental spaces bounded by the sides of the linear cross section and the wall of a tube enclosing the array. (UK)

37026 POROUS PLUGS FOR NUCLEAR FUEL RODS. (to Societe Anonyme Belgonucleaire). British Patent 1,231,129. 12 May 1971. Priority date 29 Nov 1968, Belgium.

REACTOR FUEL ELEMENTS—plugs for fast rod type, description of porous end
REACTORS, FAST—fuel elements for, description of porous end plug for rod type (D.C.C.)

37027 FUEL ELEMENT FOR A FAST BREEDER AND/OR TEST REACTOR. Lesser, Richard; Richter, Karl; Gabolde, Jean (to EURATOM). British Patent 1,233,689. 26 May 1971. Priority date 23 Apr 1969, Netherlands.

REACTOR FUEL ELEMENTS—design characteristics of helical rib spaced cylinder clad rod type, for fast breeder reactors
REACTORS, BREEDER—fuel element for fast, description of helical rib spaced cylinder clad rod type
REACTORS, FAST—fuel elements for breeder, description of helical rib spaced cylinder clad rod type (D.C.C.)

Auxiliary and Emergency Systems

Refer also to abstract 34692.

37028 (ORNL-TM-2412(Pt,10)) DESIGN CONSIDERATIONS OF REACTOR CONTAINMENT SPRAY SYSTEMS. PART X. THE STRESS CORROSION CRACKING OF TYPES 304 AND 316 STAINLESS STEEL IN BORIC ACID SOLUTIONS. Griess, J. C.; Creek, G. E. (Oak Ridge National Lab., Tenn.). May 1971. Contract W-7405-eng-26. 22p. Dep. NTIS.

The stress corrosion cracking of Types 304 and 316 stainless steel in simulated pressure-suppression and fission-product-absorption sprays was investigated. The test solutions contained 0.28M H_3BO_3 (3000 ppM B) with pH values and chloride concentrations ranging between 4.5 and 7.5, and 5 and 200 ppM, respectively. In addition one test solution contained 2 ppM iodide. All test specimens, mostly U-bends, were exposed for 1 day at 141°C and 7 days at 100°C in a recirculating spray loop and were then transferred to a tank for an additional exposure of 2 months at 82°C. The results showed that both alloys underwent cracking in all solutions. The tendency to crack was greater the lower the pH and the higher the chloride concentration. Type 316 stainless steel was somewhat more resistant to cracking than Type 304 stainless steel, and both alloys were more susceptible when sensitized than when annealed. Specimens that were sensitized in air and covered with thin oxide films cracked more frequently than similarly treated specimens that were pickled after sensitization. In all cases except one, the cracks were branching and transgranular. In one case when the solution had a pH of 6.5 and contained 20 ppM chloride and 2 ppM iodide, wide short cracks were found only in the vicinity of welds; no other localized attack was found on any other specimen. 10 references. (auth)

37029 (ORNL-TM-2412(Pt,12)) DESIGN CONSIDERATIONS OF REACTOR CONTAINMENT SPRAY SYSTEMS. PART XII. VARIABILITY OF THE DOSE REDUCTION FACTOR FOR THE REMOVAL OF ELEMENTAL IODINE. Hebble, Thomas L. (Oak Ridge National Lab., Tenn.). May 1971. Contract W-7405-eng-26. 25p. Dep. NTIS.

Pressurized water reactors have containment spray systems installed as engineered safety features. These systems serve as heat removal devices and in a number of cases function as an iodine removal system. The dose reduction factor is used in the evaluation of the containment vessel spray systems that are designed for the removal of atmospheric contaminants. The variability of this factor for the specific removal of elemental iodine is analyzed. Two aspects of variability are considered. First, a method is given for estimating the variance of the dose reduction factor as a function of two random variables; spray drop diameter and spray drop velocity. This method also provides insight into the behavior of the variability at different levels of controllable process variables. Second, an estimate of the variance is based on observations from three repeated Nuclear Safety Pilot Plant (NSPP) runs. For a spraying time of one hour, the mean dose reduction factor for the three repeated runs is 40.9 with a standard error of 2.1 ($= \sqrt{\text{Variance}}$). The corresponding factor computed from the mathematical model is 52.9 with a standard error of 9.5. Comparisons such as this are favorable for the first hour of spraying time. Beyond this period, a different I_2 removal mechanism is in force and is caused in part by the recycling spray solution. 5 references. (auth)

Operation and Economics

37030 (ORNL-TM-3243) ESTIMATED CAPITAL COSTS OF NUCLEAR AND FOSSIL POWER PLANTS. Bowers, H. I.; Myers, M. L. (Oak Ridge National Lab., Tenn.). 5 Mar 1971. 31p. Dep. NTIS.

Capital costs in $/kW(e) were estimated as a function of time for PWR, HTGR, and LMFBR nuclear electric power plants and for coal-fired and oil-fired fossil electric power plants. Costs in terms of mid-1970 dollars were projected over the 50-yr period, 1970 through 2020, taking into account estimated increases in unit size and assumed learning curves for the different types of plants. 14 references. (auth)

37031 ECONOMIC STUDIES ON STRETCH-OUT OF BURN-UP IN POWER REACTORS. Ackermann, G. Kernenergie; 14: No. 3, 67-73(Mar 1971). (In German).

The stretch-out of campaign or burnup of power reactors with batch charge of the fuel and high power-dependent negative reactivity effects seems possible when power is decreased at the end of reactor campaign. This was already realized in some nuclear power plants with pressurized water reactors. Using some simplifications, dimensionless equations are derived to evaluate in which range such a stretch-out of burnup is economical. Results prove that the use of stretch-out strategy has economical advantages. Some factors of influence neglected so far are to be taken into account for more minute studies. (auth)

37032 UTILIZATION OF NUCLEAR POWER PLANTS FOR HEAT SUPPLY OR HEAT-POWER COUPLING. Schwarz, M. (VEB Kombinat Kraftwerksanlagenbau, Dresden). Kernenergie; 14: No. 3, 57-61(Mar 1971). (In German).

Starting from the fraction of heat requirements in total power requirements, utilization of nuclear power plants for meeting the requirements of process and room heat seems inevitable. Criteria for building such plants are the demands of heat consumers for safety arrangements, parameters needed for heat power, and economics. Some notes on utilizing special chemonuclear reactors are made in addition to uses of nuclear power in conventional process and room heating plants. 10 references. (auth)

37033 PROBLEMS OF GRASPING THE WORKING BEHAVIOR OF NUCLEAR POWER PLANTS IN PRODUCTION PLANNING AND OF ITS ECONOMICAL SIMULATION. Eidam, V. (Technische Univ., Dresden); Ermlich, H.; Steinbock, P.; Weschke, P. Kernenergie; 14: No. 3, 61-6(Mar 1971). (In German).

Problems of grasping the working costs specific for nuclear power plants having influence on the simulation of the production plan of a compound mains system are discussed as a function of working regime. Qualitative features arise in grasping

XUM

the costs of nuclear fuel which are taken into account by analogy with the costs of designed preventive maintenance. Model working regimes of nuclear power plants, possibilities of economically stable startup of optimum versions of operation as well as problems to be expected in production planning of fast breeder nuclear power plants are revealed. 10 references. (auth)

37034 SITUATION OF THE NUCLEAR FUEL CYCLE INDUSTRY. Klusmann, A.; Voelcker, H. (STEAG Kernenergie, Essen). Atomkernenergie ; 17: 149-57(May 1971).

The market situation for uranium, enrichment, fuel fabrication, and reprocessing for light water reactors is summarized and the technical and economic background of this industry is described. The expected development until 1980 is outlined. 11 references. (auth)

Safety and Siting

Refer also to abstracts 34690 and 35061.

37035 (ANL-7792) PRESSURE-PULSE PROPAGATION IN TWO PHASE ONE- AND TWO-COMPONENT MIXTURES. Henry, R. E.; Grolmes, M. A.; Fauske, H. K. (Argonne National Lab., Ill.). Mar 1971. Contract W-31-109-eng-38. 86p. Dep. NTIS.

A comprehensive analytical development of the propagation velocity of small pressure pulses is presented for bubble, annular, stratified, droplet, and slug-flow regimes. Particular attention is given to the influence of flow regime on the momentum transfer between phases. Momentum transfer in bubbly, droplet, and wavy separated flows is described by consideration of the virtual mass of the discrete phase. For the smooth-interface-separated flows, no interaction is assumed between the phases. In the slug-flow regime, the distinction is made between inertially and acoustically limited pressure propagation, and a consideration of the severe attenuation of a finite pulse on crossing a vapor-liquid interface is shown to be of major importance. These analyses are compared with data obtained in this and other representative studies. Data obtained in this study are unique in that comparisons of the propagation velocity in one- and two-component mixtures are illustrated for widely different flow regimes. Characteristics of compression and rarefaction pulses in one-component flow are also described. These analyses for small pressure waves satisfactorily explain available data. 41 references. (auth)

37036 (BMI-1904) AN EVALUATION OF THE APPLICABILITY OF EXISTING DATA TO THE ANALYTICAL DESCRIPTION OF A NUCLEAR-REACTOR ACCIDENT. Quarterly Progress Report, January-March 1971. Carbiener, Wayne A.; Ritzman, Robert L. (Battelle Memorial Inst., Columbus, Ohio). Apr 1971. Contract W-7405-eng-92. 24p. Dep. NTIS.

FISSION PRODUCTS—deposition in reactor containment buildings, heat transfer model for analysis of
IODINE—deposition in reactor containment buildings, heat transfer model for analysis of
REACTOR CONTAINMENT STRUCTURES—fission product deposition in, heat transfer model for analysis of iodine
REACTOR SAFETY—coolant loss accidents in water cooled reactors, analytical description of
REACTORS, BOILING—emergency core cooling systems for, model for heat transfer analysis of top-injected spray
—coolant loss accidents in, analytical description of
REACTORS, PRESSURIZED WATER—coolant loss accidents in, analytical description of
REACTORS, WATER COOLED—coolant loss accidents in, radiolytic production of hydrogen following, (E/T)
—coolant loss accidents in, ECCSA and MUCHA codes for thermal-hydraulic analysis of (H.D.R.)

37037 (CONF-700608-36) TRANSIENT EFFECT ON LMFBR FUEL RODS BY GAS BUBBLES ENTRAINED IN THE COOLANT. Carelli, Mario D.; Shoua, Ezra D. (Westinghouse Electric Corp., Madison, Pa. Advanced Reactors Div.). [Jul 1970]. Contract AT(30-1)-4135. 18p. Dep. NTIS.

From American Nuclear Society meeting; Los Angeles, Calif. (29 Jun 1970).

The effect of the intermittent passage of gas bubbles entrained in the sodium coolant on the integrity of the fuel rod cladding is examined for typical conditions of Liquid Metal Fast Breeder Reactors. The maximum stable size of the bubbles is calculated to be of the order of 0.5 in. equivalent spherical diameter. The transient blanketing of the fuel rod due to the passage of the bubbles is studied for two extremely conservative geometrical configurations. The maximum calculated cladding temperature increase during the transient was found to be fairly limited, and the thermal fatigue effect due to the passage of a large number of bubbles was assessed. It appears that even in the most pessimistic conditions the fatigue effect is well below the failure limit. It was concluded, therefore, that gas bubbles flowing through the core do not endanger the cladding integrity and do not reduce the fuel rod lifetime. 12 references. (auth)

37038 (IN-1453) METALLURGICAL EVALUATION OF SIMULATED BWR EMERGENCY CORE COOLING TESTS. Graber, M. J.; Zelezny, W. F.; Schmunk, R. E. (Idaho Nuclear Corp., Idaho Falls). Mar 1971. Contract AT(10-1)-1230. 51p. Dep. NTIS.

Three bundles of 49 simulated boiling-water-reactor (BWR) fuel rods were exposed to emergency core cooling (ECC) tests to determine the response of Zircaloy-2 tubing. During these tests, electrically heated rods were exposed to the temperature and steam atmosphere conditions expected during emergency core cooling following a loss-of-coolant accident in a boiling water reactor. A metallurgical examination and evaluation showed that the tubes were attacked by the steam and by alumina insulator material. The reaction between the alumina and the Zircaloy-2 resulted in unexpected temperature excursions and increased embrittlement of the cladding. 13 references. (auth)

37039 (IRS-T-18(1970), pp 21-36) CRITICAL ANALYSIS OF THE EVALUATION METHODS IN REACTOR SAFETY. Seipel, H. G. (Technischer Ueberwachungs-Verein e. V., Cologne (West Germany). Institut fuer Reaktorsicherheit). 1970. (In German). NTIS (U. S. Sales Only).

The analysis compares critically the MCA-concept with the reliability method as alternative for a more objective safety evaluation. It concludes that the reliability analysis offers a first point of interest capable of development for the establishment of requirements for safety equipment of nuclear power plants. (INIS)

37040 (IRS-T-18(1970), pp 123-43) DATA ACQUISITION SYSTEM FOR THE DETERMINATION OF RELIABILITY CHARACTERISTICS. Schlothauer, D. (Technischer Ueberwachungs-Verein e. V., Cologne (West Germany). Institut fuer Reaktorsicherheit). 1970. (In German). NTIS (U. S. Sales Only).

The data acquisition system of the Institute for Reactor Safety (IRS) is described. The required operating expenditure depends on boundary conditions which must be observed, i.e., the assumptions of an exact systems analysis. With regard to the systems to be examined in reactor safety, the boundary conditions are fixed to a minimum. The completeness of the failure report is decisive for the accuracy of the calculated values. Therefore, information must be available to the personnel of the power plant from the data center at all times. As regards operating expenditure and the accuracy of data, it is favorable to introduce data acquisition before or shortly after start-up of the power plant. The IRS-data acquisition system is essentially an extension of the failure statistics of VDEW; therefore both statistics are comparable among each other and may be kept side by side. Estimates for an improvement of the data acquisition system are presented. (INIS)

37041 (IRS-T-18(1970), pp 223-39) RELIABILITY ANALYSES OF REACTOR SYSTEMS. Vetter, H. (Technischer Ueberwachungs-Verein e. V., Cologne (West Germany). Institut fuer Reaktorsicherheit). 1970. (In German). NTIS (U. S. Sales Only).

On the basis of the failure statistics of VDEW, which is described in detail, a connection between availability, reliability, and safety for the failure analysis of fossil and nuclear power plants is established. (INIS)

37042 (JAERI-Memo-4173) SUMMARY OF TECHNICAL REPORTS ON THE 1st MITI DESIGN PERMIT OF JPDR. (Japan Atomic Energy Research Inst., Tokyo). Oct 1970. 94p. (In Japanese). Dep. NTIS (U. S. Sales Only).

A summary of supplemental technical information on JPDR-2 construction permit to MITI is presented. The test described must be executed and its result must be reported to MITI. The safety regulation of JPDR-2 and the pre-operation test procedure are described. (auth)

37043 (JAERI-Memo-4174) SUMMARY OF TECHNICAL REPORTS ON THE 3rd MITI DESIGN PERMIT OF JPDR. (Japan Atomic Energy Research Inst., Tokyo). 10 Oct 1970. 90p. (In Japanese). Dep. NTIS (U. S. Sales Only).

A summary of supplemental technical information on JPDR-2 construction permit to MITI is presented. The tests described must be performed and results must be reported to MITI. The safety regulation of JPDR-2 and the pre-operation test procedures are described. (auth) (Japan)

37044 (JAERI-Memo-4260) SUMMARY OF TECHNICAL REPORTS ON THE FIFTH MITI DESIGN PERMIT OF JPDR. (Japan

XUM

Atomic Energy Research Inst., Tokyo). 10 Dec 1970. 48p. (In Japanese). Dep. NTIS (U. S. Sales Only).

A summary of supplemental technical information on JPDR-2 construction permit to MITI is presented. The test described must be executed and its result must be reported to MITI. The safety regulation of JPDR-2 and the pre-operation test procedure are described. (auth)

37045 (NP-18842) NUCLEAR POWER AND ENVIRONMENTAL POLLUTION. Davy, D. R. (Australian Atomic Energy Commission Research Establishment, Lucas Heights). [1971]. 28p. Dep. NTIS (U. S. Sales Only).

Operations which are a potential source of radioactive pollution, such as uranium mining, chemical reprocessing, transportation of spent fuel, and reactor systems, are discussed in terms of distribution of waste products within the environment. Evaluations of plant layout for the proposed Jervis Bay reactor are considered in this context, with particular reference to hydrographic studies related to the ecological effects of movement of large volumes of water, trade waste disposal, and dispersal of thermal effluent. Low level radioactive effluent is discussed with reference to discharge authorizations. For an Australian facility, biological mapping is carried out to reveal the food web most limiting in terms of allowable discharges. At the AAEC research establishment and the proposed Jervis Bay power station site, the critical foods and consumption rates are oysters (70 g/day), fish (350 g/day) and milk (1.5 pints/day/1 year old child). Comparison of permissible discharge levels with actual levels released by nuclear facilities shows reduction by a factor of $10-10^2$. It is possible to reduce Lucas Heights discharge by a factor of 10^3-10^4 below permissible levels. (Australia)

37046 (RT/ING-(70)18) NEMI: A PHYSICAL-MATHEMATICAL MODEL FOR SODIUM BOILING IN A HEATED CHANNEL. Sacco, A.; Scarano, G. (Comitato Nazionale per l'Energia Nucleare, Rome (Italy)). 1970. 36p. (CONF-700439-1). Dep. NTIS (U. S. Sales Only).

From second meeting of the Liquid Metal Boiling Working Group; Casaccia, Italy (9 Apr 1970).

The NEMI code on sodium boiling in a core channel during a loss of flow or power excursion accident is described. Results are presented for the ENA-1 experimental loop geometry, for the purpose of evaluating the reliability of the physical-mathematical model by comparison with experimental data. (auth)

37047 (TID-3525(Rev.5)(Suppl.6)) REACTOR SAFETY. A Literature Search. Raleigh, Henry D. (comp.) (Division of Technical Information Extension (AEC), Oak Ridge, Tenn.). Jun 1971. 63p. Dep. NTIS.

Included are 243 citations to references issued during 1970 on safety aspects of nuclear reactor design, siting, materials, engineered safeguards, and operating procedures. Reports cited concern hazards analyses of entire facilities to satisfy construction and operation permit requirements, evaluation of reactor systems and components reliability, and analyses of the consequences of potential accident conditions. Subject, author, corporate author, and report number-availability indexes are included. (H.D.R.)

37048 NATIONAL FIRE CODES. A COMPILATION OF NFPA CODES, STANDARDS, RECOMMENDED PRACTICES, AND MANUALS. VOLUME 9, OCCUPANCY STANDARDS AND PROCESS HAZARDS, 1970-71. Boston; National Fire Protection Association (1970). 826p. Available from National Fire Protection Association, Boston.

A selected group of standards and manuals on occupancies and process hazards is presented. Included are NFPA 801, Recommended Fire Protection Practice for Facilities Handling Radioactive Materials, and NFPA 802, Recommended Fire Protection Practice for Nuclear Reactors. (H.D.R.)

37049 PROGRAM FOR DETERMINING ENVIRONMENTAL SAFETY OF NUCLEAR POWER PLANTS. Zabka, H.; Moebert, K. (Institut fuer Kraftwerke, Berlin). Kernenergie; 14: No. 1, 21-5(Jan 1971). (In German).

Safety of plant environment against effects of ionizing radiation must be warranted in addition to safety of operational personnel when building and operating nuclear power plants. A computer program for analyzing this part of safety technology has been elaborated. The results of some examples of calculations are briefly described and evaluated. (4 references) (auth)

37050 RECOMMENDED FIRE PROTECTION PRACTICE FOR NUCLEAR REACTORS. NFPA 802 1960. Boston; National Fire Protection Association (1960). 71p. Available from National Fire Protection Association, Boston.

Potential fire and explosion hazards in nuclear reactor facilities are discussed. Fire protection practices are described and problems of specific reactor types are examined. (H.D.R.)

37051 INTRODUCTION TO NUCLEAR SAFETY. Santos, Agustin Alonso (Junta de Energia Nuclear, Madrid). Energ. Nucl. (Madrid); 15: No. 69, 16-20(Jan-Feb 1971). (In Spanish).

The concepts of nuclear safety, damage, and risks are introduced. Risks and damages are related in respect to the probabilities of accidents, and they are discussed briefly. With reference to a 1000 MW(t) nuclear power plant and considering the limits of contamination of the air and water recommended by the International Commission for Radiological Protection, a simple estimate is made of the potential damages from such installations. Finally, the difficulties inherent in the determination of the risks are presented and the probabilistic and mechanistic approximations developed for such a purpose are introduced. In conclusion, Law 25/1964 on nuclear energy is presented as an administrative mechanism for the application of nuclear safety. (tr-auth)

37052 EXPERIMENTAL RESULTS ON ACOUSTIC DETECTION OF SODIUM AND WATER BOILING. Gross, M.; Jentges, H.; Kafka, P.; Stoelben, H. Atomkernenergie; 17: No. 4, 255-60(Jul 1971).

Sodium boiling experiments were performed in a special test loop using a low sodium velocity. The sodium was made to boil at 600°C by lowering the argon gas pressure to below 1 torr. The purpose of these experiments was to investigate various acoustic methods of detecting sodium boiling in comparison with temperature and pressure shock wave measurement. Two structureborne sound pick-ups of different design were used and a capacitor microphone was immersed in the liquid sodium. Sodium boiling was found to consist of an irregular succession of individual bubbles, each producing a shock wave upon condensation. This pressure pulse was indicated simultaneously and clearly by the various acoustic sensors. A frequency analysis of the boiling noise of sodium by sound level measurements between 50 Hz and 15 kHz gave a wide-band spectrum. The measured sound pressure of the boiling shocks was between 20 and 45 DB above the general noise level, depending on the pick-up and the frequency range. To provide a comparison for the measured frequency spectra of sodium boiling noise, the same test rig and the same instrumentation were used for water boiling experiments. The frequency analysis of water boiling noise produced a similar frequency spectrum to that obtained for sodium boiling. (auth)

Power Conversion Systems

37053 NUCLEAR POWER PLANT. (to Sulzer Brothers Ltd.). British Patent 1,232,959. 26 May 1971. Priority date 13 May 1969, Switzerland.

REACTORS, GAS-COOLED—power conversion system for helium cooled, description of carbon dioxide turbine
REACTORS, POWER—power conversion system for helium cooled, description of carbon dioxide turbine
TURBINES—design parameters of carbon dioxide gas (D.C.C.)

Research and Test Reactors

Refer also to abstracts 35320, 36686, 36988, 36991, 37018, and 37114.

37054 (AECL-3738) PERFORMANCE OF UNIAXIAL CREEP MACHINES IN THE NRX AND NRU REACTORS. Anderson, P. F. (Atomic Energy of Canada Ltd., Chalk River (Ontario). Chalk River Nuclear Labs.). Feb 1971. 71p. Dep. NTIS (U. S. Sales Only). AECL $2.00.

Reactor Loops Branch began operating creep experiments in 1965. At that time, Mk-IV and Mk-VI machines were in use in NRX and NRU. Since then, a number of disposable machines have been built, resulting in the Mk-X design which may be used in either reactor. Control equipment has been automated, and data retrieval computerized. The original and re-designed equipment is described, with details of its operational reliability. 5 references. (auth)

37055 (BNL-15815) INVESTIGATION AND REPAIR OF BAFFLE PLATE DAMAGE IN THE HFBR PRIMARY HEAT EXCHANGERS. Brynda, Willam; Chow, Joe G. Y.; Hoffman, Kenneth; Tichler, Paul ([Brookhaven National Lab., Upton, N. Y.]). Jan 1970. 22p. Dep. NTIS.

Information relating to the investigation and repair of the defects in the baffle plates of the HFBR primary heat exchangers is presented. Probable cause of the defects is analyzed. (D.C.C.)

37056 (BNWL-tr-67) PURIFICATION OF THE SODIUM FOR RAPSODIE. Giraud, B. ([Commissariat a l'Energie Atomique,

Cadarache (France). Centre d'Etudes Nucleaires]). Translated by Elizabeth Appleby (Battelle-Northwest, Richland, Wash.), from report CEA-R-3395. 61p. Dep. NTIS.

General features of the fast reactor RAPSODIE are described, and properties of the liquid Na coolant are reviewed. General principles of Na purification and impurity measurement are presented. The RAPSODIE Na purification system is described in detail and data obtained from operation during the first year are presented. (H.D,R.)

37057 (CEA-R-3799) FAST NEUTRON SPECTRUM IN THE REFLECTOR OF A SWIMMING POOL REACTOR BEHIND METALLIC SLABS. Brousse, Jean-Claude (Commissariat a l'Energie Atomique, Grenoble (France). Centre d'Etudes Nucleaires). Dec 1970. 174p. (In French). Dep. NTIS (U. S. Sales Only).

Thesis. Submitted to Grenoble Univ. (France).

The experiments which were performed in the reflector of the swimming pool reactor SILOETTE, behind Pb, Al, and Fe slabs, enabled the measurement of the large perturbations introduced in the fast neutron spectrum by these materials. The neutron slowing down chiefly depends upon the inelastic reaction. The reaction cross section increases with energy which implies a spectrum softening. An attempt was made to calculate the shape of the spectrum and to fit the measurements. Calculations were made first in a one-dimensional geometry, using the NIOBE code to solve the transport equation and also the SANE Monte Carlo code. The results did not agree with the experimental values. A semi-empirical approach and a 3-dimensional geometry was then chosen; the results obtained were in perfect agreement with the measured values. The method is described. 25 references. (France)

37058 (CEA-R-4114) THERMIC CALCULATIONS ON WATER COOLED RESEARCH REACTORS. Fabrega, Serge (Commissariat a l'Energie Atomique, Grenoble (France). Centre d'Etudes Nucleaires). Mar 1971. 106p. (In French). Dep. NTIS (U. S. Sales Only).

The formulae and the more important numerical data necessary for thermic calculations on the core of a research reactor, cooled with low pressure water, are presented. Most of the problems met by the designer and the operator are dealt with (calculations margins, cooling after shutdown). Particular cases were considered (gas release, rough walls, partially rough walls, asymmetric cooling slabs, attenuation of the defects by conduction), which are not generally envisaged in works on general thermics. A list of instructions for the I.B.M. program (written in Fortran 4) is given in a supplement. This list allows real applications to be studied in a complete and precise manner when the complexity is such that the direct employment of the formulae is, in general, only adequate in the first approximation. 42 references. (auth) (France)

37059 (DOCKET-50231-83) SOUTHWEST EXPERIMENTAL FAST OXIDE REACTOR. Safety System Relay Malfunctions. (General Electric Co., Sunnyvale, Calif. Breeder Reactor Development Operation). 2 Jun 1971. 3p. Dep. NTIS.

37060 (EURFNR-889) ODILE IRRADIATION DEVICE. Fages, Denis; Lauthier, Jean-Claude; Leclere, Jacques; Lhermenier, Andre (Commissariat a l'Energie Atomique, Fontenay-aux-Roses (France). Centre d'Etudes Nucleaires). Translation of report CEA-N-1317. 41p. Dep. NTIS.

For experimental irradiations of fast reactor project fuels, a device to be used in pool type reactors, Osiris or Siloé, was designed and fabricated. Its main features are: static Na cooling, the Na being always kept liquid by electrical heaters; temperature adjustment by variable thermal barrier; flux adjustment by moving towards reactor core; and the ability to take neutrographies. Capable of evacuating more than 800 W/cm for small elements, the device Odile meets most of the requirements for fast reactor project irradiations. (auth) (France)

37061 (EURFNR-890) THE NATURAL CONVECTION IRRADIATION DEVICE "ESTHER." Leclere, Jacques; Lhermenier, Andre; Fages, Denis; Lauthier, Jean-Claude (Commissariat a l'Energie Atomique, Fontenay-aux-Roses (France). Centre d'Etudes Nucleaires). Translation of report CEA-N-1348. 39p. Dep. NTIS.

Work performed under United States–Euratom Fast Reactor Exchange Program.

In order to perform radiation experiments on fast reactor fuels, a device which was to be used in the Siloe and Osiris swimming pool reactors was designed and constructed. The Ester device is characterized by natural convection cooling. The temperature distribution is analogous to that in a reactor channel. The temperature is adjusted by a variable thermal barrier. The flux level is increased by moving towards the core. This device can dissipate between 800 and 900 W/cm. Its main interest lies in the circulation of Na or NaK along the fuel element. (auth) (France)

37062 (FMRB-32/70) ELECTRIC INSTALLATIONS AT THE FORSCHUNGS- UND MESSREAKTOR BRAUNSCHWEIG (FMRB) OF THE PHYSIKALISCH-TECHNISCHE BUNDESANSTALT. Runge, E.-G. (Physikalisch-Technische Bundesanstalt, Brunswick (West Germany)). Jan 1970. 63p. (In German). NTIS (U. S. Sales Only).

A description is given of the equipment and instrumentation of the FMRB and of its construction and function. Schematic diagrams are given to show the functions of various loops (coolant loops, auxiliary loops, ventilation installations, heavy-water system) and the corresponding control points for temperature, flow, activity, etc. As part of the signal equipment a speaker system and an industrial television device used for control of experiments are mentioned. Moreover, radiation levels in several rooms are controlled by means of stationary gamma radiation and neutron monitoring instruments. (auth) (INIS)

37063 (FMRB-35/71) EXPERIENCE REPORT ON THE OPERATION AND RADIATION PROTECTION AT THE BRAUNSCHWEIG RESEARCH AND MEASUREMENT REACTOR FOR THE YEAR 1970. Heintz, W.; Siegel, V. (Physikalisch-Technische Bundesanstalt, Brunswick (West Germany)). Feb 1971. 35p. (In German). Dep. NTIS (U. S. Sales Only).

The experience in the operation of FMRB and in radiation protection work is reported for the year 1970. No serious problems arose up to now, the generated energy amounting to 1300 MWh. (auth)

37064 (HEDL-SA-81) FTR DRIVER FUEL DEVELOPMENT PROGRAM STATUS. Hanson, J. E.; Roake, W. E. (Hanford Engineering Development Lab., Richland, Wash.). Apr 1971. Contract AT(45-1)-2170. 30p. (CONF-710414-2). Dep. NTIS.

From Conference on fast reactor fuel element technology; New Orleans, La. (13 Apr 1971).

The capability of the FTR driver fuel to perform satisfactorily at the initial operating conditions of the reactor is analyzed. Radiation testing data are reviewed. 6 references. (auth)

37065 (JAERI-Memo-4270) JFM: A CODE FOR THE JMTR FUEL ACCOUNTABILITY. Oyamade, Rokuro (Japan Atomic Energy Research Inst., Tokyo). Dec 1970. 53p. (In Japanese). Dep. NTIS (U. S. Sales Only).

The JFM is a code for accounting the JMTR fuel (except fuel specimen for irradiation test). In programming, an effort was made so that the output of the code can be used as a fuel accountability report for the nuclear fuel section by itself. (auth) (Japan)

37066 (JAERI-Memo-4356) MEASUREMENT OF CENTRAL FISSION RATIOS AND FISSION RATE DISTRIBUTIONS IN FCA. Konishi, T.; Ichimori, T.; Obu, M.; Hirakawa, N. (Japan Atomic Energy Research Inst., Tokyo). Feb 1971. 36p. (In Japanese). Dep. NTIS (U. S. Sales Only).

Measurements of central fission ratios $\sigma_f^{49}/\sigma_f^{25}$, $\sigma_f^{28}/\sigma_f^{25}$ and $\sigma_f^{37}/\sigma_f^{25}$ and the spatial distributions of fission rates in the radial direction have been performed in FCA. Absolute fission counters were employed in the measurement of central fission ratios and the standard deviations of the results were 2 to 4%. The most responsible factor for the final error is the ambiguity of the number of the fissionable atoms contained in the counters. Comparison of measured values with calculated ones suggests that the diffusion calculations with the JAERI-FAST and ABN sets give too many neutrons at high energies. As for the spatial distributions measured with relative counters, the most important point to be considered is how to correct the contributions from undesired isotopes in fission counters. In the blanket region the streaming effect through the experimental hole was observed to give no significant change on the enriched uranium counter response and to increase the natural uranium counter response by about 5% at most. Discrepancies between measured and calculated fission rate distributions can be explained neither by the isotope correction for impurities in fission counters nor by the streaming effect. 16 references. (auth) (Japan)

37067 (LB/G-3001) EXTENSION OF THE EXPERIMENTAL CAPABILITIES OF THE MR REACTOR FOR LOOP-TESTING FUEL ELEMENTS AND MATERIALS. Goncharov, V. V.; Ryazantsev, E. P.; Shavrov, P. I.; Egorenkov, P. M. (Institut Atomnoi Energii, Moscow (USSR)). Translated by R. R. Inston (Atomic Energy Research Establishment, Harwell, Eng.), from report IAE-1925. 26p. (CONF-691060-4). Dep. NTIS (U. S. Sales Only).

From Joint UK/USSR seminar on the operation and use of research and testing reactors; Harwell, England (Oct 1969).

A description is given of the main modifications that have been

XUM

carried out to the MR reactor in order to extend its experimental capabilities. As a result of the modernization of the reactor and other modifications carried out subsequently, the number of loop channels that can be installed in the reactor for testing experimental fuel elements has been more than doubled (from 13 to 27). Since its modernization, the reactor has an available power of 40 MW, or, with the loop channels, 50 MW. 2 references. (auth)

37068 (ORNL-TM-3432) HIGH FLUX ISOTOPE REACTOR QUARTERLY REPORT, JANUARY-MARCH 1971. McCord, R. V.; Corbett, B. L. (Oak Ridge National Lab., Tenn.). 17 May 1971. Contract W-7405-eng-26. 26p. Dep. NTIS.

Operation of the HFIR was routine with an on-stream time of 94.5%. An even higher operating time percentage could have been achieved but one of the four end-of-cycle shutdowns was a "long" shutdown for maintenance and semiannual inspection. Routine usage of fuel elements without plate-spacer combs was started. Operation with these elements was normal and the total system flow rate was higher as expected. (auth)

37069 (ORNL-TM-3453) BULK SHIELDING FACILITY QUARTERLY REPORT, JANUARY-MARCH 1971. Tabor, W. H.; Hurt III, S. S.; Lance, E. D. (Oak Ridge National Lab., Tenn.). 25 May 1971. Contract W-7405-eng-26. 39p. Dep. NTIS.

The BSR operated at an average power level of 1,990 kW for 33% of the time during January, February, and March of 1971. Water-quality control in both the reactor primary and secondary cooling systems was satisfactory. There were two unscheduled shutdowns both of which were caused by shim rods dropping. One was caused by a magnet failure and the other was caused by the length of the on-line magnet test pulse being too close to the magnet release time. Changes were made as authorized by Reactor Instrument and Controls Design Change Memos Nos. BSR-2Mw-27, BSR-2Mw-28, BSR-2Mw-29, and BSR-2Mw-30. The changes were as follows: the replacement of the composite amplifiers with sigma amplifiers; the replacement of the reactor exit-water radiation instrumentation with solid state gamma monitors; the replacement of the unplated armatures with nickel-plated armatures; the replacement of the high-voltage, unplated magnets with low-voltage, high-current, nickel-plated magnets; and the replacement of the magnet amplifiers with solid state module units. The Pool Critical Assembly was not used during January to March and remained in a secured condition. Preparations were started for conducting the annual experiments during the next quarter for the students of the Nuclear Engineering Departments of the University of Tennessee and Mississippi State University. (auth)

37070 (TODD-N-16) 300 POUND GAS TEST REPORT (28-IV-16006). Kenyon, Malcolm H. (comp.) (Todd Shipyards Corp., Galveston, Tex. Nuclear Div.). Apr 1970. Contract AT(45-1)-1830. 50p. Dep. NTIS.

For Battelle Memorial Inst., Pacific Northwest Lab., Richland, Wash.

The 300 Pound Gas Test was conducted as an element in a series of tests to determine the adaptability of the roller nut control rod drive mechanism to employment in an inert gas-Na vapor environment for the FAST Test Reactor program. The mechanism was cycled through 5004 rod-feet in a pure argon atmosphere at 250 to 297°F with a 314-pound drive-line weight. Inspection of the mechanism following the test indicated that: synchronizing and radial bearings, spline shaft bushing, segment arm synchronizing pins, and pivot pins showed no apparent increase in wear; leadscrew, spline shaft, and thrust bearing showed light wear; and roller nuts, inner races, and bearing balls showed considerable wear. It was concluded that variations in roller nut bearing ball diameters and possible roller nut axial tipping following wear of lower inner bearing races and balls were potential causes of high roller nut bearing wear. 5 references. (auth)

37071 (TODD-N-18) 500 POUND GAS TEST REPORT (28-IV-16008). Kenyon, Malcolm H. (comp.) (Todd Shipyards Corp., Galveston, Tex. Nuclear Div.). May 1970. Contract AT(45-1)-1830. 72p. Dep. NTIS.

For Battelle Memorial Inst., Pacific Northwest Lab., Richland, Wash.

The 500 Pound Gas Test was the second test in a series to study the adaptability of the roller nut control rod drive mechanism to use in a Na vapor-inert gas atmosphere. The test mechanism, apparatus, and procedures were essentially the same as described in the 300 Pound Gas Test with the exception of roller nut adjustment. The mechanism was cycled through 3402 rod-feet in a pure argon atmosphere at 250 to 297°F with a 498-pound driveline weight until failure of the antiscram clamp terminated the test at cycle 567. Post-test examination of the mechanism showed that: roller nuts, roller nut lower inner bearing races, and leadscrew had received heavy wear; wear was more uniformly distributed than in the 300 Pound Test; and the leadscrew was out of alignment. Qualitative models based on manufacturer's design specifications were developed, analyzed for predicted wear patterns, and compared with test observations. It was concluded that roller nut axial tipping is a verified phenomenon and indicates a probable point of mechanism failure; and that roller nut adjustment and adherence to design specifications are vitally influential on mechanism wear patterns. 4 references. (auth)

37072 (TODD-N-20) 700 POUND GAS TEST REPORT (28-IV-16009). Kenyon, Malcolm H. (comp.) (Todd Shipyards Corp., Galveston, Tex. Nuclear Div.). May 1970. Contract AT(45-1)-1830. 47p. Dep. NTIS.

For Battelle Memorial Inst., Pacific Northwest Lab., Richland, Wash.

The 700 Pound Gas Test was the third in a series of tests designed to study the adaptability of the roller nut control rod drive mechanism to operation in a Na vapor-inert gas environment. The test mechanism and apparatus were essentially the same as employed in the 300 and 500 Pound Gas Tests. The test mechanism was operated through 5000 feet of rod travel with a 682-pound driveline weight under the same conditions which prevailed during the two preceding tests. The mechanism was disassembled and inspected twice during the test, once at cycle 130 because of improper performance of the anti-scram clamps and again at cycle 201 because of malfunction of the thrust bearing. Post-test inspection indicated component wear patterns readily comparable to those observed in the 500 Pound Gas Test, and appreciably greater in magnitude. It was concluded that the wear models developed in the 500 Pound Gas Test were further verified; that the thrust bearing has been demonstrated to be the first point of mechanism failure; that the principal characteristic of wear during the first 5000 feet of rod travel is the wearing-in of the roller nut assemblies and resultant equalization of load distribution; and that driveline weight-wear correlations were too heavily effected by roller nut adjustment to be conclusive. Wear on roller nut lands as a function of driveline weight was tentatively identified as linear and thrust bearing wear as tentatively exponential. (auth)

37073 (TODD-N-21) SECOND 300 POUND GAS TEST (28-IV-16010). Kenyon, Malcolm H. (comp.) (Todd Shipyards Corp., Galveston, Tex. Nuclear Div.). Jun 1970. Contract AT(45-1)-1830. 31p. Dep. NTIS.

For Battelle Memorial Inst., Pacific Northwest Lab., Richland, Wash.

The Second 300 Pound Gas Test was the fourth test in a series designed to study the adaptability of the roller nut control rod drive mechanism to use in a Na vapor-inert gas environment, and the second test in the series to be run with a 300-pound driveline weight. The test mechanism was cycled without difficulty through an additional 5000 feet of rod travel. No pole slippage, failures, or indications of unreliable operation were encountered. Post-test inspection indicated wear patterns comparable to those observed in the 500 and 700 Pound Gas Tests, and magnitude of wear somewhat less or equal to that measured in the 500 Pound Gas Test. It was concluded that the mechanism showed no signs of imminent failure at 10,000 feet of rod travel. 3 references. (auth)

37074 (TODD-N-23) 500 POUND GAS TEST CONTINUATION SERIES REPORT (28-IV-16011). Kenyon, Malcolm H. (comp.) (Todd Shipyards Corp., Galveston, Tex. Nuclear Div.). Jun 1970. Contract AT(45-1)-1830. 53p. Dep. NTIS.

For Battelle Memorial Inst., Pacific Northwest Lab., Richland, Wash.

The 500 Pound Gas Test Continuation Series consisted of two tests, the Second and Third 500 Pound Gas Tests, designed to study the performance of the roller nut control rod drive mechanism at extended driveline travel in an inert gas atmosphere, using a 500-pound driveline weight. The mechanism was operated through an additional 5000 feet of rod travel without difficulties during the Second 500 Pound Test. The Third 500 Pound Test was terminated after 2646 feet of travel by total failure of the mechanism. Post-test inspection indicated that all four roller nut assemblies had simultaneously failed. It was concluded that diminution of the raceway base thickness of the roller nut lower inner bearing races was the direct cause of failure, that the mechanism remained capable of scramming after failure, and that the life of the mechanism to the point of total failure is on the order of 10,000 rod-feet with a 500-pound driveline load. 5 references. (auth)

37075 (TODD-N-24) GAS TEST SERIES ADDENDUM TESTS AND SYNOPTIC EVALUATIONS (28-IV-16012). Kenyon, Malcolm H. (comp.) (Todd Shipyards Corp., Galveston, Tex. Nuclear Div.). Jun 1970. Contract AT(45-1)-1830. 56p. Dep. NTIS.

For Battelle Memorial Inst., Pacific Northwest Lab., Richland, Wash.

XUM

Description of the details of three additional test series performed as addendums to the Gas Test Series is presented. A synopsis of the most pertinent observations made on the performance of the roller nut control rod drive mechanism during the six major gas tests is also included. The addendum tests were designed to study the effects of varying degrees of thrust bearing wear on the amount of torque required to turn the mechanism rotor, the effects of varying degrees of component wear on mechanism scram response, and the time response behavior of the mechanism during oscillation over short strokes with increasing rod velocities. The torque requirement tests indicated that the 700-pound roller nut/leadscrew combination offered less resistance to rotation than the 300-pound combination; that, generally, increased driveline weight produced a near-linear increase in required torque for each particular test combination; but no clear-cut relationship between thrust bearing wear and required torque was established. The scram response tests indicated that, after a certain point, wear in the roller nut assemblies actually improves scram response and that increased driveline weight reduces segment arm unlatching time. The drive and oscillation response tests indicated that response to a rod travel direction command change is almost wholly dependent on X/Y pulse frequency, reproducibility is poor, and response time is unacceptably slow for Fast Test Reactor applications; that variance in rod travel per count is high, but that reproducibility of travel is within 4 mils; and that the mechanism is limited by pole slippage to rod velocities below 19 inches per minute. The Gas Test Series synopsis discussed overall wear trends observed in the spline shaft; spline shaft bushing; pivot pins and pivot pin holes; synchronizing pins; synchronizing, radial, and thrust bearings; leadscrew; and roller nut assemblies. Design changes for the thrust bearing and roller nut assemblies were outlined, mechanism operating lives were predicted, and the need for changes to the stator and motor programmer for oscillating rod function applications was indicated. 8 references. (auth)

37076 (UARAEE-59) DETERMINATION OF THE EPITHERMAL NEUTRON SPECTRUM SHAPE IN UA-RR-1 REACTOR. Sabek, M. G.; Hamouda, I. (Atomic Energy Establishment, Cairo (Egypt). Reactor and Neutron Physics Dept.). 1968. 22p. Dep. NTIS (U. S. Sales Only).

The shape of the epithermal neutron spectrum was determined by a method based on comparison of the epithermal indices r_1 measured by different resonance detectors. This method helps to compare the actual epithermal neutron spectrum with a 1/E distribution. The energy range covered is from 1.46 to 400 eV. The detectors used were ^{115}In, ^{197}Au, ^{186}W, ^{59}Co and ^{100}Mo with resonances at 1.46, 4.90, 18.8, 132, and 367 eV respectively. The measurements were done in wet channel 24/5, displacer 5/10 and dry channel 36/6. It was found from the measurements that the epithermal neutron spectrum shape in these locations deviates slightly from the 1/E shape. 11 references. (auth)

37077 (UARAEE-63) NEW APPROACH FOR CALCULATIONS OF NUCLEAR FUEL CONSUMPTION IN THE UA-RR-1 CORE. El Mofty, O. H.; Pelepets, D. T.; Zaalouk, M. G.; Mitry, A. M. (Atomic Energy Establishment, Cairo (Egypt). Reactors Dept.). 1968. 76p. Dep. NTIS (U. S. Sales Only).

A new approach for fuel burnup calculation in UA-RR-1 is introduced. This approach is based on a known flux mapping and its variation with successive loading periods and also variable ^{235}U concentration. The calculation of burnup was carried out for the period from the reactor startup on 3/8/1961 to 5/6/1967. The calculations were carried out for every loading period of operation with unchangeable reactor core configuration. The results of calculations for fuel burnup are given in absolute quantity (gms) and per cent to the initial quantity of fuel ^{235}U in the fuel assembly. Also the total quantities of burnup by the end of each loading period of operation are given. The specific power (kw/kg ^{235}U) is presented for the UA-RR-1 during each loading period of operation. The per cent fuel burnup is presented as a function of the integral neutron flux. (auth)

37078 (UARAEE-67) CRITICAL MASS CALCULATION FOR UA-RR-1 REACTOR. Girgis, R.; Hamouda, I.; Karchava, G. (Atomic Energy Establishment, Cairo (Egypt). Reactor and Neutron Physics Dept.). 1968. 52p. Dep. NTIS (U. S. Sales Only).

A simple method to calculate water-type reactor critical parameters is presented. A combination of the two-group critical equation and four-factor formula was used as a basis for the method developed. The results of the UA-RR-1 reactor critical mass calculation as a function of lattice pitch are reported. A comparison between the calculated and experimental values yields satisfactory agreement. 39 references. (auth)

37079 (UARAEE-71) NUMERICAL STUDY OF FAST NEUTRON SPECTRA IN UA-RR-1 REACTOR CORE AND REFLECTOR. Girgis, R.; Hamouda, I.; Karchava, G. (Atomic Energy Establishment, Cairo (Egypt). Reactor and Neutron Physics Dept.). 1969. 19p. Dep. NTIS (U. S. Sales Only).

The results of fast neutron spectrum calculations in the UA-RR-1 reactor core and water reflector are summarized. Leakage from the core and reflector is found with the method suggested by Perkins. The approximate Greuling-Goertzel kernel is applied to the slowing-down equation. The results are compared with those obtained with a more rigorous approach. 15 references. (auth)

37080 (UARAEE-73) EFFECT OF DIFFERENT REFLECTORS ON UA-RR-1 REACTOR CORE CHARACTERISTICS. Abd-El-Samie, Sh.; Karchava, G. (Atomic Energy Establishment, Cairo (Egypt). Reactors Dept.). 1969. 54p. Dep. NTIS (U. S. Sales Only).

The effect of different reflectors on the main core characteristics of the UA-RR-1 reactor (water-type research with enriched fuel) is studied. The one and two-layer reflectors are considered. Ordinary water, heavy water, graphite and beryllium are investigated as a reflector material. The problem is solved in the two-group diffusion approximation by an IBM-1620 computer; the computer codes are given. The results obtained can be utilized in early stages of reactor design. (9 references) (auth)

37081 (UARAEE-83) EFFECT OF NON-UNIFORM BURN UP ON REACTOR LIFETIME. Sallam, O. H.; Karchava, G. A.; Hamouda, I. (Atomic Energy Establishment, Cairo (Egypt). Reactor and Neutron Physics Dept.). 1969. 24p. Dep. NTIS (U. S. Sales Only).

The influence of the fuel non-uniform burn up on the reactor lifetime was considered with the aid of perturbation theory. All numerical estimations were carried out in the two-group diffusion approximation for the UA-RR-1 reactor. 12 references. (auth)

37082 (UARAEE-94) PRELIMINARY REPORT ON THE AUTOMATIC START-UP SYSTEM FOR THE WWR-S. Sicivitch, I.; Azer, M. S.; Saleh, S. A. (Atomic Energy Establishment, Cairo (Egypt). Reactors Dept.). 1970. 18p. Dep. NTIS (U. S. Sales Only).

In research reactors where it is required to operate and shut down many times each day, it is preferable to have an automatic start-up system. This overcomes the difficulties of continuous power and period monitoring by the operator. A good automatic start-up system will also eliminate the possibility of scram due to inadequate rod motion which is liable in manual start-up. A schematic diagram and preliminary block diagrams for such a system are presented. (auth)

37083 (UARAEE-108) AUTOMATIC START-UP SYSTEM FOR THE UA-RR-1 REACTOR. Hassan, M. A.; Sicevitch, I. G.; Azer, M. T.; Abd-El-Megid, F. M.; Shinaishin, M. A.; Saleh, E. A. (Atomic Energy Establishment, Cairo (Egypt). Reactors Dept.). 1971. 39p. Dep. NTIS (U. S. Sales Only).

An automatic start-up system (ASS) designed and implemented for the UA-RR-1 is described. This ASS brings the reactor from deep subcriticality up to a certain criticality which sustains a required preset period. This period if fixed and power goes up to the required level; then the regulating loop is swiched on automatically to stabilize at this level. This ASS is simply a set of logic and sequencing circuits controlling the different standard components. New instruments were needed such as null organ and middle indicator, which were developed using transistors. (auth)

37084 (UARAEE-111) ESTIMATE FOR UAR RESEARCH REACTOR THERMAL INERTIA. Gaddis, E. S.; Fouad, H. Y.; Aboul-Fetouh, M. (Atomic Energy Establishment, Cairo (Egypt). Reactors Dept.). 1971. 16p. Dep. NTIS (U. S. Sales Only).

An estimate for UAR research reactor thermal inertia was obtained through experimental measurements of the transient conditions during variation of power. The coolant time constant was found to be 450 seconds, and the corresponding equivalent thermal inertia was 16.5 tons of water inside the reactor core and 28 tons of water in the whole primary circuit. (auth)

37085 (WHAN-SA-104(Rev.)) FFTF: COMPANION TEST AND DEVELOPMENT FACILITY FOR THE LMFBR PROGRAM. Gajewski, W. M.; Esselman, W. H.; Wolfe, B.; Taylor, J. J. (Hanford Engineering Development Lab., Richland, Wash.). [1970]. Contract AT(45-1)-2170. 21p. (CONF-710315-1). Dep. NTIS.

From Conference on fast reactors, Palo Alto, Calif. (7 Mar 1971).

The Fast Flux Test Facility is the reactor test complex which will be used to aid in the solution of the fuels and materials prob-

XUM

lems which are most critical to the development of a liquid metal cooled fast breeder reactor (LMFBR). The FFTF and its design features, including those that are unique to this test facility and those which are prototypic of expected future LMFBR's, are described. The operation of the FFTF is also discussed. (auth)

37086 NOISE MEASUREMENTS IN A SUBCRITICAL FACILITY BASED ON PHOTON DETECTION. Baers, B.; Markkanen, E. (Technical Univ. of Helsinki, Otaniemi, Finland). Kernenergie; 14: No. 2, 39-42(Feb 1971).

The relaxation effects associated with the spontaneous fluctuations in the neutron population and in gamma-ray emission in a subcritical nuclear reactor have been investigated based on gamma counting techniques. Estimates for the main relaxation constant (Rossi-α) could be obtained from the detection of the high-energy photon radiation with scintillation detectors both inside and in the vicinity of the reactor system. The relaxation effects obtained from out-of-pile measurements in the facility are on average faster than those obtained from photon detection inside the core. The main decay constant obtained from neutron detection in the center of the core is the smallest. The differences between the obtained relaxation effects arise from the longer relaxation length of gamma radiation compared to neutrons and from the space effects in a large facility. The detectability of the correlated noise with gamma-sensitive detectors, especially in out-of-pile measurements, is of substantial interest since it obviously opens up a wide range of practical applications. (7 references) (auth)

37087 COLD NEUTRON SOURCE OF THE FRENCH-GERMAN HIGH FLUX REACTOR IN GRENOBLE. Ageron, P.; Verdier, J. (CEA, Grenoble, France); Ewald, R.; Harig, H. D. Energ. Nucl. (Paris); 13: No. 1, 15-21(Jan-Feb 1971). (In French).

The Franco-German High Flux Reactor in Grenoble will be equipped with a cold neutron source using about 25 liters of liquid deuterium. The thermal power to be removed from this cold source will be about 7 kW at 25°K and the beam intensity for neutrons of 0.005 eV (4 Å) for example, is evaluated to be $3.5 \cdot 10^{15}$ n.s.$^{-1}$ · cm^{-2} · sterad^{-1} · eV^{-1}. The reasons for the choice of such an unusual cold moderator are given, and the essential parts and working principles of this equipment are described. Some problems which ought to be solved for the conception of the device, mainly those in regard with safety, are discussed. (auth) (France)

Rocket and Space Reactors

Refer also to abstracts 35549 and 35937.

37088 NERVA TECHNOLOGY REACTOR INTEGRATED WITH NASA LEWIS BRAYTON CYCLE SPACE POWER SYSTEMS. Boman, L. H.; Gallagher, J. G. (Westinghouse Astronuclear Lab., Pittsburgh). J. Spacecraft Rockets; 8: No. 5, 500-5(May 1971).

A conceptual design of this 2.2 MW reactor has been performed to permit integration with power conversion units which are in an advanced state of development. The reactor has flexibility for application with 25 to 600 KW(e) space power systems. Design concepts and methods utilized were developed in the NERVA program. Uranium bearing graphite fuel elements, utilizing fuel particles developed for commercial power reactors, form a cylindrical core, reflected radially, and at the inlet end by beryllium. It is controlled by rotating control drums located in the radial reflector. A manned space-base system design concept, including shielding analysis, is also discussed. 15 references. (auth)

37089 NUCLEAR SHUTTLE FOR INTERORBITAL AND TRANSPLANETARY APPLICATIONS. Johnson, Kurt P.; Holl, Richard J. (McDonnell Douglas Astronautics Co., Huntington Beach, Calif.). J. Spacecraft Rockets; 8: No. 6, 600-6(Jun 1971).

A reusable nuclear shuttle (RNS) operating out of low Earth orbit is a major element of the planned space program to provide low-cost transportation beyond Earth orbit. RNS concepts based on the 75,000 lb-thrust NERVA engine are identified which range from a large single module launched by a Saturn INT-21 to highly modularized concepts configured to be launched by the space shuttle and assembled in orbit. Operations and system implications for orbital maintenance and tanking are described. Maintenance by large-scale module replacement and direct propellant resupply by the space shuttle eliminate the requirement for expensive, permanent, manned orbital support facilities. The economic premium for reusability is established and sensitivity shown for various system parameters. The impact of the RNS and its radiation environment on associated system elements is discussed. (4 references) (auth)

37090 POWER LIMITATIONS OF AN IN-CORE THERMIONIC CELL IN STEADY-STATE OPERATION. Haug, W.; Wolf, E. (Univ., Stuttgart). Atomkernenergie; 17: No. 4, 261-6(Jul 1971). (In German).

The thermal and electrical characteristics of an incore-thermionic cell are determined with the help of a theoretical model in the steady state. For this purpose, a numerical method was developed using the analytical solution of the heat conduction problem for the cylindrical emitter body. The electrical cell data are computed by means of a converter model reported by Rasor. The limitation of electrical power output by a maximum emitter surface temperature and a maximum permissible heat generation rate is studied. 12 references. (auth)

Process Heat and Desalination Reactors

37091 (ORNL-TM-3402) ABSTRACTS OF PAPERS: DESALINATION INFORMATION MEETING, MAY 27-28, 1971. Hammond, R. P.; Johnson, J. S. (Oak Ridge National Lab., Tenn.). May 1971. Contract W-7405-eng-26. 56p. Dep. NTIS.

Abstracts are presented for 22 papers on the topics of nuclear desalination and water research. (D.C.C.)

37092 PRESENT STATUS OF MULTI-PURPOSE HIGH-TEMPERATURE GAS-COOLED REACTOR. Ishiwata, Hiroshi (Ministry of International Trade and Industry, Tokyo). Taikabutsu; 22: No. 10, 483-6(Oct 1970). (In Japanese).

In Japan, the energy consumption for iron making is tremendous: about 90% of coal is imported, while 25% of total electric power for industries is consumed by iron making. The pattern of nuclear energy utilization, and then the power generation with nuclear energy in Japan and other countries are reviewed. Multipurpose utilization of nuclear reactors is discussed. Room heating, process steam, and desalination in the world are reviewed. Description of HTGR type reactor for process heat utilization is given. In the particular circumstances in Japan, the iron making with nuclear reactors utilizing gas reduction is very attractive. (Japan)

Marine and Portable Power Reactors

37093 (CEA-CONF-1750) ANALOG STUDY OF PROPULSION POWER REACTORS. Boulven, J. (Commissariat a l'Energie Atomique, Saclay (France). Centre d'Etudes Nucleaires). 12 Feb 1971. 35p. (In French). (CONF-710214-1). Dep. NTIS (U. S. Sales Only).

From Meeting on nuclear reactors for marine propulsion; Malakoff, France (17 Feb 1971).

The analog and hybrid computer laboratory of Saclay has extensively studied ship propulsion reactors. The scheme of the physical model retained for the simulation (the core and the thermal circuits of the reactor constitute the principal parts), the physical equations, the analog study, and the program are presented. In spite of the large number of analog elements envisaged, resolution does not present any difficulties. An accuracy of about 1% was achieved. (France)

37094 (DOCKET-50238-80) N. S. SAVANNAH. Operations Report, November 9, 1970-March 31, 1971. (Maritime Administration, Washington, D. C.). 2 Jun 1971. 9p. Dep. NTIS.

37095 (IRS-T-18(1970), pp 217-21) RELIABILITY ANALYSES OF REACTOR SYSTEMS FROM THE VIEW OF PRODUCER AND OPERATOR. Ulken, D.; Kuehl, H. (Technischer Ueberwachungs-Verein e. V., Cologne (West Germany). Institut fuer Reaktorsicherheit). 1970. (In German). NTIS (U. S. Sales Only).

The maintenance of plant reliability in ship navigation depends largely on the experience and the technical skill of the operations engineer. Reliability analysis offers him and the shipowner a possibility of exact control of the plant and of optimum utilization of the invested capital. It provides the basic requirements for application of nuclear propulsion to ships with a long period of service and economical utilization. The findings of the first reliability technique applied to "N. S. Otto Hahn" will be made available to the manufacturers of nuclear ships. (INIS)

37096 LEGAL STANDARDS FOR NAVIGATION OF NUCLEAR SHIPS. de los Santos Lasuretgui, Alfonso; Palomo, Luz Corretjer (Junta de Energia Nuclear, Madrid). Energ. Nucl. (Madrid); 15: No. 69, 41-51(Jan-Feb 1971). (In Spanish).

The navigation of nuclear ships requires legal standards different from those that regulate the navigation of conventional ships. In turn, these standards, while forming part of what is called "Nuclear Law," have to be distinct from those that apply to fixed installations or to the transport of nuclear substances. This is the reason that there have been so many arrangements in connection with these ships, in spite of the small number of them, including two multilateral conventions and various bilateral accords as well as much national legislation occupied with the legal problems that surround nuclear ships. (tr-auth)

37097 ROUGH PASSAGE FOR NUCLEAR SHIPS? Clutterbuck, D. New Sci. Sci. J.; 50: No. 751, 379-81(13 May 1971).

A review is given of the present status of nuclear propelled ships, with emphasis on economic comparisons, and the plans of Germany, Japan, the United States and the UK. Diplomatic difficulties are also discussed. While Germany and Japan are making ambitious plans, the United States and UK are showing reticence. (UK)

37098 SPECIAL CONSTRUCTION, ARRANGEMENT, AND OTHER PROVISIONS FOR NUCLEAR VESSELS. 46 CFR 37 1968. Washington, D. C.; Superintendent of Documents, GPO (1968). 2p. Available from Superintendent of Documents, GPO, Washington, D. C.

Requirements for the design, construction, inspection, certification, safety, and operation of ships utilizing nuclear energy for propulsion or for any other purpose are presented. (H.D.R.)

37099 PIPING SYSTEMS AND APPURTENANCES. 46 CFR 56 1968. Washington, D. C.; Superintendent of Documents, GPO (1968). 30p. Available from Superintendent of Documents, GPO, Washington, D. C.

Specific limitations or modifications to USASI Code B31.1 for pressure and power piping to apply to ships and barges are presented. (H.D.R.)

37100 SPECIAL CONSTRUCTION, ARRANGEMENT, AND OTHER PROVISIONS FOR NUCLEAR VESSELS. 46 CFR 79 1968. Washington, D. C.; Superintendent of Documents, GPO (1968). 2p. Available from Superintendent of Documents, GPO, Washington, D. C.

Requirements for the design, construction, inspection, certification, safety, and operation of ships utilizing nuclear energy for propulsion or for any other purpose are presented. (H.D.R.)

37101 SPECIAL CONSTRUCTION, ARRANGEMENT, AND OTHER PROVISIONS FOR NUCLEAR VESSELS. 46 CFR 99 1968. Washington, D. C.; Superintendent of Documents, GPO (1968). 3p. Available from Superintendent of Documents, GPO, Washington, D. C.

Requirements for the design, construction, inspection, certification, safety, and operation of ships utilizing nuclear energy for propulsion or for any other purpose are presented. (H.D.R.)

37102 PROVISIONAL RULES FOR THE CLASSIFICATION OF NUCLEAR SHIPS. London; Lloyd's Register of Shipping (1965). 9p. Available from Lloyd's Register of Shipping, London.

Criteria for the design, fabrication, and operation of ships equipped with nuclear reactors for main propulsion are presented. Requirements are included for the hull, pressure vessels and components, reactor engineering, reactor control, complementary installations, and maintenance. (H.D.R.)

Production Reactors

37103 (BNWL-1507) ANALYSIS OF THE EFFECT OF POTENTIAL REACTOR COOLING PONDS ON THE HANFORD GROUNDWATER SYSTEM. Cearlock, D. B.; Mudd, R. D.; Reisenauer, A. E. (Battelle-Northwest, Richland, Wash. Pacific Northwest Lab.). Sep 1970. Contract AT(45-1)-1830. 20p. Dep. NTIS.

The distances separating the groundwater table (peizometric surface) from overlying waste storage tanks, cribs, trenches and swamps are an important factor in the Hanford chemical processing waste management program relative to radiological considerations. Any project that affects the Hanford groundwater system requires an evaluation to determine its effect on present and future waste management practices. Likewise, hydrological considerations are important in relation to nuclear plant siting studies at Hanford. Although a number of alternatives are available for cooling such plants, the use of cooling ponds will receive serious review due to economic and environmental factors. The potential for large seepage losses from the ponds to the groundwater system exists. These seepage losses could have a significant influence on the groundwater system and hence affect current chemical processing waste management programs. The effect on pond seepage on the groundwater system should be evaluated in conjunction with other hydrologic and geologic criteria prior to detailed siting studies. A test case involving three hypothetical unlined cooling ponds was proposed for study. An analysis of the hydrological effects of the hypothetical ponds on the Hanford groundwater system is presented. The effects of the hypothetical ponds on the Hanford groundwater system are analyzed. Also the effects in the region of the chemical processing plants in the 200 East and 200 West areas are discussed. (auth)

37104 (BNWL-SA-3713) EFFECT OF THERMAL HISTORY ON THE RESISTANCE OF COLUMBIA RIVER STEELHEAD T TROUT (SALMO GAIRDNERI) TO THERMAL STRESS. Schneider, Mark J.; Templeton, W. L. (Battelle-Northwest, Richland, Wash. Pacific Northwest Lab.). [1971]. Contract AT(45-1)-1830. 20p. (CONF-710501-14). Dep. NTIS.

From third national symposium on radioecology; Oak Ridge, Tenn. (10 May 1971).

Steelhead trout eggs were hatched and the fish raised for two years according to the temperature regime: ambient Columbia River temperature, ambient river temperature plus 1.7, 2.2, and 2.6°C. At the end of the two year period the four temperature classes were tested for thermal resistance to three lethal temperatures: 25.0, 27.0, and 29.0°C. Significant differences were found between temperature classes in the time to thermal death but not in the time to loss of equilibrium. Acclimation of a portion of each temperature class to a common 12°C removed the difference in thermal death times. 9 references. (auth)

37105 (BNWL-SA-3876) ECOLOGICAL EVALUATION: MIGRATION OF JUVENILE SALMON IN RELATION TO HEATED EFFLUENTS IN THE CENTRAL COLUMBIA RIVER. Becker, C. Dale; Coutant, Charles C.; Prentice, Earl F. (Battelle-Northwest, Richland, Wash. Pacific Northwest Lab.). [1971]. Contract AT(45-1)-1830. 26p. (CONF-710501-5). Dep. NTIS.

From third national symposium on radioecology; Oak Ridge, Tenn. (10 May 1971).

Field investigations to evaluate the effects of heated reactor discharges on juvenile salmonids passing seaward through the central Columbia River at Hanford were conducted from March to September, 1968 and 1969. Test fish held in liveboxes were drifted through the discharge areas while the encountered thermal dose (i.e., temperature increase and exposure duration) was monitored. Some mortalities resulted in shoreline drifts through areas receiving heated water via intragravel seepage from effluent retention basins. Mortalities during drifts through the main discharge plumes in midriver were insignificant except under late summer conditions. The contrasting effects between the two sites were due primarily to differences in effluent mixing patterns. Environmental features regulating thermal effects, which varied over the migration season, were prevailing river temperatures (4 to 20°C) and discharges (40,000 to 200,000 ft^3/sec). Four seasonal combinations occurred in sequence with increasing potential for thermal damage: low temperature and low discharge (early spring), low temperature–high discharge (late spring), high temperature–high discharge (early summer), and high temperature–low discharge (late summer). Juvenile salmonids produced in the Hanford area migrate seaward from April to July when low river temperatures and(or) high discharges are favorable, but delayed migrants originating above Hanford encounter less favorable conditions in July and August. 13 references. (auth)

37106 (DP-1259) IODINE RETENTION STUDIES. Progress Report, January–June 1970. Evans, A. G.; Jones, L. R. (Du Pont de Nemours (E. I.) and Co., Aiken, S. C. Savannah River Lab.). May 1971. Contract AT(07-2)-1. 24p. Dep. NTIS.

In tests simulating exposure conditions of the confinement system following power surge and loss-of-coolant accidents, the iodine retention efficiencies of carbon samples were measured. In both tests, the iodine retention efficiency decreased with increased carbon service, but was within specification for up to 42 months of service. In methyl iodide radiolysis tests, a gamma radiation field of $\sim 1.7 \times 10^7$ rads/hr did not significantly extend the effectiveness of carbon for methyl iodide adsorption. 10 references. (auth)

Reactor Theory

Refer also to abstract 37081.

XUM

37107 (INDC(NDS)-29/U) ASPECTS OF CRITICAL EVALUATION OF NUCLEAR DATA INFORMATION. Schmidt, J. J. (International Nuclear Data Committee). Dec 1970. 12p. (CONF-700949-1). Dep. NTIS (U. S. Sales Only).

From second international CODATA conference; St. Andrews, Scotland (7 Sep 1970).

Some aspects of critical evaluation of nuclear data information are discussed, particularly in relation to the data needs of nuclear-reactor designers. These aspects comprise filling gaps in experimental data, establishing and guaranteeing inner consistency among evaluated data, and detecting and removing systematic errors of experimental data. Recently, a unique computer format called EXFOR for the coding and international exchange of experimental neutron data information has been developed in a cooperative effort of the four world neutron data centers at Brookhaven, Obninsk, Saclay (ENEA), and Vienna (IAEA). This system will not only contain the experimental data together with statistical and systematic errors and the pertinent bibliographic information, but also additional detailed physical information related to the measurement conditions. These should alleviate the critical assessment and comparison of experimental data, particularly as an auxiliary tool for the evaluator. (auth)

37108 (UARAEE-52) ENERGY DISTRIBUTION OF MODERATOR ATOMS IN REACTORS. Fouad, H. Y.; El-Sayed, M. N. (Atomic Energy Establishment, Cairo (Egypt). Reactors Dept.). 1968. 25p. Dep. NTIS (U. S. Sales Only).

The velocity spectrum of moderator atoms obtained is to be used in evaluating the thermal neutron energy spectrum. It is derived by classical mechanics considering molecules to be hard spheres, interacting only through a billiard ball scattering. (auth)

37109 (UJV-2423-RF) DETERMINING REACTOR SPECTRA OF FAST NEUTRONS FROM THRESHOLD DETECTOR MEASUREMENTS. Svec, P.; Kadlec, V. (Ceskoslovenska Akademie Ved, Rez. Ustav Jaderneho Vyzkumu). 1970. 36p. (In Slovak). NTIS (U. S. Sales Only).

Methods described in literature and used to determine reactor spectra of fast neutrons from threshold detector measurements are reviewed. A mathematical discussion is given of five selected procedures tested on four model spectra. The effect of detector selection and of the number of detectors in a set on the correct plotting of measured spectra was investigated as was the effect of errors in absolute detector activities on the resulting spectrum. The following threshold reactions were used: $^{237}Np(n,f)$, $^{232}Th(n,f)$, $^{103}Rh(n,n')^{103m}Rh$, $^{115}In(n,n')^{115m}In$, $^{32}S(n,p)^{32}P$, $^{58}Ni(n,p)^{58}Co$, $^{27}Al(n,p)^{27}Mg$, $^{31}P(n,p)^{31}Si$, $^{56}Fe(n,p)^{56}Mn$, $^{28}Si(n,p)^{28}Al$, $^{24}Mg(n,p)^{24}Na$, $^{27}Al(n,\alpha)^{24}Na$. All computations were performed by a GIER computer; a description of input data for all programs is included. (auth) (INIS)

37110 DETERMINATION OF THE FAST FISSION FACTOR OF METALLIC BERYLLIUM AND OF BeO WITH THE AID OF PULSED MEASUREMENTS. Demmeler, M.; Hecker, R. (Kernforschungsanlage, Juelich, Ger.). Atomkernenergie; 17: No. 4, 223-8(Jul 1971).

With the method of a pulsed neutron source the Watt-spectrum-averaged fast-fission factor ϵ of different-sized Be- and BeO-probes was measured and compared with calculated values. The fission neutron-source was realized by a ^{235}U covered Cd-absorber, excited by the thermal neutron field in the Be-layers. Results were found to be $\epsilon_{Be} = 1.078 \pm 0.003$ and $\epsilon_{BeO} = 1.051 \pm 0.002$. 24 references. (auth)

Kinetics

Refer also to abstracts 36647, 36648, 36650, 36651, 36987, 36991, and 36992.

37111 (BNWL-1560) DERIVATION OF CORRECTIONS TO K_∞ IN THE TWO-GROUP APPROXIMATION. Lippincott, E. P. (Battelle-Northwest, Richland, Wash. Pacific Northwest Lab.). May 1971. Contract AT(45-1)-1830. 17p. Dep. NTIS.

An improved derivation of the correction terms necessary to evaluate k_∞ from experimental data in the unpoisoned and poisoned techniques is presented. Earlier derivations are extended to include epithermal fissions and correct minor errors in the earlier results. A new formula for k_∞ is derived in which the buckling has been eliminated in order to allow a more accurate value of k_∞ to be determined. 4 references. (auth)

37112 (GEAP-13672) SYN: OPERATIONAL ASPECTS OF THE COMBINED BISYN, PERT, AND BICYCL SYNTHESIS CODES. Kelley, M. D. (General Electric Co., Sunnyvale, Calif. Breeder Reactor Development Operation). Dec 1970. Contract AT-(04-3)-189. 193p. Dep. NTIS.

SYN contains two major segments, BISYN and BICYCL. The BISYN segment solves the two-dimensional multigroup neutron diffusion theory equations in r,z or x,y geometry using a noniterative synthesis method. This approach is designed to greatly reduce the computer cost of running two-dimensional multigroup problems at the risk of some loss in accuracy of the detailed flux distribution. This segment also contains a perturbation and effective delayed neutron fraction calculation. The BICYCL segment uses output from BISYN to solve the one-group neutron depletion equations. BICYCL allows the user to search on makeup or recycle isotopic compositions for a first cycle of a first core or for equilibrium concentrations. It also has provisions for fuel shuffling and the option to cycle back to BISYN in order to update the fluxes, one-group cross sections, etc. 7 references. (auth)

37113 (IN-1435) PHROG: A FORTRAN IV PROGRAM TO GENERATE FAST NEUTRON SPECTRA AND AVERAGE MULTIGROUP CONSTANTS. Curtis, R. L.; Singer, G. L.; Wheeler, F. J.; Grimesey, R. A. (Idaho Nuclear Corp., Idaho Falls). Apr 1971. Contract AT(10-1)-1230. 111p. Dep. NTIS.

PHROG is a computer code to generate energy dependent fast neutron spectra and associated average multigroup cross section data suitable for use in diffusion and transport theory reactor design analysis. The code recursively solves either a B-1 or P-1 approximation to the energy dependent transport equation utilizing cross section data obtained from a library. Logic has been incorporated to calculate both resolved and unresolved resonance data to complement the library absorption and fission data where necessary. In conjunction with the resonance calculation, an option is also available to calculate a Dancoff-Ginsburg correction factor to account for pin shadowing. The code generates up to 40 broad groups of average cross section data utilizing a 68 fine group cross section library covering an energy range from 10 MeV to .414 eV and containing data for approximately 200 materials. The code contains options for the punching of cross section and spectral data for use in future problems or in other codes. The code is written in FORTRAN and is presently operating on an IBM 360/75. A typical problem generally requires less than one minute of CPU time. 21 references. (auth)

37114 (JAERI-Memo-4276) ABSOLUTE POWER MEASUREMENT BY REACTOR NOISE ANALYSIS. Nakata, Hirokatsu (Japan Atomic Energy Research Inst., Tokyo). Jan 1971. 29p. (In Japanese). Dep. NTIS (U. S. Sales Only).

Experimental results are described on the measurement of absolute reactor power by reactor noise analysis. Reactor power is obtained by analyzing the power spectral density of output current from detector located near a reactor core. Reactor power was measured in the range from 50 mW to several hundreds watts and the effect of detector location appeared to be unimportant. Power measured by this method was smaller than power measured by the flux integral method by a factor 0.86. The power meter of JMTR was calibrated by this method before increasing power level. Thermal power was greater than power indicated by the power meter by a factor 1.12. (auth) (Japan)

37115 (RISO-234) THE NEUTRON RESONANCE REACTIONS IN THERMAL NUCLEAR REACTORS DETERMINED BY SEMI-ANALYTIC AS WELL AS NUMERICAL METHODS. Mikkelsen, Joern (Danish Atomic Energy Commission, Risoe, Research Establishment). Nov 1970. 168p. Dep. NTIS (U. S. Sales Only).

Thesis.

Methods for calculation of the neutron resonance reactions in thermal nuclear reactors are developed, verified against experiments, and mutually compared. The intention is partly to demonstrate the potential of modern computation technique in this field and partly to select those methods among the primitive approximations that show the best agreement with sophisticated calculations. The methods investigated comprise intermediate resonance semi-analytic methods, statistical treatments, and numerical heterogeneous or homogeneous slowing-down calculations with resonance overlap included or excluded. The influence of detailed spatial flux distributions, the accuracy of the equivalence principles, and methods of constructing effective group cross sections from simple resonance-integral tabulations receive special attention. It is concluded that the best way to profit from the improved resonance reaction treatments in standard multigroup reactor computation is to make use of tabulations such as those just mentioned. Apart from summarizing these studies, the report describes the RESAB program system developed in connection with the investigation. (auth)

37116 (UARAEE-56) ON THE ONE-GROUP CONSIDERATION OF MILNE PROBLEM. Hussein, A.; Novikov, A.; El-Konsol, S.; Hamouda, I. (Atomic Energy Establishment, Cairo (Egypt). Reactor and Neutron Physics Dept.). 1968. 40p. Dep. NTIS (U. S. Sales Only).

A brief review of the investigations of the Milne problem for thermal neutrons is presented. The presentation is restricted to the consideration of non-multiplying media and plane boundary with vacuum. The review is devoted to the study of neutron flux behavior at the boundary (extrapolation distance and space-angular flux distribution) in the one-group consideration. First, the solution of Milne's integral equation is given for an extremely simple case of a source-free, non-absorbing infinite halfspace with isotropic scattering. Then the corrections, stipulated by the presence of absorption, sources, anisotropy of scattering and finiteness of medium are considered. Wherever possible, comparison between calculations and experimental data is given. 28 references. (auth)

37117 (UARAEE-58) THEORY FOR ASSYMETRIC ARRAY OF CYLINDRICAL CAVITIES INSIDE A REACTOR CORE. Zaalouk, M. G.; Michaiel, M. L. (Atomic Energy Establishment, Cairo (Egypt). Reactors Dept.). 1968. 14p. Dep. NTIS (U. S. Sales Only).

A generalized theory describing the flux distribution inside a core containing an asymmetric array of cylindrical water cavities with different dimensions is presented. The two group model is used to derive the critical determinant in such cores. The choice of the 2 group analysis was made after it was proven to be satisfactory in previous work on one eccentric square cavity. Special cases of one central cavity, one eccentric cavity, a ring of cavities with no central one, and a ring of cavities with a central cavity are presented. (auth)

37118 (UARAEE-62) GENERAL REVIEW OF THERMAL NEUTRON SPECTRA INVESTIGATIONS. Elkonsol, S.; Novikov, A.; Hussein, A.; Hamouda, I. (Atomic Energy Establishment, Cairo (Egypt). Reactor and Neutron Physics Dept.). 1968. 58p. Dep. NTIS (U. S. Sales Only).

Experimental investigations of thermalization by thermal-neutron-spectra measurement are reviewed. The work is aimed at giving a general idea of the problem. The references, including books, reviews, and original articles on thermalization, while not complete, are believed to be sufficient to be used as a basis for a systematic study of the subject. (129 references) (R.W.R.)

37119 (UARAEE-64) THERMAL UTILIZATION CALCULATION WITH NEW ASYMPTOTIC DIFFUSION THEORY. Girgis, R.; Hamouda, I.; Karchava, G. (Atomic Energy Establishment, Cairo (Egypt). Reactor and Neutron Physics Dept.). 1968. 38p. Dep. NTIS (U. S. Sales Only).

The methods and results of thermal utilization factor calculation with the new asymptotic diffusion theory suggested by Clark and Pomraning are presented. The values obtained are compared to those found with ordinary diffusion theory. A three-zone cylindrical cell is considered with a variable radius of the third zone that corresponds to the variation of the reactor lattice pitch. 35 references. (auth)

37120 (UARAEE-69) NUMERICAL SOLUTION FOR THE THERMAL FLUX SPECTRUM IN A MONATOMIC MODERATOR. Fouad, H. Y.; Nasr, M. (Atomic Energy Establishment, Cairo (Egypt). Reactors Dept.). 1968. 13p. Dep. NTIS (U. S. Sales Only).

The thermal spectrum in a monatomic moderator is calculated by means of a Wigner–Wilkins differential equation for different degrees of absorption. The resulting spectrum is approximated by a Maxwellian one at an effective temperature "T_m" given by an empirical formula of the form $T_m = T_0 [1 + A \{\Sigma_a(T)/\Sigma_s\}]$ and the constant "A" was evaluated as 1.269911. (auth)

37121 (UARAEE-70) EFFECT OF PITCH VARIATION ON NUCLEAR PROPERTIES OF LIGHT WATER ASSEMBLIES USING EK-10 FUEL RODS. Fouad, H. Y.; Khazragui, A. M. (Atomic Energy Establishment, Cairo (Egypt). Reactors Dept.). 1968. 27p. Dep. NTIS (U. S. Sales Only).

Some characteristics and nuclear properties of enriched uranium light water moderated lattices were investigated as a function of the lattice pitch. The lattice pitch was changed in a broad range from 1 cm to 3 cm. Fuel elements, type EK-10, were considered which are enriched to 10%, containing 8 gm ^{235}U per element, having diameter and length of 7 mm and 500 mm respectively, canned in aluminium tube with a wall thickness of 1.5 mm. Critical dimensions and masses of these lattices were investigated applying a simple modified one group method. The different lattice parameters were investigated to show how these parameters were affected by pitch variations. Comparison with published data was made and a satisfactory agreement was found. The lattice pitch geometry was considered to be square and hexagonal. Calculations were done taking into account different values of criticality. (15 references) (auth)

37122 (UARAEE-79) TWO-GROUP TWO-REGION CRITICALITY CALCULATION DIFFUSION CODE. Fouad, H. Y.; Dimitri, F. H. (Atomic Energy Establishment, Cairo (Egypt). Reactors Dept.). 1969. 28p. Dep. NTIS (U. S. Sales Only).

A two group, two region, one dimensional diffusion code was developed operational on the I.B.M. 1620 computer. The code was made for cylindrical geometry and its modification to slab and spherical geometry is possible. (auth)

37123 (UARAEE-80) UPWARD AND DOWNWARD SCATTERING KERNELS FOR THERMAL NEUTRONS. Fouad, H. Y.; Nasr, M. (Atomic Energy Establishment, Cairo (Egypt). Reactors Dept.). 1969. 35p. Dep. NTIS (U. S. Sales Only).

For nonhydrogenous moderators, the evaluation of the effective thermal cross section and the neutron flux in the thermal range involves solving an integral equation. Neutron balance is considered and, because the moderator atoms energy distribution is comparable to that of the neutrons, both upward and downward scattering are considered. The mathematical derivation of such scattering kernels is given with numerical evaluation for two cases, one for hydrogenous moderator and another for water moderator with conditions similar to that of the UAR research reactor. (auth)

37124 (UARAEE-84) CRITICALITY EVALUATION OF HYDROGENEOUS ENRICHED LATTICES USING A THREE GROUP MODEL. El-Mofty, O. H.; El-Demerdash, A. A.; Karchava, G. A.; Zaalouk, M. G. (Atomic Energy Establishment, Cairo (Egypt). Reactors Dept.). 1969. 74p. Dep. NTIS (U. S. Sales Only).

A theoretical study of various reactor parameters was carried out to facilitate the design of hydrogenous reactors. The factors affecting these parameters (resonances, Dancoff correction, cut-off energy, disadvantage factor, and ^{235}U enrichment) were investigated. Three-group diffusion theory was used in order to attain a reasonable accuracy in which the errors in group constants may be compensated for over the energy range. Two treatments of finding diffusion coefficients for fast groups were applied. The first, for $H/^{235}U$ atomic ratios less than 150 and the second for $H/^{235}U$ greater than 150. These constants were examined in criticality calculations for different reactors and different experiments. The comparison of K_{eff} in both theoretical and experimental investigation shows satisfactory agreement and accuracy of about 1% for high and low enriched homogeneous and heterogeneous reactors. 35 references. (auth)

37125 (UARAEE-85) FOUR GROUPS FOUR REGIONS CRITICALITY CALCULATION DIFFUSION CODE. Fouad, H. Y.; Dimitri, F. H. (Atomic Energy Establishment, Cairo (Egypt). Reactors Dept.). 1969. 23p. Dep. NTIS (U. S. Sales Only).

A four groups, four regions, one-dimensional diffusion code was developed for operation on the IBM 1620 computer. The three geometries, i.e. slab, cylinder or sphere, can be treated by this code. A maximum of 21 space points can be taken into consideration. (9 references) (auth)

37126 (UARAEE-89) NUMERICAL CALCULATIONS OF K_{eff} AND NEUTRON FLUXES IN THE 2 AND 3-GROUP APPROXIMATIONS USING AN IBM-1620 CODE. Naguib, K.; Karchava, G.; Hamouda, I. (Atomic Energy Establishment, Cairo (Egypt). Reactor and Neutron Physics Dept.). 1970. 55p. Dep. NTIS (U. S. Sales Only).

An IBM-1620 code is described to calculate in the two-and three-group diffusion approximations the critical parameters of one-dimensional multiregion reactors with preset geometrical and physical core characteristics. The code permits the calculation of the central control rod worth as well as the neutron distribution in the unit lattice cell. The results of test calculations are also presented. 15 references. (auth)

37127 (UARAEE-90) MULTIGROUP MULTIREGION CRITICALITY CALCULATION DIFFUSION CODE. Fouad, H. Y.; Dimitri, F. H. (Atomic Energy Establishment, Cairo (Egypt). Reactors Dept.). 1970. 25p. Dep. NTIS (U. S. Sales Only).

A multigroup, multiregion, one-dimensional criticality calculation diffusion code was developed for operation on the IBM 1130 computer. The code treats the three geometries, i.e., slab, cylinder, and spherical. A maximum of 18 energy groups, 4 regions, and 101 space points can be handled. (auth)

XUM

37128 (UARAEE-96) SAVE: A TWO GROUP CODE FOR REFLECTOR SAVINGS OF A COMPLETELY REFLECTED CYLINDRICAL REACTOR. Nassar, S. F.; Gaafer, M. A. (Atomic Energy Establishment, Cairo (Egypt). Reactor and Neutron Physics Dept.). 1970. 27p. Dep. NTIS (U. S. Sales Only).

SAVE is a computer program code for the calculation of the reflector savings of a completely reflected cylindrical reactor in the two-group diffusion approximation. The code was designed specifically for IBM-1620. This computer has a very small capacity and an analysis of such a two-dimensional problem using a standard numerical technique is practically impossible with this device. For this reason an iterative technique was employed. The code was applied to the computation of the reflector savings of the UA-RR-1 reactor. Values of the radial and axial reflector savings were found to be 7.24 and 7.56 cm respectively. These values were found to be in a good agreement with those obtained by others. 9 references. (auth)

37129 BOUNDS OF INTEGRAL TRANSPORT OPERATORS. Ronen, Yigal (Cornell Univ., Ithaca, N. Y.). J. Nucl. Energy; 25: 27-34(Jan 1971).

A proof that the integral transport operator is always bounded in some Hilbert space is given. The boundedness is valid regardless of the type of moderator. When fission is present as well as scattering, the integral transport operator is still bounded when some physical assumptions are included. A low estimate to the norm of the integral operators is obtained. (auth) (UK)

37130 FUNCTIONALS FOR DISCONTINUOUS TRIAL FUNCTION FLUX SYNTHESIS. Lambropoulos, P.; Luco, V. (Argonne National Lab., Ill.). J. Nucl. Energy; 24: No. 11, 551-64(Dec 1970).

It is shown that the functionals originally used in variational flux synthesis with continuous trial functions can also be used with discontinuous functions, provided they are modified so as to yield physically meaningful stationary conditions at the discontinuity interfaces. It is demonstrated that various functionals proposed in the past for such use are equivalent, without any among them having any added validity. Mathematical difficulties that were attributed to the use of discontinuous trial functions are clarified and shown to have been the result of inappropriate calculational methods. (auth) (UK)

37131 EFFICIENCY OF CYLINDRICAL CONTROL RODS PARTIALLY INSERTED IN A REFLECTED REACTOR. Vukovic, Danica (Energoprojekt, Belgrade). Atomkernenergie; 17: No. 4, 235-40(Jul 1971).

Efficiency of partially inserted control rods and their effects on the distribution of the epithermal and thermal neutron fluxes in a radially reflected reactor are described. The reactor core is approximated by the homogeneous source of epithermal and thermal neutrons, and control rods by neutron sinks. The heterogeneous Feinberg-Galanin method is adopted. This method was earlier successfully applied for calculating the efficiency of infinite rods. By introducing the axial flux harmonics, the application of this method has been extended to the case of partially inserted control rods. It is further assumed that the extrapolation distances of control rods for epithermal and thermal neutrons have the same values, irrespective of the rod insertion lengths. 10 references. (auth)

37132 TIME-DEPENDENT NEUTRON THERMALIZATION IN A METAL HYDRIDE MODERATOR. Mehner, Juergen (Univ., Karlsruhe, Ger.). Atomkernenergie; 17: No. 4, 229-34(Jul 1971). (In German).

An analytic scattering model is used to describe the scattering of slow neutrons in a polycrystalline metal hydride. This model is investigated in terms of its thermalization properties. The spectrum of the thermalization operator is determined. It is shown that the thermalization in zirconium hydride may be explained by this model. Good agreement with experimental data is achieved. 15 references. (auth)

Experimental Applications

37133 (ANL-7411(Suppl.5)) ARGONNE CODE CENTER: COMPILATION OF PROGRAM ABSTRACTS. Butler, M. K.; Henline, Pamela; Legan, Marianne; Ranzini, L.; Snow, William J. (Argonne National Lab., Ill.). Feb 1971. Contract W-31-109-eng-38. 259p. Dep. NTIS.

A bibliography of computer program abstracts referring to available computer programs at the Argonne Code Center is presented. (D.C.C.)

37134 (DP-MS-70-101) EXPERIMENTAL INVESTIGATION OF THE EFFECTS OF SPACE AND REFLECTION ON THE COUNT RATE FLUCTUATION SPECTRA OF A LARGE NUCLEAR REACTOR. Thomas, Cecil Owen Jr. (Du Pont de Nemours (E. I.) and Co., Aiken, S. C. Savannah River Lab.). Mar 1971. 121p. Dep. NTIS.

Thesis. Submitted to Univ. of Tennessee, Knoxville.

The effects of space on count-rate fluctuation spectra obtained from a large nuclear reactor, the effects of a reflector on count-rate fluctuation spectra obtained from a nuclear reactor, and the spatial behavior of the correlated-to-uncorrelated ratio, which is proportional to the detector efficiency of a large nuclear reactor, were investigated. These objectives were accomplished by tape recording the output signals of neutron detectors placed along an axially-centered diameter of a large, cylindrical nuclear reactor for both reflected and non-reflected radial boundary conditions. Data were taken for cases in which the detectors were located together, for cases in which the detectors were located symmetrically, and for cases in which one detector was always located at the center of the reactor. These data were analyzed to obtain the auto-power-spectral-densities and both the magnitudes and phases of the cross-power-spectral-densities of the fluctuations of the count rates of the detectors. The correlated-to-uncorrelated ratios were inferred from the auto-power-spectral-densities. The magnitudes of the cross-power-spectral-densities were found to exhibit both space and reflector effects as evidenced by the variation of the values of their low-frequency magnitudes, break frequencies, and roll-off slopes with detector placement and boundary condition respectively. The phases of the cross-power-spectral-densities were found to deviate from zero only when the detectors were located neither together nor symmetrically. The space dependence of the correlated-to-uncorrelated ratio was found to be described by that of the average count rates obtained from the neutron detectors. 30 references. (auth)

37135 (KFK-1350) MEASUREMENT OF THE DOPPLER COEFFICIENT IN DIFFERENT FUEL SAMPLES IN A FAST AND AT FAST-THERMAL REACTOR ARRANGEMENT BY THE PILE OSCILLATOR METHOD. Barleon, L. (Kernforschungszentrum, Karlsruhe (West Germany). Institut fuer Neutronenphysik und Reaktortechnik). Dec 1970. 120p. (In German). Dep. NTIS (U. S. Sales Only).

In the critical zero energy assemblies STARK and SNEAK the pile oscillator technique was used to measure the Doppler effect with heated small samples. A detailed description of the new developed apparatus and the technique used is given. The samples are placed in fuel filled elements, in order to avoid perturbation of the neutron spectrum in the vicinity of the sample. Because such an element weighs up to 80 kg, a powerful pneumatic drive was needed to move it. Detailed calculations and experiments were made to study the temporal movement of these heavy elements. The heat losses of the heated samples were calculated and measured. Measurements of samples of depleted UO_2 and of metallic natural uranium made in STARK are reported. The experiments were compared to calculations, using various theories and nuclear data sets. (53 references) (auth)

37136 (UARAEE-66) CONTROL ROD CALCULATION WITH PERTURBATION THEORY. Sallam, O. H.; Karchava, G.; Hamouda, I. (Atomic Energy Establishment, Cairo (Egypt). Reactor and Neutron Physics Dept.). 1968. 65p. Dep. NTIS (U. S. Sales Only).

A method by which the worth of a single infinite control rod may be calculated is described. The method is based on perturbation theory and utilizes the two-group diffusion approximation. The transport-corrected boundary conditions are determined with blackness theory from a knowledge of the microscopic nuclear properties of the rod and external medium. The results of calculation of a central cylindrical boron carbide rod for the UA-RR-1 reactor are reported. The comparison of calculated and experimental results revealed good agreement. Formulas are presented for determining the reactivity difference due to water filling the central core gap and the worth of the central portion of a multiplying medium in the core. 29 references. (auth)

37137 (UARAEE-75) EFFECT OF THE PROBE TUBE ON THE THERMAL NEUTRONS SPACE-ENERGY DISTRIBUTION. El Konsol, S.; Novikov, A.; Hussein, A.; Hamouda, I. (Atomic Energy Establishment, Cairo (Egypt). Reactor and Neutron Physics Dept.). 1969. 52p. Dep. NTIS (U. S. Sales Only).

In the measurement of the neutron space-energy distribution in a moderator by the time-of-flight method, it is usually required to extract the neutron beam through an exit tube. The exit tube influence on the neutron spectrum in this tube bottom region is considered. Using a number of simplifying assumptions about the neutron space-energy distribution at the moderator, an analytical expression is obtained for the energy dependent perturba-

tion caused by the tube. The calculation has been carried out for the case of a "black" plate, immersed into an infinite water plate. The results of calculation are compared with the experimental data and satisfactory agreement is obtained. 15 references. (auth)

37138 (UARAEE-105) THEORETICAL STUDY OF THE EFFECT OF TEMPERATURE ON REACTIVITY OF EK-10 TYPE REACTORS APPLYING THREE-GROUP THEORY. El-Mofty, O. H.; El-Demerdash, A. A.; Karchava, G. A. (Atomic Energy Establishment, Cairo (Egypt). Reactors Dept.). 1970. 21p. Dep. NTIS (U. S. Sales Only).

The effect of temperature on the reactivity of a water-water reactor system with EK-10 type fuel elements is discussed. The parameters, cross-sections, thermal utilization, resonance integral, disadvantage factors, reflector saving and the number of secondary neutrons per absorption are evaluated at different temperatures and their characteristics are discussed. The range of temperature was taken from 10°C to 40°C to avoid changing the state of water. Three-group diffusion theory and the four factor formula were applied. A comparison between the obtained results and experimental measurements showed that the three-group method gave better accuracy than the four factor formula. The reactivity obtained by the three-group technique is of 1% accuracy with respect to experimental results. 8 references. (auth)

Reactor Components, Fuels, and Accessories

37139 (CONF-700211-7) PROBLEMS ABOUT FUEL CLADDING MATERIALS. STAINLESS STEEL. Hasegawa, Masayoshi (Waseda Univ., Tokyo (Japan). Dept. of Science and Engineering). [nd]. 7p. Dep. NTIS.

From Atomic Energy Society meeting; Tokyo, Japan (13 Feb 1970).

The effects of fast breeder reactor core conditions on Type 316 stainless steel fuel cans are discussed. Test data are presented on the high temperature creep properties, elongation, ductility, neutron irradiation effects, and corrosive effects of flowing sodium. (H.D.R.)

37140 (SRARI-P-96) SPECIFIC PROPERTIES OF OPERATION OF ABSORBING MATERIALS IN FAST REACTORS AND REQUIREMENTS FOR THEM. Krasnoyarov, N. V.; Gol'tsev, V. P.; Gryazev, V. M.; Guseva, T. M.; Ponomarev, V. I. (Scientific Research Atomic Reactor Inst., Melekess (USSR)). 1970. 16p. (In Russian). Dep. NTIS (U. S. Sales Only).

The possible methods of fast reactor control were investigated. The most effective method for large reactors is the use of absorbers. The control rods of different purpose and requirements for them are described. The behavior of absorbing materials from the point of view of their radiation damage and ensuring the operation reliability are considered. 15 references. (auth)

37141 NUCLEAR REACTOR CONTROL ROD DRIVE ASSEMBLY. Dempsey, John D. (to United States Atomic Energy Commission). U. S. Patent 3,575,805. 20 Apr 1971. Filed 18 Dec 1968.

A control rod drive assembly for a nuclear reactor utilizing a planetary gear system and a pair of motor drive units in continuous operation is described. Speed adjustments of one motor unit cause control rod movement for purpose of reactor control. Braking of said motor unit provides rapid rod insertion while a flywheel built into the planetary gear system provides rapid rod insertion in the event both motor units fail. (auth)

37142 PUMPS FOR NUCLEAR PLANTS. Kuendig, J. (Gebrueder Sulzer AG, Winterthur, Switzerland). Kerntech. Atomprax.; 13: No. 4, 186-8(Apr 1971). (In German).

Descriptions of various types of pumps used in reactor cooling systems are presented. (D.C.C.)

37143 NUCLEAR FUEL SUBASSEMBLIES AND COMBINATIONS THEREOF. Van Dievoet, Jean-Paul L.; DeWandeleer, Jean George; Charles, Robert Odon (to Societe Belge Pour l'Industrie Nucleaire, SA). U. S. Patent 3,567,582. 2 Mar 1971. Priority date 23 Feb 1967, Belgium.

A fuel subassembly for use in nuclear reactors comprises a support member which includes three or more elongated webs, each having one of its longitudinal edges joined with a common nexus from which the several webs radiate in an angularly spaced array, and fuel rods attached to the central support member within the thus-defined angular spaces in open lateral communication with the exterior of the subassembly. Groups of such subassemblies in which webs in different but adjoining central support members are disposed closely adjacent to one another along their outer longitudinal edges, and webs on a plurality of different central supports define cells containing fuel rods, thereby minimizing the amount of neutron-absorbing structural material required in each subassembly, are described. (Offic. Gaz.)

37144 NUCLEAR PRESSURE VESSELS. 46 CFR 55 1968. Washington, D. C.; Superintendent of Documents, GPO (1968). 3p. Available from Superintendent of Documents, GPO, Washington, D. C.

Specific limitations or modifications to Section III of the ASME Code for nuclear vessels are presented. (H.D.R.)

37145 METHOD AND APPARATUS FOR COOLING PARTS OF PUMPS IN NUCLEAR REACTORS OR THE LIKE. Gaffal, Karl (to Klein, Schanzlin, and Becker, Aktiengesellschaft). U. S. Patent 3,574,473. 13 Apr 1971. Priority date 24 Jan 1968.

A nuclear reactor pump is described wherein the shaft seals and radial bearings are cooled by cold water which is circulated by thermosiphon action when the shaft is idle and the pump chamber contains hot fluid. Streams of cold water for cooling of the bearing and of the seals are caused to flow through a common main cooler and thereupon enter the pump housing by way of a common inlet to flow toward separate outlets. The channel for the stream which cools the seals contains several flow restrictors. (auth)

37146 PULSE CHANNEL FOR REACTOR STARTUP MEASUREMENTS TYPE ILRT-1 AND ILRT-2. Ostrowski, A. (Inst. of Nuclear Research, Swierk, Poland). Kernenergie; 13: No.12, 377-80(Dec 1970).

The transistorized pulse startup channel for use with a fission chamber detector is described. Operating principles of main parts of the instrument are given together with some technical data. The channel provides for power measurements in 5 decade range (log scale 10^0 to 10^5 p/s) and for period measurements in -26 to ∞ to $+6.5$ s range. Two trip circuits for preset period levels ("warning" and "alarm") are provided, and one for signalling of the counting rate falling below minimum. The chamber is connected to a coaxial symmetrical link leading to a preamplifier by means of an adapting pulse transformer. The preamplifier is connected to a measuring panel by means of long cable (100 m or more). The panel contains measuring, signalling and supplying circuits. The channel is fed from -24 V d-c voltage in order to eliminate electrical interferences. (auth)

37147 APPARATUS AND METHOD FOR MONITORING FISSION PRODUCTS. Dady, Charles E. U. S. Patent 3,523,868. 11 Aug 1970. Filed 26 Jan 1968.

A nuclear reactor fission-product monitor having a coolant water reservoir and recirculation system for gases evolved from the water is described. The evolved gases radioactively decay to products which are removed and analyzed. (auth)

37148 NUCLEAR REACTOR ELEMENT AND ITS USE IN A REACTOR. Fonteray, Pierre-Jean; Noel, Robert; Thome, Paul (to Commissariat a l'Energie Atomique. Societe Babcock-Atlantique). French Patent 1,569,732. 11 May 1970. Filed 13 Jun 1968. 1st Addition 95,084. (In French).

The essential characteristic of the fuel elements is that the tubes are horizontally fixed, either in the two vertical parallel walls, or in any orientation between the two walls. (France)

37149 TUBULAR SUPPORTING BASE FOR A NUCLEAR REACTOR. (to Societe des Forges et Ateliers du Creusot, SA). French Patent 1,519,644. 11 May 1970. Filed 10 May 1968. 1st Addition 95,071. (In French).

Some modifications and improvements to a tubular supporting base for a nuclear reactor are described. The structure consists of a cell arrangement made up of hexagonal or cylindrical tubular elements, coaxial to the stacking columns of the reactor core. The hexagonal cell structure is provided with hexagonal gaps, each of them being formed by the free faces of the six surrounding tubular elements. The gaps enable the welded joints of the elements to be made prior to the positioning of the upper and lower horizontal pads of the supporting base on each gap. These pads are formed by the two floors which are welded to the tubular element ends and to each other. The shell structure consists of a bulkhead formed by some vertical interconnected cores which is also connected to the horizontal pads and the peripheral skirt of the supporting base forming a polygonal cell lattice in which the tubular elements are arranged in vertical rows parallel to the cell sides. (France)

37150 NUCLEAR REACTOR CONDENSER SUPPORT STRUCTURE. (to Westinghouse Electric Corp.). British Patent 1,232,957. 26 May 1971. Priority date 29 Apr 1969, United States.

XUM

REACTOR CONTAINMENT SYSTEMS—ice condenser for, description of support structure for (D.C.C.)

37151 REFUELLING MACHINE FOR A NUCLEAR REACTOR. Deacon, David; Lawson, Donald Stuart (to English Electric Co. Ltd.). British Patent 1,230,984. 5 May 1971. Filed 23 May 1967.

The refueling machine described includes a single storage compartment for a fuel rod assembly; the lower end of the compartment is open and adapted for aligned engagement with the top of a standpipe. A grab-head assembly is provided to draw the fuel rod assembly into the compartment and support it in an upper part thereof. A second grab-head assembly is adapted to support a standpipe closure plug in an enlargement at the lower end of the compartment in such a way that the plug is out of alignment with the compartment and the standpipe and also to move the plug into alignment with the standpipe when the fuel rod assembly is supported in the upper part of the compartment, and also to lower the plug into the standpipe. The machine should preferably be provided with radiation shielding around the storage compartment. (UK)

37152 GRID FOR FUEL PENCILS. Ringot, Claude (to Commissariat a l'Energie Atomique). French Patent 2,028,039. 9 Oct 1970. Filed 14 Jan 1969. (In French).

A grid for cylindrical pencils of fissile or fertile material is described. These elements are elongated (cluster type), externally clad and disposed parallel with respect to each other. The grid is machined with a radius of curvature in the region of contact with the fuel pencils slightly greater than the radius of the pencils. (France)

37153 IMPROVEMENTS IN OR RELATING TO PRESSURE VESSELS FOR NUCLEAR REACTORS. Schilling, Franz E. (to Siempelkamp GmbH). British Patent 1,230,053. 28 Apr 1971. Filed 10 Jan 1970.

The object of the pressure vessel design described is to provide a construction which is simpler than conventional designs and which avoids some of the design problems of the latter. One difficulty with conventional designs is the risk that radiation and thermal effects may damage the concrete which is employed, necessitating complicated cooling means, and waste of the associated low grade heat. The vessel described has at least its well formed from prestressed cast iron of such thickness that it effectively acts as a radiation shield. The pressure vessel and shield are in effect combined as a single unit that is largely insensitive to temperature and relatively simple as regards design consideration, and may be termed a "shielding pressure vessel". The wall may be built up from prefabricated cast iron elements extending in the length wise direction, or wall elements in the form of rings, built up from smaller castings. A baseplate and cover built up from iron castings may be provided. Pressure tight sealing means are provided at butt joints; and such joints may be interlocking. Channels may be provided within the cast iron to accommodate prestressing tension members, or external prestressing elements may be provided consisting of steel rings shrunk into position. The pressure vessels may be provided with channels, chambers or tubes for coolant, moderator material, and reflecting material. (UK)

37154 IMPROVEMENTS IN OR RELATING TO NUCLEAR REACTOR FUELLING ARRANGEMENTS. (to SNAM Progetti SpA). British Patent 1,233,695. 26 May 1971. Priority date 26 Jan 1968, Italy.

REACTOR LOADING MACHINES—design parameters of pantograph, for rotating vessel covers, (D.C.C.)

37155 SHOCK ABSORBER. Furminieux, Gilbert; Pflugrad, Kurt (to Commissariat a l'Energie Atomique). French Patent 2,036,729. 31 Dec 1970. Filed 7 Mar 1969. (In French).

A shock absorber is presented for braking and stopping a rapidly falling emergency shutdown rod. It consists of tubular elements in a multilayered arrangement, which maintain by themselves the distance between the discs separating two adjacent layers. The elements consist of cylindrical tubes made of inelastic materials radially arranged around an axis of symmetry perpendicular to the discs. (France)

XUM

GENERAL

37156 (ANL–7797) UNSTEADY COUPLED HIGH FLUX-MASS, MOMENTUM TRANSFER WITH A MOVING BOUNDARY. Kaellis, Joseph (Argonne National Lab., Ill.). Mar 1971. Contract W-31-109-eng-38. 157p. Dep. NTIS.
Thesis.

37157 (ANL–7809) MASS-SPECTROMETRIC OBSERVATIONS ON N-(ETHYLMERCURI)-p-TOLUENESULFANILIDE, CERESAN-M. Katzin, Leonard I.; Studier, Martin H. (Argonne National Lab., Ill.). May 1971. Contract W-31-109-eng-38. 4p. Dep. NTIS.

37158 (ANL/ES-CEN–1003) WORK PLAN FOR CONTINUATION OF THE PROJECT "REDUCTION OF ATMOSPHERIC POLUTION BY THE APPLICATION OF FLUIDIZED-BED COMBUSTION." Jonke, A. A.; Vogel, G. J.; Anastasia, L. J.; Jarry, R. L. (Argonne National Lab., Ill.). Apr 1971. Contract W-31-109-eng-38. 38p. Dep. NTIS.

37159 (BDX–613–161) HIGH TEMPERATURE FLAT CABLES. Quarterly Report, FY 70–4. Mosakowski, J. J.; Mitchell, M. D.; Hile, R. A.; Hilker, W. W. (Bendix Corp., Kansas City, Mo.). Nov 1970. Contract AT(29-1)-613. 46p. Dep. NTIS.

37160 (BDX–613–177) SYNTACTIC FOAM EVALUATION. Final Report. Smith, D. D. (Bendix Corp., Kansas City, Mo.). Mar 1971. Contract AT(29-1)-613. 129p. Dep. NTIS.

37161 (BDX–613–236) ELECTROFORMED GILDING METAL ROTATING BAND. Final Report. Hines, R. A. (Bendix Corp., Kansas City, Mo.). May 1971. Contract AT(29-1)-613. 29p. Dep. NTIS.

37162 (BDX–613–283) TRANSFER MOLDING OF CLOSE TOLERANCE PARTS. Quarterly Report, FY 70–4. Hishaw, R. J. (Bendix Corp., Kansas City, Mo.). May 1971. Contract AT(29-1)-613. 32p. Dep. NTIS.

37163 (BDX–613–286) CONFORMAL-COATING. Quarterly Report, FY 71-1. Moyle, W. F. (Bendix Corp., Kansas City, Mo.). Feb 1971. Contract AT(29-1)-613. 31p. Dep. NTIS.

37164 (BDX–613–294) DESIGN EVALUATION OF INSULATOR PIN. Lohr, R. D. (Bendix Corp., Kansas City, Mo.). Mar 1971. Contract AT(29-1)-613. 43p. Dep. NTIS.

37165 (BDX–613–300) POLYURETHANE FOAM MATERIAL AND PROCESS DEVELOPMENT. Quarterly Report, FY 71-2. Fender, J. R. (Bendix Corp., Kansas City, Mo.). May 1971. Contract AT(29-1)-613. 28p. Dep. NTIS.

37166 (BDX–613–313) HIGH TEMPERATURE THERMAL INSULATION. Quarterly Report, FY 71-1. Kelso, Gary L. (Bendix Corp., Kansas City, Mo.). May 1971. Contract AT(29-1)-613. 57p. Dep. NTIS.

37167 (BDX–613–320) ALUMINUM PULSE-ARC WELDING. Quarterly Report, FY71-2. Hollar, D. L. (Bendix Corp., Kansas City, Mo.). Mar 1971. Contract AT(29-1)-613. 25p. Dep. NTIS.

37168 (BDX–613–344) ELECTRONICS ENGINEERING QUARTERLY. (Bendix Corp., Kansas City, Mo.). Mar 1971. Contract AT(29-1)-613. 359p. Dep. NTIS.

37169 (BDX–613–347) HIGH FREQUENCY PARAMETER TECHNIQUES. Final Report. Martin, Dennis C. (Bendix Corp., Kansas City, Mo.). Mar 1971. Contract AT(29-1)-613. 51p. Dep. NTIS.

37170 (BDX–613–405) BLENDING OF SEVEN LOTS OF MERGINAMIDE L-425 FOR USE IN THE M300 ADHESIVE. (Bendix Corp., Kansas City, Mo.). Mar 1971. Contract AT(29-1)-613. 44p. Dep. NTIS.

37171 (BDX–613–406) THERMAL PROPERTIES OF LACTONE ESTER-BASED RIGID URETHANE FOAMS. (Bendix Corp., Kansas City, Mo.). Mar 1971. Contract AT(29-1)-613. 29p. Dep. NTIS.

37172 (BDX–613–408) PROPERTIES OF PLASMA-SPRAYED ALUMINUM COATING. Final Report. (Bendix Corp., Kansas City, Mo.). Mar 1971. Contract AT(29-1)-613. 21p. Dep. NTIS.

37173 (BDX–613–410) LINING OF COMPRESSION SET TEST FIXTURES. Interim Report. (Bendix Corp., Kansas City, Mo.). Mar 1971. Contract AT(29-1)-613. 23p. Dep. NTIS.

37174 (BNWL–B–58) PDP-9/GOULD 4800 DEVICE HANDLER AND GRAPHICS LIBRARY. Gerhardstein, L. H. (Battelle-Northwest, Richland, Wash. Pacific Northwest Lab.). Mar 1971. Contract AT(45-1)-1830. 49p. Dep. NTIS.

37175 (CALT–822–29) AN APW CALCULATION OF ENERGY BANDS IN SIMPLE CUBIC TELLURIUM. Newkirk, L. R.; Tsuei, C. C. (California Inst. of Tech., Pasadena. W. M. Keck Lab. of Engineering Materials). May 1971. Contract AT-(04-3)-822. 12p. Dep. NTIS.

37176 (CIC–E1,1-8) SPIFFY: INTERPOLATION IN TABLES OF WEIGHTED DATA. Edwards, Arthur L. (California Univ., Livermore. Lawrence Radiation Lab.). Feb 1971. 33p. Dep. NTIS.

37177 (CIC–E2,2-8) FITTER, FUNGUS, FUNNY: LINEAR LEAST SQUARES CURVE FITTING OF WEIGHTED TABULAR DATA. Edwards, Arthur L. (California Univ., Livermore. Lawrence Radiation Lab.). Dec 1970. 37p. Dep. NTIS.

37178 (CIC–P1-8) CORD, RECORD: SORTING OF TABULAR DATA. Edwards, Arthur L. (California Univ., Livermore. Lawrence Radiation Lab.). Jan 1971. 32p. Dep. NTIS.

37179 (CONF-710312–1) SANDIA LABORATORIES CARBON COMPOSITES DEVELOPMENT PROGRAM. Johnstone, J. K. (Sandia Labs., Albuquerque, N. Mex.). [nd]. 14p. Dep. NTIS.
From eighteenth refractory composites working group meeting; Huntsville, Ala. (16 Mar 1971).

37180 (COO–1489-10) CREEP IN STOICHIOMETRIC BETA NiAl. Strutt, P. R.; Rowe, G. M. (Connecticut Univ., Storrs. Dept. of Metallurgy); Dodd, R. A. (Wisconsin Univ., Madison. Dept. of Minerals and Metals Engineering). [Apr 1971]. Contract AT(11-1)-1489. 5p. (CONF-700819–12). Dep. NTIS.
From second international conference on the strength of metals and alloys; Pacific Grove, Calif. (30 Aug 1970).

37181 (COO–1693-6) SPECTRAL STUDIES OF POLYENES AND THEIR CARBONIUM IONS: IMPLICATIONS TO PHOTOBIOLOGY. Final Report. Blatz, Paul E. (Wyoming Univ., Laramie. Dept. of Chemistry). 31 Mar 1971. Contract AT(11-1)-1693. 4p. Dep. NTIS.

37182 (COO–1770-3) NUTRIENT CYCLING AND PRODUCTIVITY OF DYSTROPHIC LAKE-BOG SYSTEMS (PART B). Technical Progress Report, March 1–November 30, 1970. Griffing, Thomas C. (Notre Dame Univ., Ind. Dept. of Biology). Apr 1971. Contract AT(11-1)-1770. 43p. Dep. NTIS.

37183 (COO–1801-17) PROTEIN SYNTHESIS IN DELAYED IMPLANTING MOUSE OVA. Technical Progress Report, May 1, 1970–May 1, 1971. Weitlauf, Harry M. (Kansas Univ., Kansas City, Medical Center). Contract AT(11-1)-1801. 7p. Dep. NTIS.

37184 (COO–2094-6) ICR QUARTERLY REPORT, NO. 28. Ashenhurst, Robert L. (Chicago Univ., Ill. Inst. for Computer Research). 1 Feb 1971. Contract AT(11-1)-2094. 74p. Dep. NTIS.

37185 (DP-MS-71-25) STUDY OF MOLECULAR MOTIONS IN POLYMER SOLUTIONS BY PULSED NUCLEAR MAGNETIC RESONANCE SPECTROSCOPY. Goldstein, Lawrence O. (Du Pont de Nemours (E. I.) and Co., Aiken, S. C. Savannah River Lab.). May 1971. 60p. Dep. NTIS.
Thesis. Submitted to Clemson Univ., S. C.

37186 (GAT-Z–5046) CONTRIBUTION TO THE EVALUATION OF TEST RESULTS IN THE TESTING OF THE FIRE BEHAVIOR OF PLASTICS ON A LABORATORY SCALE. Klimke, Peter M. Translated for Goodyear Atomic Corp., Piketon, Ohio, from Plastverarbeiter; 18: No. 6, 389-98(1967). 21p. Dep. NTIS.

XUM

37187 (LA-4553) THE DIRECT SOLUTION OF THE DISCRETE POISSON EQUATION ON IRREGULAR REGIONS. Buzbee, B. L.; Dorr, F. W.; George, A.; Golub, G. H. (Los Alamos Scientific Lab., N. Mex.). May 1971. Contracts W-7405-Eng-36; AT(04-3)-326. 26p. Dep. NTIS.

37188 (LA-4655) A GENERATING OPERATOR FOR SOLUTIONS OF CERTAIN PARTIAL DIFFERENCE AND DIFFERENTIAL EQUATIONS. Hundhausen, Joan R. (Los Alamos Scientific Lab., N. Mex.). May 1971. Contract W-7405-Eng-36. 8p. Dep. NTIS.

37189 (LA-4666) ROTATING CABLE PUSHER FOR PULSED-PROPULSION SPACE VEHICLE. Cotter, T. P. (Los Alamos Scientific Lab., N. Mex.). Apr 1971. Contract W-7405-eng-36. 6p. Dep. NTIS.

37190 (LA-4682) NOVA BRANCH-DRIVER OPERATION. Biswell, Lavon R. (Los Alamos Scientific Lab., N. Mex.). May 1971. Contract W-7405-Eng-36. 7p. Dep. NTIS.

37191 (LA-tr-71-32) INCREASED SUSCEPTIBILITY OF EXPLOSIVES TO A DETONATION IMPULSE. Derzhavets, A. S. Translated by Helen J. Dahlby (Los Alamos Scientific Lab., N. Mex.), from pp 37-52 of Termostoikie Vzryvchatye Veshchestva i ikh Deistvie v Glubokikh Skvazhinakh, Izdatel'stvo Nedra, Moscow, 1969. 20p. Dep. NTIS.

37192 (MHSMP-71-31) ANALYTICAL APPLICATIONS OF LIQUID CHROMATOGRAPHY. Quinlin, W. T. (Mason and Hanger-Silas Mason Co., Inc., Amarillo, Tex.). Jan-Mar 1971. Contract DA-11-173-AMC-487(A). 4p. Dep. NTIS.

37193 (MHSMP-71-32) PHOTOGRAPHIC AND OPTICAL SYSTEMS ANALYSIS. Kelly, Stephen (Mason and Hanger-Silas Mason Co., Inc., Amarillo, Tex.). Jan-Mar 1971. Contract DA-11-173-AMC-487(A). 10p. Dep. NTIS.

37194 (MHSMP-71-33) 12.5 KJ CAPACITOR BANK. Final Report. Worley, R. D. (Mason and Hanger-Silas Mason Co., Inc., Amarillo, Tex.). Mar 1971. Contract DA-11-173-AMC-487(A). 6p. Dep. NTIS.

37195 (MHSMP-71-34) MATHEMATICAL ANALYSIS OF HE DATA. Ashcraft, R. W. (Mason and Hanger-Silas Mason Co., Inc., Amarillo, Tex.). Jan-Mar 1971. Contract DA-11-173-AMC-487(A). 5p. Dep. NTIS.

37196 (NYO-1480-171) 16 CHANNEL MEDIUM SPEED MULTIPLEXER. Prestianni, Vincent T. (New York Univ., N. Y. AEC Computing and Applied Mathematics Center). May 1971. Contract AT(30-1)-1480. 109p. Dep. NTIS.

37197 (NYO-2265-16) STUDY OF TRANSPLANTATION OF TISSUES AND ORGANS AND RELATED TOPICS IN SURGICAL RESEARCH. Part I: Technical Progress Report, June 16, 1967–June 15, 1970. Moore, Francis D. (Harvard Medical School, Boston, Mass.). 15 Jun 1970. Contract AT(30-1)-2265. 68p. Dep. NTIS.

37198 (NYO-2504-63) PRESSURE DEPENDENTS OF THE ELASTIC CONSTANTS OF NaCl AT LOW TEMPERATURE. Ghafelehbashi, M.; Koliwad, K. M. (Cornell Univ., Ithaca, N. Y. Dept. of Materials Science and Engineering). 19 Dec 1969. 15p. Dep. NTIS.

37199 (NYO-2504-74) HIGH PRESSURE-HIGH TEMPERATURE STUDY OF SPIN LATTICE RELAXATION IN PURE AND DOPED LiBr SINGLE CRYSTALS. Report No. 1243. Murty, Korukonda Linga (Cornell Univ., Ithaca, N. Y. Materials Science Center). Jan 1969. 101p. Dep. NTIS.
Thesis.

37200 (NYO-2807-91) SUMMARY OF PROGRESS, MAY 16, 1970–May 15, 1971. (Princeton Univ., N. J. Dept. of Chemical Engineering). Contract AT(30-1)-2807. 7p. Dep. NTIS.

37201 (NYO-3504-58) EXTRANEOUS GRAIN BOUNDARY DISLOCATIONS IN HIGH ANGLE (110) TWIST BOUNDARIES IN GOLD. Schober, T.; Warrington, D. H. (Cornell Univ., Ithaca, N. Y. Materials Science Center). Apr 1971. Contract AT(30-1)-3504. 23p. Dep. NTIS.

37202 (NYO-3590-8) PHYSIOPATHOLOGY OF BLOOD PLATELETS AND THE DEVELOPMENT OF EXTRACTS AND SUBSTITUTES. Three Year Progress Report, August 1, 1968–July 31, 1971. Baldini, Mario G. (Brown Univ., Providence, R. I. Div. of Hematologic Research). Contract AT(30-1)-3590. 31p. Dep. NTIS.

37203 (NYO-3597-16) AN EXPERIMENTAL STUDY OF LEAF DEVELOPMENT IN CERTAIN OF THE VASCULAR PLANTS. Kuehnert, Charles Carroll (Syracuse Univ., N. Y.). May 1971. Contract AT(30-1)-3597. 34p. Dep. NTIS.

37204 (NYO-3699-51) HIGH PRESSURE BEHAVIOR OF SOLID H_2, D_2, ^3He, ^4He, AND ^{20}Ne. Pollock, E. L.; Bruce, T. A.; Chester, G. V.; Krumhansl, J. A. (Cornell Univ., Ithaca, N. Y. Lab. of Atomic and Solid State Physics). Dec 1970. Contract AT(30-1)-3699. 38p. Dep. NTIS.

37205 (NYO-3759-18) ANNUAL PROGRESS REPORT [ON PHOTOSYNTHETIC ENERGY CONVERSION], SEPTEMBER 1, 1970–AUGUST 31, 1971. Clayton, Roderick K. (Cornell Univ., Ithaca, N. Y.). Contract AT(30-1)-3759. 8p. Dep. NTIS.

37206 (NYO-3759-30) PHOTOCHEMICAL REACTION CENTERS FROM RHODOPSEUDOMONAS SPHEROIDES. Clayton, Roderick K.; Wang, Richard T. (Cornell Univ., Ithaca, N. Y.). [nd]. 15p. Dep. NTIS.

37207 (NYO-3851-10) FIELD ION SHADOW PROJECTION MICROSCOPE AND OTHER FIM TECHNIQUES FOR VIEWING BIOMOLECULES. Final Report. Mueller, Erwin W. (Pennsylvania State Univ., University Park). Apr 1971. Contract AT(30-1)-3851. 20p. Dep. NTIS.

37208 (NYO-3995-15) ENVIRONMENTAL FACTORS AFFECTING THE STANDING CROP OF FORAMINIFERA IN SUBLITTORAL AND PSAMMONLITTORAL COMMUNITIES OF A LONG ISLAND SALT MARSH. Matera, Nicholas J.; Lee, John J. (City Coll., New York, Dept. of Biology). [nd]. Contract AT-(30-1)-3995. 83p. Dep. NTIS.

37209 (NYO-4030-9) PROTEINS IN GROWTH REGULATION DURING EARLY DEVELOPMENT OF THE CHICK EMBRYO. Comprehensive Three Year Report. Klein, Norman W. (Connecticut Univ., Storrs, Dept. of Animal Genetics). May 1971. Contract AT(30-1)-4030. 73p. Dep. NTIS.

37210 (NYO-4030-10) PROTEINS IN GROWTH REGULATION DURING EARLY DEVELOPMENT OF THE CHICK EMBRYO. Progress Report, May 1970–May 1971. Klein, Norman W. (Connecticut Univ., Storrs, Dept. of Animal Genetics). Contract AT-(30-1)-4030. 17p. Dep. NTIS.

37211 (ORNL-TM-3201) ANALYSIS OF TORISPHERICAL SHELLS SUBJECTED TO CONCENTRATED LOADS. Gwaltney, Richard C. (Oak Ridge National Lab., Tenn.). May 1971. Contract W-7405-eng-26. 82p. Dep. NTIS.
Thesis. Submitted to Univ. of Tennessee, Knoxville.

37212 (ORNL-TM-3295) COMPUTER PROGRAMS FOR SOME EDDY-CURRENT PROBLEMS, 1970. Simpson, W. A.; Luquire, J. W.; Dodd, C. V.; Spoeri, W. G. (Oak Ridge National Lab., Tenn.). Jun 1971. Contract W-7405-eng-26. 281p. Dep. NTIS.

37213 (ORNL-TM-3296) SOME FACTORS AFFECTING THE PERFORMANCE OF HYPERFILTRATION MEMBRANES. Sheppard, John D. (Oak Ridge National Lab., Tenn.). May 1971. Contract W-7405-eng-26. 163p. Dep. NTIS.
Thesis. Submitted to Univ. of Tennessee, Knoxville.

37214 (ORO-3936-4) THE VAPOR EXPLOSION-HEAT TRANSFER AND FRAGMENTATION. III. PRESSURIZATION OF A SOLIDIFYING SPHERE. Hsiao, K. H.; Cox, J. E.; Hedgcoxe, P. G.; Witte, L. C. (Houston Univ., Tex. Dept. of Mechanical Engineering). Nov 1970. Contract AT(40-1)-3936. 36p. (CONF-701102-20). Dep. NTIS.
From Meeting of the American nuclear society; Washington, D. C. (15 Nov 1970).

37215 (RLO-1725-186) RELEASE OF DISSOLVED ORGANIC MATTER FROM NATURAL POPULATIONS OF MARINE PHYTOPLANKTON. Thomas, James P. (Washington Univ., Seattle. Dept. of Oceanography). [1970]. Contract AT(45-1)-1725. 47p. Dep. NTIS.

37216 (RLO-1725-191) NUMERICAL MODEL FOR DETERMINING THE MIDDLE SCALE TIME DEPENDENT VARIATIONS IN SALINITY AND TEMPERATURE STRUCTURE IN A COASTAL ZONE PROVINCE UNDER THE INFLUENCE OF DILUTION AND UPWELLING. Duxbury, Alyn C. (Washington Univ., Seattle. Dept. of Oceanography). [1970]. 73p. Dep. NTIS.

37217 (RLO-1725-200) COLUMBIA RIVER EFFECTS IN THE NORTHEAST PACIFIC: BIOLOGICAL STUDIES. Progress Report, July 1970-May 1971. Anderson, George C. (comp.) (Washington Univ., Seattle. Dept. of Oceanography). 15 May 1971. Contract AT(45-1)-1725. 24p. Dep. NTIS.

37218 (RLO-2225-T-1-5) BIOLOGICAL HALF-LIVES FOR ZINC AND MERCURY IN THE PACIFIC OYSTER, CRASSOSTREA GIGAS. Seymour, Allyn H. (Washington Univ., Seattle. Lab. of Radiation Ecology). 10 May 1971. Contract AT(45-1)-2225-T1. 20p. (CONF-710501-15). Dep. NTIS.
From third national symposium on radioecology; Oak Ridge, Tenn. (10 May 1971).

37219 (RLO-2227-T-7-7) CENTRALIZED DATA ACQUISITION AND TIME-SHARING MESSAGE SWITCHING SYSTEM. Fryklund, J. W.; Loveland, W. A. (Oregon State Univ., Corvallis). [nd]. 5p. (CONF-700560-1). Dep. NTIS.
From second annual symposium on theory of computing; Northampton, Mass. (4 May 1970).

37220 (SC-DC-71-3821) MAGNUS DATA ON THE STANDARD 10^0 CONE CALIBRATION MODEL. Curry, Warren H.; Reed, James F. (Sandia Labs., Albuquerque, N. Mex.); Ragsdale, William C. (Naval Ordnance Lab., White Oak, Md.). Mar 1971. 24p. (CONF-710306-1). Dep. NTIS.
From thirty-fifth meeting of the supersonic tunnel association; Dallas, Tex. (8 Mar 1971).

37221 (SC-DR-70-767) ENERGY DIFFUSION IN A ONE-DIMENSIONAL FINITE SOLID WITH LINEAR HEAT LOSS. Donaldson, A. B. (Sandia Labs., Albuquerque, N. Mex.). Feb 1971. 80p. Dep. NTIS.

37222 (SC-DR-70-862) ELI-44: A COMPUTER-CONTROLLED INSTRUMENT SYSTEM. Dykes, D. G. (Sandia Labs., Albuquerque, N. Mex.). May 1971. 12p. Dep. NTIS.

37223 (SC-DR-710074) CALCULATION OF THE VAPOR PRESSURE IN DESICCATED-MULTICOMPONENT SYSTEMS. Matsko, J.; Slade, W. E.; Dungan, R. H. (Sandia Labs., Albuquerque, N. Mex.). Mar 1971. 49p. Dep. NTIS.

37224 (SC-DR-710097) ANALOG SIMULATION OF A GUIDED PARACHUTE-PAYLOAD SYSTEM. Vaughn, , R.; Reis, G. E.; Stark, J. A. (Sandia Labs., Albuquerque, N. Mex.). May 1971. 38p. Dep. NTIS.

37225 (SC-DR-710194) HIGH INTENSITY DIRECT READING HEAT FLUX GAUGE. Hardee, H. C.; Donaldson, A. B. (Sandia Labs., Albuquerque, N. Mex.). May 1971. 9p. Dep. NTIS.

37226 (SC-DR-710222) COMPUTER-BASED DISPLAY OF NONDESTRUCTIVE EVALUATION DATA. Stiefeld, B. (Sandia Labs., Albuquerque, N. Mex.). May 1971. 28p. Dep. NTIS.

37227 (SC-M-70-549) CHECKLIST OF GOOD CONTAMINATION CONTROL PRACTICES FROM A MANUFACTURING VIEWPOINT. Ballard, Douglas W. (Sandia Labs., Albuquerque, N. Mex.). Apr 1971. 42p. Dep. NTIS.

37228 (SC-R-713250) TRANSMISSION LINE COUPLED TO A CYLINDER IN AN INCIDENT FIELD. King, Ronold W. P. (Harvard Univ., Cambridge, Mass. Gordon McKay Lab. of Applied Science); Harrison, Charles W. Jr. (Sandia Labs., Albuquerque, N. Mex.). May 1971. 21p. Dep. NTIS.

37229 (SC-RR-70-742) PAN6: A COMPUTER PROGRAM FOR THE ANALYSIS OF SPACE FRAMEWORKS. Murfin, Walter B. (Sandia Labs., Albuquerque, N. Mex.). Apr 1971. 85p. Dep. NTIS.

37230 (SC-RR-710203) NUMERICAL SOLUTIONS OF NONEQUILIBRIUM REFLECTED SHOCK WAVES IN AIR WITH RADIATION. Skoglund, Victor J. (New Mexico Univ., Albuquerque); Watkins, Charles B. Jr. (Sandia Labs., Albuquerque, N. Mex.). May 1971. 110p. Dep. NTIS.

37231 (SC-RR-710296) A-STABLE BLOCK IMPLICIT ONE-STEP METHODS. Watts, Herman A. (Sandia Labs., Albuquerque, N. Mex.). May 1971. 100p. Dep. NTIS.

37232 (SC-T-713030) RELAXATION AND NONEQUILIBRIUM RADIATION BEHIND SHOCK WAVES IN AIR. Zheleznyak, M. B.; Mnatsakanyan, A. Kh.; Yakubov, I. T. Translated by T. Watt for Sandia Labs., Albuquerque, N. Mex., from Izv. Akad. Nauk SSSR, Mekh. Zhidk. Gaza.; No. 4, 161-74(1970). 39p. Dep. NTIS.

37233 (SC-T-713031) INVESTIGATION OF ISOTHERMAL COMPRESSIBILITY OF IGNEOUS ROCKS UNDER PRESSURES OF UP TO 32,000 kg(force)/cm^2. Balashov, D. B.; Volarovich, M. P. Translated by Marcel I. Weinreich (Sandia Labs., Albuquerque, N. Mex.), from Izv. Akad. Nauk SSSR, Fiz. Zemlin; No. 2, 24-32 (1971). 22p. Dep. NTIS.

37234 (SC-T-713035) SURVEY OF FILM DEVELOPERS ADAPTED FOR X-RAY INTENSITY MEASUREMENTS. Ohmasa, Masaaki; Sueno, Shigeho. Translated by O. Philippi (Sandia Labs., Albuquerque, N. Mex.), from Kobutsugaku Zasshi; 8: 304-15(1967). 19p. Dep. NTIS.

37235 (SCL-DR-710032) SANDIA LABORATORIES LIVERMORE DATA PROCESSING SYSTEM. Benton, J. D. (Sandia Labs., Livermore, Calif.). May 1971. Contract AT(29-1)-789. 22p. Dep. NTIS.

37236 (SLAC-119) TAXL: A SIMPLE HIERARCHICAL DATA STRUCTURE MANIPULATION SYSTEM. Becker, Sheldon I. (Stanford Linear Accelerator Center, Calif.). Jun 1970. Contract AT(04-3)-515. 122p. Dep. NTIS.

37237 (SRO-643-1) RNA METABOLISM IN RELATION TO THE REGULATION OF PROTEIN SYNTHESIS IN PLANTS. Key, Joe L. (Georgia Univ., Athens). [nd]. Contract AT(38-1)-643. 35p. Dep. NTIS.

37238 (TID-25714) THREE-YEAR SUMMARY, 1967-1970. (Smithsonian Institution, Washington, D. C. Radiation Biology Lab.). Contract AT(30-1)-3913. 8p. Dep. NTIS.

37239 (TID-25720) LATTICE DYNAMICS OF RUTILE. Traylor, Joseph Gibson (Oak Ridge National Lab., Tenn. Tennessee Univ., Knoxville). Dec 1970. 196p. Dep. NTIS.
Thesis.

37240 (TID-25723) ESTIMATING PLANT PRODUCTION FROM SOIL AND FLORISTIC CORRELATES IN HOT CREEK VALLEY, NEVADA. Davis, J. Barry (Nevada Univ., Reno). Jun 1971. 58p. Dep. NTIS.
Thesis.

37241 (UCID-30001) GEAR: ORDINARY DIFFERENTIAL EQUATION SYSTEM SOLVER. Hindmarsh, Alan C.; Gelinas, Robert J. (California Univ., Livermore. Lawrence Radiation Lab.). 1 Apr 1971. Contract W-7405-eng-48. 34p. Dep. NTIS.

37242 (UCID-30004) CUBRT: FAST 9-DIGIT CUBE-ROOT FUNCTION FOR THE CDC 6600. Fritsch, Fred N.; Shafer, R. E. (California Univ., Livermore. Lawrence Radiation Lab.). 5 Apr 1971. Contract W-7405-eng-48. 11p. Dep. NTIS.

37243 (UCLA-34-P-102-27) ISOTOPIC STUDIES ON STRUCTURE-FUNCTION RELATIONSHIPS OF NUCLEIC ACIDS AND ENZYMES. Progress Report, May 1, 1970-April 30, 1971. Boyer, P. D. (California Univ., Los Angeles. Dept. of Chemistry). Contract AT(04-3)-34. 11p. Dep. NTIS.

37244 (UCLA-34-P-172-2) EFFECT OF VOLUME FRACTION ON PARTICLE COARSENING: THEORETICAL CONSIDERATIONS. Ardell, A. J. (California Univ., Los Angeles. School of Engineering and Applied Science). May 1971. Contract AT(04-3)-34. 30p. (UCLA-ENG-7116). Dep. NTIS.

37245 (UCLA-34-P-177-5) STRAIN HARDENING EQUATIONS AND UNIFORM STRAIN. Vanadium Alloy Development Topical Report. Ono, K. (California Univ., Los Angeles. Dept. of Materials). Feb 1971. Contract AT(04-3)-34. 10p. Dep. NTIS.

37246 (UCRL-19861) RKM1: AN ALGOL 60 PROGRAM THAT OBTAINS THE PARAMETER DEFINING EQUATIONS FOR GENERALIZED RUNGE-KUTTA-FREY INTEGRATION SCHEMES. Close, Elon R. (California Univ., Berkeley. Lawrence Radiation Lab.). 17 Jun 1970. Contract W-7405-eng-48. 21p. (CONF-710313-1). Dep. NTIS.
From second symposium on symbolic and algebraic manipulation; Los Angeles, Calif. (23 Mar 1971).

37247 (UCRL-20528) VAPORIZATION KINETICS OF ZINC OXIDE SINGLE CRYSTALS. Galluzzo, Robert J. (California Univ., Berkeley. Lawrence Radiation Lab.). Apr 1971. Contract W-7405-Eng-48. 16p. Dep. NTIS.
Thesis.

37248 (UCRL-20535) STRUCTURES OF SULFUR-NITROGEN COMPOUNDS. Jolly, William L. (California Univ., Berkeley.

XUM

Lawrence Radiation Lab.). Mar 1971. Contract W-7405-eng-48. 19p. (CONF-710213-1). Dep. NTIS.
From Symposium on sulfur chemistry and theoretical chemistry; New Orleans, La. (18 Feb 1971).

37249 (UCRL-20538) SUPERPOSITION MODEL FOR ENVIRONMENTALLY-ASSISTED FATIGUE-CRACK PROPAGATION. Gerberich, W. W.; Birat, J. P.; Zackay, V. F. (California Univ., Berkeley. Lawrence Radiation Lab.). Mar 1971. Contract W-7405-eng-48. 44p. (CONF-710603-1). Dep. NTIS.
From International conference on corrosion fatigue; Storrs, Conn. (14 Jun 1971).

37250 (UCRL-20541) EFFECTS ON THE PROPAGATION OF OPTICAL BEAMS DUE TO SELF-INDUCED CHANGES IN INDEX OF REFRACTION. Fisher, R. A.; Taran, J-P. E.; Chiao, R. Y.; Gustafson, T. K.; Kelley, P. L. (California Univ., Berkeley. Lawrence Radiation Lab.). Mar 1971. Contract W-7405-eng-48. 52p. Dep. NTIS.

37251 (UCRL-20659) SCEPTRE USERS MANUAL. McMillan, Bradford B. (California Univ., Berkeley. Lawrence Radiation Lab.). Mar 1971. Contract W-7405-Eng-48. 69p. Dep. NTIS.
Thesis.

37252 (UCRL-20667) RECONSTRUCTION OF THE WAVE FUNCTION FROM MATRIX ELEMENTS. Garwin, Charles (California Univ., Berkeley. Lawrence Radiation Lab.). 14 Apr 1971. Contract W-7405-eng-48. 11p. Dep. NTIS.

37253 (UCRL-72637) COMPUTER GRAPHICS APPLICATION TO COMPUTER-AIDED PRINTED CIRCUIT DESIGN. Magnuson, Waldo G. Jr. (California Univ., Livermore. Lawrence Radiation Lab.). Dec 1970. 4p. (CONF-710110-2). Dep. NTIS.
From fourth international conference on systems sciences; Honolulu, Hawaii (12 Jan 1971).

37254 (UCRL-72694) HAL1903: DIGITAL LOGIC SIMULATOR. Lum, John K. Jr. (California Univ., Livermore. Lawrence Radiation Lab.). Dec 1970. 4p. (CONF-710110-1). Dep. NTIS.
From fourth international conference on systems sciences; Honolulu, Hawaii (12 Jan 1971).

37255 (UCRL-73106) THE ROLE OF NUMERICAL STABILITY IN THE COMPUTER SOLUTION OF CHEMICAL CHAIN REACTIONS. Creighton, John (California Univ., Livermore. Lawrence Radiation Lab.). 23 Mar 1971. Contract W-7405-Eng-48. 8p. (CONF-710701-1). Dep. NTIS.
From Computer simulation conference; Boston, Mass. (19 Jul 1971).

37256 (UCRL-Trans-10530) EFFECTIVENESS OF CERAMIC ARMOR PLATING. Heimke, G.; Lieber, C. O. Translated by G. Beyer for Univ. of California, Lawrence Radiation Lab., Livermore, from Naturwissenschaften; 56: No. 9, 458(1969). 3p. Dep. NTIS.

37257 (UCRL-Trans-10531) ESTIMATING SHOCK PRESSURES IN COLLISIONS BETWEEN TWO BODIES. Heimke, G.; Lieber, C. O. Translated by G. Beyer for Univ. of California, Lawrence Radiation Lab., Livermore, from Explosivstoffe; 17: No. 6, 3-6(Jun 1969). 14p. Dep. NTIS.

37258 (UR-49-1430) PROTEINS OF THE ERYTHROCYTE MEMBRANE. Juliano, Rudolph Lawrence (Rochester Univ., N. Y. Dept. of Radiation Biology and Biophysics). 1970. 71p. Dep. NTIS.

CORPORATE AUTHOR INDEX

In the Corporate Author Index, technical report literature is indexed by the organization or institution responsible for issuing the report. Entries are given for all report literature and for published literature for which a corporate author approach is especially desirable, e.g., symposium and conference proceedings.

Each entry under a corporate author gives the publication title and the *NSA* volume and abstract numbers. Report numbers, where applicable, are given in parentheses at the end of the entry.

A

AKADEMIYA NAUK SSSR, MOSCOW. INSTITUT FIZIKI.
Relativistic increase of ionization and sensitivity of nuclear emulsions, 25:34937 (CERN-Trans-71-9)
Search for elementary particles bearing a magnetic charge, 25:36379 (CERN-Trans-71-10)

AKADEMIYA NAUK UKRAINSKOI SSR, KHARKOV. FIZIKO-TEKHNICHESKII INSTITUT.
Measurement of the density of a plasma with the aid of an open resonator, 25:36089 (KHFTI-69/51)

AKADEMIYA NAUK UKRAINSKOI SSR, KIEV. INSTITUT TEORETICHESKOI FIZIKI.
Absolute, convective and global unstabilities, amplification and non-transmission of vibrations, 25:36560 (ITF-70-96-P)
Logic of conclusive explication of the quantum theory, 25:36353 (ITF-70-51-E)
Nonlinear echo phenomena in plasma, 25:36216 (ITF-70-56)

ALABAMA POWER CO., BIRMINGHAM.
Joseph M. Farley Nuclear Plant, Units 1 and 2. Preliminary safety analysis report, Amendment 15, 25:36951 (DOCKET-50348-20)

ALLIED-GULF NUCLEAR SERVICES, FLORHAM PARK, N.J.
Barnwell Nuclear Fuel Plant. Preliminary draft of supplementary data for seismic structural analysis, 25:34686 (DOCKET-50332-18)

ALLIS-CHALMERS MFG. CO., BETHESDA, MD. ATOMIC ENERGY DIV.
La Crosse Boiling Water Reactor. Nuclear instrumentation automatic gain control system, Third Addendum, 25:36895 (DOCKET-1155-116)

AMERICAN SOCIETY FOR ENGINEERING EDUCATION, URBANA, ILL.
Conference on fast reactors and the University, Troy, N. Y., 8/68, 25:36976 (CONF-680818)

AMES LAB., IOWA.
Survey of environmental radioactivity, 1--12/70, 25:34743 (IS-2541)

ARGONNE NATIONAL LAB., ILL.
Argonne code center: compilation of program abstracts, 25:37133 (ANL-7411(Suppl.5))
Bubble growth and collapse in narrow tubes with nonuniform initial temperature profiles, 25:34789 (ANL-7746)
Characteristics of a standing wave bubble or cloud chamber, 25:34955 (CONF-700623-(Vol.1), pp 408-17)
Conference on bubble chamber technology, Argonne, Ill., 6/70, 25:34956 (CONF-700623-(Vol.2))
Conference on bubble chamber technology, Argonne, Ill., 6/70, 25:34938 (CONF-700623-(Vol.1))
Empirical formula for interpolation of tabulated photon photoelectric cross sections, 25:36246 (ANL-7796)
Mass-spectrometric observations on N-(ethylmercuri)-p-toluenesulfanilide, Ceresan-M, 25:37157 (ANL-7809)
Optical constants for the ANL 12-foot bubble chamber, 25:34947 (CONF-700623-(Vol.1), pp 275-302)
Pressure-pulse propagation in two-phase one- and two-component mixtures, 25:37035 (ANL-7792)
Prog. rpt. on lithium/chalcogen secondary cells for components in electric vehicular-propulsion generating systems, semiannual, 5/23--11/22/70, 25:35275 (ANL-7777)
Results from ANL 12 ft. chamber, 25:34980 (CONF-700623-(Vol.2), pp 765-73)
Round table on experience with existing chambers, 25:34945 (CONF-700623-(Vol.1), pp 196-255)
Space-dependent transfer-function analysis of large nuclear-reactor power systems, 25:36987 (ANL-7768)
Status of the 12-foot hydrogen bubble chamber, 25:34974 (CONF-700623-(Vol.2), pp 675-95)
Survey of approximation procedures for the numerical solution of the neutron transport equation, 25:36647 (ANL-7779)
TVGP for 12 foot chamber, 25:34948 (CONF-700623-(Vol.1), pp 303-11)
Unsteady coupled high flux-mass, momentum transfer with a moving boundary, 25:37156 (ANL-7797)
Work plan for continuation of the project, reduction of atmospheric pollution by the application of fluidized-bed combustion, 25:37158 (ANL/ES-CEN-1003)

ARKANSAS POWER AND LIGHT CO., LITTLE ROCK.
Arkansas Nuclear One, Unit 1. Environmental report, operating permit stage, 25:36947 (DOCKET-50313-30)
Arkansas Nuclear One, Unit 2. Preliminary safety analysis report, Amendment 6, 25:36960 (DOCKET-50368-11)

ARKANSAS UNIV., FAYETTEVILLE. DEPT. OF CHEMISTRY.
Prog. rpt. on tracer and isotope effect studies in organic chemistry, annual, 2/1/71, 25:34572 (ORO-3224-23)

ARMY ENGINEER NUCLEAR CRATERING GROUP, LIVERMORE, CALIF.
Empirical study of behavior of clay shale slopes, 25:34768 (NCG-TR-15(Vol.1))

ASEA-ATOM, VASTERAS (SWEDEN).
COLIBRI: computer code for subchannel analysis, 25:37003 (CONF-710317-1)

ATLANTIC RICHFIELD HANFORD CO., RICHLAND, WASH.
Macroreticular ion exchange resin cleanup of Purex process TBP solvent, 25:34679 (ARH-SA-58-RD)
Technical criteria for the prevention of criticality, 25:34678 (ARH-468(Rev.))

ATOMIC ENERGY COMMISSION, WASHINGTON, D. C.
Conference on fast reactors and the University, Troy, N. Y., 8/68, 25:36976 (CONF-680818)

ATOMIC ENERGY COMMISSION COMBINED OPERATIONS PLANNING, OAK RIDGE, TENN.
Cost-benefit illustration for underground nuclear natural gas stimulation, 25:34766 (AECOP-632)

ATOMIC ENERGY ESTABLISHMENT, CAIRO (EGYPT). DEPT. OF ACCELERATORS AND PLASMA PHYSICS RESEARCH.
Axially symmetric waves in vacuum channel in plasma, 25:36218 (UARAEE-92)
Boundary conditions in the case of adjacent plasma streams, 25:36128 (UARAEE-78)
Control computer for analysis and measurement of beam quality in 50-MeV accelerator, 25:36612 (UARAEE-76)
Design and construction of a single gap high gradient column, 25:36613 (UARAEE-87)
Dielectric tensor of inhomogeneous plasma to second order with respect to space derivatives, 25:36127 (UARAEE-65)
Dynamics of THETA-pinch discharge with superimposed azimuthal magnetic field, 25:36129 (UARAEE-102)
Electromagnetic surface waves in adjacent plasma flows, 25:36219 (UARAEE-97)
Experimental studies on magnetically driven shock wave passing through a longitudinal magnetic field, 25:36117 (UARAEE-106)
Experimental studies on shock waves propagated through a longitudinal magnetic field in electrodeless discharge tubes, 25:36092 (UARAEE-101)
Instruments for measurement of the spectral lines profile and shift, 25:36091 (UARAEE-95)
Longitudinal nonlinear oscillations of hot electron magnetic plasma, 25:36217 (UARAEE-88)

ATOMIC ENERGY ESTABLISHMENT, CAIRO (EGYPT). DEPT. OF METALLURGY.
Effect of heat-treatment and cold work on the oxidation of Zr--1 percent Nb alloy in air and pressurized steam at 450-650°C, 25:35278 (UARAEE-72)
Mechanical behaviour of ni-based alloys at elevated temperatures, 25:35340 (UARAEE-55)

ATOMIC ENERGY ESTABLISHMENT, CAIRO (EGYPT). NUCLEAR CHEMISTRY DEPT.
Mechanical decladding of the Inchas fuel, 25:34780 (UARAEE-54)
Possible trends for purity control of uranium by neutron activation assay, 25:34547 (UARAEE-68)

ATOMIC ENERGY ESTABLISHMENT, CAIRO (EGYPT). RADIATION PROTECTION DEPT.
Characteristics of collimator constructed for Inchass

XUM

whole body monitor, 25:34871 (UARAEE-82)
ATOMIC ENERGY ESTABLISHMENT, CAIRO (EGYPT). REACTOR AND NEUTRON PHYSICS DEPT.
Calculation of neutron pulse shape, transmission function and resolution function in mechanical time-of-flight spectrometer, 25:34919 (UARAEE-61)
Calibration of three-crystal-NaI-pair-spectrometer, 25:34921 (UARAEE-93)
Construction of a three-crystal scintillation pair spectrometer, 25:34922 (UARAEE-100)
Control rod calculation with perturbation theory, 25:37136 (UARAEE-66)
Critical mass calculation for UA-RR-1, 25:37078 (UARAEE-67)
Determination of epithermal neutron spectrum shape in UA-RR-1 reactor, 25:37076 (UARAEE-59)
Effect of non-uniform burn up on reactor lifetime, 25:37081 (UARAEE-83)
Effect of the probe tube on the thermal neutrons space-energy distribution, 25:37137 (UARAEE-75)
Energy-dependent Milne problem, 25:36650 (UARAEE-60)
General review of thermal neutron spectra investigations, 25:37118 (UARAEE-62)
Measurement of continuous fast neutron spectra by scintillation technique, 25:34920 (UARAEE-91)
Neutron transmission through ducts perpendicular to neutron beam axis in water shields, 25:36251 (UARAEE-86)
Numerical calculations of K/sub eff/ and neutron fluxes in 2 and 3-group approximations using IBM-1620 code, 25:37126 (UARAEE-89)
Numerical study of fast neutron spectra in UA-RR-1 reactor core and reflector, 25:37079 (UARAEE-71)
One-group considerations of Milne problem, 25:37116 (UARAEE-56)
RAM-1, multigroup neutron diffusion code for IBM-1130, 25:36651 (UARAEE-107)
SAVE: two group code for reflector savings of completely reflected cylindrical reactor, 25:37128 (UARAEE-96)
Thermal neutron capture gamma-rays in iron, 25:36692 (UARAEE-103)
Thermal utilization calculation with new asymptotic diffusion theory, 25:37119 (UARAEE-64)
Transmission of slow neutrons in multiple-segment ducts in a water shield, 25:36252 (UARAEE-104)
ATOMIC ENERGY ESTABLISHMENT, CAIRO (EGYPT). REACTORS DEPT.
Automatic start-up system for UA-RR-1 reactor, 25:37083 (UARAEE-108)
Automatic start-up system for WWR-S, 25:37082 (UARAEE-94)
Cooling of a simulated fuel element by a flow of naturally circulated boiling water, 25:37009 (UARAEE-110)
Criticality evaluation of hydrogeneous enriched lattices using a three group model, 25:37124 (UARAEE-84)
Effect of different reflectors on UA-RR-1 reactor core characteristics, 25:37080 (UARAEE-73)
Effect of pitch variation on nuclear properties of light water assemblies using EK-10 fuel rods, 25:37121 (UARAEE-70)
Energy distribution of moderator atoms in reactors, 25:37108 (UARAEE-52)
Estimate for UAR research reactor thermal inertia, 25:37084 (UARAEE-111)
Experimental loop for two phase heat transfer investigations, 25:34793 (UARAEE-81)
Four groups four regions criticality calculation diffusion code, 25:37125 (UARAEE-85)
Heat transfer in annular reactor channels, 25:37008 (UARAEE-50)
Multigroup, multiregion, criticality calculation diffusion code, 25:37127 (UARAEE-90)
New approach for calculations of nuclear fuel consumption in UA-RR-1 core, 25:37077 (UARAEE-63)
Numerical solution for the thermal flux spectrum in a monatomic moderator, 25:37120 (UARAEE-69)
Station staffing requirements for operation of 150 MWe nuclear station in UAR, 25:36889 (UARAEE-98)
Theoretical study of effect of temperature on reactivity of EK-10 type reactors applying three-group theory, 25:37138 (UARAEE-105)
Theory for assymetric array of cylindrical cavities inside a reactor core, 25:37117 (UARAEE-58)
Two-group two-region criticality calculation diffusion code, 25:37122 (UARAEE-79)
Upward and downward scattering kernels for thermal neutrons, 25:37123 (UARAEE-80)
ATOMIC ENERGY ESTABLISHMENT, WINFRITH (ENGLAND).
Experience in the use of thermoluminescent dosimeters for radiation dose control purposes, 25:35023 (AEEW-M-962)
Problems of high temperature annealing of PTFE/lithium fluoride discs used for ionizing radiation dosimetry, 25:35024 (AEEW-M-991)
Reactor physics characteristics of the High Temperature Reactor, 25:36986 (AEEW-M-985)
ATOMIC ENERGY OF CANADA LTD., CHALK RIVER (ONTARIO).
Aecl research in engineering, 25:37001 (AECL-3787)
ATOMIC ENERGY OF CANADA LTD., CHALK RIVER (ONTARIO). CHALK RIVER NUCLEAR LABS.
Performance of uniaxial creep machines in NRX and NRU reactors, 25:37054 (AECL-3738)
Special arrangement shipments in Canada, 25:34843 (AECL-3804)
Valves for primary heat transport systems for Canadian power reactors, 25:37002 (AECL-3858)
ATOMIC ENERGY OF CANADA LTD., PINAWA (MANITOBA). WHITESHELL NUCLEAR RESEARCH ESTABLISHMENT.
Fabrication and burst testing of reaction-bonded silicon carbide tubes, 25:35523 (AECL-3462)
ATOMIC ENERGY RESEARCH ESTABLISHMENT, HARWELL (ENGLAND).
Revised position sensitive detector array for a charged particle spectrograph, 25:34861 (AERE-R-6776)
ATOMIC WEAPONS RESEARCH ESTABLISHMENT, ALDERMASTON (ENGLAND).
Elastic and inelastic scattering of 5.0 MeV neutrons by sodium, 25:36685 (AWRE-C-3/71)
Electrical method of assessing the suitability of silicon nitride components for use with molten plutonium, 25:35546 (AWRE-C-42-69)
Survey of the effects of porosity on the elastic moduli and strength of brittle materials with particular reference to beryllium, 25:35331 (AWRE-C-25/71)
ATOMICS INTERNATIONAL, CANOGA PARK, CALIF.
Helium production in stainless steel and its constituents as related to LMFBR development programs, 25:35503 (HEDL-SA-193)
AUSTRALIAN ATOMIC ENERGY COMMISSION RESEARCH ESTABLISHMENT, LUCAS HEIGHTS.
Burnout in forced convection boiling heat transfer, 25:37000 (AAEC/LIB/Bib-286)
Nuclear power and environmental pollution, 25:37045 (NP-18842)
Programs for the management and processing of neutron diffraction data, 25:36309 (AAEC/TM-578)
Solution of the inverse reaction problem for complex potentials, 25:36812 (AAEC/TM-586)
Tables of γ rays from (n,γ) produced nuclides, 25:36718 (AAEC/TM-585)
AUSTRALIAN NATIONAL UNIV., CANBERRA. DEPT. OF THEORETICAL PHYSICS.
Computer subprograms for scattering problems, 25:36813 (ANU-P-435)
AUSTRALIAN NATIONAL UNIV., CANBERRA. RESEARCH SCHOOL OF PHYSICAL SCIENCES.
Gamma ray analysis programs, 25:34915 (ANU-P-438)
Optical model code JIB3 (version Perey 3), 25:36814 (ANU-P-451)

B

BARI UNIV. (ITALY). ISTITUTO DI CHIMICA GENERAL ED INORGANICA.
Equilibrium compositions and thermodynamic properties of mixed plasmas. II, 25:36104 (NP-18772)
BATTELLE MEMORIAL INST., COLUMBUS, OHIO.
An evaluation of the applicability of existing data to the analytical description of a nuclear-reactor accident. Quarterly progress report, January--March 1971, 25:37036 (BMI-1904)
Evaluation of beryllium foil subjected to biaxial stresses. final report, 25:35332 (BMI-X-604)
Prog. rpt. on Amchitka bioenvironmental program on limnology studies, annual, 7/69--6/70, 25:34767 (BMI-171-125)
BATTELLE-NORTHWEST, RICHLAND, WASH. PACIFIC NORTHWEST LAB.
300 pound gas test report (28-IV-16006), 25:37070 (TODD-N-16)
500 pound gas test continuation series report (28-IV-16011), 25:37074 (TODD-N-23)
500 pound gas test report (28-IV-16008), 25:37071 (TODD-N-18)
700 pound gas test report (28-IV-16009), 25:37072 (TODD-N-20)
ALTHAEA: one-dimensional two-group diffusion code with an effective four-group burnup, 25:36862 (BNWL-462)
Analysis of air pulser performance for pulsed extraction columns, 25:34773 (BNWL-B-51)
Analysis of effect of potential reactor cooling ponds on Hanford groundwater system, 25:37103 (BNWL-1507)
Analysis of hydrological factors influencing Cable Mountain irrigation project, 25:34715 (BNWL-1502)
Bibliography of ecological publications supported by atomic energy commission related to Columbia River thermal effects studies, 25:35115 (BNWL-1543)
Derivation of corrections to K infinity in the two-group approximation, 25:37111 (BNWL-1560)
Destructive and nondestructive burnup data from natural UO_2 fuel, 25:37015 (BNWL-1568)
Ecological evaluation: migration of juvenile salmon in relation to heated effluents in central Columbia River, 25:37105 (BNWL-SA-3876)
Effect of thermal history on resistance of Columbia River steelhead trout (Salmo gairdneri) to thermal stress, 25:37104 (BNWL-SA-3713)
Gas test series addendum tests and synoptic evaluation (28-IV-16012), 25:37075 (TODD-N-24)
Measurement of the temperature dependence of K infinity for a $^{233}UO_2$--ThO_2 HTGR lattice, 25:36988 (BNWL-1561)
PDP-S/GOULD 4800 device handler and graphics library, 25:37174 (BNWL-B-58)
Prog. rpt. on isotope development, 11/70--1/71, 25:34803 (BNWL-1308-5)

Second 300 pound gas test (28-IV-16010), 25:37073 (TODD-N-21)
BAYLOR UNIV., WACO, TEX.
Prog. rpt. on radiation chemistry of high polymers, 6/70--3/71, 25:34637 (ORO-4059-1)
BENDIX CORP., KANSAS CITY, MO.
Blending of seven lots of merginamide L-425 for use in M300 adhesive, 25:37170 (BDX-613-405)
Design evaluation of insulator pin, 25:37164 (BDX-613-294)
Electroformed gilding metal rotating band, 25:37161 (BDX-613-236)
High frequency parameter techniques, 25:37169 (BDX-613-347)
Lining of compression set test fixtures, 25:37173 (BDX-613-410)
Prog. rpt. on aluminum pulse-arc welding, 3/71, 25:37167 (BDX-613-320)
Prog. rpt. on conformal-coating, 2/71, 25:37163 (BDX-613-286)
Prog. rpt. on electronics engineering, 3/71, 25:37168 (BDX-613-344)
Prog. rpt. on high temperature flat cables, 11/70, 25:37159 (BDX-613-161)
Prog. rpt. on high temperature thermal insulation, 5/71, 25:37166 (BDX-613-313)
Prog. rpt. on polyurethane foam material, 5/71, 25:37165 (BDX-613-300)
Prog. rpt. on transfer molding of close tolerance parts, 5/71, 25:37162 (BDX-613-283)
Properties of plasma-sprayed aluminum coating, 25:37172 (BDX-613-408)
Syntactic foam evaluation, 25:37160 (BDX-613-177)
Thermal properties of lactone ester-based rigid urethane foams, 25:37171 (BDX-613-406)
BETTIS ATOMIC POWER LAB., PITTSBURGH, PA.
Pressurized water reactor (PWR) project. Technical progress report, October 24, 1970--January 25, 1971, 25:36890 (WAPD-MRP-135)
Spatial distribution of indium activation in water using ^{252}Cf, 25:36652 (WAPD-TM-991)
Total and differential cross section for neutrons scattered from ^{90}Zr and Nat. Zr, 25:36740 (WAPD-T-2411)
BORDEAUX UNIV. (FRANCE). FACULTE DES SCIENCES.
Spallation of medium-mass nuclei, 25:36689 (NP-18820)
BRANDEIS UNIV., WALTHAM, MASS. DEPT. OF PHYSICS.
Prog. rpt. on research in elementary particle physics, 5/31/71, 25:36419 (NYO-3178-8)
BROOKHAVEN NATIONAL LAB., UPTON, N. Y.
7-foot bubble chamber conversion, 25:34978 (CONF-700623-(Vol.2), pp 735-49)
BNL work on Ne/H_2 targets, 25:34961 (CONF-700623-(Vol.1), pp 511-31)
Bubble chamber detection technique for gamma rays in momentum region below 1 GeV/c, 25:34964 (CONF-700623-(Vol.1), pp 555-66)
Data formats and procedures for the ENDF neutron cross section library, 25:36719 (BNL-50274)
Exploiting the parent-daughter relationship, 25:34802 (BNL-50249)
Investigation and repair of baffle plate damage in the HFBR primary heat exchangers, 25:37055 (BNL-15815)
Large superconducting magnets for bubble chambers and other detectors, 25:34999 (CONF-700623-(Vol.2), pp 1040-94)
Possible counter array for triggering a bubble chamber, 25:34968 (CONF-700623-(Vol.2), pp 593-605)
BROWN UNIV., PROVIDENCE, R. I. DEPT. OF PHYSICS.
Comment on current algebra beyond the tree approximation, 25:36482 (NYO-2262-TA-241)
BROWN UNIV., PROVIDENCE, R.I. DIV. OF HEMATOLOGIC RESEARCH.
Prog. rpt. on physiopathology of blood platelets and development of extracts and substitutes, 8/68--7/71, 25:37202 (NYO-3590-8)

C

CALIFORNIA INST. OF TECH., PASADENA.
Diffractive N* production in a triggered-bubble-chamber experiment, 25:34971 (CONF-700623-(Vol.2), pp 629-38)
Tests of an empirical rule for cuts and discussion of line reversal relations, 25:36502 (CALT-68-300)
CALIFORNIA INST. OF TECH., PASADENA. W. M. KECK LAB. OF ENGINEERING MATERIALS.
APW calculation of energy bands in simple cubic tellurium, 25:37175 (CALT-822-29)
CALIFORNIA INST. OF TECH., PASADENA. W.M. KECK LAB. OF HYDRAULICS AND WATER RESOURCES.
Longitudinal dispersion in laboratory and natural streams, 25:34719 (KH-R-12)
CALIFORNIA UNIV., BERKELEY. LAWRENCE RADIATION LAB.
(n,p) elastic scattering, 25:36661 (UCRL-20295)
Charged pion production in proton--proton interactions between 13 and 28.5 GeV/c, 25:36391 (UCRL-20632)
Effects on the propagation of optical beams due to self-induced changes in index of refraction, 25:37250 (UCRL-20541)
Eighty-lens optical camera for recording dynamic studies with the scintillation camera, 25:34872 (UCRL-20659)
Factors which will affect the cost of a superconducting synchrotron, 25:36614 (UCRL-20299)
Gamma-ray calibration standards, 25:34923 (UCRL-20476)
Neutrino physics with large H_2 chambers, 25:34941 (CONF-700623-(Vol.1), pp 56-96)
πN partial-wave amplitudes, 25:36506 (TID-25726)
Reconstruction of the wave function from matrix elements, 25:37252 (UCRL-20667)
RKM1: ALGOL 60 program that obtains the parameter defining equations for generalized Runge--Kutta--Frey integration schemes, 25:37246 (UCRL-19861)
Sceptre users manual, 25:37251 (UCRL-20659)
Stringent limits on decays $K/sub\ L/^0 \to \mu^+\mu^-$, e^+e^-, μ^+e^-+, 25:36386 (UCRL-20264)
Structures of sulfur--nitrogen compounds, 25:37248 (UCRL-20535)
Superposition model for environmentally-assisted fatigue-crack propagation, 25:37249 (UCRL-20538)
Total loss cross sections for D_2 molecules passing through H_2 gas, 25:35855 (UCRL-20099)
Vaporization kinetics of zinc oxide single crystals, 25:37247 (UCRL-20528)
CALIFORNIA UNIV., LA JOLLA, SAN DIEGO. DEPT. OF PHYSICS.
Triple Pomeron vertex, duality, and diffraction dissociation, 25:36420 (UCSD-10-P-10-78)
CALIFORNIA UNIV., LIVERMORE. LAWRENCE RADIATION LAB.
12-kilowatt output switching-type power amplifier, 25:36197 (UCRL-73047)
2X II 10-Megajoule ignitron crowbar, 25:36196 (UCRL-73031)
ac temperature technique for measuring high-temperature specific heat of metals, 25:35341 (UCRL-50962)
Astron mechanical engineering effort, 25:36198 (UCRL-73059)
Automatic data processing system for 2X II, 25:36195 (UCRL-73030)
Calculation techniques for estimating the pressure losses for conducting fluid flows in magnetic fields, 25:35938 (UCRL-51010)
Computation of plasma equilibria and stability in Astron and minimum-B mirror systems, 25:36165 (UCRL-51020)
Computer graphics application to computer-aided printed circuit design, 25:37253 (UCRL-72637)
Cord, Record: sorting of tabular data, 25:37178 (CIC-P1-8)
CUBRT: fast 9-digit cube-root function for the CDC 6600, 25:37242 (UCID-30004)
Engineering design of the 2X II, 25:36199 (UCRL-73060)
Engineering the baseball magnet system, 25:36200 (UCRL-73067)
Estimating natural terrestrial background in 17- and 60-keV energy regions from Compton continuum peak, 25:34727 (UCRL-72927)
Evaluation of beryllium foil subjected to biaxial stresses. final report, 25:35332 (BMI-X-604)
Fitter, Fungus, Funny: linear least squares curve fitting of weighted tabular data, 25:37177 (CIC-E2.2-8)
GEAR: ordinary differential equation system solver, 25:37241 (UCID-30001)
HAL1903: digital logic simulator, 25:37254 (UCRL-72694)
Loss-cone modes in inhomogeneous mirror machines, 25:36166 (UCRL-73135)
Prediction of underground nuclear explosion effects in Wagon Wheel Sandstone, 25:34770 (UCRL-50993)
Prog. rpt. on hazards control, 9--12/70, 25:34873 (UCRL-50007-70-3)
Proposal for mirror fusion experiment (MFX), 25:36194 (UCRL-51042)
Radiation damage from internal alpha decay in thorium, 25:36270 (UCRL-51009)
Recent changes in the astron fast pulsing system, 25:36201 (UCRL-73129)
SPIFFY: interpolation in tables of weighted data, 25:37176 (CIC-E1.1-8)
Structure in ^{235}U keV fission cross section, 25:36725 (UCRL-73090)
Technique for measuring pressure, volume, enthalpy, and resistance of equilibrium thermodynamic states of liquid metals at high temperatures and pressures, 25:35342 (UCRL-51035)
The role of numerical stability in the computer solution of chemical chain reactions, 25:37255 (UCRL-72106)
Two-dimensional stress-induced adiabatic flow, 25:34769 (UCRL-50987)
CALIFORNIA UNIV., LOS ANGELES. DEPT. OF CHEMISTRY.
Prog. rpt. on isotopic studies on structure-function relationships of nucleic acids and enzymes, annual, 5/1/70--4/30/71, 25:37243 (UCLA-34-P-102-27)
CALIFORNIA UNIV., LOS ANGELES. DEPT. OF MATERIALS.
Strain hardening equations and uniform strain, 25:37245 (UCLA-34-P-177-5)
CALIFORNIA UNIV., LOS ANGELES. DEPT. OF PHYSICS.
Research program of the Nuclear Consortium at the UCLA Cyclotron Laboratory, July 1970. Report AR 5, 25:36738 (UCLA-10-P-16-23)
CALIFORNIA UNIV., LOS ANGELES. SCHOOL OF ENGINEERING AND APPLIED SCIENCE.
Effect of volume fraction on particle coarsening, 25:37244 (UCLA-34-P-172-2)

XUM

CAROLINA POWER AND LIGHT CO., RALEIGH, N.C.
H. B. Robinson Unit No. 2. Environmental monitoring report, October 1, 1970--March 31, 1971, 25:36932 (DOCKET-50261-61)
H. B. Robinson Unit No. 2. Routine operating report No. 1, September 20, 1970--March 20, 1971, 25:36880 (DOCKET-50261-60)
CASE WESTERN RESERVE UNIV., CLEVELAND, OHIO. DEPT. OF CHEMISTRY.
Primary process in radiation chemistry, 25:34613 (TID-25689)
CASE-WESTERN RESERVE UNIV., CLEVELAND, OHIO. DEPT. OF PHYSICS.
Search for CP-nonconserving asymmetry in decay K/sub L/^{0} + $\pi^+\pi^-\pi^0$, 25:35550 (COO-1749-24)
CEKMECE NUCLEAR RESEARCH CENTER, ISTANBUL (TURKEY).
Manual for Turkish film dosimetry standards, 1962--69, 25:35135 (CNAEM-77)
CENTRAL ELECTRICITY GENERATING BOARD, LONDON (ENGLAND).
Nuclear power in Great Britain, 25:36863 (CONF-700653-1)
Operating experience of nuclear power-stations in UNIPEDE member countries, 25:36864 (CONF-700956-2)
CENTRE D'ETUDE DE L'ENERGIE NUCLEAIRE, MOL (BELGIUM).
Fast breeder fuel processing pyrochemical head end study, 25:34688 (EUR-4615)
Pyrochemical head end conception for fast breeder fuel processing, 25:34687 (EUR-4614)
CESKOSLOVENSKA AKADEMIE VED, REZ. USTAV JADERNEHO VYZKUMU.
Determining reactor spectra of fast neutrons from threshold detector measurements, 25:37109 (UJV-2423-RF)
Effect of radiation on the mechanical properties of concrete, 25:37007 (ORNL-tr-2470)
Fission track solid state detector, 25:34867 (NP-18845)
Plutonium hexafluoride: preparation and properties, 25:34698 (UJV-2291-Ch)
CHALMERS TEKNISKA HOGSKOLA, GOTEBORG (SWEDEN). INSTITUTIONEN FOR FYSIK.
Influence of thickness and scattering angle on stopping cross section of nitrogen, neon, and argon ions in thin carbon foils, 25:36248 (CIPR-41)
CHICAGO UNIV., ILL. INST. FOR COMPUTER RESEARCH.
Prog. rpt., 2/71, 25:37184 (COO-2094-6)
CINCINNATI GAS AND ELECTRIC CO., OHIO.
Wm. H. Zimmer Nuclear Power Station, Unit 1. Preliminary safety analysis report, Amendment 11, 25:36953 (DOCKET-50358-17)
Wm. H. Zimmer Nuclear Power Station, Unit 1. Preliminary safety analysis report, Amendment 12, 25:36954 (DOCKET-50358-18)
CITY COLL., NEW YORK. DEPT. OF BIOLOGY.
Environmental factors affecting the standing crop of foraminifera in sublittoral communities of a Long Island Salt Marsh, 25:37208 (NYO-3995-15)
CLEMSON UNIV., S. C.
Study of molecular motions in polymer solutions by pulsed nuclear magnetic resonance spectroscopy, 25:37185 (DP-MS-71-25)
COLLEGE DE FRANCE, PARIS. LABORATOIRE DE PHYSIQUE ATOMIQUE ET MOLECULAIRE.
Local models for antikaon--nucleon collisions, 25:36505 (PAM-71.1)
COLORADO UNIV., BOULDER.
Bubble chamber detection technique for gamma rays in momentum region below 1 GeV/c, 25:34964 (CONF-700623-(Vol.1), pp 555-66)
COLUMBIA UNIV., NEW YORK.
Scaling properties in e-p scattering, 25:36435 (NYO-1932(2)-189)
COLUMBUS AND SOUTHERN OHIO ELECTRIC CO., COLUMBUS, OHIO.
Wm. H. Zimmer Nuclear Power Station, Unit 1. Preliminary safety analysis report, Amendment 11, 25:36953 (DOCKET-50358-17)
Wm. H. Zimmer Nuclear Power Station, Unit 1. Preliminary safety analysis report, Amendment 12, 25:36954 (DOCKET-50358-18)
COMITATO NAZIONALE PER L'ENERGIA NUCLEARE, FRASCATI (ITALY). LABORATORI NAZIONALI DI FRASCATI.
e^+e^- annihilation into hadrons in preasymptotic region and $\mu^+\mu^-$ production in proton collisions, 25:36434 (LNF-71/5)
Heavy gas--liquid mixture bubble chamber of 70 liters volume with hydrogen internal target, 25:35007 (LNF-70/25)
Multiple e. m. processes in high energy e^-e^+ collisions, 25:36433 (LNF-71/1)
Precision of an optical spark chamber with wire electrodes, 25:35008 (LNF-70/44)
Technical--economic information on superconductors and conductors for high field magnets, 25:36607 (LNF-70/19)
COMITATO NAZIONALE PER L'ENERGIA NUCLEARE, ROME (ITALY).
Aromatic hydrocarbons as potential source of diluents for fuel reprocessing, 25:34638 (RT/CHI-(70)35)
NEMI: physical--mathematical model for sodium boiling in a heated channel, 25:37046 (RT/ING-(70)18)
Principles and methods for the derivation of a formula for the discharge of radioactive liquid wastes in surface waters, 25:34717 (EUR-4636)
Receptivity of site surrounding Casaccia CSN and disposal of radioactive waste, 25:34849 (RT/PROT-(70)36)
Seventh annual metecrological report of the Casaccia Center for Nuclear Studies, 1968, 25:34746 (RT/PROT-(70)42)
Utilization of vibrational compaction for nuclear fuel, 25:35524 (RT/ING-(70)22)
COMMISSARIAT A L'ENERGIE ATOMIQUE, CADARACHE (FRANCE). CENTRE D'ETUDES NUCLEAIRES.
Purification of sodium for RAPSODIE, 25:37056 (BNWL-tr-67)
COMMISSARIAT A L'ENERGIE ATOMIQUE, CHUSCLAN (FRANCE). CENTRE DE PRODUCTION DE PLUTONIUM DE MARCOULE.
The precipitation and filtration of trivalent plutonium oxalate, 25:34680 (CEA-R-4109)
COMMISSARIAT A L'ENERGIE ATOMIQUE, FONTENAY-AUX-ROSES (FRANCE). CENTRE D'ETUDES NUCLEAIRES.
Biasing system for treatment of deep penetration of neutrons by Monte-Carlo method, 25:36648 (CEA-R-4145)
Chemical diffusion and Kirkendall effect in the body-centered cubic phase of the system plutonium/zirconium, 25:35333 (CEA-CONF-1760)
Natural convection irradiation device ''Esther'', 25:37061 (EURFNR-890)
ODILE irradiation device, 25:37060 (EURFNR-889)
Uranium geochemistry and granitic differentiation in uranium-bearing province of Nord-Limousin, 25:34745 (CEA-R-4034)
COMMISSARIAT A L'ENERGIE ATOMIQUE, GRENOBLE (FRANCE). CENTRE D'ETUDES NUCLEAIRES.
200 MHz pulse amplitude discriminator, 25:35045 (CEA-N-1447)
Broad bandwidth differential amplifier, 25:35046 (CEA-N-1448)
Fast neutron spectrum in the reflector of a swimming pool reactor behind metallic slabs, 25:37057 (CEA-R-3755)
Nanosecond pulse amplifier with adjustable gain, working in both polarities, 25:35044 (CEA-N-1439)
Thermic calculations on water cooled research reactors, 25:37058 (CEA-R-4114)
COMMISSARIAT A L'ENERGIE ATOMIQUE, LIMEIL-BREVANNES (FRANCE). CENTRE D'ETUDES.
Use of superconductors for energy storage and discharge, 25:36074 (CEA-CONF-1736)
COMMISSARIAT A L'ENERGIE ATOMIQUE, SACLAY (FRANCE). CENTRE D'ETUDES NUCLEAIRES.
Analog study of propulsion power reactors, 25:37092 (CEA-CONF-1750)
Big hydrogen bubble chamber Mirabelle cryogenics expansion, 25:34979 (CONF-700623-(Vol.2), pp 751-64)
Characteristics of various sealing membranes for alpha activity monitoring cells used in solutions, 25:34673 (CEA-N-1440)
Gargamelle: some technical aspects, 25:35003 (CONF-700623-(Vol.2), App.I)
Isotopic electric generators, 25:34811 (ORNL-tr-2485)
Lenses and illumination system of Mirabelle, 25:34994 (CONF-700623-(Vol.2), pp 972-83)
Maintenance program for Babyline-20 dose rate meters manufactured by NARDEUX, 25:35025 (CEA-N-1435)
Mirabelle, 25:34973 (CONF-700623-(Vol.2), pp 647-74)
Optical system Mirabelle, 25:34992 (CONF-700623-(Vol.2), pp 943-58)
State of the art of producing strong magnetic fields, 25:36073 (CEA-CONF-1734)
COMMONWEALTH EDISON CO., CHICAGO, ILL.
Dresden Nuclear Power Station, Unit 2. Abnormal occurrence report: unplanned release of radioactive material, 25:36918 (DOCKET-50237-175)
Dresden Nuclear Power Station, Unit 2. Additional information concerning operation, 25:36913 (DOCKET-50237-168)
Dresden Nuclear Power Station, Unit 2. Facility License DPR-19; technical specifications Proposed Change No. 12 to Appendix A, 25:36916 (DOCKET-50237-171)
Dresden Nuclear Power Station, Unit 2. Facility License DPR-19; Proposed Change No. 11 to Appendix A, 25:36911 (DOCKET-50237-166)
Dresden Nuclear Power Station, Unit 2. Facility License DPR-19; supplementary information to Proposed Change No. 11 to Appendix A, 25:36915 (DOCKET-50237-170)
Dresden Nuclear Power Station, Unit 2. Summary technical report of secondary containment leak rate tests, October 1970--March 1971, 25:36873 (DOCKET-50237-173)
Dresden Nuclear Power Station, Unit 2. Supplementary information to special report No. 12: torus paint problems, 25:36914 (DOCKET-50237-169)
Dresden Nuclear Power Station, Unit 2. Unplanned release of radioactivity, 25:36872 (DOCKET-50237-172)
Dresden Nuclear Power Station, Unit 3. Facility Operating License No. DPR-25; technical specifications Proposed Change No. 4 to Appendix A, 25:36922 (DOCKET-50249-70)
Dresden Nuclear Power Station, Unit 3. Facility Operating License No. DPR-25; supplementary information to technical specifications Proposed Change No. 3 to Appendix A, 25:36921 (DOCKET-50249-68)
Dresden Nuclear Power Station, Unit 3. Facility Operation License No. DPR-25; technical specifications Proposed Change No. 3 to Appendix A, 25:36920 (DOCKET-50249-67)
Dresden Nuclear Power Station, Units 2 and 3. Additional information relative to safety analysis

report, Amendments 9 and 10, 25:36912 (DOCKET-50237-167)
Dresden Nuclear Power Station, Units 2 and 3. Report No. 4: modifications to off-gas system, 25:36917 (DOCKET-50237-174)
COMMONWEALTH SCIENTIFIC AND INDUSTRIAL RESEARCH ORGANIZATION, MELBOURNE (AUSTRALIA). DIV. OF METEOROLOGICAL PHYSICS.
Prog. rpt., annual, 1969--70, 25:34744 (NP-18828)
CONNECTICUT UNIV., STORRS. DEPT. OF ANIMAL GENETICS.
Prog. rpt. on proteins in growth regulation during early development of the chick embryo, 5/70--5/71, 25:37210 (NYO-4030-10)
Proteins in growth regulation during early development of the chick embryo, 25:37209 (NYO-4030-9)
CONNECTICUT UNIV., STORRS. DEPT. OF METALLURGY.
Creep in stoichiometric beta NiAl, 25:37180 (COO-1489-10)
CONNECTICUT YANKEE ATOMIC POWER CO., HADDAM.
Connecticut Yankee Atomic Power Plant. Operation report No. 71-4, April 1971, 25:36869 (DOCKET-50213-109)
CONSERVATOIRE NATIONAL DES ARTS ET METIERS, PARIS (FRANCE).
Electrostatic systems for ion transport, 25:36608 (NP-18855)
CONSIGLIO NAZIONALE DELLE RICERCHE, BARI (ITALY). CENTRO DI STUDIO PER LA CHIMICA DEI PLASMI.
Equilibrium compositions and thermodynamic properties of mixed plasmas. II, 25:36104 (NP-18772)
CONSOLIDATED EDISON CO. OF NEW YORK, INC., NEW YORK.
Indian Point Nuclear Generating Unit No. 3. Environmental report, Appendices, Vol. 2, 25:36943 (DOCKET-50286-36)
Indian Point Nuclear Generating Unit No. 3. Environmental report, 25:36941 (DOCKET-50286-34)
Indian Point Nuclear Generating Unit No. 3. Environmental report, Appendices, Vol. 1, 25:36942 (DOCKET-50286-35)
Indian Point Station, Unit No. 1. Revised schedule and plan of work on emergency core cooling system, 25:36854 (DOCKET-50003-73)
CONSUMERS POWER CO., JACKSON, MICH.
Big Rock Point Nuclear Plant. Operating with control rod drive C-3 at notch 17, 25:36906 (DOCKET-50155-82)
Big Rock Point operations report, 1/67, 25:36887 (TID-23762)
Big Rock Point operations report, 2/67, 25:36888 (TID-23819)
Palisades Plant. Failure of tube in cooling water heat exchanger, 25:36930 (DOCKET-50255-42)
Palisades Plant. Preliminary safety analysis report, Amendment 22 (includes additions and revisions to final safety analysis report), 25:36929 (DOCKET-50255-41)
CORNELL UNIV., ITHACA, N. Y.
Photochemical reaction centers from rhodopseudomonas spheroides, 25:37206 (NYO-3759-30)
Prog. rpt. on photosynthetic energy conversion, annual, 9/70--8/71, 25:37205 (NYO-3759-18)
CORNELL UNIV., ITHACA, N. Y. DEPT. OF MATERIALS SCIENCE AND ENGINEERING.
Defect structure of depleted zones in irradiated tungsten, 25:36268 (NYO-3504-50)
Pressure dependents of the elastic constants of NaCl at low temperature, 25:37198 (NYO-2504-63)
Prog. rpt. on environment and fracture, 3/20/71, 25:35337 (NYO-3975-3)
CORNELL UNIV., ITHACA, N. Y. LAB. OF ATOMIC AND SOLID STATE PHYSICS.
High pressure behavior of solid H_2, D_2, ^3He, ^4He, and ^{20}Ne, 25:37204 (NYO-3699-51)
CORNELL UNIV., ITHACA, N. Y. MATERIALS SCIENCE CENTER.
Extraneous grain boundary dislocations in high angle (110) twist boundaries in Au, 25:37201 (NYO-3504-58)
High pressure--high temperature study of spin lattice relaxation in pure and doped LiBr single crystals, 25:37199 (NYO-2504-74)

D

DAIRYLAND POWER COOPERATIVE, LA CROSSE, WIS.
La Crosse Boiling Water Reactor. Automatic gain control system: power testing I, corrected pages 5 and 7, 25:36897 (DOCKET-1155-118)
La Crosse Boiling Water Reactor. Monthly operating report, March 1971, 25:36866 (DOCKET-1155-120)
La Crosse Boiling Water Reactor. Nuclear instrumentation automatic gain control system, Third Addendum, 25:36895 (DOCKET-1155-116)
La Crosse Boiling Water Reactor. Request for technical specification changes relative to respiratory protection equipment, 25:36898 (DOCKET-1155-119)
La Crosse Boiling Water Reactor. Unplanned reactor shutdown, 25:36865 (DOCKET-1155-115)
La Crosse Boiling Water Reactor. Water level instrument behavior during main steam bypass valve malfunction incident, 25:36896 (DOCKET-1155-117)
DANISH ATOMIC ENERGY COMMISSION, RISOE. RESEARCH ESTABLISHMENT.
The neutron resonance reactions in thermal nuclear reactors determined by semi-analytic as well as numerical methods, 25:37115 (RISO-234)
DARTMOUTH COLL., HANOVER, N. H.
Prog. rpt. on cobalt sorption on surface reactive minerals in glacial environment, 8/67--2/71, 25:34722 (NYO-3912-4)
Prog. rpt. on cobalt sorption on surface reactive minerals in the glacial environment, annual, 2--12/70, 25:34721 (NYO-3912-3)
DAYTON POWER AND LIGHT CO., OHIO.
Wm. H. Zimmer Nuclear Power Station, Unit 1. Preliminary safety analysis report, Amendment 11, 25:36953 (DOCKET-50358-17)
Wm. H. Zimmer Nuclear Power Station, Unit 1. Preliminary safety analysis report, Amendment 12, 25:36954 (DOCKET-50358-18)
DEMOCRITUS NUCLEAR RESEARCH CENTER, ATHENS (GREECE).
Group velocity of high asplitude surface waves in vacuum-plasma interfaces, 25:36214 (DEMO-71/5)
Relativistic doppler effect and group velocity in homogeneous nonlinear and inhomogeneous plasma, 25:36215 (DEMO-71/6)
DEPARTMENT OF ATOMIC ENERGY, BOMBAY (INDIA). COSMIC RAYS, ASTROPHYSICS AND GEOPHYSICS COMMITTEE.
Conference on cosmic rays, astrophysics, geophysics and elementary particle physics, Delhi, 10/69, 25:35892 (CONF-691055-(Vol.1))
Conference on cosmic rays, astrophysics, geophysics and elementary particle physics, Delhi, 10/69, 25:35893 (CONF-691055-(Vol.2))
DEUTSCHE FORSCHUNGS- UND VERSUCHSANSTALT FUER LUFT- UND RAUMFAHRT E.V., STUTTGART (WEST GERMANY). INSTITUT FUER PLASMADYNAMIK.
Flow of compressible plasmas in self-induced magnetic field of arc discharges, 25:36103 (DLR-FE-70-13)
Radiative energy transport in a plasma reactor, 25:36950 (DLR-FB-70-18)
DEUTSCHES ELEKTRONEN-SYNCHROTRON, HAMBURG (WEST GERMANY).
Influence of parasitic boiling and expansion speed on the dynamic pressure in a bubble chamber, 25:34957 (CONF-700623-(Vol.1), pp 424-48)
DIVISION OF COMPLIANCE (AEC), WASHINGTON, D.C.
Connecticut Yankee Atomic Power Plant. Request to reevaluate personnel exposures to ^{131}I on April 18--22, 1971, 25:36909 (DOCKET-50213-112)
DIVISION OF REACTOR LICENSING (AEC), WASHINGTON, D. C.
Connecticut Yankee Atomic Power Plant. Change No. 17 to technical specifications of Provisional Operating License No. DPR-14, 25:36907 (DOCKET-50213-107)
Connecticut Yankee Atomic Power Plant. Change No. 18 to technical specifications of Provisional Operating License No. DPR-14, 25:36908 (DOCKET-50213-108)
Dresden Nuclear Power Station, Unit 2. Change No. 12 to technical specifications of Provisional Operating License No. DPR-19, 25:36919 (DOCKET-50237-179)
Dresden Nuclear Power Station, Unit 3. Change No. 2 to technical specifications of Facility Operating License No. DPR-25, 25:36923 (DOCKET-50249-72)
Dresden Nuclear Power Station, Unit 3. Change No. 3 to technical specifications of Facility Operating License No. DPR-25, 25:36924 (DOCKET-50249-73)
H. B. Robinson Unit No. 2. Change No. 3 to technical specifications of Provisional License No. DPR-23, 25:36931 (DOCKET-50261-59)
Humboldt Bay Power Plant, Unit No. 3. Change No. 33 to the technical specifications of the Provisional Operating License No. DPR-7, 25:36901 (DOCKET-50133-57)
Hutchinson Island Plant, Unit No. 2. Notice of receipt of application for construction permit and facility license, 25:36962 (DOCKET-50389-8)
Millstone Nuclear Power Station, Unit 2. Construction Permit No. CPPR-76, Amendment No. 1, 25:36950 (DOCKET-50336-22)
Oyster Creek Nuclear Power Plant, Unit No. 1. Notice of AEC consideration of issuance of amendment to provisional operating license, 25:36910 (DOCKET-50219-134)
Quad-Cities Station, Units 1 and 2. Preliminary safety analysis report, Amendment 23, request for additional information, 25:36928 (DOCKET-50254-37)
DIVISION OF TECHNICAL INFORMATION EXTENSION (AEC), OAK RIDGE, TENN.
Engineering materials list cumulative index, 1968--1970, 25:34779 (TID-4103(Suppl.1)(Rev.2))
Peaceful uses of nuclear energy, 25:34817
Reactor safety, literature search, 25:37047 (TID-3525(Rev.5)(Suppl.6))
DOW CHEMICAL CO., GOLDEN, COLO. ROCKY FLATS DIV.
Permeation of halogenated solvents through Drytox gloves, 25:34605 (RFP-1608)
DU PONT DE NEMOURS (E.I.) AND CO., AIKEN, S. C. SAVANNAH RIVER LAB.
ENDF/B cross section preparation and testing in the JOSHUA system, 25:36737 (TID-25690)
Experimental investigation of the effects of space and reflection on the count-rate fluctuation spectra of a large nuclear reactor, 25:37134 (DP-MS-70-101)
Iodine retention studies. Progress report, January--June 1970, 25:37106 (DP-1259)
Neutron-induced fission cross sections for ^{246} ^{248}Cm and ^{249}Cf, 25:36721 (DP-MS-70-95)
Study of molecular motions in polymer solutions by pulsed nuclear magnetic resonance spectroscopy, 25:37185 (DP-

XUM

MS-71-25)

DUKE POWER CO., CHARLOTTE, N.C.
McGuire Nuclear Station, Units 1 and 2. Preliminary safety analysis report, Amendment 6, 25:36961 (DOCKET-50369-10)

E

EBERLINE INSTRUMENT CORP., SANTA FE, N. MEX. DEPT. OF NUCLEAR SCIENCES.
H. B. Robinson Unit No. 2. Environmental monitoring report, October 1, 1970--March 31, 1971, 25:36932 (DOCKET-50261-61)

ECOLE POLYTECHNIQUE, PARIS (FRANCE).
Physics plans for Gargamelle, 25:34944 (CONF-700623-(Vol.1), pp 136-44)
Results achieved with a rapid-cycling hydrogen bubble chamber, 25:34954 (CONF-700623-(Vol.1), pp 390-407)

EG AND G, INC., LAS VEGAS, NEV.
Use of aerial surveys for determining plutonium concentration. technical report no. 1-1030, 25:34862 (EGG-1183-1517)

ELECTRICITE DE FRANCE, CLAMART.
Calculation methods for heterogeneities in reactors of the natural uranium-graphite--gas type, 25:36989 (CEA-N-1398)

ELECTRICITE DE FRANCE, PARIS.
Calculation methods for heterogeneities in reactors of the natural uranium-graphite--gas type, 25:36989 (CEA-N-1398)
Operating experience of nuclear power-stations in UNIPEDE member countries, 25:36864 (CONF-700956-2)

ENTE NAZIONALE PER L'ENERGIA ELETTRICA, ROME (ITALY).
Operating experience of nuclear power-stations in UNIPEDE member countries, 25:36864 (CONF-700956-2)

ENVIRONMENTAL SCIENCE SERVICE ADMINISTRATION, BOULDER, COLO. AERONOMY LAB.
Nonlinear theory of macroinstabilities and enhanced transport in plasmas, 25:36164 (TID-25713)

EUROPEAN ATOMIC ENERGY COMMUNITY.
Temperature stabilization in heat exchange tubes under alternating heat fluxes, 25:34775 (EUR-4634)

EUROPEAN ATOMIC ENERGY COMMUNITY, ISPRA (ITALY). JOINT NUCLEAR RESEARCH CENTER.
Laboratory guide for the selection of brazing materials, 25:35334 (EUR-4637)
Mechanical behavior of complex structures in presence of creep, thermal strains and irradiation-induced dimensional changes, 25:34774 (EUR-4629)
Temperature stabilization in heat exchange tubes under alternating heat fluxes, 25:34775 (EUR-4634)

EUROPEAN ATOMIC ENERGY COMMUNITY, KARLSRUHE (WEST GERMANY). INST. OF TRANSURANIUM ELEMENTS.
Thermogravimetric analysis (TGA) of the uranium oxide carboreduction, 25:34556 (EUR-4635)

EUROPEAN COMMUNITIES, BRUSSELS (BELGIUM). COMMISSION.
Energy outlook in community. Situation 1965, perspectives 70, 25:36855 (NP-18846)

EUROPEAN COMMUNITIES, LUXEMBOURG. COMMISSION.
Energy outlook in community. Situation 1970, perspectives 71, 25:36856 (NP-18847)

EUROPEAN COMPANY FOR THE CHEMICAL PROCESSING OF IRRADIATED FUELS, MOL (BELGIUM).
Estimation of tritium discharges into LLW-streams, 25:34719 (NP-18737)

EUROPEAN ORGANIZATION FOR NUCLEAR RESEARCH, GENEVA (SWITZERLAND).
BEBC expansion piston, 25:34985 (CONF-700623-(Vol.2), pp 836-48)
BEBC expansion servo-system, 25:34988 (CONF-700623-(Vol.2), pp 873-92)
Behaviour of transducers and gauges in high magnetic fields and at low temperatures, 25:34987 (CONF-700623-(Vol.2), pp 863-72)
Big European bubble chamber magnet progress report, 25:35001 (CONF-700623-(Vol.2), pp 1126-49)
Calibration of Gargamelle objectives, 25:34993 (CONF-700623-(Vol.2), pp 959-71)
Experimental results with the 1 m model chamber at CERN. A, 25:34982 (CONF-700623-(Vol.2), pp 790-812)
Experimental results with the 1 m model chamber. B, 25:34983 (CONF-700623-(Vol.2), pp 813-23)
Gargamelle technical aspects, 25:34959 (CONF-700623-(Vol.1), pp 460-76)
Influence of parasitic boiling and expansion speed on the dynamic pressure in a bubble chamber, 25:34957 (CONF-700623-(Vol.1), pp 424-48)
Magnetic field map of the large European bubble chamber, 25:35002 (CONF-700623-(Vol.2), pp 1150-71)
Neon--hydrogen mixtures in large cryogenic bubble chambers, 25:34962 (CONF-700623-(Vol.1), pp 532-42)
Status report of BEBC, 25:34976 (CONF-700623-(Vol.2), pp 703-13)
Track sensitive H_2 and D_2 targets in Ne--H mixtures, 25:34960 (CONF-700623-(Vol.1), pp 477-510)
Ultrasonic bubble chamber development at CERN, 25:34953 (CONF-700623-(Vol.1), pp 376-89)
Use of a computer on the CERN 2m liquid hydrogen bubble chamber, 25:34945 (CONF-700623-(Vol.1), pp 256-73)
Wide angle lens for BEBC, 25:34990 (CONF-700623-(Vol.2), pp 902-14)

F

FLORIDA POWER AND LIGHT CO.
Hutchinson Island Plant, Unit No. 2. Preliminary safety analysis report, Amendment 1, 25:36963 (DOCKET-50389-9)
Turkey Point Plant, Units No. 3 and No. 4. Preliminary safety analysis report, Amendment 35, Suppl. 35 (includes final safety analysis report, Rev. 14), 25:36925 (DOCKET-50250-44)
Turkey Point Plant, Units No. 3 and No. 4. Preliminary safety analysis report, Amendment 36, Suppl. 36 (includes final safety analysis report, Rev. 15), 25:36926 (DOCKET-50250-46)
Turkey Point Plant, Units No. 3 and No. 4. Preliminary safety analysis report, Amendment 37, Suppl. 37 (includes final safety analysis report, Rev. 16), 25:36927 (DOCKET-50250-47)

FRAUNHOFER-GESELLSCHAFT, GARMISCH-PARTENKIRCHEN (WEST GERMANY). PHYSIKALISCH-BIOKLIMATISCHE FORSCHUNGSSTELLE.
Prog. rpt. on measurement of airborne radioactivity and its meteorological application, annual, 4/69--3/70, 25:34745 (NYO-4061-2)

G

GENERAL ELECTRIC CO., PLEASANTON, CALIF. NUCLEONICS LAB.
Thermodynamic data program involving plutonia and urania at high temperatures. Quarterly report No. 14, November 1, 1970--January 31, 1971, 25:35547 (GEAP-12182)

GENERAL ELECTRIC CO., SAN JOSE, CALIF. NUCLEAR ENERGY DIV.
Midwest Fuel Recovery Plant. Preliminary safety analysis report, Amendment 11 (includes technical specifications), 25:34684 (DOCKET-50268-8)
Midwest Fuel Recovery Plant. Preliminary safety analysis report, Amendment 12, 25:34685 (DOCKET-50268-9)

GENERAL ELECTRIC CO., SAN JOSE, CALIF. REACTOR FUELS AND REPROCESSING DEPT.
Nuclear power reactor wastes and our environment, 25:34844 (CONF-700440-1)

GENERAL ELECTRIC CO., SUNNYVALE, CALIF. BREEDER REACTOR DEVELOPMENT OPERATION.
Prog rpt. on sodium technology development program, 12/70--2/71, 25:35276 (GEAP-13539-16)
Southwest Experimental Fast Oxide Reactor. Safety system relay malfunctions, 25:37059 (DOCKET-50231-83)
SYN: operational aspects of the combined BISYN, PERT, and BICYCL synthesis codes, 25:37112 (GEAP-13672)

GEOLOGICAL SURVEY, DENVER, COLO.
Radiochemical analyses of water from selected streams, wells, springs, and precipitation collected during reentry drilling, Project Rulison, 25:34728 (USGS-474-101)

GEORGIA INST. OF TECH., ATLANTA. ENGINEERING EXPERIMENT STATION.
Prog. rpt. on excitation and ionization of ions by electron impact, 9/70--5/71, 25:35833 (ORO-3027-19)

GEORGIA UNIV., ATHENS.
Prog. rpt. on RNA metabolism in relation to regulation of protein synthesis in plants, 27 May 1971, 25:37227 (SRO-643-1)

GEORGIA UNIV., ATHENS. DEPT. OF CHEMISTRY.
Prog. rpt. on radiolysis of water in wide range radiolysis source, annual, 9/1/70--6/1/71, 25:34636 (ORO-3729-4)

GOODYEAR ATOMIC CORP., PIKETON, OHIO.
Vapor pressure--temperature data for selected halogen-containing substances, 25:34602 (GAT-649)

GOSUDARSTVENNYI KOMITET PO ISPOL'ZOVANIYU ATOMNOI ENERGII SSSR, SERPUKHOV. INSTITUT FIZIKI VYSOKIKH ENERGII.
Hodoscope based on small photoelectron multipliers, FEU-85, 25:34864 (IFVE-SEF-70-17)
Increase of effectiveness of synchronized capture during bunching of beam outside the separatrix, 25:36603 (IFVE-SKU-70-20)

GRENOBLE UNIV. (FRANCE).
Fast neutron spectrum in the reflector of a swimming pool reactor behind metallic slabs, 25:37057 (CEA-R-3795)

GRENOBLE UNIV. (FRANCE). FACULTE DES SCIENCES.
Spectroscopic analysis of uranium oxide: use of halogenated carriers, 25:34504 (NP-18865)

GULF GENERAL ATOMIC CO., SAN DIEGO, CALIF.
HTGR base program quarterly progress report for the period ending February 28, 1971, 25:36977 (GA-10501)
Public Service Company of Colorado 330-MW(e) high-temperature gas-cooled reactor research and development program. Quarterly progress report for the period ending March 31, 1971, 25:36978 (GA-10560)

GULF GENERAL ATOMIC, INC., SAN DIEGO, CALIF.
Prog. rpt. on applications of neutron activation analysis in scientific crime investigation, 5/62--5/68, 25:34542 (GA-9807)
Prog. rpt. on neutron capture cross sections of Mo, Ta, and ^{238}U, final, 6/70, 25:36729 (N-70-41995)

GULF RADIATION TECHNOLOGY, SAN DIEGO, CALIF.
Fast reactor spectrum measurements. Technical summary

report, February 1, 1970--January 31, 1971, 25:36591 (GULF-RT-10523)

H

HAHN-MEITNER-INSTITUT FUER KERNFORSCHUNG, BERLIN (WEST GERMANY).
Nuclear chemistry compendium. I, 25:34863 (HMI-B-108)
HANFORD ENGINEERING DEVELOPMENT LAB., RICHLAND, WASH.
Effects of fast neutron irradiation on chromel/alumel thermocouples, 25:35072 (HEDL-SA-152)
FFTF: companion test and development facility for LMFBR program, 25:37085 (WHAN-SA-104(Rev.))
FTR driver fuel development program status, 25:37064 (HEDL-SA-81)
Neutron energy dependent cross section evaluation by a multiple foil activation method, 25:36741 (WHAN-SA-107)
Resistivity measurements of insulators using the four-probe technique, 25:36310 (HEDL-SA-119)
HARVARD MEDICAL SCHOOL, BOSTON, MASS.
Prog. rpt. on study of transplantation of tissues and organs, 6/67--6/70, 25:37197 (NYO-2265-16)
HARVARD UNIV., CAMBRIDGE, MASS. GORDON MCKAY LAB. OF APPLIED SCIENCE.
Transmission line coupled to a cylinder in an incident field, 25:37228 (SC-R-713250)
HAWAII UNIV., HONOLULU.
Proportional quantameter for the 15-foot bubble chamber, 25:34942 (CONF-700623-(Vol.1), pp 97-116)
HEIDELBERG UNIV. (WEST GERMANY).
Fiducial lines in large bubble chambers produced by laser beams, 25:34995 (CONF-700623-(Vol.2), pp 984-96)
HELSINKI UNIV. (FINLAND). RESEARCH INST. FOR THEORETICAL PHYSICS.
Improved relativistic corrections to Fermi-contact hyperfine Hamiltonian, 25:36355 (NP-18818)
HOUSTON UNIV., TEX. DEPT. OF MECHANICAL ENGINEERING.
Vapor explosion--heat transfer and fragmentation. III, 25:37214 (CRC-3936-4)

I

IDAHO NUCLEAR CORP., IDAHO FALLS.
Chemical Programs Division annual report, fiscal year 1970, 25:34690 (IN-1457)
Fast-neutron capture integral measurements of ^{99}Tc, ^{109}Ag, and other fission products, 25:36720 (CONF-710301-4)
Metallurgical evaluation of simulated BWR emergency core cooling tests, 25:37038 (IN-1453)
Optimized use of multipurpose fuel processing facilities at Idaho chemical processing plant, 25:34681 (CONF-710417-1)
PHROG: a FORTRAN IV program to generate fast neutron spectra and average multigroup constants, 25:37113 (IN-1435)
RAFFLE Monte Carlo code and its use to obtain correlated estimates of collapsed cross sections, 25:36645 (CONF-710302-11)
Treatment of radioactive waste streams at Idaho chemical processing plant by evaporation and ion exchange, 25:34682 (CONF-710509-1)
ILLINOIS UNIV., URBANA. DEPT. OF PHYSICS.
Prog. rpt. on elementary particle physics, annual, 4/70, 25:36384 (COO-1195-213)
IMPERIAL COLL. OF SCIENCE AND TECH., LONDON (ENGLAND).
Bubble chamber holography, 25:34998 (CONF-700623-(Vol.2), pp 1024-38)
Development and performance of ANL 140° camera lens, 25:34991 (CONF-700623-(Vol.2), pp 915-42)
Fisheye window concentricity problems, 25:34996 (CONF-700623-(Vol.2), pp 997-1009)
INDIANA AND MICHIGAN ELECTRIC CO., FORT WAYNE, IND.
Donald C. Cook Nuclear Plant, Units 1 and 2. Preliminary safety analysis report, Amendment 14 (includes application for transfer of construction permit), 25:36948 (DOCKET-50315-35)
INSTITUT ATOMNOI ENERGII, MOSCOW (USSR).
Extension of experimental capabilities of MR reactor for loop-testing fuel elements and materials, 25:37067 (LB/G-3001)
Fast hydrogen atom injector, 25:36186 (CTO-746)
Lepton decay of hypernucleus ^{3}H, 25:36454 (IAE-1944)
Measurements of angular correlation of neutron spin and antineutrino momentum in the decay of polarized neutrons, 25:36385 (IAE-1947)
Suppression of flute instability by means of feedback system in Phoenix II, 25:36163 (CTO-737)
INSTITUT JOZEF STEFAN, LJUBLJANA (YUGOSLAVIA).
Investigation of the systems of uranium monosulfide with some alkaline earth sulfides, 25:34603 (IJS-263)
On-line computer system for neutron physics experiments, 25:35048 (CONF-700647-, pp 183-93)
INSTITUT ZA NUKLEARNE NAUKE BORIS KIDRIC, BELGRADE (YUGOSLAVIA).
Conference on electronics and automation, Herceg-Novi, 6/70, 25:35047 (CONF-700647)
INSTITUTE FOR TELECOMMUNICATION SCIENCES AND AERONOMY, BOULDER, COLO.
Solar flare effects in ionosphere, 25:35952 (NBS-TN-326)
INSTITUTE OF NUCLEAR RESEARCH, WARSAW (POLAND).
AFST model with $\pi^+\pi^+$ and $\pi^+ p$ phase shifts and Durr--Pilkuhn form: factors applied to the reaction $\pi^+ p \to p\, 3\pi^+ 2\pi^-$ at 8 GeV/c, 25:36503 (INR-P-1265)
Binding energy of ^{3}H and n-d doublet scattering length with rank four separable potential, 25:36659 (INR-P-1234)
Bitumization of liquid radioactive wastes, 25:34845 (INR-1249)
Physico-chemical properties of lanthanide complexes with thenoyltrifluoroacetone. I, 25:34502 (INR-1247)
Properties of stainless steel 1H18N9T after aging in the power reactor temperature ranges. II, 25:35326 (INR-1255)
INSTITUTE OF NUCLEAR TECHNIQUES, KRAKOW (POLAND).
Distributions and mean values of inelasticity coefficient K/sub π^0/ for lead and graphite, 25:36389 (ITJ-5)
Estimation of energy and mean inelasticity of nuclear interactions at energies above 3.10^{12} eV, 25:36388 (ITJ-3)
Monte Carlo simulation of nuclear-electromagnetic cascade developing in an ionization spectrometer, 25:36431 (ITJ-6)
Tables of magnetic structures determined by neutron diffraction. III, 25:36311 (NP-18845)
INSTITUTO POLITECNICO NACIONAL, MEXICO CITY. ESCUELA SUPERIOR DE FISICA Y MATEMATICAS.
Isobaric analogue states between 4 and 8 MeV for reaction ^{48}Ca(p,p)^{48}Ca, 25:36690 (NP-18824)
INTERNATIONAL ATOMIC ENERGY AGENCY, VIENNA (AUSTRIA).
Investigation of reprocessing input measurement using tracer technique, 25:34689 (IAEA-R-876-F)
Nuclear well logging in hydrology, 25:34725 (STI/DOC-10/126)
Operating experience with nuclear power stations in member states, 25:36884 (IAEA-127)
INTERNATIONAL NUCLEAR DATA COMMITTEE.
Aspects of critical evaluation of nuclear data information, 25:37107 (INDC(NDS)-29/U)
ISRAEL ATOMIC ENERGY COMMISSION, TEL AVIV.
Fluctuation factors for theoretical evaluation of average neutron cross sections of fissile nuclei in the unresolved resonances region, 25:36722 (IA-1208)
ISTITUTO NAZIONALE DI FISICA NUCLEARE, MILAN (ITALY).
Projector for Gargamelle's pictures, 25:34951 (CONF-700623-(Vol.1), pp 334-44)

J

JAPAN ATOMIC ENERGY RESEARCH INST., TOKYO.
Absolute power measurement by reactor noise analysis, 25:37114 (JAERI-Memo-4276)
Impurities in processed radioisotopes produced by (n,γ) reaction: purity of ^{160}Tb, 25:34670 (JAERI-Memo-4280)
Impurities in processed radioisotopes produced by (n,γ) reaction: purity of ^{169}Yb, 25:34669 (JAERI-Memo-4279)
JFM: code for JMTR fuel accountability, 25:37065 (JAERI-Memo-4270)
Kinetics parameter calculation code: (ARGO), 25:36552 (JAERI-Memo-4331)
Measurement of central fission ratios and fission rate distributions in FCA, 25:37066 (JAERI-Memo-4356)
Prog. rpt., 1969, 25:34804 (JAERI-Memo-4285)
Second postoperation inspection on JPDR reactor pressure vessel, 25:37004 (JAERI-Memo-4330)
Summary of technical reports on 1st MITI design permit of JPDR, 25:37042 (JAERI-Memo-4173)
Summary of technical reports on 3rd MITI design permit of JPDR, 25:37043 (JAERI-Memo-4174)
Summary of technical reports on fifth MITI design permit of JPDR, 25:37044 (JAERI-Memo-4260)
JERSEY CENTRAL POWER AND LIGHT CO., MORRISTOWN, N. J.
Forked River Nuclear Generating Station, Unit 1. Preliminary safety analysis report, Amendment 10, 25:36956 (DOCKET-50363-15)
Oyster Creek Nuclear Power Plant, Unit No. 1. Isolation condenser system time delay relay failure, 25:36870 (DOCKET-50219-135)
Oyster Creek Nuclear Power Plant, Unit No. 1. Summary technical report: primary containment leakage rate test, October 1970, 25:36871 (DOCKET-50219-137)
Three Mile Island Nuclear Station, Unit 1. Preliminary safety analysis report, Amendment 20 (includes Appendix 13A and final safety analysis report modifications), 25:36944 (DOCKET-50289-35)
Three Mile Island Nuclear Station, Unit 1. Preliminary safety analysis report, Amendment 21 (includes additions and revisions to application for reactor operating license), 25:36882 (DOCKET-50289-36)
JOHNS HOPKINS UNIV., BALTIMORE, MD. DEPT. OF PHYSICS.
Prog. rpt. on research in theoretical physics, annual, 4/1/70--3/31/71, 25:36472 (NYO-4076-14)
JOINT INST. FOR NUCLEAR RESEARCH, DUBNA (USSR).
Automatic processing of information from spark chambers, 25:35004 (JINR-P10-5762)
Centralized output of spectrometry data, 25:35049 (CONF-700647-, pp 255-79)
Electron-ion bunch diagnostics by means of tremstrahlung, 25:36616 (UCRL-Trans-1440)

XUM

Experiments on acceleration of α-particles by collective method, 25:36615 (UCRL-Trans-1434)
Interaction of high-energy radiation with matter, 25:36816 (JINR-P2-5719)
Kinetic model of plane high-current electron-ion beam, 25:36604 (JINR-P9-5645)
Reaction $\pi^- + \pi^0\pi^0 n$ at 447 MeV, 25:36405 (JINR-P1-5781)
Short-lived isomers of Tb isotopes: ^{148}Tb, ^{149}Tb, ^{150}Tb, and ^{152}Tb, 25:36726 (JINR-P6-5681)

JOINT INST. FOR NUCLEAR RESEARCH, DUBNA (USSR). LAB. OF HIGH ENERGY.
Neutron--electron interaction studied by neutron diffraction on a single crystal of ^{186}W, 25:36380 (JINR-E3-5713)
System for depression of magnetic field pulsations in Dubna synchrophasotron, 25:36605 (JINR-P9-5724)

JOINT INST. FOR NUCLEAR RESEARCH, DUBNA (USSR). LAB. OF NEUTRON PHYSICS.
Effect of the optical parameters of the medium on the yield of transition radiation of non-relativistic particles, 25:36354 (JINR-P4-5734)
Synchronized chopper time-of-flight spectrometer, 25:34916 (JINR-E14-5731)

JOINT INST. FOR NUCLEAR RESEARCH, DUBNA (USSR). LAB. OF NUCLEAR PROBLEMS.
Decay of ^{139}Nd, 25:36724 (JINR-P6-5673)
Decay of ^{173}Ta, 25:36727 (JINR-P6-5704)
Decays of Nd and Pr nuclides with mass number A = 138, 25:36725 (JINR-P6-5674)
Depolarization in 612 MeV elastic pn-scattering, 25:36390 (JINR-P1-5743)
Determination of the boiling point of some isoalkyl astatides by using a glass gas chromatograph, 25:34604 (JINR-P6-5683)
Electromagnetic separation of short-lived isotopes of Rn, Xe, and Kr for spectroscopic studies, 25:34806 (JINR-P13-5757)
Hadamard: transform scintillation counter, 25:34865 (JINR-P13-5696)
Influence of ultrasound on vapor bubble dynamics in liquid H, 25:35005 (JINR-P13-5751)
New method for rare-earth isotope separation, 25:34805 (JINR-P6-5761)
Pseudo-noise sequences applicable to multiplex systems of particle detection, 25:34866 (JINR-P13-5722)
Relative yields of secondary [(p,xn)α] reactions on Bi in range E/sub p/ = 120-660 MeV, 25:36723 (JINR-P1-5530)
Shower efficiency of spark chambers, 25:35006 (JINR-P13-5810)

JOINT INST. FOR NUCLEAR RESEARCH, DUBNA (USSR). LAB. OF THEORETICAL PHYSICS.
Conformal-covariant interactions, 25:36561 (JINR-P2-5716)
Functional integration and Regge-eikonal representation of scattering amplitude, 25:36587 (JINR-P2-5768)
Gamov--Teller 1^+ excitations in odd--odd nuclei, 25:36817 (JINR-P4-5744)
Partial elimination of infrared divergences in the model of quantum field theory with degenerated vacuum, 25:36562 (JINR-P2-5760)
Q-value dependence of multinucleon transfer reactions, 25:35815 (JINR-E2-5797)
Relativistic three-particle problem in terms of three-dimensional variables, 25:36586 (JINR-E2-5771)
Spin effects at high energy in quasipotential approach. 25:36504 (JINR-E2-5770)

K

KANSAS UNIV., KANSAS CITY. MEDICAL CENTER.
Prog. rpt. on protein synthesis in delayed implanting mouse ova, 5/70--5/71, 25:37183 (COO-1801-17)

KERNFORSCHUNGSANLAGE, JUELICH (WEST GERMANY). INSTITUT FUER FESTKOERPERFORSCHUNG.
Development of a four-crystal monochromator and a rotating miniature collimator for neutron spectroscopy, 25:34917 (JUL-719-FF)

KERNFORSCHUNGSANLAGE, JUELICH (WEST GERMANY). INSTITUT FUER REAKTORENTWICKLUNG.
Method for analysis of complex and spectra in semiconductor spectroscopy, 25:34536 (JUL-709-RG)
Technical and economic state as well as prospects of atomic energy in the economy of the Federal Republic of Germany, 25:36885 (JUL-705-RG)
Temperature distribution and corrosion in the core of an advanced high-temperature reactor, 25:36980 (JUL-725-RG)

KERNFORSCHUNGSANLAGE, JUELICH (WEST GERMANY). INSTITUT FUER REAKTORWERKSTOFFE.
Irradiation experiment for testing spherical fuel elements for high-temperature reactors, 25:37018 (JUL-701-RW)

KERNFORSCHUNGSZENTRUM, KARLSRUHE (WEST GERMANY). INSTITUT FUER NEUTRONENPHYSIK UND REAKTORTECHNIK.
Measurement of Doppler coefficient in different fuel samples in a fast and at fast-thermal reactor arrangement by pile oscillator method, 25:37135 (KFK-1350)

KERNFORSCHUNGSZENTRUM, KARLSRUHE (WEST GERMANY). INSTITUT FUER RADIOCHEMIE.
Complex formation of hexivalent uranium and of pentavalent neptunium with 1,3-diketons as well as investigations on septivalent neptunium, 25:34557 (KFK-1339)
Radionuclide preparation through (n,p) and (n,α) reactions with fast reactor neutrons, 25:36686 (CONF-680986-1)

KERNFORSCHUNGSZENTRUM, KARLSRUHE (WEST GERMANY). INSTITUT FUER REAKTORENTWICKLUNG.
Contribution to experimental thermal shock analysis, 25:34776 (EURFNR-794)
Experimental investigation of the retardation of boiling of sodium on artifically roughened surfaces, 25:34791 (KFK-1332)
Inherent properties of the different primary circuits of sodium-cooled reactors, 25:37005 (KFK-1379)
Investigation of natural frequency of normal and elongated function, 25:36993 (KFK-1337)

KERNFORSCHUNGSZENTRUM, KARLSRUHE (WEST GERMANY). ZYKLOTRON-LABORATORIUM.
Improved version of Tamura's code for coupled channel calculations, 25:36818 (KFK-1333)

L

LJUBLJANA UNIV. (YUGOSLAVIA).
Investigation of the system of uranium monosulfide with some alkaline earth sulfides, 25:34603 (IJS-262)

LOS ALAMOS SCIENTIFIC LAB., N. MEX.
A generating operator for solutions of certain partial difference and differential equations, 25:37188 (LA-4655)
Bremsstrahlung emission measurement from thick tungsten targets in energy range 12 to 300 kV, 25:36249 (LA-4624)
Desalination and ion separation of sodium and potassium by bromine redox electrolysis, 25:34691 (LA-4645)
Direct solution of discrete Poisson equation on irregular regions, 25:37187 (LA-4553)
Evaluated nuclear data for hydrogen in the ENDF/B-II format, 25:36660 (LA-4574)
Geology and hydrology of Mesita del Buey, 25:34846 (LA-4660)
New method of sampling Klein--Nishina probability distribution for all incident photon energies above 1 keV, 25:36432 (LA-4663)
Nova Branch-Driver operation, 25:37190 (LA-4682)
Rotating cable pusher for pulsed-propulsion space vehicle, 25:37189 (LA-4666)

LUND INST. OF TECH. (SWEDEN). DEPT. OF NUCLEAR PHYSICS.
High energy photofission cross sections of uranium and thorium, 25:36736 (THAI-AEC-35, pp 1-8)

LYON UNIV. (FRANCE). FACULTE DES SCIENCES.
Oxidation kinetics of pure or alloyed zirconium with oxygen or water vapor, 25:35277 (NP-18833)

LYON UNIV. (FRANCE). INSTITUT DE PHYSIQUE NUCLEAIRE.
Reactions (d,α) with ^{54}Fe and ^{51}V, 25:36687 (LYCEN-7087)

M

MAGYAR TUDOMANYOS AKADEMIA KOZPONTI FIZIKAI KUTATO INTEZETE, BUDAPEST.
Survey of measurements of the fission neutron spectrum of ^{252}Cf, 25:36728 (KFKI-71-9)

MAINE YANKEE ATOMIC POWER CO., WESTBORO, MASS.
Maine Yankee Atomic Power Station. Preliminary safety analysis report, Amendment 24, 25:36945 (DOCKET-50309-35)
Maine Yankee Atomic Power Station. Preliminary safety analysis report, Amendment 25 (includes additions and revisions to final safety analysis report), 25:36946 (DOCKET-50309-36)

MARITIME ADMINISTRATION, WASHINGTON, D. C.
N. S. Savannah. Operations report, November 9, 1970--March 31, 1971, 25:37094 (DOCKET-50238-80)

MARYLAND UNIV., COLLEGE PARK.
Bubble chamber detection technique for gamma rays in momentum region below 1 GeV/c, 25:34964 (CONF-700623-(Vol.1), pp 555-66)

MARYLAND UNIV., COLLEGE PARK. DEPT. OF PHYSICS AND ASTRONOMY.
300 megacycle logic with M.E.C.L. III, 25:35009 (ORO-2504-172)

MASON AND HANGER-SILAS MASON CO., INC., AMARILLO, TEX.
12.5 KJ capacitor bank, 25:37194 (MHSMP-71-33)
Analytical applications of liquid chromatography, 25:37192 (MHSMP-71-31)
Photographic and optical systems analysis, 25:37193 (MHSMP-71-32)
Prog. rpt. on mathematical analysis of HE data, quarterly, 1--3, 1971, 25:37195 (MHSMP-71-34)

MASSACHUSETTS INST. OF TECH., CAMBRIDGE.
Counter control of bubble chamber photography, 25:34569 (CONF-700623-(Vol.2), pp 606-16)

MAX-PLANCK-INSTITUT FUER PHYSIK, MUNICH (WEST GERMANY).
Hyperon bubble chamber HYBUC, 25:34972 (CONF-700623-(Vol.2), pp 640-6)

METROPOLITAN EDISON CO., READING, PA.
Three Mile Island Nuclear Station, Unit 1. Preliminary safety analysis report, Amendment 20 (includes Appendix 13A and final safety analysis report modifications), 25:36944 (DOCKET-50289-35)
Three Mile Island Nuclear Station, Unit 1. Preliminary safety analysis report, Amendment 21 (includes additions and revisions to application for reactor operating license), 25:36882 (DOCKET-50289-36)
MICHIGAN STATE UNIV., EAST LANSING. DEPT. OF CHEMISTRY.
Prog. rpt. on ESR studies of radiation, 1--12/70, 25:34634 (COO-1385-37)
MICHIGAN UNIV., ANN ARBOR. DEPT. OF METEOROLOGY AND OCEANOGRAPHY.
Prog. rpt. on rain scavenging studies, 12/70, 25:34742 (COO-1407-38)
MILAN UNIV. (ITALY). ISTITUTO DI FISICA.
Projector for Gargamelle's pictures, 25:34951 (CONF-700623-(Vol.1), pp 334-44)
MILLSTONE POINT CO., HARTFORD, CONN.
Millstone Nuclear Power Station, Unit 1. Abnormal occurrence report No. A0-71-8, 25:36878 (DOCKET-50245-67)
Millstone Nuclear Power Station, Unit 1. Abnormal occurrence report No. A0-71-6, 25:36875 (DOCKET-50245-59)
Millstone Nuclear Power Station, Unit 1. Abnormal occurrence report No. A0-71-5, 25:36877 (DOCKET-50245-61)
Millstone Nuclear Power Station, Unit 1. Abnormal occurrence report No. A0-71-7, 25:36876 (DOCKET-50245-60)
Millstone Nuclear Power Station, Unit 1. Abnormal occurrences No. A0-71-9 and No. A0-71-10, 25:36879 (DOCKET-50245-81)
MOUND LAB., MIAMISBURG, OHIO.
Prog. rpt. on stable gaseous isotope separation and purification: October--December 1970, 25:34807 (MLM-1793)

N

NANCY UNIV. (FRANCE).
Uranium geochemistry and granitic differentiation in uranium-bearing province of Nord-Limousin, 25:34749 (CEA-R-4034)
NATIONAL ACADEMY OF SCIENCES-NATIONAL RESEARCH COUNCIL, WASHINGTON, D. C. COMMITTEE ON NUCLEAR SCIENCE.
Report on national uses and needs for separated stable isotopes, 25:34813 (TID-25705)
NATIONAL ACCELERATOR LAB., BATAVIA, ILL.
NAL plans, 25:34975 (CONF-700623-(Vol.2), pp 696-702)
Results from the BNL 7-foot chamber, 25:34981 (CONF-700623-(Vol.2), pp 774-89)
Strong interaction physics in the NAL bubble chamber, 25:34940 (CONF-700623-(Vol.1), pp 42-55)
NATIONAL INST. FOR METALLURGY, JOHANNESBURG (SOUTH AFRICA).
Determination, by neutron-activation and tracer techniques, of the losses of iridium during the fire-assay procedure for the platinum-group metals, 25:34544 (NIM-1048)
Instrumental neutron-activation analysis of samples taken at different levels of E.R.P.M. mine, 25:34543 (NIM-1013)
NATIONAL OCEAN SURVEY, LAS VEGAS, NEV.
Aleutian/Amchitka seismic program, 25:34763 (CGS-746-10)
NAVAL ORDNANCE LAB., WHITE OAK, MD.
Magnus data on standard 10° cone calibration model, 25:37220 (SC-DC-713821)
NAVAL RESEARCH LAB., WASHINGTON, D. C.
Fortran programs for (p,γ) yield calculations based on Vavilov's theory of energy loss distributions, 25:36732 (NRL-7230)
NEVADA UNIV., RENO.
Estimating plant production from soil and floristic correlates in Hot Creek Valley, Nevada, 25:37240 (TID-25723)
NEW BRUNSWICK LAB. (AEC), N. J.
Summary of results of general analytical evaluation program, 1--12/69, 25:34503 (NBL-256)
NEW MEXICO UNIV., ALBUQUERQUE.
Numerical solutions of nonequilibrium reflected shock waves in air with radiation, 25:37230 (SC-RR-710203)
NEW YORK STATE DEPT. OF ENVIRONMENTAL CONSERVATION, ALBANY, N.Y.
West Valley Reprocessing Plant. Activity in sanitary waste system effluent, 25:34683 (DOCKET-50201-73)
NEW YORK UNIV., N. Y. AEC COMPUTING AND APPLIED MATHEMATICS CENTER.
16 channel medium speed multiplexer, 25:37196 (NYO-1480-171)
Numerical solution of Boltzmann equation, 25:36126 (NYO-1480-173)
NORTH CAROLINA STATE UNIV., RALEIGH.
Computer experiment studies on mechanisms for irradiation induced defect production and annealing processes. Progress report for period ending May 31, 1970, 25:35504 (ORO-3912-4)
NORTHERN INDIANA PUBLIC SERVICE CO., HAMMOND.
Bailly Generating Station, Nuclear I. Preliminary safety analysis report, Amendment 7, 25:36957 (DOCKET-50367-14)
Bailly Generating Station, Nuclear I. Preliminary safety analysis report, Amendment 8, 25:36958 (DOCKET-50367-15)
Bailly Generating Station, Nuclear I. Preliminary safety analysis report, Amendment 9, 25:36559 (DOCKET-50367-16)
NORTHERN STATES POWER CO., MINNEAPOLIS, MINN.
Prairie Island Nuclear Generating Plant, Units 1 and 2. Preliminary safety analysis report, Amendment 10, 25:36939 (DOCKET-50282-35)
NOTRE DAME UNIV., IND. DEPT. OF BIOLOGY.
Prog. rpt. on nutrient cycling and productivity of dystrophic lake-bog systems (part B), 3--11/70, 25:37182 (COO-1770-3)

O

OAK RIDGE NATIONAL LAB., TENN.
Abstracts of papers: desalination information meeting, May 27--28, 1971, 25:37091 (ORNL-TM-3402)
An integrated system of nuclear materials control at Oak Ridge National Laboratory, 25:34847 (ORNL-4607)
Analysis of torispherical shells subjected to concentrated loads, 25:37211 (ORNL-TM-3201)
Bulk shielding facility quarterly report, January--March 1971, 25:37069 (ORNL-TM-3453)
Comparisons between predicted and measured fuel pin performance, 25:37019 (ORNL-TM-3386)
Computer programs for some eddy-current problems, 1970, 25:37212 (ORNL-TM-3295)
Design considerations of reactor containment spray systems. XII. Variability of the dose reduction factor for the removal of elemental iodine, 25:37029 (ORNL-TM-2412(Pt.12))
Design considerations of reactor containment spray systems. Part X. The stress corrosion cracking of types 304 and 316 stainless steel in boric acid solutions, 25:37028 (ORNL-TM-2412(Pt.10))
Effect of boron on ductility and strength of Inconel 600 and Types 304 and 316 stainless steel at hot metalworking temperatures, 25:35338 (ORNL-TM-3216)
Engineering development studies for Molten-Salt Breeder Reactor Processing No. 3, 25:34694 (ORNL-TM-3128)
Estimated capital costs of nuclear and fossil power plants, 25:37030 (ORNL-TM-3243)
Fueled capsule design and evaluation, safety analysis, 25:34809 (ORNL-TM-3230)
Gross strain crack tolerance of A533-B steel, 25:35225 (HSSTP-TR-14)
Lattice dynamics of rutile, 25:37239 (TID-25720)
Molten-salt fluoride volatility pilot plant: recovery of enriched uranium from aluminum-clad fuel elements, 25:34693 (ORNL-4574)
Muon transport and shielding of high-energy (less than or equal to 500 GeV) proton accelerators, 25:36610 (ORNL-TM-3353)
Neutron multiplicity for ^{239}Pu resonance fission, 25:36734 (ORNL-TM-3331)
New data system for INTEREM, 25:36193 (ORNL-TM-3401)
Oak Ridge systems analysis code (ORSAC) User's manual, 25:36886 (ORNL-TM-3223)
Operation of codes associated with MECC-3, preliminary version of intranuclear-cascade calculation for nuclear reactions, 25:36733 (ORNL-4564)
ORNL-SNAP shielding program, 25:36250 (ORNL-TM-3264)
Patent literature on process radiation and irradiator design. Part 1. United States Patents 1950 through 1968, 25:34777 (ORNL-IIC-34)
Prog. rpt. on high flux isotope reactor, 1--3/71, 25:37068 (ORNL-TM-3432)
Prog. rpt. on isotope kilowatt program, 3/31/71, 25:34810 (ORNL-TM-3394)
Radiation shielding information center user documentation, 25:36247 (CTC-48)
Some factors affecting the performance of hyperfiltration membranes, 25:37213 (ORNL-TM-3296)
Statistical technique for determining sources of variation in $(U,Pu)O_2$ oxygen-to-metal ratio, 25:36668 (ORNL-TM-3362)
Strontium-90 heat sources, 25:34808 (ORNL-IIC-36)
Survey of the materials and design of insulation for prestressed-concrete vessels for gas-cooled reactors, 25:37006 (ORNL-TM-2929)
Technical status of the radioactive waste repository: a demonstration project for solid radioactive waste disposal, 25:34848 (ORNL-4680)
Thorium ceramics data manual. Volume III. Carbides, 25:35548 (ORNL-4503(Vol.3))
OESTERREICHISCHE STUDIENGESELLSCHAFT FUER ATOMENERGIE G.M.B.H., SEIBERSDORF. PHYSIK-INSTITUT.
Mass spectrometric determination of the neutron capture cross section of isotopes of the rare earths, 25:36725 (SGAE-PH-104/1971)
OFFICE OF ATOMIC ENERGY FOR PEACE, BANGKOK (THAILAND).
Environmental isotope investigation in Totes Gebirge Styria, Austria, 25:34726 (THAI-AEC-35, pp 9-20)
Inorganic elements in human stones, 25:34546 (THAI.-AEC-39)
Soil analysis by neutron activation method, 25:34545

(THAI.-AEC-36)
Study on thermal fading characteristics of some TSEE dosimetry, 25:35026 (THAI-AEC-35, pp 21-3)
OMAHA PUBLIC POWER DISTRICT, NEBR.
Fort Calhoun Station, Unit No. 1. Preliminary safety analysis report, Amendment 25 (includes final safety analysis report, Suppl. No. 8), 25:36940 (DOCKET-50285-45)
OREGON STATE UNIV., CORVALLIS.
Centralized data acquisition and time-sharing message switching system, 25:37219 (RLO-2227-T-7-7)
OREGON STATE UNIV., CORVALLIS. DEPT. OF SOILS.
Prog. rpt. on physico-chemical properties of soils from volcanic ash, 9/70--5/71, 25:34724 (RLO-2227-T-9-1)
OREGON UNIV., EUGENE.
Prog. rpt. on diffusion controlled reactions and exchange reactions in solution, annual, 6/71, 25:34573 (RLO-2230-T-2-2)
OXFORD UNIV. (ENGLAND).
Bubble nucleation on surfaces immersed in cryogenic fluids, 25:34958 (CONF-700623-(Vol.1), pp 449-58)
Neutrino physics in heavy liquid chambers, 25:34943 (CONF-700623-(Vol.1), pp 123-35)
OXFORD UNIV. (ENGLAND). NUCLEAR PHYSICS LAB.
Bubble density in liquid helium, 25:34989 (CONF-700623-(Vol.2), pp 893-900)

P

PARIS UNIV. (FRANCE).
Biasing system for treatment of deep penetration of neutrons by Monte-Carlo method, 25:36648 (CEA-R-4145)
PARIS UNIV. (FRANCE). FACULTE DES SCIENCES.
Measurement of the A and R polarization parameters in π^--proton elastic scattering at 6 and 16 GeV/c, 25:36406 (NP-18873)
PARIS UNIV. (FRANCE). LABORATOIRE DE GENIE ELECTRIQUE.
Penetration of magnetic induction, electric field, and losses in impure superconductors, 25:36019 (CONF-700341-8)
PARIS UNIV., ORSAY (FRANCE). FACULTE DES SCIENCES.
Fission investigation using on-line mass spectrometry, 25:36730 (NP-18829)
Study of the ^{153}Sm + ^{153}Eu decay, 25:36731 (NP-18835)
PARIS UNIV., ORSAY (FRANCE). LABORATOIRE DE L'ACCELERATEUR LINEAIRE.
Device for measuring the luminoisity of Orsay storage ring, 25:36606 (LAL-1249)
Study of the ^{11}B nucleus by electron scattering, 25:36672 (LAL-1243)
PENNSYLVANIA ELECTRIC CO., JOHNSTOWN.
Three Mile Island Nuclear Station, Unit 1. Preliminary safety analysis report, Amendment 21 (includes additions and revisions to application for reactor operating license), 25:36882 (DOCKET-50289-36)
Three Mile Island Nuclear Station, Unit 1. Preliminary safety analysis report, Amendment 20 (includes Appendix 13A and final safety analysis report modifications), 25:36944 (DOCKET-50289-35)
PENNSYLVANIA STATE UNIV., UNIVERSITY PARK.
Field ion shadow projection microscope and other FIM techniques for viewing biomolecules, 25:37207 (NYO-3851-10)
PHILADELPHIA ELECTRIC CO., PA.
Limerick Generating Station, Units 1 and 2. Preliminary safety analysis report, Amendment 7, 25:36952 (DOCKET-50352-13)
Peach Bottom Atomic Power Station, Unit 1. Monthly operations report No. 61, March 1971, 25:36867 (DOCKET-50171-85)
Peach Bottom Atomic Power Station, Units 2 and 3. Environmental report, operating license stage, 25:36937 (DOCKET-50277-20)
PHYSIKALISCH-TECHNISCHE BUNDESANSTALT, BRUNSWICK (WEST GERMANY).
Electric installations at the Forschungs- und Messreaktor Braunschweig (FMRB) of the Physikalisch-Technische Bundesanstalt, 25:37062 (FMRB-32/70)
Experience report on the operation and radiation protection at the Braunschweig Research and Measurement Reactor for the year 1970, 25:37063 (FMRB-35/71)
POWER AUTHORITY OF THE STATE OF NEW YORK.
James A. Fitzpatrick Nuclear Power Plant. Environmental report, operating license stage, 25:36949 (DOCKET-50333-22)
POWER REACTOR DEVELOPMENT CO., DETROIT, MICH.
Enrico Fermi Atomic Power Plant, Unit 1. License No. DPR-9; request for authorization of Change No. 28 in the technical specifications, 25:36900 (DOCKET-50016-115)
Enrico Fermi Atomic Power Plant, Unit 1. Request increase in maximum allowable nitrogen dewpoint from minus 35 F to 0 F, 25:36899 (DOCKET-50016-114)
PRINCETON UNIV., N. J.
Bubble chamber detection technique for gamma rays in momentum region below 1 GeV/c, 25:34964 (CONF-700623-(Vol.1), pp 555-65)
PRINCETON UNIV., N. J. DEPT. OF CHEMICAL ENGINEERING.
Prog. rpt., annual, 5/16/70--5/15/71, 25:37200 (NYO-2807-91)
PRINCETON UNIV., N.J. JOSEPH HENRY LABS.
RAD swapping system for nuclear data acquisition, 25:35050 (PUC-937-396)
PRINCETON UNIV., N. J. PLASMA PHYSICS LAB.
Floating ring stabilization system, 25:36188 (MATT-839)
Lawson criteria, 25:36191 (MATT-844)
Lead shielded Dewar development, 25:36192 (MATT-846)
Optical sensors in FP-1, 25:36189 (MATT-840)
Special diagnostic devices, 25:36090 (MATT-838)
Stellarator-mirror machine target plasma reactor, 25:36190 (MATT-841)
Vacuum tube compensated flat top high-current pulse supply for symmetrical torus machine, 25:36187 (MATT-837)
PUBLIC SERVICE CO. OF COLORADO, DENVER.
Fort St. Vrain Nuclear Generating Station, Unit 1. Plans for cooperation with Bureau of Sport Fisheries and Wildlife and Colorado Game, Fish and Parks Department, 25:36935 (DOCKET-50267-30)
PUBLIC SERVICE ELECTRIC AND GAS CO., NEWARK, N.J.
Newbold Island Nuclear Generating Station, Units 1 and 2. Preliminary safety analysis report, Amendment 7, 25:36883 (DOCKET-50354-14)
PURDUE UNIV., LAFAYETTE, IND.
TVGP for track sensitive targets, 25:34949 (CONF-700623-(Vol.1), pp 312-24)

R

ROCHESTER GAS AND ELECTRIC CORP., N. Y.
Robert Emmett Ginna Nuclear Power Plant, Unit No. 1. Possible excessive gas effluent release, 25:36874 (DOCKET-50244-71)
ROCHESTER UNIV., N. Y. DEPT. OF PHYSICS AND ASTRONOMY.
Proteins of the erythrocyte membrane, 25:37258 (UR-49-1430)
RUTGERS--THE STATE UNIV., NEW BRUNSWICK, N. J.
Minimizing angle errors due to multiple scattering, 25:34950 (CONF-700623-(Vol.1), pp 325-33)
RUTHERFORD HIGH ENERGY LAB., CHILTON (ENGLAND).
1.5 metre diameter high field hydrogen chamber, 25:34977 (CONF-700623-(Vol.2), pp 714-34)
Fiber glass reinforced epoxy resin bellows, 25:34986 (CONF-700623-(Vol.2), pp 849-62)
Fisheye mounting problems, 25:34997 (CONF-700623-(Vol.2), pp 1010-23)
Magnetization current effects in coils wound from multifilament stabilized superconductor, 25:35000 (CONF-700623-(Vol.2), pp 1095-1125)
Optimization of bubble chamber design parameters for strong interaction experiments, 25:34939 (CONF-700623-(Vol.1), pp 5-41)
Refractive indices of neon and neon--hydrogen mixtures, 25:34963 (CONF-700623-(Vol.1), pp 543-54)
Resonant expansion system for the proposed high field bubble chamber, 25:34984 (CONF-700623-(Vol.2), pp 824-35)

S

SAN DIEGO GAS AND ELECTRIC CO., CALIF.
San Onofre Nuclear Generating Station, Units 2 and 3. Preliminary safety analysis report, Amendment 9, 25:36955 (DOCKET-50361-17)
SANDIA LABS., ALBUQUERQUE, N. MEX.
A-stable block implicit one-step methods, 25:37231 (SC-RR-710296)
Analog simulation of a guided parachute-payload system, 25:37224 (SC-DR-710097)
Calculated generalized oscillator strengths for atoms He--Na, 25:35844 (SC-RR-70-406)
Calculation of the vapor pressure in desiccated-multicomponent systems, 25:37223 (SC-DR-710074)
Checklist of good contamination control practices from a manufacturing viewpoint, 25:37227 (SC-M-70-549)
Comparison of turbulence intensity and stability ratio measurements to Pasquill turbulence types, 25:34747 (SC-DC-70-5443)
Computer-based display of nondestructive evaluation data, 25:37226 (SC-DR-710222)
ELI-44: computer-controlled instrument system, 25:37222 (SC-DR-70-862)
Energy diffusion in a one-dimensional finite solid with linear heat loss, 25:37221 (SC-DR-70-767)
High intensity direct reading heat flux gauge, 25:37225 (SC-DR-710194)
Ion implantation: a selective bibliography, 25:36265 (SC-B-710148)
Numerical solutions of nonequilibrium reflected shock waves in air with radiation, 25:37230 (SC-RR-710203)
PAN6: computer program for analysis of space frameworks, 25:37229 (SC-RR-70-742)
Sandia Laboratories carbon composites development program, 25:37179 (CONF-710312-1)
Solid propellant burn tests, 25:34792 (SC-DR-710084)
Transmission line coupled to a cylinder in an incident field, 25:37228 (SC-R-713250)
SANDIA LABS., LIVERMORE, CALIF.
Sandia Laboratories Livermore data processing system, 25:37235 (SCL-DR-710032)

XUM

SAXTON NUCLEAR EXPERIMENTAL CORP., PA.
Saxton Reactor. Change No. 42 to technical specifications of Provisional Operating License No. DPR-4, 25:36902 (DOCKET-50146-76)
Saxton Reactor. License No. DPR-4; technical specifications Change Request No. 46, 25:36905 (DOCKET-50146-80)
Saxton Reactor. License No. DPR-4; technical specifications Change Request No. 44, Amendment No. 1, 25:36903 (DOCKET-50146-78)
Saxton Reactor. License No. DPR-4; technical specifications Change Request No. 45, 25:36904 (DOCKET-50146-79)
SCIENTIFIC DATA SYSTEMS, LOS ANGELES, CALIF.
Conference on material testing, Budapest, 10/70, 25:34821 (CONF-701044-(Sect.2))
SCIENTIFIC RESEARCH ATOMIC REACTOR INST., MELEKESS (USSR).
Effect of acidity on the rate of cation--cation oxidation-reduction reactions of actinide elements, 25:34559 (SRARI-P-94)
Investigation of complexing of tetravalent Th, U, Np, and Pu with diethylentriaminpentaacetic acid, 25:34558 (SRARI-P-92)
Specific properties of operation of absorbing materials in fast reactors and requirements for them, 25:37140 (SRARI-P-96)
SCIENTIFIC RESEARCH INST. OF ELECTRO-PHYSICAL APPARATUS, LENINGRAD (USSR).
Calculation of the internal structure of non-laminar axially-symmetric intensive beams of charged particles, 25:36609 (NP-18860)
SKODA CONCERN, PILSEN (CZECHOSLOVAKIA). NUCLEAR POWER PLANTS DIV.
Influence of some metallurgical variables on the radiation damage sensitivity of pressure vessel steels, 25:35505 (ZJE-99)
SMITHSONIAN INSTITUTION, WASHINGTON, D. C. RADIATION BIOLOGY LAB.
Prog. rpt. on phycobiliproteins in algae, summary, 1967--70, 25:37238 (TID-25714)
SOCIETE BELGE POUR L'INDUSTRIE NUCLEAIRE, BRUSSELS.
Pyrochemical head end conception for fast breeder fuel processing, 25:34687 (EUR-4614)
SOUTHERN CALIFORNIA EDISON CO., LOS ANGELES.
San Onofre Nuclear Generating Station, Unit 1. Operation report, May 1970, 25:36868 (DOCKET-50206-113)
San Onofre Nuclear Generating Station, Units 2 and 3. Preliminary safety analysis report, Amendment 9, 25:36955 (DOCKET-50361-17)
SOUTHERN METHODIST UNIV., DALLAS, TEX. DEPT. OF PHYSICS.
Prog. rpt. on neutron cross sections for production of ^{24}Na isomer from Mg and Al, final, 10/70, 25:36688 (N-70-43042)
STAATLICHE ZENTRALE FUER STRAHLENSCHUTZ, BERLIN (EAST GERMANY).
Flocculation and sedimentation of radioactive turbid material from waste water under control of the zeta potential, 25:34696 (SZS-3/71 (pp 2-19))
Problems of instrumentation for radiation protection monitoring of waters, 25:34870 (SZS-2/71, pp 12-22)
Requirements for portable instruments for dose rate and contamination measurements, 25:34868 (SZS-2/71, pp 1-6)
Special requirements for instruments for radiation protection monitoring in nuclear power plants, 25:34869 (SZS-2/71, pp 7-11)
STANFORD LINEAR ACCELERATOR CENTER, CALIF.
Four-inch hydrogen target for 40-inch SLAC bubble chamber, 25:34965 (CONF-700623-(Vol.1), pp 567-80)
Rapid cycling bubble chamber program at SLAC, 25:34552 (CONF-700623-(Vol.1), pp 346-75)
Scintillation counter data acquisition system for use with SLAC 40'' hydrogen bubble chamber, 25:34970 (CONF-700623-(Vol.2), pp 617-26)
TAXL: a simple hierarchical data structure manipulation system, 25:37236 (SLAC-119)
Two-mile accelerator project, 25:36611 (SLAC-130)
SYRACUSE UNIV., N. Y.
Leaf development in certain of the vascular plants, 25:37203 (NYO-3597-16)
SYRACUSE UNIV., N.Y. DEPT. OF CHEMICAL ENGINEERING AND METALLURGY.
Prog. rpt. separation of krypton and xenon from reactor atmospheres by selective permeation, 1/69--12/70, 25:34692 (NYO-4057-2)
SYRACUSE UNIV., N. Y. DEPT. OF PHYSICS.
General treatment of chiral and scale breaking in SU(3) sigma model, 25:36483 (SU-1206-241)

T

TECHNISCHER UEBERWACHUNGS-VEREIN E. V., COLOGNE (WEST GERMANY). INSTITUT FUER REAKTORSICHERHEIT.
Application of statistical methods for the design of reactor systems, 25:36979 (IRS-T-18(1970), pp 205-15)
Critical analysis of the evaluation methods in reactor safety, 25:37039 (IRS-T-18(1970), pp 21-36)
Data acquisition system for the determination of reliability characteristics, 25:37040 (IRS-T-18(1970), pp 123-43)
Reliability analyses of reactor systems from the view of producer and operator, 25:37095 (IRS-T-18(1970), pp 217-21)
Reliability analyses of reactor systems, 25:37041 (IRS-T-18(1970), pp 223-39)
Versuchsatomkraftwerk Kahl; cracks in lengthening rods of control rod driving shafts, 25:36994 (INIS-mf-33)
TELEDYNE--ISOTOPES, PALO ALTO, CALIF.
Radiochemical data for STS #, Amchitka Island, Alaska, 25:34720 (NVO-1229-121)
TENNESSEE UNIV., KNOXVILLE.
Analysis of torispherical shells subjected to concentrated loads, 25:37211 (ORNL-TM-3201)
Experimental investigation of the effects of space and reflection on the count-rate fluctuation spectra of a large nuclear reactor, 25:37134 (DP-MS-70-101)
Lattice dynamics of rutile, 25:37239 (TID-25720)
Some factors affecting the performance of hyperfiltration membranes, 25:37213 (ORNL-TM-3296)
TENNESSEE VALLEY AUTHORITY, KNOXVILLE.
Watts Bar Nuclear Plant, Units 1 and 2. Draft environmental statement, 25:36969 (DOCKET-50390-E)
Watts Bar Nuclear Plant, Units 1 and 2. Preliminary safety analysis report, Vol. 4, 25:36968 (DOCKET-50390-5)
Watts Bar Nuclear Plant, Units 1 and 2. Preliminary safety analysis report, Vol. 1, 25:36965 (DOCKET-50390-2)
Watts Bar Nuclear Plant, Units 1 and 2. Preliminary safety analysis report, Vol. 2, 25:36966 (DOCKET-50390-3)
Watts Bar Nuclear Plant, Units 1 and 2. Preliminary safety analysis report, Vol. 3, 25:36967 (DOCKET-50390-4)
Watts Bar Nuclear Plant, Units 1 and 2, Rhea County, Tennessee. License application, 25:36964 (DOCKET-50390-1)
TEXAS UNIV., AUSTIN. CENTER FOR PARTICLE THEORY.
Analyticity, covariance, and unitarity in indefinite metric quantum field theories, 25:36563 (ORO-3992-26)
Deep inelastic neutrino--nucleon interactions, 25:36455 (ORO-3992-24)
Indefinite metric and shadow states in quantum field theory, 25:36564 (ORO-3992-30)
TEXAS UNIV., AUSTIN. DEPT. OF PHYSICS.
A model for dipole electromagnetic form factors, 25:36436 (ORO-3992-28)
Model for K/sub 13/ form factors and Cabibbo angle, 25:36456 (ORO-3992-39)
THOMSON-CSF, ORSAY (FRANCE).
Metallurgy of superconductors, 25:36018 (CONF-700341-7)
TODD SHIPYARDS CORP., GALVESTON, TEX. NUCLEAR DIV.
300 pound gas test report (28-IV-16006), 25:37070 (TODD-N-16)
500 pound gas test continuation series report (28-IV-16011), 25:37074 (TODD-N-23)
500 pound gas test report (28-IV-16008), 25:37071 (TODD-N-18)
700 pound gas test report (28-IV-16009), 25:37072 (TODD-N-20)
Gas test series addendum tests and synoptic evaluation (28-IV-16012), 25:37075 (TODD-N-24)
Second 300 pound gas test (28-IV-16010), 25:37073 (TODD-N-21)
TOKYO UNIV. (JAPAN).
Problems about fuel cladding materials, 25:37016 (CONF-700211-9)
TRW SYSTEMS GROUP, REDONDO BEACH, CALIF.
Gross strain crack tolerance of A533-B steel, 25:35335 (HSSTP-TR-14)

U

UNION CARBIDE CORP., OAK RIDGE, TENN. Y-12 PLANT.
Mechanical behavior of a uniaxially aligned tungsten wire-reinforced lead composite system, 25:35244 (Y-1788)
UNITED KINGDOM ATOMIC ENERGY AUTHORITY, SPRINGFIELDS (ENGLAND). PRODUCTION GROUP.
Analytical method for the general gravimetric determination of uranium in ores and concentrates, 25:34505 (PG-Report-1020)
UNITED NUCLEAR CORP., ELMSFORD, N. Y. RESEARCH AND ENGINEERING CENTER.
La Crosse Boiling Water Reactor. Water level instrument behavior during main steam bypass valve malfunction incident, 25:36896 (DOCKET-1155-117)
UNITED STATES-EURATOM FAST REACTOR EXCHANGE PROGRAM.
Contribution to experimental thermal shock analysis, 25:34776 (EURFNR-794)
Natural convection irradiation device ''Esther'', 25:37061 (EURFNR-890)
UNIVERSIDAD NACIONAL AUTONOMA DE MEXICO, MEXICO CITY. FACULTAD DE CIENCIAS.
Radiolysis of n-heptane, 25:34635 (NP-18810)
UNIVERSITY OF SOUTHERN CALIFORNIA, LOS ANGELES.
Prog. rpt. on ESR studies of thiyl free radicals relation to biological effects of radiation, annual, 3/71, 25:34639 (USC-113-F-21-3)

XUM

UTAH UNIV., SALT LAKE CITY. DEPT. OF GEOLOGICAL AND GEOPHYSICAL SCIENCES.
Carbon, oxygen, and sulfur isotopes and the origin of sandstone-type uranium deposits. Final report, 25:34750 (COO-2024-1)

V

VERMONT YANKEE NUCLEAR POWER CORP., RUTLAND.
Vermont Yankee Nuclear Power Station. Preliminary safety analysis report, Amendment 27 (includes additions and revisions to final safety analysis report), 25:36936 (DOCKET-50271-52)
VIRGINIA ELECTRIC AND POWER CO., RICHMOND.
Surry Power Station, Units 1 and 2. Preliminary safety analysis report, Amendment 22 (includes additions and revisions to final safety analysis report, Part B), 25:36938 (DOCKET-50280-40)

W

WADCO CORP., RICHLAND, WASH.
Helium production in stainless steel and its constituents as related to LMFBR development programs, 25:35503 (HEDL-SA-193)
Rotating wire spacer model in large bundle thermal-hydraulics, 25:37020 (WHAN-SA-76)
WASEDA UNIV., TOKYO (JAPAN). DEPT. OF SCIENCE AND ENGINEERING.
Problems about fuel cladding materials. Stainless steel, 25:37139 (CONF-700211-7)
WASHINGTON UNIV., SEATTLE. DEPT. OF CHEMISTRY.
Prog. rpt. on radiocarbon in sea, 8/15/68--5/1/71, 25:34723 (RLO-2225-T-20-3)
WASHINGTON UNIV., SEATTLE. DEPT. OF OCEANOGRAPHY.
Determining middle scale time dependent variations in salinity and temperature structure in coastal zone province under influence of dilution and upwelling, 25:37216 (RLO-1725-191)
Prog. rpt. on Columbia River effects in Northwest Pacific, 7/70--5/71, 25:37217 (RLO-1725-200)
Release of dissolved organic matter from natural populations of marine phytoplankton, 25:37215 (RLO-1725-186)
WASHINGTON UNIV., SEATTLE. LAB. OF RADIATION ECOLOGY.
Biological half-lives for zinc and mercury in Pacific oyster, 25:37218 (RLO-2225-T-1-5)
WEINER ASSOCIATES, INC., BALTIMORE, MD.
Test program to evaluate re-entry protection performance of metal impregnated foamed zirconia thermal switch material, 25:35549 (TID-25696)
WESTINGHOUSE ELECTRIC CORP., MADISON, PA. ADVANCED REACTORS DIV.
Effects of burnup on fuel pin thermal performance, 25:37017 (CONF-710414-1)
Status report on evaluation of sodium cross sections for ENDF/B, 25:36693 (WARD-4181-2)
Transient effect on LMFBR fuel rods by gas bubbles entrained in coolant, 25:37037 (CONF-700608-36)
WESTINGHOUSE ELECTRIC CORP., PITTSBURGH, PA. ASTRONUCLEAR LAB.
Comparison of inconel 718 and inconel 750 for elevated temperature service in a pumped NaK system, 25:35343 (WANL-TME-1857)
WESTINGHOUSE ELECTRIC CORP., PITTSBURGH, PA. NUCLEAR ENERGY SYSTEMS DIV.
Nuclear Instrumentation System: topical report, 25:36995 (WCAP-7669)
Plant instrumentation program quarterly progress report for the period ending September 30, 1970, 25:34924 (WCAP-7562-3)
Process instrumentation for Westinghouse nuclear steam supply systems (4 loop plants), 25:37010 (WCAP-7671)
WISCONSIN ELECTRIC POWER CO., MILWAUKEE.
Point Beach Nuclear Plant, Unit 1. Abnormal occurrence report: improper lineup of safety injection pump breaker, 25:36881 (DOCKET-50266-49)
Point Beach Nuclear Plant, Units 1 and 2. Preliminary safety analysis report, Amendment 12 (includes additions and revisions to final facility description and safety analysis report), 25:36933 (DOCKET-50266-48)
Point Beach Nuclear Plant, Units 1 and 2. Sensitized stainless steel in nozzles of pressurizer safety valves, 25:36934 (DOCKET-50266-50)
WISCONSIN MICHIGAN POWER CO., APPLETON, WIS.
Point Beach Nuclear Plant, Units 1 and 2. Preliminary safety analysis report, Amendment 12 (includes additions and revisions to final facility description and safety analysis report), 25:36933 (DOCKET-50266-48)
WISCONSIN UNIV., MADISON.
Neutral particle tagging facility for ANL 30'' bubble chamber, 25:34967 (CONF-700623-(Vol.2), pp 582-92)
Wisconsin rapid cycling bubble chamber, 25:34956 (CONF-700623-(Vol.1), pp 418-23)
WISCONSIN UNIV., MADISON. DEPT. OF MINERALS AND METALS ENGINEERING.
Creep in stoichiometric beta NiAl, 25:37180 (COO-1485-10)
WOODS HOLE OCEANOGRAPHIC INSTITUTION, MASS.
Prog. rpt. on general summary, 1970--1971, 25:34759 (NYO-2174-129)
WYOMING UNIV., LARAMIE. DEPT. OF CHEMISTRY.
Prog. rpt. on spectral studies of polyenes and their carbonium ions: implications to photobiology, 2/21/71, 25:37181 (COO-1693-6)

Y

YUGOSLAV FEDERAL COUNCIL FOR THE COORDINATION OF SCIENTIFIC ACTIVITIES, BELGRADE.
Conference on electronics and automation, Herceg-Novi, 6/70, 25:35047 (CONF-700647)
YUGOSLAV NUCLEAR ENERGY COMMISSION, BELGRADE.
Conference on electronics and automation, Herceg-Novi, 6/70, 25:35047 (CONF-700647)

Z

ZENTRALINSTITUT FUER KERNFORSCHUNG, ROSSENDORF BEI DRESDEN (EAST GERMANY).
Radioactive waste from the reprocessing of fast reactor irradiated fuel, 25:34697 (SZS-3/71 (pp 20-32))
ZENTRALSTELLE FUER ATOMKERNENERGIE-DOKUMENTATION, FRANKFURT AM MAIN (WEST GERMANY).
Plasma physics index. Vol. 6, No. 4, 1971, 25:36082
Surface and vacuum physics index, Vol. 6, No. 3, 1971, 25:35835
Technology index for plasmaphysics research and fusion reactors, Vol. 5, No. 4, 1971, 25:36081

PERSONAL AUTHOR INDEX

Authors' names are indexed in the form appearing in the abstracted publication. Each entry under an author's name gives the publication title and the *NSA* volume and abstract numbers. Report numbers, where applicable, are given in parentheses at the end of the entry.

Because of problems involved in the mechanical preparation of this index, all accent marks are omitted. The following changes in spelling have been introduced to reduce some of the confusion which might result from omitting the accents:

Germanic	ä appears as	ae
Germanic	ö	oe
Germanic	ü	ue
Scandinavian	ø	oe

A

AALTONEN, J., Separation of alkaline earth metal isotopes by ion exchange. I, 25:34709

ABAGYAN, G. B., Double-stage mechanism of formation of free radicals during radiolysis of frozen aqueous solutions of DNA, 25:34654

ABATUROV, L. V., Regularities in infra-red spectra (Amide A, B, I, and II bands) of globular proteins in D_2O, 25:34588

ABDELAZIZ, M. E., Control computer for analysis and measurement of beam quality in 50-MeV accelerator, 25:36612 (UARAEE-76)

Design and construction of a single gap high gradient column, 25:36613 (UARAEE-87)

ABD-EL-MEGID, F. M., Automatic start-up system for UA-RR-1 reactor, 25:37083 (UARAEE-108)

ABDEL-RASSOUL, A. A., Mechanical decladding of the Inchas fuel, 25:34780 (UARAEE-54)

Possible trends for purity control of uranium by neutron activation assay, 25:34547 (UARAEE-68)

ABD-EL-SAMIE, Sh., Effect of different reflectors on UA-RR-1 reactor core characteristics, 25:37080 (UARAEE-73)

ABDULLAEV, A. M., Facilities at Kum-bel Mountain Station for study of high-energy interactions, 25:35013

Method of projecting and studying the spatial image of complex events recorded by a spark chamber, 25:35011

Program for study of high-energy nuclear interactions of cosmic rays at Kum-bel Mountain Station, 25:36416

ABE, Hironobu, Low temperature irradiation studies on iron--boron alloys, 25:35588

ABELS, C., Thermoelectric cooling in scattering chamber 800 of Hamburg isochronous cyclotron, 25:36634

ABERS, Ernest S., Anomalous behavior of $\gamma\gamma \to \pi^0$ Lagrangians, 25:36446

ABHYANKAR, K. D., Tables of auxiliary functions for nonconservative Rayleigh phase matrix, 25:35826

ABILDAYAEV, A. M., Isotopic composition of uranium and the content of actinium in minerals and natural waters, 25:34738

ABLYAEVA, N. Kh., Hormonogenesis in thyroid by local irradiation, 25:35208

ABOUL-FETOUH, M., Estimate for UAR research reactor thermal inertia, 25:37084 (UARAEE-111)

ABRAHAMSON, Edwin W., Primary process in radiation chemistry, 25:34613 (TID-25689)

ABRAMENKO, A. N., TV system used for observations of faint variable stars, 25:35639

ABRAMOWICZ, M. A., Structure of dense stars. II, 25:35614

ABRAMS, G. S., A_2^+ mass spectrum in $\pi^+ p$ interactions at 3.7 GeV/c, 25:36411

ABRAO, Alcidio, Preparation of clear uranyl nitrate solution by fractional dissolution of sodium diuranate, 25:34699

ABU-LEILAH, M. M., RAM-1, multigroup neutron diffusion code for IBM-1130, 25:36651 (UARAEE-107)

ABU-ZEID, M. M., Calibration of three-crystal-NaI-pair-spectrometer, 25:34921 (UARAEE-93)

Construction of a three-crystal scintillation pair spectrometer, 25:34922 (UARAEE-100)

Thermal neutron capture gamma-rays in iron, 25:36692 (UARAEE-103)

ACKERMANN, G., Economic studies on stretch-out of burnup in power reactors, 25:37031

ADAIR, Attwell M., Influence of thermomechanical processing on the structure and properties of extruded Beta III titanium, 25:35398

ADAM, G., Solution of an exactly solvable quantum mechanical N-body problem, 25:36370

ADAM, M. F., Neutron diffraction cryo-orienter, 25:36080

ADAMOV, I. Yu., Azimuthal current and microwave radiation in theta pinch, 25:36122

ADAMS, J. A. S., Radon-222 emanation and high apparent Pb isotope ages in lunar dust, 25:35831

ADAMS, John A. S., Gamma-ray spectrometry of rocks, 25:34539

ADAMS, T. F., Lyman alpha emission from Galaxy, 25:35752

ADAMSON, M. G., Thermodynamic data program involving plutonia and urania at high temperatures. Quarterly report No. 14, November 1, 1970--January 31, 1971, 25:35547 (GEAP-12182)

ADE, P. A. R., Solar chromospheric activity at 400, 800, and 1200 μ, 25:35776

ADEEV, G. D., Energy surfaces of ^{238}U in parametrization of Cassinian ovaloids, 25:36793

ADIL, A. Subhan, Colorimetric determination of Au(III), 25:34521

ADOMAITENE, D., X-ray induced 8-azaguanine-resistant cells, 25:35124

AFANAS'EV, V. P., Decays of Nd and Pr nuclides with mass number A = 138, 25:36725 (JINR-P6-5674)

Electromagnetic separation of short-lived isotopes of Rn, Xe, and Kr for spectroscopic studies, 25:34806 (JINR-P13-5757)

AGARKOV, V. A., Growth and transformation of crystalline epithelium in implants following x-irradiation of donor, 25:35231

AGARWALA, Om Prakash, Effects on the alkaloid content of potatoes grown from seeds subjected to low-dose gamma irradiation, 25:35254

AGERON, P., Cold neutron source of French--German high flux reactor in Grenoble, 25:37087

AGNESE, A. G., Scale factor in cosmological homogeneous models, 25:35816

AGRAWAL, P. C., Balloon-borne instrument for studying x-ray sources in 15- to 150-keV range, 25:35014

Energy spectrum of diffuse cosmic x rays in the energy range 20 to 120 keV, 25:35921

Energy spectrum of Sco X-1 in the region 15 to 120 keV, 25:35704

AGRAWAL, S. K., Cyclic yield behavior of polycrystalline niobium, 25:35425

AGRAWAL, S. P., Variation of limiting energy of corotating cosmic rays with the solar cycle, 25:35914

AHMED, N., Shape calibration and peak-to-total ratio measurements of 5'' x 6'' NaI(Tl) scintillation detector, 25:34936

AIHARA, S., Frequency shift and suppression of ion-wave instability by high-frequency electric field, 25:36172

Optical measurement of a high-frequency electric field in a weakly ionized plasma, 25:36094

AILLERET, Pierre, Location problems for nuclear power stations, 25:36971

AITKEN, E. A., Thermodynamic data program involving plutonia and urania at high temperatures. Quarterly report No. 14, November 1, 1970--January 31, 1971, 25:35547 (GEAP-12182)

AIZENMAN, M. L., Secular stability. I, 25:35662

AKASAKA, Youichi, Paramagnetic defects induced in naphthalene and anthracene single crystals by neutron irradiation at low temperature, 25:36277

Radiation damage studies using the low temperature irradiation facility. VI, 25:36287

AKASOFU, S.-I., Results from meridian chain of observatories in Alaskan sector. I, 25:35961

AKATKIN, O. A., Device for the investigation of relative dose distributions, 25:35059

AKHIEZER, A. I., Absolute, convective and global unstabilities, amplification and non-transmission of vibrations, 25:36560 (ITF-70-96-P)

Magnetic energy pumping into a turbulent plasma, 25:36083

XUM

AKHMEDLI, M. K., Effect of the structure of mono- and bifunctional azo compounds on the analytical properties of yttrium and rare earth complex compounds, 25:34528
AKIMOV, N. I., Effect of excitation energy on yields and kinetic energies of fragments at fission of ^{239}Pu by neutrons, 25:36754
AKSELA, S., Analysis of the energy distribution in cylindrical electron spectrometers, 25:34927
ALAKSIN, V. F., Magnetic energy pumping into a turbulent plasma, 25:36083
ALANAKYAN, Yu. R., Nonlinear theory of electromagnetic-wave trapping in a plasma, 25:36230
ALBERT, P., Determination of V, Nb, and S concentrations by proton activation analysis, 25:34554
ALBERT, Roy E., X-ray fluorescence: detection of lead in wall paint, 25:35043
ALBRECHT, W., High-voltage electrophoretic separation of inorganic ions with special regard to Pt metals. III, 25:34702
ALBURGER, D. E., Properties of ^{13}B and ^{29}Na, 25:36710
ALCOCK, M. W., Stabilization of the drift-dissipative instability in a plasma by rf magnetic and electric fields, 25:36179
ALDERSON, T., Induction of mutation by γ irradiation in presence of oxygen or nitrogen, 25:35121
ALERS, G. A., Change in flow stress due to the superconducting-normal transition, 25:35389
ALEXANDER, E. C. Jr., Plutonium-244: confirmation as an extinct radioactivity, 25:35594
ALEXANDER, J. A., Techniques for fabrication of high-strength, high-modulus, low-density filament-reinforced metal matrix composites, 25:35528
ALEXANDER, Saramma, Possible correlation between atmospheric ozone content and cosmic-ray intensity variations, 25:35974
ALEXANDROV, Yu. A., Neutron--electron interaction studied by neutron diffraction on a single crystal of ^{186}W, 25:36380 (JINR-E3-5713)
ALFILLE, L., Gargamelle: some technical aspects, 25:35003 (CONF-700623-(Vol.2), App.1)
ALFVEN, H., New approach to the theory of the magnetosphere, 25:35993
ALIKHANOV, S. G., Ion shock waves in a collisionless plasma, 25:36106
ALIKHANYAN, A. I., Dynamic radiation generated in crystals by particles with ultrarelativistic energies, 25:36382
ALLADIN, Saleh Mohamed, Escape of stars from colliding galaxies, 25:35796
ALLEN, G. F. R., Spin--parity combinations in ^{22}Ne, 25:36698
ALLEWAERT, J., Experiences with a thermoluminescence dosimeter, 25:35139
ALLIO, R. J., Fuel development for power reactors, 25:35550
ALLOIN, Danielle, Spectrophotometry of NGC 3351 galaxy nucleus from 3,300 to 7,000 A, 25:35804
ALLOUSH, A. A., Characteristics of collimator constructed for Inchass whole body monitor, 25:34871 (UARAEE-82)
ALMQUIST, Ph. W., Conference on gel permeation chromatography, Miami Beach, Fla., 10/70, 25:35532
ALONSO, A., Effects of ionizing radiations on O uptake by rat liver slices, mitochondria, and mitochondrial membranes, 25:35223
ALSMILLER, F. S., Muon transport and shielding of high-energy (less than or equal to 500 GeV) proton accelerators, 25:36610 (ORNL-TM-3353)
ALSMILLER, R. G. Jr., Muon transport and shielding of high-energy (less than or equal to 500 GeV) proton accelerators, 25:36610 (ORNL-TM-3353)
ALTMANN, H., Repair of strand breaks in Chlorella-DNA caused by gamma irradiation, 25:35257
Tracer studies of synthesis of free nucleotides in yeast after β-irradiation, 25:35252
ALYAMOVSKII, S. I., Region of homogeneity of a zirconium oxynitride of NaCl structure at 1500°C, 25:35583
AMAMIYA, N., Air conditioning in the nuclear power plant, 25:34788
AMANO, H., Impurities in processed radioisotopes produced by (n,γ) reaction: purity of ^{160}Tb, 25:34670 (JAERI-Memo-4280)
Impurities in processed radioisotopes produced by (n,γ) reaction: purity of ^{169}Yb, 25:34669 (JAERI-Memo-4279)
AMANO, Muneyuki, Preparation and pulverization of hydrogenerated niobium, 25:35299
AMAVIS, R., Principles and methods for the derivation of a formula for the discharge of radioactive liquid wastes in surface waters, 25:34717 (EUR-4636)
AMBLARD, Bernard, Measurement of the A and R polarization parameters in π⁻-proton elastic scattering at 6 and 16 GeV/c, 25:36406 (NP-18873)
AMMIRAJU, P., Large-angle proton--proton scattering at high energies, 25:36534
AMMON, R. L., Comparison of inconel 718 and inconel 750 for elevated temperature service in a pumped NaK system, 25:35343 (WANL-TME-1857)
AMSEL, G., ^{18}O study of the source of oxygen in the anodic oxidation of silicon and tantalum in some organic solvents, 25:35293
Study of the oxygen growth laws of anodic oxide films on aluminum and tantalum using nuclear microanalysis of ^{18}O and ^{18}O, 25:35294
Use of nuclear microanalysis of light elements in electrochemistry, 25:34550
ANAND, K. C., Gamma radiation from the galactic center: future experiments, 25:35923
High-energy cosmic-ray electrons, 25:35920
Low-energy gamma-ray spectrum in space, 25:35922
ANANTHASWAMY, H. N., Biochemical and physiological changes in gamma-irradiated wheat during germination, 25:35102
ANASTASIA, L. J., Work plan for continuation of the project, reduction of atmospheric pollution by the application of fluidized-bed combustion, 25:37158 (ANL/ES-CEN-1003)
ANDERS, Edward, How well do we know cosmic abundances, 25:35595
ANDERS, G., Radioactive waste from the reprocessing of fast reactor irradiated fuel, 25:34697 (SZS-3/71 (pp 20-32))
ANDERSON, C. J., Engineering design of the 2X II, 25:36155 (UCRL-73060)
ANDERSON, David Vincent, Computation of plasma equilibria and stability in Astron and minimum-B mirror systems, 25:36165 (UCRL-51030)
ANDERSON, George C., Prog. rpt. on Columbia River effects in Northwest Pacific, 7/70--6/71, 25:37217 (RLO-1725-200)
ANDERSON, J. H., Total and differential cross section for neutrons scattered from ^{90}Zr and Nat. Zr, 25:36740 (WAPD-T-2411)
ANDERSON, P. F., Performance of uniaxial creep machines in NRX and NRU reactors, 25:37054 (AECL-3738)
ANDERSON, R. K., Isospin mixing in ^{8}Be, 25:36677
ANDERSON, Richard C., Transparent thoria-base ceramics containing Y_2C_3 and method for producing same, 25:35543
ANDERSON, Robert E., Aging in Hiroshima and Nagasaki atomic bomb survivors, 25:35241
ANDERSON, V. E., Relativistic ground-state energy eigenvalues of an electron-dipole system, 25:36371
ANDREEVA, O. S., Enriched U in urine, 25:34541
ANDRESEN, R. D., Electron energy distribution within a curved channel multiplier, 25:34905
ANDREWS, David, Conference on new experimental techniques in propulsion and energetics research, Munich, 9/67, 25:36107
ANDRICK, D., Angular distributions for the excitation of vibronic states by resonant electron--molecule reactions, 25:35869
ANGADI, M. A., Josephson effect in Nb--Hg contacts, 25:36068
ANGER, Hal O., Eighty-lens optical camera for recording dynamic studies with the scintillation camera, 25:34872 (UCRL-20699)
ANGIONE, Ronald J., Photoelectric sequences for brighter QSO's, 25:35679
ANKUDINOV, V. A., Oscillations of the total cross sections for inelastic processes in atomic collisions, 25:35876
ANSARI, A. R., Emission of deuterons in 24-GeV/c proton interactions with emulsion nuclei, 25:36403
ANSELL, G. S., Measurement of particle--matrix interface strength in TD-nickel, 25:35458
ANSELL, G. V., Revised position sensitive detector array for a charged particle spectrograph, 25:34861 (AERE-R-6776)
ANTONOVA, E. A., Superconductivity of niobium diselenide, 25:36041
ANTONUCCI, E., Solar effects on cosmic ray intensity observed at 70 MWE underground, 25:35731
ANTOSHIN, G. V., Isotope exchange between molecular oxygen and synthetic zeolites, 25:34580
ANTOV, G., Changes in oral cavity in chronic radiation, 25:35219
ANUCHKIN, A. M., Measurement of the concentration of oxygen dissolved in tantalum, 25:35339 (ORNL-tr-2479)
AOI, Koya, Resonance effects in metals. I and II, 25:36067
AOKI, Takashi, Influence of ambients of the reverse current of surface barrier detectors. I, 25:34897
APPENZELLER, I., Observational evidence for Parker's instability of interstellar gas and magnetic field, 25:35795
AQUILANTI, V., Mass spectrometric study of ionic reactions pertinent to the radiation chemistry of methane, 25:34645
ARAI, Shiro, Annealing effects on galvanomagnetic properties of heavily radiation-damaged graphite, 25:36314
ARAOZ, C., Some nuclear developments in Argentina, 25:35527
ARDELL, A. J., Effect of volume fraction on particle coarsening, 25:37244 (UCLA-34-P-172-2)
ARENHOEVEL, H., Electrons in strong external fields, 25:36369
ARGAN, P. E., Heavy gas--liquid mixture bubble chamber of 70 liters volume with hydrogen internal target, 25:35007 (LNF-70/25)
ARGISHEVA, A. I., Study of complex formation of Th with phthalexon S and thymolphthalexon S, 25:34532
ARIFOV, U. A., Electron emission from monocrystals of alkali-metal halide compounds, 25:35840
Influence of large doses of γ radiation on optical properties of quantum generator, 25:35082
ARIGA, Seiichi, Motion and collision of plasma blobs

produced by giant pulse laser in a transverse magnetic field, 25:36158
ARIMA, A., Stabilization of axially symmetric shape and $(pf)^2$ mixing in sd shell nuclei, 25:36822
ARL'T, R., Short-lived isomers of Tb isotopes: ^{148}Tb, ^{149}Tb, ^{150}Tb, and ^{152}Tb, 25:36726 (JINR-P6-5681)
ARMENTI, Angelo Jr., Motion of particle in gravitational monopole--quadrupole field and general theory of relativity, 25:35809
ARMINEN, E., Anomalously high collection of copper ions implanted in aluminum, 25:36295
ARMITAGE, B. H., Revised position sensitive detector array for a charged particle spectrograph, 25:34861 (AERE-R-6776)
ARMSTRONG, R. W., Dislocation substructure and strength properties of niobium single crystals, 25:35376
ARTAMONOVA, S. M., Reply to article by F. M. Spiridonov, 25:35570
ARTEAGA-ROMERO, N., Experimental conditions for $\gamma\gamma$ collisions with almost real photons, 25:36451
ARTSIMOVICH, L. A., Electronic thermal conductivity in a toroidal plasma loop, 25:36141
ASHCRAFT, R. W., Prog. rpt. on mathematical analysis of HE data, quarterly, 1--3, 1971, 25:37195 (MHSMP-71-34)
ASHENHURST, Robert L., Prog. rpt., 2/71, 25:37184 (COO-2094-6)
ASHTON, F., Characteristics of an external electrode spark chamber, 25:35021
Precision of time of flight measurements, 25:35020
ASLANOV, G. A., Arsenate method for a micro iodometric determination of scandium, 25:34508
ASSYLBAYAEV, U. H., Isotopic composition of uranium and the content of actinium in minerals and natural waters, 25:34738
ASTAKHOVA, N. K., Study of complex formation of Th with phthalexon S and thymolphthalexon S, 25:34532
ASUNDI, M. K., Internal friction due to oxygen-substitutional impurity atom complexes in zirconium, 25:35404
ATAYAN, R. R., Two aspects of oxygen influence in a radiobiological experiment, 25:35119
ATHANASSOULA, E., Group velocity of high amplitude surface waves in vacuum-plasma interfaces, 25:36214 (DEMO-71/5)
Relativistic doppler effect and group velocity in homogeneous nonlinear and inhomogeneous plasma, 25:36215 (DEMO-71/6)
ATKINS, P. W., Angular momentum coherent states, 25:36377
ATOBE, Kozo, Radiation damage studies using the low temperature irradiation facility. V, 25:36290
ATWATER, H. F., Photon attenuation coefficients for organic materials, 25:36259
AUBLE, R. L., Nuclear data sheets for A = 203, 25:36809
AUCOUTURIER, Marc, Electrochemical behavior of U electrode in contact with aqueous solutions and the nature of the phases formed as a function of pH, 25:34562
AUGER, C., Fibrosarcoma induced by alpha particle irradiation, 25:35236
AUGUST, L. S., Analysis of (p,^{3}He) and (d,α) reactions on ^{209}Bi, 25:36777
AUGUSTIN, J. E., Device for measuring the luminoisity of Orsay storage ring, 25:36606 (LAL-1249)
AULL, L. B., Cost-benefit illustration for underground nuclear natural gas stimulation, 25:34766 (AECOP-632)
AVAKYAN, Ts. M., Some reactions of the organisms to radiation in different oxygen pressures, 25:35118
AVILA CASTILLO, E., Radioactive wastes of nuclear center in Mexico, 25:34733
AVIRAM, Ira, Solution of the neutron transport equation, 25:36654
AWAL, M. A., Shape calibration and peak-to-total ratio measurements of 5'' x 6'' NaI(Tl) scintillation detector, 25:34936
AYSCOUGH, P. B., Electron spin resonance studies of fundamental processes in radiation- and photo-chemistry. VI, 25:34641
AZER, M. S., Automatic start-up system for WWR-S, 25:37082 (UARAEE-94)
AZER, M. T., Automatic start-up system for UA-RR-1 reactor, 25:37083 (UARAEE-108)
AZIMOV, S. A., Facilities at Kum-bel Mountain Station for study of high-energy interactions, 25:35013
Method of projecting and studying the spatial image of complex events recorded by a spark chamber, 25:35011
Program for study of high-energy nuclear interactions of cosmic rays at Kum-bel Mountain Station, 25:36416
AZUMA, R. E., Resonance in ^{27}Al(p,γ)^{28}Si, 25:36699

B

BAACKE, J., Backward dispersion relations for $\pi N \to \pi\Delta$ scattering and $N\Delta\gamma$ couplings, 25:36508
BABA, Nobuyoshi, Growth of anodic oxide films on Ti, Ta, and Zr, 25:35284
BABAYAN, R. S., Chromosome aberrations caused by x-irradiation, 25:35125
BABESHKIN, A. M., Consequencies of β-decay of ^{129}Te in some Te oxide compounds, 25:34674
BABIN, A. N., Development of solar flare on July 11, 1966, 25:35748
Solar radio emissions and flare of July 11, 1966, 25:35749
BABU, G. S. D., Rotational velocities and magnetic fields of A/sub p/ stars, 25:35664
BABU, Ram, Propagation and growth of weak discontinuities in magnetogasdynamics, 25:35944
BACH, P., Plastic deformation of single crystals of indium solid solutions in magnesium, 25:35387
BACHY, G., BEBC expansion servo-system, 25:34988 (CONF-700623-(Vol.2), pp 873-92)
BACK, B. B., Fission of U, Np, Pu, and Am isotopes excited in (d,p) reaction, 25:36746
BACOLLA, D., Possibilities and limitations of nuclear medicine in infant diagnostics, 25:35182
BADEWITZ, R. C., TVGP for track sensitive targets, 25:34949 (CONF-700623-(Vol.1), pp 312-24)
BAECKLIN, A., Low-energy band structure in ^{187}Os, 25:36805
BAER, H. W., Spectroscopy of states in ^{91}Zr from γ-ray transitions observed in ^{88}Sr(α,nγ)^{91}Zr reaction, 25:36757
BAERS, B., Noise measurements in a subcritical facility based on photon detection, 25:37086
BAES, C. F. Jr., Oxide chemistry of Pu in molten fluorides and free energy of formation of PuF_3 and PuF_4, 25:34566
BAGDASAROV, R. E., Prompt neutron yield in ^{238}U fission, 25:36786
BAHCALL, John N., Relative correlation of large- and small-redshift quasi-stellar objects with clusters of galaxies, 25:35693
BAHCALL, Neta A., Relative correlation of large- and small-redshift quasi-stellar objects with clusters of galaxies, 25:35693
BAIER, V. N., Electroproduction in colliding-beam experiments, 25:36446
Large angle electroproduction of electron--positron pairs, 25:36440
BAILEY, C. A., Bubble nucleation on surfaces immersed in cryogenic fluids, 25:34958 (CONF-700623-(Vol.1), pp 449-58)
BAILEY, F. P., Compressive creep of yttria rare earth stabilized zirconia storage heater refractories, 25:35555
BAINBRIDGE, Kenneth T., Uranium-235--^{207}Pb and ^{238}U--^{206}Pb mass differences, 25:36770
BAKER, D. E., Graphite as a neutron moderator and reflector material, 25:35562
BAKER, Donald M., Solar flare effects in ionosphere, 25:35952 (NBS-TN-326)
BAKER, F. L., Solid propellant burn tests, 25:34792 (SC-DR-710084)
BAKER, P. S., Patent literature on process radiation and irradiator design. Part 1. United States Patents 1950 through 1968, 25:34777 (ORNL-IIC-34)
Strontium-90 heat sources, 25:34808 (ORNL-IIC-36)
BAKHANOVICH, V. I., Influence of uranium nitrate on rabbit thyroid gland, 25:35229
BAKSHT, F. G., Effect of patchiness and increases in cathode emitting area on thermionic converter characteristics, 25:35931
BALAMUTOV, V., IAEA dose comparison program, 25:35141
BALANOV, E. I., Superconducting point contact having properties of Josephson junction, 25:36070
BALASHOV, D. B., Isothermal compressibility of igneous rocks, 25:37233 (SC-T-713031)
BALDINI, Mario G., Prog. rpt. on physiopathology of blood platelets and development of extracts and substitutes, 8/68--7/71, 25:37202 (NYC-3590-8)
BALDWIN, D. E., Loss-cone modes in inhomogeneous mirror machines, 25:36166 (UCRL-73135)
BALIEV, B. S., Arsenate method for a micro iodometric determination of scandium, 25:34508
BALL, J. B., Midstream evaluation, A = 90, 25:36801
BALLARD, Douglas W., Checklist of good contamination control practices from a manufacturing viewpoint, 25:37227 (SC-M-70-549)
BALOGH, A., Measurement of solar proton anisotropies, 25:35987
BAMBERGER, C. E., Oxide chemistry of Pu in molten fluorides and free energy of formation of PuF_3 and PuF_4, 25:34566
BANAUDI, C., Exploring cardio-respiratory function with radioactive tracers, 25:35181
BANDO, Masako, Super exclusion principle for hadronic processes. I, 25:36477
BANERJEE, H., Vector-meson dominant sum rules and low-energy kaon--nucleon scattering, 25:36519
BANKOFF, S. George, Stability of liquid flow down a heated inclined plane, 25:34800
BANKS, D. C., Empirical study of behavior of clay shale slopes, 25:34768 (NCG-TR-15(Vol.1))
BANSAL, R. C., Studies on ultra-clean carbon surfaces. III, 25:35552
BANTYSH, A. N., Isotope exchange reactions. VIII, 25:34585
BAPPA, M. K. V., Stellar chromospheres, 25:35657
BAPPU, M. K. V., K emission-line widths and the solar chromosphere, 25:35717
BARABANOVA, T. E., Studies in field of analytical chemistry of U. V, 25:34531
BARANOV, V. V., Behavior of foil specimens of NT-type alloys in external magnetic field, 25:36052

XUM

BARANOVSKII, E. A., Gas pressure gradient and transparence of sunspots, 25:35756
BARASHENKOV, V. S., Interaction of high-energy radiation with matter, 25:36816 (JINR-P2-5719)
BARAT, M., Differential measurement of the He 3³P excitation, in He⁺--He collisions, by using an ion--photon coincidence method, 25:35858
BARBARO-GALTIERI, Angela, πN partial-wave amplitudes, 25:36506 (TID-25726)
BARBASHOV, B. M., Functional integration and Regge-eikonal representation of scattering amplitude, 25:36587 (JINR-P2-5768)
BARBER, Anthony Clifford, Improvements in superconductors, 25:36066
BARBINA, V., Contribution of radioisotope techniques to the diagnosis of lung morphology, 25:35180
BARBULESCU, A., Detection of reactions taking place in pulverized mixtures of system La_2O_3--TiO_2--ZrO_2, 25:36320
BARCLAY, John Arthur, Spin--lattice relaxation by nuclear magnetic resonance on oriented nuclei, 25:36347
BARDOLLE, Jean, Oxidation kinetics of niobium--titanium alloys, 25:35282
Oxidation of polycrystalline Nb samples, 25:35280
BARIBAUD, Michel, Total cross sections for collisional detachment of one or two electrons from H^- on H_2O, 25:35867
BARISH, J., Muon transport and shielding of high-energy (less than or equal to 500 GeV) proton accelerators, 25:36610 (ORNL-TM-3353)
BARKHUDARYAN, A. V., Coulomb collisions in dense beams, 25:36640
BARKHUDARYAN, S. P., Peculiarities of the extractive-photometric determination of tantalum by basic dyestuffs, 25:34533
BARKHUDARYAN, S. R., New reagents for the extraction--photometric determination of tantalum, 25:34506
BARLEON, L., Measurement of Doppler coefficient in different fuel samples in a fast and at fast-thermal reactor arrangement by pile oscillator method, 25:37135 (KFK-1350)
BARLOW, H. C., Electrical method of assessing the suitability of silicon nitride components for use with molten plutonium, 25:35546 (AWRE-O-42-69)
BARNABY, C. F., Measurements of ^{60}Co organ burdens in rats for calculations of dose-rates to organs of man, 25:35116
BARNES, P. D., Decay modes and lifetimes of levels in ^{210}Bi, 25:36790
BARNES, R. G., Nuclear power reactor wastes and our environment, 25:34844 (CONF-700440-1)
BARNHAM, K. W. J., A_2^+ mass spectrum in π⁺p interactions at 3.7 GeV/c, 25:36411
BARON, V. V., Critical characteristics of superconducting alloys of type NT-I in a wide range of magnetic fields at different temperatures, 25:36048
Magnetization of certain Type-II superconductors, 25:36046
Physical chemistry, metallography, and metal physics of superconductors, 25:36037
Processes of superconducting solenoid into state with normal conductivity, 25:36078
Specific residual electrical resistance in S reversible N transition aspects of wire forms from superconducting materials by the resistivity method, 25:36055
Structure and superconducting properties of recrystalled and deformed alloys of Nb with 75 at. percent Ti, 25:36049
Superconducting electrolytic films of niobium, 25:36056
Transition temperature of superconducting compounds V_3Ga, V_3Si, and Nb_3Sn, 25:36040
BARONCELLI, F., Aromatic hydrocarbons as potential source of diluents for fuel reprocessing, 25:34638 (RT/CHI-(70)35)
BARONE, A., Flux-flow effect in Josephson tunnel junctions, 25:36027
BARRANDON, J. N., Determination of V, Nb, and S concentrations by proton activation analysis, 25:34554
BARRETT, R. F., Measurement of neutron mean energies of evaporation-type neutron sources, 25:34906
BARRETTO, P. M., Radon-222 emanation and high apparent Pb isotope ages in lunar dust, 25:35831
BARROWS, R. G., Equilibrium and precipitation effects in Co-rich alloys of the Co--Cr--W system, 25:35489
BARROWS, Richard Gridley, Occurrence of sigma-type phases in heat-resisting alloys, 25:35498
BARRUEL, F., Development of order of 50--50 Fe--Ni alloy irradiated by neutrons, 25:36281
BARSUKOV, V. M., Zones of corpuscular precipitations and structure of the magnetosphere, 25:35958
BARTEL, W., Inelastic electron--proton scattering in region of Δ(1236) resonance, 25:36381
BARTLETT, E. S., Oxidation protection of a chromium alloy by nickel-alloy claddings, 25:35288
BARTOLINI, W., Proton induced reactions on mass-14 nuclei, 25:36673
BASARGIN, N. N., Effect of the structure of mono- and bifunctional azo compounds on the analytical properties of yttrium and rare earth complex compounds, 25:34528
BASENDALE, J. H., Direct observation of solvation of the electron in liquid alcohols by pulse radiolysis, 25:34649
BASHKIROV, Yu. A., Plasmochemical method of synthesis of superconducting compounds with structure of A15 type, 25:36044
BASILE, M., Measurement of X^0 cross-sections in π⁻p interactions at 1.6 GeV/c, 25:36407
BASIN, L. A., Magnetic lenses with parabolic, triangular and trapezoidal distributions of linear ampere-turn density, 25:36643
BATEMAN, Benjamin Jefferson Jr., Momentum and zenithal dependence of the charge ratio of energetic cosmic-ray muons near sea level, 25:35898
BATURIN, G. N., Uranium concentration in recent oceanic sediments of water uprise zones, 25:34761
BATZER, T. H., Engineering design of the 2X II, 25:36159 (UCRL-73060)
BAUDON, J., Differential measurement of the he 3³P excitation, in He⁺--He collisions, by using an ion--photon coincidence method, 25:35858
BAUER, S. J., Dayside ionosphere of Venus, 25:35827
BAUGH, D. J., Optical model code JIE3 (version Perey 3), 25:36814 (ANU-P-451)
BAUGH, P. J., Radical processes following γ irradiation of frozen concentrated matrices of heparin and dextran sulphate, 25:34651
BAXENDALE, J. H., Pulse and γ-radiolysis of borohydride ion in aqueous solution, 25:34646
Study of oxidation and reduction of $Ru(NH_3)_5N_2^{2+}$ by γ- and electron pulse radiolysis, 25:34657
BAXTER, A. N., Spin--parity combinations in ^{22}Ne, 25:36658
BAXTER, W. V., ENDF/B cross section preparation and testing in the JOSHUA system, 25:36737 (TID-25690)
BAXTER, William J., Work function of tantalum carbide and the effects of adsorption and sputtering of cesium, 25:36335
BAYMAN, B. F., Finite-range calculation of the two-neutron transfer reaction, 25:36828
BAZHENOV, Yu. M., Safety precautions in radioactive cement storage, 25:35148
BEALS, R. J., Strengths of some uranium compounds, 25:35551
BEASLEY, C. O. Jr., Loss-cone modes in inhomogeneous mirror machines, 25:36166 (UCRL-73135)
BEASLEY, D., Survey of the effects of porosity on the elastic moduli and strength of brittle materials with particular reference to beryllium, 25:35331 (AWRE-O-25/71)
BEAUDRY, B. J., Properties, preparation, and handling of pure rare earth metals, 25:35297
BEAVAN, L. A., Defect structure of depleted zones in irradiated tungsten, 25:36268 (NYO-3504-50)
BEAVER, Wallace W., Beryllium products for nuclear, aerospace, and electronic applications, 25:35345
BECCHINI, M. F., Tumors by means of radioisotopes, 25:35185
BECK, M. S., Effects of burnup on fuel pin thermal performance, 25:37017 (CONF-710414-1)
BECKER, C. Dale, Ecological evaluation: migration of juvenile salmon in relation to heated effluents in central Columbia River, 25:37105 (ENWL-SA-2876)
BECKER, D. G., Measurement and interpretation of the luminous efficiencies of iron and copper simulated micrometeors, 25:35596
Measurements of ionization probability of Cu and LaB_6 simulated micrometeors, 25:35597
BECKER, K. H., Relative line intensities in Lyman bands of HD and H_2, 25:35848
BECKER, Martin, Conference on fast reactors and the University, Troy, N. Y., 8/68, 25:36976 (CONF-680818)
BECKER, Sheldon I., TAXL: a simple hierarchical data structure manipulation system, 25:37236 (SLAC-115)
BECKETT, C. W., High-speed (subsecond) measurement of heat capacity, electrical resistivity, and thermal radiation properties of tantalum in the range 1900 to 3200 K, 25:35477
BECKMAN, J. E., Solar chromospheric activity at 400, 800, and 1200 μ, 25:35776
BEDER, D. A., Nuclear absorption of low-energy pions, 25:36489
BEDILOV, M. R., Influence of large doses of γ radiation on optical properties of quantum generator, 25:35082
BEEBE, Herbert A., Formation of Ca II K-line core with arbitrary temperature minima, 25:35716
BEELER, J. R. Jr., Computer experiment studies on mechanisms for irradiation induced defect production and annealing processes. Progress report for period ending May 31, 1970, 25:35504 (ORO-3912-4)
BEGUM, A., Unstable intermediates. LXXXVI, 25:34667
BEGZHANOV, R. B., Angular correlation of ^{97}Nb γ radiation, 25:36763
BEISEMBAEV, P. U., Method of projecting and studying the spatial image of complex events recorded by a spark chamber, 25:35011
BEKMUKHAMETOVA, Z. U., Hormoncogenesis in thyroid by local irradiation, 25:35208
BELAN, V. G., Ion shock waves in a collisionless plasma, 25:36106
BELETSKAYA, I. P., Electrophilic substitution on aromatic carbon atom. XIV, 25:34600
BELL, R. O., Calculation of gamma-ray pulse height spectrum in a semiconductor detector in the presence of charge carrier trapping, 25:34907

BELOMESTNYKH, V. I., Tetracido-type oxalate-peroxo uranyl compounds, 25:34570
BELOV, S., Measurement of continuous fast neutron spectra by scintillation technique, 25:34920 (UARAEE-91)
Neutron transmission through ducts perpendicular to neutron beam axis in water shields, 25:36251 (UARAEE-86)
BELT, B. D., Evidence for T = 1/2 resonance in the ^{3}He system, 25:36663
BELYAEV, I. N., Reply to article by F. M. Spiridonov, 25:35570
BELYAEV, L. N., System for depression of magnetic field pulsations in Dubna synchrophasotron, 25:36605 (JINR-P9-5724)
BELYAEV, S. T., Collective excitations in nuclei, 25:36839
BELYAEV, V. B., Potentials with hard-core repulsion and nuclear three-body problem, 25:36536
BELYAKINA, T. S., Three-color photoelectric observations of Z And, 25:35634
BELYAKOVA, Z. V., Interaction of certain compounds of thorium with dimethyl sulfoxide, 25:34565
BEMALKHEDKAR, M. M., Forbush decrease in various multiplicities in Gulmarg neutron monitor, 25:35515
BEMIS, C. E. Jr., Identification of the atomic number of nobelium by an x-ray technique, 25:36778
BENAYOUN, M., Local models for antikaon--nucleon collisions, 25:36505 (PAM-71.1)
BEN-DAVID, G., Background report on fission physics, 25:36800
BENES, Konrad, Terrestrial planets and stages of their evolution, 25:35825
BENESOVSKY, F., Behavior of boron-alloyed sintered molybdenum in electron beam welding, 25:35312
Deformation anisotropy and texture of molybdenum, 25:35411
BENJAMIN, R. W., Neutron-induced fission cross sections for ^{244}Cm and ^{249}Cf, 25:36721 (DP-MS-70-95)
BENTON, J. D., Sandia Laboratories Livermore data processing system, 25:37235 (SCL-DR-710032)
BENVENUTI, A., Neutral particle tagging facility for ANL 30'' bubble chamber, 25:34967 (CONF-700623-(Vol.2), pp 582-92)
BENVENUTO, P., Heavy gas--liquid mixture bubble chamber of 70 liters volume with hydrogen internal target, 25:35007 (LNF-70/25)
BENZ, M. G., Cobalt--mischmetal--samarium permanent magnet alloys: process and properties, 25:36336
BERANGER, Gerard, Tensile behavior of polycrystalline α between 25 and 700°C, 25:35352
BERAUD, R., Microstructure effect on hyperfine interactions in Yb--Ag, 25:36332
BEREZHNYI, V. L., Azimuthal current and microwave radiation in theta pinch, 25:36122
BERG, G., Energy resolution of multiplying semiconductor detectors for soft γ spectroscopy at room temperature, 25:34918 (LB/G-3034)
BERG, H., uv inactivation of NADH, 25:35107
BERG, V., Low-energy band structure in ^{187}Os, 25:36805
BERGEDER, H. D., Radiation effects on biological membranes, 25:35210
BERGMANN, B., Technical and economic state as well as prospects of atomic energy in the economy of the Federal Republic of Germany, 25:36885 (JUL-705-RG)
BERK, H. L., Loss-cone modes in inhomogeneous mirror machines, 25:36166 (UCRL-73135)
BERKES, I., Microstructure effect on hyperfine interactions in Yb--Ag, 25:36332
BERKNER, Klaus H., Cross sections for destruction of excited H molecules in collisions with H_2 gas, 25:35874
BERLIN, L. B., Effect of cystamine on chromosome aberrations of lymphocytes in case of fractional local γ irradiation, 25:35123
BERNARD, H. W., Carbon-13 hyperfine interaction in CD_2, 25:34586
BERNHEIM, R. A., Carbon-13 hyperfine interaction in CD_2, 25:34586
BERRY, Lee Allen, Longitudinal ion-wave propagation in a magnetized plasma, 25:36222
BERTINI, H. W., Operation of codes associated with MECC-3, preliminary version of intranuclear-cascade calculation for nuclear reactions, 25:36733 (ORNL-4564)
BERTRAM, W. K., Solution of the inverse reaction problem for complex potentials, 25:36812 (AAEC/TM-586)
BERTRAND, F. E., Nuclear data sheets for A = 110, 25:36808
BESOMBES-VAILHE, J., Radiation emitted by an argon plasma produced by a low-pressure torch discharge, 25:36124
BESSONOVA, K. F., Electron energy distribution in the positive column of a helium discharge, 25:36119
BETZ, B., Training and continuous education in the radiation protection field for medicine, 25:35147
BETZ, H. D., Determination of lifetimes for multiply charged heavy ions excited in collisions with light gases, 25:35849
BEYER, G., Short-lived isomers of Tb isotopes: ^{149}Tb, ^{149}Tb, ^{150}Tb, and ^{152}Tb, 25:36726 (JINR-P6-5681)
BEYER, G. J., New method for rare-earth isotope separation, 25:34805 (JINR-P6-5761)
BEYNON, T. D., Scattering of neutrons from an excited nuclear state, 25:36707
BEZ'YAZYCHNYI, I. A., Measurement of the density of a plasma with the aid of an open resonator, 25:36085 (KHFTI-69/51)

BHADRA, Kalidas, 1s--3d excitation of atomic hydrogen by electron and proton impact, 25:35859
BHALLA, K. B., Monte Carlo calculations and the lifetime of heavy hyperfragments, 25:36535
BHANDARI, Narendra, Orbital velocities of some stone meteorites, 25:35600
BHATIA, V. B., Cosmic gamma-ray background, 25:35903
BHATIA, V. S., Charge composition of cosmic-ray nuclei of elements from Ne to Ni, 25:35910
BHATTACHARJEE, H. R., Inverse deuterium isotope effect in radiationless electronic transitions, 25:34590
BHATTACHARYA, P. K., Design and calibration of a general purpose pulse ionization chamber for mucn flux measurement, 25:35022
BHATTACHARYYA, D. P., Pion production spectrum at 12°N geomagnetic latitude, 25:35917
BHATTACHERJEE, S. K., Existence of super-heavy nuclei, 25:35592
BHIDAY, M. R., Measurement of magnetic field index n of the 5 MeV betatron by an ac potentiometer, 25:36625
BHORASKAR, V. N., Measurement of magnetic field index n of the 5 MeV betatron by an ac potentiometer, 25:36625
BHOWMIK, B., Analysis of shower particles produced in high-energy interactions, 25:36392
Neutral pions produced in 5-GeV/c antiproton interactions, 25:36404
New method for identification of shower particles in high-energy interactions, 25:36402
BHUSHAN, Vidya, Pulsed neutron and diffusion length stucy in bismuth, 25:36655
BIANCALANA, L., Contribution of isotopes to the surgery of the thyroid, 25:35190
BIANCHERIA, A., Effects of burnup on fuel pin thermal performance, 25:37017 (CONF-710414-1)
BIBRING, H., Strengthening of metals and alloys by refractory fibers grown from the melt, 25:35557
BIEBER, C. G., Structural studies and properties of a new cast high strength corrosion resistant superalloy, 25:35400
BIEDENHARN, L. C., Intrinsically self-conjugate boson structure: the symplecton, 25:36548
BIELSKI, Benon H. J., Species in irradiated oxygenated water, 25:34617
BIERMAN, E., Bubble chamber detection technique for gamma rays in momentum region below 1 GeV/c, 25:34964 (CONF-700623-(Vol.1), pp 555-66)
BIKIT, I., Penetration parameter for M1 conversion and E2 admixtures for 77 and 191 keV transitions in ^{197}Au, 25:36789
BINGHAM, C. R., Evidence for T = 1/2 resonance in the ^{3}He system, 25:36663
BINKLEY, M., Wisconsin rapid cycling bubble chamber, 25:34956 (CONF-700623-(Vol.1), pp 418-23)
BINNS, Ian Mason, Nuclear reactor fuel assemblies, 25:37025
BIONDO, C. D., Some nuclear developments in Argentina, 25:35527
BIRAT, J. P., Superposition model for environmentally-assisted fatigue-crack propagation, 25:37249 (UCRL-20538)
BIRATTARI, C., Reactions (p,xn) induced in ^{199}Tm, ^{181}Ta, and ^{209}Bi with 20 to 45 MeV protons, 25:36797
BIRYUZOVA, V. I., Early structural, ultrastructural, and functional disturbances in radiosensitive and radioresistant yeast cells under influence of ionizing radiation, 25:35247
BISELLO, D., Precision of an optical spark chamber with wire electrodes, 25:35008 (LNF-70/44)
BISWAS, S., Charge composition of cosmic-ray nuclei of elements from Ne to Ni, 25:35910
Energy spectrum of diffuse cosmic x rays in the energy range 20 to 120 keV, 25:35921
Energy spectrum of Sco X-1 in the region 15 to 120 keV, 25:35704
Relative abundance of deuterons in cosmic rays and its astrophysical significance, 25:35912
BISWELL, Lavon R., Nova Branch-Driver operation, 25:37190 (LA-4682)
BLACK, H. C., Meandering solar Type-IV burst 12/17/69, 25:35742
BLAGOV, M. I., Search for elementary particles bearing a magnetic charge, 25:36379 (CERN-Trans-71-10)
BLAGOVESHCHENSKII, V. N., Production of negative hydrogen ions in a plasma with a double sheath, 25:35842
BLAKE, Damon D., Radiation treatment of metastatic bone disease, 25:35187
BLAKE, Kenneth R., Rapid assay for nitrogen in gluten and use of reference nuclides, 25:34555
BLANC, J. M., Metallurgy of superconductors, 25:36018 (CONF-700341-7)
BLAND, M. E., Bubble nucleation on surfaces immersed in cryogenic fluids, 25:34958 (CONF-700623-(Vol.1), pp 449-58)
BLATZ, Paul E., Prog. rpt. on spectral studies of polyenes and their carbonium ions: implications to photobiology, 3/31/71, 25:37181 (COO-1693-6)
BLAZHIN, V. D., Superconductivity of a semiconductor placed in a laser light field, 25:36031
BLEACH, R. D., Evidence for multiple periodicity in x-ray emission from Cygnus X-1, 25:35690

XUM

BLECHSCHMIDT, M., Permissible limits for nuclear fuels according to atomic law and the related legal orders, 25:34857
BLINKOV, E. L., Behavior of foil specimens of NT-type alloys in external magnetic field, 25:36052
Processes of superconducting solenoid into state with normal conductivity, 25:36078
BLOECH, R., Electron beam microanalysis of complex carbides, 25:34523
BLOOM, E. E., Effects of fast neutron irradiation on the tensile properties of austenitic stainless steels, 25:35509
BLOOM, Stewart D., Effective charge and stopping power of heavy ions, 25:35261
BLUM, P. W., Interpretation of extra-terrestrial Lyman-alpha observations, 25:35593
BLUMENTHAL, George R., Spectrum of high-energy electrons undergoing Klein--Nishina losses, 25:36263
BLYTHE, H. J., Magnetic relaxation in high-purity irradiated Fe. I, 25:36294
BOARIO, U., Exploring cardio-respiratory function with radioactive tracers, 25:35181
BOBASHEV, S. V., Oscillations of the total cross sections for inelastic processes in atomic collisions, 25:35876
BOBYKIN, B. V., Magnetic lenses with parabolic, triangular and trapezoidal distributions of linear ampere-turn density, 25:36643
BOCHEV, B., Decay of ^{173}Ta, 25:36727 (JINR-P6-5704)
BOCKELMAN, C. K., Anomalous electron scattering from ^{142} ^{146} ^{150}Nd, 25:36758
BOCOLA, W., Treatment of radioactive waste in reprocessing of fuel, 25:34711
BODINE, Norman Ralph, Recoil corrections made easy, 25:36567
BOEHM, Horst, Strengthening mechanism in vanadium--titanium alloys, 25:35388
BOERNER, W., Measurement of bone density with ^{125}I-profile-scanner, 25:35171
BOGARDUS, B. J., Production and testing of superheater fuel elements, 25:37024
BOGDANKEVICH, L. S., Stability of relativistic electron beams in plasma and the problem of critical currents, 25:36169
BOGDANOVA, V. I., Calculation of the internal structure of non-laminar axially-symmetric intensive beams of charged particles, 25:36609 (NP-18860)
BOHRA, M. L., Composite sphere in general relativity, 25:36583
BOKELUND, H., Investigation of reprocessing input measurement using tracer technique, 25:34685 (IAEA-R-876-F)
BOKROS, J. C., Irradiation-induced dimensional changes and creep of isotropic carbon, 25:35585
BOLAND, B. C., Echelle spectrograph for high resolution studies of the solar vacuum ultraviolet spectrum, 25:35054
BOLDRIGHINI, C., Inclusive experiments and high-energy models, 25:36478
BOLDT, E. A., Evidence for multiple periodicity in x-ray emission from Cygnus X-1, 25:35690
BOLLAERT, A., Radiological aspects of post-radiotherapeutic colitis, 25:35158
BOLLINI, D., Measurement of X^0 cross-sections in π^-p interactions at 1.6 GeV/c, 25:36407
BOLLMEIER, A. F., Extraction of selected metallic cations by highly hindered $(GO)_2PO(OH)$ extractant in two different diluents from aqueous chloride phase, 25:34706
BOLON, Albert E., Nuclear metallurgy curriculum at Univ. of Missouri at Rolla, 25:34781
BOMAN, L. H., NERVA Technology Reactor, 25:37088
BOMAR, E. S., Lattice parameters of (U,Pu)N solid solutions, 25:35574
BOMBIK, A., Tables of magnetic structures determined by neutron diffraction. III, 25:36311 (NP-18845)
BOMKO, V. A., Features of a double-beam accelerating structure, 25:36623
BOMPIANI, C., Experiences with the shielded whole-body counter, 25:35183
BONDARENKO, L. N., Measurements of angular correlation of neutron spin and antineutrino momentum in the decay of polarized neutrons, 25:36385 (IAE-1947)
BONDARENKO, S. I., Superconducting point contact having properties of Josephson junction, 25:36070
BONDORF, J. P., Fission of U, Np, Pu, and Am isotopes excited in (d,p) reaction, 25:36746
BONE, S. J., Tables of γ rays from (n,γ) produced nuclides, 25:36718 (AAEC/TM-585)
BONK, G. J., Interactions between nuclear plant loading changes and nuclear fuel costs, 25:36893
BONNEFILLE, Robert, Laminar flow of incompressible conducting fluid in slightly divergent MHD channel, 25:35943
BONOMETTO, S., Effects of electron pair production in QSOs, 25:35678
BOOS, E. G., Quasi-two-particle reactions in proton--proton interactions at 10 GeV/c, 25:36396
BOOTH, E. S., Nuclear power in Great Britain, 25:36863 (CONF-700653-1)
BOOTH, R. S., Search for interstellar H_2CS, 25:35708
BORG, Donald C., Identification of radiation-induced hydrogen-addition radicals in adenine derivatives, 25:34652
BORGONOVI, G. M., Fast reactor spectrum measurements. Technical summary report, February 1, 1970--January 31, 1971, 25:36991 (GULF-RT-10523)
BORGSTEDT, H. U., Oxidation of Ni-V alloys in air, 25:35289
BORGSTEDT, Hans U., Grain boundary grooving of Type 304 stainless steel and Armco iron due to liquid sodium corrosion, 25:35286
BORISOV, A. A., Hodoscope based on small photoelectron multipliers, FEU-85, 25:34864 (IFVE-SEF-70-17)
BORKMAN, R. F., Deuterium effect on the phosphorescence lifetime of biacetyl crystal and vapor, 25:34593
BORKMAN, Raymond F., Single-center calculations on electronically excited states of equilateral H_3^+ ion, 25:35851
BORN, G. K., X-ray and photo-induced processes in ZnO coating material, 25:36296
BORYSOWICZ, J., Size of ^{12}C in α-particle model, 25:36681
BOSCHKO, S. A., Recrystallization of high-melting carbides, 25:35535
BOSS, J. W., Paramagnetic centres in irradiated, oxidized, and reduced Na silicate glasses, 25:36278
BOTTINELLI, L., 21-cm neutral hydrogen line and continuum study of galaxy Maffei 2, 25:35794
BOUCHARD, Jacques, Fission chamber, 25:34883
BOUDREAU, D. A., Line shapes for rf size effect in Cd, 25:36327
BOULESTEIX, C., Thin films of praseodymium sesquioxide, 25:35575
BOULTON, John, Hydriding resistant zirconium alloy components, 25:35329
BOULVEN, J., Analog study of propulsion power reactors, 25:37093 (CEA-CONF-1750)
BOURDINAUD, M., Lenses and illumination system of Mirabelle, 25:34994 (CONF-700623-(Vol.2), pp 972-83)
BOURKE, W. P., Optical model code JIB3 (version Perey 3), 25:36814 (ANU-P-451)
BOURLAND, P. D., Stopping cross sections of gases for α particles from 0.3 to 2 MeV, 25:36255
BOURRET, A., Irradiation damage in Ni and Fe in high-voltage electron microscope, 25:36301
BOVING, R., Improved electronic control unit for a motor type beam scanner, 25:36632
BOWEN, D. K., Effect of interstitial nitrogen on thermally activated flow in niobium single crystals, 25:35272
BOWEN, Vaughan T., Prog. rpt. on general summary, 1970--1971, 25:34759 (NYO-2174-129)
BOWER, J. R., Chemical Programs Division annual report, fiscal year 1970, 25:34690 (IN-1457)
BOWERS, H. I., Estimated capital costs of nuclear and fossil power plants, 25:37030 (ORNL-TM-3243)
BOWERS, R., Low-temperature electrical and thermal resistivities of tungsten, 25:36331
BOWERSOX, David F., Thermodynamics of solution of Ti, V, Cr, Fe, and Co in liquid Sn, 25:35368
BOWMAN, C. D., Structure in ^{235}U keV fission cross section, 25:36739 (UCRL-73090)
BOYARCHUK, A. A., Chemical composition of the symbiotic stars, 25:35633
BOYARCHUK, M. E., Spectrophotometric study of four K stars, 25:35636
BOYER, P. D., Prog. rpt. on isotopic studies on structure-function relationships of nucleic acids and enzymes, annual, 5/1/70--4/30/71, 25:37243 (UCLA-34-P-102-27)
BRAATZ, Ulrich, Considerations of the costs for the manufacture of fuel elements with oxide fuel for power reactors, 25:37022
BRADLEY, R. A., Statistical technique for determining sources of variation in $(U,Pu)O_2$ oxygen-to-metal ratio, 25:35568 (ORNL-TM-3362)
BRAES, L. L. E., Possible radio identification of Cygnus X-2, 25:35701
BRAHME, A., Hydromagnetic stability of a nonuniformly rotating fluid, 25:35946
BRAITHWAITE, W. J., Energy dependence of quasifree scattering in the ^{2}H(p,pn)p reaction, 25:36667
BRANCA, G., Principles and methods for the derivation of a formula for the discharge of radioactive liquid wastes in surface waters, 25:34717 (EUR-4636)
BRANSON, D., Colliding pole and branch point as model for self-consistent Poveranchuk singularity, 25:36588
BRAUN, H., Radiation effects on cell structure, 25:35205
Radionuclide preparation through (n,p) and (n,α) reactions with fast reactor neutrons, 25:36686 (CONF-680986-1)
BRAUN, Heribert, Conference on radiation protection from unsealed radioactive material and effect of radiation on the cell structure, Aachen, 10/68. IX, 25:35130
BRAY, B. G., Process for stimulating petroliferous subterranean formations with contained nuclear explosions, 25:34772
BRAY, J. A., Review of some sodium/water reaction experiments, 25:35441
BRAY, Marcel, Canonical form of the gravitational field equations, 25:36579
Some solutions of the internal problem in general relativity, 25:36578
BRAYSHAW, D. D., Singular core interactions and three-body theory, 25:36851
BRECCIA, A., Pulse and γ-radiolysis of borohydride ion in

XUM

aqueous solution, 25:34646
BREIT, G., Improvements in tests of long-range charge independence, 25:36522
BRENDLE, M., Power supply system control, 25:35068
BRENNAN, M. H., Wave propagation near the upper-hybrid frequency in a mirror-confined unstable plasma, 25:36243
BREUER, F., Principles and methods for the derivation of a formula for the discharge of radioactive liquid wastes in surface waters, 25:34717 (EUR-4636)
BREVI, R., Quality influence in post-burnout heat transfer, 25:34801
BREVIK, I., Covariant quantum electrodynamics in terms of a possible ether flow, 25:36566
BREWER, D. F., Electronic specific heat of an impure tungsten sample, 25:36312
BRIDGE, J. E. Jr., Effect of molybdenum and hardener content on gamma-prime solvus temperature in a Ni20Cr base heat-resistant alloy, 25:35460
BRIEL, U., Power supply system control, 25:35068
BRIGNOCCHI, A., Aromatic hydrocarbons as potential source of diluents for fuel reprocessing, 25:34638 (RT/CHI-(70)35)
BRINCK, Johan, Uranium: prospects and problems, 25:34758
BRINK, D. M., Coulomb energy differences in mirror nuclei in Hartree--Fock approximation, 25:36712
BRITO, Ubirajara, Thermoluminescence induced in thick targets by 3 GeV protons, 25:36298
BROCKHOUSE, B. N., Lattice vibrations in deuterated ammonium chloride at 85°K. I. Experimental, 25:36322
BROCKMANN, R., Electron--photon cascades in Pb at primary energies of 100, 200, and 400 MeV, 25:36788
BRODA, R., Decay of ^{173}Ta, 25:36727 (JINR-P6-5704)
BRODSKII, Yu. Ya., Self-trapping of powerful electromagnetic waves in a dense plasma, 25:36225
BROLLEY, John E., Elastic scattering of protons and electrons from helium atoms in the Glauber approximation, 25:35868
BRONCA, G., State of the art of producing strong magnetic fields, 25:36073 (CEA-CONF-1734)
BRONSHTEN, V. A., Noctilucent clouds, 25:35988
BROMHEAD, J. A., Racemization and ^{18}O exchange studies of heterochelate Cr(III) complexes. II, 25:34601
BROUSSE, Jean-Claude, Fast neutron spectrum in the reflector of a swimming pool reactor behind metallic slabs, 25:37057 (CEA-R-3799)
BROUW, W. N., Possible radio identification of Cygnus X-2, 25:35701
BROWN, D., Crystal structure of protactinium tetrabromide, 25:34610
Reactions of Na N,N-diethyldithiocarbamate with the chlorides and bromides of Nb(V), Ta(V), and Pa(V), 25:34568
Thermodynamics of the actinide elements. III, 25:34609
BROWN, G. E., Intermediate range nucleon--nucleon interaction, 25:36525
Landau, Brueckner--Bethe, and Migdal theories of Fermi systems, 25:36843
BROWN, R. C. A., Ultrasonic bubble chamber development at CERN, 25:34953 (CONF-700623-(Vol.1), pp 376-89)
BROWNE, J. C., Structure in ^{235}U keV fission cross section, 25:36739 (UCRL-73090)
BRUCE, A. K., Relationship of radioresistance to balanced growth-rate in Micrococcus radiodurans, 25:35263
BRUCE, T. A., High pressure behavior of solid H_2, D_2, ^{3}He, ^{4}He, and ^{20}Ne, 25:37204 (NYO-3699-51)
BRUMOVSKY, M., Influence of some metallurgical variables on the radiation damage sensitivity of pressure vessel steels, 25:35505 (ZJE-99)
BRUNE, W., Operation results of Rheinsberg nuclear power plant up to 4th refueling, 25:36891
BRUSH, A., Neutral particle tagging facility for ANL 30'' bubble chamber, 25:34967 (CONF-700623-(Vol.2), pp 582-92)
BRYNDA, William, Investigation and repair of baffle plate damage in the HFBR primary heat exchangers, 25:37055 (BNL-15815)
BUCHER, E., Electronic transitions in near-equiatomic vanadium--ruthenium alloys, 25:36339
BUCHIKHIN, A. P., Positronium atom in organic liquids, 25:35853
BUCK, O., Change in flow stress due to the superconducting-normal transition, 25:35389
BUCKLEY, R., Fluctuations in the interplanetary plasma, 25:35734
BUECKER, H., Inactivation and division delay of E. coli B/r by combined treatment with uv and vacuum, 25:35265
BUEHLER, E., CdP_2--Sn system and some properties of $CdSnP_2$ crystals, 25:35580
BUESSER, F.-W., Inelastic electron--proton scattering in region of Δ(1236) resonance, 25:36381
BUGAENKO, L. T., Appearance of H^+ ions in irradiated liquid water, 25:34668
BUGORSKII, A. P., Hodoscope based on small photoelectron multipliers, FEU-85, 25:34864 (IFVE-SEF-70-17)
BUGRIIA, A. I., Dual amplitude with Mandelstam analyticity, 25:36492
BUINOV, N. N., Structure and superconducting properties of recrystalled and deformed alloys of Nb with 75 at. percent Ti, 25:36049
BUKHALOVA, G. A., Phase diagram of the system PbO--MoO_3, 25:35581
BULANIN, V. V., Oscillations in a magnetized afterglow plasma with a transverse current, 25:36175
BULMER, R. H., Astron mechanical engineering effort, 25:36198 (UCRL-73059)
BUON, J., Device for measuring the luminosity of Orsay storage ring, 25:36606 (LAL-1249)
BURBIDGE, G. R., Relative correlation of large- and small-redshift quasi-stellar objects with clusters of galaxies, 25:35693
BURGER, J. J., Phenomenological approach to the solar modulation of cosmic rays, 25:35899
BURKHARDT, H., Smoothed Venezianc models and applications to pion--pion scattering, 25:36499
BURKHART, James A., Exploratory tests of a downstream-cathode PPD thruster, 25:36162
BURKHEAD, Martin S., Preliminary photometry of open cluster NGC 609, 25:35605
BURMAN, G. C., Technology of reactor thermal shields. I, 25:36999
BURMAN, R., Solar charge and perihelion motion of 1566 Icarus, 25:35733
BURMAN, R. R., Electromagnetism and geodesics of an Einstein Connection, 25:36443
BURNEAU, A., Vibrational spectra and anharmonicity of H_2O, D_2O, and HOD in dilute solutions, 25:34591
BURR, C. R., Anisotropic behavior of dilute magnesium--gadolinium alloys, 25:36342
BURRIS, R. W., K-meson--nucleon phase shifts near 600 MeV/c, 25:36417
BURROUGHS, W. J., Submillimetre-wave solar observations using double-output Michelson interferometer, 25:35714
BURTON, Milton, Advances in radiation chemistry. II, 25:34615
BUSCH, H., Welding peculiarities in fabrication of fuel elements for Superheat Reactor Grosswelzheim, 25:35311
BUSCHOW, K. H. J., Crystal structure of rare-earth aluminum compounds R_2Al, 25:35495
BUSSO, L., Two-body photodisintegration of ^{4}He up to 80 MeV, 25:36671
BUTLER, M. K., Argonne code center: compilation of program abstracts, 25:37133 (ANL-7411(Suppl.5))
BUTLER, Robert F., Mechanism for producing magnetic remanence in meteorites and lunar samples by cosmic-ray exposure, 25:35598
BUTLER, W. R., A_2^+ mass spectrum in π^+p interactions at 3.7 GeV/c, 25:36411
BUTORIN, G. T., Homogeneous nucleation during crystallization of supercooled tin, 25:36316
BUTSEV, V. S., Decays of Nd and Pr nuclides with mass number A = 138, 25:36725 (JINR-P6-5674)
BUTTERWORTH, J., Nuclear spin--lattice relaxation in pure and impure indium. I. Normal state, 25:36249
BUTTSEV, V. S., Decay of ^{139}Nd, 25:36724 (JINR-P6-5672)
BUTYAGIN, P. Yu., Double-stage mechanism of formation of free radicals during radiolysis of frozen aqueous solutions of DNA, 25:34654
BUZBEE, B. L., Direct solution of discrete Poisson equation on irregular regions, 25:37187 (LA-4553)
BYCHKOV, Yu. F., Fine structure of superconducting alloys of Zr with Nb, 25:36053
BYCHKOVA, M. I., Behavior of foil specimens of NT-type alloys in external magnetic field, 25:36052
Structure and superconducting properties of recrystalled and deformed alloys of Nb with 75 at. percent Ti, 25:36049
BYKOVSKII, Yu. A., Measurement of isotopic abundances by time-of-flight mass spectrometer, 25:35070
BYLINSKII, A. F., Effect of donor irradiation on appearance of nonselective markers, 25:35126

C

CABELA, E., Repair of strand breaks in Chlorella-DNA caused by gamma irradiation, 25:35257
CACACE, Fulvio, Reactions of He^3H^+ ions with gaseous hydrocarbons. IV, 25:34675
Reactions of He^3H^+ ions with gaseous hydrocarbons. II, 25:34677
Reactions of He^3H^+ ions with gaseous hydrocarbons. III, 25:34676
CAFFREY, R. E., Preparation and properties of pyrolytic zirconium dioxide films, 25:35564
CAGE, M. E., Reactions ^{39}K(^{3}He,^{3}He)^{39}K and ^{39}K(^{3}He,d)^{40}Ca at 29.3 MeV, 25:36696
CAGNETTI, P., Seventh annual meteorological report of the Casaccia Center for Nuclear Studies, 1968, 25:34746 (RT/PROT-(70)42)
CAIANIELLO, E. R., Mass equation from tadpoles, 25:36426
CAIN, Joseph C., Geomagnetic models from satellite surveys, 25:36009
CAIRNS, E. J., Prog. rpt. on lithium/chalcogen secondary cells for components in electric vehicular-propulsion generating systems, semiannual, 5/23--11/22/70, 25:35275 (ANL-7777)
CALAIS, M. D., Chemical diffusion and Kirkendall effect in the body-centered cubic phase of the system plutonium/zirconium, 25:35333 (CEA-CONF-1760)
CALARCO, J. R., Energy dependence of quasifree scattering in the ^{2}H(p,pn)p reaction, 25:36667

XUM

CALDERON, M. G., Engineering design of the 2X II, 25:36159 (UCRL-73060)
CALO, Joseph Manuel, Nanosecond studies of fluorescence in gases excited by fission fragments, 25:36254
CALVERT, J. McI, Multi-configuration frozen-core approximation. I, 25:35890
CAMERON, J. M., Energy dependence of quasifree scattering in the $^{2}H(p,pn)p$ reaction, 25:36667
CAMPBELL, J., TVGP for 12 foot chamber, 25:34948 (CONF-700623-(Vol.1), pp 303-11)
CAMPBELL, J. L., K conversion coefficient of M3 transition in ^{191}Os, 25:36804
CAMPOS, Raul Montiel, Radiolysis of n-heptane, 25:34635 (NP-18810)
CANADA, T. R., Decay modes and lifetimes of levels in ^{210}Bi, 25:36790
CANNON, C. J., Center limb observations of inhomogeneities in the solar atmosphere. II, 25:35715
CANUTO, V., Thomson scattering in a strong magnetic field, 25:36140
CAPITELLI, M., Equilibrium compositions and thermodynamic properties of mixed plasmas. II, 25:36104 (NP-18772)
CAPLAN, James Gerald, Photoelectric observations of H-alpha in late-type stars, 25:35619
CAPPELLETTI, C., Laboratory guide for the selection of brazing materials, 25:35334 (EUR-4637)
CAPPS, Richard W., Hyades membership of white-dwarf eclipsing system BD + 16°516, 25:35632
CAPRIOTTI, Eugene, Formation of condensations in planetary nebulae. I, 25:35631
CARAMIHU, D., Determination of C nucleus radius by interaction with π^- at 7 GeV, 25:36408
CARBIENER, Wayne A., An evaluation of the applicability of existing data to the analytical description of a nuclear-reactor accident. Quarterly progress report, January--March 1971, 25:37036 (BMI-1904)
CARBON, D. F., Model-atmosphere analysis of five apparently super-metal-rich K giants, 25:35649
CARBON, Duane F., Abundances in open clusters, 25:35627
CARBOTTE, J. P., Pressure dependence of specific heat of superconductor, 25:36026
Theory of weak-coupling superconductors, 25:36069
CARDMAN, L. S., Anomalous electron scattering from $^{142,144,150}Nd$, 25:36758
CARDWELL, R. G., An integrated system of nuclear materials control at Oak Ridge National Laboratory, 25:34847 (ORNL-4607)
CARELLI, Mario D., Transient effect on LMFBR fuel rods by gas bubbles entrained in coolant, 25:37037 (CONF-700608-36)
CARETTE, J.-D., Study of properties of Marmet's monokinetron by calculation of electron energy distribution profiles, 25:34926
CARLETON, Nathaniel P., Optical time-of-arrival measurements from Crab pulsar, 25:35695
CARLITZ, R., Model for Pomeranchukon couplings, 25:36512
CARLSON, A. D., Prog. rpt. on neutron capture cross sections of Mo, Ta, and ^{238}U, final, 6/70, 25:36729 (N-70-41999)
CARLSON, G. A., Calculation techniques for estimating the pressure losses for conducting fluid flows in magnetic fields, 25:35938 (UCRL-51010)
CARMONA, Francois, Variations with respect to temperature of quantities measured for neutron-irradiated carbon blacks, 25:36341
CARMONY, D. D., Evidence for splitting in Q region of $K^+\pi^+\pi^-$ mass, 25:36414
CARNUTH, W., Prog. rpt. on measurement of airborne radioactivity and its meteorological application, annual, 4/69--3/70, 25:34745 (NYO-4061-2)
CARO, P.-E., Thin films of praseodymium sesquioxide, 25:35575
CAROSELLI, Marcello, Reactions of He^3H^+ ions with gaseous hydrocarbons. III, 25:34676
CAROVILLANO, R. L., Ring current as the source region for proton auroras, 25:35995
CARPENTER, R. W., Strengthening Nb--Hf alloys by α precipitation, 25:35393
CARPENTIER, Serge, Glass having a base of metaphosphates for dosimeters which are responsive to x-rays, γ-rays, and thermal neutrons, 25:35037
CARR, W. H., Molten-salt fluoride volatility pilot plant: recovery of enriched uranium from aluminum-clad fuel elements, 25:34693 (ORNL-4574)
CARRUTHERS, George R., Far-ultraviolet interstellar absorption in Orion and Monoceros, 25:35785
CARRUTHERS, P., Broken scale invariance in particle physics, 25:36542
CARTER, T., High resolution infra-red spectra of diamond, 25:36279
CARTWRIGHT, D. G., Controlled experiment on wave--particle interactions in the ionosphere, 25:35967
CASHWELL, E. D., New method of sampling Klein--Nishina probability distribution for all incident photon energies above 1 keV, 25:36432 (LA-4663)
CASO, C., Total $\pi^+\pi^-$ cross-section for dipion energies above 1.5 GeV, 25:36509
CASSINELLI, Joseph Patrick, Extended model atmospheres for the central stars of planetary nebulae, 25:35624
CASTAGNOLA, D. C., Radiochemical data for STS A, Amchitka Island, Alaska, 25:34720 (NVO-1229-121)
CASTRILLON, J., Resolving time of a counter by the method of paired sources, 25:34890
CASWELL, J. L., Distance and spectrum of 3C 391, 25:35702
Radio spectrum of Maffei 2, 25:35803
CATALA, J., Radioactive contamination of atmosphere around Valencia measured from January 1966 till April 1968, 25:35132
CATALANO, F. A., Light curve and orbital elements of V 337 Aquilae, 25:35666
CATALANO, S., Light curve and orbital elements of V 337 Aquilae, 25:35666
CATALDO, Joseph C., Effect of pressure drifts on the plasma-column edge oscillations, 25:36245
Plasma camera diagnostics in the study of wave evolution, 25:36099
CATELLA, C., Effect of nitrogen on the linear oxidation of niobium, 25:35292
CATTANEO, M. B., Observation of solar wind heavy ions, 25:35729
CAVALLO, G., Period--luminosity function for pulsars, 25:35681
CEARLOCK, D. B., Analysis of effect of potential reactor cooling ponds on Hanford groundwater system, 25:37103 (BNWL-1507)
Analysis of hydrological factors influencing Cattle Mountain irrigation project, 25:34715 (BNWL-1502)
CELINSKI, Zdzislaw N., Electrical effects in insulating-wall boundary layer in Faraday-type MHD generator, 25:35935
CELLERINO, A. F., Exploring cardio-respiratory function with radioactive tracers, 25:35181
CESKA, M., Rapid and simple microscale separation of proteins after radioiodination, 25:34700
CEZAIRLIYAN, A., High-speed (subsecond) measurement of heat capacity, electrical resistivity, and thermal radiation properties of tantalum in the range 1900 to 3200 K, 25:35477
CHACHATY, Claude, Radical products from the radiolysis of nitroalkanes in alkaline ice glasses, 25:34643
CHAFFEE, Frederic H. Jr., Abundances in open clusters, 25:35627
CHAKRABORTY, A. K., Effect of boron on ductility and strength of Inconel 600 and Types 304 and 316 stainless steel at hot metalworking temperatures, 25:35338 (ORNL-TM-3316)
CHAMARAUX, P., 21-cm neutral hydrogen line and continuum study of galaxy Maffei 2, 25:35794
CHAMBE, G., Study of coronal condensations by means of their xuv line spectrum, 25:35768
CHAMBERLAIN, J., Submillimetre-wave solar observations using double-output Michelson interferometer, 25:35714
CHAMBEROD, A., Development of order of 50--50 Fe--Ni alloy irradiated by neutrons, 25:36281
CHAMNIROKASARNT, Darakarnt, Soil analysis by neutron activation method, 25:34545 (THAI.-AEC-36)
CHAMPIER, G., Plastic deformation of single crystals of indium solid solutions in magnesium, 25:35287
CHAN, F. C. P., Effective-range formula for form factor in K/sub 13/ decay, 25:36461
CHAN, Lydia Sing-chai, Potential of pion--nucleon scattering, 25:36510
CHAN, Shu-bon, Study of $Y_1^*(1385)$ π production near the $Y_0^*(1520)$ resonance, 25:36415
CHAND, Prakash, New SU(3) classification of vector mesons, 25:36553
CHANDLER, H. M. Jr., Vacuum tube compensated flat top high-current pulse supply for symmetrical torus machine, 25:36187 (PATT-837)
CHANDRA, S., Ion and neutral composition changes in the thermospheric region during magnetic storms, 25:35960
CHANDRASEKHARA, B. C., Magnetohydrodynamic laminar flow between porous disks, 25:35947
CHANG, Tsai Ying, Far-red light effect on ultraviolet light induced chromatid aberrations in pollen tubes of Tradescantia, 25:35120
CHANG, Zui N'yui, Isotope exchange between molecular oxygen and synthetic zeolites, 25:34580
CHANTANAKOM, Nongnooch, Study on thermal fading characteristics of some TSEE dosimetry, 25:35026 (THAI-AEC-35, pp 21-3)
CHAO, Yung-an., p--p and K^+--p scatterings, 25:36522
CHAPUIS, Anne Marie, Glass having a base of metaphosphates for dosimeters which are responsive to x-rays, γ-rays, and thermal neutrons, 25:35037
CHARASH, E., Ecological factors in siting of a nuclear power station, 25:36970
CHARBONNEAU, Serge, Calculation methods for heterogeneities in reactors of the natural uranium-graphite--gas type, 25:36989 (CEA-N-1398)
CHARGIN, A. K., Engineering the baseball magnet system, 25:36200 (UCRL-73067)
CHARLES, Robert Odon, Nuclear fuel subassemblies and combinations thereof, 25:37143
CHARLTON, L. A., Multiple-scattering theory for pion--nucleus scattering near 3,3 resonance, 25:36527
CHATRATH, M. S., Irradiation induced variation in Colletotrichum, 25:35256
CHATTERJEE, B. K., High-energy N component of extensive air showers, 25:36383
Search for high-energy gamma rays from pulsars, 25:35705
CHATTERJEE, S. D., Possible correlation between atmospheric ozone content and cosmic-ray intensity variations,

XUM

25:35974
CHATURVEDI, M., Aging behavior of Fe--30 Ni alloys containing niobium, 25:35499
CHAU, W. Y., Pulsar wobble, 25:35699
CHAUDHARI, R. D., Superplasticity in aluminum--zinc and tin--cadmium eutectoid alloys, 25:35405
CHAUMONT, Jacques, Fission investigation using on-line mass spectrometry, 25:36730 (NP-18829)
CHEADLE, B. A., Work hardening in polycrystalline alpha zirconium, 25:35394
CHEBOTAEV, P. Z., Ion shock waves in a collisionless plasma, 25:36106
CHECCUCCI, A., Coenzyme-substrate interactions, ESR study of irradiated systems, 25:34655
CHEMTOB, M., Nucleon--nucleon scattering in high waves and pion--pion dynamics, 25:36526
CHEN, C. W., Radiation hardening and radiation-anneal hardening in body-centered cubic metals, 25:35507
CHEN, Ka-wei, Two-dimensional analysis of heat transfer and fluid flow in a rod cluster with special attention to asymmetry, 25:34794
CHEN, R., Neutron-induced mutants of Pisum sativum and comparison with x-ray-induced genotypes, 25:35122
CHENEAU, Gilbert, The precipitation and filtration of trivalent plutonium oxalate, 25:34680 (CEA-R-4109)
CHENG, Wianney Kuo-chuan, Simple neutron spectrometer, 25:34925
CHERDANTSEV, P. A., Energy surfaces of ^{238}U in parametrization of Cassinian ovaloids, 25:36793
CHEREAU, Pierre, Direct measurement at 1100°C of partial molar enthalpies of O incorporation in PuO/sub 2-x/ and (U,Pu)O/sub 2+ -x/ by means of Tian--Calvet high-temperature microcalorimeter, 25:34606
CHEREL, Guy, Process and device for fuel reprocessing, 25:34713
CHERKASOVA, L. S., Early biochemical and structural changes in liver mitochondria of irradiated rats, 25:35216
CHERKESOV, A. I., Study of complex formation of Th with phthalexon S and thymolphthalexon S, 25:34532
CHERKI, C., Use of nuclear microanalysis of light elements in electrochemistry, 25:34550
CHERNAVSKII, D. S., Phase instability in scattering on random potential, 25:36599
CHERNIKOV, A. S., Y--YH_2 phase diagram at room temperature, 25:35582
CHERNOSKY, Edwin J., Response of the magnetosphere to sunspots as indicated by geomagnetic storminess levels, 25:35954
CHERNOVA, G. P., Electron paramagnetic resonance spectra of irradiated frozen aqueous solutions. XII, 25:34648
CHERNUKHO, B. M., Tungsten base metal--ceramic alloy, 25:35476
CHERNYI, G. P., Propagation of electromagnetic perturbation over a plane surface, 25:36367
CHERNYI, G. V., Deformation of laminar systems of copper--molybdenum and copper--tungsten at increases temperatures, 25:35454
Effects of composition on strength of Cu--Mo laminates, 25:35455
CHERRY, J. T., Two-dimensional stress-induced adiabatic flow, 25:34769 (UCRL-50987)
CHERTKOV, I. L., Transplantation of bone marrow to irradiated monkeys, 25:35230
CHERTOK, Robert J., Availability of radionuclides in debris from Plowshare excavation Buggy, 25:35088
Biological availability of radionuclides produced by Plowshare Event Schooner. I, 25:35090
Biological availability of radionuclides produced by Plowshare Event Schooner. II, 25:35089
CHESNOKOV, N. A., Experimental study of gas heating efficiency in sectioned plasma generator with channel adjustment, 25:35928
CHESTER, G. V., High pressure behavior of solid H_2, D_2, ^3He, ^4He, and ^{20}Ne, 25:37204 (NYO-3699-51)
CHHAJLANY, S. C., Effective-dipole form-factors for K/sub 13/-decay, 25:36459
CHI, Li Tsun, Relative yields of secondary [(p,xn)π] reactions on Bi in range E/sub p/ = 120-660 MeV, 25:36723 (JINR-P1-5530)
CHIANG, Soong Tao, Some calculations in two-body and multi-body scatterings, 25:36422
CHIAO, R. Y., Effects on the propagation of optical beams due to self-induced changes in index of refraction, 25:37250 (UCRL-20541)
CHIKOV, N., Parameters of neutron resonances of ^{233}U, ^{235}U, and ^{239}Pu, 25:35756
CHINAGLIA, B., Range of fission products in carbon, 25:36264
CHIRIVELLA, Jose, Relativistic motion of a radiating point charge in a constant electromagnetic field, 25:36363
CHISHOLM, A., T(d,n)^{4}He reaction, 25:34901
CHITNIS, E. V., Space research in India, 25:35997
CHITRE, S. M., Collapsed objects, 25:35660
CHIU, Charles B., Tests of an empirical rule for cuts and discussion of line reversal relations, 25:36502 (CALT-68-300)
CHIUDERI, Claudio, Radio model of the transition layer in solar active regions, 25:35720
CHIUDERI DRAGO, Franca, Radio model of the transition layer in solar active regions, 25:35720
CHO, Z. H., System for precise determinations of electron--gamma directional correlations, 25:34903
CHOHAN, V. S., Charge composition of cosmic-ray nuclei of elements from Ne to Ni, 25:35910
CHOI, Hyung Sup, Experimental study on the sintering of tungsten carbide powder with various metal binders, 25:35534
CHOJNOWSKI, Wladyslaw, Removal of radioactive I from milk by means of ion exchangers produced in Poland, 25:34703
CHORIN, Alexandre Joel, Numerical solution of Boltzmann equation, 25:36126 (NYO-1480-173)
CHOUDHURY, S. Rai, Anomalies in Ward identities and current commutators, 25:36427
CHOW, Joe G. Y., Investigation and repair of baffle plate damage in the HFBR primary heat exchangers, 25:37055 (BNL-15815)
CHOW, W. S., Superconductors with overlapping bands in presence of nonmagnetic impurities. II, 25:36032
CHRIMES, N. W. D., Industrial radiography with radioisotopes, 25:34841
CHRISTENSEN, D. E., Destructive and nondestructive burnup data from natural UO_2 fuel, 25:37015 (ENWL-1568)
CHRISTIAN, J. W., Plastic deformation of bcc metals, 25:35370
Solution hardening and softening in niobium--molybdenum and niobium--rhenium alloys, 25:35436
CHRISTIAN, R. S., TVGF for track sensitive targets, 25:34949 (CONF-700623-(Vol.1), pp 312-24)
CHRISTIE, R. S., Special diagnostic devices, 25:36090 (MATT-838)
CHU, C. W., Electronic transitions in near-equiatomic vanadium--ruthenium alloys, 25:36329
CHU, W. K., Stopping cross sections of gases for α particles from 0.3 to 2 MeV, 25:36255
CHUBB, T. A., X rays from Coma cluster of galaxies, 25:35799
CHUPRIN, V. A., Fine structure of superconducting alloys of Zr with Nb, 25:36053
CHURAEV, V. A., Plasma acceleration with an auxiliary stationary magnetic field , 25:36113
CHURCH, H. W., Comparison of turbulence intensity and stability ratio measurements to Pasquill turbulence types, 25:34747 (SC-DC-70-5443)
CHURCH, L. B., Zirconium-96(p,2n)^{95}Nb isomeric ratio at 400 MeV, 25:36761
CHUYANOV, V. A., Suppression of flute instability by means of feedback system in Phoenix II, 25:36162 (CTO-737)
CHWASTOWSKA, Jadwiga, Determination of Nb and Ta in products of Ta ore, 25:34510
Potentiometric determination of free nitric acid in presence of uranyl, Al, and Mg nitrates, 25:34517
CHYCZEWSKI, M., Properties of stainless steel 1H18NST after aging in the power reactor temperature ranges. II, 25:35336 (IAR-1255)
CIARANFI, E., Studies on the anti-tussor activity of aliphatic aldehydes. IV, 25:35159
CIERJACKS, S., Neutron scattering from ^{15}N. II, 25:36682
CIGNA, A. A., Principles and methods for the derivation of a formula for the discharge of radioactive liquid wastes in surface waters, 25:34717 (EUR-4636)
CINI CASTAGNOLI, G., Solar effects on cosmic ray intensity observed at 70 MWE underground, 25:35731
CIPOLLINI, Romano, Reactions of He^3H^+ ions with gaseous hydrocarbons. II, 25:34677
Reactions of He^3H^+ ions with gaseous hydrocarbons. III, 25:34676
CIRANNI, Giovanna, Reactions of He^3H^+ ions with gaseous hydrocarbons. II, 25:34677
Reactions of He^3H^+ ions with gaseous hydrocarbons. III, 25:34676
CISAK, H., Emission band spectrum of CD^+ molecule, 25:34594
CIUTI, P., Equation defining profile of non-relativistic beams with space-charge forces and finite emittance, 25:36628
CLAASSEN, Hans C., Radiochemical analyses of water from selected streams, wells, springs, and precipitation collected during reentry drilling, Project Rulison, 25:34728 (USGS-474-101)
CLARK, C. D., Solar chromospheric activity at 400, 800, and 1200 μ, 25:35776
CLARK, R. B., Radon-222 evaporation and high apparent Pb isotope ages in lunar dust, 25:35831
CLARK, Robert Beck, Deep inelastic neutrino--nucleon interactions, 25:36455 (CRO-3992-24)
CLARKSON, Jack E., Fission-excitation functions in interactions of ^{11}B, ^{12}C, ^{14}N, and ^{19}F with various targets, 25:36784
CLARKSON, R. G., Spectroscopic information from isobaric analog resonances, 25:36852
CLAUDSON, T. T., Irradiation effects on the mechanical properties of reactor structural and cladding alloys, 25:35506
CLAUER, A. H., Analysis of L and Y tilt boundary intersections formed during creep in molybdenum, 25:35402
CLAYTON, Anthony Robert King, Improvements in superconductors, 25:36066
CLAYTON, R. F., Health physics aspects of decontamination of cell line, 25:35131
CLAYTON, Roderick K., Photochemical reaction centers from rhodopseudomonas spheroides, 25:37206 (NYO-3759-30)

XUM

Prog. rpt. on photosynthetic energy conversion, annual, 9/70--8/71, 25:37205 (NYO-3759-18)
CLEE, P. T. M., Magnetization current effects in coils wound from multifilament stabilized superconductor, 25:35000 (CONF-700623-(Vol.2), pp 1095-1125)
CLEMENT, C. F., Excitation of analogue-dipole states, 25:36835
CLIFFORD, C. E., ORNL-SNAP shielding program, 25:36250 (ORNL-TM-3364)
CLIFTON, J. J., Experience in the use of thermoluminescent dosimeters for radiation dose control purposes, 25:35023 (AEEW-M-962)
CLOSE, Elon R., RKM1: ALGOL 60 program that obtains the parameter defining equations for generalized Runge--Kutta--Frey integration schemes, 25:37246 (UCRL-19861)
CLUTTERBUCK, D., Rough passage for nuclear ships, 25:37097
CNOPS, A. M., BNL work on Ne/H_2 targets, 25:34961 (CONF-700623-(Vol.1), pp 511-31)
COATS, R. B., Characteristics of an external electrode spark chamber, 25:35021
COCHAVI, S., Transition probabilities for low-lying states in ^{92}Nb, 25:36762
COCHRAN, Robert A., Occurrence and behavior of current spokes in MPD arcs, 25:36110
COFFER, H. F., Process for stimulating petroliferous subterranean formations with contained nuclear explosions, 25:34772
COFFOU, E., Symmetry of an exact three-body solution, 25:36602
COHEN, Stanley, DELPHI--SPEAKEASY system. I, 25:36357
COLDWELL, Robert Lynn, Variational calculation of electronic-or nucleonic-ordered systems, 25:36358
COLE, K. D., Formation of field-aligned irregularities in the magnetosphere, 25:35981
COLE, Ronald S., Properties of F' factor deoxyribonucleic acid transferred from ultraviolet-irradiated donors: photoreactivation in the recipient and the influence of recA, recB, recC, and uvr genes, 25:35271
COLES, R. E., Elastic and inelastic scattering of 5.0 MeV neutrons by sodium, 25:36685 (AWRE-O-3/71)
COLLERAINE, A. P., Bubble chamber detection technique for gamma rays in momentum region below 1 GeV/c, 25:34964 (CONF-700623-(Vol.1), pp 555-66)
COLLINGS, E. W., Magnetic-susceptibility and low-temperature specific-heat studies of Ti, Zr, and Hf, 25:36340
COLLINS, Leslie Edward, Improvements in ion sources, 25:36292
COMBY, G., Optical system Mirabelle, 25:34992 (CONF-700623-(Vol.2), pp 943-58)
COMER, Richard H., Radiological hazards of tritium-activated devices, 25:35138
COM-NOUGUE, Jacques, Tensile behavior of polycrystalline α between 25 and 700°C, 25:35352
COMPTON, R. N., Collisions of low-energy electrons with molecules: threshold excitation and negative-ion formation, 25:34618
CONRAD, H., Effect of purity and processing procedure on the mechanical properties of beryllium sheet, 25:35463
Effects of temperature and strain rate on the strength of beryllium sheet, 25:35459
CONSTANTINESCU, O., Radiation resistance of C--S bonds of macromolecular sulfone polyelectrolytes under the action of γ radiation, 25:34650
CONTE, F., Total $\pi^+\pi^-$ cross-section for dipion energies above 1.5 GeV, 25:36509
CONWAY, John G., Analysis of first and second spectra of dysprosium, 25:35846
COOK, J. L., Solution of the inverse reaction problem for complex potentials, 25:36812 (AAEC/TM-586)
COOKE, F. W., Effect of purity and processing procedure on the mechanical properties of beryllium sheet, 25:35463
Effects of temperature and strain rate on the strength of beryllium sheet, 25:35459
COOPER, A. S., Electronic transitions in near-equiatomic vanadium--ruthenium alloys, 25:36339
COOPER, Gilbert, Compton Fokker--Planck equation for hot plasmas, 25:36137
COOPER, J. D., Shubnikov--de Haas oscillations in neutron-irradiated graphite, 25:36284
COOPER, R. E., Survey of the effects of porosity on the elastic moduli and strength of brittle materials with particular reference to beryllium, 25:35331 (AWRE-O-25/71)
COPELAND, Edmund S., Structure-function studies of the aminothiol radioprotectants. The effect of carbon chain length in mercaptoethylamine homologs, 25:35160
CORBETT, B. L., Prog. rpt. on high flux isotope reactor, 1--3/71, 25:37068 (ORNL-TM-3432)
CORSET, J., Vibrational spectra and anharmonicity of H_2O, D_2O, and HOD in dilute solutions, 25:34591
COSTELLO, D. G., Prog. rpt. on neutron capture cross sections of Mo, Ta, and ^{238}U, final, 6/70, 25:36729 (N-70-41999)
COTTER, T. P., Rotating cable pusher for pulsed-propulsion space vehicle, 25:37189 (LA-4666)
COTTINGHAM, W. N., Smoothed Veneziano models and applications to pion--pion scattering, 25:36499
COUNSELMANN III, C. C., Multipath delay distortion of radio pulses from NP 0532, 25:35689
COURTOIS, G., Sediment dynamics and radioactive tracers: status of work in France, 25:34812 (ORNL-tr-2492)
COURTRIGHT, E. L. Jr., Mechanical behavior of a uniaxially aligned tungsten wire-reinforced lead composite system, 25:35344 (Y-1788)
COUTANT, Charles C., Bibliography of ecological publications supported by atomic energy commission related to Columbia River thermal effects studies, 25:35115 (BNWL-1543)
Ecological evaluation: migration of juvenile salmon in relation to heated effluents in central Columbia River, 25:37105 (BNWL-SA-3876)
COUTSOURADIS, D., Hardening mechanisms in multiphase alloys, 25:35396
COWLEY, E. R., Lattice vibrations in deuterated ammonium chloride at 85°K. II. Theoretical, 25:36222
COWLEY, S. W. H., Adiabatic flow model of a neutral sheet, 25:35994
COX, Allan V., Mechanism for producing magnetic remanence in meteorites and lunar samples by cosmic-ray exposure, 25:35598
COX, C. M., Comparisons between predicted and measured fuel pin performance, 25:37019 (ORNL-TM-3386)
COX, G. W., Programs for the management and processing of neutron diffraction data, 25:36309 (AAEC/TM-578)
COX, J. E., Vapor explosion--heat transfer and fragmentation. III, 25:37214 (ORO-3936-4)
COX, R., EPR identification of neutral charge state of Be vacancy in irradiated BeO, 25:36283
COX, W. Royall, Temperature dependence of electron mean free paths in cadmium and copper, 25:36328
CRAIG, R. S., Low temperature heat capacities of PrBi, PrSb, LaBi, and LaSb, crystal field effects in PrBi and PrSb, 25:35355
CRAMER, D. S., Gas target for production of monoenergetic neutrons, 25:36633
CRANBERG, L., Gas target for production of monoenergetic neutrons, 25:36633
CRAWFORD, J. H. Jr., Effect of ionizing radiation of impurity-vacancy dipoles in lead-doped NaCl and KCl, 25:36303
CREEK, G. E., Design considerations of reactor containment spray systems. Part X. The stress corrosion cracking of types 304 and 316 stainless steel in boric acid solutions, 25:37028 (ORNL-TM-2412(Pt.10))
CREIGHTON, John, The role of numerical stability in the computer solution of chemical chain reactions, 25:37255 (UCRL-73106)
CRENNELL, D. J., Λ_2^- from reaction $\pi^-p \to K/sub S/^0K^-p$ at 4.5 GeV/c, 25:36409
CRIPPA, P. R., Hese--protein interaction and radioresistance, 25:35106
CRISTOL, Stanley J., Bridged polycyclic compounds. LXV. Electrophilic addition of hydrogen chloride, acetic acid, and their deuterated analogs to benzonorbornadiene, 25:34575
CROAT, J. J., Properties, preparation, and handling of pure rare earth metals, 25:35297
CROFT, J. R., Attenuation of 14-MeV neutrons in calcium-based concrete, 25:36260
CROITORU, Petrica, Neutron generators, 25:36656
CROOK, A., Formation of stacking faults in magnesium--thorium alloys, 25:35484
CROSBIE, K. L., Fast reactor spectrum measurements. Technical summary report, February 1, 1970--January 31, 1971, 25:36991 (GULF-RT-10523)
CROSBY, Charles Edward, Improvements in and relating to the measurement of coating thickness, 25:35078
Inspection and/or measuring apparatus using radiation, 25:35041
CROSET, M., ^{18}O study of the source of oxygen in the anodic oxidation of silicon and tantalum in some organic solvents, 25:35293
Use of nuclear microanalysis of light elements in electrochemistry, 25:34550
CROSS, R. J. Jr., Interpretation of high-energy cross sections for molecular scattering, 25:35887
CROSSLEY, F. A., Microstructural analysis of a high strength martensite-beta titanium alloy, 25:35488
CROWLEY, Barbara K., Analysis of Marvel: nuclear shock-tube experiment, 25:34765
CROWTHER, R. L., Interactions between nuclear plant loading changes and nuclear fuel costs, 25:36893
CRUTCHLEY, D. E., Plastic anisotropy in bcc metals, 25:35379
CUDWORTH, Kyle M., Relative proper motions in region of open cluster NGC 2168 (M35), 25:35603
CULBERSON, O. L., Oak Ridge systems analysis code (ORSAC) User's manual, 25:36886 (ORNL-TM-3223)
CULLER, F. L., Technical status of the radioactive waste repository: a demonstration project for solid radioactive waste disposal, 25:34848 (ORNL-4680)
CUMO, M., Quality influence in post-burnout heat transfer, 25:34801
CUNNINGHAM, A. L., Techniques for fabrication of high-strength, high-modulus, low-density filament-reinforced metal matrix composites, 25:35528
CURRAN, D. J., Simple and inexpensive electronic conductivity manometer for monitoring pressure changes. Application to pressurometric titrations of iodate and ammonium ions, 25:34513
CURRY, Warren H., Magnus data on standard 10° cone calibration model, 25:37220 (SC-IC-713821)

CURTIS, C. E., Thorium ceramics data manual. Volume III. Carbides, 25:35548 (ORNL-4503(Vol.3))
CURTIS, Howell C., Reversible addition of benzoyloxy radicals to benzene, 25:34577
CURTIS, R. L., PHROG: a FORTRAN IV program to generate fast neutron spectra and average multigroup constants, 25:37113 (IN-1435)
CURTIS, T. H., Proton induced reactions on mass-14 nuclei, 25:36673
CZACHOR, A., Model of lattice dynamics for Mg, Co, and Y, 25:36333
CZARNIK, J. W., Velocity distribution of H(2S) atoms produced by dissociative excitation of H_2, 25:35864

D

DABROWSKI, J., Binding energy of ^3H and n-d doublet scattering length with rank four separable potential, 25:36659 (INR-P-1234)
DACHEV, B., Changes in oral cavity in chronic radiation, 25:35219
DACHS, J., UBV photometry of eclipsing binary zeta Phoenicis, 25:35554
DA COSTA, Jose Ribeiro, Project CEMAN, 25:34828
DADY, Charles E., Apparatus and method for monitoring fission products, 25:37147
DAGNELIE, J., Radiological aspects of post-radiotherapeutic colitis, 25:35153
DAINET, V., Reaction $\pi^- + {}^{90}Y{}^{90}n$ at 447 MeV, 25:36405 (JINR-P1-5781)
DALIBARD, Gerard, Oxidation of polycrystalline Nb samples, 25:35280
DALITZ, R. H., Shell-model analysis of Λ binding energies for p-shell hypernuclei. I, 25:36529
DALPIAZ, P., Measurement of X^0 cross-sections in π^-p interactions at 1.6 GeV/c, 25:36407
DAMLE, S. V., Gamma radiation from the galactic center: future experiments, 25:35923
DANCEWICZ, Antoni M., Significance of the intracellular distribution of enzymes in early changes of their activities after irradiation in vivo, 25:35215
DANDEKAR, B. S., Total solar eclipse of 3/7/70, 25:35764
DANIEL, H., Beta+ decay of ^{57}V, 25:36691 (ORNL-tr-2481)
DANIEL, H. R., Confinement of cosmic rays, 25:35905
DANIEL, J. S., Slip and twinning in α-uranium, 25:35382
DANIEL, R. R., Atmospheric neutrons and the Van Allen radiation belt, 25:35998
Gamma radiation from the galactic center: future experiments, 25:35923
High-energy cosmic-ray electrons, 25:35920
Search for energetic neutrons emitted during solar flares, 25:35772
TIFR balloon facility, 25:35908
DANIERE, J., Microstructure effect on hyperfine interactions in Yb--Ag, 25:36332
DAREKAR, V. S., Superplasticity in aluminum--zinc and tin--cadmium eutectoid alloys, 25:35405
DAROVSKIKH, V. F., Cesium-137 content of human body, 25:35095
DAS, G. C., Mobility of dislocations in molybdenum single crystals, 25:35485
Wave propagation in cold plasma in presence of Coriolis force, 25:36240
DAS, K. C., Nonrelativistic energy bands of double hexagonal close-packed lanthanum, 25:36352
DAS, Tapas, Recent theoretical developments in electroproduction of hadrons, 25:36452
Sign on the structure-dependent form factors in $\nu + l\nu\gamma$, 25:36469
DASS, N., Detecting radiation with a supercooled liquid, 25:35015
DATLOWE, Dayton, Relativistic electrons in solar particle events, 25:35727
DATZ, Sheldon, Excitation and dissociation of H with alkali atoms and ions from 2 to 50 eV, 25:35884
D'AURIA, J. M., Delayed states in ^{99}Nb, ^{108}Ag, and ^{110}Ag, 25:36769
DAUVERGNE, J. P., Experimental results with the 1 m model chamber at CERN. A, 25:34982 (CONF-700623-(Vol.2), pp 790-812)
DAVEY, G., Bubble nucleation on surfaces immersed in cryogenic fluids, 25:34958 (CONF-700623-(Vol.1), pp 449-58)
DAVID, C., Fast breeder fuel processing pyrochemical head end study, 25:34688 (EUR-4615)
DAVIDOV, D., Anisotropic behavior of dilute magnesium--gadolinium alloys, 25:36342
DAVIDSON, Lewis Arthur, Use of high energy ion beams for crystal analysis of ion implanted diamond, 25:36285
DAVIES, R. D., Search for interstellar H_2CS, 25:35708
Stark broadening in high-quantum-number recombination lines of hydrogen, 25:35711
DAVILA SANCHEZ, Carlos A., Molecular nature of radiobiological phenomena, 25:35101
DAVIS, A. I., Determination of mercury in biological and environmental materials by instrumental neutron activation analysis, 25:34551
DAVIS, J. Barry, Estimating plant production from soil and floristic correlates in Hot Creek Valley, Nevada, 25:37240 (TID-25723)
DAVIS, J. P., Thermionic reactor ion propulsion spacecraft for unmanned outer planet exploration, 25:35937
DAVIS, William R., Classical fields, particles, and the theory of relativity, 25:36556
DAVISON, W. D., Multi-configuration frozen-core approximation. I, 25:35890
DAVY, D. R., Ecological factors in siting of a nuclear power station, 25:36970
Nuclear power and environmental pollution, 25:37045 (NP-18842)
DAVYDOV, A. A., Critical current of superconducting alloy 65BT in fields up to 80 kOe, 25:36050
DAVYDOVA, T. A., Theory of linear transformation of waves in an inhomogeneous plasma, 25:36224
DAVYDOVSKII, V. Ya., Magnetic lenses with parabolic, triangular and trapezoidal distributions of linear ampere-turn density, 25:36643
DAWSON, J. M., Stellarator-mirror machine target plasma reactor, 25:36190 (PATT-841)
DAWSON, John M., Thermokinetic expansion theory, 25:36131
DE, A. K., Anomalous pulse spectrum of a plastic scintillator at sea level, 25:35010
DEACON, David, Refuelling machine for a nuclear reactor, 25:37151
DEAN, Guy, Direct measurement at 1100°C of partial molar enthalpies of O incorporation in PuO_{2-x} and $(U,Pu)C_{2+-x}$ by means of Tian--Calvet high-temperature microcalorimeter, 25:34606
DEAN, M. W., Magnetization current effects in coils wound from multifilament stabilized superconductor, 25:35000 (CONF-700623-(Vol.2), pp 1095-1125)
DEAN, Peter Mervyn, Radio-isotope machine, 25:34885
DE BEUKELAER, R. C., Pyrochemical head end conception for fast breeder fuel processing, 25:34687 (EUR-4614)
DE BEUKELAER, R. D., Fast breeder fuel processing pyrochemical head end study, 25:34688 (EUR-4615)
DE BORTOLI, M. C., Analysis of radioactivity in soil, 25:34500
DEBRUN, J. L., Determination of V, Nb, and S concentrations by proton activation analysis, 25:34554
DECKERT, Harald, Improvements in and relating to the coupling out of pulses from nuclear radiation detectors, 25:34914
DE CONINCK, A., Fast breeder fuel processing pyrochemical head end study, 25:34688 (EUR-4615)
Pyrochemical head end conception for fast breeder fuel processing, 25:34687 (EUR-4614)
DEENADAS, A. M., Low temperature heat capacities of PrBi, PrSb, LaBi, and LaSb, crystal field effects in PrBi and PrSb, 25:35355
DE ESTABLE-PUIG, J. F., Fibrosarcoma induced by alpha particle irradiation, 25:35236
DE ESTABLE-PUIG, R. F., Fibrosarcoma induced by alpha particle irradiation, 25:35236
DE FREITAS, C. Trench, Multispecimen hot pressing of UO_2, 25:35526
DE GIORGIO, L., Tumors by means of radioisotopes, 25:35166
DE JAGER, C., Coronae of cool stars, 25:35667
DELAND, Frank H., Scanning in cerebral vascular disease, 25:35176
DELARUE, Roger, Glass having a base of metaphosphates for dosimeters which are responsive to x-rays, γ-rays, and thermal neutrons, 25:35037
DEL BINO, G., Preparation of $^{238}PuO_2$ for neutron cross section measurements, 25:35541
DEL BOCA, R., Promotion of L-shell electrons to higher bound states in Ar^+--Ar collisions, 25:35866
DELCROS, Philippe, Results achieved with a rapid-cycling hydrogen bubble chamber, 25:34954 (CONF-700623-(Vol.1), pp 390-407)
DELHAES, Pierre, Variations with respect to temperature of quantities measured for neutron-irradiated carbon blacks, 25:36341
DELLA MEA, G., Disorder in implanted semiconductors, 25:36300
DE LOORE, C., Coronae of cool stars, 25:35667
DE LOS SANTOS LASURETGUI, Alfonso, Legal standards for navigation of nuclear ships, 25:37096
DEME, S., Synchronized chopper time-of-flight spectrometer, 25:34916 (JINR-E14-5731)
DE MEESTER, P., Model for the embrittlement and annealing of irradiated steel, 25:35508
DEMERS, Serge, Photometry of variables in globular clusters. II, 25:35610
DEMICHELIS, F., Range of fission products in carbon, 25:36264
DEMIDENKO, I. I., Ion energy spectra and lifetimes in a multipole magnetic trap, 25:36085
Plasma transport in a magnetic quadrupole field, 25:36086
DEMIRKHANOV, R. A., Production of negative hydrogen ions in a plasma with a double sheath, 25:35843
DEMISHEVA, A. G., Laboratory complex for producing homogeneous magnetic fields by superconducting magnetic systems, 25:36079
DEMMELER, M., Fast fission factor of metallic Be and of BeO, 25:37110
DEMPSEY, John D., Nuclear reactor control rod drive assembly, 25:37141
DENAULT, G. C., Corrosion of Ti--6Al--4V in HCl--methanol, 25:35287
DENHOY, B. S., Engineering the baseball magnet system,

XUM

25:36200 (UCRL-73067)
DENKER, B. I., Effects of impurities on properties of the Nb_3Sn phase, 25:36039
DENZEL, D. L., Current distribution and internal resistance in segmented MHD channels, 25:35926
DEPIREUX, J., Coenzyme-substrate interactions, ESR study of irradiated systems, 25:34655
DERENDYAEV, B. G., Isotopic exchange reaction of hydrogen in arenyl ions and their antecedents, 25:34559
DEREVSHCHIKOV, V. A., Mass and velocity spread of plasmoids in pulsed plasma accelerators, 25:36114
DE RIJK, R., Thermogravimetric analysis (TGA) of the uranium oxide carboreduction, 25:34556 (EUR-4635)
DERRE, J., Optical system Mirabelle, 25:34992 (CONF-700623-(Vol.2), pp 943-58)
DERRICK, M., Conference on bubble chamber technology, Argonne, Ill., 5/70, 25:34938 (CONF-700623-(Vol.1))
Conference on bubble chamber technology, Argonne, Ill., 6/70, 25:34966 (CONF-700623-(Vol.2))
Off-mass-shell Kw scattering phase shifts, 25:36413
DERZHAVETS, A. S., Increased susceptibility of explosives to a detonation impulse, 25:37191 (LA-tr-71-32)
DE SMET, D. J., Study of the anodic oxidation of vanadium, 25:35296
DETRAZ, C., Reaction $^{19}F(^3He,^6Li)^{16}O$ at 40 MeV, 25:36674
DE VAUCOULEURS, G., Hierarchical big-bang cosmology, 25:35817
DE VEGT, Chr, Photoelectric observations of lunar occultations, 25:35655
DE VERNEJOUL, Pierre, Measurement of the coronary flow by radiocardiography, 25:35085
DEVINNEY, Edward J., Realization of accurate close-binary light curves: application to MR Cygni, 25:35628
DEVOLD, I., COLIBRI: computer code for subchannel analysis, 25:37003 (CONF-710317-1)
DE VOLPI, A., Neutron escape from water-moderated tanks, 25:36653
DE VRIES, C., Three-magnet system for measurement of electron scattering through 180°, 25:36629
DE VRIES, H., Three-magnet system for measurement of electron scattering through 180°, 25:36629
DEWANDELEER, Jean George, Nuclear fuel subassemblies and combinations thereof, 25:37143
DHAVALE, A. T., Generalized MHD Couette flow, 25:35945
DIATLOV, V. G., Dynamics of THETA-pinch discharge with superimposed azimuthal magnetic field, 25:36129 (UARAEE-102)
DI CHIARA, F., Contribution of radioisotope techniques to the diagnosis of lung morphology, 25:35180
DICK, C. E., Production of high-intensity K x-ray beams, 25:35842
DICKEL, J. R., Supernova remnant near GX 5-1, 25:35684
DICKINSON, J. M., Use of gel permeation chromatography in the development of high-quality graphite, 25:35533
DIDENKO, A. N., Instability of ring currents, 25:35838
DIEZ, R., Radioactive contamination of atmosphere around Valencia measured from January 1966 till April 1968, 25:35132
DILULLO, C., BNL work on Ne/H_2 targets, 25:34961 (CONF-700623-(Vol.1), pp 511-31)
DIMITRI, F. H., Four groups four regions criticality calculation diffusion code, 25:37125 (UARAEE-85)
Multigroup, multiregion, criticality calculation diffusion code, 25:37127 (UARAEE-90)
Two-group two-region criticality calculation diffusion code, 25:37122 (UARAEE-79)
DINESCU, R., Thermal equilibria of phases in system MgO--TiO_2--V_2O_5, 25:35576
DINGLE, A. Nelson, Prog. rpt. on rain scavenging studies, 12/70, 25:34742 (COO-1407-38)
DIPLOCK, B. R., Fiber glass reinforced epoxy resin bellows, 25:34986 (CONF-700623-(Vol.2), pp 849-62)
DITTNER, P. F., Identification of the atomic number of nobelium by an x-ray technique, 25:36778
DITTNER, Peter F., Excitation and dissociation of H with alkali atoms and ions from 2 to 50 eV, 25:35884
DIX, W.-R., Inelastic electron--proton scattering in region of Δ(1236) resonance, 25:36381
DIXON, D. F., Valves for primary heat transport systems for Canadian power reactors, 25:37002 (AECL-3858)
DJADALI, F., Circular γ-polarization after n-capture in ^{141}Ce, ^{144}Nd, and ^{140}La, 25:36751
DJORDJEVIC, M., Electrical resistivity of graphite powder and its mixtures, 25:36334
DMITREVSKAYA, L. I., Method of calculating the number of theoretical stages of separation using a substituting line, 25:34707
DMITREVSKII, L. L., Method of calculating the number of theoretical stages of separation using a substituting line, 25:34707
DOBLE, N., Hyperon bubble chamber HYBUC, 25:34972 (CONF-700623-(Vol.2), pp 640-6)
DOBO, J., Effect of the type of polyethylene on the grafting of styrene onto polyethylene. III, 25:35591
DOBROZEMSKY, R., Mass spectrometric determination of the neutron capture cross section of isotopes of the rare earths, 25:36735 (SGAE-PH-104/1971)
DOBSON, J. C., Angular momentum coherent states, 25:36377
DODD, C. V., Computer programs for some eddy-current problems, 1970, 25:37212 (ORNL-TM-3295)
DODD, R. A., Creep in stoichiometric beta NiAl, 25:37160 (CCO-1489-10)
DODERO, M. A., Solar effects on cosmic ray intensity observed at 70 MWE underground, 25:35731
DOGGETT, LeRoy E., Fales (49) and mass of Jupiter, 25:35823
DOIDGE, P. R., Nature of transition at k/sub c2/, 25:36028
DOKSHINA, G. A., Functional state of endocrine glands in rats irradiated on 25 MeV betatron, 25:35164
DOLE, Malcolm, Prog. rpt. on radiation chemistry of high polymers, 6/70--3/71, 25:34637 (ORO-4059-1)
DOLLINS, C. C., Electron bombardment of niobium containing interstitial impurities, 25:35517
DOMINGUEZ, C. A., Asymptotic nucleon form factors from current algebra and Regge model, 25:36437
DOMKE, H., Radiation transport in a free-electron atmosphere, 25:36267
DONALDSON, A. B., Energy diffusion in a one-dimensional finite solid with linear heat loss, 25:37221 (SC-DR-70-767)
High intensity direct reading heat flux gauge, 25:37225 (SC-DR-710194)
DONALDSON, F. G., Polarization-free vacuum-ultraviolet excitation of helium by electrons, 25:35857
DONALDSON, W., Interferometric observations with baseline of 127 kilometers. II, 25:35709
DONATO, A., Treatment of radioactive waste in reprocessing of fuel, 25:34711
DONEA, J., Mechanical behavior of complex structures in presence of creep, thermal strains and irradiation-induced dimensional changes, 25:34774 (EUR-4629)
DONLAN, Vincent Louis, Two-particle fractional parentage coefficients and their application to atomic spectra, 25:35850
DONNELLY, Russell J., Measurement of the probability of nucleation of a vortex ring in helium II, 25:36017
DONOLATO, C., Structure of compounds Ag_4Sc, Ag_2Sc, Au_4Sc, Au_2Sc, and Ag_3Yb, 25:35496
DOROSHENKO, A. Z., System for depression of magnetic field pulsations in Dubna synchrophasotron, 25:36605 (JINR-PS-5724)
DORR, F. W., Direct solution of discrete Poisson equation on irregular regions, 25:37187 (LA-4553)
DORREN, J. D., N-point dual functions for mesons with physical trajectories, 25:36485
DOST, M., Spectroscopic information from isobaric analog resonances, 25:36852
DOVER, C. B., Neutron scattering from ^{15}N. II, 25:36663
DOWSETT, D. J., Off-line computer interface for a rectilinear scanner, 25:34881
DOYAMA, M., Recovery of pure platinum and dilute platinum--gold alloy electron-irradiated at liquid-nitrogen temperature, 25:36306
DRAGULESCU, C., Polarographic reduction of niobium in hydrochloric acid-thiocyanate medium, 25:34526
DRAKE, M. K., Data formats and procedures for the ENDF neutron cross section library, 25:36719 (ENL-50274)
DRAPIER, J. M., Hardening mechanisms in multiphase alloys, 25:35396
DREISS, Gerard J., Ground state correlations as variational parameters in the nuclear many-body problem, 25:36840
DREIZLER, R. M., Ground state correlations as variational parameters in the nuclear many-body problem, 25:36840
DRESCHER, Hans-Paul, Temperature distribution and corrosion in the core of an advanced high-temperature reactor, 25:36980 (JUL-725-RG)
DRIGO, A. V., Disorder in implanted semiconductors, 25:36300
DRITS, M. E., High-temperature thermomechanical treatment of magnesium--zinc--zirconium alloys, 25:35456
DROBIZ, A. M., Radioisotopic analysers for determining sulphur content in the oil-products and the experience in their exploitation, 25:35040
DROBYAZKO, V. N., Absorption-spectrophotometric determination of certain rare earth elements in the aqueous acetone solutions of dibenzoylmethane complexes, 25:34527
DROBYSHEVSKII, E. M., Nonstationary three-dimensional plasma flow in a homopolar device, 25:36205
DROZDOV, V. E., One-group method for calculating dose fields from sources of γ-radiation with complex spectrum, 25:36265
DUBENKROPP, H., Neutron scattering from ^{15}N. I, 25:36664
DUBENSKY, R. G., Stress cycling induced changes in the yield properties of molybdenum, 25:35346
DUBOSE, C. K. H., Effect of boron on ductility and strength of Inconel 600 and Types 304 and 316 stainless steel at hot metalworking temperatures, 25:35338 (ORNL-TM-3316)
DUBOV, E. E., Computation of contribution functions, 25:35757
DUBUQUOY, Claude, Separation of lanthanides by chromatography on SA-2 ion exchange paper, 25:34714
DUDEROVA, E. P., Studies in field of analytical chemistry of U. V, 25:34531
DUGLE, D. L., Gamma-ray induced strand breakage of Bacillus subtilis DNA irradiated in vivo, 25:35268
DUGLE, J. R., Gamma-ray induced strand breakage of Bacillus subtilis DNA irradiated in vivo, 25:35268
DUKE, C. B., Comparison of calculations of LEED intensities from Be(0001) and Al(001), 25:36329
DUKHOVICH, F. S., Safety precautions in radioactive cement storage, 25:35148

XUM

DULK, G. A., 80-MHz observations of harmonic Type-II solar burst, 25:35735
Distance and spectrum of 3C 391, 25:35702
Meandering solar Type-IV burst 12/17/69, 25:35742
Motions and polarization of solar Type-IV burst, 25:35740
Solar Type-II burst 10/13/69, 25:35736
DUM, Christian T., Anomalous resistivity of a turbulent plasma, 25:35145
DUMBRAIS, O. V., Verification of models of the asymptotic behavior of π^+p scattering amplitudes, 25:36511
DUMBRI, A. C., Preparation and properties of pyrolytic zirconium dioxide films, 25:35564
DUNAEV, L. M., One-group method for calculating dose fields from sources of γ-radiation with complex spectrum, 25:36265
DUNAEV, P. V., Growth and transformation of crystalline epithelium in implants following x-irradiation of donor, 25:35231
DUNCOMBE, R. L., Determination of mass of Pluto, 25:35822
DUNGAN, R. H., Calculation of the vapor pressure in desiccated-multicomponent systems, 25:37223 (SC-DR-710074)
DUNNING, K. L., Fortran programs for (p,γ) yield calculations based on Vavilov's theory of energy loss distributions, 25:36732 (NRL-7230)
DUPUY, M., Chemical diffusion and Kirkendall effect in the body-centered cubic phase of the system plutonium/zirconium, 25:35333 (CEA-CONF-1760)
DURFEE, R. C., Oak Ridge systems analysis code (ORSAC) User's manual, 25:36886 (ORNL-TM-3223)
DURNEY, B., New type of supersonic solution for the inviscid equations of the solar wind, 25:35743
DURSO, J. W., Intermediate range nucleon--nucleon interaction, 25:36525
DUSEK, J. T., Multispecimen hot pressing of UO_2, 25:35526
DUSHIN, L. A., Azimuthal current and microwave radiation in theta pinch, 25:36122
DUTOU, L., Dosimetry in cobalttherapy, 25:35136
DUTT, R., eta-X mixing in GMOR model, 25:36651
DUTTA-ROY, B., Vector-meson dominant sum rules and low-energy kaon--nucleon scattering, 25:36519
DUVAL, J. S., Radon-222 emanation and high apparent Pb isotope ages in lunar dust, 25:35831
DUVALL, D. S., Relationship of microstructure to workability in a high strength nickel-base superalloy, 25:35500
DUXBURY, Alyn C., Determining middle scale time dependent variations in salinity and temperature structure in coastal zone province under influence of dilution and upwelling, 25:37216 (RLO-1725-191)
DVORNIK, I., Effect of the type of polyethylene on the grafting of styrene onto polyethylene. III, 25:35591
DWORZECKA, M., Binding energy of ^3H and n-d doublet scattering length with rank four separable potential, 25:36659 (INR-P-1234)
D'YACHENKO, V. V., High-frequency plasma heating near the lower hybrid frequency, 25:36087
Limiting frequency for plasma absorption of high-frequency waves, 25:36238
DYCK, H. Melvin, Intrinsic polarization in K and M giants and supergiants, 25:35611
DYER, George R., Preregulation of high voltage supply circuit for a medical nuclear spectrometer, 25:34688
DYKES, D. G., ELI-44: computer-controlled instrument system, 25:37222 (SC-DR-70-862)
DYMOVICH, V. I., Measurement of isotopic abundances by time-of-flight mass spectrometer, 25:35070
DYSON, J. E., Fine structure of nebular emission lines, 25:35650
DZANTIEV, B. G., Radiative and chemical effects of accelerated multicharged ions on gaseous nitrogen-containing systems, 25:34567
DZHOLOS, R. V., Pair correlations and collective 0^+ states of nuclei. I, 25:36825
DZIEDZIELA, W., Radiation-induced grafting of styrene onto cross-linked butyl rubber, 25:34631
DZIERBA, Alex R., Diffractive N^* production in a triggered-bubble-chamber experiment, 25:34971 (CONF-700623-(Vol.2), pp 629-38)
DZYKOVICH, I. Ya., Peculiarities of formation of intermetallics in explosion-produced copper--titanium compounds, 25:35324

E

EARNEY, J. J., Phonon scattering of fast electrons by crystals, 25:36280
EAST, L. V., Precision measurement of gamma rays from ^{95}Nb decay, 25:36810
EASTHAM, A. R., Nature of transition at H/sub c2/, 25:36028
EASTHAM, D. A., Study of ^{150}Gd, 25:36775
EATHER, R. H., Ring current as the source region for proton auroras, 25:35995
EBBIGHAUSEN, E. G., Photometric elements of eclipsing binary EE Pegasi, 25:35607
ECKDAHL, C., Properties of the rotating spoke in an unstable pulsed MPD arc, 25:36111
EDELINE, J. C., Characteristics of various sealing membranes for alpha activity monitoring cells used in solutions, 25:34673 (CEA-N-1440)
EDENHOFER, B., Dislocation-pinning memory-effect in γ-irradiated and stress-annealed copper, 25:35514
EDWARDS, Arthur L., Cord, Record: sorting of tabular data, 25:37178 (CIC-P1-8)
Fitter, Fungus, Funny: linear least squares curve fitting of weighted tabular data, 25:37177 (CIC-E2.2-8)
SPIFFY: interpolation in tables of weighted data, 25:37176 (CIC-E1.1-8)
EDWARDS, B., Fisheye counting problems, 25:34957 (CONF-700623-(Vol.2), pp 1010-23)
EDWARDS, D. R., Nuclear metallurgy curriculum at Univ. of Missouri at Rolla, 25:34781
EDWARDS, H. J., Precision of time of flight measurements, 25:35020
EFANOV, V. A., Observations of 3C 273 radio source at 8 mm with maser, 25:35686
EFIMOV, Yu., Transition temperature of superconducting compounds V_3Ga, V_3Si, and Nb_3Sn, 25:36040
EFIMOV, Yu. S., Polarimetric measurements of UV Cati-type star flash radiation, 25:35637
EFIMOVA, A. N., Enriched U in urine, 25:34541
EFREMOVA, G. P., Content of artificial radioisotopes in atmosphere over Moscow during 1962--1967, 25:34748
EGORENKOV, P. M., Extension of experimental capabilities of MR reactor for loop-testing fuel elements and materials, 25:37067 (LE/G-3001)
EICHLER, J., Circular γ-polarization after n-capture in ^{141}Ce, ^{144}Nd, and ^{140}La, 25:36751
EIDAM, V., Problems of grasping the working behavior of nuclear power plants in production planning and of its economical simulation, 25:37033
EIDUS, L. Kh., Some problems of the mechanism of injury and recovery of cells, 25:35205
EISBERG, Robert M., Research progras of the Nuclear Consortium at the UCLA Cyclotron Laboratory, July 1970. Report AR 5, 25:36738 (UCLA-10-P-18-23)
EISENBERG, J. M., Multiple-scattering theory for pion--nucleus scattering near 3,3 resonance, 25:36527
EISENLOHR, H. H., IAEA dose comparison program, 25:36141
EISENSTEIN, R., Decay modes and lifetimes of levels in ^{210}Bi, 25:36790
EJIRI, H., Hindrance of charge exchange E1 transition, 25:36836
ELAGIN, V. B., Application of fast neutrons in radiation defectoscopy, 25:34825
ELCOMBE, M. M., Programs for the management and processing of neutron diffraction data, 25:36309 (AAEC/TM-578)
EL-DAHSHAN, M. E., Effect of heat-treatment and cold work on the oxidation of Zr--1 percent Nb alloy in air and pressurized steam at 450-650°C, 25:35278 (UARAEE-72)
EL-DEMERDASH, A. A., Criticality evaluation of hydrogeneous enriched lattices using a three group model, 25:37124 (UARAEE-84)
Theoretical study of effect of temperature on reactivity of EK-10 type reactors applying three-group theory, 25:37138 (UARAEE-105)
ELEONSKII, V. N., Self-focusing of a vector field, 25:36226
EL-FOULY, M., Cooling of a simulated fuel element by a flow of naturally circulated boiling water, 25:37009 (UARAEE-110)
EL-FOULY, M. F., Experimental loop for two phase heat transfer investigations, 25:34793 (UARAEE-81)
Station staffing requirements for operation of 150 Mwe nuclear station in UAR, 25:36889 (UARAEE-98)
EL-GWAILY, M. S., Experimental studies on shock waves propagated through a longitudinal magnetic field in electrodeless discharge tubes, 25:36092 (UARAEE-101)
ELIEZER, S., eta-X mixing in GMOR model, 25:36651
EL-KHALAFAWY, T. A., Dynamics of THETA-pinch discharge with superimposed azimuthal magnetic field, 25:36129 (UARAEE-102)
Experimental studies on magnetically driven shock wave passing through a longitudinal magnetic field, 25:36117 (UARAEE-106)
Experimental studies on shock waves propagated through a longitudinal magnetic field in electrodeless discharge tubes, 25:36092 (UARAEE-101)
Instruments for measurement of the spectral lines profile and shift, 25:36091 (UARAEE-95)
ELKHISHEN, M., Effect of form factors on high-energy neutrino reactions, 25:36460
EL-KONSOL, S., Calculation of neutron pulse shape, transmission function and resolution function in mechanical time-of-flight spectrometer, 25:34919 (UARAEE-61)
Effect of the probe tube on the thermal neutrons space-energy distribution, 25:37137 (UARAEE-75)
Energy-dependent Milne problem, 25:36650 (UARAEE-60)
General review of thermal neutron spectra investigations, 25:37118 (UARAEE-62)
One-group considerations of Milne problem, 25:37116 (UARAEE-56)
ELLEGAARD, C., Decay modes and lifetimes of levels in ^{210}Bi, 25:36790
ELLGEN, Paul C., Kinetics and mechanism of the reaction of nickelocene with mercaptans, 25:34597
ELLIS, B. H., Study of the anodic oxidation of vanadium, 25:35296

XUM

ELLS, C. E., Work hardening in polycrystalline alpha zirconium, 25:35394
EL-MASRY, M. A., Experimental studies on magnetically driven shock wave passing through a longitudinal magnetic field, 25:36117 (UARAEE-106)
EL-MENSHAWY, M. F., Experimental studies on magnetically driven shock wave passing through a longitudinal magnetic field, 25:36117 (UARAEE-106)
EL-MOFTY, O. H., Criticality evaluation of hydrogeneous enriched lattices using a three group model, 25:37124 (UARAEE-84)
New approach for calculations of nuclear fuel consumption in UA-RR-1 core, 25:37077 (UARAEE-63)
Theoretical study of effect of temperature on reactivity of EK-10 type reactors applying three-group theory, 25:37138 (UARAEE-105)
EL-NAGDY, M. M., Experimental study of radiation-induced boiling in superheated liquids, 25:34798
EL-NAGGAR, I. A., Boundary conditions in the case of adjacent plasma streams, 25:36128 (UARAEE-78)
Longitudinal nonlinear oscillations of hot electron magnetic plasma, 25:36217 (UARAEE-88)
EL-SAYED, M. N., Energy distribution of moderator atoms in reactors, 25:37108 (UARAEE-52)
EL-SHANSHOURY, I. A., Effect of heat-treatment and cold work on the oxidation of Zr--1 percent Nb alloy in air and pressurized steam at 450-650°C, 25:35278 (UARAEE-72)
Mechanical behaviour of ni-based alloys at elevated temperatures, 25:35340 (UARAEE-55)
EL-SIRAGY, N. M., Dielectric tensor of inhomogeneous plasma to second order with respect to space derivatives, 25:36127 (UARAEE-65)
ELSKENS, M., Improved electronic control unit for a motor type beam scanner, 25:36632
EMANUEL, N. M., Part played by radicals in radiation damage of biochemical components of cells, 25:35202
EMERSON, S. T., Hydrogen-2(p,pn)p reaction at 5.0 MeV, 25:36670
EMMERICH, W.-D., Timing with surface barrier detectors using charge and current pulses, 25:34899
ENDERLEIN, H., Post irradiation examination of a thermionic converter, 25:35936
ENDO, Yorimasa, Level structure of ^{143}Pm and ^{142}Nd, 25:36766
ENGELMANN, Ch., Experimental determination by means of activation monitors of distribution of γ photon bremsstrahlung beam produced by 25 to 45 MeV electrons, 25:34908
ENGELMANN, R., Off-mass-shell Kr scattering phase shifts, 25:36413
ENGLARO, G. C., Contribution of radioisotope techniques to the diagnosis of lung morphology, 25:35180
ENGLISH, J. J., Oxidation protection of a chromium alloy by nickel-alloy claddings, 25:35288
ENGSTROM, S. F. T., Echelle spectrograph for high resolution studies of the solar vacuum ultraviolet spectrum, 25:35054
ENOME, Shinzo, Observations of solar radio burst on 9/27/69, 25:35725
ENZMANN, H. F., Enriched uranium: report on situation in Switzerland, 25:34819
EPPLEY, R. E., Neutron-deficient Gd isotopes. III, 25:36744
ERAMZHYAN, R. A., Neutron channel in muon capture on ^{4}He, 25:36666
ERASMUS, C. S., Instrumental neutron-activation analysis of samples taken at different levels of E.R.P.M. mine, 25:34543 (NIM-1013)
ERDT, W., Experimental results with the 1 m model chamber at CERN. A, 25:34982 (CONF-700623-(Vol.2), pp 790-812)
EREMENKO, S. A., Fate of ^{76}As in rabbits with syphilis, 25:35087
EREMIN, B. G., Self-trapping of powerful electromagnetic waves in a dense plasma, 25:36225
ERICH, U., Elastic electron scattering on ^{4}He at energies between 30 and 59 MeV, 25:36658 (CERN-Trans-71-13)
ERMILOVA, V. K., Relativistic increase of ionization and sensitivity of nuclear emulsions, 25:34937 (CERN-Trans-71-9)
ERMLICH, H., Problems of grasping the working behavior of nuclear power plants in production planning and of its economical simulation, 25:37033
ERNST, R. H., Oxidation protection of a chromium alloy by nickel-alloy claddings, 25:35288
EROFEEV, V. S., Ionization instability of a self-sustaining low-pressure discharge in a strong transverse magnetic field, 25:36159
EROZOLIMSKII, B. G., Measurements of angular correlation of neutron spin and antineutrino momentum in the decay of polarized neutrons, 25:36385 (IAE-1947)
ERSHOV, B. G., Electron paramagnetic resonance spectra of irradiated frozen aqueous solutions. XII, 25:34648
ERSHOV, E. B., Distribution of ^{239}Pu in intact skin in its surface contamination, 25:35092
ERWIN, A., Neutral particle tagging facility for ANL 30'' bubble chamber, 25:34967 (CONF-700623-(Vol.2), pp 582-92)
ERYUSHEV, N. N., Observations of solar radio emission at 3.15 cm, 25:35760
ESCARAVAGE, C., Plastic deformation of single crystals of indium solid solutions in magnesium, 25:35287
ESELEVICH, V. G., Isomagnetic discontinuity in a collisionless shock wave in a plasma, 25:36125
ES'KOV, A. G., Isomagnetic discontinuity in a collisionless shock wave in a plasma, 25:36125
ESSELMAN, W. H., FFTF: companion test and development facility for LMFBR program, 25:37085 (WHAN-SA-104(Rev.))
ESSINGTON, E. H., Radiochemical data for STS A, Amchitka Island, Alaska, 25:34720 (NVO-1229-121)
ESTRADA TINAJERO, Pedro, Isobaric analogue states between 4 and 8 MeV for reaction ^{48}Ca(p,p)^{48}Ca, 25:36690 (NP-18824)
EUSTIS, R. H., Effects of electrode size on the performance of a combustion-driven MHD generator, 25:35933
EVANS, A. G., Iodine retention studies. Progress report, January--June 1970, 25:37106 (IP-1259)
EVANS, Charles Gervase Thorngate, Apparatus for carrying out processes in a controlled environment, 25:34855
EVANS, Leslie Samuel, Transport containers for radioactive materials, 25:34858
EVANS, S. M., Thermodynamic data program involving plutonia and urania at high temperatures. Quarterly report No. 14, November 1, 1970--January 31, 1971, 25:35547 (GEAP-12182)
EVERETT, C. J., New method of sampling Klein--Nishina probability distribution for all incident photon energies above 1 keV, 25:36432 (LA-4663)
EVSEEV, A. G., Stabilization of radicals formed during low-temperature radiolysis, 25:34640
EWALD, R., Cold neutron source of French--German high flux reactor in Grenoble, 25:37087
EWALDS, Klaus, Method for analysis of complex end spectra in semiconductor spectroscopy, 25:34536 (JUL-705-RC)
EXCOFFON, Jacques, Electrostatic systems for ion transport, 25:36608 (NP-18855)
EZAKI, Tadao, Josephson junctions with superconducting barriers, 25:36064
EZHELA, V. V., Constraints on growth power of the binary process amplitude, 25:36600

F

FABBRI, D., Heavy gas--liquid mixture bubble chamber of 70 liters volume with hydrogen internal target, 25:35007 (LNF-70/25)
FABIAN, A. C., Rocket observations and the cosmic x-ray background, 25:35712
FABIAN, H., Targets for particle accelerators, 25:36622
FABREGA, Serge, Thermic calculations on water cooled research reactors, 25:37058 (CEA-R-4114)
FABRITIUS, H., Ferritic Cr--Mo-steel with Nb addition usable for construction of Na-cooled nuclear reactors, 25:35407
FACSKO, Gh., Polarographic reduction of niobium in hydrochloric acid-thiocyanate medium, 25:34526
FADIN, V. S., Electroproduction in colliding-beam experiments, 25:36448
Large angle electroproduction of electron--positron pairs, 25:36440
FAELTHAMMAR, C.-G., New approach to the theory of the magnetosphere, 25:35993
FAGES, Denis, Natural convection irradiation device ''Esther'', 25:37061 (EURFNR-890)
ODILE irradiation device, 25:37060 (EURFNR-889)
FAHR, H. J., Interpretation of extra-terrestrial Lyman-alpha observations, 25:35593
FAINBERG, Joseph, Type III solar radio burst storms observed at low frequencies. III, 25:35723
FAINSHTEIN, S. M., Excitation of electromagnetic waves in a beam--plasma system with Coulomb friction, 25:36235
Instabilities in a double-stream plasma with coulomb collisions, 25:36174
FAIRCHILD, C. E., Velocity distribution of H(2S) atoms produced by dissociative excitation of H_2, 25:35864
FAIRHALL, A. W., Prog. rpt. on radiocarbon in sea, 8/15/68--5/1/71, 25:34723 (RLO-2225-T-20-3)
FANALE, Fraser P., Potassium--uranium systematics of Apollo 11 and Apollo 12 lunar samples and of some deep earth rocks, 25:35830
FARACI, G., Measurement of the surface inductance and penetration depth of superconducting aluminum, 25:36029
FARAGGI, H., Proton-pair correlation in Ti and Cr low-lying excited states, 25:36709
FARAGGIANA, R., Detailed analysis of metallic-line star 15 Vulpeculae, 25:35653
FARR, W. M., Loss-cone modes in inhomogeneous mirror machines, 25:36166 (UCRL-73135)
FARRAR IV, H., Helium production in stainless steel and its constituents as related to LMFBR development programs, 25:35503 (HEDL-SA-193)
FARRAR IV, Harry, Determination of nitrogen and hydrogen at parts-per-million levels in milligram steel samples, 25:34514
FARTUSHNYI, V. F., Experiments on acceleration of α-particles by collective method, 25:36615 (UCRL-Trans-1434)
FAUSKE, H. K., Pressure-pulse propagation in two-phase one- and two-component mixtures, 25:37035 (ANL-7792)

FAY, James A., Occurrence and behavior of current spokes in MPD arcs, 25:36110
FEDOROV, M. A., Superconductivity induced by pressure, 25:36023
FEDOROVA, N. I., Morphology of auroral electron energetic and angular distributions, 25:35982
FEDOTOV, L. N., Critical current of superconducting alloy 65BT in fields up to 80 kOe, 25:36050
Electrical resistance of Ti--Nb alloys at high pressures, 25:36321
FEDOTOV, V. P., Regulation of composition of 11-OCS by liver of dogs irradiated with gamma rays, 25:35222
FEENEY, R. K., Prog. rpt. on excitation and ionization of ions by electron impact, 9/70--5/71, 25:35833 (ORO-3027-19)
FEHRENBACHER, L. L., Compressive creep of yttria rare earth stabilized zirconia storage heater refractories, 25:35555
FEHRS, D. L., Contact potential measurements of adsorption of alkali metals on Ta(110) and W(100) crystals, 25:35359
FEINBERG, G., Decay rate for $2^3S_1 + 1^1S_0$ + one photon in He, 25:35845
FEIT, Julius, Effect of a bounded interplanetary diffusion medium on the propagation of solar flare cosmic rays, 25:35730
FELDEN, Madeleine, Excitation cross section 3s + 3p of sodium subjected to electron impact, 25:35881
FELDMANN, A., Contributions to radiation stimulation. III, 25:35248
FELS, Stephen, Anomalous behavior of $\gamma\gamma + n\pi^0$ Lagrangians, 25:36446
FENDER, J. R., Prog. rpt. on polyurethane foam material, 5/71, 25:37165 (BDX-613-300)
FERADAY, Melville Albert, Uranium--silicon fuel elements for a nuclear reactor, 25:35540
FERENCZI, G., Momentum dependence of πrho vertex, 25:36495
FERLAUTO, E. C., Gel permeation chromatographic investigation of irradiated copolymers, 25:34626
FERRARI, H. M., Fuel development for power reactors, 25:35550
FERRARI, S., Utilization of vibrational compaction for nuclear fuel, 25:35524 (RT/ING-(70)22)
FERRILL, D. A., Technical note: fatigue crack propagation in Zircaloy-2 weld metal, 25:35466
FERRIS, L. M., Distribution of transuranium elements between molten Li chloride and Li--Bi solutions. Evidence for Cf(II), 25:34705
FESSENDEN, Richard W., Electron spin resonance spectra of radiation-produced radicals, 25:34616
FET, A. I., Theory of unitary symmetry, 25:36552
FETISOV, E. P., Electron distribution function in a low-temperature plasma, 25:36134
FETISOV, V. N., Neutron channel in muon capture on ^{4}He, 25:36666
FIALA, J., Relative efficacy of intraperitoneal application of haematopoietic cells to irradiated mice, 25:35111
FIALER, Philip Anthony, Irregularities in the quiet ionosphere and their effect on propagation, 25:36003
FICHIZHYAN, B. S., Effect of radiation on the reproduction of cells of hemopoietic organs in various species of laboratory animals according to their radio-sensitivity, 25:35217
FICOCELLI V., E., Equilibrium compositions and thermodynamic properties of mixed plasmas. II, 25:36104 (NP-18772)
FIDEL'SKAYA, R. P., Intense beams with an arbitrary phase-density distribution in external focusing fields, 25:36642
FIELDS, T. H., Round table on experience with existing chambers, 25:34945 (CONF-700623-(Vol.1), pp 196-255)
FIKS, M. M., Electron-ion bunch diagnostics by means of bremstrahlung, 25:36616 (UCRL-Trans-1440)
FILBY, R. H., Determination of mercury in biological and environmental materials by instrumental neutron activation analysis, 25:34551
FILIMONOVA, G. F., Regeneration in liver after internal irradiation, 25:35221
FILIPPOVA, T. P., Abundance and characteristics of geochemistry of gold in bauxites, 25:34553
FINCH, D. R., ENDF/B cross section preparation and testing in the JOSHUA system, 25:36737 (TID-25690)
FINK, E. H., Relative line intensities in Lyman bands of HD and H_2, 25:35848
FINK, H. J., Nucleation field of a thin superconducting film on a thick normal layer, 25:36035
FINK, R. W., M/L orbital-electron-capture ratio in ^{71}Ge decay, 25:36704
FINKBEINER, H. C., Dissociation energy of diatomic cerium and predicted stability of gaseous intermetallic cerium compounds, 25:35347
FINNILA, Ronald Matti, ac temperature technique for measuring high-temperature specific heat of metals, 25:35341 (UCRL-50962)
FIORINI, E., Projector for Gargamelle's pictures, 25:34551 (CONF-700623-(Vol.1), pp 334-44)
FIRGANEK, H., Investigations of solidification front and the depth of the liquid phase in concast billets by the technique of radioactive traces, 25:34820
FISCHBECK, H. J., Spectrum shape of K-orbital shakeoff electrons and accompanying nuclear beta particles in decay of ^{143}Pr, 25:36774
FISCHEDICK, G., Cobalt-60 therapy of carcinomata of urinary bladder: five-year results, 25:35192
FISCHER, Glen Charles, Reaction $\pi^+p + K^+\Sigma^+$ from 2.75 to 14 GeV/c, 25:36410
FISCHER, Hugo B., Longitudinal dispersion in laboratory and natural streams, 25:34718 (KH-R-12)
FISCHER, K., Excitation functions of the ^{197}Au(α,xn) reactions in the energy range from 16 to 102 MeV, 25:36745
FISER, M., Decay of /sup 195m/Hg and ^{195}Hg to levels in ^{195}Au, 25:36750
FISH, L. A., Compound diffusion of cosmic rays, 25:35902
FISHER, C. M., Optimization of bubble chamber design parameters for strong interaction experiments, 25:34939 (CONF-700623-(Vol.1), pp 8-41)
FISHER, David E., Potassium--uranium systematics of Apollo 11 and Apollo 12 lunar samples and of some deep earth rocks, 25:35830
FISHER, R. A., Effects on the propagation of optical beams due to self-induced changes in index of refraction, 25:37250 (UCRL-20541)
FISHER, Roger Edwin, Spontaneous low-frequency longitudinal wave propagation in a plasma column, 25:36221
FISHMAN, L. Ya., Optimization of parameters of collimator for radioisotope scanning, 25:34880
FISK, H. E., K-meson--nucleon phase shifts near 600 MeV/c, 25:36417
FISTER, D., Influence of substichiometric carbon contents of carbide phase on properties of TiC--Mo_2C--Ni refractories, 25:35559
FLEISCHER, Robert L., Method of measuring fast neutrons by observing multipronged tracks of charged particles formed in cellulose nitrate, 25:34875
FLEMING, R. W., Empirical study of behavior of clay shale slopes, 25:34768 (NCG-TR-15(Vol.1))
FLENGHI, C., Seventh annual meteorological report of the Casaccia Center for Nuclear Studies, 1968, 25:34746 (RT/PROT-(70)42)
FLETCHER, W. H. W., Feedback stabilization of plasma instability, 25:36184
FLORENT, R., Status report of EEEC, 25:34976 (CONF-700622-(Vol.2), pp 703-13)
FLOUX, Francis, High-density and high-temperature laser-produced plasmas, 25:36156
Neutrons production in solid-deuterium laser-created plasmas, 25:36203
FLOYD, J. M., Oxygen self-diffusion and electrical transport properties of nonstichiometric ceria and ceria solid solutions, 25:35553
FOGEL, Ya. M., Luminescence spectra of excited particles knocked out of solid targets by fast Ar ions, 25:35841
FOGELBERG, B., Low-energy band structure in ^{187}Os, 25:36805
FOMENKO, V. S., Effect of the superconducting transition on the plasticity of metals, 25:35383
FOMIN, I. A., Roton viscosity and thermal conductivity of superfluid helium, 25:36015
FONTANA, Mars G., Perspectives on corrosion of materials. The 1970 Edward DeMille Campbell memorial lecture, 25:35285
FONTELL, A., Anomalously high collection of copper ions implanted in aluminum, 25:36295
FONTERAY, Pierre-Jean, Nuclear reactor element and its use in a reactor, 25:37148
FOOTE, R. S., Review of radiometric techniques in petroleum exploration, 25:34730
FOOTE, V. S. Jr., Optical sensors in FM-1, 25:36185 (MATT-840)
FORCHIONI, Alain, Radical products from the radiolysis of nitroalkanes in alkaline ice glasses, 25:34643
FORD, W. Kent Jr., Narrow band filter photographs and spectra of the planetary nebula NGC 7009, 25:35643
FORD, William Douglas, Bubble growth and collapse in narrow tubes with nonuniform initial temperature profiles, 25:34789 (AAL-7746)
FORMISANO, V., Observation of solar wind heavy ions, 25:35729
FORNWALT, D. E., Co-precipitation of $\gamma'(Ni_3Al)$ and α-Cr in a nickel-base alloy, 25:35502
FORSLOW, E. J., Radiochemical data for STS A, Amchitka Island, Alaska, 25:34720 (NVO-1229-121)
FORSTER, Harriet H., Research program of the Nuclear Consortium at the UCLA Cyclotron Laboratory, July 1970. Report AR 5, 25:36738 (UCLA-10-P-18-23)
FORSYTH, P. D., Study of ^{150}Gd, 25:36775
FOSSAN, D. B., Transition probabilities for low-lying states in ^{92}Nb, 25:36762
FOSTER, B. E., An integrated system of nuclear materials control at Oak Ridge National Laboratory, 25:34847 (ORNL-4607)
FOTHERGILL, Reginald Allen, Improvements or relating to apparatus for determining the direction of a nuclear explosion, 25:35058
FOUAD, H. Y., Effect of pitch variation on nuclear properties of light water assemblies using EK-10 fuel rods, 25:37121 (UARAEE-70)
Energy distribution of moderator atoms in reactors, 25:37108 (UARAEE-52)
Estimate for UAR research reactor thermal inertia, 25:37084 (UARAEE-111)

XUM

Four groups four regions criticality calculation diffusion code, 25:37125 (UARAEE-85)
Multigroup, multiregion, criticality calculation diffusion code, 25:37127 (UARAEE-90)
Numerical solution for the thermal flux spectrum in a monatomic moderator, 25:37120 (UARAEE-69)
Two-group two-region criticality calculation diffusion code, 25:37122 (UARAEE-79)
Upward and downward scattering kernels for thermal neutrons, 25:37123 (UARAEE-80)
FOURNET, G., Penetration of magnetic induction, electric field, and losses in impure superconductors, 25:36015 (CONF-700341-8)
FOWLER, W., NAL plans, 25:34975 (CONF-700623-(Vol.2), pp 696-702)
Results from the BNL 7-foot chamber, 25:34981 (CONF-700623-(Vol.2), pp 774-89)
FRAAS, Arthur P., Fusion by laser, 25:36211
FRAAS, L. M., Photoluminescence studies of superconducting Nb_3Sn, 25:36062
FRANA, J., Decay of /sup 195m/Hg and ^{195}Hg to levels in ^{195}Au, 25:36750
FRANCA, J. M. Jr., Preparation of clear uranyl nitrate solution by fractional dissolution of sodium diuranate, 25:34699
FRANCIS, J. E., New data system for INTEREM, 25:36193 (ORNL-TM-3401)
FRANCO, Victor, Scattering of charged particles by atoms, 25:35863
FRANCOIS, Henri, Glass having a base of metaphosphates for dosimeters which are responsive to x-rays, γ-rays, and thermal neutrons, 25:35037
FRANCOIS, P., Importance of diffusion processes in interaction between neutral waves and ionization, 25:35979
FRANCOVICCHIO, Paolo, Exchange magnetic moments of light nuclei, 25:36664
FRANK, H., Elastic electron scattering on ^{4}He at energies between 30 and 59 MeV, 25:36658 (CERN-Trans-71-13)
FRANK, I. M., Effect of the optical parameters of the medium on the yield of transition radiation of non-relativistic particles, 25:36354 (JINR-P4-5734)
FREDERICK, Carlton, Far-infrared astronomy and the galactic center, 25:35780
FREEDMAN, M. L., Relationship of radioresistance to balanced growth-rate in Micrococcus radiodurans, 25:35263
FREEDMAN, M. S., Spectrum shape of K-orbital shakeoff electrons and accompanying nuclear beta particles in decay of ^{143}Pr, 25:36774
FREISE, G., Problem of radiotherapy of the peripheral inoperable bronchial carcinoma, 25:35243
FRENCH, I. E., Effects of neutron irradiation on internal friction in Na chloride single crystals, 25:35587
FRICKE, M. P., Prog. rpt. on neutron capture cross sections of Mo, Ta, and ^{238}U, final, 6/70, 25:36729 (N-70-41999)
FRIDAY, R. G., New digitizing and memory system for wire spark chambers, 25:35016
FRIED, S., Raman spectra of technetium heptoxide, 25:34608
FRIEDMAN, F., NMR measurements in the paramagnetic state of uranium--phosphorus compounds. I. Line shifts of ^{31}P in UP and in UP/sub 1-x/S/sub x/, 25:36350
FRIEDMAN, H., X rays from Coma cluster of galaxies, 25:35799
FRIEDRICH, H., Alpha clustering and angular momentum projection before and after variation, 25:36680
FRIEDRICH, H. P., Time-dependent flux transport voltages in Nb foils, 25:36061
FRIESENHAHN, S. J., Prog. rpt. on neutron capture cross sections of Mo, Ta, and ^{238}U, final, 6/70, 25:36729 (N-70-41999)
FRIICHTENICHT, J. F., Measurement and interpretation of the luminous efficiencies of iron and copper simulated micrometeors, 25:35596
Measurements of ionization probability of Cu and LaB_6 simulated micrometeors, 25:35597
FRIK, Wolfgang, Conference on radiation protection from unsealed radioactive material and effect of radiation on the cell structure, Aachen, 10/66. IX, 25:35130
FRISCH, Henry Jonathan, Stringent limits on decays K/sub L^0 + $\mu^+\mu^-$, e^+e^-, μ^+e^+, 25:36386 (UCRL-20264)
FRITSCH, Fred N., CUBRT: fast 9-digit cube-root function for the CDC 6600, 25:37242 (UCID-30004)
FRITTELLI, L., Receptivity of site surrounding Casaccia CSN and disposal of radioactive waste, 25:34849 (RT/PROT-(70)36)
FRITZ, G., X rays from Coma cluster of galaxies, 25:35799
FRITZE, K., Decay of ^{142}La, 25:36765
FROLOV, A. M., Search for elementary particles bearing a magnetic charge, 25:36379 (CERN-Trans-71-10)
FROLOVA, A. V., Qualitative composition of radiation at depth of irradiated medium, 25:35030
FROMM, Eckehard, Equilibria in molybdenum--nitrogen solid solutions, 25:35430
Nitrogen solubility in tungsten at high temperatures, 25:35429
FRY, Arthur, Prog. rpt. on tracer and isotope effect studies in organic chemistry, annual, 2/1/71, 25:34572 (ORO-3234-23)
FRYKLUND, J. W., Centralized data acquisition and time-sharing message switching system, 25:37219 (RLO-2227-T-7-7)
FUBINI, S., Algebraic treatment of subsidiary conditions in dual resonance models, 25:36591
FUGER, J., Self-radiation effect on lattice parameter of $^{244}CmO_2$, 25:35589
Thermodynamics of the actinide elements. III, 25:34609
FUHS, A. E., Plasma diagnostic techniques, 25:36095
FUJII, Kimio, Studies on the uranium dicarbide phase, 25:35579
FUJIMOTO, M., ESR studies of restricted random motion of NH_3^+ radicals in γ-irradiated ammonium perchlorate crystals, 25:34642
FUJIMURA, Kimio, Deep inelastic structure of e--p scattering and relativistic extended particle model based on the quark model, 25:36444
FUJITAKA, K., Ionization redistribution effect of wind in nighttime ionosphere, 25:35986
FUJIWARA, Katsutoshi, Growth of anodic oxide films on Ti, Ta, and Zr, 25:35284
FUKAO, Masayuki, Wide band correlator, 25:35052
FUKUHARA, Masakatsu, Chemical and enzymatic properties of γ-irradiated subtilisin BPN, 25:35109
FULDE, Peter, Theory of superconductors containing magnetic impurities: crystalline field effects, 25:36034
FULLWOOD, R. R., Constant fraction timing adapter for a zero-crossover discriminator, 25:35064
FURMINIEUX, Gilbert, Shock absorber, 25:37155
FURNICA, G., Radiation resistance of C--S bonds of macromolecular sulfone polyelectrolytes under the action of γ radiation, 25:34650
FURTH, H. P., Stellarator-mirror machine target plasma reactor, 25:36190 (MATT-841)
FURUKAWA, Kazuo, Corrosion induced by liquid sodium, 25:35281
FUTAGAMI, Koji, Low temperature irradiation studies on iron--boron alloys, 25:35588
FYMAT, A. L., Tables of auxiliary functions for nonconservative Rayleigh phase matrix, 25:35826

G

GAAFER, M. A., SAVE: two group code for reflector savings of completely reflected cylindrical reactor, 25:37128 (UARAEE-96)
GABOLDE, Jean, Fuel element for a fast breeder and/or test reactor, 25:37027
GABOS, Z., Polarization effects in leptonic three-body decays of baryons, 25:36463
GABOVICH, M. D., Collective oscillations in a synthetic plasma composed of positive and negative ion beams, 25:36220
GABRAKOV, S. I., Gamow--Teller 1$^+$ excitations in odd--odd nuclei, 25:36817 (JINR-P4-5744)
GABRIEL, J., Effect of radiation on the mechanical properties of concrete, 25:37007 (ORNL-tr-2470)
GADALLAH, F. I., Mechanical behaviour of ni-based alloys at elevated temperatures, 25:35340 (UARAEE-55)
GADDIS, E. S., Cooling of a simulated fuel element by a flow of naturally circulated boiling water, 25:37009 (UARAEE-110)
Estimate for UAR research reactor thermal inertia, 25:37084 (UARAEE-111)
GADIOLI, E., Reactions (p,xn) induced in ^{169}Tm, ^{181}Ta, and ^{209}Bi with 20 to 45 MeV protons, 25:36797
GAFFAL, Karl, Method and apparatus for cooling parts of pumps in nuclear reactors or the like, 25:37145
GAGE, S. J., Determination of magnetic impurities in high purity copper by neutron activation analysis, 25:34546
GAILLARD, Joelle, Electron energy distribution function in weakly ionized gas, 25:36146
GAILLET, Gerard, Ionization fission chamber, 25:34884
GAIPOV, S., Electron emission from monocrystals of alkali-metal halide compounds, 25:35840
GAJEWSKI, W. M., FFTF: comparison test and development facility for LMFBR program, 25:37085 (WHAN-SA-104(Rev.))
GAL, A., Shell-model analysis of Λ binding energies for p-shell hypernuclei. I, 25:36529
GALAKTIONOV, B. B., High-frequency plasma heating near the lower hybrid frequency, 25:36087
GALAKTIONOV, B. V., Limiting frequency for plasma absorption of high-frequency waves, 25:36238
GALL, L. N., Ionization chamber for a mass-spectrometer ion source, 25:35060
GALLAGHER, J. G., NERVA Technology Reactor, 25:37088
GALLAI, Z. A., Use of N-furcylphenyl hydroxylamine for amperometric titration of Zr, 25:34535
GALLIGAN, J. M., Effect of the superconducting state on stress relaxation in lead-temperature dependence, 25:36072
GALLUZZO, Robert J., Vaporization kinetics of zinc oxide single crystals, 25:37247 (UCRL-20528)
GAL'PER, A. M., Observation of γ quanta greater than 100 MeV from 3C 120, 25:35700
GALPERIN, Yu. I., Morphology of auroral electron energetic and angular distributions, 25:35982
GAL'TSOV, D. V., Splitting of a photon in a magnetic field and polarization of hard radiation from pulsars, 25:35677
GALTSOVA, R. D., Early structural, ultrastructural, and

functional disturbances in radiosensitive and radioresistant yeast cells under influence of ionizing radiation, 25:35247
GANALYA, I. A., Energy surfaces of ^{230}U in parametrization of Cassinian ovaloids, 25:36793
GANEZO, N. V., Hypoxanthine dynamics in brain following neutron irradiation, 25:35226
GANO, Kenji, Concentration profiles of room-temperature ion-implanted indium in silicon, 25:36282
GANASSI, E. E., Some problems of the mechanism of injury and recovery of cells, 25:35205
GANDEL'MAN, G. M., Superconductivity induced by pressure, 25:36023
GANGULY, S. R., Energy spectrum of N component of cosmic rays at sea level, 25:35916
GANNITSKII, A. I., Nonstationary three-dimensional plasma flow in a homopolar device, 25:36205
GANTOIS, M., Mechanism of precipitation and plastic deformation of nickel--chromium alloys hardened by niobium and tantalum precipitation, 25:35483
GAPANOVICH, V. G., Isochronous bending magnet for a linotron, 25:36641
GARDNER, F. F., Neutral hydrogen absorption and emission in NGC 5128, 25:35789
OH-line absorption at 1665 and 1667 MHz in the direction of the Omega Nebula, 25:35696
Optical identification of PKS 0320-37, 25:35707
GARFAGNINI, R., Two-body photodisintegration of ^4He up to 80 MeV, 25:36671
GARFINKEL, A. F., Evidence for splitting in Q region of $K^+\pi^+\pi^-$ mass, 25:36414
GARIBYAN, G. M., Dynamic radiation generated in crystals by particles with ultrarelativistic energies, 25:36382
GARLAND, J. C., Low-temperature electrical and thermal resistivities of tungsten, 25:36331
GARREAU, Michel, Faradaic yield of electrolytic dissolution of Al and Be, 25:35353
GARRETT, R., T(d,n)^{4}He reaction, 25:34901
GARSEVANISHVILI, V. R., Representation for the relativistic scattering amplitude at high energies, 25:36601
Spin effects at high energy in quasipotential approach, 25:36504 (JINR-E2-5770)
GARWIN, Charles, Reconstruction of the wave function from matrix elements, 25:37252 (UCRL-20667)
GASGNIER, M., Thin films of praseodymium sesquioxide, 25:35575
GASPARINI, G. M., Aromatic hydrocarbons as potential source of diluents for fuel reprocessing, 25:34638 (RT/CHI-(70)35)
GASPARINI, Paolo, Gamma-ray spectrometry of rocks, 25:34539
GAST, P. W., Isotopic composition of lead in volcanic rocks, 25:34740
GAVENDA, J. D., Determination of magnetic impurities in high purity copper by neutron activation analysis, 25:34548
Temperature dependence of electron mean free paths in cadmium and copper, 25:36328
GAVRILOV, K. A., Radiative and chemical effects of accelerated multicharged ions on gaseous nitrogen-containing systems, 25:34567
GAY, E. C., Prog. rpt. on lithium/chalcogen secondary cells for components in electric vehicular-propulsion generating systems, semiannual, 5/23--11/22/70, 25:35275 (ANL-7777)
GEBICKI, Janusz M., Species in irradiated oxygenated water, 25:34617
GEHLBACH, R. E., Influence of titanium on the strengthening of a Ni--Mo--Cr alloy, 25:35391
GEL'D, P. V., Region of homogeneity of a zirconium oxynitride of NaCl structure at 1500°C, 25:35583
GELINAS, Robert J., GEAR: ordinary differential equation system solver, 25:37241 (UCID-30001)
GELL, Y., Bound-state models and the splitting of the A_2, 25:36497
GELLES, S. H., Evaluation of beryllium foil subjected to biaxial stresses. final report, 25:35332 (BMI-X-604)
GENEROSO, Estela E., Cytoplasmic injury in the shoot apex of maize after gamma irradiation, 25:35244
GENZ, H., M/L orbital-electron-capture ratio in ^{71}Ge decay, 25:36704
GEORGE, A., Direct solution of discrete Poisson equation on irregular regions, 25:37187 (LA-4553)
GERARD, E., 21-cm neutral hydrogen line and continuum study of galaxy Maffei 2, 25:35794
GERBERICH, W. W., Superposition model for environmentally-assisted fatigue-crack propagation, 25:37249 (UCRL-20538)
GERDANIAN, Paul, Direct measurement at 1100°C of partial molar enthalpies of O incorporation in PuO/sub 2-x/ and (U,Pu)O/sub 2+ -x/ by means of Tian--Calvet high-temperature microcalorimeter, 25:34606
GERHARDSTEIN, L. H., PDP-9/GOULD 4800 device handler and graphics library, 25:37174 (BNWL-B-58)
GERLACH, Bernd, Field theoretic criterion for particles to have mass zero, 25:36570
GERSHBERG, R. E., Flares of red dwarf stars, 25:35640
GESHEVA, M., Determination of the boiling point of some isoalkyl astatides by using a glass gas chromatograph, 25:34604 (JINR-P6-5683)
GEUE, Jean, Burnout in forced convection boiling heat transfer, 25:37000 (AAEC/LIE/Elb-286)
GEZALYAN, L. S., Effect of ionizing radiation on induced bioelectrical activity in brain of rats, 25:35235
GHAFELEHBASHI, M., Pressure dependents of the elastic constants of NaCl at low temperature, 25:37158 (NYO-2504-63)
GHOSE, Parthasarathy, Field-current identities in a gauge-invariant formulation of massive gauge fields, 25:36501
GHOSH, A. S., 1s--3d excitation of atomic hydrogen by electron and proton impact, 25:35859
GHOSH, Aparna, Nonrelativistic energy bands of double hexagonal close-packed lanthanum, 25:36352
GHOSH, M., Metabolism of nuclear basic proteins after radiation, 25:35104
GIACCO, G., Experiences with the shielded whole-body counter, 25:35183
GIANNINI, M. M., Multiple-scattering expansion of theoretical optical potential, 25:36523
GIAQUINTO, L., Utilization of vibrational coupling for nuclear fuel, 25:35524 (RT/INC-(70)22)
GIARDINI-GUIDONI, A., Mass spectrometric study of ionic reactions pertinent to the radiation chemistry of methane, 25:34645
GIBALA, R., Strength differential effect in niobium--oxygen solid solutions, 25:35373
GIDALI, Julia, Autoradiographic studies on ^3H-thymidine incorporation in liver and kidneys of irradiated mice, 25:35238
GIELISSE, P. J., Lattice vibrational spectra and physical characteristics of metals with cubic structure, 25:36319
GIERST, L., Influence of the adsorption of thiourea on electrode processes at the mercury electrode, 25:34560
GIESLER, G. C., Ge(Li)--Ge(Li) sum coincidence, 25:34932
GIFT, E. H., Oak Ridge systems analysis code (ORSAC) User's manual, 25:36886 (ORNL-TM-3223)
GILES, M. S., Ecological factors in siting of a nuclear power station, 25:36970
GILLESPIE, B. W. J., Spin--parity combinations in ^{22}Ne, 25:36698
GILLIAVOD, Norberto, Incidence of dominant lethal mutations after x-irradiation of spermatozoa of mice and rats, 25:35129
GINDIN, I. A., Effects of composition on strength of Cu--Mo laminates, 25:35455
GINGERICH, K. A., Dissociation energy of diatomic cerium and predicted stability of gaseous intermetallic cerium compounds, 25:35347
GINGERICH, Karl A., Existence of gaseous intermetallic compounds of high stability as predicted by Brewer--Engel metallic theory, 25:35350
GINOCCHIO, J. N., Approximate treatment of correlations in nuclear spectroscopy. I, 25:36806
GIRAUD, B., Purification of sodium for RAPSODIE, 25:37056 (BNWL-tr-67)
GIRGIS, R., Critical mass calculation for UA-RR-1, 25:37078 (UARAEE-67)
Numerical study of fast neutron spectra in UA-RR-1 reactor core and reflector, 25:37079 (UARAEE-71)
Thermal utilization calculation with new asymptotic diffusion theory, 25:37119 (UARAEE-64)
GIUDICI, G., Seventh annual meteorological report of the Casaccia Center for Nuclear Studies, 1968, 25:34746 (RT/PROT-(70)42)
GIULIANI, S., Mechanical behavior of complex structures in presence of creep, thermal strains and irradiation-induced dimensional changes, 25:34774 (EUR-4629)
GIVORD, Francoise, Crystallographic and magnetic properties of compounds of cobalt and lutetium, 25:36318
GIZON, Jean, E0 and E0+M1+E2 transitions of ^{179}Hf, 25:36760
GLAZER, V. M., Regeneration of in vitro x-radiation-induced injuries of DNA by polynucleotide ligase, 25:35108
GLEESON, A. M., Analyticity, covariance, and unitarity in indefinite metric quantum field theories, 25:36562 (ORO-3992-26)
GLEESON, L. J., Energy losses and modulation of galactic cosmic rays, 25:35924
GLENN, H. David, Analysis of Marvel: nuclear shock-tube experiment, 25:34765
GLENN, J. E., Spectroscopy of states in ^{91}Zr from γ-ray transitions observed in $^{88}Sr(\alpha,n\gamma)^{91}Zr$ reaction, 25:36757
GLOBENKO, Yu. G., Coulomb collisions in dense beams, 25:36640
GLONTI, L. N., Depolarization in 612 MeV elastic pn-scattering, 25:36390 (JINR-P1-5743)
GNOJEK, I., Economic aspects of prospection and exploitation of U ores in France, 25:34751
GOEHLE, B., Effect of wire parameters on the emission of hard x rays from exploding wires, 25:36326
GOEKSEL, Selahattin A., Manual for Turkish film dosimetry standards, 1962--69, 25:35135 (CNAEM-77)
GOEL, P. S., Production rates of ^{22}Na and ^3H in stone meteorites by cosmic rays, 25:35599
GOERING, R. V., Mutants of Staphylococcus aureus with increased sensitivity to ultraviolet radiation, 25:35270
GOGGIN, William R., Beryllium comes into its own, 25:35402
GOGITIDZE, G. A., Determination of ^{10}B concentrations in compounds, 25:34538

XUM

GOKHALE, G. S., Atmospheric neutrons and the Van Allen radiation belt, 25:35998
Energy spectrum of diffuse cosmic x rays in the energy range 20 to 120 keV, 25:35921
Energy spectrum of Sco X-1 in the region 15 to 120 keV, 25:35704
Search for energetic neutrons emitted during solar flares, 25:35772
TIFR balloon facility, 25:35908
GOKYU, I., Thermally activated flow in iron, low carbon steel, and other body-centered cubic metals (V and Ta), 25:35380
GOLANT, V. E., Limiting frequency for plasma absorption of high-frequency waves, 25:36238
GOL'DANSKII, V. I., Positronium atom in organic liquids, 25:35853
Radiative and chemical effects of accelerated multicharged ions on gaseous nitrogen-containing systems, 25:34567
GOLDEN, J., Generalized Veneziano model with nonlinear trajectories, 25:36493
GOLDHAMMER, Paul, Isospin mixing in ^{8}Be, 25:36677
GOLDSMITH, D. W., Heating of the interstellar medium by x rays and by cosmic rays, 25:35784
GOLDSMITH, M., Total and differential cross section for neutrons scattered from ^{90}Zr and Nat. Zr, 25:36740 (WAPD-T-2411)
GOLDSTEIN, Lawrence G., Study of molecular motions in polymer solutions by pulsed nuclear magnetic resonance spectroscopy, 25:37185 (IP-MS-71-25)
GOLLEY, M. G., Aspects of ionospheric drifts, 25:35985
GOLOSKOKOV, S. V., Spin effects at high energy in quasipotential approach, 25:36504 (JINR-E2-5770)
GOLOVIN, B. M., Automatic processing of information from spark chambers, 25:35004 (JINR-P10-5762)
GOL'TS, E. Ya, Method of obtaining short dense plasmoids, 25:36120
GOL'TSEV, V. F., Specific properties of operation of absorbing materials in fast reactors and requirements for them, 25:37140 (SRARI-P-96)
GOLUB, G. H., Direct solution of discrete Poisson equation on irregular regions, 25:37187 (LA-4553)
GOMER, Robert, Adsorption of CO on the (110) plane of W, 25:35357
GOMEZ SANTAMARIA, E., Radioactive wastes of nuclear center in Mexico, 25:34733
GOMIRATO SANDRUCCI, M., Possibilities and limitations of nuclear medicine in infant diagnostics, 25:35182
GONCHARENKO, E. N., Role of primary radiotoxins in radiation damage of a cell, 25:35200
GONCHAROV, I. N., Critical characteristics of superconducting alloys of type NT-I in a wide range of magnetic fields at different temperatures, 25:36048
GONCHAROV, V. V., Extension of experimental capabilities of MR reactor for loop-testing fuel elements and materials, 25:37067 (LB/G-3001)
GOODMAN, C. D., Identification of the atomic number of nobelium by an x-ray technique, 25:36778
Midstream evaluation, A = 88, 25:36705
GOODMAN, L., Optical studies of $^{3}(n,\pi^{*})$ magnetic sublevels in benzaldehyde, 25:34592
GOODRICH, R. G., Line shapes for rf size effect in Cd, 25:36327
GOOSMAN, D. R., Properties of ^{13}B and ^{20}Na, 25:36710
GOPALAKRISHNAN, N. V., High-energy N component of extensive air showers, 25:36383
GOPALARAMAN, C. P., Multiple ionization of cesium and barium by successive electron impacts, 25:35865
GOPALA RAO, U. V., Homologous microwave bursts and associated solar flares, 25:35774
GOPAL-AYENGAR, A. R., Enhancement of radiation lethality of bacterial cells by some sensitizers: a radiochemical approach, 25:35262
GOPASYUK, S. I., Nonuniform conductivity and force-free magnetic fields. I, 25:35755
Temporal variations of the photospheric velocity field in the active region, 25:35750
Velocity field at different levels in the solar-active regions, 25:35746
GORBUNOV, V. I., Application of fast neutrons in radiation defectoscopy, 25:34825
Optimum thickness of image-intensifying screens for radiographic inspection, 25:34824
GORDON, Geoffrey, Instrument for slicing and handling radioactive polyacrylamide gels, 25:35056
GORDON, H. A., A_{2}^{-} from reaction $\pi^{-}p$ + K/sub S/^{0}K-p at 4.5 GeV/c, 25:36409
GORDON, R. L., Resistivity measurements of insulators using the four-probe technique, 25:36316 (HEDL-SA-119)
GORIN, A. I, Experimental gamma radiography equipment for determining defects in construction materials, 25:34822
GOSHAW, A., Bubble chamber detection technique for gamma rays in momentum region below 1 GeV/c, 25:34964 (CONF-700623-(Vol.1), pp 555-66)
GOSLING, J. T., Variations in solar wind speed along the Earth's orbit, 25:35732
GOSS, W. M., Distance and spectrum of 3C 391, 25:35702
GOTO, Tetsuo, Infinite-component wave equation and scattering amplitude, 25:36557
GOTTSCHALK, W., Neutron-induced mutants of Pisum sativum and comparison with x-ray-induced genotypes, 25:35122
GOTTSTEIN, K., Hyperon bubble chamber HYBUC, 25:34572 (CONF-700623-(Vol.2), pp 640-6)
GOULD, G. W., Potentiation by halogen compounds of lethal action of γ radiation on spores of Bacillus cereus, 25:35264
GOWER, J. C., An integrated system of nuclear materials control at Oak Ridge National Laboratory, 25:34847 (ORNL-4607)
GOYER, J. P., Magnetic flection coils of Batavia accelerator, 25:36618
GRABER, M. J., Metallurgical evaluation of simulated BWR emergency core cooling tests, 25:37038 (IN-1453)
GRABIN, V. F., Peculiarities of formation of intermetallics in explosion-produced copper--titanium compounds, 25:35324
GRAEVSKII, E. Ya., Sulfhydryl groups and radiosensitivity, 25:35213
GRAFF, R. A., Kinetics of interaction of tantalum disilicide with tantalum and other metals, 25:35577
GRAHAM, E. T., Cytoplasmic injury in the shoot apex of maize after gamma irradiation, 25:35244
GRAHAM, G. M., Josephson effect in Nb--Hg contacts, 25:36068
GRASSI STRINI, A. M., Reactions (p,xn) induced in ^{169}Tm, ^{181}Ta, and ^{209}Bi with 20 to 45 MeV protons, 25:36757
GRAY, L., Evidence for existence of a narrow anti pn bound state, 25:36399
GRECO, M., Multiple e. m. processes in high energy e⁻e⁺ collisions, 25:36433 (LNF-71/1)
GREEN, Anne J., Distance and spectrum of 3C 391, 25:35702
GREEN, J. A. S., Corrosion behavior of aluminum--boron composites in aqueous chloride solutions, 25:35521
GREEN, M. B., Model for Pomeranchukon couplings, 25:36512
GREEN, Michael A., Factors which will affect the cost of a superconducting synchrotron, 25:36614 (UCRL-20299)
GREEN, R. C., Radiation shielding information center user documentation, 25:36247 (CTC-48)
GREEN, W. V., High-temperature creep of polycrystalline graphite, 25:35556
GREENBERG, J. Mayo, Interstellar grain temperatures, 25:35790
Interstellar grain temperatures, 25:35791
GREENE, D., Attenuation of 14-MeV neutrons in calcium-based concrete, 25:36260
GREENE, R. E., Patent literature on process radiation and irradiator design. Part 1. United States Patents 1950 through 1968, 25:34777 (ORNL-IIC-34)
GREENFIELD, M. A., Fracture toughness and microstructure in Ti--5.25Al--5.5V--0.9Fe--0.5Cu alloy, 25:35348
GREGORY, Carl D., Kinetics and mechanism of the reaction of nickelocene with mercaptans, 25:34597
GREHN, S., Measurement of bone density with ^{125}I-profile-scanner, 25:35171
GREIG, R. A., Tables of γ rays from (n,γ) produced nuclides, 25:36718 (AAEC/TM-585)
GREINER, W., Electrons in strong external fields, 25:36365
GRENCH, H. A., Search for 72.5s /sup 30#/Al, 25:36715
GRENNBERG, B., Corrective terms to Hartree correction formula, 25:35063
GRIESS, J. C., Design considerations of reactor containment spray systems. Part X. The stress corrosion cracking of types 304 and 316 stainless steel in boric acid solutions, 25:37028 (ORNL-TM-2412(Pt.10))
GRIFFING, Thomas C., Prog. rpt. on nutrient cycling and productivity of dystrophic lake-bog systems (part B), 3--11/70, 25:37182 (COO-1770-3)
GRIGOR'EV, V. F., Instability of ring currents, 25:35838
GRIGSBY, Ronald D., Existence of gaseous intermetallic compounds of high stability as predicted by Brewer--Engel metallic theory, 25:35350
GRIMESEY, R. A., PHROG: a FORTRAN IV program to generate fast neutron spectra and average multigroup constants, 25:37113 (IN-1435)
GRIMM, R. C., Monte-Carlo solution of Schroedinger's equation, 25:36375
GRIMM, W., Search for superheavy elements in terrestrial matter, 25:36779
GRISHIN, N. I., Noctilucent clouds, 25:35988
GRITSYNA, V. V., Luminescence spectra of excited particles knocked out of solid targets by fast Ar ions, 25:35841
GRITZNER, M. L., ORNL-SNAP shielding program, 25:36260 (ORNL-TM-3364)
GRODZINS, L., Determination of lifetimes for multiply charged heavy ions excited in collisions with light gases, 25:35849
GROENIG, Hans, Theory of a cylindrical photoionization chamber of high density, 25:36100
GROENROOS, M., Lymphoscintigraphy, gamma-venography, and histological evidence in radical operation, 25:35186
GROLMES, M. A., Pressure-pulse propagation in two-phase one- and two-component mixtures, 25:37035 (ANL-7792)
GROMOVA, I. I., Decays of Nd and Pr nuclides with mass number A = 138, 25:36725 (JINR-P6-5674)
Electromagnetic separation of short-lived isotopes of Rn, Xe, and Kr for spectroscopic studies, 25:34806 (JINR-P13-5757)
GROOS, E., Irradiation experiment for testing spherical fuel elements for high-temperature reactors, 25:37018 (JUL-701-RW)
GROSS, E. E., Charge-symmetry study with reactions ^{2}H(t,tau)nn and ^{2}H(tau,t)pp, 25:36662

p--p final-state interaction in ^{3}He(d,t)2p reaction, 25:36665
GROSS, J., Complex formation of hexivalent uranium and of pentavalent neptunium with 1,3-diketons as well as investigations on septivalent neptunium, 25:34557 (KFK-1339)
GROSS, M., Experimental results on acoustic detection of sodium and water boiling, 25:37052
GROSSIORD, Jean-Yves, Reactions (d,α) with ^{56}Fe and ^{51}V, 25:36687 (LYCEN-7087)
GROSSMUELLER, F., Rapid and simple microscale separation of proteins after radioiodination, 25:34700
GROVES, Eric Stedman, Missing mass spectrometer survey of I = 1, 0 mesons below 1.1 GeV^2, 25:36398
GRUNWALD, G., Heat transfer and hydraulic resistance in smooth and rough tubes and channels for turbulent flow, 25:34795
GRUNZWEIG-GENOSSAR, J., NMR measurements in the paramagnetic state of uranium--phosphorus compounds. I. Line shifts of ^{31}P in UP and in UP/sub 1-x/S/sub x/, 25:36350
GRUZNOV, Yu. A., Design and construction superconducting solenoids for physical investigations, 25:36076
GRYAZEV, V. M., Specific properties of operation of absorbing materials in fast reactors and requirements for them, 25:37140 (SRARI-P-96)
GUARINO, Angelo, Reactions of He^3H^+ ions with gaseous hydrocarbons. IV, 25:34675
GUERY, Marcel, Fission chamber, 25:34883
Ionization fission chamber, 25:34884
GUESEWELL, D., Experimental results with the 1 m model chamber at CERN. A, 25:34982 (CONF-700623-(Vol.2), pp 790-812)
Neon--hydrogen mixtures in large cryogenic bubble chambers, 25:34952 (CONF-700623-(Vol.1), pp 532-42)
GUILLOT, Pierre, Method and apparatus to measure the water content of a snow layer, 25:35042
GUIMIER, A., Stacking fault formation and mechanical twinning processes in a nickel-base superalloy during tensile deformation at high temperature, 25:35491
GUINAN, Edward Francis, Photometry of eclipsing systems R Canis Majoris and V1010 Oph, 25:35617
GUINN, V. P., Prog. rpt. on applications of neutron activation analysis in scientific crime investigation, 5/62--5/68, 25:34542 (GA-9807)
GUITTARD, Micheline, L_3GaS_6 compounds (L = Dy, Ho, Er, and Y), and the phase diagram of Y_2S_3--Ga_2S_3 system, 25:35571
GUJRATHI, S. C., Delayed states in ^{94}Nb, ^{108}Ag, and ^{110}Ag, 25:36769
GUNDERSON, B., Neutral particle tagging facility for ANL 30'' bubble chamber, 25:34967 (CONF-700623-(Vol.2), pp 582-92)
GUNION, John Francis, Dual description of production processes by unitarity, 25:36514
GUPTA, J. P., Irradiation induced variation in Colletotrichum, 25:35256
GUPTA, R. M., Explanation of the anomalous skin effect, 25:36138
GUPTA, U. C., Reactions ^{48}Ti(α,p)^{51}V and ^{50}Ti(^{3}He,d)^{51}V, 25:36716
GUR, Y., Fluctuation factors for theoretical evaluation of average neutron cross sections of fissile nuclei in the unresolved resonances region, 25:36722 (IA-1208)
GUREVICH, L., Existence of atoms in n-dimensional space, 25:36362
GUREVICH, S. M., Peculiarities of formation of intermetallics in explosion-produced copper--titanium compounds, 25:35324
GUROV, G. G., Increase of effectiveness of synchronized capture during bunching of beam outside the separatrix, 25:36603 (IFVE-SKU-70-20)
GURTU, A., Hypernuclei resonant states ^{5}He, ^{6}Li, and ^{9}Be, 25:36401
Some aspects of K$^-$ absorption at rest in emulsion nuclei, 25:36400
GUSEINOV, M. Dzh, Vertical distribution of magnetic field in the sunspot umbra, 25:35752
GUSEVA, T. M., Specific properties of operation of absorbing materials in fast reactors and requirements for them, 25:37140 (SRARI-P-96)
GUS'KOV, Yu. K., Ion-acoustic oscillations and transport processes in a low-temperature cesium plasma, 25:36231
GUSMINI, Simonne, Separation of lanthanides by chromatography on SA-2 ion exchange paper, 25:34714
GUSTAFSON, T. K., Effects on the propagation of optical beams due to self-induced changes in index of refraction, 25:37250 (UCRL-20541)
GUTHRIE, M. P., Operation of codes associated with MECC-3, preliminary version of intranuclear-cascade calculation for nuclear reactions, 25:36733 (ORNL-4564)
GUTT, R., Luminescence spectra of excited particles knocked out of solid targets by fast Ar ions, 25:35841
GWALTNEY, Richard C., Analysis of torispherical shells subjected to concentrated loads, 25:37211 (ORNL-TM-3201)

H

HAAG, R., Role of quantum field theory in the physics of the last decade, 25:36576
HAAGE, Horst, Conference on radiation protection from unsealed radioactive material and effect of radiation on the cell structure, Aachen, 10/68. IX, 25:35130
HAAS, D., Elastic electron scattering on ^{4}He at energies between 30 and 59 MeV, 25:36658 (CERN-Trans-71-13)
HABEGGER, L. J., Space-dependent transfer-function analysis of large nuclear-reactor power systems, 25:36587 (ANL-7788)
HABERER, G., Color indicator for the visualization of radiation fields and the beam adjustment in large irradiation plants, 25:35029
HABING, H. J., Heating of the interstellar medium by x rays and by cosmic rays, 25:35784
HABRAKEN, L., Hardening mechanisms in multiphase alloys, 25:35396
HACKSTEIN, K. G., Manufacturing fuel elements for THTR and AVR reactors, 25:35544
HAEBEL, E. U., Big European bubble chamber magnet progress report, 25:35001 (CONF-700623-(Vol.2), pp 1126-45)
HAENDEL, S. K., Effect of wire parameters on the emission of hard x rays from exploding wires, 25:36226
HAFEZ, L. A., Instruments for measurement of the spectral lines profile and shift, 25:36091 (UARAEE-95)
HAFF, K. W., Fueled capsule design and evaluation, safety analysis, 25:34809 (ORNL-TM-3230)
HAGEBOE, E., Studies of proton-induced nuclear fission, 25:36802
HAGEMANN, R., Absolute isotopic scale for deuterium analysis of natural waters, 25:34518
HAGEN, Ulrich, Alterations in the DNA structure in irradiated phages, 25:35259
HAGERTY, P., Evidence for existence of a narrow anti pn bound state, 25:36399
HAGYAN, H., Some reactions of the organism to radiation in different oxygen pressures, 25:35118
HAHN, G., Hyperon bubble chamber HYBUC, 25:34972 (CONF-700623-(Vol.2), pp 640-6)
HAISSINSKI, J., Device for measuring the luminosity of Orsay storage ring, 25:36606 (LAL-1249)
HALBERT, M. L., Evidence for T = 1/2 resonance in the ^{3}He system, 25:36663
HALL, Richard Ian, Excitation of n = 2 he levels by low-energy electrons, 25:35882
HALL, W. N., Spectral changes in the zenith skylight during total solar eclipses, 25:35765
HALLER, W. A., Determination of mercury in biological and environmental materials by instrumental neutron activation analysis, 25:34551
HALLETT, C. D., Experience in the use of thermoluminescent dosimeters for radiation dose control purposes, 25:35023 (AEEW-M-962)
HAMADA, Yasuji, Intense oscillations in the plasma heating by the large electric field, 25:36237
HAMAMOTO, Ken, Sequential brain imaging as an aid in understanding disease etiology, 25:35174
HAMILTON, J. H., Multipole admixtures of transitions from β, γ, and octupole vibrational states in ^{156}Gd, 25:36742
HAMMAD, F. H., Mechanical decladding of the Inchas fuel, 25:34780 (UARAEE-54)
HAMMOND, R. P., Abstracts of papers: desalination information meeting, May 27--28, 1971, 25:37091 (ORNL-TM-3402)
HAMOUDA, I., Calculation of neutron pulse shape, transmission function and resolution function in mechanical time-of-flight spectrometer, 25:34919 (UARAEE-61)
Control rod calculation with perturbation theory, 25:37136 (UARAEE-66)
Critical mass calculation for UA-RR-1, 25:37078 (UARAEE-67)
Determination of epithermal neutron spectrum shape in UA-RR-1 reactor, 25:37076 (UARAEE-59)
Effect of non-uniform burn up on reactor lifetime, 25:37081 (UARAEE-83)
Effect of the probe tube on the thermal neutrons space-energy distribution, 25:37137 (UARAEE-75)
Energy-dependent Milne problem, 25:36650 (UARAEE-60)
General review of thermal neutron spectra investigations, 25:37118 (UARAEE-62)
Measurement of continuous fast neutron spectra by scintillation technique, 25:34920 (UARAEE-51)
Neutron transmission through ducts perpendicular to neutron beam axis in water shields, 25:36251 (UARAEE-86)
Numerical calculations of K/sub eff/ and neutron fluxes in 2 and 3-group approximations using IEM-1620 code, 25:37126 (UARAEE-89)
Numerical study of fast neutron spectra in UA-RR-1 reactor core and reflector, 25:37079 (UARAEE-71)
One-group considerations of Milne problem, 25:37116 (UARAEE-56)
Thermal neutron capture gamma-rays in iron, 25:36652 (UARAEE-103)
Thermal utilization calculation with new asymptotic diffusion theory, 25:37119 (UARAEE-64)
Transmission of slow neutrons in multiple-segment ducts in a water shield, 25:36252 (UARAEE-104)
HANADA, Reimon, Electrical resistivity measurements of deformed metals after low-temperature neutron irradiation, 25:35501

XUM

HANDA, Hajime, Sequential brain imaging as an aid in understanding disease etiology, 25:35174
HANDA, Jyoji, Sequential brain imaging as an aid in understanding disease etiology, 25:35174
HANDLER, Thomas, Minimizing angle errors due to multiple scattering, 25:34950 (CONF-700623-(Vol.1), pp 325-33)
HANDWERK, J. H., Strengths of some uranium compounds, 25:35551
HANGAY, Gyorgy, Resistance of solid susbstances to gamma radiation, 25:34660
HANNON, M., Bonding beryllium--copper alloys with high temperature thermoplastic. A report of a program undertaken to meet the problems confronting potential users, 25:35316
HANSCHMANN, H., uv inactivation of NADH, 25:35107
HANSEN, J. E., Prog. rpt. on isotope development, 11/70--1/71, 25:34803 (BNWL-1308-5)
HANSON, J. E., FTR driver fuel development program status, 25:37064 (HEDL-SA-81)
HARA, Akio, Formation process of (W,Ti)C powder, 25:35537
Formation process of W carbide powder from W powder, 25:35536
Formation process of WC--TiC powder, 25:35531
HARBERT, John C., Radionuclide cisternography, 25:35172
HARDEE, H. C., High intensity direct reading heat flux gauge, 25:37225 (SC-DR-710194)
HARDING, R. C., Loss-cone modes in inhomogeneous mirror machines, 25:36166 (UCRL-73135)
HARGREAVES, J. K., Conjugate and closely spaced observations of auroral radio absorption. V, 25:35557
HARGROVE, G. L., Determination of nitrogen and hydrogen at parts-per-million levels in milligram steel samples, 25:34514
HARIG, H. D., Cold neutron source of French--German high flux reactor in Grenoble, 25:37087
HARIGEL, G., Experimental results with the 1 m model chamber. B, 25:34983 (CONF-700623-(Vol.2), pp 813-23)
Influence of parasitic boiling and expansion speed on the dynamic pressure in a bubble chamber, 25:34957 (CONF-700623-(Vol.1), pp 424-48)
Ultrasonic bubble chamber development at CERN, 25:34953 (CONF-700623-(Vol.1), pp 376-89)
HARKER, Y. D., Fast-neutron capture integral measurements of ^{99}Tc, ^{109}Ag, and other fission products, 25:36720 (CONF-710301-4)
HARKNESS, S. D., Study of void formation in fast neutron-irradiated metals, 25:35516
HARMAN, D. G., Effects of thermal aging and neutron irradiation on Incoloy 800, 25:35510
HAROUTUNIAN, R., Microstructure effect on hyperfine interactions in Yb--Ag, 25:36332
HARREL, H. A., Cost-benefit illustration for underground nuclear natural gas stimulation, 25:34766 (AECOP-632)
HARRIS, Frank Richard, Correlative study of radio aurora and auroral electrojet currents, 25:36006
HARRIS, M. J., Experimental study of radiation-induced boiling in superheated liquids, 25:34798
HARRIS, R. W., Effects of neutron irradiation on internal friction in Na chloride single crystals, 25:35587
HARRISON, Charles W. Jr., Inhomogeneous plasmas: on reflection and transmission of fields of arbitrary polarization, 25:36228
Transmission line coupled to a cylinder in an incident field, 25:37228 (SC-R-713250)
HARRIS-SMITH, Robbin, Apparatus for carrying out processes in a controlled environment, 25:34855
HARSHBARGER, F., Engineering the baseball magnet system, 25:36200 (UCRL-73067)
HART, Michael H., Random gravitational encounters and evolution of spherical systems. II, 25:35783
HARTECK, Paul, Introductory comments to laser interaction and related plasma phenomena, 25:36148
HARTLE, R. E., Dayside ionosphere of Venus, 25:35827
HARVEY, M., Anatomy of Hartree--Fock procedure in simple model, 25:36819
Effective operators for nuclear shell model. III, 25:36820
HARWARD, M. E., Prog. rpt. on physico-chemical properties of soils from volcanic ash, 9/70--8/71, 25:34724 (RLO-2227-T-9-1)
HASEGAWA, Masayoshi, Problems about fuel cladding materials. Stainless steel, 25:37139 (CONF-700211-7)
HASEGAWA, Seiichi, ESR studies on P$^+$ ion-implanted Si, 25:36276
HASHMI, M. H., Colorimetric determination of Au(III), 25:34521
HASSAN, A. M., Calibration of three-crystal-NaI-pair-spectrometer, 25:34921 (UARAEE-93)
Construction of a three-crystal scintillation pair spectrometer, 25:34922 (UARAEE-100)
Thermal neutron capture gamma-rays in iron, 25:36692 (UARAEE-103)
HASSAN, M. A., Automatic start-up system for UA-RR-1 reactor, 25:37083 (UARAEE-108)
HASTE, G. R., Effect of electron heating on overall efficiency of conceptual mirror fusion reactors, 25:36088
HATANO, Hiroyuki, Chemical and enzymatic properties of γ-irradiated subtilisin BPN, 25:35109
HATTEN, Bernard W., Nucleonic measuring apparatus with automatic fire safety radiation source shutter closing and locking means responsive to high temperatures for blocking the path of the shutter movement to open position, 25:35038
HATTORI, Toshihiko, Effects of the resonance-scattering amplitude in nucleon--antinucleon reactions, 25:36451
HAUG, W., Power limitations of an in-core thermionic cell in steady-state operation, 25:37090
HAUSER, Louis G., Effect of escalation on future fuel costs, 25:36861
HAVERCROFT, W. E., Nondestructive testing in Canadian governmental services, 25:34830
HAYAKAWA, S., New soft x-ray source in Aries--Taurus region, 25:35710
HAYASHI, H., Thermally activated flow in iron, low carbon steel, and other body-centered cubic metals (V and Ta), 25:35380
HAYASHI, Shu A., Fast neutron spectra from natural uranium target bombarded with high energy electrons, 25:36767
HAYASHIBE, Shogo, Level structure of ^{143}Pm and ^{143}Nd, 25:36766
HAYDEN, H. C., Promotion of L-shell electrons to higher bound states in Ar$^+$--Ar collisions, 25:35856
HAYNES, S. K., K-shell conversion electrons from 2.33-keV transition in ^{205}Pb, 25:36780
HEADLEY, F. B., 2X II 10-Megajoule ignitron crowbar, 25:36196 (UCRL-73031)
HEALY, J. H., Source parameters of Salmon and Sterling nuclear explosions, 25:34764
HEATON, L., Neutron diffraction cryo-orienter, 25:36080
HEATON, M., Virial theorem for variational functions in collision theory, 25:35871
HEBBLE, T. L., Statistical technique for determining sources of variation in $(U,Pu)O_2$ oxygen-to-metal ratio, 25:35568 (ORNL-TM-3362)
HEBBLE, Thomas L., Design considerations of reactor containment spray systems. XII. Variability of the dose reduction factor for the removal of elemental iodine, 25:37029 (ORNL-TM-2412(Pt.12))
HECKATHORN, Joy, Review of radio observations of planetary nebulae, 25:35668
HECKER, R., Fast fission factor of metallic Be and of BeO, 25:37110
HECKLEY, P. R., Reactions of Na N,N-diethyldithiocarbamate with the chlorides and bromides of Nb(V), Ta(V), and Pa(V), 25:34568
HEDGCOXE, P. G., Vapor explosion--heat transfer and fragmentation. III, 25:37214 (ORO-3936-4)
HEGER, L., Bitumization of liquid radioactive wastes, 25:34845 (IAR-1249)
HEGEWALD, H., Determination of absorbed dose of high-energy electrons by lithium fluoride detectors, 25:35027
HEIDEN, C., Time-dependent flux transport voltages in Nb foils, 25:36061
HEIKKINEN, D. W., Proton induced reactions on mass-14 nuclei, 25:36673
HEILES, C. E., Search for interstellar SH at radio frequencies, 25:35697
HEIM, W. J., Floating ring stabilization system, 25:36188 (MATT-839)
HEIMKE, G., Effectiveness of ceramic armor plating, 25:37236 (UCRL-Trans-10530)
Estimating shock pressures in collisions between two bodies, 25:37257 (UCRL-Trans-10531)
HEINTZ, W., Experience report on the operation and radiation protection at the Braunschweig Research and Measurement Reactor for the year 1970, 25:37062 (FMRB-35/71)
HEINZE, H. G., Cobalt-60 therapy of renal tumors, 25:35152
HEISENBERG, J., Inelastic electron scattering from several Ca, Ti, and Fe isotopes, 25:36695
HELLER, Michal, Construction of a relativistic model of the Universe, 25:35806
HELLRIEGEL, W., Clinical considerations of radiation protection in the handling of open radioactive material, 25:35150
Postoperative irradiation of breast cancer by fast electrons, 25:35191
HENDER, M. A., Polarization-free vacuum-ultraviolet excitation of helium by electrons, 25:35857
HENDERSON, G., Coronal line profiles observed by means of coronagraphs and a Fabry--Perot spectrometer, 25:35775
HENDRICKSON, R. A., Electron echo experiment, 25:35966
HENLEY, E. A. Jr., Model for γ decay of atomic or nuclear systems, 25:35891
HENLEY, E. M., High energy diffractive dissociation of pions and A_1, 25:36521
HENLINE, Pamela, Argonne code center: compilation of program abstracts, 25:37133 (ANL-7411(Suppl.5))
HENNING, C. D., Engineering the baseball magnet system, 25:36200 (UCRL-73067)
HENRICHS, J. M., Gas phase ESR spectra of ^{31}P, ^{75}As, ^{121}Sb, and ^{123}Sb, 25:36345
HENRIKSEN, R. N., Pulsar wobble, 25:35699
HENRY, Kenneth W., Technique for measuring pressure, volume, enthalpy, and resistance of equilibrium thermodynamic states of liquid metals at high temperatures and pressures, 25:35342 (UCRL-51035)
HENRY, L. C., Intermediate energy gamma-ray cross sections, 25:36799
HENRY, R. C., X rays from Coma cluster of galaxies,

25:35799
HENRY, R. E., Pressure-pulse propagation in two-phase one- and two-component mixtures, 25:37035 (ANL-7792)
HENRY, Richard C., Far-ultraviolet interstellar absorption in Orion and Monoceros, 25:35785
HENSLEY, D. C., Identification of the atomic number of nobelium by an x-ray technique, 25:36778
HERBISON-EVANS, D., Derivation of the orbit of a double star from observations made with an intensity interferometer, 25:35647
HERMAN, J. R., Dayside ionosphere of Venus, 25:35827
HERMAN, M., Effect of purity and processing procedure on the mechanical properties of beryllium sheet, 25:35463
HERMANN, C. W., Operation of codes associated with MECC-3, preliminary version of intranuclear-cascade calculation for nuclear reactions, 25:36733 (ORNL-4564)
HERMES, F., Excitation functions of the $^{197}Au(\alpha,xn)$ reactions in the energy range from 16 to 103 MeV, 25:35745
HERNANDEZ, G., Signature profiles of O(^{1}S) in airglow, 25:35962
HERNDON, David J., πN partial-wave amplitudes, 25:36506 (TID-25726)
HEROY, William B., Conference on unconventional methods in exploration for petroleum and natural gas, Dallas, 9/68, 25:34729
HERR, W., Thermoluminescence of lunar sample 10084 Apollo 11, 25:35824
HERRMANN, D., Requirements for portable instruments for dose rate and contamination measurements, 25:34866 (SZS-2/71, pp 1-6)
HERRMANN, E., Decay of ^{139}Nd, 25:36724 (JINR-P6-5673)
New method for rare-earth isotope separation, 25:34805 (JINR-P6-5761)
HERRMANN, G., Search for superheavy elements in terrestrial matter, 25:36779
HERTZBERG, R. W., Mechanical response of the Ni--Ni_3Nb eutectic composite. Part II. Cyclic behavior, 25:35462
Mechanical response of the Ni--Ni_3Nb eutectic composite. Part I. Monotonic behavior, 25:35461
HERVE, A., EPR identification of neutral charge state of Be vacancy in irradiated BeO, 25:36283
HERYNEK, I., Hyperon bubble chamber HYBUC, 25:34972 (CONF-700623-(Vol.2), pp 640-6)
HERZOG, Heinz, Pocket dosimeter, 25:34893
HESKIA, S., Geometrical description of generalized gauge fields. II, 25:36575
Geometrical description of generalized gauge fields. I, 25:36574
HESKIA, Said, New viewpoint on the space--time model of elementary particles. I, 25:36544
HESS, B., Thermoluminescence of lunar sample 10084 Apollo 11, 25:35824
HESSE, K. H., Long-term intensity observations on pulsars, 25:35713
HEUBERGER, A., Energy resolution of multiplying semiconductor detectors for soft γ spectroscopy at room temperature, 25:34918 (LE/G-3034)
HEULIN, Bernard, Internal friction peaks due to O in Nb--4.6 Ti alloys, 25:35410
HEYDE, K., Unified model calculations for N = 83 nuclei, 25:36749
HEYLEN, P. R., Fast breeder fuel processing pyrochemical head end study, 25:34688 (EUR-4615)
Pyrochemical head end conception for fast breeder fuel processing, 25:34687 (EUR-4614)
HEYVAERTS, J., Polarized radiation transfer in a collective plasma, 25:36143
HIBBERD, F. H., Reflection of radio waves from ionospheric irregularities at vertical incidence, 25:35978
HIBBS, S. M., Astron mechanical engineering effort, 25:36198 (UCRL-73059)
HIGGINS, C. S., Radio emission from flare stars near Orion nebula, 25:35616
HIGGY, H. R., Mechanical decladding of the Inchas fuel, 25:34780 (UARAEE-54)
HILAL, M. M., Heat transfer in annular reactor channels, 25:37068 (UARAEE-50)
HILE, R. A., Prog. rpt. on high temperature flat cables, 11/70, 25:37159 (BDX-613-161)
HILKE, H. J., Ultrasonic bubble chamber development at CERN, 25:34953 (CONF-700623-(Vol.1), pp 376-89)
HILKER, W. W., Prog. rpt. on high temperature flat cables, 11/70, 25:37159 (BDX-613-161)
HILL, D. C., Superconductivity and dislocation cell structure in niobium: stress effects, 25:36057
HINATA, Hiroshi, Conformation radiotherapy for nasopharyngeal tumor, 25:35194
HINDMARSH, Alan C., GEAR: ordinary differential equation system solver, 25:37241 (UCID-30001)
HINDMARSH, J. L., Energy levels and Lorentz invariance, 25:36374
HINES, R. A., Electroformed gilding metal rotating band, 25:37161 (BDX-613-236)
HINKLE, N. E., Radiation hardening and radiation-anneal hardening in body-centered cubic metals, 25:35507
HIPPLER, H., High-pressure region of the recombination O + C_2 + C_3, 25:34589
HIRAKAWA, N., Measurement of central fission ratios and fission rate distributions in FCA, 25:37066 (JAERI-Memo-4356)
HIRTH, J. P., Analysis of L and Y tilt boundary intersections formed during creep in molybdenum, 25:35402
HISHAW, R. J., Prog. rpt. on transfer welding of close tolerance parts, 5/71, 25:37162 (BDX-613-283)
HITTERMAN, R. L., Neutron diffraction cryo-orienter, 25:36080
HJELLMING, R. M., Black and white holes, 25:35820
HO, J. C., Magnetic-susceptibility and low-temperature specific-heat studies of Ti, Zr, and Hf, 25:36340
HO, S. T., Electron energy distribution within a curved channel multiplier, 25:34905
HODGKINS, D. J., Estimating natural terrestrial background in 17- and 60-keV energy regions from Compton continuum peak, 25:34727 (UCRL-72927)
HODISAN, T., Colorimetric determination of Ce^{++} by o-aminophenol, 25:34530
HOEGBERG, G., Influence of thickness and scattering angle on stopping cross section of nitrogen, neon, and argon ions in thin carbon foils, 25:36248 (GIPR-41)
HOEGER, T. G., Estimating natural terrestrial background in 17- and 60-keV energy regions from Compton continuum peak, 25:34727 (UCRL-72927)
HOEGGER, B., Lumped element line generator for low rf sinusoidal oscillations, 25:36229
HOEGLUND, A., Half-life measurements of excited levels in ^{121}I and ^{123}I, 25:36752
HOERZ, Gerhard, Concentration changes and metal losses during degassing by annealing of binary dilute metal--gas solutions. II, 25:35560
HOFFMAN, Kenneth, Investigation and repair of baffle plate damage in the HFBR primary heat exchangers, 25:37055 (BNL-15815)
HOFFMAN, M. A., Calculation techniques for estimating the pressure losses for conducting fluid flows in magnetic fields, 25:35938 (UCRL-51010)
HOFMANN, A., Timing with surface barrier detectors using charge and current pulses, 25:34899
HOFMANN, S., Lifetime of the 91.5 keV state in ^{151}Sm, 25:36807
HOFSTAETTER, A. B., X-ray and photo-induced processes in ZnO coating material, 25:36296
HOGE, K. G., Influence of strain rate on flow stress of tantalum, 25:35399
HOITINK, N. C., Effects of fast neutron irradiation on chromel/alumel thermocouples, 25:35072 (NEIL-SA-152)
HOLAH, D. G., Reactions of Na N,N-diethyldithiocarbamate with the chlorides and bromides of Nb(V), Ta(V), and Pa(V), 25:34568
HOLCOMB, R. S., Survey of the materials and design of insulation for prestressed-concrete vessels for gas-cooled reactors, 25:37006 (ORNL-TM-2929)
HOLL, Richard J., Nuclear shuttle for interorbital and transplanetary applications, 25:37089
HOLLAND, L., Operation of a glow discharge ion gun used for specimen thinning, 25:36639
HOLLAND, R. F., Evidence for splitting in Q region of $K^+\pi^+\pi^-$ mass, 25:36414
HOLLAR, D. L., Prog. rpt. on aluminum pulse-arc welding, 3/71, 25:37167 (BDX-613-320)
HOLLOX, G. E., Mechanical properties of TiC--VC alloys, 25:35558
HOLMAN, Kermit L., Desalination and ion separation of sodium and potassium by bromine redox electrolysis, 25:34691 (LA-4645)
HOLMBERG, L., System for precise determinations of electron--gamma directional correlations, 25:34502
HOLMES, Richard A., Value of the vertex view in brain scanning, 25:35175
HOLMQVIST, L., Rapid and simple microscale separation of proteins after radioiodination, 25:34700
HOLT, S. S., Evidence for multiple periodicity in x-ray emission from Cygnus X-1, 25:35690
HOLZAPFEL, W. B., Hall effect studies on strontium and ytterbium under high pressures, 25:36324
HOMAN, F. J., Comparisons between predicted and measured fuel pin performance, 25:37019 (ORNL-TM-3366)
HOMER, G. D., Halide--halide exchange at asymmetric silicon. New evidence against a siliconium ion-pair mechanism, 25:34579
HONDA, Yoshihide, Behavior and distribution of radioactive substances in coastal and estuarine waters, 25:34760
HONECK, H. C., ENDF/B cross section preparation and testing in the JCSHUA system, 25:36737 (TID-25690)
HOOPER, J. W., Prog. rpt. on excitation and ionization of ions by electron impact, 9/70--5/71, 25:35833 (ORO-3027-19)
HOOVER, W. R., Mechanical response of the Ni--Ni_3Nb eutectic composite. Part II. Cyclic behavior, 25:35462
Mechanical response of the Ni--Ni_3Nb eutectic composite. Part I. Monotonic behavior, 25:35461
HOPKINSON, Eric C., Method and apparatus for calibrating pulsed neutron well logging instrument, 25:35039
HOPPER, M. A., Study of the anodic oxidation of vanadium, 25:35296
HORA, Heinrich, Application of laser-produced plasmas for controlled thermonuclear fusion, 25:36155
Experimental results of free targets, 25:36152
Laser interaction and related plasma phenomena. Proceedings of the first workshop, held at East Windsor

Hill, Connecticut, June 9--13, 1969, 25:36147
Nonlinear effect of expansion of laser-produced plasmas, 25:36154
Results of the self-similarity model, 25:36132
HORAN, Paul Karl, Temperature dependence of radioinduced free-radical destruction, 25:35103
HORLITZ, G., Influence of parasitic boiling and expansion speed on the dynamic pressure in a bubble chamber, 25:34957 (CONF-700623-(Vol.1), pp 424-48)
HORNBY, C. A., Radiation-induced translocations in Prunus avium cv. Lambert, 25:35127
HORNECK, G., Inactivation and division delay of E. coli B/r by combined treatment with uv and vacuum, 25:35265
HORNSEY, Shirley, Differences in the effect of hypoxia on the radiation sensitivity of the bone marrow and the intestine in mice, 25:35161
HOROWITZ, Paul, Optical time-of-arrival measurements from Crab pulsar, 25:35695
HORSKY, J., Must it really be E = 0, 25:36581
HORVATH, J., Synchronized chopper time-of-flight spectrometer, 25:34916 (JINR-E14-5731)
HOSEA, J. C., Properties of magnetic surfaces in Model C stellarator, 25:36210
HOSEK, B., Influence of Na fluoracetate on shift of LD 50/30 value, 25:35162
HOUSE, Lewis L., Empirically corrected calculations of coronal visible lines from the $3p^23d$ configuration, 25:35744
HOUSSEAU, N., Dechanneling of α particles by dislocations occurring in Al, 25:36307
HOWER, G. L., Phase-height measurements of E region, 25:35983
HOYER, U., Atomic stopping cross section of H_2, D_2, He, N_2, and Ar for α particles, 25:36256
HRUSKA, A., Model of transverse structure of the geomagnetic tail and the reconnection process, 25:35992
HSIAO, K. H., Vapor explosion--heat transfer and fragmentation. III, 25:37214 (ORO-3936-4)
HSU, C., Space-dependent transfer-function analysis of large nuclear-reactor power systems, 25:36987 (ANL-7788)
HSU, Wu-shiung, Simple neutron spectrometer, 25:34925
HUBER, F., Spectrophotometric compositional analysis of tantalum--aluminum alloy films, 25:35303
HUDSON, H. S., Electron (10 to 100 keV) acceleration and emission from solar flares, 25:35726
HUDSON, R. D., Ultraviolet photoabsorption cross sections for molecules, 25:36013
HUDSPETH, Emmett L., Rapid assay for nitrogen in gluten and use of reference nuclides, 25:34555
HUEBER, R., Thermoluminescence of lunar sample 10084 Apollo 11, 25:35824
HUEBNER, G., Temperature dependence of growth of E. coli B in heavy water, 25:35094
HUEBNER, K., Color indicator for the visualization of radiation fields and the beam adjustment in large irradiation plants, 25:35029
HUEBNER, R. H., Collisions of low-energy electrons with molecules: threshold excitation and negative-ion formation, 25:34618
HUEGEL, H., Flow of compressible plasmas in self-induced magnetic field of arc discharges, 25:36103 (DLR-FB-70-13)
HUEGEL, J., Magnetogasdynamic properties of stationary supersonic plasma jets, 25:36108
HUGENSCHMIDT, Manfred, Achieving local thermodynamic equilibrium states in laser-induced xenon plasmas, 25:36121
HUGHES, H. L., Rapid annealing of pulse-radiation-induced space charge in silicon dioxide, 25:36302
HUGHES, J. M., Use of radioactive Xe in evaluation of pulmonary functions, 25:35170
HUGHES, T. A., Midstream evaluation, A = 88, 25:36705
HULME, E. C., Isotope-exchange reactions of ox heart phosphofructokinase, 25:34596
HUNDHAUSEN, Joan R., A generating operator for solutions of certain partial difference and differential equations, 25:37188 (LA-4655)
HUNGERFORD, E. V., Charge-symmetry study with reactions ^2H(t,tau)nn and ^2H(tau,t)pp, 25:36662
HUNKLINGER, S., Influence of impurities on laser induced breakdown in liquid ^4He, 25:36014
HUNSUCKER, Robert D., Characteristic signatures of midlatitude ionosphere, 25:35955
HUNT, W. T., Bibliographic survey of corrosion, 1960, 25:35290
HUNTINGTON, R. D., Mechanical properties of TiC--VC alloys, 25:35558
HUNZINGER, W., Estimation of tritium discharges into LLW-streams, 25:34719 (NP-18737)
HURLEY, C. A., Astron mechanical engineering effort, 25:36198 (UCRL-73059)
HURLEY, R. E., Operation of a glow discharge ion gun used for specimen thinning, 25:36639
HURT III, S. S., Bulk shielding facility quarterly report, January--March 1971, 25:37069 (ORNL-TM-3453)
HUSAIN, D., Note on the wave functions of non-local separable potentials, 25:36838
HUSON, F. R., BNL work on Ne/H_2 targets, 25:34961 (CONF-700623-(Vol.1), pp 511-31)
HUSSEIN, A., Calculation of neutron pulse shape, transmission function and resolution function in mechanical time-of-flight spectrometer, 25:34919 (UARAEE-61)
Effect of the probe tube on the thermal neutrons space-energy distribution, 25:37137 (UARAEE-75)
Energy-dependent Milne problem, 25:36650 (UARAEE-60)
General review of thermal neutron spectra investigations, 25:37118 (UARAEE-62)
One-group considerations of Milne problem, 25:37116 (UARAEE-56)
HUSSEIN, A. M., Electromagnetic surface waves in adjacent plasma flows, 25:36219 (UARAEE-97)
HUTCHINGS, W., Fabrication and burst testing of reaction-bonded silicon carbide tubes, 25:35523 (AECL-3462)
HWANG, F. S. W., Supralinearity and sensitization of thermoluminescent phosphor lithium fluoride, 25:35076

I

ICHIKAWA, Masaru, Hydrogen absorption and hydrogen exchange reactions in solution by 1:2 electron donor-acceptor complexes of anthracene with various alkali metals, 25:34578
ICHIMORI, T., Measurement of central fission ratios and fission rate distributions in FCA, 25:37066 (JAERI-Memo-4356)
IDA, M., General level structure in the dual-resonance model, 25:36474
IGATA, N., Electron bombardment of niobium containing interstitial impurities, 25:35517
IGLAR, Albert F., Hospital solid waste management, 25:34856
IKAWA, Koji, Kinetics parameter calculation code: (ARGO), 25:36992 (JAERI-Memo-4331)
IKUTA, Kazunari, Equilibrium of finite-β toroidal helices, 25:36171
INAGAKI, Michio, Studies of stainless steel cladding, 25:35315
INAKOSHI, Hideki, Conformation radiotherapy for nasopharyngeal tumor, 25:35194
IN DER SCHMITTEN, W., Irradiation experiment for testing spherical fuel elements for high-temperature reactors, 25:37018 (JUL-701-RW)
INOUYE, H., Influence of various ordered states on the mechanical properties of vanadium--cobalt--nickel ternary alloys, 25:35385
INUISHI, Yoshio, Effects of electron irradiation on photoluminescence of n-GaAs, 25:36274
IOFA, B. Z., Study of kinetics of benzoic acid extraction with toluene by isotopic exchange method, 25:34584
IONESCU-PALLAS, Nicolae, Introduction to modern theoretical mechanics, 25:36361
IOVNOVICH, M. L., Electron-ion bunch diagnostics by means of bremstrahlung, 25:36616 (UCRL-Trans-1440)
IRAC-ASTAUD, M., Perturbative solutions of renormalization groups, 25:36565
IRIARTE, Modesto Jr., In-reactor inspection and repair procedures for BONUS nuclear power plant, 25:36857
IRKAEV, S. M., Nuclear gamma resonance, 25:36343
ISAAK, S., Special solution of the field equations in the case of the characteristic [(211)], 25:36555
ISAKOV, A. I., Search for elementary particles bearing a magnetic charge, 25:36379 (CERN-Trans-71-10)
ISAKOV, V. I., Interaction of one-particle and collective excitations in odd nuclei near Pb, 25:36753
ISHII, M., Beta- and Compton-suppression for the internal conversion study, 25:34933
ISHIWATA, Hiroshi, Present status of multi-purpose high-temperature gas-cooled reactor, 25:37092
ISLAMOV, Sh. U., Effect of the structure of mono- and bifunctional azo compounds on the analytical properties of yttrium and rare earth complex compounds, 25:34528
ISLER, R. C., Polarization of H/sub α/ line produced in $He^+ + H_2$ collisions, 25:35862
ISRAEL, Harvey I., Bremsstrahlung emission measurement from thick tungsten targets in energy range 12 to 300 kV, 25:36249 (LA-4624)
ISSABAYAEV, E. A., Isotopic composition of uranium and the content of actinius in minerals and natural waters, 25:34738
ISTOMIN, L. F., TV system used for observations of faint variable stars, 25:35639
ITAGAKI, Kimio, Measurements of heats of mixing in liquid gold binary alloys, 25:35432
Measurements of heats of mixing in liquid copper binary alloys, 25:35433
ITO, Hiroshi, Sintering process for Ni--P alloy coated W, 25:35354
ITO, Katsukiyo, Gamma-ray-induced polymerization of fluorine-containing pentadiene, 25:34633
ITOH, N., Ion mass effect in dechanneling rate, 25:36289
ITOH, Noriaki, Dechanneling of MeV protons from Ge, 25:36271
IVANOV, A. A., Influence of the helicon wave upon some electrostatic instabilities of plasmas, 25:36183
IVANOV, A. N., X-ray studies of the tendency of niobium toward formation of stacking faults, 25:35493
IVANOV, G. I., Current loading and dispersion in an iris-loaded linear electron accelerator, 25:36644
IVANOV, V. V., Propagation of electromagnetic perturbation

over a plane surface, 25:36367
IVANOVA, F. A., Combined action of carbon monoxide and ionizing radiation under prolonged conditions, 25:35233
IVANOVA, G. M., Interaction of certain compounds of thorium with dimethyl sulfoxide, 25:34565
IVANOVA, T. I., Calculation of the ion trajectories in a Penning discharge, 25:36133
IVERSEN, K., High temperature brazing of reactor components, 25:35327
IVLEV, A. A., Isotope exchange reactions. VIII, 25:34585
IWAKI, Masaya, Concentration profiles of room-temperature ion-implanted indium in silicon, 25:36282
IWASAKI, Iwaji, Radium-226 distribution in hot springs and origin of highly radioactive springs. V, 25:34736
IYENGAR, V., Homogeneous nonstatic solutions of Einstein--Maxwell field-equations for isotropic space--time, 25:36559
IZEN, E. H., Magnetic circular dichroism of bands associated with the F+ center in SrO, 25:36291
IZHVANOV, L. A., Y--YH_2 phase diagram at room temperature, 25:35582
IZUMOTO, T., Spectroscopic study of (p,t) reactions from neutron-magic nuclei, 25:36794

J

JACCARINI, A., Experimental conditions for γγ collisions with almost real photons, 25:36451
JACKSON, A. D., Model space calculation of the quasiparticle interaction for nuclear matter, 25:36832
JACKSON, D. F., *Diffraction effects in high energy (p,2p) reaction*, 25:36679
JACKSON, E. S., Determination of mass of Pluto, 25:35822
JACKSON, W. R., Hydrogen-2(p,pn)p reaction at 5.0 MeV, *25:36670*
JACOB, E. H., Summary of results of general analytical evaluation program, 1--12/69, 25:34503 (NBL-256)
JACOBS, S. C., Oak Ridge systems analysis code (ORSAC) User's manual, 25:36886 (ORNL-TM-3223)
JAFFE, D., Spectrophotometric compositional analysis of tantalum--aluminum alloy films, 25:35303
JAKUBOWICZ, Antoni, Certain type of Einstein's space--times, 25:36577
JAMBOR, Ca., Approach to quantum mechanical four-body bound-state problem. II, 25:36364
JAMES, H. M., Effect of molybdenum and hardener content on gamma-prime solvus temperature in a Ni20Cr base heat-resistant alloy, 25:35460
JANECKA, J., ESR studies of restricted random motion of NH_3^+ radicals in γ-irradiated ammonium perchlorate crystals, 25:34642
JANEV, R. K., Use of Green function method for scattering of a particle on a system of bound particles, 25:36589
JANSONS, Regina A., Allometry of body weight and tail length after head x-irradiation in rats, 25:35225
JARDINE, Leslie J., Gamma-ray calibration standards, 25:34923 (UCRL-20476)
JARMAN, P. D., Ultrasonic bubble chamber development at CERN, 25:34953 (CONF-700623-(Vol.1), pp 376-89)
JARRY, R. L., Work plan for continuation of the project, reduction of atmospheric pollution by the application of fluidized-bed combustion, 25:37158 (ANL/ES-CEN-1003)
JASPER, E. W., Excitation functions of the $^{197}Au(\alpha,xn)$ reactions in the energy range from 16 to 103 MeV, 25:36745
JAULMES, Sylvie, L_3GaS_6 compounds (L = Dy, Ho, Er, and Y), and the phase diagram of Y_2S_3--Ga_2S_3 system, 25:35571
JEANMART, L., Radiological aspects of post-radiotherapeutic colitis, 25:35158
JEANNE, D., High energy particle identification by ionization measurements using single gas proportional counter, 25:35018
JEHN, Hermann, Equilibria in molybdenum--nitrogen solid solutions, 25:35430
Nitrogen solubility in tungsten at high temperatures, 25:35429
JEKI, L., Survey of measurements of the fission neutron spectrum of ^{252}Cf, 25:36728 (KFKI-71-9)
JEN, C.-L., *Model for the s-wave pion--pion phase shifts*, 25:36484
JEN, Chian-li, Comment on current algebra beyond the tree approximation, 25:36482 (NYO-2262-TA-241)
JENKOVSKII, L. L., Dual amplitude with Mandelstam analyticity, 25:36492
JENNINGS, Mark C., Intrinsic polarization in K and M giants and supergiants, 25:35611
JENSEN, A. S., Anatomy of Hartree--Fock procedure in simple model, 25:36819
JENSEN, Mead LeRoy, Carbon, oxygen, and sulfur isotopes and the origin of sandstone-type uranium deposits. Final report, 25:34750 (COO-2024-1)
JENTGES, H., Experimental results on acoustic detection of sodium and water boiling, 25:37052
JEONG, Manu, Effects of electron irradiation on photoluminescence of n-GaAs, 25:36274
JHA, S. K., Analysis of shower particles produced in high-energy interactions, 25:36392
New method for identification of shower particles in high-energy interactions, 25:36402
JIRU, P., Isotopic exchange of gaseous deuterium with lattice hydrogen of hydrides, 25:34582
JOERGENSEN, H. E., Variability of A and F main sequence stars, 25:35651
JOHANNSEN, B., Methods and use of radioimmunoassays, 25:35083
JOHANNSEN, K.-H., Flocculation and sedimentation of radioactive turbid material from waste water under control of the zeta potential, 25:34696 (SZS-3/71 (pp 2-19))
JOHANSEN, K. T., Light curve and photometric elements of β Aurigae, 25:35648
Variability of A and F main sequence stars, 25:35651
JOHNS, I. A., Meandering solar Type-IV burst 12/17/69, 25:35742
JOHNS, M. W., Midstream evaluation, A = 88, 25:36705
Midstream evaluation, A = 89, 25:36714
Midstream evaluation, A = 90, 25:36801
JOHNSON, H. H., Prog. rpt. on environment and fracture, 3/20/71, 25:35337 (NYO-3975-3)
JOHNSON, J. S., Abstracts of papers: desalination information meeting, May 27--28, 1971, 25:37091 (ORNL-TM-3402)
JOHNSON, James D., Elastic scattering of protons and electrons from helium atoms in the Glauber approximation, 25:35868
JOHNSON, Kurt P., Nuclear shuttle for intercrbital and transplanetary applications, *25:37089*
JOHNSON, R. F. Jr., Deposition and retention of inhaled Eu oxide in rat, 25:35086
JOHNSON, R. R., Reactions $^{39}K(^3He,^3He)^{39}K$ and $^{39}K(^3He,d)^{40}Ca$ at 29.3 MeV, 25:36696
JOHNSON, Rolland Paul, Weak interactions, 25:36387
JOHNSON, Thomas C., Permeation of halogenated solvents *through Drybox gloves*, 25:34605 (*RFP-1608*)
JOHNSSON, G. G., High-energy (γ,xn) reactions in ^{197}Au, 25:36785
JOHNSTON, K. J., Photoelectric observations of UU Piscium, 25:35608
JOHNSTON, W. C., K-shell conversion electrons from 2.22-keV transition in ^{205}Pb, 25:36780
JOHNSTONE, J. K., Sandia Laboratories carbon composites development program, 25:37179 (CONF-710312-1)
JOLLY, D. P., L/K electron capture ratio in decay of ^{159}Dy, 25:36771
JOLLY, William L., Structures of sulfur--nitrogen compounds, 25:37248 (UCRL-20535)
JONAS, J. J., High temperature flow stress and substructure strengthening of polycrystalline α-zirconium, 25:35401
JONES, A. D. W., Search for 72.5s /sup 30s/Al, 25:36715
JONES, B. B., Echelle spectrograph for high resolution studies of the solar vacuum ultraviolet spectrum, 25:35054
JONES, Burton F., Internal motions in Praesepe, 25:35604
JONES, C. Edward, Generalized $Q(2,1)$ expansion for asymptotically growing amplitudes, 25:36547
JONES, D. H. P., Kinematics of Scorpio--Centaurus association and Gould's belt, 25:35798
JONES, G. A., Isobaric analogue states in nuclei, 25:36676
Nuclear surface, 25:36824
JONES, J. G., Radiation shielding information center user documentation, 25:36247 (CTC-48)
JONES, J. L., Response of dosimeters to ^{60}Co and pulsed electron irradiations, 25:35034
JONES, L. R., Iodine retention studies. Progress report, January--June 1970, 25:37106 (IP-1259)
JONES, R. D., LEED intensity calculations for Be, 25:36220
JONES, T., Ratio of ^{81}Rb to /sup 81m/Kr incorporated in tissue, 25:35167
JONKE, A. A., Work plan for continuation of the project, reduction of atmospheric pollution by the application of fluidized-bed combustion, 25:37158 (ANL/ES-CEN-1003)
JORDANA, R., Effects of ionizing radiations on O uptake by rat liver slices, mitochondria, and mitochondrial membranes, 25:35223
JORDANOV, B., FG matrix treatment of normal vibrations in ethylene-like and nitromethane-like molecules, 25:34581
JOSEPH, G., *Search for energetic neutrons emitted during solar flares*, 25:35772
JOSEPH, George, Atmospheric neutrons and the Van Allen radiation belt, 25:35998
Low-energy gamma-ray spectrum in space, 25:35922
JOSHI, S. R., 2-aminobenzothiazole as gravimetric reagent: milligram level determination of Hg(II), 25:34520
JOUFFREY, B., Heterogeneous deformation of nickel single crystals at very low temperatures, 25:35378
JOUVE, Gerard, Electrochemical behavior of U electrode in contact with aqueous solutions and the nature of the phases formed as a function of pH, 25:34562
JOYCE, Glenn, Light scattering in a marginally stable plasma, 25:36144
JOYEZ, Gerard, Excitation of n = 2 He levels by low-energy electrons, 25:35882
JOZEFOWICZ, K., Energy threshold for neutron detection in a makrofol dielectric track detector, 25:34902
JUDD, G., Measurement of particle--matrix interface strength in TD-nickel, 25:35458
JULIANO, Rudolph Lawrence, Proteins of the erythrocyte membrane, 25:37258 (UR-49-1430)

JUNG, K., Temperature dependence of growth of E. coli B in heavy water, 25:35094
JUREWICZ, A., AFST model with π π and π p phase shifts and Durr--Pilkuhn form: factors applied to the reaction π⁺ p → p 3 π⁺ 2 π⁻ at 8 GeV/c, 25:36503 (INR-P-1265)
JURICKA, V., Effect of radiation on the mechanical properties of concrete, 25:37007 (ORNL-tr-2470)
JURNEY, E. T., Low-lying configurations in ²¹⁰Bi, 25:36787

K

KAAE, J. L., Irradiation-induced dimensional changes and creep of isotropic carbon, 25:35585
KAAZ, H. W., Effect of a chronic exposure to gamma radiation on shrub Ephedra nevadensis in northern Mojave Desert, 25:35249
KABAKCHI, S. A., Appearance of H⁺ ions in irradiated liquid water, 25:34668
KABAKOV, E. N., Number of epithelial cells as measure of the radiation damage and regeneration of the small intestines, 25:35220
KABENIN, V. N., Effect of excitation energy on yields and kinetic energies of fragments at fission of ²³⁹Pu by neutrons, 25:36754
KABESHEVA, E. T., Spectrographic determination of tungsten in tungsten--molybdenum alloys, 25:34516
KADLEC, V., Determining reactor spectra of fast neutrons from threshold detector measurements, 25:37109 (UJV-2423-RF)
KADMENSKII, S. G., Alpha decay of spherical nuclei, 25:36747
KADOMTSEV, B. B., Atoms in a superstrong magnetic field, 25:35644
Molecules in an ultrastrong magnetic field, 25:35645
KADYKOVA, G. N., Phase transformations in alloy 658T, 25:36051
KADYROV, N. B., Isotopic composition of uranium and the content of actinium in minerals and natural waters, 25:34738
KADYSHEVSKII, V. G., Representation for the relativistic scattering amplitude at high energies, 25:36601
KAELLIS, Joseph, Unsteady coupled high flux-mass, momentum transfer with a moving boundary, 25:37156 (ANL-7797)
KAFKA, P., Experimental results on acoustic detection of sodium and water boiling, 25:37052
KAGAN, Yu. M., Effective number of ionization and recombination events in the positive column, 25:36136
KAI, Takashi, Present state of turbo-generators for nuclear power plants, 25:36975
KAINTH, P. S., Charge composition of cosmic-ray nuclei of elements from Ne to Ni, 25:35910
KAJIMURA, Koji, Nonlinear electrical conductivity of superconducting films below the transition temperature, 25:36024
KAJZAR, F., Tables of magnetic structures determined by neutron diffraction. III, 25:36311 (NP-18845)
KAKHNYUK, V. I., Cholinesterase activity in brain of white rats following x irradiation, 25:35232
KALASHNIKOVA, V. I., Activation-analysis determination of the silver content in microcrystal centers in a photographic emulsion, 25:34549
KALBFLEISCH, G. R., Possible counter array for triggering a bubble chamber, 25:34968 (CONF-700623-(Vol.2), pp 593-605)
KALECHITS, V. E., Alpha decay of spherical nuclei, 25:36747
KALININ, V. P., Y--YH_2 phase diagram at room temperature, 25:35582
KALINNIKOV, V. G., Decay of ¹³⁹Nd, 25:36724 (JINR-P6-5673)
Decays of Nd and Pr nuclides with mass number A = 138, 25:36725 (JINR-P6-5674)
KALMYKOV, D. P., System for depression of magnetic field pulsations in Dubna synchrophasotron, 25:36605 (JINR-P9-5724)
KALOGEROPOULOS, T., Evidence for existence of a narrow anti pn bound state, 25:36399
KALYUZHNAYA, G. A., Superconductivity of niobium diselenide, 25:36041
KAMALYAN, L. A., Radiosensitivity of virus-synthesizing function of cells irradiated in vitro and in vivo, 25:35261
KAMAT, A. P., Balloon-borne instrument for studying x-ray sources in 15- to 150-keV range, 25:35014
KAMINSKAYA, A. M., Experiments on acceleration of α-particles by collective method, 25:36615 (UCRL-Trans-1434)
KAMINSKII, A. K., Experiments on acceleration of α-particles by collective method, 25:36615 (UCRL-Trans-1434)
KAMINSKY, Manfred S., Method for producing polarized atoms, 25:35836
KAMIYAMA, Hiroshi, Energy dependence of the equatorial pitch angle distribution of trapped protons, 25:36002
KAMYSHOV, V. M., Solubility of oxygen in hafnium nitride, 25:35566
KANDPAL, C. D., Photoelectric elements of eclipsing system WX Cephei, 25:35662
KANE, R. P., Modulation of galactic cosmic rays: review, 25:35907
KANEKO, Takao, Baryon--lepton correspondence and symmetry breaking, 25:36543
KANE-MAGUIRE, N., Racemization and ¹⁸O exchange studies of heterochelate Cr(III) complexes. II, 25:34601
KANG, K., Model for the s-wave pion--pion phase shifts, 25:36484
KANT, Michel, Laminar flow of incompressible conducting fluid in slightly divergent MHD channel, 25:35943
Optimization of energy exchanges between an unidirectional magnetic field and a thin conducting layer with finite dimensions, 25:35942
KANTER, H.-J., Prog. rpt. on measurement of airborne radioactivity and its meteorological application, annual, 4/69--3/70, 25:34745 (NYO-4061-2)
KANTIMATI, B., Field-gradient calculations in some metals of hexagonal close-packed structure, 25:36251
KAPER, Hans G., Survey of approximation procedures for the numerical solution of the neutron transport equation, 25:36647 (ANL-7779)
KAPFHAMMER, W. H., Moessbauer isomer shifts and hyperfine splitting of 145.4 keV γ-rays of ¹⁴¹Pr, 25:36244
KARAKOZOV, E. S., Secondary oxidation of metals after hydrogen annealing, 25:35291
KARAM, J., Thyroid scintigraphy using /sup 99m/Tc and ¹³¹I, 25:35169
KARASHIMA, S., Solution softening in Fe--Mo alloys, 25:35374
KARASHIMA, Seiichi, Stress dependence of high-temperature creep in Fe--Mo and Fe--Cr alloys, 25:35464
KARCHAVA, G., Control rod calculation with perturbation theory, 25:37136 (UARAEE-66)
Critical mass calculation for UA-RR-1, 25:37078 (UARAEE-67)
Effect of different reflectors on UA-RR-1 reactor core characteristics, 25:37080 (UARAEE-73)
Numerical calculations of K/sub eff/ and neutron fluxes in 2 and 3-group approximations using IEM-1620 code, 25:37126 (UARAEE-89)
Numerical study of fast neutron spectra in UA-RR-1 reactor core and reflector, 25:37079 (UARAEE-71)
Thermal utilization calculation with new asymptotic diffusion theory, 25:37119 (UARAEE-64)
KARCHAVA, G. A., Criticality evaluation of hydrogeneous enriched lattices using a three group model, 25:37124 (UARAEE-84)
Effect of non-uniform burn up on reactor lifetime, 25:37081 (UARAEE-83)
Theoretical study of effect of temperature on reactivity of EK-10 type reactors applying three-group theory, 25:37138 (UARAEE-105)
KARTASHEV, V. P., Focusing properties of a helical quadrupole lens, 25:36624
KARTASHOVA, L. G., Temporal variations of the photospheric velocity field in the active region, 25:35750
KASATKIN, A. P., Kinetic theory of the pinch effect, 25:36135
KASER, J. D., Analysis of air pulser performance for pulsed extraction columns, 25:34773 (ENWL-R-51)
KASHEVSKAYA, N. G., Stabilization of radicals formed during low-temperature radiolysis, 25:34640
KASTURIRANGAN, K., Atmospheric gamma-ray spectrum up to 6 gm cm⁻² over 7.6 °N geomagnetic latitude, 25:36000
KATAL'NIKOV, S. G., Method of calculating the number of theoretical stages of separation using a substituting line, 25:34707
KATRIEL, J., Solution of an exactly solvable quantum mechanical N-body problem, 25:36370
KATSUMORI, Hiroshi, Baryon electromagnetic masses, 25:36449
KATTERFELD, Gennadii N., Terrestrial planets and stages of their evolution, 25:35825
KATYAL, M., Chemical detection of zirconium and hafnium, 25:34519
KATZ, J., Broken conformal invariance, 25:36541
KATZIN, Leonard I., Mass-spectrometric observations on N-(ethylmercuri)-p-toluenesulfamilide, Ceresan-M, 25:37157 (ANL-7809)
KAUFMANN, M., Mirror instabilities in Isar I theta pinch, 25:36182
KAUL, A., Features of physico-chemical protection against exterior radiation, 25:35166
KAULA, William M., Dynamical aspects of lunar origin, 25:36010
KAWADA, Yasushi, Current status of radioactivity standardization, 25:34818
KAWAI, Hiroshi, Behavior and distribution of radioactive substances in coastal and estuarine waters, 25:34760
KAWAKAMI, Ichiro, Perturbation approach to nonlinear Vlasov equation. III, 25:36236
KAWAOKA, Kenji, Single-center calculations on electronically excited states of equilateral H_3^+ ion, 25:35851
KAYSSER, B., Activation analysis for determination of traces of magnesium and manganese in biological matrices, 25:34552
KAZARINOV, Yu. M., Depolarization in 612 MeV elastic pn-scattering, 25:36390 (JINR-P1-5743)
KEAR, B. H., Co-precipitation of γ'(Ni_3Al) and α-Cr in a nickel-base alloy, 25:35502
KEBUKAWA, Takeji, Velocity operator in many-boson systems, 25:36368
KEELY, Richard B., Impact of fuel reprocessing on health physics, 25:35140

KEEN, B. E., Feedback stabilization of plasma instability, 25:36184
Stabilization of the drift-dissipative instability in a plasma by rf magnetic and electric fields, 25:36179
KEETON, A., Comparison of inconel 718 and inconel 750 for elevated temperature service in a pumped NaK system, 25:35343 (WANL-TME-1857)
KEIL, P., Electron--photon cascades in Pb at primary energies of 100, 200, and 400 MeV, 25:36788
KEIL, R. G., *Anodization of vanadium, 25:35295*
KEIZER, S. A., Combined action of carbon monoxide and ionizing radiation under prolonged conditions, 25:35233
KELLER, H., Hazards and monitoring procedures in the handling of open radioactive material in nuclear installations, 25:35154
KELLER, Joachim, Theory of superconductors containing magnetic impurities: crystalline field effects, 25:36034
KELLERSHOHN, Claude, Measurement of the coronary flow by radiocardiography, 25:35085
KELLEY, M. D., SYN: operational aspects of the combined BISYN, PERT, and BICYCL synthesis codes, 25:37112 (GEAP-13672)
KELLEY, P. L., Effects on the propagation of optical beams due to self-induced changes in index of refraction, 25:37250 (UCRL-20541)
KELLOGG, L. S., Neutron energy dependent cross section evaluation by a multiple foil activation method, 25:36741 (WHAN-SA-107)
KELLOGG, P. J., Controlled experiment on wave--particle interactions in the ionosphere, 25:35967
KELLY, G. N., Precision of time of flight measurements, 25:35020
KELLY, J. W., Solid state diffusion, 25:35440
KELLY, R., Damage depth distribution of 15-keV Kr implanted in RbCl as obtained from diffusion measurements, 25:36272
KELLY, Stephen, Photographic and optical systems analysis, 25:37193 (MHSMP-71-32)
KELLY, W. H., Ge(Li)--Ge(Li) sum coincidence, 25:34932
N-shell conversion electrons from 2.33-keV transition in ^{205}Pb, 25:36780
Neutron-deficient Gd isotopes. III, 25:36744
KELM, S., Radiative energy transport in a plasma reactor, 25:36990 (DLR-FB-70-18)
KEL'MAN, V. M., Magnetic lenses with parabolic, triangular and trapezoidal distributions of linear ampere-turn density, 25:36643
KELSO, Gary L., Prog. rpt. on high temperature thermal insulation, 5/71, 25:37166 (BDX-613-313)
KEMP, J. C., Magnetic circular dichroism of bands associated with the F^+ center in SrO, 25:36291
KENDALL, Henry W., Structure of the proton and the neutron, 25:36445
KENNEDY, T. S., Studies on the combined effect of gamma radiation and cooking on the nutritional value of fish, 25:35272
KENNEDY, William R., Geology and hydrology of Mesita del Buey, 25:34845 (LA-4660)
KENNETT, T. J., Intermediate energy gamma-ray cross sections, 25:36799
KENT, Frederick S., X-ray fluorescence: detection of lead in wall paint, 25:35043
KENYON, Malcolm H., 300 pound gas test report (28-IV-16006), 25:37070 (TODD-N-16)
500 pound gas test continuation series report (28-IV-16011), 25:37074 (TODD-N-23)
500 pound gas test report (28-IV-16008), 25:37071 (TODD-N-18)
700 pound gas test report (28-IV-16009), 25:37072 (TODD-N-20)
Gas test series addendum tests and synoptic evaluation (28-IV-16012), 25:37075 (TODD-N-24)
Second 300 pound gas test (28-IV-16010), 25:37073 (TODD-N-21)
KEPA, R., New band system in CO molecule emission spectrum, 25:34595
KERNEL, G., Angular distributions from reaction $^{12}C(\alpha,\gamma_0)^{16}O$, 25:36675
KERR, Donald P., Uranium-235--^{207}Pb and ^{238}U--^{206}Pb mass differences, 25:36770
KERSHAW, David Stanley, Methods of the Bethe--Salpeter equation, 25:36568
KERSHAW, K., Radical processes following γ irradiation of frozen concentrated matrices of heparin and dextran sulphate, 25:34651
KERSHNER, Larry D., Proton transfer and heavy-atom reorganization in amide hydrolysis. Valence-isomeric transition states, 25:34576
KESKAR, K. S., Superconducting transition temperatures of rf-sputtered NbN films, 25:36065
KESSLER, P., Experimental conditions for γγ collisions with almost real photons, 25:36451
KEWLEY, D., Study of ^{150}Gd, 25:36775
KEY, Joe L., Prog. rpt. on RNA metabolism in relation to regulation of protein synthesis in plants, 27 May 1971, 25:37237 (SRO-643-1)
KHACHATUROV, Yu. G., Radioisotopic analysers for determining sulphur content in the oil-products and the experience in their exploitation, 25:35040
KHAIDAROV, K., Influence of large doses of γ radiation on optical properties of quantum generator, 25:35082
KHALIKOV, P. Kh., Mutation induced by gamma irradiation of chromosomes in Crepis capillaris, 25:35128
KHAMIDOV, G. Kh., Superconducting metallic compounds of rhenium, 25:36036
KHAN, M., Operating experience with nuclear power stations in member states, 25:36884 (IAEA-127)
KHANNA, F. C., Effective operators for nuclear shell model. III, 25:36820
KHARE, Avinash V., Strong-interaction dynamics based on a class of nonlinear Lagrangian models, 25:36481
KHATTAB, M., Cooling of a simulated fuel element by a flow of naturally circulated boiling water, 25:37009 (UARAEE-110)
KHATTAB, M. S., Experimental loop for two phase heat transfer investigations, 25:34793 (UARAEE-81)
KHATUN, S., Shape calibration and peak-to-total ratio measurements of 5'' x 6'' NaI(Tl) scintillation detector, 25:34936
KHAYATOV, M. R., Depolarization in 612 MeV elastic pn-scattering, 25:36390 (JINR-P1-5743)
KHAZRAGUI, A. M., Effect of pitch variation on nuclear properties of light water assemblies using EK-10 fuel rods, 25:37121 (UARAEE-70)
KHIZHNYAK, N. A., Electrode erosion in pulsed plasma accelerators, 25:36207
Wave interaction in a magnetized plasma, 25:36232
KHLYSTOVA, A. D., Spectrographic determination of tungsten in tungsten--molybdenum alloys, 25:34516
KHODUSOV, V. D., Magnetic energy pumping into a turbulent plasma, 25:36083
KHODZHAEV, A. Z., Method of obtaining short dense plasmoids, 25:36120
KHOKHLOV, Yu. K., Trajectories of particles in an isochronous cyclotron in the presence of acceleration, 25:36621
KHOPKAR, S. M., Rapid extraction of antimony with tributyl phosphate, 25:34512
KHOZE, V. A., Annihilation reaction of pair of polarized particles with spin 1/2, 25:36438
KHRYPCHANKA, I. P., Cholinesterase activity in brain of white rats following x irradiation, 25:35222
KIANG, G. C., Reaction ^{26}Mg(d,α)^{24}Ne at low energies, 25:36701
KICHIGIN, G. N., Ion shock waves in a collisionless plasma, 25:36106
KIDIN, I. N., Measurement of the concentration of oxygen dissolved in tantalum, 25:35339 (ORNL-tr-2478)
KIEFFABER, Lois M., Twilight flash of sodium, 25:35971
KIEFFER, R., Influence of substoichiometric carbon contents of carbide phase on properties of TiC--Mo_2C--Ni refractories, 25:35559
KIENLE, O., Moessbauer isomer shifts and hyperfine splitting of 145.4 keV γ-rays of ^{141}Pr, 25:36344
KIHARA, J., Thermally activated flow in iron, low carbon steel, and other body-centered cubic metals (V and Ta), 25:35380
KIKKAWA, Kyozo, Tritium content of Beppu hot spring water, 25:34732
KILLPATRICK, Allen Ross, Electron scattering from excited mercury atoms, 25:35872
KILLPATRICK, D. H., Texture and elevated temperature mechanical properties of dispersion-strengthened Ni--20Cr alloys, 25:35392
KIM, Chul-soo, EHD stability of thin liquid layer in uniform shearing action, 25:35939
KIM, J. S., Reappearance of multiple midlatitude auroral arc, 25:35969
KIM, *Kee Soon, Experimental study on the sintering of* tungsten carbide powder with various metal binders, 25:35534
KIM, Moon-uhn, EHD stability of thin liquid layer in *uniform shearing action, 25:35939*
KIMURA, Hiroshi, Point defects in body-centered cubic transition metals, 25:35492
KIMURA, Itsuro, Fast neutron spectra from natural uranium *target bombarded with high energy electrons, 25:36767*
KIMURA, Yuichiro, Behavior and distribution of radioactive substances in coastal and estuarine waters, 25:34760
KING, Chi-yu, Source parameters of Salmon and Sterling nuclear explosions, 25:34764
KING, John G., Measurement of helium--helium scattering cross section at low temperatures, 25:35860
KING, Kenneth W., Aleutian/Amchitka seismic program, 25:34763 (CGS-746-10)
KING, L. J., Molten-salt fluoride volatility pilot plant: recovery of enriched uranium from aluminum-clad fuel elements, 25:34693 (ORNL-4574)
KING, Ronold W. P., Transmission line coupled to a cylinder in an incident field, 25:37228 (SC-R-713250)
KINO, Takao, Radiation damage studies using the low temperature irradiation facility. II, 25:36286
KINTNER, Eric C., New radial velocities of galaxies from image-tube spectra, 25:35779
KIREEV, G. I., Study of kinetics of benzoic acid extraction with toluene by isotopic exchange method, 25:34584
KIREEV, V. A., Anticoincidence gamma spectrometer with shielded scintillator, 25:34928
KIRII, A. Yu., Quasilinear destabilization of dissipative parametric plasma instability in a high frequency electric field, 25:36170

XUM

KIRILLOV-UGRYUMOV, V. G., Observation of γ quanta greater than 100 MeV from 3C 120, 25:35700
KIROUAC, G. J., Neutron scattering from ^{15}N. II, 25:36683
KIRPICHANKOV, V. A., Tungsten base metal--ceramic alloy, 25:35476
KIRSCH, Lawrence, Prog. rpt. on research in elementary particle physics, 5/31/71, 25:36419 (NYO-3178-8)
KIRSH, Y., Effects of x irradiation on the ionic conductivity of doped SrF_2 crystals, 25:36304
KIRSHENINA, I. I., Electrical resistance of Ti--Nb alloys at high pressures, 25:36321
KIRSTOWSKY, E. C., Production and testing of superheater fuel elements, 25:37024
KISELEVA, K. V., Effects of impurities on properties of the Nb_3Sn phase, 25:36039
Superconductivity of niobium diselenide, 25:36041
KISLOV, A. Ya., Experimental study of a two-lens accelerator, 25:36115
KISTIAKOWSKY, V., Momentum dependence of 180° π-p charge-exchange cross section, 25:36412
KITABATAKE, Takashi, Conformation radiotherapy for nasopharyngeal tumor, 25:35194
KITAJIMA, Kazunori, Low temperature irradiation studies on iron--boron alloys, 25:35588
KITTS, F. G., Molten-salt fluoride volatility pilot plant: recovery of enriched uranium from aluminum-clad fuel elements, 25:34693 (ORNL-4574)
KIYAN, T. S., Luminescence spectra of excited particles knocked out of solid targets by fast Ar ions, 25:35841
KLEIN, Abraham, Ground state correlations as variational parameters in the nuclear many-body problem, 25:36840
KLEIN, Norman W., Prog. rpt. on proteins in growth regulation during early development of the chick embryo, 5/70--5/71, 25:37210 (NYO-4030-10)
Proteins in growth regulation during early development of the chick embryo, 25:37209 (NYO-4030-9)
KLEINERT, H., Backward dispersion relations for πN → πΔ scattering and NΔγ couplings, 25:36508
KLEPCZYNSKI, W. J., Determination of mass of Pluto, 25:35822
KLIMEK, M., Molecular weight of DNA synthesized in L-cells, 25:35207
KLIMKE, Peter M., Contribution to the evaluation of test results in the testing of the fire behavior of plastics on a laboratory scale, 25:37186 (CAT-Z-5046)
KLINOVSKAYA, T. V., Effect of the diluent on the partition coefficient and the single-stage separation factor in the extraction of rubidium and cesium salts by phenol, 25:34701
KLOBUCHAR, J. A., Simultaneous storm-time increases of ionospheric electron content and geomagnetic field in dusk sector, 25:35956
KLOSOVA, E., Mechanisms of hydrogen formation in the radiolysis of gaseous CH_3OH and CD_3OH, 25:34665
KLOTS, Cornelius E., Aspects of degradation spectra, 25:36258
KLOZENBERG, J. P., Flux content and form of the geomagnetic tail, 25:35991
KLUGE, Gy., Survey of measurements of the fission neutron spectrum of ^{252}Cf, 25:36728 (KFKI-71-9)
KLUSMANN, A., Situation of the nuclear fuel cycle industry, 25:37034
KLYGIN, A. E., Reaction of uranyl nitrate with arsenazo III in nitrate solution, 25:34524
Spectrophotometric investigation of complex formation in the system uranyl nitrate--nitric acid--water, 25:34564
KNAPP, Gillian R., H I clouds with spin temperatures less than 250°K, 25:35680
KNAPTON, John D., Radiological hazards of tritium-activated devices, 25:35138
KNAT'KO, V. A., Effect of phonon + particle doorway states in (n,γ) reaction, 25:36834
Phonon-particle doorway states in (n,γ) reactions on nuclei with A < 90, 25:36703
KNEIP, Theo. J., X-ray fluorescence: detection of lead in wall paint, 25:35043
KNOP, G., Electron--photon cascades in Pb at primary energies of 100, 200, and 400 MeV, 25:36788
KNUTSON, C. F., Process for stimulating petroliferous subterranean formations with contained nuclear explosions, 25:34772
KNUTSON, D. S., Special diagnostic devices, 25:36090 (MATT-838)
KNYAZEV, D. A., Isotope exchange reactions. VIII, 25:34585
KOBAYASHI, Katsuhei, Fast neutron spectra from natural uranium target bombarded with high energy electrons, 25:36767
KOBAYASHI, Tsunehiro, Deep inelastic structure of e--p scattering and relativistic extended particle model based on the quark model, 25:36444
Proper time formulation for the general dual amplitude, 25:36593
KOBILOV, D. Sh., Angular correlation of ^{97}Nb γ radiation, 25:36763
KOBYLINSKII, N. A., Dual amplitude with Mandelstam analyticity, 25:36492
KOBZEV, A. P., Effect of the optical parameters of the medium on the yield of transition radiation of non-relativistic particles, 25:36354 (JINR-P4-5734)
KOCH, F., Role of wave properties of isotopes in chemical kinetics, 25:34587
KOCHENOV, A. V., Uranium concentration in recent oceanic sediments of water uprise zones, 25:34761
KOCHETKOV, N. K., Racemization of α-amino acids exposed to γ radiation, 25:34622
Radiation chemistry of carbohydrates. XIV, 25:34664
KOCHURIKHIN, V. E., Isotope effects in CO_2 adsorption on zeolites, 25:34708
KODAMA, T., Optical measurement of a high-frequency electric field in a weakly ionized plasma, 25:36054
KOEHLER, J. S., Electron-irradiation effects in silicon at liquid-helium temperatures using ac hopping conductivity, 25:36305
Recovery of pure platinum and dilute platinum--gold alloy electron-irradiated at liquid-nitrogen temperature, 25:36306
KOEHLER, J. T., BNL work on Ne/H_2 targets, 25:34961 (CONF-700623-(Vol.1), pp 511-31)
KOEHLER, John, Bubble chamber detection technique for gamma rays in momentum region below 1 GeV/c, 25:34964 (CONF-700623-(Vol.1), pp 555-66)
KOEPPE, A., Behavior of boron-alloyed sintered molybdenum in electron beam welding, 25:35312
KOFOED-HANSEN, O., Investigation of nucleon--nucleon correlations by means of high-energy scattering, 25:36538
KOGA, Akito, Tritium content of Beppu hot spring water, 25:34732
KOGA, Taeko, Behavior and distribution of radioactive substances in coastal and estuarine waters, 25:34760
KOHLI, J. M., Characteristics of 17.2-GeV π⁻ interactions with emulsion nuclei, 25:36418
KOHRT, Carl, Adsorption of CO on the (110) plane of W, 25:35357
KOHYAMA, A., Electron bombardment of niobium containing interstitial impurities, 25:35517
KOIWA, Masahiro, Low temperature irradiation studies on iron--boron alloys, 25:35588
KOKES, A., Decay of /sup 195m/Hg and ^{195}Hg to levels in ^{195}Au, 25:36750
KOKUBUN, S., New polar magnetic disturbances, 25:36012
KOLACHKOVSKII, A., Determination of the boiling point of some isoalkyl astatides by using a glass gas chromatograph, 25:34604 (JINR-P6-5683)
KOLATA, J. J., Analysis of (p,^{3}He) and (d,α) reactions on ^{209}Bi, 25:36777
KOLBE, W., Liquid scintillation counting using an RCA photomultiplier Type C31 000D, 25:34895
KOLESAR, Donald C., Rotating wire spacer model in large bundle thermal-hydraulics, 25:37020 (WHAN-SA-76)
KOLESNIKOV, P. P., Influence of triple electron and ion combination on electrodynamic plasma acceleration, 25:36109
KOLESNIKOVA, L. E., Interaction of certain compounds of thorium with dimethyl sulfoxide, 25:34565
KOLIN'KO, L. E., Superconducting point contact having properties of Josephson junction, 25:36070
KOLINSKA, J., Preparation of ^{32}P applicators, 25:34671
KOLIWAD, K. M., Pressure dependents of the elastic constants of NaCl at low temperature, 25:37158 (NYO-2504-63)
KOLODNEY, M., Kinetics of interaction of tantalum disilicide with tantalum and other metals, 25:35577
KOLPAKOV, A. V., Scattering of the bremsstrahlung by the Moessbauer nuclei, 25:36346
KOLYADA, N. S., Reaction of uranyl nitrate with arsenazo III in nitrate solution, 25:34524
Spectrophotometric investigation of complex formation in the system uranyl nitrate--nitric acid--water, 25:34564
KOMAC, Milos, Investigation of the systems of uranium monosulfide with some alkaline earth sulfides, 25:34603 (IJS-263)
KOMAR, A. P., Method of measuring the polarization of an oriented hydrogen target, 25:36645
KOMAROV, O. L., Calculation of the internal structure of non-laminar axially-symmetric intensive beams of charged particles, 25:36609 (NP-18860)
KOMEL'KOV, V. S., Tandem plasma acceleration in coaxial systems, 25:36204
KONDRAT'EV, D. A., Isotope exchange between molecular oxygen and synthetic zeolites, 25:34580
KONDRATOVA, N. S., Use of N-furoylphenyl hydroxylamine for amperometric titration of Zr, 25:34535
KONDRATYUK, L. A., Allowance for Coulomb interaction in scattering of a fast charged particle by a nucleus, 25:36524
KONECNY, Charles Richard, Process for removing contaminants from zirconium surfaces, 25:34710
KONIECZNY, P. P., Relationship between alpha grain size and crack initiation fatigue strength in Ti--6Al--4V, 25:35349
KONISHI, T., Measurement of central fission ratios and fission rate distributions in FCA, 25:37066 (JAERI-Memo-4356)
KON'KOV, V. L., Kinetic theory of the pinch effect, 25:36135
KONONENKO, L. I., Absorption-spectrophotometric determination of certain rare earth elements in the aqueous acetone solutions of dibenzoylmethane complexes, 25:34527

KONONENKO, V. I., Azimuthal current and microwave radiation in theta pinch, 25:36122
KONSTANTINOV, P. V., Investigation of radiation-thermal cracking of n-tetracosane and n-heneicosane in the liquid phase, 25:34653
KONSTANTINOVA, M. M., Sulfhydryl groups and radiosensitivity, 25:35213
KONTANI, Ryozo, ESR studies on P+ ion-implanted Si, 25:36276
KONTYUG, V. A., Isotopic exchange of H α-position of alkyl groups of aromatic hydrocarbons with deuterotrifluoroacetic acid, 25:34598
KOOB, Derry D., Prog. rpt. on Amchitka bioenvironmental program on limnology studies, annual, 7/69--6/70, 25:34767 (BMI-171-129)
KOPCHAGINA, D. V., Isotopic exchange reaction of hydrogen in arenyl ions and their antecedents, 25:34599
KOPELIOVICH, V. P., Allowance for Coulomb interaction in scattering of a fast charged particle by a nucleus, 25:36524
KOPP, M., Paramagnetic centres in irradiated, oxidized, and reduced Na silicate glasses, 25:36278
KOPTYYUG, V. A., Isotopic exchange reaction of hydrogen in arenyl ions and their antecedents, 25:34599
KORBETSKII, E. V., Elastic and inelastic scattering of deuterons by nuclei, 25:36848
KORENCHENKO, S. M., Shower efficiency of spark chambers, 25:35006 (JINR-P13-5810)
KORNACKI, Kazimierz, Removal of radioactive I from milk by means of ion exchangers produced in Poland, 25:34703
KOROBKIN, V. V., Limits in detection of radiation scattered by a plasma, 25:36101
KOROBOVA, I. L., Effect of patchiness and increases in cathode emitting area on thermionic converter characteristics, 25:35931
KOROGODIN, V. I., Radiation induced damages to cells, 25:35260
KOROGODINA, Yu. V., Radiation induced damages to cells, 25:35260
KORTELING, R. G., Delayed states in ^{96}Nb, ^{108}Ag, and ^{110}Ag, 25:36769
KOSANIC, M. M., Effect of absorbed dose on the yields of radiolytic products in neutral aqueous solutions of oxalate ion and oxygen, 25:34644
KOSANKE, K. L., Ge(Li)--Ge(Li) sum coincidence, 25:34532
N-shell conversion electrons from 2.33-keV transition in ^{205}Pb, 25:36780
KOSARENKOV, V. A., Experimental study of gas heating efficiency in sectioned plasma generator with channel adjustment, 25:35928
KOSEK, S., Natural rubber latex sensitized with methane halides. II, 25:34614
KOSHKAREV, D. G., Coulomb collisions in dense beams, 25:36640
KOSTYLEV, V. A., Optimization of parameters of collimator for radioisotope scanning, 25:34880
KOTENKO, L. P., Relativistic increase of ionization and sensitivity of nuclear emulsions, 25:34937 (CERN-Trans-71-9)
KOTOV, V. A., Magnetic field and electric currents of the unipolar sunspot, 25:35751
KOTOV, V. I., Focusing properties of a helical quadrupole lens, 25:36624
KOTUKHOV, I. I., Prompt neutron yield in ^{235}U fission, 25:36786
KOTVAL, P. S., Strengthening of nickel-base superalloys by precipitation of a body-centered tetragonal γ'' phase, 25:35302
KOUSAKA, Tadako, Sequential brain imaging as an aid in understanding disease etiology, 25:35174
KOVACS, I., Angular anisotropy of fission fragments in ternary fission of ^{235}U and ^{238}U, 25:36758
KOVAL, A. G., Luminescence spectra of excited particles knocked out of solid targets by fast Ar ions, 25:35841
KOVALEV, A. I., Method of measuring the polarization of an oriented hydrogen target, 25:36645
KOVERDA, V. P., Homogeneous nucleation during crystallization of supercooled tin, 25:36316
KOWNACKI, J., 880 ns isomeric state in ^{144}Sm, 25:36752
KOYANAGI, M., Optical studies of ^{3}(n,π*) magnetic sublevels in benzaldehyde, 25:34592
KOZHAMKULOV, T. A., Interaction of one-particle and collective excitations in odd nuclei near Pb, 25:36753
KOZLOV, A. A., Study of kinetics of benzoic acid extraction with toluene by isotopic exchange method, 25:34584
KOZLOV, V. T., Stabilization of radicals formed during low-temperature radiolysis, 25:34640
KOZLOVA, N. D., Specific residual electrical resistance in S reversible N transition aspects of wire forms from superconducting materials by the resistivity method, 25:36055
KOZYREV, B. P., Thermal receiver of roentgen radiation, 25:35031
KOZYREV, V. I., Radiochemical peculiarities of granitoids of the Gissar pluton, 25:34734
KOZYREV, Yu. P., Measurement of isotopic abundances by time-of-flight mass spectrometer, 25:35070
KOZYREVA, E. V., Early biochemical and structural changes in liver mitochondria of irradiated rats, 25:35216
KRAEMER, H., Technical and economic state as well as prospects of atomic energy in the economy of the Federal Republic of Germany, 25:36885 (JUL-705-RG)
KRAINSKII, I. S., Design and construction superconducting solenoids for physical investigations, 25:36076
KRAJNIK, J., On-line computer system for neutron physics experiments, 25:35048 (CONF-700647-, pp 182-93)
KRAMER, K. H., Oxidation of Ni-V alloys in air, 25:35289
KRANE, K. S., Measurements of gamma rays emitted in decay of ^{160}Tb, 25:36776
Test of the Kumar--Baranger pairing-plus-quadrupole force model in A = 190 region, 25:36773
KRANSKY, V., Two-dimensional stress-induced adiabatic flow, 25:34769 (UCRL-50987)
KRANZ, E., Ferritic Cr--Mo-steel with Nb addition usable for construction of Na-cooled nuclear reactors, 25:35407
KRASIN, L. G., Optimum thickness of image-intensifying screens for radiographic inspection, 25:34824
KRASNOYAROV, N. V., Specific properties of operation of absorbing materials in fast reactors and requirements for them, 25:37140 (SRARI-P-96)
KRASZNOVSZKY, S., Importance of using exact forms for scattering amplitude in Regge pole theory, 25:36821
KRAT, T. V., Physical properties of solar spicules, 25:35719
KRAT, V. A., Physical properties of solar spicules, 25:35719
KRAUSE, E., Numerical solution of Navier--Stokes equations to calculate incompressible centrifuge flows, 25:34750 (CONF-700557-4)
KRAUSHAAR, J. J., Spectroscopy of states in ^{91}Zr from γ-ray transitions observed in ^{88}Sr(α,nγ)^{91}Zr reaction, 25:36757
KRAUTH, A., Problems of protective gas technology, 25:34860
KRAVCHENKO, A. T., Tungsten base metal--ceramic alloy, 25:35476
KREJS, F. R., Ground state correlations as variational parameters in the nuclear many-body problem, 25:36840
KREYE, Heinrich, Discontinuous precipitation in Cu--2 wt. percent Be, 25:35494
KRIBEL, R., Properties of the rotating spoke in an unstable pulsed MPD arc, 25:36111
KRISTIANPOLLER, N., Effects of x irradiation on the ionic conductivity of doped SrF_2 crystals, 25:36304
KRIVONOS, Yu. G., Stationary problem of cylindrical magnetoacoustic wave scattering by an ideal conducting cylinder, 25:35941
KRIVORUTSKII, E. N., Drift instabilities in a plasma in a high-frequency electromagnetic field, 25:36177
KRIVOSHEEV, M. V., Production of a high-density plasma by microwaves in a magnetic field, 25:36160
KRLIN, L., Influence of the helicon wave upon some electrostatic instabilities of plasmas, 25:36183
KROH, J., Radiation-induced grafting of styrene onto cross-linked butyl rubber, 25:34631
KROMHOUT, R. A., Lattice vibrational spectra and physical characteristics of metals with cubic structure, 25:36319
KROMPASS, R., Refabrication of nuclear fuel elements: fundamentals, plants, technology, 25:35304
KRONMUELLER, H., Magnetic relaxation in high-purity irradiated Fe. I, 25:36294
KRONRAD, L., Preparation of ^{32}P applicators, 25:34671
KROO, N., Synchronized chopper time-of-flight spectrometer, 25:34916 (JINR-E14-5731)
KRPIC, D., Penetration parameter for M1 conversion and E2 admixtures for 77 and 191 keV transitions in ^{197}Au, 25:36789
KRUEGER, W., Investigation of natural frequency of normal and elongated function, 25:36993 (KFK-1337)
KRUMHANSL, J. A., High pressure behavior of solid H_2, D_2, ^{3}He, ^{4}He, and ^{20}Ne, 25:37204 (NYO-3699-51)
KRYMSKII, G. F., Modulation of cosmic rays in interplanetary space, 25:35894
KSIAZAK, Z., Bitumization of liquid radioactive wastes, 25:34845 (INR-1249)
KUBIN, P., Heterogeneous deformation of niobium single crystals at very low temperatures, 25:35378
KUBIT, Charles John, Phase transformations in Zr--Nb alloys containing C, 25:35572
KUBOTA, M., Impurities in processed radioisotopes produced by (n,γ) reaction: purity of ^{169}Tb, 25:34670 (JAERI-Memo-4280)
Impurities in processed radioisotopes produced by (n,γ) reaction: purity of ^{169}Yb, 25:34669 (JAERI-Memo-4279)
KUCAB, M., Tables of magnetic structures determined by neutron diffraction. III, 25:36311 (NP-18845)
KUCHEROV, R. Ya., Effect of argon on thermionic converter operation at low cesium pressures, 25:35930
KUDRAUTSAVA, V. M., Use of irradiated pollen for hybridization of tulips, 25:35255
KUDRYASHOV, L. I., Appearance of H^+ ions in irradiated liquid water, 25:34668
Racemization of α-amino acids exposed to γ radiation, 25:34622
Radiation chemistry of carbohydrates. XIV, 25:34664
KUDRYASHOV, Yu. B., Role of primary radiotoxins in radiation damage of a cell, 25:35200
KUDRYAVTSEV, V. S., Atoms in a superstrong magnetic field, 25:35644
Molecules in an ultrastrong magnetic field, 25:35645
KUEHL, H., Reliability analyses of reactor systems from the

XUM

view of producer and operator, 25:37095 (IRS-T-18(1970), pp 217-21)
KUEHNER, J. A., Spin--parity combinations in ^{22}Ne, 25:36698
KUEHNERT, Charles Carroll, Leaf development in certain of the vascular plants, 25:37203 (NYU-3597-16)
KUENDIG, J., Pumps for nuclear plants, 25:37142
KULIEV, A. A., Gamov--Teller 1^+ excitations in odd--odd nuclei, 25:36817 (JINR-P4-5744)
KULIK, I. A., Machine estimate of homogeneity of magnetic fields of solenoids, 25:36077
KULIK, O. P., Chemical properties of nitrides of some transition metals, 25:35522
KULINSKII, V. I., Effect of cystamine on monoamine oxidase and catechol-O-methyltransferase, 25:35165
KULMBURG, A., Electron beam microanalysis of complex carbides, 25:34523
KULYGIN, V. M., Fast hydrogen atom injector, 25:36186 (CTC-746)
Injector for fast hydrogen atoms. I, 25:35837
KUMAR, Santosh, Nonrelativistic energy bands of double hexagonal close-packed lanthanum, 25:36352
KUMMER, M., How to avoid secular terms in classical and quantum mechanics, 25:36376
KUNAKOV, Yu. N., Investigation of compounds in the niobium--tin system obtained by means of diffusion, 25:36045
Obtaining the superconducting compound V_3Ga by means of diffusion, 25:36043
KUNTE, P. K., Balloon-borne instrument for studying x-ray sources in 15- to 150-keV range, 25:35014
KUNZ, P. D., Reactions $^{39}K(^3He,^3He)^{39}K$ and $^{39}K(^3He,d)^{40}Ca$ at 29.3 MeV, 25:36696
KUO, T. T. S., Electric dipole transitions in ^{88}Sr and ^{90}Zr, 25:36798
KUPPERMANN, Aron, Exact tunneling calculations, 25:34574
KURDYUKOV, A. A., Oxidation--reduction properties of rocks containing uranium ores in black shales, 25:34752
KUROCHKIN, V. I., Machine estimate of homogeneity of magnetic fields of solenoids, 25:36077
KUROCHKIN, V. Ya., Laboratory complex for producing homogeneous magnetic fields by superconducting magnetic systems, 25:36079
KURODA, P. K., Decay of ^{34}P and /sup 34m/Cl, 25:36700
New isotope ^{160}Lu, 25:36796
KUROV, M. A., Alpha measurement for ^{235}U and ^{239}Pu, 25:36748
KURSANOV, Yu. V., Production of negative hydrogen ions in a plasma with a double sheath, 25:35843
KURTMULLAEV, R. Kh., Isomagnetic discontinuity in a collisionless shock wave in a plasma, 25:36125
KURZ, H. E., Excitation functions of the $^{197}Au(\alpha,xn)$ reactions in the energy range from 16 to 103 MeV, 25:36745
KUSTOV, V. V., Combined action of carbon monoxide and ionizing radiation under prolonged conditions, 25:35233
KUTSENOK, T. G., Physical properties of plasma-sprayed carbides, 25:35538
KUYATT, C. E., Inelastic electron scattering from formaldehyde, 25:35883
KUZIN, A. M., Role of primary radiotoxins in radiation damage of a cell, 25:35200
KUZ'MIN, R. N., Nuclear gamma resonance, 25:36343
Scattering of the bremsstrahlung by the Moessbauer nuclei, 25:36346
KUZNETSOV, E. I., Spatial distribution of ion temperatures in Tokamak devices, 25:36097
KUZNETSOV, V. S., Calculation of the internal structure of non-laminar axially-symmetric intensive beams of charged particles, 25:36609 (NP-18860)
Intense beams with an arbitrary phase-density distribution in external focusing fields, 25:36642
KUZNETSOV, V. V., Electrical resistance of Ti--Nb alloys at high pressures, 25:36321
Short-lived isomers of Tb isotopes: ^{148}Tb, ^{149}Tb, ^{150}Tb, and ^{152}Tb, 25:36726 (JINR-P6-5681)
KUZNETSOVA, E. M., Effect of the diluent on the partition coefficient and the single-stage separation factor in the extraction of rubidium and cesium salts by phenol, 25:34701
KUZNETSOVA, G. A., Content of artificial radioisotopes in atmosphere over Moscow during 1962--1967, 25:34748
KVIN, V. E., Tungsten base metal--ceramic alloy, 25:35476
KVINIKHIDZE, A. N., Relativistic three-particle problem in terms of three-dimensional variables, 25:36586 (JINR-E2-5771)
KYLE, M. L., Prog. rpt. on lithium/chalcogen secondary cells for components in electric vehicular-propulsion generating systems, semiannual, 5/23--11/22/70, 25:35275 (ANL-7777)

L

LABAUVE, R. J., Evaluated nuclear data for hydrogen in the ENDF/B-II format, 25:36660 (LA-4574)
LABIE, E., Elastic and inelastic scattering of α particles on ^{20}Ne and ^{22}Ne, 25:36697
LA BLANCHETAIS, Ch. H., Thin films of praseodymium sesquioxide, 25:35575
LABRUM, N. R., Observations of harmonic structure in Type-III solar radio bursts, 25:35737
LABUS, J., Investigations of solidification front and the depth of the liquid phase in concast billets by the technique of radioactive traces, 25:34820
LACH, J., Strong interaction physics in the NAL bubble chamber, 25:34940 (CONF-700623-(Vol.1), pp 42-55)
LACKEY, W. J., Comparisons between predicted and measured fuel pin performance, 25:37019 (ORNL-TM-3366)
Statistical technique for determining sources of variation in $(U,Pu)O_2$ oxygen-to-metal ratio, 25:35666 (ORNL-TM-3362)
LACOMBE, P., Slip and twinning in α-uranium, 25:35282
LACOMBE, Paul, Electrochemical behavior of U electrode in contact with aqueous solutions and the nature of the phases formed as a function of pH, 25:34562
LADNER, H.-A., Safety principals in the handling of radiopharmaceuticals and radioisotope-labeled pharmaceuticals, 25:35153
LAFFERTY, Robert H. Jr., Strontium-90 heat sources, 25:34808 (ORNL-IIC-36)
LAFUMA, J., Respiratory contamination by actinides in solution, 25:35091
LAI, Kwan-wu, A_2^- from reaction $\pi^-p \to K/sub S/^0K^-p$ at 4.5 GeV/c, 25:36409
LAINER, D. I., Effects of heat treatment on the superconducting properties of Nb--Ta alloys, 25:36054
LAJTAI, A., Survey of measurements of the fission neutron spectrum of ^{252}Cf, 25:36728 (KFKI-71-9)
LAKE, Suzanne, Availability of radionuclides in debris from Plowshare excavation Buggy, 25:35088
Biological availability of radionuclides produced by Plowshare Event Schooner. I, 25:35090
Biological availability of radionuclides produced by Plowshare Event Schooner. II, 25:35089
LAKEY, J. R. A., Technology of reactor thermal shields. I, 25:36999
LAL, K. B., Emission of deuterons in 24-GeV/c proton interactions with emulsion nuclei, 25:36402
LALANNE, D., Device for measuring the luminosity of Orsay storage ring, 25:36606 (LAL-1249)
LALOU, Claude, Thermoluminescence induced in thick targets by 3 GeV protons, 25:36298
LAM, S. T., Resonance in $^{27}Al(p,\gamma)^{28}Si$, 25:36659
LAMBROPOULOS, P., Functionals for discontinuous trial function flux synthesis, 25:37130
LAMPE, M., Theory of the beam cyclotron instability in plasmas, 25:36167
LANCE, E. D., Bulk shielding facility quarterly report, January--March 1971, 25:37069 (ORNL-TM-3452)
LANCELOT, J., Isotopic composition of lead in volcanic rocks, 25:34740
LANDIN, N. A., Y--YH_2 phase diagram at room temperature, 25:35582
LANDINI, M., Soft x-ray emitting regions in the solar corona, 25:35721
LANDSBERG, P. T., Energy levels and Lorentz invariance, 25:36374
LANG, W., Contribution to experimental thermal shock analysis, 25:34776 (EURFNR-794)
LANGERON, Jean-Paul, Effect of C and O on rupture of polycrystalline Mo, 25:35409
Molybdenum decarburization by annealing at low oxygen pressures, 25:35309
LANGFORD, J. C., Particulate Pb, ^{210}Pb and ^{210}Po in the environment, 25:34762
LANORE, Jeanne-Marie, Biasing system for treatment of deep penetration of neutrons by Monte-Carlo method, 25:36648 (CEA-R-4145)
LANSIART, Alain, Gas-filled spark chamber radiation detector, 25:34876
LANZ, L., Time scales and the problem of measurement in quantum mechanics, 25:36372
LANZANO, Paolo, Relative motion of two spheroidal rigid bodies. II, 25:35665
LAPIKAS, L., Three-magnet system for measurement of electron scattering through 180°, 25:36629
LAPP, Ralph E., Four big fears about nuclear power, 25:36973
LAPSHIN, S. I., Experimental gamma radiography equipment for determining defects in construction materials, 25:34822
LARSEN, A., Coronal line profiles observed by means of coronagraphs and a Fabry--Perot spectrometer, 25:35775
LATTER, Terence David Thomas, Improvements in and relating to the measurement of coating thickness, 25:35078
Inspection and/or measuring apparatus using radiation, 25:35041
LAUDER, I., Racemization and ^{18}O exchange studies of heterochelate Cr(III) complexes. II, 25:34601
LAUER, K. F., Preparation of $^{241}PuO_2$ for neutron cross section measurements, 25:35541
LAURENSON, L., Operation of a glow discharge ion gun used for specimen thinning, 25:36639
LAURER, Gerard R., X-ray fluorescence: detection of lead in wall paint, 25:35043
LAUTHIER, Jean-Claude, Natural convection irradiation device "Esther", 25:37061 (EURFNR-890)
ODILE irradiation device, 25:37060 (EURFNR-889)
LAVAITTE, A., Broad bandwidth differential amplifier, 25:35046 (CEA-N-1448)
Nanosecond pulse amplifier with adjustable gain, working in both polarities, 25:35044 (CEA-N-1439)

LAVAKARE, P. J., Atmospheric neutrons and the Van Allen radiation belt, 25:35998
Low-energy gamma-ray spectrum in space, 25:35922
Search for energetic neutrons emitted during solar flares, 25:35772
LAVEISSIERE, Francoise, Isotopic electric generators, 25:34811 (ORNL-tr-2485)
LAWSON, Donald Stuart, Refuelling machine for a nuclear reactor, 25:37151
LAZAR, N. H., Effect of electron heating on overall efficiency of conceptual mirror fusion reactors, 25:36088
LAZAREV, E. N., Effects of diffusion interaction components on niobium--titanium alloys, 25:35325
LAZAREV, L. N., Two-particle resonance scattering in three-particle reactions, 25:36837
LAZAREV, N. F., Production of negative hydrogen ions in a plasma with a double sheath, 25:35843
LEAF, Gary K., Survey of approximation procedures for the numerical solution of the neutron transport equation, 25:36647 (ANL-7779)
LEAVENS, C. R., Theory of weak-coupling superconductors, 25:36069
LEBEDEV, M. A., Ion-acoustic oscillations and transport processes in a low-temperature cesium plasma, 25:36231
LEBEDEV, R. A., Consequencies of β-decay of ^{129}Te in some Te oxide compounds, 25:34674
LECLERCQ, Michel, Oxidation kinetics of pure or alloyed zirconium with oxygen or water vapor, 25:35277 (NP-18833)
LECLERE, Jacques, Natural convection irradiation device ''Esther'', 25:37061 (EURFNR-890)
ODILE irradiation device, 25:37060 (EURFNR-889)
LEDERER, M., Conference on gel permeation chromatography, Miami Beach, Fla., 10/70, 25:35532
LE DEVEHAT, J., Characteristics of various sealing membranes for alpha activity monitoring cells used in solutions, 25:34673 (CEA-N-1440)
LEDOVSKOI, V. P., Plasma effects in the interaction of intense electron beams with matter, 25:36157
LEE, Chung-oh, EHD stability of thin liquid layer in uniform shearing motion, 25:35939
LEE, H. C., Effective operators for nuclear shell model. III, 25:36820
LEE, John J., Environmental factors affecting the standing crop of foraminifera in sublittoral communities of a Long Island Salt Marsh, 25:37208 (NYO-3995-15)
LEE, Paul D., Photometric studies of northern galactic clusters. I, 25:35606
LEE, T. D., Scaling properties in e-p scattering, 25:36435 (NYO-1932(2)-189)
LEE, Vincent J., Preliminery photometry of open cluster NGC 609, 25:35605
LEFEBVRE, Jean-Claude, Calculation methods for heterogeneities in reactors of the natural uranium-graphite--gas type, 25:36989 (CEA-N-1398)
LEGAN, Marianne, Argonne code center: compilation of program abstracts, 25:37133 (ANL-7411(Suppl.5))
LEGG, J. R., Anomalous electron scattering from ^{142,144} ^{150}Nd, 25:36758
LEHNER, G., Problem of controlled thermonuclear fusion, 25:36212
LEHRAUS, I., High energy particle identification by ionization measurements using single gas proportional counter, 25:35018
LEHRHEUER, W., Welding and brazing techniques in the fabrication of facilities for nuclear experiments, 25:35326
LEIDERER, P., Influence of impurities on laser induced breakdown in liquid ^{4}He, 25:36014
LEIGHLY, H. P. Jr., Nuclear metallurgy curriculum at Univ. of Missouri at Rolla, 25:34781
LEIPER, W., L/K electron capture ratio in decay of ^{159}Dy, 25:36771
LEITCH, K., Aging behavior of Fe--30 Ni alloys containing niobium, 25:35499
LEITH, D. W. G. S., New digitizing and memory system for wire spark chambers, 25:35016
LELEUX, P., Elastic and inelastic scattering of α particles on ^{20}Ne and ^{22}Ne, 25:36697
LELOUP, Jean, Gas-filled spark chamber radiation detector, 25:34876
LEMAIRE, L., Co-precipitation of γ'(Ni_3Al) and α-Cr in a nickel-base alloy, 25:35502
LEMAIRE, M. C., Proton-pair correlation in Ti and Cr low-lying excited states, 25:36709
LEMAIRE, Remy, Crystallographic and magnetic properties of compounds of cobalt and lutetium, 25:36318
LEMAN, E. P., Geometric inversion and its utilization in x-radiometric and gamma--gamma method, 25:34904
LENCI, F., Coenzyme-substrate interactions, ESR study of irradiated systems, 25:34655
LENOBLE, Jacqueline, A--K supergiant stars and interstellar absorption in direction of large Magellanic Clouds, 25:35670
LENZ, D., Dislocation-pinning memory-effect in γ-irradiated and stress-annealed copper, 25:35514
LEON, J., Range and range straggling of 97-keV ^{224}Ra particles in gases, 25:36262
LEONARD, Alain, Incidence of dominant lethal mutations after x-irradiation of spermatozoa of mice and rats, 25:35129
LEONOV, A. I., Regularity in the formation of solid solutions of oxides in ZrC_2--MeO/sub n/ solutions, 25:35545
LEQUAIS, Jean, Gas-filled spark chamber radiation detector, 25:34876
LERCHE, I., Kinematic-dynamo theory. I, 25:35786
Kinematic-dynamo theory. II, 25:35787
LERIBAUX, Henri R., Space--time pair correlation function of Maxwell--Boltzmann fluid in T-approximation for temperature Green's functions. I, 25:36372
LERUSTE, Ph., Local models for antikaon--nucleon collisions, 25:36505 (FAM-71.1)
LESAGE, B., Slip and twinning in α-uranium, 25:35382
LESSER, Richard, Fuel element for a fast breeder and/or test reactor, 25:37027
LETEURTRE, J., Dechanneling of α particles by dislocations occurring in Al, 25:36307
LEUNG, Kwok-chu, Measurement of np(pp) triple scattering parameters R/sup T/(R) and R'/sup T/(R') 510 to 670 MeV, 25:36397
LEUNG, M. C., Generalized Langevin approach to evaluate ultrasonic attenuation rate in superconductors, 25:36071
LEUTZ, H., Track sensitive H_2 and D_2 targets in Ne--H mixtures, 25:34960 (CCNF-700623-(Vol.1), pp 477-510)
LEVIN, E., Role of $CHCl_3$ as a quencher for γ- and uv-excited organic solutions, 25:34624
LEVIT, Lawrence B., Search for CP-nonconserving asymmetry in decay K/sub L/^{0} → $\pi^+\pi^-\pi^0$, 25:36550 (COO-1745-24)
LEVITSKII, L. S., Interplanetary plasma and magnetic field in plane of solar equator, 25:35759
List of proton flares, polar cap absorptions, and solar microwave radio bursts, 25:35758
LEVY, I. S., Thermomechanically-produced carbide dispersion-strengthened austenitic stainless steel with improved high-temperature tensile and creep-rupture properties, 25:35300
LEWEY, S., Extraction of selected metallic cations by highly hindered $(GC)_2PC(CH)$ extractant in two different diluents from aqueous chloride phase, 25:34706
LEWIN, Walter H. G., Detection of high-energy x-ray flare from source in Crux, 25:35691
Rapid fluctuations in high-energy x-ray flux from source in Crux, 25:35692
LEWIS, D., X-rays, 25:35057
LEWIS, R. S., Plutonium-244: confirmation as an extinct radioactivity, 25:35594
LEWIS, Robert Alec, Nuclear reactor fuel assemblies, 25:37025
LEWIS, S. R., Gamma-spectrometry in marine radioactivity studies, 25:34935
LEY, F. J., Studies on the combined effect of gamma radiation and cooking on the nutritional value of fish, 25:35272
LEY-KOO, M., Radioactive wastes of nuclear center in Mexico, 25:34733
LEZAMA C, J., Laboratory for production of radioisotopes, 25:34816
LHERMENIER, Andre, Natural convection irradiation device ''Esther'', 25:37061 (EURFNR-890)
ODILE irradiation device, 25:37060 (EURFNR-889)
LI, Che-yu, Study of void formation in fast neutron-irradiated metals, 25:35516
LIEBER, C. C., Effectiveness of ceramic armor plating, 25:37256 (UCRL-Trans-10530)
Estimating shock pressures in collisions between two bodies, 25:37257 (UCRL-Trans-10531)
LIELPETER, Ya. Ya., Liquid-metal MHD induction machines, 25:35929
LIEN, Hwachii, Two-phase seeding in low-density plasma flow, 25:36116
LIER, Douglas W., Bremsstrahlung emission measurement from thick tungsten targets in energy range 12 to 300 kV, 25:36249 (LA-4624)
LIN, Chun Bin, (n,p) elastic scattering, 25:36661 (UCRL-20295)
LIN, E. C., Inverse deuterium isotope effect in radiationless electronic transitions, 25:34590
LINPERT, J. C., Plant instrumentation program quarterly progress report for the period ending September 30, 1970, 25:34924 (WCAP-7562-3)
LIN, E. K., Reaction ^{26}Mg(d,α)^{24}Na at low energies, 25:36701
LIN, R. P., Electron (10 to 100 keV) acceleration and emission from solar flares, 25:35726
LIN, S., Service of nuclear medicine, 25:35156
LIN, Tzuen-shyan, Statistics of composite beams, 25:36356
LIND, D. A., Reactions ^{39}K(^{3}He,^{8}He)^{39}K and ^{39}K(^{3}He,d)^{40}Ca at 29.3 MeV, 25:36696
LINDBERG, R. W., Microstructural analysis of a high strength martensite-beta titanium alloy, 25:35488
LINDEKEN, C. L., Estimating natural terrestrial background in 17- and 60-keV energy regions from Compton continuum peak, 25:34727 (UCRL-72927)
LINDEN, W., Effects of ultra-high-energy radiation (600 to 6000 MeV) on cell nucleus, 25:35258
LINDGREN, K., High-energy (γ,xn) reactions in ^{197}Au, 25:36785
LINDHARD, Jens, Transient fields acting on heavy ions during slowing-down in magnetized materials, 25:36846
LINDROOS, V. K., Anomalously high collection of copper ions

implanted in aluminum, 25:36295
LINDSAY, Graham Eades, Transport containers for radioactive materials, 25:34858
LINGENFELTER, R. E., Compound diffusion of cosmic rays, 25:35902
LINGERFELT, J. E., Relativistic motion of a radiating point charge in a constant electromagnetic field, 25:36363
LINSER, G., BEBC expansion piston, 25:34985 (CONF-700623-(Vol.2), pp 836-48)
LIPCHAK, J. B., Nuclear Instrumentation System: topical report, 25:36995 (WCAP-7669)
LIPPINCOTT, E. P., Derivation of corrections to K infinity in the two-group approximation, 25:37111 (BNWL-1560)
Measurement of the temperature dependence of K infinity for a $^{233}UC_2$--ThO_2 HTGR lattice, 25:36988 (BNWL-1561)
LIS, S., Physico-chemical properties of lanthanide complexes with thenoyltrifluoroacetone. I, 25:34502 (INR-1247)
LISON, R., Welding and brazing techniques in the fabrication of facilities for nuclear experiments, 25:35326
LITHERLAND, A. E., Resonance in $^{27}Al(p,\gamma)^{28}Si$, 25:36659
LITTBRAND, Bo, Dual effect of oxygen, 25:35214
LITVAK, A. G., Self-trapping of powerful electromagnetic waves in a dense plasma, 25:36225
LITVINOV, I. I., Effect of collisions on the diffusion electron current to a cylindrical probe in a magnetized plasma, 25:36098
LIU, C. T., Influence of various ordered states on the mechanical properties of vanadium--cobalt--nickel ternary alloys, 25:35385
Strengthening Nb--Hf alloys by α precipitation, 25:35353
LIU, Chelcie Bosland, Optical spectra observed during ion--molecule collisions with low-energy N_2^+ and Ar^+ beams, 25:35873
LIU, Yuen-chung, Simple neutron spectrometer, 25:34925
LIVENTSEVA, I. F., Parameters of plasma produced by fast electron beam in a magnetic field, 25:36118
LLOYD, J. W. F., Sky intensity and spectral distribution during solar eclipse of 11/12/1966 at Bage, Brazil and on aircraft, 25:35763
Summary of sky brightness measurements during eclipses of the sun, 25:35761
LODENQUAI, J., Thomson scattering in a strong magnetic field, 25:36140
LOGAN, B. A., Test of the validity of time reversal, 25:36540
LOGAN, R. K., Duality-breaking and meson spectrum, 25:36486
LOHR, R. D., Design evaluation of insulator pin, 25:37164 (BDX-613-294)
LOHSE, G. E., Treatment of radioactive waste streams at Idaho chemical processing plant by evaporation and ion exchange, 25:34532 (CONF-710509-1)
LOISEAU, B. A., Nucleon--nucleon correlation and two-pion-exchange three-body force in n force in nuclear matter, 25:36831
LOISEAUX, J. M., Proton-pair correlation in Ti and Cr low-lying excited states, 25:36709
LOKANATHAN, S., Monte Carlo calculations and the lifetime of heavy hyperfragments, 25:36535
LOKTINOV, Yu. M., Asymmetric helical magnetic configurations, 25:36206
LOMASHEVICH, C. A., Principle of formation of amplitude spectra in semiconductor nuclear radiation counters, 25:34911
LOMINO, N. S., Ion energy spectra and lifetimes in a multipole magnetic trap, 25:36085
Plasma transport in a magnetic quadrupole field, 25:36086
LOMSADZE, Yu. M., Logic of conclusive explication of the quantum theory, 25:36353 (ITF-70-61-E)
LOPES DOS SANTOS, Pedro, Determination of ^{210}Po in cigarettes and tobacco, 25:34515
LOPEZ, Natalia, Effects of ionizing radiations on I uptake by rat liver slices, mitochondria, and mitochondrial membranes, 25:35223
LOPEZ, W. M., Prog. rpt. on neutron capture cross sections of Mo, Ta, and ^{238}U, final, 6/70, 25:36729 (N-70-41999)
LORENSEN, Lyman E., Low energy radiation dosimetry method in range of 15 keV and below, 25:35033
LORENZ, K., Ferritic Cr--Mo-steel with Nb addition usable for construction of Na-cooled nuclear reactors, 25:35407
LORIKYAN, M. P., Dynamic radiation generated in crystals by particles with ultrarelativistic energies, 25:36382
LOSEVA, T. I., Isotope effects in CO_2 adsorption on zeolites, 25:34708
LOTTIN, J. C., Big hydrogen bubble chamber Mirabelle cryogenics expansion, 25:34979 (CONF-700623-(Vol.2), pp 751-64)
LOUCK, James D., Intrinsically self-conjugate boson structure: the symplecton, 25:36548
LOUTTIT, R. I., BNL work on Ne/H_2 targets, 25:34961 (CONF-700623-(Vol.1), pp 511-31)
LOVBERG, R., Properties of the rotating spoke in an unstable pulsed MPD arc, 25:36111
LOVBERG, R. H., Internal physical measurements in MHD plasma accelerators, 25:36096
LOVE, T. A., Pre-target monitor for the intensity and time distribution of a proton beam, 25:36631
LOVELAND, W. A., Centralized data acquisition and time-sharing message switching system, 25:37219 (RLO-2227-T-7-7)
LOW, F. E., Generalized O(2,1) expansion for asymptotically growing amplitudes, 25:36547
LOZAC'H, Anne-Marie, L_3GaS_6 compounds (L = Dy, Ho, Er, and Y), and the phase diagram of Y_2S_3--Ga_2S_3 system, 25:35571
LUBAROFF, David M., Attempts to abolish tolerance of skin homografts in mice with x-irradiated plasma from specifically sensitized donors, 25:35113
LUBIN, Moshe J., Fusion by laser, 25:36211
LUCAS, A. C., Production of high-intensity K x-ray beams, 25:35842
LUCAS, J., Improvements in tests of long-range charge independence, 25:36522
LUCAS, J. J., Relationship between alpha grain size and crack initiation fatigue strength in Ti--6Al--4V, 25:35349
LUCAS, J. M., Temperature variation of susceptibility of some amorphous antiferromagnetic oxides, 25:36237
LUCASSON, A., Damage production and recovery in low temperature irradiated zinc, 25:36288
LUCASSON, P., Damage production and recovery in low temperature irradiated zinc, 25:36288
LUCHKOV, B. I., Observation of γ quanta greater than 100 MeV from 3C 120, 25:35700
LUCKE, William H., Intrinsic efficiencies of some thermoluminescent-dosimetry phosphors, 25:35032
LUCO, V., Functionals for discontinuous trial function flux synthesis, 25:37130
LUDINGTON, M. A., Experimental and calculated photopeak efficiencies for coaxial Ge(Li) detector, 25:34900
LUDLOW, T. E., Thermodynamic data program involving plutonia and urania at high temperatures. Quarterly report No. 14, November 1, 1970--January 31, 1971, 25:35547 (GEAP-12182)
LUDWIG, D., Anomalous scattering of laser light from a magnetized arc plasma, 25:36123
LUDWIG, K., Anodization of vanadium, 25:35295
LUECKE, K., Dislocation-pinning memory-effect in γ-irradiated and stress-annealed copper, 25:35514
LUKATS, Bela, Resistance of solid substances to gamma radiation, 25:34660
LUKE, Stacy Wenzel, Origin of long-period micropulsations in the geomagnetic field, 25:35964
LUKENS, H. R., Prog. rpt. on applications of neutron activation analysis in scientific crime investigation, 5/62--5/68, 25:34542 (GA-9807)
LUKIN, A. M., Studies in field of analytical chemistry of U. V, 25:34531
LUKOVNIKOV, A. I., Electron distribution function in a low-temperature plasma, 25:36134
LUKS, R. K., X-ray luminescence and thermoluminescence of SrF_2 and BaF_2, 25:36317
LUK'YANOV, V. F., Studies in field of analytical chemistry of U. V, 25:34531
LUM, John K. Jr., HAL1903: digital logic simulator, 25:37254 (UCRL-72694)
LUNA, R. E., Comparison of turbulence intensity and stability ratio measurements to Pasquill turbulence types, 25:34747 (SC-DC-70-5443)
LUQUIRE, J. W., Computer programs for some eddy-current problems, 1970, 25:37212 (ORNL-TM-3295)
LUSANNA, L., Inclusive experiments and high-energy models, 25:36478
LUTON, M. J., High temperature flow stress and substructure strengthening of polycrystalline α-zirconium, 25:35401
LUTZ, H. F., Proton induced reactions on mass-14 nuclei, 25:36673
LUTZKY, M., Quadratic artificial viscosity in numerical magnetic gas dynamics, 25:35951
LWIN, Y. N., Recovery of pure platinum and dilute platinum--gold alloy electron-irradiated at liquid-nitrogen temperature, 25:36306
LYAGUSHCHENKO, R. I., Effective number of ionization and recombination events in the positive column, 25:36136
LYKHIN, V. A., Effects of impurities on properties of the Nb_3Sn phase, 25:35039
LYUL'KA, V. A., Lepton decay of hypernucleus ^3H, 25:36454 (IAE-1944)
LYUTAYA, M. D., Chemical properties of nitrides of some transition metals, 25:35522

M

MA, Te Hsiu, Far-red light effect on ultraviolet light induced chromatid aberrations in pollen tubes of Tradescantia, 25:35120
MACEK, K., Conference on gel permeation chromatography, Miami Beach, Fla., 10/70, 25:35532
MACH, K., Electron spin resonance studies of fundamental processes in radiation- and photo-chemistry. VI, 25:34641
MACHADO, Marcos E., Evidence for the photospheric origin of the flare optical continuum, 25:35722
MACHIDA, Shigeru, Super exclusion principle for hadronic processes. I, 25:36477
MACKEY, J. H., Paramagnetic centres in irradiated, oxidized, and reduced Na silicate glasses, 25:36278

MACLAUGHLIN, D. E., Nuclear spin--lattice relaxation in pure and impure indium. I. Normal state, 25:36349
MACMURDO, K. W., Neutron-induced fission cross sections for ^{244} ^{248}Cm and ^{249}Cf, 25:36721 (DP-MS-70-95)
MACQ, P., Elastic and inelastic scattering of α particles on ^{20}Ne and ^{22}Ne, 25:36697
MADSEN, D. W., Anomalous electron scattering from ^{142} ^{144} ^{150}Nd, 25:36758
MAEHLUM, B. N., Storm-time variations in high-latitude fluxes of low-energy electrons, 25:35959
MAENCHEN, G., Two-dimensional stress-induced adiabatic flow, 25:34769 (UCRL-50987)
MAES, Michel Emil, Improvements in or relating to plasma accelerators for generating propulsion thrust, 25:36105
MAFFEO, B., EPR identification of neutral charge state of Be vacancy in irradiated BeO, 25:36283
MAGARIELLO, E., Bonding beryllium--copper alloys with high temperature thermoplastic. A report of a program undertaken to meet the problems confronting potential users, 25:35316
MAGEE, John L., Advances in radiation chemistry. II, 25:34615
MAGGI, G., Contribution of isotopes to the surgery of the thyroid, 25:35190
MAGNUSON, Waldo G. Jr., Computer graphics application to computer-aided printed circuit design, 25:37253 (UCRL-72637)
MAGYARI, E., Approach to quantum mechanical four-body bound-state problem. II, 25:36364
MAHAJAN, S., Twin--slip and twin--twin interactions in Mo--35 at. percent Re alloy, 25:35481
MAHARANA, J., Charge exchange polarization (πN) in Veneziano model, 25:36517
MAHESHWARI, P. N., Reactions ^{48}Ti(α,p)^{51}V and ^{50}Ti(^{3}He,d)^{51}V, 25:36716
MAHMOUD, H. M., Experimental studies on shock waves propagated through a longitudinal magnetic field in electrodeless discharge tubes, 25:36092 (UARAEE-101)
MAHN, C., Anomalous scattering of laser light from a magnetized arc plasma, 25:36123
MAIENSCHEIN, F. C., Spectrum of photons emitted in coincidence with fission of ^{235}U by thermal neutrons, 25:36743
MAILEN, J. C., Distribution of transuranium elements between molten Li chloride and Li--Bi solutions. Evidence for Cf(II), 25:34705
MAILFERT, A., Penetration of magnetic induction, electric field, and losses in impure superconductors, 25:36019 (CONF-700341-8)
MAILLIE, H. D., Iron-59 uptake in bones of rats exposed to x irradiation, 25:35211
MAIOROV, A. N., Isotopic radiography with radiation background conditions, 25:34823
MAITA, J. P., Electronic transitions in near-equiatomic vanadium--ruthenium alloys, 25:36339
MAJID MIAN, A., Mass equations of nuclear particles, 25:36426
MAJOR, D., Attenuation of 14-MeV neutrons in calcium-based concrete, 25:36260
MAJURE, J. C., Prog. rpt. on excitation and ionization of ions by electron impact, 9/70--5/71, 25:35833 (ORO-3027-19)
MAKARIOUS, A. S., Measurement of continuous fast neutron spectra by scintillation technique, 25:34920 (UARAEE-91)
MAKHLIS, F. A., Changes in structure and properties in γ-irradiated crystallizable chloroprene rubber, 25:35590
MAKHNENKO, L. A., Current loading and dispersion in an iris-loaded linear electron accelerator, 25:36644
MAKOVSKII, L. L., Principle of formation of amplitude spectra in semiconductor nuclear radiation counters, 25:34911
MALACINSKI, George M., Instrument for slicing and handling radioactive polyacrylamide gels, 25:35056
MALAKHOVA, T. G., Transition temperature in systems Zr--V and Zr--V--Nb, 25:36042
MALANIFY, J. J., Charge-symmetry study with reactions ^{2}H(t,tau)nn and ^{2}H(tau,t)pp, 25:36662
MALEK, Emil, Past and future of heat power plants, 25:36974
MALENCHENKO, A. F., Content of I in thyroid glands and effect on uptake of ^{131}I, 25:35097
Influence of uranium nitrate on rabbit thyroid gland, 25:35229
MALLON, Barbara J., Low energy radiation dosimetry method in range of 15 keV and below, 25:35033
MALMSKOG, S. G., Half-life measurements of excited levels in ^{121}I and ^{123}I, 25:36752
Low-energy band structure in ^{187}Os, 25:36805
MAL'TSEV, V. T., Phase diagram of the system PbO--MoO_3, 25:35581
MALTSEVA, N. S., Relative yields of secondary [(p,xn)α] reactions on Bi in range E/sub p/ = 120-660 MeV, 25:36723 (JINR-P1-5530)
MALY, J., Long-range fission fragments induced by irradiation with electrons, 25:36791
MALYUTIN, A. I., Isomagnetic discontinuity in a collisionless shock wave in a plasma, 25:36125
MANABE, Shohei, Effect of fractionated x irradiation on cells in tissue culture, 25:35242
MANAKOV, V. M., Phase diagram of the system PbO--MoO_3, 25:35581
MANDZHOS, A. V., Cosmological solution of Jordan--Dicke field equations, 25:35814
MANI, H. S., Models in weak interactions, 25:36467
MANIAR, G. N., Effect of molybdenum and hardener content on gamma-prime solvus temperature in a Ni20Cr base heat-resistant alloy, 25:35460
MANN, William Anthony, Time distribution of leptonic K^0 decays, 25:36457
MANSON, A. H., Minor constituents in mesosphere and lower thermosphere during periods of ancealous absorption, 25:35984
MANSON, S. T., Ionization of L-shell of Al by fast charged particles, 25:35880
MANSOUR, H. M., Effect of form factors on high-energy neutrino reactions, 25:36460
MANSUR, L. C., Lattice vibrational spectra and physical characteristics of metals with cubic structure, 25:36319
MANTEIFEL, V. M., Early structural distrubances of nucleoproteins in radiosensitive and radioresistant cells exposed to ionizing radiation, 25:35206
MANZ, A., Hyperon bubble chamber HYBUC, 25:34972 (CONF-700623-(Vol.2), pp 640-6)
MAQUEDA, E., N--N interaction matrix elements from phase shifts and the Jost, 25:36853
MARCH, N. H., Interaction between point defects in metals, 25:36325
MARCHIDAN, Sofia, Polarographic reduction of niobium in hydrochloric acid-thiocyanate medium, 25:34526
MARENIN, Irene Renate, Ratio of ^{12}C/^{13}C and CN/C_2 in carbon stars 19 Psc and Y CVn, 25:35620
MAREST, G., Microstructure effect on hyperfine interactions in Yb--Ag, 25:36332
MARGARYAN, A. A., Radiation stability of BeF_2 glasses activated by fluorides of rare earth elements, 25:34621
MARGOLIN, H., Fracture toughness and microstructure in Ti--5.25Al--5.5V--0.9Fe--0.5Cu alloy, 25:35348
MARIK, Petr, Triple-crystal gamma scintillation spectrometer with a protective anticoincident scintillator, 25:34931
MARIN, P., Device for measuring the luminosity of Orsay storage ring, 25:36606 (LAL-1249)
MARINARO, M., Mass equation from tadpoles, 25:36425
MARINKOVIC, S., Electrical resistivity of graphite powder and its mixtures, 25:36334
MARKKANEN, E., Noise measurements in a subcritical facility based on photon detection, 25:37086
MARKS, Jnr, Thyroid ablation in young mice, 25:35084
MARKS, Robert E., Analysis of Marvel: nuclear shock-tube experiment, 25:34765
MARQUES DOS SANTOS, P., Three years statistics of simple 3 solar bursts, 25:35724
MARSDEN, R. S., RAFFLE Monte Carlo code and its use to obtain correlated estimates of collapsed cross sections, 25:36649 (CONF-710302-11)
MARSH, P. A., Corrosion of Ti--6Al--4V in HCl--methanol, 25:35287
MARSHALL, P. M., Coronal line profiles observed by means of coronagraphs and a Fabry--Perot spectrometer, 25:35775
MARTIN, D. L., Cobalt--nickel-metal--samarium permanent magnet alloys: process and properties, 25:36336
MARTIN, Dennis C., High frequency parameter techniques, 25:37169 (BDX-613-347)
MARTIN, G. D., Lead shielded Dewar development, 25:36152 (MATT-846)
MARTIN, J. A., Response of dosimeters to ^{60}Co and pulsed electron irradiations, 25:35034
MARTIN, W. R., Effect of boron on ductility and strength of Inconel 600 and Types 304 and 316 stainless steel at hot metalworking temperatures, 25:35338 (ORNL-TM-2216)
MARTINELLI, V., Seventh annual meteorological report of the Casaccia Center for Nuclear Studies, 1968, 25:34746 (RT/PROT-(70)42)
MARTINEZ, A. M., Laboratory for production of radioisotopes, 25:34816
MARTINEZ VIDAL, C. A., Some nuclear developments in Argentina, 25:35527
MARTINI MAURI, P., Possibilities and limitations of nuclear medicine in infant diagnostics, 25:35182
MARTINOLI, P., Nucleation field of a thin superconducting film on a thick normal layer, 25:36035
MARTYNOV, A. A., Alpha decay of spherical nuclei, 25:36747
MARY, Monique, Thermoluminescence induced in thick targets by 3 GeV protons, 25:36298
MASON, G. W., Extraction of selected metallic cations by highly hindered $(OC)_2PC(CH)$ extractant in two different diluents from aqueous chloride phase, 25:34706
MASON, W. M., Angular distributions from reaction ^{12}C(α,γ_0)^{16}O, 25:36675
MASOUD, M. M., Experimental studies on magnetically driven shock wave passing through a longitudinal magnetic field, 25:36117 (UARAEE-106)
Experimental studies on shock waves propagated through a longitudinal magnetic field in electrodeless discharge tubes, 25:36092 (UARAEE-101)
MASSALSKI, J., Monte Carlo simulation of nuclear-electromagnetic cascade developing in an ionization spectrometer, 25:36431 (ITJ-6)
MASSALSKI, Jerzy, Distributions and mean values of

XUM

inelasticity coefficient K/sub v⁰/ for lead and graphite, 25:36389 (ITJ-5)
Estimation of energy and mean inelasticity of nuclear interactions at energies above 3.10¹² eV, 25:36388 (ITJ-3)
MASSIN, J. P., Thyroid scintigraphy using /sup 99m/Tc and ¹³¹I, 25:35169
MASUDA, Kohzoh, Concentration profiles of room-temperature ion-implanted indium in silicon, 25:36282
Paramagnetic defects iduced in naphthalene and anthracene single crystals by neutron irradiation at low temperature, 25:36277
Radiation damage studies using the low temperature irradiation facility. VI, 25:36287
MATERA, Nicholas J., Environmental factors affecting the standing crop of foraminifera in sublittoral communities of a Long Island Salt Marsh, 25:37208 (NYO-3995-15)
MATOBA, Tohru, Motion and collision of plasma blobs produced by giant pulse laser in a transverse magnetic field, 25:36158
MATSEN, R. P., Destructive and nondestructive burnup data from natural UO_2 fuel, 25:37015 (BNWL-1568)
MATSKO, J., Calculation of the vapor pressure in desiccated-multicomponent systems, 25:37223 (SC-DR-710074)
MATSUDA, Tatsuo, Gamma-ray-induced polymerization of fluorine-containing pentadiene, 25:34633
MATSUSHITA, Teruo, Josephson junctions with superconducting barriers, 25:36064
MATSUURA, Nobuo, Production of Type 316 stainless steel cladding tubes for fast breeder reactor, 25:35305
MATSUURA, Oscar T., Three years statistics of simple 3 solar bursts, 25:35724
MATSUZAWA, Taiju, Cell population kinetics in acute intestinal radiation death, 25:35239
MATT, W., Hyperon bubble chamber HYBUC, 25:34972 (CONF-700623-(Vol.2), pp 640-6)
MATTHAEUS, Guenther, Charged particle accelerator, 25:36635
MATTHEWS, C. M. E., Ratio of ⁸¹Rb to /sup 81m/Kr incorporated in tissue, 25:35167
MATTHEWS, Lee D., Radiotracer and photoemission studies of CO chemisorbed on Mo(100), 25:35358
MATVEEV, V. A., Spin effects at high energy in quasipotential approach, 25:36504 (JINR-E2-5770)
MATVEEVA, N. M., Transition temperature in systems Zr--V and Zr--V--Nb, 25:36042
MAURER, W., Moessbauer isomer shifts and hyperfine splitting of 145.4 keV γ-rays of ¹⁴¹Pr, 25:36344
MAURO, K. D., New digitizing and memory system for wire spark chambers, 25:35016
MAURY, F., Damage production and recovery in low temperature irradiated zinc, 25:36288
MAVROMATIS, H. A., Volume, surface, and symmetry terms in semi-empirical mass formula, 25:36821
MAXIE, E. C., Irradiation of California fruits and vegetables, 25:35274
MAY, R., Welding problems connected with fabrication of moderator tank for Niederaichbach Nuclear Power Plant, 25:35322
MAZEAU, Jean, Excitation of n = 2 He levels by low-energy electrons, 25:35882
MAZZIO, Joann, Ion implantation: a selective bibliography, 25:36269 (SC-B-710148)
MAZZOLDI, P., Disorder in implanted semiconductors, 25:36300
MBIPOM, E. W., Equatorial ionospheric absorption at different longitudes, 25:35970
MCBRIDE, J. B., Theory of the beam cyclotron instability in plasmas, 25:36167
MCCARTHY, D., Use of radioactive Xe in evaluation of pulmonary functions, 25:35170
MCCARTHY, J. S., Inelastic electron scattering from several Ca, Ti, and Fe isotopes, 25:36695
MCCARTHY, S. L., Heat capacity and ac susceptibility of V_3Si, 25:36022
MCCLINTOCK, Jeffrey E., Detection of high-energy x-ray flare from source in Crux, 25:35691
Rapid fluctuations in high-energy x-ray flux from source in Crux, 25:35692
MCCLUNG, R. W., Nondestructive test development for nuclear reactor programs at ORNL, 25:34829
MCCLURE, J. L., High-speed (subsecond) measurement of heat capacity, electrical resistivity, and thermal radiation properties of tantalum in the range 1900 to 3200 K, 25:35477
MCCONE, Alan Ivins Jr., Density perturbation in a universe of collisionless particles, 25:35805
MCCONKEY, J. W., Polarization-free vacuum-ultraviolet excitation of helium by electrons, 25:35857
MCCOOK, George P., New photometric solution for TW Cassiopeiae, 25:35609
MCCORD, R. V., Prog. rpt. on high flux isotope reactor, 1--3/71, 25:37068 (ORNL-TM-3432)
MCCOY, H. E. Jr., Influence of titanium on the strengthening of a Ni--Mo--Cr alloy, 25:35391
MCCUNE, J. E., Loss-cone modes in inhomogeneous mirror machines, 25:36166 (UCRL-73135)
MCCURDY, David E., Thermoluminescent dosimeter for providing a total radiation measure of radioactivity in a fluid medium to which the dosimeter is exposed, 25:35035
MCDUFFEE, W. T., Molten-salt fluoride volatility pilot plant: recovery of enriched uranium from aluminum-clad fuel elements, 25:34693 (ORNL-4574)
MCELROY, W. N., Helium production in stainless steel and its constituents as related to LMFBR development programs, 25:35503 (HEDL-SA-193).
Neutron energy dependent cross section evaluation by a multiple foil activation method, 25:36741 (WHAN-SA-107)
MCENTIRE, R. W., Electron echo experiment, 25:35966
MCGEE, R. X., OH-line absorption at 1665 and 1667 MHz in the direction of the Omega Nebula, 25:35696
MCGUIRE, Eugene J., Calculated generalized oscillator strengths for atoms He--Na, 25:35844 (SC-RR-70-406)
MCHARRIS, Wm. C., Ge(Li)--Ge(Li) sum coincidence, 25:34932
N-shell conversion electrons from 2.33-keV transition in ²⁰⁵Pb, 25:36780
Neutron-deficient Gd isotopes. III, 25:36744
MCKEAGUE, R., Operational experience with the steam generating heavy water reactor, 25:36894
MCKEE, Christopher F., Effect of plasma instabilities in Colgate's cosmic-ray model, 25:35900
MCKEIGHEN, R. E., Electron-irradiation effects in silicon at liquid-helium temperatures using ac hopping conductivity, 25:36305
MCKEOWN, D., Re-heat cracking in high nickel alloy heat-affected zones, 25:35453
MCKINNON, N. A., Compressive creep of yttria rare earth stabilized zirconia storage heater refractories, 25:35555
MCKNIGHT, Ronald Hugh, Electron charge transfer processes by coincidence techniques, 25:35877
MCLEAN, D. J., Radioheliograph observations of harmonic Type-III solar bursts, 25:35738
MCLEAN, W. L., Proximity effect in gadolinium-backed lead films, 25:36036
MCMAHON, C. J. Jr., Microstructural aspects of fracture toughness in a cobalt-base superalloy, 25:35490
MCMILLAN, Bradford B., Sceptre users manual, 25:37251 (UCRL-20659)
MCNEESE, L. E., Engineering development studies for Molten-Salt Breeder Reactor Processing No. 3, 25:34694 (ORNL-TM-3138)
MCNELLES, L. A., K conversion coefficient of M3 transition in ¹⁹¹Os, 25:36804
MCPHERSON, D., Prog. rpt. on excitation and ionization of ions by electron impact, 9/70--5/71, 25:35833 (ORO-3027-19)
MEABURN, J., Fine structure of nebular emission lines, 25:35650
MEAD, William C., RAD swapping system for nuclear data acquisition, 25:35050 (FUC-937-396)
MEDVEDEV, S. A., Effects of impurities on properties of the Nb_3Sn phase, 25:36039
Plasmochemical method of synthesis of superconducting compounds with structure of A15 type, 25:36044
Superconductivity of niobium diselenide, 25:36041
MEEKINS, J. F., X rays from Coma cluster of galaxies, 25:35799
MEERT, A., Current flow of a condenser discharge of an electrodeless MHD motor, 25:36202
MEGAHID, R., Measurement of continuous fast neutron spectra by scintillation technique, 25:34920 (UARAEE-91)
Neutron transmission through ducts perpendicular to neutron beam axis in water shields, 25:36251 (UARAEE-86)
MEHNER, Juergen, Time-dependent neutron thermalization in a metal hydride moderator, 25:37132
MEHRA, A. L., Composite sphere in general relativity, 25:36583
MEIER, H., High-voltage electrophoretic separation of inorganic ions with special regard to Pt metals. III, 25:34702
MEISEL, M. N., Early structural distrubances of nucleoproteins in radiosensitive and radioresistant cells exposed to ionizing radiation, 25:35206
Early structural, ultrastructural, and functional disturbances in radiosensitive and radioresistant yeast cells under influence of ionizing radiation, 25:35247
MEISSNER, D., Electron irradiation experiments on Ta, 25:36273
MEKHEDOV, V. N., Relative yields of secondary [(p,xn)α] reactions on Bi in range E/sub p/ = 120-660 MeV, 25:36723 (JINR-P1-5530)
MELNICHENKO, A. K., Radiochemical peculiarities of granitoids of the Gissar pluton, 25:34734
MELTON, Charles E., Prog. rpt. on radiolysis of water in wide range radiolysis source, annual, 9/1/70--6/1/71, 25:34636 (CRC-3729-4)
MENDILLO, M., Simultaneous storm-time increases of ionospheric electron content and geomagnetic field in dusk sector, 25:35956
MENON, V. J., Pion phase shifts from backward pion--nucleon dispersion relations, 25:36520
MERCIEZ, W. Darrel, Permeation of halogenated solvents through Drybox gloves, 25:34605 (RFP-1608)
MERGELYAN, O. S., Field of a charged particle moving over a periodic dielectric structure, 25:36360
MERIADEC, B., Chemical consequences of (n,γ) reaction in K ferrocyanide, 25:34663

MERKUSHEV, G. N., Regeneration in liver after internal irradiation, 25:35221
MERMAGEN, H., Iron-59 uptake in bones of rats exposed to x irradiation, 25:35211
MERMAZ, M. C., Proton-pair correlation in Ti and Cr low-lying excited states, 25:36709
MERRILL, E. T., ALTHAEA: one-dimensional two-group diffusion code with an effective four-group burnup, 25:36862 (BNWL-462)
MERZ, E., Behavior of fission cesium in graphite-containing fuel elements, 25:35567
MERZ, M. D., Influence of grain size on the hardness of alpha plutonium, 25:35465
MERZON, G. I., Relativistic increase of ionization and sensitivity of nuclear emulsions, 25:34937 (CERN-Trans-71-9)
MESERVEY, R., Measurement of the surface inductance and penetration depth of superconducting aluminum, 25:36029
MESSING, A. W., Halide--halide exchange at asymmetric silicon. New evidence against a siliconium ion-pair mechanism, 25:34579
MESTVIRISHVILI, M. A., Constraints on growth power of the binary process amplitude, 25:36600
Vector dominance and decrease of differential cross section of lepton pair production at high energy and large scattering angles, 25:36429
METAG, V., Fission isomers in Cm and Bk isotopes, 25:36795
METHASIRI, Thamrong, High energy photofission cross sections of uranium and thorium, 25:36736 (THAI-AEC-35, pp 1-8)
METRA, S. K., Detecting radiation with a supercooled liquid, 25:35015
METTEIL, A., Problems posed by the operation of nuclear power stations, 25:36892
MEULEMAN, Johannes, Nuclear semiconductor detector and its manufacture, 25:34882
MEUREE, N., Influence of the adsorption of thiourea on electrode processes at the mercury electrode, 25:34560
MEYER, K., Reactor-physical and economical aspects of fuel burnup calculation, 25:37021
MEYERHOFF, R. W., Preparation and electrical resistivity of ultrahigh purity niobium, 25:35328
MEYN, D. A., Analysis of frequency and amplitude effects on corrosion fatigue crack propagation in Ti--8Al--1Mo--1V, 25:35279
MIAKI, Hiroshi, Effect of fractionated x irradiation on cells in tissue culture, 25:35242
MICHAIEL, M. L., Theory for assymetric array of cylindrical cavities inside a reactor core, 25:37117 (UARAEE-58)
MICHALAK, S., Effect of the optical parameters of the medium on the yield of transition radiation of non-relativistic particles, 25:36354 (JINR-P4-5734)
MICHEJDA, L., AFST model with $\pi\pi$ and πp phase shifts and Durr--Pilkuhn form: factors applied to the reaction $\pi^+ p \to p 3\pi^+ 2\pi^-$ at 8 GeV/c, 25:36503 (INR-P-1265)
MICHEL, F. Curtis, Solar-wind interaction with planetary atmospheres, 25:36011
MICHEL, Horst-Stephan, Improvements in and relating to the coupling out of pulses from nuclear radiation detectors, 25:34914
MICHEL, M. C., Plutonium-244: confirmation as an extinct radioactivity, 25:35594
MICHEL, W. L., Charge-equilibrium fractions and charge-exchange cross sections for fast ions in nitrogen and argon, 25:35866
MICIC, G. I., Effect of absorbed dose on the yields of radiolytic products in neutral aqueous solutions of oxalate ion and oxygen, 25:34644
MIDUCH, K., Attempts to apply radiography in the testing of the glass-reinforced polyester laminates, 25:34839
MIELCZAREK, S., Inelastic electron scattering from formaldehyde, 25:35883
MIHALISIN, J. R., Structural studies and properties of a new cast high strength corrosion resistant superalloy, 25:35400
MIHALOV, J. D., Flux content and form of the geomagnetic tail, 25:35991
MIHASHI, Yasuo, Sintering process for Ni--P alloy coated W, 25:35354
MIKHAILOV, B. P., Superconducting electrolytic films of niobium, 25:36056
MIKHAILOVSKII, A. B., Stability of a high-β plasma with a weak pressure gradient, 25:36176
MIKKELSEN, Joern, The neutron resonance reactions in thermal nuclear reactors determined by semi-analytic as well as numerical methods, 25:37115 (RISO-234)
MIKOSHIBA, Nobuo, Nonlinear electrical conductivity of superconducting films below the transition temperature, 25:36024
MIKULSKI, J., Separation of transition elements and actinides by means of anionite AV-17, 25:34695 (ORNL-tr-2397)
MILANOVIC, J., Penetration parameter for M1 conversion and E2 admixtures for 77 and 191 keV transitions in ^{197}Au, 25:36789
MILES, F. W., Molten-salt fluoride volatility pilot plant: recovery of enriched uranium from aluminum-clad fuel elements, 25:34693 (ORNL-4574)
MILEY, G. K., Interferometric observations with baseline of 127 kilometers. II, 25:35709
MILL, William B., Irradiation of early carcinoma of the larynx. Significance of tumor extent, 25:35188
MILLET, J., Fabrication and properties of lanthanide tungstates, 25:35529
MILLS, R. G., Lawson criteria, 25:36191 (MATT-844)
MILMAN, M., Chemical consequences of (n,γ) reaction in K ferrocyanide, 25:34663
MILNE, D. K., Supernova remnant near CX 5-1, 25:35684
MIMA, Kunioki, Theory of trapped particle instability. I, 25:36180
MINACHEV, Kh. M., Isotope exchange between molecular oxygen and synthetic zeolites, 25:34580
MINAMI, Masatsugu, Landau equations for a continuous medium and the Koba--Nielsen kernels in the generalized Veneziano formula, 25:36424
MINAMI, Shigeo, Duality, regge trajectories, and remarks on the Regge-pole model for π^0(eta) photoproduction, 25:36441
MINEL, Lee, Effect of C and O on rupture of polycrystalline Mo, 25:35409
Molybdenum decarburization by annealing at low oxygen pressures, 25:35309
MIR-KASIMOV, R. M., Representation for the relativistic scattering amplitude at high energies, 25:36601
MIRONOV, V. I., Experiments on acceleration of α-particles by collective method, 25:36615 (UCRL-Trans-1424)
MISEZHNIKOV, G. S., Observations of 3C 273 radio source at 8 mm with maser, 25:35686
MISHIMA, Yoshitsugu, Problems about fuel cladding materials, 25:37016 (CONF-700211-9)
MISHRA, R. S., Propagation and growth of weak discontinuities in magnetogasdynamics, 25:35944
MISHRA, S., Internal friction due to oxygen-substitutional impurity atom complexes in zirconium, 25:35404
MISRA, K. D., Effect of energy spectra on synchrotron radiation from the magnetosphere, 25:35976
Synchrotron radiation from electrons of various energy spectra, 25:36001
MISRA, S. P., Meson--baryon scattering in the quark model, 25:36518
MISRO, S. C., Experimental confirmation of an asymmetric Peierls barrier in the temperature dependence of yield stress in tantalum and tungsten, 25:35375
MISTRETTA, C., Neutral particle tagging facility for ANL 30'' bubble chamber, 25:34967 (CONF-700623-(Vol.2), pp 582-92)
MISUSTOVA, J., Role of hypothermy in the mechanism of radioprotective action of sodium fluoroacetate, 25:35163
MITCHELL, F. G., Irradiation of California fruits and vegetables, 25:35274
MITCHELL, John F., Radiation dosimeter, 25:35036
MITCHELL, M. D., Prog. rpt. on high temperature flat cables, 11/70, 25:37159 (EGX-613-161)
MITCHELL, T. E., Interstitial hardening and the Peierls stress in Tantalum, 25:35371
MITCHELL, Thomas G., Thyroid ablation in young mice, 25:35084
MITCHELL, Thomas P., Relativistic motion of a radiating point charge in a constant electromagnetic field, 25:36363
MITRA, A. N., Survey of resonance physics, 25:36516
MITRA, S., Anomalous pulse spectrum of a plastic scintillator at sea level, 25:35010
MITRA, Ved, Mass distribution of planets on particle accretion, 25:35832
MITRY, A. M., Heat transfer in annular reactor channels, 25:37008 (UARAEE-50)
New approach for calculations of nuclear fuel consumption in UA-RR-1 core, 25:37077 (UARAEE-63)
MITSELMAKHER, G. V., Shower efficiency of spark chambers, 25:35006 (JINR-P13-5810)
MITTAL, J. P., Light emission from the dissolution of gamma irradiated alkali halides in water, 25:34620
MITTER, H., K-mesic atoms and hypernuclei, 25:36535
MIYAKE, Masaya, Formation process of (W,Ti)C powder, 25:35537
Formation process of W carbide powder from W powder, 25:35536
Formation process of WC--TiC powder, 25:35531
MIYAMOTO, Shikao, Possible observation of the skew-symmetric tensor gauge field, 25:36571
MIYATA, Takamoto, Level structure of ^{143}Pr and ^{142}Nd, 25:36766
MIYAZONO, Shohachiro, Thermal stresses in annular disks, 25:34799
MIZER, D., Aging response of a Mg--8.7 percent Y alloy, 25:35487
MIZERA, E., Properties of stainless steel 1H18NST after aging in the power reactor temperature ranges. II, 25:35336 (INR-1255)
MLADENOV, G. M., Plasma effects in the interaction of intense electron beams with matter, 25:36157
MLADJENOVIC, M., Specific γ ray constant and γ spectrum of ^{182}Ta, 25:34815
MNATSAKANYAN, A. Kh., Relaxation and nonequilibrium radiation behind shock waves in air, 25:37232 (SC-T-713030)
MODIG, Hans G., Intracellular release of glutathione: a possible mechanism of action of radioprotective sulphydryl containing compounds, 25:35204
MODINE, F. A., Magnetic circular dichroism of bands

XUM

associated with the F+ center in SrO, 25:36291
MODROW, R. D., Optimized use of multipurpose fuel processing facilities at Idaho chemical processing plant, 25:34681 (CONF-710417-1)
MODZOLEVSKII, V. I., Tandem plasma acceleration in coaxial systems, 25:36204
MOEBERT, K., Program for determining environmental safety of nuclear power plants, 25:37049
MOECK, Edward Otto, Annular-dispersed two-phase flow and critical heat flux, 25:34797
MOEHRLE, G., Presently available methods for elimination of radioisotopes from the body and their practical application, 25:35134
MOELLER, P., Nuclear chemistry compendium. I, 25:34862 (HMI-B-108)
MOFFATT, J., Bubble density in liquid helium, 25:34989 (CONF-700623-(Vol.2), pp 893-900)
MOGAROVSKII, V. V., Radiochemical peculiarities of granitoids of the Gissar pluton, 25:34734
MOHAN, K., Homogeneous nonstatic solutions of Einstein--Maxwell field-equations for isotropic space--time, 25:36559
MOIR, A. T. B., Assay of ^{42}K in biological samples, 25:34540
MOISEEV, A. A., Cesium-137 content of human body, 25:35095
MOISEEV, I. G., Observations of 3C 273 radio source at 8 mm with maser, 25:35686
MOISEIWITSCH, B. L., Virial theorem for variational functions in collision theory, 25:35871
MOISSENKO, E. V., DNA role in cell initial radiation injury, 25:35197
MOIZHES, B. Ya., Effect of patchiness and increases in cathode emitting area on thermionic converter characteristics, 25:35931
Transition from distributed emission to a cathode spot in an arc, 25:36112
MOKLER, P. H., Energy shift of characteristic x rays induced in collisions between 15- to 60-MeV I ions and Mo, Yb, and Au targets, 25:35834
MOLDOVEANU, S., Determination of C nucleus radius by interaction with π^- at 7 GeV, 25:36408
MOLINARI, E., Equilibrium compositions and thermodynamic properties of mixed plasmas. II, 25:36104 (NP-18772)
MOLL, E., Measurement of bone density with ^{125}I-profile-scanner, 25:35171
MOLLIMARD, Daniel, Oxidation kinetics of niobium--titanium alloys, 25:35282
Oxidation of polycrystalline Nb samples, 25:35280
MOLNAR, J., Decay of ^{173}Ta, 25:36727 (JINR-P6-5704)
MOLODKIN, A. K., Interaction of certain compounds of thorium with dimethyl sulfoxide, 25:34565
MOMBELLI, L., Diagnosis of kidney function and structure by means of radioisotopes, 25:35184
MONCHKA, D., Electromagnetic separation of short-lived isotopes of Rn, Xe, and Kr for spectroscopic studies, 25:34806 (JINR-P13-5757)
MONDT, J. F., Thermionic reactor ion propulsion spacecraft for unmanned outer planet exploration, 25:35937
MONSIGNORI FOSSI, B. C., Soft x-ray emitting regions in the solar corona, 25:35721
MONTBRIAND, Leslie Edward J., Morphology of auroral hydrogen emissions during auroral substorms, 25:36005
MONTE, Jacqueline, Total cross sections for collisional detachment of one or two electrons from H^- on H_2O, 25:35867
MONTES, H., Phase-height fluctuations in the ionosphere between 130 and 250 km, 25:35977
MONTET, G. L., Threshold energy for the displacement of surface atoms in graphite, 25:35584
MOORE, F. H., Programs for the management and processing of neutron diffraction data, 25:36309 (AAEC/TM-578)
MOORE, Francis D., Prog. rpt. on study of transplantation of tissues and organs, 6/67--6/70, 25:37197 (NYO-2265-16)
MOORE, R. J., Analyticity, covariance, and unitarity in indefinite metric quantum field theories, 25:36563 (ORO-3992-26)
MOOS, W. S., IAEA dose comparison program, 25:35141
MOOY, J. H. M., Gas phase ESR spectra of ^{31}P, ^{75}As, ^{121}Sb, and ^{123}Sb, 25:36345
MORALES AMADO, A., Radioactive wastes of nuclear center in Mexico, 25:34733
MORDIKE, B. L., Asymmetry of slip in tantalum and tantalum alloys, 25:35381
Solid solution hardening of tantalum-base alloys, 25:35384
MORENO, G., Observation of solar wind heavy ions, 25:35725
MORGAN, R. E., Radical processes following γ irradiation of frozen concentrated matrices of heparin and dextran sulphate, 25:34651
MORGAN, Thomas J., Cross sections for destruction of excited H molecules in collisions with H_2 gas, 25:35874
MORGANSTERN, Kennard H., Radiation vulcanization, 25:34632
MORI, Shigeru, Thermal stability of a fusion reactor, 25:36178
MORIKAWA, T., Air conditioning in the nuclear power plant, 25:34788
MORIN, M., Respiratory contamination by actinides in solution, 25:35091
MORISHIMA, Hiroshige, Behavior and distribution of radioactive substances in coastal and estuarine waters, 25:34760
MORISHITA, Norikazu, K^+--K^0 mass difference and A_2 Regge pole, 25:36456
MORITA, K., Ion mass effect in dechanneling rate, 25:36285
MORITA, Kenji, Dechanneling of MeV protons from Ge, 25:36271
MOROZOV, A. I., Experimental study of a two-lens accelerator, 25:36115
MOROZUMI, Takashi, Influence of irradiation on corrosion, 25:35513
MORSY, S. M., Characteristics of collimator constructed for Inchass whole body monitor, 25:34871 (UARAEE-82)
MOSAKOWSKI, J. J., Prog. rpt. on high temperature flat cables, 11/70, 25:37159 (BDX-613-161)
MOSER, Z., Thermodynamic properties in Zn--In liquid solutions, 25:35442
MOSIER, H. David Jr., Allometry of body weight and tail length after head x-irradiation in rats, 25:35225
MOSIN, A. F., Antagonistic action of iodoacetate and ethanol on the recovery in yeast, 25:35251
MOSKVIN, A. I., Complex formation of Fu(IV) in sulfate solutions, 25:34563
MOSKVITIN, A. I., Behavior of foil specimens of NT-type alloys in external magnetic field, 25:36052
Processes of superconducting solenoid into state with normal conductivity, 25:36078
MOSS, C. E., Reaction $^{19}F(^3He,^6Li)^{16}O$ at 40 MeV, 25:36674
MOSTEPANENKO, V., Existence of atoms in n-dimensional space, 25:36362
MOSTOVOI, Yu. A., Measurements of angular correlation of neutron spin and antineutrino momentum in the decay of polarized neutrons, 25:36385 (IAE-1947)
MOTZ, H. T., Low-lying configurations in ^{210}Bi, 25:36787
MOTZ, J. W., Production of high-intensity K x-ray beams, 25:35842
MOULINIER, Peaceful use of nuclear fission, 25:34771
MOYLE, W. F., Prog. rpt. on conformal-coating, 2/71, 25:37163 (BDX-613-286)
MOZLEY, James M., Current status of brain scanning, 25:35177
MUBAYADZHYAN, M. A., Separation of Re from Mo and W by acetone extraction, 25:34525
MUCKENTHALER, F. J., ORNL-SNAP shielding program, 25:36250 (ORNL-TM-3364)
MUDD, R. D., Analysis of effect of potential reactor cooling ponds on Hanford groundwater system, 25:37103 (BNWL-1507)
Analysis of hydrological factors influencing Cable Mountain irrigation project, 25:34715 (BNWL-1502)
MUELLER, Erwin W., Field ion shadow projection microscope and other FIM techniques for viewing biomolecules, 25:37207 (NYO-3851-10)
MUELLER, H. J. W., Helicity conservation and duality, 25:36595
MUELLER, M. H., Neutron diffraction cryo-orienter, 25:36080
MUELLER, R. A., Inherent properties of the different primary circuits of sodium-cooled reactors, 25:37005 (KFK-1375)
MUENNICH, F., Half-life measurements of excited levels in ^{121}I and ^{123}I, 25:36752
MUGA, Marvin Luis, Improved charged particle detector, 25:34887
MUGHRABI, H., Dislocation arrangement of deformed Cu single crystals in the stress-applied state. I, 25:35520
Dislocation arrangement of deformed Cu single crystals in the stress-applied state. III, 25:35518
Dislocation arrangement of deformed Cu single crystals in the stress-applied state. II, 25:35519
MUKHEDKAR, A. J., Ir spectra and magnetic susceptibilities of uranyl complexes, 25:34612
MUKHERJEE, A. K., Experimental confirmation of an asymmetric Peierls barrier in the temperature dependence of yield stress in tantalum and tungsten, 25:35375
MUKHERJEE, S., Improvements in tests of long-range charge independence, 25:36522
MULAZZANI, Q. G., Study of oxidation and reduction of $Ru(NH_3)_5N_2^{2+}$ by γ- and electron pulse radiolysis, 25:34657
MUNRO, R. E. B., Observations at 408 MHz of radio sources. I, 25:35682
MUNTEANU, G., Determination of C nucleus radius by interaction with π^- at 7 GeV, 25:36408
MURAMATSU, Hiroshige, Gamma-ray-induced polymerization of fluorine-containing pentadiene, 25:34633
MURASHOVA, V. A., Search for elementary particles bearing a magnetic charge, 25:36375 (CERN-Trans-71-10)
MURFIN, Walter B., PANE: computer program for analysis of space frameworks, 25:37229 (SC-RR-70-742)
MURRAY, J. G., Floating ring stabilization system, 25:36188 (MATT-839)
MURTAZIN, I. A., Isotope effect for the diffusion of interstitial atoms, 25:34571 (ANL-Trans-882)
MURTHY, G. T., Search for high-energy gamma rays from pulsars, 25:35705
MURTHY, M. S. S., Shape and average energy of beta-particle spectra, 25:36841
MURTHY, P. V. Ramana, Search for high-energy gamma rays from pulsars, 25:35705
Search for tachyons in the cosmic radiation, 25:36378

MURTY, Korukonda Linga, High pressure--high temperature study of spin lattice relaxation in pure and doped LiBr single crystals, 25:37199 (NYO-2504-74)

MUSSA, G. C., Possibilities and limitations of nuclear medicine in infant diagnostics, 25:35182

MUSSET, P., Physics plans for Gargamelle, 25:34944 (CONF-700623-(Vol.1), pp 136-44)

MUSSETT, A. E., Simple programmer for an rf induction heater, with particular application to K--Ar dating, 25:34739

MUUSS, Harry, Fiducial lines in large bubble chambers produced by laser beams, 25:34995 (CONF-700623-(Vol.2), pp 984-96)

MYAE, E. A., Increase of effectiveness of synchronized capture during bunching of beam outside the separatrix, 25:36603 (IFVE-SKU-70-20)

MYALKOVSKII, V. M., Facilities at Kum-bel Mountain Station for study of high-energy interactions, 25:35013

Program for study of high-energy nuclear interactions of cosmic rays at Kum-bel Mountain Station, 25:36416

MYASNIK, M. N., Radiation induced damages to cells, 25:35260

MYERS, G. E., Threshold energy for the displacement of surface atoms in graphite, 25:35584

MYERS, M. L., Estimated capital costs of nuclear and fossil power plants, 25:37030 (ORNL-TM-3243)

MYNATT, F. R., ORNL-SNAP shielding program, 25:36250 (ORNL-TM-3364)

MYULLER, G., Reaction $\pi^- + \pi^0\pi^0 n$ at 447 MeV, 25:36405 (JINR-P1-5781)

MYZENKOVA, L. F., Specific residual electrical resistance in S reversible N transition aspects of wire forms from superconducting materials by the resistivity method, 25:36055

N

NADAI, J. P., ^{18}O study of the source of oxygen in the anodic oxidation of silicon and tantalum in some organic solvents, 25:35293

Study of the oxygen growth laws of anodic oxide films on aluminum and tantalum using nuclear microanalysis of ^{18}O and ^{18}C, 25:35294

NADZHAFKULEV, N. A., Arsenate method for a micro iodometric determination of scandium, 25:34508

NAEGELIN, R., Fuel manufacturing, Swiss aspects, 25:35313

NAGAI, Nobuyuki, Hydrogen absorption by zirconium alloy, 25:35283

NAGARAJ, Muppinalya, Massive scalar (meson) fields in geometrodynamics, 25:36582

NAGARAJAN, T., β decay and nuclear structure in A = 95 nuclei, 25:36772

Small-order deviations of ^{90}Y and ^{32}P, 25:36768

NAGASHIMA, Takashi, Spatially growing plasma waves and their nonlinear effects by beam modulation, 25:36227

NAGEL, D., State of development of nuclear power plants with pressurized-water reactors in capitalistic countries, 25:36984

NAGL, J., IAEA dose comparison program, 25:35141

NAGUIB, K., Numerical calculations of K/sub eff/ and neutron fluxes in 2 and 3-group approximations using IBM-1620 code, 25:37126 (UARAEE-89)

NAGY, L., Angular anisotropy of fission fragments in ternary fission of ^{235}U and ^{238}U, 25:36759

NAIDA, A. P., Collective oscillations in a synthetic plasma composed of positive and negative ion beams, 25:36220

NAIR, K. N., Morphology of geomagnetic field variations, 25:35990

NAIR, N. B., Slope sensitive alarm for use with fixed filter air monitors, 25:34909

NAKADA, Y., Cross slip in fcc alloys, 25:35386

NAKAGAWA, Masami, Dynamical structure of mass matrix of K^0--antiK^0 complex, 25:36466

NAKAGAWA, Masuo, Radiation damage studies using the low temperature irradiation facility. V, 25:36290

NAKAJIMA, F., Polarographic analysis of hexavalent uranium in uranium dioxide, 25:34501 (CEA-tr-X-667)

NAKAJIMA, Tetsuo, Isotopic volume effect in superconductors, 25:36060

NAKAMOTO, Shunsuke, Simplified fabrication of position sensitive detectors, 25:34896

NAKAMURA, Hisashi, Production of Type 316 stainless steel cladding tubes for fast breeder reactor, 25:35305

NAKANO, Tadao, Possible observation of the skew-symmetric tensor gauge field, 25:36571

NAKATA, Hirokatsu, Absolute power measurement by reactor noise analysis, 25:37114 (JAERI-Memo-4276)

NAMBA, Susumu, Paramagnetic defects iduced in naphthalene and anthracene single crystals by neutron irradiation at low temperature, 25:36277

NAMYSLOWSKI, J., AFST model with $\pi\pi$ and πp phase shifts and Durr--Pilkuhn form: factors applied to the reaction $\pi^+ p \to p 3\pi^+ 2\pi^-$ at 8 GeV/c, 25:36503 (INR-P-1265)

Low, intermediate, and high energies in Veneziano model for KN scattering, 25:36507

NANDI, B. C., Durgapur cosmic-ray spectrogram with two solid-iron magnets, 25:35918

Momentum spectrum and the charge ratio of vertical muons at sea level, 25:35919

Solid Fe magnets used in Durgapur cosmic ray spectrograph, 25:35012

NAQVI, A. H., Emission of deuterons in 24-GeV/c proton interactions with emulsion nuclei, 25:36402

NARANAN, S., Satellite experiments in x-ray astronomy, 25:35703

NARBUT, T. P., Superconducting point contact having properties of Josephson junction, 25:36070

NARDELLI, G., Disorder in implanted semiconductors, 25:36300

NARIAI, Hidekazu, Nonlinear effect of cosmic fluid in an expanding Universe. II, 25:35815

NASH, Douglas B., Potassium--uranium systematics of Apollo 11 and Apollo 12 lunar samples and of some deep earth rocks, 25:35830

NASIROV, R. A., Optical density of sarcosomes in animals following ionizing radiation, 25:35227

NASR, M., Numerical solution for the thermal flux spectrum in a monatomic moderator, 25:37120 (UARAEE-69)

Upward and downward scattering kernels for thermal neutrons, 25:37123 (UARAEE-80)

NASSAR, S. F., RAP-1, multigroup neutron diffusion code for IBM-1130, 25:36651 (UARAEE-107)

SAVE: two group code for reflector savings of completely reflected cylindrical reactor, 25:37128 (UARAEE-96)

NATH, G., Rayleigh problem in slip flow with transverse magnetic field, 25:35950

NATH, M., Anomalous pulse spectrum of a plastic scintillator at sea level, 25:35010

NATHAN, R. D., Polarization of H/sub α/ line produced in $He^+ + H_2$ collisions, 25:35862

NATHER, R. Edward, Observations of rapid blue variables. I, 25:35674

Observations of rapid blue variables. II, 25:35675

NAUENBERG, Uriel, Bubble chamber detection technique for gamma rays in momentum region below 1 GeV/c, 25:34964 (CONF-700623-(Vol.1), pp 555-66)

NAUMESCU, Adriana, Colorimetric determination of Ce^{++} by o-aminophenol, 25:34530

NAVALIKHIN, L. V., Anticoincidence gamma spectrometer with shielded scintillator, 25:34928

NAY, J. A., Process instrumentation for Westinghouse nuclear steam supply systems (4 loop plants), 25:37010 (WCAP-7671)

NAYAK, U. P., Effects of burnup on fuel pin thermal performance, 25:37017 (CONF-710414-1)

NECHAEV, Yu. A., Solubility of oxygen in hafnium nitride, 25:35566

NEGRI, P., Projector for Gargamelle's pictures, 25:34961 (CONF-700623-(Vol.1), pp 334-44)

NEILL, J. M., Fast reactor spectrum measurements. Technical summary report, February 1, 1970--January 31, 1971, 25:36991 (GULF-RT-10523)

NEKRASOV, K. G., Shower efficiency of spark chambers, 25:35006 (JINR-F13-5810)

NELSON, R. D., Influence of grain size on the hardness of alpha plutonium, 25:35465

NELSON, R. L., Engineering the baseball magnet system, 25:36200 (UCRL-73067)

NEMCHINSKII, V. A., Numerical solution of the quasi-linear equations for a beam--plasma system, 25:36142

NEMES, M., Nomograms for calculating optical parameters of weak magnetic quadrupolar lens systems, 25:36630

NEMETH, G., Importance of using exact forms for scattering amplitude in Regge pole theory, 25:36531

NEMETS, O. F., Mechanisms for 13.6-MeV deuteron disintegration by nuclei, 25:36713

NEMSMANN, U., Dosimetry of a gamma flash, 25:34892

NENADOVIC, M. T., Effect of absorbed dose on the yields of radiolytic products in neutral aqueous solutions of oxalate ion and oxygen, 25:34644

NENOT, J. C., Respiratory contamination by actinides in solution, 25:35091

NENOV, N., Decay of ^{173}Ta, 25:36727 (JINR-P6-5704)

NEPLYUEV, V. M., Elastic and inelastic scattering of deuterons by nuclei, 25:36848

NERSESOV, E. A., Isospin conservation and β decay of heavy nuclei, 25:36833

NESMEYANOV, An. N., Consequencies of β-decay of ^{129}Te in some Te oxide compounds, 25:34674

Study of kinetics of benzoic acid extraction with toluene by isotopic exchange method, 25:34584

NESTERENKO, V. V., Functional integration and Regge-eikonal representation of scattering amplitude, 25:36587 (JINR-P2-5768)

NESTOROV, G., Solar radiation in connection with geomagnetic disturbances in Sept. 1969, 25:36008

NEUHAUSER, J., Mirror instabilities in Ioar I theta pinch, 25:36182

NEVOLIN, V. K., Effect of argon on thermionic converter operation at low cesium pressures, 25:35930

NEVOLIN, V. N., Measurement of isotopic abundances by time-of-flight mass spectrometer, 25:35070

NEWKIRK, J. B., Equilibrium and precipitation effects in Co-rich alloys of the Co--Cr--W system, 25:35485

NEWKIRK, L. R., APW calculation of energy bands in simple cubic tellurium, 25:37175 (CALT-822-29)

NEWMEYER, J. L., Model for the production of particles with superstrong interactions, 25:36530

NEWPORT, R. W., Refractive indices of neon and neon--hydrogen mixtures, 25:34963 (CONF-700623-(Vol.1), pp 543-54)

XUM

NGUYGEN VAN GIAI, Coulomb energy differences in mirror nuclei in Hartree--Fock approximation, 25:36712
NICHOLS, J. P., Oak Ridge systems analysis code (ORSAC) User's manual, 25:36886 (ORNL-TM-3223)
NICOLIS, J. S., Group velocity of high amplitude surface waves in vacuum-plasma interfaces, 25:36214 (DEMO-71/5)
Relativistic doppler effect and group velocity in homogeneous nonlinear and inhomogeneous plasma, 25:36215 (DEMO-71/6)
NIEF, G., Absolute isotopic scale for deuterium analysis of natural waters, 25:34518
NIFONTOVA, N. V., Use of N-furoylphenyl hydroxylamine for amperometric titration of Zr, 25:34535
NIGHTINGALE, R. W., Search for 72.5s /sup 30m/Al, 25:36715
NIHEI, Isao, Corrosion induced by liquid sodium, 25:35281
NIKITIN, L. Ya., Changes in structure and properties in γ-irradiated crystallizable chloroprene rubber, 25:35590
NIKLAS, A., Formation of bands of additional absorption in ruby crystals due to x radiation, 25:36308
NIKLAS, K., Training and continuous education in the radiation protection field for medicine, 25:35147
NIKOLAEV, V. A., Fission products from spontaneous fission of ^{238}Pu, 25:36782
NILUBOL, M. L. Anong, Soil analysis by neutron activation method, 25:34545 (THAI.-AEC-36)
NINKOVIC, M., Specific γ ray constant and γ spectrum of ^{182}Ta, 25:34815
NISHIDA, A., New polar magnetic disturbances, 25:36012
NISHIGAKI, Minoru, Anomalies in the tensile properties at elevated temperatures of metastable beta titanium alloys, 25:35434
NISHIKAWA, Kyoji, Theory of trapped particle instability. I, 25:36180
NISHINO, O., Sliding pulser for rapid testing of integral linearity, 25:35066
NISHIO, Y., Welding of tantalum and newly developed tantalum-clad steel, 25:35356
NOBLE, B., Formation of stacking faults in magnesium--thorium alloys, 25:35484
NOBLE, J. V., Giant monopole state, 25:36845
NOBUKI, Minoru, Influence of high hydrostatic pressure on the flow stress of zinc and zirconium polycrystals, 25:35435
NOCI, Giancarlo, Radio model of the transition layer in solar active regions, 25:35720
NOE, M., Self-radiation effect on lattice parameter of $^{244}CmC_2$, 25:35589
NOEL, Robert, Nuclear reactor element and its use in a reactor, 25:37148
NOFAL, E. E., Instruments for measurement of the spectral lines profile and shift, 25:36091 (UARAEE-95)
NOGAMI, Y., Nucleon--nucleon correlation and two-pion-exchange three-body force in n force in nuclear matter, 25:36831
NOHARA, Ishimatsu, Radiographic examination of welded T-joint, 25:34840
NOLLE, A. W., Nuclear spin--lattice relaxation and dynamic polarization in γ-irradiated LiF, 25:36348
NOR-AREVYAN, N. G., Some reactions of the organisms to radiation in different oxygen pressures, 25:35118
NORDEMANN, Daniel, Thermoluminescence induced in thick targets by 3 GeV protons, 25:36298
NORDSIECK, Kenneth H., Further comment on the dust-radiation instability in ionized nebulae, 25:35688
NORMAN, Kenneth George, Improvements in or relating to apparatus for determining the direction of a nuclear explosion, 25:35058
NORSEEV, Yu. V., Determination of the boiling point of some isoalkyl astatides by using a glass gas chromatograph, 25:34604 (JINR-P6-5683)
NOSKOV, D. A., Explosion-like processes during impulsed treatment of materials by electron beams, 25:35515
NOSYREVA, I. A., Oscillations in a low-pressure Penning discharge, 25:36242
NOTSU, Shuzo, Radiation damage studies using the low temperature irradiation facility. II, 25:36286
NOVAK, D. L., Corrosion behavior of aluminum--boron composites in aqueous chloride solutions, 25:35521
Mechanical properties of TiC--VC alloys, 25:35558
NOVAK, Josef, Transverse oscillation of ribbed rods with a helical pitch, 25:36982
NOVAK, L., Influence of Na fluoracetate on shift of LD 50/30 value, 25:35162
Role of hypothermy in the mechanism of radioprotective action of sodium fluoroacetate, 25:35163
NOVAKOVA, J., Isotopic exchange of gaseous deuterium with lattice hydrogen of hydrides, 25:34582
NOVAKOVIC, L., Inelastic scattering of neutrons by hydrogen-bonded ferroelectrics, 25:36668
NOVIKOV, A., Calculation of neutron pulse shape, transmission function and resolution function in mechanical time-of-flight spectrometer, 25:34919 (UARAEE-61)
Effect of the probe tube on the thermal neutrons space-energy distribution, 25:37137 (UARAEE-75)
Energy-dependent Milne problem, 25:36650 (UARAEE-60)
General review of thermal neutron spectra investigations, 25:37118 (UARAEE-62)
One-group considerations of Milne problem, 25:37116 (UARAEE-56)
NOVIKOV, V. G., Experiments on acceleration of α-particles by collective method, 25:36615 (UCRL-Trans-1434)
NOVITSKAYA, M. A., Effect of donor irradiation on appearance of nonselective markers, 25:35126
NOVOTNY, J., Must it really be E = 0, 25:36581
NOWICKA-JANKOWSKA, Teresa, Indirect colorimetric determination of europium in samarium and other rare-earth oxides, 25:34507
NOYES, Richard M., Prog. rpt. on diffusion controlled reactions and exchange reactions in solution, annual, 6/71, 25:34573 (RLO-2230-T-2-2)
NURUSHEV, S. B., Hodoscope based on small photoelectron multipliers, FEU-85, 25:34864 (IFVE-SEF-70-17)

O

OATES, Daniel E., Measurement of helium--helium scattering cross section at low temperatures, 25:35860
OBERHAUSEN, E., Radiation burdens in incorporation of radioisotopes, 25:35099
OBLAK, J. M., Relationship of microstructure to workability in a high strength nickel-base superalloy, 25:35600
O'BRIEN, K., Cosmic-ray propagation in the atmosphere, 25:35925
O'BRIEN, P., K conversion coefficient of M3 transition in ^{191}Os, 25:36804
OBU, M., Measurement of central fission ratios and fission rate distributions in FCA, 25:37066 (JAERI-Memo-4286)
OCHKUR, A. P., Geometric inversion and its utilization in x-radiometric and gamma--gamma method, 25:34904
O'CONNELL, R. F., Origin of magnetic fields in white dwarfs and neutron stars, 25:35621
OESTGAARD, E., Liquid ^3He. I, 25:36016
OFFUTT, G. F., Optimized use of multipurpose fuel processing facilities at Idaho chemical processing plant, 25:34681 (CONF-710417-1)
OGAWA, M., Metabolic changes in tissues prepared from irradiated sweet potato roots with regard to ethylene effects, 25:35105
OGAWA, T., Ionization redistribution effect of wind in nighttime ionosphere, 25:35986
OGIR, M. B., Forms of motions in the chromospheric flares, 25:35747
OGUCHI, Atsushi, Influence of high hydrostatic pressure on the flow stress of zinc and zirconium polycrystals, 25:35435
OGURA, Joseph H., Irradiation of early carcinoma of the larynx. Significance of tumor extent, 25:35188
OGUSHI, Tetsuya, Flux flow as function of film thickness in Type-I superconductors, 25:36058
OHANZHANYAN, E. E., Effect of radiation on the reproduction of cells of hemopoietic organs in various species of laboratory animals according to their radio-sensitivity, 25:35217
OHKUBO, K., Electron cyclotron wave and electrostatic wave in bounded plasmas, 25:36241
OHLSSON, Harriet, EC and E0+M1+E2 transitions of ^{178}Hf, 25:36760
OHMASA, Masaaki, Survey of film developers adapted for x-ray intensity measurements, 25:37234 (SC-T-713035)
OHR, S. M., Radiation hardening and radiation-anneal hardening in body-centered cubic metals, 25:35607
OHTA, Mitsuru, Thermal stability of a fusion reactor, 25:36178
OHTSUKI, Kozo, Chemical and enzymatic properties of γ-irradiated subtilisin BPN, 25:35109
Kinetic and chemical properties of γ-irradiated subtilisin BPN, 25:35110
OKA, T., Welding of tantalum and newly developed tantalum-clad steel, 25:35356
OKABAYASHI, Takao, Gauge fields in the nonlinear realization of a group on its subgroup, 25:36658
OKADA, Moritami, Radiation damage studies using the low temperature irradiation facility. V, 25:36290
OKEL, J. G. R., Interpretation of alkali--inert-gas beam scattering with Buckingham--Corner potential, 25:35666
OKSMAN, J., Proposed annual and sunspot cycle variation of the plasmasphere, 25:35968
OKUDA, M., Reappearance of multiple midlatitude auroral arc, 25:35969
OKUDA, Shigeo, Electrical resistivity measurements of deformed metals after low-temperature neutron irradiation, 25:35501
OKUMURA, Ko, Regulation of hemocytotropic antibody formation in the rat. II. Effect of x-irradiation, 25:35112
OKUMURA, Yutaka, Cell population kinetics in acute intestinal radiation death, 25:35239
OLD, T., Reappearance of multiple midlatitude auroral arc, 25:35969
OLDENDORF, William H., Clinical applications of brain blood flow studies, 25:35178
OLDHAM, G., Gamma-radiation damage of organic scintillation materials, 25:35079
OLES, A., Tables of magnetic structures determined by neutron diffraction. III, 25:36311 (NP-18845)
OLESON, J. K., Storm-time variations in high-latitude fluxes of low-energy electrons, 25:35959
OLIVE, D. I., Operator vertices and propagators in dual theories, 25:36475
OLIVER, Young Pinckney, Total loss cross sections for D_2

molecules passing through H_2 gas, 25:35855 (UCRL-20099)
OLLERHEAD, R. W., Spin--parity combinations in ^{22}Ne, 25:36698
OLSEN, E. H., Variability of A and F main sequence stars, 25:35651
OLSEN, H., Electromagnetic interactions of particles with spin. I, 25:36450
OLSEN, R. J., Measurement of particle--matrix interface strength in TD-nickel, 25:35458
OLSHEVSKAYA, O. P., Effect of irradiation conditions on the recovery of somatic cells in mammalian organism, 25:35218
OMAE, T., Welding of tantalum and newly developed tantalum-clad steel, 25:35356
O'MARA, Robert E., Current status of brain scanning, 25:35177
O'NEILL, M. E., Source parameters of Salmon and Sterling nuclear explosions, 25:34764
ONO, K., Strain hardening equations and uniform strain, 25:37245 (UCLA-34-P-177-5)
ONODERA, Yutaka, Superconducting transition temperatures of rf-sputtered NbN films, 25:36065
ONSTOTT, E. I., Desalination and ion separation of sodium and potassium by bromine redox electrolysis, 25:34691 (LA-4645)
OPALENKO, A. A., Nuclear gamma resonance, 25:36343
OPHEL, T. R., Gamma ray analysis programs, 25:34915 (ANU-P-438)
ORBACH, R., Anisotropic behavior of dilute magnesium--gadolinium alloys, 25:36342
OREHOTSKY, R. S., Response of dosimeters to ^{60}Co and pulsed electron irradiations, 25:35034
ORENS, J. H., Theory of the beam cyclotron instability in plasmas, 25:36167
ORESHAK, O. N., Electron energy distribution in the positive column of a helium discharge, 25:36119
ORESHKINA, A. A., High-temperature thermomechanical treatment of magnesium--zinc--zirconium alloys, 25:35456
ORLENKO, N. I., One-group method for calculating dose fields from sources of γ-radiation with complex spectrum, 25:36255
ORMROD, J. H., Charge-equilibrium fractions and charge-exchange cross sections for fast ions in nitrogen and argon, 25:35866
ORTMAYER, Rudolf Max, Considerations of the costs for the manufacture of fuel elements with oxide fuel for power reactors, 25:37022
OSANOV, D. P., Distribution of ^{239}Pu in intact skin in its surface contamination, 25:35092
OSHIDA, Kenzo, Aging in Hiroshima and Nagasaki atomic bomb survivors, 25:35241
OSHIDA, Soichi, Pressure effect on the magnetic properties of superconducting La and La--Ce, 25:36021
OSIPOV, B. S., Reduction of hexavalent uranium with hydrogen sulfide in aqueous solution at high temperatures and pressures, 25:34569
OSTER, G. K., Role of $CHCl_3$ as a quencher for γ- and uv-excited organic solutions, 25:34624
OSTROWSKI, A., Pulse channel for reactor startup measurements type ILRT-1 and ILRT-2, 25:37146
OSYPOWSKI, Edward Thomas, Ward-identity techniques and low-energy pion--nucleon scattering, 25:36513
OTA, Kunio, Production of Type 316 stainless steel cladding tubes for fast breeder reactor, 25:35305
OTANI, Shitoshi, Anomalies in the tensile properties at elevated temperatures of metastable beta titanium alloys, 25:35434
OTOKOZAWA, Jun, Infinite-component wave equation and scattering amplitude, 25:36557
OTOPAL, P., Effect of radiation on the mechanical properties of concrete, 25:37007 (ORNL-tr-2470)
OTROSCHENKO, G. A., Fission of U, Np, Pu, and Am isotopes excited in (d,p) reaction, 25:36746
OTTE, V. A., Nucleon--nucleon quasi-free scattering in the p + d + p + p + n reaction at low bombarding energies, 25:36669
OVCHARENKO, C. N., Effects of heat treatment on the superconducting properties of Nb--Ta alloys, 25:36084
OVERSBY, J. P., Electron spin resonance studies of fundamental processes in radiation- and photo-chemistry. VI, 25:34641
OVERSBY, V. M., Isotopic composition of lead in volcanic rocks, 25:34740
OVSEPYAN, E. N., Extraction of U(VI)--benzoic acid anion complex by some thiazine dyestuffs, 25:34534
Investigation of reaction of acid complexes of U(VI) with basic dyes: methyl green, 25:34509
New reagents for the extraction--photometric determination of tantalum, 25:34506
Peculiarities of the extractive-photometric determination of tantalum by basic dyestuffs, 25:34533
OVSYANNIKOV, V. M., Features of a double-beam accelerating structure, 25:36623
OWCZARSKI, W. A., Relationship of microstructure to workability in a high strength nickel-base superalloy, 25:35500
OYAMADE, Rokuro, JFM: code for JMTR fuel accountability, 25:37065 (JAERI-Memo-4270)
OYANAGI, Yoshio, Veneziano amplitudes for first-excited scalars, 25:36592
OZERNOI, L. M., Magnetic field of a rotating cloud and magneto-rotational explosions, 25:35819
OZEROV, Yu. V., Observation of γ quanta greater than 100 MeV from 3C 120, 25:35700

P

PAAL, G., Global structure of Universe and distribution of quasi-stellar objects, 25:35810
PAAR, V., Diagrammatic method of particle-vibration coupling model. I, 25:36829
PABBI, S. D., Charge composition of cosmic-ray nuclei of elements from Ne to Ni, 25:35910
PACZULA, B., Investigations of solidification front and the depth of the liquid phase in concast billets by the technique of radioactive traces, 25:34820
PADALKA, V. G., Ion energy spectra and lifetimes in a multipole magnetic trap, 25:36085
Plasma transport in a magnetic quadrupole field, 25:36086
PAGE, D. E., Electron energy distribution within a curved channel multiplier, 25:34905
PAGET, T. M., Grazing-incidence spectra of Ne VII and Ne VIII, 25:35766
PAIK, N. C., Status report on evaluation of sodium cross sections for ENDF/B, 25:36693 (WARI-4181-2)
PAIS, A., Weak interactions at high energies, 25:36471
PAJANNE, E., Improved relativistic corrections to Fermi-contact hyperfine Hamiltonian, 25:36355 (NP-18818)
PAKHOMOV, V. I., Axially symmetric waves in vacuum channel in plasma, 25:36218 (UARAEE-92)
Boundary conditions in the case of adjacent plasma streams, 25:36128 (UARAEE-78)
Electromagnetic surface waves in adjacent plasma flows, 25:36219 (UARAEE-97)
PAKHOMOV, V. Ya., Effects of heat treatment on the superconducting properties of Nb--Ta alloys, 25:36084
PAL, B. K., Chemical detection of zirconium and hafnium, 25:34519
PAL, Yash, What is new in cosmic rays, 25:35904
PALME, Ch., Deformation anisotropy and texture of molybdenum, 25:35411
PALMER, H. P., Interferometric observations with baseline of 127 kilometers. II, 25:35709
PALMER, Patrick, Radio recombination line in NGC 7027, 25:35642
PALMER, Paul E., Properties, preparation, and handling of pure rare earth metals, 25:35297
PALOMO, Luz Corretjer, Legal standards for navigation of nuclear ships, 25:37096
PANASENKOV, A. A., Fast hydrogen atom injector, 25:36186 (CTC-746)
Injector for fast hydrogen atoms. I, 25:35827
PANCHENKOV, G. M., Dehydration of isopropyl alcohol on aluminum oxide irradiated by ^{60}Co gamma rays, 25:34629
Effect of preliminary irradiation on catalyst activity in decomposition of hydrogen peroxide, 25:34620
Effect of the diluent on the partition coefficient and the single-stage separation factor in the extraction of rubidium and cesium salts by phenol, 25:34701
Investigation of radiation-thermal cracking of n-tetracosane and n-heneicosane in the liquid phase, 25:34653
Radiation-catalytic dehydrogenation of cyclohexane on Al--Co--Mo catalyst, 25:34628
PANDIT, L. K., Effective-dipole form-factors for K/sub 13/-decay, 25:36459
PANKOVETS, N. G., Explosion-like processes during impulsed treatment of materials by electron beams, 25:35515
PANKRATOV, A. K., Cosmic-ray diurnal variation for periods of 1962 and 1964--1965, 25:35901
PANOFSKY, Wolfgang K. H., Structure of the proton and the neutron, 25:36445
PANSCH, E., Photoelectric observations of lunar occultations, 25:35655
PANTYUSHINA, N. N., Regulation of composition of 11-OCS by liver of dogs irradiated with gamma rays, 25:35222
PAPAGIANNIS, M. D., Simultaneous storm-time increases of ionospheric electron content and geomagnetic field in dusk sector, 25:35956
PAPALIOLIOS, Costas, Optical time-of-arrival measurements from Crab pulsar, 25:35695
PAPINEAU, A., Proton-pair correlation in Ti and Cr low-lying excited states, 25:36709
PAPOUSEK, D., FG matrix treatment of normal vibrations in ethylene-like and nitromethane-like molecules, 25:34581
PAPOYAN, S. A., Effect of radiation on the reproduction of cells of hemopoietic organs in various species of laboratory animals according to their radio-sensitivity, 25:35217
PARFENOV, L. B., Method of measuring the polarization of an oriented hydrogen target, 25:36645
PARIBOK, V. P., Radiosensitivity of cell repair systems, 25:35246
PARISI, G., e^+e^- annihilation into hadrons in preasymptotic region and $\mu^+\mu^-$ production in proton collisions, 25:36434 (LNF-71/5)
PARISI, J., Experimental conditions for $\gamma\gamma$ collisions with almost real photons, 25:36451

PARK, J. Y., Midstream evaluation, A = 89, 25:36714
PARK, Robert Turner, Veneziano partial-wave amplitude in complex s plane, 25:36487
PARK, Y., Vacuum vector of the Yukawa$_2$ model, 25:36572
PARKHOMCHUCK, V. V., Spark counter with large area, 25:35019
PARKINS, W. E., Prospects and economy of liquid-metal MHD--steam binary power plants, 25:35934
PARKS, James Edgar, Ionization of noble gases by protons, 25:35888
PARRA M, E., Laboratory for production of radioisotopes, 25:34816
PARSONS, N. R., Television imaging of fast auroral waves, 25:35965
PASHCHENKO, V. P., Ion-acoustic oscillations and transport processes in a low-temperature cesium plasma, 25:36231
PASHKOV, P. T., Increase of effectiveness of synchronized capture during bunching of beam outside the separatrix, 25:36603 (IFVE-SKU-70-20)
PASOTTI, G., Technical--economic information on superconductors and conductors for high field magnets, 25:36607 (LNF-70/19)
PASTRE, Albert, Maintenance program for Babyline-20 dose rate meters manufactured by NARDEUX, 25:35025 (CEA-N-1435)
PATEL, K. C., Variation in lipase activities during germination (in dark) of γ-irradiated castor-seeds, 25:35253
PATEL, R. D., Variation in lipase activities during germination (in dark) of γ-irradiated castor-seeds, 25:35253
PATIN, Yves, Study of the ^{153}Sm + ^{153}Eu decay, 25:36731 (NP-18835)
PATON, N. E., Deformation of body-centered-cubic titanium--vanadium single crystals, 25:35377
PATTEE, P. A., Mutants of Staphylococcus aureus with increased sensitivity to ultraviolet radiation, 25:35270
PAULEVE, J., Development of order of 50--50 Fe--Ni alloy irradiated by neutrons, 25:36281
PEARLSTEIN, L. D., Loss-cone modes in inhomogeneous mirror machines, 25:36166 (UCRL-73135)
PECHIN, W. H., Statistical technique for determining sources of variation in $(U,Pu)O_2$ oxygen-to-metal ratio, 25:35568 (ORNL-TM-3362)
PEDERSEN, J., Fission of U, Np, Pu, and Am isotopes excited in (d,p) reaction, 25:36746
PEDLAR, A., Search for interstellar H_2CS, 25:35708
Stark broadening in high-quantum-number recombination lines of hydrogen, 25:35711
PEEL, T. D., Bubble density in liquid helium, 25:34989 (CONF-700623-(Vol.2), pp 893-900)
PEELLE, R. W., Spectrum of photons emitted in coincidence with fission of ^{235}U by thermal neutrons, 25:36742
PEGEL, C., Thermoelectric cooling in scattering chamber 800 of Hamburg isochronous cyclotron, 25:36634
PEGEL, V. A., Functional state of endocrine glands in rats irradiated on 25 MeV betatron, 25:35164
PEKARSKII, G. Sh., Application of fast neutrons in radiation defectoscopy, 25:34825
PELEPETS, D. T., New approach for calculations of nuclear fuel consumption in UA-RR-1 core, 25:37077 (UARAEE-63)
PELLIONISZ, P., Double-statistical chopper for elimination of inelastic scattered neutrons in time-of-flight experiments, 25:34929
PELOVITZ, M., Floating ring stabilization system, 25:36188 (MATT-839)
PENGRA, J. G., M/L orbital-electron-capture ratio in ^{71}Ge decay, 25:36704
PENNA FRANCA, Eduardo, Determination of ^{210}Po in cigarettes and tobacco, 25:34515
PENNINGTON, M. R., Zeros in ππ amplitudes, 25:36498
PEPPARD, D. F., Extraction of selected metallic cations by highly hindered $(RO)_2PO(OH)$ extractant in two different diluents from aqueous chloride phase, 25:34706
PERDANG, J., Secular stability. I, 25:35652
PEREL, V. I., Oscillations of the total cross sections for inelastic processes in atomic collisions, 25:35876
PEREZ, Carlos A., Irradiation of early carcinoma of the larynx. Significance of tumor extent, 25:35188
PEREZ, R., Radioactive contamination of atmosphere around Valencia measured from January 1966 till April 1968, 25:35132
PEREZ, S. M., Excitation of analogue-dipole states, 25:36835
PEREZ BELLES, Rafael, Recent advances in the theory of nuclear fission, 25:36827
PERILLI, Maria L., Uranium in the world at the end of 1970, 25:34757
PERIN, A., Studies on the anti-tumour activity of aliphatic aldehydes. IV, 25:35159
PERKINS, D., Neutrino physics in heavy liquid chambers, 25:34943 (CONF-700623-(Vol.1), pp 123-35)
PERKINS, R. W., Sampler for concentrating radionuclides from natural waters, 25:34704
PERKOWSKI, Edward, Effect of ionizing radiation on the stability of some radiopaque iodine compounds, 25:34662
PERREAULT, P. D., Results from meridian chain of observatories in Alaskan sector. I, 25:35961
PERRIN, Christian, Oxidation kinetics of niobium--titanium alloys, 25:35282
Structure modifications of Nb--Ti alloy during its oxidation, 25:35482
PERRY, Charles L., Photometric studies of northern galactic clusters. I, 25:35606
PERSSON, N.-O., CCLIBRI: computer code for subchannel analysis, 25:37003 (CONF-710317-1)
PESTOV, Yu. N., Spark counter with large area, 25:35019
PETCHER, T. J., Crystal structure of protactinium tetrabromide, 25:34610
PETERS, B., Aging response of a Mg--8.7 percent Y alloy, 25:35487
PETERSEN, Henning D., Four-inch hydrogen target for 40-inch SLAC bubble chamber, 25:34965 (CONF-700623-(Vol.1), pp 567-80)
PETERSON, Alan W., Twilight flash of sodium, 25:35971
PETERSON, Sigfred, Thorium ceramics data manual. Volume III. Carbides, 25:35548 (ORNL-4503(Vol.3))
PETKAU, A., Radiation effects with a model lipid membrane, 25:34625
PETREANU, E., ^{18}O study of the source of oxygen in the anodic oxidation of silicon and tantalum in some organic solvents, 25:35293
PETROFF, P., Device for measuring the luminosity of Orsay storage ring, 25:36606 (LAL-1249)
PETROSYAN, A. A., Extraction of U(VI)--benzoic acid anion complex by some thiazine dyestuffs, 25:34534
Investigation of reaction of acid complexes of U(VI) with basic dyes: methyl green, 25:34509
PETROVYKH, N. V., Spark counter with large area, 25:35019
PETRU, Z. K., Elementary excitations in a system of charged particles in magnetic field, 25:36359
PETRUCCIANI, N., Utilization of vibrational compaction for nuclear fuel, 25:35524 (RT/ING-(70)22)
PETTY, Alan Frederick, Evolutionary considerations of binary stars, 25:35623
PETUKHOV, V. A., Search for elementary particles bearing a magnetic charge, 25:36379 (CERN-Trans-71-10)
PETZOLD, Joachim, Field theoretic criterion for particles to have mass zero, 25:36570
PEWITT, E. G., Status of the 12-foot hydrogen bubble chamber, 25:34974 (CONF-700623-(Vol.2), pp 675-95)
PFANNENSTIEL, P., Peripheral blood picture and plasma protein fractions following therapeutic incorporation of radioisotopes, 25:35189
PFEIFER, V., Separation of cerium from other fission products by extraction, 25:34522
PFISTER, J. C., Evolution of distribution of interface states in MOS structures irradiated with electrons and subjected to effect of a thermal treatment in an electric field, 25:35080
PFLUGRAD, Kurt, Shock absorber, 25:37155
PHILIPP, G., Timing with surface barrier detectors using charge and current pulses, 25:34899
PHILLIPS, E., Fabrication and burst testing of reaction-bonded silicon carbide tubes, 25:35523 (AECL-3462)
PHILLIPS, G. C., Nucleon--nucleon quasi-free scattering in the p + d → p + p + n reaction at low bombarding energies, 25:36669
PHILLIPS, G. D., Effects of γ-irradiation on sodium sulphacetamide, 25:34661
Radical processes following γ irradiation of frozen concentrated matrices of heparin and dextran sulphate, 25:34651
PHUA, K. K.-K., Smoothed Veneziano models and applications to pion--pion scattering, 25:36499
PICHLMAYER, F., Mass spectrometric determination of the neutron capture cross section of isotopes of the rare earths, 25:36735 (SGAE-PH-104/1971)
PIETRZAK-FLIS, Zofia, Dietary intake and excretion of ^{137}Cs in children, 25:35093
PIGNON, D., Strong interactions and the weak parity violating nuclear potential, 25:36458
PIGOTT, George M., Effects on the alkaloid content of potatoes grown from seeds subjected to low-dose gamma irradiation, 25:35254
PIHL, P., Rapid and simple microscale separation of proteins after radioiodination, 25:34700
PIKAEV, A. K., Electron paramagnetic resonance spectra of irradiated frozen aqueous solutions. XII, 25:34648
PIKE, T. J., Formation of stacking faults in magnesium--thorium alloys, 25:35484
PILIPENKO, A. T., Separation of Re from Mo and W by acetone extraction, 25:34525
PINTER, Gy., Importance of using exact forms for scattering amplitude in Regge pole theory, 25:36531
PINTO, R., Slope sensitive alarm for use with fixed filter air monitors, 25:34909
PIOTROWSKI, A., New method for rare-earth isotope separation, 25:34805 (JINR-P6-5761)
PIRAGINO, G., Two-body photodisintegration of ^{4}He up to 80 MeV, 25:36671
PIRSON, Sylvain J., Geological, geophysical, and chemical modifications of sediments in the environment of oil fields, 25:34731
PISAREVSKII, A. N., Some new aspects of the effect of ionizing radiation on deoxyribonucleoproteins of somatic cells, 25:35198
PISKUNOV, E. M., Investigation of complexing of tetravalent Th, U, Np, and Pu with diethylentriaminpentaacetic acid, 25:34558 (SPARI-P-92)
PISUT, J., Merging of analyticity and statistics in

extrapolations and representations of data, 25:36597
PITTERLE, T. A., Status report on evaluation of sodium cross sections for ENDF/B, 25:36693 (WARD-4181-2)
PIZER, H. I., Simple capacitor read-out for wire spark chambers in magnetic fields, 25:35017
PLACIOUS, R. C., Production of high-intensity K x-ray beams, 25:35842
PLANO, Richard J., Minimizing angle errors due to multiple scattering, 25:34950 (CONF-700623-(Vol.1), pp 325-33)
PLANT, Mary, Origin and kinetics of goblet cells in the human jejunum during irradiation, 25:35240
PLENDL, H. S., Lattice vibrational spectra and physical characteristics of metals with cubic structure, 25:36319
PLENDL, J. N., Lattice vibrational spectra and physical characteristics of metals with cubic structure, 25:36319
PLESS, I. A., Counter control of bubble chamber photography, 25:34969 (CONF-700623-(Vol.2), pp 606-16)
PLIS, Yu. A., Depolarization of protons in a phasotron with spatial variation of the magnetic field, 25:36620
PLOTNIKOVA, E. D., Some problems of the mechanism of injury and recovery of cells, 25:35205
POCSIK, G., Momentum dependence of xrhow vertex, 25:36495
PODACHIN, V. P., Effect of ionizing radiation on induced bioelectrical activity in brain of rats, 25:35235
PODTETENEVA, A. I., Laboratory complex for producing homogeneous magnetic fields by superconducting magnetic systems, 25:36079
POETZL, K., Prog. rpt. on measurement of airborne radioactivity and its meteorological application, annual, 4/69--3/70, 25:34745 (NYO-4061-2)
POGGIOLI, R. S., Model space calculation of the quasiparticle interaction for nuclear matter, 25:36832
POLIKARPOV, G. G., Marine radioecology, 25:35117
POLLOCK, E. L., High pressure behavior of solid H_2, D_2, ^3He, ^4He, and ^{20}Ne, 25:37204 (NYO-3699-51)
POLONIS, D. H., Influence of Fe and Al on precipitation of metastable Ni_3Nb in Ni--Nb system, 25:35480
POLOTSKII, I. G., Dislocation motion in monocrystals of Mo and Nb, 25:35443
POLOVIN, R. V., Absolute, convective and global unstabilities, amplification and non-transmission of vibrations, 25:36560 (ITF-70-96-P)
POLYAKOVA, A. V., Investigation of radiation-thermal cracking of n-tetracosane and n-heneicosane in the liquid phase, 25:34653
POMPILI, G., Histological changes in the uterus and ovary of albino rats after irradiation and simultaneous administration of synthetic estrogens and progestogens, 25:35237
PONASSI, A., Radioisotopic diagnosis and therapy in hematology, 25:35157
POND, P., Zeros in ww amplitudes, 25:36498
PONOMAREV, V. I., Specific properties of operation of absorbing materials in fast reactors and requirements for them, 25:37140 (SRARI-P-96)
PONTECORVO, B., Heavy leptons and neutrino astronomy, 25:36462
PONZ. F., Effects of ionizing radiations on D uptake by rat liver slices, mitochondria, and mitochondrial membranes, 25:35223
POPE, M., Role of $CHCl_3$ as a quencher for γ- and uv-excited organic solutions, 25:34624
POPE, Noel K., Space--time pair correlation function of Maxwell--Boltzmann fluid in T-approximation for temperature Green's functions. I, 25:36373
POPKOV, Yu. M., X-ray studies of the tendency of niobium toward formation of stacking faults, 25:35493
POPOV, N. F., Plasma acceleration with an auxiliary stationary magnetic field , 25:36113
POPOV, N. P., Electrode erosion in pulsed plasma accelerators, 25:36207
POPOV, V. N., Radiative and chemical effects of accelerated multicharged ions on gaseous nitrogen-containing systems, 25:34557
POPOVA, A. A., Laws of formation of single crystals of solid solutions of binary rare-earth oxides, 25:35525
POPRYADUKHIN, A. P., Determination of magnetic surfaces with a dielectric grid, 25:36208
Effect of an electric field on the motion of particles in helical fields, 25:36084
PORAI-KOSHITS, K. V., Intensity of radiation of uterus and its appendages during administration of ^{32}P, 25:35144
PORKOLAB, M., Wave propagation near the upper-hybrid frequency in a mirror-confined unstable plasma, 25:36243
PORRITT, R. E. J., Tables of γ rays from (n,γ) produced nuclides, 25:36718 (AAEC/TM-585)
PORTER, F. T., Spectrum shape of K-orbital shakeoff electrons and accompanying nuclear beta particles in decay of ^{143}Pr, 25:36774
PORTO, S. P. S., Photoluminescence studies of superconducting Nb_3Sn, 25:36062
POSSAGNO, Elvira, Reactions of He^3H^+ ions with gaseous hydrocarbons. IV, 25:34675
POSTNOVA, T. I., Regeneration of in vitro x-radiation-induced injuries of DNA by polynucleotide ligase, 25:35108
POTAP'EVA, L. E., Activation-analysis determination of the silver content in microcrystal centers in a photographic emulsion, 25:34549
POTAPOV, N. N., Phase composition, structure, and magnetic hysteresis of Nb--Sn alloys, 25:36047
POTAPOV, V. Ya., Experimental gamma radiography equipment for determining defects in construction materials, 25:34822
POTAPOVA, A. I., Functional state of endocrine glands in rats irradiated on 25 MeV betatron, 25:35164
POTETYUNKO, G. N., Spatial generalization of nomographs and use in kinematics of nuclear reactions, 25:36842
POTT, G., Irradiation experiment for testing spherical fuel elements for high-temperature reactors, 25:37018 (JUL-701-RW)
POTTON, R. J., Electronic specific heat of an impure tungsten sample, 25:36312
POUBA, Z., Uranium deposits of Central and Arsorican Massifs in France, 25:34753
POULSEN, Niel Bowman, Feasibility study to increase available TAMVEC proton and deuteron energies, 25:36637
POUPARD, Danielle, Separation of lanthanides by chromatography on SA-2 ion exchange paper, 25:34714
POUYAT, F., Experimental results with the l m model chamber. B, 25:34983 (CONF-700623-(Vol.2), pp 813-23)
POWER, D. M., Effects of γ-irradiation on sodium sulphacetamide, 25:34661
POWERS, D., Stopping cross sections of gases for α particles from 0.3 to 2 MeV, 25:36255
POWERS, William E., Irradiation of early carcinoma of the larynx. Significance of tumor extent, 25:35188
POZDNYAKOV, P. E., Device for the investigation of relative dose distributions, 25:35059
POZNANSKI, Stefan, Removal of radioactive I from milk by means of ion exchangers produced in Poland, 25:34702
PRADHAN, T., Strong-interaction dynamics based on a class of nonlinear Lagrangian models, 25:36481
PRAKASH, Y., Monte Carlo calculations and the lifetime of heavy hyperfragments, 25:36535
PRANGE, H., Elastic electron scattering on ^4He at energies between 30 and 59 MeV, 25:36658 (CERN-Trans-71-13)
PRASAD, L. S. R. K., Polynomial basis for the irreducible representations of U_6 in the chain U_6 is contained in R_6, 25:36711
PRASAD, R. Y., Generation of bremsstrahlung x rays in the lower ionosphere, 25:35999
PRASIL, Z., Mechanisms of hydrogen formation in the radiolysis of gaseous CH_3CH and CH_3OH, 25:34665
PRATT, P. L., Mobility of dislocations in molybdenum single crystals, 25:35485
PREM, L. L., Prospects and economy of liquid-metal MHD--steam binary power plants, 25:35934
PRENTICE, Earl F., Ecological evaluation: migration of juvenile salmon in relation to heated effluents in central Columbia River, 25:37105 (BNWL-SA-2876)
PREOBRAZHENSKII, A. B., Automatic processing of information from spark chambers, 25:35004 (JINR-P10-5762)
PRESNAJDER, P., Merging of analyticity and statistics in extrapolations and representations of data, 25:36597
PRESTIANNI, Vincent T., 16 channel medium speed multiplexer, 25:37196 (NYO-1480-171)
PRESTON, H. E., Experience in the use of thermoluminescent dosimeters for radiation dose control purposes, 25:35023 (AEEW-M-962)
Problems of high temperature annealing of PTFE/lithium fluoride discs used for ionizing radiation dosimetry, 25:35024 (AEEW-M-991)
PRESTON, Richard K., Effects of surface greasing in chemical reactions: the H_2^+ system, 25:35885
PRESTWICH, W. V., Decay of ^{142}La, 25:36765
PRICE, M., Calibration of Gargamelle objectives, 25:34592 (CONF-700623-(Vol.2), pp 959-71)
PRICE, Paul B., Method of measuring fast neutrons by observing multipronged tracks of charged particles formed in cellulose nitrate, 25:34875
PRIDOEHL, E., Safety problems of fast breeder sodium coolant loops, 25:37011
PRNKA, Tasilo, Contribution to the study of coherency of vanadium carbide with the matrix of alpha iron, 25:35573
PRODELL, A., Bubble chamber detection technique for gamma rays in momentum region below 1 GeV/c, 25:34564 (CONF-700623-(Vol.1), pp 555-66)
PRODELL, A. G., 7-foot bubble chamber conversion, 25:34978 (CONF-700623-(Vol.2), pp 735-49)
BNL work on Ne/H_2 targets, 25:34961 (CONF-700623-(Vol.1), pp 511-31)
Large superconducting magnets for bubble chambers and other detectors, 25:34999 (CONF-700623-(Vol.2), pp 1040-94)
PROKHOROVA, L. I., Prompt neutron yield in ^{235}U fission, 25:36786
PROKOF'EV, A. N., Method of measuring the polarization of an oriented hydrogen target, 25:36645
PROKOF'EVA, V. V., TV observations of SN 1966 (NGC 2188) and SN 1967 (NGC 3389), 25:35638
TV system used for observations of faint variable stars, 25:35639
PROKOPENKO, G. I., Dislocation motion in monocrystals of Mo and Nb, 25:35443
PROKOSHIN, A. F., Critical current of superconducting alloy 65BT in fields up to 80 kOe, 25:36050

XUN

PRONKO, P. P., Damage depth distribution of 15-keV Kr implanted in RbCl as obtained from diffusion measurements, 25:36272
PROSPERI, G. M., Time scales and the problem of measurement in quantum mechanics, 25:36372
PROVOST, G., Fabrication and properties of lanthanide tungstates, 25:35529
PRUDNIKOV, E. D., Flame-spectrophotometric microdetermination of small amounts of strontium and barium, 25:34529
PRUGNE, P., Mirabelle, 25:34973 (CONF-700623-(Vol.2), pp 647-74)
PRYOR, A. W., Programs for the management and processing of neutron diffraction data, 25:36309 (AAEC/TM-578)
PRZYBYLSKI, A., Spectrum of Large Magellanic Cloud supergiant HD 32034, 25:35673
PUDOVKIN, M. I., Zones of corpuscular precipitations and structure of the magnetosphere, 25:35958
PUGACH, V. M., Mechanisms for 13.6-MeV deuteron disintegration by nuclei, 25:36713
PUGNETTI, G., Application of alpha and beta--gamma autoradiography in shielded cells for the examination of irradiated nuclear fuels, 25:34837
PUKHOV, N. M., Phase instability in scattering on random potential, 25:36599
PUNDARI, S. Baba, Vector-meson dominant sum rules and low-energy kaon--nucleon scattering, 25:36519
PURTYMUN, William D., Geology and hydrology of Mesita del Buey, 25:34846 (LA-4660)
PUSCHMANN, H., Sorption of radionuclides by sands from rivers, 25:34737
PUSTOVALOV, G. E., Calculation of the ion trajectories in a Penning discharge, 25:36133
PUSTOVALOV, V. V., Effect of the superconducting transition on the plasticity of metals, 25:35383
PUTTICK, K. E., Observation of dislocations in cadmium by optical, x-ray, and electron microscopy, 25:35486
PUTZKI, R., Neutron scattering from ^{15}N. I, 25:36684
PYATNITSKII, L. N., Limits in detection of radiation scattered by a plasma, 25:36101
PYLE, Robert V., Cross sections for destruction of excited H molecules in collisions with H_2 gas, 25:35874
PYPER, Diane M., Short-period magnetic variable HD 133029, 25:35669
PYYKKOE, P., Improved relativistic corrections to Fermi-contact hyperfine Hamiltonian, 25:36355 (NP-18818)

Q

QUE HEE, S. S., Luminescence of water excited by ambient ionizing radiation, 25:34623
QUERE, Y., Dechanneling of α particles by dislocations occurring in Al, 25:36307
Study of crystalline defects by channeling, 25:36275
QUERU, P., Gargamelle technical aspects, 25:34959 (CONF-700623-(Vol.1), pp 460-76)
QUICKENDEN, T. I., Luminescence of water excited by ambient ionizing radiation, 25:34623
QUINLIN, W. T., Analytical applications of liquid chromatography, 25:37192 (MHSMP-71-31)
QUIST, W. E., Influence of Fe and Al on precipitation of metastable Ni_3Nb in Ni--Nb system, 25:35480

R

RAAFAT, N., Cooling of a simulated fuel element by a flow of naturally circulated boiling water, 25:37009 (UARAEE-110)
RAAFAT, N. M., Heat transfer in annular reactor channels, 25:37008 (UARAEE-50)
RABINOVICH, M. I., Excitation of electromagnetic waves in a beam--plasma system with Coulomb friction, 25:36235
Instabilities in a double-stream plasma with coulomb collisions, 25:36174
RABINOVITCH, M., Strengthening of metals and alloys by refractory fibers grown from the melt, 25:35557
RACZKA, K., Investigations of solidification front and the depth of the liquid phase in concast billets by the technique of radioactive traces, 25:34820
RADHAKRISHNAN, B., Relative abundance of deuterons in cosmic rays and its astrophysical significance, 25:35512
RADHAKRISHNAN, V., Distance and spectrum of 3C 391, 25:35702
RADOSEVICH, L. G., Gap energy of superconducting niobium carbide, 25:36030
RADUTSKII, G. M., Pion photoproduction on nucleon near threshold and the contribution for vector-meson exchange, 25:36447
RADWAN, Zofia, Direct spectrographic determination of small concentration of rare earth elements in rare earth oxides (CeO_2, La_2O_3, Nd_2O_3, Pr_6O_{11}, and Sm_2O_3), 25:34511
RADYUK, K. A., Influence of uranium nitrate on rabbit thyroid gland, 25:35229
RADZHANOV, P. S., Angular correlation of ^{97}Nb γ radiation, 25:36763
RAE, Anil C., Renormalizable model of weak interaction, 25:36468
RAESIDE, D. E., Experimental and calculated photopeak efficiencies for coaxial Ge(Li) detector, 25:34900
RAFAL'SKII, R. P., Reduction of hexavalent uranium with hydrogen sulfide in aqueous solution at high temperatures and pressures, 25:34569
RAFFO, Peter L., Thermomechanical processing of molybdenum alloys, 25:35397
RAGHAVAN, R., Resonance phenomenology, 25:36500
RAGHURAM, A. C., Dislocation substructure and strength properties of niobium single crystals, 25:35276
RAGSDALE, William C., Magnus data on standard 10° cone calibration model, 25:37220 (SC-DC-713821)
RAHM, G., Incidences of radioisotope incorporation in state of Nordrhein--Westfalen, 25:35100
RAHMAN, M. A., Shape calibration and peak-to-total ratio measurements of 5'' x 6'' NaI(Tl) scintillation detector, 25:34936
RAHMAT, G., Differential measurement of the He 2^3P excitation, in He^+--He collisions, by using an ion--photon coincidence method, 25:35858
RAI, D. K., Importance of the kinetic energy expression for the bound electron in the binary collision theory of ionization, 25:35870
RAIKO, V. J., Electromagnetic separation of short-lived isotopes of Rn, Xe, and Kr for spectroscopic studies, 25:34806 (JINR-P13-5757)
New method for rare-earth isotope separation, 25:34805 (JINR-P6-5761)
RAJA, Shanker, Cosmological world models and observational data, 25:35808
RAJAN, R. S., Ultra-heavy nuclei in cosmic rays from meteorite studies, 25:35911
RAJASEKARAN, G., Effective-dipole form-factors for K/sub 13/-decay, 25:36459
RAJCA, A., Model of lattice dynamics for Mg, Cd, and Y, 25:36333
RAKHIMOV, R. R., Electron emission from monocrystals of alkali-metal halide compounds, 25:35840
RAKOVA, T. A., Phase diagrams of the systems MoO_3--MeMoO$_4$ (Me = Mg, Ca, Sr, Ba), 25:35578
RAKOVA, V. A., Distribution of ^{239}Pu in intact skin in its surface contamination, 25:35092
RAKOVSKII, E. E., Abundance and characteristics of geochemistry of gold in bauxites, 25:34553
RAKOW, Adalbert, Measuring of the standard ionic dose in compact and liquid media during x-ray and gamma irradiation by energies between 50 keV and 3 MeV. VI, 25:35146
RALEIGH, Henry D., Reactor safety, literature search, 25:37047 (TID-3525(Rev.5)(Suppl.6))
RAMACHANDRAN, G., Is time-reversal invariance violated in electromagnetic interactions, 25:36546
RAMACHANDRAN, R., Charge exchange polarization (πN) in Veneziano model, 25:36517
RAMADURAI, S., Relative abundance of deuterons in cosmic rays and its astrophysical significance, 25:35912
RAMAN, S., Nuclear data sheets for A = 110, 25:36808
RAMATY, R., Compound diffusion of cosmic rays, 25:35902
RAMAYYA, A. V., Multipole admixtures of transitions from β, γ, and octupole vibrational states in ^{114}Cd, 25:36742
RANCHIN, Guy, Uranium geochemistry and granitic differentiation in uranium-bearing province of Nord-Limousin, 25:34749 (CEA-R-4034)
RANDALL, P. N., Gross strain crack tolerance of A533-B steel, 25:35335 (HSSTP-TR-14)
RANDIN, Jean-Paul, Differential capacitance study of stress-annealed pyrolytic graphite electrodes, 25:35563
RANDOLPH, M. L., Mechanism of inactivation of transforming deoxyribonucleic acid by x rays, 25:35269
RANDOW, F., Artificial radioactivity of fish in 1967 to 1968, 25:35096
RANGANAYAKI, P. R., Relation between sudden commencement amplitude and initial phase duration of geomagnetic storms, 25:35975
RANKIN, D. T., Current and potential opaque ceramic armor materials, 25:35554
RANKIN, J. M., Multipath delay distortion of radio pulses from NP 0532, 25:35689
RANOGAJEC, F., Effect of the type of polyethylene on the grafting of styrene onto polyethylene. III, 25:35591
RANQUET, Pierre, Spectroscopic analysis of uranium oxide: use of halogenated carriers, 25:34504 (NP-18865)
RANZINI, L., Argonne code center: compilation of program abstracts, 25:37133 (ANL-7411(Suppl.5))
RAO, N. K., Hypernuclei resonant states ^5He, ^6Li, and ^9Be, 25:36401
RAO, U. R., Cosmic-ray propagation in interplanetary space: invited review, 25:35906
Variation of limiting energy of corotating cosmic rays with the solar cycle, 25:35914
RASHERSKII, V. F., Experiments on acceleration of α-particles by collective method, 25:36615 (UCRL-Trans-1434)
RASMUSSEN, B., Fission of U, Np, Pu, and Am isotopes excited in (d,p) reaction, 25:36746
RAU, G., Behaviour of transducers and gauges in high magnetic fields and at low temperatures, 25:34987 (CONF-700623-(Vol.2), pp 863-72)
RAUH, E., Measurement of bone density with ^{125}I-profile-scanner, 25:35171
RAVI, K. V., Strength differential effect in niobium--

oxygen solid solutions, 25:35373
RAVINDRANATH, M., β decay and nuclear structure in A = 99 nuclei, 25:36772
Small-order deviations of ^{90}Y and ^{32}P, 25:36768
RAY, A. K., K-meson--nucleon phase shifts near 600 MeV/c, 25:36417
RAYCHAUDHURI, S. P., Irradiation induced variation in Colletotrichum, 25:35256
RAZAVY, M., Model for γ decay of atomic or nuclear systems, 25:35891
RAZDAN, H., Research activity at High Altitude Research Lab., Gulmarg, 25:35909
READ, F. H., Angular distributions for the excitation of vibronic states by resonant electron--molecule reactions, 25:35869
REARWIN, Stephen Dearborn, Rocket measurements of low-energy auroral electron spectra, 25:35963
REBBI, C., Off-mass-shell extrapolation of the dual-resonance amplitude, 25:36598
REBEL, H., Improved version of Tamura's code for coupled channel calculations, 25:36818 (KFK-1333)
RECHENBERG, H., Analyticity, covariance, and unitarity in indefinite metric quantum field theories, 25:36563 (ORO-3992-26)
REDDY, K. Venkata, β decay and nuclear structure in A = 99 nuclei, 25:36772
Small-order deviations of ^{90}Y and ^{32}P, 25:36768
REDHEAD, P. A., Multiple ionization of cesium and barium by successive electron impacts, 25:35865
REDKAR, R. T., TIFR balloon facility, 25:35908
REED, James F., Magnus data on standard 10° cone calibration model, 25:37220 (SC-DC-713821)
REED, R. E., Dislocation substructure and strength properties of niobium single crystals, 25:35376
REES, M. J., Effects of electron pair production in QSOs, 25:35678
REES, Martin J., Runaway stars and pulsars near Crab Nebula, 25:35694
REGNIER, Serge, Spallation of medium-mass nuclei, 25:36689 (NP-18820)
REID, C. N., Plastic anisotropy in bcc metals, 25:35379
REINHARD, B., Cobalt-60 therapy of carcinomata of urinary bladder: five-year results, 25:35192
REINHARD, H. P., Experimental results with the 1 m model chamber. B, 25:34983 (CONF-700623-(Vol.2), pp 813-23)
Wide angle lens for BEBC, 25:34990 (CONF-700623-(Vol.2), pp 902-14)
REINHARD, P.-G., Electrons in strong external fields, 25:36369
REINHARDT, Jean, Excitation of n = 2 He levels by low-energy electrons, 25:35882
REINHARDT, M., Missing mass and the gravitational lense effect, 25:35812
REIS, G. E., Analog simulation of a guided parachute-payload system, 25:37224 (SC-ER-710097)
REISENAUER, A. E., Analysis of effect of potential reactor cooling ponds on Hanford groundwater system, 25:37103 (BNWL-1507)
Analysis of hydrological factors influencing Gable Mountain irrigation project, 25:34715 (BNWL-1502)
REITAN, A., Three-neutron resonance in reaction $^{3}He(\pi^-,\pi^+)3n$, 25:36849
REITER, R., Prog. rpt. on measurement of airborne radioactivity and its meteorological application, annual, 4/69--3/70, 25:34745 (NYO-4061-2)
REIZER-STEPNIOWSKA, D., Self-quenching open-point counter as detector of positive ions, 25:34898
REJ, A. K., Regge trajectories in nuclear photoproduction, 25:36453
REK, Z., Low, intermediate, and high energies in Veneziano model for KN scattering, 25:36507
REMBIELINSKI, J., X^0 (960) meson spin--parity determination, 25:36494
REMY, C., Chemical diffusion and Kirkendall effect in the body-centered cubic phase of the system plutonium/zirconium, 25:35333 (CEA-CONF-1760)
RENDIC, D., Nucleon--nucleon quasi-free scattering in the p + d → p + p + n reaction at low bombarding energies, 25:36669
RENGARAJAN, T. N., Consequences of intense photon field around pulsar NP 0532, 25:35706
RENIER, J. P., M/L orbital-electron-capture ratio in ^{71}Ge decay, 25:36704
RENSFELT, K. G., 880 ns isomeric state in ^{144}Sm, 25:36792
REPALOW, N. S., Wave interaction in a magnetized plasma, 25:36232
REPNOW, R., Fission isomers in Cm and Bk isotopes, 25:36795
RETI, P., Development history and current state of nondestructive materials handling, 25:34635
REULE, H., Structure of compounds Ag_4Sc, Ag_2Sc, Au_4Sc, Au_2Sc, and Ag_3Yb, 25:35496
REUTOV, O. A., Electrophilic substitution on aromatic carbon atom. XIV, 25:34600
REVA, A. D., Copper and Al in tissues of the spinal cord after x irradiation of animals, 25:35228
REVESZ, Laszlo, Dual effect of oxygen, 25:35214
REVUTSKII, E. I., Features of a double-beam accelerating structure, 25:36623
REYNOLDS, J. H., Plutonium-244: confirmation as an extinct radioactivity, 25:35594
REYNOLDS, R. C. Jr., Prog. rpt. on cobalt sorption on surface reactive minerals in glacial environment, 8/67--2/71, 25:34722 (NYO-3912-4)
Prog. rpt. on cobalt sorption on surface reactive minerals in the glacial environment, annual, 2--12/70, 25:34721 (NYO-3912-3)
REZNICHENKO, V. V., Deformation of laminar systems of copper--molybdenum and copper--tungsten at increased temperatures, 25:35454
RHODES, D. W., Treatment of radioactive waste streams at Idaho chemical processing plant by evaporation and ion exchange, 25:34682 (CONF-710509-1)
RIBAUX, P. A., Handling and transport of irradiated fuel, 25:34854
RIBES, M., Concept and quality measurements of the magnetic field in connection with the important properties of the optical system considered, 25:36627
RICCIONI, N., Tumors by means of radioisotopes, 25:35165
RICHARDS, D. W., Timing observations of Crab Nebula pulsar, 25:35685
RICHARDSON, Earl C., Structure-function studies of the aminothiol radioprotectants. The effect of carbon chain length in mercaptoethylamine homologs, 25:35160
RICHARDSON, J. Reginald, Research progress of the Nuclear Consortium at the UCLA Cyclotron Laboratory, July 1970. Report AR 5, 25:36738 (UCLA-10-P-18-23)
RICHE, J., Magnetic field map of the large European tuttle chamber, 25:35002 (CONF-700623-(Vol.2), pp 1150-71)
RICHTER, A., Reaction symmetries for multiplet production, 25:36844
RICHTER, B., New digitizing and memory system for wire spark chambers, 25:35016
RICHTER, Karl, Fuel element for a fast breeder and/or test reactor, 25:37027
RICKER, George R., Rapid fluctuations in high-energy x-ray flux from source in Crux, 25:35692
RICKETT, Joe Pat, Nonlocal potentials: three-body models of /sub Λ/^{9}Be, /sub ΛΛ/^{6}He, ^{8}Be, and ^{8}Li; and model of the reaction $^{6}Li(\pi^-,nn)^{6}He$, 25:36847
RIECK, H. G., Sampler for concentrating radionuclides from natural waters, 25:34704
RIHAN, T. H., High energy approximations in potential scattering theory, 25:36590
RINDI, Alessandro, (n,p) elastic scattering, 25:36661 (UCRL-20295)
RINGOT, Claude, Grid for fuel pencils, 25:37152
RIPA, P., N--N interaction matrix elements from phase shifts and the Jost, 25:36853
RIPLEY, Charles C., Steam cooled reactor operation, 25:37013
RISEBERG, L. A., Coherence transfer in a Penning ionizing collision, 25:35875
RISK, W. S., 300 megacycle logic with M.E.C.L. III, 25:35009 (CRC-2504-172)
RISKA, D. O., Nucleon--nucleon scattering in high waves and pion--pion dynamics, 25:36526
RISKALLA, R., Study of the ^{11}E nucleus by electron scattering, 25:36672 (LAL-1243)
RISTIC, M., Operating experience with nuclear power stations in member states, 25:36884 (IAEA-127)
RITCHIE, D. R., Off-line computer interface for a rectilinear scanner, 25:34881
RITTENBERG, V., N-point dual functions for mesons with physical trajectories, 25:36485
RITTER, R. C., Cryogenic pumping gas target system, 25:36626
RITZMAN, Robert L., An evaluation of the applicability of existing data to the analytical description of a nuclear-reactor accident. Quarterly progress report, January--March 1971, 25:37036 (EMI-1904)
RIZK, H. M., Axially symmetric waves in vacuum channel in plasma, 25:36218 (UARAEE-92)
ROAF, D., Bubble density in liquid helium, 25:34589 (CONF-700623-(Vol.2), pp 893-900)
ROAKE, W. E., FTR driver fuel development program status, 25:37064 (HEDL-SA-81)
ROBERSON, James A., Influence of thermomechanical processing on the structure and properties of extruded Beta III titanium, 25:35398
ROBERT, Jack, Laminar flow of incompressible conducting fluid in slightly divergent MHD channel, 25:35942
ROBERT, R. V. D., Determination, by neutron-activation and tracer techniques, of the losses of iridium during the fire-assay procedure for the platinum-group metals, 25:34544 (NIM-1048)
ROBERTS, G. C., Attenuation of 14-MeV neutrons in calcium-based concrete, 25:36260
ROBERTS, J. A., Timing observations of Crab Nebula pulsar, 25:35685
ROBERTSON, R. G. H., Low-lying levels of ^{58}Co, 25:36694
ROBLES, Ana Maria, Control of elution and eluent from /sup 113m/In generators, 25:34672
ROBSON, D., Reaction symmetries for multiplet production, 25:36844
RODDEN, C. J., Summary of results of general analytical evaluation program, 1--12/69, 25:34503 (NEL-256)
RODGERS, M. A. J., Formation kinetics of the pyrene dimer cation observed by pulse radiolysis, 25:34658
RODONO, M., Light curve and orbital elements of V 337 Aquilae, 25:35666
RODRIGUEZ, F. A., Determination of magnetic impurities in

XUM

high purity copper by neutron activation analysis, 25:34548
ROEHR, H., Mirror instabilities in Isar I theta pinch, 25:36182
ROESLER, R., New method of interpreting the results of gamma logging of boreholes, 25:34716 (CSIRO-Trans-10088)
ROGASHKOVA, A. I., Effect of inhomogeneities in a plasma waveguide on the propagation of slow waves and on electron beam interactions, 25:36234
ROGAUSCH, K. D., Asymmetry of slip in tantalum and tantalum alloys, 25:35381
Solid solution hardening of tantalum-base alloys, 25:35384
ROGERS, A., Rapid cycling bubble chamber program at SLAC, 25:34952 (CONF-700623-(Vol.1), pp 346-75)
ROGERS, Benjamin T., Alignment telescope, 25:35069
ROGISTER, Andre, Effect of electron anisotropy on whistlers leading strong collision-free shocks, 25:35956
ROINISHVILI, N. N., Correlation between the transverse and longitudinal momenta in multiple generation, 25:36423
ROM, Frank E., Gas core nuclear reactor, 25:36985
ROMANOV, L. R., Cesium-137 content of human body, 25:35095
ROMANTSEV, E. F., Early biochemical and structural changes in liver mitochondria of irradiated rats, 25:35216
ROMNEY, E. M., Effect of a chronic exposure to gamma radiation on shrub Ephedra nevadensis in northern Mojave Desert, 25:35249
RONCHI DELLA ROCCA, S., Two-body photodisintegration of ^{4}He up to 80 MeV, 25:36671
RONEN, Yigal, Bounds of integral transport operators, 25:37129
RONGA, F., Precision of an optical spark chamber with wire electrodes, 25:35008 (LNF-70/44)
ROOSE, U. J., Dosimetry of a gamma flash, 25:34892
ROOSEN, Robert G., Gegenschein, 25:35778
ROSE, David J., Controlled nuclear fusion: status and outlook, 25:36213
ROSE, Noel R., Transfer of experimental autoimmune thyroiditis of the mouse by serum, 25:35114
ROSE, R. M., Superconductivity and dislocation cell structure in niobium: stress effects, 25:36057
ROSEN, Nathan, Complete Schwarzschild solution, 25:36580
ROSENBERG, Allan Peter, Borchers class of a local field, 25:36569
ROSENFELD, Arthur H., πN partial-wave amplitudes, 25:36506 (TID-25726)
ROSENKRANZ, F., Ionization yields of molecular and atomic I on W, W (1.6 percent ThO_2), and Pt (8 percent W) surfaces, 25:35839
ROSENTHALL, Leonard, Intravenous and intracarotid radionuclide cerebral angiography, 25:35173
ROSENZWEIG, C., Dual-resonance amplitude for spinning particles, 25:36596
ROSEO, B., Histological changes in the uterus and ovary of albino rats after irradiation and simultaneous administration of synthetic estrogens and progestogens, 25:35237
ROSINSKII, S. E., Equilibrium and stability of current-carrying plasmas in toroidal systems, 25:36181
ROSS, C. K., Nucleon--nucleon correlation and two-pion-exchange three-body force in n force in nuclear matter, 25:36831
ROSS, R. G., Oxide chemistry of Pu in molten fluorides and free energy of formation of PuF_3 and PuF_4, 25:34566
ROSSITER, D. E., Aspects of ionospheric drifts, 25:35985
ROSSOW, Terry L., 12-kilowatt output switching-type power amplifier, 25:36197 (UCRL-73047)
ROSTRON, Ira Ralph, Magnetohydrodynamics in neutron stars, 25:35601
ROTH, E., Absolute isotopic scale for deuterium analysis of natural waters, 25:34518
ROTH, S., Lead iodide nuclear particle detectors, 25:34889
ROTHFUSS, H., Device for the sealing of cylindrical containers for radioactive materials, 25:34850
ROUEFF, E., Broadening by neutral hydrogen in the solar atmosphere, 25:35770
ROUGNY, R., Microstructure effect on hyperfine interactions in Yb--Ag, 25:36332
ROUSSEAU, J. S., Interaction between point defects in metals, 25:36325
ROUSSEL, K. M., Origin of magnetic fields in white dwarfs and neutron stars, 25:35621
ROWE, G. M., Creep in stoichiometric beta NiAl, 25:37180 (CGC-1489-10)
ROWLAND, W. D., Survey of the effects of porosity on the elastic moduli and strength of brittle materials with particular reference to beryllium, 25:35331 (AWRE-O-25/71)
ROY, A. K., Electron spin resonance studies of fundamental processes in radiation- and photo-chemistry. VI, 25:34641
ROY, D., Study of properties of Marmet's monokinetron by calculation of electron energy distribution profiles, 25:34926
ROY, D. P., Duality-breaking and meson spectrum, 25:36486
ROY, S. M., Recent developments in strong-interaction theory, 25:36479
ROYER, A., Mechanism of precipitation and plastic deformation of nickel--chromium alloys hardened by niobium and tantalum precipitation, 25:35483
ROZHNOVA, T. M., Measurement of the concentration of oxygen dissolved in tantalum, 25:35339 (ORNL-tr-2475)
ROZOV, S. I., Nonstationary three-dimensional plasma flow in a homopolar device, 25:36205
RUBIN, E. S., Effects of electrode size on the performance of a combustion-driven MHD generator, 25:35933
RUBIN, R. H., Radio recombination line in NGC 7027, 25:35642
RUBIN, S. B., Kinetic model of plane high-current electron-ion beam, 25:36504 (JINR-P9-5645)
RUBIN, Vera C., Narrow band filter photgraphs and spectra of the planetary nebula NGC 7009, 25:35643
RUBINSTEIN, H. R., N-point dual functions for mesons with physical trajectories, 25:36485
RUBLEVSKII, V. F., Content of artificial radioisotopes in atmosphere over Moscow during 1962--1967, 25:34748
RUDAK, E. A., Effect of phonon + particle doorway states in (n,γ) reaction, 25:36834
Phonon-particle doorway states in (n,γ) reactions on nuclei with A < 80, 25:36703
RUDENKO, V. A., Effect of heat-treatment and cold work on the oxidation of Zr--1 percent Nb alloy in air and pressurized steam at 450-650°C, 25:35278 (UARAEE-72)
RUDERMAN, M., Thomson scattering in a strong magnetic field, 25:36140
RUDNICK, A., Evaluation of beryllium foil subjected to biaxial stresses. final report, 25:35332 (BMI-X-604)
RUDOLPH, T. D., Gymnosperm seedling sensitivity to gamma radiation: its relation to seed radiosensitivity and nuclear variables, 25:35250
RUDRAIAH, N., Magnetohydrodynamic laminar flow between porous disks, 25:35947
RUEHL, Franklin R. Jr., Method for predicting the ground state shapes of 2s--1d shell nuclides, 25:36702
RUF, R., Constructive assembly and safety principles for the primary circuit of large pressurized water reactors, 25:37012
RUFENER, F. G., Catalogue of stars measured in Geneva Observatory photometric system, 25:35646
RUFF, F., Use of radioactive Xe in evaluation of pulmonary functions, 25:35170
RUGE, I., Energy resolution of multiplying semiconductor detectors for soft γ spectroscopy at room temperature, 25:34918 (LB/G-3034)
RUH, Robert, Current and potential opaque ceramic armor materials, 25:35554
RUKHADZE, A. A., Sausage instabilities in a transparent plasma of finite conductivity, 25:36173
Stability of relativistic electron beams in plasma and the problem of critical currents, 25:36169
RUKHLIN, V. G., Equilibrium and stability of current-carrying plasmas in toroidal systems, 25:36181
RUMER, Yu. B., Theory of unitary symmetry, 25:36552
RUMPF, F., Device for measuring the luminosity of Orsay storage ring, 25:36606 (LAL-1249)
RUNCIMAN, W. A., High resolution infra-red spectra of diamond, 25:36279
RUNGE, E.-G., Electric installations at the Forschungs- und Messreaktor Braunschweig (FMRB) of the Physikalisch-Technische Bundesanstalt, 25:37062 (FMRB-32/70)
RUPONEN, S., Lymphoscintigraphy, gamma-venography, and histological evidence in radical operation, 25:35186
RUTKOWSKI, J., Effect of the optical parameters of the medium on the yield of transition radiation of non-relativistic particles, 25:36354 (JINR-P4-5734)
RUTKOWSKI, R. W., p--p final-state interaction in ^{3}He(d,t)2p reaction, 25:36665
RUUD, Clayton Olaf, Diffusion study of Cr--Mo, 25:35427
RYABOV, Yu. V., Alpha measurement for ^{235}U and ^{239}Pu, 25:36748
Parameters of neutron resonances of ^{233}U, ^{235}U, and ^{239}Pu, 25:36756
RYABTSEV, E. I., Experimental study of gas heating efficiency in sectioned plasma generator with channel adjustment, 25:35928
RYAN, D. E., Chemical detection of zirconium and hafnium, 25:34519
RYAN, E. A., Recovery of pure platinum and dilute platinum-gold alloy electron-irradiated at liquid-nitrogen temperature, 25:36306
RYAN, R. D., Cooled preamplifiers with diode current leak, 25:34910
RYAZANTSEV, E. P., Extension of experimental capabilities of MR reactor for loop-testing fuel elements and materials, 25:37067 (LB/G-3001)
RYBAKOV, A. B., Transition from distributed emission to a cathode spot in an arc, 25:36112
RYCKMAN, Stanley G., Detection of high-energy x-ray flare from source in Crux, 25:35691
RYDING, G., Determination of lifetimes for multiply charged heavy ions excited in collisions with light gases, 25:35849
RYKOV, A. G., Effect of acidity on the rate of cation--cation oxidation-reduction reactions of actinide elements, 25:34559 (SRARI-P-94)
Investigation of complexing of tetravalent Th, U, Np, and Pu with diethylentriaminpentaacetic acid, 25:34558 (SRARI-P-92)
RYTEL, M., Emission band spectrum of CD^+ molecule, 25:34594
New band system in CC molecule emission spectrum, 25:34595

RYTZ, A., Corrective terms to Hartree correction formula, 25:35063
RZAEV, R. A., Focusing properties of a helical quadrupole lens, 25:36624

S

SABBADINI, A., Time scales and the problem of measurement in quantum mechanics, 25:36372
SABEK, M. G., Determination of epithermal neutron spectrum shape in UA-RR-1 reactor, 25:37076 (UARAEE-59)
SABINOV, Kh. S., Angular correlation of ^{97}Nb γ radiation, 25:36763
SABOKAR, V. K., Peculiarities of formation of intermetallics in explosion-produced copper--titanium compounds, 25:35324
SACCHETTI, C., Radioisotopic diagnosis and therapy in hematology, 25:35157
SACCO, A., NEMI: physical--mathematical model for sodium boiling in a heated channel, 25:37046 (RT/ING-(70)18)
SACERDOTI, G., Technical--economic information on superconductors and conductors for high field magnets, 25:36607 (LNF-70/19)
SACHSE, G., Radioactive waste from the reprocessing of fast reactor irradiated fuel, 25:34697 (SZS-3/71 (pp 26-32))
SACK, S., Two-dimensional stress-induced adiabatic flow, 25:34769 (UCRL-50987)
SAFRONOV, B. G., Electrode erosion in pulsed plasma accelerators, 25:36207
SAGAN, Carl, Solar system beyond Mars, 25:35829
SAGER, D., Bubble chamber detection technique for gamma rays in momentum region below 1 GeV/c, 25:34964 (CONF-700623-(Vol.1), pp 555-66)
SAHAKARI, M. P., ir spectra and magnetic susceptibilities of uranyl complexes, 25:34612
SAHAKYAN, Zh. G., Effect of radiation on the reproduction of cells of hemopoietic organs in various species of laboratory animals according to their radiosensitivity, 25:35217
SAHOO, B., Fluoro complexes of U(IV), 25:34611
SAITO, Takeshi, Heavy nuclei in cosmic radiation above 10 GeV/nucleon, 25:35895
Interaction mean free paths of cosmic heavy nuclei above 10 GeV/nucleon, 25:36394
SAKAI, Mitsuo, Quasi-ground, quasi-beta, and quasi-gamma bands, 25:36783
SAKAI, Sunao, Twisting invariant factorization in dual resonance model. II, 25:36594
SAKAMOTO, Fumio, Thermal stresses in annular disks, 25:34799
SAKHONCHIK, Yu. A., Self-trapping of powerful electromagnetic waves in a dense plasma, 25:36225
SAKUMA, T., Solution softening in Fe--Mo alloys, 25:35374
SAKURAI, Kunitomo, Acceleration and propagation of solar cosmic rays as deduced from the relative abundance of protons to helium nuclei, 25:35728
SALAITA, George N., Prog. rpt. on neutron cross sections for production of ^{24}Na isomer from Mg and Al, final, 10/70, 25:36688 (N-70-43042)
SALAKHOV, Kh. N., Radioisotopic analysers for determining sulphur content in the oil-products and the experience in their exploitation, 25:35040
SALAMOV, D. I., Gamov--Teller 1$^+$ excitations in odd--odd nuclei, 25:36817 (JINR-P4-5744)
SALAT, Albert, Light scattering in a marginally stable plasma, 25:36144
SALEH, E. A., Automatic start-up system for UA-RR-1 reactor, 25:37083 (UARAEE-108)
SALEH, S. A., Automatic start-up system for WWR-S, 25:37082 (UARAEE-94)
SALGANIC, Yu. A., Neutron channel in muon capture on ^{4}He, 25:36666
SALLAM, O. H., Control rod calculation with perturbation theory, 25:37136 (UARAEE-66)
Effect of non-uniform burn up on reactor lifetime, 25:37081 (UARAEE-83)
SALMON, R., Oak Ridge systems analysis code (ORSAC) User's manual, 25:36886 (ORNL-TM-3223)
SALMON-CINOTTI, Tullio, (n,p) elastic scattering, 25:36661 (UCRL-20295)
SALTIEL, Jack, Reversible addition of benzoyloxy radicals to benzene, 25:34577
SALTON, D. G. M., Solid state thermoluminescent dosimetry, 25:35028
SALVARIDIS, P., Gamma-radiation damage of organic scintillation materials, 25:35079
SALVIAT, Jean, Method and apparatus for the continuous dissolution of clad nuclear fuel materials, 25:34712
SAMINADAYAR, K., Evolution of distribution of interface states in MOS structures irradiated with electrons and subjected to effect of a thermal treatment in an electric field, 25:35080
SAMOILOV, A. V., Search for elementary particles bearing a magnetic charge, 25:36379 (CERN-Trans-71-10)
SAMSONOV, G. V., Recrystallization of high-melting carbides, 25:35535
SAMUEL, D., ^{18}O study of the source of oxygen in the anodic oxidation of silicon and tantalum in some organic solvents, 25:35293
SANCHE, L., New resonances in total cross section of electrons on CO and O_2, 25:35861
SANDY, C., Thyroid ablation in young mice, 25:35084
SANFORD, P. W., Rocket observations and the cosmic x-ray background, 25:35712
SANI, Luciano, Operating experience of nuclear power-stations in UNIPEDE member countries, 25:36864 (CONF-700956-2)
SANITSKII, E. M., Physical chemistry, metallography, and metal physics of superconductors, 25:36037
SAN'KO, L. A., Quasi-two-particle reactions in proton--proton interactions at 10 GeV/c, 25:36396
SANOCHKIN, Yu. V., Ionization instability of a self-sustaining low-pressure discharge in a strong transverse magnetic field, 25:36159
SANTIAGO, E., Effects of ionizing radiations on O uptake by rat liver slices, mitochondria, and mitochondrial membranes, 25:35223
SANTORO, R. T., Pre-target scriter for the intensity and time distribution of a proton beam, 25:36621
SANTOS, Agustin Alonso, Introduction to nuclear safety, 25:37051
SANUKI, Heiji, Perturbation approach to nonlinear Vlasov equation. III, 25:36236
SAPERSTEIN, D., Role of $CHCl_3$ as a quencher for γ- and uv-excited organic solutions, 25:34624
SAPP, William Wade Jr., Picnic x-ray yields and level broadening in low-Z atoms, 25:35854
SARABHAI, V., Morphology of geomagnetic field variations, 25:35990
SARACENO, A. J., Vapor pressure--temperature data for selected halogen-containing substances, 25:34602 (CAT-649)
SARANTSEV, V. P., Electron-ion bunch diagnostics by means of bremstrahlung, 25:36616 (UCRL-Trans-1440)
Experiments on acceleration of α-particles by collective method, 25:36615 (UCRL-Trans-1434)
SARKA, K., FG matrix treatment of normal vibrations in ethylene-like and nitromethane-like molecules, 25:34581
SARMA, K. V. L., e--μ universality in absolute value ΔS = 1 processes, 25:36470
Total cross sections and elastic scattering at high energies, 25:36480
SASAKI, Yasuichi, Studies on the uranium dicarbide phase, 25:35579
SASAKI, Yasuo, Preparation and pulverization of hydrogenerated niobium, 25:35299
SASTRY, C. V., Meson--baryon scattering in the quark model, 25:36518
SASTRY, Ch. V., Observations on the scattering of decameter radio waves by solar corona, 25:35773
SASTRY, K. Shankara, Escape of stars from colliding galaxies, 25:35796
SATAPATHY, K. C., Fluoro complexes of U(IV), 25:34611
SATO, R. T., Experimental confirmation of an asymmetric Peierls barrier in the temperature dependence of yield stress in tantalum and tungsten, 25:35375
SATTAROV, M. G., Anticoincidence gamma spectrometer with shielded scintillator, 25:34928
SATTERFIELD, Marion M., Preregulation of high voltage supply circuit for a medical nuclear spectrometer, 25:34888
SAUTER, George D., Effective charge and stopping power of heavy ions, 25:36261
SAVITSKII, E. M., Behavior of foil specimens of NT-type alloys in external magnetic field, 25:36052
Critical characteristics of superconducting alloys of type NT-I in a wide range of magnetic fields at different temperatures, 25:36048
Processes of superconducting solenoid into state with normal conductivity, 25:36078
Structure and superconducting properties of recrystalled and deformed alloys of Nb with 75 at. percent Ti, 25:36049
Superconducting electrolytic films of niobium, 25:36056
Superconducting metallic compounds of rhenium, 25:36038
Transition temperature of superconducting compounds V_3Ga, V_3Si, and Nb_3Sn, 25:36040
SAVOIE, J. C., Thyroid scintigraphy using /sup 99m/Tc and ^{131}I, 25:35169
SAVOST'YANOV, E. N., Isotope exchange between molecular oxygen and synthetic zeolites, 25:34580
SAWHNEY, R. L., Kinetic approach to self modulation of an amplitude-modulated wave in magnetoplasmas, 25:36582
Optimum third-harmonic generation in magnetoplasmas, 25:36244
SAXENA, M. C., Diffusion of ^{95}Nb into Cu, 25:35406
SAYED AHMED, F. M., Neutron transmission through ducts perpendicular to neutron beam axis in water shields, 25:36251 (UARAEE-86)
Transmission of slow neutrons in multiple-segment ducts in a water shield, 25:36252 (UARAEE-104)
SCANLAN, R. M., Defect structure of depleted zones in irradiated tungsten, 25:36268 (NYO-3504-50)
SCARANO, G., NEMI: physical--mathematical model for sodium boiling in a heated channel, 25:37046 (RT/ING-(70)18)
SCARF, F. L., Pioneer 9 electric field experiment. II, 25:35767
SCARPA, G., Experiences with the shielded whole-body counter, 25:35183
SCARR, J. M., A_2^- from reaction π-p + K/sub S/°K-p at 4.5

XUM

GeV/c, 25:36409
SCHARF, H., Behavior of fission cesium in graphite-containing fuel elements, 25:35567
SCHARMANN, A. D., X-ray and photo-induced processes in ZnO coating material, 25:36296
SCHATTKE, W., Band structure in excitation spectrum of Type-II superconductors, 25:36059
SCHEARER, L. D., Coherence transfer in a Penning ionizing collision, 25:35875
SCHECHTER, J., General treatment of chiral and scale breaking in SU(3) sigma model, 25:36483 (SU-1206-241)
SCHEMMEL, R. R., Resistivity measurements of insulators using the four-probe technique, 25:36310 (HEDL-SA-119)
SCHENK, M., Defect formation energies and related properties in irradiated polymorphic materials, 25:36297
SCHENK, Max, State of radiation protection in fire departments, 25:35149
SCHERMANN, Catherine, Excitation of n = 2 He levels by low-energy electrons, 25:35882
SCHEUING, V., Hyperon bubble chamber HYBUC, 25:34972 (CONF-700623-(Vol.2), pp 640-6)
SCHIEFERDECKER, H., Detection of transuranic elements in pCi-range, 25:34537
SCHIFF, L. I., Quark selection principle. II, 25:36439
Relativity experiments in space vehicles, 25:35821
SCHIFFMACHER, G., Thin films of praseodymium sesquioxide, 25:35575
SCHILLING, Franz E., Improvements in or relating to pressure vessels for nuclear reactors, 25:37153
SCHILLING, W., Electron irradiation experiments on Ta, 25:36273
SCHINDLER, Karl, Effect of electron anisotropy on whistlers leading strong collision-free shocks, 25:35996
SCHLESINGER, H. L., Prog. rpt. on applications of neutron activation analysis in scientific crime investigation, 5/62--5/68, 25:34542 (GA-9807)
SCHLITT, K. R., Temperature stabilization in heat exchange tubes under alternating heat fluxes, 25:34775 (EUR-4634)
SCHLOTHAUER, D., Data acquisition system for the determination of reliability characteristics, 25:37040 (IRS-T-18(1970), pp 123-43)
SCHMID, J., Experimental results with the 1 m model chamber at CERN. A, 25:34982 (CONF-700623-(Vol.2), pp 790-812)
SCHMIDT, Dorn, Radiation damage from internal alpha decay in thorium, 25:35270 (UCRL-51009)
SCHMIDT, F. H., Spin dependence in the excitation of the first 2+ state of ^{54}Fe, 25:36708
SCHMIDT, Fritz, Charged particle accelerator, 25:36635
SCHMIDT, J. J., Aspects of critical evaluation of nuclear data information, 25:37107 (INDC(NDS)-29/U)
SCHMIDT, Jack, Identification of radiation-induced hydrogen-addition radicals in adenine derivatives, 25:34652
SCHMITT, M., Use of a computer on the CERN 2m liquid hydrogen bubble chamber, 25:34946 (CONF-700623-(Vol.1), pp 256-73)
SCHMUNK, R. E., Metallurgical evaluation of simulated BWR emergency core cooling tests, 25:37038 (IN-1453)
SCHNEIDER, Mark J., Effect of thermal history on resistance of Columbia River steelhead trout (Salmo gairdneri) to thermal stress, 25:37104 (BNWL-SA-3713)
SCHNEIDER, R. H., Simple binary-to-decimal or decimal-to-binary converter and adding device, 25:35067
SCHNITZER, Howard J., Prog. rpt. on research in elementary particle physics, 5/31/71, 25:36419 (NYO-3178-8)
SCHOBER, T., Extraneous grain boundary dislocations in high angle (110) twist boundaries in Au, 25:37201 (NYO-3504-58)
SCHOKNECHT, Guenter, Description of radiation fields by separation of primary and scattered radiation. IV, 25:35145
SCHOPKA, H.-J., Postoperative irradiation of breast cancer by fast electrons, 25:35191
SCHOTT, John T., SU(n) and an SU(∞) theory of elementary particles, 25:36545
SCHOWEN, Richard L., Proton transfer and heavy-atom reorganization in amide hydrolysis. Valence-isomeric transition states, 25:34576
SCHRADER, D. H., Phase-height measurements of E region, 25:35983
SCHRADER, H., Half-life measurements of excited levels in ^{121}I and ^{123}I, 25:36752
SCHRUEFER, Elmar, Reactor instrumentation, 25:36996
SCHUCHERT, H., New retentive alloys of cobalt and rare earth metals, 25:35306
SCHUESSLER, H.-D., Search for superheavy elements in terrestrial matter, 25:36779
SCHULER, Robert H., Electron spin resonance spectra of radiation-produced radicals, 25:34616
SCHULTHEISS, G. F., Experimental investigation of the retardation of boiling of sodium on artificially roughened surfaces, 25:34791 (KFK-1332)
SCHULTZ, Arnold W., Nondestructive testing of advanced fiber-reinforced composites, 25:34838
SCHULZ, G. J., New resonances in total cross section of electrons on CO and O_2, 25:35861
SCHULZ, Wallace W., Macroreticular ion exchange resin cleanup of Purex process TBP solvent, 25:34679 (ARH-SA-58-RD)
SCHULZE, H.-A., Artificial radioactivity of fish in 1967 to 1968, 25:35096
SCHUMACHER, H., Plutonium, 25:35310
SCHUMACHER, W., Organizational and architectural considerations of radiation protection during establishment of a nuclear medicine department, 25:35151
SCHUMANN, Z., Refabrication of nuclear fuel elements: fundamentals, plants, technology, 25:35204
SCHUURMANS, C. J. E., Influence of solar flares on the tropospheric circulation, 25:35973
SCHWAERZLER, B., Cobalt-60 therapy of renal tumors, 25:35193
SCHWARTZ, D. A., Evidence for multiple periodicity in x-ray emission from Cygnus X-1, 25:35690
SCHWARTZ, L. J., Kinetics of interaction of tantalum disilicide with tantalum and other metals, 25:35577
SCHWARZ, Helmut, Linear and nonlinear laser-induced emission of ions from solid targets with and without magnetic field, 25:36149
SCHWARZ, Helmut J., Laser interaction and related plasma phenomena. Proceedings of the first workshop, held at East Windsor Hill, Connecticut, June 9--13, 1969, 25:36147
SCHWARZ, M., Utilization of nuclear power plants for heat supply or heat-power coupling, 25:37032
SCHWEIMER, G. W., Improved version of Tamura's code for coupled channel calculations, 25:36818 (KFK-1333)
SCHWEMMLE, R., Investigation of natural frequency of normal and elongated function, 25:36993 (KFK-1337)
SCHWERDTEL, E., Liquid scintillation counting using an RCA photomultiplier Type C31 000D, 25:34895
SCOBIE, J., Beta energy release following thermal fission of ^{233}U and ^{235}U, 25:36764
SCOTT, B. R., Induction of mutation by γ irradiation in presence of oxygen or nitrogen, 25:35121
SCOTT, R. D., Beta energy release following thermal fission of ^{233}U and ^{235}U, 25:36764
SCOURFIELD, M. W. J., Television imaging of fast auroral waves, 25:35965
SEABORG, Glenn T., Peaceful uses of nuclear energy, 25:34817
SEAR, Reginald, Radio-isotope machine, 25:34885
SEBKO, V. P., Asymmetric helical magnetic configurations, 25:36206
SEDRIKS, A. J., Corrosion behavior of aluminum--boron composites in aqueous chloride solutions, 25:35521
SEELINGER, S. M., Effect of hydrogen on deformation and fracture processes in hafnium, 25:35457
SEGUR, Pierre, Electron energy distribution function in weakly ionized gas, 25:36146
SEIBEL, G., Strengthening of metals and alloys by refractory fibers grown from the melt, 25:35557
SEIDELMANN, P. K., Determination of mass of Pluto, 25:35822
SEIDMAN, D. N., Defect structure of depleted zones in irradiated tungsten, 25:36268 (NYO-3504-50)
SEIJKA, J., Study of the oxygen growth laws of anodic oxide films on aluminum and tantalum using nuclear microanalysis of ^{16}O and ^{18}O, 25:35294
SEIPEL, H. G., Critical analysis of the evaluation methods in reactor safety, 25:37039 (IRS-T-18(1970), pp 21-36)
SEKHON, B. S., Search for energetic neutrons emitted during solar flares, 25:35772
SEKIGUCHI, Akira, Progress of in-core instrumentation, 25:34877
SELEZOV, I. T., Stationary problem of cylindrical magnetoacoustic wave scattering by an ideal conducting cylinder, 25:35941
SELIG, H., Raman spectra of technetium heptoxide, 25:34608
SELIVANENKO, A. S., Superconductivity of a semiconductor placed in a laser light field, 25:36031
SELLEK, William Harold, Improvements in or relating to apparatus for determining the direction of a nuclear explosion, 25:35058
SELLSCHOP, J. P. F., Instrumental neutron-activation analysis of samples taken at different levels of E.R.P.M. mine, 25:34543 (NIM-1013)
SEMANS, J. P., Spatial distribution of indium activation in water using ^{252}Cf, 25:36652 (WAPD-TM-991)
SEMASHKO, N. N., Fast hydrogen atom injector, 25:36186 (CTO-746)
Injector for fast hydrogen atoms. I, 25:35837
SEMENKO, S. F., Giant dipole resonance in nuclei in transition region A approximately 90, 25:36755
SEMENOV, V. A., Giant dipole resonance in nuclei in transition region A approximately 90, 25:36755
SEMERDZHYAN, S. P., Some reactions of the organisms to radiation in different oxygen pressures, 25:35118
SEN, A., Loss-cone modes in inhomogeneous mirror machines, 25:36166 (UCRL-73135)
SEN, S. K., Prog. rpt. separation of krypton and xenon from reactor atmospheres by selective permeation, 1/69--12/70, 25:34692 (NYO-4057-2)
SENA, Edwin Andres, Composition for scintillation counting, 25:34874
SENCHENKOVA, T. M., Racemization of α-amino acids exposed to γ radiation, 25:34622
SEMENT, F., Radioactive contamination of atmosphere around Valencia measured from January 1966 till April 1968, 25:35132

SENIN, Yu. M., Uranium concentration in recent oceanic sediments of water uprise zones, 25:34761
SENKON, Hasret, Manual for Turkish film dosimetry standards, 1962--69, 25:35135 (CNAEM-77)
SENTIS, G., 200 MHz pulse amplitude discriminator, 25:35045 (CEA-N-1447)
SERDYUTSKII, V. A., Pion photoproduction on nucleon near threshold and the contribution for vector-meson exchange, 25:36447
SERENKOV, V. I., Modification of filled vulcanized polyisoprene (SKI-3) rubber by radioinduced vinyl chloride grafting, 25:34627
SERGEEV, A. P., Experiments on acceleration of α-particles by collective method, 25:36615 (UCRL-Trans-1434)
SERGIENKO, A. S., Dynamic voltage-current characteristics of d. c. plasma generators at large and small amplitudes and rates of current variation, 25:36161
SERIN, B., Proximity effect in gadolinium-backed lead films, 25:36036
SERLEMITSOS, P. J., Evidence for multiple periodicity in x-ray emission from Cygnus X-1, 25:35690
SERTORIO, L., Inclusive experiments and high-energy models, 25:36478
SERVIAN, Jorge L., Control of elution and eluent from /sup 113m/In generators, 25:34672
SESSA, A., Studies on the anti-tumour activity of aliphatic aldehydes. IV, 25:35159
SESSIONS, C. E., Influence of titanium on the strengthening of a Ni--Mo--Cr alloy, 25:35391
SETLOW, Jane K., Mechanism of inactivation of transforming deoxyribonucleic acid by x rays, 25:35269
SETTI, G., Infrared background and universal cosmic rays, 25:35818
SETTLES, R., Hyperon bubble chamber HYBUC, 25:34972 (CONF-700623-(Vol.2), pp 640-6)
SEVERIN, D., Hall effect studies on strontium and ytterbium under high pressures, 25:36324
SEVERNYI, A. B., Magnetic fields and proton flares Jul 6 and Sep 2, 1966, 25:35753
SEWART, M., Effects of γ-irradiation on sodium sulphacetamide, 25:34661
SEYMOUR, Allyn H., Biological half-lives for zinc and mercury in Pacific oyster, 25:37218 (RLO-2225-T-1-5)
SEYNA, F., Properties of stainless steel 1H18N9T after aging in the power reactor temperature ranges. II, 25:35336 (INR-1255)
SHABALIN, I. N., Secondary oxidation of metals after hydrogen annealing, 25:35291
SHACKLETTE, L. W., Gap energy of superconducting niobium carbide, 25:36030
SHAFER, R. E., CUBRT: fast 9-digit cube-root function for the CDC 6600, 25:37242 (UCID-30004)
SHAFI, M., Emission of deuterons in 24-GeV/c proton interactions with emulsion nuclei, 25:36403
SHAFRIR, N. H., Gamma-spectrometry in marine radioactivity studies, 25:34935
SHAFROTH, S. M., Midstream evaluation, A = 89, 25:36714
SHAH, G. A., Interstellar grain temperatures, 25:35751
Size-dependent resonance in Mie theory of scattering and unidentified interstellar bands, 25:35663
SHAH, K. R., Determination of mercury in biological and environmental materials by instrumental neutron activation analysis, 25:34551
SHAKHTAKHTINSKII, G. B., Arsenate method for a micro iodometric determination of scandium, 25:34508
SHAKIN, C. M., Intermediate structure and the giant-dipole resonance in ^{16}O, 25:36678
SHALTIEL, D., Anisotropic behavior of dilute magnesium--gadolinium alloys, 25:36342
SHANTAROVICH, V. P., Positronium atom in organic liquids, 25:35853
SHAPIRO, B. D., Nonlinear theory of relaxation of a monoenergetic beam in a plasma, 25:36130
SHAPIRO, P., Analysis of (p,^{3}He) and (d,α) reactions on ^{209}Bi, 25:36777
SHAPKINA, Yu. S., Flame-spectrophotometric microdetermination of small amounts of strontium and barium, 25:34529
SHARIVKER, S. Yu., Physical properties of plasma-sprayed carbides, 25:35538
SHARMA, B. D., Diffusion of ^{95}Nb into Cu, 25:35406
SHARP, W. E., Summary of sky brightness measurements during eclipses of the sun, 25:35761
SHASHKOV, A. G., Dynamic voltage-current characteristics of d. c. plasma generators at large and small amplitudes and rates of current variation, 25:36161
SHAVROV, P. I., Extension of experimental capabilities of MR reactor for loop-testing fuel elements and materials, 25:37067 (LB/G-3001)
SHAW, D. G., Recovery of pure platinum and dilute platinum--gold alloy electron-irradiated at liquid-nitrogen temperature, 25:36306
SHAW, James Scott, Photoelectric photometry of HD Telescopii and KZ Pavonis, 25:35622
SHAY, J. L., CdP_2--Sn system and some properties of $CdSnP_2$ crystals, 25:35580
SHCHEGLOV, D. A., Spatial distribution of ion temperatures in Tokamak devices, 25:36097
SHCHEKIN, Yu. K., Quantitative interpretation of radioisotope renograms, 25:35168
SHCHEKINA, G. D., Quantitative interpretation of radioisotope renograms, 25:35168
SHCHELOKOV, R. N., Tetracido-type oxalate-peroxo uranyl compounds, 25:34570
SHCHERBAKOV, A. G., Motions of fine structure features in the sunspot penumbras, 25:35745
SHCHERBININ, O. N., High-frequency plasma heating near the lower hybrid frequency, 25:36087
Limiting frequency for plasma absorption of high-frequency waves, 25:36238
SHEFFER, E. K., Galactic spurs as possible sources of soft x radiation, 25:35800
SHEFFIELD, G. V., Properties of magnetic surfaces in Model C stellarator, 25:36210
SHEINA, N. M., Use of N-furcylphenyl hydroxylamine for amperometric titration of Zr, 25:34535
SHEKHTMAN, Ya. L., DNA role in cell initial radiation injury, 25:35197
SHELINE, R. K., Low-lying configurations in ^{210}Bi, 25:36787
SHENOY, M. A., Enhancement of radiation lethality of bacterial cells by some sensitizers: a radiochemical approach, 25:35262
SHEPARD, R. C., Determination of nitrogen and hydrogen at parts-per-million levels in milligram steel samples, 25:34514
SHEPPARD, John D., Some factors affecting the performance of hyperfiltration membranes, 25:37213 (ORNL-TM-2256)
SHER, D., Estimation of the total kinetic energy of clusters of stars or galaxies, 25:35797
SHERA, E. B., Low-lying configurations in ^{210}Bi, 25:36787
SHERRER, E. N., Correlation between the transverse and longitudinal momenta in multiple generation, 25:36422
SHESTAKOV, S. V., Regeneration of in vitro x-radiation-induced injuries of DNA by polynucleotide ligase, 25:35108
SHESTAKOV, V. D., Influence of ultrasound on vapor bubble dynamics in liquid H, 25:35005 (JINR-P13-5751)
SHEV'CHENKO, V. I., Nonlinear theory of relaxation of a monoenergetic beam in a plasma, 25:36130
SHEVELEVA, T. Yu., Thermal receiver of roentgen radiation, 25:35031
SHIBATA, Toshikazu, Fast neutron spectra from natural uranium target bombarded with high energy electrons, 25:36767
SHIBUYA, Yoshio, Flux flow as function of film thickness in Type-I superconductors, 25:36058
SHIKHLAROV, K. K., Dynamic radiation generated in crystals by particles with ultrarelativistic energies, 25:36382
SHIMA, Y., Muon transport and shielding of high-energy (less than or equal to 500 GeV) proton accelerators, 25:36610 (ORNL-TM-3353)
SHIMAMURA, Isao, Harris-method calculation of electron and positron scattering by hydrogen atoms, 25:35879
SHIMIZU, Tatsuo, ESR studies on P+ ion-implanted Si, 25:36276
SHIMOJO, Hiroto, Inactivation of T antigen-forming capacities of simian virus 40 and adenovirus 12 by ultraviolet irradiation, 25:35267
SHIMURA, T., Sliding pulser for rapid testing of integral linearity, 25:35066
SHINAISHIN, M. A., Automatic start-up system for UA-RR-1 reactor, 25:37083 (UARAEE-108)
SHIPMAN, H. L., Hydrogen-rich models for horizontal-branch and post-horizontal-branch stars, 25:35626
SHIRAFUJI, Junji, Effects of electron irradiation on photoluminescence of n-GaAs, 25:36274
SHITO, Okiyasu, Model for weak interactions, 25:36464
SHKLOVSKII, I. S., Galactic spurs as possible sources of soft x radiation, 25:35800
SHKLYAREVSKII, G. M., Method of measuring the polarization of an oriented hydrogen target, 25:36645
SHKOVSKII, I. S., Pulsars and Type II supernovae, 25:35641
SHLYAK, M. P., Experimental gamma radiography equipment for determining defects in construction materials, 25:34822
SHMITT, D., Reaction $\pi^- + p^0s^0n$ at 447 MeV, 25:36405 (JINR-P1-5781)
SHMUTER, G. M., Effect of cystamine on monoamine oxidase and catechol-O-methyltransferase, 25:35165
SHMYKOV, A. A., Secondary oxidation of metals after hydrogen annealing, 25:35291
SHNOL, E. E., Theory of degenerating fermi gas in an external field, 25:36365
SHOEMAKER, V., Characteristics of a standing wave bubble or cloud chamber, 25:34955 (CONF-700623-(Vol.1), pp 408-17)
SHOR, Roberta, Strontium-90 heat sources, 25:34808 (ORNL-IIC-36)
SHORSHOROV, M. Kh., Welding of various solid state metals, 25:35321
SHOUA, Ezra D., Transient effect on LMFBR fuel rods by gas bubbles entrained in coolant, 25:37037 (CONF-700608-36)
SHTEINSHLEIGER, V. B., Observations of 3C 273 radio source at 8 mm with maser, 25:35686
SHTREMEL, M. A., Measurement of the concentration of oxygen dissolved in tantalum, 25:35339 (ORNL-tr-2479)
SHU, Frank H., Density-wave theory of galactic spirals. III, 25:35782
SHUBIN, V. G., Isotopic exchange of H α-position of alkyl groups of aromatic hydrocarbons with deuterotrifluoroacetic acid, 25:34598

Isotopic exchange reaction of hydrogen in arenyl ions and their antecedents, 25:34599
SHVARTSMAN, V. F., Electric charge of stars, 25:35615
SHVEIKIN, G. P., Region of homogeneity of a zirconium oxynitride of NaCl structure at 1500°C, 25:35583
SICEVITCH, I. G., Automatic start-up system for UA-RR-1 reactor, 25:37083 (UARAEE-108)
SICIVITCH, I., Automatic start-up system for WWR-S, 25:37082 (UARAEE-94)
SICK, I., Inelastic electron scattering from several Ca, Ti, and Fe isotopes, 25:36695
SIDHU, G. S., Structure in ^{235}U keV fission cross section, 25:36739 (UCRL-73090)
SIEGEL, V., Experience report on the operation and radiation protection at the Braunschweig Research and Measurement Reactor for the year 1970, 25:37063 (FMRB-35/71)
SIEKIERSKI, S., Physico-chemical properties of lanthanide complexes with thenoyltrifluoroacetone. I, 25:34502 (INR-1247)
SIEWIERSKI, J., Investigations of solidification front and the depth of the liquid phase in concast billets by the technique of radioactive traces, 25:34820
SIKKELAND, Torbjoern, Fission-excitation functions in interactions of ^{11}B, ^{12}C, ^{14}N, and ^{19}F with various targets, 25:36784
SIKULOVA, J., Influence of Na fluoracetate on shift of LD 50/30 value, 25:35162
SILIN, V. P., Self-focusing of a vector field, 25:36226
SILINI, Giovanni, Cellular aspects of radiation-induced bone-marrow failure, 25:35212
SILKER, W. B., Sampler for concentrating radionuclides from natural waters, 25:34704
SIL'NOV, S. M., Measurement of isotopic abundances by time-of-flight mass spectrometer, 25:35070
SILVA, E., Device for measuring the luminoisity of Orsay storage ring, 25:36606 (LAL-1249)
SILVA, R. J., Identification of the atomic number of nobelium by an x-ray technique, 25:36778
SILVER, Gary L., Variable rate neutron source, 25:36657
SILVERMAN, S. M., Sky intensity and spectral distribution during solar eclipse of 11/12/1966 at Bage, Brazil and on aircraft, 25:35763
Summary of sky brightness measurements during eclipses of the sun, 25:35761
SILVERS, Willys K., Attempts to abolish tolerance of skin homografts in mice with x-irradiated plasma from specifically sensitized donors, 25:35113
SILVESTRI, M., Developments of heat transfer and fluid flow in the nuclear field to other uses, 25:34796
SIMADER, F., Deformation anisotropy and texture of molybdenum, 25:35411
SIMMONS, R. O., Prog. rpt. on elementary particle physics, annual, 4/70, 25:36384 (COO-1195-213)
SIMOES, Jose Henriques, Iodine-131 in thyroids of cattle and sheep of Portugal, 25:35133
SIMONS, M., Rapid annealing of pulse-radiation-induced space charge in silicon dioxide, 25:36302
SIMONS, R. L., Neutron energy dependent cross section evaluation by a multiple foil activation method, 25:36741 (WHAN-SA-107)
SIMPSON, A. W., Temperature variation of susceptibility of some amorphous antiferromagnetic oxides, 25:36337
SIMPSON, D. A., Characteristics of an external electrode spark chamber, 25:35021
SIMPSON, Janet Pegdin, Electron temperatures of H II regions, 25:35683
SIMPSON, W. A., Computer programs for some eddy-current problems, 1970, 25:37212 (ORNL-TM-3295)
SINAI, Philippe, Correction of an optical system by irradiation, 25:35073
Process for correcting aberrations in optical system using irradiation and corrected optical system obtained by this process, 25:35077
SINCLAIR, R. M., Properties of magnetic surfaces in Model C stellarator, 25:36210
SINDZINGRE, Michel, French research on metallic matrix composites, 25:35431
SINGER, G. L., PHROG: a FORTRAN IV program to generate fast neutron spectra and average multigroup constants, 25:37113 (IN-1435)
SINGH, A., Optimum third-harmonic generation in magnetoplasmas, 25:36244
SINGH, A. N., Slope sensitive alarm for use with fixed filter air monitors, 25:34909
SINGH, B. B., Enhancement of radiation lethality of bacterial cells by some sensitizers: a radiochemical approach, 25:35252
SINGH, G. S., Laminar unsteady MHD flow in porous annular channel, 25:35940
SINGH, M. B., Hypernuclei resonant states ^{5}He, ^{6}Li, and ^{9}Be, 25:36401
SINGH, Om, Detecting radiation with a supercooled liquid, 25:35015
SINGH, Partap, Study of cosmic-ray modulation with neutron multiplicity analyzers, 25:35897
SINGH, R. N., Effect of energy spectra on synchrotron radiation from the magnetosphere, 25:35976
Generation of bremsstrahlung x rays in the lower ionosphere, 25:35999
Synchrotron radiation from electrons of various energy spectra, 25:36001
VLF wave amplification by wave--particle interaction, 25:35972
SINGH, R. P., Effect of energy spectra on synchrotron radiation from the magnetosphere, 25:35976
Synchrotron radiation from electrons of various energy spectra, 25:36001
VLF wave amplification by wave--particle interaction, 25:35972
SINGH, S., Analysis of shower particles produced in high-energy interactions, 25:36392
Neutral pions produced in 5-GeV/c antiproton interactions, 25:36404
New method for identification of shower particles in high-energy interactions, 25:36402
SINGH, Triyug, Monte Carlo calculations and the lifetime of heavy hyperfragments, 25:36535
SINHA, M. S., Durgapur cosmic-ray spectrograph with two solid-iron magnets, 25:35918
Momentum spectrum and the charge ratio of vertical muons at sea level, 25:35919
Solid Fe magnets used in Durgapur cosmic ray spectrograph, 25:35012
SINNIS, J., Wave propagation near the upper-hybrid frequency in a mirror-confined unstable plasma, 25:36243
SIRI-UPATHAM, Chyagrit, Inorganic elements in human stones, 25:34546 (THAI.-AEC-39)
SIRVASTAVA, J. B., Photoelectric elements of eclipsing system WX Cephei, 25:35662
SISCOE, G. L., Pioneer 9 electric field experiment. II, 25:35767
Two magnetic tail models for Uranus, 25:35828
SITENKO, A. G., Nonlinear echo phenomena in plasma, 25:36216 (ITF-70-56)
SIVARAMAN, K. R., K emission-line widths and the solar chromosphere, 25:35717
SJOEBERG, Hans Erik, Retention of ^{47}Ca in man, 25:35058
SKAALI, B., Reactions $^{26}Mg(d,p\gamma)^{27}Mg$ and $^{26}Mg(d,n\gamma)^{27}Al$, 25:36717
SKACHKOV, N. B., Representation for the relativistic scattering amplitude at high energies, 25:36601
SKARPAAS, Knut, Four-inch hydrogen target for 40-inch SLAC bubble chamber, 25:34965 (CONF-700623-(Vol.1), pp 567-80)
SKELL, P. S., Carbon-13 hyperfine interaction in CD_2, 25:34586
SKLIZKOV, G. V., Kinetic and ionization phenomena in laser-produced plasmas, 25:36150
SKOBELEV, V. V., Splitting of a photon in a magnetic field and polarization of hard radiation from pulsars, 25:35677
SKOGLUND, Victor J., Numerical solutions of nonequilibrium reflected shock waves in air with radiation, 25:37230 (SC-RR-710203)
SKRIPOV, V. P., Homogeneous nucleation during crystallization of supercooled tin, 25:36316
SKWARA, Witold, Potentiometric determination of free nitric acid in presence of uranyl, Al, and Mg nitrates, 25:34517
SLADE, W. E., Calculation of the vapor pressure in desiccated-multicomponent systems, 25:37223 (SC-DR-710074)
SLADKOVIC, R., Prog. rpt. on measurement of airborne radioactivity and its meteorological application, annual, 4/69--3/70, 25:34745 (NYO-4061-2)
SLAGGIE, E. L., Fast reactor spectrum measurements. Technical summary report, February 1, 1970--January 31, 1971, 25:36991 (GULF-RT-10523)
SLAMA, G., Coating of Nb and Nb alloys with Al. II, 25:35314
SLEE, O. B., Radio emission from flare stars near Orion nebula, 25:35616
SLEPCHENKO, L. A., Spin effects at high energy in quasipotential approach, 25:36504 (JINR-E2-5770)
SLOBODYANYUK, V. A., Ion-acoustic oscillations and transport processes in a low-temperature cesium plasma, 25:36231
SMART, W. M., Scintillation counter data acquisition system for use with SLAC 40'' hydrogen bubble chamber, 25:34970 (CONF-700623-(Vol.2), pp 617-28)
SMERD, S. F., Moving Type-IV solar burst 10/10/69, 25:35741
Solar Type-II burst 10/13/69, 25:35736
SMIALEK, R. L., Interstitial hardening and the Peierls stress in Tantalum, 25:35371
SMIRNITSKAYA, G. V., Oscillations in a low-pressure Penning discharge, 25:36242
SMIRNOV, A. A., System for depression of magnetic field pulsations in Dubna synchrophasotron, 25:36605 (JINR-P9-5724)
SMIRNOVA, I. D., Reaction of uranyl nitrate with arsenazo III in nitrate solution, 25:34524
Spectrophotometric investigation of complex formation in the system uranyl nitrate--nitric acid--water, 25:34564
SMIRNOVA, M. G., Effect of uv irradiation on hexokinase activity in skin, 25:35234
SMITH, A. J., Crystal structure of protactinium tetrabromide, 25:34610
SMITH, D. D., Syntactic foam evaluation, 25:37160 (BDX-613-177)

SMITH, Dennis Baird, Charged pion production in proton--proton interactions between 13 and 28.5 GeV/c, 25:36391 (UCRL-20632)
SMITH, Donald L., Empirical formula for interpolation of tabulated photon photoelectric cross sections, 25:36245 (ANL-7796)
SMITH, J. P., Shubnikov--de Haas oscillations in neutron-irradiated graphite, 25:36284
SMITH, J. W., Health physics aspects of decontamination of cell line, 25:35131
SMITH, Mark E., Recent changes in the astron fast pulsing system, 25:36201 (UCRL-73129)
SMITH, R. O., Proximity effect in gadolinium-backed lead films, 25:36036
SMITH, T., Measurements of ^{60}Co organ burdens in rats for calculations of dose-rates to organs of man, 25:35116
SMITH, William B., Detection of high-energy x-ray flare from source in Crux, 25:35691
SNIPES, Wallace, Temperature dependence of radioinduced free-radical destruction, 25:35103
SNOPE, A. J., Far-red light effect on ultraviolet light induced chromatid aberrations in pollen tubes of Tradescantia, 25:35120
SNOW, William J., Argonne code center: compilation of program abstracts, 25:37133 (ANL-7411(Suppl.5))
SNYDER, L., Results from meridian chain of observatories in Alaskan sector. I, 25:35961
SOBOLEVSKII, N. M., Interaction of high-energy radiation with matter, 25:36816 (JINR-P2-5719)
SOCKY, Richard B., Nondestructive testing in industry today and tomorrow, 25:34831
SODHA, M. S., Kinetic approach to self modulation of an amplitude-modulated wave in magnetoplasmas, 25:35953
Optimum third-harmonic generation in magnetoplasmas, 25:36244
SOEDERGARD, Bengt Martin, Control rod arrangement for light water nuclear reactors, 25:36998
SOERENSEN, B., Static quadrupole moment of collective octupole vibration in ^{208}Pb, 25:36803
SOFFER, J., General level structure in the dual-resonance model, 25:36474
SOKOLOV, L. F., Dehydration of isopropyl alcohol on aluminum oxide irradiated by ^{60}Co gamma rays, 25:34629
Effect of preliminary irradiation on catalyst activity in decomposition of hydrogen peroxide, 25:34630
Radiation-catalytic dehydrogenation of cyclohexane on Al--Co--Mo catalyst, 25:34628
SOKOLOV, L. S., Elastic and inelastic scattering of deuterons by nuclei, 25:36848
SOKOLOV, M. V., Mechanisms for 13.6-MeV deuteron disintegration by nuclei, 25:36713
SOKOLOV, N. A., Fine structure of superconducting alloys of Zr with Nb, 25:35053
SOKOLOV, S. N., Parametrization of phase space of N relativistic particles, 25:36428
SOKOLOV, V. I., Critical current of superconducting alloy 658T in fields up to 80 kOe, 25:36050
SOKUROVA, E. N., Radiation induced damages to cells, 25:35260
SOLACOLU, S., Detection of reactions taking place in pulverized mixtures of system La_2O_3--TiO_2--ZrO_2, 25:36320
Thermal equilibria of phases in system MgO--TiO_2--V_2O_5, 25:35576
SOLDATOV, V. P., Creep in Type-II superconductors, 25:36032
Effect of the superconducting transition on the plasticity of metals, 25:35383
SOLE, J., Use of superconductors for energy storage and discharge, 25:36074 (CEA-CONF-1736)
SOLOV'EV, V. G., Correlations between reduced neutron widths and partial radiative widths in resonances, 25:36850
SOMMER, L., Chemical detection of zirconium and hafnium, 25:34519
SOMMER, L. H., Halide--halide exchange at asymmetric silicon. New evidence against a siliconium ion-pair mechanism, 25:34579
SOMMER, N. F., Irradiation of California fruits and vegetables, 25:35274
SOMOV, A. I., Deformation of laminar systems of copper--molybdenum and copper--tungsten at increases temperatures, 25:35454
Effects of composition on strength of Cu--Mo laminates, 25:35455
SOMOV, B. V., Magnetic field of a rotating cloud and magneto-rotational explosions, 25:35819
SOMOVA, R. M., Tetracido-type oxalate-peroxo uranyl compounds, 25:34570
SONETT, C. P., Flux content and form of the geomagnetic tail, 25:35991
SOPER, J. M., Shell-model analysis of Λ binding energies for p-shell hypernuclei. I, 25:36529
SORF, F., Economic aspects of prospection and exploitation of U ores in France, 25:34751
SOROKO, L. M., Depolarization of protons in a phasotron with spatial variation of the magnetic field, 25:36620
Hadamard: transform scintillation counter, 25:34865 (JINR-P13-5696)
Pseudo-noise sequences applicable to multiplex systems of particle detection, 25:34866 (JINR-P13-5722)
SOUNDALGEKAR, V. M., Generalized MHD Couette flow, 25:35945
Hydromagnetic fluctuating flow past an infinite porous plate in slip flow regime, 25:35949
SPALEK, A., Decay of /sup 195m/Hg and ^{195}Hg to levels in ^{195}Au, 25:36750
SPARGO, A. E. C., Possible evidence for double plasmons in electron energy-loss spectra, 25:36257
SPARROW, J. H., Production of high-intensity K x-ray beams, 25:35842
SPEDDING, F. H., Properties, preparation, and handling of pure rare earth metals, 25:35297
SPENCER, G. S., Empirical study of behavior of clay shale slopes, 25:34768 (NCG-TR-15(Vol.1))
SPENCER, J. D., Neutron-induced fission cross sections for ^{248} ^{249}Cm and ^{249}Cf, 25:36721 (IP-MS-70-95)
SPEYER, Fred B., Reinforced ablative composites for extreme environments, 25:35530
SPIEWECK, F., Relativistic extension of Newton's theory of gravitation, 25:35813
SPIRIDONOV, F. P., Physicochemical properties of codeposited hydroxides of Nb and Zr and Nb and Hf, 25:35569
SPIRKO, V., FG matrix treatment of normal vibrations in ethylene-like and nitromethane-like molecules, 25:34581
SPITKOVSKII, D. M., Some new aspects of the effect of ionizing radiation on deoxyribonucleoproteins of somatic cells, 25:35198
SPITZER, Lyman Jr., Random gravitational encounters and evolution of spherical systems. II, 25:35782
SPOERI, W. G., Computer programs for some eddy-current problems, 1970, 25:37212 (ORNL-TM-3295)
SPRENG, Daniel Theodor, Radiation-enhanced diffusion in Au--Ag system, 25:35512
SPRINGER, T., Quasi-elastic scattering of neutrons for the study of random motions in solids, 25:36312
SREEKANTAN, B. V., High-energy N component of extensive air showers, 25:36383
Highlights of new astronomies, 25:35659
Search for high-energy gamma rays from pulsars, 25:35705
SREENIVASAN, A., Biochemical and physiological changes in gamma-irradiated wheat during germination, 25:35102
SRINIVASAN, V. T., Formation of free radicals in aliphatic and aromatic amino acids by trapped electrons: ESR study, 25:34647
SRIVASTAVA, P. K., 2-aminobenzothiazole as gravimetric reagent: milligram level determination of Hg(II), 25:34520
SROBODOVA, J., Preparation of ^{32}P applicators, 25:34671
STACHNIK, Robert V., Density-wave theory of galactic spirals. III, 25:35782
STALLINGS, Charles H., Finding potential distribution in cylindrically symmetric plasma, 25:36093
STAMENKOVIC, S., Inelastic scattering of neutrons by hydrogen-bonded ferroelectrics, 25:36668
STANG, Louis G. Jr., Explicit ing the parent-daughter relationship, 25:34802 (ENL-50249)
STANGE, E., Problems of instrumentation for radiation protection monitoring of waters, 25:34870 (SZS-2/71, pp 12-22)
STANSBURY, E. E., Influence of titanium on the strengthening of a Ni--Mo--Cr alloy, 25:35291
STARK, J. A., Analog simulation of a guided parachute-payload system, 25:37224 (SC-DR-710097)
STARODUBOV, Ya. D., Effects of composition on strength of Cu--Mo laminates, 25:35455
STARTSEV, V. I., Creep in Type-II superconductors, 25:36032
Effect of the superconducting transition on the plasticity of metals, 25:35383
STATHAM, C. D., Solution hardening and softening in niobium--molybdenum and niobium--rhenium alloys, 25:35436
STAUDE, Juergen, Apparent differences in magnetic field strengths measured from Zeeman splittings of molecular lines and Fe I lambda 5250.2 A, 25:35718
STEEB, S., Structure of compounds Ag_4Sc, Ag_2Sc, Au_4Sc, Au_2Sc, and Ag_3Yb, 25:35496
STEELE, B. C. H., Oxygen self-diffusion and electrical transport properties of nonstoichiometric ceria and ceria solid solutions, 25:35553
STEELE, T. W., Instrumental neutron-activation analysis of samples taken at different levels of E.R.P.M. mine, 25:34543 (NIM-1013)
STEFFEN, R. M., Measurements of gamma rays emitted in decay of ^{160}Tb, 25:36776
Test of the Kumar--Baranger pairing-plus-quadrupole force model in A = 190 region, 25:36773
STEHLIK, G., Tracer studies of synthesis of free nucleotides in yeast after β-irradiation, 25:35252
STEIGER-SHAFRIR, N. H., Range and range straggling of 87-keV ^{224}Ra particles in gases, 25:36262
STEIGER-SHAFRIR, Naftali H., Fission-excitation functions in interactions of ^{11}B, ^{12}C, ^{14}N, and ^{19}F with various targets, 25:36784
STEINBOCK, P., Problems of grasping the working behavior of nuclear power plants in production planning and of its economical simulation, 25:37033
STEINER, P., Lifetime of the 91.5 keV state in ^{191}Os, 25:36807
STEINITZ, Raphael, Short-period magnetic variable HD

XUM

133029, 25:35669
STEINKAMP, E., Remote-controlled welding of pressure tubes in Niederaichbach Nuclear Power Plant, 25:34787
STEINKOPFF, H., Refabrication of nuclear fuel elements: fundamentals, plants, technology, 25:35204
STEL'MAKH, G. P., Experimental study of gas heating efficiency in sectioned plasma generator with channel adjustment, 25:35928
STELTS, M. L., Structure in ^{235}U keV fission cross section, 25:36739 (UCRL-73090)
STENERHAG, B., Effect of wire parameters on the emission of hard x rays from exploding wires, 25:36326
STEPAKOFF, Gerald, Two-phase seeding in low-density plasma flow, 25:36116
STEPANCHUK, A. N., Reaction of TiB_2 with Ti, Zr, and V in vacuum, 25:35565
STEPANOV, A. F., Electron energy distribution in the positive column of a helium discharge, 25:36119
STEPANOV, V. A., Electron energy distribution in the positive column of a helium discharge, 25:36119
STEPANYAN, A. A., Estimation of high-energy γ-radiation fluxes from some cosmic objects, 25:35687
STEPHENS, R. I., Cyclic yield behavior of polycrystalline niobium, 25:35425
Stress cycling induced changes in the yield properties of molybdenum, 25:35346
STEPHENS, S. A., High-energy cosmic-ray electrons, 25:35920
STEPHENSON, F. R., Suspected supernova in AD 1181, 25:35676
STEPIC, R., Penetration parameter for M1 conversion and E2 admixtures for 77 and 191 keV transitions in ^{197}Au, 25:36789
STEPNIOWSKI, I., Self-quenching open-point counter as detector of positive ions, 25:34898
STERN, B. E., X-rays, 25:35057
STERN, S. Alexander, Prog. rpt. separation of krypton and xenon from reactor atmospheres by selective permeation, 1/69--12/70, 25:34692 (NYO-4057-2)
STESHENKO, N. V., Motions of fine structure features in the sunspot penumbras, 25:35745
STEVENSON, M. L., Neutrino physics with large H_2 chambers, 25:34941 (CONF-700623-(Vol.1), pp 56-96)
STEWART, L., Evaluated nuclear data for hydrogen in the ENDF/B-II format, 25:36660 (LA-4574)
STEWART, R. T., Bipolar structure in moving Type-IV solar radio burst, 25:35739
Meandering solar Type-IV burst 12/17/69, 25:35742
STEWART II, J. W., ENDF/B cross section preparation and testing in the JOSHUA system, 25:36737 (TID-25690)
STICKNEY, R. E., Contact potential measurements of adsorption of alkali metals on Ta(110) and W(100) crystals, 25:35359
STIEFELD, B., Computer-based display of nondestructive evaluation data, 25:37226 (SC-DR-710222)
STIEGLER, J. O., Effects of fast neutron irradiation on the tensile properties of austenitic stainless steels, 25:35509
STIEVE, F. E., Dose burden during fluoroscopy with image intensifier, 25:35142
STIGLICH, J. J., Current and potential opaque ceramic armor materials, 25:35554
STILLER, H., Quasi-elastic scattering of neutrons for the study of random motions in solids, 25:36313
STOBBS, J. J., Uranium market: Swiss outlook, 25:34755
STOCES, B., Effect of radiation on the mechanical properties of concrete, 25:37007 (ORNL-tr-2470)
STOCKMEYER, R., Development of a four-crystal monochromator and a rotating miniature collimator for neutron spectroscopy, 25:34917 (JUL-719-FF)
STOELBEN, H., Experimental results on acoustic detection of sodium and water boiling, 25:37052
STOKES, N. R., Variability of M stars, 25:35672
STOKES, R. A., Nuclear Instrumentation System: topical report, 25:36995 (WCAP-7669)
STOLER, P., Effect of nonuniform targets on cross sections obtained in neutron transmission experiments, 25:36811
STOLOFF, N. S., Effect of hydrogen on deformation and fracture processes in hafnium, 25:35457
STOLOV, A. L., X-ray luminescence and thermoluminescence of SrF_2 and BaF_2, 25:36317
STOLOVICH, Influence of triple electron and ion combination on electrodynamic plasma acceleration, 25:36109
STOLZ, Jean, Operating experience of nuclear power-stations in UNIPEDE member countries, 25:36864 (CONF-700956-2)
STOLZ, W., Color indicator for the visualization of radiation fields and the beam adjustment in large irradiation plants, 25:35029
STONE, R. G., Type III solar radio burst storms observed at low frequencies. III, 25:35723
STOOKSBERRY, R. W., Total and differential cross section for neutrons scattered from ^{90}Zr and Nat. Zr, 25:36740 (WAPD-T-2411)
STORER, R. G., Monte-Carlo solution of Schroedinger's equation, 25:36375
STORM, Derek W., Energy dependence of quasifree scattering in the $^2H(p,pn)p$ reaction, 25:36667
STORM, Ellery, Bremsstrahlung emission measurement from thick tungsten targets in energy range 12 to 300 kV, 25:36249 (LA-4624)
STOTT, J. P., Effect of ionizing radiation on impurity-vacancy dipoles in lead-doped NaCl and KCl, 25:36203
STOYANOV, D. Ts., Relativistic three-particle problem in terms of three-dimensional variables, 25:36586 (JINR-E2-5771)
ST-PIERRE, C., Reactions $^{48}Ti(\alpha,p)^{51}V$ and $^{50}Ti(^3He,d)^{51}V$, 25:36716
STRANG, R. M., Cryogenic pumping gas target system, 25:36626
STRASHINSKAYA, L. V., Reaction of TiB_2 with Ti, Zr, and V in vacuum, 25:35565
STRAYER, Donald M., Measurement of the probability of nucleation of a vortex ring in helium II, 25:36017
STRAZHEVSKAYA, N. B., DNA role in cell initial radiation injury, 25:35197
STREIFF, R., Effect of nitrogen on the linear oxidation of niobium, 25:35292
STRINDEHAG, Owe, Response of self-powered gamma detectors, 25:34891
STROKAN, N. B., Principle of formation of amplitude spectra in semiconductor nuclear radiation counters, 25:34511
STROM, K. M., Model-atmosphere analysis of five apparently super-metal-rich K giants, 25:35649
STROM, S. E., Model-atmosphere analysis of five apparently super-metal-rich K giants, 25:35649
STROM, Stephen E., Abundances in open clusters, 25:35627
STROMMAN, J. R., Storm-time variations in high-latitude fluxes of low-energy electrons, 25:35959
STRONSKI, I., Separation of transition elements and actinides by means of anionite AV-17, 25:34695 (ORNL-tr-2397)
STROTTMAN, D., Stabilization of axially symmetric shape and $(pf)^2$ mixing in sd shell nuclei, 25:36822
STROZIER, J. A. Jr., LEED intensity calculations for Be, 25:36330
STRUCHKOV, A. I., Mass and velocity spread of plasmoids in pulsed plasma accelerators, 25:36114
STRUDEL, J. L., Stacking fault formation and mechanical twinning processes in a nickel-base superalloy during tensile deformation at high temperature, 25:35491
STRUTT, P. R., Creep in stoichiometric beta NiAl, 25:37180 (CCG-1489-10)
STRUZHKO, V. G., Mechanisms for 13.6-MeV deuteron disintegration by nuclei, 25:36713
STUART, T. P., Use of aerial surveys for determining plutonium concentration. technical report no. 1-1030, 25:34862 (EGG-1183-1517)
STUBBE, P., Ion and neutral composition changes in the thermospheric region during magnetic storms, 25:35560
STUDIER, Martin H., Mass-spectrometric observations on N-(ethylmercuri)-p-toluenesulfanilide, Ceresan-M, 25:37157 (ANL-7809)
SU, Der-ruenn, Statistics of composite bosons, 25:36366
SUBBARAMAN, M. S., Gravitational waves: fact or fantasy, 25:36584
SUBRAMANIAN, A., Bubble chamber film-analysis facility, 25:35062
Recent interest in hadron--nucleus collisions, 25:36833
SUBRAMANIAN, S., Unstable intermediates. LXXXVI, 25:34667
SUCHER, J., Decay rate for $2^3S_1 \rightarrow 1^1S_0$ + one photon in he, 25:35845
SUDAN, R. N., Theory of the beam cyclotron instability in plasmas, 25:36167
SUDAREVA, S. V., Structure and superconducting properties of recrystalled and deformed alloys of Nb with 75 at. percent Ti, 25:36049
SUDARSHAN, E. C. G., Analyticity, covariance, and unitarity in indefinite metric quantum field theories, 25:36563 (CRC-3992-26)
Indefinite metric and shadow states in quantum field theory, 25:36564 (CRC-3992-30)
SUENAGA, M., Effect of the superconducting state on stress relaxation in lead-temperature dependence, 25:36072
SUENO, Shigeho, Survey of film developers adapted for x-ray intensity measurements, 25:37234 (SC-T-710035)
SUGANEEV, Yu. S., Welding of various solid state metals, 25:35321
SUGAR, Jack, New energy levels of triply ionized praseodymium, 25:35847
SUGIURA, A., Marker rescue with ultraviolet-inactivated influenza virus, 25:35266
SUJAK, B., Formation of bands of additional absorption in ruby crystals due to x radiation, 25:36308
Self-quenching open-point counter as detector of positive ions, 25:34898
SUKHATME, U. P., Dual-resonance amplitude for spinning particles, 25:36596
SULLIVAN, John M., Bridged polycyclic compounds. LXV. Electrophilic addition of hydrogen chloride, acetic acid, and their deuterated analogs to benzonorbornadiene, 25:34575
SUMIZU, Koichiro, Chemical and enzymatic properties of γ-irradiated subtilisin EPN, 25:35109
SUMMERS, Allan J., Device to eliminate undesirable transient effects on computer operations and the like, 25:35074
SUMMERS-GILL, R. G., Low-lying levels of ^{58}Co, 25:36654
SUNAKAWA, Sigenobu, Velocity operator in many-boson systems, 25:36368
SUNGTONG, Prapai, Soil analysis by neutron activation method, 25:34545 (THAI.-AEC-36)
SUNYAEV, R. A., Density of matter in Universe and epoch of

galaxy formation, 25:35811
SUO TON SIK, Alpha measurement for ^{235}U and ^{239}Pu, 25:36748
SUO TON SIK, N., Parameters of neutron resonances of ^{233}U, ^{235}U, and ^{239}Pu, 25:36756
SURAMLISHVILI, G. I., Wave kinetics in an anisotropic plasma. III, 25:36233
SURANYI, P., Multiplicity dependence of one-particle momentum distributions, 25:36476
SURAZHSKII, D. Ya., Methods of prospecting for U deposits, 25:34754
SUROVAYA, G. N., Phase transformations in alloy 65BT, 25:36051
SURUGUE, Jean, Conference on new experimental techniques in propulsion and energetics research, Munich, 5/67, 25:36107
SUSIC, M. V., Behavior of uranyl ion upon reduction from the ethylenedisulphurdiacetic acid solution at the dropping mercury electrode, 25:34561
SUSZYCKI, L., Monte Carlo simulation of nuclear-electromagnetic cascade developing in an ionization spectrometer, 25:36431 (ITJ-6)
SUSZYCKI, Leszek, Distributions and mean values of inelasticity coefficient K/sub v°/ for lead and graphite, 25:36389 (ITJ-5)
Estimation of energy and mean inelasticity of nuclear interactions at energies above 3.10^{12} eV, 25:36388 (ITJ-3)
SUTEU, A., Colorimetric determination of Ce^{++} by o-aminophenol, 25:34530
SUTTON, William R., Effects on the alkaloid content of potatoes grown from seeds subjected to low-dose gamma irradiation, 25:35254
SUZNJEVIC, C., Electrical resistivity of graphite powder and its mixtures, 25:36334
SUZNJEVIC, D. Z., Behavior of uranyl ion upon reduction from the ethylenedisulphurdiacetic acid solution at the dropping mercury electrode, 25:34561
SUZUKI, Shigema, Construction plan for a nuclear power plant of Chubu Electric Power Company, 25:36860
SVEC, P., Determining reactor spectra of fast neutrons from threshold detector measurements, 25:37109 (UJV-2423-RF)
SVEDBERG, R. C., Comparison of inconel 718 and inconel 750 for elevated temperature service in a pumped NaK system, 25:35343 (WANL-TME-1857)
SVESHNIKOV, A. B., Injector for fast hydrogen atoms. I, 25:35837
SVESHNIKOV, A. G., Fast hydrogen atom injector, 25:36186 (CTO-745)
SVIATSLAVSKY, I., Wisconsin rapid cycling bubble chamber, 25:34956 (CONF-700623-(Vol.1), pp 418-23)
SVIDERSKAYA, Z. A., High-temperature thermomechanical treatment of magnesium--zinc--zirconium alloys, 25:35456
SWAIN, J. H., Resonant expansion system for the proposed high field bubble chamber, 25:34984 (CONF-700623-(Vol.2), pp 824-35)
SWAMI, M. S., Hypernuclei resonant states ^{5}He, ^{6}Li, and ^{9}Be, 25:36401
Some aspects of K^- absorption at rest in emulsion nuclei, 25:36400
SWARIN, S. J., Simple and inexpensive electronic conductivity manometer for monitoring pressure changes. Application to pressuremetric titrations of iodate and ammonium ions, 25:34513
SWARTZ, Harold M., Structure-function studies of the aminothiol radioprotectants. The effect of carbon chain length in mercaptoethylamine homologs, 25:35160
SWIECKI, M., Low, intermediate, and high energies in Veneziano model for KN scattering, 25:36507
SWINDLE, D. L., New isotope ^{160}Lu, 25:36796
SYMONS, M. C. R., Unstable intermediates. LXXXV, 25:34666
Unstable intermediates. LXXXVI, 25:34667
SYREISHCHIKOVA, T. I., Search for elementary particles bearing a magnetic charge, 25:36379 (CERN-Trans-71-10)
SZEPKE, Ryszard, Beta-ray back-scattering method for coating thickness measurements, 25:34836
SZLAVIK, F., Synchronized chopper time-of-flight spectrometer, 25:34916 (JINR-E14-5731)
SZYMCZAK, Swietlana, Determination of Nb and Ta in products of Ta ore, 25:34510
SZYSZKO, Edmund, Effect of ionizing radiation on the stability of some radiopaque iodine compounds, 25:34662
SZYSZKO, Helena, Indirect colorimetric determination of europium in samarium and other rare-earth oxides, 25:34507

T

TABASSIAN, M., Radiation emitted by an argon plasma produced by a low-pressure torch discharge, 25:36124
TABATSKAYA, A. A., Isotopic exchange of H α-position of alkyl groups of aromatic hydrocarbons with deuterotrifluoroacetic acid, 25:34598
Isotopic exchange reaction of hydrogen in arenyl ions and their antecedents, 25:34599
TABOR, W. H., Bulk shielding facility quarterly report, January--March 1971, 25:37069 (ORNL-TM-3453)
TADA, Tomio, Regulation of homocytotropic antibody formation in the rat. II. Effect of x-irradiation, 25:35112
TAGAWA, Hiroaki, Studies on the uranium dicarbide phase, 25:35579
TAGGART, R., Influence of Fe and Al on precipitation of metastable Al_3Nb in Ni--Nb system, 25:35480
TAGIROV, E. A., Conformal-covariant interactions, 25:36561 (JINR-P2-5716)
TAI, Hsiang, Calculations of electron and proton collisions by atomic hydrogen, 25:35878
TAJIMA, Sakae, Growth of anodic oxide films on Ti, Ta, and Zr, 25:35284
TAKAMURA, S., Frequency shift and suppression of ion-wave instability by high-frequency electric field, 25:36172
Optical measurement of a high-frequency electric field in a weakly ionized plasma, 25:36094
TAKAMURA, Saburo, Electrical resistivity measurements of vanadium and iron deformed at 4.2°K, 25:36215
Electrical resistivity measurements of deformed metals after low-temperature neutron irradiation, 25:35501
TAKASE, Buhei, Effect of fractionated x irradiation on cells in tissue culture, 25:35242
TAKATA, Mitsuhiro, Pressure effect on the magnetic properties of superconducting La and La--Ce, 25:36021
TAKAYAMA, Tetsunobu, Flux flow as function of film thickness in Type-I superconductors, 25:36058
TAKEUCHI, Kiyoshi, Numerical solution to space-angle energy-dependent neutron integral transport equation, 25:36266
TAKEUCHI, S., Sliding pulser for rapid testing of integral linearity, 25:35066
TAKIBAEV, Zh. S., Angular distribution of particles at energies of 10 GeV, 25:36393
Quasi-two-particle reactions in proton--proton interactions at 10 GeV/c, 25:36396
TAKIMOTO, H. H., Corrosion of Ti--6Al--4V in HCl--methanol, 25:35287
TALANIN, Yu. N., Anticoincidence gamma spectrometer with shielded scintillator, 25:34928
TALWAR, S. P., Gravitohydromagnetic instability in contrastreaming plasmas, 25:35793
TAMAGUSUKU, Susumu, Sintering process for Ni--P alloy coated W, 25:35354
TAMANO, T., Properties of magnetic surfaces in Model C stellarator, 25:36210
TAMARU, Kenzi, Hydrogen absorption and hydrogen exchange reactions in solution by 1:2 electron donor-acceptor complexes of anthracene with various alkali metals, 25:34578
TAMOSAITIS, Anthony, Results from ANL 12 ft. chamber, 25:34980 (CONF-700623-(Vol.2), pp 765-73)
TAMURA, T., Spectroscopic study of (p,t) reactions from neutron-magic nuclei, 25:36794
TAMURA, Taro, Angular momentum coupling coefficients, 25:36366
TAN, C. W., Magnetohydrodynamic Couette flow with transpiration cooling, 25:35948
TANAKA, Haruo, Observations of solar radio burst on 9/27/69, 25:35725
TANAKA, S., Electron cyclotron wave and electrostatic wave in bounded plasmas, 25:36241
TANASESCU, M., Discrimination of compound signals, 25:35055
TANDON, J. N., Cosmic gamma-ray background, 25:35903
Solar corpuscular radiations and the interplanetary magnetic field, 25:35771
TANDON, S. N., 2-aminobenzothiazole as gravimetric reagent: milligram level determination of Hg(II), 25:34520
TANG, I-ming, Theory of ultrasonic attenuation in two-band superconductors, 25:36020
TANIGUCHI, Masaru, Regulation of homocytotropic antibody formation in the rat. II. Effect of x-irradiation, 25:35112
TAO, Chia-hwa, Plasma camera diagnostics in the study of wave evolution, 25:36099
TAO, L. J., Anisotropic behavior of dilute magnesium--gadolinium alloys, 25:36342
TARAFDAR, S. P., Pressure effect and absorption coefficient of H^-, 25:35661
TARAN, J-P. E., Effects on the propagation of optical beams due to self-induced changes in index of refraction, 25:37250 (UCRL-20541)
TARANTIN, N. I., Possible method of accelerating heavy ions, 25:36638
TARASENKO, A. G., Sulfhydryl groups and radiosensitivity, 25:35213
TARAYAN, V. M., Extraction of U(VI)--benzoic acid anion complex by some thiazine dyestuffs, 25:34524
Investigation of reaction of acid complexes of U(VI) with basic dyes: methyl green, 25:34509
New reagents for the extraction--photometric determination of tantalum, 25:34506
Peculiarities of the extractive-photometric determination of tantalum by basic dyestuffs, 25:34523
TARTAGLIA, A., Range of fission products in carbon, 25:36264
TARTAGLIA, Nunzio Anthony, Irregular geomagnetic micropulsations associated with geomagnetic bays in the auroral zone, 25:36004
TARUSOV, B. N., Chemiluminescence as information source

XUM

about primary reactions in biolipids by irradiation, 25:35201
TASSOUL, Jean-Louis, Nonlinear pulsations and stability of uniformly rotating spheroids, 25:35629
TASSOUL, Monique, Nonlinear pulsations and stability of uniformly rotating spheroids, 25:35629
TATARU, P. I., Gauge invariance, soft pions technique, and pion--nucleon inelastic scattering, 25:36515
TATE, E., Performance of a large-scale, nonequilibrium MHD generator with rare gases, 25:35932
TATUR, A. D., Positronium atom in organic liquids, 25:35853
TAUBER, R. N., Preparation and properties of pyrolytic zirconium dioxide films, 25:35564
TAYLOR, Clayborne D., Inhomogeneous plasmas: on reflection and transmission of fields of arbitrary polarization, 25:36228
TAYLOR, G., Effect of interstitial nitrogen on thermally activated flow in niobium single crystals, 25:35372
TAYLOR, Howard E., Improved charged particle detector, 25:34887
TAYLOR, J. J., FFTF: companion test and development facility for LMFBR program, 25:37085 (WHAN-SA-104(Rev.))
TAYLOR, R. E., Current distribution and internal resistance in segmented MHD channels, 25:35926
TAYLOR, W. R., Special arrangement shipments in Canada, 25:34843 (AECL-3804)
TAZAWA, Hisashi, Level structure of ^{143}Pm and ^{142}Nd, 25:36766
TEBBERT, H., WAK: administrative basis and commercial realization, 25:34778 (ORNL-tr-2417)
TEDROW, P. M., Measurement of the surface inductance and penetration depth of superconducting aluminum, 25:36029
TEH, H. C., Lattice vibrations in deuterated ammonium chloride at 85°K. I. Experimental, 25:36322
TEICHMANN, J., Influence of the helicon wave upon some electrostatic instabilities of plasmas, 25:36183
TEIXEIRA, Manuel Ribau, Iodine-131 in thyroids of cattle and sheep of Portugal, 25:35133
TELEKI, A., Cost-benefit illustration for underground nuclear natural gas stimulation, 25:34766 (AECDP-632)
TEL'NOV, Yu. Ya., Search for elementary particles bearing a magnetic charge, 25:36379 (CERN-Trans-71-10)
TELUSHKINA, E. L., Content of artificial radioisotopes in atmosphere over Moscow during 1962--1967, 25:34748
TEMIRALIEV, T., Quasi-two-particle reactions in proton--proton interactions at 10 GeV/c, 25:36396
TEMIRALIEV, T. T., Angular distribution of particles at energies of 10 GeV, 25:36393
TEMNY, V. V., Morphology of auroral electron energetic and angular distributions, 25:35982
TEMPLETON, W. L., Effect of thermal history on resistance of Columbia River steelhead trout (Salmo gairdneri) to thermal stress, 25:37104 (BNWL-SA-3713)
TEMPLETON, William L., Bibliography of ecological publications supported by atomic energy commission related to Columbia River thermal effects studies, 25:35115 (BNWL-1543)
TENNERY, V. J., Lattice parameters of (U,Pu)N solid solutions, 25:35574
TENNEY, F. H., Stellarator-mirror machine target plasma reactor, 25:36190 (MATT-841)
TENNEY, Gerold H., Role of nondestructive testing in materials technology and engineering, 25:34832
TENYAKOV, V. A., Abundance and characteristics of geochemistry of gold in bauxites, 25:34553
TEPLY, J., Mechanisms of hydrogen formation in the radiolysis of gaseous CH_3OH and CD_3OH, 25:34665
TERASIMA, Toyozo, Rejoining of single breaks of DNA induced by x-rays in mammalian cells, 25:35224
TEREKHIN, L. N., Experimental gamma radiography equipment for determining defects in construction materials, 25:34822
TERHUNE, Robert W., Prediction of underground nuclear explosion effects in Wagon Wheel Sandstone, 25:34770 (UCRL-50993)
TER-POGOSYAN, R. A., Radiosensitivity of virus-synthesizing function of cells irradiated in vitro and in vivo, 25:35261
TERZIAN, Yervant, Galactic nebula YM 29, 25:35630
TESKE, K., Safety problems of fast breeder sodium coolant loops, 25:37011
TESMER, J. R., Spin dependence in the excitation of the first 2$^+$ state of ^{54}Fe, 25:36708
TESTUD, J., Importance of diffusion processes in interaction between neutral waves and ionization, 25:35979
TEVEBAUGH, A. D., Prog. rpt. on lithium/chalcogen secondary cells for components in electric vehicular-propulsion generating systems, semiannual, 5/23--11/22/70, 25:35275 (ANL-7777)
THANKI, R. J., Variation in lipase activities during germination (in dark) of γ-irradiated castor-seeds, 25:35253
THENARD, J., Electronic device for Moessbauer spectrometry, 25:34934
THEYMANN, W., Irradiation experiment for testing spherical fuel elements for high-temperature reactors, 25:37018 (JUL-701-RW)
THIES, H. H., Measurement of neutron mean energies of evaporation-type neutron sources, 25:34906
THODE, Edward F., Desalination and ion separation of sodium and potassium by bromine redox electrolysis, 25:34691 (LA-4645)
THOMAS, Cecil Owen Jr., Experimental investigation of the effects of space and reflection on the count-rate fluctuation spectra of a large nuclear reactor, 25:37134 (DF-MS-70-101)
THOMAS, D. B., 1.5 metre diameter high field hydrogen chamber, 25:34977 (CONF-700623-(Vol.2), pp 714-34)
Magnetization current effects in coils wound from multifilament stabilized superconductor, 25:35000 (CONF-700623-(Vol.2), pp 1095-1125)
THOMAS, James P., Release of dissolved organic matter from natural populations of marine phytoplankton, 25:37215 (RLO-1725-186)
THOME, Paul, Nuclear reactor element and its use in a reactor, 25:37148
THOMPSON, A. W., Low temperature heat capacities of PrBi, PrSb, LaBi, and LaSb, crystal field effects in PrBi and PrSb, 25:35355
THOMPSON, B. D., Measurements of ^{60}Co organ burdens in rats for calculations of dose-rates to organs of man, 25:35116
THOMPSON, M. A., Neutral particle tagging facility for ANL 30'' bubble chamber, 25:34967 (CONF-700623-(Vol.2), pp 582-92)
THOMPSON, C. A., Interactions between nuclear plant loading changes and nuclear fuel costs, 25:36893
THOMSON, G. M., Promotion of L-shell electrons to higher bound states in Ar$^+$--Ar collisions, 25:35856
THORP II, Arthur G., Nuclear reactor structure, 25:36997
THORSLUND, Todd, Aging in Hiroshima and Nagasaki atomic bomb survivors, 25:35241
TICHLER, Paul, Investigation and repair of baffle plate damage in the HFBR primary heat exchangers, 25:37055 (BNL-15815)
TIKHOMIROV, V. S., Modification of filled vulcanized polyisoprene (SKI-3) rubber by radicinduced vinyl chloride grafting, 25:34627
TIKHONOV, N. A., Decay of ^{139}Nd, 25:36724 (JINR-P6-5672)
Decays of Nd and Pr nuclides with mass number A = 138, 25:36725 (JINR-P6-5674)
TIKHONOVA, M. N., Changes in structure and properties in γ-irradiated crystallizable chloroprene rubber, 25:35590
TIMOFEEV, G. A., Effect of acidity on the rate of cation--cation oxidation-reduction reactions of actinide elements, 25:34559 (SRARI-P-94)
TIMOFEEV-RESOVSKII, N. V., Hit and target principles in radiobiology, 25:35199
TING, Peter D., Triple Pomeron vertex, duality, and diffraction dissociation, 25:36420 (UCSD-10-P-10-78)
TIPTON, K. F., Isotope-exchange reactions of ox heart phosphofructokinase, 25:34596
TIRAPEGUI, E., Lower bounds and self-adjointness of Hamiltonians for class of models, 25:36573
TISCHLER, M., Improvements in tests of long-range charge independence, 25:36522
TISHCHENKO, M. A., Absorption-spectrophotometric determination of certain rare earth elements in the aqueous acetone solutions of dibenzoylmethane complexes, 25:34527
TISNEK, N. I., Principle of formation of amplitude spectra in semiconductor nuclear radiation counters, 25:34511
TISONE, T. C., Cross slip in fcc alloys, 25:35386
TITOV, A. A., Qualitative composition of radiation at depth of irradiated medium, 25:35030
TITOV, G. V., Optimum thickness of image-intensifying screens for radiographic inspection, 25:34824
TITTMANN, B. R., Change in flow stress due to the superconducting-normal transition, 25:35385
TIUNOV, L. A., Combined action of carbon monoxide and ionizing radiation under prolonged conditions, 25:35233
TIWARI, R. N., Solution corresponding to special field structure in Schroedinger's unified field theory, 25:36554
TKACHENKO, E. V., Phase diagrams of the systems MoO_3--$MeMoO_4$ (Me = Mg, Ca, Sr, Ba), 25:35578
TKACHEV, L. G., Influence of ultrasound on vapor bubble dynamics in liquid H, 25:35005 (JINR-P13-5751)
TKESHELAVSHILI, G. I., Effect of argon on thermionic converter operation at low cesium pressures, 25:35530
TOCHENOVA, I. N., Investigation of compounds in the niobium--tin system obtained by means of diffusion, 25:36045
Obtaining the superconducting compound V_3Ga by means of diffusion, 25:36043
TOCI, F., Thermogravimetric analysis (TGA) of the uranium oxide carboreduction, 25:34556 (EUR-4635)
TODD, J. H., Neutron multiplicity for ^{239}Pu resonance fission, 25:36734 (ORNL-TM-3331)
TOEPFFER, Christian, Q-value dependence of multinucleon transfer reactions, 25:36815 (JINR-E2-5797)
TOHMATSU, T., Ionization redistribution effect of wind in nighttime ionosphere, 25:35986
TOKAREV, Yu. V., Radio-emission background of the Metagalaxy, 25:35807
TOKARSKAYA, V. I., Radiation injury of molecular mechanisms of RNA matrix synthesis, 25:35245
TOKIN, I. B., Regeneration in liver after internal

irradiation, 25:35221
TOKUDA, Shoichi, Anomalies in the tensile properties at elevated temperatures of metastable beta titanium alloys, 25:35434
TOLSON, G. M., Production and testing of superheater fuel elements, 25:37024
TOLSTOY, I., Phase-height fluctuations in the ionosphere between 130 and 250 km, 25:35977
TOMASINI, G., Total $\pi^+\pi^-$ cross-section for dipion energies above 1.5 GeV, 25:36509
TOMIŞELLI, A., Experiences with the shielded whole-body counter, 25:35183
TOMKINS, B., Fatigue failure in high strength metals, 25:35428
TOMLINSON, R. E., Technical criteria for the prevention of criticality, 25:34678 (ARH-468(Rev.))
TONDELLO, G., Grazing-incidence spectra of Ne VII and Ne VIII, 25:35766
TONEEV, V. D., Interaction of high-energy radiation with matter, 25:36816 (JINR-P2-5719)
TONG, S. L., Decay of ^{142}La, 25:36765
TONWAR, S. C., Search for high-energy gamma rays from pulsars, 25:35705
TORIZUKA, Kanji, Sequential brain imaging as an aid in understanding disease etiology, 25:35174
TOUBOUL, Jean-Paul, Molybdenum decarburization by annealing at low oxygen pressures, 25:35309
TOUYA, Juan Jose, Control of elution and eluent from /sup 113m/In generators, 25:34672
TRAYLOR, Joseph Gibson, Lattice dynamics of rutile, 25:37239 (TID-25720)
TREACY, P. B., Computer subprograms for scattering problems, 25:36813 (ANU-P-439)
TREFIL, J. S., Model for the production of particles with superstrong interactions, 25:36530
TREFILOV, V. I., Dislocation motion in monocrystals of Mo and Nb, 25:35443
TREKHOV, E. S., Electron distribution function in a low-temperature plasma, 25:36134
TREVOROW, L. E., Prog. rpt. on lithium/chalcogen secondary cells for components in electric vehicular-propulsion generating systems, semiannual, 5/23--11/22/70, 25:35275 (ANL-7777)
TREZZA, G., Application of alpha and beta--gamma autoradiography in shielded cells for the examination of irradiated nuclear fuels, 25:34837
TRIANTIS, F. A., Momentum dependence of 180° π-p charge-exchange cross section, 25:36412
TRICHE, H., Radiation emitted by an argon plasma produced by a low-pressure torch discharge, 25:36124
TRIGER, S. A., Sausage instabilities in a transparent plasma of finite conductivity, 25:36173
TRIKHA, S. K., Pulsed neutron and diffusion length study in bismuth, 25:36655
TRIMBLE, Virginia, Runaway stars and pulsars near Crab Nebula, 25:35694
TRIPATHI, D. N., Importance of the kinetic energy expression for the bound electron in the binary collision theory of ionization, 25:35870
TRIPATHY, D. N., Collective oscillations in a dense electron gas containing a fixed point charge, 25:36239
TRIVEDI, B. M. P., Production rates of ^{22}Na and ^{3}H in stone meteorites by cosmic rays, 25:35599
TROE, J., High-pressure region of the recombination O + O_2 + O_2, 25:34589
TROFIMENKOFF, N. N., Comment on a model of parity-violating nonleptonic decays, 25:36465
TROITSKII, N. A., Effect of donor irradiation on appearance of nonselective markers, 25:35126
TRON, A. S., Deformation of laminar systems of copper--molybdenum and copper--tungsten at increases temperatures, 25:35454
TROWBRIDGE, C. W., Magnetization current effects in coils wound from multifilament stabilized superconductor, 25:35000 (CONF-700623-(Vol.2), pp 1095-1125)
TRUEMPER, J., Hadron interactions at very high energies, 25:36395
TRUHLAR, Donald G., Exact tunneling calculations, 25:34574
TSAP, T. T., Magnetic fields at different depths of the active regions of solar atmosphere, 25:35754
Velocity field at different levels in the solar-active regions, 25:35746
TSCHERDYNZEV, V. V., Isotopic composition of uranium and the content of actinium in minerals and natural waters, 25:34738
TSEGEL'NIK, L. I., Copper and Al in tissues of the spinal cord after x irradiation of animals, 25:35228
TSEITLIN, M. B., Effect of inhomogeneities in a plasma waveguide on the propagation of slow waves and on electron beam interactions, 25:36234
TSEITLIN, P. I., Some new aspects of the effect of ionizing radiation on deoxyribonucleoproteins of somatic cells, 25:35198
TSIBEREV, V. P., Effect of argon on thermionic converter operation at low cesium pressures, 25:35930
TSUBOI, Atsushi, Rejoining of single breaks of DNA induced by x-rays in mammalian cells, 25:35224
TSUEI, C. C., APW calculation of energy bands in simple cubic tellurium, 25:37175 (CALT-822-29)
TSUKERMAN, S. A., Tungsten base metal--ceramic alloy, 25:35476
TSUZUKU, Takuro, Annealing effects on galvanomagnetic properties of heavily radiation-damaged graphite, 25:36314
TSVETKOV, L. I., Observations of solar radio emission at 3.15 cm, 25:35760
TSYTOVICH, V. N., Collective beam acceleration, 25:36617 (UCRL-Trans-1443)
Drift instabilities in a plasma in a high-frequency electromagnetic field, 25:36177
TUCKER, C. W. Jr., Comparison of calculations of LEED intensities from Be(0001) and Al(001), 25:36329
TULLY, John C., Effects of surface crossing in chemical reactions: the H_3^+ system, 25:35885
TURAKULOV, Ya. Kh., Hormonogenesis in thyroid by local irradiation, 25:35208
TURCK, B., Concept and quality measurements of the magnetic field in connection with the important properties of the optical system considered, 25:36627
TURITZIN, N. M., Vacuum tube compensated flat top high-current pulse supply for symmetrical torus machine, 25:36167 (MATT-837)
TURNAU, J., AFST model with $\pi\pi$ and πp phase shifts and Durr--Pilkuhn form factors applied to the reaction $\pi^+ p \to p 3\pi^+ 2\pi^-$ at 8 GeV/c, 25:36503 (INR-P-1265)
TURNER, B. E., Anomalous CH emission from new types of galactic objects, 25:35698
Search for interstellar SH at radio frequencies, 25:35697
TURNER, G. D., New method of sampling Klein--Nishina probability distribution for all incident photon energies above 1 keV, 25:36432 (LA-4663)
TURNER, J. E., Relativistic ground-state energy eigenvalues of an electron-dipole system, 25:36371
TURNER, Ralph E., Radiography in quality control: a seventy-year progress report, 25:34834
TURNER, W., Fisheye mounting problems, 25:34997 (CONF-700623-(Vol.2), pp 1010-23)
TURTLE, J. P., Total solar eclipse of 3/7/70, 25:35764
TYBOR, W., X^0 (960) meson spin--parity determination, 25:36494
TYLER, George C., Automatic data processing system for 2X II, 25:36195 (UCRL-73030)
TYROR, J. G., Reactor physics characteristics of the High Temperature Reactor, 25:36986 (AEEW-M-985)
TYRROFF, H., New method for rare-earth isotope separation, 25:34805 (JINR-P6-5761)
TYUTYUNNIKOV, S. I., Experiments on acceleration of α-particles by collective method, 25:36615 (UCRL-Trans-1434)
TZENG, Huw-shing, Simple neutron spectrometer, 25:34925

U

UBERIO, C., Wave propagation in cold plasma in presence of Coriolis force, 25:36240
UCHIDA, Yutaka, Diagnosis of coronal magnetic structure by flare-associated hydromagnetic disturbances, 25:35777
UDAGAWA, T., Spectroscopic study of (p,t) reactions from neutron-magic nuclei, 25:36794
UDALOV, G. A., Transplantation of bone marrow to irradiated monkeys, 25:35230
UEDA, Hisashi, Inter and intramolecular charge and excitation transfer observed in irradiated polyvinyl chloride particles with surface-coated additives, 25:34656
UEDA, M., Marker rescue with ultraviolet-inactivated influenza virus, 25:35266
UEDA, Y., General treatment of chiral and scale breaking in SU(3) sigma model, 25:36483 (SU-1206-241)
UKEN, E.-A., Instrumental neutron-activation analysis of samples taken at different levels of E.R.P.M. mine, 25:34543 (NIM-1013)
ULIU, F. S., Polarization effects in leptonic three-body decays of baryons, 25:36463
ULKEN, D., Reliability analyses of reactor systems from the view of producer and operator, 25:37095 (IRS-T-18(1970), pp 217-21)
ULLAH, Nazakat, French's spectral distribution and random matrix theory, 25:36823
ULMSCHNEIDER, P., Computation of shock heated models for the solar chromosphere and corona, 25:35769
ULSETH, J. A., Neutron energy dependent cross section evaluation by a multiple foil activation method, 25:36741 (WHAK-SA-107)
ULSHMID, I., Measurement of the density of a plasma with the aid of an open resonator, 25:36089 (KHFTI-69/51)
UNGER, Emil, Autoradiographic studies on ^{3}H-thymidine incorporation in liver and kidneys of irradiated mice, 25:35238
UNGER, S., Defect formation energies and related properties in irradiated polymorphic materials, 25:36297
URBAN, K., Growth of defect clusters in thin nickel foils during electrons irradiation. I, 25:36255
URBANCOVA, Jaromira, Relative efficacy of intraperitoneal application of haematopoietic cells to irradiated mice, 25:35111
URCH, I. H., Energy losses and modulation of galactic cosmic rays, 25:35924
URITANI, I., Metabolic changes in tissues prepared from irradiated sweet potato roots with regard to ethylene effects, 25:35105

XUM

USACHEV, Yu. D., Search for elementary particles bearing a magnetic charge, 25:36379 (CERN-Trans-71-10)
USADEL, Klaus D., Magnetization of dirty superconductors near the upper critical field, 25:36025

V

VAINBLAT, T. I., Creep in Type-II superconductors, 25:36032
Effect of the superconducting transition on the plasticity of metals, 25:35383
VAKIL, U. K., Biochemical and physiological changes in gamma-irradiated wheat during germination, 25:35102
VALENTINE, K. M., Nuclear spin--lattice relaxation and dynamic polarization in γ-irradiated LiF, 25:36348
VALKOVIC, V., Hydrogen-2(p,pn)p reaction at 9.0 MeV, 25:36670
Nucleon--nucleon quasi-free scattering in the p + d → p + p + n reaction at low bombarding energies, 25:36669
VAN ALTENA, W. F., Luminosity of peculiar white dwarf Ross 640, 25:35602
VANCE, E. R., X-ray study of neutron irradiated diamonds, 25:34619
VAN DEN BERGH, S., Are the Maffei galaxies members of the local group, 25:35801
VANDEN BERGHE, G., Unified model calculations for N = 83 nuclei, 25:36749
VAN DE REE, J., Interpretation of alkali--inert-gas beam scattering with Buckingham--Corner potential, 25:35886
VAN DER GOOT, A. S., Crystal structure of rare-earth aluminum compounds R_2Al, 25:35495
VAN DER WOUDE, A., Evidence for T = 1/2 resonance in the ^{3}He system, 25:36663
VAN DE VORST, A., Formation of free radicals in aliphatic and aromatic amino acids by trapped electrons: ESR study, 25:34647
VAN DIEVOET, Jean-Paul L., Nuclear fuel subassemblies and combinations thereof, 25:37143
VANECEK, M., Uranium deposits of Central and Armorican Massifs in France, 25:34753
VANKA, M., Plutonium hexafluoride: preparation and properties, 25:34698 (UJV-2291-Ch)
VAN NIFTRIK, G. J. C., Three-magnet system for measurement of electron scattering through 180°, 25:36625
VAN PATTER, D. M., Midstream evaluation, A = 85, 25:36714
VAN REGEMORTER, H., Broadening by neutral hydrogen in the solar atmosphere, 25:35770
VAN'T VEER-MENNERET, C., Detailed analysis of metallic-line star 15 Vulpeculae, 25:35653
VAN VOORST, J. D. W., Gas phase ESR spectra of ^{31}P, ^{75}As, ^{121}Sb, and ^{123}Sb, 25:36345
VAN WYK, E., Determination, by neutron-activation and tracer techniques, of the losses of iridium during the fire-assay procedure for the platinum-group metals, 25:34544 (NIM-1048)
VAN ZURK, R., 200 MHz pulse amplitude discriminator, 25:35045 (CEA-N-1447)
VARDYA, M. S., Infrared astronomy, 25:35658
Pressure effect and absorption coefficient of H⁻, 25:35661
VARSHAVSKII, Ya. M., Regularities in infra-red spectra (Amide A, B, I, and II bands) of globular proteins in D_2O, 25:34588
VARSHNEYA, N. C., Detecting radiation with a supercooled liquid, 25:35015
VARY, James, Approximate treatment of correlations in nuclear spectroscopy. I, 25:36806
VASIL'EV, E. V., Modification of filled vulcanized polyisoprene (SKI-3) rubber by radioinduced vinyl chloride grafting, 25:34627
VASIL'EV, G. A., Combined action of carbon monoxide and ionizing radiation under prolonged conditions, 25:35233
VASIL'EV, O. V., Giant dipole resonance on nuclei in transition region N approximately 90, 25:36755
VASSILEV, G., Differential measurement of the He 3^3P excitation, in He^+--he collisions, by using an ion--photon coincidence method, 25:35858
VASTOLA, F. J., Studies on ultra-clean carbon surfaces. III, 25:35552
VATCHA, R. H., High-energy N component of extensive air showers, 25:36383
VATULIN, I. F., Laboratory complex for producing homogeneous magnetic fields by superconducting magnetic systems, 25:36079
Machine estimate of homogeneity of magnetic fields of solenoids, 25:36077
VAUGHN, H. R., Analog simulation of a guided parachute-payload system, 25:37224 (SC-DR-710097)
VAUTHERIN, D., Coulomb energy differences in mirror nuclei in Hartree--Fock approximation, 25:36712
VECLI, A., Heme--protein interaction and radioresistance, 25:35106
VELASQUEZ, D. A., Sky brightness and color change during total solar eclipse 11/12/66, 25:35762
VELINOV, P., Planetary energy introduced by galactic cosmic rays into ionosphere and atmosphere, 25:36007
VENERONI, M., Coulomb energy differences in mirror nuclei in Hartree--Fock approximation, 25:36712
VENEZIANO, G., Algebraic treatment of subsidiary conditions in dual resonance models, 25:36591
VENKATARAYUDU, T., Polynomial basis for the irreducible representations of U_4 in the chain U_4 is contained in R_4, 25:36711
VENKATAVARADAN, V. S., Interplanetary dust, 25:35913
VERBARG, Lawrence E., Device to eliminate undesirable transient effects on computer operations and the like, 25:35074
VERBEKE, R., Fast breeder fuel processing pyrochemical head end study, 25:34688 (EUR-4615)
VERCAEMER, Claude, Internal friction peaks due to O in Nb--4.6 Ti alloys, 25:35410
VERDE, Mario, Exchange magnetic moments of light nuclei, 25:36664
VERDIER, J., Cold neutron source of French--German high flux reactor in Grenoble, 25:37087
VERDIN, D., Alkoxy radical production in the radiolysis of t-butanol (2-methyl-2-propanol), 25:34659
VERDINGH, V., Preparation of $^{241}PuO_2$ for neutron cross section measurements, 25:35541
VERESHCHAGIN, V. L., Electrode erosion in pulsed plasma accelerators, 25:36207
VERGADOS, J. D., Electric dipole transitions in ^{88}Sr and ^{90}Zr, 25:36798
VERGASOVA, L. L., Effects of diffusion interaction components on niobium--titanium alloys, 25:35325
VERHEUL, H., Nuclear data sheets for A = 87, 25:36706
VERRY, Monique, Separation of lanthanides by chromatography on SA-2 ion exchange paper, 25:34714
VERSCHUUR, G. L., H I clouds with spin temperatures less than 250°K, 25:35680
VERSNYDER, F. L., Basic problems underlying high-temperature materials development, 25:35301
VESELY, T., Economic aspects of prospection and exploitation of U ores in France, 25:34751
VESELY, W. E., RAFFLE Monte Carlo code and its use to obtain correlated estimates of collapsed cross sections, 25:36549 (CONF-710302-11)
VESPALEC, Rudolf, Triple-crystal gamma scintillation spectrometer with a protective anticoincident scintillator, 25:34931
VETTER, H., Reliability analyses of reactor systems, 25:37041 (IRS-T-18(1970); pp 223-39)
VIATOUR, P., Hardening mechanisms in multiphase alloys, 25:35396
VICTOR, G., Electronic device for Mossbauer spectrometry, 25:34934
VIDAL, F., Entropy of vortices in high-kappa Type-II superconductors, 25:36063
VIEGAS, A., Colorimetric determination of Au(III), 25:34521
VIEHBOECK, F. P., Mass spectrometric determination of the neutron capture cross section of isotopes of the rare earths, 25:36735 (SGAE-PH-104/1971)
VIGNES, A., Coating of Nb and Nb alloys with Al. II, 25:35314
VIGNONI, A., Experiences with the shielded whole-body counter, 25:35183
VIKTORA, L., Relative efficacy of intraperitoneal application of haematopoietic cells to irradiated mice, 25:35111
VILCOV, N., Spontaneously fissioning isomers of transuranic nuclei, 25:36781
VINNAY, I., Angular anisotropy of fission fragments in ternary fission of ^{235}U and ^{238}U, 25:36759
VIOLA, V. E., Fission-excitation functions in interactions of ^{11}B, ^{12}C, ^{14}N, and ^{19}F with various targets, 25:36784
VISWANATHAN, R., Heat capacity and ac susceptibility of V_3Si, 25:36022
VLADIMIRSKII, B. M., Estimation of high-energy γ-radiation fluxes from some cosmic objects, 25:35687
Interplanetary plasma and magnetic field in plane of solar equator, 25:35759
VLADUTIU, Adrian C., Transfer of experimental autoimmune thyroiditis of the mouse by serum, 25:35114
VOEGELI, Paul T. Sr., Radiochemical analyses of water from selected streams, wells, springs, and precipitation collected during reentry drilling, Project Rulison, 25:34728 (USGS-474-101)
VOELCKER, H., Situation of the nuclear fuel cycle industry, 25:37034
VOGEL, G. J., Work plan for continuation of the project, reduction of atmospheric pollution by the application of fluidized-bed combustion, 25:37158 (ANL/ES-CEN-1003)
VOGTLIN, G. E., Engineering design of the 2X II, 25:36159 (UCRL-73060)
VOICE, E., Radiation-induced creep in pyrocarbon, 25:35566
VOIGT, D., Application of statistical methods for the design of reactor systems, 25:36979 (IRS-T-18(1970), pp 205-15)
VOIKHANSKAYA, N. F., Spectrophotometric study of four K stars, 25:35636
VOLARCVICH, M. P., Isothermal compressibility of igneous rocks, 25:37233 (SC-T-713031)
VOLCHENKOV, N. G., Automatic processing of information from spark chambers, 25:35004 (JINR-P10-5762)
VOLKOV, A. K., Measurement of the concentration of oxygen dissolved in tantalum, 25:35339 (ORNL-tr-2479)
VOLKOV, I. G., Investigation of compounds in the niobium--tin system obtained by means of diffusion, 25:36045

XUM

VOLKOV, Ja. F., Instruments for measurement of the spectral lines profile and shift, 25:36091 (UARAEE-95)
VOLKOV, N. V., Ion-acoustic oscillations and transport processes in a low-temperature ceslum plasma, 25:36231
VOLKOV, Ya., Experimental studies on shock waves propagated through a longitudinal magnetic field in electrodeless discharge tubes, 25:36092 (UARAEE-101)
VOLKOV, Ya. F., Dynamics of THETA-pinch discharge with superimposed azimuthal magnetic field, 25:36129 (UARAEE-102)
Experimental studies on magnetically driven shock wave passing through a longitudinal magnetic field, 25:36117 (UARAEE-106)
VOLKOVA, A. K., Changes in structure and properties in γ-irradiated crystallizable chloroprene rubber, 25:35550
VOLKOVA, C. I., Safety precautions in radioactive cement storage, 25:35148
VOLOBUEV, S. A., Observation of γ quanta greater than 100 MeV from 3C 120, 25:35700
VOLOSHKO, E. N., Qualitative composition of radiation at depth of irradiated medium, 25:35030
VOLPI, G. G., Mass spectrometric study of ionic reactions pertinent to the radiation chemistry of methane, 25:34645
VON BRENTANO, P., Fission isomers in Cm and Bk isotopes, 25:36795
Spectroscopic information from isobaric analog resonances, 25:36852
VON WIMMERSPERG, U., Angular distributions from reaction $^{12}C(\alpha,\gamma_0)^{16}O$, 25:36675
VON WITSCH, W., Nucleon--nucleon quasi-free scattering in the p + d → p + p + n reaction at low bombarding energies, 25:36669
VOROB'EVA, N. S., Obtaining the superconducting compound V_3Ga by means of diffusion, 25:36043
VOROB'EVA, V. G., Effect of excitation energy on yields and kinetic energies of fragments at fission of ^{239}Pu by neutrons, 25:36754
VORONIN, I. M., Mechanical behaviour of ni-based alloys at elevated temperatures, 25:35340 (UARAEE-55)
VOSS, Milo D., Survey of environmental radioactivity, 1--12/70, 25:34743 (IS-2541)
VOTRUBA, Josef, Transverse oscillation of ribbed rods with a helical pitch, 25:36982
VOUTILAINEN, A., Lymphoscintigraphy, gamma-venography, and histological evidence in radical operation, 25:35186
VOZNESENSKAYA, S. V., Radiation chemistry of carbohydrates. XIV, 25:34664
VRBA, P., Theory of a rotating plasma in crossed electric and magnetic fields, 25:36139
VUILLOT, Michel, Method and apparatus to measure the water content of a snow layer, 25:35042
VUJNOVIC, V., Saha equation for simultaneous determination of temperature and electron concentration, 25:36102
VUKANOVIC, R., Penetration parameter for M1 conversion and E2 admixtures for 77 and 191 keV transitions in ^{197}Au, 25:36789
VUKOVIC, Danica, Efficiency of cylindrical control rods partially inserted in a reflected reactor, 25:37131
VYGODSKAYA, A. L., Some problems of the mechanism of injury and recovery of cells, 25:35205
VYLOV, Ts., Decay of ^{139}Nd, 25:36724 (JINR-P6-5673)

W

WACHTER, J. W., Pre-target monitor for the intensity and time distribution of a proton beam, 25:36631
WAEFFLER, H., Atomic stopping cross section of H_2, D_2, He, N_2, and Ar for a particles, 25:36256
WAGEMANN, K., Technical and economic state as well as prospects of atomic energy in the economy of the Federal Republic of Germany, 25:36885 (JUL-705-RG)
WAGNER, C.-U., Electric currents and polarization fields at the base of the magnetosphere, 25:35980
WAGNER, Christian-Ulrich, Conductivity of ionospheric plasma from geomagnetic Sq variations, 25:35989
WAGNER, D. K., Low-temperature electrical and thermal resistivities of tungsten, 25:36331
WAGNER, F., Spectrum shape of K-orbital shakeoff electrons and accompanying nuclear beta particles in decay of ^{143}Pr, 25:36774
WAGNER, F. E., Moessbauer isomer shifts and hyperfine splitting of 145.4 keV γ-rays of ^{141}Pr, 25:36344
WAGNER, H. Gg., Ionization yields of molecular and atomic I on W, W (1.5 percent ThO_2), and Pt (8 percent W) surfaces, 25:35839
WAGNER, P., Thermal conductivity of Np at 300°K, 25:35424
WAGNER, William J., Empirically corrected calculations of coronal visible lines from the $3p^53d$ configuration, 25:35744
WAHBA, S. S., Possible trends for purity control of uranium by neutron activation assay, 25:34547 (UARAEE-68)
WAJDA, Stanislaw, Isotopic exchange of radiochlorine in system $[MoCl_6]^{3-}$---$^{36}Cl^-$, 25:34583
WAKANO, Masami, Effects of a finite rho width on the electromagnetic mass difference of pions, 25:36442
WALD, M., Activation analysis for determination of traces of magnesium and manganese in biological matrices, 25:34552
WALDENSTROEM, S., Electromagnetic interactions of particles with spin. I, 25:36450
WALECKA, J. D., S/sub 1/2/ doublets in hypernuclear and nuclear physics, 25:36528
WALKER, P. L. Jr., Studies on ultra-clean carbon surfaces. III, 25:35552
WALKER, R. J., Characteristics of a standing wave bubble or cloud chamber, 25:34955 (CONF-700623-(Vol.1), pp 408-17)
WALKER, Robert P., Method of measuring fast neutrons by observing multipronged tracks of charged particles formed in cellulose nitrate, 25:34875
WALKER, W. D., Neutral particle tagging facility for ANL 30'' bubble chamber, 25:34967 (CONF-700623-(Vol.2), pp 582-92)
Wisconsin rapid cycling bubble chamber, 25:34956 (CONF-700623-(Vol.1), pp 418-23)
WALLACE, A., Effect of a chronic exposure to gamma radiation on shrub Ephedra nevadensis in northern Mojave Desert, 25:35249
WALLACE, R. M., Regularities associated with the formation of lanthanide and actinide complexes, 25:34607
WALLACE, W. E., Low temperature heat capacities of PrBi, PrSb, LaBi, and LaSb, crystal field effects in PrBi and PrSb, 25:35355
WALLERSTEIN, George, Infrared excess of W Cephei and similar stars, 25:35625
WALSH, W. J., Prog. rpt. on lithius/chalcogen secondary cells for components in electric vehicular-propulsion generating systems, semiannual, 5/23--11/22/70, 25:35275 (ANL-7777)
WANG, P. S., Carbon-13 hyperfine interaction in CD_2, 25:34586
WANG, Richard T., Photochemical reaction centers from rhodopseudomonas spheroides, 25:37206 (NYO-3759-30)
WANG, W. L., Intermediate structure and the giant-dipole resonance in ^{16}C, 25:36678
WANG, W. N., Reaction $^{26}Mg(d,\alpha)^{24}Na$ at low energies, 25:36701
WARCZEWSKI, J., Monte Carlo simulation of nuclear-electromagnetic cascade developing in an ionization spectrometer, 25:36431 (ITJ-6)
WARCZEWSKI, Jerzy, Distributions and mean values of inelasticity coefficient K/sub π°/ for lead and graphite, 25:36389 (ITJ-5)
Estimation of energy and mean inelasticity of nuclear interactions at energies above 3.10^{12} eV, 25:36388 (ITJ-3)
WARD, M. D., Pulse and γ-radiolysis of borohydride ion in aqueous solution, 25:34646
WARD, T. E., Decay of ^{34}P and /sup 34s/Cl, 25:36700
New isotope ^{180}Lu, 25:36796
WARDLE, J. F. C., Structure and polarization of 3C 459 at 610 MHz, 25:35788
WARDMAN, P., Direct observation of solvation of the electron in liquid alcohols by pulse radiolysis, 25:34649
WARNER, Brian, Observations of rapid blue variables. II, 25:35675
Observations of rapid blue variables. I, 25:35674
WARNER, David Charles, Damping of plasma waves in Born approximation, 25:36223
WARNER, R. A., Ge(Li)--Ge(Li) sum coincidence, 25:34932
WAROQUIER, M., Unified model calculations for N = 82 nuclei, 25:36749
WARREN, H. S., Patent literature on process radiation and irradiator design. Part 1. United States Patents 1950 through 1968, 25:34777 (ORNL-IIC-34)
WARRINGTON, D. H., Extraneous grain boundary dislocations in high angle (110) twist boundaries in Au, 25:37201 (NYO-3504-58)
WARTELL, M. A., Interpretation of high-energy cross sections for molecular scattering, 25:35887
WATAGHIN, A., Scale factor in cosmological homogeneous models, 25:35816
WATANABE, Keiji, Dynamical structure of mass matrix of K^0--antiK^0 complex, 25:36466
WATANABE, Ringe, Boron stainless steel for JMTR fuel followers, 25:35320
WATANABE, Tadao, Stress dependence of high-temperature creep in Fe--Mo and Fe--Co alloys, 25:35464
WATANABE, Takashi, Gauge fields in the nonlinear realization of a group on its subgroup, 25:36558
WATARI, Nobuo, Energy dependence of the equatorial pitch angle distribution of trapped protons, 25:36002
WATERHOUSE, Neil, Structural and electrical properties of tantalum films sputtered in oxygen--argon mixtures, 25:36338
WATKINS, Charles B. Jr., Numerical solutions of nonequilibrium reflected shock waves in air with radiation, 25:37230 (SC-RR-710203)
WATT, Robert D., Four-inch hydrogen target for 40-inch SLAC bubble chamber, 25:34965 (CONF-700623-(Vol.1), pp 567-80)
WATTENBERG, A., Prog. rpt. on elementary particle physics, annual, 4/70, 25:36384 (COO-1195-213)
WATTERSON, J. I. W., Determination, by neutron-activation and tracer techniques, of the losses of iridium during the fire-assay procedure for the platinum-group metals, 25:34544 (NIM-1048)
WATTS, Herman A., A-stable block implicit one-step methods, 25:37231 (SC-RR-710296)
WAVE, A. R., Gamma-radiation damage of organic

scintillation materials, 25:36079
WAWRA, E., Repair of strand breaks in Chlorella-DNA caused by gamma irradiation, 25:35257
WAY, K., Midstream evaluation, A = 90, 25:36801
WAY, S., Char burning MHD systems, 25:35927
WEBBER, J. C., Radio-continuum observations of Maffei 2, 25:35802
WEBER, J., Gravitational radiation experiments, 25:36585
WEBER, Stephen V., Far-ultraviolet interstellar absorption in Orion and Monoceros, 25:35785
WEBSTER, D. S., Prog. rpt. on lithium/chalcogen secondary cells for components in electric vehicular-propulsion generating systems, semiannual, 5/23--11/22/70, 25:35275 (ANL-7777)
WEBSTER, T. H., Plastic anisotropy in bcc metals, 25:35379
WECHSLER, M. S., Radiation hardening and radiation-anneal hardening in body-centered cubic metals, 25:35507
WECKERING, Rudolf, Systematics of resonances, 25:36488
WEEKS, Robert, Operating experience of nuclear power-stations in UNIPEDE member countries, 25:36864 (CONF-700956-2)
WEERTMAN, J., High-temperature creep of polycrystalline graphite, 25:35556
WEIGUNY, A., Alpha clustering and angular momentum projection before and after variation, 25:36680
WEINBERG, Evelyn Miriam, Determination of ^{210}Po in cigarettes and tobacco, 25:34515
WEINSTOCK, Jerome, Nonlinear theory of macroinstabilities and enhanced transport in plasmas, 25:36164 (TID-25713)
WEIS, Joseph Herman, Dual resonance models for vector currents, 25:36490
WEISE, E., Lumped element line generator for low rf sinusoidal oscillations, 25:36229
WEISS, M. J., Inelastic electron scattering from formaldehyde, 25:35883
WEITKAMP, C., Versatile routing unit for measurements of time-dependent pulse-height spectra, 25:35065
WEITLAUF, Harry M., Prog. rpt. on protein synthesis in delayed implanting mouse ova, 5/70--5/71, 25:37183 (COO-1801-17)
WELCH, Robert A., Prog. rpt. on radiation chemistry of high polymers, 6/70--3/71, 25:34637 (ORO-4059-1)
WELFARE, F. G., Oak Ridge systems analysis code (ORSAC) User's manual, 25:36886 (ORNL-TM-3223)
WELFORD, W. T., Bubble chamber holography, 25:34598 (CONF-700623-(Vol.2), pp 1024-38)
Development and performance of ANL 140° camera lens, 25:34591 (CONF-700623-(Vol.2), pp 915-42)
Fisheye window concentricity problems, 25:34956 (CONF-700623-(Vol.2), pp 997-1009)
WELIN, G., Rapid evolution of LkHα 190, 25:35656
WENDHAUSEN, Henning, Irradiation planning by means of a programmable table computer, 25:35195
WENSTRAND, Terry K., Impact of fuel reprocessing on health physics, 25:35140
WENZEL, P., Substance and meaning of the nuclear fuel industry and economy, 25:36859
WERKLEIDER, Sc., Experiences with a thermoluminescence dosimeter, 25:35139
WERNICK, J. H., CdP_2--Sn system and some properties of $CdSnP_2$ crystals, 25:35580
WERTZ, J. R., Hierarchical big-bang cosmology, 25:35817
WESCHKE, P., Problems of grasping the working behavior of nuclear power plants in production planning and of its economical simulation, 25:37033
WESSELINK, A. F., Variables in NGC 1466, 25:35671
WESTON, L. W., Neutron multiplicity for ^{239}Pu resonance fission, 25:36734 (ORNL-TM-3331)
WESTWOOD, W. D., Structural and electrical properties of tantalum films sputtered in oxygen--argon mixtures, 25:36338
WEWERKA, E. M., Use of gel permeation chromatography in the development of high-quality graphite, 25:35533
WEYER, G., Lifetime of the 91.5 keV state in ^{151}Sm, 25:36807
WHEELER, B. R., Optimized use of multipurpose fuel processing facilities at Idaho chemical processing plant, 25:34581 (CONF-710417-1)
WHEELER, F. J., PHROG: a FORTRAN IV program to generate fast neutron spectra and average multigroup constants, 25:37113 (IN-1435)
RAFFLE Monte Carlo code and its use to obtain correlated estimates of collapsed cross sections, 25:36649 (CONF-710302-11)
WHELAN, E. D., Radiation-induced translocations in Prunus avium cv. Lambert, 25:35127
WHITE, A. R., Fixed-angle limit in inclusive experiments, 25:36421
WHITE, G. D., Multispecimen hot pressing of UO_2, 25:35526
WHITE, Raymond E., Secondary UBV comparison stars near some southern globular clusters. II, 25:35613
WHITEHOUSE, J. E., Defect production in n-type germanium by electron irradiation at low temperatures, 25:36293
WHITEOAK, J. B., Neutral hydrogen absorption and emission in NGC 5128, 25:35789
Optical identification of PKS 0320-37, 25:35707
WHITLOCK, L. C., Multipole admixtures of transitions from β, γ, and octupole vibrational states in ^{154}Gd, 25:36742
WHITTINGHAM, I. B., Incoherent scattering of gamma rays in heavy atoms, 25:36253
WIDENMANN, L., Radiation burden during roentgen kinematography, 25:35143
WIEDERSICH, H. W., Void formation during irradiation, 25:35511
WIERNIK, George, Origin and kinetics of goblet cells in the human jejunum during irradiation, 25:35240
WIESENACK, Guenter, Nuclear power reactors and mobile nuclear installations, 25:36858
WILD, Wolfgang, Elementary particles and symmetry, 25:36549
WILHELM, R., Experimental investigation of a toroidal diffuse pinch, 25:36168
WILKIN, C., Investigation of nucleon--nucleon correlations by means of high-energy scattering, 25:36538
WILKINSON, D. H., Properties of ^{13}B and ^{20}Ne, 25:36710
WILL, Wolfram, Measuring of the standard ionic dose in compact and liquid media during x-ray and gamma irradiation by energies between 50 keV and 3 MeV. VI, 25:35146
WILLARD, J. W., Lead shielded Dewar development, 25:36192 (MATT-846)
WILLIAMS, D. N., Oxidation protection of a chromium alloy by nickel-alloy claddings, 25:35268
WILLIAMS, Frederick C. Jr., Particle-hole state density in the uniform spacing model, 25:36830
WILLIAMS, J. C., Deformation of body-centered-cubic titanium--vanadium single crystals, 25:35377
WILLIAMS, P. F., Photoluminescence studies of superconducting Nb_3Sn, 25:36062
WILLIAMS, R. W., Chemical shifts of μ^+, 25:35852
WILLIAMS, Robert H., Nonlinear theory of macroinstabilities and enhanced transport in plasmas, 25:36164 (TID-25713)
WILLIAMS, W. T., Vacuum breakdown between superconducting electrodes, 25:36075
WILLIAMS, Wendell S., Gap energy of superconducting niobium carbide, 25:36030
WILLIAMSON, J. D., Nuclear spin--lattice relaxation in pure and impure indium. I. Normal state, 25:36345
WILLIG, W. R., Lead iodide nuclear particle detectors, 25:34889
WILLIS, A. G., Radio-continuum observations of Maffei 2, 25:35802
WILLIS, C. D., Vapor pressure--temperature data for selected halogen-containing substances, 25:34602 (GAT-649)
WILLUHN, K., Special requirements for instruments for radiation protection monitoring in nuclear power plants, 25:34869 (SZS-2/71, pp 7-11)
WILSKA, J., Preservation of fruits by radicpasteurization, 25:35273
WILSON, C. R., Results from meridian chain of observatories in Alaskan sector. I, 25:35961
WILSON, H. W., Beta energy release following thermal fission of ^{233}U and ^{235}U, 25:36764
WILSON, P. R., Center limb observations of inhomogeneities in the solar atmosphere. II, 25:35715
WILSON, R. G., Perturbation treatment of Hartree--Fock equations for ground states of 3- to 10-electron atoms, 25:35889
WILSON, Robert E., Realization of accurate close-binary light curves: application to MR Cygni, 25:35628
WINCKLER, J. R., Electron echo experiment, 25:35966
WINDELBAND, R., Determination of absorbed dose of high-energy electrons by lithium fluoride detectors, 25:35027
WINDSOR, Robert Anthony, Radio noise generation by scattering of plasma waves, 25:35896
WINKLER, C., Radioisotope selection in diagnostic nuclear medicine from the standpoint of minimal radiation burden, 25:35179
WINKLER, E., Temperature dependence of growth of E. coli B in heavy water, 25:35094
WINTHER, Aage, Transient fields acting on heavy ions during slowing-down in magnetized materials, 25:36846
WITHERS, J. C., Techniques for fabrication of high-strength, high-modulus, low-density filament-reinforced metal matrix composites, 25:35528
WITKOWSKI, S., Free targets, 25:36151
Shock-wave process and numerical calculations, 25:36152
WITT, F. J., Investigation of the structural reliability of heavy section steels for light-water reactor pressure vessel applications, 25:34827
WITTE, L. C., Vapor explosion--heat transfer and fragmentation. III, 25:37214 (ORO-3926-4)
WITTGENSTEIN, F., Big European bubble chamber magnet progress report, 25:35001 (CONF-700623-(Vol.2), pp 1126-49)
WITTKOWER, A., Determination of lifetimes for multiply charged heavy ions excited in collisions with light gases, 25:35849
WITTMAN, R. H., Explosive cladding and welding for low capital investment fabrication, 25:35298
WOLF, E., Power limitations of an in-core thermionic cell in steady-state operation, 25:37090
WOLF, George William, Elliptical polarization of starlight, 25:35618
WOLF, Walter, Prog. rpt. on ESR studies of thiyl free radicals relation to biological effects of radiation, annual, 3/71, 25:34639 (USC-113-P-21-3)
WOLFE, B., FFTF: companion test and development facility

for LMFBR program, 25:37085 (WHAN-SA-104(Rev.))
WOLFF, Richard J., uvby photometry of Ap stars, 25:35612
WOLFF, S., Influence of parasitic boiling and expansion speed on the dynasic pressure in a bubble chamber, 25:34957 (CONF-700623-(Vol.1), pp 424-48)
WOLFF, Sidney Carne, uvby photometry of Ap stars, 25:35612
WOLLENHAUPT, H., Inactivation and division delay of E. coli B/r by combined treatment with uv and vacuum, 25:35265
WOLTJER, L., Infrared background and universal cosmic rays, 25:35818
WOOD, L. S., Carbon-13 hyperfine interaction in CD_2, 25:34586
WOOD, P. M., Cost-benefit illustration for underground nuclear natural gas stimulation, 25:34766 (AECOP-632)
WOODFORD, D. A., Microstructural aspects of fracture toughness in a cobalt-base superalloy, 25:35490
WOORE, J., Shubnikov--de Haas oscillations in neutron-irradiated graphite, 25:36284
WORDEN, Earl F., Analysis of first and second spectra of dysprosium, 25:35846
WORLEY, R. D., 12.5 KJ capacitor bank, 25:37194 (MHSMP-71-33)
WORLTON, D. C., Review of selected nondestructive testing activities at Battelle Northwest Lab, 25:34833
WORWETZ, H. A., BNL work on Ne/H_2 targets, 25:34961 (CONF-700623-(Vol.1), pp 511-31)
WOZNIAK, Wanda, Effect of ionizing radiation on the stability of some radiopaque iodine compounds, 25:34662
WRIGHT, Byron T., Research program of the Nuclear Consortium at the UCLA Cyclotron Laboratory, July 1970. Report AR 5, 25:36738 (UCLA-10-P-18-23)
WRIGHT, Harvel, Aspects of degradation spectra, 25:36258
WRIGHT, Melvin C. H., Interpretation of observations of neutral hydrogen in external galaxies, 25:35781
WU, C. L., Current distribution and internal resistance in segmented MHD channels, 25:35926
WUCHERER, P., Electron--photon cascades in Pb at primary energies of 100, 200, and 400 MeV, 25:36788
WURM, J. G., Fast breeder fuel processing pyrochemical head end study, 25:34688 (EUR-4615)
Pyrochemical head end conception for fast breeder fuel processing, 25:34687 (EUR-4614)
WYLIE, Robert D., In-reactor inspection and repair procedures for BONUS nuclear power plant, 25:36857

Y

YADAV, A. A., Rapid extraction of antimony with tributyl phosphate, 25:34512
YADROSHNIKOV, V. A., Machine estimate of homogeneity of magnetic fields of solenoids, 25:36077
YAKIMENKO, M. N., Search for elementary particles bearing a magnetic charge, 25:36379 (CERN-Trans-71-10)
YAKOVLEV, K. A., Increase of effectiveness of synchronized capture during bunching of beam outside the separatrix, 25:36603 (IFVE-SKU-70-20)
YAKOVLEV, P. D., Various structural types of the molybdenum--uranium ores, 25:34756
YAKOVLEV, V. N., Oscillations in a magnetized afterglow plasma with a transverse current, 25:36175
YAKUBOV, I. T., Relaxation and nonequilibrium radiation behind shock waves in air, 25:37232 (SC-T-713030)
YAKUTOVICH, M. V., Welding of various solid state metals, 25:35321
YAMADA, Masao, A model for dipole electromagnetic form factors, 25:36436 (ORO-3992-28)
Deep inelastic neutrino--nucleon interactions, 25:36455 (ORO-3992-24)
Model for K/sub 13/ form factors and Cabibbo angle, 25:36456 (ORO-3992-39)
YAMAFUJI, Kaoru, Josephson junctions with superconducting barriers, 25:36064
YAMAJI, Kunihiko, Nonlinear electrical conductivity of superconducting films below the transition temperature, 25:36024
YAMAMOTO, Hiroshi, Inactivation of T antigen-forming capacities of simian virus 40 and adenovirus 12 by ultraviolet irradiation, 25:35267
YAMAMOTO, R. K., Momentum dependence of 180° π-p charge-exchange cross section, 25:36412
YAMAMOTO, Shuji, Fast neutron spectra from natural uranium target bombarded with high energy electrons, 25:36767
YAMAMOTO, Tsutomu, Aging in Hiroshima and Nagasaki atomic bomb survivors, 25:35241
YAMAMOTO, Y., Electron cyclotron wave and electrostatic wave in bounded plasmas, 25:36241
YAMASAKI, Shuichiro, Velocity operator in many-boson systems, 25:36368
YAMASHITA, Tsutomu, Superconducting transition temperatures of rf-sputtered NbN films, 25:36065
YAMATO, Harumi, Thermal stability of a fusion reactor, 25:36178
YAMAZAKI, Anro, Effect of fractionated x irradiation on cells in tissue culture, 25:35242
YANAVICHYUS, A. I., Interaction potential between α-particle taking into account their measurement, 25:36537
YANEVA, N., Parameters of neutron resonances of ^{233}U, ^{235}U, and ^{239}Pu, 25:36756
YANG, Chien-sheng, Electron scattering from ^{13}C, 25:36682
YARMONENKO, S. P., Effect of irradiation conditions on the recovery of somatic cells in mammalian organism, 25:35218
YAROVAYA, S. M., Radiation chemistry of carbohydrates. XIV, 25:34664
YASHIRO, Dairokuro, Inter and intramolecular charge and excitation transfer observed in irradiated polyvinyl chloride particles with surface-coated additives, 25:34656
YASUMOTO, Saburo, Effect of fractionated x irradiation on cells in tissue culture, 25:35242
YAVOR, S. Ya., Design of crossed electron-optical lenses, 25:36646
YAZAWA, Akira, Measurements of heats of mixing in liquid gold binary alloys, 25:35432
Measurements of heats of mixing in liquid copper binary alloys, 25:35433
YEAGER, Ernest, Differential capacitance study of stress-annealed pyrolytic graphite electrodes, 25:35563
YEIVIN, Yehuda, Solution of the neutron transport equation, 25:36654
YESIAN, Harry J., Triple Pomeron vertex, duality, and diffraction dissociation, 25:36420 (UCSD-10-P-10-78)
YIFTAH, S., Fluctuation factors for theoretical evaluation of average neutron cross sections of fissile nuclei in the unresolved resonances region, 25:36722 (IA-1208)
YODA, Yoichi, Concept of the marine nuclear power complex, 25:36981 (CRNL-tr-2474)
YONTS, O. C., New data system for INTEREM, 25:36193 (ORNL-TM-3401)
YOSHIDA, Hiroyuki, Low temperature irradiation studies on iron--boron alloys, 25:35588
Radiation damage studies using the low temperature irradiation facility. II, 25:36286
YOSHIDA, Susumu, Influence of high hydrostatic pressure on the flow stress of zinc and zirconium polycrystals, 25:35435
YOSHIDA, Y., Welding of tantalum and newly developed tantalum-clad steel, 25:35356
YOSHIKAWA, Nobuharu, Level structure of ^{143}Pm and ^{143}Nd, 25:36766
YOST, Jonathan C., Density-wave theory of galactic spirals. III, 25:35782
YOUMANS, Arthur H., Method and apparatus for calibrating pulsed neutron well logging instrument, 25:35039
YOUNG, Arthur, Hyades membership of white-dwarf eclipsing system BD + 16°516, 25:35632
YOUNG, D. A., Shubnikov--de Haas oscillations in neutron-irradiated graphite, 25:36284
YOUNG, J. E., Generalized C(2,1) expansion for asymptotically growing amplitudes, 25:36547
YOUNG, Jack C., Fast reactor spectrum measurements. Technical summary report, February 1, 1970--January 31, 1971, 25:36991 (GULF-RT-10523)
YOUNG, P. G., Evaluated nuclear data for hydrogen in the ENDF/B-II format, 25:36660 (LA-4574)
YOUNT, D., Proportional quantameter for the 15-foot bubble chamber, 25:34942 (CONF-700623-(Vol.1), pp 97-116)
YOUNT, S. L., Radiation shielding information center user documentation, 25:36247 (CTC-48)
YOUSSEF, A. M., Dynamics of THETA-pinch discharge with superimposed azimuthal magnetic field, 25:36129 (UARAEE-102)
YUI, Shinroku, Production of Type 316 stainless steel cladding tubes for fast breeder reactor, 25:35205
YULDASHBAEV, T. S., Method of projecting and studying the spatial image of complex events recorded by a spark chamber, 25:35011
YUROVSKII, Yu. F., Solar radio emissions and flare of July 11, 1966, 25:35749
YUTA, H., Off-mass-shell Kπ scattering phase shifts, 25:36413
Optical constants for the ANL 12-foot bubble chamber, 25:34947 (CONF-700623-(Vol.1), pp 275-302)
YUTHAMANOP, Anan, Environmental isotope investigation in Totes Gebirge Styria, Austria, 25:34726 (THAI-AEC-35, pp 9-20)

Z

ZAALOUK, M. G., Criticality evaluation of hydrogeneous enriched lattices using a three group model, 25:37124 (UARAEE-84)
New approach for calculations of nuclear fuel consumption in UA-RR-1 core, 25:37077 (UARAEE-63)
Theory for assymetric array of cylindrical cavities inside a reactor core, 25:37117 (UARAEE-58)
ZABKA, M., Program for determining environmental safety of nuclear power plants, 25:37049
ZACKAY, V. F., Superposition model for environmentally-assisted fatigue-crack propagation, 25:37249 (UCRL-20538)
ZADWORNY, Francois, Total cross sections for collisional detachment of one or two electrons from H^- on H_2O, 25:35867
ZAFAR, M., Emission of deuterons in 24-GeV/c proton interactions with emulsion nuclei, 25:36402
ZAFIRATOS, C. D., Reaction $^{19}F(^3He,^6Li)^{16}O$ at 40 MeV, 25:36674
ZAGATIN, V. I., Observations of 3C 273 radio source at 8 mm

XUM

with maser, 25:35686
ZAGORSKI, Zbigniew Pawel, Effect of ionizing radiation on the stability of some radiopaque iodine compounds, 25:34662
ZAHARESCU, Maria, Thermal equilibria of phases in system $MgO--TiO_2--V_2O_5$, 25:35576
ZAIDINS, C. S., Reaction $^{19}F(^3He,^6Li)^{16}O$ at 40 MeV, 25:36674
ZAIKINA, G. I., Phase composition, structure, and magnetic hysteresis of Nb--Sn alloys, 25:36047
ZAINULIN, Yu. G., Region of homogeneity of a zirconium oxynitride of NaCl structure at 1500°C, 25:35583
ZAKHARYCHEVA, I. I., Electrophilic substitution on aromatic carbon atom. XIV, 25:34600
ZAMKOV, V. N., Peculiarities of formation of intermetallics in explosion-produced copper--titanium compounds, 25:35324
ZAMORANI, E., Thermogravimetric analysis (TGA) of the uranium oxide carboreduction, 25:34556 (EUR-4635)
ZAMRY, V. N., Centralized output of spectrometry data, 25:35049 (CONF-700647-, pp 255-79)
ZANDER, Dennis R., Ultralinear 16-bit digital-to-analog current converter, 25:35053
ZANDRON, O., Asymptotic nucleon form factors from current algebra and Regge model, 25:36437
ZANINI, A., Two-body photodisintegration of ^4He up to 80 MeV, 25:36671
ZANNONI, R., Disorder in implanted semiconductors, 25:36300
ZARETSKII, D. F., Isospin conservation and β decay of heavy nuclei, 25:36833
ZARUBINA, O. A., Electrical resistance of Ti--Nb alloys at high pressures, 25:36321
ZARZECZNY, August, Isotopic exchange of radiochlorine in system $(MoCl_6)^{3-}--^{36}Cl^-$, 25:34583
ZASTAVENKO, L. G., Partial elimination of infrared divergences in the model of quantum field theory with degenerated vacuum, 25:36562 (JINR-P2-5760)
ZAUDERER, B., Performance of a large-scale, nonequilibrium MHD generator with rare gases, 25:35932
ZAVADIL, V., Isotopic exchange of gaseous deuterium with lattice hydrogen of hydrides, 25:34582
ZAVARYAN, E. L., Chromosome aberrations caused by x-irradiation, 25:35125
ZAYED, K. E., Boundary conditions in the case of adjacent plasma streams, 25:36128 (UARAEE-78)
ZECCHIN, R., Contribution of radioisotope techniques to the diagnosis of lung morphology, 25:35180
ZEE, A., Model for Pomeranchukon couplings, 25:36512
ZEINALOV, S. K., Study of atmospheres of supergiants. II, 25:35635
ZEITNITZ, B., Neutron scattering from ^{15}N. I, 25:36684
ZELEZNY, W. F., Metallurgical evaluation of simulated BWR emergency core cooling tests, 25:37038 (IN-1453)
ZEL'VENSKII, Ya. D., Isotope effects in CO_2 adsorption on zeolites, 25:34708
ZEMANOVA, L., Molecular weight of DNA synthesized in L-cells, 25:35207
ZHDANOV, G. S., Scattering of the bremsstrahlung by the Moessbauer nuclei, 25:36346
ZHELEZNYAK, M. B., Relaxation and nonequilibrium radiation behind shock waves in air, 25:37232 (SC-T-713030)
ZHILINSKII, A. P., Effect of a transverse electric field on the stability of a weakly ionized plasma in a magnetic field, 25:36185
Oscillations in a magnetized afterglow plasma with a transverse current, 25:36175
Parameters of plasma produced by fast electron beam in a magnetic field, 25:36118
ZHUKOVSKII, V. M., Phase diagrams of the systems $MoO_3--MeMoO_4$ (Me = Mg, Ca, Sr, Ba), 25:35578
ZHURAVLEV, G. I., Investigation of radiation-thermal cracking of n-tetracosane and n-heneicosane in the liquid phase, 25:34653
ZIELINSKI, W., Natural rubber latex sensitized with methane halides. II, 25:34614
ZIEMER, P. L., Deposition and retention of inhaled Eu oxide in rat, 25:35086
ZIJLSTRA, W. G., Gas phase ESR spectra of ^{31}P, ^{75}As, ^{121}Sb, and ^{123}Sb, 25:36345
ZIL'BERBERG, V. G., Physical properties of plasma-sprayed carbides, 25:35538
ZIMEN, K. E., Nuclear chemistry compendium. I, 25:34863 (HMI-B-108)
ZIMMERHACKL, E., High-voltage electrophoretic separation of inorganic ions with special regard to Pt metals. III, 25:34702
ZINN-JUSTIN, J., Strong interactions dynamics with Pade approximants, 25:36473
ZIVANOVIC, D., Use of Green function method for scattering of a particle on a system of bound particles, 25:36685
ZLATEVA, M., Changes in oral cavity in chronic radiation, 25:35219
ZOCCHI, F., Mass spectrometric study of ionic reactions pertinent to the radiation chemistry of methane, 25:34645
ZOELLER, R., Post irradiation examination of a thermionic converter, 25:35936
ZOLER, D., Three variants of Fermi model of particle acceleration, 25:36636
ZOLOTAREV, R. B., Radioisotopic analysers for determining sulphur content in the oil-products and the experience in their exploitation, 25:35040
ZOTIKOV, A. A., Early structural distrubances of nucleoproteins in radiosensitive and radioresistant cells exposed to ionizing radiation, 25:35206
ZSIGMOND, G., Synchronized chopper time-of-flight spectrometer, 25:34916 (JINR-E14-5731)
ZUBAREV, A. L., Potentials with hard-core repulsion and nuclear three-body problem, 25:36536
ZUBKOV, I. P., Experimental study of a two-lens accelerator, 25:36115
ZUBOV, P. I., Stabilization of radicals formed during low-temperature radiolysis, 25:34640
ZUEHLKE, P., WAK: administrative basis and commercial realization, 25:34778 (ORNL-tr-2417)
ZUKAS, E. G., High-temperature creep of polycrystalline graphite, 25:35556
ZUTZ, L., Welding peculiarities in fabrication of fuel elements for Superheat Reactor Grosswelzheim, 25:35311
ZVEREVA, A. M., Magnetic fields and proton flares Jul 6 and Sep 2, 1966, 25:35753
ZVOLSKII, I., Decay of ^{173}Ta, 25:36727 (JINR-P6-5704)
ZWARICH, R., Optical studies of $^3(n,\pi^*)$ magnetic sublevels in benzaldehyde, 25:34592
ZWICKER, H., Experimental investigation of a toroidal diffuse pinch, 25:36168
ZYKOVA, A. S., Content of artificial radioisotopes in atmosphere over Moscow during 1962--1967, 25:34748

SUBJECT INDEX

Cross references are included in cumulative subject indexes and in *Subject Headings Used by the USAEC Division of Technical Information* (USAEC report TID-5001).

The reader is also referred to *Guide to Abstracting and Indexing for Nuclear Science Abstracts* (USAEC report TID-4576).

Most headings in the subject index are specific materials, things, and processes. The headings are followed by modifiers that describe the properties of, or processes applied to, the headings.

All index entries cite *NSA* volume and abstract numbers; volume number precedes the colon and the abstract number follows it. The designation (R) following the abstract number indicates a progress report; (P) indicates a patent; and (T) indicates a translation. Abstracts for reports other than progress reports carry no letter designation. Report numbers, where applicable, are included in parentheses after the abstract number of the citation. Published literature (journal article or book) can be identified by the absence of a report number.

Ideas presented in the original literature, rather than key words, have been indexed. The indexers have selected what seemed the most probable and logical place to look for typical information. Since it is not always possible to anticipate where a user would look for information, the cumulative indexes include numerous cross references. Consideration of synonymous or closely related terms will prove valuable.

Information is indexed for the greatest use to the greatest number of users. This requires that a topic be indexed to headings that most specifically describe it and not ordinarily to the headings that describe its ultimate use or to the general class headings that include the specific headings. For example, information on boiler design for the Fermi Fast Breeder Reactor would be indexed under the headings BOILERS and FERMI FAST BREEDER REACTOR but not necessarily under the headings REACTORS, FAST or REACTORS, BREEDER.

General or broad headings are reserved for general summaries, reviews, comprehensive reports, and similar literature.

Subject Heading Styles

Generally, the direct form of subject entry is used rather than inverted headings; e.g., AMINO ACIDS rather than ACIDS, AMINO; HELIUM ISOTOPES He-4 rather than HELIUM—ISOTOPES He-4 or HELIUM—He-4 ISOTOPES. Note, however, that in some cases parenthetic modifying terms or inverted headings such as NEUTRONS, FAST, are used where the alphabetical arrangement of a direct entry would cause information to be scattered. In addition, organic compounds are usually entered in the index in the inverted form to facilitate grouping like or related compounds with the parent compounds; e.g., BENZENE, BROMO- rather than BROMOBENZENE. In general, the nomenclature used is that of the subject indexes to *Chemical Abstracts*.

Alphabetization

Subject headings are alphabetized word by word. Parenthetic qualifiers, numbers, and Greek letters within subject headings are disregarded in alphabetizing unless there are two or more headings that are otherwise identical, in which case the qualifier, numerical progression, or spelled names for the Greek letters determine the order.

Examples:

M-Capture
  see ELECTRON CAPTURE
MAGNESIUM
MAGNESIUM ALLOYS AND SYSTEMS
MANGANESE FLUORIDES
MANGANESE FLUORIDES MnF_2
MESONS
MESONS (π)
MESONS (ρ)
1-PENTANOL
2-PENTANOL

Modifying Phrases

The modifiers appearing under a subject heading are written specifically to show the relation between the item being indexed and the heading. The modifier therefore contains a maximum of useful information. Although the modifier begins with the word judged to be of greatest use to the greatest number of users, there is still need for the searcher to consider all modifiers under the heading(s) of interest.

Modifiers usually form meaningful phrases when combined with the subject heading. Some are intended to be read following the subject heading, e.g., the entry HYDROGEN—sorption by charcoal should be read "hydrogen sorption by charcoal." As a result of placing the important word first, however, many modifiers must be rearranged for smooth reading, e.g., FORMALDEHYDE—yields in radiolysis of ethyl ether, effects of deuterium on, should be read "effects of deuterium on formaldehyde yields in radiolysis of ethyl ether" and URANIUM—crystal structure of, effect of cooling rate on allotropic transformations in, should be read "effect of cooling rate on allotropic transformations in crystal structure of uranium."

Special characters are added to modifiers in the fields of physics and reactor technology; if the modifier does not establish the experimental or theoretical character of a reference, a symbol (E), (T), or (E/T) is placed immediately after the modifying phrase and before the abstract number.

XUM

Physical States and Configurations of Materials

The specific physical state, if other than normal, or the geometric configuration of the material is included in the modifying phrase; e.g., information on liquid metals is indexed under the specific metal with "liquid" in the modifier and carbon crucibles is indexed under CARBON with "crucibles" appropriately placed in the modifier. The information on carbon crucibles is also indexed under CRUCIBLES.

Nomenclature of Inorganic Compounds

Inorganic compounds are indexed to subject headings in the direct form. Cations are listed in the order of increasing valence for polycationic salts of varying valence and in alphabetic order for polycationic salts in which all cations have the same valence; e.g., SODIUM ALUMINUM SILICATES and POTASSIUM SODIUM SULFATES. If more than one anionic species is presented in a compound, the anions are arranged alphabetically, e.g., BERYLLIUM FLUORIDE HYDROXIDES.

Nomenclature of Organic Compounds

Organic compounds are indexed by subject headings based on the indexes to *Chemical Abstracts* except in the area of enzymes, in which specific enzymes, named according to the 1964 recommendations of the International Union of Biochemistry, are used. In many cases nonproprietary names for drugs are used as subject headings, and cross references are made from the systematic chemical names. Subject headings for hormones appear in the inverted style at HORMONES.

Nomenclature of Life Sciences

Subject headings for plants are names of phyla with one exception: members of the Phylum Tracheophyta are indexed under class or subclass names. Scientific names (genus and species) are used as the initial, or file, word in the modifying phrase. Scientific names are omitted only when the name is not available in the literature or cannot be found in available references.

Subject headings for animals are the names of phyla with the following exceptions: (1) members of Phylum Arthropoda and Phylum Chordata are indexed under appropriate class name, and (2) common names are used for members of Class Mammalia.

Subject headings are entered for various classes of commodities, and specific products are identified in the file-word position of the modifier. In the following examples, approved subject headings are capitalized and typical modifier file words are listed in lower case.

Example 1	Example 2
CEREALS	MEATS
bread	beef
flour	fish
oats	mutton
rice	pork
rye	poultry
wheat	seafood

Diseases, pathological conditions, and in vitro studies of atypical cells and tissues are indexed under subject headings for the organism affected, under the appropriate anatomical structure of physiological phenomenon affected, and under the appropriate disease heading. Subject headings for diseases (defined as any deviation from the norm) are DISEASES; DISEASES, INFECTIOUS; DISEASES, NEOPLASTIC; DISEASES, PHYSIOLOGICAL; DISEASES, PLANT; and DISEASES, TRAUMATIC.

Diseases of mixed etiology are treated in the following manner: neoplastic diseases that are also classified as infectious or physiological are indexed under DISEASES, NEOPLASTIC; diseases in which a microorganism is the etiologic agent are classified under DISEASES, INFECTIOUS; physiological anomalies that are neither neoplastic nor infectious are indexed under DISEASES, PHYSIOLOGICAL; the acute radiation syndrome, nonspecific radiation injuries, trauma, and wounds or incisions inflicted mechanically are indexed under DISEASES, TRAUMATIC.

Specific diseases or pathological conditions are named in the file-word position of the modifier, in the author's terminology, and are set off from the remainder of the modifier by commas. Neoplasms are designated as benign or malignant in the file-word position when more specific information is not available.

Multicomponent Alloys and Other Systems

Multicomponent alloys and systems, except well-known trade names, are indexed under a subject heading for each component in the form "element systems" for nonmetals or "element alloys and systems" for metals. The modifier begins with element symbols for each component arranged alphabetically. In addition, if significance is placed on the base metal of the alloy, this is indicated by adding "-base" to the element symbol.

Example: A 1.5C, 12Cr, 0.25V, 0.8Mo, bal Fe alloy is indexed as

```
CARBON SYSTEMS
  C--Cr--Fe-base--Mo--V, ...
CHROMIUM ALLOYS AND SYSTEMS
  C--Cr--Fe-base--Mo--V,...
IRON ALLOYS AND SYSTEMS
  C--Cr--Fe-base--Mo--V, ...
MOLYBDENUM ALLOYS AND SYSTEMS
  C--Cr--Fe-base--Mo--V, ...
VANADIUM ALLOYS AND SYSTEMS
  C--Cr--Fe-base--Mo--V, ...
```

Well-known alloys, such as ZIRCALOY-2, are indexed under the trade name; cross references from each component of the alloy to the trade name appear in cumulative indexes.

Multicomponent systems in which nonmetallic elements are present in large percentage and which are commonly referred to as systems or mixtures are indexed in a manner similar to alloys.

Example: A tungsten–silicon preparation is indexed as

```
TUNGSTEN ALLOYS AND SYSTEMS
  Si--W, ...
SILICON SYSTEMS
  Si--W, ...
```

Multicompound systems and mixtures of inorganic compounds are indexed under the subject heading for each component compound; the modifiers begin with an alphabetical listing of compound formulas.

Example: A lead titanate–lead zirconate mixture is indexed as

```
LEAD TITANATES
  PbTiO3--PbZrO3
LEAD ZIRCONATES
  PbTiO3--PbZrO3
```

A mixed system of compounds and elements is indexed by a combined form of the preceding conventions; e.g., a dispersion of copper and alumina would be indexed as

ALUMINUM OXIDES
  Al_2O_3--Cu, ...
COPPER ALLOYS AND SYSTEMS
  Al_2O_3--Cu, ...

Mixtures of organic compounds are indexed under subject headings for each component of the mixture; the modifiers begin with an alphabetical listing of compound names.

Example:

ACETIC ACID
  acetic acid--BF_3, ...
BORON FLUORIDES
  acetic acid--BF_3, ...

Example:

BENZENE, CHLORO-
  bromophenol--chlorobenzene, ...
PHENOL, BROMO-
  bromophenol--chlorobenzene, ...

If modifiers for alloys and systems are included with other modifiers under the same subject heading, they are filed last.

Example:

CARBON SYSTEMS
  deposition on nuclear fuel particles
  molecular structure of
  neutron total cross section for
  sorptive properties for xenon
  Young's modulus for
  Al--C--Cr, superconductivity in
  B--C, phase studies for
  C--U--Zr, fabrication and physical properties of

Nomenclature of High Energy Physics

Information on particle-particle events is indexed under subject headings for the specific particles involved. The modifier file word *interactions* is followed by the specific interaction written in symbolic form. Particle nomenclature and symbols follow that of Rosenfeld, et al. *Data on Particles and Resonant States,* UCRL-8030 (latest revision). For consistency the incident particle is always written first. The mass (in MeV) of a resonance state is included in parentheses after the symbol to avoid ambiguity. Hyperfragments are indicated in modifiers as in the following examples: Λ-He^5, Σ-H^3, $\Lambda\Lambda$-Be^{10}. The superscript on the right indicates the total number of baryons in the composite system.

Examples:

MESONS (π^-)
  interactions $\pi^- + p \rightarrow \Lambda + K^+ + \pi^-$ at 6 GeV/c in hydrogen bubble chamber, $\Lambda K(1700)$ enhancement in, (E)
BARYONS, RESONANCE (N^*)
  production of $\Delta^{++}(1236)$ and $\Delta^0(1236)$ from $K^- + p \rightarrow K^- + p + \pi^+ + \pi^-$ interactions at 2.63 and 2.70 GeV/c, (E)
HYPERFRAGMENTS
  binding energy of $\Lambda\Lambda$-He^6, three-body $\alpha \rightarrow \Lambda \rightarrow \Lambda$ model for

Subject headings are also provided for specific models and theories.

Examples:

ELEMENTARY PARTICLE MODELS (TRIPLET)
  hadron total cross sections in quark, numerical analysis of
CURRENT ALGEBRA
  PCAC hypothesis for A_1 and rho dominance in $\pi \rightarrow e + \nu + \gamma$ decay
REGGE POLE THEORY
  predictions for polarization in $K^- + p \rightarrow$ anti $K^0 + n$, $\pi^- + p \rightarrow \pi^0 + n$, and $\pi^- + p \rightarrow$ eta + n interactions at high energies
SYMMETRY GROUPS
  $SU(2) \times SU(4)$ intermediate-coupling model for nucleon and hyperon isobars

Nomenclature of Reactor Technology

Subject headings for reactors are of three types:

(1) Specific reactors, e.g., ARGONNE RESEARCH REACTOR, SAXTON POWER REACTOR

(2) Reactors having a common physics or engineering characteristic, e.g., REACTORS, FAST; REACTORS, ORGANIC-COOLED; REACTORS, PRESSURIZED-WATER

(3) Reactors having a common purpose, e.g., REACTORS, POWER; REACTORS, RESEARCH

Information on specific reactors, type (1), is indexed under the one specific subject heading. Information on classes or types of reactors, types (2) (characteristics) and (3) (purpose), is indexed under all applicable headings. For example, information on a heavy-water-moderated organic-cooled power reactor is indexed under REACTORS, HEAVY WATER-MODERATED; REACTORS, ORGANIC-COOLED; and REACTORS, POWER.

Subject headings exist for selected reactor components, e.g., REACTOR FUEL ELEMENTS. When applicable, headings for components are indexed even though they may have been included in a modifier under a type (1) or (2) heading. The materials in reactor components are indexed when the information is peculiar to the material.

Modifier file words under reactor headings are of two primary types: one type expresses reactor characteristics, e.g., reactivity; the other, components, e.g., control rod. If no subject heading appears for a reactor component, the heading REACTORS is used, and the component is used as the modifier file word.

XUM

A

ACCELERATOR TUBES
design of single gap high-gradient, for acceleration of 200-mA proton beams to 300 keV, 25:36613 (UARAEE-87)
design with cylindrical electrodes, 25:36635(P)
ACCELERATORS
beam dynamics in, Coulomb collisions in, 25:36640
beam--target optical alignment system for, 25:35065(P)
development of heavy-ion, using modified Alvarez acceleration method, 25:36638
magnets for linotron, calculation of isochronous bending, 25:36641
operation of collective beam, theory of, 25:36617(T) (UCRL-Trans-1443)
shielding around high-energy proton, calculations for muon, 25:36610 (ORNL-TM-3353)
theory of oscillating magnetic mirror, three variants of Fermi model, 25:36636
ACETAMIDE, 2-ICDO-
effects on γ-radioinduced inactivation of Bacillus cereus spores, potentiating, 25:35264
ACETAMIDE, N-SULFANILYL-
sodium derivative, radiation effects on, in aqueous solutions and solid state, γ, 25:34661
ACETANILIDE
complexes with uranyl ion, magnetic susceptibility and ir spectra of, 25:34612
ACETIC ACID
radiolysis of solid, ESR studies on mechanisms of γ, 25:34641
reactions with mobile electrons formed in radiolysis of aqueous perchloric acid solutions at 77°K, 25:34648
ACETIC ACID, BROMO-
reactions with mobile electrons formed in radiolysis of aqueous perchloric acid solutions at 77°K, 25:34648
ACETIC ACID, [(CARBOXYMETHYLIMINO)BIS(ETHYLENENITRILO)]TETRA-
complexes with neptunium, plutonium, thorium, or uranium, preparation and stability of, 25:34558 (SRARI-P-92)
effectiveness for removal of radioisotopes from man, 25:35134
effectiveness for removal of soluble actinide salts from human bones and lungs, 25:35091
ACETIC ACID, CHLORO-
reactions with mobile electrons formed in radiolysis of aqueous perchloric acid solutions at 77°K, 25:34648
ACETIC ACID, DIFLUORO-
ammonium salt, radiolysis of, ESR studies on γ, 25:34634(R) (COO-1385-37)
ACETIC ACID, (ETHYLENEDINITRILO)TETRA-
complexes with uranyl ion, magnetic susceptibility and ir spectra of, 25:34612
effectiveness for removal of radioisotopes from man, 25:35134
ACETIC ACID, FLUORO-
ammonium salt, radiolysis of, ESR studies on γ, 25:34634(R) (COO-1385-37)
reactions with mobile electrons formed in radiolysis of aqueous perchloric acid solutions at 77°K, 25:34648
sodium salt, radioprotective effects of, on mice, effects of hypothermia on, 25:35163
sodium salt, radioprotective effects of, on mice, x, 25:35162
ACETIC ACID, IODO-
effects on radiosensitivity of bacteria, 25:35262
effects on recovery of γ- and uv-irradiated yeast, effects of ethanol on, 25:35251
reactions with mobile electrons formed in radiolysis of aqueous perchloric acid solutions at 77°K, 25:34648
ACETIC ACID, [OXYBIS(ETHYLENENITRILO)]TETRA-
effectiveness for removal of fission product mixtures with high strontium levels from man, 25:35134
ACETIC ACID, TRICHLORO-
reactions with mobile electrons formed in radiolysis of aqueous perchloric acid solutions at 77°K, 25:34648
ACETIC ACID, TRIFLUORO-
polarographic reactions at mercury electrode, effects of thiourea on, 25:34560
ACETIC ACID, VINYL ESTER, POLYMERS
polyethylene--poly(vinyl acetate), radiation effects on crosslinking in, gel permeation chromatographic studies on effects of dose on mechanical properties of copolymer produced by γ, 25:34626
ACETONE
boiling in superheated, initiation of radiation-induced, (E), 25:34798
yields from γ radiolysis of 2-methyl-2-propanol at 30°C, 25:34659
ACETYLENE
alpha-particle stopping cross sections in gaseous, at 0.3 to 2 MeV, 25:36255
photo-absorption cross sections of, review of uv, (E/T), 25:36013
reactions with methane under simulated radiolysis conditions, mass spectrometric studies on, 25:34645
ACOUSTIC EMISSION TESTING
method for detecting deformation and fracture in reactor materials, development of in-service, 25:34833
ACRIDINE, 3,6-DIAMINO-
effects on repair of x-radiciduced single strand breaks in DNA in mouse L cells, 25:35224
ACRYLAMIDE POLYMERS
handling and slicing of radioactive gels of, instrument for, 25:35056
ACRYLIC ACID, ISOBUTYL ESTER
polyethylene--poly(isobutyl acrylate), radiation effects on crosslinking in, gel permeation chromatographic studies on effects of dose on mechanical properties of copolymer produced by γ, 25:34626
ACTINIDES
complexes, stability constants of, regularities in, 25:34607
reactions of, effects of acidity on kinetics and thermodynamics of oxidation reduction, 25:34559 (SRARI-P-94)
separation from aqueous chloride solutions by solvent extraction using bis(1-isobutyl-3-methylbutyl) phosphate, 25:34706
ACTINIUM ISOTOPES Ac-227
abundance relative to radium-226 in minerals and natural waters, 25:34738
ACTIVATION ANALYSIS
uses in forensic science, review on, 25:34542(R) (GA-9807)
ADENINE
radiolysis of deuterated and normal derivatives of, ESR studies on free radicals produced by γ, 25:34652
ADHESIVES
preparation of, blending of Merginamide L-425 for use in, 25:37170 (BDX-613-405)
AERIAL SURVEYING
instrument for determining plutonium concentration, 25:34862 (EGG-1183-1517)
methods for petroleum prospecting using gamma spectrometers, development of, 25:34730
AET
radioprotective effects of, in relation to radiotoxins in cells, 25:35200
radioprotective effects on Ehrlich ascites cells, mechanisms of, 25:35204
AGE ESTIMATION
argon/potassium method for, programmed induction heater for use in, 25:34739
AGRICULTURE
book: Peaceful Uses of Nuclear Energy, 25:34817
AIR
corrosive effects on niobium--zirconium alloy at 450 to 650°C, effects of heat treatment and cold work on, 25:35278 (UARAEE-72)
cosmic alpha particle interaction mean free paths and fragmentation probabilities above 10 GeV/nucleon in, emulsion study of, (E/T), 25:36394
cosmic nuclei interaction mean free paths and fragmentation probabilities above 10 GeV/nucleon in, emulsion study of heavy, (E/T), 25:36394
effects on corrosion fatigue crack propagation in aluminum--molybdenum--titanium--vanadium alloy, relations with stress intensity amplitude and frequency, 25:35279
reactions with aluminum--chromium--nickel--tungsten alloy-clad chromium--tungsten alloy at 2100 and 2200°F, 25:35288
reactions with nickel--vanadium alloys at high temperatures, effects of composition on kinetics of oxidation, 25:35289
AIR SAMPLERS
alarm system for fixed filter, 25:34909
effectiveness of glass bead and water bubbler, for detecting tritium oxides, 25:35138
AIRGLOW
oxygen spectral-line shapes in equatorial nighttime, in upper atmosphere, (E), 25:35962
ALAMINE 336
radiation stability of, for use as diluent in fuel reprocessing, 25:34638 (RT/CHI-(70)35)
ALANINE
radiolysis of alkaline solutions of, at 77°K, ESR studies on production of free radicals by trapped electrons produced by photoionization and x, 25:34647
ALANINE, PHENYL-
radiolysis of alkaline solutions of, at 77°K, ESR studies on production of free radicals by trapped electrons produced by photoionization and x, 25:34647
ALARM SYSTEMS
design for fixed filter air monitors, 25:34909
ALASKA
limnology of lakes of Amchitka Island, effects of Milrow Event on, 25:34767(R) (BMI-171-129)
radiation monitoring at Amchitka Island, 25:34720 (NVO-1229-121)
radioisotope dispersion, migration, and sorption in rock--water systems of Amchitka Island, 25:34720 (NVO-1229-121)
ALBUMINS
effectiveness of iodine-131- or technetium-99-labeled macroaggregated, for lung scintigraphy, 25:35180
ALCOHOLS
positron annihilation in liquid, mechanism for formation of positronium atoms in, (E/T), 25:35853

ALEUTIAN ISLANDS
seismic activity of, program for monitoring effects of Amchitka Island nuclear explosions on, 25:34763 (CGS-746-10)
ALGAE
phycobiliprotein localization and properties in, research progress on, 25:37238(R) (TID-25714)
ALKALI METAL HALIDES
radioinduced energy storage in crystals of, luminescence from aqueous release of γ, 25:34620
ALKALI METAL OXIDES
alkali metal oxides--ZrO_2, formation and properties of solid solutions of, regularity in, 25:35545
ALKALI METALS
electron reactions with atoms of, kinetic energy of bound electron in calculation of ionization cross sections for, 25:35870
scattering by rare gases, data interpretation using Buckingham--Corner potential for, (T), 25:35886
ALKALINE EARTH OXIDES
alkaline earth oxides--ZrO_2, formation and properties of solid solutions of, regularity in, 25:35545
ALKALOIDS
radiation effects on potato, following seed exposure, low-dose γ, 25:35254
ALLOYS
conference on strength of, Vol. 1, Pacific Grove, Calif., Aug. 30 to Sept. 4, 1970, 25:35369
conference on strength of, Vol. 2, Pacific Grove, Calif., Aug. 30 to Sept. 4, 1970, 25:35390
conference on strength of, Vol. 3, Pacific Grove, Calif., Aug. 30 to Sept. 4, 1970, 25:35395
fatigue-crack propagation of high strength, superposition model for environmentally-assisted, 25:37249 (UCRL-20538)
joining of, explosive bonding method for, 25:35298
particle coarsening in, effects of volume fraction on, 25:37244 (UCLA-34-P-172-2)
ALPHA DECAY
of spherical nuclei with A = 202 to 218, (T), 25:36747
ALPHA PARTICLES
abundance in solar corpuscular radiation, (E/T), 25:35728
dechanneling at 5 MeV by dislocations in aluminum, 25:36307
detection of, engineering drawings for liquid scintillation detector for, 25:34930
effects on scalp of rats, neoplastic, 25:35236
effects on thermoluminescence of Apollo 11 sample 10084, (E), 25:35824
interaction mean free paths and fragmentation probabilities above 10 GeV/nucleon in emulsion, (E), 25:36394
interaction mean free paths and fragmentation probabilities of cosmic, above 10 GeV/nucleon in air and hydrogen, emulsion study of, (E/T), 25:36394
interactions α + α, Regge theory for potential for, (T), 25:36537
modulation of primary cosmic, (T), 25:35924
monitoring in environmental waters of Amchitka Island, Alaska, 25:34720 (NVO-1229-121)
monitoring in surface waters and precipitation during reentry drilling at Project Rulison site, 25:34728 (USGS-474-101)
reactions (α,2n) with americium-243 at 26 MeV, cross sections for, (E), 25:36795
reactions (α,2n) with neodymium-142 at 31 MeV, gamma spectra and decay curves from, (E), 25:36792
reactions (α,γ) with carbon-12 at 7.6 to 8.1 MeV, gamma angular distribution and resonance parameters for, (E), 25:36675
reactions (α,nγ) with manganese-55, gamma--gamma coincidence spectra from, (E), 25:36694
reactions (α,nγ) with strontium-87 and -88 at 10.3 to 13.5 MeV, γ singles and coincidence spectra from, (E), 25:36757
reactions (α,xn) with gold-197 at 16 to 104 MeV, excitation functions for, (E), 25:36745
scattering by neon-20 and -22 at 22.5 MeV, differential cross sections for elastic and inelastic, (E), 25:36697
scattering by neon-22 at 16.5 to 21.0 MeV, energy spectra from inelastic, (E), 25:36698
stopping cross sections for gases at 0.5 to 2 MeV, atomic, (E), 25:36256
stopping cross sections in gases at 0.3 to 2 MeV, 25:36255
ALPHA SOURCES
activity monitoring in solutions, properties of various sealing membranes for on-line, 25:34673 (CEA-N-1440)
ALUMEL COUPLES
Alumel/Chromel, radiation effects on, fast neutron, 25:35072 (HEDL-SA-152)
ALUMINUM
alpha-particle dechanneling at 5 MeV by dislocations in, 25:36307
copper-ion implantation at 30 and 60 keV, anomalous collection in, 25:36295
corrosion by lithium--selenium mixtures at 375°C, 25:35275(R) (ANL-7777)
defect structure of irradiated, effects of deformation on recovery spectra of, 25:35501
determination in soils by neutron activation, 25:34545 (THAI.-AEC-36)
effects on fluorescence method for detection of hafnium and zirconium, 25:34519
effects on gravimetric determination of mercury using 2-aminobenzothiazole, 25:34520
effects on photometric determination of antimony following solvent extraction using TBP, 25:34512
effects on precipitation of metastable phases in nickel--niobium alloys, 25:35480
electric conductivity of superconducting films below T/sub c/, nonlinear excess, (E/T), 25:36024
electron-diffraction intensities of (001), inelastic-collision-model calculations of low-energy, 25:36329
inductance and penetration depth of superconducting, surface, (E), 25:36029
neutron scattering by, lattice vibrational spectra and physical characteristics of, 25:36319
oxide film growth on, oxygen-16 and oxygen-18 tracer studies of anodic, 25:35294
plasma of, production by laser irradiation of free targets, 25:36152
properties of plasma-sprayed coating of, 25:37172 (BDX-613-408)
proton reactions with, cross sections for L-shell ionization in, (T), 25:35880
radiation damage in, electric conductivity study of production rate of low-temperature neutron, 25:36286
radiation effects on content of, in functionally and morphologically different tissues in animal spinal cord, x, 25:35228
solubility of, faradaic dissolution yield of electrolytic, 25:35353
welding of, research progress on pulse-arc, 25:37167(R) (BDX-613-320)
x-ray emission induced by electrons, intense K-, 25:35842
ALUMINUM ALLOYS AND SYSTEMS
deposition on niobium and niobium alloys, study of hot dipping method for, 25:35314
properties of Type 1100, for thermal insulation on lead telluride thermoelectric units, 25:34810(R) (ORNL-TM-3394)
solidification of molten, immersed in cooling medium, analysis of pressurization in, 25:37214 (ORO-3536-4)
Al--Au, mixing at 1100°C, adiabatic calorimetric measurement of heat of, 25:35432
Al--B, fabrication and tensile properties of filament-reinforced composites of, 25:35528
Al--B, mechanical properties of composite of, 25:35421
Al--C--Co--Cr--Mo--Nb--Ni-base--Ta--Ti--Zr, properties of corrosion-resistant IN-738 superalloy, 25:35400
Al--Co--Mo, radiation effects on catalytic activity of, in dehydrogenation of cyclohexane, 25:34628
Al--Co--Mo, radiation effects on subsequent catalytic activity of, in decomposition of hydrogen peroxide, γ, 25:34630
Al--Cr--Fe--Ni-base--Ti, tensile properties at 25 to 850°C, effects of grain size, precipitates, and test time on, 25:35340 (UARAEE-55)
Al--Cr--Mo--Ni-base--Ti, solvus temperature of γ' in, effects of hardener content on, 25:35460
Al--Cr--Ni-base--Ti, solvus temperature of γ' in, effects of hardener content on, 25:35460
Al--Cr--Ni-base--Ti--W, phase precipitation in, relations of heat treatments with microstructure of, 25:35502
Al--Cr--Ni-base--W, reactions of cladding of, for chromium--tungsten alloy with air and nitrogen at 2100 and 2300°F, resistance to oxidation, 25:35288
Al--Cr--Ti-base--V, tensile properties of metastable beta, at 25 to 600°C, effects of strain rate and annealing temperature on anomalies in, 25:35434
Al--Cu, formation of Cu_2Al and $CuAl_2$ during copper-ion implantation in aluminum, 25:36295
Al--Cu, mixing at 1100°C, adiabatic calorimetric measurement of heat of, 25:35433
Al--Cu--Fe--Ti-base--V, fracture toughness of α--β, relations with microstructure, 25:35348
Al--Dy-base, crystal lattice parameters of intermetallic Dy_2Al, 25:35495
Al--Er-base, crystal lattice parameters of intermetallic Er_2Al, 25:35495
Al--Gd-base, crystal lattice parameters of intermetallic Gd_2Al, 25:35495
Al--Ho-base, crystal lattice parameters of intermetallic Ho_2Al, 25:35495
Al--Mg, welding to stainless steel, methods for, 25:35326
Al--Mo--Si, radiation effects on subsequent catalytic activity of, in decomposition of hydrogen peroxide, γ, 25:34630
Al--Mo--Ti-base--V, crack propagation in, effects of stress intensity amplitude and frequency and air, methanol, sodium chloride solution, and distilled water on corrosion fatigue, 25:35279
Al--Mo--Ti-base--V--Zr, tensile properties of metastable beta, at 25 to 600°C, effects of strain rate and annealing temperature on anomalies in, 25:35434
Al--Mo--Ti-base--Zr, tensile properties of metastable beta, at 25 to 600°C, effects of strain rate and annealing temperature on anomalies in, 25:35434

Al--Nb--Ti, heat resistance of titanium-coated, 25:35325
Al--Nd-base, crystal lattice parameters of intermetallic Nd_2Al, 25:35495
Al--Ni, creep in stoichiometric, 25:37180 (COO-1489-10)
Al--Pr-base, crystal lattice parameters of intermetallic Pr_2Al, 25:35495
Al--Sm-base, crystal lattice parameters of intermetallic Sm_2Al, 25:35495
Al--Sn--Ti-base, properties of forgings of, standard for, 25:35422
Al--Sn--Ti-base--V--Zr, microstructure of high-strength martensitic beta-phase, 25:35488
Al--Ta, preparation of thin films of, sputtering method for, 25:35303
Al--Tb-base, crystal lattice parameters of intermetallic Tb_2Al, 25:35495
Al--Ti, composition of sputtered films of, spectrophotometric determination of, 25:35303
Al--Ti-base--V, corrosion by hydrochloric acid--isopropanol incorporating sodium chloride catalyst, rates of, 25:35287
Al--Ti-base--V, corrosion by hydrochloric acid--methanol solutions, rates of, 25:35287
Al--Ti-base--V, fatigue strength of, relations of α grain size with crack initiation, 25:35349
Al--Ti-base--V, properties of forgings of, standard for, 25:35422
Al--U, fabrication of fuel elements of aluminum-clad enriched, picture frame and rolling methods for, 25:35527
Al--U, processing of irradiated, at ICPP, 25:34690(R) (IN-1457)
Al--U_3O_8, fabrication of fuel elements of aluminum-clad enriched, extrusion method for, 25:35527
Al--Y-base, crystal lattice parameters of intermetallic Y_2Al, 25:35495
Al--Zn-base, plasticity in eutectoid alloy of, at 150 to 300°C, super-, 25:35405
Al-base--B--Cu--Mg, corrosion of diffusion bonded composites of, by sodium chloride solution, effects of applied stress on, 25:35521
Al-base--Be, corrosion by lithium--selenium mixtures at 375°C, 25:35275(R) (ANL-7777)
Al-base--Mg, radiation damage in, electric conductivity study of production rate of low-temperature neutron, 25:36286

ALUMINUM CHLORIDES
vapor pressure--temperature data for, 25:34602 (GAT-645)

ALUMINUM FLUORIDES
AlF_3--BeF_2--CaF_2, radiation stability of glasses of, effects of rare earth fluorides on γ, 25:34621

ALUMINUM ISOTOPES Al-27
deuteron reactions (d,pn) at 13.6 MeV, diffraction-model analysis of proton--neutron correlations in, (E/T), 25:36713
energy levels from magnesium-26 (d,nγ) reactions and magnesium-27 beta decay, (E), 25:36717
energy-level transitions from magnesium-26 (d,nγ) reactions and magnesium-27 beta decay, branching ratios for, (E), 25:36717
neutron reactions (n,α) and (n,p) at 14.8 MeV, cross sections for, (E), 25:36688(R) (N-70-43042)
proton reactions (p,γ) at 1.724 MeV, gamma angular distributions and linear polarizations from, (E), 25:36699
proton reactions at 1 and 3 GeV, integrated cross sections for fluorine-18 and sodium-24 production in, (E/T), 25:36816 (JINR-P2-5719)
proton reactions at 450 MeV, Monte Carlo calculation of neutron spectra from, (E/T), 25:36816 (JINR-P2-5719)

ALUMINUM ISOTOPES Al-30
beta decay of, gamma spectra from, (E), 25:36715

ALUMINUM NITRATES
effects on potentiometric determination of free nitric acid, 25:34517

ALUMINUM OXIDES
argon-ion reactions at 20 keV with, luminescence spectra of excited particles knocked out from, effects of nonradiative transitions on, 25:35841
properties for use in armor materials, 25:35554
radiation effects on subsequent catalytic activity of, in decomposition of hydrogen peroxide, γ, 25:34630
radiation effects on subsequent catalytic activity of, in dehydration of 2-propanol, γ, 25:34629
Al_2O_3--Mo, properties for use as armor plate, 25:35554
Al_2O_3--Ti, properties for use as armor plate, 25:35554

AMERICIUM
determination in biological materials by α spectrometry following separation by solvent extraction using DEHPA, 25:34537
distribution and excretion following inhalation in soluble compounds, effects of DTPA on, 25:35091
separation from aqueous chloride solutions by solvent extraction using bis(1-isobutyl-3-methylbutyl) phosphate, 25:34706

AMERICIUM ISOTOPES Am-241
deuteron reactions (d,pf) at 13 MeV, analysis using double-humped barrier, (E/T), 25:36746

AMERICIUM ISOTOPES Am-243
alpha reactions (α,2n) at 26 MeV, cross sections for, (E), 25:36795
deuteron reactions (d,2n) and (d,pn) at 13 to 20 MeV, cross sections and excitation functions for, (E), 25:36795
deuteron reactions (d,pf) at 13 MeV, analysis using double-humped barrier, (E/T), 25:36746
fission of isomeric, half-life for spontaneous, (E), 25:36795
proton reactions (p,2n) and (p,3n) at 20 MeV, cross sections for, (E), 25:36795

AMES RESEARCH REACTOR
radiation monitoring of environment of, during 1970, 25:34743 (IS-2541)

AMIDE POLYMERS
properties of thin membranes of, for on-line alpha activity monitoring of solutions, 25:34673 (CEA-N-1440)

AMINO ACIDS
radiation effects on composition of, in subtilopeptidase A, γ, 25:35109
radiation effects on composition of, in subtilopeptidase A, γ, 25:35110

AMMONIA
alpha-particle stopping cross sections in gaseous, at 0.3 to 2 MeV, 25:36255
complexes with ruthenium nitrides, radiolysis of, oxidation and reduction in electron pulse and γ, 25:34657
photo-absorption cross sections of, review of uv, (E/T), 25:36013
reactions with methane under simulated radiolysis conditions, mass spectrometric studies on, 25:34645

AMMONIUM CHLORIDES
phonon dispersion curves of deuterated, neutron inelastic-scattering study of 85°K, 25:36322
phonon dispersion curves of deuterated, shell model fit of 85°K, (T), 25:36323

AMMONIUM COMPOUNDS, SUBSTITUTED
dimethylammonium fluoride, complexes with uranium tetrafluoride, magnetic susceptibilities, stability, and solubility of, 25:34611

AMMONIUM IONS
determination by pressurometric titrations using electrogenerated hypobromite, 25:34513

AMMONIUM PERCHLORATES
radiolysis of crystals of, ESR spectra of ammonium radicals from γ, 25:34642

AMPLIFIERS
design of broad bandwidth differential, 25:35046 (CEA-N-1448)
design of high-power servo-controlled, using silicon controlled rectifiers, 25:36197 (UCRL-73047)
design of nanosecond bipolar pulse, with adjustable gain, 25:35044 (CEA-N-1439)

α-AMYLASE
radiation effects on synthesis of, in germinating wheat, effects of gibberellic acid on γ, 25:35102

ANGIOSPERMIDAE
Allium sp., radioinduced chromosome aberrations in, effects of heat treatment on x, 25:35125
Crepis capillaris, radioinduced chromosome aberrations in, γ, 25:35128
Ephedra nevadensis, radiation effects on growth and flower production of, in Mojave desert, effects of chronic cesium-137 γ, 25:35249
Hordeum vulgare, radiation effects on cell nuclei in seeds of, comparison of bremsstrahlung, γ, proton, and x, 25:35258
Ipomoea batatas, radiation effects on development of peroxidase in root tissues of, effects of ethylene on γ, 25:35105
Lemna minor, radiation effects on growth of, effects of dose, light, and temperature on, 25:35248
Pisum sativum, radioinduced mutations in, for seed production, neutron and x, 25:35122
Pisum sp., radioinduced chromosome aberrations in seeds of, effects of oxygen on, 25:35119
Prunus avium, radioinduced mutations in, growth, meiosis, and pollen viability studies on, 25:35127
Ricinus communis, radiation effects on acid lipase activities in, effects of dose and germination on γ, 25:35253
Solanum sp., radiation effects on alkaloid content in, following seed exposure, low-dose γ, 25:35254
Tradescantia paludosa, radicinduced aberrations of chromosomes in pollen tubes of, effects of infrared radiation on uv, 25:35120
Triticum sp., radiation effects on synthesis of amylase and ribonuclease in germinating, effects of giberellic acid on, 25:35102
Triticum sp., radioinduced chromosome aberrations in, effects of heat treatment on x, 25:35125
Tulipa sp., radiation effects on pollen viability in, effects of dose on γ, 25:35255
Vicia faba, radiation effects on cell nuclei in seeds of, comparison of bremsstrahlung, γ, proton, and x, 25:35258
Vicia faba, radioinduced chromosome aberrations in, effects of oxygen pressure on x, 25:35118
Vicia faba, radiosensitivity of repair system of, γ and uv, 25:35246
Zea mays, radiation injuries to cytoplasm of shoot apical cells of, 25:35244

ANILINE
complexes with uranyl ion, magnetic susceptibility and ir spectra of, 25:34612
ANILINE, N,N-DIMETHYL-
hydrofluoride, complexes with uranium tetrafluoride, magnetic susceptibilities, stability, and solubility of, 25:34611
ANIMALS
effects of temperature on development and survival of, in Columbia River, 25:35115 (BNWL-1543)
radiation effects on ascorbic acid content in tissues of oral cavity in, x, 25:35219
ANTENNAS
design for determining direction to lightning or nuclear explosions by rf transients, 25:35058(P)
ANTHRACENE
effects of coatings of, on γ radiolysis products of poly(vinyl chloride), ESR studies on, 25:34656
radioinduced paramagnetic centers in single crystals of, ESR studies of 10°K neutron, 25:36287
radioinduced paramagnetic defects in single crystals of, ESR study of low-temperature neutron, 25:36277
ANTHRAQUINONE
effects of coatings of, on γ radiolysis products of poly(vinyl chloride), ESR studies on, 25:34656
ANTHRONE
effects of coatings of, on γ radiolysis products of poly(vinyl chloride), ESR studies on, 25:34656
ANTIBODIES
radiation effects on formation of mouse thyroiditis, x, 25:35114
radiation effects on formation of rat homocytotropic, x, 25:35112
ANTIMONY
determination following separation by solvent extraction using TBP, effects of diverse ions on photometric, 25:34512
effects on gravimetric determination of mercury using 2-aminobenzothiazole, 25:34520
separation of ions of, from metal ions by high-voltage electrophoresis using carboxylic and hydroxycarboxylic acids, 25:34702
ANTIMONY ALLOYS AND SYSTEMS
La--Sb, thermal capacity of intermetallic LaSb at 7 to 300°K, 25:35355
Pr--Sb, crystal field interactions in intermetallic PrSb, 25:35355
Pr--Sb, thermal capacity of intermetallic PrSb at 7 to 300°K, 25:35355
ANTIMONY FLUORIDES
vapor pressure--temperature data for, 25:34602 (CAT-645)
ANTIMONY ISOTOPES Sb-110
beta decay scheme, (E), 25:36738(R) (UCLA-10-P-18-23)
nuclear properties of, Nuclear Data Sheets for, (E), 25:36808
ANTIMONY ISOTOPES Sb-111
beta decay scheme, (E), 25:36738(R) (UCLA-10-P-18-23)
ANTIMONY ISOTOPES Sb-112
beta and electron-capture decay scheme, (E), 25:36738(R) (UCLA-10-P-18-23)
ANTIMONY ISOTOPES Sb-113
beta and electron-capture decay scheme, (E), 25:36738(R) (UCLA-10-P-18-23)
ANTIMONY ISOTOPES Sb-114
beta decay scheme, (E), 25:36738(R) (UCLA-10-P-18-23)
ANTIMONY ISOTOPES Sb-121
electron spin resonance spectra of gaseous atoms of, 25:36345
ANTIMONY ISOTOPES Sb-122
availability in peccaries following single injection of nuclear debris from Project Buggy fallout, 25:35088
ANTIMONY ISOTOPES Sb-123
electron spin resonance spectra of gaseous atoms of, 25:36345
ANTIMONY OXIDES
MnO--Nb_2O_5--PbO--$PbTiO_3$--$PbZrO_3$--Sb_2O_3, properties of piezoelectric ceramic of, for use as filter and transducer elements of mechanical filters, 25:35561(P)
MnO--PbO--$PbTiO_3$--$PbZrO_3$--Sb_2O_3--Ta_2O_5, properties of piezoelectric ceramic of, for use as filter and transducer elements of mechanical filters, 25:35561(P)
ARGON
alpha-particle stopping cross sections at 0.5 to 2 MeV, atomic, (E), 25:36256
analysis of sodium loop cover gas of, for hydrogen, chromatographic, 25:35276(R) (GEAP-13539-16)
analysis of sodium loop cover gas of, for sodium oxide, amalgamation method for, 25:35276(R) (GEAP-13539-16)
argon-ion reactions at 25 keV with, promotion of K-shell electrons to higher bound states in, (E), 25:35856
effects on operation of cesium thermionic converters, 25:35930
ion reactions at 20 to 80 keV with, charge-equilibrium fractions and charge-exchange cross sections for, (E), 25:35866
ionization by low-energy electrons in mass spectrometer, cross sections for, 25:34636(R) (ORO-3729-4)
ionization by protons at 4 MeV, pressure dependence and Jesse impurity effect in, 25:35888
plasma of, radiations from low-pressure torch discharges, 25:36124
proton reactions with, coincidence studies of charge exchange and excitation in, 25:35877
reactions in nitrogen excited by fission fragments, energy transfer rates in, 25:36254
reactions of atoms and ions of, with alkali metal halides at 0.2 to 6 keV, electron emission induced by, 25:35840
reactions with methane under simulated radiolysis conditions, mass spectrometric studies on, 25:34645
ARGON IONS
reactions of atoms and ions of, with alkali metal halides at 0.2 to 6 keV, electron emission induced by, 25:35840
reactions of multiply charged, with flowing methane--nitrogen and nitrogen--oxygen systems at 7 MeV/n, 25:34567
reactions with argon at 25 keV, production of L-shell electrons to higher bound states in, (E), 25:35856
reactions with copper, silicon, and alumina at 20 keV, luminescence spectra of excited particles knocked out by, 25:35841
reactions with gas molecules at 10 to 1000 eV, rotational and vibrational excitation and light emission from, (E), 25:35873
stopping cross sections for carbon foils, effects of thickness and scattering angle on, 25:36248 (CIPR-41)
ARGON SYSTEMS
Ar--O, thermodynamic properties between 2,000 and 35,000°K, 25:36104 (NP-18772)
ARKANSAS NUCLEAR ONE POWER REACTOR
effluents from, effects on environment of chemical, radioactive, and thermal, 25:36947 (DOCKET-50313-30)
site for, hydrological and meteorological data for, 25:36947 (DOCKET-50313-30)
ARKANSAS NUCLEAR ONE POWER REACTOR, UNIT 2
design parameters of, revised and additional data on, 25:36960 (DOCKET-50368-11)
operations aspects of, revised and additional data on, 25:36960 (DOCKET-50368-11)
ARMOR PLATE
fabrication and properties of opaque, review on, 25:35554
ARSENATES
effects on photometric determination of antimony following solvent extraction using TBP, 25:34512
ARSENIC
effects on gravimetric determination of mercury using 2-aminobenzothiazole, 25:34520
separation of ions of, from metal ions by high-voltage electrophoresis using carboxylic and hydroxycarboxylic acids, 25:34702
ARSENIC FLUORIDES
vapor pressure--temperature data for, 25:34602 (CAT-645)
ARSENIC ISOTOPES As-74
distribution in tissues of swine following field exposure to nuclear debris at Schooner Event site, fallout, 25:35090
ARSENIC ISOTOPES As-75
electron spin resonance spectra of gaseous atoms of, 25:36345
ARSENIC ISOTOPES As-76
distribution and excretion in rabbits following intravenous injection, effects of syphilis infection on, 25:35087
ARSENIC ISOTOPES As-87
nuclear properties of, Nuclear Data Sheets for, (E), 25:36706
ASCORBIC ACID
radiation effects on content of, in tissues of oral cavity in animals, x, 25:35219
ASTATINE ISOTOPES At-203
nuclear properties of, Nuclear Data Sheets for, (E), 25:36809
ASTEROIDS
exobiology survey of, (T), 25:35829
ASTRON DEVICE
accelerator for, engineering developments in fast pulsing system for, 25:36201 (UCRL-73129)
development engineering for accelerator and main chamber, 25:36198 (UCRL-73059)
plasma equilibrium and stability in, calculations for, 25:36165 (UCRL-51030)
ASTRONOMY
theory of neutrino, heavy leptons in, (T), 25:36462
ASTROPHYSICS
conference on, Delhi, India, 10/69, 25:35892 (CONF-691055-(Vol.1))
conference on, Delhi, India, 10/69, 25:35893 (CONF-691055-(Vol.2))
Lyman-α observations in, interpretation of, (T), 25:35593
ATLANTIC OCEAN
lead content of surface of, 25:34762
lead-210 content of surface of, 25:34762
plutonium-239 distribution in waters and sediment cores from, measurement of vertical, 25:34759(R) (NYO-2174-129)
polonium-210 content of surface of, 25:34762
strontium-90 content in surface waters of, (E), 25:34759(R) (NYO-2174-129)
strontium-90 distribution in waters and sediment cores from, measurement of vertical, 25:34759(R) (NYO-2174-

XUM

129)
ATMOSPHERE
air circulation in troposphere, relation with solar flares, (E/T), 25:35973
contamination by radioactive waste disposal from Casaccia site in Italy, hazards to man from, 25:34849 (RT/PROT-(70)36)
contamination of, use of fluidized-bed combustion for reduction of, 25:37158 (ANL/ES-CEN-1003)
cosmic-ray energy releases into upper, galactic, (T), 25:36007
cosmic-ray propagation and spectra in, model of hadron reactions with nuclei for, 25:35925
exchange between stratosphere and troposphere, use of beryllium-7 and phosphorus-32 as tracer for measuring, 25:34745(R) (NYO-4061-2)
gamma-ray spectrum up to 6 g cm^{-2} over 7.6° geomagnetic latitude, (E), 25:36000
neutron detection at 25 km in, high-energy solar flare-associated, (E), 25:35772
neutron flux near geomagnetic equator in high, relation to radiation-belt proton flux, (E), 25:35998
oxygen spectral-line shapes in equatorial nightglow in upper, (E), 25:35962
ozone content in, correlation with diurnal cosmic-ray meson variations, (E/T), 25:35974
radiation absorption in, submillimeter solar, (E), 25:35714
radioactive contamination of, around Valencia, Spain, January 1966 to April 1968, 25:35132
radioisotope content in Moscow, 1962 to 1967, 25:34748
stability ratio and turbulence intensity in, relations with Pasquill turbulence types, 25:34747 (SC-DC-70-5443)
ATMOSPHERIC PRECIPITATION
measurements at Casaccia, Italy during 1968, tabulated data on, 25:34746 (RT/PROT-(70)42)
tritium content of, in Vienna during 1962 to 1969, (E), 25:34726 (THAI-AEC-35, pp 9-20)
ATOMIC BEAMS
production of fast hydrogen, for thermonuclear research, 25:36186(T) (CTO-746)
production of fast hydrogen, source for, 25:35837
production of polarized, by charge transfer in foils, 25:35836(P)
ATOMIC ENERGY, LEGAL ASPECTS
legislation governing quantity of shipped or stored nuclear fuels, description of German, 25:34857
regulations for protection of uranium mining personnel in Czechoslovakia, 25:35152
regulations for shipping radioactive materials by road in UK, 25:34859
ATOMIC PHYSICS
bibliography on surface and vacuum physics, 25:35835
ATOMS
charged-particle scattering by, reduction of (3Z + 2)-dimensional integral in Glauber approximation for, 25:35863
electron--proton interactions in, in n-dimensional space, (T), 25:36362
energy of ground states of 3- to 10-electron, second- and third-order Hartree--Fock, 25:35889
energy of two-electron, multiconfiguration frozen-core approximation for, 25:35890
energy-level transitions in, exactly solvable quantum-mechanical model for, (T), 25:35891
fractional parentage coefficients for, two-particle, 25:35850
ground states of, in superstrong magnetic fields, (T), 25:35644
properties of K-mesic, review of, (E/T), 25:36539
reactions with atoms and ions, oscillations of total cross sections for inelastic processes in, (T), 25:35876
scattering by molecules at high energies, validity of spherically symmetric potential or interpretation of, 25:35887
wave functions for ground states of 3- to 10-electron, Hartree--Fock, 25:35889
AURORAE
electron fluxes at 1 to 30 keV in stable, (E), 25:35963
hydrogen emissions during auroral substorms, morphology of, (E/T), 25:36005
morphology from meridian chain through Central Alaska, new, (E), 25:35961
origin of proton, in ring current, (T), 25:35995
relation to auroral electrojet currents, radio, (T), 25:36006
wave motion in, television imaging of fast, (E), 25:35965
AURORAL ZONE
arc reappearance on Mar. 8--9, 1970 during geomagnetic-storm recovery, midlatitude multiple 6300-A, (E), 25:35969
charged-particle precipitation into four, interrelation of magnetospheric structure to phenomena of, (E/T), 25:35958
electrojets in, relation to radio aurora, (T), 25:36006
electron energy and pitch-angle distribution to 6000 km in, morphology of, (E), 25:35982
morphology from meridian chain through Central Alaska, new, (E), 25:35961
radio-wave absorption in conjugate and closely-spaced, short-term asymmetry of, (T), 25:35957
x-ray generation in ionospheric, bremsstrahlung, (E/T), 25:35999
AUSTRALIA
radiography of industrial materials in, standards for gamma, 25:34841
radioisotope shipping and use in, standards for, 25:34841
AUTORADIOGRAPHY
methods alpha and beta--gamma, for hot cell inspection of irradiated fuels, 25:34837
AVR REACTOR
fuel elements for, radiation testing of thorium carbide (ThC_2)--uranium carbide (UC_2) and uranium carbide (UC_2) particle type, 25:37018 (JUL-701-RW)
fuel for, preparation process methods for, 25:35544
AZO COMPOUNDS
properties for use in spectrophotometric determination of rare earths, 25:34528
AZOBENZENE
effects of coatings of, on γ radiolysis products of poly(vinyl chloride), ESR studies on, 25:34656
AZORES
iodine-131 content in cattle and sheep thyroid in, following Chinese nuclear tests, 25:35133
AZURE A
solvent properties for benzoic acid--uranium complex in photometric determination of uranium, 25:34534

B

BABOONS
radioinduced chromosome aberrations in transplanted bone marrow cells of, effects of dose on, 25:35230
BACKGROUND RADIATION
effects on performance of gamma radiography equipment for inspecting welded components in nuclear power plants, 25:34823
BACTERIOPHAGES
radiation effects on plaque forming ability in, 25:35265
BAILLY POWER REACTOR, UNIT 1
buildings and structures for, earthquake stress analysis for, 25:36957 (DOCKET-50367-14)
design parameters of, requested additional information on, 25:36959 (DOCKET-50367-16)
design parameters of, revised and additional data on, 25:36958 (DOCKET-50367-15)
design parameters of, revised and additional data on, 25:36957 (DOCKET-50367-14)
operations aspects of, requested additional information on, 25:36959 (DOCKET-50367-16)
operations aspects of, revised and additional data on, 25:36957 (DOCKET-50367-14)
operations aspects of, revised and additional data on, 25:36958 (DOCKET-50367-15)
BALLOONS
research using, facilities of Tata Institute for, 25:35908
BARIUM
abundance in atmospheres of four K stars, (E), 25:35636
determination in rocks by neutron activation and γ spectroscopy, 25:34543 (NIM-1013)
determination of trace amounts of, as oxide, flame spectrophotometric, 25:34529
effects on gravimetric determination of mercury using 2-aminobenzothiazole, 25:34520
effects on photometric determination of antimony following solvent extraction using TBP, 25:34512
electron reactions with, multiple ionization and formation of metastable states in, 25:35865
BARIUM FLUORIDES
thermoluminescence and x-ray luminescence spectra of gadolinium- and dysprosium-activated crystals of, (E), 25:36317
BARIUM IONS
ionization potentials for charge states up to Ba^{10+}, 25:35865
BARIUM ISOTOPES Ba-139
energy levels of, unified model calculations for, (T), 25:36749
BARIUM ISOTOPES Ba-140
availability in peccaries following single injection of nuclear debris from Project Buggy fallout, 25:35088
BARIUM MOLYBDATES
$BaMoO_4$--MoO_3, phase studies of, 25:35578
BARIUM SULFIDES
BaS--US, phase studies on, electron-probe, metallographic, and x-ray-diffraction, 25:34603 (IJS-263)
BARNWELL NUCLEAR FUEL PROCESSING PLANT
seismic studies on, 25:34686 (DOCKET-50332-18)
structural analysis of, mathematical models for, 25:34686 (DOCKET-50332-18)
BARYONS
decay of, transverse and longitudinal polarization of final baryon in leptonic three-body, (T), 25:36462
interactions with mesons, quark model for sum rules for amplitudes and cross sections of, (T), 25:36518
masses of, dispersion theory for electromagnetic, (T),

XUM

25:36449
production in leptonic three-body baryon decay, transverse and longitudinal polarization for, (T), 25:35463
symmetry for, baryon--lepton correspondence in broken SU(3) x SU(3), (T), 25:36543
BARYONS, RESONANCE
book: The Systematics of Resonances, 25:36488
theory for, dual resonance models for vector currents in, (T), 25:36490
theory for, review of quark model in, (T), 25:36500
theory for, review of, (T), 25:36516
BARYONS, RESONANCE (N*)
decay of, quark model with relativistic extended internal structure for structure functions for deep inelastic e + p interactions for total width of, (T), 25:36444
level structure of, quark model with relativistic extended internal structure for structure functions for deep inelastic e + p interactions for, 25:36444
production in deep inelastic e + p interactions, quark model with relativistic extended internal structure for, (T), 25:36444
production in p + p interactions at 10 GeV in hydrogen bubble chamber, (E), 25:36393
production of Δ and N in quasi-two-body p + p interactions at 10.01 GeV/c in hydrogen bubble chamber, momentum transfer distributions and cross sections for, (E), 25:36396
BARYONS, RESONANCE (Y*)
decay Λ(1520) → Σ(1385) + π, mixing angle for, (E/T), 25:36415
decay Λ(1520) → Σ(1385) + π, production mechanism for K⁻ + p → Σ(1385) + π interactions near Λ(1520) for, (ZT), 25:36415
production of Σ(1385) in K⁻ + p → Σ(1385) + π interactions near Λ(1520), mechanism for, 25:36415
BAUXITE
analysis for gold by neutron activation, 25:34553
BEARINGS
design of radial, for water pumps, 25:37145(P)
performance of roller nut control drive thrust, for liquid sodium cooled reactors, 25:37075 (TODD-N-24)
performance of roller nut control rod drive thrust, for liquid sodium cooled reactors, 25:37070 (TODD-N-16)
performance of roller nut control rod drive thrust, for liquid sodium cooled reactors, 25:37071 (TODD-N-18)
performance of roller nut control rod drive thrust, for liquid sodium cooled reactors, 25:37074 (TODD-N-23)
performance of roller nut control rod drive thrust, for liquid sodium cooled reactors, 25:37073 (TODD-N-21)
performance of roller nut control rod drive thrust, for liquid sodium cooled reactors, 25:37072 (TODD-N-20)
BENZANTHRACENE
effects of coatings of, on γ radiolysis products of poly(vinyl chloride), ESR studies on, 25:34656
BENZENE
boiling in superheated, initiation of radiation-induced, (E), 25:34798
reactions with benzoyloxy radicals, effects of deuterium on, 25:34577
BENZENE, tert-BUTYL-
radiation stability of, for use as diluent in fuel reprocessing, 25:34638 (RT/CHI-(70)35)
BENZENE, DIETHYL-
radiation stability of, for use as diluent in fuel reprocessing, 25:34638 (RT/CHI-(70)35)
BENZENE, ETHYNYL-
effects of coatings of, on γ radiolysis products of poly(vinyl chloride), ESR studies on, 25:34656
BENZENE, 1,3,5-TRIPHENYL-
effects of coatings of, on γ radiolysis products of poly(vinyl chloride), ESR studies on, 25:34656
BENZENEARSONIC ACID, 2,2'-[(1,8-DIHYDROXY-3,6-DISULFO-2,7-NAPHTHYLENE)BIS(AZO)]DI-
reactions with uranyl nitrates, 25:34524
BENZOIC ACID
dimerization in toluene, isotopic exchange in, 25:34584
BENZOIC ACID, 3,3'-(ADIPOYLDIIMINO)BIS[2,4,6-TRIIODO-
radiation effects on stability of, γ, 25:34662
BENZOIC ACID, 3,5-DIACETAMIDO-2,4,6-TRIIODO-
radiation effects on stability of, γ, 25:34662
BENZOIN
effects of coatings of, on γ radiolysis products of poly(vinyl chloride), ESR studies on, 25:34656
p-BENZOQUINONE
effects of coatings of, on γ radiolysis products of poly(vinyl chloride), ESR studies on, 25:34656
BERKELIUM ISOTOPES Bk-245
fission of isomeric, half-life for spontaneous, (E), 25:36795
BERYLLIUM
bend ductility of sheets of, effects of processing method and powder purity on, 25:35463
corrosion by lithium--selenium mixtures at 375°C, 25:35275(R) (ANL-7777)
effects on colorimetric determination of gold, 25:34521
effects on photometric determination of antimony following solvent extraction using TBP, 25:34512
electric field gradient in hcp, calculations, 25:36351
electron-diffraction intensities of (0001), inelastic-collision-model calculations of low-energy, 25:36325
electron-diffraction intensity calculations for, low-energy, 25:36330
mechanical properties of, effects of porosity on, 25:35331 (AWRE-C-25/71)
neutron reactions (n,2n) with, fast fission factor for, (E/T), 25:37110
oscillator strengths for excitation and ionization of, tables of calculated generalized, 25:35844 (SC-RR-70-406)
properties for use in instrumentation and optical systems, review on, 25:35403
properties of metal and compounds of, for use as engineering materials in aerospace, electronics, and nucleonics industries, 25:35345
solubility of, faradaic dissolution yield of electrolytic, 25:35353
tensile properties of compression rolled and hot upset sheet of, at 25 to 355°C, effects of strain rate on, 25:35459
tensile properties of foils of, biaxial and uniaxial, 25:35332 (BMI-X-604)
x-ray emission induced by electrons, intense K-, 25:35842
BERYLLIUM ALLOYS AND SYSTEMS
properties for use as engineering materials in aerospace, electronics, and nucleonics industries, 25:35345
Al-base--Be, corrosion by lithium--selenium mixtures at 375°C, 25:35275(R) (ANL-7777)
Be--Cu, bonding specimens of, using polyaryl sulfone adhesive, 25:35316
Be--Cu-base, precipitation of equilibrium γ phase in, effects of cold work on discontinuous, 25:35494
BERYLLIUM FLUORIDES
AlF_3--BeF_2--CaF_2, radiation stability of glasses of, effects of rare earth fluorides on γ, 25:34621
BeF_2--LiF_4--PuF_3--ThF_4, plutonium oxide precipitation in molten, equilibrated with thorium oxide, 25:34566
BeF_2--LiF--PuF_3, plutonium oxide precipitation in molten, equilibrated with beryllium oxide, 25:34566
BeF_2--LiF--PuF_3--ZrF_4, plutonium oxide precipitation in molten, equilibrated with zirconium oxide, 25:34566
BERYLLIUM ISOTOPES Be-7
use of stratospheric, as tracer for stratospheric--tropospheric air mass exchange studies, 25:34745(R) (NYO-4061-2)
BERYLLIUM ISOTOPES Be-8
energy levels in, effects of resonance interaction on, (T), 25:36837
energy levels of, alpha-particle-model calculations of rotational, (T), 25:36680
energy levels of, calculation using correlated wave functions of isospin mixing in, (T), 25:36677
BERYLLIUM ISOTOPES Be-9
binding energy of, (T), 25:36847
meson (π) reactions with, x-ray yields and level broadening from, (E), 25:35854
BERYLLIUM OXIDES
neutron reactions (n,2n) with, fast fission factor for, (E/T), 25:37110
radioinduced neutral beryllium vacancy in single crystals of, EPR identification of 3-MeV electron, 25:36282
BETA DECAY
currents in, effects of second-class, (E/T), 25:36710
spectra of forbidden, calculation of distortions in, (T), 25:36841
BETA PARTICLES
detection of, design of gas-filled spark chamber for, 25:34876(P)
dose to human female reproductive system during phosphorus-32 administration, 25:35144
dosimetry of, comparison of film badge and thermoluminescent dosimeters for, 25:35121
effects on morphological and physiological properties of fungi, mutagenic, 25:35256
effects on synthesis of free nucleotides in Saccharomyces, tracer study on, 25:35252
monitoring in environmental waters of Amchitka Island, Alaska, 25:34720 (NVO-1229-121)
monitoring in surface waters and precipitation during reentry drilling at Project Rulison site, 25:34728 (USGS-474-101)
BETA SOURCES
monitoring in sanitary waste system effluent from West Valley Processing Plant, 25:34683 (DOCKET-50201-72)
BETA SPECTROMETERS
design of conversion electron--x-ray coincidence system for beta- and Compton-suppression, 25:34932
energy distribution analysis of cylindrical electrostatic, 25:34927
properties of Mamet monokinetron, 25:34926
BETATRONS
electron--ion beam in plasma, kinetic model of plane high-current, 25:36604 (JINR-P9-5645)
magnetic field index of 5-MeV, a-c potentiometer method for measuring, 25:36625
BIBLIOGRAPHIES
on burnout in forced convection boiling heat transfer, 25:37000 (AAEC/LIB/Bib-286)
on corrosion, 1960 survey, 25:35290
on ion implantation, Jan. 1967 through Sept. 15, 1970, 25:36269 (SC-B-710148)
on plasma physics, 25:36082

XUM

on plasma physics and fusion reactors, 25:36081
on reactor physics computer programs at Argonne Code Center, 25:37133 (ANL-7411(Suppl.5))
on reactor safety, 25:37047 (TID-3525(Rev.5)(Suppl.6))
on surface and vacuum physics, 25:35835
on thermal effects on Columbia River ecosystems, 25:35115 (BNWL-1543)
BIG ROCK POINT POWER REACTOR
control rod drive malfunction at, 25:36906 (DOCKET-50155-82)
operations history for February 1967, 25:36888 (TID-23819)
operations history for January 1967, 25:36887 (TID-23762)
BIOLOGICAL MATERIALS
analysis for americium, californium, curium, and plutonium by α spectrometry following separation by solvent extraction using DEHPA, 25:34537
analysis for elements by neutron activation, 25:34546 (THAI.-AEC-39)
analysis for magnesium and manganese by thermal neutron activation, ion exchange chromatography, and γ spectrometry, 25:34552
analysis for mercury by neutron activation and γ spectrometry, 25:34551
photon attenuation coefficients at 1 to 1000 keV, (T), 25:36259
radiation effects on, role of free radicals in, 25:34639(R) (USC-113-P-21-3)
BIOLOGICAL MODELS
development of exponential and power function, for whole-body retention of europium-152, europium-153, and europium-154 in rats following inhalation of radioactive europium oxide, 25:35086
development of single exponent, for quantitative interpretation of iodine-131 kidney scans, 25:35168
BIOLOGY
stable isotope uses in, review of, 25:34813 (TID-25705)
survey of exobiology beyond Mars, (T), 25:35829
BIPHENYL
radiation effects on decomposition of, 25:34810(R) (ORNL-TM-3394)
BIPYRIDINE
complexes with uranyl ion, magnetic susceptibility and ir spectra of, 25:34612
BISMUTH
effects on colorimetric determination of gold, 25:34521
effects on gravimetric determination of mercury using 2-aminobenzothiazole, 25:34520
effects on photometric determination of antimony following solvent extraction using TBP, 25:34512
separation of ions of, from metal ions by high-voltage electrophoresis using carboxylic and hydroxycarboxylic acids, 25:34702
BISMUTH ALLOYS AND SYSTEMS
Bi--La, thermal capacity of intermetallic LaBi at 7 to 300°K, 25:35355
Bi--Li, solvent properties of liquid, for californium, 25:34705
Bi--Pr, crystal field interactions in intermetallic PrBi, 25:35355
Bi--Pr, thermal capacity of intermetallic PrBi at 7 to 300°K, 25:35355
BISMUTH ISOTOPES Bi-203
energy levels and nuclear properties of, Nuclear Data Sheets for, (E), 25:36809
BISMUTH ISOTOPES Bi-205
electron-capture decay of, N-conversion spectrum from, (E), 25:36780
BISMUTH ISOTOPES Bi-206
electron-capture decay of, N-conversion spectrum from, (E), 25:36780
BISMUTH ISOTOPES Bi-209
alpha reactions (α,xn) with, yields from proton-induced secondary, (E), 25:36723 (JINR-P1-5530)
deuteron reactions (d,α) at 20 MeV, angular distributions for, (E), 25:36777
deuteron reactions (d,pγ) at 9 MeV, gamma spectra and p--γ coincidences from, (E), 25:36790
energy levels of, two-nucleon random-phase-approximation calculation of spectroscopic factors for, (T), 25:36806
fission of, lower limit on half-life for spontaneous, (E), 25:36779
neutron scattering by, decay constants and diffusion lengths for pulsed cold-, (T), 25:36655
proton reactions (p,3n) and (p,4n) at 20 to 45 MeV, precompound and statistical contributions to excitation functions for, (E/T), 25:36797
proton reactions (p,He-3) at 40 MeV, angular distributions for, (E), 25:36777
proton-induced secondary (α,xn) reactions at 120 to 660 MeV, yields relative to astatine-211 for, (E), 25:36723 (JINR-P1-5530)
BISMUTH ISOTOPES Bi-210
energy levels from bismuth-209 (d,pγ) reactions, lifetimes and spin--parity assignments for, (E), 25:36790
energy levels from bismuth-209 neutron capture, configuration and spin--parity assignments for, (E/T), 25:36787
energy-level transitions from bismuth-209 (d,pγ) reactions, branching ratios and multipolarities for, (E), 25:36790
BITUMINOUS MATERIALS
radioactive waste fixation in Polish, feasibility studies on, 25:34845 (INR-1249)
BLACK HOLES
electric potential of, (T), 25:35615
formation of, physics of, (T), 25:35660
relation to white holes in an antiuniverse, (T), 25:35820
BLOOD
analysis for potassium-42 using Cherenkov radiation, 25:34540
circulation in human brain, radioisotope methods for clinical study of, 25:35178
flow studies in perfused tissues, use of rubidium-81 ratio to metastable krypton-81 for, 25:35167
radiation effects on human, following endolymphatic or oral iodine-131 therapy, 25:35189
radioisotope accumulation in, of swine following field exposure to nuclear debris from Schooner Event, fallout γ-emitting, 25:35090
BLOOD CELLS
radiation effects on immune response of mice to hematopoietic, following intraperitoneal and intravenous injection, x, 25:35111
radioisotope uses for diagnosis and therapy of disorders of, 25:35157
BLOOD PLASMA
analysis for potassium-42 using Cherenkov radiation, 25:34540
radiation effects on protein content of human, following endolymphatic or oral iodine-131 therapy, 25:35185
BLOOD PLATELETS
physiopathology of, research progress on, 25:37202(R) (NYO-3590-8)
BOILERS
inspection of welded T-joints in, x-radiographic method for, 25:34840
instrumentation for pressurized water reactor, review of process, 25:37010 (WCAP-7671)
packaging and shipping of radioactive, in Canada, development of special arrangement methods for, 25:34843 (AECL-3804)
testing of gas cooled reactor, pressure and temperature, 25:36978(R) (GA-10560)
BOILING
detection in liquid sodium and in water, acoustic system for, 25:37052
initiation of radiation-induced, in superheated acetone, benzene, and water, (E), 25:34798
BONE MARROW
radiation effects on mouse stem cell, lethal, 25:35212
radiosensitivity of mouse, effects of hypoxia on electron, 25:35161
BONES
density of human finger, iodine-125 scanning method for measuring, 25:35171
radiation effects on iron-59 uptake by rat, correlation between intramedullary dose and whole-body x, 25:35211
radioisotope accumulation in, of swine following field exposure to nuclear debris from Schooner Event, fallout γ-emitting, 25:35090
radiotherapy of metastases of human, effectiveness of, 25:35187
retention of soluble actinide salts in human, following inhalation, effects of DTPA on, 25:35091
BORIC ACID
corrosive effects on Type 304 and Type 316 stainless steels, (E), 25:37028 (ORNL-TM-2412(Pt.10))
BOROHYDRIDES
radiolysis of aqueous solutions of, yields from electron pulse and γ, 25:34646
BORON
effects of trace amounts of, on electron beam welding behavior of sintered molybdenum sheets, 25:35312
effects on ductility and strength of Inconel 600 and Types 304 and 316 stainless steel at high temperatures, 25:35338 (ORNL-TM-3316)
oscillator strengths for excitation and ionization of, tables of calculated generalized, 25:35844 (SC-RR-70-406)
BORON CARBIDES
oxidation in high temperature water vapor and helium environment, 25:36978(R) (GA-10560)
properties for use in armor materials, 25:35554
B_4C--SiC, properties for use as armor plate, 25:35554
BORON FLUORIDES
compounds with methyl ether, analysis for boron-10 by thermal neutron absorption method, 25:34538
BORON ISOTOPES B-10
determination in methyl ether compounds with boron trifluoride by thermal neutron absorption method, 25:34538
BORON ISOTOPES B-11
electron elastic and inelastic scattering at 100 to 300 MeV, angular distributions and spectra from, (E/T), 25:36672 (LAL-1243)
energy levels from electron inelastic scattering, form factors for, (E/T), 25:36672 (LAL-1243)
nuclear form factors from electron elastic scattering,

XUM

(E/T), 25:36672 (LAL-1243)
reactions (B-11,f) with thulium-169 and lutetium-175 up to 10.4 MeV/nucleon, excitation functions for, (E), 25:36784
BORON ISOTOPES B-13
beta decay of, half-lives and log-ft values for, (E/T), 25:36710
BORON NITRIDES
properties for use as fillers in paste-type storage battery cells, 25:35275(R) (ANL-7777)
BORON SYSTEMS
B--epoxy, testing of composites of, nondestructive methods for, 25:34838
Al--B, fabrication and tensile properties of filament-reinforced composites of, 25:35528
Al--B, mechanical properties of composite of, 25:35431
Al-base--B--Cu--Mg, corrosion of diffusion bonded composites of, by sodium chloride solution, effects of applied stress on, 25:35521
B--Fe, radiation effects on internal friction of, neutron, 25:35588
B--Mg, fabrication and tensile properties of filament-reinforced composites of, 25:35528
B--Mo, deformation anisotropy and texture of sheets of rolled and annealed, 25:35411
B--stainless steel, properties for use as JMTR fuel followers, 25:35320
BOSONS
elementary excitations in system of, in magnetic field, 25:36359
statistics of composite, quasi-spin formalism for, 25:36356
symmetry for, intrinsically self-conjugate structure in SU(2) and Sp(2), (T), 25:36548
velocity operator in many-body systems of, definition of, (T), 25:36368
BOSONS, INTERMEDIATE-VECTOR
interactions of, renormalizable model for, (T), 25:36468
BRAIN
radiation effects of bioelectric activity in rat, 25:35235
radiation effects on cholinesterase activity in rat, effects of adrenal and pituitary gland function on x, 25:35232
radiation effects on hypoxanthine content in rat, effect of dose on neutron, 25:35226
scanning of human, for blood flow, 25:35178
scanning of human, for detection of vascular accidents, 25:35176
scanning of human, intracarotid or intravenous technetium-99m for, 25:35173
scanning of human, review on radioisotope, 25:35177
scanning of human, value of uptake pattern in diagnosis during sequential technetium-99m, 25:35174
scanning of human, value of vertex view in radioisotope, 25:35175
BRAZING
methods for irradiation facility construction, 25:35326
methods for reactor components using nickel-based filler alloys, vacuum, 25:35327
BRAZING ALLOYS
composition and use of nickel-base, for reactor components, 25:35327
wetting of refractory metals by, at 700 to 1900°C, 25:35334 (EUR-4637)
BREMSSTRAHLUNG
distribution from electron-bombarded targets, activation detectors for measurement of, 25:34908
effects on cell nuclei in Hordeum vulgare and Vicia faba seeds, comparison of γ, proton, x, and, 25:35258
emission from thick tungsten targets after x irradiation at 12 to 300 kV, (E), 25:36249 (LA-4624)
reactions (γ,f) with thorium and uranium at 200 to 900 MeV, excitation functions for, (E), 25:36736 (THAI-AEC-35, pp 1-8)
reactions (γ,n) with natural uranium from electron bombardment at 18.5 to 23 MeV, energy spectra and nuclear temperatures from, (E), 25:36767
reactions (γ,xn) with A = 146 to 153 nuclei at giant resonance energies, cross sections for, (E), 25:36755
reactions (γ,xn) with gold-197 at 75 to 900 MeV, gamma spectra and yield curves and cascade--evaporation analysis of cross sections for, (E/T), 25:36785
BROMINE
effects on photometric determination of antimony following solvent extraction using TBP, 25:34512
BROMINE FLUORIDES
vapor pressure--temperature data for, 25:34602 (GAT-645)
BROMINE ISOTOPES Br-87
nuclear properties of, Nuclear Data Sheets for, (E), 25:36705
BROMOHYDROCARBONS
positron annihilation in liquid, mechanism for formation of positronium atoms in, (E/T), 25:35852
BRONZE
finishes for contact faces of pipe flanges and connecting-end flanges of valves and fittings of, standard for, 25:35418
standard for spot facing of pipe flanges of, 25:35365
BROOKHAVEN BEAM RESEARCH REACTOR
heat exchangers for, analysis and repair of baffle plate damage in primary, 25:37055 (ENL-15815)
BUBBLES
growth and stability in Freon-113 in narrow constant-diameter vertical tubes with nonuniform initial temperature profiles, (E), 25:34789 (ANL-7746)
nucleation on surfaces immersed in cryogenic fluids, effects of pressure and temperature on, 25:34958 (CONF-700623-(Vol.1), pp 449-58)
BUILDING MATERIALS
defects in, design and operation of gamma radiographic equipment for detecting, 25:34822
BULK SHIELDING FACILITY
instrumentation for, modifications to, 25:37069(R) (ORNL-TM-3453)
maintenance during January to March 1971, 25:37069(R) (ORNL-TM-3453)
operations during January to March 1971, 25:37069(R) (ORNL-TM-3453)
BURNABLE POISONS
performance of boron carbide (B_4C), in high temperature water vapor and helium environment, 25:36978(R) (GA-10560)
1,3-BUTADIENE, 2-CHLORO-
radiation effects on properties and structure of, γ, 25:35590
1,3-BUTADIENE, 2-METHYL-, POLYMERS
radioinduced polymerization of vinyl chloride on, properties of products from, 25:34627
BUTANE
ionization by low-energy electrons in mass spectrometer, cross sections for, 25:34636(R) (ORO-3729-4)
reactions with helium tritides formed by beta decay of molecular tritium, kinetic studies on, 25:34676
BUTANE, 1-ASTATO-2-METHYL-
boiling point of, gas chromatographic studies on, 25:34604 (JINR-P6-5683)
BUTANE, 1-ASTATO-3-METHYL-
boiling point of, gas chromatographic studies on, 25:34604 (JINR-P6-5683)
1,3-BUTANEDIONE, 1-(2-FURYL)-
complexes with neptunium or uranium, stability of, 25:34557 (KFK-1339)
1,3-BUTANEDIONE, 1-PHENYL-
complexes with neptunium or uranium, stability of, 25:34557 (KFK-1339)
1,3-BUTANEDIONE, 4,4,4-TRIFLUORO-1-(2-FURYL)-
complexes with neptunium or uranium, stability of, 25:34557 (KFK-1339)
1,3-BUTANEDIONE, 4,4,4-TRIFLUORO-1-PHENYL-
complexes with neptunium or uranium, stability of, 25:34557 (KFK-1339)
1,3-BUTANEDIONE, 4,4,4-TRIFLUORO-1-(2-THIENYL)-
complexes with neptunium or uranium, stability of, 25:34557 (KFK-1339)
complexes with rare earths, preparation and physicochemical properties of, 25:34502 (INR-1247)
4,4,4-trifluoro-1-(2-thienyl)-1,3-butanedione--trioctylphosphine oxide, solvent properties for cerium in fission products solutions, 25:34522
1,3-BUTANEDIONE, 1-(2-THIENYL)-
complexes with neptunium or uranium, stability of, 25:34557 (KFK-1339)
1-BUTANETHIOL, 2-AMINO-
radioprotective effects of, on Escherichia coli, function and structure studies on γ, 25:35160
1-BUTANOL
radiolysis of liquid, at low temperature, studies on electron solvation process in electron pulse, 25:34645
2-BUTANOL
yields from γ radiolysis of 2-methyl-2-propanol at 30°C, 25:34659
tert-BUTYL ETHER
yields from γ radiolysis of 2-methyl-2-propanol at 30°C, 25:34659
tert-BUTYL PEROXIDE
yields from γ radiolysis of 2-methyl-2-propanol at 30°C, 25:34659
BUTYL RUBBER
radioinduced polymerization of styrene to crosslinked, γ, 25:34631
BUTYRALDEHYDE
yields from γ radiolysis of 2-methyl-2-propanol at 30°C, 25:34659
BUTYRALDEHYDE, DIHYDROXY-
effects on survival of x-irradiated tumor-bearing mice, 25:35159
radiosensitizing effects of, on Escherichia coli, γ, 25:35159
radiosensitizing effects of, on growth of Ehrlich ascites tumors in mice and in vitro, x, 25:35159

C

CABLES
fabrication of high temperature flat, 25:37159(R) (BDX-613-161)
CADARACHE REACTORS (RAPSODIE)
coolant purification system for, design and operation of liquid sodium, 25:37056(T) (ENWL-tr-67)

XUM

CADMIUM
dislocations in monocrystalline, structure of, 25:35486
effects on colorimetric determination of gold, 25:34521
effects on gravimetric determination of mercury using 2-aminobenzothiazole, 25:34520
effects on nuclear spin--lattice relaxation in indium, 25:36349
effects on photometric determination of antimony following solvent extraction using TBP, 25:34512
electron mean free path in, magneto-acoustic attenuation study of temperature dependence of, 25:36328
Fermi surface caliper, line shape in radio-frequency size effect, 25:36327
CADMIUM ALLOYS AND SYSTEMS
Cd--P--Sn, phase diagram of CdP_2--Sn system in, 25:35580
Cd--P--Sn, properties of copper- and silver-doped crystals of, electric and optical, 25:35580
Cd--Sn-base, plasticity in eutectoid alloy of, effects of grain size on super-, 25:35405
CADMIUM ISOTOPES Cd-110
energy levels and nuclear properties of, Nuclear Data Sheets for, (E), 25:36808
CALCIUM
abundance in 15 Vul, (E/T), 25:35653
abundance in K giant stars, (E/T), 25:35649
determination in combination with magnesium in glacial waters by ion-sensitive electrode method, 25:34721(R) (NYO-3912-3)
determination in combination with magnesium in glacial waters by ion-sensitive electrode method, 25:34722(R) (NYO-3912-4)
determination in human stones by neutron activation, 25:34546 (THAI.-AEC-39)
effects on colorimetric determination of gold, 25:34521
effects on gravimetric determination of mercury using 2-aminobenzothiazole, 25:34520
effects on photometric determination of antimony following solvent extraction using TBP, 25:34512
spectral absorption bands in 4430 A interstellar bands, (E/T), 25:35663
CALCIUM FLUORIDES
AlF_3--BeF_2--CaF_2, radiation stability of glasses of, effects of rare earth fluorides on γ, 25:34621
CALCIUM ISOTOPES
separation by ion exchange, 25:34709
CALCIUM ISOTOPES Ca-40
electron elastic scattering at 250 MeV, Hartree--Fock calculations of angular distributions from, (T), 25:36712
electron inelastic scattering at 198 to 300 MeV, differential cross sections for, (E), 25:36695
energy levels from potassium-39 (He-3,d) reactions, (E), 25:36696
isospin mixing in ground state of, calculation of amount of Coulomb-induced ΔT = 1, (T), 25:36845
meson (π^+) reactions at high energies, Coulomb interaction in, (T), 25:36524
meson (π^-) reactions at high energies, Coulomb interaction in, (T), 25:36524
CALCIUM ISOTOPES Ca-42
electron inelastic scattering at 198 to 300 MeV, differential cross sections for, (E), 25:36695
CALCIUM ISOTOPES Ca-44
electron inelastic scattering at 198 to 300 MeV, differential cross sections for, (E), 25:36695
oxygen-16 reactions (O-16,C-14) at 48 MeV, cross sections for, (E), 25:36709
CALCIUM ISOTOPES Ca-47
retention in man following oral administration, effects of diseases on, 25:35098
CALCIUM ISOTOPES Ca-48
oxygen-16 reactions (O-16,C-14) at 48 MeV, cross sections for, (E), 25:36709
proton elastic scattering at 4 to 8 MeV, relative excitation function for, (E), 25:36690 (NP-18824)
CALCIUM MOLYBDATES
$CaMoO_4$--MoO_3, phase studies of, 25:35578
CALCIUM OXIDES
CaO--UO_2--ZrO_2, separation of uranium from irradiated, aqueous halide process for, 25:34690(R) (IN-1457)
CALCIUM SULFIDES
CaS--US, phase studies on, electron-probe, metallographic, and x-ray-diffraction, 25:34603 (IJS-263)
CALIFORNIUM
determination in biological materials by α spectrometry following separation by solvent extraction using DEHPA, 25:34537
distribution between molten lithium chloride and liquid bismuth--lithium alloys, 25:34705
CALIFORNIUM ISOTOPES Cf-249
carbon-12 reactions (C-12,α2n) at 77.4 MeV, alpha and x-ray spectra from products of, (E), 25:36778
neutron fission of, cross section and resonance integral of thermal, (E), 25:36721 (DP-MS-70-95)
CALIFORNIUM ISOTOPES Cf-252
fission of, background effects on measurement of Maxwellian temperature of neutron spectrum from spontaneous, (E), 25:36728 (KFKI-71-9)
use as source in neutron radiography, 25:34803(R) (BNWL-1308-5)
CAMERAS
design for plasma diagnostics in single-ended Q devices, 25:36099
CANDU REACTOR
fuel element channels for, performance of end closure seals for, 25:37001 (AECL-3787)
CARBAMIC ACID, DIETHYLDITHIO-
complexes with uranyl ion, magnetic susceptibility and ir spectra of, 25:34612
sodium salt, reactions with niobium(V), protactinium(V), and tantalum(V) bromides and chlorides, 25:34568
CARBIDES
analysis of complex, by electron beam micro methods, 25:34523
CARBOHYDRATES
radiolysis of aqueous solutions of, yields of deoxy-sugars from γ, 25:34664
CARBON
abundance of molecular, in 19 Psc and Y CVn, (E), 25:35620
density of manufactured articles of boronated and natural, standard method for measurement in air of, 25:35474
diffusion from ferritic steel, effects of niobium, titanium, and vanadium on, 25:35407
effects as an additive on properties of thermomechanically processed Type 348 stainless steel, 25:35300
effects on formation of Frenkel Pairs in neutron-irradiated nickel or alpha-iron, computer study of, 25:35504(R) (CRC-3912-4)
effects on mechanical properties of molybdenum carbide--nickel--titanium carbide solid solution, 25:35559
effects on rupture of polycrystalline molybdenum, 25:35409
fabrication and properties of composites of, research progress on, 25:37179 (CONF-710312-1)
fission fragment ranges in isotropic pyro-, uranium-235 thermal-neutron, 25:36264
ion stopping cross sections for thin foils of, effects of thickness and scattering angle on, 25:36248 (GIPR-41)
lithium-ion reactions at 2 to 10 keV with films of, energy distributions from, 25:35833(R) (ORO-3027-15)
meson (π) reactions with, x-ray yields and level broadening from, (E), 25:35854
meson (π^-) reactions at 7 GeV in bubble chamber, nuclear radius determination from, (E), 25:36408
neutron total cross section at 0.433 to 2.37 MeV, (E), 25:36740 (WAPD-T-2411)
nuclear radius of, π^- reactions with carbon at 7 GeV in bubble chamber for determination of, (E), 25:36408
oscillator strengths for excitation and ionization of, tables of calculated generalized, 25:35844 (SC-RR-70-406)
proton reactions at 450 MeV, Monte Carlo calculation of neutron spectra from, (E/T), 25:36816 (JINR-P2-5715)
radioinduced creep of fuel particle coating of pyrolytic, fast neutron, 25:35586
radioinduced dimensional changes and creep in spherically restrained and unrestrained isotropic, at 600 to 1250°C, fast neutron, 25:35585
sorptive properties for iodine and methyl iodide, effects of aging on, (E), 25:37106(R) (IP-1259)
x-ray emission induced by electrons, intense K-, 25:35842
CARBON BLACK
electron spin resonance of neutron-irradiated, temperature dependences of g factor and line width of, 25:36341
reactions with uranium oxides, kinetics of reduction in, 25:34556 (EUR-4635)
sorptive properties of activated, for hydrogen at 80 to 600°C, kinetics of chemical, 25:35552
CARBON DIOXIDES
alpha-particle stopping cross sections in gaseous, at 0.3 to 2 MeV, 25:36255
electron resonant scattering by, effects of vibronic excitation on angular distributions from, (T), 25:35869
fission-fragment reactions and ranges in, 25:36254
photo-absorption cross sections of, review of uv, (E/T), 25:36013
reactions with methane under simulated radiolysis conditions, mass spectrometric studies on, 25:34645
sorption on zeolites, isotope separation factors in, 25:34708
yields from γ radiolysis of neutral aqueous, oxygenated solutions of oxalate ions, effects of dose on, 25:34644
CARBON IONS
reactions of multiply charged, with flowing methane--nitrogen and nitrogen--oxygen systems at 7 MeV/n, 25:34567
CARBON ISOTOPES
separation by chemical exchange, distillation, and thermal diffusion, 25:34807(R) (MLM-1793)
separation factors in sorption of carbon dioxide on zeolites, 25:34708
CARBON ISOTOPES C-12
abundance in 19 Psc and Y CVn, (E), 25:35620
alpha reactions (α,γ) at 7.6 to 8.1 MeV, gamma angular distribution and resonance parameters for, (E),

XUM

25:36675
content ratio to carbon-14 in sandstone-type uranium deposits, measurement of, 25:34750(R) (COO-2024-1)
determination in thin films by nuclear reaction micro methods, 25:34550
deuteron inelastic scattering at 13.6 MeV, binding- and optical-model calculations of differential cross sections for, (T), 25:36848
energy levels in, effects of resonance interaction on, (T), 25:36837
energy levels of, alpha-particle-model calculations of rotational, (T), 25:36680
exchange with carbon-14 between adenosine 5'-diphosphate and adenosine 5'-triphosphate and between fructose 1,6-diphosphate and fructose 6-phosphate, catalytic effects of ox heart phosphofructokinase on, 25:34596
meson (π) reactions at 100 GeV, Drell--Hiida--Deck effect for 5π via A_1 and rho production in diffractive, (T), 25:36521
meson (π^+) reactions at high energies, Coulomb interaction in, (T), 25:36524
meson (π^-) reactions at high energies, Coulomb interaction in, (T), 25:36524
nuclear binding energy and radius of, alpha-particle-model calculation of, (T), 25:36681
photon reactions with, isolation of Regge trajectories in amplitudes of meson production in, (T), 25:36453
proton reactions (p,2p) at 600 MeV, diffraction-model calculation of differential cross sections for, (T), 25:36679
proton reactions (p,Li-6) at 36, 41, and 45 MeV, angular distributions for, (E), 25:36738(R) (UCLA-10-P-18-23)
reactions (C-12,3n) and (C-12,5n) with praseodymium-141 at 81 MeV, gamma spectra from, (E), 25:36726 (JINR-P6-5681)
reactions (C-12,α2n) with californium-249 at 77.4 MeV, alpha and x-ray spectra from, product of, (E), 25:36778
reactions (C-12,f) with lutetium-175, ytterbium-174, and tungsten-182 up to 10.4 MeV/nucleon, excitation functions for, (E), 25:36784

CARBON ISOTOPES C-13
abundance in 19 Psc and Y CVn, (E), 25:35620
concentration in carbon dioxide, carbon monoxide, and methane, 25:34807(R) (MLM-1793)
content in sandstone-type uranium deposits, measurement of, 25:34750(R) (COO-2024-1)
effects on emission spectra of carbon monoxide, 25:34595
effects on EPR spectra of deuterated methylene, 25:34586
effects on isomerization of cyclopropane, 25:34572(R) (ORO-3234-23)
effects on sorption of carbon dioxide on zeolites, 25:34708
electron elastic scattering by, rms charge radius ratio for carbon-13 to carbon-12 from, (E), 25:36682
electron scattering up to 20 MeV, form factors for carbon-13 energy levels from inelastic, (E), 25:36682
energy levels from carbon-14 (p,d) and (p,t) reactions, (E), 25:36673
energy levels from electron inelastic scattering up to 20 MeV, form factors for, (E), 25:36682
nuclear charge radius ratio for carbon-13 to carbon-12 from electron elastic scattering by carbon-13, (E), 25:36682

CARBON ISOTOPES C-14
content in seawater, research progress on study of, 25:34723(R) (RLO-2225-T-20-3)
content ratio to carbon-12 in sandstone-type uranium deposits, measurement of, 25:34750(R) (COO-2024-1)
effects on displacement reactions of benzyl chlorides, 25:34572(R) (ORO-3234-23)
effects on timing of bonding changes in rearrangements to positively charged carbon, 25:34572(R) (ORO-3234-23)
exchange between hexathiocyanomolybdate(III) and thiocyanates, kinetics of, 25:34583
exchange with carbon-12 between adenosine 5'-diphosphate and adenosine 5'-triphosphate and between fructose 1,6-diphosphate and fructose 6-phosphate, catalytic effects of ox heart phosphofructokinase on, 25:34596
proton elastic and inelastic scattering at 14.5 MeV, angular distributions for, (E), 25:36673
proton reactions (p,d) at 14.5 MeV, angular distributions for, (E), 25:36673
proton reactions (p,t) at 14.5 MeV, angular distributions for, (E), 25:36673

CARBON MONOXIDES
alpha-particle stopping cross sections in gaseous, at 0.3 to 2 MeV, 25:36255
band strengths in spectra of K giant stars, (E/T), 25:35649
effects on rats, combined effects of γ radiation and, 25:35233
electron reactions with, resonances in total cross sections for, (E), 25:35861
fission-fragment reactions and ranges in, 25:36254
photo-absorption cross sections of, review of uv, (E/T), 25:36013
sorption by (110) surface of tungsten, 25:35357
sorption by molybdenum (100) surface, radiotracer and photoemission studies of, 25:35358

CARBON SULFIDES
photo-absorption cross sections of, review of CS_2 uv, (E/T), 25:36013

CARBON SYSTEMS
Al--C--Co--Cr--Mo--Nb--Ni-base--Ta--Ti--Zr, properties of corrosion-resistant IN-738 superalloy, 25:35400
C--Co--Cr--Fe--Mo--Nb--Ni-base, strengthening by precipitation of body-centered tetragonal phase in, 25:35302
C--Co-base--Cr--Fe--Ni--Ta--Ti--W, fracture toughness of Mar-M-509, effects of carbide inclusions on, 25:35490
C--Cr--Fe--Mo--Nb--Ni-base, strengthening by precipitation of body-centered tetragonal phase in, 25:35302
C--Cr--Fe--V, analysis of complex carbides in, by electron beam micro methods, 25:34523
C--Fe-base, radiation effects on mechanical properties of, at 80 to 100°C, relations of composition and fast neutron, 25:35505 (ZJE-99)
C--Fe-base--Mn, radiation effects on mechanical properties of, at 80 to 100°C, relations of composition with fast neutron, 25:35505 (ZJE-99)
C--Hf--Mo-base, tensile properties of dilute, effects of thermomechanical treatments on, 25:35397
C--Mn--Si--steel, properties of plates of, for use in pressure vessels at moderate and lower temperature service, standard for, 25:35468
C--Th, phase diagram of, 25:35548 (ORNL-4503(Vol.3))
C--transition metal carbides, preparation of high-temperature composites of, methods for, 25:35530
C--UC_2, fabrication of tubular fuel elements of aluminum-clad enriched, extrusion method for, 25:35527

CARBON TETRACHLORIDE
diffusion through drybox gloves, comparison of values for other halogenated solvents with, 25:34605 (RFP-1606)
radiation effects on, and its solutions in natural rubber latex, EPR studies of γ, 25:34614

CARBON TETRAFLUORIDE
vapor pressure--temperature data for, 25:34602 (CAT-645)

CARBONYL COMPOUNDS
reactions of, mechanisms of acid-catalyzed rearrangement, 25:34572(R) (ORO-3234-23)

CARBONYL FLUORIDE
vapor pressure--temperature data for, 25:34602 (CAT-645)

CARBONYL SULFIDE
photo-absorption cross sections of molecular, review of uv, (E/T), 25:36013

CASCADE SHOWERS
development of nuclear--electromagnetic 4-TeV, in ionization spectrometer, Monte Carlo simulation for energy balance and total ionization as function of depth for, (T), 25:36431 (ITJ-6)
particle angular distributions for p + p interactions at 10 GeV in hydrogen bubble chamber, (E), 25:36393
particle identification from proton reactions with nuclei at 22.8 GeV/c in emulsions, method for, (E), 25:36402
production in p + p interactions at 10 GeV in hydrogen bubble chamber, angular distributions for, (E), 25:36393
production in proton reactions with nuclei at 22.8 GeV/c in emulsions, method for particle identification for, (E), 25:36402
production in π^- reactions with nuclei at 17.2 GeV in emulsions, (E), 25:36418

CAST IRON
finishes for contact faces of pipe flanges and connecting-end flanges of valves and fittings of, standard for, 25:35418

CATECHOL METHYLTRANSFERASE
radiation effects on activity of rat, protective effects of cystamine against, 25:35165

CATTLE
iodine-131 content in thyroid of, in Portugal following Chinese nuclear tests, 25:35133

CAVITY RESONATORS
performance of open, for plasma density measurements, (E/T), 25:36089 (KHFTI-69/51)
properties of, with two rows of drift tubes for simultaneous acceleration of two beams, 25:36623

CELL MEMBRANES
radiation effects on animal and human, review on, 25:35209

CELLS
origin of goblet, from intestinal stem cells in man during post-operative irradiation, 25:35240
radiation effect on, mechanisms of recovery following, 25:35205
radiation effects on animal and human, review on, 25:35209
radiation effects on nuclei of, in barley and bean seeds, comparison of bremsstrahlung, γ, proton, and x, 25:35258
radiation effects on number of epithelial, in rat small intestine, effects of dose on γ, 25:35220
radiation effects on structure of deoxyribonucleoproteins in somatic, 25:35198
radiation effects on structure of, conference on, 25:35130
radiation effects on, conference on, Erevan, USSR, Oct. 28 to Nov. 3, 1968, 25:35196
radiation effects on, hit and target principles for studying, 25:35199
radiation effects on, role of DNA in, 25:35197

XUM

radiation effects on, role of free radicals in, 25:35202
radiation injuries in, role of radiotoxins in, 25:35200
radiation injuries to cytoplasm of, in maize shoot apices, 25:35244
CELLS, CULTURED
radiation effects on Chinese hamster, protective and sensitizing effects of oxygen against x, 25:35214
radiation effects on Ehrlich ascites, mechanism of protective effects of cysteamine and AET against, 25:35204
radiation effects on proliferation of human osteosarcoma, effects of dose fractionation on x, 25:35242
radiation effects on structure of nucleoproteins in amnion, 25:35206
CELLS, L
radiation effects on molecular weight of DNA synthesized in pyrimidine-containing, uv, 25:35207
radioinduced mutations for 8-azaguanine resistance in, x, 25:35124
radioinduced single strand breaks in DNA from mouse, effects of metabolic inhibitors on repair of x, 25:35224
CELLULOSE ACETATES
efficiency of membranes of, for separation of krypton and xenon from reactor containment system atmospheres, 25:34692(R) (NYO-4057-2)
CEMENTS
handling and storage of cesium-137- and strontium-90-containing, protective measures for personnel during, 25:35148
CERAMIC MATERIALS
properties as armor plating, 25:37256(T) (UCRL-Trans-10530)
radiation resistance of, evaluation of, 25:34690(R) (IN-1457)
removal of layers of, electron beam method for, 25:35515
CEREBROSPINAL FLUID
cisternography of dynamics of, in hydrocephalic patients, radioisotope, 25:35172
CERIUM
determination in rare earth oxides, spectrographic, 25:34511
determination in rocks by neutron activation and γ spectroscopy, 25:34543 (NIM-1013)
determination of tetravalent, colorimetrically using o-aminophenol, 25:34530
dissociation energy and formation heat of diatomic, 25:35347
effects on colorimetric determination of gold, 25:34521
effects on photometric determination of antimony following solvent extraction using TBP, 25:34512
reactions with thiols, ESR studies on free radicals from, 25:34639(R) (USC-113-P-21-3)
separation from fission products by solvent extraction using TOPO--TTA, 25:34522
separation from other rare earths by ion exchange chromatography, 25:34714
CERIUM ALLOYS AND SYSTEMS
stability of gaseous intermetallic, predicted, 25:35347
Ce--La, magnetic properties of superconducting, pressure effect on, (E/T), 25:36021
CERIUM FLUORIDES
effects on radiation stability of beryllium fluoride glasses, 25:34621
CERIUM ISOTOPES Ce-137
sorption by human gastrointestinal tract following professional exposure, 25:35099
CERIUM ISOTOPES Ce-138
energy levels from praseodymium-138 beta and electron-capture decay, spin--parity assignments for, (E), 25:36725 (JINR-P6-5674)
energy-level transitions from praseodymium-138 beta and electron-capture decay, branching ratios, internal conversion coefficients, and multipolarities for, (E), 25:36725 (JINR-P6-5674)
CERIUM ISOTOPES Ce-140
neutron capture by, γ circular polarization from thermal, (E), 25:36751
CERIUM ISOTOPES Ce-141
availability in peccaries following single injection of nuclear debris from Project Buggy fallout, 25:35088
energy levels from cerium-140 thermal neutron capture, spin-parity assignments for, (E), 25:36751
energy levels of, unified model calculations for, (T), 25:36749
CERIUM ISOTOPES Ce-142
energy levels from lanthanum-142 decay, (E), 25:36765
CERIUM ISOTOPES Ce-144
content in atmosphere over Moscow, 1962 to 67, 25:34748
effects on rat liver regeneration, mechanism of, 25:35221
CERIUM OXIDES
diffusion of oxygen in nonstoichiometric, self-, 25:35553
electric properties of nonstoichiometric, 25:35553
CeO_2--Y_2O_3, diffusion of oxygen in nonstoichiometric solid solutions of, self-, 25:35553
CeO_2--Y_2O_3, electric properties of nonstoichiometric solid solutions of, 25:35553
CESIUM
determination in human stones by neutron activation, 25:34546 (THAI.-AEC-39)
determination in rocks by neutron activation and γ spectroscopy, 25:34543 (NIM-1013)
effects on photometric determination of antimony following solvent extraction using TBP, 25:34512
effects on radiation stability of sulfone polyelectrolytes, 25:34650
electron reactions with, multiple ionization and formation of metastable states in, 25:35865
encapsulation of fission product, for use as radiation source, method for, 25:34803(R) (BNWL-1308-5)
plasma of, ion acoustic oscillations and transport processes in low-temperature, (E), 25:36231
reactions of fission-product, with graphite in fuel elements at high temperatures, 25:35567
separation from rubidium by solvent extraction using phenol, effect of diluent on partition coefficient in, 25:34701
sorption by silts in natural waters, 25:34722(R) (NYO-3912-4)
sorption by silts in natural waters, 25:34721(R) (NYO-3912-3)
sorption by tantalum (110) and tungsten (100) crystals, contact potential measurements of, 25:35355
sorption effects on work function of tantalum carbide, 25:36335
CESIUM IODIDES
CsI--KI--LiBr--LiCl--LiI, properties of eutectics of, for use as paste electrolytes, 25:35275(R) (ANL-7777)
CESIUM IONS
ionization potentials for charge states up to Cs^{10+}, 25:35865
CESIUM ISOTOPES
determination of radioactive, in soils, 25:34500
CESIUM ISOTOPES Cs-133
neutron capture by, spectrum-averaged cross sections for pile, (E/T), 25:36720 (CONF-710301-4)
CESIUM ISOTOPES Cs-137
content in atmosphere over Moscow, 1962 to 67, 25:34748
content in fish from Baltic Sea and North Atlantic during 1967 and 1968, 25:35096
content in freshwater fish in Germany during 1967 and 1968, 25:35096
content in man, as function of age, whole-body counting of, 25:35095
content in man, evaluation of shielded whole-body counter for measuring, 25:35183
content in seawater, measurements of, 25:34759(R) (NYO-2174-129)
determination as measure of fission product concentration in spent uranium oxide (UO_2) by counting, 25:37015 (BNWL-1568)
distribution in waters of Atlantic Ocean, Mediterranean Sea, and Sargasso Sea, measurement of vertical, 25:34759(R) (NYO-2174-129)
handling and storage of cements containing, protective measures for personnel during, 25:35148
leaching from radioactive wastes after fixation in Polish bitumen, rates of, 25:34845 (INR-1249)
metabolism in children in Warsaw, 1965 to 1967 and 1969, 25:35093
removal from man, methods for, 25:35134
sorption by sediments from low terraces of Elbe, Donau, and Weser Rivers, 25:34737
uptake by human populations in Germany during 1967 and 1968 from ingestion of fish, 25:35096
CESIUM NEPTUNIUM CHLORIDES
formation heat in aqueous hydrochloric acid solutions, 25:34609
CESIUM PLUTONIUM CHLORIDES
formation heat in aqueous hydrochloric acid solutions, 25:34609
CESIUM PRASEODYMIUM FLUORIDES
praseodymium-141 Moessbauer spectra in, 25:36344
CESIUM PROTACTINIUM CHLORIDES
formation heat in aqueous hydrochloric acid solutions, 25:34609
CESIUM THORIUM CHLORIDES
formation heat in aqueous hydrochloric acid solutions, 25:34609
CESIUM URANIUM CHLORIDES
formation heat in aqueous hydrochloric acid solutions, 25:34609
CHARGED-PARTICLE BEAMS
calculations for intense, with arbitrary phase-density distribution in external focusing fields, 25:36642
focusing of, design of multipole permanent magnet lenses for, 25:36619(P)
focusing systems for, effects of magnetic field measurement errors on properties of, 25:36627
interaction with magnetosphere, vlf wave amplification in, (E), 25:35972
interactions with plasma, nonlinear theory for relaxation in, 25:36130
profile monitoring system for, electronic control unit for, 25:36632
profile of non-relativistic, with space charge forces and finite emittance, equation for, 25:36628
reactions with matter, Monte Carlo calculation of high-energy, (T), 25:36816 (JINR-P2-5719)
structure of intense non-laminar axially-symmetric,

XUM

calculation of, 25:36609 (NP-18860)
CHARGED PARTICLES
acceleration in magnetic mirrors, three variants of Fermi model for, 25:36636
channeling in crystals, dechanneling effects of defects on, 25:36275
interaction with photons near NP 0532, consequences of collision, (E/T), 25:35706
interactions with media, transition radiation from nonrelativistic, 25:36354 (JINR-P4-5734)
motion in constant electromagnetic fields, relativistic, (T), 25:36363
motion in helical magnetic fields, effect of electric fields on, (T), 25:36084
motion near periodic dielectric structure, radiations from, (T), 25:36360
precipitation into auroral zones, interrelation of magnetospheric structure to phenomena of, (E/T), 25:35958
scattering by atoms, reduction of (3Z + 2)-dimensional integral in Glauber approximation for, 25:35863
spectra measurements of, ultra-thin scintillation detector for time-of-flight, 25:34887(P)
CHEMICAL REACTIONS
kinetics of chain, role of numerical stability in computer solution of, 25:37255 (UCRL-73166)
mechanisms of homogeneous oscillating, 25:34573(R) (RLO-2230-T-2-2)
CHEMISTRY
stable isotope uses in, review of, 25:34813 (TID-25705)
CHINON REACTORS (EDF-1)
safety aspects of, 25:36892
CHINON REACTORS (EDF-2)
safety aspects of, 25:36892
CHLORAL
radiolysis of, ESR studies on, 25:34634(R) (COO-1385-37)
CHLORATES
effects on photometric determination of antimony following solvent extraction using TBP, 25:34512
CHLORIDES
determination in glacial waters by ion-sensitive electrode method, 25:34721(R) (NYO-3912-3)
determination in glacial waters by ion-sensitive electrode method, 25:34722(R) (NYO-3912-4)
CHLORINE
vapor pressure--temperature data for, 25:34602 (GAT-645)
CHLORINE FLUORIDES
vapor pressure--temperature data for, 25:34602 (GAT-645)
CHLORINE IONS
reactions with hydrogen gas at 4 MeV, charge-state distributions from, (E), 25:35849
CHLORINE ISOTOPES
separation by thermal diffusion, 25:34807(R) (MLM-1793)
CHLORINE ISOTOPES Cl-34
beta decay of ground-state and isomeric, beta and gamma spectra, branching ratios, and log-ft values for, (E), 25:36700
isomeric transition in, branching ratio for, (E), 25:36700
CHLORINE ISOTOPES Cl-36
exchange between chlorosilanes and cyclohexylamine hydrochloride, mechanisms of, 25:34579
exchange between hexachloromolybdate(III) and chlorides, kinetics of, 25:34583
CHLORINE ISOTOPES Cl-37
effects on displacement reactions of benzyl chlorides, 25:34572(R) (CRO-3234-23)
CHLORINE OXIDES
vapor pressure--temperature data for, 25:34602 (GAT-645)
yields of chlorine dioxide and chlorine trioxide from γ radiolysis of sodium chlorates, ESR studies on effects of temperature on, 25:34666
CHLORINE OXYFLUORIDES
vapor pressure--temperature data for, 25:34602 (GAT-645)
CHLOROFORM
effects on quenching of radiation-excited and uv-excited organic solutions, 25:34624
radiation effects on, and its solutions in natural rubber latex, EPR studies of γ, 25:34614
CHLOROPHYTA
Chlorella sp., radioinduced breaks in DNA of, mechanisms of repair following γ, 25:35257
CHOLANTHRENE, 3-METHYL-
effects of coatings of, on γ radiolysis products of poly(vinyl chloride), ESR studies on, 25:34656
CHOLINESTERASE
radiation effects on activity of rat brain, effects of adrenal and pituitary gland function on, 25:35232
CHROMATES
effects on photometric determination of antimony following solvent extraction using TBP, 25:34512
polarographic reactions at mercury electrode, effects of thiourea on, 25:34560
CHROMATOGRAPHY
conference on gel permeation, Miami Beach, Florida, Oct. 4 to 7, 1970, 25:35532
uses of liquid, analytical, 25:37192 (MHSMP-71-31)
CHROMEL COUPLES
Alumel/Chromel, radiation effects on, fast neutron, 25:35072 (HEDL-SA-152)
CHROMIUM
boiling superheat of sodium at surfaces of, effects of roughness on, 25:34791 (KFK-1332)
corrosion by lithium--selenium mixtures at 375°C, 25:35275(R) (ANL-7777)
determination in complex carbides by electron beam micro methods, 25:34523
determination in human stones by neutron activation, 25:34546 (THAI.-AEC-39)
determination of trace amounts of, in uranium by neutron activation, 25:34547 (UARAEE-68)
effects on colorimetric determination of gold, 25:34521
effects on gravimetric determination of mercury using 2-aminobenzothiazole, 25:34520
effects on polarographic reduction of niobium, 25:34526
plastic flow anisotropy in monocrystalline, mechanisms of, 25:35379
polarographic reactions at mercury electrode, effects of thiourea on, 25:34560
stability of powders of, in acids, 25:35522
thermodynamic properties of solution of, in liquid tin, 25:35368
CHROMIUM ALLOYS AND SYSTEMS
Al--C--Co--Cr--Mo--Nb--Ni-base--Ta--Ti--Zr, properties of corrosion-resistant IN-738 superalloy, 25:35400
Al--Cr--Fe--Ni-base--Ti, tensile properties at 25 to 850°C, effects of grain size, precipitates, and test time on, 25:35340 (UARAEE-55)
Al--Cr--Mo--Ni-base--Ti, solvus temperature of γ' in, effects of hardener content on, 25:35460
Al--Cr--Ni-base--Ti, solvus temperature of γ' in, effects of hardener content on, 25:35460
Al--Cr--Ni-base--Ti--W, phase precipitation in, relations of heat treatments with microstructure of, 25:35602
Al--Cr--Ni-base--W, reactions of cladding of, for chromium--tungsten alloy with air and nitrogen at 2100 and 2300°F, resistance to oxidation, 25:35288
Al--Cr--Ti-base--V, tensile properties of metastable beta, at 25 to 600°C, effects of strain rate and annealing temperature on anomalies in, 25:35434
C--Co--Cr--Fe--Mo--Nb--Ni-base, strengthening by precipitation of body-centered tetragonal phase in, 25:35302
C--Co-base--Cr--Fe--Ni--Ta--Ti--W, fracture toughness of Mar-M-509, effects of carbide inclusions on, 25:35490
C--Cr--Fe--Mo--Nb--Ni-base, strengthening by precipitation of body-centered tetragonal phase in, 25:35302
C--Cr--Fe--V, analysis of complex carbides in, by electron beam micro methods, 25:34523
Co--Cr--Mo--Ni, hardening of multiphase, mechanisms of, 25:35396
Co--Cr--W, phase studies of cobalt-rich, at 1350°C, 25:35489
Co--Cr--W, phase studies of, at 1350°C, 25:35498
Cr--Fe--Ni, corrosion of Unitemp 605, by lithium--selenium mixtures at 375°C, 25:35275(R) (ANL-7777)
Cr--Fe--Ni, standard for cold-drawn and hot-finished seamless pipe and tube for general corrosive service and heat-resisting uses, 25:35413
Cr--Fe--Ni, standard for hot-finished and cold-drawn rounds, squares, hexagons, and rectangles of, 25:35364
Cr--Fe--Ni, standard for plates, sheets, and strips of, 25:35360
Cr--Fe--Ni-base, tensile properties at 25 to 850°C, effects of grain size, precipitates, and test time on, 25:35340 (UARAEE-55)
Cr--Mo, diffusion in solid solutions of, at 1440 to 1603°C, solid--vapor couple measurements of, 25:35427
Cr--Nb--Ni-base, plastic deformation of precipitation hardened, 25:35483
Cr--Nb--Ni-base, precipitation in, mechanism of, 25:35483
Cr--Nb--Ni-base, strengthening by precipitation of body-centered tetragonal phase in, 25:35302
Cr--Ni--steel, welding to Inconel 625, tungsten inert gas method for, 25:35311
Cr--Ni-base, mechanical properties of dispersion-strengthened, at high temperatures, 25:35352
Cr--Ni-base--Ta, plastic deformation of precipitation hardened, 25:35483
Cr--Ni-base--Ta, precipitation in, mechanism of, 25:35483
Cr-base--W, reactions of aluminum--chromium--nickel--tungsten alloy-clad, with air and nitrogen at 2100 and 2300°F, protection from oxidation, 25:35288
CHROMIUM FLUORIDES
vapor pressure--temperature data for, 25:34602 (GAT-645)
CHROMIUM ISOTOPES Cr-51
production in (n,α) and (n,p) reactions with fast neutrons, cross sections for, (E), 25:36686 (CONF-680986-1)
CHROMIUM NITRIDES
chemical stability in water, alkali solutions, and acids, 25:35522
reaction kinetics in acids, decomposition, 25:35522
CHROMOSOMES
radioinduced aberrations in Crepis capillaris shoots, γ, 25:35128
radioinduced aberrations in onion and wheat, effects of heat treatment on x, 25:35125
radioinduced aberrations in pea seed, effects of oxygen on, 25:35119

XUM

radioinduced aberrations in Vicia faba, effects of oxygen pressure on x, 25:35118
radioinduced aberrations of human lymphocyte, protective effects of cystamine against fractionated γ, 25:35123
radioinduced aberrations of, in pollen tubes of Tradescantia, effects of infrared radiation on uv, 25:35120
radioinduced aberrations of, in transplanted monkey bone marrow, effects of dose on, 25:35230
CHROMOSPHERE
active regions in, isophotes of, (E), 25:35776
flares in, motions of, (E), 25:35747
observations of solar, extrapolation to stellar atmospheres, (T), 25:35657
shock heating of, model for, (T), 25:35769
spectra of, calcium K emission-line widths in, (T), 25:35717
spectra of, formation of Ca II K-line core in, (E/T), 25:35716
spectra of, Na D, Na 5688, and Mg I 4571 lines in, (E), 25:35715
structure of, center-limb observations of inhomogeneities in, (E), 25:35715
CHROMYL FLUORIDES
vapor pressure--temperature data for, 25:34602 (GAT-649)
CHRYSENE
effects of coatings of, on γ radiolysis products of poly(vinyl chloride), ESR studies on, 25:34656
CIRCUITS
design for determining direction to lightning or nuclear explosions by rf transients, 25:35058(P)
design of high-speed integrated 8-fold fanout, 25:35009 (ORC-2504-172)
design of printed, computer graphics system for assisting in, 25:37253 (UCRL-72637)
design of wide band correlator, 25:35052
initial conditions and transient response of electronic, SCEPTRE computer program for determining, 25:37251 (UCRL-20659)
simulation of logic, computer program for, 25:37254 (UCRL-72694)
CLAYS
stability of shale-type, in steep craters, engineering studies of, 25:34768 (NCG-TR-15(Vol.1))
CLOUDS
book: Noctilucent Clouds, 25:35988
COAL
cost analysis in U. S. for 1971 to 1985, 25:36861
COATINGS
application of conformal, research progress on, 25:37163(R) (BDX-613-286)
thickness measurement of thin, aperture platen for beta radiometric, 25:35078(P)
thickness measurement of thin, aperture platen for beta radiometric, 25:35041(P)
COBALT
complexes with ammonia, polarographic reactions at mercury electrode, effect of thiourea on, 25:34560
determination in complex carbides by electron beam micro methods, 25:34523
determination in rocks by neutron activation and γ spectroscopy, 25:34543 (NIM-1013)
determination of trace amounts of, in copper by neutron activation, 25:34548
determination of trace amounts of, in uranium by neutron activation, 25:34547 (UARAEE-68)
effects of binder of, on sintering of tungsten carbide powders, 25:35534
effects on colorimetric determination of gold, 25:34521
effects on gravimetric determination of mercury using 2-aminobenzothiazole, 25:34520
effects on photometric determination of antimony following solvent extraction using TBP, 25:34512
effects on radiation stability of sulfone polyelectrolytes, 25:34650
electric field gradient in hcp, calculations, 25:36351
lattice dynamics model of, phonon dispersion curves and frequency spectra from, 25:36333
nuclear spin--lattice relaxation times from cobalt-60 NMR at 0.004 to 0.010°K, (E/T), 25:36347
separation from other transition metals by ion exchange on anionite AV-17, 25:34695(T) (ORNL-tr-2397)
separation of ions of, from metal ions by high-voltage electrophoresis using carboxylic and hydroxycarboxylic acids, 25:34702
sorption by vermiculite in presence of interfering ions, quantitative model for, 25:34721(R) (NYO-3912-3)
sorption by vermiculite, quantitative model for, 25:34722(R) (NYO-3912-4)
sorption on surface of reactive minerals in glacial environment, research progress on, 25:34722(R) (NYO-3912-4)
sorption on surface of reactive minerals in glacial environment, research progress on, 25:34721(R) (NYO-3912-3)
thermodynamic properties of solution of, in liquid tin, 25:35368
COBALT ALLOYS AND SYSTEMS
creep and deformation of unidirectional solidified eutectic, 25:35431
Al--Co--Mo, radiation effects on catalytic activity of, in dehydrogenation of cyclohexane, 25:34628
Al--Co--Mo, radiation effects on subsequent catalytic activity of, in decomposition of hydrogen peroxide, γ, 25:34630
C--Co--Cr--Fe--Mo--Nb--Ni-base, strengthening by precipitation of body-centered tetragonal phase in, 25:35302
C--Co-base--Cr--Fe--Ni--Ta--Ti--W, fracture toughness of Mar-M-509, effects of carbide inclusions on, 25:35490
Co--Cr--Mo--Ni, hardening of multiphase, mechanisms of, 25:35396
Co--Cr--W, phase studies of cobalt-rich, at 1350°C, 25:35489
Co--Cr--W, phase studies of, at 1350°C, 25:35458
Co--Fe-base, creep at 1073°K, effects of stress on, 25:35464
Co--Lu, magnetic properties of intermetallic compounds of, (E/T), 25:36318
Co--misch metal--Sm, fabrication and magnetic properties of permanent magnets of, 25:36336
Co--Ni--V, mechanical properties of, effects of crystal ordering on, 25:35385
Co--rare earths, development of magnetic intermetallic compounds of, 25:35306
Co-base--Fe, slip in, mechanisms of creep, 25:35386
COBALT ISOTOPES Co-58
energy levels from cobalt-59 (d,t) and manganese-55 (α,nγ) reactions, spin assignments for, (E), 25:36694
excretion in feces of peccaries following single ingestion of nuclear debris from Schooner Event, fallout, 25:35089
production in (n,α) and (n,p) reactions with fast neutrons, cross sections for, (E), 25:36686 (CONF-680586-1)
COBALT ISOTOPES Co-59
deuteron reactions (d,t) at 15 and 16.5 MeV, DWBA analysis of angular distributions and l transfers from, (E), 25:36694
proton reactions (p,n) at 17 MeV, neutron spectra from, (E), 25:36676
proton reactions at 450 MeV, Monte Carlo calculation of neutron spectra from, (E/T), 25:36816 (JINR-P2-5715)
COBALT ISOTOPES Co-60
content in drinking water for compliance with ICRP organ burden standards for man, use of data from rat studies to calculate maximum permissible, 25:35116
content of organs in rats following single ingestion, calculation of equilibrium dose rate to human organs using, 25:35116
diffusion in stainless steel surfaces at 1000°C, 25:35276(R) (GEAP-13539-16)
nuclear magnetic resonance in cobalt, iron, nd nickel at 0.004 to 0.010°K, nuclear spin--lattice relaxation times from, (E/T), 25:36347
COINCIDENCE CIRCUITS
design for simultaneous measurements of electron--gamma and gamma--gamma directional correlations, 25:34903
design of conversion electron--x-ray, for beta- and Compton suppression, 25:34933
design of high-speed integrated, for liquid scintillation detector, 25:35009 (ORC-2504-172)
operation of γ--γ sum, using lithium-drifted germanium detectors, 25:34932
COLLIMATORS
design optimization for radioisotope scanners, (T), 25:34880
development of miniature rotating, for neutron time-of-flight spectroscopy, 25:34917 (JUL-719-FF)
properties of multi-slit, for whole-body counter, 25:34871 (UARAEE-82)
COLORADO
radioactivity of rainwater in central and western, during Project Rulison reentry drilling, 25:34728 (USGS-474-101)
COLUMBIA RIVER
effects in Northeast Pacific Ocean, research progress on biological studies of, 25:37217(R) (RLO-1725-200)
effects of thermal pollution on ecosystems in, bibliography on, 25:35115 (BNWL-1543)
fish population of, effects of reactor thermal effluents on migration of, 25:37105 (BNWL-SA-3876)
fish population of, effects of thermal history on effects of thermal stress on, 25:37104 (BNWL-SA-3713)
COMETS
exobiology survey of, (T), 25:35829
COMPOSITE MATERIALS
conference on strength of, Vol. 3, Pacific Grove, Calif., Aug. 30 to Sept. 4, 1970, 25:35395
fabrication for ablative environments, 25:35530
fabrication of high-strength high-modulus low-density filament-reinforced metal matrix, methods for, 25:35528
preparation by in-situ growth of refractory fibers in high-temperature alloys, 25:35557
research on metallic matrix, in France, 25:35431
testing of fiber-reinforced epoxy matrix, nondestructive methods for, 25:34838
COMPTON EFFECT
spectra of high-energy electrons undergoing Klein--Nishina losses, (T), 25:36263
COMPUTATIONAL MODULAR SYSTEMS
DELPHI, for theoretical-physics calculations, 25:36357

XUM

JOSHUA, for preparation and testing of ENDF/B neutron cross sections, 25:36737 (TID-25690)
COMPUTER PROGRAMS
ALTHAEA, for reactor fuel cycle costs, FORTRAN 2 for IBM 7090 and FORTRAN 4 for UNIVAC 1108, 25:36862 (BNWL-462)
ARGO, for fast reactor kinetics, 25:36992 (JAERI-Memo-4331)
BASFUN, for evaluating Basset function with real argument, in FORTRAN IV for IBM 360/50, 25:36813 (ANU-P-439)
bibliography of Argonne Code Center reactor physics, annotated, 25:37133 (ANL-7411(Suppl.5))
COFCOM, for evaluating ingoing and outgoing Coulomb wave functions for complex l, in FORTRAN IV for IBM 360/50, 25:36813 (ANU-P-439)
COFREG, for evaluating regular Coulomb wave functions, in FORTRAN IV for IBM 360/50, 25:36813 (ANU-P-439)
CORD and RECORD, for sorting of tabular data, 25:37178 (CIC-P1-8)
CUBRT, for fast 9-digit cube root function for CDC 6600, 25:37242 (UCID-30004)
description of, for orbit determinations on binary stars, (E/T), 25:35647
development for control of neutron diffractometers and processing neutron-diffraction data, 25:36309 (AAEC/TM-578)
DTACOR, for calculating sample-expansion effects in liquid metals, FORTRAN for CDC 6600, 25:35342 (UCRL-51035)
EOSDTA, for calculating enthalpy and electric resistance of liquid metals, FORTRAN for CDC 6600, 25:35342 (UCRL-51035)
FITTER, FUNGUS, FUNNY, for linear least squares curve fitting of weighted tabular data, 25:37177 (CIC-E2.2-8)
for analysis of gamma-ray line shapes, 25:34915 (ANU-P-438)
for calculating effects of creep, radioinduced dimensional changes, and strains in complex structures, 25:34774 (EUR-4629)
for calculation of gamma-ray pulse height spectrum in semiconductor detector, in FORTRAN for PDP-10, 25:34907
for calculation of reactor critical parameters by two- and three-group diffusion approximations, FORTRAN II for IBM 1620, 25:37126 (UARAEE-89)
for data system for INTEREM DEVICE, 25:36193 (ORNL-TM-3401)
for four-group four-region one-dimensional criticality calculations, for IBM 1620, 25:37125 (UARAEE-85)
for multigroup multiregion one-dimensional criticality calculations, for IBM 1130, 25:37127 (UARAEE-90)
for two-group two-region criticality calculations, for IBM 1620, 25:37122 (UARAEE-79)
GAMCOM, for evaluating gamma function with complex argument, in FORTRAN IV for IBM 360/50, 25:36813 (ANU-P-439)
GEOMETRICAL COEFFICIENT, for calculating geometrical coefficients in quantum theory of angular momentum, in FORTRAN IV for CDC 6600, 25:36366
HYPCOM, for evaluating Gaussian hypergeometric function with real argument and complex parameters, in FORTRAN IV for IBM 360/50, 25:36813 (ANU-P-439)
HYPLOG, for evaluating Gaussian hypergeometric function with real argument and complex parameters in logarithmic case, in FORTRAN IV for IBM 360/50, 25:36813 (ANU-P-439)
JFM, for fuel accountability for Japanese Materials Testing Reactor, 25:37065 (JAERI-Memo-4270)
JIB3, for optical-model searching, for IBM 360/50, 25:36814 (ANU-P-451)
JUPITOR KARLSRUHE VERSION, improved version of Tamura's code for coupled-channel calculations, in FORTRAN IV for IBM 360, 25:36818 (KFK-1333)
language for DELPHI system SPEAKEASY, 25:36357
MECC-3, for intranuclear-cascade calculations of nuclear reactions, in FORTRAN IV for IBM 360/75 and /91, 25:36733 (ORNL-4564)
ORSAC, for optimum economic development of nuclear power plants in U. S, 25:36886 (ORNL-TM-3223)
PAN6, for analysis of space frameworks, 25:37229 (SC-RR-70-742)
PHROG, for fast neutron spectra and average multigroup cross sections for calculation of reactor kinetics, FORTRAN 4 for IBM 360, 25:37113 (IN-1435)
PSICOM, for evaluating psi function with complex argument, in FORTRAN IV for IBM 360/50, 25:36813 (ANU-P-439)
RAFFLE, Monte Carlo neutron-transport code for obtaining collapsed cross sections and transfer matrices, in FORTRAN IV for IBM 300/75, 25:36649 (CONF-710302-11)
RAM-1, for solving multigroup, time-independent, neutron diffusion problem, in FORTRAN for IBM 1130, 25:36651 (UARAEE-107)
RKM1: for obtaining parameter defining equations for generalized Runge--Kutta--Frey integration schemes, 25:37246 (UCRL-19861)
SAVE, for two-group calculations of reflector savings of completely reflected cylindrical reactors, FORTRAN for IBM 1620, 25:37128 (UARAEE-96)
SPIFFY: interpolation in tables of weighted data, 25:37176 (CIC-E1.1-8)
SYN, for two-dimensional neutron flux synthesis, FORTRAN IV for GE 635, 25:37112 (GEAP-13672)
TAXL, simple hierarchical data structure manipulation system, 25:37236 (SLAC-119)
TENSOR, for calculating propagation of stress wave of arbitrary amplitude through two-dimensional media, FORTRAN, 25:34769 (UCRL-50987)
TVGP, modifications for reconstructing particle tracks in ANL 12-foot bubble chamber, 25:34948 (CONF-700622-(Vol.1), pp 303-11)
TVGP, modifications for reconstructing particle tracks in track-sensitive targets in bubble chambers, 25:34549 (CONF-700623-(Vol.1), pp 312-24)
VOLDTA, for analysis of volumetric data on liquid metals, for CDC 6600, 25:35342 (UCRL-51035)
WINTGRL7, for calculating energy-loss distributions according to Vavilov theory, in FORTRAN, 25:36732 (NRL-7230)
WITFUN, for evaluating Whittaker function with real argument, in FORTRAN IV for IBM 360/50, 25:36813 (ANU-P-439)
YIELD6, for calculating yields for (p,γ) reactions, in FORTRAN, 25:36732 (NRL-7230)
COMPUTERS
data in, design of magnetic temporary-storage device for elimination of undesirable transient effects on, 25:35074(P)
graphics line printer for WADCO PDP-9/AD-4 hytrid, GOULD 4800, 25:37174 (BNWL-E-58)
interface between Nova, and multicrate CAMAC system, operation and design of Branch Driver, 25:37190 (LA-4682)
multiplexer system for, 16 channel medium speed, 25:37196 (NYO-1480-171)
radiation effects on, system for monitoring possible errors from, 25:35074(P)
research progress on, 25:37184(R) (COO-2094-6)
use for analysis and measurement of beam emittance in linear accelerators, 25:36612 (UARAEE-76)
use for design and control of processes, conference on, 25:35047 (CONF-700647)
use of PDP-8 as message switching device for CDC 3300 time-sharing system, 25:37219 (RLO-2227-T-7-7)
CONCRETES
neutron attenuation by calcium-based, 14-MeV, (E), 25:36260
radiation effects on mechanical properties of prestressed, fast neutron, 25:37007(T) (ORNL-tr-2470)
CONNECTICUT YANKEE POWER REACTOR
boiler feed pumps for, periodic testing requirements for steam driven auxiliary, 25:36907 (DOCKET-50213-107)
cooling system for, in-service inspection requirements for primary, 25:36907 (DOCKET-50213-107)
effluents from, reevaluation of onsite personnel exposure to radioactive, 25:36909 (DOCKET-50213-112)
emergency core cooling system for, periodic testing requirements for, 25:36908 (DOCKET-50213-108)
emergency power system for, periodic testing requirements for, 25:36908 (DOCKET-50213-108)
instrumentation for, maximum safety settings for protective, 25:36908 (DOCKET-50213-108)
operations history for April 1971, 25:36869 (DOCKET-50213-109)
personnel of, reevaluation of iodine-131 exposure of, 25:36909 (DOCKET-50213-112)
pressure vessel for, in-service inspection requirements for, 25:36907 (DOCKET-50213-107)
CONTAMINATION
control practices from manufacturing viewpoint, checklist of good, 25:37227 (SC-M-70-549)
CONTROL SYSTEMS
performance of CRNL integrated, for processing breeder reactor fuels, 25:34847 (ORNL-4607)
CONVERSION ELECTRONS
spectroscopy of, using conversion electrons--x-ray coincidence for beta- and Compton-suppression, 25:34933
COPPER
analysis for trace amounts of cobalt or nickel by neutron activation, 25:34548
argon-ion reactions at 20 keV with, luminescence spectra of excited particles knocked out from, effects of nonradiative transitions on, 25:35841
defect structure of irradiated, effects of deformation on recovery spectra of, 25:35501
determination in soils by neutron activation, 25:34545 (THAI.-AEC-36)
determination of trace amounts of, in uranium by neutron activation, 25:34547 (UARAEE-68)
diffusion of niobium-95 in, 25:35406
effects on gravimetric determination of mercury using 2-aminobenzothiazole, 25:34520
effects on photometric determination of antimony following solvent extraction using TBP, 25:34512
electron mean free path in, magneto-acoustic attenuation study of temperature dependence of, 25:36328
electron scattering by phonons in crystals of, 25:36280
ionization probability of, in simulated micrometeors, (E), 25:35597
luminous efficiency of, in simulated micrometeors, (E),

XUM

25:35596
proton reactions at 450 MeV, Monte Carlo calculation of neutron spectra from, (E/T), 25:36816 (JINR-P2-5719)
radiation effects on content of, in functionally and morphologically different tissues in animal spinal cord, x, 25:35228
radiation effects on dislocation density of monocrystalline, in stress-applied and stress-removed states, electron microscope study of fast neutron, 25:35518
radiation effects on dislocation-pinning memory in, gamma, 25:35514
radiation effects on Stage I dislocation arrangement of deformed monocrystalline, in stress-applied state, electron microscope study of fast neutron, 25:35520
radiation effects on Stage II dislocation arrangement of deformed monocrystalline, in stress-applied state, electron microscope study of fast neutron, 25:35519
separation from other transition metals by ion exchange on anionite AV-17, 25:34695(T) (ORNL-tr-2397)
separation of ions of, from metal ions by high-voltage electrophoresis using carboxylic and hydroxycarboxylic acids, 25:34702
x-ray emission induced by electrons, intense K-, 25:35842

COPPER ALLOYS AND SYSTEMS
Ag--Cu, mixing at 1100°C, adiabatic calorimetric measurement of heat of, 25:35433
Al--Cu, formation of Cu_2Al and $CuAl_2$ during copper-ion implantation in aluminum, 25:36295
Al--Cu, mixing at 1100°C, adiabatic calorimetric measurement of heat of, 25:35433
Al--Cu--Fe--Ti-base--V, fracture toughness of α--β, relations with microstructure, 25:35348
Al-base--B--Cu--Mg, corrosion of diffusion bonded composites of, by sodium chloride solution, effects of applied stress on, 25:35521
Au--Cu, mixing at 1100°C, adiabatic calorimetric measurement of heat of, 25:35433
Be--Cu, bonding specimens of, using polyaryl sulfone adhesive, 25:35316
Be--Cu-base, precipitation of equilibrium γ phase in, effects of cold work on discontinuous, 25:35494
Cu--Ga, mixing at 1100°C, adiabatic calorimetric measurement of heat of, 25:35433
Cu--Ge, mixing at 1100°C, adiabatic calorimetric measurement of heat of, 25:35433
Cu--In, mixing at 1100°C, adiabatic calorimetric measurement of heat of, 25:35433
Cu--Mo, tensile properties of laminar systems of, at 20 to 600°C, effects of composition on, 25:35454
Cu--Mo, tensile properties of laminates of, effects of composition on, 25:35455
Cu--Sn, mixing at 1100°C, adiabatic calorimetric measurement of heat of, 25:35433
Cu--Ti, formation of intermetallic compounds of, during explosion welding, effects of niobium on, 25:35324
Cu--W, tensile properties of laminar systems of, at 20 to 600°C, effects of composition on, 25:35454

COPPER IONS
implantation in aluminum at 30 and 60 keV, anomalous collection in, 25:36295

COPPER ISOTOPES Cu-63
neutron reactions (n,α) at 0.1 MeV to 18 MeV, excitation functions for, (E), 25:36741 (WHAN-SA-107)

CORROSION
book: Bibliographic Survey of Corrosion, 1960, A Compilation of Corrosion Abstracts, 25:35290
mechanisms and methods for prevention of, review of, 25:35285

CORROSION LOOPS
design of sodium radioactive transfer test-type, 25:35276(R) (GEAP-13539-16)

COSMIC GAMMA SOURCES
detection in galactic anticenter region, (E), 25:35700

COSMIC PARTICLES
charge ratio of near-sea level energetic muons, energy and zenith angle-dependent, (E/T), 25:35858
composition of heavy primary, above 10 GeV/N, (E/T), 25:35895
effects on production of magnetic remanence in meteorites and lunar materials, (E), 25:35598
electron spectrum and charge composition of, balloon measurements of high-energy, (E), 25:35920
element abundances in, (T), 25:35595
energy losses of primary, in interplanetary space, (T), 25:35924
energy spectra of heavy primary, above 10 GeV/N, (E/T), 25:35895
hadron reactions with lead and graphite above $3(10)^{12}$ eV, distributions and mean values of inelasticity coefficient for π^0 production in, (E), 25:36389 (ITJ-5)
interaction mean free paths and fragmentation probabilities of heavy nuclei and alpha particles in air and hydrogen, emulsion study of, (E/T), 25:36394
interaction mean free paths and fragmentation probabilities of heavy nuclei and alpha particles above 10 GeV/nucleon in emulsions, (E), 25:36394
interactions N + N at 10^{11} to 10^{13} eV, proposed experiment for average characteristics and angular distributions for, (E), 25:36416
interactions π + N at 10^{11} to 10^{13} eV, proposed experiment for average characteristics and angular distributions for, (E), 25:36416
modulation by solar system, model for, (E/T), 25:35859
modulation of primary, in interplanetary space, (T), 25:35924
modulation of primary, in interplanetary space, (T), 25:35906
momentum spectrum and charge ratio of vertical muons, at sea level and 12°N geomagnetic latitude, (E), 25:35919
nucleon reactions with lead and graphite above $3(10)^{12}$ eV, ionization spectrometer study of energy and mean inelasticity for, (E), 25:36388 (ITJ-3)
production of meson (μ), proposed experiment for direct, (E), 25:36416
production spectrum of meson, near geomagnetic equator, (E/T), 25:35917
propagation of primary, in interplanetary space, (T), 25:35906
spectra of mesons (μ), mesons (π), and nucleons at sea level, model of hadron reactions with nuclei for, 25:35925
spectrum of muons at sea level and 12°N geomagnetic latitude, design of spectrograph for momentum, (E), 25:35918

COSMIC RADIATION
acceleration of primary, (T), 25:35904
book: Modulation of Cosmic Rays in Interplanetary Space, 25:35894
charge composition of, nuclei abundance of elements from neon to nickel above 250 MeV/nucleon, (E), 25:35910
conference on, Delhi, India, 10/69, 25:35892 (CONF-691055-(Vol.1))
conference on, Delhi, India, 10/69, 25:35893 (CONF-691055-(Vol.2))
confinement of primary, in galactic disk, (T), 25:35908
detection at sea level, anomalous pulse spectrum of plastic scintillation detectors for, 25:35010
diffusion of primary, compound, (T), 25:35902
distribution of primary, (T), 25:35904
effects on heating of interstellar medium by, (T), 25:35784
effects on purified water, luminescence produced by, 25:34623
energy releases by galactic, into upper atmosphere and ionospheric D region, (T), 25:36007
energy spectra of diffuse x-ray, at 20 to 120 keV, (E), 25:35921
energy spectra of N-component at sea level, ionization chamber study of, (E), 25:35916
experimental facilities at Gulmarg, 25:35909
intensity at 70 m.w.e., solar effects on, (E/T), 25:35731
intensity of N-component at sea level, ionization chamber study of, (E), 25:35916
intensity variations of primary, solar effects on, (T), 25:35907
intensity variations of, correlation with atmospheric ozone content, (E/T), 25:35974
interaction with stone meteorites, sodium-22 and tritium production rates from galactic, (E/T), 25:35899
interactions with interstellar plasma in Colgate's model, (T), 25:35900
interactions with stone meteorites, orbital velocities from track measurements of, (E/T), 25:35600
modulation of primary, solar system, (T), 25:35907
modulation of primary, solar wind, (E), 25:35759
modulation of, neutron-multiplicity analyzer data during 1968-1969 of, (E), 25:35897
nuclei abundance in, from fossil-track measurements in meteorites, ultraheavy, (E), 25:35911
origin of primary, (T), 25:35904
origin of primary, in pulsars, (T), 25:35660
origin of, infrared background in universal theory of, (T), 25:35818
particle relative abundance ratios in, deuteron and helium nuclei, (E/T), 25:35912
propagation in atmosphere, model of hadron reactions with nuclei for, 25:35925
variation of limiting energy of corotating, with solar cycle, 1958 to 1968, (E/T), 25:35914
variations of, during 1962 and 1964-65 diurnal, (E), 25:35901

COSMIC RADIO SOURCES
distance to 3C 391, (E), 25:35702
distribution of, (T), 25:35811
emission from Tau A and Vir A, occultation by solar corona, 25:35773
flux densities at 408 MHz of 4C, in declination range -7 to -3°, (E), 25:35682
identification of 100 4C, optical, (E), 25:35682
identification of 3C 58 with supernova in 1181, (T), 25:35676
identification of PKS 0320-37 with NGC 1316, optical, 25:35707
monitoring for H_2CS in directions of, (E), 25:35708
noise generation by plasma wave scattering in, 25:35856
positions at 408 MHz of 4C, in declination range -7 to -3°, (E), 25:35682
spectra of 3C 391, (E), 25:35702
structure in 3C 391, angular, (E), 25:35702

structure of, long-base-line interferometric studies of, (E), 25:35709
COSMIC-RAY SPECTROMETERS
design and performance of large-area scintillation time-of-flight, 25:35020
design of solid-iron magnetic, for muons, (E), 25:35918
magnets for, design of solid iron, 25:35012
COSMIC RAY TELESCOPES
description of, at Kum-bel Mountain Station, 25:35013
COSMIC SHOWERS
electron distribution in air, critical analysis of studies on, (E), 25:36395
electron interactions at high energies in air, review of, (E), 25:36395
hadron component of EAS, multiplate cloud chamber study of lateral distribution and charge to neutral ratio for, (E), 25:36383
hadron interactions at 1 TeV in air, review of, (E), 25:36395
meson (μ) bundles in EAS, multiplate cloud chamber study of, (E), 25:36383
tachyon production in EAS, upper limit for, (E), 25:36378
COSMIC X-RAY SOURCES
Cyg X-1, multiple periodicity in x-ray emission from, (E), 25:35690
Cyg X-2, radio identification of, (E), 25:35701
detection and measurement of, balloon-borne scintillation telescope for, (E), 25:35014
discovery of soft, in Aries--Taurus region, (E), 25:35710
GX 301-2, rapid fluctuations in high-energy flux from, (E), 25:35692
GX 304-1, x-ray flux from, (E), 25:35692
GX 5-1, identification with supernova remnant Milne 56, (E), 25:35684
Sco X-1, energy spectrum at 15 to 120 keV, (E), 25:35704
x-ray flare from, in Crux, (E), 25:35691
COSMOLOGY
cosmic fluid in expanding Universe, nonlinear effect of, (T), 25:35815
density perturbations and conformally flat expanding universe, (T), 25:35805
matter distribution in, effects of hierarchical structure of, (T), 25:35817
model featuring black hole-white hole existence, (T), 25:35820
models in, world, (T), 25:35808
models of, scale factors in homogeneous, (T), 25:35816
observational data in, (T), 25:35808
quasar distribution in, (T), 25:35810
relativistic model of Universe, construction of, (T), 25:35806
solution of Jordan--Dicke field equations, (T), 25:35814
CRAB NEBULA
light polarization from, elliptical, (E), 25:35618
CRATERS
stability of steep clay shale, engineering studies of, 25:34768 (NCG-TR-15(Vol.1))
CRITICAL ASSEMBLIES
fission ratios and rate distributions in FCA, (E/T), 25:37066 (JAERI-Memo-4356)
neutron spectra in reflector of Silouette Reactor, effects of metal slabs on perturbations in fast, (E/T), 25:37057 (CEA-R-3799)
CRITICALITY
calculations for hydrogen moderated enriched uranium fueled lattices, three-group diffusion theory model for, (E/T), 25:37124 (UARAEE-84)
calculations of, computer code for four-group four-region one-dimensional, 25:37125 (UARAEE-85)
calculations of, computer code for multigroup multiregion one-dimensional, 25:37127 (UARAEE-90)
technical criteria for, in chemical processing facilities, 25:34678 (ARH-468(Rev.))
CRYOGENICS
equipment for, design of neutron diffraction cryo-orienter, 25:36080
CRYSTALS
defect-induced changes of thermodynamic properties of polymorphic, equations for, (T), 25:36297
electron scattering by phonons in, imaginary potential calculations for fast, 25:36280
ground-state energy of electronic or nucleonic many-body system, variational calculations, 25:36358
magnetic structures determined by neutron diffraction, data tables for rhombohedral and hexagonal, 25:36311 (NP-18845)
particle dechanneling by defects in, review, 25:36275
radiation effects on, ESR studies on, 25:34634(R) (COO-1385-37)
CUMENE
radiation stability of, for use as diluent in fuel reprocessing, 25:34638 (RT/CHI-(70)35)
CUPFERRON
complexes with uranyl ion, magnetic susceptibility and ir spectra of, 25:34612
CURIUM
determination in biological materials by α spectrometry following separation by solvent extraction using DEHPA, 25:34537
distribution and excretion following inhalation in soluble compounds, effects of DTPA on, 25:35091
CURIUM ISOTOPES Cm-241
fission of isomeric, half-life for spontaneous, (E), 25:36795
CURIUM ISOTOPES Cm-242
fission of isomeric, half-life for spontaneous, (E), 25:36795
CURIUM ISOTOPES Cm-243
fission of isomeric, half-life for spontaneous, (E), 25:36795
CURIUM ISOTOPES Cm-244
neutron fission of, cross section and resonance integral of thermal, (E), 25:36721 (DP-MS-70-95)
radiation effects on lattice parameter of curium dioxide, 25:35589
CURIUM ISOTOPES Cm-245
neutron fission of, cross section and resonance integral of thermal, (E), 25:36721 (DP-MS-70-95)
CURIUM ISOTOPES Cm-246
neutron fission of, cross section and resonance integral of thermal, (E), 25:36721 (DP-MS-70-95)
CURIUM ISOTOPES Cm-247
neutron fission of, cross section and resonance integral of thermal, (E), 25:36721 (DP-MS-70-95)
CURIUM ISOTOPES Cm-248
neutron fission of, cross section and resonance integral of thermal, (E), 25:36721 (DP-MS-70-95)
CURIUM OXIDES
radioinduced expansion of $^{244}CmO_2$, self-, 25:35589
CURRENT ALGEBRA
commutators in, review of anomalies in, 25:36427
decay width ratio of $\omega \to \pi^0 + \gamma$ decay to $\pi^0 \to 2\gamma$ decay in, momentum-dependence of vector vertex function for, 25:36495
field--current identities for rho and A_1, in gauge-invariant formulation of massive gauge fields, 25:36501
Ward identities in, review of anomalies in, 25:36427
CYANOGEN
abundance in 19 Psc and Y CVn, (E), 25:35620
band strengths in spectra of K giant stars, (E/T), 25:35649
CYCLOBUTANE
reactions with helium tritides formed by beta decay of molecular tritium, kinetic studies on, 25:34675
CYCLOHEXANE
radiation effects on catalytic dehydrogenation of, on aluminum--cobalt--molybdenum catalyst, γ, 25:34628
reactions with helium tritides formed by beta decay of molecular tritium, kinetic studies on, 25:34675
CYCLOHEXIMIDE
effects on repair of x-radiation-induced single strand breaks in DNA in mouse L cells, 25:35224
CYCLONE SEPARATORS
design of, engineering drawings for, 25:34784
CYCLOPENTANE
reactions with helium tritides formed by beta decay of molecular tritium, kinetic studies on, 25:34675
CYCLOPROPANE
alpha-particle stopping cross sections in gaseous, at 0.3 to 2 MeV, 25:36255
reactions with helium tritides formed by beta decay of molecular tritium, kinetic studies on, 25:34676
CYCLOTRONS
beam energies of Texas A and M, methods for increasing deuteron and proton, (T), 25:36637
beam transport and analyzing system for UCLA, 25:36738(R) (UCLA-10-P-18-23)
particle trajectories in isochronous, effects of accelerating gaps on, (T), 25:36621
research of Nuclear Consortium at UCLA, 25:36738(R) (UCLA-10-P-18-23)
CYLINDERS
neutron leakage from water-moderated, escape fractions and reflection coefficients for, (E/T), 25:36652
CYSTAMINE
radioprotective effects on catechol methyltransferase and monoamine oxidase activity in rats, 25:35165
radioprotective effects on chromosome aberrations in man, γ, 25:35123
CYSTEAMINE
radiolysis of, ESR spectra of free radicals from electron pulse, 25:34639(R) (USC-113-P-21-3)
radioprotective effects of, in relation to radiotoxins in cells, 25:35200
radioprotective effects of, on Escherichia coli, function and structure studies on γ, 25:35160
radioprotective effects on Ehrlich ascites cells, mechanisms of, 25:35204
CYTOCHROME C
radioresistance of, relation of intramolecular excitation transfer to x, 25:35106
CYTOSINE, 5-METHYL-
radiolysis of frozen aqueous solutions of, ESR spectral studies on free radicals produced by γ, 25:34654
CZECHOSLOVAKIA
regulations for protection of uranium mining personnel, 25:35152

XUM

D

DACTINOMYCIN
effects on repair of x-radioinduced single strand breaks in DNA in mouse L cells, 25:35224
DATA ACQUISITION SYSTEMS
design for centralized output from simultaneous experiments, 25:35049 (CONF-700647-, pp 255-79)
development of on-line, for neutron physics experiments, 25:35048 (CONF-700647-, pp 183-93)
development of RAD swapping, for nuclear reaction experiments, 25:35050 (PUC-937-396)
operation of reactor safety, for determination of reliability characteristics, 25:37040 (IRS-T-18(1970), pp 123-43)
DATA PROCESSING SYSTEMS
control program and subroutines for INTEREM facility that uses PDP-12 computer, 25:36193 (ORNL-TM-3401)
description of automatic, for 2X II mirror machine, 25:36195 (UCRL-73030)
design of, for use in photometry of rapid blue variable, (E), 25:35674
development of computer, for neutron diffraction, 25:36309 (AAEC/TM-578)
development of Sandia Laboratories Livermore, 25:37235 (SCL-DR-710032)
digital filtering techniques for, 25:37195(R) (MHSMP-71-34)
power supply for, control system for, 25:35068
DATA TABULATIONS
atlas of solar flare effects in ionosphere, Sept. 1960 through Dec. 1962, 25:35952 (NBS-TN-326)
cross sections for neutron elastic scattering by hydrogen at 22.5 to 400 MeV, least-squares fit to differential, (E), 25:36661 (UCRL-20295)
energy levels and transitions of even--even Z = 6 to 82, quasi-beta, quasi-gamma, and quasi-ground, (E), 25:36783
gamma rays from nuclei produced in (n,γ) reactions, (E), 25:36718 (AAEC/TM-585)
magnetic structures determined by neutron diffraction, 25:36311 (NP-18845)
neutron cross sections of fissile nuclei in unresolved-resonances region, fluctuation factors for theoretical evaluation of average, (T), 25:36722 (IA-1208)
on mechanical and physical properties of zirconium and its alloys, 25:35439
partial-wave analyses for $\pi^- + p \to \pi^- + p$ and $\pi^+ + p \to \pi^+ + p$ interactions at 0 to 2 GeV/c, compilation of amplitudes and parameters from, 25:36506 (TID-25726)
DESALTING
bromine redox electrolysis for, operating parameters for, 25:34691 (LA-4645)
methods for, abstracts of papers on, 25:37091 (ORNL-TM-3402)
DEUTERIUM
abundance relative to hydrogen in two reference water standards, 25:34518
alpha-particle stopping cross sections at 0.5 to 2 MeV, atomic, (E), 25:36256
collisions of atomic and molecular, exact tunneling calculations for, 25:34574
determination in natural waters by mass spectrometry, 25:34518
determination in thin films by nuclear reaction micro methods, 25:34550
effects on addition of benzoyloxy radicals to benzene, 25:34577
effects on decay of vibronic bands in phosphorescence of benzaldehyde, 25:34592
effects on gas-phase hydrogen exchange reactions with halogens, 25:34572(R) (ORO-3234-23)
effects on hydrolysis of ring-substituted trifluoro-N-methylacetanilides, solvent, 25:34576
effects on isomerization of cyclopropane, 25:34572(R) (ORO-3234-23)
effects on phosphorescence lifetimes of biacetyl crystals and vapors, 25:34593
effects on quadratic force constants from fundamental frequencies of vibrations of nitromethane, 25:34581
effects on radiationless electronic transitions and intersystem crossing in anthracene, 25:34590
effects on reactions of nickelocene with mercaptans, kinetic studies on, 25:34597
effects on spectra of CH^+ in argon--acetylene systems, 25:34594
effects on vibrational spectra and anharmonicity of water in dilute solutions, 25:34591
effects on yields from γ radiolysis of deuterated and normal methanol, 25:34665
exchange and partition function ratios in hydrides, effects of chemical bond characteristics on, 25:34585
exchange between sulfuric or trifluoroacetic acids and unsaturated polyalkyl compounds, mass spectrometric and proton magnetic resonance studies on kinetics of, 25:34599
exchange of gaseous, with lattice hydrogen of hydrides, 25:34582
exchange reactions in complexes of anthracene with alkali metals, 25:34578
exchange reactions in compounds from addition of acetic or hydrochloric acids to benzonorbornadiene, 25:34575
exchange with hydrogen in a position of alkyl groups of aromatic hydrocarbons and trifluoroacetic acid, 25:34598
exchange with hydrogen in globular proteins, ir spectral studies on, 25:34588
exchange with hydrogen in γ-irradiated adenine derivatives, 25:34652
exchange with hydrogen in N,N-diethylformamide, NMR studies on internal rotation in, 25:34587
helium-3 reactions (He^3,t)2n at 19 MeV, triton spectra at 5° from, (E), 25:36662
lattice dynamics at high pressure, 25:37204 (NYO-3655-51)
plasma of, neutron spectra from laser irradiated solid target, 25:36203
plasma of, production by laser irradiation of solid, (E/T), 25:36156
potassium-atom and -ion reactions up to 50 eV with molecular, vibrational excitation and dissociation in, (E), 25:35884
properties for use in large cryogenic bubble chambers, 25:34962 (CONF-700623-(Vol.1), pp 532-42)
proton reactions (p,2p) at 4.5 to 13 MeV, impulse-approximation analysis of n--p and p--p coincidence spectra and excitation functions for, (E/T), 25:36665
proton reactions (p,pn) at 14 to 23 MeV, modified-simple-impulse-approximation calculation of proton spectra from, (E/T), 25:36667
proton reactions (p,pn) at 9.0 MeV, impulse-approximation analysis of proton spectra and peak cross sections for, (E/T), 25:36670
reactions with hydrogen gas at 3 to 45 keV, total loss cross sections for, (E), 25:35855 (UCRL-20099)
sodium-atom and -ion reactions up to 50 eV with molecular, vibrational excitation and dissociation in, (E), 25:35884
triton reactions (t,He^3)2n at 22 MeV, helium-3 spectra at 5° from, (E), 25:36662
DEUTERIUM HYDRIDES
spectra of, relative line intensities in Lyman bands of, (E), 25:35848
DEUTERONS
abundance in primary cosmic rays, relation to helium nuclei abundance, (E/T), 25:35912
dechanneling in germanium single crystals at 1.5 MeV, ion mass effect on, 25:36289
emission in proton reactions with nuclei at 24 GeV/c in emulsions, (E), 25:36403
interactions anti p + d at rest, evidence for existence of narrow anti pn bound state in,), 25:36399
interactions e + d → e + d, time reversal violation in cross sections of, (T), 25:36546
interactions $K^+ + d \to K^+ + \pi^+ + \pi^- + d(pn)$ at 9 GeV/c, $K^*(1243)$ and $K^*(1344)$ mixing in mass spectra of, (E), 25:36414
interactions n + d, calculation of doublet scattering length using rank-four separable potentials, (T), 25:36659 (IAR-P-1234)
interactions n + d, potentials with hard-core repulsion for doublet length for, (T), 25:36536
interactions p + d → ^3He + MM at 2 and 3 GeV, spectrometer study of differential cross sections versus missing mass and I = 0 and 1 meson production cross sections for, (E), 25:36398
reactions (d,2n) and (d,pn) with americium-243 at 12 to 20 MeV, cross sections and excitation functions for, (E), 25:36795
reactions (d,2n) with neptunium-237 at 12 to 18 MeV, cross sections and excitation functions for, (E), 25:36795
reactions (d,α) with bismuth-209 at 20 MeV, angular distributions for, (E), 25:36777
reactions (d,α) with iron-54 and vanadium-51 at 28 MeV, DWBA analysis of differential cross sections, l transfer, and spectra from, (E), 25:36687 (LYCEN-7087)
reactions (d,α) with magnesium-26 at 2.5 to 3.0 MeV, angular distributions, excitation functions, and spectra from, (E), 25:36701
reactions (d,He^3) with hydrogen at 20 to 45.2 MeV, evidence for T = 1/2 resonance in cross sections for, (E), 25:36663
reactions (d,nγ) and (d,pγ) with magnesium-26, gamma spectra from, (E), 25:36717
reactions (d,pf) with A = 233 to 243 nuclei at 13 MeV, analysis using double-humped barrier, (E/T), 25:36746
reactions (d,pγ) with bismuth-209 at 9 MeV, gamma spectra and p--γ coincidences from, (E), 25:36790
reactions (d,pn) with A = 27 to 197 nuclei at 13.6 MeV, diffraction-model analysis of proton--neutron correlations in, 25:36713
reactions (d,t) with cobalt-59 at 15 and 16.5 MeV, DWBA analysis of angular distributions and l transfers from, (E), 25:36694
reactions (d,t) with helium-3 at 39.1 MeV at 50, Born-approximation and Watson--Migdal analysis of final-state interactions in energy spectra from, (E), 25:36665
scattering by carbon-12 and nickel-60 at 13.6 MeV, binding- and optical-model calculations of differential

XUM

cross sections for inelastic, (T), 25:36848
scattering by even--even nuclei, effects of strong binding in elastic and inelastic, (T), 25:36848
DEWAR VESSELS
design of lead-shielded toroidal, for superconducting rings, 25:36192 (MATT-846)
DEXTRAN
sulfate, radiolysis of frozen concentrated aqueous solutions of, ESR studies on free radicals produced by, 25:34651
DIAMONDS
ion-implanted layers in Type IIa, ion-channeling analysis of phosphorus, 25:36285
radiation effects on density of single crystals of, x-ray studies on fast-neutron, 25:34619
radiation effects on infrared absorption spectra of Type-Ia, 1-MeV electron, 25:36279
removal of layers of, electron beam method for, 25:35515
DIBENZANTHRACENE
effects of coatings of, on γ radiolysis products of poly(vinyl chloride), ESR studies on, 25:34656
DIET
cesium-137 content in, of children in Warsaw, 1965 to 1967 and 1969, 25:35093
DIFFERENTIAL EQUATIONS
solution for, computer program GEAR for, 25:37241 (UCID-30001)
solution of discrete Poisson, on irregular regions, 25:37187 (LA-4553)
solution of initial value problem for, 25:37231 (SC-RR-710296)
solution of, generating operator for, 25:37188 (LA-4655)
DIFFUSION
isotope effects on interstitial, 25:34571(T) (ANL-Trans-882)
DIPHENYLAMINE
effects of coatings of, on γ radiolysis products of poly(vinyl chloride), ESR studies on, 25:34656
DISEASES
radiodiagnosis of human brain, combined contrast angiography and intracarotid injection of technetium-99m for, 25:35173
radiodiagnosis of human brain, by scanning, value of vertex view in, 25:35175
DISEASES, INFECTIOUS
syphilis, effects on distribution and excretion of injected arsenic-76 in rabbits, 25:35087
DISEASES, NEOPLASTIC
cancer, radiotherapy of human breast, development of pendular method for postoperative fast electron, 25:35191
carcinomas, diagnosis of human gynecological, comparison of lymphoscintigraphy and γ venography with microscopy during lymphadenectomy for, 25:35186
carcinomas, radiotherapy of human bladder, effectiveness of cobalt-60 in relation to survival time for, 25:35192
carcinomas, radiotherapy of human bronchial pulmonary function in comparison with surgery, 25:35243
carcinomas, radiotherapy of human larynx, effectiveness of γ, 25:35188
carcinomas, radiotherapy of human thyroid, effectiveness of radioisotopes in combination with surgery for, 25:35190
fibrosarcomas, radioinduced, in scalp of rats, x, 25:35236
lesions, radiotherapy of cervical, in man, development of rectal lesions following, 25:35158
metastases, radiotherapy of malignant bone, in humans, effectiveness of, 25:35187
radiodiagnosis of human brain, by radioisotope scanning, 25:35177
radiodiagnosis of human brain, using technetium-99m and γ scintillation camera, 25:35174
tumors, radiodiagnosis of human bone, brain, and liver, effectiveness of, 25:35185
tumors, radiosensitivity of Ehrlich ascites, in mice and in vitro, effects of dihydroxybutyraldehyde on x, 25:35159
tumors, radiotherapy of human nasopharyngeal, development of conformation method for electron and x, 25:35194
tumors, radiotherapy of human renal, effects of sex and size on cobalt-60, 25:35193
DISEASES, PHYSIOLOGICAL
effects on calcium-47 retention in man following oral administration, 25:35098
hydrocephalus, radiodiagnosis of human, cisternographic methods for study of cerebrospinal fluid dynamics in iodine-131 and technetium-99m, 25:35172
polycythemia, radiotherapy of, effectiveness of phosphorus-32, 25:35157
pulmonary edema, regional function of lungs of patients with, use of xenon-133 for determining, 25:35170
radiodiagnosis of human brain circulatory, use of γ sources for, 25:35178
radiodiagnosis of human cerebral vascular, by scanning, 25:35176
DISKS
thermal stresses in annular, at temperatures above 400°C, accuracy of strain gages for measuring, 25:34799
DISPERSION RELATIONS
amplitudes for π + π interactions in Veneziano model for partial-wave, 25:36487
analytic functions and statistics for, 25:36597
interactions π + N, phase shifts for low-energy π + π interactions from backward, 25:36520
DISSOLVERS
design for plutonium processing facility, engineering drawings for, 25:34784
DOGS
radiation effects on corticosteroid retention in liver of, effects of dose on γ, 25:35222
DONALD C. COOK POWER REACTOR, UNIT 1
construction of, transfer of permit for, 25:36948 (DOCKET-50315-35)
DONALD C. COOK POWER REACTOR, UNIT 2
construction of, transfer of permit for, 25:36948 (DOCKET-50315-35)
DRESDEN POWER REACTOR, UNIT 2
containment system for, leak rate tests for secondary, 25:36873 (DOCKET-50237-173)
coolant injection system for, pipe failure on high pressure, 25:36918 (DOCKET-50237-175)
cooling system for, paint maintenance problems for torus of, 25:36914 (DOCKET-50237-169)
emergency core cooling system for, long-term operation requirements for, 25:36916 (DOCKET-50237-171)
emergency core cooling system for, water hammer prevention in, 25:36913 (DOCKET-50237-168)
emergency core cooling system for, water level requirements for discharge piping of, 25:36916 (DOCKET-50237-171)
instrumentation for, drywell pneumatic supply system for, 25:36913 (DOCKET-50237-168)
instrumentation for, revised scram settings for APRM and IRM systems, 25:36911 (DOCKET-50237-166)
instrumentation for, scram settings for APRM and IRM systems, 25:36915 (DOCKET-50237-170)
motors for, modifications for limitorque circuit breakers and switches for, 25:36913 (DOCKET-50237-168)
operations incident of May 27, 1971, radioactivity release from pipe failure during surveillance test of emergency core cooling system, 25:36872 (DOCKET-50237-172)
pumps for, elimination of vibrations in recirculation jet, 25:36913 (DOCKET-50237-168)
pumps for, elimination of vibrations in recirculation jet, 25:36916 (DOCKET-50237-171)
radioactive waste disposal system for, modifications for off-gas, 25:36917 (DOCKET-50237-174)
steam line isolation valves for, drywell pneumatic supply system for, 25:36916 (DOCKET-50237-171)
technical specifications for, modification of auxiliary and emergency systems, 25:36919 (DOCKET-50237-176)
testing of, transient responses for loss of electrical load, 25:36912 (DOCKET-50237-167)
DRESDEN POWER REACTOR, UNIT 3
containment system for, limiting conditions for drywell pneumatic supply system for isolation valves of, 25:36922 (DOCKET-50249-70)
emergency core cooling system for, limiting conditions for discharge piping water level and long-term capability of, 25:36922 (DOCKET-50249-70)
instrumentation for, revised scram settings for APRM and IRM systems, 25:36920 (DOCKET-50249-67)
instrumentation for, scram settings for APRM and IRM systems, 25:36921 (DOCKET-50249-68)
radioactive waste disposal system for, modifications for off-gas, 25:36917 (DOCKET-50237-174)
technical specifications for, modification of reactor vessel inservice inspection, 25:36923 (DOCKET-50249-72)
technical specifications for, modification to add scram functions, 25:36924 (DOCKET-50249-73)
testing of, transient responses for loss of electrical load, 25:36912 (DOCKET-50237-167)
DUSTS
properties and behavior of radioactive and nonradioactive interplanetary, (E/T), 25:35913
DYSPROSIUM
determination as impurity in terbium oxide by neutron activation and radiochemical separation, 25:34670 (JAERI-Memo-4280)
energy levels of, from spectra analysis, 25:35846
DYSPROSIUM ALLOYS AND SYSTEMS
Al--Dy-base, crystal lattice parameters of intermetallic Dy_2Al, 25:35495
DYSPROSIUM IONS
effects of activators of, on radioluminescence and thermoluminescence spectra in strontium fluoride and barium fluoride crystals, (E), 25:36317
energy levels of Dy II from spectra analysis, 25:35846
DYSPROSIUM ISOTOPES Dy-159
electron-capture decay of, L/K capture ratio from, (E), 25:36771
DYSPROSIUM ISOTOPES Dy-160
energy levels from terbium-160 decay, spins and E2/M1 and M2/E1 multipole mixing ratios for, (E), 25:36776
neutron capture by, cross sections and resonance integrals for pile and thermal, (E), 25:36735 (SGAE-PH-104/1971)
DYSPROSIUM ISOTOPES Dy-161
neutron capture by, cross sections and resonance

integrals for pile and thermal, (E), 25:36735 (SGAE-PH-104/1971)
DYSPROSIUM ISOTOPES Dy-162
neutron capture by, cross sections and resonance integrals for pile and thermal, (E), 25:36735 (SGAE-PH-104/1971)
DYSPROSIUM ISOTOPES Dy-163
neutron capture by, cross sections and resonance integrals for pile and thermal, (E), 25:36735 (SGAE-PH-104/1971)
DYSPROSIUM OXIDES
growth of single-crystal solid solutions with another rare earth oxide by Verneuil method, formation regions in, 25:35525

E

EARTH
ionosphere of, model of solar-wind interaction with, (E/T), 25:36011
EARTHQUAKES
effects on nuclear power plants, standards for instrumentation for determining, 25:35061
ECOLOGY
book: Marine Radioecology, 25:35117
ECOSYSTEMS
effects of thermal pollution on Columbia River, bibliography on, 25:35115 (BNWL-1543)
nutrient cycling and productivity of dystrophic lake-bog, 25:37182(R) (COO-1770-3)
radiobiology research in marine, 25:35117
EDDY CURRENT TESTING
equipment and method for distinguishing inside and outside surface defects, two-frequency, 25:34833
equipment and methods for, historical development and current status of, 25:34835
equipment and methods for, of reactor materials at ORNL, development of, 25:34829
problems in, computer programs for solving, 25:37212 (ORNL-TM-3295)
ELASTOMERS
radiation effects on properties and structure of chloroprene, γ, 25:35590
ELECTRIC ARCS
cathode spots in, transition from distributed emission in, 25:36112
current spokes in magnetoplasmadynamic, occurrence and properties of, 25:36110
current spokes in magnetoplasmadynamic, rotation properties of, 25:36111
current--voltage characteristics of, for plasma production, 25:36161
plasma flow in self-induced magnetic field in, (T), 25:36103 (DLR-FB-70-13)
ELECTRIC CAPACITORS
current flow from high-voltage, time dependence of, 25:36202
description of 12.5 kJ, 25:37194 (MHSMP-71-33)
radioinduced interface states in MOS, effects of heat treatment in electric field on 1-MeV electron, 25:35080
ELECTRIC CHARGES
motion in electromagnetic field in general relativity theory, geodesics of Einstein connection for paths of, (T), 25:36443
ELECTRIC CONDUCTIVITY
effects of nonuniform, on force-free magnetic fields, (T), 25:35755
measurement of insulator, by four-probe technique, 25:36310 (HEDL-SA-119)
ELECTRIC CONTROL SYSTEMS
development of computer-controlled, 25:37222 (SC-DR-70-862)
ELECTRIC DISCHARGE
electron energy distribution in helium positive column, (E), 25:36119
ion emission from double sheath, H⁻, (E), 25:35843
ion trajectories in Penning, calculation of, 25:36133
plasma ionization instability in self-sustaining low-pressure, in magnetic fields, (E/T), 25:36159
plasma oscillations in low-pressure Penning, (E/T), 25:36242
plasma oscillations in magnetized afterglows with transverse currents, (E), 25:36175
ELECTRIC FIELDS
spectra of turbulent, in solar wind at 0.75 to 1 AU, (E), 25:35767
ELECTRIC GENERATORS
design characteristics of quadrupole, for nuclear power plants, 25:36975
ELECTRIC INSULATORS
electric conductivity measurements of refractory oxide, using four-probe technique, 25:36310 (HEDL-SA-119)
radiation effects on, guide for, 25:35081
radiation exposure limits for, standard guide for neutron and gamma, 25:35075
ELECTRIC PROBES
calibration of Langmuir, cylindrical photo-ionization chamber for, 25:36100
current flow to cylindrical, in collisional magnetoplasmas, (T), 25:36098
ELECTRODES
current--voltage characteristics of superconducting, before vacuum breakdown, 25:36075
erosion in pulsed plasma accelerators, material evaluation for, 25:36207
work functions for, effects of patchiness and surface area on, 25:35931
ELECTROJETS
relation of currents in aurora, to radio aurora, (T), 25:36006
ELECTROLYTIC CELLS
development for reductive extraction processes, 25:34694 (ORNL-TM-3138)
dissolution studies in, 25:34690(R) (IN-1457)
mass transfer in, 25:34694 (ORNL-TM-3138)
ELECTROMAGNETIC FIELDS
charged particle motion in constant, relativistic, (T), 25:36363
Einstein--Maxwell field equations in vacuo for spatially homogeneous, nonstatic solutions of, (T), 25:36585
electric charge motion in general relativity theory, geodesics of Einstein connection for paths of, (T), 25:36443
electron behavior in strong external, 25:36369
pulse propagation over plane surfaces, 25:36367
ELECTROMAGNETIC LENSES
charged-particle focusing properties of helical quadrupole, 25:36624
design of multipole permanent magnet lenses for focusing charged particle beams, 25:36619(P)
electron-optical parameters of, calculation of, 25:36643
optical parameters of antisymmetrical doublet and symmetrical triplet quadrupole, for electrons at 1 to 10 MeV, nomograms for, 25:36630
ELECTROMAGNETIC WAVES
interaction with dense plasma, self-trapping of, (E), 25:36225
modulation in magnetoplasma, kinetic theory of amplitude-modulated, (T), 25:35953
propagation along vacuum--overdense plasma interface, surface, (T), 25:36214 (DEMO-71/5)
propagation in mirror-confined plasma, near upper hybrid frequency, (E), 25:36243
propagation in nonlinear plasma, relativistic Doppler effect and group velocity in, (T), 25:36215 (DEMO-71/6)
propagation in plasma, nonlinear theory of trapping in, 25:36230
propagation in plasma, self-focusing of, (T), 25:36226
propagation in unbounded magnetoplasmas, dispersion relations for, 25:36218 (UARAEE-92)
propagation of perturbation over plane surface, 25:36367
propagation on surface of adjacent plasma flows, (T), 25:36219 (UARAEE-97)
reflection and transmission in inhomogeneous plasma, (T), 25:36228
reflection and transmission in magnetoplasmas, optimum third-harmonic generation in, (T), 25:36244
scattering on plasma, detection limits for diagnostic use of, 25:36101
ELECTRON BEAMS
interaction with ionosphere, wave--particle interactions from, (E), 25:35967
interactions with double-stream plasma, instabilities in, (T), 25:36174
interactions with plasma, beam modulation effects on wave growth in, (E), 25:36227
interactions with plasma, electromagnetic wave excitation in, (T), 25:36235
interactions with plasma, electron heating in, (E), 25:36118
interactions with plasma, potential distribution measurements from, 25:36093
interactions with plasma, quasi-linear equations for, 25:36142
interactions with plasma, stability of relativistic, 25:36169
interactions with slow waves in plasma waveguides, effect of inhomogeneities on, (T), 25:36234
reactions with ceramics, diamonds, glass, and metals, removal of material layers by, 25:35515
reactions with matter, plasma production in intense, (T), 25:36157
stability of ring currents in focusing magnetic fields, (T), 25:35838
standards for use in production and processing of foods, 25:34814
transport in antisymmetrical doublet and symmetrical triplet quadrupole electromagnetic lenses, nomograms for parameters for, 25:36630
ELECTRON-DIFFRACTION ANALYSIS
intensity calculations for low-energy, of beryllium, 25:36330
ELECTRON GAS
density of degenerate Fermi, behavior in external field, (T), 25:36365
ELECTRON LENSES
design of crossed diverging, 25:36646
ELECTRON MULTIPLIER TUBES
electron energy distribution in curved, 25:34905

XUM

ELECTRON PAIRS
production in e+ + e- and e + e interactions at high energies in colliding beams, total and differential cross sections for, (T), 25:36433 (LNF-71/1)
ELECTRON-RING ACCELERATORS
electron ring stability in, self-consistent field analysis of, 25:35838
electron--ion beam in, kinetic model of plane high-current, 25:36604 (JINR-P9-5645)
electron--ion bunch diagnostics by bremsstrahlung in, 25:36616(T) (UCRL-Trans-1440)
operation of, theory of, 25:36617(T) (UCRL-Trans-1443)
performance of model, for acceleration of alpha particles, 25:36615(T) (UCRL-Trans-1434)
ELECTRONICS
research progress on, 25:37168(R) (BDX-613-344)
ELECTRONS
acceleration of 10- to 100-keV, by solar flares, (E), 25:35726
charge composition of 12- to 30-GeV cosmic, balloon measurements of, (E), 25:35920
distribution in air showers, critical analysis of studies on, (E), 25:36395
distribution in geomagnetic field, effects on whistler propagation, (T), 25:35996
dosimetry of pulsed, response of various chemical dosimeters for, 25:35034
dosimetry of, energy response of lithium fluoride thermoluminescent dosimeters for, 25:35027
effects of pulsed, on aqueous solutions of borohydride ions, yields from, 25:34646
effects of pulsed, on cysteamine, spectra of free radicals from, 25:34639(R) (USC-113-P-21-3)
effects of pulsed, on liquid alcohols at low temperature, studies on electron solvation process in, 25:34645
effects of pulsed, on pyrene in acetone at -75°C, 25:34658
effects of pulsed, on ruthenium nitride complexes with ammonia, 25:34657
effects of pulsed, on weakly alkaline aqueous solutions, pH indicator studies on hydrogen yields from, 25:34668
effects on beryllia single crystals at 3 MeV, EPR of neutral beryllium vacancy induced in, 25:36283
effects on bone marrow and intestinal tissues of mice, effects of hypoxia on, 25:35161
effects on diffusion in gold--silver alloys at 2 MeV, 25:35512
effects on displacement of surface atoms in graphite at 100 to 200 keV, threshold energy for, 25:35584
effects on free-radical destruction in N-acetyl-DL-valine, effects of temperature on, 25:35103
effects on glucocorticoid and glycogen contents in rat endocrine glands, 25:35164
effects on hardening of interstitial-containing niobium, relations of complex defects with, 25:35517
effects on heptane, yields from, 25:34635 (NP-18810)
effects on infrared absorption spectra of Type-Ia diamonds at 1 MeV, 25:36279
effects on lead-doped sodium chloride and potassium chloride at 1.5 MeV, 25:36303
effects on MOS capacitors at 1 MeV, effects of heat treatment in electric field on interface states induced in, 25:35080
effects on n-type germanium at low temperatures, defect production in, (T), 25:36293
effects on nickel and iron foils in high-voltage electron microscope, 25:36301
effects on nickel foils at 650 keV, growth of defect clusters induced in, 25:36299
effects on photoluminescence spectrum of silicon-doped n-gallium arsenide at 1.7 MeV, annealing of, 25:36274
effects on platinum and platinum--gold alloy at 3 MeV and 90°K, annealing of, 25:36306
effects on silicon at 0.35 and 0.5 MeV and low temperatures, ac hopping conductivity study of, 25:36305
effects on silicon dioxide of pulsed, subsecond annealing of space charge induced in, 25:36302
effects on tantalum foils at 1.2 and 3 MeV at 4.5°K, influence of spontaneous recombination processes on Frenkel defect production in, 25:36273
effects on vulcanization of rubber, 25:34632
effects on zinc at 0.4 to 1.7 MeV and low temperatures, 25:36288
emission by alkali metal halides bombardment by inert-gas ions and atoms, 25:35840
emission of 10- to 100-keV, during solar flares, (E), 25:35726
energy spectra of radiating, effect on magnetospheric synchrotron radiation, (T), 25:35976
energy-loss spectra of germanium, evidence for double plasmons in, 25:36257
injection into ionosphere, echo experiment from, (E/T), 25:35966
interactions at high energies in air showers, review of, (E), 25:36395
interactions e + d + e + d, time reversal violation in cross sections of, (T), 25:36546
interactions e + e at high energies in colliding beams, total and differential cross sections for e and μ pair production in, (T), 25:36433 (LNF-71/1)
interactions e + e in colliding beams, pair production in, (T), 25:36448
interactions e + n at very high energies, neutron internal structure determination from, (E/T), 25:36445
interactions e + p at 0.80 to 1.12 GeV, cross sections for absorption of transverse and longitudinal photons in inelastic, (E), 25:36381
interactions e + p at very high energies, proton internal structure determination from, (E/T), 25:36445
interactions e + p, quark model with relativistic extended internal structure for structure functions for deep inelastic, (T), 25:36444
interactions e + p, review of parton and vector dominance models for cross sections and structure functions for hadron production in deep inelastic, (T), 25:36452
interactions e + p, scaling properties in, (T), 25:36438 (NYO-1932(2)-189)
interactions e+ + e- + e+ + e- + e+ + e-, cross section for, (T), 25:36440
interactions e+ + e- at high energies in colliding beams, total and differential cross sections for e and μ pair production in, (T), 25:36433 (LNF-71/1)
interactions e+ + e- in colliding beams, pair production in, (T), 25:36448
interactions e+ + e- in preasymptotic region, parton model predictions for hadron production in, (T), 25:36434 (LNF-71/5)
interactions e+ + e- in storage rings, experimental conditions for γ + γ interactions from, 25:36451
interactions e+ + e-, polarization effects in identical meson pair production in, (T), 25:36438
interactions γ + e + γ + e above 1 keV, Monte Carlo method of sampling Klein--Nishina probability distribution for Compton, (T), 25:36432 (LA-4663)
interactions n + e from neutron diffraction by tungsten-186, coherent amplitudes for, (E/T), 25:36280 (JINR-E3-5713)
interactions ν + e + ν + e, field exchange for, (T), 25:36571
interactions of galactic-halo, with microwave background, (E/T), 25:35903
interactions of, structure functions for vector and axial vector currents in ν + N deep inelastic interactions for deep inelastic neutrino interaction relations with deep inelastic, (T), 25:36455 (ORO-3992-24)
motion and properties in strong external fields, (T), 25:36369
production of pairs of, in quasars, (T), 25:35678
radiation from 1.3- to 4.0-GeV, passing through crystal, energy dependence of dynamic γ, (E), 25:36282
reactions of mobile radiolytic, in aqueous acid solutions at 77°K, 25:34648
reactions with alkali metal atoms, kinetic energy of bound electron in calculation of ionization cross sections for, 25:35870
reactions with barium and cesium, multiple ionization in, (E), 25:35865
reactions with carbon monoxide and oxygen molecules, resonances in total cross sections for, (E), 25:35861
reactions with helium at 30 to 50 eV, angular distributions and probabilities for allowed and forbidden transitions in, 25:35882
reactions with helium up to 2 keV, polarization-free vacuum-ultraviolet excitation cross sections for, (E), 25:35857
reactions with helium-3 and tritons, effects of exchange currents on polarization of nucleons emitted in disentegration, (T), 25:36664
reactions with hydrogen atoms at 10 to 400 eV, Glauber-approximation calculations of differential and total cross sections for 1s--3d excitation in, 25:35859
reactions with hydrogen atoms, Glauber-theory calculations of excitation cross sections for, 25:35878
reactions with hydrogen molecules, velocity distribution of metastable H atoms from dissociative excitation in, (E), 25:35864
reactions with lead at 100 to 400 MeV, angular distributions and ranges from, (E), 25:36788
reactions with molecules at low energies, review on, 25:34618
reactions with natural lead, tungsten, and uranium at 660 and 1300 MeV, fission-fragment cross sections and energies from, (E), 25:36791
reactions with sodium, excitation cross sections for, (T), 25:35881
scattering by boron-11 at 100 to 300 MeV, angular distributions and spectra from, (E/T), 25:36672 (LAL-1243)
scattering by calcium-40 at 250 MeV, Hartree--Fock calculations of angular distributions from elastic, (T), 25:36712
scattering by calcium-40, -42, -44, titanium-46, -48, -50, and iron-56 at 198 to 300 MeV, differential cross sections for inelastic, (E), 25:36695
scattering by carbon-13 up to 20 MeV, form factors for carbon-13 energy levels from inelastic, (E), 25:36682
scattering by carbon-13, rms charge radius ratio for carbon-13 to carbon-12 from elastic, (E), 25:36682
scattering by crystals of fast, calculations for phonon, 25:36280
scattering by formaldehyde at 250 eV, oscillator

XUM

strengths for transitions in inelastic, (E), 25:35883
scattering by helium at 100 and 700 eV, wave function for evaluation of Glauber amplitude for elastic, 25:35868
scattering by helium-4 at 30 to 59 MeV, differential cross sections for elastic, (E), 25:36658(T) (CERN-Trans-71-13)
scattering by hydrogen atoms, Harris-method calculation of phase shifts for s-wave elastic, 25:35879
scattering by hydrogen atoms, virial theorem for variational functions in, (T), 25:35871
scattering by mercury excited atoms at low energies, superelastic, (E), 25:35872
scattering by molecules, effects of vibronic excitation on angular distributions from resonant, (T), 25:35865
scattering by neodymium-142, -146, and -150, at 40 and 60 MeV, angular distributions for, (E), 25:36758
scattering by nuclei at 180°, magnet system for measurement of, 25:36629
slowdown in media, Monte Carlo calculations of degradation spectra for 100-keV, 25:36258
spectra of high-energy, undergoing Klein--Nishina losses, (T), 25:36263
spectra of relativistic, in solar particle events, (E), 25:35727
spectrum of 200- and >200-GeV cosmic, balloon measurements above Hyderabad, India of, (E), 25:35920
synchrotron emission from, of various energy spectra, (E/T), 25:36001
universality with mesons (μ) in two- and three-body K decays, (T), 25:36470
use for therapy of human nasopharyngeal tumors at 10 MeV, development of conformation method for, 25:35194
use of fast, for therapy of human breast cancer, development of pendular method for, 25:35191

ELECTROSTATIC GENERATORS
design of single gap high-gradient, for acceleration of 200-mA proton beams to 300 keV, 25:36613 (UARAEE-87)

ELECTROSTATIC LENSES
design for transport of ion beams, 25:36608 (NP-18855)

ELEMENT 114
properties of, atomic, (T), 25:35592

ELEMENTARY PARTICLE MODELS
absorption, polarization of Σ in $\pi^+ + p \to K^+ + \Sigma^+$ and Λ in $\pi^- + p \to K^0 + \Lambda$ interactions in, test of empirical rule for cuts and line reversal relations in, 25:36502 (CALT-68-300)
absorption, test of empirical rule for cuts and line reversal relations in strong interactions in, 25:36502 (CALT-68-300)
broken chiral SU(3) x SU(3), for angle of eta--X mixing, 25:36551
dual resonance, algebraic structure of generalized Ward identites in, 25:36591
dual resonance, twisting invariant factorization in, 25:36594
dual resonance, vector currents in, 25:36490
dual-resonance, level structure of nonspurious resonance states in, 25:36474
dual-resonance, off-mass-shell extrapolation of amplitudes in, 25:36598
eikonal, dual description of $K^- + p \to \pi^- + Y^{*+}$ and $\pi^+ + p \to K^+ + Y^{*+}$ interactions in, 25:36514
Glauber multiple scattering, for effects of short-range nucleon--nucleon correlations on hadron elastic and inelastic scattering by helium-4 at high energies, 25:36538
Glauber, review of hadron interactions with nuclei at high energies in, 25:36533
multiperipheral and multi-Regge models for inclusive interactions, 25:36478
multiperipheral, interactions $\pi^+ + p \to p + 3\pi^+ + 2\pi^-$ at 8 GeV/c in, 25:36503 (INR-P-1265)
multiperipheral, multiplicity dependence of one-particle momentum distributions in, 25:36476
multiperipheral, properties of partial cross sections for K anti K production in π + N and N + N interactions in generalized, 25:36422
parton, for proton and neutron internal structure, 25:36445
parton, predictions for hadron production in $e^+ + e^-$ interactions in preasymptotic region and structure in high-mass μ^+--μ^- pair production in p + p interactions in, 25:36434 (LNF-71/5)
parton, review of cross sections and structure functions for hadron production in deep inelastic e + p interactions in, 25:36452
vector dominance, decrease of differential cross sections for lepton pair production at high energies and large angles, 25:36429
vector dominance, review of cross sections and structure functions for hadron production in deep inelastic e + p interactions in, 25:36452
vector dominance, sum rules for K + N interactions at low energies in, 25:36519
vector dominance, vector meson exchange contributions to γ + N → π + N interactions in, 25:36447
Veneziano, amplitudes for first-excited and ground-state scalars in, 25:36592
Veneziano, asymptotic behavior of partial-wave amplitudes and dispersion relations in complex S plane for π + π interactions in, 25:36487
Veneziano, interactions π + π in smeared, 25:36459
Veneziano, interactions $\pi^+ + \pi^- \to \pi^+ + \pi^-$ in generalized, with nonlinear trajectories, 25:36493
Veneziano, Landau equations for continuous medium for Koba--Nielsen kernels in generalized formula in, 25:36424
Veneziano, N-point dual functions for mesons with physical trajectories in generalized, 25:36485
Veneziano, operator vertices and propagators in generalized, 25:36475
Veneziano, polarization in charge-exchange π + N interactions in, 25:36517
Veneziano, strong interactions in, review of, 25:36479

ELEMENTARY PARTICLE MODELS (BOOTSTRAP)
calculations for particles in, method for solving Bethe--Salpeter equation for, 25:36568

ELEMENTARY PARTICLE MODELS (TRIPLET)
decay K → π + l + ν in quark, form factors and Cabibbo angle for, 25:36456 (CRO-3992-39)
hadron dipole electromagnetic form factors in quark, 25:36436 (CRO-3992-28)
meson elastic electromagnetic form factor from quark selection principle in, pseudoscalar, 25:36439
production of quarks in superstrong final-state interactions from p + p interactions, 25:36530
resonances in quark, review of, 25:36500
structure functions for deep inelastic e + p interactions and N* level structure and total decay width in quark, with relativistic extended internal structure, 25:36444
sum rules for amplitudes and cross sections of meson interactions with baryons in quark, 25:36518

ELEMENTARY PARTICLES
bootstrap calculations for, method for solving Bethe--Salpeter equation for, (T), 25:36568
classification in SU(2), SU(3), and SU(6) symmetry, (T), 25:36549
conference on, Delhi, India, 10/69, 25:35893 (CONF-691055-(Vol.2))
conference on, Delhi, India, 10/69, 25:35892 (CONF-691055-(Vol.1))
electromagnetic interactions of two different-spin, cross sections for, 25:36450
field theoretic criterion for zero-mass, 25:36570
interactions at high energies, multiperipheral and multi-Regge models for inclusive, 25:36478
interactions of, duality compatibility with conservation of t-channel helicity in diffractive dissociation, (T), 25:36595
interactions of, duality for triple Reggeon coupling relation with low missing-mass spectrum in diffraction dissociation in two-body, (T), 25:36420 (UCSD-10-P-10-78)
interactions of, equivalent potential approach for masses and widths of rho and f^0 and I = 0 and 1 Regge trajectories in two- and many-body, (T), 25:36422
interactions of, fixed-angle limit in inclusive, 25:36421
interactions of, mass equation from tadpoles in nonpolynomial Lagrangians for self-, (T), 25:36425
interactions of, multiperipheral model for multiplicity dependence of one-particle momentum distributions in, 25:36476
mass equation from tadpoles in nonpolynomial Lagrangians for self-interactions of, (T), 25:36425
mass equations of, origin and transformations of matter from, (T), 25:36426
phase space of N relativistic, parametrization of, (T), 25:36428
production of, model for self-consistent Pomeranchuk singularity in multiple, 25:36588
research at Brandeis Univ., Sept. 1970 to April 1971, (E/T), 25:36419(R) (NYC-3178-8)
scattering by nuclei, multiple-scattering expansion of theoretical optical potential for, 25:36523
scattering on system of bound particles, Green function for optical potential model for elastic and inelastic, (T), 25:36589
search for magnetically charged, proposed experiment for, (E), 25:36379(T) (CERN-Trans-71-10)
strong interactions at high energies, review of forward elastic, (E/T), 25:36480
strong interactions at high energies, review of total cross sections for, (E/T), 25:36480
strong interactions of, class of nonlinear Lagrangian models for dynamics of, (T), 25:36481
strong interactions of, instability criterion for properties of intermediate compound systems in, (T), 25:36599
strong interactions of, Pade approximants for dynamics of, 25:36473
strong interactions of, research at Illinois Univ., fiscal 1971, (E), 25:36384(R) (COO-1195-213)
strong interactions of, research at Johns Hopkins Univ., April 1970 to March 1971 on hadron structure determination from, (T), 25:36472(R) (NYO-4076-14)
strong interactions of, review of S-matrix and Veneziano model for, (T), 25:36479
strong interactions of, test of empirical rule for cuts and line reversal relations in absorption model for, (T), 25:36502 (CALT-68-300)
symmetry for, baryon--lepton correspondence in broken

SU(3) x SU(3), (T), 25:36543
symmetry for, classification in SU(2), SU(3), and SU(6), (T), 25:36549
symmetry for, projection operator techniques for SU(S) and SU(n), (T), 25:36545
symmetry for, space--time geometry for U(3,1), 25:36544
theory for, review of anomalies in Ward identities and current commutators in, 25:36427
weak interactions of, model for, (T), 25:36464
weak interactions of, renormalizable model in W boson theories of, (T), 25:36468
weak interactions of, research at Illinois Univ., fiscal 1971, (E), 25:36384(R) (COO-1195-213)
weak interactions of, review of difficulties in models for, (T), 25:36467
ELEMENTARY PARTICLES (TRIPLET)
mass of urbaryons in broken SU(3) x SU(3) symmetry, bare, (T), 25:36543
statistics of urbaryons for super exclusion principle for hadronic processes, 25:36477
ELEMENTS
abundance of heavy, in 15 Vul, (E/T), 25:35653
photoelectric cross sections for, empirical formula for interpolation of tabulated, 25:36246 (ANL-7796)
EMBRYOS
growth and development of chick, role of nutrient proteins in regulation of, 25:37209 (NYO-4030-9)
growth and development of chick, role of proteins in regulation of, 25:37210(R) (NYO-4030-10)
ENDOCRINE GLANDS
radiation effects on glucocorticoid and glycogen contents in rat, protective effects of insulin against electron, 25:35164
ENERGY
conference on new experimental techniques in research on propulsion and, Munich, 9/67, 25:36107
storage and transfer of, system for, 25:36209
ENGINEERING
engineering materials list, cumulative index for 1968 through 1970, 25:34779 (TID-4103(Suppl.1)(Rev.2))
ENVIRONMENT
contamination by fuel reprocessing wastes, methods for controlling, 25:34844 (CONF-700440-1)
radiation monitoring of Ames Laboratory, during 1970, 25:34743 (IS-2541)
ENZYMES
structure and mechanism of, isotopic studies of, 25:37243(R) (UCLA-34-P-102-27)
EPITHELIUM
radiation effects on cell count in mouse intestinal, lethal x, 25:35239
EPOXY RESINS
B--epoxy, testing of composites of, nondestructive methods for, 25:34838
EQUIPMENT AND PROCEDURES
development for mechanical decladding of reactor fuel elements, 25:34780 (UARAEE-54)
ERBIUM
determination as impurity in terbium oxide by neutron activation and radiochemical separation, 25:34670 (JAERI-Memo-4280)
determination in aqueous acetone solutions of dibenzoylmethane complexes, absorption spectrophotometric, 25:34527
ERBIUM ALLOYS AND SYSTEMS
Al--Er-base, crystal lattice parameters of intermetallic Er_2Al, 25:35495
Er--Re, superconducting transition temperature of intermetallic compounds of, 25:36038
ERBIUM IONS
energy levels of, spin--spin and spin--other-orbit matrices for, (T), 25:35850
ERBIUM ISOTOPES Er-166
neutron capture by, cross sections and resonance integrals for pile and thermal, (E), 25:36735 (SGAE-PH-104/1971)
ERBIUM ISOTOPES Er-167
neutron capture by, cross sections and resonance integrals for pile and thermal, (E), 25:36735 (SGAE-PH-104/1971)
ERBIUM OXIDES
growth of single-crystal solid solutions with another rare earth oxide by Verneuil method, formation regions in, 25:35525
Er_2O_3--WO_3, properties of $3Er_2O_3.WO_3$, to 1500°C, electric and thermal, 25:35529
ERYTHROCYTES
radiation effects on, mechanism for, 25:35210
ESTUARIES
rare earth content of, effects of tides on, 25:34760
thorium content of, effects of tides on, 25:34760
ETHANE
alpha-particle stopping cross sections in gaseous, at 0.3 to 2 MeV, 25:36255
photo-absorption cross sections, review of uv, (E/T), 25:36013
reactions with helium tritides formed by beta decay of molecular tritium, kinetic studies on, 25:34677
reactions with methane under simulated radiolysis conditions, mass spectrometric studies on, 25:34645
yields from γ radiolysis of 2-methyl-2-propanol at 30°C, 25:34659
ETHANE, 1,2-DICHLORO-1,1,2,2-TETRAFLUORO-
vapor pressure--temperature data for, 25:34602 (CAT-645)
ETHANE, 1,1,1-TRICHLORO-
diffusion through drybox gloves, comparison of values for other halogenated solvents with, 25:34605 (RFP-1608)
ETHANE, TRICHLOROTRIFLUORO-
bubble growth and stability in, in narrow constant-diameter vertical tubes with nonuniform initial temperature profiles, (E), 25:34789 (ANL-7746)
diffusion through drybox gloves, comparison of values for other halogenated solvents with, 25:34605 (RFP-1608)
ETHANOL
effects on recovery of γ- and uv-irradiated yeast, effects of iodoacetic acid on, 25:35251
radiolysis of liquid, at low temperature, studies on electron solvation process in electron pulse, 25:34645
ETHER, tert-BUTYL METHYL
yields from γ radiolysis of 2-methyl-2-propanol at 30°C, 25:34659
ETHIONAMIDE
radiation resistance of, γ, 25:34660
ETHYLENE
alpha-particle stopping cross sections in gaseous, at 0.3 to 2 MeV, 25:36255
effects on development of peroxidase in γ-irradiated sweet potato root tissues, 25:35105
photo-absorption cross sections of, review of uv, (E/T), 25:36013
reactions with methane under simulated radiolysis conditions, mass spectrometric studies on, 25:34645
ETHYLENE, CHLORO-
radioinduced polymerization on isoprene rubber, properties of products from, 25:34627
ETHYLENE, CHLORO-, POLYMERS
radiolysis of, effects of coatings of aromatic compounds on ESR spectra of products of γ, 25:34656
ETHYLENE POLYMERS
neutron energy spectra in, comparison of calculated and measured, 25:36266
properties of thin membranes of, for on-line alpha activity monitoring of solutions, 25:34673 (CEA-N-1440)
radiation effects on alkyl radical conversion to allyl in, 25:34637(R) (ORO-4059-1)
radiation effects on subsequent grafting of styrene on, 25:35591
solvent properties for hydrogen, 25:34637(R) (ORO-4059-1)
polyethylene--poly(isobutyl acrylate), radiation effects on crosslinking in, gel permeation chromatographic studies on effects of dose on mechanical properties of copolymer produced by γ, 25:34626
polyethylene--poly(vinyl acetate), radiation effects on crosslinking in, gel permeation chromatographic stucies on effects of dose on mechanical properties of copolymer produced by γ, 25:34626
ETHYLENE, TETRACHLORO-
diffusion through drybox gloves, comparison of values for other halogenated solvents with, 25:34605 (RFP-1608)
ETHYLENE, TETRAFLUORO-, POLYMERS
properties of thin membranes of, for on-line alpha activity monitoring of solutions, 25:34673 (CEA-N-1440)
ETHYLENE, TRICHLORO-
diffusion through drybox gloves, comparison of values for other halogenated solvents with, 25:34605 (RFP-1608)
ETHYLENE, TRIPHENYL-
effects of coatings of, on γ radiolysis products of poly(vinyl chloride), ESR studies on, 25:34656
EUMYCOTA
Aspergillus nidulans, radiation induced mutations in, effects of oxygen or nitrogen on γ, 25:35121
Saccharomyces cerevisiae, radiation effects on nucleotide synthesis in, tracer study on β, 25:35252
Saccharomyces vini, radiation effects on, effects of iodoacetic acid and ethanol on recovery following γ and uv, 25:35251
yeasts, radiation effects on functional and structural characteristics of radiosensitive and radioresistant strains of, 25:35247
yeasts, radiation effects on, γ, 25:35260
EUROPE
electric power production in European Communities during 1969, 25:36855 (NP-18846)
electric power production in European Communities during 1970, 25:36856 (NP-18847)
EUROPIUM
determination as impurity in ytterbium oxide by neutron activation and radiochemical separation, 25:34665 (JAERI-Memo-4279)
determination in aqueous acetone solutions of dibenzoylmethane complexes, absorption spectrophotometric, 25:34527
determination in rocks by neutron activation and γ spectroscopy, 25:34543 (NIM-1013)
determination in samarium oxide, indirect colorimetric, 25:34507
polarographic reactions at mercury electrode, effects of thiourea on, 25:34560
separation from aqueous chloride solutions by solvent

extraction using bis(1-isobutyl-3-methylbutyl) phosphate, 25:34706
separation from other rare earths by ion exchange chromatography, 25:34714
EUROPIUM FLUORIDES
effects on radiation stability of beryllium fluoride glasses, 25:34621
EUROPIUM IONS
energy levels of, spin--spin and spin--other-orbit matrices for, (T), 25:35850
EUROPIUM ISOTOPES Eu-145
energy levels from gadolinium-145g decay, (E), 25:36744
EUROPIUM ISOTOPES Eu-151
photon reactions (γ,xn) in giant resonance region, cross sections for, (E), 25:36755
proton reactions (p,2n) at 8.0 to 13.4 MeV, gamma spectra and angular correlations for, (E), 25:36775
EUROPIUM ISOTOPES Eu-152
deposition and retention in rats following inhalation of radioactive europium oxide, whole-body, 25:35086
EUROPIUM ISOTOPES Eu-153
deposition and retention in rats following inhalation of radioactive europium oxide, whole-body, 25:35086
energy levels from samarium-153 beta decay, spin-parity assignments for, (E), 25:36731 (NP-18835)
energy-level transitions from samarium-153 beta decay, mixing ratios and multipolarities for, (E), 25:36731 (NP-18835)
photon reactions (γ,xn) in giant resonance region, cross sections for, (E), 25:36755
EUROPIUM ISOTOPES Eu-154
beta decay of, γ-γ directional correlations from, (E), 25:36742
deposition and retention in rats following inhalation of radioactive europium oxide, whole-body, 25:35086
EXPLODING WIRE PHENOMENA
x-ray emission by tungsten wires,, effects of wire parameters on, 25:36326
EXPLOSIVE FORMING
methods for joining dissimilar and similar metals and alloys, economics of, 25:35298
EXPLOSIVES
susceptibility to detonation pulse, 25:37191(T) (LA-tr-71-32)
EXPONENTIAL PILES
neutron spectrum measurements in STSF, time-of-flight methods for fast, 25:36991(R) (GULF-RT-10523)
noise measurements in, photon detection method for, 25:37086

F

FALLOUT
monitoring around Valencia, Spain, 1966 to 1968, 25:35132
FAST FLUX TEST FACILITY
design parameters of, summary of, 25:37085 (WHAN-SA-104(Rev.))
FAST TEST REACTOR
control rod drives for, 300 lb. gas test for roller nut, 25:37070 (TODD-N-16)
control rod drives for, 300 lb. gas test for roller nut, 25:37073 (TODD-N-21)
control rod drives for, 500 lb. gas test for roller nut, 25:37071 (TODD-N-18)
control rod drives for, 500 lb. gas tests for roller nut, 25:37074 (TODD-N-23)
control rod drives for, 700 lb. gas test for roller nut, 25:37072 (TODD-N-20)
control rod drives for, gas tests for roller nut, 25:37075 (TODD-N-24)
fuel cladding for, equipment for prefabrication cleaning of, 25:34783
fuel elements for, radiation testing program and performance limits for driver, (E), 25:37064 (HEDL-SA-81)
FECES
cesium-137 excretion in, of children in Warsaw, 1965 to 1967 and 1969, 25:35093
FEDERAL REPUBLIC OF GERMANY
fuel shipping and storage in, legal restrictions on, 25:34857
nuclear power plants in, economics and technical aspects of, 25:36885 (JUL-705-RG)
nuclear power plants in, review of development of, 25:35858
radioisotope incorporation in nuclear industry and research center personnel in, statistical evaluation of, 25:35100
FERMI FAST BREEDER REACTOR
shield tank for, leak rate testing frequency and nitrogen dewpoint in primary, 25:36900 (DOCKET-50016-115)
shield tank for, nitrogen dewpoint in primary, 25:36855 (DOCKET-50016-114)
FERMIONS
elementary excitations in system of, in magnetic field, 25:36359
magnetic moment of charged, skew-symmetric tensor field for anomalous, 25:36571
theory for, review of anomalies in Ward identities and current commutators in, 25:36427
FERMIUM ISOTOPES Fm-251
energy level at 191 keV from nobelium-255 alpha decay, lifetime for, (E), 25:36778
FERROMAGNETIC MATERIALS
ion slowing-down in, effects of transient magnetic fields on precession of nuclear spin of heavy, (T), 25:36846
FIELD THEORY
book: Classical Fields, Particles, and the Theory of Relativity, 25:36556
field equations for characteristic [(211)] in, special solution of, 25:36555
field structure in Schroedinger unified, exact solution corresponding to, 25:36554
gauge fields in nonlinear realization of group on its subgroup in, 25:36558
scattering amplitude for infinite-component field under scalar external field in, wave equation for, 25:36557
FILMS
stability of thin liquid, flowing down heated inclined wall, analysis of, 25:34800
FIRES
prevention in radioactive material handling facilities, standards for, 25:34853
protection practices for nuclear reactors, 25:37050
protection practices for nuclear reactors and radioactive materials handling, 25:37048
FISSION
research in, review of, (E/T), 25:36800
theory of nuclear, review of advances in, (T), 25:36827
FISSION FRAGMENTS
production from plutonium-238 spontaneous fission, average kinetic energies and masses for, (E), 25:36782
production of long-range, in electron reactions with lead, tungsten, and uranium at 550 to 1300 MeV, (E), 25:36791
ranges in pyrocarbon, from thermal-neutron fission of uranium-235, 25:36264
reactions and ranges in gases, 25:36254
FISSION PRODUCTS
deposition in reactor containment buildings, heat transfer model for analysis of, 25:37036(R) (BMI-1904)
diffusion from carbide, metallic, molten salt, and oxide *fuels*, 25:35550
effects on neutron poisoning in MSBR, 25:34694 (ORNL-TM-3138)
monitoring in reactors, Geiger--Mueller detector system for, 25:37147(P)
properties of encapsulated, for use as process radiation sources, 25:34803(R) (ENWL-1308-S)
release to atmosphere in reprocessing aluminum-clad fuel elements, 25:34693 (ORNL-4574)
separation from Purex Process TBP solvent by ion exchange using macroreticular resins, 25:34679 (ARH-SA-58-RD)
separation of cerium from, by solvent extraction using TOPO--TTA, 25:34522
FLAME CUTTING
safety in, standard provisions for, 25:35230
FLANGES
standard marking system for, 25:34786
FLUID FLOW
calculation of fully-developed longitudinal laminar, in rod bundles, 25:34794
heat transfer and hydraulic resistance in turbulent, in rough and smooth channels and tubes, generalized method for calculating, 25:34795
magneto-acoustic wave scattering by ideal conducting cylinder, (T), 25:35941
magnetohydrodynamic Couette, with heat transfer between conducting walls, 25:35945
magnetohydrodynamic Couette, with transpiration cooling, (T), 25:35948
magnetohydrodynamic laminar unsteady, in porous annular channel under radial magnetic field, (T), 25:35940
magnetohydrodynamic laminar, between porous disks, (T), 25:35947
magnetohydrodynamic slip, Rayleigh problem with transverse magnetic field in, 25:35950
magnetohydrodynamic, pressure loss calculations for lithium in fusion reactor blankets, 25:35928 (UCRL-51010)
magnetohydrodynamic, velocity profiles in slightly divergent channels for, (T), 25:35943
magnus data on standard 10° cone, 25:37220 (SC-DC-713821)
measurement through channel having dissolving walls, determination of mass and momentum boundary layers from, 25:37156 (ANL-7797)
pressure pulse propagation in two-phase mixtures, (E/T), 25:37035 (ANL-7792)
stability of nonuniformly rotating, magnetohydrodynamic, (E), 25:35946
study of two-phase, for uses in nuclear and nonnuclear fields, 25:34796
FLUORENE
effects of coatings of, on γ radiolysis products of poly(vinyl chloride), ESR studies on, 25:34656
FLUORIDE VOLATILITY PROCESSES
development of molten-salt, for uranium separation from aluminum-clad fuel elements, 25:34693 (ORNL-4574)
FLUORIDES
removal from zirconium surfaces, process for,

XUM

25:34710(P)
FLUORINE
effects on photometric determination of antimony following solvent extraction using TBP, 25:34512
oscillator strengths for excitation and ionization of, tables of calculated generalized, 25:35844 (SC-RR-70-406)
vapor pressure--temperature data for, 25:34602 (GAT-645)
FLUORINE ISOTOPES F-19
determination in thin films by nuclear reaction micro methods, 25:34550
helium-3 reactions (He-3,Li-6) at 40 MeV, differential cross sections and reaction mechanism for, (E), 25:36674
proton reactions (p,He-3) and (p,t) with, angular distributions for, (E), 25:36738(R) (UCLA-10-P-18-23)
proton reactions (p,pd) and (p,pt) with, summed energy spectra from, (E), 25:36738(R) (UCLA-10-P-18-23)
reactions (F-19,f) with terbium-159 up to 10.4 MeV/nucleon, excitation function for, (E), 25:36784
spin--lattice relaxation in gamma-irradiated lithium fluoride, 25:36348
FOAMS
evaluation of syntactic, 25:37160 (BDX-613-177)
FOOD
processing and production of, standards for safe use of radiation sources in, 25:34814
FORBUSH DECREASES
relation to various multiplicities in neutron monitor, Oct. 29, 1968 and May 14, 1969, (E/T), 25:35915
FORENSIC SCIENCE
activation analysis uses in, review on, 25:34542(R) (GA-9807)
FORKED RIVER POWER REACTOR, UNIT 1
site for, earthquake response spectra for, 25:36956 (DOCKET-50363-15)
FORMALDEHYDE
abundance in interstellar space, 25:35708
electron inelastic scattering at 250 eV by, oscillator strengths for transitions in, (E), 25:35883
FORMALDEHYDE, THIO-
abundance in interstellar space, 25:35708
search for interstellar, (E), 25:35708
FORT CALHOUN POWER REACTOR, UNIT 1
design parameters of, revised and additional data on, 25:36940 (DOCKET-50285-45)
operations aspects of, revised and additional data on, 25:36940 (DOCKET-50285-45)
FORT ST. VRAIN POWER REACTOR, UNIT 1
boilers for, pressure and temperature testing of, 25:36978(R) (GA-10560)
control elements for, reactivity worth of, 25:36978(R) (GA-10560)
control elements of, performance of boron carbide (B_4C) burnable poison, 25:36978(R) (GA-10560)
core for, properties and irradiation stability of graphite in, 25:36978(R) (GA-10560)
core physics for, 25:36978(R) (GA-10560)
fuel cycle management program for, initial loading requirements for optimum, 25:36978(R) (GA-10560)
fuel elements for, properties and irradiation stability of graphite in, 25:36978(R) (GA-10560)
fuels for, irradiation testing of coated particle, 25:36978(R) (GA-10560)
remote handling and viewing equipment for, pressure and temperature testing of in-vessel, 25:36978(R) (GA-10560)
site for, availability and distribution list for environmental radiation survey data for, 25:36935 (DOCKET-50267-30)
FRANCE
granite deposits in Nord-Limousin, geochemistry of uranium-bearing, 25:34749 (CEA-R-4034)
uranium ore prospecting in, economic aspects of, 25:34751
FRANCIUM ISOTOPES Fr-203
nuclear properties of, Nuclear Data Sheets for, (E), 25:36809
FREE RADICALS
decay in irradiated polyoxymethylene, 25:34637(R) (ORO-4059-1)
radioinduced in naphthalene crystals at 10°K, ESR studies of, 25:36287
radioinduced in naphthalene single crystals, ESR of, 25:36277
radioinduced production in coenzyme-substrate systems, ESR spectral studies on x, 25:34655
radioinduced production of, in cell proteins, mechanism of γ and uv, 25:35203
radioinduced production of, in frozen aqueous solutions of DNA, 5-methylcytosine, and thymidine, ESR spectral studies on γ, 25:34654
radioinduced production of, review on ESR studies on, 25:34616
reactions in irradiated cells, mechanism of, 25:35202
yields from γ radiolysis of adenine derivatives, ESR studies on, 25:34652
yields from γ radiolysis of frozen concentrated aqueous solutions of dextran sulfate and heparin, ESR studies on, 25:34651
yields from γ radiolysis of potassium difluorophosphate, ESR studies on, 25:34667
FRUITS
radiation processing of, quality and wholesomeness following, 25:35273
strawberries, radiation processing of, economics of γ, 25:35274
FUEL CAPSULES
design of Hastelloy C-276, for terrestrially used large radioisotope heat sources, safety evaluation of, 25:34809 (ORNL-TM-3230)
testing of radioisotope loaded, in rocket propellant combustion, 25:34792 (SC-DR-710084)

G

GADOLINIUM
determination as impurity in terbium oxide by neutron activation and radiochemical separation, 25:34670 (JAERI-Memo-4280)
GADOLINIUM ALLOYS AND SYSTEMS
Al--Gd-base, crystal lattice parameters of intermetallic Gd_2Al, 25:35495
Gd--Mg-base, magnetic resonance of single crystals of, anisotropy in, 25:36342
Gd--Re, superconducting transition temperature of intermetallic compounds of, 25:36038
GADOLINIUM FLUORIDES
effects on radiation stability of beryllium fluoride glasses, 25:34621
GADOLINIUM IONS
effects of activators of, on radioluminescence and thermoluminescence spectra in strontium fluoride and barium fluoride crystals, (E), 25:36317
energy levels of, spin--spin and spin--other-orbit matrices for, (T), 25:35850
GADOLINIUM ISOTOPES Gd-145
beta decay of ground-state, gamma spectra and scheme for, (E), 25:36744
GADOLINIUM ISOTOPES Gd-148
energy levels from terbium-148 beta and electron-capture decay, spin--parity assignments for, (E), 25:36726 (JINR-P6-5681)
GADOLINIUM ISOTOPES Gd-149
energy levels from terbium-149 beta and electron-capture decay, spin--parity assignments for, (E), 25:36726 (JINR-P6-5681)
GADOLINIUM ISOTOPES Gd-150
energy levels from europium-151 (p,2n) reactions, spins and parities of, (E), 25:36775
energy levels from terbium-150 beta and electron-capture decay, spin--parity assignments for, (E), 25:36726 (JINR-P6-5681)
GADOLINIUM ISOTOPES Gd-152
energy levels from terbium-152 beta and electron-capture decay, spin--parity assignments for, (E), 25:36726 (JINR-P6-5681)
photon reactions (γ,xn) in giant resonance region, cross sections for, (E), 25:36755
GADOLINIUM ISOTOPES Gd-154
energy levels from europium-154 decay, multipole admixtures of transitions from β, γ, and octupole vibrational, (E), 25:36742
neutron capture by, cross sections and resonance integrals for pile and thermal, (E), 25:36735 (SGAE-PH-104/1971)
photon reactions (γ,xn) in giant resonance region, cross sections for, (E), 25:36755
GADOLINIUM ISOTOPES Gd-156
neutron capture by, cross sections and resonance integrals for pile and thermal, (E), 25:36735 (SGAE-PH-104/1971)
photon reactions (γ,xn) in giant resonance region, cross sections for, (E), 25:36755
GADOLINIUM ISOTOPES Gd-158
photon reactions (γ,xn) in giant resonance region, cross sections for, (E), 25:36755
GADOLINIUM OXIDES
growth of single-crystal solid solutions with another rare earth oxide by Verneuil method, formation regions in, 25:35525
FeO--GdO, magnetic susceptibility of amorphous antiferromagnetic, temperature dependence of, (E/T), 25:36337
GAGES AND METERS
development of high intensity direct reading heat flux, 25:37225 (SC-DR-710194)
geometry effects on accuracy of x and γ radiometric, 25:34904
GALAXIES
clusters of, relation to large- and small-redshift quasars, (E/T), 25:35693
collisions of, escape of stars during, (T), 25:35756
distance modulus for NGC 1466 in LMC, (E), 25:35671
distance to IC 342, (E/T), 25:35801
distance to Maffei 2, (E), 25:35794
distance to Maffei, (E/T), 25:35801
distribution of, hierarchical structuring in, (T), 25:35817
dynamics of, instability of contrastreaming plasmas in, (T), 25:35793

XUM

energy of clusters of, total kinetic, (T), 25:35797
evolution of spherical, model for, (T), 25:35783
explosions in, magneto-rotational, (T), 25:35819
formation in early Universe, (T), 25:35811
formation of, formalism for nonlinear effects of cosmic fluid in, (T), 25:35815
gamma emission from 3C 120, (E), 25:35700
gamma emission from, proposed balloon experiments for photon flux, (E/T), 25:35923
gravitational binding in Coma cluster of, evidence for, (E/T), 25:35799
hydrogen distribution in Maffei 2, neutral, (E), 25:35794
hydrogen distribution in, neutral, (E/T), 25:35781
identification of PKS 0320-37 with NGC 1316, optical, 25:35707
light polarization from, elliptical, (E), 25:35618
mass of dark objects in clusters, detection by gravitational lens effect, (T), 25:35812
membership of IC 342 in Local Group, (E/T), 25:35801
membership of Maffei, in Local Group, (E/T), 25:35801
polarization of 3C 459 at 610 MHz, (E), 25:35788
properties of Maffei 2, physical, (E), 25:35794
radio flux densities for Maffei 2, (E), 25:35803
radio spectra of Maffei 2, (E), 25:35803
radio spectral indices and luminosities of normal, (E/T), 25:35807
radio-continuum observations of Maffei 1 and Maffei 2, (E), 25:35802
spectrophotometry of nucleus of NGC 3351 from 3300 to 7000 A, (E), 25:35804
structure in, density-wave theory of spiral, (E/T), 25:35782
structure of 3C 459 at 610 MHz, (E), 25:35788
velocities of, from image-tube spectra, radial, (E), 25:35779
x-ray emission from Coma cluster of, (E/T), 25:35795

GALL BLADDER
radioisotope accumulation in, of swine following field exposure to nuclear debris from Schooner Event, fallout γ-emitting, 25:35090

GALLIUM
effects on fluorescence method for detection of hafnium and zirconium, 25:34519
effects on gravimetric determination of mercury using 2-aminobenzothiazole, 25:34520

GALLIUM ALLOYS AND SYSTEMS
Au--Ga, mixing at 1100°C, adiabatic calorimetric measurement of heat of, 25:35432
Cu--Ga, mixing at 1100°C, adiabatic calorimetric measurement of heat of, 25:35433
Ga--Pu-base, thermal conductivity of delta-, at 300°K, 25:35424
Ga--rare earths--S, phase studies of, 25:35571
Ga--V, effects of alloying on superconducting transition temperature of intermetallic V_3Ga, 25:36040
Ga--V, preparation of superconducting intermetallic V_3Ga by diffusion, 25:36043

GALLIUM ARSENIDES
radiation effects on photoluminescence spectrum of silicon-doped n-type, annealing of 1.7-MeV electron, 25:36274

GALLIUM YTTRIUM SULFIDES
crystal structure of, 25:35571

GAMMA RADIATION
correlation measurements of, system for precise electron--gamma directional, 25:34903
cosmic background, flux above 100 MeV, (E/T), 25:35803
detection and measurement of, response of self-powered detectors for in-core, 25:34891
detection of excess flux of primary, (E), 25:35700
detection of, design of gas-filled spark chamber for, 25:34876(P)
detection of, instruments, measurement techniques, and standards for, 25:35137
distribution in water phantoms, errors due to ionization chamber air volume in measurements on, 25:35146
dose distribution in cobalt-60 therapy, use of computer and water phantom for calculating scattered, 25:35145
dose rate from sources with complex spectrum, one-group method for absorbed, (T), 25:36265
dose rate to human organs, use of cobalt-60 organ burdens in rats following single ingestion to calculate equilibrium, 25:35116
dose rates from 14-MeV neutron attenuation in calcium-based concrete, (E), 25:36260
dosimetry for cobalt therapy, calculation of cyclo- and fixed-field isodose curves during, 25:35136
dosimetry of pulsed, performance of silicon surface-barrier detector for, 25:34892
dosimetry of, development of phosphate-glass luminescent dosimeters for, 25:35037(P)
dosimetry of, response of various chemical dosimeters for, 25:35034
effectiveness for therapy of carcinomas of human larynx, 25:35188
effectiveness for therapy of human bladder carcinoma in relation to survival time, 25:35192
effectiveness for therapy of human renal tumors, effects of sex and tumor size on, 25:35193
effects on 2-methyl-2-propanol at 30°C, yields from, 25:34659
effects on alkali metal halides, luminescence from aqueous release of stored energy produced by, 25:34620
effects on alkaloid content in potatoes following seed exposure, 25:35254
effects on aluminum fluoride--beryllium fluoride--calcium fluoride glasses, effects of rare earth fluorides on, 25:34621
effects on ammonium perchlorate crystals, ESR spectra of ammonium radicals from, 25:34642
effects on aqueous perchloric acid solutions at 77°K, reactions of halogen-substituted acetic acids with mobile electrons formed in, 25:34648
effects on aqueous solutions of borohydride ions, yields from, 25:34646
effects on aqueous solutions of carbohydrates, yields of deoxy-sugars from, 25:34664
effects on bacteria and yeast, damaging, 25:35260
effects on catalytic dehydrogenation of cyclohexane, 25:34628
effects on cell nuclei in barley and bean seeds, comparison of bremsstrahlung, proton, x, and, 25:35258
effects on chemical and kinetic properties of subtilopeptidase A, 25:35110
effects on chromosomes, in Crepis capillaris shoots, aberrant, 25:35128
effects on corticosteroid retention in dog liver, 25:35222
effects on crosslinking in polyethylene and poly(isobutyl acrylate) or poly(vinyl acetate), gel permeation chromatographic studies on effects of dose on, 25:34626
effects on cytoplasm of maize shoot apical cells, 25:35244
effects on deuterated and normal adenine derivatives, ESR studies on free radicals produced by, 25:34652
effects on development of peroxidase in sweet potato root tissues, effects of ethylene on, 25:35105
effects on dihydrotriazine 4,4'-methylenebis[3-hydroxy-2-naphthoate] and ethionamide, 25:34660
effects on dislocation-pinning in copper, 25:35514
effects on DNA, 5-methylcytosine, and thymidine frozen aqueous solutions, ESR spectral studies on free radicals produced by, 25:34654
effects on Escherichia coli, function and structure studies on protective effects of cysteamine and its homologs against, 25:35160
effects on Escherichia coli, sensitizing effects of dihydroxybutyraldehyde on, 25:35159
effects on fluorescence of organic solutions, effects of chloroform on quenching of, 25:34624
effects on free radicals in cell proteins, 25:35203
effects on frequency of 2-thioxanthine resistant mutants in Aspergillus, effects of oxygen or nitrogen on, 25:35121
effects on frozen concentrated aqueous solutions of dextran sulfate and heparin, ESR studies on free radicals produced by, 25:34651
effects on gaseous, deuterated and normal methanol, kinetics of production of hydrogen from, 25:34665
effects on glassy, alkaline solutions of 2-methyl-2-nitro-1-propanol at 77°K, ESR studies on scavenging by nitromethane of paramagnetic species produced by, 25:34643
effects on growth and flower production of shrubs following chronic cesium-137 exposure in Mojave desert, 25:35249
effects on growth of gymnosperm seedlings in relation to DNA content and seed radiosensitivity, 25:35250
effects on halomethanes and their solutions in natural latex, 25:34614
effects on human lymphocyte chromosomes, effects of cystamine on aberrant fractionated dose, 25:35123
effects on hydrolytic activity of subtilopeptidase A, 25:35109
effects on inactivation of Bacillus cereus spores, potentiating effects of halogen compounds on, 25:35264
effects on inorganic and organic compounds, ESR studies on, 25:34634(R) (COO-1385-37)
effects on lipase activities in castor seeds, 25:35253
effects on morphological and physiological properties of fungi, mutagenic, 25:35256
effects on neutral aqueous, oxygenated solutions of oxalate ions, effects of dose on yields from, 25:34644
effects on number of epithelial cells in rat small intestine, evaluation of injury by, 25:35220
effects on nutritional value of codfish, combined effects of cooking and, 25:35272
effects on optical properties of neodymium-activated glass lasers, 25:35082
effects on plastic scintillation detectors, 25:35079
effects on poly(vinyl chloride), effects of coatings of aromatic compounds on ESR spectra of products of, 25:34656
effects on polymerization of fluorine-containing pentadienes at 25 to -196°C, 25:34633
effects on polymerization of styrene to crosslinked butyl rubber, 25:34631
effects on polymerization of vinyl chloride on isoprene rubber, 25:34627
effects on potassium difluorophosphate, ESR studies on radicals produced by, 25:34667

effects on properties and structure of chloroprene rubber, 25:35590
effects on racemization in frozen solutions of D- and L-glutamic acid, 25:34622
effects on rate of amino acid incorporation into proteins of rabbit lymphocytes, carbon-14 tracer study of, 25:35104
effects on rats, combined effects of carbon monoxide and, 25:35233
effects on repair systems in bacteria and plants, 25:35246
effects on RNA synthesis in plant seeds, mechanism of, 25:35245
effects on rubber at 77°K, kinetics of stabilization of radicals produced by, 25:34640
effects on ruthenium nitride complexes with ammonia, 25:34657
effects on Saccharomyces vini, effects of iodoacetic acid and ethanol on recovery following, 25:35251
effects on sodium chlorates, ESR studies on effects of temperature on yields from, 25:34666
effects on sodium sulfacetamide in aqueous solutions and solid state, 25:34661
effects on solid acetic acid, ESR studies on mechanisms of, 25:34641
effects on stability of adipiodine, diatrizoic acid, and N-methylglucamine, 25:34662
effects on stability of macromolecular sulfone polyelectrolytes, ESR studies on, 25:34650
effects on strand breaks in algae DNA, mechanisms of repair following, 25:35257
effects on strand breaks in bacteria DNA, 25:35268
effects on subsequent catalytic dehydration of 2-propanol, 25:34629
effects on synthesis of α-amylase and ribonuclease in germinating wheat, effects of gibberellic acid on, 25:35102
effects on thermal cracking of heneicosane and tetracosane, 25:34653
effects on thermoluminescence of Apollo 11 sample 10084, (E), 25:35824
effects on viability of tulip pollen, 25:35255
effects on vulcanization of rubber, 25:34632
effects on wholesomeness of California fruits and vegetables, 25:35274
emission from cosmic objects, detection of, (T), 25:35687
emission from CP 0950, CP 1133, AP 1541, and PSR 1642 pulsars, search for pulsed high-energy, (E), 25:35705
emission from galactic center, proposed balloon experiments for photon flux, (E/T), 25:35923
estimation of natural terrestrial, in 10 to 100 keV range, Compton continuum peak method for, 25:34727 (UCRL-72927)
line shapes of, computer programs for analysis of, (E), 25:34915 (ANU-P-438)
measurement of earth surface, development of petroleum prospecting methods based on airborne, 25:34730
measurements in boreholes, method for interpretation of, 25:34716(T) (CSIRO-Trans-10088)
reactions with Z = 6 to 92 nuclei at 121 keV to 10.827 MeV, cross sections for, (E), 25:36799
scattering by K-shell electrons at 662 keV in lead, energy spectrum and differential cross sections for incoherent, (T), 25:36253
spectrum in space, measurements of 0.1 to 10 MeV low-energy, (E), 25:35922
spectrum near equatorial latitude, atmospheric, (E), 25:36009
splitting in strong magnetic fields, (T), 25:35677
use for moving beam or static field therapy, development of desk computer program for planning, 25:35195

GAMMA-RAY ASTRONOMY
developments in, (T), 25:35659

GAMMA SOURCES
book: Gamma-Ray Spectrometry of Rocks, 25:34539
determination in seawater, lithium-drifted germanium spectrometer for, 25:34935
determination of, data analysis methods for lithium-drifted germanium spectrometers for spectroscopic, 25:34536 (JUL-709-RG)
gamma energies and intensities for, for detector calibration, tables of, 25:34923 (UCRL-20476)
specific constant for tantalum-182, determination of, 25:34815
standards for use in production and processing of foods, 25:34814

GAMMA SPECTROMETERS
book: Gamma-Ray Spectrometry of Rocks, 25:34539
calibration of three-crystal scintillation, 25:34921 (UARAEE-93)
calibration of, tables of gamma energies and intensities for radioisotope sources for, 25:34923 (UCRL-20476)
coincidence method for lithium-drifted germanium, sum, 25:34932
data analysis of lithium-drifted germanium, for quantitative analysis, 25:34536 (JUL-709-RG)
description of anticoincidence shielded scintillation, 25:34928
description of triple-crystal scintillation, with anticoincident circuit for background suppression, 25:34931
design and performance of lithium-drifted germanium, for determination of gamma sources in seawater, 25:34935
design and performance of three-crystal scintillation pair, 25:34922 (UARAEE-100)
performance of multiplying silicon, for low-energy gamma radiation, 25:34918(T) (LE/G-3034)
spectra shape calibration and peak-to-total ratio measurements of scintillation, 25:34936

GAMMA SPECTROSCOPY
line-shape analysis in, computer programs for, (E), 25:34915 (ANU-P-438)

GAS CENTRIFUGES
flow in, numerical solution of the Navier--Stokes equations for calculating incompressible, 25:34790(T) (CONF-700557-4)

GAS FLOW
calculation of incompressible, in centrifuges, numerical solution of Navier--Stokes equations for, 25:34790(T) (CONF-700557-4)
magnetohydrodynamic fluctuating, past infinite porous plate in slip flow regime, 25:35949
magnetohydrodynamic, energy exchange between unidirectional magnetic field and layers, 25:35942
magnetohydrodynamic, in self-induced magnetic field of arc discharges, (T), 25:36103 (ILR-FE-70-12)
magnetohydrodynamic, propagation and growth of weak discontinuities in presence of dissipative mechanisms, 25:35944
magnetohydrodynamic, quadratic artificial viscosity in numerical, 25:35951

GASES
argon-ion reactions at 10 to 1000 eV with molecular, rotational and vibrational excitation and light emission from, (E), 25:35873
nitrogen-ion (N_2^+) reactions at 10 to 1000 eV with, rotational and vibrational excitation and light emission from, (E), 25:35873
radium-244 recoil atom ranges at 96.5 keV in, (E), 25:36262
use of protective, in handling pyrophoric or toxic materials, 25:34860

GASTROINTESTINAL TRACT
cesium-137 sorption by, of personnel in nuclear medicine and research, 25:35099

GENES
radiation effects on frequency of nonselective markers in Escherichia coli, effects of dose on donor neutron, 25:35126

GEOLOGY
research programs in, review of fiscal year 1970, 25:34741

GEOMAGNETIC FIELDS
activity of, relation to sunspot cycles, (E), 25:35864
disturbances in, effect on ionospheric D-region ionization in late Sept. 1969, (E/T), 25:36008
effect on charge ratio of near-sea level cosmic-ray muons as function of energy and zenith angle, (E/T), 25:35898
kinematic-dynamo theory of, (T), 25:35786
model of, from satellite altitudes at 1500 km, (E), 25:36009
pion production spectrum near equatorial, from muon spectrum measurements, (E/T), 25:35917
pulsations in, interplanetary origin of long-period micro-, (E/T), 25:35964
pulsations in, relation of auroral geomagnetic bays to irregular micro-, (E), 25:36004
variations at low latitudes, effects of interplanetary field on diurnal, (E/T), 25:35990
variations in dusk-sector midlatitude ionosphere, relation to electron content and geomagnetic storm time, (E/T), 25:35986
variations in, barium-ion cloud and ground-based measurements of, (T), 25:35980
variations of quiet-day, ionospheric time-dependent electric conductivity from Sq, (E/T), 25:35989
variations of, morphology of, (E/T), 25:35990

GEOPHYSICS
conference on, Delhi, India, 10/69, 25:35892 (CONF-691055-(Vol.1))
conference on, Delhi, India, 10/69, 25:35893 (CONF-691055-(Vol.2))
experimental facilities at Gulmarg, 25:35909

GERMANIUM
electron energy-loss spectra of, evidence for double plasmas in, 25:36257
ion dechanneling in single crystals of, ion mass effect in 1.5-MeV, 25:36289
ion-implantation-induced lattice disorder in, channeling study of 10- to 200-keV mercury, 25:36300
proton dechanneling at 1.5 MeV from single crystals of, from backscattering spectra, 25:36271
radioinduced defects in n-type, production and recombination rates of low-temperature electron, (T), 25:36293

GERMANIUM ALLOYS AND SYSTEMS
Au--Ge, mixing at 1100°C, adiabatic calorimetric measurement of heat of, 25:35432
Cu--Ge, mixing at 1100°C, adiabatic calorimetric measurement of heat of, 25:35433
Ge--V, synthesis of superconducting A-15, 25:36044

XUM

GERMANIUM ISOTOPES Ge-71
electron-capture decay of, multiwire-proportional counter measurement of the M/L ratio in, (E), 25:36704
energy levels from (n,γ) reactions, phonon-particle doorway states in, (T), 25:36703
energy levels from germanium-70 neutron capture, analysis of anticorrelation between reduced widths and E1 transition probabilities for, (T), 25:36834
GERMANIUM ISOTOPES Ge-73
energy levels from (n,γ) reactions, phonon-particle doorway states in, (T), 25:36703
energy levels from germanium-72 neutron capture, analysis of anticorrelation between reduced widths and E1 transition probabilities for, (T), 25:36834
GLASS
radioactive waste incorporation in phosphate, in Italy, process for, 25:34711
radioinduced paramagnetic centers in oxidized and reduced sodium-silicate, EPR spectra of, 25:36278
removal of layers of, electron beam method for, 25:35515
GLOVE BOXES
design for cyclone ash separator, engineering drawings for, 25:34784
design of double-walled, for work in controlled environments, 25:34855(P)
neoprene gloves in, penetration of halogenated solvents through, 25:34605 (RFP-1608)
GLOW DISCHARGES
ionization and recombination coefficients in positive column, (T), 25:36136
GLUCITOL, 1-AMINO-1-DEOXY-
radiation effects on stability of, γ, 25:34662
GLUTAMIC ACID
radiation effects on racemization in frozen solutions of D- and L-, γ, 25:34622
radiolysis of aqueous solutions of, ESR spectral studies on free radical yields from x, 25:34655
DPN--glutamic acid, radiolysis of aqueous solutions of, ESR spectral studies on free radical yields from x, 25:34655
GLUTARIC ACID
radiolysis of aqueous solutions of, ESR spectral studies on free radical yields from x, 25:34655
DPN--glutaric acid, radiolysis of aqueous solutions of, ESR spectral studies on free radical yields from x, 25:34655
GLUTATHIONE
oxidation of, properties of free radicals from, 25:34639(R) (USC-113-P-21-3)
GLUTEN
analysis for nitrogen by neutron activation, 25:34555
GLYCINE
radiolysis of alkaline solutions of, at 77°K, ESR studies on production of free radicals by trapped electrons produced by photoionization and x, 25:34647
GLYCOLS
reactions of potassium nitrate-containing, with silicon and tantalum, oxidation, 25:35293
GOLD
defect structure of irradiated, effects of deformation on recovery spectra of, 25:35501
determination in bauxites by neutron activation, 25:34553
determination of, effects of metal ions on colorimetric, 25:34521
effects on gravimetric determination of mercury using 2-aminobenzothiazole, 25:34520
effects on photometric determination of antimony following solvent extraction using TBP, 25:34512
grain boundary dislocations in, 25:37201 (NYO-3504-58)
iodine-ion reactions at 15 to 60 MeV with, L and M x-ray spectra from, (E), 25:35834
x-ray emission induced by electrons, intense K-, 25:35842
GOLD ALLOYS AND SYSTEMS
Ag--Au, mixing at 1100°C, adiabatic calorimetric measurement of heat of, 25:35432
Ag-base--Au, radiation effects on diffusion in, 2-MeV electron, 25:35512
Al--Au, mixing at 1100°C, adiabatic calorimetric measurement of heat of, 25:35432
Au--Cu, mixing at 1100°C, adiabatic calorimetric measurement of heat of, 25:35433
Au--Ga, mixing at 1100°C, adiabatic calorimetric measurement of heat of, 25:35432
Au--Ge, mixing at 1100°C, adiabatic calorimetric measurement of heat of, 25:35432
Au--In, mixing at 1100°C, adiabatic calorimetric measurement of heat of, 25:35432
Au--Pt-base, radiation damage in, annealing of 90°K 3-MeV electron, 25:36306
Au--Sc, crystal structure of intermetallic Au_2Sc and Au_4Sc, 25:35496
Au--Sn, mixing at 1100°C, adiabatic calorimetric measurement of heat of, 25:35432
GOLD CHLORIDES
separation of ions of, from metal ions by high-voltage electrophoresis using carboxylic and hydroxycarboxylic acids, 25:34702
GOLD ISOTOPES Au-195
energy levels from mercury-195 decay, spin-parity assignments for, (E), 25:36750
energy-level transitions from mercury-195 decay, internal conversion coefficients and γ mixing ratios for, (E), 25:36750
GOLD ISOTOPES Au-196
distribution in tissues of swine following field exposure to nuclear debris at Schooner Event site, fallout, 25:35090
excretion in feces and urine of peccaries following single ingestion of nuclear debris from Schooner Event, quantitative comparison of fallout, 25:35089
GOLD ISOTOPES Au-197
alpha reactions (α,xn) at 16 to 104 MeV, excitation functions for, (E), 25:36745
deuteron reactions (d,pn) at 13.6 MeV, diffraction-model analysis of proton--neutron correlations in, (E/T), 25:36713
energy level at 268 keV from platinum-197 beta decay, spin--parity assignments for, (E), 25:36785
energy-level transitions from platinum-197 beta decay, conversion coefficients and ratios, mixing ratios, and penetration parameters from, (E), 25:36789
fission of, lower limit on half-life for spontaneous, (E), 25:36779
neutron capture at 0.01 eV to 20 MeV, excitation functions for, (E), 25:36741 (WHAN-SA-107)
photon reactions (γ,xn) at 75 to 900 MeV, cascade--evaporation analysis of cross sections and gamma spectra and yield curves for, (E/T), 25:36785
proton reactions (p,np) at 25 to 45 MeV, proton spectra and differential cross sections for, (E), 25:36738(R) (UCLA-10-P-18-23)
GOLD ISOTOPES Au-198
availability in peccaries following single injection of nuclear debris from Project Buggy fallout, 25:35088
distribution in tissues of swine following field exposure to nuclear debris at Schooner Event site, fallout, 25:35090
GOLD ISOTOPES Au-199
beta decay of, conversion-electron spectra from, (E), 25:36789
GOLD ISOTOPES Au-203
nuclear properties of, Nuclear Data Sheets for, (E), 25:36809
GRANITES
geochemistry of uranium-bearing, in Nord-Limousin, France, 25:34749 (CEA-R-4034)
GRAPHITE
cosmic hadron reactions above $3(10)^{12}$ eV, distributions and mean values of inelasticity coefficient for production of π^0 in, (E), 25:36389 (ITJ-5)
cosmic nucleon reactions above $3(10)^{12}$ eV, ionization spectrometer study of energy and mean inelasticity for, (E), 25:36388 (ITJ-3)
creep of polycrystalline, model for high-temperature, 25:35556
density of manufactured articles of boronated and natural, standard method for measurement in air of, 25:35474
development of high-quality nuclear, using furfuryl alcohol resin binders, performance of gel permeation chromatography in, 25:35533
electric capacitance of stress-annealed pyrolytic electrodes of, measurement of differential, 25:35563
electric conductivity of powdered, pressure dependence of, 25:36334
galvanomagnetic properties of irradiated polycrystalline at 77 and 300°K, effects of isothermal annealing at 473 to 2673°K on, 25:36314
neutron energy spectra in, comparison of calculated and measured, 25:36266
production and properties of nuclear-grade, for use as neutron moderator and reflector, review on, 25:35562
radiation effects on boronated and hafnated, neutron, (E), 25:36977(R) (GA-10501)
radiation effects on carrier properties of, Shubnikov--de Haas oscillation study of neutron, (E/T), 25:36284
radiation effects on, fast neutron, 25:36978(R) (GA-10560)
radioinduced displacement of surface atoms in, threshold energy for 100 to 200-keV electron, 25:35584
reactions with fission-product cesium in fuel elements at high temperatures, 25:35567
reactions with uranium oxides, kinetics of reduction in, 25:34556 (EUR-4635)
GRAPHITE SYSTEMS
graphite--SiC_2, electric conductivity of powdered, pressure dependence of, 25:36334
graphite--ZnC, electric conductivity of powdered, pressure dependence of, 25:36334
GRAVIMETERS
design of micro-, for measuring niobium oxidation kinetics, 25:35280
GRAVITATION
Einstein field equations in, canonical form of, (T), 25:36579
Newton's theory of, relativistic extension of, (T), 25:35813
solution of Jordan--Dicke field equations, (T), 25:35814
GRAVITATIONAL FIELDS
determination of missing mass in clusters of galaxies by

lens effect, (T), 25:35812
Einstein space--times for, 25:36577
field structure in Schroedinger unified field theory for, exact solution corresponding to, 25:36554
particle motion in monopole--quadrupole, (T), 25:35809
GRAVITATIONAL RADIATION
detection of, review of, (E), 25:36584
production and properties of, review of, (E/T), 25:36584
research on, review of, (E), 25:36585
GRENOBLE REACTORS (SILOE)
radiation target cans for, design parameters of liquid sodium Odile, 25:37060(T) (EURFNR-889)
radiation target cans for, design parameters of natural convection cooled Esther, 25:37061(T) (EURFNR-890)
GROUND
motion from Salmon and Sterling Events, source model for prediction of, 25:34764
GROUND WATERS
contamination by radioactive wastes from nuclear facilities, research program on, 25:34741
contamination from underground disposal of radioactive wastes at Mesita del Buey, N. M., predictions for, 25:34845 (LA-4660)
flow in Totes Gebirges area in Austria, environmental isotope tracer studies of, 25:34726 (THAI-AEC-35, pp 9-20)
flow patterns in Hanford, Wash. area, effects of cooling ponds on, 25:37103 (BNWL-1507)
flow system in Hanford area, predicted effects of Gable Mountain Irrigation Project on, 25:34715 (BNWL-1502)
isotope content of Totes Gebirges area, in Austria, measurement of oxygen-18 and tritium, 25:34726 (THAI-AEC-35, pp 9-20)
GUANIDINE, AMINO-
hydrofluoride, complexes with uranium tetrafluoride, magnetic susceptibilities, stability, and solubility of, 25:34611
GYMNOSPERMIDAE
Larix laricina, radiosensitivity of seedlings of, in relation to DNA content and seed radiosensitivity, γ, 25:35250
Picea glauca, radiosensitivity of seedlings of, in relation to DNA content and seed radiosensitivity, γ, 25:35250
Picea mariana, radiosensitivity of seedlings of, in relation to DNA content and seed radiosensitivity, γ, 25:35250
Pinus banksiana, radiosensitivity of seedlings of, in relation to DNA content and seed radiosensitivity, γ, 25:35250
Pinus contorta, radiosensitivity of seedlings of, in relation to DNA content and seed radiosensitivity, γ, 25:35250
Pinus resinosa, radiosensitivity of seedlings of, in relation to DNA content and seed radiosensitivity, γ, 25:35250
Thuja occidentalis, radiosensitivity of seedlings of, in relation to DNA content and seed radiosensitivity, γ, 25:35250

H

H.B. ROBINSON POWER REACTOR, UNIT 2
control elements for, revised technical specifications for initial physics testing part-length requirements of, 25:36931 (DOCKET-50261-59)
operations history for September 1970 to March 1971, 25:36880 (DOCKET-50261-60)
site for, environmental radioactivity survey for October 1, 1970 through March 31, 1971, 25:36932 (DOCKET-50261-61)
HI REGIONS
distribution in Maffei 2, (E), 25:35794
distribution in NGC 5128,(E), 25:35789
expansion in low spin-temperature, (E), 25:35680
spectra of low spin-temperature, emission, (E), 25:35680
temperatures of grains in, (T), 25:35790
turbulence in low spin-temperature, (E), 25:35680
HII REGIONS
distribution in spiral galaxies, (E/T), 25:35782
dust-radiation instability in, (T), 25:35688
electron temperatures of, (E/T), 25:35683
model for, numerical, (E/T), 25:35683
Stark broadening of high-quantum-number recombination lines in, (E), 25:35711
HADRONS
form factors of, quark model for dipole electromagnetic, (T), 25:36436 (ORO-3992-28)
interactions at 1 TeV in air showers, review of, (E), 25:36395
interactions of, correlation between transverse and longitudinal momenta for multiple production in, (T), 25:36423
interactions of, statistics of urbaryons for exclusion principle effects on amplitude of, (T), 25:36477
interactions with hadrons at high energies, review of total cross sections for, (E/T), 25:36480
interactions with hadrons at high energies, review of forward elastic, (E/T), 25:36480
interactions with hadrons, class of nonlinear Lagrangian models for dynamics of, (T), 25:36481
interactions with hadrons, instability criterion for properties of intermediate compound systems in, (T), 25:36599
interactions with hadrons, research at Illinois Univ., fiscal 1971, (E), 25:36384(R) (COO-1195-212)
interactions with hadrons, research at Johns Hopkins Univ., April 1970 to March 1971 on hadron structure determination from, (T), 25:36472(R) (NYO-4076-14)
interactions with hadrons, review of S-matrix and Veneziano model for, (T), 25:36479
interactions with hadrons, test of empirical rule for cuts and line reversal relations in absorption model for, (T), 25:36502 (CALT-68-300)
interactions with leptons, research at Johns Hopkins Univ., April 1970 to March 1971 on hadron structure determination from, (T), 25:36472(R) (NYO-4076-14)
production in deep inelastic e + p interactions, review of parton and vector dominance models for cross sections and structure functions for, (T), 25:36452
production in e+ + e- interactions in preasymptotic region, parton model predictions for, (T), 25:36424 (LNF-71/5)
production in γ + γ interactions in colliding beams, cross sections for, (T), 25:36433 (LNF-71/1)
reactions with lead and graphite above $3(10)^{12}$ eV, distributions and mean values of inelasticity coefficient for π^0 production in, (E), 25:36389 (ITJ-5)
reactions with nuclei at high energies, review of Glauber theory for, (E/T), 25:36533
reactions with nuclei, instability criterion for properties of intermediate compound systems in, (T), 25:36599
scattering by helium-4 at high energies, Glauber theory of multiple scattering for effects of short-range nucleon--nucleon correlations on elastic and inelastic, (T), 25:36538
structure of, research at Johns Hopkins Univ., April 1970 to March 1971 on strong and lepton--hadron interactions for determination of, (T), 25:36472(R) (NYO-4076-14)
symmetry for, book on unitary, 25:36552
HAFNIUM
deformation and fracture behavior in polycrystalline, at 77 to 298°K, effects of hydrogen on, 25:35457
determination in presence of zirconium, effects of metal ions on fluorescence method for, 25:34519
determination in rocks by neutron activation and γ spectroscopy, 25:34543 (NIM-1013)
fabrication and properties of, engineering data on, 25:35437
magnetic susceptibility of single crystals of, 25:36340
properties of chunklet and sponge, standard for, 25:35472
stability of powders of, in acids, 25:35522
thermal capacity at low temperature of single crystals of, 25:36340
HAFNIUM ALLOYS AND SYSTEMS
C--Hf--Mo-base, tensile properties of dilute, effects of thermomechanical treatments on, 25:35397
Hf--Nb, tensile properties of, effects of aging at 600 to 1000°C on, 25:35393
Hf--Pt, stability of gaseous intermetallic, 25:35250
Hf--Ta-base, hardening in solid solutions of, parameters controlling, 25:35384
HAFNIUM ISOTOPES Hf-173
energy levels from tantalum-173 beta and electron-capture-decay, lifetimes and spin--parity assignments for, (E), 25:36727 (JINR-P6-5704)
energy-level transitions from tantalum-173 beta and electron-capture, decay, conversion coefficients and multipolarities for, (E), 25:36727 (JINR-P6-5704)
HAFNIUM ISOTOPES Hf-178
energy-level transitions in, internal conversion coefficients and intensities from, (E), 25:36760
HAFNIUM NITRIDES
chemical stability in water, alkali solutions, and acids, 25:35522
reaction kinetics in acids, decomposition, 25:35522
solvent properties for oxygen at 1023 to 1073°K, 25:35566
HAMAOKA POWER REACTOR, UNIT 1
construction schedule for, 25:36860
design parameters of, 25:36860
HAMSTERS
radiation effect on reproduction of hematopoietic cells in, 25:35217
HANDBOOKS AND MANUALS
on thorium ceramics, 25:35548 (ORNL-4503(Vol.3))
HANDS
bone density in finger of human, iodine-125 scanning method for measuring, 25:35171
HANFORD PRODUCTION REACTORS
site for, effects of cooling ponds on ground water system of, 25:37103 (BNWL-1507)
thermal effluents from, effects on death rate of steelhead trout in Columbia River of, 25:37104 (BNWL-SA-3713)
thermal effluents from, effects on salmon migration in Columbia River of, 25:37105 (BNWL-SA-3876)
HASTELLOY C
properties of Type 276, for large radioisotope heat

XUM

source fuel capsules, chemical and mechanical, 25:34809 (CRNL-TM-3230)
HASTELLOY N
radiation effects on mechanical properties of, relations of environment with fast neutron, 25:35506
tensile properties of titanium-modified, 25:35391
HASTELLOY X 280
radiation effects on mechanical properties of, relations of environment with fast neutron, 25:35506
HAYNES 25 ALLOY
corrosion by lithium--selenium mixtures at 375°C, 25:35275(R) (ANL-7777)
HEALTH PHYSICS
procedures for decontamination of high-activity cell line at Harwell, 25:35131
surveillance at fuel reprocessing plant, instrumentation and methods for, 25:35140
HEART
blood flow in, use of rubidium-86 and technetium-99m-labeled erythrocytes for measuring, 25:35085
radiation effects on optical density of mitrochondria in animal, effects of hydrocortisone on, 25:35227
HEART, MECHANICAL
heat source for, radiation characteristics of isotopic, 25:34803(R) (BNWL-1308-5)
HEAT EXCHANGERS
temperature stabilization in, under variable heat flux, use of heat pipes for, (E/T), 25:34775 (EUR-4634)
HEAT EXCHANGERS (LIQUID-LIQUID)
baffles for heavy water cooled reactor primary, analysis and repair of damage to, 25:37055 (BNL-15815)
HEAT PIPES
sleeve assembly for potassium-filled, design and fabrication of nickel, 25:34810(R) (ORNL-TM-3394)
use of partially gas-filled, for temperature stabilization in heat exchanger tubes under variable heat flux, (E/T), 25:34775 (EUR-4634)
HEAT-RESISTING ALLOYS AND METALS
preparation of composites of, incorporating in-situ grown carbide fibers, 25:35557
preparation of controlled-crystal structure shapes of, by directional solidification, 25:35301
wetting by brazing alloys at 700 to 1900°C, 25:35334 (EUR-4637)
HEAT SOURCES
capsules for large radioisotopes, for terrestrial use, safety evaluation of Hastelloy C-276, 25:34809 (ORNL-TM-3230)
dose rates to man from circulatory support device isotopic, computer program for prediction of, 25:34803(R) (BNWL-1308-5)
HEAT TRANSFER
analysis for axially uniform heat generation for finite rod bundles, 25:34794
burnout in forced convection boiling, bibliography on, 25:37000 (AAEC/LIB/Bib-286)
calculation for turbulent fluid flow in rough and smooth channels and tubes, generalized method for, 25:34795
measurement of steady-state convective, in concentric annular channels during transition and turbulent flow, (E/T), 25:37008 (UARAEE-50)
research on two-phase, in BWR fuel channels, design and operation of test loop for, 25:34793 (UARAEE-81)
study of two-phase flow, for uses in nuclear and nonnuclear fields, 25:34796
HEATED EFFLUENTS
effects on Columbia River ecosystems, bibliography on, 25:35115 (BNWL-1543)
HEATERS
output control of r-f induction, design of programmer for, 25:34739
HELIUM
abundance in primary cosmic rays, relation to deuteron abundance, (E/T), 25:35912
abundance in supergiant star HD 32034, (E), 25:35673
alpha-particle stopping cross sections at 0.5 to 2 MeV, atomic, (E), 25:36256
electron elastic scattering at 100 and 700 eV by, wave function for evaluation of Glauber amplitude for, 25:35868
electron reactions at 30 to 50 eV with, angular distributions and probabilities for allowed and forbidden transitions in, 25:35882
electron reactions up to 2 keV with, polarization-free vacuum-ultraviolet excitation cross sections for, (E), 25:35857
energy levels of, calculation using multiconfiguration frozen-core approximation, 25:35890
energy-level transitions of, rate calculation for one-photon $2^3S_1 \rightarrow 1^1S_0$, 25:35845
helium-ion reactions at 200, 300, and 350 eV with, ion--photon coincidence measurements of differential cross sections for excitation in, 25:35858
ionization by protons at 4 MeV, pressure dependence and Jesse impurity effect in, 25:35888
oscillator strengths for excitation and ionization of, tables of calculated generalized, 25:35844 (SC-RR-70-406)
plasma of, electron energy distribution in positive column discharges, (E), 25:36119
plasma of, electron heating by interacting electron beams, (E), 25:36118
plasma of, optical measurement of hf electric fields in weakly ionized, 25:36094
proton elastic scattering at 1 MeV and small angles by, wave function for evaluation of Glauber amplitude for, 25:35868
proton reactions with, coincidence studies of charge exchange and excitation in, 25:35877
radioinduced production in stainless steel, methods for estimation of fast neutron, 25:35503 (HEDL-SA-193)
reactions of atoms and ions of, with alkali metal halides at 0.2 to 6 keV, electron emission induced by, 25:35840
reactions with methane under simulated radiolysis conditions, mass spectrometric studies on, 25:34645
reactions with strontium of metastable atoms of, coherence transfer to excited strontium ions formed by Penning effect in, (E), 25:35875
scattering by helium at 2.1°K, atomic-beam measurements of total effective cross sections for, 25:35860
scattering by hydrogen molecules, sudden-approximation calculations of cross sections for, 25:35887
x-ray-induced ionization of interstellar, (T), 25:35784
HELIUM IONS
dechanneling in germanium single crystals at 1.5 MeV, ion mass effect on, 25:36289
reactions of atoms and ions of, with alkali metal halides at 0.2 to 6 keV, electron emission induced by, 25:35840
reactions with helium at 200, 300, and 350 eV, ion--photon coincidence measurements of differential cross sections for excitation in, 25:35858
reactions with hydrogen molecules at 45 to 700 eV, polarization of He line produced by dissociative charge exchange in, (E), 25:35862
stopping cross sections in gases at 0.3 to 2 MeV, 25:36255
HELIUM ISOTOPES He-3
deuteron reactions (d,t) at 39.1 MeV and 50, Born-approximation and Watson--Migdal analysis of final-state interactions in energy spectra from, (E), 25:36665
electrodisintegration of, effects of exchange currents on polarization of nucleons emitted in, (T), 25:36664
lattice dynamics at high pressure, 25:37204 (NYO-3655-51)
meson reactions (π^-,π^+), production of three-nucleon resonance in, (T), 25:36849
neutron reactions (n,d) at 14.4 MeV, angular distributions for, (E), 25:36738(R) (UCLA-10-P-18-23)
nuclear charge distribution parameters from (d,t) reactions at 39.1 MeV, (E), 25:36665
proton reactions (p,d) at 12 and 46 MeV, energy spectra for, (E), 25:36738(R) (UCLA-10-P-18-23)
proton reactions (p,pd) and (p,2p) at 35 MeV, kinematic analysis of, (E), 25:36738(R) (UCLA-10-P-18-23)
reactions (He-3,d) with potassium-39 at 29.3 MeV, angular distributions for, (E), 25:36696
reactions (He-3,d) with titanium-50 at 10 MeV, DWBA analysis of angular distributions from, (E), 25:36716
reactions (He-3,Li-6) with fluorine-19 at 40 MeV differential cross section and reaction mechanisms for, (E), 25:36674
reactions (He-3,t) with deuterium at 19 MeV, triton spectra at 5° from, (E), 25:36662
scattering by potassium-39 at 29.3 MeV, angular distributions for elastic, (E), 25:36696
theories of liquid, review of Brueckner--Bethe and Landau, (T), 25:36843
HELIUM ISOTOPES He-4
binding energy from two-body correlations in liquid, (T), 25:36016
electron elastic scattering at 30 to 59 MeV, differential cross sections for, (E), 25:36658(T) (CERN-Trans-71-13)
excitation energy spectrum from two-body correlations in, (T), 25:36016
hadron elastic and inelastic scattering at high energies, Glauber theory of multiple scattering for effects of short-range nucleon--nucleon correlations on, (T), 25:36538
lattice dynamics at high pressure, 25:37204 (NYO-3655-51)
meson (μ^-) capture by, calculations of neutron spectra and asymmetries in neutron angular distributions from, (T), 25:36666
meson (π) elastic scattering near 3,3 resonance, multiple-scattering theory for differential and total cross sections for, (T), 25:36527
meson (π^+) reactions at high energies, Coulomb interaction in, (T), 25:36524
meson (π^-) reactions at high energies, Coulomb interaction in, (T), 25:36524
nuclear charge radius from electron elastic scattering, (E), 25:36658(T) (CERN-Trans-71-13)
optical breakdown in liquid, impurity effects below lambda point on threshold power of laser-induced, 25:36014
photon reactions (γ,He-3) and (γ,t) at 20 to 80 MeV, cross sections for, (E), 25:36671
roton viscosity of superfluid, (T), 25:36015
thermal conductivity of superfluid, (T), 25:36015

vortex ring nucleation probability in liquid II, (E), 25:36017
H--He-4, thermal diffusion factor for, 25:34807(R) (MLM-1793)
HELIUM TRITIDES
reactions of, produced by tritium beta decay with gaseous hydrocarbons, kinetic studies on, 25:34675
reactions of, produced by tritium beta decay with ethane and methane, kinetic studies on, 25:34677
reactions of, produced by tritium beta decay with gaseous hydrocarbons, kinetic studies on, 25:34676
HEMATOPOIETIC SYSTEM
radiation effects on cell reproduction in hamster and mouse, 25:35217
radiosensitivity of mouse, effects of dose fractionation and rate of, 25:35218
HENEICOSANE
radiation thermal cracking of liquid, γ, 25:34653
HEPARIN
radiolysis of frozen concentrated aqueous solutions of, ESR studies on free radicals produced by γ, 25:34651
HEPTANE
radiolysis of, yields from electron, 25:34635 (NP-18810)
HEXAMETHYLENETETRAMINE
complexes with uranyl ion, magnetic susceptibility and ir spectra of, 25:34612
1-HEXANETHIOL, 2-AMINO-
radioprotective effects of, on Escherichia coli, function and structure studies on γ, 25:35160
HEXOKINASE
radiation effects on activity of animal skin, protective effects of corticosteroids against uv, 25:35234
HIGH-ENERGY PHYSICS
research at Brandeis Univ., Sept. 1970 to April 1971, (E/T), 25:36419(R) (NYO-3178-8)
HIGH-TEMPERATURE LATTICE TEST REACTOR
multiplication factor for thorium oxide (ThO_2)--uranium oxide (UO_2) lattice in, temperature dependence of infinite, (E), 25:36988 (ENWL-1561)
HIROSHIMA
atomic bombing of, radiation effects on lipofuscin accumulation in man exposed to, 25:35241
HISTIDINE
effects on potentiating effects of iodine compounds on γ-radioinduced inactivation of Bacillus cereus spores, antagonistic, 25:35264
HODOSCOPES
design of, based on small photomultipliers, 25:34864 (IFVE-SEF-70-17)
HOLMIUM
determination as impurity in terbium oxide by neutron activation and radiochemical separation, 25:34670 (JAERI-Memo-4280)
determination in aqueous acetone solutions of dibenzoylmethane complexes, absorption spectrophotometric, 25:34527
HOLMIUM ALLOYS AND SYSTEMS
Al--Ho-base, crystal lattice parameters of intermetallic Ho_2Al, 25:35495
Ho--Re, superconducting transition temperature of intermetallic compounds of, 25:36038
HOLMIUM HAFNATES
crystal structure of, precipitated from hafnium and holmium hydroxides, comments on, 25:35570
crystal structure of, precipitated from hafnium and holmium hydroxides, comments on, 25:35569
HOLMIUM ISOTOPES Ho-165
neutron capture by, spectrum-averaged cross sections for pile, (E/T), 25:36720 (CONF-710301-4)
nitrogen-14 fission up to 10.4 MeV/nucleon, excitation function for, (E), 25:36784
HOLMIUM OXIDES
growth of single-crystal solid solutions with another rare earth oxide by Verneuil method, formation regions in, 25:35525
HOLMIUM ZIRCONATES
crystal structure of, precipitated from holmium and zirconium hydroxides, comments on, 25:35570
crystal structure of, precipitated from holmium and zirconium hydroxides, comments on, 25:35569
HORMONES, ADRENAL
adrenalin, effects on cholinesterase activity in x-irradiated rat brain, 25:35232
corticosteroids, radiation effects on retention of, in dog liver, γ, 25:35222
corticosteroids, radioprotective effects on hexokinase activity in animal skin, uv, 25:35234
hydrocortisone, effects on cholinesterase activity in x-irradiated rat brain, 25:35232
hydrocortisone, effects on optical density of mitrochondria in irradiated animal cardiac muscles, 25:35227
HORMONES, PANCREATIC
insulin, radioprotective effects on glucocorticoid and glycogen contents in rat endocrine glands, electron, 25:35164
HORMONES, PLANT
gibberellic acid, effects on synthesis of α-amylase and ribonuclease in γ-irradiated wheat seedlings, 25:35102
HORMONES, SEX
estrogens, effects on histology of albino rat ovaries and uterus, combined effects of x radiation and, 25:35237
progesterone, effects on histology of albino rat ovaries and uterus, combined effects of x radiation and, 25:35237
HORMONES, THYROID
radiation effects on production of, 25:35208
HOSPITALS
waste management at, equipment and methods for solid, 25:34856
HOT CELLS
decontamination at Harwell, health physics aspects of, 25:35131
HUMBOLDT BAY, POWER REACTOR
control elements for, operating limits and reactivity worth of, 25:36901 (DOCKET-50133-57)
fuel element assemblies for, design parameters of Type 2 and Type 3-2 and 3, 25:36901 (DOCKET-50133-57)
HUTCHINSON ISLAND POWER REACTOR, UNIT 2
construction of, notice of receipt of permit application for, 25:36962 (DOCKET-50389-8)
cooling water system for, revised information on component, 25:36963 (DOCKET-50389-9)
operation of, notice of receipt of license application for, 25:36962 (DOCKET-50389-8)
HYDRAULICS
uses of two-phase thermo-, in nuclear and nonnuclear fields, development of, 25:34796
HYDRAZYL, DIPHENYLPICRYL-
effects of coatings of, on γ radiolysis products of poly(vinyl chloride), ESR studies on, 25:34656
HYDROCARBONS
positron annihilation in liquid, mechanism for formation of positronium atoms in, (E/T), 25:35853
properties as diluents in fuel reprocessing, 25:34628 (RT/CHI-(70)35)
HYDROCHLORIC ACID
HCl--2-propanol, corrosive effects on aluminum--titanium--vanadium alloys, 25:35287
HCl--methanol, corrosive effects on aluminum--titanium--vanadium alloys, 25:35287
HYDROFLUORIC ACID
vapor pressure--temperature data for, 25:34602 (GAT-645)
HYDROGEN
abundance relative to deuterium in two reference water standards, 25:34518
alpha-particle stopping cross sections at 0.5 to 2 MeV, atomic, (E), 25:36256
alpha-particle stopping cross sections in gaseous, at 0.3 to 2 MeV, 25:36255
atomic beam production for plasma research, design of source for, 25:35837
atomic beams of, production for thermonuclear research, 25:36186(T) (CTC-746)
chlorine-ion reactions at 4 MeV with molecular, charge-state distributions from, (E), 25:35849
collisions of atomic and molecular, exact tunneling calculations for, 25:34574
cosmic alpha particle interaction mean free paths and fragmentation probabilities above 10 GeV/nucleon in, emulsion study of, (E/T), 25:36394
cosmic nuclei interaction mean free paths and fragmentation probabilities above 10 GeV/nucleon in, emulsion study of heavy, (E/T), 25:36394
coupling constant for atomic, potential of skew-symmetric tensor field for, (T), 25:36571
determination at ppM levels in milligram steel samples by inert gas fusion methods, 25:34514
determination in argon cover gas for sodium loops, chromatographic, 25:35276(R) (GEAP-13539-16)
determination in loop sodium, testing of in-line meter for, 25:35276(R) (GEAP-13539-16)
deuterium reactions at 3 to 45 keV with molecular, total loss cross sections for, (E), 25:35855 (UCRL-20095)
deuteron reactions (d,He-3) at 20 to 45.2 MeV, evidence for T = 1/2 resonance in cross sections for, (E), 25:36663
diffusion in water, 25:34573(R) (RLO-2230-T-2-2)
distribution of neutral, in galaxies, (E/T), 25:35781
effects of neutral, on spectral line broadening in solar atmosphere, (T), 25:35770
effects on deformation and fracture behavior in polycrystalline hafnium at 77 to 298°K, 25:35457
effects on fracture of H11 steel at -28 to +100°C, 25:35337(R) (NYO-3975-3)
effects on mechanical properties of iron whiskers, 25:35337(R) (NYO-3975-3)
electron elastic scattering by atomic, Harris-method calculation of phase shifts for s-wave, 25:35879
electron reactions at 10 to 400 eV with atomic, Glauber-approximation calculation of differential and total cross sections for 1s--3d excitation in, 25:35859
electron reactions with atomic, Glauber-theory calculation of excitation cross sections for, 25:35878
electron reactions with molecular, velocity distribution of metastable H atoms from dissociative excitation in, (E), 25:35864
electron scattering by atomic, virial theorem for variational functions in, (T), 25:35871
emissions during auroral substorms, morphology of auroral, (E/T), 25:36005
energy level shifts of atomic, potential for skew-symmetric tensor field for, (T), 25:36571

XUM

helium-atom scattering by molecular, sudden-approximation calculations of cross sections for, 25:35887
helium-ion reactions at 45 to 700 eV with molecular, polarization of Hα line produced by dissociative charge exchange in, (E), 25:35862
Lamb shift in, two-body problem in quantum electrodynamics for, (T), 25:36567
lattice dynamics at high pressure, 25:37204 (NYO-3659-51)
Lyman-alpha emission from Milky Way, (T), 25:35792
neutron capture at 10^{-5} to 10^{7} eV, cross sections evaluation for ENDF/B, 25:36660 (LA-4574)
neutron elastic scattering at 10^{-5} to 10^{7} eV, evaluation of total cross section and angular distributions for ENDF/B, 25:36660 (LA-4574)
neutron elastic scattering at 22.5 to 400 MeV, least-squares fit to differential cross sections for elastic, (E), 25:36661 (UCRL-20295)
neutron total cross section at 10^{-5} to 10^{7} eV, evaluation for ENDF/B, 25:36660 (LA-4574)
permeation in iron and steel biaxially stressed membranes, 25:35337(R) (NYO-3975-3)
photo-absorption cross sections of molecular, review of uv, (E/T), 25:36013
plasma of, hf heating near lower hybrid frequency, (E), 25:36087
plasma of, laser beam scattering from magnetized arc, (E), 25:36123
polarization of oriented targets of, method for measuring, 25:36545
positron elastic scattering by atomic, Harris-method calculation of phase shifts for s-wave, 25:35879
positron reactions with atomic, Glauber-theory calculations of excitation cross sections for, 25:35878
potassium-atom and -ion reactions up to 50 eV with molecular, vibrational excitation and dissociation in, (E), 25:35884
properties for use in large cryogenic bubble chambers, 25:34962 (CONF-700623-(Vol.1), pp 532-42)
proton reactions up to 10 eV with molecular, crossing of potential-energy surfaces in, (T), 25:35885
proton reactions up to 3 keV with atomic, Glauber-approximation calculations of differential and total cross sections for 1s--3d excitation in, 25:35859
proton reactions with atomic, Glauber-theory and multistate impact-parameter calculations of excitation cross sections for, 25:35878
radioinduced ions of, in weakly alkaline aqueous solutions, pH indicator studies on electron pulse, 25:34668
reactions with hydrogen gas at 1 to 25 keV/nucleon of excited and ground-state molecules of, cross sections for ionization and total loss in, (E), 25:35874
sodium-atom and -ion reactions up to 50 eV with molecular, vibrational excitation and dissociation in, (E), 25:35884
solubility in polyethylene, 25:34637(R) (ORO-4059-1)
sorption by activated carbon black at 80 to 600°C, kinetics of chemical, 25:35552
sorption by zirconium alloys, effects of corrosion on, 25:35283
spectra of molecular, relative line intensities in Lyman bands of, (E), 25:35848
spectra of, interpretation of extraterrestrial observations of Lyman-α, (T), 25:35593
Stark broadening of high-quantum-number recombination lines of, in H II regions, (E), 25:35711
x-ray-induced ionization of interstellar, (T), 25:35784
yields from electron pulse and γ radiolysis of aqueous solutions of borohydride ions, 25:34646
yields from γ radiolysis of 2-methyl-2-propanol at 30°C, 25:34659
yields from γ radiolysis of gaseous, deuterated and normal methanol, kinetics of, 25:34665
yields from radiolysis of frozen perchloric acid solutions, effects of halogen-substituted acetic acids on, 25:34648
i_2--Ne, index of refraction of, at 24.60 to 27.15°K and 5.83 to 22.30 mole percent neon, 25:34963 (CONF-700623-(Vol.1), pp 543-54)
H_2--Ne, properties for use in large cryogenic bubble chambers, 25:34962 (CONF-700623-(Vol.1), pp 532-42)

HYDROGEN IONS (H^-)
absorption coefficient of, effect of interparticle interaction of bound-free, (T), 25:35661
energy of ground state of, calculation using multiconfiguration frozen-core approximation, 25:35890
production in plasma discharges bounded by double sheaths, (E), 25:35843
reactions with water vapor at 5 keV, total cross sections for detachment of one and two electrons in, (E), 25:35867

HYDROGEN IONS (H_3^+)
energy levels of, single-center calculations of energies and transitions of excited states, 25:35851
potential-energy surfaces for lowest states of, 25:35885

HYDROGEN PEROXIDES
radiation effects on subsequent catalytic decomposition of, γ, 25:34630
yields from γ radiolysis of neutral aqueous, oxygenated solutions of oxalate ions, effects of dose on, 25:34644

HYDROGEN SULFIDES
photo-absorption cross sections of, review of uv, (E/T), 25:36013
reactions with uranium(VI) in aqueous solutions at 100 to 200°C, 25:34569

HYDROGEN SYSTEMS
H--He-4, thermal diffusion factor for, 25:34807(R) (MLM-1793)
H--Nb-base, preparation and pulverization of, 25:35259
H--O, effects on fracture of H11 steel at -28 to +100°C, 25:35337(R) (NYO-3975-3)

HYDROLOGY
research programs in, review of fiscal year 1970, 25:34741
well logging in, design, performance, and use of nuclear equipment and methods for, 25:34725 (STI/DOC-10/12E)

HYDROQUINONE
effects of coatings of, on γ radiolysis products of poly(vinyl chloride), ESR studies on, 25:34656

HYDROXYL (HO)
radio emission from, in direction of NGC 2438, (E), 25:35698
spectral line absorption due to, in direction of Omega Nebula, (E), 25:35696

HYDROXYLAPATITE
content in finger bones, iodine-125 scanning method for measuring, 25:35171

HYPERFRAGMENTS
binding energy of Λ-H^3, Λ-Be^9, and Λ-He^4, (T), 25:36647
decay Λ-H^3 + ^3He + 1^- + anti ν, recoil spectra, angular correlations, polarization, and lifetime for, (T), 25:36454 (IAE-1944)
decay of heavy, Monte Carlo simulation of, (T), 25:36535
decay of Λ-H^3, four-body leptonic, (T), 25:36454 (IAE-1944)
decay of Λ-He^5, Λ-Li^6, and Λ-Be^9 in emulsions, Q-value distribution for, (E), 25:36401
energy levels of heavy Λ, ground-state doublet, (T), 25:36528
hyperon (Λ) binding energies in p-shell, formulas and matrix elements for ΛN and ΛNN forces in shell model analysis of, (T), 25:36529
lifetime of heavy, Monte Carlo calculation of, (T), 25:36535
production of heavy, Monte Carlo simulation of, (T), 25:36535
production of Λ-He^5, Λ-Li^6, and Λ-Be^9 in K^- absorption by nuclei at rest in emulsions, Q-value distribution for detection of, (E), 25:36401
properties of, review of, (E/T), 25:36539

HYPERONS (Λ)
binding energies in p-shell hypernuclei, formulas and matrix elements for ΛN and ΛNN forces in shell model analysis of, (T), 25:36529
decay $\Lambda \rightarrow p + \pi^-$, model for parity-violating, (T), 25:36465
polarization in $\pi^- + p \rightarrow K^0 + \Lambda$ interactions, test of empirical rule for cuts and line reversal relations in absorption model predictions for, (T), 25:36502 (CALT-68-300)

HYPERONS (Σ)
polarization in $\pi^+ + p \rightarrow K^+ + \Sigma^+$ interactions, test of empirical rule for cuts and line reversal relations in absorption model predictions for, (T), 25:36502 (CALT-68-300)

HYPERONS (Σ^-)
decay $\Sigma^- \rightarrow n + \pi^-$, model for parity-violating, (T), 25:36465
production in K^- absorption by nuclei at rest in emulsions, properties from, (E), 25:36400

HYPERONS (Σ^+)
decay $\Sigma^+ \rightarrow n + \pi^+$, model for parity-violating, (T), 25:36465
production in K^- absorption by nuclei at rest in emulsions, properties from, (E), 25:36400

HYPERONS (Ξ^-)
decay $\Xi^- \rightarrow \Lambda + \pi^-$, model for parity-violating, (T), 25:36465

HYPOXANTHINE
radiation effects on content of, in rat brain, effects of dose on neutron, 25:35226

I

IGNEOUS ROCKS
compressibility of, study of isothermal, 25:37233(T) (SC-T-713031)

IMPACT SHOCK
pressure in collisions between two bodies, estimation of, 25:37257(T) (UCRL-Trans-10531)

IN-PILE LOOPS
design parameters for pool type research reactors, 25:37067(T) (LB/G-3001)

INCINERATORS
design of, engineering drawings for, 25:34784

INCOLOY 800
corrosion by sodium at 1300°F, 25:35276(R) (CEAP-12539-16)
radiation effects on properties of titanium-modified,

relations of thermal aging with fast neutron, 25:35510
INCONEL X750
compatibility of tubular sections of, with sodium-potassium loop at 1050 to 1310°F, 25:35343 (WANL-TME-1857)
INCONEL 600
ductility and strength of, at high temperatures, effects of boron on, 25:35338 (ORNL-TM-3316)
INCONEL 625
welding of fuel element components of, tungsten inert gas method for, 25:35311
welding to chromium--nickel--steel alloy, tungsten inert gas method for, 25:35311
INCONEL 718
compatibility of tubular sections of, with sodium-potassium loop at 1050 to 1310°F, 25:35343 (WANL-TME-1857)
radiation effects on mechanical properties of, relations of environment with fast neutron, 25:35506
INDIAN POINT POWER REACTOR, UNIT 1
emergency core cooling system for, revised plans for installation of, 25:36854 (DOCKET-50003-73)
INDIAN POINT POWER REACTOR, UNIT 3
effluents from, effects on ecology of Hudson River of chemical, radioactive, and thermal, 25:36943 (DOCKET-50286-36)
effluents from, effects on thermal plume in Hudson River of thermal, 25:36942 (DOCKET-50286-35)
effluents from, environmental effects of chemical, radioactive, and thermal, 25:36941 (DOCKET-50286-34)
site for, effects of cooling water discharge on Hudson River temperature distribution near, 25:36942 (DOCKET-50286-35)
site for, effluent effects on ecology of Hudson River near, 25:36943 (DOCKET-50286-36)
site for, hydrology and meteorology of, 25:36942 (DOCKET-50286-35)
INDIUM
content in Illinois rainwater, 1970 measurements of, 25:34742(R) (COO-1407-38)
effects on colorimetric determination of gold, 25:34521
effects on fluorescence method for detection of hafnium and zirconium, 25:34519
effects on gravimetric determination of mercury using 2-aminobenzothiazole, 25:34520
nuclear spin--lattice relaxation in pure and impure, quadrupole-resonance study of 4.2°K, 25:36349
plasticity of crystalline, effects of superconducting transition on, 25:35383
INDIUM ALLOYS AND SYSTEMS
Au--In, mixing at 1100°C, adiabatic calorimetric measurement of heat of, 25:35432
Cu--In, mixing at 1100°C, adiabatic calorimetric measurement of heat of, 25:35433
In--Mg-base, plastic deformation of solid solution monocrystals of, solute effects in, 25:35387
In--Pb, plasticity of crystalline, effects of superconducting transition on, 25:35383
In--Pb-base, creep in superconducting, 25:36032
In--Pb-base, magnetic transition at H/sub c2/ in superconducting, (E), 25:36028
In--Tl, magnetic transition at H/sub c2/ in superconducting, (E), 25:36028
In--Zn, thermodynamic properties of liquid solutions of, 25:35442
INDIUM IONS
implantation in silicon at 20 to 80 keV, content profiles of, (E/T), 25:36282
INDIUM ISOTOPES In-110
energy levels and nuclear properties of, Nuclear Data Sheets for, (E), 25:36808
INDIUM ISOTOPES In-113
production of metastable, control of elution and eluent from generators for, 25:34672
INDIUM ISOTOPES In-115
neutron capture by, spectrum-averaged cross sections for pile, (E/T), 25:36720 (CONF-710301-4)
nuclear quadrupole resonance in pure and impure indium at 4.2°K, 25:36349
INFORMATION CENTERS
evaluation of nuclear data by, procedures for critical, 25:37107 (INDC(NDS)-29/U)
INFORMATION RETRIEVAL SYSTEMS
description of, of Radiation Shielding Information Center, 25:36247 (CTC-48)
INFRARED ASTRONOMY
developments in, (T), 25:35659
observational difficulties in, (T), 25:35658
survey of results in, (T), 25:35658
INFRARED RADIATION
cosmic background, relation to universal theory of cosmic radiation, (T), 25:35818
effects on chromosomes in pollen tubes of uv-irradiated Tradescantia, aberrant, 25:35120
emission from galactic center region, (E), 25:35780
emission from stars, (T), 25:35659
emission of excess, from W Cep and similar stars, (E), 25:35625
INORGANIC COMPOUNDS
structure of, containing nitrogen and sulfur, 25:37248 (UCRL-20535)
INSTRUMENTS
radiation effects on, guide for, 25:35081
INTERSTELLAR MATERIAL
abundance of sulfur hydride and nitrogen oxide in, upper limits for, (E), 25:35697
heating by soft x rays and cosmic rays, (T), 25:35784
spectral absorption bands due to calcium, potassium, and sodium at 4430 A, (E/T), 25:35663
temperature of, effects of grain shape on, (T), 25:35791
temperatures of, effects of grain materials and radiation fields, (T), 25:35790
INTESTINES
radiation effects on epithelial cell count in mouse, lethal x, 25:35239
radiation effects on success of human, origin and kinetics of goblet cells during post-operative, 25:35240
radioinduced lesions in human, following therapy for cervical lesions, methods for diagnosis of, 25:35158
radiosensitivity of mouse, effects of hypoxia on electron, 25:35161
INVARIANCE PRINCIPLES
CP nonconserving asymmetry in $K_2^0 \rightarrow \pi^+ + \pi^- + \pi^0$ decay, search for, (E), 25:36550 (COO-1749-24)
CP violation in dynamical structure of mass matrix of K^0--anti K^0 complex, (T), 25:36466
parity violation of nuclear potentials, effect of strong interactions on weak, 25:36458
scale invariance in high-energy physics, review on broken, 25:36542
time reversal invariance in mixed dipole--quadrupole energy-level transitions, possible test for, (T), 25:36540
time reversal violation in cross sections of e + d + e + d interactions, (T), 25:36546
IODINE
deposition in reactor containment buildings, heat transfer model for analysis of, 25:37036(R) (BMI-1904)
determination as iodate by pressurometric titrations using hydrazine sulfate, manometer for, 25:34513
effects of stable, on iodine-131 uptake by human thyroid, 25:35097
excitation in photolysis of trifluoroiodoethane, 25:34613 (TID-25689)
ionization yields of molecular and atomic, on metal surfaces at 1300 to 2000°K, 25:35839
removal by carbon filters, effects of service life on, (E), 25:37106(R) (DP-1259)
removal from pressurized water reactor containment systems, effectiveness of sprays for, (E/T), 25:37025 (ORNL-TM-2412(Pt.12))
separation as iodide, from radioiodinated proteins, microscale, 25:34700
separation from milk using ion exchangers produced in Poland, 25:34703
IODINE IONS
reactions with gold, molybdenum, and yttrium at 15 to 60 MeV, L and M x-ray spectra from, (E), 25:35834
IODINE ISOTOPES
exchange between isopropyl iodide and iodine, 25:34573(R) (RLO-2230-T-2-2)
IODINE ISOTOPES I-121
energy levels from xenon-121 decay, lifetimes of, (E), 25:36752
IODINE ISOTOPES I-123
energy levels from xenon-123 decay, lifetimes of, (E), 25:36752
IODINE ISOTOPES I-125
use for measurement of bone density in fingers, 25:35171
IODINE ISOTOPES I-129
chemical state of, from beta decay of tellurium-129 in tellurium oxides and tellurates, 25:34674
IODINE ISOTOPES I-131
availability in peccaries following single injection of nuclear debris from Project Buggy fallout, 25:35088
content in thyroid of cattle and sheep in Portugal following Chinese nuclear tests, 25:35133
distribution in tissues of swine following field exposure to nuclear debris at Schooner Event site, fallout, 25:35090
effectiveness for scanning of human thyroid in comparison to technetium-99m, 25:35169
effectiveness of albumin macroaggregate-incorporated, for lung scintigraphy, 25:35180
effects on human blood and plasma proteins following endolymphatic or oral administration, 25:35189
excretion in urine of peccaries following single ingestion of nuclear debris from Schooner Event, fallout, 25:35089
release to atmosphere in reprocessing aluminum-clad fuel elements, 25:34693 (ORNL-4574)
separation from Purex Plant gaseous wastes, design of silver reactors for, 25:34785
sorption by sediments from low terraces of Elbe, Donau, and Weser Rivers, 25:34737
uptake by human thyroid gland, effects of stable iodine content on, 25:35097
use for blood flow study in human brain scanning, 25:35174
use in combination with surgery for ablation of parathyroid and thyroid glands of mice, 25:35084
use of human serum albumin incorporated, for cisternographic diagnosis of human hydrocephalus,

XUM

25:35172
IODINE ISOTOPES I-132
production of, design and performance of generator for, 25:34802 (BNL-50249)
ION BEAMS
production of highly charged, survey of possible ion sources for, 25:35833(R) (ORO-3027-19)
slowing-down in magnetized materials, effects of transient magnetic fields on precession of nuclear spin of heavy-, (T), 25:36846
transport of, electrostatic systems for, 25:36608 (NP-18855)
ION EXCHANGE MATERIALS
efficiency of macroreticular, in TBP solvent cleanup in Purex Process, 25:34679 (ARH-SA-58-RD)
ION EXCHANGERS
sorptive properties of Polish, for radioactive iodine from milk, 25:34703
ION SOURCES
design for fast hydrogen atoms, 25:35837
design of duoplasmatron, for producing ions by sputtering of solids, 25:36292(P)
design of proton, for fast hydrogen atomic beams, 25:36186(T) (CTO-746)
design optimization of electron-impact, for mass spectrometers, 25:35060
operation of cold-cathode glow-discharge gun used for specimen thinning, 25:36639
IONOSPHERE
auroral-arc reappearance on Mar 8--9, 1970 during geomagnetic-storm recovery, midlatitude multiple 6300-A, (E), 25:35969
book: Noctilucent Clouds, 25:35988
currents in, effect of lower magnetospheric electric currents and polarization fields on, (T), 25:35980
D region, cosmic-ray energy releases into, galactic, (T), 25:36007
D region, solar x ray and particle radiation in late Sept. 1969 in, effect of geomagnetic disturbances on, (E/T), 25:36006
disturbances in polar, correlation with solar wind--magnetosphere interactions, new magnetic, (E/T), 25:36012
E region, phase-height measurements over Pullman, Washington, 25:35983
electric conductivity from quiet-day geomagnetic variations, time-dependent, (E/T), 25:35989
electron flux in polar cavity of, storm-time variations of O I 6300-A associated low-energy, (E), 25:35959
electron fluxes at 1 to 30 keV in auroral, rocket measurements of, 25:35963
electron-content variations of dusk-sector midlatitude, relation to geomagnetic storm time, (E/T), 25:35956
F2 layer, relation of diffusion processes in interaction between neutral waves and ionization, (E/T), 25:35979
geomagnetic-field variations in dusk-sector midlatitude, relation to geomagnetic storm time, (E/T), 25:35956
ionization redistribution in nighttime, effect of neutral atmospheric and neutral wind on, (E/T), 25:35986
irregularities in midlatitude, uniform backscatter signature categorization of, during one-half sunspot cycle, (E), 25:35955
plasma drift in, evaluation using partial and total reflections from lower ionosphere, (E/T), 25:35985
radio-wave absorption measurements in equatorial, pulse-reflection technique for longitude and solar activity-dependent, 25:35970
radio-wave phase-height fluctuations at 130 to 250 km in, (E/T), 25:35977
radio-wave propagation in quiet, effect of irregularities on long-distance hf, (E/T), 25:36003
radio-wave reflection from irregularities in, at vertical incidence, (E/T), 25:35978
solar flare in, using high-frequency Doppler technique, Sept. 1960 to Dec. 1962, (E), 25:35952 (NBS-TN-326)
spectra of, origin of twilight flash of sodium in, (E), 25:35971
sporadic E, structure at 90 to 110 km in, relation to nighttime wind structure, (E/T), 25:35986
spread F, formation mechanism of, relation to field-aligned irregularities in magnetosphere, (T), 25:35981
wave--particle interactions in, from electron beam interactions with ionosphere, (E), 25:35967
x-ray generation at 30 to 140 km in, bremsstrahlung, (E/T), 25:35999
IONS
abundance in thermosphere during magnetic storms, varitions of, (T), 25:35960
detection of slow positive, self-quenching open-end G--M detector for, 25:34898
effects of energetic, on void growth in solids, model for, 25:35511
energy levels of multiply charged heavy, determination of radiative lifetimes of, 25:35849
energy of ground states of 3- to 10-electron, second- and third-order Hartree--Fock, 25:35889
energy of heavy, in solar wind, (E), 25:35729
energy of two-electron, multiconfiguration frozen-core approximation for, 25:35890
implantation of, bibliography on, covering Jan. 1967 through Sept. 15, 1970, 25:36269 (SC-B-710148)
reactions with argon and nitrogen at 20 to 80 keV, charge-equilibrium fractions and charge-exchange cross sections for, (E), 25:35866
reactions with atoms and ions, oscillations of total cross sections for inelastic processes in, (T), 25:35876
spectral lines due to $3p^53d$ configuration in solar corona, (E/T), 25:35744
stopping in argon and nitrogen at 20 to 80 keV, as function of ion atomic number, 25:35866
stopping of heavy, effective-charge theory for, 25:36261
IRIDIUM
determination by neutron activation of losses of, in fire-assay method for platinum group metal, 25:34844 (NIM-1048)
IRIDIUM BROMIDES
separation of ions of, from metal ions by high-voltage electrophoresis using carboxylic and hydroxycarboxylic acids, 25:34702
IRIDIUM CHLORIDES
separation of ions of, from metal ions by high-voltage electrophoresis using carboxylic and hydroxycarboxylic acids, 25:34702
IRIDIUM FLUORIDES
vapor pressure--temperature data for, 25:34602 (CAT-645)
IRIDIUM ISOTOPES Ir-184
beta decay of excited states of, log-ft values and strength functions for, (T), 25:36817 (JINR-P4-5744)
IRIDIUM ISOTOPES Ir-187
electron-capture decay of, gamma and conversion-electron spectra and ce--ce delays from, (E), 25:36805
IRON
abundance in 15 Vul, (E/T), 25:35653
abundance in F and G dwarfs in Pleiades and Hyades clusters, (E), 25:35627
corrosion of Armco, by sodium at 500 to 600°C, factors affecting, 25:35286
creep of a-, at 868 to 1073°K, effects of stress on, 25:35464
determination in complex carbides by electron beam micro methods, 25:34523
determination of trace amounts of, in uranium by neutron activation, 25:34547 (UARAEE-68)
effects of binder of, on sintering of tungsten carbide powders, 25:35534
effects of combination of oxygen and, on internal friction of zirconium alloy, 25:35404
effects on colorimetric determination of gold, 25:34521
effects on gravimetric determination of mercury using 2-aminobenzothiazole, 25:34520
effects on photometric determination of antimony following solvent extraction using TBP, 25:34512
effects on polarographic reduction of nictium, 25:34526
effects on precipitation of metastable phases in nickel--niobium alloys, 25:35480
effects on radiation stability of sulfone polyelectrolytes, 25:34650
electric conductivity of 4.2°K-deformed, recovery of, 25:36315
finishes for contact faces of pipe flanges and connecting-end flanges of valves and fittings of ductile, standard for, 25:35418
gamma dose rate in, one group method for absorbed, (T), 25:36265
luminous efficiency of, in simulated micrometeors, (E), 25:35596
mechanical properties of whiskers of, effects of hydrogen on, 25:35337(R) (NYC-3975-3)
neutron capture by, gamma spectra from thermal, (E), 25:36692 (UARAEE-103)
nuclear spin--lattice relaxation times from cobalt-60 NMR at 0.004 to 0.010°K, (E/T), 25:36347
oxidation of hydrogen-annealed, thermodynamics of, 25:35291
permeation of hydrogen in biaxially stressed membranes of, 25:35337(R) (NYC-3975-3)
plastic flow in, mechanism of thermally-activated, 25:35380
proton reactions at 600 MeV and 24 GeV, aluminum-26 production cross sections for, (E), 25:36689 (NP-18820)
radiation damage in high-purity alpha-, magnetic after-effect study of fast-neutron, 25:36294
radiation effects on mechanical properties of, at 80 to 100°C, fast neutron, 25:35505 (ZJE-99)
radioinduced defect clusters in foils of, growth of electron, 25:36301
radioinduced Frenkel Pairs in alpha, computer study of relations of carbon with neutron, 25:35504(R) (ORO-3912-4)
separation from other transition metals by ion exchange on anionite AV-17, 25:34695(T) (ORNL-tr-2297)
separation from uranium by fractional dissolution, 25:34699
separation of ions of, from metal ions by high-voltage electrophoresis using carboxylic and hydroxycarboxylic acids, 25:34702
sodium boiling superheat at surfaces of, effects of roughness on, 25:34791 (KFK-1332)
standard for spot facing of pipe flanges of, 25:35365
thermodynamic properties of solution of, in liquid tin, 25:35368

IRON ALLOYS AND SYSTEMS
Al--Cr--Fe--Ni-base--Ti, tensile properties at 25 to 850°C, effects of grain size, precipitates, and test time on, 25:35340 (UARAEE-55)
Al--Cu--Fe--Ti-base--V, fracture toughness of α--β, relations with microstructure, 25:35348
B--Fe, radiation effects on internal friction of, neutron, 25:35588
C--Co--Cr--Fe--Mo--Nb--Ni-base, strengthening by precipitation of body-centered tetragonal phase in, 25:35302
C--Co-base--Cr--Fe--Ni--Ta--Ti--W, fracture toughness of Mar-M-509, effects of carbide inclusions on, 25:35490
C--Cr--Fe--Mo--Nb--Ni-base, strengthening by precipitation of body-centered tetragonal phase in, 25:35302
C--Cr--Fe--V, analysis of complex carbides in, by electron beam micro methods, 25:34523
C--Fe-base, radiation effects on mechanical properties of, at 80 to 100°C, relations of composition and fast neutron, 25:35505 (ZJE-99)
C--Fe-base--Mn, radiation effects on mechanical properties of, at 80 to 100°C, relations of composition with fast neutron, 25:35505 (ZJE-99)
Co--Fe-base, creep at 1073°K, effects of stress on, 25:35464
Co-base--Fe, slip in, mechanisms of cross, 25:35386
Cr--Fe--Ni, corrosion of Unitemp 605, by lithium--selenium mixtures at 375°C, 25:35275(R) (ANL-7777)
Cr--Fe--Ni, standard for cold-drawn and hot-finished seamless pipe and tube for general corrosive service and heat-resisting uses, 25:35413
Cr--Fe--Ni, standard for hot-finished and cold-drawn rounds, squares, hexagons, and rectangles of, 25:35364
Cr--Fe--Ni, standard for plates, sheets, and strips of, 25:35360
Cr--Fe--Ni-base, tensile properties at 25 to 850°C, effects of grain size, precipitates, and test time on, 25:35340 (UARAEE-55)
Fe--Mo--Sn--Ti-base--Zr, crystal structure and properties of thermomechanically-processed beta-phase, 25:35398
Fe--Nb--Ni--Sn--Zr-base, properties of dilute, for use in organic cooling circuits, 25:35329(P)
Fe--Ni, radioinduced ordering in, magnetic anisotropy study of neutron, (E), 25:36281
Fe--Re, superconducting transition temperature of intermetallic compounds of, 25:36038
Fe--V_4C_3, crystal lattice coherency in, effects of particle size on, 25:35573
Fe-base--Mn, radiation effects on mechanical properties of, at 80 to 100°C, relations with fast neutron, 25:35505 (ZJE-99)
Fe-base--Mo, creep at 973 to 1153°K, effects of stress on, 25:35464
Fe-base--Mo, solution softening in dilute, at 77 to 430°K, mechanisms of, 25:35374
Fe-base--Nb--Ni, precipitation in, effects of aging at 700 to 800°C on, 25:35499
IRON FLUORIDES
iron-57 Moessbauer studies in, 25:37200(R) (NYO-2807-51)
IRON IONS
spectral line profiles due to, in solar corona, (E), 25:35775
IRON ISOTOPES Fe-54
deuteron reactions (d,α) at 28 MeV, DWBA analysis of differential cross sections, l transfer, and spectra from, (E), 25:36587 (LYCEN-7087)
proton inelastic scattering at 19.6 MeV, DWBA analysis of spin dependence in, (E/T), 25:36708
IRON ISOTOPES Fe-55
production in (n,α) and (n,p) reactions with fast neutrons, cross sections for, (E), 25:36686 (CONF-680986-1)
IRON ISOTOPES Fe-56
electron inelastic scattering at 198 to 300 MeV, differential cross sections for, (E), 25:36695
neutron inelastic scattering by excited states of, kernel for describing, (T), 25:36707
IRON ISOTOPES Fe-57
energy levels from (n,γ) reactions, phonon-particle doorway states in, (T), 25:36703
energy levels from iron-56 neutron capture, analysis of anticorrelation between reduced widths and E1 transition probabilities for, (T), 25:36834
IRON ISOTOPES Fe-59
uptake by bones of whole-body x-irradiated rats, correlation between intramedullary x-ray dose and, 25:35211
IRON OXIDES
FeO--GdO, magnetic susceptibility of amorphous antiferromagnetic, temperature dependence of, (E/T), 25:36337
FeO--YO, magnetic susceptibility of amorphous antiferromagnetic, temperature dependence of, (E/T), 25:36337
IRRADIATION FACILITIES
design of, US patents 1950 throug 1968, 25:34777 (ORNL-IIC-34)
fabrication of, brazing and welding methods for, 25:35326
ISOTOPE EFFECTS
research progress on, 25:34572(R) (ORO-3234-23)
values for, in diffusion of interstitial atoms, 25:34571(T) (ANL-Trans-882)
ISOTOPE EXCHANGE
partition function ratios in, effects of chemical bond characteristics on, 25:34585
ISOTOPE GENERATORS
design and performance of, for production of short half-life radioisotopes, 25:34802 (ENL-50249)
ISOTOPE SEPARATION METHODS
development of electromagnetic, for rare earth isotopes, 25:34805 (JINR-P6-5761)
research progress on, 25:34807(R) (MLM-1793)
theoretical stages in, method for calculation of, 25:34767

J

JAMES A. FITZPATRICK POWER REACTOR
effluents from, effects on environment of chemical, radioactive, and thermal, 25:36949 (DOCKET-50333-22)
site for, hydrological and meteorological data for, 25:36949 (DOCKET-50333-22)
JAPAN
nuclear power plants in, concepts for marine industrial complex, 25:36981(T) (ORNL-tr-2474)
radioisotopes production in, during 1969, 25:34804(R) (JAERI-Memo-4285)
tritium content in hot springs in Beppu City, 25:34732
JAPANESE MATERIALS TESTING REACTOR
fuel accountability for, computer program for, 25:37068 (JAERI-Memo-4270)
fuel followers for, fabrication and performance of boron--stainless steel, 25:35320
power of, noise analysis for measurement of absolute, 25:37114 (JAERI-Memo-4276)
JAPANESE POWER DEMONSTRATION REACTOR
pressure vessel for, inspection procedures and results for, 25:37004 (JAERI-Memo-4330)
JAPANESE POWER DEMONSTRATION REACTOR II
cooling system for, testing program for, 25:37042 (JAERI-Memo-4174)
safety aspects of, 25:37043 (JAERI-Memo-4174)
safety aspects of, review of, 25:37044 (JAERI-Memo-4260)
safety aspects of, review of, 25:37042 (JAERI-Memo-4173)
testing program for, description of pre-operational, 25:37042 (JAERI-Memo-4173)
testing program for, description of pre-operational, 25:37044 (JAERI-Memo-4260)
testing program for, description of pre-operational, 25:37043 (JAERI-Memo-4174)
JERVIS BAY POWER REACTOR, UNIT 1
radioactive effluents from, environmental effects of, 25:37045 (NP-18842)
JOSEPH M. FARLEY POWER REACTOR, UNIT 1
design parameters of, revised and additional data on, 25:36951 (DOCKET-50348-20)
operations aspects of, revised and additional data on, 25:36951 (DOCKET-50348-20)
JOSEPH M. FARLEY POWER REACTOR, UNIT 2
design parameters of, revised and additional data on, 25:36951 (DOCKET-50348-20)
operations aspects of, revised and additional data on, 25:36951 (DOCKET-50348-20)
JUPITER (PLANET)
mass of, from motion of Pales (49), (E), 25:35823

K

KIDNEYS
radiation effects on tritium incorporation in mouse, effects of time on whole-body x, 25:35238
radioisotope accumulation in, of swine following field exposure to nuclear debris from Schooner Event, fallout γ-emitting, 25:35090
scanning of human, for function and structure, radioisotopes for, 25:35184
scanning of human, using iodine-131, mathematical model for quantitative interpretation of data from, 25:35166
KRYPTON
ionization by protons at 4 MeV, pressure dependence of, 25:35888
reactions of atoms and ions of, with alkali metal halides at 0.2 to 6 keV, electron emission induced by, 25:35840
reactions with methane under simulated radiolysis conditions, mass spectrometric studies on, 25:34648
separation from reactor containment system atmospheres by selective permeation, efficiency of cellulose acetate membranes for, 25:34692(R) (NYO-4057-2)
KRYPTON IONS
implantation damage in rubidium chloride at 15 keV, depth distribution of, 25:36272
implantation in silicon at 10 to 200 keV, lattice disorder induced in, 25:36300
reactions of atoms and ions of, with alkali metal halides at 0.2 to 6 keV, electron emission induced by, 25:35840
KRYPTON ISOTOPES
separation by thermal diffusion, 25:34807(R) (MLM-1793)

XUM

separation of short-lived, electromagnetic method for, 25:34806 (JINR-P13-5757)
KRYPTON ISOTOPES Kr-81
content of metastable, relative to intravenously injected rubidium-81 in tissues, tissue perfusion blood flow studies using, 25:35167
KRYPTON ISOTOPES Kr-85
release to atmosphere in reprocessing aluminum-clad fuel elements, 25:34693 (ORNL-4574)
KRYPTON ISOTOPES Kr-86
concentration by thermal diffusion, 25:34807(R) (MLM-1793)
KRYPTON ISOTOPES Kr-87
energy levels and nuclear properties of, Nuclear Data Sheets for, (E), 25:36706

L

LA CROSSE BOILING-WATER REACTOR
instrumentation for, corrections for power testing of automatic gain control system, 25:36897 (DOCKET-1155-118)
instrumentation for, design and performance of automatic gain control system for, 25:36895 (DOCKET-1155-116)
instrumentation for, performance during main steam bypass valve malfunction of water level, 25:36896 (DOCKET-1155-117)
operation history for March 1971, 25:36866 (DOCKET-1155-120)
operations incident of May 11, 1971, unplanned shutdown actuated by power tool on 110 volt a-c outlet, 25:36865 (DOCKET-1155-115)
operations incident of May 15, 1970, low water level in core caused by main steam bypass valve malfunction, 25:36896 (DOCKET-1155-117)
personnel for, revised technical specifications for respiratory protection equipment for, 25:36898 (DOCKET-1155-119)
LABORATORIES
design for conventional and irradiation testing of nuclear materials, 25:34828
LABORATORY EQUIPMENT
description of, for production of homogeneous magnetic fields by superconducting magnetic systems, 25:36079
design and operation of, for studying two-phase heat transfer in BWR fuel channels, 25:34793 (UARAEE-81)
design and performance of pressure cell, for measuring thermodynamic properties of liquid metals, 25:35342 (UCRL-51035)
LAKES
limnology of Amchitka Island, Alaska, effects of Milrow Event on, 25:34767(R) (BMI-171-129)
LANTHANUM
determination in rare earth oxides, spectrographic, 25:34511
determination in rocks by neutron activation and γ spectroscopy, 25:34543 (NIM-1013)
effects on gravimetric determination of mercury using 2-aminobenzothiazole, 25:34520
electron band structure of double hcp, calculations using symmetrized APW functions, 25:36352
magnetic properties of superconducting, pressure effect on, (E/T), 25:36021
separation from other rare earths by ion exchange chromatography, 25:34714
LANTHANUM ALLOYS AND SYSTEMS
Bi--La, thermal capacity of intermetallic LaBi at 7 to 300°K, 25:35355
Ce--La, magnetic properties of superconducting, pressure effect on, (E/T), 25:36021
La--Sb, thermal capacity of intermetallic LaSb at 7 to 300°K, 25:35355
LANTHANUM BORIDES
ionization probability of, in simulated micrometeors, (E), 25:35597
LANTHANUM ISOTOPES La-139
neutron capture by, γ circular polarization from thermal, (E), 25:36751
oxygen-16 reactions (O-16,3n), (O-16,5n) and (O-16,7n) at 141 MeV, gamma spectra from, (E), 25:36726 (JINR-P6-5681)
LANTHANUM ISOTOPES La-140
availability in peccaries following single injection of nuclear debris from Project Buggy fallout, 25:35028
energy levels from lanthanum-139 thermal neutron capture, spin-parity assignments for, (E), 25:36751
LANTHANUM ISOTOPES La-142
beta decay of, branching ratios and gamma spectra from, (E), 25:36765
LANTHANUM OXIDES
growth of single-crystal solid solutions with another rare earth oxide by Verneuil method, formation regions in, 25:35525
reactions with titanium and zirconium oxides at high temperatures, electric conductivity detection of solid-phase, 25:36320
LARYNX
radiotherapy of carcinoma of human, effectiveness of γ, 25:35188
LASER RADIATION
conference on laser interaction and related plasma phenomena, East Windsor, Connecticut, 6/69, 25:36147
reactions with free solid targets, plasma production in, (E), 25:36152
reactions with lithium plates, plasma motion and collisions in, (E), 25:36158
reactions with solid deuterium, neutron spectra from, 25:36203
reactions with solid deuterium, plasma production from, (E/T), 25:36156
reactions with solid targets, ion emission from, 25:36149
reactions with solid targets, plasma production and heating in, 25:36150
reactions with solid targets, shock-wave kinetics from, (T), 25:36153
reactions with solid targets, techniques for plasma production, 25:36151
scattering on hydrogen arc plasmas, anomalous, (E), 25:36123
use for fusion plasma production, efficiency of, 25:36155
LASERS
development of, historical, 25:36148
optical properties of neodymium-activated glass, radiation effects on, 25:35082
use as integral part of thermonuclear power plants, 25:36211
LAVA
lead content of Canary Islands, measurement of, 25:34740
lead isotope content of Canary Islands, (E), 25:34740
uranium content of Canary Islands, measurement of, 25:34740
LEAD
content in Atlantic Ocean surface samples and at various depths in Pacific Ocean, 25:34762
content in Canary Islands lavas, measurement of, 25:34740
cosmic hadron reactions above 3(10)^{12} eV, distributions and mean values of inelasticity coefficient for production of π^0 in, (E), 25:36389 (ITJ-5)
cosmic nucleon reactions above 3(10)^{12} eV, ionization spectrometer study of energy and mean inelasticity for, (E), 25:36388 (ITJ-3)
defects in, design and performance of fast neutron defectoscopy equipment for detecting, 25:34825
determination in paint layers, equipment for x-ray fluorescence, 25:35043
effects on colorimetric determination of gold, 25:34521
effects on gravimetric determination of mercury using 2-aminobenzothiazole, 25:34520
effects on nuclear spin--lattice relaxation in indium, 25:36349
effects on photometric determination of antimony following solvent extraction using TBP, 25:34512
electron reactions at 100 to 400 MeV, angular distributions and ranges from, (E), 25:36788
electron reactions at 550 and 1300 MeV, fission-fragment cross sections and energies from, (E), 25:36791
electron scattering by phonons in crystals of, 25:36280
fission of, lower limit on half-life for spontaneous, (E), 25:36779
gamma scattering by K-shell electrons at 662 keV in, energy spectrum and differential cross sections for incoherent, (T), 25:36253
magnetic flux flow as function of film thickness, 25:36058
neutron scattering by, lattice vibrational spectra and physical characteristics of, 25:36319
plasticity of crystalline, effects of superconducting transition on, 25:35383
proximity effect in gadolinium-backed superconducting films of, 25:36036
separation of ions of, from metal ions by high-voltage electrophoresis using carboxylic and hydroxycarboxylic acids, 25:34702
superconducting state in, effect on stress relaxation in temperature dependence, (E/T), 25:36072
thermodynamic properties of liquid, at high temperatures and pressures, equipment and method for measuring, 25:35342 (UCRL-51035)
LEAD ALLOYS AND SYSTEMS
In--Pb, plasticity of crystalline, effects of superconducting transition on, 25:35383
In--Pb-base, creep in superconducting, 25:36032
In--Pb-base, magnetic transition at H/sub c2/ in superconducting, (E), 25:36028
Pb--W, mechanical properties of tungsten wire-reinforced uniaxially aligned composites of, effects of matrix variations on, 25:35344 (Y-1788)
LEAD ISOTOPES Pb-203
distribution in tissues of swine following field exposure to nuclear debris at Schooner Event site, fallout, 25:35090
energy levels and nuclear properties of, Nuclear Data Sheets for, (E), 25:36809
LEAD ISOTOPES Pb-204
content ratio to lead-206, -207, and -208 in Canary Islands lavas, (E), 25:34740
content ratio to uranium-238 in Canary Islands lavas, (E), 25:34740

LEAD ISOTOPES Pb-205
energy-level transitions from bismuth-205 electron-capture decay, N-shell internal conversion coefficients from, (E), 25:36780
LEAD ISOTOPES Pb-206
content ratio to lead-204, -207, and -208 in Canary Islands lavas, (E), 25:34740
energy level transitions in, two-nucleon random-phase-approximation calculations of decay rates and probabilities for, (T), 25:36806
energy levels of, two-nucleon random-phase-approximation calculation of wave functions and spin--parity assignments for, (T), 25:36806
nuclear mass of, relative to uranium-238, (E), 25:36770
LEAD ISOTOPES Pb-207
content ratio to lead-204 and -206 in Canary Islands lavas, (E), 25:34740
energy levels from bismuth-209 (p,He-3) and (d,α) reactions, single-neutron-hole, (E), 25:36777
energy levels of, two-nucleon random-phase-approximation calculation of spectroscopic factors for, (T), 25:36806
nuclear mass of, relative to uranium-235, (E), 25:36770
LEAD ISOTOPES Pb-208
content ratio to lead-204 and -206 in Canary Islands lavas, (E), 25:34740
energy level at 2.62 MeV, calculation of static quadrupole moment of 3-, (T), 25:36803
nuclear correlations in, two-nucleon random-phase-approximation calculation of, (T), 25:36806
proton reactions (p,np) at 30.5 MeV, angular distributions for, (E), 25:36738(R) (UCLA-10-P-18-23)
LEAD ISOTOPES Pb-209
energy levels of, two-nucleon random-phase-approximation calculation of spectroscopic factors for, (T), 25:36806
LEAD ISOTOPES Pb-210
content in Atlantic Ocean surface samples and at various depths in Pacific Ocean, 25:34762
energy levels of, two-nucleon random-phase-approximation calculation of wave functions and spin--parity assignments for, (T), 25:36806
LEAD OXIDES
MnO--Nb_2O_5--PbO--$PbTiO_3$--$PbZrO_3$--Sb_2O_3, properties of piezoelectric ceramic of, for use as filter and transducer elements of mechanical filters, 25:35561(P)
MnO--PbO--$PbTiO_3$--$PbZrO_3$--Sb_2O_3--Ta_2O_5, properties of piezoelectric ceramic of, for use as filter and transducer elements of mechanical filters, 25:35561(P)
MoO_3--PbO, phase diagram of, 25:35581
LEAD TITANATES
radioinduced defects in, thermodynamic properties of fast-neutron, 25:36297
MnO--Nb_2O_5--PbO--$PbTiO_3$--$PbZrO_3$--Sb_2O_3, properties of piezoelectric ceramic of, for use as filter and transducer elements of mechanical filters, 25:35561(P)
MnO--PbO--$PbTiO_3$--$PbZrO_3$--Sb_2O_3--Ta_2O_5, properties of piezoelectric ceramic of, for use as filter and transducer elements of mechanical filters, 25:35561(P)
LEAD ZIRCONATES
radioinduced defects in, thermodynamic properties of fast-neutron, 25:36297
MnO--Nb_2O_5--PbO--$PbTiO_3$--$PbZrO_3$--Sb_2O_3, properties of piezoelectric ceramic of, for use as filter and transducer elements of mechanical filters, 25:35561(P)
MnO--PbO--$PbTiO_3$--$PbZrO_3$--Sb_2O_3--Ta_2O_5, properties of piezoelectric ceramic of, for use as filter and transducer elements of mechanical filters, 25:35561(P)
LEPTONS
interactions with hadrons, research at Johns Hopkins Univ., April 1970 to March 1971 on hadron structure determination from, (T), 25:36472(R) (NYO-4076-14)
production of pairs at high energies at large angles, vector dominance hypothesis for decrease of differential cross sections for, (T), 25:36429
symmetry for, baryon--lepton correspondence in broken SU(3) x SU(3), (T), 25:36543
theory for heavy, in neutrino astronomy, (E), 25:36462
LEUCINE
radiation effects on incorporation of, in wheat seeds, carbon-14 tracer study of γ, 25:35102
LIGASES
effects of polynucleotide, on DNA recovery from x-radioinduced breaks, 25:35108
LIGHT
brightness and polarization of day sky during total solar eclipse, (E), 25:35764
brightness of sky and color change during total solar eclipse, (E), 25:35762
brightness of sky during total eclipse of Sun, (E), 25:35761
brightness of zenith sky and spectral distribution during total solar eclipse, (E), 25:35763
propagation of, effects of self-induced changes in index of refraction on, 25:37250 (UCRL-20541)
scattering by marginally stable plasma, (T), 25:36144
scattering in planetary atmospheres, nonconservative Rayleigh, (T), 25:35826
scattering on collisionless plasma, effect of strong magnetic fields on Thomson, (T), 25:36140
spectral changes in zenith sky, during total solar eclipse, (E), 25:35765
LIGHTNING
detection of direction to, apparatus for, 25:35058(P)
LIMERICK POWER REACTOR, UNIT 1
design parameters of, revised and additional data on, 25:36952 (DOCKET-50352-13)
operations aspects of, revised and additional data on, 25:36952 (DOCKET-50352-13)
LIMERICK POWER REACTOR, UNIT 2
design parameters of, revised and additional data on, 25:36952 (DOCKET-50352-13)
operations aspects of, revised and additional data on, 25:36952 (DOCKET-50352-13)
LINEAR ACCELERATORS
beam current loading and dispersion in iris-loaded electron, effects of space charge on, 25:36644
beam emittance of ANL 50- MeV proton, measuring method and results for, 25:36612 (UARAEE-76)
cavity resonator with two rows of drift tubes for simultaneous acceleration of two beams, 25:36622
LIPASE
radiation effects on castor seed, effects of dose and germination on γ, 25:35253
LIPIDS
radiation effects on cell, chemiluminescent studies on, 25:35201
radiation effects on membranes of, x, 25:34625
LIPOFUSCINS
radiation effects on accumulation of, in human survivors of atomic bombing of Hiroshima and Nagasaki, 25:35241
LIQUID FLOW
electrohydrodynamic stability of thin layer in, in uniform shearing motion induced by traveling electric-potential wave, (E/T), 25:35939
stability of thin film, down heated inclined wall, analysis of, 25:34800
LIQUID METAL FAST BREEDER REACTOR
costs for 1000 MW(e), analysis of 1970 to 2020 capital, 25:37030 (CRNL-TM-3243)
fuel elements for, effects of gas bubbles in coolant on integrity of cladding of, (T), 25:37037 (CONF-700608-36)
fuel elements for, performance of stainless steel clad plutonium oxide (PuO_2)--uranium oxide (UO_2) pin type, (E/T), 25:37019 (CRNL-TM-3386)
fuel pins for, effects of burnup on thermal performance of plutonium oxide (PuO_2)--uranium oxide (UO_2), 25:37017 (CONF-710414-1)
transfer functions of, analysis of space-dependent, (T), 25:36987 (ANL-7788)
LITHIUM
abundance in atmospheres of four K stars, (E), 25:35636
electric field gradient in hcp, calculations, 25:36251
magnetohydrodynamic flow in fusion reactor blankets, pressure losses in, (T), 25:35938 (UCRL-51010)
oscillator strengths for excitation and ionization of, tables of calculated generalized, 25:35844 (SC-RR-70-406)
plasma of, motion and collision of laser-produced, (E), 25:36158
properties of ingots of resolted, standard for, 25:35423
LITHIUM ALLOYS AND SYSTEMS
Ag-base--Li, slip in, mechanisms of creep, 25:35286
Bi--Li, solvent properties of liquid, for californium, 25:34705
Li--Se, corrosive effects on storage battery container materials, at 375°C, 25:35275(R) (ANL-7777)
Li--Se, phase studies of, 25:35275(R) (ANL-7777)
LITHIUM ALUMINATES
properties for use as fillers in paste-type storage battery cells, 25:35275(R) (ANL-7777)
LITHIUM BROMIDES
spin lattice relaxation in pure and doped single crystals of, high temperature and high pressure, 25:37199 (NYO-2564-74)
CsI--KI--LiBr--LiCl--LiI, properties of eutectics of, for use as paste electrolytes, 25:35275(R) (ANL-7777)
LiBr--LiSe--RbBr, phase studies, 25:35275(R) (ANL-7777)
LiBr--RbBr, properties of eutectics of, for use as paste electrolytes, 25:35275(R) (ANL-7777)
LITHIUM CHLORIDES
solvent properties of solter, for californium, 25:34705
CsI--KI--LiBr--LiCl--LiI, properties of eutectics of, for use as paste electrolytes, 25:35275(R) (ANL-7777)
LiCl--LiF--LiI, properties of eutectics of, for use as paste electrolytes, 25:35275(R) (ANL-7777)
LiCl--LiF--LiI--LiSe, phase studies of, 25:35275(R) (ANL-7777)
LITHIUM FLUORIDES
nuclear spin--lattice relaxation and dynamic polarization in gamma-irradiated, 25:36348
radioinduced color centers in single-crystal, absorption spectra and bleaching of low-temperature neutron, 25:36290
radioinduced thermoluminescence of TLD-100, supralinearity and sensitization in, 25:35076
rare-gas atom and ion reactions with, electron emission induced from single crystals by 0.2- to 6.0-keV, (E), 25:35840
BeF_2--LiF_4--PuF_3--ThF_4, plutonium oxide precipitation in molten, equilibrated with thorium oxide, 25:34566

XUM

BeF_2--LiF--PuF_3, plutonium oxide precipitation in molten, equilibrated with beryllium oxide, 25:34566
BeF_2--LiF--PuF_3--ZrF_4, plutonium oxide precipitation in molten, equilibrated with zirconium oxide, 25:34566
LiCl--LiF--LiI, properties of eutectics of, for use as paste electrolytes, 25:35275(R) (ANL-7777)
LiCl--LiF--LiI--LiSe, phase studies of, 25:35275(R) (ANL-7777)
LITHIUM IODIDES
CsI--KI--LiBr--LiCl--LiI, properties of eutectics of, for use as paste electrolytes, 25:35275(R) (ANL-7777)
LiCl--LiF--LiI, properties of eutectics of, for use as paste electrolytes, 25:35275(R) (ANL-7777)
LiCl--LiF--LiI--LiSe, phase studies of, 25:35275(R) (ANL-7777)
LITHIUM IONS
reactions with carbon films at 2 to 10 keV, energy distributions from, 25:35833(R) (ORO-3027-19)
LITHIUM ISOTOPES Li-6
binding energy of, (T), 25:36847
meson (π) reactions with, x-ray yields and level broadening from, (E), 25:35854
meson reactions (π^-,nn) with, calculation of helium-4 recoil from, (T), 25:36847
LITHIUM SELENIDES
LiBr--LiSe--RbBr, phase studies, 25:35275(R) (ANL-7777)
LiCl--LiF--LiI--LiSe, phase studies of, 25:35275(R) (ANL-7777)
LIVER
radiation effects on ascorbic acid content in animal, x, 25:35219
radiation effects on corticosteroid retention in dog, effects of dose on γ, 25:35222
radiation effects on oxygen uptake by rat, x, 25:35223
radiation effects on regeneration of rat, mechanism of cerium-144, 25:35221
radiation effects on tritium incorporation in mouse, effects of time on whole-body x, 25:35228
radioisotope accumulation in, of swine following field exposure to nuclear debris from Schooner Event, fallout γ-emitting, 25:35090
LOOPS
corrosion product deposition and transfer in sodium, development of tracer techniques for measuring, 25:35276(R) (GEAP-13539-16)
design for organic heat transfer fluid stability testing, 25:34810(R) (ORNL-TM-3394)
LUNAR MATERIALS
lead isotope ages for, (E), 25:35831
magnetic remanence in, produced by cosmic-ray exposure, (E), 25:35598
potassium abundance in, and terrestrial samples, (E), 25:35830
radon emanation rates for, (E), 25:35831
thermoluminescence of Apollo 11 sample 10084, (E), 25:35824
uranium abundance in, and terrestrial samples, (E), 25:35830
LUNGS
radiation effects on function of human, following therapy for bronchial carcinomas in comparison with surgery, 25:35243
radioisotope accumulation in, of swine following field exposure to nuclear debris from Schooner Event, fallout γ-emitting, 25:35090
regional function of, in patients with hepatic cirrhosis and pulmonary edema, use of xenon-133 for determining, 25:35170
retention of soluble actinide salts in human, following inhalation, effects of DTPA on, 25:35091
scintigraphy of human, effectiveness of iodine-131- or technetium-99-labeled albumin macroaggregates for, 25:35180
LUTETIUM
determination in rocks by neutron activation and γ spectroscopy, 25:34543 (NIM-1013)
separation from aqueous chloride solutions by solvent extraction using bis(1-isobutyl-3-methylbutyl) phosphate, 25:34706
LUTETIUM ALLOYS AND SYSTEMS
Co--Lu, magnetic properties of intermetallic compounds of, (E/T), 25:36318
LUTETIUM ISOTOPES Lu-175
boron-11 fission up to 10.4 MeV/nucleon, excitation function for, (E), 25:36784
carbon-12 fission up to 10.4 MeV/nucleon, excitation function for, (E), 25:36784
LUTETIUM ISOTOPES Lu-180
decay scheme and half-life for, (E), 25:36796
LYMPHOCYTES
radiation effects on amino acid incorporation into proteins of rabbit, carbon-14 tracer study of γ, 25:35104
radiation effects on structure of nucleoproteins in, 25:35206

M

MC GUIRE POWER REACTOR, UNIT 1
design parameters of, revised and additional data on, 25:36961 (DOCKET-50369-10)
operations aspects of, revised and additional data on, 25:36961 (DOCKET-50369-10)
MC GUIRE POWER REACTOR, UNIT 2
design parameters of, revised and additional data on, 25:36961 (DOCKET-50369-10)
operations aspects of, revised and additional data on, 25:36961 (DOCKET-50369-10)
MACHINE TOOLS
design and operation of, for mechanical decladding of reactor fuel elements, 25:34780 (UPRAEE-54)
MAGNESIUM
corrosion by lithium--selenium mixtures at 375°C, 25:35275(R) (ANL-7777)
determination in combination with calcium in glacial waters by ion-sensitive electrode method, 25:34721(R) (NYO-3912-3)
determination in combination with calcium in glacial waters by ion-sensitive electrode method, 25:34722(R) (NYO-3912-4)
determination in human stones by neutron activation, 25:34546 (THAI.-AEC-39)
determination of trace amounts of, in biological materials by thermal neutron activation, ion exchange chromatography, and γ spectrometry, 25:34552
effects on gravimetric determination of mercury using 2-aminobenzothiazole, 25:34520
lattice dynamics model of, phonon dispersion curves and frequency spectra from, 25:36333
meson (π) reactions with, x-ray yields and level broadening from, (E), 25:35854
MAGNESIUM ALLOYS AND SYSTEMS
Al--Mg, welding to stainless steel, methods for, 25:35326
Al-base--B--Cu--Mg, corrosion of diffusion bonded composites of, by sodium chloride solution, effects of applied stress on, 25:35521
Al-base--Mg, radiation damage in, electric conductivity study of production rate of low-temperature neutron, 25:36286
B--Mg, fabrication and tensile properties of filament-reinforced composites of, 25:35528
Gd--Mg-base, magnetic resonance of single crystals of, anisotropy in, 25:36342
In--Mg-base, plastic deformation of solid solution monocrystals of, solute effects in, 25:35287
Mg--Th, stacking faults in, effects of trace additions of zinc on formation of, 25:35484
Mg--Zn--Zr, mechanical properties of, effects of high-temperature thermomechanical treatment on, 25:35456
Mg--Zn--Zr, microstructure of, effects of high-temperature thermomechanical treatment on, 25:35456
Mg-base--Y, hardening and twinning in, mechanisms of, 25:35487
MAGNESIUM FLUORIDES
radioinduced color centers in single-crystal, absorption spectra and bleaching of low-temperature neutron, 25:36290
MAGNESIUM ISOTOPES
separation by ion exchange, 25:34709
MAGNESIUM ISOTOPES Mg-24
neutron reactions (n,p) at 14.8 MeV, cross sections for, (E), 25:36688(R) (N-70-43042)
MAGNESIUM ISOTOPES Mg-26
deuteron reactions (d,α) at 2.5 to 3.0 MeV, angular distributions, excitation functions, and spectra from, (E), 25:36701
deuteron reactions (d,nγ) and (d,pγ) with, gamma spectra from, (E), 25:36717
MAGNESIUM ISOTOPES Mg-27
beta decay of, beta branching ratios and gamma spectra from, (E), 25:36717
energy levels from magnesium-26 (d,pγ) reactions, 25:36717
energy-level transitions from magnesium-26 (d,pγ) reactions, branching ratios for, (E), 25:36717
MAGNESIUM MOLYBDATES
$MgMoO_4$--MoO_3, phase studies of, 25:35578
MAGNESIUM NITRATES
effects on potentiometric determination of free nitric acid, 25:34517
MAGNESIUM OXIDES
MgO--TiO_2--V_2O_5, phase studies of, 25:35576
MAGNET COILS
design and fabrication of superconducting, 25:36076
development of superconducting, 25:36073 (CEA-CONF-1734)
magnetic field homogeneity of superconducting, calculation of, 25:36077
transition processes of superconducting, changing to normal conductivity, 25:36078
MAGNETIC ANALYZERS
properties of, effects of magnetic field measurement errors on charged-particle beam, 25:36627
MAGNETIC FIELDS
atomic ground states in greater than 10^{12}G, (T), 25:35644
characteristics of interplanetary, in solar equatorial plane, (E), 25:35759
disturbances in polar, correlation with solar wind--magnetosphere interactions, (E/T), 25:36012
dynamo action in infinite media with isotropic

XUM

turbulence, (T), 25:35787
effects of interplanetary, on diurnal variations of geomagnetic field, (E/T), 25:35990
effects of transient, on heavy ions during slowing-down in magnetized materials, (T), 25:36846
effects on gages and transducers in pressure measurement in bubble chambers, 25:34987 (CONF-700623-(Vol.2), pp 863-72)
kinematic-dynamo theory of, (T), 25:35786
measurement of field index in 5-MeV betatrons, a-c potentiometer method for, 25:36625
molecule formation in ultrastrong, (T), 25:35645
origin of, in neutron stars and white dwarfs, (T), 25:35621
photon splitting in 4.41 x 10^{13} G, (T), 25:35677
production by superconducting magnetic systems, description of laboratory for, 25:36079
production of strong, state of art using Type-II superconductors for, 25:36073 (CEA-CONF-1734)
solar-particle interactions with interplanetary, (T), 25:35771
strength of stellar, relation to A/sub p/ rotational velocities, linear, (E/T), 25:35664
structure of coronal, using flare-associated hydromagnetic-disturbance formulation, (T), 25:35777
structure of force-free, effects of nonuniform conductivity on, (T), 25:35755
structure of interstellar, in vicinity of α-Per cluster, (E), 25:35795
variations of interplanetary, comparison measurements of, (E), 25:35734
variations of, in rotating plasma clouds, (T), 25:35815

MAGNETIC MIRROR MACHINES
data acquisition system for INTEREM, computer programs for, 25:36193 (ORNL-TM-3401)
data processing system for 2X II, 25:36195 (UCRL-73030)
design of 2X II, engineering, 25:36199 (UCRL-73060)
design of MFX, for fusion plasma studies, 25:36194 (UCRL-51042)
design of stellarator--mirror machine target plasma reactor, 25:36190 (MATT-841)
development engineering of baseball magnet system, 25:36200 (UCRL-73067)
efficiency of, effect of electron heating on, 25:36088
plasma equilibrium and stability in minimum-B, calculation of, 25:36165 (UCRL-51030)
plasma flute instabilities in Phoenix II, suppression by feedback, 25:36163(T) (CTC-737)
plasma instabilities in inhomogeneous, loss-cone modes of (T), 25:36166 (UCRL-73135)
switch design for 2X II, 10-MJ ignition crowbar, 25:36196 (UCRL-73031)
wave propagation in unstable plasma in, near upper hybrid frequency, (E), 25:36243

MAGNETIC MIRRORS
charged-particle acceleration in, three variants of Fermi model for, 25:36636

MAGNETIC MONOPOLES
production in superstrong final-state interactions from p + p interactions, 25:36530
search for, proposed experiment for, (E), 25:36379(T) (CERN-Trans-71-10)

MAGNETIC STORMS
effect on ion and neutral particle composition in thermosphere, (T), 25:35960
energy of auroral, relation to peak power in associated auroral geomagnetic bays, (E), 25:36004
hydrogen emissions during auroral substorms, morphology of, (E/T), 25:36005
relation of magnetospheric, to solar activity, (E), 25:35954
relation to dusk-sector midlatitude ionospheric electron content and geomagnetic-field variations, (E/T), 25:35956
relation to solar proton events, (E), 25:35758
sudden commencement amplitude of, dependence of initial phase duration on, (E), 25:35975
sudden commencements of, (E), 25:35759

MAGNETIC TESTING
equipment and methods for, historical development and current status of, 25:34835

MAGNETOHYDRODYNAMIC GENERATORS
book: Liquid-Metal MHD Induction Machines (in Russian), 25:35929
current distribution and internal resistance in segmented channels in, effects of boundary layers on, 25:35926
economics of liquid-metal, with steam in binary power plants, 25:35934
efficiency of char-burning systems for, 25:35927
electrical effects in insulating-wall boundary layer in Faraday-type, 25:35935
gas heating in, efficiency of, (E/T), 25:35928
performance of combustion-driven, electrode size effects on, 25:35933
performance of large-scale nonequilibrium, with rare gases, 25:35932

MAGNETOHYDRODYNAMICS
neutron-star properties, (T), 25:35601

MAGNETOSPHERE
charged-particle beam interactions with, vlf wave amplification in, (E), 25:35972
currents in, effects on diurnal variations of geomagnetic field, (E/T), 25:35990
electric currents and polarization fields at base of, effect on ionospheric currents, (T), 25:35580
electromagnetic-wave self-modulation in magnetoplasma, kinetic theory of amplitude-modulated, (T), 25:35982
flow model of neutral sheet, adiabatic, (T), 25:35984
geomagnetic activity in, effect of sunspots on, (E), 25:35954
irregularities in, formation and decay mechanisms of field-aligned, (T), 25:35981
particle trapping in radiation belts, proto method for origin and distribution of, (E/T), 25:35966
proton diffusion from ring current to auroral zone, (T), 25:35995
solar-wind interaction with, (T), 25:35993
solar-wind interactions with, correlation with new polar magnetic disturbances, (E/T), 25:36012
structure of, interrelation of charged-particle precipitation into auroral zones to, (E/T), 25:35958
synchrotron radiation from, effect of radiating electron energy spectra on, (T), 25:35976
variation in plasmasphere, annual and sunspot cyclic, (E/T), 25:35968

MAGNETOTAIL
field gradients in, model for, (E/T), 25:35991
field lines in, reconnection process for, (T), 25:35992
flux content and form of, (E/T), 25:35991
geomagnetic-field lines in, configuration of, (E/T), 25:35958
models for Uranus, with dipole axis parallel to solar wind, (T), 25:35828
structure of, model of transverse, (T), 25:35992

MAGNETS
cost and specifications for superconductors and conductors for high-field, 25:36607 (LNF-70/19)
design and development of superconducting, for BEBC, 25:35001 (CONF-700623-(Vol.2), pp 1126-49)
design of large superconducting, for bubble chambers, 25:34999 (CONF-700623-(Vol.2), pp 1040-94)
design of solid iron, for cosmic-ray spectrograph, 25:35012
effects of magnetization currents in multifilament superconducting, for high-field bubble chambers, 25:35000 (CONF-700623-(Vol.2), pp 1095-1125)
fabrication and properties of cobalt--misch metal--samarium permanent, 25:36336
magnetic fields of BEBC, methods for determining, 25:35002 (CONF-700623-(Vol.2), pp 1150-71)

MAINE YANKEE POWER REACTOR
design parameters of, revised and additional data on, 25:36946 (DOCKET-50309-36)
design parameters of, revised and additional data on, 25:36945 (DOCKET-50309-35)
operations aspects of, revised and additional data on, 25:36945 (DOCKET-50309-35)
operations aspects of, revised and additional data on, 25:36946 (DOCKET-50309-36)
test program for, pre-operational, 25:36945 (DOCKET-50309-35)

MALONIC ACID, BROMO-
radiolysis of, ESR studies on, 25:34634(R) (COO-1386-37)

MAN
calcium-47 retention in, following oral administration, effects of diseases on, 25:35098
cesium-137 body burden and metabolism in children of, Warsaw, 1965 to 1967 and 1969, 25:35092
cesium-137 content of, as function of age, whole-body counting of, 25:35095
inhalation of soluble actinide salts by, effects of DTPA on distribution and excretion of actinides following, 25:35091
iodine-131 uptake by thyroid gland in, effects of stable iodine content on, 25:35097
radiation dose rate to organs of, use of cobalt-60 organ burdens in rats following single ingestion to calculate equilibrium γ, 25:35116
radiation dose to female reproductive system during phosphorus-32 administration, 25:35144
radiation dose to, during fluoroscopy, review on methods for reducing, 25:35142
radiation effects on human blood and plasma proteins following endolymphatic or oral iodine-131 therapy, 25:35189
radiation effects on intestinal success of, origin and kinetics of goblet cells during post-operative, 25:35240
radiation effects on lipofuscin accumulation in, exposed to atomic bombing of Hiroshima and Nagasaki, 25:35241
radiation effects on pulmonary function in, following therapy for bronchial carcinomas in comparison with surgery, 25:35243
radiation hazards to, during diagnosis, selectivity measures for reducing, 25:35179
radiation hazards to, from radioactive waste disposal into atmosphere and surface waters near Casaccia, Italy, 25:34849 (RT/PROT-(70)36)
radiation protection of, evaluation of physicochemical methods for, 25:35166
radioinduced chromosome aberrations in lymphocytes in, protective effects of cysteine against fractionated γ, 25:35123

XUM

radioisotope contents in, evaluation of shielded whole-body counter for measuring, 25:35183
radioisotope removal from, comparison of methods for, 25:35134
radiotherapy of bladder carcinomas in, effectiveness of cobalt-60 in relation to survival time for, 25:35192
radiotherapy of breast cancer in, development of pendular method for postoperative fast electron, 25:35191
radiotherapy of carcinomas of larynx in, effectiveness of γ, 25:35188
radiotherapy of metastatic bone disease in, effectiveness of, 25:35187
radiotherapy of nasopharyngeal tumors in, development of conformation method for electron and x, 25:35194
radiotherapy of renal tumors in, effects of sex and tumor size on combined energy and cobalt-60, 25:35193
regional function of lungs of, with hepatic cirrhosis and pulmonary edema, use of xenon-133 for determining, 25:35170
scanning of thyroid of, comparison of iodine-131 and technetium-99m for, 25:35169

MANDELIC ACID
radiolysis of, ESR studies on, 25:34634(R) (COO-1385-37)
uranyl salt, magnetic susceptibility and ir spectra of, 25:34612

MANGANESE
abundance in K giant stars, (E/T), 25:35649
determination in soils by neutron activation, 25:34545 (THAI.-AEC-36)
determination of trace amounts of, in biological materials by thermal neutron activation, ion exchange chromatography, and γ spectrometry, 25:34552
determination of trace amounts of, in uranium by neutron activation, 25:34547 (UARAEE-68)
effects on colorimetric determination of gold, 25:34521
effects on gravimetric determination of mercury using 2-aminobenzothiazole, 25:34520
effects on photometric determination of antimony following solvent extraction using TBP, 25:34512
separation from other transition metals by ion exchange on anionite AV-17, 25:34695(T) (ORNL-tr-2397)
separation of ions of, from metal ions by high-voltage electrophoresis using carboxylic and hydroxycarboxylic acids, 25:34702

MANGANESE ALLOYS AND SYSTEMS
C--Fe-base--Mn, radiation effects on mechanical properties of, at 80 to 100°C, relations of composition with fast neutron, 25:35505 (ZJE-99)
C--Mn--Si--steel, properties of plates of, for use in pressure vessels at moderate and lower temperature service, standard for, 25:35468
Fe-base--Mn, radiation effects on mechanical properties of, at 80 to 100°C, relations with fast neutron, 25:35505 (ZJE-99)
Mn--Mo--Ni--steel, properties of plates of, for use in pressure vessels, standard for, 25:35473
Mn--Mo--steel, properties of plates of, for use in pressure vessels, standard for, 25:35473
Mn--W-base, crystallization at 1800 to 2000°C, 25:35476(P)
Mn--W-base, mechanical properties at 1800 to 2000°C, 25:35476(P)

MANGANESE ISOTOPES Mn-52
energy levels from iron-54 (d,α) reactions, spin--parity assignments for, (E), 25:36687 (LYCEN-7087)

MANGANESE ISOTOPES Mn-54
excretion in feces of peccaries following single ingestion of nuclear debris from Schooner Event, fallout, 25:35089
production in (n,α) and (n,p) reactions with fast neutrons, cross sections for, (E), 25:36686 (CONF-680986-1)

MANGANESE ISOTOPES Mn-55
alpha reactions (α,nγ) with, gamma--gamma coincidence spectra from, (E), 25:36694

MANGANESE ISOTOPES Mn-56
production in (n,α) and (n,p) reactions with fast neutrons, cross sections for, (E), 25:36686 (CONF-680986-1)

MANGANESE OXIDES
MnO--Nb_2O_5--PbO--$PbTiO_3$--$PbZrO_3$--Sb_2O_3, properties of piezoelectric ceramic of, for use as filter and transducer elements of mechanical filters, 25:35561(P)
MnO--PbO--$PbTiO_3$--$PbZrO_3$--Sb_2O_3--Ta_2O_5, properties of piezoelectric ceramic of, for use as filter and transducer elements of mechanical filters, 25:35561(P)

MANOMETERS
design of electronic conductivity, for monitoring pressure changes, 25:34513

MANY BODY PROBLEM
solution of three-nucleon, with simple two-body forces, 25:36375
theory for Van Hove pair correlation function in Maxwell-Boltzmann quantum fluids, 25:36373
variational calculations of ground-state energy of electronic or nucleonic systems, (T), 25:36358

MARITIME PRESSURIZED-WATER REACTOR
operations history for November 1970 to March 1971, 25:37094 (DOCKET-50238-80)

MARS (PLANET)
ionosphere of, model of solar-wind interaction with, (E/T), 25:36011

MASERS
use in determining flux densities of 3C 273, (E), 25:35686

MASS SPECTROMETERS
design and performance of on-line, for fission spectrometry, 25:36730 (NP-18829)
ion source for, design optimization of electron-impact, 25:35060
resolution of time-of-flight, with laser ion source for measurement of isotopic abundances, 25:35070

MATERIALS HANDLING
methods for pyrophoric and toxic, using protective gases, 25:34860

MATERIALS TESTING
conference on materials technology, San Antonio, Texas, May 20 to 24, 1968, 25:34826
facilities for conventional and irradiation, of nuclear materials, design of experimental, 25:34828
method for surface flammability of materials using a radiant heat energy source, standard, 25:34842
methods for heavy-section steels for use in pressure vessels for boiling water and pressurized water reactors, 25:34827

MATERIALS TESTING, NONDESTRUCTIVE
conference on equipment and methods for, Budapest, Hungary, Oct. 19 to 24, 1970, 25:34821 (CONF-701044-(Sect.2))
data from, computer-based display of, 25:37226 (SC-DR-710222)
development and uses of, by Canadian governmental services, 25:34830
development and uses of, past and present, 25:34832
equipment and method for measuring metal coating thickness, development of beta back-scattering, 25:34836
equipment for fast neutron defectoscopy, design and performance of, 25:34825
methods for radiation sources, 25:34803(R) (ENWL-1208-E)
methods for total, in present and future industry, 25:34831

MATHEMATICAL PHYSICS
transcendental functions in scattering, computer programs for evaluating, 25:36813 (ANU-P-439)

MATHEMATICS
analytic functions for extrapolations and representations of data, merging of statistics with, 25:36597

MATTER
density in Universe, lower bound to, (T), 25:35811
origin and transformations of, mass equations for elementary particles for, (T), 25:36426
particle reactions with, Monte Carlo calculation of high-energy, (T), 25:36816 (JINR-P2-5719)
structure in n-dimensional space, (T), 25:36362
transformation to antimatter in black holes, (T), 25:35820

MATTER, ANTI-
emission of, from white holes in antiuniverse, (T), 25:35820

MEATS
seafood, radiation processing of cod, nutritional value from combined effects of cooking and γ, 25:35272

MECHANICS
book: Introduction to Modern Theoretical Mechanics, 25:36361
perturbation theories in, without secular terms, 25:36376

MEDICAL PERSONNEL
radiation protection measures for, 25:35150
radiation protection measures for hospital, architectural and organizational, 25:35151
radiation protection methods for, 25:35130
radioisotope hazards to, measures for reducing, 25:35055

MEDICINE
book: Peaceful Uses of Nuclear Energy, 25:34817
developments in nuclear, for use in diagnosis and therapy, conference on, 25:35155
organization of nuclear, in Italy, 25:35156
radiation protection measures in nuclear, for patients and personnel, 25:35151
radiation protection measures in, in relation to standards for populations, 25:35147
radiodiagnosis in pediatric, review of, 25:35182
radioisotope uses in diagnostic, selectivity measures for minimal radiation burden during, 25:35179
radiopharmaceutical handling in, safety principles for, 25:35153
stable isotope uses in, review of, 25:34813 (TID-25705)

MEDITERRANEAN SEA
cesium-137 distribution in waters and sediment cores from, measurement of vertical, 25:34759(R) (NYO-2174-129)
plutonium-239 distribution in waters and sediment cores from, measurement of vertical, 25:34759(R) (NYO-2174-129)
strontium-90 distribution in waters and sediment cores from, measurement of vertical, 25:34759(R) (NYO-2174-129)

MEMBRANE FILTERS
performance of, effects of hydrodynamic boundary layer and fouling on, 25:37213 (ORNL-TM-3296)

MEMBRANES
properties of various plastic, for on-line alpha activity monitoring of solutions, 25:34673 (CEA-N-1440)
radiation effects on biological, mechanism for, 25:35210
radiation effects on model phospholipid, x, 25:34625
MERCAPTO (HS)
abundance of interstellar, upper limits for, (E), 25:35697
MERCAPTO GROUP
effects on x-radiosensitivity of Micrococcus radiodurans, 25:35263
radioprotective effects on rats, 25:35213
MERCHANT VESSELS
economics of nuclear, effects of reliability analysis on, 25:37095 (IRS-T-18(1970), pp 217-21)
MERCURY
determination by complexing with 2-aminobenzothiazole, effects of metal ions on gravimetric, 25:34520
determination in biological materials by neutron activation and γ spectrometry, 25:34551
determination in human stones by neutron activation, 25:34546 (THAI.-AEC-39)
effects on colorimetric determination of gold, 25:34521
effects on photometric determination of antimony following solvent extraction using TBP, 25:34512
electron superelastic scattering at low energies by excited atoms of, (E), 25:35872
fission of, lower limit on half-life for spontaneous, (E), 25:36779
half-life in Pacific oyster, biological, 25:37218 (RLO-2225-T-1-5)
separation of ions of, from metal ions by high-voltage electrophoresis using carboxylic and hydroxycarboxylic acids, 25:34702
stability of nonuniformly rotating, magnetohydrodynamic, (E), 25:35946
superconducting Josephson effect in contacts with niobium, ac, (E), 25:36068
MERCURY, ETHYL(N-PHENYLTOLUENESULFONAMIDO)-
mass spectrometric studies of, 25:37157 (ANL-7809)
MERCURY IONS
implantation in silicon and germanium at 10 to 200 keV, lattice disorder induced, 25:36300
MERCURY ISOTOPES Hg-195
electron-capture decay of ground-state and isomeric, γ and conversion electron spectra from, (E), 25:36750
MERCURY ISOTOPES Hg-199
energy-level transitions from gold-199 beta decay, conversion ratios, mixing ratios, and penetration parameters from, (E), 25:36789
MERCURY ISOTOPES Hg-201
exchange with mercury-203 in mercury bromide and phenylmercury bromide, 25:34600
MERCURY ISOTOPES Hg-203
energy levels and nuclear properties of, Nuclear Data Sheets for, (E), 25:36809
exchange with mercury-201 in mercury bromide and phenylmercury bromide, 25:34600
MESIC ATOMS
energy levels of low-Z π-, 25:35854
MESIC MOLECULES
meson (μ+) diamagnetic shielding in, chemical shift relative to proton, 25:35852
MESITYLENE
radiation stability of, for use as diluent in fuel reprocessing, 25:34638 (RT/CHI-(70)35)
MESONS
classification of vector, SU(3) symmetry, 25:36553
exchange of vector, in γ + N → π + N interactions near threshold, pole approximation in dispersion relations and vector dominance hypothesis for, (T), 25:36447
field geometrization over Riemann--Einstein space in general relativity, massive scalar, 25:36582
form factor for pseudoscalar, quark selection principle for elastic electromagnetic, (T), 25:36439
interactions of, N-point dual functions for, 25:36485
interactions with baryons, quark model for sum rules for amplitudes and cross sections of, (T), 25:36518
interactions with nucleons at high energies, quasipotential approach for spin effects in, (T), 25:36504 (JINR-E2-5770)
mass spectra of vector and tensor, duality breaking from, 25:36486
production of pairs of identical, in e+ + e- interactions, polarization effects in, (T), 25:36438
symmetry for vector, classification in SU(3), 25:36553
widths of scalar, chiral and scale breaking in SU(3) sigma model for, (T), 25:36483 (SU-1206-241)
MESONS (eta)
mixing with X, broken chiral SU(3) x SU(3) model for angle of, (T), 25:36551
production in γ + p → eta + p interactions, duality and meson trajectories in Regge cut model for, (T), 25:36441
production in p + d → 3He + MM interactions at 2 GeV, spectrometer study of cross sections for, (E), 25:36398
production in p + d → 3He + MM interactions at 3 GeV, spectrometer study of cross sections for, (E), 25:36398
MESONS (f)
mass and width of f0 in particle interactions, equivalent potential approach for, (T), 25:36422
MESONS (K)
decay K → 2π(3π), model for, (T), 25:36464
decay K → μ + anti ν, model for, (T), 25:36464
decay K → π + l + ν, effective dipole form factors for, 25:36459
decay K → π + l + ν, quark model in Regge pole theory for form factors and Cabibbo angle for, (T), 25:36456 (CRO-3992-39)
decay K → π + ν + l, e--μ universality hypothesis for, (T), 25:36470
decay of, e--μ universality hypothesis for two-body leptonic, 25:36470
decay of, effective-range formula for form factor in three-body leptonic, (T), 25:36461
interactions anti K + N, local models for, (T), 25:36505 (PAM-71.1)
interactions K + N → K + N at high energies, quasipotential approach for spin effects in, (T), 25:36504 (JINR-E2-5770)
interactions K + N at low energies, vector-meson-dominance sum rules for, (T), 25:36519
interactions K + N at low, intermediate, and high energies, Venezianc model for, 25:36507
interactions K + N in K+ + n → K0 + p interactions at 600 MeV in deuterium bubble chamber, K0 angular distributions and p polarization for phase shifts for, (E), 25:36417
interactions K + p, model for Pomeranchukon exchange in total cross sections for, 25:36512
interactions π + K, chiral and scale breaking in SU(3) sigma model for scattering lengths for, (T), 25:36483 (SU-1206-241)
production of anti K and K in π + N and N + N interactions, generalized multiperipheral model for properties of partial cross sections for, (T), 25:36422
MESONS (K-)
absorption by nuclei at rest in emulsions, properties of Σ- and Σ+ produced in, (E), 25:36400
absorption by nuclei at rest in emulsions, Q-value distribution for detection of A-He5, A-Li8, and A-Be9 produced in, (E), 25:36401
interactions K- + p → K- + π+ + n at 5.5 GeV/c, S-wave phase shifts for, (E), 25:36413
interactions K- + p → π- + Y0*, eikonal model with unitarity corrections for dual description of, (T), 25:36514
interactions K- + p → Σ(1385) + π near A(1520), production mechanism for, (T), 25:36415
MESONS (K0)
decay K0 → π + l(π) + ν(γ), test of ΔS = ΔQ rule in time distribution of, (T), 25:36457
decay K1 0 → π+ + π-, model for parity-violating, (T), 25:36465
decay K2 0 → e+ + e-, spectrometer study of upper limit for branching ratio for, (E), 25:36386 (UCRL-20264)
decay K2 0 → μ+ + μ-, spectrometer study of branching ratio for, (E), 25:36386 (UCRL-20264)
decay K2 0 → μ+(e+) + μ-(e-), spectrometer study of upper limits to branching ratios for, (E), 25:36387
decay K2 0 → μ+(μ-) + e-(e+), spectrometer study of upper limits to branching ratios for, (E), 25:36387
decay K2 0 → μ+(μ-) + e-(e+), spectrometer study of upper limits for branching ratios for, (E), 25:36386 (UCRL-20264)
decay K2 0 → π+ + π- + π0, search for CP-nonconserving asymmetry in, (E), 25:36550 (COO-1749-24)
mass difference (K+ - K0), contribution of A2 Regge pole to, (T), 25:36496
mass matrix of K0--anti K0 complex, CP violation in dynamical structure of, (T), 25:36466
MESONS (anti K0)
mass matrix of K0--anti K0 complex, CP violation in dynamical structure of, (T), 25:36466
MESONS (K+)
decay K+ → π+ + π0, model for parity-violating, (T), 25:36465
interactions K+ + d → K+ + π+ + π- + d(pn) at 9 GeV/c, K*(1243) and K*(1344) mixing in mass spectra of, (E), 25:36414
interactions K+ + n → K0 + p at 600 MeV/c in deuterium bubble chamber, K + N phase shifts from K0 angular distribution and p polarization in, (E), 25:36417
interactions K+ + p at 210 and 330 MeV, optimized polynomial representations for differential cross sections for coupling constants and nonspinflip amplitudes of, (T), 25:36532
interactions K+ + p in Venezianc model, differential cross sections for charge-exchange and backward elastic, 25:36507
interactions K+ + p in Venezianc model, phase shifts for, 25:36507
mass difference (K+ - K0), contribution of A2 Regge pole to, (T), 25:36496
MESONS (μ)
charge ratio of near-sea level energetic cosmic-ray, energy and zenith angle-dependent, (E/T), 25:35898
detection of, design and calibration of fast-pulse ionization chamber for, 25:35022
focusing of beams of, properties of helical quadrupole

XUM

lenses for, 25:36624
momentum spectrum and charge ratio of vertical, at sea level and 12°N geomagnetic latitude, (E), 25:35919
production of cosmic, proposed experiment for direct, (E), 25:36416
spectrum of cosmic, at sea level and 12°N geomagnetic latitude, design of spectrograph for momentum, (E), 25:35918
transport calculations for shielding around high-energy proton accelerator targets, 25:36610 (ORNL-TM-3353)
universality with electrons in two- and three-body K decays, (T), 25:36470

MESONS (μ⁻)
capture by helium-4, calculations of neutron spectra and asymmetries in neutron angular distributions from, (T), 25:36666
production of high-mass μ⁺--μ⁻ pairs in p + p interactions, parton model predictions for structure in, (T), 25:36434 (LNF-71/5)
production of μ⁺--μ⁻ pairs in e⁺ + e and e + e interactions at high energies in colliding beams, total and differential cross sections for, (T), 25:36433 (LNF-71/1)

MESONS (μ⁺)
diamagnetic shielding in mesic molecules, chemical shift relative to proton, 25:35852
production of high-mass μ⁺--μ⁻ pairs in p + p interactions, parton model predictions for structure in, (T), 25:36434 (LNF-71/5)
production of μ⁺--μ⁻ pairs in e⁺ + e and e + e interactions at high energies in colliding beams, total and differential cross sections for, (T), 25:36433 (LNF-71/1)

MESONS (ω)
decay ω → π⁰ + γ, current algebra with momentum-dependence of vertex function for πρhω for ratio of width of π⁰ → 2γ decay to width of, (T), 25:36495
production in γ reactions with carbon-12 and oxygen-16, isolation of Regge trajectories in, (T), 25:36453
production in p + d → ³He + MM interactions at 3 GeV, spectrometer study of cross sections for, (E), 25:36398
production in π⁺ + p → ω + Δ⁺⁺ interactions, test of empirical rule for cuts in density matrix elements for, (T), 25:36502 (CALT-68-300)
vertex function for πρhω, current algebra for ratio of width of ω → π⁰ + γ decay to width of π⁰ → 2γ decay from momentum-dependent, (T), 25:36495

MESONS (phi)
production in γ reactions with carbon-12 and oxygen-16, isolation of Regge trajectories in, (T), 25:36453

MESONS (π)
absorption in nuclear matter at low energy, mean free path for, (T), 25:36489
coupling constant for πN, tests of long-range charge independence in N + N interactions from, (T), 25:36522
decay π → μ + anti ν, model for, (T), 25:36464
exchange in N + N interactions, contributions of two-body, 25:36526
form factor of, model for dipole electromagnetic, (T), 25:36436 (ORO-3992-28)
interactions π + π → π + π, dual amplitude with Mandelstam analyticity for, (T), 25:36492
interactions π + K, chiral and scale breaking in SU(3) sigma model for scattering lengths for, (T), 25:36483 (SU-1206-241)
interactions π + N → π + Δ, NΔγ coupling constants and sum rules from unsubtracted dispersion relations for, 25:36508
interactions π + N → π + N at high energies, quasipotential approach for spin effects in, (T), 25:36504 (JINR-E2-5770)
interactions π + N → X⁰(960) + N*, method for determining spin--parity of X⁰(960) from forward, (T), 25:36454
interactions π + N at 0 to 700 MeV, Born approximation potential for phase shifts for, (T), 25:36510
interactions π + N at 10^{11} to 10^{13} eV, proposed experiment for average characteristics and angular distributions for, (E), 25:36416
interactions π + N at low energies, Ward identity techniques for s- and p-wave amplitudes for, (T), 25:36513
interactions π + N, gauge invariance and soft-pion techniques for constraints between π production amplitude and amplitude of, (T), 25:36515
interactions π + N, generalized multiperipheral model for properties of partial cross sections for K anti K production in, (T), 25:36422
interactions π + N, low-energy π + π phase shifts from dispersion relations for backward, (T), 25:36520
interactions π + N, model for Pomeranchukon exchange in total cross sections for, 25:36512
interactions π + N, Veneziano model for polarization in charge-exchange, (T), 25:36517
interactions π + p → A₁ + rho + p → 5π + p at 50 and 100 GeV, Drell--Hiida--Deck effect for diffractive, (T), 25:36521
interactions π + π at low energies, dispersion relations for backward π + N interactions for resonances in phase shifts for, (T), 25:36520
interactions π + π, S-wave phase shifts for, 25:36484
interactions π + π, asymptotic behavior of Veneziano partial-wave amplitude and dispersion relations in complex S plane for, (T), 25:36487
interactions π + π, chiral and scale breaking in SU(3) sigma model for scattering lengths for, (T), 25:36483 (SU-1206-241)
interactions π + π, crossing and inequality relations in solution for amplitudes of s-wave, (T), 25:36482 (NYO-2262-TA-241)
interactions π + π, smoothed Veneziano model for, 25:36499
interactions π + π, zeros in amplitudes for, 25:36485
mass difference of, effects of finite rho width on electromagnetic, (T), 25:36442
production in γ + N → π + N interactions near threshold, pole approximation in dispersion relations and vector dominance hypothesis for vector meson exchange contributions to, (T), 25:36447
production in p + d → ³He + MM interactions at 2 GeV, spectrometer study of cross sections for, (E), 25:36398
production in π + p → A₁ + rho → 5π + p interactions at 50 and 100 GeV and via A₁ and rho production in π reactions with carbon-12 at 100 GeV, Drell--Hiida--Deck effect for diffractive, (T), 25:36521
production of, gauge invariance and soft-pion techniques for constraints between π + N interaction amplitude and amplitude of, (T), 25:36515
production spectrum near geomagnetic equator, from muon spectrum measurements, (E/T), 25:35917
reactions with atoms having low Z, x-ray yields and level broadening from, (E), 25:35854
reactions with carbon-12 at 100 GeV, Drell--Hiida--Deck effects for 5π via A₁ and rho production in diffractive, (T), 25:36521
scattering by helium-4 and oxygen-16 near 3,3 resonance, multiple-scattering theory for differential and total cross sections for elastic, (T), 25:36527
vertex function for πρhω, current algebra for ratio of width of ω → π⁰ + γ decay to width of π⁰ → 2γ decay from momentum-dependent, (T), 25:36495

MESONS (π⁻)
decay π⁻ → ν + l⁻ + γ, sign of structure-dependent form factors in, (T), 25:36469
interactions π⁻ + p → 2π⁰ + n at 447 MeV, spectrometer and spark chamber study of total cross sections, neutron differential cross sections and angular distributions, and π⁰π⁰ system effective mass spectrum in, (E), 25:36405 (JINR-P1-5781)
interactions π⁻ + p → K⁰ + Λ, test of empirical rule for cuts and line reversal relations in absorption model prediction for Λ polarization in, (T), 25:36502 (CALT-68-300)
interactions π⁻ + p → K_2^0 + K⁻ + p at 4.5 GeV/c, production and decay of A_2^- from, (E), 25:36409
interactions π⁻ + p → n + π⁺ + π⁻ at 11 GeV/c, total cross section for π⁺ + π⁻ interactions from, (E/T), 25:36509
interactions π⁻ + p → π⁰ + n at 1.8 to 6.0 GeV/c, momentum dependence of differential cross sections for, (E), 25:36412
interactions π⁻ + p → π⁻ + p at 0 to 2 GeV/c, compilation of amplitudes and parameters from partial-wave analyses for, (T), 25:36506 (TID-25726)
interactions π⁻ + p → π⁻ + p at 6 and 16 GeV/c, A and R polarization parameters for, (E), 25:36406 (NP-18873)
interactions π⁻ + p → π⁻ + p at 9.85 GeV/c, angular distributions for, (T), 25:36534
interactions π⁻ + p → X⁰ + n at 1.6 GeV/c, X⁰ decay branching ratio and cross sections for, (E), 25:36407
interactions π⁻ + p at high energies, sum rule for limitation of parametrizations in models for asymptotic behavior of amplitudes of, (T), 25:36511
interactions π⁺ + π⁻ → π⁺ + π⁻, generalized Veneziano model with nonlinear trajectories for, (T), 25:36493
interactions π⁺ + π⁻ from π⁻ + p → n + π⁺ + π⁻ interactions at 11 GeV/c, total cross section for, (E/T), 25:36509
production in p + p interactions at 13 to 28.5 GeV/c in hydrogen bubble chamber, cross sections and momentum distributions for, (E), 25:36391 (UCRL-20632)
reactions (π⁻,nn) with lithium-6, calculation of helium-4 recoil from, (T), 25:36847
reactions (π⁻,π⁺) with helium-3, production of three-nucleon resonance in, (T), 25:36849
reactions with calcium-40, carbon-12, helium-4, and oxygen-16 at high energies, Coulomb interaction in, (T), 25:36524
reactions with carbon at 7 GeV in bubble chamber, nuclear radius determination from, (E), 25:36408
reactions with nuclei at 1 to 2500 MeV, computer program for intranuclear-cascade calculations of, (T), 25:36733 (CRNL-4564)
reactions with nuclei at 17.2 GeV in emulsions, properties of showers produced in, (E), 25:36418

MESONS (π⁰)
decay π⁰ → 2γ current algebra with momentum-dependence of vertex function for πρhω for ratio of width of ω → π⁰ + γ decay to width of, (T), 25:36495
production in anti p reactions with nuclei at 5 GeV/c in emulsions, angular and momentum distributions for, (E), 25:36404

XUM

production in $\gamma + p \rightarrow \pi^0 + p$ interactions, duality and meson trajectories in Regge cut model for, (T), 25:36441
production in γ reactions with carbon-12 and oxygen-16, isolation of Regge trajectories in, (T), 25:36453
production in $p + d \rightarrow {}^3He + MM$ interactions at 3 GeV, spectrometer study of cross sections for, (E), 25:36398
production in $\pi^- + p \rightarrow 2\pi^0 + n$ interactions at 447 MeV, spectrometer and spark chamber study of $\pi^0\pi^0$ system effective mass spectrum in, (E), 25:36405 (JINR-P1-5781)
production in cosmic hadron reactions with lead and graphite above $3(10)^{12}$ eV, distributions and mean values of inelasticity coefficient for, (E), 25:36385 (ITJ-5)

MESONS (π^+)
decay $\pi^+ \rightarrow \nu + l^+ + \gamma$, sign of structure-dependent form factors in, (T), 25:36469
interactions $\pi^+ + p \rightarrow 3\pi^+ + 2\pi^- + p$ at 8 GeV/c, multiperipheral model with $\pi\pi$ and πp phase shifts and form factors for, (T), 25:36503 (INR-P-1265)
interactions $\pi^+ + p \rightarrow K^+ + \Sigma^+$ at 2.75 to 14 GeV/c, forward differential cross sections and polarization for, (E), 25:36410
interactions $\pi^+ + p \rightarrow K^+ + \Sigma^+$, test of empirical rule for cuts and line reversal relations in absorption model predictions for Σ polarization in, (T), 25:36502 (CALT-68-300)
interactions $\pi^+ + p \rightarrow K^+ + Y^{*+}$, eikonal model with unitarity corrections for dual description of, (T), 25:36514
interactions $\pi^+ + p \rightarrow \omega + \Delta^{++}$, test of empirical rule for cuts in density matrix elements of ω in, (T), 25:36502 (CALT-68-300)
interactions $\pi^+ + p \rightarrow \pi^+ + p$ at 0 to 2 GeV/c, compilation of amplitudes and parameters from partial-wave analyses for, (T), 25:36506 (TID-25726)
interactions $\pi^+ + p$ at 3.7 GeV/c, mass spectra of A_2 from, (E), 25:36411
interactions $\pi^+ + p$ at high energies, sum rule for limitation of parametrizations in models for asymptotic behavior of amplitudes of, (T), 25:36511
interactions $\pi^+ + \pi^- \rightarrow \pi^+ + \pi^-$, generalized Veneziano model with nonlinear trajectories for, (T), 25:36493
interactions $\pi^+ + \pi^-$ from $\pi^- + p \rightarrow n + \pi^+ + \pi^-$ interactions at 11 GeV/c, total cross section for, (E/T), 25:36509
production in $p + p$ interactions at 13 to 28.5 GeV/c in hydrogen bubble chamber, momentum distributions for, (E), 25:36391 (UCRL-20632)
reactions with calcium-40, carbon-12, helium-4, and oxygen-16 at high energies, Coulomb interaction in, (T), 25:36524
reactions with nuclei at 1 to 2500 MeV, computer program for intranuclear-cascade calculations of, (T), 25:36733 (ORNL-4564)

MESONS (rho)
field--current identities in gauge-invariant formulation of massive gauge fields for, (T), 25:36501
mass and width in particle interactions, equivalent potential approach for, (T), 25:36422
production in γ reactions with carbon-12 and oxygen-16, isolation of Regge trajectories in, (T), 25:36453
production with A_1 in $\pi + p \rightarrow A_1 + rho \rightarrow 3\pi + p$ interactions at 50 and 100 GeV and π reactions with carbon-12 at 100 GeV, Drell--Hiida--Deck effect for 3π diffractive production in, (T), 25:36521
vertex function for $\pi rho\omega$, current algebra for ratio of width of $\omega \rightarrow \pi^0 + \gamma$ decay to width of $\pi^0 \rightarrow 2\gamma$ decay from momentum-dependent, (T), 25:36495
width effect on π electromagnetic mass difference, (T), 25:36442

MESONS (X^0)
decay $eta' \rightarrow eta + 2\pi$, chiral and scale breaking in SU(3) sigma model for, (T), 25:36483 (SU-1206-241)
decay $X^0 \rightarrow$ neutrals, branching ratio for, (E), 25:36407
mixing with eta, broken chiral SU(3) x SU(3) model for angle of, (T), 25:36551
production in $\pi^- + p \rightarrow X^0 + n$ interactions at 1.6 GeV/c, cross sections for, (E), 25:36407

MESONS, RESONANCE
book: The Systematics of Resonances, 25:36488
decay correlations of A_2^-, (E), 25:36409
effects of direct-channel, on anti $p + p \rightarrow$ anti p(anti n) + p(n) interactions at intermediate energies, (T), 25:36491
evidence for (332), (772), (775), and (800) in $\pi + \pi$ phase shift analysis, 25:36520
field--current identities for A_1, in gauge-invariant formulation of massive gauge fields, (T), 25:36501
mass and width of A_2^-, (E), 25:36409
parity and spin of $X^0(960)$ from forward $\pi + N \rightarrow X^0(960) + N^*$ interactions, method for determining, (T), 25:36454
production of 2π threshold enhancement in $p + d \rightarrow {}^3He +$ MM interactions at 2 and 3 GeV, spectrometer study of cross sections for, (E), 25:36398
production of A_1 with rho in $\pi + p \rightarrow A_1 + rho \rightarrow 3\pi + p$ interactions at 50 and 100 GeV and π reactions with carbon-12 at 100 GeV, Drell--Hiida--Deck effect for 3π diffractive production in, (T), 25:36521
production of A_2 in $\pi^+ + p$ interactions at 3.7 GeV/c, mass spectra for, (E), 25:36411
production of A_2^- from $\pi^- + p \rightarrow K_2^0 + K^- + p$ interactions at 4.5 GeV/c, (E), 25:36409
production of $K^*(1243)$ and $K^*(1344)$ in $K^+ + d \rightarrow K^+ + \pi^+ + \pi^- + d(pn)$ interactions at 9 GeV/c, (E), 25:36414
production of narrow anti pn bound state in anti $p + d$ interactions at rest, (E), 25:36399
production of X(950) in $p + d \rightarrow {}^3He +$ MM interactions at 3 GeV, spectrometer study of cross sections for, (E), 25:36398
splitting of A_2, bound-state dynamic model for, 25:36497
theory for, dual resonance models for vector currents in, (T), 25:36490
theory for, review of quark model in, (T), 25:36500
theory for, review of, (T), 25:36516

MESOSPHERE
constituent concentration and transport during anomalous absorption in, minor, (E/T), 25:35984

METAL COATINGS
thickness of, beta back-scattering equipment and method for measurement of, 25:34836

METALLURGICAL EQUIPMENT
design of tube cleaning machine for FTR fuel cladding, engineering drawings for, 25:34783

METALLURGY
conference on materials technology, San Antonio, Texas, May 20 to 24, 1968, 25:34826

METALS
abundance in K giant stars, (E/T), 25:35649
abundance in supergiant star HD 32034, (E), 25:35672
conference on strength of, Vol. 1, Pacific Grove, Calif., Aug. 30 to Sept. 4, 1970, 25:35369
conference on strength of, Vol. 2, Pacific Grove, Calif., Aug. 30 to Sept. 4, 1970, 25:35390
conference on strength of, Vol. 3, Pacific Grove, Calif., Aug. 30 to Sept. 4, 1970, 25:35395
defects in, review of interactions between point, 25:36325
deposition on titanium artillery shell case, 25:37161 (BDX-613-236)
fatigue failure in high-strength, mechanisms of, 25:35428
joining of dissimilar and similar, explosive bonding method for, 25:35298
plastic deformation mechanisms in bcc, review of models for studies of, 25:35370
radiation effects on hardening of bcc, fast neutron, 25:35507
radiation effects on, guide for, 25:35081
radiation effects on, research progress on computer study on mechanisms of neutron, 25:35504(R) (ORO-3512-4)
removal of layers of, electron beam method for, 25:35515
resonance effects in, high frequency waves and Landau Fermi-liquid, (T), 25:36067
solidification of molten, immersed in cooling medium, analysis of pressurization in, 25:37214 (ORO-3536-4)
strain hardening equations for, 25:37245 (UCLA-34-P-177-5)
tensile strength of, superconducting transition-induced changes in, 25:35389
thermal capacity of, ac temperature method for measuring high-temperature, 25:35341 (UCRL-50962)
thermal stresses in liquid, used as fast breeder reactor coolant, accuracy of strain gages for measuring, 25:34799
thermodynamic properties of liquid, at high temperatures and pressures, equipment and method for measuring, 25:35342 (UCRL-51035)

METEORITES
element abundances in chondrites, (T), 25:35595
formation of chondritic, (E), 25:35830
isotope-production rates in stone, from galactic cosmic-ray interactions, sodium-22 and tritium, (E/T), 25:35599
magnetic remanence in, produced by cosmic-ray exposure, (E), 25:35598
orbital velocities of stone, from ablation-related cosmic-ray fossil-track measurements, (E/T), 25:35600
radioinduced thermoluminescence of powdered, 2-GeV proton, 25:36298

METEOROLOGY
book: Noctilucent Clouds, 25:35988
research activities at Casaccia, Italy during 1968, 25:34746 (RT/FRCT-(70)42)
research on convective storms, rain scavenging studies in Illinois during 1970 for, 25:34742(R) (COO-1407-28)
research programs at Melbourne, Australia during 1969, 25:34744(R) (NP-18828)

METEORS
ionization probability of copper and lanthanum hexaboride simulated micro-, (E), 25:35597
luminous efficiencies of iron and copper simulated micro-, (E), 25:35596

METHANE
alpha-particle stopping cross sections in gaseous, at 0.3 to 2 MeV, 25:36255
ionization by low-energy electrons in mass spectrometer, cross sections for, 25:34636(R) (ORO-3729-4)
photo-absorption cross sections of, review of uv, (E/T), 25:36013
radiolysis of, mass spectrometric studies on ionic

XUM

reactions in, 25:34645
reactions with helium tritides formed by beta decay of molecular tritium, kinetic studies on, 25:34677
reactions with inorganic and organic compounds and rare gases under simulated radiolysis conditions, mass spectrometric studies on, 25:34645
yields from γ radiolysis of 2-methyl-2-propanol at 30°C, 25:34659
methane--N, reactions with multiply charged ions in flowing systems at 7 MeV/n, 25:34567
METHANE, DICHLORO-
diffusion through drybox gloves, comparison of values for other halogenated solvents with, 25:34605 (RFP-1608)
radiation effects on, and its solutions in natural rubber latex, EPR studies of γ, 25:34614
METHANE, DIIODO-
radiation effects on, and its solutions in natural rubber latex, EPR studies of γ, 25:34614
METHANE, HALO-
radiation effects on, and its solutions in natural rubber latex, EPR studies of γ, 25:34614
METHANE, IODO-
removal by carbon filters, effects of service life on, (E), 25:37106(R) (DP-1259)
METHANE, NITRO-
effects on paramagnetic species produced by γ radiolysis of glassy alkaline solutions of 2-methyl-2-nitro-1-propanol at 77°K, ESR studies on scavenging, 25:34643
METHANE, TRIBROMO-
radiation effects on, and its solutions in natural rubber latex, EPR studies of γ, 25:34614
METHANE, TRIFLUOROIODO-
photolysis of, emission of $I(^2P_{1/2})$ in, 25:34613 (TID-25689)
METHANOL
effects on corrosion fatigue crack propagation in aluminum--molybdenum--titanium--vanadium alloy, relations with stress intensity amplitude and frequency, 25:35279
radiolysis of gaseous, deuterated and normal, kinetics of production of hydrogen from γ, 25:34665
radiolysis of liquid, at low temperature, studies on electron solvation process in electron pulse, 25:34649
HCl--methanol, corrosive effects on aluminum--titanium--vanadium alloys, 25:35287
METHYL ETHER
compounds with boron trifluoride, analysis for boron-10 by thermal neutron absorption method, 25:34538
METHYL GREEN
reactions with uranium, extraction-photometric analysis based on, 25:34509
METHYL SULFOXIDE
reactions with hydrated tetravalent thorium compounds, properties of products from, 25:34565
METHYLENE
spectra of deuterated, carbon-13 hyperfine interaction in EPR, 25:34586
METHYLENE GREEN
solvent properties for benzoic acid--uranium complex in photometric determination of uranium, 25:34534
MICE
ablation of parathyroid and thyroid glands of, using iodine-131 combined with surgery, 25:35084
radiation effect on reproduction of hematopoietic cells in, 25:35217
radiation effects on bone marrow and intestinal tissues of, effects of hypoxia on electron, 25:35161
radiation effects on bone marrow stem cells in, lethal, 25:35212
radiation effects on cell count in intestinal epithelium in, lethal x, 25:35239
radiation effects on formation of thyroiditis antibodies in, x, 25:35114
radiation effects on immune response of, to hematopoietic cells following intraperitoneal and intravenous injection, x, 25:35111
radiation effects on survival of tumor-bearing, combined effects of dihydroxybutyraldehyde and x, 25:35159
radiation effects on survival of, protective effects of sodium fluoroacetate against x, 25:35162
radiation effects on tolerance of skin homografts of, x, 25:35113
radiation effects on tritium incorporation in kidney and liver tubulus in, effects of time on whole-body x, 25:35238
radiation effects on, role of hypothermia in protective effects of sodium fluoroacetate against, 25:35163
radioinduced dominant lethal mutations in spermatogonia of, x, 25:35129
radiosensitivity of, effects of dose fractionation and rate on, 25:35218
MICROWAVES
cosmic background, interactions with halo electrons, (E/T), 25:35903
emission from Sun, solar flare-associated homologous, (E/T), 25:35774
emission from theta-pinch plasmas, (E), 25:36122
use for plasma production in magnetic fields, (E), 25:36160
MIDWEST FUEL RECOVERY PLANT
operation of, technical specifications for application of license for, 25:34684 (DOCKET-50268-8)
radioactive wastes from, methods for controlling environmental contamination from, 25:34844 (CONF-700440-1)
safety analysis report, amendment to, 25:34685 (DOCKET-50268-9)
MILK
separation of iodine from, using ion exchange resins produced in Poland, 25:34703
MILKY WAY
cosmic-ray confinement in disk of, (T), 25:35905
infrared emission from center of, flux density of, (E), 25:35780
interstellar absorption in Orion and Monoceros, far-ultraviolet, (E), 25:35785
interstellar absorption in the direction of LMC, (E), 25:35670
interstellar gas in, instability of, (E), 25:35795
interstellar turbulence, effects on cosmic-ray diffusion, (T), 25:35902
Lyman-alpha emission from, (T), 25:35792
magnetic field in, dynamo action with isotropic turbulence, (T), 25:35787
magnetic field of, kinematic-dynamo theory of, (T), 25:35786
magnetic field, instability of, (E), 25:35795
plutonium-244 nucleosynthesis in, (E), 25:35894
stellar kinematics in Sco--Cen association and Gould's belt, (E), 25:35798
x-ray emission from North Polar Spur of, (E/T), 25:35800
MILLSTONE POINT POWER REACTOR, UNIT 1
operations incident of April 22, 1971, inoperability of gas turbine generator emergency power system, 25:36878 (DOCKET-50245-67)
operations incident of February 21, 1971, failure of gas turbine generator emergency power system to start, 25:36877 (DOCKET-50245-61)
operations incident of March 25, 1971, high flux trip during turbine control valve test, 25:36875 (DOCKET-50245-59)
operations incident of March 31, 1971, failure of motor on Loop A LPCI injection valve, 25:36876 (DOCKET-50245-60)
operations incident of May 2, 1971, cleanup system auxiliary pump bypass valve motor failure, 25:36879 (DOCKET-50245-81)
operations incident of May 5, 1971, shutdown cooling system pump suction valve motor failure, 25:36879 (DOCKET-50245-81)
MILLSTONE POINT POWER REACTOR, UNIT 2
construction permit for, environmental protection requirements of, 25:36950 (DOCKET-50336-22)
MINERALS
actinium-227/radium-226 ratio in, 25:34738
prospecting for seabed, nuclear methods for, 25:34803(R) (BNWL-1308-5)
uranium-234/uranium-238 ratio in, 25:34738
uranium-235/uranium-238 ratio in, 25:34738
MISCH METAL
development for use in permanent magnets, 25:35306
Co--misch metal--Sm, fabrication and magnetic properties of permanent magnets of, 25:36336
MITOCHONDRIA
radiation effects on optical density of animal cardiac, effects of hydrocortisone on, 25:35227
radiation effects on oxidative phosphorylation in rat brain and liver, effects of dose on x, 25:35216
radiation effects on oxygen uptake by rat, x, 25:35223
MITOSIS
radiation effects on bacteria, effects of vacuum treatment on uv, 25:35265
MOESSBAUER EFFECT
book: Nuclear Gamma Resonance (Apparatus and Methods), 25:36343
MOESSBAUER SPECTROMETERS
book: Nuclear Gamma Resonance (Apparatus and Methods), 25:36343
design of, 25:34934
MOISTURE GAGES
design of gamma radiometric, for snow layers, 25:35042(P)
MOLECULAR BEAMS
scattering of, research progress on, 25:34807(R) (MLM-1793)
MOLECULES
atom scattering at high energies by, validity of spherically symmetric potential for interpretation of, 25:35887
bound-state problem for, quantum-mechanical four-body, 25:36364
electron reactions at low energies with, review on, 25:34618
electron resonant scattering by, effects of vibronic excitation on angular distributions from, (T), 25:35869
formation in ultrastrong magnetic fields, (T), 25:35645
imagining of bio-, using field ion shadow projection microscope, 25:37207 (NYO-3851-10)
photo-absorption cross sections at less than 3000-A of astronomical major and minor constituents, uv, (E/T), 25:36013

role in description of radiobiological phenomena, 25:35101
MOLTEN SALT BREEDER REACTOR
fuel reprocessing for, engineering development studies on, 25:34694 (ORNL-TM-3138)
neutron poisoning of, effects of fission products on, 25:34694 (ORNL-TM-3138)
MOLTEN SALT REACTOR EXPERIMENT
fuel for, low-pressure distillation experiments on, 25:34694 (ORNL-TM-3138)
MOLYBDENUM
creep in monocrystalline, mechanisms of L and Y tilt boundary intersections formed in, 25:35402
decarburization of thin plates of, by low-pressure oxygen reactions at 1800°C, 25:35309
deformation anisotropy and texture of sheets of sintered, 25:35411
determination in complex carbides by electron beam micro methods, 25:34523
dislocations in monocrystalline, activation energy anisotropy of, 25:35443
dislocations in monocrystalline, mobility of edge, 25:35485
effects as an additive on properties of thermomechanically processed Type 348 stainless steel, 25:35300
effects on colorimetric determination of gold, 25:34521
effects on gravimetric determination of mercury using 2-aminobenzothiazole, 25:34520
effects on polarographic reduction of niobium, 25:34526
iodine-ion reactions at 15 to 60 MeV with, L and M x-ray spectra from, (E), 25:35834
neutron capture at 1 to 1000 keV by natural, cross sections for, (E), 25:36729(R) (N-70-41999)
oxidation of hydrogen-annealed, thermodynamics of, 25:35291
plastic flow anisotropy in monocrystalline, mechanisms of, 25:35379
rupture of polycrystalline, effects of carbon and oxygen on, 25:35409
separation from rhenium by solvent extraction using acetone and scrubbing using sodium hydroxide, 25:34525
solvent properties for nitrogen at 1600 to 2400°C and 15 to 400 torr nitrogen, equilibrium, 25:35430
sorptive properties of (100) surface of, for carbon monoxide, radiotracer and photoemission studies of, 25:35358
tensile properties of, effects of stress cycling on, 25:35346
welding behavior of sheets of sintered, effects of boron trace amounts on electron beam, 25:35312
welding to yttrium, methods for, 25:35321
MOLYBDENUM ALLOYS AND SYSTEMS
Al_2O_3--Mo, properties for use as armor plate, 25:35554
Al--C--Co--Cr--Mo--Nb--Ni-base--Ta--Ti--Zr, properties of corrosion-resistant IN-738 superalloy, 25:35400
Al--Co--Mo, radiation effects on catalytic activity of, in dehydrogenation of cyclohexane, 25:34628
Al--Co--Mo, radiation effects on subsequent catalytic activity of, in decomposition of hydrogen peroxide, γ, 25:34630
Al--Cr--Mo--Ni-base--Ti, solvus temperature of γ' in, effects of hardener content on, 25:35460
Al--Mo--Si, radiation effects on subsequent catalytic activity of, in decomposition of hydrogen peroxide, γ, 25:34630
Al--Mo--Ti-base--V, crack propagation in, effects of stress intensity amplitude and frequency and air, methanol, sodium chloride solution, and distilled water on corrosion fatigue, 25:35279
Al--Mo--Ti-base--V--Zr, tensile properties of metastable beta, at 25 to 500°C, effects of strain rate and annealing temperature on anomalies in, 25:35434
Al--Mo--Ti-base--Zr, tensile properties of metastable beta, at 25 to 600°C, effects of strain rate and annealing temperature on anomalies in, 25:35434
B--Mo, deformation anisotropy and texture of sheets of rolled and annealed, 25:35411
C--Co--Cr--Fe--Mo--Nb--Ni-base, strengthening by precipitation of body-centered tetragonal phase in, 25:35302
C--Cr--Fe--Mo--Nb--Ni-base, strengthening by precipitation of body-centered tetragonal phase in, 25:35302
C--Hf--Mo-base, tensile properties of dilute, effects of thermomechanical treatments on, 25:35397
Co--Cr--Mo--Ni, hardening of multiphase, mechanisms of, 25:35396
Cr--Mo, diffusion in solid solutions of, at 1440 to 1603°C, solid--vapor couple measurements of, 25:35427
Cu--Mo, tensile properties of laminar systems of, at 20 to 600°C, effects of composition on, 25:35454
Cu--Mo, tensile properties of laminates of, effects of composition on, 25:35455
Fe--Mo--Sn--Ti-base--Zr, crystal structure and properties of thermomechanically-processed beta-phase, 25:35398
Fe-base--Mo, creep at 973 to 1153°K, effects of stress on, 25:35464
Fe-base--Mo, solution softening in dilute, at 77 to 430°K, mechanisms of, 25:35374
Mn--Mo--Ni--steel, properties of plates of, for use in pressure vessels, standard for, 25:35473
Mn--Mo--steel, properties of plates of, for use in pressure vessels, standard for, 25:35473
Mo--Nb-base, hardening and softening of noncrystalline, mechanisms of solution, 25:35436
Mo--Ni-base, slip in, mechanisms of cross, 25:35286
Mo--Pd--Ti-base, tensile properties of metastable beta, at 25 to 800°C, effects of strain rate and annealing temperature on anomalies in, 25:35434
Mo--Sn--Ti-base, tensile properties of metastable beta, at 25 to 600°C, effects of strain rate and annealing temperature on anomalies in, 25:35434
Mo--Sn--Ti-base--Zr, tensile properties of metastable beta, at 25 to 600°C, effects of strain rate and annealing temperature on anomalies in, 25:35434
Mo--Ta, slip in crystals of, asymmetry of, 25:35281
Mo--Ta-base, hardening in solid solutions of, parameters controlling, 25:35384
Mo--Ti-base--Zr, tensile properties of metastable beta, at 25 to 800°C, effects of strain rate and annealing temperature on anomalies in, 25:35434
Mo--W, analysis for tungsten, spectrographic, 25:34516
Mo-base--Re, microstructure of twin--slip and twin--twin interactions in, 25:35481
MOLYBDENUM CARBIDES
Mo_2C--Ni--TiC, mechanical properties of solid solution of, effects of carbon and molybdenum carbide content on, 25:35559
MOLYBDENUM FLUORIDES
vapor pressure--temperature data for, 25:34602 (CAT-645)
MOLYBDENUM ISOTOPES Mo-92
proton elastic scattering by, excitation functions for, (E), 25:36676
MOLYBDENUM ISOTOPES Mo-99
availability in peccaries following single injection of nuclear debris from Project Buggy fallout, 25:35088
beta decay of, beta spectra and log ft for, (E), 25:36772
distribution in tissues of swine following field exposure to nuclear debris at Schooner Event site, fallout, 25:35090
MOLYBDENUM ORES
structure of, studies of, 25:34756
MOLYBDENUM OXIDES
separation of ions of, from metal ions by high-voltage electrophoresis using carboxylic and hydroxycarboxylic acids, 25:34702
$BaMoO_4$--MoO_3, phase studies of, 25:35578
$CaMoO_4$--MoO_3, phase studies of, 25:35578
$MgMoO_4$--MoO_3, phase studies of, 25:35578
MoO_3--PbO, phase diagram of, 25:35581
MoO_3--$SrMoO_4$, phase studies of, 25:35578
MOLYBDENUM OXYFLUORIDES
vapor pressure--temperature data for, 25:34602 (CAT-645)
MONKEYS
radioinduced chromosome aberrations in transplanted bone marrow cells of, effects of dose on, 25:35230
MONOAMINE OXIDASE
radiation effects on activity of rat, protective effects of cystamine against, 25:35165
MONTE CARLO METHOD
biasing system in, for calculation of deep penetration of neutrons, 25:36648 (CEA-R-4145)
MOON
origin of, dynamical aspects of, (E/T), 25:36010
MOUTH
radiation effects on ascorbic acid content in gingiva of, in animals, x, 25:35219
MUCOSA
radiation effects on ascorbic acid content in oral, in animals, x, 25:35219
MUONIUM
coupling constant for, potential for skew-symmetric tensor field for, (T), 25:36571
energy level shifts of, potential for skew-symmetric tensor field for, (T), 25:36571
MUSCLES
radiation effects on ascorbic acid content in animal cheek, 25:35219
MUTATIONS
radioinduced, in Aspergillus, effects of oxygen or nitrogen on γ, 25:35121
radioinduced, in fungi for morphological and physiological variations, β and γ, 25:35256
radioinduced, in L cells for 8-azaguanine resistance, x, 25:35124
radioinduced, in mouse and rat spermatogonia, dominant lethal, 25:35129
radioinduced, in sweet cherry plants, growth, meiosis, and pollen viability studies on, 25:35127
MYOGLOBIN
radiation effects on free radical yield in, role of link between heme and protein in excitation transfer during x, 25:35106
MYXOMYCOTA
Colletotrichum capsici, radioinduced mutations for morphological and physiological variations in, β and γ, 25:35256

N

NAGASAKI
atomic bombing of, radiation effects on lipofuscin accumulation in man exposed to, 25:35241
NAPHTHALENE
effects of coatings of, on γ radiolysis products of poly(vinyl chloride), ESR studies on, 25:34656
radioinduced paramagnetic centers in single crystals of, ESR studies of 10°K neutron, 25:36287
radioinduced paramagnetic defects in single crystals of, ESR study of low-temperature neutron, 25:36277
NAPHTHALENE, 1-FLUORO-
fluoronaphthalene--D, photolysis of, excitation of $C_2(^1\Sigma/sub\ g/^+)$ in, 25:34613 (TID-25689)
NAPHTHALENE, 1-NITRO-
effects of coatings of, on γ radiolysis products of poly(vinyl chloride), ESR studies on, 25:34656
2,7-NAPHTHALENEDISULFONIC ACID, 3,6-BIS[(4-CHLORO-2-PHOSPHONOPHENYL)AZO]-4,5-DIHYDROXY-
complexes with uranium, photometric determination based on, 25:34531
2,7-NAPHTHALENEDISULFONIC ACID, 4,5-DIHYDROXY-3,6-BIS[(o-PHOSPHONOPHENYL)AZO]-
complexes with uranium, photometric determination based on, 25:34531
1-NAPHTHOL, 2-NITROSO-
effects of coatings of, on γ radiolysis products of poly(vinyl chloride), ESR studies on, 25:34656
2-NAPHTHOL, 1-NITROSO-
effects of coatings of, on γ radiolysis products of poly(vinyl chloride), ESR studies on, 25:34656
1,4-NAPHTHOQUINONE
effects of coatings of, on γ radiolysis products of poly(vinyl chloride), ESR studies on, 25:34656
1-NAPHTHYLAMINE
effects of coatings of, on γ radiolysis products of poly(vinyl chloride), ESR studies on, 25:34656
NATIONAL ACCELERATOR LABORATORY SYNCHROTRON
magnet coils for, flection, 25:36618
NATURAL BACKGROUND RADIATION
measurements in petroleum-bearing soils, uses in prospecting, 25:34731
NATURAL GAS
production stimulation by Project Wagon Wheel, prediction of explosion effects on surrounding sandstone from, 25:34770 (UCRL-50993)
production stimulation using underground nuclear explosions, cost-benefit analysis of commercial, 25:34766 (AECOP-632)
NATURAL WATERS
actinium-227/radium-226 ratio in, 25:34738
origin of highly radioactive, 25:34736
radium-226 distribution in hot spring, 25:34736
tritium content of, in Beppu City, Japan, 25:34732
uranium-234/uranium-238 ratio in, 25:34738
uranium-235/uranium-238 ratio in, 25:34738
NEBULAE
dust-radiation instability in ionized, (T), 25:35688
electron temperatures in diffuse, (E/T), 25:35650
hydroxyl emission from radio-weak, anomalous, (E), 25:35698
hydroxyl line absorption at 1665 and 1667 MHz in direction of Omega, (E), 25:35696
light polarization from, elliptical, (E), 25:35618
spectra of, fine structure in emission, (E/T), 25:35650
NEODYMIUM
determination in aqueous acetone solutions of dibenzoylmethane complexes, absorption spectrophotometric, 25:34527
determination in rare earth oxides, spectrographic, 25:34511
separation from other rare earths by ion exchange chromatography, 25:34714
NEODYMIUM ALLOYS AND SYSTEMS
Al--Nd-base, crystal lattice parameters of intermetallic Nd_2Al, 25:35495
NEODYMIUM FLUORIDES
effects on radiation stability of beryllium fluoride glasses, 25:34521
NEODYMIUM IONS
energy levels of, spin--spin and spin--other-orbit matrices for, (T), 25:35850
NEODYMIUM ISOTOPES Nd-138
electron-capture decay of, branching ratios, log-ft values, and conversion-electron and gamma spectra from, (E), 25:36725 (JINR-P6-5674)
NEODYMIUM ISOTOPES Nd-139
beta and electron-capture decay of, branching ratios, log-ft values, gamma and conversion-electron spectra, and Kurie plots from, (E), 25:36724 (JINR-P6-5673)
isomeric transitions in, branching ratio relative to beta decay, (E), 25:36724 (JINR-P6-5673)
NEODYMIUM ISOTOPES Nd-142
alpha reactions (α,2n) at 31 MeV, gamma spectra and decay-curves from, (E), 25:36792
electron elastic and inelastic scattering at 40 and 60 MeV, angular distributions for, (E), 25:36758
energy levels from electron elastic and inelastic scattering, spins, parities, and transition probabilities for, (E), 25:36758
energy levels from promethium-142 beta and electron-capture decay, spin--parity assignments for, (E), 25:36766
proton reactions (p,t) at 51.7 MeV, coupled-channel Born-approximation calculation of differential cross sections for, (T), 25:36794
NEODYMIUM ISOTOPES Nd-143
energy levels of, unified model calculations for, (T), 25:36749
neutron capture by, γ circular polarization from thermal, (E), 25:36751
NEODYMIUM ISOTOPES Nd-144
energy levels fom neodymium-143 thermal neutron capture, spin-parity assignments for, (E), 25:36751
NEODYMIUM ISOTOPES Nd-146
electron elastic and inelastic scattering at 40 and 60 MeV, angular distributions for, (E), 25:36758
energy levels from electron elastic and inelastic scattering, spins, parities, and transition probabilities for, (E), 25:36758
photon reactions (γ,xn) in giant resonance region, cross sections for, (E), 25:36755
NEODYMIUM ISOTOPES Nd-148
determination as measure of fission product concentration in spent uranium oxide (UO_2) by isotope dilution, 25:37015 (BNWL-1568)
NEODYMIUM ISOTOPES Nd-150
electron elastic and inelastic scattering at 40 and 60 MeV, angular distributions for, (E), 25:36758
energy levels from electron elastic and inelastic scattering, spins, parities, and transition probabilities for, (E), 25:36758
NEODYMIUM OXIDES
growth of single-crystal solid solutions with another rare earth oxide by Verneuil method, formation regions in, 25:35525
NEON
index of refraction of, at 24.95 to 32.5°K, 25:34963 (CONF-700623-(Vol.1), pp 543-54)
ionization by protons at 4 MeV, pressure dependence of, 25:35888
oscillator strengths for excitation and ionization of, tables of calculated generalized, 25:35844 (SC-RR-70-406)
reactions of atoms and ions of, with alkali metal halides at 0.2 to 6 keV, electron emission induced by, 25:35840
reactions with methane under simulated radiolysis conditions, mass spectrometric studies on, 25:34645
H_2--Ne, index of refraction of, at 24.60 to 27.15°K and 5.83 to 22.30 mole percent neon, 25:34963 (CONF-700623-(Vol.1), pp 543-54)
H_2--Ne, properties for use in large cryogenic bubble chambers, 25:34962 (CONF-700623-(Vol.1), pp 532-42)
NEON IONS
reactions of multiply charged, with flowing methane--nitrogen and nitrogen--oxygen systems at 7 MeV/n, 25:34567
reactions with alkali metal halides at 0.2 to 6 keV, electron emission induced by, 25:35840
spectra of Ne VII and Ne VIII, grazing-incidence, (E), 25:35766
stopping cross sections for carbon foils, effects of thickness and scattering angle on, 25:36248 (GIPR-41)
NEON ISOTOPES
separation by thermal diffusion, 25:34807(R) (MLM-1793)
NEON ISOTOPES Ne-20
alpha elastic and inelastic scattering at 22.5 MeV, differential cross sections for, (E), 25:36657
energy levels of, alpha-particle-model calculations of rotational, (T), 25:36680
lattice dynamics at high pressure, 25:37204 (NYO-3655-51)
proton reactions (p,n) at 16.5 MeV, threshold energy and Q-value for, (E/T), 25:36710
NEON ISOTOPES Ne-21
concentration by thermal diffusion, 25:34807(R) (MLM-1793)
NEON ISOTOPES Ne-22
alpha elastic and inelastic scattering at 22.5 MeV, differential cross sections for, (E), 25:36657
alpha inelastic scattering at 16.5 to 21.0 MeV, energy spectra from, (E), 25:36698
concentration by thermal diffusion, 25:34807(R) (MLM-1793)
energy levels from alpha inelastic scattering, spin--parity assignments for, (E), 25:36698
energy levels of, two-hole eight-particle, (E), 25:36822
NEOPRENE
diffusion of halogenated solvents through drytox gloves of, 25:34605 (RFP-1608)
NEPTUNIUM
complexes with 1,3-diketones, stability of, 25:34557 (KFK-1339)
complexes with DTPA, preparation and stability of, 25:34558 (SRARI-P-92)
thermal conductivity of α phase of, at 300°K, 25:35424
NEPTUNIUM ISOTOPES Np-237
deuteron reactions (d,2n) at 12 to 18 MeV, cross sections and excitation functions for, (E), 25:36795

deuteron reactions (d,pf) at 13 MeV, analysis using double-humped barrier, (E/T), 25:36746
NEPTUNYL COMPOUNDS
preparation and properties of, 25:34557 (KFK-1339)
NERVES
radiation effects on fibers of, mechanism for, 25:35210
NEUTRINOS
astronomy of, heavy leptons in, (T), 25:36462
interactions $\nu + p \rightarrow \nu + p$, field exchange for, (T), 25:36571
interactions at high energies, review of semi-leptonic, (T), 25:36471
interactions $\nu + e \rightarrow \nu + e$, field exchange for, (T), 25:36571
interactions $\nu + N$, structure functions for vector and axial vector currents in deep inelastic, (T), 25:36455 (ORO-3992-24)
interactions of, structure functions for vector and axial vector currents in $\nu + N$ deep inelastic interactions for deep inelastic electron interaction relations with deep inelastic, (T), 25:36455 (ORO-3992-24)
mass--energy in early Universe due to, (T), 25:35805
research using large hydrogen bubble chambers at 15 to 80 GeV, 25:34941 (CONF-700623-(Vol.1), pp 56-96)
NEUTRINOS (anti ν/sub μ/)
interactions anti $\nu + p \rightarrow n + \mu^+$ at high energies, weak boson theory for form factor effects on, (T), 25:36460
NEUTRON CHOPPERS
characteristics for time-of-flight spectroscopy, calculation of, 25:34919 (UARAEE-61)
NEUTRON CROSS SECTIONS
data files on, formats and procedures for ENDF, (E), 25:36719 (BNL-50274)
evaluation and testing of ENDF/B, using JOSHUA system, 25:36737 (TID-25690)
evaluation for fissile nuclei in unresolved-resonances region, fluctuation factors for theoretical, (T), 25:36722 (IA-1208)
fit to scattering by hydrogen at 22.5 to 400 MeV, analytical expression from least-squares, (E), 25:36661 (UCRL-20295)
NEUTRON-DIFFRACTION ANALYSIS
cryo-orienter for, between liquid-helium and room temperatures, 25:36080
data from, programs for management and processing of, 25:36309 (AAEC/TM-578)
use in magnetic structure determinations of rhombohedral and hexagonal systems, tables from, 25:36311 (NP-18845)
NEUTRON MONOCHROMATORS
development of multicrystal, for time-of-flight spectroscopy, 25:34917 (JUL-719-FF)
NEUTRON SOURCES
design of intense, 25:36656(P)
design of variable-rate, based on (α,n) reaction using radioisotope source, 25:36657(P)
design parameters of liquid deuterium cold, for high flux reactors, 25:37087
emission rates of radioisotope, methods for measuring, (E), 25:34879
neutron angular distribution from tritium (d,n), associated particle system for measuring polarized, 25:34901
spectra from typical, (E), 25:34879
target for monoenergetic tritium (p,n), design of gas, 25:36633
NEUTRON SPECTROMETERS
design and operation of synchronized chopper time-of-flight, at IBR-30 reactor, 25:34916 (JINR-E14-5731)
design using lithium-6 fluoride and silicon surface-barrier detector for detecting tritons from lithium-6 (n,t) reaction, for neutron spectroscopy, 25:34925
operation of double statistical chopper for elimination of inelastic scattering in time-of-flight, 25:34929
performance of stilbene scintillation, 25:34920 (UARAEE-91)
resolution function for mechanical time-of-flight, calculation of, 25:34919 (UARAEE-61)
NEUTRON STARS
atomic ground states in, (T), 25:35644
electric potential of, (T), 25:35615
formation of, physics of, (T), 25:35660
gamma emission from, polarized, (T), 25:35677
magnetic fields in, origin of, (T), 25:35621
magnetohydrodynamics of, (T), 25:35601
molecule formation in, (T), 25:35645
NEUTRONS
angular distribution of polarized, from tritium (d,n) reactions, associated particle system for measuring, 25:34901
attenuation in water, activation detector measurements and Monte Carlo analysis of, 25:36652 (WAPD-TM-951)
capture by gold-197 at 0.01 eV to 20 MeV, excitation functions for, (E), 25:36741 (WHAN-SA-107)
capture by hydrogen at 10^{-5} to 10^7 eV, cross section evaluation for ENDF/B, 25:36660 (LA-4574)
capture by natural molybdenum, tantalum-181, and uranium-238 at 1 to 1000 keV, cross sections for, (E), 25:36729(R) (N-70-41999)
capture by nuclei, effect of doorway-state resonances in, (T), 25:36834
capture by technetium-99 at 1 keV to 3 MeV, excitation functions for, (T), 25:36720 (CONF-710301-4)
capture of A = 24 to 239 nuclei, tables of gamma rays from, (E), 25:36718 (AAEC/TM-585)
decay $n \rightarrow p + e + \text{anti } \nu$, angular correlations of neutron spin and antineutrino momentum in, (E), 25:36385 (IAE-1947)
detection and measurement of mean energy of, boron trifluoride ionization detector for, 25:34906
detection and measurement of, development of self-powered detectors for in-core, 25:34877
detection at 25 km in atmosphere, high-energy solar flare-associated, (E), 25:35772
detection of fast, design of cellulose nitrate dielectric track detectors for, 25:34875(P)
detection of, energy threshold of Makrofol dielectric track detectors for, 25:34902
detection of, instruments, measurement techniques, and standards for, 25:35137
diffusion in reactors, computer program for solving multigroup, (T), 25:36651 (UARAEE-107)
dosimetry of, bibliography on fission foil--dielectric track detectors for, 25:34867 (NP-18849)
effects on boronated and hafnated graphite, (E), 25:36977(R) (GA-10501)
effects on carrier properties of graphite, (E/T), 25:36284
effects on ESR of carbon black, 25:36341
effects on frequency of nonselective markers in Escherichia coli, donor, 25:35126
effects on hypoxanthine content in rat brain, 25:35226
effects on inducing boiling in superheated liquids, (E), 25:34798
effects on inorganic and organic compounds, ESR studies on, 25:34634(R) (CCC-1385-37)
effects on internal friction of boron--iron alloys, 25:35588
effects on ionic single crystals at low temperatures, bleaching of color centers induced in, 25:36290
effects on iron--nickel alloy, magnetic anisotropy study of ordering induced in, (E), 25:36281
effects on metals, research progress on computer study of mechanism of, 25:35504(R) (ORO-3912-4)
effects on naphthalene and anthracene crystals at 10°K, ESR of paramagnetic centers induced in, 25:36287
effects on naphthalene single crystals at low temperatures, ESR of paramagnetic defects induced in, 25:36277
effects on Pisum seeds, mutagenic, 25:35122
effects on production of magnetic resonance in meteorites and lunar materials, (E), 25:35598
effects on strontium oxide, magnetic circular dichroism--ESR study of F^+ center induced in, 25:36291
flux distribution in reactor cores, effects of cylindrical water cavities on, (T), 25:37117 (UARAEE-58)
flux in high-altitude equatorial atmosphere, relation to radiation-belt proton flux, (E), 25:35998
flux measurement of, standards for biological and physical applications, (E), 25:34879
flux measurements of, design of fission chamber for in-core, 25:34884(P)
flux measurements of, design of fission chamber for, 25:34883(P)
flux spectra in reactors, integral transport theory calculation of epithermal, 25:37115 (RISO-234)
flux synthesis in reactors, functionals for discontinuous-trial-function, (T), 25:37130
flux synthesis in reactors, SYN code for two-dimensional, 25:37112 (GEAF-13672)
interactions $e + n$ at very high energies, neutron internal structure determination from, (E/T), 25:36448
interactions $K^+ + n \rightarrow K^0 + p$ at 600 MeV/c in deuterium bubble chamber, K + N phase shifts from K^0 angular distribution and p polarization in, (E), 25:36417
interactions n + d, calculation of doublet scattering length using rank-four separable potentials, (T), 25:36659 (INR-P-1234)
interactions n + d, potentials with hard-core repulsion for doublet length for, (T), 25:36536
interactions n + e from neutron diffraction by tungsten-186, coherent amplitudes for, (E/T), 25:36280 (JINR-E3-5713)
interactions n + p at 510 and 600 MeV, spark chamber spectrometer study of Wolfenstein triple scattering parameters for, (E), 25:36397
interactions $p + n \rightarrow p + n$ interactions at 612 MeV, spark chamber study of depolarization in, (E), 25:36290 (JINR-P1-5743)
interactions p + n at 22.8 GeV/c, distribution of shower particles from, (E), 25:36392
leakage from water-moderated tanks, escape fractions and reflection coefficients for, (E/T), 25:36653
production in $\pi^- + p \rightarrow 2\pi^0 + n$ interactions at 447 MeV, spectrometer and spark chamber study of differential cross sections and angular distributions for, (E), 25:36405 (JINR-P1-5781)
reactions (n,2n) with beryllium and beryllium oxide, fast fission factor for, (E/T), 25:37110
reactions (n,f) with plutonium-239 up to 5.5 MeV, effect of excitation energy on fragment kinetic energies and yields from, (E), 25:36754

XUM

reactions (n,f) with uranium-235 at 12.5 to 350 keV, structure in the cross section for, (E), 25:36735 (UCRL-73090)
reactions (n,p) with nuclei with analog-dipole excitation, collective theory for, 25:36835
reactions with hydrogen at 10^{-5} to 10^{7} eV, total cross section evaluation for ENDF/B, 25:36660 (LA-4574)
reactions with nuclei at 1 to 3500 MeV, computer program for intranuclear-cascade calculations of, (T), 25:36733 (ORNL-4564)
reactions with nuclei, effect of nonuniform targets on total cross section measurements for, 25:36811
reactions with sodium-23 at 100 eV to 15 MeV, ENDF/B evaluation of total cross section for, (E), 25:36693 (WARD-4181-2)
resonance integrals in reactors, numerical and semi-analytical calculations of, 25:37115 (RISO-234)
scattering by hydrogen at 10^{-5} to 10^{7} eV, evaluation of elastic total cross section and angular distributions for ENDF/B, 25:36660 (LA-4574)
scattering by hydrogen in hydrogen-bonded ferroelectrics above the Curie point, differential cross sections for inelastic, (E), 25:36668
scattering by lattice vibrations in deuterated ammonium chloride at 85°K, inelastic, 25:36322
scattering by quantum fluid in Boltzmann statistics for temperature Green functions, (T), 25:36373
scattering by tungsten-186, n + e interactions from, (E/T), 25:36380 (JINR-E3-5713)
scattering in study of random motions in solids, review, 25:36313
spectral measurements of, standards for biological and physical applications, (E), 25:34879
structure determination from e + n interactions at very high energies, internal, (E/T), 25:36445
thermalization in reactor materials, review of, (E/T), 25:37118 (UARAEE-52)
thermalization in zirconium hydride, analytic scattering model for time-dependent, (E/T), 25:37132
transmission of slow, in multiple-segment ducts in water shield, 25:36252 (UARAEE-104)
transport equation, numerical solution to space-, angle-, energy-dependent integral, (T), 25:36266
transport in infinite two-dimensional lattices of absorption lines, one-velocity flux distribution for, (T), 25:36654
transport in matter, Monte Carlo calculation of long-range, (T), 25:36648 (CEA-R-4145)
transport in media, computer program for calculating collapsed cross sections and transfer matrices for, (T), 25:36649 (CONF-710302-11)
transport in moderators, bounds of integral operators in Hilbert space for, (T), 25:37129
transport in multidimensional heterogeneous reactor configurations, approximate procedures for numerical solution of, (T), 25:36647 (ANL-7779)

NEUTRONS, COLD
scattering by bismuth-209, decay constants and diffusion lengths for pulsed, (T), 25:36655
scattering by cubic-structure metals, lattice vibrational spectra and physical characteristics from, 25:36319

NEUTRONS, EPITHERMAL
flux distribution in radially reflected reactor, effects of partially inserted control rods on, (T), 25:37131
flux measurement of, standards for biological and physical applications, (E), 25:34879
reactions (n,f) with plutonium-239 at 14.3 to 100 eV, fission-neutron multiplicities for, (E), 25:36734 (ORNL-TM-3331)

NEUTRONS, FAST
attenuation by calcium-based concretes at 14 MeV, (E), 25:36260
capture by plutonium-239 and uranium-235, cross sections for, (E), 25:36756
effects on Alumel/Chromel thermocouples, 25:35072 (HEDL-SA-152)
effects on aluminum at low temperatures, electric conductivity study of damage production rate in, 25:36286
effects on coated particle fuels, 25:36978(R) (GA-10560)
effects on creep of fuel particle coating of pyrolytic carbon, 25:35586
effects on diamond single crystals, 25:34619
effects on dimensional changes and creep in spherically restrained and unrestrained isotropic carbon at 600 to 1250°C, 25:35585
effects on dislocation density of copper monocrystals in stress-applied and stress-removed states, electron microscope study of, 25:35518
effects on hardening in bcc metals, 25:35507
effects on helium production in stainless steel, 25:35503 (HEDL-SA-193)
effects on high-purity alpha-iron, magnetic after-effect study of, 25:36294
effects on internal friction of monocrystalline sodium chloride, relations with strain amplitude, 25:35587
effects on lead titanate and zirconate, thermodynamic properties of defects induced in, 25:36297
effects on mechanical properties of iron and carbon--iron, carbon--iron--manganese, and iron--manganese alloys at 80 to 1000°C, relations with composition, 25:35505 (ZJE-99)
effects on mechanical properties of niobium alloys, stainless steel, steel, and zirconium alloys, relations with environment, 25:35506
effects on mechanical properties of prestressed concretes, 25:37007(T) (ORNL-tr-2470)
effects on properties of graphite, 25:36978(R) (GA-10560)
effects on properties of titanium modified Incoloy 800, 25:35510
effects on Stage I dislocation arrangement of deformed copper monocrystals in stress-applied state, electron microscope study of, 25:35520
effects on Stage II dislocation arrangement of deformed copper monocrystals in stress-applied state, electron microscope study of, 25:35519
effects on tensile properties of Type 304 stainless steel, 25:35509
effects on thorium carbide (ThC_2)--uranium carbide (UC_2) and uranium carbide (UC_2) coated particles, 25:37018 (JUL-701-RW)
effects on void formation in Type 304 stainless steel at 400 to 600°C, predicted and experimental study of, 25:35516
effects on void growth in solids, model for, 25:35511
flux measurement of, standards for biological and physical applications, (E), 25:34879
reactions (n,a) and (n,p) with nuclei, cross sections for radioisotope production in, (E), 25:36686 (CONF-680986-1)
reactions (n,a) with aluminum-27, cross sections for, (E), 25:36688(R) (N-70-43042)
reactions (n,a) with copper-63 at 0.1 to 18 MeV, excitation functions for, (E), 25:36741 (WHAN-SA-107)
reactions (n,d) with helium-3 and tritium at 14.4 MeV, angular distributions for, (E), 25:36738(R) (UCLA-10-P-18-23)
reactions (n,f) with plutonium-235 and uranium-235, cross sections for, (E), 25:36756
reactions (n,f) with uranium-235 and -238 at 14 MeV, angular anisotropy of fragments from ternary, (E), 25:36759
reactions (n,f) with uranium-235 at 0.1 to 1.5 MeV, prompt-neutron yields from, (E/T), 25:36786
reactions (n,p) with aluminum-27 and magnesium-24, cross sections for, (E), 25:36688(R) (N-70-43042)
reactions (n,p) with nickel-58 at 14.8 and 22 MeV, collective treatment of analog-dipole excitations in, (T), 25:36835
reactions (n,p) with silicon-30 at 15 MeV, cross section for, (E), 25:36715
reactions with carbon, zirconium, and zirconium-90 at 0.433 to 2.37 MeV, total cross sections for, (E), 25:36740 (WAPD-T-2411)
reactions with nitrogen-15 at 0.1 to 12 MeV, coupled-channels analysis of total cross sections for, (T), 25:36683
reactions with nitrogen-15 at 0.9 to 32 MeV, R-matrix analysis of reactions with, (E), 25:36684
reactions with plutonium-239, uranium-233, and uranium-235, total cross section and resonance parameters for, (E), 25:36756
scattering by hydrogen at 22.5 to 400 MeV, least-squares fit to differential cross sections for elastic, (E), 25:36661 (UCRL-20295)
scattering by nitrogen-15 at 0.8 to 3.1 MeV, phase-shift analysis of cross-section and polarization angular distributions and excitation functions for elastic, (E), 25:36684
scattering by nitrogen-15 at 1.94 to 2.64 MeV of polarized, analyzing power from elastic, (E), 25:36684
scattering by nitrogen-15 at 2 to 3 MeV, coupled-channels analysis of differential cross sections for elastic, (T), 25:36683
scattering by sodium at 5.0 MeV, differential and integrated cross sections and spectra from elastic and inelastic, (E), 25:36685 (AWRE-O-3/71)
scattering by zirconium-90 at 2.1 and 5.17 MeV, differential cross sections for elastic, (E), 25:36740 (WAPD-T-2411)
spectra in reactors, threshold detector measurements of, (T), 25:37109 (UJV-2423-RF)
spectra in reflector of swimming pool reactor, effects of metal slabs on perturbations in, (E/T), 25:37057 (CEA-R-3799)
spectrum measurements for fast reactors, time-of-flight methods for, (E/T), 25:36991(R) (GULF-RT-10523)
use in defectoscopy, design and performance of equipment for, 25:34825

NEUTRONS, FISSION
multiplicities from plutonium-239 fission at 14.3 to 200 eV, (E), 25:36734 (ORNL-TM-3331)
spectrum from californium-252 spontaneous fission, background effects on measurement of Maxwellian temperature of, (E), 25:36728 (KFKI-71-9)

NEUTRONS, FUSION
production by laser irradiation of solid deuterium targets, 25:36203

NEUTRONS, INTERMEDIATE
flux measurement of, standards for biological and physical applications, (E), 25:34879
reactions (n,f) with plutonium-239 at 100 to 200 eV,

XUM

fission-neutron multiplicities for, (E), 25:36734 (ORNL-TM-3331)
reactions with plutonium-239 and uranium-235 at 0.1 to 30 keV, capture-to-fission ratio in, (E), 25:36748
NEUTRONS, PILE
capture by A = 147 to 173 nuclei, cross sections and resonance integrals for, (E), 25:36735 (SGAE-PH-104/1971)
capture by A = 99 to 169 nuclei, spectrum-averaged cross sections for, (E/T), 25:36720 (CONF-710301-4)
effects on corrosion of zirconium and zirconium alloys, 25:35513
effects on mechanical properties of Type A302B steel, 25:35508
NEUTRONS, PROMPT
yields from neutron fission of uranium-235 at 0.1 to 1.5 MeV, (E/T), 25:36786
NEUTRONS, THERMAL
capture by A = 147 to 173 nuclei, cross sections and resonance integrals for, (E), 25:36735 (SGAE-PH-104/1971)
capture by cerium-140, neodymium-143, lanthanum-139, γ circular polarization from thermal, (E), 25:36751
capture by iron, gamma spectra from, (E), 25:36692 (UARAEE-103)
diffusion in nonmultiplying media, review of calculations of spectra at vacuum interface of, (T), 25:36650 (UARAEE-60)
dosimetry of, development of phosphate-glass luminescent dosimeters for, 25:35037(P)
effects on potassium ferrocyanide, chemical, 25:34663
flux distribution in radially reflected reactor, effects of partially inserted control rods on, (T), 25:37131
flux measurement of, standards for biological and physical applications, (E), 25:34879
flux spectra in monatomic moderators, numerical solution of, (T), 25:37120 (UARAEE-69)
flux spectra in reactors, one-group Milne method solution of, (E/T), 25:37116 (UARAEE-56)
reactions (n,f) with uranium-233 and -235, beta energy release following, (E/T), 25:36764
reactions (n,f) with uranium-235, prompt gamma spectra in coincidence with, (E), 25:36743
reactions (n,f) with uranium-235, ranges in pyrocarbon of fragments from, 25:36264
reactions (n,γ) with curium-244, -245, -246, -247, -248 and californium-249, cross sections and resonance integrals for, (E), 25:36721 (DP-MS-70-95)
reactions (n,f) with uranium-235, cross sections for cesium and rubidium production from, (E), 25:36730 (NP-18829)
scattering by excited states of nuclei, kernel for describing inelastic, (T), 25:36707
scattering in reactor moderators, upward and downward kernels for, (T), 25:37123 (UARAEE-80)
spectra in reactor materials, review of, (E/T), 25:37118 (UARAEE-62)
spectra in reactor moderators, effects of probe on space--energy distribution of, (E/T), 25:37137 (UARAEE-75)
transmission through ducts perpendicular to neutron beam axis in water shields, (E/T), 25:36251 (UARAEE-86)
NEW MEXICO
geology and hydrology of Mesita del Buey, studies for underground disposal of radioactive wastes, 25:34846 (LA-4660)
NEWBOLD ISLAND POWER REACTOR, UNIT 1
design parameters of, revised and additional data on, 25:36883 (DOCKET-50354-14)
operations aspects of, revised and additional data on, 25:36883 (DOCKET-50354-14)
NEWBOLD ISLAND POWER REACTOR, UNIT 2
design parameters of, revised and additional data on, 25:36883 (DOCKET-50354-14)
operations aspects of, revised and additional data on, 25:36883 (DOCKET-50354-14)
NICKEL
determination of trace amounts of, in copper by neutron activation, 25:34548
determination of trace amounts of, in uranium by neutron activation, 25:34547 (UARAEE-68)
effects of binder of, on sintering of tungsten carbide powders, 25:35534
effects on colorimetric determination of gold, 25:34521
effects on gravimetric determination of mercury using 2-aminobenzothiazole, 25:34520
effects on photometric determination of antimony following solvent extraction using TBP, 25:34512
neutron scattering by, lattice vibrational spectra and physical characteristics of, 25:36319
nuclear spin--lattice relaxation times from cobalt-60 NMR at 0.004 to 0.010°K, (E/T), 25:36347
oxidation of hydrogen-annealed, thermodynamics of, 25:35291
properties for use as condenser and heat exchanger tubes, 25:35361
proton reactions at 10 to 40 MeV, activation cross sections for, (E), 25:36738(R) (UCLA-10-P-18-23)
radioinduced defect clusters in foils of, threshold energy of electron, 25:36301
radioinduced defect clusters in thin foils of, growth of 650-keV electron, 25:36299
radioinduced Frenkel Pairs in, computer study of relations of carbon with neutron, 25:35504(R) (ORO-3912-4)
separation of ions of, from metal ions by high-voltage electrophoresis using carboxylic and hydroxycarboxylic acids, 25:34702
sodium boiling superheat at surfaces of, effects of roughness on, 25:34791 (KFK-1332)
NICKEL ALLOYS AND SYSTEMS
creep and deformation of unidirectional solidified eutectic, 25:35431
properties for use as condenser and heat exchanger tubes, 25:35361
Al--C--Co--Cr--Mo--Nb--Ni-base--Ta--Ti--Zr, properties of corrosion-resistant IN-738 superalloy, 25:35400
Al--Cr--Fe--Ni-base--Ti, tensile properties at 25 to 850°C, effects of grain size, precipitates, and test time on, 25:35340 (UARAEE-55)
Al--Cr--Mo--Ni-base--Ti, solvus temperature of γ' in, effects of hardener content on, 25:35460
Al--Cr--Ni-base--Ti, solvus temperature of γ' in, effects of hardener content on, 25:35460
Al--Cr--Ni-base--Ti--W, phase precipitation in, relations of heat treatments with microstructure of, 25:35502
Al--Cr--Ni-base--W, reactions of cladding of, for chromium--tungsten alloy with air and nitrogen at 2100 and 2300°F, resistance to oxidation, 25:35288
Al--Ni, creep in stoichiometric, 25:37180 (COO-1489-10)
C--Co--Cr--Fe--Mo--Nb--Ni-base, strengthening by precipitation of body-centered tetragonal phase in, 25:35302
C--Co-base--Cr--Fe--Ni--Ta--Ti--W, fracture toughness of Mar-M-509, effects of carbide inclusions on, 25:35490
C--Cr--Fe--Mo--Nb--Ni-base, strengthening by precipitation of body-centered tetragonal phase in, 25:35302
Co--Cr--Mo--Ni, hardening of multiphase, mechanisms of, 25:35396
Co--Ni--V, mechanical properties of, effects of crystal ordering on, 25:35385
Cr--Fe--Ni, corrosion of Unitemp 605, by lithium--selenium mixtures at 375°C, 25:35275(R) (ANL-7777)
Cr--Fe--Ni, standard for cold-drawn and hot-finished seamless pipe and tube for general corrosive service and heat-resisting uses, 25:35413
Cr--Fe--Ni, standard for hot-finished and cold-drawn rounds, squares, hexagons, and rectangles of, 25:35364
Cr--Fe--Ni, standard for plates, sheets, and strips of, 25:35360
Cr--Fe--Ni-base, tensile properties at 25 to 850°C, effects of grain size, precipitates, and test time on, 25:35340 (UARAEE-55)
Cr--Nb--Ni-base, plastic deformation of precipitation hardened, 25:35483
Cr--Nb--Ni-base, precipitation in, mechanism of, 25:35483
Cr--Nb--Ni-base, strengthening by precipitation of body-centered tetragonal phase in, 25:35302
Cr--Ni--steel, welding to Inconel 625, tungsten inert gas method for, 25:35311
Cr--Ni-base, mechanical properties of dispersion-strengthened, at high temperatures, 25:35352
Cr--Ni-base--Ta, plastic deformation of precipitation hardened, 25:35483
Cr--Ni-base--Ta, precipitation in, mechanism of, 25:35483
Fe--Nb--Ni--Sn--Zr-base, properties of dilute, for use in organic cooling circuits, 25:35329(P)
Fe--Ni, radioinduced ordering in, magnetic anisotropy study of neutron, (E), 25:36281
Fe-base--Nb--Ni, precipitation in, effects of aging at 700 to 800°C on, 25:35499
Mn--Mo--Ni--steel, properties of plates of, for use in pressure vessels, standard for, 25:35473
Mo_2C--Ni--TiC, mechanical properties of solid solution of, effects of carbon and molybdenum carbide content on, 25:35559
Mo--Ni-base, slip in, mechanism of cross, 25:35286
Nb--Ni, fatigue of eutectic composite Ni--Ni_3Nb, cyclic behavior of, 25:35462
Nb--Ni, mechanical properties of eutectic composite Ni--Ni_3Nb, monotonic behavior of, 25:35461
Nb--Ni, precipitation of metastable Ni_3Nb phases in, effects of aluminum and iron on, 25:35480
Nb--Sn, effects of alloying on superconducting transition temperature of intermetallic Nb_3Sn, 25:36040
Ni--P, effects on sintering of tungsten powders, 25:35354
Ni-base--Ta, strengthening by precipitation of body-centered tetragonal phase in, 25:35302
Ni-base--V, oxidation by air at high temperatures, effects of composition on kinetics of, 25:35289
NICKEL ISOTOPES Ni-58
deuteron reactions (d,pn) at 13.6 MeV, diffraction-model analysis of proton--neutron correlations in, (E/T), 25:36713
neutron reactions (n,p) at 14.8 and 22 MeV, collective treatment of analog-dipole excitations in, (T), 25:36835
proton reactions (p,d) and (p,t) at 22 to 40 MeV, differential cross sections for, (E), 25:36738(R) (UCLA-10-P-18-23)

XUM

NICKEL ISOTOPES Ni-60
deuteron inelastic scattering at 13.6 MeV, binding- and optical-model calculations of differential cross sections for, (T), 25:36848
deuteron reactions (d,pn) at 13.6 MeV, diffraction-model analysis of proton--neutron correlations in, (E/T), 25:36713
NICKEL ISOTOPES Ni-61
deuteron reactions (d,pn) at 13.6 MeV, diffraction-model analysis of proton--neutron correlations in, (E/T), 25:36713
NICKEL ISOTOPES Ni-62
deuteron reactions (d,pn) at 13.6 MeV, proton spectra and diffraction-model analysis of proton--neutron in, (E/T), 25:36713
NICKEL ISOTOPES Ni-63
energy levels from (n,γ) reactions, phonon-particle doorway states in, (T), 25:36703
energy levels from nickel-62 neutron capture, analysis of anticorrelation between reduced widths and E1 transition probabilities for, (T), 25:36834
NICKEL ISOTOPES Ni-64
deuteron reactions (d,pn) at 13.6 MeV, diffraction-model analysis of proton--neutron correlations in, (E/T), 25:36713
NICKEL OXIDES
radiation effects on subsequent catalytic activity of, in decomposition of hydrogen peroxide, γ, 25:34630
NICOTINAMIDE-ADENINE DINUCLEOTIDE
radiolysis of aqueous solutions of, ESR spectral studies on free radical yields from x, 25:34655
reduced, radiation effects on inactivation of, mechanism of uv, 25:35107
DPN--glutamic acid, radiolysis of aqueous solutions of, ESR spectral studies on free radical yields from x, 25:34655
DPN--glutaric acid, radiolysis of aqueous solutions of, ESR spectral studies on free radical yields from x, 25:34655
NIEDERAICHBACH POWER REACTOR
moderator tank for, welding methods for, 25:35322
NIMONIC
cracking of C263 and PK33, relations of microstructure with postweld heat treatment, 25:35453
NIMONIC 80A
cracking of, relations of microstructure with postweld heat treatment, 25:35453
NIOBIUM
coating with aluminum, study of hot dipping method for, 25:35314
corrosion by lithium--selenium mixtures at 375°C, 25:35275(R) (ANL-7777)
deformation of monocrystalline, at 2.17 to 17°K, heterogeneous flow processes in, 25:35378
determination by polarography, effects of various cations on, 25:34526
determination by proton activation, 25:34554
determination of sum of tantalum and, in ore processing solutions, gravimetric, 25:34510
dislocations in monocrystalline, activation energy anisotropy of, 25:35443
effects as an additive on properties of thermomechanically processed Type 348 stainless steel, 25:35300
effects on carbon diffusion from ferritic steel, 25:35407
effects on formation of intermetallic copper--titanium compounds during explosion welding, 25:35324
electric conductivity in reversible superconducting transitions of wire samples, specific residual, 25:36055
electric conductivity of ultrahigh purity, residual, 25:35328
magnetic flux transport voltages in foils of superconducting, time-dependent, (E), 25:36061
magnetization of superconducting, 25:36046
oxidation at 450 to 1000°C, effects of nitrogen on linear, 25:35292
oxidation of polycrystalline, at 300 to 500°C, design of equipment for measuring kinetics of, 25:35280
plastic deformation at low temperatures, stress-differential effects in, 25:35373
plastic flow anisotropy in monocrystalline, mechanisms of, 25:353/9
plastic flow in monocrystalline, effects of interstitial nitrogen on thermally-activated, 25:35372
preparation of ultrahigh purity, electroplating and vacuum degassing method for, 25:35328
properties for use for consolidation or melting, standard for, 25:35449
properties of bars, rods, and wires of, standard for, 25:35448
properties of electrolytic superconducting films of, 25:36056
properties of ingots of, standard for, 25:35447
properties of seamless and welded tubes of wrought, standard for, 25:35478
properties of sheets, foils, and plates of, standard for, 25:35446
radiation effects on hardening of bcc, fast neutron, 25:35507
radioinduced hardening of interstitial-containing, relations of complex defects with electron, 25:35517
stacking faults in, x-ray studies of formation of, 25:35493
superconducting Josephson effect in contacts with mercury, ac, (E), 25:36068
superconductivity of powder composites and wires of oxygen-containing, relations with dislocation cell structure, effects of stresses on, (E/T), 25:36057
tensile properties of monocrystalline, effects of dislocation subgrain structure on, 25:35376
tensile properties of polycrystalline, effects of cyclic stressing on, 25:35425
NIOBIUM ALLOYS AND SYSTEMS
coating with aluminum, study of hot dipping method for, 25:35314
Al--C--Co--Cr--Mo--Nb--Ni-base--Ta--Ti--Zr, properties of corrosion-resistant IN-738 superalloy, 25:35400
Al--Nb--Ti, heat resistance of titanium-coated, 25:35325
C--Co--Cr--Fe--Mo--Nb--Ni-base, strengthening by precipitation of body-centered tetragonal phase in, 25:35302
C--Cr--Fe--Mo--Nb--Ni-base, strengthening by precipitation of body-centered tetragonal phase in, 25:35302
Cr--Nb--Ni-base, plastic deformation of precipitation hardened, 25:35483
Cr--Nb--Ni-base, precipitation in, mechanism of, 25:35483
Cr--Nb--Ni-base, strengthening by precipitation of body-centered tetragonal phase in, 25:35302
Fe--Nb--Ni--Sn--Zr-base, properties of dilute, for use in organic cooling circuits, 25:35329(P)
Fe-base--Nb--Ni, precipitation in, effects of aging at 700 to 800°C on, 25:35499
H--Nb-base, preparation and pulverization of, 25:35299
Hf--Nb, tensile properties of, effects of aging at 600 to 1000°C on, 25:35393
Mo--Nb-base, hardening and softening of monocrystalline, mechanisms of solution, 25:35436
N--Nb-base, degassing of dilute, by annealing, concentration changes and metal losses during, 25:35560
Nb--Ni, fatigue of eutectic composite Ni--Ni_3Nb, cyclic behavior of, 25:35462
Nb--Ni, mechanical properties of eutectic composite Ni--Ni_3Nb, monotonic behavior of, 25:35461
Nb--Ni, precipitation of metastable Ni_3Nb phases in, effects of aluminum and iron on, 25:35480
Nb--O, plastic deformation of solid solutions of, at low temperatures, stress-differential effects in, 25:35372
Nb--O--Zr, phase transformations in, 25:35572
Nb--Re, hardening and softening of monocrystalline, mechanisms of solution, 25:35436
Nb--Sn, effects of impurities and divergences from stoichiometry of properties of superconducting intermetallic Nb_3Sn, 25:36039
Nb--Sn, magnetization of, superconducting intermetallic Nb_3Sn, 25:36046
Nb--Sn, metallurgy of superconducting intermetallic Nb_3Sn, 25:36018 (CONF-700341-7)
Nb--Sn, phase composition, structure, and magnetic hysteresis of, (E), 25:36047
Nb--Sn, photoluminescence of superconducting intermetallic Nb_3Sn, 25:36062
Nb--Sn, properties of intermetallic compounds of, obtained by diffusion, (E), 25:36045
Nb--Ta, superconducting properties of, effects of heat treatment on, 25:36054
Nb--Ta-base, hardening in solid solutions of, parameters controlling, 25:35384
Nb--$TaSi_2$, tantalum trisilicide growth in, at 1150 to 1370°C, kinetics of, 25:35577
Nb--Ti, electric conductivity at high pressures, 25:36321
Nb--Ti, metallurgy of superconducting, 25:36018 (CONF-700341-7)
Nb--Ti, microstructure of, effects of oxidation at 600 to 1300°C on, 25:35482
Nb--Ti, properties of superconducting foils in external magnetic field, (E), 25:36052
Nb--Ti--Zr, phase transformations in superconducting, 25:36051
Nb--Ti-base, critical characteristics of superconducting, in wide range of magnetic fields, 25:36048
Nb--Ti-base, structure and superconducting properties of, effect of heat treatment on, 25:36049
Nb--V--Zr, superconducting transition temperature of, 25:36042
Nb--Zr, electric conductivity in reversible superconducting transitions of wire samples, specific residual, 25:36055
Nb--Zr, fine structure of superconducting, 25:36053
Nb--Zr, magnetization of superconducting, 25:36046
Nb--Zr-base, corrosion by air and pressurized steam at 450 to 650°C, effects of heat treatment and cold work on kinetics of, 25:35278 (UARAEE-72)
Nb--Zr-base, hardening behavior of, analysis of work, 25:35394
Nb--Zr-base, radiation effects on mechanical properties of, relations of environment with fast neutron, 25:35506

Nb--Zr-base, radiation effects on work hardening of, in-pile, 25:35394
Nb-base--O, degassing of dilute, by annealing, concentration changes and metal losses during, 25:35560
Nb-base--Ti, internal friction peaks in, effects of oxygen on, 25:35410
Nb-base--Ti, oxidation at 600 to 1300°C, kinetics of, 25:35282
Nb-base--Ti, preparation of, thermodiffusion method for, 25:35325
Nb-base--Ti--Zr, critical current of superconducting, in fields up to 80 kOe, 25:36050
Nb-base--Zr, corrosion by lithium--selenium mixtures at 375°C, 25:35275(R) (ANL-7777)
Nb-base--Zr, properties of bars, rods, and wires of, standard for, 25:35448
Nb-base--Zr, properties of ingots of, standard for, 25:35447
Nb-base--Zr, properties of seamless and welded tubes of wrought, standard for, 25:35478
Nb-base--Zr, properties of sheets, foils, and plates of, standard for, 25:35446

NIOBIUM BROMIDES
reactions with sodium N,N-diethyldithiocarbamate, 25:34568

NIOBIUM CARBIDES
crystallization of powdered and hot-pressed, secondary, 25:35535
properties of plasma-sprayed layers of, at 1000°C, electric and thermal, 25:35538
superconducting energy gap of, (E/T), 25:36030

NIOBIUM CHLORIDES
reactions with sodium N,N-diethyldithiocarbamate, 25:34568

NIOBIUM FLUORIDES
vapor pressure--temperature data for, 25:34602 (GAT-649)

NIOBIUM ISOTOPES Nb-90
energy levels and transitions from decay and nuclear-reaction measurements, Nuclear Data Sheets compilation of properties of, (E), 25:36801

NIOBIUM ISOTOPES Nb-92
energy levels from zirconium-92 (p,n) reactions, lifetimes and transition probabilities for, (E), 25:36762

NIOBIUM ISOTOPES Nb-94
beta decay of, precision measurement of gamma rays from, 25:36810
energy levels from niobium-93 (n,γ) reactions, lifetimes for, (E), 25:36769
energy-level transitions from niobium-93 (n,γ) reaction, (E), 25:36769

NIOBIUM ISOTOPES Nb-95
diffusion in copper, 25:35406
energy levels from zirconium-96 (p,2n) reactions, ratio of isomeric, 25:36761

NIOBIUM ISOTOPES Nb-97
energy levels from zirconium-97 beta decay, spin--parity assignments for, (E), 25:36763
energy-level transitions from zirconium-97 beta decay, γ-γ angular correlations in, (E), 25:36763

NIOBIUM NITRIDES
superconducting transition temperatures of rf-sputtered films of, (E), 25:36065

NIOBIUM OXIDES
MnO--Nb_2O_5--PbO--$PbTiO_3$--$PbZrO_3$--Sb_2O_3, properties of piezoelectric ceramic of, for use as filter and transducer elements of mechanical filters, 25:35561(P)

NIOBIUM SELENIDES
superconductivity of, 25:36041

NITRIC ACID
determination of free, in presence of aluminum, magnesium, and uranyl nitrates, potentiometric, 25:34517

NITROCELLULOSE
particle tracks in, fast-neutron detection by etching of, 25:34875(P)

NITROGEN
alpha-particle stopping cross sections at 0.5 to 2 MeV, atomic, (E), 25:36256
alpha-particle stopping cross sections in gaseous, at 0.3 to 2 MeV, 25:36255
determination at ppM levels in milligram steel samples by inert gas fusion methods, 25:34514
determination in gluten by neutron activation, 25:34585
determination in human stones by neutron activation, 25:34546 (THAI.-AEC-39)
effects of interstitial, on thermally-activated flow in monocrystalline niobium, 25:35372
effects on γ-radioinduced mutations in Aspergillus, 25:35121
effects on linear oxidation of niobium at 450 to 1000°C, 25:35292
fission-fragment reactions and ranges in, 25:36254
fluorescence excited by fission fragments, lifetimes and energy transfer rates in, 25:36254
ion reactions at 20 to 80 keV with molecular, charge-equilibrium fractions and charge-exchange cross sections for, (E), 25:35866
ionization by protons at 4 MeV, pressure dependence of, 25:35888
oscillator strengths for excitation and ionization of, tables of calculated generalized, 25:35844 (SC-RR-70-406)
photo-absorption cross sections of molecular, review of uv, (E/T), 25:36013
reactions with aluminum--chromium--nickel--tungsten alloy-clad chromium--tungsten alloy at 2100 and 2200°F, 25:35288
reactions with methane under simulated radiolysis conditions, mass spectrometric studies on, 25:34645
solubility in molybdenum at 1600 to 2400°C and 15 to 40 torr nitrogen, equilibrium, 25:35430
solubility in tungsten at 2400 to 3050°C and 15 to 40 torr nitrogen, equilibrium, 25:35429
vapor pressure--temperature data for, 25:34602 (GAT-649)

NITROGEN FLUORIDES
vapor pressure--temperature data for, 25:34602 (GAT-649)

NITROGEN IONS
reactions of multiply charged, with flowing methane--nitrogen and nitrogen--oxygen systems at 7 MeV/n, 25:34567
stopping cross sections for carbon foils, effects of thickness and scattering angle on, 25:36248 (GIPR-41)

NITROGEN IONS (N_2^+)
reactions with gases at 10 to 1000 eV, rotational and vibrational excitation and light emission from, (E), 25:35873

NITROGEN ISOTOPES N-13
energy levels from nitrogen-14 (p,d) reactions, (E), 25:36673

NITROGEN ISOTOPES N-14
determination in thin films by nuclear reaction micro methods, 25:34550
proton elastic and inelastic scattering at 14.5 MeV, angular distributions for, (E), 25:36673
proton reactions (p,d) at 14.5 MeV, angular distributions for, (E), 25:36673
reactions (N-14,f) with holmium-165 up to 10.4 MeV/nucleon, excitation function for, (E), 25:36784

NITROGEN ISOTOPES N-15
exchange reactions of, 25:34572(R) (ORO-2234-23)
neutron elastic scattering at 0.8 to 3.1 MeV, phase-shift analysis of cross-section and polarization angular distributions and excitation functions for, (E), 25:36684
neutron elastic scattering at 1.94 to 2.64 MeV, analyzing power from polarized, (E), 25:36684
neutron elastic-scattering at 2 to 3 MeV, coupled-channels analysis of differential cross sections for, (T), 25:36683
neutron total cross sections at 0.1 to 12 MeV, coupled-channels analysis of, (T), 25:36683
neutron total cross sections at 0.9 to 32 MeV, R-matrix analysis of, (E), 25:36684

NITROGEN ISOTOPES N-16
energy levels from neutron resonances in nitrogen-15, coupled-channels calculation of energies and widths for, (T), 25:36683
energy levels from neutron resonances in nitrogen-15, widths and spin--parity assignments for, (E), 25:36684

NITROGEN OXIDES NC
abundance of interstellar, upper limits for, (E), 25:35697
photo-absorption cross sections of, review of uv, (E/T), 25:36013
reactions with methane under simulated radiolysis conditions, mass spectrometric studies on, 25:34645
vapor pressure--temperature data for, 25:34602 (GAT-649)

NITROGEN OXIDES NO_2 OR N_2O_4
photo-absorption cross sections of NO_2, review of uv, (E/T), 25:36013
vapor pressure--temperature data for, 25:34602 (GAT-649)

NITROGEN OXIDES N_2O
alpha-particle stopping cross sections in gaseous, at 0.3 to 2 MeV, 25:36255
effects on yields from γ radiolysis of 2-methyl-2-propanol, 25:34659
photo-absorption cross sections of, review of uv, (E/T), 25:36013
reactions with methane under simulated radiolysis conditions, mass spectrometric studies on, 25:34645

NITROGEN SYSTEMS
methane--N, reactions with multiply charged ions in flowing systems at 7 MeV/n, 25:34567
N--Nb-base, degassing of dilute, by annealing, concentration changes and metal losses during, 25:35560
N--O, reactions with multiply charged ions in flowing systems at 7 MeV/n, 25:34567
N--Ta, stresses in, models for interstitial hardening and Peierls, 25:35371
N--Ta-base, degassing of dilute, by annealing, concentration changes and metal losses during, 25:35560

NITROSYL FLUORIDES
vapor pressure--temperature data for, 25:34602 (GAT-649)

NITRYL FLUORIDES
vapor pressure--temperature data for, 25:34602 (GAT-649)

NOBELIUM ISOTOPES No-255
alpha decay of, alpha and x-ray spectra from, (E), 25:36778

XUM

NCVAE
gamma emission from, detection of, (T), 25:35687
NRU REACTOR
experimental facilities for, design parameters and performance of machines for measuring uniaxial creep in, 25:37054 (AECL-3738)
NRX REACTOR
experimental facilities for, design parameters and performance of machines for measuring uniaxial creep in, 25:37054 (AECL-3738)
NUCLEAR AUXILIARY POWER SYSTEMS
characteristics of radioisotope-fueled, tabulated data on, 25:34811(T) (ORNL-tr-2485)
design of thermionic, for spacecraft propulsion, 25:35937
design parameters for conceptual 2.2 MW(t) NERVA Technology Reactor, with Brayton cycle, 25:37088
thermionic cells for, steady-state power limitations of in-core, (T), 25:37090
NUCLEAR CHEMISTRY
lectures on, 25:34863 (HMI-B-108)
NUCLEAR EMULSIONS
antiproton reactions with nuclei at 5 GeV/c in, angular and momentum distributions for π^0 produced in, (E), 25:36404
cosmic alpha particle mean free paths and fragmentation above 10 GeV/nucleon in, (E), 25:36394
cosmic heavy nuclei mean free paths and fragmentation above 10 GeV/nucleon in, (E), 25:36394
ionization in, relativistic increase of, 25:34937(T) (CERN-Trans-71-9)
meson (K^-) absorption by nuclei at rest in emulsions, properties of Σ^- and Σ^+ produced in, (E), 25:36400
meson (K^-) absorption by nuclei at rest in, Q-value distribution for detection of Λ-He^5, Λ-Li^6, and Λ-Be^9 produced in, (E), 25:36401
meson (π^-) reactions with nuclei at 17.2 GeV in, properties of showers produced in, (E), 25:36418
particle tracks in, relativistic increase of ionization and sensitivity for energy dependence of density of, 25:34937(T) (CERN-Trans-71-9)
proton reactions with nuclei at 22.8 GeV/c in, method for identification of shower particles from, (E), 25:36402
proton reactions with nuclei at 24 GeV/c in, deuteron emission in, (E), 25:36403
sensitivity of, relativistic increase of, 25:34937(T) (CERN-Trans-71-9)
NUCLEAR ENGINEERING
curriculum at University of Missouri at Rolla, description of, 25:34781
NUCLEAR EXPLOSIONS
detection of direction to, apparatus for, 25:35058(P)
NUCLEAR EXPLOSIONS, UNDERGROUND
effects of Amchitka Island, Alaska, on seismic activity of nearby islands, program for monitoring, 25:34763 (CGS-746-10)
effects of Milrow, on lakes of Amchitka Island, Alaska, biological, chemical, and structural, 25:34767(R) (BMI-171-129)
natural gas production stimulation by, cost-benefit analysis of commercial, 25:34766 (AECOP-632)
stress wave propagation from rock-contained, TENSOR computer program for calculating, 25:34769 (UCRL-50987)
use of contained, for petroleum production stimulation, method for, 25:34772(P)
uses of, summary of peaceful, 25:34771
NUCLEAR ISOMERS
fission of transuranic, spontaneous, 25:36781
production of, design and performance of generator for, 25:34802 (BNL-50249)
NUCLEAR MATERIALS MANAGEMENT
control system for, during processing of breeder reactor fuels at ORNL, performance of integrated, 25:34847 (ORNL-4607)
fuel accountability for Japanese Materials Testing Reactor, computer program for, 25:37065 (JAERI-Memo-4270)
NUCLEAR MATTER
binding energy of, contribution of two-pion-exchange three-body force to, (T), 25:36831
meson (π) absorption in, mean free path for low-energy, (T), 25:36489
quasiparticle interaction in, model space calculation of Landau, (T), 25:36832
theories of, review of Brueckner--Bethe, Landau, and Migdal, (T), 25:36843
NUCLEAR MODELS
optical, computer program for determining parameters of, (T), 25:36814 (ANU-P-451)
optical, method for calculating potentials from complex scattering phase shifts, (T), 25:36812 (AAEC/TM-586)
particle-vibration coupling, diagrammatic method of, (T), 25:36829
shell, analysis of Λ binding energies in p-shell hypernuclei, formulas and matrix elements for ΛN and ΛNN forces in, 25:36529
shell, E2 effective charge operators with realistic reaction matrices in, (T), 25:36820
uniform spacing, particle-hole state density in, (T), 25:36830
NUCLEAR PHYSICS
book: USA Standard Glossary of Terms in Nuclear Science and Technology, 25:36826
stable isotope uses in, review of, 25:34813 (TID-25705)
NUCLEAR POWER
book: Peaceful Uses of Nuclear Energy, 25:34817
NUCLEAR POWER PLANTS
air conditioning and ventilation of, equipment and methods for, 25:34788
costs during 1970 to 2020, estimates of capital, 25:37030 (ORNL-TM-3243)
design of U. S., quality assurance criteria for, 25:36972
development in Germany, economics and technical aspects of, 25:36885 (JUL-705-RG)
development in Germany, review of, 25:36858
development in U. S., computer program for optimum economic, 25:36886 (ORNL-TM-3223)
development of marine power complex in Japan, concepts for, 25:36981(T) (ORNL-tr-2474)
development of, advantages and hazards from, 25:34771
development of, review of, 25:36974
earthquake effects on, standards for instrumentation for determining, 25:35061
economics of, analysis for optimization of, 25:37032
economics of, effects of safety requirements on, 25:36892
effluents from, effects on ecology of radioactive and thermal, 25:36970
fuel cycle for U. S., computer program for optimization of, 25:36886 (ORNL-TM-3223)
fuel cycles for, economics of optimized, 25:36859
fuels for, cost analysis in U. S. for 1971 to 1985, 25:36861
operating experience in IAEA Member States, summary of, 25:36884 (IAEA-127)
operation in developing countries, personnel requirements for, 25:36889 (UARAEE-98)
operation in European Communities during 1969, 25:36855 (NP-18846)
operation in European Communities during 1970, 25:36856 (NP-18847)
operation in U. K., review of, 25:36863 (CONF-700652-1)
operation of European, ten year summary of, 25:36864 (CONF-700956-2)
operation of, hazards analysis for, 25:36973
operation of, safety aspects of, 25:36892
power conversion systems for, analysis of optimum, 25:36974
radiation monitoring in, requirements for instruments for, 25:34869 (SZS-2/71, pp 7-11)
safety analysis of, computer program for environmental, 25:37049
safety aspects of, review of, 25:36973
siting of, ecological factors concerning, 25:36971
space heating from, analysis of optimum economic operation for, 25:37032
thermal effluents from, effects on site selection of, 25:36971
NUCLEAR QUADRUPOLE RESONANCE
research progress on, 25:34634(R) (COO-1385-27)
NUCLEAR REACTION ANALYSIS
principles of charged particle, for light elements in electrochemistry, 25:34550
NUCLEAR REACTIONS
coupled-channel calculations of, computer program for, (T), 25:36818 (KFK-1333)
cross sections for heavy-ion multinucleon-transfer, Q-value dependence of, (T), 25:36815 (JINR-E2-5797)
data acquisition during, development of RAD swapping system for, (E), 25:35050 (PUC-937-396)
finite-range calculation of two-neutron transfer, (T), 25:36828
kinematics of three-particle, spatial generalization of nomographs and their use in, (T), 25:36842
scattering in three-particle, determination of parameters of two-particle resonance, (T), 25:36837
symmetry for isospin multiplet production in, theorem for, 25:36844
uses of fission, summary of peaceful, 25:34771
NUCLEAR REACTIONS (DIRECT)
transcendental functions in computer programs for evaluating, (T), 25:36813 (ANU-P-439)
NUCLEAR SAFETY PILOT PLANT
containment spray systems of, dose reduction factor for elemental iodine removal by, 25:37029 (ORNL-TM-2412(Pt.12))
NUCLEAR STRUCTURE
book: Collective Excitations in Nuclei, (T), 25:36835
isospin mixing in ground states, role of giant monopole state in Coulomb-induced $\Delta T = 1$, (T), 25:36845
theories of, review of Brueckner--Bethe, Landau, and Migdal, (T), 25:36843
NUCLEAR THEORY
angular momentum coupling coefficients, general computer program for, 25:36366
comparative study of French's spectral distribution and the random matrix theory, 25:36823
Hartree--Fock procedure for two particles in a four-dimensional function space, 25:36819
many-body problem in, ground-state correlations as variational parameters in, 25:36840

XUM

nuclear potential, effect of strong interactions on weak parity-violating, 25:36458
nucleon--nucleon-interaction matrix elements from phase shifts and Jost function, Born-approximation calculation of, 25:36853
potentials in, interpretation by means of equivalent local potentials of nonlocal separable, 25:36847
three-body problem in, modification of Faddeev formalism for singular core interactions in, 25:36851
volume, surface, and symmetry terms in the semi-empirical mass formula, 25:36821
wave functions of nonlocal separable potentials, comparison with equivalent local potentials, 25:36836

NUCLEI
abundance of cosmic ultra-heavy, from fossil-track measurements in meteorites, (E), 25:35911
alpha decay of spherical A = 202 to 218, (T), 25:36747
antiproton reactions at 5 GeV/c in emulsions, angular and momentum distributions for π^0 produced in, (E), 25:36404
beta decay of excited states of odd--odd deformed, Random Phase Approximation calculation of Gamow--Teller transitions in, 25:36817 (JINR-P4-5744)
beta transitions in heavy, analysis using theory of finite Fermi systems, (T), 25:36833
charge composition of cosmic, of elements from neon to nickel above 250 MeV/nucleon, (E), 25:35910
Coulomb energy differences in A = 13 to 41 mirror, Hartree--Fock calculations with isospin corrections, (T), 25:36712
detection of superheavy, (T), 25:35592
deuteron elastic and inelastic scattering by even--even, effects of strong binding in, (T), 25:36848
energy levels for A = 14, (E/T), 25:36676
energy levels in, review of isobaric analogy, (E/T), 25:36676
energy levels of 2s--1d-shell, polynomial basis in group-theory calculation of, (T), 25:36711
energy levels of even--even Z = 6 to 82, table of quasi-beta, quasi-gamma, and quasi-ground, (E), 25:36783
energy levels of heavy odd--odd, ground state doublet, (T), 25:36528
energy levels of heavy, properties of core-particle, (T), 25:36753
energy levels of odd--odd deformed, Random Phase Approximation calculation of Gamow--Teller transitions in beta decay of 1^+, (T), 25:36817 (JINR-P4-5744)
energy levels of, boson representation of pair correlations and collective 0^+, (T), 25:36825
energy levels of, collective, (T), 25:36839
energy levels of, correlations between reduced neutron and partial radiative widths for resonance, (T), 25:36850
energy levels of, proton partial widths of isobaric analog, (T), 25:36852
energy-level transitions from (n,γ) reactions, tables of, (E), 25:36718 (AAEC/TM-585)
energy-level transitions in, effects of core polarization on hindrance of charge-exchange E1, (T), 25:36836
energy-level transitions in, exactly solvable quantum-mechanical model for, (T), 25:35891
energy-level transitions in, test of time reversal invariance using mixed dipole--quadrupole, (T), 25:36540
hadron reactions at high energies, review of Glauber theory for, (E/T), 25:36533
hadron reactions with, instability criterion for properties of intermediate compound systems in, (T), 25:36599
interaction mean free paths and fragmentation probabilities of heavy, above 10 GeV/nucleon in emulsions, (E), 25:36394
interaction mean free paths and fragmentation probabilities of heavy cosmic, above 10 GeV/nucleon in air and hydrogen, emulsion study of, (E/T), 25:36394
mass formula for, volume, surface, and symmetry terms in semi-empirical, (T), 25:36821
meson (K^-) absorption at rest in emulsion, Q-value distribution for detection of Λ-He^5, Λ-Li^6, and Λ-Be^9 produced in, (E), 25:36401
meson (K^-) absorption at rest in emulsions, properties of Σ^- and Σ^+ produced in, (E), 25:36400
meson (π^+ and π^-) reactions at 1 to 2500 MeV, computer program for intranuclear-cascade calculations of, (T), 25:36733 (ORNL-4564)
meson (π^-) reactions at 17.2 GeV in emulsions, properties of showers produced in, (E), 25:36418
neutron capture by A = 24 to 239, tables of gamma rays from, (E), 25:36718 (AAEC/TM-585)
neutron capture by, effect of doorway-state resonances in, (T), 25:36834
neutron inelastic scattering by excited states of, kernel for describing, (T), 25:36707
neutron reactions (n,p) with analog-dipole excitation, collective theory for, 25:36835
neutron reactions at 1 to 3500 MeV, computer program for intranuclear-cascade calculations of, (T), 25:36733 (ORNL-4564)
neutron reactions with, effect of nonuniform targets on total cross section measurements for, 25:36811
nuclear binding energies and charge radii for even--even A = 12 to 208, Hartree--Fock calculation of, (T), 25:36712
particle scattering by, multiple-scattering expansion of theoretical optical potential for, 25:36523
photon reactions at 121 keV to 10.827 MeV with Z = 6 to 92, cross sections for, (E), 25:36799
photon reactions with Moessbauer, spectra from, (E), 25:36346
proton fission of heavy, review of, 25:36802
proton reactions (p,γ) with, computer program for calculating yields from, (T), 25:36732 (NRL-7220)
proton reactions (p,n) with analog-dipole excitation, collective theory for, 25:36835
proton reactions at 1 to 3500 MeV, computer program for intranuclear-cascade calculations of, (T), 25:36733 (ORNL-4564)
proton reactions at 22.8 GeV/c in emulsions, method for identification of shower particles from, (E), 25:36402
proton reactions at 24 GeV/c in emulsions, deuteron emission in, (E), 25:36403
proton reactions at 400 MeV to 24 GeV with intermediate, calculation of spallation cross sections for, (T), 25:36689 (NP-18820)
reactions of complex, theorem for symmetries for isospin multiplet production in, 25:36844
shapes of light even--even, general method for calculating ground-state, (T), 25:36702
stabilization of axially symmetric shape and $(pf)^2$ mixing in sd-shell, (T), 25:36822
surface of, determination of properties of, (E/T), 25:36824
tensor coupling constants for A = 12 and 20, induced, (E/T), 25:36710

NUCLEIC ACID, DEOXYRIBO-
radiation effects on molecular weight of, synthesized in L cells containing pyrimidine, uv, 25:35207
radiation effects on structure of bacteriophage, 25:35259
radiation effects on structure of cell, 25:35157
radiation effects on transferred F' factor in bacteria, effects of gene types on uv, 25:35271
radioinduced breaks in algae, mechanisms of repair following γ, 25:35257
radioinduced breaks in, effects of polynucleotide ligase on recovery from x, 25:35108
radioinduced inactivation of transforming bacteria, mechanism of x, 25:35269
radioinduced single and double strand breaks in bacteria, γ, 25:35268
radioinduced single strand breaks in mouse L cell, effects of metabolic inhibitors on repair of x, 25:35224
radiolysis of frozen aqueous solutions of, ESR spectral studies on free radicals produced by γ, 25:34654
role in radiobiological phenomena, evolution of molecular mechanisms determining, 25:35101

NUCLEIC ACID, RIBO-
radiation effects on synthesis of, in pea seeds, mechanism of γ, 25:35245

NUCLEONS
coupling constant for πN, tests of long-range charge independence in N + N interactions from, (T), 25:36522
decay N + N + π, effect of strong interaction on weak parity-violating vertex for, 25:36458
form factors from current algebra and Regge model, asymptotic, 25:36437
interactions anti K + N, local models for, (T), 25:36505 (PAM-71.1)
interactions γ + N + π + N near threshold, pole approximation in dispersion relations and vector dominance hypothesis for vector-meson-exchange contributions to, (T), 25:36447
interactions K + N + K + N at high energies, quasipotential approach for spin effects in, (T), 25:36504 (JINR-E2-5770)
interactions K + N at low energies, vector-meson-dominance sum rules for, (T), 25:36519
interactions K + N at low, intermediate, and high energies, Venezianc model for, 25:36507
interactions K + N in $K^+ + n \rightarrow K^0 + p$ interactions at 600 MeV in deuterium bubble chamber, K^0 angular distributions and p polarization for phase shifts for, (E), 25:36417
interactions N + N at 10^{11} to 10^{13} eV, proposed experiment for average characteristics and angular distributions for, (E), 25:36416
interactions N + N, coupling constant for πN for tests of long-range charge independence in, (T), 25:36522
interactions N + N, generalized multiperipheral model for properties of partial cross sections for K anti K production in, (T), 25:36422
interactions N + N, soft-pion theorem for determination of intermediate range, 25:36525
interactions N + N, two-pion exchange contribution to, 25:36526
interactions ν + N, structure functions for vector and axial vector currents in deep inelastic, (T), 25:36488 (ORO-3992-24)
interactions π + N + π + δ, $N\delta\gamma$ coupling constants and sum rules from unsubtracted dispersion relations for, 25:36508
interactions π + N + π + N at high energies,

XUM

quasipotential approach for spin effects in, (T), 25:36504 (JINR-E2-5770)
interactions ν + N → X⁰(960) + N⁺, method for determining spin--parity of X⁰(960) from forward, (T), 25:36494
interactions ν + N at 0 to 700 MeV, Born approximation potential for phase shifts for, (T), 25:36510
interactions ν + N at 10^{11} to 10^{13} eV, proposed experiment for average characteristics and angular distributions for, (E), 25:36416
interactions ν + N at low energies, Ward identity techniques for s- and p-wave amplitudes for, (T), 25:36513
interactions ν + N, gauge invariance and soft-pion techniques for constraints between ν production amplitude and amplitude of, (T), 25:36515
interactions ν + N, generalized multiperipheral model for properties of partial cross sections for K anti K production in, (T), 25:36422
interactions ν + N, low-energy ν + ν phase shifts from dispersion relations for backward, (T), 25:36520
interactions ν + N, model for Pomeranchukon exchange in total cross sections for, 25:36512
interactions ν + N, Veneziano model for polarization in charge-exchange, (T), 25:36517
interactions with mesons at high energies, quasipotential approach for spin effects in, (T), 25:36504 (JINR-E2-5770)
reactions with lead and graphite above $3(10)^{12}$ eV, ionization spectrometer study of energy and mean inelasticity for, (E), 25:36388 (ITJ-3)

NUCLEOPROTEINS
radiation effects on structure of amnion cells, lymphocytes, and Tetrahymena, 25:35206

NUCLEOPROTEINS, DEOXYRIBO-
radiation effects on structure of somatic cell, 25:35198

NUCLEOTIDES
radiation effects on synthesis of free, in Saccharomyces, carbon-14 and tritium tracer study on β, 25:35252

O

OPTICAL SYSTEMS
aberrations in lenses, irradiation method for correcting, 25:35077(P)
aberrations in lenses, irradiation method for correction of, 25:35073(P)
design of alignment telescopes, for locating points along a line from a fixed point, 25:35069(P)

ORGANIC COMPOUNDS
photon attenuation coefficients at 1 to 1000 keV, (T), 25:36259

ORGANS
radiation dose to human, from circulatory support device heat source, 25:34803(R) (BNWL-1308-5)

ORNL HIGH-FLUX ISOTOPE REACTOR
maintenance during January to March 1971, 25:37068(R) (ORNL-TM-3432)
operations during January to March 1971, 25:37068(R) (ORNL-TM-3432)

OSMIUM BROMIDES
separation of ions of, from metal ions by high-voltage electrophoresis using carboxylic and hydroxycarboxylic acids, 25:34702

OSMIUM CHLORIDES
separation of ions of, from metal ions by high-voltage electrophoresis using carboxylic and hydroxycarboxylic acids, 25:34702

OSMIUM FLUORIDES
vapor pressure--temperature data for, 25:34602 (GAT-645)

OSMIUM ISOTOPES Os-185
energy-level transitions in, comparison of E2-M1 mixing amplitudes with Kumar--Baranger pairing-plus-quadrupole force model, (E/T), 25:36773

OSMIUM ISOTOPES Os-187
energy levels from iridium-187 electron-capture decay, lifetimes and spin--parity assignments for, (E), 25:36805
energy-level transitions from iridium-187 electron-capture decay, hindrance factors, conversion coefficients, multipolarities, and probabilities for E2 and M1, (E), 25:36805

OSMIUM ISOTOPES Os-188
energy-level transitions in, comparison of E2-M1 mixing amplitudes with Kumar--Baranger pairing-plus-quadrupole force model, (E/T), 25:36773

OSMIUM ISOTOPES Os-190
energy-level transitions in, comparison of E2-M1 mixing amplitudes with Kumar--Baranger pairing-plus-quadrupole force model, (E/T), 25:36773

OSMIUM ISOTOPES Os-191
energy-level transitions in, K conversion coefficients for M3, (E), 25:36804

OSMIUM OXIDES
separation of ions of, from metal ions by high-voltage electrophoresis using carboxylic and hydroxycarboxylic acids, 25:34702

OSTEICHTHYES
Abramis Brama, radioisotope content in German, during 1967 and 1968, 25:35096
effects of temperature on development and survival of, in Columbia River, 25:35115 (BNWL-1543)
Esox lucius, radioisotope content in German, during 1967 and 1968, 25:35096
Oncorhynchus tshawytscha, effects of reactor thermal effluents on migration in Columbia River of, 25:37105 (BNWL-SA-3876)
radioisotope content in, from Baltic Sea and North Atlantic Ocean, 1967 and 1968, 25:35096
Salmo gairdneri, effects of reactor thermal history on effects of thermal stress in Columbia River, 25:37104 (BNWL-SA-3713)

OVARIES
radiation dose to human, during phosphorus-32 administration, 25:35144
radiation effects on histology of albino rat, combined effects of estrogens, progesterones, and x, 25:35237

1,3,4-OXADIAZOLE, 2-(4-BIPHENYL)-5-PHENYL-
radiation effects on fluorescence of xylene solutions of, effects of chloroform on quenching of γ and uv, 25:34624

OXALATES
radiolysis of neutral aqueous, oxygenated solutions of, effects of dose on yields from γ, 25:34644

OXAZOLE, 2,5-DIPHENYL-
radiation effects on fluorescence of xylene solutions of, effects of chloroform on quenching of γ and uv, 25:34624

OXETANE, 3,3-BIS(CHLOROMETHYL)-
polymers, radiation effects on physical properties of, for low-energy x ray dosimetry, 25:35033(P)

OXYGEN
alpha-particle stopping cross sections in gaseous, at 0.2 to 2 MeV, 25:36255
auroral-arc reappearance of 6300-A, on Mar. 8--9, 1970 during geomagnetic-storm recovery, midlatitude multiple, (E), 25:35969
determination in loop sodium, testing of in-line meter for, 25:35276(R) (GEAP-13539-16)
diffusion in nonstoichiometric cerium oxide and cerium oxide--yttrium oxide solid solutions, self-, 25:35883
diffusion in plutonium dioxide--uranium dioxide solid solutions, 25:35547(R) (GEAP-12182)
effect on radioinduced chromosome aberrations in pea seeds, 25:35119
effects of combination of iron, silicon, or tungsten and, on internal friction of zirconium alloy, 25:35404
effects of dissolved, on tensile properties of polycrystalline α-zirconium at 25 to 700°C, 25:35282
effects on electron radiosensitivity of mouse bone marrow and intestinal tissues, 25:35161
effects on γ-radioinduced mutations in Aspergillus, 25:35121
effects on internal friction peaks in niobium-base--titanium alloys, 25:35410
effects on radiolysis of water, 25:34617
effects on rupture of polycrystalline molybdenum, 25:35409
electron reactions with molecular, resonances in total cross sections for, (E), 25:35861
meson (π) reactions with, x-ray yields and level broadening from, (E), 25:35854
oscillator strengths for excitation and ionization of, tables of calculated generalized, 25:35844 (SC-RR-70-406)
photo-absorption cross sections of molecular, review of uv, (E/T), 25:36013
photosensitized production of excited singlet species of, 25:34613 (TID-25689)
radiation effects on uptake of, by rat liver slices, mitochondria, and mitochondrial membrane, x, 25:35223
radioprotective effects on Chinese hamster cells, 25:35214
reactions with hydrogen-annealed refractory metals, thermodynamics of, 25:35291
reactions with IN-738 superalloys at high temperatures, 25:35400
reactions with methane under simulated radiolysis conditions, mass spectrometric studies on, 25:34645
reactions with niobium at 450 to 1000°C, effects of nitrogen on oxidation, 25:35292
reactions with niobium--titanium alloy at 600 to 1300°C, study of microstructure from oxidation, 25:35482
reactions with niobium--titanium alloy at 600 to 1300°C, kinetics of oxidation, 25:35282
reactions with thin molybdenum plates at 1800°C and low pressure, decarburizing, 25:35309
reactions with Zircaloy-2 or zirconium, kinetics of, 25:35277 (NP-18833)
solubility in hafnium nitride at 1023 to 1073°K, 25:35566
sorption by tantalum at 77 and 298°K, 25:35339(T) (ORNL-tr-2479)
spectral red-line emission in polar cavity, time variations in O I 6300-A, (E), 25:35959
spectral-line shapes in equatorial nightglow in upper atmosphere, (E), 25:35962
vapor pressure--temperature data for, 25:34602 (GAT-645)

OXYGEN FLUORIDES
vapor pressure--temperature data for, 25:34602 (GAT-645)

OXYGEN IONS
reactions of multiply charged, with flowing methane--nitrogen and nitrogen--oxygen systems at 7 MeV/n,

XUM

25:34567
OXYGEN ISOTOPES
separation factors in sorption of carbon dioxide on zeolites, 25:34708
OXYGEN ISOTOPES O-16
determination in thin films by nuclear reaction micro methods, 25:34550
energy levels from carbon-12 (α,γ) reactors, parameters for resonances, (E), 25:36675
energy levels from fluorine-19 (he-3,Li-6) reactions, (E), 25:36674
energy levels of, alpha-particle-model calculations of rotational, (T), 25:36680
meson (π) elastic scattering near 3,3 resonance, multiple-scattering theory for differential and total cross sections for, (T), 25:36527
meson (π+) reactions at high energies, Coulomb interaction in, (T), 25:36524
meson (π-) reactions at high energies, Coulomb interaction in, (T), 25:36524
photon reactions (γ,n) at 20 to 26 MeV, 3p--3h coupling in intermediate structure of giant dipole resonance from, (T), 25:36678
photon reactions with, isolation of Regge trajectories in amplitudes of meson production in, (T), 25:36453
reactions (O-16,3n), (O-16,5n), and (O-16,7n) with lanthanum-139 at 141 MeV, gamma spectra from, (E), 25:36726 (JINR-P6-5681)
reactions (O-16,C-14) with calcium-44 and -48 and titanium-48 and -50 at 48 MeV, cross sections for, (E), 25:36709
reactions with thorium-232, cross sections and Q values for, (E), 25:36815 (JINR-E2-5797)
use as tracer for studies of anodic oxide film growth on aluminum and tantalum, 25:35294
OXYGEN ISOTOPES O-18
content in ground waters in Totes Gebirges area in Austria, 25:34726 (THAI-AEC-35, pp 9-20)
content in sandstone-type uranium deposits, measurement of, 25:34750(R) (COO-2024-1)
determination in thin films by nuclear reaction micro methods, 25:34550
effects on sorption of carbon dioxide on zeolites, 25:34708
exchange between atomic and molecular oxygen, 25:34585
exchange between molecular oxygen and synthetic zeolites, kinetics of, 25:34580
exchange reactions of, 25:34572(R) (ORO-3234-23)
exchange studies in heterochelate chromium (III) complexes, 25:34601
use as tracer for studies of anodic oxide film growth on aluminum and tantalum, 25:35294
OXYGEN SYSTEMS
Ar--O, thermodynamic properties between 2,000 and 35,000°K, 25:36104 (NP-18772)
fluoronaphthalene--O, photolysis of, excitation of $C_2(^1E/sub\ g/^+)$ in, 25:34613 (TID-25689)
H--O, effects on fracture of H11 steel at -28 to +100°C, 25:35337(R) (NYO-3975-3)
N--O, reactions with multiply charged ions in flowing systems at 7 MeV/n, 25:34567
Nb--O, plastic deformation of solid solutions of, at low temperatures, stress-differential effects in, 25:35373
Nb--O--Zr, phase transformations in, 25:35572
Nb-base--O, degassing of dilute, by annealing, concentration changes and metal losses during, 25:35560
O--Pu--U, enthalpy of oxygen incorporation in (U,Pu)O/sub 2+-x/ in, 25:34606
O--Ta-base, degassing of dilute, by annealing, concentration changes and metal losses during, 25:35560
O--V-base, degassing of dilute, by annealing, concentration changes and metal losses during, 25:35560
OYSTER CREEK POWER REACTOR, UNIT 1
containment system for, October 1970 leakage rate test for primary, 25:36871 (DOCKET-50219-137)
operative incident for, isolation condenser system time delay relay failure, 25:36870 (DOCKET-50219-135)
power level for, notice of AEC consideration of 1930 MW(t) maximum, 25:36910 (DOCKET-50219-134)
OYSTER CREEK POWER REACTOR, UNIT 2
neutron cross sections and spectra from, calculation of, 25:37115 (RISO-234)
OZONE
content in atmosphere, correlation with diurnal cosmic-ray meson variations, (E/T), 25:35974
photo-absorption cross sections of, review of uv, (E/T), 25:36013

P

PACIFIC OCEAN
lead content of, depth profile of, 25:34762
lead-210 content of, depth profile of, 25:34762
polonium-210 content of, at various depths, 25:34762
PACKAGING
methods for radioactive materials, development of special arrangement, 25:34843 (AECL-3804)
standards for radioactive materials, 25:34851
PAINTS
analysis for lead, equipment for x-ray fluorescence, 25:35043
PAIR PRODUCTION
interactions e + e and e+ + e- in colliding beams for, (T), 25:36448
PALISADES POWER REACTOR
containment spray system for, use of sodium hydroxide buffered boric acid in, 25:36929 (DOCKET-50255-41)
heat exchanger for, tube failure in component cooling water, 25:36930 (DOCKET-50255-42)
owners of, financial statements of, 25:36929 (DOCKET-50255-41)
PALLADIUM
effects on colorimetric determination of gold, 25:34521
effects on gravimetric determination of mercury using 2-aminobenzothiazole, 25:34520
effects on photometric determination of antimony following solvent extraction using TBP, 25:34512
neutron scattering by, lattice vibrational spectra and physical characteristics of, 25:36319
uses of fission product, evaluation of potential, 25:34803(R) (BNWL-1308-5)
PALLADIUM ALLOYS AND SYSTEMS
Mo--Pd--Ti-base, tensile properties of metastable beta, at 25 to 800°C, effects of strain rate and annealing temperature on anomalies in, 25:35434
Pd--Ti, stability of gaseous intermetallic, 25:35350
Pd--Zr, stability of gaseous intermetallic, 25:35350
PALLADIUM BROMIDES
separation of ions of, from metal ions by high-voltage electrophoresis using carboxylic and hydroxycarboxylic acids, 25:34702
PALLADIUM CHLORIDES
separation of ions of, from metal ions by high-voltage electrophoresis using carboxylic and hydroxycarboxylic acids, 25:34702
PALLADIUM ISOTOPES Pd-110
energy levels and nuclear properties of, Nuclear Data Sheets for, (E), 25:36808
PARACHUTES
simulation of guided, payload system, analog, 25:37224 (SC-DR-710097)
PARATHYROID GLANDS
ablation in mice using iodine-131 combined with surgery, 25:35084
PARTICLE TRACKS
analysis in track-sensitive targets in bubble chambers, computer program for, 25:34949 (CONF-700623-(Vol.1), pp 312-24)
analysis of bubble chamber, facility for film, 25:35062
analysis of bubble chamber, minimizing angle errors due to multiple scattering in, 25:34950 (CONF-700623-(Vol.1), pp 325-33)
analysis of Gargamelle bubble chamber, film projector for, 25:34951 (CONF-700623-(Vol.1), pp 334-44)
formation in liquid-helium bubble chambers, density of, 25:34989 (CONF-700623-(Vol.2), pp 893-900)
measurement of spark chamber, graphical projection method for, 25:36011
PARTICLES
abundance of neutral, in thermosphere during magnetic storms, (T), 25:35960
diffusion of fluid, in laboratory and natural streams, calculation and measurement of longitudinal, 25:34718 (KH-R-12)
motion in monopole--quadrupole gravitational fields, (T), 25:35809
PEACH BOTTOM POWER REACTOR, UNIT 1
operations history for March 1971, 25:36867 (DOCKET-50171-85)
PEACH BOTTOM POWER REACTOR, UNIT 2
effluents from, effects on environment of chemical, radioactive, and thermal, 25:36937 (DOCKET-50277-20)
site for, geological, hydrological, and meteorological data for, 25:36937 (DOCKET-50277-20)
PEACH BOTTOM POWER REACTOR, UNIT 3
effluents from, effects on environment of chemical, radioactive, and thermal, 25:36937 (DOCKET-50277-20)
site for, geological, hydrological, and meteorological data for, 25:36937 (DOCKET-50277-20)
PENETRANT TESTING
equipment and methods for, historical development and current status of, 25:34835
1,3-PENTADIENE, 2-METHYL-3,4,5,5,5-PENTAFLUORO-
radioinduced polymerization at 25 to -196°C, 25:34622
1,3-PENTADIENE, 3,4,5,5,5-PENTAFLUORO-
radioinduced polymerization at 25 to -196°C, 25:34622
PENTANE, ASTATO-
boiling point of, gas chromatographic studies on, 25:34604 (JINR-P6-5683)
2,4-PENTANEDIONE
complexes with neptunium or uranium, stability of, 25:34557 (KFK-1339)
2,4-PENTANEDIONE, 1,1,1,5,5,5-HEXAFLUORO-
complexes with neptunium or uranium, stability of, 25:34557 (KFK-1339)
2,4-PENTANEDIONE, 1,1,1-TRIFLUORO-
complexes with neptunium or uranium, stability of, 25:34557 (KFK-1339)

XUM

1-PENTANETHIOL, 2-AMINO-
radioprotective effects of, on Escherichia coli, function and structure studies on γ, 25:35160
PERCHLORIC ACID
radiolysis of, at 77°K, reactions of halogen-substituted acetic acids with mobile electrons formed in γ, 25:34648
PEROXIDASE
radiation effects on development of, in sweet potato root tissues, effects of ethylene on γ, 25:35105
PERSONNEL
radiation dose rate to fuel reprocessing, following fuel particle inhalation and skin contamination, correction factors for measuring true, 25:35140
radiation dose to hot cell, comparison of film badge and thermoluminescent dosimeters for measuring β, 25:35131
radiation dose to nuclear industry, standards for maximum permissible, 25:35154
radiation dosimetry program for, in Turkey from 1962 to 1969, 25:35135 (CNAEM-77)
radiation protection for uranium mining, Czechoslovakia standards for, 25:35152
radiation protection for, during handling and storage of cement containing cesium-137 and strontium-90, 25:35148
radiation protection measures for fire fighting, following nuclear accidents, 25:35149
radiation protection methods for nuclear industry, conference on, 25:35130
radioisotope incorporation in nuclear industry and research center, in Germany, statistics on, 25:35100
staffing requirements for nuclear power plant operation in developing countries, 25:36889 (UARAEE-98)
PERYLENE
effects of coatings of, on γ radiolysis products of poly(vinyl chloride), ESR studies on, 25:34656
PETROLEUM
analysis for sulfur, radiometric instruments for, 25:35040
production stimulation using contained underground nuclear explosions, method for, 25:34772(P)
prospecting for, comparison of soil radioactivity mapping and soil redox mapping methods of, 25:34731
prospecting for, review of radiometric methods for, 25:34730
PHANTOMS
radiation dose distribution in water, computer method for calculating scattered γ, 25:35145
radiation dose distribution in water, errors due to ionization chamber air volume in measurements on γ and x, 25:35146
radiation dose distribution measurements in liquid, detector positioning device for, 25:35059
radiation dosimetry in Plexiglas, using scintillation detectors, 25:35030
PHARMACEUTICALS
handling of radioisotope-labeled, in clinic and research, safety principals for, 25:35153
use of radioisotope-labeled, in nuclear medical service in Italy, 25:35156
PHENANTHRENE
effects of coatings of, on γ radiolysis products of poly(vinyl chloride), ESR studies on, 25:34656
PHENAZINE
photoreduction of, 25:34613 (TID-25689)
PHENOL, o-AMINO-
use as colorimetric reagent for cerium(IV), 25:34530
PHENOL, 2,6-DI-tert-BUTYL-4-METHYL-
effects on yields from γ radiolysis of 2-methyl-2-propanol, 25:34659
PHENOLPHTHALEIN, 3',3''-BIS[[BIS(CARBOXYMETHYL)AMINO]METHYL]-
complexes with thorium, spectrophotometric analyses based on, 25:34532
PHENOLPHTHALEIN, 3,3''-BIS[[BIS(CARBOXYMETHYL)AMINO]METHYL]-5',5''-DIISOPROPYL-2',2''-DIMETHYL-
complexes with thorium, spectrophotometric analyses based on, 25:34532
p-PHENYLENEDIAMINE, N,N,N',N'-TETRAMETHYL-
hydrochloride, effects of coatings of, on γ radiolysis products of poly(vinyl chloride), ESR studies on, 25:34656
PHLEOMYCIN
effects on repair of x-radioinduced single strand breaks in DNA in mouse L cells, 25:35224
PHOSPHINE OXIDE, TRIOCTYL-
solvent properties for uranium, 25:34541
4,4,4-trifluoro-1-(2-thienyl)-1,3-butanedione--trioctylphosphine oxide, solvent properties for cerium in fission products solutions, 25:34522
PHOSPHORIC ACID, 1-ISOBUTYL-3-METHYLBUTYL ESTER
solvent properties for actinides and lanthanides, 25:34706
PHOSPHORIC ACID, TRIBUTYL ESTER
solvent properties for uranium, 25:34541
PHOSPHORUS
determination in human stones by neutron activation, 25:34545 (THAI.-AEC-39)
separation from uranium by fractional dissolution, 25:34699
PHOSPHORUS FLUORIDES
vapor pressure--temperature data for, 25:34602 (CAT-645)
PHOSPHORUS IONS
implantation in diamonds at 8 to 70 keV, ion-channeling analysis of layers of, 25:36285
implantation in silicon at 100 keV, ESR study of depth distribution of, 25:36276
PHOSPHORUS ISOTOPES P-31
electron spin resonance spectra of gaseous atoms of, 25:36345
nuclear magnetic resonance line shifts in uranium phosphide and its solid solutions with uranium sulfide, 25:36350
PHOSPHORUS ISOTOPES P-32
accumulation in human female reproductive system, 25:35144
beta decay of, Fermi--Kurie plot and shape factors from, (E), 25:36768
effectiveness of sodium-phosphate-incorporated, for therapy of polycythemia, 25:35157
preparation of applicators of, by sorption on plastic anion exchange resin, 25:34671
use as tracer to study solidification of cast steel, 25:34820
use of stratospheric, as tracer for stratospheric--tropospheric air mass exchange studies, 25:34745(R) (NYO-4061-2)
PHOSPHORUS ISOTOPES P-34
beta decay of, beta and gamma spectra, branching ratios, and log-ft values for, (E), 25:36700
PHOSPHORUS SYSTEMS
Cd--P--Sn, phase diagram of CdP_2--Sn system in, 25:35880
Cd--P--Sn, properties of copper- and silver-doped crystals of, electric and optical, 25:35580
Ni--P, effects on sintering of tungsten powders, 25:35354
PHOSPHORYL FLUORIDES
vapor pressure--temperature data for, 25:34602 (CAT-645)
PHOTOELECTRIC EFFECT
cross sections for, empirical formula for interpolation of tabulated, 25:36246 (ANL-7796)
PHOTOGRAPHIC EMULSIONS
analysis of microcrystal centers in, for silver by neutron activation, 25:34549
PHOTOGRAPHIC FILM
comparison of high speed, for use in streak camera recording systems, 25:37193 (MRSMP-71-32)
processing of x-ray, study of developers used in, 25:37234(T) (SC-T-713035)
PHOTOMULTIPLIER TUBES
performance of RCA C31 000D, for liquid scintillation counting, 25:34895
PHOTONS
attenuation coefficients in organic materials at 1 to 1000 keV, (T), 25:36259
detection of <1 GeV/c, bubble-chamber technique for, 25:34964 (CONF-700623-(Vol.1), pp 555-66)
emission from 1.3- to 4.0-GeV electrons passing through crystal, energy dependence of, (E), 25:36382
interaction with photons and charged particles near NP 0532, consequences of collision, (E/T), 25:35706
interactions γ + e → γ + e above 1 keV, Monte Carlo method of sampling Klein--Nishina probability distribution for Compton, (T), 25:36432 (LA-4663)
interactions γ + γ → π^0, anomalous behavior of, 25:36446
interactions γ + γ from e^+ + e^- interactions in storage rings, experimental conditions for, 25:36451
interactions γ + γ in colliding beams, cross sections for hadron production in, (T), 25:36432 (LNF-71/1)
interactions γ + N → π + N near threshold, pole approximation in dispersion relations and vector dominance hypothesis for vector-meson-exchange contributions to, (T), 25:36447
interactions γ + p → π^0 (eta) + p, duality and meson trajectories in Regge cut model for, (T), 25:36441
interactions γ + p, model for Pomeranchukon exchange in total cross sections for, 25:36512
reactions (γ,He-3) with helium-4 at 20 to 80 MeV, cross sections for, (E), 25:36671
reactions (γ,n) with oxygen-16 at 20 to 26 MeV, 3p--3h coupling in intermediate structure of giant dipole resonance from, (T), 25:36678
reactions (γ,t) with helium-4 at 20 to 80 MeV, cross sections for, (E), 25:36671
reactions with carbon-12 and oxygen-16, isolation of Regge trajectories in amplitudes of meson production in, (T), 25:36453
PHOTOSPHERE
flare continuum in, origin of, (E), 25:35722
velocity fields in active regions, temporal variations of, (E), 25:35750
PHYSICS
book: Introduction to Modern Theoretical Mechanics, 25:36361
PIEZOELECTRIC CRYSTALS
performance for measurements in bubble chambers, effects of high magnetic fields and low temperatures on, 25:34987 (CONF-700623-(Vol.2), pp 863-72)
PINCH DEVICES
plasma instabilities in ISAR I linear theta-, m = 0 mirror, (E), 25:36182
plasma instability in toroidal diffuse, resistive, (E),

XUM

25:36168
plasma kinetics in theta-, with superimposed azimuthal magnetic fields, (T), 25:36129 (UARAEE-102)
PINCH EFFECT
kinetic theory of longitudinal, in infinite cylinders, (T), 25:36135
microwave radiations from theta, (E), 25:36122
plasma sausage instabilities in self-constricted, (T), 25:36173
shock wave propagation in conical, effect of longitudinal magnetic field on, (E), 25:36117 (UARAEE-106)
PIPE FITTINGS
standard marking system for, 25:34786
PIPES
standards for ship pressure and power systems, 25:37095
welding of ferrous, for nuclear power plant service, standard for, 25:35308
PLANETARY NEBULAE
condensations in, formation of, (T), 25:35621
dust-radiation instability in, (T), 25:35688
gravitational instabilities in, (T), 25:35621
hydroxyl emission from NGC 2438, anomalous, (E), 25:35698
light polarization from, elliptical, (E), 25:35618
models for, (E/T), 25:35668
photography of NGC 7009, narrow-band filter, (E), 25:35643
radio observations of, (E/T), 25:35668
radio recombination line in NGC 7027, (E), 25:35642
spectra of YM 29 at 318 and 606 MHz, (E), 25:35630
spectra of NGC 7009, (E), 25:35643
stars of, extended model atmospheres for central, 25:35624
PLANETS
atmospheres of, nonconservative Rayleigh scattering in, (T), 25:35826
evolution of terrestrial, (T), 25:35825
exobiology survey of Pluto and Jovian, (T), 25:35829
formation of, mass distribution during, (T), 25:35832
motion of Pales (49), use in determining mass of Jupiter, (E), 25:35823
perihelion motion of 1566 Icarus, effects of solar charge on, (E/T), 25:35733
Uranus magnetotail models with dipole axis parallel to solar wind, (T), 25:35828
PLANKTON
organic matter from, release of dissolved, 25:37215 (RLO-1725-186)
PLANTS
effects of temperature on development and survival of, in Columbia River, 25:35115 (BNWL-1543)
leaf development of vascular, 25:37203 (NYU-3897-16)
production in Hot Creek Valley, Nevada, use of soil and floristic correlates for estimating, 25:37240 (TID-25723)
protein synthesis in, RNA metabolism in relation to regulation of, 25:37237(R) (SRD-643-1)
PLASMA
bibliography on, 25:36062
bibliography on plasma physics and fusion reactors, 25:36081
charged-particle beam interactions with, vlf wave amplification in, (E), 25:35972
charged-particle motion in helical magnetic fields, effect of electric fields on, (T), 25:36084
charged-particle-beam interactions with, nonlinear theory for relaxation in, 25:36130
collisions in dense beams, Coulomb, 25:36640
conductivity of toroidal loop, thermal, (T), 25:36141
conductivity of turbulent, anomalous electric, (T), 25:36145
conference on laser interaction and related plasma phenomena, East Windsor, Connecticut, 6/69, 25:36147
confinement in magnetic mirrors, effect of electron heating on, 25:35088
confinement lifetime and ion energy spectra in multipole devices, (E), 25:36085
contraction of rotating clouds of gravitational, (T), 25:35819
cosmic-ray interaction with instellar, (T), 25:35900
diagnostic techniques for, review of, 25:36095
diagnostic techniques for, survey of, 25:36090 (MATT-838)
diagnostics in Q devices, camera for, 25:36099
diagnostics in Tokamak-5, spatial distribution of ion temperature, (E), 25:36097
diagnostics of magnetized, collisional effects on diffusion electron current to cylindrical probe in, (T), 25:36098
diagnostics of magneto-, development of microwave transient response technique for, 25:35833(R) (ORO-3027-19)
diagnostics of shocks in discharges with longitudinal magnetic fields, (E), 25:36092 (UARAEE-101)
diagnostics of weakly ionized helium, optical measurement of hf electric fields, 25:36094
diagnostics using electromagnetic wave scattering, detection limits for, 25:36101
diagnostics using electron beams, potential distribution, 25:36093
diagnostics using open resonators, density, (E/T), 25:36089 (KHFTI-69/51)
electron beam interactions with double-stream, instabilities in, (T), 25:36174
electron beam interactions with slow waves in waveguides, effect of inhomogeneities on, (T), 25:36234
electron beam interactions with, electron heating by, (E), 25:36118
electron beam interactions with, excitation of electromagnetic waves in, (T), 25:36235
electron beam interactions with, quasi-linear equations for, 25:36142
electron beam interactions with, stability of relativistic, 25:36169
electron distribution function for low-temperature, (T), 25:36134
electron energy distribution function for weakly ionized, effects of inelastic collisions on, (T), 25:36146
electron energy distribution in positive column of helium discharge, (E), 25:36119
equilibrium and stability in Astron and minimum-B mirror systems, (T), 25:36165 (UCRL-51030)
equilibrium of finite-β toroidal helices, (T), 25:36171
expansion of laser-produced, nonlinear effect of, (T), 25:36154
expansion of laser-produced, self-similarity model for, 25:36132
expansion of spherical, therskinetic theory for, 25:36131
flow in self-induced magnetic field of arc discharge, (T), 25:36103 (DLR-FB-70-13)
heating near lower hybrid frequency, hf, (E), 25:36087
heating of turbulent, by magnetic pumping, (T), 25:36083
interactions with hf electromagnetic fields, drift instabilities from, (T), 25:36177
interactions with magnetic fields, skin effect in, (T), 25:36138
ion trajectories in Penning discharges, calculation of, 25:36133
ionization and recombination coefficients in positive column glow discharges, (T), 25:36136
ionization instability of self-sustaining low-pressure discharges in strong transverse magnetic fields, (E/T), 25:36159
kinetic theory of hot, Compton Fokker--Planck equation for, 25:36137
kinetic theory of shock structure in, Boltzmann equation for, 25:36126 (NYO-1480-173)
kinetics in crossed electric and magnetic fields, theory of rotating, 25:36139
laser beam scattering on magnetized arc, anomalous, (E), 25:36123
light scattering by marginally stable, (T), 25:36144
light scattering on collisionless, effect of strong magnetic field on Thomson, (T), 25:36140
magnetic fields in rotating clouds of, (T), 25:35819
oscillations in dense electron gas containing a fixed-point charge, collective modes in, (T), 25:36239
oscillations in hot electron magnetized, longitudinal nonlinear, (T), 25:36217 (UARAEE-88)
oscillations in ion-beam-produced, collective, (E/T), 25:36220
oscillations in low-pressure Penning discharges, (E/T), 25:36242
oscillations in magnetized afterglow, with transverse currents, (E), 25:36175
oscillations in toroidal, in large electric fields, (E), 25:36237
oscillations near column edge of Q device, effects of pressure drifts on, (E), 25:36245
pinch effect in, kinetic theory of longitudinal, (T), 25:36135
production and heating by laser-irradiated solids, 25:36150
production by dc generators, dynamic current--voltage characteristics, 25:36161
production by intense electron beam interactions with matter, (T), 25:36157
production by laser irradiation of free targets, expansion properties of, (E), 25:36152
production by laser irradiation of lithium plates, motion and collision of two blobs, (E), 25:36158
production by laser irradiation of solid deuterium, neutron spectra from, 25:36203
production by laser irradiation of solid targets, techniques for, 25:36151
production by laser irradiation of solid targets, review of, 25:36149
production by laser irradiation of solids, shock-wave kinetics from, (T), 25:36153
production by laser irradiation, efficiency of, 25:36155
production by laser irradiation, high-density and high-temperature, (E/T), 25:36156
production of dense, by microwaves in magnetic fields, (E), 25:36160
properties in theta-pinch discharges, with superimposed azimuthal magnetic fields, (T), 25:36129 (UARAEE-102)
properties of inhomogeneous, dielectric tensor for, (T), 25:36127 (UARAEE-65)
radiation transport in, collective effects on polarized, (T), 25:36143
radiations from argon, in low-pressure torch discharges, 25:36124

XUM

radiations from theta-pinch, microwave, (E), 25:36122
shock wave propagation in collisionless, in absence of magnetic fields, (E/T), 25:36106
shock wave propagation in collisionless, isomagnetic discontinuities in, (E), 25:36125
shock wave propagation in discharges in longitudinal magnetic fields, (E), 25:36092 (UARAEE-101)
shock wave propagation in pinch discharge, effect of longitudinal magnetic field on, (E), 25:36117 (UARAEE-106)
spectra of, temperature and electron density determination using Saha equation, (T), 25:36102
spectral line profile and shift measurements for, instruments for, (E), 25:36091 (UARAEE-95)
stability and equilibrium in Astron and minimum-B mirror systems, (T), 25:36165 (UCRL-51030)
stability in contrastreaming, gravitohydromagnetic, (T), 25:35793
stability in current-carrying toroidal systems, (T), 25:36181
stability in hf electric fields, quasi-linear destabilization of dissipative parametric, (T), 25:36170
stability in hf electromagnetic fields, drift, (T), 25:36177
stability in inhomogeneous mirror machines, loss-cone modes, (T), 25:36166 (UCRL-73135)
stability in ISAR I linear theta-pinch, m = 0 mirror, (E), 25:36182
stability in magnetized afterglow, with transverse currents, (E), 25:36175
stability in self-constricted pinch discharges, sausage, (T), 25:36173
stability in steady-state fusion reactors, thermal, (T), 25:36178
stability in toroidal screw pinch, resistive, (E), 25:36168
stability of collisionless one-dimensional, trapped-particle, (T), 25:36180
stability of double-stream, with Coulomb collisions, (T), 25:36174
stability of high-β inhomogeneous, with weak pressure gradient, (T), 25:36176
stability of homogeneous, beam cyclotron, (T), 25:36167
stability of weakly ionized magneto-, effect of transverse electric field on, (T), 25:36185
stability of, nonlinear plasma waves and turbulence from macroinstabilities, (T), 25:36164 (TID-25713)
stabilization of drift-dissipative instabilities by rf magnetic and electric fields, (T), 25:36179
stabilization of electrostatic instabilities in nonuniform, by helicon waves, 25:36183
stabilization of flute instabilities in Phoenix II, by feedback system, 25:36163(T) (CTO-737)
stabilization of ion wave instabilities in, by hf electric fields, (E), 25:36172
stabilization using feedback by remote modulated source at ECR frequency, (E/T), 25:36184
thermodynamic equilibrium in laser-induced xenon, local, 25:36121
thermodynamic properties of argon--oxygen, between 2,000 and 35,000°K, 25:36104 (NP-18772)
thermonuclear energy from, Lawson criteria for, 25:36191 (MATT-844)
transport in magnetic quadrupole fields, 25:36086
vibrations in, review of criteria for absolute, convective, and global instability and amplification and nontransmission of, 25:36560 (ITF-70-96-P)
wave absorption between electron cyclotron and lower hybrid frequencies, limits of, (E/T), 25:36238
wave coupling in, beam cyclotron instabilities from electron cyclotron and ion acoustic, (T), 25:36167
wave damping in Born approximation for, (T), 25:36223
wave echoes in, nonlinear theory for, 25:36216 (ITF-70-56)
wave excitation and turbulence effects from macroinstabilities in, (T), 25:36164 (TID-25713)
wave excitation by probe antennas in bounded, electron cyclotron and electrostatic, (E), 25:36241
wave excitation in beam--plasma system, electromagnetic, (T), 25:36235
wave excitation in, lumped-element line generator for low-rf magnetoacoustic, 25:36229
wave growth in beam--plasma systems, beam modulation effects on, (E), 25:36227
wave interactions in magnetized, frequency multiplication in, (T), 25:36232
wave interactions with dense, self-trapping of intense electromagnetic, (E), 25:36225
wave kinetics in anisotropic, magneto-acoustic, (T), 25:36233
wave propagation along interface of vacuum--overdense, electromagnetic surface, (T), 25:36214 (DEMO-71/5)
wave propagation in cold, in presence of external magnetic field and Coriolis force, (T), 25:36240
wave propagation in collisionless one-dimensional, trapped-particle instabilities from, (T), 25:36180
wave propagation in column, spontaneous if longitudinal, (E/T), 25:36221
wave propagation in low-temperature cesium discharge, ion acoustic, (E), 25:36231
wave propagation in magnetized, longitudinal ion, (T), 25:36222
wave propagation in mirror-confined, near upper hybrid frequency, (E), 25:36243
wave propagation in nonlinear homogeneous and inhomogeneous, relativistic Doppler effect and group velocity in, (T), 25:36215 (DEMO-71/6)
wave propagation in unbounded magnetized, dispersion relations for electromagnetic, 25:36218 (UARAEE-92)
wave propagation in, perturbation solutions to nonlinear Vlasov equation for electrostatic, 25:36236
wave propagation in, self-focusing of electromagnetic, (T), 25:36226
wave reflection and transmission in inhomogeneous, electromagnetic, (T), 25:36228
wave reflection and transmission in magnetic, optimum third-harmonic generation in, (T), 25:36244
wave scattering on ultrarelativistic electrons in, radio noise generation by, 25:35896
wave transformation in inhomogeneous, theory of linear, 25:36224
wave trapping in, nonlinear theory of electromagnetic, 25:36230

PLASMA ACCELERATORS
current spokes in arc, rotation properties of, 25:36111
current spokes in arcs, occurrence and properties of, 25:36110
design for propulsion thrust, 25:36105(P)
electrode erosion in pulsed, material evaluation for, 25:36207
jet diagnostics in magnetohydrodynamic, (E), 25:36096
jet flow in homopolar, (E/T), 25:36205
performance of coaxial tandem systems, (T), 25:36204
performance of high-current two lens, (E), 25:36115
performance of MPD arc thruster with downstream cathode, 25:36162
plasmoid acceleration in inductive conical, effect of stationary magnetic field on, (T), 25:36113
plasmoid mass and velocity spread in pulsed, (E/T), 25:36114

PLASMA JETS
boundary conditions for adjacent cold, in magnetic fields, (T), 25:36128 (UARAEE-78)
diagnostics in magnetohydrodynamic accelerators, (E), 25:36096
electron--ion recombination in, effects on electrodynamic acceleration, (T), 25:36109
flow kinetics in homopolar devices, (E/T), 25:36205
plasmoid production in, using transverse electric fields, (E), 25:36120
properties of stationary supersonic, magnetohydrodynamic, 25:36108
seeding of low-density, two-phase, (T), 25:36116
wave propagation on surface of adjacent, electromagnetic, (T), 25:36219 (UARAEE-97)

PLASTIC DEFORMATION
mechanisms in bcc metals, review of models for studies of, 25:35370

PLASTICS
fire behavior of, evaluation of test results in testing of, 25:37186(T) (GAT-Z-5046)
radiation resistance of, evaluation of, 25:34690(R) (IN-1457)
transfer molding of close tolerance parts of, 25:37162(R) (BDX-613-283)

PLATINUM
effects on colorimetric determination of gold, 25:34521
effects on gravimetric determination of mercury using 2-aminobenzothiazole, 25:34520
effects on photometric determination of antimony following solvent extraction using TBP, 25:34512
fission of, lower limit on half-life for spontaneous, (E), 25:36779
radiation damage in, annealing of 90°K 3-MeV electron, 25:36306

PLATINUM ALLOYS AND SYSTEMS
Au--Pt-base, radiation damage in, annealing of 90°K 3-MeV electron, 25:36306
Hf--Pt, stability of gaseous intermetallic, 25:35350
Pt--Ti, stability of gaseous intermetallic, 25:35350
Pt--Zr, stability of gaseous intermetallic, 25:35350
Pt-base--W, iodine ionization yields at 1300 to 2000°K on surfaces of, molecular and atomic, 25:35835

PLATINUM BROMIDES
separation of ions of, from metal ions by high-voltage electrophoresis using carboxylic and hydroxycarboxylic acids, 25:34702

PLATINUM CHLORIDES
separation of ions of, from metal ions by high-voltage electrophoresis using carboxylic and hydroxycarboxylic acids, 25:34702

PLATINUM ISOTOPES Pt-194
energy-level transitions in, comparison of E2-M1 mixing amplitudes with Kumar--Baranger pairing-plus-quadrupole force model, (E/T), 25:36773

PLATINUM ISOTOPES Pt-196
energy-level transitions in, comparison of E2-M1 mixing amplitudes with Kumar--Baranger pairing-plus-quadrupole force model, (E/T), 25:36773

PLATINUM ISOTOPES Pt-197
beta decay of, conversion-electron spectra from, (E), 25:36789

PLATINUM METALS
determination by fire-assay method, neutron activation and tracer studies of iridium losses in, 25:34544 (NIM-1048)
PLOWSHARE PROJECT
effects of Project Wagon Wheel in, on surrounding sandstone, prediction of explosion, 25:34770 (UCRL-50993)
nuclear debris from Buggy excavation of, biological availability of fallout γ-emitting radioisotopes to peccaries following single injection of, 25:35088
nuclear debris from Schooner Event of, comparison of fallout γ-emitting radioisotope excretion in feces and urine of peccaries following single ingestion of, 25:35089
nuclear debris from Schooner Event of, distribution of fallout γ-emitting radioisotopes in tissues of swine following field exposure to, 25:35090
radiation monitoring of surface waters and precipitation during reentry drilling at Project Rulison site, 25:34728 (USGS-474-101)
shock waves propagation in air tunnel from Marvel Event in, analysis and measurement of, 25:34765
PLUTO (PLANET)
mass and density of, (E), 25:35822
PLUTONIUM
complex formation of tetravalent, in sulfate solutions, 25:34563
complexes with DTPA, preparation and stability of, 25:34558 (SRARI-P-92)
determination in biological materials by α spectrometry following separation by solvent extraction using DEHPA, 25:34537
determination in fuel reprocessing input using lithium-7 tracer and mass spectrometry, 25:34689 (IAEA-R-876-F)
determination in plutonium dioxide--uranium dioxide systems, 25:34503(R) (NBL-256)
determination in spent uranium oxide (UO_2) by α counting or isotope dilution, 25:37015 (BNWL-1568)
determination of, aerial surveying detector system for, 25:34862 (EGG-1183-1517)
diffusion in zirconium at 650 to 900°C, welded couple method for studying Kirkendall effect occurrence during, 25:35333 (CEA-CONF-1760)
distribution and excretion following inhalation in soluble compounds, effects of DTPA on, 25:35091
hardness of α-, at 77 to 373°K, effects of grain size on, 25:35465
monitoring in sanitary waste system effluent from West Valley Processing Plant, 25:34683 (DOCKET-50201-73)
production in Swiss power reactors, forecasts to 1990 of, 25:35310
reactions with silicon nitrides at high temperatures, effects of free silicon on, 25:35546 (AWRE-O-42-69)
separation from nitric acid solution by continuous precipitation and filtration, 25:34680 (CEA-R-4105)
separation from uranium as hexafluoride, 25:34698 (UJV-2291-Ch)
thermal conductivity of α-, at 300°K, 25:35424
PLUTONIUM ALLOYS AND SYSTEMS
Ga--Pu-base, thermal conductivity of delta-, at 300°K, 25:35424
O--Pu--U, enthalpy of oxygen incorporation in (U,Pu)O/sub 2+-x/ in, 25:34506
PLUTONIUM CARBIDES
PuC--ThC, properties of, data manual on, 25:35548 (ORNL-4503(Vol.3))
PLUTONIUM FLUORIDES PuF_3
free energy of formation of, 25:34566
BeF_2--LiF--PuF_3--ThF_4, plutonium oxide precipitation in molten, equilibrated with thorium oxide, 25:34566
BeF_2--LiF--PuF_3, plutonium oxide precipitation in molten, equilibrated with beryllium oxide, 25:34566
BeF_2--LiF--PuF_3--ZrF_4, plutonium oxide precipitation in molten, equilibrated with zirconium oxide, 25:34566
PLUTONIUM FLUORIDES PuF_4
free energy of formation of, 25:34566
PLUTONIUM FLUORIDES PuF_6
preparation and properties of, 25:34698 (UJV-2291-Ch)
vapor pressure--temperature data for, 25:34602 (GAT-645)
PLUTONIUM ISOTOPES
determination in plutonium dioxide--uranium dioxide systems, 25:34503(R) (NBL-256)
determination in spent uranium oxide (UO_2) by mass spectrometry, 25:37015 (BNWL-1568)
determination of radioactive, in soils, 25:34500
PLUTONIUM ISOTOPES Pu-237
fission of isomeric, half-life for spontaneous, (E), 25:36795
PLUTONIUM ISOTOPES Pu-238
deuteron reactions (d,pf) at 13 MeV, analysis using double-humped barrier, (E/T), 25:36746
fission of, average kinetic energies and masses of fission fragments from spontaneous, (E), 25:36782
PLUTONIUM ISOTOPES Pu-239
deuteron reactions (d,pf) at 13 MeV, analysis using double-humped barrier, (E/T), 25:36746
distribution in epidermis of swine during surface contamination, 25:35092
distribution in sediment cores and waters from Atlantic Ocean and Mediterranean Sea, measurement of vertical, 25:34759(R) (NYO-2174-129)
neutron capture by, cross section for fast, (E), 25:36756
neutron capture-to-fission ratio at 0.1 to 30 keV, 25:36748
neutron fission at 14.3 to 200 eV, fission-neutron multiplicities for, (E), 25:36734 (ORNL-TM-2231)
neutron fission of, cross section for fast, (E), 25:36756
neutron fission up to 5.5 MeV, effects of excitation energy on fragment kinetic energies and yields from, (E), 25:36754
neutron total cross section and resonance parameters for, fast, (E), 25:36756
PLUTONIUM ISOTOPES Pu-241
deuteron reactions (d,pf) at 13 MeV, analysis using double-humped barrier, (E/T), 25:36746
neutron cross sections for, preparation of oxide samples for measurement of, 25:35541
PLUTONIUM ISOTOPES Pu-244
fission of, xenon mass spectrum from spontaneous, (E), 25:35594
radioactivity of, extinct, (E), 25:35594
PLUTONIUM NITRIDES
PuN--UN, crystal lattice parameters of solid solutions of, 25:35574
PLUTONIUM OXALATES
precipitation in nitric acid solutions, method for continuous, 25:34680 (CEA-R-4109)
PLUTONIUM OXIDES
enthalpy of oxygen incorporation in PuO/sub 2-x/, 25:34606
precipitation in MSR, studies on conditions for, 25:34566
PLUTONIUM OXIDES PuO_2
preparation of samples of plutonium-241-enriched, for neutron cross section measurements, 25:35541
PuO_2--UO_2, analysis for plutonium, plutonium isotopes, and uranium, 25:34503(R) (NBL-256)
PuO_2--UO_2, diffusion of oxygen in solid solutions of, 25:35547(R) (GEAP-12182)
PuO_2--UO_2, inspection of irradiated fuels of, in hot cells, alpha and beta--gamma autoradiographic methods for, 25:34837
PuO_2--UO_2, mechanical properties of, effects of burnup on, 25:37017 (CONF-710414-1)
PuO_2--UO_2, oxygen-to-metal ratio in, statistical method for determining sources of variation in, 25:35568 (ORNL-TM-3362)
PuO_2--UO_2, uranium activity in solid solutions of, transpiration method of studying, 25:35547(R) (GEAP-12182)
PuO_2--UO_2, vaporization of solid solutions of, research progress on studies of, 25:35547(R) (GEAP-12182)
PLUTONIUM RECYCLE TEST REACTOR
fuels for, burnup data for spent natural uranium oxide (UO_2), (E), 25:37015 (BNWL-1568)
POINT BEACH POWER REACTOR, UNIT 1
operations incident of May 4, 1971, improper position of circuit breaker for safety injection pump, 25:36681 (DOCKET-50266-49)
pressurizer safety valves for, furnace sensitized stainless steel in nozzles of, 25:36934 (DOCKET-50266-50)
radioactive effluents from, revised design parameters and operations aspects to reduce, 25:36933 (DOCKET-50266-48)
radioactive waste disposal system for, revised and additional data on, 25:36933 (DOCKET-50266-48)
POINT BEACH POWER REACTOR, UNIT 2
pressurizer safety valves for, furnace sensitized stainless steel in nozzles of, 25:36934 (DOCKET-50266-50)
radioactive effluents from, revised design parameters and operations aspects to reduce, 25:36933 (DOCKET-50266-48)
radioactive waste disposal system for, revised and additional data on, 25:36933 (DOCKET-50266-48)
POLLEN
radiation effects on viability of tulip, effects of dose on γ, 25:35255
POLONIUM ISOTOPES Po-203
energy levels and nuclear properties of, Nuclear Data Sheets for, (E), 25:36809
POLONIUM ISOTOPES Po-210
content in Atlantic Ocean surface samples and at various depths in Pacific Ocean, 25:34762
determination in cigarettes and tobacco, 25:34515
POLYENES
spectra of, research progress on, 25:37181(R) (COO-1693-6)
POLYMERS
inspection of glass-reinforced laminates of ester-type, radiographic method for, 25:34839
molecular motions in solutions of, pulsed NMR spectral studies of, 25:37185 (DP-MS-71-25)
radiation chemistry of high, 25:34637(R) (ORO-4059-1)
stability of insulating, used in lithium--selenium storage battery cells, 25:35275(R) (ANL-7777)
POLYOXYMETHYLENE
radiation effects on, ESR studies of, 25:34637(R) (ORO-4059-1)

XUM

POPULATIONS
radiation protection standards for, in relation to protective measures in medicine, 25:35147
radioisotope uptake by human, in Germany during 1967 and 1968 from ingestion of fish, 25:35096
PORTUGAL
iodine-131 content in cattle and sheep thyroid in, following Chinese nuclear tests, 25:35133
POSITRONIUM
formation during positron annihilation in organic liquids, mechanism for, (E/T), 25:35853
POSITRONS
annihilation in organic liquids, mechanism for formation of positronium atoms in, (E/T), 25:35853
interactions $e^+ + e^- \rightarrow e^+ + e^- + e^+ + e^-$, cross section for, (T), 25:36440
interactions $e^+ + e^-$ at high energies in colliding beams, total and differential cross sections for e and μ pair production in, (T), 25:36433 (LNF-71/1)
interactions $e^+ + e^-$ in colliding beams, pair production in, (T), 25:36445
interactions $e^+ + e^-$ in preasymptotic region, parton model predictions for hadron production in, (T), 25:36434 (LNF-71/5)
interactions $e^+ + e^-$ in storage rings, experimental conditions for $\gamma + \gamma$ interactions from, 25:36451
interactions $e^+ + e^-$, polarization effects in identical meson pair production in, (T), 25:36438
reactions with hydrogen atoms, Glauber-theory calculations of excitation cross sections for, 25:35878
scattering by hydrogen atoms, Harris-method calculation of phase shifts for s-wave elastic, 25:35875
POTASSIUM
abundance in lunar and terrestrial materials, (E), 25:35830
determination in glacial waters by ion-sensitive electrode method, 25:34721(R) (NYO-3912-3)
determination in glacial waters by ion-sensitive electrode method, 25:34722(R) (NYO-3912-4)
effects on colorimetric determination of gold, 25:34521
effects on gravimetric determination of mercury using 2-aminobenzothiazole, 25:34520
prospecting for deposits of, gamma well logging method for, 25:34716(T) (CSIRO-Trans-10088)
reactions with deuterium and hydrogen molecules up to 50 eV, vibrational excitation and dissociation in, (E), 25:35884
separation from sodium by bromine redox electrolysis, 25:34691 (LA-4645)
sorption by tantalum (110) and tungsten (100) crystals, contact potential measurements of, 25:35359
spectral absorption bands in 4430 A interstellar bands, (E/T), 25:35663
POTASSIUM ALLOYS AND SYSTEMS
K--Na, compatibility with Inconel 718 and 750 tubular sections at 1050 to 1310°F, 25:35343 (WANL-TME-1857)
POTASSIUM ARSENIC FLUORIDES
radiolysis of, ESR studies on, 25:34634(R) (COO-1385-37)
POTASSIUM BROMIDES
rare-gas atom and ion reactions with, electron emission induced from single crystals by 0.2- to 6.0-keV, (E), 25:35840
POTASSIUM CHLORIDES
radiation effects on lead-doped crystals of, absorption spectra--ionic thermocurrent study of 1.5-MeV electron, 25:36303
POTASSIUM FERROCYANIDES
radiolysis of, chemical effects of thermal neutron, 25:34663
POTASSIUM FLUOROPHOSPHATES
radiolysis of, ESR studies on radicals produced by γ, 25:34667
POTASSIUM IODATES
effects on γ-radioinduced inactivation of Bacillus cereus spores, potentiating, 25:35264
POTASSIUM IODIDES
effects on γ-radioinduced inactivation of Bacillus cereus spores, potentiating, 25:35264
CsI--KI--LiBr--LiCl--LiI, properties of eutectics of, for use as paste electrolytes, 25:35275(R) (ANL-7777)
POTASSIUM IONS
reactions with deuterium and hydrogen molecules up to 50 eV, vibrational excitation and dissociation in, (E), 25:35884
POTASSIUM ISOTOPES K-39
helium-3 elastic scattering at 29.3 MeV, angular distributions for, (E), 25:36696
helium-3 reactions (He-3,d) at 29.3 MeV, angular distributions for, (E), 25:36696
POTASSIUM ISOTOPES K-40
content in man, evaluation of shielded whole-body counter for measuring, 25:35183
POTASSIUM ISOTOPES K-42
determination in biological materials using Cherenkov radiation, 25:34540
POTASSIUM PRASEODYMIUM FLUORIDES
praseodymium-141 Moessbauer spectra in, 25:36344
POWER PLANTS
economics of liquid-metal MHD--steam binary, 25:35934
POWER SUPPLIES
control system for data processing system, 25:35068
design of 1-MV inductive energy storage system using ignitron switching, engineering drawings for, 25:36205
PRAIRIE ISLAND POWER REACTOR, UNIT 1
operation of, estimated costs of initial five-year, 25:36939 (DOCKET-50282-35)
shutdown of, estimated maintenance costs for permanent, 25:36939 (DOCKET-50282-35)
PRAIRIE ISLAND POWER REACTOR, UNIT 2
operation of, estimated costs of initial five-year, 25:36939 (DOCKET-50282-35)
shutdown of, estimated maintenance costs for permanent, 25:36939 (DOCKET-50282-35)
PRASEODYMIUM
determination in aqueous acetone solutions of dibenzoylmethane complexes, absorption spectrophotometric, 25:34527
determination in rare earth oxides, spectrographic, 25:34511
praseodymium-141 Moessbauer spectra in, 25:36344
separation from other rare earths by ion exchange chromatography, 25:34714
PRASEODYMIUM ALLOYS AND SYSTEMS
Al--Pr-base, crystal lattice parameters of intermetallic Pr_2Al, 25:35495
Bi--Pr, crystal field interactions in intermetallic PrBi, 25:35355
Bi--Pr, thermal capacity of intermetallic PrBi at 7 to 300°K, 25:35355
Pr--Sb, crystal field interactions in intermetallic PrSb, 25:35355
Pr--Sb, thermal capacity of intermetallic PrSb at 7 to 300°K, 25:35355
PRASEODYMIUM BROMIDES
praseodymium-141 Moessbauer spectra in, 25:36344
PRASEODYMIUM CARBIDES
praseodymium-141 Moessbauer spectra in, 25:36344
PRASEODYMIUM CHLORIDES
praseodymium-141 Moessbauer spectra in, 25:36344
PRASEODYMIUM FERRATES
praseodymium-141 Moessbauer spectra in, 25:36344
PRASEODYMIUM FLUORIDES
effects on radiation stability of beryllium fluoride glasses, 25:34621
praseodymium-141 Moessbauer spectra in, 25:36344
PRASEODYMIUM HYDROXIDES
praseodymium-141 Moessbauer spectra in, 25:36344
PRASEODYMIUM IONS
energy levels of Pr IV from spectrum measurements, 25:35847
energy levels of, spin--spin and spin--other-orbit matrices for, (T), 25:35850
PRASEODYMIUM ISOTOPES Pr-138
beta and electron-capture decay of, branching ratios, log-ft values, and conversion-electron and gamma spectra from, (E), 25:36725 (JINR-P6-5674)
energy levels from neodymium-138 electron-capture decay, spin-parity assignments for, (E), 25:36725 (JINR-P6-5674)
energy-level transitions from neodymium-138 electron-capture decay, branching ratios, internal conversion coefficients, and multipolarities for, (E), 25:36725 (JINR-P6-5674)
PRASEODYMIUM ISOTOPES Pr-139
energy levels from neodymium-139 beta and electron-capture decay, spin--parity assignments for, (E), 25:36724 (JINR-P6-5673)
energy-level transitions from neodymium-139 beta and electron-capture decay, conversion coefficients and multipolarities for, (E), 25:36724 (JINR-P6-5673)
PRASEODYMIUM ISOTOPES Pr-141
carbon-12 reactions (C-12,3r) and (C-12,5n) at 81 MeV, gamma spectra from, (E), 25:36726 (JINR-P6-5681)
Moessbauer spectrum in praseodymium compounds, isomer shifts and hyperfine splitting in, 25:36344
neutron capture by, spectrum-averaged cross sections for pile, (E/T), 25:36720 (CONF-710301-4)
PRASEODYMIUM OXALATES
praseodymium-141 Moessbauer spectra in, 25:36344
PRASEODYMIUM OXIDES
phase transformation in thin films of, martensitic monoclinic--hexagonal, 25:35575
praseodymium-141 Moessbauer spectra in, 25:36344
PRASEODYMIUM SULFATES
praseodymium-141 Moessbauer spectra in, 25:36344
PREAMPLIFIERS
design and performance of high-resolution voltage-sensitive cooled, for semiconductor counters, 25:34910
PRESSURE GAGES
performance for measurements in bubble chambers, effects of high magnetic fields and low temperatures on, 25:34987 (CONF-700623-(Vol.2), pp 863-72)
PRESSURE VESSELS
design parameters of cast iron, 25:37153(P)
fabrication of nuclear, U.S. requirements for, 25:37144
inspection equipment and procedures for boiling water reactors, 25:37004 (JAERI-Memo-4330)
radiation effects on prestressed concrete, fast neutron, 25:37007(T) (ORNL-tr-2470)
structural behavior of heavy-section steel, for boiling water and pressurized water reactors, method for prediction of, 25:34827

thermal insulation for reactor prestressed concrete, survey of materials and design of, 25:37006 (ORNL-TM-2929)
PROCESS EQUIPMENT
design for conversion of uranium oxides to uranium hexafluoride, engineering drawings for, 25:34782
design of plutonium processing facility, engineering drawings for, 25:34784
PROMETHIUM
separation from other rare earths by ion exchange chromatography, 25:34714
PROMETHIUM ISOTOPES Pm-143
beta decay of, spectra shape of K-orbital shakeoff electrons and accompanying nuclear beta particles in, (E), 25:36774
energy levels from samarium-143 beta and electron-capture decay, spin--parity assignments for, (E), 25:36766
PROMETHIUM ISOTOPES Pm-151
beta decay of, gamma singles and delayed-coincidence spectra from, (E), 25:36807
PROPANE
reactions with helium tritides formed by beta decay of molecular tritium, kinetic studies on, 25:34676
reactions with methane under simulated radiolysis conditions, mass spectrometric studies on, 25:34645
PROPANE, ASTATO-
boiling point of, gas chromatographic studies on, 25:34604 (JINR-P6-5683)
PROPANE, 1,2-EPOXY-2-METHYL-
yields from γ radiolysis of 2-methyl-2-propanol at 30°C, 25:34659
PROPANE, 2-METHYL-
reactions with helium tritides formed by beta decay of molecular tritium, kinetic studies on, 25:34676
1,3-PROPANEDIONE, 1,3-DI-2-FURYL-
complexes with neptunium or uranium, stability of, 25:34557 (KFK-1339)
1,3-PROPANEDIONE, 1,3-DIPHENYL-
complexes with neptunium or uranium, stability of, 25:34557 (KFK-1339)
1,3-PROPANEDIONE, 1,3-DI-2-THIENYL-
complexes with neptunium or uranium, stability of, 25:34557 (KFK-1339)
1-PROPANETHIOL, 2-AMINO-
radioprotective effects of, on Escherichia coli, function and structure studies on γ, 25:35160
1-PROPANOL
radiolysis of liquid, at low temperature, studies on electron solvation process in electron pulse, 25:34649
2-PROPANOL
radiation effects on subsequent catalytic dehydration of, on aluminum oxide, γ, 25:34629
radiolysis of liquid, at low temperature, studies on electron solvation process in electron pulse, 25:34649
HCl--2-propanol, corrosive effects on aluminum--titanium--vanadium alloys, 25:35287
2-PROPANOL, 2-METHYL-
radiolysis at 30°C, yields from, 25:34659
1-PROPANOL, 2-METHYL-2-NITRO-
radiolysis of glassy alkaline solutions of, at 77°K, ESR studies on scavenging by nitromethane of paramagnetic species produced by γ, 25:34643
PROPELLANTS
combustion of solid, burn testing under rocket abort conditions, 25:34792 (SC-DR-710084)
PROPENE
alpha-particle stopping cross sections in gaseous, at 0.3 to 2 MeV, 25:36255
PROPENE POLYMERS
properties of thin membranes of, for on-line alpha activity monitoring of solutions, 25:34673 (CEA-N-1440)
PROPULSION
conference on new experimental techniques in research on energetics and, Munich, 9/67, 25:36107
plasma jet, accelerator design for, 25:36105(P)
PROPYNE
reactions with methane under simulated radiolysis conditions, mass spectrometric studies on, 25:34645
PROSPECTING
book: Methods of Prospecting for Uranium Deposits (In Russian), 25:34754
conference on unconventional methods for natural gas and petroleum, Dallas, Tex., Sept. 12 and 13, 1968, 25:34729
method for seabed mineral, development of neutron source for, 25:34803(R) (BNWL-1308-5)
methods for petroleum, comparison of soil radioactivity mapping and soil redox mapping, 25:34731
methods for petroleum, development of radiometric, 25:34730
PROTACTINIUM
separation from molten salt fuels by reductive extraction, 25:34694 (ORNL-TM-3138)
separation from other actinides by ion exchange on anionite AV-17, 25:34695(T) (ORNL-tr-2397)
separation from single-fluid MSBR, system performance calculations for, 25:34694 (ORNL-TM-3138)
PROTACTINIUM BROMIDES
crystal structure of, 25:34610
reactions with sodium N,N-diethyldithiocarbamate, 25:34568
PROTACTINIUM CHLORIDES
reactions with sodium N,N-diethyldithiocarbamate, 25:34568
PROTEINS
number, location, and properties of erythrocyte membrane, 25:37258 (UR-49-1430)
radiation damage to, during radioiodination, 25:34700
radiation effects on content of, in codfish, combined effects of cooking and γ, 25:35272
radiation effects on rate of amino acid incorporation into, of rabbit lymphocytes, carbon-14 tracer study of γ, 25:35104
radioinduced free radicals in cell, γ and uv, 25:35203
separation of iodides from, after radioiodination, microscale, 25:34700
spectra of globular, in heavy water, study on position of amide and peptide bands in ir, 25:34588
synthesis in delayed implanting mouse ova, 25:37183(R) (COO-1801-17)
PROTON BEAMS
monitoring of intensity and time distribution of, system for pre-target, 25:36631
PROTONS
abundance in solar corpuscular radiation, (E/T), 25:35728
dechanneling in germanium single crystals at 1.5 MeV, ion mass effect on, 25:36289
dechanneling in germanium single crystals at 1.5 MeV, 25:36271
diffusion from ring current to auroral zone, (T), 25:35995
distribution in radiation belts, adiabatic theory of energy-dependent equatorial pitch-angle, (E/T), 25:36002
effects on cell nuclei in Hordeum vulgare and Vicia faba seeds, comparison of bremsstrahlung, γ, x, and, 25:35258
effects on thermoluminescence of Apollo 11 sample 10084, (E), 25:35824
effects on thermoluminescence of meteorite powder at 3 GeV, 25:36298
emission during solar flares, (E), 25:35758
interactions ν + p → ν + p, field exchange for, (T), 25:36571
interactions anti ν + p → n + μ+ at high energies, weak boson theory for form factor effects on, (T), 25:36460
interactions anti p + p → anti p(anti n) + p(n) at intermediate energies, direct-channel resonance effects on, (T), 25:36491
interactions e + p at 0.80 to 1.12 GeV, cross sections for absorption of transverse and longitudinal photons in inelastic, (E), 25:36381
interactions e + p at very high energies, proton internal structure determination from, (E/T), 25:36445
interactions e + p, quark model with relativistic extended internal structure for structure functions for deep inelastic, (T), 25:36444
interactions e + p, review of parton and vector dominance models for cross sections and structure functions for hadron production in deep inelastic, (T), 25:36452
interactions e + p, scaling properties in, (T), 25:36425 (NYO-1932(2)-189)
interactions γ + p → π0 (eta) + p, duality and meson trajectories in Regge cut model for, (T), 25:36441
interactions γ + p, model for Pomeranchukon exchange in total cross sections for, 25:36512
interactions K + p, model for Pomeranchukon exchange in total cross sections for, 25:36512
interactions K- + p → K- + π+ + n at 5.5 GeV/c, S-wave phase shifts for, (E), 25:36413
interactions K- + p → π- + Y0*, eikonal model with unitarity corrections for dual description of, (T), 25:36514
interactions K- + p → Σ(1385) + π near Λ(1520), production mechanism for, (T), 25:36415
interactions K+ + p at 210 and 330 MeV, optimized polynomial representations for differential cross sections for coupling constants and nonspinflip amplitudes of, (T), 25:36532
interactions K+ + p in Veneziano model, differential cross sections for charge-exchange and backward elastic, 25:36507
interactions K+ + p in Veneziano model, phase shifts for, 25:36507
interactions n + p at 510 and 600 MeV, spark chamber spectrometer study of Wolfenstein triple scattering parameters for, (E), 25:36397
interactions p + d → 3He + MM at 2 and 3 GeV, spectrometer study of differential cross sections versus missing mass and I = 0 and 1 meson production cross sections for, (E), 25:36398
interactions p + n → p + n interactions at 612 MeV, spark chamber study of depolarization in, (E), 25:36390 (JINR-P1-5743)
interactions p + n at 22.8 GeV/c, distribution of shower particles from, (E), 25:36392
interactions p + p → Δ + N*(Δ) at 10.01 GeV/c in hydrogen bubble chamber, momentum transfer distributions and cross sections for, (E), 25:36396
interactions p + p → p + N*(Δ) at 10.01 GeV/c in hydrogen

XUM

bubble chamber, momentum transfer distributions and cross sections for, (E), 25:36396
interactions p + p → p + p at 5 to 13.4 GeV/c, use of exact forms for amplitude in Regge pole theory for, (T), 25:36531
interactions p + p → p + p at high energies and large angles, cross sections for, (T), 25:36534
interactions p + p at 10 GeV in hydrogen bubble chamber, angular distributions for particles in showers and N* production in, (E), 25:36393
interactions p + p at 13 to 28.5 GeV/c in hydrogen bubble chamber, cross sections and momentum distributions for π^- and π^+ production in, (E), 25:36391 (UCRL-20632)
interactions p + p at 210 and 330 MeV, optimized polynomial representations for phase shifts and differential cross sections for coupling constants and nonspinflip amplitudes of, (T), 25:36532
interactions p + p at 510 to 670 MeV, spark chamber spectrometer study of Wolfenstein triple scattering parameters for, (E), 25:36397
interactions p + p, model for Pomeranchukon exchange in total cross sections for, 25:36512
interactions p + p, model for production of quarks and magnetic monopoles in superstrong final-state interactions of, 25:36530
interactions p + p, parton model predictions for structure in high-mass μ^+--μ^- pair production in, (T), 25:36434 (LNF-71/5)
interactions π + p → A_1 + rho + p → 5π + p at 50 and 100 GeV, Drell--Hiida--Deck effect for diffractive, (T), 25:36521
interactions π^- + p → 2π^0 + n at 447 MeV, spectrometer and spark chamber study of total cross sections, neutron differential cross sections and angular distributions, and $\pi^0\pi^0$ system effective mass spectrum in, (E), 25:36405 (JINR-P1-5781)
interactions π^+ + p → 3π^+ + 2π^- + p at 8 GeV/c, multiperipheral model with $\pi\pi$ and πp phase shifts and form factors for, (T), 25:36503 (INR-P-1265)
interactions π^- + p → K^0 + Λ, test of empirical rule for cuts and line reversal relations in absorption model prediction for Λ polarization in, (T), 25:36502 (CALT-68-300)
interactions π^- + p → $K_2{}^0$ + K^- + p at 4.5 GeV/c, production and decay of $A_2{}^-$ from, (E), 25:36409
interactions π^+ + p → K^+ + Σ^+ at 2.75 to 14 GeV/c, forward differential cross sections and polarization for, (E), 25:35410
interactions π^+ + p → K^+ + Σ^+, test of empirical rule for cuts and line reversal relations in absorption model predictions for Σ polarization in, (T), 25:36502 (CALT-68-300)
interactions π^+ + p → K^+ + Y^{*+}, eikonal model with unitarity corrections for dual description of, (T), 25:36514
interactions π^- + p → n + π^+ + π^- at 11 GeV/c, total cross section for π^+ + π^- interactions from, (E/T), 25:36509
interactions π^+ + p → ω + Δ^{++}, test of empirical rule for cuts in density matrix elements of ω in, (T), 25:36502 (CALT-68-300)
interactions π^- + p → π^0 + n at 1.8 to 6.0 GeV/c, momentum dependence of differential cross sections for, (E), 25:36412
interactions π^+ + p → π^+ + p at 0 to 2 GeV/c, compilation of amplitudes and parameters from partial-wave analyses for, (T), 25:36506 (TID-25726)
interactions π^- + p → π^- + p at 0 to 2 GeV/c, compilation of amplitudes and parameters from partial-wave analyses for, (T), 25:36506 (TID-25726)
interactions π^- + p → π^- + p at 6 and 16 GeV/c, A and R polarization parameters for, (E), 25:36406 (NP-18873)
interactions π^- + p → π^- + p at 9.85 GeV/c, angular distributions for, (T), 25:36534
interactions π^- + p → X^0 + n at 1.6 GeV/c, X^0 decay branching ratio and cross sections for, (E), 25:36407
interactions π^+ + p at 3.7 GeV/c, mass spectra of A_2 from, (E), 25:36411
interactions π^+ + p at high energies, sum rule for limitation of parametrizations in models for asymptotic behavior of amplitudes of, (T), 25:36511
interactions π^- + p at high energies, sum rule for limitation of parametrizations in models for asymptotic behavior of amplitudes of, (T), 25:36511
modulation of primary cosmic, (T), 25:35924
reactions (p,2n) and (p,3n) with americium-243 at 20 MeV, cross sections for, (E), 25:36795
reactions (p,2n) with europium-151 at 8.0 to 13.4 MeV, gamma spectra and angular correlations for, (E), 25:36775
reactions (p,2n) with zirconium-96 at 400 MeV, isomeric ratio in, 25:36761
reactions (p,2p) with carbon-12 and silicon-28 at 600 MeV, diffraction-model calculation of differential cross sections for, (T), 25:36679
reactions (p,2p) with deuterium at 4.5 to 13 MeV, impulse-approximation analysis of n--p and p--p coincidence spectra and excitation functions for, (E/T), 25:36669
reactions (p,d) and (p,t) with nickel-58 at 22 to 40 MeV, differential cross sections for, (E), 25:36738(R) (UCLA-10-P-18-23)
reactions (p,d) with carbon-14 and nitrogen-14 at 14.5 MeV, angular distributions for, (E), 25:36673
reactions (p,d) with helium-3 at 12 and 46 MeV, energy spectra for, (E), 25:36738(R) (UCLA-10-P-18-23)
reactions (p,f) with heavy nuclei, review of, 25:36802
reactions (p,f) with uranium, review of, 25:36802
reactions (p,γ) with aluminum-27 at 1.724 MeV, gamma angular distributions and linear polarizations from, (E), 25:36699
reactions (p,γ) with nuclei, computer program for calculating yields from, (T), 25:36732 (NRL-7230)
reactions (p,He-3) and (p,t) with fluorine-19, angular distributions for, (E), 25:36738(R) (UCLA-10-P-18-23)
reactions (p,He-3) with bismuth-209 at 40 MeV, angular distributions for, (E), 25:36777
reactions (p,Li-6) with carbon-12 at 36, 41, and 45 MeV, angular distributions for, (E), 25:36738(R) (UCLA-10-P-18-23)
reactions (p,n) with cobalt and vanadium at 17 MeV, neutron spectra from, (E), 25:36676
reactions (p,n) with neon-20 at 16.5 MeV, threshold energy and Q-value for, (E/T), 25:36710
reactions (p,n) with nuclei with analog-dipole excitation, collective theory for, 25:36835
reactions (p,n) with strontium-88 and yttrium-88, excitation functions for, (E), 25:36676
reactions (p,np) with gold-197 and tantalum-181 at 25 to 45 MeV, proton spectra and differential cross sections for, (E), 25:36738(R) (UCLA-10-P-18-23)
reactions (p,np) with lead-208 at 30.5 MeV, angular distributions for, (E), 25:36738(R) (UCLA-10-P-18-23)
reactions (p,pd) and (p,2p) with helium-3 and tritium at 35 MeV, kinematic analysis of, (E), 25:36738(R) (UCLA-10-P-18-23)
reactions (p,pd) and (p,pt) with fluorine-19, summed energy spectra from, (E), 25:36738(R) (UCLA-10-P-18-23)
reactions (p,pn) with deuterium at 14 to 23 MeV, modified-simple-impulse-approximation calculation of proton spectra from, (E/T), 25:36667
reactions (p,pn) with deuterium at 9.0 MeV, impulse-approximation analysis of proton spectra and peak cross sections for, (E/T), 25:36670
reactions (p,t) with carbon-14 at 14.5 MeV, angular distributions from, (E), 25:36673
reactions (p,t) with neodymium-142 at 51.7 MeV, coupled-channel Born-approximation calculation of differential cross sections for, (T), 25:36794
reactions (p,xn) with bismuth-209, tantalum-181, and thulium-169 at 20 to 45 MeV, precompound and statistical contributions to excitation functions for, (E/T), 25:36797
reactions with aluminum at 1 and 3 GeV, integrated cross sections for fluorine-18 and sodium-24 production in, (E/T), 25:36816 (JINR-P2-5719)
reactions with aluminum carbon, cobalt, and copper at 450 MeV, Monte Carlo calculation of neutron spectra from, (E/T), 25:36816 (JINR-P2-5719)
reactions with aluminum, cross sections for L-shell ionization in, (T), 25:35880
reactions with argon and helium, coincidence studies of charge exchange and excitation in, 25:35877
reactions with bismuth-209 at 120 to 660 MeV, yields of secondary (a,xn) reactions relative to astatine-211 for, (E), 25:36723 (JINR-P1-5530)
reactions with hydrogen atoms up to 3 keV, Glauber-approximation calculations of differential and total cross sections for 1s--3d excitation in, 25:35859
reactions with hydrogen atoms, Glauber-theory and multistate impact-parameter calculations of excitation cross sections for, 25:35878
reactions with hydrogen molecules up to 10 eV, crossing of potential-energy surfaces in, (T), 25:35885
reactions with intermediate nuclei at 400 MeV to 24 GeV, calculation of spallation cross sections for, (T), 25:36689 (NP-18820)
reactions with iron and silicon at 600 MeV and 24 GeV, aluminum-26 production cross sections for, (E), 25:36689 (NP-18820)
reactions with natural tantalum, thorium, uranium, and vanadium at 156 MeV and 24 GeV, Monte Carlo analysis of cross sections for production of cesium, potassium, and rubidium from, (E), 25:36730 (NP-18829)
reactions with nickel at 10 to 40 MeV, activation cross sections for, (E), 25:36738(R) (UCLA-10-P-18-23)
reactions with nuclei at 1 to 3500 MeV, computer program for intranuclear-cascade calculations of, (T), 25:36733 (ORNL-4564)
reactions with nuclei at 22.8 GeV/c in emulsions, method for identification of shower particles from, (E), 25:36402
reactions with nuclei at 24 GeV/c in emulsions, deuteron emission in, (E), 25:36403
reactions with rare gases at 4 MeV, pressure and impurity effects in ionization, 25:35888
scattering by calcium-48 at 4 to 8 MeV, relative excitation function for elastic, (E), 25:36690 (NP-18824)
scattering by carbon-14 and nitrogen-14 at 14.5 MeV, angular distributions for elastic and inelastic, (E), 25:36673

scattering by helium at 1 MeV and small angles, wave function for evaluation of Glauber amplitude for elastic, 25:35868
scattering by iron-54 at 19.6 MeV, DWBA analysis of spin dependence in inelastic, (E/T), 25:36708
scattering by molybdenum-92, excitation functions for elastic, (E), 25:36676
structure determination from e + p interactions at very high energies, internal, (E/T), 25:36445
PROTONS (anti p)
interactions anti p + d at rest, evidence for existence of narrow anti pn bound state in,), 25:36399
interactions anti p + p + anti p(anti n) + p(n) at intermediate energies, direct-channel resonance effects on, (T), 25:36491
reactions with nuclei at 5 GeV/c in emulsions, angular and momentum distributions for π^0 produced in, (E), 25:36404
PROTOZOA
crop of foraminifera in sublittoral and psammonlittoral communities of Long Island salt marsh, effects of environmental conditions on standing, 25:37208 (NYO-3995-15)
Tetrahymena pyriformis, radiation effects on structure of nucleoproteins in, 25:35206
PRUSSIAN BLUE
effectiveness of orally administered, for inhibiting gastrointestinal absorption of cesium-137, 25:35134
PUERTO RICO POWER REACTOR
cooling system for, inspection and repair of preheater piping in, 25:36857
fuel elements for, fabrication process for superheater, 25:37024
PULSARS
AP 1541, pulsed gamma emission from, search for high-energy, (E), 25:35705
CP 0950, pulsed gamma emission from, search for high-energy, (E), 25:35705
CP 1133, pulsed gamma emission from, search for high-energy, (E), 25:35705
distance of, (E/T), 25:35681
intensity variations of seven, long-term, (E), 25:35713
NP 0527, relation to *NP 0531*, (E/T), 25:35694
NP 0531, relation to *NP 0527*, (E/T), 25:35694
NP 0532, long-term slowing down and periodicity perturbations for, (E), 25:35685
NP 0532, multipath delay distortion of pulses from, (E), 25:35689
NP 0532, optical time-of-arrival measurements from, (E), 25:35695
NP 0532, photon field around, collision consequences of intense, (E/T), 25:35706
oblate cores in, (T), 25:35699
oblique-rotator model for, wobble and alignment time scales in, (T), 25:35699
observational developments in, (T), 25:35659
period--age relation for, (E/T), 25:35681
period--luminosity relation for, (E/T), 25:35681
production in Type II supernovae, (T), 25:35641
PSR 1642, pulsed gamma emission from, search for high-energy, (E), 25:35705
radiation emission mechanism for, (T), 25:35660
PULSE ANALYZERS
circuit for measurement of time-dependent spectra, routing, 25:35065
pulse converter for multichannel, use of binary-to-decimal, 25:35067
PULSE COLUMNS
pulse amplitude in air, for plutonium solvent extraction, effects of reservoir air pressure and pulse frequency on, (E/T), 25:34773 (BNWL-B-51)
PULSE CONVERTERS
design and performance of ultralinear 16-bit digital-to-analog, 25:35053
use of binary-to-decimal, in vacuum tube multichannel pulse-height analyzers, 25:35067
PULSE DISCRIMINATORS
design of fast dc coupled, 25:35045 (CEA-N-1447)
operation and theory of, 25:35055
timing circuit for zero-crossover, constant fraction adapter, 25:35064
PULSE GENERATORS (ELECTRONICS)
design for integral linearity testing of analog pulse circuits, 25:35066
design of lumped-element line generator for low-rf oscillations in plasma, 25:36229
PULSE GENERATORS (PNEUMATICS)
performance for pulsed extraction columns, analysis of, 25:34773 (BNWL-B-51)
PUMPS
bearings for reactor primary, description of water cooling system for radial, 25:37145(P)
description of reactor coolant, 25:37142
design parameters of turbine, 25:37014(P)
seals for reactor primary, description of water cooling system for shaft, 25:37145(P)
PUREX PROCESS
solvent cleanup using macroreticular ion exchange resins in, 25:34679 (ARH-SA-58-RD)
PYRENE
effects of coatings of, on γ radiolysis products of poly(vinyl chloride), ESR studies on, 25:34656
radiolysis of acetone solutions of, at -75°C, dimer formation in electron pulse, 25:34658

Q

Q DEVICES
plasma diagnostics in single-ended, cusps for, 25:36055
plasma oscillations near cyclotron edge, effect of pressure drifts on, (E), 25:36245
QUAD CITIES POWER REACTOR, UNIT 1
fuel cask for, request for additional information on drop accident for, 25:36928 (DOCKET-50254-37)
instrumentation for, request for additional information on line failure for, 25:36928 (DOCKET-50254-37)
piping systems for, request for additional information on whip analysis of, 25:36928 (DOCKET-50254-37)
QUAD CITIES POWER REACTOR, UNIT 2
fuel cask for, request for additional information on drop accident for, 25:36928 (DOCKET-50254-37)
instrumentation for request for additional information on line failure for, 25:36928 (DOCKET-50254-37)
piping systems for, request for additional information on whip analysis of, 25:36928 (DOCKET-50254-37)
QUALITY CONTROL
inspection equipment and procedures for pressure vessel, 25:37004 (JAERI-Memo-4330)
QUANTUM ELECTRODYNAMICS
Lamb shift in hydrogen in, two-body problem for, 25:36567
renormalization groups in, perturbative solutions of, 25:36565
theory for covariant, ether flow in, 25:36566
two-body problem in, 25:36567
QUANTUM FIELD THEORY
Bethe--Salpeter equation in, method for solving, 25:36568
criterion for zero-mass particles in, 25:36570
field equations in, approximate conformal covariance of, 25:36561 (JINR-P2-5716)
field in, Borchers class of local, 25:36569
gauge field in, observation of skew-symmetric tensor, 25:36571
gauge fields in, chiral extension of internal holonomy group for, 25:36575
gauge vector and tensor fields, geometrical description of, 25:36574
Hamiltonians for models in, lower bounds and self-adjointness of, 25:36573
indefinite metric in relativistic, 25:36564 (ORO-3992-30)
indefinite metric in, analyticity, covariance, and unitarity in, 25:36563 (ORO-3992-26)
infrared divergences in model with degenerated vacuum, partial elimination of, 25:36562 (JINR-P2-5760)
interactions in, conformal covariance relation with gauge invariance of, 25:36561 (JINR-P2-5716)
meson field geometrization over Riemann--Einstein space in general relativity, massive scalar, 25:36582
model with degenerated vacuum in, partial elimination of infrared divergences in, 25:36562 (JINR-P2-5760)
role in physics, review of, 25:36576
shadow states in relativistic, 25:36564 (ORO-3992-30)
vibrations in, review of criteria for absolute, convective, and global instability and amplification and nontransmission of, 25:36560 (ITF-70-96-P)
Ward identities in dual resonance models in, algebraic structure of generalized, 25:36591
Yukawa, vacuum vector of Hamiltonian in, 25:36572
QUANTUM MECHANICS
eigenvalues of electron in field of electric dipole, relativistic corrections to ground-state energy, 25:36371
elementary excitations in system of charged particles in magnetic field, 25:36359
energy levels and Lorentz invariance in, 25:36374
four-body bound-state problem for identical particles, (T), 25:36364
Hamiltonian formalism for exactly solvable N-body problem, 25:36370
harmonic oscillator in, angular momentum coherent states in, 25:36377
hyperfine Hamiltonian in, improved relativistic correction to Fermi-contact, 25:36355 (NP-18818)
logic of conclusive explication of, 25:36353 (ITF-70-61-E)
measurement problem in, relation of time scales to, (T), 25:36372
perturbation theories in, without secular terms, 25:36376
Schroedinger equation in, Monte Carlo solution of, 25:36375
wave function reconstruction from matrix elements, 25:37252 (UCRL-20667)
QUASARS
charts for 22 bright, finding, (E), 25:35679
distribution of, (T), 25:35810
distribution of, (T), 25:35811
electron pair production in, observable effects of, (T), 25:35678
explosions in, magneto-rotational, (T), 25:35819

flux density of 3C 273, 25:35686
gamma emission from 3C 93, (E), 25:35700
photoelectric sequences for 22 bright, (E), 25:35675
relation of large- and small-redshift, to clusters of galaxies, (E/T), 25:35693
spectra of, absence of Lyman-α absorption in, (T), 25:35811
spectra of, photon, (T), 25:35678
spectral redshifts of, (T), 25:35810
QUINOLINE
complexes with uranyl ion, magnetic susceptibility and ir spectra of, 25:34612
8-QUINOLINOL
complexes with uranyl ion, magnetic susceptibility and ir spectra of, 25:34612

R

RABBITS
arsenic-76 distribution and excretion in chinchilla, following intravenous injection, effects of syphilis infection on,, 25:35087
radiation effects from uranium nitrate on morphofunctional state of thyroid gland of, 25:35229
RADIATION
dose rate to fuel reprocessing personnel following fuel particle inhalation and skin contamination, correction factors for measuring true, 25:35140
dose to patients during fluoroscopy, review on methods for reducing, 25:35142
effect on structure of nucleoproteins in amnion cells, lymphocytes, and Tetrahymena, 25:35206
effects on bacteria, effects of iodoacetic acid and vitamin K on lethal, 25:35262
effects on bioelectric activity in rat brain, 25:35235
effects on biological materials, mechanism for physicochemical protection against, 25:35166
effects on biological materials, role of free radicals in, 25:34639(R) (USC-113-P-21-3)
effects on biological membranes, mechanisms for, 25:35210
effects on bone marrow stem cells in mice, lethal, 25:35212
effects on catechol methyltransferase and monoamine oxidase activity in rats, inhibiting, 25:35165
effects on cell biolipids, chemiluminescent studies on, 25:35201
effects on cell structure in animals and man, review on, 25:35209
effects on cells, conference on, Erevan, USSR, Oct. 29 to Nov. 3, 1968, 25:35196
effects on cells, hit and target principles for studying, 25:35199
effects on cells, mechanisms of recovery from damaging, 25:35205
effects on cells, role of free radicals in, 25:35202
effects on cells, role of radiotoxins in, 25:35200
effects on chromosomes from transplanted babcon and monkey bone marrow cells, aberrant, 25:35230
effects on chromosomes in pea seeds, effects of oxygen on aberrant, 25:35119
effects on Ehrlich ascites tumor cells, mechanism of protective effects of cysteamine and AET against, 25:35204
effects on fruits, effects of dose, maturity, and storage temperature on, 25:35273
effects on functional and structural characteristics of radiosensitive and radioresistant yeast strains, 25:35247
effects on grafting of styrene to polyethylene, 25:35591
effects on growth of duckweed, effects of dose, light, and temperature on, 25:35248
effects on growth, meiosis, and pollen in sweet cherry plants, mutagenic, 25:35127
effects on hormone production by thyroid gland, 25:35208
effects on human pulmonary function following therapy for bronchial carcinomas in comparison with surgery, 25:35243
effects on intestinal mucosa of man, origin and kinetics of goblet cells during post-operative, 25:35240
effects on lipofuscin accumulation in man exposed to atomic bombing of Hiroshima and Nagasaki, 25:35241
effects on mice, role of hypothermia in protective effects of sodium fluoroacetate against, 25:35163
effects on mouse hematopoietic system and whole organism, effects of dose fractionation and rate on, 25:35218
effects on optical density of mitrochondria in animal cardiac muscles, 25:35227
effects on plaque forming ability in bacteriophage, inactivating, 25:35259
effects on rats, protective effects of sulfhydryl groups against damaging, 25:35213
effects on reproduction of hematopoietic cells in hamsters and mice, 25:35217
effects on structure of cells, role of DNA in, 25:35197
effects on structure of deoxyribonucleoproteins in somatic cells, degratory, 25:35198
electron-molecule reactions in, 25:34618
transport in free-electron atmosphere, 25:36267
RADIATION CHEMISTRY
book: Advances in Radiation Chemistry, Vol. 2, 25:34615
free radical production in, ESR studies on, 25:34616
processes in, research progress on primary, 25:34613 (TID-25689)
RADIATION DETECTORS
description for monitoring in nuclear power plants, 25:34869 (SZS-2/71, pp 7-11)
description of portable survey, 25:34868 (SZS-2/71, pp 1-6)
description of pressurized water reactor protection system, 25:36995 (WCAP-7669)
design and performance for radiological monitoring, NCRP recommendations for, 25:34894
development of self-powered, for in-core neutron measurements, 25:34877
development of supercooled-liquid track detector, 25:35015
geometry effects on accuracy in x and γ radiometric gages, 25:34904
lectures on, 25:34863 (HMI-B-108)
multiplex systems of, properties of pseudo-noise sequences used in, 25:34866 (JINR-P13-5722)
positioning device for dose distribution measurements in liquid phantoms, 25:35059
research at UCLRL, Sept.-Dec. 1970, 25:34873(R) (UCRL-50007-70-3)
response of self-powered, for in-core gamma detection, 25:34891
time resolution of, paired sources method for determining, 25:34890
RADIATION DETECTORS, ACTIVATION
design and performance of carbon and silver, for measuring bremsstrahlung distribution from electron-bombarded targets, 25:34908
RADIATION DETECTORS, BUBBLE CHAMBER
bubble dynamics in liquid hydrogen, effects of ultrasound on, 25:35005 (JINR-P13-5751)
bubble nucleation on metallic surfaces immersed in cryogenic fluids in, 25:34958 (CONF-700623-(Vol.1), pp 449-58)
characteristics of Gargamelle, 25:34944 (CONF-700623-(Vol.1), pp 136-44)
control system for CERN 2-meter liquid-hydrogen, description of computer, 25:34946 (CONF-700623-(Vol.1), pp 256-73)
conversion of BNL 7-foot, to 11-foot chamber, 25:34978 (CONF-700623-(Vol.2), pp 735-49)
data acquisition system for SLAC 40-inch hydrogen, description of scintillation-counter, 25:34970 (CONF-700623-(Vol.2), pp 617-28)
description of ANL 12-foot hydrogen, 25:34974 (CONF-700623-(Vol.2), pp 675-95)
description of Frascati 70-liter heavy gas--liquid, with internal hydrogen target, 25:35007 (LNF-70/25)
description of large hydrogen, for research in neutrino physics at 15 to 80 GeV, 25:34941 (CONF-700623-(Vol.1), pp 56-96)
design and construction of Gargamelle, review of technical problems in, 25:34959 (CONF-700623-(Vol.1), pp 460-76)
design and development of, conference on, 25:34938 (CONF-700623-(Vol.1))
design and development of, conference on, 25:34966 (CONF-700623-(Vol.2))
design and operation of rapid-cycling, 25:34955 (CONF-700623-(Vol.1), pp 408-17)
design and performance of Mirabelle, description of, 25:34973 (CONF-700623-(Vol.2), pp 647-74)
design considerations for BNL 11-foot, 25:34978 (CONF-700623-(Vol.2), pp 735-49)
design considerations for NAL, 25:34975 (CONF-700623-(Vol.2), pp 696-702)
design for strong-interaction experiments, parameter optimization in, 25:34939 (CONF-700623-(Vol.1), pp 5-41)
design of hyperon bubble chamber HYEUC, 25:34972 (CONF-700623-(Vol.2), pp 640-6)
design parameters of BEBC, 25:34976 (CONF-700623-(Vol.2), pp 703-13)
design specifications for proposed 1.5-meter high Field Bubble Chamber, at Rutherford High Energy Laboratory, 25:34977 (CONF-700623-(Vol.2), pp 714-34)
development and operation of ANL 12-ft, 25:34980 (CONF-700623-(Vol.2), pp 765-73)
development of BNL 7-ft, 25:34981 (CONF-700623-(Vol.2), pp 774-89)
development of neutral-particle tagging facility for ANL 30-inch, using spark chambers, 25:34967 (CONF-700623-(Vol.2), pp 582-92)
development of rapid-cycling, 25:34952 (CONF-700623-(Vol.1), pp 346-75)
development of rapid-cycling, 25:34954 (CONF-700623-(Vol.1), pp 390-407)
development of rapid-cycling, at Univ. of Wisconsin, 25:34956 (CONF-700623-(Vol.1), pp 418-23)
development of ultrasonic, 25:34953 (CONF-700623-(Vol.1), pp 376-89)
expansion system for BEBC, description of servo-controlled, 25:34988 (CONF-700623-(Vol.2), pp 872-82)
expansion system for BEBC, design criteria for piston in, 25:34985 (CONF-700623-(Vol.2), pp 836-48)
expansion system for High Field Bubble Chamber, design

and performance of fiber-glass-reinforced epoxy-resin bellows for, 25:34986 (CONF-700623-(Vol.2), pp 845-62)
expansion system for Mirabelle, design of, 25:34979 (CONF-700623-(Vol.2), pp 751-64)
expansion system for proposed Rutherford HFBC, design of resonant, 25:34984 (CONF-700623-(Vol.2), pp 824-35)
liquids for, refractive indices of neon--hydrogen mixtures and neon, 25:34963 (CONF-700623-(Vol.1), pp 543-54)
liquids in large cryogenic, properties of hydrogen--neon, 25:34962 (CONF-700623-(Vol.1), pp 532-42)
magnet for BEBC, design and development of superconducting, 25:35001 (CONF-700623-(Vol.2), pp 1126-49)
magnetic field of BEBC, methods for determination of, 25:35002 (CONF-700623-(Vol.2), pp 1150-71)
magnets for high-field, magnetization-current effects in multifilament superconducting, 25:35000 (CONF-700623-(Vol.2), pp 1095-1125)
magnets for, design of large superconducting, 25:34995 (CONF-700623-(Vol.2), pp 1040-94)
neutrino physics in heavy-liquid Gargamelle, proposed research program for 1971, 25:34943 (CONF-700623-(Vol.1), pp 123-35)
operation of existing, reports and discussion of, 25:34945 (CONF-700623-(Vol.1), pp 196-255)
optical constants for ANL 12-foot, use of tables of, 25:34947 (CONF-700623-(Vol.1), pp 275-302)
optical system for ANL 12-ft, compensation for concentricity problems in fisheye windows for, 25:34996 (CONF-700623-(Vol.2), pp 997-1009)
optical system for ANL 12-ft, development and performance of wide-angle camera lens for, 25:34991 (CONF-700623-(Vol.2), pp 915-42)
optical system for BEBC, design of wide-angle, 25:34990 (CONF-700623-(Vol.2), pp 902-14)
optical system for Gargamelle, calibration of objectives for, 25:34993 (CONF-700623-(Vol.2), pp 959-71)
optical system for Mirabelle, design and calibration of, 25:34992 (CONF-700623-(Vol.2), pp 943-58)
optical system for Mirabelle, illumination and lenses for, 25:34994 (CONF-700623-(Vol.2), pp 972-83)
optical system of Gargamelle, development of, 25:35003 (CONF-700623-(Vol.2), App.I)
optical system of High Field Bubble Chamber, mounting of fisheye windows for, 25:34997 (CONF-700623-(Vol.2), pp 1010-23)
optical systems for large liquid-hydrogen, laser-produced fiducial lines for calibration of, 25:34995 (CONF-700623-(Vol.2), pp 984-96)
optical systems for, development of holographic, 25:34998 (CONF-700623-(Vol.2), pp 1024-38)
particle tracks in ANL 12-foot, computer program for reconstructing, 25:34948 (CONF-700623-(Vol.1), pp 303-11)
particle tracks in Gargamelle, development of film projector for analyzing, 25:34951 (CONF-700623-(Vol.1), pp 334-44)
particle tracks in liquid-helium, bubble density of, 25:34989 (CONF-700623-(Vol.2), pp 893-900)
particle tracks in track-sensitive targets in, computer program for reconstructing, 25:34949 (CONF-700623-(Vol.1), pp 312-24)
particle tracks in, facility for film analysis of, 25:35062
particle tracks in, methods for minimizing angle errors due to multiple scattering in reconstruction of, 25:34950 (CONF-700623-(Vol.1), pp 325-33)
particle tracks in, optimum lengths for, 25:34940 (CONF-700623-(Vol.1), pp 42-55)
performance testing of Mirabelle, 25:34979 (CONF-700623-(Vol.2), pp 751-64)
photography in, counter control of, 25:34969 (CONF-700623-(Vol.2), pp 606-16)
pressure in rapid-cycling, effects of parasitic boiling and expansion speed on dynamic, 25:34957 (CONF-700623-(Vol.1), pp 424-48)
pressure measurement in BEBC, effects of high magnetic fields and low temperatures on gages and transducers for, 25:34987 (CONF-700623-(Vol.2), pp 863-72)
quantameter for measurement of energies of mesons (π^0) produced in NAL 15-foot, design of lead-plate proportional, 25:34942 (CONF-700623-(Vol.1), pp 97-116)
refrigeration system for Mirabelle, design of, 25:34979 (CONF-700623-(Vol.2), pp 751-64)
research program at Gargamelle, proposed, 25:34944 (CONF-700623-(Vol.1), pp 136-44)
resolution for detection of photons at <1 GeV/c, 25:34964 (CONF-700623-(Vol.1), pp 555-66)
safety features of Gargamelle, 25:35003 (CONF-700623-(Vol.2), App.I)
target for 40-inch SLAC, design and development of 4-inch hydrogen track-sensitive, 25:34965 (CONF-700623-(Vol.1), pp 567-80)
targets for BNL, development of track-sensitive, 25:34961 (CONF-700623-(Vol.1), pp 511-31)
targets in neon--hydrogen mixtures for, design of track-sensitive hydrogen and deuterium, 25:34960 (CONF-700623-(Vol.1), pp 477-510)
testing of 1-m model of BEBC, result from optics, 25:34983 (CONF-700623-(Vol.2), pp 813-23)
testing of 1-m model of BEBC, results from thermodynamics, 25:34982 (CONF-700623-(Vol.2), pp 790-812)
trigger for observing multipronged events in, design of counter-array, 25:34968 (CONF-700623-(Vol.2), pp 582-605)
triggering by wire chambers of SLAC 40-inch, for proposed study of diffractive N* production, 25:34971 (CONF-700623-(Vol.2), pp 629-38)

RADIATION DETECTORS, CLOUD CHAMBER
design and operation of rapid-cycling, 25:34956 (CONF-700623-(Vol.1), pp 408-17)

RADIATION DETECTORS, DIELECTRIC TRACK
bibliography on fission foil--dielectric track detectors for neutron dosimetry, 25:34867 (NP-18849)
design of cellulose nitrate, for fast-neutron detection by etching of multipronged alpha tracks, 25:34875(P)
energy threshold of Makrofol E, for neutrons, 25:34902

RADIATION DETECTORS, FISSION CHAMBER
design for in-core neutron flux mapping, 25:34884(P)
design of, 25:34883(P)
use with transistorized pulse channel for neutron flux measurements, 25:37146

RADIATION DETECTORS, FISSION FOIL
bibliography on fission foil--dielectric track detectors for neutron dosimetry, 25:34867 (NP-18849)

RADIATION DETECTORS, GEIGER-MUELLER
design for reactor fission product monitoring, 25:37147(P)
operation and performance of self-quenching open-end, for detection of slow positive ions, 25:34898
sensitivity for radioactivity monitoring of water, 25:34870 (SZS-2/71, pp 12-22)

RADIATION DETECTORS, IONIZATION CHAMBER
calibration and use of boron trifluoride, for measurement of mean energy of neutrons, 25:34906
circuits for coupling out of pulses from, description of, 25:34914(P)
design and calibration of fast-pulse, for muon flux measurements, 25:35022
design of pocket dosimeter, 25:34893(P)
maintenance of Babyline-20, for beta and gamma dosimetry, 25:35025 (CEA-N-1435)

RADIATION DETECTORS, PROPORTIONAL
design and performance of high-pressure, for high-energy particle identification, 25:35018
design of lead-plate quantameter for measurement of meson (π^0) energies at NAL 15-foot bubble chamber, 25:34942 (CONF-700623-(Vol.1), pp 97-116)
performance of proton recoil, for fast neutron spectrum measurements, 25:36991(R) (GULF-RT-10523)
sensitivity for radioactivity monitoring of water, 25:34870 (SZS-2/71, pp 12-22)

RADIATION DETECTORS, SCINTILLATION
circuits for large multisectioned liquid, coincidence, 25:35009 (CRO-2504-172)
composition for liquid, development of thermodynamically stable, 25:34874(P)
description for aerial surveying for determining plutonium concentrations, 25:34862 (EGG-1183-1517)
description of balloon-borne telescope for cosmic x-ray sources, (E), 25:35014
design and performance of large-area, for cosmic particle time-of-flight measurements, 25:35020
design for triggering bubble chambers, 25:34968 (CONF-700623-(Vol.2), pp 593-605)
design of automatic liquid, 25:34886(P)
design of Hadamara transform, for angular and spatial distribution measurements, 25:34865 (JINR-P13-5696)
design of lead sandwich, for measuring luminosity of Orsay storage ring, 25:36606 (LAL-1249)
design of liquid for automatic counting and display, 25:34878(P)
design of liquid, for alpha particles, engineering drawings for, 25:34930
design of ultra-thin, for time-of-flight spectroscopy of charged particles, 25:34887(P)
performance for dosimetry in Plexiglas phantoms, 25:35030
performance of sodium iodide, for noise measurements in exponential piles, 25:37086
performance of stilbene, for fast neutron spectroscopy, 25:34920 (UARAEE-91)
photomultiplier for liquid, performance of RCA C31 000D, 25:34895
pulse spectrum of plastic, for cosmic ray detection at sea level, anomalous, 25:35010
quenching effects in liquid, method for automatic compensation for, 25:34912(P)
radiation damage to plastic, gamma, 25:35079
sensitivity for radioactivity monitoring of water, 25:34870 (SZS-2/71, pp 12-22)
spectra shape calibration and peak-to-total ratio measurements of thallium-sodium iodide, 25:34936
stabilization system for, automatic drift, 25:34913(P)

RADIATION DETECTORS, SEMICONDUCTOR
cooling system for scattering chamber, 25:36634
design modification of position-sensitive array of surface-barrier, for magnetic spectrograph, 25:34861 (AERE-R-6776)
development of lead iodide, 25:34889

fabrication of well-type, 25:34882(P)
preamplifier for, design and performance of high-resolution voltage-sensitive cooled, 25:34910
pulse amplitude spectra in, principle of formation of, 25:34911
pulse height spectrum in, computer program for calculation of monoenergetic gamma, 25:34907
response functions for studying formation of amplitude spectra in, 25:34911
use for control of bubble-chamber photography, 25:34965 (CONF-700623-(Vol.2), pp 606-16)
RADIATION DETECTORS, SEMICONDUCTOR (GERMANIUM)
efficiency of coaxial lithium-drifted, photopeak, (E/T), 25:34900
RADIATION DETECTORS, SEMICONDUCTOR (SILICON)
currents in surface-barrier, surface effects on reverse, 25:34897
design of MOS, based on measurement of integrated current from post-irradiation heating for dosimetry, 25:35036(P)
fabrication of position-sensitive, 25:34896
performance of multiplying, for low-energy gamma spectroscopy at room temperature, 25:34918(T) (LB/G-3034)
performance of surface-barrier, for pulsed gamma dosimetry, 25:34892
timing with surface-barrier, using charge and current pulses, 25:34899
RADIATION DETECTORS, SPARK CHAMBER
characteristics of external electrode, for cosmic ray studies, 25:35021
data digitizing and memory system for magnetostrictive wire, 25:35016
data processing for, description of computer programs for, 25:35004 (JINR-P10-5762)
design of gas-filled, for detection of beta, gamma, and x radiation, 25:34876(P)
design of large-area high-efficiency, using electrode of high-resistive material, 25:35019
development of neutral-particle tagging facility for ANL 30-inch bubble chamber using, 25:34967 (CONF-700623-(Vol.2), pp 582-92)
efficiency of, shower, (E/T), 25:35006 (JINR-P13-5810)
particle tracks in, graphical projection method for measuring, 25:35011
performance of optical, with wire electrodes, 25:35008 (LNF-70/44)
readout for wire, in magnetic fields, capacitor, 25:35017
RADIATION DOSE
dose to human gonads and whole-body during radiodiagnosis, estimation of, 25:35179
maximum permissible, for nuclear industry personnel handling open radioactive material, 25:35154
RADIATION DOSIMETERS
design of MOS silicon, based on measurement of integrated current from post-irradiation heating, 25:35036(P)
design of plastic, based on physical property changes for x ray dosimetry below 15 keV, 25:35033(P)
research at UCLRL, Sept.-Dec. 1970, 25:34873(R) (UCRL-50007-70-3)
RADIATION DOSIMETERS, CALORIMETRIC
design and performance for x ray dosimetry at 10 to 100 keV, 25:35031
RADIATION DOSIMETERS, CHEMICAL
response of various, to gamma radiation and pulsed electrons, 25:35034
RADIATION DOSIMETERS, COLORIMETRIC
description of color indicator for beam monitoring at 0.2 to 10 Mrad, 25:35029
RADIATION DOSIMETERS, EXOELECTRON
fading characteristics of beryllium oxide, calcium sulfate, and lithium fluoride, thermal, 25:35026 (THAI-AEC-35, pp 21-3)
RADIATION DOSIMETERS, LUMINESCENT
development of phosphate-glass, sensitive to gamma rays, thermal neutrons, and x rays, 25:35037(P)
RADIATION DOSIMETERS, PHOTOGRAPHIC FILM
performance in comparison to thermoluminescent dosimeters for measuring β dose rate to personnel, 25:35131
RADIATION DOSIMETERS, THERMOLUMINESCENT
annealing of lithium fluoride--Teflon disk, 25:35024 (AEEW-M-991)
design for measuring radioactivity in fluids, 25:35035(P)
efficiencies of, measurement of intrinsic, 25:35032
operation and uses of, 25:35028
performance in comparison to film badges for measuring β dose rate to personnel, 25:35131
performance of lithium fluoride, for personnel dosimetry, 25:35023 (AEEW-M-962)
performance of lithium-fluoride, with beta and x-ray sources, 25:35139
response of lithium fluoride, for electrons, energy, 25:35027
sensitivity of lithium fluoride--Teflon disk, dependence on annealing temperature, number of cycles, and optical density of, 25:35024 (AEEW-M-991)
thermoluminescence of TLD-100 lithium fluoride, supralinearity and sensitization in, 25:35076
RADIATION DOSIMETRY
evaluation at therapy institutions, IAEA comparison program for, 25:35141
isodose curves for, using thermoluminescent dosimeters, 25:35139
methods for personnel, standards for, (E), 25:34879
methods for, survey of, 25:35137
program in Turkey, using photographic film, 1962 to 1969, 25:35135 (CNAEM-77)
RADIATION MONITORING
methods for, NCRP recommendations for, 25:34894
program for environmental, at Ames Laboratory, results of 1970, 25:34743 (IS-2541)
RADIATION PROTECTION
measures for patients and personnel in nuclear medicine, architectural and organizational, 25:35151
methods for fire fighters following nuclear accidents, 25:35149
methods for hospital personnel in nuclear medicine, 25:35150
methods for nuclear medicine patients and nuclear industry personnel, conference on, 25:35130
research at UCLRL, Sept.-Dec. 1970, 25:34873(R) (UCRL-50007-70-3)
standards for populations in relation to protective measures in medicine, 25:35147
RADIATION RATE METERS
description of portable, 25:34868 (SZS-2/71, pp 1-6)
RADIATION SOURCES
design of, U.S. patents 1950 through 1968, 25:34777 (ORNL-IIC-34)
development of advanced, 25:34803(R) (BNWL-1308-5)
production at Japan Atomic Energy Research Institute during 1969, 25:34804(R) (JAERI-Memo-4285)
testing of, methods for nondestructive, 25:34803(R) (BNWL-1308-5)
RADIATION STANDARDS AND UNITS
compilation for dosimetry and radiation detection, National Bureau of Standards, 25:35137
RADIATION TARGET CANS
design parameters for liquid metal, for swimming pool type reactors, 25:37061(T) (EURFNR-890)
design parameters for liquid sodium, for swimming pool type reactors, 25:37060(T) (EURFNR-889)
RADIATION TARGET CHAMBERS
cooling system for semiconductor detectors for, 25:36634
magnet system for measurement of electron scattering at 180°, 25:36629
RADIATION TARGETS
description of, 25:36622
design of gas, using cryogenic pumping, 25:36626
design of tritium gas, for production of monoenergetic neutrons, 25:36633
polarization measurements of oriented hydrogen, method for, 25:36645
RADIO ASTRONOMY
developments in, (T), 25:35659
RADIO GALAXIES
gamma emission from, detection of, (T), 25:35687
hydrogen absorption and emission in NGC 5128, neutral, (E), 25:35789
RADIO WAVES
absorption in conjugate and closely-spaced auroral region, short-term asymmetry of, (E), 25:35957
absorption in mesosphere and lower thermosphere, minor constituent concentration and transport during anomalous, (E/T), 25:35984
absorption measurements in equatorial ionosphere, pulse-reflection technique for longitude and solar activity-dependent, (E), 25:35970
amplification of vlf, in charged-particle beam interaction with magnetosphere, (E), 25:35972
cosmic background, spectral index of, (E/T), 25:35807
emission from stellar flares in the Orion Nebula, (E), 25:35616
emission from Sun, observations at 3.15 cm, (E), 25:35760
emission of 10-cm and 1.5-m, relation to solar flare of July 11, 1966, (E), 25:35749
propagation in quiet ionosphere, effect of irregularities on long-distance hf, (E/T), 25:36003
reflection from ionospheric irregularities, vertically incident, (E/T), 25:35978
scattering of decameter, observations of Tau A and Vir A occultation by solar corona for studying, (E/T), 25:35773
RADIOACTIVE MATERIALS
facilities for handling, standards for fire protection of, 25:34853
handling of open, in nuclear industry, toxicity classification for, 25:35154
handling of, design of double-walled glove box for safe, 25:34855(P)
handling of, fire protection practice for facilities for, 25:37048
packaging and shipping of, standards for, 25:34851
shipping by road, UK regulations for, 25:34859
shipping container for, design of sealing device for, 25:34850(P)
shipping of, design of shock-resistant steel container for, 25:34858(P)
shipping of, standards for safe air, 25:34852

RADIOACTIVE WASTE
analysis of, development of instrumentation for, 25:34924(R) (WCAP-7562-3)
calcination of, properties of products from, 25:34650(R) (IN-1457)
decontamination of evaporator condensate, by ion exchange, 25:34690(R) (IN-1457)
disposal in ground at Mesita del Buey, N. M., geologic and hydrologic studies for, 25:34846 (LA-4660)
disposal in surface waters, derivation of formula for calculation of maximum, 25:34717 (EUR-4636)
disposal into atmosphere and surface waters near Casaccia, Italy, radiation hazards to man from, 25:34849 (RT/PROT-(70)36)
disposal into Molse Nethe River, estimation of tritium content of, 25:34719 (NP-18737)
disposal of high-level solid, technical feasibility of bedded salt formations for, 25:34848 (ORNL-4680)
disposal of, safety aspects of, 25:36973
effects of fuel reprocessing, on biosphere, methods for minimizing, 25:34844 (CONF-700440-1)
effects on hydrologic environment, research program on, 25:34741
fixation in Polish bitumen, feasibility studies on, 25:34845 (INR-1249)
management at ICPP, 25:34690(R) (IN-1457)
management of solid, in US hospitals, equipment and methods for, 25:34856
processing and disposal of, at nuclear center in Mexico, 25:34733
processing and management practices at Hanford, Wash., predicted effects of Gable Mountain Irrigation Project on, 25:34715 (BNWL-1502)
processing and storage of high-activity, from fuel reprocessing, 25:34697 (SZS-3/71 (pp 20-32))
processing of aqueous, from nuclear power plants by coagulation and flocculation under control of zeta potential, 25:34696 (SZS-3/71 (pp 2-19))
processing of ICPP, by evaporation and ion exchange, 25:34682 (CONF-710509-1)
processing of Purex Plant gaseous, for iodine-131 separation, design of equipment for, 25:34785
processing of, operation of Idaho Waste Calcining facility for, 25:34690(R) (IN-1457)
release by nuclear facilities, environmental pollution from, 25:37045 (NP-18842)
solidification by phosphate glass process in Italy, 25:34711
RADIOACTIVITY
standardization of, review on, 25:34818
RADIOAPPLICATORS
design of, U.S. patents 1950 through 1968, 25:34777 (ORNL-IIC-34)
RADIOBIOLOGY
molecular mechanisms in phenomena of, 25:35101
RADIOCHEMICAL PROCESSING PLANTS
construction and operation of WAK, economic aspects of, 25:34778(T) (ORNL-tr-2417)
criticality in, technical criteria for prevention of, 25:34678 (ARH-468(Rev.))
development and optimum use of multipurpose ICPP, 25:34681 (CONF-710417-1)
plutonium input to, use of lithium-7 tracer and mass spectrometry for determination of, 25:34689 (IAEA-R-876-F)
radiation dosimetry for personnel of, correction factors for, 25:35140
radioactive waste processing at ICPP, 25:34682 (CONF-710509-1)
research and developments at ICPP, 25:34690(R) (IN-1457)
uranium input to, use of lithium-7 tracer and mass spectrometry for determination of, 25:34689 (IAEA-R-876-F)
RADIOGRAPHY, BIOMEDICAL
book: X-Rays, 25:35057
RADIOGRAPHY, INDUSTRIAL
equipment and method for gamma, using radioisotope sources, Australian standards for, 25:34841
equipment and methods for, historical development and current status of, 25:34835
equipment and methods for, review of, 25:34834
equipment for betatron, selection of optimum thickness of metallic image-intensifying screen, 25:34824
equipment for gamma, of construction materials, design and operation of, 25:34822
equipment for gamma, of welded components in nuclear power plants, effects of background radiation on performance of, 25:34823
method for glass-reinforced polyester laminates, 25:34839
method for neutron, using californium-252, development of, 25:34803(R) (BNWL-1308-5)
RADIOIMMUNOASSAY
methods and uses of, bibliographic review of, 25:35083
RADIOISOTOPE SCANNERS
circuit for spectrometer for, preregulation of high voltage supply, 25:34888(P)
collimators for, design optimization of, (T), 25:34880
data acquisition system for, off-line computer interface for, 25:34881
design with visual readout, 25:34885(P)
RADIOISOTOPE SCANNING
comparison of human lymph system, with microscopy in gynecological carcinomas, 25:35186
effectiveness of γ venography and lymphoscintigraphy, in comparison with microscopy during lymphadenectomy, 25:35186
review on developments in, of human brain, 25:35177
use for blood flow studies on human brain, 25:35178
RADIOISOTOPES
effectiveness for diagnosis and therapy, conference on developments in nuclear medicine for, 25:35155
effectiveness for diagnosis in pediatrics, review on, 25:35182
effectiveness for diagnosis of human kidney function, 25:35184
effectiveness for diagnosis of tumors in human bone, brain, and liver, 25:35185
effectiveness for scanning human cardiorespiratory system, 25:35181
effectiveness for therapy of human thyroid carcinomas before or after surgery, 25:35190
handling of pharmaceutical-incorporated, in diagnostic and therapeutic medicine, safety principles for, 25:35153
hazards to hospital personnel, measures for protection against, 25:35151
hazards to hospital personnel, methods for protection against, 25:35150
hazards to medical personnel, effects of half-life on, 25:35099
incorporation in nuclear industry and research center personnel in Germany, statistics on, 25:35100
production and properties of, for use in radiography, 25:34841
production and use of short half-life, 25:34802 (BNL-50249)
production at Japan Atomic Energy Research Institute during 1969, 25:34804(R) (JAERI-Memo-4285)
production of, facilities and equipment for, 25:34816
separation from fresh water and seawater, design of sampler for, 25:34704
shipping and use of, Australian regulations for, 25:34841
standardization of, review on, 25:34818
use as heat source in electric generators, tabulated data on, 25:34811(T) (ORNL-tr-2485)
use for diagnosis and therapy in hematology, methods for, 25:35157
uses in nuclear medicine, selectivity measures for minimal radiation burden during, 25:35179
RADIOMETRIC TESTING
equipment and methods for, of reactor materials at ORNL, development of, 25:34829
method for fiber-reinforced composites using gamma radiation, 25:34838
RADIOPROTECTIVE COMPOUNDS
evaluation for use in exterior radiation exposures, 25:35166
RADIOTHERAPY
book: X-Rays, 25:35057
developments in nuclear medicine for, conference on, 25:35155
dose distribution in cobalt-60, method for calculating scattered, 25:35145
dosimetry in, IAEA comparison program on, 25:35141
isodose curves for cyclo- and fixed-field cobalt, calculation of, 25:35136
method for human breast cancer, using fast electrons, development of pendular, 25:35191
planning for cobalt-60 moving beam or static field, use of desk computer for, 25:35195
RADIUM ISOTOPES Ra-224
range of recoil atoms of, in gases at 96.5 keV, (E), 25:36262
RADIUM ISOTOPES Ra-226
abundance relative to actinium-227 in minerals and natural waters, 25:34738
distribution in hot springs, 25:34736
sorption by human bones following professional exposure, 25:35099
RADON ISOTOPES
separation of short-lived, electromagnetic method for, 25:34806 (JINR-P13-5757)
RADON ISOTOPES Rn-203
nuclear properties of, Nuclear Data Sheets for, (E), 25:36809
RADON ISOTOPES Rn-219
emanation from lunar materials, (E), 25:35831
RADON ISOTOPES Rn-220
emanation from lunar materials, (E), 25:35831
RADON ISOTOPES Rn-222
emanation from lunar materials, (E), 25:35831
RAINWATER
deuterium/hydrogen abundance ratios in, 25:34518
indium content of Illinois, 1970 measurements of, 25:34742(R) (COO-1407-38)
particle scavenging from atmosphere by, research program on, 25:34742(R) (COO-1407-38)
radioactivity of central and western Colorado, during Project Rulison reentry drilling, 25:34728 (USGS-474-101)

RARE EARTH ALLCYS AND SYSTEMS
preparation, properties, and handling of pure, review of, 25:35297
Co--rare earths, development of magnetic intermetallic compounds of, 25:35306
Ga--rare earths--S, phase studies of, 25:35571
RARE EARTH FLUCRIDES
effects on radiation stability of beryllium fluoride glasses, 25:34621
RARE EARTH ISOTOPES
separation of radioactive, electromagnetic method for, 25:34805 (JINR-P6-5761)
RARE EARTH OXIDES
analysis for cerium, lanthanum, neodymium, praseodymium, and samarium, spectrographic, 25:34511
rare earth oxides--ZrO_2, formation and properties of solid solutions of, regularity in, 25:35545
RARE EARTH TUNGSTATES
fabrication and properties of, 25:35529
RARE EARTHS
complexes with azo compounds, spectrophotometric studies on, 25:34528
complexes with TTA, preparation and physicochemical properties of, 25:34502 (INR-1247)
complexes, stability constants of, regularities in, 25:34607
content in coastal and estuarine waters, effects of tides on, 25:34760
determination as TTA complex, 25:34502 (INR-1247)
determination in aqueous acetone solutions of dibenzoylmethane complexes, absorption spectrophotometric, 25:34527
determination using azo compounds, spectrophotometric, 25:34528
preparation, properties, and handling of pure, review of, 25:35297
separation from aqueous chloride solutions by solvent extraction using bis(1-isobutyl-3-methylbutyl) phosphate, 25:34706
separation from uranium by fractional dissolution, 25:34659
RARE GASES
alkali-metal-atom scattering by, data interpretation using Buckingham--Corner potential for, (T), 25:35886
RATS
cobalt-60 content of organs in, following single ingestion, calculation of equilibrium dose rate to human organs using, 25:35116
radiation effects on allometry of body weight and tail length in, x, 25:35225
radiation effects on bioelectric activity in brain of, 25:35235
radiation effects on catechol methyltransferase and monoamine oxidase activity in, protective effects of cystamine against, 25:35165
radiation effects on cholinesterase activity in brain of, effects of adrenal and pituitary gland function on x, 25:35232
radiation effects on enzyme activity in liver and spleen in, x, 25:35215
radiation effects on glucocorticoid and glycogen contents in endocrine glands of, protective effects of insulin against electron, 25:35164
radiation effects on growth and transformation of epithelium transplants in, x, 25:35231
radiation effects on histology of ovaries and uterus in albino, combined effects of estrogens, progesterones, and x, 25:35237
radiation effects on homocytotropic antibody formation in, x, 25:35112
radiation effects on hypoxanthine content in brain of, effects of dose on neutron, 25:35226
radiation effects on iron-59 uptake by bones of, correlation between intramedullary dose and whole-body x, 25:35211
radiation effects on liver regeneration in, mechanism of cerium-144, 25:35221
radiation effects on number of epithelial cells in small intestine in, regeneration following γ, 25:35220
radiation effects on oxidative phosphorylation in brain and liver mitochondria in, effects of dose on x, 25:35216
radiation effects on oxygen uptake in liver slices, mitochondria, and mitochondrial membranes of, x, 25:35223
radiation effects on, combined effects of carbon monoxide and γ, 25:35233
radioinduced dominant lethal mutations in spermatogonia of, x, 25:35129
radioinduced fibrosarcoma in scalp of, α, 25:35236
radioisotope deposition and retention in, following inhalation of radioactive europium oxide, whole-body europium-152, europium-153, and europium-154, 25:35086
radiosensitivity of, protective effects of sulfhydryl groups against, 25:35213
REACTION MECHANISMS
isotope effects in, role of wave properties of nuclei in, 25:34587
REACTOR CONTAINMENT STRUCTURES
fission product deposition in, heat transfer model for analysis of iodine, 25:37036(R) (BMI-1904)
REACTOR CONTAINMENT SYSTEMS
fission product removal from, selective permeation membranes for krypton and xenon, 25:34692(R) (NYO-4057-2)
ice condenser for, description of support structure for, 25:37150(P)
spray systems for, dose reduction factor for elemental iodine removal by, (E/T), 25:37029 (ORNL-TM-2412(Pt.12))
spray systems for, stress corrosion cracking of Type 304 and Type 316 stainless steel by boric acid solution in, (E), 25:37028 (ORNL-TM-2412(Pt.10))
REACTOR CONTROL ELEMENTS
design characteristics of gas cooled thimble type, for pressurized water reactors, 25:36997(P)
design of cruciform, for water cooled reactors, 25:36998(P)
drive assembly with rapid scram operation during power failure, 25:37141(P)
drives for liquid sodium cooled reactor, adaptability of pressurized water reactor roller nut, 25:37075 (TODD-N-24)
drives for liquid sodium cooled reactor, adaptability of pressurized water reactor roller nut, 25:37074 (TODD-N-23)
drives for liquid sodium cooled reactor, adaptability of pressurized water reactor roller nut, 25:37070 (TODD-N-16)
drives for liquid sodium cooled reactor, adaptability of pressurized water reactor roller nut, 25:37073 (TODD-N-21)
drives for liquid sodium cooled reactor, adaptability of pressurized water reactor roller nut, 25:37071 (TODD-N-18)
drives for liquid sodium cooled reactor, adaptability of pressurized water reactor roller nut, 25:37072 (TODD-N-20)
materials for fast, properties requirements for, 25:37140 (SEARI-P-96)
reactivity worth of cylindrical, perturbation theory calculations of, (E/T), 25:37136 (UARAEE-66)
shock absorbers for shutdown, description of disc separated radical tube, 25:37155(P)
REACTOR EXPERIMENTAL FACILITIES
measurement of uniaxial creep in heavy water moderated, design and performance of machines for, 25:37054 (AECL-3738)
REACTOR FUEL ELEMENTS
burnout in forced convection boiling heat transfer, bibliography on, 25:37000 (AAEC/LIE/Bib-286)
cladding for fast, properties of Type 316 stainless steel for, (E), 25:37139 (CONF-700211-7)
cladding for FTR, equipment for prefabrication cleaning of, 25:34783
cladding for liquid sodium cooled, corrosion problems for titanium--vanadium alloy, 25:37016 (CONF-700211-9)
cladding for sodium cooled, effects of gas bubbles in coolant on hot spots in, (T), 25:37037 (CONF-700608-36)
cladding for water cooled, effects of coolant loss accident conditions on Zircaloy-2, (E), 25:37038 (IN-1453)
cycle costs for, effects of power plant loading changes on, 25:36893
decladding of Inchas, equipment and methods for mechanical, 25:34780 (UARAEE-54)
design characteristics of cluster arranged cylinder type, for water cooled pressure tube reactors, 25:37025(P)
design characteristics of helical rib spaced cylinder clad rod type, for fast breeder reactors, 25:37027(P)
design characteristics of pressure tube type, 25:37148(P)
design of uncased subassemblies of, with interior support webs, 25:37143(P)
fabrication in Switzerland, prospects to 1980 for, 25:35313
fabrication of clad uranium silicide, method for, 25:35540(P)
fabrication of coated particle gas cooled, for recycle testing, 25:36977(R) (GA-10501)
fabrication of uranium oxide (UO_2), cost analysis for, 25:37022
fission-product cesium reactions with graphite in, 25:35567
gamma scanning of, development of instrumentation for, 25:34924(R) (WCAP-7562-3)
handling and shipping of irradiated, from Swiss reactors, performance of equipment and methods for, 25:34854
heat transfer from simulated, to natural circulation boiling water, (E), 25:37009 (UARAEE-110)
heat transfer in liquid sodium cooled bundle arranged pin type, effects of rotating wire spacers on, (E/T), 25:37020 (WHAN-SA-76)
performance limits for liquid sodium cooled pin type, (E), 25:37064 (HEDL-SA-81)
performance of liquid sodium cooled stainless steel clad plutonium oxide (PuO_2)--uranium oxide (UO_2) pin type, (E/T), 25:37019 (CRNL-TM-3386)
performance of plutonium oxide (PuO_2)--uranium oxide (UO_2) pin type, effects of burnup on thermal, 25:37017 (CONF-710414-1)
plugs for fast rod type, description of porous end,

25:37026(P)
radiation effects on, for Incore Thermionic Reactor, 25:35936
radiation effects on, one-group method for calculating γ dose fields after, 25:36265
radiation testing of thorium carbide (ThC_2)--uranium carbide (UC_2) and uranium carbide (UC_2) particle type, 25:37018 (JUL-701-RW)
radiation testing program for liquid sodium cooled pin type, (E), 25:37064 (HEDL-SA-81)
refabrication of, description of plants and technology for, 25:35304
reprocessing cycle development for gas cooled, (E), 25:36977(R) (GA-10501)
reprocessing of highly irradiated, pyrochemical head-end, 25:34585 (EUR-4615)
reprocessing of irradiated clad, apparatus and method for continuous, 25:34712(P)
reprocessing of irradiated, device and method for, 25:34713(P)
reprocessing of stainless steel-clad, pyrochemical head-end method for, 25:34687 (EUR-4614)
shipping of irradiated, design of shock-resistant steel container for, 25:34858(P)
spacer grid for clusters of pencil type, description of cylinder shaped, 25:37152(P)
thermal performance analysis in assemblies of boiling, COLIBRI code for subchannel, (E/T), 25:37003 (CONF-710317-1)
vibration in parallel flow, effects of helical ribs on transverse, (E/T), 25:36982
vibration of sodium cooled, natural frequencies and damping of, (E/T), 25:36993 (KFK-1337)

REACTOR FUELS
burnup of power reactor, economics of, 25:37021
burnup of power reactor, effects of stretch-out operation on optimum economic, 25:37031
burnup of uranium oxide (UO_2), plutonium and uranium isotopic composition and fission product concentration data from, (E), 25:37015 (BNWL-1568)
burnup of, effects on core lifetime of non-uniform, (T), 25:37081 (UARAEE-83)
compatibility of carbide and oxide, with sodium and water, 25:35550
compatibility of carbide, molten salt, and oxide, with cladding materials, 25:35550
corrosion of gas cooled pebble bed, at high temperatures, 25:35980 (JUL-725-RG)
cost analysis in U. S. for 1971 to 1985, 25:36861
cycle costs for, computer program calculation of, 25:35852 (BNWL-462)
cycle for water cooled plants, technical and economic status of, 25:37034
cycles for power reactor, economics of optimized, 25:36859
development for power reactors, technical aspects of, 25:35550
dissolution of metallic, electrolytic methods for, 25:34690(R) (IN-1457)
Doppler coefficient measurements in natural uranium and depleted uranium oxide (UO_2), pile oscillator method for, (E/T), 25:37135 (KFK-1350)
fabrication of ceramic, by vibration compaction, 25:35524 (RT/ING-(70)22)
fabrication of graphite shell particle type, for high temperature gas cooled reactors, 25:37023(P)
fission gas release from carbide, metallic, molten salt, and oxide, 25:35550
handling and storage of, use of protective gases in, 25:34860
packaging and shipping of irradiated, in Canada, development of special arrangement methods for, 25:34843 (AECL-3804)
preparation of ceramic microspheres of, method for, 25:35539(P)
preparation of, for AVR and THTR reactors, 25:35544
processing of breeder, at ORNL, performance of integrated control system for, 25:34847 (ORNL-4607)
radiation effects on coated particle, fast neutron, 25:36978(R) (GA-10560)
radiation effects testing of coated particle, 25:36977(R) (GA-10501)
reactions of pellet of, with sodium, thermodynamics of, 25:35547(R) (GEAP-12182)
reprocessing at Midwest Fuel Recovery Plant, methods for controlling environmental contamination from, 25:34844 (CONF-700440-1)
reprocessing of aluminum or zirconium, flowsheets for, 25:34690(R) (IN-1457)
reprocessing of aluminum-clad, molten-salt fluoride-volatility process for, 25:34693 (ORNL-4574)
reprocessing of coated particle, fluid bed oxidation procedures in, (E), 25:36977(R) (GA-10501)
reprocessing of graphite, pilot plant studies of head-end, 25:34690(R) (IN-1457)
reprocessing of molten salt, 25:34694 (ORNL-TM-3138)
reprocessing of, processing and storage of fuel from high-activity, 25:34697 (SZS-3/71 (pp 20-32))
reprocessing of, research at Idaho Chemical Processing Plant on, 25:34690(R) (IN-1457)
shipping and storage of, in Germany, legal restrictions on, 25:34857
swelling in carbide, metallic, and oxide, 25:35550
temperature distribution in pebble bed, at high temperatures, 25:36980 (JUL-725-RG)

REACTOR LOADING MACHINES
design characteristics of, with compartment for shielded single fuel element storage, 25:37151(P)
design parameters of pantograph, for rotating vessel covers, 25:37154(P)

REACTOR MODERATORS
atom velocity spectra in, (T), 25:37108 (UARAEE-82)
materials for, review on production and properties of graphitic, 25:35562
neutron flux spectra in scratomic, numerical solution of thermal, (T), 25:37120 (UARAEE-69)

REACTOR SAFETY
analysis of, comparison of MCA concept and reliability method for, 25:37039 (IRS-T-18(1970), pp 21-36)
analysis of, risk evaluation methods for, 25:37061
bibliography on, 25:37047 (TID-3525(Rev.6)(Suppl.6))
data acquisition system for reliability analyses in, 25:37040 (IRS-T-18(1970), pp 123-43)
fire protection practice for, 25:37050
fire protection practice for, 25:37048
reliability analyses for, use of failure statistics in, 25:37041 (IRS-T-18(1970), pp 223-39)
review of, 25:36973
systems design for, statistical methods for, 25:36975 (IRS-T-18(1970), pp 205-15)

REACTOR SAFETY EXPERIMENTS
decontamination spray system for LOFT, effects of heat losses on, 25:34690(R) (IN-1457)
fission product concentrations during LOFT, continuous sampler-monitor for measurement of, 25:34690(R) (IN-1457)

REACTOR SIMULATORS
use of analog computer, for maritime reactor kinetics and thermodynamics, 25:37093 (CEA-CONF-1750)

REACTORS
components for, method for calculation of thermal shock-induced stresses in, 25:34776(T) (EURFNR-794)
components for, vacuum brazing methods for fabrication of, 25:35327
core grid and support structure for, 25:37149(P)
critical dimensions of, code for two-group two-region calculations of, 25:37122 (UARAEE-79)
critical parameters for hydrogen moderated enriched uranium fueled, three-groups diffusion theory calculations of, (E/T), 25:37124 (UARAEE-84)
critical parameters of one-dimensional multiregion, computer code for calculation of, 25:37126 (UARAEE-85)
design of, critical evaluation and exchange of nuclear data information for, 25:37107 (INDC(NDS)-29/U)
development of, research at AECL on, 25:37001 (AECL-3787)
fission product monitoring in, Geiger--Mueller detector system for, 25:37147(P)
instrumentation for, reliability analysis of protection system, 25:36996
kinetics calculations for, computer program for fast neutron spectra and average multigroup cross sections for, 25:37113 (IN-1435)
multiplication factors for, correction terms for two--group approximation of infinite, (T), 25:37111 (BNWL-1560)
neutron diffusion in moderators, review of calculations of spectra at vacuum interface of thermal, (T), 25:36650 (UARAEE-60)
neutron flux distribution in radially reflected, effects of partially inserted control rods on epithermal and thermal, (T), 25:37131
neutron flux distribution in, effects of cylindrical water cavities on, (T), 25:37117 (UARAEE-58)
neutron flux distributions in, computer code for calculating, (T), 25:36651 (UARAEE-107)
neutron flux spectra in, integral transport theory calculation of epithermal, 25:37115 (RISO-234)
neutron flux spectra in, one-group Milne method solution of thermal, (E/T), 25:37116 (UARAEE-56)
neutron flux synthesis in, functionals for discontinuous trial function, (T), 25:37130
neutron flux synthesis in, SYN code for two-dimensional, 25:37112 (GEAP-13672)
neutron resonance cross sections for, calculation of, 25:37115 (RISO-234)
neutron resonance integrals in, numerical and semi-analytic calculations of, 25:37115 (RISO-234)
neutron scattering in, upward and downward kernels for thermal, (T), 25:37123 (UARAEE-80)
neutron spectra in, effects of probe on space--energy distribution of thermal, (E/T), 25:37137 (UARAEE-75)
neutron spectra in, review of thermal, (E/T), 25:37118 (UARAEE-62)
neutron spectra in, threshold detector measurements of fast, (T), 25:37109 (UJV-2423-RF)
neutron transport in moderators in, bounds of integral operators in Hilbert space for, (T), 25:37129
neutron transport in, approximate procedures for numerical solution of, (T), 25:36647 (ANL-7779)
noise analysis in, effects of space and reflection on count-rate fluctuation spectra from, (E), 25:37134 (DP-MS-70-101)

XUM

power of, noise analysis for measurement of absolute, 25:37114 (JAERI-Memo-4276)
pumps for, description of coolant, 25:37142
pumps for, description of water cooling system for shaft seals and radial bearings of primary, 25:37145(P)
reflector savings of completely reflected cylindrical, SAVE code for, 25:37128 (UARAEE-96)
shielding for, technology of design of thermal, 25:36999
startup of, transistorized pulse channel for neutron flux measurements during, 25:37146
thermal utilization factor for three-zone cylindrical lattice cell in, asymptotic diffusion theory calculations of, 25:37119 (UARAEE-64)
REACTORS, AGR-TYPE
development in U. K, 25:36863 (CONF-700653-1)
REACTORS, BOILING
coolant loss accidents in, analytical description of, 25:37036(R) (BMI-1904)
cooling channels for, use of Freon to model dryout in, 25:37001 (AECL-3787)
cooling system for, description of turbine pump for, 25:37014(P)
cooling system for, design requirements and performance of valves for primary, 25:37002 (AECL-3858)
emergency core cooling systems for, model for heat transfer analysis of top-injected spray, 25:37036(R) (BMI-1904)
fuel element assemblies for, COLIBRI code for subchannel thermal performance analysis in, (E/T), 25:37003 (CONF-710317-1)
fuel elements for, effects of coolant loss accident conditions on Zircaloy-2 clad, (E), 25:37038 (IN-1453)
fuel elements for, natural circulation cooling of, (E), 25:37009 (UARAEE-110)
heat transfer in fuel channels of, design and operation of test loop for studying two-phase, 25:34793 (UARAEE-81)
REACTORS, BREEDER
cladding tubes for fast, production of Type 316 stainless steel, 25:35305
coolant for liquid metal cooled fast, safety problems with liquid sodium, 25:37011
economics of, analysis for optimization of, 25:37033
fuel element cladding for liquid sodium cooled fast, corrosion problems for titanium--vanadium alloy, 25:37016 (CONF-700211-9)
fuel element for fast, description of helical rib spaced cylinder clad rod type, 25:37027(P)
fuel reprocessing for fast, pyrochemical head-end, 25:34688 (EUR-4615)
fuel reprocessing for fast, pyrochemical head-end, 25:34687 (EUR-4614)
REACTORS, CANDU-TYPE
cooling system for, design requirements and performance of valves for primary, 25:37002 (AECL-3858)
REACTORS, FAST
control elements for, properties requirements of materials for, 25:37140 (SRARI-P-96)
coolant boiling in sodium cooled, acoustic detection of, (E), 25:37052
coolant for liquid metal cooled breeder, safety problems with liquid sodium, 25:37011
cooling systems for sodium cooled, design variations in primary, 25:37005 (KFK-1379)
development of U. S., conference on role of university nuclear engineering programs in, 25:36976 (CONF-680818)
Doppler coefficient measurements in coupled fast-thermal, pile oscillator method for, (E/T), 25:37135 (KFK-1350)
Doppler coefficient measurements in, pile oscillator method for, (E/T), 25:37135 (KFK-1350)
economics of, analysis for optimization of, 25:37033
fuel element cladding for liquid sodium cooled breeder, corrosion problems for titanium--vanadium alloy, 25:37016 (CONF-700211-9)
fuel elements for breeder, description of helical rib spaced cylinder clad rod type, 25:37027(P)
fuel elements for liquid sodium cooled, effect of rotating wire spacers on heat transfer in bundle arranged pin type, (E/T), 25:37020 (WHAN-SA-76)
fuel elements for sodium cooled, properties of Type 316 stainless steel cladding for, (E), 25:37139 (CONF-700211-7)
fuel elements for, description of porous end plug for rod type, 25:37026(P)
fuel pins for Na-1 and Na-2, vibration frequencies of mockup, (E/T), 25:36993 (KFK-1337)
kinetics of, one dimensional multigroup diffusion computer program for, 25:36992 (JAERI-Memo-4331)
neutron spectrum measurements for, time-of-flight methods for fast, (E/T), 25:36991(R) (GULF-RT-10523)
transfer functions of sodium cooled, analysis of space-dependent, (T), 25:36987 (ANL-7788)
REACTORS, FRANCE
safety aspects of, 25:36892
REACTORS, GAS-COOLED
core for high temperature pebble bed, temperature distribution and corrosion in, 25:36980 (JUL-725-RG)
costs for 1000 MW(e), analysis of 1970 to 2020 capital, 25:37030 (CRNL-TM-3243)
design characteristics of gas fueled, 25:36985(P)
design characteristics of high temperature, 25:36982
development in Japan of dual purpose power and process heat, 25:37092
development of 1000 MW(e) HTGR concept during December 1970 through February 1971, 25:36977(R) (GA-10501)
fission product release and transport in high temperature, (E/T), 25:36977(R) (GA-10501)
fuel elements for high temperature, fabrication and irradiation testing of recycle, (E/T), 25:36977(R) (GA-10501)
fuel elements for high temperature, plant designs and costs for reprocessing, 25:36977(R) (GA-10501)
fuel reprocessing for high-temperature, 25:34690(R) (IN-1457)
fuels for high temperature, fabrication of graphite shell particle type, 25:37023(P)
multiplication factor for thorium oxide (ThO_2)--uranium oxide (UO_2) fueled, temperature dependence of infinite, (E), 25:36988 (BNWL-1561)
physics calculations for, methods for solution of heterogeneities in, (E/T), 25:36989 (CEA-N-1398)
physics characteristics of high temperature, summary of, 25:36986 (AEEW-M-985)
power conversion system for helium cooled, description of carbon dioxide turbine, 25:37053(P)
pressure vessels for 500 MW heavy water moderated, fast neutron radiation effects on prestressed concrete, 25:37007(T) (CRNL-tr-2470)
pressure vessels for, survey of materials and design of insulation for prestressed concrete, 25:37006 (ORNL-TM-2929)
REACTORS, GAS-FUELED
design characteristics of gas cooled, 25:36985(P)
temperature fields in plasma core, (T), 25:36990 (DLR-FB-70-18)
REACTORS, GRAPHITE-MODERATED
physics calculations for, methods for solution of heterogeneities in, (E/T), 25:36989 (CEA-N-1398)
REACTORS, GREAT BRITAIN
development of power, 25:36863 (CONF-700653-1)
physics characteristics of high temperature, summary of, 25:36986 (AEEW-M-985)
REACTORS, HEAVY WATER-MODERATED
fuel element assemblies for boiling, COLIBRI code for subchannel thermal performance analysis in, (E/T), 25:37003 (CONF-710317-1)
pressure vessels for 500 MW gas cooled, fast neutron radiation effects on prestressed concrete, 25:37007(T) (ORNL-tr-2470)
REACTORS, JAPAN
development of gas cooled dual purpose power and process heat, 25:37092
REACTORS, LIQUID METAL-COOLED
coolant boiling in sodium cooled, acoustic detection of, (E), 25:37052
coolant boiling in sodium cooled, NEMI code for thermohydraulic analysis of, (E/T), 25:37046 (RT/ING-(70)18)
coolant for fast breeder, safety problems with liquid sodium, 25:37011
cooling systems for sodium cooled, design variations in primary, 25:37005 (KFK-1379)
fuel element cladding for fast breeder, corrosion problems for titanium--vanadium alloy, 25:37016 (CONF-700211-9)
fuel elements for fast, effects of rotating wire spacers on heat transfer in bundle arranged pin type, (E/T), 25:37020 (WHAN-SA-76)
fuel elements for sodium cooled, properties of Type 316 stainless steel cladding for, (E), 25:37139 (CONF-700211-7)
safety of, effects of pressure pulse propagation in coolant two-phase mixtures on, (E/T), 25:37035 (ANL-7792)
REACTORS, MAGNOX
operation in U. K., review of, 25:36863 (CONF-700653-1)
REACTORS, MARITIME
development of, review of economics and legal aspects for, 25:37097
economics of, effects of reliability analysis on, 25:37095 (IAS-T-18(1970), pp 217-21)
kinetics of, analog computer simulation of, 25:37093 (CEA-CONF-1750)
thermodynamics of, analog computer simulation of, 25:37093 (CEA-CONF-1750)
REACTORS, MOLTEN-SALT
plutonium oxide precipitation in, studies of conditions for, 25:34566
REACTORS, PEBBLE-BED
core for high temperature gas cooled, temperature distribution and corrosion in, 25:36980 (JUL-725-RG)
REACTORS, POWER
development in Japan of dual purpose gas cooled process heat and, 25:37092
development in U. K, 25:36863 (CONF-700653-1)
development of 1000 MW(e) HTGR concept during December 1970 through February 1971, 25:36977(R) (GA-10501)
development of fast, conference on role of university nuclear engineering programs in, 25:36976 (CONF-680818)
electric generators for, design characteristics of quadrupole, 25:36975

fuel burnup in, economics of, 25:37021
fuel burnup in, effects of stretch-out operation on optimum economic, 25:37031
fuel cycle costs for, computer program calculation of, 25:36862 (BNWL-462)
fuel cycle costs for, effects of plant loading changes on, 25:36893
fuel element assemblies for boiling, COLIBRI code for subchannel thermal performance analysis in, (E/T), 25:37003 (CONF-710317-1)
fuel elements for, economics for fabrication of uranium oxide (UO_2), 25:37022
neutron flux detectors for, performance of self-powered in-core, 25:37001 (AECL-3787)
plutonium production in Swiss, forecasts to 1990 of, 25:35310
power conversion system for helium cooled, description of carbon dioxide turbine, 25:37053(P)
pressure vessels for 500 MW heavy waters moderated gas cooled, fast neutron radiation effects on prestressed concrete, 25:37007(T) (ORNL-tr-2470)
safety analysis of, comparison of MCA concept and reliability method for, 25:37039 (IRS-T-18(1970), pp 21-36)
safety of, use of failure statistics in analysis of, 25:37041 (IRS-T-18(1970), pp 223-39)
siting of, geologic and hydrologic factors in, 25:34741
uranium enrichment requirements for Swiss, forecasts to 1990 of, 25:34819
uranium requirements for Swiss, forecasts to 1990 of, 25:34755

REACTORS, PRESSURIZED-WATER
containment spray systems for, dose reduction factor for elemental iodine removal by, (E/T), 25:37029 (ORNL-TM-2412(Pt.12))
control elements for, description of gas cooled thimble type, 25:36997(P)
coolant loss accidents in, analytical description of, 25:37036(R) (BMI-1904)
cooling systems of, design requirements and safety aspects of primary, 25:37012
cooling systems of, fabrication, construction, and operation of components for, 25:37012
costs for 1000 MW(e), analysis of 1970 to 2020 capital, 25:37030 (ORNL-TM-3243)
development in U.S. and Germany, status of, 25:36984
protection system instrumentation for, description of standard, 25:36995 (WCAP-7669)
safety systems for, process instrumentation for, 25:37010 (WCAP-7671)

REACTORS, PROCESS HEAT
development in Japan of dual purpose gas cooled power and, 25:37092
development of desalination, abstracts of papers on, 25:37091 (ORNL-TM-3402)
economics of, analysis for optimization of, 25:37032

REACTORS, RESEARCH
control elements for UA-RR-1, reactivity worth of boron carbide, (E/T), 25:37136 (UARAEE-66)
coolant thermal inertia during power transients in UA-RR-1, (E), 25:37084 (UARAEE-111)
core lifetime in UA-RR-1, effects of non-uniform fuel burnup on, (T), 25:37081 (UARAEE-83)
critical mass of UA-RR-1, method for calculation of, 25:37078 (UARAEE-67)
experimental facilities of RDT Reactor, design modifications for, 25:37067(T) (LB/G-3001)
fuel burnup calculations for UA-RR-1, 25:37077 (UARAEE-63)
instrumentation for FMRB, construction and operation of, 25:37062 (FMRB-32/70)
maintenance for FMRB, during 1970, 25:37063 (FMRB-35/71)
neutron source for Franco-German High Flux Reactor, design parameters for cold, 25:37087
neutron spectra in UA-RR-1 core and reflector, numerical calculation of fast, 25:37079 (UARAEE-71)
neutron spectra in UA-RR-1, measurement of epithermal, 25:37076 (UARAEE-59)
operations for FMRB, during 1970, 25:37063 (FMRB-35/71)
physics characteristics of UA-RR-1, effects of reflector material on, (T), 25:37060 (UARAEE-73)
radioisotope production in FR-2, cross sections for (n,p) and (n,α) reactions with fast neutrons, (E), 25:36686 (CONF-680986-1)
reactivity temperature coefficient of WWR-type, three-group diffusion theory analysis of, (E/T), 25:37138 (UARAEE-105)
startup of UA-RR-1, system for automatic, 25:37083 (UARAEE-108)
startup of UA-RR-1, system for automatic, 25:37082 (UARAEE-94)
thermodynamics for water cooled, (T), 25:37058 (CEA-R-4114)

REACTORS, ROCKET
design characteristics of gas core, 25:36585(P)

REACTORS, SUPERHEATING
cooling system for steam cooled, startup procedures for, 25:37013(P)

REACTORS, SWIMMING-POOL
neutron spectra in reflector of, effects of metal slabs on perturbations in fast, (E/T), 25:37057 (CEA-R-3795)

REACTORS, THERMAL
Doppler coefficient measurements in coupled fast-thermal, pile oscillator method for, (E/T), 25:37135 (KFK-1250)

REACTORS, WATER-COOLED
containment spray systems for, effects of boric acid solution on stress corrosion cracking of Type 304 and Type 316 stainless steel in, (E), 25:37028 (ORNL-TM-2412(Pt.10))
control rods for, description of cruciform, 25:36998(P)
coolant loss accidents in, ECCSA and MUCHA codes for thermal--hydraulic analysis of, 25:37036(R) (BMI-1904)
coolant loss accidents in, radiolytic production of hydrogen following, (E/T), 25:37036(R) (BMI-1904)
cooling channels for, steady-state forced convection heat transfer in concentric annular, (E/T), 25:37008 (UARAEE-50)
fuel cycle for, technical and economic status of, 25:37034
fuel elements for pressure tube, description of cluster arranged cylinder type, 25:37025(P)
pressure vessels for, description of cast iron, 25:37153(P)
safety of, effects of pressure pulse propagation in coolant two-phase mixtures on, (E/T), 25:37035 (ANL-7752)
thermodynamics for research, (T), 25:37058 (CEA-R-4114)

REACTORS, WATER-MODERATED
physics characteristics of, effects of lattice pitch variations on, (E/T), 25:37121 (UARAEE-70)

REFRACTORY MATERIALS
preparation of composites of, incorporating in-situ grown carbide fibers, 25:35557

REGGE POLE THEORY
amplitude of p + p → p + p interactions at 5 to 13.4 GeV/c in, use of exact forms for, 25:36531
cut model for γ + p → π^0(eta) + p interactions in, duality and meson trajectories in, 25:36441
cuts from density matrix elements of ω in π^+ + p → ω + Δ^{++} interactions, test of empirical rule for, 25:36502 (CALT-68-300)
cuts in strong interactions in, test of empirical rule for, 25:36502 (CALT-68-300)
cuts in Σ polarization in π^+ + p → K^+ + Σ^+ and Λ polarization in π^- + p → K^0 + Λ interactions in, test of empirical rule for, 25:36502 (CALT-68-300)
decay K → π + l + ν in quark model in, form factors and Cabibbo angle for, 25:36456 (ORO-3992-39)
dual amplitude in, proper time formulation for general, 25:36593
dual amplitude with Mandelstam analyticity for π + π → π + π interactions in, 25:36492
dual resonance model in, twisting invariant factorization in, 25:36594
dual resonance models for vector currents in, 25:36450
dual resonance models in, algebraic structure of generalized Ward identities in, 25:36591
duality and meson trajectories in cut model for γ + p → π^0(eta) + p interactions in, 25:36441
duality compatibility with conservation of t-channel helicity in diffractive dissociation processes in, 25:36595
duality for triple Reggeon coupling relation with low missing-mass spectrum in diffractive dissociation in two-body interactions, 25:36420 (UCSD-10-P-10-78)
duality in K^- + p → π^- + Y^{*+} and π^+ + p → K^+ + Y^{*+} interactions in, eikonal model with unitarity corrections for, 25:36514
interactions a + a in, potential for, 25:36527
pole contribution to (K^+ - K^0) mass difference in, A_2, 25:36496
Pomeranchuk singularity in, colliding pole and branch point as model for self-consistent, 25:36588
Regge--eikonal representation for amplitudes of high-energy scattering in, 25:36587 (JINR-P2-5768)
Reggeon coupling relation with low missing-mass spectrum in diffraction dissociation in two-body interactions in, duality for triple, 25:36420 (UCSD-10-P-10-78)
trajectories for mesons, N-point dual functions for, 25:36485
trajectories for particle interactions in, equivalent potential approach for I = 0 and 1, 25:36422
trajectories in meson production in γ reactions with carbon-12 and oxygen-16, isolation of, (T), 25:36483

RELATIVITY THEORY
book: Classical Fields, Particles, and the Theory of Relativity, 25:36556
Einstein equations in cylindrical coordinates in general, solutions of, 25:36578
Einstein field equations in, complete Schwarzschild solution for, 25:36580
Einstein space--times in general, equations of motion and field equations for, 25:36577
electric charges in general, geodesics of Einstein connection for paths of, 25:36443
experiments in space vehicles on, review of Earth orbit and deep-space, (E/T), 25:35821
extension to Newton's theory of gravitation, (T), 25:35813
field structure in Schroediner unified field theory in, exact solution corresponding to, 25:36554
mass of closed static system in general, total, 25:36581
Riemann--Einstein space in general, massive scalar meson

XUM

field geometrization over, 25:36582
solution of Jordan--Dicke field equations, (T), 25:35814
sphere in general, field equation solution for composite, 25:36583
tests of general, effects of solar oblateness on, (T), 25:35809
REMOTE-HANDLING EQUIPMENT
testing of gas cooled reactor in-vessel, pressure and temperature, 25:36978(R) (GA-10560)
REMOTE-VIEWING EQUIPMENT
testing of gas cooled reactor in-vessel, pressure and temperature, 25:36978(R) (GA-10560)
REPRODUCTIVE SYSTEM
radiation dose to human female, during phosphorus-32 administration, 25:35144
RESISTORS
fabrication of nonstoichiometric vanadium oxide thermally sensitive, method for, 25:35542(P)
RESPIRATORY SYSTEM
scanning of human, radioisotope methods for, 25:35181
RHEINSBERG POWER REACTOR
operations during 1966 to 1970, review of, 25:36891
RHENIUM
determination of, solvent extraction process for use in, 25:34525
electric field gradient in hcp, calculations, 25:36351
separation from molybdenum and tungsten by solvent extraction using acetone and scrubbing using sodium hydroxide, 25:34525
RHENIUM ALLOYS AND SYSTEMS
Er--Re, superconducting transition temperature of intermetallic compounds of, 25:36038
Fe--Re, superconducting transition temperature of intermetallic compounds of, 25:36038
Gd--Re, superconducting transition temperature of intermetallic compounds of, 25:36038
Ho--Re, superconducting transition temperature of intermetallic compounds of, 25:36038
Mo-base--Re, microstructure of twin--slip and twin--twin interactions in, 25:35481
Nb--Re, hardening and softening of monocrystalline, mechanisms of solution, 25:35436
Re--Sc, superconducting transition temperature of intermetallic compounds of, 25:36038
Re--Ta, slip in crystals of, asymmetry of, 25:35381
Re--Ta-base, hardening in solid solutions of, parameters controlling, 25:35384
Re--Tb, superconducting transition temperature of intermetallic compounds of, 25:36038
RHENIUM CHLORIDES
separation of ions of, from metal ions by high-voltage electrophoresis using carboxylic and hydroxycarboxylic acids, 25:34702
RHENIUM FLUORIDES
vapor pressure--temperature data for, 25:34602 (GAT-649)
RHENIUM ISOTOPES Re-188
distribution in tissues of swine following field exposure to nuclear debris at Schooner Event site, fallout, 25:35090
excretion in feces and urine of peccaries following single ingestion of nuclear debris from Schooner Event, quantitative comparison of fallout, 25:35089
RHENIUM OXYFLUORIDES
vapor pressure--temperature data for, 25:34602 (GAT-649)
RHODIUM
effects on colorimetric determination of gold, 25:34521
effects on photometric determination of antimony following solvent extraction using TBP, 25:34512
uses of fission product, evaluation of potential, 25:34803(R) (BNWL-1308-5)
RHODIUM ALLOYS AND SYSTEMS
Rh--Ti, stability of gaseous intermetallic, 25:35350
Rh--Zr, stability of gaseous intermetallic, 25:35350
RHODIUM BROMIDES
separation of ions of, from metal ions by high-voltage electrophoresis using carboxylic and hydroxycarboxylic acids, 25:34702
RHODIUM CHLORIDES
separation of ions of, from metal ions by high-voltage electrophoresis using carboxylic and hydroxycarboxylic acids, 25:34702
RHODIUM ISOTOPES Rh-110
nuclear properties of, Nuclear Data Sheets for, (E), 25:36808
RIBONUCLEASE
radiation effects on synthesis of, in germinating wheat, effects of gibberellic acid on γ, 25:35102
RICHLAND AREA (WASH.)
ground water flow system in, predicted effects of Gable Mountain Irrigation Project on, 25:34715 (BNWL-1502)
RING CURRENT
origin of proton aurorae in, (T), 25:35995
RIVERS
tritium release into Moise Nethe, estimation of monthly, 25:34719 (NP-18737)
ROBERT E. GINNA POWER REACTOR, UNIT 1
operations incident of June 1 to June 5, 1971, possible excessive radioactive gas effluent release, 25:36874 (DOCKET-50244-71)
ROCKET REACTORS (NERVA)
design concepts for reusable nuclear shuttle, 25:37089
economics of reusable nuclear shuttle, 25:37089
ROCKETS
electrical equipment for, method for determining possible hazards from induced currents in, 25:37228 (SC-R-713250)
ROCKS
analysis for metals by neutron activation and γ spectroscopy, 25:34543 (AIM-1013)
book: Gamma-Ray Spectrometry of Rocks, 25:34635
thorium distribution in Central Tajikistan granitoid, 25:34734
uranium distribution in Central Tajikistan granitoid, 25:34734
RODS
heat transfer and fluid flow in bundles of, computer program for calculation of, 25:34794
RUBBER
radiation effects on solutions of halomethanes in natural latex, EPR studies of γ, 25:34614
radioinduced vulcanization of, electron or γ, 25:34632
radiolysis at 77°K, kinetics of stabilization of radicals produced by γ, 25:34640
RUBIDIUM
determination in rocks by neutron activation and γ spectroscopy, 25:34543 (AIM-1013)
effects on photometric determination of antimony following solvent extraction using TBP, 25:34512
separation from cesium by solvent extraction using phenol, effect of diluent on partition coefficient in, 25:34701
RUBIDIUM BROMIDES
LiBr--LiSe--RbBr, phase studies, 25:35275(R) (ANL-7777)
LiBr--RbBr, properties of eutectics of, for use as paste electrolytes, 25:35275(R) (ANL-7777)
RUBIDIUM CHLORIDES
ion-implantation damage in crystals of, depth distribution of 15-keV, 25:36272
RUBIDIUM ISOTOPES Rb-81
content relative to metastable krypton-81 in tissues following intravenous injection, tissue perfusion blood flow studies using, 25:35167
RUBIDIUM ISOTOPES Rb-86
production in (n,α) and (n,p) reactions with fast neutrons, cross sections for, (E), 25:36686 (CONF-680986-1)
use in radiography for measuring coronary blood flow, 25:35085
RUBIDIUM ISOTOPES Rb-87
energy levels and nuclear properties of, Nuclear Data Sheets for, (E), 25:36706
RUBIDIUM ISOTOPES Rb-88
energy levels and transitions from decay and nuclear-reaction measurements, Nuclear Data Sheets compilation of properties of, (E), 25:36705
RUBIDIUM ISOTOPES Rb-89
energy levels and transitions from decay and nuclear-reaction measurements, Nuclear Data Sheets compilation of properties of, (E), 25:36714
RUBIDIUM ISOTOPES Rb-90
energy levels and transitions from decay and nuclear-reaction measurements, Nuclear Data Sheets compilation of properties of, (E), 25:36801
RUBIES
radiation effects on absorption and photoelectron emission spectra of crystals of, x-, 25:36308
RUTHENIUM
effects on colorimetric determination of gold, 25:34521
effects on photometric determination of antimony following solvent extraction using TBP, 25:34512
release to atmosphere in reprocessing aluminum-clad fuel elements, 25:34693 (ORNL-4574)
uses of fission product, evaluation of potential, 25:34803(R) (BNWL-1308-5)
RUTHENIUM ALLOYS AND SYSTEMS
Ru--Ta-base, hardening in solid solutions of, parameters controlling, 25:35384
Ru--Ti, stability of gaseous intermetallic, 25:35350
Ru--V, electronic transition in near-equiatomic, (E), 25:36339
Ru--Zr, stability of gaseous intermetallic, 25:35350
RUTHENIUM BROMIDES
separation of ions of, from metal ions by high-voltage electrophoresis using carboxylic and hydroxycarboxylic acids, 25:34702
RUTHENIUM CHLORIDES
separation of ions of, from metal ions by high-voltage electrophoresis using carboxylic and hydroxycarboxylic acids, 25:34702
RUTHENIUM FLUORIDES
vapor pressure--temperature data for, 25:34602 (GAT-649)
RUTHENIUM ISOTOPES Ru-103
availability in peccaries following single injection of nuclear debris from Project Buggy fallout, 25:35088
distribution in tissues of swine following field exposure to nuclear debris at Schooner Event site, fallout, 25:35090
excretion in feces and urine of peccaries following single ingestion of nuclear debris from Schooner Event, quantitative comparison of fallout, 25:35089
RUTHENIUM ISOTOPES Ru-106
content in atmosphere over Moscow, 1962 to 67, 25:34748

RUTHENIUM ISOTOPES Ru-110
energy levels and nuclear properties of, Nuclear Data Sheets for, (E), 25:36808
RUTHENIUM NITRIDES
complexes with ammonia, radiolysis of, oxidation and reduction in electron pulse and γ, 25:34657
RUTHENIUM OXYFLUORIDES
vapor pressure--temperature data for, 25:34602 (GAT-645)
RUTILES
lattice dynamics of, 25:37239 (TID-25720)

S

S-MATRIX
theory for strong interactions, review of, 25:36479
SACLAY REACTORS (OSIRIS)
radiation target cans for, design parameters of liquid sodium Odile, 25:37060(T) (EURFNR-889)
radiation target cans for, design parameters of natural convection cooled Esther, 25:37061(T) (EURFNR-890)
SAFETY
standards for air transport of dangerous articles, magnetized materials, and radioactive materials, 25:34852
SAFETY HAZARDS
evaluation of solid propellant combustion, in rocket aborts, 25:34792 (SC-DR-710084)
SAINT LAURENT-DES-EAUX REACTOR (EDF-4)
safety aspects of, 25:36892
SALIVARY GLANDS
radioisotope accumulation in, of swine following field exposure to nuclear debris from Schooner Event, fallout γ-emitting, 25:35090
SALT DEPOSITS
radioactive waste disposal in, demonstration project to establish feasibility of, 25:34848 (ORNL-4680)
SAMARIUM
determination in rare earth oxides, spectrographic, 25:34511
effects on gravimetric determination of mercury using 2-aminobenzothiazole, 25:34520
separation from other rare earths by ion exchange chromatography, 25:34714
SAMARIUM ALLOYS AND SYSTEMS
Al--Sm-base, crystal lattice parameters of intermetallic Sm_2Al, 25:35495
Co--misch metal--Sm, fabrication and magnetic properties of permanent magnets of, 25:36336
SAMARIUM FLUORIDES
effects on radiation stability of beryllium fluoride glasses, 25:34621
SAMARIUM ISOTOPES Sm-142
beta and electron-capture decay of, conversion-electron and gamma spectra from, (E), 25:36766
SAMARIUM ISOTOPES Sm-143
beta and electron-capture decay of, conversion-electron and gamma spectra from, (E), 25:36766
SAMARIUM ISOTOPES Sm-144
energy level at 2323 keV from neodymium-142 (α,2n) reactions, lifetime for, (E), 25:36792
energy-level transitions from neodymium-142 (α,2n) reactions, hindrance and probabilities for E2, (E), 25:36792
SAMARIUM ISOTOPES Sm-147
neutron capture by, cross sections and resonance integrals for pile and thermal, (E), 25:36735 (SGAE-PH-104/1971)
SAMARIUM ISOTOPES Sm-148
neutron capture by, cross sections and resonance integrals for pile and thermal, (E), 25:36735 (SGAE-PH-104/1971)
photon reactions (γ,xn) in giant resonance region, cross sections for, (E), 25:36755
SAMARIUM ISOTOPES Sm-151
energy levels from promethium-151 beta decay, lifetimes for, (E), 25:36807
energy-level transitions from promethium-151 beta decay, intensities of, (E), 25:36807
SAMARIUM ISOTOPES Sm-153
beta decay of, branching ratios, log-ft values, and Auger- and conversion-electron and gamma spectra from, (E), 25:36731 (NP-18835)
SAMARIUM OXIDES
analysis for europium, indirect colorimetric, 25:34507
growth of single-crystal solid solutions with another rare earth oxide by Verneuil method, formation regions in, 25:35525
SAMPLING
equipment for radioisotope, in natural waters, design of, 25:34704
SAN ONOFRE POWER REACTOR, UNIT 1
operations history for May 1970, 25:36868 (DOCKET-50206-113)
SAN ONOFRE POWER REACTOR, UNIT 2
design parameters of, requested additional information on, 25:36955 (DOCKET-50361-17)
operations aspects of, requested additional information on, 25:36955 (DOCKET-50361-17)
SAN ONOFRE POWER REACTOR, UNIT 3
design parameters of, requested additional information on, 25:36955 (DOCKET-50361-17)
operations aspects of, requested additional information on, 25:36955 (DOCKET-50361-17)
SANDSTONE
nuclear explosion effects on, surrounding Project Wagon Wheel, prediction of underground, 25:34770 (UCRL-50993)
SARGASSO SEA
cesium-137 distribution in waters of, measurement of vertical, 25:34759(R) (NYO-2174-129)
strontium-90 distribution in waters of, measurement of vertical, 25:34759(R) (NYO-2174-129)
SATELLITES
x-ray experiments on SAS-A, (E), 25:35703
SAVANNAH RIVER PRODUCTION REACTORS
confinement system for, iodine retention efficiency of carbon in, (E), 25:37106(R) (DP-1259)
SAXTON POWER REACTOR
containment structure for, revised leak rate testing schedule for, 25:36902 (DOCKET-50146-76)
coolant for, revised technical specification for hydrogen limit in, 25:36904 (DOCKET-50146-79)
core for, revised configurations of test fuel elements in, 25:36903 (DOCKET-50146-78)
fuel element assemblies for, revised instrumentation requirements for test, 25:36905 (DOCKET-50146-80)
radioactive effluents from, revised release limits for, 25:36902 (DOCKET-50146-76)
SCANDIUM
abundance in 15 Vul, (E/T), 25:35653
determination as impurity in ytterbium oxide by neutron activation and radiochemical separation, 25:34669 (JAERI-Memo-4279)
determination by micro iodometry, arsenate method for, 25:34508
determination in rocks by neutron activation and γ spectroscopy, 25:34543 (NIM-1013)
effects on fluorescence method for detection of hafnium and zirconium, 25:34519
separation from aqueous chloride solutions by solvent extraction using bis(1-isobutyl-3-methylbutyl) phosphate, 25:34706
SCANDIUM ALLOYS AND SYSTEMS
Ag--Sc, crystal structure of intermetallic Ag_2Sc and Ag_4Sc, 25:35496
Au--Sc, crystal structure of intermetallic Au_2Sc and Au_4Sc, 25:35496
Re--Sc, superconducting transition temperature of intermetallic compounds of, 25:36038
SCANDIUM ISOTOPES Sc-49
energy levels from proton resonances in calcium-48, isobaric analog, (E), 25:36690 (NP-18824)
SCATTERING
amplitudes for first-excited and ground-state scalars in Veneziano model, 25:36592
amplitudes for spinning particles, dual-resonance, 25:36596
amplitudes in dual-resonance model, off-mass-shell extrapolation of, 25:36598
amplitudes of high-energy, functional integration method for Regge--eikonal representation for, 25:36587 (JINR-P2-5768)
amplitudes of infinite-component field under scalar external field, wave equation for, 25:36557
amplitudes of two-body, constraints on growth power of, 25:36600
amplitudes of, generalized C(2,1) expansion for asymptotically growing, 25:36547
amplitudes of, representation for relativistic, 25:36601
bound state three-body, retarded part of two-time Green function for wave functions for, 25:36586 (JINR-E2-5771)
potential, eikonal approximation and impact parameter representation for, 25:36590
potential, phase instability for random, 25:36595
theory for relativistic three-body, retarded part of two-time Green function for, 25:36586 (JINR-E2-5771)
theory of, virial theorem for variational functions in, 25:35871
three-body problem in, symmetry of solution of exactly solvable, 25:36602
transcendental functions in computer programs for evaluating, (T), 25:36813 (ANU-P-439)
SCHIZOMYCOTA
Bacillus cereus, radioinduced inactivation of spores of, potentiating effects of halogen compounds on γ, 25:35264
Bacillus subtilis, radioinduced single and double strand breaks in DNA of, γ, 25:35268
Escherichia coli, growth in heavy water, effects of temperature on, 25:35094
Escherichia coli, radiation effects on frequency of nonselective markers in genes of, effects of dose on donor neutron, 25:35126
Escherichia coli, radiation effects on transferred F' factor in DNA of, effects of gene types on uv, 25:35271
Escherichia coli, radiation effects on, function and structure studies on protective effects of cysteamine and its homologs against γ, 25:35160
Escherichia coli, radiation effects of, γ, 25:35260
Escherichia coli, radioinduced inactivation and mitotic

XUM

delay in, effects of vacuum treatment on uv, 25:35265
Escherichia coli, radiosensitivity of repair system of, γ and uv, 25:35246
Escherichia coli, radiosensitivity of, effects of iodoacetic acid and vitamin K on, 25:35262
Escherichia coli, radiosensitivity of, effects of dihydroxybutyraldehyde on γ, 25:35159
Haemophilus influenzae, radioinduced inactivation of transforming DNA in, mechanism of x, 25:35269
Micrococcus radiodurans, radiosensitivity in relation to growth rate and quantity of macromolcules, x, 25:35263
Rhodopseudomonas spheroides, photochemical reaction centers from, 25:37206 (NYO-3759-30)
Rhodopseudomonas spheroides, photosynthetic reaction centers in, research progress on, 25:37205(R) (NYO-3759-18)
Staphylococcus aureus, radiation effects on inactivation of mutants of, mechanisms of DNA dark repair in uv, 25:35270
Staphylococcus aureus, radiosensitivity of, effects of iodoacetic acid and vitamin K on, 25:35262
SCINTILLATION CAMERAS
optical camera system for, 25:34872 (UCRL-20699)
SCREENS
thickness of metallic image-intensifying, for betatron radiographic equipment, selection of optimum, 25:34824
SCRUBBERS
design of off-gas, engineering drawings for, 25:34784
SEALS AND GLANDS
design for radioactive material shipping containers, 25:34850(P)
design of water pump shaft, 25:37145(P)
development and testing of polymeric, for lithium--selenium storage battery cells, 25:35275(R) (ANL-7777)
SEAS
book: Marine Radioecology, 25:35117
rare earth content in coastal areas of, effects of tides on, 25:34760
thorium content in coastal areas of, effects of tides on, 25:34760
variations in coastal zone of, numerical model for measuring middle-scale time-dependent salinity and temperature, 25:37216 (RLO-1725-191)
SEAWATER
analysis for gamma sources, lithium-drifted germanium spectrometer for, 25:34935
carbon-14 content of, research progress on study of, 25:34723(R) (RLO-2225-T-20-3)
desalination by distillation, fluid flow and heat transfer problems in, 25:34796
deuterium/hydrogen abundance ratios in, 25:34518
radioisotope content of, measurements of cesium-137 and strontium-90, 25:34759(R) (NYO-2174-129)
separation of radioisotopes from, design of sampler for, 25:34704
SEDIMENTARY DEPOSITS
characteristics of petroleum-bearing, methods for determining chemical, geological, and geophysical, 25:34731
SEED
radiation effects on cell nuclei in barley and bean, comparison of bremsstrahlung, γ, proton, and x, 25:35258
radiation effects on RNA synthesis in pea, mechanism of γ, 25:35245
radioinduced lethal mutants in Pisum, neutron and x, 25:35122
SEEDLINGS
radiosensitivity of gymnosperm, in relation to DNA content and seed radiosensitivity, γ, 25:35250
SEIGNETTOELECTRIC MATERIALS
neutron inelastic scattering above the Curie point by hydrogen in hydrogen-bonded, differential cross sections for, (E), 25:36668
SEISMIC WAVES
effects of Amchitka Island underground nuclear explosion-generated, on seismic activity on nearby islands, program for monitoring, 25:34763 (CGS-746-10)
effects of Salmon and Sterling Event-generated, on ground motion, source model for prediction of, 25:34764
SEISMOMETERS
standards for earthquake detection, AEC safety guide, 25:35061
SELENATES
effects on photometric determination of antimony following solvent extraction using TBP, 25:34512
SELENIUM
determination in human stones by neutron activation, 25:34546 (THAI.-AEC-39)
SELENIUM FLUORIDES
vapor pressure--temperature data for, 25:34602 (GAT-649)
SELENIUM ISOTOPES Se-87
nuclear properties of, Nuclear Data Sheets for, (E), 25:36706
SELENIUM OXIDES
separation of ions of, from metal ions by high-voltage electrophoresis using carboxylic and hydroxycarboxylic acids, 25:34702
SELENIUM SYSTEMS
Li--Se, corrosive effects on storage battery container materials, at 375°C, 25:35275(R) (ANL-7777)
Li--Se, phase studies of, 25:35275(R) (ANL-7777)
SEMICONDUCTORS
superconducting of, in laser light field, (T), 25:36031
SEPARATION PROCESSES
theoretical stages in, method for calculation of, 25:34707
SERPUKHOV SYNCHROTRON
beam injection in, calculation of capture efficiency with bunching for, 25:36603 (IFVE-SKU-70-20)
SEX
effects on radiosensitivity of human renal tumors, 25:35193
SHALES
stability of clay, in steep craters, engineering studies of, 25:34768 (NCG-TR-15(Vol.1))
SHEEP
iodine-131 content in thyroid of, in Portugal following Chinese nuclear tests, 25:35133
SHELLS (GEOMETRY)
stress in torispherical, analysis of, 25:37211 (ORNL-TM-3201)
SHIELDED CONTAINERS
design of shock-resistant steel, for shipping radioactive materials, 25:34858(P)
sealing device for radioactive material shipping, design of, 25:34850(P)
SHIELDING
calculations for muon, around high-energy proton accelerator targets, 25:36610 (ORNL-TM-3353)
design of heat-block type for radioisotope powered thermoelectric converters, 25:34810(R) (ORNL-TM-3354)
design of SNAP, development of computer codes for, 25:36250 (ORNL-TM-3364)
information storage and retrieval system of RSIC, 25:36247 (CTC-48)
neutron transport equation, numerical solution to space-, angle-, energy-dependent integral, (T), 25:36266
SHIPPING
equipment and methods for irradiated fuel element, in Switzerland, performance of, 25:34854
methods for radioactive materials, development of special arrangement, 25:34843 (AECL-3804)
standards for radioactive materials, 25:34851
SHIPPINGPORT PRESSURIZED-WATER REACTOR
core 2 seed 2 for, design parameters and operating limits for, 25:36890(R) (WAPD-MRP-135)
operations during October 1970 to January 1971, 25:36890(R) (WAPD-MRP-135)
SHIPS
operation of nuclear, legal standards problems in, 25:37096
piping for, U.S. requirements for pressure and power, 25:37099
safety of nuclear, standards for, 25:37102
safety of nuclear, U.S. standards for, 25:37101
safety of nuclear, U.S. standards for, 25:37098
safety of nuclear, U.S. standards for, 25:37100
SHOCK WAVES
production by laser irradiation of solid targets, (T), 25:36153
propagation in collisionless plasma, in absence of magnetic fields, (E/T), 25:36106
propagation in collisionless plasma, isomagnetic discontinuities in, (E), 25:36125
propagation in discharges with longitudinal magnetic fields, microwave diagnostics of, 25:36092 (UARAEE-101)
propagation in geomagnetic field, whistler initiation of, (T), 25:35596
propagation in Marvel Event air tunnel, analysis and measurement of, 25:34765
propagation in pinch discharges, effect of longitudinal magnetic fields on, (E), 25:36117 (UARAEE-106)
relaxation behind, in air, 25:37232(T) (SC-T-710030)
solution of nonequilibrium, radiating, reflected, in air, numerical technique for, 25:37230 (SC-RR-710203)
structure in gas of elastic spheres, Boltzmann equation for, 25:36126 (NYC-1480-173)
SILICON
argon-ion reactions at 20 keV with, luminescence spectra of excited particles knocked out from, effects of nonradiative transitions on, 25:35841
determination in silicon nitride, electric method for, 25:35546 (AWRE-O-42-69)
effects of combination of oxygen and, on internal friction of zirconium alloy, 25:35404
indium-ion implants in antisony-doped, content profiles of 20- to 80-keV, (E/T), 25:36282
ion-implantation damage in, ESR study of depth distribution of 100-keV phosphorus, 25:36276
ion-implantation-induced lattice disorder in, channeling study of 10- to 200-keV, 25:36300
oxidation by organic solvents containing aqueous potassium nitrate, tracer study of anodic, 25:35292
proton reactions at 600 MeV and 24 GeV, aluminum-26 production cross sections for, (E), 25:36689 (NP-18820)
radiation damage in n-type, p-type, and high-purity, ac hopping conductivity study of low-temperature electron, 25:36305
separation from uranium by fractional dissolution, 25:34699

SILICON CARBIDES
fabrication and burst testing of reaction-bonded, 25:35523 (AECL-3462)
properties for use in armor materials, 25:35554
B_4C--SiC, properties for use as armor plate, 25:35554
SILICON FLUORIDES
vapor pressure--temperature data for, 25:34602 (GAT-649)
SILICON ISOTOPES Si-28
energy levels from aluminum-27 (p,γ) reactions, resonance parameters and spin--parity assignments for, (E), 25:36699
energy-level transitions from aluminum-27 (p,γ) reactions, branching ratios for, (E), 25:36699
proton reactions (p,2p) at 600 MeV, diffraction-model calculation of differential cross sections for, (T), 25:36679
SILICON ISOTOPES Si-30
neutron reactions (n,p) at 15 MeV, cross section for, (E), 25:36715
SILICON NITRIDES
analysis for unreacted silicon, electric method for, 25:35546 (AWRE-O-42-69)
reactions with molten plutonium, effects of free silicon on, 25:35546 (AWRE-O-42-69)
SILICON OXIDES
radioinduced space charge in, subsecond annealing of pulsed-electron, 25:36302
graphite--SiC_2, electric conductivity of powdered, pressure dependence of, 25:36334
SILICON SYSTEMS
Al--Mo--Si, radiation effects on subsequent catalytic activity of, in decomposition of hydrogen peroxide, γ, 25:34630
C--Mn--Si--steel, properties of plates of, for use in pressure vessels at moderate and lower temperature service, standard for, 25:35468
SILICONE RUBBERS
compression set of, effects of Kapton, Mylar, and Teflon lining on high-temperature, 25:37173 (BDX-613-410)
SILTS
cesium-137 distribution in Atlantic Ocean and Mediterranean Sea, measurement of vertical, 25:34759(R) (NYO-2174-129)
mineral deposits in seabed, nuclear methods for identifying, 25:34803(R) (BNWL-1308-5)
plutonium-239 distribution in Atlantic Ocean and Mediterranean Sea, measurement of vertical, 25:34759(R) (NYO-2174-129)
sorptive properties for cesium and cobalt, 25:34721(R) (NYO-3912-3)
sorptive properties of, from German rivers for cesium-137, iodine-131, and strontium-85, 25:34737
strontium-90 distribution in Atlantic Ocean and Mediterranean Sea, measurement of vertical, 25:34759(R) (NYO-2174-129)
transport of, development in France of radioactive tracer methods for studying, 25:34812(T) (ORNL-tr-2492)
uranium content in oceanic, of water uprise zones, 25:34761
SILVER
determination in microcrystal centers in photographic emulsions by neutron activation, 25:34549
deuteron reactions (d,pn) at 13.6 MeV, diffraction-model analysis of proton--neutron correlations in, (E/T), 25:36713
effects on colorimetric determination of gold, 25:34521
effects on gravimetric determination of mercury using 2-aminobenzothiazole, 25:34520
effects on photometric determination of antimony following solvent extraction using TBP, 25:34512
performance of foamed zirconium oxide-impregnated, as heat shield for reference design reactor reentry, 25:35549 (TID-25696)
separation of ions of, from metal ions by high-voltage electrophoresis using carboxylic and hydroxycarboxylic acids, 25:34702
x-ray emission induced by electrons, intense K-, 25:35842
SILVER ALLOYS AND SYSTEMS
Ag--Au, mixing at 1100°C, adiabatic calorimetric measurement of heat of, 25:35432
Ag--Cu, mixing at 1100°C, adiabatic calorimetric measurement of heat of, 25:35433
Ag--Sc, crystal structure of intermetallic Ag_2Sc and Ag_4Sc, 25:35496
Ag--Yb, crystal structure of intermetallic Ag_3Yb, 25:35496
Ag-base--Au, radiation effects on diffusion in, 2-MeV electron, 25:35512
Ag-base--Li, slip in, mechanisms of cross, 25:35386
Ag-base--Yb, hyperfine interactions in, study using γ--γ angular correlations of ytterbium-169 decay, 25:36332
SILVER ISOTOPES Ag-107
neutron capture by, spectrum-averaged cross sections for pile, (E/T), 25:36720 (CONF-710301-4)
SILVER ISOTOPES Ag-108
energy levels from silver-107 (n,γ) reactions, lifetimes for, (E), 25:36769
energy-level transitions from silver-107 (n,γ) reactions, (E), 25:36769
SILVER ISOTOPES Ag-109
neutron capture by, spectrum-averaged cross sections for pile, (E/T), 25:36720 (CONF-710301-4)
SILVER ISOTOPES Ag-110
energy levels and nuclear properties of, Nuclear Data Sheets for, (E), 25:36808
energy levels from silver-109 (n,γ) reactions, lifetimes for, (E), 25:36769
energy-level transitions from silver-109 (n,γ) reactions, (E), 25:36769
SKIN
plutonium-239 distribution in epidermis of pig, during surface contamination, 25:35092
radiation effects on hexokinase activity in animal, protective effects of corticosteroids against uv, 25:35234
SNOW
water content of, gamma radiometric gage for measuring, 25:35042(P)
SODIUM
abundance in K giant stars, (E/T), 25:35649
analysis for hydrogen, testing of in-line loop meter for, 25:35276(R) (GEAP-13539-16)
analysis for oxygen, testing of in-line loop meter for, 25:35276(R) (GEAP-13539-16)
boiling in heated channels, NEMI code for thermohydraulic analysis of, (E/T), 25:37046 (RT/ING-(70)18)
boiling in reactor cooling systems, accustic detection of, (E), 25:37052
boiling superheat in, effects of heating surface roughness on, 25:34791 (KFK-1332)
compatibility with carbide and oxide fuels, 25:35550
corrosive effects of liquid, on Armco iron and Type 304 stainless steel at 500 to 600°C, 25:35286
corrosive effects of liquid, on stainless steel, 25:35281
corrosive effects on austenitic stainless steels at 1300°F, 25:35276(R) (GEAP-13539-16)
corrosive effects on Inconloy 800 at 1300°F, 25:35276(R) (GEAP-13539-16)
corrosive effects on titanium--vanadium alloy, 25:37016 (CONF-700211-9)
determination in glacial waters by ion-sensitive electrode method, 25:34721(R) (NYO-3912-3)
determination in glacial waters by ion-sensitive electrode method, 25:34722(R) (NYO-3912-4)
determination in human stones by neutron activation, 25:34546 (THAI.-AEC-39)
determination in rocks by neutron activation and γ spectroscopy, 25:34543 (NIM-1013)
determination in soils by neutron activation, 25:34545 (THAI.-AEC-36)
effects on colorimetric determination of gold, 25:34521
effects on gravimetric determination of mercury using 2-aminobenzothiazole, 25:34520
effects on radiation stability of sulfone polyelectrolytes, 25:34650
electric field gradient in hcp, calculations, 25:36351
electron reactions with, excitation cross sections for, (T), 25:35881
oscillator strengths for excitation and ionization of, tables of calculated generalized, 25:35844 (SC-RR-70-406)
properties of liquid, safety problems with, 25:37011
purification of liquid, design and operation of system for, 25:37056(T) (BNWL-tr-67)
reactions with deuterium and hydrogen molecules up to 50 eV, vibrational excitation and dissociation in, (E), 25:35884
reactions with fuel pellets, thermodynamics of, 25:35547(R) (GEAP-12182)
reactions with water under reactor conditions, heat exchanger design studies from, 25:35441
separation from potassium by bromine redox electrolysis, 25:34691 (LA-4645)
sorption on tantalum (110) crystal, contact potential measurements of, 25:35359
spectral absorption bands in 4430 A interstellar bands, (E/T), 25:35663
spectral excitation in twilight ionosphere, (E), 25:35971
SODIUM ALLOYS AND SYSTEMS
K--Na, compatibility with Inconel 718 and 750 tubular sections at 1050 to 1310°F, 25:35343 (WANL-TME-1857)
SODIUM CHLORATES
radiolysis of, ESR studies on effects of temperature on yields of chlorine dioxide and chlorine trioxide from γ, 25:34666
SODIUM CHLORIDES
corrosive effects of solutions of, on diffusion bonded 2024 aluminum alloy--boron filament composite, relations with applied stress, 25:35521
corrosive effects on IN-738 superalloy at high temperatures, 25:35400
effects of solutions of, on corrosion fatigue crack propagation in aluminum--molybdenum--titanium--vanadium alloy, relations with stress intensity amplitude and frequency, 25:35279
elastic constants of single crystals of, pressure dependence of, 25:37198 (NYO-2504-63)
radiation effects on internal friction of monocrystalline, relations of strain amplitude with fast neutron, 25:35587

XUM

radiation effects on lead-doped crystals of, absorption spectra--ionic thermocurrent study of 1.5-MeV electron, 25:36303
rare-gas atom and ion reactions with, electron emission induced from single crystals by 0.2- to 6.0-keV, (E), 25:35840
SODIUM HYDRIDES
dissociation pressure of, effects on sodium coolant loop operation, 25:35276(R) (GEAP-13539-16)
SODIUM IODIDES
effects on yields from γ radiolysis of 2-methyl-2-propanol, 25:34659
SODIUM IONS
reactions with deuterium and hydrogen molecules up to 50 eV, vibrational excitation and dissociation in, (E), 25:35884
SODIUM ISOTOPES Na-20
beta decay of, half-lives and log-ft values for, (E/T), 25:36710
nuclear mass from neon-20 (p,n) reactions, (E/T), 25:36710
SODIUM ISOTOPES Na-22
production rates in stone meteorites from galactic cosmic-ray interactions, (E/T), 25:35599
SODIUM ISOTOPES Na-23
neutron elastic and inelastic scattering at 5.0 MeV, differential and integrated cross sections and spectra from, (E), 25:36685 (AWRE-0-3/71)
neutron total cross section at 100 eV to 15 MeV, evaluation for ENDF/B, 25:36693 (WARD-4181-2)
SODIUM OXIDES
determination in argon cover gas for sodium loops, amalgamation method for, 25:35276(R) (GEAP-13539-16)
SODIUM SILICATES
radioinduced paramagnetic centers in oxidized and reduced glasses of, EPR spectra of, 25:36278
SODIUM URANATES
analysis for impurities by neutron activation, 25:34547 (UARAEE-68)
separation of uranium from, by fractional dissolution, 25:34659
SOILS
analysis for aluminum, copper, manganese, sodium, and zinc by neutron activation, 25:34545 (THAI.-AEC-36)
analysis for radioactive cesium, plutonium, strontium, and uranium, 25:34500
contamination from underground disposal of radioactive wastes at Mesita del Buey, N. M., predictions for, 25:34846 (LA-4660)
gamma radiation from, use of Compton continuum peak for estimating 10 to 100 keV range natural background, 25:34727 (UCRL-72927)
properties of volcanic ash-derived, measurement of chemical and physical, 25:34724(R) (RLO-2227-T-9-1)
transport of, development in France of radioactive tracer techniques for studying, 25:34812(T) (ORNL-tr-2492)
SOLAR ACTIVE REGIONS
isophotes of chromospheric, (E), 25:35776
magnetic-field distribution in, (E), 25:35754
model of transition layer in, radio, (E/T), 25:35720
radio bursts from, Type-III, (E), 25:35723
spectra of, (E), 25:35746
velocity field at different levels in, (E), 25:35746
velocity fields in, temporal variations of photospheric, (E), 25:35750
SOLAR CORONA
electron density and temperature at base of, (T), 25:35743
magnetic structure in, using flare-associated hydromagnetic-disturbance formulation for, (T), 25:35777
shock heating of, model for, (T), 25:35769
spectra of condensations in, xuv line, (E), 25:35768
spectral line profiles, (E), 25:35775
spectral lines due to $3p^5 3d$ configuration, (E/T), 25:35744
supernovae-remnant occultation by, for studying scattering of decameter radio waves, (E/T), 25:35773
x-ray emission from regions of soft, (E), 25:35721
SOLAR FLARES
development of July 11, 1966, (E), 25:35748
effect on tropospheric circulation, (E/T), 25:35973
effects in ionosphere using high-frequency Doppler technique, Sept. 1960 to Dec. 1962, (E), 25:35952 (NBS-TN-326)
effects on cosmic-ray intensity at 70 m.w.e., (E/T), 25:35731
effects on homologous microwave emission from Sun, (E/T), 25:35774
electron acceleration and emission during, 10- to 100-keV, (E), 25:35726
electron spectra in relativistic, (E), 25:35727
magnetic fields in July 6 and Sept. 2, 1966, (E), 25:35753
motions in chromospheric, (E), 25:35747
neutron emission from, detection at 25 km of high-energy, (E), 25:35772
occurrence on Oct. 3, 1969 of west-limb, observations of Type II harmonic radio bursts from, (E), 25:35735
particle propagation in, effects of bounded interplanetary diffusion medium on, (T), 25:35730
polar cap absorption associated with, (E), 25:35758
proton intensity variations during Feb. 25, 1969, parameters affecting anisotropic measurements of, (E), 25:35987
radio burst associated with Sept. 27, 1969, (E), 25:35726
radio bursts associated with flares beyond west limb, observations at 80 MHz of Type-II, Oct. 13, 1969, (E/T), 25:35736
radio bursts associated with Oct. 26, 1968, bipolar structure in moving Type-IV, (E), 25:35739
radio bursts from Dec. 17, 1969 2B, observations of meandering plasmoid-associated Type-IV, (E), 25:35742
relation of July 11, 1966, with radio emission at 10 cm and 1.5 m, (E), 25:35749
spectra of, evidence for photospheric origin of, (E), 25:35722
x-ray emission during, (E), 25:35721
x-ray emission during, nonthermal, (E), 25:35726
SOLAR PARTICLES
acceleration and propagation of, (E/T), 25:35728
composition of, (E/T), 25:35728
intensity variations of protons during Feb. 25, 1969 event, parameters affecting anisotropic, (E), 25:35987
interactions with interplanetary magnetic field, (T), 25:35771
neutron detection at 25 km in atmosphere, high-energy solar flare-associated, (E), 25:35772
propagation of flare-produced, effects of bounded interplanetary diffusion medium on, (T), 25:35730
propagation of low-energy, (T), 25:35906
SOLAR RADIATION
absorption of submillimeter, in atmosphere, (E), 25:35714
SOLAR RADIO BURSTS
morphology of Type-III, (E), 25:35722
observation at 80 MHz of Type II harmonic, associated with Oct. 3, 1969 west-limb flare, (E), 25:35735
observations at 3.15 cm, (E), 25:35760
observations at 80 MHz of Type-II, associated with flare beyond west limb, Oct. 13, 1969, (E/T), 25:35736
observations of harmonic Type-III, radichelicograph and spectrograph, (E), 25:35738
observations of meandering plasmoid-associated Type-IV, from Dec. 17, 1969 2B solar flare, (E), 25:35742
observations of moving triple-source Type-IV, Oct. 10, 1969 radioheliograph, (E), 25:35741
origin of Sept. 27, 1969, associated with 3B or 3N flare, (E), 25:35725
polarization of moving Type-IV, relation to magnetic arch, Aug. 29--30, 1969, (E), 25:35740
relation to solar proton events, (E), 25:35758
spectral shapes of Simple-3 Type, (T), 25:35724
structure in Type-III, fundamental and second-harmonic, (E/T), 25:35737
structure of moving Type-IV, shock wave-associated bipolar, (E), 25:35739
SOLAR SPICULES
model for, 25:35719
properties of, physical, (E), 25:35719
spectra of, profiles of Hα, D3, Hβ, Ca H, and Ca K lines in, (E), 25:35719
SOLAR SYSTEM
cosmic-ray modulation by, model for primary, (E/T), 25:35899
cosmic-ray modulation by, primary, (T), 25:35907
cosmic-ray modulation in, primary, (T), 25:35924
dusts in, phenomena of radioactive and nonradioactive interplanetary, (E/T), 25:35913
element abundances in, (T), 25:35595
exobiology of asteroids, Jovian planets and moons, Pluto, and comets, survey of, (T), 25:35829
mass distribution of planets on particle accretion, (T), 25:35832
SOLAR WIND
effects on form of magnetotail, (E/T), 25:35591
equations of, supersonic solution for inviscid, (T), 25:35743
interaction with magnetosphere, (T), 25:35993
interaction with magnetosphere, correlation with new polar magnetic disturbances, (E/T), 25:36012
interaction with planetary atmospheres, and ionospheres, model of, (E/T), 25:36011
interaction with spiral interplanetary field, (T), 25:35906
ions in, heavy, (E), 25:35729
propagation in solar equatorial zone, (E), 25:35755
turbulent electric field spectrum in disturbed, (E), 25:35767
velocity of interplanetary, comparison measurements of, (E), 25:35734
velocity of, during Type-III radio bursts, (E), 25:35723
velocity variations at 1 AU, (E), 25:35732
SOLID SOLUTIONS
properties of, conference on, 25:35369
SOLIDS
diffusion in, review on theory of thermal, 25:35440
energy diffusion in one-dimensional finite, with linear heat loss, 25:37221 (SC-IR-70-767)
neutron scattering in study of random motions in, review, 25:36313
radioinduced void growth in, mechanisms of energetic ion

and neutron, 25:35511
SOLVENT EXTRACTION PROCESSES
development of reductive, in mild steel flow-through facility, 25:34694 (ORNL-TM-3138)
facility for reductive, digital simulation of flow control systems for, 25:34694 (ORNL-TM-3138)
SOLVENTS
radiation stability of Shellsol A and AB and Solvesso 100, for use as diluent in fuel reprocessing, 25:34638 (RT/CHI-(70)35)
SOUND
effects on heating of coronae of cool stars, (T), 25:35667
scattering of magneto-acoustic waves by ideal conducting cylinder, (T), 25:35941
SOUTHWEST EXPERIMENTAL FAST OXIDE REACTOR
operations incident of May 23, 1971, safety system relay malfunctions, 25:37059 (DOCKET-50231-83)
SOVIET UNION
radioisotope content in atmosphere over Moscow, 1962 to 67, 25:34748
SPACE
book: Modulation of Cosmic Rays in Interplanetary Space, 25:35894
book: Peaceful Uses of Nuclear Energy, 25:34817
gamma spectrum in, measurements of 0.1 to 10 MeV low-energy, (E), 25:35922
gas density in intergalactic, (T), 25:35818
plasma in interplanetary, collective oscillations in dense electron gas, (T), 25:36239
research programs and facilities in India, (T), 25:35997
waves in interplanetary, interaction with like-period geomagnetic-field micropulsations, (E/T), 25:35964
SPACE VEHICLES
propulsion by thermionic reactor for unmanned outer planet exploration, 25:35937
propulsion of, use of rotating cable pusher for, 25:37189 (LA-4666)
propulsion system for reusable nuclear shuttle, design concepts and economics of NERVA for, 25:37089
relativity experiments in, review of Earth orbit and deep-space, (E/T), 25:35821
SPAIN
fallout monitoring in, 1966 to 1968, 25:35132
nuclear safety regulation in, 25:37051
SPECTROMETERS
cascade shower development in ionization, Monte Carlo simulation for energy balance and total ionization as function of depth for nuclear--electromagnetic 4-TeV, 25:36431 (ITJ-6)
circuit for medical nuclear, preregulation of high voltage supply, 25:34888(F)
detectors for magnetic charged-particle, position-sensitive array of surface-barrier, 25:34861 (AERE-R-6776)
efficiency of echelle, for high-resolution studies of solar vacuum uv spectra, (E), 25:35054
magnetic field corrections for, Hartree formula for, 25:35063
SPECTROSCOPY
data acquisition from simultaneous experiments with centralized output, design of system for, 25:35045 (CONF-700647-, pp 255-79)
SPERMATOGONIA
radioinduced dominant lethal mutations in mouse and rat, comparison studies on x, 25:35129
SPHERES
neutron leakage from water-moderated, escape fractions and reflection coefficients for, (E/T), 25:36653
SPINAL CORD
radiation effects on aluminum and copper content in functionally and morphologically different structures of animal, x, 25:35228
SPORES
radioinduced inactivation of Bacillus cereus, potentiating effects of halogen compounds on γ, 25:35264
SPRAYS
effectiveness of pressurized water reactor containment system iodine removing, (E/T), 25:37029 (ORNL-TM-2412(Pt.12))
STABLE ISOTOPES
uses of separated, in U.S, 25:34813 (TID-25705)
STAINLESS STEEL
corrosion of Type 18-8, by liquid sodium, 25:35281
corrosion of Type 304, by sodium at 500 to 600°C, factors affecting, 25:35286
corrosion of Type 316, by loop sodium at 1300°F, effects of cold trap temperature and oxygen content on, 25:35276(R) (GEAP-13539-16)
corrosion of Types 304, 321, and 347, by sodium at 1300°F, 25:35276(R) (GEAP-13539-16)
diffusion of cobalt-60 in surfaces of Type 316, at 1000°C, 25:35276(R) (GEAP-13539-16)
dimensions, tolerances, and marking of wrought butt-welded fittings of, standard for, 25:35351
ductility and strength of Types 304 and 316 at high temperatures, effects of boron on, 25:35338 (ORNL-TM-3316)
fabrication and properties of boiler, superheater, heat-exchanger, and condenser tubes of welded austenitic, standard for, 25:35416
fabrication of cladding of Types 308 and 309, for Type A533B steel, welding methods for, 25:35315
microstructure of Type 1H18N9T, effects of aging on, 25:35336 (INR-1255)
preparation of dispersion-strengthened Type 348, using carbon, molybdenum, and niobium additions, 25:35300
preparation of radiation- and heat-resistant austenitic, 25:35323(P)
production of Type 316, for fast breeder reactor cladding tubes, 25:35305
properties of austenitic, for seamless boiler, superheater tubes, and heat exchanger tubes, standard for, 25:35452
properties of bolting material of austenitic, for pressure vessels, valves, flanges, and fittings for high-temperature service, 25:35408
properties of centrifugally cast cold-wrought pipe of austenitic, for high-temperature service, standard for, 25:35420
properties of centrifugally cast pipe of austenitic, for high-temperature service, standard for, 25:35426
properties of forged or rolled pipe flanges, forged fittings, valves, and parts of austenitic, for high-temperature service, standard for, 25:35470
properties of pipe of seamless and welded austenitic, for high-temperature and general corrosion service, 25:35417
properties of plates, sheets, and strips of, for use in fusion-welded unfired pressure vessels, standard for, 25:35465
properties of seamless and welded tubing of austenitic, for general service, standard for, 25:35415
properties of Type 316, for sodium cooled fast reactor fuel cans, (E), 25:37139 (CONF-700211-7)
radiation effects on helium production in, fast neutron, 25:35503 (HEDL-SA-193)
radiation effects on mechanical properties of Type 304, relations of environment with fast neutron, 25:35506
radiation effects on tensile properties of Type 304, fast neutron, 25:35509
radioinduced void formation in Type 304, at 400 to 600°C, predicted and experimental study of fast neutron, 25:35516
sodium boiling superheat at surfaces of, effects of roughness on, 25:34791 (KFK-1332)
stress corrosion cracking of Type 304 and Type 316, by boric acid solutions, (E), 25:37028 (ORNL-TM-2412(Pt.10))
testing of electric fusion-welded pipes of, for use in high-temperature service, 25:35367
testing of hot-finished and cold-drawn welded and seamless tubes of austenitic and ferritic, 25:35419
testing of nuts of austenitic, for bolts in high-pressure and high-temperature service, 25:35451
welding to aluminum--magnesium alloys, methods for, 25:35326
B--stainless steel, properties for use as JMTR fuel followers, 25:35320
STANDARDS
code of practice for the shipping of radioactive materials by road, Radioactive Substances (Great Britain) Regulations 1970, 25:34859
construction, arrangement, and other provisions for nuclear vessels, 46 CFR 79, 25:37100
construction, arrangement, and other provisions for nuclear vessels, 46 CFR 99, 25:37101
construction, arrangement, and other provisions for nuclear vessels, 46 CFR 37, 25:37098
detailed regulations governing radioactive materials, 46 CFR 146.19 1969, 25:34851
facilities handling radioactive materials, NFPA 801 1970, 25:34853
finishes for contact faces of pipe flanges and connecting-end flanges of valves and fittings, MSS SP-6 1969, 25:35418
fire protection practice for facilities handling radioactive materials, NFPA 801, 25:37048
fire protection practice for nuclear reactors, NFPA 802, 25:37048
fire protection practice for nuclear reactors, NFPA 802, 25:37050
glossary of terms in nuclear science and technology, ANSI N1.1-1967, 25:36826
instrumentation for earthquakes, AEC safety guide 12 1971, 25:35061
instruments for use in radiation fields, ISA RP 25.1 1967 standard for selection of, 25:35081
marking system for valves, fittings, flanges, and unions, MSS SP-25 1964, 25:34786
method of test for surface flammability of materials using a radiant heat energy source, ASTM E 162-67, 25:34842
neutron flux and spectra measurements for physical and biological applications, NBS Handbook 72, 25:34879
nuclear pressure vessels, 46 CFR 55, 25:37144
nuclear ships classification rules, R (C) 101--R (C) 117, 25:37102
physical aspects of irradiation, NBS Handbook 85 (ICRU Report 10b), 25:35137
piping systems and appurtenances, 46 CFR 56, 25:37099
quality assurance criteria for nuclear power plants, 10

XUM

CFR 50, 25:36972
radiation and radiation sources intended for use in the production, processing, and handling of food, 21 CFR 121G 1970, 25:34814
radiation exposure limits for electric insulators, neutron and gamma, ANSI N 4.1 1967, 25:35075
recommended practice for standard calibration and form for nuclear logs, API RP 33 1959, 25:34735
safety in welding and cutting, USAS Z49.1 1967, 25:35330
specification for alloy steel forgings for seamless drums, heads, and other pressure vessels, ASTM A 336-70a, 25:35412
specification for alloy-steel and stainless steel bolting materials for high-temperature service, ASTM A 193-70, 25:35408
specification for carbon and alloy steel nuts for bolts for high-pressure and high-temperature service, ASTM A 194-69, 25:35451
specification for carbon steel plates for pressure vessels for moderate and lower temperature service, ASTM A 516-70a, 25:35468
specification for carbon steel plates for pressure vessels for intermediate and higher temperature, ASTM A 515-70, 25:35467
specification for centrifugally cast austenitic cold-wrought pipe for high-temperature service, ASTM A 452-65, 25:35420
specification for centrifugally cast austenitic steel pipe for high-temperature service, ASTM A 451-66, 25:35426
specification for chromium--iron--nickel alloy plate, sheet, and strip, ASTM B 168-70, 25:35360
specification for chromium--iron--nickel alloy rod and bar, ASTM B 166-70, 25:35364
specification for chromium--iron--nickel alloy seamless pipe and tube, ASTM B 167-70, 25:35413
specification for electric fusion-welded austenitic chromium--nickel alloy steel pipe for high-temperature service, ASTM A 358-70, 25:35367
specification for electric-fusion-welded steel pipe for high-pressure service, ASTM A 155-70, 25:35450
specification for ferritic and austenitic steel castings for high-temperature service, ASTM A 351-70, 25:35362
specification for forged or rolled alloy-steel pipe flanges, forged fittings, and valves and parts for high-temperature service, ASTM A 182-69, 25:35470
specification for forged or rolled steel pipe flanges, forged fittings, and valves and parts for high-temperature service, ASTM A 105-68, 25:35444
specification for general requirements for carbon, ferritic alloy, and austenitic alloy steel tubes, ASTM A 450-70, 25:35419
specification for manganese--molybdenum and manganese--molybdenum--nickel alloy steel plates for pressure vessels, ASTM A 302-70, 25:35473
specification for niobium and niobium alloy bar, rod, and wire, ASTM B 392-64, 25:35448
specification for niobium and niobium alloy ingots, ASTM B 391-64, 25:35447
specification for niobium and niobium alloy seamless and welded tubes, ASTM B 394-70, 25:35478
specification for niobium and niobium alloy strip, sheet, foil, and plate, ASTM B 393-64, 25:35446
specification for nuclear grade uranium metal melt stock and nuclear grade compactible and sinterable uranium dioxide, ANSI N 5.4, 5.5, 5.6 1965, 25:35479
specification for primary hafnium metal sponge and other forms, ASTM B 414-67, 25:35472
specification for primary niobium metal, ASTM B 383-64, 25:35449
specification for remelted lithium metal in ingot form, ASTM B 357-66, 25:35423
specification for seamless and welded austenitic stainless steel tubing for general service, ASTM A 269-69, 25:35415
specification for seamless and welded austenitic stainless steel pipe, ASTM A 312-70a, 25:35417
specification for seamless and welded titanium tube for condensers and heat exchangers, ASTM B 338-65, 25:35421
specification for seamless austenitic steel pipe for high-temperature central station service, ASTM A 376-70, 25:35366
specification for seamless carbon steel pipe for high-temperature service, ASTM A 106-68, 25:35445
specification for seamless ferritic and austenitic alloy-steel boiler, superheater, and heat-exchanger tubes, ASTM A 213-70, 25:35452
specification for seamless nickel and nickel alloy condenser and heat exchanger tubes, ASTM B 163-66, 25:35361
specification for stainless and heat-resisting chromium and chromium-nickel steel plate, sheet, and strip for fusion-welded unfired pressure vessels, ASTM A 240-70, 25:35469
specification for testing for density in air of manufactured carbon and graphite articles by physical measurements, ASTM C 559-69, 25:35474
specification for titanium and titanium alloy forgings, ASTM B 381-69, 25:35422
specification for titanium and titanium alloy strip, sheet, and plate, ASTM B 265-69, 25:35362
specification for titanium sponge, ASTM B 299-69, 25:35414
specification for unalloyed uranium castings, ASTM E 419-641, 25:35471
specification for unalloyed uranium melting stock, ASTM B 420-64T, 25:35475
specification for welded austenitic steel boiler, superheater, heat-exchanger, and condenser tubes, ASTM A 249-65, 25:35416
spot facing for bronze, iron, and steel flanges, MSS SP-9 1929, 25:35365
thermocouples, sheathed, Type K, for nuclear and other high-reliability applications, ASTM E 235-67, 25:35051
transportation of dangerous articles and magnetized materials, 14 CFR 103 1963, 25:34852
welding ferrous materials for nuclear power piping, AWS D10.5-69 1969, 25:35308
wrought stainless steel butt-welding fittings, MSS SP-43 1950, 25:35351

STANFORD LINEAR ACCELERATOR
development and operation of, Oct.--Dec. 1970, 25:36611(R) (SLAC-130)

STAR CLUSTERS
age of NGC 609, 25:35605
distance of NGC 609, (E), 25:35605
energy of, total kinetic, (T), 25:35797
evolution of spherical, model for, (T), 25:35783
iron abundance in Pleiades and Hyades, (E), 25:35627
luminosity of peculiar white dwarf Ross 640, (E), 25:35602
magnetic-field structure in vicinity of α-Per, (E), 25:35795
magnitudes of colors of variable stars in M2, (E), 25:35610
membership of white dwarf eclipsing system BI + 16°516 in Hyades, (E), 25:35632
observations of NGC 188, television, (E), 25:35639
periods and light curves for variables in NGC 1466, (E), 25:35671
photometry of 46 stars in Roslund 5, (E), 25:35606
photometry of comparison stars near southern globular, (E), 25:35613
photometry of NGC 609, (E), 25:35605
photometry of variable stars in M13, (E), 25:35610
star proper motions for, in Praesepe, 91, (E), 25:35604
star relative proper motions in M35, 763, (E), 25:35603

STARS
abundance analysis of five apparently super-metal-rich K giant, (E/T), 25:35649
atmospheres for horizontal-branch and post-horizontal-branch, hydrogen-rich model, (T), 25:35626
atmospheres of γ Cyg and epsilon Peg, quantitative analysis of, (E), 25:35635
atmospheres of planetary-nebula central, extended model, (T), 25:35624
book: Flares of Red Dwarf Stars (in Russian), 25:35640
carbon isotope ratios in 19 Psc and Y CVn, (E), 25:35620
chromospheres of, characteristics of, (T), 25:35657
chromospheres of, detection of cyclic activity in, (T), 25:35717
composition of symbiotic, (E), 25:35633
curve of growth analysis of 15 Vul, (E/T), 25:35653
cyanogen abundance in 19 Psc and Y CVn, (E), 25:35620
density concentration parameter of binary, internal, (T), 25:35623
distance of variable, in NGC 1466, (E), 25:35671
electric potential of, (T), 25:35615
escape from colliding galaxies, (T), 25:35796
evolution of 1.13-solar-mass population I, (T), 25:35652
evolution of binary, (T), 25:35623
evolution of LkHα 190, period of rapid, (E), 25:35656
evolutionary age of zeta Phe, (E), 25:35654
flare activity of UV Cet-type red-dwarf, (E/T), 25:35640
formation of white-dwarf, physics of, (T), 25:35660
formation of, instability of contrastreaming plasma in, (T), 25:35793
gamma emission from, detection of, (T), 25:35687
heating in cool, coronal, (T), 25:35667
helium abundance in supergiant HD 32034, (E), 25:35673
infrared emission from, (T), 25:35659
infrared excess of W Cep and similar, (E), 25:35625
interstellar absorption in Orion and Monoceros, far-ultraviolet, (E), 25:35785
iron abundance in F and G dwarf, in Pleiades and Hyades clusters, (E), 25:35627
kinematics of, in Sco--Cen association and Gould's belt, (E), 25:35798
light curve for β Aur, (E), 25:35648
light curve for MR Cygni, (E/T), 25:35628
light curve of V 337 Aql, (E), 25:35666
light curves for close-binary, (E/T), 25:35628
light curves for ER Cep and ES Cep, (E), 25:35639
light polarization from, elliptical, (E), 25:35618
light polarization of UV Ceti-type, (E), 25:35637
light variations in 94 A and F main-sequence, (E), 25:35651
light variations of Ap, nature of, (E), 25:35612
luminosity increase in LkHα 190, (E), 25:35656
luminosity of G, K, and M, (E), 25:35619
luminosity of variable, in NGC 1466, (E), 25:35671
luminosity variations in Type M, (E), 25:35672

XUM

magnetic fields in white-dwarf, origin of, (T), 25:35621
magnitudes of, near southern globular clusters, (E), 25:35613
membership of white-dwarf eclipsing system BD + 16°516 in Hyades cluster, (E), 25:35632
metal abundance in supergiant HD 32034, (E), 25:35673
motion in binary systems, relative, (T), 25:35665
motions in spherical systems, model for, (T), 25:35783
observations of short-period variable, television, (T), 25:35639
occultations of double, lunar, (E), 25:35655
opacity of late-type, relation to absorption coefficient of negative hydrogen ions, (T), 25:35661
orbit of α Vir, computer program for, (E/T), 25:35647
orbital elements of V 337 Aql, (E), 25:35666
period of HD 133029, significance of short, (E/T), 25:35669
photoelectric measurements of WX Cep, during eclipsing, (E/T), 25:35662
photometric data on 1406, Geneva seven-color, (E), 25:35646
photometric elements of β Aur, (E), 25:35648
photometric elements of EE Peg, (E), 25:35607
photometry of 42 supergiant, (E), 25:35670
photometry of 46, in suspected cluster Ros 5, (E), 25:35606
photometry of Ap, uvby, (E), 25:35612
photometry of HC Tel and KZ Pav, (E), 25:35622
photometry of R CMa and V1010 Cph, (E), 25:35617
photometry of rapid blue variable, techniques of, (E), 25:35674
photometry of TW Cas, (E), 25:35609
photometry of U Gem, (E), 25:35675
photometry of UU Piscium, photoelectric, (E), 25:35608
photometry of Z And, three-color, (E), 25:35634
photometry of zeta Phe, UBV, (E), 25:35654
plasma rotation in, effects of Coriolis force on wave propagation of, (T), 25:36240
pulsations of uniformly rotating, nonlinear, (T), 25:35629
rotational velocities of A/sub p/, linear relationship to magnetic-field strength, (E/T), 25:35664
spectra of 1.13-solar-mass population I, secular, (T), 25:35652
spectra of G, K, and M, Hα absorption lines in, (E), 25:35619
spectra of interstellar band at 4430 A, (E/T), 25:35663
spectra of supergiant HD 32034, (E), 25:35673
spectral classification of 42 supergiant, (E), 25:35670
spectral polarization in K and M giant and supergiant, intrinsic, (E), 25:35611
spectrophotometric study of four K, (E), 25:35636
stability of dense, against radial pulsations, (T), 25:35614
stability of uniformly rotating, (T), 25:35629
structure of dense, (T), 25:35614
theory of isolated, Einstein space--times in, 25:36577

STEAM
corrosive effects on niobium--zirconium alloy under pressure at 450 to 650°C, effects of heat treatment and cold work on, 25:35278 (UARAEE-72)
H_2O--steam, flow in concentric internally heated annulus, measurement of critical heat flux and film flow rates in, 25:34797
H_2O--steam, heat transfer in upward flowing, in tubes, effects of flow quality on post-burnout, 25:34801

STEAM-GENERATING HEAVY-WATER-MODERATED REACTOR
maintenance of, review of, 25:36894
operations of, review of, 25:36894

STEAM POWER PLANTS
costs during 1970 to 2020, estimates of capital, 25:37030 (ORNL-TM-3243)
development of, review of, 25:36974

STEEL
analysis for nitrogen and hydrogen by inert gas fusion methods, 25:34514
cladding with Types 308 and 309 stainless steel, welding methods for, 25:35315
crack tolerance of A533-B, gross strain, 25:35335 (HSSTP-TR-14)
diffusion of carbon from ferritic, effects of niobium, titanium, and vanadium on, 25:35407
fatigue failure in high-strength, mechanisms of, 25:35428
finishes for contact faces of pipe flanges and connecting-end flanges of valves and fittings of, standard for, 25:35418
fracture of H11, at -28 to +100°C, effects of hydrogen and hydrogen--oxygen mixtures on, 25:35337(R) (NYO-3975-3)
mechanical properties of niobium-stabilized ferritic, relations with heat treatments, 25:35407
permeation of hydrogen in biaxially stressed membranes of, 25:35337(R) (NYO-3975-3)
plastic flow in low-carbon, mechanisms of thermally-activated, 25:35380
properties of bolting material of ferritic, for pressure vessels, valves, flanges, and fittings for high-temperature service, 25:35408
properties of castings of ferritic and austenitic, for use as valves, flanges, and fittings for corrosive and high-temperature service, 25:35363
properties of electric-fusion-welded pipe of, for use in high-pressure service, standard for, 25:35450
properties of ferritic, for seamless boiler and superheater tubes, standard for, 25:35452
properties of forged or rolled pipe flanges, forged fittings, valves, and parts of ferritic, for high-temperature service, standard for, 25:35470
properties of forged or rolled pipe flanges, forged fittings, valves, and parts of, for high-temperature service, standard for, 25:35444
properties of plates of carbon, for use for intermediate or high temperature service in boilers and pressure vessels, standard for, 25:35467
properties of seamless pipe of carbon, for high-temperature service, standard for, 25:35445
radiation effects on mechanical properties of Type A302, relations of environment with fast neutron, 25:35506
radiation effects on mechanical properties of Type A302B, pile neutron, 25:35508
solidification of cast, phosphorus-32 tracer studies of, 25:34820
spot facing of pipe flanges of, standard for, 25:35365
testing of heavy-section, for use as pressure vessels for boiling water and pressurized water reactors, 25:34827
testing of hot-finished and cold-drawn welded and seamless tubes of austenitic, carbon, and ferritic, 25:35415
testing of nuts of ferritic, for bolts in high-pressure and high-temperature service, 25:35451
testing of pressure vessel components of forged austenitic and ferritic, 25:35412
testing of seamless pipe of austenitic, for high-temperature central station service, 25:35366
welding of tantalum-clad, problems in, 25:35356
C--Mn--Si--steel, properties of plates of, for use in pressure vessels at moderate and lower temperature service, standard for, 25:35468
Cr--Ni--steel, welding to Inconel 625, tungsten inert gas method for, 25:35311
Mn--Mo--Ni--steel, properties of plates of, for use in pressure vessels, standard for, 25:35473
Mn--Mo--steel, properties of plates of, for use in pressure vessels, standard for, 25:35473

STELLAR FLARES
activity of UV Cet-type red dwarfs, (E/T), 25:35640
book: Flares of Red Dwarf Stars (in Russian), 25:35640
light polarization measurements on, (E), 25:35637
radio emission from, in the vicinity of the Crion Nebula, (E), 25:35616

STELLARATORS
design of stellarator--mirror machine target plasma reactor, 25:36190 (PATT-841)
magnetic field calculations for, axisymmetric helical, (T), 25:36206
magnetic surfaces in Tor-2, measurement using dielectric grids, (E), 25:36208
plasma instabilities in current-carrying toroidal systems, (T), 25:36181

STELLARATORS (C)
magnetic surfaces in, mapping using low-energy electrons, 25:36210

STILBENE
effects of coatings of, on γ radiolysis products of poly(vinyl chloride), ESR studies on, 25:34656

STORAGE BATTERIES
development of lithium--chalcogen, for vehicular propulsion, 25:35275(R) (ANL-7777)

STORAGE RINGS
beam dynamics in, Coulomb collisions in, 25:36640
luminosity of Orsay, lead--scintillator sandwich detectors for measuring, 25:36606 (LAL-1245)

STRAIN GAGES
performance for measurements in bubble chambers, effects of high magnetic fields and low temperatures on, 25:34987 (CONF-700623-(Vol.2), pp 863-72)
performance for measuring thermal stresses in annular disks at temperatures above 400°C, 25:34799

STRATOSPHERE
air mass exchange between troposphere and, radioactive tracer method for measuring, 25:34745(R) (NYO-4061-2)

STREAMS
diffusion of fluid particles in laboratory and natural, studies of longitudinal, (E/T), 25:34718 (KH-R-12)

STRESS
propagation through two-dimensional media, TENSOR computer program for calculating, 25:34769 (UCRL-50587)

STRONTIUM
abundance in atmospheres of four K stars, (E), 25:35636
determination of trace amounts of, as oxide, flame spectrophotometric, 25:34529
effects on gravimetric determination of mercury using 2-aminobenzothiazole, 25:34520
effects on photometric determination of antimony following solvent extraction using TBP, 25:34512
encapsulation of fission product, for use as radiation source, method for, 25:34803(R) (BNWL-1308-5)
Hall coefficient of, effects of high pressure on, 25:36324
helium-metastable-atom reactions with, coherence transfer to excited strontium ions formed by Penning effect in,

XUM

(E), 25:35875
STRONTIUM FLUORIDES
radiation effects on ionic conductivity of single crystals of pure and rare earth-doped, x-, 25:36304
thermoluminescence and x-ray luminescence spectra of gadolinium- and dysprosium-activated crystals of, (E), 25:36317
STRONTIUM ISOTOPES
determination of radioactive, in soils, 25:34500
STRONTIUM ISOTOPES Sr-85
sorption by sediments from low terraces of Elbe, Donau, and Weser Rivers, 25:34737
STRONTIUM ISOTOPES Sr-87
alpha reactions (α,nγ) at 10.3 to 13.5 MeV, γ singles and coincidence spectra from, (E), 25:36757
energy levels and nuclear properties of, Nuclear Data Sheets for, (E), 25:36706
STRONTIUM ISOTOPES Sr-88
alpha reactions (α,nγ) at 10.3 to 13.5 MeV, γ singles and coincidence spectra from, (E), 25:36757
energy levels and transitions from decay and nuclear-reaction measurements, Nuclear Data Sheets compilation of properties of, (E), 25:36705
energy-level transitions in, shell-model calculation of widths for E1, (T), 25:36798
proton reactions (p,n) with, excitation functions for, (E), 25:36676
STRONTIUM ISOTOPES Sr-89
energy levels and transitions from decay and nuclear-reaction measurements, Nuclear Data Sheets compilation of properties of, (E), 25:36714
production in (n,α) and (n,p) reactions with fast neutrons, cross sections for, (E), 25:36686 (CONF-680986-1)
STRONTIUM ISOTOPES Sr-90
beta decay of, Fermi--Kurie plot and small-order shape factor from, (E), 25:36768
content in atmosphere over Moscow, 1962 to 67, 25:34748
content in fish from Baltic Sea and North Atlantic during 1967 and 1968, 25:35096
content in freshwater fish in Germany during 1967 and 1968, 25:35096
content in seawater, measurements of, 25:34759(R) (NYO-2174-129)
content in surface waters of Atlantic Ocean, (E), 25:34759(R) (NYO-2174-129)
distribution in waters of Atlantic Ocean, Mediterranean Sea, and Sargasso Sea, measurement of vertical, 25:34759(R) (NYO-2174-129)
dose rates from shielded power sources of, (E), 25:34808 (ORNL-IIC-36)
encapsulation and testing of heat sources of, 25:34808 (ORNL-IIC-36)
energy levels and transitions from decay and nuclear-reaction measurements, Nuclear Data Sheets compilation of properties of, (E), 25:36801
handling and storage of cements containing, protective measures for personnel during, 25:35148
monitoring in sanitary waste system effluent from West Valley Processing Plant, 25:34683 (DOCKET-50201-72)
production and performance of heat sources of, 25:34808 (ORNL-IIC-36)
removal from man, methods for, 25:35134
uptake by human populations in Germany during 1967 and 1968 from ingestion of fish, 25:35096
STRONTIUM MOLYBDATES
MoO_3--SrMoO$_4$, phase studies of, 25:35578
STRONTIUM OXIDES
radioinduced F+ center in, magnetic circular dichroism--ESR study of neutron, 25:36291
STRONTIUM SULFIDES
SrS--US, phase studies on, electron-probe, metallographic, and x-ray-diffraction, 25:34603 (IJS-263)
STRONTIUM TITANATES
fabrication of thermoelectric converter fuels of, cost of, 25:34810(R) (ORNL-TM-3394)
STRUCTURES
fire protection of radioactive material handling, standards for, 25:34853
stresses and strains in complex, finite element method for calculation of, 25:34774 (EUR-4629)
STYRENE
effects of coatings of, on γ radiolysis products of poly(vinyl chloride), ESR studies on, 25:34656
radiation effects on subsequent grafting of, to polyethylene, 25:35591
radiinduced polymerization to crosslinked butyl rubber, γ, 25:34631
STYRENE POLYMERS
combustion of lead oxide-impregnated, fluidized-bed, 25:34690(R) (IN-1457)
SUBTILOPEPTIDASE A
radiation effects on chemical and kinetic properties of, γ, 25:35110
radiation effects on hydrolytic activity of, γ, 25:35109
SULFATES
determination in glacial waters by ion-sensitive electrode method, 25:34721(R) (NYO-3912-3)
determination in glacial waters by ion-sensitive electrode method, 25:34722(R) (NYO-3912-4)
SULFONES
polymers, performance in bonding beryllium--copper alloy specimens, 25:35316
radiation stability of macromolecular polyelectrolytes of, ESR studies on effects of metal ions on γ, 25:34650
SULFUR
determination by proton activation, 25:34554
determination in petroleum products, radiometric instruments for, 25:35040
SULFUR DIOXIDES
photo-absorption cross section of, review of uv, (E/T), 25:36013
SULFUR FLUORIDES
vapor pressure--temperature data for, 25:34602 (CAT-649)
SULFUR ISOTOPES S-32
content ratio to sulfur-34 in sandstone-type uranium deposits, measurement of, 25:34750(R) (COO-2024-1)
SULFUR ISOTOPES S-34
content in sandstone-type uranium deposits, measurement of, 25:34750(R) (COO-2024-1)
content ratio to sulfur-32 in sandstone-type uranium deposits, measurement of, 25:34750(R) (COO-2024-1)
energy levels from chlorine-34 and phosphorus-34 beta decay, spin--parity assignments for, (E), 25:36700
SULFUR SYSTEMS
Ga--rare earths--S, phase studies of, 25:35571
SULFURYL FLUORIDE
vapor pressure--temperature data for, 25:34602 (CAT-649)
SUN
activity of, effect on equatorial ionospheric radio-wave absorption, (E), 25:35970
cycle of 1958 to 1968, relation with variation of limiting energy of corotating cosmic radiation, (E/T), 25:35914
eclipse of, sky brightness and polarization during total, (E), 25:35764
eclipse of, sky brightness measurements during, (E), 25:35761
eclipse of, spectral changes in zenith skylight during total, (E), 25:35765
eclipse of, zenith sky brightness and color change during, (E), 25:35762
eclipse of, zenith sky intensity and spectral distribution during total, (E), 25:35763
electric charge of, effects on perihelion motion of 1566 Icarus, (E/T), 25:35733
oblateness of, effects on three tests of general relativity, (T), 25:35809
spectra of, computation of contribution functions for, (T), 25:35757
spectra of, line broadening by neutral hydrogen in, (T), 25:35770
ultraviolet spectra of, echelle grating spectrograph for, (E), 25:35054
SUNSPOTS
cycle of, effect on plasmasphere, (E/T), 25:35968
effects on daily geomagnetic activity, (E), 25:35954
electric currents in large unipolar, (E), 25:35751
fine-structure features in penumbras of, motions of, (E/T), 25:35745
gas pressure gradients in, (E/T), 25:35756
magnetic fields in large unipolar, (E), 25:35751
magnetic fields in umbra of unipolar, vertical distribution of, (E), 25:35752
opacity of, (E/T), 25:35756
relation to solar radio bursts, (E), 25:35760
spectra of, magnetic field strengths from Zeeman splittings in, (E), 25:35718
SUPERCONDUCTIVITY
pressure-induced, relation of band structure change to, (T), 25:36023
SUPERCONDUCTORS
book: Physical Chemistry, Metallography, and Metal Physics of Superconductors (in Russian), 25:36037
contacts between production and properties of point, having properties of Josephson junctions, 25:36070
critical current of alloy 65BT in fields up to 80 kOe, 25:36050
crystalline field effects in, containing magnetic impurities, 25:36034
electric conductivity in reversible transitions of wire samples, specific residual, 25:36055
electric conductivity of films below T/sub c/, nonlinear excess, (T), 25:36024
electron spin resonance in Type-I, 25:36067
excitation spectra of Type-II, band structure in, 25:36059
fabrication method for, 25:36066(P)
flux line pinning in Type-II, effects of deformation on, 25:36315
isotopic volume effect in, (T), 25:36060
Josephson junctions between, with superconducting barriers, (T), 25:36064
magnetic flux flow as function of film thickness in Type-I, (E/T), 25:36058
magnetic flux-flow effect in Josephson tunnel junctions, 25:36027
magnetic induction penetration in impure Type-II, with surface currents, electric field and losses from, (E/T), 25:36019 (CONF-700341-8)
magnetic vortices in high-kappa Type-II, entropy of,

25:36063
magnetization of dirty Type-II, near upper critical field, 25:36025
nucleation field of thin film of, on thick normal layer, 25:36035
phase transformations in alloy 65BT, 25:36051
properties of semiconductor in laser light field as, (T), 25:36031
theory of weak-coupling contribution to, 25:36069
thermal capacity of, pressure dependence of, (T), 25:36026
transition temperatures of, with overlapping bands in presence of nonmagnetic impurities, (T), 25:36033
ultrasonic attenuation rate in, Langevin approach to, 25:36071
ultrasonic attenuation theory in two-band, 25:36020
uses of, for energy storage and discharge, 25:36074 (CEA-CONF-1736)

SUPERNOVA REMNANTS
gamma emission from, detection of, (T), 25:35687
identification of 3C 58 as, from Type I supernova in 1181, (T), 25:35676
identification of Milne 56 with GX 5-1, (E), 25:35684
identification of North Polar Spur as, (E/T), 25:35800
identification of YM 29 as planetary nebula, (E), 25:35630
properties of 3C 391, (E), 25:35702
radio emissions from Tau A and Vir A, occultation by solar corona, (E/T), 25:35773

SUPERNOVAE
brightness of NGC 3198 and NGC 3389, TV observations of, (E), 25:35638
cosmic-ray ejection by, (T), 25:35900
gamma emission from, detection of, (T), 25:35687
identification of, of 1181, (T), 25:35676
mass ejection from Type II, (T), 25:35641
neutron star formation by, (T), 25:35621
production of NP 0527 and NP 0531 in binary system, (E/T), 25:35694
pulsar production in Type II, (T), 25:35641

SURFACE WATERS
contamination by radioactive waste disposal from Casaccia site in Italy, hazards to man from, 25:34849 (RT/PROT-(70)36)
quality of, abstracts of papers on maintaining, 25:37091 (ORNL-TM-3402)
radioactive waste disposal in, derivation of formula for calculation of maximum, 25:34717 (EUR-4636)
radioactivity monitoring of Amchitka Island, Alaska, 25:34720 (NVO-1229-121)
radioactivity of Project Rulison site, during reentry drilling, 25:34728 (USGS-474-101)

SURFACES
bibliography on surface and vacuum physics, 25:35835

SURRY POWER REACTOR, UNIT 1
design parameters of, revised and additional data on, 25:36938 (DOCKET-50280-40)
operations aspects of, revised and additional data on, 25:36938 (DOCKET-50280-40)
technical specifications for, revised, 25:36938 (DOCKET-50280-40)

SURRY POWER REACTOR, UNIT 2
design parameters of, revised and additional data on, 25:36938 (DOCKET-50280-40)
operations aspects of, revised and additional data on, 25:36938 (DOCKET-50280-40)
technical specifications for, revised, 25:36938 (DOCKET-50280-40)

SWEDISH REACTORS (R-2)
radiation target cans for, description of particle type fuel element, 25:37018 (JUL-701-RW)

SWINE
plutonium-239 distribution in epidermis of, during surface contamination, 25:35092
radioisotope availability in peccary, following single injection of nuclear debris from Project Buggy fallout, 25:35088
radioisotope distribution in tissues of Yorkshire, following field exposure to nuclear debris at Schooner Event site, fallout γ-emitting, 25:35090
radioisotope excretion in feces and urine of peccary, following single ingestion of nuclear debris from Schooner Event, quantitative comparison of fallout γ-emitting, 25:35089

SWITCHES
design of 10-MJ ignition crowbar, for 2X II device, 25:36196 (UCRL-73031)
development of insulated, to withstand operational shock in excess of one million g's, 25:37164 (BDX-613-294)

SWITZERLAND
plutonium production in power reactors in, forecasts to 1990 of, 25:35310
reactor fuel element fabrication in, prospects to 1980 for, 25:35313
uranium requirements in, for power reactors, forecasts to 1990 for enriched, 25:34819
uranium requirements in, for power reactors, forecasts to 1990 of, 25:34755

SYMMETRY GROUPS
book: Theory of Unitary Symmetry, 25:36552
conformal, equal-time commutator algebra for, 25:36541
nuclear reactions in, theorem for isospin multiplet production in, 25:36844
O(2,1) expansion for asymptotically growing scattering amplitudes, 25:36547
Sp(2), intrinsically self-conjugate boson structure in, 25:36548
SU(2), elementary particle classification in, 25:36549
SU(2), intrinsically self-conjugate boson structure in, 25:36548
SU(3) x S(3) broken chiral model for angle of eta--X mixing, 25:36551
SU(3) x SU(3), baryon--lepton correspondence in broken, 25:36543
SU(3) x SU(3), urbaryon bare mass in broken, 25:36543
SU(6), projection operator techniques for elementary particle theory in, 25:36545
SU(n), projection operator techniques for elementary particle theory in, 25:36545
SU(n), theorem for isospin multiplet production in nuclear reactions in, 25:36844
U(3,1), elementary particles in space--time geometry for, 25:36544
U(6), polynomial basis for irreducible representations in chain U(6) is contained in R(6), (T), 25:36711

SYMMETRY GROUPS SU(3)
breaking of chiral, in sigma model for meson properties, 25:36483 (SU-1206-241)
elementay particle classification in, 25:36549
meson classification in, vector, 25:36553
nuclear reactions in, theorem for isospin multiplet production in, 25:36844

SYMMETRY GROUPS SU(6)
elementay particle classification in, 25:36549

SYNCHROCYCLOTRONS
beam focusing in 700-MeV, depolarization of protons in, 25:36620
magnetic field pulses in Dubna, system for depression of, 25:36605 (JINR-P9-5724)

SYNCHROTRON RADIATION
emission by electrons trapped in radiation belts, rf electromagnetic wave-generated, (E/T), 25:36001
emission from magnetosphere, effect of radiating electron energy spectra on, (T), 25:35976

SYNCHROTRONS
beam injection in, calculation of capture efficiency with bunching for, 25:36603 (IFVE-SKU-70-20)
cost of superconducting, factors affecting, 25:36614 (UCRL-20259)

SYSTEMS FOR NUCLEAR AUXILIARY POWER (SNAP)
characteristics of radioisotope-fueled, tabulated data on, 25:34811(T) (CRNL-tr-2485)
shielding design for, computer codes for, 25:36250 (ORNL-TM-3364)

T

TACHYONS
production in cosmic EAS, upper limit for, (E), 25:36378

TANKS
design for plutonium processing facility, engineering drawings for, 25:34784

TANTALUM
determination as fluorotantalate by extraction and photometry using thiazine dyes, 25:34506
determination following separation of fluorotantalate anion using dyes, fluorometric, 25:34533
determination in rock by neutron activation and γ spectroscopy, 25:34543 (NIM-1013)
determination of sum of niobium and, in ore processing solutions, gravimetric, 25:34510
effects on polarographic reduction of niobium, 25:34526
electric conductivity at 1900 to 3200°K, pulsed measurements of, 25:35477
electric properties of films sputtered in oxygen--argon, relation with structures, 25:36338
oxidation by organic solvents containing aqueous potassium nitrate, tracer study of anodic, 25:35293
oxidation of, effects of electrolytes and pre-treatment on initial growth of anodic oxide films in, 25:35284
oxide film growth on, oxygen-16 and oxygen-18 tracer studies of anodic, 25:35294
plastic flow in, mechanisms of thermally-activated, 25:35380
plastic flow of, effects of strain rate on, 25:35399
preparation of thin films of, sputtering method for, 25:35303
radioinduced Frenkel defects in foils of, effects of spontaneous recombination processes on 4.5°K electron, 25:36273
slip in crystals of, asymmetry of, 25:35381
sorptive properties for oxygen at 77 and 298°K, 25:35335(T) (ORNL-tr-2479)
sorptive properties of {110} crystal of, for alkali metals, contact potential measurements of, 25:35359
stresses in, models for interstitial hardening and Peierls, 25:35371
thermal capacity at 1900 to 3200°K, pulsed measurements of, 25:35477
thermal emittance at 1900 to 3000°K, pulsed measurements of spectral and hemispherical total, 25:35477
welding of, problems in, 25:35356

XUM

yield stress in monocrystalline, effects of strain rate and temperature on, 25:35375
TANTALUM ALLOYS AND SYSTEMS
Al--C--Co--Cr--Mo--Nb--Ni-base--Ta--Ti--Zr, properties of corrosion-resistant IN-738 superalloy, 25:35400
Al--Ta, preparation of thin films of, sputtering method for, 25:35303
C--Co-base--Cr--Fe--Ni--Ta--Ti--W, fracture toughness of Mar-M-509, effects of carbide inclusions on, 25:35490
Cr--Ni-base--Ta, plastic deformation of precipitation hardened, 25:35483
Cr--Ni-base--Ta, precipitation in, mechanism of, 25:35483
Hf--Ta-base, hardening in solid solutions of, parameters controlling, 25:35384
Mo--Ta, slip in crystals of, asymmetry of, 25:35381
Mo--Ta-base, hardening in solid solutions of, parameters controlling, 25:35384
N--Ta, stresses in, models for interstitial hardening and Peierls, 25:35371
N--Ta-base, degassing of dilute, by annealing, concentration changes and metal losses during, 25:35560
Nb--Ta, superconducting properties of, effects of heat treatment on, 25:36054
Nb--Ta-base, hardening in solid solutions of, parameters controlling, 25:35384
Ni-base--Ta, strengthening by precipitation of body-centered tetragonal phase in, 25:35302
O--Ta-base, degassing of dilute, by annealing, concentration changes and metal losses during, 25:35560
Re--Ta, slip in crystals of, asymmetry of, 25:35381
Re--Ta-base, hardening in solid solutions of, parameters controlling, 25:35384
Ru--Ta-base, hardening in solid solutions of, parameters controlling, 25:35384
Ta--$TaSi_2$, tantalum trisilicide growth in, at 1150 to 1370°C, kinetics of, 25:35577
Ta-base--W, hardening in solid solutions of, parameters controlling, 25:35384
TANTALUM BROMIDES
reactions with sodium N,N-diethyldithiocarbamate, 25:34568
TANTALUM CARBIDES
work function of, effects of cesium on, 25:36335
TANTALUM CHLORIDES
reactions with sodium N,N-diethyldithiocarbamate, 25:34568
TANTALUM FLUORIDES
vapor pressure--temperature data for, 25:34602 (GAT-649)
TANTALUM ISOTOPES Ta-173
beta and electron-capture decay of, branching ratios, log-ft values, and gamma spectra from, (E), 25:36727 (JINR-P6-5704)
TANTALUM ISOTOPES Ta-181
neutron capture at 1 to 1000 keV, cross sections for, (E), 25:36729(R) (N-70-41999)
proton reactions ($p,3n$) and ($p,4n$) at 20 to 45 MeV, precompound and statistical contributions to excitation functions for, (E/T), 25:36797
proton reactions (p,np) at 25 to 45 MeV, proton spectra and differential cross sections for, (E), 25:36738(R) (UCLA-10-P-18-23)
proton reactions at 24 GeV, Monte Carlo analysis of cesium, potassium, and rubidium production cross sections from, (E), 25:36730 (NP-18829)
TANTALUM ISOTOPES Ta-182
gamma-ray constant of, calculation and tabulation of specific, 25:34815
TANTALUM ORES
analysis of products of processing of, for sum of niobium and tantalum, gravimetric, 25:34510
TANTALUM OXIDES
MnO--PbO--$PbTiO_3$--$PbZrO_3$--Sb_2O_3--Ta_2O_5, properties of piezoelectric ceramic of, for use as filter and transducer elements of mechanical filters, 25:35561(P)
TANTALUM SILICIDES
growth of Ta_5Si_3 in niobium--, tantalum--, titanium--, and zirconium--tantalum disilicide systems at 1150 to 1370°C, kinetics of, 25:35577
Nb--$TaSi_2$, tantalum trisilicide growth in, at 1150 to 1370°C, kinetics of, 25:35577
Ta--$TaSi_2$, tantalum trisilicide growth in, at 1150 to 1370°C, kinetics of, 25:35577
$TaSi_2$--Ti, tantalum trisilicide growth in, at 1150 to 1370°C, kinetics of, 25:35577
$TaSi_2$--Zr, tantalum trisilicide growth in, at 1150 to 1370°C, kinetics of, 25:35577
TD-NICKEL
strength of particle-matrix interface in, 25:35458
TD-NICKEL CHROMIUM
mechanical properties of dispersion-strengthened, at high temperatures, 25:35392
TECHNETIUM
release to atmosphere in reprocessing aluminum-clad fuel elements, 25:34693 (ORNL-4574)
uses of fission product, evaluation of potential, 25:34803(R) (BNWL-1308-5)
TECHNETIUM ISOTOPES Tc-99
effectiveness of albumin macroaggregate-incorporated, for lung scintigraphy, 25:35180
effectiveness of metastable, for scanning human thyroid in comparison to iodine-131, 25:35169
energy levels from molybdenum-99 decay, (E), 25:36772
neutron capture at 1 keV to 3 MeV, excitation functions for, (T), 25:36720 (CONF-710301-4)
neutron capture by, spectrum-averaged cross sections for pile, (E/T), 25:36720 (CONF-710301-4)
production of metastable, design and performance of generator for, 25:34802 (BNL-50249)
use of DTPA- and human serum albumin-incorporated metastable, for cisternographic diagnosis of human hydrocephalus, 25:35172
use of metastable, for human brain scanning, relation of uptake ratio to type of lesion during, 25:35174
use of metastable, for human brain scanning, value of atropine pretreatment for vertex view during, 25:35175
use of metastable, for human cerebral angiography, 25:35173
use of metastable, for labeling erythrocytes for measuring coronary blood flow, 25:35085
TECHNETIUM ISOTOPES Tc-110
nuclear properties of, Nuclear Data Sheets for, (E), 25:36808
TECHNETIUM OXIDES
spectra of gaseous, liquid, and solid Tc_2C_7, Raman, 25:34608
TELLURATES
tellurium-129 beta decay in, chemical state of iodine-129 from, 25:34674
TELLURIUM
effects on colorimetric determination of gold, 25:34521
energy bands in simple cubic, APW calculation of, 25:37175 (CALT-822-29)
separation of ions of, from metal ions by high-voltage electrophoresis using carboxylic and hydroxycarboxylic acids, 25:34702
TELLURIUM FLUORIDES
vapor pressure--temperature data for, 25:34602 (GAT-649)
TELLURIUM ISOTOPES Te-110
nuclear properties of, Nuclear Data Sheets for, (E), 25:36808
TELLURIUM ISOTOPES Te-129
beta decay in tellurium oxides and tellurates, chemical state of iodine-129 from, 25:34674
TELLURIUM ISOTOPES Te-132
availability in peccaries following single injection of nuclear debris from Project Buggy fallout, 25:35088
distribution in tissues of swine following field exposure to nuclear debris at Schooner Event site, fallout, 25:35090
TELLURIUM OXIDES
tellurium-129 beta decay in, chemical state of iodine-129 from, 25:34674
TEMPERATURE
measurements of atmospheric, at Casaccia, Italy during 1968, tabulated data on, 25:34746 (RT/PRCT-(70)42)
TERBIUM
determination as impurity in ytterbium oxide by neutron activation and radiochemical separation, 25:34669 (JAERI-Memo-4279)
TERBIUM ALLOYS AND SYSTEMS
Al--Tb-base, crystal lattice parameters of intermetallic Tb_2Al, 25:35495
Re--Tb, superconducting transition temperature of intermetallic compounds of, 25:36038
TERBIUM FLUORIDES
effects on radiation stability of beryllium fluoride glasses, 25:34621
TERBIUM IONS
energy levels of, spin--spin and spin--other-orbit matrices for, (T), 25:35850
TERBIUM ISOTOPES Tb-148
beta and electron-capture decay of isomeric, half-life and gamma spectra from, (E), 25:36726 (JINR-P6-5681)
TERBIUM ISOTOPES Tb-150
beta and electron-capture decay of isomeric, half-life and gamma spectra from, (E), 25:36726 (JINR-P6-5681)
TERBIUM ISOTOPES Tb-152
beta and electron-capture decay of isomeric, half-life and gamma spectra from, (E), 25:36726 (JINR-P6-5681)
TERBIUM ISOTOPES Tb-159
fluorine-19 fission up to 10.4 MeV/nucleon, excitation function for, (E), 25:36784
TERBIUM ISOTOPES Tb-160
beta decay of, γ--γ directional correlations in, (E), 25:36776
production by neutron irradiation of terbium oxide, radiochemical impurities formed in, 25:34670 (JAERI-Memo-4280)
TERBIUM OXIDES
analysis for impurities by neutron activation and radiochemical separation, 25:34670 (JAERI-Memo-4280)
TEREPHTHALIC ACID, POLYETHYLENE ESTERS
properties of thin membranes of, for on-line alpha activity monitoring of solutions, 25:34673 (CEA-N-1440)
m-TERPHENYL
effects of coatings of, on γ radiolysis products of poly(vinyl chloride), ESR studies on, 25:34656

o-TERPHENYL
effects of coatings of, on γ radiolysis products of poly(vinyl chloride), ESR studies on, 25:34656
p-TERPHENYL
effects of coatings of, on γ radiolysis products of poly(vinyl chloride), ESR studies on, 25:34656
radiation effects on fluorescence of xylene solutions of, effects of chloroform on quenching of γ and uv, 25:34624
TETRACOSANE
radiation thermal cracking of liquid, γ, 25:34653
TETRATHIONATES
polarographic reactions at mercury electrode, effects of thiourea on, 25:34560
THALLIUM
effects on colorimetric determination of gold, 25:34521
effects on gravimetric determination of mercury using 2-aminobenzothiazole, 25:34520
effects on nuclear spin--lattice relaxation in indium, 25:36349
effects on photometric determination of antimony following solvent extraction using TBP, 25:34512
fission of, lower limit on half-life for spontaneous, (E), 25:36779
plasticity of crystalline, effects of superconducting transition on, 25:35383
THALLIUM ALLOYS AND SYSTEMS
In--Tl, magnetic transition at H/sub c2/ in superconducting, (E), 25:36028
THALLIUM CHLORIDES
radioinduced color centers in single-crystal, absorption spectra and bleaching of low-temperature neutron, 25:36290
THALLIUM ISOTOPES Tl-203
energy levels and nuclear properties of, Nuclear Data Sheets for, (E), 25:36809
THALLIUM ISOTOPES Tl-207
energy levels of, two-nucleon random-phase-approximation calculation of spectroscopic factors for, (T), 25:36806
THERMAL DIFFUSION
theory of solid-state, review on, 25:35440
THERMAL INSULATION
design for prestressed concrete pressure vessels for gas cooled reactors, survey of, 25:37006 (ORNL-TM-2929)
fabrication of high temperature, 25:37166(R) (BDX-613-313)
materials for prestressed concrete pressure vessels for gas cooled reactors, survey of properties and performance of, 25:37006 (ORNL-TM-2929)
technology of reactor thermal shielding, 25:36999
THERMAL RADIATION SHIELDING
design and testing for isotope kilowatt program, 25:34810(R) (ORNL-TM-3394)
materials for, testing of zirconium oxide-impregnated silver, 25:35549 (TID-25696)
THERMAL STRESSES
calculation of thermal shock-induced transient, in reactor components, method for, 25:34776(T) (EURFNR-794)
measurement in annular disks at temperatures above 400°C, accuracy of strain gages for, 25:34799
THERMIONIC CONVERTERS
cathode work functions for, effects of patchiness and surface area on, 25:35931
characteristics of radioisotope-fueled, tabulated data on, 25:34811(T) (ORNL-tr-2485)
design of, for spacecraft for unmanned outer planet exploration, 25:35937
performance at low cesium pressures, effect of argon addition on, 25:35930
performance of, under irradiation in reactor, 25:35936
power output of reactor in-core, during steady-state operation, (T), 25:37090
THERMOCOUPLES
standard specification for sheathed Type-K, for nuclear and other high-reliability applications, 25:35051
THERMOELECTRIC CONVERTERS
characteristics of radioisotope-fueled, tabulated data on, 25:34811(T) (ORNL-tr-2485)
design of heat-pipe incorporating test prototype, 25:34810(R) (ORNL-TM-3394)
performance of radioisotope powered, analysis of predicted, 25:34810(R) (ORNL-TM-3394)
testing of heat-pipe incorporating module-type, 25:34810(R) (ORNL-TM-3394)
THERMONUCLEAR REACTIONS
review of controlled nuclear fusion, (E/T), 25:36213
THERMONUCLEAR REACTORS
bibliography on plasma physics and fusion reactors, 25:36081
blankets for, pressure loss calculations for lithium flow in, 25:35938 (UCRL-51010)
confinement lifetime and ion energy spectra in multipole, (E), 25:36085
development of laser-heated, review of, 25:36211
injector for, design of fast hydrogen atom, 25:36186(T) (CTC-746)
injectors for, design for fast hydrogen atoms, 25:35837
ion energy spectra and lifetime in multipole, (E), 25:36085
levitated rings in FM-1, optical sensors for analyzing, 25:36189 (MATT-840)
levitated rings in, stabilization of, 25:36188 (MATT-839)
magnetic field calculations for, axisymmetric helical, (T), 25:36206
operation of, Lawson criteria for, 25:36191 (MATT-844)
plasma instabilities in current-carrying toroidal systems, (T), 25:36181
plasma stability in steady-state, thermal, (T), 25:36178
plasma transport in magnetic quadrupole fields, 25:36086
power supplies for, design of 12-kilowatt servo-controlled amplifiers for, 25:36197 (UCRL-73047)
power supply for, design of 1-MV induction storage system using ignitron switching, 25:36209
review of problems in, 25:36212
THERMOPILES
design and performance for x ray dosimetry at 10 to 100 keV, 25:35031
THERMOSPHERE
constituent concentration and transport during ancmalous absorption in lower, minor, (E/T), 25:35984
particle composition variations during magnetic storms in, ion and neutral, (T), 25:35960
THICKNESS GAGES
design of beam aperture platen for beta radiometric, 25:35041(P)
design of beam aperture platen for beta radiometric, 25:35078(P)
development of beta back-scattering, for special metal coatings, 25:34836
safety mechanism for radiometric, design of fire-, 25:35038(P)
THIOCYANATES
effects on photometric determination of antimony following solvent extraction using TBP, 25:34512
THIOLS
oxidation by cerium ions, ESR studies on free radicals from, 25:34639(R) (USC-113-P-21-3)
THORIUM
abundance in lunar materials, (E), 25:35831
complexes with DTPA, preparation and stability of, 25:34558 (SRARI-P-92)
complexes with phenolphthalexon and thymolphthalexon, preparation and properties of, 25:34532
content in coastal and estuarine waters, effects of tides on, 25:34760
determination using phthalexon S and thymolphthalexon S, spectrophotometric, 25:34532
distribution in granitoid rocks of Central Tajikistan, USSR, 25:34734
effects on fluorescence method for detection of hafnium and zirconium, 25:34519
effects on gravimetric determination of mercury using 2-aminobenzothiazole, 25:34520
effects on photometric determination of antimony following solvent extraction using TBP, 25:34512
radiation effects in, from short-lived α-decaying dopants, damage accumulation at 4.2°K and annealing of, (E), 25:36270 (UCRL-51009)
separation from aqueous chloride solutions by solvent extraction using bis(1-isobutyl-3-methylbutyl) phosphate, 25:34706
separation from other actinides by ion exchange on anionite AV-17, 25:34695(T) (ORNL-tr-2397)
separation from uranium by fractional dissolution, 25:34699
THORIUM ALLOYS AND SYSTEMS
C--Th, phase diagram of, 25:35548 (ORNL-4503(Vol.3))
Mg--Th, stacking faults in, effects of trace additions of zinc on formation of, 25:35484
THORIUM BROMIDES $ThBr_4$
reactions of hydrated, with methyl sulfoxide, properties of products from, 25:34565
THORIUM CARBIDES
properties of, data manual on, 25:35548 (ORNL-4503(Vol.3))
PuC--ThC, properties of, data manual on, 25:35548 (ORNL-4503(Vol.3))
ThC_2--UC_2, irradiation testing of coated particles of, 25:36978(R) (GA-10560)
ThC_2--UC_2, radiation effects on coated particles, fast neutron, 25:37018 (JUL-701-RW)
ThC--UC, properties of, data manual on, 25:35548 (ORNL-4503(Vol.3))
THORIUM CHLORIDES $ThCl_4$
reactions of hydrated, with methyl sulfoxide, properties of products from, 25:34565
THORIUM DEPOSITS
occurrence of US, 1970 survey on, 25:34741
THORIUM FLUORIDES ThF_4
BeF_2--LiF_4--PuF_3--ThF_4, plutonium oxide precipitation in molten, equilibrated with thorium oxide, 25:34566
THORIUM HIGH-TEMPERATURE REACTOR
fuel for, preparation process methods for, 25:35544
THORIUM IODIDES ThI_4
reactions of hydrated, with methyl sulfoxide, properties of products from, 25:34565
THORIUM ISOTOPES Th-232
oxygen-16 reactions with, cross sections and Q values for, (E), 25:36815 (JINR-E2-5797)
photofission at 200 to 900 MeV, excitation functions for,

XUM

(E), 25:36736 (THAI-AEC-35, pp 1-8)
proton reactions at 156 MeV and 24 GeV, Monte Carlo analysis of cesium and rubidium production cross sections from, (E), 25:36730 (NP-18829)
THORIUM NITRATES
reactions of hydrated, with methyl sulfoxide, properties of products from, 25:34565
THORIUM OXALATES
reactions of hydrated, with methyl sulfoxide, properties of products from, 25:34565
THORIUM OXIDES ThO_2
ThO_2--W-base, iodine ionization yields at 1300 to 2000°K on surfaces of, molecular and atomic, 25:35839
ThO_2--Y_2O_3, preparation of transparent bodies of, method for, 25:35543(P)
THORIUM SULFATES
reactions of hydrated, with methyl sulfoxide, properties of products from, 25:34565
THREE MILE ISLAND POWER REACTOR, UNIT 1
control systems for, revised and additional data on, 25:36944 (DOCKET-50289-35)
cooling system for, revised and additional data on, 25:36944 (DOCKET-50289-35)
cost analysis for, estimated 1973 to 1977 operating, 25:36882 (DOCKET-50289-36)
engineered safeguards for, revised and additional data on, 25:36944 (DOCKET-50289-35)
instrumentation for, revised and additional data on, 25:36944 (DOCKET-50289-35)
technical specifications for, 25:36944 (DOCKET-50289-35)
testing programs for, revised and additional data on, 25:36944 (DOCKET-50289-35)
THULIUM
determination as impurity in ytterbium oxide by neutron activation and radiochemical separation, 25:34669 (JAERI-Memo-4279)
determination in aqueous acetone solutions of dibenzoylmethane complexes, absorption spectrophotometric, 25:34527
THULIUM IONS
energy levels of, spin--spin and spin--other-orbit matrices for, (T), 25:35850
THULIUM ISOTOPES Tm-169
boron-11 fission up to 10.4 MeV/nucleon, excitation function for, (E), 25:36784
hyperfine interactions in silver--ytterbium alloy from ytterbium-169 decay, 25:36332
neutron capture by, spectrum-averaged cross sections for pile, (E/T), 25:36720 (CONF-710301-4)
proton reactions (p,3n) and (p,4n) at 20 to 45 MeV, precompound and statistical contributions to excitation functions for, (E/T), 25:36797
THULIUM OXIDES
growth of single-crystal solid solutions with another rare earth oxide by Verneuil method, formation regions in, 25:35525
THYMIDINE
radiolysis of frozen aqueous solutions of, ESR spectral studies on free radicals produced by γ, 25:34654
THYROID GLAND
ablation in mice using iodine-131 combined with surgery, 25:35084
iodine-131 content in cattle and sheep, in Portugal following Chinese nuclear weapon tests, 25:35133
iodine-131 uptake by human, effects of stable iodine content on, 25:35097
radiation effects from uranium nitrate on morphofunctional state of rabbit, 25:35229
radiation effects on hormone production by, 25:35208
radiotherapy of carcinomas of human, effectiveness of radioisotopes in combination with surgery for, 25:35190
scanning of human, for diagnosis of disorders of, comparison of iodine-131 and technetium-99m for, 25:35169
TIMING CIRCUITS
design of constant fraction adapter for zero-crossover discriminator, 25:35064
TIN
crystallization of supercooled drops of, homogeneous nucleation in, 25:36316
effects on colorimetric determination of gold, 25:34521
effects on fluorescence method for detection of hafnium and zirconium, 25:34519
effects on gravimetric determination of mercury using 2-aminobenzothiazole, 25:34520
effects on nuclear spin--lattice relaxation in indium, 25:36349
effects on photometric determination of antimony following solvent extraction using TBP, 25:34512
plasticity of crystalline, effects of superconducting transition on, 25:35383
separation of ions of, from metal ions by high-voltage electrophoresis using carboxylic and hydroxycarboxylic acids, 25:34702
TIN ALLOYS AND SYSTEMS
Al--Sn--Ti-base, properties of forgings of, standard for, 25:35422
Al--Sn--Ti-base--V--Zr, microstructure of high-strength martensitic beta-phase, 25:35488
Au--Sn, mixing at 1100°C, adiabatic calorimetric measurement of heat of, 25:35432
Cd--P--Sn, phase diagram of CdP_2--Sn system in, 25:35580
Cd--P--Sn, properties of copper- and silver-doped crystals of, electric and optical, 25:35580
Cd--Sn-base, plasticity in eutectoid alloy of, effects of grain size on super-, 25:35405
Cu--Sn, mixing at 1100°C, adiabatic calorimetric measurement of heat of, 25:35433
Fe--Mo--Sn--Ti-base--Zr, crystal structure and properties of thermomechanically-processed beta-phase, 25:35398
Fe--Nb--Ni--Sn--Zr-base, properties of dilute, for use in organic cooling circuits, 25:35329(P)
Mo--Sn--Ti-base, tensile properties of metastable beta, at 25 to 600°C, effects of strain rate and annealing temperature on anomalies in, 25:35434
Mo--Sn--Ti-base--Zr, tensile properties of metastable beta, at 25 to 600°C, effects of strain rate and annealing temperature on anomalies in, 25:35434
Nb--Sn, effects of alloying on superconducting transition temperature of intermetallic Nb_3Sn, 25:36040
Nb--Sn, effects of impurities and divergences from stoichiometry of properties of superconducting intermetallic Nb_3Sn, 25:36039
Nb--Sn, magnetization of, superconducting intermetallic Nb_3Sn, 25:36046
Nb--Sn, metallurgy of superconducting intermetallic Nb_3Sn, 25:36018 (CONF-700341-7)
Nb--Sn, phase composition, structure, and magnetic hysteresis of, (E), 25:36047
Nb--Sn, photoluminescence of superconducting intermetallic Nb_3Sn, 25:36062
Nb--Sn, properties of intermetallic compounds of, obtained by diffusion, (E), 25:36045
TIN ISOTOPES Sn-110
energy levels and nuclear properties of, Nuclear Data Sheets for, (E), 25:36808
TIN ISOTOPES Sn-113
determination of abundance of, relative to indium-113m in generator eluates, 25:34672
TISSUE CULTURES
radiation effects on virus replication in, x, 25:35261
TISSUES
perfusion blood flow studies, use of rubidium-81 ratio to metastable krypton-81 for, 25:35167
TITANIUM
effects of additions of, on tensile properties of Hastelloy N, 25:35391
effects on carbon diffusion from ferritic steel, 25:35407
effects on photometric determination of antimony following solvent extraction using TBP, 25:34512
effects on polarographic reduction of niobium, 25:34526
magnetic susceptibility of single crystals of, 25:36240
meson (π) reactions with, x-ray yields and level broadening from, (E), 25:35854
oxidation of, effects of electrolytes and pre-treatment on initial growth of anodic oxide films in, 25:35284
properties of forgings of, standard for, 25:35422
properties of sponge of, standard for, 25:35414
reactions with titanium dibromide at 900 to 1700°C in vacuum, 25:35565
specification for strips, sheets, and plates of, 25:35362
stability of powders of, in acids, 25:35522
testing of seamless and welded tubes of, for condensers and heat exchangers, 25:35421
thermal capacity at low temperature of single crystals of, 25:36340
thermodynamic properties of solution of, in liquid tin, 25:35368
x-ray emission induced by electrons, intense K-, 25:35842
TITANIUM ALLOYS AND SYSTEMS
specification for strips, sheets, and plates of, 25:35362
Al_2O_3--Ti, properties for use as armor plate, 25:35554
Al--C--Co--Cr--Mo--Nb--Ni-base--Ta--Ti--Zr, properties of corrosion-resistant IN-738 superalloy, 25:35400
Al--Cr--Fe--Ni-base--Ti, tensile properties at 25 to 850°C, effects of grain size, precipitates, and test time on, 25:35340 (UARAEE-55)
Al--Cr--Mo--Ni-base--Ti, solvus temperature of γ' in, effects of hardener content on, 25:35460
Al--Cr--Ni-base--Ti, solvus temperature of γ' in, effects of hardener content on, 25:35460
Al--Cr--Ni-base--Ti--W, phase precipitation in, relations of heat treatments with microstructure of, 25:35502
Al--Cr--Ti-base--V, tensile properties of metastable beta, at 25 to 600°C, effects of strain rate and annealing temperature on anomalies in, 25:35434
Al--Cu--Fe--Ti-base--V, fracture toughness of α--β, relations with microstructure, 25:35348
Al--Mo--Ti-base--V, crack propagation in, effects of stress intensity amplitude and frequency and air, methanol, sodium chloride solution, and distilled water on corrosion fatigue, 25:35279
Al--Mo--Ti-base--V--Zr, tensile properties of metastable beta, at 25 to 600°C, effects of strain rate and annealing temperature on anomalies in, 25:35434
Al--Mo--Ti-base--Zr, tensile properties of metastable beta, at 25 to 600°C, effects of strain rate and annealing temperature on anomalies in, 25:35434

Al--Nb--Ti, heat resistance of titanium-coated, 25:35325
Al--Sn--Ti-base, properties of forgings of, standard for, 25:35422
Al--Sn--Ti-base-V--Zr, microstructure of high-strength martensitic beta-phase, 25:35488
Al--Ti, composition of sputtered films of, spectrophotometric determination of, 25:35303
Al--Ti-base--V, corrosion by hydrochloric acid--isopropanol incorporating sodium chloride catalyst, rates of, 25:35287
Al--Ti-base--V, corrosion by hydrochloric acid--methanol solutions, rates of, 25:35287
Al--Ti-base--V, fatigue strength of, relations of α grain size with crack initiation, 25:35349
Al--Ti-base--V, properties of forgings of, standard for, 25:35422
C--Co-base--Cr--Fe--Ni--Ta--Ti--W, fracture toughness of Mar-M-509, effects of carbide inclusions on, 25:35490
Cu--Ti, formation of intermetallic compounds of, during explosion welding, effects of niobium on, 25:35324
Fe--Mo--Sn--Ti-base--Zr, crystal structure and properties of thermomechanically-processed beta-phase, 25:35398
Mo--Pd--Ti-base, tensile properties of metastable beta, at 25 to 800°C, effects of strain rate and annealing temperature on anomalies in, 25:35434
Mo--Sn--Ti-base, tensile properties of metastable beta, at 25 to 600°C, effects of strain rate and annealing temperature on anomalies in, 25:35434
Mo--Sn--Ti-base--Zr, tensile properties of metastable beta, at 25 to 600°C, effects of strain rate and annealing temperature on anomalies in, 25:35434
Mo--Ti-base--Zr, tensile properties of metastable beta, at 25 to 800°C, effects of strain rate and annealing temperature on anomalies in, 25:35434
Nb--Ti, electric conductivity at high pressures, 25:36321
Nb--Ti, metallurgy of superconducting, 25:36018 (CONF-700341-7)
Nb--Ti, microstructure of, effects of oxidation at 600 to 1300°C on, 25:35482
Nb--Ti, properties of superconducting foils in external magnetic field, (E), 25:36052
Nb--Ti--Zr, phase transformations in superconducting, 25:36051
Nb--Ti-base, critical characteristics of superconducting, in wide range of magnetic fields, 25:36048
Nb--Ti-base, structure and superconducting properties of, effect of heat treatment on, 25:36049
Nb-base--Ti, internal friction peaks in, effects of oxygen on, 25:35410
Nb-base--Ti, oxidation at 600 to 1300°C, kinetics of, 25:35282
Nb-base--Ti, preparation of, thermodiffusion method for, 25:35325
Nb-base--Ti--Zr, critical current of superconducting, in fields up to 80 kOe, 25:36050
Pd--Ti, stability of gaseous intermetallic, 25:35350
Pt--Ti, stability of gaseous intermetallic, 25:35350
Rh--Ti, stability of gaseous intermetallic, 25:35350
Ru--Ti, stability of gaseous intermetallic, 25:35350
$TaSi_2$--Ti, tantalum trisilicide growth in, at 1150 to 1370°C, kinetics of, 25:35577
Ti--V, corrosion by liquid sodium, 25:37016 (CONF-700211-9)
Ti--V, deformation of bcc monocrystals of, modes and shear stresses in, 25:35377
Ti--V-base, stress rupture strength of 650 to 850°C, effects of titanium oxide formation on, 25:35388

TITANIUM BORIDES
reactions with titanium, vanadium, and zirconium at 900 to 1700°C in vacuum, 25:35565

TITANIUM CARBIDES
crystallization of powdered and hot-pressed, secondary, 25:35535
incorporation in refractory alloy composites by in-situ fiber growth, 25:35557
Mo_2C--Ni--TiC, mechanical properties of solid solution of, effects of carbon and molybdenum carbide content on, 25:35559
TiC--VC, tensile properties of monocrystalline, 25:35558
TiC--VC, uses of monocrystalline, 25:35558
TiC--WC, formation of solid solution of, mechanism of, 25:35537
TiC--WC, preparation of powders of, mechanism for, 25:35531

TITANIUM FLUORIDES
vapor pressure--temperature data for, 25:34602 (GAT-649)

TITANIUM ISOTOPES Ti-46
electron inelastic scattering at 198 to 300 MeV, differential cross sections for, (E), 25:36695

TITANIUM ISOTOPES Ti-48
electron inelastic scattering at 198 to 300 MeV, differential cross sections for, (E), 25:36695
oxygen-16 reactions (C-16,C-14) at 48 MeV, cross sections for, (E), 25:36709

TITANIUM ISOTOPES Ti-49
energy levels from vanadium-51 (d,α) reactions, spin--parity assignments for, (E), 25:36687 (LYCEN-7087)

TITANIUM ISOTOPES Ti-50
electron inelastic scattering at 198 to 300 MeV, differential cross sections for, (E), 25:36695
helium-3 reactions (He-3,d) at 10 MeV, DWBA analysis of angular distributions from, (E), 25:36716
oxygen-16 reactions (O-16,C-12) at 48 MeV, energy spectra from, (E), 25:36709
oxygen-16 reactions (O-16,C-14) at 48 MeV, differential cross sections and spectra from, (E), 25:36709
oxygen-16 reactions (O-16,N-15) at 48 MeV, energy spectra from, (E), 25:36709

TITANIUM NITRIDES
chemical stability in water, alkali solutions, and acids, 25:35522
reaction kinetics in acids, decomposition, 25:35522

TITANIUM OXIDES
reactions with zirconium and lanthanum oxides at high temperatures, electric conductivity detection of solid-phase, 25:36320
MgO--TiO_2--V_2O_5, phase studies of, 25:35576

TOBACCO (the commodity)
analysis for polonium-210, 25:34515

TOKAMAK DEVICES
ion temperature in Tokamak-5, spatial distribution of, (E), 25:36097
plasma instabilities in current-carrying toroidal systems, (T), 25:36181
plasma thermal conductivity in, electron, (T), 25:36141

TOKAMAK MODEL ST
power supplies for, vacuum tube compensated flat top high-current pulse, 25:36187 (MATT-837)

TOLUENE
radiation stability of, for use as diluent in fuel reprocessing, 25:34638 (RT/CHI-(70)36)

TOLUIDINE BLUE
solvent properties for benzoic acid--uranium complex in photometric determination of uranium, 25:34534

TONGUE
radiation effects on ascorbic acid content in animal, x, 25:35219

TOXICITY
classification for radioisotope, in nuclear industry, 25:35154

TOXINS
radioinduced reactions of, in cells, mechanism of, 25:35200

TRACER TECHNIQUES
development of radioactive, for studying sediment dynamics, review of French, 25:34812(T) (ORNL-tr-2492)
development of radioactive, for well logging in hydrology, 25:34725 (STI/DOC-10/126)
method for measuring stratospheric--tropospheric air mass exchange using stratospheric beryllium-7 and phosphorus-32, 25:34745(R) (NYO-4061-2)
method for studying solidification of cast steel using phosphorus-32, 25:34820
method for studying source of oxygen in anodic oxidation of silicon and tantalum using oxygen-18, 25:35293

TRANSACTINIDE ELEMENTS
electron behavior in fields associated with Z = 114 to 164, (T), 25:36365
existence of superheavy, (T), 25:35592
identification of atomic numbers of, x-ray method for unequivocal, 25:36778
properties of hypothetical, fission, (T), 25:36827
search for spontaneously fissioning, in terrestrial matter, (E), 25:36779

TRANSDUCERS
performance for measurements in bubble chambers, effects of high magnetic fields and low temperatures on, 25:34987 (CONF-700623-(Vol.2), pp 863-72)

TRANSISTORS
h-parameters of, development of theory, conversion factors, and operating procedures for determining, 25:37169 (BDX-613-347)

TRANSITION METAL CARBIDES
C--transition metal carbides, preparation of high-temperature composites of, methods for, 25:35530

TRANSITION METAL OXIDES
transition metal oxides--ZrO_2, formation and properties of solid solutions of, regularity in, 25:35545

TRANSITION METALS
crystal structure of body-centered cubic, review of, 25:35492

TRANSITION RADIATION
emission from nonrelativistic charged particles, effect of optical parameters of media on, 25:36354 (JINR-P4-5734)

TRANSPLANTS
radiation effects on growth and transformation of rat epithelium, x, 25:35231
radiation effects on tolerance of mouse skin, x, 25:35113
research progress on tissue and organ, 25:37197(R) (NYO-2265-16)

TRANSPORT THEORY
equations for free-electron atmosphere, 25:36267

TRANSURANIUM ELEMENTS
fission of isomers of, spontaneous, (T), 25:36781
removal from man, methods for, 25:35134

TRAPS
testing of sodium cold, under FFTF conditions, 25:35276(R) (GEAP-13539-16)

TRIAZINE, DIHYDRO-
4,4'-methylenebis[3-hydroxy-2-naphthoate], radiation

XUM

resistance of, γ, 25:34660
TRIPHENYLAMINE
effects of coatings of, on γ radiolysis products of poly(vinyl chloride), ESR studies on, 25:34656
TRIPHENYLENE
effects of coatings of, on γ radiolysis products of poly(vinyl chloride), ESR studies on, 25:34656
TRITIUM
beta decay of molecular, reactions with gaseous hydrocarbons of helium tritide ions from, 25:34675
beta decay of molecular, reactions with gaseous hydrocarbons of helium tritide ions from, 25:34676
beta decay of, reactions of ethane and methane with helium tritide ions from, 25:34677
binding energy of, effects of tensor forces in calculation with rank-four separable potential of, (T), 25:36659 (INR-F-1234)
binding energy of, potentials with hard-core repulsion for, (T), 25:36536
content in atmospheric precipitation in Vienna during 1962 to 1969, 25:34726 (THAI-AEC-35, pp 9-20)
content in ground waters in Totes Gebirges area in Austria, 25:34726 (THAI-AEC-35, pp 9-20)
content in hot springs in Beppu City, Japan, 25:34732
content in surface waters and precipitation during reentry drilling at Project Rulison site, 25:34728 (USGS-474-101)
electrodisentegration of, effects of exchange currents on polarization of nucleons emitted in, (T), 25:36664
monitoring in environmental waters of Amchitka Island, Alaska, 25:34720 (NVO-1229-121)
monitoring in sanitary waste system effluent from West Valley Processing Plant, 25:34683 (DOCKET-50201-73)
neutron reactions (n,d) at 14.4 MeV, angular distributions for, (E), 25:36738(R) (UCLA-10-P-18-23)
production rates in stone meteorites from galactic cosmic-ray interactions, (E/T), 25:35599
proton reactions (p,pd) and (p,2p) at 35 MeV, kinematic analysis of, (E), 25:36738(R) (UCLA-10-P-18-23)
radiation effects on incorporation of, in mouse kidney and liver tubulus cells, whole-body x, 25:35238
release into Molse Nethe River, estimation of monthly, 25:34719 (NP-18737)
targets of gaseous, for production of monoenergetic neutrons, 25:36633
use of environmental, for studying ground water flow in Totes Gebirges area in Austria, 25:34726 (THAI-AEC-35, pp 9-20)
TRITONS
reactions (t,He-3) with deuterium at 22 MeV, helium-3 spectra at 5° from, (E), 25:36662
TROPOSPHERE
air mass exchange between stratosphere and, radioactive tracer method for measuring, 25:34745(R) (NYO-4061-2)
circulation in upper air of, relation with solar flares, (E/T), 25:35973
TRYPTOPHAN
radiolysis of alkaline solutions of, at 77°K, ESR studies on production of free radicals by trapped electrons produced by photoionization and x, 25:34647
TUBES
heat transfer and hydraulic resistance in rough and smooth, with turbulent flow, generalized method for calculating, 25:34795
welding of pressure, tungsten inert gas equipment for remote, 25:34787
TUNGSTEN
bremsstrahlung emission from thick targets of, in energy range 12 to 300 kV, (E), 25:36249 (LA-4624)
carburization to prepare tungsten carbides, relations with microstructure, 25:35536
determination in complex carbides by electron beam micro methods, 25:34523
determination in molybdenum--tungsten alloys, spectrographic, 25:34516
effects of combination of oxygen and, on internal friction of zirconium alloy, 25:35404
effects on colorimetric determination of gold, 25:34521
effects on polarographic reduction of niobium, 25:34526
electric conductivity at low temperatures of high-purity single crystals of, temperature dependence of, 25:36331
electron reactions at 550 and 1300 MeV with natural, fission-fragment cross sections and energies from, (E), 25:36791
iodine ionization yields at 1300 to 2000°K on surfaces of, molecular and atomic, 25:35839
oxidation of hydrogen-annealed, thermodynamics of, 25:35291
radioinduced defect structure of depleted zones in high-purity, at 18°K, 20-keV W+-ion, 25:36268 (NYO-3504-50)
sintering of, effects of nickel--phosphorus alloy additions on, 25:35354
solvent properties for nitrogen at 2400 to 3050°C and 15 to 400 torr nitrogen, equilibrium, 25:35429
sorptive properties of (100) crystal of, for alkali metals, contact potential measurements of, 25:35359
sorptive properties of (110) surface of, for carbon monoxide, 25:35357
specific heat of impure, electronic, 25:36312
thermal capacity of, ac temperature method for measuring high-temperature, 25:35341 (UCRL-50962)
thermal conductivity at low temperatures of high-purity single crystals of, temperature dependence of, 25:36331
x-ray emission by exploding wires of, effects of wire parameters on, 25:36326
yield stress in monocrystalline, effects of strain rate and temperature on, 25:35375
TUNGSTEN ALLOYS AND SYSTEMS
Al--Cr--Ni-base--Ti--W, phase precipitation in, relations of heat treatments with microstructure of, 25:35502
Al--Cr--Ni-base--W, reactions of cladding of, for chromium--tungsten alloy with air and nitrogen at 2100 and 2300°F, resistance to oxidation, 25:35288
C--Co-base--Cr--Fe--Ni--Ta--Ti--W, fracture toughness of Mar-M-509, effects of carbide inclusions on, 25:35490
Co--Cr--W, phase studies of cobalt-rich, at 1350°C, 25:35489
Co--Cr--W, phase studies of, at 1350°C, 25:35498
Cr-base--W, reactions of aluminum--chromium--nickel--tungsten alloy-clad, with air and nitrogen at 2100 and 2300°F, protection from oxidation, 25:35288
Cu--W, tensile properties of laminar systems of, at 20 to 600°C, effects of composition on, 25:35454
Mn--W-base, crystallization at 1800 to 2000°C, 25:35476(P)
Mn--W-base, mechanical properties at 1800 to 2000°C, 25:35476(P)
Mo--W, analysis for tungsten, spectrographic, 25:34516
Pb--W, mechanical properties of tungsten wire-reinforced uniaxially aligned composites of, effects of matrix variations on, 25:35344 (Y-1788)
Pt-base--W, iodine ionization yields at 1300 to 2000°K on surfaces of, molecular and atomic, 25:35839
Ta-base--W, hardening in solid solutions of, parameters controlling, 25:35384
ThO_2--W-base, iodine ionization yields at 1300 to 2000°K on surfaces of, molecular and atomic, 25:35839
TUNGSTEN CARBIDES
preparation by carburization of tungsten powder at 1000 to 1900°C, relations with microstructure, 25:35536
sintering of powdered, effects of cobalt, iron, or nickel binders on, 25:35534
TiC--WC, formation of solid solution of, mechanism of, 25:35537
TiC--WC, preparation of powders of, mechanism for, 25:35531
TUNGSTEN FLUORIDES
vapor pressure--temperature data for, 25:34602 (CAT-649)
TUNGSTEN IONS
effects on defect structure of high-purity tungsten at 18°K, 20-keV W+, 25:36268 (NYO-3504-50)
TUNGSTEN ISOTOPES W-182
carbon-12 fission up to 10.4 MeV/nucleon, excitation function for, (E), 25:36784
TUNGSTEN ISOTOPES W-186
neutron scattering by, n + e interactions from, (E/T), 25:36380 (JINR-E3-5713)
TUNGSTEN ISOTOPES W-187
availability in peccaries following single injection of nuclear debris from Project Buggy fallout, 25:35088
TUNGSTEN ISOTOPES W-188
distribution in tissues of swine following field exposure to nuclear debris at Schooner Event site, fallout, 25:35090
excretion in feces and urine of peccaries following single ingestion of nuclear debris from Schooner Event, quantitative comparison of fallout, 25:35089
TUNGSTEN OXIDES
Er_2O_3--WO_3, properties of $3Er_2O_3.WO_3$, to 1500°C, electric and thermal, 25:35529
WO_3--Y_2O_3, properties of $3Y_2O_3.WO_3$, to 1500°C, electric and thermal, 25:35529
TUNGSTEN OXYFLUORIDES
vapor pressure--temperature data for, 25:34602 (CAT-649)
TURBINE BLADES
fabrication of controlled-microstructure metallic, by directional solidification, 25:35301
TURBINES
design parameters of carbon dioxide gas, 25:37053(P)
TURKEY POINT POWER REACTOR, UNIT 3
design parameters of, revised and additional data on, 25:36925 (DOCKET-50250-44)
design parameters, revised and additional data on, 25:36926 (DOCKET-50250-46)
instrumentation for, additional information on core, 25:36927 (DOCKET-50250-47)
operations aspects of, revised and additional data on, 25:36926 (DOCKET-50250-46)
operations aspects of, revised and additional data on, 25:36925 (DOCKET-50250-44)
site for, meteorological data on, 25:36927 (DOCKET-50250-47)
TURKEY POINT POWER REACTOR, UNIT 4
design parameters of, revised and additional data on, 25:36925 (DOCKET-50250-44)
design parameters, revised and additional data on, 25:36926 (DOCKET-50250-46)
instrumentation for, additional information on core, 25:36927 (DOCKET-50250-47)
operations aspects of, revised and additional data on, 25:36926 (DOCKET-50250-46)

operations aspects of, revised and additional data on, 25:36925 (DOCKET-50250-44)
site for, meteorological data on, 25:36927 (DOCKET-50250-47)
TYROSINE
radiolysis of alkaline solutions of, at 77°K, ESR studies on production of free radicals by trapped electrons produced by photoionization and x, 25:34647
TYROSINE, 3,5-DIIODO-
effects on γ-radioinduced inactivation of Bacillus cereus spores, potentiating, 25:35264

U

UDIMET 500
crystal defect formation and twinning during high-temperature deformation of, mechanisms of, 25:35491
UDIMET 700
microstructure at 1950 to above 2070°F, relations with workability, 25:35500
ULTRASONIC TESTING
development of critical angle, for detection of shifts in nil ductility transition temperature, 25:34833
equipment and methods for, historical development and current status of, 25:34835
equipment and methods for, of reactor materials at ORNL, development of, 25:34829
method for fiber-reinforced composites, 25:34838
ULTRAVIOLET ASTRONOMY
developments in, (T), 25:35659
ULTRAVIOLET RADIATION
effects on chromosomes in pollen tubes of Tradescantia, effects of infrared radiation on aberrant, 25:35120
effects on fluorescence of organic solutions, effects of chloroform on quenching of, 25:34624
effects on free radicals in cell proteins, 25:35203
effects on hexokinase activity in animal skin, protective effects of corticosteroids against, 25:35234
effects on inactivation of bacteria mutants, mechanisms of DNA dark repair in, 25:35270
effects on inactivation of NADH, mechanism of, 25:35107
effects on influenza virus plaque formation on FL cells, genetic marker for inactivating, 25:35266
effects on mitosis in bacteria, effects of vacuum treatment on inactivating, 25:35265
effects on molecular weight of DNA synthesized in L cells containing pyrimidine, 25:35207
effects on Saccharomyces vini, effects of iodoacetic acid and ethanol on recovery following, 25:35251
effects on T antigen formation by SV40 and adenoviruses, inactivating, 25:35267
effects on transferred F' factor in bacteria DNA, damaging, 25:35271
ULTRAVIOLET SOURCES
standards for use in production and processing of foods, 25:34814
UNITED KINGDOM
regulations for shipping of radioactive materials by road, 25:34859
UNIVERSE
age of, effects of variable speed of light and unit of time on estimation of, 25:35816
cosmic fluid in expanding, nonlinear effect of, (T), 25:35815
creation of antiuniverse in conjunction with, (T), 25:35820
density perturbations in collisionless-particle, (T), 25:35805
matter density in, lower bound to, (T), 25:35811
model of, construction of relativistic, (T), 25:35806
radio emission background of, spectral index for, (E/T), 25:35807
URANIUM
abundance in lunar and terrestrial materials, (E), 25:35830
abundance in lunar materials, (E), 25:35831
activity in plutonium dioxide--uranium dioxide solid solutions, transpiration method for studying, 25:35547(R) (GEAP-12182)
analysis for impurities by neutron activation, 25:34547 (UARAEE-68)
complexes with 1,3-diketones, stability of, 25:34557 (KFK-1339)
complexes with DTPA, preparation and stability of, 25:34558 (SRARI-P-92)
content in Canary Islands lavas, measurement of, 25:34740
content in oceanic sediments of water uprise zones, 25:34761
determination by reactions with methyl green, extraction, and photometry, 25:34509
determination following separation of complex with benzoic acid using Azure A, methylene green, or toluidine blue, photometric, 25:34534
determination in concentrates and ores, gravimetric, 25:34505 (PG-Report-1020)
determination in fuel reprocessing input using lithium-7 tracer and mass spectrometry, 25:34689 (IAEA-R-876-F)
determination in plutonium dioxide--uranium dioxide systems, 25:34503(R) (NBL-256)
determination in spent uranium oxide (UO_2) by sample weighing, 25:37015 (BNWL-1568)
determination in uranium oxides, polarographic, 25:34501(T) (CEA-tr-X-667)
determination of enriched, in urine by solvent extraction and counting, 25:34541
determination of radioactive, in soils, 25:34500
determination using Arsenazo III, spectrophotometric, 25:34524
determination using Phosphorazo III and Chlorophosphonazo III in acid solutions, photometric, 25:34521
distribution in granitoid rocks of Central Tajikistan, USSR, 25:34734
effects on colorimetric determination of gold, 25:34521
effects on gravimetric determination of mercury using 2-aminobenzothiazole, 25:34520
effects on photometric determination of antimony following solvent extraction using TBP, 25:34512
electrochemical behavior of electrodes of, in aqueous solutions, effects of acidity on, 25:34562
electron reactions at 550 and 1300 MeV with natural, fission-fragment cross sections and energies from, (E), 25:36791
enrichment requirements for Swiss power reactors, forecasts to 1990 of, 25:34819
monitoring in sanitary waste system effluent from West Valley Processing Plant, 25:34682 (DOCKET-50201-72)
photofission at 200 to 900 MeV, excitation functions for, (E), 25:36736 (THAI-AEC-35, pp 1-8)
photon reactions (γ,n) from electron bombardment at 18.5 to 23 MeV of natural, energy spectra and nuclear temperatures from, (E), 25:36767
production in western world, problems and prospects of, 25:34758
properties of castings of, from primary and secondary melting stock, standard for, 25:35471
properties of nuclear-grade primary metal stock of depleted, natural, or enriched uranium-235-containing, standard for, 25:35479
properties of primary and secondary melting stock of, standard for, 25:35475
proton fission of, review of, 25:36802
proton reactions at 156 MeV and 24 GeV with natural, Monte Carlo analysis of cesium, potassium, and rubidium production cross sections from, (E), 25:36730 (NP-18829)
requirements for Swiss nuclear power plants, forecasts to 1990 of, 25:34755
separation from aluminum-clad spent aluminum--uranium fuels, molten-salt fluoride-volatility process for, 25:34693 (ORNL-4574)
separation from aqueous chloride solutions by solvent extraction using bis(1-isobutyl-3-methylbutyl) phosphate, 25:34706
separation from aqueous solutions by solvent extraction using diketones, 25:34557 (KFK-1339)
separation from calcium oxide--uranium dioxide--zirconium dioxide fuel by aqueous halide process, 25:34690(R) (IN-1457)
separation from iron, phosphorus, rare earths, silicon, and thorium by fractional dissolution, 25:34695
separation from other actinides by ion exchange on anionite AV-17, 25:34695(T) (ORNL-tr-2297)
separation from plutonium as hexafluoride, 25:34698 (UJV-2291-Ch)
slip and twinning in alpha-phase, effects of dislocation and shear on, 25:35382
thermodynamic properties of liquid, at high temperatures and pressures, equipment and method for measuring, 25:35342 (UCRL-51035)
URANIUM ACETATES
analysis for impurities by neutron activation, 25:34547 (UARAEE-68)
URANIUM ALLOYS AND SYSTEMS
machining of depleted, methods for, 25:35207
Al--U, fabrication of fuel elements of aluminum-clad enriched, picture frame and rolling methods for, 25:35527
Al--U, processing of irradiated, at ICPP, 25:34690(R) (IN-1457)
O--Pu--U, enthalpy of oxygen incorporation in (U,Pu)O/sub 2+x/ in, 25:34606
U--Zr, processing of irradiated, at ICPP, 25:34690(R) (IN-1457)
URANIUM CARBIDES
crystal lattice parameters of UC_2, effects of annealing and carbon content on, 25:35579
radiation effects on coated particles, fast neutron, 25:37018 (JUL-701-RW)
ThC_2--UC_2, irradiation testing of coated particles of, 25:36978(R) (GA-10560)
ThC_2--UC_2, radiation effects on coated particles, fast neutron, 25:37018 (JUL-701-RW)
ThC--UC, properties of, data manual on, 25:35548 (ORNL-4503(Vol.3))
URANIUM CONCENTRATES
analysis for impurities by neutron activation, 25:34547 (UARAEE-68)
analysis for uranium, gravimetric, 25:34505 (PG-Report-1020)
URANIUM DEPOSITS
book: Methods of Prospecting for Uranium Deposits (In

Russian), 25:34754
geochemistry of granitic, in Nord-Limousin, France, 25:34749 (CEA-R-4034)
isotope content of sandstone-type, measurement of carbon, oxygen, and sulfur, 25:34750(R) (COO-2024-1)
mineralization of Central and Armorican Massifs in France, 25:34753
occurrence of US, 1970 survey on, 25:34741
origin and redistribution of sandstone-type, isotopic studies of, 25:34750(R) (COO-2024-1)
prospecting for deposits of, gamma well logging method for, 25:34716(T) (CSIRO-Trans-10088)
prospecting in France, economic aspects of, 25:34751
URANIUM FLUORIDES UF_4
complexes with dimethylammonium fluoride, dimethylanilinium fluoride, di-sec-butylammonium fluoride, or aminoguanidinium fluoride, 25:34611
URANIUM FLUORIDES UF_6
vapor pressure--temperature data for, 25:34602 (GAT-645)
URANIUM FLUORIDES UF_4
production by fluorination of uranium oxides, design of facility and equipment for, 25:34782
vapor pressure--temperature data for, 25:34602 (GAT-645)
URANIUM ISOTOPES
determination in spent uranium oxide (UO_2) by mass spectrometry, 25:37015 (BNWL-1568)
URANIUM ISOTOPES U-233
deuteron reactions (d,pf) at 13 MeV, analysis using double-humped barrier, (E/T), 25:36746
neutron fission of, beta energy release following thermal, (E/T), 25:36764
neutron total cross section and resonance parameters for, fast, (E), 25:36756
URANIUM ISOTOPES U-234
abundance relative to uranium-238 in minerals and natural waters, 25:34738
URANIUM ISOTOPES U-235
abundance relative to uranium-238 in minerals and natural waters, 25:34738
deuteron reactions (d,pf) at 13 MeV, analysis using double-humped barrier, (E/T), 25:36746
neutron capture by, cross section for fast, (E), 25:36756
neutron capture-to-fission ratio at 0.1 to 30 keV, 25:36748
neutron fission at 0.1 to 1.5 MeV, prompt-neutron yields from, (E/T), 25:36786
neutron fission at 12.5 to 350 keV, structure in the cross section for, (E), 25:36739 (UCRL-73090)
neutron fission at 14 MeV, angular anisotropy of fragments from ternary, (E), 25:36759
neutron fission of, beta energy release following thermal, (E/T), 25:36764
neutron fission of, cross section for fast, (E), 25:36756
neutron fission of, production cross sections for cesium and rubidium from thermal, (E), 25:36730 (NP-18825)
neutron fission of, prompt gamma spectra in coincidence with thermal, (E), 25:36743
neutron fission of, ranges in pyrocarbon of fragments from thermal, 25:36264
neutron total cross section and resonance parameters for, fast, (E), 25:36756
nuclear mass of, relative to lead-207, (E), 25:36770
URANIUM ISOTOPES U-238
abundance relative to uranium-234 and -235 in minerals and natural waters, 25:34738
content ratio to lead-204 in Canary Islands lavas, (E), 25:34740
neutron capture at 1 to 1000 keV, cross sections for, (E), 25:36729(R) (N-70-41999)
neutron fission at 14 MeV, angular anisotropy of fragments from ternary, (E), 25:36759
nuclear mass of, relative to lead-206, (E), 25:36770
potential energy surfaces of, Strutinsky-method-calculation in Cassinian-ovaloid parametrization of fission, (T), 25:36793
URANIUM NITRATES
analysis for impurities by neutron activation, 25:34547 (UARAEE-68)
effects on morphofunctional state of rabbit thyroid gland, 25:35229
URANIUM NITRIDES
PuN--UN, crystal lattice parameters of solid solutions of, 25:35574
URANIUM ORES
age and genesis of, in Central and Armorican Massifs in France, 25:34753
analysis for uranium, gravimetric, 25:34505 (PG-Report-1020)
oxidation--reduction properties of, in black shale, 25:34752
structure of, studies of, 25:34756
URANIUM OXIDES
analysis for impurities by neutron activation, 25:34547 (UARAEE-68)
conversion to uranium fluoride, design of facility and equipment for, 25:34782
URANIUM OXIDES UO_2
analysis for uranium, polarographic, 25:34501(T) (CEA-tr-X-667)
analysis of spent, for fission products, plutonium, and uranium, 25:37015 (BNWL-1568)
fabrication of fuels of, by vibration compaction, 25:35524 (RT/ING-(70)22)
inspection of irradiated fuels of, in hot cells, alpha and beta--gamma autoradiographic methods for, 25:34837
pressing of disks of, at 1400 to 1625°C, method for multispecimen hot, 25:35526
properties of nuclear-grade compactible and uranium-235-containing sinterable, standard for chemical and physical, 25:35479
reactions with carbon black or graphite, kinetics of reduction in, 25:34556 (EUR-4635)
tensile properties of sintered, at 25 to 1900°C, effects of strain rate on, 25:35551
vaporization of, research progress on studies of, 25:35547(R) (GEAP-12182)
C--UC_2, fabrication of tubular fuel elements of aluminum-clad enriched, extrusion method for, 25:35527
CaO--UO_2--ZrC_2, separation of uranium from irradiated, aqueous halide process for, 25:34690(R) (IN-1457)
PuO_2--UC_2, analysis for plutonium, plutonium isotopes, and uranium, 25:34503(R) (NEL-256)
PuO_2--UO_2, diffusion of oxygen in solid solutions of, 25:35547(R) (GEAP-12182)
PuO_2--UC_2, inspection of irradiated fuels of, in hot cells, alpha and beta--gamma autoradiographic methods for, 25:34837
PuO_2--UC_2, mechanical properties of, effects of burnup on, 25:37017 (CONF-710414-1)
PuO_2--UC_2, oxygen-to-metal ratio in, statistical method for determining sources of variation in, 25:35568 (ORNL-TM-3362)
PuO_2--UC_2, uranium activity in solid solutions of, transpiration method of studying, 25:35547(R) (GEAP-12182)
PuO_2--UC_2, vaporization of solid solutions of, research progress on studies of, 25:35547(R) (GEAP-12182)
URANIUM OXIDES UO_3
production by fluidized-bed denitration of uranyl nitrate, 25:34690(R) (IN-1457)
URANIUM OXIDES U_3O_8
analysis for impurities, evaluation of various halogenated carriers for, 25:34504 (NP-18865)
analysis for uranium, polarographic, 25:34501(T) (CEA-tr-X-667)
production of, forecasts to 1975 of worldwide capacity for, 25:34757
reactions with graphite, kinetics of reduction in, 25:34556 (EUR-4635)
Al--U_3O_8, fabrication of fuel elements of aluminum-clad enriched, extrusion method for, 25:35527
URANIUM PHOSPHIDES
phosphorus-31 NMR line shifts in, 25:36350
tensile properties of sintered, at 25 to 1900°C, effects of strain rate on, 25:35551
UP--US, phosphorus-31 NMR line shifts in solid solutions of, 25:36350
URANIUM RESERVES
development of western world, forecasts to 1983 on, 25:34758
estimates of worldwide, 25:34757
URANIUM SILICIDES
fabrication of fuel elements of, method for, 25:35540(P)
URANIUM SULFIDES
tensile properties of sintered, at 25 to 1900°C, effects of strain rate on, 25:35551
BaS--US, phase studies on, electron-probe, metallographic, and x-ray-diffraction, 25:34603 (IJS-263)
CaS--US, phase studies on, electron-probe, metallographic, and x-ray-diffraction, 25:34603 (IJS-263)
SrS--US, phase studies on, electron-probe, metallographic, and x-ray-diffraction, 25:34603 (IJS-263)
UP--US, phosphorus-31 NMR line shifts in solid solutions of, 25:36350
URANYL ACETATES
magnetic susceptibility of, 25:34612
spectra of, ir, 25:34612
URANYL CARBONATES
polarographic reactions at mercury electrode, effects of thiourea on, 25:34560
URANYL CITRATES
magnetic susceptibility of, 25:34612
spectra of, ir, 25:34612
URANYL COMPOUNDS
complexes, magnetic susceptibilities and ir spectra of, 25:34612
polarographic behavior at dropping mercury electrode in ethylenedithiodiacetic acid solution, 25:34561
URANYL FORMATES
magnetic susceptibility of, 25:34612
spectra of, ir, 25:34612
URANYL LACTATES
magnetic susceptibility of, 25:34612
spectra of, ir, 25:34612
URANYL MALATES
magnetic susceptibility of, 25:34612
spectra of, ir, 25:34612

URANYL NITRATES
complex formation in aqueous nitric acid solutions of, spectrophotometric studies on, 25:34564
complexes, magnetic susceptibilities and ir spectra of, 25:34612
denitration of, fluidized-bed process for production of uranium trioxide by, 25:34690(R) (IN-1457)
effects on potentiometric determination of free nitric acid, 25:34517
magnetic susceptibility of, 25:34612
preparation of clear and stable solutions of, 25:34659
reactions with Arsenazo III, 25:34524
spectra of, ir, 25:34612
URANYL OXALATES
complexes of, preparation of peroxo, evaluation of conditions for, 25:34570
magnetic susceptibility of, 25:34612
spectra of, ir, 25:34612
URANYL SALICYLATES
magnetic susceptibility of, 25:34612
spectra of, ir, 25:34612
URANYL SUCCINATES
magnetic susceptibility of, 25:34612
spectra of, ir, 25:34612
URANYL SULFATES
reduction of aqueous solutions of, with hydrogen sulfide at 100 to 200°C, 25:34569
URANYL TARTRATES
magnetic susceptibility of, 25:34612
spectra of, ir, 25:34612
UREA, THIO-
effects of adsorption of, on processes at mercury electrode, 25:34560
URETHAN POLYMERS
physical properties of foams of, 25:37165(R) (BDX-613-300)
URETHANS
thermal properties of lactone ester-based rigid foams of, 25:37171 (BDX-613-406)
URIDINE, 2'-DEOXY-5-FLUORO-
effects on repair of x-radioinduced single strand breaks in DNA in mouse L cells, 25:35224
URINE
analysis for enriched uranium by solvent extraction and counting, 25:34541
analysis for potassium-42 using Cherenkov radiation, 25:34540
cesium-137 excretion in, of children in Warsaw, 1965 to 1967 and 1969, 25:35093
UTERUS
radiation dose to human, during phosphorus-32 administration, 25:35144
radiation effects on histology of albino rat, combined effects of estrogens, progesterones, and x, 25:35237
radiotherapy of cervix of human, development of rectal lesions following, 25:35158

V

VACUUM
bibliography on surface and vacuum physics, 25:35835
VACUUM GAGES
performance for measurements in bubble chambers, effects of high magnetic fields and low temperatures on, 25:34987 (CONF-700623-(Vol.2), pp 863-72)
VAK REACTOR
control rod drive shafts in, detection and replacement of cracked, 25:36994 (INIS-mf-33)
VALINE, N-ACETYL-
radioinduced free radical destruction in, effects of temperature on electron, 25:35103
VALVES
design requirements of boiling reactor and heavy water moderated reactor primary cooling systems, 25:37002 (AECL-3858)
performance of boiling reactor and heavy water moderated reactor primary cooling system, 25:37002 (AECL-3858)
standard marking system for, 25:34786
VAN ALLEN RADIATION BELTS
particle trapping in, probe method for origin and distribution of, (E/), 25:35966
proton flux in, relation to neutron flux in high-altitude equatorial atmosphere, (E), 25:35998
proton pitch-angle distribution in, adiabatic theory of energy-dependent equatorial, (E/T), 25:36002
synchrotron emission from electrons trapped in, rf electromagnetic wave-generated, (E/T), 25:36001
VANADIUM
abundance in K giant stars, (E/T), 25:35649
anodization of, relations with ion current density and electrostatic field, 25:35295
determination by proton activation, 25:34554
determination in complex carbides by electron beam micro methods, 25:34523
effects on carbon diffusion from ferritic steel, 25:35407
effects on gravimetric determination of mercury using 2-aminobenzothiazole, 25:34520
effects on polarographic reduction of niobium, 25:34526
electric conductivity in reversible superconducting transitions of wire samples, specific residual, 25:36055
electric conductivity of 4.2°K-deformed, recovery of, 25:36315
neutron scattering by, lattice vibrational spectra and physical characteristics of, 25:36319
oxidation in acetic acid--sodium tetraborate solutions, anodic, 25:35296
plastic flow anisotropy in monocrystalline, mechanisms of, 25:35379
plastic flow in, mechanism of thermally-activated, 25:35380
proton reactions (p,n) at 17 MeV, neutron spectra from, (E), 25:36676
proton reactions at 24 GeV with natural, potassium production cross sections from, (E), 25:36730 (NP-18829)
reactions with titanium dibcride at 900 to 1700°C in vacuum, 25:35565
stability of powders of, in acids, 25:35522
thermodynamic properties of solution of, in liquid tin, 25:35368
VANADIUM ALLOYS AND SYSTEMS
Al--Cr--Ti-base--V, tensile properties of metastable beta, at 25 to 600°C, effects of strain rate and annealing temperature on anomalies in, 25:35434
Al--Cu--Fe--Ti-base--V, fracture toughness of α--β, relations with microstructure, 25:35348
Al--Mo--Ti-base--V, crack propagation in, effects of stress intensity amplitude and frequency and air, methanol, sodium chloride solution, and distilled water on corrosion fatigue, 25:35279
Al--Mo--Ti-base--V--Zr, tensile properties of metastable beta, at 25 to 600°C, effects of strain rate and annealing temperature on anomalies in, 25:35434
Al--Sn--Ti-base--V--Zr, microstructure of high-strength martensitic beta-phase, 25:35488
Al--Ti-base--V, corrosion by hydrochloric acid--isopropanol incorporating sodium chloride catalyst, rates of, 25:35287
Al--Ti-base--V, corrosion by hydrochloric acid--methanol solutions, rates of, 25:35287
Al--Ti-base--V, fatigue strength of, relations of α grain size with crack initiation, 25:35349
Al--Ti-base--V, properties of forgings of, standard for, 25:35422
C--Cr--Fe--V, analysis of complex carbides in, by electron beam micro methods, 25:34523
Co--Ni--V, mechanical properties of, effects of crystal ordering on, 25:35385
Ga--V, effects of alloying on superconducting transition temperature of intermetallic V_3Ga, 25:36040
Ga--V, preparation of superconducting intermetallic V_3Ga by diffusion, 25:36043
Ge--V, synthesis of superconducting A-15, 25:36044
Nb--V--Zr, superconducting transition temperature of, 25:36042
Ni-base--V, oxidation by air at high temperatures, effects of composition on kinetics of, 25:35289
O--V-base, degassing of dilute, by annealing, concentration changes and metal losses during, 25:35560
Ru--V, electronic transition in near-equiatomic, (E), 25:36339
Ti--V, corrosion by liquid sodium, 25:37016 (CONF-700211-9)
Ti--V, deformation of bcc monocrystals of, modes and shear stresses in, 25:35377
Ti--V-base, stress rupture strength of 650 to 850°C, effects of titanium oxide formation on, 25:35288
V--Zr, superconducting transition temperature of, 25:36042
VANADIUM CARBIDES
Fe--V_4C_3, crystal lattice coherency in, effects of particle size on, 25:35573
TiC--VC, tensile properties of monocrystalline, 25:35558
TiC--VC, uses of monocrystalline, 25:35558
VANADIUM FLUORIDES
vapor pressure--temperature data for, 25:34602 (GAT-645)
VANADIUM ISOTOPES V-47
beta decay of, Fermi plots, half-life, and log-ft value for, (E), 25:36691(T) (ORNL-tr-2481)
VANADIUM ISOTOPES V-51
deuteron reactions (d,α) at 28 MeV, DWBA analysis of differential cross sections, l transfer, and spectra from, (E), 25:36687 (LYCEN-7087)
energy levels from titanium-48(α,p) and titanium-50(He-3,d) reactions, angular-momentum transfer and spectroscopic factors for, (E), 25:36716
nuclear magnetic resonance in near-equiatomic ruthenium--vanadium alloys, 25:36339
VANADIUM NITRIDES
chemical stability in water, alkali solutions, and acids, 25:35522
reaction kinetics in acids, decomposition, 25:35522
VANADIUM OXIDES
fabrication of thermally sensitive resistor of nonstoichiometric, method for, 25:35542(P)
MgO--TiC_2--V_2C_3, phase studies of, 25:35576
VANADIUM SILICIDES
superconducting transition temperature of, effects of alloying on, 25:36040

XUM

superconductivity of pressed-powder compacts of V_3Si, confirmation by thermal capacity and susceptibility measurements of, 25:36022
synthesis of superconducting, of structure A-15 type, 25:36044
VAPOR PRESSURE
calculation in desiccated-multicomponent systems, 25:37223 (SC-DR-710074)
VEGETABLES
radiation processing of, economics of γ, 25:35274
VELA PROJECT
source parameters for Salmon and Sterling Events in, seismic measurements for calculation of, 25:34764
VENTILATION
equipment and methods for nuclear power plant, 25:34788
VENUS (PLANET)
ionosphere of, model of solar-wind interaction with, (E/T), 25:36011
ionosphere of, theoretical and Mariner V data of dayside, (E/T), 25:35827
VERMICULITES
formation by alteration of biotite, 25:34722(R) (NYO-3912-4)
sorptive properties for cobalt in presence of interfering ions, quantitative model for, 25:34721(R) (NYO-3912-3)
sorptive properties for cobalt, quantitative model for, 25:34722(R) (NYO-3912-4)
VERMONT YANKEE POWER REACTOR
design parameters of, requested additional information on, 25:36936 (DOCKET-50271-53)
personnel for, qualifications of power operation test program, 25:36935 (DOCKET-50271-53)
piping systems for, analysis of earthquake stresses in Class 1, 25:36936 (DOCKET-50271-53)
VESSELS
design for plutonium processing facility, engineering drawings for, 25:34784
design of silver reaction, for separation of iodine-131 from gaseous Purex Plant wastes, engineering drawings for, 25:34785
heat transfer from packed-column contactor, 25:34694 (ORNL-TM-3138)
performance of packed-column contactor, effects of axial diffusion on, 25:34694 (ORNL-TM-3138)
VIBRATIONS
damping of liquid cooled rod, (E/T), 25:36993 (KFK-1337)
frequencies in liquid cooled rods, analysis of, (E/T), 25:36993 (KFK-1337)
VIRUSES
adenovirus 12, radioinduced inactivation of T antigen in, uv, 25:35267
influenza, radiation effects on plaque formation in, genetic markers for uv, 25:35266
radiation effects on replication of, in tissue cultures, x, 25:35261
SV40, radioinduced inactivation of T antigen in, uv, 25:35267
VITAMIN B GROUP
radiation effects on content of, in codfish, combined effects of cooking and γ, 25:35272
VITAMIN K GROUP
effects on radiosensitivity of bacteria, 25:35262
VOLCANIC ASH
porosity of soils from, relation to ion retention and movement, 25:34724(R) (RLO-2227-T-9-1)
soils from, study of physico-chemical properties of, 25:34724(R) (RLO-2227-T-9-1)

W

WASPALOY
crystal defect formation and twinning during high-temperature deformation of, mechanisms of, 25:35491
WATER
analysis for deuterium by mass spectrometry, 25:34518
analysis of glacial, for calcium--magnesium, chlorides, potassium, sodium, and sulfates by ion-sensitive electrode method, 25:34721(R) (NYO-3912-3)
analysis of glacial, for calcium--magnesium, chlorides, potassium, sodium, and sulfates by ion-sensitive method, 25:34722(R) (NYO-3912-4)
boiling in reactor cooling systems, acoustic detection of, (E), 25:37052
boiling in superheated, initiation of radiation-induced, (E), 25:34798
compatibility with oxide fuels, 25:35550
diffusion of hydrogen in, 25:34573(R) (RLO-2230-T-2-2)
effects of distilled, on corrosion fatigue crack propagation in aluminum--molybdenum--titanium--vanadium alloy, relations with stress intensity amplitude and frequency, 25:35279
gamma dose rate in, one group method for absorbed, (T), 25:35265
ionization by low-energy electrons in mass spectrometer, cross sections for, 25:34636(R) (ORO-3729-4)
neutron attenuation in, activation detector measurements and Monte Carlo analysis of, 25:36652 (WAPD-TM-991)
neutron energy spectra in, comparison of calculated and measured, 25:36266
neutron transmission in multiple-segment ducts in shield of, slow, 25:36252 (UARAEE-104)
neutron transmission through ducts perpendicular to neutron beam axis in shields of, (E/T), 25:36251 (UARAEE-86)
radiation effects on oxygenated, review on formation of species from, 25:34617
radioactivity monitoring of, sensitivities of detectors for, 25:34870 (SZS-2/71, pp 12-22)
radioinduced luminescence of purified, cosmic, 25:34623
radiolysis of weakly alkaline solutions of, pH indicator studies on hydrogen yields from electron pulse, 25:34668
radiolysis of, research progress on, 25:34636(R) (ORO-3729-4)
reactions with methane under simulated radiolysis conditions, mass spectrometric studies on, 25:34645
reactions with sodium under reactor conditions, heat exchanger design studies from, 25:35441
separation of radioisotopes from, design of sampler for, 25:34704
spectra of, anharmonic constants for absorption, 25:34591
vapor pressure--temperature data for, 25:34602 (GAT-645)
H_2O--steam, flow in concentric internally heated annulus, measurement of critical heat flux and film flow rates in, 25:34797
H_2O--steam, heat transfer in upward flowing, in tubes, effects of flow quality on post-burnout, 25:34801
WATER-d
spectra of, anharmonic constants for absorption, 25:34591
WATER-d_2
effects on growth of Escherichia coli, effects of temperature on, 25:35094
effects on spectra of globular proteins, 25:34588
packaging and shipping of tritiated, in Canada, development of special arrangement methods for, 25:34843 (AECL-3804)
production by amine-hydrogen isotopic exchange, 25:37001 (AECL-3787)
spectra of, anharmonic constants for absorption, 25:34591
WATER-t
release following rupture of tritium-activated luminous device, effectiveness of glass bead and water bubbler trapping systems for detecting, 25:35138
WATER-t_2
release following rupture of tritium-activated luminous device, effectiveness of glass bead and water bubbler trapping systems for detecting, 25:35138
WATER VAPOR
hydrogen-ion (H^-) reactions at 5 keV with, total cross sections for detachment of one and two electrons in, (E), 25:35867
photo-absorption cross sections of, review of uv, (E/T), 25:36013
reactions with Zircaloy-2 or zirconium, kinetics of, 25:35277 (NF-18833)
WATTS BAR POWER REACTOR, UNIT 1
auxiliary systems for, preliminary safety analysis of, 25:36967 (DOCKET-50390-4)
construction of, permit application for, 25:36964 (DOCKET-50390-1)
containment system for, preliminary safety analysis of, 25:36966 (DOCKET-50390-3)
control system for, preliminary safety analysis of, 25:36966 (DOCKET-50390-3)
cooling system for, preliminary safety analysis of, 25:36966 (DOCKET-50390-3)
design criteria and classifications for, preliminary safety analysis of, 25:36968 (DOCKET-50390-5)
design parameters of, preliminary safety analysis of, 25:36965 (DOCKET-50390-2)
effluents from, effects on environment of chemical, radioactive, and thermal, 25:36969 (DOCKET-50390-6)
electrical systems for, preliminary safety analysis of, 25:36967 (DOCKET-50390-4)
engineered safeguards for, preliminary safety analysis of, 25:36966 (DOCKET-50390-3)
instrumentation for, preliminary safety analysis of, 25:36966 (DOCKET-50390-3)
operation aspects for, preliminary safety analysis of, 25:36967 (DOCKET-50390-4)
operation of, license application for, 25:36964 (DOCKET-50390-1)
owners of, financial statements of, 25:36964 (DOCKET-50390-1)
quality assurance program for, 25:36968 (DOCKET-50390-5)
radiation protection systems for, preliminary safety analysis of, 25:36967 (DOCKET-50390-4)
radioactive waste disposal system for, preliminary safety analysis of, 25:36967 (DOCKET-50390-4)
site for, preliminary safety analysis of, 25:36965 (DOCKET-50390-2)
steam and power conversion systems for, preliminary safety analysis of, 25:36967 (DOCKET-50390-4)
technical specifications for, proposed preliminary, 25:36968 (DOCKET-50390-5)
WATTS BAR POWER REACTOR, UNIT 2
auxiliary systems for, preliminary safety analysis of, 25:36967 (DOCKET-50390-4)
construction of, permit application for, 25:36964

(DOCKET-50390-1)
containment system for, preliminary safety analysis of, 25:36966 (DOCKET-50390-3)
control system for, preliminary safety analysis of, 25:36966 (DOCKET-50390-3)
cooling system for, preliminary safety analysis of, 25:36966 (DOCKET-50390-3)
design criteria and classifications for, preliminary safety analysis of, 25:36968 (DOCKET-50390-5)
design parameters of, preliminary safety analysis of, 25:36965 (DOCKET-50390-2)
effluents from, effects on environment of chemical, radioactive, and thermal, 25:36969 (DOCKET-50390-6)
electrical systems for, preliminary safety analysis of, 25:36967 (DOCKET-50390-4)
engineered safeguards for, preliminary safety analysis of, 25:36966 (DOCKET-50390-3)
instrumentation for, preliminary safety analysis of, 25:36966 (DOCKET-50390-3)
operation aspects for, preliminary safety analysis of, 25:36967 (DOCKET-50390-4)
operation of, license application for, 25:36964 (DOCKET-50390-1)
owners of, financial statements of, 25:36964 (DOCKET-50390-1)
quality assurance program for, 25:36968 (DOCKET-50390-5)
radiation protection systems for, preliminary safety analysis of, 25:36967 (DOCKET-50390-4)
radioactive waste disposal system for, preliminary safety analysis of, 25:36967 (DOCKET-50390-4)
site for, preliminary safety analysis of, 25:36965 (DOCKET-50390-2)
steam and power conversion systems for, preliminary safety analysis of, 25:36967 (DOCKET-50390-4)
technical specifications for, proposed preliminary, 25:36968 (DOCKET-50390-5)

WEIGHT
radiation effects on allometry of rat tail length and, x, 25:35225

WELDED JOINTS
inspection of T-, in boilers, x-radiographic method for, 25:34840

WELDING
equipment and methods for remote-controlled, of pressure tubes, tungsten inert gas, 25:34787
methods for irradiation facility construction, 25:35326
methods for reactor moderator tanks, 25:35322
safety in, standard provisions for, 25:35330
standard for ferrous materials for nuclear power piping, 25:35308

WELDS
inspection of nuclear power plant component, effects of background radiation on performance of gamma radiographic equipment for, 25:34823

WELL LOGGING
data from gamma, method for interpretation of, 25:34716(T) (CSIRO-Trans-10088)
data sheets for nuclear, standard form for, 25:34735
equipment and methods for nuclear, in hydrology, design, performance, and use of, 25:34725 (STI/DOC-10/126)
equipment for nuclear, standards for calibration of, 25:34735
equipment for pulsed neutron, method for calibrating, 25:35039(P)

WEST VALLEY PROCESSING PLANT
radioactivity in sanitary waste system effluent from, 25:34683 (DOCKET-50201-73)

WHISTLERS
effects of electron anisotropy on, leading strong collision-free shocks, (T), 25:35996
excitation by probe antennas in bounded plasmas, (E), 25:36241

WHOLE-BODY COUNTERS
collimator for, properties of multi-slit, 25:34871 (UARAEE-82)
performance of shielded, for measuring cesium-137 and potassium-40 contents in man, 25:35182

WILLIAM H. ZIMMER POWER REACTOR, UNIT 1
buildings and structures for, foundations for, 25:36953 (DOCKET-50358-17)
containment systems for, revised and additional data on, 25:36953 (DOCKET-50358-17)
control system for, revised and additional data on, 25:36953 (DOCKET-50358-17)
design parameters of, revised and additional data on, 25:36954 (DOCKET-50358-18)
electrical power systems for, revised and additional data on, 25:36953 (DOCKET-50358-17)
instrumentation for, revised and additional data for, 25:36953 (DOCKET-50358-17)
operations aspects of, revised and additional data on, 25:36954 (DOCKET-50358-18)

WIND
effect on nighttime ionospheric ionization redistribution and sporadic-E structure, neutral atmospheric and neutral, (E/T), 25:35986
measurements at Casaccia, Italy during 1968, tabulated data on, 25:34745 (RT/PROT-(70)42)

X

X RADIATION
book: X-Rays, 25:35057
cosmic background, observations in nire areas, (E), 25:35712
detection of, design of gas-filled spark chamber for, 25:34876(P)
detection of, instruments, measurement techniques, and standards for, 25:35137
distribution in water phantoms, errors due to ionization chamber air volume in measurements on, 25:35146
dosimetry below 15 keV, method based on physical property changes of plastic for, 25:35033(P)
dosimetry during diagnostic kinescopography, 25:35142
dosimetry in Plexiglas phantoms using scintillation detectors, 25:35030
dosimetry of, development of phosphate-glass luminescent dosimeters for, 25:35037(P)
effects of soft, on heating of interstellar medium, (T), 25:35784
effects on absorption and photoelectron emission spectra of ruby crystals, 25:36308
effects on alkaline solutions of aliphatic and aromatic amino acids at 77°K, ESR studies on production of free radicals by trapped electrons produced by, 25:34647
effects on allometry of body weight and tail length in rats, 25:35225
effects on aluminum and copper contents in functionally and morphologically different structures of animal spinal cords, 25:35228
effects on ascorbic acid content in tissues of oral cavity in animals, 25:35219
effects on cell count in mouse intestinal epithelium, lethal, 25:35239
effects on cell nuclei in barley and bean seeds, comparison of bremsstrahlung, γ, proton, and, 25:35258
effects on Chinese hamster cells, protective and sensitizing effects of oxygen against damaging, 25:35214
effects on cholinesterase activity in rat brain, effects of adrenal and pituitary gland function on, 25:35232
effects on chromosomes of onion and wheat seeds, aberrant, 25:35125
effects on coenzyme-substrate systems, ESR spectral studies on free radical yields from, 25:34655
effects on DNA, effects of polynucleotide ligase on recovery from, 25:35108
effects on enzymatic activity in rat liver and spleen, 25:35215
effects on formation of thyroiditis antibodies in mice, 25:35114
effects on free radical yield in cytochrome c and myoglobin, 25:35106
effects on growth and transformation of rat epithelium transplants, 25:35231
effects on growth of Ehrlich ascites tumors in mice and in vitro, sensitizing effects of dihydroxytutyraldehyde on, 25:35159
effects on histology of albino rat ovaries and uterus, combined effects of estrogens, progesterones, and, 25:35237
effects on homocytotropic antibody formation in rats, 25:35112
effects on immune response of mice to hematopoietic cells following intraperitoneal and intravenous injection, comparison of, 25:35111
effects on ionic conductivity of pure and doped strontium fluoride crystals, 25:36304
effects on iron-59 uptake by bones of rats, correlation between intramedullary dose and whole-body, 25:35211
effects on L cells, mutagenic, 25:35124
effects on Micrococcus radiodurans in relation to growth rate and quantity of macromolecules, 25:35263
effects on model phospholipid membranes, 25:34625
effects on mouse and rat spermatozoa, mutagenic, 25:35129
effects on mouse L cell DNA, degratory, 25:35224
effects on oxidative phosphorylation in rat brain and liver mitochondria, 25:35216
effects on oxygen uptake by liver slices, mitochondria, and mitochondrial membranes of rats, 25:35222
effects on photosensitive EPR signal in zinc oxide powder, 25:36296
effects on Pisum seeds, mutagenic, 25:35122
effects on proliferation of human osteosarcoma cell cultures, effects of dose fractionation on, 25:35242
effects on repair systems in bacteria and plants, 25:35246
effects on sodium silicate glass, paramagnetic centers induced in, 25:36278
effects on survival of ascites tumor-bearing mice, effects of simultaneous administration of dihydroxybutyraldehyde on, 25:35159
effects on survival of mice, protective effects of sodium fluoroacetate against, 25:35162
effects on tolerance of mouse skin homografts, 25:35113
effects on transforming DNA in bacteria, mechanism of inactivating, 25:35269
effects on tritium-labeled thymidine incorporation in mouse liver and kidney tubulus cells, effects of time on whole-body, 25:35238

XUM

effects on tungsten targets at 12 to 300 kV, bremsstrahlung emission from, (E), 25:36249 (LA-4624)
effects on Vicia faba chromosomes, effects of oxygen pressure on aberrant, 25:35118
effects on virus replication in tissue cultures, 25:35261
emission by exploding wires, 25:36326
emission during solar flares, (E), 25:35721
emission from a source in Crux, flare-like, (E), 25:35691
emission from Coma cluster of galaxies, (E/T), 25:35795
emission of nonthermal, during solar flares, 25:35726
emission of soft, from coronal regions, (E), 25:35721
emission of soft, from North Polar Spur of Milky Way, (E/T), 25:35800
energy spectra of diffuse cosmic, at 20 to 120 keV, (E), 25:35921
generation of bremsstrahlung, at 30 to 140 km in ionosphere, (E/T), 25:35999
production of intense K, by electron excitation of targets, 25:35842
scattering by Moessbauer nuclei, spectra from, (E), 25:36346
use for therapy of human nasopharyngeal tumors at 10 MeV, development of conformation method for, 25:35194

X-RAY ASTRONOMY
developments in, (T), 25:35659
experiments in, satellite, (E), 25:35702

X-RAY EMISSION ANALYSIS
book: X-Rays, 25:35057

X-RAY EQUIPMENT
book: X-Rays, 25:35057
hazards of fluoroscopic, review on methods for reducing, 25:35142

X-RAY FLUORESCENCE ANALYSIS
equipment for lead determination in paint layers, 25:35043

X-RAY SOURCES
standards for use in production and processing of foods, 25:34814

XENON
ionization by protons at 4 MeV, pressure dependence of, 25:35888
plasma of, local thermodynamic equilibrium in laser-induced, 25:36121
reactions with methane under simulated radiolysis conditions, mass spectrometric studies on, 25:34645
separation from reactor containment system atmospheres by selective permeation, efficiency of cellulose acetate membranes for, 25:34692(R) (NYO-4057-2)
uses of purified fission product, evaluation of large-scale, 25:34803(R) (ENWL-1308-5)

XENON IONS
implantation in silicon at 10 to 200 keV, lattice disorder induced in, 25:36300

XENON ISOTOPES
production in spontaneous fission of plutonium-244, isotope ratios in, (E), 25:35594
separation by thermal diffusion, 25:34807(R) (MLM-1793)
separation of short-lived, electromagnetic method for, 25:34806 (JINR-P13-5757)

XENON ISOTOPES Xe-121
beta and electron-capture decay of, γ-conversion electron delayed coincidence spectra from, (E), 25:36752

XENON ISOTOPES Xe-123
beta and electron-capture decay of, γ-conversion electron delayed coincidence spectra from, (E), 25:36752

XENON ISOTOPES Xe-131
concentration by thermal diffusion, 25:34807(R) (MLM-1793)

XENON ISOTOPES Xe-133
release to atmosphere in reprocessing aluminum-clad fuel elements, 25:34693 (ORNL-4574)
use for blood flow study in human brain scanning, 25:35174
use for determining regional lung function in patients with hepatic cirrhosis and pulmonary edema, 25:35170

XENON ISOTOPES Xe-137
energy levels of, unified model calculations for, (T), 25:36749

XYLENE
radiation stability of, for use as diluent in fuel reprocessing, 25:34638 (RT/CHI-(70)35)

Y

YTTERBIUM
determination in rocks by neutron activation and γ spectroscopy, 25:34543 (NIM-1013)
Hall coefficient of, effects of high pressure on, 25:36324
iodine-ion reactions at 15 to 60 MeV with, L and M x-ray spectra from, (E), 25:35834

YTTERBIUM ALLOYS AND SYSTEMS
Ag--Yb, crystal structure of intermetallic Ag_3Yb, 25:35496
Ag-base--Yb, hyperfine interactions in, study using γ--γ angular correlations of ytterbium-169 decay, 25:36332

YTTERBIUM FLUORIDES
effects on radiation stability of beryllium fluoride glasses, 25:34621

YTTERBIUM ISOTOPES Yb-169
electron-capture decay in silver--ytterbium alloy, γ--γ angular correlation of, 25:36332
production by neutron irradiation of ytterbium oxide, radiochemical impurities formed in, 25:34669 (JAERI-Memo-4279)

YTTERBIUM ISOTOPES Yb-170
neutron capture by, cross sections and resonance integrals for pile and thermal, (E), 25:36735 (SGAE-PH-104/1971)

YTTERBIUM ISOTOPES Yb-171
neutron capture by, cross sections and resonance integrals for pile and thermal, (E), 25:36735 (SGAE-PH-104/1971)

YTTERBIUM ISOTOPES Yb-172
neutron capture by, cross sections and resonance integrals for pile and thermal, (E), 25:36735 (SGAE-PH-104/1971)

YTTERBIUM ISOTOPES Yb-173
neutron capture by, cross sections and resonance integrals for pile and thermal, (E), 25:36735 (SGAE-PH-104/1971)

YTTERBIUM ISOTOPES Yb-174
carbon-12 fission up to 10.4 MeV/nucleon, excitation function for, (E), 25:36784

YTTERBIUM OXIDES
analysis for impurities by neutron activation and radiochemical separation, 25:34669 (JAERI-Memo-4279)
growth of single-crystal solid solutions with another rare earth oxide by Verneuil method, formation regions in, 25:35525

YTTRIUM
abundance in atmospheres of four K stars, (E), 25:35636
effects on colorimetric determination of gold, 25:34621
effects on fluorescence method for detection of hafnium and zirconium, 25:34519
lattice dynamics model of, phonon dispersion curves and frequency spectra from, 25:36333
separation from aqueous chloride solutions by solvent extraction using bis(1-isobutyl-3-methylbutyl) phosphate, 25:34706
welding to molybdenum, methods for, 25:35321

YTTRIUM ALLOYS AND SYSTEMS
Al--Y-base, crystal lattice parameters of intermetallic Y_2Al, 25:35495
Mg-base--Y, hardening and twinning in, mechanisms of, 25:35487
Y--YH_2, phase studies at room temperature, 25:35582
Y--YH_2, properties of, electric, mechanical, and physical, 25:35582

YTTRIUM HYDRIDES
Y--YH_2, phase studies at room temperature, 25:35582
Y--YH_2, properties of, electric, mechanical, and physical, 25:35582

YTTRIUM ISOTOPES Y-87
energy levels and nuclear properties of, Nuclear Data Sheets for, (E), 25:36706

YTTRIUM ISOTOPES Y-88
energy levels and transitions from decay and nuclear-reaction measurements, Nuclear Data Sheets compilation of properties of, (E), 25:36705
excretion in feces of peccaries following single ingestion of nuclear debris from Schooner Event, fallout, 25:35089

YTTRIUM ISOTOPES Y-89
energy levels and transitions from decay and nuclear-reaction measurements, Nuclear Data Sheets compilation of properties of, (E), 25:36714
proton reactions (p,n) with, excitation functions for, (E), 25:36676

YTTRIUM ISOTOPES Y-90
beta decay of, Fermi--Kurie plot and small-order shape factor from, (E), 25:36768
energy levels and transitions from decay and nuclear-reaction measurements, Nuclear Data Sheets compilation of properties of, (E), 25:36801
production of, design and performance of generator for, 25:34802 (BNL-50249)

YTTRIUM OXIDES
CeO_2--Y_2C_3, diffusion of oxygen in nonstoichiometric solid solutions of, self-, 25:35553
CeO_2--Y_2C_3, electric properties of nonstoichiometric solid solutions of, 25:35553
FeO--YO, magnetic susceptibility of amorphous antiferromagnetic, temperature dependence of, (E/T), 25:36337
ThO_2--Y_2C_3, preparation of transparent bodies of, method for, 25:35543(F)
WO_3--Y_3C_3, properties of $3Y_2O_3.WO_3$, to 1500°C, electric and thermal, 25:35529
Y_2O_3--ZrC_2, creep of rare earth-stabilized specimens of, at 1400 to 1535°C and 800 to 7500 psi, 25:35555

Z

ZINC
determination in human stones by neutron activation, 25:34546 (THAI.-AEC-39)
determination in soils by neutron activation, 25:34545

(THAI.-AEC-36)
determination of trace amounts of, in uranium by neutron activation, 25:34547 (UARAEE-68)
effects on colorimetric determination of gold, 25:34521
effects on formation of stacking faults in magnesium--thorium alloys, 25:35484
effects on gravimetric determination of mercury using 2-aminobenzothiazole, 25:34520
effects on photometric determination of antimony following solvent extraction using TBP, 25:34512
electric field gradient in hcp, calculations, 25:36351
flow stress of polycrystalline, effects of high hydrostatic pressure on, 25:35435
half-life in Pacific oyster, biological, 25:37218 (RLO-2225-T-1-5)
radiation damage in, atomic displacement process in low-temperature electron, 25:36288
separation from other transition metals by ion exchange on anionite AV-17, 25:34695(T) (ORNL-tr-2397)
separation of ions of, from metal ions by high-voltage electrophoresis using carboxylic and hydroxycarboxylic acids, 25:34702
ZINC ALLOYS AND SYSTEMS
Al--Zn-base, plasticity in eutectoid alloy of, at 150 to 300°C, super-, 25:35405
In--Zn, thermodynamic properties of liquid solutions of, 25:35442
Mg--Zn--Zr, mechanical properties of, effects of high-temperature thermomechanical treatment on, 25:35456
Mg--Zn--Zr, microstructure of, effects of high-temperature thermomechanical treatment on, 25:35456
ZINC ISOTOPES Zn-65
energy levels from (n,γ) reactions, phonon-particle doorway states in, (T), 25:36703
energy levels from zinc-64 neutron capture, analysis of anticorrelation between reduced widths and E1 transition probabilities for, (T), 25:36834
ZINC ISOTOPES Zn-67
energy levels from (n,γ) reactions, phonon-particle doorway states in, (T), 25:36703
energy levels from zinc-66 neutron capture, analysis of anticorrelation between reduced widths and E1 transition probabilities for, (T), 25:36834
ZINC OXIDES
radiation effects on EPR signal of photosensitive donor in powdered, x-, 25:36296
vaporization kinetics of single crystals of, 25:37247 (UCRL-20528)
graphite--ZnO, electric conductivity of powdered, pressure dependence of, 25:36334
ZIRCALOY-2
embrittlement of, effects of reactor coolant loss accident conditions on, (E), 25:37038 (IN-1453)
fatigue crack propagation in weld metal of, 25:35466
hardening of, analysis of work, 25:35394
oxidation by oxygen or water vapor, kinetics of, 25:35277 (NP-18833)
properties for use in nuclear industry, review on, 25:35438
properties of, data tabulation on mechanical and physical, 25:35439
radiation effects on mechanical properties of, relations of environment with fast neutron, 25:35506
radiation effects on work hardening of, in-pile, 25:35394
ZIRCALOY-4
properties for use in nuclear industry, review on, 25:35438
properties of, data tabulation on mechanical and physical, 25:35439
ZIRCONIUM
determination by amperometric titration using N-furoylphenylhydroxylamine, 25:34535
determination in indium-113m generator eluates, 25:34672
determination in presence of hafnium, effects of metal ions on fluorescence method for, 25:34519
diffusion in plutonium at 650 to 900°C, welded couple method for studying Kirkendall effect occurrence during, 25:35333 (CEA-CONF-1760)
effects on colorimetric determination of gold, 25:34521
effects on gravimetric determination of mercury using 2-aminobenzothiazole, 25:34520
effects on photometric determination of antimony following solvent extraction using TBP, 25:34512
electric conductivity in reversible superconducting transitions of wire samples, specific residual, 25:36055
electroplating of, review on, 25:35219
fabrication and properties of, engineering data on, 25:35437
fabrication by casting, drawing, and punching, review on, 25:35319
flow stress of polycrystalline, effects of high hydrostatic pressure on, 25:35435
fluoride removal from surfaces of, process for, 25:34710(P)
machining of, review of methods for, 25:35317
magnetic susceptibility of single crystals of, 25:36340
metallography and metallurgy of, review of, 25:35457
neutron total cross section at 0.433 to 2.37 MeV, (E), 25:36740 (WAPD-T-2411)
oxidation by oxygen or water vapor, kinetics of, 25:35277 (NP-18833)
oxidation of, effects of electrolytes and pre-treatment on initial growth of anodic oxide films in, 25:35264
plastic flow and microstructure strengthening in α-phase polycrystalline, measurement of high-temperature, 25:35401
powder metallurgy of, review on, 25:35319
properties for use in nuclear industry, review on, 25:35438
properties of, data tabulation on mechanical and physical, 25:35439
radiation effects on corrosion of, pile neutron, 25:35513
reactions with titanium diboride at 900 to 1700°C in vacuum, 25:35565
stability of powders of, in acids, 25:35522
tensile properties of polycrystalline α-, at 25 to 700°C, effects of dissolved oxygen on, 25:35352
thermal capacity at low temperature of single crystals of, 25:36340
welding of, review of methods for, 25:35318
ZIRCONIUM ALLOYS AND SYSTEMS
internal friction of, effects of combination of oxygen and iron, silicon, or tungsten on, 25:35404
radiation effects on corrosion of, pile neutron, 25:35513
sorptive properties for hydrogen, effects of corrosion on, 25:35283
Al--C--Co--Cr--Mo--Nb--Ni-base--Ta--Ti--Zr, properties of corrosion-resistant IN-738 superalloy, 25:35400
Al--Mo--Ti-base--V--Zr, tensile properties of metastable beta, at 25 to 600°C, effects of strain rate and annealing temperature on anomalies in, 25:35434
Al--Mo--Ti-base--Zr, tensile properties of metastable beta, at 25 to 600°C, effects of strain rate and annealing temperature on anomalies in, 25:35434
Al--Sn--Ti-base--V--Zr, microstructure of high-strength martensitic beta-phase, 25:35488
Fe--Mo--Sn--Ti-base--Zr, crystal structure and properties of thermomechanically-processed beta-phase, 25:35398
Fe--Nb--Ni--Sn--Zr-base, properties of dilute, for use in organic cooling circuits, 25:35329(P)
Mg--Zn--Zr, mechanical properties of, effects of high-temperature thermomechanical treatment on, 25:35456
Mg--Zn--Zr, microstructure of, effects of high-temperature thermomechanical treatment on, 25:35456
Mo--Sn--Ti-base--Zr, tensile properties of metastable beta, at 25 to 600°C, effects of strain rate and annealing temperature on anomalies in, 25:35434
Mo--Ti-base--Zr, tensile properties of metastable beta, at 25 to 800°C, effects of strain rate and annealing temperature on anomalies in, 25:35434
Nb--C--Zr, phase transformations in, 25:35572
Nb--Ti--Zr, phase transformations in superconducting, 25:36051
Nb--V--Zr, superconducting transition temperature of, 25:36042
Nb--Zr, fine structure of superconducting, 25:36053
Nb--Zr, magnetization of superconducting, 25:36046
Nb--Zr-base, corrosion by air and pressurized steam at 450 to 650°C, effects of heat treatment and cold work on kinetics of, 25:35278 (UARAEE-72)
Nb--Zr-base, hardening behavior of, analysis of work, 25:35394
Nb--Zr-base, radiation effects on mechanical properties of, relations of environment with fast neutron, 25:35506
Nb--Zr-base, radiation effects on work hardening of, in-pile, 25:35394
Nb-base--Ti--Zr, critical current of superconducting, in fields up to 80 kOe, 25:36050
Nb-base--Zr, corrosion by lithium--selenium mixtures at 375°C, 25:35275(R) (ANL-7777)
Nb-base--Zr, properties of bars, rods, and wires of, standard for, 25:35448
Nb-base--Zr, properties of ingots of, standard for, 25:35447
Nb-base--Zr, properties of seamless and welded tubes of wrought, standard for, 25:35478
Nb-base--Zr, properties of sheets, foils, and plates of, standard for, 25:35446
Pd--Zr, stability of gaseous intermetallic, 25:35350
Pt--Zr, stability of gaseous intermetallic, 25:35350
Rh--Zr, stability of gaseous intermetallic, 25:35350
Ru--Zr, stability of gaseous intermetallic, 25:35350
$TaSi_2$--Zr, tantalum trisilicide growth in, at 1150 to 1370°C, kinetics of, 25:35577
U--Zr, processing of irradiated, at ICPP, 25:34690(R) (IN-1457)
V--Zr, superconducting transition temperature of, 25:36042
ZIRCONIUM CARBIDES
crystallization of powdered and hot-pressed, secondary, 25:35535
properties of plasma-sprayed layers of, at 1000°C, electric and thermal, 25:35538
ZIRCONIUM FLUORIDES
BeF_2--LiF--PuF_3--ZrF_4, plutonium oxide precipitation in molten, equilibrated with zirconium oxide, 25:34566
ZIRCONIUM HYDRIDES
neutron thermalization in, analytic scattering model for

XUM

time-dependent, (E/T), 25:37132
ZIRCONIUM ISOTOPES Zr-87
nuclear properties of, Nuclear Data Sheets for, (E), 25:36706
ZIRCONIUM ISOTOPES Zr-88
energy levels and transitions from decay and nuclear-reaction measurements, Nuclear Data Sheets compilation of properties of, (E), 25:36705
ZIRCONIUM ISOTOPES Zr-89
energy levels and transitions from decay and nuclear-reaction measurements, Nuclear Data Sheets compilation of properties of, (E), 25:36714
ZIRCONIUM ISOTOPES Zr-90
energy levels and transitions from decay and nuclear-reaction measurements, Nuclear Data Sheets compilation of properties of, (E), 25:36801
energy levels from strontium-87 (α,nγ) reactions, spin assignments for, (E), 25:36757
energy-level transitions in, shell-model calculation of widths for E1, (T), 25:36798
neutron elastic scattering at 2.1 and 5.17 MeV, differential cross sections for, (E), 25:36740 (WAPD-T-2411)
neutron total cross section at 0.433 to 2.37 MeV, (E), 25:36740 (WAPD-T-2411)
ZIRCONIUM ISOTOPES Zr-91
energy levels from strontium-88 (α,nγ) reactions, spin assignments for, (E), 25:36757
ZIRCONIUM ISOTOPES Zr-96
proton reactions (p,2n) at 400 MeV, isomeric ratio in, 25:36761
ZIRCONIUM NITRIDES
chemical stability in water, alkali solutions, and acids, 25:35522
reaction kinetics in acids, decomposition, 25:35522
ZIRCONIUM OXIDES
preparation of thin pyrolytic films of, by chemical vapor deposition on silicon substrates, 25:35564
properties for use as fuel impregnation material for silver heat shields, 25:35549 (TID-2569€)
properties of thin chemical vapor-deposited films of, chemical, electric, and structural, 25:35564
reactions with titanium and lanthanum oxides at high temperatures, electric conductivity detection of solid-phase, 25:36320
alkali metal oxides--ZrO_2, formation and properties of solid solutions of, regularity in, 25:35545
alkaline earth oxides--ZrO_2, formation and properties of solid solutions of, regularity in, 25:35545
CaO--UO_2--ZrO_2, separation of uranium from irradiated, aqueous halide process for, 25:34690(R) (IN-1457)
rare earth oxides--ZrO_2, formation and properties of solid solutions of, regularity in, 25:35545
transition metal oxides--ZrO_2, formation and properties of solid solutions of, regularity in, 25:35545
Y_2O_3--ZrO_2, creep of rare earth-stabilized specimens of, at 1400 to 1535°C and 800 to 7500 psi, 25:35555
ZIRCONIUM OXYNITRIDES
crystal lattice parameters of homogeneous, at 1500°C, 25:35583
ZODIACAL LIGHT
gegenschein of, discovery history and physical parameters of, (E/T), 25:35778

REPORT NUMBER INDEX

Reports, conference papers and proceedings, numbered translations, and patents are included in this index. Each item is listed by report number; this is followed by the abstract number and a brief notation regarding public availability. The index entries show which reports are on file in the institutions listed on the back of the front cover (Dep.), which reports have been published in open-literature journals (journal citation), and which reports can be purchased (source and price). Whenever a report is identified by more than one number, the availability is given under the primary number, and a cross reference is given under the secondary report number.

The report number codes apply to USAEC reports unless designated otherwise. Non-USAEC reports are identified by parenthetical notes after the report codes; e.g., (non-AEC), (British), (Canadian), (French). The note (Misc.) identifies the codes used for both USAEC and non-USAEC reports. Patents are listed under the heading "PATENTS"; the country of origin is included in parentheses.

A comprehensive list of both USAEC and non-USAEC report codes is contained in the latest revision of TID-85, *Report Number Series Used by the Division of Technical Information in Cataloging Reports.* This information is also included in the Cumulative Report Number Index (issued annually).

Availability of USAEC Reports

All USAEC Reports abstracted in *Nuclear Science Abstracts* are available through one or more of the following sources:

(1) University and public libraries in the United States. A list of these organizations appears on the inside front cover of each issue of *NSA*.

(2) NCR Microcard Editions in Microcard and micronegative form. Orders and inquiries should be sent to: Order Processing Department, 365 South Oak Street, West Salem, Wisconsin 54669.

(3) National Technical Information Service, U. S. Department of Commerce, Springfield, Virginia 22151.

(4) Superintendent of Documents, U. S. Government Printing Office, Washington, D. C. 20402.

(5) National Cash Register Co., P. O. Box 3111, Oak Ridge, Tenn. 37830, in micronegative form. Purchase details available on request.

Availability of Non-USAEC Reports

U. S. Reports. Reports of U. S. Government agencies are available to the public from the National Technical Information Service (NTIS). If specific availability is not shown, inquiries may be directed to NTIS.

Non-U. S. Reports. Reports of atomic energy organizations of other countries are available from NTIS for U. S. sale only. Specific availability in the country of origin is shown, when known, at the report number entry. Otherwise, inquiries should be made to the organizations listed below:

AUSTRALIA

Australian Atomic Energy Commission Research Establishment. Available upon request from the Library, Australian Atomic Research Establishment, Private Mail Bag, Sutherland, New South Wales, Australia.

BELGIUM

Centre d'Étude de l'Energie Nucléaire. Available upon request to individuals and organizations from the Centre d'Etude de l'Energie Nucléaire (C.E.N.), Studiecentrum voor Kernenergie (S.C.K.), Technical Information Dept., MOL-DONK (Belgium).

CERN

CERN European Organization for Nuclear Research. Available without charge from CERN European Organization for Nuclear Research, Geneva 23, Switzerland. Copies are deposited in libraries throughout the world.

FRANCE

Commissariat à l'Energie Atomique. Inquiries for reports numbered 1-2199 should be addressed to Service Central de Documentation du C.E.A., Centre d'Etudes Nucléaires de Saclay, Boîte postale n° 2, 91. GIF-sur-YVETTE, FRANCE. Reports numbered 2200 and above are available from La Documentation Française, 31 quai Voltaire, 75, PARIS (7e), FRANCE.

Service Central de Protection contre les Rayonnements Ionisants. Copies are available from Ministère de la Santé Publique, Service Central de Protection contre les Rayonnements Ionisants, B.P. n° 78 Le Vesinet (France) Telex 25667.

GERMANY

Deutsches Elektronen-Synchrotron DESY. Copies are available from Deutsches Elektronen-Synchrotron DESY, Dokumentation, 2000 Hamburg 52, Notkestieg 1, Germany.

Gesellschaft für Kernforschung mbH (KFK). Copies are available from Gesellschaft für Kernforschung mbH, 75 Karlsruhe, Postfach 947, Germany. Copies are also deposited in many national nuclear centers in the world.

Kernforschungsanlage. Copies may be ordered from Zentralbibliothek der Kernforschungsanlage Jülich, Jülich, Bundesrepublik Deutschland.

Hahn-Meitner-Institute für Kernforschung. Available without charge from Hahn-Meitner-Institute für Kernforschung Ber-

XUM

lin, Bibliothek, Glienicker Strasse 100, 1 Berlin 39, Germany. Copies are deposited in many national nuclear centers in the world.

Johann-Wolfgang-Goethe Universität, Frankfurt Am Main, Institut für Kernphysik, (IKF). Copies are available from Gmelin Institut, 40–42 Varrentrappstrasse, Frankfurt (Main), West Germany.

ISRAEL

Israel Atomic Energy Commission. Available without charge from Israel Atomic Energy Commission, Soreq Nuclear Research Centre, Yavne, Israel.

ITALY

Centro Informazioni Studi Esperienze (CISE). For sale at CISE Press Office, Casella Postale 3986, Milano, Italy. Copies are deposited in the libraries of various nuclear centers in Italy and abroad.

Comitato Nazionale per l'Energia Nucleare. Copies are available from Comitato Nazionale per l'Energia Nucleare, Divisione Affari Internazionali e Studi Economici, Ufficio Pubblicazioni, Via Belisario, 15, Roma, Italy.

JAPAN

Japan Atomic Energy Research Institute (JAERI). Available from the Staff Supply Cooperative of Japan Atomic Energy Research Institute (JAERI), Tokai-mura, Naka-gun, Ibaraki-ken, Japan. Copies are deposited in depositories in Tokyo, Nagoya, and Osaka.

Nagoya University. Copies are available from Research Information Center, Institute of Plasma Physics, Nagoya University, Nagoya, Japan.

University of Tokyo. Available free of charge from Institute for Nuclear Study, University of Tokyo, Tanashi-Machi, Kitatama-gun, Tokyo, Japan.

NETHERLANDS

Reactor Centrum Nederland. For sale by Reactor Centrum Nederland, 112 Scheveningseweg, 's-Gravenhage, The Netherlands. Copies are deposited in university libraries in Holland and in many national nuclear centers in the world.

NEW ZEALAND

Institute of Nuclear Sciences. Copies are available from Librarian, N. Z. Institute of Nuclear Sciences, D.S.I.R., Private Bag, Lower Hutt, New Zealand. Copies are deposited in other countries.

PAKISTAN

Atomic Energy Center. Copies are available from Atomic Energy Center, P. O. Box 658, Lahore, (West Pakistan).

POLAND

Reports of the Polish nuclear institutes are published by the Nuclear Energy Information Center of the Government Commissioner for Use of Nuclear Energy. Copies are available free of charge from Nuclear Energy Information Center, Palace of Culture and Science, Warsaw, Poland.

SPAIN

Junta de Energia Nuclear. "JEN" reports are available without charge from Servicio de Documentation, Junta de Energia Nuclear, Ciudad Universitaria, Madrid (3), España.

SWITZERLAND

Eidgenössisches Institut für Reaktorforschung. "EIR" reports are available from Eidgenössisches Institut für Reaktorforschung, c/o Bibliothek, 5303 Würenlingen/Switzerland.

TURKEY

Turkish Atomic Energy Commission. Copies are available free of charge from T.A.E.C., Çekmece Nuclear Research Center, P. O. Box 1, Airport, Istanbul, Turkey.

Conferences

Published conference proceedings as well as individual unpublished papers from conferences are included in this index. A CONF number is assigned to the conference if published proceedings are received and also if only a single paper is received. The base number used is year-month-sequence. Thus, the number CONF-650101 indicates that the conference was held in 1965, in January, and that this was the first January 1965 conference so received. This number would be assigned to complete published proceedings. If individual papers are received, the base number is extended to include a paper number, e.g., CONF-650101-1. As additional papers are received, they will be assigned consecutive numbers in the series, CONF-650101-1, CONF-650101-2, etc. This numbering system ensures that all papers received from a conference will be associated with that conference in this index.

If published proceedings are received after the receipt of individual papers, the complete proceedings will be abstracted and the abstract number will appear in this index with the base CONF number.

Abbreviations Used in Availability Column

AECL — Reports of the Atomic Energy of Canada Limited are for sale by the Scientific Document Distribution Office, Atomic Energy of Canada Limited, Chalk River, Ontario, Canada.

CFSTI — See NTIS

DENM — Reports of the Atomic Energy Commission Research Establishment, Risö, are available on exchange from the Library, Danish Atomic Energy Commission, Risö, Roskilde, Denmark. Also for sale at the price shown from Jul. Gjellerup, Booksellers, 87 Sölvgade, Kobenhavn K., Denmark.

Reports of Danatom are available on loan from Research Establishment, Risö, Roskilde, Denmark. Copies are available from Danatom, Aurehojvej 2, Hellerup, Denmark.

Dep. — AEC reports so designated are maintained in the organizations listed on the inside front cover of *NSA*. Prior to July 1, 1965, reports were deposited either in printed copy form or in microform. After that time, all reports have been in the form of micronegatives.

Reports from other countries so designated are available in the United States at the organizations listed on the inside front cover of *NSA*.

DTIE Available from the U. S. Atomic Energy Commission, Division of Technical Information Extension, P. O. Box 62, Oak Ridge, Tennessee 37830. (Conference papers are available on loan only.)

EM Blueprints of AEC engineering drawings are available from NTIS, U. S. Department of Commerce, Springfield, Virginia 22151. Current prices of the CAPE-packages may be obtained from this address. TID-4100, available from the Division of Technical Information Extension, P. O. Box 62, Oak Ridge, Tennessee 37830, contains information on all the CAPE-packages for sale.

EUR For sale by Centrale de vente des publications des Communautés européennes 37, rue Glesener-Luxembourg.

GPO For sale by the Superintendent of Documents, Government Printing Office, Washington, D. C. 20402.

IAEA Available from the International Atomic Energy Agency, Vienna, Austria, and from its sales agencies in various countries throughout the world. A list of these agencies is found in each STI/DOC and STI/PUB publication.

NORW Reports from Forsvarets Forskningsinstitutt are available from Norwegian Defense Research Establishment, Library, P. O. Box 25, Kjeller, Norway.

"KR" reports are available on an exchange basis from the Library, Institutt for Atomenergi, Box 40, Kjeller, Norway.

Reports of the Norwegian Reactor School are available from the Library, Institutt for Atomenergi, P. O. Box 40, Kjeller, Norway.

NRC For sale by the National Research Council of Canada, Ottawa, Ontario, Canada.

NTIS For sale by the National Technical Information Service (NTIS), U. S. Department of Commerce, Springfield, Virginia 22151 at the following prices for eye legible copy:

1–300 pages	$3.00
301–600 pages	$6.00
601–900 pages	$9.00

Documents over 900 pages have special prices which may be obtained from NTIS. Microfiche copy of each separately bound document can be purchased for $0.95.

Reports issued by organizations outside the United States will be sold by NTIS *only to purchasers within the United States.*

Purchasers outside the United States may acquire such reports from the sources described elsewhere in these columns.

OECD Available from O. E. C. D., Publications 2, rue, André-Pascal, 75 Paris 16e, France, and from its sales agencies in various countries throughout the world. A list of these agencies is found in each OECD publication.

SWED "AE" reports are for sale from Aktiebolaget Atomenergi, Library Section, Box 43041, Stockholm 43, Sweden. Microcopy of these reports is available from the International Documentation Center, Turnba, Sweden.

Reports of the VDDIT-series may be obtained from Aktiebolaget Atomenergi, Information Office, Scientific and Technical Information, Box 43041, Stockholm 43, Sweden.

Other series are not generally available to the public. Organizations in the Atomic Energy field may obtain copies from Aktiebolaget Atomenergi.

UK United Kingdom Atomic Energy Authority reports generally may be purchased from Her Majesty's Stationery Office, P. O. Box 569, London S.E.1. Copies of many UKAEA reports (particularly earlier ones) may be purchased in microcopy form from Micro Methods Ltd., East Ardsley, Wakefield, Yorkshire, England. Copies of UKAEA reports are deposited with the National Lending Library for Science and Technology and 10 public libraries in England; with the USAEC and (through USAEC) with NTIS; and in most national nuclear centers throughout the world. In the USA, UKAEA reports are available on a subscription basis, by subject category, from UNIPUB, Inc., P. O. Box 433, New York, N. Y. 10016, USA.

UN Mail orders should be directed to the Sales Section, Room 1059, United Nations Headquarters, New York, New York 10017.

ZAED Available from Zentralstelle für Atomkernenergie Dokumentation, 6000 Frankfurt/Main 90, P. O. Box 901069, Westendstr. 21, West Germany

XUM

Report No.	Abstract No.	Availability
AAEC/LIB/Bib-	(Australian)	
286	25-37000	Dep. NTIS (U. S. Sales Only), 23p.
AAEC/TM-	(Australian)	
578	25-36309	Dep. NTIS (U. S. Sales Only), 56p.
585	25-36719	Dep. NTIS (U. S. Sales Only), 64p.
586	25-36812	Dep. NTIS (U. S. Sales Only), 5p.
ACNP-	(Misc.)	
70503.3	25-36895	See DOCKET-1155-116
AEC-	(New Zealander)	
26	25-36563	See ORO-3992-26
28	25-36435	See ORO-3992-28
30	25-36564	See ORO-3992-30
AECL-	(Canadian)	
3462	25-35523	Dep. NTIS (U. S. Sales Only). AECL $1.50, 51p.
3738	25-37054	Dep. NTIS (U. S. Sales Only). AECL $2.00, 71p.
3772	25-35865	Can. J. Phys.; 49: 606-20 (1 Mar 1971)
3787	25-37001	Dep. NTIS (U. S. Sales Only). AECL $0.50, 18p.
3804	25-34843	Dep. NTIS (U. S. Sales Only). AECL $0.20, 5p.
3828	25-35104	Can. J. Biochem.; 49: 456-62(Apr 1971)
3835	25-35258	Can. J. Microbiol.; 17: 575-83(May 1971)
3858	25-37002	Dep. NTIS (U. S. Sales Only). AECL $1.00, 23p.
AECOP-		
632	25-34766	Dep. NTIS, 31p.
AEEW-M-	(British)	
962	25-35023	Dep. NTIS (U. S. Sales Only), 8p.
985	25-36986	Dep. NTIS (U. S. Sales Only), 9p.
991	25-35024	Dep. NTIS (U. S. Sales Only), 10p.
AERE-R-	(British)	
6776	25-34861	Dep. NTIS (U. S. Sales Only). UK 9p, 6p.
ANL-		
7411(Suppl. 5)	25-37133	Dep. NTIS, 259p.
7746	25-34789	Dep. NTIS, 166p.
7777	25-35275	Dep. NTIS, 62p.
7779	25-36647	Dep. NTIS, 55p.
7788	25-36987	Dep. NTIS, 63p.
7792	25-37035	Dep. NTIS, 86p.
7796	25-36245	Dep. NTIS, 23p.
7797	25-37156	Dep. NTIS, 157p.
7809	25-37157	Dep. NTIS, 4p.
ANL/ES-CEN-		
1003	25-37158	Dep. NTIS, 38p.
ANL-Trans-		
882	25-34571	Dep. NTIS
ANU-P-	(Australian)	
438	25-34915	Dep. NTIS (U. S. Sales Only), 5p.
439	25-35813	Dep. NTIS (U. S. Sales Only), 5p.
451	25-36814	Dep. NTIS (U. S. Sales Only), 5p.
ARH-		
468(Rev.)	25-34678	Dep. NTIS, 12p.
ARH-SA-		
58-RD	25-34679	Dep. NTIS, 26p.
AWRE-O-	(British)	
3/71	25-36685	Dep. NTIS (U. S. Sales Only). UK 10p, 12p.
25/71	25-35331	Dep. NTIS (U. S. Sales Only). UK 15p, 18p.
42-69	25-35545	Dep. NTIS (U. S. Sales Only), 22p.
BDX-		
613-161	25-37159	Dep. NTIS, 46p.
613-177	25-37160	Dep. NTIS, 129p.
613-236	25-37161	Dep. NTIS, 29p.
613-263	25-37162	Dep. NTIS, 32p.
613-286	25-37163	Dep. NTIS, 31p.
613-294	25-37164	Dep. NTIS, 43p.
613-300	25-37165	Dep. NTIS, 28p.
613-313	25-37166	Dep. NTIS, 57p.
613-320	25-37167	Dep. NTIS, 25p.
613-344	25-37168	Dep. NTIS, 359p.
613-347	25-37169	Dep. NTIS, 51p.
613-405	25-37170	Dep. NTIS, 44p.
613-406	25-37171	Dep. NTIS, 29p.
613-408	25-37172	Dep. NTIS, 21p.
613-410	25-37173	Dep. NTIS, 23p.

Report No.	Abstract No.	Availability
BMI-	(Misc.)	
171-129	25-34767	Dep. NTIS, 46p.
1904	25-37036	Dep. NTIS, 24p.
BMI-X-		
604	25-35332	Dep. NTIS, 60p.
BNL-		
15815	25-37055	Dep. NTIS, 22p.
50249	25-34802	Dep. NTIS, 17p.
50274	25-36719	Dep. NTIS, 220p.
BNWL-		
462	25-36862	Dep. NTIS, 111p.
1308-5	25-34803	Dep. NTIS, 38p.
1502	25-34715	Dep. NTIS, 11p.
1507	25-37103	Dep. NTIS, 20p.
1543	25-35115	Dep. NTIS, 23p.
1560	25-37111	Dep. NTIS, 17p.
1561	25-36988	Dep. NTIS, 92p.
1568	25-37015	Dep. NTIS, 156p.
BNWL-B-		
51	25-34773	Dep. NTIS, 19p.
58	25-37174	Dep. NTIS, 49p.
BNWL-SA-		
3713	25-37104	Dep. NTIS, 20p.
3876	25-37105	Dep. NTIS, 26p.
BNWL-tr-		
67	25-37056	Dep. NTIS
CALT-		
68-360	25-36502	Dep. NTIS, 53p.
767-P-4-60	25-34574	J. Amer. Chem. Soc.; 93: 1840-51(21 Apr 1971)
822-29	25-37175	Dep. NTIS, 12p.
CAPE-		
1879	25-34930	EM
2039	25-36209	EM
2080	25-34783	EM
2081	25-34784	EM
2082	25-34785	EM
2083	25-34782	EM
CEA-Bib-	(French)	
190	25-34811	For translation see ORNL-tr-2488
CEA-CONF-	(French)	
1734	25-36073	Dep. NTIS (U. S. Sales Only), 9p.
1736	25-36074	Dep. NTIS (U. S. Sales Only), 14p.
1750	25-37093	Dep. NTIS (U. S. Sales Only), 38p.
1760	25-35333	Dep. NTIS (U. S. Sales Only), 4p.
CEA-N-	(French)	
1317	25-37060	For translation see EURFNR-885
1348	25-37061	For translation see EURFNR-850
1398	25-36989	Dep. NTIS (U. S. Sales Only), 56p.
1435	25-35025	Dep. NTIS (U. S. Sales Only), 36p.
1439	25-35044	Dep. NTIS (U. S. Sales Only), 4p.
1440	25-34673	Dep. NTIS (U. S. Sales Only), 44p.
1447	25-35045	Dep. NTIS (U. S. Sales Only), 7p.
1448	25-35046	Dep. NTIS (U. S. Sales Only), 7p.
CEA-R-	(French)	
3395	25-37056	For translation see BNWL-tr-67
3799	25-37057	Dep. NTIS (U. S. Sales Only), 174p.
4034	25-34749	Dep. NTIS (U. S. Sales Only), 357p.
4109	25-34680	Dep. NTIS (U. S. Sales Only), 62p.
4114	25-37058	Dep. NTIS (U. S. Sales Only), 106p.
4145	25-36648	Dep. NTIS (U. S. Sales Only), 73p.
CEA-tr-X-	(French)	
667	25-34501	Dep. NTIS (U. S. Sales Only)
CERN-Trans-	(European Organization for Nuclear Research)	
71-9	25-34937	Dep. NTIS (U. S. Sales Only)
71-10	25-35379	Dep. NTIS (U. S. Sales Only)
71-13	25-36658	Dep. NTIS (U. S. Sales Only)
CGS-		
746-10	25-34763	Dep. NTIS, 29p.
CIC-		
E1.1-8	25-37176	Dep. NTIS, 33p.
E2.2-8	25-37177	Dep. NTIS, 37p.
P1-8	25-37178	Dep. NTIS, 32p.
CNAEM-	(Turkish)	
77	25-35135	Dep. NTIS (U. S. Sales Only), 15p.
CONF-670999-	(Conference on New Experimental Techniques in Propulsion and Energetics Research, Munich, Germany, Sept. 11-15, 1967) 25-36107 Slough, Eng.; Technivision Services (1970). 637p	
CONF-680513-	(Inter-American Conference on Materials Technology, San Antonio, Tex., May 20-25, 1968)	

Report No.	Abstract No.	Availability
	25-34825	New York; American Society of Mechanical Engineers (1968). 647p. $27.00
CONF-680535-		(14th National Conference of the Italian Association for Health Physics and Protection from Radiation, Formia, Italy, May 29-31, 1968)
10	25-34500	Minerva Fisiconucl.; 13: 86-92(Jan-Mar 1969)
CONF-680818-		(Topical Meeting on Fast Reactors and the Universities, Troy, N.Y., Aug. 25-30, 1968)
	25-36976	Dep. NTIS, 460p.
CONF-680985-		(Symposium on Unconventional Methods in Exploration for Petroleum and Natural Gas, Dallas, Tex., Sept. 12-13, 1968)
	25-34729	Dallas; Institute for the Study of Earth and Man (1969). 251p. $10.00
CONF-680986-		(Meeting on Preparative Radiochemistry Production of Radionuclides and Labelled Compounds, Lindau Im Bodensee, Germany, Sept. 5-6, 1968)
1	25-36686	Dep. NTIS (U. S. Sales Only), 7p.
CONF-681082-		(9th Conference of the Society of German Radiation Medicine, Aachen, Germany, Oct. 11-12, 1968)
	25-35130	Strahlenschutz Forsch. Prax.; 9: 1-120(1969)
CONF-681087-		(2nd International Symposium on Initial Effects of Ionizing Radiation on a Cell II, Erivan, U.S.S.R., Oct. 29-Nov. 3, 1968)
	25-35196	Stud. Biophys.; 15-16: 1-406(1969)
CONF-690516-		(Pattern Recognition Studies Seminar, New York, June 9-10, 1969)
	25-35071	Redondo Beach, Calif.; Society of Photo-Optical Instrumentation Engineers (1969). 230p
CONF-690622-		(Laser Interaction and Related Plasma Phenomena Meeting, East Windsor Hill, Conn., June 9-13, 1969)
	25-35147	New York; Plenum Publishing Corporation (1971). 520p. $25.00
CONF-690724-		(Conference on Quantitative Relation Between Properties and Microstructure, Haifa, Israel, July 27-Aug. 1, 1969)
2	25-35333	See CEA-CONF-1760
CONF-690929-		(15th National Congress of the Italian Association for Health Physics and Protection Against Radiation, Cagliari, Italy, Sept. 29-Oct. 3, 1969)
5	25-34711	Minerva Fisiconucl.; 14: 7-16(Jan-Mar 1970)
CONF-691029-		(National Conference on the Contribution of Nuclear Medicine to Diagnosis and Therapy, Turin, Italy, Oct. 20--21, 1969)
	25-35155	Minerva Med.; 60: 4059-4166(17 Oct 1969)
CONF-691055-		(11th Symposium on Cosmic Rays, Astrophysics, Geophysics and Elementary Particle Physics, Delhi, India, Oct. 7-11, 1969)
(Vol.1)	25-35892	
(Vol.2)	25-35893	
CONF-691060-		(Joint UK/USSR Seminar on the Operation and Use of Research and Testing Reactors, Harwell, England, Oct.-Nov. 1969)
4	25-37057	See LE/G-3001
CONF-700204-		(IAEA Meeting on Research Reaction Utilization, Rome, Italy, Feb. 2-6, 1970)
8	25-36800	pp 209-24 of Research Reactor Utilization. Vol. 1. Vienna; International Atomic Energy Agency (1970)
9	25-36668	pp 177-84 of Research Reactor Utilization. Vol. 1. Vienna; International Atomic Energy Agency (1970)
CONF-700211-		(Atomic Energy Society Meeting, Tokyo, Japan, Feb. 13, 1970)
7	25-37139	Dep. NTIS, 7p.
9	25-37015	Dep. NTIS (U. S. Sales Only), 3p.
CONF-700341-		(Panel on Superconductors, Paris, France, Mar. 17-18, 1970)
1	25-36073	See CEA-CONF-1734
5	25-35074	See CEA-CONF-1736
7	25-36018	Dep. NTIS (U. S. Sales Only), 20p.
8	25-36019	Dep. NTIS (U. S. Sales Only), 26p.
CONF-700342-		(2nd International Conference on the Linear and Non-local Quantum Field Theory, Dubna, U.S.S.R., Mar. 15-20, 1970)
1	25-36561	See JINR-P2-5716
CONF-700438-		(Reactor Meeting, Berlin, Germany, Apr. 20-22, 1970)
1	25-34687	See EUR-4614
CONF-700439-		(2nd Meeting of the Liquid Metal Boiling Working Group, Casaccia, Italy, Apr. 9-10, 1970)
1	25-37046	See RT/ING-(70)18
CONF-700440-		(3rd Annual National Pollution Control Conference, San Francisco, Calif., Apr. 1-3, 1971)
1	25-34844	Dep. NTIS (U. S. Sales Only), 25p.
CONF-700505-		(2nd Congress of the International Radiation Protection Association, Brighton, England, May 3-8, 1970)
26	25-35023	See AEEW-M-962
CONF-700556-		(Italian-Polish Meeting, Warsaw, Poland, May 26-June 6, 1970)
4	25-35524	See RT/ING-(70)22
CONF-700557-		(Meeting on Mechanical Flow Processes in Gas Centrifuges, Porz-Wahn, Germany, May 14, 1970)
4	25-34790	Dep. NTIS (U. S. Sales Only)
CONF-700560-		(2nd Annual Symposium on Theory of Computing, Northampton, Mass., May 4-6, 1970)
1	25-37219	See RLO-2227-T-7-7
CONF-700608-		(American Nuclear Society Meeting, Los Angeles, Calif., June 29-July 2, 1970)
36	25-37037	Dep. NTIS, 18p.
37	25-36986	See AEEW-M-986
CONF-700623-		(International Conference on Bubble Chamber Technology, Argonne, Ill., June 10-12, 1970)
(Vol.1)	25-34938	Dep. NTIS, 591p.
(Vol.2)	25-34966	Dep. NTIS, 641p.
CONF-700630-		(Symposium on Effects of Radiation on Structural Materials, Niagara Falls, Ontario, Canada, June 29-July 2, 1970)
2	25-35505	See ZJE-99
CONF-700647-		(5th International Summer School on Electronics and Automation, Herceg-Novi, Yugoslavia, June 22-27, 1970)
	25-35047	
CONF-700651-		(European Meeting of Chemical Engineering, Frankfurt am Main, Germany, June 17-24, 1970)
1	25-34688	See EUR-4615
CONF-700653-		(Jubilee Meeting of the Association of Large Boiler Plant Operators, Essen, Germany, June 1-4, 1970)
1	25-36863	Dep. NTIS (U. S. Sales Only), 20p.
CONF-700819-		(2nd International Conference on the Strength of Metals and Alloys, Pacific Grove, Calif., Aug. 30-Sept. 4, 1970)
(Vol.1)	25-35369	Metals Park, Ohio; American Society for Metals (1970). 396p
(Vol.2)	25-35390	Metals Park, Ohio; American Society for Metals (1970). 422p
(Vol.3)	25-35395	Metals Park, Ohio; American Society for Metals (1970). 442p
12	25-37180	See CCO-1489-10
CONF-700949-		(2nd International CODATA Conference, St. Andrews, Scotland, Sept. 7-10, 1970)
1	25-37107	See INDC(NDS)-29/U
CONF-700954-		(35th Physicists Conference, Hanover, Germany, Sept. 28-Oct. 3, 1970)
	25-36430	Stuttgart; B. G. Teubner (1970). 349p
CONF-700956-		(15th International Congress of the International Union of Producers and Distributors of Electrical Energy, Cannes, France, Sept. 13-17, 1970)
2	25-36864	Dep. NTIS (U. S. Sales Only), 14p.
CONF-701044-		(5th Congress on Material Testing, Budapest, Hungary, Oct. 19-24, 1970)

XUM

Report No. (Sect.2)	Abstract No.	Availability
	25-34921	
CONF-701045-		(9th International Gel Permeation Chromatography Seminar, Miami Beach, Fla., Oct. 4-7, 1970)
	25-35532	J. Chromatogr.; 55: 1-220(17 Feb 1971)
CONF-701102-		(Meeting of the American Nuclear Society, Washington, D.C., Nov. 15-19, 1970)
20	25-37214	See ORO-3936-4
CONF-710110-		(4th International Conference on Systems Sciences, Honolulu, Hawaii, Jan. 12-14, 1971)
1	25-37254	See UCRL-72694
2	25-37253	See UCRL-72637
CONF-710111-		(HEPAP Subpanel on Advance Accelerator Technology, Berkeley, Calif., Jan. 7-9, 1971)
1	25-36514	See UCRL-20299
CONF-710210-		(Seminar on Test Requirements for Packaging for the Transport of Radioactive Materials, Vienna, Austria, Feb. 8-12, 1971)
3	25-34843	See AECL-3804
CONF-710213-		(Symposium on Sulfur Chemistry and Theoretical Chemistry, New Orleans, La., Feb. 18-20, 1971)
1	25-37249	See UCRL-20535
CONF-710214-		(Meeting on Nuclear Reactors for Marine Propulsion, Malakoff, France, Feb. 17, 1971)
1	25-37093	See CEA-CONF-1750
CONF-710301-		(3rd Conference on Neutron Cross Sections and Technology, Knoxville, Tenn., Mar. 15-17, 1971)
4	25-36720	Dep. NTIS, 9p.
11	25-36739	See UCRL-73090
12	25-36721	See DP-MS-70-95
13	25-36741	See WHAN-SA-107
14	25-36734	See ORNL-TM-3331
CONF-710302-		(Meeting on New Development in Reactor Mathematics and Applications, Idaho Falls, Idaho, Mar. 29-31, 1971)
11	25-36549	Dep. NTIS, 23p.
CONF-710304-		(Symposium on Natural and Manmade Radiation in Space, Las Vegas, Nev., Mar. 1-5, 1971)
12	25-36250	See ORNL-TM-3364
CONF-710306-		(35th Meeting of the Supersonic Tunnel Association, Dallas, Tex., Mar. 8-9, 1971)
1	25-37220	See SC-DC-713821
CONF-710312-		(18th Refractory Composites Working Group Meeting, Huntsville, Ala., Mar. 16-18, 1971)
1	25-37179	Dep. NTIS, 14p.
CONF-710313-		(2nd Symposium on Symbolic and Algebraic Manipulation, Los Angeles, Calif., Mar. 23-25, 1971)
1	25-37246	See UCRL-19861
CONF-710315-		(Conference on Fast Reactors, Palo Alto, Calif., Mar. 7-10, 1971)
1	25-37085	See WHAN-SA-104(Rev.)
CONF-710316-		(Workshop on Particle Physics at Intermediate Energies, Pasadena, Calif., Mar. 29-30, 1971)
1	25-36502	See CALT-68-300
CONF-710317-		(16th Nuclear Congress, Rome, Italy, Mar. 25-26, 1971)
1	25-37003	Dep. NTIS (U. S. Sales Only), 28p.
CONF-710401-		(Symposium on Safety in Plutonium Handling Facilities, Rocky Flats, Colo., Apr. 13-15, 1971)
1	25-34727	See UCRL-72927
2	25-34862	See EGG-1183-1517
CONF-710406-		(Conference on Air Pollution Meteorology, Raleigh, N.C., Apr. 5-9, 1971)
1	25-34747	See SC-DC-70-5443
CONF-710414-		(Conference on Fast Reactor Fuel Element Technology, New Orleans, La., Apr. 13-15, 1971)
1	25-37017	Dep. NTIS, 30p.
2	25-37054	See HEDL-SA-81
3	25-37019	See ORNL-TM-3386
CONF-710415-		(73rd Annual Meeting of the American Ceramics Society, Chicago, Ill., Apr. 26-28, 1971)
1	25-36310	See HEDL-SA-119
CONF-710417-		(International Solvent Extraction Conference, The Hague, Netherlands, Apr. 19-23, 1971)
1	25-34681	Dep. NTIS, 23p.
2	25-34679	See ARH-SA-58-RE
CONF-710418-		(4th Symposium of Engineering Problems of Fusion Research, Washington, D.C., Apr. 20-23, 1971)
1	25-36199	See UCRL-73060
2	25-36196	See UCRL-73031
3	25-36200	See UCRL-73067
4	25-36198	See UCRL-73059
5	25-36197	See UCRL-73047
6	25-36201	See UCRL-73129
7	25-36187	See MATT-837
8	25-36195	See UCRL-73030
9	25-36090	See MATT-838
10	25-36189	See MATT-840
11	25-36192	See MATT-846
12	25-36191	See MATT-844
CONF-710423-		(International Congress on Protection Against Accelerator and Space Radiation, Geneva, Switzerland, Apr. 26-30, 1971)
1	25-36610	See ORNL-TM-3353
CONF-710501-		(3rd National Symposium on Radioecology, Oak Ridge, Tenn., May 10-12, 1971)
5	25-37105	See ENWL-SA-3876
14	25-37104	See ENWL-SA-3712
15	25-37218	See RLO-2225-T-1-5
CONF-710509-		(26th Annual Purdue Industriel Waste Conference, Lafayette, Ind., May 4-6, 1971)
1	25-34682	Dep. NTIS, 15p.
CONF-710510-		(19th Annual Northwest Instrumentation Conference, Richland, Wash., May 20-21, 1971)
1	25-35072	See HEDL-SA-152
CONF-710601-		(International Conference on Radiation-Induced Voids in Metals, Albany, N.Y., June 9-11, 1971)
2	25-35503	See HEDL-SA-193
CONF-710603-		(International Conference on Corrosion Fatigue, Storrs, Conn., June 14-18, 1971)
1	25-37249	See UCRL-20538
CONF-710607-		(4th Conference on Plasma Physics and Controlled Nuclear Fusion Research, Madison, Wis., June 17-23, 1971)
1	25-36166	See UCRL-73135
CONF-710701-		(Computer Simulation Conference, Boston, Mass., July 19-21, 1971)
1	25-37255	See UCRL-73106
COO-		
1195-213	25-35384	Dep. NTIS, 27p.
1385-37	25-34634	Dep. NTIS, 6p.
1407-38	25-34742	Dep. NTIS, 81p.
1489-10	25-37180	Dep. NTIS, 5p.
1693-6	25-37181	Dep. NTIS, 4p.
1749-24	25-36550	Dep. NTIS, 94p.
1770-3	25-37182	Dep. NTIS, 43p.
1801-17	25-37183	Dep. NTIS, 7p.
2024-1	25-34750	Dep. NTIS, 121p.
2094-6	25-37184	Dep. NTIS, 74p.
CPT-	(Non-AEC)	
75	25-36455	See ORO-3992-24
77	25-36563	See ORO-3992-26
79	25-36436	See ORO-3992-28
81	25-36564	See ORO-3992-30
90	25-36456	See ORO-3992-39
CSIRO-Trans-	(Australian)	
10088	25-34716	Dep. NTIS (U. S. Sales Only)
CTC-		
48	25-35247	Dep. NTIS, 143p.
CTO-	(Non-AEC)	
737	25-36163	Dep. NTIS (U. S. Sales Only)
746	25-36186	Dep. NTIS (U. S. Sales Only)
DEMO-	(Greek)	
71/5	25-36214	Dep. NTIS (U. S. Sales Only), 6p.
71/6	25-36215	Dep. NTIS (U. S. Sales Only), 35p.
DLR-FB-	(German)	
70-13	25-35103	Dep. NTIS (U. S. Sales Only), 117p.
70-18	25-35990	Dep. NTIS (U. S. Sales Only), 54p.

Report No. Abstract No. Availability

DOCKET-1155- (LaCrosse Boiling Water Reactor) (AEC)
115 25-36865 Dep. NTIS, 2p.
116 25-36895 Dep. NTIS, 28p.
117 25-36895 Dep. NTIS, 60p.
118 25-36897 Dep. NTIS, 3p.
119 25-36898 Dep. NTIS, 11p.
120 25-36866 Dep. NTIS, 40p.

DOCKET-50003- (Indian Point Station; See Also DOCKET-50247, DOCKET-50286) (Non-AEC)
73 25-36854 Dep. NTIS, 3p.

DOCKET-50016- (Enrico Fermi Atomic Power Plant) (Non-AEC)
114 25-36899 Dep. NTIS, 2p.
115 25-36900 Dep. NTIS, 2p.

DOCKET-50133- (Humboldt Bay Power Plant) (Non-AEC)
57 25-36901 Dep. NTIS, 15p.

DOCKET-50146- (Saxton Nuclear Experimental Corporation) (Non-AEC)
76 25-36902 Dep. NTIS, 3p.
78 25-36903 Dep. NTIS, 5p.
79 25-36904 Dep. NTIS, 5p.
80 25-36905 Dep. NTIS, 4p.

DOCKET-50155- (Big Rock Point Reactor) (Misc.)
27 25-36887 See TID-23762
28 25-36888 See TID-23819
82 25-36905 Dep. NITS

DOCKET-50171- (Peach Bottom Atomic Power Station; See also DOCKET-50277 and DOCKET-50278) (Non-AEC)
85 25-36857 Dep. NTIS, 14p.

DOCKET-50201- (West Valley Reprocessing Plant--Formerly Spent Fuel Processing Plant) (Misc.)
73 25-34683 Dep. NTIS, 3p.

DOCKET-50206- (San Onofre Nuclear Generating Station) (Misc.)
113 25-36858 Dep. NTIS, 7p.

DOCKET-50213- (Haddam Neck Plant, Unit 1) (Misc.)
107 25-36907 Dep. NTIS, 11p.
108 25-36908 Dep. NTIS, 5p.
109 25-36869 Dep. NTIS, 15p.
112 25-36909 Dep. NTIS, 12p.

DOCKET-50219- (Oyster Creek Nuclear Power Plant) (Non-AEC)
134 25-36910 Dep. NTIS, 4p.
135 25-36870 Dep. NTIS, 2p.
137 25-36871 Dep. NTIS, 11p.

DOCKET-50231- (Southwest Experimental Fast Oxide Reactor) (Non-AEC)
83 25-37059 Dep. NTIS, 3p.

DOCKET-50237- (Dresden Nuclear Power Station, See also DOCKET-50249) (Non-AEC)
166 25-36911 Dep. NTIS, 6p.
167 25-36912 Dep. NTIS, 3p.
168 25-36913 Dep. NTIS, 30p.
169 25-36914 Dep. NTIS, 5p.
170 25-36915 Dep. NTIS, 3p.
171 25-36916 Dep. NTIS, 13p.
172 25-36872 Dep. NTIS, 1p.
173 25-36873 Dep. NTIS, 15p.
174 25-36917 Dep. NTIS, 15p.
175 25-36918 Dep. NTIS, 2p.
179 25-36919 Dep. NTIS, 11p.

DOCKET-50238- (N.S. Savannah Safety Assessment) (Non-AEC)
80 25-37094 Dep. NTIS, 9p.

DOCKET-50244- (Robert Emmett Ginna Nuclear Power Plant, Formerly Brookwood Nuclear Station) (Non-AEC)
71 25-36874 Dep. NTIS, 3p.

DOCKET-50245- (Millstone Point Nuclear Power Station) (Non-AEC)
59 25-36875 Dep. NTIS, 2p.
60 25-36876 Dep. NTIS, 2p.
61 25-36877 Dep. NTIS, 1p.
67 25-36878 Dep. NTIS, 2p.
81 25-36879 Dep. NTIS, 2p.

DOCKET-50249- (Dresden Nuclear Power Station; See also DOCKET-50237) (Non-AEC)
66 25-36912 See DOCKET-50237-167
67 25-36920 Dep. NTIS, 6p.
68 25-36921 Dep. NTIS, 3p.
70 25-36922 Dep. NTIS, 11p.
71 25-36917 See DOCKET-50237-174
72 25-36923 Dep. NTIS, 5p.
73 25-36924 Dep. NTIS, 13p.

DOCKET-50250- (Turkey Point, See also DOCKET-50251) (Non-AEC)
44 25-36925 Dep. NTIS, 63p.
46 25-36926 Dep. NTIS, 22p.

Report No. Abstract No. Availability
47 25-36927 Dep. NTIS, 53p.

DOCKET-50251- (Turkey Point, See also DOCKET-50250) (Non-AEC)
40 25-36925 See DOCKET-50250-44
42 25-36926 See DOCKET-50250-46
43 25-36927 See DOCKET-50250-47

DOCKET-50254- (Quad-Cities Station; See also DOCKET-50265) (Non-AEC)
37 25-36928 Dep. NTIS, 2p.

DOCKET-50255- (Palisades Plant) (Non-AEC)
41 25-36929 Dep. NTIS, 103p.
42 25-36930 Dep. NTIS, 2p.

DOCKET-50261- (H. B. Robinson) (Non-AEC)
59 25-36931 Dep. NTIS, 3p.
60 25-36880 Dep. NTIS, 68p.
61 25-36932 Dep. NTIS, 31p.

DOCKET-50265- (Quad-Cities Station; See also DOCKET-50254) (Non-AEC)
34 25-36928 See DOCKET-50254-37

DOCKET-50266- (Point Beach Nuclear Plant) (Non-AEC)
48 25-36933 Dep. NTIS, 52p.
49 25-36881 Dep. NTIS, 3p.
50 25-36934 Dep. NTIS, 2p.

DOCKET-50267- (Fort St. Vrain Nuclear Generating Station) (Non-AEC)
30 25-36935 Dep. NTIS, 3p.

DOCKET-50268- (Midwest Fuel Recovery Plant) (Non-AEC)
8 25-34684 Dep. NTIS, 92p.
9 25-34685 Dep. NTIS, 43p.

DOCKET-50271- (Vermont Yankee Nuclear Power Station) (Non-AEC)
53 25-36936 Dep. NTIS, 44p.

DOCKET-50277- (Peach Bottom Atomic Power Station; See also DOCKET-50171 and DOCKET-50278) (Non-AEC)
20 25-36937 Dep. NTIS, 358p.

DOCKET-50278- (Peach Bottom Atomic Power Station; See also DOCKET-50171 and DOCKET-50277) (Non-AEC)
20 25-36937 See DOCKET-50277-20

DOCKET-50280- (Surry Power Station, See also DOCKET-50281) (Non-AEC)
40 25-36938 Dep. NTIS, 107p.

DOCKET-50281- (Surry Power Station, See also DOCKET-50280) (Non-AEC)
40 25-36938 See DOCKET-50280-40

DOCKET-50282- (Prairie Island Nuclear Generating Plant, See also DOCKET-50306) (Non-AEC)
35 25-36939 Dep. NTIS, 5p.

DOCKET-50285- (Fort Calhoun Station) (Non-AEC)
45 25-36940 Dep. NTIS, 340p.

DOCKET-50286- (Indian Point Nuclear Plant) (Non-AEC)
34 25-36941 Dep. NTIS, 162p.
35 25-36942 Dep. NTIS, 644p.
36 25-36943 Dep. NTIS, 586p.

DOCKET-50289- (Three Mile Island Nuclear Station) (Non-AEC)
35 25-36944 Dep. NTIS, 447p.
36 25-36882 Dep. NTIS, 7p.

DOCKET-50301- (Point Beach Nuclear Plant) (Non-AEC)
31 25-36933 See DOCKET-50266-48
33 25-36934 See DOCKET-50266-50

DOCKET-50306- (Prairie Island Nuclear Generating Plant, See also DOCKET-50282) (Non-AEC)
35 25-36939 See DOCKET-50282-35

DOCKET-50309- (Maine Yankee Atomic Power Company) (Non-AEC)
35 25-36945 Dep. NTIS, 72p.
36 25-36946 Dep. NTIS, 34p.

DOCKET-50313- (Russellville Nuclear Unit) (Non-AEC)
30 25-36947 Dep. NTIS, 321p.

DOCKET-50315- (Donald C. Cook Nuclear Power Plant, See also DOCKET-50316) (Non-AEC)
35 25-36948 Dep. NTIS, 8p.

DOCKET-50316- (Donald C. Cook Nuclear Power Plant, See also DOCKET-50315) (Non-AEC)
35 25-36948 See DOCKET-50315-35

DOCKET-50332- (Barnwell Nuclear Fuel Plant) (Non-AEC)
18 25-34686 Dep. NTIS, 59p.

XUM

Report No.	Abstract No.	Availability
DOCKET-50333-	(James A. Fitzpatrick Nuclear Power Plant) (Non-AEC)	
22	25-36949	Dep. NTIS, 161p.
DOCKET-50336-	(Millstone Nuclear Power Station) (Non-AEC)	
22	25-36950	Dep. NTIS, 8p.
DOCKET-50348-	(Joseph M. Farley Nuclear Plant, Units 1 and 2, Formerly Seala Nuclear Plant, See also DOCKET-50364) (Non-AEC)	
20	25-36951	Dep. NTIS, 168p.
DOCKET-50352-	(Limerick Generating Station) (See also DOCKET-50353) (Non-AEC)	
13	25-36952	Dep. NTIS, 201p.
DOCKET-50353-	(Limerick Generating Station) (See also DOCKET-50352) (Non-AEC)	
13	25-36952	See DOCKET-50352-13
DOCKET-50354-	(Newbold Island Nuclear Generating Station) (See also DOCKET-50355) (Non-AEC)	
14	25-36883	Dep. NTIS, 275p.
DOCKET-50355-	(Newbold Island Nuclear Generating Station) (See also DOCKET-50354) (Non-AEC)	
14	25-36883	See DOCKET-50354-14
DOCKET-50358-	(Wm. H. Zimmer Nuclear Power Station, Units 1 and 2) (See also DOCKET-50359) (Non-AEC)	
17	25-36953	Dep. NTIS, 221p.
18	25-36954	Dep. NTIS, 521p.
DOCKET-50361-	(San Onofre Nuclear Generating Station) (Units 2 and 3) (See also Docket-50362) (Docket-50206) (Unit 1) (Non-AEC)	
17	25-36955	Dep. NTIS, 241p.
DOCKET-50362-	(San Onofre Nuclear Generating Station) (Units 2 and 3) (See also Docket-50361) (Docket-50206) (Unit 1) (Non-AEC)	
16	25-36955	See DOCKET-50361-17
DOCKET-50363-	(Forked River Nuclear Station) (Unit 1) (Non-AEC)	
15	25-36956	Dep. NTIS, 33p.
DOCKET-50364-	(Joseph M. Farley Nuclear Plant, Units 1 and 2, See also DOCKET-50348) (Non-AEC)	
14	25-36951	See DOCKET-50348-20
DOCKET-50367-	(Bailly Generating Station Nuclear 1), (Non-AEC)	
14	25-36957	Dep. NTIS, 549p.
15	25-36958	Dep. NTIS, 200p.
16	25-36959	Dep. NTIS, 191p.
DOCKET-50368-	(Arkansas Nuclear One) (Non-AEC) (Unit 2)	
11	25-36960	Dep. NTIS, 53p.
DOCKET-50369-	(McGuire Nuclear Station) (See also DOCKET-50370) (Non-AEC) (Units 1 and 2)	
10	25-36961	Dep. NTIS, 84p.
DOCKET-50370-	(McGuire Nuclear Station) (See also DOCKET-50369) (Non-AEC) (Units 1 and 2)	
9	25-36961	See DOCKET-50369-10
DOCKET-50389-	(Hutchinson Island Plant)(Non-AEC)	
8	25-36962	Dep. NTIS, 3p.
9	25-36963	Dep. NTIS, 5p.
DOCKET-50390-	(Watts Bar Nuclear Plant) (See Also DOCKET-50391)	
1	25-36964	Dep. NTIS, 103p.
2	25-36965	Dep. NTIS, 665p.
3	25-36966	Dep. NTIS, 507p.
4	25-36967	Dep. NTIS, 328p.
5	25-36968	Dep. NTIS, 528p.
6	25-36969	Dep. NTIS, 124p.
DOCKET-50391-	(Watts Bar Nuclear Plant) (See Also DOCKET-50390)	
1	25-36964	See DOCKET-50390-1
2	25-36965	See DOCKET-50390-2
3	25-36966	See DOCKET-50390-3
4	25-36967	See DOCKET-50390-4
5	25-36968	See DOCKET-50390-5
6	25-36969	See DOCKET-50390-6
DP-		
1259	25-37106	Dep. NTIS, 24p.
DP-MS-		
70-95	25-36721	Dep. NTIS, 6p.
70-101	25-37134	Dep. NTIS, 121p.
71-25	25-37185	Dep. NTIS, 60p.
DPC-		
71-9	25-36865	See DOCKET-1155-115
851-24	25-36866	See DOCKET-1155-120
EANDC(US)-	(European-American Nuclear Data Committee)	
151-A	25-36660	See LA-4574
EGG-		
1183-1517	25-34862	Dep. NTIS, 10p.
ENDF-		
141	25-36660	See LA-4574
ETR-	(Belgian)	
267	25-34719	See NF-18737
EUR-	(European Atomic Energy Community)	
4572	25-36993	See KFK-1337
4614	25-34687	Dep. NTIS (U. S. Sales Only). EUR F.Fr. 4.55, 20p.
4615	25-34688	Dep. NTIS (U. S. Sales Only). EUR F.Fr. 4.45, 24p.
4629	25-34774	Dep. NTIS (U. S. Sales Only). EUR FF 9,45, 66p.
4634	25-34775	Dep. NTIS (U. S. Sales Only). EUR DM,920, 78p.
4635	25-34556	Dep. NTIS (U. S. Sales Only). EUR F.Fr. 4.45, 21p.
4636	25-34717	Dep. NTIS (U. S. Sales Only). EUR F.Fr. 6.65, 43p.
4637	25-35334	Dep. NTIS (U. S. Sales Only). EUR F.Fr. 4.45, 14p.
EURFNR-	(European Atomic Energy Community)	
794	25-34776	Dep. NTIS
889	25-37060	Dep. NTIS
890	25-37061	Dep. NTIS
FMRB-	(German)	
32/70	25-37062	NTIS (U. S. Sales Only), 63p.
35/71	25-37063	Dep. NTIS (U. S. Sales Only), 25p.
GA-	(Misc.)	
9807	25-34542	Dep. NTIS, 263p.
10194	25-36729	See N-70-41999
10501	25-36977	Dep. NTIS, 107p.
10560	25-36978	Dep. NTIS, 112p.
GAT-		
649	25-34602	Dep. NTIS, 104p.
GAT-Z-		
5046	25-37186	Dep. NTIS
GEAP-	(Misc.)	
12182	25-35547	Dep. NTIS, 14p.
13539-16	25-35276	Dep. NTIS, 43p.
13672	25-37112	Dep. NTIS, 193p.
GIPR-	(Swedish)	
41	25-36248	Dep. NTIS (U. S. Sales Only), 28p.
GULF-RT-		
10523	25-36991	Dep. NTIS, 123p.
HEDL-SA-		
81	25-37064	Dep. NTIS, 30p.
119	25-36310	Dep. NTIS, 23p.
152	25-35072	Dep. NTIS, 18p.
193	25-35503	Dep. NTIS, 63p.
HMI-B-	(German)	
108	25-34863	Dep. NTIS (U. S. Sales Only), 127p.
HSSTP-TR-		
14	25-35335	Dep. NTIS, 56p.
IA-	(Israel)	
1208	25-36722	Dep. NTIS (U. S. Sales Only), 46p.
IAE-	(Russian)	
1925	25-37067	For translation see LE/G-2001
1944	25-36454	Dep. NTIS (U. S. Sales Only), 15p.
1947	25-36385	Dep. NTIS (U. S. Sales Only), 16p.
1552	25-36186	For translation see CTO-746
2012	25-36163	For translation see CTO-737
IAEA-	(International Atomic Energy Agency)	
127	25-36884	NTIS (U. S. Sales Only), 244p.
IAEA-R-	(International Atomic Energy Agency)	
876-F	25-34689	NTIS (U. S. Sales Only), 30p.
ICRU-	(Non-AEC)	
10-b	25-35137	Superintendent of Documents, GPO, Washington, D. C
IFVE-SEF-	(Russian)	
70-17	25-34864	Dep. NTIS (U. S. Sales Only), 17p.
IFVE-SKU-	(Russian)	
70-20	25-36603	Dep. NTIS (U. S. Sales Only), 16p.

XUM

Report No.	Abstract No.	Availability
IJS-	(Yugoslavian)	
263	25-34603	Dep. NTIS (U. S. Sales Only), 56p.
IN-		
1435	25-37113	Dep. NTIS, 111p.
1453	25-37038	Dep. NTIS, 51p.
1457	25-34690	Dep. NTIS, 109p.
INDC(NDS)-	(International Atomic Energy Agency)	
29/U	25-37107	Dep. NTIS (U. S. Sales Only), 12p.
INIS-mf-	(International Atomic Energy Agency)	
33	25-36994	NTIS (U. S. Sales Only), 3p.
INR-	(Non-AEC)	
1247	25-34502	Dep. NTIS (U. S. Sales Only), 14p.
1249	25-34845	Dep. NTIS (U. S. Sales Only), 44p.
1255	25-35336	Dep. NTIS (U. S. Sales Only), 12p.
INR-P-	(Polish)	
1234	25-36659	Dep. NTIS (U. S. Sales Only), 56p.
1265	25-36503	Dep. NTIS (U. S. Sales Only), 56p.
INT-	(Misc.)	
7	25-36311	See NP-18845
IS-		
2541	25-34743	Dep. NTIS, 37p.
ITF-	(Russian)	
70-56	25-36215	Dep. NTIS (U. S. Sales Only), 17p.
70-61-E	25-36353	Dep. NTIS (U. S. Sales Only), 28p.
70-96-P	25-36550	Dep. NTIS (U. S. Sales Only), 54p.
ITJ-	(Polish)	
3	25-36388	Dep. NTIS (U. S. Sales Only), 25p.
5	25-36389	Dep. NTIS (U. S. Sales Only), 11p.
6	25-36431	Dep. NTIS (U. S. Sales Only), 26p.
JAERI-Memo-	(Japanese)	
4173	25-37042	Dep. NTIS (U. S. Sales Only), 54p.
4174	25-37043	Dep. NTIS (U. S. Sales Only), 90p.
4260	25-37044	Dep. NTIS (U. S. Sales Only), 48p.
4270	25-37065	Dep. NTIS (U. S. Sales Only), 53p.
4276	25-37114	Dep. NTIS (U. S. Sales Only), 25p.
4279	25-34559	Dep. NTIS (U. S. Sales Only), 15p.
4280	25-34670	Dep. NTIS (U. S. Sales Only), 16p.
4285	25-34804	Dep. NTIS (U. S. Sales Only), 60p.
4330	25-37004	Dep. NTIS (U. S. Sales Only), 49p.
4331	25-36992	Dep. NTIS (U. S. Sales Only), 40p.
4356	25-37066	Dep. NTIS (U. S. Sales Only), 36p.
JINR-	(Russian)	
E2-5770	25-36504	Dep. NTIS (U. S. Sales Only), 15p.
E2-5771	25-36585	Dep. NTIS (U. S. Sales Only), 27p.
E2-5797	25-36815	Dep. NTIS (U. S. Sales Only), 10p.
E3-5713	25-36380	Dep. NTIS (U. S. Sales Only), 19p.
E14-5731	25-34915	Dep. NTIS (U. S. Sales Only), 31p.
P1-5530	25-36723	Dep. NTIS (U. S. Sales Only), 14p.
P1-5743	25-36390	Dep. NTIS (U. S. Sales Only), 25p.
P1-5781	25-36405	Dep. NTIS (U. S. Sales Only), 24p.
P2-5716	25-36561	Dep. NTIS (U. S. Sales Only), 16p.
P2-5719	25-36816	Dep. NTIS (U. S. Sales Only), 17p.
P2-5760	25-36552	Dep. NTIS (U. S. Sales Only), 16p.
P2-5768	25-36587	Dep. NTIS (U. S. Sales Only), 14p.
P4-5734	25-36354	Dep. NTIS (U. S. Sales Only), 16p.
P4-5744	25-36817	Dep. NTIS (U. S. Sales Only), 12p.
P6-5673	25-36724	Dep. NTIS (U. S. Sales Only), 21p.
P6-5674	25-36725	Dep. NTIS (U. S. Sales Only), 18p.
P6-5681	25-36726	Dep. NTIS (U. S. Sales Only), 15p.
P6-5683	25-34604	Dep. NTIS (U. S. Sales Only), 12p.
P6-5704	25-35727	Dep. NTIS (U. S. Sales Only), 15p.
P6-5761	25-34805	Dep. NTIS (U. S. Sales Only), 10p.
P9-4850	25-36616	For translation see UCRL-Trans-1440
P9-5091	25-36617	For translation see UCRL-Trans-1443
P9-5558	25-36615	For translation see UCRL-Trans-1434
P9-5645	25-36604	Dep. NTIS (U. S. Sales Only), 14p.
P9-5724	25-36605	Dep. NTIS (U. S. Sales Only), 11p.
P10-5762	25-35004	Dep. NTIS (U. S. Sales Only), 15p.
P13-5696	25-34865	Dep. NTIS (U. S. Sales Only), 16p.
P13-5722	25-34855	Dep. NTIS (U. S. Sales Only), 15p.
P13-5751	25-35005	Dep. NTIS (U. S. Sales Only), 19p.
P13-5757	25-34806	Dep. NTIS (U. S. Sales Only), 13p.
P13-5810	25-35005	Dep. NTIS (U. S. Sales Only), 12p.
JUL-	(German)	
701-RW	25-37018	Dep. NTIS (U. S. Sales Only), 34p.
705-RG	25-36885	Dep. NTIS (U. S. Sales Only), 55p.
709-RG	25-34535	Dep. NTIS (U. S. Sales Only), 127p.
719-FF	25-34917	Dep. NTIS (U. S. Sales Only), 27p.
725-RG	25-36980	Dep. NTIS (U. S. Sales Only), 95p.
KFK-	(German)	
1168	25-34776	For translation see EURFNR-794
1332	25-34791	Dep. NTIS (U. S. Sales Only), 100p.
1333	25-36818	Dep. NTIS (U. S. Sales Only), 78p.
1337	25-36993	Dep. NTIS (U. S. Sales Only), 54p.
1339	25-34557	Dep. NTIS (U. S. Sales Only), 98p.
1350	25-37135	Dep. NTIS (U. S. Sales Only), 120p.
1379	25-37005	Dep. NTIS (U. S. Sales Only), 27p.
KFKI-	(Hungarian)	
71-9	25-36728	Dep. NTIS (U. S. Sales Only), 18p.
KH-R-	(Non-AEC)	
12	25-34718	
KHFTI-	(Russian)	
69/51	25-36089	Dep. NTIS (U. S. Sales Only), 16p.
LA-		
4553	25-37187	Dep. NTIS, 26p.
4574	25-36660	Dep. NTIS, 18p.
4624	25-36249	Dep. NTIS, 25p.
4645	25-34691	Dep. NTIS, 16p.
4655	25-37188	Dep. NTIS, 8p.
4660	25-34846	Dep. NTIS, 12p.
4663	25-36432	Dep. NTIS, 4p.
4666	25-37189	Dep. NTIS, 6p.
4682	25-37190	Dep. NTIS, 7p.
LA-tr-		
71-32	25-37191	Dep. NTIS
LAL-	(French)	
1243	25-36672	Dep. NTIS (U. S. Sales Only), 103p.
1249	25-36606	Dep. NTIS (U. S. Sales Only), 28p.
LB/G-	(British)	
3001	25-37067	Dep. NTIS (U. S. Sales Only)
3034	25-34918	Dep. NTIS (U. S. Sales Only)
LFEN-	(Portuguese)	
115	25-35133	Zentralbl. Veterinaermed., Beih.; No. 11, 101-9(1970)
LNF-	(Italian)	
70/19	25-36607	Dep. NTIS (U. S. Sales Only), 6p.
70/25	25-35007	Dep. NTIS (U. S. Sales Only), 12p.
70/44	25-35008	Dep. NTIS (U. S. Sales Only), 5p.
71/1	25-36433	Dep. NTIS (U. S. Sales Only), 14p.
71/5	25-36434	Dep. NTIS (U. S. Sales Only), 4p.
LYCEN-	(French)	
7087	25-36687	Dep. NTIS (U. S. Sales Only), 66p.
MATT-		
837	25-36187	Dep. NTIS, 10p.
838	25-36090	Dep. NTIS, 12p.
839	25-36188	Dep. NTIS, 9p.
840	25-36189	Dep. NTIS, 12p.
841	25-36190	Dep. NTIS, 11p.
844	25-36191	Dep. NTIS, 6p.
846	25-36192	Dep. NTIS, 11p.
MHSMP-		
71-31	25-37192	Dep. NTIS, 4p.
71-32	25-37193	Dep. NTIS, 10p.
71-33	25-37194	Dep. NTIS, 6p.
71-34	25-37195	Dep. NTIS, 5p.
MLM-		
1793	25-34807	Dep. NTIS, 29p.
N-	(Misc.)	
70-41999	25-36729	NTIS, 94p.
70-43042	25-36688	NTIS, 39p.
NASA-CR-	(Misc.)	
72745	25-36729	See N-70-41999
110933	25-36688	See N-70-43042
NBL-		
256	25-34503	Dep. NTIS, 29p.
NBS-TN-	(Misc.)	
326	25-35952	GPO $0.60
NCG-TR-	(Non-AEC)	
15(Vol.1)	25-34768	Dep. NTIS, 101p.
NCRP-	(Non-AEC)	
23	25-34879	Superintendent of Documents, GPO, Washington, D. C.
NEDO-	(Non-AEC)	
14503	25-34684	See DOCKET-50268-8
NIM-	(Non-AEC)	
1013	25-34543	Dep. NTIS (U. S. Sales Only), 5p.
1048	25-34544	Dep. NTIS (U. S. Sales Only), 7p.
NP-	(AEC File No. for Non-AEC Reports)	
18733	25-35973	The Hague; Staatsdrukkerij (1965). 122p. f. 19,00
18737	25-34719	Dep. NTIS (U. S. Sales Only), 17p.
18760	25-34859	London; Her Majesty's Stationery Office (1970). 74p. Pound 0.40
18772	25-36104	Dep. NTIS (U. S. Sales Only), 129p.
18810	25-34635	Dep. NTIS (U. S. Sales Only), 65p.
18818	25-36355	Dep. NTIS (U. S. Sales Only), 12p.

XUM

Report No.	Abstract No.	Availability
18820	25-36689	Dep. NTIS (U. S. Sales Only), 38p.
18824	25-36690	Dep. NTIS (U. S. Sales Only), 79p.
18828	25-34744	Dep. NTIS (U. S. Sales Only), 41p.
18829	25-35730	Dep. NTIS (U. S. Sales Only), 97p.
18833	25-35277	Dep. NTIS (U. S. Sales Only), 177p.
18835	25-35731	Dep. NTIS (U. S. Sales Only), 70p.
18842	25-37045	Dep. NTIS (U. S. Sales Only), 28p.
18845	25-35311	Dep. NTIS (U. S. Sales Only), 86p.
18846	25-36855	Dep. NTIS (U. S. Sales Only), 174p.
18847	25-36855	Dep. NTIS (U. S. Sales Only), 58p.
18849	25-34857	Dep. NTIS (U. S. Sales Only), 9p.
18855	25-36608	Dep. NTIS (U. S. Sales Only), 61p.
18860	25-36609	Dep. NTIS (U. S. Sales Only), 20p.
18865	25-34504	Dep. NTIS (U. S. Sales Only), 87p.
18873	25-36406	Dep. NTIS (U. S. Sales Only), 87p.
NRL-	(Misc.)	
7230	25-36732	
NVO-		
1229-121	25-34720	Dep. NTIS, 62p.
NYO-		
1480-171	25-37196	Dep. NTIS, 109p.
1480-173	25-36126	Dep. NTIS, 49p.
1932(2)-189	25-36435	Dep. NTIS, 16p.
2174-129	25-34759	Dep. NTIS, 34p.
2262-TA-241	25-36482	Dep. NTIS, 12p.
2265-16	25-37197	Dep. NTIS, 68p.
2504-63	25-37198	Dep. NTIS, 15p.
2504-74	25-37199	Dep. NTIS, 101p.
2807-91	25-37200	Dep. NTIS, 7p.
3178-8	25-36419	Dep. NTIS, 12p.
3250-59	25-36869	See DOCKET-50213-109
3270-38	25-36868	See DOCKET-50206-113
3399-241	25-36483	See SU-1206-241
3504-50	25-36259	Dep. NTIS, 28p.
3504-58	25-37201	Dep. NTIS, 23p.
3590-8	25-37202	Dep. NTIS, 31p.
3597-16	25-37203	Dep. NTIS, 34p.
3699-51	25-37204	Dep. NTIS, 38p.
3759-18	25-37205	Dep. NTIS, 8p.
3759-30	25-37206	Dep. NTIS, 15p.
3851-10	25-37207	Dep. NTIS, 20p.
3912-3	25-34721	Dep. NTIS, 21p.
3912-4	25-34722	Dep. NTIS, 79p.
3975-3	25-35337	Dep. NTIS, 6p.
3995-15	25-37208	Dep. NTIS, 83p.
4030-9	25-37209	Dep. NTIS, 73p.
4030-10	25-37210	Dep. NTIS, 17p.
4057-2	25-34692	Dep. NTIS, 94p.
4061-2	25-34745	Dep. NTIS, 110p.
4076-14	25-36472	Dep. NTIS, 15p.
ORNL-		
4503(Vol.3)	25-35549	Dep. NTIS, 34p.
4564	25-35733	Dep. NTIS, 53p.
4574	25-34693	Dep. NTIS, 78p.
4607	25-34847	Dep
4680	25-34848	Dep. NTIS, 69p.
ORNL-IIC-		
34	25-34777	Dep. NTIS, 293p.
36	25-34808	Dep. NTIS, 134p.
ORNL-TM-		
2412(Pt.10)	25-37023	Dep. NTIS, 22p.
2412(Pt.12)	25-37029	Dep. NTIS, 25p.
2929	25-37006	Dep. NTIS, 92p.
3138	25-34694	Dep. NTIS, 97p.
3201	25-37211	Dep. NTIS, 82p.
3223	25-36886	Dep. NTIS, 118p.
3230	25-34809	Dep. NTIS, 60p.
3243	25-37030	Dep. NTIS, 31p.
3295	25-37212	Dep. NTIS, 281p.
3296	25-37213	Dep. NTIS, 162p.
3316	25-35338	Dep. NTIS, 15p.
3331	25-36734	Dep. NTIS, 12p.
3353	25-36610	Dep. NTIS, 41p.
3362	25-35568	Dep. NTIS, 21p.
3364	25-36250	Dep. NTIS, 29p.
3386	25-37019	Dep. NTIS, 26p.
3394	25-34810	Dep. NTIS, 26p.
3401	25-36193	Dep. NTIS, 76p.
3402	25-37091	Dep. NTIS, 56p.
3432	25-37068	Dep. NTIS, 26p.
3453	25-37069	Dep. NTIS, 39p.
ORNL-tr-		
2397	25-34695	Dep. NTIS
2417	25-34778	Dep. NTIS
2470	25-37007	Dep. NTIS
2474	25-36981	Dep. NTIS
2479	25-35339	Dep. NTIS
2481	25-36691	Dep. NTIS
2485	25-34811	Dep. NTIS
2492	25-34812	Dep. NTIS
ORO-		
2504-172	25-35009	Dep. NTIS, 37p.
3027-19	25-35833	Dep. NTIS, 34p.
3234-23	25-34572	Dep. NTIS, 66p.
3729-4	25-34636	Dep. NTIS, 39p.
3912-4	25-35504	Dep. NTIS, 23p.
3936-4	25-37214	Dep. NTIS, 36p.
3992-24	25-36455	Dep. NTIS, 11p.
3992-26	25-36563	Dep. NTIS, 38p.
3992-28	25-36436	Dep. NTIS, 25p.
3992-30	25-36564	Dep. NTIS, 13p.
3992-39	25-36456	Dep. NTIS, 15p.
4059-1	25-34637	Dep. NTIS, 8p.
PAM-	(French)	
71.1	25-36505	Dep. NTIS (U. S. Sales Only), 42p.
PATENTS	(British)	
1,164,816	25-36066	
1,168,107	25-35542	
1,181,431	25-36105	
1,218,845	25-34878	
1,220,449	25-36292	
1,222,112	25-34874	
1,223,888	25-35073	
1,224,012	25-35539	
1,224,114	25-35323	
1,225,197	25-34914	
1,225,489	25-35058	
1,225,962	25-34855	
1,226,626	25-35037	
1,226,834	25-34912	
1,226,924	25-34913	
1,228,030	25-34885	
1,228,149	25-35041	
1,228,150	25-35078	
1,228,814	25-36656	
1,229,395	25-34710	
1,229,469	25-36619	
1,230,031	25-34886	
1,230,053	25-37153	
1,230,520	25-37023	
1,230,984	25-37151	
1,231,129	25-37026	
1,232,767	25-37014	
1,232,811	25-37025	
1,232,957	25-37150	
1,232,959	25-37053	
1,233,689	25-37027	
1,233,695	25-37154	
PATENTS	(Canadian)	
865,509	25-34772	
PATENTS	(French)	
1,519,644	25-37149	
1,569,732	25-37148	
1,587,331	25-34713	
1,592,906	25-35077	
1,593,960	25-34883	
1,596,082	25-34884	
1,598,008	25-35042	
1,598,473	25-34882	
1,602,368	25-34712	
2,002,111	25-35561	
2,028,039	25-37152	
2,036,729	25-37155	
PATENTS	(German)	
1,295,723	25-34850	
1,514,804	25-34893	
1,564,583	25-36635	
PATENTS	(Russian)	
240,206	25-35476	
PATENTS	(U. S.)	
3,523,868	25-37147	
3,554,630	25-35069	
3,560,746	25-34876	
3,560,748	25-35038	
3,562,708	25-35074	
3,564,248	25-35039	
3,564,250	25-34875	
3,567,581	25-35540	
3,567,582	25-37143	
3,567,925	25-34887	
3,569,697	25-35035	
3,569,701	25-34888	
3,569,704	25-35036	
3,569,705	25-35836	
3,569,995	25-35033	
3,571,595	25-36657	
3,574,057	25-36985	
3,574,059	25-36998	
3,574,473	25-37145	
3,574,645	25-35543	
3,575,601	25-34858	
3,575,805	25-37141	
3,575,806	25-35329	
3,575,807	25-37013	
3,576,717	25-36997	

Report No.	Abstract No.	Availability
PG-Report-	(British)	
1020	25-34505	Dep. NTIS (U. S. Sales Only), 5p.
PNE-R-		
48	25-34728	See USGS-474-101
PUC-		
937-396	25-35050	Dep. NTIS, 13p.
RFP-		
1608	25-34605	Dep. NTIS, 6p.
RISO-	(Danish)	
234	25-37115	Dep. NTIS (U. S. Sales Only), 168p.
RLO-		
1725-186	25-37215	Dep. NTIS, 47p.
1725-191	25-37216	Dep. NTIS, 73p.
1725-200	25-37217	Dep. NTIS, 24p.
2225-T-1-5	25-37218	Dep. NTIS, 20p.
2225-T-20-3	25-34723	Dep. NTIS, 25p.
2227-T-7-7	25-37219	Dep. NTIS, 5p.
2227-T-9-1	25-34724	Dep. NTIS, 9p.
2230-T-2-2	25-34573	Dep. NTIS, 10p.
RT/CHI-	(Italian)	
(70)35	25-34638	Dep. NTIS (U. S. Sales Only), 24p.
RT/ING-	(Italian)	
(70)18	25-37045	Dep. NTIS (U. S. Sales Only), 36p.
(70)22	25-35524	Dep. NTIS (U. S. Sales Only), 29p.
RT/PROT-	(Italian)	
(70)17	25-34711	Minerva Fisiconucl.; 14: 7-16(Jan-Mar 1970)
(70)36	25-34849	Dep. NTIS (U. S. Sales Only), 101p.
(70)42	25-34746	Dep. NTIS (U. S. Sales Only), 100p.
SC-B-		
710148	25-36259	Dep. NTIS, 186p.
SC-DC-		
70-5443	25-34747	Dep. NTIS, 9p.
713821	25-37220	Dep. NTIS, 24p.
SC-DR-		
70-767	25-37221	Dep. NTIS, 80p.
70-862	25-37222	Dep. NTIS, 12p.
710074	25-37223	Dep. NTIS, 49p.
710084	25-34792	Dep. NTIS, 95p.
710097	25-37224	Dep. NTIS, 38p.
710194	25-37225	Dep. NTIS, 9p.
710222	25-37226	Dep. NTIS, 28p.
SC-M-		
70-549	25-37227	Dep. NTIS, 42p.
SC-R-		
713250	25-37228	Dep. NTIS, 21p.
SC-RR-		
70-406	25-35844	Dep. NTIS, 84p.
70-742	25-37229	Dep. NTIS, 85p.
710203	25-37230	Dep. NTIS, 110p.
710296	25-37231	Dep. NTIS, 100p.
SC-T-		
713030	25-37232	Dep. NTIS
713031	25-37233	Dep. NTIS
713035	25-37234	Dep. NTIS
SCL-DR-		
710032	25-37235	Dep. NTIS, 22p.
SGAE-PH-	(Austrian)	
104/1971	25-36735	Dep. NTIS (U. S. Sales Only), 31p.
SLAC-		
119	25-37236	Dep. NTIS, 122p.
130	25-36611	Dep. NTIS, 69p.
SM-	(Misc.)	
147/38	25-34843	See AECL-3804
SMU-	(Non-AEC)	
83-24	25-36588	See N-70-43042
SRARI-P-	(Russian)	
92	25-34558	Dep. NTIS (U. S. Sales Only), 20p.
94	25-34559	Dep. NTIS (U. S. Sales Only), 23p.
96	25-37140	Dep. NTIS (U. S. Sales Only), 16p.
SRD-	(Misc.)	
643-1	25-37237	Dep. NTIS, 35p.
STI/DOC-	(International Atomic Energy Agency)	
10/126	25-34725	IAEA $3.00
SU-	(Misc.)	
1206-241	25-36483	Dep. NTIS, 61p.
SZS-	(German)	

Report No.	Abstract No.	Availability
3/71 (pp 2-19)	25-34696	Dep. NTIS (U. S. Sales Only)
3/71 (pp 20-32)	25-34697	Dep. NTIS (U. S. Sales Only)
THAI.-AEC-	(Thai)	
36	25-34545	Dep. NTIS (U. S. Sales Only), 8p.
38	25-34546	Dep. NTIS (U. S. Sales Only), 15p.
TID-		
3525(Rev.5)(Suppl.6)	25-37047	Dep. NTIS, 63p.
4103(Suppl. 1)(Rev.2)	25-34779	DTIE Free
23762	25-36887	Dep. CFSTI, 20p.
23819	25-36888	Dep. CFSTI, 23p.
25689	25-34613	Dep. NTIS, 41p.
25690	25-36737	Dep. NTIS, 8p.
25696	25-35549	Dep. NTIS, 23p.
25705	25-34813	Dep. NTIS, 37p.
25713	25-36164	Dep. NTIS, 31p.
25714	25-37238	Dep. NTIS, 8p.
25720	25-37239	Dep. NTIS, 196p.
25723	25-37240	Dep. NTIS, 58p.
25726	25-36506	Dep. NTIS, 86p.
TODD-N-		
16	25-37070	Dep. NTIS, 50p.
18	25-37071	Dep. NTIS, 72p.
20	25-37072	Dep. NTIS, 47p.
21	25-37073	Dep. NTIS, 31p.
23	25-37074	Dep. NTIS, 53p.
24	25-37075	Dep. NTIS, 56p.
UARAEE-	(Egyptian)	
50	25-37008	Dep. NTIS (U. S. Sales Only), 34p.
52	25-37108	Dep. NTIS (U. S. Sales Only), 25p.
54	25-34780	Dep. NTIS (U. S. Sales Only), 45p.
55	25-35340	Dep. NTIS (U. S. Sales Only), 35p.
56	25-37116	Dep. NTIS (U. S. Sales Only), 40p.
58	25-37117	Dep. NTIS (U. S. Sales Only), 14p.
59	25-37076	Dep. NTIS (U. S. Sales Only), 22p.
60	25-36650	Dep. NTIS (U. S. Sales Only), 57p.
61	25-34919	Dep. NTIS (U. S. Sales Only), 55p.
62	25-37118	Dep. NTIS (U. S. Sales Only), 68p.
63	25-37077	Dep. NTIS (U. S. Sales Only), 76p.
64	25-37119	Dep. NTIS (U. S. Sales Only), 38p.
65	25-36127	Dep. NTIS (U. S. Sales Only), 42p.
66	25-37136	Dep. NTIS (U. S. Sales Only), 66p.
67	25-37078	Dep. NTIS (U. S. Sales Only), 52p.
68	25-34547	Dep. NTIS (U. S. Sales Only), 67p.
69	25-37120	Dep. NTIS (U. S. Sales Only), 13p.
70	25-37121	Dep. NTIS (U. S. Sales Only), 27p.
71	25-37079	Dep. NTIS (U. S. Sales Only), 15p.
72	25-35278	Dep. NTIS (U. S. Sales Only), 46p.
73	25-37080	Dep. NTIS (U. S. Sales Only), 54p.
75	25-37137	Dep. NTIS (U. S. Sales Only), 52p.
76	25-36612	Dep. NTIS (U. S. Sales Only), 17p.
78	25-36128	Dep. NTIS (U. S. Sales Only), 26p.
79	25-37122	Dep. NTIS (U. S. Sales Only), 28p.
80	25-37123	Dep. NTIS (U. S. Sales Only), 35p.
81	25-34793	Dep. NTIS (U. S. Sales Only), 50p.
82	25-34871	Dep. NTIS (U. S. Sales Only), 22p.
83	25-37081	Dep. NTIS (U. S. Sales Only), 24p.
84	25-37124	Dep. NTIS (U. S. Sales Only), 74p.
85	25-37125	Dep. NTIS (U. S. Sales Only), 23p.
86	25-36251	Dep. NTIS (U. S. Sales Only), 17p.
87	25-36613	Dep. NTIS (U. S. Sales Only), 28p.
88	25-36217	Dep. NTIS (U. S. Sales Only), 20p.
89	25-37126	Dep. NTIS (U. S. Sales Only), 55p.
90	25-37127	Dep. NTIS (U. S. Sales Only), 28p.
91	25-34920	Dep. NTIS (U. S. Sales Only), 25p.
92	25-36218	Dep. NTIS (U. S. Sales Only), 21p.
93	25-34921	Dep. NTIS (U. S. Sales Only), 24p.
94	25-37082	Dep. NTIS (U. S. Sales Only), 16p.
95	25-36091	Dep. NTIS (U. S. Sales Only), 21p.
96	25-37128	Dep. NTIS (U. S. Sales Only), 27p.
97	25-36219	Dep. NTIS (U. S. Sales Only), 38p.
98	25-36889	Dep. NTIS (U. S. Sales Only), 16p.
100	25-34922	Dep. NTIS (U. S. Sales Only), 37p.
101	25-36092	Dep. NTIS (U. S. Sales Only), 40p.
102	25-36129	Dep. NTIS (U. S. Sales Only), 26p.
103	25-36692	Dep. NTIS (U. S. Sales Only), 15p.
104	25-36252	Dep. NTIS (U. S. Sales Only), 20p.
105	25-37138	Dep. NTIS (U. S. Sales Only), 21p.
106	25-36117	Dep. NTIS (U. S. Sales Only), 40p.
107	25-36651	Dep. NTIS (U. S. Sales Only), 21p.
108	25-37083	Dep. NTIS (U. S. Sales Only), 35p.
110	25-37009	Dep. NTIS (U. S. Sales Only), 52p.
111	25-37084	Dep. NTIS (U. S. Sales Only), 16p.
UCID-		
30001	25-37241	Dep. NTIS, 34p.
30004	25-37242	Dep. NTIS, 11p.
UCLA-		
10-P-18-23	25-36738	Dep. NTIS, 195p.
34-P-172-2	25-37244	Dep. NTIS, 30p.
34-P-177-5	25-37245	Dep. NTIS, 10p.

XUM

Report No.	Abstract No.	Availability
34-P-102-27	25-37243	Dep. NTIS, 11p.
UCLA-ENG-		
7116	25-37244	See UCLA-34-P-172-2
UCRL-		
19861	25-37245	Dep. NTIS, 21p.
20099	25-35855	Dep. NTIS, 26p.
20264	25-36385	Dep. NTIS, 109p.
20295	25-36661	Dep. NTIS, 18p.
20299	25-36514	Dep. NTIS, 25p.
20476	25-34923	Dep. NTIS, 22p.
20528	25-37247	
20535	25-37248	Dep. NTIS, 19p.
20538	25-37249	Dep. NTIS, 44p.
20541	25-37250	Dep. NTIS, 52p.
20632	25-36391	Dep. NTIS, 109p.
20659	25-37251	Dep. NTIS, 69p.
20667	25-37252	Dep. NTIS, 11p.
20699	25-34872	Dep. NTIS, 9p.
50007-70-3	25-34873	Dep. NTIS, 16p.
50962	25-35341	Dep. NTIS, 71p.
50987	25-34769	Dep. NTIS, 62p.
50993	25-34770	Dep. NTIS, 24p.
51009	25-36270	Dep. NTIS, 93p.
51010	25-35939	Dep. NTIS, 40p.
51030	25-36165	Dep. NTIS, 112p.
51035	25-35342	Dep. NTIS, 203p.
51042	25-36194	Dep. NTIS, 115p.
72637	25-37253	Dep. NTIS, 4p.
72694	25-37254	Dep. NTIS, 4p.
72927	25-34727	Dep. NTIS, 12p.
73030	25-36195	Dep. NTIS, 9p.
73031	25-36196	Dep. NTIS, 18p.
73047	25-36197	Dep. NTIS, 5p.
73059	25-36198	Dep. NTIS, 13p.
73060	25-36199	Dep. NTIS, 19p.
73067	25-36200	Dep. NTIS, 11p.
73090	25-36739	Dep. NTIS, 9p.
73106	25-37255	Dep. NTIS, 8p.
73129	25-36201	Dep. NTIS, 27p.
73135	25-36155	Dep. NTIS, 30p.
UCRL-Trans-		
1434	25-36615	Dep. NTIS
1440	25-36616	Dep. NTIS
1443	25-36617	Dep. NTIS
10530	25-37256	Dep. NTIS
10531	25-37257	Dep. NTIS

Report No.	Abstract No.	Availability
UCSD-		
10-P-10-78	25-36420	Dep. NTIS, 11p.
UJV-	(Czechoslovakian)	
2291-Ch	25-34698	NTIS (U. S. Sales Only), 67p.
2390-RT	25-37007	For translation see ORNL-tr-2470
2423-RF	25-37109	NTIS (U. S. Sales Only), 36p.
UR-		
49-1211	25-35211	Health Phys.; 20: 179-85(Feb 1971)
49-1430	25-37258	Dep. NTIS, 71p.
USC-		
113-P-21-3	25-34639	Dep. NTIS, 46p.
USGS-		
474-101	25-34728	Dep. NTIS, 14p.
WAI-TR-		
70.5/AEC	25-35549	See TID-25696
WANL-TME-	(Non-AEC)	
1857	25-35343	Dep. NTIS, 44p.
WAPD-MRP-		
135	25-36890	Dep. NTIS, 18p.
WAPD-T-		
2411	25-36740	Dep. NTIS, 21p.
WAPD-TM-	(Misc.)	
991	25-36652	Dep. NTIS, 28p.
WARD-		
4181-2	25-36693	Dep. NTIS, 18p.
WCAP-	(Misc.)	
7562-3	25-34924	Dep. NTIS, 10p.
7669	25-36995	
7671	25-37010	
WHAN-SA-		
76	25-37020	Dep. NTIS, 18p.
104(Rev.)	25-37085	Dep. NTIS, 21p.
107	25-36741	Dep. NTIS, 10p.
Y-		
1788	25-35344	Dep. NTIS, 105p.
ZJE-	(Czechslovakian)	
99	25-35505	Dep. NTIS (U. S. Sales Only), 31p.

☆U. S. GOVERNMENT PRINTING OFFICE: 1971—745-058/2

XUM

UNITED STATES
GOVERNMENT PRINTING OFFICE

UNITED STATES
ATOMIC ENERGY COMMISSION
P. O. BOX 62
OAK RIDGE, TENNESSEE 37830

OFFICIAL BUSINESS

POSTAGE AND FEES PAID
U. S. ATOMIC ENERGY COMMISSION

POSTAGE AND FEES PAID
U. S. GOVERNMENT PRINTING OFFICE

UNIVERSITY MICROFILMS
SERIAL PUBLICATIONS
300 NORTH ZEEB ROAD
ANN ARBOR MICHIGAN 48106

Recent USAEC publication of special interest

TRANSPLUTONIUM ELEMENTS—A Bibliography

Prepared by Charles E. Stuber

This bibliography comprises 557 references and abstracts to the international literature compiled since the last supplement and through the period ending June 30, 1970.

Part I includes 501 references dealing with the production and chemical, nuclear, and physical properties of the elements with $Z \geqslant 95$. The references in this part are grouped by element and arranged chronologically within each group. References dealing with elements $Z \geqslant 104$ are grouped together under Transactinide Elements.

Part II includes 56 references dealing with the natural occurrence of the transplutonium elements. This collection of references discussing attempts to locate or prove the existence of the transplutonium elements in nature is also arranged chronologically.

An author and subject index are included.

Available as TID-3317(Suppl.2) for $3.00 from:

National Technical Information Service
U. S. Department of Commerce
Springfield, Virginia 22151

XUM

XUM